

## REVIEW OF METHODS FOR THE DETERMINATION OF LANTHANIDES IN GEOLOGICAL SAMPLES

CHIRAN J. KANTIPULY

Department of Earth Sciences, Memorial University of Newfoundland, St. John's, Newfoundland,  
Canada A1B 3X7

ALAN D. WESTLAND

Department of Chemistry, University of Ottawa, Ottawa, Ontario, Canada

(Received 5 December 1986. Revised 14 May 1987. Accepted 5 September 1987)

**Summary**—The following methods of determining lanthanides in geological samples are reviewed, together with the separation techniques necessarily associated with them: neutron-activation analysis, atomic-absorption and flame-emission spectrometry, plasma-source emission spectrometry, mass spectrometry, X-ray fluorescence spectrometry, and spectrophotometry.

The determination of lanthanides in geological samples is one of the most difficult and complicated analytical tasks, especially at trace levels, because of the similarity of their chemical behaviour. The elements which are frequently encountered in rock analysis are classified geochemically in Fig. 1. Those primarily associated with oxygen are termed lithophiles and the lanthanides fall into this group. Lithophilic ions have rare-gas electronic structures and consequently are not readily polarized. Secondary differentiation is influenced by the relative size of the cations, the bonding tendencies of the elements, fractional crystallization from the magma, and the densities of the compounds formed. The *f*-series metals in their usual oxidation states are bonded mainly to highly electronegative elements, usually oxygen or fluorine.

Knowledge of the fundamental laws governing the distribution and redistribution of elements during metamorphic processes, *etc.*, enables geochemists to predict the probability of the occurrence of economically interesting minerals in a particular geological environment. Particular interest is attached to the mineralization processes occurring during alteration of the rock by hydrothermal action.

In the study of ore deposits, as well as in petrology, the distribution of trace elements casts light on the genesis of ore bodies. The rare-earth elements (REE), because of their similarities, serve as a particularly suitable group of indicator elements. The determination of REE in other materials is also of interest. The presence of trace quantities of REE in high-purity metals, semiconductors and glasses has an important influence on the electrical, magnetic, mechanical, nuclear and optical properties. The mechanism of lanthanide leaching and migration is well established in the geochemical literature.<sup>1-5</sup> The light

lanthanide ions are materially larger than those of the heavy lanthanides and tend to be excluded from common rock-forming minerals during the processes of crystallization. It follows that the hydrothermal alteration of a rock may result in a change in the ratio of lighter to heavier lanthanides.

The equilibria between the solid and fluid phases will be affected by the presence of complexing species such as  $\text{Cl}^-$ ,  $\text{F}^-$ ,  $\text{CO}_3^{2-}$  and  $\text{PO}_4^{3-}$  ions, for example. The movement of the fluid phase within the geological structure will cause a displacement, not only of the REE but of all dissolved species, many of which may be metallic elements of commercial significance, *e.g.*, Cu, Pb, Au, Mo. Rational strategies of prospecting for micas, molybdenite, zircon, niobium-tantalum and lithium minerals, beryl, spinels and tourmalines, to name but a few species of interest, may depend in future on the techniques of analysis for REE.

The foundations of the classical analytical scheme for the determination of all the major elements were laid in the 19th century. By 1920, two notable textbooks on rock analysis had been published.<sup>6,7</sup> The methods described are now regarded as too time-consuming, and since about 1950 various "rapid" analytical schemes have been proposed as alternatives.<sup>8-13</sup> Interest in the minor components of silicate rocks has continued almost uninterrupted to the present day, with current work emphasizing determination of elements at below the  $\mu\text{g/g}$  (ppm) level.

To meet current geochemical requirements, multi-element analytical tools are required. The introduction of optical emission spectroscopy by Goldschmidt was followed by X-ray fluorescence and neutron-activation methods. The newest development is the use of an induced or directly coupled plasma for optical emission spectrometry and mass

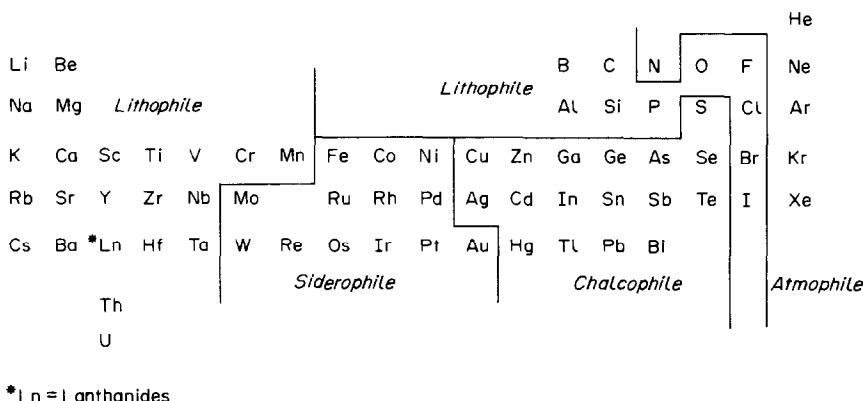


Fig. 1. Geochemical classification of the elements. Some elements display more than one type of behaviour. \*Ln = lanthanides. (Reproduced, by permission, from J. F. Ferguson, *Inorganic Chemistry and the Earth*, p. 20. Pergamon Press, Oxford, 1982.)

spectrometry. In general, these methods permit the detection of elements at below the ppm level. Classical spectrophotometers and atomic-absorption instruments have been much used for single-element determinations. Unfortunately, these instrumental methods suffer more or less from matrix or inter element interference effects, which restricts their applicability in some cases, and requires use of separation techniques. The need for and importance of separation techniques will be made evident in the next section where the matrix effects involved in neutron activation, emission spectrometry, X-ray fluorescence and spectrophotometric methods will be briefly discussed.

#### NEUTRON ACTIVATION ANALYSIS (NAA)

Neutron activation is among the most sensitive techniques for determination of the REE. The sample is irradiated with a flux of thermal neutrons, generally in a nuclear reactor. The constituent elements absorb neutrons, forming artificial radionuclides, the radioactivity spectrum of which is measured and interpreted in terms of the amounts of the various elements present. An advantage of this technique is that the detection limits can be fixed by the analyst through choice of neutron flux and irradiation time. Furthermore, multielement determinations can be performed on a single aliquot of sample without chemical separations. This is termed non-destructive instrumental neutron-activation analysis (INAA). For multielement  $\gamma$ -ray measurements, a high-resolution detector of the Ge(Li) type is used in combination with a multichannel analyser.

Geochemists have applied NAA to REE determination.<sup>14-18</sup> De Soete *et al.*<sup>19</sup> have provided a detailed discussion of all aspects of neutron activation.

The multicomparator method is used for precise work. In this method, standards containing known amounts of the element of interest are irradiated along with the samples and the induced activity is measured under the same conditions. If the matrix

elements have high absorption cross-sections, errors may arise from self-shielding effects. This type of error can be avoided by irradiating a sufficiently dilute sample or by prior separation of the elements having high absorption cross-sections. Gadolinium, for example, has the largest neutron absorption cross-section ( $4.9 \times 10^4$  barns), which results in an average neutron attenuation of 1% in a sphere of  $Gd_2O_3$  with a radius of  $0.12 \mu m$  and a mass of only  $5 \times 10^{-14}$  g. Massart and Hoste<sup>20</sup> determined Lu in a 50-mg sample of gadolinite by dissolving the sample and irradiating an aliquot of chemically separated REE solution. Turkstra and Van Droogenbroeck<sup>21</sup> reduced the effect of self-shielding in lanthanide-rich carbonatites by diluting the powdered sample with pure quartz.

The sample usually becomes highly radioactive upon irradiation and in such cases the post-irradiation treatment has to be performed with great care behind proper shielding. The  $\gamma$ -ray spectra of irradiated rock samples may be dominated by isotopes of Mn, Na, Sc, Fe, Co *etc.* from the matrix material, which swamp the  $\gamma$ -ray spectra of the REE.<sup>22</sup> The nuclide of interest may be formed by competing nuclear reactions such as (n, p), (n,  $\alpha$ ) and (n, f). For a given nuclide, of course, the  $\gamma$ -ray spectrometer cannot distinguish between the nuclei produced from the analyte of interest and those produced from interfering elements by the competing reactions.<sup>23,24</sup>

Some of the important interferences in instrumental neutron activation analysis are given in Table 1. Boynton<sup>25</sup> and Berezna<sup>26</sup> have discussed other types of interference. Among the light REE group, the nuclides that are suitable for INAA may also be formed as uranium fission products, and may be detected even when La, Ce, Nd and Sm are totally absent from the original sample. The presence of uranium in a sample enhances the values of La, Ce, Nd and Sm determined by INAA if appropriate corrections are not made for the interference. Recently, Ila *et al.*<sup>27</sup> reported that in a 5-hr irradiation,

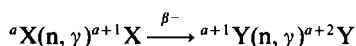


Table 1. Interferences in the NAA determination of lanthanides

Parent isotope	Product isotope	Half-life	Analytical $\gamma$ -ray, keV	Interferences to be considered for various reasons, ( $\gamma$ -ray, keV)
$^{45}\text{Sc}$	$^{46}\text{Sc}$	83.8 d	889.26	$^{160}\text{Tb}$ (879.4); $^{110\text{m}}\text{Ag}$ (884.7) $^{192}\text{Ir}$ (884.5); $^{46}\text{Ti}$ (n, p) $^{46}\text{Sc}$
$^{139}\text{La}$	$^{140}\text{La}$	40.22 hr	328.8; 1596.4	$^{235}\text{U}$ (n, f); $^{24}\text{Na}$ ; $^{239}\text{Np}$ (334.3)
$^{140}\text{Ce}$	$^{141}\text{Ce}$	32.4 d	145.4	$^{235}\text{U}$ (n, f); $^{59}\text{Fe}$ (142.4); $^{175}\text{Yb}$ (144.8) $^{133}\text{Pa}$ (145.4); $^{182}\text{Ta}$ (152.4)
$^{146}\text{Nd}$	$^{147}\text{Nd}$	10.98 d	91.03; 531.4	$^{235}\text{U}$ (n, f); $^{169}\text{Yb}$ (93.6); $^{140}\text{Ba}$ (537.2)
$^{152}\text{Sm}$	$^{153}\text{Sm}$	46.44 hr	103.2	$^{235}\text{U}$ (n, f); $^{239}\text{Np}$ (99.6, 103.8) $^{153}\text{Gd}$ (103.2); $^{182}\text{Ta}$ (100.1)
$^{151}\text{Eu}$	$^{152}\text{Eu}$	13.2 y	121.78 1408.02	$^{169}\text{Yb}$ (118.2, 130.53); $^{133}\text{Ba}$ (123.7) $^{134}\text{Cs}$ (1400.4)
$^{174}\text{Yb}$	$^{175}\text{Yb}$	101 hr	396.32	$^{233}\text{Pa}$ (398.5); $^{160}\text{Tb}$ (392.5); $^{131}\text{Ba}$ (404.3)
$^{176}\text{Lu}$	$^{177}\text{Lu}$	6.71 d	208.4	$^{239}\text{Np}$ (209.8); $^{131}\text{Ba}$ (216)

1 mg of uranium was found to be equivalent to 0.28 mg of Ce and 0.23 mg of Nd. Uranium, therefore, must be separated when REE are determined in uranium-rich minerals or ores.

Another type of interfering nuclear reaction is the second order interference, for example of the type



Interferences of this kind have been examined by Op de Beeck.<sup>28</sup> In cases where the nuclide  ${}^a\text{X}$  has a large activation cross-section, appreciable difficulties are encountered if trace amounts of the element Y are to be determined in a sample of element X by means of the radioisotope  ${}^{a+2}\text{Y}$ . If, for example, a dysprosium sample is irradiated for 22 hr at a flux of  $5 \times 10^{12}$  n. cm<sup>-2</sup>. sec<sup>-1</sup> for the determination of holmium, the  $^{166}\text{Ho}$  produced would interfere in the determination of the native holmium. Consequently this type of interference can be serious in cases where an element is to be determined in a matrix of an adjacent element.

Mosen *et al.*<sup>29</sup> and Haskin *et al.*<sup>30</sup> reported obtaining accurate results for many analyses in which the individual radionuclides were separated by ion-exchange. Their procedures are very laborious compared with the purely instrumental method of NAA. The use of lithium-drifted germanium detectors further eliminates many of the interferences.<sup>22</sup>

Melson<sup>31</sup> compared rock analyses by INAA with analyses that incorporated a radiochemical group-separation and concluded that the two methods gave essentially the same results. However, improved methods have subsequently appeared and it is evident that separation of the REE in one or more groups leads to better precision and accuracy, with errors approaching  $\pm 5\%$  or better.<sup>32-35</sup> Some authors point out that the chemical yield in precipitating REE varies widely between the various elements. Time-consuming re-irradiation of the carriers is required in order to determine the chemical yields accurately.

The simplicity of the instrumental method is very attractive but it should be emphasized that its accuracy is very dependent on the composition of the

sample. Moreover, the non-destructive technique has poorer sensitivities. A group-separation, whether based on classical or modern methods, is very desirable in order to improve the sensitivity, accuracy and confidence in the results. It may be desirable or necessary to analyse 5–10 g of sample. A chemical concentration process would then be required.

#### Separation methods

The procedures used for the separation of the REE as a group from the interfering elements have in most cases been based on classical hydroxide-fluoride or hydroxide-oxalate precipitation cycles with carriers. These procedures can be applied either before or after irradiation of the sample. A commonly used separation procedure for the REE includes the following steps.

(i) Fusion of an irradiated sample in a nickel or zirconium crucible with sodium peroxide and hydroxide in the presence of REE carriers.

(ii) Dissolution of the fusion cake with water or dilute acid.

(iii) Addition of sodium hydroxide or ammonia to precipitate REE hydroxides.

(iv) Separation of iron by extraction with diisopropyl ether from hydrochloric acid medium.

(v) Separation of scandium.

Separation of scandium is an important part of the scheme, because its isotopes have strong  $\gamma$ -ray peaks which may interfere with REE peaks. Scandium can be removed either by diethyl ether extraction in the presence of ammonium thiocyanate or by precipitating the REE fluorides, separating the precipitate by centrifugation, dissolving it in a mixture of boric acid and nitric acid, and precipitating the lanthanides as hydroxides with ammonia.<sup>29</sup> This procedure is repeated 2 or 3 times, since only about 50–80% of the scandium is separated each time. The final hydroxide precipitate is dissolved in dilute hydrochloric acid and used for  $\gamma$ -ray measurement.

Yttrium is usually not determined along with the separated lanthanides, because it lacks suitable  $\gamma$ -ray peaks. However, Steines<sup>36</sup> reported that it may be

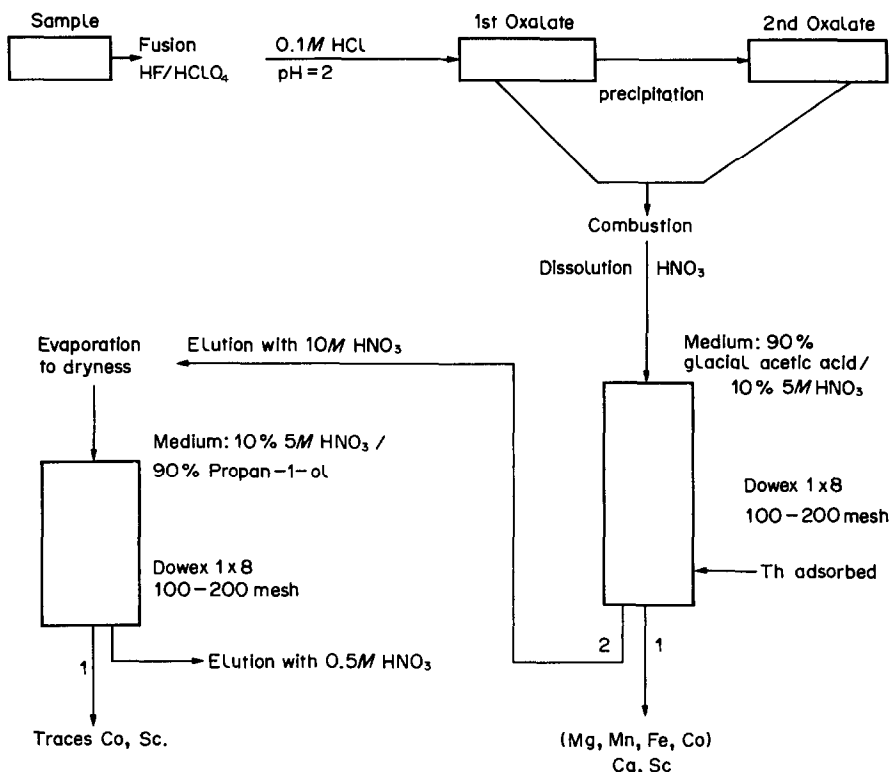


Fig. 2. Flow diagram of the pre-irradiation separation of REE from a silicate matrix.<sup>41</sup>

determined by  $\beta$ -counting of the isolated lanthanides plus yttrium fraction, but corrections for lanthanide interferences are required.

Before the advent of Ge(Li) detectors, methods based on group-separation and subsequent chromatographic separations had to be used in order to obtain reliable data for many REE simultaneously. Separations based on elution from a cation-exchange column with a suitable complexing agent have been the most popular.<sup>28</sup> Other types of separation such as anion-exchange in the presence of EDTA<sup>37</sup> and anion-exchange in mixed solvents<sup>38,39</sup> have also been used.

Separation of the REE from the matrix before irradiation is fairly uncommon in activation analysis, but is gaining popularity with the introduction of reversed-phase chromatography in inorganic analysis. In the determination of rare-earth impurities in metallic uranium, the interference due to bulk uranium has been suppressed by passing the sample through a cation-exchange column before irradiation.<sup>40</sup> The method developed by Klein<sup>41</sup> is based on digestion of the sample with hydrofluoric acid and perchloric acid, and double precipitation of the REE as oxalates to separate them from traces of Mg, Mn, Fe and Co. The REE are then separated from Sc, Th and the carrier by simple ion-exchange operations. The scheme is shown in Fig. 2.

In this type of chemical separation before activation, a blank should always be carried through the

procedure. A blank problem does not occur with post-irradiation separations. Finally, it should be mentioned that the neutron-activation technique is highly sensitive for the REE. It can be successfully employed for the determination of extremely low concentrations of REE in various natural samples when combined with chemical separations that increase the sensitivity and reduce interference.

## SPECTROCHEMICAL ANALYSIS

### Atomic absorption and flame emission

Optical emission spectrometry is the oldest instrumental method known for analysis of terrestrial matter. In principle, a minute quantity of sample is vaporized and excited sufficiently for it to emit light. The intensity of emitted radiation is measured and related to the elemental concentration. Excitation may be achieved in several ways. The classical arc and spark sources as well as glow discharges have been thoroughly reviewed by Barnes.<sup>42-44</sup> These methods have been widely used and will not be further dealt with here.

A nitrous oxide-acetylene flame with a solution nebulizer attachment has been used to determine scandium, yttrium and the lanthanides by emission spectrometry.<sup>45</sup> Spectra obtained with this excitation system are relatively simple and give much better selectivity than arc and spark source spectrometry. Inter-element interferences are eliminated in all cases

by choice of appropriate wavelengths. Greater sensitivity is achieved when the metals are converted into perchlorates and these are taken up in ethanol instead of water. Ooghe and Verbeek<sup>46</sup> have determined all the lanthanides except Ce and Pm by atomic-absorption spectrometry (AAS). They obtained good sensitivity by employing 80% methanol solutions and adding sodium or potassium chloride to suppress ionization. The method was applied to bastnasite, monazite and gadinolite. It is fortunate that the elements for which AAS is least sensitive, *e.g.*, La and Nd, are those that are more abundant in most natural samples. On the whole, however, AAS methods for the REE are less sensitive than for the majority of metals.

Van Loon *et al.*<sup>47</sup> have determined Y, Eu and elements 65–71 in minerals by AAS with aqueous sample solutions. The lowest values determined were *ca.* 0.05%. They pointed out that determination of Lu, Tb and Dy was not as sensitive as by X-ray fluorescence. Sen Gupta<sup>48,49</sup> used ethanol sample solutions and determined the more sensitive REE, Y, Nd and elements 66–70 by AAS, and La, Pr, Sm and Dy by flame emission. Microsample injection afforded a sensitivity comparable with that of electrothermal vaporization. Good results were obtained with seven standard samples, and in one of these, SY-2, the concentrations of some REE, *e.g.*, Eu, were less than 10  $\mu\text{g/g}$ .

Electrothermal vaporization from a tantalum-lined furnace has been recommended.<sup>50</sup> Both foil and sputtered tantalum have been used. The use of such a furnace improves the sensitivity and lessens memory effects. By this means, and by incorporating isolation of the REE by ion-exchange, Sen Gupta<sup>51</sup> achieved 10–40 times better sensitivity than with the simple graphite furnace applied directly. These sensitivities compared well with those achieved by NAA. Papp<sup>52</sup> has used a graphite furnace as a source for emission spectrometry.

#### *Plasma source emission spectrometry*

Electrically generated plasma sources for spectrochemical analysis are currently the subject of vigorous investigation and are being applied to the analysis of geological materials for a large variety of trace elements.

A plasma is any luminous volume of gaseous mixture in which a significant fraction of the atomic or molecular species is present as ions. There are three types of inert-gas electrical plasma sources now available, differing in the number of electrodes which are necessary to sustain the plasma.

(1) Direct-coupled argon plasma jet (DCP) with 2 or 3 electrodes.<sup>53</sup>

(2) Microwave-induced plasma (single electrode),<sup>53–55</sup> which is not widely used.

(3) Inductively-coupled torches (ICP) which are electrodeless.<sup>56,57</sup>

Inductively-coupled plasma atomic-emission spectroscopy (ICP–AES) is becoming increasingly popular. When the plasma is generated in argon, the method is sometimes designated as ICAP–AES. Mass spectrometry with a plasma source is referred to as ICP–MS.

The plasma methods provide some of the most useful and specific means for the determination of the REE elements at trace levels. Even though the chemical properties of the various lanthanides are very similar, the spectra of these elements are just as unique as those of other elements. Direct excitation of the sample with ICP or DCP provides good detectability, precision and accuracy, if the sample is sufficiently pure. Because the physical properties of these plasmas offer excellent performance and operational advantages over arc and spark emission sources, most geochemical laboratories and many others appear to favour either ICP or DCP.

In general, environmental and geochemical samples provide diverse matrices that are exceptionally complex, both chemically and physically.<sup>52</sup> The complexity of such samples raises the possibility that interelement effects of various types or spectral interferences may introduce errors in the determination of REE. Some possible interferences are listed in Table 2.

An electrical plasma is an efficient excitation source. As a consequence, all types of plasma atomic emission can be affected by many interference problems. The most significant of these are spectral interferences resulting from stray or scattered light, broad-band continuum emission, broadened matrix-element lines and direct spectral overlap. It is possible to eliminate or minimize these interferences in several ways. One involves the use of a high-dispersion, high-resolution monochromator.<sup>58,59</sup> The echelle monochromator has more than enough resolution to provide reliable determinations when there are cases of suspected interference.<sup>58</sup> The resolution and dispersion available allow a high degree of line-isolation and the effect of broad-band background radiation is minimized. However, high resolution alone cannot alleviate every kind of spectral interference. Broadening of spectral lines in electrical plasmas can occur to such an extent that some very close pairs of lines are not inherently resolvable. In some cases, alkali-metals, alkaline-earth metals, Al, Ti, Si, W, Mn, Fe and other matrix components can be so abundant that they cause significant background signals and in some instances direct spectral overlap (Table 2). In such a case the operator must select a line different from the usual one for the element of interest.

Enhancement of spectral lines by matrix constituents has been reported to occur in DC plasma jets. This effect is most likely to occur in cases in which easily ionizable elements are present in large concentration. In such situations, it is advisable to use some form of matrix-matching or matrix buffering, *e.g.*, addition of lithium or strontium to all solutions. The

Table 2. Interference data for DCP

Analyte element	Sensitive wavelength,* nm	Equivalent analyte concentration given by 100 mg/l. matrix element, mg/l.										
		Al	Ca	Fe	Mg	Ti	W	Th	U	V	Nd	La
La	408.672	0.008	0.1	0.01	0.005	—	—	—	—	—	—	—
Ce	418.660	0.06	0.3	0.1	—	—	0.3	—	2	—	—	—
Pr	440.882	0.01	0.3	0.06	0.03	—	—	4	—	8	3	2
Nd	430.538	0.04	0.4	0.05	—	—	—	1	—	—	—	—
Sm	443.432	0.06	0.9	0.05	0.01	—	—	1	—	—	2	2
Eu	381.967	—	0.02	0.01	—	—	—	0.02	—	0.03	3	—
Gd	364.619	0.008	0.02	0.4	0.02	0.2	0.4	0.5	2	—	—	0.2
Tb	367.635	—	0.04	0.1	—	0.2	0.1	3	3	0.9	—	—
Dy	353.173	—	0.008	0.01	0.1	—	—	0.3	0.3	—	—	—
Ho	404.544	0.03	0.3	1	0.02	—	2	—	—	—	—	—
Er	369.265	0.02	0.03	0.06	0.01	—	—	0.4	0.7	0.1	—	—
Tm	313.126	0.01	0.007	0.005	0.005	0.3	—	—	—	—	—	—
Yb	328.937	0.001	0.002	0.02	0.002	0.4	—	—	—	3	—	—
Lu	261.542	—	—	0.07	—	—	2	—	—	—	—	—

\*The following wavelengths, although less sensitive than those listed above, are relatively free from interferences: La 398.852; Nd 430.36; Pr 422.29; Sm 442.26; Ho 345.60; Yb 398.80.

most satisfactory method is to isolate the analytes of interest from the matrix by some kind of effective separation. A recent examination<sup>60</sup> of the application of DCP excitation to a wide selection of geological standard samples provides a good demonstration of the power and accuracy of a multielement DCP facility. Examination of the literature shows that direct-coupled plasma jets have not been studied as thoroughly as other types of emission sources. They are nevertheless being used in many laboratories to provide reliable atomic-emission analyses for a wide variety of sample constituents.

#### Mass spectrometry

Mass spectrometry is based on the separation of charged particles according to their mass/charge ratio. During the past few years, it has gained increasing significance for earth scientists, especially after spark-source mass spectrometry for geological samples was pioneered by Taylor.<sup>61,62</sup> Jackson and Strasheim<sup>63</sup> have applied the technique to geological samples.

Since the inductively-coupled argon plasma offers performance and operational advantages over arc and spark sources, a new instrument was evolved that combines ICP with a quadrupole mass spectrometer (ICP-MS). There are two principal advantages to ICP-MS; the spectra are simple to interpret and largely free from interelement interferences, and information on isotopic abundances is inherent in the method. The method is extremely useful as most of the elements in the periodic table can be detected. Although the limits of determination by ICP-MS cluster around the chondritic levels for the REE,<sup>64</sup> a preconcentration step or separation of REE into at least two groups is still desirable. The principal interferences are those due to isotopic mass overlaps, or isobaric interferences, which, being predictable from isotopic abundance tables, can easily be corrected for. Mass interferences may also arise from

other species that are present in the plasma or formed during the ion extraction stage. These include diatomic oxides, doubly-charged ions, and hydroxides or other molecular species, depending on the sample history.<sup>65</sup> The formation of these species appears to be inherent in the ICP-MS technique. They may not be eliminated despite control of the operating conditions. In addition, reagent salts dissolved in the sample solution may cause suppression of signal intensity. Although it is apparent that the presence of the easily ionized alkali-metal atoms may suppress the concentration of positive ions of the elements, a full understanding of the interferences is lacking.<sup>66</sup> Computational procedures for applying corrections for interelement interferences in spark-source mass spectrometry have been described by Bacon and Ure.<sup>67</sup>

Doherty and Vander Voet<sup>68</sup> have applied similar data-processing techniques in the ICP-MS determination of REE and yttrium in geological materials. At the Department of Earth Sciences we have recently employed ICP-MS for the determination of REE.<sup>69</sup> Although overlaps of isotopes exist in certain cases, an isotope without overlap can be found for each element. However, a more serious problem arises from the light REE forming molecular monoxide ions that cause interference in the determination of the less abundant heavy REE. The interferences are given in Table 3.

Existing ICP-source mass spectrometers exhibit problems of stability, and therefore, reproducibility. They lend themselves well to isotope dilution analysis, however, for in this technique stability is required only over a very short time scale. The use of the isotopic dilution technique has been demonstrated for geological samples, including USGS standard rocks.<sup>70,71</sup> This technique is more time-consuming, however, because the REE must be separated into two or more groups to reduce interferences, and Pr, Tb, Ho and Tm cannot be deter-

Table 3. Interference in ICP-MS

Nuclide	Abundance, %	Oxide interference
<sup>133</sup> Cs	100.00	<sup>117</sup> SnO
<sup>137</sup> Ba	11.23	<sup>121</sup> SbO
<sup>139</sup> La	99.91	<sup>123</sup> SbO
<sup>140</sup> Ce	88.48	<sup>124</sup> SnO
<sup>141</sup> Pr	100.00	<sup>125</sup> TeO
<sup>145</sup> Nd	8.30	
<sup>147</sup> Sm	15.00	
<sup>151</sup> Eu	47.8	<sup>135</sup> BaO
<sup>157</sup> Gd	15.65	<sup>141</sup> PrO
<sup>159</sup> Tb	100.00	<sup>143</sup> NdO
<sup>163</sup> Dy	24.9	<sup>147</sup> SmO
<sup>165</sup> Ho	100.00	<sup>149</sup> SmO
<sup>167</sup> Er	22.95	<sup>151</sup> EuO
<sup>169</sup> Tm	100.00	<sup>153</sup> EuO
<sup>173</sup> Yb	16.12	<sup>157</sup> GdO
<sup>175</sup> Lu	97.40	<sup>159</sup> TbO

mined, because they each possess only one stable isotope. In spite of these limitations, it is recommended as the method of choice when highly accurate data are required.

#### *Separation techniques applied in plasma source methods*

Since the REE are present in certain rock samples at or below  $\mu\text{g/g}$  levels, separation of these elements as a group should ordinarily be incorporated in the analysis. This separation not only allows for preconcentration of the REE so that lower detection limits are possible, but also simplifies the analytical problem of interference from matrix elements when geological samples of widely varying composition are encountered.

As described in the section on NAA, numerous types of separation of the REE from a matrix can be found in the literature. In most cases, ion-exchange, extraction and precipitation are suggested.<sup>46,48,72,73</sup> One of the most common techniques is to concentrate the REE with the aid of a carrier. Yttrium has been used by Hettel and Fassel<sup>74</sup> as a carrier because its ionic radius is about the same as that of  $\text{Dy}^{3+}$  and  $\text{Ho}^{3+}$ , so in chemical properties yttrium closely resembles the lanthanides. Its emission spectrum is relatively simple, so the detection limits are not affected by interfering matrix lines. Furthermore, any separation scheme devised can easily be monitored by a radioactive tracer, <sup>90</sup>Y, which is a  $\beta$ -emitter easily obtained from <sup>90</sup>Sr. It is essential to obtain a very pure supply of yttrium so as to maintain low blank values. Elements other than the lanthanides, such as calcium and aluminium, have also been used as carriers,<sup>68</sup> particularly for precipitation separations.<sup>75</sup>

Meloni *et al.*<sup>76</sup> compared carrier precipitation of REE as fluorides with cation-exchange separation. Although the chemical yields of the precipitations were inferior to the ion-exchange recoveries, the reproducibilities were superior. Buchanan and Dale<sup>77</sup> reported good results from the use of yttrium, which

served also as an internal standard. Denechaud *et al.*<sup>33</sup> believe that no single element is a quantitative carrier for all the REE. It would seem that proven methods that do not entail precipitations are to be preferred in general.

A consecutive cation- and anion-exchange separation and preconditioning scheme for the analysis of geological samples has been described by Crock and Lichte.<sup>78</sup> The method involves a low-temperature multi-acid digestion with hydrofluoric, nitric and perchloric acids. If resistant minerals such as zircon are present, a lithium metaborate fusion is used. It is claimed that the procedure minimizes interelement corrections, if not totally eliminate them. Separation of scandium from the lanthanides was not discussed, however. The procedure was applied successfully to trace analysis of certified standard geological samples for the lanthanides and yttrium. In the case of siliceous samples, silicon can be completely removed from the matrix, permitting the use of somewhat larger samples. A study of the ion-exchange procedures indicated that the recoveries of the REE were essentially quantitative and that nitric acid was a better eluent than hydrochloric acid.<sup>79</sup> Brenner *et al.* omitted the anion-exchange step.<sup>79a</sup> Yoshida and Haraguchi<sup>80</sup> employed HPLC to separate individual REE prior to determination by ICP-AES. Ammonium lactate was used to develop the chromatograms as it did not cause difficulties with the operation of the torch. The retention times of copper, zinc, nickel, sodium, potassium and lead were close to those of some of the REE. However, interferences were slight or negligible in the analysis of a standard rock sample.

The use of a phosphonate-type ion-exchanger is recommended for separating REE from other ions of significantly different radius and charge.<sup>81</sup> The phosphonate binds strongly only to large ions with multiple charges, especially lanthanides and actinides. A  $5 \times 1$  cm column packed with phenylated Kel-F powder impregnated with 2-ethylhexylphenylphosphonic acid and conditioned with 0.1M perchloric acid is used to isolate the REE as a group from the matrix elements and the REE are then determined by DC plasma emission spectroscopy. The flow-sheet for the separation of the REE is shown in Fig. 3.

In the determination of trace REE, Th, U, Zr, and Hf in certain geological materials, it is essential that the samples be completely dissolved, as current methods involving a plasma source require solution nebulization. This presents no unusual problems if the material is completely soluble in acids, but if it is necessary to resort to fusion, as in the case of tourmalines, zircon, chromite, cassiterite and other minerals, the added salt should be removed from the sample after fusion. Large quantities of added salt cause depression of the analyte signal intensity, clogging of the nebulizer, deposition on the orifice of the sampler and drift in the analyte signal. Several

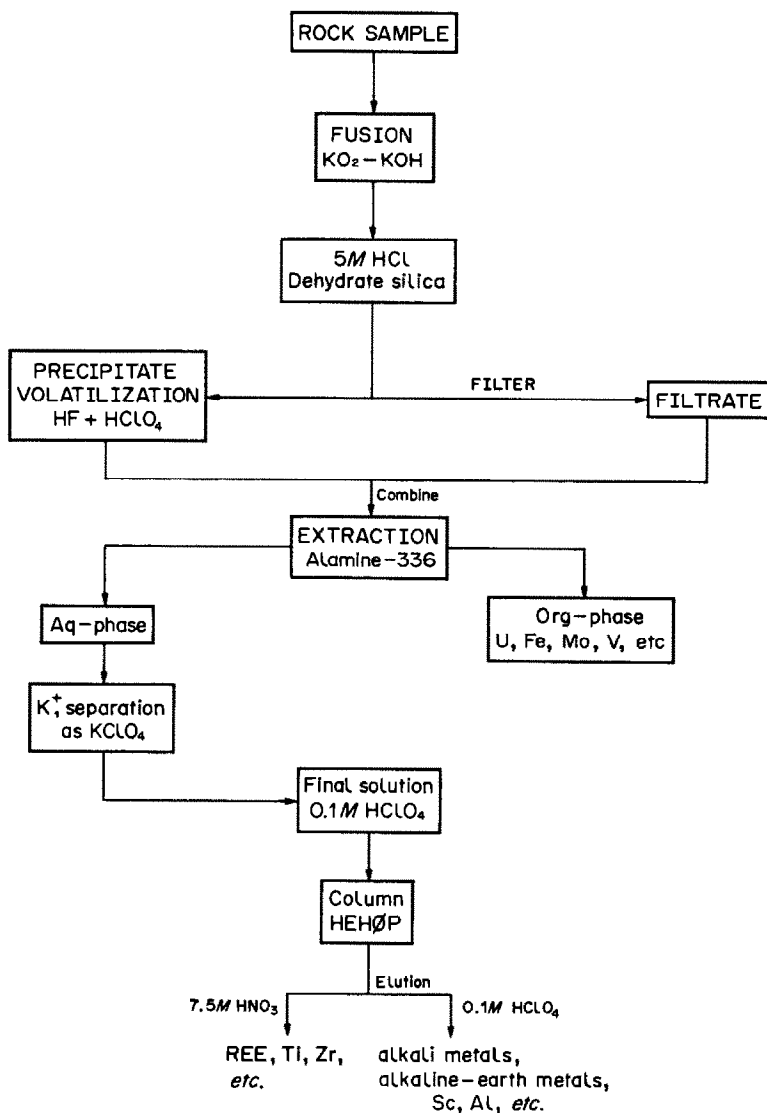


Fig. 3. Flow diagram for the determination of lanthanides in rock samples. HeHØP = 2-ethyl-hexylphenylphosphonic acid.<sup>81</sup>

users<sup>82,83</sup> have reported that the ICP-MS technique is more susceptible than ICP-AES to analyte-signal suppression by concomitant elements in the sample. These effects are severe with boron-containing fluxes such as lithium metaborate ( $\text{LiBO}_2$ ), and thus require separation of boron and lithium from the sample solution. Although boron can be volatilized as methyl borate, procedures for removal of lithium are time-consuming. Kantipuly *et al.*,<sup>84</sup> therefore, employed  $\text{K}_2\text{B}_4\text{O}_7$  as the fluxing agent in their recent work on tourmalines. The advantage of this flux is that the potassium can be easily and rapidly separated as the perchlorate, while leaving the analytes Th, U, REE, Zr and Hf in solution. The precipitate is crystalline and well-formed and will not co-precipitate the analytes of interest, which is reported to occur in work with potassium superoxide as the flux in ore and rock analysis.<sup>85</sup>

The analysis of inorganic materials by the ICP technique has a wide range of applications. A review of trace element determination in steels<sup>86</sup> discusses the use of ICP. The literature on emission techniques in the analysis of geological materials has been reviewed by Dinnin,<sup>87</sup> Boyko *et al.*<sup>88</sup> and Moore.<sup>89</sup> Kiesl<sup>90</sup> reviewed the analysis of terrestrial and extraterrestrial materials and dealt with the various steps required to obtain satisfactory results, *e.g.*, sampling and sample preparation. Emission spectroscopy and mass spectrometry are certainly the most useful analytical methods available for REE and will undoubtedly continue to be the methods of choice.

#### X-RAY FLUORESCENCE SPECTROSCOPY (XRFS)

This method is based on the analysis of the characteristic X-rays emitted by the elements of interest.

Generally, the method is limited to wavelengths between 0.03 and 0.5 nm. Recent developments in the field of X-ray fluorescence promise progress in light-element and routine trace elemental analysis. MacDonald<sup>91,92</sup> has reviewed the method extensively.

XRFS is a useful and versatile method for the determination of REE in a variety of materials. Typical applications are analyses for REE in rocks, minerals, ores and process solutions. As with other instrumental methods, XRFS is subject to spectral and other modes of interference. Since geological samples are diverse in their mineralogy composition and post-sampling history, it is difficult to prepare standards suitable for determination of low concentrations of REE elements unless a chemical separation step is included. For the final determination of analytes by XRFS it is preferable that samples be in the solid state after the concentration step.

Energy-dispersive counting with Li-doped silicon detectors has been applied to REE determinations.<sup>93</sup> Various modes of exciting the samples have been employed. The use of a secondary source and the radiation from <sup>57</sup>Co and <sup>241</sup>Am have been examined by LaBrecque *et al.*,<sup>94</sup> who claimed that the results obtained by these methods were similar and in accord with neutron-activation analysis. Havránek and Bumbalová<sup>95</sup> reported a detection limit of about 0.1 µg with a <sup>241</sup>Am source. Synchrotron radiation has also been used.<sup>96</sup> Gladney and Bower<sup>97</sup> compared XRF and NAA with the aid of several certified standard materials. XRF has been compared with atomic-absorption spectrometry<sup>98</sup> and ICP-source emission spectrometry.<sup>99</sup>

Various workers<sup>100-102</sup> have described methods that correct for matrix effects and a computer program that corrects for background interferences and mass-absorption has been provided.<sup>103</sup> Bower<sup>104</sup> has studied the precision and accuracy by analyses of ten reference rocks and reported that a 1-min counting time is optimal. The same author<sup>105</sup> has compared methods of sample preparation: lithium tetraborate discs were preferred to powder samples. Rose *et al.*<sup>106</sup> reported a precision of better than 5% with powder samples.

#### Separation methods

Generally, the chemical separation method involves fluoride precipitation or ion-exchange separation followed by lithium metaborate fusion to produce a glass disc that serves as a uniform thin support that does not interfere.

An anion-exchange procedure for preconcentration of REE from apatite has been studied.<sup>107,108</sup> A 0.5-g sample was dissolved in 1M nitric acid. The solution was evaporated to dryness, taken up in a 1:20 v/v mixture of 7M nitric acid and methanol and transferred to a screw-capped polyethylene bottle containing 0.5 g of dry anion-exchange resin in the nitrate form. The batch equilibration has the advantage over the column

technique, of homogeneous distribution of the ion of interest on the resin. Although the agreement between the results obtained by neutron-activation analysis and XRFS analysis of two phosphate samples was reasonably good, the limits of determination for the elements investigated (La, Ce, Pr, Nd) were poor. Roelandts claimed that the detection limits were not definitive and could be lowered by using longer counting times.

Various separation techniques have been described for achieving high sensitivity by producing thin sample films. Ryabukhin *et al.*<sup>109</sup> collected REE in a film of yttrium oxalate. Chinese workers<sup>110,111</sup> used ion-exchange paper or membranes (E105) and reported a detection limit of 2.5 µg.

#### SPECTROPHOTOMETRIC ANALYSIS

Spectrophotometric analyses by absorption in the visible and ultraviolet region can be performed directly on the aquo-complexes of some of the lanthanides without the use of a secondary colour-forming agent. Although the lanthanide absorption bands are sharp, their molar absorptivities are not as large as those of the coloured complexes normally used in spectrophotometric analyses. Therefore, in the determination of the lanthanides and thorium, the method normally involves complexing the analyte with a coloured organic reagent and measuring the resultant change in its optical properties. Its ease and simplicity often lead to a spectrophotometric method being selected for analysis of geological materials. In fact, colour comparison can be applied in the field without the aid of instruments.<sup>112,113</sup> The continual increase in the number of applications has been documented in excellent review articles by Hargis and Howell.<sup>114,115</sup> Comprehensive discussions of individual methods and experimental procedures for dealing with a variety of materials, including water, ores, rocks and soils are given in standard texts such as those of Sandell,<sup>116</sup> Snell and Snell,<sup>117</sup> Onishi<sup>118</sup> and Marzenko.<sup>119</sup> The book by Jeffrey and Hutchison<sup>13</sup> is a valuable source of procedures dealing with silicate rock analysis.

The molar absorptivities of most species used in trace analysis range from approximately  $10^3$  to  $10^5$  l. mole<sup>-1</sup>. cm<sup>-1</sup> at the wavelength of maximal absorption. This enables many elements to be determined in geological materials at concentrations above about 0.1 µg/g provided adequate separation from the matrix can be achieved. The presence of certain elements may cause serious interferences, as the colour reactions for REE are not specific. Interference by masking or rendering the desired colour reaction unstable may also occur. The matrix constituents may be troublesome because of their high concentrations. More extensive discussion of absorptometric errors can be found in the literature<sup>120-122</sup> and in standard analytical texts.

Table 4. Important chromogenic reagents used for REE and Th

Element	Reagent	Reaction conditions, pH	Molar absorptivity, $l.mole^{-1}.cm^{-1}$	Selectivity
Lanthanides	Arsenazo III	1-4	$5.5-6.5 \times 10^4$	low
	Arsenazo I	1-4	$1 \times 10^4$	low
	Antipyrine S	2-5	$1 \times 10^5$	low
	Alizarin Red S		$1 \times 10^4$	
	Carboxynitrazo (Ce)	2-4	$1.6 \times 10^5$	high
Thorium	Thoron (I)	0.7-1.2	$1.2 \times 10^4$	high
	Arsenazo III	1-2	$1.2 \times 10^5$	high

#### Methods of determining the rare-earth elements with chromogenic reagents

Most spectrophotometric methods for the determination of REE involve reaction with a chromogenic reagent to form a product with a high molar absorptivity. The choice of reagent is governed by many factors, such as simplicity and rapidity of the chemical procedure, chemical stability of the absorbing species, sensitivity and specificity. Several chromogenic reagents used for the determination of trivalent rare-earth ions are shown in Table 4.

None of these reagents is entirely specific for rare earths, although Arsenazo III is somewhat selective.<sup>123</sup> Cations with a radius of less than 0.7-0.8 Å show no colour reactions with Arsenazo III, and they include elements commonly found in geological sam-

ples, e.g., Al, Be, Ge, Ti and Sn. However, this reagent also forms complexes with a large number of other elements, including thorium, uranium and zirconium at low pH and iron, yttrium, scandium and other elements at higher pH. Fluoride and certain oxyanions such as phosphate and sulphate inhibit the colour formation.

Goryushina *et al.*<sup>124</sup> have developed a photometric procedure to determine the REE, in which these are first separated from all other elements that react with Arsenazo III, by precipitation as the hydroxides with ammonia, followed by precipitation as the oxalates, with calcium added as carrier.

Other methods include precipitation of the REE with sodium hydroxide to remove aluminium and the alkaline-earth elements, precipitation with

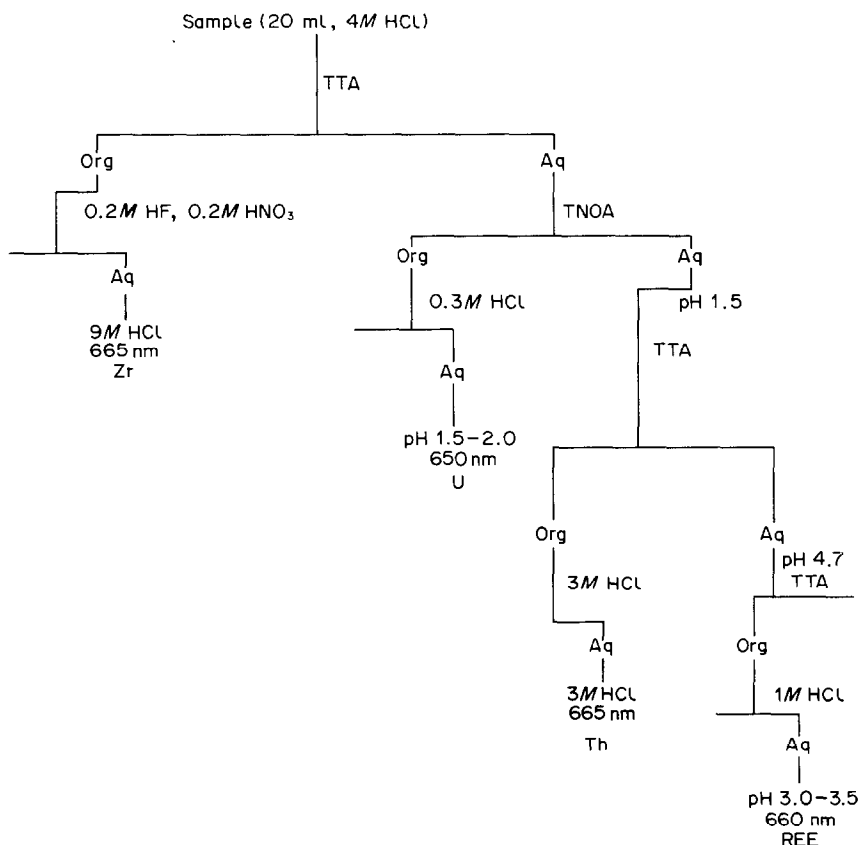


Fig. 4. Separation and determination of Zr, U, Th, and rare earths.<sup>126</sup> TTA = thenoyltrifluoroacetone, TNOA = tri-n-octylamine, Org = organic phase, Aq = aqueous phase.



hydrofluoric acid to remove iron, titanium, zirconium and other elements forming soluble fluorides, and chlorination to remove elements that form volatile chlorides including iron, titanium, aluminium and zirconium. Various procedures for determining total rare earths have been based on combinations of these separation procedures, but usually incurring a significant loss of REE amounting to 3–25%. Aladjem<sup>125</sup> has summarized much of the information prior to 1966 on the spectrophotometric determination of the REE. Cerium is the only lanthanide that can be determined selectively in the presence of the other rare earths. This is possible by oxidation of Ce(III) to Ce(IV), which quantitatively reacts with many coloured reagents and organic dyes, e.g., tris(1,10-phenanthroline)iron(II), (ferroin).

A systematic separation of zirconium, uranium, thorium and REE, and subsequent photometric determination with Arsenazo III was developed by Onishi and Sekine.<sup>126</sup> Each metal is back-extracted from the organic phase before its determination. The outline of the procedure is shown in Fig. 4.

Although some separations are inevitable, in certain cases they can be avoided by the use of masking agents. The use of such agents in spectrophotometry and other analytical procedures has been well covered in the book by Perrin.<sup>127</sup> For example, Savvin *et al.*<sup>128</sup> have described a spectrophotometric method for the determination of La, Ce, Pr and Nd in the presence of a 650-fold w/w ratio based on the colour reaction of the REE with Carboxynitrazo. Interference by Fe(II) and the heavy REE was suppressed by the addition of EDTA.

Photometric methods, especially for elements such as cerium and thorium, continue to be of interest, in spite of recent developments in use of AAS, ICP–AES and ICP–MS, which make these methods superior for the determination of trace amounts of individual rare earths. New, more sensitive and selective reagents have been synthesized. In addition, techniques such as extraction photometric methods and the use of competing ligands to improve the selectivity of chemical methods continue to make spectrophotometric methods both attractive and inexpensive. Moreover, although strong claims are made for the specificity and sensitivity of NAA, ICP–AES and ICP–MS, some of the interferences to which these methods are subject are poorly understood and continue to cause problems.

#### REFERENCES

1. A. A. Beus, *Geochemistry (USSR)*, 1958, 388.
2. D. A. Mineev, Yu. P. Dikov, B. P. Sobolev and V. L. Borutskaya, *Geokhimiya*, 1966, 468.
3. R. F. Martin, J. E. Whitley and A. R. Wooley, *Contrib. Mineral. Petrol.*, 1978, **66**, 69.
4. P. L. Hellman, R. E. Smith and P. Henderson, *ibid.*, 1979, **71**, 23.
5. H. W. Nesbitt, *Nature*, 1979, **279**, 206.
6. H. S. Washington, *Manual of the Chemical Analysis of Rocks*, 3rd Ed., Wiley, New York, 1918.
7. W. F. Hillebrand, *U.S. Geol. Surv. Bull.*, **700**, Washington, 1919.
8. R. C. Chirnside, *J. Soc. Glass Technol.*, 1959, **43**, 5T.
9. E. L. P. Mercy, *Geochim. Cosmochim. Acta*, 1956, **9**, 161.
10. E. A. Vincent, in *Methods in Geochemistry*, A. A. Smales and L. R. Wager (eds.), p. 77. Interscience, New York, 1960.
11. A. D. Maynes, *Anal. Chim. Acta*, 1965, **32**, 211.
12. W. M. Johnson and J. A. Maxwell, *Rock and Mineral Analysis*, 2nd Ed., Wiley–Interscience, New York, 1981.
13. P. G. Jeffrey and D. Hutchison, *Chemical Methods of Rock Analysis*, 3rd Ed., Pergamon Press, Oxford.
14. R. A. Schmitt, A. Mosen, C. S. Suffredini, J. E. Lasch, R. A. Sharp and D. A. Olehy, *Nature*, 1960, **186**, 863.
15. L. A. Haskin and M. A. Gehl, *J. Geophys. Res.*, 1962, **67**, 2537.
16. C. D. Coryell, J. W. Chase and J. W. Winchester, *ibid.*, 1963, **68**, 559.
17. S. Pal and D. J. Terrell, *Geostand. Newsl.*, 1978, **2**, 187.
18. M. S. Germani, I. Gokmen, A. C. Sigleo, G. S. Kowalczyk, I. Olmez, A. M. Small, D. L. Anderson, M. P. Faily, M. C. Gulovaii, C. E. Choquette, E. A. Lepel, G. E. Gordon and W. H. Zoller, *Anal. Chem.*, 1980, **52**, 240.
19. P. De Soete, R. Gijbels and J. Hoste, *Neutron Activation Analysis*, Wiley, New York, 1972.
20. D. L. Massart and J. Hoste, *Anal. Chim. Acta*, 1968, **42**, 15.
21. J. Turkstra and M. A. Van Droogenbroeck, *J. S. Afr. Chem. Inst.*, 1975, **28**, 61.
22. K. Tomura, H. Higuchi, N. Miyaji, N. Onuma and H. Hamaguchi, *Anal. Chim. Acta*, 1968, **41**, 217.
23. J. P. Op de Beeck, *J. Radioanal. Chem.*, 1969, **3**, 431.
24. I. L. Gibson and P. Jagam, in *Short Course in Neutron Activation Analysis in the Geosciences*, G. K. Meuke (ed), Chap. 5. Mineralogical Association of Canada, Toronto, 1980.
25. W. V. Boynton, in *Handbook on the Physics and Chemistry of Rare Earths*, K. A. Schneider and L. Eyring (eds.) Chap. 37F. North-Holland, New York, 1979.
26. T. Bereznai, *J. Radioanal. Chem.*, 1971, **9**, 81.
27. P. Ila, P. Jagam and G. K. Muecke, *ibid.*, 1983, **79**, 215.
28. J. P. Op de Beeck, *ibid.*, 1970, **4**, 137.
29. A. W. Mosen, R. A. Schmitt and J. Vasilevskis, *Anal. Chim. Acta*, 1961, **25**, 10.
30. L. A. Haskin, T. R. Wildeman and M. A. Haskin, *J. Radioanal. Chem.*, 1968, **1**, 337.
31. S. Melsom, *ibid.*, 1970, **4**, 355.
32. F. M. Graber, H. R. Lukens and J. K. Mackenzie, *ibid.*, 1970, **4**, 229.
33. E. B. Denechaud, P. A. Helmke and L. A. Haskin, *ibid.*, 1970, **6**, 97.
34. P. Rey, H. Wakita and R. A. Schmitt, *Anal. Chim. Acta*, 1970, **51**, 163.
35. A. O. Brunfelt, I. Roelandts and E. Steinnes, *Analyst*, 1974, **99**, 277.
36. E. Steinnes, *Talanta*, 1974, **21**, 178.
37. J. Minczewski and R. Dybczyński, *Chem. Anal. (Warsaw)*, 1965, **10**, 1113.
38. H. B. Desai, R. K. Iyer and M. S. Das, *Talanta*, 1964, **11**, 1249.
39. A. O. Brunfelt and E. Steinnes, *Analyst*, 1969, **94**, 979.
40. I. P. Alimarin, A. Z. Miklishanskii and Yu. V. Yakovlev, *J. Radioanal. Chem.*, 1970, **4**, 45.
41. P. Klein, *Thesis, Radiochemische Bestimmung der Seltenen Erdelemente in Geologischem Material (Vulkanite der Aolischen Inseln Alicudi und Filicudi)*, University of Vienna, 1975.
42. R. M. Barnes, *Anal. Chem.*, 1976, **48**, 106R.

43. *Idem, ibid.*, 1978, **50**, 100R.
44. R. M. Barnes (ed.), *Emission Spectroscopy*, Dowden, Hutchinson and Ross, Stroudsburg, PA, 1976.
45. D. N. Hingle, G. F. Kirkbright and T. S. West, *Analyst*, 1969, **94**, 864.
46. W. Ooghe and F. Verbeek, *Anal. Chim. Acta*, 1974, **73**, 87.
47. J. C. Van Loon, J. H. Galbraith and H. M. Aarden, *Analyst*, 1971, **96**, 47.
48. J. G. Sen Gupta, *Talanta*, 1976, **23**, 343.
49. *Idem, ibid.*, 1984, **31**, 1045.
50. B. V. L'vov and L. A. Pelieva, *Can. J. Spectrosc.*, 1978, **23**, 1.
51. J. G. Sen Gupta, *Talanta*, 1985, **32**, 1.
52. L. Papp, *Spectrochim. Acta*, 1983, **38B**, 1203.
53. P. Tschöpel, in *Comprehensive Analytical Chemistry*, G. Svehla (ed.), Vol. IX, Chap. 3. Elsevier, Amsterdam, 1979.
54. K. Govindaraju, G. Mevelle and C. Chouard, *Anal. Chem.*, 1976, **48**, 1325.
55. J. O. Burman and K. Boström, *ibid.*, 1979, **51**, 516.
56. V. A. Fassel, *Pure Appl. Chem.*, 1977, **49**, 1533.
57. R. M. Barnes (ed.), *Applications of Inductively Coupled Plasma to Emission Spectroscopy (1977 Analytical Symposium)*, Franklin Institute Press, Philadelphia, 1978.
58. J. A. C. Broekaert, F. Leis and K. Laqua, *Spectrochim. Acta*, 1979, **34B**, 73.
59. J. M. Mermet and C. Trassy, in *International Winter Conference of Developments in Atomic Plasma Analysis*, San Juan, Puerto Rico, 1980.
60. M. D. Feigenson and M. J. Carr, *Chem. Geol.*, 1985, **51**, 19.
61. S. R. Taylor, *Geochim. Cosmochim. Acta*, 1965, **29**, 1243.
62. *Idem*, in *Handbook on the Physics and Chemistry of Rare Earths*, K. A. Schneider and L. Eyring (eds.), Vol. 4, p. 359. North-Holland, New York, 1979.
63. P. F. S. Jackson and A. Strasheim, *Analyst*, 1974, **99**, 26.
64. N. Nakamura, *Geochim. Cosmochim. Acta*, 1974, **38**, 757.
65. A. R. Date and A. L. Gray, *Spectrochim. Acta*, 1985, **40B**, 115.
66. D. J. Douglas and R. S. Houk, *Prog. Anal. At. Spectrosc.*, 1985, **8**, 1.
67. J. R. Bacon and A. M. Ure, *Anal. Chim. Acta*, 1979, **105**, 163.
68. W. Doherty and A. Vander Voet, *Can. J. Spectrosc.*, 1986, **30**, 135.
69. H. P. Longrich, C. J. Kantipuly, B. J. Fryer and D. F. Strong, *Analysis of Rare Earths by ICP-MS, presented at 1986 Winter Conf. Plasma Spectroscopy*, Hawaii.
70. P. J. Hooker, R. K. O'Nions and R. J. Pankhurst, *Chem. Geol.*, 1975, **16**, 189.
71. F. W. E. Strelow and P. F. S. Jackson, *Anal. Chem.*, 1974, **46**, 1481.
72. A. V. Dolgorev and Y. G. Lysak, *J. Anal. Chem. U.S.S.R.*, 1975, **30**, 1644.
73. Y. K. Agrawal and H. L. Kapoor, *Talanta*, 1976, **23**, 235.
74. H. J. Hettel and V. A. Fassel, *Anal. Chem.*, 1955, **27**, 1311.
75. C. L. Waring and H. Mela, Jr., *ibid.*, 1953, **25**, 432.
76. S. Meloni, M. Oddone, A. Cecchi and G. Poli, *J. Radioanal. Chem.*, 1982, **71**, 429.
77. S. J. Buchanan and L. S. Dale, *Spectrochim. Acta*, 1986, **41B**, 237.
78. J. G. Crock and F. E. Lichte, *Anal. Chem.*, 1982, **54**, 1329.
79. J. G. Crock, F. E. Lichte and T. R. Wildeman, *Chem. Geol.*, 1984, **45**, 149.
- 79a. I. B. Brenner, E. A. Jones, A. E. Watson and T. W. Steel, *ibid.*, 1984, **45**, 135.
80. K. Yoshida and H. Haraguchi, *Anal. Chem.*, 1984, **56**, 2580.
81. C. Kantipuly, *Thesis*, University of Ottawa, 1984.
82. A. L. Gray and A. R. Date, *Analyst*, 1983, **108**, 1033.
83. J. A. Olivares and R. S. Houk, *Anal. Chem.*, 1986, **58**, 20.
84. C. J. Kantipuly, H. P. Longrich and D. F. Strong, *Determination of Thorium and Uranium in Tourmalines by ICP-MS*, presented at the 1986 Winter Conference on Plasma Spectrochemistry, Hawaii.
85. A. D. Westland and C. Kantipuly, *Anal. Chim. Acta*, 1983, **154**, 355.
86. K. H. Koch, *Radex Rundsch.*, 1982, 780.
87. J. I. Dinnin, *Anal. Chem.*, 1979, **51**, 144R.
88. W. J. Boyko, P. N. Keliher and J. M. Malloy, *ibid.*, 1980, **52**, 53R.
89. C. B. Moore, *ibid.*, 1981, **53**, 38R.
90. W. Kiesel, *CRC Crit. Rev. Anal. Chem.*, 1984, **15**, 119.
91. G. L. MacDonald, *Anal. Chem.*, 1978, **50**, 135R.
92. *Idem, ibid.*, 1980, **52**, 100R.
93. K. K. Nielson and D. R. Kalkwarf, *Electron Microsc. X-Ray Appl. Environ. Occup. Health Anal. Symp.*, 2nd, 1977, p. 31.
94. J. J. LaBrecque, J. M. Beusen and R. E. Van Grieken, *X-Ray Spectrom.*, 1986, **15**, 13.
95. E. Havránek and A. Bumbalová, *Acta Fac. Pharm. Univ. Comeniana*, 1977, **31**, 55.
96. A. V. Dubinin, I. I. Volkov, V. B. Baryshev and G. N. Kulipanov, *Geokhimiya*, 1986, 70.
97. E. S. Gladney and N. W. Bower, *Geostand. Newsl.*, 1985, **9**, 261.
98. P. C. Kennedy, B. Rosen and J. Hunt, *ibid.*, 1983, **7**, 305.
99. Hou Qing-Lie, T. C. Hughes, M. Haukka and P. Hannaker, *Talanta*, 1985, **32**, 495.
100. L. Leoni and M. Saitta, *X-Ray Spectrom.*, 1977, **6**, 181.
101. *Idem, Rend. Soc. Ital. Mineral. Petrol.*, 1976, **32**, 497.
102. Yvan-Pan Chen, *Fen Hsi Hua Hsueh*, 1981, **9**, 61.
103. E. G. Nisbet, V. J. Dietrich and A. Esenwein, *Fortschr. Mineral.*, 1979, **57**, 264.
104. N. W. Bower, *Appl. Spectrosc.*, 1985, **39**, 697.
105. N. W. Bower and G. Valentine, *X-Ray Spectrom.*, 1986, **15**, 73.
106. W. I. Rose, T. J. Bornhorst and S. J. Sivonen, *ibid.*, 1986, **15**, 55.
107. I. Roelandts, G. Duyckaerts and A. O. Brunfelt, *Anal. Chim. Acta*, 1974, **73**, 141.
108. I. Roelandts, *Anal. Chem.*, 1981, **53**, 676.
109. V. A. Ryabukhin, N. G. Gatinskaya, A. N. Ermakov and I. D. Shevaleevskii, *Zh. Analit. Khim.*, 1983, **38**, 1626.
110. Q. An, *Yanshi Kuangwu Ji Ceshi*, 1984, **3**, 162.
111. L. Feng, R. Li, Y. Zhang, Y. Wang, Z. Qian and Z. Zhao, *Diqiu Huaxue*, 1982, 35.
112. A. A. Levinson, *Introduction to Exploration Geochemistry*, p. 264. Applied Publishing, Calgary, 1974.
113. R. E. Stanton, *Analytical Methods for Use in Geochemical Exploration*, Halsted, New York, 1976.
114. L. G. Hargis and J. A. Howell, *Anal. Chem.*, 1980, **52**, 306R.
115. J. A. Howell and L. G. Hargis, *ibid.*, 1982, **54**, 171R.
116. E. B. Sandell, *Colorimetric Determination of Traces of Metals*, 3rd Ed., Interscience, New York, 1959.
117. F. D. Snell and C. T. Snell, *Colorimetric Methods of Analysis*, Vol. IIA, Van Nostrand, Princeton, 1959.
118. H. Onishi, *Photometric Determination of Traces of Metals*, 4th Ed., Part IIA, Wiley-Interscience, New York 1986.
119. Z. Marczenko, *Spectrophotometric Determination and Separation of Elements*, Horwood, Chichester, 1986.

120. G. F. Lothian, *Analyst*, 1963, **88**, 678.
121. N. T. Gridgeman, *Anal. Chem.*, 1952, **24**, 445.
122. R. Mavrodineanu, J. I. Schultz and O. Menis (eds.), *Accuracy in Spectrophometry and Luminescence Measurements*, U.S. Dept. of Commerce, Washington, 1973.
123. S. B. Savvin, *Talanta* 1961, **8**, 673; 1964, **11**, 1.
124. V. G. Goryushina, S. B. Savvin and E. V. Romanova, *Zh. Analit. Khim.*, 1963, **18**, 1340.
125. A. Aladjem, *Analytical Chemistry of Thorium and the Lanthanide Elements*, pp. 168–177. Ann Arbor-Humphrey Science Pub., Ann Arbor, 1970.
126. H. Onishi and K. Sekine, *Talanta*, 1972, **19**, 473.
127. D. D. Perrin, *Masking and Demasking of Chemical Reactions*, Wiley-Interscience, New York, 1970.
128. S. B. Savvin, T. V. Petrova and P. N. Romanov, *Zh. Analit. Khim.*, 1973, **28**, 272; 1974, **29**, 1929.

## ION-CHROMATOGRAPHIC ANALYSIS OF MIXTURES OF FERROUS AND FERRIC IRON

CARL O. MOSES\*, ALAN T. HERLIHY, JANET S. HERMAN and AARON L. MILLS  
Department of Environmental Sciences, University of Virginia, Charlottesville, VA 22903, U.S.A.

(Received 24 October 1986. Revised 13 July 1987. Accepted 25 August 1987)

**Summary**—Determinations of the aqueous iron species Fe(II) and Fe(III) are essential for a fully-informed understanding of redox processes involving iron. Most previous methods for speciation of iron have been based on the colorimetric determination of Fe(II) followed by reduction of Fe(III) and analysis for total iron. The indirect determination of Fe(III) and the consumption of relatively large sample volumes have limited the accuracy and utility of such methods. A method based on ion-chromatography has been developed for simultaneous direct determination of Fe(II) and Fe(III). Sample pretreatment involves only conventional filtration and acidification. No interferences with the iron(II) determination were found; in determination of iron(III) the only interference observed was an artifact peak (of unknown origin) that occurred only when iron(II) was present, and had an area that was a function of the iron(II) concentration and could hence be corrected for. Solutions of iron(II) free from iron(III) can be prepared by treatment with a mixture of hydrogen and nitrogen in the presence of palladium black as catalyst, to reduce the iron(III). Photoreduction of iron(III) in acidified samples increases the Fe(II)/Fe(III) ratio; no means of circumventing this effect is known, other than storing the samples in the dark and analysing them as soon as possible.

Iron is one of the most common elements in the Earth's crust, occurring in nearly all types of rock. Its redox and physiological properties make it an important component of the biogeochemical cycles of elements such as carbon, sulphur and oxygen.<sup>1-3</sup> Its reactivity also drives numerous chemical processes in natural waters, and it is a significant factor in the evaluation of water quality.<sup>4</sup>

There are many shortcomings in our understanding of the Fe-H<sub>2</sub>O system that constrain the application of equilibrium thermodynamics to the solution of problems that involve iron species in water. For example, thermochemical data for aqueous Fe(II) species are especially difficult to obtain, owing to the difficulty in eliminating oxygen and Fe(III) from the system.<sup>5</sup> In principle, the redox potential (*E*) can be used to predict the equilibrium iron speciation, given the total iron concentration, but there are many problems associated with making accurate potential measurements.<sup>6-8</sup> Even if accurate *E* values are available, their interpretation is complicated by kinetic and complexation effects that can cause the observed iron speciation to differ from the ratio of Fe(II) and Fe(III) activities predicted from the measured redox potential. The value of *E* can also be calculated from the activity ratio of another redox couple, but that ratio may not be accurately determined and the couple's redox chemistry may not be linked to that of iron. Since predictions based on equilibria can only be accurate in certain situations,

the most reliable way to acquire information on the speciation of iron is to make direct determinations of both Fe(II) and Fe(III). Unfortunately, however, finding direct analytical methods for iron species is among the problems encountered in investigation of the basic processes in the Fe-H<sub>2</sub>O system and in studies involving iron in the environment.

Atomic absorption and emission spectrometry can only determine the total iron concentration. Though some methods of electronic or resonance spectroscopy can distinguish between Fe(II) and Fe(III), they are better suited to molecules than to ions in aqueous solution. Most practical methods of analysing for aqueous iron species involve spectrophotometric determination of Fe(II).<sup>9-13</sup> Fe(III) is then reduced to Fe(II) and total iron determined, yielding the concentration of Fe(III) by difference. The main drawbacks of this approach are related to sensitivity, the level of iron to be determined, and interferences.

This paper reports the development of an ion-chromatography (IC) method for directly determining both Fe(II) and Fe(III) in water samples. It requires <1 ml of sample and no sample pretreatment other than the usual filtration and acidification of the samples. Since its introduction,<sup>14</sup> IC has become a widely-used technique for analysis of solutions<sup>15</sup> (a non-exhaustive bibliography, available from Dionex Corp., 1228 Titan Way, Sunnyvale, CA 94086, USA, lists over 500 citations up to 1984). The separation and conductimetric detection of alkali-metal and alkaline-earth metal cations are well-established, but only recently has IC technology been expanded to include transition and heavy metal determination by spectrophotometric detection.<sup>16,17</sup>

\*Author for correspondence. Present address: Department of Geological Sciences, Lehigh University, Williams Hall 31, Bethlehem, PA 18015, U.S.A.

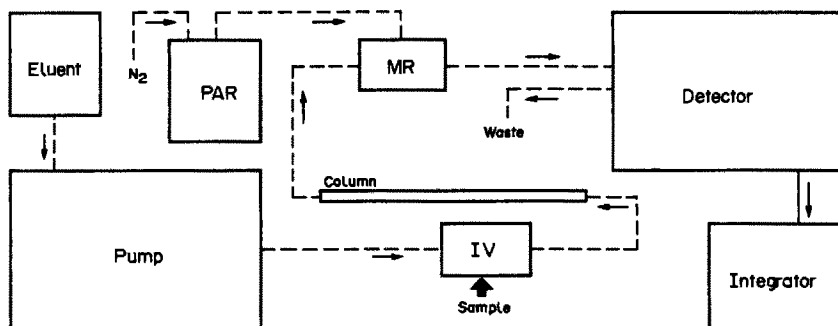


Fig. 1. Schematic of IC transition/heavy metal analytical system: IV = sample injection valve; MR = membrane reactor; dashed lines indicate fluid flow paths and the solid line indicates an electrical signal.

### Principle

In analyses for iron, a small volume (10–500  $\mu$ l) of sample is injected into an eluent stream, which carries the sample into a separator column (Fig. 1). The eluent contains a chelating agent that forms water-soluble complexes with metal ions, and the column is packed with a mixed-bed resin, which separates the complexes by differential dynamic sorption/desorption processes.<sup>18</sup> Once separated, the metal complexes are treated with a colorimetric reagent in a reactor that consists of a hollow uncharged membrane fibre bathed in the reagent. The eluent stream flows through the lumen of the fibre, where it mixes radially with reagent permeating through the membrane under pressure. Longitudinal mixing, which causes broadening of the bands, is reduced by coiling the fibre, which also enhances the radial mixing. The intensity of the resulting colour, which is proportional to the amount of metal present, is measured in a flow-through spectrophotometer cell. Since the sample volume injected is known, the original metal concentration is readily determined.

### EXPERIMENTAL

#### Sample treatment

Samples were filtered through Gelman or Millipore membranes with pore sizes no larger than 0.45  $\mu$ m. Before the sample was collected, the membrane was leached with about 500 ml of sample or demineralized water. Each filtered sample was collected in a polyethylene bottle that contained a volume of redistilled 6*M* hydrochloric acid (G.F. Smith Co.) that was 1% of that of the sample; the samples were stored at 2–5°. Analyses were completed as soon as possible after collection but always within 2 weeks (the practical length of storage is discussed below).

#### Reagents and standards

**Fe(II) standards.** A 1*mM* stock solution was prepared from  $\text{Fe}(\text{NH}_4)_2(\text{SO}_4)_2 \cdot 6\text{H}_2\text{O}$  (Aldrich) or from Fe wire (Baker). The solutions were made up with demineralized water that had been deaerated under reduced pressure. During storage, the salt was protected from exposure to air and light. The stock solution made from it (0.3921 g/l.) was acidified with a 1% v/v addition of redistilled 6*M* hydrochloric acid. For about 48 hr before use, the desired length (18 cm, ~56 mg) of 0.23-mm diameter Fe wire was soaked, with occasional ultrasonic treatment, in 0.18*M* ammonium

oxalate to remove surface coatings of hydrous Fe(III) oxide, then quickly rinsed with demineralized water and acetone, dried on a tissue, weighed to 0.01 mg, and dissolved in 10 ml of warm redistilled 6*M* hydrochloric acid. The solution was diluted to 1 litre.

Approximately 10 mg of palladium black (Aldrich; this material will be referred to as Pd-b) was added to the stock iron(II) solutions, which were then purged for 15–20 min with a mixture of hydrogen (10–30%) and nitrogen, passed through a dispersion tube at 90–120 l/hr. This procedure ensured complete reduction of the iron(III) to iron(II). The nitrogen used was passed through a column packed with "Ascarite" to remove carbon dioxide and then through a heated glass column packed with copper turnings, to remove oxygen.

After the reduction a portion of the stock iron(II) solution was filtered through a prerinsed glass-fibre or Whatman No. 1 filter, and used for preparation of calibration standards by dilution with 60*mM* hydrochloric acid. The stock solution was always reduced before use. Calibration standards were kept for no longer than 48 hr. It is not possible to use mixed Fe(II)/Fe(III) standards (see discussion).

**Fe(III) standards.** Commercial AAS standards for iron, made from iron(III) chloride dissolved in hydrochloric acid, were used as Fe(III) standards not contaminated with Fe(II). A 100-mg/l. stock solution was prepared by diluting the commercial standard with 60*mM* hydrochloric acid, and further diluted with this acid to give the calibration standards.

**Eluent.** A 6*mM* PDCA/50*mM* sodium acetate/50*mM* acetic acid solution was made by dissolving 6.8 g of sodium acetate trihydrate (Baker) in 500 ml of demineralized water, adding 1 g of PDCA (2,6-pyridinedicarboxylic acid, Aldrich), and 3 ml of glacial acetic acid (Baker), and diluting to 1 litre. The pH of this eluent was 4.5. The eluent was purged with nitrogen (stripped of  $\text{CO}_2$  and  $\text{O}_2$  as above) for about 30 min before use.

**Post-column reagent.** A 0.2*mM* PAR/3*M* ammonia/1*M* acetic acid solution was made by dissolving 43 mg of PAR in 400 ml of 7.5*M* ammonia solution and adding 600 ml of 1.67*M* acetic acid. The solution was purged with nitrogen, and stripped of  $\text{CO}_2$  and  $\text{O}_2$  for about 30 min, to prevent oxidation of the PAR, which would cause a noisy chromatographic baseline.

**Sulphite solution, 0.1*M*.** A solution of 12.6 g of anhydrous sodium sulphite (Baker) in 1 litre of demineralized water.

**CAUTION.** The inversion temperature of hydrogen is  $-80^\circ$ , so at room temperature hydrogen shows an inverted Joule-Thompson effect and becomes hot on expansion.<sup>19</sup> The explosive limits for hydrogen are 4–75% v/v in air.<sup>19</sup> During the course of our work, a rich mixture of  $\text{H}_2$  in  $\text{N}_2$  was passed through a small glass jet into an aqueous solution. When the jet was removed from the solution, a

Table 1. IC operating conditions

Eluent flow: 1.0 ml/min
Injection volume: 50 $\mu$ l
PAR delivery
pressure: 3.5–4.2 bar
flow: 0.6–0.8 ml/min
Detection wavelength: 520 nm
Recorder sensitivity: 0.16 absorbance full-scale
Time constant: 1 sec

bright orange 3-cm flame appeared at its tip, and was probably caused by a combination of heating on expansion and ignition by a static discharge as the gas passed rapidly through the small nozzle. Although the flame was easily extinguished, the incident emphasised the need for care in handling hydrogen. No problems were encountered when a gas dispersion tube was used. Palladium black is also a potential fire hazard (it is a finely divided metal, and could be pyrophoric) and quantities larger than a few mg should be stored in an inert (air-free) atmosphere. Filters containing a small amount of Pd-b (<10 mg) can be wetted with water and placed in a glass or metal dish to dry. The Pd-b will then oxidize too slowly to ignite, and once dry can be disposed of with other dry wastes.

#### Potentiometric measurements

A Ross combination pH electrode (Orion 815500) was used for pH measurements and a combination Pt electrode (Orion 967800) for redox potential measurements, with a Corning 135 pH/ion-meter. The redox electrode uses a proprietary reference electrode which has a potential of 0.246 V vs. the normal hydrogen electrode.<sup>20</sup> Redox potential values ( $E$ ) reported in this paper are referred to the normal hydrogen electrode.

#### IC methods

The IC system consisted of an APM-1 analytical pump, CG-2 precolumn, CS-5 analytical separator column, and RDM-1 reagent delivery module with membrane reactor, all from Dionex. The detector was a Knauer 87 variable-wavelength spectrophotometer with tungsten-halogen lamp, solid-state detector (photodiode), and 1-cm path-length cell (12- $\mu$ l volume). The detector output was recorded on a Kipp and Zonen dual-channel strip-chart recorder and a Hewlett-Packard 3392A integrator. All parts of the system in contact with fluid were non-metallic except for the flow passages in the detector cell. From the injection loop to the detector cell, the 0.3-mm bore PTFE connections were kept as short as possible to minimize the dead volume. Figure 1 shows the system configuration and Table 1 the operating conditions.

Before a run, 0.1M sodium sulphite was pumped through the columns at 1.0 ml/min for 1–2 hr to remove oxygen from the system. Then eluent pumping was begun and the column effluent was directed to the membrane reactor, the reagent reservoir of which was then pressurized, and from there to the detector cell. When the baseline absorbance had stabilized (30–60 min after switching to the eluent), the run could be started. Standards and samples were manually loaded into the injection loop with a plastic syringe. Acid blanks (60mM hydrochloric acid prepared with demineralized water) were used to confirm that the syringe, acid and sample loop were not contaminated, but were not used in the determination.

#### Calculations

The peak heights were measured on the strip-chart, or the peak areas by the integrator. Sample concentrations were calculated from equations fitted to the calibration curves. Linear equations were used unless a quadratic model could be shown (by the  $F$ -test) to improve the fit significantly.

The detection limit (DL) was estimated by multiplying the standard deviation ( $S$ ) of the low standard by the Student's  $t$ -value (one-tailed test) for the appropriate number of degrees of freedom at the 99% significance level ( $p = 0.01$ ). This calculation is similar to a more formal procedure<sup>21</sup> proposed by the USEPA, which is a practical approach to quantifying the detection limit as defined by IUPAC and the ACS.<sup>22</sup>

To assess the recovery, standard additions<sup>23</sup> were made to samples that contained only Fe(II) or Fe(III) or a mixture of the two. Increments of standard equivalent to 30–50% of the amount of analyte already present were added to 4–10 ml portions of sample, which were then analysed in triplicate, to give a total of 12 data points. The amount found (nmoles) was normalized to a sample volume of 10 ml and plotted against the amount added. The slope indicates the recovery and the intercepts on the two axes should give the amount initially present. A difference between the two intercepts will occur owing to imprecision in making the additions and in the procedure, and can also arise if the recovery is not 100%.

## RESULTS AND DISCUSSION

### Preparation of Fe(II) standards

The Fe wire was the preferred source of Fe(II) because ammonium iron(II) sulphate is prone to aerial oxidation. Although the degree of oxidation normally encountered is much smaller than the experimental error in the method developed, it was considered worthwhile trying to make as pure an iron(II) solution as possible for future use by us and others.

Hydroxylamine hydrochloride is widely used for the reduction of Fe(III) but was considered unsuitable because of the possibility of damage to the resin in the columns or the fibre in the membrane reactor, and the possibility that it could be retained on the columns and cause reduction of Fe(III) in subsequently-injected samples or standards.

Hydrogen is used with a catalyst to remove oxygen from the atmosphere of glove boxes or growth chambers in studies of anaerobic bacteria,<sup>24</sup> so the possibility of using this procedure was examined. In the work with anaerobic bacteria, the hydrogen, carried in nitrogen or a CO<sub>2</sub>/N<sub>2</sub> mixture, was passed over Pd-coated alumina or charcoal pellets, where it reacted with any oxygen present in it, to form water. In addition, Pd-b was suspended in the bacteriological media, which were placed in similar atmospheres. By the catalysed reaction the oxygen concentration in the atmosphere of a glove box was reduced to 0.001%, and a medium containing Pd-b and buffered at pH 7 had an  $E$  value of  $-0.29$  V.<sup>24</sup> The first step in adapting the latter procedure to preparation of Fe(III)-free solutions of Fe(II) was to determine whether hydrogen in the presence of catalyst would reduce dissolved oxygen to water in an abiotic system.

The  $E$  value of a 0.1M sodium chloride/60mM hydrochloric acid solution in equilibrium with air, measured with a combination Pt electrode, was very unstable, as expected for a solution with no reactive

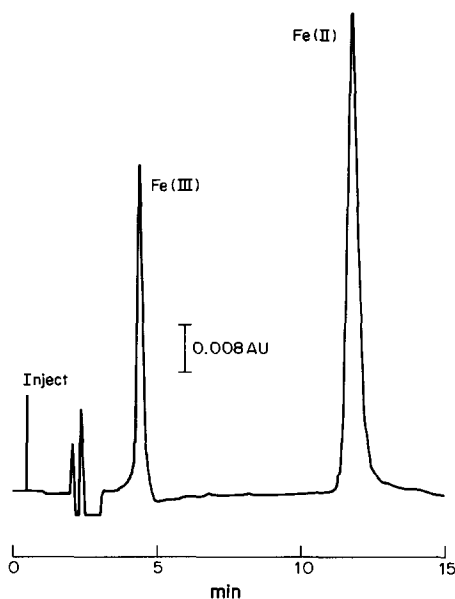


Fig. 2. Chromatogram obtained from 50  $\mu$ l injection of 4.48  $\mu$ M Fe(III)/20.0  $\mu$ M Fe(II).

redox couple, and varied between +0.3 and +0.4 V. When about 10 mg of Pd-b was suspended in the solution and this was purged with 20% hydrogen in nitrogen, the  $E$  value rapidly dropped to a steady value of  $-0.059$  V. An  $E$  of  $-0.068$  V would be predicted for a hydrogen partial pressure of 0.2 atm in equilibrium with water at pH 1.5. An  $E$  value of  $-0.059$  V would correspond to a hydrogen partial pressure of 0.1 atm. The  $E$  measurements were precise to  $\pm 0.002$  V, but the accuracy of the mixing control for the gases was probably very poor. In addition, the oxidation of hydrogen on a Pt electrode tends to attain equilibrium only slowly unless the electrode surface area is very large (which requires a platinized electrode surface). It was concluded that the  $H_2$ /Pd-b reduction procedure was successful for removal of dissolved oxygen.

The ability of  $H_2$  to reduce Fe(III) in the presence of Pd-b was then investigated. A steady  $E$  value of  $-0.03$  V was attained for a solution of 2mM Fe(II)/0.1M NaCl/60mM HCl purged for 15 min with a 20%  $H_2/N_2$  mixture in the presence of Pd-b. Similar results were obtained with a corresponding Fe(III) solution, with purging for 30 min. The computer program WATEQF<sup>25</sup> was used to calculate the equilibrium distribution of the iron under these conditions. The activity ratio Fe(II)/Fe(III) at pH 1.5 and  $E -0.03$  V was  $10^{13.5}$ , and the concentration ratio  $10^{12.9}$ . These results show that Pd-b is a suitable catalyst for the reduction of Fe(III) by hydrogen.

However, Pd also catalyses the oxidation of Fe(II),<sup>26</sup> so it is essential to filter it off from the stock iron(II) solution before mixing the calibration standards. Without the catalyst, the hydrogen that remains dissolved in solution is no longer an effective

reducing agent, and can neither damage the IC columns nor interfere with subsequent iron analyses. Since the Pd-b catalyst loses effectiveness with time, it is occasionally necessary to suspend fresh Pd-b in the solution.

#### Method performance

A typical chromatogram of a mixture of Fe(III) and Fe(II) is shown in Fig. 2. Table 2 summarizes the retention times, sensitivities and detection limits for Fe and several other metals.

Calibrations for Fe(III) were always linear. Peak-area calibrations were superior to peak-height calibrations, especially at the lowest concentrations. The calibrations for Fe(II) were usually linear but occasional large negative intercepts and curved plots of residuals indicated that a non-linear calibration model would improve the fit, especially for low concentrations, but use of quadratic models for the calibration curve improved accuracy over most of the calibration range by only about 1% or less.

The response for both species was linear up to 200  $\mu$ M. Higher concentrations were not examined, but smaller injection volumes, a higher concentration of PAR (*e.g.*, 0.4mM) and a less sensitive detector range, can be used to extend the linear range and, in some cases, avoid sample dilution. Concentrations lower than 1  $\mu$ M can be determined by increasing the injection volume (up to 500  $\mu$ l) and using a more sensitive detector range. With fresh PAR, a properly-maintained membrane reactor, and a good-quality detector, the noise in the chromatographic baseline is low enough to permit detection of concentrations at

Table 2. Method performance

Species	Retention time*, min	Sensitivity†, peak area/ $\mu$ M	DL‡, $\mu$ M
Fe(III)	3.9	$5.60 \times 10^5$ (1.3%)	1.22
Fe(II)	11.8	$4.50 \times 10^5$ (3.5%)	1.46
Cu	6.1	$2.86 \times 10^5$	
Ni	6.8	$7.00 \times 10^4$	
Zn	7.5	$1.00 \times 10^5$	
Co	8.3	$4.66 \times 10^5$	
Cd	8.9	$1.42 \times 10^4$	
Mn	10.1	$1.08 \times 10^5$	
Pb	§	—	

\*Characteristic retention time for a 20  $\mu$ M injection.

†Slope of calibration graph over 2–100  $\mu$ M range. For non-ferrous metals, sensitivities were estimated from 1 or 2 analyses and are presented for comparison only. Number in parentheses is the relative standard deviation of the slope (7 replicates). Peak area expressed in integrator counts.

‡Detection limit for 50  $\mu$ l injection volume and detector cell with 1-cm path-length; not determined for non-ferrous metals.

§No peak detected in 20 min.

least as low as 50nM ( $\sim 3 \mu\text{g/l}$ ). Analyses at this level were not examined beyond determination of their feasibility, because they require clean-laboratory conditions and great care in the preparation of reagents and standards.

The sensitivity of the method is quite high (Table 2). PAR was introduced as a colorimetric reagent when it was realized that thanks to the chromatographic separation high specificity of the reagent was no longer as important as high sensitivity.<sup>27</sup> PAR is useful for determination of cadmium, lead, uranium, and all first-row transition metals except scandium, and is well-suited to the detection of metals in IC methods, provided the metals can be separated. Besides the sensitivity, the rapidity of PAR reactions is an advantage in conjunction with the low-volume, short path-length detector cells that are desirable for chromatographic methods.

#### Separation and interferences

The CS-5 column and PDCA eluent were essential for the determination of Fe(III). Fe(II) can be determined with other combinations of column and eluent, but most other transition/heavy metal IC eluents contain components (*e.g.*, oxalate, tartrate or citrate) which can form neutral complexes with Fe(III) that are eluted in the column void volume, whereas PDCA forms an anionic complex with Fe(III) which thus undergoes retention in the CS-5 column.

Solutions of several other metals were injected to identify potential interferences. None of the metals tested showed any interference with the iron determination (Table 2), but some modification of this method may be necessary before all of them can be simultaneously resolved.

The only significant interference is a peak that overlaps that for Fe(III). Early in the development of this method, it was thought that this peak was due to Fe(III) present in the Fe(II) standards. Efforts were made to eliminate the peak by adding reductants for Fe(III), but the peak area could not be reduced below a constant value for a given Fe(II) concentration and the peak shape was different from that for pure Fe(III). The size of the peak was the same (within 3%) whether the Fe(II) standards were made from ammonium iron(II) sulphate, iron wire, a non-stoichiometric iron(II) sulphate, or a reduced Fe(III) standard, or whether the reducing agent was hydrogen (with Pd-b) or hydroxylamine hydrochloride. The cause of this peak is unknown, but it is evidently not Fe(III).

Attempts to eliminate the interference by separating the artifact from the Fe(III) peak by using eluents with less PDCA, lower pH, or both, were tried, but the main effects were merely to increase the retention time of Fe(III) slightly and that of Fe(II) considerably (to  $> 18$  min).

The interference was finally dealt with by applying an empirical correction based on the observation that the artifact area was proportional to the square root

Table 3. Analyses of mixtures

	A	B	C
Fe(II)			
expected*	4.00	8.00	20.0
found*	4.72	8.63	19.6
rsd†, %	(4.2)	(1.9)	(0.2)
recovery, %	118.0	107.9	98.0
Fe(III)			
expected	17.9	8.95	4.48
found	16.4	7.96	3.12
rsd†, %	(0.9)	(1.9)	(2.4)
recovery, %	91.6	88.9	69.6
ΣFe			
expected	21.9	17.0	24.5
found	21.1	16.6	22.7
recovery, %	96.4	97.9	92.7
Fe(II)/Fe(III)			
expected	0.223	0.894	4.464
found	0.288	1.084	6.282
recovery, %	128.8	121.3	140.7

\*All concentrations expressed in  $\mu\text{M}$ .

†Relative standard deviations ( $N = 3$ ).

of the Fe(II) concentration and the assumption that the areas of the artifact and Fe(III) peaks were additive. The Fe(II) concentration is determined, then the peak area of the artifact is calculated and subtracted from the combined artifact-Fe(III) peak area, and the concentration of Fe(III) determined from the remaining area.

#### Sample preservation and storage

Filtration is an essential step in the collection of samples. To exclude bacteria and colloidal Fe(III) species, pore sizes of 0.2  $\mu\text{m}$  or less should be used. Certain bacteria, common in environments containing Fe(II), can catalyse its oxidation.<sup>28-30</sup> Any colloidal material will partly dissolve when the sample is acidified and hence give a time-dependent and increasing value for dissolved Fe(III).<sup>31</sup> Any colloids that remain in suspension when the sample is injected into the IC are more strongly retained on the column than the dissolved Fe(III), and this may cause substantial broadening of the Fe(III) peak and eventually clogging of the column.

Oxidation of Fe(II) was quenched by acidifying samples with hydrochloric acid immediately after collection, since the rate of Fe(II) oxidation is minimal and is independent of acidity at  $\text{pH} < 3$ .<sup>26,32</sup> Re-analysis of 7 lake-sediment pore-water samples containing 100–2900  $\mu\text{M}$  Fe(II) and no detectable Fe(III) showed an average loss of 1.6% of the Fe(II) originally present, after 31 days of storage. Shortage of sample precluded detailed analysis of the variability in Fe(II) loss but the variability did not appear to be correlated with the original Fe(II) concentration and could not be distinguished from the imprecision of the technique. The concentration of hydrochloric acid used in the standards and samples, 60mM, gives a pH of 1.4–1.5 (on the activity scale, with correction for ionic strength). This is probably more than necessary to quench Fe(II) oxidation, but gives samples



Table 4. Standard-additions tests

Sample	Recovery*, %	Initial†, nmole	Actual‡, nmole
Fe(II) additions (increment = 39.4 nmole)			
8.0 $\mu$ M Fe(II)	93.0 (4.8)	80.0	86.1
Mixture B§	98.9 (4.8)	80.0	80.9
$\Sigma$ Fe in mixture	94.6 (2.6)	153.4	162.2
Fe(III) additions (increment = 17.6 nmole)			
4.48 $\mu$ M Fe(III)	97.7 (0.5)	43.5	44.6
Mixture B§	82.1 (2.9)	79.4	96.8
$\Sigma$ Fe in mixture	92.8 (6.0)	157.4	169.6

\*Slope of the line fitted to the graph of amount found ( $y$ ) vs. amount added ( $x$ ), expressed as per cent of ideal slope (1.0); numbers in parentheses are relative standard deviations ( $N = 12$ ).

†Initial amount: intercept on the  $y$ -axis, *i.e.*, amount recovered without addition, normalized to a 10-ml sample.

‡Actual amount: modulus of the intercept on the  $x$ -axis, *i.e.*, amount present calculated from intercept and recovery factor, and normalized to a 10-ml sample.

§See Table 3.

and standards having the same ionic strength and major-ion composition, which experience has shown to improve the analytical accuracy and precision in IC methods.

#### Analysis of mixtures

The chief advantage of the method is the simultaneous direct determination of Fe(II) and Fe(III). To demonstrate its performance, three mixed standards were made and analysed in triplicate (Table 3). One of these mixtures was also analysed by the standard-additions method (Table 4). In addition, a USEPA quality-control sample and a lake-sediment pore-water sample,<sup>33</sup> both of which were mixtures, were analysed by this method and the Ferrozine method<sup>13</sup> (Fig. 3).

The recoveries of Fe(II) and Fe(III) from the known mixtures sometimes differed considerably from 100%, but the absolute differences were all less than the value of the detection limit. The recovery of total iron was practically 100%, however, which in conjunction with the consistently biased value of the Fe(II)/Fe(III) ratios suggests that the distribution in the mixtures was altered and that the errors in recovery of the individual species cannot be attributed solely to the random errors of the method.

However, the standard-additions analyses (Table 4) showed that the over-recovery of Fe(II) only occurred in mixtures with Fe(III). The high ratios for the mixtures might be attributed to an under-recovery of Fe(III) caused by some error in the procedure for correcting for the artifact peak, but no

such error could be demonstrated and there was some real over-recovery of Fe(II), which would have been unaffected by the artifact. Furthermore, the comparison with the Ferrozine method (Fig. 3) showed that the IC method had no more tendency to over-recover Fe(II) or under-recover Fe(III) than did the Ferrozine method. In fact, the comparison validated the artifact correction procedure, without which the two methods would have grossly disagreed on both the Fe(III) and  $\Sigma$ Fe concentrations.

The consistent positive error in the Fe(II)/Fe(III) ratio appears to be real and not peculiar to the IC method, but is difficult to explain. The batho-phenanthroline method uses an extraction procedure to separate the two species and thus avoids any alteration of the Fe(II)/Fe(III) distribution.<sup>11</sup> An excess of ammonium fluoride has also been used with 1,10-phenanthroline,<sup>34</sup> presumably to avoid the same problem by masking the Fe(III).

It has been suggested that Fe(III) tends to be photochemically reduced in acidic systems.<sup>11</sup> Photochemical reduction of Fe(III) has been discussed previously, especially for Fe(III)-dye complexes in-

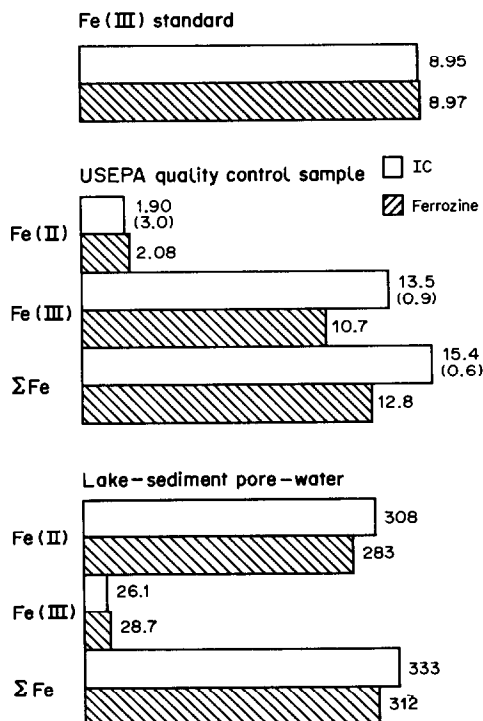


Fig. 3. Comparison of the IC method with the Ferrozine method. Concentrations in  $\mu$ M. Note the use of different scales. The USEPA quality control sample is Trace Metal I, sample 2, vial number WP481. USEPA reports the true value (for  $\Sigma$ Fe only) as 14.3  $\mu$ M and the mean recovery from performance evaluation studies as 14.1  $\mu$ M, with s.d. = 0.8  $\mu$ M. The numbers in parentheses are relative standard deviations ( $N = 3$ ). The lake-sediment pore-water sample was collected from Contrary Creek, Louisa County, Virginia, U.S.A., on 2 May 1986 and was diluted tenfold for analysis.

volving nitrogen donor atoms<sup>35</sup> or the initiation of polymerization of certain plastics.<sup>34,36</sup> It has also been observed to affect the Fe(II)/Fe(III) ratio in samples of lake water.<sup>37</sup> Since acidified Fe(III) solutions that initially contain no Fe(II) can be stored without detectable reduction, the presence of Fe(II) must be required for the photochemical reduction of Fe(III). Furthermore, since the effect has been observed in essentially pure solutions of iron(III) chloride, the process does not require agents found in natural waters, such as organic species. Simple boiling of acidified natural water samples containing Fe(II) and Fe(III) has also been shown to result in rapid conversion of Fe(III) into Fe(II),<sup>38</sup> but it is not clear from the published results whether the reaction involves species found in natural waters or is the same as the reaction observed in pure solutions. Radiolysis of aqueous solutions does produce reducing agents, chiefly electrons and hydrogen atoms,<sup>39</sup> but no experimental results are available from which to predict the possible effects of these agents on Fe(II)/Fe(III) rearrangements. The reduction of Fe(III) also proceeds in the dark,<sup>37</sup> but the effect of hydrochloric acid on the reaction is controversial, since it is stated (a) to increase the effect,<sup>37</sup> and (b) not to affect it.<sup>40</sup>

The prevention of rearrangements of Fe(II)/Fe(III) would improve the reliability of any analytical method for speciation of iron. It has been shown that FeOH<sup>2+</sup> is more susceptible to reduction than Fe<sup>3+</sup>,<sup>40,41</sup> but since at pH 0.5 the activity of FeOH<sup>2+</sup> is 2 orders of magnitude lower than the activity of Fe<sup>3+</sup>, this does not seem to be a likely reason for the problem. Until the rearrangement can be reliably prevented, the conclusion of this study is the same as that of an earlier report,<sup>37</sup> namely to avoid exposure of samples to light and to analyse them very quickly after collection.

#### CONCLUSIONS

An IC method has been developed for the simultaneous direct determination of Fe(II) and Fe(III). Sample treatment involves only filtration and acidification at the time of collection and storage at 2–5° until analysis. Detection limits for the analytical conditions considered were 1.5 μM Fe(II) and 1.2 μM Fe(III). Increasing the sample injection volume (from 50 μl) and the sensitivity of the spectrophotometric detector should lower the detection limit.

A means of preparing Fe(III)-free solutions of Fe(II) has also been developed. Hydrogen is shown to reduce both dissolved oxygen and aqueous Fe(III) in the presence of palladium black as catalyst. This procedure is useful for making accurate Fe(II) standards free from Fe(III), and should prove useful in the determination of thermodynamic data for Fe(II) and kinetic investigations of Fe(II) oxidation initiated in the absence of Fe(III).

In analysis of Fe(II)/Fe(III) mixtures, an increase in this ratio was observed and was attributed to

Fe(III) being reduced, possibly photochemically. This effect apparently requires the initial presence of Fe(II), since solutions of Fe(III) that contained no Fe(II) showed no evidence of reduction. At present, the only means of avoiding this problem is to protect samples from light and analyse them as soon as possible, preferably within a few minutes.

*Acknowledgements*—Funding was provided by the University of Virginia and by NSF awards EAR-84-18150-01 and EAR-84-17122 and a Jeffress Foundation grant to J.S.H. The advice of J. Riviello and K. Rice is appreciated. Discussions with P. Bell revealed the use of H<sub>2</sub> with Pd-b to provide anaerobic atmospheres. C. Wicks provided valuable laboratory assistance.

#### REFERENCES

1. H. Lepp (ed.), *Geochemistry of Iron*, in *Benchmark Papers in Geology*, Vol. 18. Dowden, Hutchinson, and Ross, Stroudsburg, PA, 1975.
2. H. D. Holland, *The Chemistry of the Atmosphere and Oceans*, Wiley-Interscience, New York, 1978.
3. H. D. Holland, *The Chemical Evolution of the Atmosphere and Oceans*, Princeton University Press, Princeton, 1984.
4. J. D. Hem, *U.S. Geol. Surv., Water-Supply Paper*, 2254, 1985.
5. D. K. Nordstrom, S. D. Valentine, J. W. Ball, L. N. Plummer and B. F. Jones, *U.S. Geol. Surv., Water Resources Investigations Rept.*, 84-4186, 1984.
6. M. Whitfield, *Limnol. Oceanog.*, 1970, **19**, 857.
7. J. D. Hostettler, *Am. J. Sci.*, 1984, **284**, 734.
8. R. D. Lindberg and D. D. Runnels, *Science*, 1984, **225**, 925.
9. APHA, *Standard Methods for the Examination of Water and Wastewater*, 14th Ed., American Public Health Association, Washington, D.C., 1976.
10. M. L. Moss and M. G. Mellon, *Ind. Chem. Eng., Anal. Ed.*, 1942, **14**, 862.
11. G. F. Lee and W. Stumm, *J. Am. Water Works Assoc.*, 1960, **52**, 1567.
12. M. M. Ghosh, J. T. O'Connor and R. S. Engelbrecht, *ibid.*, 1967, **59**, 897.
13. L. L. Stookey, *Anal. Chem.*, 1970, **42**, 779.
14. H. Small, T. S. Stevens and W. C. Bauman, *ibid.*, 1975, **47**, 1801.
15. C. Pohl and E. L. Johnson, *J. Chromatog. Sci.*, 1980, **18**, 442.
16. J. M. Riviello, A. Fitchett and E. Johnson, *Proc. Int. Water Conf.*, 43rd, p. 458. Eng. Soc. West. Pa., 1982.
17. R. Slingsby and J. M. Riviello, *LC Mag.*, 1983, **1**, 354.
18. J. M. Riviello, in *Ion Exchange Technology*, D. Naden and M. Streat (eds.), p. 585. Horwood, Chichester, 1984.
19. MCA, *Guide for Safety in the Chemical Laboratory*, 2nd Ed., Manufacturing Chemists' Association, Van Nostrand-Reinhold, New York, 1972.
20. D. K. Nordstrom, *Geochim. Cosmochim. Acta*, 1977, **41**, 1835.
21. J. A. Glaser, D. L. Foerster, G. D. McKee, S. A. Quave and W. L. Budde, *Environ. Sci. Technol.*, 1981, **15**, 1426. See also letters, *ibid.*, 1982, **16**, 430A–431A.
22. G. L. Long and J. D. Winefordner, *Anal. Chem.*, 1983, **55**, 712A.
23. R. Klein, Jr. and C. Hach, *Am. Lab.*, 1977, **9**, No. 7, 21.
24. A. Aranki, S. A. Syed, E. B. Kenney and R. Freter, *Appl. Microbiol.*, 1969, **17**, 568.
25. L. N. Plummer, B. F. Jones and A. H. Truesdell, *U.S. Geol. Surv., Water-Resources Investigations*, 76-13, 1976.

26. P. C. Singer and W. Stumm, *Oxygenation of Ferrous Iron*, Federal Water Quality Administration, Report 14010-06/69, 1970.
27. F. H. Pollard, P. Hanson and W. J. Geary, *Anal. Chim. Acta*, 1959, **20**, 26.
28. T. D. Brock, S. Cook, S. Petersen and J. L. Mosser, *Geochim. Cosmochim. Acta*, 1976, **40**, 493.
29. N. Lazaroff, W. Sigal and A. Wasserman, *Appl. Environ. Microbiol.*, 1982, **43**, 924.
30. S. J. Onysko, R. L. Kleinmann and P. M. Erickson, *ibid.*, 1984, **48**, 229.
31. V. C. Kennedy, G. W. Zellweger and B. F. Jones, *Water Resour. Res.*, 1974, **10**, 785.
32. P. C. Singer and W. Stumm, *Science*, 1970, **167**, 1121.
33. A. T. Herlihy and A. L. Mills, *Appl. Environ. Microbiol.*, 1985, **49**, 179.
34. M. G. Evans, M. Santappa and N. Uri, *J. Polymer Sci.*, 1951, **7**, 243.
35. G. K. Oster and G. Oster, *J. Am. Chem. Soc.*, 1959, **81**, 5543.
36. M. G. Evans and N. Uri, *Nature*, 1949, **164**, 404.
37. J. W. McMahon, *Limnol. Oceanog.*, 1967, **12**, 437.
38. J. Shapiro, *ibid.*, 1966, **11**, 293.
39. A. Appleby, G. Scholes and M. Simic, *J. Am. Chem. Soc.*, 1963, **85**, 3891.
40. P. G. David, *J. Chem. Soc., Chem. Commun.*, 1972, **23**, 1294.
41. R. Broszkiewicz and S. Minc, *Nukleonika*, 1963, **8**, 165.

## SPECTROPHOTOMETRIC DETERMINATION OF SOME ANTIAMOEBCIC AND ANTHELMINTIC DRUGS WITH METOL AND CHROMIUM(VI)

C. S. P. SASTRY, M. ARUNA and A. RAMA MOHANA RAO

Foods and Drugs Laboratories, School of Chemistry, Andhra University, Waltair 530003, India

(Received 5 May 1987. Revised 24 June 1987. Accepted 21 August 1987)

**Summary**—A sensitive spectrophotometric method is reported for the determination of tinidazole (TZ), metronidazole (MZ), benzoyl metronidazole (BMZ) or niclosamide (NS) either in pure form or in formulations. This method is based on reduction with zinc dust and hydrochloric acid followed by reaction with metol and potassium dichromate at pH  $3.0 \pm 0.2$  to give a coloured product having maximum absorbance at 720 nm (for TZ, MZ and BMZ) or 530 nm (for NS).

5-Nitroimidazoles such as tinidazole (TZ), metronidazole (MZ) and benzoyl metronidazole (BMZ), and the 4'-nitrosalicylanilide derivative niclosamide (NS) are extensively used as antiamebic and anthelmintic agents (for structures see Table 1). They have been officially determined by titrimetry with glacial acetic acid solution of perchloric acid (MZ,<sup>1-3</sup> BMZ<sup>2</sup>) or with tetrabutylammonium hydroxide (NS<sup>1,2</sup>). They have also been determined by ultraviolet spectrophotometry (TZ,<sup>4-7</sup> MZ,<sup>8-12</sup> BMZ<sup>12</sup> and NS<sup>13,14</sup>). Most of the methods for spectrophotometric determination of TZ,<sup>15-19</sup> MZ<sup>18-28</sup> and NS<sup>18</sup> in the visible region, require initial reduction by treatment with zinc and hydrochloric acid followed by application of a standard procedure to the resulting primary aromatic amine. In continuation of our investigations on the spectrophotometric determination of primary aromatic amines with metol (4-methylaminophenol sulphate) and chromium(VI),<sup>29-31</sup> we now describe the application of this combination to determination of TZ, MZ, BMZ and NS. This procedure has been applied to a wide variety of pharmaceutical preparations.

### EXPERIMENTAL

#### Reagents

All solutions were prepared in doubly distilled water. A freshly prepared 0.2% aqueous solution of metol (BDH) was always used. Potassium dichromate (Reechem) (0.01M) solution was prepared. The buffer solution (pH 2.9) was obtained by diluting a mixture of 250 ml of 0.2M potassium hydrogen phthalate (Ranbaxy) and 254 ml of 0.1M hydrochloric acid (BDH) to 1 litre with water.

**Standard drug solutions.** About 20 mg of each drug was accurately weighed and treated with 10 ml of 1M hydrochloric acid and 0.25 g of zinc dust added in portions. After standing for 20 min (for TZ, MZ and BMZ) or 45 min (for NS) at room temperature, the solution was filtered through cotton wool; the residue was washed with three 5-ml portions of solvent (water for TZ, MZ and BMZ, methanol for NS) and the filtrate was neutralized with sodium hydroxide and diluted with solvent to volume in a 100-ml standard flask.

All chemicals used were of analytical or pharmacopoeial grade.

#### Procedures

**Bulk samples.** A portion of the drug solution (0.3–3.0 ml for TZ, 0.2–2.0 ml for MZ, 0.3–4.5 ml for BMZ and 0.4–4.0 ml of NS) was accurately measured into a 25-ml standard flask. After addition of 15 ml of buffer solution, 1 ml of 0.2% metol solution and 1 ml of 0.01M potassium dichromate, the solution was diluted to the mark with water (for TZ, MZ and BMZ) or methanol (for NS) and the absorbance measured at 720 nm (for TZ, MZ or BMZ) or 530 nm (for NS) during the next 1–10 min for TZ, MZ or BMZ, or 15 min–3 hr for NS against a reagent blank prepared in a similar manner. The drug concentration was read from the appropriate calibration graph prepared under identical conditions.

**Pharmaceutical preparations.** An amount of powdered tablet or of syrup equivalent to 20 mg of drug was extracted with warm acetone (three 5-ml portions), the combined extracts were evaporated on a steam-bath and the residue was treated as for preparation of standard drug solution. This solution was then analysed as above. The results were compared with those from the Indian Pharmacopoeial non-aqueous titrimetric method using perchloric acid as titrant and Malachite Green as indicator (for MZ and BMZ), the potentiometric method using tetrabutylammonium hydroxide as titrant (for NS) and the Nagvankar spectrophotometric method<sup>4</sup> at 368 nm (for TZ). The results obtained are summarized in Table 3.

### RESULTS AND DISCUSSION

#### Absorption spectra

The absorption spectra of the reaction products from the reduced drugs show characteristic  $\lambda_{\max}$  values (Fig. 1 and 2: 720 nm for TZ, MZ and BMZ, 530 nm for NS), whereas the metol–Cr(VI) or metol–Cr(VI)–unreduced drug combinations have very low or no absorption in these regions. The calibration graphs are linear over a concentration range ( $\mu\text{g/ml}$ ) of 2.4–24.0 for TZ, 1.6–16.0 for MZ, 2.4–36.0 for BMZ and 3.2–32.0 for NS. The coloured species are stable for 1–10 min (for reduced TZ, MZ or BMZ) and 15 min–3 hr (for reduced NS); Fig. 3.

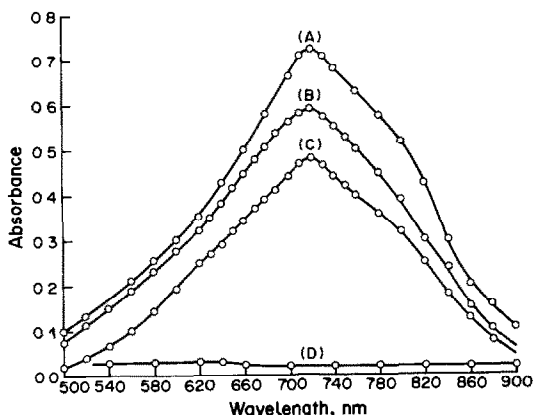


Fig. 1. Absorption spectra of benzoyl metronidazole (A), metronidazole (B) and tinidazole (C)-metol-Cr(VI) systems (concentration of benzoyl metronidazole  $1.16 \times 10^{-4}M$ , metronidazole  $8.76 \times 10^{-5}M$ , tinidazole  $6.47 \times 10^{-5}M$ , metol  $2.32 \times 10^{-4}M$  and potassium dichromate  $4.0 \times 10^{-4}M$ ): reagent blank *vs.* distilled water (D).

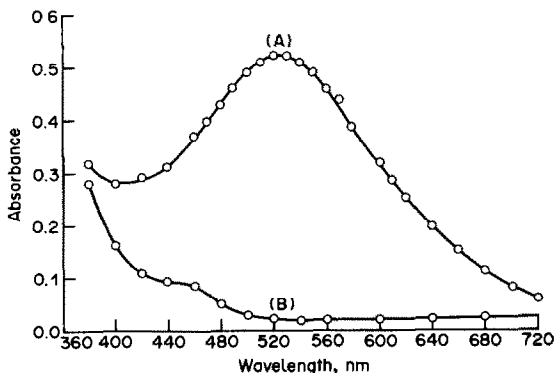


Fig. 2. Absorption spectra of niclosamide-metol-Cr(VI) system (concentration of niclosamide  $9.17 \times 10^{-5}M$ , metol  $2.32 \times 10^{-4}M$  and potassium dichromate  $4.0 \times 10^{-4}M$ ): reagent blank *vs.* distilled water (B).

The reaction conditions were established by variation of one parameter at a time. For the reduction, use of 0.5–2.0*M* hydrochloric acid and 0.2–1.0 g of zinc dust was found optimal. The reduction time was established by increasing it in increments of 5 min, and it was found that reduction for 15 min for TZ, MZ, BMZ and 40 min for NS is sufficient to yield maximum absorbance. For all four drugs use of

0.5–3.0 ml of metol solution and 0.5–2.0 ml of dichromate solution was considered optimal.

Several oxidants (potassium dichromate, sodium metaperiodate, chloramine-T, potassium ferricyanide, ferric chloride, ceric ammonium sulphate, ferric ammonium sulphate and iodine) were tried, but potassium dichromate was preferred, for the high sensitivity obtained.

#### Analytical data

The optical characteristics and figures of merit are given in Table 2. The values obtained by the proposed and reference methods for pharmaceutical preparations are compared in Table 3, together with the results of recovery experiments. Other active components such as diloxanide furoate, diiodohydroxyquinoline and furazolidone that are generally present in combined formulations did not interfere. Commonly encountered excipients such as starch, talc, lactose and magnesium stearate also did not interfere. The present method has advantages over the pharmacopeial and other reported methods in terms of simplicity, sensitivity and freedom from interferences.

The chemistry of the colour reaction may be suggested on the basis of a previously reported mechanism.<sup>32,33</sup> The nitro compound is first reduced under the proposed conditions to the corresponding amino derivative. It is probable that the *p*-*N*-methylbenzoquinone monoimine formed *in situ* from the metol-chromium(VI) combination, being a good

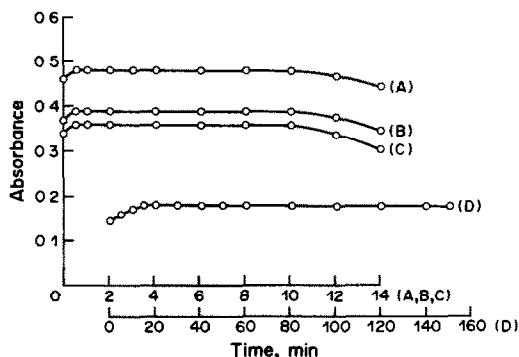


Fig. 3. Rate of colour development and stability of colour (A = benzoyl metronidazole, B = metronidazole, C = tinidazole, D = niclosamide).

Table 1. Structures of the drugs

R:—CH <sub>2</sub> CH <sub>2</sub> SO <sub>2</sub> CH <sub>2</sub> CH <sub>3</sub> —CH <sub>2</sub> CH <sub>2</sub> OH —CH <sub>2</sub> CH <sub>2</sub> OOC <sub>6</sub> H <sub>5</sub>	Tinidazole Metronidazole Benzoyl metronidazole
	Niclosamide

Table 2. Optical characteristics, precision and accuracy

Parameters	Benzoyl			
	Tinidazole	Metronidazole	metronidazole	Niclosamide
Beer's law limits, $\mu\text{g/ml}$	2.4-24.0	1.6-16.0	2.4-36.0	3.2-32.0
Molar absorptivity, $l.\text{mole}^{-1}.\text{cm}^{-1}$	$7.4 \times 10^3$	$6.82 \times 10^3$	$6.19 \times 10^3$	$5.96 \times 10^3$
*Regression equation				
Slope ( $b$ )	$2.99 \times 10^{-2}$	$3.97 \times 10^{-2}$	$2.23 \times 10^{-2}$	$1.71 \times 10^{-2}$
Intercept ( $a$ )	$4 \times 10^{-4}$	$1.6 \times 10^{-3}$	$3.4 \times 10^{-3}$	$1.12 \times 10^{-2}$
Correlation coefficient ( $r$ )	0.9998	0.9999	0.9999	0.9997
Relative standard deviation, %	1.3	1.1	0.8	0.6
Range of error, % (95% confident limit)	$\pm 1.4$	$\pm 1.1$	$\pm 0.9$	$\pm 0.6$

\* $A = a + bC$ , where  $C$  is the concentration in  $\mu\text{g/ml}$ .

Table 3. Analysis of dosage forms

Drug	Nominal amount, mg	Found, mg		Recovery by proposed method, †%
		Reference* method	Proposed method	
<b>TABLETS</b>				
Tinidazole	300	299	295	98.0
Tinidazole + DF	300	299	296	99.0
Metronidazole	200	199	198	98.9
Metronidazole + DF	200	198	197	97.9
Metronidazole + DIHQ	200	198	199	98.9
Niclosamide	500	504	508	101.0
<b>SYRUPS</b>				
Benzoyl metronidazole (7.8 ml)	500	496	496	98.6
Tinidazole + FZ	50	48.0	47.7	97.4
Benzoyl metronidazole + FZ (7.8 ml)	250	245	244	97.0

DIHQ = di-iodohydroxyquinoline 250 mg; DF = diloxanide furoate 250 mg or 500 mg; FZ = furazolidone 30 mg;

\*Reported method for TZ,<sup>4</sup> I.P. method for MZ, BMZ and NS<sup>2</sup>.

†For 100 mg added to each sample.

electron-acceptor, forms a charge-transfer complex with the amino derivatives as electron-donors. The variation in  $\lambda_{\text{max}}$  and stability of the coloured species formed from the two types of drug may be due to the difference in the ionization potential of the donor [the greater basic character of a 1-substituted-5-aminoimidazole (reduced TZ, MZ, or BMZ) relative to the primary aromatic amine (reduced NS) is due to the presence of two heterocyclic nitrogen atoms remote from the substituent].<sup>34</sup> The earlier report on the determination of aspartic acid as its imidazole derivative by treatment with metol and sodium hypochlorite<sup>35</sup> supports this proposition.

**Acknowledgements**—Thanks are due to Messrs. Biddle-Sawyer Private Limited, Bombay, and Crips Therapeutics, Waltair, for their generous gift of samples of some of the drugs.

#### REFERENCES

1. *British Pharmacopoeia, 1980*, Her Majesty's Stationery Office, London, 1980.
2. *Indian Pharmacopoeia, 1985*, Ministry of Health and Family Welfare, Govt. of India, New Delhi, 1985.
3. *United States Pharmacopoeia XX, National Formulary XV, 1980*, Mack Printing Company, Easton, 1980.
4. C. V. Nagvankar, *East. Pharm.*, 1982, **25**, 117.
5. K. N. Raut, S. D. Sabnis and S. A. Vaidya, *Indian J. Pharm. Sci.*, 1984, **46**, 98.
6. O. S. Kamalapurkar and C. Menezes, *Indian Drugs*, 1984, **22**, 164.
7. D. M. Shingbal and A. S. Khandeparkar, *ibid.*, 1987, **24**, 363.
8. C. Andras, L. Endre, A. Magdolna and G. Hedvig, *Kiserl. Orvostud.*, 1981, **33**, 166.
9. A. Samu and A. Csiba, *Proc. Hung. Ann. Meet. Biochem.*, 1979, **31**, 420.
10. Yuzhen Wang, *Yayao Gonagye*, 1985, **16**, 245; *Chem. Abstr.*, 1985, **103**, 129173.
11. A. B. Fabayo and S. K. Grudzinski, *Acta Pol. Pharm.*, 1985, **42**, 49.
12. K. P. R. Chowdary and K. T. R. Kumar, *Indian J. Pharm. Sci.*, 1983, **45**, 182.
13. Changjiu Liu, *Yaowu Fenxi Zazhi*, 1983, **3**, 56; *Chem. Abstr.*, 1983, **99**, 10966.
14. N. Bergisadi and D. Sarigul, *Acta. Pharm. Turc.*, 1986, **28**, 51.
15. N. M. Sanghavi, N. G. Joshi and D. G. Saoji, *Indian J. Pharm. Sci.*, 1979, **41**, 226.
16. T. P. Gandhi, P. R. Patel, V. C. Patel and S. C. Manakiwala, *Indian Drugs*, 1980, **18**, 76.
17. O. S. Kamalapurkar and J. J. Chudasama, *East. Pharm.*, 1983, **26**, 207.
18. N. M. Sanghavi, V. H. Sathe and M. M. Padki, *Indian Drugs*, 1983, **20**, 341.
19. M. B. Devani, C. J. Shishoo, K. Doshi and A. K. Shah, *Indian J. Pharm. Sci.*, 1981, **43**, 151.
20. N. M. Sanghavi and H. S. Chandramohan, *Indian J. Pharm.*, 1974, **36**, 151.
21. D. M. Shingbal and G. E. Natekar, *East. Pharm.*, 1979, **22**, 183.

22. R. G. Bhatkar and S. K. Chodankar, *Indian J. Pharm. Sci.*, 1980, **42**, 127.
23. B. A. Moussa, *Int. J. Pharm.*, 1982, **10**, 199.
24. O. S. Kamalapurkar and S. R. S. Priolkar, *Indian Drugs*, 1983, **20**, 391.
25. T. P. Gandhi, P. R. Patel, V. C. Patel, S. K. Patel and R. N. Gilbert, *J. Inst. Chem. India.*, 1984, **56**, 127.
26. P. Populaire, B. Decouvelaere, G. Lebreton and S. Pascal, *Ann. Pharm. Fr.*, 1968, **26**, 549.
27. J. Breinlich, *Dtsch. Apothztg.*, 1964, **104**, 535.
28. G. M. Warke, *Indian J. Pharm. Sci.*, 1974, **36**, 160.
29. R. Ramakrishna and C. S. P. Sastry, *Talanta*, 1979, **26**, 861.
30. R. Ramakrishna, P. Siraj and C. S. P. Sastry, *Acta Ciencia Indica*, 1980, **60**, 140.
31. *Idem*, *Indian J. Pharm. Sci.*, 1979, **41**, 200.
32. C. S. P. Sastry, T. M. K. Reddy and B. G. Rao, *Indian Drugs*, 1984, **21**, 145.
33. C. S. P. Sastry, B. G. Rao, B. S. Reddy and S. S. N. Murthy, *J. Indian Chem. Soc.*, 1981, **57**, 665.
34. M. R. Grimmett, in *Comprehensive Organic Chemistry*, D. Barton and W. D. Ollis, (eds.) Vol. 4, p. 366. Pergamon Press, Oxford, 1979.
35. M. K. Tummuru, K. E. Rao and C. S. P. Sastry, *Mikrochim. Acta*, 1984 **III**, 199.

# MASS SPECTROMETRIC BEHAVIOUR OF PENTACHLOROPHENYL $\beta$ -CARBOXYLENOLATE PHOSPHINO NICKEL(II) COMPLEXES: AN EXAMPLE OF THERMAL GENERATION OF A NICKEL(III) SPECIES

B. CORAIN\* and B. LONGATO

C. N. R., Centro di Studio sulla Stabilità e Reattività dei Composti di Coordinazione, c/o Dipartimento di Chimica Inorganica, Metallorganica ed Analitica, Via Marzolo 1, I35100 Padova, Italy

A. M. MACCIONI†, B. PELLI and P. TRALDI

C. N. R., Area della Ricerca di Padova, Corso Stati Uniti 4, I35100 Padova, Italy

F. R. KREISSL

Anorganisch-Chemisches Institut, T. U. München, Lichtenbergstrasse 4, D8046 Garching, West Germany

(Received 22 June 1987. Accepted 21 August 1987)

**Summary**—The mass spectral behaviour of pentachlorophenyl  $\beta$ -carboxylenolate phosphino nickel(II) square planar complexes has been investigated under electron impact (EI) and field desorption (FD) conditions. The fragmentation has been interpreted on the basis of the B/E linked scans and mass-analysed ion kinetic energy (MIKE) techniques. The acetylacetonate diphenylphosphino complex was found to undergo a solid state reaction in the probe, which led to the generation *in situ* of a nickel(III) chloro complex. Careful control of instrumental conditions and computer-assisted EI measurements made it possible to characterize the addition products as  $[\text{NiCl}(\text{C}_6\text{Cl}_5)(\text{AcAc})\text{PPh}_2\text{Me}]$  and to propose a mechanism for its solid state generation.

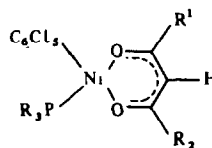
Mass spectrometry has proved to be a powerful tool for investigating the structure and reactivity of coordination and organic compounds.<sup>1,2</sup> In this connection, however, the *conditio sine qua non* for its successful utilization is the absence of undesirable chemical transformations of the analyte in the mass spectrometer, *i.e.*, in (i) the inlet system; (ii) the ion source; (iii) the analyser region.

Chemical transformations (generally isomerizations and chemical degradations) arise from the lability of the compound under study with respect to temperature and/or the ionization method employed. For these reasons, in the last decade much research has been devoted to the development of mild sample evaporation systems<sup>3</sup> and "soft" ionization methods.<sup>4-6</sup>

In previous papers we have described examples of potential errors in interpretation connected with points (ii)<sup>7</sup> and (iii).<sup>8</sup> In the former case we demonstrated the occurrence of a fast isomerization process in the ionization chamber, in the latter, by com-

parison of electron impact (EI) spectra, with B/E linked scans<sup>9</sup> and mass-analysed ion kinetic energy spectra,<sup>10</sup> we were able to describe a "slow" isomerization process, with kinetics such that it occurred only in the second field-free region of our instrument.

We report here the results obtained in a mass spectrometric investigation of some novel pentachlorophenyl  $\beta$ -carboxylenolate phosphino nickel(II) complexes<sup>11</sup> (compounds 1-9). Electron impact and field desorption (FD)<sup>12</sup> were used as ionization techniques, and fragmentations were investigated by using B/E linked scans and mass-analysed ion kinetic energy (MIKE) spectra.



\*To whom correspondence should be addressed.

†On leave from Istituto di Chimica Farmaceutica e Tossicologica dell'Università, I90100 Cagliari, Italy.

1:  $\text{PR}_3 = \text{PPh}_2\text{Me}$ ,  $\text{R}^1 = \text{R}^2 = \text{Me}$

2:  $\text{PR}_3 = \text{PPh}_2\text{Me}$ ,  $\text{R}^1 = \text{Me}$ ,  $\text{R}^2 = \text{Ph}$

3:  $\text{PR}_3 = \text{PPh}_2\text{Me}$ ,  $\text{R}^1 = \text{R}^2 = \text{t-But}$



- 4: PR<sub>3</sub> = PPh<sub>2</sub>Me, R<sup>1</sup> = t-But, R<sup>2</sup> = CF<sub>3</sub>  
 5: PR<sub>3</sub> = PPh<sub>2</sub>Me, R<sup>1</sup> = Me, R<sup>2</sup> = OEt  
 6: PR<sub>3</sub> = PPhMe<sub>2</sub>, R<sup>1</sup> = R<sup>2</sup> = Me  
 7: PR<sub>3</sub> = PPhMe<sub>2</sub>, R<sup>1</sup> = Me, R<sup>2</sup> = Ph  
 8: PR<sub>3</sub> = PMe<sub>3</sub>, R<sup>1</sup> = R<sup>2</sup> = Me  
 9: PR<sub>3</sub> = PMe<sub>3</sub>, R<sup>1</sup> = Me, R<sup>2</sup> = NHMe

We describe the unexpected behaviour of compound 1, which undergoes facile Cl<sup>•</sup> addition in the mass spectrometer. The mechanism of this reaction has been studied in detail.

### EXPERIMENTAL

Complexes 1–3 were prepared as described previously.<sup>11</sup> Mass spectrometric measurements were performed on Varian MAT 311 and VG ZAB2F<sup>13</sup> instruments with a typical ion-source temperature of 200°. The mass values refer to the <sup>58</sup>Ni and <sup>35</sup>Cl isotopic forms. The majority of the experiments on 1 were performed with the VG instrument operating in EI conditions (70 eV, 200 μA), in which the sample, contained in a glass capillary, was *ca.* 1.2 cm from the electron beam. The probe which carried the sample was usually heated to 100°. FD measurements were performed on the MAT instrument with an extraction potential of 6 kV and an ion-source temperature of 160°. Differential scanning calorimetric measurements were performed with a Perkin Elmer DSC-4 apparatus.

### RESULTS AND DISCUSSION

The most abundant and significant ionic species arising from the EI of compounds 1–3 are reported in Table 1, and the whole spectra of compounds 1–9 are available as supplementary material. All the compounds displayed easily detected molecular ions and fragment ions which are simply related to the structure of the neutral molecules. These results suggest that no isomerization processes take place on EI.

Field desorption spectra show, for all the com-

pounds, only the peaks corresponding to M<sup>+</sup> species, indicating a low proton affinity. Furthermore, the lack of fragment ions in FD conditions indicates, in principle, either that the fragmentation processes are quite slow and hence undetectable in the small time span of the field desorption experiment, or that the compounds examined exhibit a high thermal stability (it is well known that the "fragment ions" observed in FD conditions are, in fact, very often the molecular ions of pyrolysis products generated on the heated emitter).

The fragmentation pattern found for compound 1 in EI experiments, as confirmed by B/E linked scans and from the analysis of isotopic clusters, is reported in Scheme 1. Analogous fragmentation patterns occur for 2 and 3.

The only two primary decomposition pathways are due to cleavage 1, leading to the complementary ions [C<sub>6</sub>Cl<sub>5</sub>PR<sub>1</sub>R<sub>2</sub>R<sub>3</sub>]<sup>+</sup> and [M – C<sub>6</sub>Cl<sub>5</sub>PR<sub>1</sub>R<sub>2</sub>R<sub>3</sub>]<sup>+</sup>, and the cleavage of the pentachlorophenyl–Ni bond with H rearrangement, giving rise to the [C<sub>6</sub>HCl<sub>5</sub>]<sup>+</sup> ion at *m/z* 248. Further sequential Cl<sup>•</sup> losses and fragment ions related to the phosphine moiety are responsible for the other ionic species present in the mass spectra of compounds 1–3 (see Table 1).

When the probe temperature is increased from 100° to 140° compound 1 shows quite unexpected behaviour: an abundant ion at *m/z* 639, formally corresponding to [M + Cl]<sup>+</sup> ions is now present (Fig. 1). Hence, the increase in probe temperature does not seem to lead to degradative pyrolysis processes, but to a specific addition reaction which gives rise to the [M + Cl]<sup>+</sup> species. This addition reaction could arise from several different mechanisms:

(i) gas-phase, ion-molecule reactions:

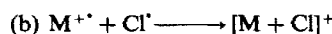
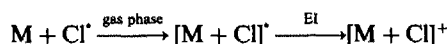
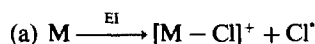


Table 1. EI mass spectra of compounds 1–3

Fragments	<i>m/z</i> (Relative abundance %)		
	Compound 1	Compound 2	Compound 3
M <sup>+</sup>	604(1.6)	542(0.3)	480(5)
[M – (Ni(AcAc))]⁺	447(1)	385(1.2)	323(65)
[M – (PhPMeCl)]⁺	446(6)	—	—
[M – (Ni(AcAc) + Cl)]⁺	412(21)	349(4)	—
[M – (Ni(AcAc) + HCl)]⁺	411(10)	350(2)	288(57)
[M – (PhPMeCl + HCl)]⁺	410(14)	—	—
[M – (Ni(AcAc) + Cl <sub>2</sub> )]⁺	377(4)	315(1.8)	253(80)
[C <sub>6</sub> Cl <sub>5</sub> H]⁺	248(10)	248(58)	—
[C <sub>6</sub> Cl <sub>4</sub> H]⁺	213(3)	213(17)	—
[M – C <sub>6</sub> Cl <sub>5</sub> ]⁺	—	—	233(15)
[PPh <sub>2</sub> Me]⁺	200(83)	—	—
[PPh <sub>2</sub> ]⁺	185(35)	—	—
[PPh <sub>2</sub> – H <sub>2</sub> ]⁺	183(100)	—	—
[C <sub>6</sub> Cl <sub>5</sub> H]⁺	178(1)	178(10)	—
[M – (C <sub>6</sub> Cl <sub>5</sub> PR <sub>3</sub> )]⁺	157(11)	157(2)	157(30)
[PPhMe <sub>2</sub> ]⁺	—	138(100)	—

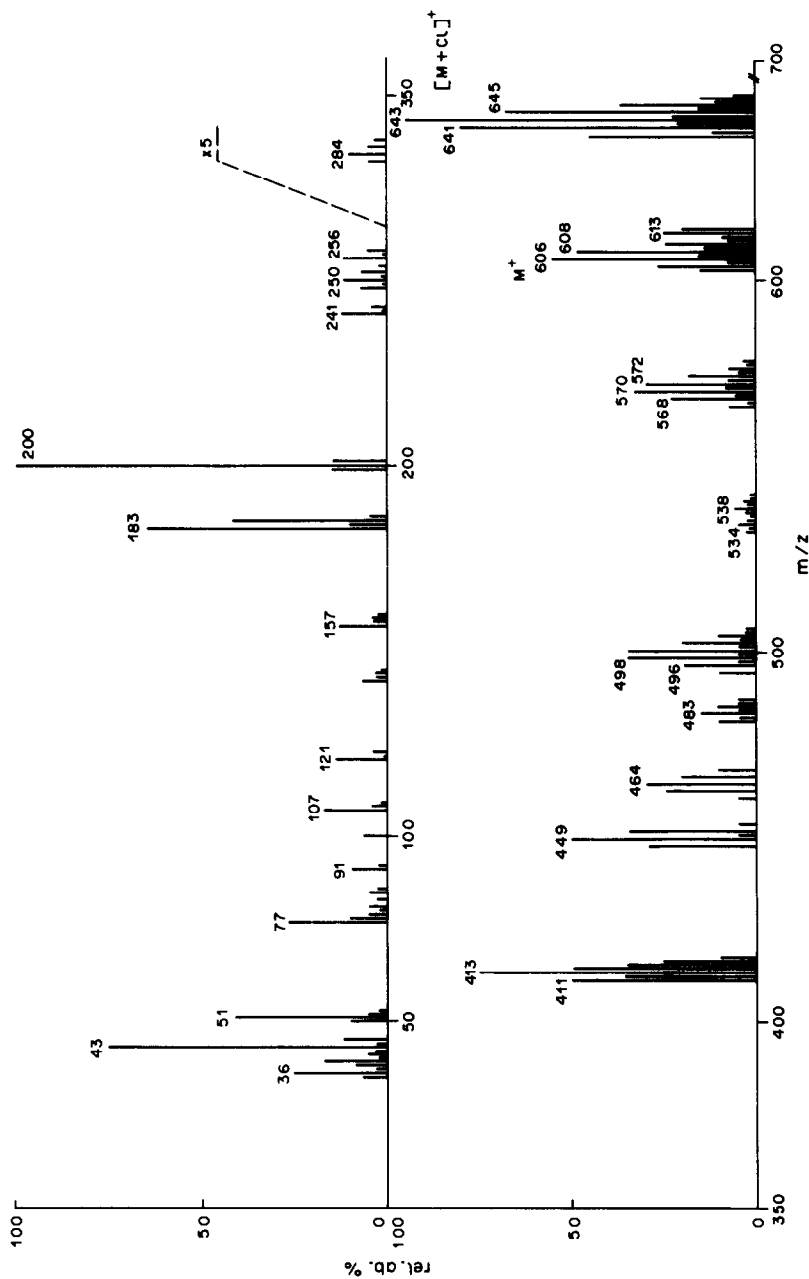
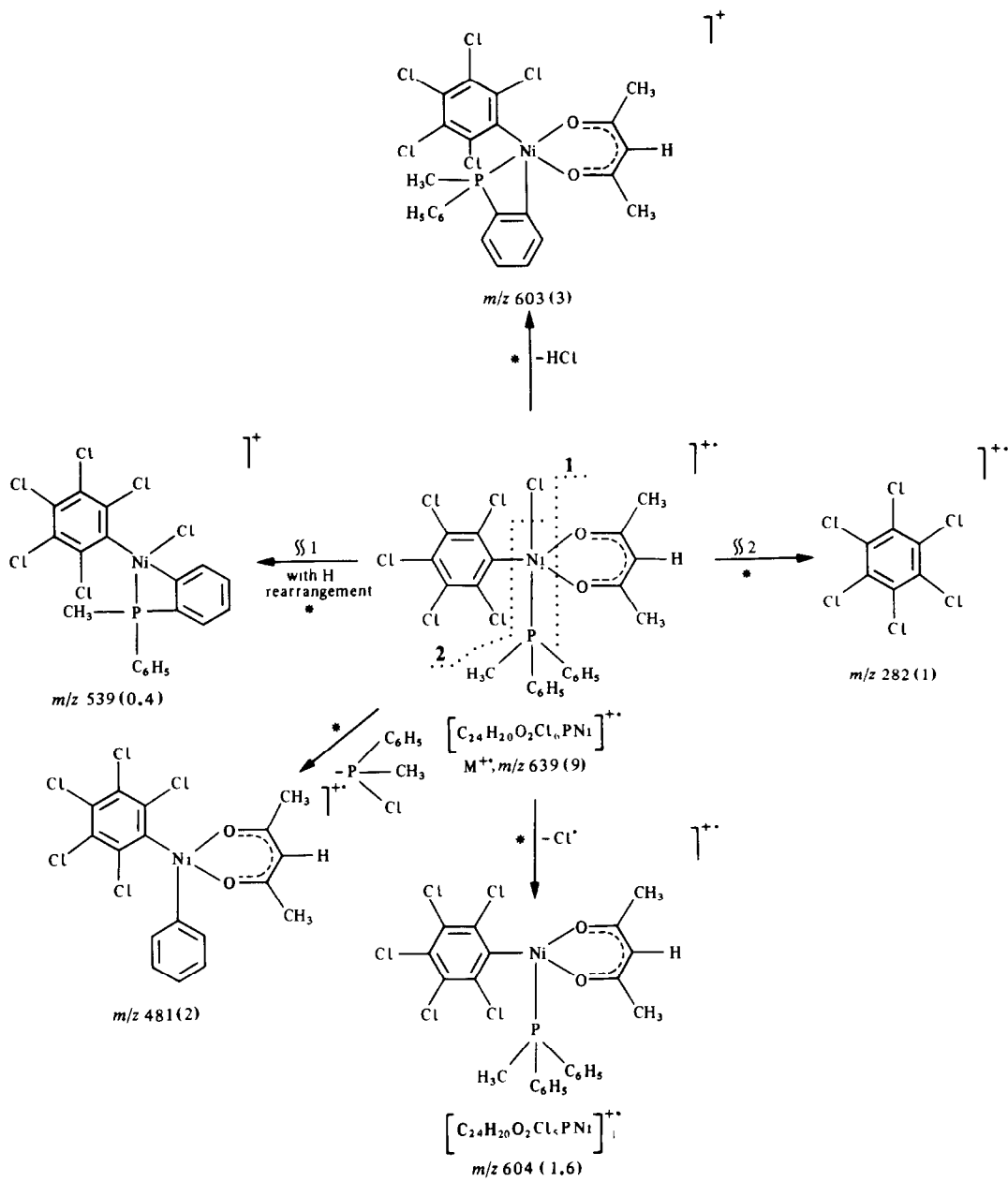
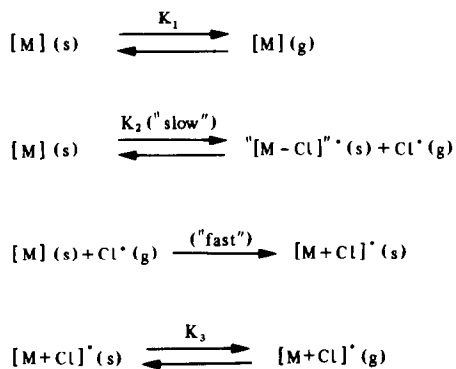


Fig. 1. 70-eV EI mass spectrum of compound 1 obtained with a probe temperature in the range 120–140°.



Scheme 2



Scheme 3

"[M - Cl]"<sub>(s)</sub>, and a chlorine radical; (ii) Cl<sup>•</sup> reacts instantaneously with the stoichiometric amount of solid 1, giving a particularly volatile nickel(III) complex, 1 + Cl; (iii) the significant presence of 1 + Cl in the EI spectrum of 1 at lower temperatures is also explained, the high vacuum conditions of the probe compartment representing the fundamental force for driving the consumption of solid 1 along a chemical route, thus leading to solid 1 + Cl; (iv) the overall effect of the probe temperature on the relative abundance of *m/z* 604 and 639 (Table 2) obviously agrees with the mechanism depicted in Scheme 3.

As a final comment, it is worthwhile noting that a slight complication in interpreting the spectrum of 1 stems from the fact that *m/z* 604 is produced not only from solid 1 but also by electron impact induced decomposition of the ionic species at *m/z* 639 (see Scheme 2).

#### REFERENCES

1. J. Charalambous, *Mass Spectrometry of Metal Compounds*, Butterworths, London, 1975.
2. J. L. Holmes, *Org. Mass Spectrom.*, 1985, **20**, 169.
3. P. Traldi, U. Vettori and F. Dragoni, *ibid.*, 1982, **17**, 587.
4. H. R. Schulten, T. Komori and T. Kawasaki, *Tetrahedron*, 1977, **33**, 2595.
5. K. Hostettmann, J. Doumas and M. Hardy, *Helv. Chim. Acta*, 1981, **64**, 297.
6. D. Fraisse, J. C. Tabet, M. Becchi and J. Raynaud, *Biomed. Environ. Mass Spectrom.*, 1986, **13**, 1.
7. S. Daolio, P. Traldi, B. Pelli, M. Basato, B. Corain and F. R. Kreissl, *Inorg. Chem.*, 1984, **23**, 4750.
8. M. Basato, B. Corain, A. C. Veronese, S. Daolio, B. Pelli and P. Traldi, *Org. Mass Spectrom.*, 1985, **20**, 46.
9. A. P. Bruins, K. R. Jennings and S. Evans, *Int. J. Mass Spectrom. Ion Phys.*, 1978, **26**, 395.
10. R. G. Cooks in *Collision Spectroscopy*, R. G. Cooks (ed.), Plenum Press, New York, 1978.
11. B. Corain, B. Longato, G. Valle and R. Angeletti, *Inorg. Chim. Acta*, 1987, **130**, 243.
12. R. Maffei-Facino, M. Carini, P. Traldi and O. Tofanetti in *Chromatography and Mass Spectrometry in Biomedical Sciences*, 2, A. Frigerio (ed.), Elsevier, Amsterdam, 1983.
13. R. P. Morgan, J. H. Beynon, R. H. Bateman and B. N. Green, *Int. J. Mass Spectrom. Ion Phys.*, 1978, **28**, 171.
14. S. Daolio, B. Facchin, C. Pagura and P. Traldi, *Org. Mass Spectrom.* 1984, **19**, 347.
15. The relevant diagram is available as supplementary material.

## SPECTROPHOTOMETRIC DETERMINATION OF TRYPTOPHAN BY REACTION WITH NITROUS ACID

KRISHNA K. VERMA and ARCHANA JAIN

Department of Chemistry, Rani Durgavati University, Jabalpur 482001, India

J. GASPARIČ

Faculty of Pharmacy, Charles University, Hradec Králové, Czechoslovakia

(Received 28 May 1986. Revised 1 June 1987. Accepted 21 August 1987)

**Summary**—The heterocyclic nucleus in tryptophan is oxidized by nitrous acid at elevated temperature to produce a phenolic intermediate which further reacts with nitrous acid to form a nitro compound that has a golden yellow colour in alkaline medium. The maximum absorbance is obtained at 400 nm with maximum molar absorptivity of  $9.44 \times 10^3 \text{ l. mole}^{-1} \text{ cm}^{-1}$ . Derivatives of tryptophan such as indole-3-acetic acid, tryptamine and tryptophanamide, as well as indole, produce the same colour, but some others, e.g., 5-hydroxytryptamine and 5-hydroxyindole-3-acetic acid do not give the colour reaction. A plausible mechanism is proposed to explain this behaviour.

Tryptophan contains an indole group. It is a vital constituent of proteins and indispensable in human nutrition for establishing and maintaining a positive nitrogen balance. Although there are several methods available<sup>1</sup> for its determination, they are tedious and the results often uncertain. Many of the spectrophotometric methods involve condensation with an aldehyde such as 4-dimethylaminobenzaldehyde and oxidation of the product. However, it is difficult to control the oxidation step to give a stable colour and reproducible results.<sup>2-8</sup> Methods have also been proposed which are based on oxidation with nitrous acid and coupling with *N*-(1-naphthyl)-ethylenediamine,<sup>9,10</sup> nitration,<sup>11</sup> or reaction with acetic anhydride<sup>12</sup> or anthrone.<sup>13</sup> Although tryptophan is normally determined after alkaline hydrolysis of proteins, improvements to prevent oxidative destruction of its indole group during acid hydrolysis have also been made.<sup>14,15</sup> 2-Hydroxy-5-nitrobenzyl bromide is thought to react with all tryptophan residues in intact proteins,<sup>16,17</sup> but low and inconsistent results have also been reported.<sup>18</sup> Methods based on the fluorescence and ultraviolet absorption properties of tryptophan<sup>19,20</sup> or their modification by reagents such as *N*-bromosuccinimide,<sup>21</sup> require the protein sample to be soluble and denatured.<sup>22</sup> Recently, a spectrophotometric method was proposed, based on colour formation when tryptophan is made to react with brucine and periodate,<sup>23</sup> but thiols and some amino-acids, e.g., cystine, glutathione and cysteine, interfere severely. There still exists a need for a rapid and accurate spectrophotometric method for determining tryptophan in a variety of soluble and insoluble proteins.

### EXPERIMENTAL

#### Reagents

Sodium nitrite, 1% aqueous solution. Sodium hydroxide, 15% solution in water.

#### Samples

The tryptophan was chromatographically pure and had a purity of 99.9% as found by the method of Basha and Roberts.<sup>9</sup> Indole-3-acetic acid, 5-hydroxytryptamine (serotonin), tryptophanamide, indole, 5-hydroxyindole-3-acetic acid and all other chemicals were obtained from Sigma Chemicals Company, U.S.A., and used as received.

#### Procedure

**Preparation of calibration graph.** Dissolve about 25 mg of tryptophan accurately weighed in water in a 250-ml standard flask and dilute to the mark. Mix 0.5–4 ml portions of this solution in 20-ml beakers with 1 ml of 6*M* hydrochloric acid and 2 ml of 1% sodium nitrite solution, dilute to about 10 ml with water and heat on a boiling water-bath for 30 min. Transfer the cooled reaction mixtures into 25-ml standard flasks, add 10 ml of 15% sodium hydroxide solution, dilute to volume with water and measure the absorbances at 400 nm against water.

**Alkaline hydrolysis of protein samples.** Heat a weighed portion (about 25 mg) of protein with 10 ml of 5*M* potassium hydroxide in a sealed glass tube at 120° for 18 hr. Acidify the cooled hydrolysate with a slight excess of hydrochloric acid, centrifuge to remove any insoluble material (and wash it with water) and dilute the supernatant solution and washings to volume in a 25-ml standard flask and analyse a suitable aliquot for tryptophan.

**Determination of tryptophan.** Treat an aliquot of test solution containing 50–500 µg of tryptophan as in the preparation of calibration graph and measure the absorbance at 400 nm against water.

#### Identification of the reaction products

A mixture of 5 ml of an aqueous solution (0.5 mg/ml) of the particular aminobenzoic or hydroxybenzoic acid, 5 ml of 6*M* hydrochloric acid and 10 ml of 1% sodium nitrite

solution was heated under a reflux condenser on a boiling water-bath for 60 min. After cooling, the reaction mixture was extracted with 10 and then 5 ml of diethyl ether, and the extract was placed in a porcelain dish.

After evaporation of the ether the residue was dissolved in one drop of ether and applied to the start-line on a Silufol precoated thin-layer chromatography sheet (Sklárny Kavalier, Votice, Czechoslovakia) and chromatographed with 1-propanol-ammonia (2:1) mixture or benzene as mobile phase. Detection was done by exposing the chromatogram to ammonia vapour or spraying with stannous chloride solution and *p*-dimethylaminobenzaldehyde.<sup>24</sup>

## RESULTS AND DISCUSSION

Treatment with nitrous acid and colour development in alkaline medium has been used earlier for the spectrophotometric determination of phenolic compounds. The stability of the nitroso chromogen of paracetamol has been reported to be increased by the addition of alcohols.<sup>25</sup> Other workers have claimed that a nitro rather than a nitroso derivative is the reaction product.<sup>26,27</sup>

However, the formation of metal chelates with the reaction product has been taken as evidence in favour of nitroso derivative formation.<sup>28</sup> The phenolic compound undergoes reaction with nitrous acid preferentially at the position *para* to the phenolic group,<sup>28</sup> or (if this position is already occupied) at the *ortho* position.<sup>29</sup>

Tryptophan is a non-phenolic compound yet has been found in the present work to undergo reaction with nitrous acid and then give colour formation in alkaline medium. Some of the tryptophan derivatives, *e.g.*, indole-3-acetic acid, tryptamine and tryptophanamide, as well as indole, behave like tryptophan but some others, *e.g.*, 5-hydroxytryptamine and 5-hydroxyindole-3-acetic acid do not response to the colour test (Fig. 1). The heterocyclic nucleus of

the tryptophan is sensitive to oxidation to kynurenine,<sup>30,31</sup> which contains an aromatic amino group and undergoes diazotization on further reaction with nitrous acid. The diazo compound formation has been confirmed by performing the nitrous acid reaction at lower temperature and coupling the product with alkaline 2-naphthol or *N*-(1-naphthyl)ethylenediamine, a dye being formed. At elevated temperatures, the diazonium group is unstable and replaced by a hydroxyl group in aqueous medium. The resulting hydroxyl compound from tryptophan *etc.*, has a free *para*-position which can undergo reaction with nitrous acid and thus give colour formation after dissociation of the aci-form in alkaline medium. The following are the probable reactions with tryptophan.

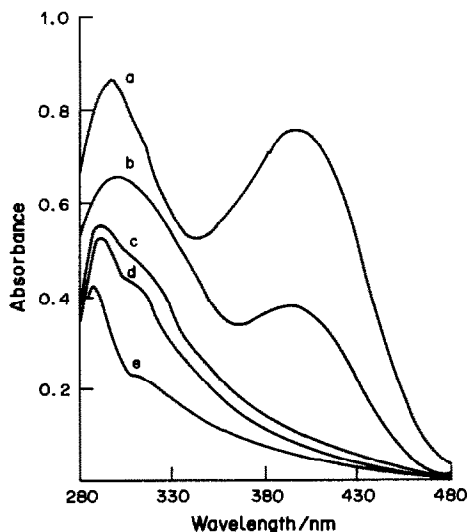
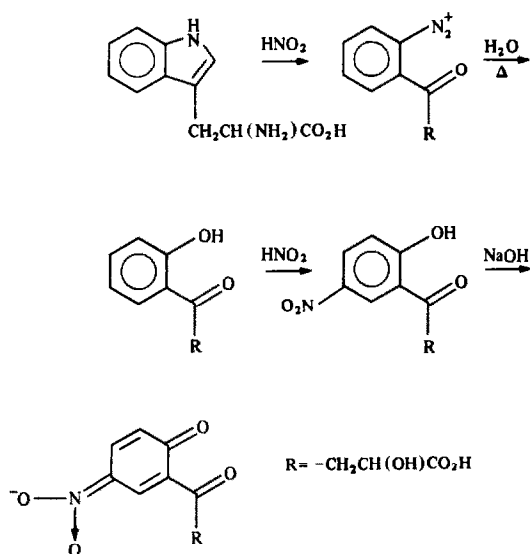


Fig. 1. Absorption spectra of chromogen obtained from (a) tryptophan, (b) indole-3-acetic acid, (c) 5-hydroxytryptamine, (d) 4-aminophenol and (e) hydroquinone.

The colour formation mechanism has been elucidated by performing the reaction with nitrous acid and the subsequent alkalization for 2- and 4-aminobenzoic acids and comparing the absorption spectra of the products with those obtained from 2- and 4-hydroxybenzoic acids under the same reaction conditions, as well as with those of the corresponding authentic nitrohydroxybenzoic acids in the same final medium (Figs. 2 and 3). The chromogen was identified by thin-layer chromatography of the ether extracts of the reaction products prior to alkalization.

The coloured solution of the salicylic acids showed four spots on the chromatograms developed with 1-propanol-ammonia (2:1) as mobile phase. The most intense corresponded to the mixture of 3-nitro- and 5-nitrosalicylic acids ( $R_F = 0.7$  and  $0.8$  respectively), a faint spot at  $R_F = 0.45$  to 3,5-dinitrosalicylic acid and the remaining two weak spots to decarboxylation products (*p*-nitrophenol and 2,4-dinitrophenol, respectively). The results were confirmed by chromatography on silica gel layers with benzene-ethyl acetate (4:1) as mobile phase. The main spot from the reaction product of

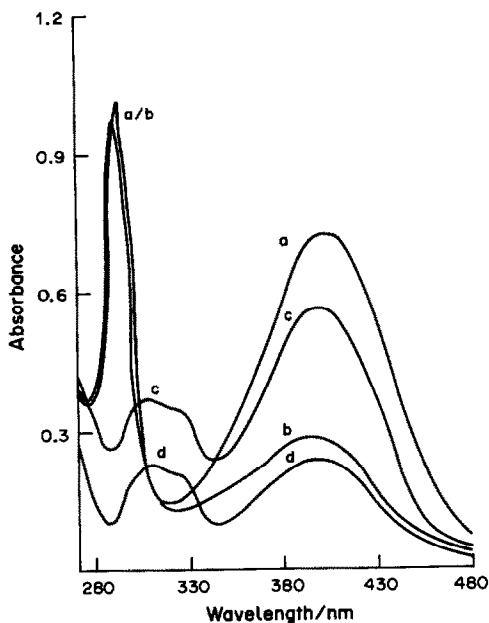
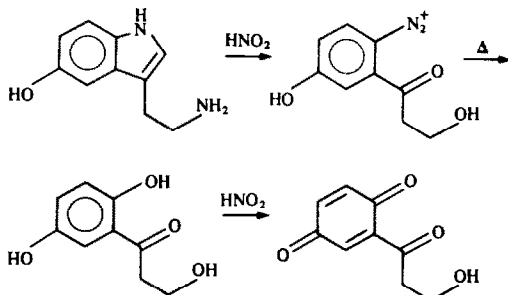


Fig. 2. Absorption spectra of chromogen produced from (a) 4-amino- and (b) 4-hydroxybenzoic acid, (c) 2-amino- and (d) 2-hydroxybenzoic acid.

*p*-hydroxybenzoic acid was identified as 3-nitro-4-hydroxybenzoic acid ( $R_F = 0.34$ ). Further weak spots were observed at  $R_F = 0.73$  and  $0.77$  corresponding to those of *p*-nitrophenol and 2,4-dinitrophenol, indicating that some decarboxylation had occurred. These results are in best accordance with the results obtained 100 years ago by Deninger.<sup>32</sup>

The failure of 5-hydroxytryptamine and 5-hydroxyindole-3-acetic acid to respond to the colour test can be attributed to the 5-hydroxyl group, which gives a benzoquinone derivative as an oxidation product rather than a nitroso or nitro derivative on reaction with nitrous acid. The possible reaction with 5-hydroxytryptamine is



This mechanism is supported by a comparison of the absorption spectrum of the benzoquinone derivative with the spectra of the reaction products from treatment of 4-aminophenol and hydroquinone with nitrous acid at elevated temperature (Fig. 1).

The golden yellow chromogen formed in the assay absorbs maximally at 400 nm. In Fig. 1, the absorp-

tion spectra of the product obtained from two model derivatives of tryptophan, *viz.* indole-3-acetic acid and 5-hydroxytryptamine, are included for comparison. Under the conditions of the determination there is a linear relationship between the absorbance at 400 nm and the amount of tryptophan present, over the concentration range 2–16 μg/ml in the final solution. The molar absorptivity has been found to be  $9.44 \times 10^3 \text{ l. mole}^{-1} \text{ cm}^{-1}$  at 400 nm.

Oxidation of the indole nucleus, deamination and the reaction with nitrous acid can be completed within 30 min at boiling water-bath temperature. Over the entire range of sample size tested, 2 ml of 1% sodium nitrite solution was found sufficient to yield maximal absorbance (Fig. 4). The possible

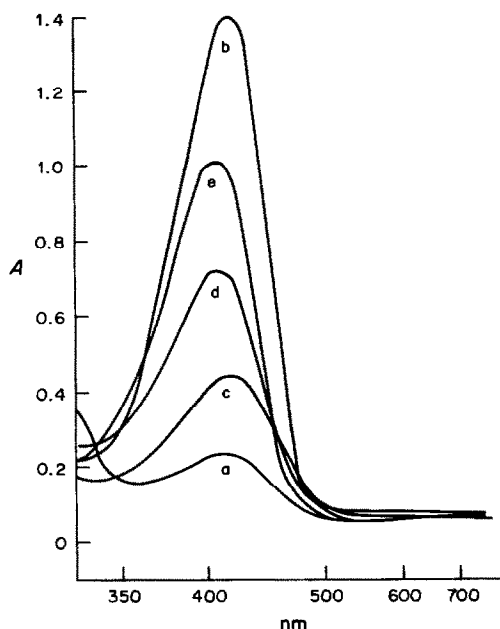


Fig. 3. Absorption spectra obtained from (a) the chromogen of salicylic acid, (b) 5-nitrosalicylic acid, (c) 3-nitro-4-hydroxybenzoic acid, (d) the chromogen of 4-hydroxybenzoic acid, (e) 4-nitrophenol.

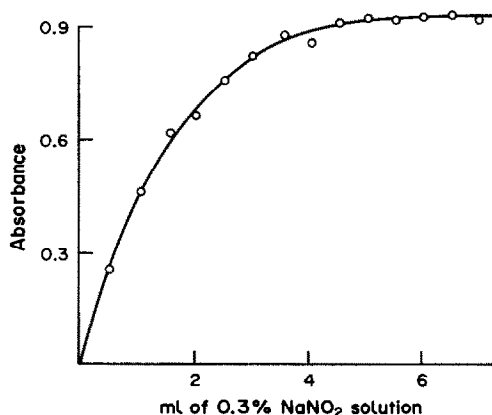


Fig. 4. Effect of sodium nitrite concentration on the colour intensity for tryptophan (21 μg/ml).

Table 1. Determination of tryptophan in pure samples and synthetic combinations

Tryptophan taken, $\mu\text{g/ml}$	Substances added*	Tryptophan found,† $\mu\text{g/ml}$	CV, %
2.05		2.08	0.9
3.42		3.39	0.8
4.86		4.91	0.6
5.99		6.01	0.5
7.65		7.60	0.4
9.21		9.19	0.4
12.39		12.29	0.5
14.66		14.73	0.6
15.98		16.08	0.8
6.42	a	6.46	0.5
7.98	b	8.05	0.4
9.40	c	9.49	0.6
12.11	d	12.06	0.5

\*Substances added were (a) glutamic acid (2 mg), asparagine (5 mg), glycine (3 mg), methionine (3 mg) and histidine (2 mg); (b) serine (5 mg), alanine (5 mg), cystine (3 mg), aspartic acid (4 mg) and lysine (3 mg); (c) glutathione (2 mg), glucose (5 mg), arabinose (2 mg) and 2-mercaptoethanol (1 mg); and (d) cysteine (2 mg), valine (4 mg) and niacinamide (2 mg).

†Average of six replicates; CV = coefficient of variation.

Table 2. Determination of tryptophan in proteins after alkaline hydrolysis

Protein	Molecular weight	mole of tryptophan/mole of protein		Reported value	Ref.
		Present method*	CV, %		
$\alpha$ -Casein	26,000	1.15	0.8	1.1	33
Myoglobin	16,890	2.16	0.7	2.0	34
Trypsin	23,800	3.35	0.9	3.2	19
Transferrin	77,000	7.76	1.1	8.0	35
Fetuin	50,750	2.21	1.0	2.0	36
Phosvitin	45,000	1.30	1.0	1.0	35

\*Average of six replicates; CV = coefficient of variation.

interference of common amino-acids and mono-saccharides which may be present along with tryptophan in tissue or protein hydrolysates has been examined. Amino-sugars, hexoses, hexuronic acids and typical amino-acids found in biological materials did not interfere with the colour development. Several amines and amides were also tested. Niacinamide, glycinamide, triethylamine, benzylamine and 1,6-diaminohexane do not interfere. 2-Mercaptoethanol and 3-mercapto propane-1,2-diol, which are commonly present in tissue extracts and solutions of proteins, do not vitiate the results. The only interfering substance found is tyrosine, which should be removed by chromatography before the analysis.

Results are given in Tables 1 and 2 for the determination of tryptophan in pure samples, synthetic combinations with other substances, and in proteins after alkaline hydrolysis.

*Acknowledgements*—Thanks are due to the University Grants Commission (New Delhi) for a Research Fellowship

to AJ, and are also due to Mrs J. Žižková for experimental assistance.

#### REFERENCES

1. M. Friedman and J. W. Finley, *J. Agr. Food Chem.*, 1971, **19**, 626.
2. J. R. Spies and D. C. Chambers, *Anal. Chem.*, 1948, **20**, 30.
3. J. R. Spies, *ibid.*, 1950, **22**, 1447.
4. J. Fischl, *J. Biol. Chem.*, 1960, **235**, 999.
5. A. Light and E. L. Smith, in *The Proteins*, H. Neurath, ed., Vol. I, p. 1. Academic Press, New York, 1963.
6. J. R. Spies, *Anal. Chem.*, 1967, **39**, 1412.
7. B. R. DasGupta, *Anal. Biochem.*, 1969, **30**, 284.
8. L. C. Gruen and D. W. Rivett, *ibid.*, 1971, **44**, 519.
9. S. M. M. Basha and R. M. Roberts, *ibid.*, 1977, **77**, 378.
10. A. K. Goswami, *Analyst*, 1974, **99**, 657.
11. S. S. M. Hassan, *Anal. Chem.*, 1975, **47**, 1429.
12. D. Arthur and T. Chia-Yi, *Anal. Biochem.*, 1975, **63**, 283.
13. Y. Nakamune, *J. Pharm. Soc. Japan*, 1961, **81**, 846.
14. H. Matsubara and R. M. Sasaki, *Biochem. Biophys. Res. Commun.*, 1969, **35**, 175.
15. T. Y. Liu and Y. H. Chang, *J. Biol. Chem.*, 1971, **246**, 2842.



16. R. H. Horton and D. E. Koshland, *J. Am. Chem. Soc.*, 1965, **87**, 1126.
17. T. E. Barman and D. E. Koshland, *J. Biol. Chem.*, 1967, **242**, 5771.
18. P. M. Burton, D. C. Hall and J. Josse, *ibid.*, 1970, **245**, 4346.
19. T. Sasaki, B. Abrams and B. L. Horecker, *Anal. Biochem.*, 1975, **65**, 396.
20. W. L. Bencze and K. Schmid, *Anal. Chem.*, 1957, **29**, 1193.
21. A. Patchornick, W. E. Lawson and B. Witkop, *J. Am. Chem. Soc.*, 1958, **80**, 4747.
22. H. Edelhoich, *Biochemistry*, 1967, **6**, 1948.
23. M. K. Tummuru, T. E. Divakar and C. S. P. Sastry, *Analyst*, 1984, **109**, 1105.
24. J. Gasparič and J. Churáček, *Laboratory Handbook of Paper and Thin-layer Chromatography*, p. 229. Horwood, Chichester, 1978.
25. M. C. Inamdar and N. N. Kadji, *Indian J. Pharm.*, 1969, **31**, 79.
26. L. Chafetz, R. E. Daly, H. Schriftman and J. J. Lomner, *J. Pharm. Sci.*, 1971, **60**, 463.
27. J. Gasparič, *Z. Anal. Chem.*, 1964, **199**, 276.
28. S. F. Belal, M. A. Elsayed, A. Elwalily and H. Abdine, *Analyst*, 1979, **104**, 919.
29. A. A. Ouf, M. I. Walash, S. M. Hassan and S. M. El-Sayed, *ibid.*, 1980, **105**, 169.
30. L. F. Fieser and M. Fieser, *Organic Chemistry*, p. 512. Asia Publishing House, Bombay, 1970.
31. K. K. Verma, *Talanta*, 1980, **27**, 541.
32. A. Deninger, *J. Prakt. Chem.*, 1890, **42**, 551.
33. T. F. Spande and B. Witkop, in *Methods in Enzymology*, C. H. W. Hirs, ed., Vol. IX, pp. 498–506. Academic Press, New York, 1967.
34. M. D. Dayhoff, *Atlas of Protein Sequence and Structure*, Vol. V, p. 418. National Biomedical Research Foundation, Washington, D.C., 1972.
35. W. C. Parker and A. G. Bearn, *J. Exp. Med.*, 1967, **115**, 83.
36. M. J. Spiro and R. G. Spiro, *J. Biol. Chem.*, 1962, **237**, 1507.

## ROOM-TEMPERATURE PHOSPHORIMETRY OF POLYAROMATIC HYDROCARBONS WITH ORGANIZED MEDIA AND PAPER SUBSTRATE: A COMPARATIVE STUDY\*

G. RAMIS RAMOS†, I. M. KHASAWNEH‡,  
M. C. GARCIA-ALVAREZ-COQUE† and J. D. WINEFORDNER§  
Department of Chemistry, University of Florida, Gainesville, FL 32611, U.S.A.

(Received 14 April 1987. Accepted 21 August 1987)

**Summary**—Room-temperature phosphorescence of some polyaromatic hydrocarbons as model compounds with stabilization by use of a microemulsion of a non-polar solvent, has been examined. Some advantage in the preparation of the solutions is achieved. A comparative study of room-temperature phosphorimetry in microemulsion and micellar media, on paper substrates and at low temperature has also been made. The spectral characteristics and analytical figures of merit are given.

Micelle-stabilized room-temperature phosphorimetry (MS-RTP) was first reported by Kalyanasundaram *et al.*<sup>1</sup> and the technique has been developed by several authors during the last decade.<sup>2-7</sup> Dramatic enhancement of RTP in solution can be achieved by incorporating the phosphors into a micellar assembly. Hydrophobic molecules are attracted into the oil-like environment of the micelle and in this way, are placed in proximity to the heavy-atom counterions, the local concentration of which is estimated to be 3–5M.<sup>8</sup> Thus, very efficient spin-orbit coupling is achieved, leading to a high phosphorescence emission.

Furthermore, the micelles can effectively screen molecules in the excited triplet state from the action of potential quenchers present in the bulk water phase. However, phosphorescence is not observed unless oxygen is removed, as it is a very efficient quencher which easily penetrates the micelles. Recently, Diaz-Garcia and Sanz-Medel<sup>9</sup> have proposed the substitution of the troublesome deoxygenation with nitrogen by chemical deoxygenation with sodium sulphite, thus avoiding foam formation and ensuring a more permanent protection of the solution against contamination with oxygen. In the presence of sulphite, however, the phosphorescence is not immediately observed. The oxygen in the bulk water phase is removed first, followed by that in the micelle pseudophases as it diffuses out. Equilibrium is achieved in a few minutes. In this work, we have adopted this simple, rapid and convenient procedure.

MS-RTP suffers from the slow dissolution of the non-polar analytes in the aqueous micellar solution. Some polyaromatic hydrocarbons (PAHs) with very low polarities and vapour pressures cannot be dissolved, even after long sonication times, which limits the applicability of MS-RTP. In this work, we propose the use of a microemulsion aqueous solution of the analyte in a non-polar solvent to circumvent this problem.

Microemulsions are formed spontaneously when appropriate amounts of water, a non-polar solvent, a surfactant and a co-surfactant (usually a C<sub>4</sub>–C<sub>6</sub> alkyl alcohol) are mixed.<sup>10</sup> If the non-polar analyte is first dissolved in a certain amount of the non-polar solvent, and this solution is gently mixed with the alcohol and then the aqueous solution of the surfactant, a clear microemulsion is obtained in a few seconds. No scattered light is observed from this solution by human eye, since the microdroplet diameters are about 10–20 nm.<sup>10</sup>

Room-temperature phosphorimetry in organized media, microemulsions and micellar solutions, is evaluated here by comparison with paper-sensitized room-temperature phosphorimetry (PS-RTP) and also with low-temperature phosphorimetry (LTP), by use of data from the literature. Spectral characteristics and analytical figures of merit are given.

### EXPERIMENTAL

#### Reagents

Hexane, heptane (high-purity solvents, Burdick and Jackson) 1-pentanol (Aldrich), sodium dodecylsulphate (SDS), reagent grade thallos nitrate and anhydrous sodium sulphite (Fisher) were used as received. Aqueous solutions were made with "nanopure" demineralized water (Barnstead).

Naphthalene and 2,3-dimethylnaphthalene were recrystallized three times from ethanol, *o*-terphenyl was recrystallized three times from methanol, and durene was vacuum-sublimed. Other PAHs from different sources were used as supplied.

\*Research supported by NIH-GM-11373-23.

†On leave from Department of Analytical Chemistry, University of Valencia, Valencia, Spain.

‡On sabbatical leave from Department of Chemistry, Yarmouk University, Irbid, Jordan.

§To whom all correspondence should be sent.

The water used for preparing sodium sulphite solutions was first deaerated with nitrogen. The solutions were prepared daily and kept in tightly stoppered containers. Micellar stock solutions were prepared by sonicating 1–5 mg of the PAHs in 20 ml of 0.5M SDS and making up to 25 ml with the same solvent. Microemulsion stock solutions were prepared by dissolving similar amounts of the analytes in 0.5 ml of heptane, adding 0.5 ml of 1-pentanol and making up to 25 ml with 0.5M SDS. Dilutions were made with enough thallium added to give a 30/70  $Tl^+$ /SDS ratio. Pure hexane solutions of the PAHs were used in the PS-RTP, with Whatman No. 1 filter paper as substrate. All experiments were done at  $20 \pm 1^\circ$ .

#### Apparatus

A Perkin-Elmer LS-5 Luminescence Spectrometer provided with a 3600 Data Base Station was used for all measurements. PS-RTP data were obtained by using a paper sample-holder attachment with four sample positions located around the central rod.<sup>11</sup> A mask with a square window ( $6 \times 6 \text{ mm}^2$ ) limited the exposed paper surface. The distance of the paper from the front of the instrument and the angle between the excitation axis and the paper are critical. Both distance and angle are adjusted for each sample until the maximum emission intensity is obtained. The distance can be easily changed by an adjustment screw located under the sample compartment. Delay and gate times were 0.03 and 9 msec, respectively. The excitation and emission slits gave 10 and 5 nm band-passes respectively, and a 305-nm cut-off filter was used in the emission-side filter holder.

#### Procedures

A 0.1-ml aliquot of the PAH stock microemulsion or micellar solution, 0.3 ml of 0.5M SDS, 0.3 ml of 0.25M thallos nitrate and 0.5 ml of 0.5M sodium sulphite are pipetted into a 10-ml standard flask and made up to volume with water. Standard 10-mm fused silica cuvettes are filled with this solution.

For PS-RTP, 10-mm diameter paper discs are cut with a paper-punch, mounted on the paper holder and spotted with  $2 \mu\text{l}$  of 0.25M thallos nitrate and  $5 \mu\text{l}$  of the analyte solution, from Hamilton syringes. The discs are dried in an oven for 20 min at  $110\text{--}120^\circ$  and allowed to cool in the sample compartment for 10 min, then the spectra are recorded. Nitrogen dried with anhydrous calcium sulphate is passed continuously through the paper holder compartment.

Phosphorescence lifetimes are measured by use of the DECAV-OBEY program. A period of 1–2 lifetimes is covered by taking six evenly spaced points, but for PS-RTP a 0.1–0.6 msec fixed period is used. The gate and integration times are 0.1 msec and 20 sec, respectively. The program is run three times for each test.

Limits of detection (LODs) are obtained by taking 16 measurements of the blank and using five standard solutions to determine the slope of the calibration graph. LOD values are calculated as the concentration corresponding to a signal that is three times the standard deviation of the blank. Similarly, the repeatability of the procedures is established by taking 16 measurements of the analyte signal at a concentration at least 10 times the corresponding LOD, and calculating their relative standard deviation.

## RESULTS AND DISCUSSION

### *Influence of 1-pentanol and heptane concentrations in microemulsion-stabilized RTP*

Several dilutions of a micellar solution of pyrene were made with 0.5M SDS, water and increasing amounts of 1-pentanol. The final concentrations of

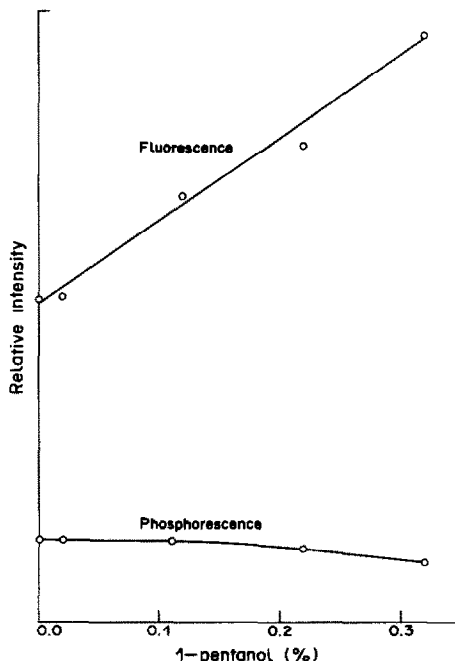


Fig. 1. Influence of 1-pentanol concentration on the luminescence of a microemulsion of  $1\text{-}\mu\text{g/ml}$  pyrene in 0.02M SDS and 0.02% heptane.

pyrene and SDS were  $1 \mu\text{g/ml}$  and 0.02M, respectively. As shown in Fig. 1, the fluorescence intensity increases almost linearly with increasing amounts of 1-pentanol and the phosphorescence decreases slightly. These effects can be attributed to a decrease in the electric charge density on the microdroplet surface. Larger amounts of co-surfactant produce a higher concentration of hydroxyl groups on the surface and, therefore, a smaller density of charged surfactant heads. This leads to a lower local concentration of the thallos ion, as the counter-ion concentration decreases.

The 1-pentanol concentration adopted for the preparation of the stock solutions of the PAHs is 2%. With this concentration, no stable microemulsions can be obtained with more than 3% heptane. Hence 2% heptane was used throughout this work. After dilution, the 1-pentanol and heptane concentrations in the final solutions were both 0.02% or less. No significant differences have been found between these solutions and pure micellar solutions with regard to fluorescence and phosphorescence spectra, phosphorescence lifetimes, limits of detection and relative standard deviations (RSDs) for all the PAHs examined in this work.

Microemulsion solutions of dibromoethane and iodoethane in 1-pentanol/SDS and 1-butanol/tetradecylammonium bromide systems have also been prepared, with a 2% concentration of the non-polar solvent and co-surfactant and a 0.5M solution of the surfactant. Although clear microemulsions, which were not destroyed by dilution, were easily obtained, no phosphorescence was observed for 20

$\mu\text{g/ml}$  pyrene in the absence of thallos nitrate in any experimental combination tested.

#### Fluorescence spectra

The excitation and emission maxima of the fluorescence spectra of some PAHs in hexane and organized media at room temperature and in heptane at 77 K are listed in Table 1. The excitation peaks in organized media are red-shifted relative to the peaks obtained in pure alkanes, the differences being bigger for the spectra obtained in hexane at room temperature. The fluorescence emission spectra for organized media also show small bathochromic shifts.

Differences in the relative intensities of the excitation peaks are also observed. The peaks at longer wavelengths are more intense in organized media. Pyrene and retene show the biggest differences in relative intensity when the medium is changed. This behaviour is probably related to the higher polarity and rigidity found in the organized media, which provide a larger stabilization of the excited singlet state.

#### Phosphorescence spectra

The phosphorescence spectral characteristics, analytical figures of merit and lifetimes observed in LTP and RTP in organized media and on paper substrate are shown in Tables 2–4.

The excitation peaks appear at the same wavelengths as for fluorescence and phosphorescence in organized media, except for *o*-terphenyl, for which the single well-defined band appears 10 nm blue-shifted when phosphorescence is measured. Shifts larger than 50 nm have been observed for other PAHs at 77 K by Inman *et al.*<sup>12</sup>

The phosphorescence excitation peaks do not show blue or red shift trends when the spectra at low temperature (77 K), in organized media and on paper substrates, are compared; the differences are smaller than 10 nm in all cases. The band half-widths are also similar, except for the 2,3-dimethylnaphthalene band, which is broader when the paper substrate is used.

The phosphorescence emission spectra show even smaller shifts than the excitation spectra, except again for 2,3-dimethylnaphthalene, which exhibits blue-shifted emission peaks at low temperature, relative to the peaks on paper and in organized media. The emission band half-widths are always slightly larger on paper substrates.

All the PAHs tested exhibited fluorescence even after addition of thallium. The phosphorescence/fluorescence intensity ratios, calculated as the ratios of the slopes of the calibration graphs, are given in Table 2. Phosphorescence was not observed for anthracene, 9-methylanthracene and durene in organized media at the 20- $\mu\text{g/ml}$  concentration level, or on paper at 0.5- $\mu\text{g}$  level. Anthracene and 9-methylanthracene exhibited a strong fluorescence which was not appreciably reduced in the presence of

thallos nitrate. Also, for naphthalene on paper a small and poorly reproducible phosphorescence signal was obtained, possibly because of loss of the compound by volatilization when the paper was dried.

The phosphorescence lifetimes were usually somewhat longer in organized media than on paper substrates, as shown in Tables 2 and 3. The abnormally long lifetime for pyrene has been confirmed with three independent solutions on different days, one of them with no heptane and 1-pentanol.

#### Analytical figures of merit

In all cases, the best LODs were obtained with the organized media. This could have been a result of the more effective heavy-atom perturbation of the analytes, together with the very low background noise, which arose from the use of a clear liquid solution and the advantageous geometry of the cell and beam positions. The RSD values for the PAHs were also smaller in the organized media than for the other media.

On the other hand, the poorer values of the LODs at low temperature could be a result of radiation scattering produced by the cracks and snow present in the frozen matrix.<sup>12</sup> The high RSD values were the result of high noise levels.

Finally, the paper substrate gave the worst results, even if absolute LODs are considered. In this case, the higher LODs arose from a lower sensitivity (slope of the calibration graph) as well as higher background noise. Sensitivities at room temperature are compared in Table 3; the values in organized media are 2–20 times greater than those for the paper substrate.

Major sources of background noise in PS-RTP are phosphorescent impurities contained in the paper, surface inhomogeneities, *i.e.*, some parts of the paper are more active than others, and changes in the alignment of both the excitation and emission monochromators.

Other sources of background noise which are often underestimated arise from the reflection properties of the surface and from interaction with the excitation radiation. Scattered radiation due to the afterglow of the flash-lamp is reflected off the paper surface, contributing to the background. Also, the reflective properties of the paper as well as the phosphorescence of the impurities decrease after irradiation.<sup>14</sup>

The analyte signal is also affected by the excitation radiation. All the PAHs examined, except pyrene, showed a decrease in intensity under exposure to the excitation radiation. The intensity losses can be as high as 25% in 10 min, as observed for retene, and could constitute the main contribution to the large RSD value for this compound. In contrast, the phosphorescence signals obtained from solutions were very stable and showed no significant intensity decrease after 15 min. If any photodecomposition

Table 1. Fluorescence spectral characteristics of PAHs obtained in alkyl hydrocarbons and organized media \*

Compound	Organized media			Hexane			Heptane at low temp.†	
	$\lambda_{exc}, nm$	$\lambda_{em}, nm$	$\lambda_{exc}, nm$	$\lambda_{em}, nm$	$\lambda_{exc}, nm$	$\lambda_{em}, nm$	$\lambda_{exc}, nm$	$\lambda_{em}, nm$
Anthracene	254(50), 343(79), 358(100), 379(80)	381(89), 402(100), 426(49), 451(14)	249	377(92), 398(100), 421(50), 446(14)	250	400		
Biphenyl	266	318(100), ~328(93)sh	246	316(100), ~328(83)sh	§	§		
<i>m,m'</i> -Bitoluene	275	320(100), ~330(82)sh	249	318(100), ~330(75)sh	§	§		
2,3-Dimethylnaphthalene	287	293(10), ~325(80)sh, 337(100)	~267(97)sh, 274(100), 306(45)	~304(19)sh ~325(88)sh, 335(100)	§	§		
Durene	279	315	273	310	§	§		
9-Methylanthracene	259(49), ~335(56)sh, 368(100), 389(74)	393(69), 415(100), 439(55), ~469(20)sh	~331(30)sh, 350(63), 367(100), 387(88)	388(89), 410(100), 435(37), 460(5)	256	412		
Naphthalene	285	~327(90)sh, 335(100)	272(100), 307(435)	324(91), 336(100), ~350(62)sh	§	§		
Pyrene	278(30), 322(73)sh, 338(100)	375(60), 390(100), 408(59)	238(100), 271(40) 335(30)	~374(76)sh, 386(100) 392(89), ~416(43)sh	335	390		
Retene	~267(60)sh ~287(89)sh 299(100), 330(20)	333(17), ~360(82)sh 370(100), ~388(80)sh	257(100), ~279(19)sh	362(87), 370(100), ~389(59)sh	264	367		
<i>o</i> -Terphenyl	292	~328(69)sh, 341(100) ~356(74)sh	248(100), ~260(94)sh	339(100), 388(92), 410(86), 435(38)	285	344		

\*Relative intensities in parentheses; sh = shoulder.

†Data taken from ref. 12.

§Not found in the literature.

Table 2. Phosphorescence characteristics in organized media at room temperature

Compound	$\lambda_{exc}^*, nm$	Half-width, † nm	$\lambda_{em}^*, nm$	Half-width, † nm	$I_p/I_F^\ddagger$	LOD, ng/ml	RSD, § %	Lifetime, msec
Biphenyl	265	28(1)	443(82), 471(100) ~500(62)sh	75(3)	0.4	2.0	1.1(0.2)	0.56 ± 0.05
<i>m,m'</i> -Bitoluene	~268(90)sh, 276(100)	34(1)	450(85), 476(100) ~505(61)sh	77(3)	0.3	2.0	0.15(0.4)	1.1 ± 0.1
2,3-Dimethylnaphthalene	287(100), ~317(15)sh	28(1)	487(96), 518(100)	69(2)	0.5	0.4	0.4(0.3)	1.02 ± 0.05
Naphthalene	284	26(1)	476(100), 511(98) 547(33)	58(2)	0.3	14	0.16(2)	0.20 ± 0.01
Pyrene	275(19), ~323(70)sh, 336(100)	31(2)	594(100), 641(20)	23(2)	0.25	0.2	2.0(0.05)	15 ± 1
Retene	266(61), ~290(85)sh, 301(100)	51(3)	482(100), 515(91)	63(2)	0.6	0.6	0.6(0.4)	1.0 ± 0.1
<i>o</i> -Terphenyl	272	33(1)	450(99), 474(100) ~500(62)sh	75(3)	0.06	2.0	0.8(0.8)	1.2 ± 0.1

\*Relative intensities in parentheses; sh = shoulder.

†In parentheses, number of bands involved.

‡Intensity ratio between the most intense phosphorescence and fluorescence peaks obtained under the same experimental conditions.

§In parentheses, concentration level in  $\mu\text{g/ml}$ .

Table 3. Phosphorescence characteristics on paper at room temperature

Compound	$\lambda_{exc}^*, nm$	Half-width, † nm	$\lambda_{em}^*, nm$	Half-width, † nm	LOD, † $\mu\text{g/ml}$	RSD§ %	Lifetime, msec	$I_{MES}^\parallel$ $I_{PS}$
Biphenyl	266	28(1) ~495(72)sh	444(71), 471(100)	82(3)	1(6)	3.8(80)	1.31 ± 0.01	2.8
<i>m,m'</i> -Bitoluene	267	31(1)	451(73), 477(100) ~500(76)sh	89(3)	2(12)	3.5(70)	1.20 ± 0.01	17
2,3-Dimethylnaphthalene	277	43(1)	495(90), 515(100)	105(2)	4(20)	2.5(70)	1.14 ± 0.01	20
Pyrene	~312(43)sh, 324(76), 337(100)	29(2)	594(100), ~605(70)sh	27(2)	0.1(0.6)	1.9(35)	1.85 ± 0.01	20
Retene	268(100), ~302(15)sh	33(2)	481(99), 514(100)	64(2)	0.5(2.5)	9(25)	1.02 ± 0.01	3.3
<i>o</i> -Terphenyl	266	32(1)	450(78), 478(100) ~500(76)sh	98(3)	0.3(1.8)	3.4(15)	0.90 ± 0.02	1.9

\*Relative intensities in parentheses; sh = shoulder.

†In parentheses, number of bands involved.

‡Absolute LOD ( $\mu\text{g}$ ) given in parentheses.§In parentheses, concentration level ( $\mu\text{g/ml}$ ).

¶Comparison of the sensitivities (slopes of the calibration curves) achieved in organized media (MES) and on paper (PS).

Table 4. Phosphorescence characteristics in heptane at 77 K

Compound	$\lambda_{exc}^*, nm$	$\lambda_{em}^*, nm$	LOD, $\mu g/ml$	RSD, %
Anthracene†	270, <u>350</u>	671	3.0	5.4
Biphenyl‡	277	437, <u>468</u> , 494	0.01	2.9
<i>m,m'</i> -Bitoluene‡	280	444, <u>476</u>	0.1	4.6
2,3-Dimethylnaphthalene‡	286	392, <u>413</u> , 436	1.0	7.6
Durene‡	277	377, 387, <u>399</u> , 410	0.02	6.2
9-Methylanthracene‡	281	414, <u>444</u> , 480	0.9	8.4
Naphthalene†	286	480, <u>510</u>	2.0	7.3
Pyrene†	<u>330</u> , 350	517, <u>555</u> , <u>592</u> , 608, 640	0.008	2.8
Retene‡	299	474, 507, 548	0.02	7.4
<i>o</i> -Terphenyl‡	281	446, <u>480</u>	0.05	6.3

\*Most intense wavelengths are underlined.

†Values taken from Ref. 13.

‡Values taken from Ref. 12.

occurs in solution, the analyte is immediately replaced by convection and diffusion, which cannot take place on the solid surface of paper.

#### CONCLUSIONS

The practical use of microemulsion solutions of the PAHs in RTP has been demonstrated. An ultrasonic bath is not necessary to dissolve the samples, and the procedure is very rapid. Also, the introduction of a new variable, the non-polar solvent, gives more versatility to the technique.

On the basis of the analytical figures of merit, phosphorescence in organized media at room temperature appears to be better than LTP and PS-RTP for chemical analysis. However, its applicability is limited to those compounds with sufficiently low polarity to prefer the hydrocarbon core of the micelles or microdroplets to the water bulk phase. The possibility of observing RTP of polar molecules, and very small sample amounts needed, are still specific advantages of PS-RTP.

*Acknowledgements*—G. Ramis Ramos and M. C. Garcia Alvarez-Coque would like to thank the "Conselleria de Cultura, Educacio i Ciencia de la Generalitat Valenciana" for the grants which made possible their stay in Gainesville.

Thanks are also due to Dr. A. Berthod from the Université Claude Bernard, Lyon I, France, for his valuable suggestions.

#### REFERENCES

1. K. Kalyanasundaram, F. Grieser and J. K. Thomas, *Chem. Phys. Lett.*, 1977, **51**, 501.
2. N. J. Turro, K. C. Liu, M. F. Chow and P. Lee, *Photophys. Photobiol.*, 1978, **22**, 523.
3. L. J. Cline Love, M. Skrilec and J. G. Habarta, *Anal. Chem.*, 1980, **52**, 754.
4. M. Skrilec and L. J. Cline Love, *ibid.*, 1980, **52**, 1559.
5. L. J. Cline Love and M. Skrilec, *ibid.*, 1981, **53**, 2103.
6. M. Skrilec and L. J. Cline Love, *J. Phys. Chem.*, 1981, **85**, 2047.
7. L. J. Cline Love, J. G. Habarta and M. Skrilec, *Anal. Chem.*, 1981, **53**, 437.
8. R. Weinberger, K. Reembish and L. J. Cline Love, *ASTM Special Technical Publ.*, 863, Philadelphia, 1985.
9. M. E. Diaz Garcia and A. Sanz-Medel, *Anal. Chem.*, 1986, **58**, 1436.
10. A. Berthod, *J. Chim. Phys.*, 1983, **80**, 407.
11. G. Scharf, B. W. Smith and J. D. Winefordner, *Anal. Chem.*, 1985, **57**, 1230.
12. E. L. Inman, Jr., A. Jurgensen and J. D. Winefordner, *Analyst*, 1982, **107**, 538.
13. *Idem*, *Talanta*, 1982, **29**, 423.
14. G. Ramis Ramos, M. C. Garcia Alvarez-Coque, A. M. O'Reilly, I. M. Khasawneh and J. D. Winefordner, unpublished results.

## DETERMINATION OF ARSENIC IN ORES, CONCENTRATES AND RELATED MATERIALS BY GRAPHITE-FURNACE ATOMIC-ABSORPTION SPECTROMETRY AFTER SEPARATION BY XANTHATE EXTRACTION

ELSIE M. DONALDSON

Mineral Sciences Laboratories, Canada Centre for Mineral and Energy Technology, Department of  
Energy, Mines and Resources, Ottawa, Canada

(Received 18 April 1987. Accepted 27 June 1987)

**Summary**—A method for determining  $\sim 0.2 \mu\text{g/g}$  or more of arsenic in ores, concentrates and related materials is described. After sample decomposition arsenic(V) is reduced to arsenic(III) with titanium(III) and separated from iron, lead, zinc, copper, uranium, tin, antimony, bismuth and other elements by cyclohexane extraction of its xanthate complex from  $\sim 8\text{--}10M$  hydrochloric acid. After washing with  $10M$  hydrochloric acid-2% thiourea solution to remove residual iron and co-extracted copper, followed by water to remove chloride, arsenic is stripped from the extract with  $16M$  nitric acid and ultimately determined in a 2% nitric acid medium by graphite-furnace atomic-absorption spectrometry, at 193.7 nm, in the presence of thiourea (which eliminates interference from sulphate) and palladium as matrix modifiers. Small amounts of gold, platinum and palladium, which are partly co-extracted as xanthates under the proposed conditions, do not interfere.

Various CANMET projects, including the Canadian Certified Reference Materials Project, (CCRMP), require the accurate determination of arsenic at trace and  $\mu\text{g/g}$ -levels in concentrates, ores, rocks, soils, processing products and related materials. Because graphite-furnace atomic-absorption spectrometry (GFAAS) is relatively sensitive for arsenic, the present investigation was undertaken to develop a reasonably rapid and accurate method that would be applicable to all these materials.

Previous investigators<sup>1-3</sup> have found that the determination of arsenic by GFAAS, at 193.7 nm, the most sensitive resonance line, is subject to strong interference from sulphate and from aluminium, potassium, sodium and various other elements. For this reason, prior separation of arsenic from matrix elements by co-precipitation with nickel pyrrolidinedithiocarbamate<sup>4</sup> or by extraction as the pyrrolidinedithiocarbamate,<sup>5-7</sup> diethyldithiophosphoric acid<sup>7</sup> or iodide complex<sup>7,8</sup> has been recommended. However, although these separation procedures may be adequate for foods, biological materials, coal, and sea and mineral waters, they are not sufficiently selective for use with such complex and diverse materials as those under consideration. Previously<sup>9</sup> in this laboratory a spectrophotometric molybdenum blue method was developed for the determination of small amounts of arsenic in concentrates, ores and copper-base alloys, based on the preliminary separation of arsenic from various matrix elements by co-

precipitation with hydrous ferric oxide, followed by its separation from iron, lead and other co-precipitated elements by a triple chloroform extraction of arsenic(III) ethyl xanthate from  $\sim 11M$  hydrochloric acid. In this, and earlier work<sup>10</sup> involving a study of the extraction of ethyl xanthate complexes from hydrochloric acid media, it was shown that the extraction of arsenic from  $\sim 8$  to at least  $11M$  hydrochloric acid is reasonably selective and that only palladium, gold, selenium and tellurium are largely or completely co-extracted as xanthates under these conditions. Copper and several other elements are partly extracted but can be essentially completely removed from the extract by suitable washing techniques, and the co-extraction of selenium and tellurium is easily prevented by reducing them to the elemental state before the extraction step. Because of the high specificity of this extraction procedure, it was considered that xanthate extraction might be very useful for the direct separation of ng and  $\mu\text{g}$  amounts of arsenic before its determination by GFAAS, particularly if quantitative extraction could be achieved in one extraction step into a solvent of specific gravity  $< 1$ . This would simplify and shorten the extraction procedure and facilitate washing of the extract to remove or reduce in concentration some co-extracted elements.

In the proposed method, arsenic is separated from matrix elements by a single extraction of its xanthate into cyclohexane from  $8\text{--}10M$  hydrochloric acid in the presence of titanium(III) as reductant. It is then stripped from the extract with  $16M$  nitric acid and ultimately determined by GFAAS in a 2% v/v nitric



acid medium in the presence of palladium and thiourea as matrix modifiers.

### EXPERIMENTAL

#### Apparatus

A Perkin-Elmer model 5000 atomic-absorption spectrophotometer, equipped with deuterium-arc background correction, an HGA-400 graphite furnace, an AS-40 auto-sampler, a Data System 10 and HGA graphics software, was used with an arsenic hollow-cathode lamp operated at 18 mA. The 193.7-nm resonance line was used with a spectral band-pass of 0.7 nm. Pyrolytically-coated graphite tubes with solid pyrolytic graphite platforms were employed and 20- $\mu$ l aliquots of the appropriate solutions were injected, followed by 5  $\mu$ l of 800  $\mu$ g/ml palladium solution as matrix modifier. Measurements were made in the peak-height mode. The instrumental conditions for the dry, char and atomization steps are given in Table 1.

#### Reagents

**Standard arsenic solution, ~100  $\mu$ g/ml.** Dissolve 0.1320 g of pure arsenic trioxide in 10 ml of 2% sodium hydroxide solution by warming. Dilute the resulting solution to 1 litre with water, then transfer it to a plastic bottle. Prepare a 1- $\mu$ g/ml solution, fresh as required, by diluting 5 ml of the stock solution to 500 ml with water.

**Titanium(III) solution, 24 mg/ml.** Add 50 ml of concentrated sulphuric acid to ~300 ml of water contained in a 1-litre beaker, marked at 500 ml. Add 12.5 g of pure titanium hydride powder, cover the beaker and heat gently until the hydride has dissolved. Cool the solution to room temperature, dilute it to the mark with water, then filter it (Whatman No. 541 paper) into a 1-litre separating funnel. Add 2 ml of freshly prepared 20% potassium ethyl xanthate solution followed by 25 ml of chloroform, stopper the funnel and shake it vigorously for 2 min. Allow the layers to separate, then drain off and discard the chloroform layer. Extract the aqueous phase twice more, in a similar manner, with 0.5 ml of xanthate solution and 15 ml of chloroform each time. Drain off the chloroform and transfer the aqueous solution to a 500-ml plastic bottle. This solution will keep for at least 2 months.

**Palladium solution, 800  $\mu$ g/ml.** Dissolve 87 mg of palladium nitrate by heating with 4 ml of concentrated nitric acid and ~0.5 ml of 30% hydrogen peroxide. Add ~10 ml of water, boil vigorously for ~10 min to destroy the excess of peroxide, then cool and dilute the solution to 50 ml with water.

**Bromine, 20% v/v solution in carbon tetrachloride.**

**Potassium ethyl xanthate, 20% w/v solution.** Prepare fresh as required.

**Hydrochloric acid, 10M.** Store in a plastic bottle.

**Thiourea, 2.5% w/v solution.**

**Hydrochloric acid (10M)-thiourea (2%) wash solution.** Dissolve 2 g of thiourea in 100 ml of 10M hydrochloric acid. Prepare a fresh solution weekly.

**Cyclohexane.** Analytical-reagent grade.

**Water, doubly-demineralized.** Demineralized water from a large-scale laboratory purification apparatus was further

purified to possess approximately 18 M $\Omega$ /cm resistivity, with a Barnstead Nanopure II purification system. All acids used were analytical-reagent grade. Teflon beakers used for sample decomposition were cleaned just before use by heating with 5-10% potassium hydroxide solution, followed by treatment with ~20% v/v nitric acid and thorough washing with doubly-demineralized water. The 100-ml beakers used for the final strip solutions were stored in 5-10% potassium hydroxide solution contained in a 4-litre beaker, then washed, just before use, with dilute nitric acid and water as described above.

#### Calibration solutions

Prepare 0.01-, 0.02-, 0.03- and 0.04- $\mu$ g/ml arsenic solutions by adding 0.5, 1, 1.5 and 2 ml, respectively, of 1- $\mu$ g/ml standard arsenic solution and 1 ml of concentrated nitric acid to 50-ml standard flasks, dilute to ~25 ml with water, add 2 ml of 2.5% thiourea solution and dilute to volume with water. Prepare a blank calibration solution in a similar manner. These solutions should be prepared fresh weekly.

#### Procedure

Transfer up to 1 g of powdered sample, accurately weighed and containing up to ~20  $\mu$ g of arsenic, to a 250-ml Teflon beaker, then cover the beaker with a Teflon cover and add 5 ml of 20% bromine solution in carbon tetrachloride (Note 1) and 10 ml of concentrated nitric acid. Mix and allow the solution to stand for ~15 min, then heat gently to remove the bromine and carbon tetrachloride. Cool, add 10 ml of concentrated hydrochloric acid and 7 ml of concentrated perchloric acid, then heat until the evolution of oxides of nitrogen ceases. Cool, remove the cover, wash down the sides of the beaker with water, then add 5 ml of concentrated hydrofluoric acid and evaporate the solution to fumes of perchloric acid. Wash down the sides of the beaker with water again and evaporate the solution to ~3 ml. Add 12 ml of water and 2 ml of concentrated hydrochloric acid, heat gently to dissolve the salts, then cool the solution to room temperature. Transfer the resulting solution to a plastic 100-ml standard flask (Note 2). Use concentrated hydrochloric acid, contained in a plastic squeeze-type wash bottle, to wash the beaker, then dilute to volume with the same solution. Run a blank through the whole procedure.

Transfer a 4-50-ml portion of the resulting solution, containing not more than 1  $\mu$ g of arsenic and ~5 mg of copper, to a 125-ml separating funnel, marked at 50 ml and, if necessary, dilute to the mark with 10M hydrochloric acid. Add sufficient titanium(III) solution to reduce all the iron(III) present (Note 3), then add 1 ml in excess, mix, and allow the solution to stand for ~15 min to ensure the complete reduction of arsenic. Add 15 ml of cyclohexane and 1 ml of freshly prepared 20% potassium ethyl xanthate solution (Note 4) and shake the solution for 2 min. Allow the layers to separate, then drain off and discard the aqueous phase. Wash the extract by shaking it for ~30 sec with 5 ml of 10M hydrochloric acid-2% thiourea solution (Note 5). Drain off the acid phase, then wash the extract three times, by shaking it for ~30 sec each time, with 5-ml portions of water to ensure the removal of chloride. Add 5

Table 1. Instrumental conditions for the determination of arsenic

Step function	1	2	3	4
	Dry	Char	Char	Atomize
Temperature ( $^{\circ}$ C)	110	300	800	2600
Ramp time (sec)	10	5	5	0
Hold time (sec)	20	20	20	5
Internal argon flow (ml/min)	300	300	300	0
Read	—	—	—	-1 sec
Baseline	—	—	—	-2 sec

ml of concentrated nitric acid to the extract, stopper the funnel tightly and, with a wrist-action shaker, shake it for 10 min. Allow the layers to separate, then drain the acid layer into a 100-ml Teflon beaker and wash the stem of the funnel with water. Wash the extract twice by shaking it for ~30 sec each time with 5-ml portions of water and add the washings to the beaker. Wash the stem of the funnel with water each time.

Carefully evaporate the resulting sample and blank solutions to 2–3 ml (Note 6) on a hot-plate, then place the beakers in a hot water-bath and evaporate until the drop remaining is ~8 mm in diameter (Note 7). Add 500  $\mu$ l of concentrated nitric acid and 7 or 8 ml of water to each beaker, heat gently for ~5 min, then allow the beakers to cool to room temperature. Transfer both the sample and blank solutions to 25-ml standard flasks, add 1 ml of 2.5% thiourea solution (Note 8), dilute to volume with water and mix thoroughly.

Measure the peak-height absorbance of the sample and blank solutions under the conditions described under "Apparatus" and in Table 1 (Notes 9 and 10). Determine the arsenic concentration of the solutions by reference to a calibration curve plotted from peak-height values obtained concurrently for the calibration solutions. Calculate the arsenic content of the solutions (in ng) and correct the result obtained for the sample solution by subtracting that obtained for the blank solution.

#### Notes

1. The use of bromine solution is not necessary if sulphides are absent.
2. If plastic standard flasks are not available, use a borosilicate flask then transfer the solution to a dry plastic bottle.
3. The solution should be distinctly purple after the reduction of iron(III) and the addition of the excess of titanium(III) solution. The same volume of titanium solution should be added to the blank solution.
4. Because of the rapid decomposition of xanthate in strongly acidic solutions, xanthate solution should only be added to two solutions at a time, followed by immediate extraction of the complex. For health reasons,<sup>11</sup> all operations involving xanthate should be performed in a fume-hood and xanthate solution should be added with an automatic pipette or with an ordinary pipette used with a suction bulb. The aqueous phase remaining after the extraction, and any excess of xanthate solution, should be treated with concentrated nitric acid and boiled vigorously to destroy the xanthate before disposal of the solution.
5. If a copper thiourea compound, indicated by a white precipitate, is present in the wash phase, wash the extract once more in a similar manner.
6. Do not allow the solution to evaporate to dryness (Note 7).
7. At this stage the drop remaining should be colourless or pale yellow. If the evaporation proceeds too far the drop will become brown or black due to carbonaceous material. This will cause erroneous results for arsenic. The analysis cannot be rescued if it goes wrong at this point, as heating with more nitric acid fails to destroy the organic matter, and perchloric acid cannot be used, because it would interfere in the GFAAS determination.
8. The thiourea solution should be added just before the GFAAS determination of arsenic because on prolonged standing white salts may precipitate and cause erroneous results. In the absence of thiourea, the solution is stable for at least 3 weeks.
9. If dilution is necessary, dilute a suitable aliquot of the solution with 2% nitric acid–0.1% thiourea solution either directly in the autosampler cup or in a standard flask of appropriate size.
10. To prevent plugging of the pipette tip with metallic

palladium, which may form on the tip after repeated injections, it should be cleaned with *aqua regia* after ~20 firings.

## RESULTS AND DISCUSSION

### *Palladium as matrix modifier*

Nickel is usually recommended as a matrix modifier for the GFAAS determination of arsenic<sup>4,12</sup> but recent work<sup>13,14</sup> has suggested that palladium may be superior. Shan Xiao-Quan *et al.*<sup>13</sup> found that the maximum charring temperature for arsenic with wall atomization is raised to ~1300° in the presence of  $\geq 2$   $\mu$ g of palladium and that the sensitivity for peak-height measurements is ~50% better than that obtained in the presence of nickel. More recently, Voth-Beach and Shrader<sup>14</sup> found that, for wall atomization in dilute hydrochloric acid solutions, palladium raises the ash temperature to ~1500°. Both palladium and nickel were investigated in the present work and platform atomization was chosen because of the greater sensitivity. Figure 1 shows that, for platform atomization from 2% nitric acid solutions, palladium gives ~25% greater sensitivity than nickel for peak-height measurements. However, peak-area results obtained for these tests were approximately the same, which indicates that there is no significant difference between palladium and nickel when peak-area is measured.<sup>12</sup> The increase in the peak appearance time caused by the presence of palladium and nickel is presumably caused by a slight delay in atomization resulting from the formation of more stable intermetallic palladium and nickel arsenides or other compounds. Palladium was chosen for further work because of the greater sensitivity in the peak-height measurement mode. The maximum permissible charring temperature found under the conditions used in this work was ~1100° but 800° was found to be adequate. Tests showed that the effect of palladium is constant from ~3 to at least 10  $\mu$ g, and in subsequent work 4  $\mu$ g, added as a 5- $\mu$ l portion of 800- $\mu$ g/ml solution, was used.

### *Separation of arsenic by extraction as the xanthate*

Preliminary work to determine the recovery of arsenic by a single extraction as the xanthate into a solvent of specific gravity <1 from ~10M hydrochloric acid was done with toluene and with titanium(III) as reductant.<sup>5</sup> In these tests, in which arsenic was stripped into water after oxidation of arsenic(III) xanthate with bromine solution in carbon tetrachloride and determined spectrophotometrically by the molybdenum blue method as described previously,<sup>9</sup> large negative errors, which increased with an increase in the volume of solvent used, were obtained for arsenic. Ultimately, it was thought that this was caused by an impurity in the toluene, which interfered with the extraction of arsenic. It was also found that toluene reacted with the added bromine, producing heat and rapid decolorization of the

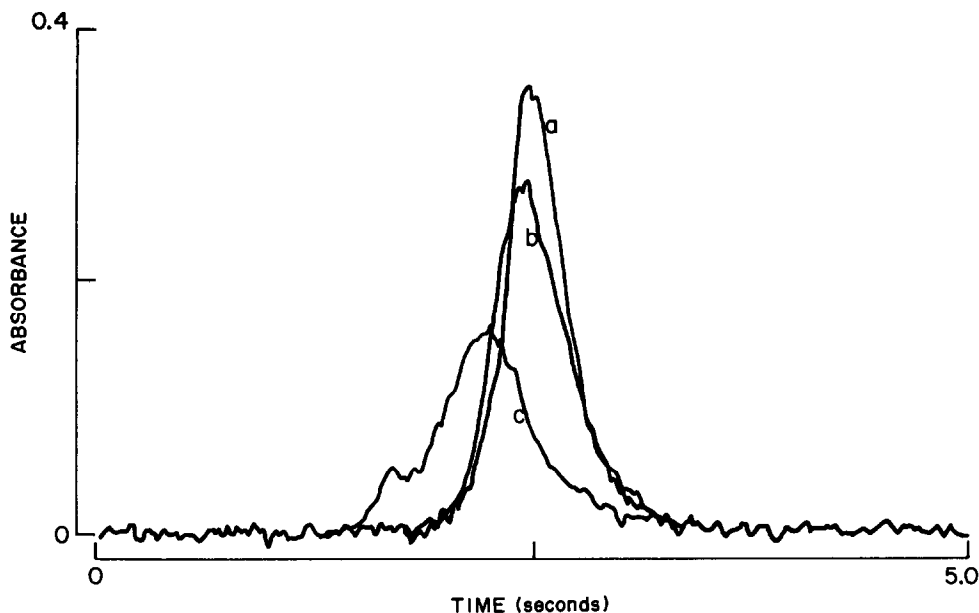


Fig. 1. Peak-height absorbance-time profiles for arsenic (0.8 ng) in 2% nitric acid in the presence and absence of matrix modifiers under the conditions given in Table 1. (a) in the presence of 4  $\mu\text{g}$  of Pd; (b) in the presence of 10  $\mu\text{g}$  of Ni; (c) in the absence of Pd and Ni.

toluene-carbon tetrachloride phase. Further work showed that cyclohexane is a suitable solvent and that up to at least 10  $\mu\text{g}$  of arsenic can be extracted quantitatively in one extraction from 6–10M hydrochloric acid when the volume ratio of the organic to aqueous phase is varied from 1:1 to at least 1:4. Some additional tests indicated that hexane should also be applicable but this was not pursued in the present work.

#### Stripping and GFAAS determination of arsenic

Although previously,<sup>9</sup> as mentioned above, arsenic was stripped into water after oxidation of arsenic(III) xanthate with bromine solution in carbon tetrachloride, this was not considered suitable for the present work because of the formation of bromide during the oxidation step. It was thought that this might cause loss of arsenic by volatilization as the bromide during the drying and charring steps. Tests showed that arsenic cannot be stripped from the extract with dilute nitric acid or hydrogen peroxide but that ~5 ml of concentrated nitric acid followed by shaking for ~10 min is effective. However, extremely low results were obtained for arsenic under these conditions. Ultimately, because the results obtained decreased with an increase in the amount of xanthate used during the extraction step, it was concluded that the error was probably caused by the presence of sulphate in the final solutions, formed by oxidation of the co-extracted xanthate during the stripping step. It is known that sulphate strongly suppresses the arsenic signal.<sup>1,2</sup> Analysis, by the barium sulphate method, of solutions obtained after extraction in the presence of 1 ml of 20% potassium

ethyl xanthate solution showed that ~90 mg of sulphate is present in the final solution under these conditions. This is equivalent to the co-extraction of ~40% of the added xanthate. In previous unpublished work involving the extraction and stripping of antimony(III) xanthate under similar conditions, essentially complete recovery of antimony—which suggests minimal or no interference from sulphate—was obtained by GFAAS when thiourea was used as a matrix modifier. Consequently, the possible use of thiourea to minimize or eliminate sulphate interference was investigated in this work. Figure 2 shows that, after the extraction of arsenic in the presence of 1 ml of 20% xanthate solution, complete recovery is obtained in the presence of 4  $\mu\text{g}$  of palladium when

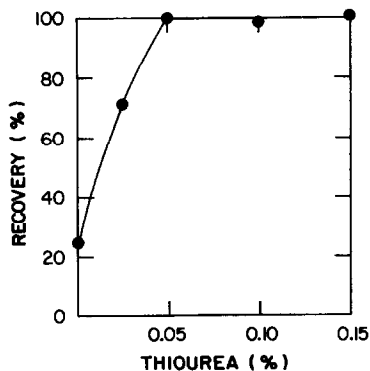


Fig. 2. Effect of thiourea on the recovery of arsenic after extraction as xanthate: As taken, 1000 ng; final volume, 25 ml; aliquot, 20  $\mu\text{l}$ ; Pd solution, 5  $\mu\text{l}$ .

$\geq 10 \mu\text{g}$  of thiourea is present in the aliquot injected into the furnace. The use of more than 1 ml of xanthate solution is not recommended, because of the resultant increase in the sulphate content of the final solution. Thiourea does not alter the shape of the atomization peak for arsenic but it reduces the peak height by  $\sim 10\text{--}15\%$ . The peak obtained in the absence of palladium is similar to that shown in Fig. 1(c) for a solution containing no palladium. A combined palladium and thiourea modifier solution cannot be prepared because of the formation of an insoluble brown palladium–thiourea complex.

While this work with thiourea was in progress, Voth-Beach and Shrader<sup>14</sup> found that a reduced-palladium matrix modifier, in which an organic reducing agent such as hydroxylamine hydrochloride or ascorbic acid is used in conjunction with palladium, is for some elements a more effective matrix modifier than palladium alone. They also found that for many elements, including arsenic, interference from sulphate can be eliminated or minimized in this way. They suggest that the reducing agent modifies the form of palladium by reducing it to the metal early in the temperature programme and that it may also influence the atomization of the analyte. Possibly thiourea may react in a somewhat similar manner in the presence of palladium. However, the mechanism for these reactions is not readily apparent.

#### *Effect of diverse ions*

Under the conditions,  $\sim 8\text{--}10 M$  hydrochloric acid, used for extraction of the arsenic, platinum and palladium are  $\sim 8$  and  $80\%$  co-extracted as xanthate complexes at the 0.2-mg level and gold is  $\sim 80\%$  extracted at the 0.5-mg level. Copper—at the 5-mg level is partly extracted but is largely removed from the extract by washing with  $10M$  hydrochloric acid containing 2% thiourea. Small amounts of co-extracted antimony, molybdenum and entrained iron are also removed in this way. The presence of more than 5 mg of copper during the extraction step is not recommended, because of the formation of insoluble yellow cuprous xanthate, which interferes mechanically with the extraction. For the same reason thiourea cannot be used to complex copper before the extraction step, because of the formation of an insoluble cuprous thiourea compound. Rhenium and germanium would probably also be partly co-extracted into cyclohexane<sup>10</sup> but they would be removed by volatilization as the heptoxide and tetrachloride during the sample decomposition step. Selenium and tellurium are not co-extracted, because they are reduced to the elemental state with titanium(III) before the extraction step. Up to 1 mg each of copper, antimony, palladium and molybdenum, 0.5 mg of gold and 0.2 mg of platinum can be present in the final solution (25 ml), either individually or collectively, without causing more than  $\sim 20\%$  error in the result. However, these amounts of gold, platinum and palladium are considerably more than would be

expected in the largest recommended aliquot (50 ml) and weight of sample (0.5 g) taken for extraction. Similarly, for the recommended maximum amount of copper and the low levels of antimony and molybdenum usually present in the samples under consideration, considerably less than 1 mg of any of these elements would be expected to be present after the extract has been washed with hydrochloric acid containing thiourea. Interference from chloride in the graphite-furnace step is avoided by washing the extract three times with water to remove entrained hydrochloric acid. However, up to  $100 \mu\text{l}$  of hydrochloric acid can be present in 25 ml of final solution without causing error in the arsenic result.

#### *Decomposition of ores*

In the previous method<sup>9</sup> the samples were treated with bromine solution in carbon tetrachloride and with nitric acid to oxidize sulphur and sulphides to sulphates, followed by the addition of hydrochloric and sulphuric acids and evaporation to fumes of sulphur trioxide to remove nitric acid and dehydrate silica. Silica was separated from arsenic during the subsequent iron collection step. However, in this work, in which this step is not used, and in which the hydrochloric acid concentration of the initial sample solution must be adjusted to  $\sim 10M$  before extraction, it was considered preferable, particularly for samples of high silica content, to remove the silica by volatilization as the fluoride during the decomposition step. As recommended by other investigators,<sup>13,15-17</sup> and because perchlorates are more soluble than sulphates, evaporation with perchloric acid was used for the removal of silicon tetrafluoride and excess of hydrofluoric acid.

#### *Applications*

Table 2 shows that the mean results obtained for arsenic in various diverse CCRMP reference materials and in several National Research Council Canada and National Bureau of Standards marine and river sediments are in excellent agreement with either the certified values, with values given for information only or with the consensus mean or tentative values obtained during interlaboratory certification programmes. They also agree reasonably well with other reported values obtained by a variety of instrumental methods. The results obtained for CCU-1, RL-1 and UTS-4 are in excellent agreement with previous results obtained in this laboratory during the respective interlaboratory certification programmes by using the iron collection–xanthate extraction–molybdenum blue spectrophotometric method.<sup>9</sup> Each of the 3 or 4 individual results obtained for these reference materials was the mean of 3 or 4 GFAAS runs each involving duplicate measurements. These were referred to a calibration curve prepared for each run as described under the procedure, for arsenic calibration solutions covering the linear range  $0\text{--}0.04 \mu\text{g/ml}$ .

Table 2. Determination of arsenic in CCRMP and other reference, ores, concentrates and related materials

Sample*	Nominal composition, %	Arsenic, µg/g		
		Certified value and 95% confidence limits	This work†	Other reported values‡
CCU-1 Copper concentrate	24.7 Cu, 3.2 Zn, 30.9 Fe, 35.4 S, 2.6 SiO <sub>2</sub>	41.0 ± 4.0	44.1 ± 0.8	44.3§
RL-1 Uranium ore	2.3 Fe, 25.3 Si, 9.2 Mg, 6.5 Al, 1.8 Ca, 0.2 U	19.6 ± 1.1	19.8 ± 2.2 (4)	19.8§
UTS-4 Uranium tailings	2.6 Fe, 6.3 Al, 1.8 Ca, 1.8 S	38.0 ± 2.0	39.6 ± 2.6 (4)	39.7§
SY-2 Syenite rock	60.1 SiO <sub>2</sub> , 12.1 Al <sub>2</sub> O <sub>3</sub> , 2.3 Fe <sub>2</sub> O <sub>3</sub> , 3.6 FeO, 2.7 MgO, 8.0 CaO	17	17.1 ± 1.3	17.6 <sup>17</sup>
SY-3 Syenite rock	59.7 SiO <sub>2</sub> , 11.8 Al <sub>2</sub> O <sub>3</sub> , 2.4 Fe <sub>2</sub> O <sub>3</sub> , 3.6 FeO, 2.7 MgO, 8.3 CaO	19	17.9 ± 1.1	19.6 <sup>17</sup>
MRG-1 Gabbro	39.3 SiO <sub>2</sub> , 8.5 Al <sub>2</sub> O <sub>3</sub> , 8.3 Fe <sub>2</sub> O <sub>3</sub> , 8.6 FeO, 13.5 MgO, 14.8 CaO 3.7 TiO <sub>2</sub>	0.5	0.5 <sub>1</sub> ± 0.0 <sub>7</sub>	0.4 <sup>17</sup>
SO-1 Regosolic soil	25.7 Si, 9.4 Al, 6.0 Fe, 2.3 Mg, 1.8 Ca, 0.5 Ti	1.9 ± 0.3¶	2.1 ± 0.3	1.7 <sup>15</sup>
SO-2 Podzolic soil	25.0 Si, 8.1 Al, 5.6 Fe, 2.0 Ca, 0.9 Ti	1.2 ± 0.2¶	1.1 ± 0.1	1.1 <sup>15</sup>
SO-3 Calcareous C Horizon soil	15.9 Si, 3.1 Al, 1.5 Fe, 5.0 Mg, 14.6 Ca	2.6 ± 0.1¶	2.5 ± 0.2	2.5 <sup>15</sup>
SO-4 Chernozemic A Horizon soil	32.0 Si, 5.5 Al, 2.4 Fe, 1.1 Ca	7.1 ± 0.7¶	6.3 ± 0.2	7.7 <sup>15</sup>
FER-1 Iron formation rock	17.0 SiO <sub>2</sub> , 49.9 Fe <sub>2</sub> O <sub>3</sub> , 23.3 FeO, 3.3 CaO	5.9 <sup>a</sup>	5.9 ± 0.4	
FER-2 Iron formation rock	49.2 SiO <sub>2</sub> , 5.2 Al, 22.5 Fe <sub>2</sub> O <sub>3</sub> , 15.2 FeO, 2.1 MgO, 2.2 CaO	1.8 <sup>a</sup>	1.6 ± 0.0	
FER-3 Iron formation rock	53.6 SiO <sub>2</sub> , 29.4 Fe <sub>2</sub> O <sub>3</sub> , 13.6 FeO, 1.0 MgO, 0.8 CaO	1.1 <sup>a</sup>	0.8 <sub>7</sub> ± 0.0 <sub>4</sub>	
FER-4 Iron formation rock	50.1 SiO <sub>2</sub> , 1.7 Al <sub>2</sub> O <sub>3</sub> , 22.7 Fe <sub>2</sub> O <sub>3</sub> , 15.5 FeO, 1.4 MgO, 2.2 CaO	3.4 <sup>a</sup>	2.9 ± 0.1	
NRCC MESS-1 Marine sediment	67.5 SiO <sub>2</sub> , 11.0 Al <sub>2</sub> O <sub>3</sub> , 4.4 Fe <sub>2</sub> O <sub>3</sub> , 1.4 MgO, 0.9 TiO <sub>2</sub> , 0.7 S	10.6 ± 1.2	10.1 ± 0.8	9.7 <sup>18</sup> , 11.5 <sup>19</sup>
NRCC BCSS-1 Marine sediment	66.1 SiO <sub>2</sub> , 11.8 Al <sub>2</sub> O <sub>3</sub> , 4.7 Fe <sub>2</sub> O <sub>3</sub> , 2.4 MgO, 0.7 TiO <sub>2</sub> , 0.4 S	11.1 ± 1.4	10.5 ± 0.4	10.2 <sup>18</sup> , 11.3 <sup>19</sup>
NBS 1645 River sediment	2.3 Al, 11.3 Fe, 3.0 Cr, 2.9 Ca, 1.1 S	66 <sup>b</sup>	64.2 ± 5.9 (4)	66.5 <sup>13</sup> , 81 <sup>20</sup> , 61 <sup>18</sup> 62.6 <sup>6</sup> , 66 <sup>15</sup> , 71 <sup>21</sup>
NBS 1646 Estuarine sediment	31 Si, 6.3 Al, 3.4 Fe, 1.1 Mg, 1.0 S, 0.5 Ti	11.6 ± 1.3	10.4 ± 0.7	11.5 <sup>18</sup> , 11.2 <sup>19</sup>

\*CCRMP reference materials except where indicated otherwise.

†Mean and standard deviation for 3 values except where indicated otherwise in parentheses.

‡Some results are the mean of several results obtained by using different decomposition methods or different finishes.

§Mean value obtained by the author during the interlaboratory certification programme.

||Most recent usable value.<sup>22</sup>

¶CCRMP value given for information only (not certified).

<sup>a</sup>Mean value obtained during the interlaboratory programme.<sup>23</sup><sup>b</sup>Tentative value.

In the proposed method, the detection limit calculated as three times the standard deviation of the reagent blank, based on a 50-ml aliquot (equivalent to a 0.5-g sample) of sample solution taken through the extraction step, is  $\sim 0.2 \mu\text{g/g}$  arsenic. The sensitivity or characteristic mass is  $\sim 12 \text{ pg}$  for 0.0044 absorbance. In this work no clean out step was required after the atomization and the pyrolytically-coated tubes and solid pyrolytic graphite platforms were used for up to  $\sim 800$  atomizations. The reagent blank varied from  $\sim 20$  to  $90 \text{ ng}$ , depending on the size of the aliquot taken. Most of this came from the hydrofluoric acid used in the decomposition step. Purification of the titanium solution by xanthate extraction<sup>11</sup> was necessary because it was found to contain a substantial amount of arsenic ( $\sim 21 \text{ ng/ml}$ ). Possibly, if required, the blank could be reduced by using ultrapure acids, particularly hydrofluoric acid. It should be possible to remove arsenic impurity from concentrated hydrochloric acid by adding some solid potassium ethyl xanthate to a suitable portion of the acid and then extracting 2 or 3 times with chloroform. A final sample solution volume of less than 25 ml is not recommended, because preconcentration would result in an increase in the sulphate concentration of the solution.

## REFERENCES

1. P. R. Walsh and J. L. Fasching, *Anal. Chem.*, 1976, **48**, 1014.
2. D. Chakraborti, W. De Jonghe and F. Adams, *Anal. Chim. Acta*, 1980, **119**, 331.
3. R. R. Brooks, D. E. Ryan and H. Zhang, *ibid.*, 1981, **131**, 1.
4. R. W. Dabeka and G. M. A. Lacroix, *Can. J. Spectrosc.*, 1985, **30**, 154.
5. C. H. Chung, E. Iwamoto, M. Yamamoto and Y. Yamamoto, *Spectrochim. Acta*, 1984, **39B**, 459.
6. F. Puttemans and D. L. Massart, *Anal. Chim. Acta*, 1982, **141**, 225.
7. F. Puttemans, P. Van Den Winkel and D. L. Massart, *ibid.*, 1983, **149**, 123.
8. P. Aruscavage, *J. Res. U.S. Geol. Survey*, 1977, **5**, 405.
9. E. M. Donaldson, *Talanta*, 1977, **24**, 105.
10. *Idem*, *ibid.*, 1976, **23**, 411.
11. *Idem*, *ibid.*, 1982, **29**, 663.
12. W. Slavin, *Graphite Furnace AAS-A Source Book*, p. 76. Perkin-Elmer Corporation, Norwalk, 1984.
13. S. Xiao-Quan, N. Zhe-Ming and Z. Li, *Anal. Chim. Acta*, 1983, **151**, 179.
14. L. M. Voth-Beach and D. E. Shrader, *Spectroscopy*, 1986, **1**, 49.
15. H. Agemian and E. Bedek, *Anal. Chim. Acta*, 1980, **119**, 323.
16. C. M. Elson, J. Milley and A. Chatt, *ibid.*, 1982, **142**, 269.
17. G. E. M. Aslin, *J. Geochem. Exploration*, 1976, **6**, 321.
18. M. Bettinelli, N. Pastorelli and U. Baroni, *Anal. Chim. Acta*, 1986, **185**, 109.
19. E. de Oliveira, J. W. McLaren and S. S. Berman, *Anal. Chem.*, 1983, **55**, 2047.
20. M. Bettinelli, *Anal. Chim. Acta*, 1983, **148**, 193.
21. H. A. Van Der Sloot, D. Hoede, Th. J. L. Klinkers and H. A. Das, *J. Radioanal. Chem.*, 1982, **71**, 463.
22. S. Abbey and E. S. Gladney, *Geostandards Newsl.*, 1986, **10**, 3.
23. S. Abbey, C. R. McLeod and W. Liang-Guo, *Geol. Surv. Canada Paper 83-19*, Geological Survey of Canada, Department of Energy, Mines and Resources, Ottawa, Canada, 1983.

## SHORT COMMUNICATIONS

# SIMULTANEOUS DETERMINATION OF LOW CONCENTRATIONS OF AMMONIUM AND POTASSIUM IONS BY CAPILLARY TYPE ISOTACHOPHORESIS

KEIICHI FUKUSHI

Kobe University of Mercantile Marine, Fukae, Higashinada, Kobe 658, Japan

KAZUO HIIRO

Government Industrial Research Institute, Osaka, Midorigaoka, Ikeda 563, Japan

(Received 16 June 1987. Accepted 5 September 1987)

**Summary**—Low concentrations of ammonium and potassium ions (<2.0 mg/l.) were determined simultaneously by capillary type isotachophoresis based on the interaction between potassium and 18-crown-6 in the aqueous leading electrolyte. The PU value of potassium ion increased with increasing concentration of 18-crown-6 up to 3mM, whereas that of the ammonium ion remained almost constant. Thus complete separation of ammonium and potassium ions could be obtained by using 1–3mM 18-crown-6. The error in the analysis of mixtures containing ammonium and potassium ions (250- $\mu$ l sample injection) was less than  $\pm 20\%$  with a leading electrolyte containing 3mM 18-crown-6. The analysis time was 18 min.

The separation of ammonium and potassium ions by capillary type isotachophoresis is possible with methanolic electrolytes, but not with aqueous electrolytes.<sup>1</sup> However, it is difficult to use a longer migration tube and to apply a higher migration current with the methanolic electrolytes.<sup>2</sup> For these reasons, when the methanolic electrolytes are used a large volume of sample solution cannot be injected into the isotachophoresis apparatus for the purpose of determination of low concentration of ions. Tazaki *et al.*<sup>3</sup> studied the isotachophoretic behaviour of mM concentrations of alkali and alkaline-earth metal ions in the presence of larger amounts of 18-crown-6 and evaluated its usefulness for their separation. Therefore, we have studied the simultaneous determination of low concentrations of ammonium and potassium ions by capillary type isotachophoresis with smaller amounts of 18-crown-6, for the purpose of determination of trace amounts of ammonia in sea-water. By using the method proposed in this paper, we have performed the separation of mixtures containing ammonium and potassium ions at concentrations less than 2.0 mg/l., within 18 min, with injection of a large volume of sample solution.

### EXPERIMENTAL

#### Reagents

All solutions were prepared with analytical-reagent grade chemicals. 18-Crown-6 was obtained from the Aldrich Chemical Co.

#### Apparatus

A Shimadzu Model IP-2A isotachophoretic analyser was used with a potential-gradient detector. The main column was a fluorinated ethylene-propylene (FEP) copolymer tube, 20 cm in length and 0.5 mm in inner diameter; the precolumn was a polytetrafluoroethylene (PTFE) tube,

20 cm in length and 1.0 mm in inner diameter for injecting a large volume of sample solution. A Hamilton Model 1725-N microsyringe was used for the injection of samples into the isotachophoresis apparatus.

### RESULTS AND DISCUSSION

#### Concentration of 18-crown-6

The concentration of 18-crown-6 in the leading electrolyte (5mM hydrochloric acid containing 30% v/v glycerol) was increased up to 5mM. The terminating electrolyte was 10mM lithium sulphate. A 250- $\mu$ l volume of a mixture containing 1.0 mg/l. ammonium and potassium ions was injected into the isotachophoresis apparatus. The migration current was maintained at 200  $\mu$ A for the first 12 min and then reduced to 50  $\mu$ A. In general, the potential unit (PU) value is used for qualitative indication of the ions, and is defined by the equation<sup>4</sup>

$$PU = \frac{PG_S - PG_L}{PG_T - PG_L}$$

where  $PG_S$ ,  $PG_L$  and  $PG_T$  are the potential gradients of the sample ion, leading ion and terminating ion, respectively.

As shown in Fig. 1, the PU value of the potassium ion increased with increasing concentration of 18-crown-6 up to 3mM. On the other hand, the PU value of the ammonium ion remained almost constant, and complete separation of ammonium and potassium ions could be obtained with 1–3mM 18-crown-6. The PU value of the potassium ion was the same as that of the sodium ion in the terminating electrolyte when its concentration was higher than 4mM. In addition, it was found that the PU value of the sodium ion was smaller than that of the calcium

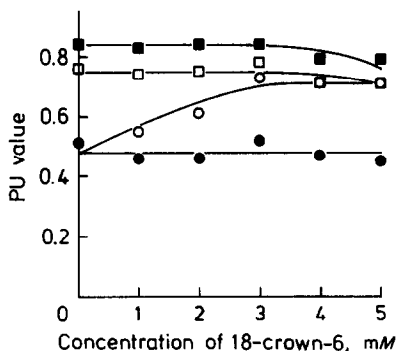


Fig. 1. Effect of the concentration of 18-crown-6 on the PU values. ● NH<sub>4</sub><sup>+</sup>; ○ K<sup>+</sup>; □ Na<sup>+</sup>; ■ Ca<sup>2+</sup>.

ion when the glycerol concentration was 20–30%, but greater than it when the glycerol concentration was less than 10%. Therefore, 3mM 18-crown-6 was selected as the concentration in the leading electrolyte.

#### Determination of low concentrations of ammonium and potassium ions

Linear working graphs were obtained for ammonium and potassium ions up to 1.0 and 2.0 mg/l., respectively, by using the leading electrolyte containing 3mM 18-crown-6. The regression equations of these graphs for ammonium and potassium ions were  $y = 34.9x - 0.08$  and  $y = 12.9x - 0.05$ , respectively. Both correlation coefficients were 1.000. In these equations,  $x$  was the concentration of the ion (mg/l.) and  $y$  the zone length (mm) when the recording speed was adjusted to 40 mm/min. The lower determination limits for ammonium and potassium ions were 2.9 and 7.8  $\mu\text{g/l.}$ , respectively, corresponding to a 0.1-mm zone length. When 250- $\mu\text{l}$  volumes of mixed solutions containing ammonium and potassium ions in various concentrations were injected and analysed by use of the working graphs, the error in the determination of these ions was less than  $\pm 20\%$ , as shown in Table 1. The isotachopherogram of mixture 6

Table 1. Analytical results for ammonium and potassium ions

Mixture	Added, mg/l.		Found, mg/l.		Error, %	
	NH <sub>4</sub> <sup>+</sup>	K <sup>+</sup>	NH <sub>4</sub> <sup>+</sup>	K <sup>+</sup>	NH <sub>4</sub> <sup>+</sup>	K <sup>+</sup>
1	0.10	2.00	0.12	2.00	+20	$\pm 0.0$
2	0.20	1.80	0.20	1.66	$\pm 0.0$	-7.8
3	0.40	1.40	0.39	1.36	-2.5	-2.9
4	0.60	1.40	0.58	1.34	-3.3	-4.3
5	0.60	0.60	0.56	0.59	-6.7	-1.7
6	0.80	0.40	0.75	0.39	-6.3	-2.5
7	1.00	2.00	1.01	0.18	+1.0	-10
8	1.00	1.00	1.02	1.03	+2.0	+3.0

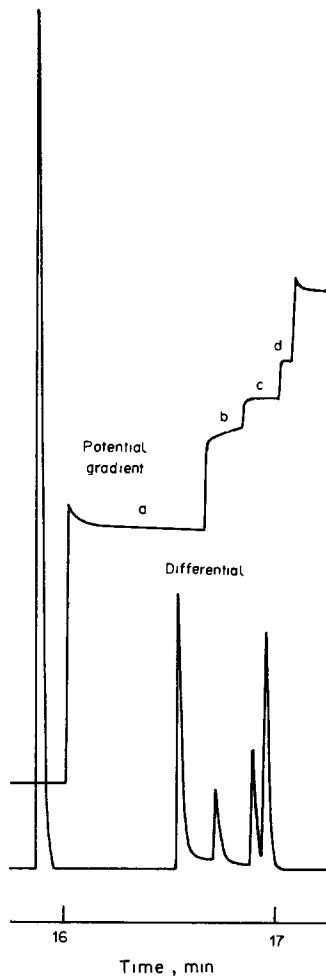


Fig. 2. Isotachopherogram of mixture 6. a, NH<sub>4</sub><sup>+</sup>; b, K<sup>+</sup>; c, Na<sup>+</sup>; d, Ca<sup>2+</sup>.

6 in Table 1 is shown in Fig. 2. In view of these results, this electrolyte system (which uses a smaller amount of 18-crown-6) can be applied to the determination of trace amounts of ammonia in sea-water after a suitable pretreatment.

#### REFERENCES

- H. Miyazaki and K. Kato, *Tosoku-Denki-Eido-Ho*, p. 56. Kodansha-Scientific, Tokyo, 1980.
- T. Hine, *4th Isotachophoresis Symposium*, Tokyo, 14 December 1984. *Abstracts*, p. 16.
- M. Tazaki, M. Takagi and K. Ueno, *Chem. Lett.*, 1982, 639.
- H. Miyazaki and K. Kato, *Tosoku-Denki-Eido-Ho*, p. 31. Kodansha-Scientific, Tokyo, 1980.



## EXTRACTIVE SPECTROPHOTOMETRIC DETERMINATION OF TRACE AMOUNTS OF IRON(III) WITH BENZYLTRIEHYLAMMONIUM CHLORIDE

K. C. BAYAN and H. K. DAS

Department of Chemistry, Gauhati University, Guwahati 781014, India

(Received 5 November 1985. Revised 16 May 1987. Accepted 2 July 1987)

**Summary**—The ion-association complex formed between a thiocyanato-iron(III) ion and a benzyltriethylammonium ion is extracted into 1,2-dichloroethane, and its absorbance at 476 nm is used for determination of the iron. Beer's law is obeyed up to about 4  $\mu\text{g/ml}$  iron concentration in the final solution. The molar absorptivity is  $2.79 \times 10^4 \text{ l. mole}^{-1} \text{ cm}^{-1}$ .

The thiocyanate method is one of the most extensively used colorimetric methods for the determination of iron, but has the disadvantage that the colour of the product fades. The complex can be extracted with various organic bases.<sup>1</sup> Here we report the use of benzyltriethylammonium chloride for the purpose; addition of a small amount of ethyl methyl ketone stabilizes and intensifies the colour.

### EXPERIMENTAL

#### Reagents

All chemicals used were of analytical grade. The stock solution of iron (100  $\mu\text{g/ml}$ ) was prepared from ferric ammonium sulphate in 0.05M sulphuric acid, and standardized by the potassium dichromate method.<sup>2</sup>

A mixture of ethyl acetate, dimethylformamide, triethylamine and benzyl chloride was refluxed to prepare the benzyltriethylammonium chloride<sup>3</sup> (BTAC), which was used as a 0.1M solution in water. A 3M potassium thiocyanate solution in water was used.

Buffers with pH-values in the range 1–6 were prepared from 0.2M hydrochloric acid, potassium hydrogen phthalate and potassium hydroxide. To 50 ml of 0.2M potassium hydrogen phthalate 20.4 ml of 0.2M hydrochloric acid were added and the mixture was diluted to 200 ml with distilled water to give a solution of pH 3.0.

#### Procedure

A portion of sample solution containing 0.8–38  $\mu\text{g}$  of iron(III) is diluted to 10 ml with potassium hydrogen phthalate buffer so that the pH is  $3.0 \pm 0.5$ . Then 2 ml of 0.1M BTAC, 0.5 ml of ethyl methyl ketone, 10 ml of 1,2-dichloroethane and 2 ml of 3M potassium thiocyanate are added. The mixture is shaken for 1 min and the organic layer separated. The absorbance of the extract is measured at 476 nm against a reagent blank. A calibration graph is prepared in the same way.

### RESULTS AND DISCUSSION

Depending on the thiocyanate concentration, a series of iron(III) complexes can be obtained. At thiocyanate concentrations higher than 0.2M, negatively charged<sup>4</sup> complexes are formed which are extractable as ion-association species with the qua-

ternary BTA ion into 1,2-dichloroethane. The extract has maximum absorption at 476 nm. Beer's law is obeyed for 0.08–3.8 ppm of iron in the final solution; the molar absorptivity is  $2.79 \times 10^4 \text{ l. mole}^{-1} \text{ cm}^{-1}$  and is constant when the pH of the aqueous layer is kept in the range 1–4.

The thiocyanate concentration is critical and must exceed 0.2M in the aqueous phase. Addition of the thiocyanate is best done after addition of the solvent, to prevent possible fading of the colour. The lower limit for the BTAC concentration in the aqueous phase is 0.01M. The presence of some ethyl methyl ketone (0.3–0.8 ml) in the reaction mixture is found to play a significant role in increasing the stability and colour intensity of the extracted species, the absorbance remaining constant for at least 3 hr. If the amount of ethyl methyl ketone added is less than 0.3 or more than 0.8 ml, the absorbance is lower.

#### Effect of foreign ions

The tolerance limit for interferences (Table 1) was set at the amount required to cause an error not exceeding about 1% in the determination of iron, but the upper concentration limit investigated was restricted to 1000-fold w/w ratio to iron.

The tolerance limits for some of the interfering species could be improved by use of masking agents, e.g., Pd(II) and Pt(IV) with thiosulphate, Mo(VI) and W(VI) with mannitol, and Cu(II) with thiourea, the tolerance level being raised to 40  $\mu\text{g}$ .

#### Application to analysis of alloys and minerals

Various samples were decomposed as outlined below, and suitable aliquots of the solutions were analysed as described above.

**Cupronickel.** A 0.5-g sample is treated with 2 ml of concentrated nitric acid. When the reaction is almost over, the mixture is warmed on a hot-plate to complete the dissolution. After addition of 1 ml of concentrated sulphuric acid the mixture is evaporated until white fumes appear, then cooled, and diluted to

Table 1. Tolerance limits for foreign ions in the extraction of 8  $\mu\text{g}$  of iron

Ions	Tolerance limit, mg	Ions	Tolerance limit, mg
Copper(II)	0.002	Manganese(VII)	0.50
Silver	0.50	Cobalt(II)	0.60
Gold(III)	0.15	Nickel	8.0
Zinc	4.0	Rhodium(III)	0.25
Cadmium	8.0	Palladium(II)	0.010
Mercury(II)	8.0	Platinum(IV)	0.005
Tin(II)	0.10	Fluoride	0.20
Tin(IV)	8.0	Bromide	8.0
Lead(II)	4.0	Iodide	0.40
Arsenic(III)	4.0	Thiosulphate	0.25
Arsenic(V)	1.0	Oxalate	0.01
Antimony(III)	0.25	Citrate	0.40
Bismuth	0.05	Tartrate	2.5
Vanadium(V)	0.25	EDTA	0.002
Chromium(III)	0.12	Thiourea	3.0
Chromium(VI)	0.050	Cyanide	0.05
Molybdenum(VI)	0.016	Perchlorate	8.0
Tungsten(VI)	0.010	Orthophosphate	2.0
Manganese(II)	4.0	Acetate	8.0

about 100 ml with 0.3M hydrochloric acid. The solution is heated almost to boiling, and hydrogen sulphide is passed through it to precipitate all the copper. The copper sulphide is filtered off and washed, and the filtrate is boiled to remove hydrogen sulphide, then evaporated to about 50 ml. Two ml of 30% hydrogen peroxide solution are added to oxidize iron(II) to iron(III), and the solution is boiled to decompose the excess of peroxide. The solution is then made up accurately to 100 ml with water.

*Aluminium alloy.* The sample is decomposed as for cupronickel.

*Gun metal.* A 1-g sample is treated with the minimum necessary volume of nitric acid (1 + 1). When the vigorous reaction is over, the mixture is slowly evaporated (on a boiling water-bath) to a volume of 5–10 ml to ensure that all the metastannic acid is precipitated. The mixture is then diluted to 50 ml and heated on the water-bath for 10–20 min, a Whatman "accelerator" is added, and the precipitate is filtered off on a Whatman No. 42 paper and washed. After addition of 1 ml of concentrated sulphuric acid the filtrate is evaporated until white fumes appear and is then cooled. After addition of 100 ml of water the solution is stirred and allowed to stand. Any precipitate is filtered off, and the filtrate (or solution) is made approximately 0.3M in hydrochloric acid, heated nearly to boiling and treated with hydrogen

Table 2. Determination of iron in alloys and minerals

Sample and composition, %	Iron found, %
Cupronickel (No. 19e)	0.840; 0.836; 0.830
Cu 67, Fe 0.83, Mn 0.80, Ni 31.2	
Aluminium alloy (No. 20b)	0.422; 0.428; 0.440
Cu 4.10, Fe 0.43, Mn 0.19,	
Ni 1.93, Si 0.29, Mg 1.61	
Gunmetal (No. 6g)	0.0202; 0.0202; 0.0208
Cu 86.4, Fe 0.02, Zn 1.30,	
Sn 10.5, Pb 1.02, Ni 0.26, P 0.11	
Lead concentrates (No. 42G)	1.38; 1.39; 1.39
Cu 0.14, Fe 1.35, Zn 3.40,	
Pb 75.6, S 14.2, As 0.32,	
Mn 0.21, Sb 0.15, Bi 0.02,	
Ag 0.074, Au 0.016	
Portland cement (No. 24b)	1.70; 1.69
CaO 62.9, MgO 2.56, Fe <sub>2</sub> O <sub>3</sub> 2.44,	
Al <sub>2</sub> O <sub>3</sub> 6.22, SiO <sub>2</sub> 20.4	
Dolomite (No. 9h)	0.143; 0.148; 0.149
CaCO <sub>3</sub> 55.2, MgCO <sub>3</sub> 43.1,	
SiO <sub>2</sub> 0.88, Fe <sub>2</sub> O <sub>3</sub> 0.21	

sulphide to precipitate the copper. The precipitate is filtered off and washed and the filtrate is evaporated to about 50 ml, then treated with hydrogen peroxide *etc.*, as for cupronickel.

*Lead concentrates.* A 0.5-g sample is dissolved in the minimum volume of nitric acid (1 + 1). Then 2 ml of concentrated sulphuric acid are added and the mixture is evaporated until white fumes appear, then cooled, diluted with water, boiled, filtered and made up to 100 ml.

*Portland cement or dolomite.* A 0.1-g sample is dissolved in the minimum of hydrochloric acid (1 + 1), the mixture is boiled and filtered, and the filtrate is made up to 100 ml with water.

The results obtained are given in Table 2.

*Acknowledgements*—The authors thank Professor A. Chaudhuri, Department of Chemistry, Gauhati University for her kind permission to work in the laboratory, and to the University Grants Commission for awarding a teacher-fellowship to K.B.

#### REFERENCES

1. E. B. Sandell, *Colorimetric Determination of Traces of Metals*, 3rd Ed., p. 533. Interscience, New York, 1959.
2. A. I. Vogel, *A Text Book of Quantitative Inorganic Analysis*, 3rd Ed., p. 309. ELBS, London, 1961.
3. A. Scola and A. Edelson, *J. Chem. Eng. Data*, 1968, 13, 453.
4. A. I. Vogel, *A Text Book of Quantitative Inorganic Analysis*, 4th Ed., p. 741. ELBS, Delhi, 1978.

## DETERMINATION OF WATER IN ORGANIC SOLVENTS BY FLOW-INJECTION ANALYSIS WITH KARL FISCHER REAGENT AND A BIAMPEROMETRIC DETECTION SYSTEM

CHEN LIANG\*, PAVEL VÁCHA† and WILLEM E. VAN DER LINDEN

University of Twente, Department of Chemical Technology, Laboratory for Chemical Analysis,  
P.O. Box 217, 7500 AE Enschede, The Netherlands

(Received 29 May 1987. Accepted 4 September 1987)

**Summary**—A flow-injection system with a biampometric flow-through detector provided with two platinum plate electrodes was tested for the determination of water with a two-component pyridine-free Karl Fischer reagent. The response was shown to be linear in the concentration range 0.03–0.11% water in methanol, ethanol or 2-propanol, with methanol as the carrier solvent. The maximum sampling frequency was about 150 samples per hr. It appeared to be possible to introduce a membrane separation step, thus allowing for the determination of water in fouled process streams. To avoid direct contact between the Karl Fischer solution and the pumping tubes, and thus extend the lifetime of the tubes, an indirect delivery system, based on replacement of the solution by pumped silicone oil, was also applied.

Since its introduction more than ten years ago, flow-injection analysis (FIA) has been widely used in many fields of chemical analysis, including the determination of water.<sup>1</sup> Compared with batchwise Karl Fischer titrations, flow-injection has several advantages: (i) reduced reagent consumption (it is reported that 2000 determinations can be done with 1 litre of reagent),<sup>2</sup> (ii) high sampling frequency (up to 250 samples per hr is possible),<sup>3</sup> and (iii) safety in applying toxic reagents because the whole analysis proceeds in a closed system. An additional advantage sometimes observed in FIA is the increased selectivity when the analyte is accompanied by more slowly reacting components. This may happen in the determination of water. A major disadvantage is the solvent effect. It has been observed that organic solvents may affect the peak shapes, thus reducing the general analytical applicability.<sup>3,4</sup> With regard to the determination of water by FIA, some authors have already reported on improvements of the manifold and particularly of the detection system.<sup>5,6</sup> In the present report this same subject is raised, including the possible application of a membrane separation step.

### EXPERIMENTAL

#### Chemicals

Two-component pyridine-free Karl Fischer reagent sol-

utions (Merck) were used. One ml of the iodine in methanol solution was equivalent to 5 mg of water. The methanol (p.a. Merck) used as the carrier stream was dried over a molecular sieve (3Å, Merck) by standing overnight. Before use the sieve beads were dried in a furnace at 300° for at least 16 hr. Standard solutions were prepared by adding demineralized water to dried methanol. The exact concentrations were checked coulometrically with a 652 KF-Coulometer (Metrohm) and Hydranal Coulomat A and C (Riedel-de Haën). All other chemicals were of analytical reagent grade.

#### Apparatus

The manifold is schematically depicted in Fig. 1. A peristaltic pump (Gilson, Minipuls 2) was used to propel the various streams. An indirect delivery system was introduced for the Karl Fischer (K.F.) solution, based on replacement of the solution by silicone oil. In this way direct contact of the pumping tubes (bore 0.5–0.6 mm) and the corrosive K.F.-solution was avoided; the pumping tubes were not affected by silicone oil. In the delivery flask the K.F.-solution and the silicone oil were separated by a thin impermeable Teflon membrane. Samples were injected man-

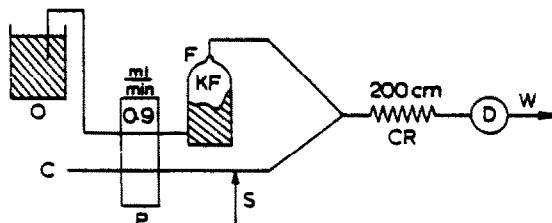


Fig. 1. Flow-injection manifold for the determination of water. P, Peristaltic pump; C, carrier stream; KF, Karl Fischer reagent; F, delivery flask; O, container with silicone oil; CR, reaction coil; D, detector; W, waste; S, injection valve.

\*Present address: Anhui University, Department of Chemistry, Hefei, Anhui, People's Republic of China.

†Present address: Department of Analytical Chemistry, Prague Institute of Chemical Technology, Prague, Czechoslovakia.

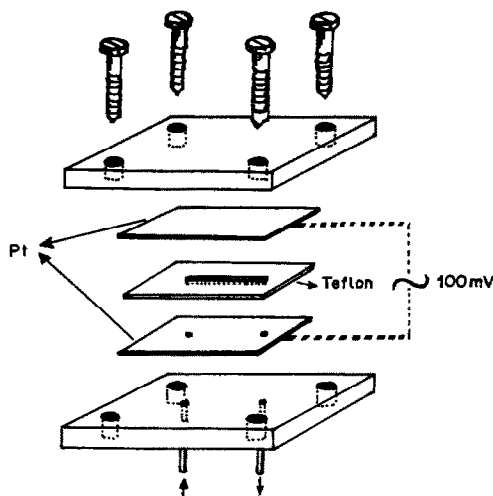


Fig. 2. Exploded view of biampereometric detector.

usually by means of a 4-way valve (Rheodyne) provided with a 30- $\mu$ l sample loop. The home-made biampereometric detection cell consisted of two thin platinum plate electrodes clamped between Perspex blocks and separated by a thin Teflon spacer (0.6 mm thick) with a groove of 10  $\times$  0.8 mm; cell volume about 5  $\mu$ l) as shown in Fig. 2. A 100-mV potential difference was applied between the two electrodes. A 585 Polarizer (Metrohm) was used as the voltage source. The output was registered on a strip-chart recorder (Kipp, BD-8). The membrane separation cell<sup>7</sup> was provided with a hydrophilic microporous polypropylene membrane (Celgard 3501, Celanese).

#### RESULTS AND DISCUSSION

The mechanism of the Karl Fischer reaction has been extensively studied<sup>8</sup> and it has been shown that the reaction goes rapidly to completion even when both reagent and water concentrations are low. Consequently, the interference of more slowly reacting concomitants can be eliminated by shortening the reaction times. By varying the concentration of the K.F.-reagent it was found that an optimum sensitivity was obtained for a 1:8 (v/v) dilution of the reagent in methanol (Table 1).

As long as sufficient K.F.-reagent is available for the reaction with a constant amount of water, constant sensitivity would be expected. However, we have observed that mixing of the carrier and reagent streams proceeds slowly for the more concentrated K.F.-solutions. This may lead to less complete reaction and, correspondingly, to decreased sensitivity. On the other hand for highly diluted K.F.-reagent

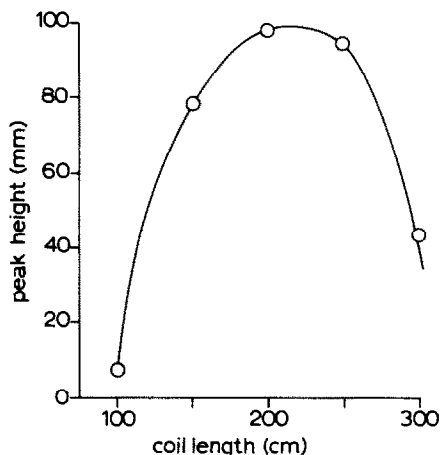


Fig. 3. Variation of peak height with reaction coil length (bore 0.5 mm). Samples contained 0.119% H<sub>2</sub>O in methanol. Flow-rate of 1:8 (v/v) diluted Karl Fischer reagent solution and carrier stream was about 0.9 ml/min.

solutions the amount of reagent limits the magnitude of the signal. Therefore there is an intermediate range of K.F.-solutions concentration that is high enough to cope with the amount of water injected but low enough for the reagent and carrier streams to be sufficiently similar for mixing to be rapid.

The relation between peak height and length of the reaction coil at a fixed flow-rate is illustrated in Fig. 3. The maximum appears at 200 cm coil length (bore 0.5 mm). Apparently, with shorter coil lengths the residence time is too short and mixing may be insufficient to ensure the reaction going to completion; with longer coil lengths the concentration sensed by the detector will decrease because of the additional dispersion. These results are in agreement with those of Kågevall *et al.*<sup>2</sup> For similar reasons the peak heights gradually decrease at flow-rates larger than about 0.8 ml/min (Fig. 4). A flow-rate of about 0.9 ml/min was selected because of the slightly better reproducibility of the peaks.

For the selected conditions (flow-rates of both reagent and carrier stream are about 0.9 ml/min; coil length is 200 cm) a linear calibration graph is obtained over the water concentration range 0.03–0.11% w/w. Without a membrane separation step, water concentrations in methanol, ethanol and 2-propanol could be determined with an accuracy that compared favourably with that obtained by coulometry (Table 2). In accordance with the work of Kågevall *et al.*<sup>2</sup> unsatisfactory results were obtained for samples of acetone.

Table 1. Dependence of peak height on concentration of Karl Fischer reagent\*

K.F.-solution: methanol, v/v	1:4	1:6	1:7	1:8	1:9	1:10	1:12
Peak height, mm	1	28	62	85	75	9	7.5

\*Samples contained 0.13% H<sub>2</sub>O in methanol; flow-rates about 0.8 ml/min.

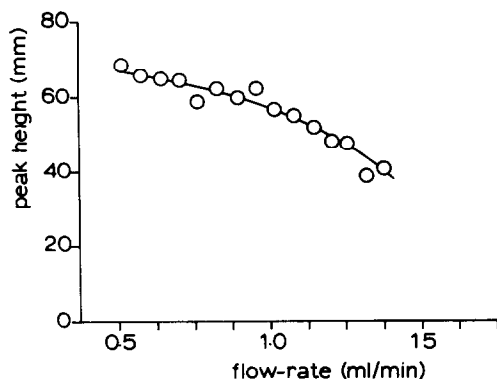


Fig. 4. Variation of peak-height with flow-rate: reaction coil length 200 cm. Samples contained 0.119% H<sub>2</sub>O in methanol.

Table 2. Comparison between results obtained by FIA and batchwise coulometry

Solvent	Water content found, % w/w	
	Coulometry	FIA
Methanol	0.039	0.041
	0.041	0.040
	0.035	0.032
	0.042	0.041
Ethanol	0.032	0.027
	0.034	0.036
	0.028	0.029
	0.050	0.049
2-Propanol	0.033	0.044
	0.037	0.036
	0.034	0.029
	0.045	0.045

If the membrane separation cell is used, the linear working range is shifted to a higher concentration level (0.1–2% w/w) because of the slow transport of water across the membrane.

#### CONCLUSION

FIA is suitable for the determination of water in methanol, ethanol and 2-propanol in the  $\mu\text{g/g}$ -range. For somewhat higher water contents a membrane separation step can be introduced, which eliminates the possibility of fouling the detection system, particularly if the sample contains solid particles.<sup>9</sup> The biamperometric detector used in this study is simple and robust but yields unsatisfactory results for water concentrations below 0.03% w/w.

*Acknowledgements*—The authors wish to express their thanks to Mr. W. Lengton, Mr. H. H. Heskamp and Ms. A. Christenhusz for their experimental help.

#### REFERENCES

1. J. Růžička and E. H. Hansen, *Flow Injection Analysis*, Wiley, New York, 1981.
2. I. Kågevall, O. Åström and A. Cedergren, *Anal. Chim. Acta*, 1980, **114**, 199.
3. I. Nordin-Andersson and A. Cedergren, *Anal. Chem.*, 1985, **57**, 2571.
4. I. Nordin-Andersson, O. Åström and A. Cedergren, *Anal. Chim. Acta*, 1984, **162**, 9.
5. R. E. A. Escott and A. F. Taylor, *Analyst*, 1985, **110**, 847.
6. H. Müller and G. Wallaschek, *Z. Chem.*, 1984, **24**, 75.
7. W. E. van der Linden, *Anal. Chim. Acta*, 1983, **151**, 359.
8. J. C. Verhoef and E. Barendrecht, *J. Electroanal. Chem.*, 1976, **71**, 305.
9. W. E. van der Linden, *Anal. Chim. Acta*, 1986, **179**, 91.

## SPECTROPHOTOMETRIC DETERMINATION OF RHENIUM WITH DITHIO-OXAMIDE IN STRONGLY ALKALINE MEDIUM

O. D. BOZHKOV and N. JORDANOV

Institute of General and Inorganic Chemistry, Bulgarian Academy of Sciences, BG-1040 Sofia, Bulgaria

L. V. BORISOVA

V. I. Vernadskii Institute of Geochemistry and Analytical Chemistry, USSR Academy of Sciences,  
Moscow, USSR

(Received 10 October 1986. Revised 6 August 1987. Accepted 21 August 1987)

**Summary**—The interaction between rhenium(VII) and dithio-oxamide in strongly alkaline medium in presence of tin(II) chloride as reductant has been studied. A purple complex is obtained, with  $\lambda_{\max}$  526 nm and  $\epsilon_{\max} = 4.0 \times 10^3$  l.mole<sup>-1</sup>.cm<sup>-1</sup>. The reaction has been applied to the determination of rhenium in tungsten-rhenium alloy after its anodic electrochemical dissolution in alkaline medium. A 1000-fold excess of molybdenum or tungsten does not interfere. A modification of the proposed method can be used as a spot-test for rapid control of rhenium content in industrial solutions.

It is often necessary to analyse strongly alkaline rhenium solutions. A spectrophotometric method is known for determination of rhenium in slightly alkaline or ammoniacal media, based on measuring the perrhenate absorbance at 230 nm.<sup>1,2</sup> Two other methods are also available for determination of rhenium in strongly alkaline medium. The first is based on the interaction between perrhenate and thiourea in the presence of tin(II) chloride as reducing agent<sup>3</sup> ( $\epsilon_{300 \text{ nm}} = 1.5 \times 10^3$  l.mole<sup>-1</sup>.cm<sup>-1</sup>) and the second on the interaction between perrhenate and hydroxylamine<sup>4</sup> ( $\epsilon_{300 \text{ nm}} = 7.9 \times 10^3$  l.mole<sup>-1</sup>.cm<sup>-1</sup>). Both procedures involve absorbance measurement in the ultraviolet region, which results in several interferences. The direct perrhenate and thiourea methods suffer from poor sensitivity and the hydroxylamine method suffers from systematic errors when large amounts of molybdenum and tungsten are present.

The interaction between rhenium(IV) and dithio-oxamide (DTO) has so far been studied only in acidic medium.<sup>5</sup> It was shown that a mixture of rhenium(IV) sulphide and elemental sulphur is obtained. The interaction between H<sub>2</sub>(ReOCl<sub>5</sub>) and DTO has also been studied in acidic medium.<sup>6</sup> A compound with composition ReOCl<sub>3</sub>(DTO)<sub>2</sub> was isolated. The Re-DTO bond was reported to be unidentate and formed with a sulphur atom of the DTO.

The present paper deals with a new possibility for rhenium determination in a strongly alkaline medium, by interaction of rhenium with DTO in the presence of a reducing agent.

### EXPERIMENTAL

#### Apparatus

A Beckman DK-2A double-beam scanning spectrophotometer was used with 1-cm fused-silica cells.

#### Reagents

**Standard rhenium solution.** Dissolve 0.1553 g of potassium perrhenate in 100 ml of distilled water; 1 ml contains 1000 µg of Re.

**Dithio-oxamide, 0.04M solution in 7M sodium hydroxide.** Dissolve 0.240 g of the reagent in 50 ml of 7M sodium hydroxide. Use only fresh solutions.

**Tin(II) chloride, 0.24M solution in 7M sodium hydroxide.** Dissolve 5.42 g of the dihydrate in a very small volume (2-3 ml) of distilled water. Add 7M sodium hydroxide (< 95 ml) with continual stirring until a clear solution is obtained, and then make up to 100 ml with more of the alkali. Use only fresh solutions.

**Hydrazine hydrochloride solution.** Dissolve 7.55 g of the hydrochloride in 100 ml of 7M sodium hydroxide. Use only fresh solution.

**Standard molybdenum and tungsten solutions.** Prepared by dissolving sodium molybdate dihydrate and sodium tungstate dihydrate in 7M sodium hydroxide.

#### Procedures

**Calibration graph.** Pipette 0.1, 0.2, 0.3, 0.4 and 0.5-ml portions of the standard rhenium solution (1000 µg/ml) into dry 10-ml graduated cylinders fitted with ground-glass stoppers. Add 1.2 ml of DTO solution and 8 ml of stannous chloride solution, make up to volume with 7M sodium hydroxide, mix, and let stand for 45 min. Measure the absorbance at 526 nm against a reagent blank. Plot the calibration graph.

**Qualitative and semiquantitative spot-test for rhenium.** Prepare a colour scale by pipetting 0, 5, 15, 25 and 40 µl of 1000-µg/ml rhenium solution into wells in a Teflon spot-test plate, and to each add 90 µl of DTO solution, 130 µl of stannous chloride solution, and make up to 260 µl with 7M sodium hydroxide and stir with a thin glass rod. To 20 µl of the unknown solution add the quantities of the reagents prescribed above. Compare the resulting colour with the reference scale. The limit of detection is 5 µg/ml. Up to 1000-fold ratio of Mo or W does not interfere with the colour reaction.

**Procedure for determination in the presence of 1000-fold ratio of Cu.** Add DTO solution to the sample solution until formation of a brownish-black precipitate ceases. Centri-

fuge, and decant the supernatant solution through a medium fast filter paper. Take an appropriate volume of this solution, add the stannous chloride solution, stir and let stand for 45 min. Measure the absorbance.

**Analysis of W-Re alloy.** Weigh 0.2 g of the alloy (chips) into a platinum spoon (to be used as anode). Place the spoon and a platinum coil (as cathode) in 20 ml of 5M sodium hydroxide. Connect to a stabilized rectifier delivering 5–6 V and 0.8–0.9 A. About 40 mg of alloy will dissolve within 20 min. Find the amount of sample dissolved, by removing, rinsing, drying and weighing the anode and residual sample after the electrolysis. Before switching off the current, reverse the polarity of the electrodes until the brown deposit of metallic rhenium on the cathode has dissolved (as little as 20  $\mu\text{g}$  of Re will darken the cathode). Make up the solution to known volume and analyse an aliquot for rhenium as described above.

**Spectrophotometric determination of rhenium in finishing product (a mixture of metallic particles of Mo-W-Re based alloy, abrasives and lubricating oil).** Treat the sample preliminarily with chloroform to eliminate the organic components and dry it to constant weight. Weigh 1 g of the treated sample and mix with 1 g of sodium hydroxide and 1 g of sodium nitrate. Stir the mixture well and place it in an iron crucible. Heat it to 600° in a muffle furnace and keep it at this temperature for 1 hr. Cool the melt and treat it with 10–15 ml of distilled water. Filter through a "rapid" filter. Transfer the clear filtrate to a 25-ml standard flask and make up to volume with distilled water. Analyse an aliquot as above.

**Spectrophotometric determination of rhenium in a sublimation product (mixture of tungsten and rhenium oxides).** Weigh 1 g of the sample into a Teflon beaker and add 10 ml of 5M sodium hydroxide. Place the beaker in an autoclave and digest the sample in oxygen at a pressure of 5–6 atm, at 110°C for 1 hr. Transfer the resulting clear solution into a 25-ml standard flask with 5M sodium hydroxide and make up to volume. Take an aliquot and analyse it as above.

## RESULTS AND DISCUSSION

When perrhenate solution is mixed with DTO solution in 1–12M sodium hydroxide medium, no colour appears but on addition of excess of reducing agent—tin(II) chloride or hydrazine hydrochloride—a purple colour is formed. The absorption spectra of

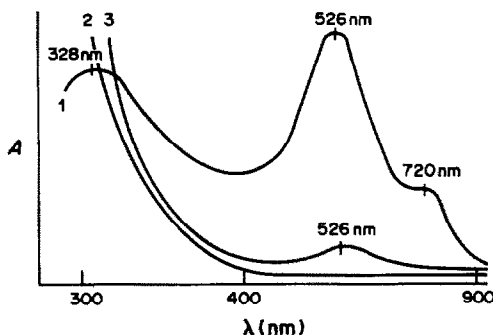


Fig. 1. Absorption spectra,  $t = 45$  min,  $l = 1$  cm, 1—Re-DTO-tin(II) chloride spectrum measured against DTO-tin(II) chloride solution,  $C_{\text{Re}} 1.61 \times 10^{-4}M$ ,  $C_{\text{DTO}} 4.8 \times 10^{-3}M$ ,  $C_{\text{Sn}} 0.19M$ ,  $C_{\text{NaOH}} 7M$ ; 2—spectrum of DTO solution in 7M NaOH recorded against distilled water,  $C_{\text{DTO}} 4.8 \times 10^{-3}M$ ; 3—spectrum of DTO + tin(II) chloride solution in 7M NaOH recorded against distilled water,  $C_{\text{DTO}} 4.8 \times 10^{-3}M$ ,  $C_{\text{Sn}} 0.192M$ .

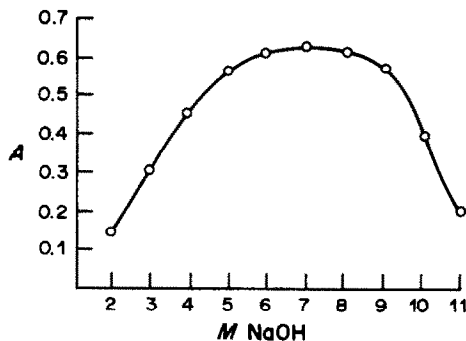


Fig. 2.  $A$  at 526 nm plotted vs.  $C_{\text{NaOH}}$ ;  $C_{\text{Re}} 1.61 \times 10^{-4}M$ ,  $C_{\text{DTO}} 4.8 \times 10^{-3}M$ ,  $C_{\text{Sn}} 8 \times 10^{-2}M$ , spectra recorded against a blank solution.

the product and the reagents are shown in Fig. 1. The spectrum of the purple solution has three absorption maxima—at 720, 526 and 328 nm. The solution containing DTO and tin(II) chloride has its absorption maximum at 526 nm, and the pure DTO solution absorbs at 315 nm. The absorbance of the rhenium-DTO complex at 526 nm can be used for the spectrophotometric determination of rhenium.

### Reaction conditions

Figure 2 shows that complex formation takes place in 1M sodium hydroxide medium but only slowly and incompletely. The rate and degree of complexation increase with hydroxide concentration, the optimal alkali concentration being 6–8M. At higher alkalinity the absorbance decreases. The reaction is still rather slow, however, maximal absorbance being attained in 40 min, then remaining constant for at least another hour or so.

A large excess of reductant (at least 500:1 molar ratio to rhenium) is needed for complete reduction of perrhenate and to provide a protective medium to prevent possible oxidation of DTO and the complex by air. A complex with identical spectral characteristics is obtained with hydrazine hydrochloride as the reductant, which shows that tin(II) chloride acts only as a reductant and does not form part of the complex.

The effect of DTO concentration is shown in Fig. 3. At low DTO:Re ratios little complex formation

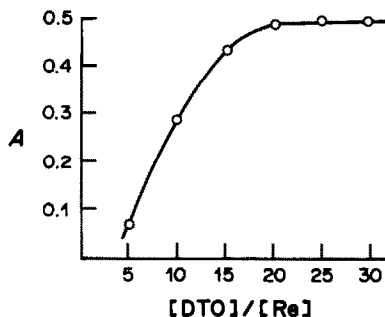


Fig. 3.  $A$  at 526 nm plotted vs.  $C_{\text{DTO}}$ ;  $C_{\text{Re}} 1.07 \times 10^{-4}M$ ,  $C_{\text{Sn}} 0.192M$ ,  $C_{\text{NaOH}} 7M$ ; spectra recorded against a blank solution.

Table 1. Determination of rhenium in various samples

Sample	Amount dissolved, mg	Number of replicates	Present method		Thiourea method	
			Mean, %	Std. devn., %	Mean, %	Std. devn., %
W-Re alloy	40	6	7.30	0.50	7.18	0.50
Mo-W-Re finishing product	1000	5	0.603	0.007	0.587	0.028
W-Re sublimation product	1000	5	0.517	0.007	—	—

takes place, precipitation of hydrolysis products being observed, since the hydroxide ions compete with the DTO reaction. At higher DTO:Re ratios the degree of complex formation increases and at 20:1 molar ratio constant absorbance is attained for a fixed amount of rhenium. Further increase in the ratio causes no shift in the absorption maximum at 526 nm, indicating formation of a single complex species in the system. For the determination a 30-fold molar ratio of DTO to rhenium is used.

#### Composition of the complex

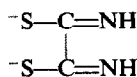
When excess of tin(II) chloride is added to an alkaline perrhenate solution a brownish black precipitate (most probably of  $\text{ReO}_2$ ) is formed. In the presence of excess of DTO no precipitate is formed, but a purple colour appears (complex formation). The same absorption spectrum is obtained with tin(II) sulphate as reductant.

Addition of excess of alkaline DTO solution to potassium hexachlororhenate(IV) solution produces a purple colour, which has an absorption maximum at 526 nm but is unstable, fading within 30 min. The addition of an excess of reductant—tin(II) chloride or hydrazine—stabilizes the colour and the absorbance at 526 nm is stable for about an hour after complete formation of the complex. The reductant will reduce higher oxidation states of rhenium and prevents both complex and ligand from oxidation by atmospheric oxygen. These facts suggest that the rhenium in the complex is in oxidation state (IV).

Ion-exchange and electrophoresis show that the complex is negatively charged. All attempts to isolate the solid complex from alkaline medium have failed. The complex is hydrophilic and is not extracted by a wide variety of organic extractants.

The Re:DTO ratio in the complex is 1:2, as determined according to the procedure of Staric and Barbanel.<sup>7</sup> The stability constant of the complex, determined by the mole-ratio and Babko<sup>7</sup> methods is  $\beta = (1.2 \pm 0.15) \times 10^6$ .

It is very likely that in strongly alkaline medium the ionized thiol form of DTO is present and the Re-DTO bond should be bidentate.



The thiol form of DTO

We therefore suggest that the composition of the complex is  $[\text{Re}(\text{OH})_2(\text{DTO})_2]^{2-}$ .

The molar absorptivity at 526 nm is  $(4.0 \pm 0.3) \times 10^3 \text{ l. mole}^{-1} \text{ cm}^{-1}$ . Beer's law is obeyed over the rhenium concentration range 5–50  $\mu\text{g/ml}$ . The standard deviation of the absorbance is 0.016 for 20 and 40  $\mu\text{g/ml}$  Re (9 replicates), and the relative standard deviations 3.6 and 1.7% respectively.

#### Interferences

Mo and W do not form complexes with DTO under the conditions described. It is found that a 1000-fold ratio of Mo and W does not interfere with the determination.

#### Applications

Three industrial samples were analysed by the proposed method. Comparison analyses of the alkaline solution were performed as follows. Rhenium was separated from the matrix by extraction with acetone from alkaline medium. The extract was evaporated to dryness. The dry residue was dissolved in distilled water and an aliquot of the resulting solution was analysed by the thiourea method.<sup>8</sup> The results are shown in Table 1.

#### REFERENCES

1. T. R. Andrew and G. H. R. Gentry, *Analyst*, 1957, **82**, 372.
2. L. V. Borisova, Yu. B. Gerlit and A. N. Ermakov, *Perspektivy razvitiya i metody izvlecheniya redkikh i rasseyannikh elementov iz rud i mestorozhdenii Armenii i Soyuza*, Izd. Akad. Nauk Arm. SSR, Erevan, 1962.
3. L. V. Borisova, A. B. Ismagulova and E. I. Ponomareva, *Zh. Kompleksnoe Ispol'zovanie Mineral'nogo sirya (Alma Ata)*, 1984, No. 12, 22.
4. L. V. Borisova, A. N. Ermakov and A. B. Ismagulova, *Analyst*, 1982, **107**, 495.
5. V. M. Tarayan and A. G. Gaibakyan, *Arm. Khim. Zh.*, 1966, **19**, 662.
6. V. Yatirajam and M. L. Kantan, *Polyhedron*, 1983, **2**, 1199.
7. M. I. Bulatov and I. P. Kalinkin, *Prakticheskoe rukovodstvo po fotometricheskim i spektrokhimicheskim metodam analiza*, pp. 222, 227. Izd. Khimiya, Leningrad, 1976.
8. L. V. Borisova and A. N. Ermakov, *Analiticheskaya khimiya reniya*, p. 101. Izd. Nauka, Moscow, 1974.



## PRECONCENTRATION AND SEPARATION OF METAL IONS BY MEANS OF AMBERLITE XAD-2 LOADED WITH PYROCATECHOL VIOLET

KRYSZYNA BRAJTER, EWA OLBRYCH-ŚLESZYŃSKA and MIECZYŚLAW STAŚKIEWICZ  
Department of Chemistry, University of Warsaw, Warsaw, Poland

(Received 19 November 1986. Revised 6 July 1987. Accepted 21 August 1987)

**Summary**—On the non-ionic sorbent Amberlite XAD-2 the sulphonated derivative of an aromatic complexing agent—Pyrocatechol Violet—was immobilized, and this chelate-forming resin was used for the preconcentration of Pb(II) and In(III) and for the separation of some metal ions. The PV-XAD-2 resin was adopted for the preconcentration of Pb(II) in tap-water. Very high preconcentration factors were obtained.

In trace metal analysis preconcentration or separation of the analyte from the matrix is frequently a necessity. Various methods and materials are recommended for preconcentration and separation. Exchange methods with highly selective resins are particularly convenient. Chelating resins prepared by the immobilization of chelating agents on various supports<sup>1-3</sup> are recommended for the purpose.

A very efficient system is provided by immobilization of the sulphonic acid derivative of an aromatic complexing agent on an anion-exchange resin.<sup>4,5</sup> In this paper we demonstrate the properties and application of such a resin, based on Amberlite XAD-2, for the preconcentration and separation of metal ions. Amberlite XAD-2 has been utilized as a support for neutral complexing agents,<sup>6,7</sup> and sorption of ionic compounds on its surface has been reported.<sup>8</sup> As the sulphonic acid derivative, we have selected Pyrocatechol Violet (PV), 3,3',4'-trihydroxyfuchson-2"-sulphonic acid (Fig. 1), and have applied the system to preconcentration of Pb(II) and In(III), and the separation of some metal ions.

### EXPERIMENTAL

#### Reagents and apparatus

The Amberlite XAD-2 (Aldrich) had a specific surface area of 330 m<sup>2</sup>/g, pore diameter 90 Å, and bead size 20-60 mesh. The Pyrocatechol Violet (BDH) was recrystallized from 10% v/v ethanol-water solution before use. PV is only slightly soluble in water (0.1% aqueous solution) but easily soluble in alcohols (59 g/l.).

Standard indium solution was prepared by dissolving 1.000 g of the metal (spectroscopic grade) in 2M hydrochloric acid and diluting the solution to volume in a 500-ml standard flask, and was further diluted as required. Metal stock standard solutions (1000 mg/l., for atomic-absorption, Merck) were diluted as required. All other chemicals were analytical grade. Doubly distilled water was used throughout.

A Beckman model 1272 atomic-absorption spectrometer was used with a Pye-Unicam GRM-1268 graphite furnace. The conditions used for determining the various elements were those recommended by the manufacturers. The glass

exchange columns, 20 cm long, 0.8, 1.0 and 1.5 cm inner diameter, had a Rotaflo tap at the bottom. The flow-rate was regulated with a peristaltic pump.

#### Preparation of PV-resin

To obtain the modified adsorbent, the XAD-2 resin was moistened with methanol, then washed with 6M hydrochloric acid, water, 2M sodium hydroxide, and water again, then shaken with  $5 \times 10^{-4}M$  PV aqueous solution until the supernatant solution became colourless. The resin was then filtered off, washed with water and alcohol, dried, and kept in the refrigerator. The modified resin contained 0.05 mmole of PV per g of Amberlite XAD-2.

#### Determination of the adsorption isotherm of PV

The sorption of PV was measured under static conditions. A 0.200-g portion of Amberlite XAD-2 was shaken for 12 hr with 20 ml of PV solution at pH 2.6. The concentration of PV was in the range  $1.4 \times 10^{-5}$ - $3.7 \times 10^{-3}M$ . After 24 hr the equilibrium concentration of dye in the solution was measured spectrophotometrically at 450 nm. The results are presented in Fig. 2.

#### The sorption of PV as a function of pH

A 0.200-g portion of resin was shaken for 12 hr with 20 ml of  $3.1 \times 10^{-3}M$  PV, and the pH was adjusted with sodium hydroxide or nitric acid to a value in the range 1.0-2.0. The equilibrium concentration of PV was measured spectrophotometrically at 450 nm after 24 hr. The results are presented in Fig. 3.

#### The stability of aqueous PV solution

Solutions of PV at 0.2% concentration are stable. At higher concentrations, even in the dark, Pyrocatechol Violet

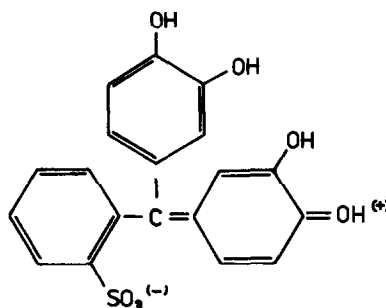


Fig. 1. 3,3',4'-Trihydroxyfuchson-2"-sulphonic acid.

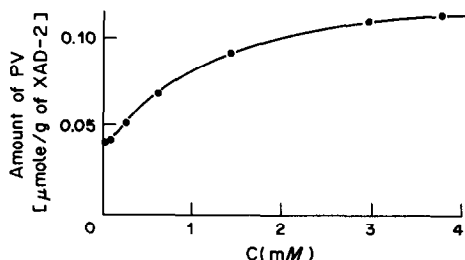


Fig. 2. Adsorption isotherm of Pyrocatechol Violet.

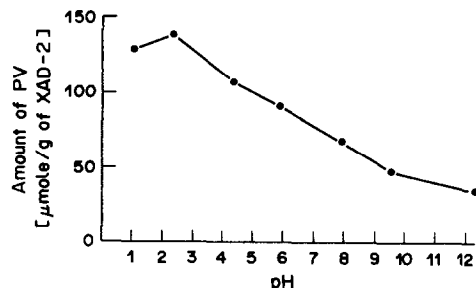


Fig. 3. The sorption of Pyrocatechol Violet as a function of pH.

decomposes slowly. To study the stability a  $6.2 \times 10^{-3} M$  solution was prepared and its absorbance was measured spectrophotometrically at 450 nm, and again 300 days later, by which time the PV concentration had decreased to 78% of its initial value.

#### Retention of metal ions as a function of pH

A constant amount (equivalent to 0.200-g dry weight) of modified resin was mixed with 1 ml of methanol and 20 ml of solution containing 0.10 mg of metal ion. The solution was adjusted to the desired pH with sodium hydroxide or nitric acid and then the mixture was shaken for 12 hr. The equilibrium hydrogen-ion and metal-ion concentrations were determined 12 hr later. The metal ions were determined by AAS.<sup>11</sup> The results are presented in Fig. 4.

#### Determination of breakthrough capacity for indium as a function of pH

Through columns (6 cm bed height) of 1.0 g of loaded Amberlite XAD-2, indium solutions (0.5 mg/l.) at various pH values were passed at a flow-rate of 1.7 ml/min.

#### Separation procedures

A 10-ml volume of solution containing a mixture of metal ions in the weight ratio In(III):Co(II):Ni(II) = 1:1000:100 (pH in the range 3.2–4.0) and a 20-ml volume of solution containing Bi(III):Cd(II):Ni(II) = 1:1500:100 (pH = 1.25) were passed through columns of PV-loaded resin. The metal ions were eluted at a flow-rate of 1.7 ml/min. A 6-cm bed height of 1.0 g of modified resin was used (column inner diameter 8 mm). The results are presented in Table 1.

## RESULTS AND DISCUSSION

It was established that Pyrocatechol Violet is adsorbed on the hydrophobic surface of the styrene-divinylbenzene type resin Amberlite XAD-2. The hydrophobic resin appears to be an excellent support for the sulphonic acid derivatives of aromatic com-

plexing agents. The sorption of PV on XAD-2 resin is due to  $\pi$ - $\pi$  dispersion forces arising from the aromatic nature of the resin and reagent. Figure 2 shows the adsorption isotherm of PV on XAD-2 at pH 2.6. The capacity of XAD-2 for PV at pH 2.6 is 0.10–0.12 mmole/g. Figure 3 shows the retention of PV on the resin as a function of pH, determined by the batch method over the pH range 1–12. The adsorption is maximal at about pH 2, and presumably specific interaction between the "potential-determining" ion<sup>8</sup> (PV) retained on the XAD-2 resin and counter-ion ( $H_3O^+$ ) increases the adsorption (the dissociation constants of PV are:<sup>9</sup>  $pK_{a1} = 0.8$ ,  $pK_{a2} = 7.80$ ,  $pK_{a3} = 9.76$ ,  $pK_{a4} = 12.83$ ). Cantwell and Puon proposed this mechanism for retention of organic ions on a non-ionic sorbent, on the basis of Grahame's modification<sup>10</sup> of the Stern-Gouy-Chapman electrical double-layer theory, and considered that if a large organic anion were used with a small cation, the anion would be adsorbed as the potential-determining ion, and the cation would serve as a counter-ion. In the work described here, specific adsorption of the anion is evident and confirms that if specific interaction occurs, the sorption of the potential-determining ion increases.

#### The retention of metal ions on XAD-2 resin modified with PV

The sorption behaviour of several transition-metal and heavy-metal ions as a function of pH was examined by the batch method. The results presented in Fig. 4 indicate that differences in retention occur.

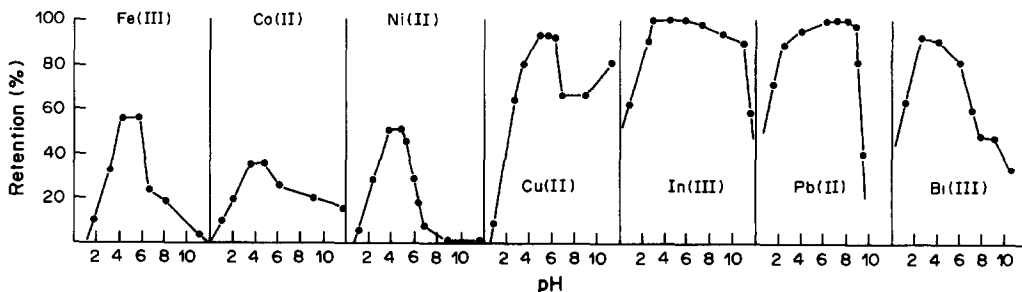


Fig. 4. Retention of metal ions on the PV-loaded resin as a function of pH.

Table 1. Separation of metal ions on PV-loaded Amberlite XAD-2 (average of 6 determinations)

Mixture	Elution agent	Amount of metal, mg	
		Added	Found*
In	0.5M HNO <sub>3</sub> , 25 ml	0.010	0.010 ± 0.0008
Co } Ni }	5 × 10 <sup>-3</sup> M tetrene, 150 ml	10.0 1.0	10.0 ± 0.077 1.02 ± 0.091
Bi	1.0M HNO <sub>3</sub> , 25 ml	0.010	0.010 ± 0.0007
Co } Ni }	5 × 10 <sup>-3</sup> M tetrene, 200 ml	15.0 1.0	14.9 ± 0.117 0.98 ± 0.054

\*Mean and range, 95% confidence limit.

At pH 1 the selectivity sequence for metal ions on the PV-XAD-2 chelating resin is: Bi(III) ≥ In(III) ≥ Pb(II) > Cu(II) > Fe(III) > Co(II) > Ni(II). As expected, the greatest affinity for PV-XAD-2 resin is exhibited by those metal ions which possess the greatest affinity for oxygen as a donor atom. The selectivity sequence is in agreement with that predictable from the stability constants of the complexes formed between PV and the metal ions: Bi(III) ≥ In(III) > Fe(III), and may indicate, to some degree, that the complexing properties of PV are not changed if it is immobilized on a resin. If a complexing agent is adsorbed as a potential-determining anion on the surface of the resin, metal ions are retained as counter-ions on the resin, according to their specific interaction with the ligand.

#### Separation of metal ions

The differences in the retention of the metal ions under study, on PV-loaded XAD-2 resin, indicate that Bi(III) and In(III) should be separable from the less strongly retained metal ions. Table 1 shows the results for separation of Bi(III) or In(III) from excess of Cu(II) and Ni(II). The separation of Bi(III) from Cu(II) is of practical interest for analysis of copper alloys. To increase the efficiency of the separation (smaller volume of eluent) tetrene was used as eluent.

#### Preconcentration of indium

Indium is firmly retained on PV-XAD-2 resin over a wide pH range (3–8). The breakthrough capacity for indium was determined under the following column operating conditions: bed-height 2 cm (0.3–0.4 g of resin), pH range 3.2–7.7, flow-rate 1.7 ml/min, column bore 8 mm, and found to be 0.3 mg of In(III).

Table 2. Determination of lead in tap-water by AAS after preconcentration on PV-resin

	Pb concentration,* µg/l.	
Sample 1	2.8 ± 0.3	3.0 ± 0.4†
Sample 2	2.6 ± 0.3	2.7 ± 0.3†

\*Mean and range of 3 determinations (95% confidence limit).

†Determination of lead by anodic stripping voltammetry (6 min preconcentration at –0.8 V vs. SCE).

From the amount of PV retained on the resin bed, the molar ratio of PV to In(III) under the given conditions is 12:1. According to Ryba *et al.*,<sup>12</sup> Pyrocatechol Violet forms 1:1 complexes with indium and some other trivalent metal ions, so in an 8-mm bore column a 6-cm bed height (1.2 g of PV-XAD-2 resin) should be able to take up 1 mg of indium, which can be eluted with nitric acid. If we assume preconcentration from 2 litres of 0.5-µg/ml indium solution, the concentration factor is 100.

#### Preconcentration of lead

With a bed height of 10 cm (2 g of resin, column bore 8 mm), passage of 2 litres of 0.05-µg/ml lead solution and elution with 25 ml of 1.5M nitric acid a concentration factor of 80 was obtained. With passage of 5 litres of the lead solution, removal of the resin from the column, and stripping with 10 ml of 1M nitric acid, a concentration factor of 500 was obtained for quantitative desorption. Only one extraction was needed. Six analyses of 5-litre samples of 0.05-µg/ml lead solution gave recovery of 0.24 ± 0.019 mg (mean and 95% confidence limit). The flow-rate for preconcentration may be as high as 5 ml/min if a 15-mm bore column is used. The PV-XAD-2 resin was used for preconcentration and determination of lead in tap-water. The results are presented in Table 2.

#### REFERENCES

1. D. E. Leyden and G. H. Luttrell, *Anal. Chem.*, 1975, **47**, 1612.
2. B. M. Vanderborcht and R. E. Van Grieken, *ibid.*, 1977, **49**, 311.
3. K. Terada, K. Matsumoto and H. Kimura, *Anal. Chim. Acta*, 1983, **153**, 237.
4. K. Brajter, *J. Chromatog.*, 1974, **102**, 385.
5. K. Brajter and E. Olbrych-Śleszyńska, *Talanta*, 1983, **30**, 355.
6. J. D. Pietrzyk, E. P. Kroeff and T. D. Rotsch, *Anal. Chem.*, 1978, **50**, 497.
7. J. D. Pietrzyk and C. H. Chu, *ibid.*, 1977, **49**, 860.
8. F. F. Cantwell and Su Puon, *ibid.*, 1979, **51**, 623.
9. A. E. Martell and R. M. Smith, *Critical Stability Constants*, Vol. 3, Plenum Press, New York, 1976.
10. D. C. Grahame, *Chem. Rev.*, 1947, **41**, 441.
11. K. Brajter and E. Olbrych-Śleszyńska, *Analyst*, 1986, **111**, 1023.
12. O. Ryba, J. Cifka, D. Ježková, M. Malát and V. Suk, *Collection Czech. Chem. Commun.*, 1958, **23**, 71.

## X-RAY PHOTOELECTRON SPECTROSCOPIC ANALYSIS OF LEAD ACCUMULATED IN AQUATIC BRYOPHYTES

M. SOMA, H. SEYAMA and K. SATAKE

The National Institute for Environmental Studies, Tsukuba, Ibaraki 305, Japan

(Received 16 March 1987. Revised 26 June 1987. Accepted 21 August 1987)

**Summary**—Lead accumulated in aquatic bryophytes, *Pohlia ludwigii*, *Scapania undulata* and *Pellia endiviifolia*, has been characterized by X-ray photoelectron spectroscopy (XPS). The well resolved Pb 4f ( $4f_{7/2}$  and  $4f_{5/2}$ ) spectra indicate that the bonding state of lead in each bryophyte is that giving a fairly narrow distribution in the binding energy. The Pb  $4f_{7/2}$  binding energy depends on the bryophyte species and is lower than that for lead sulphate. It is also possible to use XPS to detect zinc and copper accumulated in bryophytes.

A considerable number of X-ray photoelectron spectroscopic studies of biologically important substances have been reported.<sup>1</sup> However, application of XPS to real organisms without pretreatment, especially to the characterization of trace elements in living bodies, has been limited. This is perhaps because the sensitivity of XPS is too low; typically the concentration of element required is at least 0.1–1.0 atom% in the volume probed. Living organisms can concentrate elements from aquatic media and the concentration factor can sometimes be strikingly high.<sup>2</sup> Recently we have demonstrated that XPS gives some evidence for mercury–sulphur bonding in the liverwort *Jungermannia vulcanicola*.<sup>3</sup> The liverwort accumulates mercury by a factor of more than  $10^6$  (dry weight basis) from the acid stream where it lives. The XPS method opens up the possibility of characterizing the bonding state of elements accumulated in living tissues.

In this paper, XPS analyses of some bryophytes are reported. It is shown that, unlike mercury in the *J. vulcanicola*, lead in the aquatic bryophytes *Pohlia ludwigii*, *Scapania undulata* and *Pellia endiviifolia* is not bound to sulphur, but is distributed in rather uniform bonding states, as indicated by its well resolved 4f spectrum. Copper and zinc accumulated in the bryophytes are also described briefly.

### EXPERIMENTAL

#### Bryophytes

*Pellia endiviifolia* and *Pohlia ludwigii* (Spreng.) Broth., were collected in a puddle at Ginzan ("silver mountain") mine close to Lake Towada, Japan. *Scapania undulata* was sampled from a stream at Greenside mine, England. The description and elemental composition of the *P. endiviifolia*<sup>4</sup> and the *S. undulata*<sup>5</sup> are given in detail elsewhere. *Scopelophila cataractae*, known as copper moss and called Honmonji-goke (moss) in Japan, was sampled at Honmonji Temple, Tokyo.

#### XPS and ICP analyses

The X-ray photoelectron spectra and the X-ray induced Auger electron spectra were recorded on a Vacuum Gener-

ators ESCALAB 5 apparatus. The conditions for measurement have been described previously.<sup>6</sup> The bryophytes were dried in a desiccator, cut into segments of ca. 1 cm and fixed on a stainless-steel sample holder (10 mm diameter) with double-sided adhesive tape. In the case of *P. ludwigii*, a bundle about 6 cm long gave 6 segments.

The electron binding energies were standardized against the Au  $4f_{7/2}$  (83.8 eV) line from a gold film evaporated onto the sample. The uncertainty in the determination of the binding energy was  $\pm 0.2$  eV. The relative atomic abundance was calculated from the intensities of the photoelectron lines and the empirical atomic sensitivity factors.<sup>6</sup>

The elemental compositions of the bryophytes were determined by inductively-coupled plasma atomic-emission spectrometry (ICP) (Jarrel Ash Plasma Atom Comp Model 957) after digestion with concentrated nitric acid.

### RESULTS AND DISCUSSION

The survey XP-spectrum of *P. ludwigii* (segment 2–3 cm from the tip) which contained a high concentration of heavy metals (Pb, Cu and Zn; see Table 3 for the elemental composition determined by ICP and Table 2 for that determined by XPS) was obtained by scanning the binding energy range 0–1250 eV for 20 min. It revealed that, although lines due to major elements (C, N, O) predominate, the strongest lines for the minor constituents at below percent levels are detectable even in a survey spectrum. Since the C 1s line inevitably contains contributions from exogenous carbon compounds, the observations of the N 1s line (binding energy 399.6 eV) attributable mainly to amino groups are important in ensuring that real tissue is being examined.

For the *P. endiviifolia*, the Cu 2p and Zn 2p lines were detected at intensities comparable with those observed for *P. ludwigii*, but the Pb 4f lines were an order of magnitude weaker, in agreement with the ICP analysis.<sup>4</sup> The *S. undulata* exhibited the Pb 4f lines as strongly as in the *P. ludwigii*, but gave weaker Zn 2p and negligible Cu lines. The *S. cataractae* was characterized by remarkably strong Cu 2p lines, as its common name would suggest, but did not give detectable Pb and Zn lines.

Table 1. Pb  $4f_{7/2}$  binding energies in aquatic bryophytes and lead compounds

Sample	Pb $4f_{7/2}$ binding energy, eV	FWHM, eV*§
<i>Pohlia ludwigii</i>	138.7*	2.4
<i>Scapania undulata</i>	138.5*	2.3
<i>Pellia endiviifolia</i>	138.9*	—
PbSO <sub>4</sub>	139.2*†	2.2
PbS	137.5*	1.9
PbCl <sub>2</sub>	138.6*, 138.8†	2.0
Pb(CH <sub>3</sub> COO) <sub>2</sub>	138.7†	
Pb <sub>3</sub> (PO <sub>4</sub> ) <sub>2</sub>	138.4†	
PbO	137.9†	

\*This work.

†The binding energies (Ref. 7) are determined with respect to the C 1s line from a carbon contamination (285.0 eV). In this table, they were shifted 0.4 eV lower so that the binding energy of PbSO<sub>4</sub> was adjusted to give the same value as our result, which also gives a consistent C 1s binding energy (284.5 eV on PbSO<sub>4</sub> in our measurements) within experimental error.

§Full width at half-maximum.

The Pb  $4f$  spectrum of *P. ludwigii* was compared with those of PbSO<sub>4</sub> and PbS. The bryophyte sample gives well resolved  $4f_{7/2}$  and  $4f_{5/2}$  spin-orbit components with linewidths of each component similar to those shown by the pure lead compounds (Table 1). Similar well resolved Pb  $4f$  spectra were obtained for *P. endiviifolia* from the Ginzan mine and the *S. undulata* from Greenside mine. This indicates that the Pb in these bryophytes exists in homogeneous bonding states, otherwise a broader and less well resolved  $4f$  spectrum would be obtained. The comparison also shows that PbS cannot be a major lead component in the *P. ludwigii*. The observation contrasts with the case of Hg in the *J. vulcanicola*, for which XPS gave evidence of Hg-S bonding.<sup>3</sup>

Table 1 lists the Pb  $4f_{7/2}$  binding energies found in the bryophytes, together with those of some lead compounds.<sup>7</sup> The Pb  $4f_{7/2}$  binding energies in the three bryophytes are slightly different, the lowest (138.5 eV) being found for the *S. undulata*. Since the average C 1s binding energies are the same ( $284.7 \pm 0.1$  eV) for all the bryophytes, the differences are considered to be significant. Similarly the binding energies in the *P. ludwigii* and *S. undulata* are different from that of PbSO<sub>4</sub>.

The *P. ludwigii* also exhibited well resolved Cu and Zn  $2p$  spin-orbit components. However, the Cu  $2p$  spectrum (Cu  $2p_{3/2}$  binding energy 932.8 eV) suffered from X-ray induced reduction<sup>8</sup> and lost satellites characteristic of Cu<sup>2+</sup>.<sup>9</sup> With lowered X-ray intensity, the characteristic satellite structure was observed for the *S. cataractae*. For the *P. ludwigii*, the characteristic ESR spectrum of paramagnetic Cu<sup>2+</sup> was obtained. As is known, the Zn  $2p_{3/2}$  binding energy (1022.0 eV for the *P. ludwigii*) alone does not give much information on the bonding state of Zn.<sup>10</sup>

Table 2 shows an example of a semi-quantitative analysis of the *P. ludwigii* by XPS. The atomic abundances of Pb, Cu and Zn relative to C are consistent with their bulk concentrations in the 0.1–1% level (Table 3). Accordingly, since the probing depth of XPS is limited to the surface layers (<100 Å) of the solid samples, it is suggested that the heavy metals are not significantly concentrated in the surface layers of the bryophyte samples. The concentration of Zn is constant throughout the segments whereas that of Pb and Cu varies.

As can be seen from Table 2, XPS can determine the sulphate-S and sulphide-S (mostly attributable to protein-S in this case) separately, owing to the chem-

Table 2. Atomic concentrations relative to carbon (=1000, based on C 1s line) in *P. ludwigii* determined by XPS

Element	Line	Segment*					
		0-1	1-2	2-3	3-4	4-5	5-6
O	1s	210	250	280	240	310	350
N	1s	47	43	55	40	49	69
Si	2s	2.0	3.4	5.1	6.7	10	14
P	2p	2.0	2.8	3.9	1.9	2.4	2.4
S (+VI)	2p	0.47	1.2	0.92	0.80	1.6	1.9
(-II)	2p	0.60	0.58	0.87	0.40	0.72	0.62
Pb	4f	0.12	0.61	0.73	0.44	0.45	0.61
Cu	2p <sub>3/2</sub>	0.86	2.1	3.6	2.8	2.9	5.6
Zn	2p <sub>3/2</sub>	1.6	1.2	1.1	1.0	1.5	1.5

\*Lengths (cm) from the tip of bundle of the *P. ludwigii*.

Table 3. Elemental composition of the shoot of *P. ludwigii* and water samples from Ginzan (3 Nov. 1983) determined by ICP analysis

Element	Shoot, mg/kg				Water, mg/l.
	0-1 cm	1-2 cm	2-3 cm	0-3 cm	
Na	197	177	200	193	4.7
Mg	$2.14 \times 10^3$	$1.84 \times 10^3$	$2.02 \times 10^3$	$1.98 \times 10^3$	4.5 0.91
Al	935	794	$1.09 \times 10^3$	973	0.89 <0.1
P	$6.05 \times 10^3$	$5.06 \times 10^3$	$6.88 \times 10^3$	$5.75 \times 10^3$	<0.1 <0.5
K	$3.21 \times 10^4$	$3.52 \times 10^4$	$3.12 \times 10^4$	$3.09 \times 10^4$	<0.5 0.73
Ca	$5.41 \times 10^3$	$5.04 \times 10^3$	$6.02 \times 10^3$	$5.17 \times 10^3$	0.79 2.85
Mn	22	18	40	26	2.80 <0.02
Fe	597	516	666	640	<0.02 <0.02
Cu	$5.76 \times 10^3$	$1.04 \times 10^4$	$1.15 \times 10^4$	$8.56 \times 10^3$	<0.02 0.02
Zn	$3.72 \times 10^3$	$4.33 \times 10^3$	$4.91 \times 10^3$	$4.05 \times 10^3$	0.66 0.66
Pb	$2.67 \times 10^3$	$6.09 \times 10^3$	$8.36 \times 10^3$	$5.35 \times 10^3$	0.02* 0.03*

\*Values between determination and detection limit of ICP analysis.

ical shift in the S 2p line for the two species.<sup>11</sup> This capability is useful in the speciation of sulphur in the biological sample, especially when the sample contains chalcophile metals. The peak at higher binding energy (168.4 eV) can be attributed to sulphate-S and the lower one (162.9 eV) to sulphide-S. X-ray induced changes in the S 2p spectra<sup>12</sup> were not observed.

For the *P. ludwigii*, the total atomic concentration of Pb, Cu and Zn always exceeded the total amount of sulphur. Therefore, if one-to-one stoichiometry is assumed, the total amount of heavy metals cannot be involved in bonding with the sulphur-containing ligands. As stated above, dominant presence of PbS is not likely on the basis of the Pb 4f<sub>7/2</sub> binding energy. The binding energy in the bryophytes ranges from a value fairly close to that of PbSO<sub>4</sub> (*P. endiviifolia*) to a significantly different one (*S. undulata*). For the *S. undulata* the sulphate-S/Pb ratio was 2.2 for one sample but was less than unity (0.6) for a second sample. A close correlation between the Pb and sulphate-S concentrations is not observed for the *P. ludwigii* (Table 2). Therefore, it is unlikely that the sulphate ion is the sole binding ligand for Pb in these bryophytes. Table 2 shows that the concentration of Pb has no correlation with that of other elements (except Cu). Apparently more information

is required to establish the bonding state of lead in bryophytes.

*Acknowledgements*—We thank Dr. H. Ochi for identification of the *P. ludwigii*. Thanks are also due to Mr. M. Nishikawa for the ICP analysis.

#### REFERENCES

1. M. M. Millard, *Adv. Exp. Med. Biol.*, 1974, **48**, 589; D. M. Hercules, *Anal. Chem.*, 1976, **48**, 294R; A. D. Baker, M. A. Brisk and D. C. Liotta, *ibid.*, 1978, **50**, 328R; 1980, **52**, 161R.
2. H. J. M. Bowen, *Environmental Chemistry of Elements*, Academic Press, London, 1979.
3. K. Satake, M. Soma, H. Seyama and T. Uehiro, *Arch. Hydrobiol.*, 1983, **99**, 80.
4. K. Satake, M. Nishikawa and K. Shibata, *Hydrobiologia*, 1987, **148**, 131.
5. K. Satake, submitted to *J. Bryology*.
6. M. Soma, H. Seyama and K. Okamoto, *Talanta*, 1985, **32**, 177.
7. N. I. Nevedov, Ya. V. Salyn' and H. Keller, *Zh. Neorgan. Khim.*, 1984, **24**, 2564.
8. J. C. Klein, C. P. Li, D. M. Hercules and J. F. Black, *Appl. Spectrosc.*, 1984, **38**, 729.
9. D. C. Frost, A. Ishitani and C. A. McDowell, *Mol. Phys.*, 1972, **24**, 861.
10. C. D. Wagner, W. M. Riggs, L. E. Davis, J. F. Moulder and G. E. Mullenberg, *Handbook of X-ray Photoelectron Spectroscopy*, Perkin-Elmer, 1979.
11. B. J. Lindberg, *Int. J. Sulfur Chem.*, 1972, **C7**, 33.
12. M. Thompson, R. B. Lennox and D. J. Zemon, *Anal. Chem.*, 1979, **51**, 2260.

## APPLICATION OF REVERSE PULSE POLAROGRAPHY TO THE DETERMINATION OF SUBSTANCES WHICH FORM FILMS ELECTROCHEMICALLY ON THE MERCURY ELECTRODE\*

J. M. LOPEZ FONSECA, A. OTERO and J. C. GARCIA MONTEAGUDO

Depto. de Química Física, Facultad de Farmacia, Universidad de Santiago de Compostela,  
Santiago de Compostela, Spain

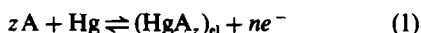
(Received 20 February 1987. Revised 4 May 1987. Accepted 2 July 1987)

**Summary**—The application of reverse pulse polarography to the determination of substances which form films electrochemically on the mercury electrode is illustrated with penicillamine and cysteine. The dependence of the peak current on several variables is reported and compared with theoretical predictions. It is shown that under optimal instrumental conditions (long drop times and short effective pulses) reverse pulse polarography compares favourably with both normal pulse polarography and differential pulse polarography for the determination of penicillamine and cysteine, concentrations of penicillamine as low as  $5 \times 10^{-8} M$  being readily determined in the presence of copper(II).

Reverse pulse polarography ("scan-reversal pulse polarography, RPP") is a variant of normal pulse polarography in which the initial potential is held at a value at which the electrode reaction being studied takes place, and pulses of increasing potential are applied. This technique holds great promise for the characterization of electrode reactions, including investigation of their polarographic reversibility<sup>1,2</sup> and identification and determination of their intermediate and final products.<sup>2</sup> Amperometric RPP has been employed in conjunction with flow-injection analysis for the determination of a variety of species.<sup>3,4</sup> The present paper describes the use of RPP for the determination of substances that take part in the electrochemical formation of films of mercury compounds on the electrode surface. The results presented concern two substances of biological interest, cysteine and penicillamine. The technique described is a form of cathodic stripping voltammetry, and shares its inherent sensitivity.

### THEORY

In polarography, any species A that forms an insoluble compound with mercury ions produces an anodic wave due to oxidation of the mercury of the electrode according to the reaction



where the subscript el indicates that the reaction occurs at the surface of the electrode. If the concentration of A is such that the maximum surface

concentration of  $\text{HgA}_z$  is attained, this wave may be followed by a second at more positive potentials.

When RPP is employed with an initial potential  $E_i$  kept constant at a value yielding the limiting current of the anodic wave, the reaction above takes place during the time that elapses between the electrode drop beginning to form and the potential pulse being applied. An analysis of the process, similar to that by Koryta,<sup>5</sup> shows the number  $N$  of moles of product formed under conditions in which the electrode surface is not saturated, is given by

$$N = 0.85 m^{2/3} t_0^{2/3} \Gamma = 0.627 \times 10^{-3} C_A D_A^{1/2} m^{2/3} t_0^{7/6} / z \quad (2)$$

where  $m$  is the mercury flow-rate,  $\Gamma$  the surface concentration of  $\text{HgA}_z$ ,  $C_A$  the molar concentration and  $D_A$  the diffusion coefficient of A.

Applying sufficiently large negative potential pulses drives reaction (1) backward, reducing the mercury in the compound concentrated on the electrode surface. The situation is thus analogous to that of reactant adsorption in normal pulse polarography, in which the current-potential curves present a characteristic peak shape.<sup>6-11</sup> The appearance of this peak is a consequence of measuring the current at a fixed time  $t_p$  towards the end of the pulse. As the pulse potential is made increasingly negative the current first increases as more mercury(II) in the adsorbed film is reduced to mercury, but eventually decreases when the potential pulse is sufficiently negative to cause increasingly complete reduction of the adsorbed film before the current is measured. The peak current will decrease with increase in the time  $t_p$  that elapses between the moment at which the potential pulse is applied and that at which the current is measured (*i.e.*, the effective pulse duration). For a plane stationary electrode and low electrode surface coverage,

\*Part of this work was presented at the 36th Meeting of the International Society of Electrochemistry, Salamanca, Spain, 1985.

theoretical calculations show that  $i_p = kt_p^{-0.95}$  for reversible redox reactions and  $i_p = kt_p^{-1.0}$  if the reaction is totally irreversible.<sup>8-11</sup> The system is shown schematically in Fig. 1.

These considerations have an important consequence for the analytical determination of the species A, since if  $t_p$  is short, then the peak current recorded in RPP, which is proportional to the quantity of  $\text{HgA}_2$  deposited on the electrode, may be expected to be greater than in normal pulse polarography or differential pulse polarography, in which the current is dependent only on the diffusion of A.

#### EXPERIMENTAL

Polarographic measurements were made with a Tacussel Type PRG5 polarograph in conjunction with a three-electrode cell system having a saturated calomel electrode as reference and a platinum counter-electrode. The drop-time of the dropping mercury electrode,  $t_d$  was mechanically maintained at a constant value in the range 1.0–9.9 sec. The effective pulse duration  $t_p$  was maintained at a constant value between 14 and 80 msec. A scan-rate of 1 mV/sec was usually employed. In the differential pulse polarography a pulse amplitude of +100 mV was used.

Measurements were made at  $25 \pm 0.1^\circ$ . Solutions were deaerated by passage of oxygen-free nitrogen for about 10 min. The pH-values were measured with a Radiometer Model 26 pH-meter.

A stock aqueous solution ( $2 \times 10^{-3}M$ ) of cysteine (Sigma) or penicillamine (Ega-Chemie) was prepared daily by dissolving the compound in water that had been deaerated by passage of nitrogen. All other chemicals were Merck analytical reagent grade. Water was purified by a Millipore-Milli Q system.

#### RESULTS AND DISCUSSION

Polarograms a' and b' in Fig. 2 were obtained by RPP for  $5 \times 10^{-6}M$  penicillamine (a') or cysteine (b') in  $0.06M$  sodium tetraborate buffer. In each case  $E_i$  was set at a value that would give the limiting current

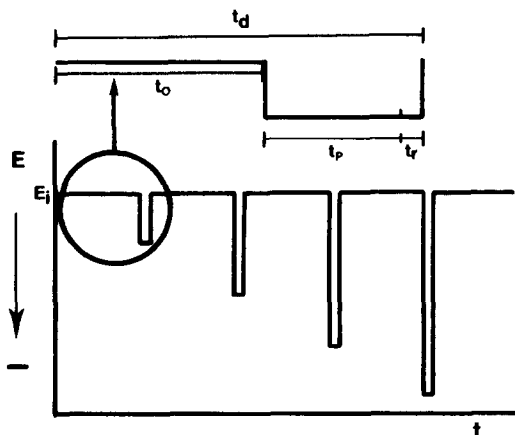


Fig. 1. Schematic representation of potential-time signal (not to scale) in RPP;  $t_d$  is the drop time,  $t_0$  the time over which the initial potential is applied,  $t_p$  the time that elapses between the moment at which the potential pulse is applied and the instant at which the current is measured, and  $t_r$  the time between this latter instant and the moment at which the potential pulse ends.

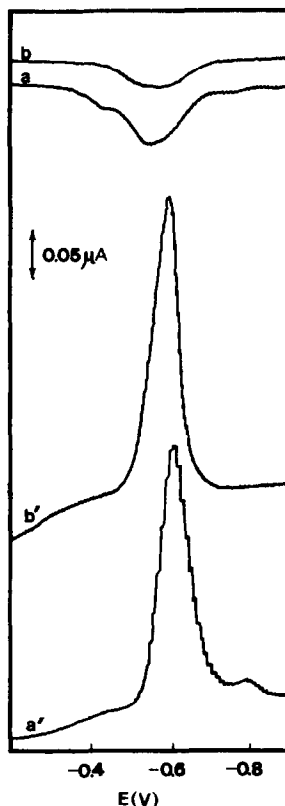


Fig. 2. Polarograms obtained for the systems  $5 \times 10^{-6}M$  penicillamine– $0.06M$  sodium tetraborate, pH 9.2 (a and a') and  $5 \times 10^{-6}M$  cysteine– $0.06M$  sodium tetraborate, pH 9.2 (b and b'). a, b: differential pulse polarograms ( $E_i$  –0.9 V;  $t_d$  9.9 sec;  $t_p$  14 msec), recording begun at –0.9 V. a', b': reverse pulse polarograms ( $E_i$  –0.2 V;  $t_d$  9.9 sec;  $t_p$  14 msec). In recording b' the scan rate was 0.4 mV/sec.

of the anodic wave in normal pulse polarography. As predicted, a well-defined peak is observed when the increasingly negative potential pulses are applied, the peak potential being close to the half-wave potential of the anodic wave observed in normal pulse polarography. Varying  $E_i$  between –0.1 and –0.4 V had no significant effect on  $i_p$ .

The dependence of  $i_p$  on  $t_0$ , the time elapsed prior to application of the pulse, which is controlled by varying  $t_d$  mechanically, was evaluated. The slopes of the straight lines obtained in graphs of  $\log i_p$  vs.  $\log t_0$  (1.12 for penicillamine and 1.14 for cysteine) were close to the values predicted by equation (1), confirming that  $i_p$  is proportional to the quantity of mercury compound deposited on the electrode. The same conclusion may be inferred from the proportionality between  $i_p$  and the concentration of thiol compound present in the medium (Fig. 3) which likewise complied with equation (2).

The slopes of the straight lines obtained on plotting of  $\log i_p$  against  $\log t_p$  (–0.98 for penicillamine and –1.01 for cysteine) indicate that the dependence of  $i_p$  on  $t_p$  is close to that predicted for reversible redox reactions,<sup>11</sup> even though this prediction is not strictly



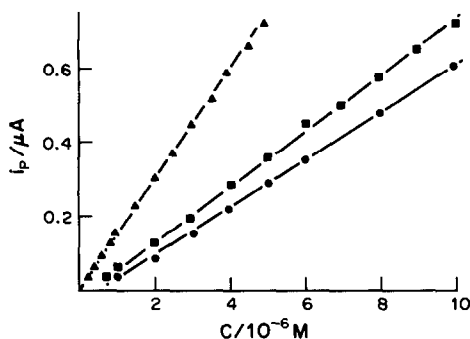


Fig. 3. Dependence of the peak current in reverse pulse polarography on the concentration of penicillamine (●) or cysteine (■) in 0.06M sodium tetraborate, and on the concentration of penicillamine in the system  $1 \times 10^{-5}M$  Cu(II)-0.06M sodium tetraborate (▲);  $t_d$  9.9 sec;  $t_p$  14 msec.

applicable to the dropping mercury electrode used in this work.

The results obtained show that with optimal instrumental settings ( $t_d$  9.9 sec,  $t_p$  14 msec) RPP is a more sensitive technique than either normal pulse polarography or differential pulse polarography for determination of the two model substances. In comparison with normal pulse polarography, for  $5 \times 10^{-6}M$  thiol compound the ratio  $i_p(\text{RPP})/i_p(\text{NPP})$  is about 5, and RPP has the additional advantage of providing peaks instead of waves. In comparison with differential pulse polarography the ratio  $i_p(\text{RPP})/i_p(\text{DPP})$  is about 8, and the RPP peaks are better defined, with half-peak amplitudes of 70 mV (penicillamine) and 65 mV (cysteine) as against 120 and 150 mV respectively in differential pulse polarography (Fig. 2), though it should be remembered that for such sensitivity RPP requires an instrument capable of providing low values of  $t_p$ .

The determination of sub- $\mu M$  concentrations of penicillamine and cysteine by RPP is complicated by the appearance of an extra peak at a more negative potential (Fig. 4, curve a). This peak is attributed to the reduction of complexes formed in solution by reaction of the thiol compounds with Cu(II) ions present as impurities in the media and adsorbed on the electrode surface.<sup>12</sup> This problem can be overcome by adding enough Cu(II) to complex all the thiol compound present, in which case the polarograms exhibit only the more negative of the two

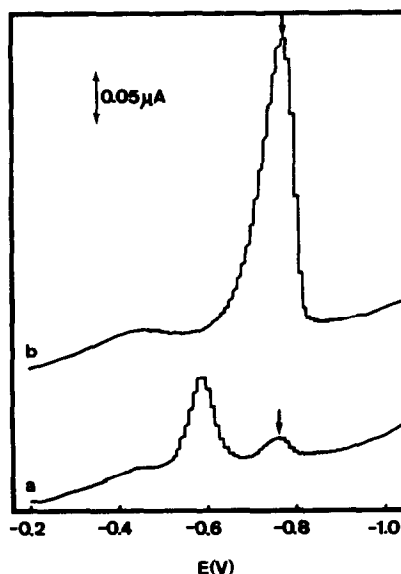


Fig. 4. Reverse pulse polarograms obtained in the systems  $2 \times 10^{-6}M$  penicillamine-0.06M sodium tetraborate (a) and  $2 \times 10^{-6}M$  penicillamine- $2 \times 10^{-6}M$  Cu(II)-0.06M sodium tetraborate (b);  $t_d$  9.9 sec;  $t_p$  14 msec.

peaks (Fig. 4, curve b). Figure 3 shows the proportionality between the  $i_p$  of this new peak and the concentration of penicillamine, and that values of the latter as low as  $5 \times 10^{-8}M$  are readily determined.

#### REFERENCES

1. K. B. Oldham and E. P. Parry, *Anal. Chem.*, 1970, **42**, 229.
2. J. Osteryoung and E. Kirowa-Eisner, *ibid.*, 1980, **52**, 62.
3. P. Maizota and D. C. Johnson, *Anal. Chim. Acta*, 1980, **118**, 233.
4. J. Wang and H. D. Dewald, *Talanta*, 1982, **29**, 901.
5. J. Koryta, *Collection Czech. Chem. Commun.*, 1953, **18**, 206.
6. G. C. Barker and J. A. Bolzan, *Z. Anal. Chem.*, 1966, **216**, 215.
7. J. B. Flanagan, K. Takahashi and F. C. Anson, *J. Electroanal. Chem.*, 1977, **85**, 257.
8. J. Puy, F. Mas, F. Sanz and J. Virgili, *ibid.*, 1985, **183**, 27.
9. F. Mas, J. Puy, F. Sanz and J. Virgili, *ibid.*, 1985, **183**, 73.
10. M. Lovrić, *ibid.*, 1984, **170**, 143; 1984, **181**, 35.
11. S. Komorsky-Lovrić and M. Lovrić, *ibid.*, 1985, **190**, 1.
12. U. Forsman, *ibid.*, 1980, **111**, 325; 1981, **122**, 215; 1983, **152**, 241.

## CHEMICAL MEASUREMENTS WITH OPTICAL FIBERS FOR PROCESS CONTROL

GILBERT BOISDE, FLOREAL BLANC and JEAN-JACQUES PEREZ

DGR-SEP Groupe Instrumentation et Automatisation, Centre d'Etude Nucléaires de Fontenay-aux-Roses, BP No. 6, 92265 Fontenay-aux-Roses Cedex, France

(Received 20 May 1987. Revised 7 September 1987. Accepted 14 September 1987)

**Summary**—Several aspects of remote *in situ* spectrophotometric measurement by means of optical fibers are considered in the context of chemical process control. The technique makes it possible to measure a species in a particular oxidation state, such as plutonium(VI), sequentially, under the stringent conditions of automated analysis. For the control of several species in solution, measurements at discrete wavelengths on the sides of the absorption peaks serve to increase the dynamic range. Examples are given concerning the isotopic separation of uranium in the Chemex process. The chemical control of complex solutions containing numerous mutually interfering species requires a more elaborate spectral scan and real-time processing to determine the chemical kinetics. Photodiode array spectrophotometers are therefore ideal for analysing the uranium and plutonium solutions of the Purex process. Remote on-line control by ultraviolet monitoring exhibits limitations chiefly due to Rayleigh scattering in the optical fibers. The measurement of pH in acidic (0.8–3.2) and basic media (10–13) has also been attempted. Prior calibration, signal processing and optical spectra modeling are also discussed.

The value of optical fibers for chemical process control in irradiated nuclear fuel reprocessing installations was demonstrated more than ten years ago with glass fibers.<sup>1</sup> The production of silica fibers usable over long distances (several hundred m) and the evaluation of their behavior under ionizing radiation<sup>2,3</sup> were vital for the industrial operation of remote *in situ* spectrophotometry.<sup>4</sup> The simultaneous on-line control of uranium and nitrates in solution by the method of Bostick *et al.*<sup>5</sup> was generalized<sup>6</sup> at the CEA (French Atomic Energy Commission) through the coupling of optical fibers with commercial instruments.<sup>7</sup>

Investigations in nuclear environments in the U.S.A.,<sup>8–10</sup> West Germany<sup>11</sup> and France,<sup>12</sup> and the measurement of copper *in situ* in electroplating baths<sup>13</sup> are typical examples of recent industrial developments in on-line control by use of optical fibers. The contribution of data-processing also allows the modeling of optical spectra<sup>6</sup> and their use according to the principles of chemometrics.<sup>14</sup>

Although the term "optrode" has been proposed<sup>15</sup> for optical fiber chemical sensors, we prefer the term "optode", the earlier designation,<sup>16</sup> which in our opinion is etymologically more appropriate (from the Greek *optixos* = optic and *odos* = path). The sensors which are based on absorption, light scattering,<sup>17</sup> fluorescence<sup>8,18</sup> and Raman spectrometry,<sup>19</sup> and use optical fibers as simple light guides, are called "passive optodes". The latest investigations concern so-called "active" optodes which take advantage of fiber-environment effects and of selective chemical reactions on part of the fiber length or at its end. After the first reviews by Chabay<sup>20</sup> and Seitz,<sup>21</sup> the considerable development of active optodes has ne-

cessitated new reviews in the fields of chemistry<sup>22,23</sup> and biochemistry.<sup>24</sup> The latest approaches in enzymology<sup>25</sup> and in continuous measurement are characteristic of process control requirements.

This study reviews the recent research at CEA on passive and active optodes. In the first category, the most significant examples concern *in situ* control of chemical species, alone and in mixtures. An extension of the measurement system to the ultraviolet reveals applications to the control of pharmaceutical products. An active optode for pH measurement in acidic and basic media is also described. Calibration, the determination of complexation constants, and signal processing are also discussed.

### EXPERIMENTAL

#### Instrumentation

Four types of instruments were employed in this investigation, chosen according to the complexity of the problem.

**Telephot®.** This interference filter photometer simultaneously measures  $(n + 1)$  wavelengths, where  $n$  is the number of variables. The complementary wavelength which serves as a reference is generally an absorption valley. In a two-wavelength version for high absorbance solutions, the detectors are photomultipliers (Hamamatsu R928). In a four-wavelength version, photomultipliers are preferable in the 400–600 nm range, and photodiodes are adequate in the near infrared. The measurement cell, placed at a distance of 60 m from the measuring instrument, is illuminated with white light from long-life quartz-halogen lamps (2000–5000 hr, depending on the power supply voltage). These instruments are marketed under CEA licence by the Seres Company (Z.I. Aix-en-Provence, 13763 Les Milles Cedex, France).

**Optical fiber couplers.** Optical couplers on spectral scan spectrophotometers (Beckman 5740, DU7, Varian 2300 *etc.*) and diode-array spectrophotometers (HP 8450 and 8451),

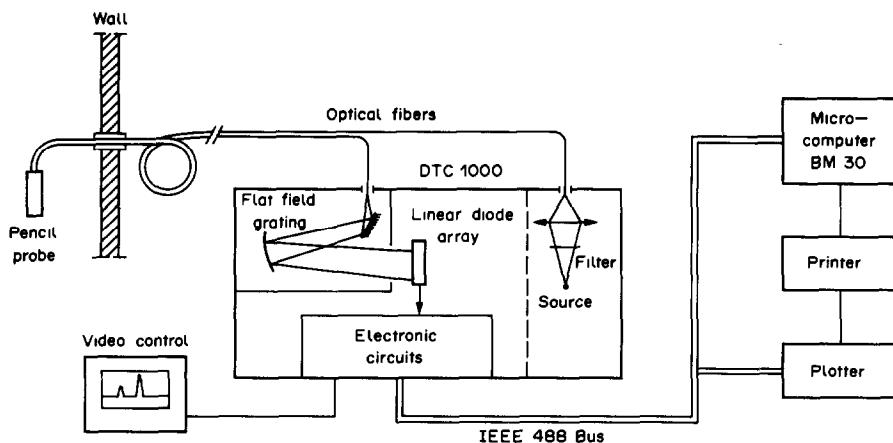


Fig. 1. Block diagram of DTC 1000 spectrophotometer.

marketed under CEA licence (by the Photonetics Company, 52 avenue de l'Europe, 78160 Marly-le-Roi, France), give insertion losses of about 10 dB. The remaining dynamic range is about 15–20 dB, but decreases sharply in the ultraviolet.

**DTC 1000.** Commercial spectrophotometers are unsuitable for measurements with optical fibers or are inoperative in the near infrared. The new instrument called the DTC 1000 was developed at the CEA for the 0.4–1  $\mu\text{m}$  range. It is designed for the real-time on-line control of plutonium(VI), for which the width of the absorption peak at mid-height is 2.7 nm. This measurement requires good resolution at 831 nm, and is described elsewhere.<sup>26</sup>

The linear photodiode array (1728 pixels) serves to give sufficient resolution as well as the analytical speed needed for the determination of chemical kinetics. The stationary character of the instrument guarantees good measurement repeatability. Optical fibers allow the DTC 1000 to make measurements in aggressive (nuclear) environments and for on-line industrial control. The spectrophotometer is of the single-beam type, and the main components (Fig. 1) are a halogen source (20 W), PCS 1000 optical fibers (Society Quartz et Silice), a CEA pencil probe, a Jobin Yvon flat-field grating, a Thomson Th7801 diode array, electronic circuitry with IEEE 488 interface, and a Bull-Mical 30 microcomputer (compatible with IBM PC-XT). All this equipment is also marketed under CEA licence by the Photonetics Company.

The performance characteristics of the instrument are as follows:

- spectral range 700–930 nm (potentially 500–1000 nm)
- resolution: 0.5–1 mm
- measurement range: 3 absorbance units
- video recurrence: 10 msec spectrum
- transfer time: 100 msec spectrum

The following functions are executed by the software:

- acquisition reference and sample spectra as the mean of  $n$  measurements
- optical density computation and smoothing
- peak identification
- output on screen, printer and plotter
- back-up on floppy disk.

**DEL-PIN sensor.** Designed in our laboratories<sup>27</sup> for several operations (object detection, optical fiber sensor), this inexpensive instrument has an LED of appropriate wavelength as a light-source (RTC.CQF 24). The LED is frequency-modulated at 10 kHz. The detector, a photodiode (PIN type RTC-BPF 24) is synchronized with the trans-

mitter. The amplification and filtering circuits are designed to measure a few tens of pW. A typical signal of 200–2500 mV is obtained, depending on the geometric configuration of the pH optode.

#### Operating conditions

The tests described here were conducted at various industrial sites of the CEA group, by several laboratories.

Plutonium(VI) determinations utilized the well-known technique of plutonium(IV) oxidation by  $\text{AgO}^{28}$  or ceric nitrate,<sup>29</sup> with neodymium as spectral reference,<sup>30</sup> in an automated analytical device designed in our laboratories.<sup>31</sup>

Measurement of uranium(III), (IV) and (VI) in the Chemex isotopic separation process was made with a two- or four-wavelength "Telephot".<sup>32</sup> In this process the aqueous phases are 3–7M hydrochloric acid (depending on operating conditions). The U(III) and U(IV) mixture is determined at the electrolyzer outlet (reduction) and at isotopic-exchange equilibrium by using a 4-wavelength "Telephot" [3 unknowns, U(III), U(IV),  $\text{Cl}^-$ , and one reference]. Traces of U(III) and U(VI) in U(IV) (oxidation test) and of U(IV) (at extractor outlet) are determined by using a 2-wavelength "Telephot". The measurement cells, connected by optical fibers (distance 30–60 m), have optical paths (1–50 cm) adjusted to the desired sensitivity. They are made of corrosion-resistant poly(vinyl difluoride), PVDF.

Spectral determination of uranium(VI),<sup>12</sup> uranium(IV) and plutonium(III) in the Purex process were achieved by using an HP 8450 spectrophotometer.<sup>33</sup> To separate plutonium and uranium by selective extraction, plutonium(IV) is reduced to plutonium(III) by the combined action of hydroxylamine nitrate and uranium(IV) in the presence of hydrazine nitrate as stabilizer. Chemical determinations of uranium (0.5–50 g/l.) and plutonium (0.5–30 g/l.) are performed *in situ* in nitric acid (calibration in the 0.5–5M range as total nitrates).

For all on-line controls, the optical probes (pencil type) had fixed optical path-lengths irrespective of the concentration of the medium. The probe<sup>4</sup> consists of two optical monofibers for two-way light travel, a silica lens and a "multivex" anticorrosion-coated concave mirror (made by MTO, Massy 91302, France) for measurements in nitric acid. This probe is also marketed under CEA licence by the Photonetics Company. Operational optical fibers for process control are of the PCS (Plastic Cladding Silicone) type with a 1000- $\mu\text{m}$  core (Society Quartz et Silice) containing 30 ppm of hydroxyl ions, or even 300–1200 ppm for measurements in the ultraviolet.

The pH optodes were examined successively with a Beckman 5740 spectrophotometer equipped with optical fibers,

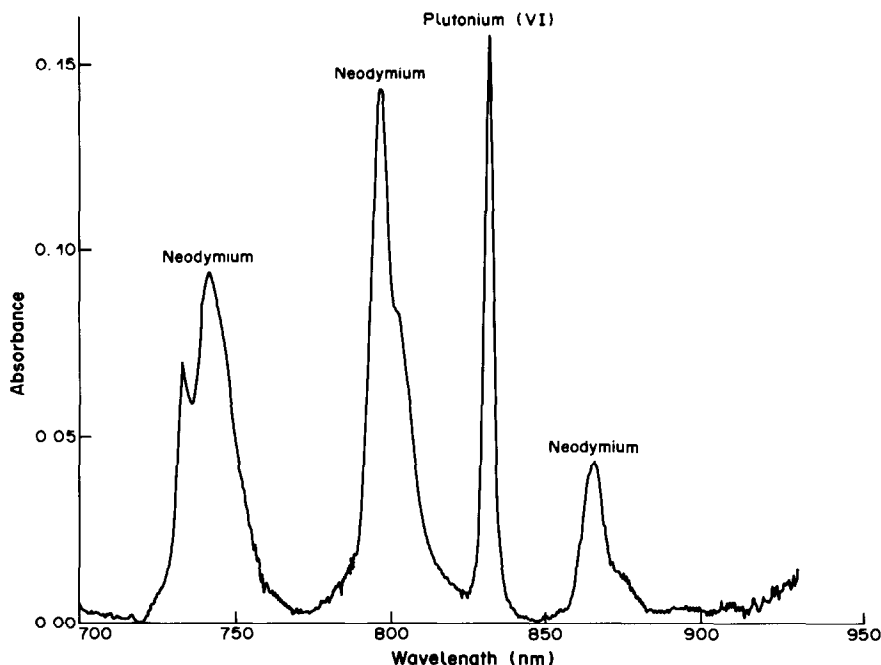


Fig. 2. Measurement (DTC 1000 spectrophotometer) of plutonium(VI) (40 mg/l.) with neodymium as internal reference.

a two-wavelength "Telephot" and the DEL-PIN sensor. The 1–1.5 mm diameter optode has no membrane. One fiber transmits the light onto a single active microsphere. The scattered and reflected light is collected by 1–6 fibers, depending on the detector (photomultiplier or PIN photodiode). The solution to be analysed is in contact with the reagent immobilized by drilling a hole through a hypodermic needle used as a support. The dye, Thymol Blue or Bromophenol Blue (Products Kuhlmann), dissolved in 0.1% alcohol solution is immobilized on an Amberlite XAD microsphere (Fluka A.G.) by contact with it for about 30–40 sec, followed by rinsing with distilled water.

For these active optodes, all-silica QSF 200/280 fibers (Quartz et Silice) are preferable because of the desired miniaturization and the industrial fabrication of reproducible standardized connectors (optical telecommunications systems).

## RESULTS

Remote on-line control with optical fibers has many aspects.<sup>6</sup> The concepts are more clearly understood in the light of the recent work described above.

### *Measurement of an isolated species with automated sampling*

Although the analytical automation device may be complex and good repeatability of the sampling is essential, on-line measurement is often calibrated by the addition of an internal reference. This applies to the measurement of plutonium(VI), which has a narrow spectrum (half-height band-width of about 2.7 nm, influenced by the acidity of the medium) that is compared with a neodymium internal reference. Figure 2 shows the spectrum obtained with the DTC 1000.

With an optical path of 1 cm, the detection limit for plutonium is 1 mg/l. (absorbance 0.004) and the corresponding background noise is about 0.5 mg/l. in the same conditions. The monitoring of traces of plutonium(VI) (a few mg/l.) during the dissolution of irradiated fuels has proved promising.

### *Simultaneous measurement of two "interactive" species*

Figure 3 shows the absorption spectra (400–1000 nm) of uranium(III) and (IV) in hydrochloric acid medium.<sup>32</sup> The peak at 723–726 nm, characteristic of U(III), corresponds to a deep absorption valley for U(IV). Since solutions with a high total uranium concentration absorb very strongly, U(III) is measured at 746 and 754 nm on the sides of this absorption peak. Uranium(IV) is determined at 655 nm and the internal reference is selected at a common valley of the U(III) and U(IV) spectra at 780 nm. The absorbance of each of the species varies linearly with the concentration of hydrochloric acid. Thus the net absorbance ( $A_\lambda - A_\nu$ ) for measurement at wavelength  $\lambda$  and of the absorption valley at wavelength  $\nu$  is

$$(A_\lambda - A_\nu) = [\text{U(III)}](a[\text{H}^+] + b) + [\text{U(IV)}](c[\text{H}^+] + d) \quad (1)$$

where  $a$ ,  $b$ ,  $c$  and  $d$  are constants determined by calibration.

Data-acquisition by a four-wavelength Telephot<sup>®</sup> (3 unknowns and 1 reference) allows the concentrations of U(III) and U(IV) to be computed.

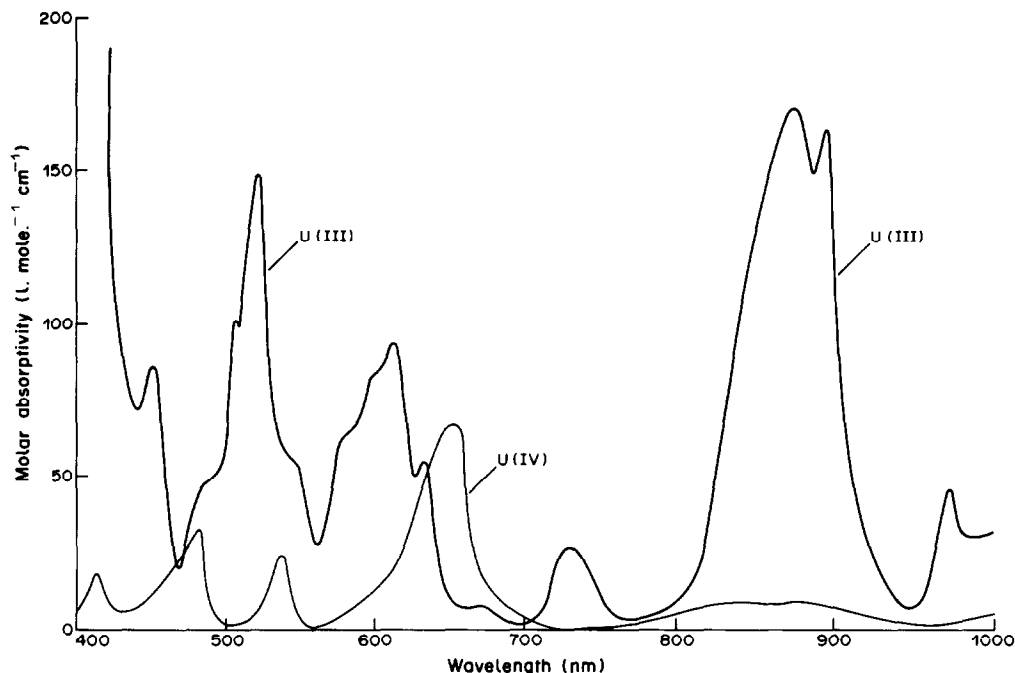


Fig. 3. Absorption spectra of uranium(III) and (IV) in hydrochloric acid medium.

The large relative error (Table 1) in the measurement of U(IV) results from its low concentration (less than 0.1M) in comparison with U(III) (1.5M).

*Determination of traces of a species in a solution containing another species in high concentration*

Figure 4 shows how a two-wavelength "Telephot" can be used to measure traces of uranium(III) or (VI) in a highly concentrated solution of uranium(IV). The Beer-Lambert law must be verified for measurements on the low-wavelength sides of the absorption peaks, because of the high absorbances at the peaks (about 20). For uranium(VI), for example, it is possible to select the wavelengths corresponding to isoabsorbance between the U(IV) + U(VI) and U(IV) zones. The use of a 0.5-cm optical path-length cell thus allows the measurement, at 412 and 775 nm (or 407 and 700 or 760 nm), as shown in Fig. 5, of about 0.004M uranium(VI) in 1.3M uranium(IV). This performance is still unrivalled by any other *in situ* technique. Uranium(III) can similarly be determined in presence of uranium(IV) by proper choice of wavelengths for measurement.

*Determination of several species in solution*

The uranium-plutonium partition in the Purex

process can be optimized by on-line *in situ* spectrophotometric determination of the species U(VI), U(IV) and Pu(III) in the mixer-settler batteries.<sup>33</sup> The comparative spectrum of each of the species has already been reported.<sup>6</sup> As a first approximation, the general absorbance function is:

$$(A_{\lambda} - A_{\nu}) = [U(VI)](a[NO_3^-] + b) + [U(IV)](c[NO_3^-] + d) + [Pu(III)](e[NO_3^-] + f) \quad (2)$$

where  $a$ ,  $b$ ,  $c$ ,  $d$ ,  $e$  and  $f$  are constants determined by calibration at wavelength  $\lambda$  relative to the wavelength ( $\nu$ ) of the absorption valley selected as reference (e.g., 530 nm). Note that the values of the coefficient  $e$  may change sign depending on the wavelength, as shown in Fig. 6 for plutonium(III). This results from the spectral changes caused by variation in the acidity ( $[H^+]$ ) and ionic strength of the medium (nitrate content), because several nitrate complexes exist in solution.

In this type of measurement, a photodiode-array spectrometer offers the advantage of the ability to obtain several on-line spectra which can be mutually correlated by the associated computer data-processing.

Table 1

Telephot measurements, M			Chemical control, M		
U(III)	U(IV)	U total	U(III)	U(IV)	U total
1.559	0.014	1.573	1.56	0.01	1.57
1.485	0.036	1.520	1.47	0.05	1.52

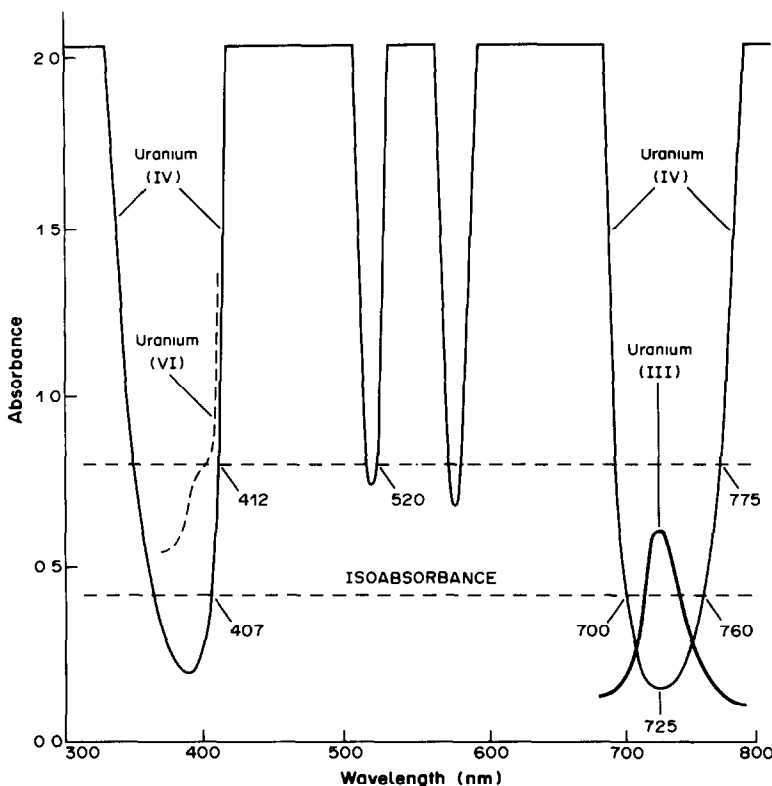


Fig. 4. Determination of traces of uranium(VI) or (III) in a high concentration (1.5M) of uranium(IV), in a 0.5-cm optical path-length cell. Selection of wavelengths by use of an isoabsorbance line.

#### In situ measurements in the ultraviolet (0.2–0.4 $\mu\text{m}$ )

Several limitations are observed for ultraviolet measurements when optical fibers are coupled with spectrophotometers. Thus it is necessary to compile a balance sheet to evaluate the losses in the optical circuit. It must include the insertion losses, losses due to Rayleigh scattering (function  $K/\lambda^4$ ) in the fibers and at their ends, losses due to specific absorption (impurities), and those resulting from imperfections of the waveguide. An overall balance sheet was recently compiled for the *in situ* control of the dissolution of pharmaceutical products.<sup>34</sup>

The dynamic range of the measuring instrument must also be taken into account. It may be necessary to use a photomultiplier sensitive to 200-nm radiation. However, this is liable to increase the background and the instability of the measurement in extreme conditions of use.

For PCS fibers (type QSF 1000 doped with OH), Fig. 7 shows the length limits as a function of measurement wavelength, considering the available dynamic range of 10, 20 or 30 dB. Thus with 30 m ( $2 \times 15$ ) of PCS 1000 ultraviolet type optical fibers and a "pencil" probe with an ultraviolet transmitting mirror, a wavelength of 280 nm was reached with an HP 8451 spectrophotometer (scale range 30 dB). A Beckman DU 7 spectrophotometer with a scale

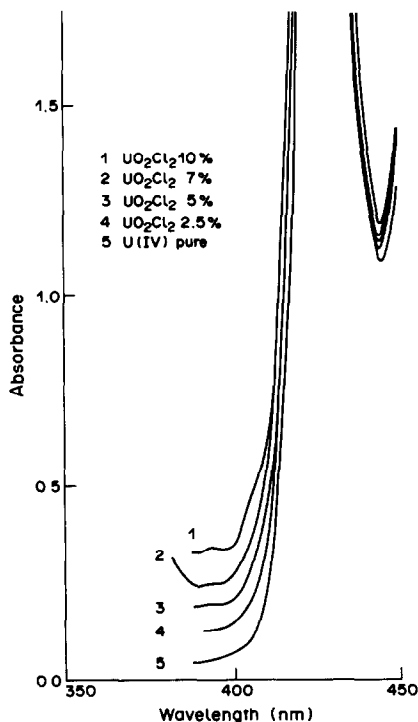


Fig. 5. Influence of  $\text{UO}_2\text{Cl}_2$  on uranium(IV) spectrum in hydrochloric acid medium.

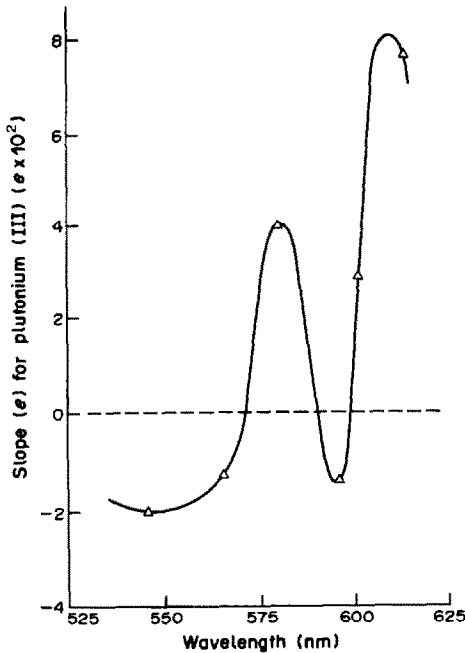


Fig. 6. Variation with wavelength of the slope ( $e$ ) of the empirical nitrate-plutonium(III) equation  $\Delta A = [\text{Pu(III)}](e[\text{NO}_3^-] + f)$  in on-line process control. The dashed line intersects the curve at the wavelengths for the isobestic points ( $e = 0$ ) of the Pu(III)- $\text{HNO}_3$  system.

range of 45 dB allows measurements to be taken at wavelengths down to 240 nm.

Significant efforts still need to be made to improve fiber purity, in order to obtain a good measurement margin at 200 nm over distances of 10–20 m.

#### *pH optode for in situ control*

A miniature optode was built according to the principles of Peterson *et al.*<sup>35</sup> and of Kirkbright *et al.*<sup>36</sup> to measure the variation in absorption and light-scattering by an immobilized pH-sensitive dye, its special feature being the absence of a membrane. The results have been reported elsewhere.<sup>37</sup> The dyes used were Thymol Blue for the two pH ranges 0.8–3.2 (absorbance peak at 555 nm) and 10–13 (peak at 600 nm), and Bromophenol Blue for pH between 3.2 and 7 (peak at 604 nm). Figure 8 shows an example of the use of Thymol Blue in both ranges.

The general absorbance-pH function is given by the equation:

$$\text{pH} = \text{p}K - \log\left[\frac{\epsilon_1 IT - A}{A - \epsilon_{\text{IH}} IT}\right] \quad (3)$$

for the reversible reaction



where  $\epsilon_1$  and  $\epsilon_{\text{IH}}$  are the molar absorptivities of the forms  $\text{I}^-$  and  $\text{IH}$ ,  $T$  the concentration of the immo-

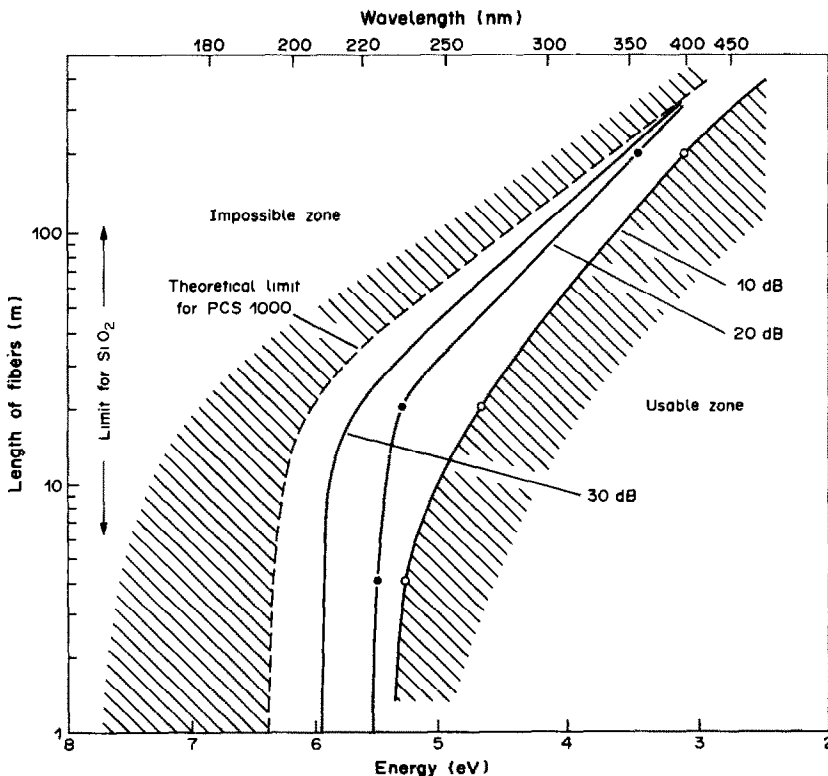


Fig. 7. Usable length of optical fibers (PCS) in relation to wavelength in ultraviolet for available dynamic ranges of 10, 20 and 30 dB. Theoretical limit for a QSF 1000 W fiber without impurities.

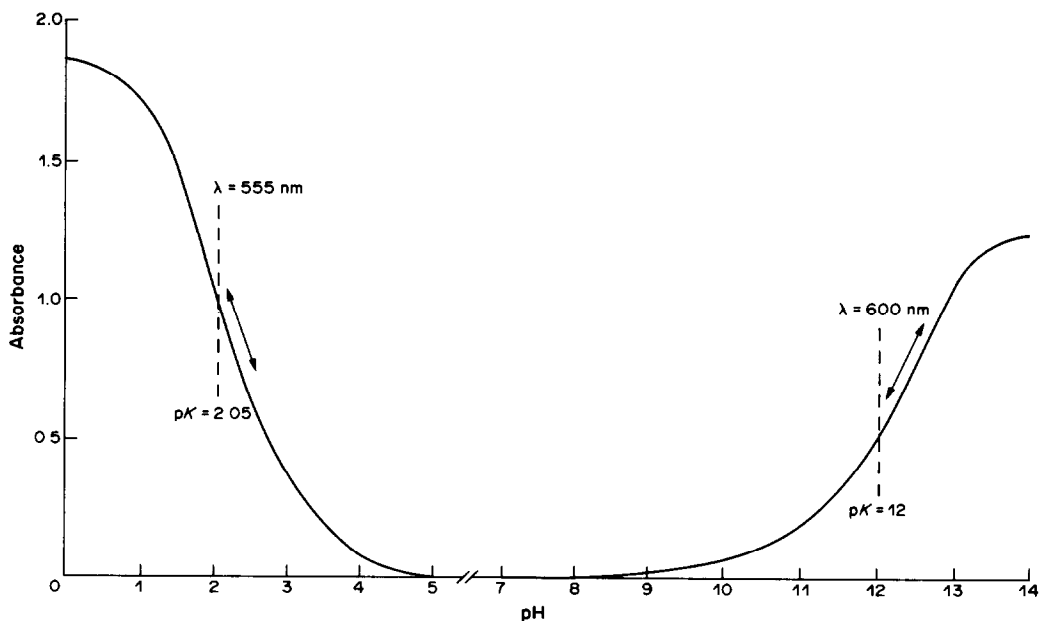


Fig. 8. Typical response of a Thymol Blue optode in acid and basic media.

bilized dye,  $A$  the absorbance measured, and  $l$  a constant related to the optical path-length and hence of the system employed ( $\epsilon_1, \epsilon_{1H}$  and  $A$  refer to the same wavelength).

Note that the kinetics of the dye-medium reaction to be analyzed will become faster (1 min) and the reversibility better as the pH becomes more acidic or more basic. The lifetime of this optode is about 2 weeks.

#### DISCUSSION

On-line control with passive optodes is a technique that plant operators are beginning to adopt because of the many advantages it provides (real-time measurement, ease of operation). However, the reliability of the measurement probe in industrial conditions must be demonstrated. The choice of the spectrophotometer is still the prerogative of the analyst. Rugged instruments such as the "Telephot" can be used by the process operators, but procedures have to be devised to check the absence of drift and for calibrations, implying a close knowledge of the process limits.

Remote multistation measurement from a central laboratory is perfectly consistent with the use of optical fibers and with optical multiplexing. In process control, this can justify the use of top-of-the-range instruments, and hence also of *in situ* fluorescence and Raman spectrometry techniques.

One vital prerequisite for *in situ* industrial control by optical fibers is to design an optical line with all the components fixed, particularly the measurement cells and the spectrometer components (gratings *etc.*). In addition to real-time measurement, this is one of

the advantages of the DTC 1000 and the photodiode-array HP 8451, which use fixed optical path-length cells. The measurement wavelength can be selected in accordance with the minimum (lower detection limit) and maximum of the dynamic range. Figure 9 shows one example for uranium(IV) measured with a 4-cm optical path-length immersion probe.

Computerized data-processing allows the modeling of optical spectra and facilitates the detection of interference. Calibration, a detailed knowledge of the process, and of potential deviations from the setpoint are nevertheless indispensable.

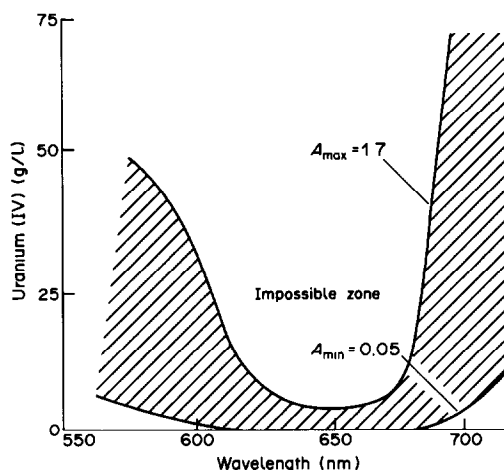


Fig. 9. Usable zone (hatching) in on-line control of uranium(IV) with a 4-cm optical path-length pencil probe.  $A_{max}$  represents the maximum for the dynamic range;  $A_{min}$  is the detection limit set by the signal to noise ratio.



The modeling of optical spectra from empirical functions of polynomial type presents the drawback of intrinsic limits (wide measurement differences if the functions are of second or higher order). A more rigorous approach based on the determination of the complexation constants and of the influence of the ionic strength, *etc.*, helps to develop a coherent mathematical model, as demonstrated for uranium(VI),<sup>38</sup> but the application of this technique is difficult for industrial solutions.

There is considerable hope for on-line *in situ* control with active optodes. The design of inexpensive instruments is now within our reach. However, for industrial operation it is still necessary to acquire basic knowledge about the mechanisms involved. Some examples are dye diffusion into supports, optode behavior during temperature variations, influence of the dye concentration and ionic strength of the medium, optode lifetime, *etc.* Finally, optode miniaturization is important for the easy adaptation of optodes, for example, in parallel, to broaden the measurement range and to allow several simultaneous measurements.<sup>39</sup>

#### CONCLUSIONS

Remote *in-situ* chemical control with passive optodes has become an industrial reality. Thus, more than 1 km of fibers has been installed at the CEA for some 20 work-stations and specific spectrometric equipment has been designed for these applications. The most varied aspects can be encountered: measurement of a single species in a restricted analytical medium, simultaneous determination of several species, possibly with mutual interference, trace measurements in a complex medium, a wide range of wavelengths from 200 to 1800 nm for gas analysis<sup>40</sup> with silica fibers. However, the use of this technique by plant operators under the supervision of a central laboratory is only beginning, and it is still necessary to overcome a certain degree of reluctance to change old habits.

Active optodes are still too recent to be applied industrially in process control. However, the many research projects under way throughout the world in all fields (medicine, enzymology, pollution, nuclear) is an undeniable sign of their importance. Much progress still has to be made. Nevertheless, the possibilities of building all-optical networks of sensors, spatial multiplexing with a centralized top quality measuring instrument, and insensitivity to electromagnetic environments, are definite advantages arising from the introduction of optical fibers in the chemical industry.

#### REFERENCES

- J. J. Perez, G. Boisdé, P. Dedaldechamp and B. Durault, *CEA-CR-11*, p. 69. Saclay, 1975.
- E. J. Friebele, K. J. Long, C. G. Askins, M. E. Gingerich, M. J. Marrone and D. L. Griscom, *Proc. SPIE—Int. Soc. Opt. Eng.*, 1985, **541**, 70.
- G. Boisdé, C. Bonnejean, J. J. Perez, V. Neuman, B. Wurier and D. Boucher, *ibid.*, 1984, **404**, 17.
- J. J. Perez, G. Boisdé, M. Goujon de Beauviver, G. Chevalier and M. Isaac, *Analysis*, 1980, **8**, 344.
- D. T. Bostick, *U.S. At. Energy Comm. Rept.*, ORNL-TM 6292, 1978; *NBS Special Publ.*, 1980, **582**, 121.
- G. Boisdé and J. J. Perez, *Proc. SPIE—Int. Soc. Opt. Eng.*, 1984, **514**, 227.
- G. Boisdé, C. Linger, G. Chevalier and J. J. Perez, *ibid.*, 1983, **403**, 153.
- F. P. Milanovich and T. Hirschfeld, *Adv. Instrum.*, 1983, **38**, 404.
- R. A. Malstrom, T. Hirschfeld and T. Deaton, *U.S. At. Energy Comm. Rept.*, DP. MS 82-38, 1982.
- D. R. Van Hare and W. S. Prather, *ibid.*, DP-1714, 1986.
- P. Groll, M. Persohn, J. Roemer and B. Schuler, KFK-3843, 1984.
- G. Boisdé, C. Linger and J. J. Perez, *5th Ann. Symp. Safeguards Nuclear Mat. Manag.* p. 203. ESARDA, Versailles, 1983.
- J. E. Freeman, A. G. Childers, A. W. Steele and G. M. Hieftje, *Anal. Chim. Acta*, 1985, **177**, 121.
- T. Hirschfeld, J. B. Callis and B. R. Kowalski, *Science*, 1984, **226**, 312.
- S. A. Borman, *Anal. Chem.*, 1981, **53**, 1616A.
- D. W. Lübbers and N. Z. Opitz, *Z. Naturforsch.*, 1975, **30c**, 532.
- D. Snell and G. D. Pitt, *Int. Conf. Optical Techniques Process Control, BHRA*, p. 27. SIRA, Cranfield, 1983.
- D. L. Perry, S. M. Klainer, H. R. Bowman, F. P. Milanovich, T. Hirschfeld and S. Miller, *Anal. Chem.*, 1981, **53**, 1048.
- McGeery, M. Fleischmann and P. Hendra, *ibid.*, 1983, **55**, 146.
- I. Chabay, *ibid.*, 1982, **54**, 1071A.
- W. R. Seitz, *ibid.*, 1984, **56**, 16A.
- A. L. Harmer, *Int. Summer School Erice, Optical Fibre Sensors*, Italy, May, 1986, S. Martelucci and A. M. Scheggi (eds.), in the press.
- G. Boisdé and J. J. Perez, *Congrès Société Française de Chimie Paris*, 8–12 Sept. 1986, Microfilm CEA-Conf. 8701, 1986.
- J. I. Peterson and G. G. Vurek, *Science*, 1984, **224**, 123.
- M. A. Arnold and T. J. Ostler, *Anal. Chem.*, 1986, **58**, 1137.
- F. Blanc, P. Vernet and J. J. Perez, *Rept., CEA, French Atomic Commission*, in the press.
- F. Blanc, C. Bonnejean and G. Boisdé, *French Conf. S.E.E. (Société Electriciens Electroniciens Paris)*, June 1986, Microfilm CEA-Conf. 8437, 1986.
- P. Cauchetier, *Analysis*, 1980, **8**, 336.
- Idem*, *Anal. Chim. Acta*, 1981, **124**, 449.
- M. C. Bouzou and A. A. Brutus, *NBS Spec. Publ.*, 1980, **582**, 497.
- J. J. Perez, *Europ. Conf. Industrial Line Spectrographic Analysis, Rouen 1985*, 2–1.
- R. M. Costes, G. Boisdé, A. Travert, C. Bonnejean, M. Girard and P. Levy, *ibid.*, 5–1.
- G. Boisdé, A. Deroite, G. Mus and M. Tachon, *ibid.*, 7–1.
- G. Boisdé, S. Rougeault and J. J. Perez, *Opto. 86*, p. 71. Masson, Paris, 1986; Microfilm CEA-Conf. 8572, 1986.
- J. I. Peterson, S. R. Goldstein, R. V. Fitzgerald and D. K. Buckhold, *Anal. Chem.*, 1980, **52**, 864.
- G. F. Kirkbright, R. Narayanaswamy and N. A. Welti, *Analyst*, 1984, **109**, 1025.
- G. Boisdé and J. J. Perez, *Proc SPIE—Int. Soc. Opt. Eng.* 1987, **798**, in the press.
- J. P. Corriou and G. Boisdé, *Anal. Chim. Acta*, 1986, **190**, 255.
- O. S. Wolfbeis, *Z. Anal. Chem.*, 1986, **325**, 387.
- K. Chan, H. Ito and H. Inaba, *Appl. Opt.*, 1984, **23**, 3415.

## OPTICAL-FIBRE SENSING OF FLUORIDE IONS IN A FLOW-STREAM

R. NARAYANASWAMY\*, D. A. RUSSELL and F. SEVILLA, III†

Department of Instrumentation and Analytical Science, UMIST, P.O. Box 88, Manchester, England

(Received 20 May 1987. Revised 4 August 1987. Accepted 23 September 1987)

**Summary**—The Alizarin Fluorine Blue method for the determination of fluoride has been adapted for use with optical fibres. The reagent was immobilized on a polymer matrix, Amberlite XAD-2, and the reflectance of this reagent phase was measured as a function of fluoride concentration by use of a flow-cell assembly and a bifurcated fibre-optic system. A linear response was obtained for 0.16–0.95mM fluoride at a pH of 4.1, with a response time of approximately 12 min.

The concept of using an immobilized reagent at the tip of an optical fibre to detect a chemical species has led to the development of a new class of sensor.<sup>1,2</sup> These devices are based on the detection of a change of colour or luminescence of the immobilized reagent in the presence of an analyte, by transmission of the radiation through the fibre. Optical-fibre sensors have the advantages of an internal reference system, suitability for remote monitoring and freedom from electromagnetic interference.

Numerous optical-fibre chemical sensors have been reported for a variety of species, both gaseous and in solution. Sensors for pH,<sup>3-6</sup> sulphide<sup>7,8</sup> and some cations<sup>9-11</sup> have been constructed for measurements on solutions. An optical sensor has also been fabricated for chloride, bromide and iodide,<sup>12</sup> but no sensor for fluoride has been reported. This paper describes a method for determining fluoride in a flowing stream by use of an immobilized reagent phase and a fibre-optic detection system.

Most of the colour reactions of fluoride depend on ligand-exchange reactions in which fluoride forms a complex with the cation of a coloured binary complex, and thus bleaches the colour. Only a few reactions of fluoride involve development of a colour. These are based on the formation of a coloured ternary complex by fluoride with a binary complex, such as the cerium(III) complex of Alizarin Complexone<sup>13</sup> (also known as Alizarin Fluorine Blue, AFB) (Fig. 1). Some other lanthanides exhibit a similar reaction.<sup>14</sup> A spectrophotometric method based on this reaction<sup>15-17</sup> has been established as a reliable and sensitive method for fluoride measurement, far superior to most procedures based on the bleaching reactions of fluoride.<sup>18</sup>

No optical-fibre sensor has yet been reported that is based on the use of a ternary complex. The high

sensitivity and reasonable selectivity of the AFB method for determination of fluoride suggested its investigation for development of an optical-fibre fluoride sensor.

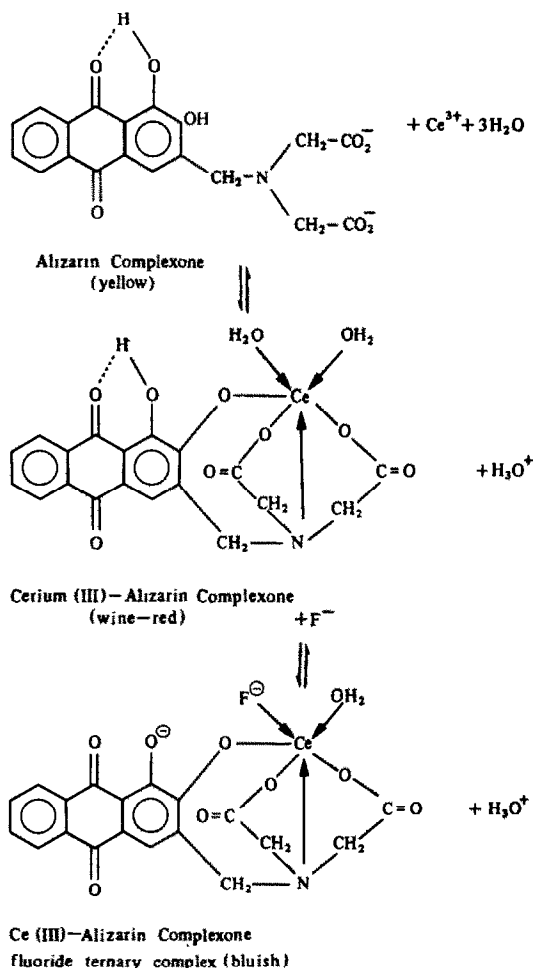


Fig. 1. Formation of the cerium(III) chelate and fluoride ternary complex from Alizarin Complexone.

\*To whom correspondence should be addressed.

†Present address; University of Santo Tomas, Espana, Manila, Philippines.

## EXPERIMENTAL

*Reagents*

Alizarin Complexone solution was prepared by dissolving 0.1 g of the reagent in 50 ml of water containing 0.25 ml of concentrated ammonia solution, then adding 0.25 ml of glacial acetic acid and diluting to 100 ml.

Acetate buffer solution (pH 4.1) was prepared by dissolving 60 g of sodium acetate trihydrate in 500 ml of water, adding 115 ml of glacial acetic acid and diluting to 1 litre. Acetate buffer (pH 5.1) was similarly prepared with 80 g of sodium acetate trihydrate, 15 ml of glacial acetic acid, and dilution to 1 litre.

Cerium(III) nitrate and lanthanum nitrate stock solutions (0.01 *M*) were prepared by dissolving 2.171 g of cerium(III) nitrate hexahydrate and 2.165 g of lanthanum nitrate hexahydrate respectively, in 500 ml of water.

Fluoride solutions were prepared by diluting a standard sodium fluoride solution (1000  $\mu\text{g}$  of fluoride per ml) to the required concentration with acetate buffer.

The substrate for immobilization was Amberlite XAD-2, a cross-linked copolymer of styrene and divinylbenzene. All reagents were BDH "AnalaR" grade. Demineralized, distilled water was used throughout.

*Immobilization procedure*

The XAD-2 polymer beads were washed with water, then with acetone, and air-dried. They were next soaked in methanol for 15 min and then in water to wet them. The beads (5.0 g) were placed in 400 ml of a 1:1 mixture of Alizarin Complexone solution and pH-4.1 acetate buffer, left there overnight and then washed well with water. The polymer beads with Alizarin Complexone adsorbed on them were kept in 100 ml of a 1:1 mixture of 0.01 *M* cerium(III) nitrate and pH-4.1 acetate buffer for 2 hr, then washed with water.

The corresponding immobilized lanthanum chelate was similarly prepared but with the pH-5.1 buffer.

*Instrumentation*

The instrumentation (Fig. 2) was a modified version of a system previously described.<sup>4</sup> Light from a quartz-halogen lamp (12 V, 100 W) was passed down one branch of a bifurcated optical fibre system, constructed from a bundle of 16 polymer fibres (Optronics). The light was focused onto the end of the fibre (which was protected by a heat-absorbing filter) by a series of lenses. To remove interference from ambient light, the light was modulated by an optical chopper (Bentham 218) set at a frequency of 360 Hz.

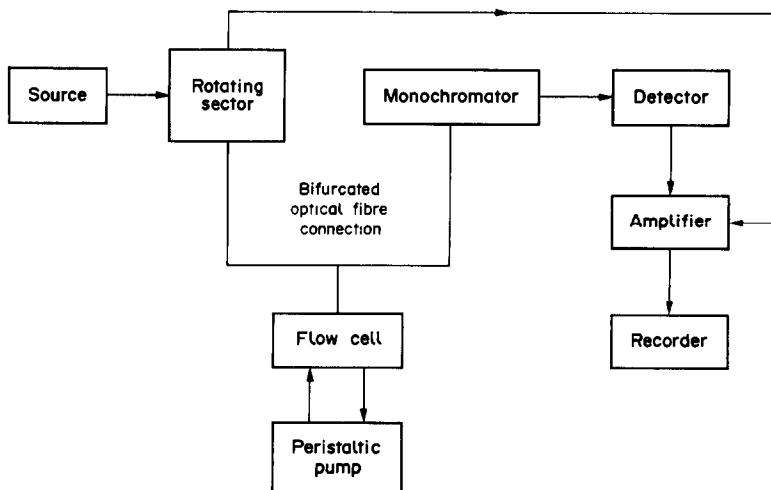


Fig. 2. Schematic diagram of the instrumentation used for reflectance measurements.

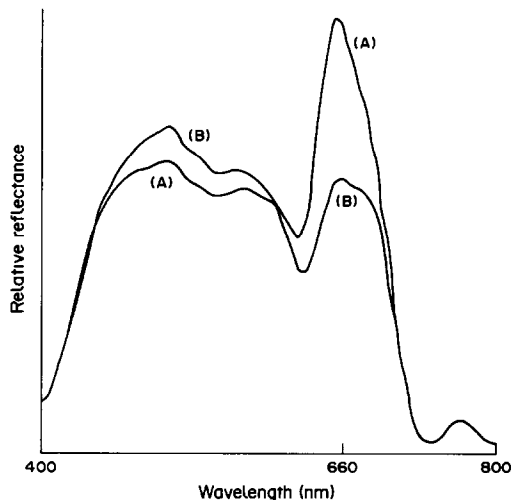


Fig. 3. Reflectance spectra from (A) the immobilized cerium(III) chelate and (B) the immobilized ternary fluoride complex.

The beads carrying the immobilized chelate were packed in a flow-cell constructed as described previously.<sup>19</sup> A peristaltic pump (Watson Marlow 502S) was used to pass the buffer and other solutions over the reagent phase at a rate of 0.5 ml/min. The reagent phase was irradiated with light from one branch of the optical fibre, and the light reflected from it was collected and guided to a monochromator (ISA Jobin-Yvon H-1061) by the second branch of the bifurcated optical fibre and subsequently detected by a photomultiplier (Hamamatsu R446). The signal was enhanced by a current amplifier (Bentham 286) and a lock-in amplifier (Bentham 223) synchronized with the optical chopper frequency. The output of the amplifier was proportional to the intensity of the reflected light and was recorded on a chart recorder (BBC SE120).

The reference signal was obtained from an optical fibre surrounded by XAD-2 polymer beads without any immobilized reagent.

*Reflectance measurements*

The reflectance spectrum of the immobilized binary cerium(III) chelate was recorded before and after its reaction with fluoride (Fig. 3). The maximum divergence between the

two spectra was at 660 nm, and this wavelength was therefore used for subsequent reflectance measurements. The same wavelength was optimal for use with the lanthanum complex (Fig. 3).

The measurements were expressed as relative reflectances, *i.e.*, the reflectance of the binary lanthanide or of the fluoride ternary complex relative to that of the undyed polymer beads as reference. The analytical signal used is then the difference between these relative values ( $\Delta$  relative reflectance).

## RESULTS AND DISCUSSION

### *Immobilization of the reagent phase*

Amberlite XAD-2 was selected as the immobilizing agent because of its hydrophobic nature, which imparts to it an ability to interact with the non-polar portion of the chelate molecule. Two methods (A and B) for immobilization of the reagent were tried. In method A the XAD-2 was soaked in a solution of the lanthanide chelate, and in B the Alizarin Complexone was immobilized first and then treated with the lanthanide solution.

Both methods produced adsorption of the wine-red chelate on XAD-2, but the product from method A did not react with fluoride, whereas the chelate formed by method B produced a colour change in the presence of fluoride.

The failure of the product formed by method A could be attributed to the manner in which the chelate molecule is held on the surface of the XAD-2 beads. If the fluoride-sensitive portion of the chelate, *i.e.*, the portion containing the lanthanide ion, were bound to the polymeric structure, it would be inaccessible for reaction with the fluoride. The polarity of this end of the Alizarin Complexone molecule might be sufficiently reduced by the chelation for hydrophobic interactions or  $d-\pi$  charge-transfer complexation to take place. Similar observations have been made on the reaction of sulphide with the silver-dithiofluorescein complex.<sup>19</sup>

When method B was used, the yellow Alizarin Complexone was adsorbed on the XAD-2, but some leaching occurred when the dyed beads were placed in fresh water, indicating weak adsorption. When placed in lanthanide solution the yellow beads became wine-red as the lanthanide chelate formed. The chelate was not leached by water, presumably because the decrease in polarity on chelation increased the strength of bonding to the XAD-2.

The colour change of the immobilized chelate from wine-red to lilac-blue in the presence of fluoride shows that the chelated group was not bound to the XAD-2 and thus was able to form the ternary complex. At the pH used (4.1) Alizarin Complexone is doubly negatively charged and can be held on the XAD-2 surface only through the hydrophobic portion of the ring structure, with the ionic end directed away from the polymer surface. Since the lanthanide ion interacts with the ionic end of the Alizarin Complexone, and the reaction does not alter the

orientation on the XAD-2, the chelate grouping will be oriented away from the surface of the polymer and available for reaction with fluoride.

The amount of the cerium chelate immobilized was found by removing the cerium(III) from it with 0.05M sulphuric acid (5 ml per g of XAD-2) and determining the cerium(III) spectrophotometrically.<sup>20</sup> On addition of the sulphuric acid the dyed beads became yellow, showing that the cerium(III) had been removed, leaving the Alizarin Complexone immobilized. It was assumed that the ratio of cerium(III) to Alizarin Complexone was 1:1, but this was confirmed by desorbing the Alizarin Complexone from the XAD-2 with methanol, and determining it spectrophotometrically. The chelate loading was found to be 36  $\mu$ mole per g of XAD-2.

### *Formation constant of the ternary complex in the immobilized phase*

The reaction can be written as  $A + F \rightleftharpoons AF$  where A is the metal chelate of Alizarin Complexone, F is fluoride and AF the ternary complex. The conditional formation constant ( $K$ ) is given by

$$K = C_{AF}/C_A C_F \quad (1)$$

where  $C_A$  and  $C_{AF}$  are the equilibrium concentrations of metal chelate and ternary complex respectively, and  $C_F$  the fluoride concentration of the solution continuously flooding the reagent phase.

The reflectance spectra can be described by the Kubelka-Munk theory,<sup>21</sup> by means of which the reflectance values ( $R$ ) obtained can be related to the concentration of the ternary complex ( $C_{AF}$ ) by

$$F(R) = (1 - R)^2/2R = kC_{AF} \quad (2)$$

where  $F(R)$  is the Kubelka-Munk function and  $k$  is a constant combining the absorption and scattering constants.

The initial concentration of the reagent phase ( $C_T$ ) is related to  $C_A$  and  $C_{AF}$  at any instant by the equation

$$C_T = C_A + C_{AF} \quad (3)$$

Combining equations (1)–(3) gives

$$1/F(R) = (1/kC_T K C_F) + (1/kC_T) \quad (4)$$

A plot of  $1/F(R)$  vs.  $1/C_F$  should give a linear relationship from which  $K$  could be calculated by dividing the intercept by the slope. By use of such a plot and equation (4) the conditional formation constants for the ternary complexes of fluoride with the immobilized cerium(III) and lanthanum Alizarin Complexone chelates were evaluated as  $4.7 \times 10^3 \text{ M}^{-1}$  and  $8.5 \times 10^3 \text{ M}^{-1}$ , respectively. The measured values of the slope and intercept may be substituted into equation (4) to predict the reflectance response of the immobilized reagent phase to the concentration of fluoride present (Fig. 4). It is apparent from Fig. 4 that equation (4) is not applicable at low

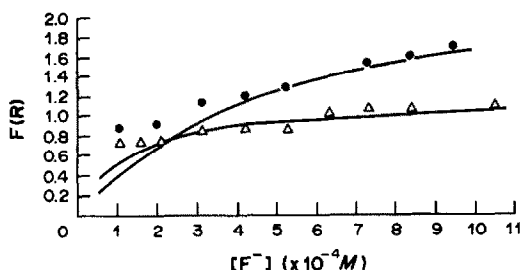


Fig. 4. Theoretical response of the metal chelates as predicted by equation (4) (—), compared with the experimentally determined values for the cerium(III) chelate (●) and the lanthanum chelate (△).

fluoride concentrations. The linear portion of the plot of  $F(R)$  vs. fluoride concentration represents the region in which the Kubelka–Munk theory would be applicable.

It has been reported<sup>22</sup> that in solution the lanthanum ternary complex exists as a ring-form dimer (Alizarin Complexone–lanthanum)<sub>2</sub> to which two fluoride ions are attached. The conditional formation constant for this complex was reported as  $6.3 \times 10^{13}$  at pH 4.5. This type of dimeric structure would not be possible with the immobilized Alizarin Complexone because the orientation of the immobilized chromophore would not permit the formation of the ring structure with the metal ions. Hence only the monomeric complex and the corresponding fluoride would be formed. The conditional formation constant for the monomeric ternary complex is reported<sup>22</sup> to be  $3.6 \times 10^4$ , in reasonable agreement with our value for the immobilized complex.

#### Response to fluoride ions

The response of the immobilized Alizarin Complexone chelates of cerium(III) and lanthanum to varying concentrations of fluoride is shown in Fig. 5. The reflectance decreased as the binary chelate was converted into the ternary complex. Plots of the relative reflectance vs. logarithm of the fluoride ion concentration appeared sigmoidal, but reasonably linear sections could be defined for the ranges 0.16–0.95 mM fluoride for the cerium(III) chelate and 0.16–0.84 mM fluoride for the lanthanum chelate. The

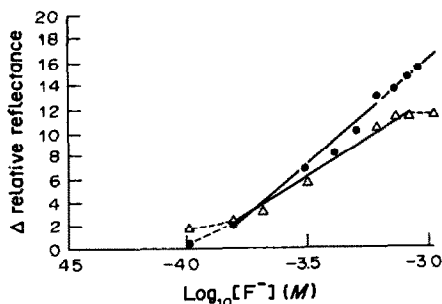


Fig. 5. Change in reflectance of immobilized cerium(III) chelate (●) and immobilized lanthanum chelate (△) as a function of logarithm of the fluoride concentration.

limit of detection of fluoride, defined as the concentration equivalent to a signal four times the standard deviation of the blank, was estimated as 0.11 mM for both chelates.

It has been reported<sup>23</sup> that the lanthanum complex has greater sensitivity than the cerium(III) complex for fluoride when measurement is made at 281 nm, but this wavelength could not be used with the polymer optical fibres as this type of fibre has a high attenuation at wavelengths shorter than 400 nm.

#### Response time

The time taken to attain steady-state response was observed to be 12 min for the cerium(III) chelate and 22 min for the lanthanum chelate. The steady-state response time for the cerium(III) chelate was much shorter than that observed for the reaction in solution and was of the same order of magnitude as that reported for the solution reaction in the presence of an organic solvent.<sup>16,17</sup> The XAD-2 adsorbent may be considered to behave as a solid solvent for organic reagents containing the benzene ring and thus affect the speed of formation of the ternary complex.<sup>24</sup> This is similar to the effect observed in an organic solvent.<sup>13,14</sup> Immobilization of a reagent has also been shown to produce medium effects on acid–base equilibria.<sup>25</sup>

The reflectance decreases exponentially with time, which implies a first-order reaction, with the rate dependent only on the fluoride concentration. The rate of reaction is zero order with respect to the immobilized reagent, since this is present in a large excess.

Further studies were concentrated on the cerium(III) chelate because it exhibited faster response and a broader linear range than the lanthanum chelate.

#### Effect of pH

The decrease in reflectance on formation of the ternary complex was measured at several pH values, of which pH 4.1 gave the greatest decrease (Fig. 6). Immobilization of the reagent is presumed to have the same effect as adding an organic solvent to the reaction mixture (see above). The optimal pH is reported to be 5.0–5.1 when an organic solvent is

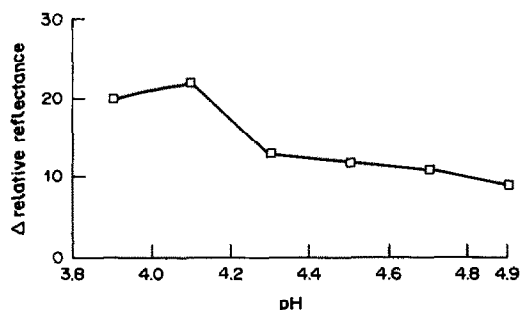


Fig. 6. The effect of pH on formation of the ternary complex from the cerium(III)–Alizarin Complexone chelate.

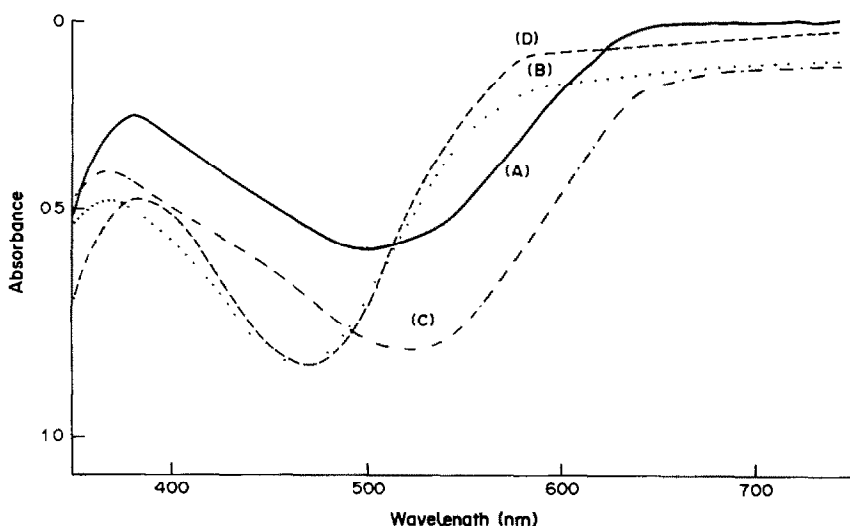


Fig. 7. Absorption spectra obtained from a solution of the ternary fluoride complex of cerium(III) containing (A) a low concentration of aluminium ions ( $10^{-4}M$ ), (B) a high concentration of aluminium ions ( $10^{-2}M$ ) and from a solution of the chelate of Alizarin Complexone with (C) cerium(III) and (D) aluminium.

absent and 4.1–4.3 when it is present,<sup>16,17</sup> (which was why pH 4.1 was selected for the initial work).

#### Reversibility studies

Regeneration of the reagent phase after use is essential unless a new fibre is to be used for each analysis. Regeneration might be achieved by removing the fluoride from the ternary complex *e.g.*, by formation of a sufficiently stable fluoro-complex, such as hexafluoroaluminate. Use of  $10^{-5}$ – $10^{-1}M$  aluminium solutions was investigated. Beads that had been treated with  $10^{-3}$ – $10^{-1}M$  aluminium, although restored to their original wine-red, showed no colour change with fluoride solution. However, the beads obtained by using  $10^{-4}$  or  $10^{-5}M$  aluminium produced the expected change to blue on reaction with fluoride. The reason for this difference in behaviour was realized after spectral studies on the reaction in a homogeneous system. Figure 7 shows the spectra of the ternary complex in the presence of low (A) and high (B) aluminium concentrations. Comparison of these spectra with those of the cerium (C) and aluminium (D) chelates of Alizarin Complexone suggests that (i) a low concentration of aluminium removes the fluoride from the ternary complex, leaving behind the cerium chelate, (ii) a high concentration of aluminium displaces the cerium as well as the fluoride ion from the complex, yielding the aluminium chelate of Alizarin Complexone.

Consequently only very dilute solutions of aluminium ( $10^{-5}$ – $10^{-4}M$ ) should be used to regenerate the reagent phase. The regeneration takes approximately 1 hr (indicated by a constant reflectance response). The response of the regeneration reagent to fluoride was lower than that of fresh immobilized reagent phase, suggesting that either some of the cerium may have been replaced by aluminium or that some

leaching of the adsorbed phase occurred during the regeneration.

Desorption of the immobilized reagent phase was not observed during other parts of this investigation.

#### Reproducibility of immobilized reagent response

The reproducibility of the response from the immobilized cerium(III) chelate to  $0.53mM$  fluoride was studied with 11 samples from the same batch of beads; the relative standard deviation found was 10%.

Table 1. Effect of diverse ions

Foreign ion	Added as	Molarity	Error, %
Chloride	NaCl	0.530	+12
		0.053	0
Bromide	NaBr	0.530*	0
Iodide	NaI	0.530	+18
		0.053	0
Nitrate	NaNO <sub>3</sub>	0.530*	0
Sulphate	Na <sub>2</sub> SO <sub>4</sub>	0.530	-7
		0.053	0
		0.053	-72
Phosphate	Na <sub>3</sub> PO <sub>4</sub>	$5.3 \times 10^{-4}$	-28
		$5.3 \times 10^{-6}$	0
		0.530	+37
Chlorate	NaClO <sub>3</sub>	0.530	+37
		0.053	0
Aluminium	Al(NO <sub>3</sub> ) <sub>3</sub>	0.053	-57
		$5.3 \times 10^{-4}$	-23
		$5.3 \times 10^{-6}$	0
Barium	BaCl <sub>2</sub>	0.053*	0
Calcium	Ca(NO <sub>3</sub> ) <sub>2</sub>	0.053*	0
Iron(III)	Fe(NO <sub>3</sub> ) <sub>3</sub>	0.053	+48
		$5.3 \times 10^{-4}$	+12
		$5.3 \times 10^{-6}$	0
Magnesium	Mg(NO <sub>3</sub> ) <sub>2</sub>	0.053*	0

\*The effect of higher concentrations of these ions could not be determined because of problems associated with dissolving the salts in the buffer solution.

*Interference studies*

The ions examined were chosen on the basis of their occurrence with fluoride in natural waters. They were incorporated into the buffer system used in the preparation of a 0.53mM fluoride solution, at concentrations successively decreased by a factor of 10. The criterion for interference was an error greater than twice the standard deviation obtained in the absence of the foreign ion.<sup>26</sup> Table 1 shows the results obtained. Aluminium, iron and phosphate are the ions which interfere the most.

*Conclusions*

The method is applicable to the determination of fluoride in the range 0.16–0.95mM, with a relative standard deviation of approximately 10%. The response time is about 12 min. The reaction is pH-dependent and liable to interference from phosphate, iron and aluminium ions, which would need to be eliminated before the analysis. The sample would also need to be buffered to the optimum pH. The reagent phase can be regenerated by treatment with an aluminium solution of concentration not greater than  $10^{-4}M$ , but at the cost of reduced response and extended analysis time.

## REFERENCES

1. W. R. Seitz, *Anal. Chem.*, 1984, **56**, 16A.
2. R. Narayanaswamy, *Anal. Proc.*, 1985, **22**, 204.
3. J. I. Peterson, S. R. Goldstein, R. F. Fitzgerald and D. K. Buckhold, *Anal. Chem.*, 1980, **52**, 864.
4. G. F. Kirkbright, R. Narayanaswamy and N. A. Welti, *Analyst*, 1984, **109**, 1025.
5. L. A. Saari and W. R. Seitz, *Anal. Chem.*, 1982, **54**, 821.
6. Z. Zhujun and W. R. Seitz, *Anal. Chim. Acta*, 1984, **160**, 47.
7. R. Narayanaswamy and F. Sevilla III, *Int. J. Optical Sensors*, 1986, **1**, 403.
8. A. Martínez, M. C. Moreno and C. Cámara, *Anal. Chem.*, 1986, **58**, 1877.
9. L. A. Saari and W. R. Seitz, *ibid.*, 1983, **55**, 667.
10. *Idem*, *Analyst*, 1984, **109**, 655.
11. Z. Zhujun and W. R. Seitz, *Anal. Chim. Acta*, 1985, **171**, 251.
12. E. Urbano, H. Offenbacher and O. S. Wolfbeis, *Anal. Chem.*, 1984, **56**, 427.
13. R. Belcher, M. A. Leonard and T. S. West, *Talanta*, 1959, **2**, 92.
14. M. A. Leonard and T. S. West, *J. Chem. Soc.*, 1960, 4477.
15. R. Belcher and T. S. West, *Talanta*, 1961, **8**, 853.
16. S. S. Yamamura, M. A. Wade and J. H. Sikes, *Anal. Chem.*, 1962, **34**, 1308.
17. M. Hanocq and L. Molle, *Anal. Chim. Acta*, 1968, **40**, 13.
18. N. T. Crosby, A. L. Dennis and J. G. Stevens, *Analyst*, 1968, **93**, 643.
19. R. Narayanaswamy and F. Sevilla III, *ibid.*, 1986, **111**, 1085.
20. H. L. Greenhaus, A. M. Feibush and L. Gordon, *Anal. Chem.*, 1957, **29**, 1531.
21. P. Kubelka and F. Munk, *Z. Tech. Phys.*, 1931, **12**, 593.
22. F. J. Langmyhr, K. S. Klausen and M. H. Nouri-Nekoui, *Anal. Chim. Acta*, 1971, **57**, 341.
23. R. Belcher and T. S. West, *Talanta*, 1961, **8**, 863.
24. P. Larson, E. Murgia, T. J. Hsu and H. F. Walton, *Anal. Chem.*, 1973, **45**, 2306.
25. R. Narayanaswamy and F. Sevilla III, *Anal. Chim. Acta*, 1986, **189**, 365.
26. G. F. Kirkbright, *Talanta*, 1966, **13**, 1.

## OPTICAL AND FIBRE-OPTIC SENSORS FOR VAPOURS OF POLAR SOLVENTS

HERMANN E. POSCH and OTTO S. WOLFBEIS

Analytical Division, Institute of Organic Chemistry, Karl-Franzens-University, A-8010 Graz, Austria

JOHANNES PUSTERHOFER

AVL-Ges.m.b.H., Postfach 15, A-8011 Graz, Austria

(Received 20 May 1987. Accepted 18 September 1987)

**Summary**—An optical sensor is described which continuously measures the concentration of vapours of polar organic solvents such as alcohols, ethers, esters and ketones, but does not respond to hydrocarbons and chlorinated hydrocarbons. The detection is based on reversible decolorization of the blue thermal printer paper used in graphic plotters. Two sensing principles are exploited. In the first, a sensor sheet is placed in a flow-through cell. An LED acts as a source of yellow light and a phototransistor measures the light transmitted. In the second, the sensing membrane is placed at the end of a bifurcated fibre-optic and its diffuse reflectance is measured. The sensitivity of the devices towards various kinds of vapours has been studied and the detection limits vary from 10 to 1000 ppm for some of the most common technical solvents.

The development of optical and fibre-optic sensors is at present one of the fastest growing research areas in analytical chemistry. This is mainly due to the advantages of fibre-optic sensors, which include small size, freedom from electrical interference, and remote-sensing capabilities. The state of the art has been discussed in several useful reviews.<sup>1-8</sup>

Following the development of sensors for oxygen,<sup>9</sup> halides,<sup>10</sup> halothane and/or oxygen,<sup>11</sup> pH,<sup>12</sup> ionic strength,<sup>13</sup> ammonia,<sup>14</sup> electrolytes,<sup>15</sup> hydrogen peroxide<sup>16</sup> and enzyme activities<sup>17</sup> we present here a sensor capable of continuous monitoring of vapours which may be toxic or form mixtures with air.

We have taken advantage of the observation that thermal printer paper (of the types used in plotters and printers) assumes a blue or almost black colour when immersed in liquid organic polar solvents or their vapours. The resulting blue paper is then reversibly decolorized by vapours of the same solvents. This led to the design and construction of the sensor described below.

### EXPERIMENTAL

#### Solvents and vapours

All solvents used in this work were freshly distilled. Vapour mixtures were prepared by bubbling air through the solvent. Except for n-butanol, the vapour pressure of the solvent ( $p$ ) as a function of absolute temperature ( $T$ ) was calculated according to equation (1), which is a simplified version of equation (2):

$$\log p = -A/T + B \quad (1)$$

Values of  $A$  and  $B$  were taken from a handbook,<sup>18</sup> for methanol ( $A = 1984$ ,  $B = 8.740$ ), ethanol (2457, 9.543), toluene (2866, 27.647), diethyl ether (1546, 7.909), tetra-

hydrofuran (1644, 7.721), dioxan (1890, 7.930), acetone (1687, 8.005), ethyl acetate (1962, 8.556). The vapour pressure of n-butanol must be calculated by using equation (2):

$$\log p = -A/T + B + C(\log T) \quad (2)$$

because the additional term  $C(\log T)$  is not negligible in this case.<sup>18</sup> The values of  $A$ ,  $B$  and  $C$  are 4100, 40.211 and  $-10.35$  respectively for n-butanol.

#### Sensing membranes

The following commercially available thermal printer papers were tested for their utility in vapour sensing: Hewlett-Packard printer papers Nos. 9270-0479, 5580-8735 and 9270-0962, for use in the HP printer models 9815, 3380 and 85, respectively; Perkin Elmer Lambda 5 spectrophotometer printer papers (Part Nos. 119849 and BO 126708); Kontron Anacomp integrator type 220 printer paper (Chart No. TO 2227).

#### Construction of the flow-through cell

A schematic top view of the flow-through cell is shown in Fig. 1. It consists of an aluminium block with a hole along the axis for the gas-flow, and two holes at right angles for mounting the LED (6) and phototransistor (2). The mounting for the LED is removable to allow quick and easy change of the sensing membranes. To protect the phototransistor from ambient light, the gas-supply tubes are bent helically and the rear of the LED is covered with black "Plexiglas". The opto-electronic parts are listed in Table 1.

#### Fibre-optic vapour sensor

In the fibre-optic approach, light of wavelength 580 nm from a 250 W tungsten halogen lamp (incorporated in an Aminco SPF 500 spectrofluorimeter) is focused onto one end of a bifurcated optical fibre (150 cm long and 4 mm in internal diameter at the common end) made from poly(methyl methacrylate) with statistically mixed bundles (Faseroptik Henning, D-8501 Allersburg, FRG). The common end of the two arms is covered with the sensing material. Reflected light returns through the second arm of the optical fibre and is guided to the photomultiplier tube (PMT) of the fluorimeter. The change in the reflectance of the sensing



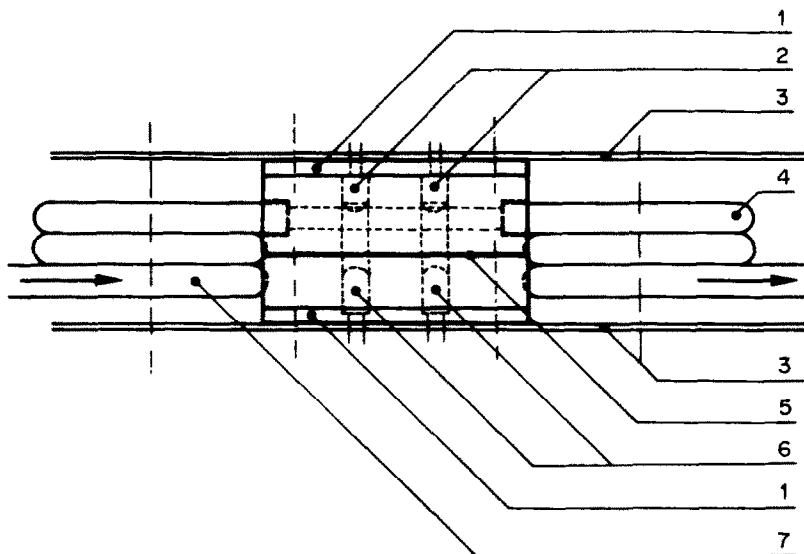


Fig. 1. Top view of the flow-through cell. (1) Light-proof cover; (2) phototransistors; (3) printed electronic circuit; (4) gas outlet coils (optically isolated); (5) sensor membranes (one white and one blue); (6) LEDs; (7) gas inlet coil (optically isolated).

membrane after exposure to various levels of vapours is detected by the PMT, the output from which is plotted on an *X/Y* recorder (HP 7525A).

## RESULTS

### *Construction of the detector cell*

The optical system of the flow-through cell (Fig. 1) consists of two LEDs fixed in an aluminium block; one is covered with the blue sensing-membrane and the other (the reference) with white paper possessing transmission characteristics similar to those of the untreated printer paper. Two phototransistors on the other side of the flow-through cell measure the light intensity transmitted by the two layers of paper. The two optical systems (LEDs and phototransistors) are optically isolated, so that no mutual interference is possible. The current produced by the two photodetectors is amplified and displayed on a FLUKE

multimeter 27 or recorded on a plotter. The electronic circuit of the detection system is outlined in Fig. 2.

### *Sensing membranes*

Thermal papers from various sources were immersed in an atmosphere of ether for a period of at least 5 min to produce a blue or almost black colour. The absorption spectra of the blue papers are similar, with maxima between 605 and 610 nm. The black thermal papers have similar maxima but with an additional weaker band at around 470 nm. Consequently, an LED with an emission maximum at around 580 nm was considered a suitable light-source. At this wavelength, all the papers investigated have an absorbance that is approximately 95% of that at the wavelength of maximum absorption.

When the blue papers thus produced are exposed to vapours of polar solvents the colour intensity is diminished. Table 2 summarizes the changes in the

Table 1. List of parts used in construction of the vapour sensor\*

Part	Specification	Part	Specification	Part	Specification
IC1	LM 317T	R1	1 k $\Omega$	P1	200 $\Omega$
IC2	LF 351	R2	330 $\Omega$	P2	200 $\Omega$
IC3	LF 351	R3	195 $\Omega$	P3	10 k $\Omega$
IC4	LF 351	R4	195 $\Omega$	P4	10 k $\Omega$
IC5	LF 351	R5	100 k $\Omega$	P5	10 k $\Omega$
IC6	LF 351	R6	100 k $\Omega$		
		R7	27 k $\Omega$	T1	BF 246
C1	0.22 $\mu$ F Ta	R8	3.01 k $\Omega$	T2	BF 246
C2	2 $\times$ 47 $\mu$ F Ta	R9	27 k $\Omega$	T3	BPW 14B
C3	10 $\mu$ F Ta	R10	3.01 k $\Omega$	T4	BPW 14B
C4	10 $\mu$ F Ta	R11	1 k $\Omega$		
		R12	1 k $\Omega$		
		R13	1 k $\Omega$		
		R14	1 k $\Omega$		
		R15	100 k $\Omega$		

\*Data correspond to the components given in Fig. 2.

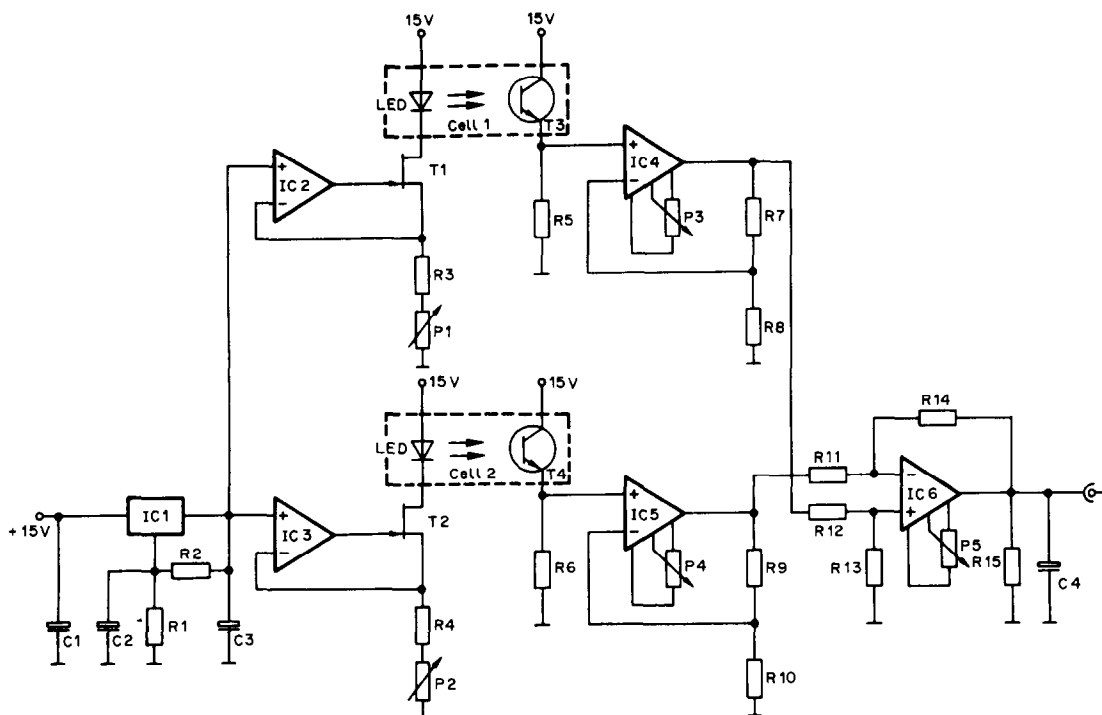


Fig. 2. Electronic circuit of the temperature-compensated flow-through cell.

optical signal obtained with various papers exposed to acetone-saturated air (21% acetone, v/v at 18°).

#### Electronic circuit

Figure 2 shows the circuit of the temperature-compensated sensor. Independent current sources were produced by using a resistance-programmable voltage regulator serving as a voltage reference, and two operational amplifiers (op-amps) combined with appropriate field-effect transistors. By tuning of P1 and P2, the current can be adjusted to between 12.5 and 25 mA.

The reference cell contains a strip of white paper, the transmission of which is not affected by the

vapour of polar solvents. The sample cell contains the blue sensor strip, the colour of which changes in accordance with the gas composition. The voltage-follower stages, consisting of two sensitive phototransistors, give two signals at the emitter resistances R5 and R6, and these are amplified by IC4 and IC5. The output signal of op-amp IC6 is proportional to the difference in measured light transmission of the reference and sample cells. The lower the vapour concentration in the sample cell, the lower will be the output signal obtained from the electronic circuit. This signal can even be negative if the decolorized sensor strip has a higher transmission than the reference strip. This can be compensated for by zero adjustment.

Table 2. Colour, absorbances, and signal changes of various thermal printer papers after exposure to acetone-saturated air at 18°, corresponding to 21% (v/v) acetone in air

Thermal printing paper	Colour	Signal change, mV	$\log I_0/I$ at absorption max*
HP, 9815 Part No. 9270-0479	blue	980	1.99
HP, 3380 Part No. 5580-8735		1100	1.52
HP, 85 Part No. 9270-0962	blue	940	1.51
Perkin Elmer, Lambda 5 Part No. 119 849	blue	760	1.10
Kontron, Anacomp 220 CHART No. TO 2227	black	690	1.39
Perkin Elmer, Lambda 5 Part No. BO 126 708	black	640	1.14

\*White paper was used in the reference beam.

Table 3. Signal changes ( $\Delta V$ ) of the Hewlett-Packard 8388 thermal printer paper on exposure to vapours of technical solvents

Solvent	Concentration,		$\Delta V, mV$	$\Delta V \cdot \%^{-1}, * mV$
	% v/v			
dichloromethane	49.6		540 (irrev.)	—
chloroform	21.1		55	2.6
tetrachloromethane	12.6		24	1.9
cyclohexane	10.1		0	0
toluene	2.8		0	0
diethyl ether	50.7		949	28.7
tetrahydrofuran	18.7		1227	65.6
dioxan	4.2		1233	294
methanol	12.4		450	36.3
ethanol	5.7		680	119
n-butanol	0.68		748	1153
acetone	21.0		1100	52.4
ethyl acetate	9.4		1060	113

\*Change in absorbance per % solvent in air.

Because of the use of a reference cell and two identical phototransistors, a very stable and temperature-independent signal is obtained. Even small changes (usually a decrease) in the light intensity of the LED, shortly after switching on, are compensated by this technique. The maximum signal drift over 48 hr was  $\pm 1.5$  mV which is negligible with respect to a total signal change of over 1000 mV (for instance with tetrahydrofuran).

#### Sensor response

The paper found to have the best response was the HP 3380 thermal printer paper (Table 2). It displays

an almost complete and reversible decolorization after exposure to vapours of polar solvents. The degree of decolorization is dependent on the nature of the solvent and is highest for alcohols, esters and ethers, when expressed as signal change per % solvent in air. Hydrocarbons and chlorinated hydrocarbons are either without effect or, as in the case of dichloromethane, give irreversible bleaching. The data obtained with 13 frequently employed solvents are collected in Table 3. Contrary to our expectations, the anaesthetic gases Forane and Ethrane (which are ethers) do not affect the colour of the membranes. It was also found that an increase in temperature leads

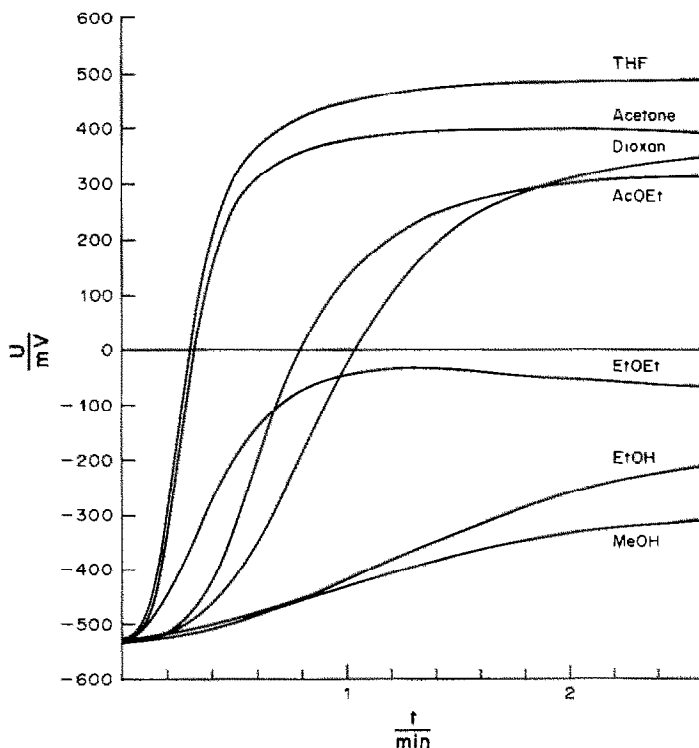


Fig. 3. Change of signal with time, obtained for air saturated with vapours of various solvents, at 18°. THF, tetrahydrofuran; AcOEt, ethyl acetate; EtOEt, diethyl ether; EtOH, ethanol; MeOH, methanol.

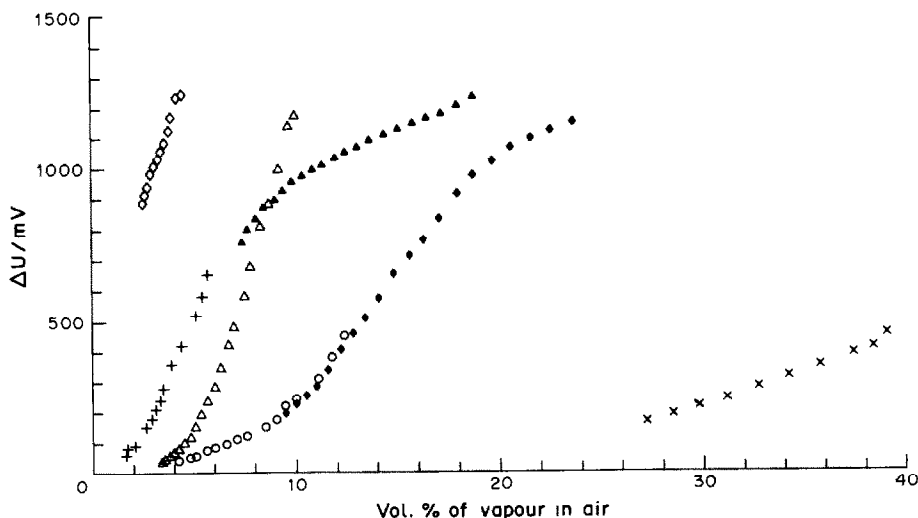


Fig. 4. Dependence of phototransistor signal on vapour concentration of several frequently used solvents. (◆) acetone, (×) diethyl ether, (▲) tetrahydrofuran, (◇) dioxan, (△) ethyl acetate, (+) ethanol, (○) methanol. The vapour-air mixtures were prepared by bubbling air through liquid solvent reservoirs at a defined temperature. The initial values were obtained at 0°, the final values at 20°.

to decolorization, the process being irreversible at above 60°.

The response time depends on the nature of the solvent and the sample flow-rate. Figure 3 shows the change in signal obtained as the sensor is exposed to solvent-saturated air at a flow-rate of 60 ml/min. The response to vapours of aprotic solvents is more rapid than that to alcohols (which itself is quick enough to be of practical utility in process control). Typical response times (99% of final signal) are 30 sec for acetone and 3–4 min for methanol. Interestingly, after passage of pure air again, the initial value is reached only after a much longer time (acetone *ca.* 2 min, methanol *ca.* 7 min). Thus, the recovery time can range from 1 min (for diethyl ether) to 7 min (for methanol). The response and recovery times both depend slightly on the vapour concentration, but this was not studied in detail.

The relation between vapour concentration in the sample and relative signal change is shown in Fig. 4 for various vapour-air mixtures. There are large differences in response, despite the similarities in the chemical structure of the solvents.

#### Sensitivity

Given a signal resolution of 1 mV, the sensor is capable of indicating ppm amounts of solvent vapours in air. Typical detection limits are 10 ppm for *n*-butanol, 250 ppm for ethanol, 1000 ppm for diethyl ether and 30 ppm for dioxan.

#### Fibre-optic approach

The change in the diffuse reflectance of the blue membrane was measured by attaching the paper membrane to the distal end of a fibre. The relative signal change per % of organic vapour in the air stream was, however, only half that obtained with the

optical sensor cell, where transmission intensity was measured. Consequently, the resolution of the fibre-optic sensor is somewhat poorer than that of the conventional opto-sensor. The fibre-optic arrangement was found to have no drift problems, although no reference cell was used, the initial value always being restored.

Response and recovery times were about half those for the measurements made in the transmission mode, although an almost identical flow-through cell was employed and the detection limits were almost the same.

#### DISCUSSION

The sensor described here measures concentrations of solvent vapours in air from the ppm level up to saturation. It is therefore of potential utility in process control and related fields. Its response depends on the nature of the solvent. Long-chain alcohols are more efficient colour "quencher" than are short-chain alcohols. Ethers and ethyl acetate are comparable in their response, but chlorinated hydrocarbons are without effect (or lead to irreversible decolorization). The lack of response of some anaesthetic gases frustrated our initial objective, which was to develop a sensor for these gases.

To the best of our knowledge, the colour-forming capability of thermal printer papers is based on the colour change of micro-encapsulated carboxylic acid dyes, such as Crystal Violet, in their (colourless) lactone form. When released by thermal action, they assume the blue colour of the triphenylmethane dye. The equilibrium between dye and colourless lactone is known to be dependent on the polarity of the solvent. No attempts have been made to improve the material with respect to dye and solid support.

Although a number of tests are available for

detection and determination of hazardous or toxic gases, and a number of test kits are marketed by various companies, we think that our vapour sensor offers two decisive advantages. It allows continuous measurement of vapour concentration and it can be applied to a number of solvent vapours.

The sensors introduced here demonstrate the advantages of opto-sensors. The fibre-optic method has considerable advantages in the detection of vapours since fibres have no electrical links and therefore do not present a risk in a potentially explosive atmosphere. Since the transmission of optical signals *via* fibres is possible over large distances, the instrument can remain in the benign atmosphere of the laboratory, while the sensor head can be exposed without risk to the environment to be probed.

#### REFERENCES

1. T. Giallorenzi, J. A. Bucarro, A. Dandridge, G. H. Sigel, J. H. Cole, S. C. Rashleigh and R. G. Priest, *IEEE J. Quantum. Electron.*, 1982, **QE-18**, 626.
2. T. Hirschfeld, T. Deaton, F. Milanovich and S. Klainer, *Opt. Eng.*, 1983, **22**, 527.
3. D. W. Lübbers and N. Opitz, *Sens. Actuators*, 1984, **4**, 641.
4. J. I. Peterson and G. G. Vurek, *Science*, 1984, **224**, 123.
5. T. Hirschfeld, J. B. Callis and R. B. Kowalski, *ibid.*, 1984, **226**, 312.
6. O. S. Wolfbeis, *Trends Anal. Chem.*, 1985, **4**, 184.
7. W. R. Seitz, *Anal. Chem.*, 1984, **56**, 16A.
8. J. F. Place, R. M. Sutherland and C. Dähne, *Biosensors*, 1985, **1**, 321.
9. O. S. Wolfbeis, H. Offenbacher, H. Kroneis and H. Marsoner, *Mikrochim. Acta*, 1984 **1**, 153.
10. E. Urbano, H. Offenbacher and O. S. Wolfbeis, *Anal. Chem.*, 1984, **56**, 427.
11. O. S. Wolfbeis, H. E. Posch and H. Kroneis, *ibid.*, 1985, **57**, 2556.
12. H. Offenbacher, O. S. Wolfbeis and E. Furlinger, *Sens. Actuators*, 1986, **9**, 73.
13. O. S. Wolfbeis and H. Offenbacher, *ibid.*, 1986, **9**, 85.
14. O. S. Wolfbeis and H. Posch, *Anal. Chim. Acta*, 1986, **185**, 321.
15. O. S. Wolfbeis and P. Hochmuth, *Eur. Pat.* 198,815 (22.10.1986).
16. H. E. Posch, M. J. P. Leiner and O. S. Wolfbeis, *Ind. Intl. Symp. on Quant. Luminescence Spectrometry in Biomed. Sci.*, Ghent (Belgium), 11–14 May 1987.
17. O. S. Wolfbeis, *Anal. Chem.*, 1986, **58**, 2874.
18. Landolt-Börnstein, *Zahlenwerte und Funktionen*, Part 2a, p. 89ff. Springer Verlag, Berlin, 1960.

## MULTI-ELEMENT OPTICAL WAVEGUIDE SENSOR: GENERAL CONCEPT AND DESIGN

RICHARD R. SMARDZEWSKI

Analytical Division, Research Directorate, U.S. Army Chemical Research, Development and Engineering Center, Aberdeen Proving Ground, MD 21010-5423, U.S.A.

(Received 20 May 1987. Accepted 26 August 1987)

**Summary**—A prototype of a self-contained multi-element optical waveguide sensor for detection and identification of the constituents of gaseous or liquid mixtures has been fabricated. The device consists of eight optical waveguides, each coated with a thin film known to react specifically with one or more components in a multicomponent system. An array of eight sequentially-activated light-emitting diodes is attached to the waveguide assembly in such a fashion as to activate each detection channel separately. Each waveguide is a fiber-optic coupled to a single high-gain, low-noise photomultiplier tube or photodiode/operational amplifier detector. The amplified signals can be displayed visually or input to a microprocessor pattern-recognition algorithm. CMOS analog switches/multiplexers are used in feedback loops to control automatic gain-ranging, light-level adjustment and channel-sequencing. Preliminary experiments involving the monitoring of redox/pH changes are discussed.

Colorimetric and fluorimetric coatings for detection and identification of gaseous species have been used for over 100 years, one of the earliest being the cobalt(II) chloride moisture test.<sup>1</sup> A general review of the literature up to 1966 is available in Ruch's annotated bibliography.<sup>2</sup> A more quantitative discussion of the various tests (without references) can also be found in the Dräger detector tube handbook.<sup>3</sup> Generally speaking, the analyte of interest reacts with a particular organic dye to produce a visible color change, which can be monitored by absorption, transmission or fluorescence measurement. High sensitivity and specificity are the desired objectives but compromises always have to be made.

The advent of optical fibres soon saw their application as "light pipes" in conventional oxygen determination (measurement of oxyhemoglobin),<sup>4</sup> dye dilution measurements,<sup>5</sup> laser-Doppler velocity measurement,<sup>6</sup> fluorimetry,<sup>7</sup> and physical sensors.<sup>8-10</sup> The recent use of fiber-optic waveguides for chemical analyses is based, for the most part, on light-intensity changes in an indicator material immobilized at or near the "business-end" of the fiber. Single, dual, multiple, bifurcated and trifurcated optical fibers are used to carry probe-photons to and information-containing photons from the analyte-probe interface. Reviews by Seitz<sup>11</sup> and Peterson *et al.*<sup>12</sup> have summarized the state of the art to 1984, the latter focusing more on biomedical applications while the former deals primarily with chemical sensors. Two additional reviews of chemical microsensors in general (optical waveguides being one type) are those by Wohltjen<sup>13</sup> and Hirschfeld *et al.*<sup>14</sup>

Table 1 lists examples of species which have been spectroscopically monitored by means of their interaction with a reagent phase immobilized on an optical waveguide.

The basic principle of the optical waveguide sensor is chemically-selective induction of a refractive index change at the waveguide/thin detector-layer interface which effectively increases or decreases the evanescent wave coupling into the external medium.<sup>29</sup> This change is monitored as an increase/decrease in waveguide transmittance. Ease of miniaturization, portability, low cost and low power requirements are the driving forces behind the development of this particular type of chemical sensor. Recent reports<sup>20,30</sup> have demonstrated its potential for detection of certain vapors at ppm levels.

### Waveguide assembly

In an extension of this principle, a prototype of a self-contained multi-element optical waveguide sensor for detection and identification of the components of gas or fluid mixtures has been fabricated. The device consists of eight optical waveguides, each comprised of a 9-cm length of thin-walled (0.3 mm) cylindrical glass capillary tube (0.8 mm bore), sealed at one end. All eight waveguides are fitted into a gasketed sampling chamber of low dead-volume. An array of eight sequentially-activated light-sources (LEDs) is attached to the waveguide assembly in such a fashion as to activate each detection channel separately. Thin chemically-selective coatings are applied to the exterior surface of each waveguide. In certain cases, organized molecular assemblies are deposited in stepwise fashion by successive Langmuir-Blodgett (LB) dip cycles. Silane-coupling agents are used in other cases, where a chemically-selective film is immobilized on the glass surface. All the coatings used at present rely on a color change caused by selective adsorption and/or reaction, and this is monitored by miniature 0.5-in. outer diameter end-on photomultiplier tubes or solid-state silicon diodes operating

Table 1

Analyte	Reagent phase	Monitored optical change	Reference
pH	Phenol Red/polyacrylamide	Reflectance (reversible)	15
pH	Fluoresceinamine/cellulose	Fluorescence (reversible)	16
CO <sub>2</sub>	pH dye/CO <sub>2</sub> -permeable membrane	Fluorescence	17
Moisture	CoCl <sub>2</sub> /gelatin	ATR/transmission	18
Oil in water	Organophilic coating	ATR/transmission	19
NH <sub>3</sub>	Oxazine dye	ATR/transmission	20
Al <sup>3+</sup> , Mg <sup>2+</sup> , Zn <sup>2+</sup>	8-Quinolinol-5-sulfonate	Fluorescence	21
Halothane	Decacyclene/silicone	Fluorescence quenching	22
Bilirubin	None	Absorbance	23
IgG	IgG-Ab	Fluoroimmunoassay	24, 25
O <sub>2</sub>	Hemoglobin	Reflectance	26
Halide ion	Quinoline indicators	Fluorescence quenching	27
<i>p</i> -Nitrophenyl phosphate	Enzyme (phosphatase)	Product absorbance	28

in either the photoconductive or photovoltaic mode to measure the light intensity transmitted from the appropriate LED.

#### Electro-optic configuration

As outlined in Fig. 1, two general detection approaches were taken (single and multiple detectors). In this report, however, only the single-detector version is discussed.

The electronic configuration for each channel is depicted in Fig. 2. The current to each individual LED is controlled by a discrete pulse transistor

(2N222) driven by an appropriate TTL pulse from a single-board computer (SBC). Optical-fiber bundles are used to couple the individual waveguide outputs to a single photodetector. Separate potentiometers are used to adjust the brightness of each LED, to suit individual reaction, channel and detector characteristics. Visible-radiation LEDs are used, two each for the red, green and yellow, and one each for the orange and blue regions of the spectrum. Except for the blue-emitting type (Siemens LBD 5410), they are of the standard GaP, GaAsP variety (Pacom Electronics, L-32 types). The photometric outputs vary with the particular type of LED, in the general range

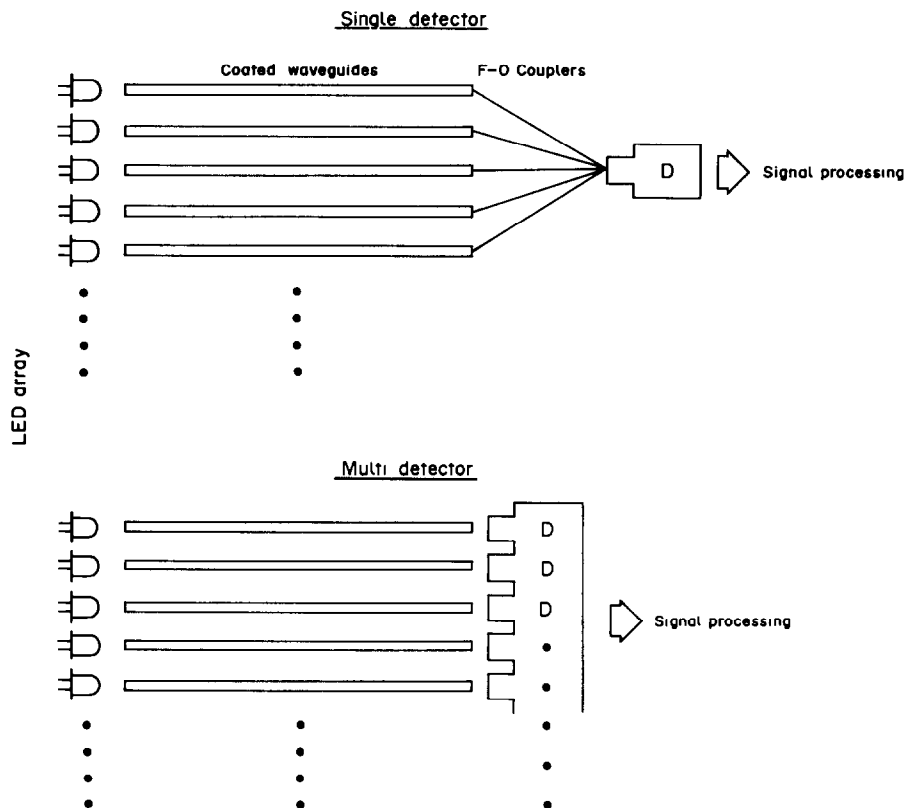


Fig. 1. Multi-element detection strategies.

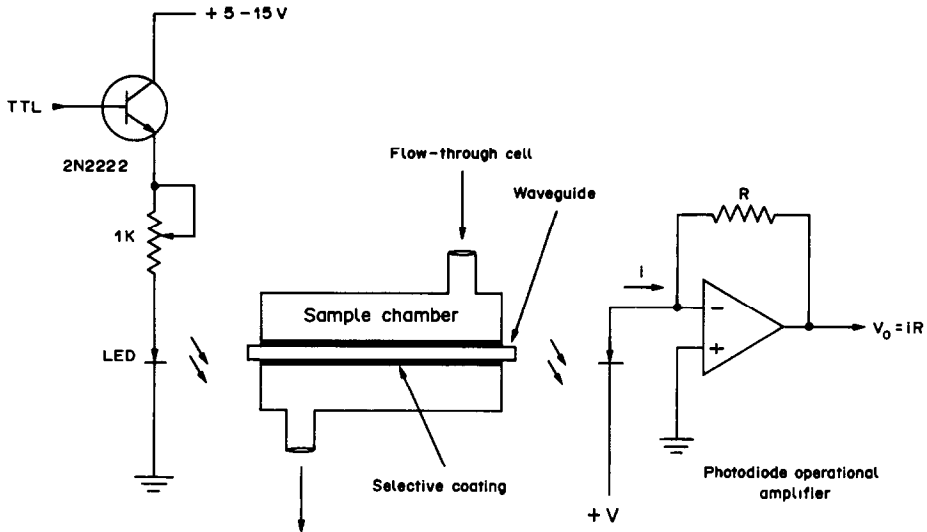


Fig. 2. Electro-optic configuration of a single channel.

2-12 mcd. The bandwidths (FWHM) are about 32 nm (green), 46 nm (yellow, orange), 25 nm (red) and 70 nm (blue).

The drive transistors and the digitized (12-bit) detector output are connected to a 6522 NMOS interface adaptor situated in a 6502-driven AIM-65 microcomputer (Fig. 3).

An assembly-language algorithm (shown as a flow-sheet in Fig. 4) is used to activate the individual channels for selected on/off times and acquire and store the digitized detector outputs for subsequent

processing. In the configuration used, the minimum on-times for LED output stabilization are about 1-2 msec. In a typical data-cycle, a single LED is activated and, after a suitable delay period, the amplified detector output is digitized and stored in memory. Shortly thereafter, the LED is deactivated and the remaining channels similarly examined.

Attempts were made to pulse the LEDs at a faster rate. However, as indicated in Fig. 5, reasonable square-wave outputs were achieved only with switching times longer than *ca.* 1 msec. This is most likely

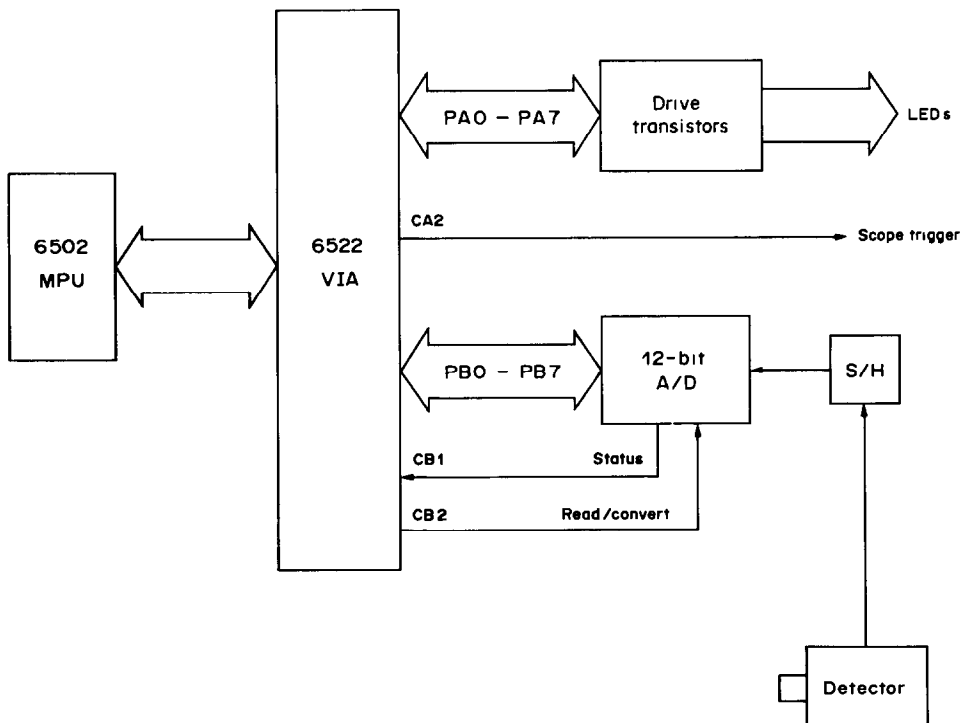


Fig. 3. Microcomputer interface.



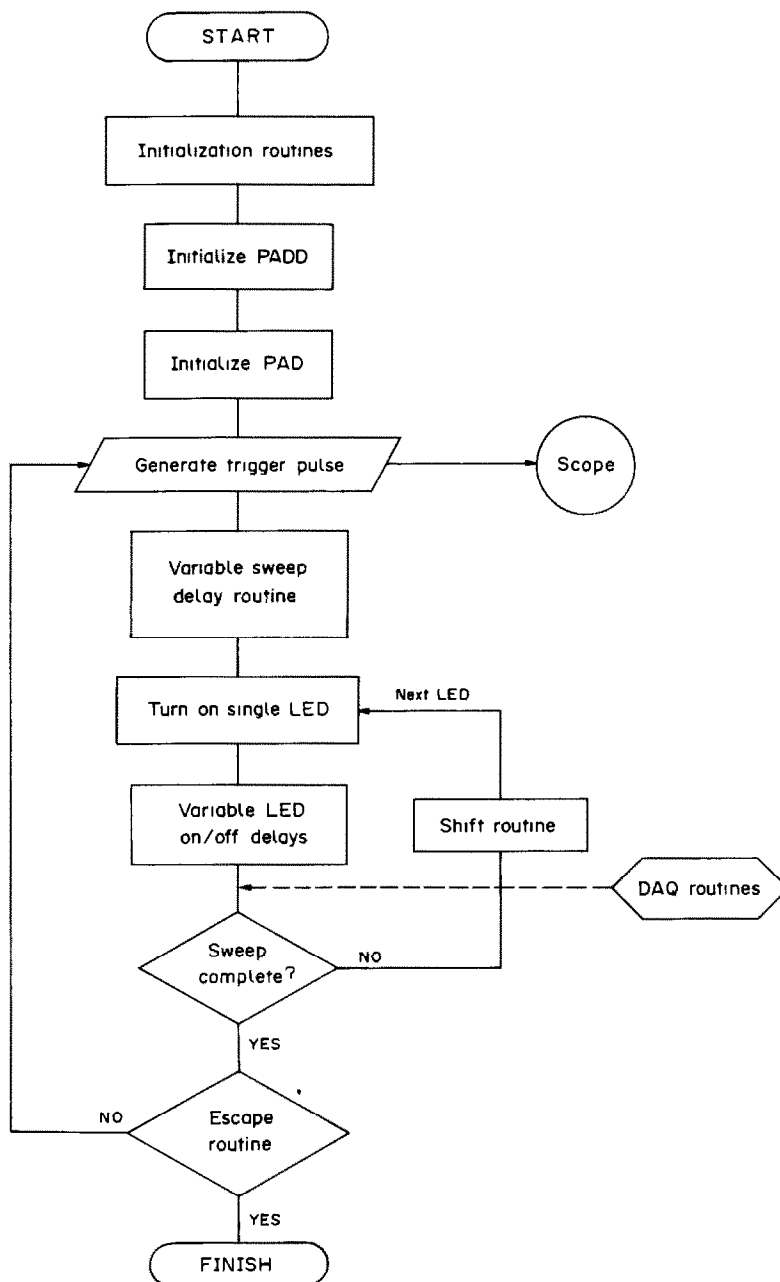


Fig. 4. Flow-sheet for data acquisition and LED control. PAD = Port A data register; PADD = Port A data direction register; DAQ = data acquisition routines.

a consequence of  $RC$  time-constant limitations in the LED/current-limiting resistor combinations.

#### Display of signals from the various channels

For display purposes, the signals from the various channels were output to an analog oscilloscope to produce a bar-graph pattern, the individual bar heights being proportional to the detector output for the corresponding channel. This is illustrated in Fig. 6 for the 8-channel waveguide. Here, the optical waveguide in channel 3 (channels labeled from left to right) was coated with a 50-nm thick film of a

silane-coupled benzyl viologen dye derivative which served as a redox indicator. The particular derivative used was  $N,N'$ -bis( $p$ -trimethoxysilyl)benzyl)-4,4'-bipyridinium dichloride (or BPQ<sup>2+</sup>),<sup>31,32</sup> which was known from earlier studies<sup>33</sup> to undergo a reversible color change in the presence of a reducing agent (see Fig. 7). It was covalently linked to the glass optical waveguide by soaking the waveguide for several days in a 10% water/acetonitrile solution containing several milligrams of the dye derivative. Surplus dye and the solvent were removed by flushing with water. The final coatings were observed to be extremely

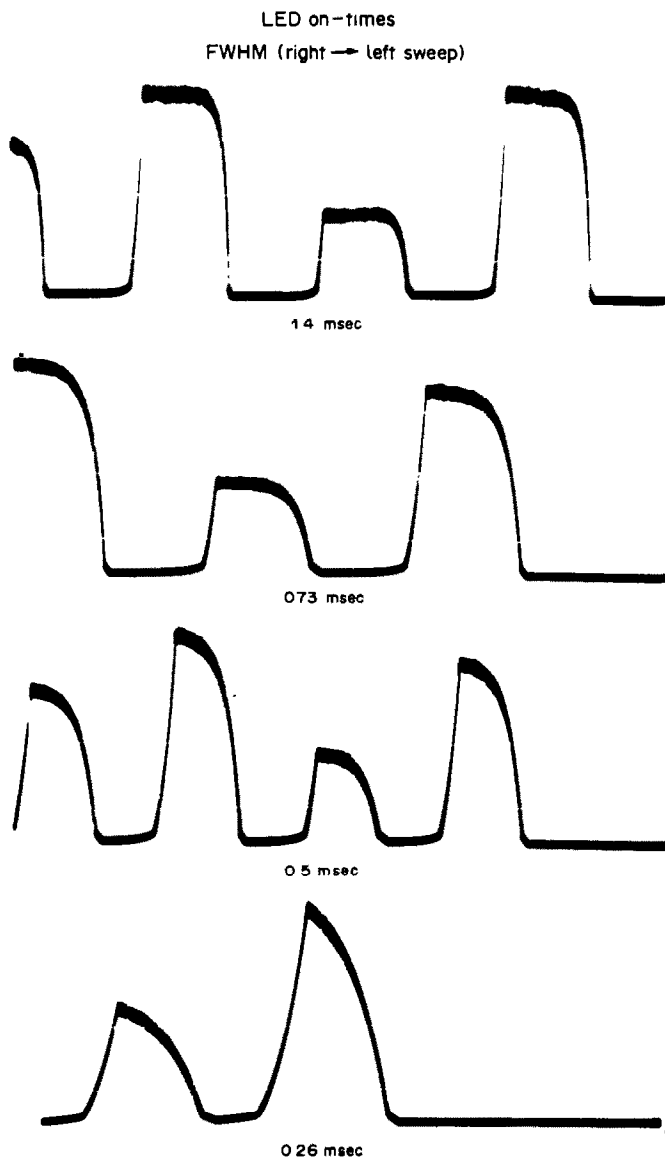


Fig. 5. Optical output (PMT-response) of pulsed LEDs. FWHM (right-to-left sweeps).

durable and maintained their effectiveness even after months of exposure to ambient air. Upon exposure of the 8-channel waveguide to a reducing solution (70 mg/l.  $\text{Na}_2\text{S}_2\text{O}_4$ ), the colorless viologen film became blue.

The light-beam from the red-emitting LED in channel 3 was thereby attenuated as depicted in Fig. 6 (middle trace). The corresponding waveguide in channel 6 was coated with an insoluble pH-sensing dye film, some  $\mu\text{m}$  thick. The active ingredient, Alizarin Yellow, undergoes a yellow  $\rightarrow$  red transition at pH 10–12. This can be seen in Fig. 6 (bottom trace), for the response when the reducing solution has been purged and replaced by a basic (pH > 10) aqueous solution. The light from a green-emitting LED in channel 6 is attenuated, while the light-

intensity in channel 3 resumes its original value as a consequence of the oxidation, by dissolved oxygen, of the viologen coating on optical waveguide 3, to the colorless form. The response time for pH was 0.5 sec.

#### CONCLUSIONS

Multi-element optical waveguide sensors are relatively simple devices which can ultimately be used as small, portable chemical detectors/identifiers in a gas or fluid environment. The diagnostic scheme demonstrated here relies on a colorimetric change in the coatings immobilized on the waveguides. Other systems which hold promise for development as chemical microsensors include:

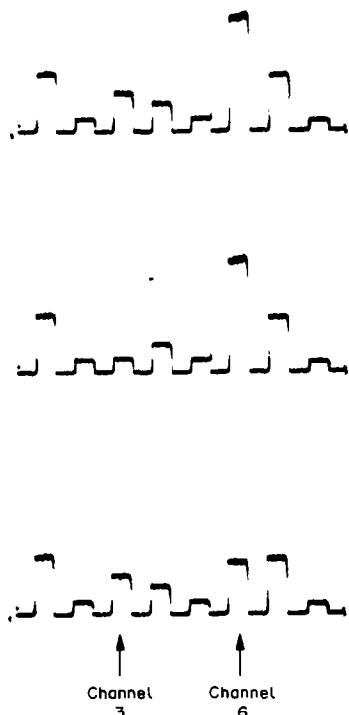


Fig. 6. Response of an 8-element optical waveguide to neutral (top), reducing (middle) and basic (bottom) solutions.

#### Immobilized fluorophore/dynamic chemiluminescence<sup>34</sup>

#### Grating couplers<sup>35</sup>

#### Fluorescent excitation transfer immunoassay<sup>36</sup>

#### Reflectometry<sup>37</sup>

#### Indium slide immunoassay<sup>38</sup>

#### Chemically-induced physical effects<sup>39</sup>

In addition to use of different detection techniques, future adaptations may employ advanced waveguide geometries (integrated optics). The recent advances in optical computing<sup>40</sup> may well drive researchers in this

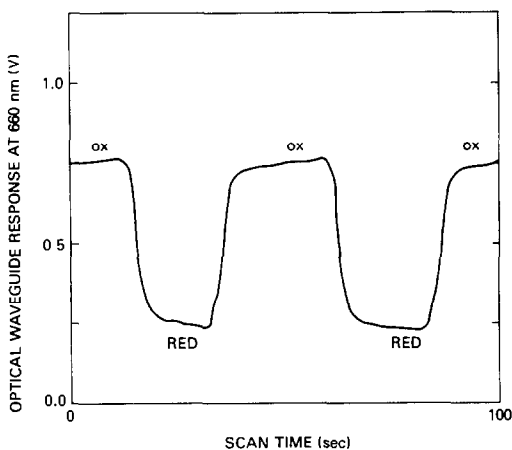


Fig. 7. Throughput (at 660 nm) of a single optical waveguide coated with silane-coupled BPQ<sup>2+</sup> and periodically exposed to a sodium dithionite reducing solution (70 mg/l).

direction. In any case, it is not an overstatement to say that there exists a variety of imaginative approaches to the "hardware" design and fabrication of optical chemical microsensors. Their chief limitation, however, appears to reside in their "software", *i.e.*, the chemically sensitive and selective reagent coatings. For the most part, traditional colorimetric/fluorimetric assays have been employed in the majority of the current generation of optical devices, which brings us to where we are today. As in most, if not all chemical sensors, the Achilles heel is the chemically sensitive/selective coating. Depending on the number of different sensing elements used, the selectivity problem can be solved. What remains to be developed is the extension of sensitivity to the sub-ppm region.

**Acknowledgements**—The author is grateful to Dr. Anna Johnson-Winegar, U.S. Army Medical Research and Development Command for support of this work and to Mr. John F. Giuliani of the Naval Research Laboratory for many helpful discussions. Special thanks are also accorded to Dr. William R. Barger of the Naval Research Laboratory for immobilizing the viologen coatings on the waveguide and to Professor Mark Wrighton of the Massachusetts Institute of Technology for supplying the silaned derivatives.

#### REFERENCES

1. C. Winkler, *J. Prakt. Chem.*, 1864, **91**, 209.
2. *Chemical Detection of Gaseous Pollutants*, W. E. Ruch (ed.), Ann Arbor Publishers, Ann Arbor, MI, 1966.
3. *Detector Tube Handbook*, 4th Ed., Drägerwerk AG, Lubeck, FRG, 1979.
4. C. C. Johnson, *Biomed. Sci. Instrum.*, 1974, **10**, 45.
5. M. L. Polanyi and R. M. Hehir, *Rev. Sci. Instrum.*, 1962, **33**, 1050.
6. H. Nishihara, J. Kiyama, N. Hoki, F. Kajiya, M. Hironaga and M. Kano, *Appl. Opt.*, 1982, **21**, 1785.
7. A. Mayevsky and B. Chance, *Science*, **217**, 537, 1982.
8. D. A. Krohn, *Adv. Instrum.*, 1983, **38**, 877.
9. K. H. Wanser and R. E. Wagoner, *Photonics Spectra*, October 1983, 61.
10. D. A. Krohn, *Electronics Products*, 12 December 1984, 93.
11. W. R. Seitz, *Anal. Chem.*, 1984, **56**, 16A.
12. J. I. Peterson and G. G. Vurek, *Science*, 1984, **224**, 123.
13. H. Wohltjen, *Anal. Chem.*, 1984, **56**, 87A.
14. T. Hirschfeld, J. B. Callis and B. R. Kowalski, *Science*, 1984, **226**, 312.
15. J. I. Peterson, S. R. Goldstein, R. V. Fitzgerald and D. K. Buckhold, *Anal. Chem.*, 1980, **52**, 864.
16. L. A. Saari and W. R. Seitz, *ibid.*, 1982, **54**, 821.
17. Z. Zhujun and W. R. Seitz, *Anal. Chim. Acta*, 1984, **160**, 305.
18. A. P. Russell and K. S. Fletcher, *ibid.*, 1985, **170**, 209.
19. F. K. Kawahara, R. A. Fiutem, H. S. Silvus, F. M. Newman and J. H. Frazer, *ibid.*, 1983, **151**, 315.
20. J. F. Giuliani, H. Wohltjen and N. L. Jarvis, *Opt. Lett.*, 1983, **8**, 54.
21. Z. Zhujun and W. R. Seitz, *Anal. Chim. Acta*, 1985, **171**, 251.
22. O. S. Wolfbeis, H. E. Posch and H. W. Kroneis, *Anal. Chem.*, 1985, **57**, 2556.
23. J. T. Coleman, J. F. Eastham and M. J. Sepaniak, *ibid.*, 1984, **56**, 2246.
24. R. M. Sutherland, C. Dahne, J. F. Place and A. S. Ringose, *Clin. Chem.*, 1984, **30**, 1533.

25. J. D. Andrade, R. A. Vanwagenen, D. E. Gregonis, K. Newby and J. N. Lin, *IEEE Trans. Electron. Dev.*, 1985, **ED-32**, 1175.
26. Z. Zhujun and W. R. Seitz, *Anal. Chem.*, 1986, **58**, 220.
27. E. Urbano, H. Offenbacher and O. Wolfbeis, *ibid.*, 1984, **56**, 427.
28. M. A. Arnold, *ibid.*, 1985, **57**, 565.
29. N. J. Harrick, *Internal Reflection Spectroscopy*, Interscience, New York, 1967.
30. J. F. Giuliani and N. L. Jarvis, *Sens. Actuators*, 1984, **6**, 107.
31. R. N. Dominey, T. J. Lewis and M. S. Wrighton, *J. Phys. Chem.*, 1983, **87**, 5345.
32. T. J. Lewis, H. S. White and M. S. Wrighton, *J. Am. Chem. Soc.*, 1984, **106**, 6947.
33. J. F. Giuliani, D. Dominguez, W. Barger, P. Bey, Jr., E. Barbano and R. R. Smardzewski, *Optical Waveguide Studies of Viologen Films Exposed to Redox Reagents*, in *Proc. 1985 Sci. Conf. Chemical Defense Research*, CRDEC, APG, MD, 19–22 November 1985.
34. G. Gubitz, P. Van Zoonen, C. Gooijer, N. H. Velthorst and R. W. Frei, *Anal. Chem.*, 1985, **57**, 2071.
35. K. Tiefenthaler and W. Lukosz, *Thin Solid Films*, 1985, **126**, 205.
36. E. F. Ullman, M. Schwarzberg and K. E. Rubenstein, *J. Biol. Chem.*, 1976, **251**, 4172.
37. S. Welin, H. Elwing, H. Arwin, I. Lundstrom and M. Wikstrom, *Anal. Chim. Acta*, 1984, **163**, 263.
38. I. Giaever, *J. Immunol.*, 1973, **110**, 1424.
39. *A New Kind of Sensor*, *Photonics Spectra*, October 1984, 36.
40. J. Hecht, *Optical Computers, High Technology*, February 1987.

## DETERMINATION OF pH WITH ACID-BASE INDICATORS: IMPLICATIONS FOR OPTICAL FIBRE PROBES

T. E. EDMONDS, N. J. FLATTERS, C. F. JONES and J. N. MILLER

Department of Chemistry, Loughborough University of Technology, Loughborough, England

(Received 10 February 1987. Revised 24 June 1987. Accepted 21 August 1987)

**Summary**—Results are presented which clearly illustrate the possibilities and limitations of the use of indicators immobilized on optical fibres, in the determination of pH.

In recent years a number of pH-probes for use in aqueous systems have been based on attaching an immobilized colorimetric indicator to the end of an optical fibre.<sup>1</sup> The indicator is usually immobilized on a solid support such as polystyrene,<sup>2</sup> polyacrylamide<sup>3,4</sup> or porous glass beads,<sup>5</sup> by adsorption or covalent bonding. The support is held in place at the end of the optical fibre by some form of porous membrane. Most of the pH-probes that have been developed use immobilized acid-base indicators, such as Phenol Red,<sup>3</sup> Bromothymol Blue<sup>2,4</sup> and others,<sup>6</sup> although a few have been based on use of a fluorescent dye, e.g., fluorescamine.<sup>5</sup> The optical property measured (reflectance, absorbance or fluorescence) depends on the configuration of the device and the nature of the indicator.

The development of these fibre-optic pH-probes is no more than an extension of the relatively simple chemistry involved in the spectrophotometric determination of pH. The pH of a solution may be determined spectrophotometrically by measuring the concentration ratio of the undissociated indicator species, HA, to the dissociated species A<sup>-</sup>; the system may be calibrated by making measurements in a series of non-absorbing buffer solutions. Provided that the total concentration of indicator remains constant, an expression based on the Henderson-Hasselbalch equation<sup>7</sup> can be developed which relates solution absorbance to pH.

$$pK'_a = \text{pH} + \log[\text{HA}]/[\text{A}^-] \quad (1)$$

where  $pK'_a$  is the concentration indicator constant and is related to the thermodynamic value  $pK_a$  by

$$pK'_a = pK_a + \log \gamma_{\text{HA}}/\gamma_{\text{A}} \quad (2)$$

where  $\gamma_x$  is the activity coefficient of species x.

The reason for using equation (1) is that absorbance measurements are a linear function of the solute concentration and not its activity. It would be possible to determine pH spectrophotometrically by measurements at two different wavelengths, at one of which only the dissociated form absorbs and at the

other only the undissociated form. Measurement of the absorbance at a single wavelength is simpler, however. For example, if the absorbance of the undissociated form of the indicator is negligible at the selected wavelength, the equation

$$pK'_a = \text{pH} + \log(A_{\text{max}} - A)/A \quad (3)$$

can be used, where  $A_{\text{max}}$  is the absorbance at a pH high enough to ensure complete dissociation of the indicator and  $A$  is the absorbance at any given pH, the total indicator concentration being constant.

The work described in this paper was undertaken to determine the reliability of spectrophotometric pH and  $pK'_a$  measurements in aqueous systems, and of those made with immobilized indicators.

### EXPERIMENTAL

#### Apparatus

Absorption spectra were measured with a Pye-Unicam PU8600 UV/VIS spectrophotometer, interfaced with a BBC microcomputer by the PU8600 series scanning software program.<sup>8</sup> The pH of the buffer solutions was measured with a Corning 140 pH-meter with a combination electrode (RS components 424-557). Solutions were kept at  $25.0 \pm 0.1^\circ$ .

#### Reagents

Solutions of Bromocresol Purple, Bromocresol Green, Bromophenol Blue, Bromothymol Blue and Phenol Red (Fisons), Cresol Red and Methyl Red (BDH) were prepared in dilute sodium hydroxide solution as described by Bishop.<sup>9</sup> The buffer solutions were made from Fisons and BDH reagent-grade chemicals and distilled water. The pH buffers (ionic strength of 0.01 M) were prepared according to Perrin and Dempsey.<sup>10</sup> The indicator and buffer solutions were stored in 100-ml polyethylene bottles.

#### Procedure

The pH of each buffer solution at  $25.0^\circ$  was checked against NBS buffers by use of a glass electrode and a standard potentiometric procedure.<sup>11</sup> For spectrophotometric determination of pH 10 ml of buffer solution were mixed in a stoppered sample-tube (to prevent evaporation), with 1 ml of Phenol Red, Bromophenol Blue, Bromothymol Blue or Bromocresol Purple, or 0.5 ml of Cresol Red, or 0.1 ml of Methyl Red solution. Addition of the indicator caused no perceptible change in the pH of the buffer. Between measurements the sample tubes were kept sealed and partly submerged in a water-bath maintained at  $25.0 \pm 0.1^\circ$ .

The spectrophotometer was programmed to record the absorbance at every 2 nm between 300 and 700 nm. The absorption spectrum for the appropriate reference buffer solution was scanned and stored. The same cuvette (path-length 1 cm) was used in recording the absorption spectrum for the buffered solution of indicator. These two measurements were repeated over a range of pH values. For each pH, the logarithms of the transmittances of the sample (buffer plus indicator),  $T_s$ , and reference solution (buffer only),  $T_b$ , were printed out for each wavelength, along with the difference  $\log T_b - \log T_s$  (*i.e.*, the absorbance), enabling the isosbestic point and absorbance at the analytical wavelength to be accurately determined.

## RESULTS AND DISCUSSION

### Preliminary measurements

The precision of the spectrophotometer was checked by measuring the absorbance of cobalt ammonium sulphate solutions (36.69mM, in 1% v/v sulphuric acid) at 500 nm against a water blank. A series of ten replicates gave a relative standard deviation (RSD) of 0.3%.

### Determination of $pK'_a$

For solution absorbance measurements, the incident intensity,  $I_0$ , is estimated by measurement of the transmittance ( $T_b$ ) of a reference solution (a reagent blank is commonly used) at the same wavelength as the transmittance ( $T_s$ ) of the sample solution. When an optical fibre pH probe is used, this method of estimating  $T_b$  is impracticable, and it becomes necessary to use a wavelength at which the transmittance of neither the acid nor the base form of the indicator changes with pH, *i.e.*, the isosbestic point, or at some wavelength at which neither form absorbs radiation. The transmittance at this wavelength is assumed to compensate adequately for any optical and instrumental variations. We decided to calculate the absorbance data by use of both the normal reference intensity,  $I_0$ , measured at the analytical wavelength for the appropriate buffer solution, and the isosbestic reference intensity  $I_{ob}$ . For a given indicator, the isosbestic point showed a small wavelength shift (a few nm in most cases), depending on pH, buffer composition and ionic strength. In order to maintain a reasonable analogy between the solution measurements and fibre-optic measurements, the isosbestic point transmittance was recorded at a fixed wavelength.

To check the validity of this approach a series of transmittance measurements was made for each of the indicators at the selected wavelength corresponding to the isosbestic point. The transmittance ( $I_{ob}$ ) of the indicator was measured in each of the buffers used subsequently for  $pK'_a$  determination, along with the transmittance ( $I_{ref}$ ) for each buffer alone. Thus, for each of the five indicators tested six  $I_{ob}$  and six  $I_{ref}$  values were recorded. The mean and standard deviations for each group of six transmittance values were obtained, and from these data the relative standard deviation (RSD) was calculated. The RSD is a measure of the variation in the transmittance within each group of measurements ( $I_{ob}$  or  $I_{ref}$ ). The RSD values for  $I_{ref}$  shows the variation in transmittance of the different buffers; those for  $I_{ob}$  show the variation in transmittance of the different buffers plus any variation in the transmittance of the indicator arising from a shift of the isosbestic point. Ideally, repeated measurements of the transmittance for a given solution should be constant: measurements made with cobalt ammonium sulphate solutions indicated that there would in fact be an RSD of  $\sim 0.3\%$ .

The mean and standard deviation for the five  $I_{ob}$  RSDs were 3.0% and 1.3% respectively and those for the  $I_{ref}$  RSDs were 2.4% and 1.2%. A two-tailed *F*-test failed to show a significant difference between the two standard deviations, and a *t*-test failed to distinguish between the means. In other words these values appear to have been drawn from the same population. Accordingly we can say that the variation in transmittance of an indicator at the selected, fixed wavelength corresponding to its isosbestic point was indistinguishable from the variation in the transmittance of the different buffers in which the indicator was present. Consequently, use of  $I_{ob}$  instead of  $I_{ref}$  for calculation of the solution absorbance is a valid procedure.

The  $pK'_a$  values for the indicators were calculated by using an expression similar in nature to equation (3):<sup>12,13</sup>

$$pK'_a = \text{pH} + \log[(A_{\text{max}} - A)/(A - A_{\text{HA}})] \quad (4)$$

where  $A_{\text{HA}}$  is the absorbance of the indicator at the analytical wavelength and very low pH (*i.e.*, the indicator can be assumed to be totally undissociated).

The accuracy and precision of the  $pK'_a$  value

Table 1. Measured values obtained by using standard ( $^{\text{a}}pK'_a$ ) and isosbestic ( $^{\text{b}}pK'_a$ ) wavelength references (ionic strength 0.01M, temperature  $25.0 \pm 0.1^\circ\text{C}$ )

Indicator	Indicator concentration, M	Wavelength, nm		$^{\text{a}}pK'_a$ (standard reference) $\pm$ s.d.	$^{\text{b}}pK'_a$ (isosbestic reference) $\pm$ s.d.	$\Delta pK'_a = (^{\text{a}}pK'_a - ^{\text{b}}pK'_a)$
		Analytical	Isosbestic			
Bromophenol Blue	$5.4 \times 10^{-3}$	590	494	$3.99 \pm 0.07$	$4.03 \pm 0.04$	-0.04
Bromothymol Blue	$5.8 \times 10^{-4}$	615	500	$6.88 \pm 0.19$	$6.84 \pm 0.13$	0.04
Bromocresol Green	$5.2 \times 10^{-5}$	616	508	$4.57 \pm 0.03$	$4.69 \pm 0.10$	-0.12
Bromocresol Purple	$6.7 \times 10^{-4}$	588	486	$6.30 \pm 0.05$	$6.17 \pm 0.07$	0.13
Cresol Red	$5.0 \times 10^{-3}$	570	485	$7.96 \pm 0.09$	$7.82 \pm 0.15$	0.14
Methyl Red	$3.7 \times 10^{-5}$	518	460	$4.86 \pm 0.05$	$4.98 \pm 0.13$	-0.12
Phenol Red	$1.1 \times 10^{-5}$	560	480	$7.65 \pm 0.04$	$7.55 \pm 0.18$	0.10

Table 2. Results obtained for  $pK'_a$  with changing ionic strength, at 25°C

Ionic strength, $M$	0.01	0.10	0.50	1.00	1.50	2.00	3.00
Bromophenol Blue	3.94	4.41	4.37	4.40	4.42	4.45	4.51
Bromocresol Green	4.57	4.65	4.65	4.68	4.71	4.75	4.82
Bromocresol Purple	6.26	5.67	5.67	5.71	5.74	5.75	5.76
Methyl Red	4.90	5.04	5.08	5.13	5.31	5.07	5.01
Phenol Red	7.46	6.96	6.52	6.37	6.39	6.55	6.44

calculated from equation (4) depends on a number of conditions.

(i) The path-length, concentration and ionic strength of the indicator solution, and the temperature, must be kept constant for all the measurements.

(ii) The solution matrix must remain the same for each measurement (in practice this is impossible to achieve when different buffer compositions are used).

(iii) The pH value used for the calculation must be accurate.

The two sets of  $pK'_a$  values obtained in this work were analysed statistically to decide whether the use of different reference intensities caused significant differences.<sup>14</sup> A  $t$ -test indicated that the difference between the  ${}^s pK'_a$  and  ${}^b pK'_a$  values (Table 1) at the 95% ( $P = 0.05$ ) confidence level was *not* significant. Thus, the isosbestic reference intensity  $I_{ob}$  can be used to calculate  $pK'_a$  without introducing a significant systematic error [if equation (4) is used].

#### Effect of ionic strength and temperature on the $pK'_a$ value

The spectrophotometrically determined  $pK'_a$  value is a function of the activity coefficients,  $\gamma$ , of the dissociated and undissociated indicator species [equation (2)]. Consequently any factor that influences the magnitude of  $\gamma_{HA}$  and  $\gamma_{A^-}$  will also affect the measured  $pK'_a$  value.

From the Debye–Hückel equation,<sup>15</sup>

$$-\log \gamma_i = \frac{AZ_i^2 \sqrt{I}}{1 + B a_i \sqrt{I}} \quad (5)$$

where  $A$  and  $B$  are constants that vary with the temperature and dielectric constant of the solvent,  $Z$  is the charge of the ion  $i$ ,  $a_i$  is the ion-size parameter, and  $I$  the ionic strength, it is evident that the ionic strength and temperature of the system affect the magnitude of the activity coefficient,  $\gamma$ , and thus the  $pK'_a$  value calculated.

If the solvent matrix and system temperature are kept constant then the effect on the  $pK'_a$  value of

changing the ionic strength can be observed. The results in Table 2 were obtained by varying the ionic strength of a single buffer solution [of  $pH \approx pK'_a$  ( $I = 0.01M$ ) for each indicator] from 0.01 to 3.0M by introducing a background electrolyte (sodium chloride) into the buffer solution. The results show that the change in ionic strength can affect the  $pK'_a$  value by as much as 1.23. Clearly it is important that the ionic strength of the system under analysis should be recorded, and that it should remain constant during pH-measurement procedures.

In both the ionic strength and temperature studies (which follow), the  $pK'_a$  values have been obtained by using a conventional reference solution for the absorbance measurements. We have not attempted to use the isosbestic point reference for calculation of absorbance. The variation in wavelength of this point with solution parameters would have entailed making extra measurements to establish the correct wavelength of the isosbestic point. It is worth noting at this stage that such a procedure would be out of the question for a sensor containing immobilized reagents. Table 3 gives examples of the change in  $pK'_a$  caused by a temperature increase of 5° (from 25° to 30°); the general increase in the  $pK'_a$  value is about 0.2.

#### Measurement of pH

Once the  $pK'_a$  value for an indicator is known, equation (4) can be used to determine, from absorbance measurements the pH of a solution containing the indicator. This kind of measurement can be performed without recourse to calibration if the ionic strength, temperature and buffer capacity of the solution are known. The effect of the first two of these quantities has been described. The buffer capacity will reflect the extent to which dissociation of the acid–base indicator itself will influence the pH of the solution. Results for a series of spectrophotometric estimations of pH are given in Table 4. Methyl Red, Bromophenol Blue and Bromothymol Blue were used, and the pH estimations were made on the basis of both calculated  $pK'_a$  values, i.e.,  ${}^s pK'_a$  and  ${}^b pK'_a$

Table 3. Effect of temperature on the calculated  $pK'_a$  ( $\pm$  s.d.)

	${}^b pK'_a$ , equation (4)		${}^s pK'_a$ , equation (3)	
	25°C	30°C	25°C	30°C
Cresol Red	7.96 $\pm$ 0.09	8.30 $\pm$ 0.15	7.95 $\pm$ 0.05	8.13 $\pm$ 0.04
Phenol Red	7.65 $\pm$ 0.04	7.81 $\pm$ 0.02	7.61 $\pm$ 0.05	7.79 $\pm$ 0.03
Bromocresol Green	4.57 $\pm$ 0.03	4.77 $\pm$ 0.03	4.57 $\pm$ 0.03	4.71 $\pm$ 0.03
Bromothymol Blue	6.88 $\pm$ 0.19	7.09 $\pm$ 0.02	6.82 $\pm$ 0.20	7.04 $\pm$ 0.01

Table 4. Values for pH determined potentiometrically, and spectrophotometrically with different references

	pH <sub>m</sub>	pH <sub>c</sub> <sup>s</sup>	pH <sub>c</sub> <sup>s</sup>	pH <sub>c</sub> <sup>ib</sup>	pH <sub>c</sub> <sup>ib</sup>
Methyl Red	4.55	4.55	4.58	4.69	4.81
	4.82	4.78	4.81	4.84	4.92
	5.02	5.04	5.05	5.12	5.08
	5.28	5.22	5.22	5.21	5.13
	5.40	5.46	5.43	5.21	5.13
Bromophenol Blue	3.69	3.72	3.73	3.76	3.95
	3.90	3.90	3.91	3.91	4.04
	4.09	4.07	4.07	4.08	4.14
	4.38	4.28	4.29	4.34	4.34
	4.52	4.60	4.60	4.49	4.46
Bromothymol Blue	5.80	5.82	5.92	6.00	6.32
	6.02	6.20	6.22	5.86	6.29
	6.58	6.42	6.41	6.68	6.57
	6.78	6.51	6.60	6.72	6.59
	6.93	6.89	6.77	6.86	6.68
	7.67	7.94	7.90	7.67	7.34

pH<sub>m</sub> is the pH measured by standard potentiometric procedures.

pH<sub>c</sub><sup>s</sup> is the pH (standard reference) calculated with equation (4).

pH<sub>c</sub><sup>ib</sup> is the pH (isosbestic reference) calculated with equation (4).

pH<sub>c</sub><sup>s</sup> and pH<sub>c</sub><sup>ib</sup> are the pH values (standard and isosbestic references respectively) calculated with equation (3).

[calculated by using equation (4)]. The ionic strength of these solutions was kept constant at 0.01M, and all measurements were performed at 25.0 ± 0.1°. Under these circumstances variation of the wavelength of the isosbestic point is caused solely by variation in the pH. It was shown earlier that this does not have a statistically significant effect on the measured pK'<sub>a</sub> value.

Although non-parametric statistical tests such as the Wilcoxon signed rank test failed to demonstrate significant systematic differences between the first and second, and the first and fourth columns of Table 4, it is clear that the spectrophotometric estimation of pH to within 0.05 of the potentiometric value is obtained in only a few instances. It should be borne in mind that all these measurements were made at carefully controlled ionic strength and temperature, and with solutions of high buffer capacity. In addition, the conditions for spectrophotometric measurement were good, and adequate correction for non-zero background absorbance was made by the use of equation (4). Suppose that instead we use

equation (3), in which the undissociated form of the acid-base indicator is assumed to give a negligible absorbance at the analytical wavelength. Then re-arranging equation (3) gives:

$$A = A_{\max}/(10^{-D} + 1) \quad (6)$$

where  $D = \text{pH} - \text{pK}'_a$ .

Values for pK'<sub>a</sub> and pH calculated on the basis of equation (3) are shown in Tables 5 and 4 respectively. The initial absorbance data used to calculate the results in Tables 1 and 4 [by equation (4)] are used to calculate the results in Tables 5 and 4 [by equation (3)]. Comparison of the results (Table 5) indicates that the pK'<sub>a</sub> values calculated by using the standard reference are significantly more precise than those calculated by using the isosbestic reference. The difference ( $\Delta\text{pK}'_a = {}^s\text{pK}'_a - {}^{\text{ib}}\text{pK}'_a$ ) between the two pK'<sub>a</sub> values ranges from -0.72 to 0.86. Statistical analysis of the pK'<sub>a</sub> values at the 99% ( $P = 0.01$ ) level indicates that the difference between the two is significant. This result is expected because the  $A_{\text{HA}}$  value is *not* negligible if the isosbestic reference is used. However, statistical analysis of the  ${}^s\text{pK}'_a$  (standard reference) values obtained by use of equations (4) and (3) shows that there is *no* significant difference between the values at the 95% level. Thus, the only significant difference between all four pK'<sub>a</sub> values for each indicator occurs when the isosbestic reference is used in conjunction with equation (3). The pH results obtained by using equation (5) are also given in Table 4. Again Wilcoxon signed rank tests failed to establish any significant systematic differences between the columns. However it is manifest that there are large errors associated with these estimates of pH, ranging from -0.52 + 0.33 when equation (3) is used with the isosbestic point reference.

#### Implications for use of fibre-optic pH-probes

It has been shown<sup>3</sup> that the response of a fibre-optic probe based on immobilized acid-base indicators can be described by the equation

$$\log(I_t/I_{\text{ob}}) = \log r [-K^P/(10^{-D} + 1)] \quad (7)$$

where  $I$  is the transmitted power measured at the analytical wavelength,  $I_{\text{ob}}$  the transmitted power measured at an isosbestic wavelength,  $r$  a constant (the ratio of the incident power at the analytical wavelength to the incident power at the isosbestic wave-

Table 5. Measured pK'<sub>a</sub> values (±s.d.) obtained by using both standard and isosbestic wavelength references, and equation (3)

Indicator	<sup>s</sup> pK' <sub>a</sub> (standard reference)	<sup>ib</sup> pK' <sub>a</sub> (isosbestic reference)	$\Delta\text{pK}'_a = {}^s\text{pK}'_a - {}^{\text{ib}}\text{pK}'_a$
Bromophenol Blue	3.99 ± 0.06	3.60 ± 0.15	0.43
Bromothymol Blue	6.82 ± 0.20	6.12 ± 0.33	0.72
Bromocresol Green	4.57 ± 0.03	4.20 ± 0.14	0.49
Bromocresol Purple	6.30 ± 0.04	5.71 ± 0.07	0.46
Cresol Red	7.95 ± 0.05	7.12 ± 0.40	0.70
Methyl Red	4.92 ± 0.04	5.70 ± 0.21	-0.72
Phenol Red	7.61 ± 0.05	6.69 ± 0.61	0.86



length), and  $K^P$  a probe constant given by  $S\xi/l$ , where  $S$  is the total indicator concentration in the probe,  $l$  is the effective path-length for the probe and  $\xi$  is the molar absorptivity of the indicator at the analytical wavelength.

Equations (6) and (7) are identical in operation, if not in form. The probe constant of (7) performs the same function as  $A_{\max}$  in (6), and the necessity of estimating other incident power in the case of a fibre-optic probe introduces the constant  $r$ , and the term  $I_{00}$  in (7). If we make the assumption that  $r$  and  $K^P$  are constant for a given probe, and can be determined in a straightforward manner (just like measuring  $A_{\max}$  for a solution), then the errors involved in the determination of pH by the fibre-optic probes may be discussed in terms of the errors in pH estimation that have been noted in the solution work.

First it is apparent that operation of a fibre-optic probe is analogous to the determination of pH by an indicator, with equation (3) for calculation and the isosbestic point as a reference. Under these conditions, in the conventional spectrophotometric measurements, not only was the measured value of  $pK'_a$  shown to be significantly different from the other estimates of  $pK'_a$ , but also the largest range of differences between potentiometrically and spectrophotometrically estimated pH values (from  $-0.57$  to  $+0.33$ ) was observed. The similarity between equations (6) and (7) indicates that under the same conditions, a comparable range in the estimation of pH by a fibre-optic probe might be expected. The results of Tables 2 and 3, although showing the change in the  $pK'_a$  value with change in temperature or ionic strength, are of direct consequence to pH-measurement with fibre-optic probes, because of the part played by  $pK'_a$  in the factor  $D$  of equation (7). In fact this problem is compounded in the case of fibre-optic probes. Not only do the solution parameters affect the pH-estimation through variation in the activity coefficients, but also through variation in the wavelength of the isosbestic point.

Accordingly, direct use of a fibre-optic probe for the determination of pH in an unknown solution with an accuracy of  $\pm 0.1$  (let alone  $\pm 0.01$ ) is unrealistic. Calibration of a probe with appropriate buffers may be used to decrease the error, but this sort of approach runs counter to the principles of this kind of sensor, *viz.* that the device should be dipped into a

solution and a reading taken that directly, rapidly and accurately indicates the pH. Formulating appropriate buffers for one type of sample is tedious enough, but if samples of differing ionic strength and temperature are to be tested, yet another set of buffers would have to be made up and the probe recalibrated.

We have not investigated pH-measurements with indicators on samples of low buffer capacity. It is evident from the theory of weak acids and bases that a significant concentration of indicator species could have radical effects on the pH of such a sample. Finally, the probe constant of equation (7) depends to a large extent on  $l$  and  $S$ . Proper control of  $l$  in the context of probes based on indicators immobilized on small beads or particles is not straightforward, and small changes in geometry could have radical effects on the probe response.

Unless the errors discussed above can be rigorously compensated for, and fibre-optic probe construction radically improves so that quantities such as the effective path-length and total indicator concentration can be rigorously controlled, the future of this type of sensor appears to be very limited.

#### REFERENCES

1. R. Narayanaswamy, *Anal. Proc.*, 1985, **22**, 204.
2. G. F. Kirkbright, R. Narayanaswamy and N. A. Welti, *Analyst*, 1984, **109**, 15.
3. J. I. Peterson, S. R. Goldstein, R. V. Fitzgerald and D. K. Buckhold, *Anal. Chem.*, 1980, **52**, 864.
4. T. E. Edmonds and I. D. Ross, *Anal. Proc.*, 1985, **22**, 206.
5. L. A. Saari and W. R. Seitz, *Anal. Chem.*, 1982, **54**, 823.
6. G. F. Kirkbright, R. Narayanaswamy and N. A. Welti, *Analyst*, 1984, **109**, 1025.
7. D. J. Pietrzyk and C. W. Frank, *Analytical Chemistry*, 2nd Ed., Academic Press, London, 1979.
8. P. Ganns, *Pu 8600 Series Scanning Software*, Pye Unicam, Cambridge, 1984.
9. E. Bishop, *Indicators*, Pergamon Press, Oxford, 1972.
10. D. D. Perrin and B. Dempsey, *Buffers for pH and Metal Ion Control*, Chapman & Hall, London, 1979.
11. *British Standard 1647: 1961, Specification for pH Scale*, British Standards Institution, London, 1961.
12. A. I. Vogel, *A Textbook of Quantitative Analysis*, 4th Ed., Longmans, London, 1979.
13. A. Albert and E. P. Serjeant, *The Determination of Ionization Constants: A Laboratory Manual*, 3rd Ed., Chapman & Hall, London, 1984.
14. J. C. Miller and J. N. Miller, *Statistics for Analytical Chemistry*, 2nd Ed., Ellis Horwood, Chichester, 1988.
15. H. A. Laitinen and W. E. Harris, *Chemical Analysis*, 2nd Ed., McGraw-Hill, New York, 1975.

## A FIBER-OPTIC SENSOR FOR CO<sub>2</sub> MEASUREMENT

CHRISTIANE MUNKHOLM and DAVID R. WALT\*

Max Tishler Laboratory for Organic Chemistry, Department of Chemistry, Tufts University, Medford,  
MA 02155, U.S.A.

FRED P. MILANOVICH

Lawrence Livermore National Laboratory, Livermore, CA 94550, U.S.A.

(Received 20 May 1987. Accepted 21 August 1987)

**Summary**—A fiber-optic sensor has been prepared which responds to carbon dioxide at physiologically significant concentrations. It is based on pH modulation by dissolved carbon dioxide in a sensing layer of fluorescent dye. By use of a previously developed methodology by which the sensing chemistry is bonded directly to the glass fiber tip, the miniature size of the sensor is preserved. This method involves consecutive applications of solution polymers to the fiber tip rather than mechanical attachment of sensor reagents. Preparations of polymer-immobilized dyes and polymer membranes are described.

The entry of optical fibers into the field of analytical chemistry has extended the ability to perform real-time analysis. A chemical species can now be detected without separation from its natural matrix. Many of these sensors operate by changes in the luminescent properties of a sensing layer on interaction with the analyte. This enormous potential for continuous monitoring of physiological, biological and environmental systems is now limited only by the ingenuity required to convert chemical changes into luminescent ones. A second but exceedingly important advantage of optical fibers is their very small size, with typical diameters of 100–500  $\mu\text{m}$ . This feature permits positioning in similarly sized locations. In the development of fiber-optic sensor technology, it is desirable to preserve continuous reversible sensor chemistry and the miniature size of the sensors.

Numerous prototype sensors have already been demonstrated that are based on immobilizing fluorescent indicator dyes at the distal tip of the optical fiber.<sup>1–7</sup> With many of these, various mechanical and adhesive methods have been used to fix the sensor in the vicinity of the fiber tip. Our approach is different in an important way: we have succeeded in covalently bonding the sensor directly to the fiber tip.<sup>3,8</sup> The miniature size of the fiber is preserved and the response times are greatly shortened. A fiber-optic pH-sensor based on fluorescein immobilized by using this method of attachment has a response time of less than 5 sec and is reversible and reproducible.<sup>3</sup>

Other researchers have made gas-sensing fiber-optic sensors in either of two designs: (1) the reagent is mechanically fixed to the fiber tip, resulting

in a large device with slow response times<sup>4–6</sup> or (2) the indicator layer is fixed on a transparent “Plexiglas” window in contact with the optical fiber.<sup>9,10</sup> Although the latter arrangement gives fast response times, neither approach preserves the miniature dimensions needed for *in vivo* application.

It is well known that carbon dioxide will dissolve in water, according to the equation



Since dissolution of CO<sub>2</sub> results in a change in solution pH, the conversion of our fiber-optic pH-sensor into a carbon dioxide sensor was a logical extension. For such a sensor (Fig. 1) the pH-sensitive fluorescent dye must be sequestered from the sensing environment. Thus, a semipermeable membrane is required to exclude protons and allow CO<sub>2</sub> to enter the pH-sensing region, where it reacts with water in the hydrophilic microenvironment of the dye-containing polymer matrix, changes the pH and thereby alters the fluorescence intensity.

We have extended our amplification technique to the preparation of a CO<sub>2</sub>-sensitive fiber by the consecutive application of polymer material to the optical fiber tip. This device is of the size (300  $\mu\text{m}$ ) needed for *in vivo* venous, arterial or other biological locations, and compares favourably with a miniature potentiometric CO<sub>2</sub>-sensing catheter recently described for *in vivo* monitoring, which has an outer diameter of 1.1 mm.<sup>11</sup>

Three carbon dioxide sensors prepared in this way will be described. They differ in the polymer and dye materials used to construct the pH-sensitive layer: (1) fluorescein copolymerized with acrylamide, (2) fluorescein copolymerized with 2-hydroxyethyl methacrylate (HEMA) and (3) hydroxypyrenetrisulphonic acid (HPTS) adsorbed on acrylamide. They all use a

\*To whom correspondence should be addressed.

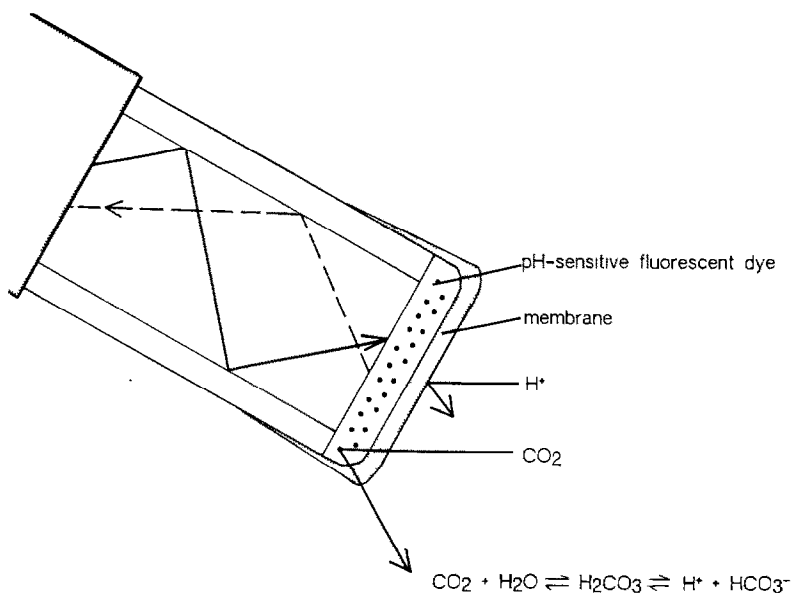


Fig. 1. Model of fiber-optic  $\text{CO}_2$ -sensor.

coating of dimethylsiloxane-bisphenol A carbonate copolymer as the semipermeable membrane used to exclude protons from the sample itself.

## EXPERIMENTAL

### Instrumentation

The instrument used for measuring fluorescence with optical fibers has been described previously.<sup>3</sup> Briefly, a Spectra-Physics Model 162A-04 argon-ion laser provides the excitation radiation (typically 488 nm), which is passed through a neutral density filter and a dichroic mirror to the coupled fiber. The returning fluorescence signal (red-shifted) returns via the same fiber, and is deflected through 90° by the front surface of the angled dichroic mirror. This signal beam is filtered (long-wavelength band-pass), focused, and passed through a slit into a single-grating monochromator. The resulting wavelength-dispersed signal is measured with a photo-counting detection system (Pacific Instruments, Model 126). The intensity of the fluorescence is measured in photon counts per second as a function of time or of the wavelength examined.

### Materials

Glass-on-glass fibers (200/250  $\mu\text{m}$ ), approximately 1 m long, were terminated at one end with AMP connectors. The other ends, from which a length of approximately 2 cm of sheathing was removed, were washed in concentrated sulphuric acid and rinsed with distilled water. The connector ends were polished and the stripped ends cut square, as verified by microscopic examination.

Dimethylsiloxane-bisphenol A carbonate (DMS-BPAC) block copolymer was obtained from Petrarch Systems, Bristol, PA, sodium 8-hydroxyppyrene-1,3,6-trisulphonate from Molecular Probes, Eugene, OR, and fluoresceinamine (Isomer I or II) from Sigma. All other chemicals were obtained from Aldrich Chemical Co. and were used without further purification.

### Preparation of pH probes

The optical-fiber tips require treatment to activate the glass surface with a polymerizable double bond. Three different surface activation systems have been described.<sup>3</sup>

After surface preparation, the fiber tip can be converted into a pH probe in any of the following ways.

1. *Fluorescein copolymerized with acrylamide.* This method has been described before,<sup>3</sup> but we have found that better results can be obtained by allowing the monomer dye solution to stand for 12 hr prior to polymer initiation. This allows the dye to become solubilized and greatly improves the incorporation of the dye derivative into the resulting polymer.

2. *Fluorescein copolymerized with 2-hydroxyethyl methacrylate (HEMA).* To form the polymer, 2-hydroxyethyl methacrylate (20 ml), ethylene glycol dimethacrylate (400  $\mu\text{l}$ ), acrylated fluorescein<sup>3</sup> (1 ml of solution in tetrahydrofuran) and demineralized water (20 ml) are mixed and allowed to stand overnight. Surface-activated optical fibers are positioned in the monomer dye solution and ammonium persulphate (15 mg) and riboflavin (15 mg) are added. The system is kept in a nitrogen atmosphere and exposed to white light from an 8-W fluorescent light bulb. Since the polyHEMA is a more resilient polymer than polyacrylamide, the removal of the glass fibers from the polymer gel can result in complete stripping of the polymer material from the glass surface. Therefore, it is critical to remove the fibers at an appropriate moment before gelation occurs.

3. *Hydroxyppyrenetrisulphonate (HPTS) adsorbed on acrylamide.* Allylamine (105  $\mu\text{l}$ ) and a dye solution (50 mg of HPTS in 2 ml of water) were added to the stock acrylamide-methylenebisacrylamide solution<sup>3</sup> (100 ml). Polymerization was initiated with ammonium persulphate (15 mg). After the polymer had formed, the optical fibers were removed and treated immediately with a membrane material.

### Preparation of carbon dioxide probes

The membrane coating was prepared with a 4% solution of DMS-BPAC block copolymer in a mixture of dichloromethane and n-hexane (1:1). Before application, the pH sensors were soaked in 1mM sodium bicarbonate solution. For membrane treatment the DMS-BPAC solution was pipetted onto the fiber tip, and allowed to dry at room temperature for 24 hr. The membrane was then tested by placing the sensor in different pH buffers and measuring the fluorescence intensity. If the intensity signals were not constant, the membrane was not pinhole free and the entire

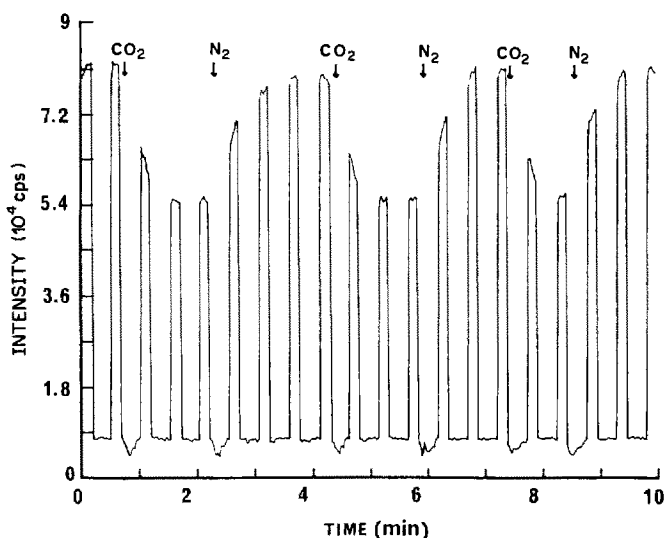


Fig. 2. CO<sub>2</sub> tests on sensor with acrylamide and fluorescein as the pH-sensing material:  $\lambda_{\text{ex}} = 488 \text{ nm}$ ,  $1.5 \mu\text{W}$ ;  $\lambda_{\text{em}} = 530 \text{ nm}$ .

process was repeated, including the soaking in bicarbonate solution. Sometimes a third treatment was required. The fabricated sensor was then stored with the fiber tip in water, allowing rehydration of the sensor microenvironment.

#### Measurements

Before being tested with CO<sub>2</sub>, the integrity of the membrane was checked by making fluorescence measurements in different pH buffers. The sensor was then placed in a flask of water through which nitrogen was bubbled. A measurement was made and was assigned the value 0% CO<sub>2</sub>. The sensor was then moved to another flask with carbon dioxide bubbling through the water. Measurements were taken until an equilibrium value was achieved. The sensor was then returned to the first flask and measurements were taken until equilibrium was re-established.

### RESULTS AND DISCUSSION

Figure 2 presents a typical time scan of a fiber-optic CO<sub>2</sub>-sensor tested with a 5% CO<sub>2</sub> gas mixture (with nitrogen) bubbled through the test solution. The initial fluorescence signal,  $8.0 \times 10^4 \text{ cps}$ , represents the intrinsic fluorescence of the sensor microenvironment before introduction of CO<sub>2</sub>. When CO<sub>2</sub> diffuses through the membrane it generates protons and bicarbonate ions and the fluorescence signal of the pH-sensitive dye is quenched. Equilibrium is reached at  $5.4 \times 10^4 \text{ cps}$ . The sensor is then degassed by returning the fiber to the flask of water

with nitrogen bubbling through it and the fluorescence intensity is re-established at  $8.0 \times 10^4 \text{ cps}$  as the original condition of the sensor microenvironment is restored. In Fig. 2 the response to CO<sub>2</sub> is 70% complete in 30 sec and at equilibrium in 60 sec. The recovery rate is similar.

A problem with the sensor has been a progressive loss of fluorescence signal after cycling at high CO<sub>2</sub> concentrations. At CO<sub>2</sub> concentrations of less than 5% the effect is mitigated and this loss is not expected to be a severe problem in monitoring of physiologically significant concentrations of CO<sub>2</sub>.

The data in Fig. 2 were obtained with a pH-sensing material formed from fluorescein copolymerized with acrylamide. If the fluorescein is copolymerized with HEMA the intensity change at a given CO<sub>2</sub> concentration is almost double that of the acrylamide-based sensor (Table 1). We have observed this increased dynamic range with the HEMA fiber-optic pH-sensor as well, but cannot explain it.

A third CO<sub>2</sub>-sensor was prepared with the pH-sensitive dye HPTS, adsorbed on and/or encapsulated in a cross-linked acrylamide matrix. This approach was taken since formation of a derivative of the dye had a detrimental effect on the sensitivity to pH. The suitability of this dye for determination of CO<sub>2</sub> by use of fiber optics has already been

Table 1. Relative response of different polymer-dye matrices to CO<sub>2</sub>, expressed as  $I/I_0$  when exposed to a CO<sub>2</sub> solution

CO <sub>2</sub> , %	Sensor material		
	Fluorescein/acrylamide	Fluorescein/HEMA	HPTS/acrylamide
99.0	0.6	0.2	0.4
3.5	0.9	0.75	0.8

described.<sup>10</sup> When adsorbing the dye, however, it is necessary to proceed immediately with the membrane treatment. If sodium bicarbonate solution is to be included it must be added during the polymerization reaction, since the NaHCO<sub>3</sub> concentration has been found to be an important parameter in CO<sub>2</sub> response.<sup>10</sup>

Our initial results indicate that the HPTS may be the superior dye for the CO<sub>2</sub>-sensor as it has a more dynamic response to the pH established by the carbonic acid/bicarbonate system. Because of the enhancement of the fluorescein response in the HEMA matrix we are now trying to combine the HEMA with HPTS.

The limiting factor in the development of this sensor has been the membrane formation chemistry. Numerous attempts were made to polymerize a siloxane prepolymer (carrying functional groups) onto the pH-sensor polymer but the treatments needed had a detrimental effect on the dyes. Several solvent-cast polymer materials have been examined, but although more successful than the siloxane approach, they suffer from the following limitations: (1) acidification of the pH-sensitive dye, resulting in a probe insensitive to CO<sub>2</sub>, (2) mechanical weakness, producing leaks, both immediate and eventual, (3) lack of reproducibility in the coating thickness, (4) attack on the membrane carbonate by base in the pH sensor. The application technique can also be critical when attempts are made to join hydrophobic and hydrophilic polymer layers.

## CONCLUSIONS

In the preparation of this fiber-optic CO<sub>2</sub>-sensor, we have preserved the miniature size of the fiber so that its suitability for *in vivo* applications is not compromised. The response is rapid and reversible, and can be optimized by suitable choice of the polymer and dye used for the pH-sensor material. Once a dependable membrane system has been incorporated into the sensor design, the possibility of continuously monitoring subtle physiological changes in dissolved CO<sub>2</sub> with a fiber-optic sensor will be realized.

## REFERENCES

1. J. I. Peterson and G. G. Vurek, *Science*, 1984, **224**, 123.
2. L. A. Saari and W. R. Seitz, *Anal. Chem.*, 1982, **54**, 821.
3. C. Munkholm, D. R. Walt, F. P. Milanovich and S. M. Klainer, *ibid.*, 1986, **58**, 1427.
4. O. S. Wolfbeis, *Z. Anal. Chem.*, 1986, **325**, 387.
5. J. I. Peterson, R. V. Fitzgerald and D. K. Buckhold, *Anal. Chem.*, 1984, **56**, 62.
6. Z. Zhujun and W. R. Seitz, *ibid.*, 1986, **58**, 220.
7. J. L. Gehrich, D. W. Lübbers, N. Opitz, D. R. Hansmann, W. W. Miller, J. K. Tusa and M. Yafusi, *IEEE Trans. Biomed. Eng.*, 1986, **BME-33**, 117.
8. D. Jordan, D. R. Walt and F. P. Milanovich, *Anal. Chem.*, 1987, **59**, 437.
9. D. W. Lübbers and N. Opitz, *Z. Naturforsch C, Biosci.*, 1975, **30C**, 532.
10. N. Opitz and D. W. Lübbers, *Adv. Exp. Med. Biol.*, 1984, **180**, 757.
11. W. N. Opdycke and M. E. Meyerhoff, *Anal. Chem.*, 1986, **58**, 950.

## A NEW ION SENSOR BASED ON FIBER OPTICS

FRANK V. BRIGHT, GREG E. POIRIER and GARY M. HIEFTJE\*

Department of Chemistry, Indiana University, Bloomington, IN 47405, U.S.A.

(Received 20 May 1987. Accepted 28 August 1987)

**Summary**—A fluorimetric ion sensor based on fiber optics has been developed that employs Rhodamine 6G hydrophobically and electrostatically “trapped” on a Nafion film. The sensor is based on the measurement of quenching or enhancement of the Rhodamine 6G fluorescence by various ions. It was found that ions such as  $\text{Co}^{2+}$ ,  $\text{Cr}^{3+}$ ,  $\text{Fe}^{2+}$ ,  $\text{Fe}^{3+}$ ,  $\text{Cu}^{2+}$ ,  $\text{Ni}^{2+}$  and  $\text{NH}_4^+$  rapidly quench the Rhodamine 6G fluorescence at an initial rate that depends on the concentration of the ion. This quenching is then readily reversed by the addition of “reverser” ions such as  $\text{H}^+$ ,  $\text{Li}^+$ ,  $\text{Na}^+$ ,  $\text{K}^+$ ,  $\text{Ba}^{2+}$ ,  $\text{Ca}^{2+}$ ,  $\text{Mn}^{2+}$ ,  $\text{Zn}^{2+}$  and  $\text{Mg}^{2+}$ . Again, the initial rate for the attainment of the original fluorescence was found to depend on the concentration of the reverser ion. Therefore, by monitoring the quenching directly the concentration of quencher ions can be determined. In addition, by loading the film with quencher and monitoring the initial rate of return towards the original baseline signal, it is possible to determine non-quenching ions.

The area of fiber-optic sensors has bloomed over the past five years. The recent advances and trends in fiber-optic sensors have been described in several excellent reviews.<sup>1-10</sup> Assuredly, most of the interest in fiber-optic sensors arises not only from their ability to identify and determine chemical species, but also from their potential in remote sensing. One of the stumbling blocks in the development of effective sensors has been finding immobilized reagent phases which respond with sufficient sensitivity and selectivity to the target analyte(s). Ideally, these immobilized reagents should also have reversible behavior and be very durable.

Narayanaswamy and Serilla<sup>11</sup> have developed a reflectance-type sensor for the determination of sulfide, with detection limits in the mM range. Other reflectance-type sensors have been developed for pH,<sup>12</sup> ammonia<sup>13</sup> and moisture.<sup>14</sup> Fluorescence sensors have been described for determination of oxygen<sup>15</sup> and halide ions.<sup>16,17</sup> Saari and Seitz have developed a complexometric sensor for the determination of beryllium that employs immobilized morin<sup>18</sup> and offers detection limits in the  $\mu\text{M}$  range. The same authors applied this sensor to the determination of aluminium and again obtained detection limits at the  $\mu\text{M}$  level.<sup>19</sup> However, they noted interference from  $\text{Co}^{2+}$ ,  $\text{Mg}^{2+}$ ,  $\text{Cu}^{2+}$  and  $\text{Fe}^{3+}$ . Zhujun and Seitz have described a complexometric fluorescence-based sensor which utilizes 8-hydroxyquinoline-5-sulfonic acid for the determination of  $\text{Al}^{3+}$ ,  $\text{Mg}^{2+}$ ,  $\text{Zn}^{2+}$ ,  $\text{Cd}^{2+}$ ,  $\text{Ca}^{2+}$ ,  $\text{Be}^{2+}$  and  $\text{Sr}^{2+}$ .<sup>20</sup> Detection limits were again of  $\mu\text{M}$  order. Unfortunately, the spectral character of the complexes was such that mixtures could not be resolved, although it was proposed that derivative spectroscopy might be employed for this purpose.

Recently, Seitz and co-workers have described a selective complexometric sensor for the determination of  $\text{Na}^+$  that offers a detection limit of 20mM.<sup>20</sup> This sensor employed 8-anilino-1-naphthalenesulfonic acid,  $\text{Cu(II)}$ -polyethyleneimine and a commercial sodium-selective ionophore immobilized on silica.<sup>21</sup> In this case selectivity was provided by the selective ionophore.

In the present paper we describe a new fluorimetric fiber-optic sensor for the determination of several ionic species. The sensor employs as the reagent phase a fluorophore trapped on a Nafion film. To our knowledge, this is the first application of Nafion-trapped species to fiber-optic sensing. Nafion is a perfluorinated polysulfate polymer. It has been proposed<sup>22</sup> that “ionopores” are formed within Nafion as the solvent evaporates and the charged sulfate groups agglomerate in the developing film. These pores act as cation-selective “holes” in the Nafion membrane. Cationic dye molecules can then reside on the Nafion membrane with their organic portions hydrophobically bound to the bulk membrane while their charged groups reside in the ionopore.

Immobilization of Rhodamine 6G on Nafion is especially attractive because the dye is both electrostatically and hydrophobically bound to the Nafion polyanion in aqueous solution. Furthermore, because of the anionic character of Nafion, positively charged ions are preferentially permitted to approach the fluorophore, so anionic interferences are minimal. Also, Nafion-based fluorimetric fiber-optic sensors can be fashioned simply and rapidly, and are quite durable.

In this study, ionic species such as  $\text{Co}^{2+}$ ,  $\text{Cr}^{3+}$ ,  $\text{Fe}^{3+}$ ,  $\text{Cu}^{2+}$ ,  $\text{Fe}^{2+}$ ,  $\text{Ni}^{2+}$  and  $\text{NH}_4^+$  were found to enter the ionopores and to quench the fluorescence of the

\*To whom correspondence should be addressed.

immobilized Rhodamine 6G. This is not too unlike the effects observed previously for rhodamine dyes in bulk solution.<sup>23</sup> In contrast, ions such as  $H^+$ ,  $K^+$ ,  $Li^+$ ,  $Na^+$ ,  $Ba^{2+}$ ,  $Ca^{2+}$ ,  $Mn^{2+}$ ,  $Zn^{2+}$  and  $Mg^+$  did not quench the fluorescence, but instead served as "reversers" in that they displaced the quencher ions and helped to re-establish the original level of fluorescence. The reversers can easily be determined from the initial rate of fluorescence increase after the film has been loaded with a quencher ion.

### THEORY

Fluorescence from the Nafion/Rhodamine 6G sensor is quenched, as described above, by various positive ions. In the case of the reverser ions, a competition occurs for ionophoric sites occupied by the quenching ions; reverser ions can kinetically displace the quenchers and thereby regenerate the original fluorescence signal.

The rate ( $d[Q_N]/dt$ ) at which the quencher diffuses into the Nafion film, reaches the ionophoric sites, and quenches the Rhodamine 6G fluorescence, is described by the expression

$$\frac{d[Q_N]}{dt} = k_1 F [Q_S] \quad (1)$$

where  $[Q]$  is the equilibrium quencher concentration, subscripts S and N represent the ions in solution or in the Nafion, respectively,  $k_1$  is the rate coefficient for the "transfer" of the quenching ion from the bulk solution into the Nafion, and  $F$  is the fraction of Rhodamine-laden ionophoric sites available to the quencher ions. If the observed fluorescence intensity as a function of time ( $dI/dt$ ) depends on  $[Q_N]$ , then:

$$\frac{d[Q_N]}{dt} = -k_2 \frac{dI}{dt} \quad (2)$$

where  $k_2$  is a new proportionality constant that incorporates the dependence of  $[Q_N]$ ,  $F$  and  $k_1$  on  $dI/dt$ . Upon combination of equations (1) and (2) the fluorescence intensity can be related to the quencher concentration in the bulk solution ( $[Q_S]$ ) by

$$\frac{dI}{dt} = -\frac{k_1}{k_2} F [Q_S] \quad (3)$$

At time  $t = 0$  the available fraction of ionophoric sites within the Nafion ( $F$ ) is constant (for a given Nafion/Rhodamine 6G sensor) and  $(dI/dt)_{t=0}$  (the initial rate of quenching) is given by:

$$\left(\frac{dI}{dt}\right)_{t=0} = -k [Q_S]_{t=0} \quad (4)$$

where  $k = k_1 F / k_2$  and  $[Q_S]_{t=0}$  is simply the concentration of quencher species in the bulk solution at time zero. A similar equation can be derived for the reverser ion:

$$\left(\frac{dI}{dt}\right)'_{t=0} = k' [R_S]_{t=0} \quad (5)$$

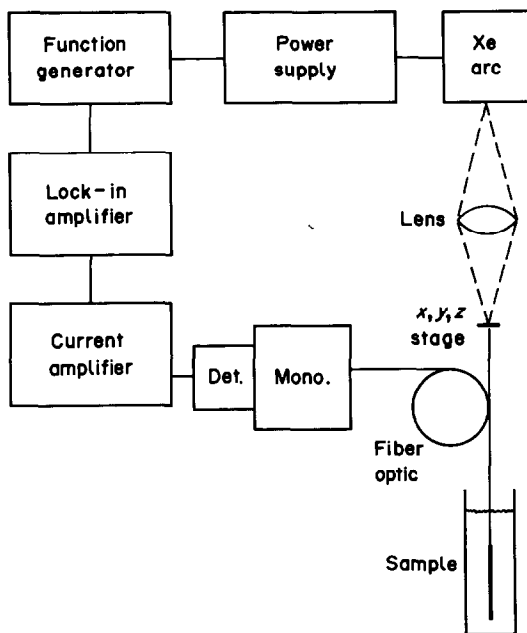


Fig. 1. Schematic diagram of the instrument. Mono. = monochromator. Det. = photomultiplier tube detection.

where  $R$  denotes a reverser ion. Therefore, a plot of  $(dI/dt)_{t=0}$  vs. quencher ion concentration or  $(dI/dt)'_{t=0}$  vs. reverser ion concentration will be linear. These linear plots can then be employed as working curves for determinations of either the quencher or reverser ions, respectively.

### EXPERIMENTAL

#### Reagents

The analyte cations were obtained from readily available reagent-grade materials. Initially, the chlorides were used, but later studies showed little dependence of the response on the counter-ion. All solutions were prepared in distilled demineralized water. A 0.100M stock solution of each metal ion was prepared and working solutions were prepared by serial dilution. Rhodamine 6G was purchased (Exciton Co.) and used as received. Nafion (perfluorinated ion-exchange powder) was purchased as a 5% solution in a mixture of aliphatic alcohols and water (Aldrich; cat. no. 27470-4). Hydrofluoric acid (70:30 HF:pyridine) was also supplied by Aldrich.

#### Instrumentation

All absorption spectra were recorded on a Hewlett-Packard model 8450 diode-array spectrophotometer.

Figure 1 shows a schematic diagram of the fiber-optic instrument used in these studies. The excitation source consists of an intensity-modulated xenon arc lamp system (Varian EIMAC model PS 300-1 power supply and model 300-2 lamp unit). Early versions of the instrument employed a continuous-wave argon-ion laser (Spectra Physics model 171), but satisfactory results were also achieved with the xenon arc lamp. The xenon lamp intensity is modulated by a square wave from a function generator (Krohn-Hite model 1600 lin/log sweep generator). For all results presented here, the average lamp current was 17 A (peak current 22 A) at a modulation frequency of 150 Hz.

The excitation wavelength is selected by a 15-nm band-pass filter centered at 500 nm. The filtered excitation light

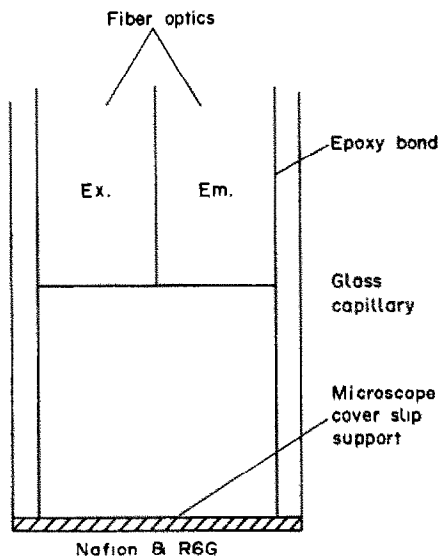


Fig. 2. Schematic diagram of the fiber-optic sensor. Ex. = optical fiber that carries exciting light to the fluorophore. Em. = optical fiber that carries emitted fluorescence radiation from the sensor to the photometric system. Open space indicated between microscope cover slip and fiber optic is an air-gap.

is then focused by a lens (focal length 60 mm) into one end of the bifurcated fiber-optic sensor (Fig. 2). The sensor consists of two identical 2-m lengths of 400- $\mu\text{m}$  diameter UV-transmitting fiber (General Fiber Optics part no. 14-400). Similar results were also achieved with 200- $\mu\text{m}$  diameter UV-grade fibers from Galileo Fiber Optics. The distal ends of the fibers are cemented together with epoxy resin (Epotek 320) within a 3-mm bore glass capillary. The glass capillary extends 1 cm below the end of the excitation and emission fibers, in order to ensure that the entire reagent surface is illuminated by the exciting light. A microscope cover slip is then glued (Superglue) over the opening of the glass capillary as shown in Fig. 2. This cover slip serves as a support for the Nafion/Rhodamine 6G membrane.

The fluorescence is collected by the second fiber optic (Em. in Fig. 2) and led to a monochromator (Kratos model GM 100-1) with band-pass centered at 550 nm. The resulting photon flux is detected by a photomultiplier tube (Hamamatsu model R928) operated at a biasing voltage of  $\sim 1000$  V dc. The output from the photomultiplier is then sent to a fast current-amplifier (Keithley model 840 Auto Loc). The TTL output from the function generator serves as the reference for the lock-in amplifier.

The output from the lock-in amplifier is directed to a computer (Digital Equipment Co. model MINC 11/23) which collects and analyzes the data by an interactive BASIC subroutine. The program consists essentially of two parts: (1) data collection (fluorescence intensity *vs.* time); (2) least-squares fitting of the initial portion of the data set (determination of initial rate).

#### Fiber preparation

The Nafion/Rhodamine 6G film is immobilized at the distal end of the optical fiber by means of a variant of the method proposed by Rubenstein and Bard.<sup>22</sup> The microscope cover slip, attached to the fiber's distal end, is first treated with a 70% solution of HF in pyridine for 30–60 sec. (It is important to note that an HF treatment time of longer than 2 min would result in both dissolution of the support glue and destruction of the microscope cover slip.) This HF

etching serves to produce a roughened surface which helps the Nafion to adhere to the microscope cover slip.

The reagent phase is produced by pipetting (Rainin Inc. pipet) between 25 and 50  $\mu\text{l}$  of the Nafion solution onto the microscope cover slip. The solvents are allowed to evaporate at room temperature over a 1-hr period and the sensor is then rinsed repeatedly with distilled demineralized water. The Nafion-coated cover slip is then quickly dipped in 1.00mM solution of Rhodamine 6G in 10% ethanol, removed, immersed in distilled demineralized water, removed and allowed to dry in air for 10 min, and rinsed again with water. For long-term storage, the fiber is immersed in water. This sensor is simple to produce and quite durable and gives a reproducible response over a period of several weeks, in both acidic (1M hydrochloric acid) and basic (1M ammonia) media. However, the film will separate or peel from the cover slip if the sensor is allowed to become completely dry.

#### General operation

For initial optimization, the detected fluorescence signal is maximized while the sensor is immersed in a water blank. This optimization usually consists of simply repositioning the excitation fiber with respect to the exciting light, or of minor readjustment of the lock-in amplifier phase setting. Following this initial optimization the system is stable (long-term signal drift  $<5\%$ ) for well over 4 hr.

For all the quencher ions studied, the Rhodamine 6G fluorescence decreases at a rate that is dependent on the quenching-ion concentration. Unfortunately, the quenching is not reversed simply by replacing the sensor in water, but must be reversed by the use of another ion ( $\text{H}^+$ ,  $\text{Na}^+$  or  $\text{Li}^+$ ) to displace the quencher. At first it might seem as if this lack of immediate reversibility is a detriment, but in fact it allows us to determine also those ions which reverse the quenching process.

Let us first consider the case of an ionic species ( $\text{Co}^{2+}$ ,  $\text{Cr}^{3+}$ ,  $\text{Fe}^{3+}$ ,  $\text{Fe}^{2+}$ ,  $\text{Cu}^{2+}$ ,  $\text{Ni}^{2+}$  or  $\text{NH}_4^+$ ) which quenches the fluorescence. As the quenching metal ion diffuses into the Nafion it reduces the Rhodamine 6G fluorescence. The rate of this quenching is dependent on two parameters: the solution concentration and identity of the quenching ion. From the plot of fluorescence intensity *vs.* time, the initial rate ( $V_i$ ) for the quenching process is determined and can be related to the initial concentration of quencher. The original fluorescence intensity can then be restored by immersing the sensor in a solution of one of the reversing ions ( $\text{H}^+$ ,  $\text{Na}^+$  or  $\text{Li}^+$ ).

To determine the concentration of a reverser ion, the fiber is first immersed in a solution of a quenching ion (e.g.,  $\text{Cu}^{2+}$ ) and the fluorescence quenched. The sensor is then removed from this solution, rinsed with water, and placed in the reversing-ion sample solution. The rate at which the fluorescence returns to its original level is again dependent on the two parameters mentioned above (concentration and identity of the ion). Consequently, the concentration of the reverser ion can be determined from the initial rate for restoration of fluorescence. A working curve of  $V_i$  *vs.* ion concentration can readily be constructed.

## RESULTS AND DISCUSSION

#### Quencher ions

Figure 3 shows a typical time-response trace for the sensor operating in the quencher mode. It is apparent that quenching by  $10^{-4}$  M  $\text{Cu}^{2+}$  is very rapid and requires less than 1 min to reach a nearly steady-state level. Table 1 compiles detection limits for all the quencher ions studied. The detection limit was defined as that concentration of metal ion which



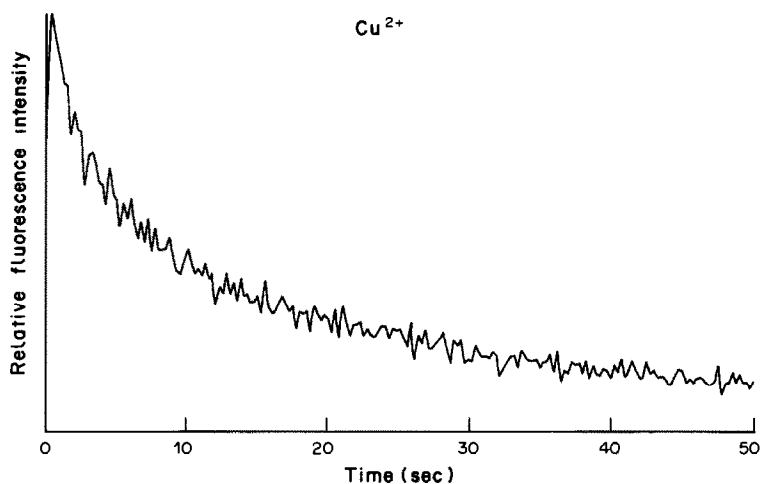


Fig. 3. Time-dependence of quenching of immobilized Rhodamine 6G caused by  $10^{-4}M$   $Cu^{2+}$ .

Table 1. Detection limits for quencher ions

Ion	Detection limit, $\mu M$
$Co^{2+}$	0.74
$Cr^{3+}$	0.82
$Fe^{3+}$	0.80
$Cu^{2+}$	1.2
$Fe^{2+}$	1.9
$Ni^{2+}$	2.1

Table 2. Statistical information for quencher-ion linear working graphs

Ion	Slope	Intercept	Correlation coefficient ( $r^2$ )	Std. error of estimate
$Co^{2+}$	3.81	0.12	0.981	0.16
$Cr^{3+}$	3.46	0.10	0.976	0.18
$Fe^{3+}$	3.14	0.09	0.992	0.09
$Cu^{2+}$	2.83	0.08	0.973	0.17
$Fe^{2+}$	2.51	0.04	0.991	0.11
$Ni^{2+}$	2.10	0.02	0.997	0.13

gave an initial rate of fluorescence decay that was twice the standard deviation of the steady-state fluorescence measured with the sensor immersed in water. The linear dynamic range for the determination of quencher ions extends over more than 4 orders of magnitude. Table 2 shows the results from

a least-squares analysis of a working graph for each ion. The detection limits parallel the initial rates of quenching as follows:  $Co^{2+} > Cr^{3+} > Fe^{3+} > Cu^{2+} > NH_4^+ > Fe^{2+} > Ni^{2+}$ . Because these quenching rates were dependent on the identity of the ionic species we chose to explore this feature in more detail.

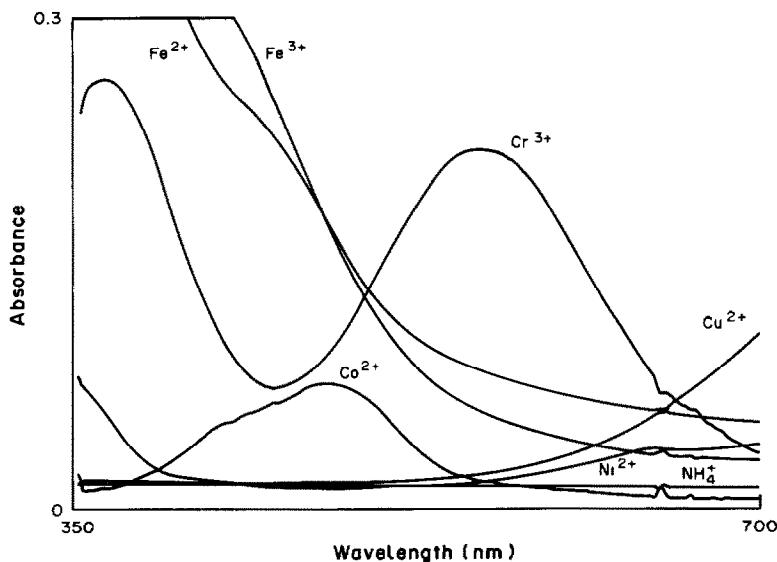


Fig. 4. Absorption spectra of quencher ions ( $10^{-2}M$  in aqueous solution).

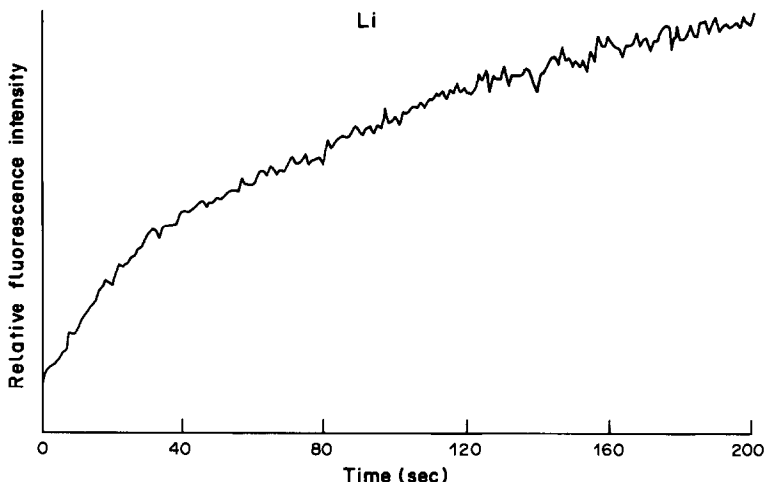


Fig. 5. Reverser-ion effect for  $10^{-4}M$   $Li^+$ ; other reverser ions behave similarly. The quenching by  $10^{-5}M$   $Cu^{2+}$  is being reversed.

Unfortunately, we did not find any physical parameter that correlated well with the initial rate of fluorescence decay caused by the quencher ion. For example, the crystal ionic radii, the approximate effective ionic radii, magnetic moments, and fluorescence lifetimes for each of the ions with the sensor do not correlate with the initial rate. Also, energy transfer to the absorption bands of the ions can be ruled out as a major contributor because of the very weak absorbances of all the quenching ions near 550 nm (Fig. 4). Rhodamine 6G has an emission spectrum centered at 550 nm with 120 nm full width at half maximum. Of the ions studied,  $Cr^{3+}$  would be the most likely to exhibit energy transfer (*cf.* Fig. 4), but no correlation was found between the degree of spectral overlap and initial quenching rates.

Regardless of the mechanism(s) involved in the quenching, it is clear that the quenching-based sensor is quite rapid, has excellent sensitivity, and is simple to operate. The instrumentation is rather simple to set up and not very expensive. Interference from traditional fluorescence quenchers (halides) is non-existent

because the ionopores of the Nafion film do not allow the halide to approach within the Rhodamine 6G interaction volume. For example, the bromide and chloride of a given cation gave approximately the same response.

*Reverse ions*

Figure 5 shows a typical response curve for a reverser ion; in this case  $10^{-4}M$   $Li^+$  is used to reverse the quenching caused by  $10^{-5}M$   $Cu^{2+}$ . Table 3 lists the detection limits calculated for the reverser ions in the same way as for quencher ions. In this mode of operation the linear dynamic range of the sensor is again over 4 orders of magnitude. Table 4 gives the results from a least-squares analysis of the linear working graphs. For completeness, the initial rate of enhancement was studied in more detail in an effort to gain insight into the mechanism.

The initial rates of reversal follow the order  $Ba^{2+} > K^+ > Ca^{2+} > Na^+ > Mn^{2+} > Zn^{2+} > Li^+ > Mg^{2+}$ , the same as the trend in both crystal ionic radii and approximate effective ionic radii. Figure 6 shows a plot of initial rate of enhancement *vs.* crystal ionic radii,<sup>24</sup> for  $Cs^+$ ,  $K^+$ ,  $Na^+$ ,  $Li^+$ ,  $Ba^{2+}$ ,  $Mn^{2+}$ ,  $Zn^{2+}$

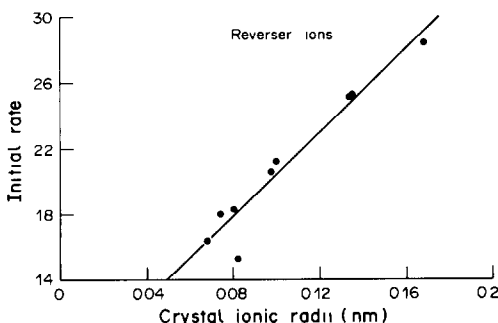


Fig. 6. Initial slope of the plot of fluorescence intensity *vs.* time (initial rate) as a function of the crystal ionic radii of the reverser ions. The quenching by  $10^{-5}M$   $Cu^{2+}$  is being reversed. Correlation coefficient is 0.932.

Table 3. Detection limits for reverser ions

Ion	Detection limit, $\mu M$
$Cs^+$	0.74
$K^+$	0.82
$Na^+$	1.4
$Li^+$	1.7
$H^+$	0.94
$Ba^{2+}$	0.81
$Ca^{2+}$	1.2
$Mn^{2+}$	1.5
$Zn^{2+}$	1.6
$Mg^{2+}$	1.8

Table 4. Statistical information for reverser-ion linear working graphs

Ion	Slope	Intercept	Correlation coefficient ( $r^2$ )	Std. error of estimate
Cs <sup>+</sup>	3.82	0.13	0.991	0.21
K <sup>+</sup>	3.69	0.14	0.997	0.12
Na <sup>+</sup>	2.73	0.08	0.990	0.13
Li <sup>+</sup>	2.02	-0.02	0.975	0.27
H <sup>+</sup>	3.31	0.16	0.982	0.21
Ba <sup>2+</sup>	3.71	0.18	0.952	0.41
Ca <sup>2+</sup>	2.93	0.16	0.966	0.42
Mn <sup>2+</sup>	2.42	0.01	0.967	0.33
Zn <sup>2+</sup>	2.13	0.10	0.983	0.25
Mg <sup>2+</sup>	1.81	-0.12	0.976	0.32

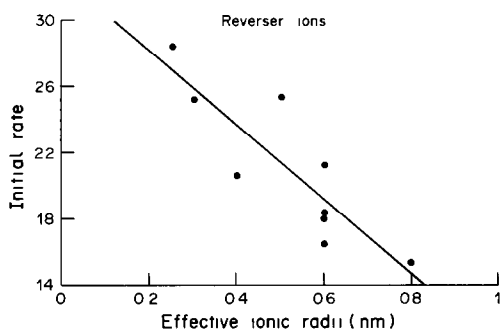


Fig. 7. Initial slope of the plot of fluorescence intensity *vs.* time (initial rate) as a function of the effective ionic radii of the reverser ions. Correlation coefficient is 0.745. The quenching by  $10^{-5}M$   $Cu^{2+}$  is being reversed.

and  $Mg^{2+}$  at the  $10^{-4}M$  level. Clearly, a linear relationship exists (correlation coefficient = 0.932) between size of the ion and the rate at which it restores the fluorescence intensity of  $Cu^{2+}$ -quenched Rhodamine 6G. Figure 7 shows a plot of the initial rate *vs.* effective ionic radii<sup>25</sup> for all the reverser ions studied. In this case the correlation coefficient is only 0.745. Thus it appears that the size of the reverser ion plays a critical role in the rate of the enhancement (displacement) process; however, such a trend is not readily apparent for the quencher ions.

#### CONCLUSION

The new sensor described can determine several ion species, and is simple to make, easy to operate, durable and rapid. Common measurement times are

20 and 70 sec for quencher and reverser ions respectively. The worst relative standard deviations observed were 4.5% for quencher ions and 5.8% for reverser ions. Unfortunately, the sensor is non-selective, but several of the ions have quenching or enhancement rates which differ by 40–50%. For this reason the sensor might be especially useful when applied in a sensor array.<sup>26</sup>

*Acknowledgements*—This work was supported in part by the Office of Naval Research, The Upjohn Company, and the National Science Foundation through grant 83-20053. The authors would like to thank Galileo Fiber Optics for providing the 200- $\mu m$  UV-grade fiber.

#### REFERENCES

1. F. P. Milanovich and T. Hirschfeld, *Adv. Instrum.*, 1986, **38**, 407.
2. W. R. Seitz, *Sensors*, 1985, **2**, 6.
3. O. S. Wolfbeis, *Trends Anal. Chem.*, 1985, **4**, 184.
4. R. Narayanaswamy, *Anal. Proc.*, 1985, **22**, 204.
5. T. E. Edmonds and I. D. Ross, *ibid.*, 1985, **22**, 206.
6. J. I. Peterson and G. G. Vurek, *Science*, 1984, **224**, 123.
7. I. Chabay, *Anal. Chem.*, 1982, **54**, 1071A.
8. F. E. Alder, *Z. Anal. Chem.*, 1986, **324**, 372.
9. T. Hirschfeld, *ibid.*, 1986, **324**, 618.
10. W. R. Seitz, *Anal. Chem.*, 1984, **56**, 16A.
11. R. Narayanaswamy and F. Sevilla III, *Analyst*, 1986, **111**, 1085.
12. G. F. Kirkbright, R. Narayanaswamy and N. A. Welti, *ibid.*, 1984, **109**, 1025.
13. J. F. Giuliani, H. Wohltjen and N. L. Jarvis, *Optics Lett.*, 1983, **8**, 54.
14. A. P. Russell and K. S. Fletcher, *Anal. Chim. Acta*, 1985, **170**, 209.
15. O. S. Wolfbeis, H. Offenbacher, H. Kroneis and H. Marsoner, *Mikrochim. Acta*, 1984 **I**, 153.
16. E. Urbano, H. Offenbacher and O. S. Wolfbeis, *Anal. Chem.*, 1984, **56**, 427.
17. W. A. Wyatt, G. E. Poirier, F. V. Bright and G. M. Hieftje, *ibid.*, 1987, **59**, 572.
18. L. A. Saari and W. R. Seitz, *Analyst*, 1984, **109**, 655.
19. *Idem*, *Anal. Chem.*, 1983, **55**, 667.
20. Z. Zhujun and W. R. Seitz, *Anal. Chim. Acta*, 1985, **171**, 251.
21. Z. Zhujun, J. L. Mullin and W. R. Seitz, *ibid.*, 1986, **184**, 251.
22. I. Rubenstein and A. J. Bard, *J. Am. Chem. Soc.*, 1980, **102**, 6641.
23. *CRC Handbook of Organic Analytical Reagents*, K. L. Cheng, K. Uno and T. Imamura (eds.), p. 465. CRC Press, Boca Raton, 1982.
24. *CRC Handbook of Chemistry and Physics*, 63rd Ed., p. F165. CRC Press, Boca Raton.
25. *Handbook of Analytical Chemistry*, L. Meites (ed.), p. 1. McGraw-Hill, New York, 1963.
26. W. P. Carey, K. R. Beebe, B. R. Kowalski, D. L. Illman and T. Hirschfeld, *Anal. Chem.*, 1986, **58**, 149.

## AN OPTICAL IONIC-STRENGTH SENSOR BASED ON POLYELECTROLYTE ASSOCIATION AND FLUORESCENCE ENERGY TRANSFER

LYNN M. CHRISTIAN and W. RUDOLF SEITZ

Department of Chemistry, University of New Hampshire, Durham, NH 03824, U.S.A.

(Received 20 May 1987. Accepted 21 August 1987)

**Summary**—The optical ionic-strength sensor is based on an indicator phase consisting of an aqueous solution of fluorescein-labelled dextran and polyethyleneimine labelled with Sulforhodamine 101 (Texas Red), confined behind a dialysis membrane. At low ionic strength the polymers associate and the average distance between the fluorescein and Texas Red is short enough for efficient energy transfer to occur. With increasing ionic strength the polymers dissociate and the efficiency of energy transfer decreases. The measured parameter is the ratio of the emission intensity at 520 nm, where fluorescein fluorescence is maximal, to the intensity at 620 nm, where the Texas Red emission is strong. The increase in the intensity ratio as a function of ionic strength is similar but not quite the same for different ions, suggesting that the mechanism of response involves more than a simple ionic strength effect.

We are interested in developing reversible indicators for use in fiber-optic sensors. These sensors offer several potential advantages over electrical sensors, including freedom from electrical interference and better stability with respect to calibration. Recent reviews provide a perspective of the field.<sup>1-3</sup>

Because there is a limited number of reversible indicators that have optical properties which change on interaction with analytes, we have become interested in the possibility of developing more complex indicator systems involving two or more components which combine or dissociate as a function of analyte concentration. We believe that this will provide a useful response to analytes for which there are no available direct indicators. Furthermore, by varying the relative concentrations of the components of the indicator system, it is possible to vary the effective equilibrium constant and thus the range of analyte concentrations sensed by the indicator.

The first reported reversible two-component indicator designed for use in a fiber-optic sensor was the glucose indicator system developed by Schultz *et al.*,<sup>4</sup> in which increasing glucose concentrations bring about the dissociation of fluoresceinated dextran and Concanavalin A. The Concanavalin A was immobilized outside the area illuminated through the fiber. Dissociation allowed the fluoresceinated dextran to diffuse into the zone of illumination, thus leading to an increase in the observed fluorescence intensity.

Here we report an indicator system based on the dissociation of two water-soluble polymers, dextran (C<sub>6</sub>H<sub>12</sub>O<sub>6</sub>)<sub>n</sub> and polyethyleneimine (CH<sub>2</sub>CH<sub>2</sub>NH)<sub>n</sub>. At pH 7 and low ionic strength the dextran (dex) and polyethyleneimine (PEI) associate. The effect of added ions is to cause them to dissociate. The primary interaction is between the added ions and the

protonated amino groups on the PEI. The reaction may be represented as



Fluorescence energy transfer is used to obtain a measurable optical parameter that is related to the degree of association between the dextran and PEI. One polymer is labelled with a fluorescent donor and the other with a fluorescent acceptor. When the two polymers are dissociated, the average distance between the donor and acceptor is too large for significant energy transfer to occur. However, upon association the distance decreases and energy is transferred to the acceptor. This leads to a decrease in donor fluorescence intensity and an increase in acceptor fluorescence intensity. When fluorescence energy transfer has been used for homogeneous immunoassay,<sup>5,6</sup> the parameter measured has been the decrease in donor emission. However, in the context of a sensor the ratio of donor to acceptor emission intensities should be measured since this parameter will not be affected by instrumental drift.

### EXPERIMENTAL

#### Apparatus

The fiber-optic fluorimeter differs from the instrument used in earlier work<sup>7</sup> only in having a filter wheel in the emission channel to allow rapid sequential measurements of emission intensities at two different wavelengths. Otherwise, the components include a tungsten-halogen light-source, interference filters for wavelength selection, a bifurcated fiber-optic bundle, and a photomultiplier as the detector.

Perkin-Elmer models 204 and MPF2A spectrofluorimeters were used to obtain fluorescence excitation and emission spectra. All pH measurements were made with an Orion Ross combination pH-electrode coupled to an Orion model 501 digital Ionalyzer.

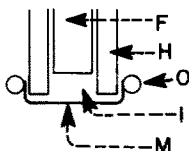


Fig. 1. Diagram of sensor tip. F = common end of bifurcated fiber-optic bundle, H = holder for common end of bundle, O = an O-ring that holds the dialysis membrane (M) in place to separate indicator solution (I) from the sample.

### Materials

Fluorescamine (FLRA), Rhodamine isothiocyanate (RITC), and dextran (MW  $1.89 \times 10^4$ ) labelled with fluorescein isothiocyanate (FITC) were obtained from Sigma. The sulfonyl chloride derivative of Sulforhodamine 101 (Texas Red) was obtained from Molecular Probes. Polyethyleneimine (PEI) with an average molecular weight of  $5.0 \times 10^4$  was obtained as a 50% w/w aqueous solution from Aldrich. It is a highly branched polymer containing an approximately 1:2:1 ratio of primary to secondary to tertiary nitrogens. Response to various anions was tested with reagent grade sodium salts.

### Procedures

Literature procedures were used to label PEI with FLRA,<sup>6</sup> RITC<sup>6</sup> and Texas Red.<sup>9</sup> Excess of reagent was separated from the labelled polymer by dialysis. A 5:1 mole ratio of Texas Red to polymer was used to prepare the PEI for use in the sensor.

To prepare a sensor, 25  $\mu$ l of a reagent solution 1.3  $\mu$ M in dextran and 1.6  $\mu$ M in PEI and adjusted to pH 7.4 with dilute hydrochloric acid were confined behind a dialysis membrane (10,000 MWCO from Spectrum Industries) on the common end of the bifurcated fiber-optic bundle as shown in Fig. 1. Response of the sensor to various anions was determined by inserting the common end of the sensor in 10.0 ml of water and making a series of standard additions of small volumes of 1.0M stock solutions of anion. After each addition the fluorescence intensities at both 520 nm and 620 nm were measured. Reversibility of response was confirmed by replacing the final salt solution with water.

## RESULTS

### Choice of labelling system

Three donor-acceptor pairs, FLRA/FITC, FITC/RITC and FITC/Texas Red, were evaluated for use in the ionic-strength sensor. The FLRA/FITC system has favorable characteristics for energy transfer applications.<sup>10</sup> However, PEI labelled with FLRA was only very weakly fluorescent, presumably because the secondary amine groups on the PEI interfere with the labelling reaction.<sup>11</sup> FITC/RITC has been used for homogeneous immunoassay applications based on energy transfer, in which the measured parameter is the decrease in FITC emission intensity when the FITC and RITC-labelled components of the assay system are bound to each other.<sup>6</sup> RITC-labelled PEI was observed to quench the fluorescein emission efficiently when bound to FITC-labelled dextran. However, the Rhodamine emission resulting from energy transfer is weak and is barely observable as a perturbation on the long-wavelength tail of the stronger fluorescein emission.

Fluorescein/Texas Red was chosen as the donor/acceptor system for the sensor because the Texas Red emission maximum is at a longer wavelength than that of RITC and thus can be more readily distinguished from the tail of the fluorescein emission.<sup>12</sup> To maximize both the extent of energy transfer and the intensity of Texas Red emission, the PEI was labelled at a 5:1 Texas Red/PEI mole ratio.

### Spectra

Figure 2 shows the fluorescence emission spectra for FITC-labelled dextran by itself (curve 1) and in the presence of Texas Red-labelled PEI (curve 2). The large decrease in fluorescein emission accompanying the addition of Texas Red-labelled PEI is evidence that the dextran and PEI are binding to each other sufficiently for efficient energy transfer to take place. The Texas Red emission band at 600 nm is excited partly by energy transfer from FITC and partly by direct excitation at 488 nm, the wavelength used for FITC excitation.

Figure 2 also includes the fluorescence emission spectrum observed when the solution of FITC-dextran and Texas Red-PEI is made 1.0M in sodium chloride (curve 3). The addition of the salt restores the fluorescein emission intensity to nearly its original value in the absence of Texas Red-PEI, indicating that the added salt is causing the dextran and PEI to dissociate. There is also an increase in the emission at 600 nm, which is due to the long-wavelength tail of the fluorescein emission rather than to Texas Red emission. At wavelengths longer than 650 nm, where the fluorescein emission is negligible but Texas Red still emits, the emission intensity decreases on addition of salt to the solution. This is to be expected if the salt causes the dextran and PEI to dissociate since Texas Red will no longer be excited by energy transfer.

On the basis of the spectra in Fig. 2, interference filters with transmission maxima at 520 and 620 nm

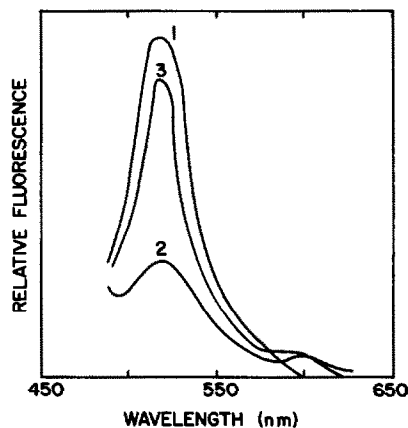


Fig. 2. Fluorescence emission spectra for 1.3  $\mu$ M fluorescein-labelled dextran by itself (1), in the presence of 1.6  $\mu$ M PEI (2) and in the presence of both 1.6  $\mu$ M PEI and 1.0M NaCl (3). Fluorescence was excited at 493 nm.

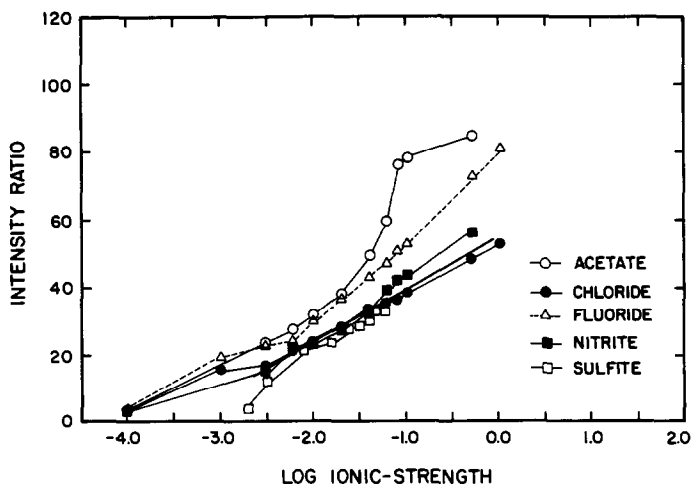


Fig. 3. Intensity ratio as a function of ionic strength for added fluoride, chloride, nitrite, sulfite and acetate.

were selected for the two-wavelength sensor measurement: 520 nm is the wavelength of maximum fluorescein emission, and although 620 nm is a longer wavelength than that of the Texas Red emission maximum, it was chosen because the emission ratio of Texas Red to fluorescein is higher there than at 600 nm.

Towards the end of this study it was discovered that the 488 nm excitation filter used for the sensor measurement had a weak transmission band (6.7% maximum transmittance) centered at 608 nm. Because of the transmission overlap between this band and the 620 nm transmission band of the emission filter, the signal measured at 620 nm with the fiber-optic fluorimeter was due primarily to scattered excitation radiation rather than to Texas Red emission. Although the original goal was to use the intensity of the acceptor emission as a reference signal, the intensity of the scattered radiation also serves as an adequate reference to compensate for instrumental fluctuations.

#### Effect of added ions

Figure 3 shows the effect of added ions on the 520/620 nm intensity ratio. The variation in intensity ratio with the log of the ionic strength is almost linear at ionic strengths from 3.0 mM to 1.0 M. The effects of added sulfite, nitrite and chloride are similar. At all concentrations the intensity ratios are higher for fluoride than for the other inorganic ions, indicating that fluoride is more effective at disrupting energy transfer.

Acetate is even more effective than fluoride at disrupting energy transfer, suggesting that hydrophobic interactions between the anion and protonated PEI may facilitate the PEI-dextran dissociation. With acetate, an ionic strength of 0.1 M is sufficient to cause almost complete dissociation.

Higher ionic strengths cause only a slight further increase in intensity ratio.

In all cases the response is reversible. The response time is about 5 min. It mainly consists of the time required for mass transfer into the reagent phase and could be significantly reduced by improved engineering.

#### DISCUSSION

We have demonstrated the possibility of using fluorescence energy transfer to obtain spectral shifts accompanying polymer-polymer binding. This makes it possible to relate the measured parameter to an intensity ratio. Accordingly, we feel that fluorescence energy transfer is very well suited for use with indicator systems based on competitive binding.

In principle this idea is broadly applicable. Selectivity can be obtained by modifying one of the polymers with a selective reagent. Binding of analyte would be detected through its effect on the polymer-polymer interaction. In practice, however, these interactions are affected both by pH and ionic strength, severely limiting the scope of possible applications. Furthermore, the complexity of polymer-polymer interactions makes it very difficult to predict the response for a particular system.

*Acknowledgement*—Partial support for this research was provided by NSF Grant CHE85-02061.

#### REFERENCES

1. J. I. Peterson and C. G. Vurek, *Science*, 1984, **224**, 123.
2. W. R. Seitz, *Anal. Chem.*, 1984, **56**, 16A.
3. O. S. Wolfbeis, *Z. Anal. Chem.*, 1986, **325**, 387.
4. J. S. Schultz, S. Mansoure and I. J. Goldstein, *Diabetes Care*, 1982, **5D**, 245.

5. L. Winfrey and B. S. Wagman, *Am. Clin. Prod. Rev.*, 1984, **3**, No. 6, 31.
6. E. F. Ullman, M. Schwarzberg and K. E. Rubinstein, *J. Biol. Chem.*, 1976, **251**, 4172.
7. L. A. Saari and W. R. Seitz, *Anal. Chem.*, 1982, **54**, 821.
8. M. Weigele, S. De Bernardo, W. Leimbruber, R. Cleeland and E. Grunberg, *Biochem. Biophys. Res. Commun.*, 1973, **54**, 899.
9. V. E. Handschin and W. J. Ritschard, *Anal. Biochem.*, 1976, **71**, 143.
10. J. N. Miller, C. S. Lim and W. J. Bridges, *Analyst*, 1980, **105**, 91.
11. S. Stein, P. Bohlen, J. Stone, W. Dairman and S. Udenfriend, *Arch. Biochem. Biophys.*, 1973, **155**, 202.
12. J. E. Titus, R. Haugland, S. O. Sharrow and D. M. Segal, *J. Immun. Meth.*, 1982, **50**, 193.

## ELECTROCHROMIC DYES, ENZYME REACTIONS AND HORMONE-PROTEIN INTERACTIONS IN FLUORESCENCE OPTIC SENSOR (OPTODE) TECHNOLOGY

N. OPITZ and D. W. LÜBBERS

Max-Planck-Institut für Systemphysiologie, 4600 Dortmund 1, Federal Republic of Germany

(Received 20 May 1987. Accepted 28 August 1987)

**Summary**—The analytical potential of fluorescence-based optochemical sensors (optodes) has been expanded by use of (1) electrochromic dyes incorporated in thin polymeric multilayers by means of Langmuir-Blodgett film techniques, (2) enzyme-catalysed biochemical reactions and (3) antibody-linked immunological reactions. Fluorescence optical biosensors have been developed for the determination of electrical potentials (*e.g.*, those produced by ion-selective membranes) and of hormones (*e.g.*, thyroxine) and metabolites (*e.g.*, lactate, glucose, xanthine and ethanol).

During the past decade, research on and development of sensors and their associated instrumentation have gained increased attention because of advances in data acquisition and processing offered by microprocessors and microcomputers. Special emphasis has been placed on the development of new sensors for continuous monitoring of chemical and biological substances. Fluorescence-based optochemical sensors are of special interest because of their broad applicability and technical advantages in connection with fibre-optic spectrophotometric instruments. In particular, the fluorescence optical sensors "optodes", introduced by us in 1975,<sup>1,2</sup> enable a variety of different substances or parameters to be determined, *e.g.*, oxygen, carbon dioxide, hydrogen-ion activity,<sup>3</sup> ionic strength<sup>4</sup> and related parameters such as osmolality or osmotic pressure. A fibre-optic catheter for intravascular measurements of pH, pCO<sub>2</sub> and pO<sub>2</sub> has also been described.<sup>5</sup> With suitable fluorescent indicators or chelate complexes, the activities of K<sup>+</sup>, Na<sup>+</sup>, Ca<sup>2+</sup> and Cl<sup>-</sup> may also be determined. Fibre-optic fluorescence sensors have been described for determination of ammonia, halothane, moisture and enzyme activities.<sup>6-8</sup> These examples clearly demonstrate the great potential of optochemical sensors as a basis for analytical determinations. We will discuss the application of electrochromic dyes for measuring electrical potentials, as well as enzyme-coupled biochemical and antibody-linked immunological reactions leading to the development of fluorescence optical biosensors for the determination of hormones and metabolites.

### ELECTROCHROMIC DYES INCORPORATED IN POLYMERIZED LANGMUIR-BLODGETT LAYERS AS A BASIS FOR OPTICAL MEASUREMENT OF ELECTRICAL POTENTIALS

Electrochromic dyes incorporated into plasma membranes of living cells are able to monitor the

electrical potential between two electrolyte solutions separated by these membranes.<sup>9,10</sup> The physical principle is based on the Stark effect, *i.e.*, an electric-field induction of a wavelength shift in the absorption and emission spectra. As Graf *et al.*<sup>11</sup> showed, the corresponding frequency shift can be well approximated<sup>12,13</sup> by

$$\Delta\nu \approx -\Delta\vec{\mu}\vec{F}_e/(hc) \quad (1)$$

where  $\Delta\nu$  = frequency shift,  $\Delta\vec{\mu} = \vec{\mu}_e - \vec{\mu}_g$ ,  $\vec{\mu}_e$  and  $\vec{\mu}_g$  = permanent dipole moments of the excited and ground states, respectively,  $F_e$  = electric field strength,  $h$  = Planck's constant and  $c$  = velocity of light.

If a signal is to be detectable, equation (1) implies that

- (1) the transition moment of the dye should be parallel to the electric field,
- (2) the absolute field strength should exceed 10<sup>5</sup> V/cm,
- (3) the dye should show a large change in dipole moment on excitation.

Therefore, the membrane layers used as dye matrices require certain properties.

- (1) They have to possess a high electrical resistance and be very thin ( $\leq 10$  nm), because typical biological potential differences are of the order of 100 mV.
- (2) Since the transition moment of the dye has to be oriented parallel to the electric field, the membrane should have a highly ordered structure.
- (3) To ensure stability and chemical resistance, the membranes should be polymeric.

Graf<sup>14</sup> has demonstrated that all these features are given by Langmuir-Blodgett (L-B) multilayers made of long-chain diacetylenic acids such as pentacosanoic acid<sup>15</sup> (Fig. 1a). In our work, electrochromic dyes were synthesized as described by Loew



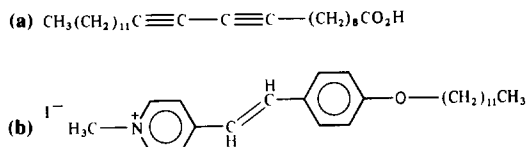


Fig. 1. (a) Structure of pentacosadiynoic acid. (b) Structure of 12-POE.

and Simpson,<sup>16</sup> and to obtain the high surface activity necessary for using the L-B techniques, the side-chains and polar headgroups were carefully selected. Figure 1b shows the structure of *trans*-4-[4-(dodecyloxy)phenylethylenyl]-*N*-methylpyridinium iodide (12-POE), which gave the best results.

Multilayer samples were built according to the L-B technique described elsewhere.<sup>17,18</sup> Fatty acids and the dyes were spread on a clean water surface on a commercial film balance and the resulting monomolecular film was reduced in area and transferred to a solid substrate. Multilayers consisting of 9 layers of ultraviolet-polymerized pentacosadiynoic acid and one dye layer (in the middle) were built up on platinum-coated semitransparent glass slides. As indicated in Fig. 2, the electric field was applied by means of two droplets of electrolyte solution in contact with Ag/AgCl electrodes.

Optical measurements of fluorescence and electrochromism were made with an SLM-8000 S spectrophotometer. In this set-up, light entered the multilayer at an angle of 30° to the plane of the layer, and the fluorescence was detected at an angle of less than 10°. Polymerized multilayers free of cracks and inhomogeneities showed a resistance of about 1 GΩ/cm<sup>2</sup>. Electric fields of approximately 10<sup>6</sup> V/cm could be applied without electrical breakdown. Samples with these properties were suitable for electro-optical experiments.

First, the difference spectrum, *i.e.*, intensity difference per wavelength unit with and without an electric field applied, was compared with the first derivative of the unperturbed emission spectrum. Applying the theories of Liptay<sup>12</sup> and Loew *et al.*<sup>13</sup> enabled the difference spectrum to be fitted very well by the derivative spectrum (Fig. 3). The wavelength shift of the emission spectrum depended linearly on the applied field strength up to  $1.3 \times 10^6$  V/cm and

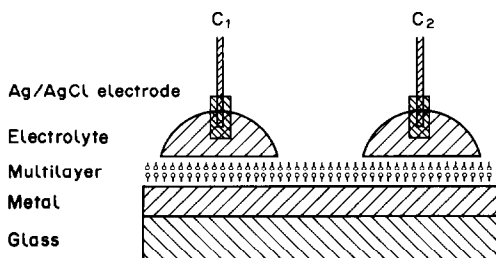


Fig. 2. Set-up for electrical measurements on multilayer samples<sup>14</sup> ( $C_1$ ,  $C_2$  = Ag/AgCl electrodes).

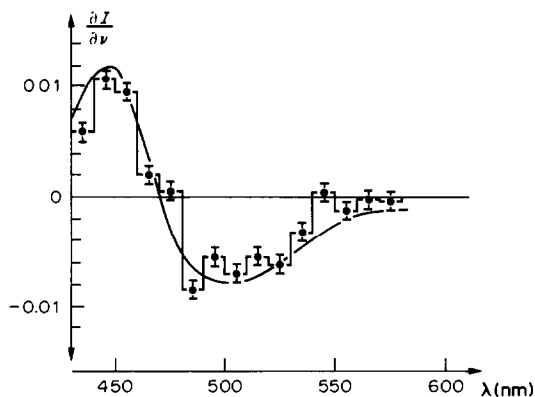


Fig. 3. Difference spectrum and first derivative of the emission spectrum of a multilayer sample of 12-POE (field strength 10<sup>6</sup> V/cm).<sup>11</sup> (Reprinted by permission of the copyright holders).

reached a maximum value of 3.5 nm. As can be seen in Fig. 4, no significant nonlinear dependence of the electrochromism on the applied voltage could be detected.

The signal-to-noise ratio in these experiments was about 50, but could be improved by reducing the film thickness and optimizing the optical detection system, which in our experimental conditions collected less than 0.1% of the emitted light. Optical detection of electrical potentials by using electrochromic dyes in combination with ion-selective membranes would enable highly selective determinations of ionic activities to be made without the problems caused by the reference electrodes needed for use with ion-selective electrodes, and could be used in remote sensing.

#### FLUORESCENCE OPTICAL BIOSENSORS USING ENZYME-CATALYSED BIOCHEMICAL AND ANTIBODY-LINKED IMMUNOLOGICAL REACTIONS

The concept of fluorescence-based optochemical sensors can be extended to the determination of biological substances such as hormones and metabo-

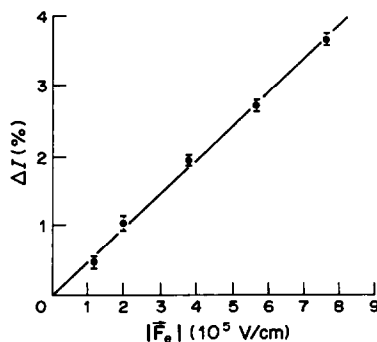


Fig. 4. Calibration curve for optical measurement of electrical potentials with electrochromic dyes incorporated into L-B multilayers<sup>11</sup> ( $E_e$  = electric field strength;  $I$  = fluorescence intensity). (Reprinted by permission of the copyright holders).

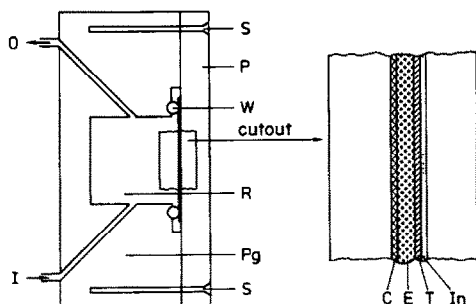


Fig. 5. Schematic representation of an enzyme optode.<sup>23</sup> (C = cellophane membrane, E = enzyme gel layer, In = indicator gel, T = PTFE membrane, S = screw, P<sub>g</sub> = Plexiglas, W = washer, P = UV-permeable Plexiglas, I = inlet, O = outlet, r = reaction cuvette).

lites, if suitable biochemical and immunological reactions are involved. For the sake of simplicity we use the terms enzyme optodes and immune optodes, depending on the biological reaction involved.

#### Enzyme optodes

By analogy with enzyme electrodes, enzyme optodes<sup>19-21</sup> are optodes coated with suitable enzyme layers that generate the signal to be monitored by the optode. For instance, for the continuous monitoring of glucose concentrations, glucose oxidase is immobilized within a thin layer ( $\sim 50 \mu\text{m}$ ) of bovine serum albumin cross-linked by glutaraldehyde. This thin layer is directly attached to an O<sub>2</sub> optode by means of an additional cellophane membrane (Fig. 5). The measuring device consists of a flow-through cuvette with the enzyme optode clamped to its side. The O<sub>2</sub>-sensitive film consists of an indicator gel of  $10^{-2}M$  pyrenebutyric acid dissolved in bis(2-ethylhexyl) phthalate, stabilized by addition of 1% ethyl cellulose and covered by a  $6.5 \mu\text{m}$  PTFE membrane.

Provided that sufficient oxygen is available within the sample, such a combined sensor allows the determination of glucose concentrations, since glucose and oxygen diffuse into the enzyme layer, where glucose is oxidized to gluconic acid. This biochemical reaction consumes oxygen, generating a pO<sub>2</sub> gradient across the enzyme layer, corresponding to the amount of glucose oxidized. When steady-state

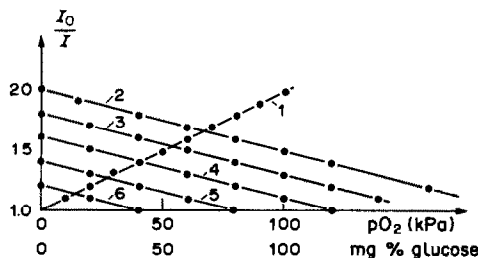


Fig. 6. Calibration curves of an enzyme optode for glucose at different oxygen partial pressures of the medium<sup>23</sup>: (2) 100 kPa O<sub>2</sub>, (3) 80 kPa O<sub>2</sub>, (4) 60 kPa O<sub>2</sub>, (5) 40 kPa O<sub>2</sub>, (6) 20 kPa O<sub>2</sub>. Curve (1) shows the optode's oxygen calibration.

diffusion conditions have been reached, the amount of glucose determines the pO<sub>2</sub> within the O<sub>2</sub>-sensitive layer of the O<sub>2</sub> optode (for theoretical considerations see Lübbers *et al.*<sup>22</sup>) and, therefore, the degree of fluorescence quenching, which is monitored photometrically. Figure 6 shows calibration curves for a glucose optode monitored at different oxygen partial pressures in the medium, together with its oxygen calibration curve.<sup>23</sup> The glucose calibration curves (decreasing with increasing glucose concentration) are almost parallel and can be closely approximated by the equation

$$(I_0/I) = 1 + KpO_2 - K'c_{\text{gluc}} \quad (2)$$

where  $I$  and  $I_0$  are the fluorescence intensities in the presence and absence of glucose,  $K$  the overall quenching constant,  $K'$  the sensitivity for glucose, pO<sub>2</sub> the oxygen partial pressure in the sample, and  $c_{\text{gluc}}$  the glucose concentration.

The range of concentrations that can be measured is determined by the pO<sub>2</sub> of the medium, the enzyme activity and the permeability of the outer cellophane membrane. Since the activity of enzymes shows a significant pH-dependence, the pH of the film also has to be carefully adjusted to achieve maximum enzyme activity. Moreover, traces of catalase have to be included in the enzyme layer to remove hydrogen peroxide, which would inhibit the glucose oxidase activity. The 90% response time of such enzyme optodes is about 1 min.

The principles of the enzyme optode for glucose can be extended to other substances if suitable oxidases are available. Examples are shown in Fig. 7 for lactate, xanthine and ethanol.

An advantage of these enzyme optodes over enzyme electrodes is that the fluorescence optical O<sub>2</sub>-sensor does not itself consume oxygen, so the diffusion of oxygen across the enzyme layer is not subject to the effect of any additional oxygen consumption.

Moreover, the O<sub>2</sub>-sensor surface is not in direct contact with biological fluid, so the calibration curve is not affected by changes in the diffusion properties of the O<sub>2</sub>-sensor membrane due to clogging by proteins and other biomolecules. Finally, owing to the transparency of the different sandwiched layers, the pO<sub>2</sub> gradient developed across the enzyme layer can be determined directly by means of a second O<sub>2</sub>-sensitive indicator layer arranged in series, as described in detail in the literature.<sup>22</sup>

#### Immune optodes

Analytical methods for the determination of hormones generally require specific reagents such as antibodies or other receptors with a high selectivity. Thus, the integration of the principle of fluorescence immunoassays into the optode appeared to be of interest. In our study with Reck and Himmelsbach,<sup>24</sup> the applicability of an optode device for continuous hormone measurements was tested with thyroxine

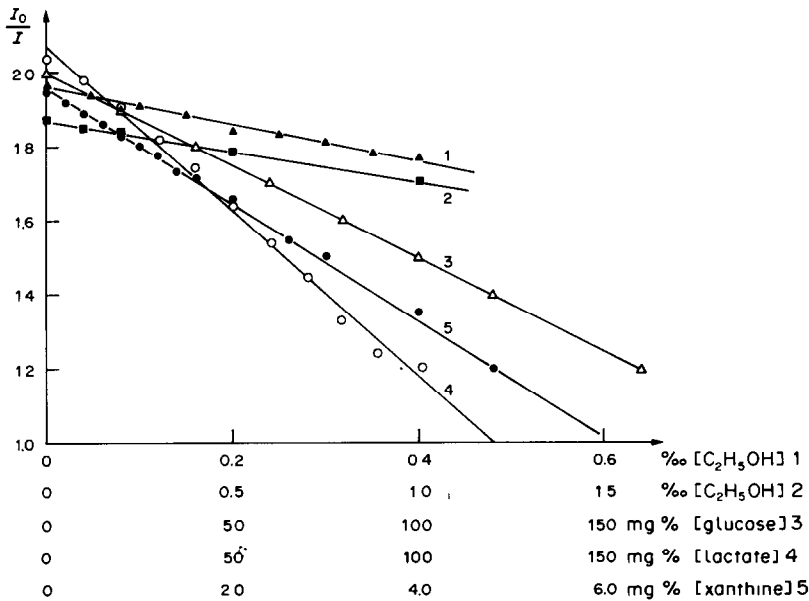


Fig. 7. Calibration curves of enzyme optodes for lactate, xanthine, ethanol and glucose<sup>23</sup> monitored at a pO<sub>2</sub> of 100 kPa. (In the case of ethanol measurements the influence of the diffusion properties of the outer membrane upon the calibration curves is demonstrated by applying (1) a cellophane membrane and (2) a dialysis membrane.

(T<sub>4</sub>) and its specific carrier, thyroxine-binding globulin (TBG), as a model system. A favourable property of this system is the specific 1:1 strong binding of the ligand by the protein ( $K_{\text{ass}} = 4 \times 10^{10}$ ). Furthermore, the binding causes a marked quenching of the protein's intrinsic fluorescence, and this can be used for optode measurements. The immune optode consisted of two compartments separated by a semipermeable Visking dialysis membrane. One of these compartments served as indicator chamber for TBG solutions, and the other contained the sample, which could be changed by continuous flow during measurements. The indicator compartment was irradiated only during measuring intervals of about 5 sec in order to protect the protein as far as possible against photodecomposition by ultraviolet light. The

face of the device used for fluorescence measurements was made of "Plexiglas", which is transparent to ultraviolet radiation. The preparation of T<sub>4</sub> solutions and characterization of human TBG have been described by Reck.<sup>25</sup>

Fluorescence curves obtained with different T<sub>4</sub> concentrations in the sample chamber are shown in Fig. 8. As can be seen, the intensity of the TBG fluorescence decreased in all three experiments almost linearly with increasing T<sub>4</sub> concentration. When the TBG was nearly saturated with ligand, the calibration curves levelled off. This result can be explained by the high association constant of the TBG-T<sub>4</sub> complex, and the rapid and almost complete binding of T<sub>4</sub> molecules within the indicator chamber. Hence, when the binding capacity of TBG molecules is not exhausted, the free T<sub>4</sub> concentration in the indicator chamber is always rather low compared with that in the sample chamber. Therefore, it can be assumed that there is an almost constant flow of T<sub>4</sub> molecules from the sample chamber into the indicator chamber, which causes a linear decrease of the fluorescence intensity with time at a given ligand concentration in the sample chamber. Thus, the rate of decrease in fluorescence is proportional to the T<sub>4</sub> concentration of the sample for a given amount of TBG molecules and defined diffusion properties of the dialysis membrane. A change in the T<sub>4</sub> concentration within the sample chamber produces a new steady state within a few minutes. The rate of change in the fluorescence corresponds to the new T<sub>4</sub> concentration, whether the concentration is increased or decreased. Such dynamic experiments can be continued until saturation of the binding protein is reached.

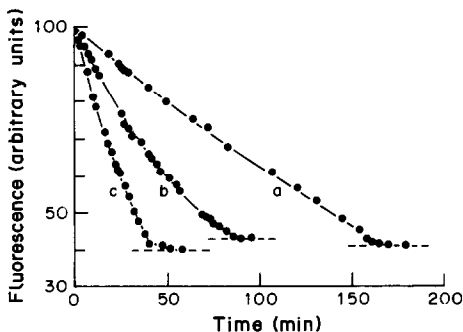


Fig. 8. Time course of normalized fluorescence intensities during a typical series of experiments with TBG as indicator<sup>25</sup> using an optode inlet of 0.65 mm depth ( $\lambda_{\text{ex}} = 290$  nm,  $\lambda_{\text{em}} = 340$  nm). Indicator solution 5  $\mu$ M TBG in 0.06 M KH<sub>2</sub>PO<sub>4</sub>, 0.7 mM EDTA, pH 7.4; T<sub>4</sub> solution (a) 1  $\mu$ M, (b) 2  $\mu$ M, (c) 5  $\mu$ M; flow rate = 2 ml/min.

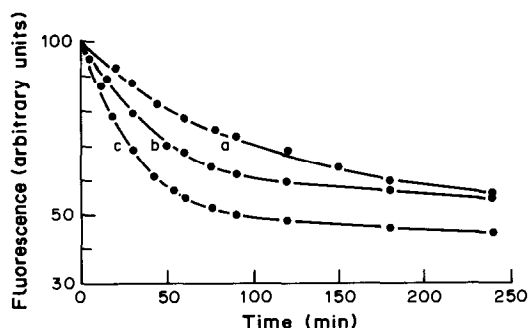


Fig. 9. Time course of normalized fluorescence intensities during a series of experiments with a  $5\mu\text{M}$  BSA solution in the indicator chamber of the optode.<sup>23</sup> ( $\text{T}_4$  solution (a)  $1\mu\text{M}$ , (b)  $2\mu\text{M}$ , (c)  $5\mu\text{M}$ ; other experimental conditions as in Fig. 8).

If other binding proteins with lower affinities for  $\text{T}_4$  are used instead of TBG, the linear range of the immune optode is narrower. Figure 9 shows the effect of replacing TBG by bovine serum albumin (BSA) possessing a binding site with an association constant of about  $10^6$  for  $\text{T}_4$  and three or more sites of lower affinity.<sup>26</sup> Even the highest of these association constants is about 4 orders of magnitude lower than the association constant of TBG. As a consequence, the change in fluorescence is a non-linear function of time almost from the beginning. This is because lower affinity of the BSA molecules for the ligand results in accumulation of unbound  $\text{T}_4$  molecules within the indicator chamber, causing a decrease in ligand flux across the dialysis membrane because of the smaller  $\text{T}_4$  gradients. Therefore, in Fig. 9 the curves level out to constant fluorescence intensities, which represent the equilibrium states determined by the corresponding ligand concentrations within the sample chamber. Neither method, however, can be used for continuous measurements. In the case of TBG (and probably for any other high-affinity binding protein) the dissociation of the ligand receptor complex proceeds far too slowly to allow monitoring of changing ligand concentrations at thermodynamic equilibrium within reasonable response times. On the other hand, choosing a substrate with lower affinity for the ligand would increase the time resolution but decrease the sensitivity. This dilemma appears to be inherent in the use of specific binding biomolecules in biosensor systems. If fast measurements at or close to equilibrium are desired, the binding must be weak in order to avoid unduly long response times. Highly selective but low-affinity monoclonal antibodies in combination with sensitive reporter groups, as proposed by North,<sup>27</sup> might provide a promising way to solve this problem.

In earlier experiments it was shown that the application of fluorescence indicators, for instance to

measure  $\text{pO}_2$ ,  $\text{pCO}_2$ , and pH, had distinct advantages over the use of conventional electrodes, particularly in regard to miniaturization, stability, and easy handling. The fluorescence optical measurements of small electrical potentials and the combination with enzyme and immune reactions described above demonstrate that the optode technique can be successfully extended to a wider range of analytical applications.

#### REFERENCES

1. D. W. Lübbers and N. Opitz, *Z. Naturforsch. C, Biosci.*, 1975, **30c**, 532.
2. N. Opitz and D. W. Lübbers, *Pflügers Arch.*, 1975, **355**, R120.
3. D. W. Lübbers, N. Opitz, P. P. Speiser and H. J. Bisson, *Z. Naturforsch. C, Biosci.*, 1977, **32c**, 133.
4. N. Opitz and D. W. Lübbers, *Sens. Actuators*, 1983, **4**, 473.
5. J. L. Gehrich, D. W. Lübbers, N. Opitz, D. R. Hansmann, W. W. Miller, J. K. Tusa and M. Yafuso, *IEEE Trans. Biomed. Eng.*, 1986, **33**, 117.
6. O. S. Wolfbeis and H. E. Posch, *Anal. Chim. Acta*, 1986, **185**, 321.
7. O. S. Wolfbeis, H. E. Posch and H. W. Kroneis, *Anal. Chem.*, 1985, **57**, 2556.
8. O. S. Wolfbeis, *ibid.*, 1986, **58**, 2874.
9. N. Bennett, M. Michel-Villaz and Y. Dupont, *Eur. J. Biochem.*, 1980, **111**, 105.
10. H. V. Davila, B. M. Salzberg, L. B. Cohen and A. S. Waggoner, *Nature, New Biology*, 1973, **241**, 159.
11. H.-J. Graf, N. Opitz and D. W. Lübbers, *Proc. 2nd Int. Meeting Chemical Sensors*, Bordeaux, 1986, p. 696.
12. W. Liptay, *Angew. Chem.*, 1969, **8**, 195.
13. L. M. Loew, G. W. Bonneville and J. Surow, *Biochem.*, 1978, **17**, 4065.
14. H.-J. Graf, *Thesis*, University of Dortmund, FRG, 1986.
15. D. S. Johnston, S. Sanghera, M. Pons and D. Chapman, *Biochim. Biophys. Acta*, 1980, **602**, 57.
16. L. M. Loew and L. L. Simpson, *Biophys. J.*, 1981, **34**, 353.
17. K. B. Blodgett, *J. Am. Chem. Soc.*, 1935, **57**, 1007.
18. G. L. Gaines, *Insoluble Monolayers at Gas-Liquid Interfaces*, Wiley, New York, 1966.
19. K.-P. Völkl, N. Opitz and D. W. Lübbers, *Z. Anal. Chem.*, 1980, **301**, 162.
20. K.-P. Völkl, U. Grossmann, N. Opitz and D. W. Lübbers, *Adv. Physiol. Sci., Proc. 28th Int. Congr.*, 1980, **25**, 99. A. G. B. Kovách, E. Dóra and M. Kessler (eds.), Akademiai Kiadó, Budapest, 1981.
21. N. Uwira, N. Opitz and D. W. Lübbers, *Adv. Exp. Med. Biol.*, 1984, **169**, 913.
22. D. W. Lübbers, K.-P. Völkl, U. Grossmann and N. Opitz, in *Progress in Enzyme and Ion-Selective Electrodes*, D. W. Lübbers, H. Acker, R. P. Buck, G. Eisenman, M. Kessler and W. Simon (eds.), p. 67. Springer, Berlin, 1981.
23. K.-P. Völkl, *Thesis*, University of Bochum, FRG, 1980.
24. B. Reck, K. Himmelpach, N. Opitz and D. W. Lübbers, *Pflügers Arch.*, 1985, **405**, R64.
25. B. Reck, *Thesis*, University of Freiburg i.B., FRG, 1983.
26. R. F. Steiner, J. Roth and J. Robbins, *J. Biol. Chem.*, 1966, **241**, 560.
27. J. R. North, *Trends Biotechnol.*, 1985, **3**, 180.

## TOWARDS A FLUORESCENT CHEMORECEPTIVE LIPID MEMBRANE-BASED OPTODE

ULRICH J. KRULL\*, R. S. BROWN, R. F. DEBONO and B. D. HOUGHAM  
Chemical Sensors Group, Department of Chemistry, Erindale College, University of Toronto,  
Mississauga Road, Mississauga, Ontario, Canada

(Received 20 May 1987. Accepted 28 August 1987)

**Summary**—Lipid membranes have been deposited on the surface of glass slides and quartz fibres for the development of optical chemical sensors. The fluorescence properties of probes embedded within ordered lipid matrices were sensitive to physical and electrostatic environmental alterations of the membrane caused by various non-selective processes. This work reports criteria for surface deposition of monolayers of phosphatidylcholine-steroid mixtures and stearic acid by Langmuir-Blodgett techniques. The fluorophores 1-anilino-naphthalene-8-sulphonate and 12-(9-anthroyloxy)stearic acid were incorporated into the monolayers for determination of the physical characteristics of the membranes. Interactions of the membranes with the perturbing species phloretin and valinomycin in aqueous solution, and with chloroform, n-hexane and *N,N*-dimethylaniline in the gas phase, are described. An evanescent-wave intrinsic fibre-optic sensor based on lipid membrane excitation is reported.

Fibre-optic chemical sensors have received widespread attention as dedicated sensitive and selective devices capable of remote operation without significant susceptibility to electronic and magnetic interference.<sup>1-4</sup> Extrinsic fibre sensors are by far the most common type of such devices reported to date, and consist of chemically selective solution cells interfaced to optical waveguides. The fibre acts only to transmit optical radiation to and from a chemical reaction system. The selective reaction usually occurs in a closed microscopic volume physically located in close proximity to one end of the fibre. Innovations in fibre-optic sensor research have recently appeared in the area of selective chemical analysis for inorganic ions or molecules by means of specialized reagents,<sup>5-7</sup> but few advances in optical biosensor research have been reported. The selective biochemical methods which have been applied to fibre-optic sensing<sup>8,9</sup> are generally limited in their chemical applicability, and also by physical restrictions such as low sensitivity due to the limited path-length of miniature solution cells. The work described here is directed towards the investigation and development of a generic biosensor based on the transduction of artificial chemoreceptive processes in an intrinsic fibre-optic mode.

Previous work in the area of biosensors introduced the manipulation of the properties of ordered bilayer lipid membranes (BLMs) for implementation of a generic transduction mechanism suitable for electrochemical sensing of selective receptor-binding events taking place within the sensing membrane.<sup>10-12</sup> The binding of proteinaceous receptors with analyte

causes perturbation of the lipid membrane structure and electrostatic fields, which in turn control the permeability of the membrane for ions. The change in ion current is related to the degree of perturbation of the membrane by receptor complexation, and has provided an analytical signal for analyte concentrations as low as  $10^{-13} M$  in some cases.<sup>11</sup>

Even though the BLM is ideal for sensitive response, and assists in maintenance of an environment suitable for maximizing receptor-binding activity, the electrochemical transduction is limited by extreme sensitivity to electrical noise and requires complete structural integrity of the lipid membrane. It is possible to avoid these practical limitations by non-electrochemical analytical exploitation of the membrane perturbation. The method of choice presented here makes use of the high sensitivity of fluorescence spectrophotometry and the ability of membrane-embedded fluorophores to respond to perturbation of the membrane potential and lipid molecular packing/fluidity. The physical thickness of a lipid monolayer or bilayer is less than 10 nm, and therefore restricts the analytical utility which can be achieved by adsorbing the layer on an optic fibre. However, the membrane thickness is ideal for interaction with the evanescent-wave which is generated by total internal reflection in all optical fibres.<sup>13,14</sup>

### THEORY OF INTRINSIC LIPID-MEMBRANE OPTICAL BIOSENSORS

Intrinsic fibre-optic biosensors are based on the coupling of selective chemistry with the optical radiation available along the surface length of an optical waveguide. At the points of total internal reflection,

\*To whom correspondence should be addressed.

a standing wave of electromagnetic radiation can be envisaged within the fibre. A useful property of this standing wave is that its amplitude does not decay to zero at the fibre surface, but has an external component, known as the evanescent wave, which decays exponentially along the  $Z$ -axis perpendicular to the fibre surface. The intensity of the radiation,  $I$ , is related to the incident angle  $\theta$ , a transmission factor  $T(\theta)$ , and a characteristic penetration depth,  $d_p$ :

$$I = T(\theta)\exp(-2Z/d_p) \quad (1)$$

The term  $d_p$  is related to the refractive index of the fibre,  $n_1$ , the refractive index of the external environment,  $n_2$ , and the wavelength of the optical radiation,  $\lambda$ :

$$d_p = \frac{\lambda}{2\pi n_1 [\sin^2 \theta - (n_2/n_1)^2]^{1/2}} \quad (2)$$

These relationships indicate that a significant intensity of optical radiation can penetrate to depths of a few hundred nm for wavelengths in the visible portion of the electromagnetic spectrum. It is therefore possible to coat an optical fibre with a thin film of selective reagent, and generate an analytical signal by excitation of the reagent with an evanescent wave. This system is ideal for adjusting the sensitivity of the sensor by simply varying the length of coated fibre. Furthermore, the selective chemistry takes place only in a defined surface region, avoiding bulk solution interference, and permitting use of specialized reagents which optimally operate as molecular monolayers.

Perturbation of the fluorescence signal resulting from a sensor of this configuration may be realized either by surface interaction with a fluorescent analyte or by altering the intrinsic surface-layer fluorescence through analyte interactions. Since most analytes do not fluoresce, the latter strategy offers greater versatility. Fluorescence in membranes will respond to characteristics such as structure and phase, fluidity, hydration, electric fields, and accessibility of fluorescent moieties to external quenching agents.

This work investigated monolayer membranes of phospholipid and stearic acid deposited onto borosilicate glass and quartz optical supports.<sup>15-17</sup> The fluorophore 1-anilinoanthracene-8-sulphonate was incorporated to respond to hydration and potential fields in the vicinity of the polar head-group region of the membrane. The fluorophore 12-(9-anthroiloxy)stearic acid was incorporated to study variations in fluidity in the hydrocarbon region of the membrane. Overall membrane structure was varied by use of different controlled monolayer surface pressures during membrane deposition. Exposure to membrane perturbants and fluorescence-quenching agents, in both gas and liquid phase environments, was also studied.

## EXPERIMENTAL

### Chemicals

Phosphatidylcholine (PC) from egg yolk (Avanti Biochemicals, Birmingham, AL, USA) and cholesterol (C) (Sigma Chemical Company, St. Louis, MO, USA) were used for making the phospholipid membranes. Stearic acid (Sigma) was employed to prepare fatty acid membranes. The fluorophores 1-anilinoanthracene-8-sulphonate (ANS) (Eastman Kodak, Rochester, NY, USA), 12-(9-anthroiloxy)stearic acid (12-ASA) (Molecular Probes Inc., Eugene, OR, USA), and the membrane perturbants phloretin and valinomycin (Sigma) were all used as received, without further purification. The membrane stimulants chloroform, *n*-hexane and *N,N*-dimethylaniline, and all other solvents, were of analytical reagent grade. All water was obtained from a five-stage Milli-Q (Millipore® Water System) cartridge-filtering system and had a specific resistivity of not less than 18 M $\Omega$ /cm. The surface silanizing agent octadecyltrichlorosilane (OTS) (Aldrich, Milwaukee, WI, USA) was stored under anhydrous conditions.

### Apparatus

A Lauda Model 1974 thin-film balance (Brinkman Instruments, Toronto, Canada) was used in association with a home-made film lift<sup>18</sup> for deposition of lipid monolayers onto glass and quartz surfaces. Glass wafers were cut to dimensions of 0.5  $\times$  3 cm from plain borosilicate microscope slides of thickness 0.1 cm (Fisher Scientific, Toronto, Canada). Quartz wafers, 0.8  $\times$  6 cm, were cut from 1.5-mm thick quartz plates (Heraeus Amersil, Sayerville, NJ).

Fluorescence measurements of the monolayer-coated wafers incorporating ANS were made with a Turner Model 111 fluorimeter (Turner, Palo Alto, CA, USA). The wafers were supported in a Pyrex tube which could be rotated to provide reproducible excitation illumination angles. For experiments with the fluorescence probe ANS, the primary excitation filter chosen had a 50-nm band-pass centred at 360 nm, and the secondary emission filter had a 485 nm short-wavelength cut-off. Gas phase experiments made use of a capped Pyrex sample holder, which was connected to a thermally regulated headspace vessel as shown in Fig. 1. Syringes were used for reproducible sampling and quantitative transfer of small volumes of gas within the closed assembly.

Fluorescence studies of stearic acid/12-ASA monolayers deposited onto quartz wafers were performed with a pulsed (300 psec) model LN 103 nitrogen laser operating at 337 nm (PRA, London, Ontario, Canada). Fluorescence was analysed with a SPEX 1700II monochromator and an RCA 7625 photomultiplier tube operated at 2000 V. The output was monitored by a gated integrator/boxcar averager system (EG&G, PAR, Princeton, NJ) with 50  $\Omega$  input impedance, interfaced with an Apple II computer. The detection system was triggered optically by a fast photodiode.

The optical fibres used were commercial silica fibres of 400  $\mu$ m diameter (PCS 400, Tasso, Montreal, Canada). The fibre-based fluorescence spectra were collected by using the above-mentioned nitrogen laser, a Heath EU 700 monochromator (Schlumberger, Mississauga, Canada), an R928 photomultiplier tube (Hamamatsu, Bridgewater, NJ), and a P477415 power supply/photometer (Zeiss, FRG) operated at 1 kV.

### Procedures

The phospholipid solutions consisted of 2.5 mg of PC and 2.5 mg of cholesterol in 5.0 ml of hexane. These solutions were stored under nitrogen in darkness at  $-20^\circ$  when not being used. The fatty acid solutions consisted of 2 mg of stearic acid in 5.0 ml of hexane, and were stored in the same way as the phospholipid solutions. The incorporation of the anthroiloxy-labelled fatty acid probes into these solutions was achieved by first preparing a 1 mg/ml stock solution of

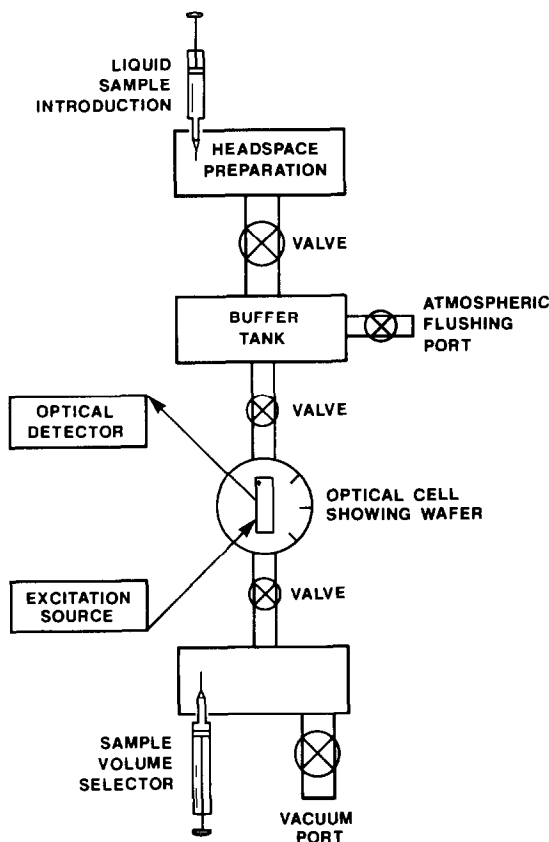


Fig. 1. Gas-phase sampling apparatus showing location of the production of a headspace of known partial-pressure and the sample-wafer housing illustrating the angular alignment of the excitation beam.

the fluorescent probe in ethanol. A fixed quantity of the ethanolic solution (10–100  $\mu\text{l}$ ) was transferred to a separate vial and evaporated to dryness under nitrogen. The residual film was incorporated into the phospholipid or fatty acid solution by addition of a fixed volume of the appropriate hexane solution to the vial. Molecular ratios of lipid to fluorescent probe in the range from 100:1 to 20:1 were investigated.

The lipid solutions were characterized by production of experimental pressure–area isotherms for lipid monolayers. Approximately 70  $\mu\text{l}$  of the lipid solution was added dropwise (by syringe) over a period of 30 sec to the surface of 900 ml of degassed water in a Lauda trough at fixed temperature. After a period of 15 min (to allow the hexane to evaporate) the monolayer was compressed at a speed of 0.9 cm/min until the collapse pressure was attained.

The glass wafers were cut by scoring with a diamond-tipped scribe and then cleaving to the required size. The wafers were then sonicated in a 2% aqueous solution of sodium dodecylsulphate detergent for 1 hr, rinsed with distilled water, soaked in chromic acid for at least 1 hr, rinsed extensively with water and then stored in a dust-free environment. The monolayer on the trough was initially compressed to the desired surface pressure and allowed to equilibrate for 15 min. Monolayers were cast onto glass wafers at a surface pressure of 20–40 mN/m, which was held constant during the entire casting procedure. A monolayer was transferred to a wafer by immersing the wafer by means of an automatic casting elevator at a speed of 0.85 cm/min through the air–water interface at an angle of 90°. At the end of the immersion the wafer was allowed to soak in

the aqueous phase for 5 min before being withdrawn at 0.85 cm/min.

The fluorophore ANS was introduced into the phospholipid monolayers by two different methods. One consisted of casting the monolayers onto the wafers from an aqueous  $10^{-4}\text{M}$  ANS subphase in the Lauda trough. The second method consisted of casting a monolayer of PC/C on the wafers from a water subphase, and subsequently soaking these wafers in a solution of  $10^{-4}\text{M}$  ANS for 24–72 hr, the wafers being manually lowered into the interaction vial, but removed slowly with the casting elevator in order to allow the water to drain completely from the surface.

All monolayer-coated optical components were stored in a desiccator in darkness, but were not protected by low temperatures or an inert gas atmosphere. Experiments to observe the fluorescence from wafers consisted of suspension of the coated glass in an aqueous solution and introduction of the membrane perturbants valinomycin or phloretin as concentrated methanolic solutions. The utility of the fluorescent membranes as gas-phase sensors was demonstrated by providing variable atmospheres containing membrane perturbants and fluorescence quenching agents such as *N,N*-dimethylaniline for the anthroyloxy probes.

The quartz wafers and fibres were first alkylated with OTS.<sup>19</sup> The alkylated surfaces were characterized by contact-angle measurements; the values found were near 90°, and were unaffected by subjecting the alkylated wafers to the original glass-cleaning procedure.

Monolayers of stearic acid and 12-ASA were deposited onto these surfaces from a Langmuir–Blodgett trough at surface pressures of 13–38 mN/m. The stearic acid:12-ASA ratio was 27:1. Deposition was monitored by observing the trough barrier movement during operation at constant pressure. Spectral and temporal data for the quartz wafer surface-fluorescence were collected by inserting the wafer into a fluorescence spectrometer. The laser beam was first split by a quartz plate, a small portion of the beam being sent to a fast (<nsec) photodiode which triggered the data collection. The beam struck the sample at 70° to the normal. The reflected beam was directed onto a fluorescent target, to ensure reproducible alignment of the wafer. The fluorescence was detected at 90° to the incident laser beam, with averaging of 50 pulses for each data point to reduce noise in the output. Measurements for optical fibres were made with a similar instrument configuration, with the fibre inserted into the path of the laser. This assembly did not allow collection of temporal data.

## RESULTS AND DISCUSSION

### Monolayer compression

The pressure–area isotherms of monolayers provide a facile method of physical structure characterization, and interpretation of molecular interaction.<sup>12</sup> The collapse pressures and corresponding areas, as well as the average molecular areas at 16 and 32 mN/m pressure are summarized in Table 1. Each of the compression curves showed zones of loose association (low surface pressure), partial condensation, complete condensation and then collapse as the surface pressure increased.<sup>20</sup>

Consideration of the average molecular area data provides an indication of chemical bonding interactions within the monolayer as well as physical volume criteria.<sup>20</sup> At the lipid-to-probe molecular ratios of approximately 22:1 used to obtain the results shown in Table 1, it is apparent that the

Table 1. Compression pressure–area results for lipid monolayer films at an air–water interface

Monolayer composition (over water subphase), temperature	Molecular area, $nm^2$ , at		
	Pressure collapse	32 mN/m	16 mN/m
PC/C, 26°C	$0.43 \pm 0.02$	$0.44 \pm 0.02$	$0.48 \pm 0.02$
PC/C, 36°C	$0.44 \pm 0.01$	$0.45 \pm 0.01$	$0.53 \pm 0.01$
PC/C, $10^{-4}M$ ANS in water subphase 26°C	$0.38 \pm 0.01$	$0.40 \pm 0.01$	$0.51 \pm 0.01$
PC/C: 12-ASA (22:1 lipid-to-probe molecular ratio), 26°C	$0.47 \pm 0.01$	$0.50 \pm 0.01$	$0.58 \pm 0.01$

12-ASA fatty acid probe is causing a distinct physical perturbation leading to an expanded monolayer. The physical area that would be swept out by rotation of the 12-ASA probe in the plane of the monolayer implies that the lateral projection of the bulky anthroxyloxy group should cause a general increase in molecular area.

The action of ANS on the membrane indicates that it may participate in a bonding interaction, since it actually produces a membrane contraction rather than simply a physical volume displacement. It is difficult to identify the action of ANS on the membrane since the probe is not fixed in location or orientation, and can be distributed throughout the ordered matrix. The charge which ANS may bring to the surface of the membrane can dramatically alter the surface dipolar interactions and local hydrogen-bonding interactions which affect structure.<sup>12,20</sup>

The ANS and 12-ASA fluorophores may differentially partition into domain structures, which are likely to be present in the membranes described in this work.<sup>21,22</sup> Therefore the chemistry of the fluorophores may be relatively complicated at the molecular level and consequently analytical data obtained from fluorescence lifetime or polarization experiments may be questionable. However, the reproducible compression curves indicate that reliable average film properties can be obtained, and this indicates that parameters such as total fluorescence intensity and maximum emission wavelength should be relatively consistent between experiments.

#### *Monolayer deposition on plain wafers*

Monolayer deposition of phospholipid and stearic acid consisted of a three-phase cycle: immersion, a 5-min soaking period to allow free silanol groups on the substrate surface to become deprotonated and provide a negative charge on the surfaces of the wafer,<sup>23</sup> and withdrawal.

The conclusion that only a monolayer was deposited during the casting sequence is based on observations from

- (1) monitoring of the casting;
- (2) the transfer function = (loss of trough area)/(substrate area);
- (3) the wetting characteristics of the coated wafers.

During all casting sequences the movement of the monolayer compression barrier was accurately moni-

tored by recording its position as it moved to provide constant surface pressure. During the immersion and soaking sequence, minimal movement of the barrier was observed. Only during the withdrawal did the barrier compress the film to maintain a constant surface pressure. The transfer function found from 15 casting sequences (3–5 wafers coated per sequence) was  $1.2 \pm 0.1$ . Ideally the transfer function should be 1.0, so a small amount of leakage at the moving barrier or the measuring barrier probably occurred.

The wetting characteristics of the coated and uncoated wafers with aqueous solution were observed. Upon removal from solution the monolayer-coated wafers exhibited either no wetting or the presence of discrete droplets. The uncoated wafers exhibited such a high degree of wetting that a thin film of water was drawn up as they were removed. Hence the wetting characteristics of the coated wafers indicated that these had a hydrophobic external surface.

The observations above suggest that a monolayer was deposited, with the polar (hydrophilic) head-groups adjacent to the substrate surface and the acyl chain (hydrophobic) region at the air–monolayer interface. Diffusion measurements of bilayers and monolayers of lipids on glass wafers have provided evidence that a hydration layer exists between the monolayer and the surface of the wafer.<sup>23</sup> The monolayer lipid film may be held onto the wafer through an interfacial potential due to the separation of charge existing in the zwitterionic head-groups and the negatively charged wafer surface.

#### *Monolayer deposition on alkylated wafers*

Deposition onto the alkylated wafers was similar to that onto plain wafers, except that monolayer transfer occurred only during insertion of the substrate through the surface liquid in the trough. This indicated that only a monolayer was transferred, and that it was oriented with its acyl chains adjacent to the wafer and the polar head-group region facing the atmosphere.<sup>24</sup> Transfer ratios were close to unity, but the values found were unreliable owing to monolayer leakage and instability.

#### *Relationship of fluorescence to membrane properties*

The ability of a lipid membrane to act as a fluorescent transducer implies that the membrane structure must affect the characteristics of a suitable fluorophore. Two primary physical characteristics



Table 2. Fluorescence values for glass wafers coated with PC/C monolayers and treated with 1-anilinonaphthalene-8-sulphate

Glass wafer preparation	Relative fluorescence signal, of wafer in air at various monolayer casting pressures				
	Uncoated	at 25.5 mN/m*	at 29.5 mN/m*	at 34.6 mN/m*	at 37.6 mN/m†
Cleaned	0 ± 2	—	—	—	—
PC/C monolayer	—	0	0	0	26 ± 10
PC/C monolayer, wafer soaked in 10 <sup>-4</sup> M ANS	—	18 ± 5	20 ± 2	26 ± 1	52 ± 16
PC/C monolayer prepared over 10 <sup>-4</sup> M ANS subphase	-2 ± 2	—	—	—	56 ± 18

\*Excitation angle 45°.

†Excitation angle 50°.

which are interdependent and can be perturbed in a lipid membrane are the packing/fluidity parameters and the membrane potential.<sup>12</sup> Different degrees of monolayer compression will alter these two parameters and provide an indication of fluorophore sensitivity to structural alterations of the membrane. The principle of casting at various surface pressures is based on the assumption that the monolayer's microstructure on the trough can be successfully transferred to a wafer without alteration. Casting at different compression pressures would therefore allow structurally different monolayers to be deposited.

Phospholipid monolayers deposited onto plain borosilicate wafers and incorporating ANS gave the fluorescence results in Table 2. In general, the fluorescence is expected to increase upon incorporation of the molecule into the membrane.<sup>23</sup> This is due to the decrease in polarity of the ANS environment, because ANS responds to local levels of hydration, as well as to polarity associated with the potential fields of ions present in the vicinity of the probe. Increases in fluorescence with monolayer pressure were attributed mainly to further decreases in hydration of the probe environment. The negatively charged ANS is probably located near the head-group region of the membrane, and thus the decrease in hydration may be

interpreted as a decrease in the penetration of external solution into the membrane. In the head-group region, the probe will also respond to changes in local charge distribution, though the relative contributions of this and the hydration effect is not known.

Changes in the partitioning of ANS into the membrane were also considered as a source of variation in fluorescence intensity. Increasing the surface pressure increases the negative electrostatic charge on the surface, and also the steric hindrance of the membrane to probe penetration. Either effect would cause a decrease in the amount of partitioning into the membrane, and therefore these were not regarded as major factors. One possible result of these effects would be variation in the location of the ANS probe molecules within the membrane, but this was not discernible from the results.

Table 3 provides a summary of the trends observed in the fluorescence signals from these wafers. All values quoted in tables were obtained with a 45° incident angle unless specified otherwise.

Though detailed interpretation of the results for ANS fluorescence in phospholipid membranes was not possible, measurable response to variations in bulk membrane structure were observed. These systems are therefore viable for transduction of selec-

Table 3. Fluorescence dependence on excitation radiation incident angle for glass wafers coated with PC/C monolayers containing 1-anilinonaphthalene-8-sulphonate

Glass wafer preparation*	Relative fluorescence for various incident angles					
	0°	15°	30°	60°	75°	90°
Cleaned, uncoated	-1	3	36	34	1	1
PC/C monolayer	1 ± 2	3 ± 3	41 ± 9	28 ± 9	-2 ± 2	-2 ± 2
PC/C monolayer, wafer soaked in 10 <sup>-4</sup> M ANS	-2	3	56	26	-1	-1
PC/C monolayer prepared over 10 <sup>-4</sup> M ANS subphase	-1	7	63	45	1	-1
PC/C monolayer 12-ASA (22:1 lipid:probe molar ratio)	10	35	>104	80	1	-2

\*Monolayer cast onto wafer at surface pressure of 37.6 mN/m.

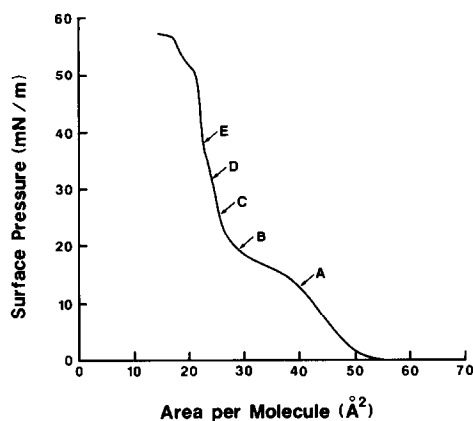


Fig. 2. Compression isotherm of a stearic acid/12-ASA monolayer (27:1 molar ratio) on a 0.1M KCl subphase. Labelled arrows indicate pressures at which samples were deposited (see Table 4).

tive membrane receptor-binding events where similar structural variations are induced.

Monolayers containing stearic acid and 12-ASA in 27:1 molar ratio were deposited onto alkylated quartz wafers to yield a characterizable system. This system had 18-carbon *n*-alkyl chains bound to the surface and covered with a monolayer of stearic acid adsorbed with the fluorescent moiety anchored in the interior of the hydrocarbon zone, and the head-group at the exterior.

The monolayer was characterized by means of the isotherm for its surface pressure *vs.* area per molecule (Fig. 2), obtained with the Langmuir-Blodgett film balance. The monolayer pressure during deposition was controlled at the values indicated in Table 4 and Fig. 2. Some structural information about the monolayer was gained by examination of the compression isotherm. The prominent shoulder at a pressure of 15–17 mN/m is characteristic of monolayers of stearic acid containing 12-ASA and is completely absent when pure stearic acid is used. This shoulder therefore indicated a rearrangement of the monolayer packing, which was somehow dependent on the presence of the anthroxyloxy group. An inflection point was observed at 36–38 mN/m. The increasing slope on the higher-pressure portion of the curve indicated a phase of lower compressibility. This suggested that the monolayer underwent or completed a phase transition from a fluid to a relatively solid phase.

Table 4. Fluorescence of stearic acid/12-ASA (27:1 molar ratio) monolayers deposited onto alkylated quartz wafers at the indicated surface pressures

Wafer	Surface pressure, mN/m	Relative fluorescence, %
A	12.8	61
B	19.2	18
C	25.6	100
D	32.0	85
E	38.4	88

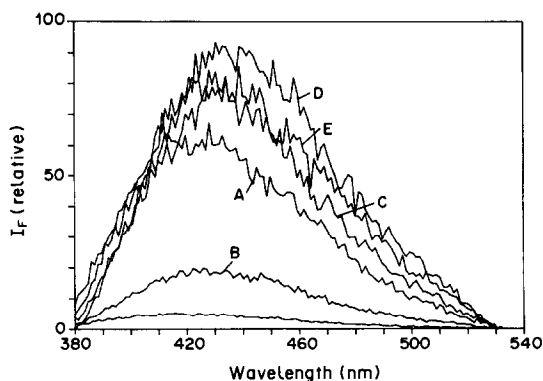


Fig. 3. Fluorescence spectra of stearic acid/12-ASA monolayers (27:1 molar ratio) deposited onto alkylated quartz wafers. Labels indicate the monolayer pressure during deposition (see Table 4). Bottom curve indicates background spectrum. Curves are averaged from 50 points, and corrected for differences in surface density of the fluorophore in the monolayer.

Monolayer collapse was observed at 51 mN/m, indicating the pressure at which the monolayer was no longer stable, because of shear of sections into multilayers or loss of material into the subphase.

The fluorescence intensity results shown in Table 4 and Fig. 3 indicate an emission response to the structural assessments made above. Intensities were corrected for differences in surface density (area per molecule) between samples.

The pressure increase from A to B caused a decrease in fluorescence. The most likely cause of such a decrease is local concentration of the anthroxyloxy moiety, allowing the formation of dimers.<sup>25</sup> This effect could occur by the partitioning of 12-ASA into one phase of a multi-domain monolayer, or by the formation of separate 12-ASA domains in the monolayer. The magnitude of the decrease suggests the latter, and is supported by the extent of the rearrangement observed in the compression curve. Consideration must also be given to the possibility that deposition was simply less efficient at the surface pressure of sample B, though transfer ratio measurements did not indicate this.

This increase in pressure to point C caused an increase in the fluorescence signal. This indicated a redistribution of the 12-ASA molecules away from localized concentration. The increase in intensity relative to sample A indicated that this was a more condensed phase, reducing non-radiative collisional quenching of the excited 12-ASA molecules. The differences between samples C, D and E were negligible, suggesting that collisional deactivation did not change dramatically upon increase of the pressure beyond point C.

The lack of a shift in peak wavelength of the spectra was consistent with the assumption that the polarity of the environment of the fluorophore (the hydrocarbon region of the membrane), did not vary significantly.

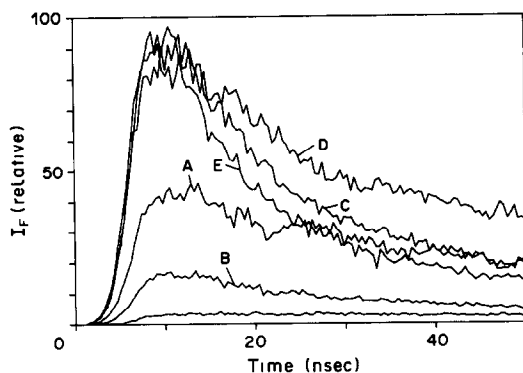


Fig. 4. Fluorescence decay curves of stearic acid/12-ASA monolayers (27:1 molar ratio) deposited onto alkylated quartz wafers. Labels indicate the monolayer pressure during deposition (see Table 4). Bottom curve indicates background. Curves are averaged from 50 points, and corrected for differences in surface density of the fluorophore in the monolayer.

Figure 4 indicates the temporal fluorescence curves obtained from monolayers formed at different compression pressures. The temporal curves were difficult to interpret. The decay was multiexponential in nature, and the large noise level inherent in the nitrogen laser pulse prevented reliable curve fitting analyses. Qualitatively, the decay of wafers C, D and E showed a complex profile, indicating that the 12-ASA molecules were probably located in a variety of local environments or domains. The extended decay of wafer D suggested that a greater number of domains existed in that sample than in those obtained at higher or lower pressures. This was consistent with the observation of an inflection point in the pressure isotherm between points D and E. Sample C was dominated by the fluid phase and sample E was dominated by the more solid phase, giving each a similar decay profile. Sample D, exhibiting domain structures of both phases as well as interfacial regions, indicates a more complicated decay profile in terms of membrane structure, and may require a distributed-lifetime treatment of the results.<sup>26</sup>

#### Membrane perturbation in solution

In order to test the alteration of the fluorescence of

supported lipid monolayers as a function of perturbation of membrane packing/fluidity and electrical potential parameters, the experimentation included subjecting the membrane to interaction with the dipolar potential-probe phloretin and the structural-perturbant valinomycin. Phloretin (molecular weight 275) has a large dipole moment ( $\mu = 5.6$  D) and is known to align itself against the inherent trans-membrane dipolar potential.<sup>10</sup> Recent evidence has also indicated that it may enter the membrane and align near the surface at low concentrations, or may penetrate deeply at higher concentrations, thereby producing a structural perturbation. Valinomycin (molecular weight 1111) is a cyclic polypeptide capable of complexing and transporting Group I cations through a lipid membrane. It has previously been observed to cause significant electrochemical signals due to its perturbation of the membrane structure.<sup>27</sup> Table 5 summarizes the effect of various concentrations of the membrane perturbants on the fluorescence of ANS in ordered phospholipid membranes. The detection limits for both phloretin and valinomycin are consistent with their membrane perturbation abilities as previously observed electrochemically.<sup>10</sup>

The mode of fluorescence decrease is attributed to a change in polarity of the ANS local environment. This would be caused by a combination of structural perturbation and introduction of polar species, whether the perturbants themselves or accompanying ions.

#### Membrane perturbation in the gas phase

The initial concentrations of the various gases used for experimentation were >20 ppt (parts per thousand, v/v) chloroform, 200 ppt hexane and 2 ppt DMA. The response was noted as the gas sample was drawn from the sampling flask through the wafer holder and into the receiving flask. The membranes used were PC/C monolayers containing a fluorescent probe deposited onto glass wafers.

No response was obtained for the ANS-doped monolayers for chloroform or hexane. The result for the hexane system was consistent with the non-polar nature of hexane. Chloroform is an established quenching agent,<sup>28</sup> and also had no effect on the

Table 5. Fluorescence response to phloretin and valinomycin of 1-anilinonaphthalene-8-sulphonate in phospholipid membranes\* supported on glass

Membrane perturbants	Relative fluorescence signal	
	Initial	Chemical equilibrium (> 5 min)
Phloretin ( $10^{-6}M$ )	$11 \pm 2$	$10 \pm 2$
	$14 \pm 3$	$5 \pm 2$
	$12 \pm 2$	$2 \pm 1$
Valinomycin ( $10^{-8}M$ )	$10 \pm 1$	$2 \pm 1$
	$11 \pm 2$	$5 \pm 2$
	$12 \pm 1$	$8 \pm 2$

\*Lipid membranes coated at approximately 35 mN/m surface pressure, monolayer cast over  $10^{-4}M$  ANS subphase.

fluorescence. This provided support for the assumption that the ANS was located near the head-groups at the glass surface, and was shielded by the hydrocarbon zone.

A large fluorescence increase was obtained from PC/C monolayers containing 12-ASA, upon exposure to air, chloroform and hexane. This response was almost always transient, returning to the baseline value within 1 min. This was observed for chloroform concentrations as low as 25 ppt. The transient behaviour is probably due to a process such as a phase transition, where the presence of interfacial regions between phases causes an increase in fluorescence. This transition would be expected to occur from a more dense to a less dense phase on incorporation of the organic molecules, altering the overall structure of the membrane. Similar transient phenomena have been observed for lipid membranes in electrochemical<sup>27</sup> and piezoelectric<sup>29</sup> experiments, where transitory alterations in dipolar potential and microviscosity occur on exposure of the membrane to non-selective interaction with probes.

The reagent *N,N*-dimethylaniline (DMA) is a known quencher of the anthroyloxy probes<sup>30</sup> and caused a significant decrease in the fluorescence signal. Again the signal was transient, and a rapid significant decrease in fluorescence over a period of 1 min was observed, followed by an increase in signal to some steady state, usually less than the initial fluorescence. The decrease in fluorescence may be related to the concentration of the quencher [Q] by the Stern–Volmer equation:<sup>26</sup>

$$\frac{F_0}{F} = 1 + K[Q] \quad (3)$$

where  $K$  is the quenching constant, and  $F_0$  and  $F$  are the fluorescence intensities of the fluorophore in the absence and presence of the quencher respectively. The Stern–Volmer equation is only valid for purely dynamic or collisional quenching occurring in the absence of any significant inner-filter effects.<sup>28</sup> The inner-filter effect arises when the quencher absorbs at the wavelength of either excitation or emission of the fluorophore.

A Stern–Volmer plot for DMA is shown in Fig. 5; a linear plot with a correlation factor of 0.89 was obtained over a significant concentration range.

The fact that a linear plot was obtained rules out any significant inner-filter effect. The Stern–Volmer plot does not indicate whether dynamic or static quenching is occurring.

#### *An intrinsic fibre-optic sensor*

The fluorescence results for stabilized phospholipid monolayers coated onto glass wafers clearly indicate that significant analytical signals can be derived from membrane perturbation processes. The equipment used for these experiments was very limited in sensitivity, and demonstrated that an ample signal could

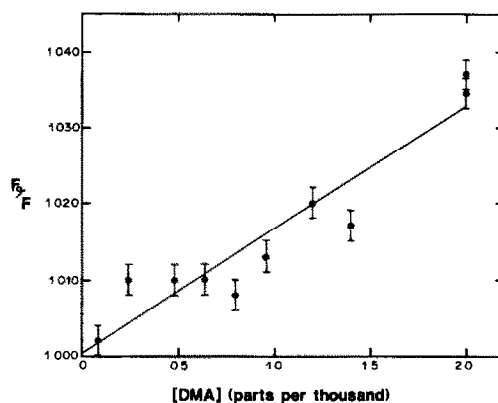


Fig. 5. A Stern–Volmer plot for the fluorescence quenching agent *N,N*-dimethylaniline. The fluorescent matrix was a monolayer of phospholipid containing 12-ASA (22:1 molecular ratio of lipid-to-probe) deposited at 35 mM/m onto a borosilicate glass wafer.

be obtained from monolayers with a total area of less than 3 cm<sup>2</sup>.

Figure 6 shows a fluorescence spectrum obtained by evanescent excitation of a 12-ASA/stearic acid monolayer on an alkylated silica fibre. This spectrum indicated that the results of the wafer experiments described previously should be applicable to fibre-based sensors. Note that the blue component now observed in the spectrum is probably due to intrinsic fluorescence of the fibre, which is of lower quality material than the wafers used.

Some of the instrumentation used in this study was large and expensive, which made it less desirable for most sensor applications. Such a complete study is necessary, however, as it allows for optimization of future, simplified and less expensive systems, and anticipates technological developments which may make measurements such as fluorescence lifetimes possible on a miniaturized instrument.

Sensitivity of fluorescence to membrane structural parameters has been demonstrated. True biosensor development requires the further demonstration that

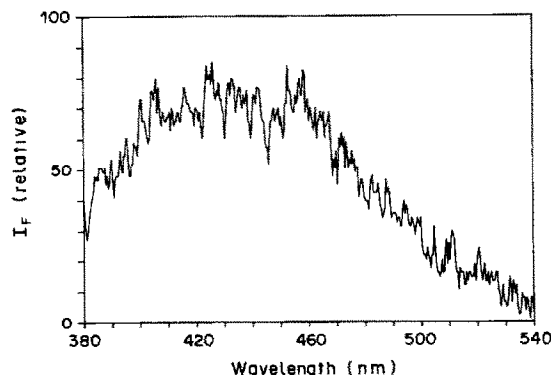


Fig. 6. Fluorescence spectrum obtained from the stearic acid/12-ASA monolayer deposited on a 400- $\mu$ m alkylated silica fibre at 30 mN/m. The large underlying blue component is the intrinsic fluorescence of lower quality quartz.

receptor-analyte interactions can induce structural variations of this nature. Further work is proceeding towards the permanent deposition of lipid membranes onto fibres, and the development of new receptor molecules capable of extensive membrane perturbation.

*Acknowledgements*—We are indebted to the Natural Sciences and Engineering Research Council of Canada for support for this work, to Drs. Raymond Measures and Mark Cappelli, of the University of Toronto, Institute for Aerospace Studies, for the use of the fluorescence lifetime instrumentation, and Mr. Roberto Nespolo for technical assistance.

#### REFERENCES

1. W. R. Seitz, *Anal. Chem.*, 1984, **56**, 16A.
2. O. S. Wolfbeis, *Trends Anal. Chem.*, 1985, **4**, 184.
3. T. Hirschfeld, *Z. Anal. Chem.*, 1986; **324**, 618; *In Tech.*, 1986, **33**, No. 2, 45.
4. R. Th. Kersten and R. Kist (eds.), *Proceedings of the International Conference on Optical Fiber Sensors*, VDE-Verlag, Berlin, 1984.
5. Z. Zhujun, J. L. Mullin and W. R. Seitz, *Anal. Chim. Acta*, 1986, **184**, 251.
6. O. S. Wolfbeis, H. E. Posch and H. W. Kroneis, *Anal. Chem.*, 1985, **57**, 2556.
7. R. Narayanaswamy and F. Sevilla, *Analyst*, 1986, **111**, 1085.
8. J. S. Schultz, *U.S. Patent* 4344438, 1982.
9. B. L. Liu and J. S. Schultz, *IEEE Trans. Biomed. Eng.*, 1986, **33**, 133.
10. M. Thompson and U. J. Krull, *Anal. Chim. Acta*, 1983, **147**, 1.
11. U. J. Krull and M. Thompson, *IEEE Trans. Electron Devices*, 1985, **32**, 1180.
12. U. J. Krull, M. Thompson and H. E. Wong, *Bioelectrochem. Bioenerg.*, 1986, **15**, 371.
13. J. F. Place, R. M. Sutherland and C. Dähne, *Biosensors*, 1985, **1**, 321.
14. J. D. Andrade, R. A. VanWagenen, D. E. Gregonis, K. Newby and J.-N. Lin, *IEEE Trans. Electron Devices*, 1985, **32**, 1175.
15. R. M. Weis, K. Balakrishnan, B. A. Smith and H. M. McConnell, *J. Biol. Chem.*, 1982, **257**, 6440.
16. V. Von Tschärner and H. M. McConnell, *Biophys. J.*, 1981, **36**, 409.
17. U. J. Krull, C. Bloore and G. Gumbs, *Analyst*, 1986, **111**, 259.
18. U. J. Krull, M. Thompson and H. E. Wong, *ibid.*, 1985, **110**, 1299.
19. J. Sagiv, *J. Am. Chem. Soc.*, 1980, **102**, 92.
20. U. J. Krull, M. Thompson, E. T. Vandenberg and H. E. Wong, *Anal. Chim. Acta*, 1985, **174**, 83.
21. V. T. Moy, D. J. Keller, H. E. Gaub and H. M. McConnell, *J. Phys. Chem.*, 1986, **90**, 3198.
22. L. A. Sklar, B. S. Hudson and R. D. Simoni, *Biochemistry*, 1977, **16**, 819.
23. L. K. Tamm and H. M. McConnell, *Biophys. J.*, 1985, **47**, 105.
24. V. von Tschärner and H. M. McConnell, *ibid.*, 1981, **36**, 421.
25. A. E. McGrath, C. G. Morgan and G. K. Radda, *Biochim. Biophys. Acta*, 1976, **426**, 173.
26. D. R. James and W. R. Ware, *Chem. Phys. Lett.*, 1986, **126**, 7.
27. M. Thompson and U. J. Krull, *Anal. Chim. Acta*, 1982, **141**, 33.
28. C.-N. Ho, G. Patonay and I. M. Warner, *Trends Anal. Chem.*, 1986, **5**, 37.
29. M. Thompson, C. L. Arthur and G. K. Dhaliwal, *Anal. Chem.*, 1986, **58**, 1206.
30. J. R. Lakowicz, *Principles of Fluorescence Spectroscopy*, Chap. 9. Plenum Press, New York, 1983.

## FIBER-OPTIC TIME-RESOLVED FLUORIMETRY FOR IMMUNOASSAYS

RANDY D. PETREA and MICHAEL J. SEPANIAK\*

Department of Chemistry, University of Tennessee, Knoxville, TN 37996-1600, U.S.A.

TUAN VO-DINH

Health and Safety Research Division, Oak Ridge National Laboratory, P.O. Box X, Oak Ridge,  
TN 37831, U.S.A.

(Received 20 May 1987. Accepted 12 August 1987)

**Summary**—Rare-earth metal chelates used as fluorescent labels for immunoassays possess extremely long fluorescence lifetimes and permit the effective use of time-resolved detection. This is very important in fiber-optic fluorimetry, a technique that ordinarily exhibits large signal backgrounds from back-scattered radiation. With time-resolved detection to reject the back-scattered radiation, the limit of detection for Eu 2-naphthyltrifluoroacetate is  $10^{-12}M$ , nearly three orders of magnitude lower than for the fiber-optic measurement of the most common fluorescent label, fluorescein isothiocyanate. Commercially available reagents labeled with an europium chelate are used to demonstrate the potential utility of time-resolved fluorimetry in fiber-optic immunoassays. Rabbit immunoglobulin G (IgG) is covalently bonded to the distal end of quartz optical fibers prior to exposure to anti-rabbit IgG labelled with europium chelate. The limit of detection for the assay is approximately  $0.1 \mu\text{g/ml}$ .

A number of fiber-optic devices have been developed for bioanalysis.<sup>1-12</sup> Though practical and routine use of these devices for *in situ* measurements of biochemicals has not been realized, there is promise that reliable fiber-optic sensors will be developed that can be implanted in living systems to provide sensitive, site-specific, and rapid (or preferably continuous) analyses for biochemicals.

Design features for various types of fiber-optic sensors have been described and reviewed.<sup>8,13,14</sup> Sensors which measure the intrinsic absorbance, scattering, or fluorescence of the analytes of interest are generally referred to as "optical" sensors.<sup>13</sup> Better analytical selectivity is achieved with fiber-optic "chemical" sensors (FOCS), which employ an immobilized reagent phase.<sup>8</sup> The spectroscopic signals obtained with FOCS are the result of specific interactions between the immobilized reagents and the analytes. The interaction must be reversible if continuous monitoring is to be accomplished. Immobilization is achieved by a variety of methods, including trapping of reagent within a membrane,<sup>15-17</sup> direct covalent bonding of reagent to the distal end of the fiber,<sup>18</sup> and incorporating the reagent into a polymer phase that is covalently bonded to the fiber's distal end.<sup>12</sup> The method of immobilization and the amount of reagent phase can influence the FOCS response characteristics.<sup>8,12,18</sup>

When compared to multiple (bifurcated) fiber designs, sensors that utilize a single optical fiber to transmit excitation radiation to the sample, and

signal radiation from the sample to the detector, have the advantages of better signal collection efficiency and smaller size. The latter attribute can be important in their eventual *in vivo* use. Unfortunately, single-fiber sensors are usually plagued by high optical background levels. This is due to the fact that a significant amount of excitation radiation is reflected at the fiber faces and is not easily rejected by spatial filtering. Attempts to circumvent this back-scatter radiation problem have included employing high rejection-ratio double monochromators<sup>12</sup> and grinding fiber faces at angles that minimize the reflected optical background.<sup>19</sup> Limitations to these correction techniques include the low throughputs of double monochromators and the difficult, irreproducible nature of "angling" small quartz surfaces.

Recently, the principles of solid-phase immunoassay have been applied to FOCS design.<sup>10,18,20-22</sup> The fiber and immobilized receptors form a fluoroimmunosensor (FIS), that can be used to perform *in situ* fluoroimmunoassays. The FISs offer the potential for excellent analytical selectivity by exploiting the specificity of antibody-antigen reactions.<sup>23</sup> FISs have been developed for direct assays of natural fluorophores<sup>22</sup> and for competitive binding assays.<sup>21</sup> Furthermore, it should be possible to design FISs to perform "sandwich assays" and, by using relatively low avidity antibodies to improve response times, for continuous monitoring.

Fluorescein isothiocyanate (FITC) is the most commonly used labelling fluorophore in fluoroimmunoassays.<sup>23</sup> Though FITC has a reasonably large fluorescence quantum efficiency, it has the

\*To whom correspondence should be addressed.

disadvantage of possessing a relatively small Stokes shift (approximately 30 nm). Hence, simple spectral rejection of back-scatter radiation is not very efficient and large optical background levels have been observed in our previous FIS work, particularly when intense laser radiation was employed for excitation.

An alternative type of fluorescent label, rare-earth metal chelates, offers some unique and important characteristics for fluoroimmunoassays.<sup>23-25</sup> The metal chelates which are used most often in fluoroimmunoassays are those of Eu(III) and Tb(III) complexed with  $\beta$ -diketones and EDTA derivatives.<sup>23</sup> Excitation with these labels involves absorption in the near-ultraviolet spectral region by the ligand. This is followed by energy transfer from the ligand's excited singlet state, through its triplet state, to the resonance levels of the rare-earth ion. The metal-ion emission exhibits a narrow band in the green-red visible spectral region. Concomitant with this energy transfer process is an unusually large Stokes shift (typically 200–300 nm) and an extremely long emission lifetime (typically 0.1–1.0 msec). The former characteristic facilitates efficient spectral rejection of the back-scattered radiation, while the latter characteristic permits virtual elimination of optical background, including sample matrix fluorescence, by the use of time-resolved detection. This time-resolved technique has been used in performing very sensitive-fluoroimmunoassays of a variety of antigens.<sup>26-30</sup> Unfortunately, assays using these metal chelate labels do have problems, the most significant of which are fluorescence quenching by water in the solvation sphere of the rare-earth ion, and the general instability of complexes of rare-earth ions. These problems can necessitate fairly complicated assay procedures.

In this paper we report our preliminary investigations of fiber-optic measurements with Eu-chelate labels and time-resolved detection. Temporal rejection of back-scatter from the fiber optic is shown to be effective and allows much more sensitive measurements for Eu 2-naphthoyltrifluoroacetone than for FITC. Commercially available immunochemicals labelled with rare-earth chelate are used to demonstrate the potential utility of time-resolved fluorimetry in FIS measurements.

## EXPERIMENTAL

### Materials

Sheep anti-rabbit immunoglobulin G (IgG) labelled with Eu-chelate, enhancement solution, wash concentrate, and assay buffer were purchased from LKB Instruments, Inc., Gaithersburg, MA. The composition of the enhancement solution was 1.0 g/l. Triton X-100, 6.8mM potassium hydrogen phthalate, 0.1mM acetic acid, 50 $\mu$ M tri-n-octylphosphine oxide (TOPO), and 15 $\mu$ M 2-naphthoyltrifluoroacetone. Rabbit IgG and ovalbumin were purchased from Cooper Biomedical Inc., Malvern, PA. 3-Glycidioxypropyltrimethoxysilane (GOPS) was acquired from Aldrich Chemical Co., Milwaukee, WI. All other reagents were supplied by Sigma Chemical Co., St. Louis, MO.

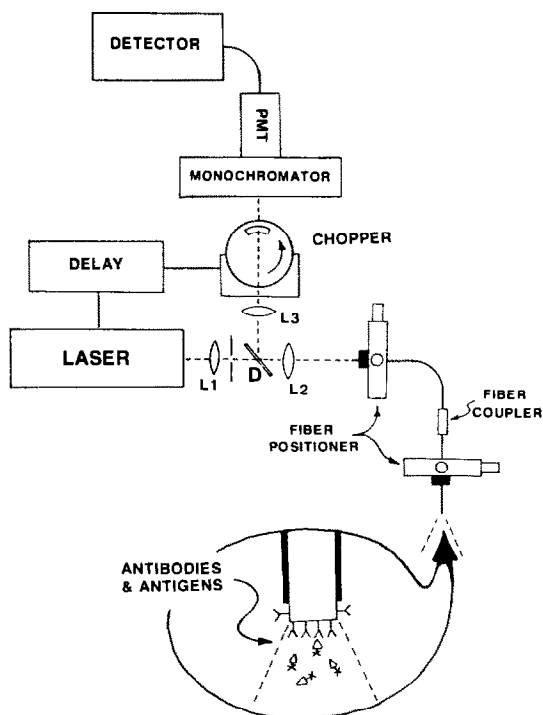


Fig. 1. Diagram of apparatus used for FIS measurements.

Multi-mode fused-silica 600- $\mu$ m core diameter optical fibers (numerical aperture = 0.22) were obtained from Math Associates, Westbury, NY. These fibers were cut into 75-cm lengths and terminated at one end with an SMA connector (Math Associates). The ends were then successively polished with 15- $\mu$ m, 3- $\mu$ m and 0.3- $\mu$ m lapping film.

### Apparatus

A Perkin-Elmer 650-40 spectrofluorimeter was used to evaluate the IgG binding capacity of FIS sensors. All time-resolved fluorescence measurements with optical fibers were performed with the apparatus shown in Fig. 1. A Lambda Physik Model 50B excimer laser (308 nm) was used as the excitation source. The laser was operated in this work at 20 Hz and produced 10-nsec duration output pulses of approximately 20 mJ energy. The laser radiation was focused by a 38-mm diam. ( $f$  4.7) lens,  $L_1$ , through an iris opening of approximately 2 mm. The iris aperture served to limit the beam diameter and reduce the incident power to levels that did not damage the optical fibers. The radiation was then passed through a custom-made dichroic filter, D, (Newport Corporation, Fountain Valley, CA), with 90% transmission at 308 nm, and focused by a 25-mm diam. ( $f$  2) lens,  $L_2$ , onto the incident end of the fiber optic. The Eu-chelate fluorescence ( $\lambda = 613$  nm) arising from excitation at the distal end of the fiber, was partially collected by the fiber, transmitted to and collimated by  $L_2$ , and reflected by the dichroic filter (reflectivity = 60% at 613 nm). The collimated radiation was focused by a 25-mm diam. ( $f$  4) lens,  $L_3$ , through a modified chopper (Ortec Model 9479) onto the entrance slit of an Instruments SA, Model H-10, monochromator ( $f$  3.5). Photocurrents generated by a cooled ( $\sim -25^\circ$ ) RCA C31034B photomultiplier tube (PMT), operated at 1800 V, were measured by either a Pacific Precision Instruments Model 126 quantum photometer in the current or photon-count mode, or by an EG&G Model 165 boxcar detector. Data were collected and recorded on a strip-chart recorder.

The chopper modification involved replacing the stock aperture wheel with one that contained a single 1/15th sector

aperture. Thus, operation at 20 Hz resulted in a 3-msec optical gate. The synchronous output of the chopper was fed to a laboratory-built delay circuit, which then triggered the laser. The temporal relationship between the chopper gate and laser pulse was adjusted with the delay circuit. The delay timing was optimized by placing the distal end of the fiber alternately in Eu-chelate solution and in solvent and adjusting the delay to maximize the signal to background ratio. The size of the imaged signal at the chopper wheel was slightly less than 2 mm and this resulted in an effective gate-opening time of about 100  $\mu$ sec. Detectability with this gated detection system was ultimately limited by timing jitter, which was approximately a few hundred  $\mu$ sec, as observed with an oscilloscope at the synchronous output of the laser.

#### Procedures

**Fiber silanation with 3-glycidoxypropyltrimethoxysilane.** The outer claddings of the fibers were stripped back 3 mm from one end in order to expose the silica core. The stripped ends were then rinsed first in hot nitric acid, then with distilled water, and submerged in 10% aqueous GOPS solution at 90° for 3 hr. The pH of the solution was maintained at 3 by additions of 1M hydrochloric acid. The "GOPS fibers" were then dried overnight at 105°.

**Fiber activation and protein attachment.** The GOPS fibers were immersed in 0.1M periodic acid for 1 hr at room temperature to oxidize the GOPS, then washed with distilled water and phosphate-buffered saline (PBS), pH 7.4, before being suspended for 24 hr at 4° in polypropylene vials containing 1 ml of 5-mg/ml rabbit IgG. During this time, covalent bonds between the aldehyde groups of the oxidized GOPS and the amino groups of the protein were formed by Schiff's base reactions. The fibers were then placed in 1 ml of PBS, and three 2-mg portions of NaBH<sub>4</sub> were added at 15-min intervals, to reduce the Schiff's bases. The fibers were finally stored in a 1% solution of ovalbumin in PBS at 4°.

**Determination of fiber binding capacity.** The plastic cladding on the optical fibers was stripped from the core in order to expose 1-cm sections of fiber. Rabbit IgG was bonded to the sections by the procedure described above. After incubation of the sections in a 0.01-mg/ml solution of Eu-chelate labelled anti-rabbit IgG for 48 hr at 4°, the sections were rinsed with PBS and placed in 1.5 ml of the enhancement solution. It was assumed that this long incubation resulted in complete saturation of the fiber surface with anti-rabbit IgG. In the enhancement solution, the Eu ion dissociates from the antibody-bound chelate and forms a highly fluorescent chelate with the 2-naphthoyltrifluoroacetone in the enhancement solution. The binding capacity was determined by measuring the resulting Eu 2-naphthoyltrifluoroacetate fluorescence ( $\lambda_{ex} = 337$  nm,  $\lambda_{em} = 613$  nm) with the Perkin-Elmer 650-40 spectrofluorimeter and comparing it with a standard curve. A value of 1  $\mu$ g of labelled IgG per cm<sup>2</sup> of silica fiber surface was obtained.

**Comparison of limits of detection by conventional FITC and time-resolved Eu-chelate fluoroimmunoassays.** Limits of detection for FITC were determined for standard cuvette and fiber-optic measurements. Excitation was provided by a Spectra Physics Model 171 Argon ion laser ( $\lambda = 488$  nm, 30 mW). For the cuvette measurements, the laser radiation was focused by a 25-mm diam. ( $f$  2.0) lens through a 1.0-cm cuvette. The FITC fluorescence ( $\lambda_{max} = 523$  nm) was collected at 90° with a 25-mm diam. ( $f$  4) lens and imaged onto the entrance slit of the monochromator. Photocurrents generated by an RCA 1P28 PMT, operated at 700 V, were measured. The instrumental arrangement shown in Fig. 1 and described above was used for the fiber-optic measurements, except that the laser, dichroic filter, lenses and PMT (see above) used were suitable for the measurement of FITC. Calibration plots prepared with standard solutions

of FITC in pH-9.3 borate buffer, were obtained and limits of detection were determined as the concentration yielding a signal that was twice the noise obtained with a blank.

By similar procedures, with the laser and optical components described above, the limits of detection for Eu 2-naphthoyltrifluoroacetate were also determined for standard cuvette and fiber-optic measurements. Three different forms of signal recovery were employed: (1) electronically gated detection with a boxcar, (2) optically gated detection with a photometer and (3) optically gated detection with a photon counter.

**Time-resolved fluorescence measurements with FIS.** FISs prepared in accordance with the aforementioned procedure, were incubated in varying concentrations of anti-rabbit IgG labelled with Eu-diazophenyl-EDTA for 14 hr (overnight) at 4°. The sensors were then rinsed with and stored in wash concentrate until needed for use. The sensors were then coupled to the apparatus shown in Fig. 1, and the fibers were inserted 1 mm into 1.5-mm diameter micro-wells, drilled in a Teflon pad. The micro-wells were filled with 10  $\mu$ l of enhancement solution. The fibers were left in this position for 1 min, then moved back to a predetermined position, and the fluorescence was measured after a 1-min interval. Each fiber was then removed from its micro-well and both fiber and micro-well were thoroughly washed with enhancement solution. The fiber was returned to the well for measurement of the optical background.

## RESULTS AND DISCUSSION

The data presented in Table 1 illustrate the efficacy of time-resolved detection in improving detectability in fiber-optic fluorimetry. No immunochemicals were employed in the initial study. The limits of detection for cuvette measurements demonstrate the excellent sensitivity of laser fluorimetry. Although the optical systems (lasers, lens, etc.) and detectors were different for the FITC (conventional) and Eu 2-naphthoyltrifluoroacetate (time-resolved) measurements, the limits of detection are comparable and extremely low. The Eu-chelate molar absorptivity at the excimer laser output (308 nm) is approximately 40% of its value at  $\lambda_{max}$ . Furthermore, the pulse-to-pulse energy reproducibility of the excimer is rather poor ( $\pm 5$ –10%). If these factors are corrected, the time-resolved detection of the Eu-chelate might exhibit a lower limit of detection than that for FITC.

The time-resolved cuvette measurements were performed with a boxcar detector. Considering the extremely long lifetime of the Eu-chelate it was a

Table 1. Comparison of limits of detection

	FITC*	Eu 2-naphthoyl trifluoroacetate†
Cuvette	$4 \times 10^{-14} M$	$8 \times 10^{-14} M^a$
Fiber optic	$7 \times 10^{-10} M$	$3 \times 10^{-8} M^a$ $2 \times 10^{-12} M^b$ $1 \times 10^{-12} M^c$

\*Excitation by argon ion laser, 488 nm, 30 mW. Emission at 520 nm, monitored with photometer.

†Excitation by excimer laser, 308 nm, 20 Hz,  $\sim 20$  mJ/pulse. Emission at 613 nm, monitored with (a) boxcar detector, (b) optical gating and photometer, or (c) optical gating and photon counter.



relatively simple matter to temporally reject the laser specular scatter and the Rayleigh and Raman scatter of the solvent. A 1- $\mu$ sec delay and 1- $\mu$ sec gate window were employed with the detector. Moreover, the specular scatter occurring at the cuvette walls was easily rejected spatially by imaging the path of the laser beam through the cuvette onto the monochromator so that the fluorescence passed through the entrance slit but the specular scatter was blocked.

As discussed previously, spatial rejection of back-scatter radiation is not easily accomplished when fiber-optic measurements are performed. Thus, a larger optical background was observed for the fiber-optic case, and this partially accounts for the much poorer limits of detection when measurements were performed by placing the distal end of an untreated fiber in the fluorophore solutions. The fluorescence collection efficiency is also poorer for the fiber-optic case. It is interesting that the time-resolved measurements with the boxcar detector resulted in very poor detectability. Electronically gated detection with the boxcar is not effective in the fiber-optic case because the intense back-scatter radiation coincident with the excimer laser pulse is not spatially filtered and tends to "blind" the PMT. When the boxcar gate opens, the PMT response to the Eu-chelate fluorescence is severely damped. Detectability is improved by several orders of magnitude, and is much better than for the fiber-optic FITC measurement, when optical gating is used with the chopper arrangement shown in Fig. 1. Background levels were very low (approximately 100 cps for photon counting and 2 nA for the dc photocurrent measurement). Thus further electronic gating was not necessary and, owing to the low radiation levels, slightly lower limits of detection were observed for the photon counting case.

Reducing the timing jitter for the optical gating should improve the limits of detection. The low background levels given above were achieved by adjusting the temporal position of the optical gate to block all the back-scatter radiation coincident with the laser pulse. This results in a reduction of signal, since much of the fluorescence during the first few hundred  $\mu$ sec following the laser pulses is blocked. By using more sophisticated mechanical shutters or electro-optical gating it should be possible to reduce the jitter and thereby improve detectability.

A standard curve was prepared for the fiber-optic measurements of Eu 2-naphthoyltrifluoroacetate. A correlation coefficient of 0.9998 was obtained over the range from the limit of detection to  $7 \times 10^{-7} M$ . In this work the linear dynamic range is limited by photometer saturation and not by fluorescence inner-filter effects.<sup>4</sup> The input stage of the photometer contains a diode clamp circuit that protects the instrument from damage, by shunting large input currents to ground.

The excimer laser used in this work has several

disadvantages. The high powers ( $> 1$  MW at the output of the laser) associated with short duration pulses eventually damaged the optical fibers and, more critically, tended to photodegrade the samples. Measurements were performed by exposing the sample to the laser for 3-sec intervals so as to minimize the degradation. This made it necessary to use relatively short (1 sec) detector time-constants. Noise levels for the non-immunochemical measurements discussed above were determined as the standard deviations for peak signals resulting from multiple laser exposures of the solvent. The high peak power and low repetition rate of the laser resulted in large peak signals with a low duty cycle ( $\sim 2\%$ ). This contributed to the photometer saturation problem described above. Finally, the pulse-to-pulse and long term stability of the laser was poor, thereby contributing to noise and calibration problems.

A CW helium-cadmium laser would be more appropriate for these measurements. Its 325-nm output is closer to the  $\lambda_{\max}$  of the Eu 2-naphthoyltrifluoroacetate absorption than is the 308-nm output of the excimer laser. The helium-cadmium laser is characterized by moderate power (typically  $\sim 10$  mW) and excellent stability. It could be synchronously modulated at a few hundred Hz to produce stable time-resolved signals with a fairly high duty cycle.

Several sandwich assay kits based on time-resolved fluorimetry are commercially available. In a solid-phase sandwich assay a "first" antibody to the antigen of interest is immobilized on a substrate, incubation with the antigen is effected, then a "second," fluorescently labelled, antibody is added. In some cases the antigen and second antibody can be added simultaneously. The second antibody is specific for a different antigenic determinant than is the first, and the two antibodies together sandwich the antigen. After appropriate washing steps, the fluorescence of the labelled second antibody is measured. The sandwich assay procedure could easily be adapted to FIS measurements, with the possibility of performing the initial incubation *in vivo*.

For any given sandwich assay system, adaptation to FIS measurements would require systematic optimization of the immobilization and incubation procedures. To avoid such complications in these preliminary studies we employed a single antibody-antigen system. We had previously demonstrated that rabbit IgG could be covalently bonded to fibers by the GOPS procedure, while maintaining significant activity for polyclonal FITC-labelled anti-rabbit IgG.<sup>21</sup> The binding capacity,  $\sim 1 \mu\text{g}/\text{cm}^2$ , of the Eu-chelate labelled immunochemicals used in this work (see experimental section) is comparable to that obtained in the previous work, and corresponds to approximately  $10^{-13}$  mole of Eu-labelled antibody on the sensing portion of 600- $\mu\text{m}$  fiber. As our measurements are performed (see experimental section), this corresponds to the antibody on the end and the

first mm of the sides of the fiber. Except for the fact that antigen, instead of the first antibody, was covalently bonded to the fiber, the procedure for the time-resolved FIS measurements described here is similar to that which would be employed in an actual sandwich FIS assay.

The analytical characteristics which are of greatest interest in this FIS developmental work are the sensitivity, reproducibility and dynamic range of the FIS measurements. Our preliminary experiments were aimed at assessing these characteristics for the simple immunochemical system investigated.

The antibody-bound Eu-chelate used in this work does not have a sufficiently high fluorescence quantum efficiency to be used directly for measurement. Instead, after incubation, the Eu is released into an enhancement solution which contains another chelating agent, 2-naphthoyltrifluoroacetone, as well as surfactant and other compounds which serve to exclude water from the Eu solvation sphere, and thereby increase the fluorescence signals. Detection limits for Eu in this enhancement solution (see Table 1) are much lower than those reported for direct measurements that involve a single ligand for protein conjugation and for fluorescence measurement.<sup>29</sup>

The amount of Eu released into the enhancement solution depends on the FIS experimental conditions, but is ultimately limited by the modest binding capacity of the fibers. Assuming that several Eu-chelate molecules are bonded to each labelled protein molecule,<sup>29</sup> the amount of Eu bonded at saturation is approximately  $10^{-12}$  mole. For reasons of sensitivity it is advantageous to restrict the released Eu to a small volume of enhancement solution at the distal end of the fiber. Several approaches were investigated before settling on the micro-well technique used in this work. The micro-well was nearly filled by the 10  $\mu$ l of enhancement solution. The release of  $10^{-12}$  mole of Eu then resulted in the formation of a  $10^{-7}M$  solution of Eu 2-naphthoyltrifluoroacetate. Saturated fibers, when placed in 10  $\mu$ l of enhancement solution, yielded signal levels which were roughly equal to those of the  $10^{-7}M$  Eu-chelate standard solutions used in the non-immunochemical work.

Reproducibility for time-resolved FIS measurements was evaluated by incubating eight prepared fibers overnight with 0.005-mg/ml Eu-chelate labelled anti-rabbit IgG. The incubated fibers were sequentially aligned in the apparatus shown in Fig. 1, the bound Eu was released into 10  $\mu$ l of enhancement solutions, and the fluorescence signals were measured with the photometer. Once the signal measurement was complete the fiber and micro-well were thoroughly washed with enhancement solution, the micro-well was filled with fresh enhancement solution and the background measured. With the present arrangement it is difficult to center the fiber within the micro-well. To compensate for signal variations resulting from changes in laser power, fiber position and other factors, we filled the micro-well with a dilute Eu-

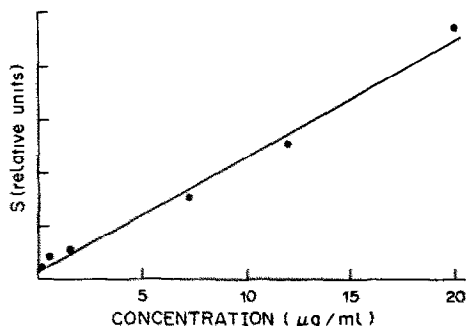


Fig. 2. Standard curve for measurements of Eu-chelate labelled anti-rabbit IgG. Each data-point is the average of four measurements.

chelate standard solution after the background was determined, and a normalization fluorescence signal was measured. Sample signals,  $S$ , were then determined by using the equation.

$$S = \frac{I_f - I_b}{I_n} \quad (1)$$

where  $I_f$ ,  $I_b$  and  $I_n$  are the fluorescence, blank and normalization signals, respectively. The relative standard deviation of the sample signal for the eight fibers was 19%. Both chemical and physical factors contribute to the creation of noise in these measurements. The chemical factors include the reproducibility of silanating and activating the fibers, bonding protein to the fibers (quantity and condition of the bonded protein) and the incubation step. The physical factors include the reproducibility of the laser output, coupling the fibers and positioning them in the micro-wells. By consideration of these factors we are exploring methods for improving the reproducibility of FIS measurements.

Utilization of FISs for actual assays will require the use of calibration graphs. The standard curve shown in Fig. 2 was obtained for incubations with standard solutions of Eu-chelate labelled anti-rabbit IgG over the range from 0.5 to 20  $\mu$ g/ml. The signal-to-noise ratio ( $S/N$ ) for the lowest concentration standard (0.1  $\mu$ g/ml) is approximately 2, with the noise determined as the standard deviation of the blanks in the reproducibility study. Although these measurements were performed with 300- $\mu$ l sample volumes, we have previously demonstrated the ability to perform competitive binding FIS measurements with sample volumes as small as 10  $\mu$ l.<sup>21</sup> Working with 10- $\mu$ l sample volumes, the absolute limit of detection would be approximately 6 fmoles. The actual amount of bound anti-rabbit IgG is probably considerably less than this.

In conclusion, we have demonstrated the efficacy of time-resolved detection in improving detectability in fiber-optic fluorimetry. Rare-earth metal chelates, with their extremely long fluorescence lifetimes, offer advantages as fluorescent labels for immunoassays. We have presented preliminary data indicating that

sensitive, low-volume, *in situ* immunoassays can be performed with rare-earth metal chelate labels and fiber-optic time-resolved fluorimetry.

*Acknowledgements*—The authors wish to thank M. J. Frantz, visiting summer undergraduate student from Wittenberg University, for his assistance in evaluating the binding capacity of the treated fibers, and B. J. Tromberg of the University of Tennessee for his advice concerning the preparation of FISs. This work was supported by the National Institutes of Health under contract number GM 34730 with the University of Tennessee, Knoxville.

#### REFERENCES

1. B. Chance, V. Legallais, J. Sorge and N. Graham, *Anal. Biochem.*, 1975, **66**, 498.
2. S. Goldstein, R. Bonner, R. Dedrick, E. Grantham, P. Gullino, C. Gibson and D. McGuire, *J. Biomech. Eng.*, 1980, **102**, 265.
3. G. Renault, E. Raynal and M. Sinet, *Opt. Laser Technol.*, 1982, June, 143.
4. B. Tromberg, J. Eastham and M. Sepaniak, *Clin. Chem.*, 1983, **29**, 1678.
5. J. Coleman, J. Eastham and M. Sepaniak, *Anal. Chem.*, 1984, **56**, 2246.
6. S. Schwab and R. McGreery, *ibid.*, 1984, **56**, 2199.
7. J. Schultz, S. Mansouri and I. Goldstein, *Diabetes Care*, 1982, **160**, 47.
8. W. Seitz, *Anal. Chem.*, 1984, **56**, 16A.
9. J. Peterson, R. Fitzgerald and D. Buckhold, *ibid.*, 1984, **56**, 62.
10. J. Andrade, R. Vanwagenen, D. Gregonis, K. Newby and J. Lin, *IEEE Trans. Electron Devices*, 1985, **ED-32**, 1175.
11. M. Arnold, *Anal. Chem.*, 1985, **57**, 565.
12. C. Munkholm, D. Walt, F. Milanovich and S. Klainer, *ibid.*, 1986, **58**, 1427.
13. J. Peterson and G. Vurek, *Science*, 1984, **224**, 123.
14. O. Wolfbeis, *Z. Anal. Chem.*, 1986, **325**, 387.
15. J. Peterson, R. Fitzgerald and D. Buckhold, *Anal. Chem.*, 1984, **56**, 62.
16. L. Saari and W. Seitz, *ibid.*, 1983, **55**, 667.
17. Z. Zhujun and W. Seitz, *Anal. Chim. Acta*, 1984, **160**, 47.
18. B. Liu and J. Schultz, *IEEE Trans. Biomed. Eng.*, 1986, **BME-33**, 133.
19. G. Renault, E. Raynal and E. Cornilliant, *J. Biomed. Eng.*, 1983, **5**, 243.
20. R. Sutherland, C. Dähme, J. Place and A. Ringrose, *Clin. Chem.*, 1984, **30**, 1533.
21. B. Tromberg, M. Sepaniak, T. Vo-Dinh and G. Griffin, *Anal. Chem.*, 1987, **59**, 1226.
22. T. Vo-Dinh, B. Tromberg, G. Griffin, K. Ambrose, M. Sepaniak and E. Gardenhire, *Appl. Spectrosc.*, in press.
23. I. Hemmilä, *Clin. Chem.*, 1985, **31**, 359.
24. E. Soini and I. Hemmilä, *ibid.*, 1979, **25**, 353.
25. I. Hemmilä, S. Dakubu, V. Mikkala, H. Siitari and T. Lövgren, *Anal. Biochem.*, 1984, **137**, 335.
26. J. Eskola, T. Nevalainen and T. Lövgren, *Clin. Chem.*, 1983, **29**, 1777.
27. K. Pettersson, H. Siitari, I. Hemmila, E. Soini, T. Lövgren, V. Hanninen, P. Tanner and U. Stenman, 1983, **29**, 60.
28. T. Lövgren, I. Hemmilä, K. Pettersson, J. Eskola and E. Bertoft, *Talanta*, 1984, **31**, 909.
29. J. E. Kuo, K. H. Milby, W. D. Hinsberg III, P. R. Poole, V. L. McGuffin and R. N. Zare, *Clin. Chem.*, 1985, **31**, 50.
30. H. Kaihola, K. Irjala, J. Viikari and V. Nääntö, *ibid.*, 1985, **31**, 1706.

## FIBER-OPTIC BIOSENSORS BASED ON FLUORESCENCE ENERGY TRANSFER

DAVID MEADOWS and JEROME S. SCHULTZ\*

Department of Chemical Engineering, University of Michigan, Ann Arbor, MI 48109, U.S.A.

(Received 20 May 1987. Revised 1 July 1987. Accepted 19 August 1987)

**Summary**—A new optical homogeneous biochemical method for the assay of glucose has been developed, based on fluorescence energy transfer between a glucose analog, dextran labeled with fluorescein isothiocyanate (FITC-dextran), and a glucose-receptor protein, Rhodamine-labeled Concanavalin A (Rh-ConA). When FITC-dextran binds to Rh-ConA in solution, and is light-activated, the FITC label transfers its absorbed energy to the Rhodamine label, which then emits light according to its own characteristic fluorescence spectrum. When glucose is added to this solution, the FITC fluorescence intensity increases as FITC-dextran is released from the Rh-ConA and is replaced by glucose. Thus it is possible to determine glucose concentrations directly from the level of FITC fluorescence.

One of the key elements in the diagnosis and management of disease is the measurement of (a) specific endogenous substances which either control homeostatic mechanisms or reflect the malfunction of these mechanisms and (b) the blood concentrations of drugs used to remedy the disorders. Most clinical analytical methods are based on techniques which require blood samples to be withdrawn from the patient and taken to laboratories for analysis, and consequently only periodic information is available. Because of the skills needed for their performance, most such analyses cannot be done outside the laboratory, *e.g.*, in the home or workplace.

There are a number of reasons for an intense interest in developing simple, accurate, and rapid clinical assays which can be used by non-analytical chemists, *e.g.*, physicians, nurses, patients. In the intensive care setting, where there is a high level of expertise, there is a need for continuous monitoring of blood for metabolites (*e.g.*, glucose) and relatively toxic drugs (*e.g.*, methotrexate, gentamicin). There is also an increasing need for patient self-monitoring, such as blood glucose by diabetics, and at the intermediate level, clinical analysis to be performed in the doctor's office to help in rapid diagnosis.

Until very recently, most approaches for miniature continuous biosensors have been based on electrochemical detectors. These can be broadly classified as potentiometric or amperometric devices.<sup>1,2</sup> The usual electrochemical biosensor consists of a "biochemical" layer containing enzymes, organelles, or cells which are held in place in front of an electrode by a dialysis membrane. The literature is extensive, the groups of Rechnitz<sup>3</sup> and Suzuki<sup>4</sup> being particularly prolific.

Recently, increasing attention is being given to miniaturization of these electrochemical sensors by use of thin-film integrated circuit technology.<sup>5-7</sup>

There are several problems with electrochemical sensors that have not yet been overcome, however.

1. For potentiometric detectors there is usually persistent drift of the working-cell potential with time, resulting in a need for frequent standardization with solutions of known analyte concentration.

2. The effect of consumption of analyte in the measurement is aggravated for amperometric devices because of the limitations in diffusional transport between the transducer compartment and the detector element.

Thus, enzyme electrodes have had only a "minor impact on medical measurement",<sup>8</sup> because the use of electrochemical biosensors has mainly been in off-line systems where samples can be alternated with standards.

A primary focus of our research on biosensors has been to utilize an optical analytical method that will be an alternative to the electrochemical biosensor for on-line concentration measurements. There are some inherent advantages to use of spectrophotometry, fluorimetry and light-scattering for analytical purposes, because of the higher information content of the optical domain compared to electrochemical phenomena. Thus spectral features such as absorption or fluorescence at selective frequencies, provide additional degrees of freedom to characterize and quantify a given analyte in a mixture with other substances.

By use of optical-fiber waveguides, spectrophotometric methods can be miniaturized to monitor very small samples, since the active portion of the sensor is about 1  $\mu$ l in volume. This capability has

\*To whom correspondence should be addressed.

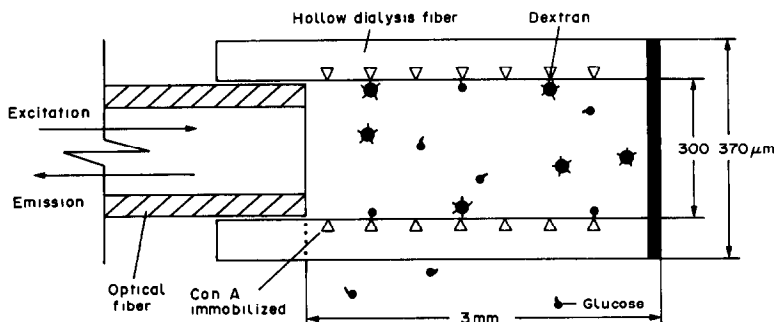


Fig. 1. Schematic of heterogeneous affinity sensor transducer element.

become especially significant in recent years owing to the ready availability of a variety of optical fibers and optoelectronic devices for light-sources and detectors.<sup>9</sup> Optical fibers have been used to fabricate micro-colorimeters and micro-fluorimeters,<sup>10</sup> but it is only recently that optical-fiber detector elements have been coupled to biochemical reactions for the purpose of developing miniaturized biosensors.<sup>11</sup>

The required selectivity was conferred on the biosensor by using a selective bioreceptor (Concanavalin A) and competitive binding between an analog-analyte (FITC-dextran) and the analyte (glucose).<sup>12</sup> A schematic diagram of the optical biosensor is shown in Fig. 1, along with typical dimensions of the active transducer element. In this sensor, the receptor is immobilized on the inner wall of the hollow dialysis fiber. Some typical calibration curves with different analytes are shown in Fig. 2. The response of the sensor displays the expected pattern for a competitive assay, namely a more or less linear response at low concentration and a leveling off at higher concentrations as the competing analyte is displaced from receptor sites. In addition, the different curves demonstrate that the sensitivity of the sensor is related to

the equilibrium binding constant between analyte and receptor; the higher the binding constant, the greater the sensitivity.

A major concern in the performance of any sensor is its rate of response to changes in concentration. There are three physical/chemical processes that contribute to the dynamic behavior of this sensor: (a) diffusion of the analyte through the wall of the hollow fiber, (b) the competitive displacement reaction between analyte, competing analyte and receptor sites, and (c) diffusion of the various species within the hollow-fiber compartment. The time constants for 90% completion of these individual steps have been estimated or measured<sup>12</sup> and found to be about 5 min for glucose diffusion through the wall of the dialysis fiber, about 1 sec for the displacement reaction (at the concentration conditions within the lumen), and about 3 min for the diffusion of components within the lumen. The overall time constant for various fabricated sensors ranged from 6 to 12 min. The analyses indicated that faster response could be achieved by making the sensors with hollow fibers with a smaller lumen diameter and/or thinner walls.

The Schultz and Mansouri sensor gave very good short-term stability during *in vivo* glucose monitoring in a heparinized dog, and good long-term stability during *in vitro* experiments. However, further testing of the sensor raised several pertinent questions about long-term *in vitro* stability. In our most recent work, we have been trying to improve on the design.

One major simplification of the sensor is to eliminate the need for chemical immobilization of the bioreceptor (ConA) on the hollow fiber wall to achieve spatial separation of the free and bound forms of FITC-dextran. The chemical immobilization has often been difficult to reproduce and the alignment of the optical and dialysis fibers must also be carefully maintained. If the chemical immobilization step could be eliminated, physical degradation of the dialysis fiber would no longer be a factor. Also, the Schultz and Mansouri sensor is not capable of automatic on-line recalibration to correct for drift of the optical and electrical components. Any shift in the calibration must be corrected by

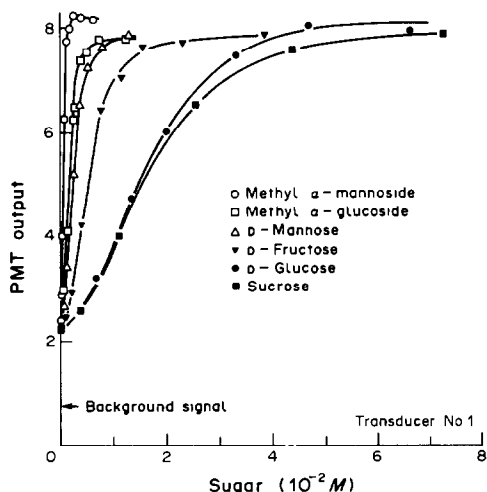
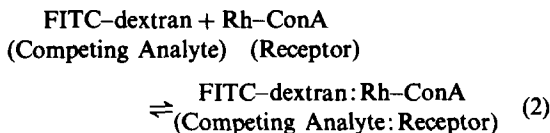
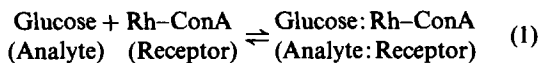


Fig. 2. Effect of binding constant on sensor response.

using a series of standard glucose solutions. We believe that a new optical homogeneous assay which we have recently developed for glucose may be used in the design of an improved sensor.

The new assay has all the reaction species in one phase and is based on a fluorescence energy transfer technique. Most such methods have been developed for haptens bearing a chromophore that can quench the intrinsic ultraviolet fluorescence of antibody tryptophan residues<sup>13-15</sup> as the hapten and antibody bind together. However, the technique has received relatively little attention for fluorophores that absorb in the visible region.<sup>16,17</sup> Our approach employs two labels that absorb and fluoresce in the visible region, FITC-dextran as a donor (fluorescer) and Rhodamine-labeled ConA (Rh-ConA) as the acceptor (quencher). The competing reactions for the system are given in equations (1) and (2).



The efficiency of the energy transfer process is directly related to the overlap of the emission spectrum of the donor with the absorption spectrum of the acceptor. The hatched region in Fig. 3 shows that there is relatively good spectral overlap of the fluorescein emission spectrum, maximum at 520 nm, with the Rhodamine absorption spectrum, maximum

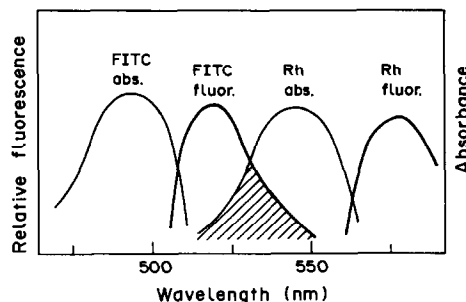


Fig. 3. Overlap of FITC emission spectrum with Rhodamine absorption spectrum.

at 550 nm. Increasing the overlap of the spectra should increase the efficiency of resonance energy transfer between the chromophore pair. When FITC-dextran reversibly binds to Rh-ConA, the two chromophores are close enough together (< 50 Å) for a significant portion of the fluorescein signal to be quenched by the Rhodamine. As glucose is added to the system, FITC-dextran is liberated from the Rh-ConA, causing the fluorescein signal to increase. With this system, it is possible to measure a wide range of glucose concentrations by adjusting the concentrations of each component to give the highest sensitivity over the desired glucose range. An added feature of the system is that the Rhodamine fluorescence signal is not significantly affected by the energy transfer, so it can be used as the internal reference for calibration purposes. Because the assay is homogeneous, it is possible to eliminate all immobilization steps and to scale down the assay from the 1-10 ml bench scale to the 1-μl sensor level. Figure

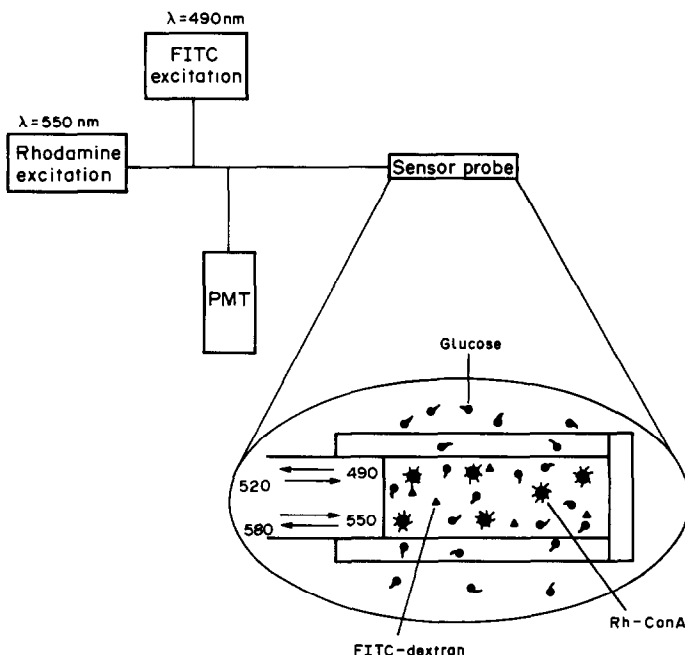


Fig. 4. Schematic of affinity sensor transducer element modified for homogeneous assay.

4 shows how the sensor would be constructed. Light at two different wavelengths, 490 and 550 nm, would be alternately passed into the fiber, and the resulting signal recorded. A change in the Rhodamine signal would indicate a drift in the light-source or detector, and a change in the FITC signal would indicate a change in the glucose concentration. This flexibility will make it easy to develop sensors for many other low molecular weight (<1000) analyte systems by utilizing a selection of commercially available antibodies,  $F_{AB}$  fragments, binding proteins, etc.

#### EXPERIMENTAL

All fluorescence measurements were made with a specially designed spectrofluorimeter operated in the ratio mode. For measuring fluorescein quenching during energy transfer experiments, the excitation and emission wavelengths were 470 and 520 nm, respectively. All experiments were performed at 25° in 0.05M phosphate buffer (containing 0.15M sodium chloride) at pH 7.4. For the quenching curves, a sample containing the desired FITC-dextran concentration was added to a cuvette in the spectrofluorimeter. The fluorescence intensity of the fluorescein was recorded at a single wavelength, 520 nm, after each Rh-ConA addition. Additions were made without removing the cuvette from the holder, and corrections were made for dilution and the inner filter effect from Rhodamine. Glucose titrations were performed similarly, except that the initial solutions contained both FITC-dextran and Rh-ConA at the desired levels. There was approximately a 5-min delay between each addition of glucose of Rh-ConA to ensure that the binding reaction had reached equilibrium.

FITC-labeled dextran, MW  $7.0 \times 10^4$ , was obtained from Pharmacia (Piscataway, NJ), and Rh-ConA from Sigma (St. Louis, MO), U.S. Biochemicals (Cleveland, OH) and Polysciences (Warrington, PA).

#### RESULTS

Energy transfer between fluorescein and Rhodamine was demonstrated by stepwise addition of a pH-7.4 buffered solution of Rh-ConA to a solution of the FITC-dextran. Figure 5 shows that the fluorescein signal significantly decreased as the Rh-ConA concentration was increased. As much as 45% of the fluorescence was quenched at an Rh-ConA concentration of 0.33 mg/ml. The data are replotted (Fig. 6) in terms of the Rh-ConA/FITC-dextran ratio after correction for non-specific

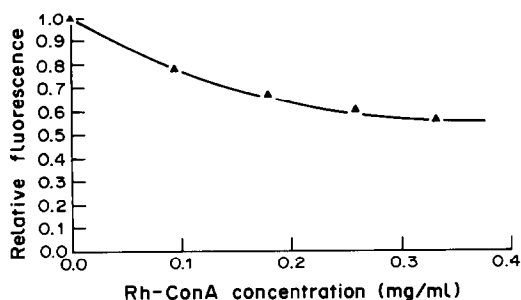


Fig. 5. Quenching effect of Rh-ConA on FITC fluorescence.

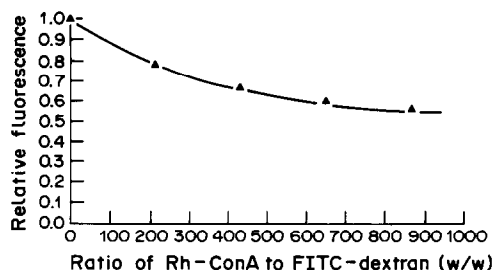


Fig. 6. Normalized quenching effect of Rh-ConA on FITC fluorescence.

absorption of FITC fluorescence, *i.e.*, the inner filter effect. It is easy to see from the figure that the relatively weak binding between ConA and dextran makes it important to have a large excess of Rh-ConA in relation to FITC-dextran in order to achieve a significant amount of fluorescence quenching.

When glucose was titrated (reverse titration) by addition to a solution of Rh-ConA and FITC-dextran, there was the expected increase in fluorescence as the glucose displaced FITC-dextran from the ConA binding sites. Figure 7 shows the fraction of the theoretical maximum fluorescein signal recovered during glucose addition to two solutions with different Rh-ConA/FITC-dextran ratios. The theoretical maximum fluorescein signal was deduced from Fig. 6 for each Rh-ConA/FITC-dextran ratio by assuming that all the quenched signal would be restored when a large excess of glucose was added to the sample. For a weight ratio of 217 for Rh-ConA/FITC-dextran, the fluorescence approached the theoretical maximum more rapidly than when the ratio was 870. At a glucose concentration of 3.00 mg/ml, 60% of the signal was recovered with the 217-ratio system, whereas only ~50% was recovered with the 870-ratio system. As expected from the law of mass action, to achieve the largest signal response within a given glucose range, lower Rh-ConA/FITC-dextran ratios should be used for low glucose concentrations and higher ratios for larger glucose concentrations. Although the relative signal change at low ratios is large for small changes

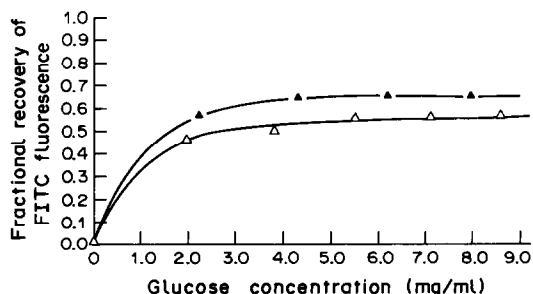


Fig. 7. Recovery of FITC fluorescence during glucose titration: —▲— Rh-ConA/FITC-dextran = 217 w/w; —△— Rh-ConA/FITC-dextran = 870 w/w.

in glucose concentration, the absolute change is smaller. Therefore, both the detector sensitivity and the level of background fluorescence must be considered when specifying the Rh-ConA/FITC-dextran ratio.

#### DISCUSSION

The new optical homogeneous assay currently has a working range up to 2.00 mg/ml (Fig. 7). The linear region of the glucose titration curve can be arranged to cover a particular concentration range by adjusting the Rh-ConA/FITC-dextran ratio. For a larger ratio, the titration curve will be linear to higher levels of glucose, but the sensitivity to small concentration changes will be diminished. There are several other ways of adjusting the sensitivity besides changing the reactant ratios. If the binding constant is increased, then better sensitivities are possible. The sensitivity can also be improved by adjusting the exciter/quencher ratio, or by changing the fluorochrome pair so that the spectral overlap is larger, without adversely affecting the absorptivity. Finally, the size of the ligand analog can be decreased so that the fluorochromes are closer together on binding, which would permit more efficient energy transfer.

There is a practical lower limit to the assay, however. For measuring low glucose concentrations, the FITC-dextran concentration must also be low, making the fluorescein signal smaller and more prone to noise effects. Therefore, the FITC-dextran concentration must be large enough to ensure a good signal-to-noise ratio. We have typically used FITC-dextran concentrations of 0.5–5.0  $\mu\text{g/ml}$  with very good results.

An upper limit to the dynamic range of the homogeneous glucose biosensor is set by the solubility of Rh-ConA. Because the sensor would initially be calibrated with all the components in solution, it is essential that the components are stable for the duration of the experiment. This means that the solution must not form insoluble aggregates, or the calibration would be changed. For the Rh-ConA/FITC-dextran system, this is particularly critical because over a period of hours at 25° ConA will become irreversibly aggregated and form precipitates. This process is even more rapid at 37°. We have performed several experiments to determine whether the stability of Rh-ConA could be increased by physical means such as changes in temperature, ionic strength, pH, or addition of synthetic polymers, but none of these methods was able to significantly increase the stability of ConA. We are currently trying several chemical modification methods, some of which have extended the stability of ConA to as long as two weeks at 37° without adversely affecting the glucose binding. It is expected that there will be an optimum set of conditions for the modification procedure since there is a limited number of reaction sites on native ConA. The greater the number of reaction sites used

during the chemical modification step, the fewer the number of remaining reaction sites available for Rhodamine labeling. We will be reporting on this work in a subsequent paper.

#### CONCLUSIONS

Our approach to the construction of fiber-optic biosensors based on competitive reactions for a bioreceptor between an analyte and a fluorescent analog-analyte has been extended by the use of homogeneous fluorescence quenching techniques. The approach described has several advantages over the heterogeneous systems previously reported.

1. It allows simultaneous monitoring of glucose concentrations from the FITC signal and continuous internal calibration from the Rhodamine signal to correct for light-source and detector sensitivity fluctuations.

2. The receptor does not have to be immobilized on the interior wall of the dialysis fiber, so the alignment between the optical and dialysis fibers is less critical.

3. Physical degradation of the dialysis fiber caused by the immobilization procedure is no longer important.

4. The assay can be easily scaled down from bench experiments to the sensor probe configuration because all the reaction components are in a single homogeneous solution.

5. The technique is general in nature, and any suitable Rhodamine-labeled bioreceptor, e.g., an antibody,  $F_{AB}$  fragment, binding protein, can be added directly to the hollow fiber lumen along with the macromolecular ligand analog. This makes the sensor much more versatile for measuring hormones, metabolites and drugs, since there is no immobilization chemistry to be developed for each assay system.

On the other hand, in order to achieve the most efficient quenching, the overlap of the spectra for the two fluorophores needs to be optimized along with the relative concentrations of the two fluorophores. A higher quenching efficiency will increase the detection limit of the assay by increasing the signal-to-noise ratio. There are additional considerations that must be taken into account when designing a sensor, with regard to the relative concentrations and solubilities of the bioreceptor and the analyte-analog in the sensor compartment. The binding constant must be such that the assay gives a linear response over the desired analyte range when the bioreceptor and analyte analog are used at maximum solubility.

#### REFERENCES

1. M. Aizawa, *Proc. Int. Mtg. Chem. Sensors*, pp. 683–692. Elsevier, Amsterdam, 1983.
2. T. C. Pinkerton and B. L. Lawson, *Clin. Chem.*, 1982, **28**, 1946.
3. G. A. Rechnitz, *Science*, 1981, **214**, 287.



4. S. Suzuki, I. Satow and I. Karube, *Appl. Biochem. Biotechnol.*, 1982, **7**, 147.
5. J. Janata and R. J. Huber, *Ion-Selective Electrode Rev.*, 1979, **1**, 31.
6. I. Lauks, *SPIE Int. Soc. Optical Eng. Proc. Critical Reviews of Technology: Stratified Media*, 1983, **387**.
7. P. W. Cheung, W. J. Ko, D. J. Fung and S. H. Wong, *Theory, Design and Biomedical Application of Solid State Chemical Sensors*, P. W. Cheung, G. Fleming, W. H. Ko, M. R. Newman, (eds.), CRC Press, Cleveland, 1978.
8. P. Vadgama, *J. Med. Eng. Technol.*, 1951 **5**, 293.
9. I. Chabay, *Anal. Chem.*, 1982, **54**, 1071A.
10. G. G. Vurek and R. L. Bowman, *Anal. Biochem.*, 1969, **29**, 238.
11. J. S. Schultz and G. Sims, *Biotechnol. Bioeng. Symp.*, 1979, **9**, 65.
12. J. S. Schultz, S. Mansouri and I. J. Goldstein, *Diabetes Care*, 1982, **5**, 245.
13. L. Stryer, *Radiat Res. Suppl.*, 1960, **2**, 432.
14. *Idem*, *Ann. Rev. Biochem.*, 1978, **47**, 819.
15. N. M. Green, *Biochem. J.*, 1964, **90**, 564.
16. E. F. Ullman, M. Schwarzenberg and K. E. Rubens, *J. Biol. Chem.*, 1976, **251**, 4172.
17. P. L. Khanna and E. F. Ullman, *Anal. Biochem.*, 1980, **108**, 156.

## FIBER-OPTIC BIOSENSOR FOR ETHANOL, BASED ON AN INTERNAL ENZYME CONCEPT

BONNIE S. WALTERS, TIMOTHY J. NIELSEN  
and MARK A. ARNOLD\*

Department of Chemistry, University of Iowa, Iowa City, IA 52242, U.S.A.

(Received 20 May 1987. Accepted 22 June 1987)

**Summary**—A new type of biosensor is introduced, based on a novel internal enzyme system which separates the sample solution from the analytical reaction. The bioanalyte diffuses through a gas-permeable membrane into the internal enzyme solution. A reaction that includes the bioanalyte is catalyzed and the rate of this reaction is related to the bioanalyte concentration. The first example of this type of biosensor is illustrated by the development of a fiber-optic internal enzyme biosensor for ethanol. Alcohol dehydrogenase is the enzyme and the rate of production of reduced nicotinamide adenine dinucleotide is measured. Results that demonstrate the feasibility of the internal enzyme system are presented and the relative merits of this type of biosensor are discussed.

Fiber-optic chemical sensors (FOCSs) are based on the immobilization of an analytical reagent at the distal tip of either a single optical fiber or a bundle of fibers. An optical property of this reagent changes in response to the analyte concentration and this change is measured through the optical fiber device. Fiber-optic biosensors have been developed, involving the immobilization of a biomolecule such as an enzyme or antibody at the sensor tip. A new type of fiber-optic biosensor which is based on a novel concept of an "internal enzyme" biosensor system is reported here. This arrangement protects the enzyme from a sample solution, which provides several advantages from an analytical point of view.

Conventional biosensors are based on the immobilization of a biocatalyst at the sensing tip of a transducer. The biocatalytic layer serves to convert the bioanalyte into a transducer-measurable species. A steady-state condition is established when the rate of product formation is counterbalanced by the rate of product diffusion away from the sensor tip. The steady-state signal from the transducer can be related to the bioanalyte concentration by means of a calibration curve. Alternatively, the consumption of a measurable co-substrate can be measured. Many examples of conventional biosensors have been reported, in which an amperometric or a potentiometric membrane electrode serves as the transducer.<sup>1-3</sup> An example of a fiber-optic biosensor based on the production of a coloured product at the tip of a bifurcated optical-fiber bundle has been reported.<sup>4</sup>

Several problems are common for conventional biosensors. The biocatalytic layer of a conventional biosensor is directly exposed to the sample solution. This arrangement makes the system susceptible to

interference by components in the sample that can alter or modulate the activity of the immobilized biocatalyst. Many substances are known to inhibit or activate enzymatic reactions. For example, trace amounts of heavy metals can either activate or inhibit an enzyme, depending on the particular system involved. Modification of the immobilized biocatalytic activity between sensor calibration and sample measurement can produce significant errors. Exposure to irreversible inhibitors can render the sensor useless by completely inactivating the enzyme. Reagents are often used to protect the biocatalytic layer from activity modulators; an example is the addition of EDTA to complex heavy metals. In addition, the pH of the sample must be adjusted to the optimum for the biosensor. The need to add reagents to protect the enzyme and to provide optimal conditions for the analytical reaction makes it difficult to develop reagent-less biosensors. Reagentless sensors are preferred, however, to minimize sample perturbations during measurements. Finally, conventional biosensors are generally slow in responding to changes in the bioanalyte concentration. This slow response is due to the need to establish a steady-state concentration of the measurable product at the sensor tip. Response times of several minutes are common, and return to the base-line between measurements can be quite lengthy (30-60 min) depending on the type of transducer employed.<sup>5,6</sup>

An internal enzyme biosensor system is introduced here, which can eliminate the above-mentioned limitations of conventional biosensors. It is demonstrated for the first time with an internal enzyme fiber-optic biosensor for ethanol. Figure 1 shows a schematic representation of this ethanol biosensor. A gas-permeable membrane separates the sample solution from the internal enzyme solution. The principal components of this internal enzyme solution are the

\*To whom correspondence should be addressed.

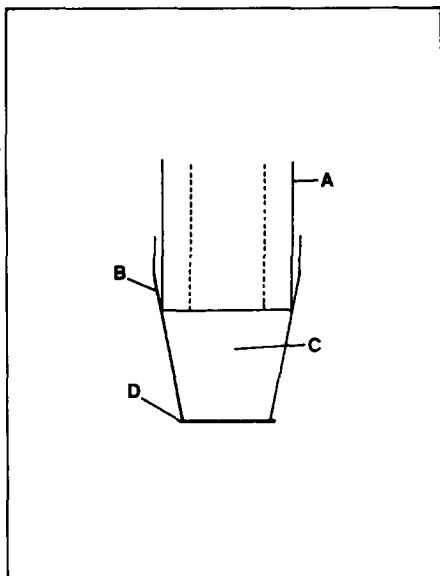


Fig. 1. Schematic diagram of fiber-optic internal enzyme biosensor for ethanol: A, bifurcated optical-fiber bundle; B, sensor body; C, internal enzyme solution; D, gas-permeable membrane.

enzyme alcohol dehydrogenase and oxidized nicotinamide adenine dinucleotide ( $\text{NAD}^+$ ). Ethanol in the sample diffuses through the gas-permeable membrane and enters the internal solution where it is oxidized to acetaldehyde, with the formation of reduced nicotinamide adenine dinucleotide (NADH). Production of NADH is followed fluorimetrically with a bifurcated optical-fiber bundle positioned in the internal solution. The rate of NADH production is measured and this rate is related to the sample ethanol concentration.

#### EXPERIMENTAL

##### Optical arrangement

Figure 2 shows a block diagram of the optical arrangement used for this fiber-optic biosensor. The light source was a 100-W quartz halogen-tungsten lamp (Oriental model 6333) supplied from a constant-voltage transformer (Oriental model 6393). Light from this source passed through an infrared-blocking filter and a 50-nm band-pass filter with transmission centered at 350 nm (Aminco Type UG-1). The resulting excitation radiation was focused into one arm of a bifurcated optical-fiber probe (Oriental model 77540) composed of fused-silica fibers. The excitation radiation traveled through the bundle and irradiated the internal enzyme solution. A portion of the NADH emission was collected by the second half of the bifurcated probe. The returning radiation was passed through a high band-pass filter with a cut-off for  $\lambda < 450$  nm (Aminco Type KV-470), to select the NADH emission. The emitted light was detected by a photomultiplier tube (Oriental model 77340) and a photometer (Oriental model 7070). The photomultiplier was operated at  $-500$  V, and the fluorescent intensities were recorded on a strip-chart recorder (Sargent Welch model XKR).

##### Sensor construction

Ethanol sensors were constructed from a plastic tube that was tapered at one end to an outer diameter of 6 mm. A square of microporous Teflon (0.02  $\mu\text{m}$  porosity; Gore & Associates, Elkton, MD) was stretched across the opening

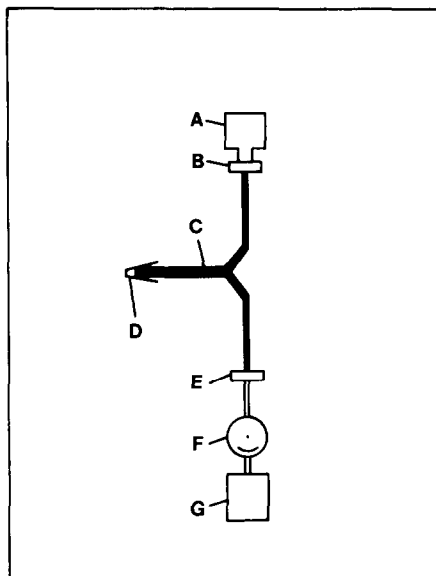


Fig. 2. Block diagram of fiber-optical arrangement: A, light source; B, filters; C, bifurcated optical-fiber bundle; D, sensor tip; E, filter; F, photomultiplier tube detector system; G, strip-chart recorder.

of this tapered end and the membrane was held in position with a plastic O-ring. The internal solution was placed inside the sensor and the common end of the bifurcated fiber-optic probe was positioned just above the internal solution.

The internal solution was prepared by combining stock solutions of  $\text{NAD}^+$  and alcohol dehydrogenase with the buffer. Unless otherwise noted, the buffer was composed of 0.3M Tris and 0.022M glycine, adjusted to pH 8.7 with hydrochloric acid. Stock solutions of  $\text{NAD}^+$  were prepared by dissolving 0.50 g of  $\text{NAD}^+$  (Grade III; Sigma Chemical Co., St. Louis, MO) in 5.00 ml of water. Stock solutions of alcohol dehydrogenase (275 units/mg; Sigma Chemical Co., St. Louis, MO) were made by dissolving approximately 1.5 mg of enzyme in 1 ml of cold buffer. Both  $\text{NAD}^+$  and alcohol dehydrogenase stock solutions were prepared immediately before use. The internal solution was prepared by combining 2.6 ml of buffer, 2.0 ml of the  $\text{NAD}^+$  solution and 0.5 ml of the alcohol dehydrogenase solution. The final composition of the internal solution was 0.15M Tris/0.011M glycine/HCl, 0.006M  $\text{NAD}^+$  and 40.4 units/ml alcohol dehydrogenase; 0.51 ml of this internal solution was employed in the sensor, giving approximately 21 units of enzyme at the sensor tip. For preparation of all solutions freshly distilled demineralized water was employed.

##### Sensor response

Sensor responses were obtained by immersing the tip of the ethanol sensor in 10 ml of an external solution which was either water or buffer (0.1M Tris + HCl, pH 7.5). The external solution was placed in a glass-jacketed cell kept at 25° with a thermostatic water-bath, and stirred with a small magnetic stirring bar. To start, the intensity of the probe was monitored without ethanol present, until a steady-state baseline value was established. A standard amount of an ethanol standard was then added to the external solution, and the intensity *vs.* time data were collected on the strip-chart recorder for several minutes before the sensor was removed and the next measurement started.

Various methods were employed to calculate the rate of NADH formation. Initial rates were calculated either by drawing a line through the intensity-time curve and determining its slope, or by performing a least-squares analysis of the initial intensity-time data. In the latter case, intensity

values were read directly from the photometer at specific time intervals. Alternatively, rates were calculated by using both variable and fixed time procedures. No significant differences were detected between the results obtained by these various methods. Generally, the graphical initial-rate method was employed.

### RESULTS AND DISCUSSION

The analytical use of the internal enzyme ethanol biosensor is based on the relationship between the rate of NADH formation and the sample ethanol concentration. Figure 3 shows an ethanol calibration curve where the rate of intensity change is plotted as a function of the sample ethanol concentration. A linear relationship is observed over an ethanol concentration range from 0.9 to 9mM. The clinically important range for ethanol in serum is approximately one order of magnitude higher than the linear region of this calibration curve. These results suggest that application of this internal enzyme fiber-optic biosensor for serum ethanol measurement is possible with a simple dilution.

Because reagents are consumed during operation of the sensor, the operating conditions continually change during and between measurements. To avoid this problem during characterization studies, a new sensor was constructed before each measurement. Sensor reproducibility was thus a major factor when data from the sensors were combined to give the various response profiles. Table 1 summarizes a reproducibility study in which sensor responses were compared for specific ethanol concentrations over the concentration range of interest. Overall, the relative standard deviation for between-sensor re-

Table 1. Between-sensor reproducibility for fiber-optic ethanol biosensors

Sensor	[Ethanol], mM	Rate, nA/min	Average*
1	1.51	0.24	
2	1.51	0.35	0.30 ± 0.04
3	1.51	0.30	(7.5%)
4	1.74	0.44	
5	1.74	0.43	0.44 ± 0.01
6	1.74	0.45	(2.3%)
7	1.93	0.46	
8	1.93	0.54	0.47 ± 0.05
9	1.93	0.41	(10.6%)
10	2.28	0.47	
11	2.28	0.51	0.51 ± 0.04
12	2.28	0.56	(7.8%)
13	2.51	0.56	
14	2.51	0.52	0.53 ± 0.02
15	2.51	0.53	(3.8%)

\*Average ± standard deviation (relative standard deviation). Rates are expressed in terms of the current output from the photomultiplier as a function of time.

producibility ranged from 2.3 to 10.6% with an average of 6.4%.

Several parameters have been investigated to determine their effect on the sensor response. Figure 4 shows the effect of NAD<sup>+</sup> concentration on the rate of NADH formation. The rate became constant with NAD<sup>+</sup> concentrations above 5mM. In subsequent studies, 6mM NAD<sup>+</sup> was used in constructing the sensor, to minimize variations in sensor response with slight differences in NAD<sup>+</sup> concentration.

The effects of pH and the buffer composition were examined. The optimum pH for the internal solution is between 8.7 and 8.8, which agrees with previous investigations of this enzymatic reaction.<sup>7</sup> The com-

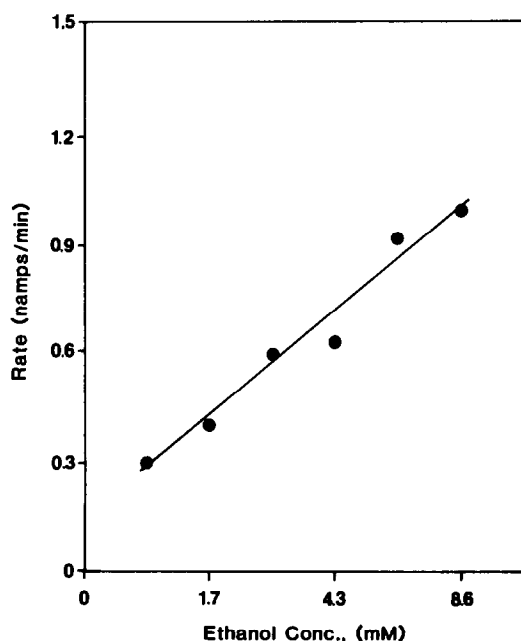


Fig. 3. Calibration of fiber-optic internal enzyme biosensor for ethanol.

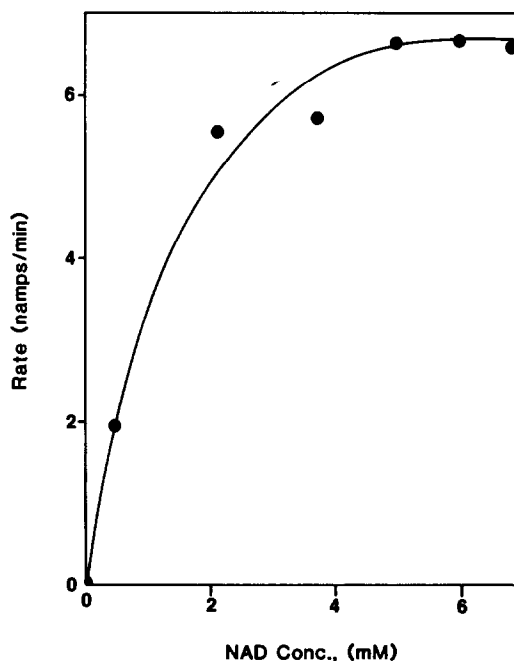


Fig. 4. Effect of NAD<sup>+</sup> concentration on the rate of sensor response.

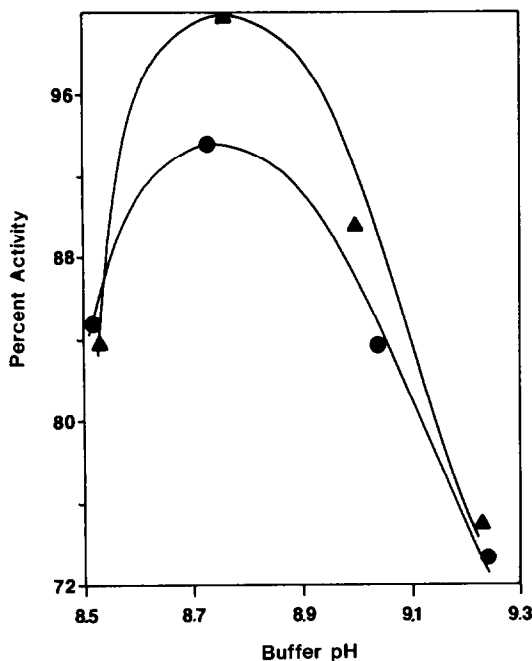
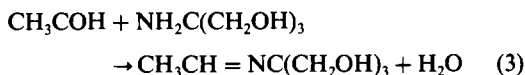
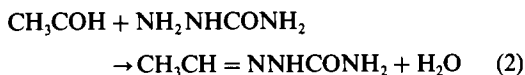


Fig. 5. Effects of pH and buffer composition on sensor response. ▲, Tris buffer alone; ●, Tris buffer with 0.038M semicarbazide.

position of the buffer is important because the reaction catalyzed by alcohol dehydrogenase must be forced towards the production of NADH. Thermodynamically, this reaction favours the production of ethanol and  $\text{NAD}^+$  ( $K_{\text{eq}} = 10^{-14}$  for ethanol and  $\text{NAD}^+$  as reactants). In order to employ this reaction for analytical purposes, it must be driven towards the production of NADH by removing acetaldehyde as fast as it is formed. This can be achieved by reaction of the acetaldehyde with semicarbazide<sup>7</sup> or with the primary amino group of Tris. The following reactions were investigated with various buffer compositions:



where (1) is the analytical reaction catalyzed by alcohol dehydrogenase, (2) represents removal of acetaldehyde with semicarbazide, and (3) involves removal of acetaldehyde with Tris. The pH profiles for sensors with and without 0.038M semicarbazide in 0.15M Tris/HCl buffer are shown in Fig. 5. Although the rates in these two buffer systems are comparable, slightly faster rates are obtained without the semicarbazide. On the basis of these pH profiles and the toxic nature of semicarbazide, a 0.15M Tris/HCl buffer without semicarbazide is recommended.

Numerous advantages can be expected for internal enzyme biosensors. Reagentless probes can be developed because the analytical reaction is physically separated from the sample solution. This separation allows the use of optimal conditions for the analytical reaction without altering the sample. This advantage is a key feature of the internal enzyme concept because it allows *in situ* biomeasurements without perturbation of the system.

Rapid response times are expected for this sensor because it is based on a rate measurement which can be made shortly after the sensor is placed in contact with the sample. Also, there is no need for the sensor response to return to the baseline before the next assay. This absence of a recovery step is a major advantage over conventional biosensors, which often require many minutes to recover before the next measurement can be made.<sup>5,6</sup>

Excellent selectivity is expected for this type of biosensor because there are two selectivity factors which discriminate against possible interferences. First, a highly selective enzyme is employed as the catalytic component. Secondly, the gas-permeable membrane prevents non-volatile interferences from entering the analytical solution. This latter feature protects the system from common enzyme inhibitors and activators. In addition, sample turbidity is not a problem because particulate material cannot pass through the gas-permeable membrane and enter the analytical solution.

Several disadvantages are expected, however. First, the bioanalyte must be capable of passing through the gas-permeable membrane, which restricts this type of biosensor to volatile substrates. This restriction drastically limits the number of bioanalytes for which internal enzyme biosensors can be developed. A potential limitation is the consumption of reagent by the sensor. Many strategies can be developed to deal with this problem. One is to develop disposable biosensors, a batch of sensors being prepared and the entire batch calibrated by testing a representative sample. Each remaining sensor is used once and then discarded. Such an approach requires a high degree of reproducibility between sensors within a batch. Alternatively, sufficient reagent can be added to the internal solution to allow several measurements (including calibrations) to be made with a single sensor. A further approach involves continuous pumping of fresh reagents to the sensor tip.

The data presented here clearly illustrate the feasibility of the internal enzyme biosensor approach. Biosensors of this type are not restricted to use with fiber-optic detection and other transducers can be used to monitor the rate of the biocatalyzed reaction. We plan to continue our development of this ethanol biosensing probe and to extend the internal enzyme concept to other biosensing systems.

*Acknowledgements*—Acknowledgement is made to the donors of The Petroleum Research Fund, administered by

the American Chemical Society, for partial support of this research. Also, the financial support of the National Institutes of Health (GM 35487) is acknowledged.

#### REFERENCES

1. M. A. Arnold, *Am. Lab.*, 1983, **15**, No. 6, 34.
2. P. W. Carr and L. D. Bowers, *Immobilized Enzymes in Analytical and Clinical Chemistry*, Wiley, New York, 1980.
3. R. K. Kobos, In *Ion-Selective Electrodes in Analytical Chemistry*, H. Freiser (ed.), Vol. II, Chap. 1. Plenum Press, New York, 1980.
4. M. A. Arnold, *Anal. Chem.*, 1985, **57**, 565.
5. M. E. Collison and M. A. Arnold, *Anal. Lett.*, 1986, **19**, 1759.
6. M. A. Arnold, *Ion-Selective Electrode Rev.*, 1986, **8**, 85.
7. F. Lindquist, in *Methods of Biochemical Analysis*, D. Glick (ed.), Vol. VII, p. 217. Interscience, New York, 1959.

## SOLID-STATE INSTRUMENTATION FOR USE WITH OPTICAL-FIBRE CHEMICAL-SENSORS

A. J. GUTHRIE, R. NARAYANASWAMY\* and N. A. WELT†

Department of Instrumentation and Analytical Science, UMIST, P.O. Box 88, Manchester, England

(Received 20 May 1987. Accepted 21 August 1987)

**Summary**—A solid-state instrument has been developed for use with optical-fibre pH-sensors, which incorporates light-emitting diode sources and a photodiode detector. The instrument has an internal reference. The optical and electronic principles are described. The responses of the sensor and instrument are reported and compared with those obtained with conventional instrumentation.

The use of optical fibres for chemical sensing is a recent development, and offers some advantages over other systems, such as electrical isolation, suitability for use in hazardous environments, potentially small sensor size and freedom from electrical interference. A number of sensors for various chemical species have been reported.<sup>1-3</sup>

Many systems have been used to retrieve information from this type of sensor and a number of these have been based on conventional spectrophotometers or similar equipment, which utilize incandescent sources, a wavelength-selecting element (filter, grating or prism) and a detector (photomultiplier or photodiode).<sup>4,5</sup>

We have already reported the development of a pH-sensor,<sup>1</sup> based on the use of a pH-sensitive dye immobilized at the tip of an optical fibre. The instrumentation employed in this development study was rather large and consisted of a broad-band light source (tungsten-halogen incandescent lamp), a mechanical modulator, monochromator, photomultiplier, demodulator and amplifier. This system, though suitable for development studies and evaluation of sensing-probe systems, would not be of practical use as a portable pH-measuring system. There is a need for simple instrumentation suitable for use with optical-fibre chemical-sensors.

Solid-state sources have been used<sup>6</sup> as a source of continuous illumination, and their use may be susceptible to interference from variation in ambient light. A sensing system using a modulated solid-state source and solid-state detector has also been reported<sup>7</sup> but without the incorporation of a reference system. Systems using solid-state sources and detectors used in conjunction with remote absorption cells have also been reported.<sup>8,9</sup> Optical-fibre chemical-sensor instrumentation incorporating a reference system has been reported by Peterson,<sup>2</sup> which

uses an incandescent light-source, interference filters for wavelength selection, and mechanical modulation. Here we report the construction of a dedicated instrument for use with optical-fibre pH-sensors. This instrument employs solid-state sources and detector, which allows it to be small, portable and of low power consumption. The use of modulated sources allows the sensors to be used without any shielding from ambient light. A reference system is incorporated to compensate for any optical losses due to fibre coupling or bending, for example.

### INSTRUMENTATION

#### Sources

Light-emitting diodes (LEDs) were chosen as the light-sources, because they have a reasonably narrow band-width (typically 30 nm) and low power consumption, may be modulated electronically, and are available for wavelengths that are suitable for use with several indicator dye systems. The measuring LED has an emission wavelength of 635 nm and the reference LED (a "sweet spot" device) has an emission wavelength of 820 nm. Ideally the reference and measuring wavelengths should be derived from the same source, but since LEDs are narrow-band sources this was not possible. The light from the two sources was combined and then followed the same optical path, through the sensor to the detector.

#### Detector

The detector used was a silicon photodiode. Photodiodes that respond in the wavelength region of interest are small, robust, cheap and do not require the high-voltage supply associated with photomultiplier tubes. However, they do not have the gain of photomultiplier tubes and are, therefore, less sensitive.

In the application described here, the light-signal detected was intense enough to allow photodiodes to be used. The response of photodiodes extends into the near infrared regions.

#### Reference system

In an optical-fibre chemical-sensing system, changes in a signal intensity which may be due to non-chemical causes, for example, fibre bending or changes at fibre connections *etc.*, will produce an output change which may be erroneously considered to be of chemical origin. A reference system is therefore necessary to correct for these effects. The system used in the instrument described here utilizes a

\*To whom correspondence should be addressed.

†Present address: Department of Electrical Engineering, Monash University, Clayton 3168, Victoria, Australia.

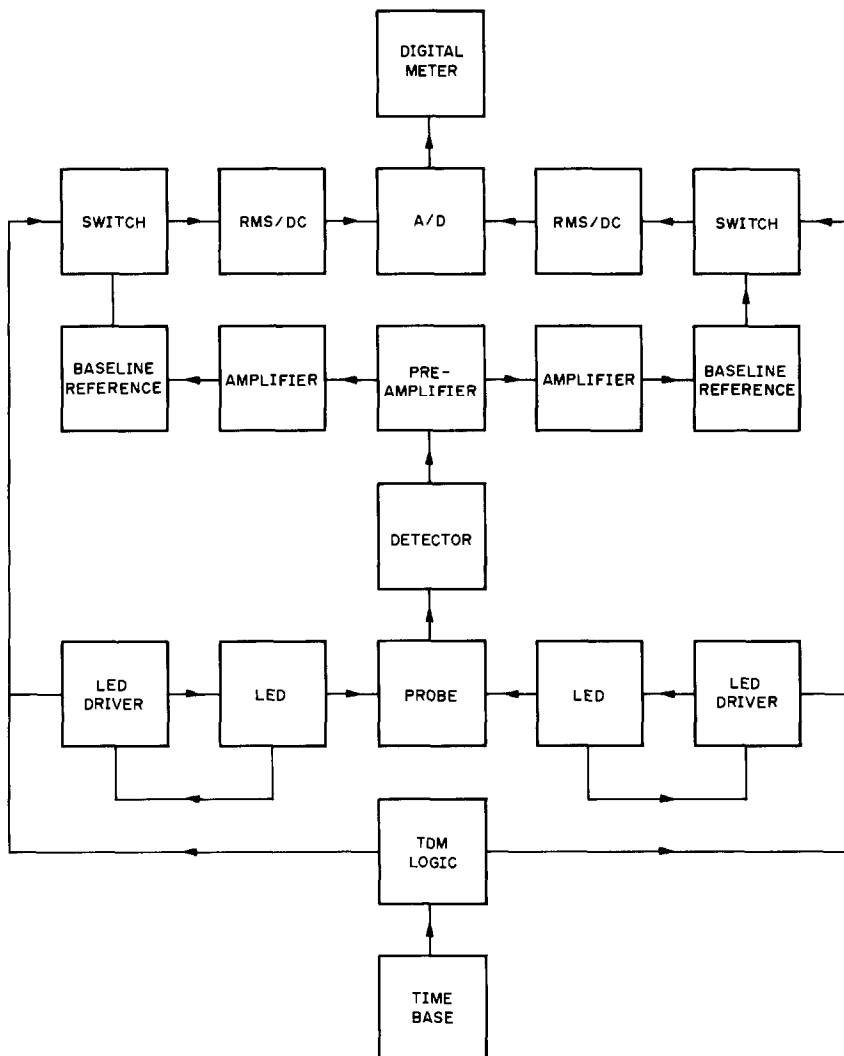


Fig. 1. Block diagram of the optoelectronic instrument.

second light-source which emits at a wavelength that is not absorbed by the immobilized indicator reagent. The reflected light intensity at this "reference" wavelength will be independent of the state of the indicator, and will depend only on the optical losses in the system. Thus, dividing the signal intensity obtained at the measurement wavelength by the signal intensity at the reference wavelength gives a measurement that depends only on the indicator state. The measurement and reference information is separated by using time-division multiplexing. The sources are pulsed alternately at approximately 2 kHz. The signal from the detector is a train of pulses, with alternate pulses corresponding to signals from one of the sources, thus allowing the optically encoded information to be separated. The two signals are amplified and converted into dc signals, and the ratio of their intensities is then displayed on a meter. Experiments were made with different modulation frequencies for each source, and narrow-band filters were used to separate the measuring and reference information; the channel separation achieved, however, was less satisfactory.

The instrument may be divided into the optical system and the electronic system.

#### Optical system

The optical system consists of the two source LEDs, the photodiode detector and the interconnecting optical fibres.

The measuring LED source was modified for connection to an optical fibre by removal of part of its body, so that there was a flat, polished surface perpendicular to the direction of light emission and very close to the emitting junction. A spherical glass bead (approx. 1 mm diameter), which acted as a focusing lens, was cemented in an indentation made over the emitting area. Both LED sources were cemented onto modified optical-fibre connectors. The signal was received by a photodiode, which was cemented to an optical fibre connector similarly to the LEDs. The light from the sources was combined by using a bifurcated polymer optical-fibre bundle (Optronics, "Crofon" fibre) consisting of sixteen fibres, with eight fibres going to each source.

#### Electronic system

The system, illustrated in a block diagram (Fig. 1), consists of two parts: the source timing and driving circuits in one part and the detection circuits in the other. A timer is used to provide the time base, which is divided by using logic circuits (JK flip-flop and OR gates) to provide two signals which are 180° out of phase with each other and have a mark-to-space ratio of 1 to 3. These signals were used to drive the LED sources, so the two LEDs operated alternately. A synchronization signal was also derived from the logic circuits, which controlled the analogue switches in the detection circuits. The signals detected by the photodiode



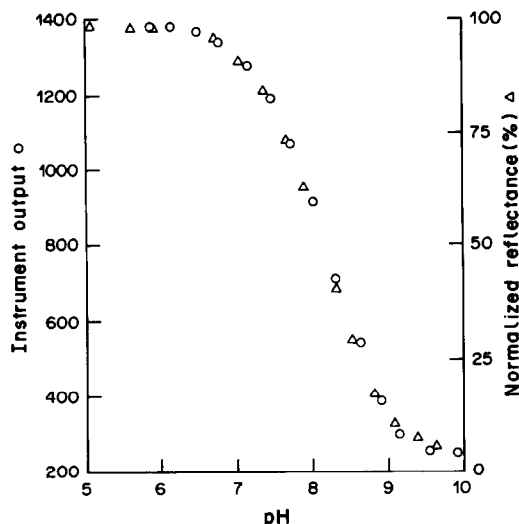


Fig. 2. Probe response vs. pH. O Measured with optoelectronic instrument described.  $\Delta$  Measured with conventional instrumentation.<sup>4</sup>

were amplified and split into two identical channels, each of which was earthed to minimize switching noise. The signals were then passed to the analogue switches, which were controlled by the timing logic to allow alternate pulses to pass into each RMS-DC converter such that each channel corresponded to one LED. The ratio of the d.c. levels from the RMS-DC converters was displayed on the digital panel meter.

All components were supplied by RS Components Ltd.

#### The pH-sensing probe

An optical-fibre pH-sensor incorporating Bromothymol Blue was used in conjunction with this instrument. The probe was constructed and tested as described previously.<sup>1</sup> The pH-sensor was placed in a buffered solution and the pH of this solution was varied between 6 and 10. The instrument output was plotted against the solution pH (Fig. 2). The pH of the solution was monitored with a glass electrode (EIL) and a pH-meter (EDT model ecm 201). All reagents were obtained from BDH Chemicals Ltd.

#### RESULTS AND DISCUSSION

As shown in Fig. 2, the instrument output shows good agreement with the results obtained by using the conventional system described previously<sup>1</sup> at a single wavelength. After suitable calibration this instrument may be used to monitor the response of an

optical-fibre pH-sensor of the type described. The response is linear over a range of approximately 2.0 pH units with a resolution of 0.01; the range and resolution would of course depend on the indicator used in the sensor.<sup>4</sup> The instrument showed a random drift of  $\pm 2\%$  of reading over a 3-hr period, which may be attributed to thermal effects on the system.

#### CONCLUSIONS

We have shown that a solid-state instrument can be developed and constructed for use with optical-fibre chemical-sensors. This instrument offers the advantages of being small, portable, with low power consumption, and of low cost when compared to the conventional instrumentation that can be used with these sensors. Though the instrument described was developed for use with optical-fibre pH-sensors, it could also be adapted for use with other optical chemical-sensors based on the use of immobilized colorimetric reagents and suitable light sources.

The instrument could also be converted to provide a direct pH read-out. Any problems associated with drift of the two source outputs may be overcome by the incorporation of a monitoring and control system so that the source outputs can be maintained constant with respect to each other.

*Acknowledgement*—The partial support of Elf (UK) plc for this work is acknowledged. Elf (UK) plc hold proprietary rights on this instrument.

#### REFERENCES

1. G. F. Kirkbright, R. Narayanaswamy and N. A. Welti, *Analyst*, 1984, **109**, 1025.
2. J. I. Peterson, S. R. Goldstein and R. V. Fitzgerald, *J. Biomech. Eng.*, 1980, **102**, 141.
3. W. R. Seitz, *Anal. Chem.*, 1984, **56**, 16A.
4. G. F. Kirkbright, R. Narayanaswamy and N. A. Welti, *Analyst*, 1984, **109**, 15.
5. L. A. Saari and W. R. Seitz, *Anal. Chem.*, 1982, **54**, 821.
6. T. E. Edmonds and I. D. Ross, *Anal. Proc.*, 1985, **22**, 206.
7. J. F. Giuliani, H. Wohltjen and N. L. Jarvis, *Optics Lett.*, 1983, **8**, 54.
8. H. Inaba, K. Chan and H. Ito, *SPIE 514*, 2nd Int. Conf. OFS, 5-7 Sept. 1984, 211.
9. N. Benaim, K. T. V. Grattan and A. W. Palmer, *Analyst*, 1986, **111**, 1095.

## DETERMINATION OF URANIUM AT TRACE LEVELS BY RADIOCHEMICAL NEUTRON-ACTIVATION ANALYSIS EMPLOYING RADIOISOTOPIC YIELD EVALUATION

A. R. BYRNE and L. BENEDIK

"J. Stefan" Institute, "E. Kardelj" University, 61000 Ljubljana, Yugoslavia

(Received 14 August 1987. Accepted 26 October 1987)

**Summary**—Nanogram and picogram quantities of uranium were determined in biological materials by radiochemical neutron-activation analysis. Two different approaches using either  $^{239}\text{U}$  or  $^{239}\text{Np}$  were employed for cross-checking, and the question of negative errors due to incomplete acid dissolution of any possible inorganic (siliceous) fraction was studied. In the first and main approach, radiochemical separation of the short-lived  $^{239}\text{U}$  (23.5 min) nuclide was based on TBP extraction following rapid conventional wet-ashing. Addition of large amounts of uranium carrier (ca. 50 mg) allowed the chemical yield to be evaluated from the gamma spectrum of the isolated fraction by means of the 186 keV peak of  $^{235}\text{U}$ . In the second approach, the longer-lived  $^{239}\text{Np}$  (56.5 hr) daughter was separated by anion-exchange; this nuclide allowed use of lengthier dissolution procedures employing total decomposition with hydrofluoric acid. Nanogram quantities of  $^{237}\text{Np}$  were irradiated simultaneously with the sample and an aliquot of the resulting solution containing  $^{237}\text{Np}$  and  $^{238}\text{Np}$  (51 hr) was added prior to sample destruction, these isotopes serving as carrier and yield tracer, respectively. Results are presented for a series of reference materials. The methodologies and results from the two approaches are discussed and evaluated.

There are considerable amounts of data in the literature on the low concentrations of uranium found in foodstuffs and human tissues: nevertheless, it is apparent from a recent review by Wrenn *et al.*<sup>1</sup> and from other papers<sup>2-4</sup> that there is still disagreement over the concentrations in bone, and few and conflicting values for soft tissues and blood. This is probably due at least in part to the fact that none of these studies included verification of the analytical methods by the use of certified reference materials (SRMs, CRMs), which have only recently become available from the US National Bureau of Standards (NBS), Washington, and that few of them used any other forms of quality control, such as the standard additions method, analysis of precision, or inter-laboratory intercomparisons.

Though there are several very sensitive analytical techniques for uranium, such as isotope-dilution mass spectrometry,<sup>5</sup> neutron-induced track counting<sup>6,7</sup> or fluorimetry<sup>8,9</sup> (commercial instruments using laser-induced fluorescence are now available), neutron-activation analysis (NAA) possesses the not inconsiderable advantage, at ultratrace or sub-nanogram levels, of being essentially a blank-free and matrix-insensitive technique. It was the aim of the present study to develop a radiochemical NAA method suitable for the analysis of the types of tissue mentioned above, and applicable to work in our co-operative project with the NBS, to assist in the certification of the uranium content of biological reference materials (or candidate RMs). For this purpose a technique using the short-lived (23.5 min half-life)  $^{239}\text{U}$  radioisotope of uranium and solvent extraction with tri-n-butyl phosphate (TBP) follow-

ing neutron irradiation and rapid wet-ashing, was developed, based on earlier work by Steines<sup>10,11</sup> and in our laboratory.<sup>12</sup> A novel feature was the addition of large amounts of uranium carrier (ca. 50 mg) which allowed the chemical yield of the separation to be evaluated from the gamma-ray spectrum of the isolated uranium fraction (used for quantification of the 74.7 keV peak of  $^{239}\text{U}$ ) by counting the 185.7 keV gamma-rays of the naturally radioactive  $^{235}\text{U}$  isotope of the carrier.

Arising from the desirability of verifying this method and the results it produced, a second approach using the longer-lived daughter of  $^{239}\text{U}$ ,  $^{239}\text{Np}$ , with a half-life of 56.5 hr, was also developed, based on anion-exchange separation of neptunium. This not only allowed cross-checking of results, but also enabled a lengthier, total dissolution of the sample to be used. This allowed us to investigate whether results obtained for certain materials by the  $^{239}\text{U}$  technique with conventional wet-ashing might be subject to negative errors due to incomplete dissolution of any possible lithogenous or siliceous uranium-containing fraction, for example, in botanical materials perhaps contaminated by soil or dust. In this second approach, a radioisotopic technique for measurement of the chemical yield was also employed. Some tens of ng of  $^{237}\text{Np}$  (half-life  $2.1 \times 10^6$  yr) were irradiated simultaneously with the sample and an aliquot of the resulting solution containing  $^{237}\text{Np}$  and the induced gamma-emitter  $^{238}\text{Np}$  (half-life 50.8 hr) was added prior to sample destruction, these isotopes serving as carrier and yield tracer, respectively.

Results for a series of biological SRMs, mainly from the NBS, are given and the results and meth-

odologies of the two approaches are discussed and evaluated.

### EXPERIMENTAL

#### Reagents and materials

A 25% (v/v) solution of TBP in toluene was prepared. A 5M nitric acid solution containing 2 ml of 40% hydrofluoric acid per litre was prepared and stored in a polythene bottle. Hydrochloric acid (9M, 4.5M and 0.5M) and 7M nitric acid solutions were prepared.

Anion-exchange columns, 10 cm long and 1 cm in diameter, were prepared in glass tubes fitted with a stopcock, by slurring Dowex-1  $\times 4$ , 50–100 mesh (or Dowex-1  $\times 8$ , 100–200 mesh) in the  $\text{Cl}^-$  form. The columns were well washed with water and 0.5M hydrochloric acid and preconditioned immediately before use, first with 4.5M and then 50 ml of 9M hydrochloric acid. The columns were re-used after washing well with 0.5M hydrochloric acid, water and 0.5M hydrochloric acid and preconditioning as above.

$^{237}\text{Np}$  solution, 1 nCi (37 Bq) per ml, was diluted with 7M nitric acid to give a concentration of 0.1 nCi/g equivalent to about 140 ng/g. [The specific activity of  $^{237}\text{Np}$  is 0.7 pCi (26 mBq) per ng of Np.]

#### Irradiations

For analysis using  $^{239}\text{U}$ , samples and uranium standards were irradiated in the pneumatic transfer system (rabbit) of the Institute's TRIGA MK II reactor in the "F" ring at a neutron flux of  $4 \times 10^{12}$  n.cm $^{-2}$ .sec $^{-1}$  for up to 30 min, depending on the uranium content.

For analysis using  $^{239}\text{Np}$ , samples and uranium standards and a 200- $\mu\text{l}$  aliquot of  $^{237}\text{Np}$  solution were irradiated in the rotating rack position (Lazy Susan) at a neutron flux of  $2 \times 10^{12}$  n.cm $^{-2}$ .sec $^{-1}$  for about 20 hr and cooled for a further 24 hr before commencing the procedure.

#### Samples

Materials were weighed and sealed into polythene ampoules that had been cleaned by soaking for several hours in 7M nitric acid and rinsing well, and then dried. The sealed ampoules were further encapsulated in polythene foil to avoid superficial contamination during irradiation and handling. The sample weights ranged from 250 mg to 1 g for the lowest uranium concentrations ( $^{239}\text{U}$  method).

#### Standards

Working irradiation standards of 1  $\mu\text{g/ml}$  uranium (for  $^{239}\text{U}$ ), and 5  $\mu\text{g/ml}$  (for  $^{239}\text{Np}$ ), both in 1% v/v nitric acid, were prepared at frequent intervals by dilution of a stock 0.1 mg/ml solution prepared from uranyl nitrate hexahydrate. This was checked against a second standard prepared from uranyl acetate from a different supplier. A carrier solution of 50 mg/ml uranium was also prepared from uranyl nitrate. All these materials were of natural isotopic composition. About 200  $\mu\text{l}$  of irradiation standard for  $^{239}\text{U}$  were sealed in a polythene tube, 2 mm in bore. After irradiation, a 100- $\mu\text{l}$  aliquot was pipetted out, weighed and made up to the same volume (10 ml) as the extracted sample fraction, with acidified carrier solution. For  $^{239}\text{Np}$ , about 200  $\mu\text{l}$  of the more concentrated uranium solution (5  $\mu\text{g/ml}$ ) were weighed and sealed in a silica tube (bore 2 mm). After irradiation, the contents were quantitatively transferred to a counting bottle with the aid of 1 ml of 9M hydrochloric acid containing a few drops of hydrofluoric acid (to complex Np and assist in leaching the walls of the tube) with which the silica tube was rinsed several times, being allowed to stand for some time filled with the rinsing solution for each wash. The solution was then made up to 10 ml with 4.5M hydrochloric acid. About 200  $\mu\text{l}$  (the exact amount need not be known) of  $^{237}\text{Np}$  solution in a similar silica tube was irradiated together with the uranium ( $^{239}\text{Np}$ ) standard. After irradiation it was transferred and diluted to volume

with 7M nitric acid in a 10-ml standard flask. Aliquots of 1 ml give a suitable activity of  $^{238}\text{Np}$  for tracer purposes (about 1 cps at the 984 keV peak).

#### Activity measurements

Gamma-ray spectroscopy of 10-ml volumes contained in 50-ml polythene bottles (diameter 45 mm) was performed by measurement directly on the top of an ORTEC intrinsic Ge detector (17% efficiency, 1.8 keV resolution at 1332 keV) connected to a Canberra 80 multichannel analyser system.

**Uranium-239.** Total peak areas of the 74.7 keV peak of  $^{239}\text{U}$  (in the sample and standard) and the 185.7 keV peak of  $^{235}\text{U}$  (in the sample) were measured immediately after the end of the radiochemical procedure. The peak of  $^{235}\text{U}$  at 185.7 keV was used to evaluate the chemical yield by reference to the count rate of an unprocessed aliquot of uranium carrier solution (50 mg/ml). The count rate of the 185.7 keV peak under our conditions was about 1.5 cps for 50 mg of natural uranium. The counting time of the sample was normally 1200 sec, or 1800 sec near the limit of detection. Thus to achieve good statistics, the sample fraction was normally counted again for about 5000 sec to determine the yield with higher precision (though for routine use the first count would be acceptable). The amount of uranium carrier added (50 mg) gave a compromise between precise evaluation of the chemical yield without lengthy counting, and reduced accuracy in the evaluation of the 74.7 keV  $^{239}\text{U}$  peak at low activities due to an increase in the Compton background under this peak, from  $^{235}\text{U}$  activity. Corrections were applied to make allowance for decay between the standard and sample countings, and to the sample count when it was not short relative to the half-life of  $^{239}\text{U}$ . In addition, for samples with very low uranium contents, a very small correction was applied to the 74.7 keV peak area to allow for X-rays at this energy, induced from heavy elements (mainly in the detector itself) by the activity of the sample (largely  $^{235}\text{U}$ ) and the background.

**Neptunium-239.** The peak of  $^{239}\text{Np}$  at 277.6 keV, and that of  $^{238}\text{Np}$  at 984.4 and the doublet at 1026 and 1028.5 keV were counted under the same conditions as for  $^{239}\text{U}$  (see above).

The chemical yield was evaluated from the weights used and the relative count rates of  $^{238}\text{Np}$  (as the sum of the 984.4 and 1026 + 1028.5 keV doublet peaks), from the sample and from an untreated aliquot of the  $^{238}\text{Np}$  solution used for spiking the samples.

The 228.2 keV peak of  $^{239}\text{Np}$  is not suitable for determination of uranium, as this peak has a contribution from the fission product  $^{132}\text{Te}$ . On the other hand, the 103.7 and/or 106.1 keV peaks of  $^{239}\text{Np}$  may be used, and in fact offer a higher sensitivity than the 277.6 keV peak. However, account should be taken of the small contribution to the 103.7 keV peak from  $^{238}\text{Np}$  (103.8 keV, 0.33%), and the possibility of a contribution to the 106 keV peak from  $^{153}\text{Sm}$ , if present as a radiochemical impurity.

#### Radiochemical procedure

**$^{239}\text{U}$  method.** The irradiated sample was rapidly wet-ashed over a gas flame in a 100-ml long-necked silica Kjeldahl flask already containing 3 ml of 9M sulphuric acid and 50 mg of U (1 ml of carrier solution) by heating with repeated additions of concentrated nitric acid until a pale yellow-green colour was obtained which did not darken on heating. The flask was then cooled by being plunged into water, 1–2 ml of concentrated perchloric acid was added, and the flask reheated to evaporate the perchloric acid as dense white fumes. (Note. If the use of perchloric acid is precluded by the fume-hood design or safety regulations, the wet-ashing can also be satisfactorily completed by dropwise addition of 30% hydrogen peroxide at this stage, and the excess destroyed by boiling.) The contents of the flask were transferred to a 50-ml separatory funnel with 19 ml of 5M nitric acid (measuring cylinder), added in two portions.

Uranium was extracted by vigorous shaking for 30–40 sec with 10 ml of 25% TBP solution in toluene, and the aqueous phase was run off and discarded. The organic phase was washed briefly with two 5-ml portions of 5M nitric acid containing 2 ml of hydrofluoric acid per litre. The organic phase was drawn off by pipette, run into a 50-ml polythene measuring bottle (diameter 45 mm) and counted directly on the top of the Ge detector. The separation procedure takes about 15 min to perform.

**<sup>239</sup>Np method.** For destruction by wet-ashing without hydrofluoric acid, the irradiated sample was transferred to a Kjeldahl flask already containing 2 ml of concentrated sulphuric acid and a weighed aliquot of the <sup>237+238</sup>Np tracer (see above, standards), and wet-ashed as described for the <sup>239</sup>U method.

If total dissolution with the aid of hydrofluoric acid was to be used, the irradiated sample was transferred to a 100-ml Teflon beaker containing the <sup>237+238</sup>Np spike, and 5 ml of concentrated nitric acid were added. It was covered with a watch-glass and allowed to simmer on a hot-plate for 1 hr. Then 5 ml of concentrated perchloric acid were added and the heating was continued. More nitric acid was added from time to time as necessary. When a clear yellow solution was obtained, 5 ml of 40% hydrofluoric acid were added and allowed to boil off from the uncovered beaker. Another 5 ml of hydrofluoric acid were added and heating was continued until the volume was reduced to 1–2 ml.

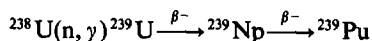
In both procedures, 20 ml of 9M hydrochloric acid were then added, followed by about 0.5 g of hydroxylamine hydrochloride, and the solution was warmed gently for about 10 min to ensure that Np was present as Np(IV). When the hydrofluoric acid system was used, about 0.5 g of boric acid was also added to complex any remaining trace of fluoride, which would otherwise decrease the sorption of Np on the anion-exchanger.

The solution was then transferred to the top of the anion-exchange column and allowed to flow through it at about 1 ml/min. (If there is a precipitate, it will dissolve during the subsequent elution.) The column was then washed with 50 ml of 9M hydrochloric acid, and 50 ml of 7M nitric acid. The Np was finally eluted from the column with 50 ml of 4.5M hydrochloric acid and collected in a clean Kjeldahl flask. The volume was reduced to a few ml by boiling and the solution transferred with 4.5M hydrochloric acid to a counting bottle to give a volume of 10 ml for gamma-spectroscopy.

## RESULTS AND DISCUSSION

### The <sup>239</sup>U method

The neutron-capture reaction



and successive beta decay offer two possibilities for NAA of uranium, by use of either the short-lived <sup>239</sup>U or its longer lived <sup>239</sup>Np daughter. In the procedure developed by Steinnes,<sup>10,11</sup> <sup>239</sup>U was separated by solvent extraction with TBP; however, it was reported that some of the heavier rare-earth elements were partially co-extracted, as might be expected from the data of Peppard.<sup>13</sup> Dermelj *et al.*,<sup>12</sup> in this laboratory, showed that the use of a 5M nitric acid solution containing a small amount of hydrofluoric acid (0.2% v/v) was very effective in improving the radiochemical purity by removing traces of radionuclides other than those of uranium, which is important if an NaI(Tl) well-type detector, with high

efficiency but low resolution, is to be used to measure the 74.7 keV gamma-rays of <sup>239</sup>U. In that work, the chemical yield was determined by re-activation. In the present modification, the yield is more simply determined by counting the 185.7 keV gamma-rays of <sup>235</sup>U in the separated uranium fraction, after addition of large amounts (*ca.* 50 mg) of uranium carrier at the beginning of the radiochemical procedure. In this case the use of a Ge or Ge(Li) high-resolution detector is preferable. The clean-up washes containing hydrofluoric acid substantially reduce the Compton background under the 74.7 keV peak measured on the Ge detector, and are also very effective in stripping <sup>234</sup>Th, <sup>231</sup>Th and <sup>234</sup>Pa, the gamma-emitting progeny in radioactive equilibrium with the added natural uranium carrier, leaving only <sup>235</sup>U gamma-rays. Fortunately, <sup>239</sup>U, apart from a gamma-ray at 43.5 keV (5.6%), has no significant gamma-rays other than the main peak at 74.7 keV (59.3%). These aspects are illustrated in Fig. 1. The spectrum of <sup>239</sup>U separated from NBS Bovine Liver demonstrates the sensitivity and radiochemical purity achieved with the method.

Preliminary experiments on the extraction of uranium from wet-ashed residues were performed to optimize the chemical yield. The presence of sulphuric acid lowers the extraction of uranium with TBP from nitric acid media, but 3 ml of 9M sulphuric acid in 20 ml of the aqueous phase (*i.e.*, yielding 5M nitric acid and 1.3M sulphuric acid) still gives a good recovery, as shown in Table 1. The amount of sulphuric acid used is a compromise between speed of wet-ashing on the one hand, and chemical yield on the other. If smaller amounts of sulphuric acid are used, the wet-ashing is slower and the higher extraction is offset by the increased decay of <sup>239</sup>U. The chemical yield for the method, with biological materials and using only 2 ml of 9M sulphuric acid, was found to be 86 ± 2.5% (10 replicates), and when the quantity of sulphuric acid was increased to 3 ml to speed up the wet-ashing, especially for large sample aliquots, the yield found was 83 ± 2% (10 replicates).

The results obtained by the <sup>239</sup>U method for a range of reference materials, mostly from the NBS, are shown in Table 2. (Some of these results and a preliminary version of the method were reported earlier.<sup>20</sup>)

Excellent agreement with the certified values was found for NBS Oyster Tissue and New Bovine Liver; for Pine Needles our result was somewhat lower, but the uncertainty of the certified value is high. Also, in the compilation of literature values for NBS Reference Materials published by Gladney *et al.*,<sup>16</sup> the results of four other laboratories for Pine Needles (13, 15, 15 and 18 ng/g), all obtained by NAA, give a mean of 15 ± 2 ng/g.

Kelly and Fassett<sup>5</sup> have described an isotope-dilution mass-spectrometric (IDMS) method, which as a reference method of high accuracy and sensitivity, was used for the certification of uranium in the

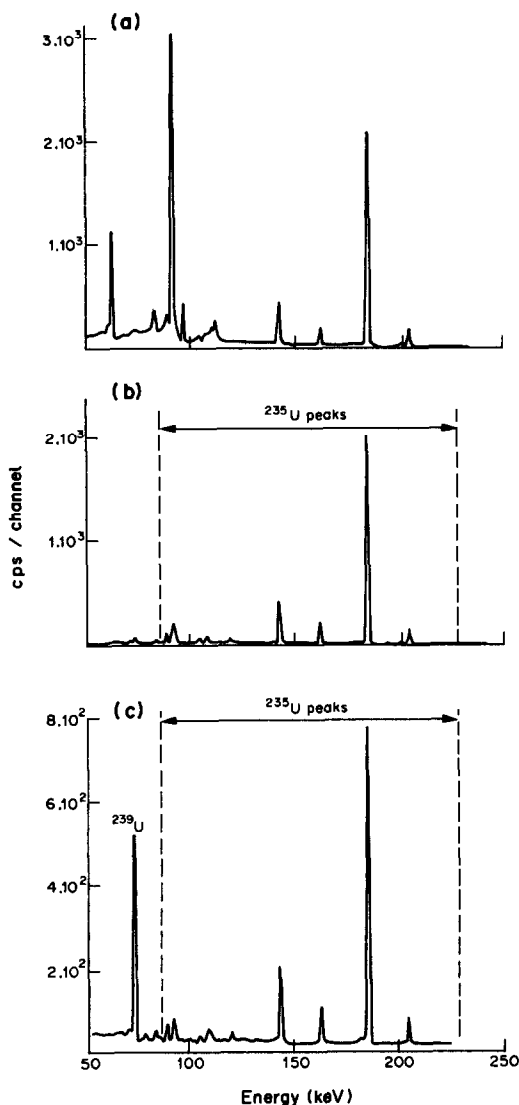


Fig. 1. Gamma-spectra of: (a), uranium carrier, showing peaks of  $^{235}\text{U}$  and daughters of  $^{238}\text{U}$  and  $^{235}\text{U}$  ( $^{234}\text{Th}$ ,  $^{234}\text{Pa}$ ;  $^{231}\text{Th}$ ); (b), uranium after TBP extraction, showing only  $^{235}\text{U}$  peaks; (c), uranium fraction (about 0.5 ng of U) extracted from neutron-irradiated NBS Bovine Liver SRM 1577a, showing  $^{239}\text{U}$  peak at 74.7 keV and peaks of  $^{235}\text{U}$  as in (b).

new Bovine Liver SRM 1577a at NBS. By our method, besides obtaining good results for Bovine Liver, we were able to analyse NBS Wheat Flour SRM 1567a, Rice Flour SRM 1568a, and Non-fat Milk Powder SRM 1549, the last-named being found to contain only a quarter of the uranium in 1577a (see Table 2). For this ultratrace material, an NaI(Tl)

Table 1. Extraction of uranium (%) by 25% TBP in toluene from mixed  $\text{HNO}_3$ - $\text{H}_2\text{SO}_4$  media at a phase ratio of 1:1

$[\text{H}_2\text{SO}_4], M$	$[\text{HNO}_3], M$	3.5	5.25	7.0
0.9		93.7	93.3	93.3
1.8		89.0	87.0	84.0
3.6		70.4	67.0	63.0

well-type detector was used to increase the efficiency of counting, only 100  $\mu\text{g}$  of uranium carrier being added to reduce the background signal under the peak, and the yield was determined by the re-activation technique. The net areas of the  $^{239}\text{U}$  peak for the Milk Powder sample (about 900 mg) were around 2000 counts, and a good standard deviation was achieved even at this very low level. If available, a well-type Ge detector would be ideal for such ultratrace work and would enable the  $^{235}\text{U}$  isotopic-yield technique to be applied.

Notwithstanding the discussion above of our results for Pine Needles, these values aroused our suspicions that the difference from the certified value could be due to the fact that total dissolution with hydrofluoric acid was not used, and stimulated us to develop the alternative  $^{239}\text{Np}$  procedure. For certification work, total dissolution is mandatory. It is also worth pointing out that the  $^{239}\text{U}$  method involves handling large quantities of uranium as carrier, so the possibility of contamination should be borne in mind. Good housekeeping and the use of separate areas for preparation of samples and for radiochemical work avoid this potential danger.

#### The $^{239}\text{Np}$ method

This method was developed largely as a check on the correctness of the results produced by the more rapid and sensitive  $^{239}\text{U}$  technique. Apart from its use as a back-up method, it has some advantages in its own right, largely due to the longer half-life of  $^{239}\text{Np}$  (56.5 hr), which allows more elaborate sample decomposition and radiochemistry to be applied (in particular, total dissolution with the aid of hydrofluoric acid).

The major disadvantage of working with  $^{239}\text{Np}$  in earlier methods,<sup>14,15</sup> was the fact that when used as a carrier-free nuclide it is very prone to co-adsorption and co-precipitation losses, and the chemical yield is difficult or impossible to measure. These problems were completely overcome in our method by addition of neutron-irradiated  $^{237}\text{Np}$  to the sample before starting the procedure. The long-lived alpha-emitter  $^{237}\text{Np}$  ( $2.14 \times 10^6$  yr) is of very low specific activity and sufficient can be added to act as a carrier: several ng of Np are added to each sample. The  $^{238}\text{Np}$  produced by neutron-capture during irradiation is a gamma-emitter of half-life 50.8 hr, which acts as a tracer to allow the determination of the chemical yield of the Np separation.

The use of the isotopes of Np as mutual tracers has several interesting applications. Thus Niese and Niese<sup>21</sup> used  $^{239}\text{Np}$  and  $^{238}\text{Np}$  to monitor the recovery of  $^{237}\text{Np}$  separated from spent nuclear fuel, with subsequent non-destructive NAA to measure the concentration of  $^{237}\text{Np}$ , by means of  $^{238}\text{Np}$ . In the case of reactor water,  $^{238}\text{Np}$  was used<sup>22</sup> to monitor the recovery of  $^{239}\text{Np}$  in NAA of the uranium content. Byrne<sup>23</sup> used  $^{239}\text{Np}$  to measure the recovery of  $^{237}\text{Np}$  separated from Cumbrian sediments, and then, fol-

Table 2. Concentrations of uranium found by the  $^{239}\text{U}$  method in biological reference materials, ( $\mu\text{g}/\text{kg}$  dry weight)

Material	Found*	Certified	Literature
NBS SRM-1566			
Oyster Tissue	$111 \pm 3$ (6)	$116 \pm 6$	
NBS SRM-1575			
Pine Needles	$14.5 \pm 0.6$ (5)	$20 \pm 4$	
NBS SRM-1577a			
New Bovine Liver	$0.70 \pm 0.035$ (5)	$0.71 \pm 0.03$	
NBS SRM-1549			
Non-fat Milk Powder	$0.17 \pm 0.01$ (5)	—	
NBS SRM-1567a			
Wheat Flour	$0.29 \pm 0.04$ (7)	—	
NBS SRM-1568a			
Rice Flour	$0.27 \pm 0.02$ (7)	—	
NBS RM-8431			
Mixed diet	$2.4 \pm 0.3$ (3)	—	$3.1 \pm 1.2^{19}$
IAEA CRM H-9			
Mixed human diet	$5.3 \pm 0.2$ (3)	—	$5.0 \pm 0.6^{19}$

\*Mean and standard deviation, number of replicates in parentheses.

lowing neutron-irradiation,  $^{239}\text{Np}$  again to measure the yield of  $^{238}\text{Np}$  in the post-irradiation radiochemical separation. In the present technique,  $^{238}\text{Np}$  is used to monitor the yield of  $^{239}\text{Np}$  produced by neutron-irradiation of uranium. The gamma-energies of  $^{238}\text{Np}$  and  $^{239}\text{Np}$  are very compatible for gamma-spectroscopy, as the former has virtually no low-energy gamma-rays, while the latter has no high-energy gamma-rays. It should also be noted that the absolute activity of  $^{238}\text{Np}$  (or of  $^{237}\text{Np}$ ) is not required, as the chemical yield measurement is based purely on relative measurements of the gamma-peaks of  $^{238}\text{Np}$  in an unprocessed aliquot (as standard) and in the sample fraction separated according to the procedure above.

This radiochemical separation is based on well known ion-exchange behaviour; the anion-exchange separation of  $\text{Np(IV)}$ , which closely resembles  $\text{Pu(IV)}$  in its behaviour, is based on the fact, used in very many published methods for Pu determination, that a combination of concentrated hydrochloric acid ( $\geq 9M$ ) and 7–8M nitric acid elutes virtually every other element from an anion-exchange column and is thus very selective for  $\text{Np(IV)}$  and  $\text{Pu(IV)}$ . Both may be stripped with dilute hydrochloric acid or mineral acid containing hydrofluoric acid [or in the case of Pu, by elution as  $\text{Pu(III)}$  with a reducing agent such as iodide]. In Edgington's procedure<sup>14</sup> for NAA of U

and Th, anion-exchange was used to separate  $^{239}\text{Np}$  (and  $^{233}\text{Pa}$ ), but only hydrochloric acid was used to elute impurities from the anion-exchanger.

The radiochemical purity of the separated  $^{239}\text{Np}$  was excellent; only traces of  $^{233}\text{Pa}$  (from Th),  $^{187}\text{W}$  and occasionally  $^{122}\text{Sb}$  were observed in the spectra. The radiochemical yield averaged around 80%.

The total dissolution of biological materials in a Teflon beaker (or bomb) with nitric, perchloric and hydrofluoric acid mixtures is relatively slow and tedious, particularly when compared with wet-ashing in a Kjeldahl flask (5–10 min). However, the longer half-life of  $^{239}\text{Np}$  is compatible with such procedures and with the lengthier anion-exchanger separation.

#### Comparison of the $^{239}\text{U}$ and $^{239}\text{Np}$ methods

As mentioned above, it was of particular interest to compare results from the  $^{239}\text{U}$  method with those obtained by the  $^{239}\text{Np}$  procedure, both with and without the use of total dissolution with hydrofluoric acid. Table 3 shows such results for three NBS botanical reference materials. Noteworthy is the very good agreement between the two methods when the same type of initial wet-ashing technique was used, and the small but significant increase in the concentrations found in these plant materials following total dissolution. From these results we may also deduce something about the relative size of the endogenous,

Table 3. Comparison of uranium concentrations in botanical reference materials found by  $^{239}\text{U}$  method with those from  $^{239}\text{Np}$  method with and without HF dissolution, ( $\mu\text{g}/\text{kg}$  dry weight)

Material	$^{239}\text{U}$	$^{239}\text{Np}$		Certified	Literature
		(without HF)	(with HF)		
NMS SRM-1575					
Pine Needles	$14.5 \pm 0.6$ (5)	$14.9 \pm 1.0$ (4)	$17.8 \pm 0.9$ (6)	$20 \pm 4$	$15 \pm 2^{16}$ (4)†
NBS SRM-1527					
Citrus Leaves	$29.9 \pm 0.7$ (4)	$31.2 \pm 1.0$ (6)	$36.3 \pm 2.2$ (6)	$\leq 150$	$32.3 \pm 3.4^{19}$
NBS SRM-1571					
Orchard Leaves	$23.5 \pm 1.5$ (6)	$23.2 \pm 1.2$ (3)	$29.3 \pm 1.6$ (6)	$29 \pm 5$	

\*Mean and standard deviation, number of replicates in parentheses.

†Mean of results from four laboratories.

biological (soluble) fraction and the residual, insoluble fraction, presumably due to soil or dust contamination on leaf surfaces. Assuming a crustal abundance of 2 mg/kg for uranium, and an endogenous biological uranium content of about 20 µg/kg in the plant material, soil contamination of 1 part per 1000 (0.1%) would increase the uranium content by 10% to 22 µg/kg. Heydorn *et al.*<sup>17</sup> showed in the case of vanadium that discrepancies in the results for Orchard Leaves could be largely attributed to the same cause, namely, incomplete dissolution of the substantial visible siliceous residue.

There are of course two viewpoints on this question; while the producers of reference materials may feel that a warning (caveat emptor!) to the user, which indeed appears in the Certificate, that total dissolution is necessary, fulfils his obligations, it is also reasonable that users of biological reference materials could expect them to be just that, and not a mixture of biological and inorganic/geological materials. On the other hand, some real samples arriving in the laboratory will suffer from similar problems, and the analyst should be aware of the possibility of negative errors if total dissolution of botanical specimens is not used. However, further discussion of the philosophy of the preparation and use of reference materials is beyond the scope of this paper.

#### CONCLUSION

It would perhaps be a mistake to overemphasize this problem of inorganic contamination, as the majority of sample types of interest (biological materials with trace uranium contents), such as tissues, organs, body fluids, most foodstuffs, *etc.*, will not be affected by it. The <sup>239</sup>U technique described is rapid, very sensitive, has a convenient and accurate chemical yield measurement, and as demonstrated in Table 2 produces results of good accuracy. The <sup>239</sup>Np method is slower and less sensitive, but is more amenable to use of total dissolution of the sample. The addition of a <sup>237+238</sup>Np spike also increases the accuracy and convenience of working with <sup>239</sup>Np. It should also prove useful for NAA of geological materials with low uranium contents, which can be more easily handled after 2 or 3 days cooling, and for other samples with somewhat higher uranium contents where non-destructive NAA using gamma-spectroscopy of <sup>239</sup>Np is difficult or impossible, owing to high matrix radioactivity.

The <sup>238</sup>U method will be the method of choice for most samples of the type mentioned above, though the possibility of an insoluble fraction should be borne in mind and investigated. Further work to develop rapid total dissolution of biological materials in combination with the <sup>239</sup>U method is in progress, including investigation of alkaline fusion, as used in the NAA determination of iodine in biological materials.<sup>18</sup>

*Acknowledgements*—The financial support of the National Bureau of Standards (NBS), Washington, DC, under contract JFP-692, and of the Slovenian Research Council, is gratefully acknowledged.

#### REFERENCES

1. M. E. Wrenn, P. W. Durbin, B. Howard, J. Lipsztein, J. Rundo, E. T. Still and D. L. Willis, *Health Phys.*, 1985, **48**, 601.
2. I. M. Fisenne and G. A. Welford, *ibid.*, 1986, **50**, 739.
3. I. M. Fisenne and P. M. Perry, *ibid.*, 1985, **49**, 1272.
4. Y. Igrashi, A. Yamakana, R. Seki and N. Ikeda, *ibid.*, 1985, **49**, 707.
5. W. R. Kelly and J. D. Fassett, *Anal. Chem.*, 1983, **55**, 1040.
6. R. L. Fleischer, P. B. Price and R. M. Walker, *Nuclear Tracks in Solids: Principles and Applications*, Univ. of California Press, Berkeley, 1975.
7. E. I. Hamilton, *Applied Geochronology*, p. 267. Academic Press, 1965.
8. G. R. Price, R. J. Ferretti and S. Schwarz, *Anal. Chem.*, 1953, **25**, 322.
9. J. C. Veselsky and A. Wölfl, *Anal. Chim. Acta*, 1976, **85**, 135.
10. E. Steinnes, *Talanta*, 1975, **22**, 1041.
11. *Idem*, *Anal. Chim. Acta*, 1975, **76**, 461.
12. M. Dermelj, J. Novak, V. Ravnik and L. Kosta, *J. Radioanal. Chem.*, 1978, **44**, 271.
13. D. F. Peppard, W. J. Driscoll, R. J. Sironen and S. McCarthy, *J. Inorg. Nucl. Chem.*, 1957, **4**, 326.
14. D. N. Edgington, *Int. J. Appl. Radiat. Isot.*, 1967, **18**, 11.
15. M. Picer and P. Strohal, *Anal. Chim. Acta*, 1968, **40**, 131.
16. E. S. Gladney, C. E. Burns, D. R. Perrin, I. Roelandts and T. E. Gills, *Concentration Data for NBS Biological and Environmental Standard Reference Materials*, NBS, Washington, March 1984.
17. K. Heydorn, E. Damsgaard and B. Rietz, *Anal. Chem.*, 1980, **52**, 1045.
18. E. Steinnes, *Analyst*, 1976, **101**, 455.
19. H. S. Dang and A. Chatt, *Trans. Am. Nucl. Soc.*, 1986, **59**, 169; and A. Chatt, personal communication, 1987.
20. A. R. Byrne and M. Dermelj, *Vestn. Slov. Kem. Drus.*, 1986, **33**, 423.
21. U. Niese and S. Niese, *J. Trace Microprobe Techniques*, 1982–83, **1**, 339.
22. *Idem*, *J. Radioanal. Nucl. Chem.* 1985, **91**, 17.
23. A. R. Byrne, *J. Environ. Radioactivity*, 1986, **4**, 133.

# ION-PAIR LIQUID-SOLID EXTRACTION FOR THE PRECONCENTRATION OF TRACE METAL IONS

## OPTIMIZATION OF EXPERIMENTAL CONDITIONS

VALERIO PORTA, EDOARDO MENTASTI, CORRADO SARZANINI and MARIA CARLA GENNARO  
Dipartimento di Chimica Analitica, Università di Torino, Via Pietro Giuria 5, 10125 Torino, Italy

(Received 18 April 1987. Revised 28 June 1987. Accepted 23 October 1987)

**Summary**—Cu(II) has been recovered from dilute solutions (0.1 µg/ml) by adsorbing the ion-pairs formed between different quaternary ammonium salts and the Cu-8-hydroxyquinoline-5-sulphonic acid complex on adsorbent resins, namely XAD 8 and S 862. Both batch and column techniques have been used, the first of which gave superior recovery and precision. It has also been shown that XAD 8 resin can be transformed into an ion-exchanger suitable for preconcentration of Cu(II). The results obtained have been compared with those of reversed-phase ion-pair chromatography and a model is proposed.

Preconcentration is becoming a necessary and decisive step in the determination of traces and especially ultratraces of metal ions. In recent years many efforts have been made to increase the recovery of traces from very diluted samples and to optimize the separation from the matrix and interferents. Many methods have been developed that use complexation on and subsequent elution from chemically treated silica,<sup>1</sup> ion-exchange resin,<sup>2,3</sup> silica gel or synthetic resins loaded with a chelating agent,<sup>4,5</sup> for extraction of a water-insoluble complex<sup>6</sup>.

Many of the methods proposed utilized long-chain quaternary ammonium salts for the extraction of ionic or polar water-soluble chelating agents such as PAR (pyridylazoresorcinol),<sup>7</sup> Cryptand 2.2.2,<sup>8,9</sup> and Catechol Violet<sup>10</sup> into organic solvents. High recoveries and good separations from the matrix are achieved with these methods, but the rather low preconcentration factor (maximum 100) limits their applicability for the enrichment of dilute samples.

On the other hand, Aliquat 336 and Eriochrome Black T coupled with silica gel have been found to be useful in liquid-solid extraction of some bivalent and trivalent metal ions.<sup>11</sup>

In this paper we evaluate the suitability of the less polar sorbents XAD 8 and Duolite S 682, coupled with different quaternary ammonium salts, for liquid-solid extraction.

A reversed-phase interaction, similar to reversed-phase ion-pair chromatography, must be considered as the mechanism of the process and the two techniques show similar behaviour.<sup>12</sup>

8-Hydroxyquinoline-5-sulphonic acid has been chosen as the chelating agent, since it forms stable complexes with a large number of metal ions.

### EXPERIMENTAL

#### Apparatus

Absorbance measurements were made with a Hitachi 150-20 double-beam spectrophotometer and metal concen-

trations were evaluated by inductively-coupled plasma atomic-emission spectrometry (Plasma 300, Allied Analytical System). Measurements of copper were made at 324.75 nm with background correction. Blanks were run with every sample in order to detect specific interferences with the analytical peak. All laboratory glassware and polyethylene and polypropylene equipment was washed with 6M nitric acid and repeatedly rinsed with high-purity water (HPW). A peristaltic pump equipped with a variable-speed control was used to ensure a constant flow in the range up to 11 ml/min, when required.

#### Reagents

Analytical-grade Amberlite XAD 8 (Fluka), 20-50 mesh, a macroporous acrylic ester adsorbent resin (specific surface 180 m<sup>2</sup>/g), Duolite S 862 (Duolite), 20-50 mesh, a macroporous styrene-divinylbenzene adsorbent resin (specific surface 650 m<sup>2</sup>/g), and Silica Gel 60 (Merck), 70-230 mesh, were used. The two resins were washed with methanol and water, dried in an oven at 60-80° and stored in a desiccator. The silica gel was purified by washing with 12M hydrochloric acid, to remove iron and other impurities, then rinsed with water until the washings gave a negative test for chloride, and finally dried in an oven at 100-120° and stored in a desiccator.

A standard copper solution (Merck, 1000 µg/ml metal concentration) was diluted to the desired concentration. High-purity water (HPW) was obtained by treating demineralized water with a Milli-Q purification system (Millipore, Bedford, MS).

Cetyltrimethylammonium bromide (Merck) (CTAB), tri-caprylmethylammonium chloride (Fluka) (Aliquat), and tetrabutylammonium chloride (Fluka) (TBAC) were used as received; 8-hydroxyquinoline-5-sulphonic acid (Aldrich) (SOX) was an analytical-grade product. All other reagents were of analytical grade.

#### Procedures

**Adsorption isotherms.** The adsorption isotherms were evaluated for SOX and the Cu-SOX complex, which was prepared by dissolving the stoichiometric amount of ligand and cupric chloride required to form the Cu(SOX)<sub>2</sub> complex. Then 100.0 ml samples [SOX or Cu(SOX)<sub>2</sub>, 0.25 × 10<sup>-4</sup>-3.00 × 10<sup>-4</sup>M] containing 50.0 ml of 5.50 × 10<sup>-4</sup>M CTAB were brought to pH 6.0 for the ligand test and pH 10.0 for the complex examination respectively. At pH 6 there is no protonation of the nitrogen atom or dissociation of the hydroxyl group of the ligand. Then



0.50 g of an adsorbent was added and the mixture was shaken vigorously for 100 min. All adsorption experiments with silica gel were performed at pH 6.0 to avoid dissociation of its silanol groups. After the adsorption, the adsorbent was removed with a filtration membrane filter (pore size 3.0  $\mu\text{m}$ ) and the residual concentration of ligand or complex was determined spectrophotometrically, at 239.6 and 260.0 nm respectively.

Adsorption on silica gel as a function of pH was evaluated by using 100.0 ml of solution containing 5.00  $\mu\text{moles}$  of  $\text{Cu}(\text{SOX})_2$  and 27.4  $\mu\text{moles}$  of CTAB and adding 0.50 g of silica gel.

Each experiment was done in triplicate and the relative standard deviation was always within 5%.

**Eluent, pH and contact time.** To find the best stripping agent, 0.50 g of XAD 8 or S 862 was added to 100.0 ml of solution brought to pH 6.5 and containing 10  $\mu\text{g}$  of copper, 27.4  $\mu\text{moles}$  of CTAB and 3.50  $\mu\text{moles}$  of SOX. After 100 min stirring the resin was transferred into a glass column and washed with HPW at the pH of the test solution. Table 1 shows the results for different eluting agents and that 2.0M hydrochloric acid is the most efficient for recovery of copper from both resins. After the elution, S 862 can be washed with an appropriate amount of methanol and re-used, whereas XAD 8, after washing with methanol, gives a reduced recovery (95%) and must be renewed.

With the optimum stripping agent, experiments were performed with the same metal, ligand and surfactant concentrations and contact time to evaluate the effect of pH on the adsorption. The optimum pH range is 6–9, see below.

The best contact time for adsorption was then examined and complete metal recovery was obtained with 60 or more min of stirring.

**Choice of tetralkylammonium salt.** The effect of CTAB, Aliquat and TBAC at different concentrations was investigated with 100.0 ml of solution at pH 6.5, containing the amounts of SOX,  $\text{Cu}(\text{II})$  and resin used for the pH optimization tests and varied concentrations of the quaternary ammonium salts. The mixtures were shaken for 80–90 min and the metal was recovered with 2.0M hydrochloric acid.

**Column experiments.** Two procedures were tested. In the first, a glass column filled with 1.00 g of raw resin was washed with 20 ml of methanol and 50 ml of HPW. The metal recovery was evaluated by passage of 100.0 ml of solution containing 10.0  $\mu\text{g}$  of  $\text{Cu}(\text{II})$ , 3.50  $\mu\text{moles}$  of SOX and 27.4  $\mu\text{moles}$  of CTAB or 8.00  $\mu\text{moles}$  of Aliquat. The flow was kept constant in the range 0.5–10.0 ml/min and the copper was stripped with 2.0M hydrochloric acid.

In the second procedure, 0.50 g of resin was washed as described above, then added as a batch to 50.0 ml of

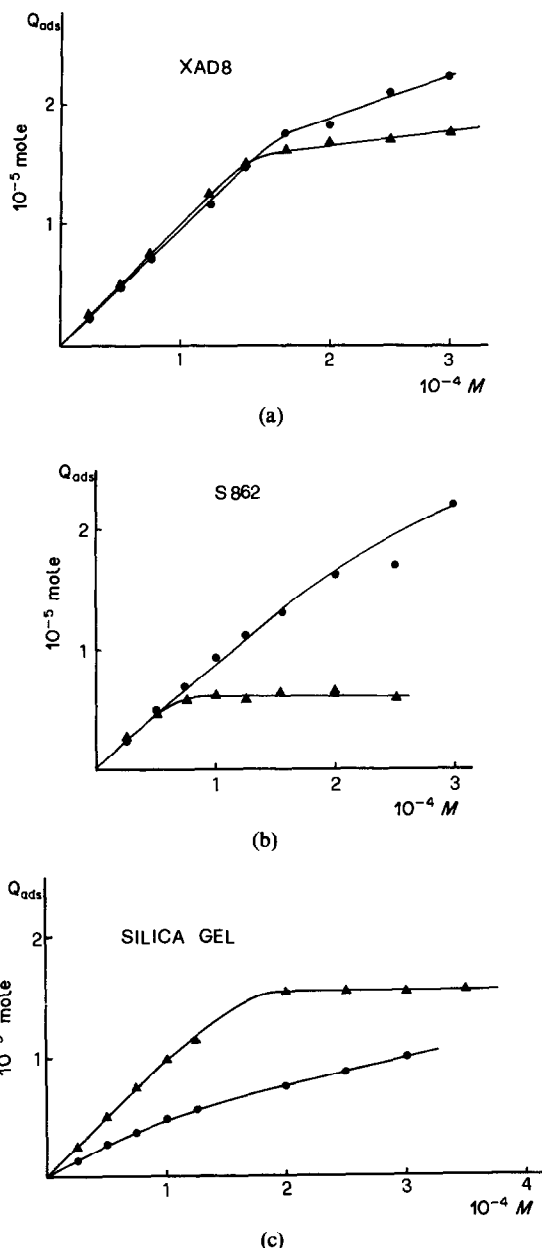


Fig. 1. (a) Moles of ligand adsorbed on XAD 8; (b) S 862; (c) silica gel, as a function of the concentration of ligand in solution: (●) adsorption of free ligand; (▲) adsorption of ligand as its Cu complex.

Table 1. Efficiency of different stripping agents for the recovery of  $\text{Cu}(\text{II})$  from XAD 8 and S 862

Stripping agent	$\text{Cu}(\text{II})$ recovery, %	
	XAD 8	S 862
0.1M HCl	93.0 $\pm$ 0.7	93.1 $\pm$ 1.5
0.5M HCl	94.5 $\pm$ 1.1	97.7 $\pm$ 1.6
1.0M HCl	96.4 $\pm$ 1.6	97.1 $\pm$ 2.8
2.0M HCl	98.3 $\pm$ 1.2	96.6 $\pm$ 0.6
4.0M HCl	*	98.6 $\pm$ 1.5
1.0M $\text{HClO}_4$	95.6 $\pm$ 1.1	90.9 $\pm$ 2.2
2.0M $\text{HClO}_4$	90.7 $\pm$ 0.6	85.4 $\pm$ 2.3
1.0M $\text{HNO}_3$	96.6 $\pm$ 1.2	81.2 $\pm$ 0.5
2.0M $\text{HNO}_3$	98.4 $\pm$ 1.7	93.1 $\pm$ 1.5
0.5M $\text{H}_2\text{SO}_4$	88.2 $\pm$ 1.0	96.7 $\pm$ 1.5
$\text{CH}_3\text{OH}$	73.4 $\pm$ 0.3	*
$\text{CHCl}_3$	*	*

\*Irreproducible results.

solution containing different concentrations of CTAB or Aliquat. The resin was then transferred into a glass tube and washed with HPW at pH 6.5 to remove the fraction of organic cation not adsorbed.

The efficiency of this "ion-exchange" resin was evaluated by passage (at 5.0 ml/min) of 100.0 ml of solution containing 10.0  $\mu\text{g}$  of  $\text{Cu}(\text{II})$  and 3.50  $\mu\text{moles}$  of SOX at pH 6.5.  $\text{Cu}(\text{II})$  was stripped with 2.0M hydrochloric acid.

## RESULTS AND DISCUSSION

Adsorption isotherms were evaluated in order to quantify the affinity and nature of the interaction of

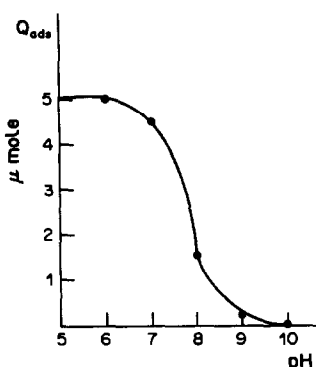


Fig. 2. Moles of ligand, as the Cu complex, adsorbed on silica gel, as a function of pH.

the adsorbents (XAD 8, S 862, silica gel) with the ligand (SOX) or metal complex [Cu(SOX)] coupled with a quaternary ammonium salt (CTAB) at constant concentration. Figure 1 shows the results. The isotherms for the different adsorbents are strictly dependent on the structure and polarity of the adsorbent. The polar adsorbents XAD 8 and silica gel show higher affinity for the metal complex, whereas the S 862 resin, characterized by a non-polar structure, gives higher adsorption for the ligand. This is probably due to interaction between the complexed metal ion, which is not fully co-ordinated, and the co-ordinating groups of the resin (carboxylate) or the silica gel (silanol). This effect is similar to the synergic effect shown by some solvents in the liquid-liquid extraction of metal complexes with quaternary ammonium salts.<sup>13</sup> The strong interaction of S 862 resin with the aromatic part of the ligand is reduced when the ligand is restricted within the rigid structure of the complex.

Comparison of the adsorption isotherms for the ligand and its metal complex shows that silica gel, which enhances the difference in interaction, is the most suitable adsorbent. On the other hand the adsorption on silica (Fig. 2) is affected by pH over a wider range than that on the resins. This can be attributed to an ion-exchange between the quaternary

ammonium cation in solution and the proton of the silanol groups, which reduces the concentration of the organic cation available for association with the copper complex. Since quantitative recovery of ions such as  $Pb^{2+}$ ,  $Co^{2+}$  and  $Mn^{2+}$ , which form complexes of low stability with SOX, requires high pH values, silica gel cannot be used for their preconcentration and the choice is limited to XAD 8 and S 862.

The isotherms also indicate that the capacity of all the adsorbents is limited, but sufficient for preconcentration of trace elements.

The optimum conditions for the method were evaluated to enhance the preconcentration yield and metal recovery.

**Elution.** The metal fixed on the column can be stripped in two ways: (a) destruction of the complex by protonating the ligand by acidic elution; (b) desorption of the ion-association complex by elution with a solvent of low polarity.

Both possibilities were evaluated with (a) various mineral acids at different concentrations, and (b) methanol and chloroform. Table 1 shows that the best results are obtained by using an acidic eluent, whereas methanol gives a recovery of only 70% from XAD 8 and irreproducible values with S 862. Other solvents such as chloroform are unsuitable because they are not inert towards the resin.

**Contact time.** The stirring time, in batch experiments, is a limiting parameter. Figure 3 shows the metal recovery *vs.* contact time. The results were similar for both resins XAD 8 or S 862 and typical of the kinetics of adsorption at trace levels.

**Effect of  $NR_4^+$  concentration.** The quaternary ammonium salt structure and concentration can affect the metal recovery. Figures 4–6 show the recoveries as a function of surfactant concentration. The XAD 8 resin gave the best results in all cases; in the presence of CTAB 100% recoveries were obtained even at low concentrations of surfactant; for Aliquat only XAD 8 gave suitable results, and S 862 resin gave inconsistent values. Moreover at high concentrations of Aliquat an insoluble product separated, which militates against the use of ammonium salts of

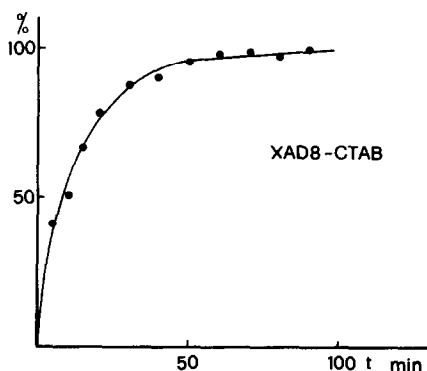


Fig. 3. Recovery of Cu(II) from XAD 8 as a function of stirring time, with CTAB as counter-ion.

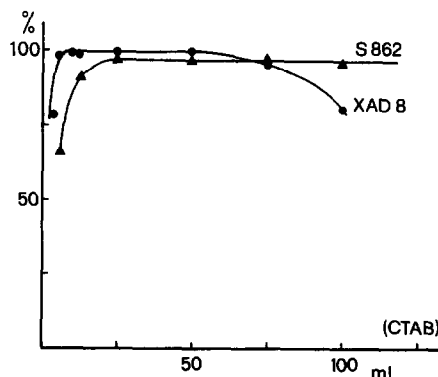


Fig. 4. Recovery of Cu(II) from XAD 8 and S 862 as a function of volume of  $5.5 \times 10^{-4} M$  CTAB added.

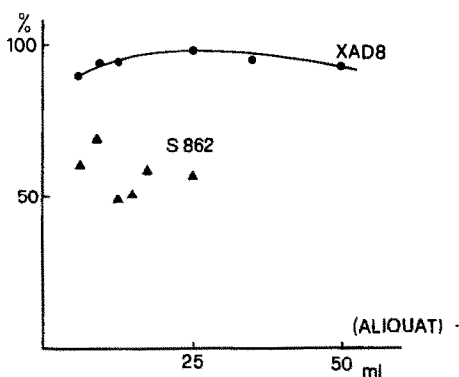


Fig. 5. Recovery of Cu(II) from XAD 8 and S 862 as a function of volume of  $4.0 \times 10^{-4} M$  Aliquat added.

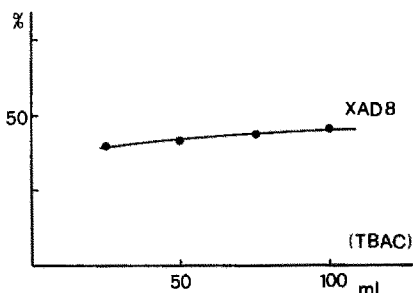


Fig. 6. Recovery of Cu(II) from XAD 8 as a function of volume of  $4.0 \times 10^{-4} M$  TBAC added.

higher molecular weight. In all cases TBAC gave the lowest recovery.

The difference in the behaviour of the resins at high concentrations of CTAB, must also be pointed out probably because of their different specific surfaces. The lower recovery with CTAB and XAD 8 forced us to pay attention to the quantity of ligand, organic cation and resin used in the preconcentration of larger volumes.

*Column experiments.* Elution from a column is more suitable in preconcentration techniques because

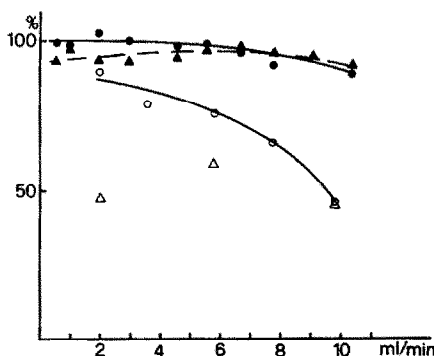


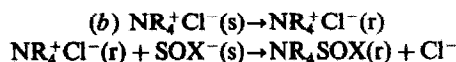
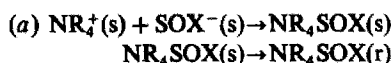
Fig. 7. Recovery of Cu(II) from XAD 8 and S 862 as a function of elution rate with CTAB and Aliquat 366: (●) XAD 8-CTAB; (▲) S 862-CTAB; (○) XAD 8-Aliquat; (△) S 862-Aliquat.

larger volumes of sample can be examined without much manipulation (which could produce losses and contamination). The limiting parameter in this case is the elution rate and Fig. 7 shows the metal recovery with different resins and surfactants as a function of elution rate. XAD 8 and S 862 give good results when CTAB is used but the recovery in the presence of Aliquat is strongly dependent on flow-rate for XAD 8 and gives inconsistent values with S 862 (quadruplicated experiments). However, the column experiments show a precision of 3.5% which is poor compared with the value of 1.5% found for the batch experiments.

The possibility of modifying the adsorbent resins into a specific ion-exchanger was also considered. The XAD 8 or S 862 resin was loaded with a suitable amount of CTAB or Aliquat solution. The resins thus obtained were able to exchange bromide or chloride counter-ions with the SOX anion. These SOX-loaded resins have been used for preconcentration of Cu(II) and Fig. 8 shows the recovery as a function of the volumes of CTAB or Aliquat solution used for the experiments.

In this case also, recoveries above 90% were achieved even when the XAD 8 was loaded with CTAB below the stoichiometric 1:1 molar ratio with respect to SOX, whereas S 862 gave irreproducible results.

*Proposed mechanisms.* To account for the differences in behaviour observed in the experiments described, the following mechanism, similar to those in reversed-phase ion-pair chromatography,<sup>12</sup> can be proposed:



where (s) = solution, (r) = resin.

In the first case a neutral species, namely the  $\text{NR}_4\text{SOX}$  ion-pair, is adsorbed on the resin in a liquid-solid extraction step. The second mechanism involves two steps: the ammonium salt is adsorbed on the resin and the subsequent reaction can be con-

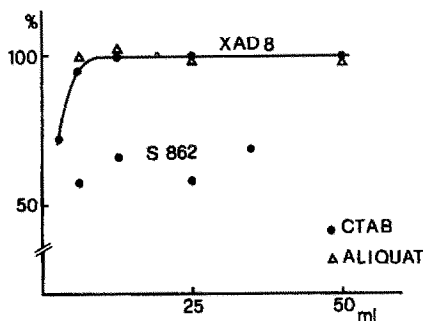


Fig. 8. Recovery of Cu(II) from loaded XAD 8 as a function of volume of  $5.5 \times 10^{-4} M$  CTAB or  $4 \times 10^{-4} M$  Aliquat added.

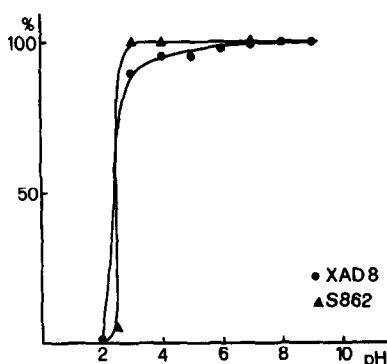


Fig. 9. Recovery of Cu(II) from XAD 8 and S 862, as a function of pH.

sidered as an ion-exchange process involving the modified resin and the ligand or the complex.

Both mechanisms can act simultaneously in the preconcentration but the predominance of one or the other seems to be a function of the structure and type of the ammonium salt and resin used. This is shown in the experiments with loaded resins, where the first mechanism is obviously excluded and the second is divided into two distinct steps. This enables us to show, Fig. 8, that the S 862 resin is not able to act through the second mechanism, because the styrene-divinylbenzene resin preferentially adsorbs neutral organic molecules possessing aromatic rings, but not charged quaternary ammonium salts with linear chains. On the other hand higher interaction between the  $\text{NR}_4^+$  and the linear and polar structure of the XAD 8 must be expected and, in fact total recovery is obtained with this resin over the whole range of CTAB and Aliquat concentrations investigated.

The differences in adsorption behaviour of CTAB and Aliquat on XAD 8 and S 862, Figs. 4 and 5, is not clearly defined by the previous arguments. The results and the similarity to liquid-liquid extraction<sup>13</sup> must be taken into account. It is well known that quaternary ammonium salts produce highly stable ion-pairs, especially when the substituent groups are small; this is the case, in our experiments, for CTAB, the molecule of which has three methyl groups and one longer linear chain. So Aliquat, which has only one methyl group and three long-chain alkyl groups, making it less effective for ion-pair association. This reason, and the fact that the S 862 resin acts only through the first mechanism, explain why the highest recoveries are obtained when this resin is coupled with CTAB.

In the column experiments, where the kinetics of adsorption is the most important parameter, mechanism (a) is expected to be operative, since it

occurs in a single step. Here also, in fact, CTAB, which as already said forms ion-pairs of higher stability, gives the best results with both resins, but the recovery with Aliquat is strongly affected by the elution rate, Fig. 7.

Finally, the recovery as a function of pH was evaluated for both resins, with the results shown in Fig. 9. The behaviour, in this case, is quite similar, showing that the recovery is independent of the structure of the adsorbent but related to the stability constants of the complex.

## CONCLUSIONS

The results obtained show that this method can be applied successfully to the preconcentration of copper from very dilute solutions. For this purpose the batch procedure appears superior. Moreover, comparison of the recovery, as a function of pH, with that obtained with an anion-exchange resin and the same ligand,<sup>3</sup> suggests that the method could be extended to other metal ions of interest, even in the presence of potential interferents, such as high background electrolyte concentrations or competing ligands, which could reduce the efficiency.

*Acknowledgements*—The financial support of the Ministero della Pubblica Istruzione (MPI) and Consiglio Nazionale delle Ricerche (CNR) is gratefully acknowledged.

## REFERENCES

1. H. Watanabe, K. Goto, S. Taguchi, J. W. McLaren, S. S. Berman and D. S. Russell, *Anal. Chem.*, 1981, **53**, 738.
2. C. Sarzanini, E. Mentasti, M. C. Gennaro and E. Marengo, *ibid.*, 1985, **57**, 1960.
3. E. Mentasti, C. Sarzanini and V. Porta, unpublished results.
4. M. A. Marshall and H. A. Mottola, *Anal. Chem.*, 1983, **55**, 2089.
5. S. N. Willie, R. E. Sturgeon and S. S. Berman, *Anal. Chim. Acta*, 1983, **149**, 59.
6. R. E. Sturgeon, S. S. Berman, J. A. H. Desaulniers, A. P. Mykytiuk, J. W. McLaren and D. S. Russell, *Anal. Chem.*, 1980, **52**, 1585.
7. D. Nonova and K. Stoyanov, *Anal. Chim. Acta*, 1982, **138**, 321.
8. W. Szczepaniak and B. Juskowiak, *Anal. Chim. Acta*, 1982, **140**, 261.
9. D. Blanco Gomis, E. Fuente Alonso and A. Sanz-Medel, *Talanta*, 1985, **32**, 915.
10. S. Przeszlakowski and H. Wydra, *ibid.*, 1984, **31**, 401.
11. S. Przeszlakowski and R. Kojan, *Analyst*, 1985, **110**, 1077.
12. C. Horvath, *HPLC: Advances and Perspective*, p. 179. Academic Press, New York, 1980.
13. J. Minczewski, J. Chwastowska and R. Dybczyński, *Separation and Preconcentration Methods in Inorganic Trace Analysis*, p. 163. Ellis Horwood, Chichester, 1982.

# DETERMINATION OF FLUORINE AND CHLORINE IN GEOLOGICAL MATERIALS BY INDUCTION FURNACE PYROHYDROLYSIS AND STANDARD-ADDITION ION-SELECTIVE ELECTRODE MEASUREMENT\*

T. DENIS RICE

Mineral Resources Development Laboratory, New South Wales Department of Mineral Resources,  
Post Office Box 76, Lidcombe, 2141, Australia

(Received 4 June 1987. Revised 5 October 1987. Accepted 16 October 1987)

**Summary**—Fluorine and chlorine in geological materials are volatilized by pyrohydrolysis at about 1150° in a stream of oxygen (1000 ml/min) plus steam in an induction furnace. The catalyst is a 7:2:1 mixture of silica gel, tungstic oxide and potassium dihydrogen phosphate. The sample/catalyst mixture is pyrohydrolysed in a re-usable alumina crucible (already containing four drops of 1 + 3 phosphoric acid) inserted in a silica-enclosed graphite crucible. The absorption solution is buffered at pH 6.5 and spiked with 1.6 µg of fluoride and 16 µg of chloride per g of solution, to ensure rapid and linear electrode response during subsequent standard-addition measurement. The simple plastic absorption vessel has >99.5% efficiency. The 3s limits of detection are 5–10 µg/g and 40–100 µg/g for fluorine and chlorine respectively. The procedure is unsuitable for determining chlorine in coal.

Since about 1954,<sup>1</sup> various pyrohydrolysis procedures have been used for volatilizing fluoride and chloride from solid samples. That a recent report on analytical methods for fluorine in environmental samples<sup>2</sup> does not mention pyrohydrolysis but advocates a lengthy ashing, fusion and distillation procedure, suggests that pyrohydrolysis has yet to be widely accepted as the decomposition method of choice in determination of fluorine in solid samples. Unlike some other pyrohydrolysis procedures, the method described has such features as an effective and low-toxicity catalyst (containing tungstic oxide instead of the more hazardous<sup>3</sup> vanadium pentoxide), employment of a reusable alumina crucible, and a simple, efficient absorption vessel.

Both tube furnaces<sup>1,4–11</sup> and induction furnaces<sup>12–14</sup> have been used for pyrohydrolysis. The first reported use of an induction furnace in determination of fluorine and chlorine (as well as bromine and sulphur)<sup>15</sup> involved pyrolysis as distinct from pyrohydrolysis. Although about twice as expensive as a tube furnace, an induction furnace is more convenient for pyrohydrolysis because of its greater ease of operation. Laboratories having induction furnaces that are no longer in use can employ them for pyrohydrolysis.

Before the era of the ion-selective electrode (ISE) and ion-chromatography, titration and neutron-activation were used<sup>4</sup> for determining fluoride and chloride, respectively, in pyrohydrolysates. Chloride, unlike fluoride, can be determined in solution

by either spectrophotometry<sup>9,16</sup> or ion-chromatography<sup>10,13</sup> with greater sensitivity and probably greater precision than by ISE, but the present work examines use of the chloride as well as the fluoride ISE in the analysis of pyrohydrolysates.

## EXPERIMENTAL

### Reagents

**Catalyst.** A finely ground mixture of 7 parts by weight silica gel, 2 parts tungstic oxide and 1 part potassium dihydrogen phosphate.

**Spiked buffered absorption solution (1.600 µg of F and 16.00 µg of Cl per g, pH 6.5).** This contains 10 g of potassium nitrate, 115 g of ammonium acetate and 16.00 g of Standard Solution B (see below) in 2000 g.

**Unspiked buffer solution (pH 6.5).** Prepared as above but without Standard Solution B.

**Standard Solution A (2000 µg of both F and Cl per g).** Weigh out 2.212 g of sodium fluoride and 1.650 g of sodium chloride (both dried at 105°) and transfer them through a polyethylene funnel into a tared 600-ml polyethylene bottle, rinsing in with water. Add 250.0 g of unspiked buffer solution and dilute with water to a total solution weight of 500.0 g. Swirl occasionally during a 1-hr period to ensure complete dissolution. Transfer about 180 ml of this solution to a 250-ml polyethylene dispensing bottle.<sup>17</sup>

**Standard Solution B (200.0 µg of F and 2000 µg of Cl per g).** Add  $m = 50–52$  g (weighed to the nearest 0.01 g) of Standard Solution A to a 600-ml polyethylene bottle. Transfer 0.02970m g of sodium chloride (dried at 105°) into this bottle through a polyethylene funnel. Add 4.5m g of unspiked buffer solution and dilute with water to a total solution weight of 10m g. Swirl occasionally during a 10-min period to ensure complete dissolution. Transfer about 180 ml of this solution to a 250-ml polyethylene dispensing bottle.

**Other reagents.** Phosphoric acid (1 + 3), containing 0.1% Triton X-100 surfactant; spiked blank solution prepared by 2-fold gravimetric dilution of about 25 g of spiked absorption solution; 5M sodium hydroxide, conveniently prepared

\*Presented in part at the 9th Australian Symposium on Analytical Chemistry, Sydney, April 1987.

by diluting 1 volume of technical grade 60% w/v sodium hydroxide solution with 2 volumes of water; nitric acid, (1 + 9) and (1 + 99); oxygen, industrial grade. Use demineralized water throughout.

#### Apparatus

**Glass vials.** Capacity 10 ml, with tightly fitting snap-on plastic caps, thoroughly washed with water and dried.

**Polystyrene vials.** Capacity 70 ml, with unlined leak-proof polyethylene screw caps, tared. To minimize contamination and condition them for storage of dilute fluoride and chloride solutions, they are rinsed well with water, then filled with nitric acid (1 + 99) and let stand with occasional shaking for at least 24 hr. Just before use, they are emptied and rinsed well with water.

**Absorption vessel.** This consists (right-hand side of Fig. 1) of a 70-ml polystyrene vial with two holes in its cap, into which two pieces of polyethylene tubing (o.d. 6.3 mm, i.d. 4 mm, lengths 85 and 280 mm) are fitted. The end of the longer tube is 6–8 mm above the base of the vial; the end of the other is about 3 mm below the underside of the cap. The longer piece of polyethylene tubing is butt-joined to silica tubing (o.d. 6 mm, i.d. 4 mm, length 150 mm) with silicone tubing (i.d. 4.7 mm).

**Steam generator.** This consists of a 1-litre round-bottomed flask containing a few boiling chips and 0.2 g of sodium hydroxide<sup>18</sup> dissolved in 800 ml of water; a 1-litre heating mantle; a non-return valve, glass tubing and T-piece, silicone tubing and drain bottle (Fig. 1). The length of tubing from the top of the flask to the combustion tube inlet is 1.0 m.

**Induction furnace and accessories.** A Leco 623-300 induction furnace; timer; gas control unit; Leco 521-084 variable transformer; Leco 519-005 igniter; crucible pair comprising a Leco 550-182 silica-enclosed graphite crucible and an alumina crucible of height 25 mm and outer diameter 18 mm (Cat. No. CN-4, Ceramic Oxide Fabricators Pty Ltd., 83 Wood Street, Eaglehawk, Vic., 3556, Australia); custom-made silica connecting piece (containing loosely packed silica wool) butt-joined by silicone tubing to Leco 519-004 combustion tube and to absorption vessel (Fig. 1). For cooling purposes, the vial of the absorption vessel is half-immersed in a 1-litre beaker of water (not shown in Fig. 1), and kept in position with a ring-clip.

**Potentiometric system.** Orion 811 pH/mV meter, 94-09 fluoride and 94-17B chloride electrodes, 90-02 double-junction reference electrode, 91-70-03 temperature probe, 605 electrode switch, PTFE-coated stirrer bar length 20 mm, magnetic stirrer with thermal insulation mat.

#### Procedures

**Avoidance of contamination.** Minimize fluorine and chlorine contamination by appropriate care at all stages of the procedure. For example, always handle crucibles with tongs or tweezers. Occasionally, clean the crucibles, igniter and combustion tubes thoroughly by immersion in warm 5M sodium hydroxide for 10 min, rinsing with water, immersion in nitric acid (1 + 9) for 10 min, rinsing again with water and drying in the oven. Material strongly adhering to alumina crucibles can be removed by prolonged heating in 5M sodium hydroxide.

**Sample preparation.** Accurately weigh  $250 \pm 1$  mg of finely ground sample and mix well with  $500 \pm 1$  mg of catalyst in a glass vial. If the F or Cl content exceeds 0.5%, weigh proportionately less sample. Run blank determinations at the beginning (duplicate), middle and end of a batch of samples.

**Apparatus conditioning.** Bring the steam generator to a gentle boil. After 20–30 pyrohydrolyses, insert a fresh, loosely packed quantity of silica wool into the wider end of the silica connecting piece. Turn on the furnace and connect (at A, Fig. 1) a spare absorption vessel containing about 25 ml of water. Add 4 drops of phosphoric acid (1 + 3) to

an alumina crucible in a silica-enclosed graphite crucible, place the crucible pair in the furnace and heat it at near maximum plate current (480–500 mA) for 3 min with oxygen passing through the steam generator into the furnace at 1000 ml/min; remove the crucible pair from the furnace and allow it to cool. Leave the furnace assembly in stand-by mode (steam-generator heating-mantle turned down very low, oxygen flow about 50 ml/min) until ready for a pyrohydrolysis.

**Pyrohydrolysis.** With the aid of a dispensing bottle<sup>17</sup> add  $25 \pm 0.5$  g of spiked buffered absorption solution to a clean polystyrene vial; record the weight of solution to the nearest 0.02 g. Seal the vial with a water-rinsed absorption vessel cap (setting aside the original vial cap upright on a clean bench). Place the assembled absorption vessel in a dry 1000-ml tall-form glass beaker and record the weight of the beaker plus vessel to the nearest 0.2 g. Connect the absorption vessel at A (Fig. 1) with the vial half-immersed in water and kept in position with a ring-clip.

Add 4 drops of phosphoric acid (1 + 3) to an alumina crucible in a silica-enclosed graphite crucible. Transfer the sample/catalyst mixture from the glass vial into the insert crucible.

With the steam-generator mantle set appropriately (typically at 30% of maximum setting), the timer set at 14 min, the variable transformer set to give near maximum plate current (480–500 mA), place the loaded crucible pair in the furnace (with tongs) and raise the oxygen flow-rate to 1000 ml/min. Press the timer button to start the pyrohydrolysis. (The steam-generator mantle must not be set so high that the polyethylene inlet tube of the absorption vessel melts because of too rapid transfer of steam.)

After 30 sec (when the crucible and igniter appear red hot but before rapid release of volatiles) turn the variable transformer down so that the crucible is just below very dull red heat (plate current typically 240 mA). Two min later, increase the transformer setting to about 60 so that the plate current is about 310 mA. One min later, with the crucible dull red, increase this setting to about 75 (plate current about 390 mA). Thirty sec later, increase the setting to 95 so that nearly maximum plate current (480–500 mA) is obtained. Maintain the oxygen flow at 1000 ml/min throughout the pyrohydrolysis. (For samples other than those high in combustible material, such as coal or sulphide ores, the slow increase in temperature is not required and nearly maximum plate current is used throughout the pyrohydrolysis.)

When the furnace switches off, wait 1 min before decreasing the oxygen flow to about 50 ml/min. Then remove the crucible, disconnect the absorption vessel at A (Fig. 1), wipe the water from the outside of the vial and reweigh the absorption vessel in the dry 1-litre beaker to obtain the steam yield, which should be between 1 and 7 g. (When it has cooled, prepare the crucible pair for re-use by scraping out most of the residue with a metal spatula, holding the crucible in tongs.)

**Pyrohydrolysate treatment.** Rinse down all inner surfaces of the absorption vessel with a fine jet of water and then remove the absorption vessel cap/tubing assembly from the vial. Dilute the pyrohydrolysate plus rinsings to 50–55 g with water, weighing to the nearest 0.1 g. Set the sealed vial aside to cool from typically 30° to room temperature.

**Electrode care and conditioning.** When not in use, store the two ISEs dry, and keep the tip of the reference electrode immersed in water. To keep the response time of the F electrode at 2 min, the sensing element must be polished at least weekly, when in use, with 0.5- $\mu$ m alumina<sup>19</sup> (Metrohm EA 1085) or 0.25- $\mu$ m diamond dust. The ISEs must be conditioned for at least 30 min before use and for at least 30 sec between measurements, by insertion into spiked blank solution stirred so that a vortex just fails to form. The inner-chamber solution of the double-junction reference electrode should be replaced weekly, and the outer-chamber

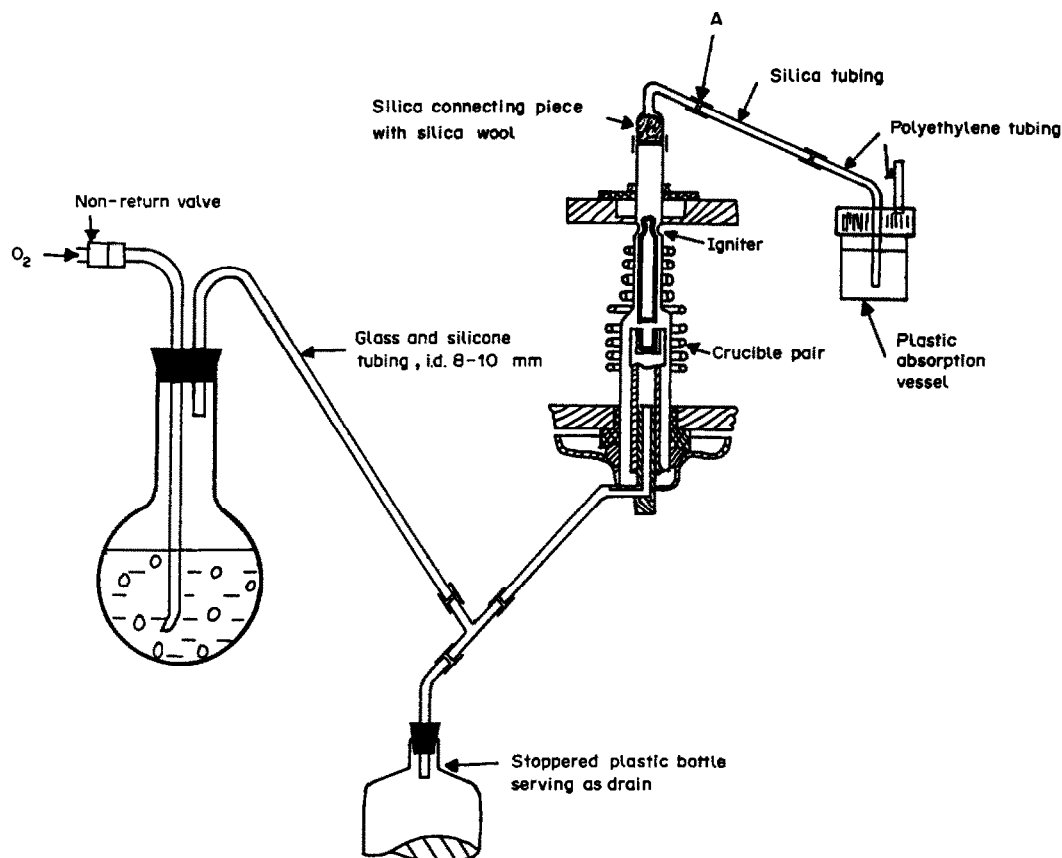


Fig. 1. Schematic of induction furnace pyrohydrolysis apparatus.

solution (spiked blank solution) at the beginning of each day of use.

**Emf measurement.** Remove the electrodes from the stirred conditioning solution and stir the test solution for 5–10 sec before inserting the electrodes into it to a depth of 20 mm and dislodging any air-bubbles from the sensing elements. During this 5–10 sec gently shake off most of the adhering solution from the electrode tips; do not use a tissue. Record the electrode potentials to the nearest 0.1 mV after 2 min; they should not change by more than 0.1 mV during the next 2 min.

Depending on the fluoride concentration, add between 0.5 and 3 g—measured to the nearest mg—of Standard Solution A or B so that the fluoride ISE potential falls by 20–40 mV. After 2 min, record the potential to the nearest 0.1 mV. Remove the electrodes, rinse them with water and place them in stirred conditioning solution for at least 20 sec before use in the next measurement as described above. Record the temperature of the measured solution to the nearest 0.2°. During each batch of measurements, check the electrode-response slopes by double standard-addition.<sup>20</sup> (For the electrodes used in the present work these slopes at 25° were  $59.1 \pm 0.2$  and  $57.5 \pm 0.5$  mV/decade for F and Cl respectively.)

Calculate the results by formulae similar to those already published,<sup>20</sup> with correction for the blank.

## RESULTS AND DISCUSSION

### Results for reference samples

Table 1 shows that the results obtained for fluorine in selected reference samples are generally in accept-

able agreement with the results of others. It remains to be established why the PIGE (proton-induced gamma-ray emission spectrometry) results for some samples, notably GXR-1 and NBS 1633a, are appreciably higher than the pyrohydrolysis results; PIGE analysis of the pyrohydrolysis residues from GXR-1 revealed that the pyrohydrolysis result for GXR-1 may be low by not more than 100  $\mu\text{g/g}$ . The good agreement between the PIGE and pyrohydrolysis results for the four coal samples in Table 1 is noteworthy.

The results for chlorine (Table 2) are also in acceptable agreement with other results except the result for BE-N, which is low by about 25% and the result for GXR-1 which is higher than the only other reported result by about 60%.

### Interferences

The results for chlorine in coal samples by this procedure were always erratically higher, typically by a factor of two or three, than the recommended values. This appears to be because other species which the chloride ISE senses, such as thiocyanate, are formed during pyrohydrolysis of coal and probably of other organic materials. Ion-chromatography may enable chlorine to be determined in coal pyro-

Table 1. Fluorine in selected reference samples

Sample	F, $\mu\text{g/g}^a$	
	This work <sup>b</sup>	Other values
GSP-1 granodiorite	3767 $\pm$ 98	3700 <sup>c</sup> 3477 <sup>d</sup> 3659 <sup>e</sup> 3567 <sup>f</sup> 3746 <sup>g</sup> 3798 <sup>h</sup>
GXR-1 jasperoid	1290 $\pm$ 12	1200 $\pm$ 190 <sup>i</sup> 1390 <sup>j</sup> 1961 <sup>d</sup>
NIM-L lujavrite	4393 $\pm$ 87	4400 <sup>c</sup> 4783 <sup>d</sup>
BE-N basalt	1110 $\pm$ 21	1000 <sup>k</sup> 1242 <sup>d</sup> 1130 <sup>j</sup> 1065 <sup>f</sup>
GSR-2 andesite	281 $\pm$ 6	275 <sup>l</sup> 307 <sup>m</sup>
GSR-6 carbonate	404 $\pm$ 6	400 <sup>l</sup> 460 <sup>m</sup>
IGS 38 barite ore	$(2.94 \pm 0.03) \times 10^4$	$(2.89 \pm 0.02) \times 10^{4n}$
NBS 120b phosphate rock	$(3.89 \pm 0.03) \times 10^4$	$3.84 \times 10^{4o}$
NBS 1632a coal	177 $\pm$ 2	176 <sup>p</sup> 176 <sup>q</sup> 178 <sup>r</sup>
NBS 1633a fly ash	73 $\pm$ 2	81 <sup>h</sup> 82 <sup>q</sup> 109 <sup>r</sup>
SARM 18 coal	107 $\pm$ 3	115 <sup>p</sup> 116 <sup>q</sup> 114 <sup>j</sup> 41–116 <sup>s</sup>
SARM 19 coal	95 $\pm$ 8	96 <sup>p</sup> 105 <sup>q</sup> 93 <sup>j</sup> 28–105 <sup>s</sup>
SARM 20 coal	142 $\pm$ 4	148 <sup>p</sup> 156 <sup>q</sup> 153 <sup>j</sup> 44–156 <sup>t</sup>

<sup>a</sup>Sample dried at 105°C.

<sup>b</sup>Mean  $\pm$  standard deviation of 4 determinations done on different days.

<sup>c</sup>Usable value.<sup>21</sup>

<sup>d</sup>Proton-induced gamma-ray emission spectrometry (PIGE).<sup>22</sup>

<sup>e</sup>Induction furnace pyrohydrolysis (IFP).<sup>23</sup>

<sup>f</sup>Tube furnace pyrohydrolysis (TFP).<sup>9</sup>

<sup>g</sup>IFP.<sup>24</sup>

<sup>h</sup>TFP.<sup>25</sup>

<sup>i</sup>Proposed value.<sup>26</sup>

<sup>j</sup>PIGE.<sup>27</sup>

<sup>k</sup>Working value.<sup>28</sup>

<sup>l</sup>Usable value.<sup>29</sup>

<sup>m</sup>PIGE.<sup>30</sup>

<sup>n</sup>Recommended value.<sup>31</sup>

<sup>o</sup>Certificate value.

<sup>p</sup>TFP.<sup>11</sup>

<sup>q</sup>TFP.<sup>32</sup>

<sup>r</sup>PIGE.<sup>33</sup>

<sup>s</sup>Range of mean results from 8 laboratories, only two of which, those reporting the highest results, used pyrohydrolysis.<sup>34</sup>

hydrolysates and give greater sensitivity than the ISE procedure.

The present work has confirmed the findings of others<sup>6,9</sup> that fluoride can be measured by ISE in pyrohydrolysates without addition of DCTA. No interference has been observed when this procedure is used for determining fluorine in samples containing up to 2000  $\mu\text{g/g}$  boron.

#### Efficiency of the absorption vessel

Pyrohydrolyses of many synthetic and natural samples with high F or Cl contents, with use of two absorption vessels connected in series, have shown that the first absorption vessel has a collection efficiency of  $>99.5\%$ . A lower collection efficiency has been found when the end of the vessel's longer

piece of polyethylene tubing is not the prescribed 6–8 mm above the base of the vial.

#### Recovery of F and Cl

Recoveries close to 100% for Cl but only 80–90% for F (probably because of appreciable retention of fluoride in the slag from the catalyst used) have been observed by others.<sup>10,13</sup> Pyrohydrolyses by the present procedure, of 250 mg of international or in-house reference sample with about 1 mg of NaF or added NaCl, have always resulted in at least 95% of the added fluoride or chloride being recovered, except for the reference carbonate rock GSR-6,<sup>29</sup> for which recovery of only 52–60% of the added fluoride was consistently found. This finding is somewhat puzzling in view of the good agreement between the usable



Table 2. Chlorine in selected reference samples

Sample	Cl, $\mu\text{g/g}^a$	
	This work <sup>b</sup>	Other values
GSP-1 granodiorite	355 $\pm$ 24	340 <sup>c</sup> 338 <sup>d</sup> 327 <sup>e</sup>
GXR-1 jasperoid	182 $\pm$ 28	110 <sup>f</sup>
NIM-L lujavrite	1183 $\pm$ 26	1200 <sup>c</sup> 1290 <sup>d</sup>
BE-N basalt	224 $\pm$ 14	300 <sup>g</sup> 295 <sup>d</sup> 285 <sup>h</sup>
GSR-2 andesite	70 $\pm$ 22	42 <sup>h</sup>
GSR-6 carbonate	65 $\pm$ 24	80 <sup>h</sup>
NBS-1633a fly ash	< 50	—

<sup>a</sup>Sample dried at 105°.

<sup>b</sup>Mean  $\pm$  standard deviation of 4 determinations done on different days.

<sup>c</sup>Usable value.<sup>21</sup>

<sup>d</sup>Fusion/spectrophotometry.<sup>35</sup>

<sup>e</sup>TFP.<sup>10</sup>

<sup>f</sup>Instrumental thermal-neutron activation.<sup>26</sup>

<sup>g</sup>TFP.<sup>9</sup>

<sup>h</sup>Proposed value.<sup>36</sup>

value and the result obtained by this procedure for sample GSR-6 (Table 1).

#### Pyrohydrolysis conditions

Addition of phosphoric acid<sup>37</sup> has been found to allow reduction of the pyrohydrolysis time from 20 to 14 min and to reduce considerably the variability of the blank, and memory effects (possibly caused by absorption of fluoride and chloride at "alkaline hot spots" in the silica tubing).

Phosphoric acid may also enhance the catalytic effect of the tungstic oxide. Experiments with various sample weights have shown that the amount of sample pyrohydrolysed does not have to be lowered from 250 mg unless the F or Cl content exceeds at least the 0.5% level specified in the procedure, *i.e.*, the amounts of phosphoric acid and catalyst used appear to suffice for the complete pyrohydrolysis of at least 1250  $\mu\text{g}$  of the halide.

Blanks run immediately after samples with high fluorine or chlorine contents have shown that no more than 0.5% of the halide from such samples remains in the pyrohydrolysis train. It is therefore recommended that samples containing < 1000  $\mu\text{g/g}$  F or Cl should be decomposed separately (in a batch) from those containing higher levels of F or Cl. The re-use of the crucible pair after emptying out most of the previously pyrohydrolysed material has been found to result in no contamination problems.

The results in Table 3 for the phosphate rock sample NBS 120b justify the use of the mixed catalyst as a safeguard against possible lowering, with time, of the induction furnace temperature at near maximum (500 mA) plate current. These results indicate that a "silica gel + phosphoric acid" catalyst would be satisfactory for fluorine determination if the induction furnace consistently gave a temperature of 1170°. However, tungstic oxide is required for complete pyrohydrolysis of chloride.<sup>25,38</sup> Too low a temperature (about 1000°) and an ineffective catalyst

may explain the low pyrohydrolysis results obtained for fluorine by others.<sup>39</sup>

#### Electrode measurement technique

Conditioning the fluoride electrode in a blank solution spiked with 0.8  $\mu\text{g/g}$  fluoride, as described in the procedure, has been found to be as effective as the previously recommended<sup>20</sup> conditioning with 0.06M lanthanum nitrate solution at pH 2.0–2.3. The simple measurement technique described requires about 5 min per solution.

#### Electrode performance

Recording the potential readings for the spiked conditioning solution, between standard-addition measurements, allows observation of the drift of the electrodes. If the drift is equal and in the same direction for both the F and Cl ISEs, and the temperature is constant to within 0.3°, it is likely that the reference electrode is causing the drift. Renewing the outer chamber solution or replacing the reference electrode may eliminate such drift.

In the present work an electrode switch was found very useful in comparing the performance of various fluoride ISEs (the chloride ISE being replaced by a second fluoride ISE). It was found that a fluoride ISE would give accurate standard-addition results only if the potential drifted in a negative direction, typically by 0.2 mV, in the period between 30 and 120 sec after insertion into a solution or after standard addition. Perhaps the undesirable drift in a positive direction could be reversed by replacement of the internal solution of the electrode with a solid, as described by Komljenović *et al.*<sup>40</sup>

#### Blank and detection limits

From many batches of analyses by this procedure, typical mean absolute blanks were 3  $\mu\text{g}$  for fluoride and 62  $\mu\text{g}$  for chloride, with standard deviation ranges of 0.4–0.8 and 3–8  $\mu\text{g}$  respectively. The 3 $\sigma$  detection limits for 250-mg solid samples analysed by this procedure are therefore 5–10  $\mu\text{g/g}$  for fluorine and 40–100  $\mu\text{g/g}$  for chlorine.

Table 3. Effect of pyrohydrolysis temperature and catalyst composition on fluorine recovery from NBS 120b, Florida phosphate rock

Pyrohydrolysis temperature, <sup>a</sup> °C	Plate current, mA	Observed F content, <sup>b</sup> %		
		Catalyst 1 <sup>c</sup>	Catalyst 2	Catalyst 3
1010	380	2.81	3.02	3.81
1090	440	3.69	3.89	3.90
1170	500	3.91	3.90	3.91

<sup>a</sup>Measured on outside of crucible through radiofrequency shield by optical pyrometer.

<sup>b</sup>Pyrohydrolysis of 25-mg sample mixed with 500 mg of catalyst and 4 drops of 1 + 3 H<sub>3</sub>PO<sub>4</sub>.

<sup>c</sup>Catalyst 1 = SiO<sub>2</sub> gel.

Catalyst 2 = 7:3 SiO<sub>2</sub> gel/KH<sub>2</sub>PO<sub>4</sub>.

Catalyst 3 = 7:2:1 SiO<sub>2</sub> gel/WO<sub>3</sub>/KH<sub>2</sub>PO<sub>4</sub>.

## CONCLUSIONS

The procedure for fluorine determination described in this paper is sensitive, simple and reliable and, with an alternative tube-furnace procedure,<sup>11,32</sup> is the basis of a draft Standards Association of Australia procedure for fluorine in coal, coke and fly-ash. The ISE procedure for Cl lacks sensitivity and cannot be used for coal, because of interference.

Use of a different absorption solution, such as 0.01M potassium dihydrogen phosphate at pH 6.0, with subsequent ion-chromatographic measurement, remains to be studied. The experience of others<sup>10,13</sup> indicates that the pyrohydrolysis decomposition procedure described in this paper could be followed by ion-chromatography to enable sensitive and reliable determination of total F, Cl and S in geological materials.

*Acknowledgements*—The author thanks B. Carruthers for making the silica connecting piece for the combustion tube, E. Clayton for the PIGE analysis of pyrohydrolysis residues, and K. Johnson for help with some of the experimental work.

## REFERENCES

1. J. C. Warf, V. D. Cline and R. D. Tevebaugh, *Anal. Chem.*, 1954, **26**, 342.
2. The Analytical Working Group of the Comité Technique Européen du Fluor, *Anal. Chim. Acta*, 1986, **182**, 1.
3. N. I. Sax, *Dangerous Properties of Industrial Materials*, 6th Ed., pp. 2704, 2717–2719, Van Nostrand-Reinhold, New York, 1984.
4. M. Gillberg, *Geochim. Cosmochim. Acta*, 1964, **28**, 495.
5. M. J. Nardozzi and L. L. Lewis, *Anal. Chem.*, 1961, **33**, 1261.
6. R. L. Clements, G. A. Sergeant and P. J. Webb, *Analyst*, 1971, **96**, 51.
7. J. C. Mills, K. J. Doolan and A. C. Knott, *Rept. Part 4, NERDDP Grant No. 80/0220*, 1983.
8. G. Gao, B. Yan and L. Yang, *Fuel*, 1984, **63**, 1552.
9. D. Whitehead and J. E. Thomas, *Anal. Chem.*, 1985, **57**, 2421.
10. G. E. M. Hall, A. I. MacLaurin and J. Vaive, *J. Geochem. Explor.*, 1986, **26**, 177.
11. W. C. Godbeer and D. J. Swaine, *Fuel*, 1987, **66**, 794.
12. A. Farzaneh and G. Troll, *Geochem. J.*, 1977, **11**, 177.
13. K. L. Evans, J. G. Tarter and C. B. Moore, *Anal. Chem.*, 1981, **53**, 925.
14. M. Bettinelli, *Analyst*, 1983, **108**, 404.
15. A. L. Conrad, J. K. Evans and V. F. Gaylor, *Anal. Chem.*, 1959, **31**, 422.
16. G. Troll and A. Farzaneh, *Geostds. Newsl.*, 1980, **4**, 37.
17. T. D. Rice, *Anal. Chim. Acta*, 1978, **97**, 213.
18. C. A. Horton, in *Treatise on Analytical Chemistry*, I. M. Kolthoff and P. J. Elving (eds.), Part II, Vol. 7, pp. 207–334. Interscience, New York, 1961.
19. W. J. van Oort and E. J. J. M. van Eerd, *Anal. Chim. Acta*, 1983, **155**, 21.
20. T. D. Rice, *ibid.*, 1983, **151**, 383.
21. S. Abbey, *Geol. Surv. Canada, Paper 83-15*, 1983.
22. I. Roelandts, G. Robaye, G. Weber and J. M. Delbrouck, *Geostds. Newsl.*, 1985, **9**, 191.
23. G. Troll and A. Farzaneh, *ibid.*, 1978, **2**, 43.
24. E. Kiss, Research School of Earth Sciences, Australian National University, Canberra, Australia, personal communication.
25. W. C. Godbeer, CSIRO Division of Fossil Fuels, North Ryde, Australia, personal communication.
26. E. S. Gladney, C. E. Burns and I. Roelandts, *Geostds. Newsl.*, 1984, **8**, 119.
27. E. Clayton, Applied Physics Division, Australian Atomic Energy Commission, Menai, Australia, personal communication.
28. K. Govindaraju, *Geostds. Newsl.*, 1980, **4**, 49.
29. Xie Xuejing, Yan Mingcai, Li Lianzhong and Shen Huijun, *ibid.*, 1985, **9**, 277.
30. I. Roelandts, G. Robaye, P. Aloupogiannis, G. Weber and J. M. Delbrouck-Habaru, *ibid.*, 1987, **11**, 79.
31. B. Lister, *ibid.*, 1986, **10**, 177.
32. K. J. Doolan, BHP Central Research Laboratories, Shortland, Australia, personal communication.
33. E. Clayton and L. S. Dale, *Anal. Lett.*, 1985, **18**, 1533.
34. E. J. Ring and R. G. Hansen, *Mintek Rept. No. M169*, 1984.
35. R. Fuge, *Geostds. Newsl.*, 1985, **9**, 209.
36. Xie Xuejing, Institute of Geophysical and Geochemical Exploration, Langfang, Hebei, People's Republic of China, personal communication.
37. W. J. Kirsten, *Anal. Chem.*, 1979, **51**, 2064.
38. M. C. Grondelle and P. J. Zeen, *Anal. Chim. Acta*, 1980, **116**, 397.
39. M. A. Peters and D. M. Ladd, *Talanta*, 1971, **18**, 655.
40. J. Komljenović, S. Krka and N. Radić, *Anal. Chem.*, 1986, **58**, 2893.

## A COMPARISON OF GLASSY-CARBON AND CARBON-POLYMER COMPOSITE ELECTRODES INCORPORATED INTO ELECTROCHEMICAL DETECTION SYSTEMS FOR HIGH- PERFORMANCE LIQUID CHROMATOGRAPHY

J.-M. KAUFFMANN, C. R. LINDERS and G. J. PATRIARCHE\*

Institut de Pharmacie, Université Libre de Bruxelles, Campus Plaine 205/6, Boulevard de Triomphe,  
B-1050 Bruxelles, Belgium

MALCOLM R. SMYTH

School of Chemical Sciences, NIHE Dublin, Glasnevin, Dublin 9, Eire

(Received 14 September 1987. Accepted 16 October 1987)

**Summary**—A comparison has been made of the performance of a novel composite carbon-polymer electrode and a glassy-carbon electrode for use as working electrodes in an electrochemical detector for HPLC. The composite electrode was found to be comparable to the glassy-carbon electrode in terms of current response, superior in terms of cost, machinability, noise levels, stabilization time and accessible potential range, and inferior in terms of the potentials required for the oxidation of certain model compounds such as epinephrine and norepinephrine.

To date, electrochemical detection systems for use in high-performance liquid chromatography (HPLC) have found wide application for the determination of many compounds of biological and environmental significance.<sup>1-3</sup> Several electrode materials have been incorporated into a variety of detector designs. The most common electrode materials are based on solid carbon, *e.g.*, glassy carbon, pyrolytic carbon *etc.*, or on carbon particles (carbon black, graphite) mixed with an appropriate binder. The latter types of electrode material include carbon paste, as well as other composite materials obtained by mixing carbon particles with Teflon,<sup>4-6</sup> Kel-F,<sup>7-9</sup> polyethylene,<sup>10-14</sup> polypropylene,<sup>15</sup> PVC,<sup>16</sup> and chloroprene.<sup>16</sup> The performance of this type of composite electrode compared to that of glassy carbon is still a matter of debate.<sup>5,7</sup> We have therefore investigated the use of a new composite electrode material based on a mixture of a copolymer of ethylenevinyl acetate with 9% vinyl acetate, and various amounts of carbon black. We have previously investigated such material in terms of its electrochemical properties in different supporting electrolytes,<sup>14,17</sup> and used it for the determination of some compounds of pharmaceutical interest.<sup>17-19</sup> We have therefore decided to investigate the use of this material as a working electrode in an electrochemical detector for HPLC, and compared its performance with that of glassy carbon.

### EXPERIMENTAL

Cyclic voltammetric measurements were performed with a PAR 174A-175 polarograph associated with an RE 0074 recorder. A three-electrode cell was used, containing the saturated calomel electrode, the platinum auxiliary electrode and the working electrode [either glassy carbon (Metrohm AG) or a composite electrode]. Oxygen was removed by passing purified nitrogen through the solution before the experiments and over the solution during them. The composite polymer-carbon material was prepared by heating for 12 min at 150°, with stirring at 60 rpm, a mixture of carbon black (KETCHENBLACK) and the polymer (copolymer of ethylenevinyl acetate with 9% vinyl acetate) in appropriate amounts, with a Brabender Plasti-Corder PLE 330 internal mixer. Thin disks (thickness 1.5 mm) were obtained by pressing the final mixture through a Davenport Press at 170° and 200 kg/cm<sup>2</sup> pressure. Details of the electrode construction were reported previously.<sup>14</sup>

Measurements were made at room temperature and all current values scaled to identical electrode surface area. The chromatographic apparatus consisted of Bruker LC 31-B and LC 21-B high-performance liquid chromatography, a Rheodyne 7125 sample injector fitted with a 20- $\mu$ l loop and a Bruker model E 230 electrochemical detector. The LC column was an IBM 5- $\mu$ m octadecyl, 250  $\times$  4.5 mm. The working and auxiliary electrodes, housed in the electrochemical flow-through cell, were glassy-carbon electrodes, the reference electrode was a saturated calomel electrode. The design of the home-made electrolytic cell containing the composite electrode is identical to that of the Bruker detector (see Fig. 1). The cell blocks were made of Plexiglas and separated by a 55- $\mu$ m Teflon spacer to form the thin-layer channel. The carbon-polymer composite was machined and inserted mechanically into the Plexiglas block of the detector. The diameter of the working electrode was 6 mm. All working electrodes used were polished manually to a mirror finish with a smooth cloth and alumina powder suspension (Metrohm EA 267A). During experiments, the

\*To whom correspondence should be addressed.

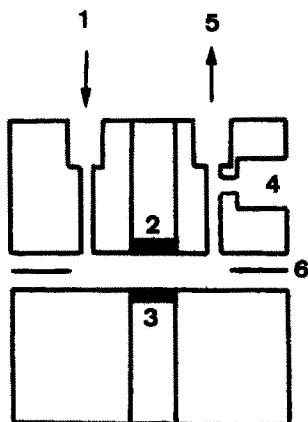


Fig. 1. Schematic diagram of the thin layer electrochemical detector. 1, Mobile-phase inlet; 2, auxiliary electrode; 3, working electrode; 4, reference electrode housing; 5, mobile-phase outlet; 6, Teflon spacer.

electrode surface was renewed by gentle polishing on a filter paper impregnated with methanol. The flow-rate of the mobile phase (which consisted of 5 g of ammonium sulphate, 3 g of acetic acid and 0.25 g of ethylenediaminetetraacetic acid per litre of triply distilled water) was 1 ml/min. Before use the mobile phase was deaerated by purging with purified helium. Epinephrine (A) and norepinephrine (NA) from Bio-Rad were used as test substances in the HPLC. Other products and reagents were of Merck analytical grade.

## RESULTS AND DISCUSSION

### Study of accessible potential range

A comparison was made of the accessible potential range of a glassy-carbon electrode and various carbon-polymer composite electrode formulations (containing 20, 25 and 30% carbon) in various electrolytes, by cyclic voltammetry (CV). The results are summarized in Table 1. The potential ranges shown are for the region giving a current of at least  $2.5 \mu\text{A}$ . These results show that all the composite electrodes tested increase the range on the anodic side by 300–400 mV. This allows the detection of compounds which are difficult to oxidize at the glassy-carbon electrode.<sup>14,18</sup> All the composite electrodes tested were less able than the glassy-carbon electrode to detect compounds which undergo reduction at carbon electrodes.

### Comparison of electrode characteristics

The carbon-polymer composite electrodes were compared with the glassy-carbon electrode in terms of the current obtained, the oxidation potential and the peak shape for four model compounds commonly determined by using HPLC with electrochemical detection (ED). These compounds were ascorbic acid, L-dopa, tryptophan and tyrosine. The results obtained by CV are summarized in Table 2.

In terms of current response, and hence sensitivity of the various electrode materials towards the com-

Table 1. Potential limits of glassy-carbon and carbon-polymer electrodes, *V* vs. SCE

Medium	Glassy carbon		Composite (20% C)		Composite (25% C)		Composite (30% C)	
0.1M H <sub>2</sub> SO <sub>4</sub>	-0.78	+0.97	-0.80	+1.42	-0.64	+1.34	-0.45	+1.22
0.1M Acetate buffer, pH 3.55	-0.87	+0.90	-0.76	+1.26	-0.68	+1.26	-0.54	+1.11
0.05M Phosphate buffer, pH 5.05	-1.07	+0.93	-0.75	+1.38	-0.83	+1.27	-0.74	+1.15
0.038M (NH <sub>2</sub> ) <sub>2</sub> SO <sub>4</sub> + 0.05M CH <sub>3</sub> COOH	-0.93	+0.98	-0.87	+1.49	-0.75	+1.42	-0.63	+1.23

Table 2. Response characteristics of glassy-carbon and composite electrodes towards several compounds in 0.1M H<sub>2</sub>SO<sub>4</sub>: drug concentration  $5 \times 10^{-4}\text{M}$ ; scan-rate 20 mV/sec; potentials vs. SCE

Compounds	Parameters	Glassy carbon	Composite (20% C)	Composite (25% C)	Composite (30% C)
Ascorbic acid	$E_p$ (V)	+0.420	+0.830	+0.630	+0.650
	$i_p$ ( $\mu\text{A}$ )	36	26	30	31
	$E_p - E_{p/2}$ (mV)	75	160	110	110
L-Dopa	$E_p$ (V)	+0.570	+0.790	+0.670	+0.680
	$i_p$ ( $\mu\text{A}$ )	56	38	55	59
	$E_p - E_{p/2}$ (mV)	50	110	60	60
Tryptophan	$E_p$ (V)	+0.980	+1.120	+1.020	+1.020
	$i_p$ ( $\mu\text{A}$ )	84	35	72	83
	$E_p - E_{p/2}$ (mV)	70	140	85	90
Tyrosine	$E_p$ (V)	+1.020	+1.200	+1.080	+1.070
	$i_p$ ( $\mu\text{A}$ )	65	18	42	46
	$E_p - E_{p/2}$ (mV)	50	120	70	70

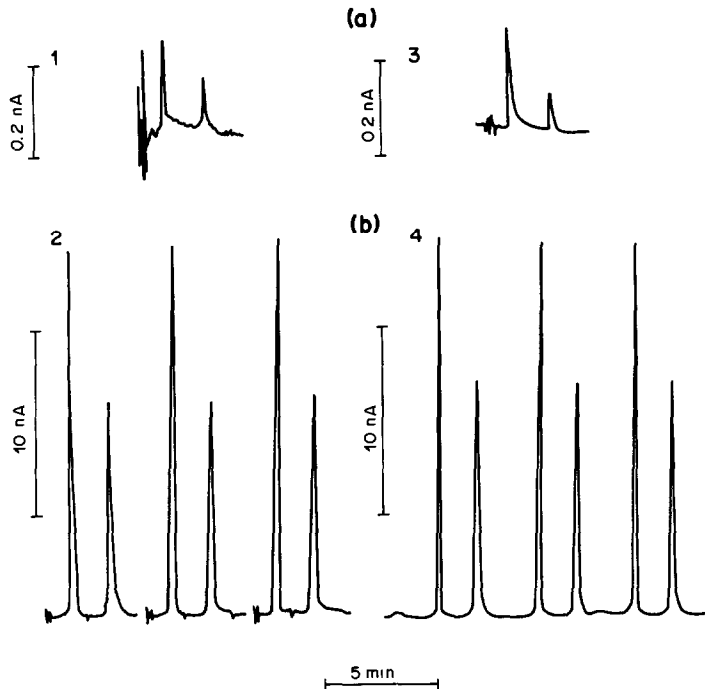


Fig. 2. Typical chromatograms of norepinephrine (NA) (first peak) and epinephrine (A) (second peak) detected amperometrically. Working electrodes: 1, 2, glassy carbon; 3, 4, composite electrode (25% carbon); flow-rate 1 ml/min, injection of 20  $\mu$ l containing: (a) 10  $\mu$ g each of NA and A, (b) 1 ng each of NA and A.

pounds in question, it can be seen that the glassy-carbon electrode gives a larger current than any of the composite electrodes, except in the case of L-dopa and the composite electrode containing 30% carbon. The currents obtained for the composite electrodes increased with increasing carbon content in the formulation. This is to be expected since increasing the carbon content increases the active surface area available for oxidation to occur. For all the compounds studied, the current responses of the composite electrode containing only 20% carbon were much lower than those obtained at the glassy-carbon electrode. The composite electrodes containing 25 or 30% carbon, however, gave sensitivities comparable to those with the glassy carbon. In terms of ease of oxidation, all the composite electrodes gave higher potentials for the oxidation of the four compounds studied. Increasing the carbon content from 20 to 25 or 30% improved the situation somewhat, but the peak potential values for L-dopa, tryptophan and tyrosine were all greater by 50–100 mV than with the glassy-carbon electrode. In the case of ascorbic acid, the difference was more pronounced, and could lead to greater interference from naturally-occurring matrix constituents in the determination of ascorbic acid in biological materials.

In terms of peak shape (as measured by  $E_p - E_{p/2}$  values), all the composite electrodes were inferior to the glassy-carbon electrode, especially the composite electrode containing 20% carbon. For the composite electrodes containing 25 or 30% carbon, the slope of

the voltammetric response was slightly higher for L-dopa, tryptophan and tyrosine, but much higher for ascorbic acid.

It can be seen, therefore, that the best composite electrode formulation in terms of current response, peak shape and accessible potential range is the one containing 25% carbon. This was chosen, therefore, for further investigation as a detector material for HPLC, with the cell shown in Fig. 1.

#### *Performance of the composite electrode material as a detector in HPLC*

To test the performance of the novel carbon-polymer composite electrode as a detector in HPLC, the determination of epinephrine and norepinephrine was investigated. These compounds are normally used for such studies, since the determination of neurotransmitters is a major application of HPLC-ED.

First, the carbon-polymer composite electrode was compared with a conventional glassy-carbon electrode (both materials having been incorporated in identical cells, Fig. 1) in terms of the baseline currents obtained at various applied potentials. From this it can be seen that the currents obtained with the glassy-carbon electrode were in all cases higher than those obtained with the composite electrode. In addition, the potential of the composite electrode reached any applied potential value in about a fifth of the time (on average) needed by the glassy-carbon electrode at

the same applied potential. This is of obvious importance when chromatovoltammetric curves are being constructed, where potential values have to be changed following injection, and when the electrode material requires to be cleaned or replaced.

The current response of the two electrode materials at potential values on the plateau of the chromatovoltammetric curves for both compounds (+0.65 V for the glassy carbon electrode and +0.75 V for the composite electrode) was investigated. For both compounds, the currents obtained were similar with both electrode materials.

With regard to noise, the composite electrode gave much steadier baselines, especially when the detectors were operated near the limit of detection for the two compounds (Fig. 2).

Both electrode materials gave linear response between 5 pg and 20 ng for both compounds. The limit of detection in both cases was about 2 pg.

The reproducibility of both detectors was checked by using 8 successive 200-pg injection of both compounds, and the coefficients of variation were found to be 3.4 and 3.0% for norepinephrine and epinephrine respectively for the glassy-carbon electrode, and 2.9 and 2.8% respectively for the composite electrode.

#### CONCLUSIONS

The results from this study have shown that the carbon-polymer electrode is comparable to the glassy-carbon electrode with respect to current response (and hence sensitivity). It is superior to the glassy-carbon electrode with respect to noise levels, stabilization time and accessible potential range, but inferior in terms of requiring a higher potential for the oxidation of model compounds, and in terms of kinetics of electron transfer.

This new material, however, is much easier to machine than glassy carbon, and is cheaper. It is expected that this new electrode will find many

applications for the determination of oxidizable compounds of biological and environmental significance.

*Acknowledgements*—Thanks are expressed to the Bruker Company (Brussels) for technical support and to the "Fonds National de la Recherche Scientifique" (F.N.R.S. Belgium) for support to one of us (G.J.P.). This research was performed within the framework of the program PREST (Contract No. 278/84) and the SPPS program (Belgium Politic Research, ARC, Contract No. 86/91-89).

#### REFERENCES

1. C. M. Selavka and I. S. Krull, *J. Liquid Chromatog.*, 1987, **10**, 345.
2. D. C. Johnson, S. G. Weber, A. M. Bond, R. M. Wightman, R. E. Shoup and I. S. Krull, *Anal. Chim. Acta*, 1986, **180**, 187.
3. K. Štulík and V. Pacáková, *J. Electroanal. Chem.*, 1981, **129**, 1.
4. M. H. Shah and I. L. Honiberg, *Anal. Lett.*, 1983, **16**, 1149.
5. D. N. Armentrout, J. D. McLean and M. W. Long, *Anal. Chem.*, 1979, **51**, 1039.
6. L. N. Klatt, D. R. Connell, R. E. Adams, I. L. Honiberg and J. C. Price, *ibid.*, 1975, **47**, 2470.
7. D. E. Tallman and D. E. Weisshaar, *J. Liquid Chromatog.*, 1983, **6**, 2157.
8. J. E. Anderson, D. E. Tallman, D. J. Chesney and J. L. Anderson, *Anal. Chem.*, 1978, **50**, 1051.
9. J. L. Anderson, K. K. Whiten, J. D. Brewster, T. Yuan Ou and W. K. Nonidez, *ibid.*, 1985, **57**, 1367.
10. M. Mascini, F. Pallozzi and A. Liberti, *Anal. Chim. Acta*, 1973, **43**, 126.
11. A. Liberti, C. Morgia and M. Mascini, *ibid.*, 1985, **173**, 157.
12. J. D. McLean, *Anal. Chem.*, 1982, **54**, 1169.
13. J. B. Nair, M. N. Munk and J. D. McLean, *J. Chromatog.*, 1987, **416**, 340.
14. M. P. Prete, J.-M. Kauffmann, J.-C. Vire, G. J. Patriarche, B. Debye and G. Geuskens, *Anal. Lett.*, 1984, **17**, 1391.
15. S. G. Weber and W. C. Purdy, *Anal. Chim. Acta*, 1978, **100**, 531.
16. K. Štulík, V. Pacáková and B. Starková, *J. Chromatog.*, 1981, **213**, 41.
17. G. J. Patriarche, J.-M. Kauffmann and J.-C. Vire, *J. Pharm. Biomed. Anal.*, 1983, **1**, 469.
18. J.-M. Kauffmann, M. P. Prete, J.-C. Vire and G. J. Patriarche, *Z. Anal. Chem.*, 1985, **321**, 172.
19. G. J. Patriarche, *J. Pharm. Biomed. Anal.*, 1986, **4**, 789.

## DETERMINATION OF ARSENIC AND ANTIMONY IN BIOLOGICAL MATERIALS BY SOLVENT EXTRACTION AND NEUTRON ACTIVATION

W. M. MOK and C. M. WAI\*

Department of Chemistry, University of Idaho, Moscow, ID 83843, U.S.A.

(Received 20 June 1987. Revised 14 September 1987. Accepted 16 October 1987)

**Summary**—Arsenic and antimony in digested biological samples can be extracted with pyrrolidinecarbo-dithioate at pH 1 into chloroform and stripped with nitric acid for neutron-activation analysis (NAA). The extraction method eliminates interferences from matrix species, including Br and Na, making the accurate determination of low levels of As and Sb in biological materials feasible. The detection limits under the experimental conditions used are 0.005 and 0.006  $\mu\text{g/g}$  for arsenic and antimony, respectively. A comparison of the results obtained for As and Sb in NBS biological standards by this method and by non-destructive instrumental neutron-activation analysis (INAA) is also given.

The determination of trace quantities of arsenic and antimony in the environment is of considerable importance because of toxicological concern.<sup>1-4</sup> Accurate determination of low levels of As and Sb in biological samples can be accomplished only by techniques that are very sensitive and selective. Neutron-activation analysis (NAA) usually meets these requirements. Under interference-free conditions, the sensitivity of NAA for As and Sb is of the order of several nanograms. However, the applicability of non-destructive instrumental neutron-activation analysis (INAA) to biological samples is often limited by spectral interferences from matrix elements, including Na, K, P, and Br. The detection limits of As and Sb by INAA in biological systems may be raised to a level higher than that required for analysing small samples. In general, INAA can determine As down to about 2  $\mu\text{g/g}$  in most biological materials, assuming a sample weight of 1 g, an irradiation time of 1 hr and a counting time of 10 min.<sup>5</sup> Many biological materials contain less than 2  $\mu\text{g/g}$  As and the concentrations of Sb in these materials are generally even lower. Therefore, in biological materials with low levels of As and Sb, chemical separation, either before or after irradiation, is necessary in order to achieve maximum sensitivity and accuracy for the determination of these two elements by NAA.

Preconcentration of trace metals by solvent extraction prior to neutron irradiation has been applied to natural waters and biological materials in our laboratory.<sup>6-9</sup> Chemical separation before irradiation has the advantages of giving a larger concentration factor for trace elements, allowing sufficient time for laboratory operation, and minimizing exposure of the

analysts to radiation. This paper describes such a procedure for the separation of As and Sb from biological materials. The As and Sb concentrations in a number of NBS biological standards have been determined and compared with those from direct INAA. Conditions under which chemical separation for NAA becomes mandatory for accurate determination of these trace elements are discussed.

### EXPERIMENTAL

#### Reagents and instruments

The concentrated nitric and sulphuric acids used in the sample digestion were Baker Ultrex Reagent grade. Chloroform used in the extraction was EM Science Omnisolv grade. All other chemicals were Baker Analytical grade. Distilled demineralized water was used for making all solutions. All glassware was cleaned by soaking in 10% v/v nitric acid for at least 24 hr, rinsed with demineralized water and dried in a class-100 clean hood equipped with a vertical laminar flow filter (CCI).

Standard As and Sb solutions (1000 mg/l) were prepared by dissolving  $\text{As}_2\text{O}_3$  and  $\text{Sb}_2\text{O}_3$ , respectively, according to the procedures given earlier.<sup>9</sup> Ammonium pyrrolidinecarbo-dithioate (APCDT) solution was prepared by dissolving 7.5 g of reagent in 100 ml of demineralized water, filtering, and then extracting with chloroform for purification. Disodium ethylenediaminetetra-acetate (EDTA) solution was prepared by dissolving 12.5 g in 100 ml of demineralized water.

All samples and standards were normally irradiated for 2 hr in a 1-MW TRIGA reactor at a steady neutron flux of  $6 \times 10^{12}$  n.cm<sup>-2</sup>.sec<sup>-1</sup> followed by one day of cooling. A large-volume coaxial ORTEC Ge(Li) detector with a resolution of about 2.3 keV at the 1332 keV  $\gamma$ -ray of <sup>60</sup>Co was used for activity measurements. The detector output was fed into an EG&G ORTEC ADCAM (model 918) multichannel analyser. The data from the analyser were processed by EG&G ORTEC software on an IBM-PC.

#### Sample digestion and extraction procedure

The biological sample was digested in a round-bottomed flask fitted with a reflux reservoir and condenser as de-

\*To whom correspondence should be addressed.

scribed by Mok *et al.*<sup>8</sup> Usually 1.0–2.0 g of material was placed in a 50-ml round-bottomed flask and a few glass beads were added. A mixture of concentrated nitric and sulphuric acids (5:4 v/v) was added to cover the sample, and the mixture was left overnight. The digestion started with gentle heating on a heating mantle until foaming ceased. The heat was then increased, and small amounts of the condensed nitric acid were admitted from the condenser whenever a slight darkening of the digest occurred. This operation was repeated until no darkening was observed, and white fumes were evolved, after which heating was continued for another 5 min and the apparatus then allowed to cool. The sample solution was diluted with 10 ml of water and boiled for another 5 min. The solution was then transferred into a 100-ml standard flask and the apparatus rinsed. The rinsing solution was added to the flask and the solution made up to volume with demineralized water.

A 30-ml portion of the digest solution was transferred into a 125-ml polyethylene bottle, diluted to about 100 ml and adjusted to pH 1. One ml of 25% sodium thiosulphate solution and 1 ml of 20% potassium iodide solution were added to reduce quinquivalent As and Sb to their trivalent states. After a waiting period of 15–30 min, 4 ml of EDTA solution, 10 ml of chloroform and 2 ml of APCDT solution were added. The mixture was shaken vigorously for 10 min on a wrist-action mechanical shaker and the phases were allowed to separate. To strip As and Sb, 8 ml of the organic phase were transferred to a 20-ml Beckman polyvial and 2 ml of 50% v/v nitric acid were added. The vial was shaken vigorously for 10 min. After phase separation, 1.5 ml of the acid were taken for neutron irradiation. A complete blank was run in the same manner as the samples in each set of experiments. The sample sealing, irradiation and transfer procedures have been described elsewhere.<sup>8,9</sup> Each sample was usually counted for 2000–4000 sec. When the As content in a sample was much higher than that of Sb, the sample was normally recounted after 2–3 days. Appropriate quantities of standards were prepared to cover the expected ranges of As and Sb in the samples. This series of As and Sb standards was analysed by the procedure above and calibration curves were prepared. The elements were determined by comparing the net photopeak areas with those of the standards.

For INAA, about 100–200 mg of material was irradiated for each sample. Irradiation of more than 200 mg of biological materials per sample often resulted in high levels of radiation from matrix species, making the sample difficult to handle experimentally. Each activated sample was usually counted twice, 2–3 days and 5–6 days after the end of irradiation.

## RESULTS AND DISCUSSION

### Spectral interferences

The nuclear data and major interferences for determination of As and Sb by NAA are given in Table 1.

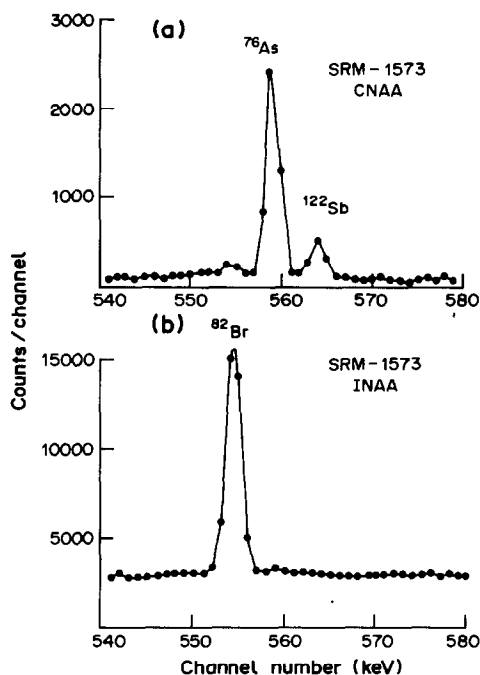


Fig. 1. Gamma-spectra of NBS SRM-1573 (Tomato Leaves) in the energy range 540–580 keV. (a) CNA with APCDT extraction, sample weight 2 g, (b) INAA, sample weight 0.1 g.

The gamma peaks which provide the greatest sensitivity are at 564.1 keV for <sup>122</sup>Sb ( $t_{1/2} = 67.2$  hr) and 559.1 keV for <sup>76</sup>As ( $t_{1/2} = 26.4$  hr). A major interference for <sup>122</sup>Sb and <sup>76</sup>As is from the 554.3 keV peak from the decay of <sup>82</sup>Br ( $t_{1/2} = 35.3$  hr). The Ge(Li) detector, which has a resolution of about 2.3 keV (FWHM), is capable of resolving these three peaks. However, when the concentration of Br in a sample is high, the greater background and the tailing of the 554.3 keV peak may affect the measurements of <sup>76</sup>As and <sup>122</sup>Sb. This is illustrated in Fig. 1 which shows the gamma spectra in the region of interest for NBS-SRM-1573 (Tomato Leaves) obtained from INAA, and from CNA by the separation procedure described. The Br concentration in SRM-1573 is 26  $\mu\text{g/g}$ , which is apparently high enough to raise the background, causing a serious problem for Sb and As determination by INAA (Fig. 1b). Another prominent feature of the spectrum is the high background radiation caused primarily by the presence of high

Table 1. Nuclear data for neutron activation of As and Sb, and major spectral interferences

Nuclide	Abundance of parent, %	Cross section, <i>barus</i>	Half-life of daughter	Major gamma peak, keV
<sup>76</sup> As	100	4.5	26.4 hr	559.1
<sup>122</sup> Sb	57.3	6	67.2 hr	564.1
<sup>24</sup> Na	100	0.53	15.0 hr	1368.5
<sup>42</sup> K	6.8	1.2	12.4 hr	1524.6
<sup>82</sup> Br	49.5	3	35.3 hr	554.3
<sup>32</sup> P	100	0.18	14.28 d	bremsstrahlung



Table 2. Determination of As and Sb in some NBS standard reference materials by INAA and by the proposed CNAA

Reference material	As, $\mu\text{g/g}$			Sb, $\mu\text{g/g}$		
	CNAA	INAA	NBS value	CNAA	INAA	NBS value
Orchard Leaves 1571	$8.84 \pm 0.11$	$10.8 \pm 0.2$	$10 \pm 2$	$3.04 \pm 0.10$	$2.83 \pm 0.04$	(2.9)*
Pine Needles 1575	$0.24 \pm 0.01$	$0.22 \pm 0.01$	$0.21 \pm 0.04$	$0.19 \pm 0.01$	$0.20 \pm 0.01$	(0.2)
Citrus Leaves 1572	$2.89 \pm 0.03$	$3.07 \pm 0.02$	$3.1 \pm 0.3$	$0.068 \pm 0.003$	N.D.	(0.04)
Tomato Leaves 1573	$0.25 \pm 0.01$	N.D.	$0.27 \pm 0.05$	$0.047 \pm 0.003$	N.D.	no values given

\*Values in parentheses are not certified, but are given for reference by NBS.

All values are based on triplicate analyses.

N.D., not detected.

levels of  $^{24}\text{Na}$ ,  $^{42}\text{K}$ , and  $^{32}\text{P}$  in the system. This high background radiation would also raise the detection limits of As and Sb significantly. The APCDT extraction procedure effectively removes the alkali metal ions, halides and phosphorus species from the system. As shown in Fig. 1a, the  $^{82}\text{Br}$  peak in SRM-1573 after the extraction was barely detectable and the background radiation was significantly reduced. The 559.1 keV peak of  $^{76}\text{As}$  and the 564.1 keV peak of  $^{122}\text{Sb}$  are well resolved in Fig. 1a, and the detection limits of As and Sb approach those expected under interference-free conditions. With a sample weight of 2 g, under the experimental conditions described in this paper, the detection limits of As and Sb, calculated as the amounts equivalent to 3 times the standard deviation of the background under the appropriate photopeaks, are 0.005 and 0.006  $\mu\text{g/g}$  respectively. The detection limits can be further lowered by increasing the sample weight, the irradiation time and the counting time.

Generally speaking, As concentrations in biological materials are several times higher than those for Sb. If the ratio of As/Sb in a sample is large, then a minor peak of  $^{76}\text{As}$  at 562.8 keV (2.7% relative to the 559.1 keV major peak) may cause appreciable interference with the 564.1 keV peak of  $^{122}\text{Sb}$ . In general, a correction should be applied to the  $^{122}\text{Sb}$  peak by using the intensity ratios of the As peaks at 559.1 and 562.8 keV. The interference of  $^{76}\text{As}$  with  $^{122}\text{Sb}$  can be minimized by recounting after allowing the former to decay. Since the half-life of  $^{122}\text{Sb}$  is about 2.5 times that of  $^{76}\text{As}$ , we normally recounted samples with high As/Sb ratios 3–4 days after the first counting, to obtain more reliable  $^{122}\text{Sb}$  data.

#### INAA vs. CNAA for As and Sb determination in biological samples

The concentrations of As and Sb in four NBS standard biological reference materials, determined by INAA and by CNAA with the proposed separation method are given in Table 2. The bromine contents of these standard reference materials vary from 9  $\mu\text{g/g}$  in SRM-1575 (Pine Needles) to 26  $\mu\text{g/g}$  in SRM-1573 (Tomato Leaves). In samples with high As and Sb contents, such as SRM-1571, or with low bromine content as in SRM-1575, the As and Sb values obtained by INAA are in good agreement with

the values given by NBS. In samples with high bromine and low As and Sb contents, as in SRM-1573, INAA failed to provide meaningful As and Sb values. In order to determine low levels of As and Sb in biological materials by NAA, chemical separation appears necessary. The As and Sb values in the four standard reference materials determined by the APCDT separation and NAA are in good agreement with the values given by NBS (Table 2). Antimony is generally more difficult to determine than arsenic because of its low concentrations in biological systems. In the case of SRM-1572 (Citrus Leaves), the As/Sb ratio approaches 44 and Sb can be determined accurately only by CNAA. It should be pointed out that the NBS Sb values quoted are not certified values, but values for reference only. The Sb concentration in SRM-1573 (Tomato Leaves) has not been reported before in the literature.

This CNAA method has been applied to the analysis of sagebrush samples collected from Idaho Falls (Table 3). The As and Sb levels in these samples are low, comparable to those found in SRM-1573 (Tomato Leaves). Without pre-irradiation separation, As and Sb in sagebrush are hardly detectable by INAA. With the APCDT extraction method, well resolved  $^{76}\text{As}$  and  $^{122}\text{Sb}$  peaks with low background radiation were observed for these samples. The concentrations of Sb in the sagebrush samples were determined by CNAA to be in the range 41–49 ng/g.

#### CONCLUSION

The APCDT extraction procedure eliminates matrix interferences and concentrates As and Sb from plant digests for NAA. The detection limits for As and Sb in biological materials are estimated to be 0.005 and 0.006  $\mu\text{g/g}$ , respectively. The proposed

Table 3. As and Sb in three sagebrush samples, determined by the proposed CNAA method\*

Sample	As, $\mu\text{g/g}$	Sb, $\mu\text{g/g}$
1	$0.156 \pm 0.003$	$0.041 \pm 0.003$
2	$0.188 \pm 0.003$	$0.049 \pm 0.002$
3	$0.160 \pm 0.002$	$0.041 \pm 0.002$

\*All values are based on triplicate analyses.

Samples were collected from Idaho Falls, Idaho, in Nov. 1986.

CNAAs technique proves to be a sensitive and reliable method for the accurate determination of low levels of As and Sb in biological samples, as demonstrated by the results obtained from NBS standards.

*Acknowledgements*—This work was supported in part by a grant from the Westinghouse Idaho Nuclear Company, Inc. Neutron irradiations were performed at the Washington State University Nuclear Radiation Center under the Reactor Sharing Program supported by the Department of Energy.

#### REFERENCES

1. J. M. Harrington, J. P. Middaugh, D. L. Morse and J. Houseworth, *Am. J. Epidemiol.*, 1978, **108**, 377.
2. S. Hernberg, in *Origins of Human Cancer*, H. H. Hiatt (ed.), Vol. 4, pp. 147–157. Cold Spring Harbour Laboratories, New York, 1977.
3. C. D. Rail and W. M. Hadley, *J. Environ. Health*, 1976, **39**, 173.
4. T. D. Luckey and B. Venugopal, *Metal Toxicity in Mammals*, Vol. 1, p. 139. Plenum Press, New York, 1977.
5. R. R. Brooks, D. E. Ryan and H. Zhang, *Anal. Chim. Acta*, 1981, **131**, 1.
6. W. M. Mok and C. M. Wai, *Anal. Chem.*, 1984, **56**, 27.
7. J. C. Yu and C. M. Wai, *ibid.*, 1984, **56**, 1689.
8. W. M. Mok, H. Willmes and C. M. Wai, *ibid.*, 1984, **56**, 2623.
9. W. M. Mok and C. M. Wai, *ibid.*, 1987, **59**, 233.

## METAL-ION CHROMATOGRAPHY ON SILICA-IMMOBILIZED 2-PYRIDINECARBOXYALDEHYDE PHENYLHYDRAZONE

NINUS SIMONZADEH and A. A. SCHILT

Department of Chemistry, Northern Illinois University, DeKalb, IL 60115, U.S.A.

(Received 23 July 1987. Revised 27 August 1987. Accepted 16 October 1987)

**Summary**—The chromatographic properties of silica-immobilized 2-pyridinecarboxyaldehyde phenylhydrazone as stationary phase for separation of aqueous metal-ion mixtures containing various combinations of Mn(II), Fe(II), Cd(II), Zn(II), Co(II), Pb(II), and Cu(II) are described. Separations were achieved in many cases by using mobile phases containing chloride or perchlorate anions, at moderate flow-rates. Quantitative chromatographic analysis was possible for a variety of sample types over a wide range of metal-ion concentrations.

Incorporation of chelating agents in various column-packing materials has been increasingly investigated. Various reagents have been chemically bonded to surfaces of silica supports by silylation reactions.<sup>1-4</sup> Such surface-modified silica supports have in many cases given more efficient and selective metal-ion separations than conventional ion-exchange resins.

In an earlier report<sup>1</sup> we described separations of some transition-metal ions on 2-pyridinecarboxyaldehyde phenylhydrazone (PAPH) immobilized on 37-74- $\mu\text{m}$  particles of silica. In the present work we have attached PAPH covalently to a 5- $\mu\text{m}$  silica support and characterized the product (denoted as Chromosorb-PAPH) for its effectiveness in chromatographic analysis of metal-ion mixtures by HPLC with post-column detection.

### EXPERIMENTAL

#### Reagents and materials

Chromosorb LC-6, 5- $\mu\text{m}$  particle size, 400 +  $\text{m}^2/\text{g}$  specific surface area, 120  $\text{\AA}$  pore size, was obtained from Johns-Manville Co. Aminophenyltrimethoxysilane (mixed isomers) and trimethylchlorosilane were purchased from Petrarch System Inc., Bristol, PA. The aminophenyltrimethoxysilane was distilled twice at reduced pressure, and refrigerated before use. Pyridine-2-carboxyaldehyde was purchased from Aldrich Chemical Co. and used without further purification. PAR [4-(2-pyridylazo)resorcinol, monosodium salt monohydrate] was obtained from Aldrich Chemical Co. and used as received. PAR was generally used as a  $1.12 \times 10^{-4} M$  solution prepared in pH-11 (0.05M  $\text{NH}_4^+/\text{NH}_3$ ) buffer. NBS standard reference material No. 1573 (Tomato Leaves) was obtained from the National Bureau of Standards, "One-A-Day" Maximum Formula vitamin tablets (Miles Laboratories, Inc., Elkhart, IN) were purchased locally. Metal-ion sample solutions were prepared from the nitrates, for zinc, lead, cobalt, and cadmium. Iron was used as ferrous ammonium sulphate, copper as cupric sulphate, and manganese as manganese chloride.

#### Apparatus

The chromatographic system used in this study was assembled as shown in Fig. 1. The liquid chromatograph

was a Bioanalytical System LC-150 (Bioanalytical Systems, Inc., West Lafayette, IN) equipped with a 20- $\mu\text{l}$  injection loop. A post-column reaction system was used for detection of metal ions in the effluent. The effluent was directed to a low-volume T-junction where it mixed with the reagent solution (the eluent and the PAR solution were pumped through 1/18 in. o.d. stainless-steel tubing. Reciprocating pumps (Model 396, Milton Roy Co.) were used in conjunction with the liquid chromatograph. The PAR chelates were monitored at 550 nm by a flow-through photometric detector (Bioanalytical Systems LC-6). The stationary phase was slurry-packed (carbon tetrachloride as medium) into a standard 250 mm  $\times$  4.6 mm i.d. stainless-steel column at Altech Associates Inc., Deerfield, IL. The length of tubing from the injection valve to column inlet and from the column outlet to the T-junction was kept as short as possible to minimize band broadening due to diffusion. The tubing from the T-junction to the detector was approximately 20 in. long and coiled to ensure complete mixing. Solution absorbances were measured with a Varian Model 2290 recording spectrophotometer.

#### Immobilization procedure

The synthetic steps used for the attachment of the desired reactive groups to the silica support, and the chelation capacity studies, have been described previously.<sup>1</sup>

#### Separations

A pH-4.5 acetate buffer eluent, and eluents containing sulphate, chloride and perchlorate, all at pH 4.5 and 0.041M in conjugate-base concentration, were used to elute metal-ion mixtures containing certain combinations of manganese, iron, cadmium, zinc, lead and cobalt. The pH of the eluents was adjusted to  $4.5 \pm 0.02$  by addition of a sufficient amount of the appropriate conjugate acid. All eluents contained 0.1% of hydroxylamine hydrochloride as reductant. Eluent and PAR flow-rates of  $0.47 \pm 0.02$  ml/min and  $0.60 \pm 0.03$  ml/min, respectively, were maintained. Metal-ion mixtures containing copper were chromatographed with 0.060M sodium oxalate adjusted to pH 4.5 with perchloric acid (1 + 1).

#### Quantitative analysis

Synthetic samples were prepared, containing various known amounts of manganese, iron, cadmium, zinc, lead, cobalt and copper. NBS Tomato Leaves and "One-A-Day" vitamin tablets were dry-ashed and the residues dissolved in acid according to a procedure described elsewhere.<sup>5</sup> From

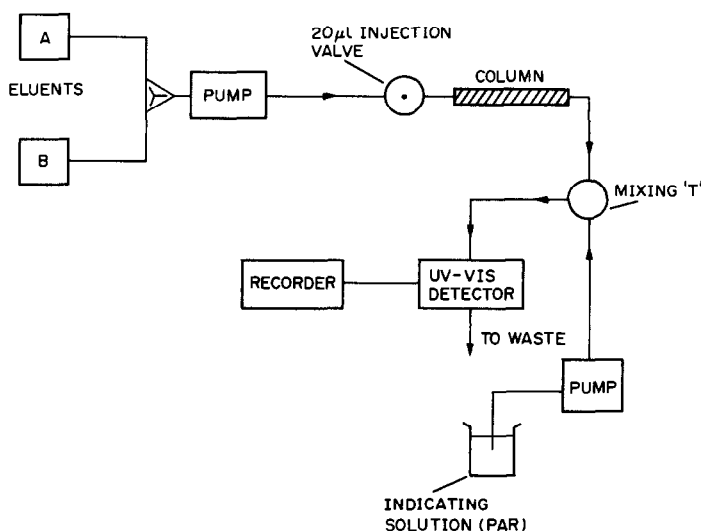


Fig. 1. Schematic diagram of the liquid chromatograph and the post-column reaction system.

calibration graphs for various metal-ion standards, constructed by plotting peak area *vs.* metal-ion concentration for the 0.02–30mM range, the concentrations of the metal ions present in the various samples were determined.

#### RESULTS AND DISCUSSION

Table 1 lists the characteristics of the Chromosorb–PAPH column. The agreement, within experimental error, of the capacity data obtained from the copper sorption study and the acid–base titration indicates that the basic sites are equally accessible to protons and metal ions, presumably because they are located on the surface rather than in narrow pores. An argument for the 1:1 stoichiometry of the immobilized metal–ligand complex has been proposed previously.<sup>1</sup>

#### Metal-ion chromatography

At pH 3 or below, all of the metal ions tested were eluted in the void volume. A pH of 4.5 proved satisfactory for optimal chromatographic retention

Table 1. Characteristics of the Chromosorb–PAPH column

Particle size, $\mu\text{m}$	5*
Specific surface area, $\text{m}^2/\text{g}$	> 400*
Pore diameter, $\text{\AA}$	120*
Weight of packing in column, g	1.8
Void volume, ml	$3.3 \pm 0.1$
Bonded PAPH, $\mu\text{mole/g}$	$19^\dagger \pm 3$
	$18^\S \pm 2$
Surface coverage, $\mu\text{mole}/\text{m}^2$	0.048†
Column capacity, $\mu\text{mole PAPH}$	34†
Column length, mm	250
Column bore, mm	4.6

\*Manufacturer's values.

†Based on copper uptake at pH 4.5.

§Based on acid–base titration.

and separation. Effects of anions on resolution were examined to allow selection of the most appropriate eluent components. Acetate resulted in considerable overlap of the bands for zinc, lead and cobalt. Sulphate gave good resolution of zinc from lead but

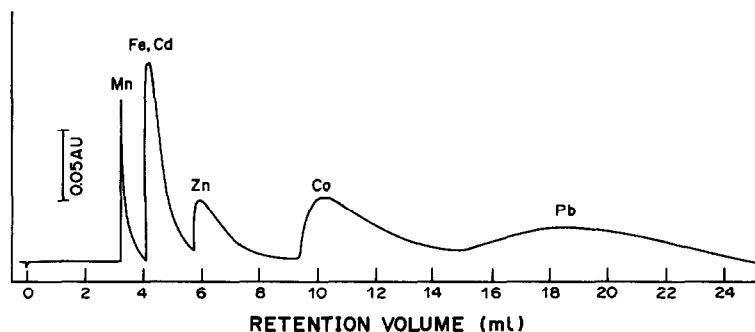


Fig. 2. Chromatograph of a sample containing manganese, iron, cadmium, zinc, cobalt and lead. Eluent: pH-4.5 sodium perchlorate/perchloric acid; flow-rate:  $0.47 \pm 0.02$  ml/min. Concentrations used: 0.2mM for Mn(II), and 0.8mM each for Fe(II), Cd(II), Zn(II), Co(II), and Pb(II).

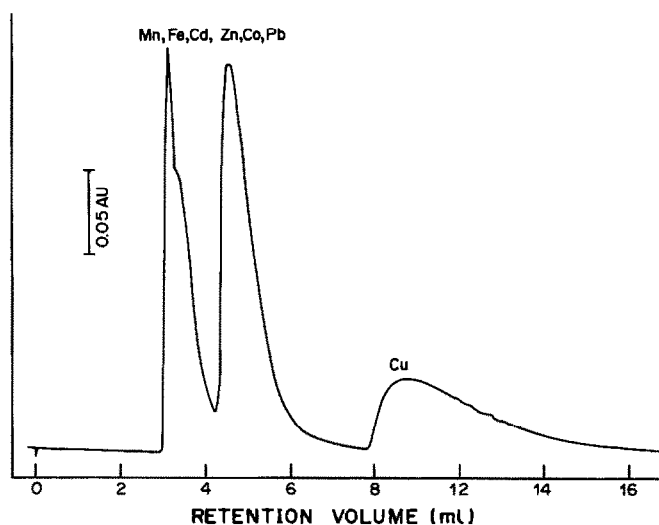


Fig. 3. Chromatogram of a sample containing manganese, iron, cadmium, zinc, cobalt, lead and copper. Eluent: pH-4.5 oxalate buffer; flow-rate:  $0.70 \pm 0.02$  ml/min. Concentrations used:  $0.8mM$  for copper, and  $0.5mM$  each for Mn(II), Fe(II), Cd(II), Zn(II), Co(II) and Pb(II).

not of lead from cobalt. Chloride and perchlorate gave similar results, each proving suitable for resolution of manganese, iron (with cadmium), zinc, cobalt and lead (in that order) as seen in Fig. 2. Copper was strongly retained at pH 4.5 but could be eluted with a pH 4.5 oxalate buffer (Fig. 3).

All the chromatograms exhibited broad and asymmetric peaks, due in part to the use of post-column reaction detection. For example, the peak due to manganese(II) in Fig. 2 is distorted primarily by effects associated with injection of the post-column reagent solution and its mixing with the eluent. An additional contribution to band broadening occurs during the elution of the other metal ions, since they are retained by chelation and must be displaced or dissociated from the silica-bound ligand. Slow kinetics was observed for these in separate experiments, which explains the broadness of the peaks. Some improvement in peak shape might be afforded by use of an elevated temperature or an eluent pH-gradient.

#### Quantitative analysis

Table 2 lists the results obtained for the various

samples. The results are in reasonable agreement, within experimental error, with the known amounts of metal present in each type of sample. Lead, cobalt and cadmium, if present in the tomato leaves and vitamin tablets, were at concentrations too low to be determined by this method. The results demonstrate that the Chromosorb-PAPH stationary phase can be used effectively to determine various metal ions, in a variety of sample types, over a wide range of metal-ion concentrations.

#### Evaluation of the Chromosorb-PAPH stationary phase

The Chromosorb-PAPH stationary phase was used successfully for the separation of up to seven metal ions in aqueous solution. Significant improvement in chromatographic resolution was noted with this stationary phase when a  $5\text{-}\mu\text{m}$  support was used instead of the larger particle support reported previously.<sup>1</sup> The column was used for a total of 160 hr, over a period of about 19 weeks, without apparent loss in chromatographic resolution. It was stored in demineralized water when not in use.

Table 2. Chromatographic analysis of samples\*

Metal ion	Synthetic sample, <i>mM</i>		Tomato leaves, $\mu\text{g/g}$		Vitamin tablets, <i>mg/tablet</i>	
	True	Found	True	Found	True	Found
Mn	0.197	$0.20 \pm 0.01$	$238 \pm 7$	$245 \pm 12$	2.5	$2.1 \pm 0.2$
Fe	0.500	$0.54 \pm 0.02$	$690 \pm 25$	$730 \pm 50$	18	$15 \pm 1$
Zn	0.100	$0.10 \pm 0.01$	$62 \pm 6$	$57 \pm 5$	15	$14 \pm 1$
Pb	0.300	$0.31 \pm 0.01$	—	—	—	—
Co	0.100	$0.10 \pm 0.01$	—	—	—	—
Cd	0.200	$0.20 \pm 0.01$	—	—	—	—
Cu	0.600	$0.58 \pm 0.03$	—	—	1.89	$1.8 \pm 0.1$

\*Values found are averages, with average deviations specified, based on four replicate determinations for the synthetic sample and two for the others.

## REFERENCES

1. S. Watanek and A. A. Schilt, *Talanta*, 1986, **33**, 895.
2. J. R. Jezorek and H. Freiser, *Anal. Chem.*, 1979, **51**, 366.
3. S. Imai, M. Muroi, A. Hamaguchi and M. Koyama, *ibid.*, 1983, **55**, 1215.
4. J. R. Parish, *ibid.*, 1982, **54**, 1890.
5. A. A. Schilt, *Perchloric Acid and Perchlorates*, G. F. Smith Chemical Company, Columbus, Ohio, 1979.
6. L. G. Sillén and A. E. Martell, *Stability Constants of Metal-Ion Complexes*, Chemical Society, London, 1964.
7. L. R. Snyder and J. J. Kirkland, *Introduction to Modern Liquid Chromatography*, Wiley, New York, 1979.
8. E. B. Sandell and H. Onishi, *Photometric Determination of Traces of Metals: General Aspects*, Chapter 6. Wiley, New York, 1978.

## ELECTROCHEMICAL MASKING FOR REMOVAL OF THE TITANIUM MATRIX EFFECT IN DPASV DETERMINATION OF THALLIUM

ALEKSANDER CISZEWSKI and ZENON LUKASZEWSKI  
Institute of Chemistry, Technical University of Poznan, Poland

(Received 30 January 1987. Revised 21 March 1987. Accepted 16 October 1987)

**Summary**—The possibilities for eliminating the matrix effect caused by large concentrations of titanium in an EDTA-based electrolyte have been examined. In these solutions titanium gives a DPASV peak, the height of which decreases with increase in preconcentration time. This effect depends on the pH and is probably caused by impurities in the EDTA. Complete damping of the titanium peak by means of this effect is not possible. The influence of the following surfactants on the DPASV peak for titanium in 0.2M EDTA at pH 4.5 was investigated: polyoxyethylated alkylphenols having an average of 3 and 9.5 ethylene oxide sub-units; polyoxyethylene (glycerol mono-oleate) ether having an average of 20 ethylene oxide sub-units; polyoxyethylene (sorbitol mono-oleate) ether having an average of 20 ethylene oxide sub-units; poly(ethylene oxide) having M.W.  $5.0 \times 10^6$ ; poly(ethylene oxide)poly(propylene oxide) block copolymer having M.W.  $1.625 \times 10^6$ ; *N,N,N,N',N',N'*-hexamethylhexamethylenediammonium bromide (HMB); benzyl(dibutylphenoxylethoxy)dimethylammonium chloride; hexadecyltrimethylammonium bromide; tetrabutylammonium chloride (TBAC); hexadecyldimethylbenzylammonium chloride, hexadecyltributylphosphonium bromide; tetraphenylphosphonium bromide; sodium dodecylsulphate; sodium stearate; sodium dodecylbenzenesulphonate; sodium octadecyloxyethylene ether sulphate; sodium octadecyloxyethylene ether malonate (Malester). Except for TBAC and HMB all the surfactants investigated decreased the titanium peak, although to different degrees. Generally the effect increased in the sequence cationic surfactants < non-ionic surfactants < anionic surfactants. The more hydrophobic non-ionic surfactants decreased the titanium peak more strongly than did the less hydrophobic ones. Malester was found the best of the investigated surfactants for this purpose. Sodium dodecylbenzenesulphonate also gave good results, although in this case an additional peak appeared. In the presence of these last two surfactants iron(III) does not substantially disturb the base-line current.

Titanium is one of the main components of many mineral matrices. Its content in the lithosphere is 5.7 mg/g,<sup>1</sup> and its average content in soils is approximately 5.0 mg/g.<sup>2</sup> Full decomposition of gram amounts of such samples can introduce several mg of titanium into the solution obtained. Even when such samples are treated with acids, to dissolve only the heavy metals, the solutions will have an appreciable concentration of titanium.<sup>3</sup> Such concentrations can interfere in the determination of thallium by anodic stripping methods. Although the titanium does not undergo accumulation in the mercury drop during the usual preconcentration, in many complexing base electrolytes its presence causes the appearance of a large additional peak which makes the determination of thallium impossible. This applies to EDTA solutions. Of course, it is possible not to use such complexing electrolytes and thus avoid the problems connected with the presence of titanium. However, another very difficult problem in electroanalysis, *viz.* the determination of thallium in the presence of an excess of lead, is easily solved only by use of complexing base electrolytes, the best being an EDTA solution. The complexing action of EDTA alone can substantially increase the tolerance for lead in the

determination of thallium.<sup>4</sup> Extremely high excesses of lead can be tolerated if the lead is "electrochemically masked" by the addition of the surfactant tetrabutylammonium chloride (TBAC) to the EDTA solution.<sup>5</sup> Besides EDTA and TBAC, Triton X-100 and DCTA can be used.<sup>6</sup> Hence, the problem appears to be to eliminate the influence of titanium on the determination of thallium without giving up the use of EDTA as the base electrolyte, or else to eliminate the influence of lead on the determination of thallium in a non-complexing base electrolyte. The first alternative seems the easier to realize.

The purpose of this work was removal of the titanium matrix effect on the determination of thallium in DPASV while retaining the tolerance for a large excess of lead. This is part of our ultimate aim, the development of a highly selective method for the determination of thallium, especially in such matrices of practical importance as soil.

EDTA solutions have been used in voltammetric determination of titanium for a very long time.<sup>7</sup> The influence of surfactants on the behaviour of titanium in d.c. and a.c.-polarography (at the DME) with a citrate base electrolyte has also been examined with the aim of increasing the sensitivity of the deter-

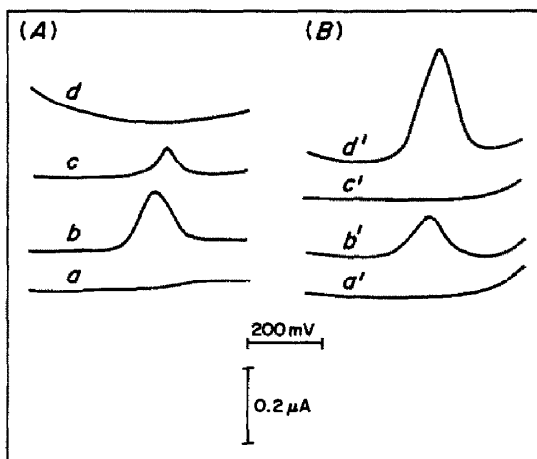


Fig. 1. Voltamperograms of thallium ( $b$  and  $b'$ ), lead ( $c$  and  $c'$ ) and titanium ( $d$  and  $d'$ ) in non-complexing ( $A$ ) and complexing ( $B$ ) base electrolyte. Base-line ( $a$  and  $a'$ ). Base electrolytes ( $A$ )  $0.1M$  acetic buffer (pH 4.6); ( $B$ )  $0.2M$  EDTA (pH 4.6).  $[Ti]$   $0.2\mu M$ ;  $[Pb]$   $0.1\mu M$ ;  $[Tl]$   $50\mu M$ . Preconcentration potential  $-0.800$  V; preconcentration time ( $a-c'$ ): 300 sec; ( $d$  and  $d'$ ) 0 sec.

mination,<sup>8</sup> but the matrix effect of titanium in anodic stripping voltammetry, as well as the removal of that effect, has not yet been sufficiently examined.

#### EXPERIMENTAL

##### Apparatus

A Telpod (Poland) pulse polarograph model PP-04 was used. Voltamperograms were displayed on an Endim (GDR) 620.02 XY-recorder. The differential pulse amplitude was 50 mV and the scan-rate 11.1 mV/sec. Radiometer controlled-temperature electrode equipment was used. The surface area of the hanging mercury drop was 2.1 mm<sup>2</sup>. The auxiliary electrode was a platinum wire and the reference electrode an SCE. All potentials reported in this paper were referred to the SCE.

##### Reagents

The non-ionic surfactants Triton X-100 (Merck), Rokafenol N-3 (Rokita), Pluronic F108 (Serva), poly(ethylene oxide)  $5.0 \times 10^6$  (BDH), BRIJ 35 (Riedel de Haen), Tagat 02 (Goldschmidt), Tween 80 (Schuchardt), Oxetal T105 (Zschimmer and Schwarz), the cationic surfactants  $N,N,N',N',N',N'$ -hexamethylhexamethylenediammonium bromide (HMB) (Fluka), benzyl(di-isobutylphenoxyethoxy)dimethylammonium chloride (Hyamine 1622) (Serva), hexadecyltrimethylammonium bromide (HDTMAB) (Merck), tetrabutylammonium chloride (TBAC) (Fluka), hexadecyldimethylbenzylammonium chloride (HDDMBAC) (Fluka), hexadecyltributylphosphonium bromide (HDTBPB) (Fluka), tetraphenylphosphonium bromide (TPPB) (Merck) and the anionic surfactants sodium dodecylsulphate (Serva), sodium stearate (Seva), sodium kerylbenzenesulphonate (Oswiecim), sodium dodecylbenzenesulphonate (BDH). Sulforokanol (Rokita) and Malester (Pollena-Strzemieszycze) were used without additional purification.

The supporting electrolyte was  $0.2M$  EDTA, which was usually prepared from the analytical grade reagent (POCh). However, in some experiments a purified reagent (precipitated from acidic solution<sup>9</sup>) as well as an analytical grade reagent (Merck) was used. The pH of the EDTA solutions

was adjusted with sodium hydroxide solution (Merck). The standard solutions of Tl(I) were prepared from thallium(I) nitrate and the standard solutions of titanium from titanium(III) chloride. All solutions were prepared in water triply distilled in a fused-silica apparatus.

##### Procedure

The solutions examined were deaerated by passage of purified nitrogen before measurement. In all the experiments preconcentration was done at a potential of  $-0.800$  V with the solution stirred. The voltamperograms were recorded after a 30-sec quiescent period.

#### RESULTS

##### Behaviour of titanium in surfactant-free EDTA solutions

The positions of the peaks of thallium, lead and titanium on voltamperograms in  $0.1M$  acetic buffer and in  $0.2M$  EDTA solution (in both cases pH = 4.6) are presented in Fig. 1. In the acetate buffer, i.e., the base electrolyte without strong complexing properties, titanium (curve  $d$ ) does not give a peak; however, lead gives a peak which coincides with the thallium peak (curve  $b$ ). Because in the most real samples the content of lead is much higher than that of thallium, the determination of the latter is impossible. In the EDTA solution lead (see curve  $c'$ ) does not give a peak, but there is a clear peak for titanium (curve  $d'$ ). In this case the determination of thallium is again impossible, without removal of the titanium

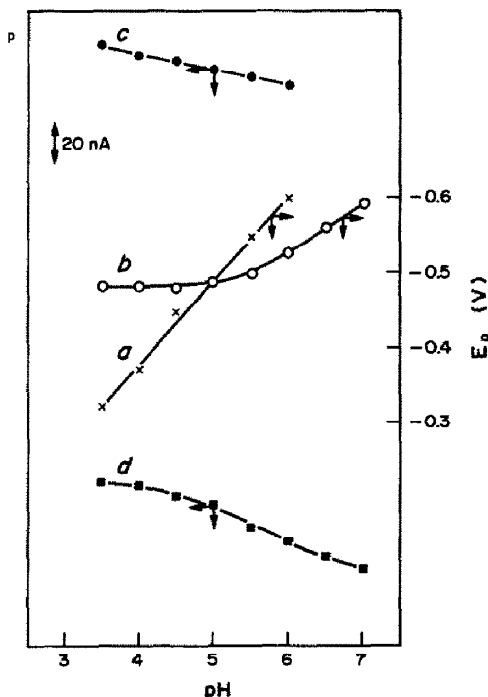


Fig. 2. Dependence of the peak potential ( $a$  and  $b$ ) and peak height ( $c$  and  $d$ ) on pH for titanium ( $a$  and  $c$ ) and thallium ( $b$  and  $d$ ) in  $0.2M$  EDTA base electrolyte.  $[Ti]$   $50\mu M$ ;  $[Tl]$   $0.1\mu M$ . Preconcentration potential  $-0.800$  V; preconcentration time ( $a$  and  $c$ ) 0 sec, ( $b$  and  $d$ ) 300 sec.



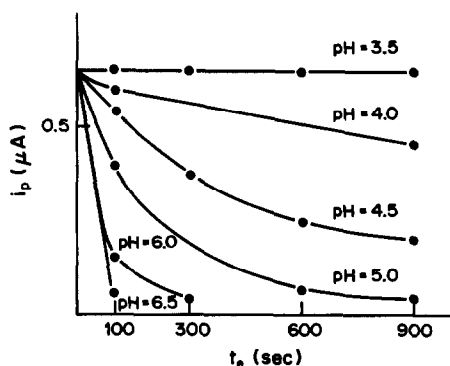


Fig. 3. Dependence of the titanium peak height on preconcentration time in EDTA solutions of different pH values. [Ti] 0.1mM. Preconcentration potential  $-0.800$  V.

peak, because the usual content of titanium is several orders of magnitude higher than the thallium content.

An attempt to remove the titanium effect by changing the pH was tried first, the pH being changed over the range 3.5–6 in increments of 0.5. Voltamperograms for titanium were recorded without preconcentration, and for thallium after 300 sec of preconcentration. The results obtained are shown in Fig. 2. Although the positions of the peaks shifted with change of pH, no great difference between the peak potentials was produced. The resolution was best at pH 3.5 (about 150 mV). Lower pH might offer more promise, but too much acidification could cause precipitation of the EDTA, on account of its relatively high concentration.

A very important role in the behaviour of the titanium peak is played by the preconcentration time. This is surprising since it seems that there is no preconcentration of titanium on the electrode surface, and therefore the preconcentration time should not influence the peak height. This effect was therefore investigated for different pH values, and preconcentration times ranging from 0 to 900 sec. The results are shown in Fig. 3 and several voltamperograms obtained for different preconcentration times at pH 5 are shown in Fig. 4 (curves *b*, *c* and *d*). It is obvious that the peak height for titanium decreases with prolongation of preconcentration time, and this effect strongly increases with pH. This behaviour suggests that blocking of the electrode surface may be occurring. Several experiments were made to find the substance which blocked the electrode surface. EDTA from different sources, or specially purified, gave very similar results. In another experiment the titanium was added after normal preconcentration for 840 sec (at pH 5), and the preconcentration was then continued for another 60 sec. The voltamperogram (Fig. 4, curve *e*) shows that the mercury surface was already blocked before the titanium was added. For this reason the titanium peak is almost completely eliminated. It should be added that in linear

sweep ASV increase of preconcentration time gives the same effect on the titanium peak.

#### *Influence of surfactants on the titanium peak*

All experiments on the influence of surfactants on the titanium peak were performed in 0.2M EDTA at pH 4.5. The preconcentration time was varied, taking into account its influence on the formation of the surfactant layer as well as the effect considered above.

The experiments with non-ionic surfactants were conducted at a titanium concentration of 0.12mM and a concentration of surfactant of 10 mg/l. Each of the non-ionic surfactants investigated causes very strong decrease of the titanium peak. An example is shown in Fig. 5, for Triton X-100. Curve *a* was obtained with a surfactant-free solution without preconcentration. Curve *b*, obtained from a solution containing Triton X-100 but also without preconcentration, shows complete disappearance of the titanium peak. The same results occur with preconcentration for 300 sec (curve *c*), but with tenfold higher recording sensitivity a small titanium

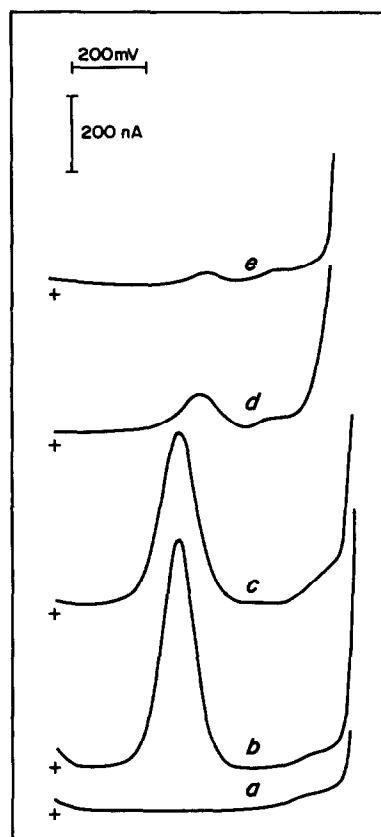


Fig. 4. Voltamperograms for 0.1mM titanium in 0.2M EDTA (pH 5.0) performed after different preconcentration times (curves *b*, *c*, *d* and *e*). Curve *a* is the base-line without titanium. Preconcentration potential:  $-0.800$  V; preconcentration time: (*a* and *b*) 0 sec, (*c*) 100 sec, (*d* and *e*) 900 sec. For curve *e* titanium was added after 840 sec of preconcentration in titanium-free base electrolyte.

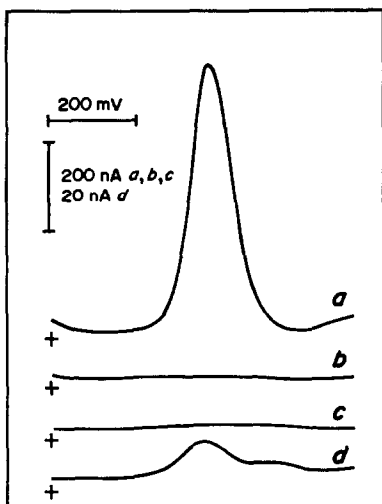


Fig. 5. Voltamperograms for 0.12mM titanium in 0.2M EDTA (pH 4.5) in the presence of 10 mg/l. Triton X-100. Curve *a* is for a surfactant-free solution. Preconcentration time (*a* and *b*) 0 sec, (*c* and *d*) 300 sec.

peak is seen (curve *d*). Such an increase in the sensitivity is necessary if very low concentrations of thallium are to be determined. At such sensitivity it is possible to compare the damping of the

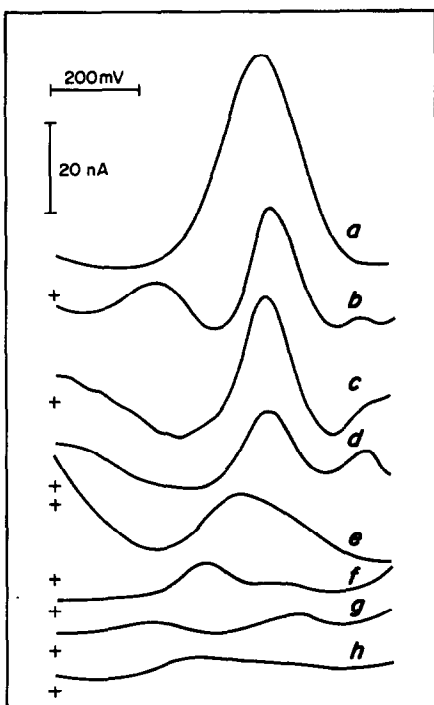


Fig. 6. Voltamperograms for 0.12mM titanium in 0.2M EDTA (pH 4.5) in the presence of 10 mg/l. concentrations of different non-ionic surfactants: (*a*) Pluronic F 108, (*b*) Tagat 02, (*c*) BRIJ 35, (*d*) PEO 5,000,000, (*e*) Oxetal T105, (*f*) Triton X-100, (*g*) Tween 80 and (*h*) Rokafenol N-3. Preconcentration potential  $-0.800$  V; preconcentration time 300 sec.

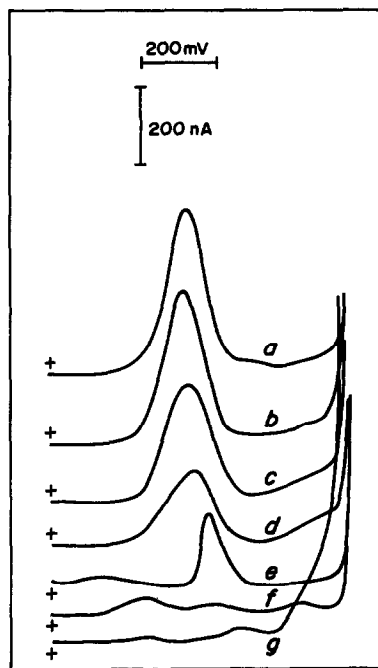


Fig. 7. Voltamperograms for 0.12mM titanium in 0.2M EDTA (pH 4.5) in the presence of 0.1mM concentration of different cationic surfactants: (*a*) TBAC, (*b*) HMB, (*c*) HDTMAB, (*d*) TPPB, (*e*) HDDMBAB, (*f*) Hyamine 1622 and (*g*) HDTBPB. Preconcentration potential  $-0.800$  V; preconcentration time 300 sec.

titanium peak by different surfactants (Fig. 6), the sequence of damping efficiency being Pluronic F-108 < Tagat 02 < BRIJ 35 < poly(ethylene glycol)  $5 \times 10^6$  < Oxetal T105 < Triton X-100 < Tween 80 < Rokafenol N-3. With Rokafenol N-3 and Tween 80 the titanium peak is almost completely damped.

The experiments with cationic surfactants were conducted with 0.12mM titanium and 0.1mM surfactant. In contrast to the non-ionic and anionic surfactants, which are generally polydisperse mixtures or technical products, the cationic surfactants used were pure substances, which justifies use of molar concentration units (0.1mM solutions of these substances contain  $\sim 10$  mg/l.) Except for TBAC and HMB, which had no damping action, the cationic surfactants only partially damp the titanium peak, their action differs considerably (Fig. 7, voltamperograms recorded at a tenth of the sensitivity used for Fig. 6). The damping efficiencies are in the sequence TBAC = HMB < HDTMAB < TPPB < HDDMBAB < Hyamine 1622 < HDTBPB. Although in the last two curves the titanium peak seems to be substantially damped, at the higher sensitivity necessary for the trace thallium determination, the base-line current would be seriously affected.

The experiments with anionic surfactants were done with 0.25mM titanium and 100 mg/l. surfactant (except concentration for sodium stearate, for which

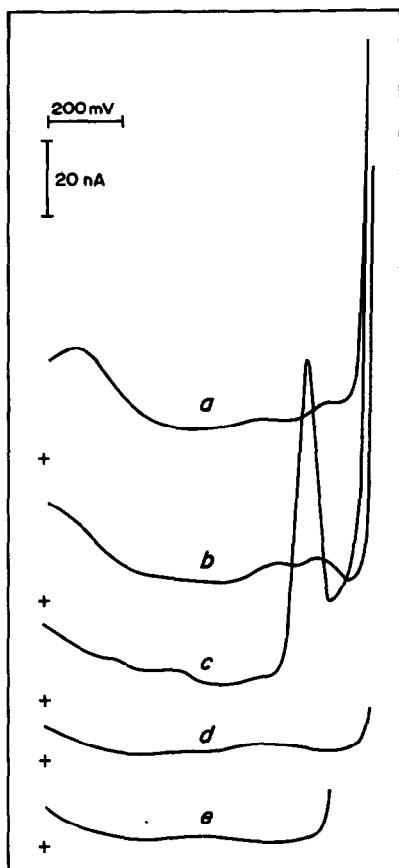


Fig. 8. Voltamperograms for 0.25mM titanium in 0.2M EDTA (pH 4.5) in the presence of different anionic surfactants: (a) sodium stearate, (b) Sulforokanol, (c) sodium dodecylbenzenesulphonate, (d) sodium dodecylsulphate and (e) Malester. Concentration of surfactant: (a) 10 mg/l., (b, c, d and e) 100 mg/l. Preconcentration potential  $-0.800$  V; preconcentration time: 300 sec.

it was 10 mg/l. because of the limited solubility). All these surfactants strongly but not completely damp the titanium peak (Fig. 8). Sodium dodecylbenzenesulphonate (curve c) gives an additional peak, which is connected with the nature of this surfactant. Sodium kerylbenzenesulphonate, which is a commercial technical product of similar structure, gives a similar effect.

As the base current for the 0.25mM titanium solution seems to be promising when an anionic surfactant is present, a series of experiments with the simultaneous presence of 10mM thallium and 0.25mM titanium was performed. The preconcentration time was 300 sec. The results obtained are shown in Fig. 9. With Sulforokanol (curve b) or sodium dodecylsulphate (curve d) present, the thallium peak is higher than in a surfactant-free solution (curve f). This is a result of the additivity of the remaining current of the incompletely damped titanium peak and the thallium peak current. With sodium stearate present (curve a) the height of the

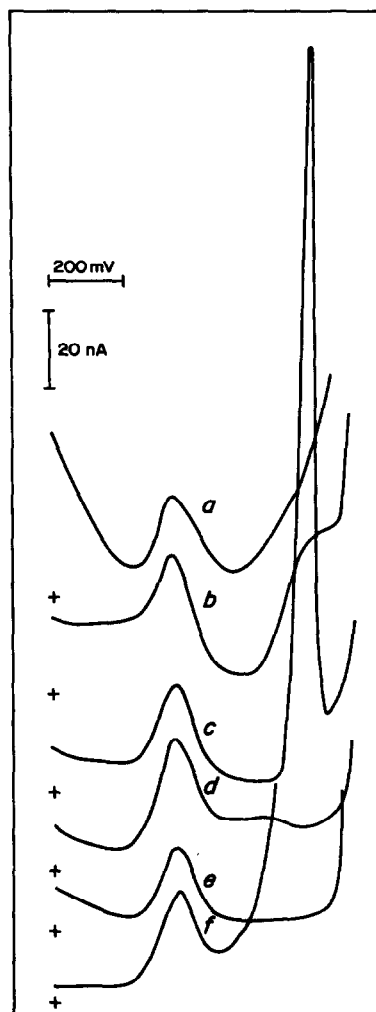


Fig. 9. Peaks for thallium in the presence of an excess of titanium in 0.2M EDTA (pH 4.5) containing different anionic surfactants: (a) sodium stearate, (b) Sulforokanol, (c) sodium kerylbenzenesulphonate, (d) sodium dodecylsulphate and (e) Malester. Curve f is for solution free from titanium and surfactant. [Ti] 10mM; [Ti] 0.25mM; [surfactant] (a) 10 mg/l., (b, c, d and e) 100 mg/l., (f) 0. Preconcentration potential  $-0.800$  V; preconcentration time 900 sec.

thallium peak is unchanged, but the base current seems disappointingly high. Sodium kerylbenzenesulphonate causes the appearance of an additional very high peak on the voltamperogram (curve c), as with pure sodium dodecylbenzenesulphonate (compare with curve c in Fig. 8); however, the position of this peak does not hinder the evaluation of the thallium peak. The base current seems better with commercial sodium kerylbenzenesulphonate than with pure sodium dodecylbenzenesulphonate. The best conditions for thallium determination are in the solution with Malester (curve e).

Iron(III) influences the base current of the voltamperograms in a similar way to titanium, i.e., it also does not undergo accumulation in the mercury drop.

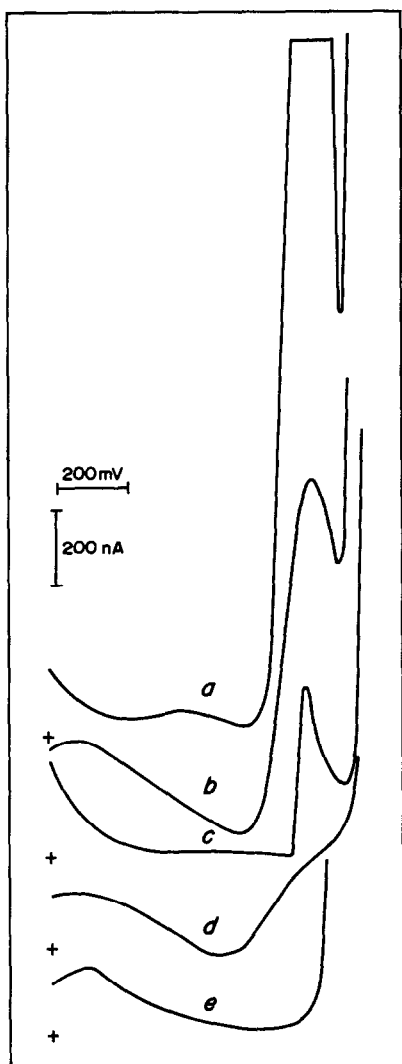


Fig. 10. Voltamperogram for 0.25mM titanium and 1mM iron(III) in 0.2M EDTA (pH 4.5) in the presence of different anionic surfactants: (a) sodium stearate, (b) Sulforokanol, (c) sodium kerylbenzenesulphonate, (d) sodium dodecylsulphate and (e) Malester. [Surfactant] (a) 10 mg/l., (b, c, d and e) 100 mg/l. Preconcentration potential  $-0.800$  V; preconcentration time 100 sec.

Moreover, the simultaneous presence of iron(III) and some surfactants causes the appearance of new injurious effects in the base current. It should be mentioned that iron(III) is almost always present in samples, which is why the investigations were undertaken with anionic surfactants and iron(III). They were performed with 1mM iron(III), 0.25mM titanium, and 100 mg/l. surfactant concentration (except for sodium stearate, the concentration of which was 10 mg/l.). The results obtained are shown in Fig. 10. The voltamperogram of the sodium stearate system (curve a) show a large peak for oxidation of iron(III) and the remains of the peak for titanium, and for this reason such conditions are unsuitable for the determination of thallium. The

curves for Sulforokanol (b) and sodium dodecylsulphate (d) also show a very bad base line current. Comparatively good base line currents are obtained with Malester (curve e) and kerylbenzenesulphonate (curve c), although in the last case an additional peak appears.

#### DISCUSSION

Almost all the surfactants investigated damped the titanium peak. This suppressive action increases in the sequence: cationic surfactants < non-ionic surfactants < anionic surfactants, but there are great differences between the effects of surfactants within a given group. A similar sequence was observed by Hoff and Jacobsen<sup>10</sup> for titanium in a citrate base electrolyte in a.c. polarography, although they found an increase in titanium peak height in the case of cationic surfactants. In our case most of the cationic surfactants damped the titanium peak, but less so than other surfactants. Jacobsen explains the difference in the action of cationic surfactants and anionic surfactants (for titanium as well as bismuth and indium) as connected with the charges of the surfactant and of the complex to be reduced on the electrode.<sup>8,10</sup> If the surfactant and the complex have the same type of charge, strong inhibition is observed, but in the opposite case, an increase in the peak or wave height can be observed. In our case titanium is present in the solution in the form of the negatively charged complex  $Ti(OH)_2Y^{2-}$ . The peak considered is caused by oxidation of the titanium(III) complex, which is probably also anionic but with lower charge. Hence in this case the effect according to Jacobsen's model appears as the much weaker damping of the titanium peak, instead of an increase in the peak. This difference can be explained as caused by the different degrees of coverage of the mercury surface with cationic surfactant in the two cases. With the DME, the mercury surface is renewed at each drop and lower surface concentrations of surfactant are achieved. In the case of the HMDE, even if there is no separate preconcentration, accumulation of the surfactant on the electrode occurs during the recording of the voltamperogram. On the other hand, it is necessary to look at the Jacobsen model slightly sceptically because there are many examples of completely opposite behaviour of the systems examined. For example, the peak for the negatively charged complex of lead(II) in EDTA solution is extremely inhibited by the positively charged TBAC.<sup>5</sup>

The reasons for the differences in behaviour of surfactants of the same charge type are very complicated. In the case of non-ionic surfactants a certain inhibiting role is played by the hydrophobicity of the surfactant. The least hydrophobic of the surfactants investigated, Pluronic F 108, which has an HLB value of 27.0, is also less efficient in terms of its inhibitory effect (see Fig. 6). The most hydrophobic, Rokafenol N-3, which has an HLB value of about 8, is the most

efficient inhibitor. Of the pair Triton X-100 and Rokafenol N-3, both of which are characterized by a similar chemical structure [they are (octyl/nonyl)-phenolpolyoxyethylene monoethers], but different lengths of the oxyethylene chain, the more hydrophobic Rokafenol N-3 damps the titanium peak more efficiently. The same is observed in the case of the oxyethylated alcohols, BRIJ 35 and Oxetal T105. The less hydrophobic BRIJ 35, which has the longer oxyethylene chain, damps the titanium peak more weakly than does the more hydrophobic Oxetal T105. Among the anionic surfactants, the sulphates seem to be less efficient inhibitors than the others. The case of sodium stearate is exceptional because of the low solubility of this surfactant in water.

The behaviour of titanium in a surfactant-free solution is also very interesting, particularly the decrease in the peak height observed when the preconcentration time is increased. This effect is more pronounced in a solution having a higher pH value, and for a pH of 3.5 is almost negligible. Undoubtedly, the surface of the electrode is blocked by a species of accidental origin. However, the question arises as to what this inhibitor is or at least what is its nature; is it a component of the base electrolyte or is it connected with the titanium? The experiment resulting in voltamperogram *e* in Fig. 4 gives a partial answer to this question. Accumulation of the inhibitor was evidenced for a titanium-free EDTA solution. The peak for the titanium added to the solution for the last 60 sec preconcentration, was almost completely damped. Hence, the inhibitor was contained in titanium-free EDTA solution. At the moment of addition of the titanium the electrode surface was already covered by a layer of unknown surfactant. That is why the damping of the titanium peak was very high in spite of the short time the titanium was present in the preconcentrated solution. Since the action of the inhibitor increases with increase in preconcentration time (see Fig. 3), there is evidence that the concentration of inhibitor in the solution is comparatively small. Otherwise the coverage of the electrode surface should be immediate and the time of preconcentration should then not play any role in the inhibition. It is also clear that the damping is pH-dependent, indicating that the concentration of inhibitor increases with increase in pH. This means that the inhibitor is the base in the acid-base couple. These properties show that the effect could not be caused by the anion  $H_2Y^{2-}$ , because its concentration is high and decreases with increase in pH. Also, other EDTA species (specifically  $HY^{3-}$  and  $Y^{4-}$ ) could not have caused the effect, because of the very quick replacement (by solution equilibria processes) of the amounts of these

species adsorbed. Hence, it seems probable that the inhibitor is some impurity of EDTA. However, there is no evidence of a significant difference in the action of EDTA from different sources. Hence, all these reagents presumably contain the inhibitor.

The effect discussed above could be useful analytically because with sufficiently long preconcentration times (which are always necessary in the determination of thallium traces) the titanium matrix effect is sufficiently lowered without the use of any additional reagents. The fact that the effect may depend on the content of an impurity in the EDTA is of no practical importance, because the action of EDTA reagents from different sources is the same. More important from the analytical point of view is the incomplete damping of the titanium peak under these conditions. That is why the effect discussed above can be used together with "electrochemical masking" by the addition of an anionic surfactant. The best of the surfactants investigated is Malester, although even in this case the base line current is not ideal. Sodium dodecylbenzenesulphonate could also be used, in spite of the additional high peak produced on voltamperograms in its presence (curve *c* in Fig. 8). Perhaps, a further search for more effective anionic surfactants would be fruitful.

A very important advantage of anionic surfactants in comparison with non-ionic surfactants is the fact that they do not cause the appearance of additional peaks in the presence of iron(III), whereas non-ionic surfactants do.<sup>11</sup> For that reason non-ionic surfactants cannot be used for "electrochemical masking" of titanium in the case of samples containing iron.

*Acknowledgement*—This work was supported by Research Program CPBP 01.17.

#### REFERENCES

1. R. D. Reeves and R. R. Brooks, *Trace Element Analysis of Geological Materials*, Wiley, New York, 1978.
2. A. Cottenie and M. Verloo, *Z. Anal. Chem.*, 1984, **317**, 389.
3. A. Wolf, P. Schramel, G. Lill and H. Hohn, *ibid.*, 1984, **317**, 512.
4. V. Gemmer-Colos, I. Kiehnast, J. Trenner and R. Neeb, *ibid.*, 1981, **306**, 144.
5. A. Ciszewski and Z. Lukaszewski, *Talanta*, 1983, **30**, 873.
6. N. You and R. Neeb, *Z. Anal. Chem.*, 1983, **314**, 394.
7. E. Görlich, Z. Kowalski and H. Przewlocka, *Chem. Anal. (Warsaw)*, 1954, **6**, 120.
8. H. K. Hoff and E. Jacobsen, *Anal. Chim. Acta*, 1971, **54**, 511.
9. A. J. Barnard Jr., E. F. Joy, K. Little and J. D. Brooks, *Talanta*, 1970, **17**, 785.
10. E. Jacobsen and H. Lindseth, *Anal. Chim. Acta*, 1976, **86**, 123.
11. A. Ciszewski and Z. Lukaszewski, to be published.

## CATALYTIC SPECTROPHOTOMETRIC DETERMINATION OF TRACE AMOUNTS OF COPPER(II) WITH 3-HYDROXY-2-NAPHTHOIC ACID

E. CASASSAS\*, A. IZQUIERDO-RIDORSA and L. PUIGNOU

Department of Analytical Chemistry, Faculty of Chemistry, University of Barcelona, Diagonal 647, 08028 Barcelona, Spain

(Received 10 November 1986. Revised 13 May 1987. Accepted 7 October 1987)

**Summary**—A very sensitive catalytic spectrophotometric method for the determination of copper(II) concentrations as low as 0.06 ng/ml is described. This method is based on the oxidation of 3-hydroxy-2-naphthoic acid by hydrogen peroxide in ammoniacal medium, catalysed by copper(II). The results of an exhaustive study of interferences are given. The new method is applied to determination of copper in atmospheric aerosol samples. A qualitative study of the mechanism by means of electron paramagnetic resonance spectroscopy is also included.

Many spectrophotometric methods that use *o*-hydroxycarboxylic aromatic compounds as reagents have been reported for the determination of trace amounts of metal ions,<sup>1-4</sup> one of the most sensitive being that of Minzl and Hainberger<sup>5</sup> for the determination of copper(II) with salicylic acid and hydrogen peroxide in ammoniacal medium, with a detection limit of 5 ng/ml. Examination of other *o*-hydroxycarboxylic aromatic acids in that system has led to a new and more sensitive procedure for copper(II) determination, with 3-hydroxy-2-naphthoic acid (HNA) as reagent. Copper(II) concentrations lower than 1 ng/ml can be determined.

Many catalytic methods have been proposed for copper(II) determination. In most, high sensitivity is accompanied by poor selectivity,<sup>6-9</sup> usually because several transition metal ions show similar catalytic effects. Methods with good selectivity usually have poor limits of detection.<sup>10,11</sup> The new method has good selectivity as well as high sensitivity, the only interferent ion being iron(III).

The reddish colour produced in the reaction may be due to an oxidation product of the 3-hydroxy-2-naphthoic acid. Minzl and Hainberger, however, reported that a salicylatocopper(III) complex was the compound responsible for the reddish colour developed in their procedure. As no other copper(III) complexes of aromatic *o*-hydroxycarboxylic acids have been described, some measurements have been made by electron paramagnetic resonance (EPR) spectroscopy to determine whether a salicylatocopper(III) complex actually forms, and to ascertain whether an analogous compound is produced in the 3-hydroxy-2-naphthoate system or the colour is due to oxidation of the organic reagent, catalysed by copper(II), as our results seem to suggest.

### EXPERIMENTAL

#### Instrumentation

Beckman Acta M-VII double-beam spectrophotometer equipped with 1-cm silica cells. Radiometer PHM 64 pH-meter, with a Radiometer GK 2401 B combined electrode (glass electrode plus saturated calomel electrode). Electron paramagnetic resonance spectrometer (Varian E.P.R. E-109 E), equipped with silica cells (Varian E-248) and coupled to an HP 9835 B microcomputer. Atomic-absorption spectrophotometer, Perkin-Elmer 4000.

#### Chemicals

3-Hydroxy-2-naphthoic acid (Merck) was purified by precipitation with water from ethanolic solutions treated with active charcoal. Hydrogen peroxide 30% (Fluka). Copper(II) oxide (Merck). All chemicals and metal salts were of analytical-reagent grade. Ultrapure water with a resistivity of 18.3 M $\Omega$ /cm was obtained from a Culligan Water Purification System.

#### Solutions

Copper(II) stock solution, 480  $\mu$ g/ml, was prepared from copper oxide and distilled nitric acid, standardized iodometrically, and diluted with ultrapure water as required. 3-Hydroxy-2-naphthoic acid solution, 0.4M in 15% v/v (8.6M) ammonia solution. Hydrogen peroxide solution, 2%. The last two solutions must be prepared daily. Pyrex glassware and polypropylene volumetric ware, cleaned according to the most stringent standards,<sup>12</sup> was used throughout.

#### Procedure

Into a 100-ml glass-stoppered standard flask, introduce 1.00 ml of test solution containing between 6 and 60 ng of copper(II), followed by 2.00 ml of 2% hydrogen peroxide solution and 5.00 ml of the 3-hydroxy-2-naphthoic acid solution. Heat the flask and its contents for 20 min in a water-bath maintained at 80°. Cool, make up to the mark with ultrapure water and mix. After 15 min, read the absorbance at 425 nm against a blank, prepared in the same way but with 1.00 ml of ultrapure water instead of the copper(II) solution. Read the copper(II) concentration from a calibration graph prepared by treating copper(II) standards in the same way, or use the standard-additions method.

\*To whom correspondence should be addressed.

*Analysis of aerosol samples*

Mineralize the filter containing the aerosol sample (or an appropriate fraction of the filter) with concentrated nitric acid (Merck, p.a.) on a hot-plate, dilute the solution, filter it through a Whatman No. 41 paper and evaporate the filtrate to dryness. Dissolve the residue in 5 ml of 7–8*M* hydrochloric acid, transfer the solution into an extraction tube and extract it twice with 5-ml portions of di-isopropyl ether. Transfer the aqueous phase into a 50-ml standard flask, dilute to the mark with water and determine the copper in a 1-ml aliquot as above.

**RESULTS AND DISCUSSION***Absorption spectrum*

The absorption spectrum of the reaction product is given in Fig. 1. It exhibits absorption maxima at 390 and 425 nm. The maximum at 390 nm is irreproducible because it represents the difference between two strong absorptions. For analytical purposes, the absorbance at 425 nm must be used. In the Minzl and Hainberger method the absorbance is read at 376 nm, on the rising portion of an absorption band.

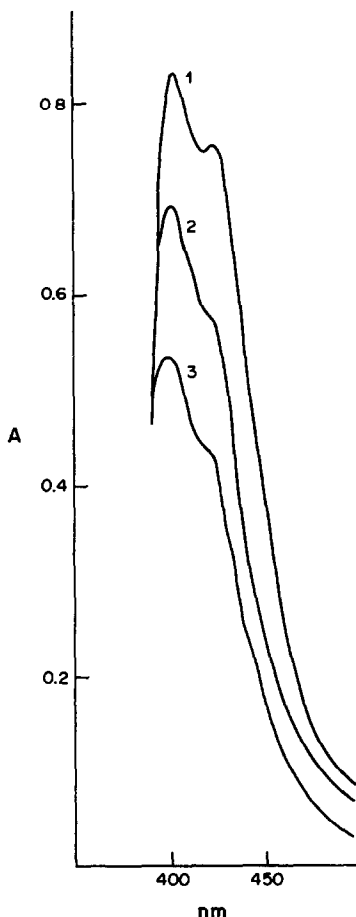


Fig. 1. Absorption spectrum of the reaction solution against its blank. [HNA] = 0.020*M*; [H<sub>2</sub>O<sub>2</sub>] = 0.04%. 1, [Cu(II)] = 0.039 μg/ml; 2, [Cu(II)] = 0.029 μg/ml; 3, [Cu(II)] = 0.019 μg/ml.

Table 1. Effect of hydrogen peroxide concentration on absorbance at 425 nm; [Cu(II)] = 0.96 ng/ml; [HNA] = 0.025*M*

H <sub>2</sub> O <sub>2</sub> , %	A*
0	0
0.005	0.553
0.01	0.896
0.02	1.046
0.03	1.104
0.04	1.153
0.06	1.149
0.10	1.023
0.18	0.877
0.30	0.441
0.60	0.224

\*Absorbance of the copper(II)-containing solution against a blank.

Because of the high absorbance of the reference blank, the reaction solution must be diluted as stated in the *Procedure* to bring the absorbance into a measurable range.

*Effect of reagent concentrations*

Table 1 shows that the net absorbance is maximal with a final hydrogen peroxide concentration in the range 0.04–0.06%.

The absorbance is strongly dependent on the final concentration of 3-hydroxy-2-naphthoic acid up to 0.020*M*, above which it is constant. Because of the high absorbance of the reference blank at the working wavelength, use of the lower limit of this constancy range, 0.020*M*, is best. The reagent must be dissolved in 8.6*M* ammonia to prevent its precipitation.

The coloured product is also obtained when tris-(hydroxymethyl)aminomethane, dimethylamine or methylamine is used as the base, but use of 0.5*M* sodium hydroxide, 60% ethylenediamine solution, or 15% monoethanolamine, diethanolamine or triethanolamine solutions fails to produce the reaction. Other nitrogen bases, such as pyridine, do not show the activating effect reported for other catalytic reactions, *e.g.*, the oxidation of hydroquinone by hydrogen peroxide proposed by Dolmanova *et al.*<sup>13</sup> in one of the best existing methods for copper determination.

*Effect of temperature and heating time*

In the range of copper(II) concentrations used in the procedure, the coloured reaction product is not formed at room temperature. As Table 2 shows, the absorbance increases exponentially with temperature. An analogous increase is observed for the blank solutions. A reaction temperature of 80° has been adopted as a compromise but rigorous control of the temperature and duration of heating is essential if reproducible results are to be obtained. Heating for 20 min is convenient.

Table 2. Effect of temperature on absorbance at 425 nm; [Cu(II)] = 0.96 ng/ml; [HNA] = 0.025M; [H<sub>2</sub>O<sub>2</sub>] = 0.3%

Temperature, °C	A
17	0.000
38.5	0.021
60.5	0.132
77	0.404
82	0.669
92	1.445

After the solutions have been heated, the absorbance continues to increase for a while, but measurements can be made about 15 min after the end of the heating, when the absorbance has become stable.

#### Calibration graph

The relationship between absorbance and copper(II) concentration in the final solution is linear from 0.06 to 1.0 ng/ml but the calibration line does not pass through the origin.

The detection limit, evaluated according to the IUPAC convention,<sup>14</sup> was 0.046 ng/ml, and the quantification limit (evaluated as 10 times the copper concentration corresponding to the standard deviation of the blank absorbance) was 0.22 ng/ml. The relative standard deviation for 0.29 ng/ml copper (8 replicates) was 4%.

The sensitivity, expressed as the slope of the calibration function, was very high,  $1.07 \times 10^8$  l./mole. In spite of the high blank and lengthy heating time, features it has in common with the MnZl and Hainberger procedure, the new method has the practical advantages of a lower detection limit and higher sensitivity.

Table 3. Study of interferences; [Cu(II)] = 0.29 ng/ml; [HNA] = 0.020M; [H<sub>2</sub>O<sub>2</sub>] = 0.04%

Ion	Limiting concentration ratio, interfering ion:Cu(II)
Fe(III)	10:1
Zn(II)	10 <sup>3</sup> :1
Pb(II)	10 <sup>3</sup> :1
Co(II)	10 <sup>3</sup> :1
Ni(II)	10 <sup>2</sup> :1
Mn(II)	10 <sup>2</sup> :1
Cr(III)	10 <sup>3</sup> :1
Ce(IV)	10 <sup>2</sup> :1
PO <sub>4</sub> <sup>3-</sup>	10 <sup>3</sup> :1
S <sub>2</sub> O <sub>8</sub> <sup>2-</sup>	10 <sup>2</sup> :1
Citrate	10 <sup>2</sup> :1
Tartrate	10 <sup>2</sup> :1

\*Other ions that do not interfere at the levels studied are: Al(III), Ca(II), Mg(II), Hg(II), Sr(II), Ba(II), K(I), Na(I), AsO<sub>4</sub><sup>3-</sup>, acetate, F<sup>-</sup>, Cl<sup>-</sup>, NO<sub>3</sub><sup>-</sup>, EDTA, oxalate, I<sup>-</sup>, SCN<sup>-</sup>, SO<sub>4</sub><sup>2-</sup>.

#### Interferences

The effect of about 30 foreign ions has been investigated; Table 3 shows the tolerable concentration ratios to copper, the criterion of interference being a relative deviation of 4% in the absorbance for a solution containing 0.29 ng/ml copper(II). The results in Table 3 show that, of the cations investigated, Fe(III) interferes seriously, when present in 10-fold w/w ratio to copper. Ni(II), Mn(II) and Ce(IV) interfere at 100-fold ratio to copper. All other metal ions studied do not interfere at the levels tested. Among the anions, peroxodisulphate, citrate and tartrate interfere when they are present in 100-fold ratio to copper. Citrate and tartrate decrease the absorbance, probably by formation of a copper(II) complex, whereas peroxodisulphate, which is a strong oxidant, causes the absorbance to increase.

#### Application of the method to atmospheric aerosol samples

The method was applied to analysis of some atmospheric aerosol samples, which were also analysed by standard AAS methods.<sup>12</sup> The samples were collected on glass-fibre filters in a high-volume sampler for 24-hr periods, at a suburban sampling point (Molins de Rei, Barcelona) near to a heavy-traffic highway. The average contents ( $\mu\text{g}/\text{m}^3$ ) in the samples collected were: Cu 0.30, Zn 19, Cd 0.07, Pb 1.27, Ca 7.3, Mg 0.6, Fe 5.5, Mn 0.1.

For copper(II) determination by AAS the whole sample was needed; the much more sensitive catalytic method required only a small fraction of the 24-hr sample and dilution steps, or even of a sample collected in a much shorter period of time (actually, the full procedure can be performed on a tenth of a sample collected in 1 hr). This is an important advantage of the present method, if the interest is mainly in fluctuations of concentration with time, rather than daily average.

When the aerosol sample contains iron, its interfering effect cannot be masked by addition of fluoride, EDTA or other common masking agents, but can be eliminated by prior extraction of the iron with di-isopropyl ether from strongly acidified solutions.

Table 4 shows the AAS results for copper(II) in three different 24-hr samples, together with the results obtained by the new method for samples collected between 9 and 10 a.m. on the days concerned. All the

Table 4. Copper(II) contents of some urban atmospheric aerosol samples

Sample number	Copper(II) content, $\mu\text{g}/\text{m}^3$	
	AAS (24-hr sample)	New method (1-hr sample)
1	0.29	0.42
2	0.18	0.23
3	0.15	0.24



Table 5. Recovery of copper(II) added to some atmospheric aerosol samples

Sample number	Cu(II) added*, ng/ml	Cu(II) found*, ng/ml	Recovery, %
4	0	0.31 ± 0.02	
4	0.13	0.43 ± 0.01	92
5	0	0.41 ± 0.01	
5	0.13	0.56 ± 0.02	115

\*Concentrations in the spectrophotometer cell.

results are the means of 4 determinations. Although the values obtained from both methods are of the same order of magnitude, the differences observed in Table 4 are relatively important. They are probably due to differences between hourly and daily averages.

Table 5 shows the results (also means of 4 determinations) obtained for 1-hr samples, before and after the addition of known amounts of copper. The recovery is good. The individual values which were averaged did not differ by more than  $\pm 8\%$  from these means. This is consistent with the expected precision of the method when it includes an extraction step.

#### Mechanism of the chemical process

Copper(II) ions are paramagnetic and give an EPR signal<sup>15-18</sup> split into four lines due to the coupling of the unpaired electron with the copper nucleus. Copper(III) ions are diamagnetic and do not give an EPR signal.

Figure 2 shows the EPR spectrum (curve A) for a solution containing 3-hydroxy-2-naphthoic acid, hydrogen peroxide and copper(II) nitrate in 3%

ammonia, in which the reaction has taken place. Curve B shows the spectrum for a solution identically prepared and processed, except that it does not contain hydrogen peroxide. Both spectra were recorded 1 hr after the solutions had been prepared. Three important features are observable. (a) The four bands ( $g$  about 2.14) have the same total area in each spectrum. This shows that the reaction does not alter the copper(II) concentration and that there is no appreciable formation of a copper(III) complex. (b) In spectrum A there are five additional sharp lines that appear at a higher field ( $g = 2.0062$ ), which suggests the appearance of a new species containing an unpaired electron. This is consistent with the formation of an organic free radical obtained by the oxidation of 3-hydroxy-2-naphthoic acid. The low intensity and the area ratios (approximately 1:4:6:4:1) of these bands show that only a small fraction of the 3-hydroxy-2-naphthoic acid is present as a free radical and that the unpaired electron is coupled with four equivalent hydrogen atoms. (c) The form of the four bands in spectrum A does not suggest the existence of a complex between copper(II) and the new organic compound formed. These bands are due only to the copper(II) complexes which are formed in solutions containing ammonia and 3-hydroxy-2-naphthoic acid.

Features (a) and (c) are also applicable to the salicylate system, but feature (b) is not: the EPR spectrum obtained after the reaction has taken place does not show the existence of a new species containing an unpaired electron. This must imply, if the mechanism of the reaction is the same for both systems, that for the salicylate system the radical

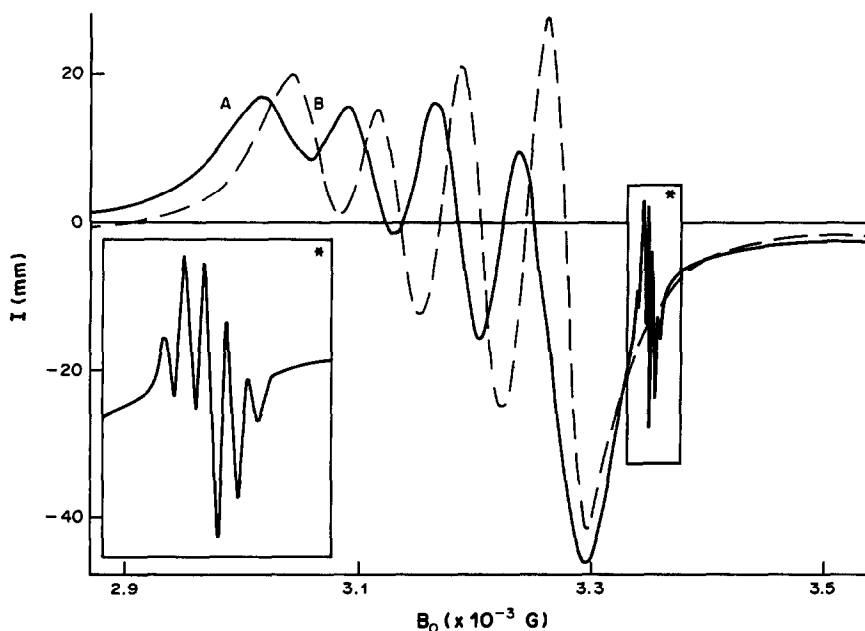


Fig. 2. Electron paramagnetic resonance spectra. Solution A  $[\text{Cu(II)}] = 10^{-2} M$ ;  $[\text{H}_2\text{O}_2] = 0.3\%$ ;  $[\text{HNA}] = 0.08 M$ ;  $[\text{NH}_3] = 1.72 M$ . Solution B  $[\text{Cu(II)}]$ ,  $[\text{HNA}]$ ,  $[\text{NH}_3]$  as in Solution A, hydrogen peroxide absent. (The signal at  $B_0 = 3.39 \times 10^3 G$  is shown at a higher amplification in the insert.)

formed is unstable and rapidly reacts to yield a stable molecule.

All the results obtained confirm the catalytic nature of the reaction, which is the oxidation of the organic reagent. The first step in the reaction is the decarboxylation of the organic acid, catalysed by copper(II).<sup>19-21</sup> This is shown by the fact that the chromogenic reaction also takes place when 3-hydroxy-2-naphthoic acid is replaced by 2-naphthol. The fact that there is no formation of a copper(II) complex with the oxidation product is a further proof of the absence of the chelating carboxylate group.

Aromatic compounds with free phenolic groups are oxidized in basic media in the presence of a transition metal ion. This catalyses the reaction, giving oxidative coupling reactions,<sup>22-24</sup> with radical intermediates. The reaction under study takes place in a similar way, yielding a stable free radical intermediate which is highly coloured due to electron delocalization. This intermediate eventually leads to a stable, highly coloured final product. Both compounds contribute to the colour developed in the reaction.

Further investigations are being carried out to elucidate the nature of the free radical and the final oxidation product.

*Acknowledgement*—The authors gratefully acknowledge Professor Manuel Ballester's fruitful discussions.

#### REFERENCES

1. A. I. Cherkasov and T. S. Zhigalkina, *Tr. Astrakh. Tekh. Inst. Rybn. Prom. Khoz.*, 1962, **8**, 25.
2. S. L. Gupta and R. N. Soni, *J. Indian Chem. Soc.*, 1966, **43**, 473.
3. *Idem, ibid.*, 1967, **44**, 195.
4. *Idem, J. Inst. Chem. (India)*, 1968, **40**, 126.
5. E. Minzl and L. Hainberger, *Mikrochim. Acta*, 1975 **II**, 353.
6. K. Khalifa, *Analyst*, 1970, **95**, 207.
7. A. A. Alexiev, P. R. Bontchev and S. Gantcheva, *Mikrochim. Acta*, 1976 **II**, 487.
8. J. L. Ferrer-Herranz and D. Pérez-Bendito, *Anal. Chim. Acta*, 1981, **132**, 157.
9. S. Hiraoka and D. Yamamoto, *Bunseki Kagaku*, 1983, **32**, 434.
10. M. N. Orlova, *Vopr. Med. Khim.*, 1972, **17**, 16.
11. V. F. Toropova, M. G. Gabdullin, A. R. Garifzyanov and R. A. Cherkasov, *Zh. Analit. Khim.*, 1984, **39**, 267.
12. Method No. P. & CAM 173, *General Procedure for Metals*, Vol. 5, N.I.O.S.H. *Manual of Analytical Methods*, 1979.
13. I. F. Dolmanova, O. I. Mel'nikova, G. I. Tsizin and T. N. Shekhovtsova, *Zh. Analit. Khim.*, 1980, **35**, 728.
14. I.U.P.A.C., *Compendium of Analytical Nomenclature, Definitive Rules 1977*, Pergamon Press, Oxford, 1978.
15. J. F. Boas, R. H. Dunhill, J. R. Pilbrow, R. C. Srivastava and T. D. Smith, *J. Chem. Soc. A*, 1969, 94.
16. B. A. Goodman, D. B. McPhail and H. K. J. Powell, *J. Chem. Soc. Dalton*, 1981, 822.
17. E. R. Werner and B. M. Rode, *Inorg. Chim. Acta*, 1984, **91**, 217.
18. R. Tauler, E. Casassas and B. M. Rode, *ibid.*, 1986, **114**, 203.
19. D. M. Hughes and J. C. Ried, *J. Org. Chem.*, 1949, **14**, 522.
20. A. Cairncross, J. R. Roland, R. M. Henderson and W. A. Sheppard, *J. Am. Chem. Soc.*, 1970, **92**, 3187.
21. B. M. Trost and P. L. Kinson, *J. Org. Chem.*, 1972, **37**, 1273.
22. T. J. Stone and W. A. Waters, *J. Chem. Soc.*, 1964, **213**, 4302.
23. D. Barton, *Chem. in Britain*, 1967, **3**, 330.
24. D. G. Hewitt, *J. Chem. Soc. C*, 1971, 1750.

## CHEMICAL AND ELECTROCHEMICAL BEHAVIOUR OF NITRIC AND NITROUS ACIDS IN SULPHOLANE

A. BOUGHRIET\* and M. WARTEL

Laboratoire de Chimie Analytique et Marine, Université des Sciences et Techniques de Lille,  
Flandres-Artois, 59655 Villeneuve d'Ascq Cedex, France

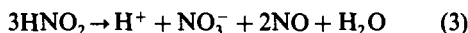
(Received 30 June 1986. Revised 22 September 1987. Accepted 3 October 1987)

**Summary**—With a glass electrode filled with mercury as indicator electrode for hydrogen ions, the acidity constant of nitric acid and the stability constants of the complexes  $HA_2^-$  ( $A = Cl^-, NO_3^-$ ) in sulpholane at 303 K have been determined potentiometrically. The acidity constant of nitrous acid has also been determined in sulpholane medium because of the low stability of this acid in aprotic media. On the basis of the results, some aspects of the electrochemical and thermodynamic properties of oxygen-nitrogen compounds are discussed in order to explain the catalytic effect of  $NO^+$  in aromatic nitration by  $N_2O_4$  and/or  $N_2O_3$  in aprotic solvents.

The dissociation constants  $K_A$  of nitrous and nitric acids:



are of interest<sup>1</sup> as a link in the determination of equilibria involving oxides of nitrogen such as  $NO_2$ ,  $NO$ ,  $N_2O_3$ ,  $N_2O_4$ . The species  $HNO_3$  is a strong acid in dilute acid media:<sup>2,3</sup>  $pK_A = -1.3$  at 298 K.<sup>2</sup> Sampoli *et al.*<sup>4</sup> have shown that the value of  $pK_A(HNO_3)$  in concentrated acid solutions [or non-ideal acid media,  $pK_A(HNO_3) = -1.9$ ] appears not to be very different from the  $pK_A$  data in the literature<sup>5-11</sup> or determined in ideal acid media.<sup>2,3</sup> Nitrous acid is a relatively weak acid in dilute acid solution, with  $pK_A(HNO_2)$  reported as 3.0-3.5.<sup>4,12-16</sup> Moreover, the instability of  $HNO_2$  in dilute acid media to disproportionation by the reaction



complicates the chemical phenomena.<sup>1</sup> The kinetics of this decomposition has been examined in detail by Abel and Schmid.<sup>17</sup> Furthermore, under a pressure of 1 atm of  $NO$ ,  $HNO_2$  can be considered a stable species.<sup>1</sup> The chemical behaviour of  $HNO_3$  and  $HNO_2$  in acid media has also been of interest in the interpretation of the mechanism of diazotization of amines<sup>18</sup> and nitration of aromatics.<sup>19-24</sup>

In aprotic solvents such as acetonitrile, nitromethane, dimethylsulphoxide and sulpholane, the acidity of protic acids<sup>2,3,25-27</sup> has been found to be much weaker than in aqueous or acid media.<sup>2,3,14</sup> This phenomenon is mainly due to the weak solvating character of these solvents relative to that of water, as suggested by Gutmann *et al.*<sup>28,29</sup> Thus, aromatic compounds undergo nitration under mild conditions

on treatment with oxygen-nitrogen compounds in these solvents.<sup>30-42</sup> In view of the difficulties which have arisen (because of the occurrence of several equilibria involving the solvent molecule) when working with diluted nitrating agents in acid medium to obtain critical mechanistic information, it appears that aromatic nitration by  $N_2O_4$  and/or  $N_2O_3$  in the presence of a catalytic precursor in aprotic media is a potentially valuable means of preparing nitrated aromatic compounds.<sup>33-37,42</sup> The explanation of the nitration mechanism necessitates knowledge of the electrochemical and thermodynamic properties of oxygen-nitrogen compounds, and especially the acidity constants of nitric and nitrous acids. Likewise, these acidity constants are important for interpretation of numerous electrochemical processes in aprotic media.<sup>43-45</sup>

These considerations have led us to undertake the determination of the acidity constants of  $HNO_3$  and  $HNO_2$  in aprotic media.

### EXPERIMENTAL

#### Chemicals

The purification of sulpholane (Prolabo) has already been described.<sup>26</sup> Prior to use, the solvent was filtered through a dry alumina column under argon (neutral alumina dried in a vacuum at 573 K for one week). Pure nitric acid was prepared by distillation of fuming nitric acid under reduced pressure.<sup>46</sup> Piperidine was distilled under reduced pressure, and the distillate was passed through a column of dry alumina. The  $HCl$  gas was prepared by heating sodium chloride with orthophosphoric acid. Solutions of hydrogen chloride in sulpholane were obtained by passing a slow stream of the  $HCl$  gas (dried by passage through a column filled with phosphorus pentoxide) through weighed amounts of this solvent. The concentration of the solution was established by weighing to find the amount of  $HCl$  dissolved, and also by dissolving a known volume of the solution in water and titrating the acid with a standard base.

#### Procedures

Voltammetric half-wave reduction potential measurements were made with a Tacussel PRT 20-10 potentiostat in

\*Author for correspondence.

combination with a Tacussel UAP4 universal programmer. Rotating-disc electrode voltamperograms were recorded on a Sefram TGM 164 X-Y recorder. The cell and electrodes used for the voltammetric measurements were very similar to those described in previous publications.<sup>44,47</sup>

Potentiometric measurements were made by means of a Tacussel ISIS 20000 millivoltmeter which was combined with a Tacussel EPL 2 recorder in order to follow the stability of the derivative ( $dE/dt$ ). The indicator electrode was a mercury-filled glass electrode (Tacussel Hg B10).

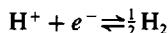
All the potentiometric experiments were performed with a watertight cell kept at  $303.0 \pm 0.2$  K in a water-jacketed vessel. Stirring was continuous during the titration. A 2-ml Gilmont microburette was used for the addition of the basic titrant (piperidine) to avoid introduction of moisture.

All potentials were referred to the half-wave oxidation potential of a ferrocene solution in sulpholane. This  $E_{1/2}$  potential can be taken as the origin of the potential scale (as suggested by Koepf *et al.*<sup>48</sup>).

All manipulations of materials and preparation of solutions were performed in an efficient dry-box. The water content in the sulpholane was determined by an automatic Karl Fischer titration before use.

## RESULTS AND DISCUSSION

First, using a voltammetric technique, we studied the electrochemical properties of  $\text{HNO}_3$  and  $\text{HNO}_2$  at the Pt electrode in aprotic media. As mentioned previously,<sup>49-51</sup> the  $\text{HNO}_3$  and  $\text{HNO}_2$  species undergo the following reactions in these solvents:



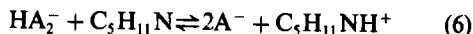
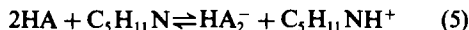
However, the overall processes are not reversible, and it has not been possible to use them to determine the acidity constants of  $\text{HNO}_2$  and  $\text{HNO}_3$  by this method. We then attempted to analyse  $\text{HNO}_3$  solutions potentiometrically after addition of a strong base solution in an aprotic solvent. This method has allowed us to follow the differences in acidity of this medium by measuring the variation of potential between a glass electrode and the  $\text{Ag}/\text{Ag}^+$  reference electrode.

Analytically pure nitric acid solutions in sulpholane have been studied potentiometrically with the mercury-filled glass electrode as indicator electrode for hydrogen ions.<sup>52</sup> The equilibrium potential is given by

$$E = E^\circ + \frac{RT}{F} \ln[\text{H}^+] \quad (4)$$

This electrode had been used extensively in non-aqueous media for the determination of acidity constants.<sup>52</sup> However, Coetzee and Bertozzi<sup>53</sup> noted that the glass electrode gave poor performance in the electrochemical study of a strong acid such as  $\text{HSbCl}_6$  in aprotic media. We have chosen to take the acidity constant  $\text{p}K_{\text{HCl}}^{\text{H}^+}$  of the weak acid HCl in sulpholane as the origin of the  $\text{p}K$  scale ( $\text{p}K_{\text{HCl}}^{\text{H}^+} = 14.5$ , determined by Coetzee and Bertozzi<sup>53</sup>). Thus, we have examined the neutralization of an  $\text{HNO}_3$  solution by a piperidine solution (which is one of the stronger of

the weak bases in sulpholane), with 0.1M tetraethylammonium perchlorate as supporting electrolyte (Fig. 1). The curve for potentiometric titration of HCl with piperidine in sulpholane is also reported in Fig. 1. Since the potentiometric curve for the  $\text{HNO}_3$  titration lies below that for the HCl titration, we can already affirm that  $\text{HNO}_3$  is a weaker acid than HCl in sulpholane, *i.e.*,  $\text{p}K_{\text{HNO}_3}^{\text{H}^+} > \text{p}K_{\text{HCl}}^{\text{H}^+}$ . On each of these curves, two potential jumps occur at [piperidine]/[acid] ratios equal to 0.5 and 1.0. This observation proves the formation of the  $\text{HA}_2^-$  species ( $\text{A} = \text{NO}_3, \text{Cl}$ ) as mentioned previously by Alder *et al.*<sup>54</sup> in the case of HCl. We can therefore write the reactions



The Nernst equation, applied to reactions (5) and (6), gives

$$\begin{aligned} E &= E^\circ(2\text{AH}) + \frac{RT}{F} \ln \frac{[\text{HA}]^2}{[\text{HA}_2^-]} \\ &= \left[ E^\circ + \frac{RT}{F} \ln K_{2\text{AH}}^{\text{H}^+} \right] + \frac{RT}{F} \ln \frac{[\text{AH}]^2}{[\text{HA}_2^-]} \quad (7) \end{aligned}$$

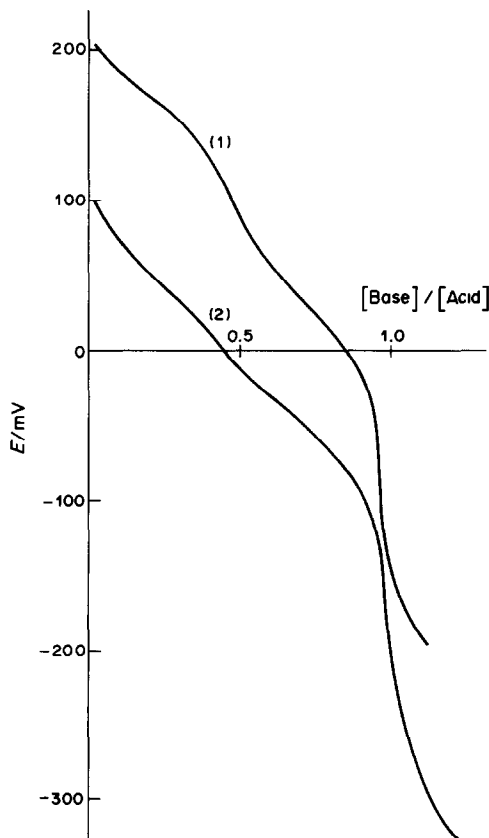


Fig. 1. Neutralization curves (glass indicator electrode filled with mercury) of  $\text{HNO}_3$  and HCl (0.020M) with 0.2M piperidine solution in sulpholane at 303 K: (1) HCl (2)  $\text{HNO}_3$ . Supporting electrolyte 0.1M  $(\text{C}_2\text{H}_5)_4\text{NClO}_4$

Table 1. Values of the acidity constants  $K_{AH}^{H^+}$  and  $K_{HA_2^-}^{H^+}$  corresponding to the reactions  $AH \rightleftharpoons A^- + H^+$  and  $HA_2^- \rightleftharpoons H^+ + 2A^-$  respectively ( $A = NO_3$  and Cl), in sulpholane at 303 K (references in parentheses)

Equilibria	HClO <sub>4</sub>	HSO <sub>3</sub> F	HSO <sub>3</sub> Cl	H <sub>2</sub> S <sub>2</sub> O <sub>7</sub>	H <sub>2</sub> SO <sub>4</sub>	HCl	HNO <sub>3</sub>	HNO <sub>2</sub>
$AH \rightleftharpoons A^- + H^+$ $pK_{AH}^{H^+}$	2.7 (55) 3.0 (25)	3.3 (55)	4.4 (26)	5.0 (26)	12.9 (56)	14.5 (25)	16.0 ± 0.6	~20.6
$HA_2^- \rightleftharpoons H^+ + 2A^-$ $pK_{HA_2^-}^{H^+}$	—	—	—	—	16.4 ± 0.4	17.5 ± 0.5	18.6 ± 0.8	—
$E_{1/2}, V^*$	-0.45 ± 0.03	—	—	-0.60 ± 0.03	-0.60 ± 0.03	-0.65 ± 0.04	-0.80 (43)	-1.45 (43)

\*Versus the half-wave potential of the ferrocene/ferricinium couple. The  $E_{1/2}$  value for reduction of the proton of AH is obtained with 0.01M AH solutions in sulpholane.

and

$$E = E^\circ(HA_2^-) + \frac{RT}{F} \ln \frac{[HA_2^-]}{[A^-]^2}$$

$$= \left[ E^\circ + \frac{RT}{F} \ln K_{HA_2^-}^{H^+} \right] + \frac{RT}{F} \ln \frac{[HA_2^-]}{[A^-]^2} \quad (8)$$

where  $K_{2AH}^{H^+}$  and  $K_{HA_2^-}^{H^+}$  are the acidity constants for the reactions  $2AH \rightleftharpoons HA_2^- + H^+$  and  $HA_2^- \rightleftharpoons 2A^- + H^+$ , respectively. The standard potentials  $E^\circ(2AH)$  and  $E^\circ(HA_2^-)$  are expressed as a function of  $E^\circ$ ,  $K_{2AH}^{H^+}$  or  $K_{HA_2^-}^{H^+}$ . In order to establish the reversibility of the electrochemical processes, we studied the two sections of each potentiometric curve, corresponding to reactions (5) and (6). We found a linear  $E$  vs.  $\log[x/(1-2x)^2]$  plot for  $0 < x < 0.5$  (1st wave) and  $E$  vs.  $\log[(1-x)/(2x-1)^2]$  plot for  $0.5 < x < 1$  (2nd wave), where  $x$  is the concentration ratio [piperidine]/[acid] during the titration. The line slope is equal to  $55 \pm 3$  mV/log unit, which is near the theoretical value of  $2.303RT/F$ . Thus, the standard potentials  $E^\circ(2AH)$  and  $E^\circ(HA_2^-)$  can be calculated by extrapolation of the linear plots. Hence, the two potential differences:

$$\Delta E_1 = E^\circ(2AH) - E^\circ(HA_2^-)$$

$$= \frac{RT}{F} \ln \frac{K_{2AH}^{H^+}}{K_{HA_2^-}^{H^+}} = -\frac{RT}{F} \ln K_{AH}^*$$

and

$$\Delta E_2 = E^\circ[H(NO_3)_2^-] - E^\circ(HCl_2^-)$$

$$= \frac{RT}{F} \ln \frac{K_{HNO_3}^{H^+}}{K_{HCl_2^-}^{H^+}} = \frac{RT}{F} \ln \frac{K_{HNO_3}^{H^+} K_{HNO_3}^*}{K_{HCl}^{H^+} K_{HCl}^*}$$

allow us to derive the equilibrium constant  $K_{AH}^*$  corresponding to the reaction



and the acidity constants  $K_{HNO_3}^{H^+}$  and  $K_{HA_2^-}^{H^+}$  of HNO<sub>3</sub> and the complex  $HA_2^-$ , respectively, taking into account the  $pK_{HCl}^{H^+}$  value (14.5).<sup>25</sup> All the results are reported in Tables 1 and 2.

We cannot strictly determine the acidity constant of nitrous acid because of its low stability in aprotic media. However, it can be noted that the difference in  $pK$  between HCl and HNO<sub>3</sub> determined in (H<sub>2</sub>O + acid) media,<sup>12-16</sup>  $pK_{HNO_3}^{H^+} - pK_{HCl}^{H^+} = 1.7$ , is

Table 2. Value of the equilibrium constant  $K_{AH}^*$  corresponding to the reaction  $HA_2^- \rightleftharpoons HA + A^-$  ( $A = NO_3, Cl$ ) in some aprotic solvents (references in parentheses)

Protic acid (AH)	$HA_2^- \rightleftharpoons HA + A^-$ $pK_{AH}^*$		
	Nitromethane at 298 K	Acetonitrile at 298 K	Sulpholane at 303 K
H <sub>2</sub> SO <sub>4</sub>	3.7 (57)	3.1 (58)	3.5 (57)
HSO <sub>3</sub> CH <sub>3</sub>	3.1 (57)	—	—
HCl	3.5 (57)	2.3 (58)	3.0 ± 0.4 3.1 (57)
HNO <sub>3</sub>	—	2.3 (58)	2.65 ± 0.40 3.1 ± 0.3*

\*Previously determined potentiometrically with the silver/silver chloride indicator electrode.<sup>47</sup>

nearly identical with that found in sulpholane medium ( $\Delta pK = 1.5$ ). Hence, we have assumed that the difference of 4.6 in  $pK$  between HNO<sub>2</sub> and HNO<sub>3</sub> in (H<sub>2</sub>O + acid) media<sup>2,3,14</sup> ( $pK_{HNO_2}^{H^+} = -1.3$ ,<sup>2</sup> and an average value of  $pK_{HNO_2}^{H^+}$  is  $\sim +3.3 \pm 0.3$ <sup>4,12-16</sup>), will be the same for sulpholane. In that case, the acidity constant  $pK_{HNO_2}^{H^+}$  of nitrous acid in sulpholane is  $> 20.6$  at 303 K.

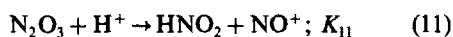
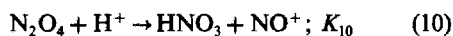
These acidity constants are reported in Tables 1 and 2 along with those found for some protic acids commonly used. It should be noted that, since the  $E_{1/2}$  reduction potential of the acid AH diminishes with  $pK_{AH}^{H^+}$ , the facility to reduce the H<sup>+</sup> ion of the protic acids,  $H^+ + e^- \rightarrow \frac{1}{2}H_2$ , is related in part to their  $pK^{H^+}$  values (Table 1).

However, the overall reduction process for protic acids is complicated by the hydrogen-bond formation leading to the relatively stable  $HA_2^-$  species (Table 2).

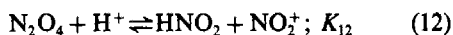
#### USE OF THE ACIDITY CONSTANTS IN THE EXPLANATION OF SOME ELECTROCHEMICAL AND CHEMICAL PROCESSES IN SULPHOLANE

Recently, nitration of aromatics by oxygen compounds of nitrogen(IV) and/or (III) has been studied by several authors.<sup>19-21,23,24,38-40</sup> Redox processes were proposed to interpret the catalytic pathway involving the nitrogen(III):<sup>19-24</sup> nitrosation plus oxidation,<sup>59,60</sup> or electron transfer from the aromatic substrate to NO<sup>+</sup> followed by radical cation reactions,<sup>19,20</sup> in a catalytic mechanism of the type first substantiated by

Giffney and co-workers.<sup>61,62</sup> More recently, we have reported preliminary results on the nitration of naphthalene by  $N_2O_4$  and/or  $N_2O_3$ , catalysed by  $NO^+$  in aprotic media.<sup>42</sup> For highly activated aromatics such as naphthalene, nitration by way of nitroso intermediates is a commonly accepted mechanism. However, the possibility of a nitrosonium-arene complex<sup>21,63</sup> or of radical cation intermediates<sup>64</sup> in aromatic nitration has also been suggested. Insufficient data are available to specify the nature of the intermediate step in more detail. However, in all cases, in order to explain the nitration mechanism catalysed by nitrogen(III), a redox process followed by elimination of a hydrogen ion from the aromatic substrate has been proposed. Little attention has been focused on the redox products and the catalytic mechanism by which they and the nitro compounds are formed in aprotic media. We recently related the efficiency of  $NO^+$  in nitration of aromatics by  $N_2O_4$  and/or  $N_2O_3$  in sulpholane to the possibility of the recycling of the nitrosonium ion in the medium.<sup>42,65,66</sup> Indeed, this phenomenon can be explained, in part, by the high values of the constants for the two reactions (after elimination of an  $H^+$  ion in the aromatic substrate):



owing to the very weak ionic dissociations of nitric acid and nitrous acid in sulpholane. We have calculated  $K_{10}$  and  $K_{11}$  by means of the equations  $K_{10} = K_{N_2O_4}^1 / K_{HNO_3}^{H^+}$  and  $K_{11} = K_{N_2O_3}^1 / K_{HNO_2}^{H^+}$  where  $K_{N_2O_4}^1$  and  $K_{N_2O_3}^1$  are the ionic disproportionation constants of  $N_2O_4$  ( $N_2O_4 \rightleftharpoons NO^+ + NO_2^-$ ) and  $N_2O_3$  ( $N_2O_3 \rightleftharpoons NO^+ + NO_2^-$ ), respectively, obtaining the values  $K_{N_2O_4}^1 = 7.1 \times 10^{-8}$  and  $K_{N_2O_3}^1 = 6.3 \times 10^{-12}$  at 303 K, in sulpholane.<sup>47,67</sup> Thereby, we obtain  $K_{10} = 6 \times 10^8$  and  $K_{11} = 2.5 \times 10^9$  at 303 K, in sulpholane. It is worth noting that the intervention of the nitronium ion has been excluded in the nitration process, on account of its low concentration in  $N_2O_4$  solutions in aprotic media,<sup>44</sup>  $K_{N_2O_4}^2 = [NO_2^+][NO_2^-] / [N_2O_4] = 10^{-22}$  at 303 K, in sulpholane,<sup>44</sup> and the low value of the constant for the reaction (after elimination of an  $H^+$  ion in the aromatic substrate):



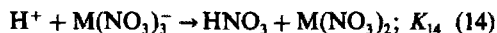
$K_{12} = K_{N_2O_4}^2 / K_{HNO_2}^{H^+} \approx 4 \times 10^{-2}$  at 303 K, in sulpholane.

This low value explains why the infrared spectra of mixtures of  $N_2O_4$  and  $H^+$  in sulpholane do not exhibit the antisymmetric stretching band (at about  $2400 \text{ cm}^{-1}$ ) of the  $NO_2^+$  ion.

Likewise, we have observed a catalytic effect of some metal nitrates  $M(NO_3)_2$  ( $M = Cu, Zn$  and  $UO_2$ ) on the nitration of naphthalene by  $N_2O_4$  in sulpholane.<sup>42</sup> This activation has also been ascribed to catalysis by  $NO^+$  formed through the reaction<sup>68</sup>



and regenerated continuously in the medium during the nitration, according to

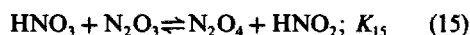


followed by reaction (13). We have calculated  $K_{14}$  by means of the equation

$$K_{14} = 1 / K_M^* K_{HNO_3}^{H^+}$$

where  $K_M^*$  is the stability constant of the complex  $M(NO_3)_3^-$ ;  $K_M^* = [M(NO_3)_3^-] / [M(NO_3)_2][NO_3^-]$ ;  $K_{Zn}^* = 2.9 \times 10^7$ ,  $K_{Cu}^* = 4.0 \times 10^7$ ,  $K_{UO_2}^* = 2.7 \times 10^7$  at 303 K, in sulpholane.<sup>68</sup> Hence, we obtain  $K_{14} = 3.4 \times 10^8$ ,  $2.5 \times 10^8$ ,  $3.7 \times 10^8$  for  $M = Zn, Cu$  and  $UO_2$  respectively.

However, the nitric acid formed by reactions (10) and/or (14) cannot be considered as one of the end-products of the aromatic nitration by mixtures of  $N_2O_4 + NO^+$  in sulpholane. Indeed, the electrochemical study of the nitration reaction has allowed us to identify  $HNO_3$  as an intermediate which is afterwards consumed by  $N_2O_3$  (this species is provided by the redox step of the nitration) through the reaction<sup>42,65,66</sup>



Thus, we observed that the cathodic wave attributed to the reduction of  $HNO_3$  diminishes, whereas the wave corresponding to the reduction of the  $HNO_2$  proton increases. The stoichiometry of the aromatic nitration by  $N_2O_4$  can therefore be written overall as



The value of the constant for reaction (15) is:  $K_{15} = K_{HNO_3}^{H^+} K_{N_2O_3}^1 / K_{HNO_2}^{H^+} K_{N_2O_4}^1 \approx 3.5$  at 303 K, in sulpholane.

It should be noted that the equilibrium constant for reaction (15) has been of great interest, for some time, in the interpretation of the decomposition of nitrous acid in sulpholane,<sup>43</sup> and also for a better understanding of the redox processes of  $N_2O_4$  alone and with water in aprotic solvents.<sup>45</sup>

## CONCLUSION

By use of the glass electrode filled with mercury, as an indicator electrode for the hydrogen ion, the acidity constant  $K_{HNO_3}^{H^+}$  of nitric acid and the equilibrium constants  $K_{HA_2^-}^{H^+}$  and  $K_{AH}^*$  corresponding to the reactions  $HA_2^- \rightleftharpoons H^+ + 2A^-$  and  $HA_2^- \rightleftharpoons A^- + AH$  ( $A = Cl, NO_3$ ) have been determined potentiometrically in sulpholane (Tables 1 and 2). The results show the very weak acid character of  $HNO_3$  and the relative stability of the entity  $HA_2^-$  formed by hydrogen bonding  $(A-H-A)^-$  in sulpholane. It has not been possible to determine the acidity constants  $K_{HNO_2}^{H^+}$  of  $HNO_2$  by this method on account of the low stability of nitrous acid in aprotic media. However, the  $K_{HNO_2}^{H^+}$  value has been estimated as  $K_{HNO_2}^{H^+} \approx 20.6$  at 303 K, in sulpholane. The knowl-

edge of the acidity constants of  $\text{HNO}_2$  and  $\text{HNO}_3$  has allowed us to account for the decomposition of nitrous acid and for the electrochemical properties of  $\text{N}_2\text{O}_4$  alone and in the presence of water in aprotic media.<sup>43-45</sup> However, agreement on the precise nitration mechanism of aromatics, catalysed by  $\text{N(III)}$ , has not yet been reached, because of the lack of data on the chemical and electrochemical behaviour of the reactants and end-products in the solvent used. Therefore, it appears necessary to take another approach to examining the nitration reaction. Thus, in order to elucidate the mechanism of aromatic nitration by  $\text{N}_2\text{O}_4$  and/or  $\text{N}_2\text{O}_3$  in sulpholane, taking into account the electrochemical and thermodynamic properties of oxygen-nitrogen compounds and especially those of  $\text{HNO}_2$  and  $\text{HNO}_3$  in this solvent, we have attempted to explain the stoichiometry of the nitration reaction and the catalytic role of  $\text{NO}^+$ .<sup>42,65,66</sup> However, many questions of the nitration mechanism are yet to be resolved. We are pursuing the investigations on the nitration of aromatics by  $\text{N}_2\text{O}_4$  and/or  $\text{N}_2\text{O}_3$  in sulpholane, and the mechanistic aspects with particular emphasis on the nature of the reactive intermediates in the nitration pathway. The results will be reported in another paper.

## REFERENCES

- G. Y. Markovits, S. E. Schwartz and L. Newman, *Inorg. Chem.*, 1981, **20**, 445.
- A. Collumeau, *Bull. Soc. Chim. France*, 1968, **12**, 5087.
- S. Ahrland, in *The Chemistry of Nonaqueous Solvents*, J. J. Lagowski (ed.), Vol. VA, p. 30. Academic Press, New York, 1978.
- M. Sampoli, A. D. Santis and N. C. Marziano, *J. Chem. Soc., Chem. Commun.*, 1985, 110.
- H. A. C. McKay, *Trans. Faraday Soc.*, 1956, **52**, 1568.
- R. C. Axtmann, W. E. Schuler, and B. B. Murray, *J. Phys. Chem.*, 1960, **64**, 57.
- J. G. Dawber and P. A. H. Wyatt, *J. Chem. Soc.*, 1960, 3589.
- G. C. Hood and C. A. Reilly, *J. Chem. Phys.*, 1960, **32**, 127.
- W. Davis, Jr. and H. J. Bruin, *J. Inorg. Nucl. Chem.*, 1964, **26**, 1069.
- O. Redlich, R. W. Duerst and A. Merbach, *J. Chem. Phys.*, 1968, **49**, 2986.
- H. Strehlov, I. Wagner and P. Hildebrandt, *Ber. Bunsenges. Phys. Chem.*, 1983, **87**, 516.
- H. Schmid, R. Marchgraber and F. Dunkl, *Z. Elektrochem.*, 1937, **43**, 337.
- E. G. Vassian and W. H. Eberhardt, *J. Phys. Chem.*, 1958, **62**, 84.
- G. Charlot, *Les Méthodes de la Chimie Analytique—Analyse Quantitative Minérale*, p. 8. Masson, Paris, 1961.
- P. Lumme and J. Tummavuori, *Acta Chem. Scand.*, 1965, **19**, 617.
- Wu-Hsiung Ho, *Proc. Natl. Sci. Council, (China)*, 1977, No. 10, Part 1, 175.
- E. Abel and H. Schmid, *Z. Phys. Chem. (Leipzig)*, 1928, **134**, 279.
- J. H. Ridd, *Q. Rev. Chem. Soc.*, 1961, **15**, 418.
- D. S. Ross, G. P. Hum and W. G. Blucher, *J. Chem. Soc., Chem. Commun.*, 1980, 532.
- L. Main, R. B. Moodie and K. Schofield, *ibid.*, 1982, **48** and references therein.
- B. Milligan, *J. Org. Chem.*, 1983, **48**, 1495.
- D. S. Ross, K. F. Kuhlmann and R. Malhotra, *J. Am. Chem. Soc.*, 1983, **105**, 4299.
- D. S. Ross, K. D. Moran and R. Malhotra, *J. Org. Chem.*, 1983, **48**, 2118.
- U. Al-Obaidi and B. B. Moodie, *J. Chem. Soc. Perkin Trans. II*, 1985, 467.
- J. F. Coetzee and R. J. Bertozzi, *Anal. Chem.*, 1973, **45**, 1064.
- P. Pierens, Y. Auger, J. C. Fischer and M. Wartel, *Can. J. Chem.*, 1975, **53**, 2989.
- M. Wartel, Y. Auger, G. Delesalle, J. C. Fischer and P. Pierens, *J. Electroanal. Chem.*, 1977, **85**, 47.
- U. Mayer and V. Gutmann, *Structure and Bonding*, Vol. 12, p. 113. Springer-Verlag, Heidelberg, 1972.
- V. Gutmann, *Chem. Tech.*, 1977, 255.
- G. R. Underwood, R. S. Silverman and A. Vanderwalde, *J. Chem. Soc. Perkins Trans. II*, 1973, 1178.
- C. L. Perrin, *J. Am. Chem. Soc.*, 1977, **99**, 5516.
- J. M. Achord and C. L. Hussey, *J. Electrochem. Soc.*, 1981, **123**, 2556.
- L. Ebersson, L. Jonsson and F. Radner, *Acta Chem. Scand.*, 1978, **B32**, 749.
- L. Ebersson and F. Radner, *ibid.*, 1980, **B34**, 739.
- Idem*, *ibid.*, 1984, **B38**, 861.
- Idem*, *ibid.*, 1985, **B39**, 343 and references therein.
- Idem*, *ibid.*, 1985, **B39**, 357.
- G. A. Olah and S. J. Kuhn, *Friedel-Crafts and Related Reactions: Acylation and Related Reactions*, Vol. III, Part 2, p. 1404. Interscience, New York, 1964.
- G. A. Olah, H. C. Henry, J. A. Olah and S. C. Narang, *Proc. Natl. Acad. Sci. USA*, 1978, **75**, 1045.
- G. A. Olah, S. C. Narang and J. A. Olah, *ibid.*, 1981, **78**, 3298.
- G. A. Olah, S. C. Narang, J. A. Olah and K. Lammertsma, *ibid.*, 1982, **79**, 4487.
- A. Boughriet, J. C. Fischer, M. Wartel and C. Bremard, *Nouv. J. Chim.*, 1985, **9**, 651.
- A. Boughriet, J. C. Fischer, G. Leman and M. Wartel, *Bull. Soc. Chim. France*, 1985, **1**, 8.
- A. Boughriet, M. Wartel, J. C. Fischer and C. Bremard, *J. Electroanal. Chem.*, 1985, **190**, 103.
- A. Boughriet, M. Wartel and J. C. Fischer, *Talanta*, 1986, **33**, 385.
- G. Brauer, *Handbook of Preparative Inorganic Chemistry*, 2nd Ed., Vol. I, p. 491. Academic Press, New York, 1963.
- M. Wartel, A. Boughriet and J. C. Fischer, *Anal. Chim. Acta*, 1979, **110**, 211.
- M. M. Koepf, H. Wendt and H. Strehlov, *Z. Electrochem.*, 1960, **64**, 483.
- G. Bontempelli, G. A. Mazzochin and F. Magno, *J. Electroanal. Chem.*, 1974, **55**, 91.
- D. Serve, *Thesis*, Grenoble (France), A07174, 1972.
- G. Cauquis and D. Serve, *C.R. Acad. Sci. Paris*, 1970, **270C**, 1773.
- J. C. Fischer, Y. Auger, G. Delesalle and M. Wartel, *J. Electroanal. Chem.*, 1978, **88**, 91, and references therein.
- J. F. Coetzee and R. J. Bertozzi, *Anal. Chem.*, 1971, **43**, 961.
- R. W. Alder, G. R. Chakley and M. C. Whiting, *Chem. Commun.*, 1966, **13**, 405.
- R. L. Benoit, C. Buisson and G. Choux, *Can. J. Chem.*, 1970, **48**, 2353.
- Y. Auger, *Thesis*, Lille, 1978.
- J. C. Fischer, *Thesis*, Lille, 1976.
- I. M. Kolthoff, S. Bruckenstein and M. K. Chantooni, *J. Am. Chem. Soc.*, 1961, **83**, 3927.
- J. Hoggett, R. B. Moodie, J. R. Penton and K.

- Schofield, *Nitration and Aromatic Reactivity*, p. 57. Cambridge University Press, Cambridge, 1971.
60. R. G. Coombes, J. G. Golding and P. Hadjigeorgiou, *J. Chem. Soc., Perkin Trans. II*, 1979, 1451.
61. J. C. Giffney and J. H. Ridd, *ibid.*, 1979, 618.
62. F. Al-Omran, K. Fujiwara, J. C. Giffney and J. H. Ridd, *ibid.*, 1980, 518.
63. Z. J. Allan, J. Podstata, D. Šnobl and J. Jarkovský, *Collection Czech. Chem. Commun.*, 1967, 32, 1449.
64. J. M. Tedder and G. Theaker, *Tetrahedron*, 1969, 5, 288.
65. A. Boughriet, C. Bremard and M. Wartel, *Nouv. J. Chim.*, 1987, 11, 245.
66. *Idem*, *J. Electroanal. Chem.*, 1987, 225, 125.
67. A. Boughriet, M. Wartel, J. C. Fischer and Y. Auger, *ibid.*, 1985, 186, 201.
68. A. Boughriet, M. Wartel and J. C. Fischer, *Can. J. Chem.*, 1986, 64, 5.



# THE EFFECT OF SURFACTANTS ON THE DISSOCIATION CONSTANTS OF PHENOTHIAZINE DERIVATIVES

## ALKALIMETRIC DETERMINATION OF DIETHAZINE AND CHLORPROMAZINE

P. RYCHLOVSKÝ and I. NĚMCOVÁ

Department of Analytical Chemistry, Charles University, Albertov 2030, 128 40 Prague 2, Czechoslovakia

(Received 14 April 1987. Revised 24 September 1987. Accepted 2 October 1987)

**Summary**—The effect of a cationic, an anionic and a non-ionic surfactant on the acid–base equilibria of the phenothiazine derivatives, diethazine hydrochloride and chlorpromazine hydrochloride, has been studied. It has been found that the presence of cationic and non-ionic surfactants strongly enhances the dissociation of the two derivatives, whereas the anionic surfactant decreases the dissociation constant. These effects are in agreement with a theory based on a pseudophase, ion-exchange model of micelles. From the dissociation-constant values as a function of the surfactant concentration, the binding constants for diethazine and chlorpromazine with the surfactants Septonex and sodium dodecylsulphate have been calculated. The ability of cationic surfactants to solubilize the free bases of the phenothiazine derivatives and to increase their dissociation constants has been utilized to develop a new method for alkalimetric determination of the derivatives in a micellar medium. The method has been applied to determination of the content of the active component in pharmaceutical preparations.

Phenothiazine derivatives are often studied in pharmacology and recently have also been investigated in connection with photo-redox processes in micellar systems (construction of photogalvanic cells).<sup>1,2</sup> There are generalized methods for determining these substances<sup>3,4</sup> and many of the compounds have been used as spectrophotometric reagents<sup>5,6</sup> or redox indicators.<sup>7</sup>

As it is well known that micellar media formed by surfactants significantly affect many analytically useful reactions,<sup>8</sup> we have studied the effect of surfactants on the absorption spectra of some phenothiazine derivatives and on the stability of their oxidation products,<sup>9</sup> as well as on their reactions with metal ions.<sup>10</sup> This paper deals with the effects of surfactants on the acid–base properties of phenothiazine derivatives, as effects on the dissociation constant have been demonstrated for other substances in surfactant solutions<sup>11,12</sup> and utilized analytically.<sup>13,14</sup>

Phenothiazine derivatives are usually prepared as the hydrochlorides or maleates and behave as very weak acids. Their dissociation equilibrium can be expressed by the equation

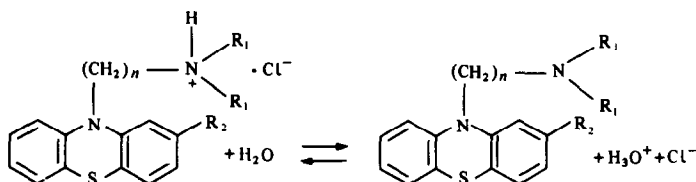
In an aqueous medium not containing a surfactant the base formed is insoluble. To determine the dissociation constants  $K_a$  for such substances, the method of non-logarithmic linear titration curves<sup>15</sup> can be employed; it has been applied to some phenothiazine derivatives.<sup>16</sup> If the free base is not precipitated, then the method yields the equation,

$$Z = A - \frac{Z[H_3O^+]}{K_a} \quad (1)$$

where  $Z$  is the number of moles of substance neutralized and  $A$  is the analytical concentration of the weak base. Plotting  $Z$  against  $Z[H_3O^+]$  yields a straight line with slope  $1/K_a$ . If the base precipitates, then  $K_a$  is obtained from the slope of the straight line,

$$Z = A - \frac{B[H_3O^+]}{K_a} \quad (2)$$

where  $B$  is the concentration of the dissolved portion of the free base, obtained spectrophotometrically. The method permits the determination of  $pK_a$  with a standard deviation of  $\leq 0.03$ .<sup>15</sup>



Diethazine·HCl:  $R_1 = C_2H_5$ ,  $R_2 = H$ ,  $n = 2$   
 Chlorpromazine·HCl:  $R_1 = CH_3$ ,  $R_2 = Cl$ ,  $n = 3$

## EXPERIMENTAL

## Apparatus

The pH was measured with a PHM 64 instrument (Radiometer, Denmark) with a GK 2401 B glass combined electrode that was calibrated with aqueous buffers supplied by the same company. The titrations were performed on TTT 11 titrator with an ABU 13 autoburette (2.5 ml) (Radiometer). The absorption spectra were measured on a PU 8800 instrument (Pye-Unicam Philips, England). The solutions were kept at constant temperature with a U 15 thermostat (VEB Prüfgeräte, GDR).

## Reagents

Stock solutions ( $5 \times 10^{-3} M$ ) of chlorpromazine hydrochloride (LPC, London; m.w. 355.47) and diethazine hydrochloride (Léčiva, Czechoslovakia; m.w. 334.47) were obtained by dissolving the substances in distilled water. The purity of the substances was checked by melting point measurements in a Kofler block and by TLC with a methanol-chloroform (1:1 v/v) mobile phase. The stock solutions of diethazine and chlorpromazine were stored in the dark, in closed vessels, to prevent their oxidation.

Stock solutions ( $5 \times 10^{-2} M$ ) of 1-carboxypentadecyltrimethylammonium bromide (Septonex; Spofa, Czechoslovakia; m.w. 422.48), sodium dodecylsulphate (SDS; Serva, FRG; m.w. 288.37) and *p*-octylphenol polyoxyethylene ( $n = 30$ , Triton X-305; Carlo Erba, Italy; m.w. 1510) were prepared by dissolving the substances in distilled water. The Septonex was first dried for several days in a vacuum desiccator.

The titrations were performed with a standard 0.2M sodium hydroxide solution, free from carbonate and standardized with oxalic acid. The ionic strength of solutions was adjusted with potassium chloride.

## Procedures

**Determination of the  $pK_a$  values.** Solutions of the two hydrochlorides ( $5 \times 10^{-4} M$ ), with ionic strength  $I = 0.1$  (KCl), were titrated with the standard 0.2M alkali in surfactant micellar solutions at  $25 \pm 0.5^\circ$ , except for the measurements with SDS, where the temperature was  $35 \pm 0.5^\circ$  because SDS precipitated at lower temperatures. The measurements were made in the dark, with vigorous stirring and continuous passage of nitrogen through the solution, the titrant being added in 10- $\mu$ l portions. The pH was allowed to stabilize before each addition of titrant.

In the absence of surfactants and at surfactant concentrations below the critical micelle concentration (cmc), a fine white precipitate of the free base appeared during the titration. A large amount of alkali was then added after the attainment of the equivalence point, to ensure complete deprotonation of the phenothiazine derivative, the liquid was centrifuged and the concentrations of the free diethazine (DE) and chlorpromazine (CP) bases in solution were determined spectrophotometrically in the clear supernatant ( $\lambda_{\max}$  DE = 250 nm and  $\lambda_{\max}$  CP = 254 nm; five measurements, with a precision of 2%). The  $K_a$  values were then obtained from equation (2). With supercritical surfactant concentrations the free bases were solubilized by the micelles and equation (1) could be used to determine  $K_a$ .

**Determination of phenothiazine derivatives in the commercial substances and pharmaceutical preparations.** An accurately weighed amount of ( $\sim 0.85$  g) of the hydrochloride is dissolved in 10 ml of 0.1M Septonex, 5 ml of 1M potassium chloride are added and the mixture is diluted to 50 ml with water. The solution is titrated with 0.2M sodium hydroxide in the dark, with vigorous stirring and passage of nitrogen through the solution.

A weighed amount of powdered tablet equivalent to about 0.25 mmole of active component is stirred with about 20 ml of water for 15 min, the solution is filtered through cotton-wool, 10 ml of 0.1M Septonex and 5 ml of 1M

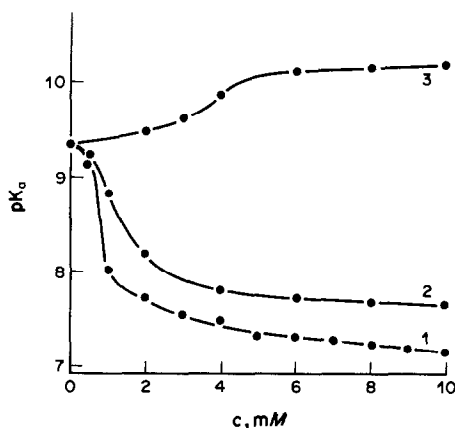


Fig. 1. Dependence of the  $pK_a$  value for diethazine·HCl on the surfactant concentration.  $c_{DE} = 5 \times 10^{-4} M$ ,  $c_{KCl} = 0.1 M$ : 1—Septonex, 2—Triton X-305, 3—SDS.

potassium chloride are added, the solution is diluted with water to 50 ml and the titration is performed as above.

## RESULTS AND DISCUSSION

*Effect of surfactants on the  $pK_a$  values of phenothiazine derivatives*

We studied the effects of the cationic surfactant Septonex, anionic surfactant SDS and non-ionic surfactant Triton X-305, over a concentration range from  $5 \times 10^{-4}$  to  $1 \times 10^{-2} M$ . The  $pK_a$  values of protonated diethazine and chlorpromazine are plotted in Figs. 1 and 2 as a function of the surfactant concentration. It can be seen that the presence of the cationic and the non-ionic surfactant leads to a sharp decrease in the  $pK_a$  values of both derivatives at around the surfactant critical micelle concentration (cmc); the cmc values are roughly  $1.1 \times 10^{-4} M$  for Septonex in a medium of 0.1M strong electrolyte<sup>17</sup> and  $5 \times 10^{-4} M$  for Triton X-305, the cmc of which is little affected by the presence of salts.<sup>18</sup> On the other

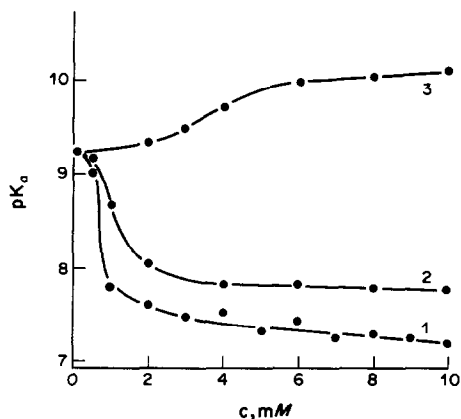


Fig. 2. Dependence of the  $pK_a$  value for chlorpromazine·HCl on the surfactant concentration.  $c_{CP} = 5 \times 10^{-4} M$ ,  $c_{KCl} = 0.1 M$ : 1—Septonex, 2—Triton X-305, 3—SDS.

hand, the  $pK_a$  values of the derivatives considerably increase in the vicinity of the cmc value (under the present conditions *ca.*  $1.3 \times 10^{-3} M$ )<sup>19</sup> of the anionic surfactant SDS.

The decrease in the  $pK_a$  value (an enhancement of dissociation) of protonated diethazine and chlorpromazine in the presence of the cationic and non-ionic surfactant and the increase in  $pK_a$  value (suppression of the dissociation) in the presence of the anionic surfactant are in agreement with the results given in the literature for the acid-base equilibria of other organic systems<sup>12-14,20</sup> and correspond to Hartley's findings<sup>11</sup> and to the theory employing a pseudophase, ion-exchange model.<sup>21,22</sup> According to this model, both the acid-base forms of the organic molecule are bound to the micelles through hydrophobic interactions. The ability of the cationic micelles to bind  $OH^-$  ions by electrostatic forces and thus to concentrate them within the small volume of the micellar pseudophase then favours dissociation of a weak acid on the micelle surface. The binding of the organic molecules to the micelles of an anionic surfactant suppresses the dissociation, as  $OH^-$  ions are not bound to the negatively charged micelle surface and deprotonation of the acid is thus not favoured. The  $OH^-$  ions are probably bound to the micelles of non-ionic surfactants, but the interaction is weaker and thus the enhancement of dissociation is less pronounced than with cationic surfactants.

#### *Equilibrium constants for binding of the hydrochlorides with Septonex and sodium dodecylsulphate*

The  $K_a$  values obtained for protonated diethazine and chlorpromazine, as a function of the surfactant concentration, make it possible to determine the constants for binding these species with the surfactants.<sup>20</sup>

For the dissociation of a weak acid,  $HA^+ \rightleftharpoons H^+ + A$ , and the distribution of the species between the micellar and the aqueous pseudophase, the dissociation constant  $K_m$  (in the presence of the surfactant) can be expressed by

$$K_m = K_w(1 + K_A[C]) / (1 + K_{HA^+}[C]) \quad (3)$$

where  $K_w$  is the dissociation constant in the absence of the surfactant and  $[C]$  is the difference between the actual surfactant concentration and the cmc value. The  $K_A$  and  $K_{HA^+}$  values are the binding constants for the substance in the deprotonated and protonated form, respectively, with the micelles, given by the relationship

$$K = [S_m] / [S_w] ([C] - [S_w]) \quad (4)$$

where subscripts m and w for substrate S refer to the micellar and aqueous phase, respectively.

In the study of the effect of the anionic surfactant SDS on the acid-base equilibria of some methyl-substituted derivatives of phenol (an equilibrium of the  $HA \rightleftharpoons H^+ + A^-$  type), to determine the constant for the binding of these derivatives with SDS from the

values of the dissociation constants in the micellar medium, an assumption was made<sup>20</sup> which simplifies equation (3) and permits the determination of the binding constant; it is also applicable to our measurements. This assumption is that the positive charge on the protonated form of the phenothiazine derivatives exhibits a greater tendency to associate with the anionic surfactant SDS than does the base ( $K_A[C] \ll 1$ ) and thus equation (3) can be simplified to yield

$$K_m = K_w(1 + K_{HA^+}[C]) \quad (5)$$

Analogously, for the cationic surfactant Septonex it is possible to assume that the positive charge on the protonated form of the phenothiazine derivatives has little tendency to associate with the surfactant, compared with the free base ( $K_{HA^+}[C] \ll 1$ ) and equation (3) is converted into the form

$$K_m = K_w(1 + K_A[C]) \quad (6)$$

Plotting  $K_m/K_w$  against  $[C]$  for the anionic surfactant and  $K_m/K_w$  against  $[C]$  for the cationic surfactant yields straight lines with slopes equal to the appropriate binding constants with the surfactants.

By this method, the values  $K_A = 1 \times 10^4$  and  $9.5 \pm 1 \times 10^3$  have been obtained for the interaction of diethazine and chlorpromazine, respectively, with Septonex. For the reaction with the SDS surfactant, the value  $K_{HA^+} = 4 \pm 1 \times 10^2$  has been obtained for both the phenothiazine derivatives.

These binding constants are of the same order of magnitude as those for unsubstituted phenothiazine and the cationic surfactant cetyltrimethylammonium bromide ( $3 \times 10^4$ ) and the anionic surfactant SDS ( $1 \times 10^3$ ), obtained from the kinetic equations for the phenothiazine reaction with Fe(III).<sup>26</sup> Similar results have been obtained in studies of the interactions of other aromatics with cationic and anionic surfactants.<sup>27,28</sup>

It follows from the values obtained for the binding constants that unsubstituted phenothiazine and the bases of the derivatives studied in this work are bound to the micelles of cationic surfactants more strongly than phenothiazine and the protonated form  $HA^+$  are bound to those of anionic surfactants, although it could be assumed that the  $HA^+$  species might interact electrostatically with the negative charge on the SDS micelle surface. These findings are also in agreement with the results obtained in the first part of this work, indicating that Septonex causes greater changes in the  $pK_a$  values than SDS does (see Figs. 1 and 2). The results obtained thus again confirm that hydrophobic interactions predominate in the interactions of organic molecules with surfactants.

#### *Alkalimetric determination of phenothiazine derivative in micellar solutions*

We have utilized the ability of the surfactant to solubilize the free bases of the phenothiazine deriva-

Table 1. Determination of diethazine·HCl and chlorpromazine·HCl in the commercial substances

	Diethazine·HCl*, %	Chlorpromazine·HCl*, %
Classical potentiometry	100.4 ± 0.3	99.9 ± 0.1
Automatic titrator	100.5 ± 0.6	99.9 ± 0.6
HClO <sub>4</sub> titration in CH <sub>3</sub> COOH	100.1 ± 0.3	100.0 ± 0.1
Ce(SO <sub>4</sub> ) <sub>2</sub> titration	100.5 ± 0.5	99.9 ± 0.5

\*Referred to nominal amount taken, ± standard deviation.

Table 2. Determination of diethazine·HCl and chlorpromazine·HCl in pharmaceutical preparations

	Deparkin*, %	Plegomazin*, %
Titration in Septonex	98.9 ± 0.9	98.9 ± 0.8
Heterogeneous titration	99.1 ± 0.9	98.9 ± 0.8
UV spectrophotometry	99.9 ± 0.6	99.0 ± 0.6

\*Percentage of the nominal content, ± standard deviation.

tives and to increase the dissociation constants  $K_a$  of their protonated forms (by up to two orders of magnitude) for the development of an alkalimetric determination of phenothiazine derivatives in the form of the hydrochlorides by titration with standard sodium hydroxide solution, in presence of the cationic surfactant Septonex. The titration can be done potentiometrically, with  $\text{pH}_{\text{eq}} = 9.5$  for automatic titrations.

The mean results obtained from ten parallel determinations of the two hydrochlorides are given in Table 1. They are in good agreement with those obtained by titration with standard perchloric acid solution in anhydrous acetic acid<sup>23</sup> and by redox titration with standard ceric sulphate solution<sup>24</sup> (see Table 1). Analysis of the pharmaceutical preparations Deparkin (Spofa, Czechoslovakia; active component diethazine) and Plegomazin (Egyt, Hungary; active component chlorpromazine) gave the results reported in Table 2. Automatic titration was used, and the results were compared with those obtained by heterogeneous titration<sup>25</sup> and spectrophotometry.<sup>4</sup> The other substances in the preparations (carbohydrates, dyes, waxes) did not interfere in the determination.

The proposed alkalimetric determination is simpler and faster than the titrations in non-aqueous and heterogeneous media that are often used for the determination of phenothiazine derivatives.

## REFERENCES

1. S. A. Alkaitis, G. Beck and M. Grätzel, *J. Am. Chem. Soc.*, 1975, **97**, 5723.
2. M. Grätzel, *Israel J. Chem.*, 1979, **18**, 364.
3. G. Cimbura, *J. Chromatog. Sci.*, 1972, **10**, 287.
4. J. Blažek, A. Dyměš and L. Stejskal, *Pharmazie*, 1976, **31**, 681.
5. L. Kum-Tatt and Ai-Mee Seet, *Mikrochim. Acta*, 1974, 955.
6. H. S. Gowda and A. T. Gowda, *J. Indian Chem. Soc.*, 1982, **59**, 1201.
7. H. Puzanowska-Tarasiewicz and M. Tarasiewicz, *Dev. Neurosci. (Amsterdam)*, 1980, **7**, 49.
8. M. E. Díaz García and A. Sanz-Medel, *Talanta*, 1986, **33**, 255.
9. I. Němcová, J. Novotný and V. Horská, *Microchem. J.*, 1986, **34**, 180.
10. V. Horská, *Diploma Thesis*, Charles University, Prague, 1983.
11. G. S. Hartley, *Trans. Faraday Soc.*, 1934, **30**, 444.
12. N. Funasaki, *Nippon Kagaku Kaishi*, 1976, 722.
13. E. Pelizzetti and E. Pramauro, *Anal. Chim. Acta*, 1980, **117**, 403.
14. *Idem, ibid.*, 1981, **128**, 273.
15. H. R. Levy and M. Rowland, *J. Pharm. Sci.*, 1971, **60**, 1155.
16. A. Hulshoff and J. H. Perrin, *Pharm. Acta Helv.*, 1976, **51**, 65.
17. L. Čermáková, J. Rosendorfova and M. Malát, *Collection Czech. Chem. Commun.*, 1980, **45**, 210.
18. A. Ray and G. Nemethy, *J. Am. Chem. Soc.*, 1971, **93**, 6787.
19. M. J. Corrin and W. D. Harkins, *ibid.*, 1947, **69**, 683.
20. E. Pramauro and E. Pelizzetti, *Anal. Chim. Acta*, 1981, **126**, 253.
21. F. H. Quina and H. Chaimovich, *J. Phys. Chem.*, 1979, **83**, 1844.
22. C. A. Bunton, L. S. Romsted and L. Sepulveda, *ibid.*, 1980, **84**, 2611.
23. J. Blažek and V. Špinková, *Ceskoslov. Farm.* 1974, **23**, 3.
24. H. Basinska and K. Nowakowski, *Acta Pol. Pharm.*, 1972, **29**, 463.
25. J. Blažek and M. Pinkasová, *Ceskoslov. Farm.*, 1979, **28**, 367.
26. E. Pelizzetti and E. Pramauro, *Ber. Bunsenges. Phys. Chem.*, 1979, **83**, 996.
27. C. Hirose and L. Sepulveda, *J. Phys. Chem.*, 1981, **85**, 3689.
28. E. Pelizzetti and E. Pramauro, *ibid.*, 1984, **88**, 990.

## EVALUATION OF AN OVERDETERMINED SYSTEM BASED ON MULTIPLE ION-SELECTIVE ELECTRODES OF THE SAME TYPE

SCOTT A. GLAZIER and MARK A. ARNOLD\*

Department of Chemistry, University of Iowa, Iowa City, IA 52242, U.S.A.

JEFFERY P. GLAZIER

Department of Welding Engineering, Ohio State University, 190 W. 19th Ave., Columbus,  
OH 43210, U.S.A.

(Received 10 March 1987. Revised 24 June 1987. Accepted 23 September 1987)

**Summary**—Possible advantages of using multiple ion-selective electrodes of the same type for the determination of analyte ions in multicomponent mixtures are investigated. Specifically, potassium and ammonium ions are determined in model multicomponent mixtures with a combination of four valinomycin and four nonactin polymeric membrane electrodes. The electrode potentials are monitored by a specially designed data-acquisition system, and conventional matrix operations are used to calculate the ion concentrations. The results indicate that greater confidence in the analyses can be obtained from an overdetermined system of this type.

Otto and Thomas<sup>1</sup> recently evaluated an experimental design in which up to eight different ion-selective membrane electrodes were used simultaneously for the determination of sodium, potassium, calcium, and magnesium ions in clinically important solutions. They showed that such an overdetermined approach to the problem of multiple ion determination is feasible and that an overdetermined system provides better predictability than an exactly determined one (four electrodes, one for each of the four cations). The theoretical advantages of overdetermined systems have been discussed in detail.<sup>2</sup>

The overdetermined system studied by Otto and Thomas consisted of eight electrodes, each with a different selectivity pattern. An alternative approach, which has yet to be evaluated, involves use of groups of electrodes with nominally identical selectivity patterns. An overdetermined system of this nature might be able to provide greater confidence in the determination of a particular ion in solution. This approach is of special interest because of the continuing advances in microfabrication technology, which can provide arrays of many individual electrodes made of the same material.

The purpose of our investigation was to establish the merits of using multiple ion-selective electrodes of the same type for the determination of ions in solution. Four valinomycin and four nonactin polymer-membrane electrodes were employed for the simultaneous determination of potassium and ammonium

ions in a single sample. A novel data-acquisition system was developed to facilitate data-collection and analysis. This system automatically collects data from up to sixteen individual electrodes in conjunction with a single reference element, and uses conventional matrix operations and regression techniques to calculate the ion concentrations. We have found that results from this type of overdetermined system are more reliable than those from individual electrode pairs.

### EXPERIMENTAL

#### Reagents

High molecular-weight poly(vinyl chloride) (PVC) and Gold Label tetrahydrofuran (THF) (Aldrich), dibutyl sebacate (Eastman Kodak), nonactin, valinomycin, and Sigma 7-9 Tris (Sigma) were used. All other chemicals were of analytical reagent grade. Demineralized distilled water was used in the preparation of standard and sample solutions.

#### Preparation of polymeric membrane electrodes

Nonactin and valinomycin polymer-membrane electrodes were constructed from disposable plastic pipette tips with small lengths (approximately 0.5–1.0 cm) of Nalgene tubing pressed onto the ends. The end of the tubing was dipped into the appropriate coating solution ten times, the solvent being allowed to evaporate between dips. The nonactin coating solution consisted of 11.6 mg of nonactin, 130.2 mg of PVC, 250  $\mu$ l of dibutyl sebacate, and 3 ml of THF. The valinomycin coating solution consisted of 5.6 mg of valinomycin, 130.6 mg of PVC, 250  $\mu$ l of dibutyl sebacate, and 3 ml of THF. Both types of electrode were stored in test-tubes that contained 100  $\mu$ l of 0.1999M potassium chloride (in 0.1M Tris-HCl buffer, pH 7.50) when not in use; this solution composition was also used for the internal electrolyte for the electrodes. Silver wires coated with silver

\*To whom correspondence should be addressed.

chloride were used as internal reference electrodes. Electrode potentials were measured relative to that of an Ag/AgCl double-junction reference electrode with 1M lithium acetate in the outer junction.

#### Preparation of standards and samples

Potassium and ammonium ion standards for calibration of the nonactin and valinomycin electrodes were prepared by dissolving the corresponding chlorides in 0.1M Tris-HCl (pH 7.50) buffer.

Model samples 1 and 2, prepared by dissolving potassium and ammonium chlorides in 0.1M Tris-HCl (pH 7.50) buffer, had the following compositions.

Sample 1:  $5.95 \times 10^{-4}M$  KCl,  $1.00 \times 10^{-3}M$   $NH_4Cl$

Sample 2:  $5.95 \times 10^{-4}M$  KCl,  $8.78 \times 10^{-4}M$   $NH_4Cl$

#### Determination of potassium and ammonium in samples

Potassium and ammonium ions in the samples were simultaneously determined by direct potentiometric analysis. Initially, four valinomycin and four nonactin electrodes were simultaneously calibrated with standard potassium solutions with activities ranging from  $2.798 \times 10^{-4}$  to  $1.193 \times 10^{-2}M$ . Selectivity coefficients for these electrodes were then determined, by means of additions of potassium and ammonium standards to 50 ml of the Tris buffer, the resulting concentrations being as follows:

Addition	$[K^+], M$	$[NH_4^+], M$
1	$4.79 \times 10^{-4}$	$3.59 \times 10^{-4}$
2	$8.36 \times 10^{-4}$	$6.27 \times 10^{-4}$
3	$1.192 \times 10^{-3}$	$8.94 \times 10^{-4}$
4	$1.547 \times 10^{-3}$	$1.160 \times 10^{-3}$

The model samples were analysed by immersing all eight electrodes in the sample solution. The resulting steady-state potentials were monitored simultaneously by the data-acquisition system. The data were analysed by combining the responses of various electrodes into different sets, as described below.

## RESULTS AND DISCUSSION

### Hardware design

Numerous articles deal with, at least in part, the design and use of computer-controlled data-acquisition instrumentation for ion-selective elec-

trodes.<sup>3-10</sup> With so many systems proposed, it may prove difficult to choose the best design for a particular need. The advantages of the present system are: (1) the ability to monitor 16 indicator electrodes relative to a single reference electrode, (2) use of an inexpensive integrated-circuit analogue multiplexer instead of separate relays for electrode monitoring, (3) use of a kit-based analogue-to-digital converter (ADC) that is simple to assemble and calibrate and provides high resolution, and (4) an RS232C output for remote positioning of the acquisition system and easy adaptability to a variety of computers.

The acquisition system is illustrated schematically in Fig. 1. Each indicator electrode is connected to a CA3140AS operational amplifier, which serves to increase the input impedance of the acquisition system. The electrode amplifiers are electrically connected, in random or sequential order, to the ADC by an IH6116CPI integrated-circuit multiplexer.

Analogue electrode potentials are converted into BCD (binary coded decimals) by the ICL7135 which is part of the ADC kit (ICL7135 EV/KIT, Hamilton Avnet Electronics, Cedar Rapids, IA). The converter offers a maximum conversion rate of about 2-3 Hz. It has 4.5-digit precision which allows a resolution of  $\pm 0.1$  mV at a full scale span of  $\pm 2$  V. Since the converter has an auto-zero function, calibration consists of input of a stable voltage and setting the adjustment potentiometer to give the appropriate digital output. The converter kit is available on a 4.5 x 6 inch printed circuit board with edge connector. There are several signals accessible from the connector, including (1) the under-range, over-range, and polarity lines, which contain information about the magnitude and polarity of the potential input, (2) the strobe line, which is the main handshake signal for data output, (3) five digit drives, which correspond to the five BCD values used to represent the five decimal places in the output digital reading, (4) the four BCD data lines and (5) a run/hold line to allow conversion to be started at will.

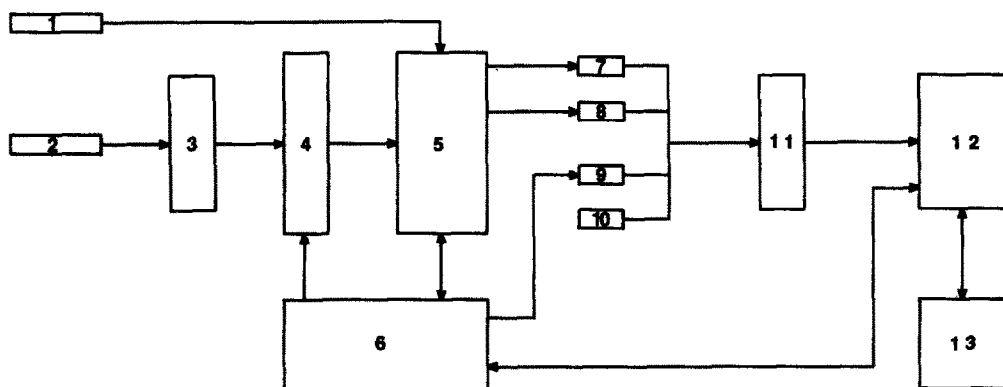


Fig. 1. Schematic of the data-acquisition system: (1) reference electrode, (2) indicator electrodes, (3) input amplifiers, (4) multiplexer, (5) ADC, (6) control circuitry, (7-10) output registers, (11) output buffers, (12) universal asynchronous receiver/transmitter, (13) port SER01 IBM 9000.

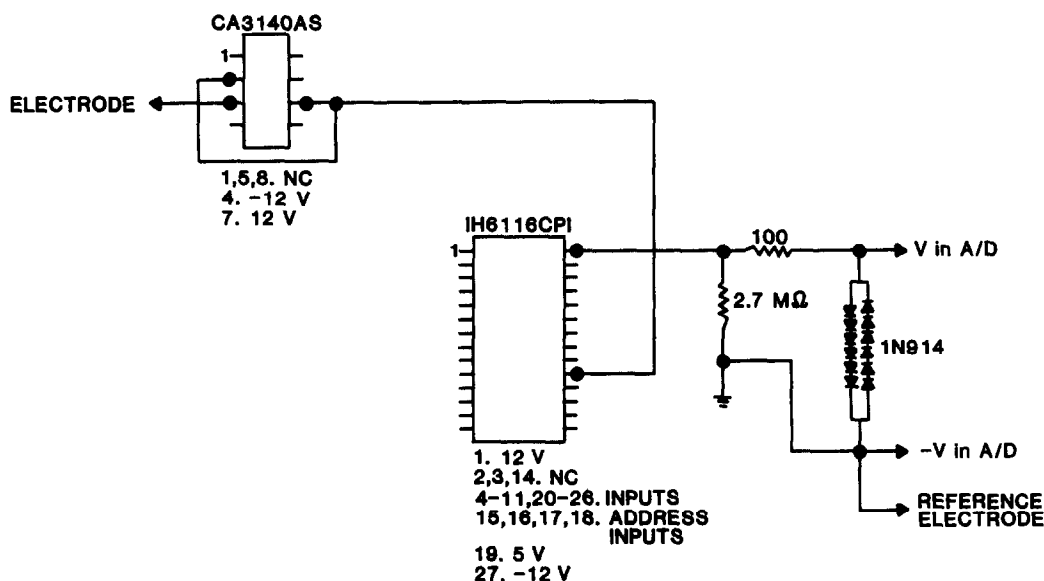


Fig. 2. Schematic of the analogue portion of the data-acquisition system: shown below each integrated circuit are the connections which could not be represented schematically.

Perhaps the most novel aspect of this acquisition system is the portion of the circuitry from the electrode amplifiers to the ADC; this simple arrangement is shown in Fig. 2. Listed below each integrated circuit are the connections which could not be represented schematically. One resistor ( $2.7\text{ M}\Omega$ ) is necessary to compensate for the internal resistance of each multiplexer channel. The other resistor, in conjunction with the set of diodes, acts to protect the ADC by limiting the absolute value of the input voltage.

The internal functioning of the acquisition system is straightforward and easily understood. First, the sampling rate,  $0.018\text{--}2.34\text{ Hz}$ , is loaded into the sample-rate generator. Next, the beginning and ending multiplexer channels for sequential scanning are loaded into the multiplexer counter and end-of-scan comparator, respectively. A pulse sent to the ADC begins the conversion. All five BCD data bytes are encoded separately into ASCII values between 48 and 57. These are converted into RS232C format and sent to the computer. The polarity, over-range, and under-range signals are encoded into a single ASCII value. Likewise, the current multiplexer channel and a communications terminator are encoded as separate values and sent. Finally, the current channel-number is compared to that for the end of scan. If they are equal, acquisition returns to the beginning, otherwise, the multiplexer channel is simply incremented. The four control registers indicated contain the information to be sent to the computer. One contains the BCD data, a second holds the polarity and over-range/under-range information, a third holds the value of the current multiplexer channel, and the fourth stores the communications terminator.

#### Computer and software design

The computer used for data-collection was the IBM System 9000. All programming was performed in version 1.2 System 9000 Basic. In the data-acquisition algorithm, the steady-state response of the electrodes was determined by a simple method. First, ten potentials (read to  $0.1\text{ mV}$ ) were collected (at a rate of  $2.343\text{ Hz}$ ) from each of the eight electrodes connected to the acquisition system. The standard deviations of the sets of potentials were calculated and compared with the limit of  $0.3\text{ mV}$ . If all the standard deviations were below this limit (no provision has been made for the case that the standard deviations never fall below the limit), the sets were averaged individually, and the averages stored as the steady-state potentials. Otherwise, new data were taken from each of the electrodes and processed in the same manner.

#### Calculations

The determination of two ions with ion-selective electrodes in the present procedure requires, initially, a mathematical model to describe the response of the electrodes to the presence of the ions in solution. The model examined in this work, the extended Nernst equation, is a convenient function (written here for response to potassium and ammonium ions):

$$E = E_c + S \log([K^+] + k_{KNH_4}[NH_4^+]) \quad (1)$$

where  $E$  = electrode potential,  $E_c$  = electrode potential constant,  $S$  = slope of electrode linear response to potassium ions, and  $k_{KNH_4}$  = the selectivity coefficient of the electrode for ammonium ions relative to potassium ions.

$E_c$  and  $S$  for each electrode can be obtained by a simple two-parameter least-squares fit of the potential data obtained in calibration with potassium standards.  $k_{\text{K}^+/\text{NH}_4^+}$ , the only unknown remaining, is determined by calibration of the electrodes with standards that contain both potassium and ammonium ions, followed by least-squares calculations. In these calculations, equation (1) is transformed into a linear function with respect to  $[\text{K}^+]$  and  $[\text{NH}_4^+]$ .

$$10^{(E-E_c)/S} = [\text{K}^+] + k_{\text{K}^+/\text{NH}_4^+}[\text{NH}_4^+] \quad (2)$$

Since equation (2) is a linear combination of  $[\text{K}^+]$  and  $[\text{NH}_4^+]$ , it is possible to consider a set of such equations represented in matrix notation:

$$\mathbf{R}_{A,B} = \mathbf{C}_{A,2} \mathbf{K}_{2,B} \quad (3)$$

where

$\mathbf{R}_{A,B}$  = matrix of  $10^{(E-E_c)/S}$  values obtained with  $B$  electrodes for  $A$  standard solutions containing both analytes,

$\mathbf{C}_{A,2}$  = matrix of concentrations in  $A$  standard solutions of both analytes,

$\mathbf{K}_{2,B}$  = matrix of selectivity coefficients for both analytes from  $B$  electrodes.

The matrix  $\mathbf{K}$  is then

$$\mathbf{K} = (\mathbf{C}^T \mathbf{C})^{-1} (\mathbf{C}^T \mathbf{R}) \quad (4)$$

where  $\mathbf{C}^T$  is the transpose of  $\mathbf{C}$  and  $(\mathbf{C}^T \mathbf{C})^{-1}$  is the inverse of  $\mathbf{C}^T \mathbf{C}$ . The coefficient preceding the potassium ion concentration term in the extended Nernst equation is simply unity, so in practice  $[\text{K}^+]$  is subtracted from each response,  $10^{(E-E_c)/S}$ . It should be noted that the potentials measured for the standards

containing both ions must be within the linear response region of potassium calibration for the electrodes used. Also, the number of standard solutions used to determine the coefficients must be greater than or equal to the number of analytes of interest.

To determine the concentrations of potassium and ammonium ions in an unknown solution, it is necessary to measure the potential of each electrode in the solution. Then the coefficient for potassium ion (unity) must be placed into the  $\mathbf{K}$  matrix. Finally, if the number of electrodes equals the number of analytes to be determined, the following relationship is used:

$$\mathbf{C}^*_{1,2} = \mathbf{R}^*_{1,2} \mathbf{K}^{-1} \quad (5)$$

where  $\mathbf{R}^*$  is the matrix of the responses,  $10^{(E-E_c)/S}$ , to the unknown by each of the electrodes, and  $\mathbf{C}^*$  is the matrix of unknown analyte concentrations. If the number of electrodes used is greater than the number of analytes to be determined, the following relationship must be used:

$$\mathbf{C}^* = \mathbf{R}^* \mathbf{K}^T (\mathbf{K} \mathbf{K}^T)^{-1} \quad (6)$$

Multicomponent analyses based on these types of computation are discussed thoroughly by Kowalski *et al.*<sup>2</sup>

#### Determination of potassium and ammonium ions in samples

Table 1 summarizes the results obtained. Sixteen different electrode pairs can be combined from the individual electrodes (4 valinomycin,  $Av-Dv$ , and 4 nonactin,  $An-Dn$ ). Concentrations of potassium and ammonium ions have been calculated from the re-

Table 1. Ion concentration measurements from various electrode combinations\*

Data set	Electrodes	Sample 1						Sample 2					
		[K]	C.I.	%Error	$[\text{NH}_4^+]$	C.I.	%Error	[K]	C.I.	%Error	$[\text{NH}_4^+]$	C.I.	%Error
1	<i>Av/An</i>	5.9	1.4	-1.7	10.5	3.9	5.0	5.3	0.26	-10.9	8.5	0.06	-3.2
2	<i>Bv/An</i>	5.9	0.9	-1.7	10.5	4.0	5.0	5.5	0.43	-7.6	8.5	0.07	-3.2
3	<i>Cv/An</i>	5.8	1.4	-3.3	10.5	4.0	5.0	5.5	0.55	-7.6	8.5	0.07	-3.2
4	<i>Dv/An</i>	6.0	1.2	0.0	10.5	4.0	5.0	5.9	0.58	-0.8	8.4	0.07	-4.3
5	<i>Av/Bn</i>	5.9	1.5	-1.7	9.8	2.1	-2.0	5.3	0.25	-10.9	8.2	0.43	-6.6
6	<i>Bv/Bn</i>	6.0	1.0	0.0	9.8	2.1	-2.0	5.5	0.40	-7.6	8.2	0.43	-6.6
7	<i>Cv/Bn</i>	5.8	1.4	-3.3	9.8	2.1	-2.0	5.5	0.53	-7.6	8.2	0.39	-6.6
8	<i>Dv/Bn</i>	6.0	1.2	0.0	9.8	2.1	-2.0	5.9	0.54	-0.8	8.1	0.38	-7.7
9	<i>Av/Cn</i>	5.9	1.5	-1.7	10.0	3.1	0.0	5.3	0.25	-10.9	8.5	0.68	-3.2
10	<i>Bv/Cn</i>	5.9	1.0	-1.7	10.0	3.1	0.0	5.5	0.42	-7.6	8.4	0.68	-4.3
11	<i>Cv/Cn</i>	5.8	1.4	-3.3	10.0	3.1	0.0	5.5	0.53	-7.6	8.4	0.73	-4.3
12	<i>Dv/Cn</i>	6.0	1.2	0.0	10.0	3.1	0.0	5.9	0.55	-0.8	8.4	0.73	-4.3
13	<i>Av/Dn</i>	5.9	1.5	-1.7	9.9	2.7	-1.0	5.3	0.24	-10.9	8.2	0.63	-6.6
14	<i>Bv/Dn</i>	5.9	1.0	-1.7	9.9	2.8	-1.0	5.5	0.39	-7.6	8.2	0.63	-6.6
15	<i>Cv/Dn</i>	5.8	1.4	-3.3	9.9	2.8	-1.0	5.5	0.51	-7.6	8.2	0.67	-6.6
16	<i>Dv/Dn</i>	6.0	1.2	0.0	9.9	2.7	-1.0	5.9	0.52	-0.8	8.1	0.68	-7.7
	Average	5.9	1.3	-1.6	10.1	3.0	0.5	5.6	0.43	-6.7	8.3	0.46	-5.3
	Maximum	6.0	1.5	0.0	10.5	4.0	5.0	5.9	0.58	-0.8	8.5	0.73	-3.2
	Minimum	5.8	0.9	-3.3	9.8	2.1	-2.0	5.3	0.24	-10.9	8.1	0.06	-7.7
	Array of all 8 electrodes	6.0	1.3	0.0	10.0	3.0	0.0	5.6	0.41	-6.7	8.3	0.23	-5.5

\*Concentration and confidence interval values have units of  $10^{-4}M$ ; C.I. is the 95% confidence interval; and %error is per cent relative error.



sponse for each electrode pair. The precision of each electrode pair is given by the resulting 95% confidence interval (C.I. in the table represents half the range of this confidence interval). Accuracy is measured as relative error. The true values for potassium and ammonium ions, respectively are taken to be  $5.95 \times 10^{-4}$  and  $1.00 \times 10^{-3}M$  for sample 1, and  $5.95 \times 10^{-4}$  and  $8.78 \times 10^{-4}M$  for sample 2. Results calculated by combining the responses from all eight electrodes are also listed. In all cases, the reported values are based on pooled values from three separate measurements.

For the two-electrode systems, both the accuracy and precision are heavily dependent on the particular electrodes used. Confidence intervals and relative errors are nearly the same for the ammonium ion concentrations when a particular nonactin electrode is coupled with any of the valinomycin electrodes (data sets 1–4). Likewise, similar values are obtained for potassium ion concentrations when a particular valinomycin electrode is coupled with any nonactin electrode (data sets 1, 5, 9 and 13). This is not surprising, in view of the selectivities of the respective electrodes for these cations.

The best set of electrodes can be identified from the results in Table 1. For the determination of potassium ions in model sample 1, electrode *Dv* was the best with respect to accuracy, whereas electrode *Bv* was best from the standpoint of precision. For the determination of ammonium ions in sample 1, electrodes *Cn* and *Bn* gave the best accuracy and precision, respectively. The best combinations of electrodes for sample 1 were sets 12 (*Dv/Cn*) for accuracy and 6 (*Bv/Bn*) for precision. It is important to note that no single combination of two electrodes gave the best results with respect to both accuracy and precision. Of course, the electrode set which provides the highest degree of accuracy should be selected, if it can be properly identified.

A different set of optimal electrodes was indicated in the analysis of sample 2. Although exactly the same electrodes were used as before, considerable variation in electrode performance was observed. The highest accuracy was obtained with electrodes *Dv* and *An*, and best precision with electrodes *Av* and *An* for potassium and ammonium ions, respectively. The large negative errors for sample 2 clearly indicate a systematic error during these measurements. The most probable cause of this error was a significant drift in the response curves between electrode cali-

bration and sample analysis. It is evident that variations in electrode response between samples are significant. Overall, it is difficult, if not impossible, to pick out the best combination of electrodes because of this inconsistency in electrode response.

Results from the entire array of eight electrodes provide values that are close to the average values given by the individual electrode pairs. The use of an overdetermined system effectively averages the response of the individual electrodes, thus reducing the dependence of the final answer on any single element in the array.

Overdetermined systems of this type do not provide the best or the worst result. The best and worst results are given by the combination of the best and worst electrodes. Selection of the best individual electrodes is not possible, however, because of the significant variability in the electrode response between samples. The overdetermined system, on the other hand, provides an average result that is based on all electrodes used. Although this average does not match the best possible response, it does represent the best practical response in view of the electrodes' inconsistency. Overall, greater confidence can be placed in results from an overdetermined system based on electrodes of the same type. This enhanced reliability might prove to be of the greatest benefit of using arrays of multiple ion-selective membrane electrodes.

*Acknowledgement*—Acknowledgement is made to the donors of The Petroleum Research Fund, administered by the American Chemical Society, for support of this research.

#### REFERENCES

1. M. Otto and J. D. R. Thomas, *Anal. Chem.*, 1985, **57**, 2647.
2. M. A. Sharaf, D. L. Illman and B. R. Kowalski, *Chemometrics*, pp. 135–139. Wiley, New York, 1986.
3. J. M. Ariano and W. F. Gutknecht, *Anal. Chem.*, 1976, **48**, 281.
4. N. Busch, P. Freyer and H. Szameit, *ibid.*, 1978, **50**, 2166.
5. A. H. B. Wu and H. V. Malmstadt, *ibid.*, 1978, **50**, 2090.
6. C. R. Martin and H. Freiser, *ibid.*, 1979, **51**, 803.
7. D. Betteridge, E. L. Dagless, P. David, D. R. Deans, G. E. Penketh and P. Shawcross, *Analyst*, 1976, **101**, 409.
8. A. Gustavsson and P. Nylén, *Anal. Chim. Acta*, 1981, **125**, 65.
9. J. Slanina, F. Bakker, J. J. Möls, J. E. Ordeman and A. G. M. Bruyn-Hes, *ibid.*, 1979, **112**, 45.
10. L. P. Rigdon, C. L. Pomernacki, D. J. Balaban and J. W. Frazer, *ibid.*, 1979, **112**, 397.

## FLUORESCENCE DRAINAGE PROFILES OF THIN LIQUID FILMS

RAY VON WANDRUSZKA\* and JAMES D. WINEFORDNER†

Department of Chemistry, University of Florida, Gainesville, FL 32611, U.S.A.

(Received 18 August 1987. Accepted 9 September 1987)

**Summary**—Fluorescence drainage-profiles of thin liquid films formed from Rhodamine solutions containing anionic, cationic and non-ionic surfactants have been investigated. It is found that the influence of system variables such as electrolyte concentration, dye concentration, film environment and solution viscosity can be evaluated by means of the profiles. The addition of sodium chloride leads to the expansion (non-ionic surfactant), or contraction (anionic surfactant) of the profiles. In the case of the cationic surfactant, it reduces the number of fringes in the profiles. The height of selected fringes changes linearly with dye concentration, and no fringes are observed when the films are submerged in non-polar solvents. The influence of solution viscosity on film thickness and drainage rate is demonstrated by the number and frequency of fringes in the profile. The formation of first and second “black films” from solutions containing varying concentrations of sodium chloride can be shown.

Recent work on the fluorescence of dyes in thin liquid films<sup>1,2</sup> has dealt with the appearance of interference fringes during the draining (thinning) of films in vertical frames. The fringes arise because of optical interference between the fluorescence emissions from the dye molecules accumulated at the two film surfaces. Fluorescence drainage-profiles have been generated<sup>1</sup> by monitoring the fluorescence intensities over a period of time. The profiles and fringes are similar to those obtained by reflectance measurements (Fig. 1), with the notable exception that the intensity of the reflectance fringes increases, whereas that of the fluorescence fringes decreases as the profile develops. Also, the fluorescence fringes are generally more clearly resolved.

An interpretation of the shapes of fluorescence drainage-profiles has been presented.<sup>2</sup> It was concluded that the total number of fringes in a profile is determined by the initial film thickness, the fringe width and spacing depend on the drainage rate of the aqueous film core, and the fluorescence intensities are dependent on a combination of factors related to dye accumulation in, and drainage from, the core and the surfaces.

In this paper, a description is given of the use of fluorescence profiles as an alternative method for the analysis of thin films.

### EXPERIMENTAL

The experimental details have already been fully described<sup>1</sup> and will only be summarized briefly here.

Surfactant solutions—sodium lauryl sulphate (SL, 1.3%), tetradecyltrimethylammonium bromide (TTAB, 1%) and

Brij 99 (1%)—were prepared from analytical-grade reagents. Rhodamine B dye ( $5.6 \times 10^{-5}M$  solution) was of laser grade and other chemicals were of analytical grade. The films were formed in a thick-walled closed cell made of blackened brass, with a circular stainless-steel frame attached to the Teflon lid. The solution was drained from the bottom of this cell and measurements were started as the film formed in the frame. No special temperature control was implemented.

A 1-mm<sup>2</sup> spot on the film was excited with 514.5 nm radiation (from an argon-ion laser) incident at 45° to the surface and the fluorescence was measured (also at 45° to the surface) after dispersion with a double monochromator. The emission was monitored at a fixed wavelength over the lifetime of the film and fluorescence drainage-profiles over periods extending from a few minutes to more than an hour were obtained.

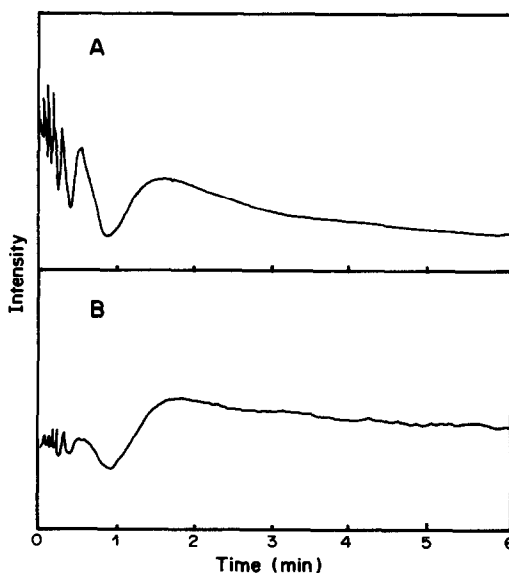


Fig. 1. Fluorescence (A) and reflectance (B) drainage profiles of a Brij 99 film.

\*On leave from Department of Chemistry, University of Witwatersrand, Johannesburg, South Africa.

†Author for correspondence. Work supported by grant: NIH-GM11373-23.

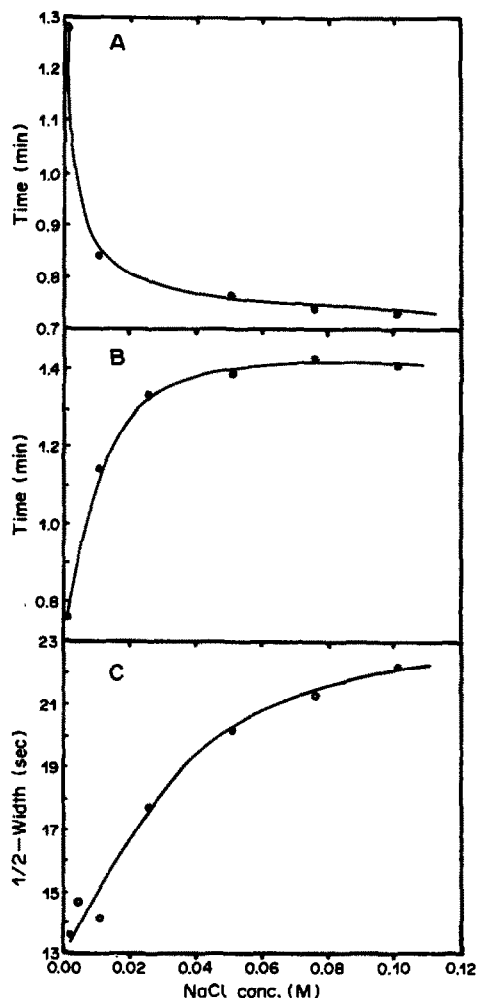


Fig. 2. Variation of (A) SLS film draining time, (B) Brij 99 film (B) drainage time, and (c) penultimate fringe half-width for TTAB, with NaCl concentration.

## RESULTS AND DISCUSSION

### *Influence of electrolyte*

The fluorescence drainage-profiles obtained with three major categories of surfactants (cationic, anionic and non-ionic) were affected differently by electrolytes. The outstanding feature of a series of SLS (anionic) films was a contraction of the profile with increasing sodium chloride concentration. The total number of fringes remained the same, but they were more closely spaced at higher sodium chloride concentrations. This means<sup>2</sup> that the initial film thickness was the same in all cases, but the rate of film thinning increased with the salt concentration. Figure 2 shows the variation of drainage time with sodium chloride concentration, where drainage time is defined as the time elapsed between the beginning of the profile and the apex of the last fringe but one. It was chosen because the very last fringe is rather broad and ill-defined (see Fig. 1).

The opposite effect was found with Brij 99 (non-

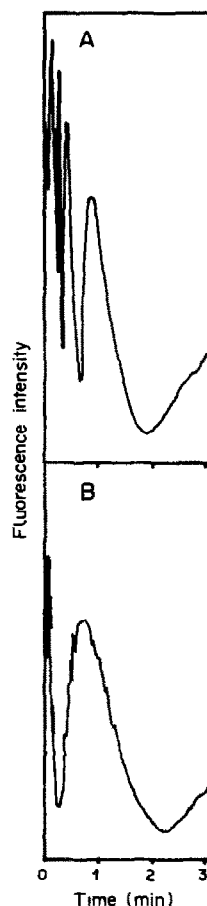


Fig. 3. Fluorescence drainage-profiles of (A) TTAB film and (B) TTAB/0.1M NaCl film.

ionic) films or with different sodium chloride concentrations: the fluorescence drainage-profiles expanded with increasing salt concentration, again without a change in the total number of fringes. Clearly, in this case the addition of sodium chloride decreased the rate of film thinning (Fig. 2).

The effect of an electrolyte on films formed with TTAB was not reflected in the length of the fluorescence drainage-profile. The penultimate fringe appeared after approximately the same time at all sodium chloride concentrations, but the number of fringes decreased significantly with increasing salt concentration (Fig. 3). The time and the appearance of the second to last fringe indicate that the drainage (thinning) rate of the film had not been affected by the sodium chloride. However, the absence of earlier fringes at higher salt concentrations suggests that the movement of dye from the interior of the film to the surfaces had been disturbed. The appearance of a fringe pattern requires that there be both an accumulation of dye molecules at the film surfaces and constantly decreasing distance between these surfaces. Since the latter seems to be occurring, it must be concluded that the former is not. As explained elsewhere,<sup>2</sup> during the first seconds of film life there is a net movement of dye molecules from the interior

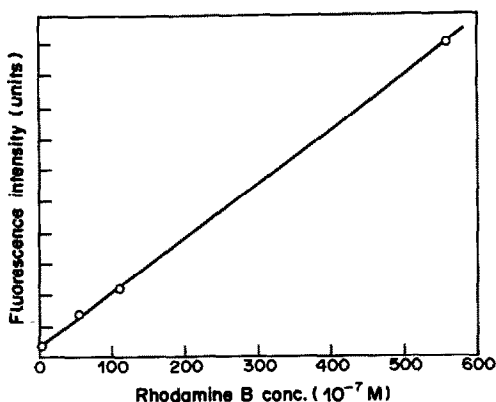


Fig. 4. Variation of penultimate fringe height with dye concentration for SLS film.

to the film surfaces. If this movement is disturbed or delayed, well-defined fringes will not be observed. The half-width of the penultimate fringe varied markedly with sodium chloride concentration in the TTAB solution (Fig. 2).

#### Dye concentration

Varying the Rhodamine dye concentration between  $5.6 \times 10^{-5} M$  and  $5.6 \times 10^{-7} M$  in an SLS solution did not affect the relative shape of the fluorescence profile, but decreased the intensity. Again, the penultimate fringe, being the most reproducible, was chosen to assess the concentration effect. The fringe height (measured from the bottom of the following trough) was found to vary fairly linearly with dye concentration (Fig. 4). It is not clear at this stage why the plot has a positive intercept on the ordinate.

#### Films in hydrocarbon solvents

Aqueous surfactant films were preserved intact upon submersion in hydrocarbon solvents. Films of Brij 99 in pentane, n-hexane, iso-octane and n-nonane exhibited long-term stability, but showed slowly decreasing Rhodamine B fluorescence intensities without interference patterns (Fig. 5). This indicates that a film in a non-polar environment of this kind quickly ceases to drain and attains a stable thickness well above that of the black film.<sup>3</sup> The effect is due to the drag on both film surfaces caused by the interaction of hydrophobic surfactant groups with the hydrocarbon solvent. The slow decrease in fluorescence intensity probably arises because of gradual specific drainage of dye from the surface and a small amount of leaching of dye into the bulk solvent.

#### Viscosity of solution

The viscosities of the surfactant/dye solutions were varied by incorporation of different amounts of glycerol. TTAB solutions with 0–20% glycerol (viscosities 1–14.4 cP) gave profiles of similar shapes and with the same number of fringes. The profiles ex-

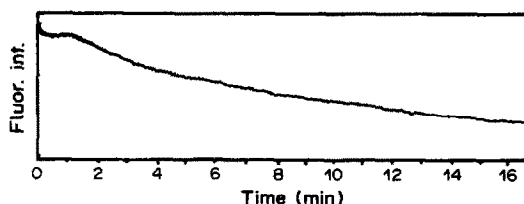


Fig. 5. Fluorescence drainage-profile of a Brij 99 film in n-nonane solution.

panded somewhat with increasing glycerol content, indicating a slowing down of the film-drainage process without increase of initial film thickness. However, solutions with 40% (15.7 cP) and 50% (21.7 cP) glycerol gave vastly expanded profiles with large numbers of fringes. Figure 6 shows a comparison between 20% and 60% glycerol solutions. It should be noted that in the latter a very large number of fringes is compressed into the first 10 sec of film life and is followed by numerous more widely spaced fringes. This profile is indicative of great initial film thickness; the heavy film drains rapidly for about 45 sec, losing most of its bulk during this time. Subsequently, drainage proceeds at a slow pace,

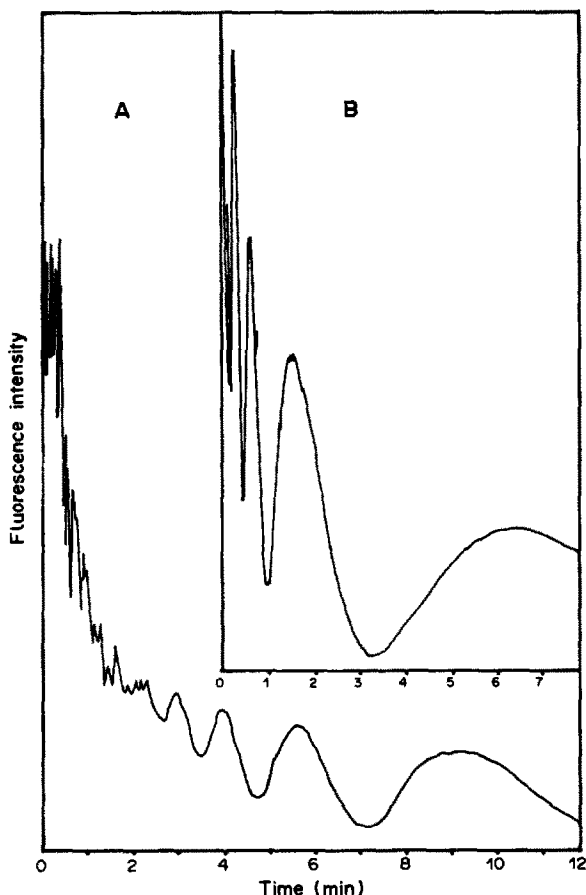


Fig. 6. Fluorescence drainage-profiles of TTAB films containing (A) 60% glycerol and (B) 20% glycerol.

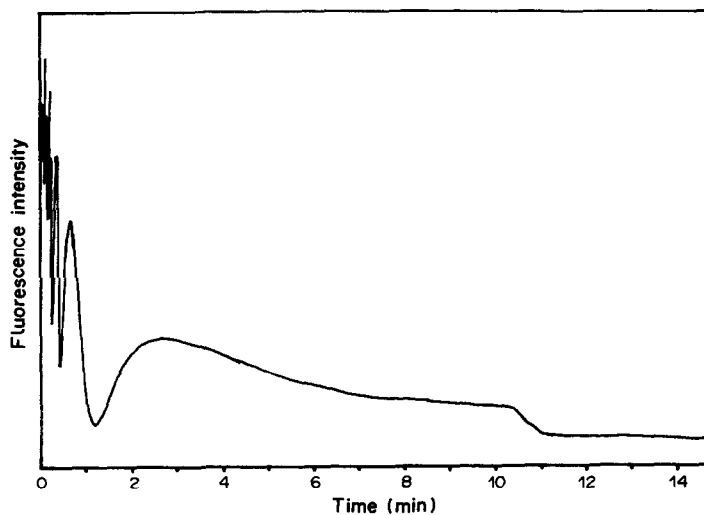


Fig. 7. Fluorescence profile of a TTAB film, showing black film formation.

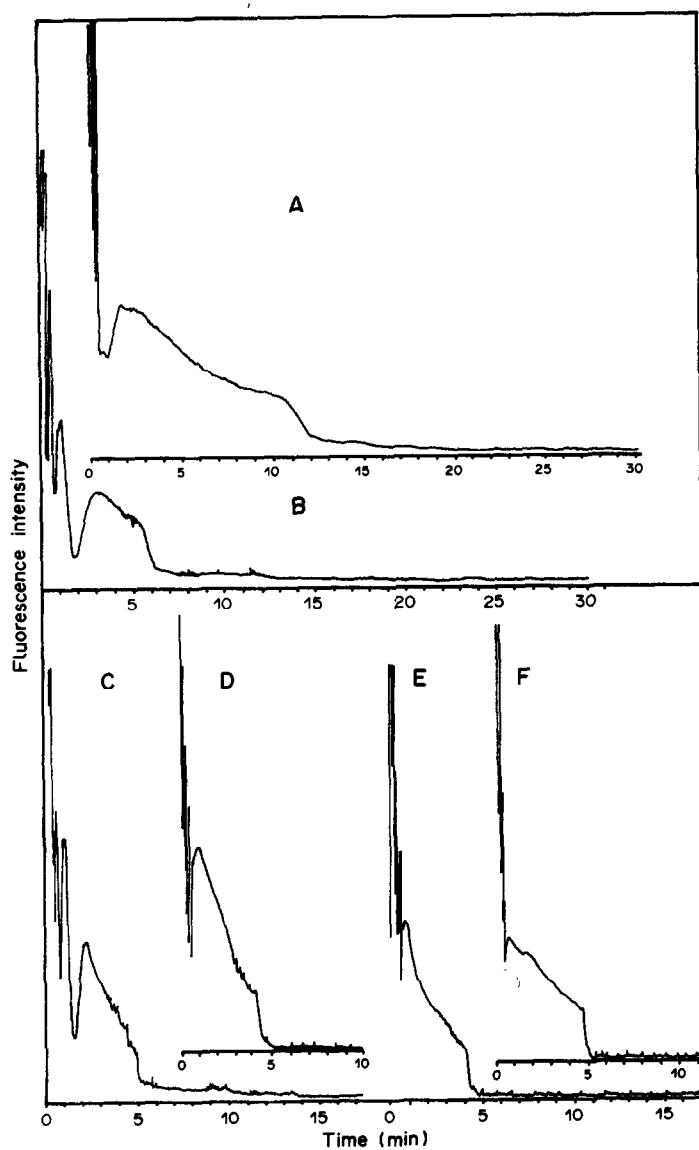


Fig. 8. Black film formation in fluorescence drainage-profiles of SLS films containing (A) 0.0M, (B) 0.02M, (C) 0.038M, (D) 0.075M, (E) 0.15M and (F) 0.3M NaCl.

consistent with the glycerol content, and about 5 broader fluorescence fringes are formed.

### Black film

The fluorescence drainage-profiles clearly show the occurrence of black soap films (Fig. 7). Formation of the black film leads to a sharp decrease in fluorescence intensity, occurring after several minutes of film life, when interference fringes no longer exist. Earlier work<sup>1</sup> showed that at this stage, the contribution to the overall fluorescence intensity by dye in the film interior is minimal. The 4-fold drop in intensity must therefore be due to a relatively sudden decrease of dye concentration at the surfaces when the black film is formed. It may be surmised that the close proximity of the surfaces (< 50 nm) causes the dye molecules to be displaced from their positions near the surface and carried down with the bulk of the aqueous core as it is being "squeezed out".

Early studies<sup>4,5</sup> revealed the existence of a "second" black film, a still thinner region in the "first" black film. It has been found to form from the first black film by evaporation<sup>6</sup> or to arise spontaneously when a surfactant solution of high electrolyte concentration is used.<sup>7</sup> It has been studied thoroughly by FT-IR spectroscopy.<sup>8</sup> The fluorescence drainage-profile of an SLS film, extending into the black film region, is shown in Fig. 8.

A sharp transition occurs after about 10 min of film life and lasts slightly less than 2 min. The fluorescence of the resulting film (which appears black in room light) continues to decrease at an ever slower rate for at least another hour. This is the first black film, thinning slowly after formation. No distinct transition to another type of black film is observed. A 0.02M sodium chloride concentration in the SLS solution (Fig. 8) led to accelerated black film formation, the black film appearing after about 5 min. The transition was somewhat sharper than in the previous case and the black film was slightly thinner. Its drainage behaviour remained relatively unchanged, except for the appearance of some "noise" spikes on the profile. These result from a

complex alternating pattern of coloured patches that arise in black films containing salts. The effect has been termed "irregular behaviour"<sup>6</sup> and was reported to occur mainly in the boundary regions between different types of films.<sup>7</sup>

With sodium chloride concentrations of 0.15M and 0.3M, the black film transitions were notably sharp and the resulting films extremely thin and invariant in time. In these cases, the second black film was formed immediately.<sup>7</sup> A 0.038M sodium chloride concentration gave some slight indication of a transition between the first and second black films (Fig. 8); the first black film was formed after 5 min of film life, and the transition to the invariant state (second black film) took place in the period from 10 to 12 min. However, this appears to be a relatively gradual process of thinning, unlike the abrupt first black film formation.

### CONCLUSION

Fluorescence drainage-profiles present an interesting and convenient way of studying liquid films. Film stability, relative rate of draining and sensitivity to system variables can be easily monitored. Though the results obtained with flat vertical films may be applied to foam lamellae in general, further investigations of foams by this method are needed.

### REFERENCES

1. R. von Wandruszka and J. D. Winefordner, *Talanta*, 1986, **33**, 871.
2. *Idem*, *ibid.*, 1987, **34**, 971.
3. J. T. G. Overbeek, *J. Phys. Chem.*, 1960, **64**, 1178.
4. I. Newton, *Opticks*, Book II, Part I, Smith and Walford, London, 1704.
5. J. W. Gibbs, *Trans. Connecticut Acad.*, 1876-8, **3**, 343.
6. K. J. Mysels, K. Shinoda and S. P. Frankel, *Soap Films—Studies of Their Thinning, and a Bibliography*, Pergamon Press, London, 1959.
7. M. N. Jones, K. J. Mysels and P. C. Scholten, *Trans. Faraday Soc.*, 1966, **62**, 1336.
8. J. Umemura, M. Matsumoto, T. Kawai and T. Takenaka, *Can. J. Chem.*, 1985, **63**, 1713.

## RADIOMETRIC DETERMINATION OF URANIUM ACCUMULATED IN BACTERIAL CELLS

M. CHWISTEK, J. CHMIELOWSKI\* and I. TOMZA†

Department of Biochemistry, University of Silesia, 40-032 Katowice, Poland

(Received 25 March 1987. Revised 8 July 1987. Accepted 9 September 1987)

**Summary**—A method for the radiometric determination of uranium accumulated in bacterial cells was investigated. *Pseudomonas putida* ATCC 33015 was grown in a medium containing uranium in the form of  $UO_2(NO_3)_2$ . The cells were harvested by centrifugation, washed, resuspended in a buffer solution, ultrasonically disrupted and then suspended in Unisolve-1. The radiation emitted by natural uranium isotopes (mainly  $^{238}U$  and  $^{234}U$ ) was measured by liquid scintillation counting with natural uranium as an internal standard. Mineralization of the samples was not required. Determination of the uranium content of bacterial cells was done either by comparing the radioactivity of the sample with that of standard samples or by using a calibration graph. The method was also used for determination of uranium in isolated subcellular fractions. Most of the uranium was associated with components of the cell membrane (lipids and polysaccharides), but part was bound to nucleic acids and microsomes. The relative standard deviation of the radiometric measurements did not exceed 5%.

Several papers dealing with metal accumulation by micro-organisms have been published in recent years.<sup>1,2</sup> The process of metal bioaccumulation has been utilized in order to concentrate heavy metals, including uranium,<sup>3-6</sup> in microbial cells, or to remove these metals from aqueous environments. Some attempts have been made to develop methods for use in recovery of uranium dispersed in aqueous systems and for the decontamination of waste waters derived from processing of nuclear fuel. Various methods of uranium determination have been applied in these studies. A spectrophotometric method, with Arsenazo III<sup>7</sup> was adopted in the investigation of uranium accumulation by the yeast *Saccharomyces cerevisiae*<sup>3</sup> and the fungus *Rhizopus arrhizus*.<sup>4</sup> The uptake of uranium by the alga *Chlorella regularis* has been investigated by X-ray fluorescence.<sup>8</sup> The recovery of uranium from sea-water by algae, and by fungi from waste waters derived from uranium-ore treatment has been monitored by neutron activation.<sup>9-11</sup>

The purpose of this study was to use the liquid scintillation technique for the radiometric determination of uranium in intact *Pseudomonas putida* cells and in their subcellular fractions.

### EXPERIMENTAL

#### Apparatus

The counting was performed with an LKB 1215 Rack-Beta liquid scintillation counter. All the measurements were made within the energy range corresponding to the energy of alpha-particles emitted mainly by  $^{238}U$  and  $^{234}U$  (background 18 cpm). The bacterial cells were disrupted with a

Techpan model UD-11 ultrasonic disintegrator. A Beckman L5-75 ultracentrifuge was used to separate the subcellular fractions of the uranium-loaded cells.

#### Reagents

Uranyl nitrate hexahydrate (Johnson-Matthey) was separated from uranium decay products by means of Dowex 1 × 8. Unisolve-1 (Koch-Light) and Dimilume-30 (Packard) liquid scintillators were used. All the reagents used to prepare the nutrients were of analytical grade.

#### Culture conditions

The organism used in this study was a wild strain of *Pseudomonas putida* ATCC 33015. The bacteria were grown in a chemostat (model Biostat, Braun) under aerobic conditions at 30° in a mineral medium<sup>12</sup> (devoid of yeast extract) supplemented with catechol (4 mM) as sole source of carbon. The mineral medium consisted of  $K_2HPO_4$  (0.15%),  $KH_2PO_4$  (0.05%),  $MgSO_4 \cdot 7H_2O$  (0.02%) and  $NH_4Cl$  (0.5%); the pH was adjusted to 7.3. The bacteria were adapted to the biodegradation of 4 mM catechol by induction, i.e., by growth in the presence of a gradually increasing concentration of catechol. The pH of the growth medium was maintained at 7.3. The outflow of the chemostat was collected in a sterile flask. A 500-ml portion of the suspension was centrifuged to separate the cells from the growth medium. The cells were then washed twice with the mineral medium.

#### Determination of uranium in samples

The washed cells, free from extraneous nutrients, were suspended in 500 ml of saline uranyl nitrate solution (0.1 or 0.5 mM). This suspension was incubated at 30° and aerated by shaking. At the desired time, cells were separately harvested from two 10-ml aliquots of the suspension, by centrifugation for 20 min at 5000 g. The pellets were washed twice with distilled water and centrifuged. Each batch of washed cells was then resuspended in 4 ml of distilled water and sonicated for 1 min at 0° with a Techpan model UD-11 ultrasonic disintegrator. The sonicated suspensions (each 4 ml) were placed in separate glass vials, then 6 ml of gelling scintillator (Unisolve-1) were added to each vial and the mixture was vigorously shaken in order to obtain a homogeneous gel. The radioactivity of the samples was determined

\*Author for correspondence.

†Present address: Radiometry Laboratory, Central Mining Institute, 40-166 Katowice, Poland.

Table 1. Comparison of radiometric determinations of uranium in sonicated and untreated cells of *Pseudomonas putida*

Parameter	Uranium count rate in bacterial suspension	
	Sonicated	Untreated
Mean value $\bar{x}$ (5 samples), <i>cpm</i>	580	575
Standard deviation, <i>s</i> , <i>cpm</i>	3	29
Relative standard deviation, <i>s</i> , %	0.5	5.0
Confidence interval ( $\bar{x} \pm t_{0.95} s / \sqrt{n}$ ), <i>cpm</i>	580 $\pm$ 4	575 $\pm$ 36

by measuring the integrated count rate with the LKB 1215 RackBeta liquid scintillation counter, with natural uranium added to one vial as an internal standard. The uranium in the bacterial cells was determined either by comparing the count rate (in cpm) of the sample with that of the corresponding sample plus internal standard or by use of a calibration graph obtained for a series of standard samples of known uranium content.

#### RESULTS AND DISCUSSION

The radioactivity of the samples was measured exactly 3 days after their preparation, to avoid errors resulting from a rise in the activity of the samples due to the appearance of uranium decay products (Pa).

Liquid scintillation measurements usually require thorough homogenization of any biological material and its even distribution in the scintillation cocktail. In this study the use of ultrasonication for disruption of cells and release of cytoplasm and cell membrane material, appeared to be a relatively simple and efficient method of homogenization. The efficiency of homogenization was checked spectrophotometrically.<sup>13</sup> Ultrasonication for 60 sec at 0° was found to be sufficient to produce a homogeneous suspension suitable for the radiometric measurements.<sup>14</sup>

The effect of homogenization of the samples on the reliability of the radiometric measurements was examined statistically. Ten samples containing equal amounts of cells (3.0 mg dry weight) and uranium (1.3  $\mu$ mole) were counted, half previously sonicated and the rest untreated. The results are presented in Table 1. Statistical analysis of the experimental data by Snedecor's test showed that the reliability of counting was significantly enhanced after sonication of the sample. The same could be concluded from comparison of the standard deviations for the measurements, but the means of the two sets of measurements did not differ at the 95% significance level (Student's *t*-test). It can be concluded that homogenization of a bacterial suspension with 20-kHz ultrasound for 1 min is sufficient to ensure adequate accuracy of the radiometric determination of uranium in bacterial cells. The relative standard deviation of the radiometric measurement with the LKB liquid scintillation counter was preset at 5%, which

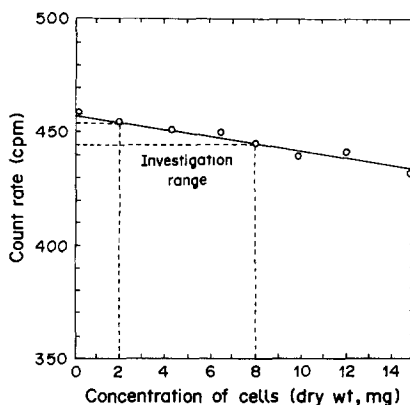


Fig. 1. The effect of cell concentration (dry weight) on the quenching of the scintillation process. Each sample contained 1  $\mu$ mole of uranium.

was achieved by preselecting the number of counts to be accumulated before data print-out (1  $\mu$ mole of uranium gave 450 cpm, and the counting time for this was 3 min). There is a possibility that the bacterial biomass might quench the scintillation process and decrease the counting efficiency. To examine this possibility the effect of the concentration of bacterial cells on the measurement efficiency was determined (Fig. 1), and found that to be insignificant. Within the biomass concentration range 200–800 mg/l. (dry weight) the calculated change in the efficiency of counting was 2.3%.

The uranium associated with the cells was determined from a calibration graph obtained for a series of standard solutions containing various amounts of uranium (0.1–1.5  $\mu$ mole) and 3.5 mg of cells (dry weight) per vial. The standard solutions were then homogenized by sonication. The calibration graph is presented in Fig. 2. A calibration graph for uranium

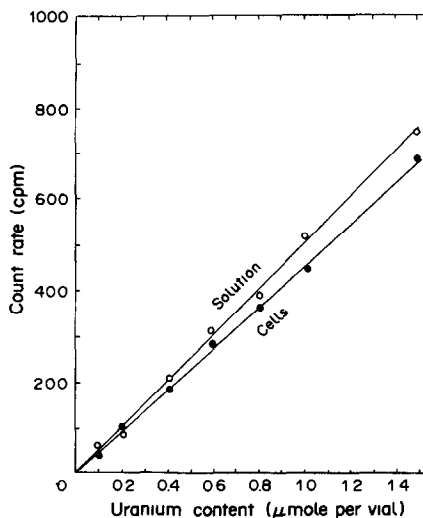


Fig. 2. Calibration graphs for the radiometric determination of uranium: (A) in bacterial cells (3.5 mg dry weight) (●—●), (B) in solution (○—○).



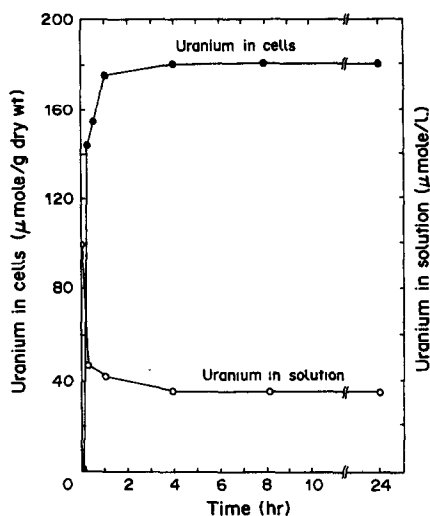


Fig. 3. Uranium accumulation by *Pseudomonas putida* ATCC 33015. The initial uranium concentration was 0.1 mM, concentration of cells (dry weight) 350 mg/l., pH 5.0.

in the supernatant liquid obtained after separation of the bacteria by centrifugation was prepared similarly, but with the microbial cells omitted from the standard samples. A linear relationship was obtained for 0.1–1.5  $\mu\text{mole}$  of uranium per vial (see Fig. 2).

The method described here was used to study uranium accumulation in *Pseudomonas putida* cells. The changes in uranium content in the intact cells and in the incubation medium during a 24-hr exposure are shown in Fig. 3. The cells exposed to uranium were able to accumulate 180  $\mu\text{mole}$  of uranium per g dry weight of cells. The accumulation level reached the saturation plateau after 1 hr of incubation and remained practically unchanged during further exposure to uranium.

The uranium in the cell fractions isolated by the procedure of Horitsu *et al.*<sup>15</sup> was determined in a similar way. The samples containing subcellular fractions differed slightly in colour and turbidity. Because these factors might cause an increase in the quench

level and decrease the counting efficiency, and hence affect the measured count rates, an internal standard was used in the radiometric measurements. The samples (in duplicate, 4 ml each) were placed in two scintillation vials and 6 ml of the scintillation solution (Unisolve-1 or Dimilume-30) were added to each. Then 0.1 ml of 0.01 mM uranyl nitrate was added to one vial. The number of counts per  $\mu\text{mole}$  of uranium was calculated as the difference between the count rates obtained for the pair of samples. The same procedure was used for each cell fraction isolated by the Horitsu method from the uranium-loaded *Pseudomonas putida* cells. These results are summarized in Table 2. Uranium was found in various cell components but most of it (82.5%) was distributed in the lipid and the polyphosphate–polysaccharide fraction. The remaining cell membrane heteropolymers such as lipopolysaccharides, mucopeptide and poly- $\beta$ -hydroxybutyrate bound only 3.5% of the total cell-associated uranium. A small amount of uranium (4.9%) was found in the microsomal fraction and the nucleic acids.

The large proportion of uranium found in the lipid and the polyphosphate–polysaccharide fraction did not appear to have any significant effect on the permeability or other properties of the cell envelope. However, the accumulation of many metals by DNA can lead to marked effects on genome function, as has been previously noted in studies on *Bacillus subtilis*.<sup>16</sup>

## CONCLUSIONS

The method presented in this paper enables trace amounts of uranium ( $10^{-7}$ – $10^{-6}$  mole) to be determined, as well as higher concentrations of this element dissolved in aqueous media or associated with whole cells and the subcellular fractions of bacteria.

The use of ultrasonic cell disruption for homogenization of samples allowed mineralization of bacterial cells to be avoided. The sonication of samples resulted in enhancement of counting efficiency and improvement in the accuracy and reliability of the measurements.

Table 2. Distribution of uranium in cellular components of uranium-loaded *Pseudomonas putida* ATCC 33015 cells; the cells (350 mg/l. dry weight) were fractionated by the Horitsu method<sup>15</sup> after 1 hr incubation in the presence of 0.5 mM  $\text{UO}_2^{2+}$  at pH 5.0

Uranium distribution in cellular components		
Fractions	$\mu\text{mole/g}$ (dry weight) of cells	%
Whole cells	830	100.0
Lipids	348	42.0
Polysaccharides, polyphosphates	336	40.5
Lipopolysaccharides, mucopeptide, poly- $\beta$ -hydroxybutyrate	29.0	3.5
Nucleic acids	18.3	2.2
Proteins	5.0	0.6
Microsomal fraction	22.4	2.7
Undetermined losses	60.7	8.5

With whole bacterial cells in a sample the uranium count rate was affected by a slight quenching of the scintillation process. For the cell concentration range 200–800 mg/l. (dry weight) the counting efficiency was decreased by about 2%.

*Acknowledgements*—This work was supported by the Polish Research Programme CPBP 03.08. The radiometric measurements were performed at the Radiometry Laboratory, Central Mining Institute, Katowice.

#### REFERENCES

1. A. O. Summer and S. Silver, *Ann. Rev. Microbiol.*, 1978, **32**, 637.
2. S. R. Hutchins, M. S. Davidson, J. A. Brierley and C. L. Brierley, *ibid.*, 1986, **40**, 311.
3. G. W. Strandberg, S. C. Shumate and J. R. Parrot, *Appl. Environ. Microbiol.*, 1981, **41**, 237.
4. M. Tsezos and B. Volesky, *Biotechnol. Bioeng.*, 1982, **24**, 385.
5. T. Horikoshi, A. Nakajima and T. Sakaguchi, *Eur. J. Appl. Microbiol. Biotechnol.*, 1981, **12**, 90.
6. M. Galun, P. Keller, D. Malki, H. Feldstein, E. Galun, S. Siegel and B. Siegel, *Water Air Soil. Pollut.*, 1983 **20**, 221.
7. S. B. Savvin, *Talanta*, 1961, **8**, 673.
8. T. Horikoshi, A. Nakajima and T. Sakaguchi, *Agric. Biol. Chem.*, 1979, **43**, 617.
9. T. Sakaguchi, T. Horikoshi and A. Nakajima, *J. Ferment. Technol.*, 1978, **56**, 561.
10. T. Horikoshi, A. Nakajima and T. Sakaguchi, *ibid.*, 1979, **57**, 19.
11. M. Tsezos, *Biotechnol. Bioeng.*, 1984, **26**, 973.
12. Y. Kojima, N. Itada and O. Hayaishi, *Biochem. J.*, 1961, **236**, 2223.
13. D. G. Hegeman, *J. Bacteriol.*, 1966, **91**, 1140.
14. M. Chwistek, J. Chmielowski, A. Danch and B. Klapcińska, *Chem. Anal.*, (Warsaw), 1981, **26**, 141.
15. H. Horitsu, M. Takago and M. Tomojeda, *Eur. J. Appl. Microbiol. Biotechnol.*, 1978, **5**, 279.
16. T. Kada, K. Hirano and Y. Shirasu, in *Chemical Mutagens*, F. J. de Serres and A. Hollaender (eds.), Vol. 6, p. 149. Plenum Press, New York, 1980.

## DETERMINATION OF SEMIMICRO AMOUNTS OF CALCIUM IN THE PRESENCE OF OTHER ALKALINE-EARTH METALS

NIRMAL MAITRA, ALBERT W. HERLINGER and BRUNO JASELSKIS

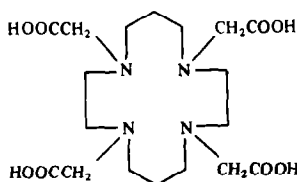
Department of Chemistry, Loyola University of Chicago, 6525 North Sheridan Rd, Chicago, IL 60626, U.S.A.

(Received 15 December 1986. Revised 16 July 1987. Accepted 29 August 1987)

**Summary**—Cyclam tetraacetic acid (CTA) is used to determine semimicro quantities of calcium in the presence of other alkaline-earth metals in natural and synthetic water samples. End-point detection is achieved amperometrically with  $Zn(en)_2^{2+}$  as the indicator. Magnesium and barium do not interfere. In the presence of strontium, two distinct end-points are obtained when its concentration is comparable with that of the calcium. If the concentrations are substantially different, calcium and strontium appear to be titrated together.

Calcium can be determined in the presence of magnesium gravimetrically, and by titrimetric methods using ethylenediaminetetraacetic acid (EDTA) or its analogues.<sup>1–6</sup> Fluorescence,<sup>6</sup> atomic absorption,<sup>7</sup> spectrophotometric,<sup>8–10</sup> ion-specific electrode potentiometric,<sup>11</sup> and thermometric<sup>12</sup> techniques have also been used. The titrimetric methods in general are based on either titration of calcium after separation from magnesium or after precipitation of magnesium hydroxide at high pH, and use of indicators such as calcein.<sup>13</sup> The latter method obviates the need for prior separation. End-point detection can also be achieved amperometrically by using electroactive species as described by Laitinen and Simpson,<sup>14</sup> Ringbom and Wilkman,<sup>15</sup> Reilly *et al.*,<sup>16</sup> and Kainz and Sontag.<sup>17</sup> In the direct titration of calcium at high pH, the amount of calcium found is less than the theoretical value, and this error increases at calcium concentrations less than millimolar.

In the present study, 1,4,8,11-tetraazacyclotetradecane-*N,N',N'',N'''*-tetraacetic acid, a relatively new analytical reagent,<sup>18</sup> is used for the direct titration of calcium in the presence of magnesium and other alkaline-earth metal ions. Cyclam tetraacetic acid (CTA) is a trivial name we use to designate this reagent.



CTA

End-point detection is achieved amperometrically with tris(ethylenediamine)zinc(II),  $Zn(en)_3^{2+}$ , as the indicator. By this method, submilligram amounts of calcium in synthetic and natural (Chicago) water

samples, and strontium in the presence of calcium, have been determined.

### EXPERIMENTAL

#### Apparatus

A PAR Model 170 electrochemical unit with a three-electrode system was used for the amperometric determinations. Titrant was delivered to the polarographic cell from a precision micrometer burette.

#### Reagents

All chemicals used were of analytical or primary standard grade unless otherwise noted. Cyclam tetraacetic acid was prepared by the reaction of 1,4,8,11-tetraazacyclotetradecane with monochloroacetic acid in aqueous alkaline medium.<sup>19</sup> Reaction conditions were identical to those described by Desreux for the synthesis of the related tetraazatetra-acetic acid macrocycle DOTA.<sup>18</sup> The CTA was purified by precipitation from aqueous solution at the isoelectric point and standardized against 0.0200M calcium solution (prepared by dissolving 1.002 g of dried calcium carbonate in 500 ml of 0.100M hydrochloric acid), with amperometric end-point detection. The supporting electrolyte was prepared by mixing equal volumes of 0.9M aqueous solution of ethylenediamine and 2.0M potassium chloride solution and adjusting the final pH to 11 with 2M hydrochloric acid. An approximately 0.02M amperometric indicator solution was prepared by dissolving 275 mg (2.0 mmole) of anhydrous zinc chloride in 100 ml of the supporting electrolyte. Standard 0.020M solutions of magnesium, strontium and barium were prepared from the chlorides.

#### Procedure

Amperometric titrations were done in a standard polarographic cell. Known volumes (0.050–2.00 ml) of the solution to be titrated, along with 0.500 ml of the indicator solution and 25 ml of the supporting electrolyte were placed in the cell and deaerated by purging with nitrogen for 5 min. The polarogram was then recorded over the potential range from  $-1.2$  to  $-1.6$  V vs. the saturated calomel electrode (SCE). The reduction current for the zinc-ethylenediamine indicator complex was measured at  $-1.60$  V. Titrant was then added to the polarographic cell in 0.050 or 0.100 ml increments from a precision micrometer burette. After each addition of titrant, nitrogen was bubbled through the solution for about 1 min before the diffusion current was measured. The end-point of the titration was obtained from the intersection of the best straight lines drawn through the

Table 1. Titration of synthetic and Chicago water samples with CTA\*

Amount taken, mg			Amount found, mg	
Ca <sup>2+</sup>	Mg <sup>2+</sup>	Sr <sup>2+</sup>	Ca <sup>2+</sup>	Sr <sup>2+</sup>
<b>Synthetic samples</b>				
0.320	—	—	0.318 ± 0.008	—
0.410	0.25	—	0.407 ± 0.009	—
0.820	0.05	—	0.816 ± 0.010	—
0.041	0.25	—	0.042 ± 0.005	—
—	—	0.438	0.435 ± 0.013	—
0.410	—	0.438	0.409 ± 0.009	0.431 ± 0.013
0.820	—	0.438	0.818 ± 0.010	0.431 ± 0.013
0.410	—	0.876	0.407 ± 0.010	0.868 ± 0.012
<b>City water†</b>				
0.185	0.050	0.001	0.187 ± 0.006	

\*Portions of calcium and other alkaline-earth metal ion solutions were added to 25 ml of supporting electrolyte solution plus 0.500 ml of the zinc-ethylenediamine complex.

†The amount of calcium, magnesium and strontium in 5.00 ml of City water as reported by the Department of Water Purification Laboratories for the City of Chicago.

data points in a plot of diffusion current *vs.* volume of standard CTA solution added. The diffusion currents were corrected for the dilution factor when the volume of titrant used exceeded 1 ml.

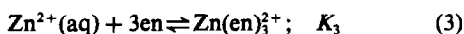
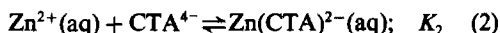
#### Determination of calcium in Chicago water

A 5.00-ml sample of Chicago tap water was added to 25 ml of the supporting electrolyte and 0.500 ml of the indicator solution. After deaeration the solution was titrated with CTA as described above. Total calcium and magnesium in the water sample was determined by titration with EDTA, with calmagite as indicator. The magnesium present was determined by difference.

## RESULTS AND DISCUSSION

Synthetic and Chicago water samples containing calcium, magnesium, strontium and barium were analysed by the procedure described. The results summarized in Table 1 are the average of six determinations.

The success of a direct determination of calcium in the presence of other alkaline-earth metals ions depends upon the magnitude of the formation constants of the complex ions in solution during the titration. With CTA as the titrant and tris(ethylenediamine)-zinc(II) as the amperometric indicator, the important complexation reactions to consider are:



The formation constants and the calculated conditional constants for these reactions are shown in Table 2. For  $Zn(en)_3^{2+}$  to be a useful indicator for the determination, CTA must readily displace the ethylenediamine from it at the end-point and the magnitude of the equilibrium constant for the reaction

Table 2. Formation constants and calculated conditional constants\*

Ion	log $K_f$	log $K'_f$	log $K_5$	log $K'_5$
Mg(CTA) <sup>2-</sup>	3.02†	2.67	0.690	1.88
Ca(CTA) <sup>2-</sup>	9.48†	9.13	-5.77	-4.58
Sr(CTA) <sup>2-</sup>	6.15†	5.80	-2.44	-1.25
Ba(CTA) <sup>2-</sup>	4.32†	3.97	-0.61	0.580
Zn(CTA) <sup>2-</sup>	15.81†	15.46		
Zn(en) <sub>3</sub> <sup>2+</sup>	12.10‡	10.91§		

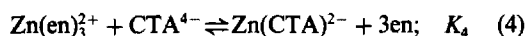
\*The conditional constants,  $K'$ , have been calculated for pH 11, from the formation constants for the CTA-metal complexes and the successive  $pK_a$  values for CTA, *viz.* 3.46, 4.31, 9.75 and 11.07.

†From reference 19.

‡From reference 20.

§Zinc-ethylenediamine conditional constant calculated for pH 11 and an ethylenediamine concentration of 0.4M.

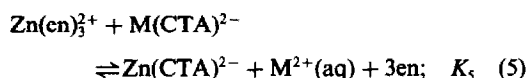
[equation (4)] should be relatively large.



The value of this equilibrium constant,  $K_4$ , is obtained from the equilibrium constants for the reactions shown in equations (2) and (3), in the usual way;

$$K_4 = \frac{[Zn(CTA)^{2-}][en]^3}{[Zn(en)_3^{2+}][CTA^{4-}]} = \frac{K_2}{K_3}$$

The conditional equilibrium constant  $K'_4$  was calculated to be  $10^{4.55}$  at pH 11 and an ethylenediamine concentration of 0.4M. A further requirement is that the competitive equilibrium between  $Zn^{2+}$  and analyte ( $M^{2+}$ ) for CTA should favour the analyte. Specifically, the equilibrium constant for the reaction between the indicator complex and the CTA-analyte complex, equation (5), must be relatively small.



The value of this equilibrium constant,  $K_5$ , is calculated from the formation constants for the reactions shown in equations (1)–(3):

$$K_5 = \frac{[Zn(CTA)^{2-}][M^{2+}][en]^3}{[Zn(en)_3^{2+}][M(CTA)^{2-}]} = \frac{K_2}{K_3 K_1}$$

As seen in Table 2, the conditional constant  $K_5$  is relatively small for  $M = Ca^{2+}$  or  $Sr^{2+}$  and these ions are titrated with CTA prior to  $Zn(en)_3^{2+}$  in the determination. Further, because of the small formation constants of the magnesium and barium complexes with CTA, these ions do not interfere in the direct determination of calcium or strontium by this method.

The zinc-ethylenediamine reduction currents observed during the titration of alkaline-earth metal ions with CTA are shown in Fig. 1. The pM values for calcium, strontium, and barium calculated by using the appropriate conditional formation constants are shown in Fig. 2. It can be seen from these figures that the titration of calcium and strontium

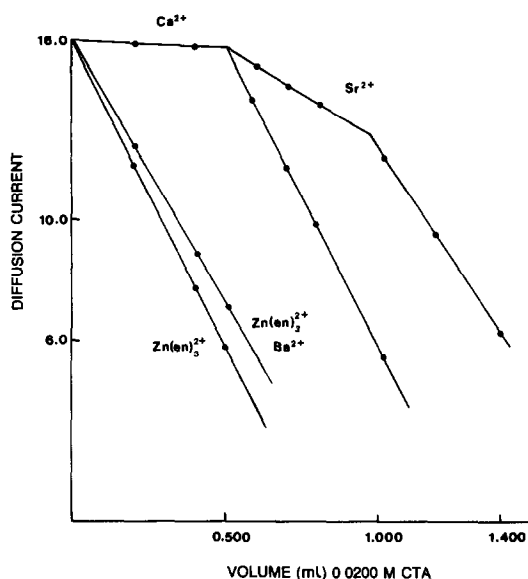


Fig. 1. Amperometric titration of calcium, strontium, barium and zinc-ethylenediamine.

with CTA is feasible and that satisfactory end-points can be obtained with  $\text{Zn(en)}_2^{2+}$  as the indicator. The amperometric titrations show that though the observed diffusion current for the indicator complex with barium ion is present is somewhat higher than when this ion is absent, barium does not interfere in the determination of calcium or strontium. It is also apparent that complexation of zinc from the indicator by CTA occurs only after the titration of calcium and strontium is complete. The sharpness of the end-point in the titration of solutions containing calcium and strontium depends upon the concen-

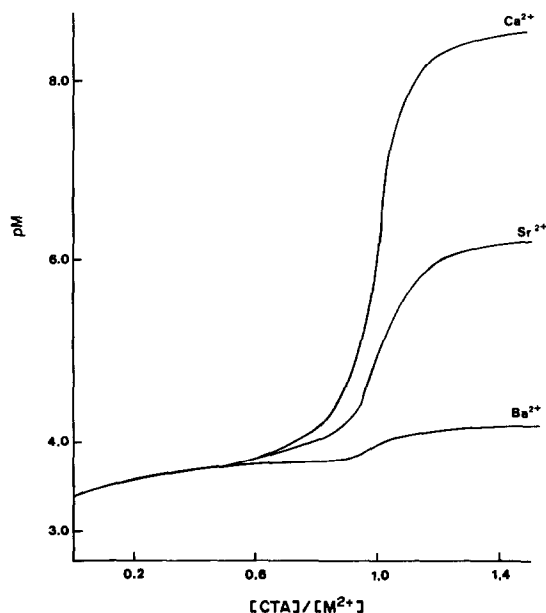


Fig. 2. Theoretical titration curves for 0.0004M calcium, strontium and barium with 0.0200M CTA.

tration of both ions present. Two distinct end-points are observed when the concentrations of these ions are comparable. Both ions may be determined sequentially provided the amount of calcium and strontium present is greater than 0.15 mg and the amount of strontium is less than 1.2 mg in the solution in the titration cell. However, when the concentrations are substantially different, calcium and strontium appear to be titrated together. If this situation prevails, only the total concentration of the ions may be obtained.

Calcium in natural (City of Chicago) and synthetic water samples has been determined with an approximate precision of  $\pm 6 \mu\text{g}$ . This corresponds to a range of  $\pm 0.008 \text{ ml}$  of 0.02M CTA at the intersection of the two best lines defined by the data points in the amperometric titration. This is comparable to the precision obtainable by visual end-point detection. In general, the relative error decreases with increasing amounts of calcium titrated.

At pH 11 or below, up to 0.5 mg of magnesium will remain in solution in the 25 ml or so of electrolyte in the polarographic cell, and even at higher concentrations magnesium does not interfere. At this pH, aluminium is not complexed by CTA and therefore does not interfere.

Transition-metal ions in general have relatively large formation constants with CTA.<sup>19</sup> These ions will be co-titrated with calcium and if present should be removed prior to the calcium determination either by electrolysis at a mercury cathode or by other methods such as liquid-liquid extraction, ion-exchange or precipitation, or they should be masked.<sup>4</sup>

Phosphate, fluoride and other anions which form precipitates with calcium and strontium in alkaline solution interfere. Carbonate in the amounts normally present in natural samples does not interfere, nor does it interfere in analysis of dolomite or limestone, since carbonate is eliminated during acid dissolution of the sample.

#### REFERENCES

1. R. W. Schmidt and C. N. Reilly, *Anal. Chem.*, 1957, **29**, 264.
2. P. B. Sweetser and C. E. Bricker, *ibid.*, 1954, **26**, 195.
3. A. J. Courtoisier, F. Forestier and A. Ray, *Ann. Technol. Agric.*, 1977, **26**, 1.
4. R. Přibil, *Applied Compleximetry*, Pergamon Press, Oxford, 1982.
5. F. S. Sadek, R. W. Schmidt and C. N. Reilly, *Talanta*, 1959, **2**, 38.
6. H. Diehl, *Calcein, Calmagite and o,o'-Dihydroxyazobenzene: Titrimetric, Colorimetric and Fluorimetric Reagents for Calcium and Magnesium*, G. Frederick Smith Chemical Co., Columbus, 1964.
7. A. N. Turanov and G. F. Telegin, *Zavodsk. Lab.*, 1983, **49**, No. 8, 33.
8. H. Flaschka and J. Ganchoff, *Talanta*, 1961, **8**, 720.
9. R. Přibil and J. Adam, *ibid.*, 1977, **24**, 117.
10. V. V. Abramov, S. M. Chesnokova and P. A. Andreev, *Zh. Analit. Khim.*, 1975, **30**, 2255.
11. M. M. Emara, N. A. Farid and A. Wasfi, *Electrochim. Acta*, 1981, **26**, 1705.

12. Sun Hong Kim, *Punsok Hwahak*, 1973, **11**, 188.
13. H. Diehl and J. L. Ellingboe, *Anal. Chem.*, 1956, **28**, 882.
14. H. A. Laitinen and R. F. Sympton, *ibid.*, 1954, **26**, 556.
15. A. Ringbom and B. Wilkman, *Acta Chem. Scand.*, 1949, **3**, 22.
16. C. N. Reilley, A. Scribner and C. Temple, *Anal. Chem.*, 1956, **28**, 450.
17. G. Kainz and G. Sontag, *Z. Anal. Chem.*, 1974, **269**, 267.
18. J. F. Desreux and M. F. Lonein, *Inorg. Chem.*, 1986, **25**, 69.
19. H. Stetter and W. Frank, *Angew. Chem.*, 1976, **15**, 686.
20. I. M. Kolthoff, E. B. Sandell, E. J. Meehan and S. Bruckenstein, *Quantitative Analysis*, 4th Ed., p. 1147. Macmillan, London, 1969.

## SHORT COMMUNICATIONS

# DIFFERENTIAL PULSE POLAROGRAPHIC DETERMINATION OF THE HERBICIDES ATRAZINE, PROMETRINE AND SIMAZINE

M. T. LIPPOLIS and V. CONCIALINI

Dipartimento di Chimica "G. Ciamician", Università di Bologna, Via Selmi 2, 40126 Bologna, Italy

(Received 15 July 1987. Accepted 23 October 1987)

**Summary**—A differential pulse polarographic method, using the dropping mercury electrode, for the determination of the herbicides atrazine, prometrine and simazine is described. The optimum pH is 2. The limit of detection is  $8 \times 10^{-8} M$ , corresponding to about  $15 \mu g/l$ . The electrochemical behaviour of the compounds on glassy-carbon and mercury-coated glassy-carbon electrodes was also examined with a view to its use for electrochemical detection of the herbicides after their separation by HPLC.

Derivatives of *s*-triazine are used extensively in agriculture as herbicides. Several analytical procedures for their determination are available,<sup>1</sup> particularly chromatographic methods.<sup>2-6</sup> Extensive studies of the use of HPLC have been published by York and Roth<sup>5</sup> and by Dufek.<sup>7</sup> A recent paper on the determination of triazines by capillary gas chromatography<sup>8</sup> gives references to analysis for them in water.

Electroanalytical techniques<sup>9-12</sup> have also been used and the present work is concerned with application of pulse polarography to determination of atrazine, simazine and prometrine.

### EXPERIMENTAL

An Amel model 466 polarograph was used with a three-electrode cell containing a dropping mercury electrode (DME), with mechanical detachment of the drop from the capillary, a platinum counter-electrode and a calomel reference electrode. An Amel 492/GC3 glassy-carbon electrode was also used. The polarograms were recorded on a Hewlett-Packard X-Y recorder, model 7040 A.

A stream of nitrogen was used to deoxygenate the solutions and keep them oxygen-free. Measurements of pH were made directly in the polarographic cell.

The glassy-carbon electrode was mercury-coated by electro-deposition at  $-0.7 V$  (*vs.* SCE), with stirring, from a deaerated  $10^{-3} M$  mercury(II) solution in  $0.1 M$  potassium nitrate. The electrode surface area was  $0.03 \text{ cm}^2$  and the mercury film was about  $1 \mu m$  thick, requiring about 10 min to form. The film appeared grey, and the surface was prepared for each test by wiping with a soft paper tissue. The reproducibility was quite good.<sup>14</sup>

Triazine stock solutions were prepared in methanol and were found to be stable for at least two months.

The pH of the polarographic solutions was adjusted to  $< 2$  with hydrochloric acid and increased by addition of sodium acetate as required.

All solutions were prepared from analytical grade chemicals with doubly distilled water.

### RESULTS AND DISCUSSION

#### *Polarographic behaviour of atrazine, prometrine and simazine*

The electroanalytical behaviour of the triazines was strongly dependent on the pH of the solution. Figure 1 indicates (from peak current as a function of pH) that the protonated form is reduced in acid solution; it also shows the variation of  $E_p$  *vs.* pH.

Analysis of the d.c. polarograms at pH 2.0 suggests that the reduction process is irreversible ( $E/\log[(i_0 - i)/i] = 70 \text{ mV}$ ).

The peak currents show a maximum at about pH 2, which is recommended as the working pH.

#### *Effects of modulation amplitude*

Figure 2 shows the dependence of  $i_p$  and  $E_p$  on the pulse amplitude. The peak height increases with pulse amplitude, but  $E = 50 \text{ mV}$  is recommended to avoid

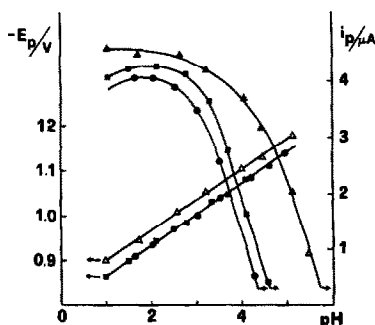


Fig. 1. Effect of pH on the wave heights and peak potentials for  $2 \times 10^{-5} M$  atrazine (●), simazine (■) and prometrine (Δ) in  $0.05 M$  KCl containing HCl and  $\text{CH}_3\text{COONa}$ . Scan-rate  $2 \text{ mV/sec}$ ; modulation amplitude  $-50 \text{ mV}$ .

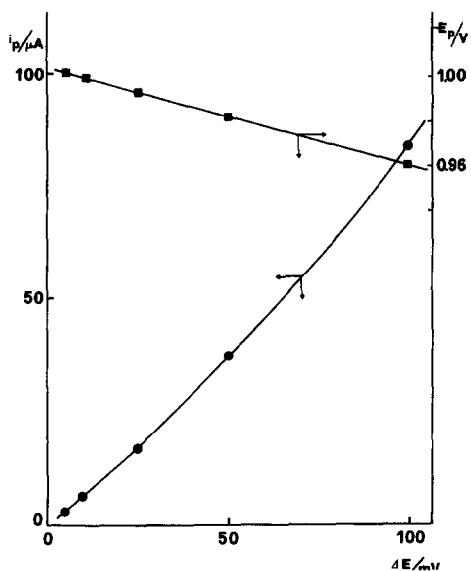


Fig. 2. Dependence of the peak heights and peak potentials on the modulation amplitude for  $10^{-4}M$  atrazine in  $0.05M$  KCl at pH 2.2.

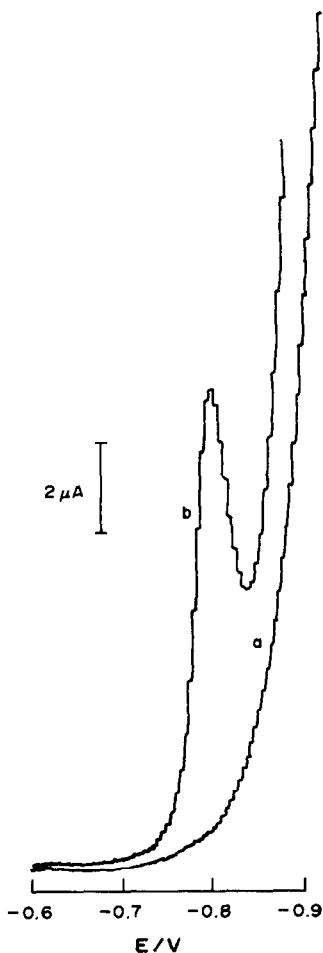


Fig. 3. Differential pulse polarograms of  $10^{-4}M$  atrazine in  $0.05M$  KCl at pH 2.2. (a) Glassy-carbon working electrode with periodic renewal of the diffusion layer. (b) Mercury-coated glassy-carbon electrode. Scan-rate  $2\text{ mV/sec}$ ; modulation amplitude  $-50\text{ mV}$ .

having an  $E_p$  too close to that for discharge of hydrogen ions.

Figure 2 also shows the dependence of the peak potentials on the pulse amplitude. The slope is 0.4, consistent with irreversibility of the reduction.

#### Calibration curves and detection limits

Calibration plots for the compounds examined were linear up to  $10^{-6}M$  when the dropping mercury electrode was used with a scan-rate of  $2\text{ mV/sec}$  and a modulation amplitude of  $-50\text{ mV}$  at pH 2.2.

The detection limit was taken as  $3S_b/m$  where  $S_b$  is the standard deviation of the background current and  $m$  the slope of the calibration curve.  $S_b$  was estimated to be  $7\text{ nA}$ , which gives detection limits of  $8 \times 10^{-8}M$  for atrazine and simazine and  $7 \times 10^{-8}M$  for prometryne. The detection limits correspond to about  $15\text{ μg/l.}$  for each of the three herbicides.

#### Behaviour of glassy-carbon and mercury-coated glassy-carbon electrodes

With regard to the possible utilization of electrochemical detection after HPLC separation of the triazines, their behaviour at the glassy-carbon electrode (GCE) (with and without mercury coating) was studied.

Figure 3 shows the voltammetric curve for the GCE and  $10^{-4}M$  atrazine. No reduction waves appear, so this type of electrode is useless for triazine detection after HPLC. However, if a mercury-coated GCE is used, a reduction wave, attributable to atrazine, appears before the hydrogen discharge.

Work is in progress to explore the applicability of this electrode for electrochemical detection of *s*-triazines in HPLC.

#### REFERENCES

1. H. Gysin and E. Knüsli, in *Advances in Pest Control Research*, R. L. Metcalf (ed.), Vol. 3, p. 289. Wiley-Interscience, New York, 1971.
2. L. Fishbein, *Chromatog. Rev.*, 1970, **12**, 167.
3. W. P. Cochrane and R. Purkayastha, *Toxicol. Envir. Chem. Rev.*, 1973, **1**, 137.
4. T. H. Byast and E. G. Cotterill, *J. Chromatog.*, 1975, **104**, 211.
5. H. York and B. Roth, *ibid.*, 1977, **144**, 39.
6. P. Dufek and V. Pacáková, *ibid.*, 1980, **187**, 341.
7. P. Dufek, V. Pacáková and E. Tesařová, *ibid.*, 1980, **191**, 115.
8. P. C. Bardalaye and W. B. Wheeler, *Intern. J. Environ. Anal. Chem.*, 1986, **25**, 105.
9. R. J. Hance, *Pestic. Sci.*, 1970, **1**, 112.
10. C. E. McKone, T. H. Byast and R. J. Hance, *Analyst*, 1972, **97**, 653.
11. H. Beňadiková, M. Stastny and R. Volf, *Sp. Vedec. Praci. VSCHT, Prague*, 1979, **14**, 67.
12. J. Hernández Méndez, R. Carabias Martínez, M. E. González López and M. Cuesta González, *Anal. Chim. Acta*, 1985, **176**, 121.
13. A. M. Bond, *Modern Polarographic Methods in Analytical Chemistry*, Chap. 6. Dekker, New York, 1980.
14. T. M. Florence, *J. Electroanal. Chem.*, 1970, **27**, 273.
15. L. Meites, *Polarographic Techniques*, p. 240. Wiley, New York, 1965.



## A SIMPLE SPECTROPHOTOMETRIC METHOD FOR DETERMINATION OF ISOXSUPRINE HYDROCHLORIDE IN PHARMACEUTICALS

C. V. RAJESWARI\*, D. V. NAIDU, N. V. S. NAIDU and P. R. NAIDU  
Department of Chemistry, S.V. University, Tirupati-517502, India

(Received 20 May 1987. Revised 26 September 1987. Accepted 16 October 1987)

**Summary**—A spectrophotometric method has been developed for the determination of isoxsuprine hydrochloride and its dosage forms, based on its coupling reaction with diazotized sulphanilic acid. The yellow chromophore has an absorption maximum at 440 nm. Beer's law holds over the range 0.8–8  $\mu\text{g/ml}$  in the final solution.

Isoxsuprinehydrochloride is an orally and par-  
enterally active peripheral and cerebral vasodilator.  
In addition to adrenergic action, it has a direct  
relaxant effect on the smooth muscular tissue of the  
blood vessels and of the uterus.<sup>1</sup> A spec-  
trophotometric method<sup>2</sup> and a column chro-  
matographic method<sup>3</sup> for its determination have been  
described. Colorimetric methods available make  
use of sodium cobaltinitrite,<sup>4</sup> 2,6-dichloroquinone-  
chloroimide,<sup>5</sup> Bromophenol Blue, Bromocresol Pur-  
ple, Bromocresol Green, Bromothymol Blue  
and Methyl Orange.<sup>6</sup> Spectrophotometric methods  
using diazotized benzocaine<sup>1</sup> or D-nitroaniline,<sup>7</sup> an  
infrared absorption method<sup>8</sup> and an ultraviolet spec-  
trophotometric method<sup>9</sup> employing an automatic  
analyser system have also been reported. Other meth-  
ods include gas chromatography<sup>10</sup> and HPLC cou-  
pled with colorimetry.<sup>11</sup>

We report here a new spectrophotometric method  
employing diazotized sulphanilic acid as a coupling  
agent in alkaline medium.

### EXPERIMENTAL

#### Reagents

**Standard drug solution.** Isoxsuprine hydrochloride was checked for purity and strength according to the U.S.P. specification and found to meet those requirements. The sample used in the investigation was  $99.6 \pm 0.5\%$  pure. A standard solution was prepared by dissolving 20 mg of the pure substance in 100 ml of distilled water.

**Diazotized sulphanilic acid solution.** Add dropwise 20 ml of freshly prepared 2% sodium nitrite solution to 40 ml of 1% sulphanilic acid solution in 1M hydrochloric acid. This reagent should be used within 1 hr after preparation.

#### Preparation of samples

**Tablets.** Weigh and powder 20 tablets. Weigh out an amount of the equivalent to about 20 mg of isoxsuprine hydrochloride and extract it with 100 ml of distilled water.

**Injections.** Pipette out a volume of injection equivalent to about 20 mg of isoxsuprine hydrochloride and dilute it to 100 ml with distilled water.

#### General procedure

Transfer volumes of 0, 0.1, 0.2, 0.3, . . . 1.0 ml of standard drug solution into 25-ml standard flasks with a suitable micropipette. To each flask add 4 ml of diazotized sulphanilic acid solution and 5 ml of 5% sodium hydroxide solution and make up to the mark with distilled water.

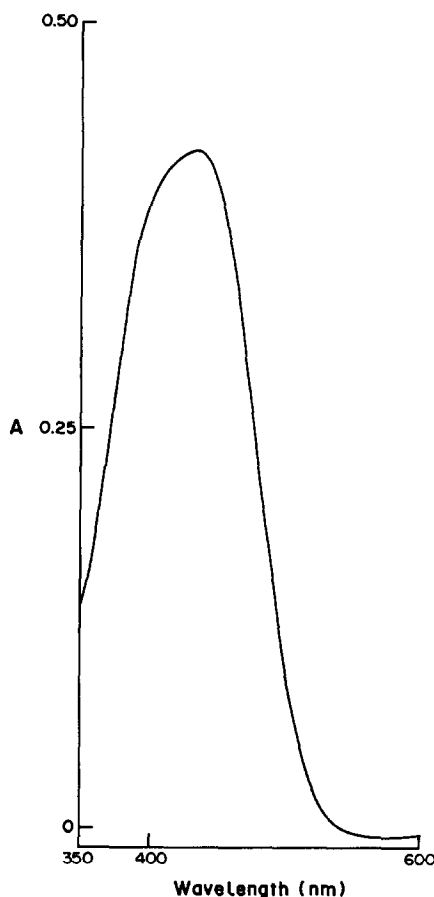


Fig. 1. Absorption spectrum of azo-dye formed by reaction of isoxsuprine hydrochloride and diazotized sulphanilic acid.

\*Author for correspondence.

Table 1

Samples	Nominal amount of ISH, mg	Amount found by present method*	Amount of ISH added, mg	Found, mg	Recovery, %
<i>Tablets</i>					
(T <sub>1</sub> ) ISH	10	9.84 ± 0.05	20	20.20 ± 0.03	101.0
(T <sub>2</sub> ) ISH	10	9.84 ± 0.07	40	40.12 ± 0.02	100.3
(T <sub>3</sub> ) ISH† (MTS, ETD)	10	9.79 ± 0.06	20	19.85 ± 0.06	99.2
(T <sub>4</sub> ) ISH	20	19.86 ± 0.06	60	59.74 ± 0.06	99.6
<i>Injections</i>					
(I <sub>1</sub> ) ISH	10 mg/2 ml	9.86 ± 0.05	20	19.86 ± 0.06	99.3
(I <sub>2</sub> ) ISH	10 mg/2 ml	9.85 ± 0.06	40	41.52 ± 0.04	103.8

\*Each result is the mean of ten replicates, ± standard deviation.

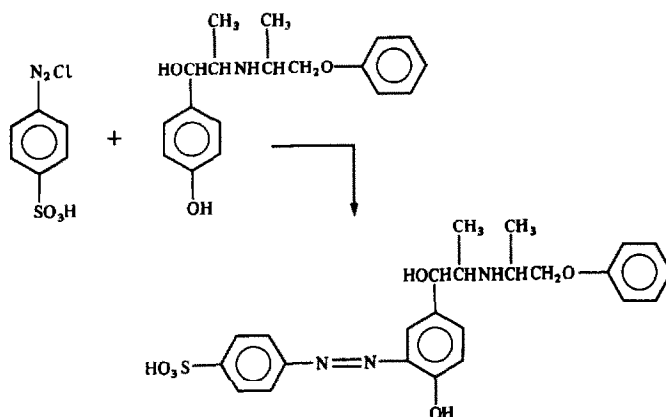
†Laboratory preparation.

ISH Isoxsuprine hydrochloride. MTS Methyltestosterone. ETD Ethinyloestradiol.

Measure the absorbance at 440 nm against a reagent blank. Construct a calibration plot. Beer's law is obeyed in the range 0.8–8 µg/ml in the final solution. Use the same procedure to analyse the sample solutions.

## RESULTS AND DISCUSSION

The method is based on the reaction of the diazonium salt of sulphanic acid with isoxsuprine hydrochloride to produce a yellow species with  $\lambda_{\max}$  at 440 nm. The absorption spectrum of the coloured compound is shown in Fig. 1. The coupling reaction is shown below.



The colour develops instantaneously and is stable for more than 4 hr. The diazotization and coupling reactions could be performed at room temperature, and excess of sodium nitrite does not interfere. This method does not suffer interference from common excipients such as starch, talc, etc. or from methyltestosterone and ethinyloestradiol in analysis of tablets. The recoveries obtained in standard addition experiments ranged between 99 and 103% and are comparable to those reported in the literature.<sup>1,7</sup> The proposed method is simple, rapid and reproducible, and suitable for quality-control analysis of pharmaceutical formulations containing the drug.

*Acknowledgements*—The authors are thankful to M/s. Duphar-Interfran Ltd., Bombay, for providing necessary reference standards of the drug. One of the authors (C.V.R.) is grateful to C.S.I.R., New Delhi, for the award of a Senior Research Fellowship.

## REFERENCES

1. R. T. Sane, V. G. Nayak and V. B. Malkar, *Talanta*, 1985, **32**, 31.
2. *National Formulary*, XIV Ed., p. 372. American Pharmaceutical Association, Washington, 1975.
3. *United States Pharmacopeia*, 20th Rev., p. 434. Mack Printing Co., Easton, 1980.
4. D. M. Shingbal and G. B. Natekar, *East. Pharm.*, 1980, **23**, 109.
5. D. M. Shingbal and V. S. Velingkar, *Indian J. Pharm. Sci.*, 1980, **42**, 122.
6. R. T. Sane, V. G. Nayak and A. Y. Dhamankar, *Indian Drugs*, 1982, **19**, 284.
7. D. M. Shingbal and R. M. Agni, *ibid.*, 1983, **20**, 203.
8. *British Pharmacopoeia* 1980, Vol. II, p. 628. HMSO, Cambridge, 1980.
9. R. R. Bryant, D. E. Mantle, D. L. Timma and D. S. Yoder, *J. Pharm. Sci.*, 1968, **57**, 658.
10. F. Volpe, J. Zintel and D. Spiegel, *ibid.*, 1979, **68**, 1264.
11. L. B. Hakes, T. C. Corby and B. J. Meakin, *J. Pharm. Pharmacol.*, 1979, **31** (Suppl.), 25.

## MODIFIED REVERSE PULSE POLAROGRAPHIC BEHAVIOUR OF MAGNESIUM ION IN AQUEOUS SOLUTION

MINORU HARA and NOBORU NOMURA

Faculty of Education, Toyama University, Gofuku, Toyama 930, Japan

(Received 19 March 1987. Revised 25 September 1987. Accepted 22 October 1987)

**Summary**—Modified reverse pulse polarography (MRPP) is proposed for measuring the quantity of a reduction product formed at the initial potential in reverse pulse polarography. A double potential-step method is employed for this purpose. MRPP has been applied to the study of the electrochemical behaviour of magnesium in aqueous solution. For magnesium the height of the MRPP anodic wave was proportional to concentration at low pH, but not in unbuffered neutral solution. This difference is attributed to formation of hydroxo-magnesium complexes because of depletion of hydrogen ions near the electrode in a neutral solution.

In scan-reversal normal pulse polarography, also called reverse pulse polarography (RPP),<sup>1</sup> diffusion-controlled reduction of a substance of interest takes place at the initial electrode potential and then a potential pulse is applied in a positive direction and the current sampled. It is useful for studying the electrochemical behaviour of reduction products generated at an electrode held at the initial potential. RPP has been used not only for the study of electrode processes but also for analytical purposes.<sup>1,2</sup> It is well-known that for a neutral magnesium solution a large reduction current without a limiting value appears in the d.c. polarogram and that hydrogen is evolved during the measurement.<sup>3</sup> As the reduction current cannot be used for determination of the

magnesium, many indirect polarographic methods have been reported.<sup>4,5</sup> We have already tried to apply RPP to direct polarographic determination of magnesium,<sup>6</sup> but obtained only an ill-defined anodic wave, considered to arise from oxidation of amalgamated magnesium. It is difficult, however, to obtain reproducible RP-polarograms of magnesium even in neutral solutions, because hydrogen bubbles generated during application of the initial potential adhere to the mercury electrode and disturb the measurement. This difficulty in RPP results from the long reduction period, so this is avoided in MRPP by applying only a short reduction period towards the end of the life of the mercury drop. Figure 1 shows the timing sequences for RPP and MRPP. In MRPP,

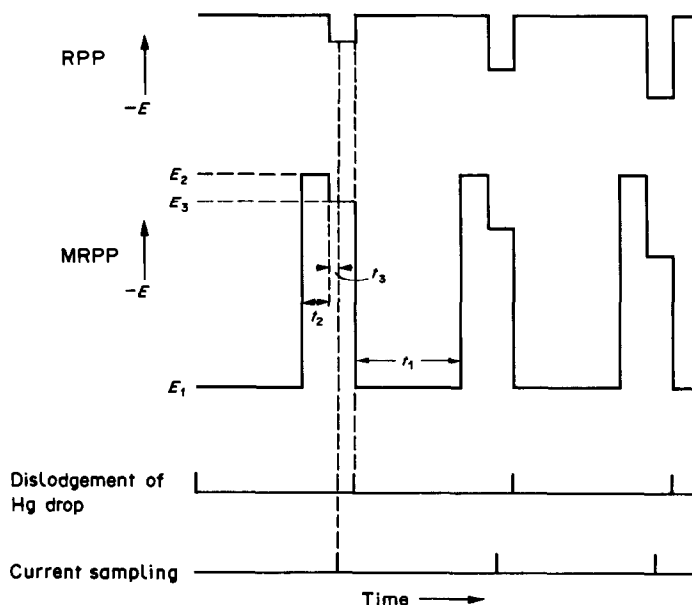


Fig. 1. Potential-time sequences in RPP and MRPP.

three potentials are successively applied during the lifetime of one mercury drop, and are denoted by  $E_1$ ,  $E_2$  and  $E_3$ .  $E_1$  and  $E_2$  are fixed during a run, and  $E_3$  is changed steadily in a positive direction from one drop to the next.  $E_1$  is held for period  $t_1$ ,  $E_2$  for period  $t_2$ , and the electrolysis current is sampled at a time  $t_3$  during the application of potential  $E_3$ . Potentials  $E_1$  and  $E_2$  are selected so that no reaction occurs at  $E_1$  and diffusion-controlled reduction of the substance of interest takes place at  $E_2$ .

This paper describes the application of MRPP, normal pulse polarography (NPP) and modified normal pulse polarography (MNPP)<sup>6,7</sup> for determination of magnesium in aqueous solutions.

### EXPERIMENTAL

#### Apparatus

The polarograph used in this study was constructed in our laboratory. The potentiostat had a positive feedback circuit for compensating the  $iR$ -drop<sup>7</sup> and could supply up to 60 mA electrolysis current. It was controlled by a Fujitsu FM-77 8-bit personal computer, with an MBL68B09 central processing unit. The applied potential was generated by an Analog Devices AD7524 8-bit DA converter. The electrolysis current was amplified by an Analog Devices AD524 instrumentation amplifier, placed between a potential controller and a counter-electrode. The output signal of the amplifier was fed to a National Semiconductor ADC 0804 8-bit analogue-to-digital converter through an active filter and a Harris HA1-2425 sample-hold circuit and stored in the memory of the computer. The sampled current was not averaged—the instantaneous value was recorded. After the complete measurement cycle, the polarogram was printed out by a dot-matrix printer. The mercury flow-rate of the DME was kept at 0.630 mg/sec, and the drop lifetime was controlled by the computer and a solenoid knocker. The current was sampled 2.0 msec after application of potential  $E_3$ . Time intervals were measured with a Matsushita VP-4546A electronic counter.

#### Reagents

The solutions of magnesium and calcium chloride were standardized by EDTA titration with Eriochrome Black T as indicator. Reagent-grade tetramethylammonium bromide ( $\text{Me}_4\text{NBr}$ ) was used as supporting electrolyte without further purification. The sample solutions were deaerated by the passage of nitrogen in the usual manner.

### RESULTS AND DISCUSSION

Use of RPP for determining calcium, strontium and barium was reported in our previous paper.<sup>6</sup> Since calcium required the most negative potential for reduction the initial study of MRPP was performed with calcium as the model test substance. The diffusion-controlled reduction of calcium proceeds at potentials more negative than  $-2.35$  V, and the limiting oxidation current for amalgamated calcium appears at potentials more positive than  $-0.85$  V. The effect of varying the reduction period,  $t_2$ , is shown in Fig. 2. The sum of  $t_1$  and  $t_2$  was kept constant in this experiment in order to compare the calcium wave-heights for the same surface area of the mercury drop. The extreme right point on the curve in Fig. 2 indicates the wave height in RPP. Evidently

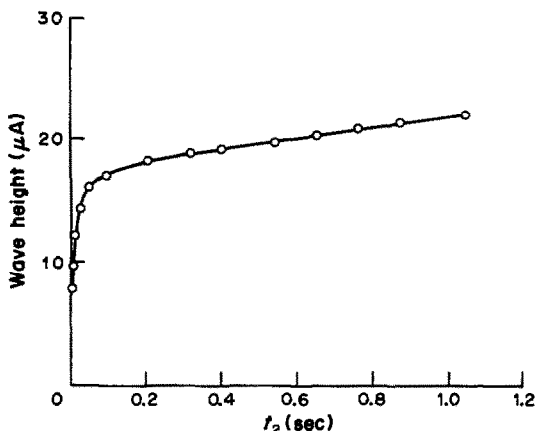


Fig. 2. Effect of reduction period,  $t_2$ , in MRPP on the anodic wave height for calcium:  $4.16 \times 10^{-4} M$   $\text{CaCl}_2$ ,  $0.1 M$   $\text{Me}_4\text{NBr}$ , pH 5.7,  $t_1 + t_2 = 1.047$  sec,  $E_1 = -1.00$  V,  $E_2 = -2.50$  V.

decreasing  $t_2$  in MRPP causes little loss in sensitivity. Moreover, it is very convenient for the polarography of alkaline-earth metal ions at low pH, because it minimizes the evolution of hydrogen bubbles, which adhere to the mercury electrode and interfere in measurement of the polarograms. Hence 46.0 msec was selected for  $t_2$  in subsequent experiments.

Figure 3 shows three types of pulse polarogram for magnesium in an unbuffered pH-5.5 aqueous solution. They are similar to those reported previously.<sup>6</sup> The MRP-polarogram is more reproducible than the RP-polarogram because the evolution of hydrogen is suppressed by the shortening of the reduction period,  $t_2$ . The ill-defined anodic wave in MRPP results from oxidation of the amalgamated magnesium formed by electrolysis at potential  $E_2$ . The NPP and MNPP waves for magnesium have no limiting value and are very different in magnitude, because the NPP current contains the large reduction current for the evolution of hydrogen but the MNPP current does not. The NPP current at fixed potential for magnesium in neutral solution increased abnormally with increase

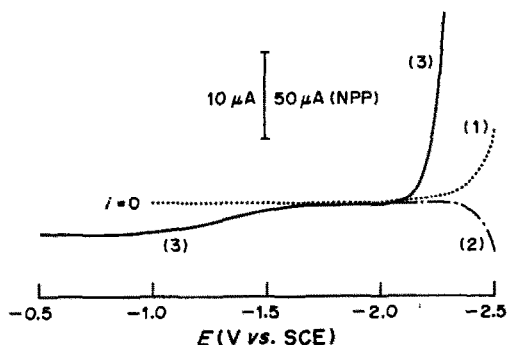


Fig. 3. Three types of pulse polarogram for magnesium in a neutral solution: pH = 5.5,  $4.57 \times 10^{-4} M$   $\text{MgCl}_2$ ,  $0.1 M$   $\text{Me}_4\text{NBr}$ ,  $t_1 = 1.00$  sec,  $t_2 = 46.0$  msec, (1) NPP,  $E_1 = -1.00$  V; (2) MNPP,  $E_1 = -1.00$  V,  $E_3 = -0.70$  V; (3) MRPP,  $E_1 = -1.00$  V,  $E_2 = -2.48$  V.

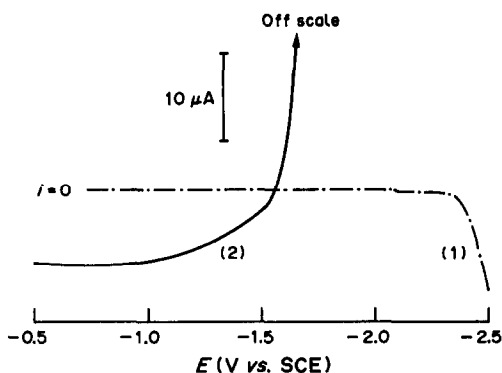


Fig. 4. Two types of pulse polarogram for magnesium at pH 2:  $4.57 \times 10^{-4} M$   $MgCl_2$ ,  $0.1 M$   $Me_4NBr$ ,  $t_1 = 1.00$  sec,  $t_2 = 46.0$  msec, (1) MNPP,  $E_1 = E_2 = -0.70$  V, scanned from  $-0.7$  V; (2) MRPP,  $E_1 = -1.00$  V,  $E_2 = -2.48$  V, scanned from  $-2.48$  V.

in magnesium concentration, whereas the MNPP wave height was almost independent of magnesium concentration above  $2 \times 10^{-4} M$ .

Two types of pulse polarogram for magnesium at low pH are shown in Fig. 4. The anodic current in MNPP at pH 2 (curve 1) does not have a limiting value. With decrease in pH, the MNPP wave becomes higher and steeper, and the anodic MRPP wave also becomes higher. In unbuffered neutral solutions, the magnesium ions at the electrode surface may form hydroxo-complexes because of local increase in pH, due to depletion of hydrogen ions at the electrode surface by evolution of hydrogen. The hydroxo-magnesium species cannot be reduced at the electrode, so the wave height for magnesium is lower for neutral solution than at low pH.

The dependence of the MRPP anodic current at  $-0.80$  V on the concentration of magnesium was investigated as a function of pH and the results are shown in Fig. 5. The reduction potential,  $E_2$ , was held at  $-2.48$  V throughout. The relationship was linear at pH 2, but non-linear at pH 3.0 or 5.5. The non-linearity at higher pH can be attributed to the formation of magnesium hydroxo-complexes at the electrode surface. The anodic current in MNPP at pH 2 increases with magnesium concentration. The relative standard deviation of the wave height in MRPP for  $4.57 \times 10^{-4} M$  magnesium at pH 2.0 was 5.6% (five replicates). Because the reduction of magnesium at  $E_1$  in MRPP is not diffusion-controlled, the reproducibility of the anodic wave height for magnesium in MRPP is not so good, but that of the other

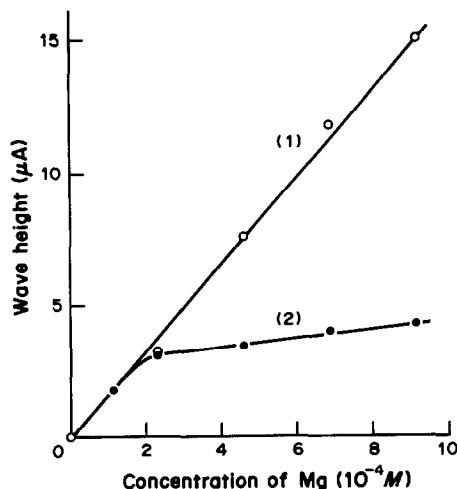


Fig. 5. Relationships between the anodic wave height in MRPP and concentration of magnesium ion:  $0.1 M$   $Me_4NBr$ ,  $E_1 = -1.00$  V,  $E_2 = -2.48$  V,  $t_1 = 1.00$  sec,  $t_2 = 46.0$  msec, (1) pH = 2.0, (2) pH = 5.5.

alkaline-earth metals is diffusion-controlled and hence their anodic oxidation is very reproducible.

Thus MRPP is well suited to the study of the electrochemical behaviour of a reduction product formed at an extremely negative potential and accompanied by evolution of hydrogen. When tetramethylammonium chloride is used as supporting electrolyte for amperometric determinations by MRPP, neither dissolved oxygen nor hydrogen ions interfere in the determination of magnesium, just as in MNPP.<sup>6</sup> However, many metal ions, especially those of the alkali, alkaline earth and heavy metals, interfere in the determination of magnesium, so a prior separation would be required. Amperometric detection by MRPP would probably prove very useful for the determination of the four alkaline earths by ion-chromatography.

#### REFERENCES

1. J. Osteryoung and E. Kirowa-Eisner, *Anal. Chem.*, 1980, **52**, 62.
2. A. Brestovisky, E. Kirowa-Eisner and J. Osteryoung, *ibid.*, 1983, **55**, 2063.
3. I. Zlotowski and I. M. Kolthoff, *J. Phys. Chem.*, 1945, **49**, 386.
4. R. Přebil and E. Vicenová, *Chem. Listy*, 1952, **46**, 535.
5. B. Fleet, Soe Win and T. S. West, *Analyst*, 1969, **94**, 269.
6. M. Hara and N. Nomura, *Talanta*, 1986, **33**, 857.
7. M. Hara, *ibid.*, 1985, **32**, 41.

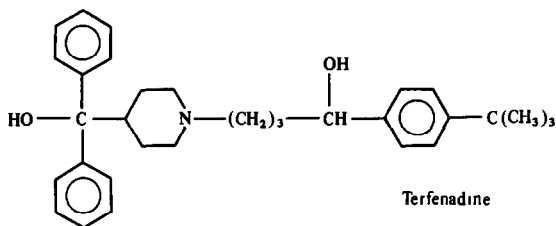
## UTILITY OF IODINE AND 7,7,8,8-TETRACYANOQUINODIMETHANE FOR DETERMINATION OF TERFENADINE

MOHAMED E. ABDEL-HAMID\* and MUSTAFA A. ABUIRJEIE  
Jordan University of Science and Technology, Faculty of Pharmacy, Irbid, Jordan

(Received 21 January 1987. Revised 25 May 1987. Accepted 14 October 1987)

**Summary**—Simple and sensitive spectrophotometric methods for the assay of terfenadine are described. The first is based on the reaction of terfenadine with iodine to give a molecular charge-transfer complex, the terfenadine acting as an  $n$ -electron donor and iodine as a  $\sigma$ -electron acceptor. The second depends on the formation of a highly coloured stable radical anion between terfenadine and 7,7,8,8-tetracyanoquinodimethane (TCNQ) as a  $\pi$ -electron acceptor. Beer's law is obeyed over the terfenadine concentration range 0.2–1.2 mg/100 ml. The proposed methods have been successfully applied to the analysis of commercial terfenadine tablets.

Terfenadine is a new selective histamine  $H_1$ -receptor antagonist devoid of the sedative and anticholinergic properties commonly associated with antihistamine therapy.



As it is a relatively new drug, few procedures have been described for its determination. A radio-immunoassay method<sup>1</sup> has been reported for its determination in human plasma. Iodine and 7,7,8,8-tetracyanoquinodimethane (TCNQ) have proved to be useful reagents for the analysis of a wide range of pharmaceutical compounds,<sup>2-5</sup> and their application for spectrophotometric determination of terfenadine is described here.

### EXPERIMENTAL

#### Reagents

Pharmaceutical grade terfenadine powder was used as a 1-mg/ml solution in anhydrous chloroform as a stock standard, and diluted tenfold as required. Iodine solution, 0.025%, in chloroform and TCNQ solution, 0.2%, in acetonitrile were utilized as chromogenic reagents. All reagents and solvents used were of analytical grade.

#### Calibration graphs

**Iodine method.** Various volumes (1–6 ml) of 0.1 mg/ml working standard terfenadine solution were transferred into 50-ml standard flasks. The solution in each flask was mixed with 5 ml of iodine solution and diluted to volume with the

same solvent. The solutions were left in the dark for 30 min and their absorbances were measured at 290 and 365 nm, against chloroform as a blank.

**TCNQ method.** Various volumes (1–6 ml) of working standard solution (0.1 mg/ml) were transferred into 50-ml standard flasks. The solvent was removed by immersing the flasks in a water-bath at 70°. The flasks were cooled and the residues dissolved in about 10 ml of acetonitrile. A 2.5-ml portion of TCNQ solution was added to each flask and the volume made up to 50 ml with acetonitrile. The solutions were left at room temperature for 30 min and the absorbances measured at 845 nm against a blank prepared simultaneously without terfenadine solution.

#### Tablet analysis

An accurately weighed quantity of the well mixed powder from 20 tablets, equivalent to about 60 mg of terfenadine, was transferred into a 50-ml standard flask. The base was then extracted by sonic treatment of the powder with 30 ml of chloroform for 20 min. The mixture was diluted to volume, thoroughly mixed and filtered. The first 10-ml portion of filtrate was rejected and the remainder was collected. An aliquot (10 ml) was accurately diluted to 50 ml with chloroform. A 5-ml aliquot of this solution was analysed by the procedure for calibration with iodine, and a 4-ml aliquot was used for analysis with TCNQ. Completeness of extraction of terfenadine base from the powdered tablets was confirmed by TLC. A negative test was obtained with chloroform:methanol (90:10) as mobile phase and iodine vapour as detecting agent.

#### Stoichiometric relationship

Master solutions of terfenadine and iodine ( $0.5 \times 10^{-4} M$ ) in anhydrous chloroform were prepared. A series of 10-ml quantities of mixtures containing a total volume of 10 ml of the master solutions in different proportions (from 0:10 to 10:0) were made up in 10-ml standard flasks. The flasks were left in the dark for 30 min and the absorbances were measured at 290 nm against chloroform.

#### Association constant and molar absorptivity

Terfenadine solutions in chloroform were prepared ( $1.5, 2.0, 3.0 \dots 6 \times 10^{-4} M$ ). These solutions and an iodine solution in chloroform ( $8 \times 10^{-3} M$ ) were placed in a water-bath at 25°. Then 5-ml volumes of the iodine solution were rapidly mixed with the same volume of each terfenadine solution and the absorbance was measured at 290 nm against chloroform.

\*Author for correspondence.

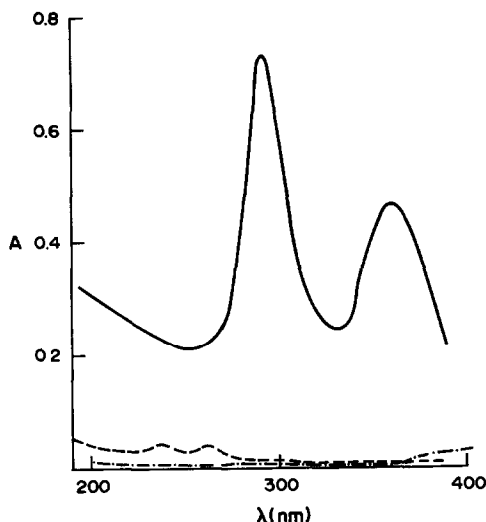


Fig. 1. Absorption spectra of (-----) terfenadine, (-.-.-) iodine and (—) terfenadine-iodine complex in chloroform (terfenadine 10  $\mu\text{g/ml}$ ).

#### RESULTS AND DISCUSSION

Terfenadine, being an  $n$ -electron donor, reacts instantaneously with either iodine or TCNQ, giving characteristic coloured reaction products. Upon reaction of terfenadine with a chloroform solution of iodine, a yellowish purple or yellow colour is formed, depending on the terfenadine concentration. The reaction product is distinguished from slow oxidation or substitution reaction products of iodine with amines by being easily dissociated on dilution with solvents of high polarity. The absorption spectrum of the coloured product exhibits intense bands at 290 and 365 nm (Fig. 1). Terfenadine and iodine have almost negligible absorbances at these wavelengths. The product is assumed to be a molecular charge-transfer (CT) complex.<sup>2</sup>

The mole ratio of the reactants in the CT complex

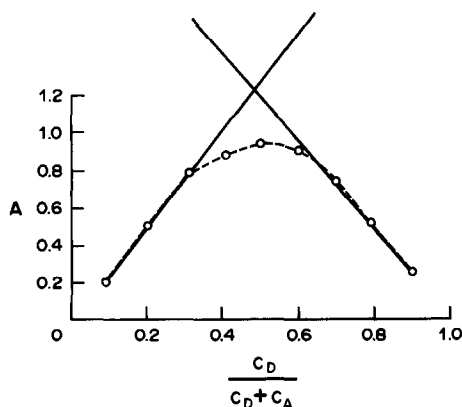


Fig. 2. Continuous variations plot for terfenadine and iodine in chloroform ( $0.5 \times 10^{-4} M$ ).

Table 1. Effect of time on the absorbance of the terfenadine products

Time after mixing, min	Iodine method, 290 nm	TCNQ method, 845 nm
0	0.750	0.350
10	0.810	0.430
20	0.845	0.510
30	0.860	0.580
40	0.860	0.582
50	0.848	0.580
60	0.830	0.577
100	0.820	0.570
120	0.815	0.566

was determined by the method of continuous variations,<sup>6</sup> and found to be 1:1 (Fig. 2). This is in agreement with the presence of a single tertiary nitrogen atom in the terfenadine molecule. The association constant and molar absorptivity of the terfenadine-iodine complex were determined by using the Benesi-Hildebrand equation.<sup>7</sup> The iodine concentration was kept constant, and lower than the varied concentration of terfenadine. The association constant and molar absorptivity were found to be  $1.1 \times 10^4$  and  $0.4 \times 10^4 \text{ l.mole}^{-1} \cdot \text{cm}^{-1}$ , respectively. Although the complex was formed rapidly, constant absorbance readings were obtained only after the solution had stood for 30 min in the dark (Table 1), and remained constant for about a further hour. At 290 and 365 nm, linear calibration graphs ( $r$  0.9984 and 0.9989) were obtained over the concentration range 2–12  $\mu\text{g/ml}$  in the final solution measured.

The reproducibility of the procedure was determined by measuring replicate samples (10  $\mu\text{g/ml}$  terfenadine in the final test solution) at 290 and 365 nm (Table 2). At this concentration level the coefficients of variation were 0.5% and 0.7% respectively.

Interaction of terfenadine with TCNQ gives a bluish-green chromogen with a strong absorbance maximum at 845 nm (Fig. 3). The bands developed in the spectrum were attributed to formation of the TCNQ radical anion by complete transfer of  $n$ -electrons from the terfenadine molecule to TCNQ in polar medium.<sup>5</sup> Maximum absorbance was attained

Table 2. Precision study of the iodine and TCNQ methods

	Iodine method (10 $\mu\text{g/ml}$ )		TCNQ method (8 $\mu\text{g/ml}$ ), 845 nm
	290 nm	365 nm	
	0.740	0.461	0.631
	0.750	0.471	0.634
	0.748	0.466	0.639
	0.744	0.465	0.632
	0.745	0.463	0.636
	0.752	0.460	0.633
Average	0.747	0.464	0.634
SD	0.004	0.003	0.003

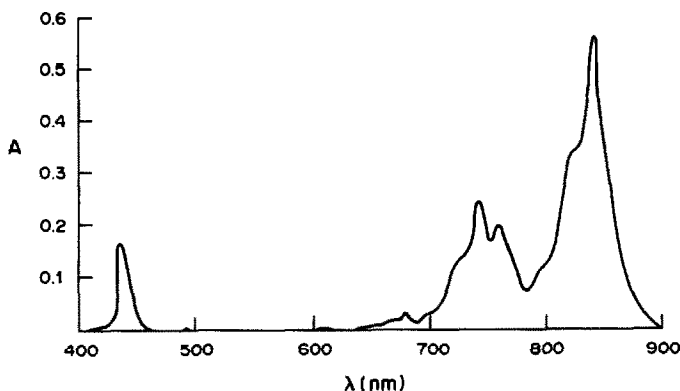


Fig. 3. Absorption spectrum of terfenadine-TCNQ reaction product measured against reagent blank in acetonitrile (terfenadine 8  $\mu\text{g/ml}$ ).

Table 3. Recovery studies on known terfenadine samples and commercially available tablets (Teldane®)\* by the iodine (1) and TCNQ (2) methods

Amount taken, or claimed per tablet, mg	Concentration level, $\mu\text{g/ml}$		Amount found, mg		Recovery %	
	(1)	(2)	(1)	(2)	(1)	(2)
<i>Known samples</i>						
40.0	8.0	8.0	39.9	39.9	99.8	99.5
45.0	9.0	9.0	44.8	44.5	99.6	98.9
50.0	10.0	10.0	50.2	50.2	100.4	100.4
60.0	12.0	8.4	60.5	60.1	100.8	100.2
Overall recovery, %					100.2	99.7
SD					0.55	0.6
Theoretical <i>t</i> -value ( $P = 0.05$ ) = 2.31					$t_{\text{calc}} = 1.24$	
<i>Commercial tablets</i>						
60.0	12.0	8.4	59.2	58.9	98.7	98.2
60.0	12.0	8.4	59.9	60.3	99.3	100.5
60.0	12.0	8.4	59.7	59.6	99.5	99.3
60.0	12.0	8.4	60.2	59.8	100.3	99.7

\*Each tablet contains 60 mg of terfenadine (Merrell Dow, France).

after 30 min and the colour remained stable for at least 2 hr (Table 1). Acetonitrile is ideal as the solvent, as it offers good solvating capacity for TCNQ, and gives the highest yield of the radical anion. A concentration of 5.0 mg of TCNQ in the total volume of 50 ml solution was considered optimum for colour formation. Under the experimental conditions described, a linear calibration graph ( $r = 0.9995$ ) over the terfenadine concentration range of 2–12  $\mu\text{g/ml}$  in the final solution was obtained.

The reproducibility of the TCNQ procedure was found by running 6 replicate samples, each containing 8  $\mu\text{g/ml}$  terfenadine in the final solution (Table 2). At this concentration level, the CV was 0.5%.

Table 3 shows the accuracy of the proposed methods. Recovery studies were performed with four different concentration levels of terfenadine. The overall recovery was 100.2 and 99.7% for the iodine and TCNQ procedures, respectively. The results given by the two methods were statistically compared by the Student *t*-test and found not to differ signifi-

cantly. Commercially available terfenadine tablets were analysed by the proposed methods. The results obtained are also presented in Table 3.

The suggested methods are rapid and simple, and suitable for routine analysis of terfenadine tablets in drug control laboratories.

#### REFERENCES

1. C. E. Cook, D. L. Williams, M. Myers, C. R. Tallent, G. A. Leeson, R. A. Okerholm and G. J. Wright, *J. Pharm. Sci.*, 1980, **69**, 1419.
2. R. Foster, *Organic Charge Transfer Complexes*, Academic Press, London, 1969.
3. A. M. Taha, A. K. S. Ahmed, C. S. Goma and H. M. El-Fataury, *J. Pharm. Sci.*, 1974, **63**, 1853.
4. S. Belal, M. A. Elsayed, M. E. Abdel-Hamid, H. Abdine, *ibid.*, 1981, **70**, 127.
5. K. A. Kovar and M. Abdel-Hamid, *Arch. Pharm.*, 1984, **317**, 246.
6. J. Rose, *Advanced Physico-Chemical Experiments*, Pitman, London, 1964.
7. H. A. Benesi and J. H. Hildebrand, *J. Am. Chem. Soc.*, 1949, **71**, 2703.



## THE DETERMINATION OF NITRATE AND SULPHATE IN 50% SODIUM HYDROXIDE SOLUTION BY ION-CHROMATOGRAPHY

JARL M. PETTERSEN

Norsk Hydro Research Center, N-3900 Porsgrunn, Norway

HANNE G. JOHNSEN and WALTER LUND

Department of Chemistry, University of Oslo, Oslo 3, Norway

(Received 10 August 1987. Accepted 25 September 1987)

**Summary**—Electrolysis in combination with a cation-selective membrane is used to reduce the concentration of sodium hydroxide in the sample, prior to the ion-chromatographic determination of nitrate and sulphate. The advantage and disadvantage of this type of sample pretreatment are discussed.

A 50% w/w sodium hydroxide solution (s.g. 1.54) cannot be easily analysed for trace anions by direct injection into an ion-chromatograph, because the anion peaks will be strongly distorted. Therefore, the concentration of sodium hydroxide must be decreased before the sample is injected into the chromatograph. In many cases a 1:100 dilution of the sample will allow a satisfactory determination of chloride, nitrate and sulphate. However, such a high dilution cannot be used if the concentration of anions in the original sample is close to the instrumental detection limits. This situation may be encountered when sodium hydroxide samples produced by the amalgam process are analysed. Such samples, which frequently contain less than 10  $\mu\text{g/g}$  nitrate or sulphate, were of particular interest in this work.

Instead of dilution, the 50% sodium hydroxide solution can be passed through a cation-exchange resin in the hydrogen form, which will remove the sodium hydroxide. However, in the procedure described by Hill<sup>1</sup> the anions were washed through the column with water, resulting in a 25-fold dilution of the sample. In some preliminary experiments we tried to analyse the eluate from a cation-exchange resin directly, without elution with water, using a small amount of resin, and bromide as internal standard, but reproducible results could not be obtained.

It was therefore of interest to find an alternative method of decreasing the high concentration of sodium and hydroxide ions, without dilution of the sample. The use of electrolysis in combination with a cation-selective membrane seemed an attractive approach. The use of this sample pretreatment technique is discussed below.

### EXPERIMENTAL

#### Apparatus

The electrolysis cell, which was made from Teflon, consisted of a 1-ml anode compartment and a 5-ml cathode

compartment. A cation-selective membrane (Nafion 901; Du Pont), 0.1 mm thick and with an exposed area of 0.8  $\text{cm}^2$ , separated the two parts, which were held together by screws. A small platinum-gauze electrode, with a surface area of ca. 1  $\text{cm}^2$ , was placed inside each of the two cell compartments. A double-junction reference electrode (Hg/HgO/0.5M NaOH; Ingold) was placed in the anode compartment, and a Teflon-covered magnet, for stirring, in the cathode compartment. An Amel 551 potentiostat was used for the controlled-potential electrolysis.

The chromatograph was a Dionex model 12, with a QIC pump, a 184- $\mu\text{l}$  double-stack injection valve, an AS4 separator column and a hollow-fibre suppressor column. The eluent was 0.003M sodium bicarbonate/0.0024M sodium carbonate, and the suppressor solution was 0.02M sulphuric acid.

#### Procedure

Rinse the cell with dilute acetic acid and then with water. Transfer 1.0 ml of the 50% sodium hydroxide sample to the anode compartment, and fill the cathode compartment with 5 ml of 0.5M sodium hydroxide solution. Start the stirrer and electrolyse for 3 hr, using an anode potential of +0.8 V vs. Hg/HgO, and adding water to the anode compartment as required, to maintain the volume at ca. 1.0 ml. The current limit for the membrane, 0.2  $\text{A}/\text{cm}^2$ , should not be exceeded. Check that the final concentration of sodium hydroxide is below 0.3M, by titrating a 50- $\mu\text{l}$  aliquot with standard acid. Terminate the electrolysis, add water to make up to the original volume (1.0 ml) and inject an aliquot of the neutralized sample into the ion chromatograph. Calculate the concentration of the anions from standard curves.

If chromate is used as internal standard, the adjustment of the final sample volume prior to the analysis can be omitted.

### RESULTS AND DISCUSSION

#### The electrolysis step

Perfluorinated Nafion membranes exhibit remarkable ion selectivity.<sup>2</sup> In this material, the anion transport is very much less than the cation transport. The membranes are widely used industrially, in chlor-alkali electrolysis cells. A particularly high current

efficiency is obtained with membranes that are sulphonated on one side, and carboxylated on the other, like the one used in this work. The present work illustrates that these membranes can be useful also for analytical purposes.

During the electrolysis, the hydroxide ions are oxidized at the anode according to the reaction  $4\text{OH}^- \rightarrow \text{O}_2 + \text{H}_2\text{O} + 4e^-$ . Simultaneously, the sodium ions move from the anode compartment through the cation-selective membrane to the cathode. The reaction at the cathode is  $4\text{H}_2\text{O} + 4e^- \rightarrow 2\text{H}_2 + 4\text{OH}^-$ . The membrane prevents the hydroxide ions from moving to the anode.

The result of these processes is a decrease in the concentration of sodium hydroxide in the anode compartment, and a corresponding increase in its concentration in the cathode compartment. Therefore, the cathode compartment should be larger than the anode compartment, to keep the concentration in the cathode compartment reasonably low.

During the experiments, it was noticed that the solution volume decreased in the anode compartment, and increased in the cathode compartment. From the redox equations the opposite effect would be expected, because water is produced at the anode and consumed at the cathode. However, the sodium ions are transported through the membrane in hydrated form, carrying 3.7 mole of water per mole of cation, according to the manufacturer.<sup>3</sup> This process will predominate over the redox process, which only contributes 0.5 mole of water per mole of the hydroxide (or sodium) ion. Therefore, water has to be added to the anode compartment, or the cell would go dry before the completion of the electrolysis.

Generally a complete neutralization of the 50% sodium hydroxide solution was not attempted. The electrolysis was terminated when the concentration had been decreased to *ca.* 1% sodium hydroxide (*i.e.*, the concentration was decreased from 19M to 0.3M). At this level the sodium hydroxide did not interfere with the chromatographic response of the anions of interest. The time needed to reach this concentration depended on the electrolysis current, which in turn was a function of the electrolysis potential. Normally an anode potential of +0.8 V *vs.* Hg/HgO was used. The current was then 0.15 A and the electrolysis time 3 hr. A higher current was avoided, because the current limit of the membrane, 0.2 A/cm<sup>2</sup>, would then be exceeded. In such a case a slight release of sulphate from the membrane was observed. If necessary, the final concentration of sodium hydroxide was checked by titrating a 50- $\mu$ l aliquot with a standard acid.

The Nafion 901 membrane is carboxylated on one side and sulphonated on the other. Reversing the membrane in the cell did not affect the results.

#### Internal standard

Because of the change in the sample volume during the electrolysis, the use of an internal standard, which could be added prior to the electrolysis, would be

desirable. It would permit a direct analysis of the neutralized sample, with no need for adjustment of the final sample volume prior to the injection into the ion-chromatograph. Bromide seemed a possible choice, because of its absence in the sodium hydroxide samples analysed in this work, and its suitable retention time. However, when bromide was added to the sample, no bromide peak was observed after the electrolysis, indicating that the ion was oxidized during the electrolysis. A poor recovery was also obtained for bromate added to the sample prior to the electrolysis. The best results were obtained with chromate as internal standard. When a sodium hydroxide solution was spiked with chromate, a quantitative recovery was obtained. The chromatographic response was the same for the electrolysed sample as for a standard solution of chromate.

The disadvantage of using chromate as internal standard is its long retention time, *ca.* 40 min, compared to 5–10 min for nitrate and sulphate. Also the peak area should be used for the chromate ion, instead of the peak height.

#### Analysis of 50% sodium hydroxide

A typical chromatogram obtained after the electrochemical neutralization is shown in Fig. 1. The peaks correspond to chloride, nitrate, sulphate and chromate, respectively. As can be seen from the figure,

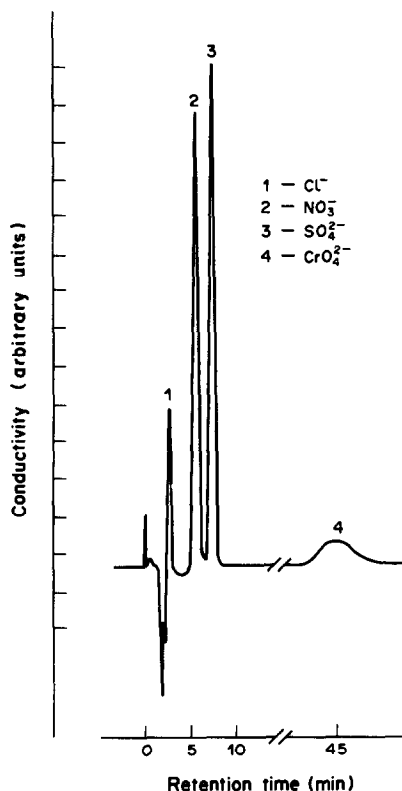


Fig. 1. Chromatogram obtained after electrochemical neutralization of a 50% sodium hydroxide sample containing 13.5  $\mu\text{g/g}$  nitrate and 7.5  $\mu\text{g/g}$  sulphate.

Table 1. Recovery tests for 50% sodium hydroxide solution

Chloride			Nitrate			Sulphate		
Added, $\mu\text{g/g}$	Found, $\mu\text{g/g}$	Recovery, %	Added, $\mu\text{g/g}$	Found, $\mu\text{g/g}$	Recovery, %	Added, $\mu\text{g/g}$	Found, $\mu\text{g/g}$	Recovery, %
0	0.4	—	0	6.5	—	0	16.9	—
5	2.0	32	5	11.4	98	5	22.1	104
10	2.9	25	10	17.0	105	10	26.5	96

Table 2. Results obtained for 50% sodium hydroxide from three manufacturers

Manufacturer	Nitrate			Sulphate		
	$n$	$\bar{x}$ , $\mu\text{g/g}$	$S_r$ , %	$n$	$\bar{x}$ , $\mu\text{g/g}$	$S_r$ , %
A	6	6.8	3.6	6	16.3	6.4
B	3	6.9	3.6	3	5.1	10.8
C	3	18.0	1.8	3	5.7–10.7*	—

$n$  = number of analyses;  $\bar{x}$  = mean ( $\mu\text{g}$  per g of 50% NaOH solution);  $S_r$  = relative standard deviation.

\*Three different batches were analysed.

well defined peaks were obtained for nitrate and sulphate, even though the 50% sodium hydroxide sample contained only 13.5  $\mu\text{g/g}$  nitrate, and 7.5  $\mu\text{g/g}$  sulphate. The results of a recovery test for chloride, nitrate and sulphate are given in Table 1. The test was made by spiking the 50% sodium hydroxide with known amounts of the anions. The values were calculated from the linear standard graphs obtained for aqueous solutions of the respective anions. Chromate was used as internal standard. The values found before the addition of the anion spikes correspond to the original concentration of the anions in the sodium hydroxide used for the test. As can be seen from Table 1, a satisfactory recovery was obtained for nitrate and sulphate, but not for chloride.

Table 2 gives the results for 50% sodium hydroxide samples obtained from three different manufacturers. The sodium hydroxide samples were produced by the amalgam process, and thus contained low levels of anions, which originated primarily from the water used in the process.

The number of analyses indicated in Table 2 refers to the number of complete neutralization and chromatographic detection sequences. As can be seen from Table 2 the precision of the method was of the order of 5–10%.

Only nitrate and sulphate are determined by the present method, because these anions contain the respective elements in their highest oxidation states. The corresponding anions of lower oxidation states,

such as nitrite and sulphite, will be oxidized during the electrolysis, and will thus appear as nitrate and sulphate. However, in the sodium hydroxide samples analysed in this work the concentration of nitrite and sulphite was probably very low.

In principle, the results obtained for nitrate and sulphate represent the total amount of nitrogen and sulphur in the sample. Therefore, if samples were analysed by this technique, as well as by a direct method (e.g., after a dilution of the sample), any significant difference between the results obtained by the two procedures should correspond to the concentration of the lower oxidation state anions in the sample.

Halide ions could not be determined by the technique, owing to oxidation during the electrolysis, as indicated by poor recoveries for chloride, bromide and bromate. However, the presence of perchlorate and perbromate ions could not be detected.

*Acknowledgements*—We would like to thank Mr. K. Hamberg for help with designing the cell and Mr. R. Dahl for technical assistance.

#### REFERENCES

1. R. A. Hill, *J. High Resol. Chromatog. Chromatog. Commun.*, 1983, **6**, 275.
2. A. Lindheimer, J. Molenat and C. Gavach, *J. Electroanal. Chem.*, 1987, **216**, 71.
3. *Nafion Product Bulletin*, Du Pont, 1984.

## A COMPUTATIONAL METHOD FOR APPROXIMATE EVALUATION OF IONIZATION CONSTANTS FROM POTENTIOMETRIC DATA

A. GUSTAVO GONZALEZ, DANIEL ROSALES, JOSE L. GOMEZ ARIZA and A. GUIRAUM PEREZ  
 Department of Analytical Chemistry, Faculty of Chemistry, University of Sevilla, 41012-Sevilla, Spain

(Received 9 March 1987. Revised 25 August 1987. Accepted 23 November 1987)

**Summary**—A general equation is given for the evaluation of proton dissociation constants from potentiometric data. The method is applicable to monobasic acids, and also polybasic acids, where the successive dissociation steps may or may not overlap. A computer program was employed for the calculations. The method was tested by evaluation of the constants for 22 acids, from monobasic to octobasic, with satisfactory agreement with literature data.

Potentiometric titrations have been widely used in the determination of ionization constants of acids, and many books and monographs have been devoted to this topic.<sup>1</sup> Recently, computational methods have been reviewed by Leggett.<sup>2</sup>

Our method is based on an equation proposed by Rossotti and Rossotti,<sup>3</sup> originally intended for the graphical evaluation of stability constants in mono-nuclear complex systems. With some modifications, and the help of a personal computer, the simultaneous computation of up to eight ionization constants is possible.

### EXPERIMENTAL

Analytical grade reagents were used without further purification. The titrations were done with stirring and a protective stream of nitrogen, though both were stopped during readings. The temperature and ionic strength were kept constant. The glass electrode was calibrated before each titration, against buffers of pH 4, 7 and 10.

### THEORY

The following symbols are used:

- $\beta_i$ —overall protonation constant of acid H<sub>i</sub>L
- $h$ —free hydrogen-ion concentration
- $K_w$ —dissociation constant of water
- $K$ —number of ionizable protons
- $\bar{n}$ —Bjerrum formation function
- $\alpha$ —fraction of acid titrated
- $L$ —total acid concentration
- $B$ —titrant concentration
- $V$ —volume of titrant
- $V_0$ —initial volume of acid

The Bjerrum function, the average number of protons ligand-bound per ligand, can be expressed

by:

$$\bar{n} = \frac{\sum_{i=0}^K i\beta_i h^i}{\sum_{i=0}^K \beta_i h^i}$$

or

$$\bar{n} \sum_{i=0}^K \beta_i h^i = \sum_{i=0}^K i\beta_i h^i$$

Because, by definition,  $\beta_0 = 1$ , we obtain;

$$\bar{n} \left( 1 + \sum_{i=1}^K \beta_i h^i \right) = \sum_{i=1}^K i\beta_i h^i$$

and on rearranging:

$$\begin{aligned} \bar{n} + \sum_{i=1}^K \bar{n}\beta_i h^i &= \sum_{i=1}^K i\beta_i h^i \\ \bar{n} \sum_{i=1}^K (i - \bar{n}) \beta_i h^i &= (1 - \bar{n})\beta_1 h + (2 - \bar{n})\beta_2 h^2 + \dots \\ &+ (K - \bar{n})\beta_K h^K \end{aligned} \quad (1)$$

For  $h \leq 10^{-2}M$ , terms in  $h^i$  for  $i \geq 3$  can be neglected, and the equation reduces to:

$$\bar{n} = (1 - \bar{n})\beta_1 h + (2 - \bar{n})\beta_2 h^2 \quad (2)$$

Dividing equation (2) throughout by  $(1 - \bar{n})h$ , we obtain:

$$\frac{\bar{n}}{(1 - \bar{n})h} = \beta_1 + \frac{(2 - \bar{n})h}{(1 - \bar{n})} \beta_2$$

Then, if we plot

$$Y(1, 2) = \frac{\bar{n}}{(1 - \bar{n})h} \text{ vs. } X(1, 2) = \frac{(2 - \bar{n})h}{(1 - \bar{n})}$$

the intercept at  $X = 0$  gives  $\beta_1$  and the slope of the straight line obtained gives  $\beta_2$ .

Once  $\beta_1$  and  $\beta_2$  are evaluated, if the  $h'$  terms in equation (1), for  $i \geq 5$ , are neglected, we obtain:

$$\bar{n} = (1 - \bar{n})\beta_1 h + (2 - \bar{n})\beta_2 h^2 + (3 - \bar{n})\beta_3 h^3 + (4 - \bar{n})\beta_4 h^4$$

Dividing this equation throughout by  $(3 - \bar{n})h^3$  and rearranging, we obtain:

$$\frac{\bar{n} + (n - 1)\beta_1 h + (\bar{n} - 2)\beta_2 h^2}{(3 - \bar{n})h^3} = \beta_3 + \frac{(4 - \bar{n})h}{(3 - \bar{n})} \beta_4$$

Then the straight line obtained by plotting

$$Y(3, 4) = \frac{\bar{n} + (\bar{n} - 1)\beta_1 h + (\bar{n} - 2)\beta_2 h^2}{(3 - \bar{n})h^3} \text{ vs. } X(3, 4) = \frac{(4 - \bar{n})h}{(3 - \bar{n})}$$

yields  $\beta_3$  and  $\beta_4$ .

In general, we can obtain any pair of formation constants ( $\beta_i, \beta_{i+1}$ ) by plotting:

$$Y(i, i + 1) = \frac{\sum_{j=0}^{i-1} (\bar{n} - j)\beta_j h^j}{(i - \bar{n})h^i} \text{ vs. } X(i, i + 1) = \frac{(i + 1 - \bar{n})}{(i - \bar{n})} h \quad (3)$$

When  $K$  is an odd number, two different methods

can be applied:  $\beta_1, \beta_2, \dots, \beta_{K-1}$  can be evaluated from (3), where  $i \leq K - 1$ , then  $\beta_K$  is evaluated by plotting

$$Y(K) = \frac{\sum_{j=0}^{K-1} (\bar{n} - j)\beta_j h^j}{(K - \bar{n})h^{K-1}} \text{ vs. } X(K) = h$$

or instead,  $\beta_1$  can be evaluated by plotting

$$Y(1) = \frac{\bar{n}}{(1 - \bar{n})} \text{ vs. } X(1) = h$$

and the rest of the overall protonation constants evaluated from (3), where  $i \geq 2$ .

From titration data (volume of titrant added and pH of solution), the experimental  $\bar{n}$  values are obtained from the expression

$$\bar{n} = (K - a) + \frac{Kw}{h} - \frac{h}{L}$$

where  $a$  is given by:

$$a = \frac{VB}{V_0 L}$$

From the overall formation constants, the ionization constants are obtained from the expression:

$$K_{a_i} = \frac{\beta_{k-i}}{\beta_{k-i+1}}$$

Table 1. Comparison between evaluated and reported  $pK_a$  values

Type	Reagent	$pK_a$ found*	$pK_a$ reported*	Ref.
HL	<i>p</i> -Chloroanilium ion	3.91	3.93	1
HL	Benzoic acid	4.14	4.12	1
HL	Acetic acid	4.79	4.75	4
HL	Cyclohexanone-2-pyridylhydrazone ion	6.88	6.89	5
HL	Tris	8.16	8.18	1
HL	Boric acid	9.27	9.27	1
HL	Ammonium ion	9.30	9.25	4
HL	Glycine	9.88	9.88	1
HL	<i>p</i> -Cresol	10.13	10.14	1
H <sub>2</sub> L	Oxalic acid	1.47; 3.86	1.40; 3.80	6
H <sub>2</sub> L	Succinic acid	4.19; 5.50	4.16; 5.61	7
H <sub>2</sub> L	Adipic acid	4.43; 5.36	4.42; 5.42	8
H <sub>2</sub> L	Cyclohexane-1,2-dione-2-pyridylhydrazone ion	4.98; 6.51	4.95; 6.47	5
H <sub>2</sub> L	Cyclohexane-1,3-dione-2-pyridylhydrazone ion	2.72; 4.62; 8.48	2.70; 4.63; 8.50	5
H <sub>3</sub> L	Citric acid	3.02; 4.41; 5.88	3.08; 4.39; 5.82	9
H <sub>4</sub> L	Ethylenediaminetetra-acetic acid	1.93; 2.86; 6.31; 10.12	2.07; 2.75; 6.24; 10.34	6
H <sub>4</sub> L	<i>p</i> -Phenylenediaminetetra-acetic acid	2.51; 3.48; 5.39; 6.86	2.58; 3.37; 5.39; 6.85	10
H <sub>4</sub> L	Phosphinidynetripionic acid	2.89; 3.77; 4.50;	2.89; 3.81; 4.70;	8
H <sub>5</sub> L	Anthrapurpurin complexone	2.92; 4.96; 7.61; 9.84; 10.64	3.0; 5.3; 7.6; 10.0; 10.7	11
H <sub>5</sub> L	Diethylenetriaminepenta-acetic acid	1.38; 2.17; 4.53; 8.47; 10.50	1.80; 2.55; 4.33; 8.60; 10.58	12
H <sub>6</sub> L	Triethylenetetraminehexa-acetic acid	2.38; 2.80; 4.23; 6.17; 9.46; 10.14	2.42; 2.95; 4.16; 6.16; 9.40; 10.19	13
H <sub>8</sub> L	<i>N,N,N',N'</i> -Tetrakis-phosphonomethyl-1,2-cyclohexanediamine	2.75; 4.04; 5.85; 6.67; 7.34; 7.77; 9.31; 10.37	2.40; 3.70; 5.32; 6.46; 6.97; 7.69; 9.39; 10.89	13

\*For temperature and ionic strength conditions, see the corresponding references.

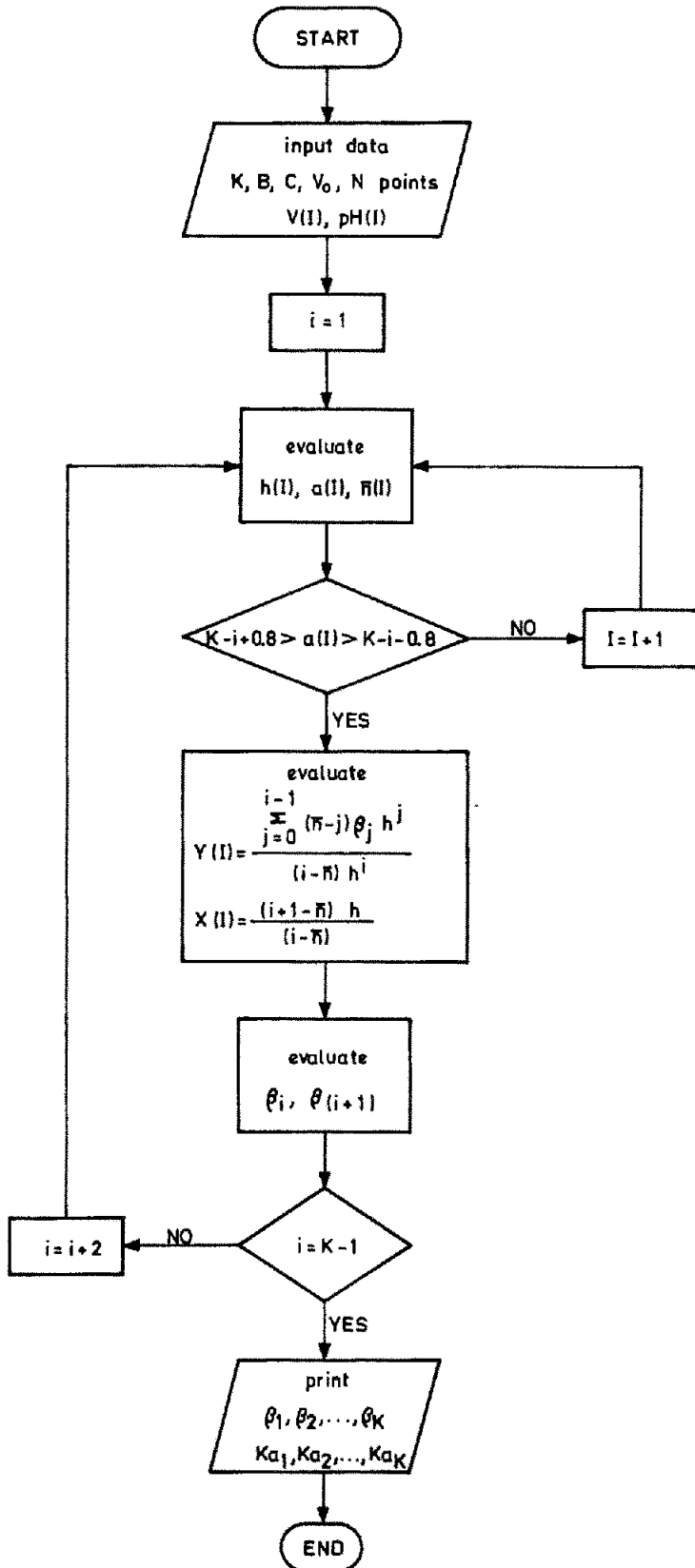


Fig. 1

## RESULTS AND DISCUSSION

A program called POTEVK written in BASIC was used to evaluate the ionization constants of up to octobasic acids, with a TOSHIBA T-100 personal computer. The program needed about 16 kbytes of memory. Figure 1 is a flow diagram for the program.

In the evaluation of any pair of constants ( $\beta_i, \beta_{i+1}$ ) of an acid  $H_KL$ , the program uses only the experimental data fulfilling the condition  $K - i + 0.8 > a > K - i - 0.8$ .

The neglect in equation (1) of terms in  $h^i$  for  $i \geq 2$  is satisfactory, since for  $H_4L$  with  $pK_a = 4$ , even at pH 2 the variation between the  $\bar{n}$  values obtained from equations (1) and (2) will not differ by more than 7%.

Any bias in the evaluation of  $\beta_1, \beta_2, \dots, \beta_{K-2}$  would accumulate in the evaluation of  $\beta_{K-1}$  and  $\beta_K$ . Therefore, careful experimental work is required to ensure that reliable results are obtained.

The method was used to evaluate the ionization constants of 22 acids, many of them polyprotic acids with overlapping constants. In some cases, the experimental data of other authors were used. The results obtained, summarized in Table 1, agree reasonably well with the reported values. Correlation coefficients of the straight lines were always higher than 0.990, and the standard deviations of  $pK_a$ , calculated from the linear regression, were about 0.02. The standard deviations obtained from several titrations of the same sample were 0.01–0.16.

The method is a computerized version of a graphical approach, and as such it cannot give results that give as good a fit to the data as a multiparametric curve-fitting program, but it would be very useful in conjunction with one of those programs, such as SUPERQUAD, as a means of finding suitable starting estimates for the  $\beta$ -values.

The program has the advantages that the computation takes less than 1 min, even for the octoprotic acid and 50 data points, and can be easily modified for use with data from an automatic titrator unit.

Listings of POTEVK are available from the authors on request.

*Acknowledgements*—We thank Dr. A. G. Asuero for valuable discussion and Mrs. M. V. Medina for the titration of some samples.

## REFERENCES

1. A. Albert and E. P. Serjeant, *The Determination of Ionization Constants*, 3rd Ed., Chapman & Hall, London, 1983, and references therein.
2. D. J. Leggett (ed.), *Computational Methods for the Determination of Formation Constants*, Plenum Press, New York, 1985.
3. F. Rossotti and H. Rossotti, *The Determination of Stability Constants*, McGraw-Hill, New York, 1961.
4. G. Charlot, *Less Réactions Chimiques en Solution*, 6th Ed., Masson, Paris, 1969.
5. D. Rosales, J. A. Muñoz Leyva and J. L. Gómez Ariza, *Quim. Anal.*, 1983, **2**, 277.
6. J. Inczedy, *Analytical Applications of Complex Equilibria*, Ellis Horwood, Chichester, 1976.
7. R. C. Weast (ed.), *Handbook of Chemistry and Physics*, 65th Ed., p. D-166. CRC Press, Boca Raton, 1984–85.
8. D. Litchinsky, N. Purdie, M. B. Tomson and W. D. White, *Anal. Chem.*, 1969, **41**, 1726.
9. G. Schwarzenbach and H. Ackermann, *Helv. Chim. Acta*, 1949, **32**, 1684.
10. B. Rodríguez Ríos, A. Peralonso Uruña and A. Mederos Pérez, *An. Quim.*, 1968, **61B**, 717.
11. J. L. Vilchez Quero, *Ph.D. Thesis*, University of Granada, 1977.
12. T. Moeller and L. C. Thompson, *J. Inorg. Nucl. Chem.*, 1962, **24**, 499.
13. T. A. Bohigian Jr. and A. E. Martell, *Inorg. Chem.*, 1965, **4**, 1269.
14. C. V. Banks and R. E. Yerrick, *Anal. Chim. Acta*, 1959, **20**, 301.

## EXTRACTION-SPECTROPHOTOMETRIC DETERMINATION OF IRON(II) BY TERNARY COMPLEX FORMATION WITH PYROCATECHOL VIOLET AND CETYLTRIMETHYLAMMONIUM BROMIDE

M. TAREK M. ZAKI\*, W. H. MAHMOUD and A. Y. EL-SAYED

Department of Chemistry, Faculty of Science, Ain Shams University, Abbassia, Cairo, Egypt

(Received 23 March 1987. Revised 18 July 1987. Accepted 23 November 1987)

**Summary**—A method for iron(II) determination based on reaction with Pyrocatechol Violet to form a 1:2 binary complex at pH 5-7 is described and has been extended to an extraction-spectrophotometric procedure for the determination of iron(II) by formation of the 1:2:2 iron(II)-Pyrocatechol Violet-cetyltrimethylammonium bromide ternary complex. The molar absorptivities of the binary and ternary complexes at 595 and 605 nm are  $6.55 \times 10^4$  and  $1.35 \times 10^5$  l. mole<sup>-1</sup>. cm<sup>-1</sup>, respectively. The method has been successfully applied to the determination of iron in felspar, Portland cement and sodium hydroxide.

Triphenylmethane dyes such as Xylenol Orange,<sup>1-4</sup> Methylthymol Blue,<sup>5,6</sup> Eriochrome Cyanine R,<sup>7,8</sup> Pyrocatechol Violet,<sup>9-11</sup> Pontachrome Azur Blue B,<sup>12</sup> Chrome Azurol S,<sup>13,14</sup> Chromoxane Violet R,<sup>15</sup> Proline Thymol Blue,<sup>16</sup> Methyl Xylenol Blue<sup>17</sup> and Aluminon<sup>18</sup> have been used for the spectrophotometric determination of iron(III), and Methylthymol Blue has been used for determination of iron(II).<sup>19</sup>

The sensitivity of such methods is significantly increased by addition of long-chain cationic surfactants to the reaction system, e.g., determination of iron(III) as a ternary complex with Chrome Azurol S and cetyltrimethylammonium bromide (CTAB),<sup>20-22</sup> Eriochrome Cyanine R and CTAB<sup>22,23</sup> or tridodecyl-ethylammonium bromide (TDEAB),<sup>24</sup> Pyrogallol Red and zephiramine,<sup>25</sup> Bromopyrogallol Red and CTAB,<sup>26</sup> Chromal Blue G and CTAB,<sup>27</sup> and Pyrocatechol Violet and TDEAB.<sup>28</sup>

In the present work, the reaction of iron(II) with Pyrocatechol Violet was studied, and also the ternary complex involving CTAB. The method developed was applied to the analysis of complex matrices for iron.

### EXPERIMENTAL

#### Reagents

All chemicals used were analytical-reagent grade and doubly-distilled water was used.

**Iron(II) solution**,  $1.00 \times 10^{-3}$ M. Prepared by dissolving 0.0980 g of ammonium iron(II) sulphate hexahydrate in 250 ml of 0.1M hydrochloric acid. A working standard solution was prepared from it by dilution.

**Hydroxylamine hydrochloride solution**, 5%.

**Pyrocatechol Violet solution (PV)**,  $1.00 \times 10^{-3}$ M. Pre-

pared by dissolving 0.0966 g of PV (Aldrich) in 250 ml of water.

**Cetyltrimethylammonium bromide (CTAB) solution**,  $1 \times 10^{-3}$ M. Prepared by dissolving 0.0911 g of CTAB (Fluka) in 250 ml of chloroform.

**Acetate buffers**, 0.4M.

**Iron-free hydrochloric acid**. Purified by removing iron by the Jackson and Phillips method.<sup>29</sup>

#### Apparatus

A Perkin-Elmer Model Lambda 3B double-beam spectrophotometer with 10-mm fused silica cells and a Schott Geräte pH-meter Model CG 710 with a combination of glass-calomel electrode were used.

#### Procedures

**Determination of iron(II) as PV binary complex.** For calibration, 0.2-20 µg of iron(II) was mixed with 2.0 ml of hydroxylamine hydrochloride solution in a 25-ml standard flask. After 5 min, 5.0 ml of PV solution were added and the solution was made up to volume with acetate buffer (pH 6.0). After 30 min the absorbance was measured at 595 nm against a reagent blank.

**Determination of iron(II) as PV-CTAB ternary complex.** A solution containing not more than 4.0 µg of iron(II) and 2.0 ml of hydroxylamine hydrochloride solution was mixed in a 50-ml separatory funnel. After 5 min, 5.0 ml of PV solution and 10.0 ml of acetate buffer (pH 5.15) were added. After 30 min, 10.0 ml of  $5 \times 10^{-4}$ M CTAB in chloroform solution were added and the mixture was vigorously shaken for 5 min. The organic phase was separated and centrifuged at 3000 rpm for 2 min, then its absorbance was measured at 605 nm against a reagent blank prepared in the same way.

**Determination of iron in felspar and Portland cement.** About 0.2 g of sample was accurately weighed, mixed with 5 ml of concentrated hydrochloric acid and 1.0 ml of concentrated nitric acid in a porcelain dish, and the mixture was evaporated to dryness on a steam-bath. The dry mass was moistened with 5 ml of concentrated hydrochloric acid, and warmed on a steam-bath for 10 min, then 20 ml of hot water were added. Any residue was filtered off and washed, the filtrate and washings being collected in a 250-ml standard flask. A suitable aliquot of this solution was

\*To whom all correspondence should be addressed.



treated with 1.0 ml of 0.2M malonic acid, 2.0 ml each of 0.01M ammonium citrate and tartrate solutions, and analysed for iron as described above.

**Determination of iron in sodium hydroxide.** About 0.2–0.4 g of sample was weighed and prepared according to the Marzenko and Kalowska method.<sup>22</sup> The iron was determined as the PV–CTAB ternary complex after addition of 2.0 ml of 0.01M ammonium tartrate solution.

## RESULTS AND DISCUSSION

Several authors have studied the reaction of triphenylmethane dyes with iron(III), but little attention has been paid to the reactions with iron(II). In a preliminary study, experiments were performed to see whether addition of Xylenol Orange, Eriochrome Cyanine R and PV to iron(II) would show better sensitivity than that for iron(III). PV was the only one that did. Trials to increase the sensitivity further were made by addition of aqueous CTAB solution, but little improvement was found. Much better results were obtained by using a chloroform solution of CTAB for extraction of the binary complex. The ternary iron(II)–PV–CTAB complex formed in the organic phase had more than double the molar absorptivity of the aqueous binary complex.

### Absorption spectra

The absorption spectra of the binary and ternary complexes and the reagent blanks are shown in Fig. 1. The green iron(II)–PV complex has an absorp-

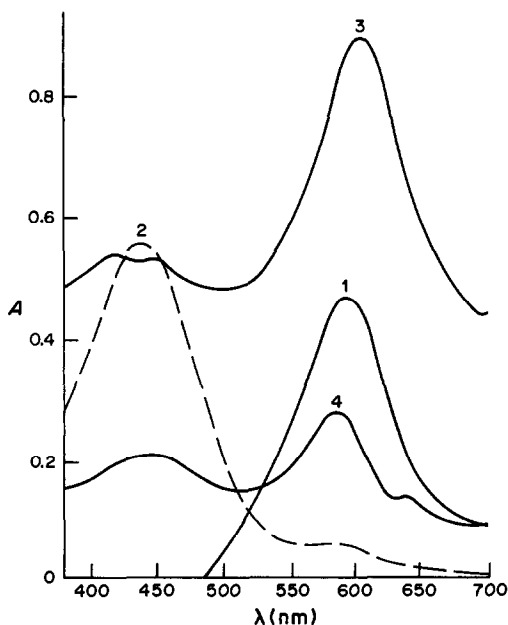


Fig. 1. Absorption spectra of iron(II)–PV in aqueous medium, iron(II)–PV–CTAB in chloroform, and their reagent blank.  $[PV]_{aq} = 2 \times 10^{-4}M$ , 2.0 ml of 5%  $NH_2OH \cdot HCl$ , pH = 6 for aq. measurements, pH = 5.15 for extraction, 1.00-cm cells. Curve 1, iron(II)–PV in aqueous medium,  $[Fe^{2+}] = 7 \times 10^{-6}M$ , vs. blank; 2, PV in aqueous medium vs. buffer (pH = 6); 3, iron(II)–PV–CTAB in chloroform,  $[Fe^{2+}]_{aq} = 6.5 \times 10^{-6}M$ ,  $[CTAB]_o = 5 \times 10^{-4}M$ , vs. blank; 4, PV–CTAB in chloroform vs. blank.

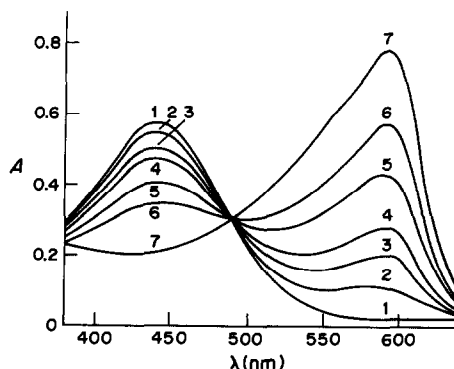


Fig. 2. Absorption spectra of PV at various pH values.  $[PV] = 3.5 \times 10^{-5}M$ , 1.00-cm cells, pH values: curve 1, 5.0; 2, 6.4; 3, 7.0; 4, 7.2; 5, 7.6; 6, 8.0; 7, 9.0.

tion maximum at 595 nm in neutral or slightly acidic media. The extracted ternary complex shows a shift of the absorption maximum to 605 nm, with an increase in absorbance.

### Effect of pH

The absorption spectra of  $3.5 \times 10^{-5}M$  PV at different pH values are given in Fig. 2, and have an isosbestic point at 490 nm. The effect of pH on the absorbance of the binary complex at 595 nm is shown in Fig. 3 (curve 1). The absorbance reaches its maximum value at pH 5.0 and remains constant up to pH 7.0. Therefore, acetate buffer of pH 6.0 was used for formation of the binary complex.

Figure 4 shows the effect of pH on the extraction of  $4.6 \times 10^{-5}M$  aqueous PV with 10.0 ml of  $5 \times 10^{-4}M$  CTAB in chloroform. The absorption

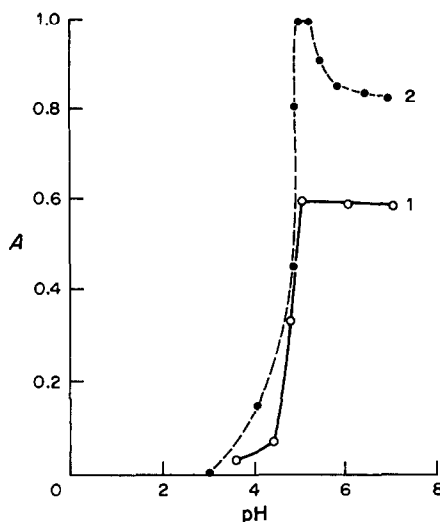


Fig. 3. Effect of pH on the absorbance of aqueous iron(II)–PV complex and the extraction of iron(II)–PV–CTAB complex into chloroform: 2.0 ml of 5%  $NH_2OH \cdot HCl$ , 1.00-cm cells. Curve 1, iron(II)–PV complex,  $[Fe^{2+}]_{aq} = 9 \times 10^{-6}M$ ,  $[PV]_{aq} = 2 \times 10^{-4}M$ , wavelength = 595 nm; 2, iron(II)–PV–CTAB complex in chloroform,  $V_{aq} = 25$  ml,  $V_o = 10.0$  ml,  $[Fe^{2+}]_{aq} = 7.4 \times 10^{-6}M$ ,  $[PV]_{aq} = 2 \times 10^{-4}M$ ,  $[CTAB]_o = 5 \times 10^{-4}M$ , wavelength = 605 nm.

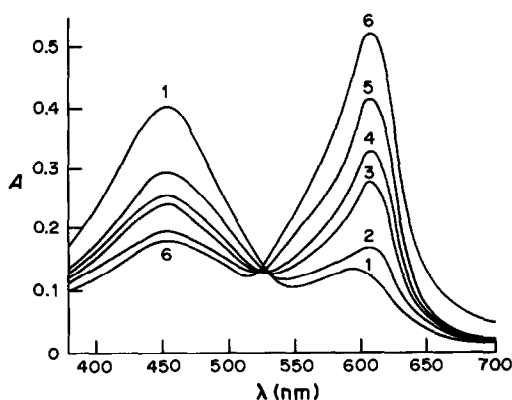


Fig. 4. Absorption spectra of extracted PV-CTAB in chloroform as function of pH of the aqueous media.  $[PV]_{aq} = 4.6 \times 10^{-5} M$ ,  $[CTAB]_o = 5 \times 10^{-4} M$ , 1.00-cm cells, pH values: curve 1, 5.6; 2, 6.2; 3, 6.6; 4, 6.8; 5, 7.0; 6, 7.2.

band at 590 nm in the aqueous phase is shifted to 610 nm in the organic phase. However, the spectral interference of the reagent blank with the ternary complex (which absorbs at 605 nm) is minimized in the presence of hydroxylamine hydrochloride, cf. Fig. 1, curve 4.

The absorbance of the ternary complex in chloroform is dependent on the pH of the aqueous phase from which it is extracted (Fig. 3, curve 2). The optimum pH for quantitative extraction is 4.9–5.4 and pH 5.1–5.2 is recommended.

#### Effect of PV concentration

The optimum concentration of reagent for quantitative formation of the binary complex from 20  $\mu g$  of iron(II) was found to be  $2 \times 10^{-4} M$ . The same concentration was used in the aqueous phase to prepare the ternary complex. Deviation from this concentration decreased the absorbance of the organic phase.

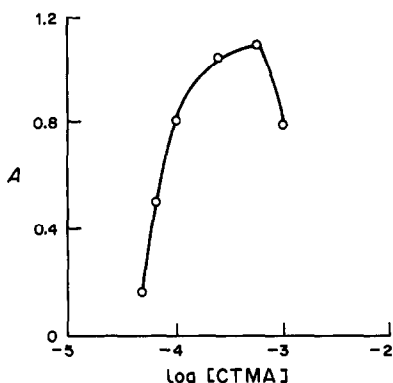


Fig. 5. Effect of CTAB concentration in chloroform on the formation and extraction of iron(II)-PV-CTAB complex.  $[Fe^{2+}]_{aq} = 8 \times 10^{-6} M$ ,  $[PV]_{aq} = 2 \times 10^{-4} M$ ,  $[NH_2OH.HCl]_{aq} = 0.72 M$ , pH = 5.15, 1.00-cm cells, wavelength = 605 nm.

#### Extraction solvents

Solutions of CTAB in benzene, toluene, xylene, carbon tetrachloride, n-butyl acetate and nitrobenzene were not useful for extracting the ternary complex, which either formed at the interface between the aqueous and organic layers or was incompletely extracted. Extraction was quantitative with chloroform as solvent, however.

#### Effect of CTAB concentration

Figure 5 shows that a CTAB concentration between  $4 \times 10^{-4}$  and  $5 \times 10^{-4} M$  in chloroform is optimum for quantitative extraction; the  $5 \times 10^{-4} M$  solution is used in the recommended procedure. Concentrations outside this range give lower absorbances for the ternary complex. Concentrations  $> 10^{-3} M$  produce a stable emulsion on shaking and the two phases do not separate.

#### Shaking time, degree of extraction and stability

Shaking for 4–10 min gives the same absorbance; shaking for 5 min was selected for the procedure.

A repeated extraction of an aqueous solution of the binary complex showed that 98.7% of the binary complex formed with 2.2  $\mu g$  of iron(II) in 25 ml of aqueous phase is removed in one extraction with 10.0 ml of  $5 \times 10^{-4} M$  CTAB in chloroform.

The absorbance of the binary complex gradually increased during the first 20 min after mixing and then remained constant for more than 3 hr. The absorbance of the ternary complex remained constant for about 90 min after the extraction.

#### Calibration, molar absorptivities and precision

In determination of iron(II) as the binary and ternary complexes Beer's law is obeyed up to 0.8 and 0.35  $\mu g/ml$  iron respectively in the final solution measured. The molar absorptivities of the binary

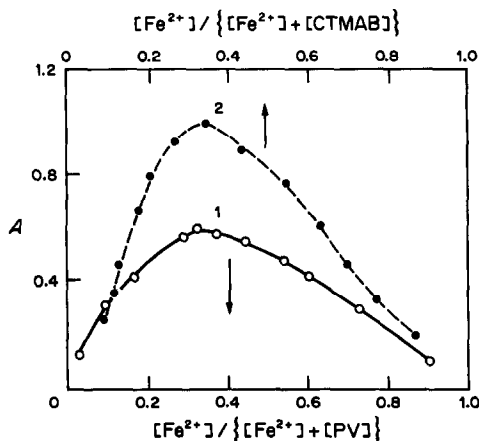


Fig. 6. Continuous-variation study of iron(II)-PV and iron(II)-PV-CTAB systems. Curve 1,  $[Fe^{2+}]_{aq} + [PV]_{aq} = 2.7 \times 10^{-5} M$ , pH = 6.0, 1.00-cm cells, wavelength = 595 nm; 2,  $[Fe^{2+}]_{aq} + [CTAB]_o = 2.2 \times 10^{-6} M$ , pH = 5.15, 1.00-cm cells, wavelength = 605 nm.

Table 1. Effect of diverse ions on the determination of 2 µg of iron(II) as the ternary complex

Tolerance limit, [Ion]/[Fe <sup>2+</sup> ]	Diverse ions
1000	Ba <sup>2+</sup> , Be <sup>2+</sup> , Bi <sup>3+</sup> <sup>a</sup> , Ca <sup>2+</sup> , Cd <sup>2+</sup> , Co <sup>2+</sup> , Cu <sup>2+</sup> , Mg <sup>2+</sup> , Mn <sup>2+</sup> , Ni <sup>2+</sup> , Pd <sup>2+</sup> , Zn <sup>2+</sup> , Cl <sup>-</sup> , NO <sub>3</sub> <sup>-</sup> , SO <sub>4</sub> <sup>2-</sup> , ascorbate, citrate, malonate, oxalate, tartrate
500	As <sup>5+</sup> , Pb <sup>2+</sup> , Ti <sup>4+</sup>
200	Al <sup>3+</sup> <sup>b</sup> , Mo <sup>6+</sup> <sup>c</sup> , Th <sup>4+</sup> <sup>d</sup>
100	Cr <sup>3+</sup> <sup>d</sup> , Gd <sup>3+</sup> , Hf <sup>4+</sup> <sup>d</sup> , In <sup>3+</sup> <sup>c</sup> , La <sup>3+</sup> , Nb <sup>5+</sup> <sup>e</sup> , Pr <sup>3+</sup> , Sb <sup>3+</sup> <sup>d</sup> , Sc <sup>3+</sup> <sup>d</sup> , Sm <sup>3+</sup> , Sn <sup>4+</sup> <sup>e</sup> , Ta <sup>5+</sup> <sup>e</sup> , V <sup>5+</sup> <sup>f</sup> , W <sup>6+</sup> <sup>e</sup> , Zr <sup>4+</sup> <sup>d</sup>
< 0.5	Ga <sup>3+</sup> , Ge <sup>4+</sup>

## \*Masking agents

<sup>a</sup>1 ml of 0.1M sodium chloride.<sup>b</sup>1 ml of 0.4M malonic acid.<sup>c</sup>1 ml of 10% thioglycollic acid solution.<sup>d</sup>2 ml of 0.01M ammonium citrate.<sup>e</sup>2 ml of 0.01M ammonium tartrate.<sup>f</sup>3 ml of 10% hydroxylamine hydrochloride solution.

Table 2. Determination of iron in felspar and Portland cement

Sample	Fe <sub>2</sub> O <sub>3</sub>		No. of determinations	Relative standard deviation, %
	Certified, %	Found, %		
Felspar	0.10	0.099	10	0.5
Portland cement	2.05	2.04	10	0.4

and ternary complexes, found by least-squares analysis of 15 results, were  $6.55 \times 10^4$  and  $1.35 \times 10^5$  l.mole<sup>-1</sup>.cm<sup>-1</sup>, respectively.

However, the molar absorptivity of the ternary iron(III)-PV-CTAB complex in chloroform was only  $7.4 \times 10^4$  l.mole<sup>-1</sup>.cm<sup>-1</sup> at 615 nm. This value is close to that reported by Shijo<sup>28</sup> for the iron(III)-PV-TDEAB ternary complex in methyl isobutyl ketone ( $\epsilon = 7.76 \times 10^4$  l.mole<sup>-1</sup>.cm<sup>-1</sup> at 623 nm).

*Composition of the binary and ternary complexes*

Job's method<sup>30</sup> indicated that the Fe(II):PV molar ratio in the binary complex was 1:2 and that the molar ratios in the ternary iron(II)-PV-CTAB complex were 1:2:2 (Fig. 6). The ternary complex is probably [Fe(PV)<sub>2</sub>]<sup>2-</sup>.(CTA<sup>+</sup>)<sub>2</sub>.

*Interferences*

The effect of more than 40 ions on the determination of iron(II) as the ternary complex was studied. The tolerance limit was taken as the amount that caused  $\pm 2\%$  error in the absorbance. Interference of some ions such as Al(III), Cr(III), Hf(IV), In(III), Mo(VI), Nb(V), Sb(III), Sc(III), Sn(IV), Ta(V), Th(IV), V(V), W(VI) and Zr(IV) was eliminated by the addition of suitable masking agents (Table 1). Bismuth(III) was precipitated as the oxychloride and did not interfere. However, gallium(III) and germanium(IV) interfered when their concentration exceeded half that of iron(II). Trials to mask these ions were unsuccessful.

*Application of the method*

The ternary complex method was successfully applied to the determination of iron in felspar and Portland cement, the interference of aluminium(III) and titanium(IV) being eliminated by the addition of malonate, tartrate and citrate as masking agents. The results (Table 2) were in good agreement with those from standard chemical and X-ray fluorescence methods.

Determination of iron in sodium hydroxide required preliminary separation by extraction as the thiocyanate complex into methyl isobutyl ketone.<sup>22</sup> The organic solvent was evaporated, the residue mineralized with concentrated sulphuric acid and iron determined by the iron(II)-PV-CTAB method. Table 3 show the results for analysis of sodium hydroxide samples, together with recoveries of known added amounts of iron.

Table 3. Determination of iron (10 replicates) in pure sodium hydroxide

Sample weight, g	Iron			Relative standard deviation, %
	Added, µg	Found		
	µg	µg	%	
0.2	—	1.22	$6.0 \times 10^{-4}$	0.7
0.2	2.6	3.59		0.5
0.4	—	2.50	$6.35 \times 10^{-4}$	0.7
0.4	1.3	3.76		0.5

## REFERENCES

1. K. L. Cheng, *Talanta*, 1959, **3**, 147.
2. B. Buděšínský, *Z. Anal. Chem.*, 1962, **188**, 266.
3. M. Otomo, *Bunseki Kagaku*, 1965, **14**, 677.
4. H. Nishida, T. Nishida and T. Segawa, *ibid.*, 1979, **28**, 379.
5. K. Tonosaki, *Bull. Chem. Soc. Japan*, 1966, **39**, 425.
6. B. Karadakov, D. Kantcheva and P. Nonova, *Talanta*, 1968, **15**, 525.
7. F. J. Langmyhr and T. Stumpe, *Anal. Chim. Acta*, 1965, **32**, 535.
8. V. N. Tikhonova and T. M. Anisimova, *Zh. Analit. Khim.*, 1983, **38**, 778.
9. I. I. Birmantas and E. I. Yasinskene, *ibid.*, 1965, **20**, 811.
10. T. Ishito and S. Ichinohe, *Bunseki Kagaku*, 1972, **21**, 1207.
11. Y. Ichinohe, *Kagaku No Jikken*, 1972, **23**, 117.
12. Y. Katsube, K. Uesugi and J. H. Yoe, *Bull. Chem. Soc. Japan*, 1961, **34**, 72.
13. F. J. Langmyhr and K. S. Klausen, *Anal. Chim. Acta*, 1963, **29**, 149.
14. T. M. Maljutina, V. A. Orlova and B. Ya. Spivakov, *Zh. Analit. Khim.*, 1974, **29**, 790.
15. I. S. Mustafin and N. F. Lisenko, *ibid.*, 1962, **17**, 1052.
16. M. Koch and I. Kochová, *Acta Univ. Agr., Fac. Agron., Brno*, 1968, **16**, 167.
17. M. Deguchi and M. Yashiki, *Hiroshima Daigaku Igaku Zasshi*, 1970, **18**, 113.
18. S. P. Sangal, *Chim. Anal. (Paris)*, 1965, **47**, 288.
19. K. C. Srivastava and S. K. Banerji, *Microchem. J.*, 1968, **13**, 621.
20. Y. Shijo and T. Takeuchi, *Bunseki Kagaku*, 1968, **17**, 1519.
21. Y. Nakamura, H. Nagai, O. Kubota and S. Himeno *ibid.*, 1973, **22**, 1156.
22. Z. Marzenko and H. Kalowska, *Anal. Chim. Acta*, 1981, **123** 279.
23. Y. Shijo and T. Takeuchi, *Bunseki Kagaku*, 1971, **20**, 980.
24. Y. Shijo, *Bull. Chem. Soc. Japan*, 1975, **84**, 2793.
25. T. Korenaga, S. Motomizu and K. Toei, *Anal. Chim. Acta*, 1979, **104**, 369.
26. H. Xi-Wen and D. P. Poe, *Talanta*, 1981, **28**, 419.
27. M. Miyawaki and K. Uesugi, *Mikrochim. Acta*, 1985 **I**, 135.
28. Y. Shijo, *Bull. Chem. Soc. Japan*, 1977, **50**, 1013.
29. H. Jackson and D. S. Phillips, *Analyst*, 1962, **87**, 718.
30. P. Job, *Ann. Chim. (Paris)*, 1928, **9**, 113.

# DETERMINATION OF THE SUM OF RARE-EARTH ELEMENTS BY FLOW-INJECTION ANALYSIS WITH ARSENAZO III, 4-(2-PYRIDYLAZO)RESORCINOL, CHROME AZUROL S AND 5-BROMO-2-(2-PYRIDYLAZO)-5-DIETHYLAMINOPHENOL SPECTROPHOTOMETRIC REAGENTS

D. B. GLADILOVICH\*, V. KUBÁŇ and L. SOMMER

Department of Analytical Chemistry, J. E. Purkyně University, 611 37 Brno, Czechoslovakia

(Received 21 August 1987. Accepted 21 November 1987)

**Summary**—The reactivity of Arsenazo III, Chrome Azurol S in the presence of cetyltrimethylammonium or cetylpyridinium bromide, 4-(2-pyridylazo)resorcinol and 5-bromo-2-(2-pyridylazo)-5-diethylaminophenol with various rare-earth elements (REE) has been studied and the optimum conditions have been established for the spectrophotometric determination of REE with stationary and flow systems. Arsenazo III is the most suitable for the determination of the sum of REE, especially La, Ce, Nd, by FIA with spectrophotometric detection at 660 nm, in systems containing 0.04 mM reagent and 0.2M formate buffer (pH 3) and for sample volumes of 30  $\mu$ l. The detection limits are 10.8 ng La, 11.0 ng Ce and 9.4 ng Nd in 30  $\mu$ l. Limited amounts of Fe(III) and Al(III) are screened with 10 mM ascorbic and 5-sulphosalicylic acids. The sum of the REE is obtained from calibration plots prepared with La(III) standard solutions. The method has been successfully used for apatites and REE oxide concentrates after various kinds of decomposition.

The rare-earth elements (REE) have recently become important components of metallurgical materials and in some special technologies. The determination of the sum of REE in geological samples, concentrates and various technological materials has limited significance but is often demanded for characterization. Among the analytical methods used for these purposes spectrophotometry is rapid and convenient. The sensitivity of procedures using various azo, bisazo or triphenylmethane dyes as reagents<sup>1–16</sup> is high enough, the molar absorptivities being in the range  $5–8 \times 10^4$  l.mole<sup>-1</sup>.cm<sup>-1</sup> but the selectivity is poor, and sophisticated masking or prior separation of REE from common interferents in samples with complicated matrices is necessary.<sup>17</sup>

In the work reported in this paper the frequently used reagents Arsenazo III, 4-(2-pyridylazo)-resorcinol (PAR), Chrome Azurol S (CAS) in the presence of cetylpyridinium and cetyltrimethylammonium bromide, and 5-bromo-2-(2-pyridylazo)-5-diethylaminophenol (BrPADAP) were examined in combination with flow-injection analysis (FIA) for the determination of REE. FIA has become very popular because of its reduced sample and reagent consumption, its rapidity and the possibility of full automation. The kinetic aspects of complex formation may also be followed by this technique.<sup>18</sup> Since there is generally no considerable difference in complex formation by various REE with a particular reagent, the interaction of the four reagents was

studied in detail only with lanthanum, to find the optimum conditions for their use as spectrophotometric reagents in FIA of the REE. These studies are also of interest for the post-column detection of REE in ion-exchange chromatography or HPLC.<sup>19–24</sup>

## EXPERIMENTAL

### Reagents

Stock solutions of REE (10 mM) were prepared by dissolving accurately known weights of the spectrally pure nitrates (La, Ce, Pr, Nd, Tb, Ho), oxides (Sm, Er, Y, Tm, Lu) or carbonates (Eu, Gd, Dy, Yb) in 1M nitric acid and diluting with doubly distilled water to give an acid concentration of 0.1M. The solutions were standardized by chelometric titration, with Xylenol Orange as indicator.<sup>25</sup>

Chrome Azurol S (CAS) trisodium salt (Merck) was carefully purified and converted into the free acid dihydrate.<sup>26</sup> The chromatographically pure sample contained 85.0% of active substance (calculated as the acid). A 5 mM solution was prepared in water alkalinized by 10–15 drops of 15M ammonia solution.

5-Bromo-2-(2-pyridylazo)-5-diethylaminophenol (BrPADAP, chromatographically pure, Merck) was used as 0.1–1 mM stock solutions in ethanol or dimethylformamide.

4-(2-Pyridylazo)resorcinol (PAR, Lachema Chem. Co., Brno) was recrystallized several times from methanol;<sup>27</sup> the product contained 89.7% of the active substance; 0.1–1 mM aqueous stock solutions were prepared.

Arsenazo III [2,7-bis-(*o*-arsonophenylazo)-1,8-dihydroxynaphthalene-3,6-disulphonic acid, disodium salt]; 0.1–1 mM stock solutions of the chromatographically pure acid<sup>28</sup> were prepared.

Cetylpyridinium bromide (CP) and cetyltrimethylammonium bromide (CTMA), (Lachema, Brno), were reprecipitated as the pure substances from ethanolic solutions by addition of diethyl ether, and used as 20% stock solutions in ethanol and water respectively.

\*On leave from the Department of Analytical Chemistry, A. A. Zhdanov University, 199164 Leningrad, U.S.S.R.

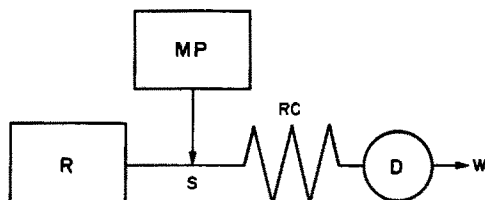


Fig. 1. Flow diagram of FIA manifold. R—reagent solution (flow-rate,  $F_m = 1$  ml/min, hydrostatic overpressure); MP—membrane pump, RC—reaction coil ( $L_r = 30$  cm, i.d. 0.6 cm), D—spectrophotometric detector (18  $\mu$ l flow-cell, 330–850 nm), W—waste.

Ethanol containing 5% (v/v) methanol was purified by distillation from solid EDTA disodium salt (1 g per litre). Dimethylformamide (Reachim, U.S.S.R.) was distilled at  $56^\circ/22$  mm Hg.

All dyestuff concentrations given are the true values (*i.e.*, corrected for purity). All water used was doubly distilled in silica apparatus.

#### Apparatus

Radelkis OP-208/1 pH-meter with OP 0718 P glass electrode and OP 0830 P SCE, regularly calibrated with NBS buffers, pH 2.18–7.01. A Specord M 40 double-beam spectrophotometer with 10-mm silica cuvettes (Zeiss, Jena) was used at  $24 \pm 1^\circ$ .

A block scheme of the FIA manifold is shown in Fig. 1. It uses a loop injector for 8–100  $\mu$ l sample volumes or a chromatographic six-way cock with a 30- $\mu$ l sampling loop. The loops were filled with solution by means of a diaphragm pump (Varian, Switzerland). A Spekol 21 single-beam spectrophotometer with a Z-shaped flow-cell (10 mm optical path-length, 18  $\mu$ l volume) was used for detection at 335–800 nm in combination with a K 201 recorder (1 scale unit = 0.005 absorbance). Teflon capillaries (bore 0.6 mm) were used for connections. The carrier stream containing the reagent, buffer, masking agent(s) and inert electrolyte was pulselessly transported from a reservoir by hydrostatic pressure at a flow-rate of 0.5–3 ml/min. Peristaltic or diaphragm pumps failed to give the required repeatability of flow-rate (0.1–1.0%). The maximum yield of reaction product in the various systems was obtained with a carrier flow-rate of 1.0 ml/min, injected sample volume 30  $\mu$ l, length of reaction capillary *ca.* 40 cm between injection port and detector cell, and degree of dispersion  $D = c_0/c_m \sim 7$ , where  $c_0$  is the signal for zero dispersion and  $c_m$  the signal maximum when the sample zone passes through the detector.<sup>18</sup>

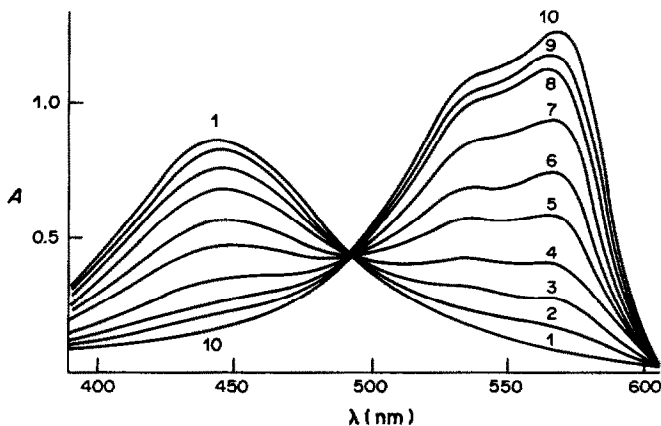


Fig. 2. Absorption spectra of BrPADAP solution with  $\text{La}^{3+}$  in excess.  $c_L = 20 \mu\text{M}$ ,  $c_M = 2 \text{mM}$ , 30% dimethylformamide,  $I = 0.1$  ( $\text{HNO}_3 + \text{NH}_3$ ) pH: curve 1, 4.34; 2, 5.26; 3, 5.67; 4, 5.98; 5, 6.32; 6, 6.65; 7, 7.01; 8, 7.30; 9, 7.45; 10, 8.13.

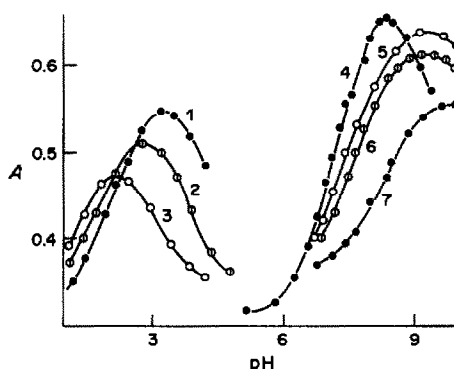


Fig. 3. Absorbance vs. pH plots for various stationary systems of reagent and  $\text{La}^{3+}$ .  $c_M = 10 \mu\text{M}$ ,  $I = 0.10$  ( $\text{KNO}_3 + \text{NH}_3$ ). Arsenazo III: 650 nm; curve 1,  $c_L = 20 \mu\text{M}$ ; 2,  $c_L = 50 \mu\text{M}$ ;  $c_L = 100 \mu\text{M}$ . BrPADAP;  $\lambda$  560 nm; curve 4,  $c_L = 100 \mu\text{M}$ , 30% dimethylformamide. CAS + CP:  $\lambda$  620 nm; curve 5,  $c_L = 75 \mu\text{M}$ , surfactant 200  $\mu\text{M}$ . CAS + CTMA:  $\lambda$  620 nm; curve 6,  $c_L = 75 \mu\text{M}$ , surfactant 200  $\mu\text{M}$ . PAR: 520 nm; curve 7,  $c_L = 400 \mu\text{M}$ .

Calibration plots were prepared from the heights of the peak maxima and the parameters were evaluated by linear regression analysis. The detection limits were based on the  $3s_{xy}$  criterion, where  $s_{xy}$  is the standard deviation of the spread of points around the calibration plot. The variances of several series of results were evaluated by means of the Cochran criterion, for 8 parallel determinations. The arithmetic means were compared by the *Student* or *Dean* and *Dixon* criteria.<sup>29</sup>

## RESULTS AND DISCUSSION

### Stationary systems

**Interaction of  $\text{La}^{3+}$  with BrPADAP.** A characteristic double absorption maximum at 540 and 565 nm indicates complex formation from pH < 4 in 30% (v/v) dimethylformamide, especially in solutions with excess of metal ion (2.0mM  $\text{La}^{3+}$  + 20  $\mu\text{M}$  BrPADAP, Fig. 2). The absorbance vs. pH plots reach a plateau at pH 8.0–8.2 for solutions with 40–100  $\mu\text{M}$  BrPADAP in excess (curve 4 in Fig. 3). At higher pH, the complex species decomposes on standing. A computer analysis of the results indicated stepwise

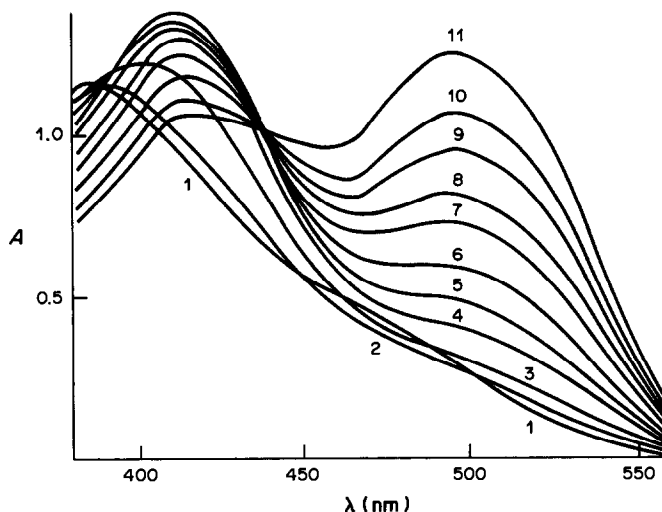


Fig. 4. Absorption spectra of PAR solution with  $\text{La}^{3+}$  in excess.  $c_L = 17.9 \mu\text{M}$ ,  $c_M = 200 \mu\text{M}$ ; pH curve 1, 3.77; 2, 4.56; 3, 5.11; 4, 5.63; 5, 6.00; 6, 6.23; 7, 6.38; 8, 6.50; 9, 6.83; 10, 7.01; 11, 7.25.

formation of ML (at pH < 4) and  $\text{ML}_2$  (at pH 4–8) in solutions with reagent excess (L is the fully dissociated anion of BrPADAP).<sup>5</sup> The optimum conditions for spectrophotometric determination would be  $\text{pH } 8.1 \pm 0.1$  ( $0.1 \text{M } \text{NH}_3/\text{NH}_4^+$  buffer) with  $0.4 \text{mM}$  BrPADAP and 30% dimethylformamide (conditional absorptivity  $6.1 \times 10^4 \text{ l. mole}^{-1} \cdot \text{cm}^{-1}$  at 568 nm, but the hydrolytic decomposition of  $\text{ML}_2$  under these conditions makes the reagent unsuitable for the identification or determination of  $\text{La}^{3+}$  or other REE.

**Interaction of  $\text{La}^{3+}$  with PAR.** The complex formation in aqueous solution with excess of  $\text{La}^{3+}$  ( $0.2 \text{mM } \text{La}^{3+} + 17.5 \mu\text{M}$  PAR) at pH 4–8 is characterized by  $\lambda_{\text{max}}$  509 nm (Fig. 4). The  $\Delta A$  vs. pH plots for solutions with reagent excess ( $10 \mu\text{M } \text{La}^{3+} + 0.2\text{--}0.4 \text{mM}$  PAR) reach a plateau at pH 9–10 (curve 7 in Fig. 3). The absorbance is constant 5 min after mixing of the components but in the next 5 min decreases by 5% at pH 8.0–9.5 or 20% at pH 9.0–9.5, so the absorbance was read during the first 5 min. The computer treatment of the absorbance data at 390–560 nm for solutions with reagent excess indicates a mixture of ML and  $\text{MLH}$  complexes at pH 3.0–6.2 and a more absorptive chelate  $\text{ML}_2$  at pH 6.2–9.5. The last chelate easily hydrolyses to  $\text{M(OH)L}$  and further hydrolytic products.<sup>5</sup> For the determination of  $\text{La}^{3+}$  or other REE the  $\text{ML}_2$  chelate is optimal at pH 9.0–9.5 in solutions containing  $0.2 \text{mM}$  PAR and  $0.1 \text{M } \text{NH}_3/\text{NH}_4^+$  buffer, with conditional molar absorptivity  $\epsilon = 3.8 \times 10^4 \text{ l. mole}^{-1} \cdot \text{cm}^{-1}$  at 510 nm.

**Interaction of  $\text{La}^{3+}$  with Chrome Azurol S in the presence of cationic surfactant.** At least two ternary species,  $\text{La}^{3+}$ –CAS–CTMA (or CP) with  $\lambda_{\text{max}}$  620 and 650 nm are evident from the absorption spectra of aqueous solutions containing  $74.6 \mu\text{M}$  CAS and  $0.5 \text{mM}$  CTMA or  $0.1 \text{mM}$  CP with increasing pH (Fig. 5) and from the  $\Delta A$  vs. pH plots for solutions with the same reagent concentration and variable

surfactant concentration,  $0.05\text{--}1 \text{mM}$  CTMA or CP (curves 5 and 6 in Fig. 3). The first species ( $\lambda_{\text{max}}$  620 nm,  $\epsilon' = 6.3\text{--}7.2 \times 10^4 \text{ l. mole}^{-1} \cdot \text{cm}^{-1}$ ) is quantitatively formed at pH 8.8–9.6 in the presence of  $0.1\text{--}0.2 \text{mM}$  CTMA or CP. The optimum surfactant concentration and pH interval depend on the total concentration of CAS for a particular REE concentration, e.g.,  $0.4\text{--}0.5 \text{mM}$  CTMA or CP for  $0.15\text{--}0.20 \text{mM}$  CAS and  $10 \mu\text{M } \text{La}^{3+}$  at pH 9.2–9.6. The ratio  $c_{\text{surfactant}}/c_{\text{CAS}} = 2\text{--}3$  should always be maintained. The same is valid for  $\text{Y}^{3+}$ ,  $\text{Yb}^{3+}$ ,  $\text{Gd}^{3+}$ . Optimum conditions for the method correspond to  $80 \mu\text{M}$  CAS and  $0.2 \text{mM}$  CTMA or CP at  $\text{pH } 9.4 \pm 0.2$  ( $0.1 \text{M } \text{NH}_3/\text{NH}_4^+$  buffer) for the concentration interval  $2\text{--}10 \mu\text{M}$  REE. Another ternary species with  $\epsilon' = 9.2\text{--}9.6 \times 10^4 \text{ l. mole}^{-1} \cdot \text{cm}^{-1}$  at 650 nm is formed at pH 9.8–10.2 in solutions containing  $40\text{--}80 \mu\text{M}$  CAS and  $0.10\text{--}0.15 \text{mM}$  CTMA or CP for all REE examined. The formation of such species is, however, slower with CTMA or CP concentrations

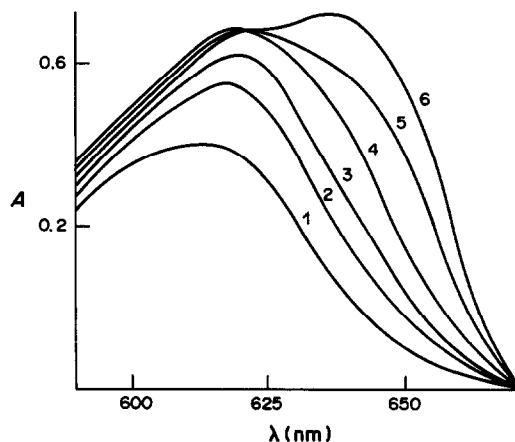


Fig. 5. Absorption spectra in the system CAS–CTMA– $\text{La}^{3+}$ .  $c_L = 75 \mu\text{M}$ , surfactant  $200 \mu\text{M}$ ,  $c_M = 10 \mu\text{M}$ ,  $I = 0.10$ ; pH, curve 1, 7.63; 2, 8.10; 3, 8.41; 4, 8.73; 5, 9.14; 6, 9.27.

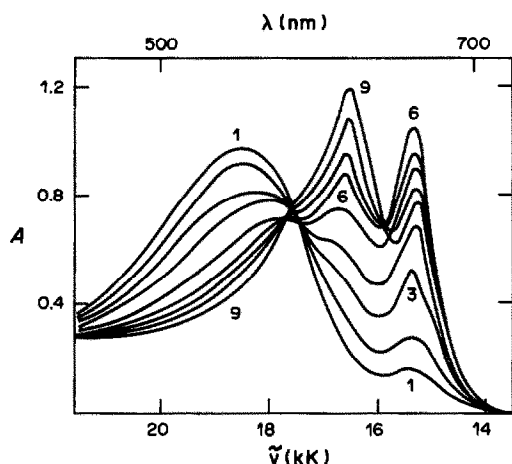


Fig. 6. Absorption spectra of Arsenazo III solutions with  $\text{La}^{3+}$ .  $c_L = 50\mu\text{M}$ ,  $c_M = 20\mu\text{M}$ ;  $I = 0.10$ ; pH, curve 1, 1.25; 2, 1.69; 3, 2.06; 4, 2.33; 5, 2.70; 6, 3.01; 7, 3.61; 8, 4.51; 9, 5.35.

greater than  $0.15\text{mM}$ . Small changes in the concentration of the reacting components may cause deformations of the linear calibration plots for small concentrations of REE.<sup>11</sup>

**Interaction of  $\text{La}^{3+}$  with Arsenazo III.** A double absorption peak at 610 and 660 nm in solutions containing  $50\mu\text{M}$  Arsenazo III and  $20\mu\text{M}$   $\text{La}^{3+}$  at pH 1–7 is typical for the complex formation (Fig. 6). The absorbance at 660 nm reaches a constant maximum value at pH 3.0–3.4 in  $20\mu\text{M}$  equimolar solutions, at pH 2.8–3.1 for threefold and pH 2.2–2.4 for fivefold reagent excess, in contrast to pH 6–7, where a constant maximum absorbance value is reached at 610 nm (Fig. 3). This is in agreement with earlier data in the literature.<sup>12–15</sup> The conditional molar absorptivity at 660 nm and pH 3.0 with  $20\mu\text{M}$  reagent is  $4.98 \times 10^4 \text{ l. mole}^{-1} \text{ cm}^{-1}$ . The two  $\lambda_{\text{max}}$  values indicate two different metal complexes, but the use of the shorter-wavelength  $\lambda_{\text{max}}$  belonging to the more strongly absorbing  $\text{ML}_2$  complex is less suitable for the determination because of the higher reagent background and greater interferences.<sup>12–14</sup> The optimum conditions for the ML complex at 660 nm are pH 3.0–3.3,  $0.1\text{M}$  formate buffer and  $2.0\mu\text{M}$  reagent for all REE, and the Lambert–Beer Law is obeyed for 1– $8\mu\text{M}$  REE.

**Summarizing notes.** The sensitivity of the aforementioned reagents for REE is greatly influenced by pH and the concentration of reagent in excess. CAS (with cationic surfactant), BrPADAP and PAR show the greatest sensitivity, which may differ considerably for various REE (Table 1) with PAR under the optimum conditions. BrPADAP is not suitable because of the easy decomposition of its REE chelates in alkaline medium. The colour contrast  $\Delta\lambda_{\text{max}} = \lambda_{\text{max(chelate)}} - \lambda_{\text{max(reagent)}}$  is 80 nm for PAR, 115 nm for BrPADAP, 190 nm for CAS plus CTMA or CP and 130 nm for Arsenazo III. The lowest spread of points around the calibration plot is for Arsenazo III, and its average value of  $s_{xy} = 0.012$  absorbance is

equivalent to 21 ng/ml for  $\text{Y}^{3+}$ , 33 ng/ml for  $\text{La}^{3+}$ , 35 ng/ml for  $\text{Ce}^{3+}$ , 35 ng/ml for  $\text{Gd}^{3+}$  or 46 ng/ml for  $\text{Lu}^{3+}$  respectively. It also leads to the best detection limit of all reagents tested for Eu and Dy, in spite of the molar absorptivities being lowest for the Arsenazo III complexes. The differences in  $s_{xy}$  and derived parameters for various REE and a particular reagent are negligible.

#### Flow systems

Metal ion solution ( $30\mu\text{l}$ ) was injected into the carrier solution containing the reagent in optimal concentration,  $0.2\text{M}$  buffer, and the surfactant if necessary. The flow-rate was always 1 ml/min. The necessary parameters for the system are summarized for  $\text{La}^{3+}$ ,  $\text{Ce}^{3+}$  and  $\text{Nd}^{3+}$  with Arsenazo III, CAS + CTMA, CAS + CP or PAR in Table 2. Calibration plots were linear for 4– $20\mu\text{M}$  REE if the peak height was read from the detector record. BrPADAP is not recommended, because of the low repeatability of the measurements (relative standard deviation 15–20% for 10 parallel measurements) and the easy decomposition of its REE chelates in alkaline medium.

Arsenazo III showed the best properties for the FIA determination of REE. It gives the best detection limit, a surprisingly high apparent molar absorptivity in comparison to CAS plus cationic surfactant, or PAR, in contrast to the stationary systems (cf. Tables 1 and 2). Moreover, 0.8 mg of Al(III) or 1.5 mg of Fe(III) in  $30\mu\text{l}$  may be screened with 10 mM ascorbic and 5-sulphosalicylic acids in the determination of 10–80 ng of REE at pH 3.0. Calibration plots were again linear but the slopes were 10–20% lower. Linear plots with decreased slopes were also obtained when  $0.2\text{M}$  2-DL-hydroxyisobutyric acid (which is often used as a complexing eluent in ion-exchange or high-performance liquid chromatography of REE) was present.

Of the reagents tested, only Arsenazo III may be used for the determination of the sum of REE in various raw materials and oxide concentrates, especially when the light REE such as La, Ce, Nd predominate in the sample. Parameters of the calibration plots for these particular elements differ only negligibly, which is not the case when PAR or CAS + CTMA or CAS + CP are used for the determination of REE by FIA. Thus, a fairly small relative error (–3.4% for Ce or +2.8% for Nd) is found if their concentration is evaluated from the calibration plot for  $\text{La}^{3+}$ , and the variation in the contents of these three elements in the sample has negligible effect on this error. In contrast, considerable errors result if CAS (plus cationic surfactant) or PAR is used (Table 3).

#### Determination of the sum of REE in oxide concentrates and apatites

Three procedures were compared for the decomposition of oxide concentrates (procedure A) and



Table 1. Molar absorptivities and detection limits for various REE with Arsenazo III, CAS/cationic surfactant and PAR in optimal conditions in stationary systems<sup>a</sup>

Element	Arsenazo III <sup>b</sup>			CAS/CTMA <sup>c</sup>			CAS/CP <sup>d</sup>			PAR <sup>e</sup>		
	$\epsilon, 10^4 \text{ l. mole}^{-1} \text{ cm}^{-1}$	D.L., $\mu\text{M}$	$\epsilon, 10^4 \text{ l. mole}^{-1} \text{ cm}^{-1}$	D.L., $\mu\text{M}$	$\epsilon, 10^4 \text{ l. mole}^{-1} \text{ cm}^{-1}$	D.L., $\mu\text{M}$	$\epsilon, 10^4 \text{ l. mole}^{-1} \text{ cm}^{-1}$	D.L., $\mu\text{M}$	$\epsilon, 10^4 \text{ l. mole}^{-1} \text{ cm}^{-1}$	D.L., $\mu\text{M}$	$\epsilon, 10^4 \text{ l. mole}^{-1} \text{ cm}^{-1}$	D.L., $\mu\text{M}$
La	4.98 ± 0.04	0.6	6.33 ± 0.20	0.9	6.81 ± 0.14	0.5	4.59 ± 0.06	1.0				
Ce	4.86 ± 0.05	0.8	6.58 ± 0.12	0.5	6.95 ± 0.18	0.6	6.35 ± 0.11	0.7				
Pr	4.95 ± 0.06	0.9	6.64 ± 0.22	0.7	7.58 ± 0.22	0.6	7.05 ± 0.15	1.0				
Nd	4.93 ± 0.04	0.6	6.88 ± 0.18	0.6 <sub>5</sub>	7.57 ± 0.13	0.5	7.70 ± 0.14	0.8				
Sm	4.73 ± 0.05	0.8	6.70 ± 0.17	0.6	7.29 ± 0.11	0.4	8.48 ± 0.20	1.1				
Eu	5.36 ± 0.03	0.4 <sub>5</sub>	6.66 ± 0.15	0.7	7.58 ± 0.20	0.5 <sub>5</sub>	8.98 ± 0.23	1.2				
Gd	5.41 ± 0.06	0.8	6.85 ± 0.17	0.6	7.91 ± 0.15	0.5	9.18 ± 0.18	0.9				
Tb	5.22 ± 0.04	0.6	6.61 ± 0.16	0.6	7.71 ± 0.09	0.5	9.05 ± 0.22	1.1				
Dy	5.25 ± 0.03	0.4	6.96 ± 0.15	0.5	7.67 ± 0.24	0.5	9.45 ± 0.16	0.8				
Ho	5.23 ± 0.05	0.7	6.50 ± 0.19	0.6	7.98 ± 0.11	0.4	9.57 ± 0.15	0.7				
Er	4.99 ± 0.04	0.7	6.75 ± 0.13	0.5	7.82 ± 0.29	0.5	9.30 ± 0.21	1.0				
Tm	4.83 ± 0.06	0.9 <sub>5</sub>	6.64 ± 0.18	0.6	7.86 ± 0.20	0.5	9.19 ± 0.25	1.2				
Yb	5.12 ± 0.06	0.9	7.05 ± 0.18	0.5	7.84 ± 0.15	0.4	9.06 ± 0.26	1.3				
Lu	4.60 ± 0.05	0.9	6.80 ± 0.20	1.1 <sub>5</sub>	7.96 ± 0.18	0.4	9.01 ± 0.19	1.0				
Y	5.03 ± 0.06	0.8 <sub>5</sub>	7.01 ± 0.17	0.6	8.07 ± 0.13	0.4	8.87 ± 0.18	0.9				

<sup>a</sup>Data from linear regression of calibration plots; <sup>b</sup> $s_{xy(A)} = 0.008-0.015$ , 660 nm, 20 $\mu\text{M}$  reagent, pH 3.0-3.3, 0.1M formate; <sup>c</sup>620 nm, 80 $\mu\text{M}$  reagent, 0.2mM CTMA, pH 8.8-9.6, <sup>d</sup>620 nm, 80 $\mu\text{M}$  reagent, 0.2mM CP, pH 9.2-9.5; <sup>e</sup> $s_{xy(A)} = 0.010-0.020$ , 0.1M  $\text{NH}_4^+/\text{NH}_3$  buffer; <sup>f</sup>520 nm, 400 $\mu\text{M}$  reagent, pH 9.0-9.5, 0.1M  $\text{NH}_4^+/\text{NH}_3$  buffer,  $s_{xy} = 0.010-0.015$ ; <sup>g</sup>detection limit, D.L. ( $\mu\text{M}$ ) =  $3 \times 10^6 s_{xy(A)}/\epsilon$ .

apatites (procedures B, C). Several interfering components, e.g., phosphates, are removed by the use of a cation-exchanger during procedure B.

*Procedure A.*<sup>30</sup> Weigh 5 or 50 mg of finely ground sample and dissolve it in 10 ml of hydrochloric acid (1 + 100) or (1 + 10) containing 2-3 or 30-40 drops respectively of 30% hydrogen peroxide. Heat the mixture for 2-3 min, to boiling, cool, transfer quantitatively into a 100-ml standard flask and dilute with water to the mark. Pipette an aliquot into a 25-ml standard flask, add 2.5 ml of 0.1M ascorbic acid and 5-sulphosalicylic acid and make up to the mark with water. Inject a 30- $\mu\text{l}$  aliquot into the flow stream containing 40 $\mu\text{M}$  Arsenazo III in 0.2M formate buffer (pH 3) and flowing at 1 ml/min.

*Procedure B.*<sup>31</sup> Weigh 50-100 mg of finely ground apatite sample containing 0.1-1% of REE, mix it with 2 g of Dowex cation-exchanger 50W x 8(50-100 mesh) in the H<sup>+</sup> form, and 25 ml of water in an Erlenmeyer flask or test-tube provided with a ground joint, and stopper the tube. Shake the mixture vigorously for 3 hr at 50-60°, transfer it quantitatively to form a column in a glass tube, wash the column with 100 ml of water, and elute the REE with 50 ml of 8M nitric acid. Evaporate the eluate almost to dryness and dissolve the residue in water and dilute it to volume in a 100-ml standard flask. Dilute a 5-ml aliquot of this solution to the mark in a 25-ml standard flask and inject a 30- $\mu\text{l}$  aliquot into the FIA manifold. Then continue as for procedure A.

*Procedure C.*<sup>30</sup> Weigh 50-100 mg of sample containing 0.5-1% REE and dissolve it in 10 ml of nitric acid (1 + 1), dilute to 200 ml with water, add 10 ml of 0.1M calcium chloride, 1.5 g of solid oxalic acid dihydrate, and heat to 70-80° with stirring. Neutralize with dilute ammonia solution until a precipitate just appears, and redissolve this by adding several drops of dilute hydrochloric acid. Add a few drops of Methyl Orange indicator and then dilute ammonia solution until the yellow colour of the indicator appears. Filter off the precipitate after 3 hr and wash it with 1% oxalic acid solution neutralized to pH 4 with ammonia. Dry, calcine and ignite for 10 min at 600° in a porcelain crucible. Dissolve the residue in 10 ml of nitric acid (1 + 50), dilute the solution with water to the mark in a 100-ml standard flask and inject a 30- $\mu\text{l}$  aliquot into the FIA manifold.

The preparation of a sample for the FIA takes 10-15 min after decomposition and a further 20 sec suffices for the analysis. The sum of REE is evaluated from calibration plots prepared from lanthanum nitrate standard solutions and expressed as the lanthanum content, the small differences in the apparent molar absorptivities and the atomic weights being ignored. Thus, a sample containing 0.24% La, 0.33% Ce and 0.12% Nd (i.e., theoretical sum 0.69%) gave 0.676 ± 0.007%, 0.650 ± 0.006% and 0.693 ± 0.007% for the total content of REE when the results were evaluated from calibration plots prepared from La<sup>3+</sup>, Ce<sup>3+</sup> and Nd<sup>3+</sup> standard solutions respectively. This indicates relative deviations such as -3.8% or +2.5% only when the results from the cerium and neodymium calibration plots are compared with those obtained from the lanthanum plot. Use of the neodymium plot might be best.

Results for oxide concentrates agreed well for samples of various weights or for various standard additions of lanthanum nitrate to the sample solution (Table 4), and were tested by the Cochran and Student criteria respectively. Similarly the differences

Table 2. Determination of La, Ce and Nd by means of FIA with various spectrophotometric indicators (injected volume: 30  $\mu$ l, flow-rate 1 ml/min)

	Arsenazo III <sup>a</sup>			CAS/CTMA <sup>b</sup>			CAS/CP <sup>b</sup>			PAR <sup>h</sup>		
	La	Ce	Nd	La	Ce	Nd	La	Ce	Nd	La	Ce	Nd
a		660			620			620			520	
b	0.288	0.343	0.309	0.261	0.181	0.168	0.252	0.174	0.172	0.200	0.160	0.170
c	10.8	11.0	9.4	13.7	17.2	21.3	14.5	14.8	13.0	23.1	18.1	28.7
d	2.2	2.6	1.5	3.4	4.7	6.0	3.5	5.4	5.0	3.0	5.3	3.7
e	2.5–20	2.5–20	2.5–20	5–25	7.5–25	7.5–25	5–25	7.5–25	7.5–25	5–30	5–30	5–30
f		40			160			160			800	

<sup>a</sup>Wavelength (nm) used for indication; <sup>b</sup>apparent molar absorption coefficient,  $\epsilon'$ , ( $10^4$  l.mole<sup>-1</sup>.cm<sup>-1</sup>) recalculated from the peak height vs. REE concentration plots for 30  $\mu$ l injection; <sup>c</sup>detection limit (ng/30  $\mu$ l) calculated from D.L. =  $3 s_{x(H)}/k_w$  where  $H$  is peak height (recorder scale units) and  $k_w$  is the slope of the plot of peak height vs. REE contents in 30  $\mu$ l; <sup>d</sup>relative standard deviation (%) for 82.2 ng La, 85.7 ng Ce and 87.2 ng Nd per 30  $\mu$ l, from 8 parallel analyses; <sup>e</sup>optimum REE concentration range ( $\mu$ M); <sup>f</sup>reagent concentration ( $\mu$ M); <sup>g</sup>0.2M formate buffer (pH 3.0); <sup>h</sup>0.2M NH<sub>4</sub><sup>+</sup>/NH<sub>3</sub> buffer; <sup>i</sup>0.4mM surfactant solution.

Table 3. Contents of La, Ce, Nd related to the same absorbance signal and relative deviations for La if taken from calibration plots for Ce and Nd (50 recorder scale units; for conditions see Table 2)

Reagent	Found, ng/30 $\mu$ l			Relative deviation (%) for La taken from plots for	
	La	Ce	Nd	Ce	Nd
Arsenazo III	28.6	27.6	29.4	-3.4	+2.8
CAS + CP	45.4	70.0	72.2	+54	+59
CAS + CTMA	50.7	71.0	78.3	+40	+55
PAR	89.3	111.3	106.1	+25	+19

Table 4. Determination of the sum of REE in samples mainly containing La, Ce, Nd, with Arsenazo III by means of FIA<sup>a</sup> (working conditions in Table 2)

Sample	Decomposition procedure	Sample taken, mg	Sum of REE found, % <sup>b</sup>	Relative standard deviation, %
Oxide concentrate I	A	32.7	69.8 $\pm$ 3.3	5.5
	A	66.6	70.7 $\pm$ 0.8	1.4
	A	4.15	70.9 $\pm$ 1.2	2.0
	A	4.99	68.6 $\pm$ 1.7	2.9
Oxide concentrate II	A	4.56	68.6 $\pm$ 1.0	1.8
	A	7.99	66.2 $\pm$ 0.7	1.3
	A	4.16 <sup>c</sup>	68.2 $\pm$ 1.5	2.7
	A	4.37 <sup>d</sup>	68.8 $\pm$ 1.6	2.8
Apatite	B	80.0	0.676 $\pm$ 0.007	1.2
	B	41.2	0.654 $\pm$ 0.017	3.1
	C	103.9	0.661 $\pm$ 0.008	1.4
	C	58.3	0.637 $\pm$ 0.011	2.2
	C	40.6 <sup>e</sup>	0.667 $\pm$ 0.020	3.7

<sup>a</sup>8 parallel analyses; <sup>b</sup>confidence interval with  $t(\alpha = 0.05, \nu = 7)$ ; standard additions: <sup>c</sup>1.37 mg of La<sup>3+</sup>, <sup>d</sup>2.47 mg of La<sup>3+</sup>, <sup>e</sup>0.685 mg of La<sup>3+</sup>.

in variances and arithmetic means were negligible for apatite samples analysed by both decomposition variants (B, C). The results for the apatite sample were in good agreement with the sum of content of La, Ce and Nd (the content of other REE oxides was less than 0.001%) obtained separately by atomic-emission spectrometry of high resolution with an N<sub>2</sub>O-acetylene flame, AAS, RFA, and ICP and DCP spectrometry during interlaboratory tests.<sup>31</sup>

## REFERENCES

1. S. Shibata and I. Isiguro, *Rept. Gov. Ind. Res. Inst. Nagoya*, 1962, 11, 318.
2. L. Sommer and H. Novotná, *Talanta*, 1967, 14, 457.
3. E. Ohyoshi, *Anal. Chem.*, 1983, 55, 2404.
4. *Idem*, *Talanta*, 1984, 31, 1129.
5. D. B. Gladilovich, V. Kubaň and J. Havel, *Collection Czech. Chem. Commun.*, 1988, 53, in the press.
6. G. J. Klopff and K. D. Cook, *Anal. Chim. Acta*, 1984, 162, 293.
7. C. Vekhande and K. N. Munshi, *Indian J. Chem.*, 1976, 14A, 189.
8. *Idem*, *Microchem. J.*, 1978, 23, 28.
9. L. Němcová, P. Plocková and Tran Hong Con, *Collection Czech. Chem. Commun.*, 1982, 47, 503.
10. M. Jarosz and Z. Marczenko, *Anal. Chim. Acta*, 1984, 159, 309.
11. D. B. Gladilovich and V. Kubaň, *Chem. Papers*, 1988, in the press.
12. S. B. Savvin, *Organicheskie reagenty gruppy Arsenazo III*, Atomizdat, Moscow, 1971.

13. I. G. Surin, P. K. Spitsyn and V. F. Barkovskii, *Zh. Analit. Khim.*, 1974, **34**, 1103.
14. B. Buděšínský, *Collection Czech. Chem. Commun.*, 1963, **28**, 2902.
15. D. B. Gladilovich and V. Kubáň, *Scr. Fac. Sci. Natur. Univ. Brun.*, in the press.
16. M. Procházka, *Thesis*, Charles University, Prague, 1985.
17. K. K. Unger, *Chromatographia*, 1984, **18**, 46.
18. J. Růžička and E. H. Hansen, *Flow Injection Analysis*, Wiley, New York, 1981.
19. S. Elchuk and R. M. Cassidy, *Anal. Chem.*, 1979, **51**, 1434.
20. A. Mazzucotelli, A. Dodone, R. Fracke and F. Baffi, *Chromatographia*, 1982, **15**, 1982.
21. *Idem*, *J. Chromatog.*, 1985, **349**, 137.
22. D. J. Barkley, M. Blanchette, R. M. Cassidy and S. Elchuk, *Anal. Chem.*, 1986, **58**, 2222.
23. R. M. Cassidy, S. Elchuk and P. K. Dasgupta, *ibid.*, 1987, **59**, 85.
24. V. Kubáň, L. Sommer and D. B. Gladilovich, *Zh. Analit. Khim.*, in the press.
25. J. Kinnunen and B. Wennestrand, *Chemist-Analyst*, 1957, **46**, 92.
26. N. Mouková, D. Gotzmannová, V. Kubáň and L. Sommer, *Collection Czech. Chem. Commun.*, 1981, **46**, 354.
27. M. Langová, I. Klabenešová, K. Kasiura and L. Sommer, *ibid.*, 1976, **41**, 2386.
28. V. Radil, private communication.
29. K. Eckschlager and V. Štěpánek, *Information Theory as Applied to Chemical Analysis*, Wiley-Interscience, New York, 1979.
30. A. Špačková (ed.), *Chemical Analysis in Geology*, Geological Survey, Prague, 1985.
31. V. Otruba, private communication.

# LUMINESCENCE CHARACTERISTICS OF DIBENZOFURAN AND SEVERAL POLYCHLORINATED DIBENZOFURANS AND DIBENZO-*p*-DIOXINS

I. M. KHASAWNEH\* and J. D. WINEFORDNER†

Department of Chemistry, University of Florida, Gainesville, FL 32611, U.S.A.

(Received 10 September 1987. Accepted 18 November 1987)

**Summary**—The room-temperature fluorescence (RTF), low-temperature phosphorescence (LTP) and room-temperature phosphorescence (RTP) characteristics of dibenzofuran and several polychlorinated dibenzofurans and dibenzo-*p*-dioxins are presented and are shown to be suitable for the determination of these compounds. The limits of detection are as low as 0.02, 0.2 and 0.7 for RTF, LTP and RTP, respectively. The relative standard deviations are between 1 and 4% for RTP.

Polychlorinated dibenzofurans (PCDFs) and dibenzo-*p*-dioxins (PCDDs) have been the subject of great concern for many environmentalists and analysts in recent years. These two groups of compounds exhibit similar physical, chemical and biological properties.<sup>1</sup> The compounds are very stable and are found in fly-ash from municipal incinerators,<sup>2-5</sup> many chemicals such as chlorinated phenols and phenoxy acids and chlorobenzenes,<sup>6,7</sup> outdoor air,<sup>8</sup> metal chlorides<sup>9</sup> and herbicides.<sup>10-12</sup> The sources and fates of PCDFs and PCDDs have been reported.<sup>9,13-15</sup> Some of these compounds have highly toxic, teratogenic, mutagenic, and potentially carcinogenic properties<sup>14,16</sup> and these properties differ from one isomer to another. Because of the complexity and toxicity of PCDFs and PCDDs, and their presence with other compounds such as pesticides, highly sensitive and selective analytical techniques are required for their determination and measurement. The most widely used methods for the analysis and determination of these compounds are high-resolution gas chromatography and mass spectrometry.<sup>8,17-25</sup> The determination of these compounds requires many preliminary steps such as extraction, concentration, and sometimes separation from similar chlorinated organic compounds.

Luminescence spectrometry is a selective and sensitive technique, *e.g.*, Moye *et al.*<sup>26</sup> have reported the phosphorescence characteristics of 52 pesticides, but little work has been done on the determination of PCDFs and PCDDs. In previous studies,<sup>27-29</sup> we reported the luminescence properties of biphenyl and several polychlorinated biphenyl isomers and their mixtures, examined by room-temperature fluorescence (RTF), low-temperature phosphorescence (LTP), and room-temperature phosphorescence

(RTP) with and without the presence of external heavy atoms and found that luminescence spectrometry is selective and sensitive for polychlorinated biphenyls (PCBs). Because of their similarity to PCBs in structural, physical and chemical properties, we decided to study the RTF, LTP and RTP properties of several PCDF and PCDD isomers, and also those of dibenzofuran. Although identification and measurement of the PCDF and PCDD isomers require use of separation techniques, luminescence spectrometry could be combined with gas chromatography (GC) or liquid chromatography (LC). Other luminescence spectrometric techniques such as time-resolved spectroscopy, phase-resolved spectroscopy and synchronous spectroscopy can be used for the determination of mixtures of these compounds.

## EXPERIMENTAL

### Apparatus

All RTF and RTP measurements were made with a Perkin-Elmer LS-5 spectrofluorometer. This instrument is microprocessor-controlled and equipped with a xenon arc lamp (pulsed at ac line frequency) as an excitation source. A Perkin-Elmer data station 3600 interfaced with the LS-5 spectrofluorometer was used to obtain all excitation and emission spectra, and these were printed by a Perkin-Elmer printer (600).

In the RTF measurements, quartz cuvettes (10 × 10 mm) were used in the sample compartment, which has four different positions to accommodate the cuvettes. A 305-nm cut-off filter was used before the emission monochromator. The excitation and emission band-passes were adjusted at 10 and 5 nm, respectively, for all measurements.

In the RTP measurements, a paper-sample holder designed in our laboratory and described elsewhere<sup>28,30</sup> was used to hold the filter paper. The distance of the filter paper surface from the front of the instrument and the angle between the excitation axis and the paper surface were critical and were adjusted for each sample to yield the highest RTP signal. The excitation and emission band-passes were again 10 and 5 nm, respectively. Delay and gate times used were 0.03 and 9 msec, respectively. A cut-off filter (305 nm) was used in the emission-side filter holder.

\*Present address: Chemistry Department, Yarmouk University, Irbid, Jordan.

†To whom all correspondence should be addressed.

Table 1. Room-temperature fluorescence characteristics of dibenzofuran and several polychlorinated dibenzofurans and dibenzo-*p*-dioxins

Compound	Excitation wavelength,* <i>nm</i>	Emission wavelength,* <i>nm</i>	Limit of detection,† <i>ng/ml</i>	RSD,§‡ %	BRSD,§ %
Dibenzofuran	246, <u>285</u>	<u>316</u> , 327	0.020	1.0	3.0
1,2,3,4-Tetrachlorodibenzofuran	252, <u>292</u>	<u>338</u> , 407	0.15	1.0	6.0
2,3,7,8-Tetrachlorodibenzofuran	257, <u>307</u>	340	0.025	1.2	1.0
1,2,3,4-Tetrachlorodibenzo- <i>p</i> -dioxin	230	<u>342</u> , 418	2.0	2.0	5.0
1,2,7,8-Tetrachlorodibenzo- <i>p</i> -dioxin	230	346	0.70	2.0	8.0
1,3,7,8-Tetrachlorodibenzo- <i>p</i> -dioxin	232	343	4.0	2.0	5.0
2,3,7,8-Tetrachlorodibenzo- <i>p</i> -dioxin	235	343	1.3	2.0	4.0
1,2,3,7,8-Pentachlorodibenzo- <i>p</i> -dioxin	232	<u>342</u> , 416	1.8	2.0	3.0
1,2,4,7,8-Pentachlorodibenzo- <i>p</i> -dioxin	232	343	5.5	4.0	3.0
1,2,3,4,7,8-Hexachlorodibenzo- <i>p</i> -dioxin	230	<u>340</u> , 409	4.5	4.0	7.0
1,2,3,4,6,7,8-Heptachlorodibenzo- <i>p</i> -dioxin	232	<u>343</u> , 405	0.50	2.0	8.0
1,2,3,4,6,7,8,9-Octachlorodibenzo- <i>p</i> -dioxin	232	341	2.5	2.5	8.0

\*The wavelength of the most intense peak is underlined ( $\pm 2$  nm).

†LOD is the concentration that gives a signal 3 times the standard deviation of 16 blanks.

§Based on 16 measurements.

‡Independent of analyte concentration.

In the LTP measurements, an Aminco-Bowman spectrofluorometer was used to obtain the spectra of all compounds. This instrument is equipped with a 150-W xenon arc-lamp and an RCA IP28 photomultiplier tube operated at  $-800$  V (American Instrument Co., Silver Spring, MD). A phosphoroscope designed in our laboratory<sup>31</sup> was used to obtain the LTP signal. This phosphoroscope uses a rotating can driven by a motor connected to a variable auto-transformer (Type 2PF 1010, Staco Inc., Dayton, OH) to control the rotation rate. The sample cell was a silica tube about 25 cm long and 3 mm in bore. A silica Dewar flask filled with liquid nitrogen was used to freeze the sample, and a stream of nitrogen gas (dried in a gas drying unit filled with anhydrous calcium sulphate, W. A. Hammond Drierite Co., Xenia, OH) was passed continuously into the sample compartment to prevent frost formation. The volume used for each measurement was about 150  $\mu$ l, and the volume illuminated was about 50  $\mu$ l. All spectra were recorded with a Fisher Recordall Series 5000 recorder. The instrumental settings used were: entrance and exit slit-widths 1 mm each, sensitivity 3, and response time 4.

#### Materials

The compounds were all  $\geq 99\%$  pure except for 1,2,3,4-tetrachlorodibenzofuran, 1,3,7,8-tetrachlorodibenzo-*p*-dioxin and 1,2,3,4,6,7,8-heptachlorodibenzo-*p*-dioxin, which were 95% pure. Dibenzofuran was obtained from the Environmental Protection Agency (Research Triangle Park, NC 27709, USA), and the other PCDFs and PCDDs were from Accustandard Inc. (New Haven, CT 06511). The hexane and iso-octane were high-purity solvents (Burdick and Jackson Laboratories, Inc., Muskegon, MI 49442). Thallium nitrate (Fisher Scientific Co., Fair Lawn, NJ) was used to provide the heavy atom in RTP measurements. The filter paper used for the RTP was Whatman No. 1.

#### Procedure

For RTF and LTP measurements, working solutions were prepared by successive dilution of 50  $\mu$ g/ml solutions with hexane. For RTP, the 50  $\mu$ g/ml solutions were used, with iso-octane as the blank. The filter paper was cut into squares (6  $\times$  6 mm), placed on the sample holder and secured by two small screws; a 5- $\mu$ l portion of analyte or blank was spotted on the filter paper by syringe and the paper dried at 110° for 15 min, then cooled in a pure nitrogen gas stream inside the sample compartment for 10 min. In examination of heavy-atom effects, 2  $\mu$ l of 0.2M thallium nitrate were spotted directly onto the paper before the analyte or blank was added.

LTP lifetimes were measured by recording the decay curve of the analytes after excitation had been stopped, and correcting for the response time of the instrument. RTP lifetimes were measured with the LS-5 spectrofluorometer and the "Decay-Obey" program. Gate and integration times were 0.1 msec and 20 sec respectively.

## RESULTS AND DISCUSSION

### RTF measurements

The RTF characteristics of dibenzofuran and several PCDF and PCDD isomers are shown in Table 1. The excitation and emission wavelengths for the PCDF isomers become longer as the number of chlorine atoms increases. However, for the PCDD isomers, increase in the number of chlorine atoms causes only small shifts. This may be a result of localization of the electron density around the oxygen and chlorine atoms, which behave as electron-withdrawing groups. This electron localization increases the energy required to excite the molecule, causing the excitation wavelengths of PCDDs to be shorter than those of the PCDFs.

Column 4 of Table 1 shows the limits of detection, defined as the concentration of a compound that would give a signal equal to three times the standard deviation of 16 blanks. In general, as the number of chlorine atoms increases, the limits of detection become poorer, because the presence of chlorine in a molecule decreases the fluorescence intensity and increases the phosphorescence by increasing inter-system crossing (ISC).

Column 5 shows the relative standard deviation (RSD) for each compound and this is practically independent of analyte concentration. Column 6 gives the relative standard deviation of the blank (BRSD). These values were obtained by taking 16 measurements of the analyte and blank at the maximum excitation and emission wavelength of the analyte. The precision of RTF seems to be good,

Table 2. Low-temperature phosphorescence characteristics of dibenzofuran and several polychlorinated dibenzofurans and dibenzo-*p*-dioxins

Compound	Excitation wavelength,* nm	Emission wavelength,* nm	Limit of detection,† ng/ml	Lifetime, sec	RSD,‡ %	BRSD,§ %
Dibenzofuran	<u>234</u> , 287	462	0.60	0.90 ± 0.07	5.0	9.5
1,2,3,4-Tetrachlorodibenzofuran	263	484	0.25	0.85 ± 0.13	9.0	9.0
2,3,7,8-Tetrachlorodibenzofuran	<u>258</u> , 316	450, <u>470</u>	1.2	0.70 ± 0.09	6.0	9.0
1,2,3,4-Tetrachlorodibenzo- <i>p</i> -dioxin	<u>240</u> , 314	480	12.0	1.03 ± 0.07	2.0	2.0
1,2,7,8-Tetrachlorodibenzo- <i>p</i> -dioxin	<u>236</u> , 306	<u>412</u> , 430	2.0	1.55 ± 0.17	10.0	8.0
1,3,7,8-Tetrachlorodibenzo- <i>p</i> -dioxin	<u>243</u> , 310	415, <u>440</u>	2.5	1.40 ± 0.15	7.0	7.0
2,3,7,8-Tetrachlorodibenzo- <i>p</i> -dioxin	<u>238</u> , 316	415, 435	3.0	1.40 ± 0.13	6.0	6.0
1,2,3,7,8-Pentachlorodibenzo- <i>p</i> -dioxin	<u>242</u> , 317	420, 430	1.0	1.30 ± 0.06	4.0	7.5
1,2,4,7,8-Pentachlorodibenzo- <i>p</i> -dioxin	<u>246</u> , 312	<u>415</u> , 440	4.0	1.25 ± 0.11	5.0	7.5
1,2,3,4,7,8-Hexachlorodibenzo- <i>p</i> -dioxin	<u>248</u> , 310	452	3.5	1.1 ± 0.09	3.0	8.0
1,2,3,4,6,7,8-Heptachlorodibenzo- <i>p</i> -dioxin	<u>248</u> , 309	425, 453	3.5	1.0 ± 0.09	2.5	8.0
1,2,3,4,6,7,8,9-Octachlorodibenzo- <i>p</i> -dioxin	251	430, 457				

\*The wavelength at the most intense peak is underlined ( $\pm 3$  nm).

†LOD is the concentration that gives a signal 3 times the standard deviation of 16 blanks.

§Based on 16 measurements.

‡Independent of analyte concentration.

the RSD being between 1 and 4% and the BRSD between 1 and 8%.

#### LTP measurements

The LTP (at 77 K) characteristics of dibenzofuran and the PCDFs and PCDDs studied in this work are shown in Table 2. The excitation and emission wavelengths again became longer as the number of chlorine atoms on the rings increases. This trend is clearer for the excitation wavelengths than the emission wavelengths. The excitation and emission wavelengths for the PCDF isomers are clearly longer than for the PCDD isomers. This may be because localization of change on the two oxygen atoms in the PCDD isomers makes excitation more difficult, hence requiring shorter excitation wavelengths. The differences in excitation wavelength between the LTP values in Table 2 and the RTP values in Table 3 are primarily the result of the lack of instrumental

correction in the LTP measurements (Aminco SPF) as opposed to the RTP measurements (Perkin-Elmer LS-5); also, the uncertainty in all wavelengths for the two instruments is  $\pm 2$  nm.

Column 4 of Table 2 shows the limits of detection and demonstrates that LTP is quite sensitive but RTP is more sensitive for most compounds. Columns 6 and 9 give the RSDs and BRSDs; the precision of LTP is not as good as that of RTP but is still reasonable ( $\leq 10\%$ ). Poorer precision may result from the use of liquid nitrogen causing condensation of moisture on the walls of the Dewar flask and to cracking during freezing of the sample.

#### RTP measurements

Table 3 shows the RTP characteristics of the PCDF and PCDD isomers on Whatman No. 1 filter paper with and without thallium nitrate to prove an external heavy-atom effect. It can be seen that the

Table 3. Room-temperature phosphorescence characteristics of dibenzofuran and several polychlorinated dibenzofurans and dibenzo-*p*-dioxins on filter paper with and without heavy atom present

Compound	Excitation wavelength,* nm	Emission wavelength,* nm	Enhancement factor,† F	Limit of detection,§ ng	Lifetime, msec	RSD,‡,¶ %	BRSD,‡ %
Dibenzofuran							
Without Tl	231, 248, <u>280</u>	417, <u>434</u> , 461	—	2.5	1.65	6.0	3.0
With Tl	251, <u>282</u>	415, 442	4.5	0.75	0.50	1.0	2.0
1,2,3,4-Tetrachlorodibenzofuran							
Without Tl	286	472	—	10.5	1.05	2.0	3.0
With Tl	287	<u>472</u> , 502	2.0	9.0	0.95	2.0	2.0
2,3,7,8-Tetrachlorodibenzofuran							
Without Tl	231, 258, <u>303</u>	471	—	1.0	1.55	8.0	2.0
With Tl	231, 260, <u>304</u>	472	1.2	0.70	1.30	4.0	2.0
Polychlorinated dibenzo- <i>p</i> -dioxins	No useful RTP is detected						

\*The wavelength of the most intense peak is underlined ( $\pm 2$  nm).

†F is the intensity of emission from the analyte in the presence of heavy-atom divided by the intensity of the same concentration without heavy atom.

§LOD is the concentration that gives a signal 3 times the standard deviation of 16 blanks.

‡Based on 16 measurements.

¶Independent of analyte concentration.

PCDF isomers exhibit RTP but the PCDD isomers do not. The lack of phosphorescence may be due to instrumental limitations combined with short excited-state lifetimes for the PCDD isomers. We examined the addition of an external heavy atom to enhance the RTP signal, but the PCDD isomers still did not give any reasonable RTP under the experimental conditions used. Although the LS-5 delay time could have been decreased to examine instantaneous luminescence, this was not done.

Columns 2 and 3 in Table 3 show that the excitation and emission wavelengths became longer when chlorine atoms are attached to the two aromatic rings of dibenzofuran, but the positions of the chlorine atoms have a greater effect on the excitation wavelengths than on the emission wavelengths. The external heavy atom makes both the excitation and emission wavelengths longer, and enhances the RTP intensity of PCDF isomers (column 4). The enhancement is greater for dibenzofuran than for the PCDF isomers, which may be due to the chlorine atoms behaving as internal heavy atoms.

The limits of detection (column 5) are lower for all compounds in the presence of the heavy atom but the decrease is more noticeable for dibenzofuran than the PCDF isomers. The RSD and BRSD values (2–8 and 1–3%, respectively) indicate good precision.

#### Phosphorescence lifetime measurements

The phosphorescence lifetimes were measured at 77 K and at room temperature with and without the presence of an external heavy atom. Column 5 in Table 2 shows the lifetimes of the PCDFs and PCDDs studied, corrected for instrumental response. The lifetimes decrease as the number of chlorine atoms on the rings increases and, the lifetimes of the PCDFs are shorter than those of the PCDDs. The difference in lifetimes may be insufficient for resolution of mixtures. Column 6 in Table 3 shows the lifetimes of PCDFs which exhibit RTP with and without thallium present. The lifetimes of these compounds are decreased by a factor of 3 in the presence of thallium. The decrease in lifetimes and increase in sensitivities caused by presence of an external heavy atom may be utilized to separate the emissions of these compounds in mixtures.

#### CONCLUSION

Luminescence spectrometry has been shown to be a sensitive and selective technique for the determination of PCDF and PCDD isomers. RTF is known to be more sensitive than LTP and RTP, but the phosphorimetric methods are more selective. Although the PCDDs cannot be determined by RTP under the experimental conditions described, this technique is still promising for the determination of many similar compounds, and if the external heavy-

atom effect is utilized or the differences in excited-state lifetimes are exploited, RTP it can provide a selective, sensitive, inexpensive and fast method for the analysis of their mixtures.

*Acknowledgement*—This research was supported by NIH-5-R01-GM11373-23.

#### REFERENCES

1. C. Rappe, *Environ. Sci. Technol.*, 1984, **13**, 78A.
2. J. W. A. Lustenhouw, K. Olie and O. Hutzinger, *Chemosphere*, 1980, **9**, 501.
3. K. Olie, P. L. Vermeulen and O. Hutzinger, *ibid.*, 1977, **6**, 455.
4. H. R. Buser, H. P. Bosshardt and C. Rappe, *ibid.*, 1978, **7**, 165.
5. G. A. Eiceman, R. E. Clement and F. W. Karasek, *Anal. Chem.*, 1979, **51**, 2343.
6. C. Rappe, S. Marklund, H. R. Buser and H. P. Bosshardt, *Chemosphere*, 1978, **7**, 269.
7. H. R. Buser, *ibid.*, 1979, **8**, 415.
8. M. Oehme, S. Mano and A. Mikalsen, *ibid.*, 1976, **15**, 607.
9. A. Heindl and O. Hutzinger, *ibid.*, 1986, **15**, 653.
10. C. Rappe, H. R. Buser and H. P. Bosshardt, *ibid.*, 1978, **7**, 431.
11. H. R. Buser and H. P. Bosshardt, *J. Chromatog.*, 1974, **90**, 71.
12. T. Yamagishi, T. Miyazaki, K. Akiyama, M. Morita, J. Nakagawa, S. Horii and S. Kaneko, *Chemosphere*, 1981, **10**, 1137.
13. O. Hutzinger, M. J. Blumich, M. van den Berg and K. Olie, *ibid.*, 1985, **121**, 581.
14. J. M. Czuczwa and R. A. Hites, *Environ. Sci. Technol.*, 1984, **18**, 444.
15. R. R. Bumb, W. B. Crummett, S. S. Cutie, J. R. Gledhill, R. H. Hummel, R. O. Kagel, L. L. Lamparski, E. V. Luoma, D. L. Miller, T. J. Nestrick, L. A. Shadoff, R. H. Stehl and J. S. Woods, *Science*, 1980, **210**, 385.
16. H. R. Buser and C. Rappe, *Anal. Chem.*, 1980, **52**, 2257.
17. F. W. Karasek and F. I. Onaska, *ibid.*, 1982, **54**, 309A.
18. C. Rappe, H. R. Buser, H. Kuroki and Y. Masacla, *Chemosphere*, 1979, **8**, 259.
19. H. R. Buser, *Anal. Chem.*, 1976, **48**, 1553.
20. *Idem*, *ibid.*, 1977, **49**, 918.
21. D. W. Kuehl, P. M. Cook, A. R. Batterman and B. C. Butterworth, *Chemosphere*, 1987, **16**, 657.
22. D. W. Kuehl, P. M. Cook, A. R. Batterman, D. Lothenback and B. C. Butterworth, *ibid.*, 1987, **16**, 667.
23. R. Masse and B. Pelletier, *ibid.*, 1987, **16**, 7.
24. S. Markland, C. Rappe, M. Tyskling and K. Egeback, *ibid.*, 1987, **16**, 29.
25. J. J. Nestrick and L. L. Lamparski, *Anal. Chem.*, 1982, **54**, 2292.
26. H. A. Moye and J. D. Winefordner, *J. Agric. Food Chem.*, 1965, **13**, 518.
27. I. M. Khasawneh and J. D. Winefordner, *Microchem. J.*, in the press.
28. *Idem*, *ibid.*, in the press.
29. I. M. Khasawneh, M. Chamsaz and J. D. Winefordner, *Anal. Lett.*, in the press.
30. G. Scharf, B. W. Smith and J. D. Winefordner, *Anal. Chem.*, 1985, **57**, 1230.
31. I. M. Khasawneh, J. Kerkhoff, D. Siegel, A. Jurgensen, E. Inman and J. D. Winefordner, *Microchem. J.*, 1985, **31**, 281.

## DETERMINATION OF BORATE ION-PAIR STABILITY CONSTANTS BY POTENTIOMETRY AND NON-APPROXIMATIVE LINEARIZATION OF TITRATION DATA

HOWARD R. ROGERS\* and CONSTANT M. G. VAN DEN BERG  
Oceanography Department, University of Liverpool, Liverpool, England

(Received 6 January 1986. Revised 28 October 1987. Accepted 10 November 1987)

**Summary**—Borate anions,  $B(OH)_4^-$ , are known to associate with alkali and alkaline-earth metal cations in sea-water. The borate cation ion-pairs are of the general form  $MB(OH)_4^{(n-1)+}$ , where  $M^{n+}$  is the cation. In this work, the cation borate stability constants ( $K_{MB}^*$ ) have been evaluated for  $Na^+$ ,  $Li^+$ ,  $Mg^{2+}$ ,  $Ca^{2+}$  and  $Sr^{2+}$  where  $K_{MB}^* = [MB(OH)_4^{(n-1)+}]/[M^{n+}][B(OH)_4^-]$ . The  $K_{MB}^*$  values were obtained from values found for the stability constant of boric acid ( $K_B^*$ ) in various electrolyte media at 25° and an ionic strength of 0.7. Acid–base potentiometric titrations were performed in the electrolyte media with a standard Pt/H<sub>2</sub> electrode and a junctionless Ag/AgCl reference electrode to monitor the emf. A non-approximative equation was used to linearize the titration data. The values obtained were:  $K_{LiB}^* = 0.89 \pm 0.02$ ,  $K_{NaB}^* = 0.44 \pm 0.01$ ,  $K_{MgB}^* = 13.6 \pm 0.7$ ,  $K_{CaB}^* = 11.4 \pm 0.15$ ,  $K_{SrB}^* = 3.47 \pm 0.06$ . The values for  $K_{MB}^*$  correlate with the charge-density parameter  $z^2/(r + 0.85)$ , where  $r$  is the radius of the cation. The speciation of boron in sea-water was predicted from the  $K_{MB}^*$  data for the major cations present.

Nearly all the investigations of the chemistry of boron in sea-water have been concerned with the contribution of borate to the total alkalinity.<sup>1–5</sup> The alkalinity has become particularly important in recent years owing to widespread concern over the increase in atmospheric carbon dioxide caused by fossil-fuel combustion, and the relevance of the oceans as global sinks for carbon dioxide.<sup>6</sup> Apart from work on the contribution of borate anions to the buffer mechanism of sea-water, some interest has been focused on the compounds formed by borate ions with the major cations present in sea-water,  $Na^+$ ,  $Ca^{2+}$  and  $Mg^{2+}$ .<sup>3,7</sup> Data for discrete ion-pair associations between major cations and anions in sea-water are essential for speciation calculations.<sup>8</sup>

The practical determination of the stability constants for ion-pairs of borate with cations has always been done potentiometrically.<sup>3,7</sup> However, as in all investigations of proton-transfer equilibria in sea-water, direct intercomparison of data is made difficult by the use of three definitions for pH in sea-water: the NBS scale, the pH (SWS) or “total” hydrogen-ion concentration scale, and the “free” hydrogen-ion concentration scale.<sup>9</sup> The first attempt to determine the stability constants of the ion-pairs of borate with  $Na^+$ ,  $Mg^{2+}$  and  $Ca^{2+}$  was made by using a “constant pH” method, and the NBS pH scale.<sup>7</sup> The method involved addition of sodium tetraborate to aqueous solutions of the chlorides of  $Na^+$ ,  $Mg^{2+}$ ,  $Ca^{2+}$  and  $K^+$ , until a constant pH was achieved. The constant pH value (measured by a glass and calomel electrode pair) was equal to the apparent dissociation constant

of boric acid in the saline medium. The stability constants ( $K_{MB}^*$ ) for the borate cation ion-pairs were calculated by assuming that association of potassium with borate was negligible.<sup>7</sup> Other work, by Swedish workers using an acid–base titration procedure and the program LETAGROP, yielded a value for  $K_{MgB(OH)_4}^*$ .<sup>3</sup>

In our investigations, potentiometric acid–base titrations were performed in electrolyte solutions with a Pt/H<sub>2</sub> and Ag/AgCl (sleeveless) electrode pair. This choice of electrode couple, although inappropriate for *in situ* oceanographic measurements, is ideal for laboratory studies. Provided that oxidizing or reducing solutes are absent, the Pt/H<sub>2</sub> electrode exhibits Nernstian response. (Glass electrodes are subject to interference from sodium ions at high pH, and to changes in the asymmetry potential of the glass membrane.) Junction-potential variations that occur when electrode pairs are calibrated in low ionic-strength NBS buffers and then transferred to high ionic-strength solutions were avoided by calibrating the electrode system in the acid pH region during the titrations, by using an incremental method.<sup>4,5</sup>

Values for the stability constant of boric acid ( $K_B^*$ ) in the simple aqueous electrolyte solutions were calculated by using a non-approximative equation to linearize the titration data and these  $K_B^*$  values were then used to evaluate stability constants ( $K_{MB}^*$ ) for each cation borate ion-pair.

### EXPERIMENTAL

#### Reagents

All the salts and the boric acid used were of analytical grade. The aqueous solutions were made with water that had been distilled once, then passed through mixed-bed

\*Present address: Water Research Centre, Henley Road, Medmenham, P.O. Box 16, Marlow, Bucks, England.



ion-exchange resins, an activated carbon filter, and finally a membrane filter. The purified water had a resistivity of  $>10$   $M\Omega\cdot\text{cm}$ . The solutions of the alkali and alkaline-earth metal chlorides were irradiated with ultraviolet light for 3 hr in preweighed fused-silica ampoules with a 1-kW mercury lamp to remove any trace of organic material.<sup>11</sup> This extra purification step was necessary to avoid poisoning or deactivation of the hydrogen electrode by reducible contaminants. Any small loss of water by evaporation during irradiation was compensated for by adjusting the weight by dropwise addition of irradiated distilled water. The chloride solutions were then acidified to pH 3.3 with "Aristar" hydrochloric acid, and the boric acid was added and dissolved. The solutions were made  $4 \times 10^{-3}M$  with respect to boric acid, and had a total ionic strength of 0.7. Before the titrations, hydrogen was bubbled vigorously through the solution to purge any residual carbon dioxide produced during the acidification. The sodium hydroxide titrant solutions were prepared by dilution of a filtered 12.5M stock solution. The titrant reservoir was guarded from carbon dioxide by a vent-tube filled with Carbosorb AS (6–12 mesh, 63%  $\text{Na}_2\text{O}$ ) granules. A standard potassium hydrogen phthalate solution was used to standardize the sodium hydroxide solution, which was freshly prepared daily.

#### Instrumentation

The potentiometric titrations were conducted in a glass reaction vessel, sealed with a perspex lid held with G-clamps, and placed in a 100-l. water-bath. The desired temperature was maintained ( $\pm 0.03^\circ$ ) by circulating water from a refrigeration unit in tandem with a thermostatically-controlled heating coil. The temperature of the water-bath was measured with a mercury thermometer, and checked periodically with an electronic thermometer. The reaction vessel was soaked in 5% "Decon 90" detergent, washed with concentrated hydrochloric acid and rinsed with copious amounts of ultrapure water, then dried at  $100^\circ$  in an oven.

Samples were transferred to the cooled reaction vessel with a calibrated 100-ml pipette. The potentials were measured with a Schlumberger/Solartron A210 digital voltmeter (accurate to 0.01 mV), supplied with a voltage follower to increase the input impedance, and coupled with a Solartron A291 recorder drive unit and tape-punch unit. Titrant was delivered by a Radiometer ABU12 Autoburette (2.5-ml) in 30- $\mu\text{l}$  portions, each addition taking 45 sec, during which the sample was stirred continuously.

The sample was stirred for a further 45 sec to allow the electrodes to equilibrate, then the stirrer was switched off and two successive readings of potential were recorded over a 4-sec period. The cycle was repeated for each addition.

#### Gas-scrubbing

Precautions were taken to avoid erroneous responses from the  $\text{Pt}/\text{H}_2$  electrode, caused by the presence of impurities in the hydrogen stream. The hydrogen was passed through copper piping into a trap containing Carbosorb AS (6–12 mesh) granules to remove any carbon dioxide, an acidic ammonium vanadate/zinc amalgam trap to remove traces of oxygen (oxygen is reduced at the  $\text{Pt}/\text{H}_2$  electrode), and finally through 0.6M sodium chloride/1M sodium hydroxide solution to remove any carry-over of acid from the vanadium solution.

#### Electrodes

The Pt electrode was prepared by electroplating Pt foil for 5 min with platinum black from a 1% platinum(IV) chloride/0.02% lead acetate solution by making it the anode at 2.5 V and 6.5 mA (the cathode was a Pt wire). After each experiment the Pt black was stripped off with boiling *aqua regia*.

The clean Pt foil was then placed in 1M sulphuric acid and made the cathode at a potential of  $-2.5$  V (Pt wire anode) for 10 min. (If the Pt surface was perfectly clean,

hydrogen bubbles streamed from the whole foil surface; if not, the *aqua regia* cleaning was repeated.) The presence of lead acetate during the plating ensured adherence of the Pt black to the clean Pt foil.<sup>12</sup> However, because lead may be leached from the platinum surface and cause poisoning of the active surface by reduction under acidic conditions, any lead was removed from the electrode surface after the plating. This was achieved by soaking the freshly plated electrode in 1M perchloric acid for 2 hr. When the plating was completed the electrodes had a characteristic black velvet texture indicative of an active Pt surface, and were free from lead. The electrodes were then thoroughly rinsed and kept in irradiated ultrapure water until required. Nernstian behaviour of the hydrogen electrode was checked by plotting the measured emf values against  $\log [\text{H}^+]$  in the acidic region of the titrations. The slope was typically within 0.3% of the theoretical 59.16 mV at  $25^\circ$ . The Ag/AgCl electrodes were prepared from 1-mm diameter silver wire. The wire was cleaned with concentrated nitric acid and rinsed with ultrapure water, then made the anode against another silver wire in 1M hydrochloric acid, at a potential of 2.5 V, for 30 sec, to form the AgCl coating. The Ag/AgCl electrode was stored, between experiments, in a saturated potassium chloride solution to which a few drops of 1M silver nitrate solution had been added.

#### Procedures

**Electrode calibration.** Samples of electrolyte solutions were measured into the reaction vessel with a calibrated 100-ml pipette. Each  $K_{\text{W}}^{\#}$  determination was preceded by acidification of the sample to pH 3.3 with hydrochloric acid, followed by purging with hydrogen to remove residual carbon dioxide. The solution was then titrated with 0.12M sodium hydroxide/0.6M sodium chloride which had previously been standardized with a standard potassium hydrogen phthalate solution. The standard electrode potential of the  $\text{Pt}/\text{H}_2$  electrode vs. the Ag/AgCl reference electrode was calculated by use of a Gran function for the acidic part of the titration; the equivalence volume was calculated with the same function.<sup>13</sup>

**$K_{\text{W}}^{\#}$  and  $K_{\text{B}}^{\#}$  determinations.** Because the non-approximate linearization plots used for  $K_{\text{B}}^{\#}$  estimations required  $K_{\text{W}}^{\#}$  values for each electrolyte medium, the latter were determined in media without boric acid present, by using Gran plots. This method of  $K_{\text{W}}^{\#}$  estimation has been used by other workers.<sup>3</sup>

The values of  $K_{\text{B}}^{\#}$  were determined by titrating the  $4 \times 10^{-3}M$  boric acid/0.7M electrolyte solutions with 0.12M sodium hydroxide/0.6M sodium chloride solution. The electrode potentials used for the  $K_{\text{B}}^{\#}$  evaluations typically related to pH values between 7 and 9. The Gran plots and the Hofstee algorithm used to linearize the data are discussed in the next section.

#### Theory and calculations

Simple Gran functions have long been recognized as a useful means of linearizing potentiometric titration data. The Gran functions that were initially applied to sea-water alkalinity titrations did not, however, allow for minor protonation reactions,<sup>16</sup> and this led to systematic errors. Errors of 12  $\mu\text{mole}/\text{kg}$  for sea-water samples taken during the GEOSECS program were estimated to occur from neglecting minor side-reactions.<sup>17</sup> Of these minor protonation reactions, those with borate ions are the most significant, but the contribution of orthophosphate to the alkalinity may become relevant in deep ocean waters (particularly the Pacific Ocean), in areas of upwelling, and in anoxic bottom waters where orthophosphate is released from underlying sediments (e.g., the Baltic Sea). Modifications of the early Gran algorithms can avoid such systematic errors.<sup>18</sup>

Although Gran functions are a useful means of linearizing potentiometric titration data, they cannot be used to evalu-

ate acidity constants with values near  $10^{-7}$ , because of the assumption that  $[H^+] > [OH^-]$  or *vice versa*<sup>14,15</sup> they therefore lose their linearity when the buffer action is minimal.

In this work, titrations were performed in simple electrolyte media and minor side-reactions were not a problem. The Hofstee equation used to linearize the potentiometric data and to obtain values for stability constants was first used to study enzyme-substrate equilibria,<sup>10</sup> where the end-point is usually unknown. Other workers have since recommended that the same equation be used to linearize data over the full pH range of an acid-base titration.<sup>14,19</sup> Both the Gran and the Hofstee equations are derived from simple mass-balance equations, and each takes into account the effect of volume changes during the course of a titration. The essential difference between the Gran and Hofstee linearization methods is that standard electrode potentials need to be determined before the  $K_{HA}$  evaluations in the Hofstee procedure. This is because absolute  $[H^+]$  values, and not simply values proportional to  $[H^+]$ , need to be included in the linearization calculations. Derivation of the Hofstee equation is based on the electroneutrality condition of the solution:

$$[H^+] + [Na^+] = [OH^-] + [B(OH)_4^-] \quad (1)$$

where  $[Na^+]$  is the concentration of base (NaOH) added to the solution. The following relationships are also valid

$$K_B^* = [B(OH)_3]/[B(OH)_4^-][H^+] \quad (2)$$

where  $K_B^*$  is the stability constant of boric acid. The total boric acid concentration  $C_B^*$ , after the addition of  $V$  ml of base (of concentration  $C_{Na}$ ) to  $V_0$  ml of boric acid solution of concentration  $C_B$  is

$$C_B^* = C_B V_0 / (V + V_0) \quad (3)$$

$$= [B(OH)_3] + [B(OH)_4^-] \quad (4)$$

and the sodium concentration is

$$[Na^+] = V C_{Na} / (V + V_0) \quad (5)$$

At the equivalence point,  $V_e$  ml, the amount of base added is equal to the amount of titratable boric acid:

$$V_e C_{Na} = V_0 C_B \quad (6)$$

Combination of equations (1)–(6) produces a non-approximate equation of the form

$$r K_B^* + s = V_e \quad (7)$$

where

$$r = V[H^+] + [(V_0 + V)[H^+]^2 - (V_0 + V)K_W^*] / C_{Na} \quad (8)$$

and

$$s = (V_0 + V)[H^+] / C_{Na} - K_W^* / [H^+] + V \quad (9)$$

A value for  $K_B^*$  is obtained from the slope of a plot of  $r$  against  $s$ , by use of a value of  $K_W^*$  valid for the same electrolyte medium. The necessary  $K_W^*$  values were determined by titration of the electrolyte solutions with sodium hydroxide in the absence of boric acid (Table 4). Although equation (7) is non-approximate, it requires a knowledge of absolute  $[H^+]$  values and not simply values proportional to  $[H^+]$  (as used in the Gran method). Hydrogen-ion concentrations were computed from the measured electrode potentials and the standard electrode potentials determined previously. All measured electrode potentials were corrected for the slight decrease in the chloride-ion concentration in the course of the titration, as the reference electrode (Ag/satd. AgCl) had no sleeve. The corrected  $[Cl^-]$  at any point is given by

$$[Cl^-] = (0.6V + 0.7V_0) / (V_0 + V). \quad (10)$$

This equation is used to calculate corrected values for the measured e.m.f. ( $E_m$ ) and the Gran function:

$$E_{corr} = E_m - 0.059159 \log [Cl^-], \quad (11)$$

and

$$F_1 = (V_0 + V) 10^{E_{corr}/k} / C_{Na} \quad (12)$$

where  $k = (RT/F) \ln 10$ . The Gran plot of  $F_1$  vs.  $V$  yielded a value for  $E_0$  from titration data in the range from pH 3 to neutral, as

$$E_{0(corr)} = -k \log(\text{slope}). \quad (13)$$

After the equivalence point, titrations were continued into the alkaline region to provide data for  $K_W^*$  estimation. The Gran function used to evaluate  $K_W^*$  was

$$F_2 = (V_0 + V) 10^{(E_0(corr) - E_{corr})/k} / C_{Na} \quad (14)$$

A plot of  $F_2$  vs  $V$  has a slope of  $1/K_W^*$ .

Data for the  $K_B^*$  estimations were fitted to equation (7) by using a linear least-squares regression, run on an IBM 4341 mainframe computer.

An attempt was made to estimate the effect of errors in  $V_0$ ,  $K_W^*$ ,  $T$  and other parameters on the value of  $K_B^*$  obtained from the plot of  $r$  vs.  $s$ . This was achieved by generating theoretical  $[H^+]$  and  $V$  values, inserting them into equations (8) and (9), and then estimating the effect of possible errors in  $K_W^*$ ,  $T$ ,  $C_{Na}$  and  $V_0$  on the calculated value for  $K_B^*$ . The theoretical  $[H^+]$  and  $V$  values were generated by computer from a quadratic equation derived from mass-balance equations, with selected values for  $K_W^*$  and  $K_B^*$ . It was found that a 0.3% error in  $V_0$  caused an error of 0.002 in  $pK_B^*$ , a 0.2° error in  $T$  one of 0.003 in  $pK_B^*$ , and a 2% error in  $K_W^*$  one of less than 0.001 in  $pK_B^*$ . The method is, therefore, very insensitive to errors in  $K_W^*$ . Stoichiometric ion-pairing constants ( $K_{MB}^*$ ) for the ion-pairing of  $B(OH)_4^-$  with cations  $M^{n+}$  were calculated from the equation:

$$K_B^* = K_{KCl}^* / (1 + \Sigma [M^{n+}] K_{MB}^*) \quad (15)$$

where  $K_{KCl}^*$  is the stability constant for boric acid in 0.7M potassium chloride medium. Values for  $K_{MB}^*$  were calculated by assuming that borate ion-pairing with potassium cations is negligible (*cf.* Byrne and Kester<sup>7</sup>).

Because the titrations were done with sodium hydroxide/sodium chloride solution, there will be a slight error in the  $K_{KCl}^*$  value, because of sodium-borate ion-pairing, and this may have caused an overestimate of up to 1% in values for  $K_B^*$ , *i.e.* the  $pK_B^*$  values in Table 1 may be too large by up to 0.005. We did not correct for this as the effect is small, and it does not affect the values for  $K_{MB}^*$  (Table 2) which are calculated from the ratio of  $K_B^*/K_{KCl}^*$  in equation (15).

## RESULTS

The results of the  $K_B^*$  determinations in the electrolytes used are presented in Table 1. Each value is the average of three or four determinations; the results varied over a range of less than  $\pm 0.003$ . The concentration of  $Mg^{2+}$  (0.02M) in the mixed electrolyte was

Table 1. Values of  $pK_B^*$  in artificial electrolytes at 25°

Medium	$pK_B^*$	Reference
0.7M NaCl	8.850	this work
0.7M <sub>w</sub> NaCl†	8.859	3
0.68M NaCl	8.853	7
0.725M NaCl	8.832	2
0.7M KCl	8.966	this work
	8.996	7
0.7M LiCl	8.754	this work
0.056M CaCl <sub>2</sub> /0.53M NaCl	8.694	this work
0.02M MgCl <sub>2</sub> /0.64M NaCl	8.775	this work
0.056M SrCl <sub>2</sub> /0.53M NaCl	8.812	this work

†  $M_w$  = mole/kg of solution.

less than that of the other bivalent cations (0.056M) because precipitation of  $Mg(OH)_2$  at higher magnesium concentrations caused curvature of the Hofstee plot. Potential readings used for the Hofstee plots typically corresponded to pH values between 7 and 9. Ion-pair stability constants,  $K_{MB}^*$ , were calculated from  $K_B^*$  data by using equation (15), and assuming that ion-pairing of potassium and borate in 0.7M potassium chloride medium is negligible.

The assumption that  $K_{KB}^*$  is zero or negligible when compared with the stability constants for the complexes of the other major cations has been made by other workers.<sup>7</sup> However, this assumption is based on theoretical calculations using estimated and uncertain activity coefficients for  $B(OH)_3$  and  $B(OH)_4^-$ , and this assumption is disputable. Nevertheless, the  $K_{MB}^*$  data obtained for the metal-borate complexes can be rationalized in terms of simple electrostatic and charge-density or polarization arguments. From the  $pK_w^*$  data in Table 4 it is evident that a lowering in  $pK_w^*$  accompanies the introduction of a more strongly polarizing cation into the medium. The polarizing power of a cation is useful for predicting the degree of hydrolysis in aqueous solutions and is given by (cation charge)<sup>2</sup>/(cation radius + 0.85). (The term 0.85 is an empirical correction to the Born function  $z^2/r$ ; it is the radius of the oxygen atom in a water molecule.<sup>8</sup>) An increase in hydrolysis occurs with increasing polarizing power, in the order  $K^+ < Na^+ < Li^+ < Sr^{2+} < Ca^{2+} < Mg^{2+}$ . The  $pK_w^*$  data in Table 4 confirm that the greater the cation polarizing power, the stronger are the M-O interactions (hydration), and the more acidic are the protons of the ligand water molecules *i.e.*, the lower is  $pK_w^*$ .

It is clear from the values for  $K_{MB}^*$  in Table 2 that the stability of the metal-borate ion-pairs also depends on the polarizing power of the cation. This trend can be explained by the same coulombic arguments that apply to cation hydrolysis. Figure 1 shows the correlation between  $K_{MB}^*$  and  $z^2/(r + 0.85)$ . Other workers have also used this means of rationalizing stability-constant data.<sup>8</sup> From the  $K_{MB}^*$  data obtained in this study it is clear that the alkali-metal ions form relatively weaker borate ion-pairs than the alkaline-earth metal ions do.  $Li^+$  and  $Na^+$  display weak association with borate, and  $K^+$  shows little or

Table 2. Stability constants for the formation of ion-pairs with borate ions at 25°

Ion-pair	This work (0.7M NaCl)	Byrne and Kester <sup>7</sup> (0.68M NaCl)	Dyrssen and Hansson <sup>1</sup> (0.7M <sub>w</sub> NaCl)
$LiB(OH)_4$	$0.89 \pm 0.02$	—	—
$NaB(OH)_4$	$0.44 \pm 0.01$	$0.57 \pm 0.02$	—
$MgB(OH)_4^+$	$13.6 \pm 0.7$	$8.03 \pm 0.15$	$5.4 \pm 0.2$
$CaB(OH)_4^+$	$11.4 \pm 0.15$	$13.0 \pm 0.15$	—
$SrB(OH)_4^+$	$3.47 \pm 0.06$	—	—

\*M<sub>w</sub> = mole/kg of solvent.

Table 3. Inorganic speciation of boron in sea-water at 25°, 35‰ salinity and pH 8.2; values given as % of total boron

Ion	This work	Constant pH method <sup>7</sup>
$B(OH)_3$	59.7	76.4
$B(OH)_4^-$	21.2	13.3
$MgB(OH)_4^+$	12.6	5.1
$NaB(OH)_4$	4.4	3.6
$CaB(OH)_4^+$	2.1	1.6
$SrB(OH)_4^+$	0.005	—

negligible borate ion-pairing. However, the underlying assumption that the activity coefficients of free ions are independent of the electrolyte composition at constant ionic strength may explain the observed apparent differences in ion-pairing with  $Li^+$ ,  $Na^+$  and  $K^+$ . In fact borate ion-pairing with these cations may be negligible. Improved Debye-Hückel equations such as the Pitzer equations<sup>23</sup> can make possible the calculation of activity coefficients of ions in high ionic-strength electrolytes. Pitzer interaction coefficients for the association of  $Ca^{2+}$ ,  $Mg^{2+}$  and borate ions have recently been calculated at ionic strengths from 0.5 to 6, and the negative Pitzer coefficients for the  $Ca^{2+}$ -borate and  $Mg^{2+}$ -borate interactions indicate some degree of ion-pairing.<sup>24</sup>

In contrast to the alkali-metal ions,  $Mg^{2+}$ ,  $Ca^{2+}$  and  $Sr^{2+}$  show stronger and significant associations with borate anions, the strength of interaction decreasing with increasing ionic radius (presumably because of the decreasing charge density).

The ion-pairing stability constants have been used to deduce the speciation of boron in sea-water, and the distribution obtained can be compared with that yielded by using the constant-pH method<sup>7</sup> (Table 3). The sea-water distribution is derived by using the equation

$$K_{(sw)}^* = K_{(KCl)}^* (1 + K_{NaB}^* [Na^+] + K_{MgB}^* [Mg^{2+}] + K_{CaB}^* [Ca^{2+}] + K_{SrB}^* [Sr^{2+}] + K_{LiB}^* [Li^+]) \quad (16)$$

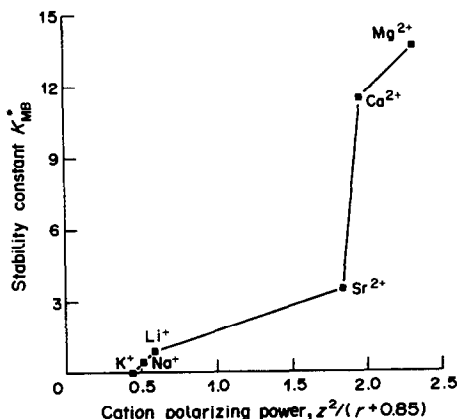


Fig. 1. Correlation of  $K_{MB}^*$  with cation polarizing power.

Table 4. Values of  $\log K_{\text{B}}^*$  in various electrolyte solutions at 25°

Medium	This work	Dyrssen and Hansson <sup>3</sup>	Harned and Owen <sup>21</sup>	Sjoberg <i>et al.</i> <sup>22</sup>
0.7M LiCl	13.630 ± 0.003		13.636 ( <i>I</i> = 0.5)	
0.7M NaCl	13.739 ± 0.006	13.77		13.727 ± 0.001 ( <i>I</i> = 0.6)
0.7M KCl	13.774 ± 0.007		13.77 ( <i>I</i> = 1.01)	
0.53M NaCl/0.056M CaCl <sub>2</sub>	13.688			
0.53M NaCl/0.02M MgCl <sub>2</sub>	13.295			

where  $K_{\text{B}}^*$  is the stability constant for boric acid in sea-water.

For sea-water of salinity 35‰ the cations concerned have the following concentrations:  $[\text{Na}^+] = 0.479M$ ;  $[\text{Mg}^{2+}] = 0.054M$ ;  $[\text{Ca}^{2+}] = 0.011M$ ;  $[\text{Sr}^{2+}] = 9 \times 10^{-5}M$ ;  $[\text{Li}^+] = 2.6 \times 10^{-5}M$ . Our value for  $K_{\text{B}}^*$  obtained from equation (16) is  $2.242 \times 10^{-9}$ . It is evident from Table 3 that although  $\text{Sr}^{2+}$  shows significant association with borate, this ion-pair is unimportant in sea-water owing to the low concentration of  $\text{Sr}^{2+}$ . Lithium ion-pairing in sea-water is even less significant. The general pattern of speciation in sea-water is comparable with that outlined by Byrne and Kester.<sup>7</sup> However, our value for  $\log 1/K_{\text{B}}^*$  (8.649) differs from that obtained by Byrne and Kester<sup>7</sup> (8.736), and consequently  $\text{H}_3\text{BO}_3$  is less important in our system. Discrepancies between the speciation predicted from this work, and that suggested by Byrne and Kester<sup>7</sup> are probably due to our adoption of the free hydrogen-ion pH scale, to residual liquid-junction effects, and to Byrne and Kester's use of single data-point titrations. Nevertheless, both our study and that of Byrne and Kester<sup>7</sup> confirm that the ion-pair  $\text{MgB}(\text{OH})_4^+$  is the predominant cation-associated species in sea water.

#### CONCLUSIONS

The aim of this investigation was to measure the stability constants ( $K_{\text{MB}}^*$ ) for the ion-pairs formed by borate and "major sea-water cations". It was achieved by using a procedure that avoided a major problem of marine electrochemical pH-measurements, the residual liquid junction potential effect. The free hydrogen-ion pH scale was used. The potentiometric titration data were linearized with a non-approximative equation for data points over a range of pH (7–9), rather than by a single point method.<sup>7</sup> The resultant  $K_{\text{MB}}^*$  data were reasonably rationalized by using cation polarizing power arguments.

The method in this study could not be extended to

direct  $K_{\text{B}}^*$  determinations in sea-water because of magnesium hydroxide precipitation. However, the incorporation of the cation-borate stability-constant data into a simplified "sea-water borate" speciation scheme provided a distribution comparable with that outlined in previous work that used the NBS reference scale. The procedures adopted in our work could be extended to investigate the speciation of other weak acids in saline media.

#### REFERENCES

1. K. Buch, *J. Cons. Perm. Int. Explor. Mer.*, 1933, **8**, 309.
2. B. B. Owen and E. J. King, *J. Am. Chem. Soc.*, 1943, **65**, 1612.
3. D. Dyrssen and I. Hansson, *Mar. Chem.*, 1973, **1**, 137.
4. I. Hansson, *Deep Sea Res.*, 1973, **20**, 461.
5. *Idem*, *Acta Chem. Scand.*, 1973, **27**, 924.
6. E. P. Jones and E. M. Levy, *J. Mar. Res.*, 1980, **39**, 405.
7. R. H. Byrne and D. R. Kester, *ibid.*, 1974, **32**, 119.
8. D. R. Turner, M. Whitfield and A. G. Dickson, *Geochim. Cosmochim. Acta*, 1981, **45**, 855.
9. A. G. Dickson, *ibid.*, 1984, **48**, 2299.
10. B. H. J. Hofstee, *Science*, 1960, **131**, 39.
11. F. A. J. Armstrong, P. M. Williams and J. D. H. Strickland, *Nature*, 1966, **211**, 481.
12. A. M. Feltham and M. Spiro, *Chem. Rev.*, 1971, **71**, 177.
13. G. Gran, *Analyst*, 1952, **77**, 661.
14. F. Ingman and E. Still, *Talanta*, 1966, **13**, 1431.
15. L. Pehrsson, F. Ingman and A. Johansson, *ibid.*, 1976, **23**, 769.
16. D. Dyrssen, *Acta Chem. Scand.*, 1965, **19**, 1265.
17. A. L. Bradshaw, P. G. Brewer, D. K. Shafer and R. T. Williams, *Earth Plan. Sci. Lett.*, 1981, **55**, 99.
18. I. Hansson and D. Jagner, *Anal. Chim. Acta*, 1973, **65**, 363.
19. A. Johansson, *Analyst*, 1970, **95**, 535.
20. M. Whitfield and D. R. Turner, in *Marine Electrochemistry*, M. Whitfield and D. Jagner (eds.), p. 66. Wiley, New York, 1981.
21. H. S. Harned and B. B. Owen, *The Physical Chemistry of Electrolyte Solutions*, Ed., p. 633. Reinhold, New York, 1958.
22. S. Sjoberg, Y. Hagglund, A. Nordin and N. Ingri, *Mar. Chem.*, 1983, **13**, 35.
23. K. S. Pitzer and G. Mayorga, *J. Phys. Chem.*, 1973, **77**, 2300.
24. P. J. Hershey, M. Fernandez, P. J. Milne and F. J. Millero, *Geochim. Cosmochim. Acta*, 1986, **50**, 143.

# PRECONCENTRATION AND VOLTAMMETRIC MEASUREMENT OF MERCURY WITH A CROWN-ETHER MODIFIED CARBON-PASTE ELECTRODE

JOSEPH WANG and MOJTABA BONAKDAR

Department of Chemistry, New Mexico State University, Las Cruces, New Mexico 88003, U.S.A.

(Received 22 July 1987. Revised 8 September 1987. Accepted 31 October 1987)

**Summary**—Carbon-paste electrodes modified with crown-ethers were constructed by mixing the crown-ethers into a graphite powder/Nujol oil matrix. The electrodes so formed were able to bind mercuric ions chemically, and gave greater voltammetric response to mercury than that of ordinary carbon-paste electrodes. The response was characterized with respect to paste composition, crown-ether, preconcentration period, mercury concentration, reproducibility, possible interferences, and other variables. Best results were obtained with 18-crown-6 and an acetate buffer (pH 4.0). The electrode gave good linearity for  $1 \times 10^{-5}$ – $6 \times 10^{-5} M$  mercury, a detection limit of  $2 \times 10^{-6} M$ , and a relative standard deviation of 11%. The investigation may lead to a new class of modified (complexing) electrodes, with different patterns of reactivity.

The application of chemically modified electrodes (CMEs) in electroanalytical measurements is now a practical proposition. One promising approach involves attachment of a preconcentration agent to the surface, to accumulate analytes chemically prior to voltammetric measurement.<sup>1</sup> This concept is important because it can allow construction of sensitive voltammetric sensors that are specific (or at least selective) for an analyte. The approach is analogous to anodic stripping voltammetry in that a preconcentration step is employed to enhance the sensitivity and selectivity. It can also enhance the scope of stripping measurements, as it utilizes a chemical (non-electrolytic) step for the accumulation. The preconcentration agent may be introduced in the carbon-paste matrix<sup>2,3</sup> or by substitution in an appropriate polymeric coating.<sup>4,5</sup> The modifier is commonly a ligand possessing high affinity for the analyte, or an ion-exchanger (resin or polyelectrolyte).

In this paper, we describe a preliminary investigation of crown-ethers as electrode modifiers for preconcentration/voltammetric measurements. Crown-ethers are macrocyclic polyethers that have received considerable attention,<sup>6</sup> and are highly suitable neutral carriers for ion-selective electrodes (*e.g.*, the valinomycin-based potassium electrode). Voltammetric applications of crown-ethers are rare however. Several groups, particularly those of Koryta,<sup>7</sup> Peter,<sup>8</sup> and Luca,<sup>9</sup> have used polarography and cyclic voltammetry to study the redox behaviour and thermodynamic stability of various crown-ether metal complexes in different organic solvents. However, the utility of crown-ethers in voltammetric analysis in general, and as electrode modifiers for the preconcentration/voltammetric concept in particular, has not been explored, although this approach appears very promising as it should combine the

inherent selectivity of macrocyclic reagents with the high sensitivity of preconcentration/voltammetric measurements. In the work described below, the electrodes were modified by mixing the desired amount of crown-ether with a carbon-paste matrix; this allows easy variation of the modifier content and renewal of the electrode surface. The crown-ethers and their complexes remain stably incorporated in the carbon-paste matrix because of their very limited solubility in aqueous solutions. Mercury(II) was used as model analyte, but the concept can be extended to determination of other metal ions through a judicious choice of the crown-ether (provided the reactivity at the electrode surface is the same as that in solution).

## EXPERIMENTAL

### Apparatus

A Bioanalytical Systems Model VC-2 electrochemical cell was employed. The working electrode, reference electrode (Ag/AgCl, Model RE-1, Bioanalytical Systems), and platinum-wire auxiliary electrode were inserted into the cell through holes in its Teflon cover. The cell was placed on a magnetic stirrer and a 2.2-cm long stirring bar was used. Current-voltage data were recorded with an EG&G PAR Model 264A voltammetric analyser and a EG&G PAR Model 0073 X-Y recorder.

Chemically modified carbon-paste electrodes were prepared by grinding the crown-ether crystals (Aldrich) with a mortar and pestle, then adding the graphite powder; after additional grinding of the mixture, nujol oil was added and the whole was thoroughly hand-mixed. In most studies the final composition was 54:36:10% w/w graphite/oil/modifier. The paste was packed into one end of a glass tube (3 mm bore, 1 mm wall), to make contact with a copper wire inserted in the tube. Plain (unmodified) carbon paste was prepared in the usual manner, and contained 40% Nujol oil.

### Reagents

All solutions were prepared with demineralized water. Stock solutions,  $1 \times 10^{-3} M$ , of various metal nitrates were prepared and stored in polyethylene bottles. The supporting electrolyte was 0.1M acetate buffer (pH 4.0).

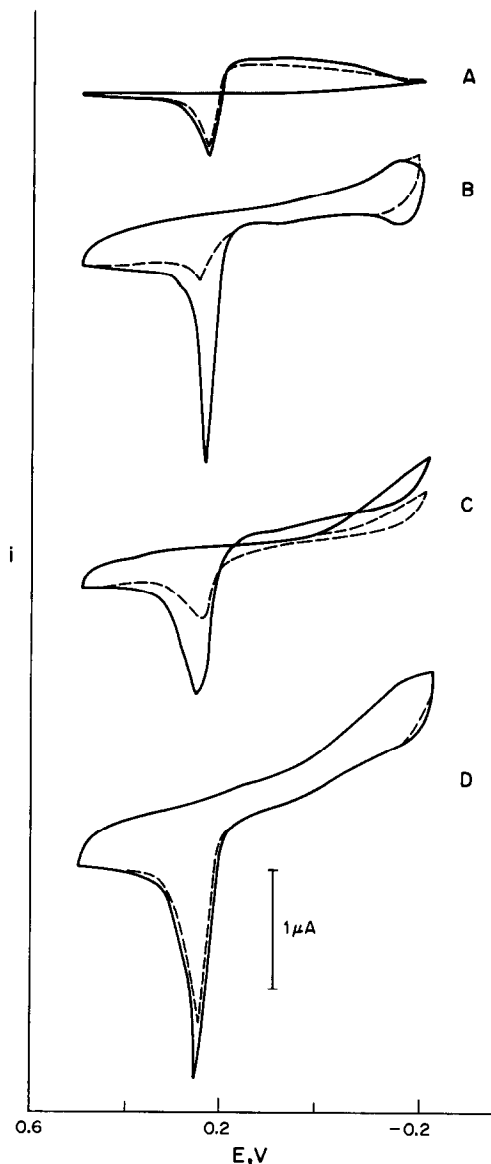


Fig. 1. Cyclic voltamperograms for  $5 \times 10^{-5} M$  Hg(II) obtained after 120 sec stirring at  $+0.5 V$  vs. Ag/AgCl, with (A) unmodified carbon paste, and pastes modified with (B) 10% w/w 18-crown-6, (C) dicyclohexano-18-crown-6, and (D) 15-crown-5. Scan-rate, 50 mV/sec; electrolyte, acetate buffer (pH 4.0). The dashed lines represent the response without accumulation.

#### Procedure

A fresh working-electrode surface was used for each preconcentration/voltammetric cycle, and smoothed with a computer card. For the preconcentration step, the working electrode was immersed in 10 ml of stirred sample solution for a given time, during which it was held at  $+0.5 V$  vs. Ag/AgCl. (Though it was possible to accumulate mercury at open-circuit, this required a long equilibration time for a stable current to be achieved before the scan). After the preconcentration, the stirring was stopped, and the accumulated ion measured by cycling the potential between  $+0.5$  and  $-0.2 V$ , and recording the cyclic voltamperogram. The surface was then renewed by removing the outer 2 mm and refilling with fresh paste (this ensured a "mercury-free" surface and thus absence of memory effects).

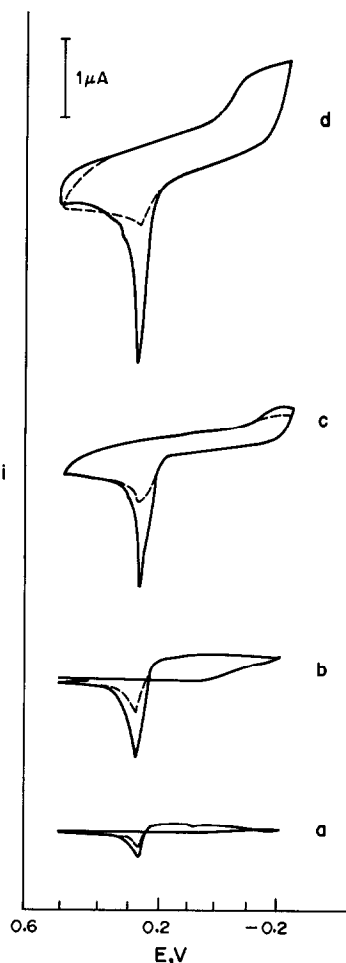


Fig. 2. Effect of carbon-paste composition on the cyclic voltammetric response for  $5 \times 10^{-5} M$  Hg(II) following 120 sec stirring at  $+0.5 V$  vs. Ag/AgCl. Amount of 18-crown-6 in paste: (a) 0; (b) 0.05, (c) 0.20 and (d) 0.40 g. The dashed lines represent the response without accumulation.

#### RESULTS AND DISCUSSION

Figure 1 shows cyclic voltamperograms obtained with ordinary (A) and various crown-ether modified (B–D) carbon-paste electrodes that had been immersed for 2 min in a stirred  $5 \times 10^{-5} M$  Hg(II) solution. During the stirring period the electrode was held at  $+0.5 V$  vs. Ag/AgCl, at which electrolytic plating could not occur. The dotted lines represent the analogous response without the stirring period. A small mercury oxidation peak, which is not affected by the stirring period, is obtained with the ordinary electrode. In contrast, the crown-ether electrodes exhibit substantially larger mercury peaks, which are strongly influenced by the stirring period, hence indicating an effective non-electrolytic uptake of mercury. Notice that though the ordinary electrode exhibits a current "cross-over" point, characteristic of an electrolytic deposition–stripping mechanism, no such behaviour is observed for the 18-crown-6 and 15-crown-5 modified electrodes. Most subsequent

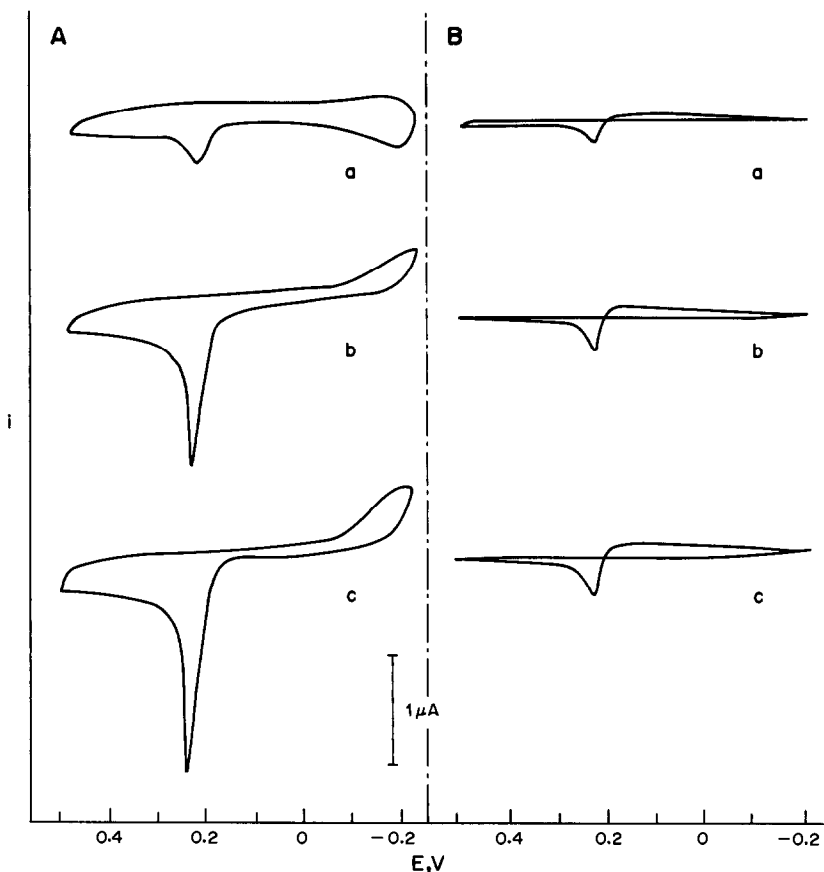


Fig. 3. Effect of preconcentration period on the cyclic voltammetric response for  $5 \times 10^{-5} M$  Hg(II), with (A) 18-crown-6 modified carbon paste and (B) unmodified carbon paste. Preconcentration period: (a) 0, (b) 2 and (c) 5 min. Other conditions as in Fig. 1B.

work was performed with 18-crown-6 as modifier, because it yielded the best signal-to-background characteristics. This compound is known to be an extracting reagent for the separation of mercury.<sup>6</sup> Electrodes modified with dibenzo-18-crown-6 yielded a response similar to that of the ordinary electrode (not shown).

Figure 2 shows the effect of the paste composition on the preconcentration/voltammetric response. Carbon-paste electrodes containing 0.05, 0.2 and 0.4 g of 18-crown-6 (together with 1.2 g of graphite powder and 0.8 g of Nujol oil) were employed. As expected from the increased complexing capacity of the electrode, the amount of mercury ion accumulated and the resulting voltammetric peak, increased (non-linearly) with the amount of crown-ether in the paste. For example, the electrodes containing 0.05, 0.2 and 0.4 g of modifier yielded peak current enhancement by factors of 2.1, 3.8 and 5.6, respectively, relative to the response without accumulation (shown as a dashed line). The corresponding voltamperogram at the unmodified electrode (a) exhibits a substantially smaller mercury peak. Notice also that the extent of the current cross-over decreases when the amount of modifier is increased. The electrode containing 0.2 g of modifier was employed for the

majority of the work because of its better signal-to-background characteristics.

Because crown-ethers, being neutral compounds, form cationic complexes with metal ions, we initially expected to monitor a reductive process following the accumulation at +0.5 V, but only a small peak at ca. -0.18 V was obtained, that was not analytically useful. In contrast, on reversal of the scan direction (at -0.2 V), the reduced form of the complex undergoes an oxidation step to yield the well-defined anodic peak (shown in Figs. 1 and 2). This peak must be distinguished from the stripping peak associated with electrolytic deposition (during the preceding cathodic scan). For example, with the 18-crown-6 electrode the complex undergoes oxidation at +0.26 V but the stripping process occurs at +0.31 V. Subsequent scans result in a sharp decrease of the oxidation peak for the complex, but a gradual increase of the stripping peak (as complete stripping does not occur).

Figure 3 shows cyclic voltamperograms for  $5 \times 10^{-5} M$  mercury(II) after different preconcentration times. A rapid increase of the peak with increasing preconcentration time is observed for the modified electrode, indicating an enhancement of the mercury concentration on the surface. With 5-min

preconcentration, a 7-fold peak current enhancement was observed. Longer times did not affect the response (not shown), possibly because of saturation of the binding sites. The response of the ordinary electrode is not affected by the change in preconcentration time. Again, note the different shapes of the voltamperograms obtained with the modified and ordinary electrodes (the latter exhibiting the characteristic "cross-over" point). The precision of the results was estimated by six successive measurements of  $5 \times 10^{-5} M$  mercury (conditions as in Fig. 1B). The mean peak current found was  $1.62 \mu A$  with a range of  $1.44$ – $1.85 \mu A$  and a relative standard deviation of 11%. These data indicate that the electrode renewal gives a relatively reproducible surface. Such precision is commonly observed for other modified electrodes utilizing the preconcentration/voltammetric scheme. Possible interferences from coexisting metal ions capable of binding to 18-crown-6 were evaluated. Measurements of  $5 \times 10^{-5} M$  mercury(II) were not affected by the addition of  $5 \times 10^{-5} M$  lead(II), silver(I), nickel(II), zinc(II), iron(II), cadmium(II) and copper(II). Similarly, the large concentration excess of the supporting electrolyte cation (sodium) did not interfere. The effect of various electrolytes, such as potassium chloride, hydrochloric acid, potassium nitrate, or acetate, borate and phosphate buffers, was examined. Best results were obtained with the acetate buffer solution, but no response was observed for the chloride solutions (chloride ions compete with crown-ethers for the mercuric ions,  $\log K_{HgCl_2} = 16.9$ ). The unstirred solution yielded a substantially lower response (by a factor of 5), indicating the strong effect of mass-transport on the mercury uptake.

Figure 4 shows the analytical signals of the modified carbon-paste electrode in a standard-additions experiment with 120-sec accumulation from acetate buffer spiked with  $1 \times 10^{-5} M$  (a),  $2 \times 10^{-5} M$  (b), and  $3 \times 10^{-5} M$  (c) mercury(II). The response is proportional to the mercury concentration, and is substantially larger than the corresponding response without accumulation (shown as dashed lines), or with the unmodified carbon-paste electrode (not shown). These three measurements were part of a set for six concentration increments ranging from  $1 \times 10^{-5}$  to  $6 \times 10^{-5} M$ . Linearity between the peak current and concentration was obtained. A least-squares treatment yielded a slope of  $390 \text{ nA} \cdot 1. \mu \text{mole}^{-1}$  (correlation coefficient, 0.992). A detection limit near  $2 \times 10^{-6} M$  is estimated, based on the signal corresponding to three times the noise of the response shown in voltamperogram a. Further lowering of the detection limit may be achieved by using longer preconcentration times or advanced voltammetric waveforms.

In conclusion, although this study should be considered preliminary, it serves to illustrate the potential utility of electrodes modified with crown-ethers, for voltammetric analysis. The incorporation of other crown-ethers into the carbon paste matrix appears to

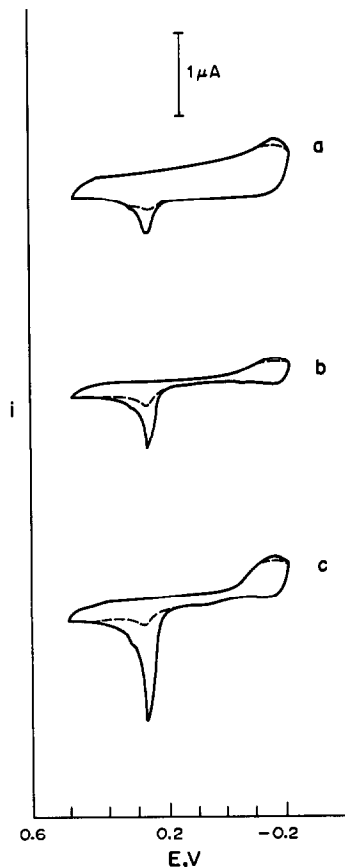


Fig. 4. Cyclic voltamperograms for solutions containing (a)  $1 \times 10^{-5} M$ , (b)  $2 \times 10^{-5} M$ , and (c)  $3 \times 10^{-5} M$  Hg(II), with the 18-crown-6 modified carbon-paste electrode. Other conditions as in Fig. 1.

provide a promising route for preconcentration/voltammetric measurements of other metal ions at CMEs by an analogue of stripping voltammetry. In particular, sulphur- and nitrogen-containing macrocycles should be extremely useful for the uptake and determination of various heavy or transition metals.

*Acknowledgement*—This work was supported by the National Institutes of Health, under Grant No. GM 30313-04.

#### REFERENCES

1. A. R. Guadalupe and H. D. Abruna, *Anal. Chem.*, 1985, **57**, 142.
2. J. Wang, B. Greene and C. Morgan, *Anal. Chim. Acta*, 1984, **158**, 15.
3. K. Kalcher, *ibid.*, 1985, **177**, 175.
4. D. M. T. O'Riordan and G. G. Wallace, *Anal. Chem.*, 1986, **58**, 128.
5. J. A. Cox and P. J. Kulesza, *Anal. Chim. Acta*, 1983, **154**, 71.
6. I. M. Kolthoff, *Anal. Chem.*, 1979, **51**, 1R.
7. J. Koryta and M. L. Mittal, *J. Electroanal. Chem.*, 1972, **36**, 14.
8. F. Peter, M. Gross, L. Pospíšil and J. Kůta, *ibid.*, 1978, **90**, 239.
9. M. M. Khalil, I. Tănasa and C. Luca, *Talanta*, 1985, **32**, 1151.



## INTERPRETATION OF THE SELECTIVITY AND DETECTION LIMIT OF LIQUID ION-EXCHANGER ELECTRODES

MAGDALENA MAJ-ŻURAWSKA, TOMASZ SOKALSKI and ADAM HULANICKI\*  
 Department of Chemistry, Warsaw University, Warsaw, Poland

(Received 17 March 1987. Revised 16 October 1987. Accepted 30 October 1987)

**Summary**—An equation has been derived which describes the e.m.f. of a liquid ion-exchanger membrane electrode in conditions of low concentration levels of the primary and interfering ions. The equation is based on the assumption that if the external solution contains no excess of ions which may exchange with the organic phase, then the concentration of the exchanger at the interface decreases, and this is responsible for formation of a diffusion layer inside the membrane. Therefore the potential response depends on the initial concentration of the ion-exchanger in the membrane phase, on the thicknesses of the diffusion layer on both sides of the interface, and on the diffusion coefficients of the species in both phases. This equation explains the non-Nernstian behaviour of the electrode in the presence of interferents, as well as the variation of the conditional selectivity coefficients. The parameters mentioned also influence the detection limit of an electrode. The electrode behaviour has been tested in unstirred solutions and in solutions stirred at different rates. Through its influence on the diffusion layer thickness, the stirring also influences the electrode potential and the characteristics of the electrode.

Electrodes based on liquid ion-exchangers have found numerous practical applications in analysis and their behaviour has been widely discussed.<sup>1–8</sup> Initially it was assumed that the selectivity coefficient which follows from the Nikolskii equation is a constant unequivocally defined by the thermodynamic characteristics of the system, namely the ratio of the partition coefficients of individual ions or more generally the equilibrium constant of the exchange reaction. Nevertheless it has been shown that selectivity coefficients cannot be regarded as constants, because they change not only with the long-term changes in membrane composition<sup>9</sup> but also with the activity level of the ion in solution. It has been established<sup>10</sup> that with decreasing activity of the interfering ion the selectivity coefficients tend to approach a value of unity, regardless of whether they are greater or smaller than unity at higher levels of the interfering ions. Jyo and Ishibashi<sup>11</sup> have suggested a quantitative model for this effect, which shows good agreement with experimental findings in the high and medium concentration range ( $> 10^{-4}M$ ), but fails for lower concentrations.

In this paper another model is proposed which is in relatively good agreement with the experimental data over the whole concentration range accessible for ion-selective electrode measurements. The effect of solution stirring is also discussed and experimentally verified. This effect could also be predicted on the basis of the Jyo and Ishibashi<sup>11</sup> model, which takes into account the thickness of the diffusion layer,

which in turn depends on the stirring rate, but these authors have not mentioned the effect of stirring rate on the electrode response.

### THEORY

The model given by Jyo and Ishibashi<sup>11</sup> assumes that the apparent changes in selectivity coefficients are due to differences between the ion activities in the bulk of the solution ( $a_i, a_j$ ), and those at the membrane surface in the external solution [ $a_i(0), a_j(0)$ ] (Fig. 1) as well as to differences between the concentration of exchanger sites occupied by given ions inside the membrane ( $c_i, c_j$ ) and at the interface [ $c_i(0), c_j(0)$ ]. When ion-association is predominant in the

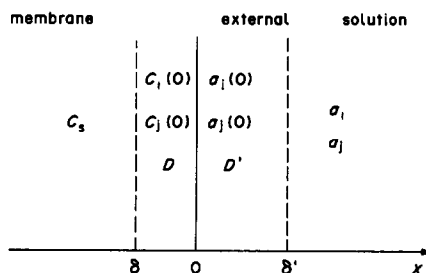


Fig. 1. Scheme of the membrane-external solution interface:  $c_s$ —ion-exchanger concentration;  $c_i(0), c_j(0)$ —concentrations of ions I and J in the membrane at the interface, respectively;  $a_i, a_j, a_i(0), a_j(0)$ —activities of ions I and J in the external solution in the bulk and at the interface, respectively;  $D, D'$ —diffusion coefficients of ions in the membrane and in the external solution;  $\delta, \delta'$ —the thicknesses of the Nernstian diffusion layers inside the membrane and in the external solution, respectively.

\*Author to whom correspondence should be addressed.

membrane the concentrations should refer to the respective ion-associates ( $c_{is}$  and  $c_{js}$ ).

Like Jyo and Ishibashi,<sup>11</sup> we assume that the case presented refers to univalent ions ( $z_i = z_j = \pm 1$ ), with equal mobilities of free ions in the membrane ( $u_i = u_j$ ) as well as equal mobilities of the corresponding ion-associates ( $u_{is} = u_{js}$ ) for the membranes where association plays a significant role. We also assume that the association inside the membrane does not influence partition of the ion, *i.e.*, it is either negligible or non-specific.

Under these conditions the theoretical selectivity coefficients are defined by the actual activities and concentrations at the membrane interface. Thus for negligible association

$$K_{ij} = \frac{a_i(0)c_j(0)}{c_i(0)a_j(0)} \quad (1a)$$

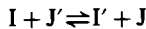
and for negligible dissociation

$$K_{ij} = \frac{a_i(0)c_{js}(0)}{c_{is}(0)a_j(0)} \quad (1b)$$

Because the fluxes of all species at steady-state follow Fick's law, then

$$D' \left[ \frac{a(0) - a}{\delta'} \right] = D \left[ \frac{c - c(0)}{\delta} \right] \quad (2)$$

where  $D'$  and  $D$  are the diffusion coefficients in the external solution and in the membrane, respectively, and  $\delta'$  and  $\delta$  correspond to the thickness of the diffusion layers in the external solution and in the membrane, respectively. Equation (2) for each ion participating in the exchange reaction



where the primed symbols refer to the external solution and the unprimed to the membrane phase, can be transformed for each ion into the following relationships

$$a_i(0) = a_i + \frac{D\delta'}{D'\delta} [c_i - c_i(0)] \quad (3a)$$

$$a_j(0) = a_j + \frac{D\delta'}{D'\delta} [c_j - c_j(0)] \quad (3b)$$

On introduction of  $c_s$  which represents the total concentration of ion-exchanger sites inside the membrane, equations (3a) and (3b) can be expressed in terms of the mole fractions of exchanger sites [ $x_i, x_j, x_i(0), x_j(0)$ ] inside the membrane and at the membrane interface. Thus writing

$$C = \frac{D\delta'}{D'\delta} c_s \quad (4)$$

yields

$$a_i(0) = a_i + C[x_i - x_i(0)] \quad (5a)$$

$$a_j(0) = a_j + C[x_j - x_j(0)] \quad (5b)$$

The model presented by Jyo and Ishibashi,<sup>11</sup> amongst other things, assumes that the number of

exchanger sites in the membrane remains constant. As a consequence, and taking into account electro-neutrality, we obtain

$$c_i(l) + c_j(l) + c_{is}(l) + c_{js}(l) = c_s = \text{const.}(l) \quad (6)$$

and hence

$$x_i(l) + x_j(l) = 1 \quad (7)$$

where  $(l)$  denotes distance from the interface (thickness  $d$ ) inside the membrane ( $0 \leq l \leq d$ ).

Then  $x_i$  and  $x_j$  denote the mole fractions

$$x_i = \frac{c_i + c_{is}}{c_s} \quad (8a)$$

$$x_j = \frac{c_j + c_{js}}{c_s} \quad (8b)$$

In our model, however, the constancy of the number of exchanger sites in the membrane is not assumed, but leakage of ion-exchanger from the membrane is, so

$$c_i(l) + c_j(l) + c_{is}(l) + c_{js}(l) = c_s(l) \quad (9)$$

where

$$c_s(l) = c_s - \Delta c_s \quad (10)$$

The term  $\Delta c_s$  denotes the decrease in exchanger concentration due to leakage from the membrane, and

$$x_i(l) + x_j(l) + x_{\Delta}(l) = 1 \quad (11)$$

where

$$x_{\Delta} = \frac{\Delta c_s}{c_s} \quad (12)$$

In the membrane at a diffusion layer depth  $l = \delta$ , we have  $x_i = 1$ ,  $x_j = 0$  and  $x_{\Delta} = 0$ , but at the interface,  $l = 0$ ,  $x_i + x_j < 1$  and  $x_{\Delta} \neq 0$ .

Introduction of equation (11) along with (1) and (5) allows calculation of the unknown boundary values of the ion activities  $a_i(0)$  and  $a_j(0)$  in terms of the bulk activities,  $a_i$  and  $a_j$ , the theoretical selectivity coefficient  $K_{ij}$ , parameter  $C$  and the mole fraction  $x_{\Delta}(0)$ . In this relationship the actual activities at the membrane surface,  $a_i(0)$ ,  $a_j(0)$  and the theoretical selectivity coefficient  $K_{ij}$  can be correlated to the bulk activities,  $a_i$ ,  $a_j$  and the experimental (conditional) selectivity coefficient  $K_{ij}^{\text{pot}}$ . Thus

$$\begin{aligned} a_i(0) + K_{ij} a_j(0) &= a_i + K_{ij}^{\text{pot}} a_j \\ &= \frac{1}{2}(a_i + K_{ij} a_j - K_{ij} C) \\ &\quad + \frac{1}{2} x_{\Delta}(0) C (K_{ij} + 1) + \frac{1}{2} \sqrt{\Delta} \end{aligned} \quad (13)$$

where

$$\begin{aligned} \Delta &= (a_i + K_{ij} a_j - K_{ij} C)^2 + 2K_{ij} C [2 - x_{\Delta}(0)] (a_i + a_j) \\ &\quad + C^2 \{ [K_{ij} x_{\Delta}(0) + 1]^2 + x_{\Delta}(0)^2 (K_{ij} - 1)^2 \\ &\quad - K_{ij}^2 [x_{\Delta}(0) + 1]^2 + K_{ij}^2 - 1 \} \\ &\quad + 2x_{\Delta}(0) C a_i + 2K_{ij}^2 x_{\Delta}(0) C a_j \end{aligned} \quad (14)$$

When  $x_{\Delta}(0) = 0$ , this equation is reduced to the one presented by Jyo and Ishibashi.<sup>11</sup>

When the external solution contains only the primary ion, then all terms containing  $a_i$  disappear and the primary ion activity at the membrane surface  $a_i(0)$  is given by

$$a_i(0) = a_i + x_{\Delta}(0)C \quad (15)$$

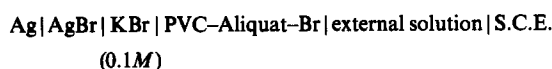
This means that when the analytical concentration, and in consequence the activity, is equal to 0, then the limit of detection,  $L$ , can be expressed as

$$L = x_{\Delta}(0)C - x_{\Delta}(0)c_s \frac{D\delta'}{D'\delta} \quad (16)$$

and depends on the concentration of ion-exchanger in the membrane,  $c_s$ , and on  $x_{\Delta}(0)$ , as well as on the term which contains the characteristics of both diffusion layers. Because  $x_{\Delta}(0)$  depends on the partition coefficient  $k_i$ , it can be shown that this agrees with the derivation presented by Kamo *et al.*<sup>3,4</sup> In their notation, the detection limit is related to  $\sqrt{A_x}$ , where  $A_x = 4\sigma^2/b_x$ ,  $\sigma$  being the total concentration of ion-exchanger in the membrane and  $b_x$  the difference between the standard chemical potentials of the exchanger in the aqueous and membrane phases. In their equation Jyo and Ishibashi<sup>11</sup> do not explicitly mention the detection limit, but in their earlier paper<sup>12</sup> it was suggested that the limit of detection is determined by the leakage of the ion-exchanger into the aqueous solution. The experimental proof of the dependence on the exchanger concentration was also reported.<sup>3,12,13</sup>

#### EXPERIMENTAL

The electrode membrane was prepared as described elsewhere,<sup>10</sup> with 67% Aliquat-Br and 33% PVC. The total Aliquat concentration in the membrane was 0.002M. The e.m.f. was measured in the cell



with an LM1604 DC digital voltmeter (Solartron).

The external solution was either unstirred (velocity  $v_0$ ) or stirred with a magnetic bar at three different velocities ( $v_1, v_2, v_3$ ), the rate of rotation ( $\omega$ ) of the stirring bar being 2.4, 10.4 and 20 rps respectively. The electrode was situated at a distance  $r = 2$  cm from the stirring axis, so the linear velocity under the electrode could be assumed as constant and equal to 30, 130 and 250 cm/sec for  $v_1, v_2$  and  $v_3$  respectively.

Potential response functions were obtained in solutions of potassium chloride, bromide and thiocyanate. Between measurements the electrode was removed from the solution, then again immersed after appropriate additions and thorough mixing. A selected stirring rate was then applied, and the potential response was recorded after 5 min. During the last minute the drift of e.m.f. was not larger than 0.5 mV.

The ion activities were calculated by using the Debye-Hückel theory as shown by Meier *et al.*<sup>14</sup>

The selectivity coefficients  $K_{Br, X}^{Br}$  were evaluated by the separate solution method with 0.1M KCl, KBr or KSCN. For chloride and thiocyanate as interferents the selectivity coefficients were 0.16 and 80, respectively.

The membrane composition was estimated by HPLC with the Trilab 2000 chromatography data system, a Bruker LC

21-B pump and a Perkin-Elmer LC-55 spectrophotometer. The column packing used was PL-Gel 100A, 5  $\mu\text{m}$ . Chloroform was used as eluent at a flow-rate of 1 ml/min and a pressure of 4.6–4.7 MPa.

#### RESULTS AND DISCUSSION

The potential response function of the Aliquat-Br electrode in chloride, bromide and thiocyanate solutions was measured with and without stirring (Fig. 2). The values of  $C$  and  $x_{\Delta}(0)$  were obtained as follows. For each stirring rate three curves based on equation (13) (for  $\text{Cl}^-$ ,  $\text{Br}^-$ ,  $\text{SCN}^-$ ) were fitted to the three sets of experimental points simultaneously, *i.e.*, the sum of the squares of the residuals was minimized. The values of  $C$  and  $x_{\Delta}(0)$  for different ions are

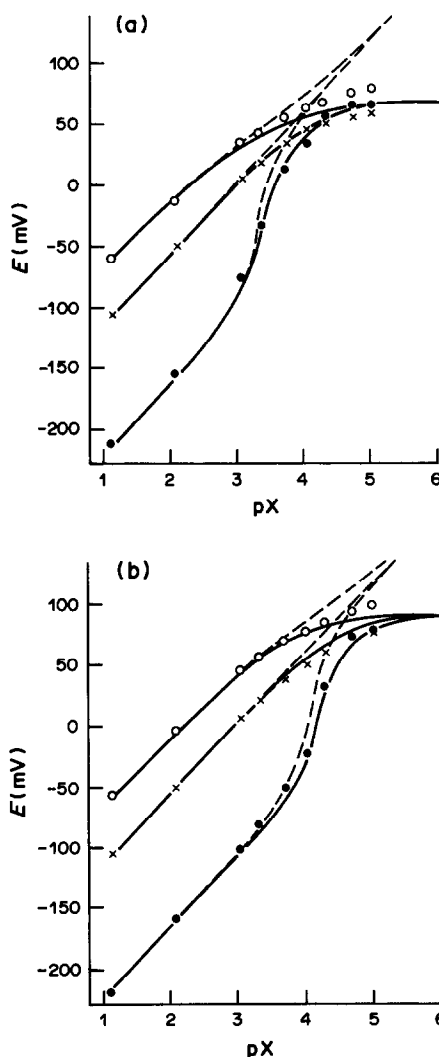


Fig. 2. Response pattern of bromide liquid-membrane electrode Aliquat 336S-Br, PVC: a, unstirred solution; b, maximal stirring rate ( $v_3$ ). Experimental points:  $\circ$ — $\text{Cl}^-$ ,  $\times$ — $\text{Br}^-$ ,  $\circ$ — $\text{SCN}^-$ ; solid lines—theoretical curves calculated from equation (13); dashed lines—theoretical curves calculated from the Jyo and Ishibashi equation.<sup>11</sup> Set of parameters: a,  $x_{\Delta}(0) = 0.14$ ,  $C = 5.3 \times 10^{-4}$ ; b,  $x_{\Delta}(0) = 0.32$ ,  $C = 9.0 \times 10^{-5}$ .

Table 1. Calculated and experimental values of  $x_A(0)$ 

pBr	Stirring rate	$\Delta a_i \times 10^5$	$x_A(0)$	
			calc.	exper.
5.0	$v_3$	3.5	0.43	0.32
4.7		3.9		
4.3		4.0		
4.0		4.2		
5.0	$v_2$	4.3	0.36	0.27
4.7		4.5		
4.3		4.4		
4.0		4.3		
5.0	$v_1$	7.5	0.29	0.22
4.7		7.4		
4.3		6.2		
4.0		6.6		
5.0	$v_0$	9.6	0.16	0.14
4.7		9.4		
4.3		7.8		
4.0		7.1		

assumed to be equal at constant stirring rate. The values of  $K_{\text{Br,Cl}} = 0.16$ ,  $K_{\text{Br,SCN}} = 80$ ,  $E^0 = -170.06$  mV and  $S = 57.97$  mV/decade used were those obtained from the experiments.

Comparison of the curves calculated according to equation (13) and the equation used by Jyo and Ishibashi<sup>11</sup> shows excellent agreement for concentrations higher than  $10^{-3}M$ . The functions calculated with the aid of both equations practically coincide. For lower ion activities, however, the curves based on equation (13) fit the experimental points well, whereas the curves calculated according to Jyo and Ishibashi do not. This discrepancy can be attributed to these authors' invalid assumption of constancy of the ion-exchanger concentration in the membrane cross-section. When both activities  $a_i$  and  $a_j$  approach zero, then according to the Jyo and Ishibashi model<sup>11</sup> the logarithmic term in the Nikolskii equation tends to minus infinity, which is in obvious disagreement with the experimental results. At limitingly low activities, the potential response in the absence of all interferents approaches a definite limiting potential value which is due to partition of the electrode-active material between the membrane and the external solution.

Table 2. The set of parameters evaluated for various stirring rates: exchange reaction constants  $K_{\text{Br,Cl}} = 0.16$ ,  $K_{\text{Br,SCN}} = 30$ ,  $E^0 = -170.06$  mV,  $S = 57.97$  mV/decade (experimental values)

Stirring rate	$x_A(0)$	$C$
$v_0$	0.14	$6.3 \times 10^{-4}$
$v_1$	0.22	$2.4 \times 10^{-4}$
$v_2$	0.27	$1.2 \times 10^{-4}$
$v_3$	0.32	$9.0 \times 10^{-5}$

The role of this partition is usually underestimated in analytical practice, as well as in theoretical considerations, in spite of the fact that there is general agreement that such processes have a pronounced effect on the limit of detection.

Clear evidence for a drastic change in membrane composition was obtained by gel permeation chromatography, for a membrane kept for 7 days in continuously stirred water. Removal of the ion-exchanger from the membrane was nearly quantitative. The changes in membrane composition were also investigated with neutral carrier membranes by a similar procedure.<sup>15</sup> The results were confirmed by elemental analysis of membranes freshly prepared and after leaching for 5 days with water. During this period the decrease in Aliquat 336S content, as measured by the nitrogen content, was close to 50%. In all these experiments, the equilibrium concentration of Aliquat 336S in the water, calculated from the amount leached out of the membrane, was in the range  $2-4 \times 10^{-5}M$ . This is in fair agreement with the  $\Delta a_i = a_i(0) - a_i$  values (Table 1) obtained from the potentiometric measurements.

The depletion of ion-exchanger in the diffusion layer of the membrane compared with the concentration on the inside of the membrane is represented by the mole fraction  $x_A$ , in our theoretical presentation. For given experimental conditions (stirring rate) the value of  $x_A$  was assumed to be constant, and independent of the ion-activity in the bulk of the external solution. This is only an approximation because an increase of ion-activity would without doubt inhibit the loss of ion-exchanger from the membrane, and thus decrease the value of  $x_A(0)$ . Despite that, the assumption made seems to be justified by the fact that for concentrations above  $10^{-3}M$  the potential response functions calculated by using equation (13) and that of Jyo and Ishibashi<sup>11</sup> are the same, and the estimated value of  $x_A(0)$  in the range from  $10^{-5}$ – $10^{-4}M$  potassium bromide is practically constant under given experimental conditions (Table 1).

The estimation of  $x_A(0)$  was based on the difference  $\Delta a_i = a_i(0) - a_i$  measured experimentally in the range  $10^{-5}$ – $10^{-4}M$  bromide at fixed stirring rate. From equation (5a), assuming  $x_i(\delta) = 1$ , and  $x_i(0) = 1 - x_A(0)$ , the depletion fraction can be calculated as

$$x_A(0) = \frac{\Delta a_i}{C} \quad (17)$$

where  $C$  is constant under given conditions. The value of  $C$  was taken as one of the two parameters of the curves calculated by using equation (13).

The agreement between the experimental points and the curve calculated by using equation (13) was tested for the unstirred solution and for three different stirring rates. The points fit sufficiently well in all cases, as shown for the unstirred solution and for the highest stirring rate,  $v_3$  (Fig. 2). The trend of

the empirical parameters  $x_A(0)$  and  $C$  is in accord with expectation (Table 2). The value of  $C$  given by Morf<sup>2</sup> according to Jyo and Ishibashi<sup>11</sup> is  $1.8 \times 10^{-4}$ , which is of the same order of magnitude as our results in Table 2. The more rapid stirring decreases the

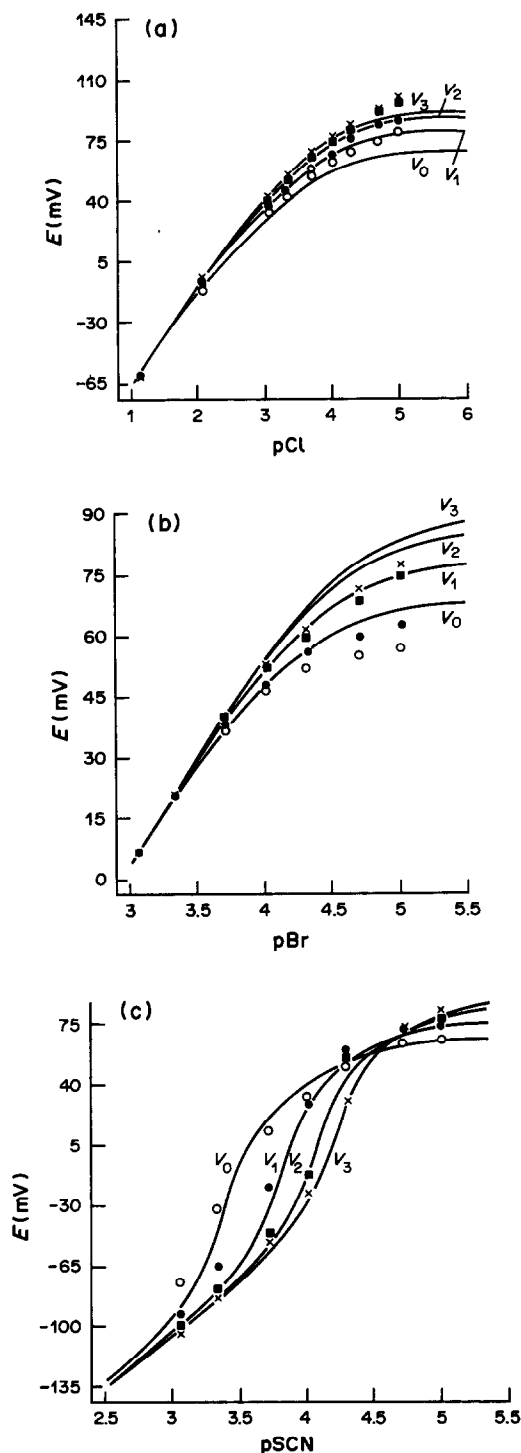


Fig. 3. Response pattern of bromide electrode in unstirred ( $v_0$ ) and stirred ( $v_1, v_2, v_3$ ) solutions: a, in chloride; b, in bromide; c, in thiocyanate solutions. Set of parameters: see Table 2.

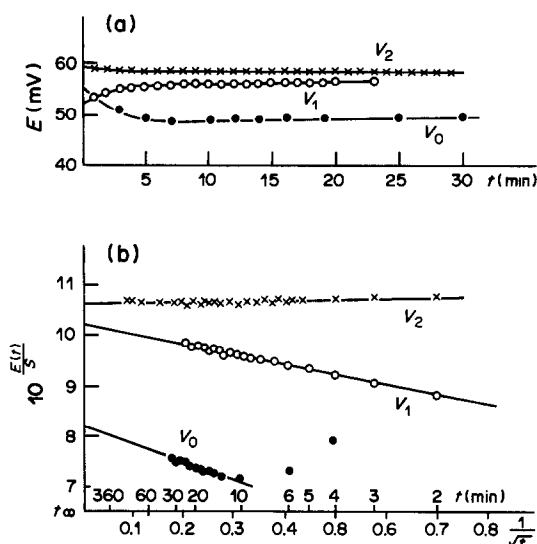


Fig. 4. Determination of steady-state potential of bromide electrode (unstirred— $v_0$ , stirred— $v_1, v_2$ ) in  $5 \times 10^{-5} M$  KBr: a, changes of potential values with time; b, extrapolation of  $10^{E(t)/S}$  to  $t \rightarrow \infty$  by linear regression (curve fit based on  $E(t) = E(\infty) + S \log(c/\sqrt{t})$ ).

thickness of the diffusion layer,  $\delta'$  in the external solution and thus  $C$  becomes smaller. Similarly  $x_A(0)$  increases, indicating more vigorous removal of the exchanger from the membrane.

The ratios of the experimentally observed  $C$  values for the different stirring rates  $v_1, v_2$  and  $v_3$  are  $C_1:C_2:C_3 = 20:12:9$ . If the thicknesses of the diffusion layer are inversely proportional to the square root of the flow velocities then these ratios should be  $C_1:C_2:C_3 = 20:14.4:6.9$ .

The predicted changes of potential response for the various stirring rates are in fair agreement with the experimental data (Fig. 3). Over the range of stirring rates investigated the measured potential changes by significant amounts, from approximately 20 mV for chloride and bromide, to several tens of mV for thiocyanate. Such a potential shift, which is observed for concentrations below  $10^{-3} M$  was until now underestimated. The general opinion was that in stirred solution the equilibrium potential is attained more rapidly but its value should not differ from that in unstirred solution. A better fit of the theoretical curves to the experimental points could be obtained by individual calculation, but only at the cost of losing the assumed constancy of  $C$  and  $x_A(0)$  and hence loss of insight into the mechanism.

The rate of attainment of a steady potential in the  $5 \times 10^{-5} M$  potassium bromide solution is different for various stirring rates (Fig. 4a). By extrapolation of  $10^{E(t)/S}$  as a function of  $1/\sqrt{t}$  (Fig 4b) it can be shown that  $E(\infty)$ , i.e., the potential response after a sufficiently long time  $t(\infty)$ , differs by even more than 10 mV, thus also influencing the limit of detection.

This discussion may also lead to some practical analytical consequences. In solutions stirred at a

constant but relatively high rate, the limit of detection for the primary ion can be improved. On the other hand, measurements in the presence of interferents with  $K_{ij} \gg 1$  are less affected by interference when the solution is not stirred.

*Acknowledgements*—The authors are greatly indebted to Dr. Daniel Ammann and Dr. Urs Oesch (ETH, Zürich) for fruitful discussions and to Miss Gabriela Suter (ETH, Zürich) for performing the gel permeation chromatography.

This research was partially supported by projects MR-I-32 and CPBP-01-17.

#### REFERENCES

1. H. Freiser (ed.), *Ion-selective Electrodes in Analytical Chemistry*, Plenum Press, New York, 1978.
2. W. E. Morf, *The Principles of Ion-selective Electrodes and of Membrane Transport*, Akadémiai Kiadó, Budapest; Elsevier, Amsterdam, 1981.
3. N. Kamo, N. Hazemoto and Y. Kobatake, *Talanta*, 1977, **24**, 111.
4. N. Kamo, Y. Kobatake and K. Tsuda, *ibid.*, 1980, **27**, 205.
5. D. Midgley, *Anal. Chem.*, 1977, **49**, 1211.
6. S. Kihara and Z. Yoshida, *Talanta*, 1984, **31**, 789.
7. T. Kakiuchi and M. Senda, *Bull. Chem. Soc. Japan*, 1984, **57**, 1801.
8. T. Kakiuchi, I. Obi and M. Senda, *ibid.*, 1985, **58**, 1636.
9. A. Hulanicki and Z. Augustowska, *Anal. Chim. Acta*, 1975, **78**, 261.
10. A. Hulanicki and R. Lewandowski, *Chem. Anal. Warsaw*, 1974, **19**, 53.
11. A. Jyo and N. Ishibashi, private communication in ref. 2, p. 262.
12. N. Ishibashi and A. Jyo, *Microchem. J.*, 1973, **18**, 220.
13. N. Ishibashi, H. Kohara and N. Uemura, *Bunseki Kagaku*, 1972, **21**, 1072.
14. P. C. Meier, D. Ammann, W. E. Morf and W. Simon, in *Medical and Biological Applications of Electrochemical Devices*, J. Koryta (ed.) Wiley, Chichester, 1980.
15. D. Ammann, *Ion-Selective Microelectrodes*, Springer-Verlag, Berlin, 1986.

## MEASUREMENT OF NANOMOLAR LEVELS OF PSYCHOACTIVE DRUGS IN URINE BY ADSORPTIVE STRIPPING VOLTAMMETRY

LUCAS HERNANDEZ, ANTONIO ZAPARDIEL, JOSE ANTONIO PEREZ LOPEZ  
and ESPERANZA BERMEJO

Department of Chemistry, Autonoma University, 28049 Madrid, Spain

(Received 10 August 1987. Accepted 30 October 1987)

**Summary**—Adsorptive stripping voltammetry was used to determine nanomolar levels of the benzodiazepines pinazepam, camazepam, bromazepam and thienodiazepine (BrTDO) in urine. Measurements were made by differential pulse voltammetry at a hanging mercury drop electrode. The influences of various operational conditions on the stripping response were examined. The optimum accumulation potentials and accumulation times were  $-0.40$  V and up to 60 sec for pinazepam,  $-0.60$  V and up to 40 sec for camazepam,  $-0.40$  V and up to 30 sec for bromazepam and  $-0.60$  V and up to 60 sec for BrTDO, respectively. The effects of various urine components on the voltammetric response were also studied, and preliminary separation of the drugs was found necessary because of interference by creatinine and uric acid. The proposed method is appropriate for the determination of the four drugs in urine up to the 1000 ng/ml level with short accumulation periods (10–60 sec). The relative standard deviation for the 500 ng/ml level of the drugs in urine (30-sec accumulation) was less than 3%.

Benzodiazepines are a group of drugs primarily used as anxiolytics and hypnotics. Administration is usually oral, absorption varies from 0.5 to 6 hr, depending on the compound, and excretion takes place through the kidney. The extensive use made nowadays of benzodiazepine derivatives calls for control of such compounds in biological fluids since, despite having a wide therapeutic margin, they are not completely free from contraindications and adverse side-effects. Dose adjustment, toxicological control and evaluation of the interferences of these drugs in other laboratory analyses are all factors that justify the need for such determinations. Urine is widely analysed as an aid to diagnosis and to check the treatments prescribed for various diseases, because it provides relevant information on metabolic disorders, drug overuse and identification of toxicological states, and offers the great advantage of being the only practical laboratory sample available for diagnosing the severity of certain types of poisoning. Many drugs, including the benzodiazepines, interfere with common laboratory analyses, giving false readings for barbiturates, alkaloids, corticosteroids, glucose, etc. Knowledge of their presence in urine is therefore important if wrong results and mistaken diagnoses are to be avoided.

Adsorptive stripping voltammetry is a relatively recent technique that has proved sensitive for the determination of a great number of pharmaceutical compounds that can be adsorbed at an electrode surface. The technique uses controlled interfacial accumulation of the analyte on the working electrode as a preconcentration step before the voltammetric measurement of the surface-bound species. Pro-

cedures for determining important drugs, at down to  $10^{-10}$ – $10^{-9}$  M levels, have been reported for cardiac glycosides,<sup>1</sup> tetracyclines,<sup>2</sup> tricyclic antidepressants,<sup>3</sup> streptomycin,<sup>4</sup> nitrazepam and diazepam,<sup>5</sup> diltiazem,<sup>6</sup> antitumour agents,<sup>7–9</sup> benzodiazepines and thienodiazepines in human serum,<sup>10,11</sup> and many other drugs.<sup>12,13</sup>

Gas and liquid chromatography, thin-layer chromatography and HPLC with different detectors are the techniques most frequently used for detection and determination of the drugs under study in biological fluids.<sup>10,11</sup> Voltammetric and polarographic methods, usually differential pulse polarography, have also been described, but are generally not sensitive enough.<sup>10,11,14,15</sup>

In the present work the determination of benzodiazepines and thienodiazepines in urine was studied by adsorptive stripping voltammetry. Nanomolar levels of pinazepam, camazepam, bromazepam and BrTDO in urine can be measured after controlled analyte accumulation at the hanging mercury drop electrode. The structures of the drugs used are shown in Fig. 1. Conditions for enhancing the surface concentration of the drugs have been carefully optimized. In addition to the analytical utility of the study, the interfacial redox data found can offer a better understanding of the drugs' activity in urine.

### EXPERIMENTAL

#### Apparatus

To allow complete automation of the stripping procedure a Metrohm 646 VA processor, together with a 647 VA stand was chosen. The hanging mercury drop electrode used was a multimode type (Metrohm 6.1246.020), and the surface

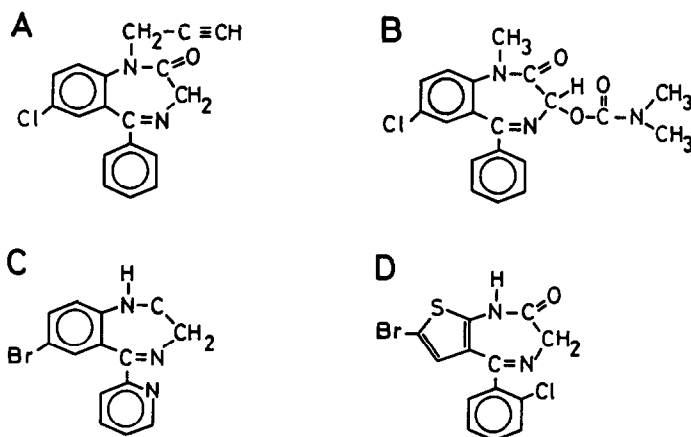


Fig. 1. Structures of the drugs: (A) pinazepam, (B) camazepam, (C) bromazepam and (D) BrTDO.

area of the drop was 0.60 mm<sup>2</sup>. The auxiliary electrode was a glassy-carbon rod (2 × 65 mm) and an Ag/AgCl/3M KCl reference electrode was used. The solution was stirred with a built-in rotor. All measurements were performed at room temperature and all potentials are expressed with respect to the Ag/AgCl/3M KCl electrode.

#### Reagents

Stock solutions (1.00 × 10<sup>-3</sup>M) of pure pinazepam (Zambeletti), camazepam (Farmasimes), bromazepam and BrTDO (Roche) were prepared by dissolving the compounds in methanol. The solutions were stored in the dark under refrigeration to minimize the risk of decomposition; 1.00 × 10<sup>-5</sup>M solutions were prepared daily from the stock solutions.

The supporting electrolytes were Britton–Robinson, acetate and phosphate buffers, of different ionic strengths. All chemicals were analytical-reagent grade (Merck). Aqueous solutions were prepared in purified water (Milli Q and Milli Ro, Millipore). Urine samples from five human subjects were combined for use.

#### Procedures

**Treatment of urine samples.** A Waters Associates Sep-pak C<sub>18</sub> cartridge was activated with 5 ml of methanol and rinsed twice with 3 ml of water. The cartridge was then buffered at pH 7.0 with 2 ml of 0.04M Britton–Robinson buffer (for bromazepam, pinazepam and BrTDO) or at pH 9.2 with 2 ml of 0.01M sodium tetraborate (for camazepam), after which the drug was separated by passing 1 ml of urine (containing 100–1000 ng of the drug) through the cartridge, where the drug was retained. The cartridge was washed with 4 ml of a methanol/water mixture (1:3 v/v) and then rinsed with 2 ml of water. The drugs were eluted with two 2-ml portions of diethyl ether and the combined eluent was evaporated under a stream of nitrogen. The resultant residue was dissolved in 200 μl of methanol and diluted to 25 ml with Britton–Robinson buffer of pH 4.0 (for pinazepam), or pH 5.0 (for bromazepam and BrTDO) or with acetate buffer of pH 5.0 (for camazepam). The solutions thus obtained were ready for voltammetric analysis.

**Adsorptive stripping voltammetry.** Adequate deoxygenation was obtained by passing nitrogen through the solution for 10 min before the initial cycle and for 30 sec before each successive cycle. The accumulation potential appropriate for each drug was applied to the working electrode (HMDE) while the solution was continuously stirred. After a 10-sec rest-time a scan towards more negative potentials was initiated for differential pulse voltammetry (pulse amplitude 70 mV and scan-rate 20 mV/sec) or by linear scan voltammetry (scan-rate 40 mV/sec) and the corresponding voltamperograms were recorded.

#### RESULTS AND DISCUSSION

The electrochemical studies conducted on the drugs under consideration indicate that adsorption takes place on the electrode surface during the drug reduction. This adsorption can be used as an effective preconcentration step prior to voltammetric measurement.

Figure 2 shows repetitive cyclic voltamperograms for 1.06 × 10<sup>-7</sup>M camazepam in 0.04M acetate buffer at pH 5.0 and for 1.28 × 10<sup>-7</sup>M bromazepam in 0.04M Britton–Robinson buffer at pH 5.0.

When the solutions were stirred for 180 sec at -0.60 V for camazepam and 90 sec at -0.40 V for bromazepam before the cyclic potential scans were started, only one irreversible cathodic peak, at -0.93 V for camazepam and at -0.58 V for bromazepam, was observed in the first scan (marked 1 in Fig. 2). Similar peaks were obtained for pinazepam at -0.81 V and BrTDO at -0.89 V, but they are not shown in the figure. Such peaks can be attributed to the reduction of the azomethine group of the adsorbed species. The second and third scans (marked 2 and 3 in Fig. 2) showed a drastic reduction in the heights of the cathodic peaks, with a slight shift towards more positive values, which is an indication of the quick desorption of the product from the electrode surface. Subsequent scans also gave the same response, the peak being smaller by a factor of 36.5 for camazepam and 35 for bromazepam than that obtained in the initial scan.

For the drugs under discussion, the voltammetric responses obtained with the linear scan and differential pulse waveforms make it advisable to use the differential pulse stripping mode because, although the peak shapes are similar in both cases, the peak height is about 5 times greater.

Figure 3 shows differential pulse voltamperograms for 1.21 × 10<sup>-7</sup>M pinazepam, 1.06 × 10<sup>-7</sup>M camazepam, 1.28 × 10<sup>-7</sup>M bromazepam and 8.13 × 10<sup>-8</sup>M BrTDO, with accumulation times of 180, 180, 90 and 480 sec, respectively; the voltamperograms without accumulation are shown by broken lines. Short accu-



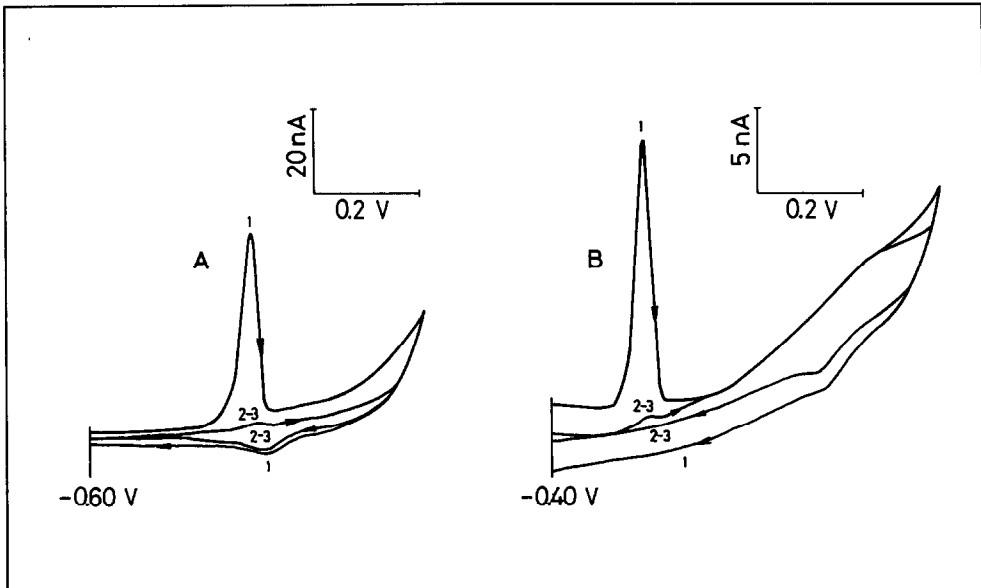


Fig. 2. Repetitive cyclic voltamperograms for: (A)  $1.06 \times 10^{-7} M$  camazepam in  $0.04 M$  acetate buffer at pH 5.0 (180 sec at  $-0.60 V$ ) and (B)  $1.28 \times 10^{-7} M$  bromazepam in  $0.04 M$  Britton-Robinson buffer at pH 5.0 (90 sec at  $-0.40 V$ ). Scan-rate  $40 mV/sec$ .

mulation periods cause a substantial enhancement in peak height under the conditions stated in Fig. 3 (14 times higher for pinazepam, 15 for camazepam, 13 for bromazepam and 33 for BrTDO). Well-defined stripping peaks were observed for all the compounds. Stripping potentials were  $-0.85 V$  for pinazepam,  $-0.92 V$  for camazepam,  $-0.57 V$  for bromazepam

and  $-0.89 V$  for BrTDO. With the procedure above, highly sensitive determinations of the compounds can be achieved by differential pulse adsorptive stripping voltammetry.

Results in adsorptive stripping voltammetry are often complicated by the presence of other substances capable of adsorption at the electrode surface, which

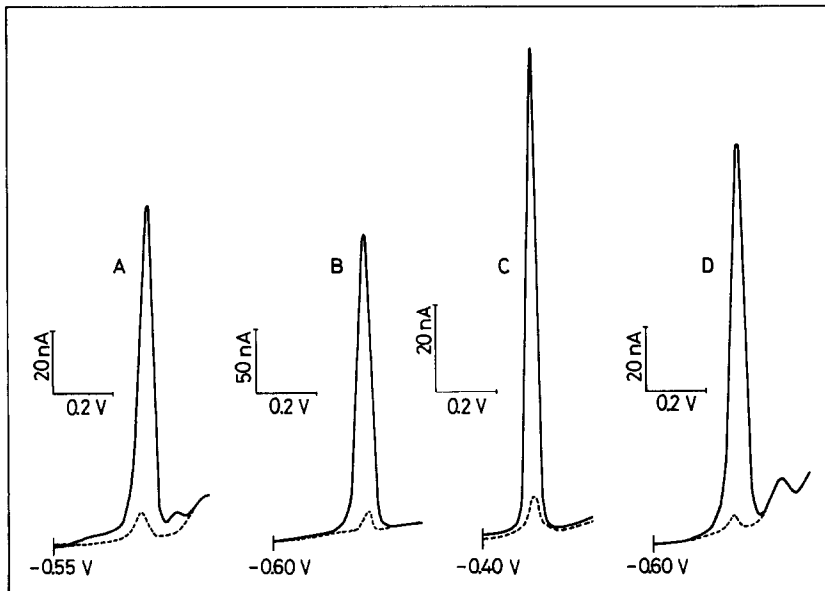


Fig. 3. Differential-pulse adsorptive stripping voltamperograms: (A)  $1.21 \times 10^{-7} M$  pinazepam in  $0.04 M$  Britton-Robinson buffer at pH 4.0 (180 sec at  $-0.55 V$ ), (B)  $1.06 \times 10^{-7} M$  camazepam in  $0.04 M$  acetate buffer at pH 5.0 (180 sec at  $-0.60 V$ ), (C)  $1.28 \times 10^{-7} M$  bromazepam in  $0.04 M$  Britton-Robinson buffer at pH 5.0 (90 sec at  $-0.40 V$ ) and (D)  $8.13 \times 10^{-8} M$  BrTDO in  $0.04 M$  Britton-Robinson buffer at pH 5.0 (480 sec at  $-0.60 V$ ). Scan-rate  $20 mV/sec$ ; pulse amplitude  $70 mV$ . The broken line represents the voltamperograms obtained without accumulation.

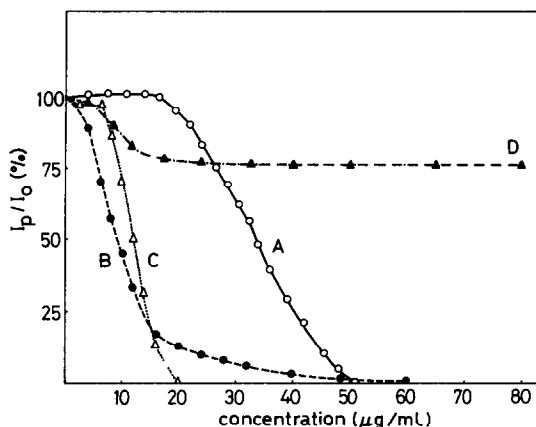


Fig. 4. Effects of various urine components on stripping peak current for  $5.34 \times 10^{-8} M$  camazepam, with 30 sec accumulation time at  $-0.60 V$ : (A) creatinine, (B) uric acid, (C) albumin and (D) glucose. Other conditions as in Fig. 3.

prevent the analytes from being adsorbed. For that reason, a study was made of the influence of various urine components on the stripping peak currents of the drugs. The following urine constituents were selected: creatinine ( $60 \mu g/ml$ ), glucose ( $4 \mu g/ml$ ), albumin ( $3.2 \mu g/ml$ ), uric acid ( $32 \mu g/ml$ ), urea ( $1200 \mu g/ml$ ), phosphate ( $40 \mu g/ml$ ), chloride ( $284 \mu g/ml$ ), potassium ( $125 \mu g/ml$ ) and lead ( $4 \mu g/ml$ ). The concentrations in brackets correspond to average values in the urine of healthy subjects, allowing for the 1:25 dilution for analysis adopted throughout this work.

Figure 4 shows the variation of the ratio between the peak current for camazepam after addition of a certain amount of each urine constituent and that in the absence of the constituent. The presence of creatinine and uric acid at concentrations of 9 and  $34 \mu g/ml$ , respectively, lowered the voltammetric response by 50% and at normal concentrations caused it to disappear almost entirely. Albumin and glucose at the low levels at which they are usually present in urine lower the signal only by 3 and 2%, respectively, causing almost no interference. It has also been proved that there is no interference from phosphate, chloride, potassium, lead and urea (not shown in Fig. 4) in amounts at least 4 times higher than those usually found in urine. The effect on the remaining drugs is similar to that on camazepam. The interferences caused by creatinine and uric acid necessitate the pretreatment of urine samples to isolate the drugs of interest.

For determination of the drugs in urine and optimization of the accumulation conditions, several factors must be investigated: nature of the solvent, ionic strength, mass transport, pH, potential and time. Some of these, and also some instrumental conditions, directly affect the voltammetric response, mainly the shape and reproducibility of the waves.

The effect of the pH and ionic strength of the electrolyte used was studied with different electrolytes

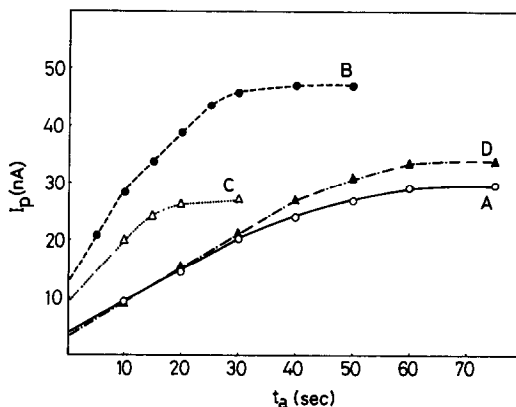


Fig. 5. Influence of accumulation time on voltamperogram peak current for drugs in urine: (A) pinazepam ( $661 \text{ ng/ml}$ ), (B) camazepam ( $700 \text{ ng/ml}$ ), (C) bromazepam ( $711 \text{ ng/ml}$ ) and (D) BrTDO ( $728 \text{ ng/ml}$ ). Other conditions as in Fig. 3.

(Britton–Robinson, acetate and phosphate buffers of different pH and ionic strength) to find the best conditions for obtaining the corresponding voltamperograms. The results showed that even though voltamperograms could be obtained for all four compounds with all the electrolytes tested, the largest peaks were obtained with  $0.04 M$  acetate buffer (pH 5.0) for camazepam,  $0.04 M$  Britton–Robinson buffer (pH 5.0) for bromazepam and BrTDO and  $0.04 M$  Britton–Robinson buffer (pH 4.0) for pinazepam. These optimal drug–buffer combinations were used for the rest of the study.

The influence of accumulation time on peak current was studied, with the results for drugs in urine shown in Fig. 5. An initial region of linear de-

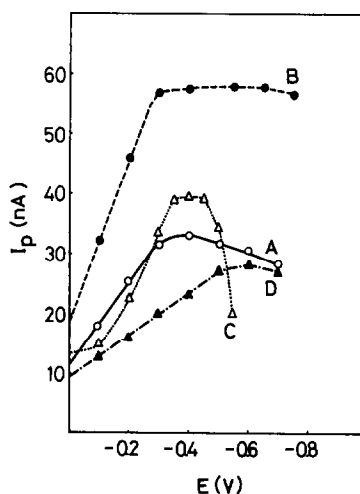


Fig. 6. Influence of accumulation potential on stripping peak current for drugs in urine: (A) pinazepam ( $944 \text{ ng/ml}$ ), (B) camazepam ( $1000 \text{ ng/ml}$ ), (C) bromazepam ( $1016 \text{ ng/ml}$ ) and (D) BrTDO ( $1040 \text{ ng/ml}$ ). Accumulation time 30 sec. Other conditions as in Fig. 3.

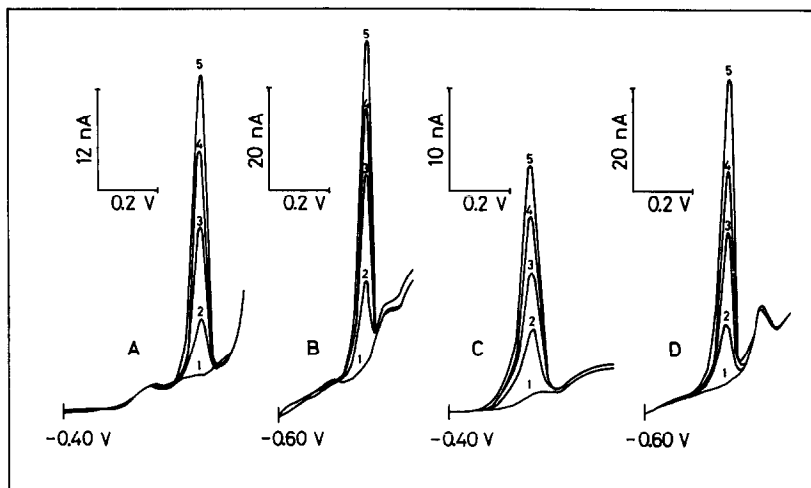


Fig. 7. Stripping peaks for different concentrations of (A) pinazepam ( $t_a = 30$  sec), (B) camazepam ( $t_a = 30$  sec), (C) bromazepam ( $t_a = 10$  sec) and (D) BrTDO ( $t_a = 60$  sec): (1) without drugs; (2) 283, 200, 203 and 208; (3) 472, 400, 406 and 520; (4) 661, 500, 610 and 728; and (5) 944, 700, 813 and 1040 ng per ml or urine, respectively. Other conditions as in Fig. 3.

pendence between peak current and accumulation time can be observed up to 30 sec (slope 0.53 nA/sec) for 661 ng/ml pinazepam, up to 10 sec (slope 1.80 nA/sec) for 700 ng/ml camazepam, up to 15 sec (slope 1.10 nA/sec) for 711 ng/ml bromazepam and up to 40 sec (slope 0.59 nA/sec) for 728 ng/ml BrTDO.

The results indicated the maximum accumulation times for drug concentrations up to 1000 ng/ml in urine to be 60 sec for pinazepam and BrTDO, 30 sec for bromazepam and 40 sec for camazepam.

The influence of accumulation potential on stripping peak current was studied at potentials between 0.0 and  $-0.75$  V for the four compounds. Figure 6 gives the results obtained and allows determination of the optimum accumulation potentials as  $-0.40$  V for bromazepam and pinazepam and  $-0.60$  V for BrTDO and camazepam.

The instrumental conditions that can affect voltammetric measurement—rest-time, drop size, stirring speed, pulse amplitude, scan-rate and pulse repetition—were all studied. The peak current remained constant when rest-times of 0–15 sec were used; a value of 10 sec was used in the rest of the study. For the remaining conditions, the optimum values were: 1920 rpm stirring speed, drop size (surface area)  $0.60$  mm<sup>2</sup>, pulse amplitude 70 mV, scan-rate 20 mV/sec and pulse repetition 0.4 sec.

Under the above-mentioned conditions, calibration plots were obtained for each of the four drugs. Table 1 summarizes the results obtained for different accumulation times, including characteristics of calibration plots, detection limits (estimated as the concentration corresponding to a signal to noise ratio of 3) and recovery tests.

Table 1. Results obtained for the determination of pinazepam, camazepam, bromazepam and BrTDO in urine at accumulation potentials of  $-0.40$ ,  $-0.60$ ,  $-0.40$  and  $-0.60$  V, respectively

Drug	Parameter	Accumulation time, sec				
		10	20	30	40	60
Pinazepam (recovery 89–92%)	Sensitivity, nA.ml.ng <sup>-1</sup>	0.015	0.024	0.031	0.039	0.047
	Correlation coefficient	0.9998	0.9997	0.9992	0.9996	0.9996
	Detection limit, ng/ml	50	30	25	20	15
	Linear response, ng/ml	200–1000	200–1000	100–1000	100–1000	100–700
Camazepam (recovery 89–93%)	Sensitivity, nA.ml.ng <sup>-1</sup>	0.040	0.060	0.068	0.079	—
	Correlation coefficient	0.990	0.991	0.992	0.995	—
	Detection limit, ng/ml	25	20	15	10	—
	Linear response, ng/ml	200–1000	100–1000	100–1000	100–1000	—
Bromazepam (recovery 92–96%)	Sensitivity, nA.ml.ng <sup>-1</sup>	0.026	0.035	0.041	—	—
	Correlation coefficient	0.9996	0.998	0.997	—	—
	Detection limit, ng/ml	30	25	20	—	—
	Linear response, ng/ml	100–1000	100–1000	100–1000	—	—
BrTDO (recovery 90–92%)	Sensitivity, nA.ml.ng <sup>-1</sup>	—	0.022	0.030	0.038	0.050
	Correlation coefficient	—	0.998	0.998	0.9991	0.9992
	Detection limit, ng/ml	—	45	30	25	20
	Linear response, ng/ml	—	100–1000	100–1000	100–1000	100–1000

The procedure described allows determination of the drugs in urine in the range 100–1000 ng/ml, with sensitivities of 0.015–0.079 nA.ml.ng<sup>-1</sup> ( $r = 0.990$ – $0.9998$ ). The mean relative errors are less than 5.5%, the determination limits between 40 and 170 ng/ml in urine, and recoveries in the range 89–96%. The method, moreover, is quick and fairly reproducible (relative standard deviations typically less than 3% for ten 500-ng/ml samples).

If necessary, higher amounts of the drugs can be determined by taking smaller volumes of sample. The standard addition method could also be used in the concentration range in which the response is linear.

*Acknowledgement*—The authors wish to thank CAICYT for financial support for this project (No. 2077-83).

#### REFERENCES

1. J. Wang, J. S. Mahmoud and P. A. M. Farias, *Analyst*, 1985, **110**, 855.
2. J. Wang, T. Peng and M. S. Lin, *Bioelectrochem. Bioenerg.*, 1986, **15**, 147.
3. J. Wang, M. Bonakdar and C. Morgan, *Anal. Chem.*, 1986, **58**, 1024.
4. J. Wang and J. S. Mahmoud, *Anal. Chim. Acta*, 1986, **186**, 31.
5. R. Kaldova, *ibid.*, 1984, **162**, 197.
6. J. Wang, P. A. M. Farias and J. S. Mahmoud, *Analyst*, 1986, **111**, 837.
7. J. Wang, Peng Tuzhi, M. S. Lin and T. Tapia, *Talanta*, 1986, **33**, 707.
8. J. Wang, M. S. Lin and V. Villa, *Analyst*, 1987, **112**, 247.
9. J. Wang, Tuzhi Peng and M. S. Lin, *Bioelectrochem. Bioenerg.*, 1986, **16**, 395.
10. L. Hernández, A. Zapardiel, J. A. Pérez López and E. Bermejo, *Analyst*, 1987, **112**, 1149.
11. *Idem*, *Bioelectrochem. Bioenerg.*, submitted for publication.
12. J. Wang, *Am. Lab.*, 1985, **17**, No. 5, 41.
13. W. F. Smyth, in *Electrochemistry, Sensors and Analysis*, M. R. Smyth and J. G. Vos (eds.), p. 29. Elsevier, Amsterdam, 1986.
14. H. Oelschläger, *Bioelectrochem. Bioenerg.*, 1983, **10**, 25.
15. M. A. Fernández Arciniega, *Ph.D. Thesis*, Autonoma University, Madrid, 1984.

# SIMULTANEOUS SPECTROPHOTOMETRIC DETERMINATION OF ERBIUM AND PRASEODYMIUM WITH 1-(2-PYRIDYLAZO)-2-NAPHTHOL IN THE PRESENCE OF OCTYLPHENOL POLY(ETHYLENEGLYCOL) ETHER (TX-100)

J. HERNANDEZ MENDEZ\*, B. MORENO CORDERO and J. L. PEREZ PAVON

Department of Analytical Chemistry, Faculty of Chemistry, University of Salamanca, Salamanca, Spain

(Received 5 November 1986. Revised 5 June 1987. Accepted 30 October 1987)

**Summary**—The optimum conditions for formation of Er-PAN and Pr-PAN complexes in micelles of TX-100 are described, and methods proposed for spectrophotometric determination of the two elements. The molar absorptivities were  $5.0 \times 10^4 \text{ l. mole}^{-1} \text{ cm}^{-1}$  for Er and  $4.6 \times 10^4 \text{ l. mole}^{-1} \text{ cm}^{-1}$  for Pr. A simple method is proposed for simultaneous determination of Er and Pr without previous separation, based on a micellar masking process.

For several years, the use of micellar media of tertiary metal-chromophore-surfactant systems has been a common practice in the spectrophotometric determination of metal ions, with a view to enhancing sensitivity and/or selectivity.<sup>1-4</sup> The solubilizing power of micellar systems has allowed investigators to speed up and simplify many common analytical procedures when the chromophore or chelate formed is insoluble or only slightly soluble in water, thus avoiding costly and tedious extractions and allowing determination in homogeneous medium.<sup>5,6</sup>

The growing importance of the rare-earth elements in advanced engineering and high-technology ceramics<sup>7-9</sup> and in special glasses has made it necessary to develop simple and rapid analytical methods for determining traces of these elements.

1-(2-Pyridylazo)-2-naphthol (PAN) has been widely employed both for the spectrophotometric determination of trace elements<sup>10</sup> and for the extraction and separation of lanthanides.<sup>11-13</sup> However, since the chelates obtained are insoluble in water, they are usually made in aqueous alcohol media or extracted into non-polar solvents.<sup>11,14,15</sup>

In the present work we describe the spectrophotometric behaviour of the Er-PAN and Pr-PAN systems solubilized in micelles of TX-100. A method is also proposed for the simultaneous determination of Er and Pr without their previous separation.

## EXPERIMENTAL

### Reagents

Standard solutions of Er and Pr were prepared by dissolution of suitable amounts of the oxides (99.9% pure, Sigma) in small volumes of concentrated hydrochloric acid,

followed by dilution with distilled water. The  $4 \times 10^{-3} M$  solution of PAN (Merck, 99% pure) was prepared by dissolving 0.100 g in 100 ml of absolute ethanol. Aqueous solutions of octylphenol poly(ethylene glycol) ether (TX-100, Merck) (100 g/l), and tris(hydroxymethyl) aminomethane (tris) (1M) and boric acid/borate (0.20M) buffer solutions were also prepared.

### Apparatus

A Varian Techtron spectrophotometer model 635 with a Radiometer Rec.61 recorder and 1.0-cm optical path cuvettes was used. The pH values were measured with a PHM 51 pH-meter.

### General procedure

For calibration for the individual elements, add to 5.0 ml of buffer solution, in the following order,  $x$  ml of  $4 \times 10^{-3} M$  PAN (5.0 ml for Er and 10.0 ml for Pr), a sufficient amount of TX-100 for the TX-100/PAN w/w ratio to be 100 for Er and 75 for Pr, and various amounts of the element of interest, and let stand for 30 min. Measure the absorbance at 535 nm against a blank. Analyse samples containing either Er or Pr (but not both), by the same procedure.

For simultaneous determinations, obtain the sum of Er and Pr by measuring the absorbance at 535 nm in a medium buffered at pH 9.2 (boric acid/borate) and a TX-100/PAN w/w ratio of 75. To determine Er in the presence of Pr buffer the medium at pH 7.6 (tris buffer) and make the TX-100/PAN w/w ratio 50. In both cases measure the absorbance at 535 nm after 30 min.

## RESULTS AND DISCUSSION

### Absorption spectra

Figure 1 shows the absorption spectra of the Er-PAN and Pr-PAN systems in 0.02M boric acid borate medium (pH 9.2) in the presence (—) and absence of TX-100 (---) following extraction of the chelates into diethyl ether, which according to Shibata<sup>11</sup> is the most suitable medium for the individual determination of these elements. For both Er and

\*Author for correspondence.

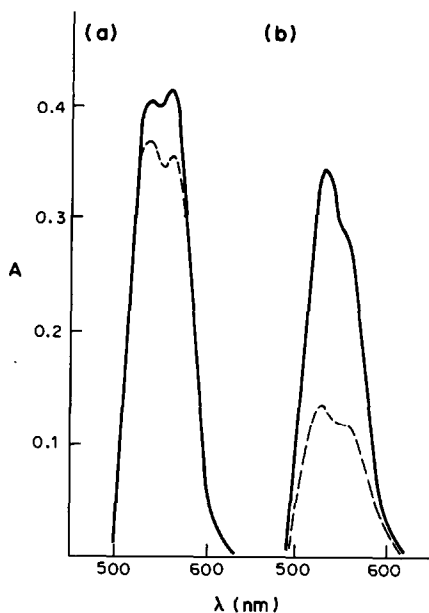


Fig. 1. Absorption spectra of Er-PAN (a) and Pr-PAN (b): (—) in the presence of TX-100; (---) extracts in diethyl ether. (a)  $8.0 \times 10^{-6}M$  Er,  $8.0 \times 10^{-5}M$  PAN, 0.10 g/mg TX-100/PAN. (b)  $8.0 \times 10^{-6}M$  Pr,  $8.0 \times 10^{-5}M$  PAN, 0.075 g/mg TX-100/PAN.

Pr the spectra obtained under the two sets of conditions were similar; Er exhibits two absorption maxima at 535 and 560 nm and Pr shows a maximum at 535 and a shoulder at 560 nm. However, it should be noted that the chelates are unstable in diethyl ether medium, particularly that of Pr. This is a drawback for analytical purposes.

In the presence of micelles of TX-100, the behaviour of both systems is modified: the absorbance increases with time until a constant value is reached, and the solutions are stable.

It should be stressed that both the time needed for the colour to develop and the maximum absorbance reached do not depend, as is usually the case, on the total concentration of surfactant, but rather on the TX-100/PAN ratio; this is the starting point for the simultaneous determination of both elements, since

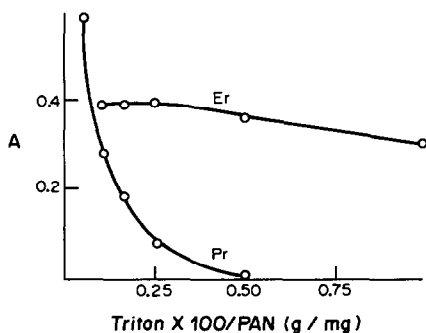


Fig. 2. Effect of TX-100/PAN ratio on the absorbance:  $8.0 \times 10^{-6}M$  Er,  $1.6 \times 10^{-5}M$  Pr,  $8.0 \times 10^{-5}M$  PAN, pH = 9.2 (0.02M borate buffer),  $\lambda = 535$  nm,  $t = 30$  min.

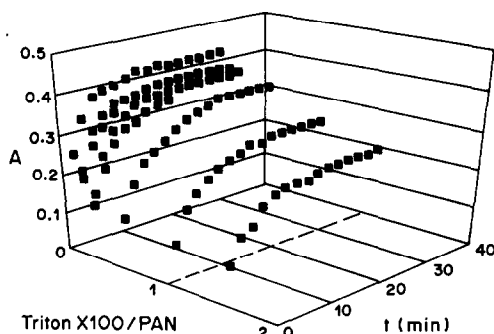


Fig. 3. Variations of absorbance with time and TX-100/PAN ratio:  $8.0 \times 10^{-6}M$  Er,  $8.0 \times 10^{-5}M$  PAN, pH = 9.2 (0.02M borate buffer),  $\lambda = 535$  nm.

the Pr signal disappears as a result of micellar masking when the TX-100/PAN w/w ratio is greater than 50 (Fig. 2). The influence of the reaction time and TX-100/PAN ratio on the Er-PAN and Pr-PAN systems is shown in Figs. 3 and 4.

The absorbance of the Er-PAN and Pr-PAN systems in the presence of TX-100 is strongly affected by the pH of the medium (Fig. 5); for both systems bell-shaped curves are obtained with plateaux at pH values between 7 and 9 for Er, and 8 and 10 for Pr. This difference could be utilized alone for determination of both elements in the same solution, but in this work was used in conjunction with micellar masking of the Pr signal.

The mole-ratio and slope-ratio methods show that the stoichiometry of both complexes is 1:3 (Me: PAN). This ratio differs from the values reported by other authors. Shibata<sup>11</sup> found a stoichiometry of 1:2 for the chelates extracted into diethyl ether; Czakis-Sulikowska *et al.*<sup>12,13</sup> found it to be 1:1 in several alcohol-water media, and Navratil<sup>16</sup> found a ratio 1:4. However, Rao *et al.*<sup>17,18</sup> describe a 1:3 complex in 20% (v/v) ethanol. The different stoichiometry found for the chelates formed in micellar media can be ascribed to a rearrangement of the water molecules surrounding the metal ion, which would modify their co-ordination capacity. Similar effects have been reported by other authors.<sup>19</sup>

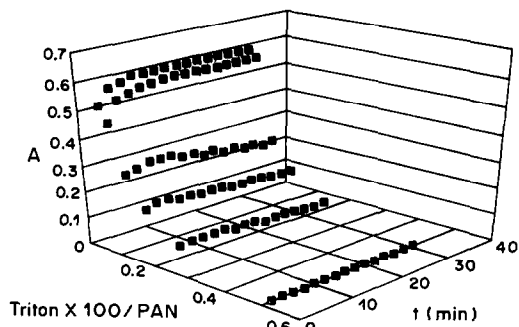


Fig. 4. Variations of absorbance with time and TX-100/PAN ratio.  $1.6 \times 10^{-5}M$  Pr,  $8.0 \times 10^{-5}M$  PAN, pH = 9.2 (0.02M borate buffer),  $\lambda = 535$  nm.

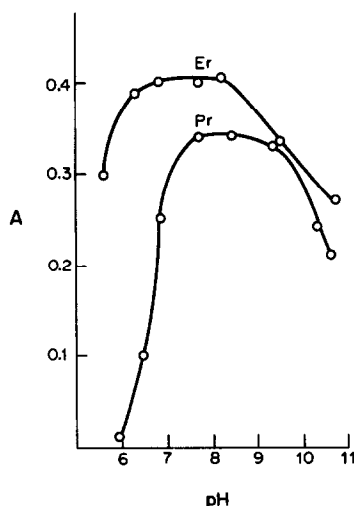


Fig. 5. Effect of pH on the absorbance:  $8.0 \times 10^{-6} M$  Er and Pr,  $8.0 \times 10^{-5} M$  PAN, 0.10 g/mg TX-100/PAN for Er and 0.075 g/mg TX-100/PAN for Pr,  $\lambda = 535$  nm.

#### Analytical characteristics of the individual determinations

The Er-PAN system obeys Beer's law up to 6.0  $\mu\text{g/ml}$  in the final solution, at 535 nm in buffered medium at pH 9.2 and in the presence of a TX-100/PAN w/w ratio of 100. For the Pr-PAN system, with a TX-100/PAN w/w ratio of 75, and otherwise identical conditions Beer's law is obeyed up to 5.5  $\mu\text{g/ml}$ . The detection limit (defined as the concentrations equivalent to the blank plus three times its standard deviation) is 0.03  $\mu\text{g/ml}$  for Er and Pr.

#### Analytical characteristics of the simultaneous determinations

The sum of Er and Pr was obtained by measuring the absorbance at 535 nm in a medium buffered at pH

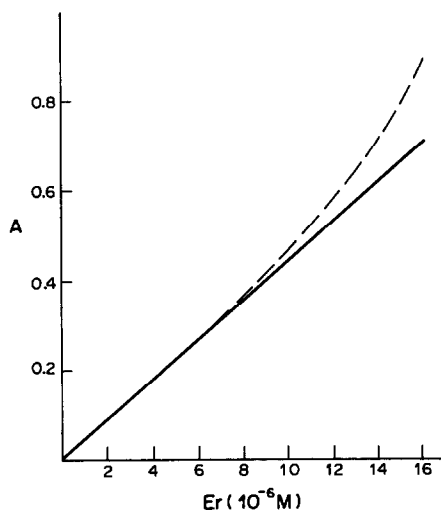


Fig. 6. Calibration graphs: (—) Er; (---) Er + Pr (Pr/Er = 10); 0.075 g/mg TX-100/PAN, pH = 9.2 (0.02 M borate buffer),  $\lambda = 535$  nm.

9.2 (boric acid/borate) and a TX-100/PAN w/w ratio of 75. For the determination of Er in the presence of Pr the TX-100/PAN ratio and pH were optimized by the modified simplex method with final concentrations of  $4.0 \times 10^{-6} M$  Er and  $4.0 \times 10^{-5} M$  Pr, and minimizing  $(A_{Er+Pr} - A_{Er})/A_{Er}$ , (where  $A$  = absorbances, and found to be 75 and pH 7.2 respectively.

Several later experiments showed that the conditions obtained were optimum if the final concentration of Er was less than 0.67  $\mu\text{g/ml}$  that is, to a certain extent the optimum experimental conditions depend on the Er concentration. The system was thus reinvestigated, optimizing the variables one by one, the new optimal values being pH 7.6, TX-100/PAN ratio of 50, and reaction time 30 min. Under these conditions the Er-PAN-TX-100 system obeys Beer's law for final concentrations up to 6.8  $\mu\text{g/ml}$ . The amount of Pr was obtained by using the expression:

$$C_{Pr} = [A_{9.2} - A_{7.6} \epsilon_{Er_{9.2}} / \epsilon_{Er_{7.6}}] / \epsilon_{Pr_{9.2}}$$

where the numerical subscripts indicate the pH values at which the absorbances and molar absorptivities were obtained.

For Er concentrations greater than 1.3  $\mu\text{g/ml}$ , however, a certain anomaly may be seen when there is Pr in the solution: under the conditions in which the tertiary system Pr-PAN-TX-100 does not exhibit absorption, an increase in the signal of the Er-PAN-TX-100 system is observed (Fig. 6). This can be accounted for in terms of formation of a quaternary Er-Pr-PAN-TX-100 system (the molar absorptivity of which is greater than that of the Er-PAN-TX-100 system). The complex is formed only above a certain concentration of Er, since in the experiments detailed in Fig. 6, the Pr/Er ratio remains constant and equal to ten. The formation of this compound could easily explain the high errors reported in the literature for simultaneous determination of lanthanides.

Table 1 shows the results obtained in the determination of 0.67  $\mu\text{g/ml}$  Er in the presence of various concentrations of Pr. It may be seen that for Pr/Er ratios below 20, the error due to the presence of Pr is not very high (about 3%). Table 2 shows the results obtained in the simultaneous determination of both

Table 1. Spectrophotometric determination of 0.67  $\mu\text{g/ml}$  erbium with PAN in TX-100 micelles and the presence of praseodymium

Pr added, $\mu\text{g/ml}$	Er found,* $\mu\text{g/ml}$	Recovery, %
	0.67	100
0.67	0.67	100
6.7	0.67	100
13.4	0.69	103
20.1	0.76	113

\*Mean value of three determinations.  $\lambda$  535 nm,  $t$  30 min.

Table 2. Simultaneous spectrophotometric determination of erbium and praseodymium

Metal ions added, $\mu\text{g/ml}$		Metal ions found,* $\mu\text{g/ml}$	
Er	Pr	Er	Pr
1.0	0.28	0.99	0.27
0.67	0.56	0.66	0.57
0.33	0.85	0.31	0.87

\*Mean value of three determinations.

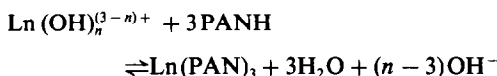
Table 3. Spectroscopic characteristics of Ln-PAN-Triton X-100 systems\*

Lanthanide	$\lambda$ , nm	$\epsilon$ , $10^4 \text{ l. mole}^{-1} \cdot \text{cm}^{-1}$
Nd	535	4.3
Sm	535	4.9
Eu	560	4.6
Gd	535	4.3
Tb	560	5.1
Dy	560	5.3
Ho	560	4.6
Tm	560	4.9
Yb	560	5.1
Lu	560	4.9

\*Conditions: pH 9.2 (0.04M borate buffer), Triton X-100/PAN ratio 100 w/w.

lanthanides at varied but not very different concentrations.

Of the three forms of PAN in equilibrium ( $\text{PANH}_2^+$ ,  $\text{PANH}$  and  $\text{PAN}^-$ ) only the un-ionized form ( $\text{PANH}$ ) is insoluble in water, though it dissolves well in water-alcohol and dioxan-water mixtures, and in ionic or non-ionic micelles. The micellization induces modifications in the protonation and dissociation constants<sup>20,21</sup> as a function of the concentration of surfactant in solution. However, since the dissociation constant, under our experimental conditions, should decrease ( $\text{p}K$  increased) the PAN must be present mainly in the undissociated form. Because the lanthanide would be present in the form of a hydroxo-complex, the complexing reaction may be expressed by:



An experimental detail which should be noted is the decrease in the signal of both systems when the concentration of TX-100 is increased; the effect is more pronounced in the case of Pr. This could be accounted for by bearing in mind that an increase in the number of micelles would lead to a decrease in the concentration of the chromophore per micelle. Similar findings have been reported by other authors.<sup>22,23</sup>

The difference in the behaviour of Pr and Er as a function of the surfactant concentration can be re-

lated to the higher formation constant of the Er-PAN system.

### Selectivity

Under the working experimental conditions for both the individual and simultaneous determinations, all the other lanthanides interfere in that they form coloured chelates with absorption maxima at wavelengths close to 535 nm (Table 3), and therefore must be absent.

All the heavy elements also produce a positive or negative interference, according to the charge of their ions. This interference is eliminated by extraction of the corresponding diethyldithiocarbamates from acid medium with a 1:1 mixture of ethyl acetate and chloroform, into which the excess reagent is also extracted. The alkaline-earth and alkali metal cations do not interfere up to concentrations close to 0.01 and 0.1M, respectively.

*Acknowledgement*—The authors thank F. Becerro Dominguez for his kind help with the modified simplex method.

### REFERENCES

1. B. K. Chernova, *J. Anal. Chem. U.S.S.R.*, 1977, **32**, 1171.
2. W. L. Hinze, in K. L. Mittal (ed.), *Solution Chemistry of Surfactants*, Vol. 1, Plenum Press, New York, 1979.
3. S. B. Savvin, *Crit. Rev. Anal. Chem.*, 1979, **8**, 55.
4. E. Pelizzetti and E. Pramauro, *Anal. Chim. Acta*, 1985, **169**, 1.
5. H. Watanabe, in K. L. Mittal, and E. J. Fendler (eds.), *Solution Behaviour of Surfactants: Theoretical and Applied Aspects*, Vol. II, Part VII, Plenum Press, New York, 1982.
6. D. W. Armstrong, *Sepr. Purif. Meth.*, 1985, **13**, 213.
7. B. T. Kilbourn, *J. Less-Common Metals*, 1985, **111**, 1.
8. G. Yoldjian, *ibid.*, 1985, **111**, 17.
9. P. Falconnet, *ibid.*, 1985, **111**, 9.
10. Z. Marczenko, *Spectrophotometric Determination of Elements*, Horwood, Chichester, 1976.
11. S. Shibata, *Anal. Chim. Acta*, 1959, **22**, 470; 1960, **23**, 367; 1961, **25**, 348; 1963, **28**, 388.
12. N. Pustelnik, B. Kuźnik and D. M. Czakis-Sulikowska, *Acta Chim. Hung.*, 1985, **118**, 93.
13. D. M. Czakis-Sulikowska and A. Malinowska, *ibid.*, 1985, **118**, 121.
14. J. Starý, *The Solvent Extraction of Metal Chelates*, Pergamon Press, Oxford, 1964.
15. B. Kuźnik, *J. Inorg. Nucl. Chem.*, 1981, **43**, 3363.
16. O. Navrátil, *Collection Czech. Chem. Commun.*, 1966, **31**, 2492.
17. J. M. Rao and D. Satyanarayana, *J. Indian Chem. Soc.*, 1980, **57**, 1132.
18. J. M. Rao, D. Satyanarayana and A. Umesh, *Bull. Chem. Soc. Japan*, 1979, **52**, 588.
19. S. B. Savvin, R. K. Chernova and L. M. Kudryavtesera, *J. Anal. Chem. U.S.S.R.*, 1979, **34**, 51.
20. B. F. Pease and M. B. Williams, *Anal. Chem.*, 1959, **31**, 1147.
21. L. A. Al'botá, *J. Anal. Chem. U.S.S.R.*, 1985, **40**, 771.
22. H. Kohara, *Bunseki Kagaku*, 1974, **23**, 39.
23. J. Rosendorfová and L. Čermáková, *Talanta*, 1980, **27**, 705.



# DETERMINATION OF ARSENIC IN ORES, CONCENTRATES AND RELATED MATERIALS BY CONTINUOUS HYDRIDE-GENERATION ATOMIC-ABSORPTION SPECTROMETRY AFTER SEPARATION BY XANTHATE EXTRACTION

ELSIE M. DONALDSON and MAUREEN E. LEAVER

Mineral Sciences Laboratories, Canada Centre for Mineral and Energy Technology,  
Department of Energy, Mines and Resources, Ottawa, Canada

(Received 23 September 1987. Accepted 29 October 1987)

**Summary**—A recent graphite-furnace atomic-absorption method for determining  $\sim 0.2 \mu\text{g/g}$  or more of arsenic in ores, concentrates, rocks, soils and sediments, after separation from matrix elements by cyclohexane extraction of arsenic(III) xanthate from  $\sim 8\text{--}10M$  hydrochloric acid, has been modified to include an alternative hydride-generation atomic-absorption finish. After the extract has been washed with  $10M$  hydrochloric acid–2% thiourea solution to remove co-extracted copper and residual iron, arsenic(III) in the extract is oxidized to arsenic(V) with bromine solution in carbon tetrachloride and stripped into water. Following the removal of bromine by evaporation of the solution, arsenic is reduced to arsenic(III) with potassium iodide in  $\sim 4M$  hydrochloric acid and ultimately determined by hydride-generation atomic-absorption spectrometry at 193.7 nm, with sodium borohydride as reductant. Interference from gold, platinum and palladium, which are partly co-extracted as xanthates under the proposed conditions, is eliminated by complexing them with thiosemicarbazide before the iodide reduction step. The detection limit for ores and related materials is  $\sim 0.1 \mu\text{g}$  of arsenic per g. Results obtained by this method are compared with those obtained previously by the graphite-furnace method.

The accurate determination of arsenic at trace and  $\mu\text{g/g}$ -levels in ores, concentrates, rocks, soils, processing products and related materials is important in many CANMET projects, including the Canadian Certified Reference Materials Project (CCRMP), and recently in this laboratory a relatively rapid graphite-furnace atomic-absorption spectrometric (GFAAS) method was developed for the determination of  $\sim 0.2 \mu\text{g/g}$  or more of arsenic in these materials.<sup>1</sup> This method involves the preliminary separation of arsenic, after its reduction with titanium(III), from iron, lead, zinc, copper and other matrix elements by cyclohexane extraction of arsenic(III) xanthate from  $\sim 8\text{--}10M$  hydrochloric acid. After several washing steps to remove co-extracted copper, residual iron and chloride, arsenic is stripped from the extract with  $16M$  nitric acid and ultimately determined by GFAAS in a 2% nitric acid–0.1% thiourea medium with palladium as matrix modifier. It was considered that, with an alternative stripping step involving bromine oxidation of arsenic(III) in the extract followed by back-extraction into water, as described in an earlier method for arsenic based on xanthate extraction and a spectrophotometric molybdenum blue finish,<sup>2</sup> this method could easily be modified to include a hydride-generation atomic-absorption (HGAAS) finish which would be very useful for

routine work. Results obtained for various reference materials by this modified method are compared with those obtained previously by the GFAAS method. An advantage of the proposed method for arsenic over many other HGAAS methods is that arsenic is separated from other interfering hydride-forming elements, *viz.* lead, tin, bismuth, antimony, selenium and tellurium.

## EXPERIMENTAL

### Apparatus

A Varian-Techtron model AA6 spectrometer, equipped with a 10-cm laminar-flow air-acetylene burner and an arsenic hollow-cathode lamp, was used in this work. It was interfaced with a Varian model VGA-76 automated vapour-generation accessory, which features a continuous-flow design incorporating a peristaltic pump and is coupled with a flame-heated silica absorption cell. With this system, the sample solution, hydrochloric acid and sodium borohydride solution are pumped through a reaction or mixing coil and the arsine and other gaseous reaction products formed are then swept by means of a stream of nitrogen into a gas-liquid separator to remove liquid and water vapour. From there they are swept into the silica cell—heated by an air-acetylene flame—where the arsine is thermally decomposed and where, after a suitable delay period to allow the production of a steady-state atomic-absorption signal, the absorbance is integrated for a suitable time. A schematic diagram and a detailed description of the development of this accessory can be found elsewhere.<sup>3</sup> The spectrometer and vapour generator were used under the following conditions.

Wavelength: 193.7 nm  
Lamp current: 8 mA  
Spectral band-width: 0.5 nm

Air flowmeter reading: 6.5 (~11 l./min)  
 Acetylene flowmeter reading: 3.0 (~2 l./min)  
 Integration period for absorbance measurement:  
 3 sec after ~40 sec delay time  
 Hydrochloric acid (10M) uptake rate: ~1 ml/min  
 Sodium borohydride solution uptake rate: ~1 ml/min  
 Sample solution uptake rate: ~8 ml/min  
 Nitrogen flow-rate: ~90 ml/min

#### Reagents

*Sodium borohydride, 0.6% solution containing ~0.5% sodium hydroxide.* Store in a plastic bottle. Prepare a fresh solution every two days.

*Thiosemicarbazide solution, 2.5%.* Dissolve 2.5 g of the reagent by heating with 100 ml of water containing 2 ml of concentrated hydrochloric acid. Cool and filter the solution into a plastic bottle. Prepare a fresh solution every three days.

*Potassium iodide (10%)–ascorbic acid (1%) solution.* Store in a plastic bottle.

*Hydrochloric acid, 10M.* Store in a plastic bottle.

Doubly demineralized water was used throughout and 100- and 1- $\mu$ g/ml arsenic solutions and all other solutions used in the extraction step were prepared as described previously.<sup>1</sup>

#### Calibration solutions

Prepare 0.005-, 0.01-, 0.015- and 0.02- $\mu$ g/ml arsenic solutions by adding 0.5, 1, 1.5 and 2 ml, respectively, of 1- $\mu$ g/ml standard arsenic solution to 100-ml standard flasks. Dilute each solution to ~15 ml with water, then add 10 ml of concentrated hydrochloric acid and 4 ml of 2.5% thiosemicarbazide solution and mix thoroughly. Add 1 ml of 10% potassium iodide–1% ascorbic acid solution, mix and allow the solutions to stand for ~45 min to ensure the complete reduction of arsenic (Note 1). Add 10 ml more of concentrated hydrochloric acid to each solution, then dilute to volume with water. Prepare a zero calibration solution in a similar manner (Note 2).

#### Procedure

After sample decomposition (including a blank) and the extraction of up to ~1  $\mu$ g of arsenic, contained in a suitable aliquot of the initial 10M hydrochloric acid sample solution, as described previously,<sup>1</sup> wash the extract once (or twice if necessary) with 5 ml of 10M hydrochloric acid–2% thiourea solution, as described, to remove co-extracted copper. Drain off the acid phase, then add 3 ml of 20% bromine solution in carbon tetrachloride to the extract, stopper the funnel and mix thoroughly. Allow the solution to stand for ~5 min to ensure the complete oxidation of arsenic(II) to arsenic(V), then add 5 ml of water and shake the funnel for ~30 sec. Allow the layers to separate, then drain the aqueous phase into a 100-ml Teflon beaker. Wash the stem of the funnel with water and collect the washings in the beaker. Repeat the stripping step twice more, washing the stem of the funnel with water each time.

Evaporate the resulting blank and sample solutions to ~10 ml (Notes 3 and 4), then dilute them to ~15 ml with water, add 10 ml of concentrated hydrochloric acid and proceed with the reduction of arsenic as described above, using half the volumes of thiosemicarbazide and potassium iodide solutions recommended for the calibration solutions. After the 45-min reduction period, transfer the resulting solutions, without further addition of concentrated hydrochloric acid, to 50-ml standard flasks, then dilute them to volume with water and mix.

Using the zero calibration solution to zero the spectrometer, measure the absorbance generated by the calibration solutions, followed by the blank and sample solutions (Note 5), under the conditions described under "Apparatus". Determine the arsenic concentration of both solutions either by reference to a graph plotted from the absorbance values obtained for the calibration solutions or calculate the

concentrations from the values obtained for the calibration solutions that bracket the sample and blank concentrations (Note 6). Calculate the arsenic content of both solutions in ng and correct the result obtained for the sample solution by subtracting that obtained for the blank solution.

#### Notes

1. A standard arsenic solution prepared by dissolving arsenic(III) oxide in sodium hydroxide solution as recommended previously<sup>1</sup> may contain some arsenic(V) if it has stood for a considerable length of time, because arsenite is slowly oxidized by air to arsenate in an alkaline medium.<sup>4</sup> However, this will not cause problems in tests involving arsenic(III) as long as the test solution is taken through the reduction step.

2. Although the calibration solutions become deep yellow on standing they are still stable for at least five days.

3. At this point the solution should be colourless, indicating that all the bromine has been removed. If some remains it will interfere with the reduction of arsenic(V) to arsenic(III) by iodide. This will produce a low result for arsenic.

4. For samples of low arsenic content, a 25-ml final sample solution volume can be used, if desired, instead of 50 ml as recommended in the procedure. However, in this case the solution should be evaporated to ~7 or 8 ml, followed by the addition of 5 ml of concentrated hydrochloric acid, 1 ml of thiosemicarbazide solution and 0.25 ml of potassium iodide–ascorbic acid solution for the reduction step. For samples of high arsenic content, a 100-ml final volume can be used under the conditions described for the calibration solutions.

5. If dilution is necessary, dilute suitable aliquots of both the blank and sample solutions with freshly prepared zero calibration solution and correct the result (ng of arsenic) obtained for the diluted sample solution by subtracting that obtained for the diluted blank solution.

6. Although the calibration graph is not linear it was found that more accurate results, with minimal positive error, were obtained for arsenic if they were calculated on the basis of linearity between two calibration solutions that closely bracket the sample concentration. Much greater errors were obtained when calibration curves were used. This problem should not occur with the newer microprocessor-controlled atomic-absorption spectrometers which feature direct concentration read-out with curve linearization.

## RESULTS AND DISCUSSION

### Stripping and HGAAS determination of arsenic

Previously<sup>1</sup> arsenic(III) xanthate in the cyclohexane extract was oxidized with, and stripped into, 16M nitric acid before the ultimate determination of arsenic by GFAAS. However, treatment of the extract with bromine solution in carbon tetrachloride, followed by stripping of the arsenic into water as described in earlier work,<sup>2</sup> was considered advantageous for hydride-generation work because the residual bromine in the strip solution can be more quickly and efficiently removed by heating and evaporation of the solution than can nitric acid, which requires fuming of the solution with sulphuric or perchloric acid. Reduction of the resultant arsenic(V) to the trivalent state required for the hydride-generation step is readily accomplished by making the solution ~4M in hydrochloric acid, adding potassium iodide and allowing ~45 min for complete reduction.<sup>5,6</sup> A potassium iodide concentration of ~0.4% during the

reduction step was found to be adequate. As recommended by other investigators,<sup>3,6</sup> using the same hydride-generation accessory, 10M hydrochloric acid and 0.6% sodium borohydride solution, which was confirmed to be the optimum concentration, were used in the acid and borohydride channels of the hydride-generator. Under these conditions, the final hydrochloric acid concentration of the sample solution, after the iodide reduction and dilution of the solution to volume with water, can vary from ~0.5 to at least 10M without affecting the sensitivity for arsenic. At the pumping rates specified, this corresponds to hydrochloric acid concentrations in the range ~1.4–9M during the arsine generation step. Other workers<sup>7–9</sup> have also found that hydrochloric acid concentrations  $\geq 1M$  have no significant effect on the reaction. For convenience a final hydrochloric acid concentration of 2M was chosen for the sample and calibration solutions in this work.

#### Effect of diverse ions

As found previously,<sup>1</sup> platinum is slightly co-extracted and palladium and gold are largely co-extracted as xanthate complexes under the conditions, ~8–10M hydrochloric acid, used for the extraction of arsenic. Copper, which is also partly co-extracted, is largely removed from the extract by washing it with 10M hydrochloric acid containing thiourea. Although easily reducible elements such as these and

the other platinum-group elements are known to interfere severely in the determination of arsenic by hydride-generation,<sup>10</sup> interference from these elements can be eliminated or minimized by complexing them with thiosemicarbazide.<sup>5,9,11</sup> Tests showed that, when 2 ml of 2.5% thiosemicarbazide solution were added before the iodide reduction step, up to at least 0.2 mg of gold, platinum and palladium and 2 mg of copper can be present individually in the final solution (50 ml), or half these amounts of these elements can be present collectively, without causing significant error in the result. However, as mentioned previously,<sup>1</sup> these amounts of gold, platinum and palladium are considerably more than would be expected in the final sample solution on the basis of the largest sample taken and the largest aliquot used for extraction. Similarly, considerably less than 1 mg of copper would be present after the extract is washed as described above. Low results were obtained for arsenic in the presence of palladium and copper when the thiosemicarbazide solution was added after the potassium iodide solution. Under these conditions palladium and copper form iodide complexes.

#### Applications

Table 1 shows that the mean results obtained for arsenic in various CCRMP reference materials and in several National Research Council Canada and National Bureau of Standards marine and river

Table 1. Determination of arsenic in CCRMP and other reference ores, concentrates and related materials

Sample*	Certified value and 95% confidence limits, As, $\mu\text{g/g}$	As found, $\mu\text{g/g}$	
		GFAAS method†	Proposed method‡
CCU-1 Copper concentrate	41.0 $\pm$ 4.0	44.1 $\pm$ 0.8	44.1 $\pm$ 3.0 (5)
CCU-1a Copper concentrate	53 $\pm$ 5§	48.7 $\pm$ 0.7 #	48.6 $\pm$ 1.4 (5) #
RL-1 Uranium ore	19.6 $\pm$ 1.1	19.8 $\pm$ 2.2	21.5 $\pm$ 0.4 (4)
UTS-4 Uranium tailings	38.0 $\pm$ 2.0	39.6 $\pm$ 2.6	40.5 $\pm$ 1.8 (5)
SY-2 Syenite rock	17¶	17.1 $\pm$ 1.3	16.1 $\pm$ 0.9
SY-3 Syenite rock	19¶	17.9 $\pm$ 1.1	17.9 $\pm$ 1.7
MRG-1 Gabbro	0.5¶	0.5 <sub>1</sub> $\pm$ 0.0 <sub>7</sub>	0.7 <sub>3</sub> $\pm$ 0.0 <sub>3</sub>
SO-1 Regosolic soil	1.9 $\pm$ 0.3 <sup>a</sup>	2.1 $\pm$ 0.3	2.1 $\pm$ 0.2
SO-2 Podzolic soil	1.2 $\pm$ 0.2 <sup>a</sup>	1.1 $\pm$ 0.1	1.2 $\pm$ 0.2
SO-3 Calcareous C Horizon soil	2.6 $\pm$ 0.1 <sup>a</sup>	2.5 $\pm$ 0.2	2.4 $\pm$ 0.3
SO-4 Chernozemic A Horizon soil	7.1 $\pm$ 0.7 <sup>a</sup>	6.3 $\pm$ 0.2	6.7 $\pm$ 0.6
FER-1 Iron formation rock	5.9 <sup>b</sup>	5.9 $\pm$ 0.4	6.0 $\pm$ 0.5 (4)
FER-2 Iron formation rock	1.8 <sup>b</sup>	1.6 $\pm$ 0.0	1.9 $\pm$ 0.2
FER-3 Iron formation rock	1.1 <sup>b</sup>	0.8 <sub>7</sub> $\pm$ 0.0 <sub>4</sub>	1.1 $\pm$ 0.1
FER-4 Iron formation rock	3.4 <sup>b</sup>	2.9 $\pm$ 0.1	3.4 $\pm$ 0.4 (4)
NRCC MESS-1 Marine sediment	10.6 $\pm$ 1.2	10.1 $\pm$ 0.8	9.8 $\pm$ 0.7
NRCC BCSS-1 Marine sediment	11.1 $\pm$ 1.4	10.5 $\pm$ 0.4	10.2 $\pm$ 0.5
NBS 1645 River sediment	66 <sup>c</sup>	64.2 $\pm$ 5.9	69.9 $\pm$ 3.4 (6)
NBS 1646 Estuarine sediment	11.6 $\pm$ 1.3	10.4 $\pm$ 0.7	10.2 $\pm$ 0.4

\*CCRMP reference materials except where indicated otherwise. Except for CCU-1a nominal compositions are given in the previous work.<sup>1</sup> The approximate percentage chemical composition of CCU-1a is ~27 Cu, ~27 Fe, ~3 Zn and ~35 S.

†Mean values and standard deviations obtained previously.<sup>1</sup>

‡Mean and standard deviation for 3 values except where indicated otherwise in parentheses.

§Consensus mean value (excluding gross outliers) obtained during the interlaboratory certification programme.

# Mean of 5 results obtained by the authors during the interlaboratory certification programme.

¶Most recent usable value.<sup>12</sup>

<sup>a</sup>CCRMP value given for information only (not certified).

<sup>b</sup>Mean value obtained during the interlaboratory programme.<sup>13</sup>

<sup>c</sup>Tentative value.

sediments are, in most cases, in good agreement with the certified values, with values given for information only or with the consensus mean or tentative values obtained during interlaboratory certification programmes. Except for NBS 1645, they are also in excellent agreement with the results obtained previously by the GFAAS method and with other reported values.<sup>1</sup> Although the mean value obtained for NBS 1645 is slightly higher than the GFAAS value, it is still within the wide range of values (61–81  $\mu\text{g/g}$ ) reported by other workers.<sup>1</sup> The mean result obtained for CCU-1a, and which is at present undergoing certification by the CCRMP, which was not included in the previous work,<sup>1</sup> is in excellent agreement with the mean GFAAS value obtained in this laboratory for certification purposes, but slightly lower than the current consensus mean value. In the present work, each of the individual results obtained for the reference materials was the mean of 3 or 4 HGAAS runs involving duplicate measurements each time.

The precision for arsenic by the proposed HGAAS method (Table 1) is comparable with that obtained by the GFAAS method. However, the practical detection limit, calculated as three times the amount of arsenic equivalent to the standard deviation of the reagent blank, based on a 50-ml aliquot (0.5 g) of sample solution taken through the extraction step, is  $\sim 0.1 \mu\text{g}$  of arsenic per g. This is about half the limit

found for the GFAAS method.<sup>1</sup> The sensitivity or characteristic concentration is  $\sim 0.16 \text{ ng}$  of arsenic per ml for 0.0044 absorbance. The reagent blank varied from  $\sim 5$  to 90 ng, depending on the size of the aliquot taken for extraction. This is comparable with the blanks obtained with the GFAAS method.<sup>1</sup>

#### REFERENCES

1. E. M. Donaldson, *Talanta*, 1988, **35**, 47.
2. *Idem, ibid.*, 1977, **24**, 105.
3. B. T. Sturman, *Appl. Spectrosc.*, 1985, **39**, 48.
4. I. M. Kolthoff and E. B. Sandell, *Textbook of Quantitative Inorganic Analysis*, 2nd Ed., p. 591. Macmillan, New York, 1948.
5. S. P. Kellerman, *MINTEK Report NO. M39, Council for Mineral Technology, Randburg, South Africa*, 1982.
6. K. Brodie, B. Frary, B. Sturman and L. Voth, *Varian Instruments at Work*, 1983, No. AA-38.
7. L. Ebdon, J. R. Wilkinson and K. W. Jackson, *Anal. Chim. Acta*, 1982, **136**, 191.
8. E. de Oliveira, J. W. McLaren and S. S. Berman, *Anal. Chem.*, 1983, **55**, 2047.
9. R. K. Anderson, M. Thompson and E. Culbard, *Analyst*, 1986, **111**, 1143.
10. L. M. Voth-Beach and D. E. Shrader, *Spectroscopy*, 1985, **1**, 60.
11. G. F. Kirkbright and M. Taddia, *Anal. Chim. Acta*, 1978, **100**, 145.
12. S. Abbey and E. S. Gladney, *Geostds. Newsl.*, 1986, **10**, 3.
13. S. Abbey, C. R. McLeod and W. Liang-Guo, *Geol. Surv. Canada Paper* 83–19, 1983.

## DETERMINATION OF Mo(VI) IN TAP-WATER AND SEA-WATER BY DIFFERENTIAL-PULSE POLAROGRAPHY AND CO-FLOTATION

J. L. HIDALGO, M. A. GOMEZ, M. CABALLERO, R. CELA and J. A. PEREZ-BUSTAMANTE  
Department of Analytical Chemistry, Faculty of Sciences, University of Cádiz, Spain

(Received 27 February 1987. Revised 6 October 1987. Accepted 27 October 1987)

**Summary**—A new method is described for the microdetermination of Mo(VI) in natural waters and sea-water by differential-pulse polarography based on the catalytic wave caused by Mo(VI) in nitrate medium following preconcentration by co-flotation on Fe(III) hydroxide. In the case of sea-water samples, hexadecyltrimethylammonium bromide (HTAB) was used together with octadecylamine as the surfactant. For the analysis of natural water samples only HTAB is needed. Molybdenum in the range 0.7–5.7 ng/ml has been determined.

It has been shown that the molybdate ion can be reduced polarographically only at pH less than 6.<sup>1,2</sup> Stern<sup>3</sup> found that in acid solutions containing nitrate, a very large wave appeared, owing to a catalytic reduction process involving Mo(VI).<sup>4-7</sup> This wave was used by Lanza *et al.*<sup>8</sup> in a procedure for the determination of molybdenum in steel by differential-pulse polarography (DPP).

Classical polarographic methods have not been used very much for the determination of trace elements in sea-water, because the sensitivity is generally not good enough—stripping voltammetric methods are to be preferred.<sup>9</sup> Prabhu *et al.*<sup>10</sup> have used DPP following preconcentration by co-precipitation.

Co-flotation is a technique which has received a great deal of attention in recent years<sup>11-13</sup> for separating and preconcentrating trace elements from natural waters, waste waters and sea-water. Kim and Zeitlin<sup>14</sup> have determined molybdate in waters by co-flotation with Fe(III) hydroxide, with sodium dodecylsulphate as surfactant, and spectrophotometric measurement. However, the combination of polarography and flotation does not seem to have been used for the determination of trace metals. This approach should be very interesting because the high concentration factor obtained by flotation should make it possible to use the polarographic methods for determination of trace metals levels below the detection limits normally attainable by these techniques. The combination should also allow some interferences to be eliminated.

The probable reason for earlier neglect of this combination of methods is that the surfactants needed in the flotation may suppress not only maxima on polarographic waves, but even the waves themselves.

This paper describes application of the combina-

tion for the microdetermination of Mo(VI) in natural waters and sea-water by means of DPP, utilizing the catalytic wave produced by Mo(VI) with nitrate, following preconcentration by co-flotation with Fe(III) hydroxide by means of the surfactants hexadecyltrimethylammonium bromide and octadecylamine.

### EXPERIMENTAL

#### Reagents

All reagents used were of analytical grade, without further purification. The working solutions were prepared weekly by diluting aqueous stock solutions [1000 µg/ml Mo(VI), 0.05M Fe(III), 4M ammonium nitrate, 0.005M hexadecyltrimethylammonium bromide (HTAB), 5M nitric acid], and 3-g/l. ethanolic solution of octadecylamine (OA). Solutions of possible interfering ions and of several other surfactants were also prepared. Amberlite IR-120 resin (300–1000 µm) was used as the ion-exchanger.

#### Apparatus

The polarographic measurements were made with a Metrohm E506 polarograph, E505 stand, EA427 Ag/AgCl reference electrode and EA285 platinum auxiliary electrode. All pH-measurements were made with a Metrohm 654 pH-meter. The flotation device used has been described previously.<sup>15,16</sup>

#### Procedures

Place 500 ml of the water sample in a 600-ml beaker, and add 1.0 ml of HTAB solution and 1.0 ml of OA solution. In another beaker, precipitate Fe(III) hydroxide by adding 2.0 ml of 2M ammonia to 1.0 ml of 0.005M Fe(III), and transfer the precipitate to the beaker containing the water sample. Adjust the pH to 4.00 ± 0.1 by careful addition of nitric acid, stirring the mixture for 17 min. Transfer the contents of the beaker quantitatively into the flotation column, already containing 2.0 ml of ethanol, and set the air flow-rate to 32 ml/min, to allow co-flotation to take place. After 5 min interrupt the air flow and discharge the solution in the column (mostly through the side-trap of the column, the remainder by suction through the sintered-glass plate

at the bottom of the column. Dissolve the precipitate with 12 ml of 1.25M nitric acid then wash the column walls with more nitric acid, and dilute the combined solution and washings to 25 ml with distilled water.

Pass this solution through a  $2 \times 20$  cm column packed with Amberlite IR-120 resin, previously washed with 200 ml of 0.5M nitric acid, collecting the effluent in a 50-ml standard flask containing 8.0 g of ammonium nitrate. Elute with 0.5M nitric acid, collecting the eluate in the same standard flask until the solution reaches the mark.

Transfer some of the eluate to a polarographic cell, and analyse by DPP, with initial potential 0.0 V, drop-time 0.6 sec, scan-rate  $-8.3$  mV/sec, recorder sensitivity 1.5 mA/mm, mercury column height 57.0 cm, pulse amplitude  $-50$  mV.

Determine the concentration of molybdenum by making standard additions of 1000 ng/ml Mo(VI) solution.

Use the same procedure for natural waters and waste waters of low salinity, but with only HTAB as surfactant.

## RESULTS AND DISCUSSION

### The catalytic wave in saline medium

A calibration curve was constructed by the method described by Lanza *et al.*,<sup>8</sup> but with a medium containing 35 g of sodium chloride per litre. Under these conditions a well-defined peak with  $E_p - 0.13$  V (Fig. 1) was obtained. The relationship between the Mo(VI) concentration and the intensity of the peak was a linear function of the molybdenum concentration in the range 0.01–10.0  $\mu\text{g/ml}$ .

The effect of several surfactants on the polarographic behaviour was then investigated to find the most suitable from a polarographic point of view: these were then tested in the co-floitation process. The test solutions contained 1 mg of Mo(VI) and 35 g of sodium chloride per litre of 2M ammonium nitrate/0.25M nitric acid. Increasing quantities of the surfactants HTAB, Triton X-100, Aliquat 336, benzyltrimethyltetradecylammonium chloride (zefiramine); sodium oleate, tetramethylammonium bromide and octadecylamine were tried, and changes in peak potential and peak height were noted for DPP and of the half-wave potential for d.c. polarography. The results obtained for peak height are shown in Fig. 2.

The half-wave potential was shifted to more negative values by HTAB concentrations above 125 mg/l. The same effect was observed for more than 12 mg/l. Triton X-100. Zefiramine, sodium oleate and Aliquat 336 produced precipitates in the medium, which caused oscillations of the polarographic current, making measurements difficult. Octadecylamine also caused turbidity in the solution but the polarographic determination was not affected until the surfactant concentration exceeded 120 mg/l. Such observations, and the results given in Fig. 2, indicated that HTAB would be the most convenient surfactant because it did not affect the polarography and was excellent in the co-floitation process for solutions of low salinity.<sup>10</sup> In solutions of high salinity, it proved necessary to add octadecylamine as well.

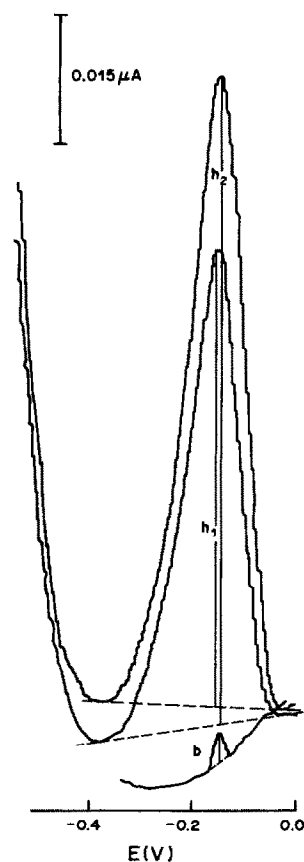


Fig. 1. DPP peak corresponding to a sea-water sample ( $h_1$ , unspiked sample;  $h_2$ , sample spiked with 2.0 ng/ml Mo; b blank).

Next, a systematic study was made of possible interferences in presence of HTAB. Different cationic and anionic species were selected either because they could form complexes with Mo(VI) or because they are normally present in natural waters or sea-water.

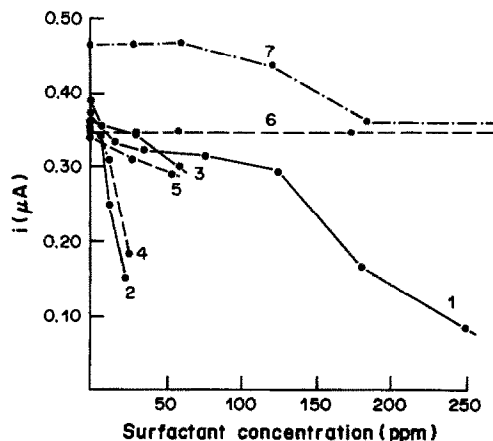


Fig. 2. Variation in DPP peak intensity for Mo(VI) determination, as a function of the nature and quantity of surfactant added (1, HTAB; 2, Triton X-100; 3, Aliquat 336; 4, zefiramine; 5, sodium oleate; 6, tetramethylammonium bromide; 7, octadecylamine).

Table 1. Study of interferences in the polarographic determination of molybdenum (interference positive if an error exceeding  $\pm 3\%$  is observed)

Species	Interference	Concentration ratio, ion:Mo(VI)
Cu(II)	+	>0.5:1
Pb(II)	-	100:1
Cd(II)	-	100:1
Zn(II)	-	100:1
Ni(II)	-	100:1
Co(II)	-	100:1
Hg(II)	-	100:1
Mn(II)	+	>0.5:1
Mg(II)	+	>1:1
Fe(III)	+	>100:1
Cr(VI)	-	100:1
bromide	-	1000:1
iodide	+	>5:1
nitrite	-	100:1
phosphate	-	1500:1
oxalate	-	100:1
tartrate	-	100:1

The results are shown in Table 1. In each case the concentration range studied was determined by the interferent:analyte ratio usually found in sea-water. Cu(II), Mn(II),  $Mg^{2+}$  and iodide interfered seriously. Fe(III) caused an appreciable reduction in peak height when present at  $\geq 100$ -fold ratio to Mo(VI) but it was still possible to measure the Mo(VI) quantitatively by the standard-additions method, up to an Fe(III):Mo(VI) ratio of 200:1. These interferences and the sensitivity levels achieved made it evident that the polarographic method could not be used directly for sea-water, and that a preconcentration would be essential to improve the sensitivity and eliminate the interferences.

#### Co-flotation

The preconcentration step was optimized in two stages. In the first, synthetic samples containing 5 mg/l. Mo(VI) were used because it was then easier to monitor the kinetics and the yield of the process by measurement of the residual Mo(VI) in the bulk solution at different times during the co-flotation. Once optimum conditions had been found in this way, the second stage was commenced, in which the co-floated molybdenum was determined polarographically, its initial concentration being progressively reduced until ng/ml levels were reached. The optimum conditions obtained in the first stage served

only as a guide in the second stage, because the Mo(VI):co-precipitant and Mo(VI):surfactant ratios were very different in the two series of experiments.

#### Natural and low-salinity waters

HTAB was used as the surfactant and Fe(III) hydroxide as the co-precipitant (because this was the most commonly used co-precipitant in co-flotation procedures<sup>16,17</sup> and is convenient because its colour can be used for monitoring the flotation). An initial pH of 4.0 was used for the co-flotation, to eliminate most interferences. [The optimum pH-range for co-flotation of Cu(II) with Fe(III) hydroxide is  $>7$ ,<sup>18</sup> and Mn(II) is floated as the hydroxide by dodecylsulphate<sup>19</sup> at pH 11.5; neither Mn(II) nor iodide seems to be floated at this pH.<sup>20,21</sup>] Moreover, colloidal Fe(III) hydroxide has maximum positive charge at this pH and is capable of quantitatively adsorbing the anionic Mo(VI) present in solution, at pH  $> 1.0$ .<sup>17</sup>

The experimental conditions were optimized by means of the simplex program COFLOT.<sup>22</sup> The air flow-rate, co-precipitant and surfactant concentrations, pH and induction time were the variables. Table 2 gives the initial simplex for this investigation. For samples containing Mo(VI) at the  $\mu\text{g/ml}$  level the optimum set of values, obtained after 21 experiments, was air flow-rate 32 ml/min, co-precipitant 2.26 ml of 0.05M Fe(III), surfactant 2.46 ml of 0.005M BHTA, pH 3.75, induction time 17 min.

Further experiments were then performed for fine adjustment of the operating conditions, starting with those provided by COFLOT, and confirmed the optimal ranges yielded by the program. These experiments also showed that the co-flotation was initially faster when the gas flow in the column was increased, as shown in Table 3, but the foam consistency became poorer as the air flow-rate increased, causing the precipitate to settle back into the solution. The conditions found by using COFLOT were indeed optimal, but not all critical; 30% variation of the amount of surfactant or co-precipitant or in the induction produced no appreciable difference in the co-flotation yield, but the pH-value had to be strictly controlled within the range  $4.0 \pm 0.1$  for reproducible results to be obtained.

Under these conditions triplicate experiments gave yields of 93.0, 92.9 and 93.6%. The best results were obtained by co-flotation at  $17 \pm 3^\circ$ . As already stated,

Table 2. Initial simplex for optimization of Mo(VI) co-flotation in low-salinity waters

Vertex	Air flow-rate ml/min	Co-precipitant, ml	Surfactant (HTABr), ml	pH	Induction time, min	Mo(VI) recovery, %
1	100	1.0	3.0	4.0	10	83.0
2	45	1.0	3.0	4.0	10	90.9
3	100	2.0	3.0	4.0	10	91.3
4	100	1.0	2.0	4.0	10	84.0
5	100	1.0	3.0	9.0	10	13.6
6	100	1.0	3.0	4.0	5	84.2

Table 3. Effect of the gas flow-rate in the column on the kinetics of Mo(VI) co-floitation [recovery of Mo(VI) as a function of the time elapsed in the co-floitation process]

Flow, ml/min	Time, min				
	0.5	1.0	5.0	10.0	15.0
32.0	31.6	86.0	92.0	92.0	93.0
60.0	29.4	72.0	90.5	90.5	90.5
80.0	76.0	90.4	92.0	92.0	92.0
100.0	77.7	86.7	89.2	90.0	90.0

after the co-floitation only the presence of iron causes problems with the Mo(VI) determination. Other impurities in the reagents do not produce peaks in the working potential range, and the typical blank value of 0.25 ng/ml is satisfactory.

Obviously the use of thorium or aluminium hydroxides as co-precipitant should eliminate the interference experienced with iron(III) in the DDP technique. However, use of thorium hydroxide as co-precipitant showed a significant lack of reproducibility, the average recoveries of Mo(VI) ranging around 70%. Use of aluminium hydroxide was even worse, only 20% of the Mo(VI) being recovered at best.

#### Saline waters

When the experimental conditions given above for low-salinity samples were used to preconcentrate molybdenum from high-salinity samples, 10.4% of the Mo(VI) added was recovered. We have reported previously on the inability of HTAB-metal hydroxide systems to separate trace metals by co-floitation from media with salinity similar to that of sea-water.

For such samples, the HTAB-OA combination (based on previous results)<sup>23</sup> proved to be the best for the co-floitation. Octadecylamine has low solubility in aqueous media, so to get good recovery in the co-floitation it was necessary to use it at the lowest concentration that was still efficient. It was found

Table 4. Results for analysis of synthetic samples

No.	Sample*	Mo(VI) added, ng/ml	Mo(VI) found, ng/ml	Recovery, %
1	LS	1.00	0.86	86
2	LS	1.00	1.00	100
3	LS	1.00	0.93	93
4	LS	1.00	0.82	82
5	LS	1.00	0.98	98
6	LS	1.00	1.20	120
7	LS	1.00	0.98	98
8	HS	2.00	1.92	96
9	HS	2.00	2.00	100
10	HS	2.00	1.75	87.5
11	HS	2.00	1.92	96
12	HS	2.00	1.78	89
13	HS	2.00	1.77	88.5
14	HS	2.00	2.06	103

\*LS = low salinity sample (distilled water); HS = high salinity sample (synthetic sea-water).

Table 5. Results for analysis of two real samples

No.	Sample type*	Mo(VI) found, ng/ml
1	TW	0.72
2	TW	0.67
3	TW	0.70
4	SW	5.5
5	SW	5.8
6	SW	5.8

\*TW = tap-water; SW = sea-water samples taken from Cádiz Bay.

that 12 mg/l. octadecylamine in the bulk solution and a concentration of HTAB similar to that used for non-saline media gave good separation without difficulty. A higher concentration of OA in the samples did not improve the co-floitation yield and interfered in the final DPP analysis.

A series of optimization experiments showed that the best results are obtained under conditions similar to those previously established for non-saline waters, so those conditions (plus addition of 12 mg of octadecylamine per litre) were adopted for subsequent fine-tuning optimization.

#### Substrate analysis

In the second stage of the optimization process, polarographic analysis was used to determine the co-floitation yield after 5 min of flotation. Synthetic saline and non-saline samples with Mo(VI) contents of 100 and 10 ng/ml were tested. With decreasing Mo(VI) concentration, the results became less satisfactory because the polarographic wave was seriously affected by the high levels of surfactant species and co-precipitant. Also, the pH-value initially selected (3.75) then caused rather poor reproducibility. A flotation pH of 4.0 and use of lower quantities of surfactant and co-precipitant were found to provide less critical conditions for the precipitation, and satisfactory results were obtained. Even under these conditions, however, Mo(VI) concentrations of 1 ng/ml could not be determined properly, because the high Fe(III):Mo(VI) ratio of 2800 seriously affected the polarographic signal. The Fe(III) and Mo(VI) were therefore separated by ion-exchange, and the conditions given in the experimental section were established as optimal for samples with low concentrations of Mo(VI) (1–100 ng/ml). The results obtained under these conditions for the analysis of synthetic samples are shown in Table 4.

#### Determination of Mo(VI) in real samples

Once suitable experimental conditions had been found for the determination of trace levels of Mo(VI), samples of tap-water and sea-water were analysed. The results are shown in Table 5. Good reproducibility was obtained, with average values of 0.7 ng/ml for the tap-water samples and 5.7 ng/ml for the sea-water.



## REFERENCES

1. Ya. P. Hokhshtein, *J. Gen. Chem. USSR*, 1940, **10**, 1725.
2. R. Holtje and R. Geyer, *Z. Anorg. Allgem. Chem.*, 1941, **246**, 258.
3. A. Stern, *Ind. Eng. Chem.*, 1942, **14**, 74.
4. M. G. Johnson and R. J. Robinson, *Anal. Chem.*, 1952, **24**, 366.
5. G. P. Haight, *Acta Chem. Scand.*, 1961, **15**, 2013.
6. I. M. Kolthoff and I. H. Hodara, *J. Electroanal. Chem.*, 1963, **5**, 2.
7. A. T. Violanda and W. D. Cooke, *Anal. Chem.*, 1964, **36**, 2287.
8. P. Lanza, D. Ferri and P. L. Buldini, *Analyst*, 1980, **105**, 379.
9. M. G. C. van den Berg, *Anal. Chem.*, 1983, **57**, 1532.
10. V. G. Prabhu, L. R. Zarapkar and M. S. Das, *Mikrochim. Acta*, 1980 **II**, 67.
11. A. A. Clarke and D. J. Wilson, *Sepr. Purif. Methods*, 1978, **7**, 55.
12. M. Hiraide and A. Mizuike, *Rev. Anal. Chem.*, 1982, **6**, 151.
13. A. Mizuike and M. Hiraide, *Pure Appl. Chem.*, 1982, **54**, 1956.
14. Y. S. Kim and H. Zeitlin, *Sepr. Sci.*, 1971, **6**, 505.
15. R. Cela and J. A. Pérez-Bustamante, *Afinidad*, 1982, **39**, 124.
16. L. M. Cabezón, R. Cela and J. A. Pérez-Bustamante, *ibid.*, 1983, **40**, 144.
17. Y. S. Kim and H. Zeitlin, *Anal. Chim. Acta*, 1969, **46**, 1.
18. G. T. McIntyre, J. J. Rodriguez, E. L. Tackston and D. J. Wilson, *Report* 1981, W-82-06708, OWRT-A-064; *Chem. Abstr.*, 1982, **97**, 77619q.
19. T. Inoue, T. Shiba and S. Takiuchi, *Sogo Shikensho Nenpo*, 1980, **3a**, 185; *Chem. Abstr.*, 1981, **94**, 49638u.
20. E. H. de Carlo, H. Zeitlin and Q. Fernando, *Anal. Chem.*, 1982, **54**, 898.
21. M. Caballero, *Doctoral Thesis*, Univ. of Cádiz, Spain, 1986.
22. M. Caballero, R. Cela and J. A. Pérez-Bustamante, *Sepr. Sci. Technol.*, 1986, **21**, 39.
23. L. M. Cabezón, M. Caballero, R. Cela and J. A. Pérez-Bustamante, *Talanta*, 1984, **31**, 597.

## SEPARATION OF OXYANIONS OF SULPHUR BY SINGLE-COLUMN ION-CHROMATOGRAPHY

A. BEVERIDGE, W. F. PICKERING\* and J. SLAVEK

Department of Chemistry, University of Newcastle, N.S.W. 2308, Australia

(Received 5 May 1987. Revised 30 June 1987. Accepted 23 August 1987)

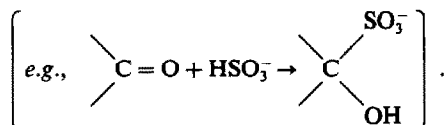
**Summary**—After stabilization of sulphite by addition of a five-fold excess of formaldehyde, mixtures of sulphite, sulphate and thiosulphate are readily separated by HPLC. For use with Vydac columns (302IC or 300IC) a suitable eluent is 1–3mM phthalic acid (pH 5–6), and the eluted ions may be detected by means of the change in refractive index or the absorbance at 290 nm. With a flow-rate of 2 ml/min, anion elution times are about 2.7 (0.7) min for HOCH<sub>2</sub>SO<sub>3</sub><sup>-</sup>, 7.5 (2.6) min for SO<sub>4</sub><sup>2-</sup> and 8.4 (5.2) min for S<sub>2</sub>O<sub>3</sub><sup>2-</sup>, the values in parentheses being those for the shorter 300IC column. Detection limits for sulphite and sulphate were around 1 mg/l., with relative standard deviations of 2–3% at higher levels. The sensitivity for S<sub>2</sub>O<sub>3</sub><sup>2-</sup> was an order of magnitude lower. The proposed method has advantages over earlier procedures based on alkaline eluents.

The determination of sulphite in solutions containing other oxyanions of sulphur is of interest in many areas. For example, sodium sulphite is added to boiler waters to scavenge residual oxygen, and the sulphite to sulphate ratio provides an indication of the effectiveness of feed-water deaeration. In the food and pharmaceutical industries, sulphite is widely used to minimize oxidation and bacterial growth, and the addition of this ion to photographic fixers and developers retards oxidation of other components. Photographic products (and diluted effluent samples) also contain high levels of thiosulphate.

Ion-chromatography can be used to determine low levels of sulphur anions such as sulphate, sulphite and thiosulphate,<sup>1</sup> but application of this technique is limited by rapid oxidation of sulphite to sulphate during the analytical cycle<sup>2</sup> and long thiosulphate retention times.

Sulphite oxidation can result from dissolved oxygen in the diluent water, interaction at sample/air interfaces, or even oxygen diffusion through the PTFE tubing used in some instruments. The process is catalysed by Fe(III) and Cu(II) salts.<sup>2</sup> Purging solutions with nitrogen or argon retards (but does not eliminate) sulphate formation. The observed ratio of sulphate to sulphite varies with the concentration of sulphite injected<sup>2</sup> and this introduces errors if attempts are made to correct for sample oxidation by subtracting the sulphate level detected in standards (a procedure used in boiler water studies<sup>3</sup>).

Sulphite in solution can be stabilized through interaction with aldehydes or ketones to form hydroxysulphonic acids



\*Author for correspondence.

The efficiency of different stabilizers for ion-chromatography studies has been investigated<sup>4</sup> and found to decrease in the order HCHO > other carbonyls > alcohols > saccharides. The addition of equimolar quantities of HCHO stabilized sulphite solutions for up to 72 hr, and almost no oxidation was observed in chromatographic runs provided the sample was directly injected into deaerated eluent. However, the size of the sulphite peak was found to depend on the HCHO:SO<sub>3</sub><sup>2-</sup> ratio as well as on the sulphite concentration.

For stabilization of the SO<sub>3</sub><sup>2-</sup> content of photographic materials addition of 2% (v/v) formalin (38% HCHO, 10% CH<sub>3</sub>OH) has been recommended.<sup>5</sup>

Most studies have used Dionex® separation columns in conjunction with a suppressor column, conductimetric detection and a basic eluent (e.g., 3mM NaHCO<sub>3</sub>/2.4mM Na<sub>2</sub>CO<sub>3</sub><sup>4,5</sup> or 5mM Na<sub>2</sub>CO<sub>3</sub>/4mM NaOH<sup>3</sup>). Unfortunately, at high pH the formaldehyde/sulphite adduct hydrolyses. This leads to an elution peak located near the normal sulphite position, with a size and shape influenced by the stabilizer concentration, and it has been suggested that it reflects an average retention time for sulphite partially oxidized to sulphate. With weakly basic eluents (e.g., 1mM NaHCO<sub>3</sub>), and excess of formaldehyde (or formalin) in the eluent, a new peak (for the stabilized HOCH<sub>2</sub>SO<sub>3</sub><sup>-</sup>) appears, with a short retention time. This peak is clearly separated from any organic acids present (as in photographic samples<sup>5</sup>) but elution of sulphate and thiosulphate is extremely slow, and regular flushing of the column with 50mM Na<sub>2</sub>CO<sub>3</sub> is required to remove accumulations of these ions.

Since the instability of sulphite solutions prior to injection into the chromatograph is a major problem, HOCH<sub>2</sub>SO<sub>3</sub>Na has been recommended as the sulphite standard.<sup>2,4,6</sup> This compound is stable towards aerial oxidation and hydrolysis, and the stability in pH 4 buffer has been found to be excellent.<sup>7</sup>

On this evidence, it was predicted that use of a weak acid eluent and a single column might effectively separate  $\text{HOCH}_2\text{SO}_3^-$  from sulphate, and this paper describes the results of our investigation of this modified approach.

With standard alkaline eluent mixtures the retention time for the thiosulphate ion is much longer than that of sulphate and the peaks tend to tail badly. Chromatograms showing sulphate and thiosulphate well separated have appeared in the literature<sup>8,9</sup> (with an  $\text{S}_2\text{O}_3^{2-}$  retention time of around 12 min) but the reported retention times imply poor separation of  $\text{SO}_3^{2-}$  and  $\text{SO}_4^{2-}$ . With a very short column and a high eluent flow-rate,  $\text{S}_2\text{O}_3^{2-}$  can be eluted in about 4 min, but all other anions present (including  $\text{SO}_4^{2-}$ ) are eluted as a single early peak.<sup>10</sup> To overcome these problems, it has been proposed<sup>11</sup> that determination of sulphite/sulphate and thiosulphate contents be based on separate IC runs, with the eluents most suitable for each. To separate the three anions on a single chromatogram in a time period of less than 15 min, gradient elution has been recommended.<sup>6</sup> Two Dionex separator columns were joined in series and the basicity of the eluent was increased from 4.8mM  $\text{NaHCO}_3$ /4.8mM  $\text{Na}_2\text{CO}_3$  to 6.9mM  $\text{NaHCO}_3$ /8.6mM  $\text{Na}_2\text{CO}_3$ . Even with optimized gradient conditions, however, the thiosulphate peak broadens and tails, indicating partial decomposition in the suppressor column. This effect was not pronounced when a weakly acid eluent was used.

#### EXPERIMENTAL

The liquid chromatography unit used for the single-column anion separations consisted of a Kortex pumping unit, a Vydac<sup>®</sup> anion column (either a 25-cm 302 IC or a 5-cm 300 IC), a sample loop (50 or 500  $\mu\text{l}$ ) and an Erma ERC-751 refractive-index detector unit. The eluent (1–3mM phthalic acid, adjusted to pH 5.6) was delivered at 2 ml/min. Some comparison studies were made with a Waters liquid chromatograph fitted with a Lambda-Max Model 481LC spectrophotometer detection unit. With this system, the anion peaks were identified by the indirect ultraviolet absorption method (wavelength set at 290 nm).

Standard solutions containing millimolar concentrations of sulphite, sulphate, thiosulphate, dithionite and tetrathionate ions were prepared from analytical-grade sodium salts. Stabilized sulphite solutions were prepared from the sodium salt of hydroxymethylsulphonic acid. Sulphite ions present in test samples were stabilized by the addition of excess of formaldehyde (*e.g.*, five times the sulphite level). Tetrathionate ions were not detected after their introduction into the column and dithionite solutions were visibly unstable.

The dilute phthalic acid eluent solutions, containing analytical grade reagent, were adjusted to the desired pH range (5–6) by addition of sodium hydroxide solution before being degassed by filtration under vacuum through a 0.45- $\mu\text{m}$  membrane.

Before introduction of sample the separation columns were equilibrated with eluent for several hours to ensure a stable baseline. With thiosulphate and excess of HCHO present, performance declined after several days of continuous use, and regular back-flushing of the column was needed to maintain sharp peaks and clear separations. The sensitivity of the detection units was adjusted to give peaks of measurable size for each anion concentration examined.

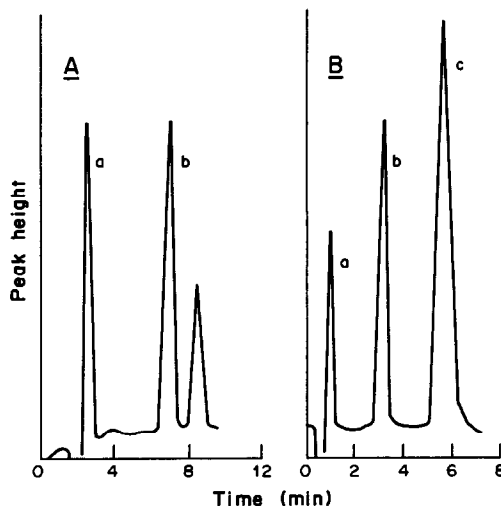


Fig. 1. Elution pattern showing separation of a mixture containing sulphite (a), sulphate (b) and thiosulphate (c), at room temperature. A, Each ion present at 1mM level in 5mM HCHO; Vydac 302 IC column, 2mM phthalic acid (pH 5) eluent flowing at 2 ml/min; refractive index detection. B, Separation of 2mM  $\text{SO}_3^{2-}$  (a), 3mM  $\text{SO}_4^{2-}$  (b) and 4mM  $\text{S}_2\text{O}_3^{2-}$  (c) in 10mM HCHO on a Vydac 300 IC column. Eluent 3mM phthalic acid (pH 6), flow-rate 2 ml/min. Indirect detection at 290 nm.

The experimental variables studied included eluent concentration, pH and flow-rate, relative concentrations of anions, precision and sensitivity, and effect of different detection modes.

#### RESULTS AND DISCUSSION

As shown in Fig. 1, mixtures of sulphite, sulphate and thiosulphate can be successfully separated in less than 10 min by using a Vydac column, 1–3mM phthalic acid as eluent, and formaldehyde stabilization of sulphite. Optimum conditions varied slightly with type of column used and detection mode.

Without HCHO stabilization, mg/l. concentrations of sulphite were rapidly oxidized to sulfate (*e.g.*, in minutes), whereas in stabilized solutions the  $\text{HOCH}_2\text{SO}_3^-$  ion was eluted close to the initial negative system-peaks, with no significant sulphate response. The presence of HCHO (the minimum excess required was fivefold) did not affect either the sulphate or thiosulphate peak responses.

With the Vydac 302 IC (25-cm) column the elution times for 1mM ion levels were about 2.5 ( $\text{HOCH}_2\text{SO}_3^-$ ) 6.9 ( $\text{SO}_4^{2-}$ ) and 8.4 min ( $\text{S}_2\text{O}_3^{2-}$ ) (*cf.* Fig. 1A). With the shorter (5-cm) 300 IC column and optimized conditions (*e.g.*, 3mM phthalic acid, pH 6, flowing at 2–2.5 ml/min) the elution times were reduced to 0.8, 3.5 and 6.9 min for  $\text{SO}_3^{2-}$ ,  $\text{SO}_4^{2-}$  and  $\text{S}_2\text{O}_3^{2-}$ , respectively (*cf.* Fig. 1B). The peak shape was sensitive to eluent pH, as shown in studies with 2mM phthalic acid as displacing agent. At pH < 6, the  $\text{S}_2\text{O}_3^{2-}$  peak tailed and had an accompanying negative trough; at pH > 6.5 the sulphite-formaldehyde adduct peak merged into the solvent-system peak. At

flow-rates below 2 ml/min, the elution times were doubled and the thiosulphate response greatly broadened. At pH 6, increasing the organic acid concentration from 1 to 3mM reduced the elution times, but use of still higher concentrations again caused overlap of  $\text{HOCH}_2\text{SO}_3^-$  with the solvent peak.

With ion concentrations not exceeding 2mM ( $\text{SO}_3^{2-}$  or  $\text{SO}_4^{2-}$ ) or 5mM ( $\text{S}_2\text{O}_3^{2-}$ ), varying the relative concentration of two ions had no significant effect on the peak size for the third. In other words, no interaction effects were observed.

In precision studies, the relative standard deviations of peak height measurements were found to be around 1.5% for sulphate peaks and less than 3.0% for the sulphite and thiosulphate peaks (with 2–6 cm peak heights).

With 500- $\mu\text{l}$  samples the detection limit for sulphite and sulphate was around 1 mg/l. (*i.e.*, 10 $\mu\text{M}$ ), but the high detector amplification required for these low levels resulted in a noisy background. With ion concentrations > 10mM the column was overloaded, and broad distorted peaks were obtained. The thiosulphate ion responses tended to level off slowly at concentrations > 3mM (*i.e.*, > 350 mg/l.).

Linear calibration curves were obtained for sulphite and sulphate over the 1–50 mg/l. range (*i.e.*, up to 500 $\mu\text{M}$ ). The intercepts calculated from regression line plots (peak height *vs.* ion concentration) were generally small (a few mm), and the correlation coefficients were around 0.99. The slope of the regression lines varied with eluent concentration (and pH), detector amplification setting, sample volume and ion of interest. For example, with 2mM phthalic acid (pH 5) as eluent and refractive-index detection, the slopes for sulphate were 25 cm.l.mmole<sup>-1</sup> with 50- $\mu\text{l}$  samples and 195 cm.l.mmole<sup>-1</sup> with 500- $\mu\text{l}$  samples. Changing the eluent to 1.5mM phthalic acid (pH 5.5) reduced the slope to 21 cm.l.mmole<sup>-1</sup> and the sulphite adduct slope to 19 cm.l.mmole<sup>-1</sup>. With these conditions the initial baseline was difficult to establish, the sulphite intercept was large (~1 cm) and the points were more scattered. A plot which did not pass through the origin was also obtained by using indirect ultraviolet detection and sulphite levels of 0.2–1mM (*i.e.*, up to 80 mg/l.  $\text{SO}_3^{2-}$ ), again owing to the adduct peaks partially overlapping the trough corresponding to the solvent. The slope of the calibration plots prepared by using ultraviolet detection was much smaller. For example, with 3mM phthalic acid (pH 6) as eluent, slopes of around 2.5 cm.l.mmole<sup>-1</sup> ( $\text{SO}_3^{2-}$  or  $\text{SO}_4^{2-}$ ) or 1.8 cm.l.mmole<sup>-1</sup> ( $\text{S}_2\text{O}_3^{2-}$ ) were observed for 50- $\mu\text{l}$  samples.

With a liquid chromatograph fitted with an ultraviolet detector, however, the 300 IC column did yield well defined peaks (as shown in Fig. 1B) with elution times shorter than those observed with the other instrument (*e.g.*, with a mixture of 2mM  $\text{HOCH}_2\text{SO}_3^-$ , 1mM  $\text{SO}_4^{2-}$  and 4mM  $\text{S}_2\text{O}_3^{2-}$  the corresponding peaks appeared after 0.7, 2.6 and 5.2 min).

The need for a sulphite stabilizer when using

degassed acidic eluents was quickly apparent. For example, with freshly prepared 100 mg/l. sodium sulphite solution, a second 50- $\mu\text{l}$  injection made just 3 min after the first was found to yield a large sulphate peak preceded by a small (~5 mm) sulphite peak. The same standard, stabilized with HCHO, yielded an  $\text{HOCH}_2\text{SO}_3^-$  peak ~175 mm high.

In comparison studies made with 10mM sodium sulphite containing varying amounts of HCHO, it was found that the sulphate peak height decreased to a minimum value as the aldehyde level was increased from 1 to 50mM, the adduct peak sharpening and attaining a maximum value at the same point. It was concluded that a five-fold molar excess was the minimum amount of stabilizer needed to inhibit aerial oxidation of sulphite. Though the presence of this amount of stabilizer reduced sulphate blanks to a minimum, it was observed that the calibration graphs for sulphite did not necessarily pass through the origin. Some of the shift is due to the difficulty in defining a baseline when the peak is preceded by a negative signal for the solvent. To try to improve the situation, the eluent flow-rate (usually 2 ml/min) was reduced, but this resulted in peak broadening without any shift in peak position. Varied weights of phthalic acid were also added to the sulphite samples, but instead of eliminating the negative solvent signal, this procedure added a shoulder on the leading edge of the sulphite peak.

The suitability of other sulphite stabilizers mentioned by previous authors<sup>4</sup> was re-examined, and yielded dismal results. With solutions initially 10mM in  $\text{SO}_3^{2-}$ , large excesses of fructose, propan-2-ol or glycerol failed to prevent oxidation, and the baseline was distorted by a broad peak just preceding the sulphate peak. The inclusion of increasing amounts of acetone resulted in smaller sulphate peaks, but no adduct peak was detected, probably because this additive caused broadening of the initial negative solvent signal.

Comparison of the retention times for other anions under similar operating conditions indicated that a peak for fluoride would overlap the  $\text{HOCH}_2\text{SO}_3^-$  peak, but subsequent peaks due to ions such as chloride (overlap with  $\text{H}_2\text{PO}_4^-$  peak), nitrite (overlap with bromide) and nitrate should all precede the  $\text{SO}_4^{2-}$  and  $\text{S}_2\text{O}_3^{2-}$  peaks.

With the 300 IC column it was found that the operating conditions had to be modified to achieve separation of the sulphite–HCHO adduct from chloride. As shown in Fig. 2, operating at a higher pH (*e.g.*, 6.5) yielded a separation time of around 0.2 min. The presence of chloride reduced the adduct peak size, and the calibration plots indicated that the standard sulphite solutions used should also contain chloride if this ion is present in the sample. Varying the relative amounts of  $\text{SO}_3^{2-}$  (0.5–2mM) and  $\text{Cl}^-$  (0.25–1mM) showed that such variations did not affect measurement of the individual peak heights. As might be expected, the position of the phosphate ion

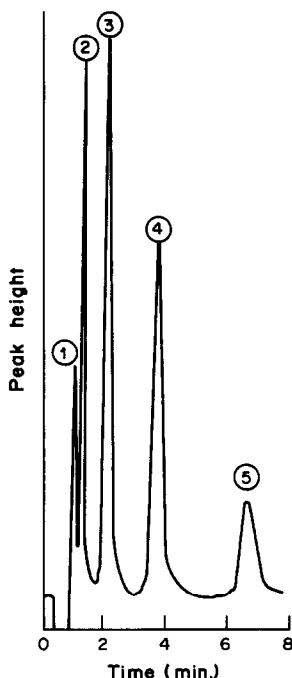


Fig. 2. Elution pattern showing separation of a mixture containing  $1\text{mM}$  levels of  $\text{HOCH}_2\text{SO}_3^-$  (1);  $\text{Cl}^-$  (2);  $\text{NO}_3^-$  (3);  $\text{SO}_4^{2-}$  (4); and  $\text{S}_2\text{O}_3^{2-}$  (5). Room temperature; Vydac 3001C column;  $2\text{mM}$  phthalic acid (pH 6.5) eluent, flow-rate  $1.5\text{ ml/min}$ ;  $50\text{ }\mu\text{l}$  sample; refractive index detection.

peak varied with eluent pH, coming before that of nitrate at pH 6.5, but after it at pH 8.6.

The separation of sulphate and thiosulphate by single-column chromatography appears to yield better results than the procedures outlined by earlier investigators.<sup>6,8-11</sup> With alkaline eluents the retention time for thiosulphate is usually unacceptably long when ion-chromatography conditions ideal for sulphite/sulphate separation are used. One answer is to have two separate runs with different eluents, but this is time-consuming and inconvenient. The other alternative proposed is stepwise gradient elution<sup>6</sup> but nearly 15 min will still be required for total thiosulphate displacement, and the peak is distorted

by tailing. When thiosulphate present in a sample is not to be determined, it is recommended that the column be flushed with a stronger eluent followed by water after every 30 injections.<sup>5</sup> As noted earlier, regular back-flushing of the Vydac columns is also recommended to remove some ill-defined secondary products that slowly reduce the column efficiency. Two possible contaminants are colloidal sulphur and polymerized formaldehyde, but this aspect has yet to be investigated. It was estimated that owing to the noisy background and lower sensitivity of detection, the detection limit for thiosulphate would normally be around  $250\text{ }\mu\text{M}$  ( $\sim 60\text{ mg/l}$ ). The upper limit was set by the column becoming overloaded with ion concentrations  $>10\text{mM}$  (broad peaks) and non-linear calibration curves being obtained.

Practical applications have yet to be tested, but areas of potential interest are the determination of sulphite/sulphate ratios in boiler waters, and analysis of photographic solutions.

#### REFERENCES

1. H. Small, T. S. Stevens and W. C. Bauman, *Anal. Chem.*, 1975, **47**, 1801.
2. L. D. Hansen, B. E. Richter, D. K. Rollins, J. D. Lamb and D. J. Eatough, *ibid.*, 1979, **51**, 633.
3. T. S. Stevens, V. T. Turkelson and W. R. Albe, *ibid.*, 1977, **49**, 1176.
4. M. Lindgren, A. Cedergren and J. Lindberg, *Anal. Chim. Acta*, 1982, **141**, 279.
5. M. J. McCormick and L. M. Dixon, *J. Chromatog.*, 1985, **322**, 478.
6. T. Sundén, M. Lindgren, A. Cedergren and D. D. Siemer, *Anal. Chem.*, 1983, **55**, 2.
7. P. K. Dasgupta, K. de Cesare and J. C. Ullrey, *ibid.*, 1980, **52**, 1912.
8. D. T. Gjerde, J. S. Fritz and G. Schmuckler, *J. Chromatog.*, 1979, **186**, 590.
9. D. T. Gjerde, G. Schmuckler and J. S. Fritz, *ibid.*, 1980, **187**, 35.
10. F. J. Trujillo, M. M. Miller, R. K. Skogerboe, H. E. Taylor and C. L. Grant, *Anal. Chem.*, 1981, **53**, 1944.
11. L. J. Holcombe, B. F. Jones, E. E. Ellsworth and F. B. Meserole, in *Ion Chromatographic Analysis of Environmental Pollutants*, Vol. 2, p. 401. Ann Arbor Science, Ann Arbor, 1979.

## SHORT COMMUNICATIONS

# SPECTROPHOTOMETRIC MICRODETERMINATION OF BISMUTH IN ORGANIC COMPOUNDS AFTER OXYGEN-FLASK COMBUSTION

H. N. A. HASSAN, M. E. M. HASSOUNA\* and Y. A. GAWARGIOUS†  
Microanalytical Research Laboratory, National Research Centre, Dokki, Cairo, Egypt

(Received 26 June 1987. Revised 24 November 1987. Accepted 8 December 1987)

**Summary**—A method has been developed for the micro and submicro determination of bismuth in organic compounds, based on combustion in an oxygen-filled flask, provided with a silica spiral instead of the conventional platinum holder (which alloys with bismuth). After absorption of the products in hydrochloric acid (1 + 1), the solution is chemically treated to convert the bismuth into the orange-yellow  $\text{BiI}_4^-$  complex, then the absorbance is measured at 465 nm. Analysis of 12 organic compounds containing 28–74% of bismuth yielded satisfactory results with a maximum standard deviation of 0.4%.

Bismuth is used in medicinal compounds, pharmaceutical preparations,<sup>1</sup> and many synthetic industrial products. The methods available for its determination employ Parr-bomb fusion or wet digestion for decomposition of organobismuth compounds, followed by gravimetric,<sup>2</sup> titrimetric,<sup>3,4</sup> polarographic,<sup>4</sup> spectrophotometric<sup>4</sup> or other<sup>4</sup> measurements.

Although reasonable attention has been paid to the spectrophotometric determination<sup>4,5</sup> of traces of inorganic bismuth, no simpler and faster means for the decomposition of organobismuth compounds have been described. The present work has extended the use of oxygen-flask combustion to bismuth compounds, followed by spectrophotometric measurement of bismuth as the orange-yellow iodide complex,<sup>5</sup>  $\text{BiI}_4^-$ , at 465 nm.

### EXPERIMENTAL

#### Apparatus

The combustion flask is a 500-ml "Schöniger" flask, the stopper of which carries a spiral of 5–6 turns made of 2-mm diameter silica or borosilicate glass rod, the free end of which is 7–8 cm distant from the stopper.

#### Reagents

Except where otherwise stated, all reagents were of analytical grade and doubly distilled water was always used. A 1 mg/ml standard bismuth solution was made by dissolving 0.2321 g of  $\text{Bi}(\text{NO}_3)_3$  in 50 ml of nitric acid (1 + 1) and diluting to 1 litre with water. This solution was diluted further as required.

#### Sample pretreatment for pharmaceutical preparations

*Bismonil*. Bismuth subsalicylate was kindly supplied by The Nile Co. for Pharmaceutical & Chemical Industries, El-Amiria, Cairo, Egypt, as an oil suspension in ampoules,

each containing 0.2 g of  $\text{C}_7\text{H}_5\text{O}_4\text{Bi}$ . To extract the active ingredient the contents of the ampoule were transferred to a porosity-3 sintered-glass disk, suction was applied, and the residue on the disk was washed with diethyl ether and then with alcohol until the powder was freed completely from the oil. It was dried at 105° and stored.

*De-Nol*. Tripotassium dicitratobismuthate ( $\text{C}_{12}\text{H}_{10}\text{O}_{16}\text{K}_3\text{Bi}$ ), was produced by Gist-Brocades nv (Delft, Netherlands) and provided as a suspension. To extract the active ingredient, 20 ml of the suspension were heated on a steam-bath until a sticky semi-solid was left. This was covered with alcohol, crushed with a thick glass rod, heated to remove the alcohol, then dried at 105°.

#### Procedure

Weigh 3–5 mg of the organobismuth compound and transfer it onto a piece of ashless filter paper. Fold the paper into a cylindrical shape, and fix it tightly in the silica spiral. Light the fuse and burn the sample in the usual way in a 500-ml oxygen-filled flask containing 10 ml of hydrochloric acid (1 + 1). Shake the flask for 10 min, rinse the stopper, add 1 ml of concentrated sulphuric acid, and evaporate the solution, first on a hot-plate and then on a steam-bath, nearly to dryness. Transfer the flask contents quantitatively with water into a 50-ml standard flask, then add 3 ml of sulphuric acid (1 + 1), 2 ml of 2% ascorbic acid solution and 5 ml of fresh 20% potassium iodide solution, in that order, and dilute to the mark with water. Mix well and after 5 min, measure the absorbance of the orange-yellow iodide complex at 465 nm against a blank. Determine the weight of bismuth by reference to a graph covering the range 0.1–2.5 mg of bismuth and prepared by treatment of 0.1–2.5 ml of standard bismuth solution with 5 ml of sulphuric acid (1 + 1), ascorbic acid and potassium iodide, and dilution to 50 ml, as above.

### RESULTS AND DISCUSSION

The first combustions, conducted in 250-ml oxygen-flasks, yielded bismuth recoveries that were low by 30–40%, in agreement with Macdonald and Sirichanya,<sup>3</sup> who reported some alloying with platinum even in the presence of fusion agents such as

\*Present address: Chemistry Department, Faculty of Science at Beni-Suef, Cairo University, Beni-Suef, Egypt.

†To whom correspondence should be addressed.

Table 1. Spectrophotometric determination of Bi in organobismuth compounds after oxygen-flask combustion

Compound and formula	Concentration measured,* $\mu\text{g/ml}$	Bi, %		Standard deviation,* Bi, %
		Theory	Found*	
Triphenylbismuth, $\text{C}_{18}\text{H}_{15}\text{Bi}$	12.0–35.3†	47.46	47.3–47.5†	0.1†
Bismuth oxalate, $\text{C}_6\text{O}_{12}\text{Bi}_2$	15.0–31.2	61.28	61.5–61.6	0.3
Bismuth citrate, $\text{C}_6\text{H}_5\text{O}_7\text{Bi}$	18.2–31.3	52.50	52.3–52.8	0.3
Bismuth pyrogallate, $\text{C}_6\text{H}_3\text{O}_3\text{Bi}$	12.4–30.7	62.93	62.7–63.2	0.4
Bismuth subacetate, $\text{C}_2\text{H}_3\text{O}_3\text{Bi}$	20.5–31.8	73.58	73.3–73.9	0.3
Bismuth oxinate, $\text{C}_{27}\text{H}_{18}\text{O}_3\text{N}_3\text{Bi}$	17.2–36.8	31.69	31.5–31.8	0.2
Bi dimethylglyoximate, $\text{C}_4\text{H}_6\text{N}_2\text{O}_4\text{Bi}_2$	12.6–36.0	74.09	74.0–74.7	0.3
2,2'-Bipyridylbismuth trichloride, $\text{C}_{10}\text{H}_8\text{N}_2\text{BiCl}_3$	21.0–32.2	44.32	44.1–44.6	0.3
Bi diethyldithiocarbamate, $\text{C}_{15}\text{H}_{30}\text{N}_3\text{S}_6\text{Bi}$	14.7–30.1	31.97	31.8–32.3	0.3
Bi tetramethylenedithiocarbamate, $\text{C}_{15}\text{H}_{24}\text{N}_3\text{S}_6\text{Bi}$	21.2–33.2	32.26	32.1–32.5	0.2
Bismuth subsalicylate (Bismonil), $\text{C}_7\text{H}_5\text{O}_4\text{Bi}$	24.1–30.7	57.71	57.4–58.0	0.4
Tripotassium dicitratobismuthate (De-Nol), $\text{C}_{12}\text{H}_{10}\text{O}_{16}\text{K}_3\text{Bi}$	13.1–27.4	28.37	28.2–28.5	0.2

\*Four determinations; concentrations refer to final solution.

†Ten determinations.

sodium peroxide, and therefore applied wet combustion instead. Other workers<sup>3,6-9</sup> also found alloy formation or insoluble oxide formation with closed-flask decomposition of organic bismuth, antimony, arsenic, lead, iron and copper compounds, causing seriously low results. This alloy formation was assumed to occur only in the reducing atmosphere formed around the platinum contact surface<sup>6</sup> by partial combustion of the carbon-rich filter paper. Surprisingly, ignition of ashless filter paper alone, after addition of bismuth nitrate solution to the hydrochloric acid absorption solution, also resulted in low bismuth values. Thus, it seems that hot platinum can alloy with bismuth even on contact with the bismuth solution during the shaking. This is in accordance with a report<sup>10</sup> of bismuth losses of 20–90% during the decomposition of silicates in platinum ware. No improvement was achieved on boiling the platinum sample holder in the acid absorbent for periods even longer than 10 min. Benzoyl peroxide as auxiliary oxidant has been reported<sup>11</sup> to prevent platinum alloying with arsenic when the absorption solution is aqueous iodine alone,<sup>11</sup> or containing four drops of 0.5M nitric acid.<sup>12</sup> Use of this procedure for bismuth compounds did not raise the low bismuth figures, however.

Further combustions were performed with use of a quartz spiral, as utilized for arsenic compounds,<sup>9,13-16</sup> with iodine<sup>11</sup> or iodine–nitric acid mixture<sup>12</sup> for absorption, but low bismuth results were still obtained even with shaking periods of up to 30 min. This was ascribed to incomplete dissolution of the yellowish traces of  $\text{Bi}_2\text{O}_3$  deposited on the quartz spiral.

When 10 ml of hydrochloric acid (1 + 1) were used as absorbent, the ashless filter paper was reduced in size, and more oxygen was made available by use of 500-ml flasks, combustion of 3–5 mg samples yielded correct bismuth analyses. Although the use of 10 ml

of nitric acid (1 + 1) as absorbent proved equally satisfactory, hydrochloric acid was preferred for generality because it was also suitable for organonickel<sup>8</sup> and copper compounds.<sup>17</sup> For comparison, some wet digestions with the conventional  $\text{H}_2\text{SO}_4\text{--H}_2\text{O}_2$  mixture were performed, but the results were no better.

Use of this relatively unselective spectrophotometric finish is possible because organic compounds containing more than one metal are unusual. Also, high sensitivity is not essential since the micro procedure requires use of at least a 3-mg sample of the bismuth compounds. The iodide method selected has adequate sensitivity and selectivity, is rapid and simple, and uses inexpensive readily available reagents. Chloride interference is eliminated by removal as hydrogen chloride by heating with sulphuric acid; other possible interferences<sup>5</sup> are not observed in the proposed procedure.

New organic reagents for bismuth<sup>18-20</sup> are not necessary for this application.

Analysis of triphenylbismuth by the proposed procedure (10 determinations) gave a maximum error of  $\pm 0.5\%$ . Four analyses of each of another 11 organic bismuth compounds (28–74% Bi), including two pharmaceutical preparations, yielded satisfactory results (Table 1) (average standard deviation 0.3%).

#### REFERENCES

1. T. S. Ma and R. C. Rittner, *Modern Organic Elemental Analysis*, p. 235. Dekker, New York, 1979.
2. R. Belcher, D. Gibbons and A. Sykes, *Mikrochim. Acta*, 1952, **40**, 76.
3. A. M. G. Macdonald and P. Sirichanya, *Microchem. J.*, 1969, **14**, 199.
4. J. S. Fritz, in *Treatise on Analytical Chemistry*, I. M. Kolthoff and P. J. Elving (eds.), Part, II, Volume 8, p. 148. Interscience, New York, 1965.
5. Z. Marczenko, *Spectrophotometric Determination of Elements*, Chapter 9, Ellis Horwood, Chichester, 1976.

6. R. Belcher, A. M. G. Macdonald and T. S. West, *Talanta*, 1958, **1**, 408.
7. A. M. G. Macdonald, *Analyst*, 1961, **83**, 3.
8. S. W. Bishara, Y. A. Gawargious and B. N. Faltaoos, *Anal. Chem.*, 1974, **46**, 1103.
9. Y. A. Gawargious, L. S. Boulos and B. N. Faltaoos, *Talanta*, 1976, **23**, 513.
10. E. B. Sandell and H. Onishi, *Photometric Determination of Traces of Metals, Part I: General Aspects*, p. 83. Wiley, New York, 1978.
11. E. Celon, S. Degetto, G. Marangoni and L. Sindellari, *Mikrochim. Acta*, 1976 **I**, 113.
12. Xiang Lijuan, Hou Xiaming and Hu Zhenyuan, *Fenxi Huaxue*, 1982, **10**, 243.
13. W. Merz, *Mikrochim. Acta*, 1959, 640.
14. M. Corner, *Analyst*, 1959, **84**, 41.
15. K. Eder, *Mikrochim. Acta*, 1960, 471.
16. R. Püschel and Z. Štefanac, *ibid.*, 1962, 1108.
17. Y. A. Gawargious, M. E. M. Hassouna and H. N. A. Hassan, *ibid.*, 1986 **III**, 15.
18. V. E. Poladyan, S. F. Pakhol'chuk, L. M. Avlasovich and A. M. Andrianov, *Ukr. Khim. Zh.*, 1985, **51**, 743.
19. H. Sun and C. Li, *Fenxi Huaxue*, 1983, **11**, 767.
20. Ru-Qin Yu, Zheng-Qi Zhang and Zhi-Hua Zhang, *Talanta*, 1984, **31**, 1121.



## EXTRAKTION VON GINSENOSIDEN MIT AMMONIAK UND KOHLENSÄURE UNTER ERHÖHTEM DRUCK

J. R. KIM\* und H. LENTZ

Universität-Gesamthochschule Siegen, Fachbereich Chemie, Postfach 101240, D-5900 Siegen, BRD

(Eingegangen am 23. September 1987. Angenommen am 21. November 1987)

**Zusammenfassung**—Die Extrahierbarkeit von Ginsenosiden aus Ginsengpflanzen durch Ammoniak und durch Kohlensäure wurde untersucht. Kohlensäure kann Ginsenoside praktisch nicht extrahieren, auch dann nicht, wenn Wasser zugesetzt wird. Die mit Ammoniak gewonnenen Extrakte haben einen deutlich höheren Ginsenosidanteil als Extrakte, die mit Wasser oder Methanol gewonnen wurden. Mit Ammoniak ließ sich eine Ginsenosidkomponente mehr gewinnen als mit Wasser.

**Summary**—Extraction of ginsenosides from plant material with carbon dioxide and ammonia has been examined. Carbon dioxide cannot extract the ginsenosides from either dry or wet material, but ammonia gives a higher yield of the ginsenoside fraction than conventional extraction with water or methanol, and extracts one more component than water does.

Als wirksame Inhaltsstoffe der Ginsengarten gelten Triterpen-Saponine oder Ginsenoside.<sup>1</sup> Diese wurden von Shibata *et al.* mittels Dünnschichtchromatographie getrennt und als Ginsenoside Rx klassifiziert.<sup>2,3</sup> Ginsenoside sind durch die Hydroxylgruppen in den Glucosidringen gut in polaren Lösungsmitteln löslich, so daß Ginsengextrakte normalerweise durch die Extraktion mit Alkohol oder Wasser gewonnen werden.<sup>4</sup>

In neuerer Zeit ist für viele empfindliche Inhaltsstoffe als wirksames und schonendes Extraktionsverfahren die Extraktion mit komprimierten Lösungsmitteln angewandt worden. Das gilt besonders für das Lösungsmittel Kohlendioxid, das im industriellen Maßstab zur Decoffeinierung von Kaffee und zur Gewinnung von Hopfeninhaltsstoffen eingesetzt wird. Die Kohlensäure kann dabei überkritisch ("Extraktion mit überkritischen Gasen") aber auch unterkritisch sein, z.B. unter dem eigenen Dampfdruck stehen.

Aus Versuchen, eine Chromatographie mit überkritischen Lösungsmitteln durchzuführen, ist be-

kannt,<sup>5</sup> daß Ammoniak (kritische Temperatur 132°, kritischer Druck 113,5 bar) viele Stoffe und besonders stickstoffhaltige Substanzen gut lösen kann. Beispielsweise ist die Löslichkeit von Coffein in Ammoniak<sup>6</sup> deutlich größer als dessen Löslichkeit in Kohlensäure.<sup>7</sup> Sehr oft jedoch ist die Reaktivität des Ammoniaks für die Anwendung als Extraktionsmittel schädlich.

In der vorliegenden Arbeit sollte die Möglichkeit einer Extraktion von Ginsenosiden durch Kohlensäure und durch Ammoniak untersucht werden. Dabei wurden die Versuche mit Ammoniak auf die Bedingungen 100° und 100 bar beschränkt, da eine Variation der Versuchsbedingungen erst sinnvoll erscheint, wenn das Verfahren wirtschaftlich vielversprechend ist, so daß optimale Bedingungen gesucht werden müssen.

### EXPERIMENTELLES

Die Ginsengwurzeln stammten aus Korea (Panax Ginseng C. A. Meyer). Sie wurden grob zerkleinert und dann der Extraktion unterzogen.

Als Extraktionsgefäß diente ein Autoklav aus V4A-Stahl mit einem Innendurchmesser von 17 mm, einem Außendurchmesser von 25 mm und einer Höhe von 410 mm. Der Autoklav wurde elektrisch beheizt und die Temperatur elektronisch auf  $\pm 1^\circ$  geregelt. Der Druck wurde durch eine Dosierpumpe erzeugt und mit Federmanometern

\*Ständige Anschrift: Department of Chemistry, Hanyang University, 396 Daehak-dong, Ansan, Kyongki-do, Republic of Korea.

Tabelle 1. Bedingungen und Ausbeuten der Ginsenosidextraktionen

Extraktionsmittel	Druck, bar	Temperatur, °C	Extraktionszeit, min	Ausbeute, Gew. %
Methanol (80%ig)	1	50	90	33
Wasser	1	70	90	34
Ammoniak	100	104	15	19
Ammoniak (zu 21,5% feuchter Ginseng)	100	104	20	20
Kohlendioxid	200	104	60	<1
Kohlendioxid (feuchter Ginseng)	150	51	40	<1

Tabelle 2. Prozentuale Verteilung der Ginsenoside ( $R_x$ )<sup>2,3</sup>,  $R_p$ -Werte (in Klammern), Gesamtfläche der Flecken (in mm<sup>2</sup>) und der Ginsenosidanteil am Extrakt (%)

Extraktionsmittel	Rb <sub>1</sub>	Rb <sub>2</sub>	Rc	Rd	Re	Rf	Rg <sub>1</sub>	Rg <sub>2</sub>	R'	R''	Fläche	Ginsenosidanteil
*—*	12,5 (0,04)	11,7 (0,08)	12,1 (0,11)	10,1 (0,25)	15,0 (0,18)	14,0 (0,29)	11,3 (0,49)	13,4 (0,68)	—	—	146	1,0
Methanol (80%)	20,3 (0,03)	17,4 (0,07)	15,4 (0,11)	7,7 (0,25)	23,1 (0,18)	16,1 (0,29)	—	—	—	—	78	0,5
Wasser	14,4 (0,04)	15,1 (0,07)	14,2 (0,11)	13,0 (0,25)	9,9 (0,17)	9,2 (0,29)	6,5 (0,49)	8,7 (0,68)	9,1 (0,39)	—	96	0,65
Ammoniak	11,3 (0,04)	9,7 (0,08)	7,5 (0,11)	8,1 (0,25)	6,5 (0,18)	11,7 (0,30)	8,6 (0,49)	12,1 (0,68)	9,2 (0,39)	15,3 (0,57)	171	1,2
Ammoniak (feuchter Ginseng)	12,4 (0,04)	9,5 (0,08)	9,0 (0,11)	10,9 (0,25)	9,7 (0,18)	9,5 (0,29)	8,0 (0,50)	11,2 (0,68)	8,6 (0,39)	11,4 (0,57)	193	1,3

\*Ginsana—Kapsel—Inhalt als Standard.

gemessen. Das Extraktionsmittel durchströmte den Autoklaven und wurde durch ein geregeltes Ventil in ein Glasgefäß hinein entspannt. Dabei fiel der gelöste Extrakt aus. Das verbrauchte Gas konnte nach der Entspannung ebenfalls bestimmt werden. Die Apparatur ist im Detail an anderer Stelle beschrieben.<sup>8</sup>

Ein Teil der zerkleinerten Ginsengwurzeln wurde mit Methanol bzw. Wasser in einer Soxhlet-Apparatur extrahiert, um Vergleichsproben zu haben. Die Analyse der Extrakte erfolgte durch Dünnschichtchromatographie. Als Standard wurde der Inhalt von Ginsana Weichgelatine-Kapseln (Weimer, Rastatt) verwendet. Die Dünnschichtchromatographie wurde auf DC-Aluminiumfolien, Typ Kieselgel 60 F<sub>254</sub> (Merck) mit einem Laufmittel aus Chloroform, Methanol und Wasser im Verhältnis 65:35:10 durchgeführt.<sup>1</sup> Nach der Trennung wurde die Platte getrocknet, mit einer Mischung aus Essigsäureanhydrid, Schwefelsäure und Ethanol (5:5:90) besprüht und bei 105° 10 Minuten nachgetrocknet.

#### ERGEBNISSE UND DISKUSSION

Die Ausbeuten (trockene Extraktgewichte bezogen auf die eingesetzten trockenen Ginsengmengen) der Extraktionsversuche sind mit den Drucken, Temperaturen und Extraktionszeiten in Tabelle 1 angegeben.

Die Ausbeute an Extrakt ist noch nicht die Ausbeute an Ginsenosiden. Durch die Aufnahme von Verdünnungsreihen wurde ein linearer Zusammenhang zwischen den Substanzmengen und den Flächen auf der Dünnschichtplatte gefunden. Deshalb kann aus diesen Flächen auf die einzelnen Ginsenosidfraktionen und auf den gesamten Ginsenosidanteil zurückgeschlossen werden. Für jeden Extrakt wurde die gleiche Menge (3 µl) auf die Dünnschichtplatte gegeben. Die prozentuale Verteilung der Ginsenoside ( $\pm 0,2$ ) und ihre Retentionswerte ( $R_f$ ) sind in Tabelle 2 angegeben. Aus der Gesamtgröße der Flecken läßt sich der Ginsenosidanteil angeben, indem der Inhalt der Ginsana-Kapseln als Vergleichssubstanz benutzt wird. Deren Ginsenosidanteil ist nach Herstellerangaben 1,0%; nämlich 4 mg Ginsenosid auf 400 mg Kapselinhalt. Die letzte Spalte der Tabelle 2 ergibt sich also aus dem Flächenvergleich der Extrakte zum benutzten Standardpräparat und ist nur eine relative Angabe.

Die vorliegenden Ergebnisse lassen sich dahin zusammenfassen, daß überkritische Kohlensäure nicht als Extraktionsmittel für Ginsenoside geeignet ist. Ammoniak dagegen scheint für ein Extraktionsverfahren der Ginsenoside wegen seiner guten Selektivität und seines geringen Zeitbedarfes brauchbar zu sein. Mit Ammoniak läßt sich ein Ginsenosid mehr extrahieren als selbst mit Wasser. Es könnte sich zwar auch um eine Modifizierung eines Ginsenosids durch Reaktion mit Ammoniak handeln. Jedoch ist das den Prozentzahlen nach unwahrscheinlich. Die Verwendbarkeit von Ammoniak als Extraktionsmittel für Naturstoffe ist vermutlich selten gegeben. Denn oft stört die Reaktivität des Ammoniaks. So werden Hopfeninhaltsstoffe ab-

gebaut und Kaffeebohnen durch Amidbildung geschädigt.<sup>8</sup>

*Danksagung*—Wir sind Herrn Dr. U. Liedtke für die gute Zusammenarbeit dankbar. Der Deutschen Forschungsgemeinschaft und dem Fonds der Chemischen Industrie danken wir für die finanzielle Förderung. Wir danken der koreanischen Forschungsorganisation KOSEF für ein Forschungsstipendium (J.R.K.).

#### LITERATUR

1. H. R. Schulten and F. Soldati, *J. Chromatog.*, 1981, **212**, 37.
2. S. Shibata, S. Sanada, N. Kondo, J. Shoji and O. Tanaka, *Chem. Pharm. Bull.*, 1974, **22**, 421.
3. K. Kappstein, *Das Buch vom Ginseng*, Morzsiany Verlag, Bern, 1980.
4. F. Soldati and O. Sticher, *Planta Med.*, 1980, **38**, 348.
5. J. C. Giddings, M. N. Myers, L. McLaren and R. A. Keller, *Science*, 1968, **159**, 67.
6. J. R. Kim and H. Lentz, submitted to *Fluid Phase Equilibria*, 1987.
7. H. Lentz, M. Gehrig and J. Schulmeyer, *Physica*, 1986, **139/140B**, 70.
8. U. Liedtke, *Ammoniak als Extraktionsmittel*, Dissertation, Siegen, 1987.

## CORRELATION OF SPECTRAL-LINE INTENSITY-RATIO FLUCTUATIONS OF DIFFERENT ELEMENTS

BO THELIN

Swedish Institute of Space Physics,\* P.O. Box 812, S-981 28 Kiruna, Sweden

(Received 22 June 1987. Revised 16 October 1987. Accepted 14 November 1987)

**Summary**—Reasonably linear correlations have been obtained for spectral lines from different elements in an double-chamber hollow-cathode lamp when the spectral-line intensity-ratio fluctuations are plotted vs. the photon energies and ionization energies of these lines. When these fluctuations are plotted as a function of the upper level energies, no linear relation at all is obtained. The analyses were done by using a computerized image-dissector echelle-spectrometer system.

The principle of use of internal standards in spectrometry is based on relating the intensity ratio of selected spectral lines of the analyte and internal-standard elements to concentration ratios and was introduced by Gerlach.<sup>1</sup> In later work there was a tendency to exclude "bad" line-pairs from the analysis, without giving any satisfactory explanation. In a theoretical paper by Barnett *et al.*<sup>2</sup> the principles behind choosing analyte and internal-standard lines were given. Suckewer<sup>3</sup> studied the essential sources of spectroanalytical errors connected with the determination of the density ratios in plasmas for different elements. These authors and others assume that the line intensity from an atomic transition  $E_m \rightarrow E_n$  is proportional to the Boltzmann factor  $\exp(-E_m/kT)$ , where  $E_m$  is the energy of the upper energy level, and  $h\nu_{mn} = E_m - E_n$  is the energy of the emitted photon. Thus the conventional intensity formula is written

$$I_{mn}^a = C_{mn}^a \exp(-E_m^a/kT) / \sum_i g_i \exp(-E_i^a/kT) \quad (1)$$

where  $I_{mn}^a$  is the intensity of light with photon energy  $h\nu_{mn}$  from sample constituent "a",  $C_{mn}^a$  is a composite of factors derived from the transition probability, electron and atomic densities, density, quenching, absorption effects, sample geometry, and apparatus constants,  $\sum_i g_i \exp(-E_i^a/kT)$  is the partition sum of all energy levels of an atom, and  $g_i$  is the statistical weight of an energy level.

In the work described here the spectral-line intensity-ratio fluctuations have been studied with use of a double-chamber hollow-cathode lamp (DCHC).<sup>4</sup> The results show that the data fit badly to equation (1) but fit fairly well to a formula with a new exponential factor instead of the one in (1).

### EXPERIMENTAL

The experimental work was done at the Swedish Institute for Metals Research, Stockholm, where a double-chamber hollow-cathode (DCHC) lamp was studied for spectro-

analytical purposes together with an image-dissector echelle-spectrometer system (IDES). This DCHC lamp is a new excitation source in optical emission spectroscopy and is used for trace element analysis of steel samples. The operating conditions used are given in Table 1. The hollow steel sample was sputtered from both ends in the lamp and the elements studied were Mn, V, Ni, Al, Si, Cu, Ti, Mo, Cr, W, Co, Ag, Ca and Fe. The spectral lines used are listed in Table 2. The steel samples used were JK5A, 7A, 2B, and 1B for the 170-W experiment and JK 2B and 6A for the 250-W experiment.

As registration system the image-dissector echelle-spectrometer (IDES) system<sup>5</sup> was used. This system, which works with photon counting, is very versatile and consists of an echelle spectrograph with high resolution, an image-dissector tube, and a minicomputer system which controls the peak measurements.

Table 1. Experimental parameters

<i>DCHC-lamp</i>	
Flush time	60 sec
Preburn time	60 sec
Pressure, Ne	1 mmHg
Current	1100 and 700 mA
Power	250 and 170 W
<i>Sample</i>	
Tube-shaped, 30 × 4 mm bore	
<i>Spectrometer</i>	
Type	Echelle (IDES)
Wavelength region	200–800 nm
Linear dispersion	0.16 nm/mm at 200 nm 0.32 nm/mm at 400 nm
Entrance and exit slits	35 μm
Integration time	60 sec
Integration time per line	1.5 sec
Integration time per measurement point	0.1 sec

Table 2. Spectral lines used

Element	Wavelength, nm	Element	Wavelength, nm
Mn	279.5	Mo	386.4
V	438.0	Cr	425.5
Ni	341.5	W	429.5
Al	396.2	Co	345.4
Si	288.2	Ag	328.1
Cu	324.8	Ca	396.9
Ti	375.3	Fe	372.0

\*Formerly "Kiruna Geophysical Institute".

Every spectral line was measured 15 times, each for 0.1 sec at the peak of the integrated signal, equivalent to a total integration time of 1.5 sec, long enough to give adequately precise results.

### RESULTS AND DISCUSSION

In previous papers<sup>6-8</sup> a new method of analysis was presented, where the fluctuations of the intensity ratios from two simultaneously measured spectral lines were studied, with ICP light-sources ("end-on" and "side-on") and a hollow-cathode lamp for flat metal samples (FSHC)<sup>9,10</sup> together with two different IDES systems.

From the ratio between the intensities of two simultaneously measured lines from sample constituents "a" and "b" respectively, and differentiation of the logarithmic form of equation (1), we obtain

$$\frac{d(I_{mn}^a/I_{m'n'}^b)}{(I_{mn}^a/I_{m'n'}^b)} = \frac{d(C_{mn}^a/C_{m'n'}^b)}{(C_{mn}^a/C_{m'n'}^b)} + \left(\frac{1}{kT}\right) \frac{dT}{T} (E_m^a - E_{m'}^b - \bar{E}^a + \bar{E}^b) \quad (2)$$

where  $\bar{E}^a$  is the Boltzmann mean value

$$\left[ \sum_i g_i E_i \exp(-E_i/kT) \right] / \left[ \sum_i g_i \exp(-E_i/kT) \right]$$

estimated from the term scheme of each element.<sup>11</sup>

In this and the previous papers the absolute values of the derivatives have been identified as the maximum relative deviations in the observed data set. These data have been obtained from a series of repeated simultaneous measurements of line intensities. The ratios of pairs of simultaneously measured line intensities are averaged for each line-pair. The maximum relative deviation from the average value of each line-pair ratio is taken as the absolute value of  $d(I_{mn}^a/I_{m'n'}^b)/(I_{mn}^a/I_{m'n'}^b)$  in equation (2).

If  $R$  is used as an abbreviation for the maximum relative deviation, and  $|E_m^a - E_{m'}^b - \bar{E}^a + \bar{E}^b|$  is denoted by  $D(E)$ , we can write equation (2) in the form

$$R(I_{mn}^a/I_{m'n'}^b) = R(C_{mn}^a/C_{m'n'}^b) + D(E)R(T)/kT \quad (3)$$

According to this equation it should be mathematically possible to obtain a straight line with slope  $R(T)/kT$  by plotting  $R(I_{mn}^a/I_{m'n'}^b)$  vs.  $D(E)$  for spectral line-pairs of elements a and b.

From repeated intensity measurements of different spectral lines with the ICP-IDES and FSHC-IDES systems<sup>6-8</sup> it was discovered that no linear relationship could be obtained for the data points by use of equation (3). A much better result was obtained with an intensity formula with an exponential factor  $\exp[-(J^a + hv_{mn}^a)/kT]$ , giving

$$D(E) = |J^a - J^b + hv_{mn}^a - hv_{m'n'}^b| \quad (4)$$

than by the standard formula, which is based on the assumption of local thermal equilibrium (LTE).  $J$  is the ionization energy and  $hv_{mn}$  is the photon energy. These papers also give a more profound discussion of

the statistics and how the different parts of equation (3) relate to each other. Theoretical considerations and work by S. Yngström<sup>12</sup> have given strong support to this method of fluctuation analysis of line-pairs from different elements.

Similar linear and non-linear relationships for different  $D(E)$ -expressions, as mentioned above, have also been obtained with the DCHC lamp, as shown in Figs. 1 and 2. Four different steel samples were run

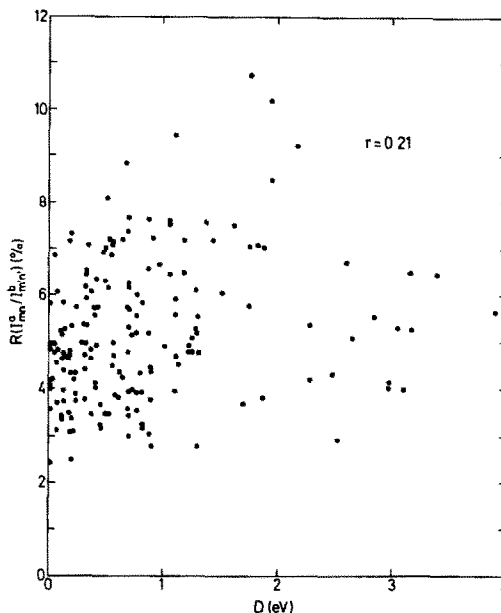


Fig. 1. Relative fluctuations of spectral line-pair intensity ratios plotted vs.  $D(E) = |E_m^a - E_{m'}^b - \bar{E}^a + \bar{E}^b|$ , for use of the DCHC-lamp at 170 W. For information about samples and runs see text.

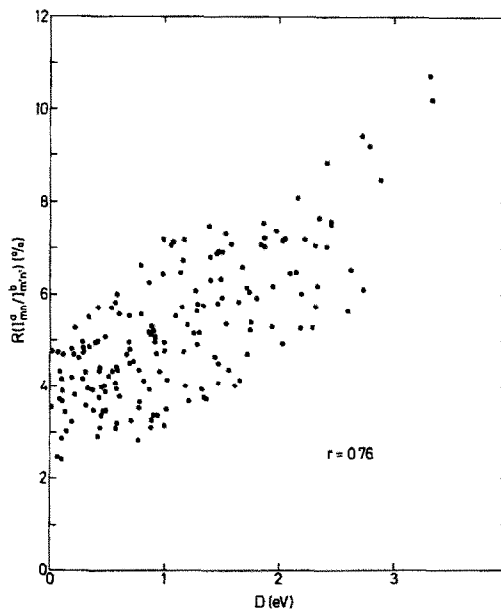


Fig. 2. Relative fluctuations of spectral line-pair intensity ratios plotted vs.  $D(E) = |J^a - J^b + hv_{mn}^a - hv_{m'n'}^b|$  for use of the DCHC-lamp at 170 W.

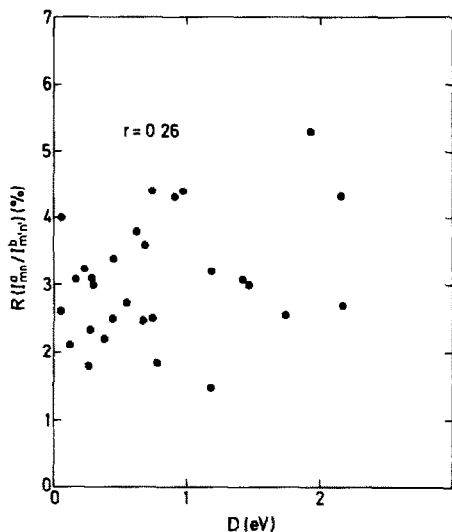


Fig. 3. Plot for Fig. 1, for DCHC-lamp run at 250 W.

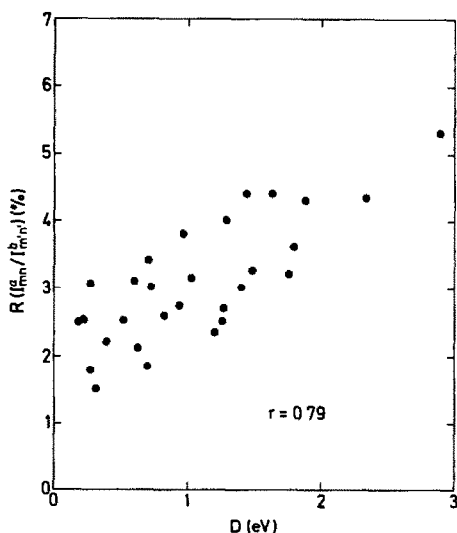


Fig. 4. Plot as for Fig. 2, for DCHC-lamp run at 250 W.

5 times each in succession at a power of 170 W, and analysed for 14 different elements. Hence each point in these graphs has "collected" intensity ratio fluctuations from 20 measurements. From this data set it is possible to compare the two exponents in the graphs. As in the previous work, the data correlate badly with the old LTE formula (1)—see Fig. 1—but

show good correlation with an intensity formula with the factor  $\exp[-(J^a + hv_{mn}^a)/kT]$ , see Fig. 2. The same phenomenon is also clearly seen from the plots in Figs. 3 and 4, where two different steel samples were run 10 times each in succession at a power of 250 W. For these figures 10 different elements were studied.

As seen from Figs. 2 and 4, moderately good correlation coefficients are obtained. The slope in Fig. 2 is larger than that in Fig. 4, since  $R(T)/kT$  is larger for Fig. 2 because of the lower mean temperature. The correlation coefficients for use of  $D(E) = |E_m^a - E_m^b - \bar{E}^a + \bar{E}^b|$ , Figs. 1 and 3 are extremely poor.

Another conclusion from this investigation is that in analytical work it is important to use line-pairs with  $D(E)$ -values that are as small as possible, to make them temperature-independent. This can be done very easily with the IDES-system, giving good analytical precision. The results obtained agree well with those in the previous papers and also with those of a study for seventeen elements, involving absolute intensities from standard intensity tables.<sup>13</sup>

*Acknowledgements*—The author thanks Dr. S. Yngström at IRF for valuable discussions and crucial theoretical suggestions and Prof. B. Hultqvist for his kind support of this project. The author also thanks the staff at the Swedish Institute for Metals Research in Stockholm and at Sandvik AB, Sandviken for providing laboratory facilities.

#### REFERENCES

1. W. Gerlach, *Z. Anorg. Allg. Chem.*, 1925, **142**, 383.
2. W. B. Barnett, V. A. Fassel and R. N. Kniseley, *Spectrochim. Acta*, 1968, **23B**, 643.
3. S. Suckewer, *ibid.*, 1971, **26B**, 515.
4. B. Berglund and B. Thelin, *Analyst*, 1982, **107**, 867.
5. A. Danielsson and P. Lindblom, *Appl. Spectrosc.*, 1976, **30**, 151.
6. B. Thelin, *Preprint 063*, Kiruna Geophysical Institute, Sweden, 1983.
7. *Idem*, *Analyst*, 1986, **111**, 419.
8. *Idem*, *ibid.*, 1987, **112**, 623.
9. *Idem*, *Jernkontorets Forskning Series D*, Swedish Institute for Metals Research, Stockholm, 1981, No. 355.
10. L. Danielsson and B. Thelin, *Proc. 4th Commission Européenne d'Etude et d'Application de Travaux de l'Analyse en Siderurgie*, Liège, Belgium, 1981.
11. W. F. Meggers, C. H. Corliss and F. Stribner, *Natl. Bur. Stds. Monograph*, No. 32, Part I, 1961.
12. S. Yngström and B. Thelin, *Preprint 062*, Kiruna Geophysical Institute, Sweden, 1983.
13. B. Thelin and S. Yngström, *Spectrochim. Acta*, 1986, **41B**, 403.

## EVALUATION OF CERTAIN PHARMACEUTICALS WITH HEXA-AMMINECOBALT(III) TRICARBONATOCOBALTATE(III)—I

### DETERMINATION OF SOME *N*-SUBSTITUTED PHENOTHIAZINE DERIVATIVES

M. I. WALASH, F. BELAL\* and F. A. ALY

Department of Analytical Chemistry, Faculty of Pharmacy, University of Mansoura, Mansoura, Egypt

(Received 22 July 1987. Revised 12 September 1987. Accepted 29 October 1987)

**Summary**—Hexa-amminecobalt(III) tricarbonatocobaltate(III) (HCTC) has been used for the determination of six *N*-substituted phenothiazine derivatives. The drugs in 10% v/v sulphuric acid medium were titrated with  $5 \times 10^{-3}M$  HCTC with visual or spectrophotometric end-point detection. The stoichiometry of the reaction was assumed and a reaction mechanism suggested. The methods were applied to the analysis of dosage forms with results comparable to those given by the official methods.

Certain salts of trivalent cobalt have high oxidation potentials, which if properly utilized could be useful in the determination of many compounds.<sup>1</sup> Several cobalt(III) compounds have been reported as analytical reagents, viz. cobalt(III) acetate,<sup>2</sup> cobalt(III) sulphate in sulphuric acid<sup>3</sup> and cobalt(III) mixed-ligand complexes.<sup>4</sup> These reagents are either unstable or not easily prepared. Moreover, their oxidation potential is markedly decreased by the presence of complexing agents.

The complex hexa-amminecobalt(III) tricarbonatocobaltate(III) (HCTC) was first described, evaluated and used as an analytical reagent by Baur and Bricker.<sup>5</sup> It is stable in suitably buffered solutions for more than a month, and for years in the dry state. It has been used for determination of several organic and inorganic compounds.<sup>6-10</sup> The purpose of our investigation was to extend the applications to include some pharmaceuticals, specifically phenothiazines.

#### EXPERIMENTAL

##### Reagents

HCTC was prepared as described by Baur and Bricker<sup>5</sup> and used as a  $5 \times 10^{-3}M$  solution made by dissolving 3.0 g of the dry powder in 1 litre of water saturated with sodium bicarbonate, by stirring for 2-3 hr, after which it was filtered, and standardized iodometrically.

Sodium thiosulphate solution,  $5 \times 10^{-3}M$ .

Potassium iodide, 10% solution.

Sulphuric acid, 10% v/v.

Phenothiazines. Pure drug samples were kindly provided by several pharmaceutical companies, and used as received. Dosage forms containing the compounds studied were collected from commercial sources. Standard solutions of the phenothiazines were prepared in 10% v/v sulphuric acid.

##### Procedures

**Visual titrations.** A convenient volume of the phenothiazine solution, accurately measured (about 5 ml), is transferred to a 50-ml conical flask. The titrant is added slowly, with continuous stirring by magnetic stirrer. At first a red or orange colour develops, and the titration is continued until this colour has completely disappeared.

**Spectrophotometric titration.** Aliquots (5 ml) of the sample solution are transferred to 50-ml standard flasks. Titrant is added to each flask, in increasing volumes, followed by dilution to the mark with 10% v/v sulphuric acid. The absorbances are measured at the specified  $\lambda_{\text{max}}$  (Table 1) against water as a blank. The titrant is initially added in volumes increasing in 1-ml increments until the colour intensity is seen to begin to decrease, and then in 0.2-ml increments. The end-point is determined by plotting absorbance vs. volume of titrant added.

The amount of the drug is calculated from

$$\text{Amount of drug} = VMR/N \text{ mg}$$

where  $V$  = ml of HCTC used in the titration,  $M$  = molecular weight of the drug,  $R$  = molarity of HCTC,  $N$  = number of moles of HCTC reacting with 1 mole of analyte.

##### Procedures for dosage forms

**Tablets.** Weigh and pulverize 20 tablets. Weigh accurately an amount of the powder equivalent to about 100 mg of the pure drug. Extract this with three 30-ml portions of 10% v/v sulphuric acid, and filter into a 100-ml standard flask. Wash the filter and dilute to the mark with the acid. Apply either visual or spectrophotometric titration to a suitable aliquot of the solution.

**Ampoules.** Mix the contents of 20 ampoules. Transfer an accurately measured volume equivalent to 100 mg of the pure drug into a 100-ml standard flask, complete to the mark with 10% v/v sulphuric acid, mix, and analyse an aliquot as for tablets.

#### RESULTS AND DISCUSSION

The method is based on the fact that cobalt(III), released from tricarbonatocobaltate(III) in acidic me-

\*To whom correspondence should be addressed.

Table 1. Determination of phenothiazines by the proposed and official methods\*

Compound	Molar ratio	Visual titration		Spectrophotometric titration			Official method, <sup>11,12</sup> %
		Recovery, %	Range, mg	$\lambda_{\max}$ , mm	Range, mg	Recovery, %	
Promazine·HCl	1:2	99.9 (1.6)	2-15	510	1-10	100.5 (0.4)	99.7 (0.6)
Promethazine·HCl	1:2	101.4 (0.6)	2-15	510	1-5	100.9 (0.7)	101.2 (0.6)
Levomepromazine·HCl	1:2	98.8 (1.0)	2-15	570	—	—	101 (1.6)
Perphenazine	1:2	101.6 (0.4)	2-15	525	1-9	100.8 (0.9)	100.7 (0.8)
Fluphenazine·2HCl	1:2	100.6 (0.3)	2-15	495	1-7	101.9 (0.5)	101 (0.5)
Mesoridazine besylate	1:2	101.5 (1.7)	2-15	520	1-10	101.4 (0.7)	102.5 (1.7)

\*The figures in parentheses are the coefficients of variation. The results given are the averages of 15 separate determinations.

dium, directly oxidizes phenothiazines first to red phenothiazonium free radicals, and finally to the colourless sulphoxides. A proposed mechanism is presented in Fig. 1, in accordance with the 1:2 reaction ratio observed. The mechanism of oxidation of chlorpromazine in aqueous medium was reported by Merkle and Discher.<sup>13</sup>

For visual detection of the end-point, the titration must be performed slowly, with continuous and efficient stirring to avoid local excess of the reagent and hence the possible oxidation of water.<sup>5</sup>

The spectrophotometric titration seems to be more accurate. In the final part of the plot of absorbance *vs.* volume added, two straight lines are produced, and their intersection corresponds to the end-point. Potentiometric titration was attempted, but the end-point was sluggish and the results were inaccurate, either because of further oxidation of the phenothiazine sulphoxides to the corresponding sulphone,<sup>14</sup> or because of oxidation of water.

Interference from drugs likely to be present together with the phenothiazines in formulations was

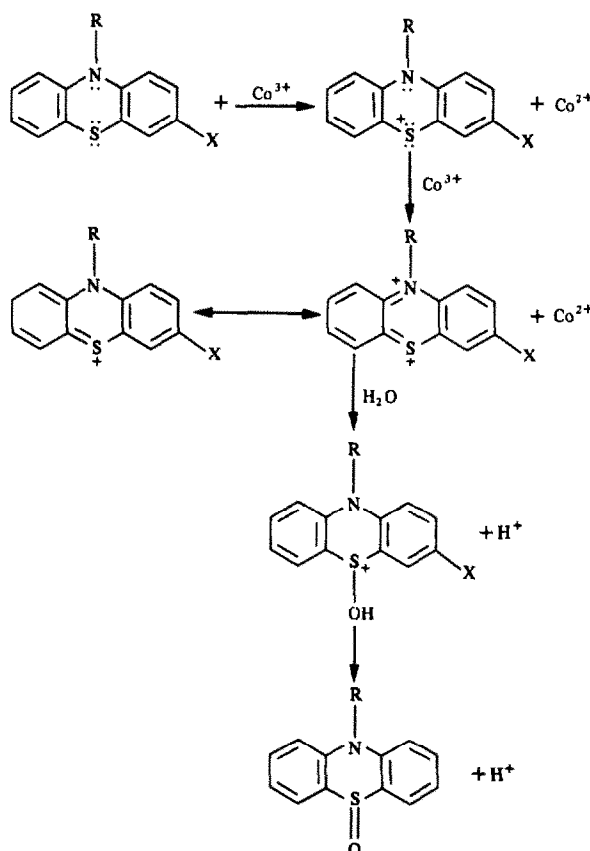


Fig. 1. Proposed mechanism of reaction between phenothiazines and HCTC.



Table 2. Determination of phenothiazines in their dosage forms\*

Preparation	Proposed method recovery, %		Official method, <sup>11,12</sup> recovery, %
	Visual titration	Spectrophotometric titration	
Sparine vial	99.3	99.6	99.5
(Promazine·HCl 50 mg/ml)	(1.0)	(0.4)	(1.6)
Promantine ampoules	106.1	106.0	106.7
(Promethazine·HCl 25 mg/ampoule)	(0.9)	(0.1)	(1.3)
Levomepromazine·HCl tablet	98.1	—	100.7
(Levomepromazine·HCl 25 mg/tablet)	(1.7)	—	(1.5)
Trilafon tablets	102.1	101.8	102.5
(Perphenazine 8 mg/tablet)	(1.1)	(0.7)	(0.5)
Moditen tablets	90.2	89.9	90.6
(Fluphenazine·2HCl 1 mg/tablet)	(0.9)	(0.7)	(2.7)
Mesoridazine besylate tablets	101.5	102.1	102.8
(Mesoridazine besylate 5 mg/tablet)	(0.8)	(0.7)	(2.3)

\*The figures in parentheses are the coefficients of variation. The results given are the averages of 10 separate determinations.

studied; codeine, ephedrine, citric acid, paracetamol, atropine, pethidine and amitryptiline did not interfere under the described conditions. This is due to the preferential reaction of phenothiazines with the reagent, and the self-indication system provided by the phenothiazonium free radicals. Chloride was also found not to interfere with the determination.

The suggested method was applied to the determination of the studied compounds in dosage forms. The results in Table 2 indicate that the method gives good accuracy and precision, with satisfactory agreement with the results given by the official methods.<sup>11,12</sup>

Statistical analysis of the results by the *F*- and *t*-tests showed no significant difference between the performance of the methods.<sup>15</sup>

Although phenothiazines have been determined by a variety of techniques,<sup>16-18</sup> the method described here is rapid, convenient and does not require special working conditions, unlike many other reagents. Moreover, owing to the stability of the solid reagent and reasonable stability of its buffered solution,<sup>19</sup> the titrant can be used for routine analysis.

#### REFERENCES

1. A. Berka, J. Vulterin and J. Zýka, *Newer Redox Titrants*, p. 49. Pergamon Press, Oxford, 1965.
2. M. Hanif, J. Doležal and J. Zýka, *Microchem. J.*, 1971, **16**, 291.
3. Z. Sheikh, J. Doležal and J. Zýka, *ibid.*, 1971, **16**, 395.
4. H. Khalifa, M. A. Zayed and A. A. Ali, *ibid.*, 1984, **30**, 319.
5. J. A. Bauer and C. E. Bricker, *Anal. Chem.*, 1965, **37**, 1461.
6. M. F. M. El Ghandour and A. Abd El-Razek, *Microchem. J.*, 1984, **30**, 201.
7. M. Hanif, M. Saleem, Z. Sheikh and J. Zýka, *Mikrochim. Acta*, 1976 **II**, 625.
8. M. Vasatová and J. Zýka, *Microchem. J.*, 1977, **22**, 34.
9. T. A. Nasser and M. Saleem, *J. Chem. Soc. Pakistan*, 1983, **5**, 119.
10. M. Hanif, I. Ijaz, M. Ahmad and S. Dureshi, *Pakistan J. Sci. Ind. Res.*, 1983, **26**, 13.
11. *The British Pharmacopoeia*, H.M. Stationery Office, London, 1980.
12. *The United States Pharmacopoeia*, XXI Revision, American Pharmaceutical Association, Washington, D.C., 1985.
13. F. H. Merkle and C. A. Discher, *J. Pharm. Sci.*, 1964, **53**, 620.
14. J. Wallace and J. Biggs, *ibid.*, 1971, **60**, 1346.
15. D. H. Sanders, A. F. Murph and R. J. Eng, *Statistics*, McGraw-Hill, New York, 1976.
16. J. Blažek, *Pharmazie*, 1967, **22**, 129.
17. J. Blažek, A. Dymeš and Z. Stejskal, *ibid.*, 1976, **31**, 10.
18. J. E. Fairbrother, *Pharm. J.*, 1979, **222**, 271.
19. M. Hanif and M. Saleem, *Pakistan J. Sci. Ind. Res.*, 1976, **19**, 9.

## ANALYTICAL DETERMINATION OF DIMETHYL SULPHOXIDE BY COMPLEX FORMATION WITH THE PENTACYANOFERRATE(II) ION

HENRIQUE E. TOMA, DENISE OLIVEIRA and AMERICO T. MEENOCHITE  
Instituto de Quimica, Universidade de São Paulo, C. Postal 20.780, São Paulo, SP, Brazil

(Received 10 September 1987. Accepted 23 October 1987)

**Summary**—A method for determination of small amounts of dimethyl sulphoxide and non-hindered sulphoxides is proposed, based on selective reaction with the aquapentacyanoferrate(II) ion, leading to stable complexes which can be detected electrochemically.

Dimethyl sulphoxide (dmsO) is a very important solvent for many inorganic and organic compounds.<sup>1,2</sup> In co-ordination chemistry, it behaves as an ambidentate ligand which may bind to metal ions through either the sulphur or the oxygen atom,<sup>3</sup> and as a leaving group, it has found interesting applications in transition-metal chemotherapy.<sup>4</sup>

The methods for determination of dmsO in aqueous solution are mainly based on redox reactions, e.g., with permanganate.<sup>5</sup> In general, however, they are susceptible to interference, even from mild reducing species such as alcohols and unsaturated compounds. In this work we propose an alternative method based on the reaction of dmsO with the aquapentacyanoferrate(II) ion, yielding the  $[\text{Fe}(\text{CN})_5\text{dmsO}]^{3-}$  complex.<sup>6</sup> The starting complex and the product exhibit reversible redox behaviour in aqueous solutions, and can easily be detected by electrochemical techniques, such as cyclic voltammetry.

### EXPERIMENTAL

#### Reagents

The complex  $\text{Na}_3[\text{Fe}(\text{CN})_5\text{NH}_3] \cdot 3\text{H}_2\text{O}$  was prepared from  $\text{Na}_2[\text{Fe}(\text{CN})_5\text{NO}] \cdot 2\text{H}_2\text{O}$  (Carlo Erba), according to the conventional procedure.<sup>7</sup>  $\text{C}_5\text{H}_9\text{N}_6\text{O}_3\text{FeNa}_3$  requires C 18.42%, N 25.77%, H 2.76%; analysis gave C 18.6%, N 25.8%, H 2.77%. Aminopentacyanoferrate(II) complex solution (0.1M) was freshly prepared by dissolving the solid in deaerated water. All other reagents were of high purity and were used as supplied.

$[\text{RuCl}_2(\text{dmsO})_4]$  was prepared from  $\text{RuCl}_3 \cdot 3\text{H}_2\text{O}$  and dmsO by the procedure of Bora and Singh.<sup>8</sup>  $\text{C}_8\text{H}_{24}\text{O}_4\text{S}_4\text{Cl}_2\text{Ru}$  requires C 19.83%, H 4.99%; analysis gave C 19.6%, H 4.9%.

#### Measurements

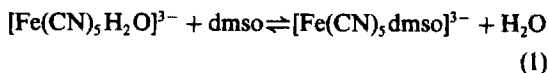
Cyclic voltammetry measurements were made with a Princeton Applied Research instrument, consisting of a Model 173 potentiostat and a Model 175 universal programmer. A gold disk electrode was employed for the measurements, along with the conventional Luggin capillary with an Ag/AgCl (1M KCl) reference electrode. The auxiliary electrode was a platinum wire dipping into the electrolyte solution (0.5M KCl) in a small compartment separated from the working solution by a fine glass frit. The measured

potentials were converted onto the normal hydrogen electrode (NHE) scale by adding 0.222 V.

The titrations were performed according to the following procedure: a 3.00-ml sample, containing dmsO (1–5mM), and the electrolyte solution (0.1M KCl), were transferred into the electrochemical cell and kept under an argon atmosphere for about 10 min. The aminopentacyanoferrate(II) complex (0.1M) was added stepwise, with a Gilmont ultraprecision micrometer syringe. After each addition, the solution was stirred for 5 min, and a cyclic voltamperogram was recorded in the range 0–1 V vs. NHE, at a typical potential scan-rate of 50 mV/sec.

### RESULTS AND DISCUSSION

Dimethyl sulphoxide forms a very stable complex with the aquapentacyanoferrate(II) ion, by co-ordinating specifically through the sulphur atom.<sup>6</sup> The reaction is very rapid,<sup>6,9</sup> proceeding with a specific rate of  $380 \text{ l.mole}^{-1}.\text{sec}^{-1}$  at 25°. The product is rather inert to substitution,<sup>6</sup> exhibiting a dissociation kinetic constant of  $7.5 \times 10^{-5} \text{ sec}^{-1}$ . The equilibrium constant for<sup>9</sup> the formation of the  $[\text{Fe}(\text{CN})_5\text{dmsO}]^{3-}$  complex, equation (1), is  $4.9 \times 10^6$  (ionic strength 0.1M).



The dmsO complex absorbs radiation only slightly in the visible-ultraviolet region. The ligand-field band<sup>6,9</sup> which appears at 352 nm ( $\epsilon = 210 \text{ l.mole}^{-1}.\text{cm}^{-1}$ ), is not suitable for direct spectrophotometric analysis because of its weak intensity, and the strong overlap with the absorption spectrum of the aquapentacyanoferrate(II) ion.

In aqueous solution, the dmsO-pentacyanoferrate(II) complex exhibits reversible electrochemical behaviour,<sup>10</sup> with a redox potential of 0.850 V vs. NHE, which is much higher than that of the aquapentacyanoferrate(II) ion,<sup>9</sup> 0.370 V. Consequently, electrochemical methods are more appropriate than spectrophotometric ones for detection of the dmsO complex.

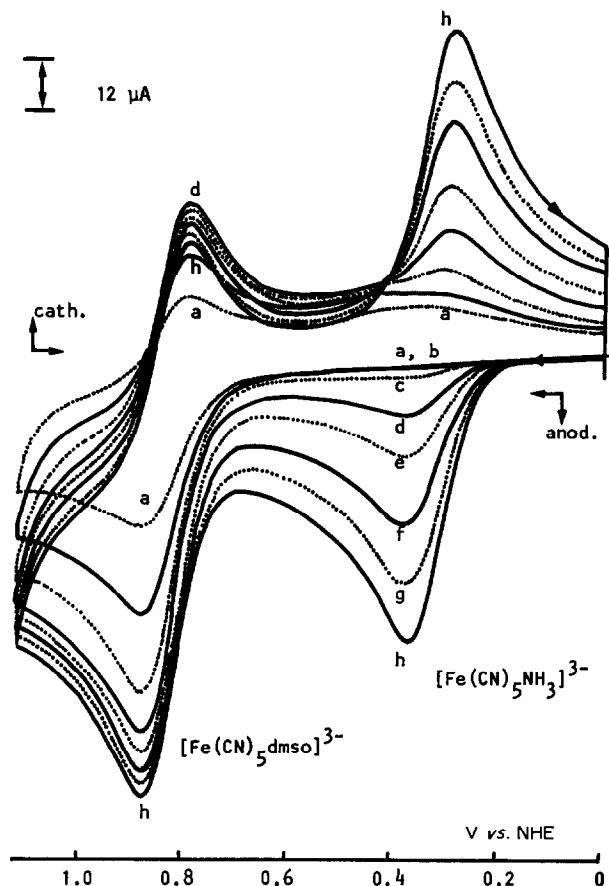
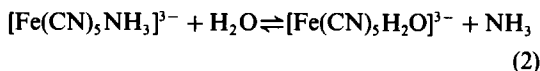


Fig. 1. Titration of dmsoligated ferrocyanide with aminopentacyanoferrate(II) complex, monitored by cyclic voltammetry at 25° in 0.1M KCl medium (a–h correspond to the measurements after successive additions of 0.040 ml of the cyanoferrate complex (0.115M) to 3.8 ml of 4.2mM dmsoligated ferrocyanide).

Unfortunately, the aquapentacyanoferrate(II) ion cannot be obtained with reasonable purity in the solid state owing to its tendency to dimerize and decompose in aqueous solution.<sup>11,12</sup> For this reason, the aminopentacyanoferrate(II) complex has been used as a convenient source of the aquapentacyanoferrate(II) ion.<sup>13</sup> This complex can be easily obtained in pure form.<sup>7</sup> It undergoes rapid dissociation in aqueous solution,<sup>13</sup> yielding the aquapentacyanoferrate(II) ion, as in equation (2).



The dissociation equilibrium is completely shifted to the right in highly dilute solutions, or in the presence of acids or buffers. The redox potential of the aminopentacyanoferrate(II) complex<sup>9</sup> is 0.340 V, much lower than that of the dimethyl sulphoxide complex.

A typical titration of dmsoligated ferrocyanide with the aminopentacyanoferrate(II) ion, monitored by cyclic voltammetry, is shown in Fig. 1. Initially, the titration leads to a systematic increase of the electrochemical waves at around 0.85 V, corresponding to the one-electron

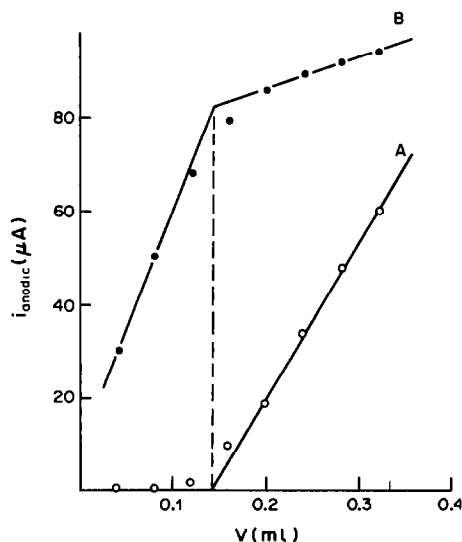
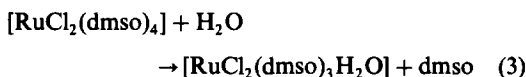


Fig. 2. Plots of the anodic peak currents measured at (A) 0.36 and (B) 0.88 V against the volume of 0.115M aminopentacyanoferrate(II) complex solution added in the titration of 3.8 ml of 4.2mM dmsoligated ferrocyanide aqueous solution.

oxidation of the  $[\text{Fe}(\text{CN})_5\text{dmsO}]^{3-}$  complex. As the titration proceeds, the excess of the aminopentacyanoferrate(II) complex gives rise to a peak at 0.34 V in the cyclic voltamperograms. In this way, the equivalence point can be obtained in duplicate from plots of the anodic peak currents, corrected by the dilution factor, against the volumes of titrant added, as shown in Fig. 2. The reproducibility and error obtained with this method were better than 2%.

As an interesting application of this method, we investigated the dissociation reactions of the  $[\text{RuCl}_2(\text{dmsO})_4]$  complex<sup>15</sup> in aqueous solution. This complex has three dmsO ligands co-ordinated through the sulphur atom, and one labile dmsO ligand co-ordinated through the oxygen atom.<sup>15</sup> The redox potential of the  $[\text{RuCl}_2(\text{dmsO})]$  couple is 1.55 V in dichloromethane,<sup>16</sup> and no electrochemical wave has been observed for it in the range of potentials from 0 to 1 V, in aqueous solution. Titration of freshly prepared solutions of the  $[\text{RuCl}_2(\text{dmsO})_4]$  complex with the aminopentacyanoferrate(II) ion led to equivalence points corresponding exactly to 1:1 stoichiometry, confirming the dissociation of one dmsO ligand, as previously proposed in the literature<sup>14</sup> [equation (3)].



The method was also successfully employed in the determination of dimethyl sulphoxide in several solvent mixtures, containing, for instance, methanol, ethanol, 2-propanol, or acetone. It can be extended to non-hindered sulphoxides, such as methyl alkyl sulphoxides and tetramethylene sulphoxide. *N*-Heterocyclic bases, such as pyridine and pyrazine and

their derivatives, also form strong complexes with the pentacyanoferrate(II) ion, but they would be better detected by spectroscopic methods, owing to the occurrence of strong charge-transfer bands in the visible region.<sup>17</sup>

*Acknowledgements*—We thank CNPq, FAPESP and FINEP for financial support.

#### REFERENCES

1. D. Martin, A. Weise and H.-J. Niclas, *Angew. Chem. Intern. Ed.*, 1967, **6**, 318.
2. H. L. Schläfer and W. Schaffernicht, *Angew. Chem.*, 1960, **72**, 618.
3. W. L. Reynolds, *Prog. Inorg. Chem.*, 1970, **12**, 1.
4. N. Farrell, *J. Chem. Soc., Chem. Commun.*, 1982, 331.
5. V. Krishnan and C. C. Patel, *J. Inorg. Nucl. Chem.*, 1964, **26**, 2201.
6. H. E. Toma, J. M. Malin and E. Giesbrecht, *Inorg. Chem.*, 1973, **12**, 2084.
7. G. Brauer, *Handbook of Preparative Inorganic Chemistry*, Vol. 2, 2nd Ed., p. 1511. Academic Press, New York, 1965.
8. T. Bora and M. M. Singh, *J. Inorg. Nucl. Chem.*, 1976, **38**, 1815.
9. H. E. Toma, A. A. Batista and H. B. Gray, *J. Am. Chem. Soc.*, 1982, **104**, 7509.
10. H. E. Toma and C. Creutz, *Inorg. Chem.*, 1977, **16**, 545.
11. H. E. Toma, *Inorg. Chim. Acta*, 1975, **15**, 205.
12. G. Emschwiller, *Compt. Rend. Acad. Sci. (Paris)*, 1967, **265C**, 281.
13. H. E. Toma and J. M. Malin, *Inorg. Chem.*, 1973, **12**, 2080.
14. N. Farrell and N. G. Oliveira, *Inorg. Chim. Acta*, 1980, **44**, L255.
15. A. Mercer and J. Trotter, *J. Chem. Soc., Dalton*, 1975, 2480.
16. D. P. Riley, *Inorg. Chim. Acta*, 1985, **99**, 5.
17. H. E. Toma and J. M. Malin, *Inorg. Chem.*, 1973, **12**, 1039.

## A NOVEL URUSHI MATRIX CHLORIDE ION-SELECTIVE FIELD EFFECT TRANSISTOR

SHIN-ICHI WAKIDA, MASATAKA YAMANE and KAZUO HIRO

Government Industrial Research Institute, Osaka, Midorigaoka 1-8-31, Ikeda City,  
Osaka Pref., 563, Japan

(Received 14 August 1987. Accepted 23 October 1987)

**Summary**—A durable chloride ion-selective field effect transistor (ISFET) is proposed with Urushi as the membrane matrix. The chloride ion-sensing material is a quaternary ammonium chloride: trioctylmethylammonium chloride (TOMA-Cl) or tridodecylmethylammonium chloride (TDMA-Cl). The optimum composition of the Urushi membrane was found by use of Urushi ion-selective electrodes. The mixture with the most favourable composition was coated on the gate region of the FET device. The Urushi ISFET with TDMA-Cl proved to be superior to that with TOMA-Cl, in sensitivity, linearity and selectivity. The Urushi ISFET with TDMA-Cl showed a linear response of about  $-51$  mV per decade change of chloride ion activity in the range  $10^{-4}$ – $1M$ . The Urushi ISFET showed excellent stability and durability for over two months, because of strong adhesion of the membrane to the  $Si_3N_4$  gate.

Recently, various kinds of chemical sensor sensitive to chemical species have been investigated.<sup>1</sup> Ion-selective electrodes (ISEs) and ion-selective field effect transistors (ISFETs) are well-known as ion sensors. It is hoped that ion sensors can be routinely used for continuous *in vivo* monitoring of biological fluid electrolytes. ISFETs are miniature ion sensors developed from the ISE and solid-state microelectronics technologies and have been attracting much attention for clinical and biological applications.

Despite the advantages of ISFETs, their widespread commercial use has been delayed. Brown *et al.*<sup>2</sup> have pointed out that ISFETs suffer from serious problems; lack of calibration stability, inaccuracy due to chemical cross-sensitivity, difficulty of encapsulation, and poor membrane adhesion, the last of which is the most serious. Although many of the better ion-sensing materials are organic compounds, ISFETs with organic gate coatings have short lifetimes and are unreliable because of poor adhesion of the membrane to the gate of the device.<sup>3</sup>

To resolve this problem, Blackburn and Janata<sup>4</sup> used the suspended mesh method and Kawakami *et al.*<sup>5</sup> proposed use of photoresist matrix membranes cross-linked by photopolymerization. Oesch *et al.*<sup>6</sup> used highly lipophilic plasticizers in the matrix to achieve the same effect. We have proposed durable ISFETs with Urushi as the membrane matrix.<sup>7</sup> Urushi is a natural oriental lacquer used for lacquerware<sup>8</sup> and has Urushiol (60–80%), water (10–30%), rubber substances (7–8%), nitrogen compounds (2–3%) and laccase, an oxidizing enzyme, as its components.<sup>9</sup> Since Urushi lacquer shows excellent durability and mechanical strength, we have used it as the membrane matrix to make very durable ISEs.<sup>10,11</sup> As the Urushi matrix membrane is hard, lustrous and smooth, the lifetimes of Urushi electrodes exceed 1000 hr.

Shiramizu *et al.* reported chloride ISFETs made with AgCl and AgCl–Ag<sub>2</sub>S membranes and polyfluorinated polyphosphazene as the membrane matrix.<sup>12</sup> Vlasov *et al.* reported chloride ISFETs with vacuum-deposited AgCl–AgBr membranes.<sup>13</sup> Marsoner *et al.* studied a chloride ISE more suitable for clinical use than such chloride-sensing materials as AgCl, neutral carriers and quaternary ammonium chlorides,<sup>14</sup> but found that the last-named sensors yielded the best selectivity.

In our work, the best composition for a chloride ion-sensing membrane containing quaternary ammonium chloride and Urushi was estimated by use of an Urushi ISE. Urushi ISFETs were then fabricated by coating the gates of the devices with the optimal Urushi mixture. We report the electrochemical characteristics of the Urushi ISFET.

### EXPERIMENTAL

#### *Fabrication of Urushi ISEs*

The quaternary ammonium chloride, *i.e.*, trioctylmethylammonium chloride (TOMA-Cl, Dojin Research Laboratories Co. Ltd.) or tridodecylmethylammonium chloride (TDMA-Cl, Polysciences Inc.) was mixed in different portions with Urushi latex (Saito Co. Ltd.) on a watch-glass. The mixture was coated onto a copper base (10 mm in diameter) which was then fitted to the end of the polycarbonate electrode body<sup>10</sup> (12 mm diameter, 120 mm long). After the coating, the Urushi membrane was hardened for 10 days at 30° at 90% relative humidity. The surface of the Urushi membrane was lustrous and smooth.

#### *Fabrication of Urushi ISFETs*

The mixture of quaternary ammonium chloride and Urushi latex found optimal for ISEs was coated on the gate of the device<sup>15</sup> ( $0.5 \times 6.5 \times 0.23$  mm; donated by the Central Research Laboratory, Shimadzu Corporation). After coating, the Urushi membrane was hardened in the same way as for the Urushi ISE. The Urushi matrix membrane is lustrous, smooth, and strongly adhesive to the  $Si_3N_4$  gate.

### Measurements with Urushi ISEs

After the prepared Urushi ISE was conditioned in  $10^{-3}M$  chloride solution for a few hours, its potential response was measured vs. a silver-silver chloride double-junction reference electrode with an outer chamber filling solution of  $0.1M$  lithium acetate (Orion Research model 90-02) in stirred solutions. The chloride activity was calculated by the Debye-Hückel equation.

### Measurements with Urushi ISFETs

The Urushi ISFET response was measured with a source-follower circuit in the dark (because of some photosensitivity) and without stirring [stirring affected the potentials by  $\leq 0.2$  mV (up to 500 r.p.m.)]

## RESULTS AND DISCUSSION

### Composition of chloride-sensing Urushi membranes

The best composition for chloride-sensing Urushi membranes (TOMA-Cl/Urushi or TDMA-Cl/Urushi) was estimated from the response of Urushi ISEs. The electrochemical characteristics of the two series of chloride ISEs are summarized in Tables 1 and 2. The ion-sensing membranes made with equal weights of quarternary ammonium chloride Urushi showed the best electrochemical characteristics for both TOMA-Cl and TDMA-Cl.

### Electrochemical characteristics of Urushi ISFETs

The Urushi ISFET was fabricated by coating the best Urushi mixture on the gate of the ISFET. The potential response of an Urushi ISFET with TOMA-Cl is shown in Fig. 1; the response to chloride activity was linear from  $1M$  down to  $10^{-3.5}M$  with a slope factor of ca. 46 mV/pCl. The Urushi ISFET with TDMA-Cl showed a linear response in the  $10^{-4}$ – $1M$  range, with slope of ca. 51 mV/pCl (Fig. 2). The Urushi ISFET with TDMA-Cl was superior to that with TOMA-Cl in sensitivity and linear response range.

### Selectivity of the Urushi ISFET

The selectivity of the Urushi ISFET is represented by the selectivity coefficients  $K_{ClX}^{pot}$  defined by the

Table 1. Electrochemical characteristics of Urushi ISEs with TOMA-Cl

Weight ratio of TOMA-Cl and Urushi	Slope, mV/pCl	Linear range, $a_{Cl}$ , M
40:60	36	$10^{-3}$ –1
45:55	36	$10^{-3}$ –1
50:50	44	$10^{-3.5}$ –1
55:45	43	$10^{-3.5}$ –1

Table 2. Electrochemical characteristics of Urushi ISEs with TDMA-Cl

Weight ratio of TDMA-Cl and Urushi	Slope, mV/pCl	Linear range $a_{Cl}$ , M
40:60	50	$10^{-4}$ –1
45:55	50	$10^{-4}$ –1
50:50	54	$10^{-4}$ –1
55:45	51	$10^{-4}$ –1

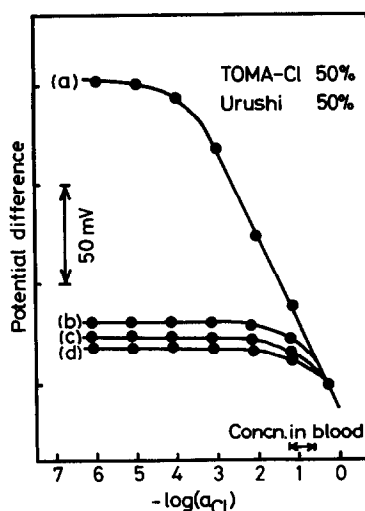


Fig. 1. Potential response of Urushi ISFET in presence of (a) no interferences, (b)  $0.1M$   $SO_4^{2-}$ , (c)  $0.1M$   $HPO_4^{2-}$ , (d)  $0.1M$   $HCO_3^-$ .

Nikolskii-Eisenman equation. Selectivity coefficients for the electrolytes in blood were measured by the mixed-solution method. The responses of Urushi ISFETs to  $0.1M$  concentrations of interfering ions ( $HCO_3^-$ ,  $HPO_4^{2-}$  and  $SO_4^{2-}$ ) are shown in Figs. 1 and 2. The selectivity coefficients calculated by the conventional graphical method are summarized in Table 3: the Urushi ISFET with TDMA-Cl was more selective than that with TOMA-Cl. The selectivity of the Urushi matrix ISFET is the same as that of the corresponding PVC matrix ISFET.<sup>16</sup> It is considered that the selectivity is independent of the matrix materials. In view of these selectivities (and the absence of interference from cations), the Urushi ISFET with TDMA-Cl should be capable of operat-

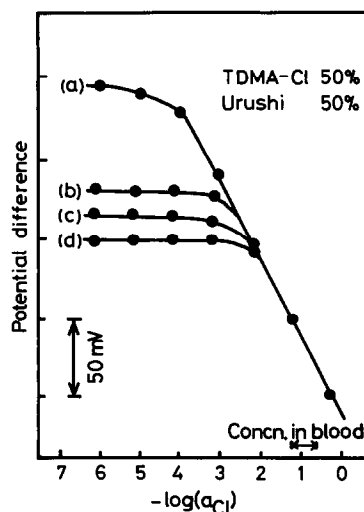


Fig. 2. Potential response of Urushi ISFET in presence of (a) no interferences, (b)  $0.1M$   $HCO_3^-$ , (c)  $0.1M$   $HPO_4^{2-}$ , (d)  $0.1M$   $SO_4^{2-}$ .

Table 3. Selectivity coefficients,  $K_{ClX}^{pot}$ 

Interfering ion (X)	Concn. in blood, $M$	$a$	$\log K_{ClX}^{pot}$	
			$b$	$c$
$HCO_3^-$	$2.1 \times 10^{-2}$ – $2.9 \times 10^{-2}$	0.5	–1.6	–1.5
$HPO_4^{2-}$	$5.3 \times 10^{-4}$ – $1.6 \times 10^{-3}$	1.0	–1.6	–1.3
$SO_4^{2-}$	$1.0 \times 10^{-4}$ – $9.9 \times 10^{-3}$	0.8	–1.2	–1.2
$Br^-$	$8.8 \times 10^{-6}$ – $1.7 \times 10^{-4}$	1.4	0.2	1.1
$SCN^-$	$4.7 \times 10^{-7}$ – $9.8 \times 10^{-6}$	2.3	2.2	3.5
$F^-$	$3.2 \times 10^{-7}$ – $1.2 \times 10^{-6}$	0.2	–1.7	—
$I^-$	$3.0 \times 10^{-7}$ – $4.8 \times 10^{-7}$	2.8	2.3	2.7

$a$  TOMA-Cl/Urushi,  $b$  TDMA-Cl/Urushi,  $c$  TDMA-Cl/PVC.<sup>16</sup>

ing without interference from the electrolytes in blood. The problem of its becoming coated with protein when monitoring biological fluids remains to be solved, however.

#### Durability of the Urushi ISFET

The Urushi ISFETs maintained the same potential response for over two months, indicating that the membrane was adhering strongly to the  $Si_3N_4$  gate.

**Acknowledgement**—We thank Dr. Ujihira, Faculty of Engineering, University of Tokyo, for encouragement throughout the studies.

#### REFERENCES

1. J. Janata and R. J. Huber, *Solid State Chemical Sensors*, Academic Press, New York, 1985.
2. R. B. Brown, R. J. Huber, D. Petelenz and J. Janata, *Proc. 3rd Int. Conf. Solid-State Sensors Actuators*, p. 125, Philadelphia, 1985.
3. Yu. G. Vlasov, *Proc. 4th Ion-Selective Electrodes*, p. 245. *Matrafüred, Hungary, 1984*, Akadémiai Kiadó, Budapest, 1985.
4. G. Blackburn and J. Janata, *J. Electrochem. Soc.*, 1982, **129**, 2580.
5. S. Kawakami, T. Akiyama and Y. Ujihira, *Z. Anal. Chem.*, 1984, **318**, 349.
6. U. Oesch, A. Xu, Z. Brzózka, G. Suter and W. Simon, *Chimia*, 1986, **40**, 351.
7. S. Wakida, T. Tanaka, A. Kawahara, M. Yamane and K. Hiroy, *Analyst*, 1986, **111**, 795.
8. *Kirth-Othmer Encyclopaedia of Chemical Technology*, 2nd Ed., Vol. 17, p. 387. Wiley, New York, 1968.
9. *Encyclopaedia Chimica*, Vol. 1, p. 807. Kyoritsu Pub. Co., Tokyo, 1960.
10. K. Hiroy, A. Kawahara and T. Tanaka, *Anal. Chim. Acta*, 1979, **110**, 321.
11. K. Hiroy, T. Tanaka, A. Kawahara and S. Wakida, *Anal. Sci.*, 1986, **2**, 145.
12. B. Shiramizu, J. Janata and S. D. Moss, *Anal. Chim. Acta*, 1979, **108**, 161.
13. Yu. G. Vlasov, D. E. Hackleman and R. P. Buck, *Anal. Chem.*, 1979, **51**, 1570.
14. M. J. Marsoner, C. Ritter and M. Ghahramani, *Proc. Int. Symp. Ion-Selective Electrodes*, Shanghai, p. 36, 1985.
15. T. Matsuo and M. Esashi, *Sensors Actuators*, 1981, **1**, 77.
16. K. Tsukada, M. Sebata, T. Maruizumi, Y. Miyahara and H. Miyagi, *Proc. 4th Int. Conf. Solid-State Sensors Actuators*, p. 155. Tokyo, 1987.

# DETERMINATION OF COPPER IN THE PRESENCE OF A LARGE EXCESS OF BISMUTH BY DIFFERENTIAL-PULSE ANODIC-STRIPPING VOLTAMMETRY WITHOUT PRELIMINARY SEPARATION

ALEKSANDER CISZEWSKI

Institute of General Chemistry, Technical University of Poznań, 60-965 Poznań, Poland

(Received 20 March 1987. Revised 10 June 1987. Accepted 23 October 1987)

**Summary**—Conditions have been found which make possible the determination of copper in the presence of a large excess of bismuth by differential-pulse and anodic-stripping voltammetry without preliminary separation. The electrochemical activity of the bismuth, which usually interferes in the determination of copper, is inhibited by using tetrabutylammonium chloride (TBAC) as surfactant. In 0.2M EDTA and 0.01M ascorbic acid at pH 4.5 as supporting electrolyte without the surfactant present, trace levels of copper ( $1.5 \times 10^{-8}M$ ) can be determined accurately if the molar ratio of bismuth to copper is not higher than 3, but if the electrolyte also contains TBAC at 0.01M concentration, bismuth can be tolerated in concentrations up to  $10^{-4}M$ , and the height of the copper peak is unaffected.

Differential-pulse anodic-stripping voltammetry (DPASV) is widely used for determination of trace metals in environmental, biological and industrial samples, but its application is sometimes difficult or even impossible because of interference. The most frequent problem is overlap of the peaks for the analyte and interferent, e.g., in the determination of thallium in the presence of lead or of indium in the presence of cadmium. Another cause of difficulty arises in determination of a trace metal in the presence of a large excess of another substance which gives an anodic peak in the stripping step, at less negative potential than the ion of interest. Though in this case the stripping peaks are quite far apart a high concentration of the foreign ion will substantially increase the background current, thus causing interference, e.g., the determination of thallium in the presence of bismuth or copper. Similar difficulties occur when the deposition of the analyte is accompanied by a simultaneous electrode reaction (in solution) of another substance, present in excess. During the stripping process, the substance in solution undergoes the reverse electrode reaction, which may cause interference by producing a peak in the vicinity of the peak of interest.

The objective of the present study was to apply electrochemical masking<sup>1-4</sup> to DPASV determination of copper in the presence of a large excess of bismuth, without preliminary separation. In most solutions both copper and bismuth give well developed waves or peaks in the vicinity of  $-0.1$  V vs. SCE, which causes difficulty in determination of one in the presence of the other. Up till now, the problem has been solved by solution exchange after the deposition step<sup>5,6</sup> or by using surfactants.<sup>2,7</sup> In the last case 3,4-dichlorobenzyltriphenylphosphonium chloride was used as surfactant in 0.05M EDTA or 0.05M

DPTE solution, which allowed determination of copper in the presence of 25- or 300-fold excess of bismuth, respectively.<sup>7</sup>

In the present study a common reagent—tetrabutylammonium chloride (TBAC)—was used as surfactant for the electrochemical masking of bismuth,<sup>3</sup> with EDTA as complexing agent.

## EXPERIMENTAL

### Apparatus

Anodic stripping voltamperograms were obtained with a Telpod (Poland) pulse polarograph model PP-04, and an Endim (GDR) 620.02 XY recorder. A classical three-electrode system was employed. The hanging mercury-drop electrode (HMDE) was a Radiometer Kemula Equipment E69 model with a drop size corresponding to 3 divisions travel of the micrometer screw. A platinum wire was used as auxiliary electrode and an SCE as reference. The differential-pulse amplitude was 50 mV and scan-rate 11.1 mV/sec. During the deposition step the solutions were stirred. All potentials reported are referred to the SCE.

### Reagents

Merck TBAC, EDTA (disodium salt) and ascorbic acid were used. Standard solutions of bismuth and copper ( $10^{-2}M$ ) were prepared by dissolving the metals in nitric acid, and diluted to give concentrations below  $10^{-3}M$  just before use. Water was doubly distilled in a silica still. The background electrolyte was 0.2M EDTA + 0.01M ascorbic acid + 0.01M TBAC, pH  $4.5 \pm 0.2$ , adjusted with purified potassium hydroxide solution. Before measurement all solutions were brought to  $20 \pm 0.5^\circ$  in a thermostat.

### Determination of copper in the presence of bismuth

Adjust the mixture of 1 ml of tested sample plus 20 ml of 0.25M EDTA, 0.25 ml of 1M ascorbic acid and 0.25 ml of 1M tetrabutylammonium chloride to pH  $4.5 \pm 0.2$  by dropwise addition of 10% potassium hydroxide solution, transfer the solution to a 25-ml standard flask and make up to the mark with water. Transfer the solution into the electrochemical cell and pass purified nitrogen or argon through it for 15 min. Stop the flow of gas, form a mercury drop at the capillary tip of the working electrode and start the



stirrer. Perform the electrolytic deposition at  $-0.900$  V vs. SCE for a few minutes, depending on the expected copper content. After the deposition, switch off the stirrer, change the potential to  $-0.400$  V, wait for 20 sec, then record the voltamperogram from  $-0.400$  to  $0$  V. Repeat the measurement cycle twice more on the same solution, with a new mercury drop each time. Estimate the copper by the standard-addition method, by making three successive additions of a known fixed volume of copper standard solution to the same solution, repeating the measurement cycle each time, beginning from the deposition stage. From the linear plot of peak height vs. amount of copper standard added, read the amount of copper in the sample.

## RESULTS AND DISCUSSION

A  $0.2M$  EDTA +  $0.01M$  ascorbic acid +  $0.01M$  TBAC solution, pH 4.5 was chosen as background electrolyte.

The copper deposited on an HMDE under these conditions gives a stripping peak at  $-0.22$  V with peak-width 55 mV. Figure 1 shows that the proposed medium allows satisfactory determination of copper at a concentration of about  $10^{-8}M$ . A deposition potential of  $-0.900$  V was chosen as optimal. A linear relation of peak-current to copper concentration was found over the range  $1 \times 10^{-8}$ – $1 \times 10^{-6}M$ . The plot of peak-current vs. deposition

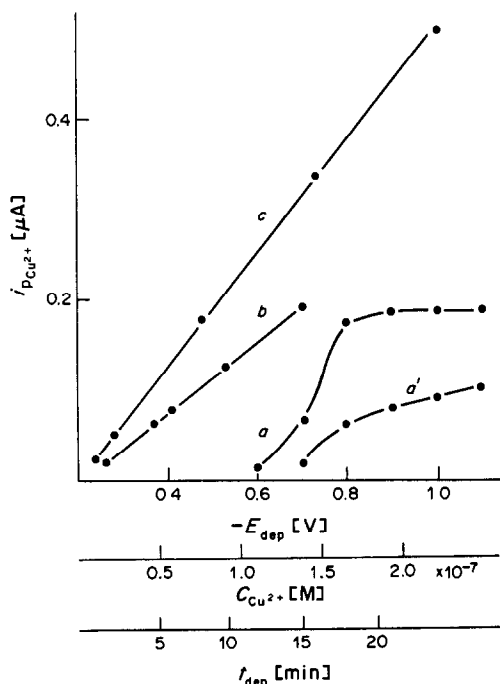


Fig. 1. Dependence of the differential-pulse anodic-stripping peak current for copper on the deposition potential *a*, deposition time *b* and copper concentration *c*, [Cu]; *a*, *b*,  $7.5 \times 10^{-8}M$ . Deposition potential; *b*, *c*,  $-0.900$  V. Deposition time: *a*, *c*, 900 sec. Curve *a'* shows the dependence of the differential-pulse anodic-stripping peak current for bismuth on the deposition potential; [Bi]  $1 \times 10^{-7}M$ , deposition time 900 sec.

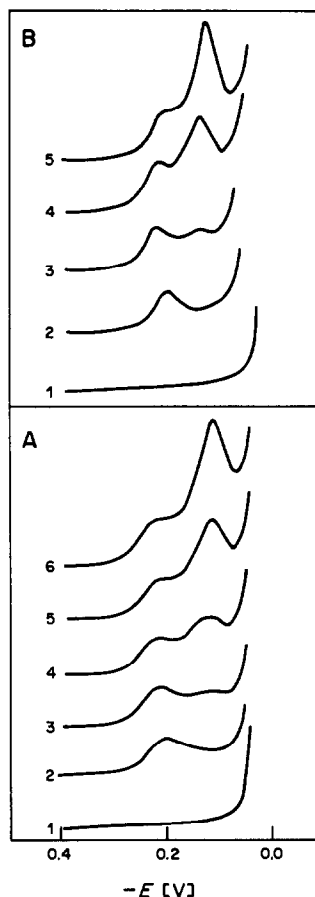


Fig. 2. Voltamperograms for copper and bismuth in the absence (A) and presence (B) of TBAC. Deposition potential  $-0.900$  V. Deposition time 900 sec. (A) [Cu]: 1, 0; 2–6,  $1.5 \times 10^{-8}M$ . [Bi]: 1, 2, 0; 3,  $1 \times 10^{-8}M$ ; 4,  $2 \times 10^{-8}M$ ; 5,  $3 \times 10^{-8}M$ ; 6,  $4 \times 10^{-8}M$ . (B) [Cu]: 1, 0; 2–5,  $1.5 \times 10^{-8}M$ . [Bi]: 1, 0; 2,  $1 \times 10^{-4}M$ ; 3,  $2 \times 10^{-4}M$ ; 4,  $3 \times 10^{-4}M$ ; 5,  $4 \times 10^{-4}M$ .

time was linear for deposition periods ranging from 1 to 15 min.

Bismuth, in the chosen background electrolyte but in the absence of TBAC, gives a stripping peak at  $-0.13$  V. Figure 1, curve *a'*, shows the dependence of the bismuth peak-current on the deposition potential. From the shape of curves *a* and *a'* it is evident that the simultaneous presence of copper and bismuth will result in two peaks on the voltamperogram, and difficulty in the determination because the peaks overlap.

The purpose of the study was determination of copper in the presence of bismuth. Figure 2A shows a few differential-pulse anodic-stripping curves for test solutions with a constant concentration of copper ( $1.5 \times 10^{-8}M$ ) and increasing concentration of bismuth (from  $1 \times 10^{-8}$  to  $4 \times 10^{-8}M$ ). It was estimated that if the molar ratio of bismuth to copper is higher than 3, the determination of the copper will be incorrect. Greater tolerance for bismuth was achieved by introducing TBAC into the background electro-

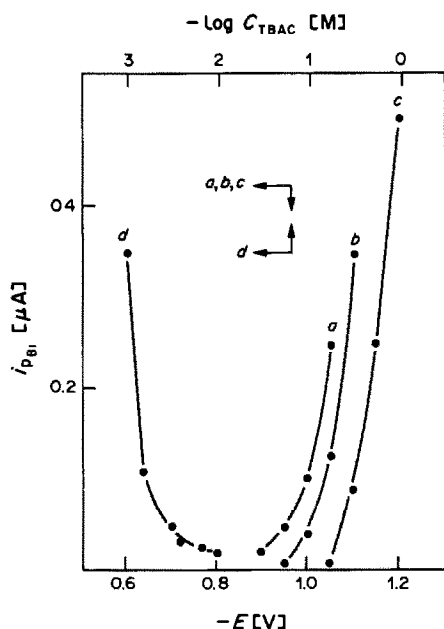


Fig. 3. Variation in the size of the bismuth peak vs. deposition potential and TBAC concentration. [Bi]: *a, d*,  $2 \times 10^{-4}M$ ; *b*,  $1 \times 10^{-4}M$ ; *c*,  $5 \times 10^{-5}M$ . [TBAC]: *a-c*  $0.01M$ . Deposition potential: *d*,  $-0.900V$ . Deposition time: *a-d*, 300 sec.

lyte. This surface-active agent does not influence the anodic peak-current of copper, and its influence on that of bismuth depends on the bismuth concentration, TBAC concentration and deposition potential, as shown in Fig. 3. It is shown that in the presence of  $0.01M$  TBAC and at a deposition potential of  $-0.900V$  the peak-current of bismuth is completely damped for concentrations of  $1 \times 10^{-4}M$  and below without affecting the copper peak. This makes possible the determination of traces of copper in the presence of a several thousand-fold excess of bismuth. Figure 2B shows differential-pulse anodic

Table I. Accuracy and precision of the determination of copper in the presence of bismuth and TBAC (7 replicates)

Series	Added		Cu found, ng/ml	Std. devn., ng/ml	Relative std. devn., %
	Bi, $\mu\text{g/ml}$	Cu, ng/ml			
I	—	1.9	1.7	0.48	28
II	20.8	1.9	1.6	0.55	34
III	41.6	31.0	31.0	1.66	5

stripping curves for test solutions containing  $1.5 \times 10^{-8}M$  copper,  $0.01M$  TBAC and increasing concentrations of bismuth. The shapes of these curves are identical to those in Fig. 2A but the concentrations of bismuth are higher by a factor of  $10^4$ . Hence use of these conditions meets the aim of the work.

The precision and recovery for the determination of copper in the presence of a large excess of bismuth were examined near the limiting conditions. The results, given in Table I, show the precision for the determination of copper in the presence of a  $10^4$ -fold ratio of bismuth to be typical for such voltammetric measurements. Better results were obtained when the concentration ratio of bismuth to copper was about  $10^3$ .

*Acknowledgement*—This work was supported by Research Program MR-I-32.

#### REFERENCES

1. J. Georges, *Anal. Chim. Acta*, 1981, **127**, 233.
2. R. Neeb and I. Kiehnast, *Naturwissenschaften*, 1970, **57**, 37.
3. A. Ciszewski, *Talanta*, 1985, **32**, 1051.
4. A. Ciszewski and Z. Łukaszewski, *ibid.*, 1983, **30**, 873.
5. V. F. Yankauskas, V. M. Pichugina, A. A. Kaplin and V. I. Kuleshov, *Izv. Tomsk. Politekh. Inst.*, 1969, **169**, 118.
6. I. Šinko and S. Gomišček, *Anal. Chim. Acta*, 1971, **54**, 253.
7. N. You and R. Neeb, *Z. Anal. Chem.*, 1983, **314**, 158.

## LETTER TO THE EDITOR

Sir,

We were surprised to find in Harju's paper in the September 1987 issue of Talanta (page 820) the statement:

"For calcium complexes with glycine, Daniele *et al.* reported [1] the formation constants  $K_{Ca, GLY} = 10^{1.05}$  and  $K_{CaGLY, H} = 10^{8.80}$ . From the co-ordination chemistry point of view, the high stability constant reported for the protonated species, CaHGLY, seems doubtful. The corresponding constant for the protonated calcium complex with EDTA..... for instance, is  $10^{3.18}$ ."

This statement seems to us to arise from a misunderstanding, and is not correct in its implication about the validity of our work. For one thing, the constant  $10^{8.80}$  is the protonation constant of  $CaGLY^+$ , not the equilibrium  $Ca^{2+} + HGLY = CaHGLY^{2+}$ ). For another, the comparison with the EDTA complex is not of like with like, and hence misleading and useless. In fact, the protonation constant simply reflects the ability of the complex to bind a proton, which is generally inversely proportional to the stability of the unprotonated complex, for a certain series of ligands, as shown by the examples reported in the Table.

Table

Equilibrium	log $K$	T, °C	I, M	Ref.
Amino-carboxylic ligands-----				
$Ca^{2+} + GLY^- = CaGLY^+$	1.05	25	0.25	1
$CaGLY^+ + H^+ = CaHGLY^{2+}$	8.80	25	0.25	1
$Ca^{2+} + TMDTA^{4-} = CaTMDTA^{2-}$	7.28	20	0.1	2
$CaTMDTA^{2-} + H^+ = CaHTMDTA^-$	6.34	20	0.1	2
$Ca^{2+} + L^{4-} = CaL^{2-}$	9.60	20	0.1	2
$CaL^{2-} + H^+ = CaHL^-$	4.47	20	0.1	2
$Ca^{2+} + EDTA^{4-} = CaEDTA^{2-}$	10.69	20	0.1	2
$CaEDTA^{2-} + H^+ = CaHEDTA^-$	3.18	20	0.1	2
Dicarboxylic ligands-----				
$Ca^{2+} + Succ^{2-} = CaSucc$	1.45	25	0.25	1
$CaSucc + H^+ = CaHSucc^+$	4.51	25	0.25	1
$Ca^{2+} + Mal^{2-} = CaMal$	1.64	25	0.25	1
$CaMal + H^+ = CaMal$	4.26	25	0.25	1
$Ca^{2+} + ODA^{2-} = CaODA$	3.46	25	0.25	1
$CaODA + H^+ = CaHODA^-$	2.92	25	0.25	1

L = meso-(1,2-dimethylethylene)dinitrotetra-acetate;

Succ = succinate; Mal = malonate; ODA = oxydiacetate

## REFERENCES

- [1] P.G. Daniele, A. De Robertis, C. De Stefano, S. Sammartano and C. Rigano, J. Chem., Soc. Dalton Trans., 1985, 2353.
- [2] A.E. Martell and R.M. Smith, Critical Stability Constants, Vol. 1, Amino-Acids, Plenum Press, New York, 1974.

\*Dipartimento di Chimica Analitica  
dell'Università, via P. Giuria, 5,  
10125 Torino, Italy

†Istituto di Chimica Analitica dell'Università,  
Salita Sperone 31, 98166 Messina S. Agata, Italy

§Dipartimento di Scienze Chimiche dell'Università,  
viale A. Doria 6, 95125 Catania, Italy

Pier G. Daniele\*  
Alessandro De Robertis†  
Concetta De Stefano†  
Silvio Sammartano†  
Carmelo Rigano§

29 January 1988

## SOFTWARE SURVEY SECTION

---

### Software package TAL-001/88

#### FLUOPAC1

Contributors: F. Garcia Sanchez and A.L. Ramos, University of Malaga, Dept. of Analytical Chemistry, The University, Malaga 29071, Spain; and M.T. Oms and V. Cerda, University of Baleares, Spain.

Brief description: The software package is for use in research in spectrofluorimetry. The first step in FLUOPAC1 is data acquisition: excitation - emission fluorescence spectra are digitized and stored in disc files. The stored data may then be presented either as an isometric representation (contour map), or in three-dimensional representation. A new option is the measurement of asynchronous variable-angle fluorescence spectra. The contour plots are useful as a guide in the design of optimal variable angle spectra. The package is particularly valuable for the manipulation and analysis of multicomponent samples with overlapping fluorescence spectra, for which conventional or synchronous spectrometry would be unable to accomplish the analysis.

Potential users: Analytical chemists, molecular luminescence spectroscopists

Fields of interest: Analytical and environmental chemistry

This package has been developed for the IBM PC, and is written in BASIC (compiled), to run under PC-DOS. It is available on 5.25-in disc. The memory required is 256K.

Distributed by the contributors.

An IBM-PC computer, or clone, is required, along with a Perkin-Elmer LS-5 Spectrofluorimeter with RS232 interface, and a suitable printer. No modifications are required to the instrument or computer. The package is self-documenting. The source code is not available. The package has been fully operational for about 1 year. The contributors are willing to deal with enquiries.

### Software package TAL-004/88

#### FLEET STREET EDITOR/FLEET STREET PUBLISHER

Contributor: Mirrorsoft Ltd.

Brief description: A range of desk-top publishing software.

Potential users: Any workers requiring high quality integrated text and graphics. The packages are suitable for both the novice and experienced professional user.

This range of software is now available for Atari Mega 2 or 4 ST, BBC Micro, IBM PC and compatibles, and the Amstrad PCW. The Atari package can be used with the SLM804 laser printer.

Distributed by Mirrorsoft Ltd, 01-337 4837.

Software package TAL-002/88

SOPHD

Contributors: R. Sambasiva Rao, A. Satyanarayana and P.V. Krishna Rao, School of Chemistry, Andhra University, Waltair-530 003, India.

Brief description: SOPHD simulates pH vs. volume data for proton - ligand and metal - ligand complexes, including protonated and hydroxylated complexes. These data are useful for validating chemical models and investigating the effects of systematic and random errors in calculating equilibrium constants. The algorithm is based on the Gauss-Newton method. Theoretical distribution diagrams are drawn, and optimal experimental conditions for determination of stability constants are predicted. The algorithm was described in Proc. Summer Simul. Conf., 1985, 359.

Potential users: Researchers in complex equilibria and simulations.

Fields of interest: Complex equilibria, chemometrics.

This program is written in FORTRAN 77, and it will run on an IBM PC or compatible, or a Microvax II, under MS-DOS or UNIX. It is available on 5.25-in disc. The memory required is 256K.

Distributed by the contributors.

The program has extensive external documentation. The source code is available. The program has been fully operational for 3 years. The contributors are willing to deal with enquiries.

Software package TAL-003/88

GHS

Contributors: P.V. Krishna Rao, R. Sambasiva Rao and A. Satyanarayana, School of Chemistry, Andhra University, Waltair-530 003, India.

Brief description: GHS is a computer program for evaluation of thermodynamic parameters of complex equilibria, including change in free energy, enthalpy and entropy. The original version was implemented in FORTRAN IV for a mainframe computer, but now a user-friendly version has been written in MS FORTRAN 77. Change in enthalpy is calculated by assuming the logarithm of the equilibrium constant to be a Harned's parabolic function or a polynomial in temperature. Data can be input from the keyboard or from a data file.

Potential users: Researchers in equilibrium constants calculation.

Fields of interest: Complex equilibria, chemometrics.

This program is written in FORTRAN 77, and it will run on an IBM PC or compatible, or a Microvax II, under MS-DOS or UNIX. It is available on 5.25-in disc. The memory required is 256K.

Distributed by the contributors.

The program is self-documenting. The source code is available. The contributors are willing to deal with enquiries.

## DETERMINATION OF LEAD IN FLY-ASH FROM A GARBAGE INCINERATOR BY ATOMIC-ABSORPTION AND X-RAY FLUORESCENCE SPECTROMETRY

MARIT ANDERSSON, CHRISTINA ERICZON and ÅKE OLIN

Department of Analytical Chemistry, Uppsala University, P.O. Box 531, S-751 21 Uppsala, Sweden

(Received 17 September 1987. Revised 4 January 1988. Accepted 13 January 1988)

**Summary**—The lead content in fly-ash collected by an electrostatic precipitator has been determined by atomic-absorption spectrometry (AAS) after decomposition by four different leaching/dissolution techniques, and also determined by X-ray fluorescence spectrometry (XRFS) by the standard-addition method. The XRFS data were evaluated by non-linear regression since the standard additions affected the attenuation coefficient of the sample. Good agreement was obtained between the results obtained with AAS and XRFS. It is concluded that lead is quantitatively extracted by hot 1M nitric acid or treatment with hydrofluoric acid/nitric acid. Direct measurement of briquetted samples by XRFS is suggested for rapid monitoring of the lead content in fly-ash from garbage incineration.

Because of the high cost of fuels for energy production, the expense of management of waste, and the scarcity of suitable land-filling sites for solid waste, there is increasing use of incineration to reduce the volume of garbage and, at the same time, to provide an additional energy resource. Refuse incinerators create problems, however, because the fly-ash usually contains considerable amounts of heavy metals. Toxic organic compounds, such as dioxins, can also be formed under improper combustion conditions. Most of the fly-ash is collected by electrostatic precipitators and scrubbers, but some of it will enter into the atmosphere. There will also be problems connected with disposal of the fly-ash and bottom-ash. Leaching of the ashes could cause increased concentrations of heavy metals in ground water and vegetation at the disposal sites. Hence there is a need for a simple and rapid method for monitoring the content of heavy metals in fly-ash. Lead is ubiquitously present in fly-ash, often at a substantial concentration. This metal may therefore be selected as a convenient indicator of the heavy metal content of fly-ash. Atomic-absorption spectrometry (AAS) and X-ray fluorescence spectrometry (XRFS) have been studied in this work, as the means for determination of lead in fly-ash from an incinerator for household refuse.

The AAS technique requires that some dissolution/leaching method is included in the analytical procedure. Many investigators have used digestion with strong acids in a bomb. A combination of nitric, hydrochloric and hydrofluoric acid has been used for coal fly-ash<sup>1,2</sup> and coal and fly-ash.<sup>3</sup> A mixture of nitric and hydrofluoric acids has been used for coal or coal ash<sup>4-6</sup> and dust.<sup>7</sup> Extraction with nitric acid at various temperatures has been described for analysis of stabilized coal waste,<sup>8</sup> coal fly-ash,<sup>1</sup> fly-ash collected on filter paper,<sup>4,5</sup> fly-ash from

garbage incineration collected on a filter<sup>9</sup> and bottom- and fly-ash from garbage incineration.<sup>10</sup> A room-temperature dissolution method employing hydrofluoric and boric acid has been presented for coal fly-ash<sup>11</sup> and stabilized coal waste.<sup>8</sup>

Fusion with lithium tetraborate and caesium iodide, followed by dissolution in acid, has been used for coal and fly-ash<sup>3</sup> and fusion with lithium metaborate followed by dissolution in 1.6M hydrochloric acid has been used for coal fly-ash.<sup>12</sup> Behel *et al.*<sup>13</sup> have studied many combinations of hydrochloric, nitric, sulphuric, perchloric and hydrofluoric acids for digestion or extraction of mixed bottom- and fly-ash from garbage incineration, to determine the total content of cadmium and lead. They concluded that extraction with 1.0M hydrochloric acid was the best procedure with respect to simplicity and reproducibility, but it gave slightly lower results for cadmium than some of the other methods did.

In the XRFS methods, pressed briquettes, with or without some diluent, have been used for analysis of coal and coal fly-ash<sup>12,14,15</sup> and raw and stabilized coal wastes.<sup>8</sup> Fusion with lithium tetraborate and lanthanum oxide or tungstic oxide has been used for urban dusts and fly-ash.<sup>7</sup> Purdue and Williams<sup>16</sup> used a smear technique, with an internal standard, to prepare thin films for powdered samples such as furnace dust, and Davison *et al.*<sup>2</sup> suspended coal fly-ash in propanol and dispersed it ultrasonically before its collection on 0.4  $\mu\text{m}$  Millipore membrane filters.

### EFFECT OF STANDARD ADDITIONS ON XRFS LINE INTENSITIES

In quantitative XRFS the concentrations of the analytes are generally evaluated by mathematical treatment of the intensities of the characteristic lines,

with a large computer program. Calibration with standards is also necessary in order to obtain accurate results. Suitable standards for fly-ash are not readily available. In addition the general method is less attractive when a single element is to be determined in samples which may have very different overall composition. The method of standard additions is then an alternative, especially when the samples are fine powders. It has been used for the determination of low concentrations of lead (<300  $\mu\text{g/g}$ ) in powdered samples.<sup>17</sup> The additions can be made directly and no treatment is needed other than drying and mixing before pressing the briquette.

The expression for the intensity of a fluorescence line excited by a continuous spectrum is complicated. In the present study two simplifications can be made. First, a heavy metal, lead, is to be determined in a matrix where all the main components are light elements. Therefore enhancement effects can be neglected. Secondly, the concentration of the analyte is small, about 1%, and the matrix will only be moderately changed by the standard additions. The equivalent wavelength, *i.e.*, the wavelength of monochromatic radiation representative of the polychromatic distribution of wavelengths exciting the sample, will then remain almost constant<sup>18</sup> and the expression for the line intensity of an analyte X,  $I_x$ , can be written<sup>19</sup>

$$I_x = Q_x \frac{C_x}{\mu_s^*} \quad (1)$$

where  $Q_x$  is a proportionality constant,  $C_x$  the concentration of the analyte expressed as a mass fraction, and  $\mu_s^*$  the effective mass-attenuation coefficient of the specimen.

In the standard addition,  $B$  g of a compound containing the analyte at concentration  $C_0$  is added to  $A$  g of the sample. The analyte concentration in the "spiked" specimen will then be

$$C = \frac{AC_x + BC_0}{A + B} \quad (2)$$

The effective attenuation coefficient is

$$\mu_s^* = \frac{A\mu_A^* + B\mu_B^*}{A + B} \quad (3)$$

where  $\mu_A^*$  and  $\mu_B^*$  represent the corresponding coefficients of the original sample and the added compound, respectively. From equations (1)–(3) we obtain

$$I_x = Q_x \left( \frac{AC_x + BC_0}{A\mu_A^* + B\mu_B^*} \right) = \frac{Q_x C_0 (C_x/C_0 + y)}{\mu_A^* (1 + y\mu_B^*/\mu_A^*)} \quad (4)$$

where  $y$  is the ratio  $B/A$ . The subscript  $x$  will now be dropped, for simplicity.

The line intensity is thus a non-linear function of  $y$ , containing three parameters. The analyte concentration can be found by fitting equation (4) to the experimental data ( $I; y$ ) by non-linear least-squares methods. Since linear regression programs are more

readily available, the following approximate variant of equation (4) has been developed. Provided the second term in the denominator of the equation is small compared to 1, terms of higher order than two can be omitted, and

$$I = a_0 + a_1 y + a_2 y^2 \quad (5)$$

with

$$\begin{aligned} a_0 &= C \frac{Q}{\mu_A^*}; \\ a_1 &= \left( C_0 - C \frac{\mu_B^*}{\mu_A^*} \right) \frac{Q}{\mu_A^*}; \\ a_2 &= -C_0 \frac{\mu_B^* Q}{\mu_A^* \mu_A^*} \end{aligned} \quad (6)$$

The coefficients  $a_0$ ,  $a_1$ ,  $a_2$  can be found by fitting equation (5) to the data by linear regression.  $C$  is then obtained by solving the equation

$$C^2 - \left( \frac{a_1 C_0}{a_2} \right) C + \frac{a_0 C_0^2}{a_2} = 0. \quad (7)$$

In applications of the standard-additions method it is generally assumed that  $\mu_s^*$  in equation (1) is constant. From equation (4) it is seen that this assumption is fulfilled when  $A\mu_A^* \gg B\mu_B^*$  or  $\mu_A^* \approx \mu_B^*$ . The first case represents the determination of very low concentrations of the analyte. The corresponding standard-addition functions are

$$I = Q'(C + yC_0); \quad Q' = Q/\mu_A^* \quad (8)$$

and

$$(1 + y)I = Q'(C + yC_0) \quad (9)$$

When the condition  $A\mu_A^* \gg B\mu_B^*$  does not hold, the plot of equation (8) will be non-linear, with a slope decreasing with increasing  $y$ . The regression line will then yield an erroneous analytical result. A somewhat more correct result may be obtained from equation (9), which partly compensates for the non-linearity. In practice, however, this equation can hardly be expected to be followed exactly. Therefore equation (4) should be tried if equation (8) leads to a non-linear plot. If the range of the standard additions is small, then the non-linearity may be difficult to detect.

A linear variation of equation (4) would be

$$I \left( 1 + y \frac{\mu_B^*}{\mu_A^*} \right) = Q'(C + yC_0) \quad (10)$$

which is of limited use since it requires calculation of the effective attenuation coefficients and hence requires a knowledge of the concentrations of the major components of the sample.

## EXPERIMENTAL

Six fly-ash samples collected at different times were examined. The samples were homogenized and agglomerates were broken up in a mixer.



### Reagents

All reagents were of p.a. quality. Standard solutions of lead were prepared from the nitrate. The standards for AAS were made up with 1% v/v nitric acid and for XRFS with demineralized water.

### Apparatus

The atomic-absorption measurements were performed with a Perkin-Elmer 2380 atomic-absorption spectrometer at 217.0 nm, with use of a deuterium lamp for background correction. The operating conditions recommended by the manufacturer were used. For the X-ray measurements a Philips PW 1410 X-ray spectrometer equipped with a PW 1710 processor was used. The  $PbL_{\alpha}$ ,  $PbL_{\beta}$  and background intensities were measured with a chromium-target X-ray tube operated at 60 kV/36 mA, a lithium fluoride crystal (200) and a scintillation detector. The counting time was 5 sec for each line and background.

### Dissolution-extraction methods for the AAS determinations

**A. Leaching with nitric acid.** About 100 mg of ash was weighed into a Teflon tube and 25 ml of 1M nitric acid were added. The tube was capped and allowed to stand overnight at 90°. The solution was diluted to 100 ml with demineralized water and filtered (Munktell 11-cm OOH paper). Finally, the solution was diluted to contain about 4  $\mu$ g/ml lead.

**B. Leaching with EDTA in acetic acid/acetate buffer.** A 75–100 mg portion of ash was weighed into a Teflon tube, 25 ml of 0.1M EDTA in acetic acid/acetate (0.7M/0.5M) buffer, pH 4.5, were added and the tube was allowed to stand overnight at 90°, after which 10 ml of 1M nitric acid were added before dilution to 100 ml with demineralized water and filtration. Before measurement the solution was diluted to contain about 4  $\mu$ g/ml lead.

**C. Leaching with hydrofluoric/boric acid.** A 30–50 mg sample of fly-ash was weighed into a Teflon tube, and 10 ml of demineralized water and 2 ml of hydrofluoric acid (48% w/v) were added. The tube was shaken at room temperature for 48 hr, then 20 ml of saturated boric acid solution were added and the tube was shaken for another 48 hr at room temperature, and finally in an ultrasonic bath for 1 hr. The solution was diluted to 100 ml with saturated boric acid solution and filtered. This procedure is a modification of published methods for coal fly-ash<sup>11</sup> and stabilized coal waste.<sup>8</sup>

**D. Leaching with hydrofluoric/nitric acid.** A 50-mg portion of ash was weighed into a Teflon tube. A few drops of water were added to wet the sample, followed by 2 ml of hydrofluoric acid (48% w/v). The tube was shaken at room temperature for 3 hr and then the hydrofluoric acid was driven off by heating at 100° overnight. Twenty ml of 1M nitric acid were added, and the tube was allowed to stand at 90° for 2–5 hr, then in an ultrasonic bath for 2 hr, and finally shaken at room temperature overnight (16 hr). The solution was then diluted to 100 ml with demineralized water, filtered, and diluted further to a lead concentration of about 2  $\mu$ g/ml before measurement.

Reagent blanks were carried through all steps of the different dissolution methods and were used to prepare calibration graphs. The lead content of the ash was evaluated from these plots. Two determinations were made on each ash.

### Sample preparation for the X-ray measurements

A 4.000-g sample of ash was weighed into each of six Teflon containers holding two steel balls (diameter 11 mm). Standard additions of 0–1.00 ml of a standard lead solution (about 160 mg/ml) were then made. The spiked samples were dried at 110° overnight and allowed to cool at room temperature for 1–2 hr. The containers were shaken for 5 min in a Braun "Mikro-dismembrator II" (West Germany) to mix and grind the samples. Briquettes were made by

Table 1. Results (%) from the determinations of lead in fly-ash by AAS after different dissolution methods

Ash	Method			
	A	B	C	D
1	1.23; 1.20	1.15; 1.15	—; 1.18	1.23; 1.21
2	1.06; 1.06	1.00; 1.00	1.05; 1.03	1.08; 1.05
3	1.01; 1.00	0.95; 0.93	1.01; 0.99	1.03; 1.03
4	1.33; 1.32	1.26; 1.26	1.34; 1.33	1.34; 1.31
5	1.08; 1.09	1.04; 1.02	1.08; 1.16	1.10; 1.07
6	—	—	—	0.83; 0.84

transferring a 2.00-g sample to a die. The sample surface was smoothed and 1.0 g of cellulose powder was added to act as a backing. The die was subjected to a pressure of 11 MPa for 1 min. The briquettes were covered with mylar film. The  $PbL_{\alpha}$  and  $PbL_{\beta}$  lines were measured together with two background counts for each line. The net intensities were used to evaluate the lead content. All determinations were made in duplicate. A standard of leaded glass was repeatedly measured to check the stability of the instrument.

## RESULTS AND DISCUSSION

The results from the AAS determinations of the lead content of six ashes are presented in Table 1. Leaching with nitric acid (A), hydrofluoric/boric acid (C) or hydrofluoric/nitric acid (D) gives about the same results. With method (C) greater signal noise was observed, caused by the presence of boric acid. It is better to drive off the hydrofluoric acid if elements which do not form volatile compounds are to be determined. Leaching with EDTA (B) gives lower results than the other methods. This is not surprising, since this is a rather gentle method.

The results from the XRFS measurements are shown in Table 2. There is no significant difference between the results from the  $PbL_{\beta}$  and  $PbL_{\alpha}$  lines. A systematic difference would be expected if a substantial amount of arsenic is present in the sample, because the  $PbL_{\alpha}$  and  $AsK_{\alpha}$  lines overlap. The X-ray spectra of the samples indicate that small amounts of arsenic were present in some of the samples, but were too low to affect the determination of lead.

A typical standard addition plot according to equation (9) is shown in Fig. 1. The plot is curved.

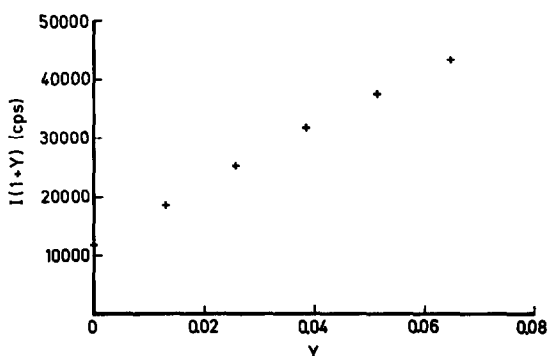


Fig. 1. Standard-addition plot according to equation (9).

Table 2. Results (%) from the determinations of lead in fly-ash with XRFs and different evaluation methods

Ash	Equation (4)				Equations (5), (7)				Equation (9)				Equation (10)					
	$L_\beta$	$L_\alpha$	$L_\beta$	$L_\alpha$	$L_\beta$	$L_\alpha$	$L_\beta$	$L_\alpha$	$L_\beta$	$L_\alpha$	$L_\beta$	$L_\alpha$	$L_\beta$ ( $L_{III}$ )	$L_\beta$ ( $L_{II}$ )	$L_\alpha$			
1	1.20	1.22	1.23	1.21	1.26	1.28	1.28	1.26	1.54	1.55	1.52	1.50	1.22	1.24	1.26	1.28	1.27	1.25
2	1.06	1.06	1.08	1.08	1.09	1.10	1.12	1.12	1.34	1.34	1.31	1.32	1.06	1.06	1.10	1.10	1.09	1.10
3	0.95	0.98	0.99	1.01	0.99	1.02	1.02	1.04	1.28	1.30	1.27	1.28	1.02	1.02	1.05	1.06	1.06	1.06
4	1.28	1.36	1.25	1.36	1.33	1.40	1.30	1.40	1.65	1.63	1.61	1.60	1.32	1.29	1.36	1.33	1.35	1.33
5	1.11	1.14	1.19	1.16	1.15	1.18	1.22	1.20	1.41	1.41	1.38	1.40	1.12	1.13	1.16	1.16	1.15	1.17
6	0.82	0.89	0.83	0.91	0.85	0.91	0.85	0.93	1.07	1.07	1.07	1.07	0.85	0.85	0.88	0.88	0.89	0.89

Hence the assumptions behind equations (8) and (9) are not valid and the results obtained with this approach will be too high, as confirmed by the results presented in Table 2.

The analytical results obtained when the data were fitted to equation (4) are given as the first entry in Table 2. They are compared with those from the AAS determinations in Fig. 2. In this comparison the mean of the concentrations found from the  $PbL_\alpha$  and  $PbL_\beta$  lines has been used. The AAS concentrations are those obtained by leaching with hydrofluoric/nitric acid and nitric acid. The agreement between the two methods is good. It can be seen from Table 2 that the reproducibility of the X-ray results is not quite satisfactory in some cases. An inspection of the primary data revealed that they agreed much better than did the analytical results calculated from them. It is therefore suspected that evaluation according to equation (4) is sensitive to small errors in the measurements. This point will be further investigated.

Results obtained by means of extraction methods *A* and *D* and AAS analysis thus agree with the determinations by XRFs. This indicates that lead is quantitatively extracted from the fly-ash with 1M nitric acid. This is contrary to the results for stabilized coal waste.<sup>8</sup> Low recoveries were obtained for all elements when the leaching was done with concentrated nitric acid. Low results were also found for coal fly-ash treated with boiling nitric acid (1 + 1).<sup>1</sup> The dissimilarity in behaviour between coal fly-ash and incinerator fly-ash is caused by a difference in the

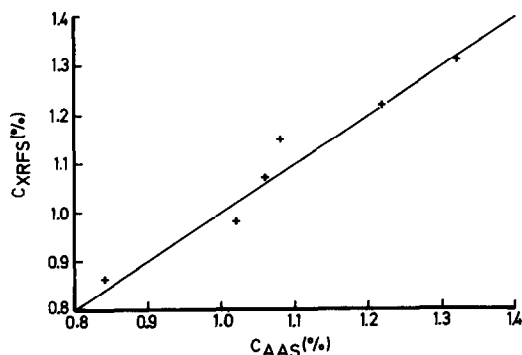


Fig. 2. Comparison between analytical results obtained with XRFs [equation (4),  $L_\alpha$  and  $L_\beta$ ] and AAS (dissolution methods *A* and *D*). A line of unit slope passing through the origin has been drawn.

location of the lead in the two types of ash. In coal fly-ash a considerable part of the element is apparently present in the interior of the particles, whereas it is present on the surface of the incinerator fly-ash, as a result of condensation from the gas phase.<sup>20</sup>

The results from the leaching with EDTA, where recoveries of about 95% were obtained, also show the ready availability of the lead. However, a word of caution might be added here. In our preliminary work with the extraction methods there were indications that the recovery dropped when a large amount of sample was taken. This could be due to the formation of slightly soluble lead compounds when the concentrations in the extracts become too high. For instance, lead sulphate could form, as the amount of sulphur is quite high in the ashes.

The XRFs data were also evaluated according to equations (5) and (7). As seen from Table 2 the analytical results are high by about 4%. It can be shown that a systematic error of this magnitude is introduced by neglect of the terms of higher order in the series expansion of equation (4).

One ash was analysed for the major elements (Table 3). The results were employed in an evaluation of the XRFs measurements according to equation (10). The concept of the effective excitation wavelength was utilized in the calculation of the effective mass attenuation coefficients. As the effective wavelength, 2/3 of the wavelength of the appropriate absorption edge was used.<sup>21</sup> For  $PbL_\beta$ , calculations were performed for the  $L_{II}$  and  $L_{III}$  edges, since the corresponding  $PbL_\beta$  lines were not resolved. Mass attenuation coefficients were taken from Thin and Leroux.<sup>22</sup> The data for the other ashes were also evaluated by using the composition in Table 3. The rationale for this is the moderate change in  $\mu^*$  caused by changes in the concentrations of the major elements. Theoretical calculations indicated that if 10% of one of the two main elements, calcium and potassium, was exchanged for an equivalent amount of magnesium and sodium, respectively,  $\mu^*$  changed by only 2%. As can be seen from Table 2, fairly accurate results were obtained despite the crude assumptions involved.

Table 3. Concentration of major elements in ash No. 5 (%)

Al	Ca	Cl	Fe	K	Mg	Na	S	Si	Ti
4.0	8.5	10.5	0.3	13.5	1.1	3.6	1.5	11.6	~2

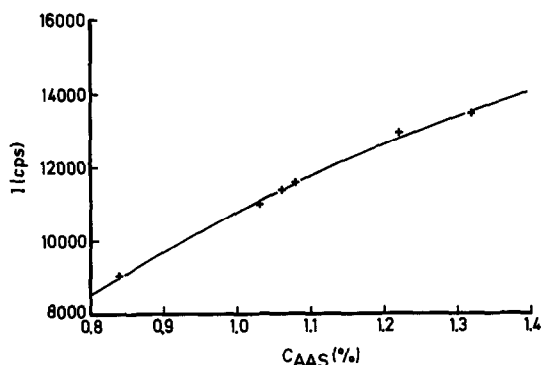


Fig. 3. Calibration graph obtained from ashes 1–6.

Fly-ash from a garbage incinerator typically contains 0.5–2% lead. It is evident from the results in Table 2 that X-ray measurements of standard additions made directly to such ashes will provide accurate analytical results if evaluated by equation (4). However, it is a time-consuming method. The moderate influence, on  $\mu^*$ , of changes in the amounts of the main components, suggests that properly analysed samples could be used to establish a calibration curve. Figure 3 shows the calibration plot obtained from the six samples analysed here. It has been used to evaluate XRFS measurements on additional samples taken from the same incinerator. Data obtained for ashes spanning the concentration range of the calibration graph are presented in Table 4. They indicate that the lead content so obtained is accurate to within about 5%. Direct XRFS

Table 4. Comparison of lead (%) determination in fly-ash [XRFS measurements ( $PbL_{\beta}$ ) evaluated from a calibration curve]

Ash	AAS	XRFS
7	1.34	1.29
8	1.04	1.00
9	0.88	0.93

measurements of briquetted samples would thus constitute a rapid method for monitoring the lead content of the fly-ash.

*Acknowledgements*—Thanks are due to Pertti Knuutila for the determination of major elements in fly-ash and to Roland Forsberg for putting the samples at our disposal.

#### REFERENCES

1. M. Reuss, *Water Sci. Technol.*, 1983, **15**, 193.
2. R. L. Davison, D. F. S. Natusch and J. R. Wallace, *Environ. Sci. Technol.*, 1974, **8**, 1107.
3. R. A. Nadkarni, *Anal. Chem.*, 1980, **52**, 929.
4. C. Block, *Anal. Chim. Acta*, 1975, **80**, 369.
5. C. Block and R. Dams, *Water, Air, Soil Pollut.*, 1975, **5**, 207.
6. A. M. Hartstein, R. W. Freedman and D. W. Platter, *Anal. Chem.*, 1973, **45**, 611.
7. W. Wegscheider, K. E. Lorber and K. Müller, *Int. J. Environ. Anal. Chem.*, 1978, **5**, 171.
8. M. G. Heaton, J. S. Buyer, J. P. Hershey and I. W. Duedall, *Environ. Technol. Lett.*, 1982, **3**, 529.
9. R. R. Greenberg, G. E. Gordon, W. H. Zoller, R. B. Jacko, D. W. Neuendorf and K. J. Yost, *Environ. Sci. Technol.*, 1978, **12**, 1329.
10. W. Weisweiler, B. Hochstein and E. Schwarzbach, *Staub-Reinhalt. Luft*, 1986, **46**, 60.
11. D. Silberman and G. L. Fisher, *Anal. Chim. Acta*, 1979, **106**, 299.
12. J. A. Campbell, J. C. Laul, K. Nielson and R. D. Smith, *Anal. Chem.*, 1978, **50**, 1032.
13. D. Behel Jr., P. M. Giordano and D. R. Stephenson, *Commun. Soil Sci. Plant Anal.*, 1986, **17**, 385.
14. R. D. Giaquic, R. B. Garrett and L. Y. Goda, *Anal. Chem.*, 1977, **49**, 1012.
15. J. A. Cooper, B. D. Wheeler, G. J. Wolfe, D. M. Bartell and D. B. Schlafke, *Adv. X-Ray Anal.*, 1977, **20**, 431.
16. G. E. Purdue and R. W. Williams, *X-Ray Spectrom.*, 1985, **14**, 102.
17. N. Pind, *Talanta*, 1984, **31**, 1118.
18. R. Tertian and F. Claisse, *Principles of Quantitative X-Ray Fluorescence Analysis*, p. 84. Heyden, London, 1982.
19. R. Tertian and F. Claisse, *op. cit.*, p. 71.
20. J. W. Kaakinen, R. M. Jorden, M. H. Lawasani and R. E. West, *Environ. Sci. Technol.*, 1975, **9**, 862.
21. R. Jenkins, *An Introduction to X-Ray Spectrometry*, p. 127. Wiley, New York, 1983.
22. T. P. Thinh and J. Leroux, *X-Ray Spectrom.*, 1979, **8**, 85.

## SPECTROPHOTOMETRIC DETERMINATION OF GALLIUM IN ALLOYS AND FLY-ASH WITH PYRIDOXAL DERIVATIVES OF THIOCARBOHYDRAZIDE AND CARBOHYDRAZIDE

F. J. BARRAGAN DE LA ROSA, R. ESCOBAR GODOY and J. L. GOMEZ ARIZA†  
 Department of Analytical Chemistry, Faculty of Chemistry, University of Seville, 41012-Seville, Spain

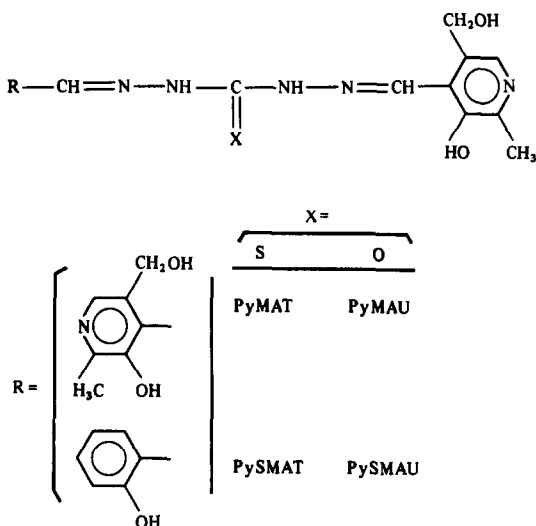
(Received 25 May 1987. Revised 2 December 1987. Accepted 10 December 1987)

**Summary**—The symmetric derivatives of pyridoxal with thiocarbohydrazide and carbohydrazide, and the asymmetric derivatives of pyridoxal and salicylaldehyde with the same hydrazides have been synthesized and their analytical potential for spectrophotometric and kinetic fluorimetric determination of metal ions was studied. Gallium(III) and PyMAU(1,3-bis{[4-(2-methyl-3-hydroxy-5-hydroxymethyl)pyridyl]methyl}eneaminourea at pH = 4.2 form a complex with a single absorption maximum at 425 nm, which can be extracted into cyclohexanone in the presence of a controlled amount of sodium perchlorate. The extract has maximum absorbance at 435 nm. Both systems can be used for determining gallium. The optimal range of gallium concentration for measurement in a 1-cm cell is 0.5–1.25 µg/ml for the procedure in homogeneous medium ( $\epsilon_{425} = 3.76 \times 10^4 \text{ l. mole}^{-1} \cdot \text{cm}^{-1}$ ) and 0.25–1.25 µg/ml for the extraction procedure ( $\epsilon_{435} = 5.30 \times 10^4 \text{ l. mole}^{-1} \cdot \text{cm}^{-1}$ ). The latter procedure has been applied to the determination of gallium in alloys and fly-ash.

Numerous thiocarbohydrazones and carbohydrazones have been used in trace analysis<sup>1-5</sup> and sensitive and selective procedures proposed for several metals.<sup>6-14</sup>

Attention has now turned to pyridoxal derivatives<sup>15</sup> and in the present work four compounds have been synthesized and studied:

used in the electronic industry and as antitumour agents,<sup>16-18</sup> and sensitive analytical methods are needed for its determination. Spectrophotometric<sup>19-21</sup> and fluorimetric<sup>19,20</sup> methods using organic reagents have been employed for determining gallium in various types of sample. The procedure proposed here is sensitive and suitable for estimation of gallium in nickel and aluminium alloys and in fly-ash.



PyMAU gives a good reaction with gallium, which is considered in detail, since gallium compounds are

### EXPERIMENTAL

#### Apparatus

Perkin-Elmer 1310 and Varian XL 200 spectrometers were used for recording infrared and NMR spectra. Absorbances were measured with a Perkin-Elmer 554 spectrophotometer and fluorescence with a Perkin-Elmer LS-5 spectrofluorimeter, equipped with an 8.3-W xenon discharge lamp pulsed at line frequency. A K5 ultrathermostatic water-bath circulator (Colora Messtechnik GmbH) and 1 × 1-cm silica cells were used.

**Reagent solutions.** Stock solutions of the organic reagents ( $1.25 \times 10^{-3} M$ ), containing 10% v/v DMF were used for the absorbance-pH studies and for the fluorimetric investigations of the catalytic effect of metal ions on the oxidation of the reagents. For photometric studies of the metal-ion complexes formed, 0.05% solutions of the reagents, containing 10% v/v DMF, were used (but in the recommended procedure for gallium determination the DMF is unnecessary). These solutions are stable for a week if stored in an amber bottle in a refrigerator.

**Gallium stock solution.** Prepared by dissolving 3.211 g of GaCl<sub>3</sub> in 100 ml of 1M hydrochloric acid. This solution was standardized by EDTA titration, and diluted with distilled water as required.

**Buffer solution, pH 3.8.** Sodium acetate-acetic acid (0.8M).

†To whom correspondence should be addressed.

**Titanium(III) chloride stock solution (15%) in 1M hydrochloric acid (Merck).** All other solutions or solvents were prepared from analytical-reagent grade salts or materials, and distilled demineralized water was used throughout.

### Reagents

**Preparation of the thiocarbonylhydrazide and carbonylhydrazide derivatives.** The symmetric reagents were prepared by condensation of thiocarbonylhydrazide or carbonylhydrazide with pyridoxal in the usual way for Schiff's bases. For synthesis of the asymmetric derivatives a previous step is necessary, to obtain the corresponding monosalicylaldehyde derivative by the method described by Brown *et al.*,<sup>22</sup> and this product is used to prepare the final reagent by condensation with pyridoxal.

For PyMAU and PyMAT, carbonylhydrazide or thiocarbonylhydrazide (0.025 mole) was dissolved in 10 ml of water, 0.5 ml of concentrated hydrochloric acid was added and the solution was gently heated, 0.05 mole of pyridoxal hydrochloride in 50 ml of ethanol was slowly added, and the mixture was heated for 10 min. A crude yellow precipitate was formed, filtered off and recrystallized from ethanol:water (4:1) acidified with hydrochloric acid.

For PySMAU and PySMAT, mono(salicylidene) carbonylhydrazide or thiocarbonylhydrazide (0.025 mole) was dissolved in 50 ml of ethanol acidified with 1 ml of glacial acetic acid, then 0.025 mole of pyridoxal hydrochloride dissolved in 10 ml of water containing 0.5 ml of concentrated hydrochloric acid was added. The mixture was refluxed until a crude precipitate appeared. The product was recrystallized from ethanol-water (2:1).

Elemental analysis gave the following results:

PyMAU (m.p. 264–5°) C<sub>17</sub>H<sub>20</sub>N<sub>6</sub>O<sub>5</sub> · 2HCl · H<sub>2</sub>O

	C	H	N	Cl
Calculated, %	42.58	5.01	17.50	14.80
Found, %	41.9	5.1	17.2	14.8

PyMAT (m.p. 255–7°) C<sub>17</sub>H<sub>20</sub>N<sub>6</sub>O<sub>4</sub>S · 2HCl

	C	H	N	S	Cl
Calculated, %	42.77	4.61	17.61	14.88	15.18
Found, %	42.4	4.3	17.8	15.2	16.3

PySMAU (m.p. 222–3°) C<sub>16</sub>H<sub>17</sub>N<sub>5</sub>O<sub>4</sub> · HCl

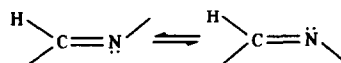
	C	H	N	Cl
Calculated, %	50.60	4.74	18.44	9.35
Found, %	50.6	4.9	18.2	9.6

PySMAT (m.p. 217–8°) C<sub>16</sub>H<sub>17</sub>N<sub>5</sub>O<sub>3</sub>S · HCl · H<sub>2</sub>O

	C	H	N	S	Cl
Calculated, %	46.43	4.84	16.92	7.73	8.50
Found, %	45.5	5.0	16.4	7.2	8.6

The compounds are readily soluble in water, especially the carbonylhydrazide derivatives. The infrared spectra (KBr discs) show the characteristic stretching vibration bands of the structure assigned to these reagents (Table 1).

Some features of the <sup>1</sup>H NMR spectra (Table 2) in *d*<sub>6</sub>-dimethylsulphoxide indicate the structure of the reagents. The integrated signals agree with the number of hydrogen atoms in the molecules. For the azomethine protons (positions 1 and 5), the asymmetric compounds exhibit two signals as expected. In general, the azomethine signals are doublets suggesting the existence of *Z-E* isomers, analogously to oximes, with the equilibrium:



except for PyMAU, which shows only a singlet, probably because of formation of a hydrogen bond between the electron pairs of these nitrogen atoms and the phenol groups on the pyridoxal rings, which causes greater rigidity of the molecule, especially for PyMAU. Finally, the peaks of the imine protons (positions 2 and 4) disappear on deuteration, which confirms their nature.

The ultraviolet spectra of aqueous solutions of the reagents are red-shifted when the pH is increased (Table 3).

The ionization constants were determined by classical spectrophotometric methods,<sup>23,24</sup> but the presence of several equilibria made it difficult to interpret the results from Fig. 1. The thiocarbonylhydrazide derivatives show *pK* values corresponding to the pyridinium, thioimidol and phenol groups. For PySMAT the values were 3.8, 7.7 and 9.6 respectively. The symmetric derivative PyMAT exhibits overlapping dissociation equilibria for the two pyridinium groups, the *pK* values of which were 3.4 and 5.0; as shown in Fig. 1(A) the curve for *A* vs. pH at 360 nm shows an inflection point and the *pK* values were evaluated one at each side of it, the Buděšinský method<sup>25</sup> being used to prove that only one proton is liberated before and one after this inflection point. The other equilibria for this reagent are

Table 1. Infrared bands\* (cm<sup>-1</sup>)

Reagent					Assignments
PyMAU	PySMAU	PyMAT	PySMAT		
3500–2600 m	3500–2500 m	3500–2600 m	3400–2700 m		N—H, O—H and C—H (aromatic) stretch
1725 s	1680 s	—	—		C=O (amide I) stretch
1615 w	1605–1620 w	1615 w	1605 w		C=N stretch
1540 s	1530 s	1540 s	1535 s		N—H (amide II) in plane deformation
1600–1450 m	1600–1450 m	1600–1450 m	1600–1450 m		C=C (aromatic) stretch
1360 m	1360 m	—	—		CO—N (amide III) stretch
—	—	1200 s	1170 s		C=S stretch
750 m	755 m	745 m	760 m		C—H (aromatic) in plane deformation

\*Abbreviations: s, strong; m, medium; w, weak.

Table 2.  $^1\text{H}$  NMR spectra in  $d_6$ -dimethylsulphoxide\*,  $\delta$  (ppm)

Reagent	Assignments						
	H ( $-\text{CH}_3$ )	H ( $-\text{CH}_2-$ )	H (2-hydroxyphenyl)	H (OH-, pyridoxal)	H ( $-\text{CH}=\text{O}$ )	H (OH-, 2-hydroxyphenyl)	H ( $-\text{NH}-$ )
PyMAU	2.68 s	4.80 s	—	8.90 s	8.15 s	—	12.15 s
PySMAU	2.62 s	4.76 s	6.90 } 7.34 } 7.95 }	m	8.34 s	8.15 d 8.70 d	10.20 s 11.27 s 11.77 s
PyMAT†	2.62 d	4.77 d	—	8.85 s	8.19 d	—	—
PySMAT	2.85 d	5.02 d	6.95 } 7.45 } 8.05 }	m	9.30 s	8.48 d 8.80 d	10.20 s 12.90 s 13.35 s

\*Abbreviations: s, singlet; d, doublet; m, multiplet.

†Sparingly soluble in dimethylsulphoxide.

Table 3. Spectral characteristics at various pH values

	pH					
	1.76		7.50		12.62	
	$\lambda_{\text{max}}^*$	$\epsilon^\dagger$	$\lambda_{\text{max}}^*$	$\epsilon^\dagger$	$\lambda_{\text{max}}^*$	$\epsilon^\dagger$
PyMAU	340	2.5	385	2.5	390	2.9
PySMAU	330	1.7	335	2.1	370	2.1
PyMAT	362	3.0	396	2.5	405	2.9
PySMAT	355	2.8	360	2.5	395	2.9

\*nm.

† $10^4 \text{ l. mole}^{-1} \cdot \text{cm}^{-1}$ .

characterized by pK values of 6.8 (thioimidol) and 9.2 (phenol group). The carbohydrazide derivatives have pK values of 4.9 and 4.4 for the pyridinium groups of PySMAU and PyMAU respectively; and 7.5 and 9.5 for the hydroxy group of the pyridoxal and the phenol group of PySMAU, the higher acidity of the OH-group of pyridoxal being in accord with the literature.<sup>26</sup> The pyridoxal OH-groups of PyMAU yield two pK values, at 8.2 (Fig. 1D,  $\lambda = 305 \text{ nm}$ ) and 8.8 (Fig. 1D,  $\lambda = 360 \text{ nm}$ ).

The solutions of the reagents in water are readily oxidized or reduced (Table 4), the thiocarbohydrazide derivatives being especially unstable in alkaline medium. The catalytic effect of numerous metal ions on the oxidation of the reagent by hydrogen peroxide was tested in acetate and

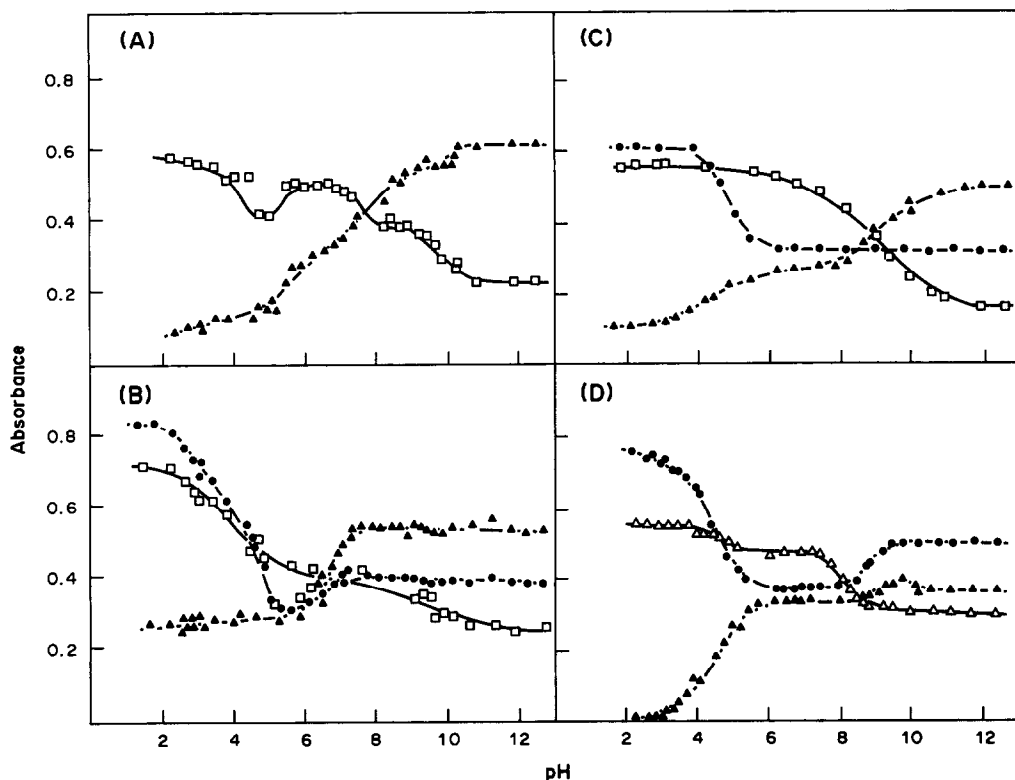


Fig. 1. Effect of pH on absorbance of the reagents ( $2.5 \times 10^{-5} \text{ M}$ ): A, PySMAT; B, PyMAT; C, PySMAU; D, PyMAU.  $\Delta$  305 nm;  $\square$  330 nm;  $\bullet$  360 nm;  $\blacktriangle$  396 nm.

Table 4. Effect of oxidation and reduction on the absorption spectra of the reagents (decrease in absorbance in 1 hr, %)

Reagent	Ascorbic acid (0.12%)		Hydrogen peroxide (0.16%)	
	pH = 4.5	pH = 9.5	pH = 4.5	pH = 9.5
PyMAU	5	9	7	22
PySMAU	17	7	23	23
PyMAT	10	25	10	45
PySMAT	7	14	50	56

ammonia buffers, and several were found to catalyse the oxidation of the reagents (particularly in ammonia medium) to fluorescent products, which can potentially be used for the kinetic determination of these elements (Table 5).

#### Procedures

**Determination of gallium in homogeneous medium.** Into a 25-ml standard flask transfer a suitable volume of sample solution containing 15–30  $\mu\text{g}$  of gallium, and add 4 ml of aqueous 0.05% PyMAU solution, adjust to pH 3–5 with 3 ml of buffer solution (sodium acetate–acetic acid) and mix. Then dilute to volume and measure the absorbance at 425 nm against a reagent blank.

**Determination of gallium by extraction into cyclohexanone.** To an aqueous solution of gallium (2.5–10  $\mu\text{g}$ ) in a separating funnel, add 3 ml of sodium acetate–acetic acid buffer solution to adjust the pH to 4–5, 2 ml of 2M sodium perchlorate, and 1.5 ml of 0.05% PyMAU solution and dilute to 10 ml with distilled water. Shake the solution vigorously with 5 ml of cyclohexanone (accurately measured) for 2 min, collect the organic phase, and shake the aqueous phase with another 5 ml of cyclohexanone. Dry the combined extracts with anhydrous sodium sulphate. Measure the absorbance at 435 nm against a blank similarly prepared.

**Dissolution and preparation of samples.** Weigh 1 g of nickel alloy into a conical beaker and dissolve it in 20 ml of *aqua regia* and 2 ml of saturated bromine water. Evaporate to dryness on a sand-bath, cool to room temperature, dissolve the residue in 2 ml of concentrated sulphuric acid and evaporate until white fumes appear. Cool again to room temperature, and take up the residue in a little 6M hydrochloric acid, filter off the silica, wash it and dilute to 50 ml with 6M hydrochloric acid.

Weigh 1 g of aluminium alloy into a conical beaker, dissolve it in 6M hydrochloric acid, and dilute the solution to 50 ml with 6M hydrochloric acid.

Weigh 0.5 g of fly-ash (previously calcined at 800° for 2 hr), dissolve it in 6M hydrochloric acid, and filter off and wash the silica residue. Dilute accurately to 50 ml with 6M hydrochloric acid.

**Separation of gallium from the samples.** Treat the samples thus prepared, by the method proposed by Busev *et al.*<sup>20</sup> to separate the gallium. Transfer the prepared 50-ml sample into a separating funnel, rinsing the beaker with 2–3 ml of 6M hydrochloric acid. Carefully add titanium(III) solution until a violet colour persists. Allow the solution to stand for 2–3 min, then add 30 ml of diethyl ether, and shake the mixture vigorously for 1 min. Discard the lower layer and wash the extract with two 2-ml portions of 6M hydrochloric acid. Strip the gallium with two 10–15 ml portions of water, shaking for 1 min each time, and place the combined strippings in a porcelain dish containing 0.1 g of sodium chloride, and evaporate the solution to dryness on a sand-bath. Dissolve the residue in water and transfer the solution into a 25-ml standard flask for aluminium and nickel alloys and a 50-ml flask for fly-ash, and finally dilute to the mark with distilled water.

## RESULTS AND DISCUSSION

### Reaction with metal ions

The chromogenic properties of the reagent on reaction with metal ions were tested in both hydrochloric acid/potassium chloride (pH 2.1) and acetic acid/sodium acetate (pH 4.5) media (Table 6 summarizes the most important results). The reactivity is favoured by the presence of a sulphur atom in the molecule of the reagent, the reactions being more sensitive at pH 2.1. PyMAU is more interesting as a spectrophotometric reagent, because its solution in water is more stable, the absorbance of the blank is lower, and the selectivity greater than for the other reagents. In addition the absorption maximum of the gallium chelate with PyMAU at pH 2.1 shows a bathochromic shift relative to the outer metal complexes.

### Study of the gallium–PyMAU system

Gallium solutions rapidly form a yellow chelate with an excess of PyMAU in aqueous medium, and the absorbance remains stable for 60 min. This chelate can be extracted into non-aqueous solvents such as cyclohexanol and cyclohexanone, but the extraction is complete only with the latter (in the presence of sodium perchlorate). Other solvents such as chloroform, methyl isobutyl ketone, ether, 2-propanol, isobutanol and isoamyl alcohol have proved inefficient for extraction of the chelate from the aqueous medium.

Table 5. Catalytic effect of metal ions (1  $\mu\text{g}/\text{ml}$ ) on oxidation of the reagent at pH = 9.2 with 0.06%  $\text{H}_2\text{O}_2$ 

Reagent	$\lambda_{\text{ex}}$ , nm	$\lambda_{\text{em}}$ , nm	Metal ions and relative catalytic activity*
PyMAU	349	431	$\text{Cu}^{2+}(2.42) > \text{Mn}^{2+}(1.00) > \text{Co}^{2+}(0.53)$
PySMAU	350	455	$\text{Mn}^{2+}(1.00) > \text{Cu}^{2+}(0.91) > \text{V}^{5+}(0.24) > \text{Co}^{2+}(0.19)$
PyMAT	380	499	$\text{Co}^{2+}(1.42) > \text{Mn}^{2+}(1.00) > \text{Au}^{3+}(0.68) > \text{Ti}^{4+}(0.62) > \text{Cu}^{2+}(0.55)$
PySMAT	348	438	$\text{Ti}^{4+}(2.25) > \text{Pd}^{2+}(1.80) > \text{Ce}^{4+}(1.74) > \text{Cr}^{3+}(1.57) > \text{Mn}^{2+}(1.00) > \text{Cu}^{2+}(0.96) > \text{Zr}^{4+}(1.95) > \text{Au}^{3+}(0.64)$

\*The fluorescence obtained after 5 min in presence of  $\text{Mn}^{2+}$  is taken as 1.00.

Table 6. Photometric characteristics of the complexes in solution\*

Cations	PyMAU				PySMAU				PyMAT				PySMAT			
	pH = 2.1		pH = 4.5		pH = 2.1		pH = 4.5		pH = 2.1		pH = 4.5		pH = 2.1		pH = 4.5	
	$\lambda$	$\epsilon$	$\lambda$	$\epsilon$	$\lambda$	$\epsilon$	$\lambda$	$\epsilon$	$\lambda$	$\epsilon$	$\lambda$	$\epsilon$	$\lambda$	$\epsilon$	$\lambda$	$\epsilon$
Cu(II)	405	1.0	405	1.1	—	—	—	—	405	1.4	—	—	430	1.1	440	0.6
Ga(III)	452	0.8	425	3.3	420	3.0	—	—	425	1.3	—	—	420	0.7	—	—
Ni(II)	—	—	405	0.6	—	—	—	—	—	—	—	—	—	—	—	—
Co(II)	—	—	—	—	—	—	—	—	—	—	—	—	430	0.9	440	1.3
U(VI)	—	—	—	—	420	4.3	—	—	—	—	—	—	—	—	—	—
Fe(III)	—	—	—	—	—	—	—	—	410	1.0	—	—	—	—	430	1.1
Al(III)	—	—	—	—	—	—	415	2.6	—	—	—	—	—	—	—	—
Au(III)	—	—	—	—	—	—	—	—	415	5.1	—	—	—	—	—	—
Zr(IV)	425	1.2	425	2.0	—	—	—	—	—	—	—	—	—	—	—	—
V(V)	390	1.2	—	—	—	—	—	—	—	—	—	—	—	—	—	—

\* $\lambda_{\max}$  (nm) and  $\epsilon_{\max}$  ( $10^4$  l. mole<sup>-1</sup>. cm<sup>-1</sup>).

The absorption spectra of the gallium chelate in water and cyclohexanone are shown in Fig. 2. They show only one absorption maximum at 425 nm in water, which shifts to 435 nm in a less polar solvent such as cyclohexanone.

#### Influence of pH

The effect of pH on colour development was studied by preparing a series of samples at different pH values in the range from 1.5 to 11 (Fig. 3A), and the absorbance was found to be independent of pH in the interval 3.0–5.0. When solvent extraction is used this plateau is restricted to pH 4.0–5.0 (Fig. 3B) and the absorbance is higher, suggesting that the sensitivity and selectivity in the determination of gallium will be increased by use of extraction. For adjustment of the pH to a suitable range for both cases an acetic acid/acetate buffer of pH 3.8 was selected.

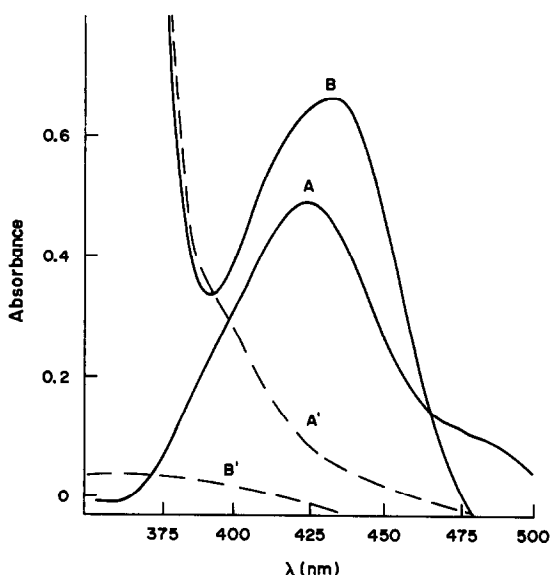


Fig. 2. Absorption spectra of gallium(III)-PyMAU complex: A, in aqueous solution; A', blank; B, in cyclohexanone; B', blank. Gallium 1  $\mu$ g/ml, pH 4.2.

#### Stoichiometry of the complex

The Ga(III)-PyMAU chelate in both the homogeneous and extraction systems was found to have 1:1 composition.

#### Other variables studied

The influence of several factors which can affect the absorbance, such as type and amount of buffer solution, ionic strength adjuster, order of addition of the reagents, and concentration of PyMAU was examined.

Other variables were tested in the extraction procedure. The concentration of perchlorate as counterion is critical and must be between 0.2 and 0.6M; a lower concentration does not completely extract the chelate and a higher one causes a decrease in the absorbance and prevents separation of the two layers. A shaking-time of at least 2 min was found adequate for extraction of the complex into cyclohexanone. The optimum volume ratio was established as 2:1 aqueous phase:organic phase for double extraction of the aqueous phase.

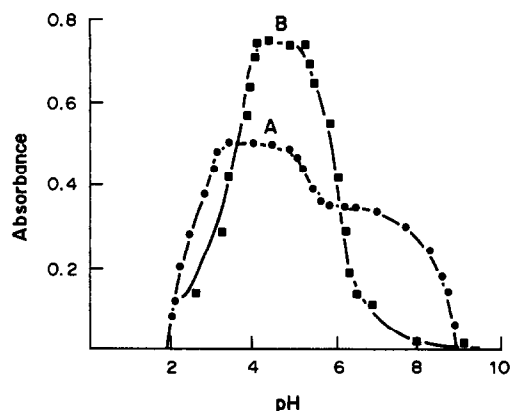


Fig. 3. Absorbance vs. pH curves for the gallium(III)-PyMAU complex: A, in aqueous solution, at 425 nm; B, in cyclohexanone at 435 nm. Gallium 1  $\mu$ g/ml.



Table 7. Tolerance limits for interferences in the spectrophotometric determination of 1 µg/ml Ga in homogeneous medium with PyMAU at pH 4.3

Foreign ions	Amount tolerated, µg/ml
Co(II), Ni(II), Cu(II), Al(III), Fe(III)*, Th(IV), Zr(IV), V(V), citrate, EDTA, C <sub>2</sub> O <sub>4</sub> <sup>2-</sup> †, P <sub>2</sub> O <sub>7</sub> <sup>4-</sup> †	1
Ni(II)†, U(VI), Au(III), In(III), Ti(IV), Zr(IV)†, Mo(VI)	2
U(VI)†, Pt(IV), P <sub>2</sub> O <sub>7</sub> <sup>4-</sup>	5
Ag(I), Co(II)†, Fe(II), Pd(II), Sn(II), Cr(III), In(III)†, NO <sub>3</sub> <sup>-</sup> , F <sup>-</sup> , tartrate	10
Be(II), Zn(II), Sb(III), Au(III)†, Ti(IV)†, Pt(IV)†, Ce(IV), W(VI), Mo(VI)†	25
Ti(O), Hg(O), Cd(II), Bi(III), As(III), S <sub>2</sub> O <sub>3</sub> <sup>2-</sup> , IO <sub>4</sub> <sup>-</sup>	50
Pb(II), Hg(II), La(III), Ce(III), SO <sub>3</sub> <sup>2-</sup> , bicine	100
Mn(II), Se(IV), PO <sub>4</sub> <sup>3-</sup>	200
S <sub>2</sub> O <sub>8</sub> <sup>2-</sup>	500
Ca <sup>2+</sup> , Mg <sup>2+</sup> , thiourea, thiosemicarbazide, Br <sup>-</sup> , I <sup>-</sup>	1000
B <sub>4</sub> O <sub>7</sub> <sup>2-</sup> , AsO <sub>4</sub> <sup>3-</sup> , ClO <sub>4</sub> <sup>-</sup> , IO <sub>3</sub> <sup>-</sup> , CN <sup>-</sup>	2000
Na <sup>+</sup> , K <sup>+</sup> , Cs <sup>+</sup> , Ba <sup>2+</sup> , Sr <sup>2+</sup> , SCN <sup>-</sup>	4000
Cl <sup>-</sup> , BrO <sub>3</sub> <sup>-</sup> , ClO <sub>3</sub> <sup>-</sup>	

\*The interference is significantly reduced by addition of ascorbic acid.

†Procedure with extraction in cyclohexanone.

Table 8. Determination of gallium in alloys and fly-ash

Standard sample	Composition, %	Ga added, %	Ga found, %
Aluminium alloy (1)	Fe 0.08%, SiO <sub>2</sub> 0.03%, Cu 0.01%, Ti 0.002%, V 0.004%, Zn 0.015%, Ga 0.009%.	—	0.0084 ± 0.0005
Nickel alloy (2)	Co 15%, Cr 10%, Al 5.5%, Ti 5%, Mo 3%, V 1%, C 0.15%, Pb 0.0021%, Bi 0.001%, Ag 0.0035%, Sb 0.0047%, As 0.0050%, Mg 0.0147%, Sn 0.0091%, Zn 0.0091%, Ga 0.0050%.	—	0.0060 ± 0.0003
Fly-ash I (3)	SiO <sub>2</sub> 48.81%, Al <sub>2</sub> O <sub>3</sub> 32.20%, Fe <sub>2</sub> O <sub>3</sub> 5.15%, CaO 4.62%, MgO 1.57%, Na <sub>2</sub> O 0.96%, K <sub>2</sub> O 3.54%, MnO <sub>2</sub> 0.04%, TiO <sub>2</sub> 1.96%, P <sub>2</sub> O <sub>5</sub> 1.07%.	0.553	0.548 ± 0.010
Fly-ash II (4)	SiO <sub>2</sub> 51.67%, Al <sub>2</sub> O <sub>3</sub> 37.08%, Fe <sub>2</sub> O <sub>3</sub> 3.41%, CaO 1.00%, MgO 0.41%, Na <sub>2</sub> O 0.6%, K <sub>2</sub> O 0.99%, TiO <sub>2</sub> 2.04%, P <sub>2</sub> O <sub>5</sub> 0.76%.	0.558	0.563 ± 0.012

(1) and (2) Certified analysis of National Bureau of Standards.

(3) and (4) The composition was determined by atomic-absorption spectrometry and a gallium spike was added to the sample solution.

### Spectrophotometric determination of gallium with PyMAU

*Without extraction.* Beer's law is obeyed over the gallium range 0.1–2.0  $\mu\text{g/ml}$ , and the optimum concentration range evaluated by a Ringbom plot is 0.5–1.25  $\mu\text{g/ml}$ . The molar absorptivity at 425 nm is  $3.76 \times 10^4 \text{ l.mole}^{-1}.\text{cm}^{-1}$  and the relative standard deviation is 0.4% for 0.75  $\mu\text{g/ml}$  (11 samples).

*With extraction.* Beer's law is obeyed for gallium concentrations between 0.1 and 1.5  $\mu\text{g/ml}$  at 435 nm ( $\epsilon_{435} = 5.3 \times 10^4 \text{ l.mole}^{-1}.\text{cm}^{-1}$ ) and the optimum concentration range is 0.25–1.25  $\mu\text{g/ml}$ , the relative error being 2.9%.

The results of interference studies on both methods are given in Table 7. The tolerance limit for a foreign ion was considered to be the greatest amount that caused an error of not more than 5% of the absorbance of a 0.75- $\mu\text{g/ml}$  pure gallium solution. An upper test limit of 100  $\mu\text{g/ml}$  was fixed in the study for cations and 1000  $\mu\text{g/ml}$  for anions.

In general, there is higher tolerance for several species such as Co(II), Ni, Zr, V(V), Mo(VI) and Ti(IV) in the extraction procedure, but the interference of oxalate and pyrophosphate is more severe. Because of its better selectivity, the extraction procedure is preferable, even though it is more tedious.

### Determination of gallium in alloys and fly-ash

Gallium was determined by the extractive photometric method in aliquots of the solutions prepared as described. The results are shown in Table 8. For the fly-ash samples, which did not contain gallium, a spike of 2.5 mg of gallium was added to the 50 ml of sample solution in order to test the recovery.

### Conclusions

Pyridoxal derivatives of thiocarbohydrazide and carbohydrazide show a higher sensitivity for the spectrophotometric determination of metal ions, particularly for gallium, which can be selectively determined with PyMAU, especially if the method is combined with Busev's method for prior separation of gallium. Of the four reagents considered, PyMAU is the best for gallium determination, because it exhibits higher solubility and stability, and the blanks are lower. In addition, the method can be applied either in homogeneous medium or with solvent ex-

traction (which decreases the interferences). Finally, PyMAU compares favourably in sensitivity with classical reagents for gallium such as Rhodamine, Gallion, Xylenol Orange and Malachite Green, with which the use of solvent extraction is also necessary.

### REFERENCES

1. F. J. Barragán de la Rosa, J. L. Gómez Ariza and F. Pino, *Talanta*, 1983, **30**, 555.
2. D. Rosales, G. González and J. L. Gómez Ariza, *ibid.*, 1985, **32**, 467.
3. M. T. Montaña González, J. L. Gómez Ariza and A. Garcia de Torres, *Anal. Quim.*, 1984, **80**, 129.
4. G. Galán, M. T. Morales, M. T. Montaña and J. L. Gómez Ariza, *J. Mol. Struct.*, 1986, **143**, 517.
5. E. Sánchez Romero, J. L. Gómez Ariza and A. Guiraúm, *ibid.*, 1986, **143**, 509.
6. F. J. Barragán de la Rosa, J. L. Gómez Ariza and F. Pino, *Mikrochim. Acta*, 1983 **II**, 455.
7. *Idem*, *ibid.*, 1983 **III**, 159.
8. D. Rosales, J. L. Gómez Ariza and J. A. Muñoz Leyva, *ibid.*, 1985 **I**, 77.
9. F. J. Barragán de la Rosa, J. L. Gómez Ariza and F. Pino, *ibid.*, 1984 **I**, 171.
10. J. L. Gómez Ariza, F. J. Barragán de la Rosa and M. T. Montaña González, *ibid.*, 1984 **II**, 407.
11. D. Rosales and J. L. Gómez Ariza, *Anal. Chim. Acta*, 1985, **169**, 367.
12. *Idem*, *Anal. Chem.*, 1985, **57**, 1411.
13. D. Rosales, J. L. Gómez Ariza and A. G. Asuero, *Analyst*, 1986, **111**, 449.
14. D. Rosales, I. Millán and J. L. Gómez Ariza, *Talanta*, 1986, **33**, 607.
15. R. Escobar Godoy, F. J. Barragán de la Rosa and J. L. Gómez Ariza, *J. Mol. Struct.*, 1986, **143**, 505.
16. M. M. Hart and R. H. Adamson, *Proc. Natl. Acad. Sci., U.S.A.* 1971, **68**, 1623.
17. R. C. Hayes, *J. Nucl. Med.*, 1970, **18**, 740.
18. R. A. Zweidinger and L. Barnett, *Anal. Chem.*, 1973, **45**, 1563.
19. F. D. Snell, *Photometric and Fluorimetric Methods of Analysis*, Part I, pp. 497–534. Wiley, New York, 1978.
20. A. I. Busev, V. G. Tipsova and V. M. Ivanov, *Analytical Chemistry of Rare Elements*, Mir, Moscow, 1981.
21. Z. Marczenko, *Spectrophotometric Determination of Elements*, pp. 267–273. Horwood, Chichester, 1976.
22. A. C. Brown, E. C. Pickering and F. J. Wilson, *J. Chem. Soc.*, 1927, 107.
23. J. P. Phillips and L. L. Merritt, Jr., *J. Am. Chem. Soc.*, 1948, **70**, 410.
24. L. Sommer, *Folia Fac. Sci. Nat. Univ. Purk., Brno*, 1964, **5**, 1.
25. B. Buděšinský, *Talanta*, 1969, **16**, 1277.
26. A. K. Lunn and R. A. Morton, *Analyst*, 1952, **77**, 718.

## EXTRACTION-SPECTROPHOTOMETRIC DETERMINATION OF BORON WITH 4,6-DI-*tert*-BUTYL-3- METHOXYCATECHOL AND ETHYL VIOLET

MITSUKO OSHIMA, KIYOMI SHIBATA, TAKAKO GYOUTEN,  
SHOJI MOTOMIZU and KYOJI TÔEI

Department of Chemistry, Faculty of Science, Okayama University, 3-1-1 Tsushimanaka, Okayama-shi,  
700 Japan

(Received 9 July 1986. Revised 25 November 1987. Accepted 10 December 1987)

**Summary**—4,6-Di-*tert*-butyl-3-methoxycatechol (DBMC) has been developed as a new reagent for boron, the complex anion formed being extracted as an ion-associate with Ethyl Violet into toluene, and the absorbance measured at 610 nm. The calibration graph is linear up to 0.43  $\mu\text{g}$  of boron, the molar absorptivity is  $1.02 \times 10^5 \text{ l. mole}^{-1} \text{ cm}^{-1}$  and the relative standard deviation 1.2%. The method has been applied to the determination of boron in sea-water and river water with satisfactory results.

Spectrophotometric determination of boron by measurement of an extracted ion-associate formed between an anionic boron-reagent complex and a cationic dye will be sensitive if the dye cation has high molar absorptivity. As complexing reagents for boron, fluoride,<sup>1</sup> various  $\alpha$ -hydroxy-acids,<sup>2</sup> benzoic acids,<sup>3,4</sup> catechols<sup>5</sup> and naphthols<sup>6</sup> are available. Of these, fluoride is the most popular. However, the method based on fluoride and Methylene Blue requires close control of the acid concentration, reaction time and temperature in formation of the tetrafluoroborate. Moreover, there is a large reagent blank, which is a general disadvantage of such extraction-spectrophotometric procedures. We reported earlier a method<sup>7</sup> based on complexation of boron with 3,5-di-*tert*-butyl-catechol and extraction of the ion-associate formed with Ethyl Violet, the high absorbance of the reagent blank being lowered by treatment with hydrogen peroxide. To eliminate the peroxide treatment, we have synthesized a new complexing reagent, 4,6-di-*tert*-butyl-3-methoxycatechol (DBMC), which with Ethyl Violet gives a highly sensitive method for boron determination.

### EXPERIMENTAL

#### Reagents

**Standard boron solution** ( $1 \times 10^{-2} \text{ M}$ ). Dissolve 0.1546 g of boric acid in 250 ml of demineralized water. Prepare working solutions by accurate dilution.

**DBMC.** Synthesized similarly to 3,5-di-*tert*-butyl-catechol.<sup>8</sup> Dissolve 14 g of 3-methoxycatechol in 35 ml of *tert*-butyl alcohol and carefully add 10 ml of concentrated sulphuric acid, keeping the temperature below 20°; use fused-silica (not borosilicate) apparatus. Disperse the solid product in water, collect it, wash it with water, then recrystallize it three times from petroleum ether (b.p. 30–70°). White plates are obtained (m.p. 129–131°). The identity of the product has been confirmed by <sup>1</sup>H NMR (CDCl<sub>3</sub>):  $\delta = 1.35$  (18H, s), 3.80 (3H, s), 6.75 (1H, s), and

the mass spectrum [ $m/z$  252 ( $\text{M}^+$ )]. The DBMC is used as a  $3.5 \times 10^{-2} \text{ M}$  solution in toluene.

**Ethyl Violet.** Prepare a  $4 \times 10^{-4} \text{ M}$  solution in water.

Use analytical-grade reagents and demineralized water. Store all solutions in polyethylene bottles, except the toluene solution. For the extractions use 20-ml stoppered test-tubes made of soda glass or fused silica.

#### Procedure

Transfer 2 ml of sample solution (containing up to 2  $\mu\text{g}$  of boron) to the extraction tube, and add 0.5 ml of phosphate buffer solution (0.1M, pH 8), 0.5 ml of  $4 \times 10^{-4} \text{ M}$  Ethyl Violet, and 5 ml of  $3.5 \times 10^{-2} \text{ M}$  DBMC solution in toluene, then shake the mixture on a mechanical shaker, for 50 min. Measure the absorbance of the toluene layer at 610 nm. If fused-silica extraction tubes are used, shaking for 30 min is enough.

### RESULTS AND DISCUSSION

#### Selection of catechol derivative

In our earlier work,<sup>7</sup> we tested 8 catechols and chose 3,5-di-*tert*-butylcatechol for the determination of boron with Ethyl Violet as counter-ion. The molar absorptivity was high ( $1.05 \times 10^5 \text{ l. mole}^{-1} \text{ cm}^{-1}$ ) but so was the absorbance of the reagent blank, necessitating the addition of hydrogen peroxide and subsequent centrifuging to decrease the blank. In trying to find more useful reagents for boron, we tried synthesizing other catechol derivatives by reacting *tert*-butyl alcohol with 3-methyl-, 3-isopropyl- and 3-methoxycatechol in a similar way to the synthesis of 3,5-di-*tert*-butylcatechol. No product was obtained from *tert*-butyl alcohol and 4-methylcatechol and the product from isoamyl alcohol and catechol was a pale violet tar. The catechol derivatives obtained were examined by essentially the procedure described above. DBMC was chosen because it was the only one of the reagents tested that did not necessitate a special procedure to minimize the reagent blank. The results are shown in Table 1.

Table 1. Comparison of catechol derivatives

Optimal conditions	Catechol substituents			
	3-methyl	3-methyl-5- <i>tert</i> -butyl	3-isopropyl-5- <i>tert</i> -butyl	3-methoxy-4,6-di- <i>tert</i> -butyl
Extraction pH	5.5	6.0	8.0	8.0
[Ethyl Violet], <i>M</i>	$5 \times 10^{-4}$	$8 \times 10^{-4}$	$8 \times 10^{-4}$	$4 \times 10^{-4}$
[Reagent] <i>M</i>	0.3	0.07	0.03	0.035
[H <sub>2</sub> O <sub>2</sub> ] %*	17.5	17.5	3.5	—
Standing time, min†	40	30	15	—
Blank absorbance	0.143	0.237	0.422	0.080
Molar absorptivity, $10^4 \text{ l. mole}^{-1} \text{ cm}^{-1}$	8.9	10.0	8.5	10.2

Aqueous phase: 2 ml of boric acid solution + 0.5 ml of buffer solution + 0.5 ml of Ethyl Violet solution; organic phase: 5 ml of DBMC solution in toluene.

\*One ml was added to diminish the reagent blank.

†Time elapsed between addition of H<sub>2</sub>O<sub>2</sub> and measurement of absorbance.

### Absorption spectra

The absorption spectra of the ion-associate formed between the boron-DBMC complex anion and Ethyl Violet in toluene, and of the reagent blank, are shown in Fig. 1. The absorption maximum is at 610 nm. The molar absorptivity is  $1.02 \times 10^5 \text{ l. mole}^{-1} \text{ cm}^{-1}$ . The mean absorbance for 0.216  $\mu\text{g}$  of boron (10 replicates) was 0.479 (relative standard deviation 1.2%). The blank absorbance was about 0.08.

### Effect of experimental variables

**Contamination from reaction vessels.** Borosilicate (from suppliers A and B), fused-silica and soda-glass test-tubes were tested. The results are shown in Table 2. Borosilicate glass causes considerable and variable contamination, but the silica and soda-glass tubes cause practically no contamination. In practice, soda-glass test-tubes are recommended on grounds of lower cost.

**Effect of pH.** This is shown in Fig. 2. Citrate buffer was used for pH 4.0–5.0, phosphate buffer for pH 6.0–8.5, ammonia buffer for pH 9.0–10.0. Maximum and constant absorbance was obtained at pH 7.0–8.5, so pH 8 is recommended for use.

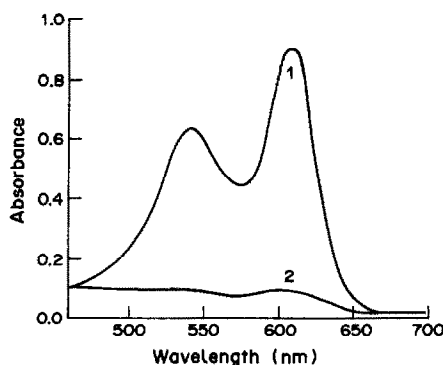


Fig. 1. Absorption spectra in toluene: 1, boron 0.432  $\mu\text{g}$ , reference toluene; 2, reagent blank, reference toluene.

Table 2. Contamination from the extraction vessels

Extraction tube	Absorbance*	
	B 0.423 $\mu\text{g}$	Reagent blank
Borosilicate glass A (20 ml)	0.907	0.141
	0.955	0.138
	0.899	0.180
B	0.886	0.258
	0.932	0.184
	0.936	0.167
Fused silica (20 ml)	0.870	0.080
Soda glass (11.5 ml)	0.876	0.085

\*Reference: toluene.

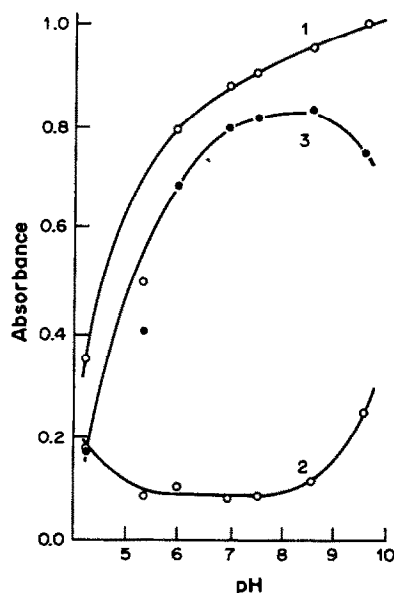


Fig. 2. Effect of pH on reaction and extraction: 1, boron 0.432  $\mu\text{g}$ , reference toluene; 2, reagent blank, reference toluene; 3, boron 0.432  $\mu\text{g}$ , reference reagent blank.

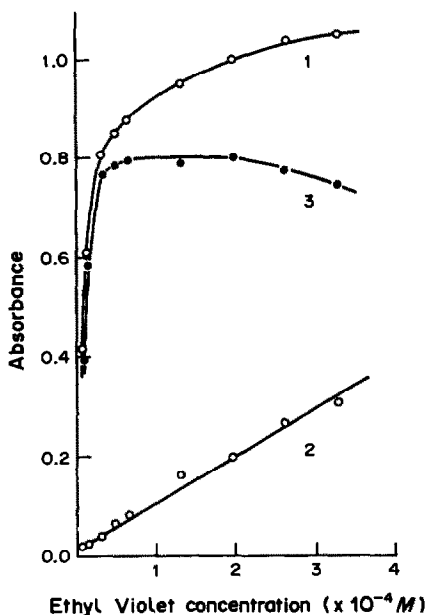


Fig. 3. Effect of Ethyl Violet concentration: 1, boron 0.432  $\mu\text{g}$ , reference toluene; 2, reagent blank, reference toluene; 3, boron 0.432  $\mu\text{g}$ , reference reagent blank.

**Effect of Ethyl Violet concentration.** Ethyl Violet was chosen as counter-ion on the basis of the previous work. The effect of its concentration is shown in Fig. 3. Maximum and constant blank absorbance is obtained with  $0.5 \times 10^{-4}$ – $2 \times 10^{-4} M$  Ethyl Violet concentration in the aqueous phase, so use of 0.5 ml of  $4 \times 10^{-4} M$  solution is recommended ( $\cong 0.7 \times 10^{-4} M$  in the aqueous phase).

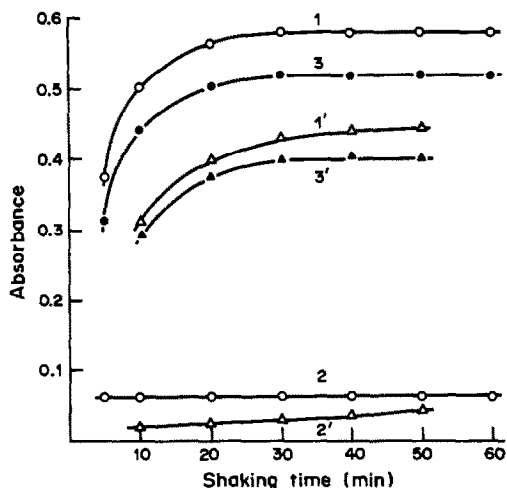


Fig. 5. Effect of shaking time. Curves 1, 2 and 3, aqueous phase 2 ml of boric acid solution + 0.5 ml of buffer solution + 0.5 ml of Ethyl Violet solution; organic phase 4 ml of DBMC toluene solution, with soda-glass test-tube. Curves 1', 2' and 3', aqueous phase 5 ml of boric acid solution + 0.5 ml of buffer solution + 0.5 ml of Ethyl Violet solution, organic phase 5 ml of DBMC toluene solution, with fused-silica test-tube. 1,1', boron 0.262  $\mu\text{g}$ , reference toluene; 2,2', reagent blank, reference toluene; 3,3', boron 0.262  $\mu\text{g}$ , reference reagent blank.

**Shaking time.** Figures 4 and 5 show that constant absorbance was obtained with 30 min shaking except when small-volume (11.5 ml) test-tubes were used with 5 ml of organic phase and 3 ml of aqueous phase (because the mixing was then less efficient). The shaking time is fixed at 50 min for safety.

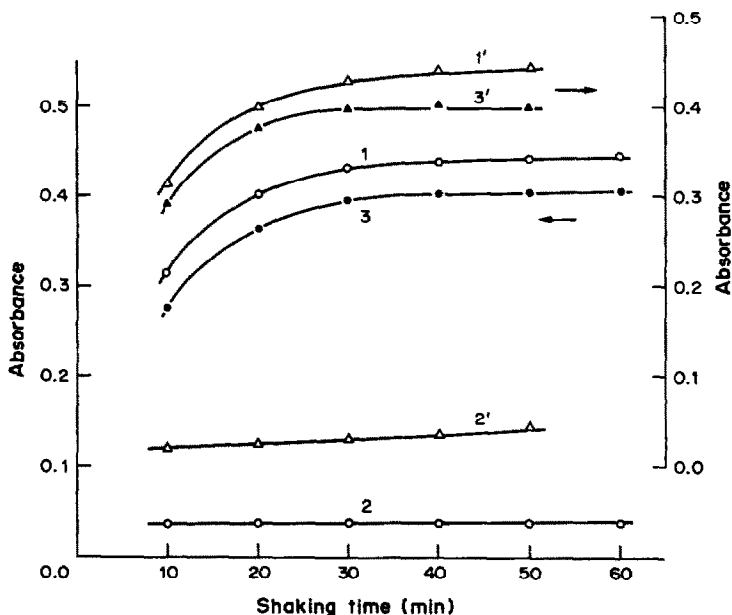


Fig. 4. Effect of shaking time. Curves 1, 2 and 3, with 11.5 ml soda-glass test-tubes (left-hand scale); curves 1', 2' and 3', with 20-ml fused-silica test-tubes (right-hand scale): 1, 1', boron 0.262  $\mu\text{g}$ , reference toluene; 2, 2', reagent blank, reference toluene; 3, 3', boron 0.262  $\mu\text{g}$ , reference reagent blank. Aqueous phase 2 ml of boric acid solution + 0.5 ml of buffer solution + 0.5 ml of Ethyl Violet solution; organic phase 5 ml of DBMC solution in toluene.

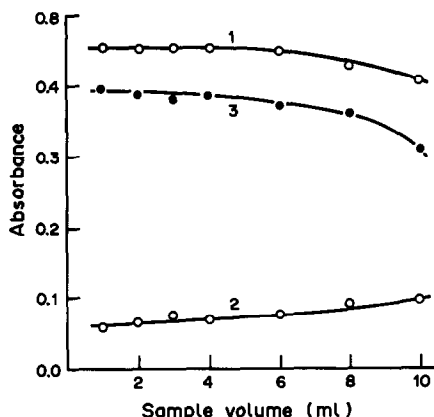


Fig. 6. Effect of sample volume: 1, boron 0.262  $\mu\text{g}$ , reference toluene; 2, reagent blank, reference toluene; 3, boron 0.262  $\mu\text{g}$ , reference reagent blank. Aqueous phase:  $x$  ml of boric acid + 0.5 ml of buffer solution + 0.5 ml of Ethyl Violet solution; organic phase 5 ml of DBMC toluene solution.

**Effect of sample volume.** Figure 6 shows that increasing the sample volume from 1 to 10 ml decreases the absorbance because of the decreasing concentration of the reagents, but linear calibration graphs are obtained for sample volumes up to 5 ml, and up to 0.43  $\mu\text{g}$  of boron. If the following procedure is adopted, 10 ml of sample solution can be analysed: transfer 10 ml of sample solution to a 20-ml fused-silica test-tube, and add 0.5 ml of 0.5M phosphate buffer (pH 8), 0.5 ml of  $6 \times 10^{-4}$ M Ethyl Violet, and 5 ml of  $4 \times 10^{-2}$ M DBMC solution; then shake the mixture for 40 min and measure the absorbance of the toluene phase at 610 nm.

### Interferences

The effect of concomitant ions was examined and the results are shown in Table 3. The metal ions which can precipitate as hydroxide at pH 8 were kept in solution by addition of 0.5 ml of 0.01M EDTA adjusted to pH 8 with sodium hydroxide. EDTA at this concentration does not interfere with the determination.

### Application to practical samples

Boron in sea-water and river water sampled in Okayama Prefecture was determined by the proposed method. The results are shown in Table 4. Sea-waters were diluted 20 times with demineralized water and the river water at Ogawa bridge (which was mixed with sea-water) was diluted 10 times. As the concentrations of other ions present in the sample solutions were less than those listed in Table 3, addition of EDTA was not necessary. The boron contents of these sample solutions were also determined by an HPLC method.<sup>9</sup> The results obtained by both methods were in good agreement, as shown in Table 4.

### Conclusion

Some new complexing reagents for boron have been synthesized by introduction of *tert*-butyl groups into catechol derivatives. DBMC (4,6-di-*tert*-butyl-3-methoxycatechol) was found the most useful because synthesis and purification of the reagent are easy, use of a washing procedure to reduce the reagent blank is unnecessary, and the determination of boron is simple. Moreover, the proposed method is highly sensitive ( $\epsilon = 1.02 \times 10^5$  l.mole<sup>-1</sup>.cm<sup>-1</sup>). Boron in

Table 3. Effect of other species

Without EDTA		With EDTA (0.0014M)	
Ions	Tolerance level, M	Ions	Tolerable level, M
$\text{NH}_4^+$	$1 \times 10^{-1}$	$\text{Zn}^{2+}$	$2.5 \times 10^{-3}$
$\text{Na}^+, \text{K}^+$	$5 \times 10^{-2}$	$\text{Ni}^{2+}$	$2 \times 10^{-3}$
$\text{Cl}^-, \text{Br}^-, \text{I}^-$ ,		$\text{Al}^{3+}, \text{Pb}^{2+}$	$1 \times 10^{-3}$
$\text{NO}_3^-, \text{SO}_4^{2-}$		$\text{Mn}^{2+}$	$5 \times 10^{-4}$
$\text{Mg}^{2+}, \text{HCO}_3^-$	$5 \times 10^{-3}$	$\text{Fe}^{3+}$	$1 \times 10^{-4}$
$\text{Ca}^{2+}$	$1 \times 10^{-3}$	$\text{Co}^{2+}, \text{Cu}^{2+}$	$5 \times 10^{-5}$
$\text{CO}_3^{2-}, \text{SCN}^-$	$2.5 \times 10^{-4}$	Dodecylsulphate	$2.5 \times 10^{-7}$
$\text{Sr}^{2+}, \text{ClO}_4^-$	$1 \times 10^{-4}$		

Table 4. Determination of boron in sea-water and river waters

Sample	Dilution	Absorbance*	Boron found, $\mu\text{g/ml}$	
			This method	HPLC
Sea-water				
Shin Okayama Port	1/20	$0.791 \pm 0.008$	$3.85 \pm 0.15$	3.85
Ushimado	1/20	$0.885 \pm 0.004$	$4.45 \pm 0.03$	4.31
Kuban	1/20	$0.687 \pm 0.010$	$3.35 \pm 0.04$	3.34
River water				
Ogawa Bridge	1/10	$0.352 \pm 0.002$	$0.704 \pm 0.006$	0.77
Yuujou Bridge	—	$0.118 \pm 0.001$	$0.0132 \pm 0.0002$	0.0125

\*Mean and range of three measurements.

sea-water and river water has been determined with satisfactory results.

#### REFERENCES

1. L. Ducret, *Anal. Chim. Acta*, 1957, **17**, 213.
2. S. Sato, *ibid.*, 1983, **151**, 465.
3. J. Bassett and P. J. Matthews. *Analyst*, 1974, **99**, 1.
4. M. Oshima, S. Motomizu and K. Tōei, *Bunseki Kagaku*, 1983, **32**, 458.
5. E. J. Hakoila and J. J. Kankare, *Anal. Chem.*, 1972, **44**, 1857.
6. S. Sato and S. Uchikawa, *Anal. Chim. Acta*, 1982, **143**, 283.
7. M. Oshima, S. Motomizu and K. Tōei, *Anal. Chem.*, 1984, **56**, 948.
8. H. Schulze and W. Flaig, *Liebigs Annalen*, 1952, **575**, 231.
9. S. Motomizu, I. Sawatani, M. Oshima and K. Tōei, *Anal. Chem.*, 1983, **55**, 1629.

## SEPARATION OF GALLIUM, INDIUM AND THALLIUM BY EXTRACTION WITH *n*-OCTYLANILINE IN CHLOROFORM

SHASHIKANT R. KUCHEKAR and MANOHAR B. CHAVAN\*

Analytical Chemistry Laboratory, Department of Chemistry, Marathwada University,  
Aurangabad 431004, India

(Received 18 March 1986. Received 25 November 1987. Accepted 10 December 1987)

**Summary**—Extraction of gallium(III), indium(III) and thallium(III) with *n*-octylaniline in chloroform at various concentrations of hydrogen halide acids (HCl, HBr, HI) has been studied and a scheme for their separation proposed. The procedure can be successfully applied to the separation and determination of gallium in presence of mercury, bismuth, manganese, zinc and lead; indium in presence of bismuth, antimony, lead, mercury, cadmium and zinc; and thallium in presence of mercury, cadmium, manganese, aluminium, tin and antimony. The advantage of the method is that the reagent can be recovered for reuse. The method is simple, rapid, and effects clear-cut separation.

Liquid ion-exchangers have been used for the solvent extraction of many metals.<sup>1,2</sup> Liquid anion-exchangers are based on primary, secondary and tertiary aliphatic amines. Owing to their generally greater solubility, primary amines are used less frequently than secondary amines. The presence of an octyl group in the *para* position in aniline renders this amine more basic and less soluble in water, and *p*-*n*-octylaniline has been used as a group extractant for the noble metals.<sup>3,4</sup> However, this application had limitations, such as the difficulty caused by the tendency of the reagent, which was synthesized from octylbenzene, to form emulsions. Later<sup>5</sup> it was reported that the formation of emulsions is minimal if the reagent is synthesized from *n*-octanol and aniline. Here, the use of *p*-*n*-octylaniline as an extractant for gallium, indium and thallium(III) from hydrogen halide acids is reported. The advantage of the method is that the reagent can be recovered for reuse without loss of extraction efficiency.

Other extractants useful for gallium, indium and thallium(III) include TBP,<sup>6</sup> *N*-benzylaniline,<sup>7</sup> mesityl oxide,<sup>8</sup> 4-methylpentan-2-ol,<sup>9</sup> trioctylamine<sup>10</sup> and Aliquat 336,<sup>10</sup> but all are subject to limitations.<sup>10</sup> The method described here offers a rapid and clear-cut separation of gallium, indium and thallium(III) from each other.

### EXPERIMENTAL

#### Reagents

*Standard solution of gallium(III) and indium(III)*. Prepared as described earlier.<sup>11,12</sup>

*Standard solution of thallium(III)*. Prepared by dissolution of the hydroxide in concentrated hydrochloric acid, and dilution. Standardized complexometrically after addition of bromine water to ensure all the thallium was in the tervalent state.<sup>13</sup>

*Buffer solution*. Prepared by dissolving 27.2 g of sodium acetate tetrahydrate in 400 ml of water, adding 17 ml of glacial acetic acid and diluting to one litre.

*Reagent solution*. *p*-*n*-Octylaniline was prepared according to the method given by Pohlandt,<sup>5</sup> and used as a 10% v/v solution in chloroform, and diluted further as required.

The chloroform and all other materials used were of guaranteed grade. Doubly distilled water was used throughout.

#### *Extraction of the individual elements (in the absence of the others)*

Adjust the hydrochloric acid concentration to 8.0M for gallium (40–360 µg/ml), 2.0M for indium (40–320 µg/ml; 8.0M lithium chloride medium), and 0.1M for thallium (20–80 µg/ml). Shake 25 ml of test solution for 1 min with 10 ml of 3, 8 and 1.5% reagent solution in chloroform for Ga, In and Tl respectively. Allow the phases to separate. Strip gallium and indium from the organic phase by shaking it for 1 min with two 25-ml portions of distilled water. For Tl(III) use two 35-ml portions of acetate buffer for stripping. Determine the metal ion in the aqueous phase complexometrically.

#### *Recovery of reagent*

Shake the residual organic phase two or three times with 10-ml portions of ammonia solution (s.g. 0.88 solution diluted 1:1 with water), and then with distilled water. Distil off the chloroform, and treat the *p*-*n*-octylaniline with sodium hydroxide pellets to remove the last traces of water. After decantation, distil the reagent under reduced pressure before use.

### RESULTS AND DISCUSSION

Gallium, indium and thallium were extracted from their solutions in hydrochloric, hydrobromic or hydroiodic acid, with different concentrations of *p*-*n*-octylaniline solution in chloroform. Figure 1 shows the results. The effect of lithium chloride as salting-out agent on extraction of gallium and indium from hydrochloric acid is shown in Fig. 2. The results given in Fig. 1 and Table 1 show that it is possible to separate the three elements by appropriate choice of

\*Author to whom correspondence should be addressed.



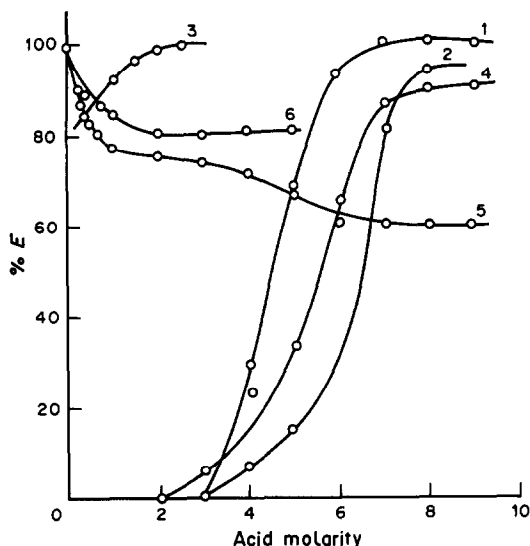


Fig. 1. Extraction of Ga (1.4 mg), In (2.6 mg), Tl (2.0 mg) with *n*-octylaniline (R) as a function of HCl, HBr or HI concentration. 1, Ga, HCl 3% R; 2, Ga, HBr, 3% R; 3, In, HI, 1.5% R; 4, In, HCl, 7% R; 5, Tl, HCl, 1.5% R; 6, Tl, HBr, 1.5% R.

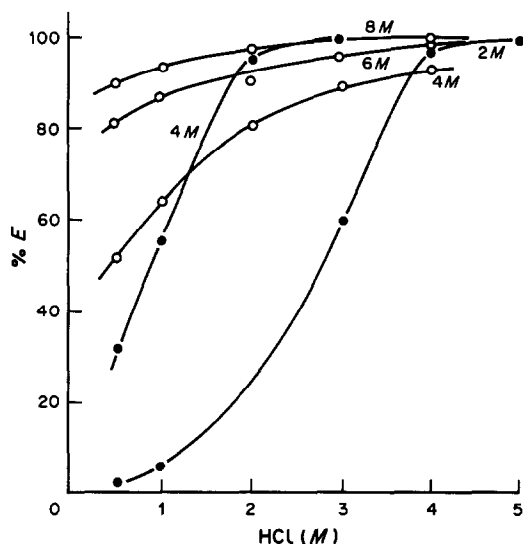


Fig. 2. Extraction of Ga (1.4 mg) and In (2.6 mg) as a function of salting-out agent (LiCl) concentration: ●—Ga; ○—In.

conditions. Because thallium(III) is reduced to thallium(I) by iodide, it is essential to remove thallium before hydriodic acid is used in the separation scheme. Fortunately gallium and indium are not extracted at all at low enough hydrochloric acid concentration, whereas thallium can be completely extracted if the concentration of the organic base is high enough. Gallium is not extracted at all from hydriodic acid solution, whereas indium is completely extractable from a 1.5*M* solution of potassium iodide in 2.5*M* sulphuric acid. Finally, gallium can be extracted from 8*M* hydrochloric acid. The method is shown as a flow-chart in Fig. 3.

Gallium is extracted quantitatively when the total chloride concentration is about 8*M*. For quantitative extraction of indium(III) from 2*M* hydrochloric acid in a single step it is necessary to use 8*M* lithium chloride as the salting-out agent. Other salting-out agents such as ammonium chloride and magnesium chloride have no significant effect on the extraction of gallium and indium. However, aluminium chloride cannot be used, as it interferes in the final determination.

Log-log plots of distribution coefficients *vs.* amine concentration at fixed acidity for gallium, indium and thallium indicate a 1:1 limiting mole ratio of amine to metal, which suggests that the species extracted is

Table I. Percentage extraction and distribution coefficient (in brackets) as the function of *n*-octylaniline concentration in chloroform (*R*)

<i>R</i> , %	Ga(III)*	In(III)†	In(III)‡	Tl(III)*
0.5	53.0 (2.8)	25.0 (0.8)	comp. ext.	92.7 (31.8)
1.0	69.2 (5.7)	37.0 (1.5)	comp. ext.	comp. ext.
1.5	90.2 (23.0)	48.0 (2.3)	comp. ext.	comp. ext.
2.0	91.0 (25.3)	60.0 (3.8)	—	comp. ext.
2.5	93.0 (33.2)	71.0 (6.1)	—	comp. ext.
3.0	94.0 (39.3)	80.3 (10.2)	—	—
5.0	98.0 (125.0)	96.4 (66.7)	—	—
7.0	comp. ext.	comp. ext.	—	—
10.0	comp. ext.	comp. ext.	—	—

Ga, In, Tl taken, 1.4, 2.6 and 2.0 mg, respectively.

\*Ga(III), 6*M* HCl; Tl(III) 0.1*M* HCl.

†In(III), 2*M* HCl + 8*M* LiCl.

‡In(III), 1.5*M* KI + 2.5*M* H<sub>2</sub>SO<sub>4</sub>.

Ga(III) 1-9 mg, In(III) 1-8 mg, Tl(III) 0.5-2.0 mg

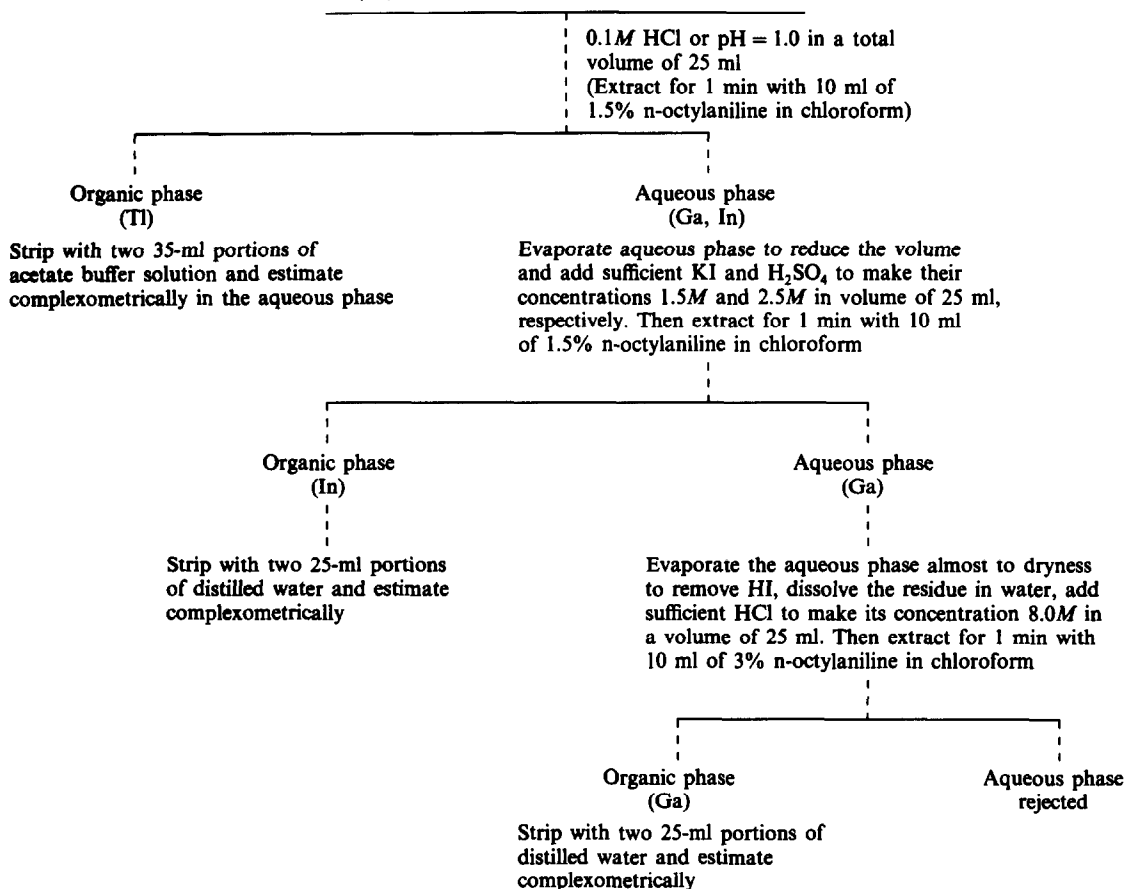


Fig. 3. Flow-chart for separation.

Table 2. Effect of diverse ions

Diverse ion added	Amount tolerated, mg			Diverse ion added	Amount tolerated, mg		
	Ga(III)	In(III)	Tl(III)		Ga(III)	In(III)	Tl(III)
Mn(II)	20	15	20	Au(III)	10	2	5
Hg(II)	20	5	20	Ag(I)	5	5	5
V(V)	20	20	10	Pt(IV)	2	5	5
U(VI)	20	5	20	Pd(II)	5	5	2
Tl(III)	co-ext.	co-ext.	—	Ru(III)	2	2	5
In(III)	co-ext.	—	20	Rh(III)	5	5	5
Ga(III)	—	co-ext.	20	Te(IV)	2	5	5
W(VI)	20	5	20	Fe(II)	co-ext.	co-ext.	10
Cr(VI)	20	15	10	Fe(III)	co-ext.	co-ext.	20§
Mo(VI)	20	5	5	Fluoride	200	100	100
Zn(II)	20	5	5	Citrate	200	200	100
Sn(II)	co-ext.	5	5	Ascorbate	200	100	Int.
Cd(II)	20	5	5	Acetate	100	200	200
Bi(III)	15	15	co-ext.	Phosphate	100	200	200
Sb(III)	10	10	20	Thiourea	100	50	Int.
Pb(II)	10	15	co-ext.	Thiocyanate	100	50	Int.
Ti(IV)	5	5	10	Tartrate	100	200	200
Co(II)	5	5	10	H <sub>2</sub> O <sub>2</sub> , 30% (100 vol.)	1 ml	1 ml	1.5 ml
Cu(II)	5	5	10	Thiosulphate	80	200	Int.
Ni(II)	5	20	10	Oxalate	50	100	200
Al(III)	5	20†	5	EDTA	25	25	100
As(III)	5	5	10	Malonate	80	100	80
Mg(II)	5	5	20	Salicylate	100	200	200
Re(VII)	15	15	10				

Ga, In, Tl taken, 1.4, 2.6 and 2.0 mg, respectively.

\*Masked with ascorbate. †Masked with thiosulphate. §Masked with fluoride.

Table 3. Separation and determination of gallium, indium and thallium

Elements taken, mg			Elements found, mg		
Ga	In	Tl	Ga	In	Tl
1.40	2.57	2.31	1.39	2.57	2.31
2.80	2.57	2.31	2.78	2.57	2.31
7.11	7.71	1.15	7.07	7.67	1.15
5.67	5.14	2.31	5.61	5.09	2.31
9.95	5.14	1.15	9.88	5.14	1.15
2.81	7.71	2.31	2.80	7.70	2.31

probably  $\text{RNH}_3^+ \cdot \text{MCl}_4^-$  where R is  $\text{C}_8\text{H}_{17}\text{C}_6\text{H}_4$ , and M is Ga, In or Tl.

Extraction was found to be more than 99.9% complete in 30 sec, so a 1-min shaking period is recommended for all three extractions.

#### Effect of diverse ions

Several ions were examined for interference (Table 2) in the proposed method. An error of  $\pm 1.5\%$  in analyte recovery was considered tolerable. The species which seriously affect the extraction are Tl(III), In(III), Sn(II) and Fe(II, III) for gallium; Tl(III), Ga(III) and Fe(II, III) for indium; Pb(II), Bi(III), thiosulphate, thiocyanate, thiourea and ascorbate for thallium.

#### Separation and determination of Ga, In and Tl

Tables 3 and 4 show the results for analysis of mixtures containing the three elements, and for analysis of mixtures containing only one of them.

**Acknowledgements**—Thanks are due to the U.G.C., New Delhi, for providing a fellowship for SRK. The authors express their deep sense of gratitude to Dr R. A. Chalmers for his valuable suggestions in the preparation of the manuscript.

Table 4. Determination of gallium, indium and thallium in synthetic mixtures: results of three determinations of each sample

Diverse elements taken, mg	Ga, In or Tl, mg	
	Taken	Found
Hg(II) 10, Bi 5,	1.40 Ga	1.40, 1.40, 1.39
Mn(II) 10, Zn 5	1.40 Ga	1.39, 1.42, 1.42
Mn(II), 15, Pb 5		
Bi 5, Sb(III) 5	2.57 In	2.57, 2.53, 2.55
Hg(II) 5, Cd 5,	2.57 In	2.49, 2.52, 2.52
Pb 5, Zn 5		
Hg(II) 5, Cd 2,	2.31 Tl	2.25, 2.23, 2.30
Mn(II) 10		
Al 2.5, Sn(II) 5,	2.31 Tl	2.31, 2.30, 2.31
Sb(III) 10		

#### REFERENCES

1. A. R. Prabhu and S. M. Khopkar, *J. Sci. Ind. Research*, 1971, **30**, 16.
2. J. Starý, *The Solvent Extraction of Metal Chelates*, Pergamon Press, Oxford, 1964.
3. A. A. Vasilyeva, I. G. Yudelevich, L. M. Gindin, T. V. Labian, S. R. Shulman, I. L. Kotlarevsky and V. N. Andrievsky, *Talanta*, 1975, **22**, 745.
4. C. Pohlandt and T. W. Steele, *Natl. Inst. Metallurgy, Johannesburg, Rept. No. 1881*, 1977.
5. C. Pohlandt, *Talanta*, 1979, **26**, 199.
6. A. K. De and A. K. Sen, *ibid.*, 1967, **19**, 629.
7. M. M. L. Khosla, S. R. Singh and S. P. Rao, *ibid.*, 1974, **21**, 411.
8. M. B. Chavan and V. M. Shinde, *Chem. Anal. (Warsaw)*, 1974, **19**, 1183.
9. S. B. Gawali and V. M. Shinde, *Anal. Chem.*, 1976, **48**, 62.
10. S. D. Shete and V. M. Shinde, *Analyst*, 1982, **107**, 225.
11. M. B. Chavan and V. M. Shinde, *Anal. Chim. Acta*, 1972, **59**, 165.
12. *Idem*, *Sepr. Sci.*, 1973, **8**, 285.
13. F. J. Welcher, *The Analytical Uses of Ethylenediamine-tetraacetic Acid*, pp. 177, 180, 183. Van Nostrand, New York, 1961.

## A NEW LIQUID MEMBRANE ELECTRODE FOR THE SELECTIVE DETERMINATION OF PERRHENATE

SAAD S. M. HASSAN\* and M. A. HAMADA

Department of Chemistry, Faculty of Science, Qatar University, Doha, Qatar

(Received 5 October 1987. Accepted 10 December 1987)

**Summary**—A new perrhenate ion-selective electrode has been developed, incorporating a nitrobenzene solution of nitron perrhenate as a liquid membrane. The electrode gives near-Nernstian response to  $3 \times 10^{-5}$ – $10^{-2} M$  perrhenate over the pH range 3–8. Most common anions (except for periodate and perchlorate) give little interference. The electrode has been satisfactory for direct potentiometric determination of as little as  $10 \mu\text{g/ml}$  rhenium. The average recovery and standard deviation were 99% and 2.1%, respectively. Measurements of the solubility products of some sparingly soluble perrhenates gave results that agreed closely with those recorded in the literature and obtained by other procedures.

Rhenium is used for the production of some hard corrosion-resistant alloys and as a catalyst for industrial hydrogenation and dehydrogenation reactions.<sup>1</sup> Most of the procedures for its determination involve conversion with hydrogen peroxide into perrhenate, which can be assessed by gravimetric,<sup>2,4</sup> spectrophotometric,<sup>5,8</sup> indirect atomic-absorption spectrometric,<sup>9</sup> polarographic,<sup>10</sup> and isotopic dilution<sup>11</sup> methods. Most of these techniques involve several time-consuming manipulation steps and are neither selective nor sensitive.

It has been reported that the commercial perchlorate<sup>12</sup> and nitrate<sup>13</sup> ion-selective electrodes with membranes containing nickel bathophenanthroline perchlorate and tributyloctadecylphosphonium nitrate, respectively, can be used, after appropriate membrane conditioning, as perrhenate sensors. Electrodes responsive to perrhenate as a primary ion have been based on the ion-pair complexes of perrhenate with tetraoctylammonium,<sup>14</sup> tetradecylammonium,<sup>15</sup> triheptyldodecylammonium,<sup>16</sup> tetraphenylarsonium,<sup>17,18</sup> triaquo-oxahexakis(stearato)-trichromium(III)<sup>19</sup> and some basic dyes<sup>20</sup> dispersed in lipophilic solvents or polymer matrices. Many of these electrode systems, however, suffer from serious interference by  $\text{Cl}^-$ ,  $\text{NO}_3^-$ ,  $\text{SCN}^-$ ,  $\text{I}^-$ ,  $\text{ClO}_4^-$ ,  $\text{WO}_4^{2-}$ ,  $\text{VO}_4^{3-}$  and  $\text{MoO}_4^{2-}$  ions.<sup>12,13,15,17,19</sup>

Recently we described some membrane electrode systems for  $\text{IO}_4^-$ ,<sup>21</sup>  $\text{ClO}_4^-$ ,<sup>22</sup>  $\text{BF}_4^-$ <sup>23</sup> and  $\text{SCN}^-$ <sup>24</sup> based on the ion-pair complexes of these ions with nitron. In this investigation, the nitron-perrhenate ion-pair complex was prepared and tested as electroactive species for use in an electrode responsive to perrhenate. A liquid membrane consisting of a nitrobenzene solution of nitron perrhenate was found to respond to  $3 \times 10^{-5}$ – $10^{-2} M$   $\text{ReO}_4^-$  over the pH

range 3–8 with minimal interference from many anions.

### EXPERIMENTAL

#### Apparatus

All EMF measurements were made at  $25 \pm 1^\circ$  with the nitron perrhenate liquid membrane electrode and a Corning pH/ion meter (Model 135). An Orion Ag/AgCl double junction reference electrode (Model 90-02) with the outer barrel filled with 10% potassium nitrate solution completed the cell. An Orion combined glass electrode was used for pH adjustment. The electrochemical cell used for potential measurements was: Ag-AgCl/ $10^{-2} M$  aqueous  $\text{NH}_4\text{ReO}_4 + 10^{-2} M$  NaCl/ $10^{-2} M$  nitron perrhenate in nitrobenzene//porous membrane// $\text{ReO}_4^-$  test solution/Ag-AgCl reference electrode.

#### Reagents

All reagents were of analytical grade unless otherwise stated and doubly distilled water was used throughout. A  $10^{-2} M$  nitron solution was prepared in 10% v/v acetic acid. A  $10^{-2} M$  aqueous perrhenate stock solution was prepared from ammonium perrhenate of purity not less than 99.8%. Dilute perrhenate solutions ( $10^{-6}$ – $10^{-3} M$ ) were freshly prepared by serial dilution.

Nitron perrhenate complex was prepared by mixing about 20 ml of  $10^{-2} M$  ammonium perrhenate and 25 ml  $10^{-2} M$  nitron acetate. The grey precipitate was collected in a G4 sintered-glass crucible, washed with cold water, dried at  $80^\circ$  for 1 hr and ground to a fine powder. Elemental analysis of the precipitate gave C 42.4%, H 2.9% and N 9.7%;  $\text{C}_{20}\text{H}_{16}\text{N}_4 \cdot \text{HReO}_4$ ; C 42.6%, H 2.9% and N 9.7%. The most significant absorption bands in the infrared spectrum of the precipitate were those at  $3240$ – $3260 \text{ cm}^{-1}$  and  $920$ – $940 \text{ cm}^{-1}$ , assigned to stretching vibrations of the secondary amine and perrhenate groups, respectively.

#### Electrode preparation and calibration

An Orion electrode barrel (Model 92) was used with an Orion microporous membrane (92-06-04) to separate the organic and aqueous phases. The organic ion-exchanger liquid membrane was a  $10^{-2} M$  solution of the nitron perrhenate complex in nitrobenzene, and the internal reference solution was a mixture of equal volumes of aqueous  $10^{-2} M$  ammonium perrhenate and sodium chloride solutions. The electrode was conditioned after preparation, by being soaked in  $10^{-3} M$  ammonium perrhenate for at least 24 hr and was stored in the same solution when not in use.

\*To whom correspondence should be addressed.

The perrhenate electrode and the reference electrode were immersed in approximately 20 ml of  $10^{-6}$ – $10^{-2}M$  standard perrhenate solution in a 50-ml beaker. The emf readings were recorded when stable to  $\pm 1$  mV and plotted as a function of  $p\text{ReO}_4$ .

#### Measurement of solubility products

About 0.5 g of a freshly prepared sparingly soluble perrhenate was suspended in 20 ml of doubly distilled water and kept in an airtight Erlenmeyer flask. The mixture was shaken vigorously for 3 hr in a thermostat adjusted to  $25 \pm 1^\circ$  and allowed to stand for 1 hr before the potential was measured. The concentration of perrhenate in solution and hence the solubility product was calculated.

## RESULTS AND DISCUSSION

### Electrode response and stability

The performance of the electrode system was characterized by measuring the useful linear response range, slope, effect of pH, response time, membrane selectivity and electrode stability. The IUPAC recommendations<sup>25</sup> were used for evaluating these parameters. In pure aqueous ammonium perrhenate solutions, the electrode displayed near-Nernstian response for  $3 \times 10^{-5}$ – $10^{-2}M$  perrhenate with a slope of a 56 mV/ $p\text{ReO}_4$ . The limit of detection was  $4.5 \times 10^{-5}M$ . Figure 1 shows the dependence of the electrode potentials on  $p\text{ReO}_4$ . Similar results were obtained for perrhenate solutions in 0.1M sodium chloride.

Least-squares analysis of data collected for 3 different electrodes over 3 months gave the relationship:  $E$  (mV) =  $(-56 \pm 0.6) \log C - (12 \pm 0.8)$ , the standard deviation being 1.2 mV. The reproducibility of the potential readings from day-to-day measurements for the same solutions was within  $\pm 2$  mV and the variation in the slope did not exceed 2 mV/ $p\text{ReO}_4$  over a period of 6 weeks. The useful lifetime of the electrode is 5–6 weeks, after which the membrane of the electrode should be renewed. The

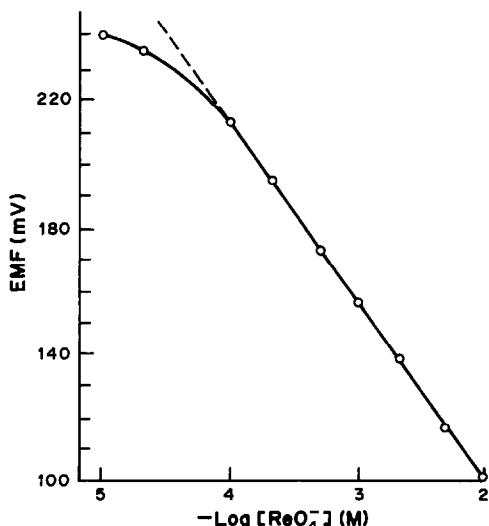


Fig. 1. Potential-response curve for the nitron perrhenate liquid membrane electrode.

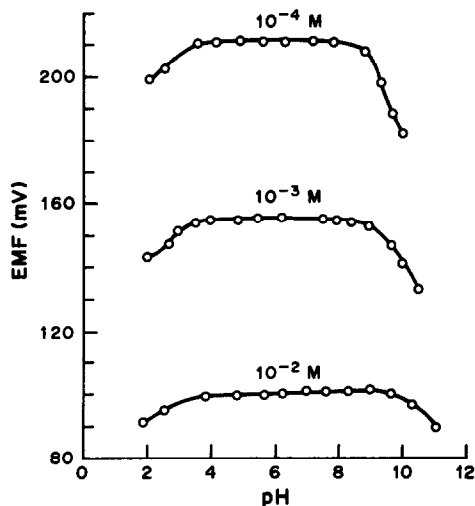


Fig. 2. Effect of pH on the potential response of the nitron perrhenate liquid membrane electrode.

electrode was stored in doubly distilled water between measurements and in  $10^{-3}M$  ammonium perrhenate when not in use. The stability of the nitron perrhenate membrane is attributed to the stable aromatic structure of the triazolium cation of nitron, which is closely related to the well known stable tetrazolium cation.<sup>26</sup>

The static response time of the electrode was evaluated by exposing the electrode to a rapid change in perrhenate concentration and recording the resulting emf as a function of time. Steady potentials were established after 30 sec for concentrations  $\geq 10^{-3}M$ , 50 sec between  $10^{-3}$  and  $10^{-4}M$ , and 80 sec for concentrations  $\leq 10^{-4}M$ . The potential readings remained stable within  $\pm 2$  mV for at least 5 min.

### Effect of pH and foreign ions

The effect of pH on the electrode potential readings was studied for  $10^{-2}$ – $10^{-4}M$  perrhenate adjusted to different pH values with sodium hydroxide solution or hydrochloric acid. The potential–pH plots (Fig. 2) indicate that the potentials were almost independent of pH in the range 3–8. At low pH there is hydrogen-ion interference, and at high pH the emf decreases, probably owing to dissociation of the membrane material.

The effect of some common anions on the potential response of the electrode was tested by determining the selectivity coefficients of the membrane by the separate solutions method, as described previously.<sup>21–25</sup> The results (Table 1) show good selectivity relative to 14 common anions at the  $10^{-2}M$  level. The electrode shows poor selectivity, however, with respect to periodate and perchlorate, both of which also interfere with some previously described perrhenate electrodes.<sup>15,19</sup>

Rhenium is commonly associated with molybdenum and tungsten in its ores and alloys. Prior separation by solvent extraction<sup>27,28</sup> or

Table 1. Potentiometric selectivity coefficients for some anions, obtained by the separate solution method

Interferent (B)*	$K_{\text{ReO}_4, \text{B}}^{\text{pot}}$
Cl <sup>-</sup>	$5.1 \times 10^{-3}$
ClO <sub>3</sub> <sup>-</sup>	$6.7 \times 10^{-3}$
ClO <sub>4</sub> <sup>-</sup>	0.76
Br <sup>-</sup>	$3.5 \times 10^{-3}$
I <sup>-</sup>	$2.1 \times 10^{-2}$
IO <sub>4</sub> <sup>-</sup>	0.91
NO <sub>2</sub> <sup>-</sup>	$4.2 \times 10^{-3}$
NO <sub>3</sub> <sup>-</sup>	$4.6 \times 10^{-3}$
SCN <sup>-</sup>	$4.0 \times 10^{-2}$
SO <sub>3</sub> <sup>2-</sup>	$5.6 \times 10^{-3}$
S <sub>2</sub> O <sub>3</sub> <sup>2-</sup>	$3.1 \times 10^{-3}$
SO <sub>4</sub> <sup>2-</sup>	$3.8 \times 10^{-3}$
MoO <sub>4</sub> <sup>2-</sup>	$4.8 \times 10^{-3}$
WO <sub>4</sub> <sup>2-</sup>	$1.5 \times 10^{-3}$
Acetate	$3.8 \times 10^{-3}$
Oxalate	$1.1 \times 10^{-3}$

\*All tested at  $10^{-2}M$  level.

chromatography<sup>29,30</sup> is thus an unavoidable step in almost all previous procedures for analysis of rhenium–molybdenum and rhenium–tungsten mixtures. Molybdate and tungstate seriously interfere with some perrhenate membrane electrodes,<sup>19</sup> but have negligible effect on the response of the proposed nitron perrhenate electrode. Up to a 200-fold molar ratio of either ammonium molybdate or ammonium tungstate to  $10^{-5}$ – $10^{-3}M$  ammonium perrhenate has no significant effect on the electrode potential.

#### Determination of perrhenates

Analysis of 10–2000- $\mu\text{g/ml}$  rhenium solutions prepared from standard sodium perrhenate solutions, in triplicate, by direct potentiometry with the membrane electrode and a calibration graph prepared with ammonium perrhenate solutions gave the results shown in Table 2. The average recovery was 98.7% and mean relative standard deviation 2.1%.

The solubility products of some sparingly soluble perrhenates were also determined as described, and the results (given in Table 3) agreed fairly well with the reported values.<sup>31,32</sup> For silver perrhenate, how-

Table 2. Direct potentiometric determination of perrhenate

Rhenium added, $\mu\text{g/ml}$	Recovery,* %	Standard deviation, %
10.0	98.8	2.1
30.0	99.1	2.0
70.0	98.9	1.9
100	99.5	2.2
150	98.1	2.1
200	99.5	1.9
400	98.1	1.8
800	98.7	2.0
1200	98.2	2.2
1800	98.0	2.3

\*Mean of 3 measurements.

Table 3. Direct potentiometric determination of the solubility products of some sparingly soluble perrhenates

Compound	$K_{\text{sp}}$		Reference
	Electrode method ( $n = 4$ )	Literature values	
KReO <sub>4</sub>	$2.6 \pm 0.1 \times 10^{-3}$	$1.9 \times 10^{-3}$	31
CsReO <sub>4</sub>	$4.0 \pm 0.3 \times 10^{-4}$	$4.0 \times 10^{-4}$	31,32
TlReO <sub>4</sub>	$1.2 \pm 0.2 \times 10^{-5}$	$1.2 \times 10^{-5}$	31
AgReO <sub>4</sub>	$6.8 \pm 0.2 \times 10^{-4}$	$7.9 \times 10^{-5}$	31
Nitron-HReO <sub>4</sub>	$6.3 \pm 0.3 \times 10^{-8}$	$9.0 \times 10^{-8}$	2

ever, the value found was  $6.8 \times 10^{-4}$  (literature value  $7.9 \times 10^{-5}$ ). The value found by measuring the silver ion concentration with a silver sulphide ion-selective electrode (Orion 94-16) was  $6.3 \times 10^{-4}$ , close to the value obtained with the perrhenate electrode.

The results show that direct potentiometric measurement of perrhenate with the nitron perrhenate electrode gives a simple and rapid determination of this ion. The electrode system proposed shows useful sensitivity, reasonable selectivity, fast response times and adequate stability. The method involves minimal sample pretreatment, compared with many of the previously described procedures.<sup>2-11</sup>

#### REFERENCES

- J. C. Bailar, Jr., H. J. Emeleus, R. Nyholm and A. F. Trotman-Dickenson (eds.), *Comprehensive Inorganic Chemistry*, pp. 905–911. Pergamon Press, Oxford, 1975.
- W. Geilmann and A. Voigt, *Z. Anorg. Allgem. Chem.*, 1930, **193**, 311.
- H. H. Willard and G. M. Smith, *Ind. Eng. Chem., Anal. Ed.*, 1939, **11**, 305.
- T. C. Chadwick, *Anal. Chem.*, 1976, **48**, 1201.
- J. B. Headridge, *Analyst*, 1958, **83**, 690.
- J. L. Kassner, S. F. Ting and E. L. Grove, *Talanta*, 1961, **7**, 269.
- W. Bakowski and A. Bakowski, *Microchem. J.*, 1984, **29**, 137.
- V. M. Tarayan, F. V. Mirzoyan and Zh. V. Sarkisyan, *Dokl. Akad. Nauk. Arm. SSR*, 1976, **63**, 36; *Anal. Abstr.*, 1977, **33**, 2B134.
- P. Senise and L. G. Silva, *Anal. Chim. Acta*, 1975, **80**, 319.
- R. Colton, J. Dalziel, W. P. Griffith and G. Wilkinson, *J. Chem. Soc.*, 1960, 71.
- R. A. Pacer and S. M. Benecke, *Anal. Chem.*, 1981, **53**, 1160.
- R. F. Hirsch and J. D. Portock, *Anal. Lett.*, 1969, **2**, 295.
- M. Geissler and R. Kunze, *Anal. Chim. Acta*, 1986, **189**, 245.
- V. N. Golubev and T. A. Filatova, *Elektrokhimiya*, 1974, **10**, 1123.
- Sh. K. Norov, V. V. Pal'chevskii and E. S. Gureev, *Zh. Analit. Khim.*, 1977, **32**, 2394.
- D. Feng and Z. Xie, *Huaxue Tongbao*, 1983, No. 6, 22; *Anal. Abstr.*, 1984, **46**, 3J108.
- V. A. Zarinskii, L. K. Shpigun, V. M. Trepalina and I. V. Volobueva, *Zavodsk. Lab.*, 1977, **43**, 941.
- V. A. Zarinskii, L. K. Shpigun, O. M. Petrakhin and V. M. Trepalina, *Zh. Analit. Khim.*, 1976, **31**, 1191.
- M. M. Mansurov, G. L. Semenova, Kh. M. Yakubov and A. A. Pendin, *ibid.*, 1985, **40**, 1267.

20. J. Pan, F. Hao, W. Wang and H. Wang, *Gaodeng Xuexiao Huaxue Xuebao*, 1984, **5**, 473; *Chem. Abstr.*, 1984, **101**, 142975z.
21. S. S. M. Hassan and M. M. Elsaied, *Analyst*, 1987, **112**, 545.
22. *Idem*, *Talanta*, 1986, **33**, 679.
23. S. S. M. Hassan and M. A. F. Elmosalamy, *Z. Anal. Chem.*, 1986, **325**, 178.
24. *Idem*, *Analyst*, 1987, **112**, 1709.
25. IUPAC Analytical Chemistry Division, Commission on Analytical Nomenclature, *Pure Appl. Chem.*, 1976, **48**, 127.
26. G. A. Olaii, *J. Inorg. Nucl. Chem.*, 1961, **16**, 225.
27. S. Tribalat, *Anal. Chim. Acta*, 1950, **4**, 258.
28. S. J. Rimshaw and G. F. Malling, *Anal. Chem.*, 1961, **33**, 751.
29. E. F. Huffman, R. L. Oswald and L. A. Williams, *J. Inorg. Nucl. Chem.*, 1956, **3**, 49.
30. D. S. Gaibakyan and S. D. Bagdasaryan, *Arm. Khim. Zh.*, 1984, **37**, 9; *Anal. Abstr.*, 1984, **46**, 11B15.
31. Ju. Lurie, *Handbook of Analytical Chemistry*, p. 105. Mir, Moscow, 1978.
32. J. A. Dean (ed.), *Lange's Handbook of Chemistry*. 12th Ed., Sec. 5.7. McGraw-Hill, New York, 1979.

## A SIMPLE OPERATIONAL RELATIONSHIP BETWEEN DROP-TIME AND INTERFACIAL TENSION AT A CHARGED MERCURY/AQUEOUS SOLUTION INTERFACE

JAMES B. CRAIG\* and CARLANN MACKAY

Department of Chemistry, University of Aberdeen, Meston Walk, Old Aberdeen, Scotland

(Received 3 November 1987. Accepted 9 December 1987)

**Summary**—This paper describes a simple operational relationship between the drop-time of a dropping mercury electrode and the interfacial tension at a charged mercury/aqueous solution interface. An apparatus and technique for measuring drop-times is reported, and examples are given of the fit of experimental drop-times to literature values of interfacial tensions. The operational relationship is independent of temperature in the range 293–313 K.

The adsorption of organic molecules at charged interfaces has been widely studied because of its practical and theoretical importance in bioelectrochemistry. The main methods of obtaining quantitative information on adsorption at a charged mercury/aqueous solution interface, as a function of the electrical potential difference applied across the interface, are based on the determination of the interfacial tension or the differential capacity. In general terms, the interfacial tension is difficult to measure experimentally but, being a direct thermodynamic parameter, is relatively easy to interpret and to use in adsorption isotherms. On the other hand, with a modest amount of electronic equipment the differential capacity is relatively easy to measure but, being an indirect thermodynamic parameter, is less easy to interpret.

There are many techniques for determining liquid/liquid interfacial tensions, ranging from absolute, static methods, such as the pendant and sessile drop techniques, to relative, dynamic methods, such as those based on drop-weight, drop-volume, and drop-time. The former methods are usually delicate and tedious to operate, whereas the experimental parameters of the latter methods can be measured easily.

In electrocapillary studies of low molecular-weight organic and inorganic species at charged mercury/aqueous solution interfaces, the drop-time method has received much attention because (a) it is simple to operate, (b) measurement is independent of the mercury/solution/glass contact angle, (c) little mercury is used, (d) large amounts of data are produced rapidly, (e) there are many types of sensitive drop-fall detectors available,<sup>1</sup> and (f) the whole process can be automated.<sup>2</sup> The method, however, suffers from one serious disadvantage: the relationship between drop-time and interfacial tension is inexact, and therefore the conversion of drop-time data is complicated.

The basic equation (1), derived by Smith<sup>3</sup> and used by Barradas and Kimmerle,<sup>4</sup> equates the weight of a mercury drop immediately prior to its detachment from the glass capillary, with the difference between the upward force of the interfacial tension around the circumference of the capillary orifice and the “back-pressure effect”, due to the curvature of the drop, which opposes the upward force, *i.e.*,

$$\left(\frac{D-d}{D}\right)Mg = 2\pi r\gamma - \frac{2\pi r^2\gamma}{R} \quad (1)$$

where  $D$  = density of the heavy phase (mercury),  $d$  = density of the light phase (aqueous solution),  $M$  = mass of the mercury drop,  $g$  = gravitational acceleration constant,  $\gamma$  is the interfacial tension,  $r$  = radius of the capillary orifice and  $R$  = radius of the mercury drop (assumed to be spherical just prior to detachment).

The last term in equation (1) is the correction for the back-pressure, which is more pronounced during the early stages of drop growth. The  $(D-d)/D$  term is the correction for the buoyancy of the drop.

Equation (1) can be rearranged to give:

$$\gamma = \left(\frac{D-d}{D}\right)\left(\frac{Mg}{2\pi r}\right)\left(\frac{R}{R-r}\right) \quad (2)$$

Harkins and Brown<sup>5</sup> derived for their drop-weight experiments a similar equation which can be expressed in a similar form:

$$\gamma = \left(\frac{D-d}{D}\right)\left(\frac{Mg}{2\pi r}\right)(f) \quad (3)$$

where  $f$  is a function which will be discussed later. Barradas and Kimmerle used equation (2) in the form:

$$\gamma = \left(\frac{D-d}{D}\right)\left(\frac{Mg}{2\pi r}\right)(1+a) \quad (4)$$

where  $a = r/(R-r)$ .

There are three disadvantages in applying equation (2) to drop-time data. The first is due to the assump-

\*To whom correspondence should be addressed.



tion that just prior to detachment the drop is spherical, the second is due to the assumption that the whole of the spherical drop falls on detachment: both assumptions have been shown by high-speed photography<sup>6</sup> to be invalid. The third disadvantage is that, as a result of the back-pressure effect, the mercury flow-rate is not constant but varies with drop growth. Barradas and Kimmerle used an average back-pressure,  $b$ , and flow-rate, and related all drop-times to that,  $t_{\text{ref}}$ , of a solution of known interfacial tension,  $\gamma_{\text{ref}}$ , for example, the electrocapillary maximum of 0.1M potassium chloride at 298 K, to obtain the expression:

$$\frac{\gamma}{\gamma_{\text{ref}}} = \frac{t}{t_{\text{ref}}} \left\{ \left( \frac{t}{t_{\text{ref}}} \right)^{-\left[ \frac{3Kb}{3h-b} + \frac{Ka}{3(1-a)} \right]} \right\} \quad (5)$$

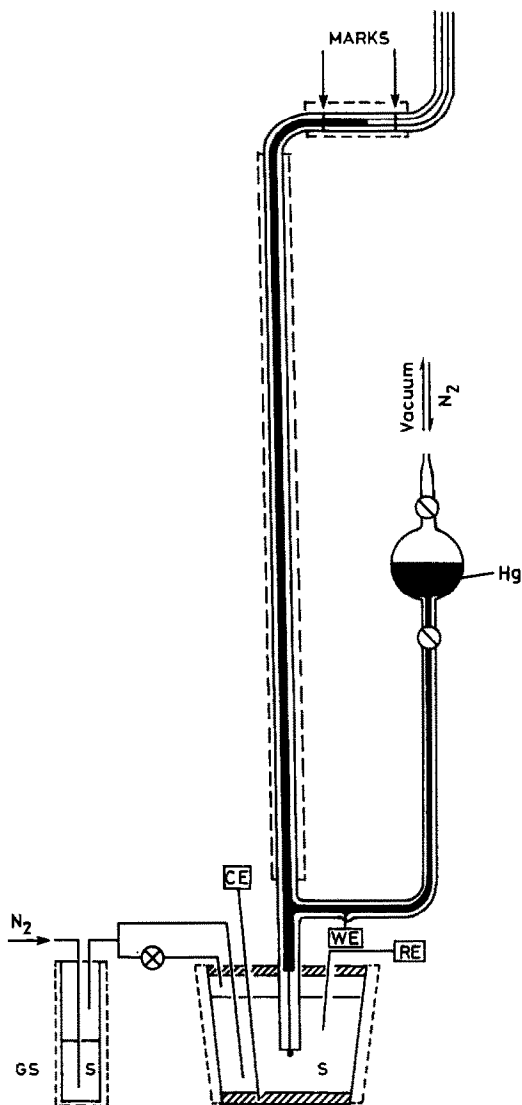


Fig. 1. Dropping mercury electrode. Hg = mercury reservoir; WE, RE and CE = working, reference and counter electrodes; GS = gas scrubber; S = solution; "MARKS" = limit of horizontal travel of head of mercury; dotted lines indicate thermostatically controlled regions.

where  $K$  is a constant and  $h$  is the hydrostatic head of mercury in the electrometer column. An initial value of  $K = 1$  is assumed, from which the primary values of  $a$  and  $b$  are determined. Equation (5) is then re-evaluated by an iterative process until a constant value of  $K$  is obtained.

Corbuser and Gierst<sup>7</sup> had earlier derived a simpler relationship which may be expressed in the differential form:

$$\frac{\Delta\gamma}{\gamma} = K' \frac{\Delta t}{t} \quad (6)$$

where  $K'$  was found to tend to a value of unity for small-bore capillaries and large hydrostatic heads of mercury ( $K' = 0.973$  when  $r \sim 30 \mu\text{m}$  and  $h \sim 80 \text{ cm}$ ). We have found equation (5) to be accurate but inconvenient to use and equation (6) to be progressively less accurate as the drop-time  $t$  differs from  $t_{\text{ref}}$ .

Smith<sup>3</sup> has shown that  $M$  can be expressed in terms of a time series, or more simply by:

$$M = \alpha_1 t^{\beta_1} \quad (7)$$

where  $\alpha_1$  and  $\beta_1$  are constants. Thus equation (2) becomes:

$$\gamma = \alpha_2 \left( \frac{D-d}{D} \right) \left( \frac{R}{R-r} \right) t^{\beta_1} \quad (8)$$

where  $\alpha_2 = \alpha_1 g / 2\pi r$ .

Harkins and Brown realized that the Tate equation<sup>6</sup> relating  $\gamma$  and  $M$  was only an approximation because of the invalidity of the assumptions regarding drop shape and mode of detachment, and their correction factor,  $f$  in equation (3), a function of  $r$  and drop volume, was found quite empirically from an analysis of drop-times of solutions of known surface tension. In a similar empirical manner, we have found that:

$$\frac{R}{R-r} = \alpha_3 t^{\beta_2} \quad (9)$$

where  $\alpha_3$  and  $\beta_2$  are constants. For a reference solution with density  $d_{\text{ref}}$ , equation (2) reduces to the simple relationship:

$$\gamma = \alpha_4 t^{\beta} \left( \frac{D-d_{\text{ref}}}{D} \right) = \alpha t^{\beta} \quad (10)$$

where  $\alpha_4 = \alpha_2 \alpha_3$ ,  $\beta = \beta_1 + \beta_2$ , and  $\alpha = \alpha_4 (D - d_{\text{ref}}) / D$ . For a solution of density  $d_s$ , equation (10) yields

$$\gamma = \alpha \left( \frac{D-d_s}{D-d_{\text{ref}}} \right) t^{\beta} \quad (11)$$

## EXPERIMENTAL

### Reagents

Potassium chloride, AnalaR grade (BDH), was dried before use; water was doubly distilled in Pyrex apparatus; mercury was washed with dilute nitric acid, rinsed with distilled water, dried, filtered, and triply-distilled under

high vacuum; dimethyldichlorosilane (BDH) was used as received.

#### Apparatus

The glass electrometer shown in Fig. 1 consisted of a tall (~80 cm) column with a horizontal arm at the top to provide a constant head of mercury during operations. The bottom of the column ended in a glass capillary (bore ~30  $\mu\text{m}$ ) serving as a dropping mercury electrode (DME). The inner bore of the DME was silicone-coated with dimethyldichlorosilane. The reference electrode was a 0.1M KCl/calomel electrode but all electrode potentials were reported with respect to the standard hydrogen electrode (see Fig. 2 and Table 1).

#### Electronics

The potentiometer consisted of a 1.5-V d.c. source and a 1-k $\Omega$  10-turn helipot, the voltage being applied to the working and counter electrodes. A high-impedance 4 $\frac{1}{2}$ -digit voltmeter (Weston 2462) was used to monitor the potential between the working and the reference electrodes. The precision drop-fall detector is described in a separate paper.<sup>8</sup> The lifetime of consecutive drops was measured by feeding the output pulse (+5 V, TTL-compatible) from the detector into the first of the one-bit inputs of an Apple IIe microcomputer<sup>9</sup> fitted with a 1-MHz computer clock (Mountain, card number MTN008). A back-up counting device consisted of a pair of TTL-compatible digital counters (Newport Electronics 6130A) desynchronized so that one counted the odd-numbered drops, and the other the even-numbered drops. Drop-times for our particular capillary were about 8–9 sec (see Table 1) and were reproducible to better than  $\pm 5$  msec. For each experiment, at least 135

Table 1. Drop-time–interfacial tension data for 0.1M KCl at 298 K

Electrical potential,* V	Drop-time,† sec	Interfacial tension, mN/m	
		D&P‡	This work‡
0.334	8.160	378.5	378.8
0.284	8.373	388.0	387.6
0.234	8.557	396.2	395.8
0.184	8.718	403.3	403.2
0.134	8.855	409.5	409.6
0.084	8.971	414.6	414.9
0.034	9.066	418.8	419.1
-0.016	9.139	422.1	422.3
-0.066	9.192	424.4	424.5
-0.116	9.222	425.8	425.8
-0.166	9.237	426.4	426.3
-0.216	9.232	426.2	426.0
-0.266	9.211	425.2	425.1
-0.316	9.175	423.6	423.6
-0.366	9.126	421.5	421.5
-0.416	9.066	418.8	418.9
-0.466	8.996	415.7	415.8
-0.516	8.917	412.2	412.3
-0.566	8.829	408.3	408.3
-0.616	8.733	404.0	404.0
-0.666	8.628	399.4	399.2
-0.716	8.514	394.3	394.0
-0.766	8.389	388.7	388.5
-0.816	8.253	382.7	382.6
-0.866	8.108	376.2	376.3
-0.916	7.954	369.3	369.6
-0.966	7.796	362.3	362.3

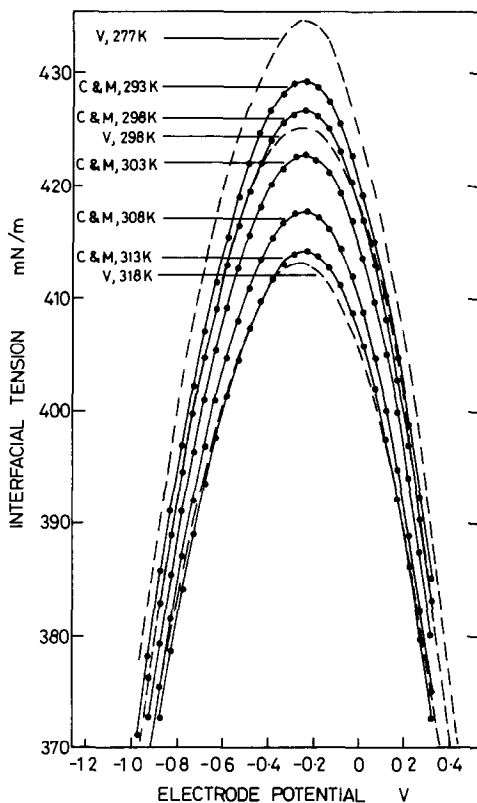


Fig. 2. Electrocapillary curves for 0.1M  $\text{KNO}_3$  at various temperatures. V from Vanel;<sup>13</sup> C&M, this work. The potential of the mercury electrode is given with respect to the standard hydrogen electrode.

\*The potential of the DME was measured with respect to a 0.1M KCl/Hg<sub>2</sub>Cl<sub>2</sub>/Hg electrode but is reported here relative to the standard hydrogen electrode.

†Each drop-time is an average of 5 observations.

‡Interfacial tension values of Devanathan and Peries.<sup>10</sup> Regression analysis of  $\ln \gamma$  (D&P) vs.  $\ln t$  (experimental) gave  $\alpha = 50.344$ ,  $\beta = 0.96099$ , and a correlation coefficient of 0.99995.

‡Computed from  $t$  with  $\alpha = 50.344$  and  $\beta = 0.96099$ .

drop-times were used in the evaluation of the polynomials in equation (12b).

#### Data processing

The data of Devanathan and Peries<sup>10</sup> for 0.1M potassium chloride at 298 K were chosen as standard data for instrument calibration. Processing of data can be done at two levels, elementary and advanced. If the cell reference electrode has the same characteristics as those of the electrode used by Devanathan and Peries, then the drop-time data are inserted into equation (10) to obtain the instrument parameters  $\alpha$  and  $\beta$ . We have found, however, that the cell reference electrode potential can vary by a few mV from day to day, so a more complicated process of evaluation is required. The  $\gamma$  vs.  $E$  and  $t$  vs.  $E$  data are separately analysed by a computer<sup>11</sup> to obtain the coefficients of the seventh order polynomials:

$$\gamma = a_1 + b_1 E + c_1 E^2 + \dots + h_1 E^7 \quad (12a)$$

$$t = a_2 + b_2 E + c_2 E^2 + \dots + h_2 E^7 \quad (12b)$$

The multiple correlation coefficients ( $R^2$ ), which give an indication of the degree of fit of the polynomial to the data, for the 7th–10th orders were respectively 0.99998, 0.99998, 0.99999, and 0.99999, so the seventh order polynomials were chosen for routine calibration purposes.

Equations (12a) and (12b) were differentiated<sup>12</sup> to obtain the respective potentials of zero charge,  $E_{pzc}(\gamma)$  and  $E_{pzc}(t)$ .

These potentials may differ by  $\Delta E$ :

$$\Delta E = E_{\text{pzc}}(\gamma) - E_{\text{pzc}}(t) \quad (13)$$

The drop-time potentials were then increased by  $\Delta E$  and drop-times evaluated with equation (12b) for potentials corresponding to those selected by Devanathan and Peries, and the shifted drop-times were inserted into equation (10). The computer program<sup>12</sup> contains a subroutine to increase and decrease  $\Delta E$  by successive increments of 0.5 mV to see whether there are any improvements in the correlation coefficients. Any further shift found necessary allows for either  $E_{\text{pzc}}$  value being miscalculated because of scatter in the data in the vicinity of these potentials.

## RESULTS

The drop-time data for a 0.1M potassium chloride solution at 298 K are given in Table 1, together with the values of  $\alpha$  and  $\beta$  obtained by regression analysis of the logarithm of the experimental drop-times against the logarithm of the interfacial tension data of Devanathan and Peries. The correlation coefficient in this case was 0.99995. The terms  $\alpha$  and  $\beta$  have been found to be relatively temperature-independent in the interval 293–313 K, *i.e.*, from laboratory to body temperature, the region of importance in our study of the electrocapillary properties of biomedical molecules. The instrument can therefore be calibrated with a 0.1M potassium chloride solution at 298 K to obtain  $\alpha$  and  $\beta$ ; thereafter, only the solution densities are needed in order to transform drop-times into interfacial tensions. To demonstrate this, the electrocapillary curves of 0.1M potassium nitrate at 293, 298, 303, 308 and 313 K, calculated in this way, are compared in Fig. 2 with those obtained at 277, 298 and 318 K by Vanel.<sup>13</sup> Agreement between the two sets of curves is good.

## CONCLUSION

The relationship between the drop-times of a drop-

ping mercury electrode and interfacial tensions is inexact. Of the two commonly employed relationships, equation (5) is accurate but difficult to use, whereas equation (6) is easy to use but is progressively inaccurate as the potential differs from the potential of zero charge. However, equation (11) has both the accuracy of equation (5) and the simplicity of equation (6). The experimental procedure is simple, efficient and economic in terms of time and material, and its use in the study of the electrocapillary properties of amino-acids and peptides will be reported in later papers.

*Acknowledgement*—This work was supported by the Science and Engineering Research Council, U.K., under the specially promoted programme on medical engineering, Grant Number GR/B/0616.1.

## REFERENCES

1. P. D. Tyma, M. J. Weaver and C. G. Enke, *Anal. Chem.*, 1979, **51**, 2300.
2. E. T. Verdier, R. Grand and P. Vanel, *J. Chim. Phys.*, 1969, **66**, 376.
3. G. S. Smith, *Trans. Faraday Soc.*, 1951, **47**, 63.
4. R. G. Barradas and F. M. Kimmerle, *Can. J. Chem.*, 1967, **45**, 109.
5. W. Harkins and F. Brown, *J. Am. Chem. Soc.*, 1919, **41**, 499.
6. T. Tate, *Phil. Mag.*, 1864, **27**, 176.
7. P. Corbusier and L. Gierst, *Anal. Chim. Acta*, 1956, **15**, 254.
8. J. B. Craig, D. Hopkins and A. R. Howie, *Talanta*, 1988, **35**, 401.
9. An Applesoft Basic computer program for timing and recording drop lifetimes is available on request from the authors.
10. M. A. V. Devanathan and P. Peries, *Trans. Faraday Soc.*, 1954, **50**, 1236.
11. Biomedical Statistical Package BMDP5R, University of California, 1979.
12. Fortran program Centre is available on request from the authors.
13. P. Vanel, *C.R. Acad. Sci.*, 1972, **274C**, 237.

## SOME OBSERVATIONS ON THE KERR EFFECT IN SUSPENSIONS OF BENTONITE

JAMES B. KING and ROGER STEPHENS

Department of Chemistry, Dalhousie University, Halifax, Nova Scotia, Canada

(Received 31 July 1987. Accepted 23 November 1987)

**Summary**—Apparatus is described which allows continuous electro-optic signals to be obtained from aqueous suspensions of bentonite. A radiofrequency-field generator and external electrodes are used to allow the suspension to be contained in an all-glass cell. The magnitude of the response is found to depend both on cation charge and on concentration. There appears to be little chemical selectivity save under circumstances which cause the ion population available to the suspension to be depleted.

Bentonite clays are found in many areas of the world, and are widely employed in a variety of technical applications.<sup>1,2</sup> The material consists primarily of montmorillonite, which is a layered structure built up of units comprising two sheets of silica tetrahedra with a central sheet of aluminium–oxygen octahedra between them, the three sheets forming one layer. The sheets are permeable to aqueous solutions, resulting in a high degree of swelling of the material and causing the interior to become accessible to ions present in the solution. The physical and chemical properties of the clay depend on the origin and history of the sample because, for instance, up to a maximum of about 15% of the silicon atoms can be replaced, normally by aluminium, within the tetrahedral sheets,<sup>1,2</sup> and the aluminium in the octahedral sheet can be replaced by various ions of lower valency. This behaviour is primarily responsible for the cation-exchange capacity of the clay.

In water, bentonite readily forms a polydisperse suspension within which the individual particles take the form of thin flakes, as a result of cleavage of the layered structure, with widths in the size range of  $\sim 0.01$ – $10 \mu\text{m}$ . The surfaces are hydrated, the innermost water dipoles being mutually aligned.<sup>3</sup> In addition, each particle carries an overall negative charge and is surrounded by co- and counter-ions. The innermost ionic layer is considered to be bound. The ionic distribution around each particle is regarded as an electric double or triple layer.<sup>3,4</sup>

Montmorillonite shows a cation-exchange capacity of 0.8–1.5 meq/g.<sup>2</sup> The primary reasons for this have been mentioned; the substitution of silicon and aluminium produces a charge imbalance which makes cation adsorption sites available, and the permeability of the layered structure makes these accessible to the solution. Minor exchange can also occur at the broken edges of the particles. The latter mechanism accounts for about 20% of the total cation-exchange capacity.<sup>2</sup> It also provides one of the mechanisms for anion-exchange (0.2–0.3 meq/g in montmorillonite<sup>2</sup>). The ionic environment of the clay

particles associated with ion-exchange processes strongly influences the properties of the material. In particular, it is its effect on the induced dipole moment which is of present interest.

In aqueous suspension the clay particles adopt a random orientation, but undergo partial alignment in the presence of an external electric field, as a result of field–dipole interactions.<sup>5</sup> The alignment of physically anisotropic particles causes the suspension to become optically active, *i.e.*, the material shows a Kerr effect. The Kerr effect in bentonite exhibits various unusual features, such as its low frequency response and the reversal of birefringence at high field strengths.<sup>6,7</sup> Of particular interest, however, is the observation that significant optical rotation can be obtained at field strengths down to 5 or 10 V/cm; a result which requires a remarkably high value for the Kerr coefficient. The sensitivity which is implied by this behaviour has not been examined for any possible analytical utility. The present work describes some preliminary results from such an examination.

### EXPERIMENTAL

The apparatus used is shown in Fig. 1. The outer dimensions of the cell were 7.5 cm length  $\times$  5 mm width  $\times$  2.5 cm depth. The cell was built from glass microscope slides of 1 mm thickness, glued with silicone rubber to minimize stress birefringence in the end-windows. Aluminium foil was taped outside the two longest faces of the cell to serve as electrodes. The electric field was produced by a radio-frequency supply which delivered up to 5 kV peak-to-trough at 2.2 MHz. This arrangement prevented direct contact between the electrodes and the suspension. The maximum frequency response of the suspension ( $\sim 100$  Hz) is insufficient to allow the electro-optic response to follow the RF field. Thus the alignment of the clay particles in this cell is entirely the result of interactions between the applied field and an induced dipole. Hence the electro-optic signals are expected to show a 4th-power dependence on the field strength, and to carry no RF modulation.

The remaining apparatus comprised a quartz–halogen lamp (Sylvania BXT), dichroic sheet polarizers with an extinction ratio of  $1 \times 10^{-4}$ , and a Jarrell–Ash 82-410 monochromator, reciprocal dispersion 3.2 nm/mm, slit-width  $100 \mu\text{m}$ . The light was chopped at 72 Hz. Signals were

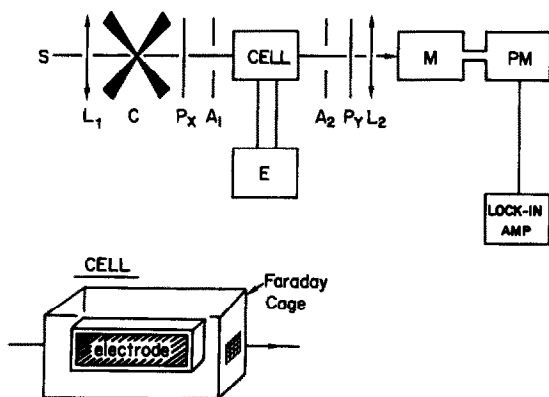


Fig. 1. Apparatus. S: source. L1, L2: lenses.  $P_x$ ,  $P_y$ : polarizer and analyser. C: chopper. E: RF field supply. M, PM: monochromator, photomultiplier. A1, A2: limiting apertures, used to prevent scattering and depolarization of the incident beam by the cell walls.

detected by a 1 P 28 photomultiplier. Electronics were built in the laboratory.

Bentonite suspensions were prepared by adding about 1 g of bentonite (Anachemia) to 500 ml of 1M sodium nitrate. After stirring for 24 hr the suspension was allowed to settle. The bulk of the solution was decanted and the clay desalted by dialysis against demineralized distilled water for 3–6 days. The clay was then resuspended in a graduated cylinder containing 2 litres of distilled water, and allowed to settle for one week. The top 500 ml were removed for use as a stock suspension, to be diluted as required later on. The stock concentrations were typically between 2 and 3 g/l. A problem encountered at this stage was the ability of the suspension to adsorb cations after prolonged exposure to glass (e.g., 1–2 weeks). This required the stock suspension to be periodically checked and renewed: it also required the sample cell to be soaked with suspension prior to use, to clean the inner surfaces.

## RESULTS

### General behaviour

In operation all glassware was first cleaned with fresh suspension, which was then discarded. The test suspension was diluted to the required level. If any salts were to be added, the addition was normally made at this stage. Finally the suspension was transferred to the cell by pipette. To obtain a response the RF supply was switched on for a few seconds, the resulting signal being compared with that from distilled water.

The most satisfactory results were obtained for suspension concentrations in the range 10–100 mg/l., with a path-length of 7.5 cm. At lower concentrations the signals were too weak to allow a satisfactory working range to be found, and at higher concentrations the conductivity of the solutions tended to increase sufficiently to cause over-heating of the cell. Within the stated range the particular concentration used did not appear to be critical.

The types of response seen are illustrated by the signals shown in Fig. 2. It is clear that the relaxation of the suspension is not always the simple thermal

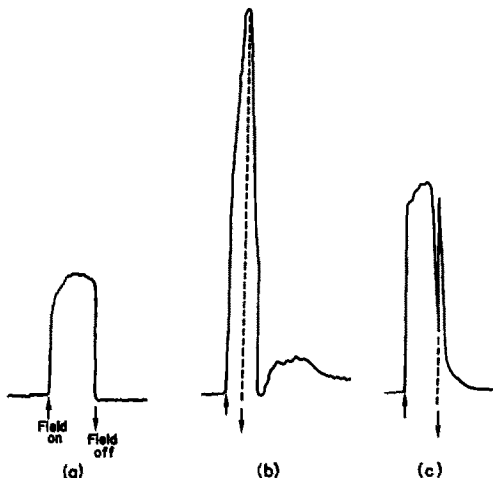


Fig. 2. Examples of different types of response: (a) 'normal'; (b) steady drift under constant field conditions; (c) memory effect following the decay of the applied field.

randomization implied by Fig. 2(a). However, apart from a few general observations, such as a greater tendency towards more complex behaviour with increasing field strengths, we were unable to define reproducible conditions under which a particular type of response would be obtained. Quantitative measurements were made on the signal amplitude at a fixed time (10 sec) after the field was switched on.

The signals were found to depend on the bentonite suspension concentration and on field strength more or less in the manner expected on the basis of a particle alignment resulting from field-induced-dipole interactions. Thus the dependence on concentration (Fig. 3) was approximately quadratic, and the curve appears to be fairly normal save for the initial minimum (a result induced by a reduction in the background transmission of the apparatus when the field was applied with a suspension of low concentration in the cell). The dependence on field strength

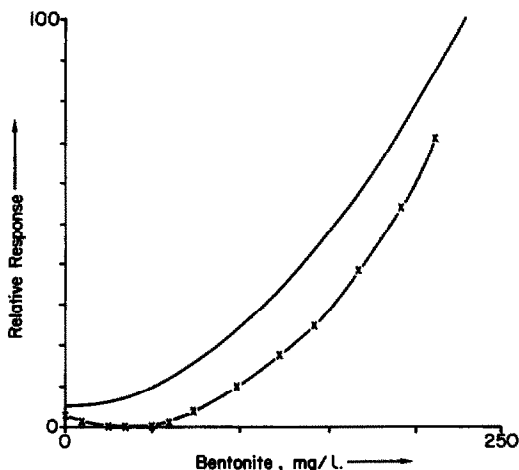


Fig. 3. Response vs. bentonite concentration. Lower curve: experimental behaviour. The upper curve is the function  $y = x^2$ .

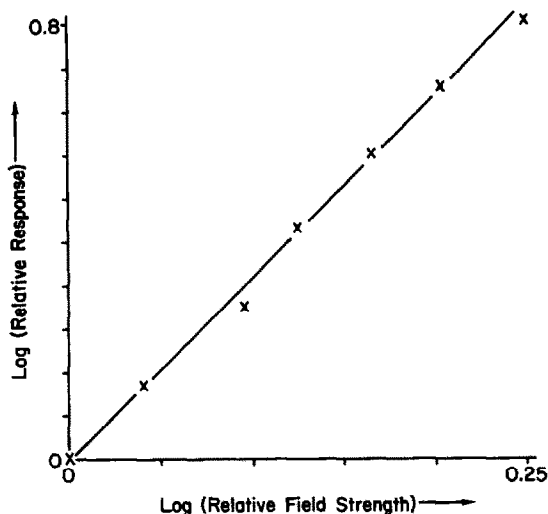


Fig. 4. Response vs. field strength up to the maximum supply voltage.

(Fig. 4) gave an exponent of 3.1 at 5 kV rather than the expected value of 4. The exponent increased to 3.6 when the supply voltage was reduced to 2 kV, results which indicate the onset of a saturation effect for the alignment process. Deviations from Kerr's law at high field strengths have been reported by earlier workers.<sup>5,6,8</sup>

The wavelength response of the electro-optic signal is shown in Fig. 5. The profile was found to be independent of the nature of any material adsorbed on the clay; the observations provide no spectral selectivity. This probably results from the combination of low concentration and the low absorption coefficient of the species studied, rather than from any inherent property of the system. The maximum in the electro-optic response corresponds quite well

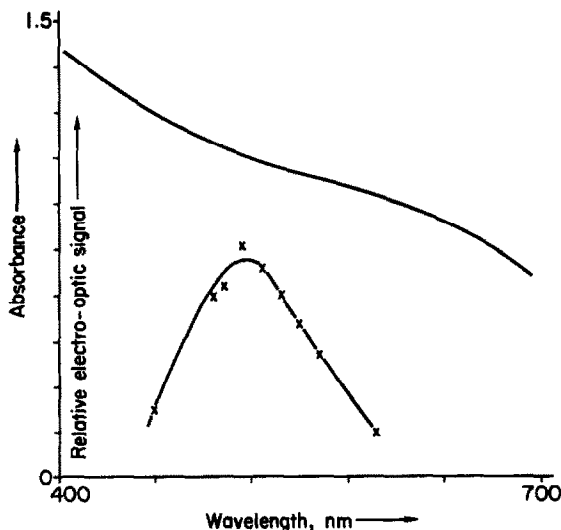


Fig. 5. Wavelength-dependence. Upper curve: absorbance. Lower curve: uncorrected electro-optic response. The red-end decay is the result of reduced photomultiplier sensitivity.

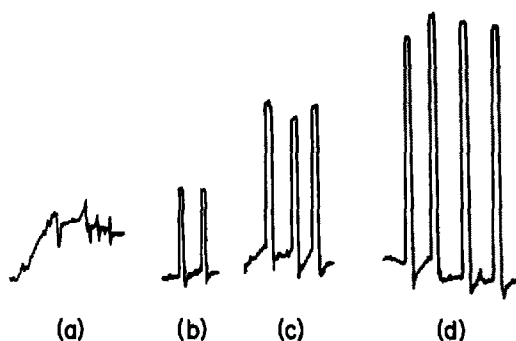


Fig. 6. Blank (a) and signals for solutions containing 4, 8, 12  $\mu\text{g/l. Pb}^{2+}$ , as  $\text{Pb}(\text{NO}_3)_2$  (b, c, d, respectively).

with the emission peak of a quartz-halogen lamp, and allows good sensitivity to be obtained by use of an optical system of low resolving power and large aperture.

*Effect of cations*

The electro-optic response of a freshly prepared suspension of bentonite was found to be very weak, being barely detectable over the background transmission of the polarizers. However, the addition of small concentrations of cations produced strong enhancements of the signal (Figs. 6 and 7). The enhancement is approximately quadratic at low concentrations; the levelling off in Fig. 7 is probably the result of saturation of the available adsorption sites, since it occurs at cation concentrations of the order of the CEC. The curves in Fig. 7 show a marked dependence on cationic charge. This trend is further

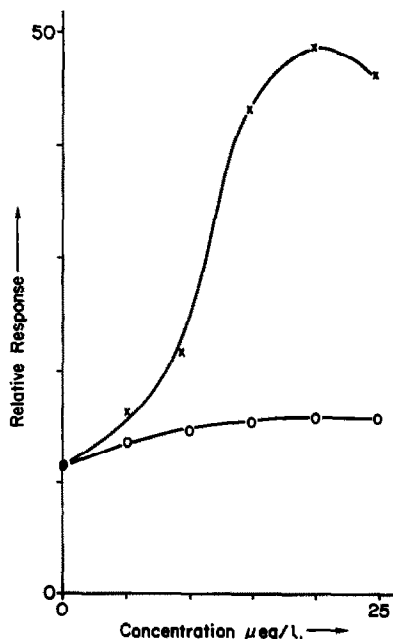


Fig. 7. Response vs. cation concentration. Points  $\times$ ,  $\circ$  are for  $\text{La}^{3+}$  and  $\text{Na}^+$ , respectively, as their chlorides.

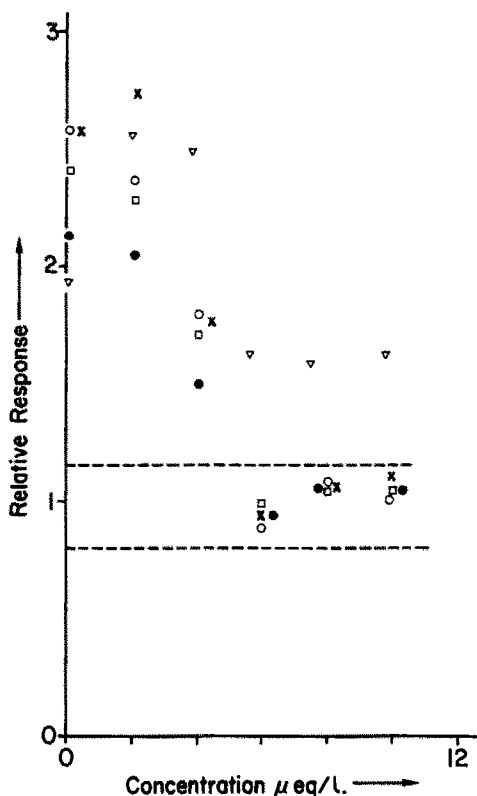


Fig. 8. Response vs. concentration for univalent cations. Points  $\square$ ,  $\circ$ ,  $\bullet$ ,  $\nabla$ ,  $\times$  are for  $\text{Na}^+$ ,  $\text{Li}^+$ ,  $\text{K}^+$ ,  $\text{Cs}^+$ ,  $\text{NH}_4^+$ , as the chlorides.

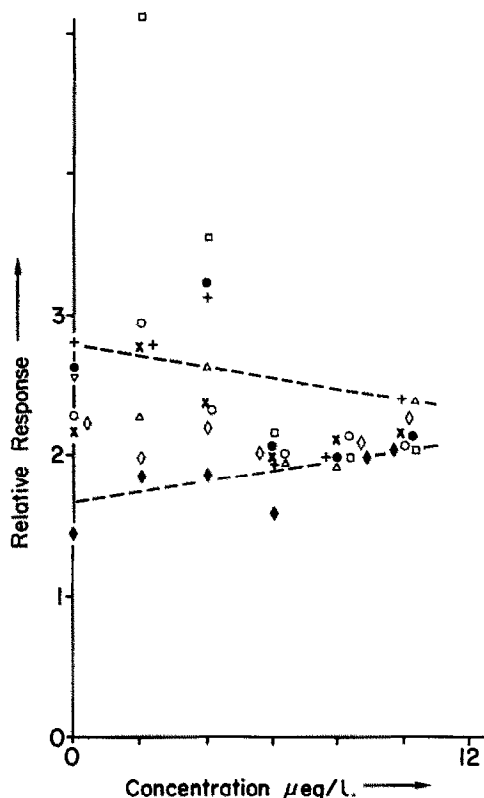


Fig. 9. Response vs. concentration for bivalent cations. Points  $\times$ ,  $\circ$ ,  $\bullet$ ,  $\square$ ,  $+$ ,  $\nabla$ ,  $\blacklozenge$ ,  $\diamond$  are for  $\text{Cu}^{2+}$ ,  $\text{Ni}^{2+}$ ,  $\text{Cd}^{2+}$ ,  $\text{Fe}^{2+}$ ,  $\text{Mg}^{2+}$ ,  $\text{Ca}^{2+}$ ,  $\text{Sr}^{2+}$ ,  $\text{Ba}^{2+}$ , as the chlorides.

illustrated by the results in Figs. 8–10, in which the ratio of the electro-optic response relative to that for  $\text{La}^{3+}$  is given for groups of uni-, bi- and trivalent species. These curves tend towards limiting values of 1, 2 and 3 respectively at the high end of the concentration range (corresponding to the region of peak response in Fig. 7). Thus the magnitude of the response apparently yields information on the magnitude of the ionic charge rather than the nature of the cation.

The limits observed in these figures cover a range of values, which is to be expected unless chemical effects are completely absent. Thus, for example, the results for  $\text{Cs}^+$  are uniformly high, which might reasonably be interpreted as arising from the unusually strong binding of this ion to montmorillonite.<sup>1,2</sup> Similarly the values for  $\text{Fe}^{3+}$  are consistently

low, which is interpreted below as the result of hydrolysis in solution.

The nature of the anion was not found to exert any obvious effect on the magnitude of the response (Fig. 11), possibly because of the relative scarcity of anion-exchange sites.

#### Effect of pH

Hydrogen ions can influence the electro-optic response directly, effectively converting the clay into a weak polyprotic acid, or indirectly by their effect on the aqueous equilibria which influence the nature of the available cation population. The latter type of effect is illustrated in Fig. 12, in which the electro-optic signals for  $\text{Fe}^{3+}$  and  $\text{La}^{3+}$  in the presence of different amounts of hydrochloric acid are shown. The anomaly in the response of  $\text{Fe}^{3+}$  (Fig. 10) is seen

Table 1. Relative responses for the oxidation of  $\text{Fe}^{2+}$  and  $\text{Fe}^{2+}$ -clay systems with  $\text{H}_2\text{O}_2$

Order of mixing	Response in water		Response in $5 \times 10^{-4}M$ HCl	
	A = twice distilled water	A = $\text{H}_2\text{O}_2$	A = twice distilled water	A = $\text{H}_2\text{O}_2$
A + clay	0.78	0.85	0.68	0.67
(A + $\text{Fe}^{2+}$ ) + clay	1.9	0.89	1.6	2.7
(clay + $\text{Fe}^{2+}$ ) + A	2.0	2.2	1.5	2.7
(A + $\text{La}^{3+}$ ) + clay	3.0	3.0	3.0	3.0
(clay + $\text{La}^{3+}$ ) + A	3.0	3.0	3.0	3.0

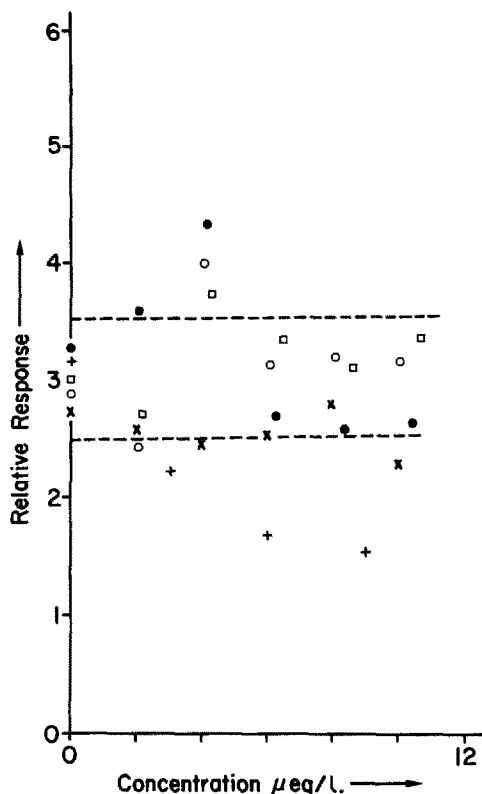


Fig. 10. Response vs. concentration for trivalent cations. Points  $\times$ ,  $O$ ,  $\bullet$ ,  $\square$ ,  $+$  are for  $Al^{3+}$ ,  $Y^{3+}$ ,  $Sc^{3+}$ ,  $Pr^{3+}$ ,  $Fe^{3+}$ , as the chlorides.

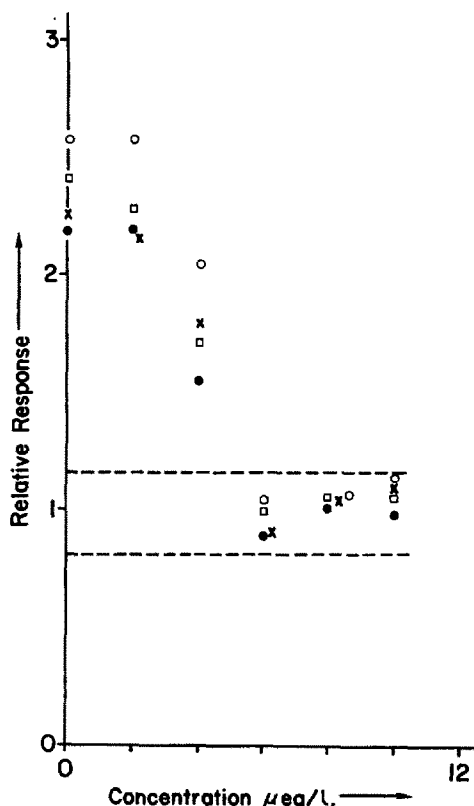


Fig. 11. Response vs. concentration for various sodium salts. Points  $\square$ ,  $O$ ,  $\bullet$ ,  $+$ ,  $\times$  are for  $Cl^-$ ,  $SO_4^{2-}$ ,  $Br^-$ ,  $PO_4^{3-}$ ,  $NO_3^-$ .

in Fig. 12 to become less apparent as the pH is lowered. This is interpreted as the result of reduced hydrolysis in the solution, leading to an increase in the amount of  $Fe^{2+}$  available to the clay.

An indirect effect of pH was observed during the oxidation of  $Fe^{2+}$  by  $H_2O_2$ . A series of measurements was made in which  $Fe^{2+}$ ,  $H_2O_2$  and clay were mixed, in different sequences, in water and in hydrochloric acid. The results are summarized in Table 1. In the absence of the acid the signal of  $Fe^{2+}$  pre-adsorbed on the clay remained constant and at a level characteristic of a bivalent ion even after addition of  $H_2O_2$ . However, no signal was observed when  $Fe^{2+}$  was mixed with  $H_2O_2$  prior to addition of the clay. The behaviour in the presence of hydrochloric acid was quite different. The magnitude of the signal no longer depended on whether the  $H_2O_2$  was added to the solution of  $Fe^{2+}$  before or after addition of the clay, and in both cases the size of the signal was closer to the range characteristic of a trivalent than of a bivalent ion. These results suggest that  $Fe^{2+}$  ions which are pre-adsorbed onto the clay are protected from oxidation in the absence of hydrochloric acid, but appear to become more mobile in the acidified solution. These results are primarily of interest because they illustrate the non-invasive nature of the electro-optic technique, which allows it to probe directly at the environment within the clay particles without perturbing the chemistry of the system.

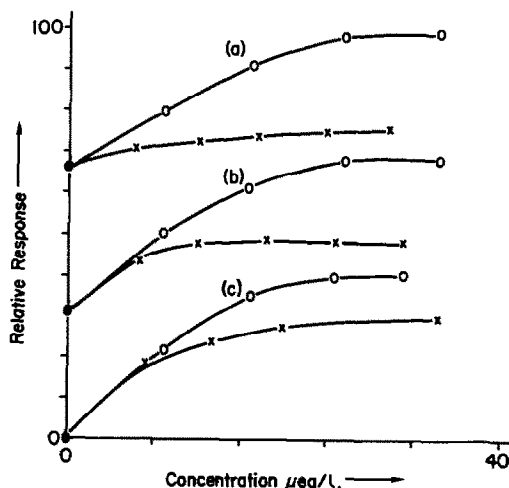


Fig. 12. Response of  $La^{3+}$  ( $O$ ) and  $Fe^{3+}$  ( $\times$ ). Curves (a), (b), (c) were measured for distilled water,  $1 \times 10^{-4} M$  HCl,  $5 \times 10^{-4} M$  HCl media, respectively.

#### CONCLUSIONS

A number of problems have emerged with the electro-optic procedure in the form described here. These problems are mainly associated with the nature of the clay suspension. Samples must be prepared in an identical manner in order for consistent results



to be obtained, and even minor departure from a particular procedure can lead to a marked variability in behaviour. Certain aspects of this variability, such as the memory effect which can be observed as the electric field decays, remain unclear both as to their origins and method of control. Even when a consistent preparation is achieved, the useful lifetime of the material is limited because of ion-exchange between the suspension and the walls of the container.

Despite the experimental difficulties observed in this work, the electro-optic technique is felt to be of potential value. The inherent sensitivity of the method is high, and it is likely that further improvements are possible (for instance by the use of optical linearization procedures<sup>9</sup>). The ability of the technique to give information on the oxidation state of adsorbed cations is also of interest, since such measurements are made by an essentially spectroscopic probe which introduces a minimal degree of perturbation into the system under study.

*Acknowledgements*—The authors are indebted to the Natural Sciences and Engineering Research Council of Canada for support of this work. One of them (JBK) thanks the Sumner Foundation and Dalhousie University for graduate support.

#### REFERENCES

1. R. E. Grim, *Applied Clay Mineralogy*, McGraw-Hill, New York, 1962.
2. W. Eitel, *Silicate Science*, Vol. 1, Academic Press, New York, 1964.
3. J. O'M. Bockris and A. K. N. Reddy, *Modern Electrochemistry*, Plenum Press, New York, 1970.
4. J. O. Robertson, Jr., *Ph.D. Thesis*, University of Southern California, 1975.
5. C. T. O'Konski, K. Yoshioka and W. H. Orttung, *J. Phys. Chem.*, 1959, **63**, 1558.
6. M. J. Shah, D. C. Thompson and C. M. Hart, *ibid.*, 1963, **67**, 1170.
7. G. B. Thurston and D. I. Bowling, *J. Coll. Interface Sci.*, 1969, **30**, 34.
8. M. J. Shah, *J. Phys. Chem.*, 1963, **67**, 2215.
9. R. Stephens, *Spectrochim. Acta*, 1983, **38B**, 1077.

## COMPLEXOMETRIC-SPECTROPHOTOMETRIC ASSAY OF TETRACYCLINES IN DRUG FORMULATIONS

SALAH M. SULTAN, IBRAHIM Z. ALZAMIL and NAWAL A. ALARFAJ  
Chemistry Department, College of Science, King Saud University, Riyadh 11451, P.O. Box 2455,  
Saudi Arabia

(Received 3 October 1986. Revised 15 April 1987. Accepted 23 November 1987)

**Summary**—An accurate, rapid and very simple spectrophotometric method for the assay of tetracyclines (tetracycline.HCl, chlorotetracycline.HCl, demeclocycline, oxytetracycline.HCl and doxycycline) has been developed. The method is based on the complexation of iron(III) with tetracyclines in 0.001M sulphuric acid. It has been successfully applied to the assay of tetracyclines in drug formulations, and the interferences of excipients have been examined. The results have been statistically compared with those obtained by two standard methods and found to be very satisfactory.

The tetracyclines and their derivatives (tetracycline, oxytetracycline, chlorotetracycline, demeclocycline and doxycycline) are extensively employed as bacteriostatic antibiotic drugs. Various methods for their determination have been reviewed.<sup>1</sup> In the British Pharmacopoeia<sup>2</sup> a biological assay for tetracycline is given but it is an elaborate method not suitable for routine analysis. Iron(III) was early recommended in the U.S. Pharmacopoeia<sup>3</sup> for the determination of oxytetracycline. A simple spectrophotometric method for the assay of tetracycline was recently described<sup>1</sup> but it is not suitable for the assay of other derivatives. Two spectrophotometric methods for the assay of some tetracycline derivatives have been described based on oxidation with ammonium vanadate<sup>4</sup> and sodium cobaltinitrite,<sup>5</sup> but neither is specific.

The present work is based on the ability of tetracyclines to form metal-ion complexes.<sup>6,7</sup> Chelation with cations such as iron(III), aluminium, copper(II), nickel, cobalt(II), zinc, vanadium(III), thorium, lanthanum, magnesium and calcium is well established.<sup>8-18</sup> It has been reported that iron(III) has higher affinity than other cations for chelation with tetracyclines *in vitro*.<sup>6,8-14,19</sup>

In the method presented here, tetracycline is added to iron(III) and the absorbance of the brown complex formed is measured.

### EXPERIMENTAL

#### Apparatus

A Varian Model DMS 100 Spectrophotometer connected to a Varian Model DS 15 Data Station and a Hewlett-Packard Model 82905 B Printer was used for all absorbance measurements. Matched sets of 10-mm cells were used throughout.

#### Reagents

High-purity distilled water was used throughout. Stock solutions were prepared from analytical or pharmaceutical grade chemicals, and working solutions were prepared from these by appropriate dilution.

Ferric ammonium sulphate solution (1 mg/ml) was prepared by dissolving about 1 g, accurately weighed, in a litre of 0.001M sulphuric acid.

Tetracycline solution (1 mg/ml) was freshly prepared by dissolving the required amount in 0.001M sulphuric acid by warming, then cooling and making up to volume in a standard flask. For analysis of capsules, the contents of 10 were mixed and weighed and a quantity of the powder equivalent to 250 mg of tetracycline was accurately weighed out, and stirred with 200 ml of 0.001M sulphuric acid for 10 min, with warming, then the solution was filtered (Whatman No. 41 filter-paper), the paper was washed with hot 0.001M sulphuric acid and the filtrate and washings were diluted to volume with 0.001M sulphuric acid in a 250-ml standard flask after cooling to room temperature.

#### General procedure

Place 10 ml of ferric ammonium sulphate solution and an appropriate amount of tetracycline solution in a 50-ml standard flask. Swirl and leave for 20 min for tetracycline hydrochloride but only 5 min for the other derivatives, then dilute to the mark with 0.001M sulphuric acid. Measure the absorbance at the appropriate wavelength against a reagent blank treated similarly.

### RESULTS AND DISCUSSION

#### Mechanism

The tetracyclines were added to iron(III) solution in sulphuric acid of different concentrations. A brown soluble compound was always obtained, with each derivative giving a characteristic wavelength of maximum absorption, at 423 nm for tetracycline and 435 nm for the four derivatives examined. The maxima can be attributed to complex formation of iron(III) with the tetracyclines. When iron(II) was used no colour change was observed. The tetracycline structure contains numerous sites at which chelation with metal cations might occur, the most important of these being in the portion of the molecule which contains the two enolized 1,3-diketone groupings.<sup>6,20-22</sup> Such enol groups readily form six-membered rings with metal ions, with the two oxygen atoms as donors.<sup>21,22</sup> Job's method<sup>23,24</sup> showed that

the ratio of iron(III) to tetracycline is 1:2. This ratio has also been reported for combination of copper(II), nickel and zinc with tetracycline.<sup>20</sup> Accordingly, it is suggested that iron(III) chelates with tetracycline as follows:

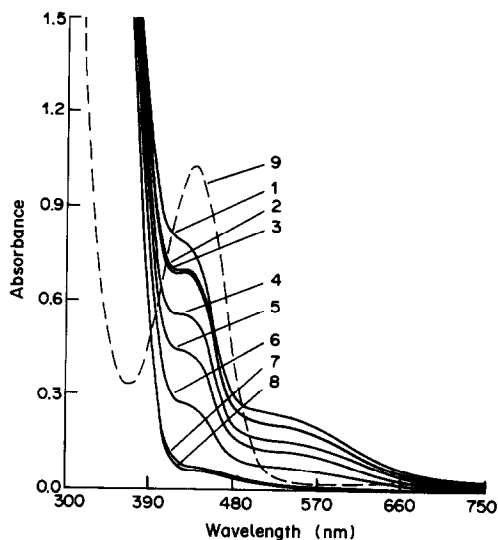
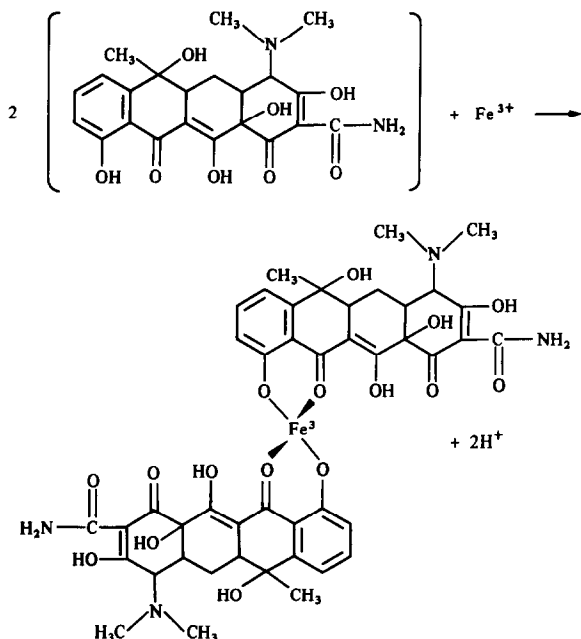


Fig. 1. Absorption spectra for reactants [3 mg of tetracycline + 6 mg of iron(III)] in 50 ml of solution, measured against a reagent blank at different sulphuric acid molarities: 1—0.0001; 2—0.0005; 3—0.001; 4—0.003; 5—0.005; 6—0.01; 7—0.05; 8—0.10; 9—2.

All the iron(III) complexes thus formed are stable for 24 hr. Figure 1 shows that the absorbance of the tetracycline-iron(III) complex at 423 nm decreases as the sulphuric acid concentration is increased, becoming minimal at 0.1M acidity. In the sulphuric acid range 0.0005–0.002M the absorbance is almost constant and 0.001M acidity is optimal. At sulphuric acid concentrations >0.1M protonation of the tetracycline molecule is possible and an absorbance peak for the protonated form appears at 441 nm as in curve 9. At acidities lower than 0.0005M, hydrolysis of iron(III) is expected and the maximum is not as well defined (curve 1). For this reason, 0.001M sulphuric acid was selected as optimum.

#### Spectral data

Beer's law was found to hold over the range 10–200 µg/ml for all five compounds examined. Table 1 gives the molar absorptivities at the wavelength of maximum absorption.

#### Applications

The method was applied to the assay of tetracyclines in drug formulations (commercial products randomly collected from local pharmacies). Typical results are given in Table 2 and show good agreement with those obtained by other methods. The sodium molybdate method was used for tetracycline, and the sodium cobaltinitrite method<sup>3</sup> for the other four compounds. The *t*-values (Table 3) showed no significant difference between the means obtained (95% confidence limit).

#### Interferences

The results for analysis of the compounds in drug formulations with the constituents listed in Table 2 indicate that the excipients usually present in dosage forms, such as starch, lactose and glucose, did not interfere. Troleandomycin, glucosamine.HCl and vitamin K<sub>3</sub> did not interfere with the determination of tetracycline. Thiamine, pyridoxine and folic acid did not interfere with the determination of oxytetracycline. Vitamins B<sub>1</sub>, B<sub>2</sub>, B<sub>6</sub>, B<sub>12</sub>, nicotinamide and calcium pantothenate did not interfere with the determination of tetracycline or oxytetracycline. Sulphamethizole and phenazopyridine.HCl, however,

Table 1. Analytical appraisal for compounds (in pure form) investigated

Generic name	Supplier	$\lambda_{\max}$ , nm	$\epsilon$ , l. mole <sup>-1</sup> . cm <sup>-1</sup>
Tetracycline.HCl	Lederle	423	4646
Demethylchlorotetracycline	Lederle	435	5190
Chlorotetracycline.HCl	Lederle	435	5533
Oxytetracycline.HCl	Pfizer	435	5240
Doxycycline	Pfizer	435	4922

Table 2. Results for all drugs investigated by the proposed method and/or the sodium molybdate<sup>4</sup> and sodium cobaltinitrite<sup>5</sup> methods

Drug proprietary name, and supplier	Generic name	Nominal composition, mg	Proposed method		Standard method, found, mg
			Found per capsule, mg*	Error, %†	
Tetrerba, Carlo Erba	Tetracycline	250 tetracycline.HCl	262	+4.9	262 <sup>a</sup>
Uropol, Bristol-Myers	Tetracycline	125 tetracycline.HCl 250 sulphamethizole 50 phenazopyridine.HCl	429	+243	302 <sup>a</sup>
Dumocycline, Dumex	Tetracycline	250 tetracycline.HCl	257	+2.6	258 <sup>a</sup>
Tetrambezim, Lepetit	Tetracycline	250 tetracycline.HCl	251	+0.5	253 <sup>a</sup>
Sigmamycin, Pfizer	Tetracycline	167 tetracycline.HCl 83 troleandomycin	155	-7.0	155 <sup>a</sup>
Achromycin, Lederle,	Tetracycline	250 tetracycline.HCl	249	-0.3	249 <sup>a</sup>
Laticin, Biochemie	Tetracycline	250 tetracycline.HCl 250 glucosamine.HCl 2.5 Vit. B <sub>1</sub> 2.5 Vit. B <sub>2</sub> 2.5 Vit. B <sub>6</sub> 2.5 Vit. B <sub>12</sub> 75 Vit. C 0.5 Vit. K <sub>3</sub> 25 nicotinamide 5 calcium pantothenate	149	-40	263 <sup>a</sup>
Vibramycin, Pfizer,	Doxycyclin	100 doxycycline	102	+1.5	102 <sup>b</sup>
Urobiotic, Pfizer	Oxytetracycline.HCl	125 oxytetracycline.HCl 250 sulphamethiazole 50 phenazopyridine.HCl	478	+282	330 <sup>b</sup>
Terramycin S.F., Pfizer	Oxytetracycline.HCl	250 oxytetracycline.HCl 2.5 thiamine 2.5 riboflavin 25 niacinamide 5 calcium pantothenate 0.5 pyridoxine 0.375 folic acid 1 Vit. B <sub>12</sub> 75 ascorbic acid	173	-31	381 <sup>b</sup>
Terramycin, Pfizer	Oxytetracycline.HCl	250 oxytetracycline	259	+4.0	260 <sup>b</sup>
Demeclocycline, Lederle	Demethylchloro-tetracycline	pure analytical reagent (another batch)	—	-1.4	—
Chlorotetracycline	Chlorotetracycline.HCl	pure analytical reagent (another batch)	—	-0.5	—

\*Mean of 7 determinations.

†Difference from nominal content.

Table 3. Statistical comparison of the results obtained (7 replicates) by the proposed method with results obtained by the sodium molybdate<sup>4</sup> and/or sodium cobaltinitrite<sup>5</sup> method

Drug proprietary name	Recovery $\pm$ standard deviation, %			
	Method*	Method†	Method§	t Calculated‡
Tetrerba	104.8 $\pm$ 0.9	105.0 $\pm$ 0.2	—	0.38
Dumocycline	102.6 $\pm$ 0.6	103.2 $\pm$ 0.2	—	1.71
Achromycin V	99.8 $\pm$ 0.7	99.5 $\pm$ 0.4	—	0.81
Tetrambezim	100.5 $\pm$ 0.7	101.2 $\pm$ 0.4	—	1.75
Sigmamycin	93.0 $\pm$ 0.2	93.0 $\pm$ 0.8	—	0.51
Vibramycin	101.6 $\pm$ 0.4	—	102.0 $\pm$ 0.5	0.68
Terramycin	103.6 $\pm$ 0.6	—	104.1 $\pm$ 0.8	0.56
Demeclocycline	99.1 $\pm$ 0.2	—	99.5 $\pm$ 0.2	1.10
Chlorotetracycline.HCl	95.3 $\pm$ 0.6	—	94.9 $\pm$ 0.5	0.43

\*Proposed method.

†Sodium molybdate method.

§Sodium cobaltinitrite method.

‡Theoretical value = 2.45 ( $P = 0.05$ ).

gave a large positive error in the determination of both tetracycline and oxytetracycline.

Vitamin C also interfered with the determination of tetracycline and oxytetracycline, but with a negative systematic error. This may be due to decrease in the iron(III) concentration by reduction with ascorbic acid, but addition of extra iron(III) failed to eliminate the interference.

#### Conclusion

This method is accurate, simple, rapid and suitable for routine analysis of all commonly used tetracyclines. There is no interference from most compounds added to drug formulations containing tetracyclines.

*Acknowledgements*—The authors thank Lederle Laboratories and Pfizer Corporation, for supplying the standard samples. Mrs Nawal A. Alarfaj thanks King Saud University for offering a chance to read for the M.Sc. degree.

#### REFERENCES

1. S. M. Sultan, *Analyst*, 1986, **111**, 97.
2. *British Pharmacopoeia*, H.M.S.O., London, 1980.
3. *U.S. Pharmacopeia*, 15th Revision, Mack, Easton PA, 1955.
4. M. M. Abdel-Khalek and M. S. Mahrous, *Talanta*, 1983, **30**, 792.
5. M. S. Mahrous and M. M. Abdel-Khalek, *ibid.*, 1984, **31**, 289.
6. P. J. Neuvonen, *Drugs*, 1976, **11**, 45.
7. J. J. Stezowski, *Jerusalem Symp. Quantum Chem. Biochem.*, 1977, **9**, 375.
8. A. Albert, *Nature*, 1953, **172**, 201.
9. A. Albert and C. W. Rees, *ibid.*, 1956, **177**, 433.
10. *Idem, ibid.*, 1963, **172**, 201.
11. P. J. Neuvonen, G. Gothoni, R. Hackman and K. Bjorksten, *Brit. Med. J.*, 1970, **4**, 532.
12. P. J. Neuvonen, P. J. Pentikainen and G. Gothoni, *Brit. J. Clin. Pharmacol.*, 1975, **2**, 94.
13. T. F. Chin and J. L. Lach, *Am. J. Hosp. Pharm.*, 1975, **32**, 625.
14. T. Sakaguchi, M. Toma, T. Yoshida and H. Takasu, *Pharm. Bull.*, 1958, **78**, 177.
15. M. Saiki and F. W. Lima, *J. Radioanal. Chem.*, 1977, **36**, 435.
16. D. E. Williamson and G. W. Everett, Jr., *J. Am. Chem. Soc.*, 1975, **97**, 2397.
17. F. A. Hochstein, C. R. Stephens and L. H. Conover, *ibid.*, 1953, **75**, 5455.
18. H. Ibsen, M. R. Urist and S. Ugeno, *Proc. Soc. Eptl. Biol. Med.*, 1962, **109**, 797.
19. J. J. Silva and H. M. Dias, *Rev. Port. Quim.*, 1972, **14**, 159.
20. J. T. Doluisio and A. N. Martin, *J. Med. Chem.*, 1963, **6**, 16.
21. L. A. Mitscher, A. C. Bonacci, B. Slater-Eng, A. K. Hacker and T. D. Sokoloski, *Antimicrob. Ag. Chemother.*, 1969, **1**, 111.
22. L. A. Mitscher, B. Slater-Eng and T. D. Sokoloski, *ibid.*, 1972, **2**, 66.
23. P. Job, *Ann. Chim. (Paris)*, 1928, **9**, 113.
24. *Idem, ibid.*, 1936, **17**, 97.

# DETERMINATION OF RESIDUAL AROMATIC AMINE HYDROCHLORIDES IN PROCESS SAMPLES OF DI-ISOCYANATE USED IN THE MANUFACTURE OF POLYURETHANE

## A COMPARISON OF ELECTROANALYTICAL METHODS

PAOLO UGO and SALVATORE DANIELE

Department of Spectroscopy, Electrochemistry and Physical Chemistry, University of Venice,  
S. Marta 2137, 30123 Venice, Italy

GINO BONTEMPELLI

Institute of Chemistry, University of Udine, viale Ungheria 43, 33100 Udine, Italy

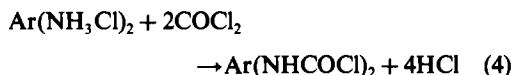
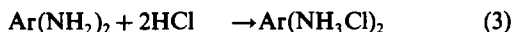
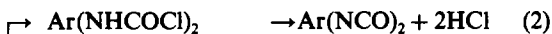
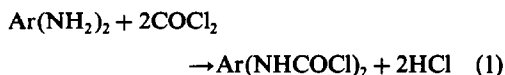
ANTONIO BECCARI

Montedipe S.p.a., Portomarghera, 30100 Venice, Italy

(Received 10 June 1987. Revised 29 October 1987. Accepted 14 November 1987)

**Summary**—Aromatic diamine hydrochlorides have been determined in the presence of different amounts of hydrochloric acid by acid–base titration followed potentiometrically, by linear sweep voltammetry, by differential pulse voltammetry and also by direct DPV measurement. Tests on simulated and production samples have shown that the best results are obtained by using DPV at a mercury electrode, because of its good resolution, which makes it possible to achieve good accuracy (error < -1%) and good precision (rsd 1.5%) at 0.1M levels. Moreover, it has the advantage that neither preliminary treatment of the sample nor a trial titration is required.

Aromatic di-isocyanates are of great commercial interest as precursors of polyurethanes, which are polymers with many practical applications. Di-isocyanates are generally produced industrially by reacting the corresponding aromatic diamines with phosgene:



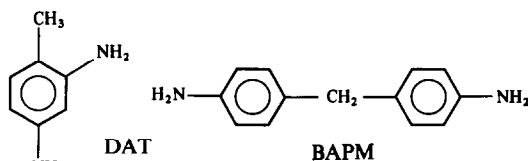
The presence of appreciable amounts of residual unreacted aromatic diamine hydrochloride in the final product indicates both that the process is not running efficiently, and also that the product is sufficiently contaminated to be only of low commercial value. Consequently, there is a need for a simple and fast method for determining aromatic amine hydrochlorides (moderately weak acids) in the presence of large amounts of a strong acid such as the

hydrochloric acid formed in the process above. Such a method could be employed not only to test the purity of di-isocyanate samples, but also to help optimize the process so as to avoid the production of undesired substituted-urea derivatives as by-products. This second goal is usually achieved by using mathematical models to relate the parameters regulating process conditions (flow-rate, temperature and pressure) to the concentrations of all the species involved (monitored on samples suitably chosen from the process stream), the determination of which also requires reliable analytical procedures.

Aromatic diamine hydrochlorides are usually determined in industrial practice by potentiometric acid–base titration either directly, or by back-titration. Samples are pretreated with methanol or propanol to eliminate the residual phosgene and to convert the di-isocyanates into the corresponding urethanes.<sup>1,2</sup> It is difficult with such procedures to distinguish between the hydrochloric acid and the aromatic amine hydrochlorides, so the accuracy and precision are poor, and only a total acid content is usually reported for commercially available di-isocyanates.

With the aim of devising a more convenient method for this analysis, we compared the performance offered by potentiometry with that given by

more sophisticated electroanalytical techniques such as differential pulse and linear sweep voltammetry. The tests were made on mixtures of hydrochloric acid and either 2,4-diaminotoluene (DAT) or bis(4-aminophenyl)methane (BAPM), corresponding to samples drawn from the process streams of two commonly employed di-isocyanates supplied by Montedipe, Italy.

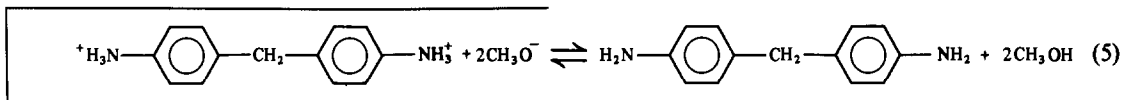


This paper reports the relevant findings.

### EXPERIMENTAL

#### Chemicals

All the chemicals used were of reagent-grade quality. BAPM.2HCl and DAT.2HCl were prepared by slightly modifying a method reported elsewhere.<sup>3</sup> Methanolic hydrogen chloride solution (made by bubbling the gas through methanol, and standardized by titration with methanolic sodium methoxide solution) was added to the appropriate diamine in methanol and the resulting solution was concentrated by evaporation. The white crystals produced were filtered off and dried under vacuum at 50°. Stock solutions of sodium methoxide in methanol were obtained by reacting metallic sodium with an excess of methanol, and were standardized by titration with hydrochloric acid.



#### Apparatus and procedure

All measurements were made on methanol solutions at 20°. Samples drawn from the process stream, as well as samples of the final product, were reacted first with methanol to eliminate residual phosgene and to convert di-isocyanates into the corresponding urethanes.

Voltammetric experiments were done in a three-electrode cell: the working electrode was surrounded by a platinum spiral counter-electrode and its potential was probed by use of a Luggin-capillary reference-electrode compartment made adjustable in position by being mounted on a syringe barrel. An aqueous SCE was used as the reference electrode.

For the linear sweep voltammetry (LSV) the working electrode was either a gold sphere freshly covered with mercury or a platinum disc mirror-polished with graded alumina powder. In the latter case the most reproducible voltamperograms were obtained when the platinum working electrode was pre-anodized at an appropriate activation potential (+1.1 V *vs.* SCE) for 4 sec prior to each voltammetric scan (no improvement in performance was obtained with longer pre-anodization times). After pre-anodization the solution was stirred for 15 sec at +0.1 V *vs.* SCE to reduce the PtO formed<sup>4,5</sup> and to re-equilibrate the solution. The pre-anodization procedure seemed to be more effective when large amounts of chloride ions were present, probably thanks to the cleaning effect of the chlorine evolved at the platinum surface. This observation suggested to us the use of tetrabutylammonium chloride (TBACl) as the supporting electrolyte.

The differential pulse voltammetry (DPV) was performed at either a dropping mercury electrode (DME) with mech-

anical control of the drop-time or a platinum disc pre-activated as described above.

An Amel 552 potentiostat in conjunction with an Amel 568 digital logic-function generator was used in the LSV measurements, and the DPV experiments were performed with an Amel 472 multipolarographic unit. DPV tests on platinum were also performed with this last unit coupled to an Amel 568 function generator to ensure that any scan was automatically preceded by the pre-activation sequence described above. Voltamperograms were recorded on an Amel 863 X-Y recorder.

Preliminary DPV tests at the DME showed that the best peak-separation was obtained with drop-time = 1 sec, pulse height = 20 mV, scan-rate = 2 mV/sec. Lowering the scan-rate led to peak broadening, probably because of the quite long electrode-solution contact time, which caused progressive poisoning of the activated platinum surface.<sup>6,7</sup>

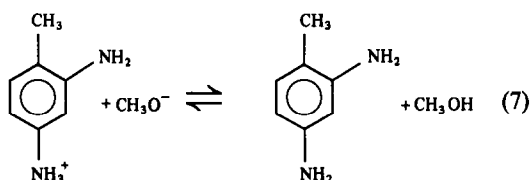
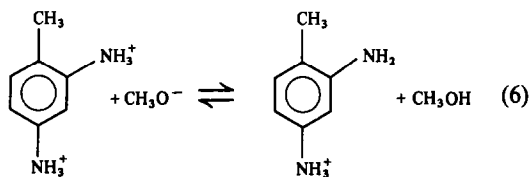
Potentiometric titrations were done with a glass electrode and a Beckman 5000 pH-meter; the equivalence points were determined by the first-derivative method.

### RESULTS AND DISCUSSION

#### Potentiometric titrations

Figure 1 shows the curves obtained when BAPM.2HCl (line a) and DAT.2HCl (line b) were titrated with sodium methoxide solution in methanol. In BAPM.2HCl, the two protonated amine functional groups behave as relatively weak acids of equal strength, as expected on the basis of the lack of conjugation between the two aromatic rings, and the titration curve displays only one potential break, corresponding to the reaction:

In contrast, the curve for DAT.2HCl shows that the two protonated amine groups have different acid strengths ( $\Delta pK_a \approx ca. 3.1$ ), so that two equivalence points are detected, corresponding to the reactions



The higher acidity of the protonated *o*-amino group, expected on the basis of combined mesomeric, inductive and steric effects,<sup>8</sup> is comparable with that of hydrogen chloride in methanol medium (line c in Fig. 1). The protonated *p*-amino group shows a relatively lower acid strength, comparable with that displayed by BAPM.2HCl. The accuracy and precision of these titrations are summarized in Table 1.

Table 1. Accuracy and precision of potentiometric and monoamperometric titrations on HCl/amine solutions

Analytical procedure	Protonated amine*	Accuracy, † %	Relative standard deviation, %
Potentiometric titration in HCl-free soln.	BAPM.2HCl	+ 1.1	1.5
	DAT.2HCl	+ 1.0	1.7
Potentiometric titration after evaporation	BAPM.2HCl	+ 2.0	2.8
	DAT.2HCl	+ 3.5	4.7
Monoamperometric titration	BAPM.2HCl	+ 2.0	3.1
	DAT.2HCl	+ 2.2	3.2

\*Concentration = 1mM.

†Mean error of five replicate measurements.

The addition of increasing amounts of methanolic hydrogen chloride solution to these solutions of protonated amines caused a progressive worsening in the resolution of the end-points on the titration curves, eventually making it impossible to distinguish the end-point for the protonated amine from that for the hydrogen chloride when the HCl:amine molar ratio was about 10 (see line d in Fig. 1 for DAT). The direct potentiometric titration of the protonated amines in samples containing an excess of hydrogen chloride is therefore not possible unless a preliminary treatment for eliminating the excess of hydrogen chloride is used. As we have shown, a simple evaporation under vacuum is sufficient to bring the ratio below this critical level.

Titration done after this pretreatment give satisfactory accuracy and precision, as shown in Table 1.

#### Linear sweep voltammetry

The cathodic voltammetric behaviour of both BAPM.2HCl and DAT.2HCl agrees with that expected on the basis of the potentiometric titrations. As shown in Fig. 2, line a, the voltamperogram for BAPM.2HCl at a platinum working electrode is characterized by one cathodic peak at  $-0.520$  V, which corresponds to the simultaneous reduction of both protons linked to the amine groups.

For DAT.2HCl (line b), however, two separate cathodic peaks (at  $-0.300$  and  $-0.520$  V) are detected, in agreement with the different basicity of the *o*- and *p*-positions, mentioned above. Moreover, the potential of the first of these two peaks coincides with the reduction potential for methanolic hydrogen chloride solutions.

When a mercury-covered gold electrode is used as the working electrode, the voltamperograms obtained (lines c and d in Fig. 2) differ from those recorded with a platinum electrode only by the typical overpotential affecting the reduction of protons on Hg.

All the peaks mentioned are diffusion-controlled in the scan-rate and concentration ranges explored by us (25–500 mV/sec and 0.4–8.0mM), so they can be used for analytical determinations.

An excess of hydrogen chloride interferes in these measurements too, precluding the direct voltammetric determination of the protonated amine unless the hydrogen chloride is first removed by evaporation under vacuum.

However, if LSV is used to detect the end-points in acid-base titrations of the original sample, quite satisfactory results are obtained, allowing the time-consuming and troublesome evaporation step to be

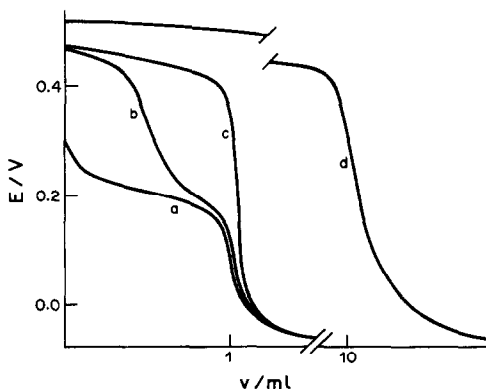


Fig. 1. Potentiometric titration curves of methanol solutions containing: 1mM BAPM.2HCl (curve a); 1mM DAT.2HCl (curve b); 2mM HCl (curve c); 1mM DAT.2HCl and 10mM HCl (curve d). Titrant 10mM  $\text{CH}_3\text{ONa}$  solution in methanol.

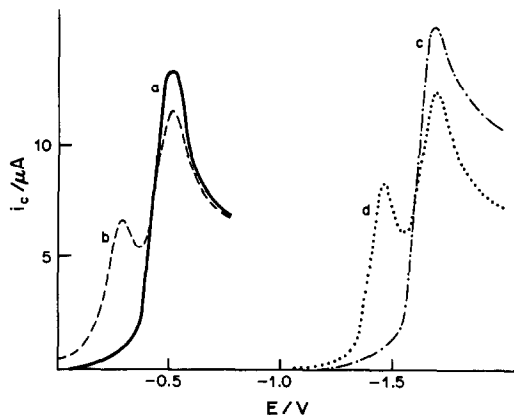


Fig. 2. Linear sweep voltamperograms recorded with a platinum electrode (curves a and b) and with a mercury-covered gold electrode (curves c and d) for 0.1M TBACl solutions in methanol, containing 1mM BAPM.2HCl (curves a and c) and 1mM DAT.2HCl (curves b and d). Scan-rate 50 mV/sec.



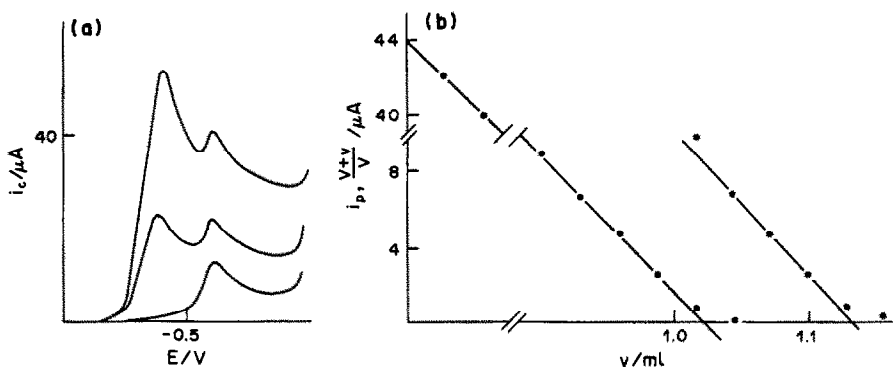


Fig. 3. (a) Sequence of voltamperograms recorded during the monoamperometric titration of a 0.1M TBACl solution in methanol, initially containing 0.5mM BAPM.2HCl and 5mM HCl. Working electrode platinum; scan-rate 50 mV/sec; titrant 40mM  $\text{CH}_3\text{ONa}$  solution in methanol. (b) Monoamperometric titration curve drawn from voltammetric curves. Working potential:  $-0.300\text{ V}$  (●—●);  $-0.520\text{ V}$  (\*—\*).  $V$  = initial volume,  $v$  = volume added.

omitted. Figure 3a shows a succession of voltamperograms recorded during such a titration.

The stronger acid (HCl) is progressively neutralized until only the protonated amine remains. This can be determined easily by linear extrapolation of a plot of  $i_p$  vs. volume of titrant added (see Fig. 3,b). The accuracy and precision for this type of amperometric titration are reported in Table 1. Similar results should be obtained more simply by monitoring the titration amperometrically at a fixed potential, first at  $-0.3\text{ V}$  to detect the end-point for hydrogen chloride and then at about  $-0.52\text{ V}$  to determine the amine.

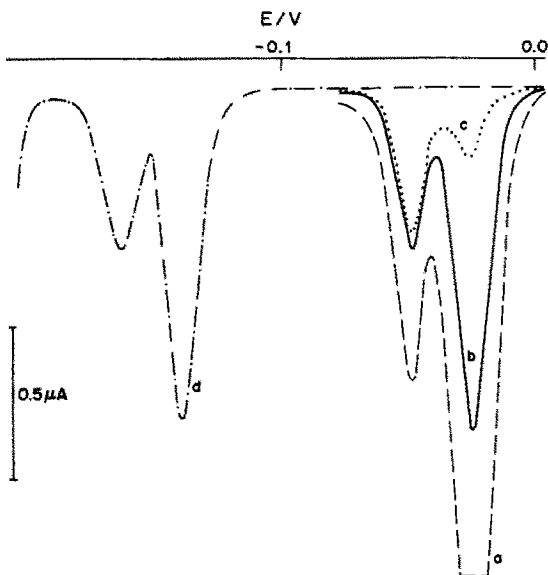


Fig. 4. Differential pulse voltamperograms recorded on a 0.1M TBACl solution in methanol: 0.1mM BAPM.2HCl and 5.0mM HCl (curve a); 0.1mM BAPM.2HCl and 0.8mM HCl (curves b and d); 0.1mM BAPM.2HCl and 0.02mM HCl (curve c). For curves a,b,c: working electrode platinum; pulse height 20 mV; scan-rate = 20 mV/sec. For curve d: working electrode DME; drop-time 1 sec; pulse height 20 mV; scan-rate = 2 mV/sec.

#### Differential pulse voltammetry

As the differential pulse technique offers higher resolution of close peaks than does the linear scan method, an attempt was made to determine the protonated amines directly in the presence of an excess of hydrogen chloride, without titration, thus avoiding any preliminary treatment of samples.

Figure 4, lines a–c, shows three differential pulse voltamperograms recorded at a platinum working electrode for mixtures of hydrogen chloride and BAPM.2HCl in different molar ratios. Two well separated peaks ( $\Delta E_p = 0.240\text{ V}$ ) are obtained, the less negative of which is due to reduction of the free hydrogen chloride. Such a separation allows good resolution to be achieved when comparable concentrations of the two components are present (line b in Fig. 4), but the resolution becomes poorer as the ratio departs markedly from unity (lines a and c in Fig. 4).

A similar pattern is observed when a mercury working electrode is used (line d in Fig. 4), the only difference being a cathodic shift of both peaks owing to the well known overpotential for proton discharge on mercury, already mentioned for the LSV experiments.

The results obtained by this technique for a series of simulated samples confirm the conclusions drawn

Table 2. Accuracy and precision of DPV determinations on HCl/amine solutions

HCl/amine molar ratio*	Accuracy, %†		Relative standard deviation, %	
	Pt electrode	DME	Pt electrode	DME
0.2	+1.1	+0.8	3.2	3.0
1	-0.7	-0.5	1.2	0.8
10	-0.8	-0.5	1.5	0.8
20	-1.0	-0.7	2.0	1.4
50	-1.0	-0.8	2.2	1.4
100	-1.3	-1.0	3.4	2.2

\*The amine concentration was kept constant at 0.1mM. †Mean error of five replicate measurements.

Table 3. Relative standard deviation for the analysis of process samples

Analytical procedure	Relative standard deviation, %			
	BAPM. 2HCl		DAT. 2HCl	
	min	max	min	max
Potentiometric titration after evaporation	3.3	3.9	5.1	5.5
Monoamperometric titration on Pt electrode	3.1	4.0	3.0	4.1
Monoamperometric titration on Au/Hg electrode	3.3	4.2	3.3	4.1
DPV (Pt)	2.2	3.8	2.4	4.0
DPV (DME)	2.0	3.1	2.1	3.3

from Fig. 4, that the accuracy and precision depend on the HCl:amine molar ratios (see Table 2), though they are satisfactory over a wide range of ratios. However, it is worth noting that when a dropping mercury electrode is used instead of a platinum one for the DPV, the results are better thanks to the good reproducibility of the electrode surface and the slightly improved resolution between peaks, gained by employing a slower scan-rate (see experimental section).

#### Analysis of process samples

The electroanalytical methods used above for simulated samples of known concentration were also applied to process samples and finished products, since other matrix components (such as chlorobenzene and urethanes) are unlikely to cause interference.

Measured volumes of samples drawn from the process stream were reacted with an excess of methanol to convert isocyanates into urethanes and to destroy the dissolved phosgene, according to the ASTM recommendations.<sup>1</sup> The protonated amines were then present in the mM concentration range in the methanol solutions and accompanied by a 10–100-fold excess of hydrogen chloride. Consequently, any of the electroanalytical methods described above could be used, though a higher dilution was required for the more sensitive DPV technique, and pretreatment under reduced pressure was required with the other methods. In all tests, the reproducibility was good, as can be seen from Table 3.

Agreement between the results obtained for the same sample by the different methods employed was satisfactory, the maximum relative difference between the concentrations found for the protonated amines being about 7%. This must be considered in the

context of industrial practice, where a precision of  $\pm 5\%$  is regarded as satisfactory.

For the refined or crude finished products, only analysis by DPV gave reliable results, owing to the quite low concentrations of acid species resulting from dissolving even large amounts of these samples in methanol. DPV analyses of solutions in which the total acid concentration was not less than *ca.* 0.2mM (irrespective of the HCl:amine ratio) had relative standard deviations that in the worst case were 6–8% for use of platinum electrodes and 5–6% for mercury electrodes. The relative standard deviation was considerably higher when solutions of real samples with total acid content below *ca.* 0.2mM were analysed. Again the precision is satisfactory for process work, since a  $\pm 10\%$  error is acceptable for 10–50 ppm amine content (as in the samples examined by us). For refined products with 200–1000 ppm amine content the acceptable error range is  $\pm 5\%$ .

*Acknowledgements*—We wish to thank Professor P. Lanza (Bologna) for his useful suggestions. The financial aid of the Italian Research Council (C.N.R.) and of the Ministry of Public Education is gratefully acknowledged.

#### REFERENCES

1. Plastics II, in *Book of Methods of the American Society for Testing and Materials*, Vol. 08.02, pp. 40–60. ASTM, Easton, 1983.
2. *Recueil de normes francaises des plastiques*, Vol. 4, AFNOR, Paris, 1982.
3. I. Konstantinov and A. I. Kormucheshkina, *Zh. Priklad. Khimi.*, 1976, **49**, 596.
4. A. V. Tripković and R. R. Adžić, *J. Electroanal. Chem.*, 1986, **205**, 335.
5. W. C. Barrette, Jr. and D. T. Sawyer, *Anal. Chem.*, 1984, **56**, 653.
6. R. F. Lane and A. T. Hubbard, *J. Phys. Chem.*, 1977, **81**, 734.
7. P. Ugo, S. Daniele, G. A. Mazzocchin and G. Bontempelli, *Anal. Chim. Acta*, 1986, **189**, 253.
8. J. W. Smith, in *The Chemistry of the Amine Group*, S. Patai (ed.), Chap. 4. Wiley, New York, 1968.

## DISTRIBUTION COEFFICIENTS AND ION-EXCHANGE SELECTIVITIES FOR 46 ELEMENTS WITH A MACROPOROUS CATION-EXCHANGE RESIN IN HYDROCHLORIC ACID-ACETONE MEDIUM

FRANZ W. E. STRELOW

National Chemical Research Laboratory, Council for Scientific and Industrial Research, P.O. Box 395, Pretoria, 0001 Republic of South Africa

(Received 3 October 1987. Accepted 10 November 1987)

**Summary**—Distribution coefficients with the macroporous cation-exchange resin AG MP-50 in HCl-acetone mixtures ranging from 0.2 to 4.0M HCl and from 0 to 95% acetone have been determined for 46 elements. The ion-exchange behaviour of the elements is discussed, some possible separations are indicated, and elution curves demonstrating separations of the combinations Au(III)-Bi-Zn-Pb-Sr; Rh(III)-In-Ga-Cu-Ni and Cd-Fe(III)-Li-Al-Yb are presented.

For the planning of ion-exchange separations systematic information (in the form of tables) about distribution coefficients is of great value. In the case of gel-type microporous cation-exchangers such information is available for aqueous HCl,<sup>1,2</sup> HNO<sub>3</sub>,<sup>3</sup> H<sub>2</sub>SO<sub>4</sub>,<sup>3</sup> HBr,<sup>4,5</sup> HClO<sub>4</sub>,<sup>2,6</sup> HCl-HClO<sub>4</sub> mixtures,<sup>7</sup> HF,<sup>8,9</sup> HF-HNO<sub>3</sub> mixtures,<sup>10</sup> HF-H<sub>2</sub>SO<sub>4</sub> mixtures,<sup>10</sup> HF-H<sub>3</sub>BO<sub>3</sub> mixtures,<sup>11</sup> acetic acid<sup>12</sup> and tartaric acid or tartrate media<sup>13-15</sup> as well as for HCl-ethanol,<sup>16</sup> HCl-acetone,<sup>17-19</sup> HBr-acetone<sup>4,20</sup> and various other systems. For the so-called macroporous or macroporous cation-exchangers this kind of systematic information is to a large extent lacking. The early work of Fritz and Kawazu and their co-workers,<sup>21-23</sup> who used a macroporous resin to minimize resin-volume changes during high-pressure liquid chromatography, and HCl-organic solvent mixtures to elute elements having tendencies to chloride-complex formation, contains only limited information. The coefficients published relate almost entirely to a few elements with medium strong chloride-complex formation tendencies, and to use of acetone media.

Marsh *et al.*<sup>24</sup> have published a study of distribution coefficients for 53 elements with a microporous resin in nitric acid. Unfortunately, the results are presented as percentage of sorption, in the form of small graphs without experimental points, and allow only an approximate estimation of the actual values of the coefficients. This is not very satisfactory for estimating optimum conditions for critical separations. Studies of distribution coefficients and the ion-exchange behaviour of 46 elements with a microporous resin in aqueous hydrochloric acid<sup>25</sup> and for 46 elements in hydrochloric acid-methanol mixtures<sup>26</sup> were published earlier, and numerical values of the coefficients were given.

Acetone, because of its lower dielectric constant,

promotes chloride-complex formation considerably more strongly than does methanol and therefore should provide conditions favourable for separations at considerably lower solvent or hydrochloric acid concentrations. In addition, cation-exchange separations of many elements with relatively weak tendencies to chloride-complex formation, which are difficult or impossible with HCl-methanol mixtures, are greatly facilitated and often become very easy. Since no comprehensive study of distribution coefficients and exchange behaviour of cations with a macroporous cation-exchange resin in HCl-acetone mixtures (or other low dielectric constant solvents) seems to be available at present, the results of such a study are presented here.

### EXPERIMENTAL

#### Reagents

The AG MP-50 macroporous sulphonated polystyrene cation-exchanger (100-200 mesh) marketed by Bio-Rad Laboratories, Richmond, California, was used. The resin as received was found to contain appreciable amounts of calcium (about 1 mg/g of dry resin). For purification it was packed into large columns (3 cm diameter) and then washed with 5M nitric acid until the effluent was free from calcium. All water was distilled and, for further purification, passed through an Elgastat demineralizer. Only chemicals of analytical-reagent quality were used.

Standard solutions were mainly prepared from the chlorides of the elements, but the nitrates were used for Hg(II), Pb(II), U(VI) and Ti(I), and for Sc, Y and the lanthanides the oxides were dissolved and converted into the dry chlorides. Gold and platinum metals were dissolved in *aqua regia*, a pressure bomb lined with Teflon being used for dissolving Rh and Ir, to yield Rh(III) and Ir(III/IV). Most standard solutions were made up in 5.0M hydrochloric acid, but for the alkali metals only the 2.5M acid was used. The Ti(IV) solution was prepared in 2.5M hydrochloric acid and V(V), Mo(VI) and W(VI) solutions were made up in 0.5M hydrochloric acid, all four with hydrogen peroxide added for stabilization.

### Equipment

Borosilicate glass tubes (16.5 mm bore, length about 400 mm) were used as columns, fitted with a No. 1 porosity sintered-glass disc and a burette tap at the bottom, and a B19 joint at the top. The columns were filled with a slurry of the AG MP-50 resin in the hydrogen form to give a bed volume of 27 ml of settled resin, corresponding to 10 g of dry resin. The resin was purified by passage of about 500 ml of 5M nitric acid at a flow-rate of 2–3 ml/min, followed by 100 ml of demineralized water.

Atomic-absorption measurements were made with a Varian-Techtron AA-5 instrument, with air-acetylene or nitrous oxide-acetylene flames. A Zeiss PMQII instrument was used for spectrophotometric measurements.

### Distribution coefficients

The cleaned resin was dried in a vacuum pistol with magnesium perchlorate (anhydrous) and kept over anhydrous in a desiccator. Residual water was determined by drying at 120° and the weights of resin were corrected accordingly.

Distribution coefficients were determined by equilibrating 2.500 g of dry resin in the hydrogen form with 250 ml of solution by shaking for 24 hr at  $20 \pm 1^\circ$  in a mechanical shaker. The solutions contained 2 meq of the cation and the concentrations of hydrochloric acid and acetone indicated in the tables. For example, "0.5M HCl containing 80% acetone" was prepared by mixing 12.5 ml of 10M hydrochloric acid with 27.5 ml of water, 200 ml of acetone and 10 ml of standard solution (added last). Volume changes on mixing were disregarded. When the standard solution already contained free acid, the amounts of 10M acid and water used were adjusted accordingly. In a few cases [Pb(II), Tl(I), Bi(III) and Sb(III)] amounts smaller than 2 meq were used because of the limited solubility of these ions in chloride media.

After equilibration, the resin was separated by filtration and the amounts of the element in the aqueous and resin phases were determined. In most cases filtration was done with a sintered-glass plate in a glass column and the element retained was eluted with a suitable reagent. In some cases, when quantitative elution of an element appeared difficult (Th, Zr, Hf, Sc, lanthanides and Ba) a filter paper was used, the resin was ashed and the ash either dissolved for subsequent analysis or weighed directly after ignition at a

suitable temperature. From the results, the equilibrium distribution coefficients<sup>1</sup> were calculated.

### Elution curves

In order to explore the separation possibilities of HCl-acetone mixtures with the macroporous resin, elution curves of some multi-element mixtures were prepared.

**Separation of Au(III)-Bi-Zn-Pb-Sr** (Fig. 1). A solution containing about 0.2 mmole of each element in 50 ml of 0.2M hydrochloric acid was loaded on the column of 27 ml (10 g) of the purified resin (H+ form), followed by small portions of 0.2M hydrochloric acid, and the gold(III) eluted with a total of 100 ml of the same acid. Then bismuth was eluted with 150 ml of 0.5M HCl in 30% acetone, zinc with 150 ml of 0.50M HCl in 60% acetone, lead with 150 ml of 1.0M HCl in 80% acetone and strontium with 150 ml of aqueous 5M HNO<sub>3</sub>. The flow-rate was  $2.5 \pm 0.5$  ml/min throughout. Fractions (10 ml in volume) were collected with an automatic fraction-collector from the beginning of the sorption step, because gold is not sorbed and passes through. The elements in the fractions were determined by flame atomic-absorption spectrometry after evaporation of the organic solvents, dissolution and dilution as required.

**Separation of Rh(III)-In-Ga-Cu-Ni** (Fig. 2). A mixture of 0.3 mmole of rhodium(III) and 0.2 mmole each of indium, gallium, copper and nickel was separated by the procedure just described, and the elution sequence 100 ml of 0.20M aqueous HCl for rhodium; 150 ml of 0.50M HCl in 60% acetone for indium; 150 ml of 0.50M HCl in 75% acetone for gallium; 150 ml of 0.50M HCl in 90% acetone for copper, and 150 ml of aqueous 3.0M HCl for nickel. Again fractions were collected starting from the beginning of the sorption step and flame atomic-absorption spectrometry was used for determination of all the elements.

**Separation of Cd-Fe(III)-Li-Al-Yb** (0.2 mmole of each), Fig. 3. Sorption took place from 50 ml of 0.05M HCl in this case, and the elements were washed into the resin with the same reagent. The elution sequence was 150 ml of 0.20M HCl in 70% acetone for cadmium; 150 ml of 0.50M HCl in 80% acetone for iron(III); 150 ml of 1.00M aqueous HCl for lithium; 150 ml of 3.0M HCl in 20% acetone for aluminium and 150 ml of aqueous 6.0M HCl for ytterbium. The fractions (10 ml) were taken from the start of the elution step. Again flame atomic-absorption spectrometry was used for determination of the elements.

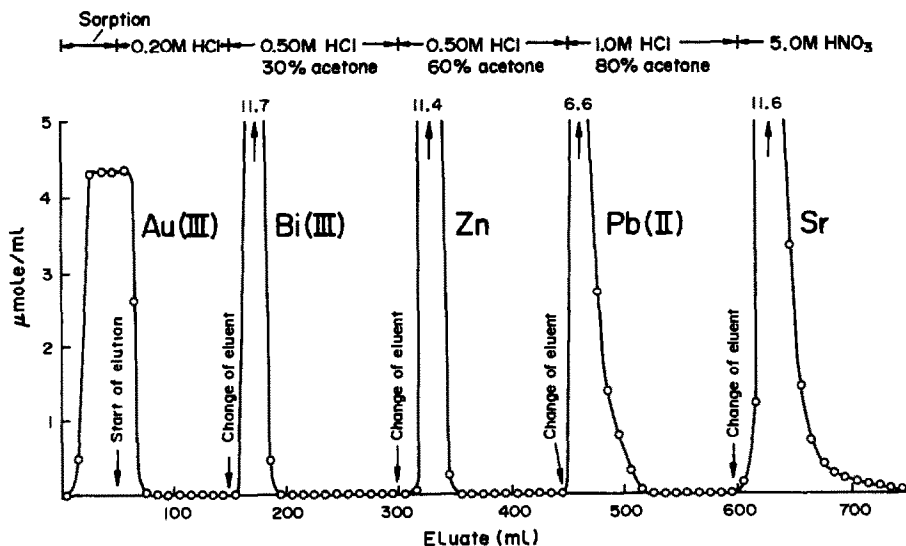


Fig. 1. Elution curve for Au(III)-Bi-Zn-Pb-Sr. Column of 27 ml (10 g) of AG MP-50 resin, 100–200 mesh,  $127 \times 16.5$  mm. Flow-rate  $2.5 \pm 0.5$  ml/min; 0.2 mmole of each element.

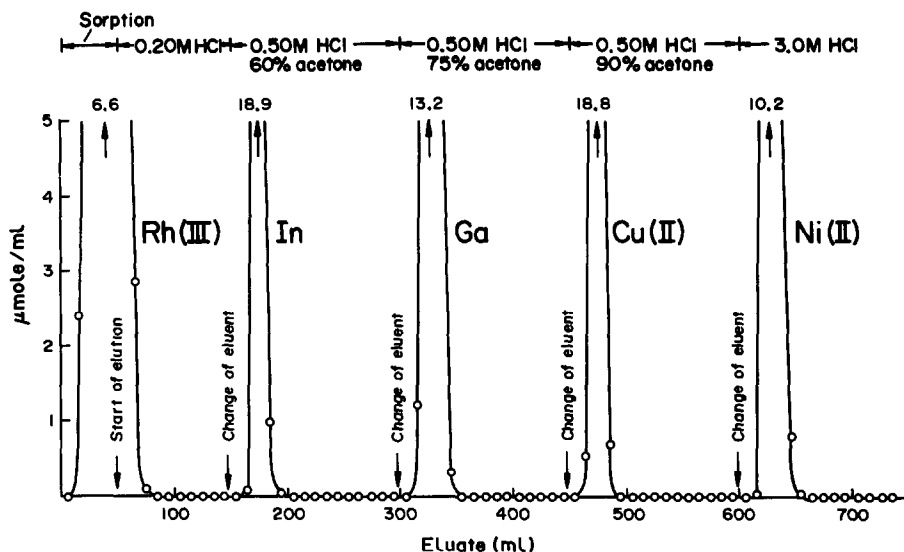


Fig. 2. Elution curve for Rh(III)-In-Ga-Cu(II)-Ni. Column and flow-rate similar to those for Fig. 1; 0.3 mmole of Rh and 0.2 mmole of each other element.

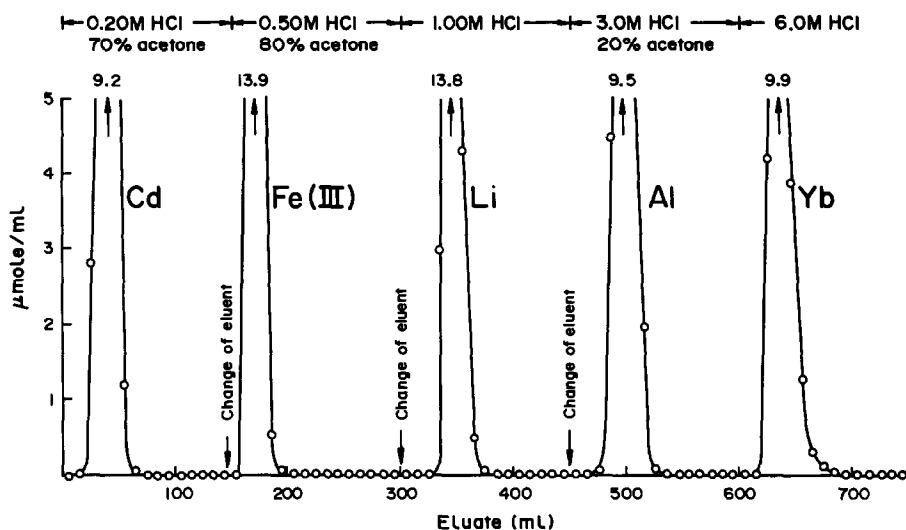


Fig. 3. Elution curve for Cd-Fe(III)-Li-Al-Yb. Column and flow-rate similar to those for Fig. 1; 0.2 mmole of each element.

## RESULTS AND DISCUSSION

The results for the distribution coefficients are shown in Tables 1-6, in each of which the ions are arbitrarily arranged according to their distribution coefficients in aqueous solution, except for Sb(III), which is given last because it is believed that its distribution is partially due (high values in Tables 1 and 2) to effects other than ion-exchange, probably precipitation inside the resin pores, where the hydrochloric acid concentration is lower than that outside.

The cation-exchange distribution coefficients generally decrease with increasing acid concentration from 0.20 to 4.00M HCl and they increase with increasing acetone concentration until the hydration

field around the cation is weakened sufficiently to allow replacement of the water molecules in the co-ordination shell by chloride ions. This causes a sudden decrease in the value of the coefficients on further increase in acetone concentration. In the HCl-acetone mixtures, this decrease takes place at considerably lower HCl and/or solvent concentrations than in the corresponding HCl-methanol mixtures,<sup>26</sup> because acetone, owing to its lower dielectric constant, promotes chloride-complex formation much more effectively. Numerous separations of ion-pairs such as Fe(III)-Cu(II), Cu(II)-Co(II), and Co(II)-Mn(II), which are difficult or even impossible with a macroporous resin in HCl-methanol mixtures, therefore become easy with HCl-acetone.

Table 1. Distribution coefficients with AG MP-50 resin in 0.2M HCl with various amounts of acetone

Species	Acetone, %						
	0	20	40	60	80	90	95
Th	>10 <sup>5</sup>	>10 <sup>5</sup>	>10 <sup>5</sup>	>10 <sup>5</sup>	>10 <sup>5</sup>	>10 <sup>5</sup>	>10 <sup>5</sup>
Zr	>10 <sup>5</sup>	>10 <sup>5</sup>	>10 <sup>5</sup>	>10 <sup>5</sup>	>10 <sup>5</sup>	4.30 × 10 <sup>4</sup>	3000
Hf	>10 <sup>5</sup>	>10 <sup>5</sup>	>10 <sup>5</sup>	>10 <sup>5</sup>	>10 <sup>5</sup>	8.00 × 10 <sup>4</sup>	5800
La	>10 <sup>5</sup>	>10 <sup>5</sup>	>10 <sup>5</sup>	>10 <sup>5</sup>	>10 <sup>5</sup>	>10 <sup>5</sup>	>10 <sup>5</sup>
Sc	>10 <sup>5</sup>	>10 <sup>5</sup>	>10 <sup>5</sup>	>10 <sup>5</sup>	>10 <sup>5</sup>	>10 <sup>5</sup>	>10 <sup>5</sup>
Y	~6.00 × 10 <sup>4</sup>	>10 <sup>5</sup>	>10 <sup>5</sup>	>10 <sup>5</sup>	>10 <sup>5</sup>	>10 <sup>5</sup>	>10 <sup>5</sup>
Yb	~6.00 × 10 <sup>4</sup>	~10 <sup>5</sup>	>10 <sup>5</sup>	>10 <sup>5</sup>	>10 <sup>5</sup>	>10 <sup>5</sup>	>10 <sup>5</sup>
Ba	2.80 × 10 <sup>4</sup>	5.00 × 10 <sup>4</sup>	~10 <sup>5</sup>	>10 <sup>5</sup>	>10 <sup>5</sup>	>10 <sup>5</sup>	>10 <sup>5</sup>
Pb(II)*	2.30 × 10 <sup>4</sup>	3.30 × 10 <sup>4</sup>	3.00 × 10 <sup>4</sup>	8.90 × 10 <sup>3</sup>	137	3.4	3.5
Ga	1.50 × 10 <sup>4</sup>	3.00 × 10 <sup>4</sup>	~10 <sup>5</sup>	~10 <sup>5</sup>	19.4	2.1	2.2
Al	1.10 × 10 <sup>4</sup>	2.20 × 10 <sup>4</sup>	5.60 × 10 <sup>4</sup>	>10 <sup>5</sup>	>10 <sup>5</sup>	>10 <sup>5</sup>	>10 <sup>5</sup>
Fe(III)	6.60 × 10 <sup>3</sup>	9.00 × 10 <sup>3</sup>	2.20 × 10 <sup>4</sup>	3.30 × 10 <sup>3</sup>	27.1	2.1	5.2
Sr	5.70 × 10 <sup>3</sup>	1.10 × 10 <sup>4</sup>	>10 <sup>4</sup>	>10 <sup>4</sup>	>10 <sup>4</sup>	>10 <sup>4</sup>	>10 <sup>4</sup>
Ca	3.70 × 10 <sup>3</sup>	7.20 × 10 <sup>3</sup>	>10 <sup>4</sup>	>10 <sup>4</sup>	>10 <sup>4</sup>	>10 <sup>4</sup>	>10 <sup>4</sup>
Tl(I)†	1.26 × 10 <sup>3</sup>	1.75 × 10 <sup>3</sup>	2.62 × 10 <sup>3</sup>	3.09 × 10 <sup>3</sup>	1540	1168	558
Bi(III)‡	1.79 × 10 <sup>3</sup>	486	60	41	2.2	1.9	1.8
Mn(II)	1.07 × 10 <sup>3</sup>	1.93 × 10 <sup>3</sup>	4.70 × 10 <sup>3</sup>	1.00 × 10 <sup>4</sup>	1.20 × 10 <sup>4</sup>	2.54 × 10 <sup>3</sup>	147
U(VI)	970	1.64 × 10 <sup>3</sup>	3.25 × 10 <sup>3</sup>	5.10 × 10 <sup>3</sup>	920	25.1	3.7
Cu(II)	740	1.21 × 10 <sup>3</sup>	2.09 × 10 <sup>3</sup>	4.01 × 10 <sup>3</sup>	500	11.4	1.9
Fe(II)	710	1.27 × 10 <sup>3</sup>	3.20 × 10 <sup>3</sup>	7.30 × 10 <sup>3</sup>	1.85 × 10 <sup>3</sup>	11.4	1.5
Zn	690	1.12 × 10 <sup>3</sup>	1.25 × 10 <sup>3</sup>	89	3.4	1.6	1.8
Co(II)	670	1.08 × 10 <sup>3</sup>	2.65 × 10 <sup>3</sup>	5.60 × 10 <sup>3</sup>	7.60 × 10 <sup>3</sup>	287	9.8
Ni(II)	580	770	1.06 × 10 <sup>3</sup>	1.75 × 10 <sup>3</sup>	1.91 × 10 <sup>3</sup>	1.93 × 10 <sup>3</sup>	1.11 × 10 <sup>3</sup>
Mg	469	790	1.81 × 10 <sup>3</sup>	4.93 × 10 <sup>3</sup>	7.11 × 10 <sup>3</sup>	5.80 × 10 <sup>3</sup>	5.80 × 10 <sup>3</sup>
Sn(IV)	385	81	16.9	1.9	2.0	2.0	1.8
Be	307	398	640	1.09 × 10 <sup>3</sup>	1.18 × 10 <sup>3</sup>	790	620
In	286	216	128	31.5	1.9	1.8	1.9
V(IV)	236	366	720	1.53 × 10 <sup>3</sup>	1.82 × 10 <sup>3</sup>	720	203
Cs	228	340	650	1.18 × 10 <sup>3</sup>	2.27 × 10 <sup>3</sup>	2.75 × 10 <sup>3</sup>	2.38 × 10 <sup>3</sup>
Rb	201	321	660	1.30 × 10 <sup>3</sup>	2.50 × 10 <sup>3</sup>	3.00 × 10 <sup>3</sup>	2.60 × 10 <sup>3</sup>
Ti(IV)¶	197	339	810	2.00 × 10 <sup>3</sup>	2.70 × 10 <sup>3</sup>	2.80 × 10 <sup>3</sup>	2.20 × 10 <sup>3</sup>
Cd	171	203	152	12.9	2.0	2.0	2.1
K	165	294	560	1.71 × 10 <sup>3</sup>	4.10 × 10 <sup>3</sup>	4.80 × 10 <sup>3</sup>	4.30 × 10 <sup>3</sup>
Na	64	105	199	560	1.27 × 10 <sup>3</sup>	1.44 × 10 <sup>3</sup>	1.41 × 10 <sup>3</sup>
Li	22.3	33.3	61	110	201	283	337
Te(IV)	15.5	22.6	38.2	55	2.5	1.6	1.6
Au(III)	2.2	1.2	1.3	0.8	1.1	0.8	0.7
Rh(III) #	1.8	1.4	1.7	1.5	1.6	1.5	2.3
Ir(III/IV) #	1.8	1.6	1.8	2.2	2.1	1.5	2.2
Pd(II) #	1.8	2.6	1.8	1.6	1.6	1.7	1.4
Pt(IV) #	1.1	0.8	1.2	0.9	1.1	0.7	1.0
Tl(III)	0.9	1.0	1.0	0.8	0.7	0.6	0.6
W(VI)**	0.8	0.7	0.9	0.9	0.7	0.8	0.9
Mo(VI)**	0.5	0.4	0.6	0.5	0.4	0.3	0.4
V(V)††	0.4	0.5	0.9	2.0	4.1	2.4	1.7
Hg(II)							
As(III)							
As(V)							
Se(IV)							
Sb(III)*	464	580	540	6.5	1.1	0.9	1.4

\*0.2 mmole.

†0.05 mmole.

‡0.1 mmole.

§Visible precipitation.

¶0.5 mmole, 0.3% H<sub>2</sub>O<sub>2</sub>.

# Equilibration time, 2 hr.

\*\*0.3% H<sub>2</sub>O<sub>2</sub>.††0.3% H<sub>2</sub>O<sub>2</sub>, 2 hr equilibration time.

As with the 8% cross-linked microporous resin used earlier,<sup>18</sup> some elements with quite strong tendencies to chloride-complex formation, such as Hg(II), Au(III), Tl(III), Rh(III), Pd(II), Pt(IV) and Ir(III/IV), show little or no sorption over the whole range of acetone concentrations at the lowest HCl concentration. The same applies to elements which tend to form oxyanions, e.g., Mo(VI), W(VI), V(V), As(III) and As(V). The first three of these require the presence of hydrogen peroxide for stabilization, and V(V) shows signs of some reduction to V(IV) at a concentration of 60% or more acetone, even when

the equilibration time is reduced to 2 hr. Bi(III), Cd, In and Sn(IV), which also form relatively stable chloride complexes, are strongly sorbed from 0.2M HCl and only weakly from 0.5M HCl. Their distribution coefficients decrease with increase of concentration of acetone. The relatively large distribution coefficient for Sn(IV) in aqueous 0.2M HCl could be partially due to hydrolysis inside the resin pores, because of the strong tendency of this ion to hydrolyse. The distribution coefficients of many other elements with medium or low tendency to form chloride complexes show an initial increase with

Table 2. Distribution coefficients with AG MP-50 resin in 0.5M HCl with various amounts of acetone

Species	Acetone, %					
	0	20	40	60	80	90
Th	> 10 <sup>5</sup>	> 10 <sup>5</sup>	> 10 <sup>5</sup>	> 10 <sup>5</sup>	> 10 <sup>5</sup>	> 10 <sup>5</sup>
Zr	> 10 <sup>5</sup>	> 10 <sup>5</sup>	> 10 <sup>5</sup>	> 10 <sup>5</sup>	> 10 <sup>5</sup>	4.90 × 10 <sup>3</sup>
Hf	~ 10 <sup>5</sup>	> 10 <sup>5</sup>	> 10 <sup>5</sup>	> 10 <sup>5</sup>	> 10 <sup>5</sup>	8.70 × 10 <sup>3</sup>
La	6.80 × 10 <sup>4</sup>	> 10 <sup>5</sup>	> 10 <sup>5</sup>	> 10 <sup>5</sup>	> 10 <sup>5</sup>	> 10 <sup>5</sup>
Sc	1.80 × 10 <sup>4</sup>	3.70 × 10 <sup>4</sup>	8.00 × 10 <sup>4</sup>	> 10 <sup>5</sup>	> 10 <sup>5</sup>	> 10 <sup>5</sup>
Y	7.40 × 10 <sup>3</sup>	1.70 × 10 <sup>4</sup>	> 10 <sup>4</sup>	> 10 <sup>4</sup>	> 10 <sup>4</sup>	> 10 <sup>4</sup>
Yb	7.10 × 10 <sup>3</sup>	1.50 × 10 <sup>4</sup>	3.00 × 10 <sup>4</sup>	~ 10 <sup>5</sup>	> 10 <sup>5</sup>	> 10 <sup>5</sup>
Ba	4.80 × 10 <sup>3</sup>	8.40 × 10 <sup>3</sup>	1.60 × 10 <sup>4</sup>	3.10 × 10 <sup>4</sup>	6.30 × 10 <sup>4</sup>	~ 10 <sup>5</sup>
Pb(II)*	1.39 × 10 <sup>3</sup>	1.59 × 10 <sup>3</sup>	1.07 × 10 <sup>3</sup>	219	4.6	2.1
Sr	990	1.89 × 10 <sup>3</sup>	5.40 × 10 <sup>3</sup>	> 10 <sup>4</sup>	> 10 <sup>4</sup>	> 10 <sup>4</sup>
Ga	890	1.64 × 10 <sup>3</sup>	4.35 × 10 <sup>3</sup>	610	1.8	2.6
Fe(III)	810	980	1.79 × 10 <sup>3</sup>	378	2.3	1.9
Al	720	1.44 × 10 <sup>3</sup>	3.40 × 10 <sup>3</sup>	9.10 × 10 <sup>3</sup>	1.10 × 10 <sup>4</sup>	6.60 × 10 <sup>3</sup>
Ca	640	1.26 × 10 <sup>3</sup>	3.30 × 10 <sup>3</sup>	8.50 × 10 <sup>3</sup>	> 10 <sup>4</sup>	> 10 <sup>4</sup>
Ti(I)†	345	435	560	590	178	59
U(VI)	201	314	520	610	54	3.3
Mn(II)	172	293	630	1.37 × 10 <sup>3</sup>	1.33 × 10 <sup>3</sup>	54
Cu(II)	117	179	311	338	22.7	1.7
Fe(II)	116	198	413	860	101	0.7
Co(II)	108	188	410	920	540	5.6
Cs	102	149	259	488	860	800
Ni(II)	101	158	251	415	459	320
Zn	101	128	40.2	3.2	1.8	1.6
Rb	89	138	253	498	910	1.01 × 10 <sup>3</sup>
Mg	88	139	284	700	1.19 × 10 <sup>3</sup>	1.08 × 10 <sup>3</sup>
K	75	136	279	820	1.98 × 10 <sup>3</sup>	1.91 × 10 <sup>3</sup>
Be	51	52	72	109	159	162
V(IV)	42.2	62	119	230	254	74
Ti(IV)§	36.0	59	129	349	740	1.04 × 10 <sup>3</sup>
Na	28.3	49.6	98	260	378	380
Cd	15.2	14.9	5.4	2.0	2.1	1.9
Bi(III)‡	10.5	5.8	4.3	3.1	1.9	1.6
In	10.1	7.5	5.0	2.2	2.2	2.1
Li	9.8	13.9	23.2	49.1	84	130
Te(IV)	5.5	7.9	10.9	8.2	1.5	1.3
Sn(IV)	5.0	3.1	2.1	1.9	1.7	1.8
Au(III)	1.3	1.4	1.1	0.8	0.9	0.7
Rh(III)¶	1.3	1.5	1.4	1.2	1.4	1.7
Ir(III/IV)¶	1.2	1.3	1.4	1.1	1.4	1.5
Pd(II)¶	1.2	1.4	1.2	1.3	1.4	1.1
Pt(IV)¶	1.0	0.8	0.9	1.0	0.7	0.8
Tl(III)	0.7	0.9	0.8	0.7	0.6	0.5
W(VI) #	0.7	0.8	0.8	0.7	0.6	1.0
V(V)**	0.5	0.6	0.7	1.2	2.3	2.2
Mo(VI) #	0.4	0.4	0.3	0.4	0.3	0.4
Hg(II)						
As(III)						
As(V)	< 0.5	< 0.5	< 0.5	< 0.5	< 0.5	< 0.5
Se(IV)						
Sb(III)*	218	135	1.0	1.2	1.1	0.7

\*0.2 mmole.

†0.05 mmole.

§0.5 mmole, 0.3% H<sub>2</sub>O<sub>2</sub>.

‡0.1 mmole.

¶Equilibration time, 2 hr.

# 0.3% H<sub>2</sub>O<sub>2</sub>.\*\*0.3% H<sub>2</sub>O<sub>2</sub>, 2 hr equilibration time.

increasing concentration of acetone but a decrease at still higher acetone concentrations. The position of the maximum is a good indication of the tendency of the cation to chloride-complex formation in acetone. Even ions with rather small or negligible tendencies to chloride-complex formation, such as Zr, Hf, Al, Be and Ni, show a slight decrease in distribution coefficient in 0.2 and 0.5M HCl at the highest acetone concentrations. At higher acid concentration (> 1M) these ions mostly show an increase in distribution coefficient with increase in acetone concentration.

Some ions such as Ca, Sr, Ba, Pb, Sc, Th and the

lanthanides have much larger distribution coefficients with the macroporous resin than with the micro-porous resin. The values can increase by factors ranging from 3 to about 20 (Pb) which stretches the selectivity scale considerably. Some of these ions, e.g., Pb, U(VI), Sc and the heavy alkali-metals, change their position in the selectivity sequence compared with that obtained on a gel-type resin. As a result zinc and lead can easily be separated with the macroporous resin in HCl-acetone (Fig. 1), a separation which is not possible with a gel-type resin, with which their distribution coefficients in HCl-acetone do not show much difference.

Table 3. Distribution coefficients with AG MP-50 resin in 1.0M HCl with various amounts of acetone

Species	Acetone, %				
	0	20	40	60	80
Th	$4.40 \times 10^4$	$9.40 \times 10^4$	$> 10^5$	$> 10^5$	$> 10^5$
Zr	$1.90 \times 10^4$	$5.30 \times 10^4$	$> 10^5$	$> 10^5$	$6.00 \times 10^4$
Hf	$5.60 \times 10^3$	$1.60 \times 10^4$	$4.20 \times 10^4$	$> 10^5$	$> 10^5$
La	$4.50 \times 10^3$	$9.8 \times 10^3$	$2.80 \times 10^4$	$\sim 10^5$	$> 10^5$
Sc	$2.18 \times 10^3$	$5.4 \times 10^3$	$1.50 \times 10^4$	$4.40 \times 10^4$	$\sim 10^5$
Ba	$1.18 \times 10^3$	$2.82 \times 10^3$	$6.80 \times 10^3$	$1.60 \times 10^4$	$3.80 \times 10^4$
Y	740	$1.26 \times 10^3$	$2.70 \times 10^3$	$7.90 \times 10^3$	$> 10^4$
Yb	710	$1.54 \times 10^3$	$5.40 \times 10^3$	$1.60 \times 10^4$	$2.10 \times 10^4$
Sr	233	440	$1.38 \times 10^3$	$6.5 \times 10^3$	$> 10^4$
Ca	154	276	670	$1.88 \times 10^3$	$7.10 \times 10^3$
Ga	118	202	429	7.4	2.0
Tl(I)*	101	118	134	116	107
Pb(II)†	100	91	50	8.9	1.8
Al	89	165	550	$1.04 \times 10^3$	$1.44 \times 10^3$
Fe(III)	87	111	138	10.9	1.4
U(VI)	67	101	143	124	3.7
Cs	53	74	120	209	326
Mn(II)	45.6	75	147	287	103
Rb	44.8	75	123	243	401
K	36.9	61	128	285	321
Co(II)	30.0	48.9	95	193	14.3
Fe(II)	29.0	47.7	91	156	1.5
Cu(II)	27.7	41.4	61	39.9	1.7
Ni(II)	27.5	47.3	76	128	142
Mg	23.8	37.8	76	186	314
Zn	19.7	13.6	2.4	1.5	1.5
Be	14.5	14.9	20.0	29.2	54
Na	14.4	23.0	48.4	106	155
V(IV)	12.1	17.1	30.4	58	38.0
Ti(IV)§	10.7	18.4	40.0	113	426
Li	5.1	7.6	12.1	21.5	44.2
Te(IV)	2.5	2.9	3.8	2.9	1.4
Cd	2.1	1.8	1.1	0.6	0.7
Bi(III)‡	1.6	1.2	1.0	0.9	0.9
In	1.4	1.6	1.2	0.9	0.8
Sn(IV)	1.1	1.3	1.2	1.0	1.1
W(VI)¶	0.7	0.8	0.6	0.6	0.7
V(V)‡	0.4	0.5	0.6	1.1	1.2
Mo(VI)¶	0.4	0.3	0.3	0.3	0.4
Hg(II)	} <0.5	<0.5	<0.5	<0.5	<0.5
As(III)					
As(V)					
Se(IV)					
Sb(III)†	1.1	1.2	0.9	0.7	0.7

\*0.05 mmole.

†0.2 mmole.

§0.5 mmole, 0.3% H<sub>2</sub>O<sub>2</sub>.

‡0.1 mmole.

¶0.3% H<sub>2</sub>O<sub>2</sub>.# 0.3% H<sub>2</sub>O<sub>2</sub>, 2 hr equilibration time.

### Summary of ion-exchange behaviour

**Alkali metals.** All the distribution coefficients and especially those of lithium increase with increasing acetone concentration faster than they do with methanol concentration. For this reason methanol is a better organic solvent for separating lithium from sodium or the heavier alkali metals. A separation factor of  $\alpha_{Li}^{Na} = 6$  can nevertheless be obtained in 2.0M HCl containing 60% acetone, which is better than  $\alpha_{Li}^{Na} = 5$  in 1.0M HCl containing 80% methanol with a gel-type AG50W-X8 resin. Elements with relatively strong tendencies to chloride-complex for-

mation [Zn, Cd, In, Bi(III), Sn(IV) and Tl(III)] can be separated by elution with 0.2M HCl in 85% acetone, whereas the alkali metals are strongly retained ( $D_{Li} = 245$ ). For the elution of Au(III), Tl(III), Hg(II), As(III), Se(IV) and the platinum metals, 0.1M HCl in 90% acetone is quite satisfactory; lithium ( $D > 500$ ) is even more strongly retained under these conditions.

**Beryllium, magnesium and the alkaline-earth metals.** Distribution coefficients for all five increase with acetone concentration and follow the same pattern as observed for HCl-methanol mixtures.<sup>26</sup> When beryllium is eluted with 2.0M HCl in 60% acetone, Mg,



Table 4. Distribution coefficients with AG MP-50 resin in 2.0M HCl with various amounts of acetone

Species	Acetone, %				
	0	20	30	60	70
Th	$1.00 \times 10^4$	$2.60 \times 10^4$	$5.30 \times 10^4$	$7.80 \times 10^4$	$9.00 \times 10^4$
Zr	800	$2.12 \times 10^3$	$6.80 \times 10^3$	$2.80 \times 10^4$	$8.80 \times 10^3$
La	481	752	$1.32 \times 10^3$	$3.20 \times 10^3$	$5.70 \times 10^3$
Hf	447	$1.24 \times 10^3$	$4.20 \times 10^3$	$1.20 \times 10^4$	$1.20 \times 10^4$
Sc	287	720	$2.35 \times 10^3$	$8.60 \times 10^3$	$1.80 \times 10^4$
Ba	282	635	$1.93 \times 10^3$	$5.40 \times 10^3$	$1.04 \times 10^4$
Y	97	165	345	950	$1.72 \times 10^3$
Yb	83	156	424	$1.41 \times 10^3$	$2.40 \times 10^3$
Sr	74	135	321	920	$1.75 \times 10^3$
Ca	50	84	173	510	$1.05 \times 10^3$
Cs	24.2	31.9	48.8	81	108
U(VI)	24.1	30.0	38.0	11.1	2.4
Ti(I)*	20.6	23.3	19.3	13.1	11.2
Rb	20.1	29.7	49.0	99	133
K	16.9	31.9	66	135	151
Ga	15.4	24.5	16.5	1.9	1.5
Al	14.4	21.3	51	138	198
Mn(II)	11.5	18.1	31.5	54	25.3
Fe(III)	10.1	11.4	9.3	6.1	2.3
Na	8.3	13.4	26.9	63	99
Co(II)	7.1	10.7	18.9	22.3	3.1
Fe(II)	7.1	10.9	16.9	2.7	1.2
Mg	7.0	10.1	18.6	46.2	74
Ni(II)	6.9	11.9	19.4	38.9	55
Cu(II)	5.7	6.7	6.4	1.7	1.8
Pb(II)†	4.9	3.8	2.3	1.1	1.1
Be	4.5	5.2	7.7	12.5	16.1
Ti(IV)‡	3.9	6.9	14.8	46.2	110
V(IV)	3.8	5.2	8.7	16.5	15.8
Li	2.6	3.4	5.3	10.6	15.4
Zn	1.8	1.1	0.9	1.3	1.1
Cd	1.4	1.0	0.7	0.5	0.6
In	1.2	1.3	0.9	0.7	0.8

\*0.05 mmole.

†0.2 mmole.

‡0.5 mmole, 0.3% H<sub>2</sub>O<sub>2</sub>.

Ca, Sr, Ba, Ni, Mn(II), Na, K, Rb, Cs, Al, Sc, Y, the lanthanides, Ti, Zr, Hf and Th will be retained, but the separations of some of these elements from beryllium are not as good as in HCl-methanol and fairly large columns are required for these. Cobalt(II) and U(VI) accompany beryllium. Zn, Cd, In, Bi, Sn(IV), Te(IV), Hg(II), Au(III), Pd(II), Rh(III), Ir(III), Tl(III), As(III) and Se(IV) can be eluted very easily with 0.2M HCl in 85% acetone, and Be and the alkaline-earth ions are retained very strongly. This separation is more effective than the corresponding one in HCl-methanol and can be carried out on much smaller columns.

*Cu(II), Fe(II), Co(II), Mn(II), Ni(II).* All five show some degree of chloride-complex formation in dilute HCl at high acetone concentrations. The tendency to form chloride complexes is relatively strong for Cu(II) and Fe(II) whereas that for Ni(II) is almost negligible. Copper(II), Fe(II) and Co(II) can be eluted with 0.5M HCl in 90% acetone, while Mn(II) and Ni(II) are retained together with many other ions, including Li and the other alkali-metal ions, Be and the alkaline-earth metal ions, Ti(IV), V(IV), Al, Sc, Y, the lanthanides and other species not forming chloride complexes. Zn, Cd, In and the other ions

named above, which form stable chloride complexes, can be eluted easily with 0.2M HCl in 85% acetone or with 0.5M HCl in 65% acetone, while copper(II) and the other metal ions are strongly retained. With 0.2M HCl in 92% acetone copper(II) can be eluted while Co(II) is retained together with Mn(II) and Ni(II). All five ions can be eluted effectively with 4.0M HCl in 45% acetone while Ca, Sr, Ba, Sc, Y, Zr, Hf, Th and the lanthanides are retained.

*Sc, Yb, La, Zr, Hf, Th.* All are very strongly sorbed and show considerably increased distribution coefficients with increasing concentration of acetone. Zr and to a lesser degree Hf, show a slight tendency towards decreased distribution coefficients at the highest acetone concentration, indicating some chloride-complex formation. Th and Sc cannot be eluted by hydrochloric acid of any concentration and elution of the light lanthanides is very difficult and prolonged. Mixtures of a good replacing cation and a complexing agent such as ammonium acetate plus EDTA or DPTA are required for effective elution of these elements, as has been demonstrated for the very strongly adsorbed scandium.<sup>25</sup> As has been pointed out, the selectivity scale for the lanthanides from ytterbium to lanthanum is considerably larger for the

Table 5. Distribution coefficients with AG MP-50 resin in 3.0M HCl with various amounts of acetone

Species	Acetone, %			
	0	20	40	60
Th	$1.91 \times 10^3$	$6.20 \times 10^3$	$2.10 \times 10^4$	$5.00 \times 10^4$
La	128	250	600	$1.92 \times 10^3$
Zr	122	346	$1.27 \times 10^3$	$2.80 \times 10^3$
Sc	121	282	880	$3.60 \times 10^3$
Ba	117	250	710	$2.78 \times 10^3$
Hf	71	208	760	$3.40 \times 10^3$
Y	37.6	63	127	328
Sr	36.8	69	162	500
Yb	26.3	53	134	488
Ca	23.0	41.3	91	280
Cs	13.4	17.2	28.1	49.2
U(VI)	12.0	16.0	13.7	2.4
Rb	11.9	17.1	30.3	55
K	10.7	17.4	31.4	58
Tl(I)*	6.3	5.5	4.4	3.2
Na	5.4	9.0	19.8	45.0
Mn(II)	4.7	6.0	9.7	9.9
Ga	4.6	6.5	1.5	1.5
Al	4.5	6.6	15.6	55.0
Ni(II)	3.9	4.8	8.2	13.0
Mg	3.3	5.2	8.4	23.1
Co(II)	3.1	4.5	7.1	2.4
Fe(II)	2.9	3.9	4.8	1.0
Be	2.5	2.9	4.4	6.5
Ti(IV)†	2.3	4.1	11.2	42.6
Fe(III)	2.2	2.3	1.8	1.2
V(IV)	2.1	3.0	4.7	6.9
Li	1.9	2.6	3.6	7.6
Cu(II)	1.9	2.0	1.5	1.4
Pb(II)‡	1.6	1.4	0.9	0.8
Zn	1.0	0.9	1.1	0.8
In	0.8	0.7	0.9	0.6
Cd	0.7	0.8	0.7	0.6

\*0.05 mmole.

†0.5 mmole, 0.3% H<sub>2</sub>O<sub>2</sub>.

‡0.2 mmole.

macroporous resin than for the a gel-type resin such as AG50W-X8,<sup>26</sup> but as in the case of methanol there is not much further improvement on addition of acetone. The separation of the lanthanides from aluminium is not as good as that in HCl-methanol. The separation factors for ytterbium and scandium from aluminium are 9.9 and 67 respectively in 4.0M HCl containing 40% acetone, as compared with 12.6 and 89 in 3.0M HCl containing 40% methanol. The major cause for the decreased separation factor is the fact that the distribution coefficients of aluminium increase more with acetone than with methanol concentration. This is also the reason why a higher HCl concentration is required for fast elution of aluminium when acetone mixtures are used. Iron(III) and gallium are much more effectively separated from Sc *etc.* in HCl-acetone. A lower concentration of HCl can be used and elution is very fast with 0.5M HCl in 85% acetone, while scandium *etc.* are retained extremely strongly, with distribution coefficients  $>10^4$ . With 1.0M HCl in 85% acetone even uranium(VI), which is difficult to elute with HCl-methanol mixtures, is eluted effectively. Te(IV),

Mn(II), Fe(II), Mg, Ni, Co(II), Cu(II), Ti(IV), V(IV), Be, Li, Cd, In, Bi and several other species have lower distribution coefficients than aluminium, and are eluted very easily with 4.0M HCl in 40% acetone and accompany aluminium. Most of them can be eluted effectively at considerably lower concentrations of HCl with much larger separation factors when the separation of aluminium is not required. Zr, Hf and Th accompany the lanthanides and Sc. The elution of K, Rb and Cs with 4.0M HCl in 40% acetone is prolonged and shows considerable tailing. Better separation is possible in 4.0M HCl containing 20% of acetone or methanol, though ytterbium and the heavy lanthanides are less strongly retained under these conditions, so larger columns are required.

*Al, Fe(III), Ga, U(VI), V(IV), Ti(IV).* The decrease in distribution coefficients with solvent concentration for iron(III) and gallium is very much more pronounced in acetone mixtures than in methanol. Both can be effectively eluted with 0.2M HCl in 90% acetone or with 0.5M HCl in 80% or even 75% acetone (Figs. 2 and 3), while Co(II), Mn(II), Ni, Li and the other alkali-metals, Be and all the alkaline-

Table 6. Distribution coefficients with AG MP-50 resin in 4.0M HCl with various amounts of acetone

Species	Acetone, %			
	0	20	40	50
Th	580	$1.95 \times 10^3$	$7.60 \times 10^3$	$1.60 \times 10^4$
Ba	72	159	406	890
Sc	77	180	498	960
La	67	122	308	580
Zr	37.1	108	413	770
Sr	22.2	41.5	110	246
Hf	20.6	66	292	$1.31 \times 10^3$
Y	19.0	35.7	87	155
Ca	14.2	26.0	65	120
Yb	12.2	26.0	73	141
Cs	8.8	10.9	20.6	27.2
Rb	7.9	11.6	19.1	25.3
U(VI)	7.9	8.9	7.4	2.1
K	7.6	11.9	23.0	36.2
Na	3.9	6.3	14.5	22.8
Ti(I)*	3.0	2.7	2.4	1.9
Mg	2.8	4.1	6.3	9.4
Ni(II)	2.8	3.5	5.2	5.9
Ga	2.7	3.6	1.4	1.4
Mn(II)	2.5	3.4	4.4	4.5
Al	2.4	3.5	7.4	15.9
Co(II)	2.0	2.7	2.8	1.4
Be	1.9	2.2	2.9	3.7
Fe(II)	1.9	2.1	1.8	1.0
Ti(IV)†	1.8	3.6	10.7	18.3
V(IV)	1.7	2.2	3.2	4.0
Li	1.5	1.9	3.0	3.5
Fe(III)	0.9	1.0	0.8	0.8
In, Cd, Zn } Cu(II) Pb(II)	<1	<1	<1	<1

\*0.05 mmole.

†0.5 mmole, 0.3% H<sub>2</sub>O<sub>2</sub>.

earth metals, Ti(IV), Zr, Hf, Th, Al, Sc, Y and the lanthanides are strongly retained. When 0.5M HCl in 75% acetone is used for elution, Cu(II) and U(VI) are also retained.

V(IV) and Ti(IV) can easily be eluted with aqueous 1.0M HCl containing hydrogen peroxide, while Al, Ga, Fe(III), U(VI) and also Pb, Ca, Sr, Ba, Sc, Y, Zr, Hf, Th and the lanthanides are retained. All the species in this group, including uranium(VI), can be eluted together, with 4M HCl in 40% acetone, while Ca, Sr, Ba, Sc, Hf, Zr, Th, Y and the lanthanides are retained. Uranium(VI) can be eluted with 0.5M HCl in 91% acetone and separated from V(IV), Ti(IV), Ni(II), Mn(II), Li and the other alkali-metals, Be and the alkaline-earth metals, Al and all species with negligible tendency to form chloride complexes.

Zn, Cd, Hg(II), In. Zinc shows an initial slight increase followed by a decrease in sorption with increasing acetone concentration in 0.2 and 0.5M HCl. At higher acidities the decrease in sorption is continuous with increasing acetone concentration. Sorption of cadmium and indium decreases continuously with increasing acetone concentration at all concentrations of HCl. Mercury(II) is virtually not sorbed from any HCl-acetone combination investigated. Separations can be achieved by eluting

Hg(II) with aqueous 0.2M HCl, Cd with 0.5M HCl in 35% acetone and Zn with 0.5M HCl in 60% acetone. Indium accompanies cadmium. Ga, Fe(III), Pb(II), Cu(II), Co(II), Ni, Mn(II), V(IV), Ti(IV), Be, Mg, Al and many other species are retained when zinc is eluted as described.

Pb(II), Bi(III), Sn(IV), Te(IV). Lead is much more strongly sorbed by the macroporous resin than by AG50W-X8. From 0.2 and 0.5M HCl the sorption increases with acetone concentration up to about 30% and then decreases. Good separations with quite large separation factors comparable to those obtained with 0.5M HCl containing 40% methanol are possible by eluting Bi, Sn(IV) and Te(IV) with 0.5M HCl in 30% acetone. Lead is strongly retained but can be easily eluted with 3.0M HCl. Many other metal ions, e.g., Au(III), Hg(II), In, Se(IV), As(III) and the platinum metals are also eluted with 0.5M HCl in 30% acetone and separated from lead. For Cd and Zn, 0.5M HCl in 60% acetone provides faster elution and better separation. Though lead is not retained as strongly, the separation is nevertheless satisfactory, provided a 5 or 10 g resin column is used (Fig. 1). When hydrogen peroxide is present, small amounts of V(IV), Mo(IV) and W(VI) can also be eluted with 0.5M HCl in 30% acetone and separated

from Pb. Larger amounts of lead, together with larger amounts of these elements, will tend to precipitate. With 1.0M HCl in 80% acetone lead can be eluted quite effectively, while Li and the other alkali-metal ions, Be and the alkaline-earth metal ions, Ni, Mn(II), Ti(IV), Zr, Hf, Th, Al, Sc, Y and the lanthanides are still retained.

*Au(III), Pt(IV), Pd(II), Rh(III), Ir(III/IV), As(III), As(V), and Se(IV).* As with other resins and HCl-methanol these species are sorbed only slightly or not at all at any acidities. Acetone does not seem to cause any significant changes of the distribution coefficients in 0.2 and 0.5M HCl, the only acidities investigated for these elements. These species can be eluted with aqueous 0.1 or 0.2M hydrochloric acid and thus separated from most other ions, including In, Cd and small amounts of Bi. Problems can be caused by ions which tend to hydrolyse, precipitate or polymerize, such as Sn(IV), Sb(III), and large amounts of Bi, Mo(VI), W(VI) and V(V), though the last three can be stabilized by hydrogen peroxide when gold is absent. Hg(II) accompanies Au(III) and the other metal ions. Au(III), Se(IV), As(III), As(V), Pt(IV) and Pd(II) can be separated from Te(IV) by elution with 0.2M HCl in 60% acetone, Te(IV) being retained, as described for an AG50W-X8 resin.<sup>27</sup> The macroporous resin retains the tellurium slightly more strongly and the low-level tailing of Au(III), Pd(II), Rh(III) and Ir(III/IV) is considerably reduced when acetone is used instead of methanol.

*V(V), Mo(VI), W(VI).* These require the presence of hydrogen peroxide to prevent polymerization or precipitation from causing difficulties in the ion-exchange process. Mo(IV) and W(VI) are virtually not sorbed from 0.2 and 0.5M HCl at any concentration of acetone. V(V) is slightly sorbed at acetone concentrations  $\geq 60\%$ . This is probably due to reduction to V(IV) as indicated by a slight greenish discoloration of the resin. When the equilibration time is increased to 24 hr, a more complete reduction can be observed. For the elution of these species 0.01M HCl containing 0.15% hydrogen peroxide is very effective and separates them from all others except mercury(II) and the platinum metals above. Gold(III) will be reduced to the metal. Species which hydrolyse easily, such as Sn(IV) and Ti(IV) should be absent; when they are present, the concentration of hydrochloric acid has to be increased. W(VI) precipitates at an HCl concentration  $> 2M$ , even in the presence of hydrogen peroxide.

*Sb(III) and Tl(I).* These two ions cause special problems because of their tendency to precipitate in hydrochloric acid medium. Visible precipitates are formed when larger amounts of Tl(I) are present in dilute hydrochloric acid ( $\leq 1M$ ) at all acetone concentrations. With the 0.05 mmole of thallium used for this work, visible precipitation occurred only in 0.2M HCl containing 90 and 95% of acetone. It is suspected that precipitation may have occurred inside the resin particles and that the solution outside may

also have contained some semi-stable colloidal thallium(I) chloride. It was observed in elution experiments that thallium(I), in 0.2M aqueous HCl or its mixtures with acetone, partially passes through the column despite the quite large distribution coefficient (Table 1). The "sorbed" part of the thallium(I) on the other hand is difficult to elute and shows very prolonged tailing. Precipitation and/or colloidal precipitate formation are also suspected for Sb(III) in aqueous 0.2 and 0.5M HCl, 0.2M HCl containing 20% and 40% of acetone, and 0.5M HCl containing 20% acetone. Sb(III) also passes partially through the column with these eluents, despite fairly large distribution coefficients (Tables 1 and 2).

#### General aspects

Comparison of the results presented in this paper with those available for HCl-methanol mixtures<sup>26</sup> clearly shows the greater ability of acetone to promote chloride-complex formation in the external phase, with a resulting decrease in the distribution coefficients, which, in the case of acetone, can often be quite dramatic. The distribution coefficients in 0.5M HCl containing 80% methanol or acetone are 830 and 2.3 respectively for Fe(III) and 1310 and 1.8 for Ga, and for Cu(II) in 0.5 M HCl containing 90% of these solvents are 48 and 1.7. As a result these three species and others such as Co(II) and U(VI), which otherwise require 2, 3 or even 4M aqueous HCl or 2M HCl in 70% methanol [Fe(III), Ga, Cu(II)] for elution, can easily be eluted with 0.5M or even with 0.2M HCl (Table 1) when acetone is used as the chloride complexation-promoting solvent. This opens up various possibilities for new separations with the macroporous resin, that are not possible with methanol as solvent.

It also appears that many ions, including Bi, Cd, In, Ga, Zn, Fe(III) and Cu(II), are eluted very sharply by HCl-acetone mixtures (Figs. 1-3). The peaks show almost no tailing and the exchange kinetics seem to be better for HCl-acetone than in HCl-methanol mixtures.<sup>26</sup> Furthermore, in addition to the marked change in selectivity for some species such as Pb, Sr, Ba, Sc, U(VI) and the lanthanides, from that with an 8% cross-linked gel-type resin,<sup>26</sup> there are also some smaller changes in selectivity which could lead to improved separations by use of a macroporous resin.

The best separation between Co(II) and Mn(II) by cation-exchange in HCl-acetone has been described by Victor.<sup>28</sup> The optimal separation factor in 0.35M HCl containing 90% acetone was 7. A separation factor of 15 seems to be possible in 0.2M HCl-95% acetone and of 10 in 0.5M HCl-90% acetone with the macroporous resin (Tables 1 and 2). The reason is that Mn(II) is distinctly more strongly sorbed than Co(II) by the macroporous resin ( $\alpha_{Co}^{Mn} \approx 1.5$  for 0.2-1.0M HCl). With a gel-type resin both elements are almost equally strongly sorbed in this acid range. Many other new separations should become possible

and others improved considerably by use of a macroporous resin with HCl-acetone mixtures as eluting agents. In other cases a gel-type resin or another eluent system may offer advantages. Which resin or eluting system provides the best separation for a given problem has to be decided from case to case by intelligent use of available tables of distribution coefficients and consideration of the kinetic exchange behaviour of the elements involved.

*Acknowledgements*—I should like to thank Miss E. Smuts and Mr R. Verheij for carrying out parts of the experimental work for this paper.

#### REFERENCES

1. F. W. E. Strelow, *Anal. Chem.*, 1960, **32**, 1185.
2. F. Nelson, T. Murase and K. Kraus, *J. Chromatog.*, 1964, **13**, 503.
3. F. W. E. Strelow, R. Rethemeyer and C. J. C. Bothma, *Anal. Chem.*, 1965, **37**, 106.
4. F. W. E. Strelow, M. D. Hanekom, A. H. Victor and C. Eloff, *Anal. Chim. Acta*, 1975, **76**, 377.
5. F. Nelson and D. C. Michelson, *J. Chromatog.*, 1966, **25**, 414.
6. F. W. E. Strelow and H. Sondorp, *Talanta*, 1972, **19**, 1113.
7. F. Nelson and K. Kraus, *J. Chromatog.*, 1979, **178**, 163.
8. J. S. Fritz, B. B. Garralda and S. K. Karraker, *Anal. Chem.*, 1961, **33**, 882.
9. R. Caletka and V. Krivan, *Talanta*, 1983, **30**, 543.
10. L. Danielsson, *Acta Chem. Scand.*, 1965, **19**, 1859.
11. T. Adachi, *Bull. Chem. Soc. Japan*, 1982, **55**, 802.
12. S. K. Jha, F. de Corte and J. Hoste, *Anal. Chim. Acta*, 1970, **62**, 163.
13. J. C. Rouchaud and G. Revel, *J. Radioanal. Chem.*, 1973, **16**, 221.
14. A. Dadone, F. Baffi and R. Fraché, *Talanta*, 1976, **23**, 593.
15. F. W. E. Strelow and T. N. van der Walt, *Anal. Chem.*, 1982, **54**, 457.
16. F. W. E. Strelow, C. R. van Zyl and C. J. C. Bothma, *Anal. Chim. Acta*, 1969, **45**, 81.
17. J. S. Fritz and T. Rettig, *Anal. Chem.*, 1962, **34**, 1562.
18. F. W. E. Strelow, A. H. Victor, C. R. van Zyl and C. L. Eloff, *ibid.*, 1971, **43**, 870.
19. J. Korkisch and S. S. Ahluwalia, *Talanta*, 1967, **14**, 155.
20. J. Korkisch and E. Klakl, *ibid.*, 1969, **16**, 377.
21. K. Kawazu and J. S. Fritz, *J. Chromatog.*, 1973, **77**, 397.
22. J. S. Fritz and J. N. Story, *Anal. Chem.*, 1974, **46**, 825.
23. K. Kawazu, M. Shibata and H. Kakijama, *J. Chromatog.*, 1975, **115**, 543.
24. S. F. Marsh, J. E. Alarid, C. F. Hammond, M. J. McLeod, F. R. Roensch and J. E. Rein, *Los Alamos Scientific Laboratory Report LA-7083*, Feb. 1978.
25. F. W. E. Strelow, *Anal. Chem.*, 1984, **56**, 1053.
26. *Idem*, *Anal. Chim. Acta*, 1984, **160**, 31.
27. *Idem*, *Anal. Chem.*, 1984, **56**, 2069.
28. A. H. Victor, *S. Afr. J. Chem.*, 1983, **36**, 76.

## KINETIC DETERMINATION OF Hg(II) IN DIFFERENT MATERIALS, BASED ON ITS INHIBITORY EFFECT ON A CATALYSED PROCESS

C. SANCHEZ-PEDREÑO\*, M. I. ALBERO and M. S. GARCIA

Department of Analytical Chemistry, Faculty of Sciences, University of Murcia, Murcia, Spain

(Received 17 March 1987. Revised 18 August 1987. Accepted 25 September 1987)

**Summary**—A new kinetic method for the determination of Hg(II) based on its inhibitory effect on the Pd(II)-catalysed reaction between Co(III)-EDTA and hypophosphite is proposed. The reaction is followed spectrophotometrically at 540 nm by measuring the induction period. Both the influence of the reaction variables and the interference of many ions have been studied. A mechanism for the inhibition process is also proposed. Under the selected experimental conditions of  $2.7 \times 10^{-3} M$  Co(III)-EDTA, pH-3.2 Britton-Robinson buffer,  $0.3 M$   $H_2PO_2^-$ ,  $0.35 \mu g/ml$  Pd(II), and temperature  $18 \pm 0.2^\circ$ , Hg(II) was determined in the range 13–120 ng/ml. The method was applied to the determination of Hg(II) in sphalerites and pharmaceuticals.

In an earlier paper<sup>1</sup> we reported on the Pd(II)-catalysed reduction of the Co(III)-ethylenediaminetetra-acetate complex by hypophosphite, and this led us to propose a new kinetic method for the determination of palladium. The interferences studied showed that Hg(II) exerted a strong inhibitory effect, appearing as an induction period which was related to the Hg(II) concentration.

The toxicity of mercury salts and vapours has fostered the development of a number of micro-methods for the determination of this element. Most of these methods have been listed in reviews.<sup>2-11</sup> A significant number of them are based on the catalytic action of Hg(II) on ligand-exchange reactions<sup>12-16</sup> and slow redox processes,<sup>17-21</sup> or on their inhibitory effect on catalytic indicator systems.<sup>22-25</sup> In this paper we describe a kinetic method for the determination of Hg(II) based on its inhibitory effect on the  $H_2PO_2^-$ -[Co(III)-EDTA]-Pd(II) system. The procedure has been successfully applied to the determination of mercury in sphalerites with low mercury contents, as well as in pharmaceuticals.

### EXPERIMENTAL

#### Apparatus

Absorbance-time ( $A-t$ ) curves were recorded on a Perkin-Elmer 550SE dual-beam spectrophotometer with 1-cm cells, kept at constant temperature by means of a Colora Minicyostat MC III. A Radiometer PHM 63 pH-meter was used for pH measurements.

#### Reagents

Co(III)-EDTA, 0.04 M. Exactly 50 ml of 0.1 M cobaltous nitrate and 50 ml of 0.1 M EDTA were pipetted into a 250-ml beaker. After addition of 3 g of potassium peroxodisulphate the solution was adjusted to pH 6 with a 1:1

v/v dilution of s.g. 0.88 ammonia solution, and boiled gently for about 20 min to decompose the excess of peroxodisulphate. Finally, the solution was made up to volume in a 125-ml standard flask.<sup>26</sup>

Sodium hypophosphite solution 3M. Prepared weekly and stored in a dark bottle.

PdCl<sub>2</sub> solution,  $5 \times 10^{-3} M$ . Prepared in 0.2 M hydrochloric acid.

Mercuric nitrate solution,  $10^{-3} M$ . Prepared in 0.5 M sulphuric acid, and standardized according to the method given by Schwarzenbach and Flaschka.<sup>27</sup>

Britton-Robinson buffer, pH 3.2. Solutions of metal nitrates and sodium salts of several anions were used for interference studies. All reagents were of analytical-grade and solutions were prepared with doubly distilled water. Lower concentrations were obtained by appropriate dilution before use.

#### General procedure

The experiment was started by placing 0.4 ml of 0.02 M Co(III)-EDTA, 1 ml of Britton-Robinson buffer and 0.4 ml of  $2.5 \times 10^{-3} M$  palladium chloride (in that order) in spectrophotometric cells, and then adding appropriate volumes of  $2 \times 10^{-6} M$  mercuric nitrate so that the final Hg(II) concentrations were between 13 and 120 ng/ml. The solutions were diluted to 2.7 ml with water. The cells were placed in a thermostatic bath at  $18 \pm 0.2^\circ$  for about 10 min. Then, 0.3 ml of sodium hypophosphite solution was added to the test cell and the spectrophotometer recorder was started. The solution was shaken, the cell placed in the spectrophotometer, and the  $A-t$  curve at 540 nm recorded. The data obtained were used to plot the calibration graph of induction period vs. Hg(II) concentration.

Cells were cleaned after use by immersion in nitric acid (1 + 1) for 15 min to remove traces of palladium adsorbed on their walls.

#### Procedure for determination of mercury in sphalerites

A 0.1-g sample was dissolved in 1.5 ml of hydrochloric acid (1 + 1) and 2 ml of concentrated nitric acid, added consecutively, with gentle heating during the process. Once the sample was dissolved, 2 ml of concentrated sulphuric acid were added and heating was continued until persistent white fumes appeared. After transfer of the solution to a 200-ml standard flask and dilution to volume, mercury was determined by the recommended procedure.

\*To whom correspondence should be addressed.

### Procedure for determination of mercury in pharmaceuticals

For determination of Hg(II) in cleaning solutions for contact lenses, samples of 5–10 ml were treated with 1 ml of concentrated sulphuric acid and 10 ml of concentrated nitric acid, and the mixtures were heated until persistent white fumes appeared. They were then made up to volume with water in 250-ml standard flasks and mercury was determined by the recommended procedure.

## RESULTS AND DISCUSSION

Previous work demonstrated that over a wide pH-range hypophosphite does not reduce Co(III)–EDTA at an appreciable rate, but that Pd(II) is a sensitive catalyst for this process. We have found that Hg(II) has no effect on the  $\text{H}_2\text{PO}_2^-$ –[Co(III)–EDTA] system. On the other hand, it has a strong inhibitory effect on the Pd(II)-catalysed reaction, manifested as an induction period associated with the Hg(II) concentration.

The reaction is followed spectrophotometrically by measuring the time elapsed until the absorbance of Co(III)–EDTA starts to decrease. Figure 1 shows  $A-t$  curves corresponding to mixtures at pH 3.2 with concentrations of  $2.7 \times 10^{-3} M$  Co(III)–EDTA,  $0.3 M$  hypophosphite,  $0.35 \mu\text{g/ml}$  Pd(II) and up to  $147 \text{ ng/ml}$  Hg(II). Once the induction period has elapsed, the reaction rate is similar to that observed in the absence of Hg(II).

### Influence of pH

The influence of pH on the inhibited reaction was studied with reactant concentrations similar to those described above, and solutions containing  $53 \text{ ng/ml}$  Hg(II). The pH was adjusted to between 1.5 and 4.0 with Britton–Robinson buffer. As seen in Fig. 2, the induction period remains unchanged over the pH range 2.1–3.6. All subsequent investigations were performed at pH 3.2.

### Influence of various variables

The influence of the Co(III)–EDTA concentration [other conditions:  $0.3 M$  hypophosphite,  $0.35 \mu\text{g/ml}$  Pd(II) and  $53 \text{ ng/ml}$  Hg(II), pH 3.2] was studied in

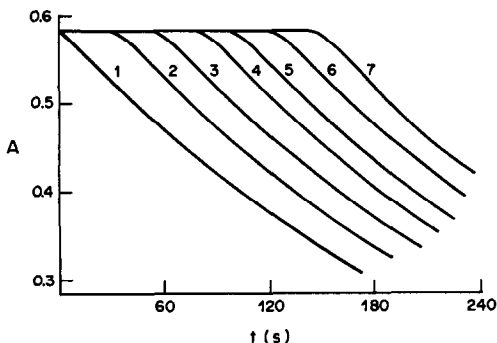


Fig. 1. Absorbance–time curves:  $2.7 \times 10^{-3} M$  Co(III)–EDTA;  $0.3 M$   $\text{H}_2\text{PO}_2^-$ ;  $0.35 \mu\text{g/ml}$  Pd(II); pH 3.2;  $18^\circ$  [Hg(II)], ng/ml: (1) 0; (2) 13; (3) 40; (4) 67; (5) 93; (6) 120; (7) 147.

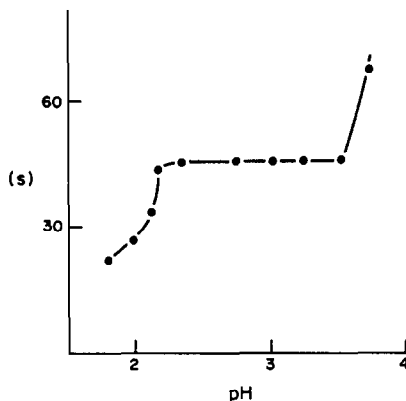


Fig. 2. Variation of induction period with pH:  $2.7 \times 10^{-3} M$  Co(III)–EDTA;  $0.3 M$   $\text{H}_2\text{PO}_2^-$ ;  $0.35 \mu\text{g/ml}$  Pd(II);  $53 \text{ ng/ml}$  Hg(II);  $18^\circ$ .

the range  $6.7 \times 10^{-4}$ – $4 \times 10^{-3} M$ . The induction period increases with Co(III)–EDTA concentration up to  $2 \times 10^{-3} M$  and then becomes constant. A concentration of Co(III)–EDTA of  $2.7 \times 10^{-3} M$ , which yielded suitable absorbance values, was selected.

The influence of the hypophosphite concentration was similarly studied in the range  $0.1$ – $0.6 M$ . The induction period decreases rapidly with increasing hypophosphite concentration in the range  $0.1$ – $0.2 M$  and becomes constant at concentrations  $> 0.2 M$ . A concentration of  $0.3 M$  was therefore selected.

Figure 3 shows the influence of temperature on the induction period; a temperature of  $18 \pm 0.2^\circ$  was selected for further experiments. In the absence of Pd(II) the reaction does not take place, even at the highest temperature tested ( $60^\circ$ ).

Figure 4 shows that the induction period decreases with increasing Pd(II) concentration.

The two graphs in Fig. 5 correspond to two series of experiments with the selected concentrations of Co(III)–EDTA and hypophosphite, pH and temperature, and containing  $0.35 \mu\text{g/ml}$  (curve 1) and

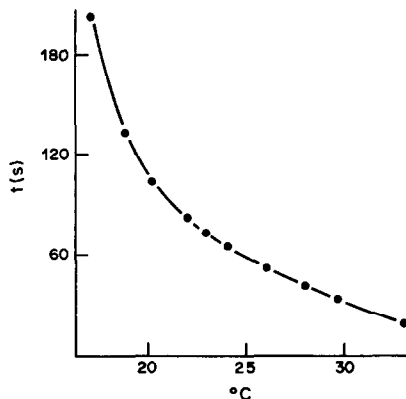


Fig. 3. Variation of induction period with temperature:  $2.7 \times 10^{-3} M$  Co(III)–EDTA;  $0.3 M$   $\text{H}_2\text{PO}_2^-$ ; pH 3.2;  $0.35 \mu\text{g/ml}$  Pd(II);  $106 \text{ ng/ml}$  Hg(III).

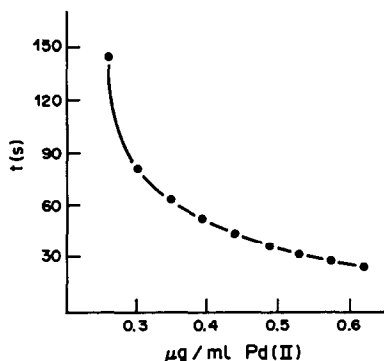


Fig. 4. Dependence of induction period on Pd(II) concentration:  $2.7 \times 10^{-3}M$  Co(III)-EDTA;  $0.3M$   $H_2PO_2^-$ ; pH 3.2;  $18^\circ$ ; 53 ng/ml Hg(II).

0.53  $\mu g/ml$  (curve 2) Pd(II) and varied Hg(II) concentration. The use of 0.35  $\mu g/ml$  Pd(II) gives greater sensitivity and better reproducibility. The calibration graph is linear from 13 to 120 ng/ml Hg(II).

The coefficient of variation for the determination of 68 ng/ml Hg(II) (10 determinations) was 1.2%.

#### Mechanism of the inhibited reaction

In the earlier work<sup>1</sup> we found that the catalytic effect of Pd(II) on the reduction of Co(III)-EDTA by hypophosphite seems to be due to heterogeneous catalysis attributable to elemental Pd formed in the fast reduction of Pd(II) by hypophosphite. This palladium catalytically decomposes the excess of hypophosphite, yielding active hydrogen ( $H^*$ ) which rapidly reduces the Co(III)-EDTA, as in some processes involving hypophosphite and dyes and catalysed by Pd(II).<sup>28,29</sup>

The mechanism of the process inhibited by Hg(II) is thought to be similar to that suggested for an analogous process:<sup>30</sup> the hypophosphite reduction of Pd(II) induces simultaneous reduction of Hg(II). The Hg formed is in close contact with Pd, thereby

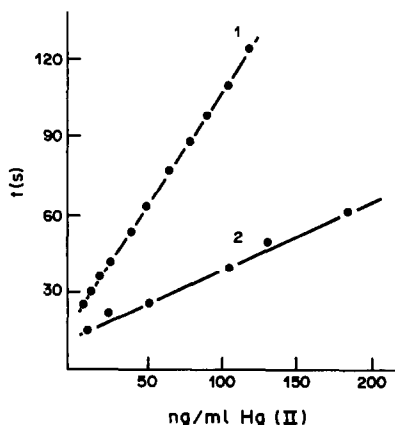


Fig. 5. Calibration graphs for Hg(II):  $2.7 \times 10^{-3}M$  Co(III)-EDTA;  $0.3M$   $H_2PO_2^-$ ; pH 3.2;  $18^\circ$ ; [Pd(II)],  $\mu g/ml$ : (1) 0.35; (2) 0.53.

Table 1. Interference of foreign ions in the determination of 80 ng/ml of Hg(II)

Ion added*	Limiting molar ratio, [Ion]/[Hg(II)]
Cd(II)	16000
Zn(II); Ni(II)	8000
$HHPO_2^-$	5000
$F^-$ ; Cr(III)	2000
$Cl^-$	700
Fe(III), Au(III)	50
Mn(II)	10
Cu(II)	5
Pb(II); Bi(III); Ag(I); V(V)	1
$I^-$ ; $Br^-$ ; Pt(IV); Sn(II)	< 0.5

\* $ClO_4^-$ ;  $SO_4^{2-}$ ;  $NO_3^-$  do not interfere.

reducing the active surface of the latter. Thus, it takes some time (induction period) to produce the threshold amount of  $H^*$  needed to act upon the Co(III)-EDTA complex. When this amount is reached, the catalysed reduction of the complex begins and proceeds at the same rate as in the absence of Hg(II). The induction period is a linear function of the  $[Hg(II)]/[Pd(II)]$  ratio, so at fixed temperature, pH and concentrations of Co(III)-EDTA, hypophosphite and Pd(II), the induction period depends on the Hg(II) concentration, so allowing the kinetic determination of this ion.

#### Effect of other ions

The determination of 80 ng/ml Hg(II) tolerates the presence of foreign ions at the levels given in Table 1, the criterion for interference being an error greater than 4% in the determination of Hg(II).

#### Application

The proposed method was satisfactorily applied to the determination of mercury in cleaning solutions for contact lenses, where it is present as phenylmercury nitrate (certified content 0.0033%, found 0.0030%) or sodium ethylmercurithiosalicylate, thiomersal, (certified content 0.004%, found 0.004%). The coefficients of variation (5 determinations) were 3.4 and 2.9%, respectively.

The procedure has also been applied to the determination of mercury in sphalerites. The results found (0.069 and 0.064% mercury) are comparable with those obtained by atomic-absorption spectrometry (0.068 and 0.064% mercury, respectively). The coefficients of variation (5 determinations) were 2.8% and 3.5%, respectively.

#### REFERENCES

- C. Sánchez-Pedrño, M. S. Garcia and M. I. Alberó, *An. Quim.*, 1987, **83B**, 78.
- Analytical Methods Committee, *Analyst*, 1965, **90**, 515.
- S. Chilov, *Talanta*, 1975, **22**, 205.
- Mercury Analysis Working Party of BITC, *Anal. Chim. Acta*, 1974, **72**, 37; 1976, **84**, 231.
- M. López-Rivadulla and E. Fernández Gómez, *Quim. Anal.*, 1976, **30**, 251.



6. N. Crosby, *Analyst*, 1977, **102**, 225.
7. F. D. Snell, *Photometric and Fluorimetric Methods of Analysis*, Part. 1, p. 101. Wiley, New York, 1978.
8. K. Heinz, *Z. Chem.*, 1981, **21**, 201.
9. A. K. Shrivastava and S. G. Tandon, *Toxicol. Environ. Chem.*, 1982, **5**, 311.
10. Y. Agrawal and G. Mehd, *Rev. Anal. Chem.*, 1982, **6**, 185.
11. IUPAC, *Pure Appl. Chem.*, 1984, **56**, 1477.
12. M. K. Gadia and M. Mehra, *Microchem. J.*, 1978, **23**, 278.
13. N. Lis and M. Katz, *An Assoc. Quím. Argent.*, 1981, **69**, 1.
14. A. Miloaz, J. Majewska and H. Krzystek, *Chem. Anal. Warsaw*, 1971, **16**, 1085.
15. M. Phull, H. C. Bajaj and P. C. Nigam, *Talanta*, 1981, **28**, 610.
16. M. Mehra, M. Satake and M. Katyal, *Indian J. Chem.*, 1984, **23A**, 860.
17. L. I. Dubovenko and T. A. Bogoslovskaya, *Ukr. Khim. Zh.*, 1971, **37**, 1057.
18. T. E. Gaytan, A. Carta and Yu. A. Zhukov, *Centro Ser. Quím. Technol. Quím.*, 1978, **6**, 81.
19. P. J. Ke and R. J. Thibert, *Mikrochim. Acta*, 1972, 768.
20. F. Lázaro, M. Luque de Castro and M. Valcárcel, *Z. Anal. Chem.*, 1985, **320**, 128.
21. F. Grases, J. G. March and R. Forteza, *Microchem. J.*, 1985, **32**, 367.
22. I. A. Il'icheva, N. L. Antul'skaya, I. F. Dolmanova and L. A. Petrukhina, *Metody Anal. Kontrol'ya Kach. Prod. Khim. Promsil.*, 1979, **8**, 43; *Chem. Abstr.*, 1979, **91**, 44052b.
23. J. Masłowska and J. Leszczyńska, *Talanta*, 1985, **32**, 883.
24. A. Papanastasiou-Dimandi and P. A. Siskos, *Microchem. J.*, 1985, **32**, 237.
25. K. Sriramam, B. S. R. Sarma, K. Kalidas and P. Ravindranath, *Analisis*, 1986, **14**, 99.
26. F. Ch. Chang and K. L. Cheng, *Mikrochim. Acta*, 1979 **II**, 219.
27. G. Schwarzenbach and H. Flaschka, *Complexometric Titrations*, p. 272. Methuen, London, 1969.
28. V. V. S. Eswara Dutt and H. A. Mottola, *Anal. Chem.*, 1976, **48**, 80.
29. C. Sánchez-Pedreño, M. Hernández Córdoba and G. Martínez Tudela, *An. Quím.*, 1979, **75**, 536.
30. *Idem, ibid.*, 1981, **77**, 68.

## SHORT COMMUNICATIONS

# A PRECISION DROP-FALL DETECTOR FOR POLAROGRAPHIC AND ELECTROCAPILLARY WORK

J. B. CRAIG\*, D. HOPKINS and R. A. HOWIE

Department of Chemistry, University of Aberdeen, Meston Walk, Old Aberdeen, Scotland

(Received 3 November 1987. Accepted 9 December 1987)

**Summary**—This paper describes the construction of a rugged yet very precise detector for use in polarographic and electrocapillary work. It employs an a.c. bridge technique to utilize the large and abrupt change in capacitance on drop-detachment. Timing and recording of drop-times is achieved with a laboratory microcomputer or a counter/timer.

In polarographic and electrocapillary experiments the lifetime of a natural drop from a dropping mercury electrode needs to be known with millesimal precision. Currently, drop-fall detectors use a superimposed a.c. voltage, or a light pulse,<sup>1</sup> or a frequency-modulated transmitter where the DME forms part of the antenna.<sup>2</sup> This paper describes the construction of a rugged yet sensitive drop-fall detector based on the a.c. bridge technique commonly used in differential capacity measurements. Its output is compatible with a laboratory computer to time, record and manipulate data for consecutive drops.

\*To whom correspondence should be addressed.

## EXPERIMENTAL

### Apparatus

The four arms of the Wheatstone bridge, Fig. 1, are formed by resistors R1 and R2, the cell, and the variable resistance VR1 in series with switched capacitors C1-C5, this last arrangement allowing a wide range of C/R ratios to be selected to balance the bridge. The out-of-balance signal appearing across the bridge is fed to a preamplifier stage (TR1) through an isolatory screened transformer (TX1). The signal is further amplified by an operational amplifier stage (IC1) which has its gain manually controlled by VR2. The Y output signal can be viewed on an oscilloscope, and is also applied to a full-wave rectifier stage (IC7, D5, D6, and associated components). The d.c. voltage appearing across C24 is used to drive the meter M2, thus giving visual indication of the out-of-balance signal. The Y output signal is also fed to a squaring circuit (TR2, D1), the

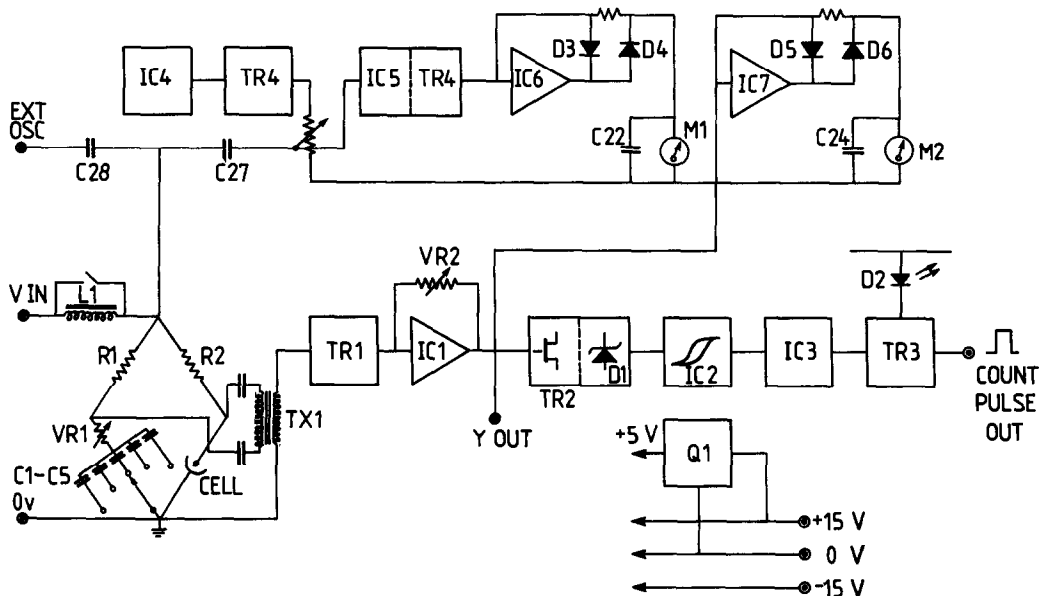


Fig. 1. Block diagram of the drop-fall detector.

Table 1. Drop-times of a dropping mercury electrode in 0.1M potassium chloride at 25°. Potentials were measured with respect to a 0.1M potassium chloride/calomel electrode but are reported here with respect to the standard hydrogen electrode

Potential, V	Drop time, sec				
	Drop 1	Drop 2	Drop 3	Drop 4	Drop 5
0.334	5.095	5.094	5.098	5.095	5.097
0.284	5.307	5.305	5.304	5.307	5.307
0.234	5.450	5.454	5.451	5.452	5.449
0.184	5.578	5.575	5.573	5.576	5.574
0.134	5.677	5.680	5.683	5.678	5.680
0.084	5.769	5.769	5.771	5.773	5.770
0.034	5.844	5.850	5.847	5.845	5.845
-0.016	5.908	5.907	5.911	5.908	5.905
-0.066	5.955	5.954	5.954	5.954	5.951
-0.116	5.990	5.989	5.985	5.988	5.987
-0.166	6.006	6.008	6.011	6.007	6.007
-0.216	6.015	6.017	6.015	6.015	6.015
-0.266	6.008	6.013	6.011	6.011	6.018
-0.316	5.997	6.001	6.001	6.000	6.004
-0.366	5.978	5.977	5.976	5.981	5.977
-0.416	5.944	5.948	5.948	5.945	5.947
-0.466	5.909	5.910	5.910	5.910	5.907
-0.516	5.865	5.867	5.861	5.869	5.860
-0.566	5.818	5.813	5.813	5.817	5.815
-0.616	5.758	5.758	5.756	5.760	5.755
-0.666	5.694	5.697	5.694	5.697	5.695
-0.716	5.625	5.621	5.624	5.628	5.625
-0.766	5.549	5.550	5.549	5.551	5.547
-0.816	5.473	5.468	5.470	5.469	5.468
-0.866	5.383	5.385	5.383	5.384	5.381
-0.916	5.291	5.290	5.293	5.291	5.293
-0.966	5.191	5.197	5.192	5.196	5.194

resultant signal being applied to a Schmitt trigger (IC2) to provide a clean output pulse for triggering the monostable oscillator (IC3). The time constant of IC3 is set at 2 sec and during this period the light-emitting diode (D2) is lit and a TTL +5-V pulse is available at the emitter of the buffer stage (TR3). In this particular case the output is fed to two counting devices: the first contains a pair of counters (Newport Universal, Model 6130A), one counting the odd-numbered and the other the even-numbered drops; in the second device, the signal is fed into the first of the one-bit inputs of an Apple IIe microcomputer fitted with a Mountain computer 1-MHz clock (card number MTN008).

The a.c. signal (10 mV, 100 Hz) applied to the bridge is derived from either an internal oscillator (IC4) through a buffer stage (TR4) or an external oscillator through C28. The d.c. polarizing voltage is applied to the bridge through L1, which presents a high impedance to the a.c. signal, thereby preventing this signal from being shunted by the external d.c. supply. To provide an indication of the amplitude of the a.c. signal, this is amplified (IC5, TR4) and rectified (IC6), and the magnitude of the resultant d.c. signal can be observed on the meter M1. The power supply consists of a  $\pm 15$ -V rail with a +5-V regulated supply from a voltage regulator (Q1).

The a.c. bridge can be set so that a zero out-of-balance signal is obtained either at the birth of the drop or at the point of its detachment. The first option was chosen in the present studies of the electrocapillary properties of bio-medical components where large changes in differential capacity and interfacial tension, and hence in drop times and sizes, were observed. The drop-fall detector is very rugged and has required no maintenance in two years of constant use. It has the advantage that the out-of-balance signal is constantly monitored, allowing the bridge cap-

acitors to be switched to maintain optimum operating conditions.

With addition of a simple timer/drop-knocker unit, replacement of C1-C5 with a series of decade capacitors, and display of the Y-out signal on an oscilloscope, the detector may be used to obtain differential capacity measurements by the method of Hills and Payne.<sup>3</sup>

## RESULTS

Table 1 shows typical drop-times in 0.1M potassium chloride, at 25°, as a function of electrical potential. A simple operational relationship between drop-times and interfacial tensions is given in a separate paper.<sup>4</sup> A detailed circuit diagram and computer program are available on request.

*Acknowledgement*—This work was sponsored by the United Kingdom Science and Engineering Research Council's programme on tissue-implant interactions, grant number GR/B/0616.1.

## REFERENCES

1. P. D. Tyma, *J. Electrochem. Soc.*, 1978, **125**, 284C.
2. C. Yarnitsky, C. A. Wijnhorst, B. Van der Laar, H. Reyn and J. H. Sluyters, *J. Electroanal. Chem.*, 1977, **77**, 391.
3. G. J. Hills and R. Payne, *Trans. Faraday Soc.*, 1965, **61**, 326.
4. J. B. Craig and C. Mackay, *Talanta*, 1988, **35**, 365.

## THE INFLUENCE OF ATOMIZATION PRESSURE ON THE BEHAVIOUR OF ALUMINIUM IN ELECTROTHERMAL ATOMIC-ABSORPTION SPECTROMETRY

JÁNOS FAZAKAS

C.P. 2-104, R-78200 Bucharest 2, Romania

MICHEL HOENIG

Institut de Recherches Chimiques, Ministère de l'Agriculture, Museumlaan 5, 1980 Tervuren, Belgium

(Received 21 August 1987. Revised 14 November 1987. Accepted 18 December 1987)

**Summary**—Pressurized atomization in argon purge gas considerably enhances the peak area in AAS determination of aluminium, owing to the decrease in the diffusion rate of atoms with increasing pressure. If lower heating rates are used, the diffusional loss mechanism becomes more important. Thus pressure then has an even more pronounced influence on signal strength. Atomization under pressure in argon purge gas is shown to be beneficial only for light elements. It can be expected that if instrumental matrix modification is made by using hydrogen as purge gas, increasing the atomization pressure may prove beneficial for all elements.

Earlier papers from both our laboratories<sup>1-7</sup> discussed the effect of pressure on the signals from several elements in electrothermal atomic-absorption spectrometry (ETAAS). The present paper continues our work by examining the case of aluminium and drawing some general conclusions as to the usefulness of pressurized atomization.

### EXPERIMENTAL

We used the Instrumentation Laboratory IL-555B CTF and the IL-655 electrothermal atomizers, both in the temperature-feedback mode. These atomizers are similar in design, the only important difference from the point of view of the present paper being that with Ramp 0, the heating rates are *ca.* 1100°/sec and 800°/sec respectively. Pyrocoated graphite tubes were used as supplied by the manufacturer.

Ashing and atomization were done at the temperatures recommended by the manufacturer<sup>8</sup> (1000° and 2500° respectively). Argon was used as purge gas. The atomization pressure was read on the built-in manometer of the furnace power supply. When not pressurized, the argon flow-rate was 5 l./min.

Absorbance signals were monitored with an IL-551 Video I or an IL-951 Video II spectrometer. The primary radiation source was an IL hollow-cathode lamp operated at 10 mA. The 309.3 nm quasi-resonance\* line was used with a spectral band-width of 0.5 nm. The peak shapes were followed on the video display of the spectrometers.

Samples were deposited from an aerosol by means of an IL-254-FASTAC autosampler into the furnaces preheated to 150°.

Stock standard solutions were prepared from oxysalts, though it has been shown<sup>9</sup> that when the aerosol deposition technique is used the chemical form of the sample is not of paramount importance. Dilute standards were prepared just before use and contained 0.05% v/v concentrated nitric

acid. Some experiments were repeated with an IL-257 spectrometer and an IL-555B CTF electrothermal atomizer.

### RESULTS

Figure 1 shows the relative effect of pressure on the peak-height and peak-area signals of aluminium, when the IL-655 atomizer was used. Though the peak-height is only insignificantly affected, the peak area increases threefold as the pressure is raised from atmospheric to 4 kg/cm<sup>2</sup>. Similar results were obtained with the IL-555B CTF atomizer, but the enhancement factors were somewhat lower. The reasons for this will be discussed later.

Figure 2 shows the shapes of the absorption peaks obtained with normal and pressurized atomization with the IL-555B CTF atomizer. The whole evolution of the peak, and especially the removal of atoms, is slower with pressurized atomization. Similar peak shapes were obtained with the IL-655 atomizer.

Figure 3 shows the calibration plots for aluminium at various pressures and heating rates of the furnace. When lower heating rates (Ramp 5, *ca.* 300°/sec) are used, the enhancement factors are much more pronounced than with the high heating rates (Ramp 0). It should also be noted that with the lower ramp rates there is also significant enhancement of the peak-height with increasing pressures. This is contrary to what we have observed at high heating rates (see Fig. 1).

### DISCUSSION

The slower evolution of the atomic vapour in pressurized atomization (Fig. 2) inherently means that:

(a) the relative time-resolution of the detection system improves with increasing atomization pres-

\*The 309.3 nm line actually originates at 112 cm<sup>-1</sup> above the ground state. However, for all practical purposes it still behaves as a resonance line, hence the name quasi-resonance line.

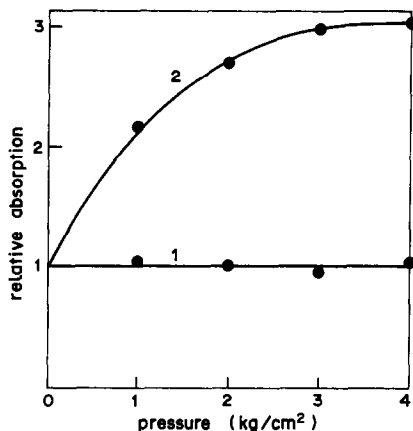


Fig. 1. Relative influence of pressure on the determination of aluminium by ETAAS with an IL-655 atomizer. 1—peak-height; 2—peak-area.

sure, with a consequent improvement of precision and accuracy, and

(b) the slower evolution of the absorption signal also means that the atom-vapour temperature will be higher, so any vapour phase dissociation should be more complete.

It is quite clear that several factors affect the behaviour of a given analyte vis-à-vis atomization pressure. The most important of these are as follows.

(a) The Lorentz broadening and the accompanying shift (to the red in argon) of the absorption lines with increasing pressure. This should result in a decrease of absorption since the centre of the absorption lines will be shifted away from the wavelength of the hollow-cathode lamp emission line.

(b) The reduction of the diffusion coefficient of the atoms with increasing pressure. In the case of aluminium the reduction of the diffusion rate is quite evidently so important that it more than compensates for the effect of line broadening and shift.

Our previous works<sup>1-6</sup> on the effect of pressure on various analytes were based on the misconception that pressure should prove beneficial in the case of

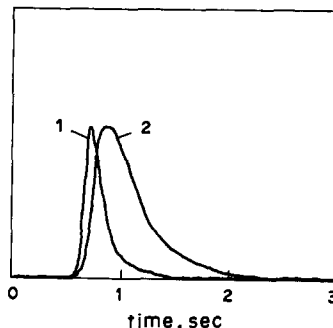


Fig. 2. Peak shapes for aluminium with normal and pressurized atomization (IL-551 Video I+IL-555 B CTF). 1—atomization at ambient pressure; 2—atomization at 4 kg/cm<sup>2</sup>.

volatile elements. Our only excuse may be that we were following the footsteps of other workers<sup>10</sup> who could not avoid the same pitfall. It was only after our experience with beryllium<sup>7</sup> that we finally realized that pressurized atomization may enhance signals only in the case of light elements and only when the removal of atoms from the furnace is mostly diffusion-controlled. The volatile elements studied by us (cadmium,<sup>1,6</sup> silver,<sup>2</sup> thallium<sup>4</sup> and lead<sup>1</sup>) will leave the furnace mostly by convective effects and pressure can have little if any influence on this. In such cases the predominant effect of pressure is the Lorentz shift and broadening, with a resultant worsening of sensitivity. It should be noted here that all the volatile elements studied by us,<sup>1-6</sup> as well as those studied by others,<sup>10</sup> are all heavy elements, so their diffusion coefficients are already very small. As a consequence, any reduction of the diffusion rate by an increase in pressure will have insignificant effects. In view of this, it is to be expected that pressurized atomization in an argon atmosphere would also be beneficial for light elements such as lithium and boron.

As the heating rate of the electrothermal atomizer decreases, the convective losses become less important, while the diffusional losses become more important. This is probably why, with the lower ramp rates, the enhancement factors are much more pro-

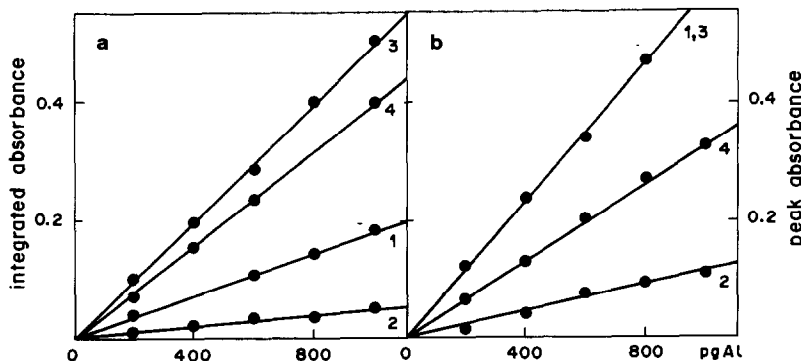


Fig. 3. Calibration plots for aluminium in the peak-area (a) and the peak-height (b) modes as obtained with an IL-655 atomizer. 1—ambient pressure atomization, ramp 0; 2—ambient pressure atomization, ramp 5; 3—atomization at 4 kg/cm<sup>2</sup>, ramp 0; 4—atomization at 4 kg/cm<sup>2</sup>, ramp 5.

nounced for aluminium, as shown in Fig. 3. It may also be the reason why we have seen some enhancement of the cadmium signal<sup>11</sup> with the IL-655 atomizer (heating rate 800°/sec) and a decrease of signal with the IL-555B CTF (heating rate 1100°/sec).

Since the diffusion coefficient plays such a significant role in the behaviour of analytes as a function of pressure, it is to be expected that the nature of the purge gas is also of importance. Thus if the purge gas is hydrogen or helium the diffusion of atoms will be very rapid. This should mean that pressurized atomization would prove beneficial in such cases, in enhancing signals.

Some readers may believe that it requires a rather special mentality to use hydrogen as purge gas. The term "instrumental matrix modification" has been defined and discussed in a recent paper.<sup>12</sup> The use of hydrogen during atomization<sup>13</sup> is an unjustly neglected means of instrumental matrix modification. The use of hydrogen overcomes many interferences and also reduces background absorption. However, not unexpectedly<sup>13</sup> the signal obtained in hydrogen is much smaller than that in argon. As a consequence we believe it could be beneficial to use pressurized atomization in such cases in order to restore the signal to the magnitude normally recorded in argon.

It is still unclear to us why different lines of the same element<sup>3</sup> behave differently in atomization under pressure. However, in the light of our findings we believe that it is worthwhile to study further the various theoretical and practical implications of pressurized atomization.

#### CONCLUSIONS

Pressurized atomization has been shown to be beneficial for the determination of aluminium. The explanation is that aluminium is a light element and the analyte loss from the atom reservoir is mostly diffusion-controlled. Thus an increase of atomization pressure will lower the diffusion rate, hence improving the peak-area signal for aluminium.

The heating rate of the atomizer is an important factor in considering the effect of pressure on various analytes. The lower the heating rate, the more important the diffusional atom loss, hence the more significant the effect of pressure.

In the light of our experience, pressurized atomization in an argon atmosphere can only be useful for light elements. However, pressurized atomization may prove beneficial for all elements if hydrogen is used as purge gas. Further investigations of various theoretical and practical aspects of pressurized atomization would certainly be a worthwhile venture.

We have previously reported<sup>3</sup> different enhancement factors for various aluminium lines, but this observation was later found to be due to an instrumental artifact.

*Acknowledgements*—One of the authors (J.F.) wishes to thank Instrumentation Laboratory—Austria GmbH for the loan of part of the instrumentation used in the work. The same author also wishes to thank Mrs. Maria Avramescu for permission to repeat some experiments with the IL-257 spectrometer and the IL-555B CTF atomizer.

#### REFERENCES

1. M. Hoenig, R. Vanderstappen and P. Van Hoeyweghen, *Analisis*, 1978, **6**, 433.
2. J. Fazakas, *Mikrochim. Acta*, 1983 **I**, 249.
3. *Idem*, *Spectrochim. Acta*, 1982, **37B**, 921.
4. *Idem*, *Anal. Lett.*, 1982, **15**, 1523.
5. *Idem*, *Rev. Roum. Chim.*, 1982, **27**, 685.
6. *Idem*, *Spectrochim. Acta*, 1983, **38B**, 455; *Magy. Kém. Folyoirat*, 1985, **91**, 365.
7. *Idem*, *Mikrochim. Acta*, 1983 **II**, 217.
8. *Atomic Absorption Methods Manual*, Vol. 2, *Flameless Operations*, Instrumentation Laboratory Inc., Wilmington, Mass., December 1976.
9. J. Fazakas, *Spectrosc. Lett.*, 1982, **15**, 221.
10. R. E. Sturgeon, C. L. Chakrabarti and P. C. Bertels, *Spectrochim. Acta*, 1977, **32B**, 257.
11. M. Hoenig and R. Wollast, *ibid.*, 1982, **37B**, 399.
12. L. Brazdes and J. Fazakas, *Acta Chim. Hung.*, in the press.
13. R. D. Beaty and M. M. Cooksey, *At. Abs. Newslett.*, 1978, **17**, 53.

## DETERMINATION OF ANTIMONY IN ROCKS AND SULPHIDE ORES BY FLAME AND ELECTROTHERMAL ATOMIC-ABSORPTION SPECTROMETRY

N. K. ROY and A. K. DAS

Geological Survey of India, Central Chemical Laboratory, Calcutta 700016, India

(Received 19 June 1987. Revised 16 November 1987. Accepted 8 December 1987)

**Summary**—Atomic-absorption methods for determination of antimony at  $\mu\text{g/g}$  levels in rocks and sulphide ores by flame atomization (FAA) and electrothermal atomization (ETAA) have been described. The FAA method involves the separation of antimony from matrix elements by extraction as the iodide into methyl isobutyl ketone containing tri-*n*-octylphosphine oxide, from dilute hydrochloric acid solution, followed by direct aspiration of the extract into an air-acetylene flame. If necessary, antimony is first separated from copper and lead by co-precipitation with hydrous ferric oxide from ammoniacal medium and by precipitation of lead as lead sulphate. The ETAA method involves co-precipitation of antimony with hydrous ferric oxide followed by dissolution of the precipitate in dilute nitric acid, mixing with nickel solution as releasing agent, and ETAA measurement by use of a tungsten strip atomizer.

Antimony is a comparatively rare element, occurring only at  $\mu\text{g/g}$  levels in certain rocks and minerals. Flame atomic-absorption (FAA) methods have not sufficient sensitivity to permit its determination at such low levels. Electrothermal atomic-absorption (ETAA) methods have the requisite sensitivity but are subject to various interferences. Obviously the FAA determination requires a preconcentration step, and both FAA and ETAA require a separation step to remove potential interferents. With ETAA methods interferents may also be dealt with by addition of matrix modifiers. Welsch and Chao,<sup>1</sup> and Donaldson and Wang,<sup>2</sup> have proposed FAA methods involving extraction of antimony iodide into methyl isobutyl ketone (MIBK) and stripping into an aqueous phase. Here we describe an extraction FAA method which is essentially similar to one proposed by Burke<sup>3</sup> for determination of low amounts of antimony in iron-, aluminium- and nickel-base alloys. It has enabled us to reach much lower detection limits for determination of antimony in rocks and minerals. We have also developed an ETAA method for the determination.

### EXPERIMENTAL

#### Apparatus

Flame AA measurements were made at 217.6 nm with a Varian AA-6 atomic-absorption spectrometer and hollow-cathode lamp. An air-acetylene flame was used. ETAA measurements were made with a Scintrex AAZ-2 Zeeman-modulated atomic-absorption spectrometer, with sample atomization on a heated tungsten strip. The conditions used were as follows.

Source	H.C. lamp (Varian)
Wavelength	217.6 nm
Purge gas	Argon

Volume of solution injected	10 $\mu\text{l}$
Dry at	120°
Ash at	500° (for 10 sec)
Ramp	50°/sec
Atomize at	2000°

#### Reagents

A standard antimony solution (1000  $\mu\text{g/ml}$ ) was prepared by dissolving the metal (99.9% purity) in nitric acid, and diluted, as required, with 5% v/v nitric acid. Nickel (1000  $\mu\text{g/ml}$ ) and iron(III) solutions (1000  $\mu\text{g/ml}$ ) were prepared by dissolving the 99.9% pure metals in the minimum amount of *aqua regia*, and diluting with nitric acid (5% v/v). TOPO-MIBK reagent was prepared by dissolving 1 g of tri-*n*-octylphosphine oxide in 100 ml of methyl isobutyl ketone.

#### Sample decomposition

Powdered sample (silicate rock or sulphide ore, 0.5–1 g) is weighed into a Teflon beaker and treated with a mixture of concentrated nitric acid (5 ml), 48% w/v hydrofluoric acid (10 ml) and concentrated perchloric acid (5 ml). The mixture is slowly evaporated to dryness on a hot-plate. The dried mass is treated with perchloric acid (2 ml) and again evaporated to dryness. This operation is repeated and the residue is dissolved in 20 ml of 50% v/v hydrochloric acid and diluted to volume in a 100-ml standard flask.

For silicate rock samples, this solution is directly used for liquid-liquid extraction and FAA measurement. For sulphide ores, it is subjected to further treatment, as described below, before liquid-liquid extraction and FAA measurement.

**Copper sulphide ores.** An aliquot of sample solution containing 5–50  $\mu\text{g}$  of antimony is diluted to about 100 ml. Iron(III) solution (1000  $\mu\text{g/ml}$ , 5 ml) is added, followed by the dropwise addition of dilute ammonia solution until the solution is distinctly alkaline, then 5 ml more ammonia solution. The mixture is boiled for a minute, let cool to room temperature, and filtered. The precipitate is washed several times with water and then dissolved in 20 ml of 50% v/v hydrochloric acid. This solution is used for the liquid-liquid extraction and FAA measurement.

**Lead sulphide ores.** An aliquot of sample solution containing 5–50  $\mu\text{g}$  of antimony is diluted with water to about 100 ml and heated to boiling. Sulphuric acid (25% v/v, 5 ml) is added to the hot solution with stirring, and the precipitate formed is allowed to settle for an hour, then filtered off and washed several times with hot water. The filtrate and washings are evaporated to about 50 ml and this solution is used for the liquid–liquid extraction and FAA measurements.

If this solution is likely to contain 5 mg of copper or more, it is further treated as described above for copper ores.

#### Extraction and FAA measurement

To the solution obtained after separation of copper or lead, or an aliquot of silicate-rock sample solution containing 5–50  $\mu\text{g}$  of antimony, 5 ml of concentrated hydrochloric acid are added and the volume is brought to about 60 ml by addition of water or by evaporation, as required. Ascorbic acid (2 g) and potassium iodide (1 g) are added and dissolved then the solution is transferred to a separatory funnel and shaken vigorously with 5 ml of TOPO–MIBK reagent for 1 min. The phases are allowed to separate and the aqueous phase is rejected. The organic phase is collected in a dry test-tube containing about 1 g of anhydrous sodium sulphate. The clear liquid is directly aspirated into a lean flame for FAA measurement.

For calibration, standard solutions containing 0–50  $\mu\text{g}$  of antimony are mixed with 10 ml of concentrated hydrochloric acid, diluted to 60 ml with water, and after addition of ascorbic acid (2 g) and potassium iodide (1 g) are extracted with 5 ml of TOPO–MIBK reagent as above. A complete reagent blank is run through the whole procedure and appropriate blank corrections are made.

#### ETAA measurement

An aliquot of the sample solution containing 2–10  $\mu\text{g}$  of antimony is mixed with 5 ml of 1000- $\mu\text{g}/\text{ml}$  iron(III) solution and hydrous ferric oxide is precipitated as described for copper sulphide ores. The precipitate is filtered off, washed with hot water, and dissolved in 10 ml of 50% v/v nitric acid. The solution is mixed with 5 ml of 1000- $\mu\text{g}/\text{ml}$  nickel solution and diluted to volume in a 50-ml standard flask. A 10- $\mu\text{l}$  aliquot of this solution is injected into the furnace for ETAA measurement.

Calibration solutions are prepared by taking 0, 2, 4, 6, 8 and 10  $\mu\text{g}$  of antimony in 50-ml standard flasks, adding 5 ml each of the 1000- $\mu\text{g}/\text{ml}$  iron(III) and nickel solutions and diluting to volume with 5% v/v nitric acid. Ten- $\mu\text{l}$  aliquots are then taken for ETAA measurement. A blank is run along with the experimental solutions and appropriate blank corrections are made. All measurements should be made in triplicate and the average used.

## RESULTS AND DISCUSSION

### Interferences

Extraction of antimony by TOPO–MIBK mixture is adversely affected by the presence of large amounts of copper and lead, which are likely to be present in many sulphide ores, so separation of the antimony from copper and lead is necessary when these are present in amounts exceeding 5 mg in the sample aliquots. Antimony is separated from copper by co-precipitation with hydrous ferric oxide, and from lead by precipitation of lead sulphate. We have found no loss of antimony in these separations. The antimony iodide extraction is reasonably quantitative over a wide range of hydrochloric acid concentration (1–4M). Other elements forming extractable iodides, (mercury, bismuth, cadmium, indium *etc.*) are also partly extracted but do not cause any interference if present in low amounts (below 5 mg), which is normally the case with common sulphide ores.

The ETAA method employing tungsten strip atomization is subject to severe interelement interferences (Table 1). We observed that iron reduces the

Table 1. Effect of foreign ions on ETAA measurements for antimony (Sb taken 10  $\mu\text{g}$ , final volume of solution 50 ml)

Foreign ion*	Amount,	
	mg	Sb absorbance†
None		0.090
Fe <sup>3+</sup>	1	0.086
Fe <sup>3+</sup>	5	0.078
Fe <sup>3+</sup>	10	0.076
Fe <sup>3+</sup>	20	0.078
Ni <sup>2+</sup>	1	0.104
Ni <sup>2+</sup>	5	0.123
Ni <sup>2+</sup>	10	0.126
Cu <sup>2+</sup>	5	0.080
Pb <sup>2+</sup>	5	0.095
Al <sup>3+</sup>	5	0.087
Mg <sup>2+</sup>	5	0.092
Ca <sup>2+</sup>	5	0.075
K <sup>+</sup>	5	0.057
Na <sup>+</sup>	5	0.068

\*The nitrates were used.

†Average of three measurements.

Table 2. Determination of antimony in rocks and minerals

Sample	Sb, $\mu\text{g}/\text{g}$		
	This work, FAA method	This work, ETAA method	Reported value
Copper sulphide ore 1	12	14	—
Copper sulphide ore 2	35	32	—
Lead sulphide ore 1	7.2	8.0	—
Lead sulphide ore 2	31	32	—
Lead sulphide ore 3	205	197	—
Granodiorite, GSP-1 (USGS)	3.3	3.8	3.2*
Andesite, AGV-1 (USGS)	4.5	5.1	4.4*
Granite, B-26 (GSI)	3.5	3.0	3.6†
Copper concentrate IGS-44	$3.4 \times 10^3$	—	$3.5 \times 10^3$ §

\*Recommended value from Gladney *et al.*<sup>5</sup>

†Consensus value obtained by different other methods.

§Recommended value (0.35%) from Lister.<sup>4</sup>



antimony absorbance but the effect levels out for iron concentrations of 100  $\mu\text{g/ml}$  and above. Nickel has an enhancement effect which becomes maximal at a nickel concentration of about 100  $\mu\text{g/ml}$  in the solution. Alkali metals and calcium cause serious interference in the ETAA determination of antimony. So removal of alkali and alkaline-earth metals from the measurement solution, and maintenance of an optimum concentration of nickel and iron is essential in the ETAA determination.

#### *Applications*

The proposed methods have been applied to the determination of antimony in a number of materials of different types, such as copper sulphide ores, lead sulphide ores, silicate rocks *etc.*, and the results are shown in Table 2. The methods have been validated by analysis of standard reference samples. Replicate analyses of our own Geological Survey of India reference sample (Granite, B-26) showed that the relative standard deviation (rsd) of the FAA method (5.8%) was much superior to that of the ETAA

method (13.7%). The large rsd for the ETAA method was partly due to the uncertainty of measurement of the 10- $\mu\text{l}$  samples and partly to the instrumental noise in the measurements. The rsd of the FAA results was due slightly more to the chemical processing than to the instrumental noise. The only advantage of the ETAA method is that it can be applied to much smaller amounts of sample. The FAA method can be used for determination of antimony down to 2  $\mu\text{g/ml}$  in geological samples.

*Acknowledgement*—The authors are thankful to the Director General, Geological Survey of India for his kind permission to publish this work.

#### REFERENCES

1. E. P. Welsch and T. T. Chao, *Anal. Chim. Acta*, 1975, **76**, 65.
2. E. M. Donaldson and M. Wang, *Talanta*, 1986, **33**, 233.
3. K. E. Burke, *Analyst*, 1972, **97**, 19.
4. B. Lister, *Geostds. Newsl.*, 1987, **11**, 11.
5. E. S. Gladney and C. E. Burns, *ibid.*, 1983, **7**, 3.

## SPECTROPHOTOMETRIC DETERMINATION OF PRIMARY AROMATIC AMINES WITH 4-*N*-METHYLAMINOPHENOL AND 2-IODYLBENZOATE

KRISHNA K. VERMA, SUNIL K. SANGHI and ARCHANA JAIN  
Department of Chemistry, Rani Durgavati University, Jabalpur 482001, India

(Received 1 July 1987. Accepted 23 November 1987)

**Summary**—2-Iodylbenzoate is proposed as an oxidimetric agent, in the presence of 4-*N*-methylaminophenol, for the spectrophotometric determination of primary aromatic amines. The purple-red product absorbs maximally at 525 nm and Beer's law is obeyed over a range corresponding to 4–32 µg/ml amine in the final solution. In contrast to dichromate or *N*-bromosuccinimide, previously used as the oxidant, 2-iodylbenzoate avoids errors arising from too large an excess of the oxidant, instability of the coupling intermediate, and the oxidation of the amine.

The widespread use of primary aromatic amines as raw materials, intermediates and finished products necessitates simple and accurate methods for their determination.<sup>1</sup> The most frequently used spectrophotometric methods are based on diazotization and coupling,<sup>2-4</sup> Schiff's base formation<sup>5,6</sup> and oxidative coupling.<sup>7-10</sup> A very sensitive method of general applicability involves the formation of a purple-red colour when primary aromatic amines are made to react with 4-*N*-methylaminophenol (metol) and an oxidizing agent, which may be dichromate,<sup>11,12</sup> *N*-bromosuccinimide,<sup>13</sup> or iodate, hexacyanoferrate(III), chloramine-T or peroxydisulphate.<sup>14</sup> The order of addition of the reagents and the amount of oxidant used play critical roles. The recommended order of addition is oxidant, 4-*N*-methylaminophenol and the primary aromatic amine. Any delay in the addition of amine, or change in the order of addition of the reagents, causes lower absorbance values. The colour is completely bleached when more than the requisite amount of oxidant (for which there is a narrow tolerance range) is added. We have used 2-iodylbenzoate as an oxidimetric reagent in a number of analytical determinations<sup>15-18</sup> and now report its use to circumvent this problem.

### EXPERIMENTAL

#### Reagents

2-Iodylbenzoic acid was synthesized by the procedure described by Fieser and Fieser,<sup>19</sup> and by the bromate oxidation method of Banerjee *et al.*,<sup>20</sup> modified as follows. To a boiling mixture of 12 g of 2-iodobenzoic acid, 50 ml of anhydrous acetic acid and 100 ml of 40% v/v sulphuric acid, slowly add, over a period of 20 min (with vigorous stirring, in a fume-chamber) a solution of 9 g of potassium bromate in 100 ml of warm water. Reflux the mixture for 90 min, during which all the bromine evolved will be removed. Cool, filter off the product and wash it with water. Yield 13 g (90%) of 2-iodylbenzoic acid, m.p. 222° (decomposition), purity ~95% (determined by iodometry<sup>21</sup>).

**2-Iodylbenzoate, 0.4% solution.** Dissolve 0.4 g of the free acid in a slight excess of potassium hydroxide solution (0.2 g in 25 ml of water), and dilute to volume in a 100-ml standard flask.

**4-*N*-Methylaminophenol sulphate (0.2%) solution, freshly prepared.**

**Acetic acid, 1% v/v.**

**Test samples.** Solutions of individual primary aromatic amines prepared by stirring an accurately weighed mass of the amine with 2 drops of 10% v/v hydrochloric acid, diluting to volume in a standard flask, standardizing by previously reported procedures,<sup>3,5,22-26</sup> and diluting appropriately with water.

#### Procedures

**Preparation of calibration graph.** Prepare a 200-µg/ml standard solution of the primary aromatic amine as described above. Treat 0.5–4 ml volumes of this solution with 2 ml of 0.2% 4-*N*-methylaminophenol solution, 1 ml of 1% acetic acid and 1 ml of 0.4% 2-iodylbenzoate solution, dilute to about 10 ml with water, allow to stand for 20 min, dilute to volume in a 25-ml standard flask and measure the absorbance at 525 nm against a reagent blank.

**Drug samples.** Weigh a known number of tablets and grind them to a fine powder. Accurately weigh a portion containing about 50 mg of analyte, stir it with 2 drops of 10% hydrochloric acid, dilute to about 100 ml with water, filter off any insoluble matter (starch, *etc.*) (Whatman No. 41 filter paper) and wash it with water. Dilute the combined filtrate and washings to volume in a 250-ml standard flask. Take a portion of the solution containing 100–800 µg of analyte, and analyse it as described for the preparation of the calibration graph.

### RESULTS AND DISCUSSION

The absorption spectrum of the chromogen obtained on reacting the amine with the product of oxidizing 4-*N*-methylaminophenol with 2-iodylbenzoate shows a maximum in the range 520–530 nm; the absorbance is measured at 525 nm for all amines. The reagent blank has only negligible absorbance. The optimum pH range for obtaining maximum colour intensity is 2.5–4. For convenience, 1 ml of 1% acetic acid is used. Though larger volumes do not

affect the absorbance values, 2 ml of 0.2% 4-*N*-methylaminophenol solution and 1 ml of 0.4% 2-iodylbenzoate solution will yield maximum colour intensity.

The first step in the colour development is oxidation of the 4-*N*-methylaminophenol to 1,4-benzoquinonemethylimine (which has a short life in aqueous solution, being prone to hydrolysis to 1,4-benzoquinone and methylamine<sup>27</sup>) and then its coupling with the primary aromatic amine. Neither

1,4-benzoquinone nor a mixture of hydroquinone and 2-iodylbenzoate will couple with amine to give a colour. Dichromate,<sup>11,12</sup> *N*-bromosuccinimide,<sup>13</sup> or other oxidants used previously,<sup>14</sup> react with primary aromatic amines and if the amine is not added last, lower absorbance values are produced. Thus the 4-*N*-methylaminophenol and oxidant (order immaterial) must be mixed first, and then the amine added. Because of the appreciable loss of 1,4-benzoquinonemethylimine by its rapid hydrolysis, any

Table 1. Determination of primary aromatic amines in pure solutions

Amine	[Amine], $\mu\text{g/ml}$		RSD† %	Molar absorptivity, $10^3 \text{ l. mole}^{-1} \text{ cm}^{-1}$
	Taken	Found by present method*		
Sulphanilic acid	4.02	4.05	0.3	7.3
	14.07	14.11		
	20.30	20.19		
	28.14	27.96		
4-Aminobenzoic acid	5.21	5.25	0.3	7.2
	15.62	15.56		
	26.05	26.12		
	31.25	31.01		
4-Aminosalicylic acid	3.38	3.42	0.3	6.4
	6.76	6.72		
	13.52	13.46		
	18.24	18.39		
	23.63	23.75		
	31.04	31.19		
Sulphadiazine	3.86	3.92	0.2	7.2
	9.21	9.13		
	16.80	16.75		
	22.54	22.41		
Sulphanilamide	5.26	5.20	0.2	7.0
	12.31	12.29		
	19.06	19.10		
	25.73	25.81		
Sulphaphenazole	4.58	4.53	0.4	6.6
	13.91	13.86		
	25.13	25.04		
	30.62	30.82		
Sulphamoxole	5.03	5.07	0.4	7.0
	14.71	14.67		
	26.59	26.68		
	31.21	31.10		
Sulphasomidine	4.98	5.04	0.5	6.5
	17.61	17.56		
	25.80	25.92		
	32.11	31.95		
Sulphamethoxy pyridazine	5.52	5.55	0.6	7.1
	12.39	12.43		
	19.06	19.00		
	29.32	29.12		
Sulphadimethoxine	6.15	6.10	0.5	6.9
	18.42	18.41		
	26.71	16.55		
	30.59	30.27		
Sulphacetamide	4.13	4.18	0.2	6.4
	16.06	16.19		
	21.55	21.43		
	28.90	28.72		
Sulphamethiazole	4.82	4.78	0.5	6.0
	16.39	16.49		
	27.52	27.38		
	31.68	31.42		

\*Mean of 6 replicates.

†Average RSD for entire concentration range.

Table 2. Analysis of sulpha drugs

Sulpha drug formulation*	Sulphonamide present	Amount, mg		
		Nominal amount	Present method†	Comparison method (reference)
Diastrep <sup>a</sup>	sulphadiazine	100	108 ± 0.4	105 (26)
Sulfuno	sulphamoxole	500	510 ± 0.5	514 (22)
Orisul	sulphaphenazole	500	510 ± 0.4	507 (22)
Urolocosil	sulphamethiazole	500	509 ± 0.4	513 (22)
Elkosin	sulphasomidine	500	525 ± 0.6	521 (23)
LAS	sulphamethoxy pyridazine	500	536 ± 0.6	530 (26)
Lasibon	sulphadimethoxine	500	490 ± 0.5	495 (23)
Nebasulf <sup>b</sup>	sulphacetamide	60	65 ± 0.4	68 (26)

\*The drugs also contained (a) chloramphenicol (125 mg) and streptomycin sulphate (125 mg); (b) nocomycin sulphate (5 mg) and bacitracin (250 units).

†Mean ± relative standard deviation (%) for 6 replicates.

delay in addition of the amine also results in low (and variable) absorbance values.<sup>11-14</sup> Since 2-iodylbenzoate does not react with primary aromatic amines,<sup>15</sup> both errors (due to reaction of the oxidant with amines, and the instability of 1,4-benzoquinone-methylimine) can be avoided. Any order of addition of reagents, excepting premixing of the 2-iodylbenzoate and 4-*N*-methylaminophenol, can be used.

Beer's law is valid over a range corresponding to 4-32 µg/ml primary aromatic amine in the final solution. Results are given in Table 1 for the assay of individual amines in pure solutions, and in Table 2 for the analysis of sulpha drugs.

*Acknowledgement*—Sincere thanks are due to the Council of Scientific and Industrial Research (New Delhi) for award of a Senior Research Fellowship to AJ.

## REFERENCES

- H. Abdine, M. A. Korany, A. M. Wahibi and F. El-Yazbi, *Talanta*, 1979, **26**, 1046.
- G. Norwitz and P. N. Keliher, *Anal. Chem.*, 1981, **53**, 1238.
- Idem, ibid.*, 1982, **54**, 807.
- Idem, Talanta*, 1982, **29**, 407.
- H. S. I. Tan and D. Shelton, *J. Pharm. Sci.*, 1974, **63**, 916.
- M. Qureshi and I. A. Khan, *Anal. Chim. Acta*, 1976, **86**, 309.
- C. T. H. Ellcock and A. G. Fogg, *Lab. Pract.*, 1974, **23**, 555.
- D. N. Krammer and L. U. Tolentino, *Anal. Chem.*, 1971, **43**, 834.
- D. N. Krammer and E. B. Hackley, *Anal. Lett.*, 1971, **4**, 223.
- R. Tawa and S. Hirose, *Chem. Pharm. Bull.*, 1980, **28**, 2136.
- R. R. Krishna and C. S. P. Sastry, *Talanta*, 1979, **26**, 861.
- R. R. Krishna, P. Siraj and C. S. P. Sastry, *Indian J. Pharm. Sci.*, 1979, **41**, 200.
- C. S. P. Sastry, B. G. Rao, B. S. Reddy and S. N. S. Murthy, *J. Indian Chem. Soc.*, 1981, **58**, 655.
- R. R. Krishna, P. Siraj and C. S. P. Sastry, *Acta Cienc. Indica, Ser. Chem.*, 1980, **6**, 140.
- K. K. Verma and A. K. Gulati, *Anal. Chem.*, 1982, **54**, 2550.
- K. K. Verma, A. K. Gulati, S. Palod and P. Tyagi, *Analyst*, 1984, **109**, 735.
- K. K. Verma and P. Tyagi, *Anal. Chem.*, 1984, **56**, 2157.
- K. K. Verma and A. Jain, *ibid.*, 1986, **58**, 821.
- L. F. Fieser and M. Fieser, *Reagents for Organic Synthesis*, Vol. 1, p. 511. Wiley-Interscience, New York, 1967.
- A. Banerjee, G. C. Banerjee, S. Bhattacharya, S. Banerjee and H. Samaddar, *J. Indian Chem. Soc.*, 1981, **58**, 605.
- L. F. Fieser and M. Fieser, *op. cit.*, p. 507.
- A. C. Bratton and E. K. Marshall, *J. Biol. Chem.*, 1939, **128**, 537.
- V. M. S. Ramanujam, N. M. M. Gowda, N. M. Trieff and M. S. Legator, *Microchem. J.*, 1980, **25**, 295.
- N. M. Trieff, V. M. S. Ramanujam and G. C. Forti, *Talanta*, 1977, **24**, 188.
- B. Jayaram and N. M. M. Gowda, *Analyst*, 1985, **110**, 985.
- K. K. Verma, P. Tyagi and A. K. Gulati, *J. Pharm. Biomed. Anal.*, 1987, **5**, 51.
- D. Amin, *Analyst*, 1985, **110**, 211.

## ANALYTICAL DATA

# SOLVENT EXTRACTION OF Cd(II) WITH N-CYCLOHEXYL-N-NITROSOHYDROXYLAMINE AND 4-METHYLPYRIDINE INTO METHYL ISOBUTYL KETONE

G. RAURET, L. PINEDA, R. CASAS and R. COMPAÑO

Department of Analytical Chemistry, University of Barcelona, Barcelona, Spain

A. SANCHEZ-REYES

Department of Fundamental Physics, University of Barcelona, Barcelona, Spain

(Received 14 August 1987. Revised 6 October 1987. Accepted 8 December 1987)

**Summary**—The distribution equilibria of the complexes cadmium-cnha and cadmium-cnha-4-methylpyridine in the water-methyl isobutyl ketone system have been studied at 25°, by using <sup>109</sup>Cd as a radiotracer to measure the metal distribution ratio. A very sensitive method for detection of <sup>109</sup>Cd, based on the use of a liquid scintillator, has been developed. From the graphical treatment of the equilibrium data, it has been deduced that CdL<sub>2</sub> is the complex extracted in the absence of 4-methylpyridine, and that the adduct CdL<sub>2</sub>B is extracted when the second ligand is present. This model has been checked by treating the data with the program LETAGROP-DISTR and the following equilibrium constants have been obtained: stability constants of CdL<sub>2</sub>, log β<sub>1</sub> = 2.82 ± 0.14, log β<sub>2</sub> = 5.981 ± 0.004; distribution constant of CdL<sub>2</sub>, log K<sub>DC</sub> = -0.49 ± 0.01; adduct formation constant of CdL<sub>2</sub>B, log K<sub>i</sub> = 2.70 ± 0.07.

The industrial applications of cadmium have increased considerably in recent years.<sup>1</sup> Because this element is highly toxic even at very low concentrations it must be determined in environmental samples.

Although some analytical methods for cadmium determination are very sensitive, low concentrations are generally determined after use of a preconcentration technique such as solvent extraction. Several authors have proposed systems for cadmium extraction.<sup>2-13</sup> Reagents such as dithizone,<sup>2,3</sup> thiooxine,<sup>3</sup> and some dithiocarbamates,<sup>4,6,7</sup> co-ordinating through sulphur atoms, have often been studied. When the co-ordination takes place through nitrogen or oxygen atoms, a second ligand (pyridine, picolines, 1,10-phenanthroline, TOPO, TBP, ...) has often been added to the system to enhance the extraction as a result of formation of a ternary complex.<sup>8-10,12</sup>

In the present paper, as a part of a wider study to assess the utility of *N*-cyclohexyl-*N*-nitrosohydroxylamine (cnha) as an agent for extracting metals into methyl isobutyl ketone (MIBK),<sup>14,15</sup> we report the study of the distribution equilibria of Cd-cnha and Cd-cnha-4-methylpyridine complexes. The cnha-MIBK system has proved useful for the determination of Cu(II) in river water by atomic-absorption spectrometry<sup>14</sup> and its application to the determination of other heavy metals in natural and waste waters is now being studied.

The use of radioactive tracers is one of the best methods for studying the distribution of metals be-

tween immiscible phases. In the present work, <sup>109</sup>Cd was used and a very sensitive method for its detection, based on the use of a liquid scintillator, has been developed.

## EXPERIMENTAL

### Reagents

The sodium salt of *N*-cyclohexyl-*N*-nitrosohydroxylamine was obtained from the potassium salt (BASF) as described earlier.<sup>14</sup>

A stock solution of cadmium (1 g/l.) was made by dissolving the metal (analytical-reagent grade) in a small volume of concentrated nitric acid, then adding perchloric acid and boiling until white fumes were evolved. The solution was cooled, transferred to a 1-litre standard flask and diluted to the mark.

Carrier-free <sup>109</sup>Cd (*t*<sub>1/2</sub> 453 d) was supplied by Amersham International as CdCl<sub>2</sub>. The radiotracer was added to the cadmium solution before the extraction.

Analytical-reagent grade pyridine (Fluka), tri-*n*-butyl phosphate (Carlo Erba), tri-*n*-octylphosphine oxide (Merck) and benzyltrimethyltetradecylammonium chloride (Fluka). Triethylamine, 95% (Merck) and 4-methylpyridine, 96% (Fluka). The content of 4-methylpyridine in the commercially available product was checked by gas chromatography. Liquid scintillation cocktail Insta-Gel (Packard).

All other chemicals were of analytical grade and were used without further purification.

### Apparatus

A coaxial Ge(Li) semiconductor detector (Ortec), with an effective volume of 58 cm<sup>3</sup>, connected to a 4092-channel multichannel analyser (Silena) was used for gamma-ray measurements. A dual liquid-scintillation counter (Bertold LB 5040) was used for beta particle measurements.

A pH-meter (Radiometer PHM 64), equipped with a glass-calomel electrode pair, and standardized with buffer solutions at pH 4.008 and 6.865 (25°) prepared from Merck salts according to DIN 19266, was used.

#### Procedure

Ten ml of aqueous phase saturated with the organic solvent and containing an appropriate concentration of cadmium (labelled with  $^{109}\text{Cd}$ ), the sodium salt of cnha and 4-methylpyridine (the last only when the distribution of the ternary complex was studied) were shaken with 10 ml of MIBK, saturated with water, in a thermostatic bath at  $25.0 \pm 0.1^\circ$  for 15 min. The pH of the aqueous phase was adjusted with either perchloric acid or an acetic acid-sodium acetate buffer, and sodium perchlorate was added to give a constant ionic strength of 0.1. After phase separation, the metal distribution ratio ( $D$ ) was measured by one of the following procedures.

(a) For  $D > 0.1$  equal volumes (4 ml) of both phases were measured by pipette into suitable counting tubes and their activities measured at constant geometry. Then

$$D = A_o/A_w \quad (1)$$

where  $A_o$  and  $A_w$  are the activities of the organic and aqueous phases respectively.

(b) For  $D < 0.1$ , 4 ml of each aqueous phase were taken and their  $\gamma$ -activities determined; the same volume of each organic phase was mixed with 15 ml of the liquid scintillator and the activity measured. The distribution ratio was calculated by means of the expression

$$D = \frac{A_o (\text{liquid scintillator}) \times F}{A_w (\text{gamma})} \quad (2)$$

where  $F$  is defined as

$$F = \frac{\text{Activity of organic phase (gamma)}}{\text{Activity of organic phase (liquid scintillator)}} \quad (3)$$

and is found for each series of experiments by use of organic phases with activities measurable accurately by means of both techniques.

The quench of the samples was determined by the channel ratio-external standard method. All the samples of each series showed the same quench.

## RESULTS AND DISCUSSION

### Measurement of $^{109}\text{Cd}$ activity

The nuclear transformation of  $^{109}\text{Cd}$  takes place by electron capture to give  $^{109\text{m}}\text{Ag}$ , which decays to the ground state by an 88-keV gamma transition ( $\sim 3.8\%$ ) or emission of internal conversion electrons ( $\sim 96.2\%$ ).<sup>16</sup> When the metal solution is labelled with  $^{109}\text{Cd}$ , the distribution ratio may be determined, after phase equilibration, as the ratio of the gamma activity of the organic phase to that of the aqueous phase. However, the low probability of gamma-ray emission, together with the low efficiency ( $\sim 4\%$ ) of the Ge(Li) detector for the geometry used, made it necessary, when  $D$  was lower than 0.1, to increase the quantity of radiotracer added to the system or to use long counting periods in order to measure the activity of the organic phase with adequate accuracy.

The advantageous features of liquid scintillation measurements for detecting low-energy beta emitters seemed favourable for the detection of internal conversion electrons of  $^{109}\text{Cd}$  and also the subsequent Auger electrons. Since these electrons are mono-energetic, their pulse-height distribution curve will be

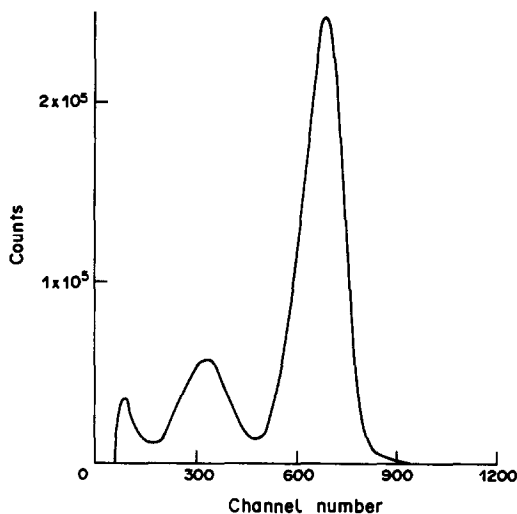


Fig. 1. Spectrum of the Auger and internal conversion electrons of  $^{109}\text{Cd}$ .

peak-shaped and the area under the curve will give their total number. Figure 1 shows the spectrum obtained by mixing a solution of known activity of  $^{109}\text{Cd}$  with the liquid scintillator. The lowest energy peak, at 18 keV, corresponds to the Auger electrons and the 65 and 84 keV peaks correspond to the internal conversion electrons. The spectrum may contain a small contribution from the gamma-rays, which can interact with the scintillator and produce an electric pulse.

From the total number of counts, obtained from integration of the spectrum and the activity of the  $^{109}\text{Cd}$  solution, an overall apparent efficiency of 120% was obtained, because of the simultaneous detection of the Auger and internal conversion electrons. Hence, this method is 800 times as sensitive as the Ge(Li) detector method, for the same counting time, and is suitable for measuring the activity of the organic phases when the distribution ratio is very low.

### Distribution of the cadmium-cnha binary complex in the water-MIBK system

**Influence of shaking time.** The distribution ratio values obtained at pH 7.20, with shaking times between 1 and 60 min, show that the distribution equilibrium is attained after 5 min of shaking. In subsequent experiments an extraction time of 15 min was adopted.

**Influence of ionic strength.** The ionic strength of the aqueous phase was varied over the range 0.01–1.0M by the addition of sodium perchlorate. The distribution ratio, at constant pH and cnha concentration, was independent of ionic strength up to 0.3M; at higher values, the distribution ratio slightly decreased. In the rest of the work the ionic strength was adjusted to 0.1M.

**Influence of metal concentration.** Varying the cadmium concentration between  $8.93 \times 10^{-6}\text{M}$  and

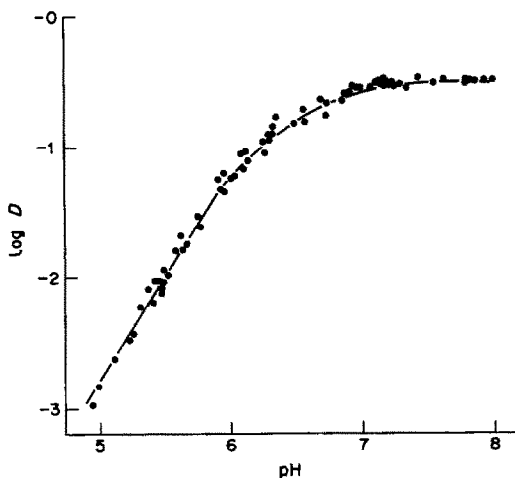


Fig. 2. Influence of pH on the distribution ratio.  $c_{\text{cnha}} = 1.0 \times 10^{-2} M$ .  $c_{\text{Cd}} = 9.0 \times 10^{-5} M$ .

$7.14 \times 10^{-4} M$ , at pH 7.1 and with a reagent concentration of  $1.0 \times 10^{-2} M$ , had no effect on the distribution ratio, suggesting that only mononuclear species were extracted.

**Influence of pH and ligand concentration.** The influence of pH on the distribution ratio was studied for  $1.0 \times 10^{-2} M$  cnha. The various pH values were obtained by addition of dilute perchloric acid to the aqueous phase. The results are plotted in Fig. 2. Because of the low buffer capacity of the aqueous phases, the pH measurements were very slow; therefore, in the subsequent experiments an acetic acid-acetate mixture, at total concentration  $6.0 \times 10^{-2} M$ , was added to the aqueous phases to facilitate the pH measurement.

Figure 3 shows values of  $\log D$ , obtained for four different ligand concentrations, plotted vs. pH. If the curve in Fig. 2 is compared with that for the same reagent concentration in Fig. 3, it is evident that the curve for the acetate medium is displaced by about 0.4 pH units to higher values, although both curves coincide in the region of maximum extraction. This

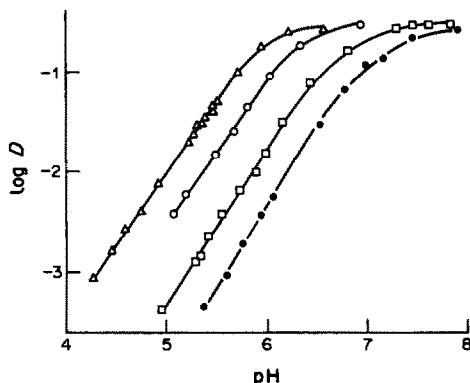


Fig. 3. Influence of pH on the distribution ratio in the presence of an acetic acid-acetate buffer.  $c_{\text{Cd}} = 9.0 \times 10^{-5} M$ .  $c_{\text{cnha}} = \bullet 5.0 \times 10^{-3} M$ ;  $\square 1.0 \times 10^{-2} M$ ;  $\circ 2.5 \times 10^{-2} M$ ;  $\triangle 5.0 \times 10^{-2} M$ .

suggests that acetate forms non-extractable cadmium complexes in the aqueous phase, and that this decreases the distribution ratio. A later series of experiments done in the absence of cnha confirmed that cadmium is not extracted with acetate into MIBK.

**Composition of the extracted species and calculation of the equilibrium constants.** Since variation of the cadmium concentration demonstrated that only mononuclear species are extracted, the metal distribution ratio is given by

$$D = \frac{\sum_n \sum_m [\text{ML}_n(\text{HL})_m]_o}{[\text{M}]_w + \sum_p [\text{ML}_p]_w + \sum_q [\text{MX}_q]_w} \quad (4)$$

where M represents the metal, HL the extracting agent, X another ligand present in the aqueous phase and the subscripts o and w denote the organic and the aqueous phases respectively. Charges have been omitted for simplicity.

If only the species  $\text{ML}_n(\text{HL})_m$  is extracted and the metal is present in the aqueous phase predominantly as the cation  $\text{M}^{n+}$ , the following equation can be obtained:

$$\log D = \log K_{\text{ex}} + n\text{pH} + (m+n)\log[\text{HL}]_o \quad (5)$$

where  $K_{\text{ex}}$ , the extraction constant of  $\text{ML}_n(\text{HL})_m$ , is  $K_m K_{\text{DC}} \beta_n K_a^n / K_{\text{DR}}^m$  ( $\beta_n$  = formation constant of  $\text{ML}_n$ ;  $K_{\text{DC}}$  = distribution constant of  $\text{ML}_n$ ;  $K_m$  = adduct formation constant in the organic phase,  $K_a$  and  $K_{\text{DR}}$  = dissociation and distribution constants of the reagent, respectively).

When species other than  $\text{ML}_n$  can be neglected in the aqueous phase, the following equation is valid:

$$\log D = \log(K_m K_{\text{DC}}) + m \log[\text{HL}]_o \quad (6)$$

#### (a) Graphical treatment

The curve shown in Fig. 2 is linear up to pH 5.8, with a slope of 1.7. In accordance with equation (5), this suggests that  $n = 2$ , although the presence of a mixture of  $\text{Cd}^{2+}$  and  $\text{CdL}^+$  in the aqueous phase must be considered. The small variations of  $[\text{HL}]_o$  over the pH range 4.9–5.8 have been neglected in the slope analysis of the curve  $\log D$  vs. pH. At higher pH values the slope of this curve decreases and finally, at pH 7.0, the distribution ratio becomes independent of the pH, pointing to the validity of equation (7).

The curves obtained in the presence of acetate in the aqueous phase (Fig. 3) are very similar to the curve in Fig. 2, with a linear segment having a slope of 1.5–1.6.

To examine the influence of cnha concentration on the distribution ratio, at constant pH, the values of  $\log D$  corresponding to each reagent concentration were calculated from the curves in Fig. 3 at pH 5.10, 5.40, 5.50, 5.70, 5.90 and 6.00. These values, plotted against  $\log[\text{HL}]_o$ , give straight lines with slopes of 1.8–1.9, and this, according to equation (5), suggests

Table 1. Survey of the equilibrium constants for the extraction of Cd(II) with *cnha* into methyl isobutyl ketone

Method	$\log K_{DC}$	$\log \beta_1$	$\log \beta_2$	$\log K_1$	$\sigma(\log D)$
Graphical	-0.49	3.0	6.0	2.60	
LETAGROP-	$-0.49 \pm 0.01$		$5.981 \pm 0.004$		0.0146
DISTR		$2.82 \pm 0.14$			0.0618
		$3.35 \pm 0.14^*$			0.0680
				$2.70 \pm 0.07$	0.0673

\*Value obtained in the presence of acetate in the aqueous phase.

The limits given for the constants correspond to  $\log[\beta \pm 3\sigma(\beta)]$ ;  $\sigma(\log D) = (\Sigma(\log D_{\text{exp}} - \log D_{\text{calc}})^2/N)^{1/2}$

that  $m + n = 2$ . Since all the curves in Fig. 3 tend to the same maximum value of  $\log D$ , it is unlikely that any adduct species is extracted, so  $m = 0$  and  $n = 2$  and

$$\log D = \log K_{DC} \quad (7)$$

The slopes of the distribution curves suggest that the species extracted is the simple 1:2 chelate  $\text{CdL}_2$ . Its distribution constant, evaluated as the average of the distribution ratio values obtained at pH values above 7.0, is  $\log K_{DC} = -0.489 \pm 0.008$ .

To check the proposed model, as well as to calculate  $K_{DC}$  and the stability constants  $\beta_1$  and  $\beta_2$  of  $\text{CdL}_2$  in the aqueous phase, Sillén's curve-fitting method<sup>17</sup> was applied to the data obtained in the absence of acetate. The normalized curves are given by

$$D^* = u^2/(1 + pu + u^2) \quad (8)$$

where the normalized variables and the parameter  $p$  are defined by  $D^* = D/K_{DC}$ ,  $u = \beta_2^{1/2}[\text{L}^-]$  and  $p = \beta_1/\beta_2^{1/2}$ .

The values of the constants obtained by this method are given in Table 1. The good agreement between the experimental points and one of the normalized curves confirms the proposed model.

#### (b) Numerical treatment

The values of the constants obtained graphically were refined by means of the program LETAGROP-DISTR.<sup>18</sup> The data obtained in the absence of acetate were subdivided into two groups. From the group of points obtained at pH above 7.0,  $K_{DC}$  and  $\beta_2$  were refined. The points at lower pH were used to obtain  $\beta_1$ . Treatment of all the data at once leads to less precise values of  $\beta_2$  and  $K_{DC}$ . The results are given in Table 1.

In the computer treatment of the data obtained in the presence of acetate in the aqueous phase, the formation of cadmium-acetate complexes must be taken into account. Literature values for the stability constants of these complexes<sup>19</sup> were adjusted for an ionic strength of 0.1 by the method of Linder and Murray.<sup>20</sup>

The data obtained in the presence of acetate were used only to find the constant  $\beta_1$ ; the other constants were not refined because, as can be seen in Fig. 3, there were few experimental points for the condi-

tions where the complex  $\text{CdL}_2$  is the predominant species in both phases. The final value of  $\beta_1$  is given in Table 1.

The distribution of cadmium among the various species was calculated by HÅLTAFALL.<sup>21</sup> Figures 4 and 5 show distribution diagrams calculated for an aqueous phase with and without acetate.

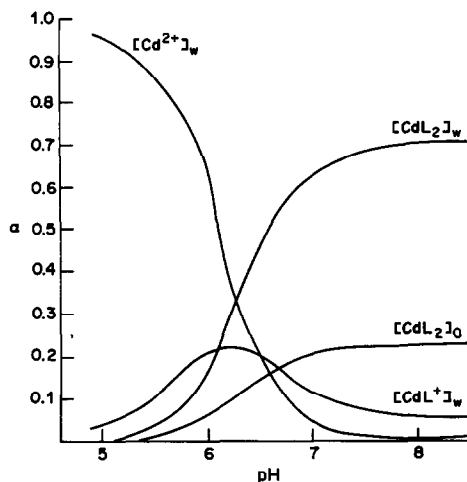
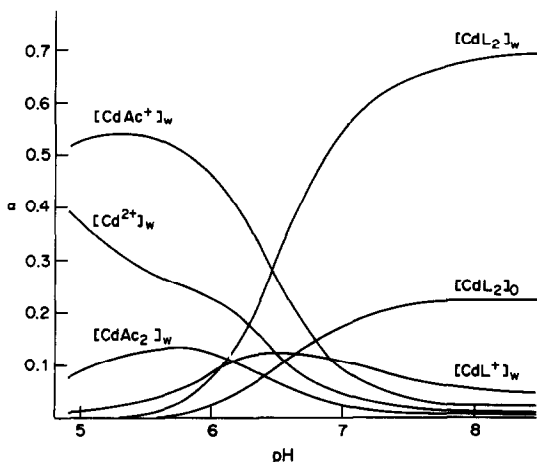
Fig. 4. Distribution diagram of species.  $c_{\text{cnha}} = 1.0 \times 10^{-2} M$ .Fig. 5. Distribution diagram of species in the presence of acetate.  $c_{\text{cnha}} = 1.0 \times 10^{-2} M$ ;  $c_{\text{acetate}} = 0.06 M$ .



Table 2. Influence of the presence of a second ligand on the degree of extraction ( $R$ ) of cadmium;  $c_{\text{cnha}} = 1.0 \times 10^{-2} M$

Ligand	Concentration	pH	$R$ , %
Triocetylamine	$5.0 \times 10^{-2} M$	7.73	44
Pyridine	$1.0 \times 10^{-3} M$	7.82	25
	$5.0 \times 10^{-2} M$	7.96	71
4-Methylpyridine	$1.0 \times 10^{-3} M$	7.92	25
	$5.0 \times 10^{-2} M$	8.06	88
Zephiramine	$5.0 \times 10^{-2} M$	7.40	59
Tributyl phosphate	$1.0 \times 10^{-3} M$	7.98	25
	$5.0 \times 10^{-2} M$	7.92	28
Triocetylphosphine oxide	$1.0 \times 10^{-3} M$	8.02	25
	$5.0 \times 10^{-2} M$	7.73	93

#### DISTRIBUTION OF CADMIUM-CNHA-4-METHYLPYRIDINE TERNARY COMPLEX IN THE WATER-MIBK SYSTEM

To enhance the extraction of cadmium by formation of a ternary complex, a second ligand was added to the system. The influence of various compounds on the degree of metal extraction was studied and the results are shown in Table 2. Of the substances found to enhance extraction, 4-methylpyridine ( $\gamma$ -picoline) was chosen as synergic agent because it is more readily available.

To find out whether any cadmium- $\gamma$ -picoline complexes are extracted into MIBK in the absence of cnha, some extractions for pH = 5.4–7.5, [metal] =  $9.0 \times 10^{-5} M$  and [ $\gamma$ -picoline] =  $5.0 \times 10^{-2} M$ , were tried. Since  $99.0 \pm 0.5\%$  of cadmium remained in the aqueous phase at all pH values, the extraction of cadmium in the absence of cnha can be neglected.

#### Effect of pH and cnha concentration

Three series of extractions at varied pH were performed, each series corresponding to one ligand concentration. In all the experiments the cadmium

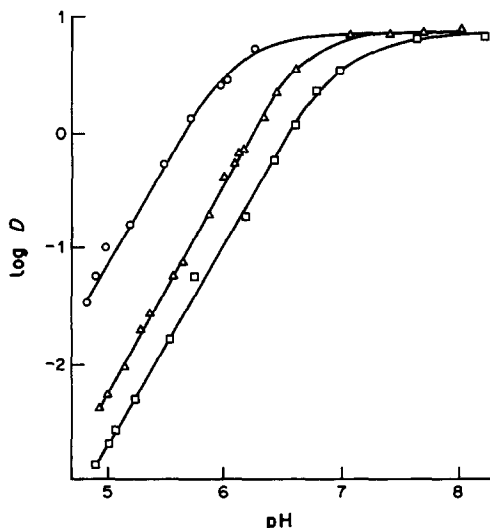


Fig. 6. Influence of pH on the distribution ratio for the ternary complex.  $c_{\text{Cd}} = 9.0 \times 10^{-5} M$ .  $c_{\gamma\text{-picoline}} = 5.0 \times 10^{-2} M$ .  $c_{\text{cnha}} = \square 5.0 \times 10^{-3} M$ ;  $\triangle 1.0 \times 10^{-2} M$ ;  $\circ 5.0 \times 10^{-2} M$ .

and  $\gamma$ -picoline concentrations were kept constant at  $9.0 \times 10^{-5} M$  and  $5.0 \times 10^{-2} M$ , respectively. The results are shown in Fig. 6.

#### Effect of pH and $\gamma$ -picoline concentration

Similarly, three series of extractions at varied pH and different  $\gamma$ -picoline concentrations were carried out. The metal concentration was  $9.0 \times 10^{-5} M$  and that of cnha  $1.0 \times 10^{-2} M$  in all cases. These results are shown in Fig. 7.

The influence of  $\gamma$ -picoline concentration, in the region where the distribution ratio is independent of pH, was also studied.  $[B]_o$  was calculated from the values of the distribution constant of  $\gamma$ -picoline (6.59) and the dissociation constant of the picolinium ion ( $7.00 \times 10^{-7}$ ) previously determined.<sup>22</sup> Figure 8 shows a plot of  $\log D$  vs.  $\log[B]_o$ .

#### Composition of species extracted and calculation of the adduct formation constant

Taking into account the formation of ternary complexes with  $\gamma$ -picoline, the metal distribution ratio is given by

$$D = \frac{[ML_n]_o + \sum_s [ML_n B_s]_o}{[M]_w + \sum_p [ML_p]_w + \sum_q [MX_q]_w + \sum_r [MB_r]_w} = \frac{\left(1 + \sum_s K_s [B]_o^s\right) K_{DC} \beta_n K_a^n [HL]_o^n}{K_{DR}^n [H]_w^n \left\{1 + \sum_p \beta_p [L]_w^p + \sum_q \beta_q [X]_w^q + \sum_r \beta_r [B]_w^r\right\}} \quad (9)$$

where, besides the symbols previously defined, B represents  $\gamma$ -picoline and  $K_s$  is the adduct formation constant in the organic phase. When the cation  $M^{n+}$  is the predominant species in the aqueous phase and  $[B]_o$  is kept constant,

$$\log D = \log K + n \log [HL]_o + n \text{pH} \quad (10)$$

where

$$K = \left(1 + \sum_s K_s [B]_o^s\right) \frac{K_{DC} \beta_n K_a^n}{K_{DR}^n} \quad (11)$$

If the metal is present in the aqueous phase predominantly as the complex  $ML_n$ , equation (12) is deduced:

$$D = K_{DC} + K_{DC} \sum_s K_s [B]_o^s \quad (12)$$

#### (a) Graphical treatment

The curves of  $\log D$  vs. pH, plotted in Fig. 6, have linear segments with slope 1.8, so according to equation (10), it is probable that  $n = 2$ . At higher pH values the slope decreases progressively to zero and the three curves coincide, a fact which confirms that self-adduct complexes with cnha are not extracted.

The slope of the linear segments of the curves of  $\log D$  vs. pH in Fig. 7 is 1.8. The values of  $\log D$  corresponding to each  $\gamma$ -picoline concentration were

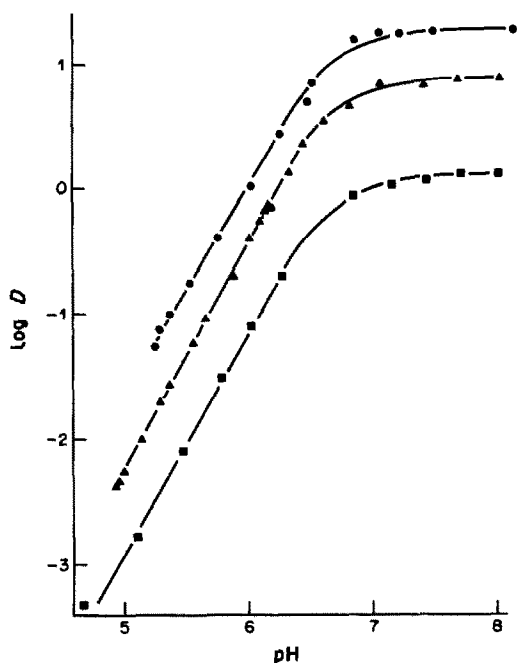
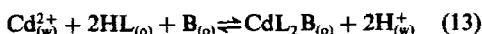


Fig. 7. Influence of pH on the distribution ratio for the ternary complex.  $c_{\text{Cd}} = 9.0 \times 10^{-3} M$ .  $c_{\text{cnha}} = 1.0 \times 10^{-2} M$ .  $c_{\gamma\text{-picoline}} = \blacksquare 1.0 \times 10^{-2} M$ ;  $\blacktriangle 5.0 \times 10^{-2} M$ ;  $\bullet 1.0 \times 10^{-1} M$ .

calculated from the curves in Fig. 7 at pH 5.30, 5.60, 5.90 and 6.20. These values, plotted against  $\log [B]_o$ , give straight lines with a slope of 1.1.

The former results suggest that, in the presence of  $\gamma$ -picoline, the distribution equilibrium can be represented by the equation



The data plotted in Fig. 8 were obtained in conditions where  $s = 1$  in equation (12). At low  $\gamma$ -picoline

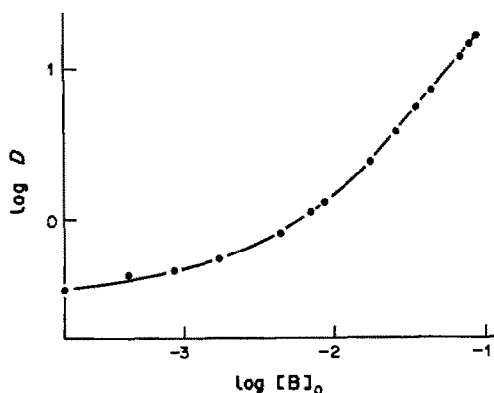


Fig. 8. Distribution of Cd(II) as a function of the equilibrium concentration of  $\gamma$ -picoline in the organic phase.  $c_{\text{Cd}} = 9.0 \times 10^{-3} M$ .  $c_{\text{cnha}} = 1.0 \times 10^{-2} M$ . pH = 7.65–7.95.

concentration, the complex  $\text{CdL}_2$  is the predominant species in both phases and equation (12) becomes  $\log D = K_{\text{DC}}$ ; at higher concentrations the adduct  $\text{CdL}_2\text{B}$  is the main species in the organic phase and equation (12) becomes

$$\log D = \log(K_{\text{DC}}K_s) + \log[B]_o \quad (14)$$

which explains the existence of a linear segment with a slope close to 1.

To calculate the adduct formation constant, a curve-fitting method<sup>17</sup> was applied to the data of Fig. 8. The normalized curve  $D^* = 1 + u$  was obtained by substituting the normalized variables  $D^* = D/K_{\text{DC}}$  and  $u = K_s[B]_o$  in equation (12) for  $s = 1$ . The value  $\log K_s = 2.60$  was obtained.

#### (b) Numerical treatment

The value of  $K_s$  was refined by means of the program LETAGROP-DISTR,<sup>18</sup> the final result being  $\log K_s = 2.70 \pm 0.07$  with  $\sigma(\log d) = 0.0673$  (Table 1).

#### REFERENCES

1. J. W. Moore and S. Ramamoorthy, *Heavy Metals in Natural Waters: Applied Monitoring and Impact Assessment*, pp. 29–31. Springer Verlag, New York, 1984.
2. T. Sekine and Y. Hasegawa, *Solvent Extraction Chemistry; Fundamentals and Applications*, pp. 615–617. Dekker, New York, 1977.
3. H. Onishi, *Photometric Determination of Traces of Metals, Part IIA*, 4th Ed., pp. 305–315. Wiley, New York, 1986.
4. A. Dorneman and H. Kleist, *Analyst*, 1979, **104**, 1030.
5. J. Kommarek, J. Havel and L. Sommer, *Collection Czech. Chem. Commun.*, 1979, **44**, 3241.
6. R. E. Sturgeon, S. S. Berman, A. Desaulniers and D. S. Russell, *Talanta*, 1980, **27**, 85.
7. B. Nikolova and N. Jordanov, *ibid.*, 1982, **29**, 861.
8. E. Yamada, E. Nakayama, T. Kuwamoto and T. Fujinaga, *Anal. Chim. Acta*, 1982, **138**, 409.
9. *Idem*, *Bull. Chem. Soc. Japan*, 1982, **55**, 3155.
10. G. N. Rao and R. Lahiri, *Proc. Indian Acad. Sci. Ser. Chem. Sci.*, 1983, **92A**, 167.
11. M. Silva and M. Valcárcel, *Mikrochim. Acta*, 1983 **I**, 315.
12. T. A. Onishchenko, Yu. K. Onishchenko, I. V. Pyatnitskii and V. V. Sukhan, *Zh. Analit. Khim.*, 1986, **41**, 1040.
13. Y. K. Agrawal and T. A. Desai, *Analyst*, 1986, **111**, 305.
14. G. Rauret, L. Pineda, M. Ventura and R. Compañó, *Talanta*, 1986, **33**, 141.
15. G. Rauret, R. Compañó, L. Pineda and J. M. Falgueras, *An. Quim.*, 1987, **83**, 82.
16. C. M. Lederer and V. S. Shirley (eds), *Table of Isotopes*, 7th Ed., p. 503. Wiley, New York, 1978.
17. L. G. Sillén, *Acta Chem. Scand.*, 1956, **10**, 186.
18. D. Hay Liem, *ibid.*, 1971, **25**, 1521.
19. A. E. Martell and R. M. Smith, *Critical Stability Constants*, Vol. 3, Plenum Press, New York, 1977.
20. P. W. Linder and K. Murray, *Talanta*, 1982, **29**, 377.
21. N. Ingri, W. Kakolowicz, L. G. Sillén and B. Warnquist, *Talanta*, 1967, **14**, 1261; errata, 1968, **15**, No. 3, ix.
22. G. Rauret, L. Pineda and R. Compañó, *An. Quim.*, in the press.

## 1,2-NAPHTHOQUINONE-2-THIOSEMICARBAZONE AS A NEW ACID-BASE INDICATOR IN ISOPROPYL AND *tert*-BUTYL ALCOHOL MEDIA

ELISABETH BOSCH and MARTI ROSES

Department of Analytical Chemistry, University of Barcelona, Avda. Diagonal 647,  
08028 Barcelona, Spain

(Received 15 September 1986. Revised 10 November 1987. Accepted 21 November 1987)

**Summary**—1,2-Naphthoquinone-2-thiosemicarbazone is proposed as an acid-base indicator for use in isopropyl and *tert*-butyl alcohol media. The dissociation constants have been determined in both media and the colour transition, sensitivity and sharpness of the indicator are described by means of chromatic parameters. The indicator has been used for determination of some organic acids, with errors of less than 1%.

1,2-Naphthoquinone-2-thiosemicarbazone (NQT), mixed with picric acid and Sandolan Turquoise E-AS, has been proposed as a screened acid-base indicator for use in aqueous solution.<sup>1</sup> It is now shown to be useful in isopropyl and *tert*-butyl alcohol media as well.

Isopropyl alcohol ( $K_a = 10^{-20.8}$ ,  $\epsilon = 19.9$  at 25°) and *tert*-butyl alcohol ( $K_a = 10^{-28.5}$ ,  $\epsilon = 10.0$  at 30°) show good acid-strength differentiating ability, hydrogen-bond accepting capability<sup>2,3</sup> and very good solvating power which prevents homoconjugation phenomena. In addition, their low volatility and wide availability in highly purified form make them excellent media for titration of acids.<sup>4</sup>

The present work deals with a spectrophotometric study of NQT in these alcohols, and the determination of its  $pK_a$  values and colour change intervals by means of the CIE and complementary systems.<sup>5-7</sup> The optimum concentration for the indicator has been determined according to the Kotrlý and Vytřas method.<sup>8,9</sup> This method has been applied to the CIELAB and CIELUV co-ordinates for the indicator transition<sup>10</sup> and the colour change sensitivity has been measured in terms of SCD values.<sup>11</sup>

The behaviour of the indicator has been tested by titration of some acids in both solvents and the results are precise, accurate and similar to those obtained by titrations in aqueous method, with visual indicators.

### EXPERIMENTAL

#### Apparatus

A Beckman Acta M-VII spectrophotometer with 10-mm cells was used for recording spectra, and a Hewlett-Packard Series 200 computer for calculations. A Radiometer PHM 64 pH-meter with glass/calomel electrodes was used for pH measurements. For work with isopropyl alcohol solutions the calomel electrode was filled with a saturated solution of potassium chloride in methanol and used with a salt bridge containing a saturated solution of tetramethylammonium chloride in isopropyl alcohol.<sup>12</sup> For work with *tert*-butyl alcohol solutions a reference electrode similar

to this, and used successfully by Marple *et al.*,<sup>13</sup> was prepared. The SCE was immersed in the aqueous phase of a water/*tert*-butyl alcohol mixture saturated with potassium chloride. The organic phase of the mixture was in contact with a 1M solution of tetrabutylammonium bromide in *tert*-butyl alcohol containing 5% v/v isopropyl alcohol to prevent freezing or variations in concentration with temperature drop. The electrode was kept at 30°. The measurements obtained show good reproducibility. A Gibson Minipuls 2 peristaltic pump was used to circulate the solutions.

#### Reagents

NQT was prepared and purified according to Luque de Castro *et al.*<sup>14</sup> and its characteristics have been reported.<sup>1</sup> Merck GR grade isopropyl alcohol and *tert*-butyl alcohol were used, and their water content was determined by the Karl Fischer method and found to be 0.076 and 0.073% respectively. A 0.1M tetrabutylammonium hydroxide (TBAH) solution in isopropyl alcohol (Carlo Erba), with a methanol content of 8% (determined by gas chromatography), was used; it was standardized against benzoic acid. Picric acid (Doesder AR-ACS grade, vacuum-dried) and benzoic acid and veronal (Merck GR grade) were used.

#### Determination of standard potentials

The potentiometric systems were calibrated by titration of picric acid with TBAH,<sup>12,15</sup> because the dissociation constants of picric acid and tetrabutylammonium picrate in both solvents are known.<sup>16,17</sup>

#### Procedure

Indicator solutions (approximately  $5 \times 10^{-5}M$ ) buffered with veronal were titrated with TBAH solution, and monitored simultaneously by potentiometry and continuous measurement of the absorbance values at 10-nm intervals between 380 and 770 nm. The solutions were stirred with a stream of nitrogen and continuously circulated between the titration vessel and the spectrophotometer cell by means of a peristaltic pump. The absorbance characteristics of the completely undissociated and dissociated forms of the indicator were determined with its solution in sulphuric or benzoic acid and TBAH media, respectively. The temperature was  $25 \pm 0.2^\circ$  for work with isopropyl alcohol solutions and  $30 \pm 0.2^\circ$  for *tert*-butyl alcohol solutions.

#### Computation methods

To calculate the standard potentials from the titration data the program ACETERISO,<sup>17</sup> written in BASIC, was

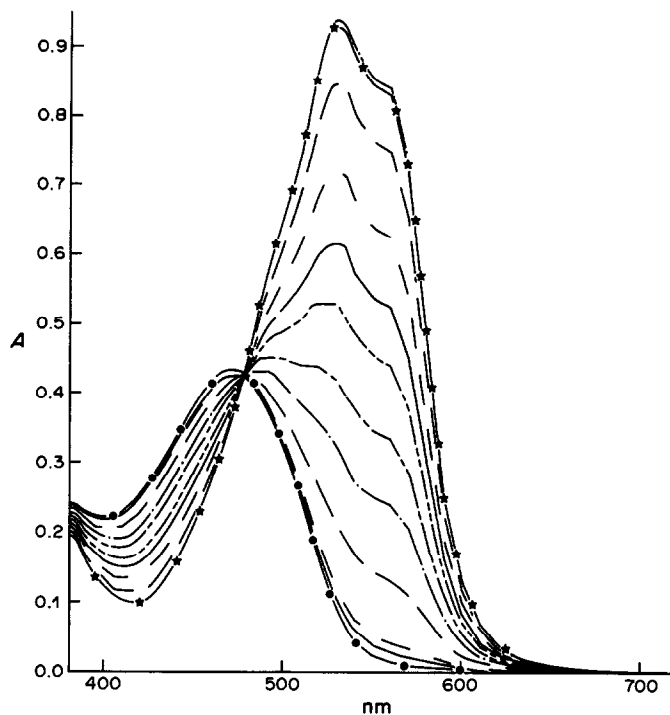


Fig. 1. Visible spectra of NQT in *i*-PrOH at some pH values in the transition range. Acidic form —●—, basic form —★—. Intermediate pH values: 9.71; 10.54; 11.56; 12.02; 12.26; 12.51; 12.69; 12.91; 13.32 and 14.80.

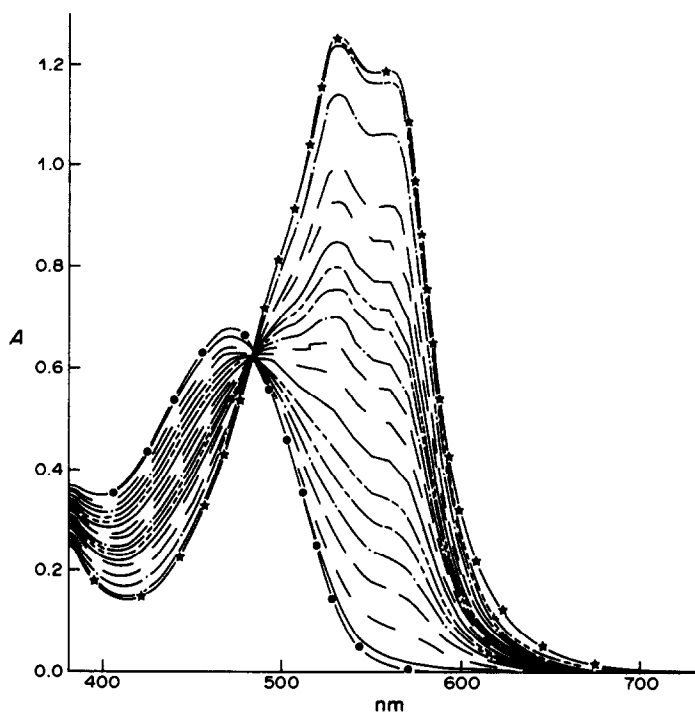


Fig. 2. Visible spectra of NQT in *t*-BuOH at some pH values in the transition range. Acidic form —●—, basic form —★—. Intermediate pH values: 10.53; 14.65; 14.99; 15.16; 15.27; 15.35; 15.45; 15.52; 15.59; 15.65; 15.71; 15.77; 15.83; 15.90; 16.04; 16.31; 16.78 and 17.52.

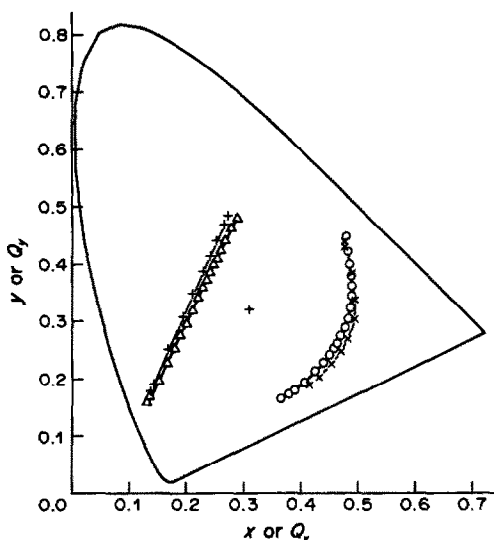


Fig. 3. Experimental transition colour points in the CIE ( $x$ ,  $y$ ) chromaticity system at the optimum concentration:  $\times \times \times$  NQT in  $i$ -PrOH;  $\circ \circ \circ$  NQT in  $t$ -BuOH. Experimental transition complementary colour points ( $Q_x$ ,  $Q_y$ ):  $+++$  NQT in  $i$ -PrOH;  $\Delta \Delta \Delta$  NQT in  $t$ -BuOH. pH values as in Figs. 1 and 2.

used. To determine the chromaticity parameters, the weighted-ordinate method with the coefficients for standard illuminant C and  $10^\circ$  angle of vision were employed. The  $pK_a$  values were calculated from complementary chromaticity co-ordinates, by use of the SUPERCOLOR program,<sup>17</sup> written in BASIC.

## RESULTS AND DISCUSSION

The visible spectra of NQT at selected pH-values in the transition range are given in Figs. 1 and 2. The stability with time in  $5 \times 10^{-5} M$  isopropyl alcohol solutions was tested by continuous measurement at the absorption maxima. NQT shows no decomposition during at least one week in isopropyl alcohol solution, a day in acidic medium and 2 hr in basic solution. Because room temperature is normally lower than the  $30^\circ$  required for titrations in  $tert$ -butyl alcohol media, no stability study was performed, and it is recommended to use isopropyl alcohol solutions in everyday titrations.

The NQT colour changes are described by means of the CIE (1976), CIELAB and CIELUV chromaticity co-ordinates, and the complementary chromaticity coordinates for the limits and some intermediate points of the transition range, Figs. 3 and 4. The chromaticity co-ordinate values are given for the optimal indicator concentrations for titrations and were determined from the CIELAB and CIELUV coordinates.<sup>10</sup> Both systems show no significant differences in the results obtained. Figure 5 shows the colour-change perceptibility index as a function of indicator concentration. The minima of the curves show the optimum concentration for use. In both

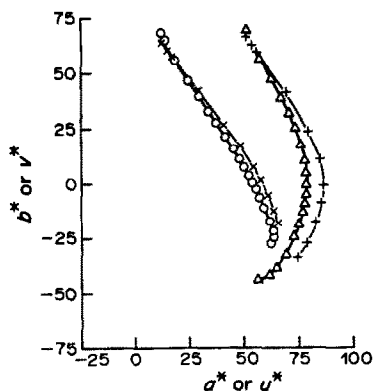


Fig. 4. Experimental transition colour points in the CIE-LAB chromaticity system ( $a^*$ ,  $b^*$ ):  $\times \times \times$  NQT in  $i$ -PrOH;  $\circ \circ \circ$  NQT in  $t$ -BuOH. Experimental transition colour points in the CIELUV chromaticity system ( $u^*$ ,  $v^*$ ):  $+++$  NQT in  $i$ -PrOH;  $\Delta \Delta \Delta$  NQT in  $t$ -BuOH. All the points (pH values as in Figs. 1 and 2) are plotted for the optimum concentration.

media studied, this value was  $10^{-4} M$ . It is not specified more closely because of the wide minima, as normally found.<sup>9</sup>

The  $pK_a$  values given in Table 1 are the average of those obtained from  $Q_x$ ,  $Q_y$  and  $Q_z$  because all these parameters show an adequate variation in the transition ranges. The values agree with those calculated from the standard absorbance method at 530 and 410 nm.

Figure 6 shows the plot of  $\Delta E$ , the total colour difference between any point in the transition range and the colour point of the acidic form of the

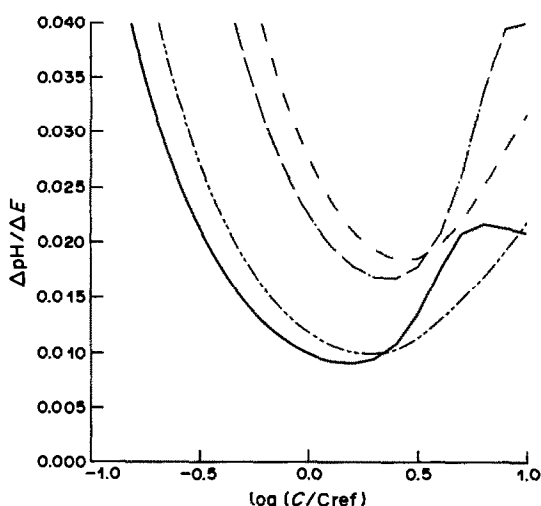


Fig. 5. Dependence of the index of colour change perceptibility on the relative change of indicator concentration. The reference concentration was  $3.63 \times 10^{-5} M$  for  $i$ -PrOH and  $5.48 \times 10^{-5} M$  for  $t$ -BuOH solutions. From CIELAB coordinates:  $---$  NQT in  $i$ -PrOH;  $----$  NQT in  $t$ -BuOH. From CIELUV coordinates:  $---$  NQT in  $i$ -PrOH;  $----$  NQT in  $t$ -BuOH.

Table 1

Medium	Isopropyl alcohol	<i>tert</i> -Butyl alcohol
Optimum concentration	$10^{-4}M$	$10^{-4}M$
$pK_a$	$12.44 \pm 0.05$	$15.73 \pm 0.10$
SCD	55 (CIELAB); 59 (CIELUV)	99 (CIELAB); 106 (CIELUV)
$pH_{mcc}$	12.2	15.5
$pH_{mcc} - pK_a$	-0.2	-0.2
$\Delta pH_{1/2SCD}$	1.7	0.9
Transition range	10.4-13.9	14.5-16.2

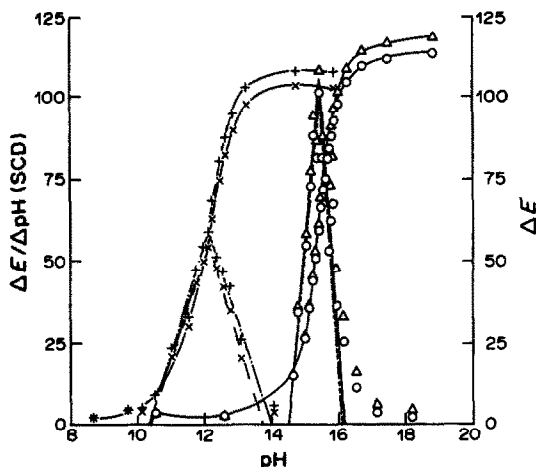


Fig. 6. Change in the chromatic difference values ( $\Delta E$ ) and SCD values ( $\Delta E/\Delta pH$ ) with pH. Symbols as in Figs. 4 and 5. pH values as in Figs. 1 and 2.

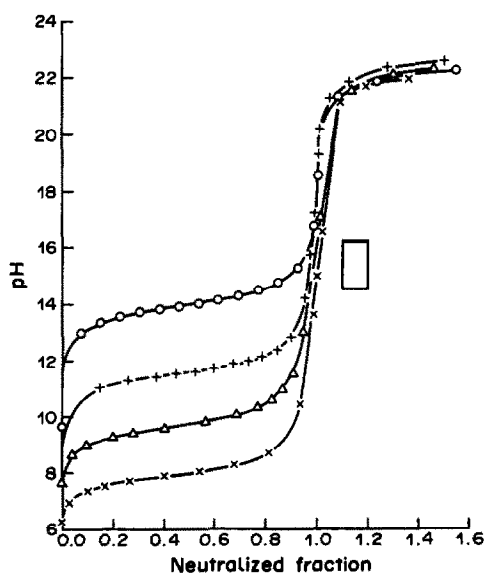


Fig. 7. Titration curves for some acetic acids in *tert*-butyl alcohol.  $\circ$  Acetic acid,  $+$  chloroacetic acid,  $\Delta$  dichloroacetic acid and  $\times$  trichloroacetic acid.  $\square$  Transition range of NQT in *tert*-butyl alcohol.

indicator, *vs.* pH, and also the derivative curve. The derivative curve shows the specific colour discrimination (SCD) of the indicator, calculated from the CIELAB and CIELUV systems. The sensitivity, expressed as SCD values, and sharpness, calculated at the half-bandwidth, ( $\Delta pH_{1/2SCD}$ ), of the SCD peak, are given in Table 1.

NQT shows good indicator properties in both alcohols, with greater sensitivity and narrower transition range in *tert*-butyl alcohol than in isopropyl alcohol. This behaviour agrees with that of the usual acid-base indicators.<sup>12,15</sup> In both media the maximum colour change occurs at a pH value very near the  $pK_a$  value and the optimum concentrations, referred to a 10-mm path-length, are the same.

Finally, to evaluate the practical usefulness of NQT, various acidic organic substances were titrated. Amounts of about 100 mg were dissolved in isopropyl or *tert*-butyl alcohol and titrated with TBAH, with NQT as indicator at the optimum concentration. The results obtained show that salicylic, ascorbic, benzoic and nicotinic acids can be determined with good accuracy in both *tert*-butyl and isopropyl alcohols, with relative standard deviations smaller than 1%. As an example of the use of NQT as indicator, Fig. 7 shows the titration curves (for *tert*-butyl alcohol medium) of a set of acids of the same chemical family which differ in acid strength. Trichloroacetic, dichloroacetic and chloroacetic acids are strong enough to be titrated with NQT as indicator with good accuracy and precision, but acetic acid, being the weakest of the series, cannot be titrated successfully.

## REFERENCES

1. E. Bosch, E. Casassas, A. Izquierdo and M. Rosés, *Anal. Chem.*, 1984, **56**, 1422.
2. R. W. Taft and M. J. Kamlet, *J. Am. Chem. Soc.*, 1976, **98**, 377.
3. *Idem, ibid.*, 1976, **98**, 2886.
4. M. J. Kamlet, J. L. M. Abboud, R. W. Taft and M. H. Abraham, *ibid.*, 1981, **103**, 6067.
5. F. W. Billmeyer Jr. and M. Saltzman, *Principles of Color Technology*, 2nd Ed., Wiley, New York, 1981.
6. C. Reilley, H. Flaschka, S. Laurent and B. Laurent, *Anal. Chem.*, 1960, **32**, 1218.
7. C. Reilley and E. Smith, *ibid.*, 1960, **32**, 1233.
8. K. Vytas, *Chem. Zvesti*, 1974, **28**, 252.

9. S. Kotrlý and K. Vytřas, in *Essays on Analytical Chemistry*, E. Wänninen (ed.), pp. 259–280. Pergamon Press, Oxford, 1977.
10. J. Barbosa, E. Bosch and R. Carrera, *Talanta*, 1985, **32**, 1077.
11. V. M. Bhuchar and A. K. Agrawal, *Analyst*, 1982, **107**, 1439.
12. J. Barbosa, E. Bosch and F. Suárez, *ibid.*, 1985, **110**, 1473.
13. L. W. Marple and J. S. Fritz, *Anal. Chem.*, 1962, **34**, 796.
14. M. D. Luque de Castro, E. Cosano, M. D. Pérez-Bendito and M. Valcárcel, *An. Quim.*, 1978, **75**, 861.
15. J. Barbosa, E. Bosch and M. Rosés, *Analyst*, 1987, **112**, 179.
16. I. M. Kolthoff and M. K. Chantooni, *J. Phys. Chem.*, 1978, **82**, 944.
17. M. Rosés, *Ph.D. Thesis*, University of Barcelona, 1986.

## POTENTIAL OF THE FLOW-GRADIENT FUNCTION IN FIA WITH A MULTIFUNCTION PUMP DELIVERY SYSTEM

JUN'ICHI TOEI

Scientific Instrument Division, Tosoh Corporation, 2743-1 Hayakawa, Ayase-shi, Kanagawa, 252 Japan

(Received 9 January 1987. Revised 20 January 1988. Accepted 29 January 1988)

**Summary**—By use of a multifunction pump delivery system with which any flow patterns are easily programmed, the potential of the flow-gradient function in FIA has been investigated. The mechanical stability and reproducibility of the pump system are very high because of the use of a central programming unit, and this enabled further and closer investigation of the function. A new parameter (dispersion volume) is proposed for evaluation of flow-gradient systems.

Flow-injection analysis (FIA) has been extensively developed and is now a widely applied technique.<sup>1,2</sup> In the usual FIA system the flow-rate of the carrier is kept constant because constant flow is simple and easily controlled. Recently Ríos *et al.*<sup>3</sup> reported a fundamental study of a new gradient technique in which the flow-rate of the carrier is varied, and proved that it had many advantages. In particular, it has a high washing effect and gives sharper peaks. However, the instrument was rather complex and no further applications have appeared.

In high-performance liquid chromatography (HPLC), programmed flow-rate systems are commonplace and are used in combination with reversed-phase chromatography to afford better resolution in elution of organic and biological compounds.<sup>4,5</sup> Moreover, a high-quality multifunction pump delivery system for use in HPLC and FIA has been produced commercially<sup>6</sup> and provides highly precise analysis with reversed-phase chromatography. The system can also be used to give a flow-rate gradient.

In earlier work<sup>7,8</sup> flow-control was obtained with a reservoir of carrier at a given height, and Ríos *et al.* used a reservoir that was raised or lowered.<sup>3</sup> However, with these gravity-flow arrangements accurate programming of the flow-rate gradient was difficult.

In the multifunction pump system the flow-rate is accurately programmed by a central programming unit (CPU) which controls the movement of a plunger by means of a high-quality pulse motor, giving a precise flow-gradient. In this paper the fundamental characteristics of the flow-gradient technique are described, along with the gradient dispersion characteristics for a non-reacting system, a fast chemical reaction and a slow biological reaction. For slow reactions, a combined flow-gradient and stopped-flow technique is particularly suitable.

### EXPERIMENTAL

#### Reagents

Arsenazo III was obtained from Dojinkagakukenkyusho (Japan) and used without further purification. Commercial

calcium (1000 mg/l.) and glucose (2000 and 5000 mg/l.) standard solutions were diluted with demineralized water as required. For the determination of glucose a Wako C Glucose Test kit (Wako Pure Chemicals, Japan) was modified and used as in earlier work. The carrier streams used were as follows.

*Dispersion study:* demineralized water.

*Determination of calcium:* 0.05M NaH<sub>2</sub>PO<sub>4</sub>/Na<sub>2</sub>HPO<sub>4</sub> (pH 5.0, 5.5, 6.0); 4 × 10<sup>-5</sup>M Arsenazo III.

*Determination of glucose:* 0.1M NaH<sub>2</sub>PO<sub>4</sub>/Na<sub>2</sub>HPO<sub>4</sub>, pH 7.4; 0.025% phenol; 3000 U/l. glucose oxidase (E.C.1.1.3.4) from *A. Niger*; 400 U/l. peroxidase (E.C.1.11.1.7) from horseradish; 66.6 U/l. mutarotase (E.C.5.1.3.3) from hog-kidney cortex; 0.26mM 4-aminoantipyrine

#### Apparatus

The system consisted of a CCPM multifunction (metal-free; Tosoh Co.), a Rheodyne 7125 injection valve (equipped with a 100- $\mu$ l Teflon loop) or a Rheodyne 7413 injection valve, a reactor tube (0.4 mm bore × 250 cm) and a back-pressure tube (0.2 mm bore × 200 cm) after the detector flow-cell. The absorbance was monitored with a UV-8000 spectrophotometer (Tosoh Co.) equipped with an 8- $\mu$ l flow-cell, and the results were recorded on a CP-8000 data station (Tosoh Co.). A signal from a marker fitted to the injection valve started the programmed flow-gradient and the FIA data-acquisition simultaneously and automatically. The pressure change in the flow system was measured with a pressure sensor fitted to the pump. A typical FIA manifold is shown in Fig. 1.

#### Interpretation of the data

The flow-gradient parameters are as follows:  $Q$  (ml/min) = slope of the flow-gradient,  $f$  (ml/min) = flow-rate for isocratic elution,  $F$  (ml/min) = flow-rate when the peak maximum is passing through the detector under gradient flow,  $F_0$  (ml/min) = initial flow-rate on injection into the gradient flow,  $H$  (mV) = peak height,  $A$  ( $V \times \text{msec}$ ) = peak area,  $T$  (min) = residence time,  $W$  (sec) = peak width at half height,  $D$  = dispersion coefficient.

### RESULTS AND DISCUSSION

#### System without chemical reaction

The study was started by determining the mechanical stability and reproducibility of the FIA system with isocratic and flow-gradient elution, for  $Q = 0.5$  ( $F_0 = 0$ ), 0 ( $F_0 = 0.5$ ) and  $-0.5$  ( $F_0 = 1$ ), *i.e.*, for positive, zero (isocratic) and negative gradient. The



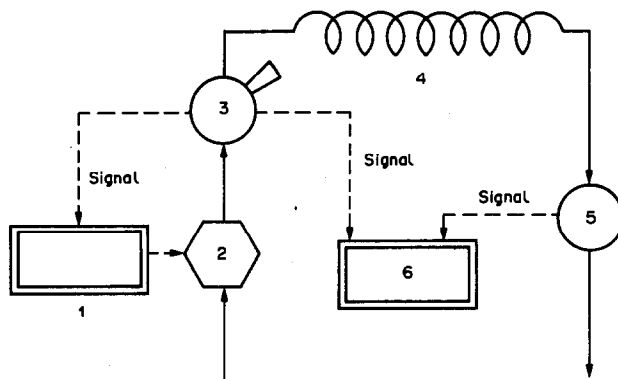


Fig. 1. Schematic diagram of flow system: 1, pump controller; 2, pump delivery system; 3, injector; 4, reaction tubing; 5, detector; 6, data station.

Table 1. Reproducibility (7 replicates) of the flow-gradient system with a non-chemical system

$Q$ , $ml/min^2$	$F_0$ , $ml/min$	Time, $min$	R.S.D., %	Peak height, $mV$	R.S.D., %	Peak area*	R.S.D., %
0.5	0	1.34	0.35	35.2	0.90	4.97	2.16
0	0.5	0.72	0.00	33.7	2.45	6.11	2.78
-0.5	1.0	0.39	0.00	34.9	1.46	3.91	2.56

Sample, 0.1% aqueous acetone solution: sample volume 20  $\mu$ l; reaction tube, 0.4 mm bore  $\times$  250 cm; back-pressure tube, 0.2 mm bore  $\times$  200 cm; detector wavelength, 254 nm.

\*Integrated value, units are  $10^3$  mV. sec.

carrier was demineralized water and the sample solution 0.1% v/v acetone solution in water. The absorbance was monitored at 254 nm and the results are summarized in Table 1. The reproducibility was slightly better for the positive gradient than for the others, partly because of the larger residence time and lower initial flow-rate ( $F_0$ ).

The fundamental parameters of the positive gradient were next investigated. The results are summarized in Table 2. Both peak width and height were decreased as  $Q$  was increased, in agreement with Ríos *et al.*<sup>3</sup> who called this the "washing effect". It is one of the advantages of the flow-gradient method. A positive gradient decreases tailing and shortens the time needed to return to the baseline (Fig. 2).

The washing effect is explainable by the usual dispersion theory for isocratic FIA systems. In these

systems dispersion has been mainly investigated by means of the dispersion coefficient  $D = H_{ss}/H_{max}$ , where  $H_{ss}$  is the steady-state signal and  $H_{max}$  the peak height. However, in the study of gradient flow  $H_{ss}$  is identical for every gradient slope and the use of  $D$  is sometimes nonsense. Hence  $H_{max}$  is used first as a coefficient for evaluation. In isocratic FIA,  $D$  is

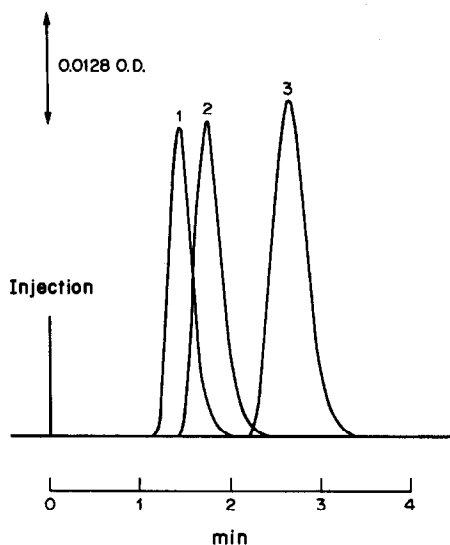


Fig. 2. Typical recorder traces for positive flow-gradient. Slope: 1, 0.6  $ml/min^2$ ; 2, 0.4  $ml/min^2$ ; 3, 0.2  $ml/min^2$ ; sample, 0.1% aqueous acetone solution; sample volume, 20  $\mu$ l; reaction tubing, 0.4 mm bore  $\times$  250 cm; detector wavelength, 254 nm; first flow-rate, 0  $ml/min$ .

Table 2. The results for positive flow-gradient (details as in Table 1)

$Q$ , $ml/min^2$	Time, $min$	Peak height, $mV$	Peak width, $sec$
0.2	2.35	40.7	15.4
0.25	2.02	40.2	14.3
0.3	1.76	38.8	14.2
0.35	1.65	37.7	13.4
0.4	1.49	38.6	13.2
0.45	1.42	37.4	13.9
0.5	1.33	36.9	12.2
0.55	1.26	36.0	11.6
0.6	1.19	36.3	11.2
0.7	1.09	35.8	10.8

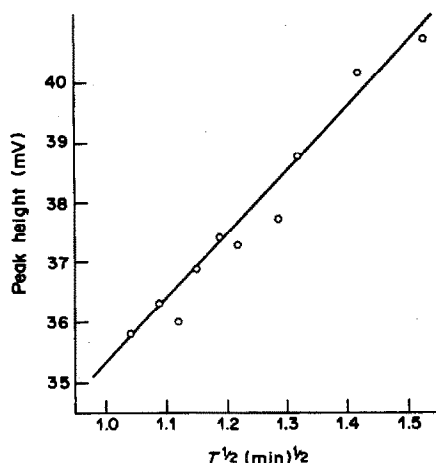


Fig. 3. Relation between peak height and  $\sqrt{T}$  for positive flow-gradient. Details as in Table 2.

roughly proportional to  $\sqrt{T}$  ( $T$  = residence time), so the relation between  $H_{\max}$  and  $\sqrt{T}$  was examined (Fig. 3), and found to be linear. So the usual dispersion theory applicable to isocratic FIA might be thought applicable to flow-gradient FIA. Unfortunately, however, the peak height was sometimes unstable when  $F$  was increased, so a new parameter was tried, the dispersion volume,  $K = WF$ , which should behave like  $D$ . If the dispersion of the injected sample is large,  $K$  is large. Figure 4 shows that  $K$  is inversely proportional to  $\sqrt{T}$ , suggesting that  $K$  can be used as a fundamental parameter in flow-gradient FIA. The same relation was observed for the negative gradient, but the correlation was much poorer ( $r = 0.7850$ ) than that for the positive gradient ( $r = 0.9815$ ), because of the shorter residence time and relatively high initial flow-rate.

The results for the effect of injection volume are summarized in Table 3, and suggest that in flow-gradient FIA peak height is proportional to injection volume, as in isocratic FIA. For both methods the signal was a linear function of volume up to 50  $\mu$ l. The results, however, suggest another ad-

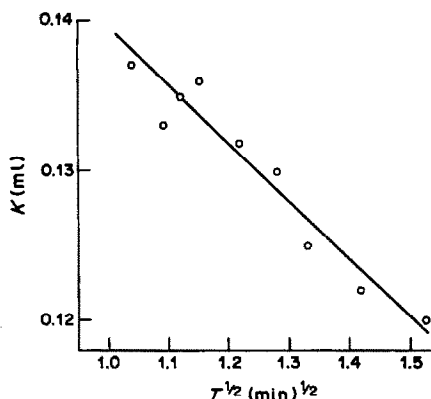


Fig. 4. Relation between  $K$  (dispersion volume) and  $\sqrt{T}$  for positive flow-gradient. Details as in Table 2.

vantage of flow-gradient FIA. That is, the peak width is reduced although the residence time in flow-gradient FIA is longer than that in isocratic FIA.

#### System with chemical reaction

Several investigations with a fast chemical reaction were performed with FIA parameters based upon the results for the system without chemical reaction. Arsenazo III has been used as a component of the mobile phase in determination of calcium by ion-exchange chromatography,<sup>10</sup> so this system was adopted as a model reaction for investigation of flow-gradient FIA. The reactions of Arsenazo III are known to be fast.<sup>11,12</sup> The sample solution was a 20  $\mu$ g/ml standard calcium solution and the absorbance was monitored at 600 nm.

The effect of pH on  $H_{\max}$  vs.  $\sqrt{T}$  was investigated over the range 5–6, but the correlation was very poor and an inverse relation was obtained only at pH 6.0. The results suggest that  $D$  cannot be adopted as a main parameter for the system evaluation of flow-gradient FIA. In contrast, plots of  $K$  vs.  $\sqrt{T}$  were linear for both pH 5.5 and 6.0 (Fig. 5). Evidently  $K$  (the dispersion volume) is a suitable parameter for the evaluation of flow-gradient FIA.

Table 3. Effect of injection volume (details as in Table 1)

Mode	$Q_0$ , ml/min <sup>2</sup>	$F_0$ , ml/min	Volume, $\mu$ l	Time, min	Peak height, mV	Peak width, sec	Peak area*
Isocratic	0	1	5	1.19	6.9	22.0	1.68
			10	1.16	15.5	21.5	3.69
			20	1.14	29.3	20.8	6.73
			30	1.11	42.5	21.6	10.58
			50	1.06	67.9	22.6	19.20
$H_m(\text{mV}) = 1.34V(\mu\text{l}) + 1.56; r = 0.9991$							
Gradient	0.4	0	5	1.48	8.9	8.9	0.81
			10	1.48	17.5	8.3	1.68
			20	1.47	35.9	8.4	3.38
			30	1.44	54.2	8.6	5.19
			50	1.43	83.6	9.0	8.31
$H_m(\text{mV}) = 1.67V(\mu\text{l}) + 1.54; r = 0.9984$							

\*Units are  $10^3$  mV·sec.

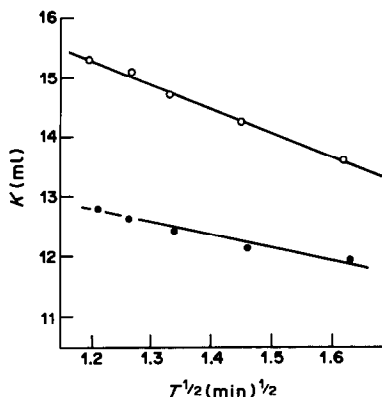


Fig. 5. Relation between  $K$  and  $\sqrt{T}$  for positive flow-gradient. Sample, 20 ppm calcium; sample volume, 20  $\mu\text{l}$ ; carrier, 0.05N  $\text{NaH}_2\text{PO}_4/\text{Na}_2\text{HPO}_4$ ; pH,  $\bullet$  5.5,  $\circ$  6.0; detector wavelength, 600 nm. Other details as in Table 2.

It was established that when a chemical reaction takes place in the flow-gradient system the dispersion is different from that when no chemical reaction occurs, so various types of flow-gradient were investigated with the same reaction.

Stepwise change in flow-gradient is widely used in HPLC, but does not seem to have been used in FIA, so this was investigated first. Typical flow-gradient patterns are shown in Fig. 6(a). The flow-rate was kept constant at 1 ml/min for 18 sec (by which time the sample plug had almost reached the detector) after the injection and thereafter changed to various values in the range 0.5–2.5 ml/min and kept constant at the new value. Figure 7 shows that  $K$  is roughly inversely proportional to  $\sqrt{T}$ , suggesting that both flow-rates affect the dispersion in the same way.

Next, flow-gradients with the same slope  $Q$  but different initial flow-rate  $F_0$  were investigated. Typical

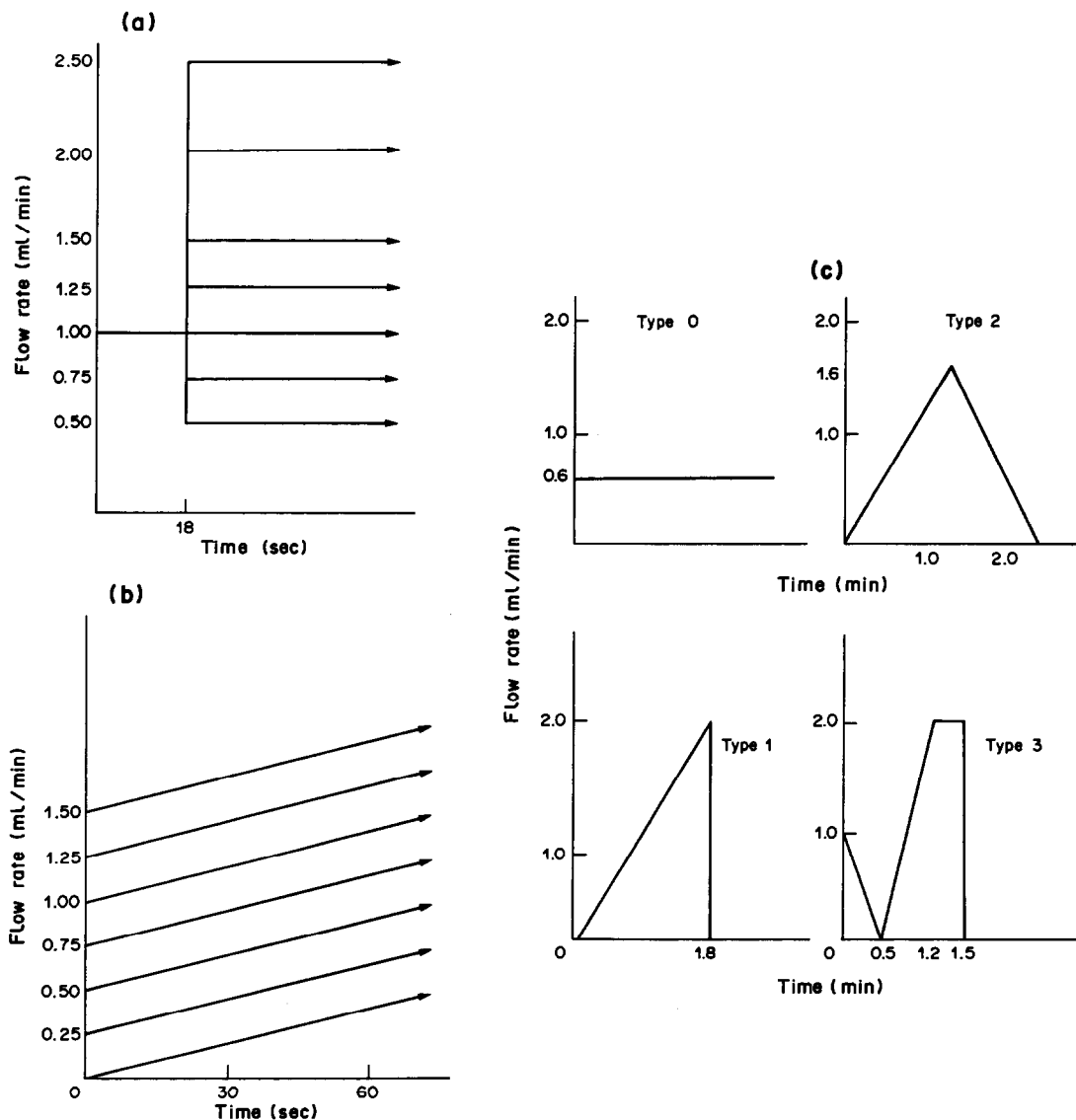


Fig. 6. Typical flow patterns for (a) step gradient, (b) positive flow-gradient with the same slope, (c) positive and negative flow-gradient; carrier, pH 6.0; other details as in Fig. 5.

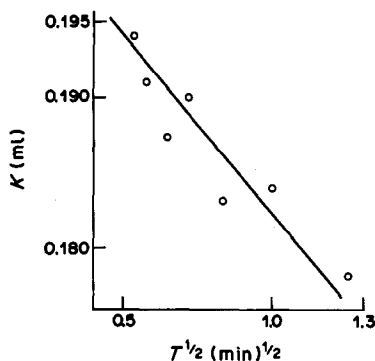


Fig. 7. Relation between  $K$  and  $\sqrt{T}$  for step gradient.

flow patterns are shown in Fig. 6(b). When  $F_0$  was increased, the residence time and peak width were decreased. Again  $K$  was roughly inversely proportional to  $\sqrt{T}$ . However, when  $F_0$  was not zero, the scatter was larger and the stability worse, because the sample was injected into a flowing solution (in which case a difference between the carrier and sample flow-rates results in more variable dispersion).

When a flow-gradient is used with fast reactions, higher  $Q$  is preferred because of the sharper peak shape and shorter analysis time. However, in analyses with slow reactions such as enzymatic assays, where a longer reaction time is needed, higher  $Q$  is not always preferred. Further work was therefore undertaken with the same residence time (0.98 min) and the same fast reaction, but with three flow-gradient patterns [Fig. 6(c)] and an isocratic system. To ensure

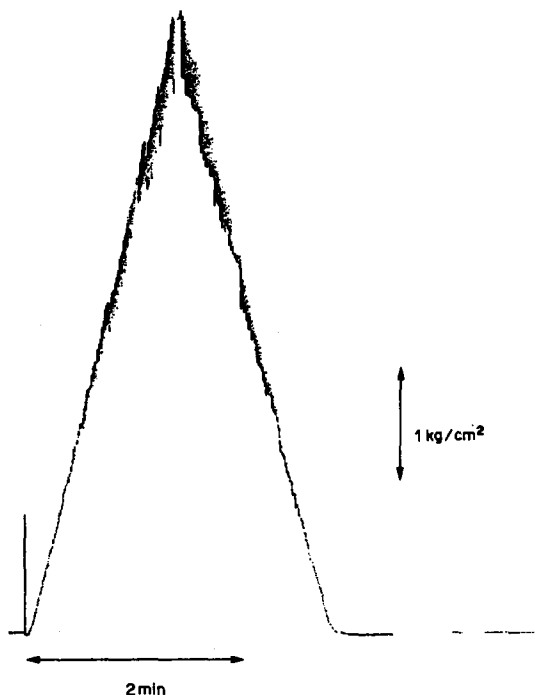


Fig. 8. Recorder traces for the pressure change in pattern 2 in Fig. 6(c).

Table 4. The results for various flow patterns

Type [in Fig. 6(c)]	Time, min	R.S.D., % ( $n = 5$ )	Peak height, mV	R.S.D., % ( $n = 5$ )	$N$
0	0.97	0.64	336	1.17	14
1	0.98	0	298	0.93	51
2	0.98	0.76	302	2.06	51
3	0.97	0.51	332	1.14	84

Sample, Ca 20 ppm; sample volume, 20  $\mu$ l; detector wavelength, 600 nm.

that the pump delivery system gave the correct flow-gradient function, the pressure change was measured with a pressure sensor in the pump (Fig. 8). The flow-gradient was found to be performed with high precision.

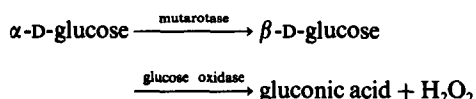
The results in Table 4 shows that the reproducibility of the peak height was poorer for the complex flow patterns (types 2 and 3) than for the others. As the residence time was almost the same throughout, the peak shape could be evaluated mathematically by using the theoretical plate number  $N$ , which is usually used for evaluation of resolution in HPLC:

$$N = 5.54 (T/W)^2$$

where  $T$  is the residence time and  $W$  is the half-width of the peak.  $N$  was lowest for isocratic flow and higher for flow-pattern 2, presumably because  $Q$  was then maximal and the flow-rate was higher when the peak maximum was passing through the detector cell.

#### Slow biological reaction

The specific reaction of glucose oxidase with  $\beta$ -D-glucose<sup>13,14</sup> proceeds in two steps



and has been successfully used for the determination of glucose in serum. Okuda *et al.*<sup>15</sup> used the reaction of  $\text{H}_2\text{O}_2$  with 4-aminoantipyrine and phenol, catalysed by peroxidase, to determine glucose, and this reaction was employed to test the flow-gradient FIA system.

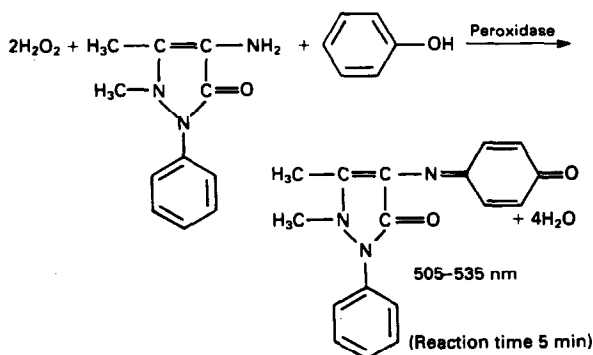


Table 5. Effect of gradient slopes for the enzymatic assay

$Q$ , ml/min <sup>2</sup>	Time, min	Peak height, mV	Peak width, sec	Peak area*	Analysis time, sec
0.2	2.31	215	24.5	5.56	188
0.4	1.55	167	17.6	3.16	130
0.6	1.25	140	15.0	2.22	102

Carrier as shown in test; sample, glucose 2 g/l.; sample volume, 0.5  $\mu$ l; detector wavelength, 505 nm.

\*Units are  $10^3$  mV.sec.

First, a positive flow-gradient was investigated by varying  $Q$  from 0.2 to 0.6 ml/min.<sup>2</sup> The results in Table 5 show that as  $Q$  is increased the peak height is decreased and the residence time shortened, and hence with high  $Q$  the reaction time was much too short for the enzymatic reaction to proceed very far. Although linear calibration plots were obtained for lower  $Q$  (they were non-linear for higher  $Q$ ), both the residence time and analysis time were very long, so new flow patterns were sought for fast determination of glucose in clinical samples.

Stopped-flow was an obvious possibility, and the pump delivery system had a facility for combining this with use of the flow-gradient. The flow patterns used are shown in Fig. 9, and are based on type 3 in Fig. 6(c). The "stopped-flow" pattern was applied only after the injection. A shorter reaction tube (0.4 mm bore  $\times$  80 cm) was used in order to reduce analysis time and reagent consumption. In earlier work the sample volume was relatively large (20  $\mu$ l), resulting in high sensitivity, but in the present work a low sample volume (0.5  $\mu$ l) is adopted in order to reduce sample and reagent consumption, so a short reaction tube and low maximum flow-rate can be used. The effect of reaction time on peak height was investigated by varying the duration of stopped-flow and the results are shown in Fig. 10. In the previous work it took 5 min to reach a steady-state for the reaction, but in the present case only 2-3 min because of the small sample volume. The calibration plots were found to be linear up to about 5 mg/ml

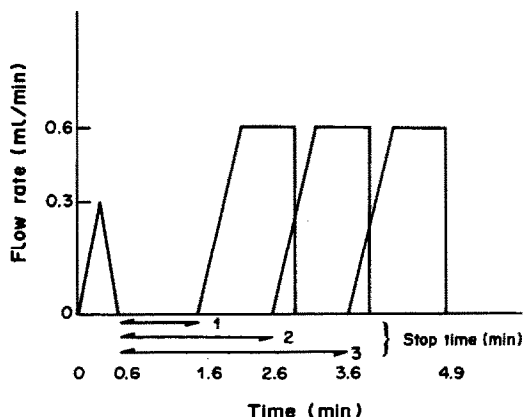


Fig. 9. Typical flow patterns for the determination of glucose by enzymatic assay: reaction tubing 0.4 mm bore  $\times$  80 cm; detector wavelength, 505 nm.

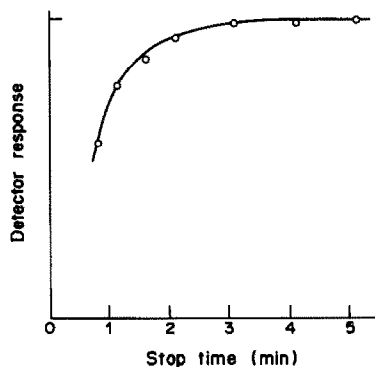


Fig. 10. Effect of stop time on peak height: sample, 2 g/l. glucose; sample volume, 0.5  $\mu$ l; other details as in Fig. 9.

glucose in the sample (*i.e.*, the normal range for serum samples), for stop times ranging from 1 to 2 min, but the linearity was the poorer, the shorter the stop time. A time of 1.5 min was selected to give a compromise between short analysis time and higher linearity. The detection limit was low enough to allow serum samples to be diluted by a factor of 20, and the analysis could be performed at the rate of 30 injections per hour.

## CONCLUSIONS

A new type of flow function, of successive positive and negative flow-gradients, followed by a positive flow-gradient combined with stopped-flow, has been found to give high sensitivity (peak height) and reproducibility. The method is applicable to clinical analysis of glucose by enzymatic assay, and should be generally useful for biological assays.

## REFERENCES

1. J. Růžička and E. H. Hansen, *Flow Injection Analysis*, Wiley, New York, 1981.
2. M. Varcárcel and M. D. Luque de Castro, *Flow-Injection Analysis: Principles and Applications*, Horwood, Chichester, 1987.
3. A. Ríos, M. D. Luque de Castro and M. Varcárcel, *Talanta*, 1985, **32**, 845.
4. L. R. Snyder, J. W. Doran and J. R. Grant, *J. Chromatog.*, 1979, **165**, 3.
5. Y. Kato, T. Kitayama and T. Hashimoto, *ibid.*, 1985, **333**, 93.
6. J. Toei and N. Baba, *ibid.*, 1986, **361**, 368.
7. J. Wang and B. A. Freiha, *Anal. Chem.*, 1983, **55**, 1285.
8. R. W. Pratt and D. C. Johnson, *Anal. Chim. Acta*, 1983, **148**, 87.
9. J. Toei and N. Baba, *Bunseki Kagaku*, 1986, **35**, 411.
10. J. Toei, *HRC & CC*, 1987, **10**, 111.
11. E. G. Lamkin and M. B. Williams, *Anal. Chem.*, 1965, **37**, 1029.
12. K. L. Cheng, K. Ueno and T. Imamura, *Handbook of Organic Analytical Reagents*, CRC Press, Baton Roca, 1982.
13. A. S. Casten and R. Brandt, *Anal. Biochem.*, 1963, **6**, 461.
14. J. B. Bill, *J. Appl. Physiol.*, 1965, **20**, 749.
15. J. Okuda, I. Miwa, K. Masuda and K. Tokui, *Carbohydrate Res.*, 1977, **58**, 267.

## SORPTION OF PROTONS AND METAL IONS FROM AQUEOUS SOLUTIONS BY A STRONG-BASE ANION-EXCHANGE RESIN LOADED WITH SULPHONATED AZO-DYES

MARIA PESAVENTO\* and ANTONELLA PROFUMO

Dipartimento di Chimica Generale, Università di Pavia, Pavia, Italy

RAFFAELA BIESUZ

IRSI, Istituto Ricerche Sicurezza Industriale, Milano, Italy

(Received 9 May 1987. Revised 12 January 1988. Accepted 22 January 1988)

**Summary**—Two sulphonated azo-dyes, which bear a nitrogen donor atom in the diazo group and are known to complex many heavy metal ions in aqueous solution, have been found to be sorbed by a strong-base anion-exchange resin (Dowex 1-X8) simply by ion-exchange. The resin containing the dyes behaves like a chelating resin, able to sorb copper(II) and nickel(II) from aqueous solution, if the proper conditions are chosen. The acidity, ionic composition and volume of the aqueous solution, and the amount and nature of the sorbed ligand are the factors which determine the fraction of metal ion sorbed when the batch technique is used. The experimental results are interpreted by using a model of the resin based on the Donnan equilibrium concept, which allows prediction of the sorption conditions on the basis of some independently determined quantities, such as the protonation and complex formation constants in aqueous solution, and the activity of the counter-ion in the resin phase. The exchange of protons between the resin and the aqueous solution can also be explained with this model.

In the present paper the sorption properties of a strong-base anion-exchange resin, Dowex 1-X8, loaded with a suitable azo-dye, for hydrogen ions and copper(II) and nickel(II) ions are described. Two sulphonated azo-dyes were considered: T-azo-R [1-(tetrazolylazo)-2-hydroxynaphthalene-3,6-disulphonic acid] and T-azo-C [2-(tetrazolylazo)-1,8-dihydroxynaphthalene-3,6-disulphonic acid]. Their synthesis and use as spectrophotometric reagents for a number of metal ions were reported earlier.<sup>1-3</sup> Owing to the presence of the two sulphonic acid groups, the dyes are easily sorbed from aqueous solutions by an anion-exchanger. Some preliminary observations showed that Dowex 1-X8, loaded with one of these two azo-dyes, is able to sorb heavy metal ions from aqueous solution of proper acidity. Sorption systems of this kind can be very useful, because the active part is easily varied, without recourse to the sometimes difficult and time-consuming procedures needed for covalently linking the reagent to the skeleton of the resin.

There are many chelating agents which incorporate an anionic group that is not involved in the chelation of metal ions, for instance a sulphonate group. Some of them have already been used as loading agents on anion-exchangers, e.g., azothiopyrine disulphonic acid, for uptake of mercury, copper and cadmium

from aqueous solutions,<sup>4</sup> and Pyrocatechol Violet for preconcentration of aluminium from drinking water.<sup>5</sup>

The aim of this paper is not only to describe an effective method for separating copper and nickel from aqueous solutions, but also to point out the factors which affect the exchange properties of the loaded resin and to correlate them with the protonation and complex formation constants of the reagents in aqueous solution, and with some properties of the resin, measured independently.

The practical importance of this point is evident. For example, it should be possible to predict the best conditions for analytical operations such as separation or preconcentration of metal ions by the batch technique.

From this point of view, the most suitable model is probably that first proposed by Gregor<sup>6</sup> and now widely accepted,<sup>7</sup> that the resin is treated as an aqueous phase, separated from the external solution by a boundary across which all the molecular and ionic components of the system, except the fixed quaternary ammonium groups, can diffuse. Electro-neutrality must be maintained in both phases, but at the boundary an electric potential (Donnan potential) is set up, owing to the difference in the activities of the ionic components in the two phases. It can be demonstrated<sup>8,9</sup> that for any strong electrolyte  $A_xC_y$ , the following relationship (the Donnan equilibrium) holds

\*Author for correspondence.

$$\{A\}^a\{C\}^c = \{\bar{A}\}^a\{\bar{C}\}^c \quad (1)$$

where {A} and {C} are the activities of the ions A and C and a bar over a symbol indicates that the resin phase is referred to. The reference and standard states are the same in both the solution and the resin phase.<sup>10</sup>

Using a Donnan-based model, Marinsky and co-workers<sup>8,11,12</sup> were able to demonstrate that the internal protonation and complex formation constants of each monomeric component of a number of resins are equal to those of the related water-soluble monomeric analogues, despite the fact that the apparent constants alter as the reactions proceed, and the composition of the aqueous solution changes.

In the systems considered here, the active groups are fixed inside the resin simply by ion-exchange instead of being covalently bound, as in the resins investigated by Marinsky, and thus it must be demonstrated that equation (1) holds in this case too.

## EXPERIMENTAL

### Reagents

T-azo-R and T-azo-C were synthesized as previously described,<sup>1,2</sup> and their standard solutions prepared by direct weighing of the solid. All other reagents were of analytical grade.

Dowex 1-X8, 100–200 mesh, in chloride form (which has benzyltrimethylammonium groups as the active fixed groups) was obtained from Bio-Rad, and purified by a procedure similar to that proposed by Gregor,<sup>13</sup> before use. The resin was stirred for 10 hr in 0.1M sodium hydroxide, then for 10 hr in 0.1M hydrochloric acid (or nitric acid), and finally washed with water until the washings were neutral. The purified resin was dried at 60° to constant weight<sup>8</sup> and stored in a desiccator. With this treatment the impurities leachable from the resin were drastically reduced.

The total capacity of the resin for anions, and its water content (g of water per g of dry resin after equilibration in the test solution) were determined by the usual methods.<sup>13,14</sup> The capacity was found to be 3.20 meq/g of dry resin. The modified resin was prepared simply by stirring a weighed amount of Dowex 1-X8 with an aqueous solution containing the required amount of dyestuff. The sorption could be followed spectrophotometrically. The loaded resin was filtered off, dried at 60°, and stored in a desiccator.

### Procedures

The protonation of the resin was studied by potentiometric titrations in aqueous solutions of different ionic strengths, at fixed temperature (25.0°) and under a small nitrogen overpressure, in a cell equipped with a Ross glass electrode (Orion 810-100) and a Wilhelm-type<sup>15</sup> reference electrode, in which the filling solution of the bridge had the

same composition as the external solution in order to minimize variation in the liquid-junction potential. Contact with the test solution was made through a porous glass membrane, in order to avoid diffusion of the resin inside the reference electrode. The test solution, at an ionic strength ranging from 0.010 to 2.500M sodium chloride, held in suspension a known amount of loaded resin. Before each titration, the cell was standardized as previously described,<sup>1</sup> by determining the standard potential  $E_0$ , the liquid-junction potential  $E_j$ , and the ionic product of water  $K_w$ . The titrations were performed automatically, under control by a specifically designed microcomputer, with the titrant delivered by a Metrohm 655 DOSIMAT automatic burette. An Orion 701 A digital potentiometer was used to measure the potential of the cell at each titration point.

To study the sorption of metal ions, the same procedure was used, and in addition a known volume of the clear solution was removed at each titration point, and analysed for its metal ion content by standard atomic-absorption spectrometry (AAS) procedures with an air/acetylene flame or electrothermal atomization (IL model 551 spectrophotometer).

Both the proton and metal-ion exchanges are slow reactions: 1–2 hr is required for equilibrium to be reached after each addition of titrant. The equilibrium was considered as established when the drift of the potential of the glass electrode was less than 0.2 mV in 10 min.

## RESULTS AND DISCUSSION

### Swelling of the resin and uptake of salts

Some data on swelling and water and salt uptake of Dowex 1-X8 are reported in Table 1 for different compositions of the external aqueous solution. Because of the rigidity of the resin, its external volume increases only slightly with the ionic strength of the solution, even when the water content decreases. On the other hand, the external volume is influenced by a change of the counter-ion from chloride to perchlorate.

Strong electrolytes enter the resin phase also by diffusion, but this invasion is notable only when the molal ionic strength of the external solution is higher than 1m. It can be calculated by applying the Donnan relationship.<sup>1</sup> When  $a = c = 1$ , the equation reduces to

$$[A][C] = [\bar{A}][\bar{C}] \quad (2)$$

where the concentrations ( $[ ]$ ) are expressed as molalities and C is the co-ion (cation). Equation (2) is valid when the ratio of the activity coefficients is

Table 1. Sorption of water and sodium chloride by Dowex 1-X8

Composition of the solution	Water sorbed by 1 g of dry resin,* g	NaCl sorbed by 1 g of dry resin,* mmole	NaCl sorbed by 1 g of dry resin,† mmole	Volume of 1 g of dry resin after equilibration,* ml
Pure water	0.60			1.26
0.010m NaCl	0.60	$1.1 \times 10^{-5}$		
0.110m NaCl	0.59	$1.1 \times 10^{-3}$	0.01	1.36
1.000m NaCl	0.46	0.06	0.09	1.38
1.000m NaClO <sub>4</sub>	0.23			1.05

\*Experimentally found values.

†Values calculated by equation (3).

equal to 1, which can be considered true for sodium chloride solutions. Suppose that the resin Dowex 1 in the chloride form is suspended in aqueous 1*m* sodium chloride. Some sodium chloride diffuses into the resin owing to the difference in the ion activities in the two phases, and as electroneutrality of the resin phase must be maintained, equation (2) becomes

$$I^2 = (\overline{[Q]} + \overline{[Na]})\overline{[Na]} \quad (3)$$

where  $\overline{[Q]}$  is the "concentration" of the quaternary ammonium groups in the resin phase. The concentration of sodium in the resin is a measure of the salt invasion. The values calculated by equation (3) are reported in Table 1, where the experimentally found values are also shown. The most interesting point is that the chloride concentration inside the resin from ionic invasion is negligible relative to that due to the neutralization of the fixed quaternary ammonium groups, for external electrolyte concentrations up to 1*m*.

#### Proton sorption by Dowex 1-X8

The titration curve of Dowex 1-X8, Fig. 1, shows that some weakly basic groups (0.05 meq/g of dry resin), which are neutralized at pH 3–9, are still present even after the purification. This confirms an early observation of Gregor<sup>16</sup> that 0.02 meq of weak base per g of dry resin is titrated at pH 3–7, and 0.03 meq/g at higher pH. The protonations of the resin itself must, of course, be taken into account as concomitant equilibria when the protonation of the sorbed reagents is studied.

#### Sorption of azo-dyes on Dowex 1-X8

When T-azo-R and T-azo-C are sorbed by the

resin, three counter-ions are displaced by each azo-dye molecule. The maximum capacity of the resin for these reagents is 1.07 mmole/g of dry resin. Therefore, in spite of their large size, the two azo-dyes are able to neutralize all the positive charges in the resin (3.20 meq/g of dry resin).

The capacity is independent of the acidity of the external solution over the pH range 2–12, but depends on its anionic composition, particularly at ionic strengths higher than 0.1*m*. For instance, in 1*m* sodium chloride the maximum capacity for the two azo-dyes is reduced to 0.1 mmole/g of dry resin. This is because all the anions can be sorbed by the exchanger, and therefore displace more or less the azo-dyes, depending on their activities in the aqueous and resin phases. The selectivity coefficients of T-azo-C and T-azo-R with respect to some common univalent anions were determined spectrophotometrically, and are reported in Table 2. They are almost constant for resin-phase forms ranging from 100% azo-dye to 100% univalent anion, and are in

Table 2. Selectivity coefficients of azo-dyes (L) with respect to univalent anions (A) on Dowex 1-X8

Anion (A)	$\log K_{A,L}^*$ T-azo-C	$\log K_{A,L}^*$ T-azo-R
Acetate	-6.0	
Chloride	-2.7	
Bromide	-0.8	
Nitrate	-0.8	
Perchlorate	+2.2	+3.7

$$*K_{A,L} = \frac{([A]^2[L])}{([L],[A]^2)}$$

All concentrations are expressed in molality.

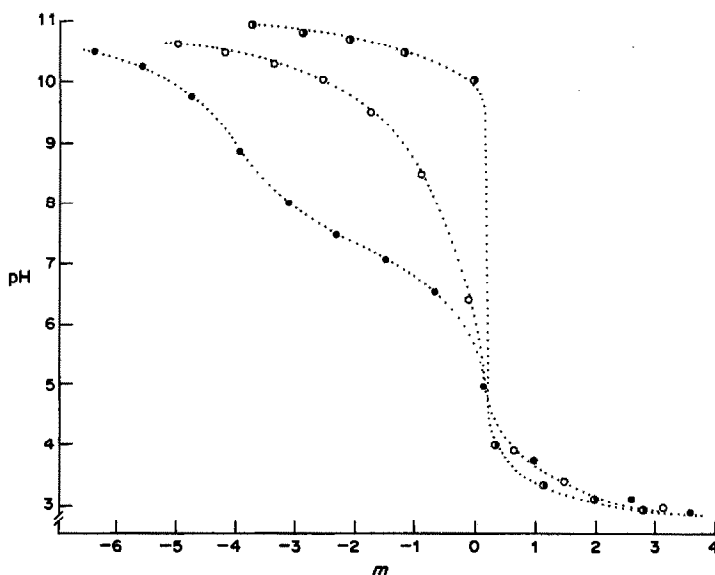


Fig. 1. Potentiometric titration of Dowex 1-X8:  $m \times 10 = \mu\text{moles of H}^+$  in analytical excess;  $\odot$ : 25 ml of 0.010*m* sodium chloride, containing 0.0400 mmole of hydrochloric acid (solution A);  $\circ$ : solution A, containing also 1.1000 g of Dowex 1-X8;  $\bullet$ : solution A, containing also 1.1000 g of Dowex 1-X8 and 0.0300 meq of T-azo-C.



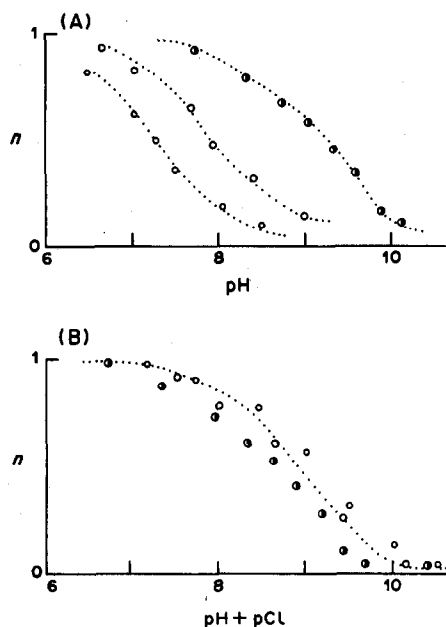


Fig. 2. Protonation curve of T-azo-C sorbed on Dowex 1-X8, in sodium chloride solutions of different concentrations.  $V = 25$  ml, 1.1000 g of Dowex 1-X8, 0.0300 meq of T-azo-C. Curves A:  $n$  vs. pH. Curves B:  $n$  vs.  $\text{pH} + \text{pCl}$ .  
 ○:  $I = 2.500m$ ; □:  $I = 0.100m$ ; ●:  $I = 0.010m$ .

good agreement with those reported by the manufacturer of the resin.

Knowledge of the numerical value of the selectivity coefficients is important because it allows calculation of the azo-dye/counter-ion ratio inside the resin at which the reagent is sorbed simply by ion-exchange.

Some bivalent anions (sulphate, monohydrogen phosphate, carbonate) have also been considered. They are not able to displace the azo-dyes from the resin, even at concentrations as high as 3M.

#### Exchange of protons by Dowex 1-X8 loaded with T-azo-C and T-azo-R

The titration curve in Fig. 1 shows that, as expected, one proton is exchanged for each molecule of reagent present in the resin phase.

When dealing with such equilibria in aqueous solutions, it is usual to calculate a protonation curve<sup>17</sup> of  $n$  vs. pH, where  $n$  is the average number of neutralizable protons linked to each molecule of ligand. The same treatment can be applied to the two-phase equilibria considered here. Some protonation curves ( $n$  vs. pH) for T-azo-C at different ionic strengths of the solution are shown in Fig. 2, and the corresponding data for T-azo-R are reported in Table 3. It is evident that the composition of the external solution strongly affects the position of the curves, and therefore the observed protonation constants ( $K_{a1}$ ) which can be calculated from them. This is usually the case for acidic groups fixed in a solid phase (either natural, such as iron hydroxide, silicates, etc., or synthetic)<sup>11,12</sup> and finds an explanation in the Donnan-based model of the resin reported above.

By definition,  $n$  is given by

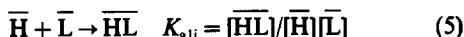
$$n = \frac{[\overline{\text{HL}}]_t}{[\overline{\text{L}}]_t} \quad (4)$$

where  $[\overline{\text{L}}]_t$  is the total ligand molality in the resin phase ( $[\overline{\text{L}}]_t = [\overline{\text{HL}}] + [\overline{\text{L}}]$ ).

Table 3. Protonation of T-azo-R sorbed on Dowex 1-X8, suspended in solutions containing different concentrations of sodium chloride ( $V = 50$  ml; 0.0760 mmole of ligand; 1.0218 g of resin)

$I = 0.015m$ NaCl			$I = 0.096m$ NaCl		
pH	$n$	$\log K_{a1} - \log [\overline{\text{A}}]$	pH	$n$	$\log K_{a1} - \log [\overline{\text{A}}]$
7.25	0.85	9.81	7.55	0.93	9.68
7.50	0.73	9.74	7.95	0.83	9.65
7.72	0.61	9.72	8.20	0.72	9.62
7.95	0.48	9.72	8.43	0.62	9.65
8.20	0.36	9.76	8.65	0.50	9.66
8.55	0.28	9.95	8.87	0.40	9.70
			9.12	0.29	9.74
			9.40	0.19	9.78
			9.70	0.10	9.76
$I = 0.964m$ NaCl			$I = 1.929m$ NaCl		
pH	$n$	$\log K_{a1} - \log [\overline{\text{A}}]$	pH	$n$	$\log K_{a1} - \log [\overline{\text{A}}]$
8.50	0.93	9.64	8.60	0.93	9.44
8.75	0.80	9.38	9.02	0.83	9.43
9.05	0.77	9.59	9.33	0.72	9.45
9.23	0.66	9.51	9.55	0.62	9.48
9.43	0.56	9.55	9.75	0.51	9.48
9.68	0.41	9.54	9.92	0.41	9.48
9.85	0.36	9.62	10.10	0.31	9.47
10.05	0.27	9.64	10.25	0.25	9.49
10.22	0.18	9.58	10.42	0.19	9.50

In the resin phase the protonation equilibrium (charges omitted for simplicity) is



which is more or less shifted to the right, depending on the equilibrium constant values and  $[\bar{H}]$ , which in turn depends on the composition of the external solution, according to the Donnan equation

$$[\bar{H}][A] = [\bar{H}][\bar{A}]. \quad (6)$$

Thus the intrinsic protonation constant  $K_{a1i}$  and the observed protonation constant  $K_{a1}$  are related by the equation

$$K_{a1i} = K_{a1} \frac{[\bar{A}]}{[A]} \quad (7)$$

and  $n$  is given by

$$n = K_{a1i} [\bar{H}][A][\bar{A}] / (K_{a1i} [\bar{H}][A][\bar{A}] + 1) \quad (8)$$

from which the curves of  $n$  vs. pH are expected to depend on  $[A]$ , whereas the curves for  $n$  vs. (pH + pA) should be independent of the ionic composition of the external solution insofar as  $[A]$  is independent of it. In the cases considered here, the plots of  $n$  vs. (pH + pA) are indeed almost identical. An example is reported in Fig. 2 (B). This is a further demonstration that the ionic invasion is practically negligible up to about 1M sodium chloride concentration. Similar results were obtained for T-azo-R (Table 3).

It is worth stressing that these values, for both T-azo-C and T-azo-R, are independent of the degree of protonation. This behaviour is quite different from that of most polymeric materials, though similar results have been obtained for a series of insoluble poly(amidoamines).<sup>18</sup>

Comparison with other systems of similar structure is not possible at the moment, because no investigations on the protonation properties of reagents fixed on a resin by ion-exchange have been found by us in the literature. However, such behaviour can be expected, because  $[A]$  is still constant when the degree of protonation changes [equation (7)]. This is because in the systems investigated here the amount of ligand sorbed is usually only a small fraction of the total amount of chloride inside the resin, so that the change in the counter-ion concentration required to maintain electroneutrality of the resin phase<sup>19</sup> is negligible.

The mean values of the protonation constants obtained from four independent titrations with different amounts of ligand sorbed on different amounts of resin are  $\log K_{a1i} = 8.93 \pm 0.08$  for T-azo-C, and  $9.62 \pm 0.09$  for T-azo-R, which are very similar to the values in aqueous 0.1M sodium perchlorate medium,<sup>3</sup> 8.30 and 9.10, respectively. This indicates that the activity of the chloride counter-ion inside the resin phase ( $\{\bar{A}\}$ ) is around 1M, much lower than its concentration, which should be 5.45–7.11M, depending on the amount of water sorbed.

The activity of the chloride in the resin can be

evaluated by the specific interaction theory.<sup>20,21</sup> The activity coefficient  $\gamma_{Cl}$  of the chloride ion is given by

$$\log \gamma_{Cl} = -D + b(Cl, Q)[\bar{Q}] \quad (9)$$

where  $D = 0.51\sqrt{I}/(1 + 1.5\sqrt{I})$  at 25°,  $[\bar{Q}]$  represents the molal concentration of ammonium groups inside the resin, and  $b(Cl, Q)$  is the interaction coefficient of chloride and the ammonium groups (Q) and can be assumed to be equal to  $-0.05$ , which is the interaction coefficient of chloride and glycine in aqueous solution, reported by Ciavatta.<sup>21</sup>

The activity of chloride in the resin phase can thus be estimated to be 1.6m (at  $I = 5.45m$ ), in reasonable agreement with the expected value of 1m. However, further investigation is required to confirm this point, for instance to give a better estimate of the specific interaction coefficient.

#### *Sorption of copper(II) and nickel(II) by Dowex 1-X8 loaded with T-azo-R and T-azo-C*

The capacity of the loaded resin for copper(II) and nickel(II) depends on the acidity of the external solution and its maximum value was found to be equal to the number of mmoles of T-azo-R or T-azo-C sorbed per g of dry resin. This indicates that the metal ion can be sorbed only by chelation.

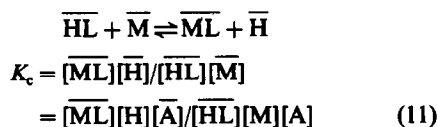
The fraction ( $f$ ) of total metal ion sorbed on the resin at a particular acidity of the solution was experimentally determined. Data for sorption of copper(II), under different conditions, on Dowex 1-X8 loaded with T-azo-C, are reported in Table 4. Copper(II) is so strongly sorbed by Dowex 1-X8 loaded with T-azo-R that it is impossible to elute it even at pH < 1. Therefore this system was not further investigated.

The corresponding data for nickel(II) are reported in Table 5. To reproduce analytical conditions, the ligand is always in large excess with respect to metal ions. It can be seen from Tables 4 and 5 that the factors which mainly influence the sorption of metal ions are the composition and volume of the solution phase, and the amount of sorbed ligand. This can be explained on the basis of the model proposed above: if the metal ion can enter the resin phase only by reacting with the azo-dye, and is present in the solution phase only as the aquo-ion, then  $f$  is given by

$$f = \frac{[\bar{M}L]g}{([\bar{M}L]g + [M]V)} \quad (10)$$

where  $g$  indicates the number of grams of water in the resin in equilibrium with  $V$  ml of metal ion solution of concentration  $[M]$ .

The complexation reaction and its equilibrium constant inside the resin are



where the second form of the complexation constant

Table 4. Sorption of copper(II) from aqueous solutions at different sodium chloride concentration on Dowex 1-X8 loaded with T-azo-C

$I = 0.030m$  NaCl;  $V = 25$  ml; 0.0506 mmole of ligand;  
0.0050 mmole of copper(II);  
1.4930 g of resin

pH	$f$	$\log K_c - \log [\bar{A}]$
2.31	0.56	2.01
2.60	0.75	2.09
2.80	0.84	2.14
2.98	0.86	2.02

$I = 0.100m$  NaCl;  $V = 25$  ml; 0.0506 mmole of ligand;  
0.0050 mmole of copper(II);  
1.4930 g of resin

pH	$f$	$\log K_c - \log [\bar{A}]$
1.38	0.34	2.02
1.53	0.47	2.11
1.75	0.60	2.12
2.07	0.70	1.99
2.75	0.88	1.81

$V = 100$  ml; 0.0500 mmole of ligand;  
0.0010 mmole of copper(II);  
0.1500 g of resin

pH	$f$	$\log K_c - \log [\bar{A}]$
1.50	0.16	2.08
1.82	0.31	2.13
2.09	0.41	2.05
2.55	0.62	1.96
2.53	0.65	2.04
2.97	0.86	2.12
3.55	0.94	1.95

$V = 100$  ml; 0.1000 mmole of ligand;  
0.0010 mmole of copper(II);  
0.2050 g of resin

pH	$f$	$\log K_c - \log [\bar{A}]$
1.69	0.33	2.00
1.89	0.50	2.11
2.13	0.59	2.03
2.55	0.78	2.00
3.27	0.95	2.01

$V = 500$  ml; 0.0500 mmole of ligand;  
0.0050 mmole of copper(II);  
0.7610 g of resin

pH	$f$	$\log K_c - \log [\bar{A}]$
2.03	0.12	2.10
2.55	0.29	2.06
2.55	0.46	2.10
3.00	0.59	2.16
3.60	0.71	1.79
4.00	0.92	2.06

$I = 1.000m$  NaCl  $V = 25$  ml; 0.0500 mmole of ligand;  
0.0050 mmole of copper(II);  
0.7610 g of resin

pH	$f$	$\log K_c - \log [\bar{A}]$
1.04	0.23	1.11
1.58	0.43	0.97
2.08	0.63	0.83
2.52	0.84	0.88
3.03	0.96	1.03

Table 4—continued

$V = 25$  ml; 0.0527 mmole of ligand;  
0.0050 mmole of copper(II);  
0.3140 g of resin

pH	$f$	$\log K_c - \log [\bar{A}]$
1.16	0.20	0.91
1.55	0.45	1.04
2.03	0.65	0.91
2.30	0.75	0.85
2.57	0.88	1.03

Table 5. Sorption of nickel(II) from aqueous solution at different sodium chloride concentrations on Dowex 1-X8 loaded with T-azo-C and T-azo-R

T-azo-C  
 $V = 50$  ml; 0.0102 mmole of ligand;  
0.0010 mmole of nickel(II);  
0.3000 g of resin  
 $I = 0.060m$

pH	$f$	$\log K_c - \log [\bar{A}]$
5.00	0.16	-0.81
5.72	0.54	-0.74
6.54	0.75	-1.15

$I = 0.100m$

pH	$f$	$\log K_c - \log [\bar{A}]$
4.93	0.19	-0.87
6.12	0.70	-1.06
6.66	0.87	-1.14

$I = 2.00m$

pH	$f$	$\log K_c - \log [\bar{A}]$
3.93	0.13	-1.37
4.93	0.53	-1.49
6.16	0.95	-1.49

T-azo-R

$V = 50$  ml; 0.2052 mmole of ligand;  
0.0010 mmole of nickel(II);  
0.035 g of resin  
 $I = 0.100m$ .

pH	$f$	$\log K_c - \log [\bar{A}]$
1.70	0.24	1.19
2.10	0.46	1.22
2.64	0.69	1.09
3.03	0.80	0.96

is obtained by applying the Donnan equilibrium to the exchange of protons and bivalent metal ions.

As in the acidity range considered the sorbed ligand is present only as HL,  $f$  is given by

$$f = 1/(1 + [H][\bar{A}]V/\bar{L}_t[A]K_c) \quad (12)$$

and insofar as  $[\bar{A}]$  is constant, is a unique function of  $pH - pA$ . Equation (12) also shows that the volume of the solution ( $V$ ) and the total amount of sorbed ligand ( $\bar{L}_t$  strongly affect the sorption of metal ions. On the other hand, the total amount of resin is not expected to be important, which is also verified in practice.

The data reported in Tables 4 and 5 allow evaluation of  $\log K_c - \log [A]$  by use of equation (12). The

continued

results, reported in the third column of Tables 4 and 5, show an acceptable agreement with the complexation constants of the corresponding complexes in 0.1M sodium perchlorate [ $\log K_c = 1.63$  and  $-0.88$ , respectively, for the complexes of copper(II) and nickel(II) with T-azo-C, and  $\log K_c = 1.27$  for the nickel(II)/T-azo-R complex]. This further confirms that the activity of the counter-ion inside the resin must be about 1m.

The calculated complexation constant of Cu/T-azo-C in 1.000m sodium chloride solutions is somewhat lower than expected, probably owing to the competing complexation of copper(II) by chloride ions. Indeed early published values<sup>22</sup> of the stability constants of the copper(II)/chloride complexes account for the observed difference for 1.000m sodium chloride media. This is further confirmed by the fact that this difference is not observed for sorption of nickel(II) ions, which form weaker complexes with chloride.

The conclusion that can be drawn from the results obtained in the present research is that equation (12) is really useful to calculate the fraction of metal ion sorbed on a properly loaded anion-exchange resin. The quantities which must be known are the total amount of chelating reagent sorbed, the compositions of the aqueous solution and of the resin phase (capacity and water sorbed), volume and acidity of the aqueous phase, and the complex formation and protonation constants in the aqueous phase of the particular complex considered. All of these are either already known, or easily determinable.

*Acknowledgement*—This research was partially supported by the National Research Council (CNR) of Italy.

## REFERENCES

1. M. Pesavento, C. Riolo, T. Soldi and R. Garzia, *Ann. Chim. (Rome)*, 1982, **72**, 217.
2. M. Pesavento, *ibid.*, 1983, **73**, 173.
3. M. Pesavento and T. Soldi, *Analyst*, 1983, **108**, 1128.
4. M. Nakayama, M. Chikuma and H. Tanaka, *Talanta*, 1982, **29**, 503.
5. C. Sarzanini, E. Mentasti, V. Porta and M. C. Gennaro, *Anal. Chem.*, 1987, **59**, 484.
6. H. P. Gregor, *J. Am. Chem. Soc.*, 1951, **73**, 642.
7. F. Helfferich, *Ion Exchange*, p. 97. McGraw-Hill, New York, 1962.
8. J. A. Marinsky, Fu Grand Lin and K.-S. Chung, *J. Phys. Chem.*, 1983, **87**, 3139.
9. F. Helfferich, *op. cit.*, p. 134.
10. *Idem*, *op. cit.*, p. 142, footnote.
11. J. A. Marinsky and Y. Merle, *Talanta*, 1984, **31**, 199.
12. S. Alegret, J. A. Marinsky and M. T. Escales, *ibid.*, 1984, **31**, 683.
13. H. P. Gregor, J. Belle and R. A. Marcus, *J. Am. Chem. Soc.*, 1954, **76**, 1884.
14. M. Marhol, *Ion Exchangers in Analytical Chemistry*, pp. 94 and 98. Elsevier, Amsterdam, 1982.
15. W. Forsling, S. Hietanen and L. G. Sillén, *Acta Chem. Scand.*, 1952, **6**, 901.
16. H. P. Gregor, J. Belle and R. A. Marcus, *J. Am. Chem. Soc.*, 1955, **77**, 2713.
17. J. Bjerrum, *Metal Ammine Formation in Aqueous Solution*, p. 20. Haase, Copenhagen, 1957.
18. R. Barbucci, M. Casolaro, M. C. Beni, P. Ferruti, M. Pesavento, T. Soldi and C. Riolo, *J. Am. Chem. Soc.*, 1981, **103**, 2559.
19. Ö. Szabadka, *Talanta*, 1982, **29**, 181.
20. G. Biedermann, *Dahlem Workshop on the Nature of Seawater*, p. 339. Dahlem Konferenzen, Berlin, 1975.
21. L. Ciavatta, *Ann. Chim. (Rome)*, 1980, **70**, 551.
22. L. G. Sillén and E. A. Martell, *Stability Constants of Metal-ion Complexes*, Special Publ. 17 and 25, The Chemical Society, London, 1964, 1971.

## SYNTHESIS AND ANALYTICAL CHARACTERIZATION OF A CHELATING RESIN LOADED WITH DITHIZONE

J. CHWASTOWSKA and E. KOSIARSKA

Department of Analytical Chemistry, Faculty of Chemistry, Technical University of Warsaw,  
Warsaw, Poland

(Received 5 September 1986. Revised 16 November 1987. Accepted 22 January 1988)

**Summary**—A chelating sorbent loaded with dithizone was obtained by chemical reaction with styrene-DVB (5%) copolymer as matrix. The analytical characteristics of the sorbent were established and optimum sorption conditions for Ag, Cu, Cd, Pb, Ni, Co and Zn under static and dynamic conditions determined. The sorbent was applied to determination of copper and lead in river water and of silver in electrolytic copper. After separation of traces of metals on the sorbent and desorption with hydrochloric acid, the metals were determined in the effluent by atomic-absorption spectrophotometry.

It is to be expected that a chelating sorbent loaded with dithizone would be useful in analysis, because dithizone is one of the most versatile chelating reagents forming complexes with heavy metals. Such sorbents have been prepared by deposition of dithizone on polyurethane foam<sup>1,2</sup> and polystyrene beads,<sup>3</sup> and used for preconcentration of mercury from sea-water, but the recovery was not always good enough, because of instability of the sorbent. The best dithizone-resin on polystyrene beads<sup>3</sup> had to be kept in the refrigerator for a few days. Braun and Farag have also deposited dithizone on polyurethane foam and used the sorbent for collection of silver<sup>4</sup> and mercury<sup>5</sup> and detection of zinc and lead.<sup>6</sup>

A chelating resin was prepared by Tanaka *et al.*<sup>7</sup> by treatment of a strongly basic anion-exchanger (Amberlite IRA 400) with a sulphonic acid derivative of dithizone.

Another way of preparing chelating resins is by chemical reaction. Griesbach and Lieser<sup>8</sup> have described the synthesis of fifteen sorbents, including one loaded with dithizone, but the products were not analysed and the properties of the sorbents obtained were not studied.

In the present work a chelating resin loaded with dithizone was made by chemical reaction. A matrix (a styrene-divinylbenzene copolymer) was nitrated, reduced, diazotized and coupled with dithizone. It is possible to couple with dithizone because in weak acid medium its amine groups are able to activate the benzene ring for electrophilic substitution. The conditions for each stage of synthesis were adopted from Davies *et al.*<sup>9</sup> The conditions given by Griesbach and Lieser (especially for the coupling) did not yield good results.

### EXPERIMENTAL

#### Reagents

Standard 1-mg/ml stock solutions of Cu, Pb, Bi, Zn, Cd, Co, Ni, Ag were prepared by dissolving the metals or

appropriate salts in a suitable acid or acidified distilled water.

#### Synthesis

The method was the same as that for production of a chelating sorbent loaded with Arsenazo I.<sup>10</sup> The styrene-DVB (5%) copolymer (10 g) was nitrated with a 5:2 v/v mixture of concentrated sulphuric and nitric acids at 60° for 30 min, and reduced to the amine by treatment with a mixture of 80 g of tin(II) chloride dihydrate, 90 ml of concentrated hydrochloric acid and 100 ml of ethanol for 10 hr at 90°. After washing, about half of the reduction product was diazotized by alternate slow additions of equal amounts of 2M hydrochloric acid and 2M sodium nitrite at 0°, then washed with cold water and introduced into a cold solution of 2.5 g of dithizone in 450 ml of glacial acetic acid and 200 ml of acetone (the dithizone was initially purified according to Marczenko,<sup>11</sup> then precipitated with 6M hydrochloric acid and collected). The coupling reaction was conducted at 0 ± 3° for 24 hr. The sorbent was filtered off and washed, then treated with hypophosphorous acid for 10 min. The product was dark brown.

#### Experimental techniques

The sorption of various metals was examined under static and dynamic conditions. To determine the capacity and stability of the sorbent, optimum sorption conditions (kinetics, pH) and desorption conditions, the static method was used. To determine optimum pH, flow-rate, and sample volume in the column process, the dynamic method was used.

The degree of sorption was determined by atomic-absorption spectrophotometric determination of the test element in the effluent and the eluate. An air-acetylene flame was used, with observation at 10 mm above the burner, with the following wavelengths (nm): Cu 324.8; Pb 217; Cd 228.8; Zn 213.9; Co 240.7; Ni 232; Bi 223.1; Ag 328.1.

**Sorption kinetics.** Samples (10 ml) of 10<sup>-4</sup>M copper or zinc, at pH 6.0-6.1 were shaken for 30, 60, 90 and 120 min with 0.5 g of the sorbent in separatory funnels.

**Desorption conditions.** Portions of resin (0.5 g) were shaken for 60 min with 10-ml portions of 10<sup>-4</sup>M copper (pH 6.0) and then stripped by shaking for different times with 10 ml of 2M or 4M hydrochloric acid. The stripping solutions were analysed by AAS.

**Total sorption capacity.** This was determined under the following conditions: amount of sorbent 0.5 g, volume of solution 10 ml, amount of metal 2.5 mg, pH appropriate for the element concerned, time of shaking 60 min. The resin

was separated, washed with water of appropriate pH and stripped with 4M hydrochloric acid. The metals in the strippings were determined by AAS.

**Sorption under dynamic conditions.** A column 9 mm in diameter was made with 2 g of the sorbent, and washed with water of appropriate pH. Then a 50-ml volume of test solution of appropriate pH containing a fixed amount of metals was passed through the resin at a flow-rate of 2 ml/min. The resin was next washed with water at appropriate pH, and the metal ions were eluted with 15 ml of 4M hydrochloric acid and 20 ml of water and determined by AAS. The effect of flow-rate on the sorption was studied over the range 2–5 ml/min. The influence of the sample volume was studied by passing 50, 100, 200, 500 and 1000 ml volumes of metal solutions through the column at a constant flow-rate of 2 ml/min. In the examination of group sorption of metals, bismuth could not be examined because of its hydrolysis under the conditions used.

**Analysis of water samples.** A 1-litre sample of water was filtered and its pH adjusted to 4.5. A column, 9 mm in diameter, of 4 g of sorbent was initially washed with 20 ml of redistilled water adjusted to pH 4.5. The sample was then passed through the column at 5 ml/min, followed by 20 ml of redistilled water (pH 4.5). The trace metals were eluted with 15 ml of 4M hydrochloric acid and 20 ml of water. After evaporation to low bulk the eluate was diluted to volume in a 10-ml or 25-ml standard flask, as appropriate for the amount of element to be determined and the sensitivity, and analysed by AAS.

**Determination of silver in cathode copper.** The copper sample (1–3 g) was dissolved in concentrated nitric acid, and the solution was heated to remove nitrogen oxides and then evaporated until copper nitrate began to crystallize. The residue was dissolved in water and enough nitric acid to give a 2M concentration of acid after dilution to volume in a 50-ml standard flask.

A column, 3 mm in diameter, of 0.5 g of the sorbent was washed with 15 ml of 2M nitric acid, and a 5- or 10-ml aliquot of sample solution was passed through it at 2 ml/min. The column was washed with water until the pH of the effluent was about 3. The silver sorbed was then eluted with 10 ml of 0.5M sodium thiosulphate, and after dilution of the eluate to volume in a 25-ml standard flask was determined by AAS.

## RESULTS AND DISCUSSION

### Characteristics of the reagent

The results of elemental analysis of the amine-derivative of resin and the final product of synthesis are given in Table 1. The results for nitrogen (9.8–10.6%) in the final product suggest incomplete reduction (the amount of nitrogen corresponding to the amount of sulphur determined is 8.4%).

The metal-ion capacity ranges from 0.03 mmole/g of dry sorbent for bismuth to 0.08 mmole/g for copper (Table 2), and is lower than expected from the

Table 1. Elemental analysis of products of synthesis

Element	Content, %	
	Amine-derivative	Dithizone-resin
C	62.6–63.8	56.3–56.9
H	5.9–6.1	4.5–4.7
N	14.0–14.3	9.8–10.6
S	—	3.0–3.2

Table 2. Total sorption capacity, mmole/g of sorbent

Ion	pH	Capacity
Cu(II)	5.5	0.08
Pb(II)	4.8	0.05
Zn(II)	6.4	0.04
Ni(II)	6.0	0.04
Cd(II)	6.0	0.05
Co(II)	6.1	0.06
Ag(I)	0 (1M HNO <sub>3</sub> )	0.06
Bi(III)	2.5	0.03

amount of sulphur determined, suggesting that there is steric hindrance.

The infrared spectra of the styrene–divinylbenzene copolymer (curve 1), dithizone alone (curve 2) and the synthesis product (curve 3) are shown in Fig. 1. The absorption bands at 1200–1300 cm<sup>-1</sup>, characteristic for —SH groups, are very intense in the spectrum of dithizone and also prominent in the spectrum of the dithizone-resin (but not so intense, of course), and may be taken as proof of the presence of the dithizone-group in the product.

The sorbent is highly stable and can be used repeatedly. A sample used 25 times in succession under static conditions did not decrease in sorption efficiency. A column of sorbent was used continuously for about 6 months with good results. Our findings are quite different from those previously published for sorbents prepared by deposition of dithizone on polymer beads.<sup>1–3</sup>

### Sorption under static conditions

The study of the sorption kinetics showed that shaking for 1 hr is needed for equilibrium to be reached. From the sorption curves (Fig. 2) it can be seen that all the elements studied are almost quantitatively sorbed (sorption 90–100%). According to

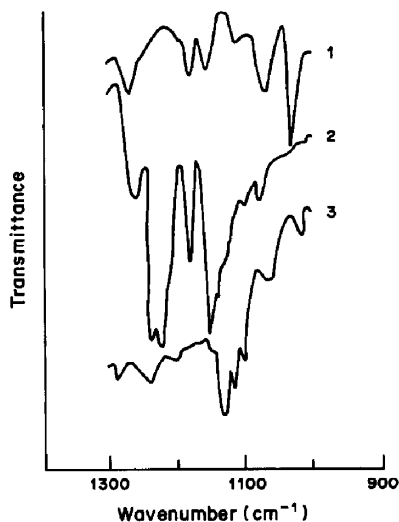


Fig. 1. Infrared spectra (oil medium): 1—the matrix, 2—dithizone, 3—the dithizone-resin.

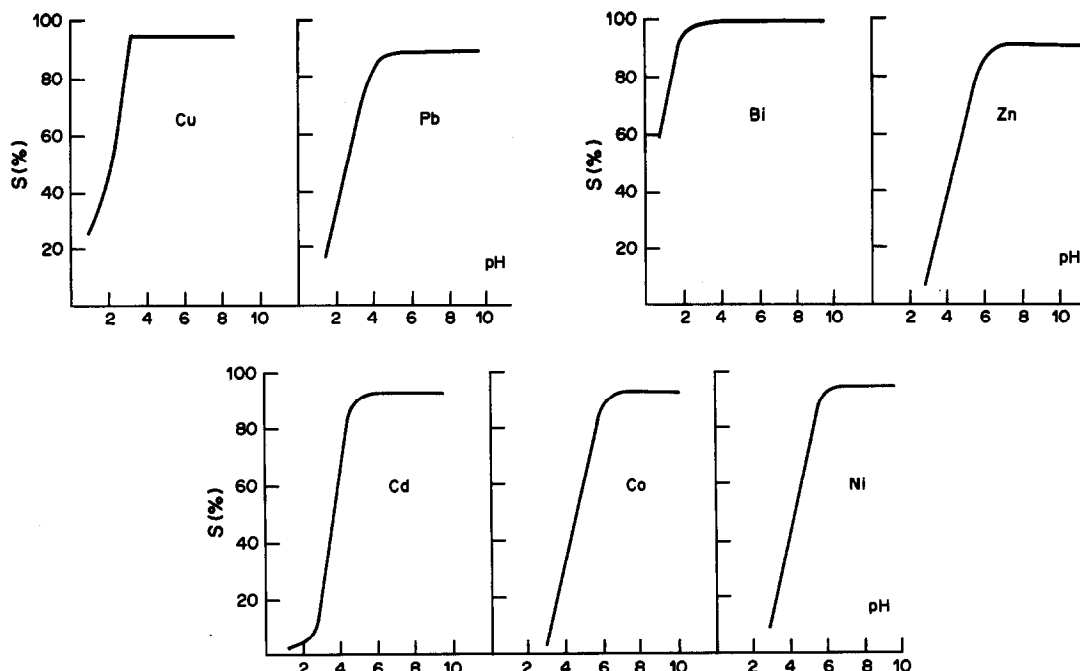


Fig. 2. Relationship between sorption and solution pH.

the optimum pH of sorption, the metals studied can be divided into three groups:

- metals which are quantitatively sorbed only in alkaline medium: nickel, cobalt, zinc and cadmium;
- metals which are quantitatively sorbed both in alkaline and acid medium: copper, bismuth and lead;
- metals which are quantitatively sorbed only in acid medium: silver.

The dithizone sorbent is selective for silver, which can be separated in aqueous acidic solution from each of the other metals studied. The sorbent can be applied to isolation of a group of metals, e.g. pH 5–6.5 is optimum for sorption of Cu, Pb, Cd, Co, Ni, Zn.

All the elements retained by the sorbent, except silver, are easily stripped by shaking with three portions of 4M hydrochloric acid, each for 10 min.

Silver is desorbed by shaking with three portions of 0.5M sodium thiosulphate, each for 10 min.

#### Column method

The results for sorption of a group of metals (Cu, Pb, Cd, Co, Ni, Zn) at different pH values (Table 3) show that the column method is more efficient than the static method, all six elements being sorbed quantitatively at  $\text{pH} \geq 5$ . The flow-rate affects the degree of sorption, except for copper and lead (Table 4). Also, increase in the sample volume decreases the degree of sorption (except of copper and lead) for a fixed amount of sorbent and fixed total amount (50  $\mu\text{g}$ ) of metal (Table 5). Thus for the group separation of all the elements the optimum flow-rate is 2 ml/min and the optimum sample volume is 50 ml.

The results obtained show that copper and lead are the best sorbed. The optimum pH for sorption of

Table 3. Group column sorption of metals at different pH values; 50 ml of solution, flow-rate 2 ml/min, amount of each metal 50  $\mu\text{g}$

pH	Sorption, %					
	Cu	Pb	Zn	Cd	Co	Ni
4.0	100	100	95.5	100	74.0	93.0
5.1	100	100	100	100	100	100
6.5	100	100	98.6	98.5	100	100

Table 4. The influence of the flow-rate on the degree of sorption at pH 5.1

Flow-rate, ml/min	Sorption, %					
	Cu	Pb	Zn	Cd	Co	Ni
2	100	100	100	100	100	100
5	100	100	63.5	62.5	43.0	45.0

Table 5. The influence of the sample volume on the degree of sorption at pH 5.2; flow-rate 2 ml/min; 50 µg of metal

Sample volume, ml	Sorption, %					
	Cu	Pb	Zn	Cd	Co	Ni
50	100	100	100	100	100	100
100	100	100	89.5	91.0	73.0	77.5
200	100	100	87.5	91.5	73.5	73.5
500	100	100	75.2	78.5	50.0	50.0
1000	100	100	69.5	64.0	44.0	45.0

Table 6. Analysis of synthetic water; pH 5.2; sample 100 ml, flow-rate 5 ml/min

Element	Added,	Found,	Recovery,	n
	µg	µg	%	
Cu	25	24.3	97.2	6
	15	14.6	97.0	4
Pb	50	49.5	99.0	6
	25	24.7	98.8	4

copper and lead in the column method is lower than for the other elements (Table 3). Also the effectiveness of sorption of copper and lead does not depend on the flow-rate and the sample volume. These facts suggest that the copper and lead complexes in the system studied are much more stable than the complexes of the other elements. However, stability of the complex is only one of the many factors which affect the affinity of an ion for the sorbent.

#### Applications

Our investigations show that the dithizone-resin can be applied to the separation of copper and lead from water and to the separation of silver from other metals, and results for the determination of copper and lead in river water and of silver in copper cathode metal are given below.

**Analysis of water.** A synthetic water sample having the composition (mg/l.) Na<sup>+</sup> 30, K<sup>+</sup> 8, Mg<sup>2+</sup> 40, Ca<sup>2+</sup> 110, Cl<sup>-</sup> 248, SO<sub>4</sub><sup>2-</sup> 158, conforming to acceptable limits for drinking water, was analysed for two levels of copper and lead, and the results in Table 6

show that the salts present in the water do not affect the degree of sorption of copper and lead. Analysis of a river water gave a relative standard deviation of about 1.5% for both copper and lead at the 5.3 and 7.8 µg/l. level respectively.

**Analysis of cathode copper.** The results of determination of silver in copper by separation with the dithizone-resin and analysis by AAS were in good agreement with those obtained by the independent method described by Boguszewska *et al.*,<sup>12</sup> as shown in Table 7.

**Acknowledgement**—This work was performed in connection with problem MR. I-32.

#### REFERENCES

1. A. Chow and D. Buksak, *Can. J. Chem.*, 1975, **5**, 137.
2. Y. K. Lee, K. J. Whang and K. Ueno, *Talanta*, 1975, **22**, 535.
3. A. G. Howard and M. H. Abbab-Zavar, *ibid.*, 1979, **26**, 895.
4. T. Braun and A. B. Farag, *Anal. Chim. Acta*, 1974, **69**, 85.
5. *Idem*, *ibid.*, 1974, **75**, 133.
6. *Idem*, *ibid.*, 1974, **73**, 301.
7. H. Tanaka, M. Chikuma, A. Harada, T. Ueda and S. Yube, *Talanta*, 1976, **23**, 489.
8. M. Griesbach and K. H. Lieser, *Angew. Makromol. Chim.*, 1980, **90**, 143.
9. R. V. Davies, J. Kennedy, E. S. Lane and J. L. Willans, *J. Appl. Chem.*, 1959, **9**, 368.
10. J. Chwastowska, *Chem. Anal. Warsaw*, 1987, **32**, 643.
11. Z. Marczenko, *Separation and Spectrophotometric Determination of Elements*, pp. 92, 93, Horwood, Chichester, 1986.
12. Z. Boguszewska, M. Krasiejko and B. Palmowska-Kuś, *Talanta*, 1986, **33**, 155.

Table 7. Results of determination of silver in electrolytic copper

Method		n	Silver found, 10 <sup>-3</sup> %	Relative std. devn., %
Separation	Determination			
Electrolysis	Spectrophotometry	4	1.04*	4
Sorption	AAS	6	1.14	5

\*Results from Boguszewska *et al.*<sup>12</sup>



# DETERMINATION OF ANTIMONY IN LEAD, ZINC CONCENTRATES AND OTHER SMELTER PRODUCTS BY ATOMIC-ABSORPTION SPECTROPHOTOMETRY AFTER SEPARATION BY *n*-BUTYL ACETATE EXTRACTION OF THE CHLORO-COMPLEX

S. S. MURTI and S. C. S. RAJAN\*

Process Laboratory, Hindustan Zinc Limited, Visakhapatnam-530 015, A.P., India

J. SUBRAHMANYAM

College of Engineering, Andhra University, Waltair-530 003, A.P., India

(Received 8 May 1987. Revised 21 August 1987. Accepted 22 January 1988)

**Summary**—An extractive atomic-absorption spectrophotometric (AAS) procedure is developed for fast and accurate determination of up to 20  $\mu\text{g/g}$  antimony in lead and zinc concentrates and other smelter products. The procedure involves digestion of the sample with potassium bisulphate and sulphuric acid, addition of hydrazine to reduce all antimony to Sb(III), reoxidation to Sb(V), extraction of the chloro-complex of antimony(V) with *n*-butyl acetate, and AAS analysis of the organic phase for antimony.

Determination of antimony by atomic-absorption spectrophotometry (AAS) has been dealt with in fair detail in the literature.<sup>1-5</sup> Donaldson<sup>1</sup> has developed several methods for the determination of small amounts of antimony in copper, nickel, lead, zinc and molybdenum concentrates and related materials. These methods involve preliminary separation of antimony(III) from the matrix elements by coprecipitation with hydrous ferric and lanthanum oxides. The precipitate is dissolved in dilute hydrochloric acid and antimony is determined either by AAS or, if the sample contains <100  $\mu\text{g/g}$  antimony, by the spectrophotometric iodide method after further separation from iron, lead and other co-extracted elements, by chloroform extraction as antimony xanthate. Although these methods yield accurate results for antimony, they are time-consuming, particularly the spectrophotometric method, and the AAS method is not applicable to samples of high lead and iron contents. Recently Donaldson and Wang<sup>6</sup> published another method for the determination of 5  $\mu\text{g/g}$  or more of antimony as well as small amounts of bismuth, indium, copper and cadmium in ores and related materials. However, this method is also not rapid, because it involves an iron co-precipitation step to recover antimony retained by lead and calcium sulphates, followed by methyl isobutyl ketone (MIBK) extraction, and stripping of the iodide complex before the AAS determination.

In general, the sensitivity of antimony determination in aqueous solutions by AAS is not very

high. Solvent extraction not only helps in separating and concentrating the desired species, but also increases the sensitivity.<sup>2</sup> Several workers have employed ketones and esters, *viz.* amyl acetate, MIBK and *n*-butyl acetate for the extraction of the chloro-complex of antimony(V) from hydrochloric acid solutions and determined antimony by aspirating the organic phase into the flame.<sup>3-5</sup> These procedures were developed mainly for metallurgical samples and geological prospecting.

We have worked out a procedure for the determination of antimony in our lead and zinc smelter products, *viz.* concentrates, lead sinter, blast furnace slag and zinc calcine. The procedure involves suitable decomposition of the sample, and taking up the salts in 6*M* hydrochloric acid. Sodium nitrite is added to oxidize antimony(III) and the chloro-complex of antimony(V) is immediately extracted with *n*-butyl acetate, the extract then being aspirated into the flame. *n*-Butyl acetate was chosen as solvent because its solubility in hydrochloric acid of high concentration is much less than that of MIBK,<sup>5</sup> and it still gives a good sensitivity enhancement.<sup>2</sup> The time interval between oxidation and extraction is too short for problems to arise from hydrolysis of antimony(V). This procedure is found to be fast and reliable.

## EXPERIMENTAL

### Apparatus

A Varian Techtron AA-275 instrument was used. The air-flow was set at 8.5 and a pressure of 40 psig, and the acetylene-flow was set at 2.0 on the gas manifold, with pressure 10 psig. The aspiration rate was 3.5-4.0 ml/min and the measurements were made at 217.6 nm.

\*Author for correspondence.

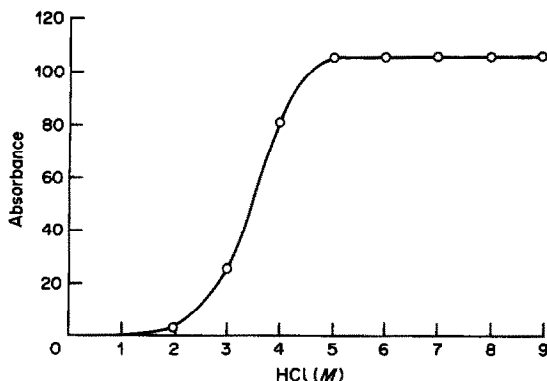


Fig. 1. Effect of HCl concentration on the extraction and determination of 50  $\mu\text{g}$  antimony. Aqueous phase, 50 ml; n-butyl acetate, 10 ml; 5%  $\text{NaNO}_2$  solution added 0.5 ml.

#### Reagents

**Standard antimony solution.** Pure antimony metal (1.0000 g) is heated with 10 ml of concentrated sulphuric acid in a 250-ml beaker on a hot-plate till dense white fumes are evolved. The beaker is cooled, a little water and 1 g of hydrazine sulphate are added and the solution is heated again till dense white fumes have evolved for 15 min. The beaker is then cooled in ice-water, 100 ml of 2M hydrochloric acid are added and the mixture is allowed to attain room temperature. The contents of the beaker are transferred to a 1-litre standard flask and made up to the mark with 2M hydrochloric acid. This solution contains 1 mg/ml antimony, and is diluted with 6M hydrochloric acid to give a 10- $\mu\text{g}$ /ml working standard.

**Sodium nitrite solution, 25%.** Freshly prepared.

#### Procedures

**Calibration.** To 40 ml of 6M hydrochloric acid in each of six 125-ml separating funnels 0, 2, 4, 6, 8 and 10 ml of antimony working standard solution are added from a burette, and the total volume is made up to 50 ml by addition of the required quantity of 6M hydrochloric acid. One ml of sodium nitrite solution is added to each separating funnel, followed immediately by 10 ml of n-butyl acetate from a safety pipette. The separating funnels are shaken gently for 30 sec and the layers are allowed to separate. The lower aqueous layers are drained off and the organic layers are washed with 10 ml of 10% v/v hydrochloric acid solution. The aqueous layers are discarded and the organic layers are drained off into test-tubes through rolled-up filter paper placed in the stems of the separating funnels. The organic solutions then measured by AAS, with pure n-butyl acetate used for setting the zero. The absorbance of the blank (zero added antimony), if any, is deducted from the absorbance values of the standards.

**Sample treatment.** Depending on the antimony content, 0.1–1.0 g of the sample is weighed accurately and into a 250-ml beaker. One g of potassium bisulphate and 10 ml of concentrated sulphuric acid are added and the beaker is covered with a watch-glass (Note 1). The beaker is heated for 1 hr on a hot-plate. The beaker is cooled and its walls are washed down with a small quantity of water (10 ml). One g of hydrazine sulphate is added and the heating is repeated till dense white fumes are evolved. The beaker is cooled in ice-water, 50 ml of 6M hydrochloric acid are added and the beaker is warmed just enough for the salts to dissolve, and is then cooled. The contents of the beaker are transferred to a 100-ml standard flask and made up to the mark with 6M hydrochloric acid (Note 2). An aliquot containing 20–100  $\mu\text{g}$  of antimony is taken in a 125-ml separating funnel and 6M hydrochloric acid is added to

make up the volume to 50 ml. The solution is then processed as described under calibration, starting from the addition of sodium nitrite. Antimony is determined in the organic solutions by comparing with standard solutions (Note 3).

#### Notes

(1) In the case of blast furnace slag, the sample is taken in a Teflon beaker, and 15 ml of concentrated hydrofluoric acid are added after the potassium bisulphate and sulphuric acid.

(2) For samples containing less than 0.01% antimony, a 1-g sample is processed and the whole sample solution is used without dilution to 100 ml.

(3) The organic extracts are quite stable and can be read even on the next day provided the tubes containing them are tightly stoppered.

#### DISCUSSION

##### *Effect of hydrochloric acid concentration on the extraction of antimony*

It is well known that the degree of extraction of antimony(V) increases with hydrochloric acid concentration. Hannaker and Hughes<sup>5</sup> recommended 8M hydrochloric acid for extraction with n-butyl acetate, but in general, the higher the acid concentration, the greater the mutual solubility of the two phases. Figure 1 shows that the antimony extraction into n-butyl acetate is complete even from 5M hydrochloric acid. Hence an acid concentration of 6M is recommended.

##### *Effect of sodium nitrite concentration*

Nitrite is generally preferred for the oxidation of antimony prior to extraction.<sup>3,4,7,8</sup> Yanagisawa *et al.*<sup>4</sup> noted that when excess of sodium nitrite is used, with MIBK as solvent, the organic layer becomes brownish yellow and the antimony signal is lowered. With n-butyl acetate as solvent, we found that although a brownish yellow colour developed with increasing sodium nitrite concentration, there was no effect on the antimony signals (Fig. 2). Further, washing the organic phase with 10% v/v hydrochloric acid to remove any co-extracted iron also removed the brownish yellow colour completely, although it failed to do so when MIBK was used as the extractant. It is interesting that Walker *et al.*<sup>3</sup> did not record any such effect even though more nitrite was used (2 ml

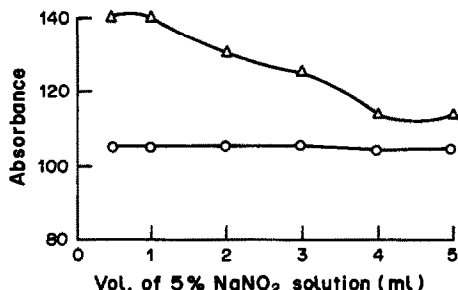


Fig. 2. Effect of sodium nitrate on the determination of 50  $\mu\text{g}$  of antimony. O, n-butyl acetate;  $\Delta$ , MIBK.

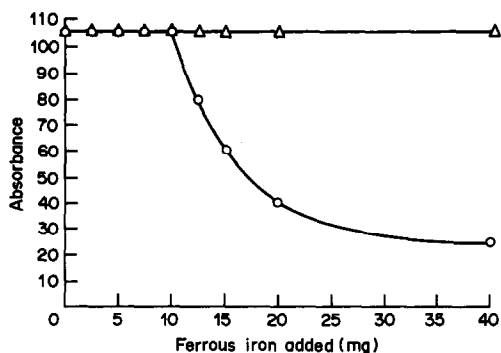


Fig. 3. Effect of ferrous iron on the determination of 50  $\mu\text{g}$  of antimony.  $\Delta$ , 1 ml of 25%  $\text{NaNO}_2$  solution;  $\circ$ , 0.5 ml of 5%  $\text{NaNO}_2$  solution.

of 20% potassium nitrite solution) with n-amyl acetate as solvent. When amyl acetate is used in our method, washing the organic layer again removes the brownish yellow colour that is formed initially.

*Effect of ferrous iron concentration*

In the initial studies, when only 0.5 ml of 5% sodium nitrite solution was used, the antimony results for lead blast furnace slag were very low. Since this slag contained 30–35% iron, mostly as ferrous oxide, it was suspected that the sodium nitrite was being consumed by the ferrous iron, thus inhibiting the oxidation of antimony, and this was confirmed experimentally. Different quantities of ferrous iron to a known quantity of antimony at two different concentrations of sodium nitrite (Fig. 3). Hence, the quantity of sodium nitrite added was increased to 1 ml of 25% solution.

*Effect of decomposition procedure*

Decomposition with potassium bisulphate-sulphuric acid mixture gave smooth decomposition for all samples. In the case of highly siliceous samples such as blast furnace slag, though the silica gel produced did not affect the final results, it caused a separate phase during extraction, creating difficulties in transfer of the organic layer. This was overcome by treating the sample according to Note 1. With zinc calcine, the digestion procedure yielded very low values for antimony. It was suspected that in zinc calcine, a product from the fluidized bed roaster, the antimony was probably present in its higher oxidation state. Addition of hydrazine sulphate during the digestion resulted in complete recovery of the antimony, confirming that part of the antimony was probably in the quinquevalent state. It is well known that for quantitative extraction of antimony(V), the antimony(III) must be oxidized just before the extraction, to avoid the problem of hydrolysis.<sup>3,9-11</sup> Similar behaviour was expected for the lead sinter, but in this case addition or exclusion of hydrazine sulphate did not appreciably affect the analytical values (Table 1). This may be due to the fact that lead sinter is not

Table 1. Effect of various decomposition methods on the determination of antimony

Sample	Antimony found, %						Certified* value	By alternative AAS method
	$\text{KHSO}_4\text{-H}_2\text{SO}_4\text{-hydrazine}$	$\text{KHSO}_4\text{-H}_2\text{SO}_4$	$\text{HNO}_3\text{-H}_2\text{SO}_4$	$\text{HNO}_3\text{-H}_2\text{SO}_4\text{-hydrazine}$	0.054	0.052		
1. Zinc concentrate (CZN-1)	0.054	0.055	0.043	—	—	0.052	0.055	
2. Zinc concentrate (Zawar Mines)	0.0025	0.0025	—	—	—	—	—	
3. Zinc calcine	0.035	0.022	0.003	0.029	0.006	—	0.032	
4. Lead concentrate (Agnigundala Mines)	0.0064	—	0.004	—	—	—	—	
5. Lead concentrate (Zawar Mines)	0.035	0.038	0.0083	0.028	—	—	0.034	
6. Lead concentrate (CPB-1)	0.374	0.380	0.219	0.35	—	0.36	0.370	
7. Lead sinter (1)	0.225	0.210	0.107	0.210	—	—	0.228	
8. Lead sinter (2)	0.226	0.222	—	—	—	—	0.228	

\*Reference 1.

Table 2. Antimony results obtained for lead-zinc concentrates and other related products with the recommended method

Sample	*Antimony found, %	Standard deviation	Certified Sb value and range, %	†Sb found by AAS method <sup>1</sup> , %
1. Zinc concentrate CZN-1	0.054	0.002	0.052 (0.050-0.055)	0.055
2. Zinc concentrate (Zawar Mines)	0.0025	0.0004	—	—
3. Zinc calcine	0.035	0.004	—	0.032
4. Lead concentrate (Agnigundula Mines)	0.0064	0.0005	—	—
5. Lead concentrate (Zawar Mines)	0.035	0.002	—	0.034
6. Lead concentrate (CPB-1)	0.374	0.004	0.360 (0.34-0.39)	0.370
7. Lead sinter (1)	0.225	0.004	—	0.228
8. Lead sinter (2)	0.226	0.002	—	0.228
9. Lead blast furnace slag	0.025	0.001	—	0.025

\*Average of five results.

†Reference 1.

subject to such severe oxidative treatment as the zinc calcine. However, the addition of hydrazine sulphate is still recommended as a general precaution for dealing with quinquevalent antimony present in the sample or arising during the decomposition.<sup>1,11</sup>

Digestions involving nitric acid, followed by fuming with sulphuric acid, yielded low values for antimony. Addition of hydrazine sulphate during the fuming stage improved the antimony values, but they were still always marginally low (Table 1). As suggested by Donaldson,<sup>1</sup> this effect, which occurs whether hydrazine sulphate is added or not (Table 2), is caused by the formation of an unreactive mixed antimony (III + V) species, which is formed in the presence of oxidizing acids and is not readily reduced with hydrazine sulphate.

### Results

Table 2 gives the results obtained for antimony in zinc concentrates, lead concentrates, calcine, lead sinter and lead blast furnace slag. The values for Canmet CZN-1 (Zinc concentrate) and CPB-1 (Lead concentrate) are comparable with the certified values. For the lead sinter, zinc calcine, blast furnace slag and other concentrates, the values were checked by Donaldson's iron-lanthanum collection/AAS method. The samples containing <100 µg/g antimony (samples 2 and 4) were checked by the standard-addition technique. The results show that

the method can be conveniently applied for determination of antimony in lead and zinc concentrates and its various smelter products. An analyst can comfortably complete the analysis of 6-8 samples in less than 8 hr (one shift).

*Acknowledgement*—One of the authors (S. S. Murti) thanks the management of Hindustan Zinc Limited, Visakhapatnam, for permission to carry out research leading to the Ph.D. degree, of which the present work forms a part.

### REFERENCES

1. E. M. Donaldson, *Talanta*, 1979, **26**, 999.
2. J. C. Chambers and B. E. McClellan, *Anal. Chem.*, 1976, **48**, 2061.
3. C. R. Walker, O. A. Vita and R. W. Sparks, *Anal. Chim. Acta*, 1969, **47**, 1.
4. M. Yanagisawa, M. Suzuki and T. Takeuchi, *ibid.*, 1969, **47**, 121.
5. P. Hannaker and T. C. Hughes, *Anal. Chem.*, 1977, **49**, 1485.
6. E. M. Donaldson and M. Wang, *Talanta*, 1986, **33**, 233.
7. R. Greenhalgh and J. P. Riley, *Anal. Chim. Acta*, 1962, **27**, 305.
8. R. E. Stanton and A. J. McDonald, *Analyst*, 1962, **87**, 299.
9. A. G. Fogg, J. Jillings, D. R. Marriott and D. T. Burns, *ibid.*, 1969, **94**, 768.
10. E. B. Sandell, *Colorimetric Determination of Traces of Metals*, 3rd Ed., pp. 258-265. Interscience, New York, 1959.
11. C. L. Luke, *Anal. Chem.*, 1953, **25**, 674.

## COMBINATION pH ELECTRODES OF SPECIAL DESIGN: TEMPERATURE CHARACTERISTICS AND PERFORMANCE IN POORLY-BUFFERED WATERS

DEREK MIDGLEY

CEGB, Central Electricity Research Laboratories, Kelvin Avenue, Leatherhead, Surrey, England

(Received 21 October 1987. Accepted 13 January 1988)

**Summary**—The performance of 5 combination pH electrodes with special design features has been assessed. Two electrodes were intended for measurements in low-conductivity waters, two were designed to have a rapid and stable temperature response and one electrode shared both features. The performance in low-conductivity waters was either poor or merely acceptable; better results have been obtained with separate glass and reference electrodes. The electrodes designed to have good temperature response were better in this respect than conventional combination electrodes, but the same or better performance can be obtained by use of separate glass and remote-junction reference electrodes. It should be noted that the temperature coefficients of these combination electrodes were the same as for almost all pH electrodes: any improvement was only in the rate and stability of response.

Combination pH electrodes have the glass membrane electrode and the reference electrode built into a common body. In studies of pH measurement in poorly buffered, poorly conducting, waters,<sup>1-6</sup> such electrodes have tended to give larger errors than are obtained with separate glass and reference electrodes. The errors are associated with the reference half of the combination electrode,<sup>2,4,5</sup> the design of which is a compromise to make it fit into the standard electrode body, particularly so with regard to the liquid junction. Nevertheless, combination electrodes appeal to users because they are thought to be convenient to handle. A few combination electrodes from the wide range commercially available have, therefore, been selected for testing. On the basis of previous work with reference electrodes in general, certain types were not expected to be satisfactory and these were excluded from the tests, namely electrodes with reference filling solutions immobilized in any way,<sup>4,7,8</sup> and electrodes in which solutions saturated with silver chloride contact a ceramic-frit junction.<sup>4,5,9</sup> Those selected have features designed to improve on "standard" electrodes with regard to temperature response or errors in poorly buffered media. The test procedures have been described elsewhere.<sup>4,10</sup>

### THEORY

#### pH response

At constant temperature, the pH response of a combination electrode is given by a form of the Nernst equation:

$$E = E_{gl}^0 - E_{ref}^0 - k \text{ pH} + E_j \quad (1)$$

where  $E_{gl}^0$  and  $E_{ref}^0$  are the standard potentials of the glass and reference electrodes, respectively,  $E_j$  is the liquid-junction potential and  $k$  is the slope factor,

theoretically equal to  $2.303 RT/F$  with  $R$  the gas constant,  $F$  the Faraday constant and  $T$  the absolute temperature. The pH at which  $E = 0$  is the zero-point pH for the electrode and is denoted by  $E^0$  pH.

#### Temperature response

The e.m.f. of an electrode over a range of temperatures can be approximated by use of the isopotential coefficient,<sup>11,12</sup>  $\text{pH}_{iso}$ . The derivation and limitations of this approach have been discussed.<sup>13</sup> Equation (1) can be re-expressed as

$$E \approx E_s - k(\text{pH} - \text{pH}_{iso}) \quad (2)$$

where  $E_s$  contains the temperature-invariant components of  $E_{gl}^0$ ,  $E_{ref}^0$  and  $E_j$ , and  $\text{pH}_{iso}$  allows for the temperature-dependent components.

### EXPERIMENTAL

#### Apparatus

E.m.f. values were measured with a digital pH meter reading to 0.1 mV. The temperature was controlled by means of a Techne C-100 thermocirculator connected, when necessary, to a Techne 1000 refrigerator unit.

#### Reagents

Standard NBS buffers were prepared from BDH "AnalaR" materials: 0.05M potassium hydrogen phthalate (pH 4.005 at 25°) and 0.025M potassium dihydrogen phosphate/0.025M disodium hydrogen phosphate (pH 6.865 at 25°). Dilute mineral acid solutions ( $10^{-4}N$  and  $3 \times 10^{-5}N$ ) were prepared by dilution of a stock solution made up from an ampoule of concentrated volumetric reagent (BDH).

#### Electrodes tested

The manufacturers' descriptions of the electrodes tested are summarized in columns 1-7 of Table 1. All the electrodes conformed to the "standard" body size (12 mm in diameter and 90-100 mm head of filling solution). The distinctive features of their design are listed in columns 8 and 9 of Table 1.

## RESULTS

Table 1. Manufacturers' specifications for the electrodes tested

Electrode	Inner reference	External reference	Junction*	E <sup>o</sup> pH	pH <sub>iso</sub>	Membrane resistance, MΩ	Special features		Code
							For low-conductivity waters	Temperature response	
Orion "Ross" 81-02	Pt/I <sub>2</sub> , I <sub>3</sub> <sup>-</sup>	Pt/I <sub>2</sub> , I <sub>3</sub> <sup>-</sup>	Ceramic frit	7 ± 0.5	7		No AgCl in bridge solution to block frit <sup>4,9</sup>	Rapid, because e.m.f. of remote matched internal and external reference electrodes should shift in parallel <sup>14</sup>	XI XXI
Orion "Ross" 81-62	Pt/I <sub>2</sub> , I <sub>3</sub> <sup>-</sup>	Pt/I <sub>2</sub> , I <sub>3</sub> <sup>-</sup>	Fixed glass sleeve	7 ± 0.5	7		No AgCl in bridge solution to block junction; high flow-rate for low-conductivity waters		XII
Ingold 405-EQ (Equithal)	Ag/AgCl	Ag/AgCl	Ceramic frit	7	7	400	No AgCl in bridge solution, but can dissolve from electrode	Rapid because of matched, equally immersed internal and external reference electrodes	XV
Ingold 405-88TE	Ag/AgCl	Ag/AgCl	PTFE sleeve on glass	7	7	400	Annular junction specially for high-precision measurements.	None; long chloride-coated Ag wire reference electrodes neither remote nor easily equilibrated	XVI
Russell CETL-LCW	Ag/AgCl	Hg/Hg <sub>2</sub> Cl <sub>2</sub>	Fixed plastic sleeve	6.84		19	Calomel avoids AgCl blockage of frit; <sup>4,9</sup> high rate of flow of reference solution	Problem of calomel electrode hysteresis <sup>10</sup>	XXII

\*All these electrodes have 3M KCl bridge solutions.

There are no agreed tolerances for the performance of pH electrodes, even in standard documents,<sup>15,16</sup> although what constitutes an acceptable total error inevitably depends on the purposes and conditions of the analysis. The criteria in Table 2 are proposed by the author as practical measures for assessing electrodes, based on tests of commercial pH and reference electrodes.<sup>4,5,10</sup> Other criteria could be proposed, especially with regard to changes in performance with age, but the working analyst is unlikely to have time for more than spot checks, and an undamaged electrode should be capable of working for 6–12 months unless exposed to especially hostile physical or chemical conditions. By application of these criteria it should at least be possible to avoid the worst electrodes.

#### Tests on low-conductivity waters

The results are summarized in Table 3. Comparison with Table 2 shows that electrodes XI and XII were unacceptable in almost every respect and the replacement electrode XXI was the only one meeting all the criteria. Electrodes XVI and XXII were good or acceptable except with respect to noise. Electrode XXII was peculiar in that medium-term (0.5–1 min cycle) rather than short-term (<5 sec cycle) instability was the main problem and that this also occurred in unstirred solution: it may be that the rate of outflow of filling solution was too high to produce a stable junction.

These results show the difficulty of predicting *a priori* whether an electrode will be good or bad for a given application. Selection on the basis of geometry of the liquid junction (frit or sleeve) is clearly unreliable since good and bad electrodes of both types were found. In the nominally identical electrodes XXI and XI, the junctions had very similar flow-rates and electrical resistances, yet differed grossly in the important characteristics of junction bias and response. The two electrodes with plastic sleeves (XVI and XXII) differed by factors of 100 in flow-rates and 10 in electrical resistance, but showed considerable similarity in the way their potentials behaved. The uselessness of anything but extremes of flow-rate and electrical resistance in the prediction of performance has been noted before.<sup>4,5</sup>

#### Temperature tests

A reliable pair of separate electrodes was included for comparison: a Corning 00311101J glass electrode (XIV in Ref. 10) and a calomel electrode with a remote ceramic frit junction (VIII in Refs. 4 and 10). In these tests the electrodes were generally immersed just sufficiently to ensure electrical continuity, so there was no question of the whole electrode being at thermal equilibrium. Electrode XV, however, was immersed up to the level of the internal baffle, so the temperature of the glass and reference half-cells

Table 2. Proposed criteria of acceptability for pH and reference electrodes

Performance characteristic*	Electrode classification	
	"Good"	"Acceptable"
Slope factor† (mV/pH) at 298.15 K	58.8 ± 59.4	57.5–60.0
Noise‡ (mV)	<0.1	≤ 0.2
Shift on stirring§ (mV)	<0.2	≤ 0.3
Response time§ (sec)	≤ 20	≤ 60
Junction bias†§ (mV)	1.5–2.0	≤ 3
$E^0$ pH (difference from expected value)	± 0.2	± 0.5
Isopotential pH (difference from expected value)	± 0.2	± 0.5

\*The following approximate equivalences may be useful: 1 mV  $\approx$  0.017 pH, 0.01 pH  $\approx$  0.6 mV.

†It may be noted when calculating these characteristics that good buffer solutions have a tolerance of  $\pm 0.003$  pH<sup>17</sup> and some commercial buffer powders may give a tolerance no better than  $\pm 0.02$  pH.

§See footnotes to Table 3.

Table 3. Measured characteristics of combination electrodes at 25°

Electrode	Flow-rate, $\mu\text{l/hr}$	Junction electrical resistance, $k\Omega$	Slope factor <sup>a</sup> , $\text{mV/pH}$	Noise <sup>b</sup> , $\text{mV}$	Shift on stirring <sup>c</sup> , $\text{mV}$	Response time <sup>d</sup> , $\text{sec}$	Junction bias <sup>e</sup> , $\text{mV}$	$E^0$ pH
XI*	4.4	0.3	58.8	0.4	0.5	90,60	6.9	7.89
XXI	4.7	0.3	58.6	0.2	-0.3	9,18	1.1	7.13
XII*	17	2.1	58.8	1.5	0.8†	600,180	5.4	7.05
XV	0.4	1.8	58.5	1.6	0.7	120,—	2.5	7.12
XVI	0.2	11	59.4	0.8	0.3	40,200	1.0	7.03
XXII	190	1.1	58.6	0.1/1.2§	0.4	30,3	0.9	7.11

\*Measured in pH-4 and pH-7 buffer solution.

<sup>b</sup>Peak-to-trough in stirred  $3 \times 10^{-5}N$  H<sub>2</sub>SO<sub>4</sub>.

<sup>c</sup>E.m.f. (stirred)—e.m.f. (quiescent) in  $10^{-4}N$  H<sub>2</sub>SO<sub>4</sub>.

<sup>d</sup>Time to reach equilibrium after (a) stopping and (b) restarting stirring in  $10^{-4}N$  H<sub>2</sub>SO<sub>4</sub>.

<sup>e</sup>E.m.f. in pH-4.005 phthalate buffer—e.m.f. in quiescent pH-4.006 ( $10^{-4}N$ ) H<sub>2</sub>SO<sub>4</sub>.

\*Data on reference half-cell from Ref. 4.

†After transient of -5 mV.

§The higher figure represents slow ( $\sim 30$  sec) fluctuations. These also occurred at an amplitude of about 0.3 mV in unstirred solution.

should have been very close to that of the solution (cf. electrode I in Ref. 10). Each electrode of the separate electrode pair should have been at thermal equilibrium, but there would have been a temperature gradient along the junction tube, except at 25°. These arrangements correspond to normal practice.

*Temperature coefficient of the slope factor.* The ratios of the observed to theoretical values of  $\partial k/\partial T$  obtained in several experiments are shown in Table 4. As with separate glass and reference electrodes,<sup>10</sup> the observed values do not differ from the theoretical ones within experimental error.

*Recovery of original e.m.f.* The changes in e.m.f. as the electrodes were taken through temperature cycles

starting and finishing at 25° were generally less than 1 mV (Table 5) and so hysteresis was of little or no significance. Over 3 or 4 runs like those in Table 5, the electrodes (with the exception of XVI) usually gave larger changes on the first cycle, especially after a period of storage. These differences may arise from the condition of the junction after storage, because they were smaller for the fast-flowing junction of electrode XII and random for electrode XVI, in which the junction is re-formed for each immersion.

*Time course of the temperature response.* Figure 1 shows how the e.m.f. found in potassium hydrogen phthalate buffer solution varied with temperature for various electrodes. Figures 1A and 1B show the e.m.f.

Table 4. Temperature coefficient of the slope factor

Electrode	XXI	XV	XVI	XXII	XIV + VIII
Temp. range (°C)	9–50	11–72	9–50	9–50	9–50
Observed/theoretical*	1.000	0.997	1.000	0.996	1.001
Std. devn.	0.004	0.004	0.007	0.004	0.005
No. of trials	5	5	4	5	7

\*  $\frac{\Delta k/\Delta T}{2.303R/F}$

Table 5. Evidence for thermal hysteresis

Extreme temp.,	Cycle no.	Electrodes					
		XII	XXI	XV	XVI	XXII	XIV + VIII
Change in e.m.f. on return to 25°C, mV							
50	1	1.8	3.6	-0.3*	0.0	-0.8	0.7
	2		-0.8	0.2*	0.6	0.0	0.0
10 ± 1	1	0.4†	0.2	-0.2	0.3	0.6	0.3
	2	0.5†	-0.4	-0.4	0.0	-0.4	-0.6

\*Extreme temperature = 72°C.

†Extreme temperature = 15°C.

responses in successive cycles as the temperature was varied smoothly. Electrodes XV and XXII tended to overshoot and electrode XXII showed considerable instability on the first cycle. Figure 1C shows the responses for a direct transfer from solution at 25° to an identical solution at 40°: those of electrodes XVI and XXII went through a maximum and that of electrode XXI showed instability. Figure 1D shows a direct transfer between solutions at 25° and 74°: electrode XV overshoot slightly but the separate pair (XIV + VIII) responded very sharply. Electrodes XVI and XXII always gave responses that went through a maximum on an increase in temperature (or a minimum for a decrease) and this reflects the different thermal capacities and positions of the glass and reference halves of these electrodes. Figure 1A shows electrode XXII at its worst: generally the potential changed smoothly. The response of electrode XXI sometimes changed smoothly and sometimes as in Fig. 1C: the thermal matching of the two halves of the electrode was seemingly imperfect. Electrode XV had a relatively small tendency to overshoot, showing the near-equivalence of the two parts of the electrode.

The advantages of matching the internal and external reference elements are shown by the better performance of electrodes XV and XXI compared with electrodes XVI and XXII, although the performance of the former pair also showed that the matching was imperfect. Figure 1D shows that if electrodes were switched between solutions at different temperatures, then using a glass electrode with a small thermal capacity and a remote junction reference electrode (XVI + VIII) gave a sharper response than was obtained even with a thermally matched combination electrode.

*Isopotential pH.* Table 6 shows the results calculated for ranges of temperature either side of 25°. In the higher range the results for combination electrodes are grouped closely around the expected value of 7, but the values in the lower range are much smaller. This discrepancy arises from two main sources.

(a) The temperature coefficients of the standard potentials are not truly linear.<sup>13</sup>

(b) The thermal gradients inside the electrodes are different for hot and cold test solutions, because of convection.<sup>10</sup>

In the case of the separate pair of electrodes (XIV + VIII), the difference should arise only from non-linearity of the temperature coefficient of the glass electrode's standard potential, because the reference electrode was at a constant temperature and the glass electrode should have been in thermal equilibrium with the test solution.

#### DISCUSSION

The various performance characteristics have already been discussed in terms of the construction of the electrodes, and these will now be considered individually.

#### Ross electrodes

One example with a frit junction (XI) had a poor performance in low-conductivity waters, whereas the other (XXI) was highly acceptable. The version specifically designed for such measurements (XII) was the worst of all those included in these tests. Two electrodes (XI and XII) deteriorated rapidly, with

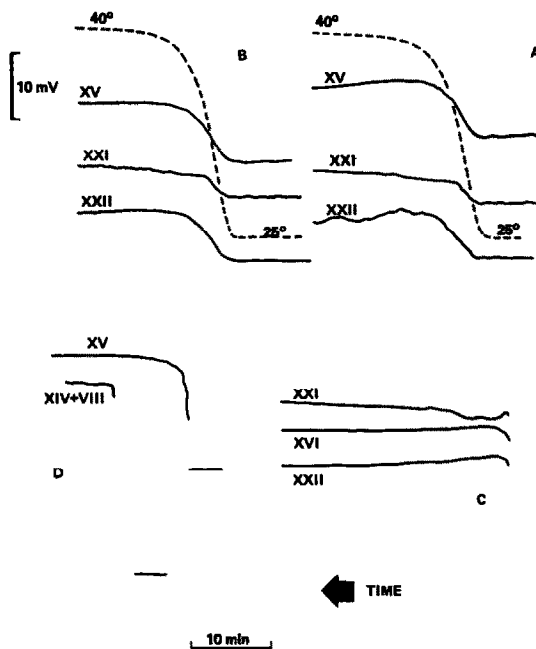


Fig. 1. Response to changes in temperature in pH 4 buffer. A, B and C 25–40°; D 25–74°.



Table 6. Isopotential pH

Temp range, °C		Electrode						
		XXI	XI	XII	XV	XVI	XXII	XIV + VIII
25–50	pH <sub>iso</sub>	7.08	7.15*	7.3*	7.18	6.74	6.84	7.90
	s.d.	0.65	—	1.3	0.44	0.31	0.23	0.18
	n	8	1	3	3	7	6	4
25–10 ± 1	pH <sub>iso</sub>	6.30	6.67	6.50	6.15	5.27	5.69	7.28
	s.d.	0.30	—	0.90	0.17	0.33	0.42	0.49
	n	3	1	5	3	3	3	3

\*Range 25–35°C.

visible changes in the reference half-cell. The reference filling solution changed from yellow-brown to an opalescent pale yellow (at which stage  $E^0$  had shifted by about 50 mV, but the slope factor was unchanged) and finally, about 3 months after purchase, became colourless, and a steady e.m.f. could then not be obtained. The iodine in the reference solution had apparently been consumed and in the absence of a well-poised redox couple a steady e.m.f. could not be expected. The solution inside the glass-electrode half of the combination electrode was not visibly changed and measurement of the individual half-cell potentials *vs.* a separate calomel electrode showed that only the reference half was faulty. This fault prevented the full range of tests being applied to electrodes XI and XII. There was no access to the reference half-cell to allow the solution to be analysed or replaced. With a replacement electrode (XXI) the same problem had not arisen within a space of 6 months, during which the standard potential changed by  $-8$  mV.

Since these electrodes are designed to have superior temperature characteristics, their performance in this respect was disappointing. Table 6 shows that the isopotential pH was determined with less precision than for other electrodes and the discrepancy in response to warm and cold solutions, although smaller than for the other combination electrodes, was no better than that obtained with a glass electrode and a separate remote junction reference electrode. The expected simple and rapid responses to changes in temperature were not always obtained, as exemplified by Fig. 1C. Electrode XI also showed the largest discrepancy between  $E^0$ pH and pH<sub>iso</sub>, which with many pH meters leads to inaccurate temperature compensation: this was probably because of the deteriorating reference half-cell.

It should be noted that the design of this electrode does *not* reduce the temperature coefficient of the cell: the temperature coefficient of the slope factor is a true constant that is not under the analyst's control and the temperature coefficient of the standard potential (expressed as pH<sub>iso</sub>) is designed to be the same as that for all standard commercial electrodes (pH<sub>iso</sub> = 7). Description<sup>18</sup> of these electrodes as being "virtually temperature insensitive" is very misleading.

#### Ingold 405-EQ (Equithal)

The Equithal electrode is not optimized for use in low-conductivity waters, and its performance in this regard was only modest. After one year, despite being stored in 3M potassium chloride when not in use, its slope factor suddenly dropped to 52 mV/pH, which is typical of a frit becoming blocked with precipitated silver chloride (electrodes II and III in Ref. 4). Although initially the filling solution is not saturated with silver chloride, it is always possible for silver chloride to dissolve from the electrode itself and be transported to the frit, especially when the electrode is being stored and there is no outflow of filling solution. Measurement against a calomel electrode confirmed that the reference half of the combination electrode was at fault. Some recovery in performance was evident when the filling solution was replaced by fresh 3M potassium chloride and the electrode was soaked for 1 month in the same solution.

The electrode is designed to have good thermal properties, and Fig. 1 shows that the e.m.f. changed smoothly with temperature, with only a slight overshoot of e.m.f. on change of temperature, *i.e.*, the glass and reference half-cells were well (but not perfectly) balanced. The results for isopotentials in Table 6, however, showed that the precision of pH<sub>iso</sub> and its variation with temperature were unremarkable.

#### Ingold 405-88TE

This electrode has a liquid junction designed for high-precision measurements. It had a fairly acceptable performance in low-conductivity waters, but use of a separate reference electrode with a similar type of junction gave even better performance.<sup>4</sup> Although the reference electrode is of the silver-silver chloride type, the junction is relatively immune to clogging with silver chloride and can easily be cleaned if necessary. The consumption of internal filling solution is remarkably low for a sleeve-junction electrode and this is of considerable convenience.

The thermal properties of the electrode have not been optimized and the e.m.f. always overshoot when the temperature was changed, because of temperature gradients within the electrode. The variation of iso-

potential with temperature was greater than for the Equithal electrode or a separate glass/remote reference arrangement.

#### *Russell CE7L-LCW*

This electrode is designed for use in low-conductivity waters and the bias in such solutions was small, although this was the only electrode to show slow fluctuations of potential in such solutions. The high rate of outflow of the reference solution poses problems in monitoring over periods of more than an hour or two because enough potassium chloride may leak into a small volume of test solution to affect the activity coefficients and the liquid-junction potential, and hence the indicated pH. The head of electrolyte solution drops fairly quickly and the properties of the electrode may change, until it ceases to work because the calomel element is no longer immersed. Keeping the reservoir full would be an insignificant maintenance burden in laboratory use but inconvenient for any permanent installation. Previous tests with a variety of electrodes<sup>4,5</sup> do not suggest that such a high flow-rate is necessary.

The use of a calomel reference half-cell should avoid the junction blockages found with the silver chloride types, but is unlikely to confer good thermal properties. In fact, the electrode's thermal performance was better than might have been expected from measurements with separate calomel reference electrodes,<sup>10</sup> although the isopotential pH varied considerably with temperature and the e.m.f. always overshot the equilibrium values on changes in temperature. Hysteresis was not a problem in these tests. The calomel element was "semi-remote" from the glass bulb, and this probably explains the thermal characteristics. Increasing its remoteness would improve the performance.

#### CONCLUSIONS

None of the combination electrodes had an outstandingly good performance in measuring pH in low-conductivity waters, although the Ingold 405-88TE and one example of the Ross 82-01 were acceptable. Electrodes expressly sold as being suitable for this purpose were no better than the others, as has been found for other makes of electrode.<sup>5,6</sup>

The Ross and Equithal type of combination electrodes showed rather better temperature response than other combination electrodes, in that the problem of overshooting the equilibrium e.m.f. was much reduced, but neither the constancy of  $\text{pH}_{\text{iso}}$  with temperature nor its reproducibility within a fixed temperature range was exceptionally good. There was no evidence that these electrodes are better than separate glass and remote-junction reference electrodes.

Only small numbers of electrodes have been tested and recommendations for or against individual types are not proposed: each offers at least one character-

istic that could make it preferable to "standard" combination electrodes in particular applications and in some cases more generally. The results reinforce the view that, before use in poorly buffered waters, *individual* electrodes should be tested for their suitability<sup>4,5</sup> and that when temperature-compensation is required the precision and accuracy of the  $\text{pH}_{\text{iso}}$  value should not be taken for granted.<sup>10,13</sup>

It may be instructive to try to draw from these and other<sup>4,5,7-10</sup> results an outline of an "optimal" combination electrode for general use, within the constraints imposed by the properties of available materials. Little can be said about the glass membrane and the internal filling solution from tests on commercial electrodes, because the exact compositions of these components are not available. There are, however, indications<sup>10</sup> that the temperature coefficients of the filling solutions could be improved. Most problems arose from the reference half-cell, because of liquid-junction potentials<sup>4,5</sup> and temperature gradients.<sup>10</sup>

#### *Liquid junction*

As noted here and elsewhere,<sup>4,5</sup> the geometry of the junction and its gross characteristics such as flow-rate and electrical resistance are poor predictors of satisfactory performance, and each electrode needs to be tested individually in some sort of secondary standard similar to the test sample, e.g.,  $10^{-4}N$  strong acid in the case of poorly buffered, poorly conducting waters.

There is ample evidence<sup>4,7,8</sup> that immobilized filling solutions are associated with large errors, but a low rate of loss of filling solution is desirable, both for convenience and to minimize contamination of the sample. Frit junctions are generally better than sleeve junctions in this respect, but the PTFE-on-glass arrangement in electrode XVI combined a low rate of flow with fairly good performance. Frits always seem to become blocked with silver chloride eventually, even if the filling solution is not pre-saturated with silver chloride (as in electrode XV): a double-junction arrangement would delay the onset of the problem, but would complicate construction of the electrode. The easily-cleaned sleeve junction avoids this problem in the short term, but is not necessarily satisfactory over long periods.<sup>19</sup>

An ion-exchange barrier has been proposed<sup>9</sup> to prevent silver chloride (as  $\text{AgCl}_2^-$ ) from reaching the frit, but the use of calomel electrodes appears to avoid junction blockage completely. The other commonly used reference elements, of the Thalamid and Ross types, require double-junction arrangements and so do not directly affect the junction with the test solution.

#### *Temperature effects*

These tests confirm that placing the inner and outer reference electrodes symmetrically to minimize the thermal gradient between them has advantages of speed and smoothness of response to temperature

changes. No preference can yet be expressed between arrangements in which both electrodes are at the same temperature as the test solution (XV, with Ag–AgCl electrodes) and those in which both are remote from the test solution (XI, XII, XXI: Ross electrodes); in both types a small degree of asymmetry was still evident from the results. There is no fundamental reason for associating one arrangement with a particular type of electrode; indeed silver–silver chloride electrodes have been used successfully in separate “doubly remote” glass and reference electrodes.<sup>20</sup> Because of its thermal hysteresis, the calomel electrode is the least suited for measurements at sharply varying temperatures, but might be acceptable in the doubly remote configuration. These configurations have so far not improved the constancy or precision of the isopotential pH compared with other arrangements and more attention may need to be paid to glass electrode filling solutions.<sup>13</sup>

It may be noted that the opposite extreme of configuration (with a remote reference electrode) works very well with separate electrodes (XIV and VIII) and may be applicable to combination types. Electrode XXII approached this configuration and had a better temperature response than expected. The glass electrode should have a minimal volume of filling solution (and hence low thermal capacity) and a silver–silver chloride inner reference. The outer reference electrode should be mounted high up the stem and a baffle placed between one third and halfway up the stem to reduce convective heating.<sup>10</sup> In this position, the electrode is vulnerable to drying out and a low rate of outflow of filling solution is therefore desirable; a double-junction arrangement would make the electrode more reliable, but would complicate the construction. As the temperature of the reference electrode is intended to be practically constant (at least over the period of calibration and a few measurements), the calomel electrode should be acceptable in this application. If the temperature does change, however, the change in apparent pH reading obtained with a silver–silver chloride electrode would be less than one fifth of that with a calomel electrode.<sup>10</sup> Provided the liquid junction can be kept clear, as discussed above, the silver–silver chloride electrode would be preferred.

Almost all the desirable features mentioned above (symmetrical configuration, protection of electrodes by double-junction arrangements, reduction of convection and prevention of silver chloride contamination) complicate the design and manufacture of electrodes, especially if they are to be made to

standard dimensions. All these features are available with commercial electrodes, although not collectively. The choice of liquid junction still seems largely empirical, however, and even nominally identical electrodes can differ appreciably in their electrochemical properties.

The Ross electrode shows that new reference systems are possible and many others may be worthy of consideration. Cells incorporating more reactive redox systems than silver- and mercury-based electrodes, however, may need protection from oxygen or other contaminants and the stability of such systems over long periods may need investigation. Improvement of traditional systems is still possible and may be implemented more speedily.

*Acknowledgement*—This work was carried out at the Central Electricity Research Laboratories and is published by permission of the Central Electricity Generating Board.

#### REFERENCES

1. A. K. Covington, P. D. Whalley and W. Davidson, *Analyst*, 1983, **108**, 1528.
2. W. F. Koch and G. Marinenko, *Sampling and Analysis of Rain*, ASTM STP 823, S. A. Campbell (ed.), p. 10. American Society for Testing and Materials, Philadelphia, 1983.
3. W. Davison and M. J. Gardner, *Anal. Chim. Acta*, 1986, **182**, 17.
4. D. Midgley, *Atmos. Environ.*, 1987, **21**, 173.
5. W. Davison and C. Woof, *Anal. Chem.*, 1985, **57**, 2567.
6. C. Jones, D. R. Williams and F. Marsicano, *Sci. Total Environ.*, 1987, **64**, 211.
7. D. Midgley and K. Torrance, *Analyst*, 1976, **101**, 833.
8. D. P. Brezinski, *ibid.*, 1983, **108**, 425.
9. *Idem*, *Anal. Chim. Acta*, 1982, **134**, 247.
10. D. Midgley, *Analyst*, 1987, **112**, 581.
11. J. Jackson, *Chem. Ind. London*, 1948, 7.
12. A. K. Covington, *CRC Crit. Rev. Anal. Chem.*, 1974, **3**, 355.
13. D. Midgley, *Analyst*, 1987, **112**, 573.
14. J. W. Ross, *U.S. Patent* 4495050, 1985.
15. BS 2586, *Glass and Reference Electrodes for the Measurement of pH*, British Standards Institution, London, 1979.
16. BS 6438: Part 2, *Electrochemical Analyzers, Part 2, Method for Specifying Performance of pH Value Analyzers*, British Standards Institution, London, 1984.
17. BS 1647: Part 2, *pH Measurement Part 2, Specification for Reference Value Standard Solutions and Operational Reference Standard Solutions*, British Standards Institution, London, 1984.
18. P. F. Boyle, J. W. Ross, J. C. Synnott and C. L. James, *Impact of Acid Rain and Deposition on Aquatic Biological Systems*, ASTM STP 928, B. G. Isom, S. D. Dennis and J. M. Bates (eds.), p. 98. American Society for Testing and Materials, Philadelphia, 1986.
19. G. B. Marshall and D. Midgley, *Analyst*, 1978, **103**, 438.
20. K. Torrance, *ibid.*, 1984, **109**, 1555.

## AMPEROMETRIC FLOW DETECTION WITH A COPPER WORKING ELECTRODE—RESPONSE MECHANISM AND APPLICATION TO VARIOUS COMPOUNDS

KAREL ŠTULÍK and VĚRA PACÁKOVÁ

Department of Analytical Chemistry, Charles University, Albertov 2030, 128 40 Prague 2, Czechoslovakia

KANG LE

Central Iron and Steel Research Institute, Beijing, China

BAS HENNISSSEN

Laboratory of Instrumental Analysis, Technical University of Eindhoven, The Netherlands

(Received 23 October 1987. Revised 30 November 1987. Accepted 12 January 1988)

**Summary**—The mechanism of amperometric detection with a copper electrode has been studied with four amino-acids in four different carrier liquids containing aqueous buffer and methanol. It is concluded that the response is produced by complexation of the test substances with cupric ions in the outer, porous layer of the passivating film, with formation of  $\text{CuL}^+$  species. The increase in detector current is primarily determined by the complexation kinetics and to a lesser degree by the stability of the complex formed. The complexation rate strongly decreases with increasing amounts of organic solvent in the carrier liquid. The optimal detection conditions are discussed on the basis of the detection mechanism. Results are given for the detection of various structural types of amines and amino-alcohols.

Considerable attention has recently been paid to the use of complexation reactions of various substances with cupric ions for electrochemical flow detection of the ligands. As a means of detection, equilibrium potentials of cupric ion-selective electrodes,<sup>1-4</sup> and copper metal tubular<sup>5,6</sup> or wire<sup>7-14</sup> electrodes have been monitored. Alternatively, measurements can be made amperometrically with a copper metal electrode in wall-jet,<sup>15-18</sup> tubular<sup>19</sup> or copper fibre-array<sup>19</sup> systems. This type of detection has been applied mainly to amino-acids, but other ligands have also been studied, e.g., organic acids,<sup>7,8</sup> inorganic anions,<sup>9,12</sup> choline<sup>19</sup> and proteins.<sup>14</sup> Various inorganic ions have been detected indirectly,<sup>12</sup> including those of the alkaline-earth metals.<sup>10,11,13</sup> Most of the papers deal with HPLC detection, but the technique is also applicable to flow-injection measurements and continuous monitoring.

The principal drawback of potentiometric measurement is sluggish response of the sensor, which is especially undesirable in HPLC, as it broadens the elution curve. Moreover, potentiometric measurement is not particularly sensitive and the calibration plot is non-linear.

It has been shown by Hitchman and Nyasulu<sup>14</sup> that cathodic electrochemical pretreatment is necessary for reliable functioning of copper potentiometric sensors; the authors conclude that the response is based on interaction of the ligand with copper adatoms on the electrode surface. In amperometric measurements<sup>15-19</sup> the electrode is also cathodically pretreated to clean the surface and to produce a fresh, active copper layer, but then it is polarized in a

solution of pH about 6 or higher, at mildly positive potentials (typically +0.15 V vs. Ag/AgCl), at which a passive oxide/hydroxide layer is formed. It is assumed that the sensor response arises from the interaction of the ligand with the cupric ions contained in the passive layer and this model has been studied by batch experiments with a rotating disk electrode<sup>15</sup> and in flow-through systems of the wall-jet,<sup>16</sup> tubular<sup>19</sup> and fibre-array electrode<sup>19</sup> type.

In view of the potential applicability of this principle to a wide range of substances, and also of the complexity of a detection mechanism involving mass transport and complexation kinetics and thermodynamics, the present paper deals with the detection mechanism and the selection of the optimal experimental conditions and also gives experimental data on detection of various classes of compounds.

### EXPERIMENTAL

#### Apparatus

The measurements were made with apparatus consisting of either an MHPP 20 (Laboratorní Přístroje, Czechoslovakia), or a 2150 (LKB, Sweden) HPLC pump, an LCI-30 injection valve with 0.5 and 3.0  $\mu\text{l}$  sample loops, cells with copper tubular or fibre-array electrodes (internal volumes of 0.6 and 0.2  $\mu\text{l}$ , respectively),<sup>19,20</sup> an ADLC 1 meter and TZ 4100 line recorder (all from Laboratorní Přístroje). The individual parts of the apparatus were connected by short stainless-steel capillaries 0.2 mm in internal diameter. A stainless-steel counter-electrode and a saturated silver/silver chloride reference electrode were used. All the potential values are referred to this reference electrode.

The stopped-flow spectrophotometric measurements of the complexation reaction rates were made with a Durrum (USA) instrument, at the appropriate absorption maxima.

### Chemicals

Four different carrier solutions were used: 0.025M potassium dihydrogen phosphate, in 10% v/v methanol/water adjusted to pH 6.8 (A) or pH 3.0 (B); 0.025M potassium dihydrogen phosphate in 50% v/v aqueous methanol at pH 6.8 (C); 0.025M potassium borate in 10% v/v methanol/water at pH 6.8 (D). The pH values were adjusted with phosphoric acid and potassium hydroxide solutions and are the meter-readings. All the substances were of *p.a.* grade and were not further purified.

The pure test substances were obtained from various manufacturers. The liquid substances were purified by distillation.

Stock solutions of the test substances (and of cupric nitrate for stopped-flow kinetic measurements) were prepared at a concentration of  $10^{-3}M$  in the appropriate carrier solution and were diluted, as required, with the carrier solution prior to measurement.

### Procedure

Before each series of measurements (or more often, if necessary) the working electrode was activated by polarization for 15 min at  $-0.3V$  in the given carrier solution. Unless otherwise stated, the measurements were made at  $+0.15V$  (which lies in the optimal potential region, see below) after stabilization of the baseline. The hydrodynamic voltamperograms were obtained in the flow-through cell, point-by-point, allowing for stabilization of the current. In some experiments, the solution was deaerated by passage of nitrogen that was freed from traces of oxygen in traps containing anthraquinone- $\beta$ -sulphonate and alkaline pyrogallol solutions, continuously regenerated by amalgamated zinc granules.

The measurements were made at laboratory temperature ( $22 \pm 2^\circ$ ). The calibration plots were obtained by linear regression and the limits of detection are the absolute amounts of analyte in the injected volume producing currents equal to twice the average noise amplitude.

## RESULTS AND DISCUSSION

### Detection mechanism and optimal conditions

It has repeatedly been shown<sup>15,16,19</sup> that a copper electrode responds to complexing agents only at a solution pH greater than *ca.* 6, that the measuring sensitivity increases with increasing pH and decreasing ionic strength, strongly depends on the kind of ions in solution (high sensitivity in phosphate or carbonate, poor sensitivity in borate media) and that the response is not obtained at electrode potentials below  $-0.1V$  vs. Ag/AgCl.<sup>19</sup>

As demonstrated in the extensive literature<sup>21</sup> the passive layer on copper is formed by oxidation at pH 3–4. First a compact, highly insoluble layer of  $Cu_2O$  is formed and then a loose amorphous layer consisting of  $CuO$ ,  $Cu(OH)_2$  and basic cupric salts, its composition depending on the solution composition.<sup>22</sup> This layer is much more soluble and thus a certain constant thickness of the bilayer film is eventually attained, when oxidation of the copper metal is counterbalanced by dissolution of  $CuO$ . The amperometric response of copper electrodes thus results from the interaction of complexing agents with  $Cu^{2+}$  ions contained in the porous outer layer, leading to enhanced solubility of the film.

Therefore, the magnitude of the current at a copper electrode depends on a number of parameters.

A. *Thermodynamic*: the stability of the complex formed between  $Cu^{2+}$  and the test substance.

B. *Kinetic*:

(a) rate of formation and dissolution of the passivating bilayer;

(b) rate of transport of the test substance in solution;

(c) rate of transport of the test substance and  $Cu^{2+}$  in the outer porous layer of the passivating film;

(d) rate of complex formation.

The relative importance of these factors can be assessed from the dependences of the background current and the signal on the experimental conditions and on the rate and stability constants for the complexation reaction. Using the results of our previous work,<sup>19</sup> we selected four carrier solution compositions, involving a dihydrogen phosphate solution permitting sensitive detection (A), the same solution, but with a low pH (B) or containing more methanol (C) and a borate solution (D), in which poor detection sensitivity is obtained. Methanol was added to the solution because an organic modifier is usually required in HPLC separations. Four L-amino-acids were chosen as test substances giving different sensitivities, as detection of amino-acids has been studied most thoroughly.

The effect of the carrier solution on the rate of formation and dissolution of the passivating film is demonstrated in Fig. 1. It is evident that at low pH no passivating layer is formed and the current corresponds to direct oxidation of Cu to  $Cu^{2+}$  (curve 1). In phosphate at pH 6.8 (curve 2), the formation of the passive layer is demonstrated. The presence of a higher amount of organic solvent of low polarity (curve 3) evidently suppresses the solubility of the passivating film. In the presence of borate (curve 4), the solubility of the passivating film is progressively enhanced at higher electrode potentials. These dependences illustrate the suitability of the phosphate medium at pH 6.8. From the point of view of the background value in detection, higher contents of organic solvents have a favourable effect.

The signals of the test substances, corrected for the background, in these carrier solutions, are plotted in Fig. 2 as functions of the electrode potentials. It can be seen that, unfortunately, the presence of higher contents of organic solvents also strongly suppresses the interaction of the test substances with the passivating film. No signals were obtained from these substances in the medium at pH 3.0. The optimal electrode potential is between 0.1 and 0.2 V, as at higher values the current is poorly reproducible and the baseline noise is high.

It has been shown<sup>23</sup> that in the reaction of histidine with cupric ions, the  $Cu^{2+}$  species predominates in solution at pH 5–7 and that the  $Cu(OH)hist$  and  $Cu_2(OH)_2hist_2$  species predominate at higher pH values. The  $Cu^{2+}$  species content attains a max-

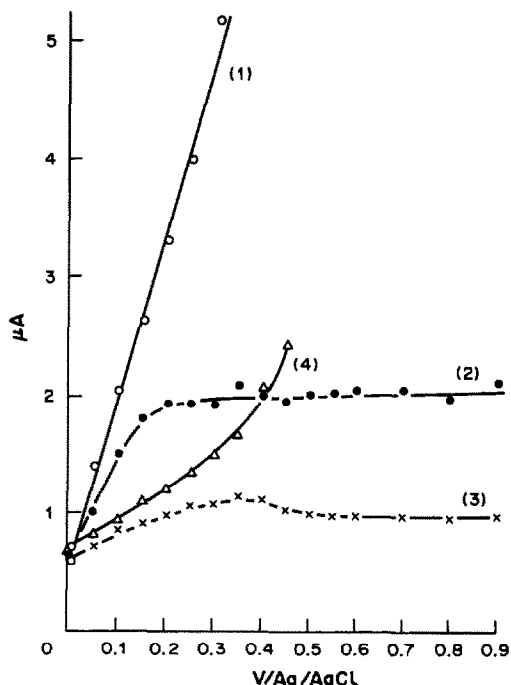
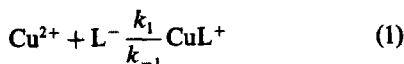


Fig. 1. Dependence of the background current on electrode potential in the carrier liquids studied. (1) Solution B; (2) solution A; (3) solution C; (4) solution D. Flow-rate, 20  $\mu\text{l}/\text{min}$ .

imum of ca. 7% at ca. pH 6.5. Assuming analogous behaviour of the other amino-acids, the complexation reaction,



can be considered to be responsible for the detector response. Table 1 lists the stability constants taken from the literature,<sup>24</sup> the homogeneous complexation reaction half-times obtained by using the stopped-flow method with the carrier liquids studied, the rate constants  $k_1$  calculated from the half-times assuming that the reaction is second order, the experimental detection sensitivities (slopes of the calibration plots) and the detection limits.

The rate constants in the media studied are substantially lower than the values given for three amino-acids in the literature, for purely aqueous solutions at 25° and ionic strength,  $I = 0.1M$  (L-leucine,<sup>25</sup>  $k_1 = 1.6 \times 10^9 \text{ l. mole}^{-1} \text{ sec}^{-1}$ ; L-serine,<sup>26</sup>  $k_1 = 2.5 \times 10^9 \text{ l. mole}^{-1} \text{ sec}^{-1}$ ; N-methylglycine,<sup>27</sup>  $k_1 = 2.8 \times 10^9 \text{ l. mole}^{-1} \text{ sec}^{-1}$ , by a temperature jump method), but are similar to the values that were selected<sup>15</sup> to fit the experimental current-values in work with a copper rotating disk electrode. As follows from the high values of the stability constants, reaction (1) is strongly shifted to the right. The overall rate of the complexation reaction at a copper electrode will be somewhat lower than that of the homogeneous reaction, as transport of the reactants within the porous oxide/hydroxide layer is also involved. This contribution is constant under constant experimental conditions.

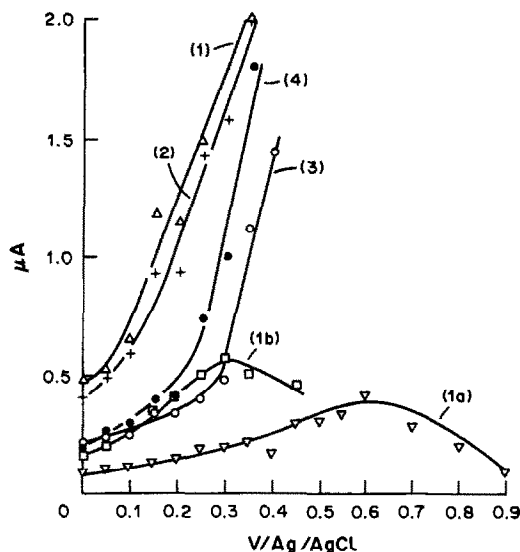


Fig. 2. Dependences of the signal magnitude for the test substances on electrode potential in the carrier liquids studied. (1) Histidine, solution A; (1a) histidine, solution C; (1b) histidine, solution D; (2) serine, solution A; (3) valine, solution A; (4) aspartic acid, solution A. Flow-rate, 20  $\mu\text{l}/\text{min}$ . Injected volume, 0.5  $\mu\text{l}$ . Solute concentrations: histidine, 5.24 mg/ml; serine, 7.33 mg/ml; valine, 4.95 mg/ml; aspartic acid, 5.79 mg/ml. The background value was subtracted from the signal.

A comparison of the rate and stability constants with the measuring sensitivities and the detection limits (Table 1) indicates the decisive effect of the complexation kinetics. The complex stability has a less pronounced influence. These effects are more perceptible with the sensitivity values. In agreement with the literature,<sup>23</sup> there is no complexation reaction at pH 3.0 (free  $\text{Cu}^{2+}$  greatly predominates). An increased content of organic solvent leads to a pronounced decrease in the complexation reaction rate (see Table 1), and this is also reflected in the substantially decreased measuring sensitivity. This effect is apparently due to a decrease in the relative permittivity in the presence of organic solvents, which generally causes a decrease in the rate constants for ionic reactions. On the other hand, the effect of the ionic strength should be small, as ions of opposite signs are involved in the reaction (*cf.* standard literature on reaction kinetics).

Our results are somewhat at variance with those reported elsewhere,<sup>15</sup> in which the formation of  $\text{CuL}_2$  complexes was assumed and it was concluded that the complexation reaction rates were so high that the convective-diffusional transport of the ligand in solution controlled the overall rate of the process. Of course, there is a substantial difference between the conditions with a rotating disk electrode (RDE), where the electrode is in continuous contact with the test substance, and those of flow detection<sup>19</sup> in which the electrode is only exposed to separate zones of the ligands, as in our work. Furthermore, the RDE

Table 1. Complexation rates, complex stabilities, detection sensitivities and detection limits for the test substances

Carrier solution* Solute	A				B	C	D
	Histidine	Serine	Valine	Aspartic acid	Histidine	Histidine	Histidine
Reaction half-time at 25°C, $\tau_{1/2}$ , sec	0.4	1.5	1.9	2.3	no reaction	very slow reaction	very slow reaction
Rate constant, $k_1$ , l.mole <sup>-1</sup> .sec <sup>-1</sup>	$2.5 \times 10^4$	$6.7 \times 10^3$	$5.3 \times 10^3$	$4.3 \times 10^3$	—	—	—
Stability constant <sup>24</sup>	10.20	7.89	8.11	8.57	—	—	—
$\log \beta_1$	18.10	14.48	14.90	15.35	—	—	—
$\log \beta_2$	4.6	2.5	1.5	1.4	—	0.86	0.70
Sensitivity, nA/ng	0.4	0.5	4.1	13.0	—	2.5	3.0
Detection limit, ng	—	—	—	—	—	—	—

\*See Experimental.

results were obtained in purely aqueous solutions where the complexation rate should be higher than in our work with at least 10% methanol present. This is also confirmed by some results with a wall-jet detector,<sup>15</sup> where a buffer containing 10% methanol was used (see Fig. 9 in that paper); the signal increased with increasing flow-rate only for the amino-acids with the fastest complexation reactions.

In our experiments we found that the detector signal always decreased with increasing flow-rate (from 5 to 100  $\mu\text{l}/\text{min}$ , cf. Fig. 3 in Štulík *et al.*<sup>19</sup>) and was independent of the cell geometry (copper fibres or copper tube), indicating that the overall process is controlled by the complexation kinetics. This is understandable when the reaction half-times in Table 1 are considered. Assuming that the reaction is complete after a period of  $10\tau_{1/2}$ , the required times range from 4.0 to 23.0 sec. The residence times of the test substance in the detector cells with volumes of 0.2 and 0.6  $\mu\text{l}$  were only 2.4 and 7.2 sec, respectively, for the lowest flow-rate studied (5  $\mu\text{l}/\text{min}$ ). Obviously, the convective-diffusional transport may become the rate-determining step when large cells or extremely low flow-rates are used.

Sensitive detection is thus possible with substances rapidly forming sufficiently stable complexes with  $\text{Cu}^{2+}$  under the conditions for passive layer formation on the electrode. The solution should contain the smallest possible amount of organic solvent and the flow-rate should be low (useful in microcolumn HPLC). The ionic strength of the solution is of little importance. The effect of atmospheric oxygen dissolved in the solutions was also tested, in view of the fact that the dissolution of copper in complex-forming media often depends on the presence of oxidants.<sup>21</sup> However, no change occurred when oxygen was removed by passage of nitrogen. Hence, the presence of atmospheric oxygen does not affect the detection.

#### Detection of various substances

On the basis of the considerations above and the literature on their complexation properties, the detection of various amines, amino-alcohols and peptides has been tested. The detection of peptides has been studied together with the conditions for their HPLC separation, with the results described elsewhere.<sup>28</sup>

Various structural types of amines were tested. The calibration curve parameters and detection limits are given in Table 2. The amount of methanol in the carrier liquid had to be increased to enhance the solubility of the test substances. Primary, secondary and tertiary amines can be detected, but the sensitivity is not particularly high and is independent of the primary amine structure. The detection is substantially more sensitive for diamines than for monoamines, the sensitivity decreasing with increasing chain length and with increasing number of substituents on the nitrogen atom. Hence there is a possibility

Table 2. Calibration curve parameters for various amines and amino-alcohols with carrier liquid, 0.025M  $\text{KH}_2\text{PO}_4$  + 30% methanol, pH 7.0; flow-rate, 20  $\mu\text{l}/\text{min}$ ; injected amount, 0.5  $\mu\text{l}$ ; applied potential, +0.15 V

Solute	Corr. coeff	Slope, $\mu\text{A}/\mu\text{g}$	Detection limit, ng
Allylamine	—	—	50
Butylamine	0.973	0.152	60
Isobutylamine	0.970	0.406	40
Isopropylamine	0.977	0.406	40
Cyclohexylamine	0.969	0.125	65
Benzylamine	0.981	0.397	40
Diethylamine	0.968	0.128	65
Di-isopropylamine	0.997	0.063	400
Allylethylamine	—	—	55
Allylcyclohexylamine	—	—	48
Piperidine	—	—	63
Ethyl-di-isopropylamine	0.995	0.163	60
Triethylamine	0.995	0.088	200
Allyldiethylamine	—	—	43
Allyldimethylamine	—	—	40
Diallylethylamine	—	—	28
Diallybutylamine	—	—	30
Diallylcyclohexylamine	—	—	28
Trilaurylamine	—	—	27
Dimethylphenylamine	—	—	27
Hydrazine sulphate	0.998	4.40	2.5
Ethylenediamine sulphate	0.996	2.90	4.0
<i>N,N</i> -Dimethylethylenediamine	0.993	7.0	1.0
<i>N,N'</i> -Dimethylethylenediamine	0.975	5.30	4.0
<i>N,N,N'</i> -Trimethylethylenediamine	0.960	4.40	4.0
<i>N,N,N,N'</i> -Tetramethylethylenediamine	0.999	1.40	8.0
<i>N,N,N,N'</i> -Tetramethylpropylenediamine	0.982	0.10	140
<i>o</i> -Phenylenediamine	0.992	3.4	0.3
Ethanolamine	0.960	0.7	29
<i>N</i> -Dimethylaminobutanol	0.989	0.1	100
Diethanolamine	0.972	0.40	44
Triethanolamine	0.960	4.4	3.0

Table 3. Correlation of the detection limits with the stability constants of the  $\text{Cu}^{2+}$  complexes for some diamines

Diamine	Stability constants <sup>24</sup>		Detection limit, ng
	$\log \beta_1$	$\log \beta_2$	
Ethylenediamine	—	11.2	4.0
<i>N,N</i> -Dimethylethylenediamine	9.33	16.40	1.0
<i>N,N'</i> -Dimethylethylenediamine	10.15	17.36	2.0
<i>N,N,N,N'</i> -Tetramethylethylenediamine	7.20	11.87	8.0

of determining diamines in the presence of monoamines and of differentiating diamines according to their structure. Amino-alcohols can also be detected, with a sensitivity decreasing with increasing length of the carbon chain. Triethanolamine can be detected with the highest sensitivity and hence with the possibility of selective determination.

Data on the stabilities of the complexes involved are scarce and no kinetic data are available. General correlation of the detection sensitivity with the stability and rate constants is thus impossible. However, the few available stability constants correlate with the detection limits (see Table 3) and thus it can be assumed that the complexation rates of these substances are similar.

*Acknowledgements*—The authors are grateful to Dr J. Pristach of the Institute of Haematology and Blood Transfusion, Faculty of Medicine, Charles University, for kindly providing the apparatus for stopped-flow measurements and his great help with the measurements.

#### REFERENCES

1. A. Libický and L. Wünsch, *Collection Czech. Chem. Commun.*, 1961, **26**, 2663.
2. Y. A. Gawargious, A. Besada and M. E. M. Hassouna, *Microchim. Acta*, 1974, 1003.
3. C. R. Lascombe, G. B. Box and J. A. W. Dalziel, *J. Chromatog.*, 1978, **166**, 403.
4. E. M. Athanasiou-Malaki and M. A. Koupparis, *Anal. Chim. Acta*, 1984, **161**, 349.



5. P. W. Alexander, P. R. Haddad, G. K. C. Low and C. Maitra, *J. Chromatog.*, 1981, **209**, 29.
6. P. W. Alexander and C. Maitra, *Anal. Chem.*, 1981, **53**, 1590.
7. P. R. Haddad, P. W. Alexander and M. Trojanowicz, *J. Chromatog.*, 1984, **315**, 261.
8. P. W. Alexander, P. R. Haddad and M. Trojanowicz, *Austral. Electrochemistry Conf.*, Geelong, Victoria, 1984.
9. *Idem*, *Anal. Chem.*, 1984, **56**, 2417.
10. P. W. Alexander, M. Trojanowicz and P. R. Haddad, *Anal. Lett.*, 1984, **17**, 309.
11. P. R. Haddad, P. W. Alexander and M. Trojanowicz, *J. Chromatog.*, 1984, **294**, 397.
12. *Idem*, *ibid.*, 1985, **321**, 363.
13. *Idem*, *ibid.*, 1985, **324**, 319.
14. M. L. Hitchman and F. W. M. Nyasulu, *J. Chem. Soc., Faraday Trans.*, 1986, **82**, 1223.
15. W. Th. Kok, H. B. Hanekamp, P. Bos and R. W. Frei, *Anal. Chim. Acta*, 1982, **142**, 31.
16. W. Th. Kok, U. A. Th. Brinkman and R. W. Frei, *J. Chromatog.*, 1983, **256**, 17.
17. *Idem*, *J. Pharm. Biomed. Anal.*, 1983, **1**, 369.
18. W. Th. Kok, G. Groenendijk, U. A. Th. Brinkman and R. W. Frei, *J. Chromatog.*, 1984, **315**, 271.
19. K. Štulík, V. Pacáková, M. Weingart and M. Podolák, *ibid.*, 1986, **367**, 311.
20. K. Štulík, V. Pacáková and M. Podolák, *ibid.*, 1984, **298**, 225.
21. U. Bertocci and D. R. Turner, in *Encyclopedia of Electrochemistry of the Elements*, Vol. II, pp. 384–497. Dekker, New York, 1974.
22. G. Bianchi and P. Longhi, *Corros. Sci.*, 1973, **13**, 853.
23. D. D. Perrin and V. S. Sharma, *J. Chem. Soc. (A)*, 1967, 724.
24. A. E. Martell and R. M. Smith, *Critical Stability Constants*, Vols. 1 and 2, Plenum, New York, 1974, 1975.
25. R. F. Pasternack, E. Gibbs and J. C. Cassatt, *J. Phys. Chem.*, 1969, **73**, 3814.
26. R. L. Karpel, K. Kustin and R. F. Pasternack, *Biochim. Biophys. Acta*, 1969, **177**, 434.
27. R. F. Pasternack, K. Kustin, L. A. Hughes and E. Gibbs, *J. Am. Chem. Soc.*, 1969, **91**, 4401.
28. K. Štulík, V. Pacáková and G. Jokuszies, *J. Chromatog.*, 1988, **436**, 334.

## HPLC SEPARATION OF HETEROCYCLIC $\beta$ -DIKETONATES OF ACTINIDE, LANTHANIDE AND TRANSITION METALS\*

RAUL MORALES†, C. S. BARTHOLDI and P. T. CUNNINGHAM  
Analytical Chemistry Group, MS G740, Los Alamos National Laboratory, Los Alamos,  
NM 87545, U.S.A.

(Received 2 October 1987. Accepted 8 January 1988)

**Summary**—Liquid-chromatography conditions for the separation of neutral chelates of 1-phenyl-3-methyl-4-benzoyl-5-pyrazolone with transition metals, lanthanides and actinides have been established. The use of reverse-phase liquid chromatography, instead of ion-exchange, is a novel approach for actinide separation. The high molar absorptivities of the  $\beta$ -diketonates in the ultraviolet region allow for their detection at the nanogram level. The potential exists, therefore, for the rapid solvent extraction, concentration and determination of traces of actinides and other metals.

In the last 10 years modern liquid chromatography has played a successful role in the determination of trace metals. Although the emphasis has been on the use of ion-chromatography, the application of reversed-phase high-performance liquid chromatography (HPLC) for the separation and detection of neutral metal chelates and organometallics is also well documented.<sup>1-4</sup> Most studies and applications involving modern liquid chromatography have focused on metals other than those of the lanthanide and actinide series. The *f*-elements have also been investigated<sup>5-11</sup> but only to a more limited extent.

Because of the hydrolytic nature of actinide and lanthanide ions, organic compounds that form stable complexes with them in acidic solutions are desirable both as extractants and photometric reagents. However, the analytical applications of such reagents,  $\beta$ -diketones in particular, have been primarily in the field of solvent extraction. The diketones are effective extractants but somewhat unselective and generally do not yield chelates with spectral characteristics useful for the selective determination of given metal ions. Normally, the spectra of the chelates do not exhibit definitive wavelength maxima in the visible region. In the ultraviolet region, the spectra of the ligand and its complexes are very similar. These factors, therefore, have relegated  $\beta$ -diketones to solvent extraction applications. HPLC, however, has already demonstrated its potential for separating metal complexes<sup>1-4</sup> and using similar spectral charac-

teristics to advantage by allowing a common wavelength to be used for monitoring purposes.

Thenoyltrifluoroacetone (TTA) and 1-phenyl-3-methyl-4-benzoyl-5-pyrazolone (HPMBP) are the two heterocyclic  $\beta$ -diketones most often associated with the extraction of metals in actinide matrices. The objective of this study was to evaluate the chromatographic behaviour of metal chelates of these  $\beta$ -diketones. HPMBP was selected as the starting ligand because of its reported<sup>12-17</sup> better stability in acids and on storage, lipophilic characteristics, high extraction capacity at high acid concentrations, fast reactions with metal ions and the high molar absorptivities expected for its complexes.

### EXPERIMENTAL

The liquid chromatograph used consisted of an M510 pump, U6K injector, RCM-100 radial compression module, model 490 programmable multiwavelength detector, and a model 680 automated gradient controller, all from Waters Associates. A Spectra Physics SP 4270 was used for peak area integration. A Waters Associates Nova-Pak C<sub>18</sub> Radial Pak, 5 mm  $\times$  10 cm cartridge was used for the separations. Spectral studies were conducted with a Perkin-Elmer model 559 spectrophotometer.

HPMBP was obtained from Aldrich Chemical Co. and used as received. Chromatographic solvents were obtained from Burdick and Jackson. The metal chelates Fe(PMBP)<sub>3</sub>, Ga(PMBP)<sub>3</sub>, Nd(PMBP)<sub>3</sub>·3H<sub>2</sub>O, Gd(PMBP)<sub>3</sub>·3H<sub>2</sub>O, Th(PMBP)<sub>4</sub>, and UO<sub>2</sub>(PMBP)<sub>2</sub>·2C<sub>2</sub>H<sub>5</sub>OH were prepared by methods previously described,<sup>18,19</sup> with minor modifications.<sup>20</sup> The <sup>237</sup>Np(PMBP)<sub>4</sub> chelate<sup>21</sup> was prepared by equilibrating 20 ml of  $1 \times 10^{-3}M$  Np(NO<sub>3</sub>)<sub>4</sub> in 0.5M nitric acid with 15 ml of 0.1M HPMBP in chloroform. The excess of HPMBP in the chloroform phase was stripped with 0.1M sodium hydroxide. The chloroform was then evaporated, leaving a yellow, viscous liquid that failed to crystallize even after 2 weeks. The liquid was redissolved in chloroform and an aliquot was counted on a scintillation counter to ascertain the presence of <sup>237</sup>Np. This neptunium solution was used for qualitative chromatographic purposes. A Cu(II) chelate solution was prepared and used in a similar manner.

\*Presented in part at the Tenth International Symposium on Column Liquid Chromatography (HPLC, 1986). Work performed by the Los Alamos National Laboratory operated under the U.S. Department of Energy, Contract No. W-7405-ENG 36.

†Author for correspondence.

## RESULTS AND DISCUSSION

Before studying the chromatographic behaviour of HPMBP and its chelates, it was necessary to conduct limited solubility and stability studies with the solvents we expected to evaluate as eluents. All compounds were found to be readily soluble in chloroform, so  $1 \times 10^{-3} M$  stock solutions were prepared. Similar concentrations were prepared for the ligand in acetonitrile and for the ligand and the lanthanide chelates in ethanol. However, millimolar solutions of the other complexes in either acetonitrile or ethanol could not be prepared because of their limited solubilities. Stock solutions of such compounds were therefore prepared by initial dissolution in chloroform, followed by dilution with ethanol or acetonitrile to yield a final solvent composition of 4% v/v chloroform. None of the compounds was found to dissolve in water.

The absorption spectra of the chelates in the 190–800 nm region were found to be qualitatively similar to the spectrum of HPMBP, with the exception of the uranyl chelate, in which the longer wavelength band is unresolved and appears as a shoulder (Fig. 1). Although the uranyl and iron complexes were highly coloured (orange and burgundy, respectively), they exhibited no  $\lambda_{\max}$  in the visible region. Ethanol (95 or 100 v/v) solutions of all chelates, except those of uranium(VI), iron(III) and gallium, displayed spectral shifts (towards the spectrum of HPMBP), as a function of either concentration or time, suggesting dissociation of the complexes. The rate of spectral change generally decreased with increase in concentration. All compounds displayed greater stability in acetonitrile, with those of the lanthanides still the most unstable. The spectra of the chloroform solutions remained constant for 2 weeks for all chelates except those of the lanthanides. Even freshly prepared solutions of the lanthanide complexes were unstable in all solvents, as demonstrated by the different spectra obtained as a function of concentration. Molar absorptivities for the chelates in acetonitrile are given in Table 1.

Initially, silica columns were used to study the chromatographic behaviour of the chelates listed in Table 1. When Porasil (Waters Associates), Partisil 5-PAC (Whatman), and various combinations of

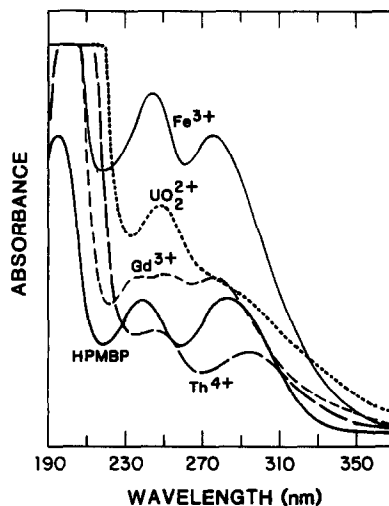


Fig. 1. Absorption spectra of metal-PMBP chelates in acetonitrile. Chelates run at different concentrations and sensitivity.

n-hexane, 2-propanol, methylene chloride, acetonitrile and tetrahydrofuran were used as eluents, there was either poor column selectivity or complete retention of certain compounds. An amino column (IBM) with combinations of chloroform, ethanol and n-butanol as eluents gave similar results.

Reverse-phase chromatography of the chelates was attempted with Chromegabond fluoroether (ES Industries),  $\mu$ Bondapak phenyl,  $\mu$ Bondapak C<sub>18</sub>, and Nova-Pak C<sub>18</sub> Radial Pak (Waters Associates) columns. No selectivity was obtained with the fluoroether column and acetonitrile/water systems. Although the other columns provided some selectivity with mobile phases containing water, the Nova-Pak C<sub>18</sub> columns, especially when they were new, produced peaks that did not tail as badly. This column was therefore selected for further studies.

Although spectrophotometric calibration curves could be obtained at either of the wavelengths cited in Table 1 for the complexes, 250 nm was selected as the common wavelength for monitoring all complexes by HPLC. The primary reason for this was the better defined  $\lambda_{\max}$  for the uranyl chelate at 249 nm. With the Nova-Pak C<sub>18</sub> column, binary mobile phases consisting of water with methanol, ethanol,

Table 1. Molar absorptivities of HPMBP and its metal chelates in acetonitrile\*

Compound	$\lambda_1$ , nm	$\epsilon$ , $10^4 l. mole^{-1} cm^{-1}$	$\lambda_2$ , nm	$\epsilon$ , $10^4 l. mole^{-1} cm^{-1}$
HPMBP	239	$1.86 \pm 0.05$	277†	$1.93 \pm 0.06$
Nd(PMBP) <sub>3</sub> ·3H <sub>2</sub> O	undefined	—	277	$5.34 \pm 0.07$
Gd(PMBP) <sub>3</sub> ·3H <sub>2</sub> O	undefined	—	277	$5.03 \pm 0.06$
Ga(PMBP) <sub>3</sub>	243	$4.91 \pm 0.12$	291	$5.64 \pm 0.27$
Fe(PMBP) <sub>3</sub>	245	$5.72 \pm 0.13$	277	$5.08 \pm 0.13$
Th(PMBP) <sub>4</sub>	246	$7.12 \pm 0.27$	293	$5.92 \pm 0.39$
UO <sub>2</sub> (PMBP) <sub>2</sub> ·2EtOH	249	$5.20 \pm 0.18$	shoulder	—

\*Based on a minimum of 3 values.

†Band sometimes found at 284 nm depending on degree of keto-enol isomerization.

2-propanol, acetonitrile and tetrahydrofuran produced tailing peaks, multiple peaks, insufficient selectivity or irreproducible retention times. Column regeneration was necessary in many instances. Since these results indicated the chelates to be kinetically unstable, HPMBP was added to the mobile phase to minimize or eliminate complex dissociation. The best separations were obtained by using a mobile phase consisting of  $1.2 \times 10^{-5} M$  HPMBP in 3% water/acetonitrile under the conditions described in Fig. 2a. Under these chromatographic conditions, the chelates of  $Nd^{3+}$ ,  $Gd^{3+}$ , and  $UO_2^{2+}$  are essentially unretained. The order of retention for the other chelates is  $Cu^{2+} < Ga^{3+} \sim Th^{4+} < Fe^{3+} < Np^{4+}$ . This order suggests that polar complexes are eluted first. The thorium complex may contain co-ordinated water<sup>22</sup> and is eluted earlier than expected. The copper complex yielded two peaks, the first having the same retention time as that of the uranyl complex. Increasing the water content of the mobile phase resulted in better resolution (Fig. 2b) but after 6 hr the column lost its original selectivity and efficiency. A decrease in sensitivity was also observed at the higher water content, probably due to  $\lambda_{max}$  shifts resulting from the different solvent environment.

The quantitative potential of HPLC of the chelates was also explored. Since the metal complexes exhibit molar absorptivities ( $\epsilon$ ) in the  $10^4$  l.mole<sup>-1</sup>.cm<sup>-1</sup> range, HPLC should be a viable technique for their trace determination. The calibration curves for the chelates of gallium, iron and thorium were linear up to 0.4, 0.3 and 0.8  $\mu g$  of complex per  $\mu l$  injected, respectively. Equally important, the curves pass through the origin, indicating minimal material loss as the compounds pass through the column. To confirm this minimal loss, various volumes of three different thorium chelate standard solutions were injected into the chromatograph. The eluted fractions corresponding to the chelate peaks were collected, and evaporated in a stream of air, and the residues were dissolved in 5 ml of 1M nitric acid. The acid solutions were analysed for thorium by ICP-MS.

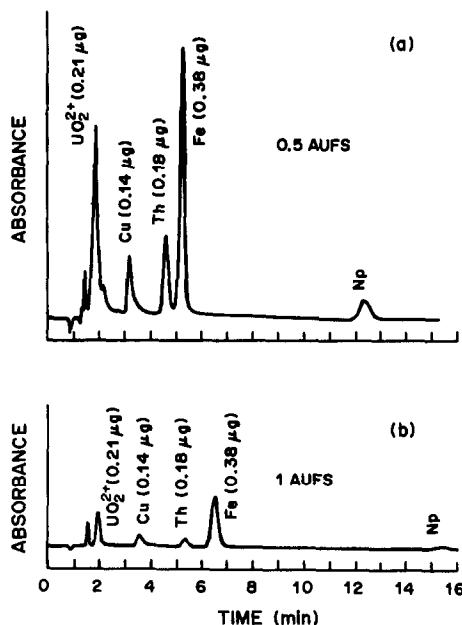


Fig. 2. Effect of mobile phase composition on the chromatographic behaviour of PMBP chelates of  $UO_2^{2+}$ ,  $Cu^{2+}$ ,  $Th^{4+}$ ,  $Fe^{3+}$  and  $Np^{4+}$ . Nova-Pak  $C_{18}$  Radial Pak, 1 ml/min, 250 nm. (a)  $1.2 \times 10^{-5} M$  HPMBP in 3%  $H_2O/CH_3CN$ , (b)  $1.2 \times 10^{-5} M$  HPMBP in 5%  $H_2O/CH_3CN$ . Microgram amounts refer to the chelates.

Controls, *i.e.*, unchromatographed solutions, were analysed in the same way as the eluates. Table 2 shows thorium recoveries of  $\geq 90\%$ , with  $\bar{x} = 100.2\%$  and  $s = 8.0\%$ . The recoveries calculated from the chromatographic peak areas averaged  $95.9 \pm 9.0\%$ .

The detection limits obtainable by using the higher sensitivity settings of the HPLC detector have not yet been investigated, but nanograms of metal can easily be determined at a setting of 0.5 absorbance for full-scale reading. Chromatography of HPMBP/chloroform extracts from 0.1M hydrochloric acid spiked with gallium, iron and thorium yields peaks consistent with the retention times of standards made by direct dissolution of the complexes.

Table 2. Thorium separation by HPLC and determination by ICP-MS

Sample	Concentration, $\mu g/\mu l$	Volume injected, $nl$	Amount injected, $ng$	Amount found by ICP-MS, $ng$	Recovery, %
1	0.0374	2	0.075	0.070	93
2	0.0374	2	0.075	0.070	93
3	0.0374	3	0.112	0.115	103
4	0.0748	2	0.150	0.135	90
5	0.1123	2	0.225	0.250	111
6	0.1123	2	0.225	0.240	96
7	0.1123	3	0.337	0.380	113
8	0.1123	10	1.123	1.130	101
9	0.1123	10	1.123	1.140	102
10*	0.0374	(2)	(0.075)	0.075	100
11*	0.0748	(2)	(0.150)	0.150	100
12*	0.1123	(2)	(0.225)	0.235	104

$$\bar{x} = 100.2 \pm 8.0\%$$

\*Unchromatographed solutions which served as controls.

## CONCLUSIONS

Work reported in the literature has already demonstrated the usefulness of compounds such as HPMBP for the extraction of metals that readily hydrolyse or polymerize in solution. The HPLC investigations reported here extend the potential of such extractants, by allowing further separations when interfering metals are co-extracted. Furthermore, the simultaneous separation and determination of several metals becomes possible and is particularly attractive for trace analysis. The use of masking agents and pH control should provide even greater selectivity in such determinations. Our investigations also suggest that group separations by HPLC may be possible, *e.g.*, of lanthanides from other  $M^{3+}$  metals as well as from actinides, especially if the latter are in the  $M^{4+}$  state.

*Acknowledgements*—The authors wish to thank D. Hobart and P. Palmer for the preparation of chemically pure Np(IV), B. Smith and G. Jarvinen for the synthesis of the metal chelates used in this study, and G. Bentley for the thorium determinations by ICP-MS.

## REFERENCES

1. J. W. O'Laughlin, *J. Liq. Chromatog.*, 1984, **7**, 127.
2. B. R. Willeford and H. Veening, *J. Chromatog.*, 1982, **251**, 61.
3. G. Schwedt, *Chromatographia*, 1979, **12**, 613.
4. C. A. Tollinche and T. H. Risby, *J. Chromatog. Sci.*, 1978, **16**, 448.
5. D. O. Campbell, *Transplutonium Elements—Production and Recovery*, J. D. Navratie and W. W. Schulz (eds.), pp. 189–201. ACS, Washington DC, 1981.
6. N. R. Larsen and W. B. Pedersen, *J. Radioanal. Chem.*, 1978, **45**, 135.
7. S. Elchuck and R. M. Cassidy, *Anal. Chem.*, 1979, **51**, 1434.
8. C. H. Knight, R. M. Cassidy, B. M. Recoskie and L. W. Green, *ibid.*, 1984, **56**, 474.
9. R. M. Cassidy, S. Elchuck, N. L. Elliot, L. W. Green, C. H. Knight and B. M. Recoskie, *ibid.*, 1986, **58**, 1181.
10. M. Schadel, N. Troutmann and G. Hermann, *Radiochim. Acta*, 1977, **24**, 27.
11. A. Casoli, A. Mangia and G. Predieri, *Anal. Chem.*, 1985, **57**, 563.
12. B. Skytte-Jensen, *Acta Chem. Scand.*, 1959, **13**, 1668, 1890.
13. Yu. A. Zolotov, M. K. Chmutova and P. N. Paler, *Russian J. Anal. Chem.*, 1968, **23**, 1298.
14. Yu. A. Zolotov, N. T. Sizonenko, E. S. Zolotovskaya and E. I. Yakovenko, *ibid.*, 1969, **24**, 15.
15. G. N. Rao and J. S. Thakur, *J. Sci. Ind. Res.*, 1975, **34**, 110.
16. J. N. Mathur and P. K. Khopkar, *Sepr. Sci. Technol.*, 1982, **17**, 985.
17. Yu. P. Novikov, S. A. Ivanova and B. F. Myasoedov, *Radiochem. Radioanal. Lett.*, 1982, **52**, 155.
18. E. C. Okafor, *J. Inorg. Nucl. Chem.*, 1980, **42**, 1155.
19. *Idem*, *Polyhedron*, 1983, **2**, 309.
20. G. D. Jarvinen, R. R. Ryan, B. F. Smith and J. M. Ritchey, *Inorg. Chim. Acta*, submitted for publication.
21. L. I. Moseev and B. V. Monakhov, *Radiokhimiya*, 1968, **10**, 293. (English translation).
22. W. Wenging, L. Qingliang, M. S. Careia, G. R. Chopin, D. Yuwen and Y. Min, *Solvent Extr. Ion Exch.*, 1986, **4**, 663.

## COMPUTATIONAL ELIMINATION OF INTERFERENT EFFECTS IN FLAME ATOMIC-ABSORPTION SPECTROMETRY

L. PSZONICKI, A. LECHOTYCKI and M. KRUPIŃSKI

Institute of Nuclear Chemistry and Technology, Dorodna 16, 03-195 Warsaw, Poland

(Received 18 October 1984. Revised 28 July 1987. Accepted 18 December 1987)

**Summary**—Empirical formulae, which describe quantitatively the interferent effects in flame atomic-absorption analysis, have been proposed. The formulae enable calculation of the total multi-interferent effect of a complex system, on the basis of characteristic coefficients established for simple analyte-interferent pairs. The approach may be used for the computational elimination of interferent effects and for correction of analytical results. Experimental verification has confirmed that the corrected results are consistent with the actual concentrations.

Atomic-absorption spectrometry, like most analytical methods, is sensitive to interference effects caused by various components of the samples to be analysed. Usually these effects are eliminated or at least minimized by choosing the optimal conditions for each type of material, separation of interferents, use of buffers. All these manipulations are time-consuming when applied to large series of samples and not always effective, especially when the concentration of a strong interferent varies over a wide range in a series of samples. Therefore, the idea of eliminating the interferences by computation seems very attractive. Some general proposals of this type have already been made<sup>1-3</sup> but their application to atomic-absorption analysis is limited since either the complex system which exists in atomic-absorption atomization does not fulfil the required simplifying assumptions<sup>3</sup> or a large number of coefficients must be re-determined after any change in composition of the system.<sup>1,2</sup>

The processes responsible for the absorption and emission of electromagnetic radiation in the flame may be described quantitatively by thermodynamic equations, but only for simple and well-defined systems. The flames used in atomic-absorption spectrometry form, together with the analytical samples, very complex systems, and their quantitative description by the thermodynamic formulae is hardly possible. We have assumed, therefore, that the evaluation of interferent effects on this basis does not promise success.

The proposal of Parczewski and Rokosz<sup>4</sup> to calculate the interferent effects in atomic-absorption analysis on the basis of a set of empirical polynomial equations seems to be very useful for analytical systems with an exactly defined number of components, but when this number is changed, a new set of equations must be formed and the coefficients determined.

The aim of this work was to consider some general regularities observed in the interference effects occurring in two-component systems composed of an analyte and one interferent, and to describe these effects by a general equation. The parameters of such an equation, found experimentally to be constant for every system, may be considered as coefficients characterizing the effects of individual interferents and may form the basis for description of multi-component systems analysed by flame atomic-absorption spectrometry.

### CHARACTERISTICS OF INTERFERENCE EFFECTS

#### *The effect of individual interferents*

Information on the effect of individual interferents as a function of their concentration may be found in many papers and handbooks on atomic-absorption analysis. The careful examination of this information has suggested some general regularities, which have been confirmed by our experiments.

The effect of aluminium on the calibration curve for strontium is shown in Fig. 1 and represents one of the most typical examples of a strong interferent effect. The total analytical signal  $R$  may be considered as a sum of the signal  $R_A$  produced by the pure analyte (the signal obtained in the absence of interferent) and of the signal  $R_I$  produced by an interferent (difference between the signals obtained with and without interferent present). For any given concentration of the analyte ( $c_A$ ) and interferent ( $c_I$ ) the value of  $R_I$  is given by

$$R_I = R - R_A \quad (1)$$

$R_I$  is positive when the analyte signal is enhanced by an interferent or negative (as in Fig. 1) when the analyte signal is suppressed.

In atomic-absorption spectrometry (AAS) the calibration curves are seldom linear over a large range of

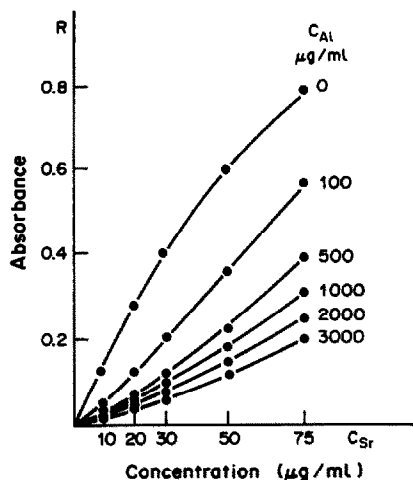


Fig. 1. Effect of various concentrations of aluminium ( $c_{Al}$ ) on analytical signals  $R$  of strontium concentration ( $c_{Sr}$ ).

concentration and this additionally complicates the picture. The analyst, however, is not interested in the deformation of analytical signals themselves but in the bias of the final analytical results. Therefore, it is more convenient to consider the interferent effect as a bias of results expressed in concentration units ( $\Delta c$ ) and to transform equation (1) into the form:

$$\Delta c = c_{AP} - c_A \quad (2)$$

where  $c_{AP}$  is the apparent concentration of an analyte determined in the presence of an interferent and  $c_A$  is the actual concentration of the analyte. The curves showing the effect of aluminium on strontium (Fig. 1) may then be presented in the new form (Fig. 2). In this system the function  $c_{AP} = f(c_A)$  is always linear when  $c_I = 0$  since  $c_{AP} = c_A$ . The values of  $\Delta c$  represented by the distances between the calibration curves obtained in the presence and absence of the interferent are a function of both  $c_A$  and  $c_I$ .

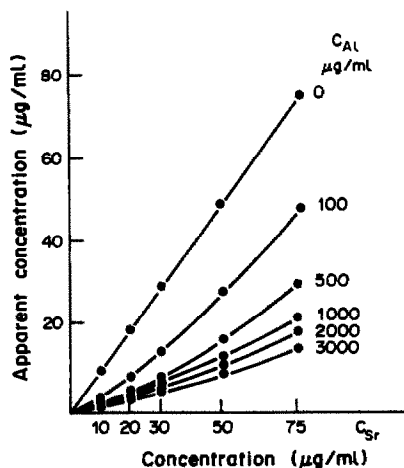


Fig. 2. Apparent concentration of strontium as a function of its actual concentration ( $c_{Sr}$ ) and the concentration of aluminium ( $c_{Al}$ ).

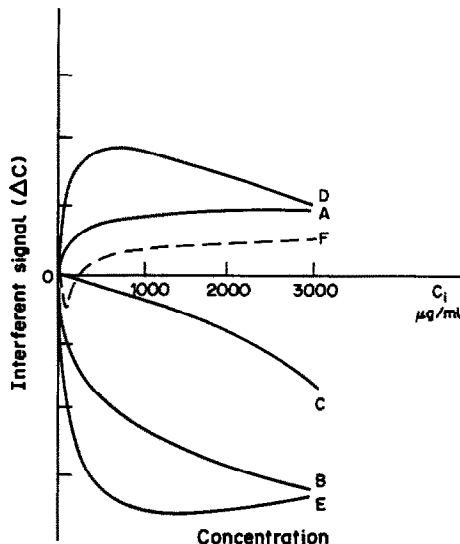


Fig. 3. The curves representing various types of interferent effects ( $\Delta c$ ) as functions of interferent concentration ( $c_I$ ) at a constant analyte concentration.

The various types of interferent effects, caused either by cations or anions and represented by the  $\Delta c$ -function at constant  $c_A$ , are shown schematically in Fig. 3. The dominant type of these effects is represented by curves A and B. Both may be well approximated by the equation of the saturation curve:

$$\Delta c = \bar{d}c_I / (\bar{a} + c_I) = c_I / (a + dc_I) \quad (3)$$

where  $a = \bar{a}/\bar{d}$  and  $d = 1/\bar{d}$ .

The parameters of the equation for curve A are  $a > 0$  and  $d > 0$ , and for curve B are  $a < 0$  and  $d < 0$ . The effects represented by curve C, which occur very seldom in their pure form, may also be described by equation (3) with  $a < 0$  and  $d > 0$  (the positive mirror image of curve C will be given by  $a > 0$  and  $d < 0$ ); in both cases  $|a|$  must be  $> |dc|$ . The only shortcoming of this function is its discontinuity at  $a = -dc$  or  $-a = dc$ . This point, however, is always outside the range delimited by the experimental data and the fitting procedure.

Exact examination of the experimental data showed that only a small group of analyte–interferent systems may be described quantitatively by equation (3), *e.g.*, the effect of vanadium on chromium and strontium or the effect of calcium on magnesium. For these systems the interferent effect is also simply proportional to the analyte concentration. The other group of interferent effects, *e.g.*, the effect of aluminium on strontium or titanium, may be characterized quantitatively by a similar function in which at constant  $c_A$ ,  $\Delta c$  is dependent on the concentration ratio ( $c_R$ ) of interferent to analyte:  $c_R = c_I/c_A$ . This function has the form:

$$\Delta c = c_R / (a + dc_R) = c_I / (ac_A + dc_I) \quad (4)$$

In this case the dependence on the analyte concen-

tration is more complex since  $c_A$  also occurs in the denominator.

Equations (3) and (4) describe two extreme types of interferent effects and the differences between them are caused, most probably, by their mechanisms of operation being different. The interferent effect observed for most systems seems to be a result of competition of these two component effects and may be considered as their sum:

$$\Delta c = c_A c_1 \left[ \frac{1}{(a_1 + d_1 c_1)} + \frac{1}{(a_2 c_A + d_2 c_1)} \right] \quad (5)$$

This formula describes very well all types of interferent effects presented in Fig. 3, and is valid for any analyte concentration within the concentration range investigated. Its only shortcoming is the fact that  $a_1$ ,  $a_2$ ,  $d_1$  and  $d_2$  cannot be estimated unambiguously on the basis of experimental data by the iteration method, so the formula may hardly be applied for practical purposes.

The interferent effects represented by curve F (Fig. 3) seldom occur, and then only in a very rich or very lean flame or when increasing the interferent concentration radically changes the basic parameters of the system investigated, *e.g.*, the pH, viscosity, *etc.* For the flames usually used in analysis, and when the parameters are kept approximately constant, the interferent effects of this type may be excluded from consideration, and equation (5) may be replaced by the empirical formula

$$\Delta c = c_A c_1 / (\alpha + \delta c_A + \beta c_1 + \epsilon c_A^2 + \rho c_A c_1 + \gamma c_1^2) \quad (6)$$

This formula may be readily transformed into linear form and its parameters calculated from experimental data by simple regression. Equation (6) describes well all types of interferent effects (with the exception of type F) over the whole range of analyte concentration of interest and very seldom needs to be used

in its general form, *e.g.*, for description of the effect of aluminium on vanadium. Usually some of the coefficients are equal to zero and the number of components in the brackets is reduced to four, three or two (see Table 2). If only  $\alpha$  or  $\beta$  or  $\delta$  and  $\beta$  are not equal to zero, equation (6) is transformed into equation (3) or (4), respectively.

The coefficients of equation (6) ( $\alpha, \delta, \beta, \epsilon, \rho, \gamma$ ) are constant (and thus may be considered as characteristic coefficients) for a given analyte–single interferent system, but only for the concentration ranges  $c_A$  and  $c_1$  for which the system was calibrated, and for the given parameters of the atomizer. Nevertheless, it has been found that these coefficients are significantly less sensitive than the absolute values of analytical signals to small deviations in the flame composition and the other parameters which are difficult to regulate precisely, and they are therefore effectively constant over long periods of time.

#### THE EFFECTS IN MULTI-INTERFERENT SYSTEMS

An analytical sample usually forms a multi-component system and many of these components can affect not only the analytical signal of the analyte but also the activity of other interferents. The mathematical description of their effects, on the basis of coefficients characterizing the total system, requires time-consuming calibration work, and the coefficients established are usually useless when the number of components is changed. This difficulty might be overcome by an approach based on utilization of the characteristic coefficients for the individual interferents.

Our search for such an approach was based on the following observations:

(i) The total effect of a multi-interferent system is never smaller than the individual effect of the strongest interferent, and never larger (in practice always smaller) than the sum of the individual effects of all the interferents present in the system.

(ii) Buffers and releasing agents affect the analyte signal and this effect will strongly depend on their concentration, and at low concentrations they may be considered as strong interferents.

(iii) Components which do not affect the analyte signal individually also have no effect on it when the sample contains combinations of them.

The total effect ( $\Delta c_T$ ) of a two-interferent system at a constant analyte concentration may be presented graphically as a plane OBDA in three-dimensional space (Fig. 4). It is a function of the individual interferent concentrations  $c_a$  and  $c_b$ . The curves OA and OB represent the individual effects of interferents "a" and "b", respectively. For various systems the plane OBDA can shift in the range delimited by planes OBA'A and OBEA. Plane OBA'A represents the situation when the effect of the stronger interferent decides the value of  $\Delta c_T$  and  $\Delta c_T = \Delta c_a$ . Plane OBEA represents the sum of the individual effects  $\Delta c_a$

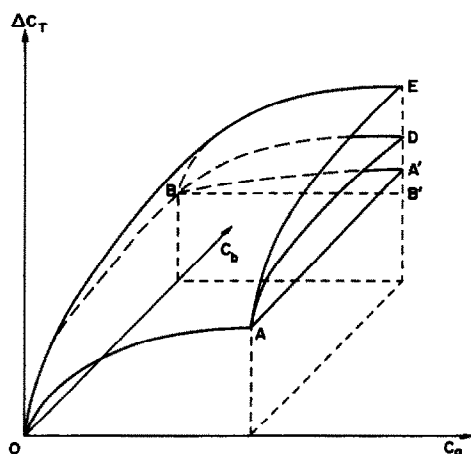


Fig. 4. Complex effect ( $\Delta c_T$ ) of two interferents as a function of their concentrations. Plane OBA'A—complex effect dominated by interferent "a". Plane OBEA—sum of the individual effects of the interferents "a" and "b". Plane OBDA—complex effect which occurs most frequently.



and  $\Delta c_b$  at any given point ( $\Delta c_T = \Delta c_a + \Delta c_b$ ). For an  $m$ -interferent system  $\Delta c_T$  may be considered as a plane in  $(m + 1)$ -dimensional space.

The total multi-interferent effect may be considered as the sum of the partial effects contributed by all interferents present. The partial effect  $\Delta c_{pk}$  of the  $k$ th interferent in the mixture of  $n$  interferents may be calculated from a modified version of empirical equation (6) in which all the  $c_A$ -values and the parameter  $\alpha$  are multiplied by a quantity  $A_k$ :

$$\Delta c_{pk} = A_k c_A c_{A_k} / (\alpha_k A_k + \delta_k A_k c_A + \beta_k c_{i_k} + \epsilon_k A_k^2 c_A^2 + \rho_k A_k c_A c_{i_k} + \gamma_k c_{i_k}^2) \quad (7)$$

where  $\alpha_k$ ,  $\delta_k$ ,  $\beta_k$ ,  $\epsilon_k$ ,  $\rho_k$  and  $\gamma_k$  are coefficients corresponding to those in equation (6), but characterizing effect of the individual interferent.

The constant  $A_k$  characterizes the contribution of the  $k$ th interferent to the overall effect of the given multi-interferent system and is calculated as the ratio of the absolute value of the individual effect of the  $k$ th interferent to the sum of the absolute values of the individual effects of all interferents in the system:

$$A_k = |\Delta c_k| / \sum_{i=1}^n |\Delta c_i|$$

$$k = 1, 2, \dots, n$$

The total interferent effect is equal to the sum of the partial effects of all interferents:

$$\Delta c_T = \sum_{i=1}^n \Delta c_{p_i} \quad (8)$$

If a strong interferent is present in large excess in a system then its  $A$ -value is approximately equal to unity, whereas the  $A$  values of all the other interferents are very small. In consequence the total effect is approximately equal to the partial effect of this strong interferent.

The empirical formula (8) was chosen as the best approximation of the experimentally found  $\Delta c$ -values and tested with a wide range of analyte-multi-interferent systems. In all cases the calculated  $\Delta c$ -values were found to lie within the confidence limits of the values determined experimentally.

#### POSSIBILITIES OF APPLICATION OF THE APPROACH

The approach presented may be used for the computational correction of analytical results obtained in the presence of interferents. However, as with application of all other approaches of this type, this is reasonable only in the analysis of large series of samples of similar analyte content, when the concentration of a limited number of components varies over a large range. The time needed for calibration of the system is then shorter, sometimes significantly, than that necessary for elimination of the interferences individually for each sample.

When only one component of a sample affects the measured signal and its concentration is known, then

the corrected concentration may be easily calculated from equation (6). In practice, however, such a situation happens only seldom. More frequently an analyte varying over a large range of concentration is determined in the presence of a matrix of approximately constant composition. In this case the whole matrix may be treated as one component. Its concentration is known since it depends on the weight of sample analysed and is equal to  $c_1$ . By putting  $\Delta c = c_{AP} - c_A$ , equation (6) is transformed into

$$A c_A^3 + B c_A^2 + D c_A + E = 0 \quad (9)$$

where:

$$A = \epsilon$$

$$B = \delta + \rho c_1 - \epsilon c_{AP}$$

$$D = \alpha + \beta c_1 + \gamma c_1^2 - c_{AP}(\delta + \rho c_1)$$

$$E = c_{AP}(\alpha + \beta c_1 + \gamma c_1^2)$$

$c_{AP}$  is the uncorrected measured value

The corrected concentration  $c_A$  may easily be found from equation (9) by the Newton-Raphson iteration method.<sup>5,6</sup>

For multicomponent systems with known concentrations of interferents the corrected analyte concentration may be found in a similar way by using equation (8).

The main field of application of the approach is to multicomponent analysis when there is mutual interference between the components to be determined. The corrected values for all of them may then be found by the following iteration procedure.

(i) The uncorrected (apparent) concentrations of the individual components are determined by suitable analytical methods.

(ii) The first approximation of the corrected concentration of any individual component is calculated from equation (8), using as  $c_1$  the uncorrected concentrations found for other components acting as interferents.

(iii) The second and subsequent approximations of the corrected values are calculated in the same way, using each time the last approximation of the corrected values of the other component, until convergence is obtained.

The main shortcoming of the approach is that the concentration of all components contributing to the total interferent effect should be known or determined. In practice the situation is not so complicated. The partial effect of each individual interferent depends on its characteristic value  $A$  (which is a function of the concentration of all interferents) and the constant coefficients. Only the strong interferents present in a sufficiently large concentration make a significant contribution to the total effect and, usually, only two or three of them need be taken into account. The effect of the others may be neglected.

#### EXPERIMENTAL

##### *Instrumentation and analytical conditions*

A Jarrell-Ash atomic-absorption spectrometer (JA 82-811) equipped with hollow-cathode lamps and air-

Table 1. Measurement conditions

Analyte	$\lambda$ , nm	Distance above the burner top, mm	Bandpass, nm	Flame
Ca	422.7	6.0	0.2	C <sub>2</sub> H <sub>2</sub> -N <sub>2</sub> O
Cr	357.9	5.0	0.1	C <sub>2</sub> H <sub>2</sub> -air
Mg	285.2	6.0	0.2	C <sub>2</sub> H <sub>2</sub> -air
Mo	313.3	5.5	0.2	C <sub>2</sub> H <sub>2</sub> -N <sub>2</sub> O
Mo	313.3	7.0	0.2	C <sub>2</sub> H <sub>2</sub> -N <sub>2</sub> O
Na	589.0	6.0	0.4	C <sub>2</sub> H <sub>2</sub> -air
Pt	265.9	7.0	0.2	C <sub>2</sub> H <sub>2</sub> -air
Rh	343.5	7.0	0.2	C <sub>2</sub> H <sub>2</sub> -air
Sr	460.7	6.0	0.2	C <sub>2</sub> H <sub>2</sub> -air
Ti	364.3	6.0	0.1	C <sub>2</sub> H <sub>2</sub> -N <sub>2</sub> O
V	318.5	8.0	0.1	C <sub>2</sub> H <sub>2</sub> -N <sub>2</sub> O

acetylene and nitrous oxide-acetylene burners was used. The analytical conditions used are presented in Table 1. All samples were measured in 1M hydrochloric acid medium and the values corrected for the blank. The concentration of the major background anion (chloride) was kept approximately constant. Background correction could be neglected in all cases considered.

#### Reagents

All reagents were of "suprapur" grade. The water was doubly distilled in silica apparatus.

Stock standard solutions of the elements (10 mg/ml) were prepared in 1M hydrochloric acid except for titanium, which was prepared in 8M hydrochloric acid. Working solutions were prepared just before use, by dilution of the stock solutions with 1M hydrochloric acid (3M for titanium).

#### Choice of analyte-interferent systems

The systems used for testing the approach were chosen according to the following criteria.

(i) The interferent effect should be large. The errors resulting from the random dispersion of analytical measurements may then be neglected.

(ii) Spectral interferences in the system, such as overlap of spectral lines, or background absorption, should be small enough to be neglected.

#### Experimental design

Estimation of the coefficients characterizing any analyte-interferent pair requires the preparation of several calibration curves, each on the basis of  $j$  standard solutions, for the pure analyte and in the presence of  $m$  different concentrations of interferent in the range of interest. The total number of standard solutions which must be measured is  $m(j+1)$ . In our experiments  $j$  and  $m$  were usually both equal to 5 and the total number of standard solutions was 30.

The quality of description of a multi-interferent system by equation (8) may usually be tested on the basis of only a few standard solutions (5-10) corresponding to the points located at the centre and the peripheral area of the multidimensional plane representing the function  $\Delta c = f(c_A, c_{I1}, \dots, c_{In})$ .

#### Calculation of characteristic coefficients

The coefficients  $\alpha$ ,  $\delta$ ,  $\beta$ ,  $\epsilon$ ,  $\rho$  and  $\gamma$  characterizing any analyte-interferent system are estimated on the basis of experimental data and equation (6). For this purpose the equation must be transformed into linear form:

$$c_A c_i / \Delta c = \alpha + \delta c_A + \beta c_i + \epsilon c_A^2 + \rho c_A c_i + \gamma c_i^2 \quad (10)$$

The concentrations  $c_A$  and  $c_i$  are known for all standard solutions,  $\Delta c = c_{AP} - c_A$  results from the measurements, and the characteristic coefficients in the equation may be esti-

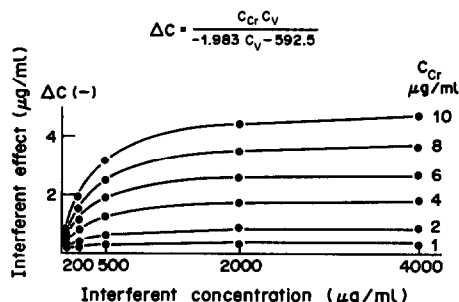


Fig. 5. Effect of vanadium on the determination of chromium.

mated by linear regression. Since fitting the same experimental points to the transformed function may affect their form in a different way than use of the untransformed function, the best coefficients found for equation (10) may not be the best for equation (6). This difficulty may be dealt with by multiplying the value of every data point by its transformed statistical weight as proposed by Jurs.<sup>7</sup> If the statistical weights are the same for all points, as in our experiments, it is convenient to assume all their values to be equal to 1 and then the transformed statistical weight of the  $i$ th point may be calculated from the equation:

$$w_i = (\Delta c_i)^4 / (c_A^2 c_i^2) \quad (11)$$

The regression coefficients may then be calculated from the set of equations (10) written in matrix form:<sup>8,9</sup>

$$[B] = ([X]^T [W] [X])^{-1} [X]^T [W] [Y] \quad (12)$$

where

[B] = matrix of regression coefficients  
 [X] = matrix of independent variables  
 [W] = matrix of statistical weights  
 [Y] = matrix of dependent variables

The columns of matrix [X] are equal to  $c_i$ ,  $c_A$ , 1,  $c_i^2$ ,  $c_A c_i$ ,  $c_A^2$ . All calculations were done with a PDP-11/45 minicomputer.

## RESULTS AND DISCUSSION

Typical examples of individual interferent effects are shown in Figs. 5-8. The black points marked in the plots represent the experimental values, and the continuous lines represent the values calculated from equation (6) in its full form (Fig. 8) or in the reduced form containing three (Fig. 7) or two (Figs. 5 and 6) constant coefficients. It should be noted that Figs. 5

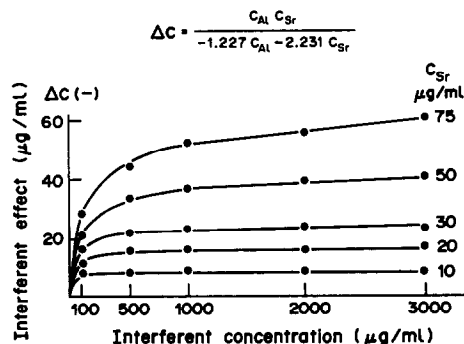


Fig. 6. Effect of aluminium on the determination of strontium.

Table 2. Parameters characterizing individual analyte-interferent system

No.	Analyte		Interferent							Correlation coefficient, $r_{xy}$	
	Element	Range, $\mu\text{g/ml}$	Element	Range, $\mu\text{g/ml}$	$\alpha$	$\delta$	$\beta$	$\epsilon \times 10^2$	$\rho \times 10^3$		$\gamma \times 10^5$
1	Ca	0.5-4.0	Mg	100-3000	300	—	1.40	—	180	—	0.9860
2	Ca	0.5-4.0	Na	50-1000	22	—	1.02	—	180	—	0.9964
3	Cr	1.0-10.0	V	25-4000	-590	—	-1.98	—	—	—	0.9993
4	Mg	0.25-3.0	Al	100-3000	150	—	-3.43	—	—	38	0.9953
5	Mg	0.25-3.0	Ti	100-3000	2	—	-1.42	-40	—	2.7	0.9999
6	Mg	0.5-3.0	Ca	100-2000	650	—	7.60	—	1600	—	0.9910
7	Mg	0.5-3.0	Na	100-2000	850	—	4.54	—	—	—	0.9932
8	Mo	4-80	Al	40-3000	100	1.9	0.992	—	29	—	0.9932
9	Mo	10-75	Ni	100-3000	250	3.8	2.18	—	8.1	16	0.9962
10	Mo	10-75	Cu	100-3000	320	-0.56	1.40	—	—	—	0.9827
11	Na	0.5-4.0	Mg	5-100	90	-18.0	0.614	—	730	—	0.9963
12	Na	0.5-4.0	Ca	5-100	48	-55.0	0.238	2000	560	0.7	0.9521
13	Pt	20-200	Rh	40-2000	-25	-0.085	-1.14	—	—	—	0.9992
14	Pt	40-400	Pd	50-2000	—	-1.7	-0.912	-0.1	13	-18	0.9990
15	Pt	10-200	Mo	500-5000	—	-4.7	-1.46	10	—	2.9	0.9992
16	Pt	10-200	Ni	500-5000	—	-7.1	-0.874	—	2.1	-8.0	0.9977
17	Rh	5-40	Pt	50-2000	820	4.0	0.435	—	-17	27	0.9968
18	Sr	10-75	Al	100-3000	—	-2.2	-1.23	—	—	—	0.9981
19	Sr	10-75	Ti	100-3000	—	-1.3	-0.952	—	—	—	0.9983
20	Sr	10-75	V	100-3000	-41	—	-1.06	—	—	—	0.9992
21	Sr	10-75	Fe	100-3000	—	-20.0	-1.54	—	7.4	—	0.9982
22	Sr	10-75	Mo	100-3000	-1600	3.7	-1.55	—	—	—	0.9965
23	Sr	10-75	Mn	100-3000	—	-31.0	-1.10	—	3.9	—	0.9979
24	Ti	20-300	Al	100-3000	51	1.1	0.677	—	1.3	16	0.9974
25	V	25-150	Mg	100-3000	460	0.63	1.26	—	5.7	-8.4	0.9966
26	V	25-150	La	100-3000	210	1.9	1.27	—	-0.55	4.2	0.9917
27	V	20-200	Al	100-3000	80	-1.0	1.22	0.7	5.9	6.0	0.9971
28	V	25-150	Cr	10-3000	800	-13.0	1.67	8.0	8.9	-13	0.9921
29	V	25-150	Sr	50-3000	460	—	1.85	—	27	—	0.9938

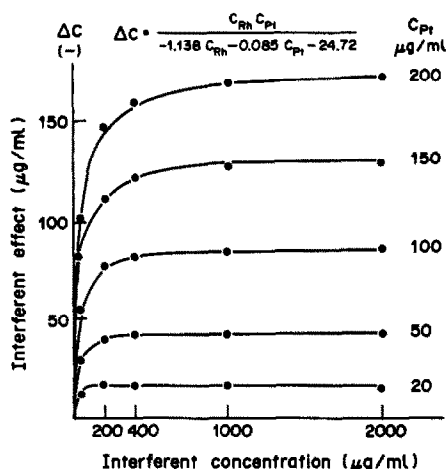


Fig. 7. Effect of rhodium on the determination of platinum.

and 6 demonstrate the extreme cases of interferents in their pure forms, which are dependent only on the absolute ( $c_i$ ) or relative ( $c_r$ ) interferent concentration and can be described by equations (3) or (4), respectively. All plots show good agreement of experimental and calculated data. The largest deviation, occurring for the effect of aluminium on the vanadium determination, does not exceed 2% of the actual vanadium concentration, whereas the uncorrected interferent effect amounts to about 38%. A similar situation occurs for all other analyte–interferent pairs investigated. The coefficients characterizing these pairs are listed in Table 2. Their quality is described by the correlation coefficients given in the last column, referring to the fitting of equation (6) to the experimental data. All examples mentioned indicate that equation (6) well describes various types of interferent effects occurring in flame atomic-absorption spectrometry, and caused by individual interferents.

Figure 9 shows the description of the multi-interferent effect of four components by equation (8). In order to enable its presentation in a two-dimensional plot the concentrations of all interferents are equal (value represented by the abscissa) for each data point. The agreement between the calculated

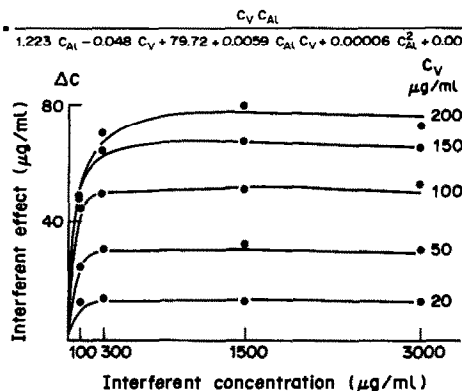


Fig. 8. Effect of aluminium on the determination of vanadium.

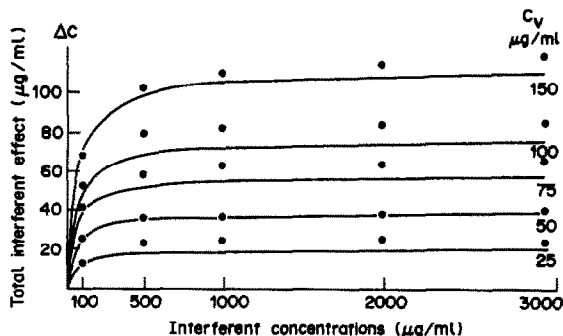


Fig. 9. Total effect of lanthanum, magnesium, chromium and aluminium on the determination of vanadium.

and experimental data is satisfactory. The maximal deviation does not exceed 10% of the actual analyte concentration, whereas the total uncorrected interferent effect is about 80%.

The comparison of corrected and uncorrected results of multicomponent analysis for some systems is shown in Table 3. All corrected results can be accepted as satisfactory, even for such large interferent effects as for molybdenum in sample 2 or strontium in sample 3.

CONCLUSIONS

The experimental results have confirmed the assumption that, excluding some particularly complicated cases, the various types of individual interferent effects may be described by the general equation (6). The coefficients in this equation, estimated on an experimental basis, may be used as the coefficients quantitatively characterizing the effects observed for individual analyte–interferent pairs. They also enable computation of the effects of complex multi-interferent systems, by application of equation (8).

The values of the characteristic coefficients are valid only for the analytical conditions and atomization parameters with which they were established. They are, however, insensitive to small changes in these parameters and are constant over long time intervals. Under normal laboratory conditions they should be checked every few months.

Table 3. Multicomponent analysis; comparison of actual ( $C_A$ ), uncorrected determined ( $C_{AP}$ ) and corrected determined ( $C_C$ ) values of concentrations

Sample composition	Concentration, µg/ml		
	$C_A$	$C_{AP}$	$C_C$
Ca	3.0	3.4	2.9
Mg	3.5	3.5	3.5
Na	3.5	4.0	3.3
Pt	200	183	201
Mo	50	71	52
Ni	20	20	20
Sr	50	16	51
V	100	108	100
Rh	40	48	39
Pt	200	109	200

The proposed approach allows computational correction for the interferences occurring in atomic-absorption analysis. It requires the estimation of a set of characteristic coefficients, and the concentration of all active interferences present in the sample. Since these operations are time-consuming, the most reasonable application of the approach is to analysis of large series of samples of the same type, particularly for multicomponent analysis, when all interfering components are determined.

When a laboratory has collected a large set of coefficients for many analyte-interferent pairs, it is able to estimate *a priori* on the basis the magnitude of the expected interference effect for a new sample, the composition of which is approximately known.

## REFERENCES

1. J. Swietoslawska, *Chem. Anal. Warsaw*, 1971, **15**, 337.
2. H. Kaiser, *Z. Anal. Chem.*, 1972, **260**, 252.
3. L. Pszonicki, *Talanta*, 1977, **24**, 613.
4. A. Parczewski and A. Rokosz, *Chem. Anal. Warsaw*, 1978, **23**, 225.
5. D. D. McCracken, *A Guide to Fortran IV Programming*, Wiley, New York, 1970.
6. H. J. Bartsch, *Mathematische Formeln*, VEB Fachbuchverlag, Leipzig, 1976.
7. P. C. Jurs, *Anal. Chem.*, 1970, **42**, 747.
8. R. M. Draper and H. Smith, *Applied Regression Analysis*, Wiley, New York, 1973.
9. D. M. Himmelblau, *Process Analysis by Statistical Methods*, Wiley, New York, 1970.

# DETERMINATION OF TWO METALS FROM A SINGLE POTENTIOMETRIC TITRATION CURVE

## THE APPLICATION OF TWO INDICATOR ELECTRODES

A. PARCZEWSKI

Department of Analytical Chemistry, Jagiellonian University, Kraków, Poland

(Received 14 August 1987. Revised 15 October 1987. Accepted 8 December 1987)

**Summary**—The advantages of applying two indicator electrodes in complexometric potentiometric multicomponent titration are shown by means of simulated titration curves. Two measurement arrangements have been considered, one in which the indicator electrodes are directly connected to a voltmeter and the other in which the electrodes are connected to the voltmeter through a summing operational amplifier. They have been compared with the conventional arrangement of a single indicator electrode and a reference electrode. The influence of the stability constants of the complexes in solution and of the electrode parameters on the shape of titration curves has been examined. It is shown that the use of two indicator electrodes may significantly increase the applicability of multicomponent potentiometric titrations.

Multicomponent titration, in which the analytes are determined from a single titration curve, seems to be a very attractive analytical method which can easily be computerized and automated. Multicomponent titration methods appear especially useful in routine analysis and the development of these techniques is therefore worthy of more attention. The development of multicomponent procedures for routine analysis has to be preceded by theoretical and practical examinations, including optimization of the experimental conditions.

Complexometric titration appears to be a useful method which can be applied both for moderate (mg) and low ( $\mu\text{g}$ ) amounts of metals in solution. Various methods of end-point detection have been applied in complexometric multicomponent (usually two-component) titrations, e.g., potentiometric, amperometric, and photometric. The experimental and theoretical examination of potentiometric titrations has so far been concerned with the conventional measuring arrangement with a single indicating electrode.<sup>1-4</sup> However, data concerning the influence of electrode parameters on the titration curve are scarce. The use of ion-selective electrodes as "mutual reference electrodes" in potentiometry has been suggested.<sup>5</sup>

In the present paper, various arrangements of electrodes for potentiometric titrations are considered: the conventional ones in which indicator and reference electrodes or two different indicator electrodes are connected directly to the voltmeter, and an unconventional one in which a pair of different indicator electrodes and a third (here, a reference) electrode, are connected to the voltmeter through an

electronic summing operational amplifier.<sup>6</sup> The following factors affecting the titration have been considered in the present investigations: solution equilibria (stability constants of the complexes that the titrant complexone forms with the metals), electrode parameters (response slope, selectivity coefficients, detection limits), and summing operational amplifier parameters (weights of electrode signals contributing to the amplifier output). The influence of these factors on the shapes of titration curves has been examined by computer-simulation based on the physico-chemical model of the titration process. The advantages of using the summing operational amplifier are discussed.

### METHOD

#### Assumptions

(a) Complexone ligands,  $Y$ , form 1:1 complexes with the metal ions,  $M_j$ ;  $j = 1, \dots, N$ , where  $N$  is the number of metal ions considered:



where  $K_j$  is the appropriate conditional stability constant.<sup>3</sup>

(b) The potential of an indicator electrode is described by the Nernst equation. For the membrane electrode, the Nikolskii equation is applicable:<sup>3,7</sup>

$$E_i = E_i^0 \pm S \log([M_i] + \sum k_{i,j} [M_j]^{r_{i,j}} + L_i) \quad (2)$$

where:  $E_i^0$ ,  $S$ ,  $K_{i,j}$ , and  $L_i$  respectively denote a constant, the slope factor of the electrode response, the conditional selectivity coefficient, and the limit of detection.<sup>3</sup> (For the sake of simplicity  $L_i$  was assumed to be constant: selectivity coefficients and detection limits in real analytical systems<sup>8,9</sup> may show some variation.) The exponent  $r_{i,j} = z_i/z_j$ ;  $z_i$  and  $z_j$  are the charges of the metal ions  $i$  and  $j$ , respectively.

(c) Equilibrium is achieved during the titration (kinetic effects are negligible).

(d) The effect of dilution may be neglected.

### Model

The following formula can be derived from assumptions (a), (c) and (d):

$$F = \frac{vC_T}{V_0} = C - \sum_{j=1}^N [M_j] + \frac{C_1 - [M_1]}{K_1[M_1]} \quad (3)$$

where

$$[M_j] = \frac{C_j}{\left(\frac{C_1}{M_1} - 1\right) \frac{K_j}{K_1} + 1} \quad \text{and} \quad C = \sum_{j=1}^N C_j$$

where  $F$  is the total concentration of complexone titrant in the sample solution (titration parameter multiplied by  $C$ ),  $C_j$  is the total concentration of metal  $J$ ,  $C_T$  denotes the concentration of the titrant solution, and  $v$  and  $V_0$  denote the volume of titrant added and the volume of sample solution before titration, respectively. In this paper only two-component systems are considered, *i.e.*,  $N = 2$ .

### Electrode sets

**Set A.** A conventional system in which a single indicator electrode and a reference electrode are connected directly to the voltmeter. The potential difference between the electrodes is measured during the titration:

$$E = E_I - E_R \quad (I = 1 \text{ or } 2) \quad (4)$$

where  $E_R$  is the potential of the reference electrode.

**Set B.** A pair of indicator electrodes is connected directly to the voltmeter and

$$E = E_1 - E_2 \quad (5)$$

**Set C.** An unconventional system in which a pair of indicator electrodes and the reference electrode are connected to the voltmeter through the electronic summing operational amplifier described elsewhere.<sup>6</sup> A simplified circuit is presented in Fig. 1. (N.B. resistances R1, R2 and RF correspond to R5, R6 and R7 respectively, in the previous description.<sup>6</sup>) In this case the weighted sum of the potentials of the indicator electrodes is measured during the titration:

$$E = W_1 E_1 + W_2 E_2 + \text{constant} \quad (6)$$

In practice the weights  $W_1$  and  $W_2$  can be selected by appropriate adjustment of the resistances R1 and R2 (Fig. 1):  $W_1 \approx RF/R1$ ,  $W_2 \approx RF/R2$ . In this way the ratio of the potential jumps at the end-points in the titration curve can be adjusted so as to "improve" the shape of the curve.

### Calculations

The titration curves shown in Figs. 2–6 were calculated as follows. The constant parameters  $K_1$ ,  $K_2$ ,  $C_1$ ,  $C_2$ ,  $C_T$ ,  $V_0$ ,  $E_1^0$ ,  $E_2^0$ ,  $S_1$ ,  $S_2$ ,  $k_{1,2}$ ,  $k_{2,1}$ ,  $L_1$ ,  $L_2$ ,  $r_{1,2}$  and  $r_{2,1}$  corresponding to the curve under consideration were inserted into equa-

tions (2) and (3). Next, concentration  $M_2$ , and electrode potential,  $E_I$  [equation (2)], and the titrant volume,  $v$  [equation (3)] were calculated for successive given values of  $[M_1]$ , decreasing in geometric progression starting at  $[M_1] = C_1$ . The calculations were performed on an AM-STRAD 6128 microcomputer, and the curves were printed with a Schneider DMP2000 matrix printer.

### RESULTS

The influence of various factors on the shapes of the titration curves is shown in Figs. 2–6 for the electrode sets A, B and C (see above). To facilitate comparison of the simulated curves the scales of the ordinates (potential change) have been made the same. However, the origin of the ordinate has been selected arbitrarily ( $E_1^0$  and  $E_2^0$  in equation (2) are given arbitrary values). In all cases,  $C_1 = C_2 = 0.0001M$ ,  $C_T = 0.01M$ , and  $V_0 = 20$  ml. The equivalence points have been marked at the top and bottom of each set of curves.

### DISCUSSION

It should be borne in mind that the model assumed in this paper describes real analytical systems only approximately, and its adequacy depends on the nature and concentration of the sample solution components and on the kind of electrodes used. Nevertheless, the selected curves presented in Figs. 2–6 give a general idea of how the experimental parameters influence two-component potentiometric titrations in which single or dual indicator electrodes are applied. Some additional information will be given in the discussion below. For the sake of convenience the metal which forms the stronger complex with the titrant ligand is termed the "first" metal, and the corresponding end-point and electrode are also labelled "first".

It is seen from Fig. 2 that for "ideal" electrodes, which are specific ( $k_{I,J} = 0$ ) and unaffected by the detection limit (*i.e.*,  $L_I = 0$ ), there is no evident advantage of the two-electrode measuring systems (B and C) over the conventional one (A). Actually, for  $S_1 = S_2$  it is not possible to determine the second metal (sum of metal content) with set B, because the changes in potential of the two electrodes are in the same direction and cancel each other, at least partially. For  $S_1 < S_2$ , at the second end-point the potential change of the second electrode exceeds that of the first, the result being a U-shaped curve, as mentioned elsewhere.<sup>6</sup> If  $K_1 = K_2$  (not shown in Fig. 2) then only the sum of both metals can be determined (not the individual metals); with set B and  $S_1 = S_2$  (and  $k_{1,2} = k_{2,1}$ ,  $L_1 = L_2$ ) even the sum of the metals content cannot be found. The cases presented in Figs. 3–6, which refer to realistic situations ( $K_{I,J} \neq 0$ ,  $L_I \neq 0$ ), are much more interesting. Figure 3 shows that, if  $L_1$  exceeds a limiting value that depends on other experimental factors, set A is useless in two-component potentiometric titration. Two-electrode sets have advantages in such cases, set C being the

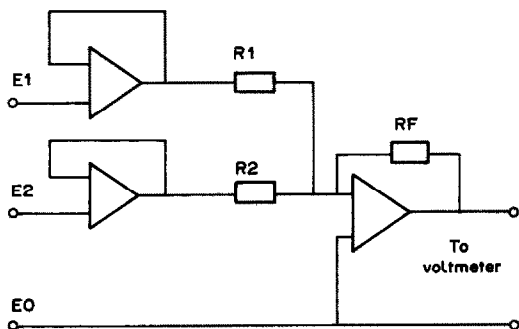


Fig. 1. Summing operational amplifier used to obtain weighted sum of potentials. E0, E1 and E2 denote inputs for the electrodes (E0 is the input for the reference electrode); R1, R2 and RF are resistances.

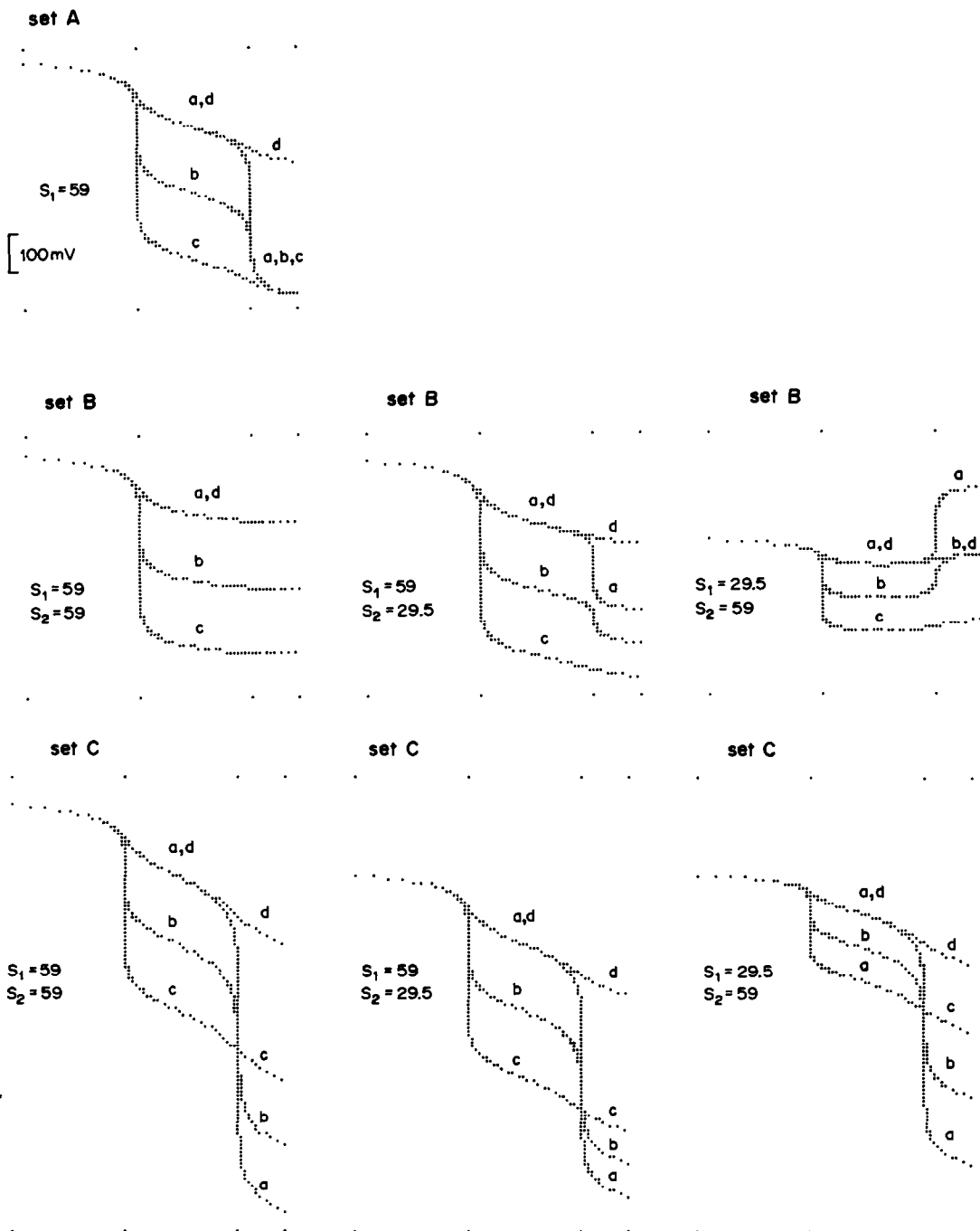


Fig. 2. Influence of the stability constants,  $K_1$ ,  $K_2$ , and slope factors,  $S_1$ ,  $S_2$ , on the shape of the titration curves. The curves correspond to the following  $\log K_1$  and  $\log K_2$  values: a: 15 and 12, b: 15 and 9, c: 15 and 6, d: 9 and 6.  $S_1$  and  $S_2$  are given in mV. In all cases  $L_1 = L_2 = k_{1,2} = k_{2,1} = 0$  [see equation (2)], and  $W_1 = W_2 = 1$  [see equation (6)].

more reliable (for some  $L_1$  and  $L_2$  values set B may also be useless). For  $L_1 \neq 0$  (but greater than a limiting value) set B also leads to U-shaped curves for  $S_1 > S_2$ . The reason is that at the detection limit  $L_1$ , the potential of the first electrode will scarcely change, so the potential changes of the second electrode predominate. It is worthwhile keeping in mind that in the model [see equations (1) and (2)] the

detection limits  $L_1$  and  $L_2$  may include the influence of solution components (other than the analytes) which affect the electrode potential but are not bound by the titrant, *i.e.*, their concentration does not change during the titration.  $L_1$  and  $L_2$  may then assume relatively high values in specific instances of analytical samples.

In Fig. 4 the mutual influence of  $L_1$  and  $L_2$  on the



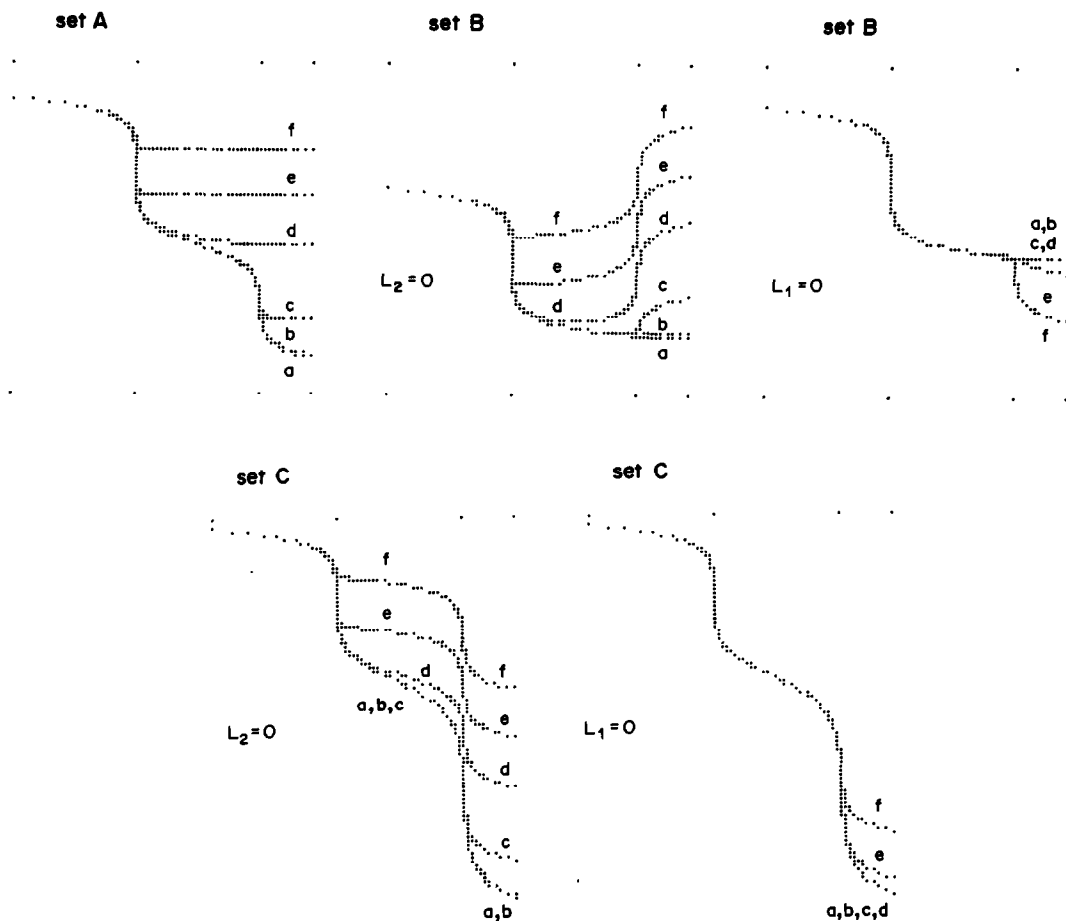


Fig. 3. Influence of the detection limits,  $L_1$ ,  $L_2$ , on the shape of the titration curves. In all cases  $\log K_1 = 15$ ,  $\log K_2 = 9$ ,  $S_1 = S_2 = 59$ , and  $k_{1,2} = k_{2,1} = 0$ . The curves correspond to the following values of  $L_1$  or  $L_2$ : a: 0, b:  $10^{-15} M$ , c:  $10^{-13} M$ , d:  $10^{-10} M$ , e:  $10^{-8} M$ , f:  $10^{-6} M$ .

titration curves is presented for sets B and C. The shape of the titration curve is very sensitive to these parameters for set B (the same "strange" shapes can also be obtained for other values of  $L_2$ ). For set C the curve corresponding to  $L_1 = L_2 = 10^{-15}$  is not

presented; it overlaps curve b up to the second end-point, but the potential jump at this point is much greater. It is evident that a titration curve obtained for  $L_1 \neq 0$  and  $L_2 \neq 0$  is not a simple superposition of the corresponding curves in Fig. 3.

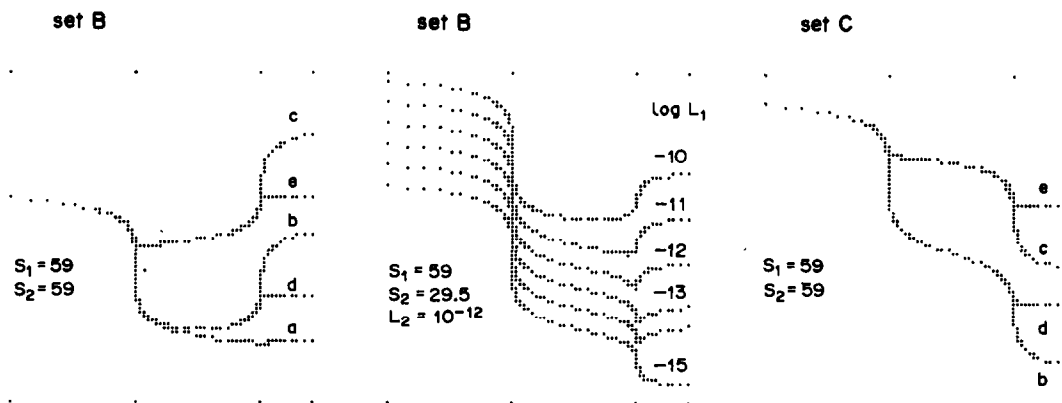


Fig. 4. Mutual influence of the detection limits  $L_1$  and  $L_2$  on the shape of the titration curves. In all cases  $\log K_1 = 15$ ,  $\log K_2 = 9$ ,  $k_{1,2} = k_{2,1} = 0$ . The curves presented in the left- and right-hand sets correspond to the following  $\log L_1$  and  $\log L_2$  values: a: -15 and -15, b: -10 and -10, c: -6 and -10, d: -10 and -6, e: -6 and -6.

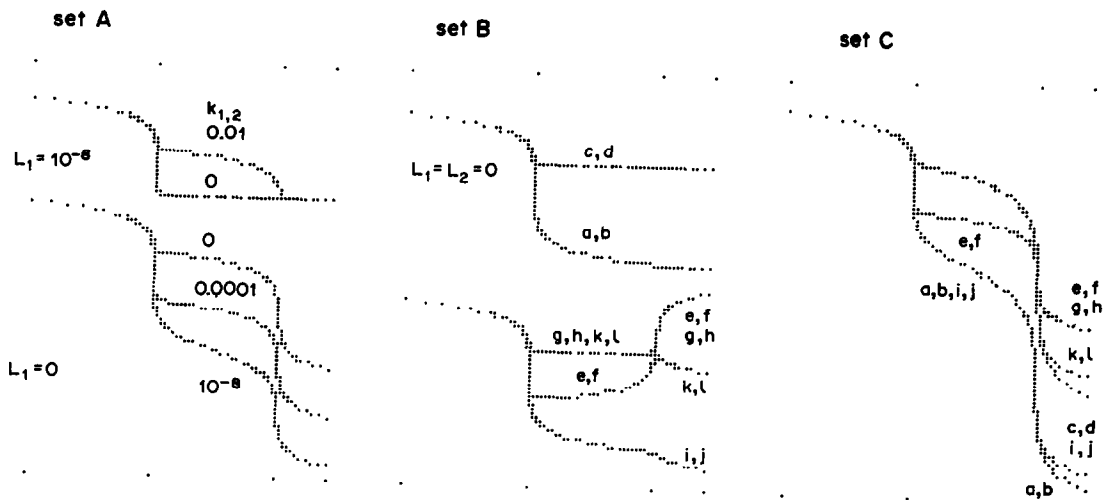


Fig. 5. Influence of selectivity coefficients,  $k_{i,j}$ , on the shape of the titration curves. In all cases  $\log K_1 = 15$ ,  $\log K_2 = 9$ ,  $S_1 = S_2 = 59$ . The curves correspond to the following values of  $k_{1,2}$  and  $k_{2,1}$ : a,e,i: 0 and 0; b,f,j: 0 and 0.01, c,g,k: 0.01 and 0; d,h,l: 0.01 and 0.01. Moreover, curves a,b,c,d correspond to  $L_1 = L_2 = 0$ ; e,f,g,h to  $L_1 = 10^{-6} M$  and  $L_2 = 0$ ; i,j,k,l to  $L_1 = 0$  and  $L_2 = 10^{-8} M$ . In the case of set A the curves are explained in the figure.

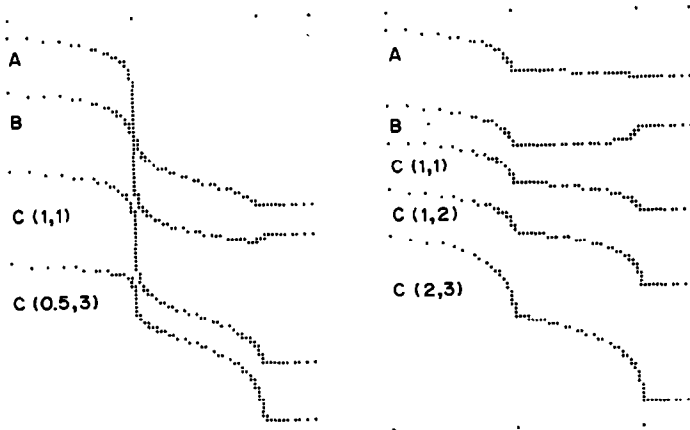


Fig. 6. Comparison of the titration curves obtained with sets A, B and C. For set C the weights  $W_1, W_2$  [see equation (6)] are given in parenthesis. In both examples  $\log K_1 = 15$ ,  $\log K_2 = 9$ ,  $S_1 = 59$ ,  $S_2 = 29.5$ . The first example (left) corresponds to  $k_{1,2} = k_{2,1} = 0$ ,  $L_1 = 10^{-11} M$ ,  $L_2 = 10^{-6} M$ , and the second example (right) to  $k_{1,2} = 0.0001$ ,  $k_{2,1} = 0.01$ ,  $L_1 = L_2 = 10^{-6} M$ .

Figure 5 shows the influence of the selectivity coefficients,  $k_{i,j}$ , on the shape of titration curves at various levels of  $L_1$  and  $L_2$ . It is seen that for  $k_{i,j} \neq 0$  an electrode with a relatively high  $L_1$  value may be useful for two-component titration even with set A. Finally, in Fig. 6 two examples which illustrate the advantages of two-electrode set C are presented, showing how the shape of the curves can be adjusted in order to obtain comparable potential jumps at the two end-points. It can also be proved that, in all cases, the higher the metal and titrant concentrations, the more pronounced are the potential jumps at the end-points. This obvious fact is not illustrated.

The experimental data for complexometric titration of Fe(III) and Cu(II) with use of sets A, B and

C have been presented elsewhere.<sup>6</sup> Platinum and copper ion-selective electrodes were applied in that case. [Actually the Pt electrode responds to the Fe(III)/Fe(II) concentration ratio, but the curves obtained resemble those presented above<sup>6,10</sup> The use of Pt electrodes in sets A, B and C will be considered separately.] Some further information relating to the theoretical considerations in this paper can now be added. With the arrangement B, in which, apart from the Pt electrode, copper-selective electrodes of different origin (Orion, Crytur, Aquaion, Reflex) were successively used, U-shaped titration curves were obtained, including those of the "strange" shape shown in Fig. 4. It was also proved that different pretreatments of the membrane surface can lead to

quite significant changes in the shapes of titration curves obtained with set *B*. The titration curves obtained with set *C* appeared to be much less sensitive to these changes in experimental conditions.

#### CONCLUSIONS

The discussion above shows that two-electrode measuring sets may significantly increase the scope of multi-component potentiometric titrations. Set *C* is especially useful, because the resultant curves are less sensitive to changes in electrode parameters than is set *B*. It is also more reliable than set *B*, which may give only a very small jump or none at all at the second end-point (see Figs. 2–6). Moreover, set *C* makes it possible to adjust the potential jumps at the end-points. In practice the best way is to have all possibilities at hand, and this is easily attainable as the additional equipment for set *C* is simple and cheap.<sup>6</sup> The arrangement may also be developed to make it still more flexible and useful, especially in

conjunction with other procedural modifications, including the application of compound titrants.<sup>10</sup>

*Acknowledgement*—The investigations were supported financially within the scope of project CPBP 01.17.

#### REFERENCES

1. U. Hannema and G. den Boef, *Anal. Chim. Acta*, 1967, **39**, 167.
2. *Idem*, *ibid.*, 1967, **39**, 479.
3. J. M. van der Meer, G. den Boef and W. E. van der Linden, *ibid.*, 1975, **76**, 261.
4. T. F. Christiansen, J. E. Busch and S. C. Krogh, *Anal. Chem.*, 1976, **48**, 1051.
5. Zeng Binli, *Zhongnan Kuangye Xueyuan Xuebao*, 1982, **3**, 89, *Chem. Abstr.*, 1983, **98**, 154446k.
6. A. Parczewski, *Talanta*, 1987, **34**, 586.
7. A. Hulanicki, *Chem. Anal. (Warsaw)*, 1972, **17**, 217.
8. P. Kivalo, R. Virtanen, K. Wickström, M. Wilson, E. Pungor, K. Tóth and G. Sundholm, *Anal. Chim. Acta*, 1976, **87**, 387.
9. P. Kivalo, R. Virtanen, K. Wickström, M. Wilson, E. Pungor, G. Horvai and K. Tóth, *ibid.*, 1976, **87**, 401.
10. A. Parczewski, submitted to *Analisis* (also presented at EUROANALYSIS VI, Paris, 6–12 September 1987).

## INFLUENCE OF CARBON DIOXIDE IN THE DETERMINATION OF OXYGEN IN COPPER BY REDUCTION FUSION

LI MANLING, TANG MEIER and SUN ZHENGCAI

Shanghai Electrical Apparatus Research Institute, Ministry of Machine Building Industry,  
Shanghai, China

WU LINGYE, TANG SUNMING and WANG GUOWEI

Shanghai Research Institute of Materials, Ministry of Machine Building Industry, Shanghai, China

HE HUANNAN, YAN RONGHUA, ZHAO GUNADI and LU QINGREN

Shanghai Institute of Metallurgy, Academy of Sciences of China, Shanghai, China

(Received 20 June 1987. Revised 4 November 1987. Accepted 21 November 1987)

**Summary**—It has been reported that copper melted in a graphite crucible at high temperature will give off its oxygen content mainly as CO and partially as CO<sub>2</sub>. Thus if oxygen in copper is determined by means of apparatus designed to measure only CO as the reaction product, the results are obviously liable to error. Methods of suppressing formation of CO<sub>2</sub> during the fusion process are proposed. When the oxygen is determined by gas chromatography, formation of CO<sub>2</sub> can be suppressed by adding a 0.5% Si-1.5% Ni-Cu bath-alloy together with the copper sample or by inserting a spectrographically pure carbon rod into the graphite crucible used for the fusion. When the oxygen is determined by coulometry, formation of CO<sub>2</sub> can be suppressed by the addition of the Si-Ni-Cu bath-alloy or by appropriate modification of the graphite crucible to obtain an optimum working temperature. The results obtained by either method are in agreement with those obtained by a modified vacuum fusion method in which CO and CO<sub>2</sub> can both be measured. These methods have been validated by analysis of two standard reference materials.

The oxygen content of copper has a significant effect on its electrical conductivity and mechanical properties<sup>1</sup> and must be kept at a reasonable level to guarantee a good quality of product. Therefore, it is necessary to determine the oxygen accurately. In the current methods used for metal analysis the oxygen content is always calculated on the assumption that it has been wholly converted into carbon monoxide during the fusion of the metal, either under vacuum or in an inert gas atmosphere, but this assumption cannot be applied to copper samples, because part of the oxygen in copper is converted into carbon dioxide.<sup>2,3</sup> Obviously this leads to an error in determinations made with instruments which measure only CO. To solve this problem, it is necessary to modify the method either by suppressing completely the formation of CO<sub>2</sub> or by providing some means of measuring both the CO and the CO<sub>2</sub> formed. The object of this study was to find some easy ways to suppress the formation of CO<sub>2</sub> and to ensure the complete conversion of oxygen in the sample into only CO.

To suppress the CO<sub>2</sub> formation, McLauchlan,<sup>4</sup> Kraft,<sup>5</sup> Kraft and Kahles,<sup>6,7</sup> Paessold<sup>8</sup> and Froberg<sup>9</sup> have added bath materials with strong oxygen affinity, such as cast aluminium and 0.5% Cr-15% Ni-Cu alloy, and Kraft and Kahles<sup>6,7</sup> also increased the size of the graphite crucible or used post-

reduction of the CO<sub>2</sub> in a furnace containing carbon granules heated to approximately 1200°.

Whether the oxygen is determined by gas chromatography, coulometry or manometric techniques, part of the oxygen content of the copper will be evolved as CO<sub>2</sub> when the sample is decomposed by fusion in a graphite crucible in an inert gas atmosphere or under vacuum.

We have investigated three different ways of suppressing the formation of CO<sub>2</sub> in the inert-gas fusion method: (1) by adding a bath-alloy, (2) by increasing the carbon contact surface, and (3) raising the working temperature of the fusion.

In the vacuum-fusion method, the CO and CO<sub>2</sub> evolved can both be measured, so there is no necessity to suppress the formation of CO<sub>2</sub>. However, appropriate modifications have been made to the vacuum-fusion method and it is now used as a check for the other two methods.

### EXPERIMENTAL

#### Sample preparation

Pieces of copper (0.5-2 g) with oxygen contents in the range 7.6-961 µg/g, were taken for the analyses. The individual pieces were etched in a mixture of 50 ml of phosphoric acid (s.g. = 1.7), 28 ml of acetic acid (>96%) and 22 ml of nitric acid (s.g. = 1.4), at room temperature for 1 min.<sup>10</sup> The BCR reference materials were etched first in

Table 1. Dimensions and surface areas of the graphite crucibles

Length, mm	Bore, mm	Wall thickness, mm	Surface area, cm <sup>2</sup>	Remarks
60	14	3	27.9	Used for the inert-gas fusion method and modified vacuum-fusion method
23	7	1.4	5.4	Used for the impulse heating coulometric method
23	7 ± 0.1	1.25 ± 0.05	5.4	Used for impulse heating in the "reduction within the crucible" method
23	10	1.4	8	Used for impulse-heating in the "bath-alloy" method

concentrated hydrochloric acid (s.g. = 1.2) at 20° for 3 min, and then in a mixture of equal volumes of nitric acid (s.g. = 1.4), acetic acid (>96%) and phosphoric acid (s.g. = 1.7) at 70° for 1 min. All samples were rinsed well with water, then methanol, and finally dried in a stream of warm air.<sup>11</sup>

#### Apparatus

Three types of instrument were used: (A) an inert-gas fusion/gas chromatograph,<sup>10</sup> (B) an MCS-805 impulse heating coulometric analyser,<sup>12</sup> (C) a vacuum-fusion apparatus.<sup>13</sup> The dimensions and surface areas of the graphite crucibles are given in Table 1.

#### Procedures

(A) *Gas chromatographic method.* Samples to be analysed are transferred from the storage desiccator to the sampling arm. The graphite crucible is set in the quartz furnace tube and thoroughly outgassed in a stream of purified helium (at 200 ml/min) at approximately 2100–2200° for about 3–4 hr. Then the temperature is lowered to 1600–1650° until the blank is reduced to less than 0.1 µg of oxygen per 5 min. The sample is dropped into the crucible and the helium line from the furnace is connected to the enrichment column (packed with silica gel, 20–40 mesh and cooled to –196°) for 5 min. The gas subsequently liberated from the column by heating is transferred in the helium stream at 40 ml/min into the analytical column (also 20–40 mesh silica gel) of the gas chromatograph (held at 70°). The amount of carbon dioxide is estimated from the chromatogram.

The procedure for the determination of CO was described earlier.<sup>10</sup>

(B) *Coulometric method.* The graphite crucible is outgassed by three heating cycles at a current of 700 A (at 8 V) for 45 sec, in a stream of purified argon flowing at 2 l./min. The current is then decreased to 660 A for 30 sec and the argon flow reduced to 160 ml/min. The blank is determined over a 3-min period. This process must be repeated until the blank is less than 10 µg of oxygen. The sample is heated at 660 A for 30 sec. The carbon monoxide extracted is oxidized with CuO to form CO<sub>2</sub> for measurement by coulometry.

(C) *Modified vacuum-fusion method.* The samples and the packed graphite crucible are installed in the same quartz

furnace tube as in procedure (A). The furnace is then slowly evacuated and the entire system continuously pumped until a high vacuum of 10<sup>-5</sup> mmHg is attained. A high-frequency field is applied and the temperature in the crucible is gradually raised to 2100–2200°. The out-gassing takes about 2–3 hr. The temperature is then lowered to the operating level of 1400–1450° to yield a low and stable blank (<0.5 ppm). One extraction takes about 7–10 min. After the total gas pressure  $P_1$ , in the known volume of the analytical system, has been measured on the McLeod gauge, the liquid nitrogen bath is placed around the trap for about 2 min to freeze out the carbon dioxide, and the pressure  $P_2$  is measured. The quantity of CO<sub>2</sub> removed ( $P_{CO_2}$ ), can readily be calculated from the pressure difference  $P_1 - P_2$ . The gas mixture is then passed through a heated column of CuO, the CO<sub>2</sub> and H<sub>2</sub>O produced (H<sub>2</sub>O from H<sub>2</sub> from the copper) are frozen out in a liquid-nitrogen trap, and the inert gas is pumped off. The liquid-nitrogen bath is replaced by a dry-ice/acetone bath, and the CO<sub>2</sub> evolved is measured manometrically, and is equivalent to the CO produced from the sample. The oxygen content can then be calculated.

## RESULTS AND DISCUSSION

### Amounts of CO<sub>2</sub> produced

In the reducing fusion procedure, the amount of CO<sub>2</sub> accompanying the CO is a function of contact time, temperature and surface area of the crucible, *i.e.*, it depends on the analytical conditions and instrument used. The yields of CO<sub>2</sub> obtained under various analytical conditions with different instruments are summarized in Table 2. It can be seen that the higher the oxygen content the more CO<sub>2</sub> is evolved in all three instruments.

### Addition of bath-alloy

The following bath-alloys were tested for their efficiency in eliminating formation of CO<sub>2</sub>: (1) 1% Mn–Cu, (2) 0.5% Si–0.5% Cr–15% Ni–Cu, (3) 0.5%

Table 2. Amount of oxygen (µg per g of sample) evolved as CO<sub>2</sub> from the sample

No.	Oxygen content of copper sample, µg/g	Sample weight, g	Oxygen evolved, µg/g		
			Inert-gas fusion/gas chromatography apparatus	Impulse heating coulometric apparatus*	Vacuum-fusion apparatus
1	7.6	2	0	0	1–2
2	272	0.5	0–10	10–27	28–66
3	552	0.5	1–16	16–59	47–82
4	961	0.5	—	38–92	129–143

\*For samples containing below 30 µg/g oxygen the formation of CO<sub>2</sub> is negligible.

Table 3. Amount of oxygen evolved as CO<sub>2</sub> from samples treated with 0.5% Si-1.5% Ni-Cu bath alloy

No.	Analytical conditions	Oxygen content of copper sample, $\mu\text{g/g}$	Sample weight, g	Cu/bath-alloy w/w ratio	Oxygen evolved, $\mu\text{g/g}$
1	Inductive-heating, inert-gas fusion at 1600-1650° for 8-10 min	552	0.5	1:4	0
				1:5	0
		327	0.5	1:3	0
2	Impulse heating, inert-gas fusion at 800 A for 30 sec	272	0.5	1:2	0
		552	0.5	2:1	20 ~ 58
				1:2	4-14
				1:3	0

Table 4. Amount of oxygen ( $\mu\text{g}$  per g of sample) extracted as CO<sub>2</sub> from copper in the inert-gas fusion/gas chromatography apparatus with different carbon surface areas

Oxygen content of copper sample, $\mu\text{g/g}$	Oxygen extracted, $\mu\text{g/g}$			
	Carbon powder (2 g, 10-20 mesh), 1700-1750°	Carbon powder (2 g, 10-20 mesh) + Cu, 14 g 1700-1750°	Carbon granules, 5 x 6 mm, 6 grains 1700-1750°	Carbon rod, 6 x 15 mm 1600-1650°
552	10-16	7-8	<2	<1
272	1-9	0-1	<2	<1

Table 5. The efficiency of the carbon reactor

Carbon reactor temperature, °C	Amount of CO <sub>2</sub> injected, at NPT, ml	Volume of unreacted CO <sub>2</sub> , at NPT, ml
16	47.8	47.8
1200	47.8	24.7-29.7
1250	47.8	5.7-7.4
1300	47.8	0
1300	95.6	0
1300	239	0

Si-Cu, (4) 1% Si-Cu, (5) 0.5% Si-1.5% Ni-Cu, (6) 0.5% Si-1.5% Ni-Cu. All these alloys are of low oxygen content and have strong oxygen affinity, forming metal oxides which then yield CO with the graphite crucible. They are added to the graphite crucible together with the copper sample. The 0.5% Si-1.5% Ni-Cu alloy proved the best, as shown in Table 3.

#### Effect of increasing the carbon contact surface area

The use of carbon powder, carbon granules or a carbon rod to increase the contact surface area was tested. As shown in Table 4, once CO<sub>2</sub> is evolved from the sample, it comes into contact with the additional carbon surface, where it reacts to give CO through the reaction  $\text{CO}_2 + \text{C} = 2\text{CO}$ .

Table 4 shows that the best results will be obtained by inserting a carbon rod into the graphite crucible at 1600-1650° for 6 min.

Table 6. Yield of CO<sub>2</sub> as a function of temperature in the inert-gas fusion/gas chromatography apparatus

Fusion temperature, °C	CO <sub>2</sub> extracted (expressed as O, $\mu\text{g/g}$ )
1550-1600	1-16
1700-1750	1-7
1800-1850	0-3

The use of a carbon reactor was also tested as a means of suppressing CO<sub>2</sub> formation. The reactor consists of a fused-silica tube 8 mm in diameter and 620 mm long, filled with spectrographic carbon granules (10-20 mesh). It is inserted into a tube furnace in which the temperature of the 110-mm long heating zone can be raised to 1300°. One end of the silica tube is connected to the outlet from the impulse heating furnace and the other to the coulometric detector. Its efficiency was tested by connecting it to the detector, injecting known amounts of carbon dioxide into it, and measuring the amount escaping reduction. Table 5 shows the results.

Table 7. Effect of the design of crucibles

Oxygen content of copper sample, $\mu\text{g/g}$	Crucible type (see Fig. 1)	Heating current, A	CO <sub>2</sub> extracted (expressed as O, $\mu\text{g/g}$ )
552	U3	620	2-12
552	U3	780	0-13
552	H3	720	4-17
552	U2	660	2-18
552	U2	700	0-2
552	H2	660	0
552	H2	700	0
961	H2	660	0-0.5

Table 8. Comparison of results for use of modified methods (A) and (B) with suppression of CO<sub>2</sub> and of (C) without it, for determination of oxygen in copper

No.	Sample*	A			B			C
		Addition of bath-alloy	Increasing the carbon area	Raising the operating temperature	Addition of bath-alloy	Increasing the carbon area	Reduction within crucible	
1	C-deoxidized Cu No. 1	$\bar{X} = 559$ $n = 16$ $S = 15$			$\bar{X} = 545$ $n = 7$ $S = 7$	$\bar{X} = 548$ $n = 10$ $S = 4$	$\bar{X} = 559$ $n = 6$ $S = 11$	
2	Continuous cast Cu No. 1	$\bar{X} = 283$ $n = 7$ $S = 6$	$\bar{X} = 281$ $n = 29$ $S = 5$	$\bar{X} = 281$ $n = 14$ $S = 9$		$\bar{X} = 278$ $n = 5$ $S = 3$	$\bar{X} = 277$ $n = 8$ $S = 6$	$\bar{X} = 285$ $n = 4$ $S = 4$
3	Continuous cast Cu No. 2	$\bar{X} = 327$ $n = 8$ $S = 8$	$\bar{X} = 331$ $n = 17$ $S = 8$	$\bar{X} = 331$ $n = 11$ $S = 6$		$\bar{X} = 327$ $n = 6$ $S = 5$	$\bar{X} = 326$ $n = 31$ $S = 10$	$\bar{X} = 322$ $n = 17$ $S = 10$
4	Electrolytic tough-pitch Cu BCR No. 22 (138 ± 7 µg/g)		137 139 140 140		139 138 139 142	141 141 142 145	137 142 138 135	140 140 140 144
5	Continuous cast Cu BCR No. 58 (390 ± 12 µg/g)		402 401 401 399		396 386 385 383	398 396 390 391	386 395 395 386	400 399 398 387
6	Cu wire ingot					964 948	$\bar{X} = 961$ $n = 9$ $S = 12$	958 962 985

\*Weight of sample taken, 0.5 g; all results expressed as µg of oxygen per g of copper;  $\bar{X}$  = average value;  $n$  = number of measurements;  $S$  = standard deviation.

The results show that passing the gases through a carbon reactor at 1300° can reduce all the carbon dioxide. The efficiency was checked with a sample containing 552 ppm of oxygen. No CO<sub>2</sub> was detected in the gaseous products from the reactor.

#### Effect of operating temperature

Thermodynamic data for the conversion of carbon monoxide into the dioxide indicate that the production of CO<sub>2</sub> should decrease as the temperature is increased. This is confirmed by the results shown in Table 6, for a sample containing 552 µg/g oxygen.

Another method for suppressing CO<sub>2</sub> formation, modification of the graphite crucible design in various ways, was also tested. The crucible is modified so that two temperature zones are obtained within the crucible. In the low temperature zone (at the bottom of the crucible), the copper sample is melted and its oxygen content is converted mainly into CO and partially into CO<sub>2</sub>. The gas mixture then passes through a high-temperature zone (in the middle of the crucible), where the CO<sub>2</sub> evolved is completely reduced to CO (hence we call this the "reduction within the crucible" method). Several designs have been tested and the results obtained are listed in Table 7.

It is evident from Table 7 that the best design for the crucible is a type H2 (Fig. 1), with which the formation of CO<sub>2</sub> in the fusion process can be completely eliminated. Since the use of the "reduction within the crucible" method is more convenient than the carbon reactor method, it is recommended for use in routine and referee analysis.

#### Validation

BCR reference materials and copper samples with different oxygen contents were analysed by the inert-

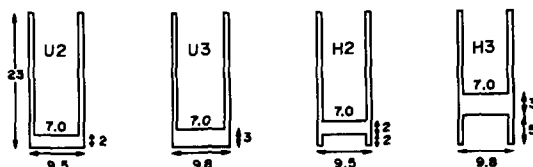


Fig. 1. Dimensions of crucibles for "reduction within crucible" method. Dimensions in mm. For wall thickness see Table 1.

gas fusion/gas-chromatography method (A), the impulse-heating coulometric method (B) and the modified vacuum-fusion method (C). The results obtained are shown in Table 8; the reproducibility is good.

#### REFERENCES

1. G. Kraft, *Eurisotop Office Information Booklet 59*, Eurisotop, Brussels, 1972.
2. M. G. Frohberg and H. Leygraf, *Balzer High Vacuum Report*, No. 8, 1967.
3. A. Colombo, *Anal. Chim. Acta*, 1976, **81**, 397.
4. E. J. McLauchlan, *Metall. Met. Form.*, 1975, **42**, No. 2, 32.
5. G. Kraft, *Analysis of Non-Metals in Metals*, p. 425. De Gruyter, Berlin, 1981.
6. G. Kraft and A. Kahles, *Erzmetall*, 1969, **22**, 429.
7. *Idem, ibid.*, 1976, **29**, 334.
8. G. Paessold, *Proc. Third Balzers Conference Liechtenstein*, 1967, 42.
9. M. G. Frohberg, *ibid.*, 1967, 41.
10. Li Manling, Sun Zhengcai, Ren Huizhen, Qi Genfu, Yan Yufen, Tang Meier, *Fenxi Huaxue*, 1983, **11**, 930.
11. J. Pauwels, *BCR-Rept.* EUR 6241, Comm. Europ. Communities, 1979.
12. Shen Jia Jun, Wu Lingye and Tang Sunming, *Physical Testing and Chemical Analysis*, 1983, **19**, No. 4, 44.
13. Li Xiuqi and He Huannan, *ibid.*, 1966, T32, 58.



## SHORT COMMUNICATIONS

# SPECTROPHOTOMETRIC DETERMINATION OF NICKEL IN COPPER-BASE ALLOY WITH 2-(2-THIAZOLYLAZO)-*p*-CRESOL

SERGIO LUIS COSTA FERREIRA

Department of Analytical Chemistry, Federal University of Bahia, Salvador, Bahia, Brazil

(Received 22 May 1986. Revised 10 June 1987. Accepted 23 October 1987)

**Summary**—A spectrophotometric method for determination of nickel in copper-base alloy with 2-(2-thiazolylozo)-*p*-cresol (TAC) is described. The interferences of foreign ions can be eliminated by masking with a mixture of sodium tartrate and sodium thiosulphate. The nickel-TAC complex has low solubility in water, but is soluble in aqueous ethanol. Beer's law is obeyed for 20–70  $\mu\text{g}$  of nickel in 50 ml of solution, at pH 5.7. The molar absorptivity at 580 nm is  $2.6 \times 10^4 \text{ l. mole}^{-1} \cdot \text{cm}^{-1}$ . The method has been applied successfully to determination of nickel in reference samples.

2-(2-Thiazolylozo)-*p*-cresol (TAC) forms coloured complexes with several metal ions but its use as a colorimetric reagent is limited. It was initially used for determination of copper by Gusev *et al.*<sup>1</sup> and Sommer *et al.*<sup>2</sup> Gusev *et al.* have also proposed use of TAC for determination of nickel in a uranium-base alloy, with chloroform extraction of the complex and absorbance measurement at 610 nm. The present work describes the use of TAC for colorimetric determination of nickel in copper-base alloys, but with use of an aqueous ethanol system.

### EXPERIMENTAL

#### Reagents

TAC solution, 0.1 g in 100 ml of ethanol. Standard nickel solutions: 25 mg/ml and 25  $\mu\text{g}$ /ml. Buffer solution, pH 5.9, prepared by mixing 1.0M sodium acetate and 1.0M acetic acid in appropriate ratios. Masking solution, consisting of 16.7 g of sodium thiosulphate pentahydrate and 0.15 g of sodium tartrate dissolved in 250 ml of distilled water.

#### General procedure

Into a 50-ml standard flask transfer a portion of sample solution containing up to 70  $\mu\text{g}$  of nickel. Add 10.0 ml of acetate buffer, 5.0 ml of ethanol, 5.0 ml of masking solution and 2.0 ml of TAC solution, dilute to the mark with water, mix, and after 10 min measure the absorbance at 580 nm in a 1-cm cell against a solution prepared in the same way but without the addition of TAC.

Prepare a calibration graph with appropriate standards.

### RESULTS AND DISCUSSION

The absorption maximum of the complex is at 580–600 nm and that of the reagent blank is at 350–380 nm; the spectra do not overlap. Maximal and constant absorbance is obtained for 50  $\mu\text{g}$  of nickel with 1.2 ml of 0.1% TAC solution per 50 ml, so 2.0 ml of TAC solution is selected as optimal. The absorbance is also maximal and constant with 2.0–10.0 ml of ethanol per 50 ml, so use of 5.0 ml is

recommended. The maximum allowable amount of masking reagent per 50 ml of solution was found to be 5.0 ml.

#### Characteristics of the nickel-TAC complex

The absorbance of the complex is pH-dependent, but constant in the range 5.7–6.0. Beer's law is obeyed at 580 nm for 20–70  $\mu\text{g}$  of nickel in 50 ml of solution, at pH 5.7, and the apparent molar absorptivity is  $2.6 \times 10^4 \text{ l. mole}^{-1} \cdot \text{cm}^{-1}$ .

The order of addition of the reactants does not influence formation of the complex. Complete colour development takes 10 min and the colour is then stable for at least 24 hr.

#### Interferences

The selectivity was investigated by determination of 25  $\mu\text{g}$  of nickel in presence of various amounts of other ions. Iron(II), iron(III) and cobalt(II) interfere.

The interference of copper(II), bismuth, tin(IV), manganese(II), cadmium, molybdenum(VI), lead and aluminium may be reduced somewhat by the masking solution; the tolerance limits are given in Table 1.

Table 1. Effect of foreign ions on determination of 25.1  $\mu\text{g}$  of Ni in presence of mixed masking reagents

Ion	Added, $\mu\text{g}$	Ion/Ni ratio, w/w	Ni found, $\mu\text{g}$	Error, $\mu\text{g}$
Al <sup>3+</sup>	376	15	24.5	-0.6
Mg <sup>2+</sup>	1063	43	25.3	+0.2
Ca <sup>2+</sup>	1873	75	25.6	+0.5
Cd <sup>2+</sup>	81	3	24.9	-0.2
Pd <sup>2+</sup>	307	12	25.7	+0.6
Cr <sup>3+</sup>	731	29	26.2	+1.1
Bi <sup>3+</sup>	387	15	25.2	+0.1
Mo(VI)	732	29	25.3	+0.2
Zn <sup>2+</sup>	101	4	25.4	+0.3
Cu <sup>2+</sup>	4516	181	25.4	+0.3

Table 2. Analysis of various samples

Sample	Nickel present, %	Nickel found, %
Cast Bronze NBS.52.C	0.76	0.77, 0.78, 0.78
Nickel-Copper Alloy NBS.162a	64.0	63.2, 63.3, 63.5
Copper-Nickel- Zinc-Alloy NBS.157	11.82	11.8, 11.9, 11.8
Bronze 239 CEPED standard	0.30	0.30, 0.30, 0.30

#### Determination of nickel in bronzes and brasses

Pipette into a 50-ml standard flask an aliquot of the sample solution, containing 20–70  $\mu\text{g}$  of nickel. Add 10.0 ml of pH 5.70 acetate buffer, 5.0 ml of ethanol,

5.0 ml of masking solution and 2.0 ml of TAC (0.1%) solution, dilute to the mark with water, mix, and after 10 min measure the absorbance at 580 nm in a 1-cm cell against a solution prepared in the same way but without the addition of TAC.

Results obtained by applying the proposed method to several standard samples agree well with the certified values (Table 2).

*Acknowledgement*—The author is greatly indebted to Professor Antonio Celso Spinola Costa, Federal University of Bahia, for many helpful discussions and suggestions during this study.

#### REFERENCES

1. S. I. Gusev, I. N. Glushkova and L. A. Ketova, *Uch. Zap. Perm. Gos. Univ.*, 1973, **289**, 255.
2. L. Sommer, M. Langová and V. Kubáň, *Collection Czech. Chem. Commun.*, 1976, **41**, 1317.
3. S. I. Gusev, M. V. Zhvakina, I. A. Kozhevnikova and L. S. Mal'tseva, *Zavodsk. Lab.*, 1976, **42**, 19.
4. E. B. Sandell, *Colorimetric Determination of Traces of Metals*, 3rd Ed., p. 83. Interscience, New York, 1959.

## HYDRALAZINE-SELECTIVE PVC MEMBRANE ELECTRODE BASED ON HYDRALAZINIUM TETRAPHENYLBORATE

S. S. BADAWY\*, A. F. SHOUKRY, M. S. RIZK and M. M. OMAR  
Department of Chemistry, Faculty of Science, Cairo University, Giza, Egypt

(Received 5 December 1986. Revised 27 April 1987. Accepted 22 January 1988)

**Summary**—A hydralazine ion-selective PVC membrane electrode based on hydralazinium tetraphenylborate has been prepared with dioctyl phthalate as plasticizer. The electrode showed linear response with a slope factor of 57.5 mV/concentration decade at 20° over the concentration range from  $4 \times 10^{-4}$  to  $10^{-1}M$  hydralazine. The effects, on the electrode performance, of membrane composition, pH of the test solution and the time of soaking were studied. The electrode exhibited good selectivity for hydralazine with respect to a large number of inorganic cations and organic substances of biological importance. The standard-addition method and potentiometric titrations were used to determine hydralazine concentrations in pure solutions and in a pharmaceutical preparation, with satisfactory results.

Ion-selective electrodes based on lipophilic salts of tetraphenylborate (TPB) with various organic cations of pharmaceutical importance have been investigated.<sup>1-5</sup> Hydralazine hydrochloride (HL.HCl; 1-hydrazinophthalazine hydrochloride) is an important pharmaceutical compound used as a vasodilator in the treatment of hypertension. Several methods for its determination have been reported, including fluorimetry,<sup>6</sup> HPLC,<sup>7,8</sup> polarography,<sup>9</sup> GLC<sup>10-13</sup> and spectrophotometry.<sup>14</sup> The low cost and ease of operation of potentiometric instrumentation make its use for the determination of HL a useful alternative. For these reasons we have investigated the performance characteristics of an HL-selective membrane electrode based on incorporation of hydralazinium-tetraphenylborate (HL-TPB) into a poly(vinyl chloride) (PVC) matrix and used this electrode for the determination of hydralazine in pure solutions and in pharmaceutical preparations such as Ser-Ap-Es antihypertension tablets, which contain hydralazine hydrochloride.

### EXPERIMENTAL

#### Reagents

All reagents were of the highest purity available. The TPB solution was standardized as previously described.<sup>15</sup> The HL-TPB was prepared by a method similar to that described previously.<sup>3</sup>

#### Membrane preparation

Four membranes were prepared in which the concentration of HL-TPB was varied in order to find the optimal composition. A selected amount (25, 50, 75 or 100 mg) of the salt was dissolved in a mixture of 15 ml of tetrahydrofuran (THF), 0.5 g of PVC and 0.5 g of dioctyl phthalate. The resulting solution was poured into a Petri dish (9.5 cm in diameter) and left at room temperature for the THF to evaporate. A transparent membrane about 0.2 mm in thickness was obtained, from which a disc of about

12 mm diameter was cut. The disc was glued to the polished end of a PVC tube by means of PVC solution in THF. The electrode body was then filled with 0.1M sodium chloride/0.001M HL as the internal solution.

#### Potential measurements

The electrochemical system was as follows: Ag,AgCl/internal filling solution/membrane/test solution/saturated KCl salt bridge/saturated calomel electrode. The potential was measured, at a constant temperature of 20°, with a Chemtrix type 62 digital pH/mV-meter, the test solution being continuously stirred.

#### Selectivity of the electrode

The selectivity coefficients were evaluated by the separate solutions method,<sup>4</sup> with  $10^{-3}M$  solutions of HL and the interferent.

#### Potentiometric determination of HL

Small increments of 0.1M HL were added to 100-ml samples of various concentrations. The change in emf was recorded after each addition and used to calculate the concentration of the HL sample solution.

For the analysis of HL formulations, 20 tablets were ground up and 140-250 mg portions of the powder were quantitatively transferred to 150-ml beakers containing 100 ml of distilled water. The mixture was stirred vigorously until dissolution seemed complete, and the standard-addition technique was applied as above.

#### Potentiometric titration of HL

An aliquot of solution containing 5-20 mg of HL was transferred to a 150-ml beaker and the volume made up to 100 ml with distilled water. This solution was titrated with  $5 \times 10^{-3}M$  standard NaTPB solution, the HL membrane electrode being used as the sensor.

For HL in Ser-Ap-Es tablets, 120-290 mg portions of the powdered tablets were transferred to 100-ml beakers containing 50 ml of water and titrated as above.

### RESULTS AND DISCUSSION

The response characteristics of the membranes investigated are summarized in Table 1 and the calibration graphs are given in Fig. 1. It is clear that electrode *b* was the best, giving a calibration plot with almost Nernstian slope over a relatively wide range of

\*Author to whom correspondence should be addressed.

Table 1. Composition and response characteristics of PVC-matrix membranes

Membrane	Ion-pair content, %	Potential response			
		Slope, mV/decade	Linear detection region, M	Response time, sec	Intercept at pHL = 0, mV
a	2.44	47.0	$8.0 \times 10^{-4}$ – $6.3 \times 10^{-2}$	10–20	140
b	4.76	57.5	$4.0 \times 10^{-4}$ – $1.0 \times 10^{-1}$	10–15	164
c	6.98	44.5	$4.0 \times 10^{-4}$ – $6.3 \times 10^{-2}$	10–15	163
d	9.09	44.0	$1.6 \times 10^{-3}$ – $5.0 \times 10^{-2}$	15–20	132

concentration and having a fast response. Electrode *b* was therefore used for all subsequent studies.

### Effect of pH

The effect of the pH of the test solution ( $10^{-2}M$  HL,  $0.1M$  NaCl) on the electrode potential was investigated by following the variation in emf with change in pH produced by the addition of very small volumes of  $0.01$ – $0.1M$  sodium hydroxide or hydrochloric acid. Figure 2 shows that the electrode can be used at pH 2.1–6.0 for HL determination. At pH < 2.1 the potential decreases, presumably because of formation of the diprotonated species. At pH > 6.0 the decrease in potential can be attributed to the conversion of  $HL^+$  into HL.

### Effect of soaking

Calibration graphs (pHL vs. *E*) were obtained by use of the electrode after it had been soaked in

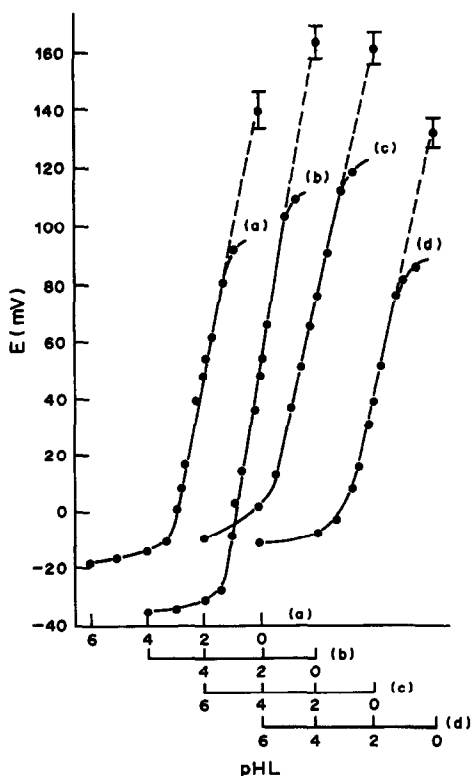
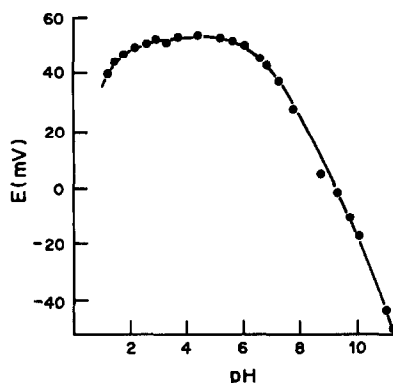


Fig. 1. Calibration plots of the HL electrodes.

Fig. 2. Effect of pH on the potential of electrode *b*.

$10^{-3}M$  HL for periods of 5 min, 0.5, 1.0, 1.5, 2.0, 3.0, 6.0 and 24 hr. The optimum soaking time was found to be 1–2 hr, the slopes of the calibration curves being 57.5–55.5 mV/pHL at  $20^\circ$ . Soaking for longer than 2 hr is not recommended and the electrode should be kept dry in an opaque closed vessel in a refrigerator when not in use.

### Selectivity

None of the species (J) investigated interfered (Table 2), as indicated by the very small values of  $K_{HL^+, J}^{pot}$ . The inorganic cations did not interfere because of differences in ionic size, mobility and permeability compared with  $HL^+$ . In the case of sugars, amino-acids and amines, the high selectivity is mainly attributed to their different polarity and lipophilic nature compared with hydralazine.

### Analytical applications

The electrode was used successfully for the determination of HL in pure solutions and in Ser-Ap-Es

Table 2. Selectivity coefficients for the hydralazine electrode

Interferent	$K_{HL^+, J}^{pot}$	Interferent	$K_{HL^+, J}^{pot}$
$NH_4^+$	$2.7 \times 10^{-2}$	phenylalanine	$1.0 \times 10^{-2}$
$Na^+$	$2.3 \times 10^{-2}$	$(Et)_3NH^+$	$5.5 \times 10^{-2}$
$K^+$	$3.5 \times 10^{-2}$	$(Et)_2NH_2^+$	$3.5 \times 10^{-1}$
$Ca^{2+}$	$7.9 \times 10^{-4}$	$(Me)_2NH_2^+$	$2.4 \times 10^{-1}$
$Mg^{2+}$	$8.5 \times 10^{-4}$	$(Me)_4N^+$	$4.3 \times 10^{-2}$
$Fe^{2+}$	$6.6 \times 10^{-3}$	lactose	$2.4 \times 10^{-2}$
$Fe^{3+}$	$4.8 \times 10^{-3}$	sucrose	$2.7 \times 10^{-2}$
glycine	$7.4 \times 10^{-3}$	maltose	$4.2 \times 10^{-2}$
alanine	$6.5 \times 10^{-3}$		

Table 3. Potentiometric determination of hydralazine

Solution	Standard-addition method			Potentiometric titration		
	Taken, mg	Mean recovery, %	Standard deviation, %	Taken, mg	Mean recovery, %	Standard deviation, %
Pure HL	9.83-29.79	99.6	1.5	5-20	98.9	0.9
Ser-Ap-Es*	12.03-21.49	101.1	2.4	10-25	98.0	1.0

\*Swisspharma-Cairo, under licence from Ciba-Geigy Ltd., Basle, Switzerland.

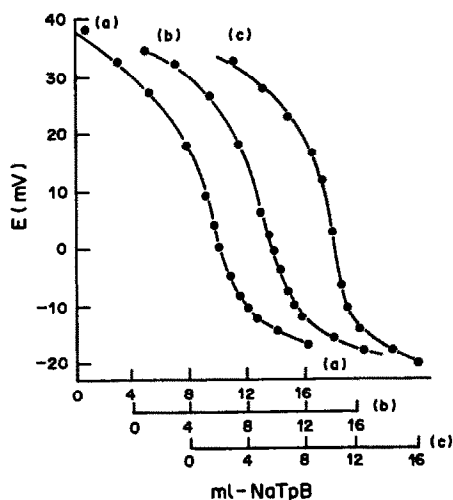


Fig. 3. Potentiometric titration of solutions containing powdered Ser-Ap-Es tablets (10 mg of HL) with  $5 \times 10^{-3} M$  NaTPB.

tablets by the standard-addition method and potentiometric titration (Table 3). Representative replicate titration curves are given in Fig. 3. The standard deviations and recoveries in Table 3 reveal the reasonably good precision and accuracy of the pro-

posed methods and indicate that the excipients in the Ser-Ap-Es tablets do not interfere.

*Acknowledgement*—Many thanks to Professor M. M. Khater of Cairo University for her kind interest in this work.

## REFERENCES

1. J. Anzai, C. Isomura and T. Osa, *Chem. Pharm. Bull.*, 1985, **33**, 236.
2. H. Chi and T. Zhou, *Yaoxue Xuebao*, 1983, **18**, 278.
3. S. S. Badawy, A. F. Shoukry and Y. M. Issa, *Analyst*, 1986, **111**, 1363.
4. V. V. Coşofreţ and R. P. Buck, *ibid.*, 1984, **109**, 1321.
5. S. Yao, G. Shen and H. Wu, *Yaowu Fenxi Zazhi*, 1984, **4**, 281.
6. N. D. Danielson and R. G. Bartolo, *Anal. Lett.*, 1983, **16**, 343.
7. T. M. Ludden, L. K. Goggin, J. L. McNay, K. D. Haegle and A. M. M. Shepherd, *J. Pharm. Sci.*, 1979, **68**, 1423.
8. G. R. Rao, S. Raghuvver, Y. P. Rao and K. R. Mohan, *Indian Drugs*, 1983, **20**, 285.
9. Z. Fijalek and E. Szyszko, *Acta Pol. Pharm.*, 1981, **38**, 439.
10. P. H. Degen, *J. Chromatog.*, 1979, **176**, 375.
11. W. J. Proveaux, J. P. O'Donnell and J. K. H. Ma, *ibid.*, 1979, **176**, 480.
12. K. M. Smith, R. N. Johnson and B. T. Kho, *ibid.*, 1977, **137**, 431.
13. K. D. Haegle, H. B. Skrdlant, N. W. Robie, D. Lalka and J. L. McNay, *ibid.*, 1976, **126**, 517.
14. M. C. Dutt, T. L. Ng and L. T. Long, *J. Assoc. Off. Anal. Chem.*, 1983, **66**, 1455.
15. T. K. Christopoulos, E. P. Diamandis and T. P. Hadjiannou, *Anal. Chim. Acta*, 1982, **143**, 143.

## IRON(II) TITRATION OF SOME METAL IONS, WITH OXAZINE DYES AS REDOX INDICATORS

K. VIJAYA RAJU\* and G. MADHU GAUTAM

Department of Engineering Chemistry, Andhra University, Waltair 530 003, India

(Received 2 December 1987. Accepted 21 January 1988)

**Summary**—The use of oxazine dyes as redox indicators in the determination of uranium(VI), copper(II), osmium(VIII), iridium(IV) and thallium(III) with iron(II) as redox titrant in phosphoric acid medium has been investigated. The determination of copper in brass and the analysis of the binary mixtures of U(VI) and U(IV), and of Tl(III) and Tl(I) with this reductant and these indicators have been studied.

Several metal ions, such as U(VI),<sup>1</sup> Mo(VI),<sup>2</sup> V(IV),<sup>3</sup> Tl(III),<sup>4</sup> Cu(II),<sup>5</sup> Sb(V),<sup>6</sup> As(V),<sup>7</sup> Os(VIII) and Ir(IV)<sup>8</sup> have been determined by titration with iron(II) in phosphoric acid medium. The only redox indicators so far employed in these titrations appear to be a few of the thiazine group of dyes<sup>1-10</sup> and cacotheline.<sup>9</sup> However, these methods are not free from drawbacks. Very recently the use of oxazine dyes as redox indicators in some of these determinations, e.g., of V(IV) and Mo(VI)<sup>11</sup> and Sb(V) and As(V)<sup>12</sup> has been reported from our laboratories. The present communication describes the use of six oxazine dyes as advantageous redox indicators in the determination of U(VI), Cu(II), Os(VIII), Ir(IV) and Tl(III) with iron(II) in phosphoric acid medium. The methods developed have been applied to analysis of brass for copper and for analysis of binary U(VI)-U(IV) and Tl(III)-Tl(I) mixtures.

### EXPERIMENTAL

#### Reagents

All solutions were prepared with distilled water and all chemicals were of analytical reagent grade unless otherwise stated.

Approximately 0.1M solutions of iron(II) ammonium sulphate hexahydrate and cerium(IV) sulphate were prepared and standardized,<sup>13,14</sup> and portions were further diluted to 0.01M and 0.04M respectively.

Solutions of 0.1M copper(II) sulphate,<sup>15</sup> 0.01M sodium hexachloroiridate(IV)<sup>16</sup> and 0.0025M osmic acid<sup>16</sup> were prepared<sup>8</sup> and standardized iodometrically.

Solutions of 0.05M and 0.1M uranium(VI) and 0.1M uranium(IV) (made by using a Jones reductor<sup>17</sup>) were prepared from uranyl acetate and standardized.<sup>18</sup> Solutions of thallium(III) 0.005M and 0.01M and 0.01M thallium(I) were prepared from laboratory grade thallium(I) carbonate as described earlier<sup>19</sup> and standardized.<sup>19</sup>

Aqueous solutions (0.1 g per 100 ml) of the dyes (Gurr & Co., England) Brilliant Cresyl Blue (BCB), Capri Blue (CPB), Gallocyanine (GC), Gallamine Blue (GB), Celestin Blue (CLB) and Sevron Blue 5G (SB 5G) (Colour Index Nos. 51010, 51015, 51030, 51045, 51050 and 51004 respectively) were prepared. Phosphoric acid of GR grade (Merck) was used.

#### General procedure

A known volume of metal ion solution (2-10 ml) was treated with enough orthophosphoric acid to give the required overall acidity near the equivalence point. After addition of 0.2-0.3 ml of indicator solution, the reaction mixture was titrated with 0.1M iron(II) [0.01M for Ir(IV), Os(VIII) and Tl(III)]; the solution was continuously stirred by means of a magnetic stirrer, and a carbon dioxide atmosphere was maintained throughout the titration to prevent aerial oxidation of iron(II) and the leuco dye. The colour change at the end-point is from green to pale yellow with BCB and CPB (the leuco bases are pale yellow)<sup>20</sup> and from pink to colourless with the rest of the dyes except in titration of Cu(II), where the appearance of a white-cream colour (with a light yellow tinge with BCB and CPB) marks the end-point. An indicator correction of 0.10 ml of iron(II) was applied in the titrations with 0.01M iron(II). The Os(VIII) solution was prepared with phosphoric acid cooled in ice-water, and titrated at 20-25°, because of risk of loss by volatilization<sup>8</sup> at the laboratory temperature ( $\geq 28^\circ$ ). In the determination of Cu(II), it was necessary for the reaction medium to be 0.005-0.01M in potassium thiocyanate<sup>5</sup> in addition to 9.0-10.5M in phosphoric acid, and it was best to add the indicator just before the equivalence point, as it is partly destroyed<sup>5</sup> if added at the beginning.

#### Brass analysis

Dissolve 0.5-1.0 g of sample in 15-25 ml of nitric acid (1 + 1), add 5-10 ml of concentrated sulphuric acid and then evaporate the mixture to fumes. Dilute to about 70 ml with water and filter off and wash any precipitate. Add a few ml of bromine water to the combined filtrate and washings and boil off the excess of bromine. Cool, dilute to volume in a 100-ml standard flask and analyse a fraction as already described.

#### Analysis of U(VI)-U(IV) or Tl(III)-Tl(I) mixtures

The total concentration of the metal ion should not exceed 0.06M for uranium and 0.006M for thallium when the solution is diluted to 50 ml. Titrate a 10-ml portion of the mixture with 0.1M iron(II) for U (0.01M for Tl), employing any of the six oxazine dyes as indicator, and the general procedure and reaction conditions of Table 1. This gives the content of U(VI) or Tl(III) present in the mixture. Titrate another 10 ml with cerium(IV) sulphate [0.1M for U(IV) and 0.04M for Tl(I)] as described by Rao<sup>21</sup> [3-4M hydrochloric acid and 1-1.5M phosphoric acid medium, with GC as indicator, for U(IV)] and as outlined by Sagi<sup>19</sup> [0.6-0.7M hydrochloric acid medium at 80-90° to the pale

yellow colour, for Tl(I) U(VI) or U(IV) in the range 0.12–0.60 g and Tl(III) or Tl(I) in the range 10–50 mg (in a total volume of 50 ml) have been determined with an error of  $\pm 0.6\%$ , with the six oxazine dyes as indicators.

### RESULTS AND DISCUSSION

Table 1 gives the titration conditions, range of metal ion determined, and the conditional redox potentials of the couples concerned.<sup>1,5,8,22</sup> The colour transitions of the indicators are sharp and reversible at the equivalence point, which corresponds to the complete reduction of U(VI), Cu(II), Os(VIII), Ir(IV) and Tl(III) to U(IV), Cu(I), Os(IV), Ir(III) and Tl(I) respectively, the indicators being reduced to their leuco bases in a 2-electron reaction.<sup>20</sup> The conditional redox potential of the metal ion couples are in the range 0.70–1.10 V, while that of the iron(III)/iron(II) couple in 9–12M phosphoric acid media (the range used) is 0.410–0.390 V. Therefore, any redox indicator having a transition potential in the range 0.55–0.75 V should function satisfactorily in these titrations. As the standard redox potentials of most of the oxazine dyes lie in this range<sup>22</sup> the use of these indicators in these determinations was investigated. Other dyes of this type such as Nile Blue, Meldola's Blue, Resorufin *etc.*, which have a standard redox potential<sup>23</sup> less than 0.50 V, were found to be unsatisfactory. Since the performance of a redox indicator can be better judged from its transition potential than from its standard potential, the transi-

tion potentials of the dyes used were determined<sup>24</sup> and are presented in Table 2.

The error of these methods with each indicator has been found not to exceed  $\pm 0.5\%$ . The precision was determined for six replicate titrations of 59.5, 31.77, 2.38, 9.60 and 5.10 mg of U(VI), Cu(II), Os(VIII), Ir(IV) and Tl(III) respectively, and the relative standard deviations<sup>25</sup> were all in the range 0.3–0.4%.

In the earlier methods,<sup>1,2,9,10</sup> in which thiazine dyes were used as redox indicators, the colour transition at the end-point, from green to pale yellow green, made detection of the end-point difficult and some of the indicators underwent partial destruction and needed to be added near the end-point. The present methods obviate both these difficulties [except for the Cu(II) titration] and the colour change at the end-point, for GC, GB and CLB, from pink to colourless, can be easily detected. The relative cheapness, solubility in water and stability of the aqueous (2–3 months) and acid (1 week) solutions<sup>20</sup> of these dyes are added advantages.

### Interferences

Large amounts of Mn(II), Pb(II), Zn(II), Sn(IV),  $\text{SO}_4^{2-}$ ,  $\text{Cl}^-$  [except  $\text{Cl}^-$  in the determination of Tl(III)],  $\text{CH}_3\text{COO}^-$  and  $\text{ClO}_4^-$  do not interfere. The colours of Cr(III) and Ni(II) do not interfere when less than 0.8 and 4 mg of these ions respectively are present per ml of titration mixture. The colour of Co(II) up to 2 mg/ml does not interfere with BCB and

Table 1. Determination of metal ions with oxazine dyes as indicators

Metal ion	Reaction medium, $[\text{H}_3\text{PO}_4]$ , M	Range of metal ion determined, mg	Conditional redox potential, V ( $\pm 5$ mV)
U(VI)	11–12	24–120	0.730 [U(VI)/U(IV)] <sup>1</sup>
Cu(II)	9–10.5	13–64	0.700 [Cu(II)/Cu(I)] <sup>5</sup>
Os(VIII)	9–12	1–5	Not available [Os(VIII)/Os(IV)] <sup>8</sup>
Ir(IV)	9–11	4–20	0.880 [Ir(IV)/Ir(III)] <sup>8</sup>
Tl(III)	11–12	2–10	1.10 [Tl(III)/Tl(I)] <sup>22</sup>

Table 2. Determination of metal ions with oxazine dyes as indicators

Indicator	Transition potential, V ( $\pm 5$ mV)				
	U(IV)	Cu(II)	Os(VIII)	Ir(IV)	Tl(III)
BCB	0.552	0.570	0.581	0.594	0.610
CPB	0.536	0.586	0.575	0.583	0.630
GC	0.546	0.552	0.609	0.582	0.594
GB	0.550	0.544	0.616	0.596	0.625
CLB	0.603	0.588	0.594	0.589	0.615
SB5G	0.615	0.594	0.573	0.588	not found suitable

Table 3. Determination of copper in brass

Copper content found by the iodometric method, <sup>26</sup> %	Copper content found by the present method*, %					
	BCB	CPB	GC	GB	CLB	SB 5G
59.9	60.15 $\pm$ 0.15	59.70 $\pm$ 0.20	60.14 $\pm$ 0.16	59.63 $\pm$ 0.18	60.08 $\pm$ 0.12	59.60 $\pm$ 0.19

\*Average  $\pm$  s.d. of 6 determinations.

CPB (up to 0.3 mg/ml with the rest of the indicators). W(VI) gives a white precipitate but does not interfere. Nitrate interferes at all concentrations.

In view of the non-interference of the other metals normally present in brass, the methods have been applied to the determination of copper in brass (Table 3). The indicators have also been examined for use in the analysis of binary mixtures consisting of U(VI)–U(IV) or Ti(III)–Ti(I).

*Acknowledgements*—The authors wish to express their grateful thanks to the authorities of the University for research facilities provided, and to Professor N. Krishna Murthy for his interest shown and encouragement given during the progress of the work.

#### REFERENCES

- G. G. Rao and S. R. Sagi, *Talanta*, 1962 **9**, 715.
- Idem, ibid.*, 1963, **10**, 169.
- G. G. Rao and L. S. A. Dikshitulu, *ibid.*, 1963, **10**, 295.
- S. R. Sagi, K. V. Ramana and G. S. P. Raju, *Z. Anal. Chem.*, 1974, **272**, 208.
- N. K. Murthy and Y. P. Rao, *Indian J. Chem.*, 1976, **14A**, 721.
- L. S. A. Dikshitulu and K. V. Raju, *J. Indian. Chem. Soc.*, 1978, **55**, 346.
- Idem, Indian J. Chem.*, 1978, **16A**, 978.
- L. S. A. Dikshitulu, K. V. Raju and S. N. Dindi, *J. Indian Chem. Soc.*, 1981, **58**, 415.
- N. K. Murthy and Y. P. Rao, *Indian J. Chem.*, 1976, **14A**, 1023.
- N. K. Murthy and V. Satyanarayana, *Acta Ciencia Indica*, 1977, **3**, 201.
- K. V. Raju and K. Ramesh, *J. Inst. Chem. (India)*, 1987, **59**, 116.
- K. V. Raju and K. R. Babu, *Acta Ciencia Indica*, 1987, **13**, in the press.
- A. I. Vogel, *A Text Book of Quantitative Inorganic Analysis*, 3rd Ed., p. 319. Longmans, London, 1961.
- H. H. Willard and P. Young, *J. Am. Chem. Soc.*, 1930, **52**, 36.
- A. I. Vogel, *op. cit.*, p. 358.
- F. E. Beamish, *The Analytical Chemistry of the Noble Metals*, pp. 325 and 331. Pergamon Press, London, 1966.
- A. I. Vogel, *op. cit.*, pp. 289 and 291.
- V. P. Rao, B. V. S. R. Murty and G. G. Rao, *Z. Anal. Chem.*, 1956, **150**, 401.
- S. R. Sagi and K. V. Ramana, *Talanta*, 1969, **16**, 1217.
- L. S. A. Dikshitulu, K. V. Raju and V. H. Rao, *Indian J. Chem.*, 1980, **19A**, 1031.
- N. V. Rao, K. R. K. Murty and C. K. Sastry, *Proc. Natl. Acad. Sci. India*, 1973, **43A**, 122.
- S. R. Sagi, G. S. P. Raju and K. V. Ramana, *Talanta*, 1975, **22**, 93.
- E. Bishop, *Indicators*, p. 498. Pergamon Press, Oxford, 1972.
- R. Belcher, A. Nutton and I. W. Stephen, *J. Chem. Soc.*, 1952, 3857.
- R. B. Dean and W. J. Dixon, *Anal. Chem.*, 1951, **23**, 634.
- W. Scott, *Standard Methods of Chemical Analysis*, 1st Ed., Vol. 1, pp. 371 and 398. Van Nostrand, Princeton 1925.



## EVALUATION OF TWO NEW ASYMMETRIC DERIVATIVES OF THIOCARBOHYDRAZIDE AS SPECTROPHOTOMETRIC ANALYTICAL REAGENTS

FERNANDO ALVAREZ, FERNANDO DE PABLOS\* and JOSE LUIS GOMEZ ARIZA

Department of Analytical Chemistry, Faculty of Chemistry, University of Sevilla, 41012-Sevilla, Spain

(Received 10 August 1987. Accepted 21 January 1988)

**Summary**—The synthesis and analytical properties of 1-(2-pyridylmethylideneamino)-3-(4-hydroxybenzylideneamino)thiourea PHT and 1-(2-pyridylmethylideneamino)-3-(2,4-dihydroxybenzylideneamino)thiourea PDT have been studied. A spectrophotometric method has been used to determine the protonation constants of the reagents and a spectrophotometric survey of the reactions of various cations with PHT and PDT has been made.

Thiocarbohydrazide can easily be obtained by reacting carbon sulphide with hydrazinium hydroxide.<sup>1</sup> It can be used in analytical chemistry for organic functional group analysis,<sup>2</sup> colour tests for anions and cations,<sup>3-5</sup> and gravimetric determinations and separations of metals.<sup>4,5</sup> Several symmetric<sup>6-8</sup> and asymmetric<sup>9-12</sup> derivatives of thiocarbohydrazide have been proposed as analytical reagents for trace metal analysis, spectrophotometric determination of zinc,<sup>13,14</sup> iron,<sup>15,16</sup> palladium,<sup>17</sup> mercury,<sup>18</sup> indium<sup>19</sup> and cobalt,<sup>20</sup> and fluorimetric determination of gallium.<sup>21</sup>

This paper deals with the synthesis and possible analytical applications of two new asymmetric derivatives of thiocarbohydrazide: 1-(2-pyridylmethylideneamino)-3-(4-hydroxybenzylideneamino)thiourea (PHT) and 1-(2-pyridylmethylideneamino)-3-(2,4-dihydroxybenzylideneamino)thiourea (PDT).

In each case 2 ml of glacial acetic acid and 0.7 ml of pyridinecarboxaldehyde were then added and the mixture was refluxed for 1 hr. When the solution had cooled, 200 ml of water were added and the mixture was cooled in a refrigerator. The yellow products were filtered off and recrystallized from 1:1 v/v aqueous ethanol.

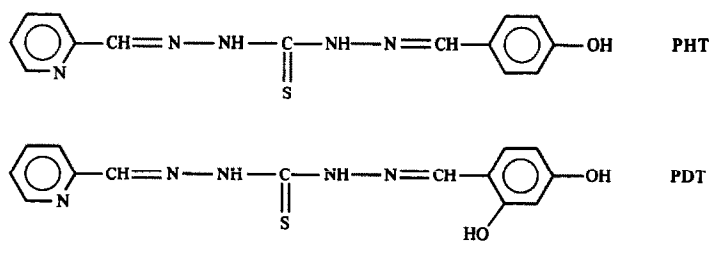
The microanalytical results were as follows:

PHT (m.p. 215–216°)	C	H	N	S
Required for C <sub>14</sub> H <sub>13</sub> N <sub>3</sub> O <sub>2</sub> S, %	56.2	4.4	23.4	10.7
Found, %	56.4	4.6	23.7	10.2

PDT (m.p. 209–210°)	C	H	N	S
Required for C <sub>14</sub> H <sub>13</sub> N <sub>3</sub> O <sub>2</sub> S, %	53.4	4.1	22.2	10.1
Found, %	53.3	3.9	22.1	9.5

### Other reagents

Salts and solvents of analytical reagent grade purity or better were used throughout. All metal ion solutions were standardized by appropriate methods.



### EXPERIMENTAL

#### Synthesis of the reagents

The reagents were obtained in two steps. First, the monoderivatives of thiocarbohydrazide with 4-hydroxybenzaldehyde and 2,4-dihydroxybenzaldehyde, respectively, were obtained by the method described by Brown *et al.*<sup>22</sup> In the second step these derivatives were condensed with 2-pyridinecarboxaldehyde in the usual way for Schiff bases, but with some modifications. For PHT, 5 mmoles of the 4-hydroxy derivative were dissolved in 100 ml of boiling ethanol; for PDT, 4 mmoles were similarly dissolved.

### RESULTS AND DISCUSSION

The solubility of the reagents in water and in organic solvents is very low [except for dimethylformamide (DMF) in which it is 10 g/l.]. Their solutions in DMF are stable for at least a week.

The infrared spectra (KBr discs) of the reagents are complicated because the aromatic portion of the molecules gives rise to numerous bands, the overlap of which makes detailed assignments difficult. The principal bands and their assignments are given in Table 1. The assignments for the spectrum of pyridine

\*To whom all correspondence should be addressed.

Table 1. Infrared spectral data

Frequency, $cm^{-1}$		
PHT	PDT	Assignment
3370 m	3440 m	N—H stretch
3120 w	3150 w	—OH intramolecular hydrogen bond
1620 s	1640 s	C=N stretch
1570–1440*	1595–1440*	aromatic C=C stretch
1170 m	1170 m	C=S stretch
1250–900*	1230–900*	pyridine C—H in-plane deformation
900–690*	885–680*	pyridine C—H out-of-plane deformation

\*Multiplet.

are well established,<sup>23-25</sup> and also the bands due to C=N, aromatic C=C and C=S stretches.

The ultraviolet spectra of solutions of both reagents show an absorption maximum at between 325 and 345 nm. For aqueous solutions the maximum is at 326 nm and the spectra are pH-dependent. The changes can be attributed to protonation of the pyridine nitrogen atom in acid medium, the dissociation of the thioimidol group in neutral medium and the dissociation of the aromatic hydroxyl groups in alkaline medium. The  $pK_a$  values were calculated from pH vs. absorbance plots and the first dissociation constants,  $K_{a1}$  were evaluated by the Lunn–Morton<sup>26</sup> and Maroni–Calmon<sup>27</sup> methods. The values of  $K_{a2}$  and  $K_{a3}$  are too close together for use of these methods, and the Roth–Bunnett method<sup>28</sup> was used instead. The value of  $K_{a4}$  for PDT has not been calculated because deprotonation of the second hydroxyl group can occur only in strongly alkaline medium and in this medium PDT is unstable. The  $pK_a$  values found are: PHT,  $pK_{a1} = 3.5$ ,  $pK_{a2} = 7.0$ ,  $pK_{a3} = 8.1$ ; PDT,  $pK_{a1} = 3.5$ ,  $pK_{a2} = 7.1$ ,  $pK_{a3} = 8.4$ .

The reagents are readily oxidized by hydrogen peroxide or ammonium persulphate in acid, neutral and alkaline media, but are not easily reducible.

Table 2. Spectrophotometric characteristics of the PHT and PRT complexes\*

Reagent	Cation	$\lambda_{max}$ , nm	Optimum	$\epsilon$ , $10^{-3} l. mole^{-1} cm^{-1}$
			pH†	
PHT	Bi(III)	408	4.0–4.5	73.1
	Zn(II)	400	7.0–7.5	57.2
	Ga(III)	415	3.7–4.0	58.5
	Hg(II)	380	6.5–7.0	58.4
	Ni(II)	408	6.8–7.6	44.2
	Co(II)	406	3.5–5.5	46.7
PRT	Cu(II)	404	4.3–5.2	28.6
	In(III)	408	5.8–6.5	66.6
	Bi(III)	412	5.8–6.4	57.1
	Bi(III)§	427	4.8–6.2	137.0*
	Ga(III)	413	6.0–7.0	57.4
	Pd(II)‡	408	4.8–6.7	137.0*

\*For 40%, v/v dimethylformamide medium.

†pH-meter reading.

§Extracted into chloroform in the presence of perchlorate.

‡Extracted into chloroform.

\* Apparent molar absorptivity (phase-volume ratio 5:2, aqueous phase: organic phase).

Neither reagent shows fluorescence in DMF or in acid, neutral or alkaline aqueous media.

#### Reactions with metal ions

The analytical characteristics of the more interesting reactions are summarized in Table 2. Both reagents act as general chromogenic ligands yielding high molar absorptivities, although they are not selective, the absorption maxima for the complexes all being located around 400 nm.

Remarkable sensitivities can be obtained for Bi(III), Zn(II), Ga(III), and Hg(II) with PHT, and for In(III), Ga(III), Bi(III) and Pd(II) with PDT. The sensitivities for Bi(III) and Pd(II) with PDT can be improved by extracting the complex into chloroform.

In Table 3, PHT and PDT are compared with symmetric and asymmetric derivatives of thio-carbohydrazide derived from salicylaldehyde and 2-pyridinecarboxaldehyde. In general, higher molar

Table 3. Comparison of the spectrophotometric characteristics of some chelates of thiocarbohydrazone reagents\*

Cation	PMAT†		SAT§		PST‡		PHT		PDT	
	$\lambda_{max}$	$\epsilon$	$\lambda_{max}$	$\epsilon$	$\lambda_{max}$	$\epsilon$	$\lambda_{max}$	$\epsilon$	$\lambda_{max}$	$\epsilon$
Co(II)	395	58.8	410	27.3	410	50.9	406	46.7	405	47.7
Cu(II)	400	16.5	400	22.2	410	18.0	404	28.6	388	24.9
Pd(II)	392	23.4	390	12.0	400	24.5	382	46.6	390	63.8
Zn(II)	394	11.2	390	12.0	410	67.5	393	49.0	398	61.6
Ni(II)	410	21.1	420	18.4	405	51.7	392	47.8	387	43.2
Hg(II)	396	57.7	382	37.1	400	64.2	380	69.2	—	—
Ga(III)	—	—	—	—	—	—	415	31.2	422	42.3
In(III)	410	37.2	404	47.6	415	63.4	392	59.7	408	66.6
Bi(III)	400	12.6	—	—	415	50.2	406	69.0	406	68.2
V(V)	430	7.3	396	19.3	400	15.9	442	13.5	398	40.2
Fe(II)	384	34.4	390	22.8	400	65.0	392	64.2	393	55.5
	620	4.5	550	4.0	635	5.6	620	6.4	630	6.1

\*Acetate-buffered medium,  $\lambda_{max}$  in nm,  $\epsilon$  in  $10^{-3} l. mole^{-1} cm^{-1}$ .†1,3-Bis(2-pyridylmethylideneamino)thiourea.<sup>6</sup>§1,3-Bis(salicylideneamino)thiourea.<sup>7</sup>‡1-(2-pyridylmethylideneamino)-3-(salicylideneamino)thiourea.<sup>9</sup>

absorptivities are obtained with the asymmetric derivatives and this confirms the results obtained by Rosales *et al.*<sup>9</sup> Because of the stronger chromophore effect of the 4-phenol and 2,4-diphenol groupings compared to the 2-phenol group, higher molar absorptivities would be expected for PHT and PDT chelates than for PST chelates. This trend is marked in only certain cases, such as for Cu(II), Pd(II), Bi(III), V(V). Its advantage, however, is offset by a correspondingly higher molar absorptivity of the two reagents at the maximum absorbance wavelengths of the complexes; the values (l. mole<sup>-1</sup> cm<sup>-1</sup>) measured at 400 nm *vs.* distilled water, are, approximately, 480 for PHT, 790 for PDT and 95 for PST.

In any case, PHT and PDT can form the basis of sensitive methods for the determination of various metal ions, and extraction steps are not necessary because the complexes are soluble in water-dimethylformamide mixtures. It is noteworthy that PHT and PDT react with Ga(III), but the other derivatives compared do not.

## REFERENCES

1. N. P. Bun-Hoi, T. B. Loc and N. D. Xuong, *Bull. Soc. Chim. France*, 1955, 694.
2. C. Duval and N. D. Xuong, *Mikrochim. Acta*, 1956, 747.
3. D. Williams and F. M. Nakhla, *Bull. Inst. Mining Met.*, 1951, No. 533, 257; *Chem. Abstr.*, 1951, 45, 6956 g.
4. C. Duval and T. B. Loc, *Compt. Rend.*, 1955, 240, 1097.
5. *Idem*, *Mikrochim. Acta*, 1956, 458.
6. F. J. Barragan de la Rosa, J. L. Gómez Ariza and F. Pino, *Talanta*, 1983, 30, 555.
7. M. T. Montaña, J. L. Gómez Ariza and A. García de Torres, *An. Quim. Ser. B*, 1984, 80, 129.
8. J. R. Bonilla Abascal, A. García de Torres and J. M. Cano Pavón, *Microchem. J.*, 1983, 28, 132.
9. D. Rosales, G. González and J. L. Gómez Ariza, *Talanta*, 1985, 32, 467.
10. G. Galán, M. T. Morales, M. T. Montaña and J. L. Gómez Ariza, *J. Molec. Struct.*, 1986, 143, 517.
11. R. Escobar, F. J. Barragán de la Rosa and J. L. Gómez Ariza, *ibid.*, 1986, 143, 505.
12. E. Sánchez, J. L. Gómez Ariza and A. Guiraum, *ibid.*, 1986, 143, 509.
13. M. T. Morales, M. T. Montaña, G. Galán and J. L. Gómez Ariza, *Analyst*, 1987, 112, 467.
14. D. Rosales and J. L. Gómez Ariza, *Anal. Chim. Acta*, 1985, 169, 367.
15. F. J. Barragán de la Rosa, J. L. Gómez Ariza and F. Pino, *Mikrochim. Acta*, 1983 III, 159.
16. D. Rosales, J. L. Gómez Ariza and J. A. Muñoz Leyva, *ibid.*, 1985 I, 77.
17. D. Rosales, J. L. Gómez Ariza and A. G. Asuero, *Analyst*, 1986, 111, 449.
18. D. Rosales and J. L. Gómez Ariza, *Anal. Chem.*, 1985, 57, 1411.
19. D. Rosales, I. Millán and J. L. Gómez Ariza, *Talanta*, 1986, 33, 607.
20. F. J. Barragán de la Rosa, J. L. Gómez Ariza and F. Pino, *Mikrochim. Acta*, 1983 II, 455.
21. E. Ureña, A. García de Torres, J. M. Cano Pavón and J. L. Gómez Ariza, *Anal. Chem.*, 1985, 57, 2309.
22. A. C. Brown, E. C. Pickering and F. J. Wilson, *J. Chem. Soc.*, 1927, 107.
23. C. H. Kline and J. Turkevich, *J. Chem. Phys.*, 1944, 12, 300.
24. L. Corssin, B. J. Fax and R. C. Lord, *ibid.*, 1953, 21, 1170.
25. J. K. Wimshurst and H. J. Bernstein, *Can. J. Chem.*, 1957, 35, 1185.
26. A. K. Lunn and R. A. Morton, *Analyst*, 1952, 77, 718.
27. P. Maroni and J. P. Calmon, *Bull. Soc. Chim. France*, 1964, 519.
28. B. Roth and J. F. Bunnett, *J. Am. Chem. Soc.*, 1965, 87, 334.

## SEPARATION AND DETERMINATION OF SELENIUM(IV) AND MOLYBDENUM(VI) IN MIXTURES BY SELECTIVE PRECIPITATION WITH POTASSIUM THIOCARBONATE

M. YUSUF, A. C. SARKI, S. B. IDRIS, G. A. AYOKO and K. SINGH\*  
Department of Chemistry, Ahmadu Bello University, Zaria, Nigeria

(Received 23 October 1986. Revised 30 November 1987. Accepted 12 January 1988)

**Summary**—A simple method for the separation and determination of selenium(IV) and molybdenum(VI) in mixtures, based on selective precipitation with potassium thiocarbonate, has been developed. The procedure allows quantitative determination of 10–100 mg of selenium or 10–70 mg of molybdenum at pH 0.5–1.0. No interference by a wide range of other metal ions is observed.

Potassium thiocarbonate (PTC) has been used as an alternative to hydrogen sulphide in a wide variety of analytical procedures.<sup>1–8</sup> Its attraction as a reagent lies in its stability and the ease of preparation and standardization of its aqueous solution. It can also act as both a precipitant and a complexing and masking agent.<sup>3</sup> It has been used for the separation and determination of copper, lead, silver, cadmium, thallium and bismuth in the presence of EDTA and other complexones,<sup>9</sup> and for analysis of ternary mixtures of silver, copper and platinum or gold.<sup>10</sup>

Its reactions with molybdenum(VI) and selenium(IV) over a wide pH range, and its use for their separation from mixtures with other metal ions have now been examined and are presented in this paper.

### EXPERIMENTAL

#### Reagents

All solutions were prepared with analytical reagent grade chemicals and doubly demineralized water, unless otherwise stated.

*Potassium thiocarbonate (PTC) stock solution, 1M.* Prepared and standardized as described previously,<sup>1</sup> and diluted as required.

*Metal-ion solutions, 1 mg/ml.* Prepared by dissolving appropriate quantities of metal compounds in water, or as required,<sup>1</sup> and standardized gravimetrically.<sup>11</sup> The compounds used were silver, copper, lead, bismuth, and zirconium nitrates, chromium(III), nickel, thorium and beryllium chlorides, cobalt(II) bromide, zinc and manganese sulphates, ferrous ammonium sulphate (later oxidized), sodium selenite and tellurite, cadmium oxide, titanium dioxide, aluminium hydroxide and ammonium molybdate.

#### Procedures

*Effect of pH on the precipitation of selenium(IV) and molybdenum(VI) with PTC.* To an aliquot of solution con-

taining 40 mg of selenium(IV) or 50 mg of molybdenum(VI), adjusted to pH 0.5–10 with 3M sulphuric acid and/or 8M ammonia solution, 0.5M PTC solution was added dropwise until precipitation was complete. After digestion for 30 min on a hot water-bath, the precipitate was filtered off on Whatman No. 42 filter paper, and washed first with water and then with alcohol.

The selenium(IV) precipitate was dried at 105° and weighed as SeS<sub>2</sub>. The molybdenum(VI) precipitate was transferred to a platinum crucible and ignited at 600–750° to convert MoS<sub>3</sub> into MoO<sub>3</sub>, which was used as the weighing form. The conversion factors are 0.552 for Se/SeS<sub>2</sub> and 0.667 for Mo/MoO<sub>3</sub>.

*Determination of selenium(IV) in mixtures.* Appropriate volumes of the metal-ion solutions to provide (a) 10–20 mg of zirconium, chromium, iron, and thorium or (b) 5–20 mg of beryllium, cobalt, manganese, nickel, and zinc were added to solutions containing 10–50 mg of selenium(IV). The pH was adjusted to 0.5–1.0 with 3M sulphuric acid, and 0.5M PTC was added dropwise with constant stirring until precipitation was complete. The precipitates were collected, dried and weighed as described above.

*Determination of molybdenum(VI) in mixtures.* The procedures for separation and determination of molybdenum(VI) were tested with three groups of metals.

Group A—cobalt, zinc, nickel and iron.

Group B—silver, lead, bismuth, cadmium, and copper.

Group C—titanium, chromium, aluminium, and thorium.

Aliquots of the standard metal ion solutions containing the group A or group C metals (5–10 mg of each metal) were added to aliquots of solutions containing 5–60 mg of molybdenum(VI). The mixtures were made acidic (pH 0.5–1.0) with 3M sulphuric acid and 0.5M PTC was added dropwise with constant stirring till precipitation was complete. The precipitates were collected, ignited and weighed as described above.

For group B metals (5–10 mg each), a slightly different procedure was used. The metal ion solutions were mixed with aliquots containing molybdenum(VI) (10–50 mg) and the mixture was made slightly alkaline (pH 8) with 0.1M sodium hydroxide. PTC solution was then added dropwise until all the foreign metal ions were precipitated and molybdenum(VI) remained as its thiocarbonate complex. The precipitate was filtered off and the filtrate acidified to pH 0.5–1.0, the molybdenum being precipitated as MoS<sub>3</sub>, which was collected, ignited and weighed as described above.

\*Author to whom correspondence should be addressed.

Table 1. Effect of pH on precipitation of Se(IV) and Mo(VI) with PTC\*

pH	Metal ion taken, mg		Product obtained, mg		Recovery, %	
	Se(IV)	Mo(VI)	SeS <sub>2</sub>	MoO <sub>3</sub>	Se(IV)	Mo(VI)
0.5	40	50	72.3	75.0	99.9	99.9
1.0	40	50	72.1	75.0	99.6	99.9
1.5	40	50	72.0	74.3	99.4	99.0
2.0	40	50	66.9	69.0	92.4	92.0
2.5	40	50	65.3	66.0	90.2	88.0
3.0	40	50	60.7	63.0	83.8	88.0
3.5	40	50	57.0	61.5	78.7	82.0
4.0	40	50	53.2	60.0	73.6	80.0
4.5	40	50	49.3	56.3	68.0	75.0
5.0	40	50	45.3	52.5	62.5	70.4
6.0	40	50	37.2	0.0	51.3	0.0
≥7.0	40	50	0.0	0.0	0.0	0.0

\*Each result is an average of three determinations.

## RESULTS AND DISCUSSION

### Effect of pH

PTC precipitates molybdenum(VI) and selenium(IV) as the thiocarbonates in alkaline medium and sulphides in acidic medium.<sup>9</sup> Table 1 shows that the precipitation of selenium(IV) and molybdenum(VI) is quantitative at pH 0.5–1.0; however, at pH 1.5–6.0 (for selenium) and pH 1.5–5.0 (for molybdenum), the composition of the precipitate is uncertain, but is probably a mixture of thiocarbonate and sulphide, and at pH greater than 6 no precipitate is obtained.

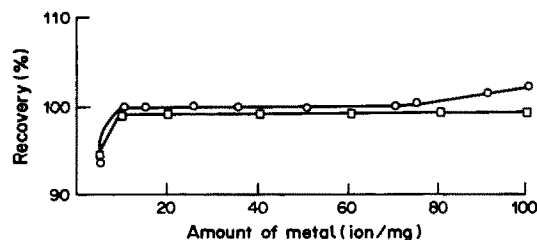


Fig. 1. Effect of amounts of selenium(IV) (□) and molybdenum(VI) (○) on their precipitation by PTC at pH 0.5–1.0.

### Effect of selenium and molybdenum concentrations

Figure 1 shows that at least 10 mg of selenium or molybdenum must be present for recovery to be quantitative. Precipitation is quantitative for up to 100 mg of selenium, but positive errors are obtained for molybdenum in amounts greater than 70 mg, possibly because of incomplete conversion into MoO<sub>3</sub> on ignition. Hence, a range of 10–50 mg is recommended.

### Separation and determination of selenium(IV) and molybdenum(VI) in mixtures

In acidic medium selenium(IV) and molybdenum(VI) are precipitated as sulphides whereas the other metal ions in the mixtures tested remain in solution. In alkaline medium, on the other hand, silver, lead, bismuth, cadmium, and copper are precipitated as the thiocarbonates while molybdenum(VI) remains in solution as its thiocarbonate complex, but is precipitated as MoS<sub>3</sub> on acidification. Dropwise addition of PTC provides and regulates an adequate supply of hydrogen sulphide without polluting the laboratory atmosphere. The efficiency and selectivity achieved with the reagent is illustrated by the results in Tables 2 and 3.

Table 2. Separation and determination of Se(IV) in presence of other metals\*

Se(IV) taken, mg	Other metals, mg					SeS <sub>2</sub> obtained, mg	Se(IV) recovered, %
	Al	Zr	Cr(III)	Fe(III)	Th		
10.00	15	10	15	10	10	18.0	99.6
20.00	20	15	8	15	5	36.1	99.6
30.00	15	20	20	8	15	53.9	99.3
40.00	8	10	5	20	15	72.0	99.5
50.00	10	5	10	8	20	90.0	99.4
	Be	Co	Mn	Ni	Zn		
10.00	10	20	10	20	20	18.0	99.6
20.00	15	5	20	15	10	36.0	99.4
30.00	20	10	15	20	15	54.0	99.5
40.00	15	20	10	5	8	72.1	99.6
50.00	10	15	10	10	10	90.1	99.6

\*Average of triplicate determinations.

Table 3. Separation and determination of Mo(VI) in presence of other metals\*

Mo(VI) taken, mg	Other metals, mg					MoO <sub>3</sub> obtained, mg	Mo(VI) recovered, %
	Co	Zn	Fe(III)	Ni			
50.00	10	11	10	10		75.0	100
30.00	10	5	10	10		45.0	99.9
15.00	10	15	10	15		23.0	99.9
10.00	10	5	8	6		15.0	99.9
	Ag	Pb	Cd	Cu	Bi		
50.00	15	15	10	5	10	74.9	99.9
30.00	10	10	10	10	10	44.9	99.9
15.00	5	5	10	10	6	22.5	99.8
10.00	20	5	20	20	15	15.0	99.8
	Ti	Al	Th	Cr(III)			
50.00	10	10	10	10		75.0	100
30.00	10	5	10	10		45.0	99.9
15.00	10	6	9	9		22.5	99.9
10.00	10	9	10	10		15.0	99.9

\*Average of three determinations.

Compared with other gravimetric reagents and methods for the separation and determination of selenium(IV) and molybdenum,<sup>12,13</sup> the method described is simple, economical and quantitative.

## REFERENCES

1. K. N. Johri and K. Singh, *Indian J. Chem.*, 1965, 3, 158.
2. K. N. Johri, *Macro and Semimicro Chemical Analysis Without H<sub>2</sub>S, Using Potassium Trithiocarbonate*, 2nd Ed., Asia Publishing House, Bombay, 1968.
3. K. N. Johri and K. Singh, *Bull. Chem. Soc. Japan*, 1967, 40, 990.
4. *Idem*, *Analyst*, 1965, 90, 745.
5. K. N. Johri, N. K. Kaushik and K. Singh, *Talanta*, 1969, 16, 432; *J. Thermal Anal.*, 1970, 2, 37.
6. K. N. Johri and N. K. Kaushik, *Chromatographia*, 1976, 9, 326.
7. K. N. Johri and K. Singh, *Mikrochim. Acta*, 1970, 1.
8. K. N. Johri, N. K. Kaushik and K. Singh, *ibid.*, 1969, 737.
9. K. Singh, R. D. Gupta and P. G. Bhatia, *Acta Chim. Acad. Sci. Hung.*, 1983, 113, 3.
10. *Idem*, *Analyst*, 1982, 107, 832.
11. A. I. Vogel, *A Textbook of Quantitative Inorganic Analysis*, 3rd Ed., Longmans, London, 1973.
12. B. V. Narayana and N. A. Raju, *Analyst*, 1982, 107, 392.
13. R. S. Young, *Separation Procedures in Inorganic Analysis*, 1st Ed., pp. 299-318, 392-398. Griffin, London, 1980.

# ON THE DETERMINATION OF TOTAL DISSOLVED TIN IN NATURAL WATERS BY DIRECT HYDRIDE GENERATION AND NON-DISPERSIVE ATOMIC-FLUORESCENCE SPECTROMETRY

ALESSANDRO D'ULIVO

Istituto di Chimica Analitica Strumentale del C.N.R., Via Risorgimento, 35, 56100 Pisa, Italy

(Received 27 May 1987. Revised 14 September 1987. Accepted 18 December 1987)

**Summary**—The analytical response of inorganic tin and of eleven organotin compounds of the type  $R_nSnX_{4-n}$  (with  $n = 1, 2, 3$  and  $R =$  methyl, ethyl, butyl and phenyl) was compared for direct hydride generation with non-dispersive atomic fluorescence detection. Most of these compounds showed behaviour resembling that of inorganic tin, with the exception of tributyltin and the phenyltin compounds. A simple pretreatment with  $10^{-3}M$  bromine and  $0.033M$  nitric acid at  $70^\circ$  for 60 min prevents any risk of underestimation and the total dissolved tin in natural waters can be determined with recoveries better than 90%, with inorganic tin as calibration standard.

The problems associated with organotin pollution, and the circulation and degradation of tin compounds in the aquatic environment, are well documented in the literature.<sup>1-3</sup> One of the most powerful analytical methods for the determination of tin compounds at trace level comprises hydride generation followed by gas chromatographic separation and selective detection.<sup>4-6</sup> Few efforts have so far been devoted, however, to solving the problem of total tin determination by hydride generation with direct sweeping of the evolved hydrides to the atomizer.<sup>7</sup>

This paper reports an investigation of the limitations and risks of direct hydride generation combined with non-dispersive atomic-fluorescence detection (NDAFS), in the determination of total dissolved tin in natural water samples and proposes a relatively simple procedure to avoid them.

## EXPERIMENTAL

### Apparatus

The NDAF spectrometer and the experimental parameters were similar to those previously described.<sup>8,9</sup> The atomizer, the gas transfer line and the reduction procedure were similar to those reported previously for lead<sup>10</sup> and alkyl-lead compounds<sup>11</sup> except for the use of magnetic stirring. A reaction vessel of 100 ml volume was employed to allow direct hydride generation from a 10-ml sample volume. Some experimental parameters were reoptimized to obtain maximum sensitivity for tin, and the best conditions were found to be use of  $0.02$ – $0.03M$  nitric acid and 1 ml of 1% sodium tetrahydroborate solution with gas flow-rates of 0.25 and 0.8 l./min for hydrogen and argon respectively. Detection limits of 25 pg of tin (three times the standard deviation of the blank signal) and 13 ng/l. (three times the standard deviation of the blank after the bromination) were obtained, very much lower than the corresponding values for the multielement mode.<sup>8</sup>

### Reagents

An inorganic stock tin solution (100  $\mu$ g/ml) was prepared from pure tin metal (Baker) and stored in  $1M$  hydrochloric

acid/8% citric acid medium. Alkyltin and aryltin compounds were obtained from Ventron and were dissolved in absolute ethanol to give 20–100  $\mu$ g/ml stock tin solutions, depending on their solubility. These solutions were kept refrigerated and in the dark, and diluted just before use.

Sodium tetrahydroborate stock solution (5%) was prepared by dissolving the solid reagent (BDH, reagent for AAS, pellets) in  $0.1M$  sodium hydroxide and filtering with a  $0.45$ - $\mu$ m membrane. This solution was freed from tin by co-precipitation with lanthanum hydroxide.

The potassium bromide/potassium bromate solution was prepared by dissolving 2.9 g of the bromide (Merck, Suprapur grade) and 0.8 g of the bromate (Erba, ACS grade) in 100 ml of demineralized water. A  $5M$  hydrazine hydroxide solution (Merck, Suprapur grade) was used to destroy the excess of bromine. Aqueous sample solutions were acidified with  $15M$  nitric acid (Merck, Suprapur grade) which gave a lower blank than did hydrochloric acid of the same degree of purity. Doubly distilled water was further purified with a Millipore-Q system.

### Sample pretreatment

This was similar to that reported by Farey *et al.*<sup>12</sup> for the determination of total mercury, modified as follows. Two ml of bromide/bromate solution were placed in a 100-ml glass-stoppered borosilicate standard flask. Then 0.22 ml of  $15M$  nitric acid were added and the mixture was swirled gently for a few seconds. Bromine was rapidly evolved and the water sample was then added up to the mark (warning: this operation should be performed under the fume hood). The resulting solution was about  $0.033M$  in nitric acid and  $10^{-3}M$  in bromine. The flask was kept in a water-bath at  $70^\circ C$  for 60 minutes then cooled to room temperature and treated with 40  $\mu$ l of  $5M$  hydrazine hydroxide solution. The sample was then ready for hydride generation without further manipulations.

Natural water samples were filtered ( $0.45$   $\mu$ m membrane), made  $10^{-3}M$  in nitric acid, stored in polyethylene bottles at  $4^\circ$  and used within a few days.

## DISCUSSION AND CONCLUSIONS

Figure 1 shows the peak height for fixed amounts of tin and organotin compounds as a function of the acidity. Except for the phenyltin compounds and

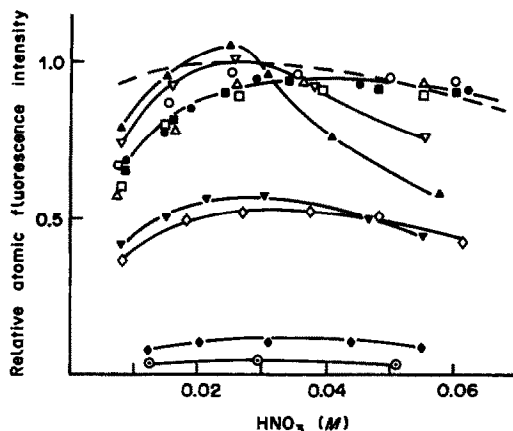


Fig. 1. Effect of acidity on the atomic-fluorescence signal obtained by the reduction of several tin compounds each present at 650 ng/l. level as tin. Inorganic tin (---), methyltin trichloride (■), dimethyltin dichloride (□), trimethyltin chloride (▽), diethyltin dichloride (△), triethyltin bromide (▲), butyltin trichloride (○), dibutyltin dichloride (●), tributyltin acetate (▼), phenyltin trichloride (◇), di-phenyltin dichloride (◆) and triphenyltin acetate (⊙).

tributyltin, there is a range of acidity, centred at about 0.03M nitric acid, over which the signal is almost independent of the acidity. Also, the peak shape is similar to that obtained with inorganic tin, and both peak height and peak area measurements lead to similar results in terms of relative analytical responses. For tributyltin and monophenyltin, however, owing to marked tailing of the signal generated from their reduction, peak area measurement gives about 60% greater response than that of peak height

measurement, but the response is significantly lower than that obtained with inorganic tin. Di- and triphenyltin generate peaks with such severe tailing that even peak area measurements are devoid of meaning. These species must therefore be decomposed before the hydride generation, if the evaluation of total tin is to be correct.

The bromination procedure, applied to pure standard solutions (Sn 1 ng/ml), gave quantitative recovery for tributyltin at 70° in less than 30 min, and for the phenyltin compounds at 60° in less than 15 min. Furthermore it did not affect the analytical response and recovery of inorganic tin. These results were partly confirmed for aqueous samples spiked with different tin compounds (see Table 1). The discrepancies observed for tributyltin are probably due to the fact that the bromine concentration available depends on the chemical oxygen demand of the sample. Pretreatment for 60 min at 70° is considered necessary to ensure quantitative recoveries of every tin compound.

Figure 1 indicates that the pretreatment converts the phenyltin compounds into inorganic tin. For tributyltin nothing can be said about the nature of the degradation product, since the analytical responses for monobutyltin, dibutyltin and inorganic tin are all very similar.

These results show that direct hydride generation combined with NDAFS can be safely used for the determination of total dissolved tin in natural uncontaminated waters in which only tin and methyltin species are present. For polluted natural waters the method may give large errors if tributyltin and phenyltins are present, but use of the bromination pretreatment will give correct results, and inorganic tin can be used as the calibration standard.

Table 1. Effect of bromination on the recovery of tin in spiked natural water samples

Sample	Compound added	Sn added, ng/l.	Tin recovered*, %		
			Without bromination	With bromination at 70°C Reaction time, min	
Sea-water	Sn(IV)	5000	94.0 ± 3.1	30	93.2 ± 3.5
	Me <sub>3</sub> SnCl	5000	93.6 ± 3.8	30	96.5 ± 3.6
	Et <sub>3</sub> SnBr	1500	98.2 ± 3.0	30	97.2 ± 3.9
	Bu <sub>3</sub> Sn(COOCH <sub>3</sub> )	3000	49.2 ± 3.3	30	102.7 ± 5.5
	Ph <sub>3</sub> Sn(COOH <sub>3</sub> )	3000	4.7 ± 0.5	30	98.7 ± 7.3
River water	Sn(IV)	100	87 ± 3.7	30	98 ± 7.0
	Me <sub>3</sub> SnCl	300	95.0 ± 5.3	30	96.6 ± 4.9
	Bu <sub>3</sub> Sn(COOCH <sub>3</sub> )	500	45.4 ± 3.0	30	80.8 ± 3.5
		500	46.4 ± 4.2	60	94.0 ± 4.7
	Ph <sub>3</sub> Sn(COOCH <sub>3</sub> )	500	0	30	90.6 ± 3.8
Tap water	Sn(IV)	500	96.9 ± 3.8	30	96.0 ± 5.0
	Me <sub>3</sub> SnCl	500	101.6 ± 3.6	30	98.6 ± 5.4
	Et <sub>3</sub> SnCl	1500	98.2 ± 3.1	30	99.3 ± 3.5
	Bu <sub>3</sub> (COOCH <sub>3</sub> )	2000	49.7 ± 2.9	30	70.8 ± 3.2
		2000	47.4 ± 2.2	60	91.0 ± 4.9
	Ph <sub>3</sub> Sn(COOH <sub>3</sub> )	1000	5.2 ± 1.2	30	95.1 ± 5.8

\*Means and standard deviations (3 determinations) calculated on the basis of calibration with inorganic tin.



## REFERENCES

1. S. J. Blunden, L. A. Hobbs and P. J. Smith, in *Environmental Chemistry*, Vol. 3, pp. 49-77. Royal Society of Chemistry, London, 1984.
2. W. P. Ridley, L. J. Dizikies and J. M. Wood, *Science*, 1977, **197**, 329.
3. S. J. Blunden and A. H. Chapman, *Environ. Technol. Lett.*, 1982, **3**, 267.
4. R. S. Braman and M. A. Thompkins, *Anal. Chem.*, 1979, **51**, 12.
5. M. O. Andreae and J. T. Byrd, *Anal. Chim. Acta*, 1984, **156**, 147.
6. O. F. X. Donard, S. Rapsomanikis and J. H. Weber, *Anal. Chem.*, 1986, **58**, 772.
7. M. Camail, B. Loiseau, A. Margailan and J. L. Vermet, *Anahsis*, 1983, **11**, 358.
8. A. D'Ulivo, R. Fuoco and P. Papoff, *Talanta*, 1985, **32**, 103.
9. A. D'Ulivo, C. Festa and P. Papoff, *ibid.*, 1983, **30**, 907.
10. A. D'Ulivo and P. Papoff, *ibid.*, 1985, **32**, 383.
11. A. D'Ulivo, R. Fuoco and P. Papoff, *ibid.*, 1986, **33**, 401.
12. B. J. Farey, L. A. Nelson and M. G. Rolph, *Analyst*, 1978, **103**, 656.

## RAPID SPECTROPHOTOMETRIC DETERMINATION OF ZIRCONIUM WITH 2-(5-BROMO-2-PYRIDYLAZO)-5-DIETHYLAMINOPHENOL

G. V. RATHAIAH and M. C. ESHWAR\*

Department of Chemistry, Indian Institute of Technology, Bombay-400 076, India

(Received 3 October 1986. Revised 16 July 1987. Accepted 23 August 1987)

**Summary**—Zirconium reacts with 2-(5-bromo-2-pyridylazo)-5-diethylaminophenol in the pH range 3.8–5.8 to form a red chelate that is soluble in methanol–water mixtures. The absorbance of the 1:3 complex obeys Beer's law over the zirconium concentration range 0.02–0.44  $\mu\text{g/ml}$  and has a molar absorptivity of  $1.54 \times 10^5 \text{ l.mole}^{-1}.\text{cm}^{-1}$  at 585 nm. The formation constant is  $\log \beta_3 = 16.15$ . Of 59 species studied, only EDTA, Ga, In, Ti, Hf and V(V) interfere seriously.

Pyridylazo dyes have been found useful for spectrophotometric determination of zirconium. The absorbance of the complex formed with 1-(2-pyridylazo)-2-naphthol (PAN) in a non-polar phase has been measured after 45 min<sup>1</sup> and 1 hr.<sup>2</sup> Several methods of varying sensitivity<sup>3-7</sup> have been based on reaction with 4-(2-pyridylazo)resorcinol (PAR). The complexes formed by zirconium with 1-[3-(1-methyl-2-piperidyl)-2-pyridylazo]-2-naphthol<sup>8</sup> and 2-[3-(1-methyl-2-piperidyl)-2-pyridylazo]-3,4-xyleneol<sup>9</sup> have very low molar absorptivity. 2-(3,5-Dibromo-2-pyridylazo)-5-diethylaminophenol (3,5-dibromo-PADAP)<sup>10</sup> is the most sensitive pyridylazo dye reported so far ( $\epsilon = 1.06 \times 10^5 \text{ l.mole}^{-1}.\text{cm}^{-1}$ ) for spectrophotometric determination of zirconium. Since 2-(5-bromo-2-pyridylazo)-5-diethylaminophenol (5-Br-PADAP) is a highly sensitive reagent for spectrophotometric determination of metal ions,<sup>11-14</sup> its reaction with zirconium has now been studied.

### EXPERIMENTAL

#### Apparatus

The apparatus employed was the same as described earlier.<sup>15</sup>

#### Reagents

**Zirconium solution.** Stock solution was prepared by heating 0.588 g of zirconium nitrate pentahydrate with 100 ml of 4M nitric acid, cooling, and diluting to 250 ml with 4M nitric acid. The solution was standardized complexometrically, and working solutions were prepared by appropriate dilution with 0.4M nitric acid.

**5-Br-PADAP solution.** A 0.1% solution in methanol was prepared.

**Buffer solution.** A 0.5M acetate buffer of pH 4.5 was prepared by dissolving 17.0 g of sodium acetate trihydrate

in 150 ml of distilled water, adjusting the pH to 4.5 with 0.5M acetic acid and diluting to 250 ml.

#### Procedure

To an aliquot of solution containing <11.0  $\mu\text{g}$  of zirconium, add 1 ml of 5-Br-PADAP solution and 5 ml of acetate buffer (pH 4.5). Add 10 ml of methanol to dissolve the complex, make up to volume in a 25-ml standard flask with distilled water and measure the absorbance at 585 nm against a reagent blank prepared under identical conditions.

### RESULTS AND DISCUSSION

#### Spectral characteristics

The wavelength of the maximum absorption changes slightly with increase in pH, but is effectively constant at 573 nm at pH > 8.0 (Table 1). The absorbance is also pH-dependent but constant at 585 nm over the pH range 3.8–5.8 (Fig. 1). Hence measurement at 585 nm and pH 4.5 is recommended. The amount of buffer (pH 4.5) added can be varied from 2 to 12 ml without effect on the absorbance, and use of 5 ml is recommended.

Figure 2 shows the absorption spectra of the complex and the reagent. Beer's law is obeyed over the zirconium range 0.5–11  $\mu\text{g}$ , and the molar absorptivity is  $1.54 \times 10^5 \text{ l.mole}^{-1}.\text{cm}^{-1}$ . The complex forms instantaneously and the absorbance is stable for at least 72 hr. Table 2 shows that only chloro-

Table 1. Effect of pH on absorption maximum

pH	$\lambda_{\text{max}}$ , nm	pH	$\lambda_{\text{max}}$ , nm
1.0	591	6.0	575
2.0	590	7.0	574
3.0	586	8.0	573
4.0	584	9.0	573
5.0	581	10.0	573

\*Author for correspondence.

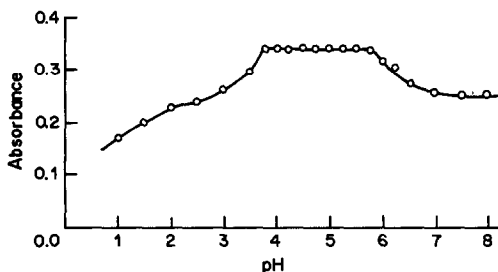


Fig. 1. Effect of pH on absorbance of Zr-5-Br-PADAP complex at 585 nm.

phosphonazo III and 2-(6-bromobenzothiazol-2-ylazo)-5-diethylaminophenol give methods of higher sensitivity. The relative standard deviation for determination of 5  $\mu\text{g}$  of zirconium was 1.0% (10 variates).

#### Effect of initial pH of zirconium solution

As zirconium tends to undergo irreversible hydrolysis even at low pH, the effect of the initial pH on complexation was studied. The absorbance of the complex was found to be lower when the initial pH of the zirconium solution was  $>0.75$  (Fig. 3). Hence a 0.4M nitric acid medium is recommended.

#### Reaction conditions

One mg of 5-Br-PADAP (1 ml of 0.1% solution)

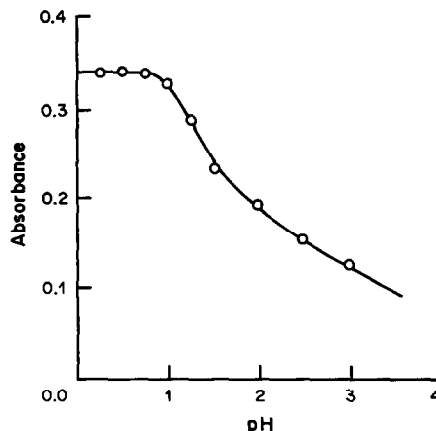


Fig. 3. Effect of initial pH of Zr(IV) solution on absorbance of Zr-5-Br-PADAP complex.

is an ample excess for reaction with up to 11  $\mu\text{g}$  of zirconium. It is essential to add the buffer after the zirconium solution and the reagent have been mixed.

The complex is only sparingly soluble in aqueous medium but soluble in various polar organic solvents, such as methanol, ethanol, acetone, dimethylformamide, tert-butyl alcohol and dioxan. A minimum 1:3 v/v ratio of solvent to water is sufficient for dissolution of the complex but ratios  $>1:2$  give higher and constant absorbance. Hence, use of 40% v/v methanol is recommended.

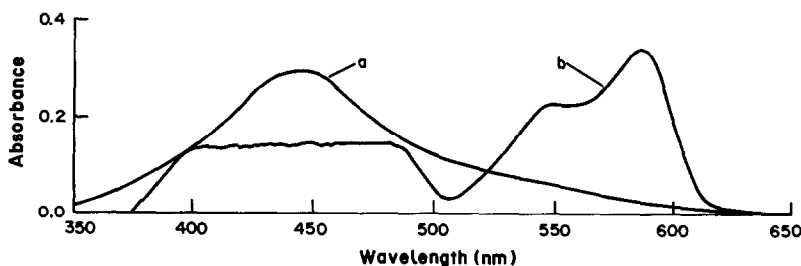


Fig. 2. Absorption spectra. Curve a, reagent blank vs. solvent,  $[5\text{-Br-PADAP}] = 5.72 \times 10^{-6} M$ ; curve b, Zr-5-Br-PADAP complex vs. reagent blank,  $[\text{Zr}] = 2.23 \times 10^{-6} M$ ,  $[5\text{-Br-PADAP}] = 1.14 \times 10^{-4} M$ .

Table 2. Comparison with other methods

Reagent	$\lambda_{\text{max}}$ , nm	$\epsilon$ , $10^4 \text{ l. mole}^{-1} \cdot \text{cm}^{-1}$	Reference
Arsenazo III	665	12.0	16
2-(6-Bromobenzothiazol-2-ylazo)-5-diethylaminophenol	520	44.0	17
Bromopyrogallol Red	670	7.0	18
Chlorophosphonazo III	675	21.0	19
Chrome Azurol S	555	4.76	20
3,5-Dibromo-PADAP	590	10.6	10
PAN	555	3.6	2
PAR	530	6.6	7
Stilbazo	560	6.3	21
2-(2-Thiazolylazo)-5-dimethylaminophenol	595	10.5	22
1-(2-Thiazolylazo)-2-naphthol	590	3.36	23
4-(2-Thiazolylazo)resorcinol	550	6.4	24
Xylenol Orange	570	5.2	21
5-Br-PADAP	585	15.4	Present method

Table 3. Effect of diverse ions (zirconium 5 µg/25 ml)

Foreign species added	Tolerance limit, µg
Cl <sup>-</sup> , Br <sup>-</sup> , I <sup>-</sup> , SO <sub>4</sub> <sup>2-</sup> , NH <sub>4</sub> <sup>+</sup> , Mg <sup>2+</sup> , Ca <sup>2+</sup> , Sr <sup>2+</sup> , Ba <sup>2+</sup>	> 30,000
S <sub>2</sub> O <sub>3</sub> <sup>2-</sup>	15,000
Urea, thiourea, CO <sub>3</sub> <sup>2-</sup> , La <sup>3+</sup>	10,000
Succinate, Be <sup>2+</sup> , Al <sup>3+</sup> , Mn <sup>2+</sup> , As(III), Se(IV), Mo(VI), Ag <sup>+</sup> , W(VI)	5000
NH <sub>2</sub> OH.HCl, N <sub>2</sub> H <sub>4</sub> .H <sub>2</sub> SO <sub>4</sub>	3000
Cd <sup>2+</sup>	2500
CN <sup>-</sup> , Pt(IV)	1500
F <sup>-</sup> , SCN <sup>-</sup> , Y <sup>3+</sup> , Pb <sup>2+</sup> , Th <sup>4+</sup>	1000
Sc <sup>3+</sup> , Sb(III)	750
Cr(III)	500
Rh(III)	400
Citrate, tartrate, PO <sub>4</sub> <sup>3-</sup> , Pd(II) <sup>b</sup> , Zn <sup>2+</sup>	200
Ni <sup>2+</sup> , Au(III), Hg(II) <sup>b</sup>	100
Oxalate, Cu <sup>2+</sup> , Ce <sup>3+</sup>	75
Fe(III) <sup>b</sup> , Co(II) <sup>b</sup> , U(VI)	50
Tl <sup>3+</sup> , Bi <sup>3+</sup>	5

<sup>a</sup>Masked with S<sub>2</sub>O<sub>3</sub><sup>2-</sup>.

<sup>b</sup>Masked with CN<sup>-</sup>.

#### Composition of the complex

Both the continuous-variation and mole-ratio methods showed the metal-to-ligand ratio in the complex to be 1:3. The formation constant (log β<sub>3</sub>) was found to be 16.15 by the mole-ratio method.

#### Interferences

The effect of various ions was studied, and the tolerance limit was set at the amount causing an error of ±2.0% in determination of 5 µg of zirconium. EDTA caused negative interference, whereas positive interference was caused by V(V), Ti(IV), Hf, Ga and In at all levels. Cyanide and thiosulphate were used to mask some of the interfering cations. The tolerance limits are presented in Table 3.

#### Application to analysis of zircon

About 0.3 g of zircon was fused with 4.0 g of borax in a platinum crucible. After cooling, the mass was lixiviated with 2M hydrochloric acid and the solution diluted to 250 ml with distilled water. Twenty-five ml of this solution were mixed with 25 ml of concentrated hydrochloric acid and the solution was boiled to convert the bulk of the silicon into silica gel, which was filtered off and washed. The filtrate was evaporated until all hydrogen chloride had been evolved. The residue was treated with 10 ml of concentrated nitric acid and the solution evaporated to dryness. The residue was leached and accurately made up to 250 ml with 0.4M nitric acid. An aliquot of this

solution was taken and zirconium determined as in the procedure. The results obtained from duplicate analysis gave the zirconium content as 48.2 and 48.1%, compared to the theoretical value of 47.9% (ZrO<sub>2</sub> 64.70%). Other constituents of the ore were Al<sub>2</sub>O<sub>3</sub> (2.90%), TiO<sub>2</sub> (0.55%), Fe<sub>2</sub>O<sub>3</sub> (0.06%), U<sub>3</sub>O<sub>8</sub> (0.032%) and SiO<sub>2</sub> (rest).

*Acknowledgement*—The authors express their grateful thanks to the Council of Scientific and Industrial Research (India) for awarding a Senior Research Fellowship to one of them (GVR).

#### REFERENCES

1. R. F. Rolf, *Anal. Chem.*, 1961, **33**, 125.
2. R. E. Ross, V. M. Drabek and R. P. Sarsen, *Talanta*, 1969, **16**, 748.
3. Yu. K. Tselinksii and E. V. Lapitskaya, *Tr. Vses. Nauch-Issled Inst. Khim. Reaktivov Osobo. Khim. Veshchestv*, 1969, **31**, 310; *Chem. Abstr.*, 1971, **75**, 126025d.
4. O. A. Tataev and E. A. Yarysheva, *Sb. Nauch. Soobshch. Dagestan. Univ. Kafedra Khim.*, 1969, **6**, 58; *Chem. Abstr.*, 1972, **77**, 69661y.
5. S. G. Nagarkar and M. C. Eshwar, *Mikrochim. Acta*, 1974, 747.
6. O. V. Mandzhgaladze, N. S. Mgeladze and K. G. Bazierashvili, *Izv. Akad. Nauk. Gruz. SSR. Ser. Khim.*, 1980, **67**, 27; *Anal. Abstr.*, 1981, **41**, 4B105.
7. S. Kalyanaraman and T. Fukasawa, *Anal. Chem.*, 1983, **55**, 2239.
8. M. Abdurakhmanov, R. Kh. Dzhiyanabaeva and Sh. T. Talipov, *Tr. Tashkentisk. Gos. Univ.*, 1967, **288**, 83; *Anal. Abstr.*, 1968, **15**, 3283.
9. K. Rakhmatullaev, M. A. Rakhmatullaev, Sh. T. Talipov and Kh. Tashmatov, *Uzbek. Khim. Zh.*, 1969, **6**, 118; *Anal. Abstr.*, 1971, **20**, 2399.
10. S. I. Gusev, N. F. Gavrilova and L. V. Poplevina, *Zh. Analit. Khim.*, 1977, **32**, 1363.
11. D. A. Johnson and T. M. Florence, *Talanta*, 1975, **22**, 253.
12. F. S. Wei, Y. R. Zhu and F. Yin, *Anal. Lett.*, 1980, **13**, 1533.
13. V. Kubáň and M. Macka, *Collection Czech. Chem. Commun.*, 1983, **48**, 52.
14. A. Z. Abu-Zuhri, *Microchem. J.*, 1984, **29**, 345.
15. G. V. Rathaiah and M. C. Eshwar, *Analyst*, 1986, **111**, 61.
16. S. B. Savvin, *Talanta*, 1961, **8**, 673.
17. C. P. Zang, D. Y. Qi and T. Z. Zhou, *ibid.*, 1982, **28**, 1119.
18. S. Takayoshi and F. Yuko, *Bull. Chem. Soc. Japan*, 1969, **42**, 2272.
19. T. Yamamoto, H. Muto and Y. Kato, *Bunseki Kagaku*, 1977, **26**, 575.
20. Y. Koriuchi and H. Nishida, *ibid.*, 1967, **16**, 20.
21. A. K. Babko and V. T. Vasilenko, *Zavodsk. Lab.*, 1961, **27**, 640.
22. T. Chikao, *Bunseki Kagaku*, 1977, **26**, 260.
23. S. Kalyanaraman, A. Sugiyama and T. Fukasawa, *Analyst*, 1985, **110**, 213.
24. B. Subrahmanyam and M. C. Eshwar, *Indian J. Chem.*, 1977, **15A**, 66.

## SOFTWARE SURVEY SECTION

---

### Software package TAL-005/88

#### MULTIVARIATE LINEAR REGRESSION FOR CALIBRATION AND TESTING OF ANALYTICAL METHODS

Contributor: Leslaw Wawrzonek, Institute of Nuclear Chemistry and Technology, 03-195 Warsaw, Dorodna 16, Poland.

Brief description: The software comprises five programs, with functions as follows:

(1). A program for preparing an input data matrix. This matrix consists of the concentrations of the elements in the reference materials, measured variables, and also new variables computed by this program, which are functions of the measured variables (e.g. product, quotient, etc.). The matrix can have up to 50 rows (samples) and 50 columns (variables).

(2). A program for calculation of single-variable linear regression for four models: ordinary regression, weighted regression, regression through the centroid ( $y = a + bx$ ) or regression through the origin ( $y = bx$ ). The program calculates basic statistical parameters of the calibration function, identifies the outliers, calculates confidence intervals for  $x$  and  $y$ , and analyses the residuals.

(3). A program for calculation of a multivariate regression model for variables chosen from the input data matrix. All basic statistical parameters are calculated, with partial  $F$  coefficients and confidence intervals for the dependent variable. The model can have up to 10 variables.

(4) and (5). Programs for calculation of concentrations of elements in unknown samples (corresponding to programs (2) and (3) respectively), with confidence intervals, and the possibility of comparing the results with analyses done by reference methods.

The programs run interactively. A "sort" option is used to print the results in increasing order of the dependent variable. Programs (2) and (3) can produce graphs of the residuals versus any variable from the input matrix.

Potential users: Analytical chemists, all users of the linear calibration method.

Fields of interest: Analytical chemistry, physics (especially X-ray fluorescence).

This program has been developed in FORTRAN for the PDP 11 or IBM PC AT, to run under RSX 11 or PC-DOS. It is available on 0.5-inch magnetic tape, or 5.25-inch double-sided floppy disc. The memory required is 256 Kb.

Distributed by the Institute of Nuclear Chemistry and Technology.

A 132-character printer is required. The program is user-friendly and self-documenting, with minimal external documentation. The software is fully operational and has been in use for three years at four sites. The contributor is willing to deal with enquiries. Please write to him at 02-765 Warsaw, Kuratowskiego 4/8, Poland.

## MICROCOMPUTER APPLICATION OF NON-LINEAR REGRESSION ANALYSIS TO METAL-LIGAND EQUILIBRIA

PAUL D. TAYLOR\*, IAN E. G. MORRISON and ROBERT C. HIDER

Department of Chemistry and Biological Chemistry, University of Essex, Wivenhoe Park,  
Colchester, England

(Received 5 October 1987. Revised 14 January 1988. Accepted 17 February 1988)

**Summary**—A non-linear least-squares regression program is described which is suitable for PC-compatible microcomputers. The program is written in GWBASIC, but compiled to run with the Intel 8087 fast numeric processor. Subroutines which simulate functions are compiled separately from the main program. Parameters are optimized by a Gauss-Newton-Marquardt algorithm which can be provided with either analytically or numerically calculated partial derivatives. Multi-component potentiometric titrations are simulated and parameters optimized by using analytical derivatives. Spectrophotometric titrations are also simulated, but absorptivities are optimized by linear regression while stability constants are optimized non-linearly by using numerical derivatives. Provision is made for "global analysis" of parameters. The experimental points can be displayed on screen, along with the "best" fit and the speciation. The program is demonstrated here by the determination of the  $pK_a$  values and stability constants of a hydroxy-pyridinone ligand and its complexes with Fe(III).

Despite an established library of powerful mainframe computer programs for the determination of stability constants from titrimetric data,<sup>1</sup> efforts have been made by numerous workers<sup>2-8</sup> to optimize stability constants by use of microcomputers. The impetus for this is convenience, especially with the increasing use of microcomputers for the control of automated systems, in which data are saved on disc and directly input to data-processing programs in the laboratory. Despite its faults, BASIC is a good language for such programs, because it is widely understood and accessible to adaptation by those who are not computer experts.

The computer program NONLIN15, written in Microsoft GWBASIC, was conceived as a laboratory tool for the determination of stability constants of multi-component equilibria from data gathered by an automated titrator. This system, which will be described in a later paper, simultaneously obtains equilibrium readings of glass electrode emf and optical absorbance at a single wavelength, for incremental titrant additions. To speed up NONLIN15 it is compiled to operate on a PC-compatible computer (Opus PCII) equipped with an Intel 8087 fast numeric processor, by the Microway 8087 BASIC/INLINE software Version 1.15, using its facility for separately compiled subroutines, which allows new functions to be included with minimal effort. A speed that is more than 50 times that with interpreted BASIC is achieved.

### PROGRAM STRUCTURE

#### *Simulation of functions*

The separately compiled subroutines which simulate chosen functions perform the input of all function parameters, calculation of statistical weights, generation of  $y$  as a function of  $x$ , and calculation of analytical partial derivatives of this function with respect to specific parameters.

#### *Simulation of potentiometric titrations*

The chemical system modelled consists of a metal ion and ligand in equilibrium with a series of complexes which tend to dissociate as the hydrogen-ion concentration is increased. The computer simulation of this model involves the solution of the set of simultaneous equations representing the conservation equations and equilibrium quotients. The free metal ion, ligand and hydrogen-ion concentrations in this system are calculated by Newton-Raphson iteration. The three appropriate root equations shown below use the following terms:

$\beta(j)$	Cumulative formation constant for the $j$ th associated species.
$S(j)$	Concentration of the $j$ th associated species.
$e(i, j)$	Stoichiometric coefficient of the $i$ th component in the $j$ th associated species.
$Ct(i)$	Total analytical concentration of the $i$ th component.
$c(i)$	Free concentration of the $i$ th component.

\*Author for correspondence.

$Mt, Lt, Ht$	Total analytical concentrations of metal ion, ligand and hydrogen ion respectively.
$m, l, h$	Free metal ion, ligand and hydrogen-ion concentrations respectively.
$NC$	Total number of components.
$NS$	Total number of associated species.
$Kw$	Ionization constant of water $[H^+][OH^-]$ .
$\epsilon(j)$	Absorptivity of the $j$ th species

$$Mt = m + \sum_{j=1}^{NS} e(m, j)S(j) \quad (1)$$

$$Lt = l + \sum e(l, j)S(j) \quad (2)$$

$$Ht = h + \sum e(h, j)S(j) - Kw/h \quad (3)$$

where

$$S(j) = \beta(j) \prod_{i=1}^{NC} c(i)^{\alpha(i, j)} \quad (4)$$

The  $3 \times 3$  Jacobian matrix of partial derivatives<sup>9</sup> of each total analytical concentration  $Mt$ ,  $Lt$  and  $Ht$  with respect to the logarithm of the concentration of the free components  $m$ ,  $l$  and  $h$  [equations (5) and (6)] has been shown to be a symmetrical matrix,<sup>10</sup> so calculation is reduced by one third. The use of logarithmic space also helps to avoid computer overflow and underflow errors.

$$J = \begin{pmatrix} \left( \frac{\partial Mt}{\partial \log m} \right)_{l, h} & \left( \frac{\partial Mt}{\partial \log l} \right)_{m, h} & \left( \frac{\partial Mt}{\partial \log h} \right)_{m, l} \\ \left( \frac{\partial Lt}{\partial \log m} \right)_{l, h} & \left( \frac{\partial Lt}{\partial \log l} \right)_{m, h} & \left( \frac{\partial Lt}{\partial \log h} \right)_{m, l} \\ \left( \frac{\partial Ht}{\partial \log m} \right)_{l, h} & \left( \frac{\partial Ht}{\partial \log l} \right)_{m, h} & \left( \frac{\partial Ht}{\partial \log h} \right)_{m, l} \end{pmatrix} \quad (5)$$

$$J = \begin{pmatrix} m + \sum_{j=1}^{NS} e(m, j)^2 S(j) & \sum e(m, j)e(l, j)S(j) & \sum e(m, j)e(h, j)S(j) \\ \sum e(m, j)e(l, j)S(j) & l + \sum e(l, j)^2 S(j) & \sum e(l, j)e(h, j)S(j) \\ \sum e(m, j)e(h, j)S(j) & \sum e(l, j)e(h, j)S(j) & h + \frac{Kw}{h} + \sum e(h, j)^2 S(j) \end{pmatrix} \quad (6)$$

The vector  $X_{n+1}$  giving the next improved estimate of  $\log m$ ,  $\log l$  and  $\log h$  is calculated from the previous estimate by equations (7) or (8) where  $J$  is the Jacobian matrix and  $F_{nn}$  is the column vector consisting of the current solution of the root equations.

$$J(X_{n+1} - X_n) = -F_{nn} \quad (7)$$

$$X_{n+1} = X_n - J^{-1}F_{nn} \quad (8)$$

Solution of simultaneous equations by full matrix inversion as shown in equation (8) is computationally inefficient<sup>9</sup> and unnecessary at this stage. Choleski's method<sup>9</sup> is employed instead. Iteration continues until the equations are solved with an accuracy better

than 0.01% of the analytical concentrations  $Mt$ ,  $Lt$  and  $Ht$ . At this point the concentrations of all the complex species and the value of  $-\log h$  corresponding to a given volume of acid or base titrant will have been calculated from the current estimates of the stability constants. Also at this point, the Jacobian matrix is fully inverted by using the last steps of the Choleski algorithm. The inverse Jacobian thus generated is used, as described by Avdeef and Raymond,<sup>10</sup> to generate the analytical partial derivatives required for the Gauss-Newton-Marquardt optimization algorithm. Values for  $\partial \log h / \partial Mt$ ,  $\partial \log h / \partial Lt$  and  $\partial \log h / \partial Ht$  are obtained directly from the inverse Jacobian, whereas terms for  $\partial \log h / \partial \log \beta(j)$  are obtained from equation (9).

$$\frac{\partial \log h}{\partial \log \beta(j)} = \sum_{i=1}^{NC} \frac{\partial \log h}{\partial Ct(i)} \frac{\partial Ct(i)}{\partial \log \beta(j)} \quad (9)$$

The inverse Jacobian matrix is also used to extrapolate the titration curve to give better initial estimates for free component concentrations at the next point.<sup>11</sup> The statistical weighting scheme suggested by Avdeef<sup>12</sup> is used. Rigorous statistical weighting is vital when the sum-of-squares of emf or pH is minimized.

#### Simulation of spectrophotometric titrations

Calculation of absorbance as a function of  $-\log h$  involves solution of one less simultaneous equation than for potentiometric titrations. A  $2 \times 2$  Jacobian matrix is therefore employed. In other respects the algorithm to generate speciation is identical to that already described. Absorbance is then calculated from equation (10).

$$A = \sum_{j=1}^{NS} \epsilon(j)S(j) + \epsilon_0 \quad (10)$$

The analytical derivatives for absorptivities supplied to the Gauss-Newton optimization algorithm are simply the relevant species concentrations as shown in equation (11).

$$\frac{\partial A}{\partial \epsilon(j)} = S(j) \quad (11)$$

The remaining parameters describing spectrophotometric titrations are optimized by using numerically obtained derivatives for simplicity (see next section).

### Optimization of parameters by the Gauss–Newton–Marquardt algorithm

Minimization of the sum-of-squares of residuals is performed by a standard Gauss–Newton algorithm developed from the program GENFIT.<sup>13</sup> The Marquardt algorithm<sup>14</sup> has recently been introduced into the program and functions by multiplying the diagonal terms of the Hessian matrix by the factor  $(1 + x)$ . The value of  $x$  is initially 0.1 and is reduced by a factor of three each time the sum-of-squares of residuals is reduced in an iteration. When convergence fails, the parameters of the previous iteration are restored and  $x$  is repeatedly increased by a factor of three until convergence is regained. Up to ten variables may be refined simultaneously. Some may be held constant for a sequence of operations and freed for variation later. If analytical derivatives have not been supplied by the function simulation algorithm than a standard numerical differentiation method is employed. Once convergence has been established (tested by the ratio of successive iterations) the statistical parameters chi-squared and the Hamilton  $R$  factor<sup>15</sup> are calculated. In both potentiometric and spectrophotometric analyses the stepwise stability constants are optimized rather than the overall stability constants.

A special modification to the Gauss–Newton algorithm has been made to deal with linear parameters such as absorptivities. The method is based on that reported for the program ELORMA.<sup>3</sup> Numerical derivatives for non-linear parameters such as stability constants are calculated by the usual perturbation method, but immediately after the speciation has been generated the absorptivities are replaced by their best linear least-squares values. This separate treatment of linear and non-linear parameters gives more reliable and more rapid convergence.<sup>4</sup> Zuberbühler *et al.* have employed a highly sophisticated mathematical technique in their program SPECFIT which enables the use of analytical derivatives for non-linear parameters to be retained<sup>4</sup> during this two-stage process.

### Global optimization

Global optimization of the parameters common to a set of experiments gives more reliable values and a better chance of rejection of a spurious model function. Parameters such as equilibrium constants must by definition (assuming ideality) be constant and therefore common to a set of titrations. For parameters which are not constant throughout a set of titrations, another method of global optimization is required. The method used recognizes the experimental ease with which some variables such as concentration may be increased by a known factor even when the absolute values are not known. For example, in a set of titrations in which the metal concentration is increased between titrations by addition of 1, 2, 3 ml, *etc.*, of a stock solution, the factors

1, 2, 3, *etc.*, may be input into NONLIN15 and held constant while the metal concentration is optimized. Experimentally this is performed by repetitive titration of a single sample solution but with addition of say 1 ml of stock metal or ligand solution between titrations. Dilution effects from these additions and from the titrant volume are all handled by the program. This process can help to eliminate small systematic errors.

### Utilization of combined potentiometric and spectrophotometric data

Programs which perform non-linear regression analysis simultaneously on potentiometric and spectrophotometric data have been described in the literature,<sup>16</sup> but this approach requires the weighting of the two types of data to be in the correct proportion. A different approach is used in NONLIN15, in that the two sets of data are analysed in a two-stage process which exploits the properties of each.

The parameters for initial acid concentration, titrant concentration,  $pK_w$  and carbonate concentration have no effect on the plot of absorbance *vs.* Nernstian electrode response. Furthermore, the process of resolving the absorbance into the contributions made by each absorbing species is independent of the electrode  $E_0$ . The spectrophotometric data may therefore be used in isolation to optimize speciation. An arbitrary  $E_0$  value may then be used to give apparent but erroneous values of the equilibrium constants. The way in which errors in  $E_0$  are transformed into errors in these apparent equilibrium constants is shown in equation (14). This function is dependent on the proton stoichiometry as well as the error  $E_t$  in the arbitrary  $E_0$ . The automated spectrophotometric/potentiometric titrator described earlier gathers the data for emf *vs.* titrant volume point by point, simultaneously with the spectrophotometric data. The potentiometric data are then used to perform an internal calibration by optimization of  $E_0$  and adjustment of the equilibrium constants according to equation (14), while the absorbing species concentrations are held constant at the levels determined spectrophotometrically. The initial guesses for this second stage are the arbitrary  $E_0$  used in the analysis of the spectrophotometric data and the corresponding apparent equilibrium constants. The analytical derivative supplied to the Gauss–Newton–Marquardt algorithm is shown in equation (16).

$$\log S(j) = \log \beta(j) + e(m, j) \log m + e(l, j) \log l + e(h, j) \log h \quad (12)$$

$$\text{emf} = E_0 + E_t + S \log h \quad (13)$$

where  $S$  is the electrode slope.

For fixed speciation:

$$\log \beta(j) = \text{const} + e(h, j)(\text{emf} - E_0 - E_t)/S \quad (14)$$

$$d \log \beta(j)/d E_t = -e(h, j)/S \quad (15)$$



Table 1. Comparison of data<sup>17</sup> analysed by MINQUAD<sup>6</sup> and NONLIN15; the standard error of the emf was taken as 0.6 mV, that of the titrant volume as 0.010 ml; these values were substituted into the weighting equation of Avdeef<sup>12</sup>

Program	Titration	$\log \beta_{0,1,1}$	$\log \beta_{0,2,1}$	$\log \beta_{1,0,1}$	$\log \beta_{1,0,2}$	$\log \beta_{1,0,3}$
MINIQUAD <sup>6</sup>	5	9.659	12.071	5.636 (8)*	10.396 (7)*	13.824 (13)*
	6			5.646 (14)	10.408 (14)	13.849 (21)
	7			5.614 (15)	10.368 (14)	13.736 (22)
	8			5.635 (3)	10.391 (4)	13.811 (25)
	9			5.616 (2)	10.366 (6)	—
NONLIN15	5			5.636 (11)	10.396 (11)	13.822 (15)
	6			5.648 (11)	10.407 (11)	13.848 (10)
	7			5.614 (10)	10.367 (9)	13.745 (9)
	8			5.634 (2)	10.392 (4)	13.797 (2)
	9			5.615 (2)	10.361 (10)	—

\*The digits in parentheses are  $10^3$  times the standard deviations of the mantissas of the  $\log \beta$  values.

From equation (13)

$$\begin{aligned} \frac{d \text{emf}}{dE_r} &= 1 + S \sum_{j=1}^{NS} \left[ \frac{\partial \log h}{\partial \log \beta(j)} \right] \left[ \frac{d \log \beta(j)}{dE_r} \right] \\ &= 1 - \sum_{j=1}^{NS} \left[ \frac{\partial \log h}{\partial \log \beta(j)} \right] e(h, j) \end{aligned} \quad (16)$$

The partial derivative  $\partial \log h / \partial \log \beta(j)$  can be found from the inverse Jacobian matrix as already described. The remaining parameters for initial acidity, titrant concentration,  $pK_w$  and carbonate concentration may be optimized along with  $E_r$  if desired. A model must give an acceptable fit with both the spectrophotometric and potentiometric data if it is not to be rejected.

The method is found to be particularly advantageous for measuring dissociation occurring at pH values greater than 10 or less than 4. In these circumstances potentiometric titration becomes less reliable as  $\partial \log h / \partial \log \beta(j) \ll 1$ . The method also avoids independent optimization of highly correlated variables such as initial acidity and  $\log \beta(j)$  for a minor species undergoing dissociation at pH values near 7.

The technique can be used to optimize  $E_r$  in titration of metal–ligand systems. However, it is not then possible to hold constant any  $pK_a$  values which produce significant speciation change over the titration range. The method demands that all appreciable proton-dependent speciation be optimized simultaneously from the spectrophotometric data.

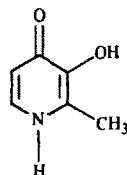
#### Validation

NONLIN15 has been validated by repeating the analysis of the potentiometric titration data of the nickel–glycinate system studied by Braibanti *et al.*<sup>17</sup> NONLIN15 optimizes the logarithms of stepwise stability constants, which are summed in Table 1 for comparison with the overall logarithms of the stability constants obtained with MINIQUAD.<sup>6</sup> The standard errors given here for NONLIN15 are similarly obtained by summation of the stepwise standard errors. This gives a pessimistic estimate of the true

standard error.<sup>18</sup> Convergence for titration 7, consisting of 97 points, occurred from initial estimates of  $\log \beta_{1,0,1} = 5$ ,  $\log \beta_{1,0,2} = 9$  and  $\log \beta_{1,0,3} = 12$  in 3 iterations, taking a total time of 9 sec.

#### Application

The use of the program is briefly demonstrated here for determination of the stability constants of the bidentate ligand 3-hydroxy-2-methyl-4-(1H)-pyridinone (I).



I

#### EXPERIMENTAL

Nitric acid (0.2M) and potassium hydroxide solution (0.2M) were prepared from BDH "Convof" ampoules. Ionic strength was maintained at 0.2 with potassium nitrate (BDH Aristar grade). All solutions were made up with 18-M $\Omega$ /cm water from a Millipore Milli-Q system. Temperature was maintained at  $22.5 \pm 0.1^\circ$  with a Churchill thermocirculator. Ambient temperature was also kept at 22.50. The ferric ion solution was prepared from the Fisons analytical grade nitrate and standardized by EDTA titration according to established procedures.<sup>19</sup> The ligand 3-hydroxy-2-methyl-4(1H)-pyridinone was synthesized and purified in this department.<sup>20</sup> Glass electrode performance was first checked by titrating with potassium hydroxide solution (0.2M) a 25-ml volume of potassium nitrate solution (0.2M) acidified with nitric acid, and making a Grans plot.<sup>21</sup> The ligand solution was then added, and the  $pK_a$  values were determined from three titrations, without removal of the electrode, each performed after addition of a further 2 ml of nominally 5mM ligand solution. Absorbance was monitored at 270 nm. In a separate experiment 5 ml of nominally 5mM ligand and 1 ml of nominally 5mM ferric nitrate were added to 25 ml of potassium nitrate solution (0.2M) before titration with potassium hydroxide (0.2M). Subsequent titrations were performed after addition of a further 1 ml of ferric nitrate solution, until a total of 3 ml had been added. Absorbance was monitored at a wavelength of 305 nm, where the uncomplexed ligand has a low absorbance compared with the complex.

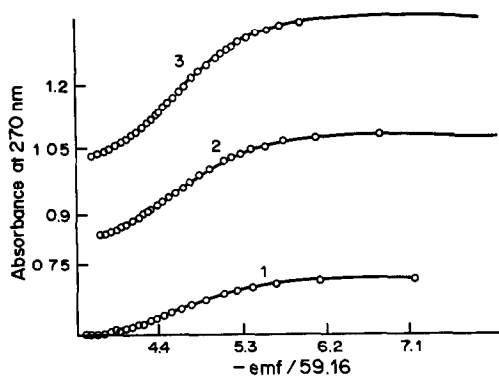


Fig. 1. Spectrophotometric titrations of the ligand (I). Absorbance at 270 nm vs. measured  $-emf/59.16$ . A further 2 ml of ligand solution was added between titrations. The solid line is the function simulated from the globally optimized parameters below.  $E_0$  was fixed at zero.

Iteration 5, Chi-squared =  $1.13 \times 10^{-3}$ ,  $R = 1.16 \times 10^{-3}$   
Error limit  $1.1116 \times 10^{-3}$

$$\begin{aligned} \epsilon \text{ for LH} &= 1262.8 \pm 0.5 \text{ l. mole}^{-1} \cdot \text{cm}^{-1} \\ \epsilon \text{ for LH}_2^+ &= 796.3 \pm 0.5 \text{ l. mole}^{-1} \cdot \text{cm}^{-1} \\ \text{Absorbance zero} &= 0.3119 \pm 0.003 \\ pK_a &= 4.609 \pm 0.001 \end{aligned}$$

## RESULTS

Experimental points and the simulated curves generated by the computer with optimized parameters are shown in Figs. 1–3, and the speciation at convergence is shown in Fig. 4. The optimized parameters are given in the legend to each figure. The slope of the glass electrode response as a fraction of the theoretical Nernstian response at 25° was optimized from spectrophotometric titration of a highly purified ref-

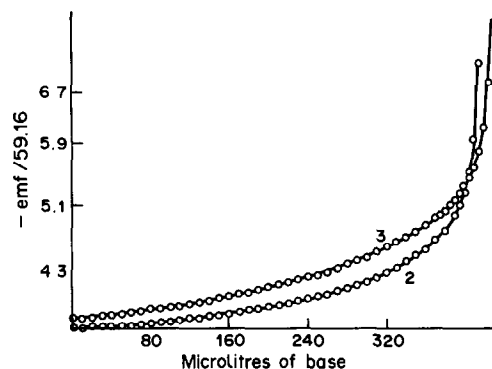


Fig. 2. Potentiometric titrations obtained simultaneously with the absorbance data shown in Fig. 1. The error  $E_r$  in  $E_0$  used for Fig. 1 was optimized by using the derivative shown in equation (16), and the  $pK_a$  was adjusted according to equation (14). The solid line is the function simulated from the globally optimized parameters below.

Iteration 8, Chi-squared = 0.370,  $R = 9.58 \times 10^{-4}$   
Error limit 0.3621

$$\begin{aligned} \text{Initial acid conc.} &= 4.348 \times 10^{-4} \pm 3 \times 10^{-7} M \\ E_0 &= 0.9086 \pm 0.0005 \\ \text{Added acid} &= 419 \pm 0.1 \mu\text{l} \\ pK_a &= 3.700 \pm 0.0015 \end{aligned}$$

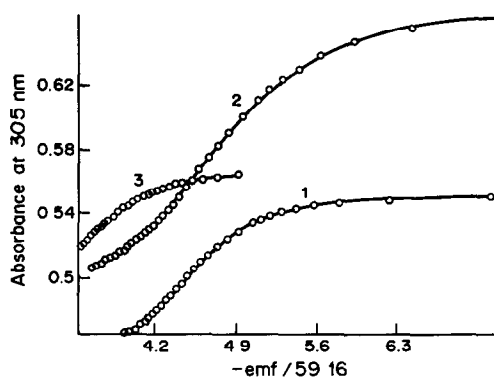


Fig. 3. Spectrophotometric titration of ligand (I) in the presence of 1, 2 and 3 ml of ferric nitrate solution.  $Mt:Lt = (1) 1:5.809; (2) 1:2.905; (3) 1:1.936$ . The solid line is the function simulated from the globally optimized parameters below.

Iteration 5, Chi-squared =  $7.59 \times 10^{-4}$ ,  $R = 1.36 \times 10^{-3}$   
Error limit  $7.3509 \times 10^{-4}$

$$\begin{aligned} \epsilon \text{ for ML}_2^+ &= 290 \pm 1 \text{ l. mole}^{-1} \cdot \text{cm}^{-1} \\ \epsilon \text{ for ML}_2^+ &= 674.7 \pm 0.6 \text{ l. mole}^{-1} \cdot \text{cm}^{-1} \\ \epsilon \text{ for ML}_3 &= 1354 \pm 1.4 \text{ l. mole}^{-1} \cdot \text{cm}^{-1} \\ \epsilon \text{ for LH} &= 118.2 \pm 0.8 \text{ l. mole}^{-1} \cdot \text{cm}^{-1} \\ \epsilon \text{ for LH}_2^+ &= 93.2 \pm 0.5 \text{ l. mole}^{-1} \cdot \text{cm}^{-1} \\ \text{Log } K_2 &= 12.027 \pm 0.001 \\ \text{Log } K_3 &= 9.734 \pm 0.001 \end{aligned}$$

erence ligand with a single  $pK_a$  (maltol). The  $pK_a$  of the ligand 3-hydroxy-2-methyl-4(1H)-pyridinone was first globally optimized from the spectrophotometric titration curves by using an assumed electrode  $E_0$  of zero. The error  $E_r$  in  $E_0$  was then optimized from the simultaneously measured data for  $emf$  vs. titrant volume [equations (14) and (16)]. The stability constants for the complexes of the ligand with Fe(III) were optimized from the spectrophotometric titration of the metal–ligand system, by using the  $pK_a$  values, electrode slope and  $E_0$ -value determined above.

### Comparison with other programs

The program NONLIN15 has many similarities to the BASIC program MICMAC.<sup>8</sup> Both are in modu-

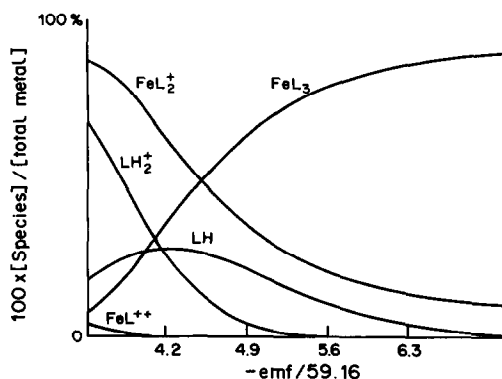


Fig. 4. Speciation plot for the titration shown in Fig. 3, curve 2, in which 2 ml of ferric nitrate were added.  $Mt:Lt = 1:2.905$ .

lar form to simplify the inclusion of new model functions, but NONLIN15 can use analytical derivatives, and this speeds operation and improves the reliability of convergence. When potentiometric titrations are modelled these analytical derivatives are used to optimize the total component concentrations,  $E_0$ -values and other parameters, as well as the logarithms of all the equilibrium constants. In this respect it is similar to the program TITFIT.<sup>2</sup> However, potentiometric parameters are optimized in NONLIN15 by minimizing the squared residuals of emf rather than titrant volume. A rigorous slope-dependent weighting scheme is used. Minimization with respect to titrant volume inherently gives the equivalence regions less weight by virtue of the slope-dependent density of points, and this method or the method adopted in NONLIN15 have been found by other workers to give closely comparable statistical parameters.<sup>22</sup> A recent publication<sup>23</sup> describes the FORTRAN program PROTAF with the features above, which minimizes the sum of square residuals of titrant volume and emf or pH.

The presence of carbonate in the basic titrant is included in the potentiometric model used for NONLIN15.

When NONLIN15 is used to analyse spectrophotometric data, the optimization of absorptivities proceeds by a method similar to that used in the program ELORMA,<sup>3</sup> as discussed previously. A recent publication<sup>24</sup> describes the FORTRAN 77 program CFTSP which optimizes stability constants and absorptivities, but without the distinction between the linear and non-linear parameters. Finally, a simple method of utilizing simultaneously measured spectrophotometric and potentiometric data has been included in the program. Satisfactory speed of operation on a microcomputer is achieved by use of the Intel 8087 coprocessor. Several improvements to the program are currently being considered. One of these is the inclusion of a general speciation program called MLGEN19,<sup>25</sup> which is routinely used in this department to simulate speciation in any three-component system with up to thirty complexes. Currently, however, NONLIN15 offers a menu of fixed but comprehensive equilibrium models in which non-existent species may be suppressed by use of large negative log  $K$  or p $K_a$  values.

The GWBASIC program listing is available on request.

*Acknowledgement*—This research was supported by the British Technology Group.

#### REFERENCES

1. D. J. Leggett (ed.), *Computational Methods for the Determination of Stability Constants*, Chap. 1. Plenum, New York, 1985, and references therein.
2. A. D. Zuberbühler and A. T. Kaden, *Talanta*, 1982, **29**, 201.
3. H. Gampp, M. Maeder and A. D. Zuberbühler, *ibid.*, 1980, **27**, 1037.
4. H. Gampp, M. Maeder, C. J. Mayer and A. D. Zuberbühler, *ibid.*, 1985, **32**, 257.
5. R. J. Motekaitis and A. E. Martell, *Can. J. Chem.*, 1982, **60**, 168.
6. A. Sabatini, A. Vacca and P. Gans, *Talanta*, 1974, **21**, 53 (original mainframe program); A. P. Arnold, S. A. Daignault and D. L. Rabenstein, *Anal. Chem.*, 1985, **57**, 1112 (Microcomputer version).
7. A. Izquierdo and J. L. Bettran, *Anal. Chim. Acta*, 1986, **181**, 87.
8. A. Laouenan and E. Suet, *Talanta*, 1985, **32**, 245.
9. G. H. Golub and F. C. Van Loan, *Matrix Computations*, North Oxford Academic, Oxford, 1983.
10. A. Avdeef and K. N. Raymond, *Inorg. Chem.*, 1979, **18**, 1605.
11. D. J. Leggett, *op. cit.*, p. 295.
12. A. Avdeef, *Anal. Chim. Acta*, 1983, **148**, 237.
13. I. E. G. Morrison, unpublished program.
14. D. W. Marquardt, *J. Soc. Ind. Appl. Math.*, 1963, **11**, 431; W. H. Press, B. P. Flannery, S. A. Teukolsky and W. T. Vetterling, *Numerical Recipes: The Art of Scientific Computing*, Cambridge University Press, Cambridge, 1986.
15. M. Jaskolski and L. Lomozik, *Talanta*, 1985, **32**, 511.
16. D. J. Leggett, *op. cit.*, p. 293.
17. A. Braibanti, F. Dallavalle and G. Mori, *Ann. Chim., Rome*, 1978, **68**, 861.
18. M. Micheloni, A. Sabatina and A. Vacca, *Inorg. Chim. Acta*, 1977, **25**, 41.
19. A. I. Vogel, *A Textbook of Quantitative Inorganic Analysis*, 3rd Ed., Longmans, London, 1961.
20. 3-Hydroxy-2-methyl-4-(1H)-pyridinone was synthesized by P. Sarpong at the University of Essex.
21. G. Grans, *Acta Chem. Scand.*, 1950, **4**, 559; *Analyst*, 1952, **77**, 661.
22. A. D. Zuberbühler, Personal communication.
23. R. Fournaise and C. Pettifaux, *Talanta*, 1987, **34**, 385.
24. L. Lampugnani, L. Meites, P. Papoff and T. Rotunno, *Anal. Chim. Acta*, 1987, **77**, 194.
25. P. D. Taylor, *Ph.D. Thesis*, University of Essex, 1987.

## ANALYSIS OF MIXTURES OF PURINES AND PYRIMIDINES BY FIRST- AND SECOND-DERIVATIVE ULTRAVIOLET SPECTROMETRY

JEAN-JACQUES AARON\* and MAME DIABOU GAYE

Institut de Topologie et de Dynamique des Systèmes, associé au C.N.R.S., Université Paris 7, 1, rue Guy de la Brosse, 75005 Paris, France

(Received 21 December 1987. Revised 20 January 1988. Accepted 15 February 1988)

**Summary**—Zero-order, first-derivative and second-derivative ultraviolet absorption spectra of a series of purines, pyrimidines and their binary mixtures in aqueous solution have been recorded at 298 K. It is shown that second-derivative spectra can be used for the identification of eight mixtures of purines and pyrimidines. Several graphical procedures are tested for evaluating derivative spectra in quantitative measurements of single compounds and mixtures. Linear log-log calibration plots are obtained with correlation coefficients generally larger than 0.99. Second-derivative spectra appear to provide a precise and simple method for determination of purines and pyrimidines, at concentrations ranging between  $5 \times 10^{-6}$  and  $5 \times 10^{-4}M$ .

The use of zero-order ultraviolet spectrometry for qualitative and quantitative analysis of mixtures where the components present overlapping spectral bands, is generally very difficult. Derivative techniques have been applied to ultraviolet spectrometry in order to reduce spectral interferences and to increase the sensitivity of detection.<sup>1</sup> Among other advantages, the experimental procedure is easy to handle and time-saving. Derivative ultraviolet spectrometry has recently been shown to be useful for characterizing and analysing mixtures of organic compounds.<sup>2-11</sup>

In a preliminary study, we showed the value of these derivative techniques for the unequivocal identification of several purines and pyrimidines in single-component aqueous solutions.<sup>12</sup> The present paper describes the application of first- and second-derivative ultraviolet spectrometry to the analysis of selected binary mixtures of purines and pyrimidines. Several graphical methods are compared for evaluating the precision of derivative ultraviolet spectrometry in quantitative studies.

### EXPERIMENTAL

#### Reagents

Adenine, 6-chloropurine, 6-mercaptopurine, hypoxanthine, cytosine, 5-fluorouracil and theophylline were purchased from United States Biochemical Corp. Purine and 6-methylpurine were obtained from C.D.C. Chemicals. Caffeine, theobromine and uric acid were obtained from Eastman Kodak. Thymine, uracil, 5-aminouracil and 5-bromouracil were purchased from Aldrich Chemical Co. 6-Iodopurine was obtained from Sigma Chemical Co. Demineralized water was used as solvent.

#### Apparatus

Zero-order, first- and second-derivative absorption spec-

tra were obtained at room temperature (298 K) between 400 and 200 nm, with a Beckman model 3600 recording spectrophotometer and a Beckman series 30 derivative accessory. Solutions under study were put in silica cells of 1-cm path-length. Spectral band-widths were automatically adjusted to between 0.2 and 5 nm. The wavelength scanning speed was set at 100 nm/min and the chart speed at 13 cm/min. The absorbance scale was set to 2, and the time constant was 4 sec for derivative spectra. The derivative accessory was set, for first- and second-derivative spectral measurements, at sensitivities of 1, 30, 100 or 200, depending on the concentration of the solution. The analogue signals from the spectrophotometer were processed by the classical, built-in electronic differentiator circuit of the Beckman derivative accessory, to provide derivative spectra.

#### Preparation of solutions

Stock solutions of single compounds of purines and pyrimidines and their two-component mixtures were prepared in demineralized water. For quantitative studies, a series of standard solutions was made by appropriate dilution or mixing of the stock solutions. Concentrations were between  $5 \times 10^{-6}$  and  $5 \times 10^{-4}M$ .

### RESULTS AND DISCUSSION

#### Zero-order, first-derivative and second-derivative ultraviolet spectra of adenine, purine and their mixtures

To test the efficiency of the first- and second-derivative spectra compared to zero-order spectra for the identification of purines and pyrimidines in mixtures, adenine and purine were selected for a detailed study.

The absorption spectra of adenine and purine are characterized by broad bands with  $\lambda_{max}$  at about 260 and 262 nm, respectively. The first-derivative spectrum of adenine shows a maximum (peak) at about 271 nm and a minimum (trough) at 246 nm, while that of purine has maxima at 270 and 203 nm,

\*Author to whom correspondence should be addressed.

Table 1. Effect of varying proportions of components on the first- and second-derivative ultraviolet spectra of binary mixtures of adenine (A) and purine (P)\*

Single compounds and mixtures	Wavelength, nm		
	Zero-order	First-derivative†	Second-derivative†
Adenine ( $10^{-4}M$ )	260	<u>271</u> ; (266); 246	<u>282</u> ; <u>273</u> ; 267; 260; (245); (238); (234); (230); 215; 205
Purine ( $10^{-4}M$ )	262	(275); <u>270</u> ; 253; (234); <u>203</u>	<u>278</u> ; <u>272</u> ; (265); 261; <u>247</u> ; (226); (211); 208; (205).
Adenine-purine ( $10^{-5}$ - $9 \times 10^{-5}M$ )	261	(276)P; 270A + P; 252P; (234)P; <u>204</u>	(281)A; 278P; (275); 271A; 265A; 260A + P; 246P; (230); (211)P; 208P; (206)P
Adenine-purine ( $2 \times 10^{-5}$ - $8 \times 10^{-5}M$ )	257	(276); 270A; 251P; (232)P; <u>205</u>	(282)A; 278P; 275A + P; <u>271A</u> ; 265A; 258A; 245P; (230); (214)A; 212P; 208P
Adenine-purine ( $3 \times 10^{-5}$ - $7 \times 10^{-5}M$ )	262	270A; 250A + P; <u>208</u>	(282)A; 278A + P; (276); <u>272A</u> ; 266A; 259A; (244)P; (229); 215A; 212P
Adenine-purine ( $4 \times 10^{-5}$ - $6 \times 10^{-5}M$ )	262	<u>270A</u> ; 250A + P; <u>210</u>	(282)A; (279)A + P; (275); <u>272A</u> ; 265A; 258A; (246)P; <u>214A</u>
Adenine-purine ( $5 \times 10^{-5}$ - $5 \times 10^{-5}M$ )	260	<u>270</u> ; 248	(282)A; (279)A + P; <u>272A</u> ; 267A; 260A; 216A

\*In aqueous solution at 298 K.

†Wavelengths of maxima are underlined, other wavelengths correspond to minima. Those for shoulders are given in brackets.

shoulders at 275 and 234 nm, and a minimum at 253 nm (Table 1). The second-derivative spectrum of adenine presents maxima at 282 and 273 nm, shoulders at 245, 238, 234 and 230 nm, and minima at 267, 260, 215 and 205 nm, while that of purine shows maxima at 278, 272, 247 and 208 nm, shoulders at 226, 211 and 205 nm, and minima at 265 and 261 nm (Table 1).

We have studied the zero-order, first-derivative and second-derivative ultraviolet spectra of mixtures of adenine and purine of various compositions, but constant total molar concentration of the two compounds (Table 1). As expected, the zero-order absorption spectra of all the mixtures are characterized by a strong overlap of the absorption bands of adenine and purine, which prevents determination of the individual components in such mixtures.

The first-derivative ultraviolet spectra of the mixtures show several maxima and minima (Table 1) but peaks (or troughs) could be identified unequivocally as belonging to purine only for certain compositions (Fig. 1). Although first-derivative spectra give better resolution than zero-order spectra do, they cannot be used for analysis of mixtures of adenine and purine.

The second-derivative spectra of the mixtures display a larger number of maxima and minima (Table 1, Fig. 1), and peaks (or troughs) can be attributed unequivocally to purine or to adenine, for all the compositions examined. Hence spectroscopic identification of adenine and purine in mixtures is possible only when the second-derivative spectra are used. The detection power for both adenine and purine in mixtures is also enhanced by the differentiation. A similar conclusion was recently

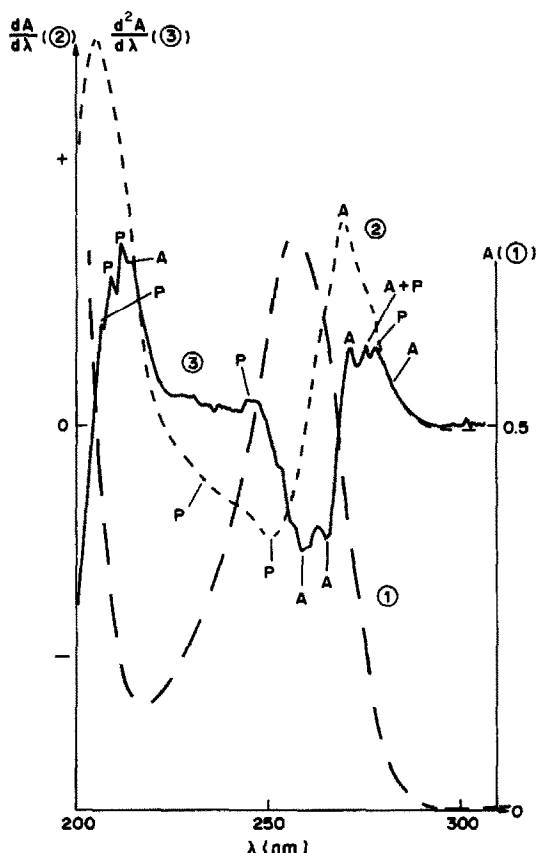


Fig. 1. Zero-order (curve 1), first-derivative (curve 2) and second-derivative (curve 3) ultraviolet spectra of a mixture of adenine ( $2 \times 10^{-5}M$ ) and purine ( $8 \times 10^{-5}M$ ). The peaks, troughs and shoulders characterizing the compounds are denoted P (purine) and A (adenine).

Table 2. Identification of binary mixtures of purines and pyrimidines by using second derivative UV spectra\*

Composition	Wavelength†, nm
<b>Single compounds‡</b>	
Adenine	<u>282</u> , <u>273</u> , <u>267</u> , <u>260</u> , (245), (238), (234), (230), <u>215</u> , <u>205</u>
Caffeine	<u>291</u> , <u>271</u> , <u>243</u> , <u>230</u> , <u>216</u> , <u>202</u>
Cytosine	<u>285</u> , <u>267</u> , <u>245</u> , <u>216</u> , <u>202</u>
6-Methylpurine	<u>277</u> , <u>270</u> , (264), <u>260</u> , <u>248</u> , (230), <u>210</u>
Purine	<u>278</u> , <u>272</u> , (265), <u>261</u> , <u>247</u> , (226), (211), <u>208</u> , (205)
Thymine	<u>289</u> , <u>286</u> , <u>265</u> , <u>227</u> , <u>210</u>
Uracil	<u>279</u> , <u>258</u> , <u>222</u> , (217), <u>205</u>
Uric acid	<u>306</u> , (299), <u>286</u> , <u>252</u> , <u>231</u> , <u>210</u> , (208), (206)
<b>Mixtures</b>	
Adenine(A)-cytosine(C) ( $1 \times 10^{-5}$ - $9 \times 10^{-5}M$ )	(285)C, (283)A, (276)A, 267A + C, 260A, <u>246C</u> , <u>216A</u> , 208, 203C
Adenine(A)-purine(P) ( $2 \times 10^{-5}$ - $8 \times 10^{-5}M$ )	(282)A, 278P, 275A + P, 271A, 265A, 258A, <u>245P</u> , (230) (214)A, <u>212P</u> , <u>208P</u>
Caffeine(CAF)-6-methylpurine(MP) ( $5 \times 10^{-5}$ - $5 \times 10^{-5}M$ )	288CAF, 275MP, 270CAF, 263MP, <u>244</u> , 229CAF, (215)CAF, <u>211MP</u> , (208)MP
Cytosine(C)-thymine(T) ( $5 \times 10^{-5}$ - $5 \times 10^{-5}M$ )	<u>286T</u> , <u>283C</u> , 267C + T, <u>248C</u> , <u>228T</u> , <u>215C</u> , 210T, <u>203C</u>
6-Methylpurine(MP)-uracil(U) ( $1 \times 10^{-5}$ - $9 \times 10^{-5}M$ )	(279)U, <u>276MP</u> , 260MP, (222)U, <u>212P</u> , 201MP
Uric acid(UA)-purine(P) ( $5 \times 10^{-5}$ - $5 \times 10^{-5}M$ )	306UA, 289UA, 227P, 271P, (266)P, (262)P, <u>250UA</u> , <u>233UA</u> , (211), 209, (206)
Uric acid(UA)-caffeine(CAF) ( $5 \times 10^{-5}$ - $5 \times 10^{-5}M$ )	306UA, (290)CAF, 276CAF, <u>250UA</u> , 229, <u>216CAF</u> , (212)UA, (208)UA, 201CAF
Uric acid(UA)-uracil(U) ( $5 \times 10^{-5}$ - $5 \times 10^{-5}M$ )	306UA, 287UA, 278U, 260U, <u>250UA</u> , 232UA, (216)U, (208)UA, (205)UA

\*In aqueous solution at 298 K.

†Wavelengths of maxima are underlined, other wavelengths correspond to minima. Those for shoulders are given in brackets.

‡Concentration:  $5 \times 10^{-5}M$ .

reached by Gil *et al.*,<sup>7</sup> for an equimolar mixture of cytosine and adenine.

#### Second-derivative ultraviolet spectra of purines and pyrimidines and their binary mixtures

The characteristics of the second-derivative ultraviolet spectra for selected purines, pyrimidines and their binary mixtures are given in Table 2. The spectra of the individual compounds show several maxima and minima. It can be seen that most of the peaks and troughs observed in the mixtures are attributable unambiguously to each component (Table 2). Therefore, the second-derivative spectra can be used for the qualitative analysis of binary mixtures of purines and pyrimidines, whereas the zero-order and first-derivative spectra are unsatisfactory for the purpose. For example, it can be seen, in Fig. 2, that the zero-order and first-derivative spectra of a mixture of cytosine and thymine (curves 1 and 2) do not provide any useful information for identifying these two compounds, whereas the second-derivative spectrum (curve 3) gives seven characteristic wavelength values for cytosine or thymine. In the case of a mixture of caffeine and 6-methylpurine (Fig. 3), the first-derivative spectrum provides only four specific wavelength values, but the second-derivative spectrum is characterized by eight wavelength values allowing identification of these purines.

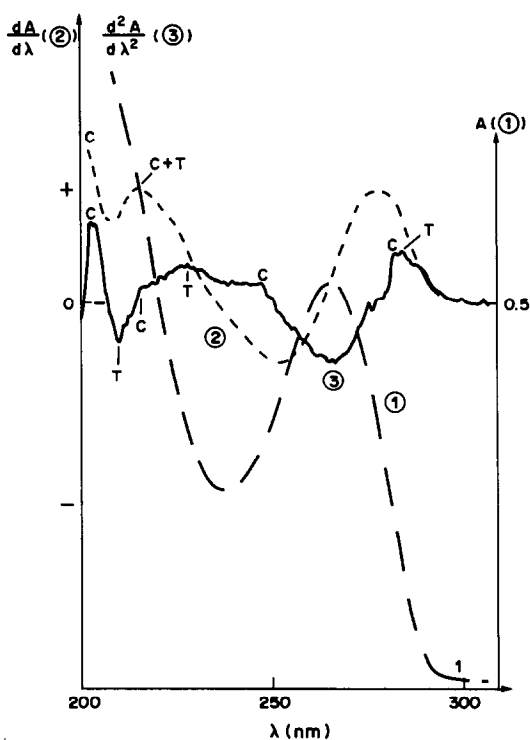


Fig. 2. Zero-order (curve 1), first-derivative (curve 2) and second-derivative (curve 3) ultraviolet spectra of a mixture of cytosine (C) ( $5 \times 10^{-5}M$ ) and thymine (T) ( $5 \times 10^{-5}M$ ).

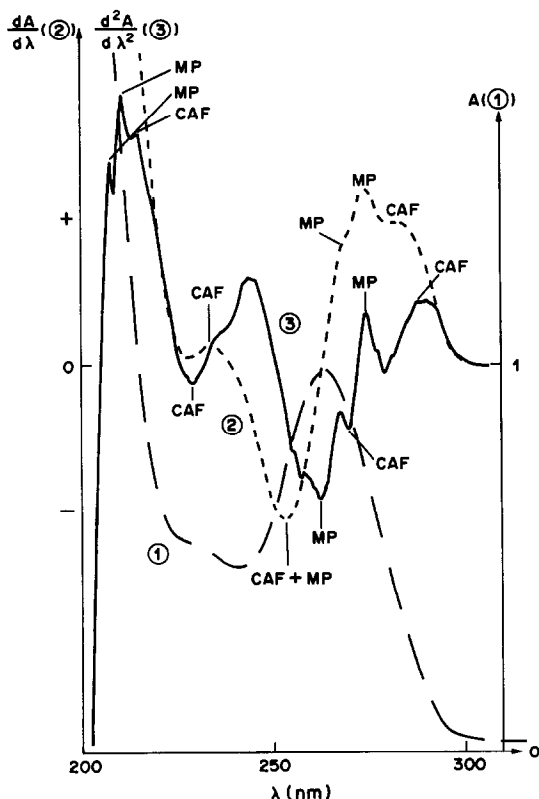


Fig. 3. Zero-order (curve 1), first-derivative (curve 2) and second-derivative (curve 3) ultraviolet spectra of a mixture of caffeine (CAF) ( $5 \times 10^{-5}M$ ) and 6-methylpurine (MP) ( $5 \times 10^{-5}M$ ).

*Evaluation of first- and second-derivative ultraviolet spectra of purines and pyrimidines for quantitative measurements*

Several methods of evaluation of derivative spectra

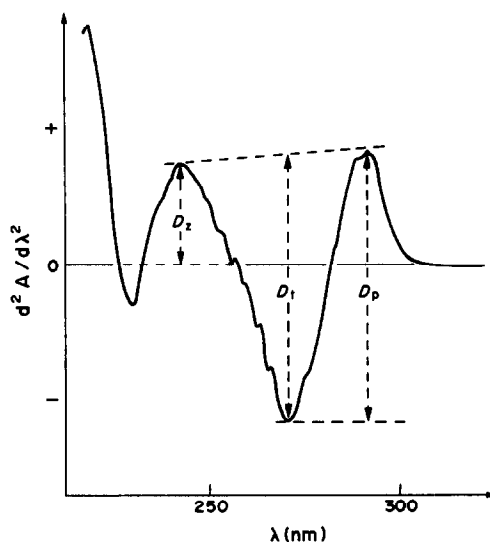


Fig. 4. Evaluation of the second-order derivative spectrum of caffeine ( $5 \times 10^{-5}M$ ) for quantitative measurements. Tangent method ( $D_t$ ), peak-to-trough method ( $D_p$ ) and zero-crossing method ( $D_z$ ).

have been proposed for the determination of analytes.<sup>1-3</sup> The tangent (t) method consists of drawing a common tangent to two neighbouring maxima or minima, and measuring a distance  $D_t$  to the intermediate extremum value, parallel to the ordinate. The peak-to-trough (p) method is based on the measurement of the distance  $D_p$  between two extrema (a minimum and a maximum); it is mainly used for quantitative analysis of multicomponent mixtures. Finally, the zero-crossing (z) method consists of evaluating the vertical distance  $D_z$  from a peak to the

Table 3. Statistical treatment of analytical data obtained from the first derivative spectral measurement of purines and pyrimidines using several evaluation procedures

Compound	Peak-to-trough method ( $D_p$ )				Zero-crossing method ( $D_z$ )			
	LDR*	Slope†	Intercept†	Correlation† coefficient	LDR*	Slope†	Intercept†	Correlation† coefficient
Adenine	20	0.91	6.96	0.998	20	0.92	6.54	0.999
5-Aminouracil	40	0.93	6.54	0.999	40	0.92	6.21	0.999
5-Bromouracil	20	0.88	6.67	0.999	40	0.93	6.09	0.999
Caffeine	40	0.89	6.51	0.999	40	0.92	6.62	0.999
6-Chloropurine	20	0.74	6.06	0.989	20	0.86	6.42	0.998
Cytosine	40	0.94	6.75	0.997	40	0.99	6.76	0.999
5-Fluorouracil	20	0.97	6.61	0.998	40	0.93	5.78	0.995
Hypoxanthine	20	1.05	7.35	0.995	40	1.04	6.99	0.996
6-Iodopurine	20	0.94	6.96	0.998	20	0.92	6.67	0.999
6-Mercaptopurine	10	0.83	6.73	0.997	10	0.92	6.41	0.998
6-Methylpurine	20	0.90	6.73	0.999	40	0.81	6.11	0.999
Purine	20	0.93	7.02	0.993	20	0.96	6.93	0.995
Theobromine	20	1.01	7.42	0.995	20	1.01	6.70	0.991
Theophylline	20	0.92	6.84	0.998	40	0.91	6.40	0.998
Thymine	40	0.90	6.61	0.999	40	0.95	6.20	0.998
Uracil	40	0.87	6.55	0.995	40	0.95	6.52	0.999
Uric acid	20	0.85	6.65	0.995	40	0.83	5.95	0.995

\*LDR = linear dynamic range, corresponding to the ratio of the upper concentration of linearity (within 5%) and the limit of detection.

†Values calculated by the statistical treatment of 5-7 measurements for each log-log calibration plot.

Table 4. Statistical treatment of analytical data obtained from the second derivative spectral measurements of purines and pyrimidines by several evaluation procedures

Compound	Peak-to-trough method ( $D_p$ )			Zero-crossing method ( $D_z$ )			Tangent method ( $D_t$ )				
	LDR* Slope†	Intercept†	Correlation† coefficient	LDR* Slope†	Intercept†	Correlation† coefficient	LDR* Slope†	Intercept†	Correlation† coefficient		
Adenine	—	—	—	20	0.86	6.36	0.997	20	0.80§	6.42§	0.999§
5-Aminouracil	20	0.87	0.998	10	1.07	6.43	0.999	20	0.82	5.67	0.992
5-Bromouracil	20	0.84	0.998	20	0.89	6.09	0.999	20	0.82	6.08	0.997
Caffeine	40	0.90	0.999	40	0.98	6.64	0.998	40	0.26	3.59	0.843
6-Chloropurine	20	0.88	0.999	40	0.90	6.39	0.996	40	1.43	8.81	0.898
Cytosine	40	0.78	0.992	40	0.86	5.93	0.996	40	0.72	5.55	0.991
5-Fluorouracil	40	0.90	0.999	10	0.94	6.12	0.986	40	0.83	5.84	0.999
Hypoxanthine	—	—	—	20	1.06	7.07	0.992	15§	0.97§	6.85§	0.996§
6-Iodopurine	—	—	—	20	0.92	6.27	0.999	20§	0.78§	6.18§	0.992§
6-Mercaptopurine	10	0.78	0.995	10	0.74	5.65	0.998	10	0.79	6.24	0.993
6-Methylpurine	—	—	—	20	0.83	6.11	0.999	40	0.78§	6.30§	0.997§
Purine	—	—	—	20	0.88	6.36	0.995	10	0.85§	6.60§	0.988§
Theobromine	20	0.97	0.995	20	0.82	6.07	0.999	20	0.94	6.90	0.996
Theophylline	40	0.90	0.998	20	0.78	5.56	0.998	40	0.83	6.27	0.997
Thymine	40	0.89	0.998	40	0.82	5.87	0.999	40	0.89	6.40	0.998
Uracil	20	0.87	0.999	40	0.83	5.97	0.998	20	0.86	6.34	0.999
Uric acid	40	0.81	0.995	40	0.85	5.89	0.989	40	0.79	6.06	0.992

\*LDR = linear dynamic range, corresponding to the ratio of the upper concentration of linearity (within 5%) and the limit of detection.

†Values calculated by the statistical treatment of 5-7 measurements for each log-log calibration plot.

§Because of the shape of the peaks, amplitudes  $D_t$  were extrapolated for these compounds.



Table 5. Analytical data obtained from the second derivative spectral measurement of mixtures of purines and pyrimidines\*

Mixtures	Compound	$\lambda_{AN}^\dagger$ , nm	Slope $^\ddagger$	Intercept $^\ddagger$	Correlation $^\ddagger$ coefficient
Adenine-cytosine (A) (C)	A	216	0.84	6.65	0.999
	C	246	0.58	4.35	0.918
Adenine-purine (A) (P)	A	272	1.09	7.34	0.999
	P	246	1.20	6.85	0.943
6-Methylpurine-uracil (MP) (U)	MP	276	0.80	6.02	0.985
	U	—	—	—	—
Cytosine-thymine (C) (T)	C	202	1.31	8.07	0.996
	T	—	—	—	—

\*All measurements were made by the zero-crossing method and corrected for the presence of the overlapping peaks of the other component where necessary.

$\dagger\lambda_{AN}$  = analytical wavelength of the peak (or trough) used for the calibration curve of the particular compound in the mixture.

$\ddagger$ Values calculated by the statistical treatment of 4–5 measurements for each calibration graph.

zero (base) line. We present an example of the application of these three methods to the second-order derivative spectrum of caffeine (Fig. 4).

We have calculated  $D_i$ ,  $D_p$  and  $D_z$  values for selected purines and pyrimidines. These quantities have been correlated with the absolute concentration of the single compounds in solution, in the range from  $5 \times 10^{-6}$  to  $2 \times 10^{-4}M$ . The statistical treatment of the analytical data obtained from selected wavelength values of the first- and second-derivative spectral measurements is given in Tables 3 and 4, respectively. The data show that, for first-derivative spectra, log-log correlations are excellent between the purine (or pyrimidine) concentration and  $D_p$  and  $D_z$ . The correlation coefficients are larger than 0.99 in all cases, and the slopes are close to unity. The linear dynamic ranges (LDR) (upper/lower limit ratio) vary between 10 and 40 (Table 3). Studies with second-derivative spectra also indicate that the concentrations of purines (or pyrimidines) correlate well with the peak-to-trough amplitudes,  $D_p$ , and the peak-to-baseline amplitudes  $D_z$  (Table 4). The calibration plots obtained by the tangent method ( $D_i$  values) provide poorer log-log correlations, with correlation coefficients ranging between 0.84 and 0.99, according to the compounds. For this method a better precision was achieved by using an extrapolation procedure for the heights of the peaks. The LDR values are between 10 and 40 (Table 4).

#### Quantitative analysis of mixtures of purines and pyrimidines

The statistical treatment of the analytical data obtained from the second-derivative spectral measurements of selected mixtures of purines and pyrimidines (Table 5) reveals that the concentrations of adenine, cytosine, purine and 6-methylpurine (ranging between  $10^{-5}$  and  $10^{-4}M$ ) correlate well with the peak-to-baseline amplitudes,  $D_z$ , determined at selected wavelength values. In most cases, the correlation coefficients are larger than 0.99, and the

slopes are close to unity, as they are for the individual compounds. This indicates that the second-derivative spectra maxima and minima of purines are resolved sufficiently to allow quantitative analysis of mixtures. However, for 6-methylpurine-uracil and cytosine-thymine mixtures, no meaningful correction relative to the uracil and thymine components could be obtained. This is probably due to the partial overlapping of the peaks selected for determining these particular compounds.

#### CONCLUSION

Second-derivative ultraviolet spectrometry is a convenient technique for identifying most purines and pyrimidines in two-component mixtures. First- and second-derivative spectra give practically the same satisfactory precision for the log-log correlations between concentrations of the simple compounds and the peak-to-trough or peak-to-baseline amplitudes. Quantitative correlations are also found for the second-derivative spectral measurements of the individual components in binary mixtures of purines.

#### REFERENCES

1. A. F. Fell, *Trends Anal. Chem.*, 1983, **2**, 63.
2. T. C. O'Haver and G. L. Green, *Anal. Chem.*, 1976, **48**, 312.
3. G. Talsky, L. Mayring and H. Kreuzer, *Angew. Chem. Int. Ed. Engl.*, 1978, **17**, 785.
4. B. Morrelli, *Analyst*, 1982, **107**, 282.
5. *Idem, ibid.*, 1983, **108**, 870.
6. *Idem, ibid.*, 1983, **108**, 1506.
7. M. Gil, N. Iza and J. Morcillo, *An. Quim. Ser. A.*, 1983, **79**, 473.
8. M. A. Korany, A. M. Wahbi, M. A. Elsayed and S. Mandour, *Anal. Lett.*, 1984, **17**, 1373.
9. P. S. Ramanathan and V. S. Sarang, *Indian J. Chem.*, 1984, **23A**, 37.
10. A. H. Lawrence and J. Kovar, *Anal. Chem.* 1984, **56**, 1731.
11. K. Kitamura and R. Majima, *ibid.*, 1983, **55**, 54.
12. J. J. Aaron and D. Gningue, *Analisis*, 1985, **13**, 426.

## SPECIATION AND DETERMINATION OF TIN(IV) AND ORGANOTIN COMPOUNDS IN SEA-WATER BY HYDRIDE GENERATION-ATOMIC-ABSORPTION SPECTROMETRY WITH AN ELECTRICALLY HEATED LONG ABSORPTION CELL

M. CHAMSAZ\*, I. M. KHASAWNEH† and J. D. WINEFORDNER‡  
Department of Chemistry, University of Florida, Gainesville, FL 32611, U.S.A.

(Received 23 September 1987. Revised 26 January 1988. Accepted 5 February 1988)

**Summary**—A method is described for the determination of nanogram or subnanogram amounts of Sn(IV) and the halides of methyltin, dimethyltin, trimethyltin, n-butyltin, dibutyltin, and tributyltin. These compounds are volatilized from water samples by hydride generation, collected on a chromatographic stationary phase, desorbed in order of increasing boiling point, and detected by atomic-absorption spectrometry with atomization in a long electrothermally heated alumina tube furnace. The absolute detection limits are in the range 0.4–1.5 ng with a reproducibility of 4–15% for inorganic tin and organotin compounds.

In recent years, there has been growing interest in the analysis and speciation of tin derivatives in the environment. Organotin compounds have been widely used for a variety of commercial applications such as fungicides,<sup>1</sup> wood preservatives,<sup>2</sup> and stabilizers in plastics.<sup>3</sup> Organotin compounds with short alkyl chains generally exhibit considerable toxicity toward both aquatic organisms and mammals. For example, the tributyltin compounds used as anti-fouling agents in paints for the hulls of ships<sup>4</sup> have been found to have sublethal and lethal effects on fish,<sup>5</sup> crab,<sup>6</sup> shrimp,<sup>7</sup> and oyster,<sup>8</sup> even at ng/ml levels or lower in sea-water. Although total tin determination has been possible for many years, it is only within the past decade that speciation methods have been developed for sensitive measurements of tin derivatives. Most of these speciation techniques involve separation by gas chromatography<sup>9–18</sup> or adsorptive collection of the hydrides followed by separation based on sequential desorption in order of increasing boiling point,<sup>9,19–26</sup> coupled with some sort of element-specific detection system, such as flame atomic-absorption spectrometry (AAS),<sup>9,11,21–25</sup> electrothermal atomic-absorption spectrometry,<sup>26,27</sup> atomic-emission spectrometry,<sup>10,28,29</sup> mass spectrometry,<sup>12,15,30</sup> or flame photometric detection.<sup>14,16,31–33</sup> Recently, high-performance liquid chromatography followed by electrothermal<sup>34,35</sup> or flame<sup>36</sup> atomic-absorption spectrometry or hydride-generation-direct current plasma emission

spectrometry<sup>37</sup> have been widely employed for speciation and measurement of organotin compounds in aquatic environments.

Hydride-generation with trap collection followed by atomic-absorption detection has received much attention and has been shown to be a very simple and sensitive method for speciation and determination of organotin compounds at nanogram and lower levels. Many types of atomization cells have been employed, including flames, flame-in-tube atomizers, flame-heated silica tubes, electrothermally heated silica tubes, and graphite furnace atomizers. Electrically heated silica tubes have been found to give higher sensitivity as the result of longer residence time of the atom clouds in the optical path, lower dilution and reduced noise levels. Another advantage of this type of atomizer is that it is possible to control the temperature and to obtain an optimum temperature for each element. The electrothermal atomizer used for this study consisted of an alumina tube inserted inside an electrically heated graphite tube furnace. The present work describes the experimental procedure of generation, trapping and separation of organotin hydrides on a chromatographic stationary phase, and AAS detection by use of a heated alumina tube, together with the optimization of different parameters and the results obtained.

### EXPERIMENTAL

#### Apparatus

The trapping system included a 500-ml gas-washing bottle with a 29/42 tapered glass joint, a glass U-tube water trap (40 cm × 1.2 cm o.d.), and a Pyrex U-tube hydride trap (25 cm × 6.5 mm o.d.). The hydride trap was packed for 2/3 of its length with either glass wool or chromatographic material and wrapped with nichrome wire (26 gauge). Flexible Teflon tubing (2.5 mm i.d.) and 1/4–1/8 in. Teflon Swagelok

\*On sabbatical leave from Chemistry Department, Faculty of Sciences, Mashhad University, Mashhad, Iran.

†On sabbatical leave from Chemistry Department, Yarmouk University, Irbid, Jordan.

‡Author to whom all correspondence should be sent.

reducing unions were used to connect the whole system to the furnace. The power supply to the wire round the trap was supplied by a variable transformer. The furnace, similar to the one described by Wang *et al.*,<sup>38</sup> consisted of a central graphite tube (14 cm × 7 mm i.d.) as the resistive heating element. Two graphite electrodes held the heater-tube ends, allowing for expansion as well as providing good electrical contact, and two brass electrodes with internal water cooling held the graphite electrodes. A sample-gas inlet tube made of alumina, which was held by a threaded graphite-tube holder, was inserted into the inner tube. The entire absorption cell was housed inside a silica cylinder which was flushed with argon as sheath gas at a flow-rate of 3 l./min. An inner tube made of alumina, silica or graphite (20 cm × 4.5 mm) was placed inside the central tube to act as the absorption cell. Two electric cables connected the 2.5-kW SCR Power Supply (Model SCR 20-250, Electronic Measurements Inc., Neptune, NY) to the brass electrodes. Tin in the organotin hydrides was determined by means of a Hitachi 180-80 polarized Zeeman atomic-absorption spectrometer. A Fisher Scientific high spectral-output tin hollow-cathode lamp operated at 7 mA was used as the light-source. All measurements were made at the 224.6 nm resonance line with a spectrometer bandwidth of 0.4 nm. Peak heights were used as the measurement parameter. The signals from the photomultiplier were processed by a micro-processor and analytical results were recorded on a Hitachi Model 056 strip-chart recorder set at 10 mV to give full scale deflection for an absorbance of 0.2, with a chart speed of 2 cm/min.

#### Reagents

Demineralized water was used in all experiments. All glassware used for preparation, storage and dilutions was cleaned by soaking in 10% v/v nitric acid for 10 hr, followed by rinsing with demineralized water. Hydrochloric acid (5M) was prepared from ACS Fisher Scientific concentrated hydrochloric acid. Aqueous 4% sodium borohydride solution was made from the Alfa Ventron 99% pure salt, filtered through a 0.2 μm filter paper, purged with argon for 30 min, and allowed to stand for 12 hr in a glass flask to reduce the tin blank and ensure optimum reproducibility. Fisher certified ACS spectroanalysed grade methanol was used.

#### Standards

Organotin compounds were purchased from Alfa Ventron Chemical; 1000 μg/ml stock solutions of methyltin and butyltin chlorides were prepared in 10% hydrochloric acid (made with demineralized water) and methanol respectively. A 1000 mg/ml stock solution of inorganic tin was prepared by dissolving 1.000 g of 99.9% purity tin (Fisher Scientific) in 10 ml of concentrated hydrochloric acid and diluting to 100.0 ml with demineralized water. Working standards were freshly prepared before measurement, by dilution with demineralized water for inorganic tin and methyltins, and methanol for butyltins. Artificial sea-water of salinity 35‰

was prepared with analytical grade sodium sulphate and sodium, potassium, calcium and magnesium chlorides.<sup>39</sup>

#### Procedure

Samples (500 ml) of sea-water spiked with inorganic tin and organotin compounds were introduced into the reaction flask. They were acidified with 3 ml of 5M hydrochloric acid, the magnetic stirrer was started, and helium was bubbled through the sample for a few minutes to remove oxygen, during which time the hydride trap was cooled in liquid nitrogen. Five ml of 4% sodium borohydride solution were injected over a period of 60 sec into the hydride-generation flask through a rubber septum on the vessel side-arm, producing a smooth evolution of hydrogen bubbles which effectively stripped the hydrides from the solution in 5 min. The hydride trap was then removed from the liquid nitrogen and the collected hydrides were volatilized, in order of their boiling points, into a heated alumina or silica tube and the tin was measured by atomic-absorption spectrometry.

## RESULTS AND DISCUSSION

### Hydride generation

Inorganic tin and alkyltin compounds react with sodium borohydride under acidic conditions to yield the corresponding hydrides. In this study, different acids at different concentrations were evaluated as reaction media for hydride generation from stannic chloride and all the alkyltin compounds listed in Table 1. Hydrochloric acid (addition of 3 ml of the 5.0M acid resulted in pH ~ 2) was found to give greater sensitivity than a corresponding addition of acetic acid. Addition of 1 ml or 10 ml of 5M hydrochloric acid resulted in a sensitivity lower by about 55%; the optimal volume was 3 ml (±0.3). A second injection of sodium borohydride after a 5-min (or longer) cooling period produced no change in sensitivity. To assess the recovery of inorganic tin and organotin compounds from sea-water, the same procedure was applied to the tin compounds in demineralized water; there was an average difference of only 4% between the two sets of results.

### Carrier lines and water traps

Use of small (2–5 mm) diameter carrier lines contributed to the overall high sensitivity of the system, as a result of the lower dead volume. The

Table 1. Analytical figures of merit for tin and organotin chlorides<sup>a</sup>

Compound	Linear range, ng <sup>b</sup>	Sensitivity, ng <sup>c</sup>	Detection limit, ng <sup>d</sup>	RSD% <sup>e</sup>
SnCl <sub>4</sub>	0.4–50	1.1	0.4	6
CH <sub>3</sub> SnCl <sub>3</sub>	0.4–50	1.2	0.4	5
(CH <sub>3</sub> ) <sub>2</sub> SnCl <sub>2</sub>	0.5–50	1.3	0.5	4
(CH <sub>3</sub> ) <sub>3</sub> SnCl	0.6–50	1.7	0.6	7
C <sub>4</sub> H <sub>9</sub> SnCl <sub>3</sub>	0.5–50	1.3	0.5	6
(C <sub>4</sub> H <sub>9</sub> ) <sub>2</sub> SnCl <sub>2</sub>	0.9–50	2.6	0.9	9
(C <sub>4</sub> H <sub>9</sub> ) <sub>3</sub> SnCl	1.5–50	4.5	1.5	15

<sup>a</sup>Analytical figures of merit are for individual compounds (not mixtures).

<sup>b</sup>From detection limit to limit of linearity.

<sup>c</sup>Concentration which gives 0.0044 absorbance.

<sup>d</sup>Based on concentration giving a signal = 3 × standard deviation of the blank signal.

<sup>e</sup>For seven replicate determinations at the 10-ng level.

length of the carrier lines was kept to 35 cm to avoid loss of water vapour by condensation on the tube surface. The water trap was necessary to remove water vapour and hence to extend the lifetime of the adsorbent phase. For the determination of inorganic tin and methyltin compounds, the Pyrex U-tube, immersed in dry-ice/acetone ( $-78^{\circ}$ ) efficiently removed water from the system, allowing up to 50 determinations before changing of the trap became necessary. However, when butyltin compounds are to be determined, the trap should not be cooled, as they would then be retained in the trap. When the water trap was not used, the sensitivity for butyltins was sharply reduced after 3 sample runs. In order to remove traces of water completely from the trap, at the end of each determination the trap was connected to the argon line and heated to about  $100^{\circ}$  by the nichrome wire wrapped round it, and argon was passed through the system for about 2 min. When this was done, no loss of sensitivity was observed, and the packing material did not have to be changed during a series of 50 measurements.

#### *Furnace optimization*

Silica, alumina and graphite tubes of the same lengths and diameters were evaluated as the atomization units. A graphite tube gave much lower sensitivity, even if impregnated with sodium tungstate or zirconium chloride. A silica tube gave 10–20% higher sensitivity than an alumina tube for inorganic tin and organotin compounds. The higher sensitivity could have been due to the faster heating-rate of the silica tube. The surface of the silica tube deteriorated rapidly, however, resulting in decreased sensitivity, as noticed by others.<sup>40</sup> The sensitivity could be regained by soaking the silica tube in 10% hydrofluoric acid. The alumina tube showed no deterioration effects, and so was chosen for use. Measurement with an optical pyrometer showed the furnace temperature to be  $1400^{\circ}$ .

#### *Influence of gas flow-rate*

The collection efficiency and speciation of organotin hydrides depended on the helium carrier-gas flow-rate. Low flow-rates could be used for determination of methyltin compounds, with good separation efficiency. For the less volatile butyltin compounds, higher gas flow-rates were necessary, at the expense of reduced separation efficiency. A flow-rate of 15 ml/min was found to be optimal for all the organotin compounds with regard to both sensitivity and speciation. Addition of hydrogen and oxygen to the furnace gas has been known to greatly enhance the sensitivity.<sup>41,42</sup> Addition of hydrogen through a port placed at the edge of the furnace significantly increased the sensitivities for inorganic tin and all the organotin derivatives. Introducing oxygen into the furnace further increased the sensitivity by an average of 50%. This suggests that the atomization in the furnace occurred through collisions with H and OH

radicals in a rich hydrogen–oxygen flame.<sup>39,41</sup> The optimal flow-rates of oxygen and hydrogen were 180 and 670 ml/min, respectively.

#### *Separation of inorganic tin and organotins*

Tin hydride and organotin hydrides evolved from the hydride trap in a manner which allowed their separation and identification by means of their retention times. The retention times of these hydrides are related to their boiling points,  $\text{SnH}_4$  ( $-52^{\circ}$ ),  $\text{CH}_3\text{SnH}_3$  ( $1.4^{\circ}$ ),  $(\text{CH}_3)_2\text{SnH}_2$  ( $35^{\circ}$ ),  $(\text{CH}_3)_3\text{SnH}$  ( $59^{\circ}$ ),  $\text{C}_4\text{H}_9\text{SnH}_3$  ( $100^{\circ}$ ),  $(\text{C}_4\text{H}_9)_2\text{SnH}_2$  ( $250^{\circ}$ ) and  $(\text{C}_4\text{H}_9)_3\text{SnH}$  ( $280^{\circ}$ ). Three adsorbents were tested. The initial experiments were with glass wool. Resolution of the stannane, methylstannanes and butylstannanes signals was possible with good sensitivities. The other two adsorbents were Chromosorb GAW-DMCs and Chromosorb WAW-DMCs (60–80 mesh) coated with 3% silicone OV-101 and OV-3, respectively. Both acted similarly and resulted in improved separation of inorganic tin and organic hydrides. Figure 1 represents typical simultaneous separation of inorganic tin, three methyltins and three butyltins. The hydride trap was slowly warmed for the release of the dibutyltin and tributyltin compounds.

#### *Calibration graphs, sensitivity, detection limits and precision*

The calibration plots for tin(IV), methyltin and butyltin compounds were linear over the concentration ranges shown in Table 1; all results in Table 1 are for the compounds run individually. The linear range is up to two orders of magnitude and can be further increased by using the 235.48 nm wavelength. Inorganic tin, methyltin and monobutyltin compounds have similar sensitivities. The sensitivities for dibutyltin and tributyltin compounds are generally lower, which could be the result of reduced efficiency of tin atomization through collision of H and OH radicals with the larger alkyl groups. Use of peak area instead of peak height increased the sensitivity for tributyltin hydride by a factor of 3. The detection limits (three times the standard deviation of the blank) varied from 0.4 to 1.5 ng for 500-ml samples. The precision (relative standard deviation) for five replicate determinations of each compound at the 10-ng level ranged from 4 to 15%. The reproducibility could possibly be improved by using the peak area instead of peak height.

#### CONCLUSION

The combination of hydride generation with electrothermal atomization in a long absorption tube provides a simple and very sensitive method for speciation and determination of inorganic tin and organotin compounds. Good separation of these compounds can be achieved by use of chromatographic stationary phases in the hydride trap.

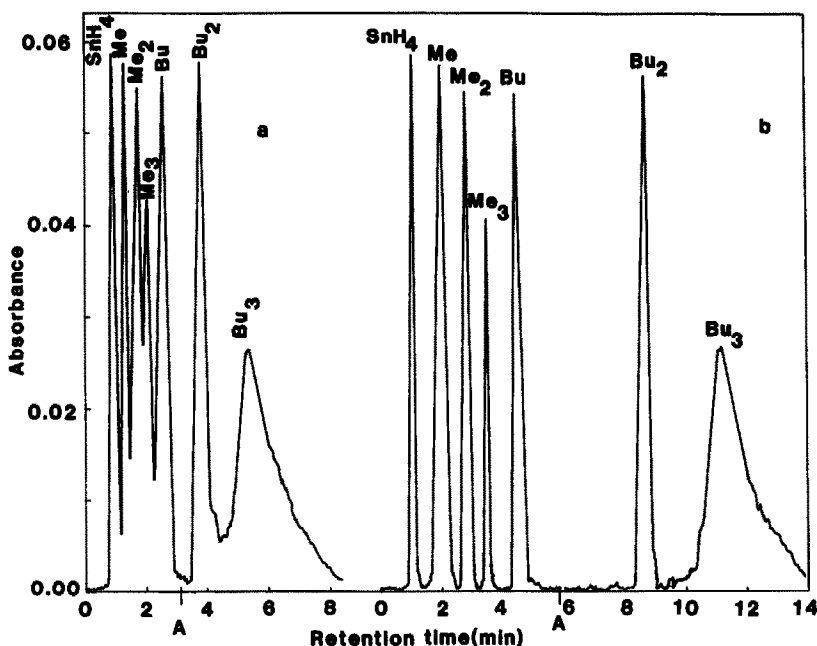


Fig. 1. Speciation of inorganic tin, methyltin and butyltin compounds in 500 ml of artificial sea-water by using (a) glass wool (b) chromatographic material in the hydride trap. Me = methyl, Bu = n-butyl. The amount of each compound present is Sn(IV), 15 ng; MeSnCl<sub>3</sub>, 15 ng; Me<sub>2</sub>SnCl<sub>3</sub>, 15 ng; Me<sub>3</sub>SnCl<sub>3</sub>, 15 ng; BuSnCl<sub>3</sub>, 15 ng; Bu<sub>2</sub>SnCl<sub>3</sub>, 30 ng; Bu<sub>3</sub>SnCl<sub>3</sub>, 60 ng. Dibutyltin and tributyltin hydrides are released from the hydride trap after the evolution of monobutyltin hydride by slowly warming the trap at the time indicated by A.

No standard sea-water was available for examining the merits of this technique, but replicate analyses resulted in highly consistent calibration graphs. The results show that this technique could be used for determination of organotin compounds in aquatic environments at the ng/ml level.

*Acknowledgement*—This research was supported by NIH-GM11373-25.

#### REFERENCES

1. A. G. Davies and P. J. Smith, in *Comprehensive Organometallic Chemistry*, G. Wilkinson (ed.), Vol. 2, Pergamon Press, Oxford, 1982.
2. I. G. Thaper and K. V. Mariwala, *Painindia Ann.*, 1978, **80**, 85.
3. E. A. Loktev, V. M. Goldberg, M. L. Kerber and M. S. Akutin, *Izv. Vyssh. Uchebn. Zaved. Khim. Tekhnol.*, 1979, **22**, 723.
4. M. H. Gitlitz, *J. Coatings Technol.*, 1981, **53**, 46.
5. V. Seinen, T. Helder, H. Vernig, A. Penninks and P. Leeuwangh, *Sci. Total Environ.*, 1981, **19**, 155.
6. R. B. Laughlin, W. French, R. B. Johannesen, H. E. Gaurd and F. E. Brinckman, *Chemosphere*, 1984, **13**, 575.
7. M. M. Salazar and S. M. Salazar, in *Proceedings of the 11th US-Japan Experts Meeting in Management of Sediments Containing Toxic Substances*, 4-6 November 1985, Seattle, WA.
8. M. J. Waldock and T. E. Thain, *Mar. Pollut. Bull.*, 1983, **14**, 411.
9. R. J. Maguire and R. J. T. Katz, *J. Chromatog.*, 1983, **268**, 99.
10. R. J. Maguire, Y. K. Chau, G. A. Rengert, E. T. Halk, P. T. S. Wong and O. Kramer, *Environ. Sci. Technol.*, 1982, **16**, 698.
11. Y. K. Chau, P. T. S. Wong and G. A. Bengert, *Anal. Chem.*, 1982, **54**, 246.
12. C. C. Gilmour, J. M. Tuttle and J. C. Means, *ibid.*, 1986, **58**, 1848.
13. A. Woolins and W. A. Cullen, *Analyst*, 1984, **109**, 1527.
14. G. I. Olson, F. E. Brinckman and J. A. Jackson, *Int. J. Environ. Anal. Chem.*, 1983, **15**, 249.
15. J. C. Means and K. L. Huleback, *Neurotoxicology*, 1983, **4**, 37.
16. J. A. Jackson, W. R. Bluir, F. E. Brinckman and W. P. Iverson, *Environ. Sci. Technol.*, 1982, **16**, 110.
17. G. Newbert and H. Andreas, *Z. Anal. Chem.*, 1976, **280**, 31.
18. G. Newbert and H. O. Wirth, *ibid.*, 1975, **273**, 19.
19. A. O. Valkirs, M. P. F. Seligman, G. J. Olson, F. E. Brinckman, C. L. Mathias and J. M. Bellamo, *Analyst*, 1987, **112**, 17.
20. V. F. Hodge, S. L. Seidel and F. D. Godberg, *Anal. Chem.*, 1979, **51**, 1256.
21. H. D. Fleming and R. G. Ide, *Anal. Chim. Acta*, 1970, **83**, 67.
22. A. O. Valkirs, P. F. Seligman, G. Vaga, P. M. Stang, V. Homer and S. H. Lieberman, *Technical Report*, No. 1037, Naval Ocean Systems Center, San Diego, CA, 1985.
23. A. O. Valkirs, P. F. Seligman, P. M. Stang, V. Homer, S. H. Lieberman, G. Vaga and C. A. Dooley, *Mar. Pollut. Bull.*, 1986, **17**, 319.
24. S. Tugral, T. I. Bulkas, E. D. Goldberg and I. Salihoglu, *J. Elud. Pollut. Mar. Mediterr.*, 1982, **6**, 497.
25. D. T. Burns, F. Glockling and M. Harriott, *Analyst*, 1981, **106**, 921.
26. O. F. Y. Donard, S. Rapsomanikis and J. H. Weber, *Anal. Chem.*, 1986, **58**, 772.

27. M. O. Andreae and J. T. Byrd, *Anal. Chim. Acta*, 1986, **156**, 147.
28. R. S. Braman and M. A. Thompkins, *Anal. Chem.*, 1979, **51**, 12.
29. C. L. Mathias, G. J. Olson, F. E. Brinckman and J. M. Bellama, *Environ. Sci. Technol.*, 1986, **20**, 609.
30. T. E. Stewart and R. D. Cannizaro, in *Pesticide Analytical Methodology*, J. Harvey, Jr. and G. Zweig (eds.), p. 367. ACS, Washington DC, 1986.
31. S. Kapila and C. R. Vogt, *J. Chromatog. Sci.*, 1986, **18**, 144.
32. B. W. Wright, M. L. Lee and G. M. Both, *HRC&CC*, 1979, **2**, 189.
33. W. A. Aue and C. G. Flinn, *J. Chromatog.*, 1986, **142**, 145.
34. K. L. Jewett and F. E. Brinckman, *J. Chromatog. Sci.*, 1981, **19**, 583.
35. T. M. Vickery, H. E. Huston, E. Howell, G. V. Harrison and G. J. Ramelow, *Anal. Chem.*, 1980, **52**, 1743.
36. L. Ebdon, S. J. Hill and P. Jones, *Analyst*, 1985, **110**, 515.
37. I. S. Krull and K. W. Panaro, *Appl. Spectrosc.*, 1985, **39**, 960.
38. W. J. Wang, S. Hanamura and J. D. Winefordner, *Anal. Chim. Acta*, 1986, **184**, 213.
39. K. H. Khoo, R. W. Ramette, C. H. Culberson and R. G. Bates, *Anal. Chem.*, 1977, **49**, 29.
40. B. Welz and M. Melcher, *Analyst*, 1983, **108**, 213.
41. J. Dedina and I. Rubeska, *Spectrochim. Acta*, 1980, **35B**, 119.
42. T. Nakahara, *Prog. Anal. At. Spectrosc.*, 1983, **6**, 163.

## COMPUTERIZED FLOW CONSTANT-CURRENT STRIPPING ANALYSIS FOR SOME ELECTROACTIVE ORGANIC COMPOUNDS

### APPLICATION TO THE DETERMINATION OF ERYTHROMYCIN IN URINE

CHI HUA, DANIEL JAGNER and LARS RENMAN

Department of Technical Analytical Chemistry, Chemical Centre, University of Lund, P.O. Box 124,  
S-221 00 Lund, Sweden

(Received 2 December 1987. Accepted 5 February 1988)

**Summary**—The possibility of determining various electroactive organic compounds, *e.g.*, erythromycin and riboflavin, by adsorptive preconcentration at constant potential on a mercury-coated carbon-fibre electrode in a flow system prior to stripping with a reductive constant current, is demonstrated. The advantages of measuring the electrode potential *vs.* time instead of current *vs.* electrode potential during stripping, the possibility of operating with non-deoxygenated solutions, the increased linear calibration range in the multiple scanning mode, and the possibility of using the technique for detection in liquid chromatography, are discussed. An analytical procedure for the determination of erythromycin at the  $10^{-6}M$  level in urine after extraction with diethyl ether is described.

Electrochemical stripping analysis can be performed with three different methods of preconcentration. In the most frequently used of these, normally referred to as anodic stripping voltammetry, the trace analytes are reduced potentiostatically to the metals, which are simultaneously dissolved in the mercury or plated on the gold electrode material, and subsequently re-oxidized by an oxidative potential ramp. In cathodic stripping voltammetry, the analytes react with mercury(I) or mercury(II) ions formed by anodic oxidation of a mercury electrode under potentiostatic control, to form insoluble salts, *e.g.*, mercury(II) selenide or calomel, the mercury ions in which are then reduced by a reductive potential ramp. In the third method, adsorptive stripping voltammetry, the analytes are adsorbed on a mercury electrode surface held under potentiostatic control, and are subsequently reduced or oxidized by a potential ramp. By this method, either adsorbable electroactive organic compounds or trace elements forming adsorbable and reducible complexes with organic reagents can be determined.

The three methods have in common that the useful analytical information is obtained by monitoring the oxidative or reductive current *vs.* the electrode potential during stripping. The height or area of the current peaks caused by reduction or oxidation is taken as a measure of the analyte concentration in the sample.

Although very much less frequently used in practice, owing mainly to lack of suitable commercial instrumentation, analytical information can also be obtained by monitoring the electrode potential *vs.*

time during stripping. The necessary change in working electrode potential can be initiated either by spontaneous chemical oxidation, as in potentiometric stripping analysis, or by applying a constant oxidative or reductive current through the working electrode, here referred to as constant-current stripping. Potentiometric stripping analysis, exploiting the preconcentration method used in anodic stripping voltammetry, has proved useful for the determination of several trace elements in various kinds of sample.<sup>1-5</sup> Reductive constant-current stripping has been applied to the determination of selenium in whole blood<sup>6</sup> after preconcentration in the cathodic-stripping mode, and to the determination of nickel,<sup>7</sup> cobalt,<sup>7</sup> uranium,<sup>8</sup> molybdenum<sup>9</sup> and iron<sup>10</sup> in natural waters, after preconcentration in the adsorptive-stripping mode.

As has been shown for potentiometric stripping analysis, the monitoring of potential *vs.* time instead of current *vs.* potential offers some unique advantages, *e.g.*, the possibility of analysing oxygenated solutions, lower susceptibility to organic matter present in the sample, simple instrumentation, and easy operation in connection with fibre electrodes<sup>11</sup> and flow systems.<sup>12</sup> A major disadvantage, however, is that in the determination of low analyte concentrations, the potential *vs.* time transient signal is very rapid, lasting typically less than 1 sec. Thus it must be monitored by a recording device with a more rapid response rate than a normal strip-chart recorder. This problem can be overcome by the use of modern personal computers.<sup>12</sup> Computerized measurement of potential *vs.* time is simpler than that of current *vs.*

potential, since time is an inherent parameter of any computer system.

Reductive constant-current stripping analysis has not hitherto been applied to the determination of electroactive organic compounds. For this reason it was thought worthwhile to attempt to modify some published procedures for the determination of various organic compounds, based on current *vs.* potential monitoring and mercury drop electrodes, for use in the constant-current stripping mode with mercury-film coated carbon-fibre flow electrodes.<sup>11</sup> The advantage would be operation with oxygenated solutions and thus a simpler analytical procedure. In conjunction with a low dead-volume fibre flow-electrode it might also serve as a detection device in liquid chromatography. The computerized constant-current stripping approach would also make it possible to overcome a serious disadvantage inherent in adsorptive preconcentration, namely the very limited linear calibration range. This could be facilitated by applying the "multiple scanning" mode previously used in the determination of uranium(VI).<sup>8</sup> In this mode, constant-current stripping is initiated after a short period of potentiostatic preconcentration, typically 10 sec. The stripping curve is stored in the computer, together with a background stripping curve obtained after typically 1 sec of potentiostatic deposition. This procedure can be repeated any desired number of times, after which the accumulated background scans are subtracted digitally from the accumulated analytical scans. In this way the linear calibration range can be extended by at least one order of magnitude.

Since the main purpose of this communication is to demonstrate the feasibility of constant-current stripping analysis for organic compounds, the choice of analyte is of minor importance. To facilitate comparison between the monitoring of time and monitoring of current, analytes which have been determined by means of current *vs.* electrode potential measurements and stripping techniques have been chosen. They include erythromycin,<sup>13</sup> novobiocin,<sup>13</sup> digitoxin,<sup>14</sup> riboflavin<sup>15</sup> and the copper(II) complex of benzylpenicillamine. A complete analytical procedure for the determination of erythromycin in urine has also been developed.

## EXPERIMENTAL

### Instrumentation

A computerized potentiometric and constant-current stripping analyser described elsewhere<sup>12</sup> was used in all experiments. In this analyser six different solutions can be drawn into the flow-cell in any desired order. During an analysis, the working electrode potential, flow-rate, magnitude of stripping current, and the opening and closing of magnetic inlet valves is under computer control. After real-time acquisition of the stripping and background data at a sampling rate of 25.6 kHz and digital filtration, the stripping curves are displayed either on a printer/plotter or on a strip-chart recorder. In all experiments an averaging filter of 30 mV and a Savitsky-Golay filter of 18 mV were used, and the potential resolution in the measurements was 2 mV.

### Electrodes

A 10- $\mu$ m diameter carbon fibre, inserted perpendicular to the flow direction in a polyethylene tube with an inner diameter of 0.80 mm, as described elsewhere,<sup>11</sup> was used as the working electrode in all the flow experiments. A platinum tube mounted downstream from the carbon fibre was used as counter-electrode, and a thin-layer saturated calomel electrode (SCE) as reference.<sup>12</sup>

A Princeton Research Model 303 hanging mercury drop working electrode (small drop size) and a platinum wire counter-electrode were used in the batch experiments. All potentials given in this paper are expressed *vs.* SCE.

### Reagents

The reagents used were of analytical grade except for the mineral acids, sodium chloride and sodium acetate, which were of Suprapur grade (Merck). All dilutions were made with "Millipore Q" water. Stock aqueous solutions (0.1M) of erythromycin, digitoxin, digitoxigenin, novobiocin and riboflavin (all from Sigma) and the potassium salt of benzylpenicillin (Fluka) were prepared daily.

### Plating the mercury film

Before each electrolysis/stripping cycle a fresh film of mercury was plated onto the carbon-fibre electrode from a 100-mg/l. solution of mercury(II) nitrate in 0.10M nitric acid flowing at 2.40 ml/min. The first step in the mercury film renewal was electrochemical removal of the used film by application of a potential of 0.60 V for 40 sec. A fresh film of mercury was then plated onto the carbon fibre by electrolysis at  $-1.50$  V for 120 sec.

### Flow-rates

All flow-rates were 0.40 ml/min unless otherwise stated.

### Determination of erythromycin in urine

Place 1 ml of the urine in a centrifuge tube and add 0.15 ml of saturated sodium carbonate solution and 5 ml of diethyl ether. Stopper the tube and shake it for 30 sec, then centrifuge it at 3000 rpm for 3 min. Transfer the ether phase to a beaker, and repeat the extraction with another 5 ml of diethyl ether. Combine the extracts and evaporate the ether with a stream of air. Add 30 ml of supporting electrolyte consisting of 0.10M sodium chloride and 0.01M boric acid, then adjust the pH to 11.0. Repeat the whole procedure with another 1-ml portion of the urine to which a standard addition of erythrocymin of suitable magnitude has been made. The standard addition should preferably increase the erythromycin content of the sample by a factor of 2-5.

Place the two solutions at two inlets of the analyser, perform the mercury film renewal procedure then admit the sample to the flow cell and electrolyse it at  $-1.0$  V for 2 sec, prior to stripping with a constant current of 5  $\mu$ A until a potential of  $-2.0$  V is reached. Electrolyse again at  $-1.0$  V for 0.1 sec and register a background stripping scan. Keep the electrode at  $-2.0$  V for 1 sec and repeat the analytical and background stripping scans as above, a further 19 times. Repeat the complete procedure with the spiked sample, identify the stripping peaks from the two samples, and evaluate the stripping-peak areas, integrating over the potential region  $\pm 0.13$  V around the peak stripping potential. Finally, evaluate the concentration in the sample by means of the normal equations for standard addition. Clean the fibre electrode by electrolysis at  $-2.50$  V for 60 sec in 1M sodium hydroxide solution in 50% v/v aqueous ethanol before starting the next analysis.

## RESULTS

### Erythromycin

The two main experimental parameters in adsorptive stripping analysis are the sample pH and the



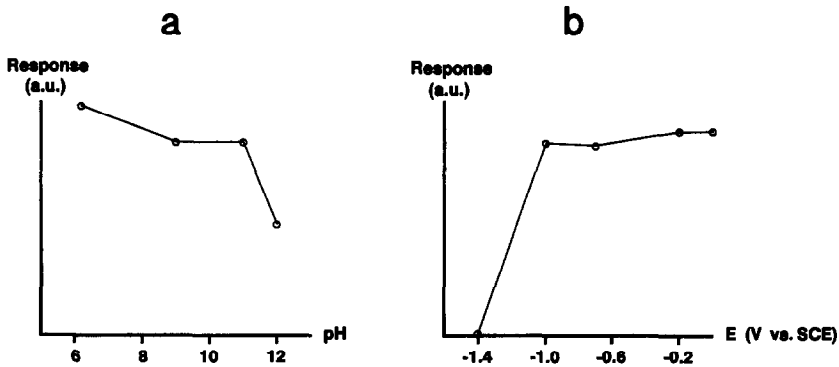


Fig. 1. Dependence of erythromycin constant-current stripping peak area on (a) pH and (b) electrolysis potential.

deposition potential. The effect of pH was investigated over the range 6.2–12 (controlled by adding acetic acid, boric acid and sodium hydroxide as required) for samples containing  $10^{-6}M$  erythromycin and  $0.10M$  sodium chloride. Twenty stripping scans, each obtained after electrolysis at  $-1.00V$  for 2 sec, were used and the results are shown in Fig. 1(a). The pH is not critical in the range 9–11 so pH 11.0 was chosen to avoid the risk of decomposition at lower pH.

The electrolysis potential was optimized by varying it between  $-0.10$  and  $-1.40V$  in a solution containing  $5 \times 10^{-7}M$  erythromycin in  $0.10M$  sodium chloride adjusted to pH 11 with sodium hydroxide, and examining the mean of seven stripping scans, each obtained after electrolysis for 8 sec. The results are shown in Fig. 1(b). Obviously the sensitivity for erythromycin is reasonably constant for electrolysis potentials in the range from  $-0.20$  to  $-1.00V$ . To decrease the risk of competitive adsorption of other adsorbable species in the sample the electrolysis potential should be kept as negative as possible and

for this reason an electrolysis potential of  $-1.00V$  was chosen.

As mentioned above, the range of linear response is normally very narrow in adsorptive stripping analysis. The difference between the single and multiple scanning modes is illustrated in Fig. 2. Here a total electrolysis time of 40 sec has been used, with  $0-20 \times 10^{-7}M$  erythromycin solutions buffered at pH 11.0. In the multiple scanning mode (curve b) the electrolysis time was subdivided into twenty periods of 2 sec. The difference in linear range between the multiple and single scan (curve a) modes is obvious.

Figure 3 shows the constant-current stripping curves for a urine sample (obtained from a person not using the drug) spiked to have  $3.0 \times 10^{-5}$  and  $6.0 \times 10^{-5}M$  concentrations of erythromycin. By using the standard-addition equation and assuming the  $3.0 \times 10^{-5}M$  erythromycin sample to be the unknown, eight repetitive analyses yielded a mean value of  $2.9 \times 10^{-5}M$  with a standard deviation of  $0.3 \times 10^{-5}M$ .

Constant-current stripping analysis for erythro-

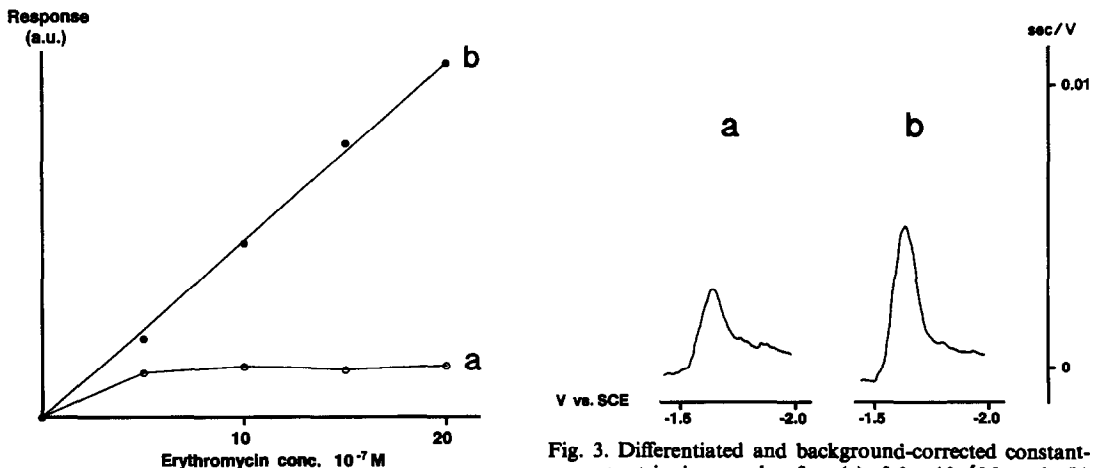


Fig. 2. Comparison between single and multiple constant-current stripping for erythromycin. Electrolysis for 40 sec at  $-1.0V$  (a) and the sum of 20 electrolyses at  $-1.0V$  for 2 sec each (b).

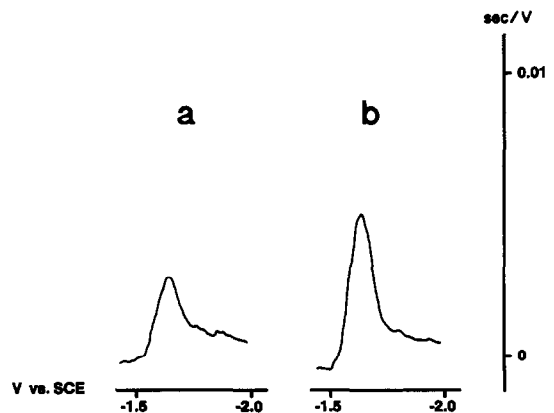


Fig. 3. Differentiated and background-corrected constant-current stripping peaks for (a)  $3.0 \times 10^{-5}M$  and (b)  $6.0 \times 10^{-5}M$  erythromycin in urine subsequent to extraction with diethyl ether, evaporation and dissolution in 30 ml of pH 11.0 buffer. Twenty accumulated stripping curves, each obtained after electrolysis for 2 sec at  $-1.0V$ .

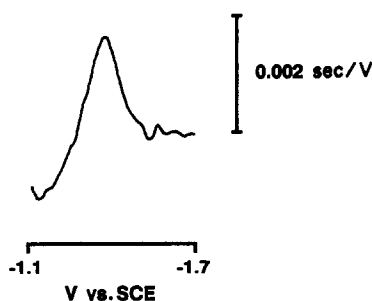


Fig. 4. Differentiated and background-corrected constant-current stripping curve obtained on a hanging mercury drop electrode in quiescent solution. Twenty accumulated scans, each obtained after 2 sec of electrolysis at  $-1.0$  V, of  $10^{-6}M$  erythromycin at pH 11.0.

mycin is subject to two kinds of interference, namely competitive adsorption of other organic compounds present in the sample and the presence of species which can be reduced at potentials close to that of erythromycin, *e.g.*, zinc ions. Obviously zinc does not interfere if the erythromycin is determined subsequent to the extraction procedure described above. Even so, the interference from zinc was investigated, by adding zinc at 2-mg/l. level to the solution obtained after extraction of erythromycin. The constant-current stripping peak then obtained for the reduction of zinc could be eliminated completely by addition of sufficient  $10^{-2}M$  EDTA. Competitive adsorption was investigated by the addition of albumin, gelatin and camphor at 20-mg/l. level to  $3 \times 10^{-5}M$  erythromycin before the extraction. No effect on the erythromycin response could be detected.

The mercury drop is by far the most frequently used working electrode in adsorptive stripping analysis. Whether or not this electrode could be used in combination with the constant-current stripping technique in oxygenated solutions was therefore investigated. That it could is obvious from Fig. 4, which shows the sum of twenty background-corrected constant-current stripping scans, each obtained after electrolysis of a  $10^{-6}M$  erythromycin solution in

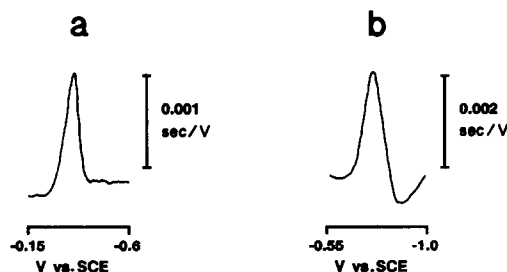


Fig. 6. Differentiated and background-corrected constant-current stripping curves for (a)  $10^{-7}M$  riboflavin (electrolysis for 30 sec at  $-0.15$  V at pH 6.0) and (b)  $4 \times 10^{-6}M$  benzylpenicilloic acid and  $10^{-5}M$  copper(II) (electrolysis for 10 sec at  $-0.10$  V at pH 4.6).

$0.10M$  sodium chloride (pH = 11) at  $-1.0$  V for 2 sec in quiescent solution and with a constant current of  $20 \mu A$ . The peak potential obtained for erythromycin,  $-1.38$  V, is close to that obtained on the mercury-film coated carbon-fibre electrode (Fig. 3) and approximately  $0.20$  V cathodic relative to that obtained by Wang.<sup>13</sup>

*Novobiocin, digitoxin, digitoxigenin, riboflavin and benzylpenicilloic acid*

Figure 5(a) shows the accumulated and background-corrected constant-current ( $3.4 \mu A$ ) stripping curves obtained from ten consecutive scans, each after electrolysis for 5 sec at  $-0.90$  V of  $10^{-6}M$  novobiocin in  $0.10M$  sodium chloride at pH 7.4. Also shown in Fig. 5 are single-scan constant-current ( $3.4 \mu A$ ) stripping curves obtained after 10 sec of electrolysis in pH-11.7  $0.10M$  sodium chloride solutions of (b)  $2 \times 10^{-6}M$  digitoxin and (c)  $10^{-6}M$  digitoxigenin, at  $-1.40$  V for (b) and  $-0.90$  V for (c). The single-scan constant-current ( $1.2 \mu A$ ) stripping peak for  $10^{-7}M$  riboflavin at pH 6.0 after electrolysis at  $-0.15$  V for 30 sec in  $0.10M$  sodium chloride solution is shown in Fig. 6(a) and that for  $4 \times 10^{-6}M$  benzylpenicilloic acid/ $10^{-5}M$  copper(II) ( $2 \mu A$ ) at pH 4.6 after electrolysis for 10 sec at  $-0.10$  V in the same medium is shown in Fig. 6(b).

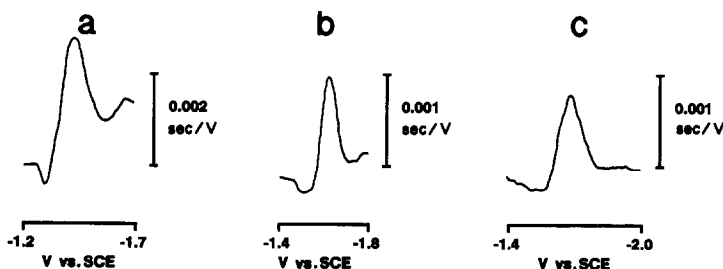


Fig. 5. Differentiated and background-corrected constant-current stripping curves for (a)  $10^{-6}M$  novobiocin (ten accumulated scans, each obtained at pH 7.4) after electrolysis for 5 sec at  $-0.90$  V, (b)  $2 \times 10^{-6}M$  digitoxin (electrolysis at  $-1.40$  V for 10 sec at pH 11.7) and (c)  $10^{-6}M$  digitoxigenin (electrolysis at  $-0.90$  V for 10 sec at pH 11.7).

## DISCUSSION

The results obtained clearly show that the constant-current stripping mode in combination with adsorptive accumulation can be exploited successfully for the determination of adsorbable electroactive compounds in oxygenated solutions, with a mercury-film coated carbon fibre or a mercury drop electrode as sensor. The sensitivity is, however, lower than that obtained with current *vs.* voltage stripping techniques, by approximately a factor of five. Considering the very high sensitivity inherent in adsorptive stripping this is a minor problem. For example, the optimum concentration range for the determination of erythromycin in urine is  $0.1\text{--}10 \times 10^{-5}M$  (Fig. 3), which is sensitive enough to cover the normal range ( $1.4\text{--}60 \times 10^{-5}M$ ) of concentration in the urine of persons under treatment with this drug.<sup>17</sup> In most applications the loss in sensitivity is more than compensated for by the possibility of operating in oxygenated solutions and the increased linear concentration range obtainable in the multiple scanning mode.

## REFERENCES

1. E. Mortensen, E. Quizel, H. J. Skov and L. Kryger, *Anal. Chim. Acta*, 1979, **112**, 297.
2. J. K. Christensen and L. Kryger, *ibid.*, 1980, **118**, 53.
3. D. Jagner, M. Josefson and S. Westerlund, *ibid.*, 1981, **129**, 153.
4. *Idem*, *ibid.*, 1981, **128**, 155.
5. D. Jagner, M. Josefson, S. Westerlund and K. Årén, *Anal. Chem.*, 1981, **53**, 1406.
6. C. Hua, D. Jagner and L. Renman, *Anal. Chim. Acta*, 1987, in the press.
7. H. Eskilsson, C. Haraldsson and D. Jagner, *ibid.*, 1985, **175**, 79.
8. C. Hua, D. Jagner and L. Renman, *ibid.*, submitted for publication.
9. *Idem*, *ibid.*, 1987, **192**, 103.
10. *Idem*, *ibid.*, submitted for publication.
11. H. Huiliang, C. Hua, D. Jagner and L. Renman, *ibid.*, 1987, **193**, 61.
12. L. Renman, D. Jagner and R. Berglund, *ibid.*, 1986, **188**, 137.
13. J. Wang and J. S. Mahmoud, *ibid.*, 1986, **186**, 31.
14. J. Wang, J. S. Mahmoud and P. A. Farias, *Analyst*, 1985, **110**, 855.
15. J. Wang, D. Luo, P. A. M. Farias and J. S. Mahmoud, *Anal. Chem.*, 1985, **57**, 158.
16. U. Forsman, *Anal. Chim. Acta*, 1983, **146**, 71.
17. L. D. Sabath, D. A. Gerstein, P. B. Loder and M. Finland, *J. Lab. Clin. Med.*, 1968, **72**, 916.

## DETERMINATION OF THE OPTIMUM WORKING RANGE IN SPECTROPHOTOMETRIC PROCEDURES

A. G. ASUERO\*

Department of Bromatology, Toxicology, and Applied Chemical Analysis, Faculty of Pharmacy,  
The University of Seville, 41012 Seville, Spain

G. GONZALEZ, F. DE PABLOS and J. L. GOMEZ ARIZA

Department of Analytical Chemistry, Faculty of Chemistry, The University of Seville, 41012 Seville, Spain

(Received 11 November 1985. Revised 17 January 1988. Accepted 2 February 1988)

**Summary**—A brief introduction to the topics of covariance and variance is given in this paper. An abstract vectorial space, the "precision pattern space" is introduced in order to find the general expression for the law of random error propagation. A new approach to the determination of the optimum working range in spectrophotometric procedures has been developed. The method involves the use of the calibration curve and the application of the Laplacian operator to concentration. The general expression reported for the relative error in concentration tends towards the classical photometric error expression in limiting cases.

The determination of the optimum working range (OWR) in spectrophotometric procedures is a classical problem in chemical analysis. Several authors<sup>1-15</sup> have reported different expressions for evaluation of the concentration range in which photometric error is at a minimum. Careful scrutiny of these papers reveals that most authors have considered only the standard deviation of the transmittance, and few of them<sup>10,12,14</sup> have considered the contribution of the standard deviations of the intercept and slope of the calibration line, to the analytical error. Nevertheless, as pointed out by Mandel and Linning,<sup>16</sup> a strong correlation exists between the estimated slope and intercept of a straight line obtained by least squares calculations. Accordingly, the usual method for the derivation of the confidence intervals for the slope and intercept of fitted straight line equations may lead to erroneous conclusions.

The main sources of error in analytical methods based on the absorption of radiation are: (i) error in reading the test solution; (ii) error in setting the instrument to read 0% and 100% transmittance (baseline). Because of the logarithmic relationship between transmittance and concentration, small errors in measuring the transmittance cause large relative errors in the calculated concentration at low and high transmittances. With modern spectrophotometers, the errors due to setting of 0% transmittance and the baseline are often considered to be zero, since these two settings are made at the start of a run and not reset for each individual measurement.<sup>12</sup> The main source of indeterminate

error is then regarded as the measurement of the absorbance. This seems, however, to ignore the possibility of instrumental drift.

There is no doubt that the effect of experimental variables may be found more efficiently through a statistical approach than by traditional methods. In this paper a new approach to the determination of the OWR from calibration graphs is developed. The general expression reported below for the relative error in concentration tends towards the classical photometric error expression<sup>3</sup> in limiting cases. The covariance of measurements can be as important as the variances<sup>17</sup> and both contribute significantly to the total analytical error, so a brief introduction to these important topics is given in the following.

The covariance between two random variables  $x$  and  $y$  (with a joint distribution) is defined as the expected value of the product of the deviations of  $x$  and  $y$  from their expected values (true or population means  $\mu_x$  and  $\mu_y$ , respectively):

$$\text{Cov}(x, y) = E[(x - \mu_x)(y - \mu_y)] \quad (1)$$

The unbiased estimates for the unknown means  $\mu_x$  and  $\mu_y$  are the sample means  $\bar{x}$  and  $\bar{y}$ , respectively:

$$\bar{x} = \frac{1}{N} \sum x_i \quad \text{and} \quad \bar{y} = \frac{1}{N} \sum y_i \quad (2)$$

where  $N$  is the number of pairs of observations  $(x_i, y_i)$ .

By simple algebra, we can write

$$\begin{aligned} \sum (x_i - \bar{x})(y_i - \bar{y}) &= \sum [(x_i - \mu_x) \\ &\quad - (\bar{x} - \mu_x)][(y_i - \mu_y) - (\bar{y} - \mu_y)] \\ &= \sum (x_i - \mu_x)(y_i - \mu_y) \\ &\quad - N(\bar{x} - \mu_x)(\bar{y} - \mu_y) \end{aligned} \quad (3a)$$

\*To whom correspondence should be addressed.

Taking expectations of both sides of equation (3a) gives

$$E \left[ \sum (x_i - \bar{x})(y_i - \bar{y}) \right] = \sum \text{Cov}(x_i, y_i) - N \text{Cov}(\bar{x}, \bar{y}) \quad (3b)$$

Since all replicates belong to the same statistical population, it follows that

$$\text{Cov}(x_i, y_i) = \text{Cov}(x, y), \quad (4a)$$

and since

$$\text{Cov}(\bar{x}, \bar{y}) = \frac{\text{Cov}(x, y)}{N}, \quad (4b)$$

combining equations (3b) and (4b) and rearranging gives

$$\text{Cov}(x, y) = E \left[ \frac{\sum (x_i - \bar{x})(y_i - \bar{y})}{N - 1} \right] \quad (5a)$$

This expectation value is an unbiased estimate of the population covariance, so it is identical with the sample covariance  $\text{Cov}(x, y)$  and

$$\text{Cov}(x, y) = \frac{1}{N - 1} \sum (x_i - \bar{x})(y_i - \bar{y}) \quad (5b)$$

(where  $N - 1$  is the number of degrees of freedom). The covariance is a measure of the correlation between  $x$  and  $y$ . If  $x$  and  $y$  are independent, *i.e.*, not correlated, the covariance is zero. However, the converse is not necessarily true.<sup>19</sup>

The variance is the special case of the covariance of a random variable,  $R$ , with itself

$$\text{Var}(R) = E[(R - \mu_R)^2] = \sigma_R^2 \quad (6a)$$

It then follows directly from previous results that the sample variance is given by

$$\begin{aligned} \text{Var}(x) &= \frac{1}{N - 1} \sum (x_i - \bar{x})^2 \\ &= \frac{1}{N - 1} \left| \sum x_i^2 - \frac{(\sum x_i)^2}{N} \right| = s_x^2 \end{aligned} \quad (6b)$$

The square root of the variance is called the standard deviation (denoted by  $\sigma$  for the population and by  $s$  for the sample) and is always positive.

By dividing the sample covariance by the product of the sample standard deviations of  $x$  and  $y$ ,  $s_x$  and  $s_y$ , respectively, we obtain the sample correlation coefficient  $r_{xy}$  (or the covariance between two standardized variables  $x^*$  and  $y^*$ ), which is independent of the scales chosen:

$$\begin{aligned} r_{xy} &= \frac{\text{Cov}(x, y)}{s_x s_y} \\ &= \frac{1}{N - 1} \sum \left[ \frac{x_i - \bar{x}}{s_x} \right] \left[ \frac{y_i - \bar{y}}{s_y} \right] \end{aligned}$$

$$\begin{aligned} &= \frac{1}{N - 1} \sum x_i^* y_i^* \\ &= \frac{\sum (x_i - \bar{x})(y_i - \bar{y})}{\sqrt{\sum (x_i - \bar{x})^2 \sum (y_i - \bar{y})^2}} \\ &= \frac{\sum x_i y_i - \frac{\sum x_i \sum y_i}{N}}{\sqrt{\left[ \sum x_i^2 - \frac{(\sum x_i)^2}{N} \right] \left[ \sum y_i^2 - \frac{(\sum y_i)^2}{N} \right]}} \\ &= \frac{S_{XY}}{\sqrt{S_{XX} S_{YY}}} \end{aligned} \quad (7)$$

where  $S_{XX}$  and  $S_{YY}$  are the sums of the squares of deviations from the mean for the two variables ( $x$  and  $y$ ) and  $S_{XY}$  is the corresponding sum of the cross-products.

All analytical measurements are random variables and therefore the information they provide will have a certain imprecision. However, the quantities that are of interest to the analytical chemist are usually functions of a set of observations and it is often desired to know how the mean and variance of these functions are related to the means, variances and covariances of the original measurements. The relationship for the error of an arbitrary function of several variables, known as the law of random-error propagation, is perhaps the most important relation in the theory of errors, because we are mainly concerned with the error of the final results, rather than the error of individual measurements. The problem is how to calculate the error of a final result obtained from experimental values by means of a certain functional relation. In the following discussion, a new approach to the derivation of the law of random-error propagation, based on the application of linear algebra, is given. The effects of systematic errors—the assessment of which is frequently the most difficult aspect of a chemical measurement—are not considered here.

For convenience, we introduce an abstract vectorial space which we call the "precision pattern space (PPS)", which is  $n$ -dimensional if there are  $n$  random variables. The moduli of its  $n$  basic vectors coincide with the standard deviations,  $\sigma_i$ , of the corresponding random variables. Suppose we have a continuous function of the physical quantities  $x_1, x_2, \dots, x_N$

$$R = f(x_1, x_2, \dots, x_N) \quad (8)$$

and that the experimentally determined  $x_i$  values are normally distributed about the value  $\mu_i$  with variance  $\sigma_i^2$ . The standard error associated with the measurement of  $x_i$  will be given by the sample standard deviation  $s_i$ , and all the  $s_i$  values will contribute to the total random error in  $R$ ,  $s_R$  (because  $s_R$  is the error estimate of a quantity  $R$  which is derived from the original observations, it is often termed the standard

error). The question is how these errors ( $s_i$ ) are propagated in the calculation of  $R$ .

To answer this question, we will use an  $N$ -dimensional subspace of the PPS, denoted by PPSV, where  $N$  is the number of variables that  $R$  depends on. The PPSV is formed by  $N$  vectors, the moduli of which coincide with the standard deviations  $\sigma_i$  of the variables  $x_i$ . The PPS and its subspaces have euclidean structure, so the scalar product of any two basic vectors,  $\epsilon_i$  and  $\epsilon_j$ , is given by

$$d_{ij} = \epsilon_i \epsilon_j = |\epsilon_i| |\epsilon_j| \cos \theta_{ij} \tag{9}$$

where  $\theta_{ij}$  is the angle between  $\epsilon_i$  and  $\epsilon_j$ . When  $i = j$  we obtain

$$d_{ii} = (\epsilon_i)^2 = \sigma_i^2 = \text{Var}(x_i) \tag{10a}$$

If  $i \neq j$ , then

$$d_{ij} = \text{Cov}(x_i, x_j) \tag{10b}$$

and  $\cos \theta_{ij}$  coincides with the population correlation coefficient  $\rho_{ij}$  between  $x_i$  and  $x_j$

$$\rho_{ij} = \frac{d_{ij}}{\sqrt{d_{ii}d_{jj}}} = \frac{\text{Cov}(x_i, x_j)}{\sqrt{\sigma_x^2 \sigma_y^2}} \tag{11}$$

It is fairly easy to show that  $-1 \leq \rho_{ij} \leq 1$ . Application of the Cauchy inequality<sup>20</sup> gives

$$|\epsilon_i \epsilon_j| \leq |\epsilon_i| |\epsilon_j| \tag{12a}$$

and hence

$$\frac{|\epsilon_i \epsilon_j|}{|\epsilon_i| |\epsilon_j|} \leq 1 \tag{12b}$$

Since  $\sigma_i$  and  $\sigma_j$  are always positive, combining equations (9)–(12) yields

$$|\rho_{ij}| \leq 1 \quad \text{and} \quad -1 \leq \rho_{ij} \leq 1 \tag{13}$$

The correlation coefficient gives a measure of the degree of relationship between two variables. Equation (11) is the infinite sample-population analogue of equation (7) (which applies to a finite sample population).

The basis of the PPS and its subspaces is non-orthonormal, so

$$d_{ij} \neq \delta_{ij} \tag{14}$$

where  $\delta_{ij}$  is the Kronecker delta,<sup>21</sup>  $\delta_{ij} = 0$  for  $i \neq j$ ,  $\delta_{ij} = 1$  for  $i = j$ . Any vector of the PPSV can be expressed as a linear combination of basic vectors

$$V = a_1 \epsilon_1 + a_2 \epsilon_2 + \dots + a_N \epsilon_N \tag{15}$$

where the coefficients  $a_i$  ( $i = 1-N$ ) are constants. The set of all linear combinations of  $\epsilon_1, \epsilon_2, \dots, \epsilon_N$  is a subspace of the PPSV. The scalar product  $VV$  is given by

$$\begin{aligned} VV &= (a_1 \epsilon_1 + a_2 \epsilon_2 + \dots + a_N \epsilon_N)^2 \\ &= a_1^2 \epsilon_1^2 + a_2^2 \epsilon_2^2 + \dots + a_N^2 \epsilon_N^2 \\ &\quad + 2a_1 a_2 \epsilon_1 \epsilon_2 + 2a_1 a_3 \epsilon_1 \epsilon_3 + \dots \end{aligned} \tag{16a}$$

and, taking into account equations (10a) and (10b)

$$VV = \sum a_i^2 \sigma_i^2 + 2 \sum_{i < j} a_i a_j \text{Cov}(x_i, x_j) \tag{16b}$$

There will be  $N$  squared terms like  $a_i^2 \sigma_i^2$ , and  $N(N-1)/2$  cross-product terms like  $2a_i a_j \text{Cov}(x_i, x_j)$ . As the basic vectors are non-orthonormal the cross-product terms differ from zero. The square root of the scalar product of  $V$  with itself or the euclidean norm<sup>22</sup> (or length) is identical with the standard deviation,  $\sigma_R$ , of a quantity  $R$  that is a linear function of  $N$  quantities  $x_i$ :

$$R = a_1 x_1 + a_2 x_2 + \dots + a_N x_N \tag{17}$$

This follows from equation (6a), since

$$\begin{aligned} \text{Var}(R) &= E\{[R - E(a_1 x_1 + a_2 x_2 \\ &\quad + \dots + a_N x_N)]^2\} \\ &= E\left\{\left[\sum a_i (x_i - \mu_i)\right]^2\right\} \\ &= E\left[\sum a_i^2 (x_i - \mu_i)^2 \right. \\ &\quad \left. + 2 \sum_{i < j} a_i a_j (x_i - \mu_i)(x_j - \mu_j)\right] \\ &= \sum a_i^2 \sigma_i^2 + 2 \sum_{i < j} a_i a_j \text{Cov}(x_i, x_j) \end{aligned} \tag{18}$$

which is identical with expression (16b).

The simplest case to consider is the variance of an algebraic sum

$$R = x_1 \pm x_2 \tag{19}$$

for which the general equation (16b) reduces to

$$VV = (\epsilon_1 \pm \epsilon_2)^2 = \sigma_1^2 + \sigma_2^2 \pm 2\text{Cov}(x_1, x_2) = \sigma_R^2 \tag{20}$$

If the variables are statistically correlated it is not permissible simply to add their variances.

If  $a_1 = a_2 = \dots = a_N = 1/N$  and the random variables are non-correlated (in this case the basic vectors are orthogonal), then

$$R = \frac{x_1 + x_2 + \dots + x_N}{N} \tag{21a}$$

and

$$V = \frac{1}{N}(\epsilon_1 + \epsilon_2 + \dots + \epsilon_N) \tag{21b}$$

so

$$V^2 = \frac{1}{N^2}(\sigma_1^2 + \sigma_2^2 + \dots + \sigma_N^2) = \sigma_R^2 \tag{22}$$

If the variance of the data points is uniform (homoscedastic)

$$\sigma_1^2 = \sigma_2^2 = \dots = \sigma_N^2 = \sigma_x^2 \tag{23}$$

and

$$\sigma_R^2 = \frac{\sigma_x^2}{N} \tag{24a}$$

When all the population mean values are the same,  $\sigma_R^2$  is identical with  $\sigma_x^2$ , and thus the standard deviation of  $\bar{x}$  (standard error of the mean) is

$$\sigma_{\bar{x}} = \sigma_x / \sqrt{N} \quad (24b)$$

Equation (24b) applies also to finite sample populations if  $\sigma_{\bar{x}}$  and  $\sigma_x$  are replaced by  $s_{\bar{x}}$  and  $s_x$ .

The gradient operator in the PPSV has the form

$$\nabla = \epsilon_1 \frac{\partial}{\partial x_1} + \epsilon_2 \frac{\partial}{\partial x_2} + \cdots + \epsilon_N \frac{\partial}{\partial x_N} \quad (25)$$

so the divergence of any vector of the PPSV is given by

$$\begin{aligned} \nabla \mathbf{V} &= \left[ \sum \epsilon_i \frac{\partial}{\partial x_i} \right] \left[ \sum a_i \epsilon_i \right] \\ &= \left[ \epsilon_1 \frac{\partial}{\partial x_1} + \epsilon_2 \frac{\partial}{\partial x_2} + \cdots \right] \\ &\quad \times [a_1 \epsilon_1 + a_2 \epsilon_2 + \cdots] \\ &= \epsilon_1^2 \frac{\partial a_1}{\partial x_1} + \epsilon_1 \epsilon_2 \frac{\partial a_2}{\partial x_1} \\ &\quad + \cdots + \epsilon_2 \epsilon_1 \frac{\partial a_1}{\partial x_2} + \epsilon_2^2 \frac{\partial a_2}{\partial x_2} + \cdots \\ &= \sum \frac{\partial a_i}{\partial x_i} \sigma_i^2 + \sum_{i < j} \left[ \frac{\partial a_i}{\partial x_j} + \frac{\partial a_j}{\partial x_i} \right] \text{Cov}(x_i, x_j) \end{aligned} \quad (26)$$

and equals zero because the coefficients  $a_i$  are arbitrary numbers, or arbitrary functions independent of the  $x_i$  random variables. In other words, the vectors of the PPS are solenoidal. For this reason we seek an operator which acts on scalars and not on vectors.

The Laplacian in the PPSV is given by

$$\begin{aligned} \nabla^2 &= \left[ \sum_i^N \epsilon_i \frac{\partial}{\partial x_i} \right] \left[ \sum_j^N \epsilon_j \frac{\partial}{\partial x_j} \right] \\ &= \left[ \epsilon_1 \frac{\partial}{\partial x_1} + \epsilon_2 \frac{\partial}{\partial x_2} + \cdots + \epsilon_N \frac{\partial}{\partial x_N} \right]^2 \\ &= \epsilon_1^2 \left[ \frac{\partial}{\partial x_1} \right]^2 + \epsilon_2^2 \left[ \frac{\partial}{\partial x_2} \right]^2 \\ &\quad + \cdots + 2\epsilon_1 \epsilon_2 \left[ \frac{\partial}{\partial x_1} \right] \left[ \frac{\partial}{\partial x_2} \right] \\ &\quad + 2\epsilon_1 \epsilon_3 \left[ \frac{\partial}{\partial x_1} \right] \left[ \frac{\partial}{\partial x_3} \right] + \cdots \\ &= \sum_i^N \left[ \frac{\partial}{\partial x_i} \right]^2 \sigma_i^2 \\ &\quad + 2 \sum_{i < j}^N \left[ \frac{\partial}{\partial x_i} \right] \left[ \frac{\partial}{\partial x_j} \right] \text{Cov}(x_i, x_j) \end{aligned} \quad (27)$$

The application of the Laplacian to an arbitrary

function  $R$  such as equation (8) leads to

$$\begin{aligned} \nabla^2(R) &= \sum_i^N \left[ \frac{\partial R}{\partial x_i} \right] \sigma_i^2 + 2 \sum_{i < j}^N \left[ \frac{\partial R}{\partial x_i} \right] \\ &\quad \times \left[ \frac{\partial R}{\partial x_j} \right] \text{Cov}(x_i, x_j) \end{aligned} \quad (28)$$

The general expression for the law of random error propagation in  $R$  is in this way easily derived. The variance of the quantities evaluated by indirect measurements can be directly obtained by computing the Laplacian of  $R$

$$\nabla^2(R) = \sigma_R^2 \quad (29)$$

In the particular case where the variables  $x_i$  are mutually independent, all the covariances are zero and equation (28) reduces to

$$\sigma_R^2 = \sum_i^N \left[ \frac{\partial R}{\partial x_i} \right]^2 \sigma_i^2 \quad (30)$$

If the function  $R$  is linear,

$$R = a_1 x_1 + a_2 x_2 + \cdots + a_N x_N,$$

the Laplacian of  $R$  coincides with the square of the euclidean norm of the corresponding vector,

$$\mathbf{V} = a_1 \epsilon_1 + a_2 \epsilon_2 + \cdots + a_N \epsilon_N:$$

$$\nabla^2(R) = |\mathbf{V}\mathbf{V}| \quad (31)$$

The familiar route to the derivation of the law of random error propagation is as follows. To prove equation (28) we can expand

$$\mu_R = R(\mu_{x_1}, \mu_{x_2}, \dots, \mu_{x_N}) = f(\mu) \quad (32)$$

in a Taylor series about the point  $(\mu_{x_1}, \mu_{x_2}, \dots, \mu_{x_N})$ :

$$\begin{aligned} R &= \mu_R + \frac{\partial f(\mu)}{\partial x_1} (x_1 - \mu_1) \\ &\quad + \frac{\partial f(\mu)}{\partial x_2} (x_2 - \mu_2) \\ &\quad + \cdots + \frac{\partial f(\mu)}{\partial x_N} (x_N - \mu_N) \\ &\quad + \text{higher order terms} \end{aligned} \quad (33)$$

From the definition of variance and the properties of expectation,<sup>18</sup> by neglecting all but the first-order terms in equation (33) we obtain

$$\begin{aligned} \sigma_R^2 &= \text{Var}(R) = E \left[ \left( \mu_R + \sum \frac{\partial f(\mu)}{\partial x_i} (x_i - \mu_i) - \mu_R \right)^2 \right] \\ &= \sum \left[ \frac{\partial f(\mu)}{\partial x_i} \right]^2 E[(x_i - \mu_i)^2] + 2 \sum_{i < j} \left[ \frac{\partial f(\mu)}{\partial x_i} \right] \\ &\quad \times \left[ \frac{\partial f(\mu)}{\partial x_j} \right] E[(x_i - \mu_i)(x_j - \mu_j)] \\ &= \sum \sigma_i^2 \left[ \frac{\partial f(\mu)}{\partial x_i} \right]^2 + 2 \sum_{i < j} \left[ \frac{\partial f(\mu)}{\partial x_i} \right] \end{aligned}$$

$$\times \left[ \frac{\partial f(\mu)}{\partial x_j} \right] \text{Cov}(x_i, x_j) \quad (34)$$

As the partial derivatives of  $f$  with respect to  $x_i$  are evaluated at the point  $\mu_{x_i}$  we have

$$\left[ \frac{\partial f}{\partial x_i} \right]_{\mu} = \frac{\partial R}{\partial x_i} \quad (35)$$

Thus equation (34) is identical with the expression for the Laplacian of  $R$  given by equation (28). The variance of an indirect measurement is found in the same manner as the population variance, but the deviations are taken about the mean of the indirect measurement (sample mean). However, the formula expressing the variance of  $R$  is of general validity and in no way depends on the size of the sample.

The continuing interest in, and importance of, calibration in analytical chemistry is indicated by the number of publications that appear each year.<sup>17,23,24</sup>

Calibration involves a very special type of modelling and parameter estimation,<sup>23</sup> in that chemical measurements are converted into chemical information, and it lies at the heart of nearly every analysis.<sup>24</sup>

The absorbances,  $A$ , of a set of samples:

$$A = A_{\text{sample}} - A_{\text{blank}} = -\log(T_{\text{sample}}/T_{\text{ref}}) + \log(T_{\text{blank}}/T_{\text{ref}}) = \log T_{(b/s)} \quad (36)$$

are related to the concentrations  $C$  by means of the calibration equation, usually obtained by single linear regression:

$$A = b_0 + b_1 C \quad (37)$$

where  $b_1$  and  $b_0$  are the slope and intercept of the regression line, respectively (estimated by the least-squares method). Two basic assumptions are involved in single linear regression analysis: the first is that the dependent variable ( $y$ ) has a random error of measurement, whereas the independent variable ( $x$ ) is free from error because it is set by the experimenter; the second is that the variance of the response is normally distributed and homoscedastic (homogeneous) over the entire range of calibration. Both assumptions are usually taken as valid in the context of analytical calibration,<sup>25</sup> though they may not in fact be so. However, as parameters estimated in least-squares methods are always linear combinations of the observations, their variances are linear combinations of the random measurement error. Because  $b_0$  and  $b_1$  are estimated from the same set of experimental data, the estimated errors are very likely to be correlated. Obviously, correlation between the slope and intercept implies that covariance between them is significant.

The slope and intercept of a straight line  $y = b_0 + b_1 x$  are given by<sup>26</sup>

$$b_1 = \frac{S_{XY}}{S_{XX}} \quad \text{and} \quad b_0 = \bar{y} - b_1 \bar{x} \quad (38)$$

where  $(\bar{x}, \bar{y})$  is the centroidal point.<sup>27</sup>

The variance of the regression line for  $N$  observations is given by

$$s_{y_x}^2 = \frac{Q}{N-2} \quad (39)$$

$Q$  being the sum of the squares of the residuals

$$Q = \sum (y_i - \hat{y}_i)^2 = S_{YY} - b_1^2 S_{XX} \quad (40)$$

where  $\hat{y}$  is the predicted value of  $y$  for a given  $x$ . The variances of the slope ( $s_{b_1}^2$ ) and intercept ( $s_{b_0}^2$ ), as well as the covariance of the slope and intercept,  $\text{Cov}(b_0, b_1)$  can easily be evaluated from the variance-covariance matrix.

Let  $E[\mathbf{B}]$  designate the expected value of  $\mathbf{B}$ , the column vector of the regression coefficients

$$\mathbf{B} = \begin{bmatrix} b_0 \\ b_1 \end{bmatrix} \quad (41)$$

The variance-covariance matrix is defined by<sup>26,28</sup>

$$\begin{aligned} \text{Var}(\mathbf{B}) &= E\{(\mathbf{B} - E[\mathbf{B}])(\mathbf{B} - E[\mathbf{B}])'\} \\ &= \begin{vmatrix} s_{b_0}^2 & \text{Cov}(b_0, b_1) \\ \text{Cov}(b_1, b_0) & s_{b_1}^2 \end{vmatrix} \\ &= (\mathbf{X}'\mathbf{X})^{-1} s_{y_x}^2 \end{aligned} \quad (42)$$

where  $\mathbf{X}$  is the matrix of the independent variables and  $\mathbf{X}'$  its transpose.

$$\mathbf{X} = \begin{bmatrix} 1 & x_1 \\ 1 & x_2 \\ \vdots & \vdots \\ 1 & x_N \end{bmatrix} \quad (43)$$

The vector  $\mathbf{B}$  is related to the observation vector  $\mathbf{Y}$  by means of

$$\mathbf{Y} = \mathbf{B}\mathbf{X} \quad (44a)$$

$$\begin{bmatrix} y_1 \\ y_2 \\ \vdots \\ y_N \end{bmatrix} = \begin{bmatrix} b_0 \\ b_1 \end{bmatrix} \begin{bmatrix} 1 & x_1 \\ 1 & x_2 \\ \vdots & \vdots \\ 1 & x_N \end{bmatrix} \quad (44b)$$

Substituting in equation (42) for  $(\mathbf{X}'\mathbf{X})^{-1}$  we obtain

$$\begin{aligned} \text{Var}(\mathbf{B}) &= \frac{1}{N \sum x_i^2 - \left(\sum x_i\right)^2} \\ &\times \begin{vmatrix} \sum x_i^2 & -\sum x_i \\ -\sum x_i & N \end{vmatrix} s_{y_x}^2 \end{aligned} \quad (45)$$

and from equation (42) and (45)

$$s_{b_0}^2 = \frac{\left(\sum x_i^2\right) s_{y_x}^2}{N S_{XX}} \quad (46)$$

$$s_{b_1}^2 = \frac{s_{y_x}^2}{S_{XX}} \quad (47)$$



$$\text{Cov}(b_0, b_1) = \text{Cov}(b_1, b_0) = \frac{-\bar{x}s_{yz}^2}{S_{XX}} \quad (48)$$

An approach to the evaluation of covariance different from the one described here is given by Foucart and Lafaye.<sup>29</sup>

The calibration curve is interesting in that it may be used both for the estimation of unknown concentrations and for the evaluation of the optimum working range, the latter in connection with reproducibility studies. Assuming that the determination of unknown concentrations is affected only by random errors, the application of the PPSV-Laplacian to  $C$  gives

$$\begin{aligned} \nabla^2(C) = s_C^2 = & \frac{s_A^2}{b_1^2} + \frac{s_{b_0}^2}{b_1^2} \\ & + (A - b_0)^2 \frac{s_{b_1}^2}{b_1^4} + 2 \frac{\text{Cov}(b_0, b_1)}{b_1^3} (A - b_0) \quad (49) \end{aligned}$$

The variance of the absorbance is related to the variance of the transmittance

$$s_A^2 = 0.4343^2 \frac{s_{T(b/s)}^2}{T_{(b/s)}^2} \quad (50)$$

Inserting equations (48) and (50) into (49), dividing by  $C^2$  and extracting square roots on both sides, we get the relative concentration error  $s_C/C$ .

$$\begin{aligned} \frac{s_C}{C} = & \left[ \frac{0.4343^2 s_{T(b/s)}^2}{T_{(b/s)}^2 (A - b_0)^2} + \frac{s_{b_0}^2}{(A - b_0)^2} \right. \\ & \left. + \frac{s_{b_1}^2}{b_1^2} - \frac{2\bar{x}s_{yz}^2}{S_{XX}(A - b_0)b_1} \right]^{1/2} \quad (51a) \end{aligned}$$

Substitution from equations (46) and (47) converts this expression into

$$\begin{aligned} \frac{s_C}{C} = & \left\{ \frac{0.4343^2 s_{T(b/s)}^2}{T_{(b/s)}^2 (A - b_0)^2} \right. \\ & \left. + \frac{s_{yz}^2}{S_{XX}} \left[ \frac{\sum x_i^2}{N(A - b_0)^2} + \frac{1}{b_1^2} - \frac{2\bar{x}}{(A - b_0)b_1} \right] \right\}^{1/2} \quad (51b) \end{aligned}$$

However, the practical importance of the general theory of error lies not only in the calculation of errors, but also in the search for ideal conditions, under which the error associated with the measurement process will be minimal.<sup>30</sup> In a plot of  $s_C/C$  against  $T$ , the portion of the curve where  $s_C/C$  shows a minimum gives the optimum working range. The necessary calculations involved in equation (51b) can easily be done on a programmable calculator. Differentiation of  $s_C/C$  with respect to  $T$  and equating to zero gives

$$-\log T_{(b/s)} = \frac{0.4343^2 s_{T(b/s)}^2 + T_{(b/s)}^2 \frac{\sum x_i^2 s_{yz}^2}{N S_{XX}}}{0.4343 s_{T(b/s)}^2 + T_{(b/s)}^2 \frac{\bar{x}s_{yz}^2}{b_1 S_{XX}}} + b_0 \quad (52a)$$

A more compact version of equation (52a) can be obtained by using the slope and intercept standard deviations instead of the regression standard deviation:

$$A = -\log T_{(b/s)} = \frac{0.4343^2 s_{T(b/s)}^2 + T_{(b/s)}^2 s_{b_0}^2}{0.4343 s_{T(b/s)}^2 + T_{(b/s)}^2 \frac{\bar{x}}{b_1} s_{b_1}^2} + b_0 \quad (52b)$$

If it is assumed that (i) the random errors involved in the calibration straight line parameters are negligible with respect to the random errors in reading the transmittance, and (ii)  $b_0$  is not significant, equation (52b) leads to 0.434 as the absorbance at which the photometric error is at a minimum, in accordance with the classical treatment by Ringbom.<sup>3</sup>

The application of the equations described in this paper to several practical systems is now in progress and will be reported later.

**Acknowledgements**—One of the authors (A. G. Asuero) would like to acknowledge the support provided by the "Dirección General de Investigación Científica y Técnica de España (DGICYT)" through Project No. PB-86-0611.

#### REFERENCES

1. F. Twyman and G. F. Lothian, *Proc. Phys. Soc. (London)*, 1933, **45**, 643.
2. T. R. Hogness, F. P. Zscheile and A. E. Sidwell, *J. Phys. Chem.*, 1937 **41**, 404.
3. A. Ringbom, *Z. Anal. Chem.*, 1939, **115**, 332.
4. G. H. Ayres, *Anal. Chem.*, 1949, **21**, 652.
5. C. F. Hiskey, *ibid.*, 1949, **21**, 1440.
6. D. Z. Robinson, *ibid.*, 1951, **23**, 273.
7. W. A. E. McBryde, *ibid.*, 1952, **24**, 1639.
8. N. T. Gridgeman, *ibid.*, 1952, **24**, 445.
9. C. M. Crawford, *ibid.*, 1959, **31**, 343.
10. G. Svehla, A. Páll and L. Erdey, *Talanta*, 1963, **10**, 719.
11. J. D. Ingle, Jr., *Anal. Chem.*, 1973, **45**, 861.
12. D. Whitehead, *Talanta*, 1973, **20**, 193.
13. H. L. Youmans and Van H. Brown, *Anal. Chem.*, 1976, **48**, 1152.
14. C. Jordan, *Anal. Proc.*, 1980, **17**, 18.
15. O. Grossmann, *Z. Anal. Chem.*, 1985, **320**, 112.
16. J. Mandel and F. J. Linning, *Anal. Chem.*, 1957, **29**, 743.
17. B. R. Kowalski, *ibid.*, 1980, **52**, 112R.
18. S. Akhnazarova and V. Kafarov, *Experiment Optimization in Chemistry and Chemical Engineering*, pp. 28, 15. Mir, Moscow, 1982.
19. K. A. Brownlee, *Statistical Theory and Methodology in Science and Engineering*, p. 79. Wiley, New York, 1965.
20. G. W. Stewart, *Introduction to Matrix Computations*, p. 164. Academic Press, Orlando, Florida, 1973.
21. G. Dahlquist and A. Björck, *Numerical Methods*, p. 138. Prentice Hall, Englewood Cliffs, New Jersey, 1974.
22. C. L. Lawson and R. J. Hanson, *Solving Least Squares Problems*, p. 234. Prentice Hall, Englewood Cliffs, New Jersey, 1974.
23. I. E. Frank and B. R. Kowalski, *Anal. Chem.*, 1982, **54**, 232R.
24. M. F. Delaney, *ibid.*, 1984, **56**, 261R.
25. J. Agterdenbos, *Anal. Chim. Acta*, 1979, **108**, 315.
26. N. Draper and H. Smith, *Applied Regression Analysis*, 2nd Ed., pp. 14, 83. Wiley, New York, 1981.
27. J. B. Kennedy and A. M. Neville, *Basic Statistical*

- Methods for Engineers and Scientists*, 2nd Ed., p. 256. Harper & Row, New York, 1976.
28. R. Tomassone, E. Lesquoy and C. Millier, *La regression, nouveaux regards sur une ancienne méthode statistique*, p. 75. Masson, Paris, 1983.
29. T. Foucart and J.-Y. Lafaye, *Regression linéaire sur micro-ordinateurs*, pp. 99–100. Masson, Paris, 1983.
30. K. Eckschlager, *Errors, Measurement and Results in Chemical Analysis*, p. 13. Van Nostrand-Reinhold, London, 1969.

## DETERMINATION OF ORGANOTINS IN NATURAL WATERS BY TOLUENE EXTRACTION AND GRAPHITE FURNACE AAS

S. C. APTE and M. J. GARDNER

Water Research Centre, P.O. Box 16, Henley Road, Medmenham, Marlow, Bucks., England

(Received 22 July 1987. Revised 26 January 1988. Accepted 29 January 1988)

**Summary**—The determination of tributyltin in natural waters by extraction into toluene and graphite-furnace AAS measurement of tin has been investigated. The effect of pH on the extraction of mono-, di- and tributyltin and triphenyltin has been examined and the optimum conditions for the estimation of tributyltin assessed. The AAS performance is greatly improved by using furnace tubes pretreated by soaking in sodium tungstate solution. Such pretreatment is essential if low detection limits are to be attained. Extraction of the tributyltin from aqueous media resulted in a marked signal enhancement (irrespective of the type of furnace tube), which varied according to the nature of the aqueous solution. The enhancement is believed to result from water in the toluene extract activating the tube surface. Methods for the estimation of tributyltin in waters, appropriate for screening samples as part of routine monitoring programmes, are described. With a 1-litre sample, a limit of detection of ~4 ng/l. was attained for tin. The relative standard deviation of six replicate analyses of sea-water containing 170 ng/l. tin (present as tributyltin) was 1.5%.

Tributyltin (TBT) is the active biocidal constituent of many antifouling preparations currently used to coat the hulls of boats. Much concern has recently been expressed over the potentially harmful effects of tributyltin on many forms of marine life, even when this substance is present at low ng/l. concentrations. For instance, lethal TBT concentrations as low as 100 ng/l. for shellfish have been reported,<sup>1</sup> and damaging sub-lethal effects, such as shell thickening in the oyster<sup>1,2</sup> and imposex in the dog whelk,<sup>3</sup> are known to occur as a result of exposure to TBT concentrations in the 2–50 ng/l. range. Concern is highest in areas having a high density of pleasure craft, where the boats are moored for long periods of time and the circulation of water is often restricted. As a result, the UK Government has proposed a provisional ambient water target concentration of 20 ng/l. for TBT in waters.<sup>1</sup> Even more stringent water-quality standards are being considered. Sensitive and accurate analytical methods are therefore required for routine TBT monitoring purposes, with detection limits in the low ng/l. range.

Several methods have been developed for the determination of butyltin compounds in waters, involving extraction, derivative formation and gas chromatographic separation, and selective detection by flame photometry,<sup>4–6</sup> atomic-absorption spectrometry (AAS)<sup>7–9</sup> or mass spectrometry.<sup>10,11</sup> Whilst these techniques are capable of attaining the required low ng/l. detection limits, a considerable drawback to their use is their complexity and low sample throughput. For routine monitoring purposes, much simpler and more rapid methods are desirable.

Several studies have made use of a relatively simple method for the determination of organotins, involving liquid extraction into a neutral organic solvent such as a toluene, and determination of the tin

content of the extract by graphite furnace AAS.<sup>12,13</sup> Despite the reported use of this method in TBT monitoring,<sup>2,3,14,15</sup> there is little information available in the open literature regarding optimization of the analytical conditions and on the typical analytical performance.

In this paper, we report the results of our evaluation of solvent-extraction/GFAAS methods for tributyltin determination. The work had the aim of developing a simple method appropriate for routine monitoring purposes, with low ng/l. detection limits. It included an assessment of interferences arising from the co-extraction of other organotins that may be present in waters: triphenyltin, and mono- and dibutyltin. The last two are known breakdown products of tributyltin in waters,<sup>16</sup> and are considerably less toxic. The recommended analytical conditions and the analytical performance data are presented.

### EXPERIMENTAL

#### Apparatus

A Perkin Elmer 4000 atomic-absorption spectrometer, equipped with a tin hollow-cathode lamp, deuterium lamp background correction and an HGA 400 furnace-programmer, was used for the determination of tin. Initially, a Perkin Elmer AS-40 autosampler was used for sample introduction into the furnace, but high blank concentrations were observed (presumably caused by leaching of inorganic tin from worn pump components), so its use was abandoned in favour of manual sample injection with a micropipette. The measurement wavelength was 286.3 nm, spectral bandwidth 0.2 nm. The furnace programme was:

Step	Temperature, °C	Ramp time, sec	Hold time, sec
Dry	120	10	10
Ash	900	10	10
Atomize	2500	max. rate	3
Clean-out	2700	max. rate	3

The injection volume was 20  $\mu$ l. To maximize sensitivity, the argon gas flow was stopped during atomization. Except in comparison of peak profiles, peak height measurements were used throughout.

The graphite tubes were pretreated by soaking for at least 24 hr in sodium tungstate solution (5% w/v). Prior to use, the tubes were dried in an oven at 110° for about 30 min and conditioned in the furnace itself by heating at progressively increasing temperature up to 2700°. For prolonged storage, the tubes were kept in the tungstate solution until required. The tube life was greater than 300 firings.

All glassware was cleaned by soaking in 10% v/v nitric acid solution, rinsing first with demineralized water, then with methanol, and drying before use. Extraction funnels were rinsed with methanol, then copious quantities of demineralized water, between extractions.

#### Reagents

Stock standard solutions in methanol were prepared from tributyltin chloride (BDH Chemicals), dibutyltin chloride (DBT), monobutyltin chloride (MBT) and triphenyltin chloride (TPT) (Aldrich Chemicals) at a concentration of 1000 ppm tin. These were found stable for several months when stored in the dark. Working standards (Sn 1 and 10 mg/l.) were prepared in methanol and were kept for a few days. Aristar-grade toluene (BDH Chemicals) and HPLC-grade pentane (Rathburn Chemicals) were used for solvent extractions. The nominal purity of the MBT and TPT was stated by the suppliers to be 95%. The TBT and DBT were checked for the presence of other butyltin compounds by the method described by Mathias *et al.*<sup>5</sup> and estimated to be at least 95% pure.

During the investigation of furnace conditions and extraction procedures, standards were prepared by spiking 10 ml of aqueous sample with the organotin compound followed by extraction (in a 25-ml pyrex glass bottle) for 5 min with 10 ml of toluene. The phases were not separated prior to analysis, and care was taken to withdraw test samples from only the upper toluene layer. The extract systems could be stored in the bottles for at least a week without observable change in concentration.

Sea-water for performance tests was collected from the Solent, England, and filtered (0.45- $\mu$ m membrane) on return to the laboratory. In preliminary experiments, such as investigation of the effect of pH on extraction, artificial sea-water<sup>17</sup> was used.

#### Toluene extraction

The sample was filtered (0.45- $\mu$ m membrane filter), and 1 litre was vigorously shaken for 10 min in a glass separating funnel with 2 or 5 ml of toluene (depending on the desired detection limit). The mixture was allowed to settle for 10 min before the bulk of the water was discarded and the toluene and remaining aqueous phase was transferred to a glass sample vial equipped with a PTFE liner in the cap. No effort was made to separate the two liquid phases completely (care was taken to pipette from only the toluene phase). If an emulsion formed in the organic phase on extraction, it was transferred to a glass centrifuge tube (and the walls of the funnel were washed with clean sea-water if necessary) and broken down by centrifugation at 2000 rpm for 5 min prior to transfer to a clean sample vial. Calibration was done by spiking a river or sea-water sample with tributyltin and extracting in the same manner as for samples. The maximum volume of methanolic spiking solution (TBT standard) added to 1 litre of aqueous solution was kept below 200  $\mu$ l. Over the salinity range 3–35‰ calibration should be done with standards prepared in clean sea-water. In analysis of freshwaters, samples should be arranged into groups having similar bulk compositions, and calibration done with standards prepared with a chemically similar freshwater, and treated in the same manner as the samples.

#### Pentane extraction

One litre of water was extracted with 10 ml of pentane in the same manner as described above. After discard of the aqueous phase and collection of the organic phase, the funnel was washed with a further 10 ml of pentane and the extracts were combined. The extract was dried by freezing at -15° for at least 3 hr, and the pentane phase was pipetted into a dry vial, then evaporated to dryness under a gentle stream of nitrogen, and the residue was redissolved in 0.5 ml of toluene.

## RESULTS AND DISCUSSION

### Optimization of furnace conditions

Furnace conditions were optimized with TBT standards prepared directly in toluene. The type of furnace tube used was found to have a profound effect on sensitivity (Fig. 1). Pyrolytically coated tubes gave very poor sensitivity and non-pyrolytic tubes were only slightly better. About threefold increase in sensitivity was obtained by soaking the tubes in sodium tungstate solution.<sup>18–20</sup> This treatment had the additional advantages of increasing tube life and improving precision. Tungstate-coated pyrolytically-coated tubes gave slightly better sensitivity than non-pyrolytic ones and were therefore used in subsequent work. Pretreatment of furnace tubes with other transition metal salts (*e.g.*, of zirconium, vanadium and molybdenum) as used by other workers<sup>18–20</sup> was not evaluated, but these may be equally as effective.

Irrespective of furnace tube type, TBT was found stable on ashing at up to 600° (900° in a tungstate-treated furnace tube). This indicates stabilization of tributyltin compounds in the furnace, as the boiling points of these compounds [tributyltin chloride 171–173°, bis(tributyltin) oxide 180°] would suggest that volatilization should occur. Signal response was constant for atomization temperatures in the range 2300–2600°. The optimum furnace conditions are those given in the experimental section.

With the furnace conditions optimized for TBT, standards of TPT and DBT in toluene gave the same signal response as TBT. The signal response obtained

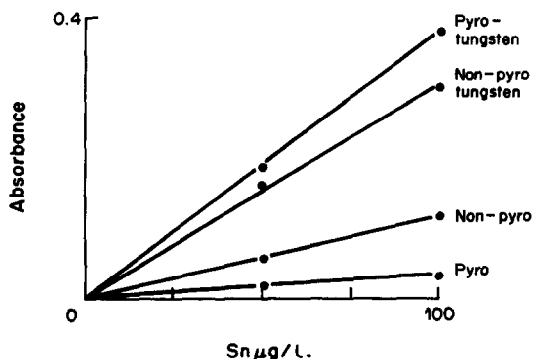


Fig. 1. Effect of furnace tube type on sensitivity.

for MBT however, was only about a third of that for the other organotins.

#### Effect of extraction on signal response

It was apparent that toluene extracts of TBT from aqueous solution gave markedly higher AAS signals than those for corresponding standards prepared directly in toluene, but different degrees of enhancement were obtained for tributyltin extracted from demineralized water, sea-water and 3% saline solution (Fig. 2). Typically, extraction from sea-water resulted in a 40% signal enhancement, but the degree of enhancement was variable from day to day (enhancement effects were studied on at least 10 days). In addition, the response obtained for standards prepared directly in toluene decreased during the course of the working day (Fig. 2), whereas the response for extracted standards remained the same throughout the day. The enhancement effect was found to be independent of tube type (non-pyrolytic, pyrolytic, L'vov platform, with or without tungstate pretreatment). To see whether the enhancement effect was related to the solvent used, the experiments were repeated with 1,1,1-trichloroethane. The results were similar, but the sensitivity was lower.

This set of experiments demonstrated the importance of preparing standards by extraction from a similar matrix to that of the sample. Calibration with standards prepared directly in toluene, which in any case would be questionable analytical practice, could lead to an overestimation of the organotin concentration. Furthermore, calibration with extraction as for the samples should compensate for the solubility of toluene in water, as shown below.

The effect of variation of salt content in the sample, as would be found in estuarine waters, was checked by comparing calibrations obtained with full strength sea-water and the same sea-water diluted tenfold. The results indicated that bias caused by variations in salinity over this range was not important.

It was then thought that the differences in degree of enhancement observed for extracts from different

aqueous solutions might be due to variation in the water content of the toluene extracts. The difference in response for extraction from 3% saline solution and sea-water (Fig. 2) led us to think a surfactant mechanism might increase transport of water into the toluene layer from sea-water samples; however, repetition of the experiments with ultraviolet-irradiated aliquots of the same sea-water showed no difference in response. Perhaps the most illuminating experiment involved pretreatment of the furnace tube by evaporation of demineralized water in the tube before analysis of a TBT standard prepared directly in toluene (Table 1). The results clearly demonstrated an enhancement effect related to the presence of water in the tube. Examination of the absorbance-time profiles during the atomization step showed no observable difference in peak shape between extracted standards and those made up directly in toluene. We can only conclude from our limited experiments that water present in the toluene extract in some way activates the tube surface, possibly affecting the efficiency of the ashing step. As this aspect was outside the main purpose of the work, it was not pursued further.

#### Effect of pH on the extraction

The effect of pH on the extraction behaviour of tributyltin, dibutyltin, monobutyltin and triphenyltin from artificial sea-water solutions was investigated over the range 0–10, obtained by addition of dilute acid or base. The results (Fig. 3) showed some interesting differences in behaviour. Similar results were obtained for TBT and TPT, which showed little variation in extraction over the pH range investigated, whereas DBT gave a similar extraction over the pH range 0–4, above which it fell rapidly. The MBT extraction was uniformly low over the whole pH range investigated.

Since some workers<sup>3,12</sup> separate DBT from other organotins in organic extracts by stripping with alkali, this method was investigated. Shaking a 10-ml toluene extract (containing 0.5  $\mu\text{g}$  of DBT) with 10 ml of 0.1M sodium hydroxide for 5 min gave practically complete stripping. A similar test with

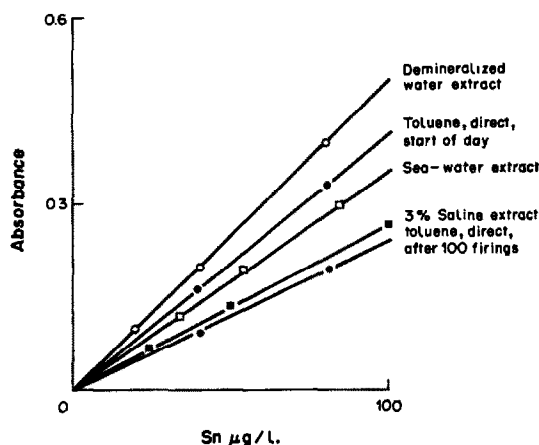


Fig. 2. Effect of extraction on GFAAS signal response.

Table 1. Effect of tube pretreatment with demineralized water on signal response

Run	Signal response (absorbance)	Conditions
1	0.200	water added
2	0.102	no water
3	0.231	water added
4	0.091	no water

Sample tributyltin chloride (Sn 50  $\mu\text{g/l}$ .) dissolved in toluene. Water pretreatment involved pipetting 20  $\mu\text{l}$  of demineralized water into the furnace, followed by heating at 100° until dry. The sample was then analysed as soon as the tube had cooled to room temperature. The samples were analysed consecutively, with a maximum delay of 2 min.

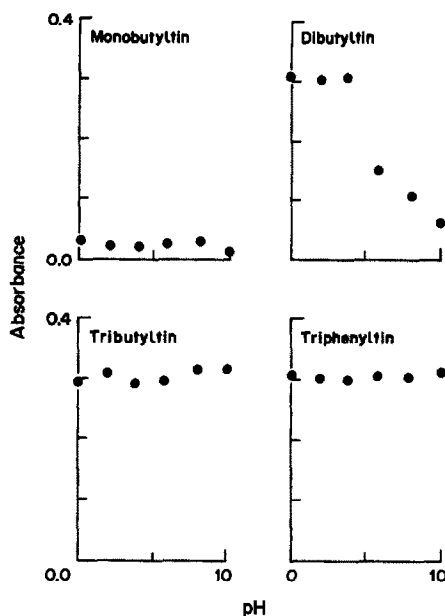


Fig. 3. Effect of extraction pH on signal response: 10 ml of artificial sea-water spiked with 50  $\mu\text{g/l}$ . tin for each organotin standard, and extracted with the same volume of toluene.

TBT standard showed no back-extraction. This step may therefore be included to improve the accuracy of the TBT determination, or to give an estimation of DBT content. Alternatively, dibutyltin and tributyltin may be determined together, if the extraction is done at  $\text{pH} < 4$ , and then the TBT can be determined after stripping of DBT with alkali. The stripping step was not included in our final method, for simplicity. It was deemed acceptable to extract samples at  $\text{pH} 8$  and accept the possible inclusion of a small fraction of DBT.

TPT was found to be potentially the most serious source of bias amongst the organotin compounds tested. However, the co-extraction of TPT with butyltin compounds is not likely to present serious problems in analysis of most natural samples, as this

Table 2. Within-batch performance data for 1-litre samples

Precision (5 ml toluene extraction):	
Sea-water, 170 ng/l. Sn (6 replicates), 1.5% relative standard deviation	
Sea-water, 55 ng/l. Sn (7 replicates), 5% relative standard deviation	
Detection limits:	
5 ml toluene extraction: 4.0 ng/l. Sn (6 replicates)	
2 ml toluene extraction: 1.9 ng/l. Sn (6 replicates)	
(based on 4.65 times the standard deviation of the blank) <sup>21</sup>	
Linear range:	
Up to at least 100 $\mu\text{g/l}$ . Sn in the organic extract	
i.e., 0–500 ng/l. Sn for 5 ml toluene extraction	
0–200 ng/l. Sn for 2 ml toluene extraction	

compound is at present a relatively minor constituent of antifouling preparations.

#### Performance characteristics

Within-batch performance data for the toluene extraction method are presented in Table 2. Detection limits below 5 ng/l. for tin were easily attainable (Table 2). The precision for 100 ng/l. tin was excellent. The assessment of recovery was made difficult by the signal enhancement effects caused by the extraction, and the solubility of toluene in water. The latter significantly affects the final volume of the organic extract when large volumes of water are equilibrated with small volumes of toluene. The solubility of toluene in distilled water at 20° is about 0.05% w/w, and so is that of water in toluene. Thus the volume of a 5-ml portion of toluene equilibrated with 1 litre of water will decrease by about 10%. The effect is even more marked for extraction with 2 ml of toluene. Approximate recoveries of TBT (at the 250 ng/ml Sn level) from 1 litre of sea-water by extraction with 5 ml of toluene were estimated by comparing the tin content of the extract with that of the organic phase obtained from extraction of 10 ml of sea-water containing 500 ng of tin (as TBT) with 10 ml of toluene (conditions under which extraction of TBT could be assumed to be 100% complete). After correction for the solubility effect, the true recovery was estimated as  $82 \pm 3\%$  (4 replicates). However, if all calibration is done by application of the full procedure to 1-litre volumes of suitably prepared standards, there should be inherent compensation for the apparent loss, evaluated by comparison with a standard solution obtained by a 1:1 phase-volume ratio extraction of 10 ml of spiked sea-water. This approach was used to overcome the difficulties created by signal enhancement on extraction. At a concentration of 250 ng Sn/l., recovery was estimated as  $91 \pm 3\%$  (4 replicates).

In this work, all performance data were obtained with filtered samples, i.e., the performance relates to dissolved organotins. Recoveries from unfiltered samples could be lower, for example, if the extraction procedure does not completely release any TBT which may be adsorbed on particulates. This is a problem common to all analytical methods for organotins that do not make a distinction between dissolved and particulate forms.

Interferences other than those arising from the co-extraction of other organotin compounds were not investigated. The presence of substances such as surfactants, oil or grease in contaminated samples may well affect extraction efficiency and/or GFAAS detection. If interferences are suspected, their presence should be checked by the standard-addition method.

#### Sample storage

A brief examination was made of sample storage. Pyrex glass and polycarbonate bottles were evalu-

ated. Polyethylene bottles were not tested, as these had already been shown to be unsuitable.<sup>22</sup> Pyrex and polycarbonate bottles (250-ml capacity) were rinsed in warm detergent solution, thoroughly washed with demineralized water and soaked for at least 24 hr in 5% (w/v) hydrochloric acid. After rinsing with demineralized water and drying, each bottle was filled with clean sea-water (settled, but not filtered) and spiked with 1  $\mu\text{g/l}$ . tin (as tributyltin). All solutions were prepared in triplicate and stored for five days in the dark at room temperature. On analysis, the final tin concentrations were  $0.76 \pm 0.01 \mu\text{g/l}$ . for the polycarbonate bottles and  $1.01 \pm 0.11 \mu\text{g/l}$ . for the pyrex glass bottles. In contrast to recommendations in the literature,<sup>16,23</sup> the polycarbonate containers were found unsuitable for sample storage, and in the absence of information to the contrary, it is advised that samples should be stored in pyrex glass and analysed as soon as possible.

#### *Extraction with pentane*

To obtain detection limits for tin below 2 ng/l., it was found impractical to reduce the volume of toluene used to much below 2 ml, owing to losses on the funnel walls, problems with emulsion formation, and the solubility effect mentioned above. Emulsions could be broken down to some extent by centrifugation, but turbid samples presented serious problems in recovering the organic phase. As a result, an alternative method for obtaining a low detection limit was evaluated. This involved initial extraction with pentane, which is less prone than toluene to emulsion formation, followed by evaporation of the solvent from the extract by a stream of nitrogen and dissolution of the residue in toluene (because the high volatility of pentane, and the difficulties associated with pipetting it, make it unsuitable for introduction into the graphite furnace).

The efficiency of this approach was investigated by evaporating 5 ml of pentane containing 25 ng/l. tin (as TBT) and redissolving the residue in 500  $\mu\text{l}$  of toluene. The mean recovery (five replicates) was  $98 \pm 7\%$ . Initially, it was thought that the main source of imprecision was loss of TBT during complete evaporation to dryness. However, when 25- $\mu\text{l}$  aliquots of methanol containing 25 ng of TBT were similarly evaporated to dryness and maintained under the nitrogen stream for a further minute before redissolution of the TBT in toluene, the results indicated  $98 \pm 1.5\%$  recovery (three replicates), confirming that this step was satisfactory. An overall detection limit of 0.75 ng/l. for tin (evaluated as 4.65 times the standard deviation of the blank,<sup>21</sup> 6 replicates) was obtained. Recovery was evaluated with sea-water samples spiked with 25 ng/l. tin (seven replicates) and was 83.4%, with a relative standard deviation of 9.0%. Further work is required to improve the precision. It was thought that improvement might be obtained by using a more sophisticated preconcentration step involving use of

a Kuderna Danish apparatus, but time and other factors did not allow us to pursue this further. In our experiments, a maximum sample volume of 1 litre was used with a single extraction with 5 ml of pentane and a final volume of 500  $\mu\text{l}$  of toluene solution, giving a preconcentration factor of 2000. It would, however, be possible to increase the sample volume and extract with several portions of solvent, if improved detection limits are desired.

#### CONCLUSIONS

By use of toluene extraction of tributyltin and determination of tin by graphite furnace AAS, limits of detection of below 4 ng/l. tin have been attained. Enhancement of the GFAAS sensitivity by pre-treatment of the graphite tube is an essential step if low detection limits are required. The relative standard deviation for six replicate analyses of sea-water containing 170 ng/l. tin (as tributyltin) was 1.5%.

A significant GFAAS signal enhancement effect is observed when tributyltin is extracted from aqueous samples. It is therefore essential to prepare standards with matrices similar to those of the samples, and to apply the complete procedure to them. In the case of estuarine samples, there was little observed difference in signal response between samples of 35‰ and 3.5‰ salinity. Estuarine samples may therefore be analysed with calibration based on standards prepared in a full strength sea-water matrix, low in TBT.

The extraction studies indicated that in determination of TBT, the co-extraction of MBT is a relatively unimportant source of bias. The co-extraction of DBT may be reduced by adjustment of the sample pH to  $>8$ . Alternatively, DBT may be quantitatively removed from the extract by washing with sodium hydroxide solution. TPT appears to be the potentially most important source of bias, as it has extraction behaviour similar to that of TBT.

The methods described in this paper may be used to screen aqueous samples for TBT. Samples identified as containing high levels of organotins may then be submitted to a more detailed, but time-consuming, determination of the specific organotin species present.

Preliminary investigations suggest that extraction into pentane, followed by evaporation and redissolution in toluene, may allow the attainment of sub-ng/l. detection limits.

#### REFERENCES

1. UK Department of the Environment, Pollution Paper No. 24, *Organotin in antifouling paints: environmental considerations*, HMSO, July 1986.
2. J. J. Cleary and A. R. D. Stebbing, *Mar. Poll. Bull.*, 1987, **18**, 238.
3. G. W. Bryan, P. E. Gibbs, L. G. Hummerstone and G. R. Burt, *J. Mar. Biol. Ass. UK*, 1986, **66**, 611.
4. R. J. Maguire and H. Huneault, *J. Chromatog.*, 1981, **209**, 458.

5. C. L. Mathias, J. M. Bellama, G. J. Olson and F. E. Brinckman, *Environ. Sci. Technol.*, 1986, **20**, 609.
6. M. D. Muller, *Anal. Chem.*, 1987, **59**, 617.
7. M. O. Andrae and J. T. Byrd, *Anal. Chim. Acta*, 1984, **156**, 147.
8. L. Randall, O. F. X. Donard and J. H. Weber, *ibid.*, 1986, **184**, 197.
9. V. F. Hodges, S. L. Seidel and E. D. Goldberg, *Anal. Chem.*, 1979, **51**, 1256.
10. M. D. Mueller, *Z. Anal. Chem.*, 1984, **317**, 32.
11. H. A. Meinema, T. Burger-Wiersma, G. Versluis De-Haan and E. C. Gevers, *Environ. Sci. Technol.*, 1978, **12**, 288.
12. *M&T Chemicals, 1976, Standard Test Method TA-37*, M&T Chem. Inc., Rahway, New Jersey.
13. E. J. Parks, W. R. Blair and F. E. Brinckman, *Talanta*, 1982, **32**, 633.
14. J. J. Cleary and A. R. D. Stebbing, *Mar. Poll. Bull.*, 1985, **16**, 350.
15. M. J. Waldock and D. Miller, *International Council for the Exploration of the Sea, Copenhagen, Paper CM 1983/E:12*, 1983.
16. P. F. Seligman, A. O. Valkirs and R. F. Lee, *Environ. Sci. Technol.*, 1986, **20**, 1229.
17. K. Grasshof, M. Ehrhardt and K. Kremling, *Methods of Seawater Analysis*, p. 398. Verlag Chemie, Weinheim, 1983.
18. T. M. Vickrey, H. E. Howell, G. V. Harrison and G. J. Ramelow, *Anal. Chem.*, 1980, **52**, 1743.
19. T. M. Vickrey, G. V. Harrison, G. J. Ramelow and J. C. Carver, *Anal. Lett.*, 1981, **13**, 781.
20. T. M. Vickrey, G. V. Harrison and G. J. Ramelow, *Anal. Chem.*, 1981, **53**, 1573.
21. A. L. Wilson, *Talanta*, 1973, **20**, 725.
22. W. R. Blair, G. J. Olsen, F. E. Brinckman, R. C. Paule and D. A. Becker, *Natl. Bur. Stds. Rept. NBSIR-86/3321*, 1986.
23. A. O. Valkirs, P. F. Seligman, G. J. Olsen, F. E. Brinckman, C. L. Mathias and J. M. Bellama, *Analyst*, 1987, **112**, 17.



## TRACE METAL DETERMINATION IN ANIMAL TISSUES: AN INTERLABORATORY COMPARISON

R. WAGEMANN\* and F. A. J. ARMSTRONG

Department of Fisheries and Oceans, Central and Arctic Region, Freshwater Institute, 501 University Crescent, Winnipeg, Manitoba, Canada

(Received 6 August 1986. Revised 15 January 1988. Accepted 28 January 1988)

**Summary**—Two dried and powdered preparations of narwhal liver and muscle were distributed to 13 laboratories for analysis for Cu, Cd, Zn, Pb, Hg, and Se. Laboratories chose their own methods, using atomic-absorption spectrometry, atomic-emission spectrometry with a direct-current or inductively-coupled plasma, anodic stripping voltammetry (ASV), neutron activation analysis (NAA), and gas chromatography. The coefficients of variation ranged from 2 to 5% for Cu, Cd, Zn, Hg in liver, but were somewhat higher for Zn by ASV and NAA. In muscle, the precision for Zn was similar to that for liver, but was poorer for Cu (8.8%) and Cd (19%). For Pb, the overall precision was 15% and 21% for liver and muscle respectively. Selenium in both tissues was determined with an overall precision of 6–7%, except by NAA, for which it was considerably worse, at 21–26%.

There are numerous interlaboratory comparisons of analyses for trace elements in plant and animal tissues<sup>1–10</sup> and they are valuable in showing what confidence can be put in such analyses, as well as giving information on methods and on statistical treatment. They give useful information on precision, but can rarely say much about accuracy, since there are few analytical procedures which can give bias-free results. Isotope-dilution mass-spectrometry or neutron-activation analysis have this capability, but they require special facilities.

In the early work, differences between laboratories were discouragingly large, and though these have somewhat decreased,<sup>9</sup> they still exist,<sup>10</sup> and the aims of such comparison studies must be considered when laboratories are chosen. For example, for validation of reference materials, laboratories are often selected on the basis of reputation or past performance, whereas for an overall view, as many laboratories as possible should be chosen, without special regard to their facilities or experience.

In the study reported here we have tried to find out what the best achievable results might now be in conventional laboratories, *i.e.*, those not having an ultraclean installation, but chosen with regard to the experience and reputation of the participants. Thirteen laboratories from Europe and North America (Appendix) participated, together with our own, using various work-up methods and instrumental techniques.

We prepared two materials (similar to those that such laboratories might handle regularly), with some-

what different trace metal concentrations. These were narwhal liver and narwhal muscle, prepared with care to avoid contamination, and representative, as nearly as we could ensure, of dried natural materials in composition. A reference material such as NBS Bovine Liver was not thought entirely suitable for inclusion as an "unknown", partly because its composition is not the same as the narwhal materials, and also because it is easily recognized.

Participants were to choose their own methods and the number of replications (which varied from two, for some laborious methods, to ten, with an overall average of about five). Laboratories provided short summaries of their work-up procedures, which are not included; only differences between procedures are indicated.

### EXPERIMENTAL

#### *Sample preparation*

Large tissue samples, comprising a whole liver nearly one metre across, and about 20 kg of dorsal muscle as well as some other whole organs from a narwhal (*Monodon monoceros*), were obtained for this study by the Management Research Section, Central and Arctic Region, Department of Fisheries and Oceans, Winnipeg. The samples were cut out in the field at the site of kill with a cleaned knife, put into acid-washed plastic bags, frozen, and transported on ice to the Freshwater Institute for subsampling. The tissues were then handled only with polyethylene-gloved hands on acid-washed Teflon® sheets, and were cut with a cleaned (acid-washed and rinsed) knife. Portions of each organ (50–100 mm square, depending on the organ) were removed from defined locations in the specimen with minimal handling. Bulk composite samples, amounting to half of the original quantities, were put in shallow, acid-washed polyethylene boxes for freeze-drying and distribution; other representative samples were set aside for moisture determination. The tissues were dried at –20° in a commercial large-volume freeze drier, over a period of four weeks. The dried muscle, which was light, fibrous and friable, was easily powdered by rubbing the dried pieces of tissue together

\*Author for correspondence.

Crown copyright reserved. Authors R. Wagemann and F. A. J. Armstrong, for the Department of Fisheries and Oceans, Government of Canada.

between (gloved) hands to yield material of which 80% passed easily through a 1-mm (nylon) mesh. The residue was hard and twig-like, quite irreducible by hand, and may have consisted of portions of blood vessels. This residue was discarded, since the object was to obtain homogeneous material. The dried liver was dense and tough, and could only be pulverized after freezing in liquid nitrogen. A Teflon® roller on a Teflon® board was used for this purpose. The material which passed through the 1-mm screen was retained for distribution and analysis. Exposure to the atmosphere during this treatment was probably responsible for the 6–7% moisture found in the samples by the participating laboratories and ourselves.

#### Statistical treatment

The weighted means were calculated from

$$[\text{weighted mean}] = \frac{\sum_1^k (\bar{X}_i/s_i^2)}{\sum_1^k 1/s_i^2}$$

where  $\bar{X}_i$  is the laboratory mean for a particular method, and  $s_i^2$  is the corresponding variance.

#### Outliers

Two criteria, which had to be satisfied simultaneously, were used to exclude questionable laboratory means from the overall mean in Tables 2 and 3.

1. The mean in question had to be well distant in the upper left or lower right quadrants from the diagonal in a Youden<sup>11</sup> plot.

2. The mean in question had to be significantly different at the 90% confidence level ( $\alpha = 0.1$ ) from all other means according to a multimeans comparison test,<sup>12</sup> based on the formula

$$(\bar{Y}_i - \bar{Y}_{i+x}) = S[\text{MSE}(1/n_i + 1/n_{i+x})]^{1/2}$$

where  $i$  is the running index for the  $k$  groups (means) being compared,  $x$  is an incremental integer,

$$S = [(k-1)F_{k-1, n-k, 1-\alpha}]^{1/2}$$

and MSE is a pooled variance which can be expressed as

$$\text{MSE} = \frac{[(n_1 - 1)s_1^2 + (n_2 - 1)s_2^2 + \dots + (n_k - 1)s_k^2]}{(n_1 + n_2 + n_3 + \dots + n_k - k)}$$

The outcome of the test is indicated in the figures by error bars; where these overlap, the corresponding means do not differ significantly. Scheffé's method is applicable to unequal sample sizes, and is the most conservative of such tests.

## RESULTS

### Moisture

Portions were distributed in sealed plastic vials, and to enable proper comparison of trace metal results, drying for 24 hr at 80° was recommended. Reporting of loss of weight on drying was requested together with metal concentrations on a dry-weight basis. Moisture was apparently not determined in a few cases (Table 1), and for these we assume that the material was analysed as received, and the results were reported on that basis. This would give trace metal results lower by 6–8% than they would have been if the drying instruction had been followed. We report here results as received. On average, the liver lost 7.1% in weight on redrying, and the muscle 6.0% (Table 1), with coefficients of variation of 13 and 10% respectively.

The loss in weight on drying of the original, undried, raw tissue at 80° for 24 hr, determined in

Table 1. Loss of weight of samples on drying in each laboratory

Lab. No.*	Loss, %†	
	Liver	Muscle
1	6.99	6.19
2	8.0	4.7
3	7.45	6.35
4	7.4	6.5
5	8.6	6.4
6	5.8	5.1
7	6	6
8	7.4	5.9
9	nd§	nd
10	7.8	6.5
12	nd	nd
13	nd	nd
14	6.02	5.93
Mean and SD	7.14 ± 0.94	5.97 ± 0.61

\*The laboratory numbers were arbitrarily assigned.

†The raw liver and muscle lost roughly 70% weight on initial drying; see results section. Some of this loss may have been due to volatilization of organics.

§nd = not determined.

our laboratory, was 71.3% for the muscle, and 69.9% for the liver. These numbers may be used for recalculation of results from a dry-weight to a wet-weight basis. Some earlier work for narwhal tissues<sup>13</sup> reported 71.9 and 74.3% loss in weight for muscle and liver respectively.

### Intermethod comparison

Five basically different instrumental techniques were used by the various laboratories for the analyses, namely, atomic-absorption spectrometry (in three variants: with flame atomization, FAA, cold vapour atomization, CVAA, and electrothermal atomization, ETAA), atomic-emission spectrometry (AE) with a direct-current (DCP) or inductively coupled (ICP) plasma, anodic stripping voltammetry (ASV), neutron activation analysis (NAA), and gas chromatography (GC). Laboratories used their own methods, and some used two different ones. ASV and GC were each used by only one laboratory, so that interlaboratory comparison for these is impossible. The data are summarized in Tables 2 and 3.

Copper was determined by FAA, AE, or ASV, with close agreement for the liver by all three methods, but for muscle, although the FAA and AE results agreed closely, a significantly lower result was obtained by ASV (Fig. 1).

Cadmium was determined by FAA, ETAA, AE, and ASV. The AE and FAA results agreed closely for both tissues. Both ETAA and ASV yielded a significantly higher result than the other two methods (Fig. 2), but the Youden plot<sup>11</sup> indicated an outlier only for ASV (Fig. 1). For the muscle, ETAA gave a slightly higher result (not significant at the 90% confidence level) than the other two spectrometric

Table 2. Means, SD values (number of determinations) and [weighted means] for results from all laboratories, for six elements ( $\mu\text{g/g}$ , dry weight) in liver

Method	Cu	Cd	Zn	Pb	Hg	Se
FAA	25.5 $\pm$ 1.0 (50) [25.3 $\pm$ 0.6]	225 $\pm$ 7.3 (55) [223 $\pm$ 3.4]	190 $\pm$ 3.7 (55) [219 $\pm$ 0.3]	0.26 $\pm$ 0.08 (7) [0.37 $\pm$ 0.06]	—	—
CVAA	—	—	—	—	63.2 $\pm$ 3.4 (52) [65.1 $\pm$ 0.7]	—
ETAA	—	258* (3)	—	0.44 $\pm$ 0.05 (20) [0.42 $\pm$ 0.03]	—	29.8 $\pm$ 1.7 (28) [29.6 $\pm$ 1.0]
AE	26.5 $\pm$ 0.7 (33) [29.6 $\pm$ 0.5]	216 $\pm$ 5.3 (33) [233 $\pm$ 2.9]	181 $\pm$ 8.3 (33) [202 $\pm$ 1.8]	—	—	31.6 $\pm$ 2.1 (14) [28.4 $\pm$ 2.1]
ASV†	26.1 (2)	270 (3)	287§ (2)	0.30 (2)	—	—
NAA†	—	—	177 (2)	—	—	24.9 (3)
GC†	—	—	—	—	—	31.9 $\pm$ 1.3 (4)
Overall mean and SD	25.9 $\pm$ 0.9	224 $\pm$ 7	186 $\pm$ 6	0.39 $\pm$ 0.06	—	30.3 $\pm$ 2.0

\*Standard deviations were not calculated for fewer than four results.

†A weighted mean was not calculated when only one laboratory was involved or when too few results were available to calculate the SD.

§Not included in overall mean.

methods (Fig. 3). ASV gave a significantly lower result. The cadmium concentration in muscle was much lower than in liver, making its determination by AE apparently more demanding (as shown by the greater standard deviation) than by other methods.

Zinc was determined in both tissues by FAA, AE, ASV, and NAA. The results were not significantly different by any of these methods (Fig. 3), but ASV gave high values for the liver.

Lead was determined by FAA and ETAA, and

ASV. The results agreed reasonably well. This was encouraging since lead is notoriously difficult to determine precisely and accurately at trace levels.<sup>10,14</sup>

Mercury was determined only by CVAA. NAA might have provided a valuable check, but was not used.

Selenium was determined most commonly by ETAA (hydride method), and also by AE (directly, without preconcentration), NAA and GC. The results obtained by the various methods agreed reason-

Table 3. Means, SD values (number of determinations) and [weighted means] for results from all laboratories for six elements ( $\mu\text{g/g}$ , dry weight) in muscle

Method	Cu	Cd	Zn	Pb	Hg	Se
FAA	2.33 $\pm$ 0.15 (53) [2.48 $\pm$ 0.08]	1.50 $\pm$ 0.10 (57) [1.40 $\pm$ 0.05]	59.9 $\pm$ 2.4 (55) [56.3 $\pm$ 0.9]	0.37 $\pm$ 0.10 (19) [0.31 $\pm$ 0.09]	—	—
CVAA	—	—	—	—	3.34 $\pm$ 0.16 (51) [3.32 $\pm$ 0.08]	—
ETAA	—	1.73 $\pm$ 0.23 (7) [1.85 $\pm$ 0.23]	—	0.40 $\pm$ 0.06 (23) [0.39 $\pm$ 0.04]	—	1.14 $\pm$ 0.06 (24) [0.92 $\pm$ 0.04]
AE	2.47 $\pm$ 0.28 (32) [2.39 $\pm$ 0.03]	1.45 $\pm$ 0.53 (23) [1.56 $\pm$ 0.17]	60.6 $\pm$ 1.5 (32) [59.9 $\pm$ 0.20]	—	—	1.50 $\pm$ 0.1 (4)*
ASV*	1.66† (2)	0.19† (2)	64.0 (2)	0.57 (2)	—	—
NAA*	—	—	56.1 (2)	—	—	2.03† (2)
GC*	—	—	—	—	—	1.43 $\pm$ 0.08 (4)
Overall mean and SD	2.38 $\pm$ 0.21	1.51 $\pm$ 0.29	60.2 $\pm$ 2.2	0.39 $\pm$ 0.08	—	1.22 $\pm$ 0.07

\*A weighted mean was not calculated when only one laboratory was involved or when too few results were available.

†Not included in overall mean; standard deviations not calculated when fewer than four results available.

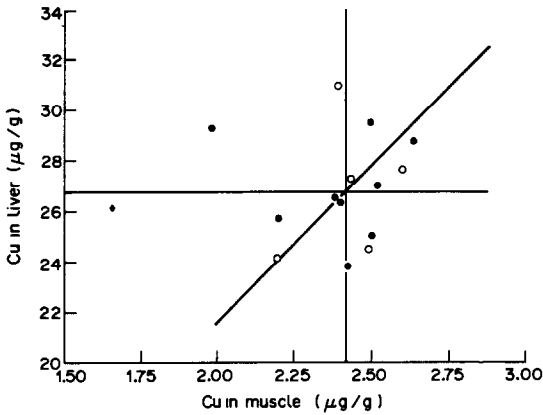


Fig. 1. Concentration of copper in liver *vs.* concentration of copper in muscle by FAA (●), AE (○) and ASV (◆).

ably well (Tables 2 and 3), except for those by NAA, which gave the lowest result for liver, and the highest result for muscle.

The criteria for presence of outliers were both met for four of the means, which were therefore excluded from the overall means in Tables 2 and 3. These were the means for selenium in muscle by NAA, for zinc in liver, and for copper and cadmium in muscle by

ASV, used by only one laboratory; we therefore excluded ASV from further discussion.

*Interlaboratory comparison*

Agreement between laboratories using FAA, CVAA, ETAA and AE was generally good for all elements. Zinc was also measured by NAA by two laboratories, with reasonably good agreement between them for muscle, but poor agreement for liver. The two laboratories also used this method for Se in liver, with good agreement between them and with the overall mean. Only one laboratory used NAA for Se in muscle (where this element was present at a much lower concentration than in liver), and produced a high outlier. One laboratory used GC for Se and, for both tissues, the values were in good agreement with the overall means.

Mercury was determined only by CVAA by all laboratories, with good agreement for both tissues.

Nine laboratories produced a quantitative result for lead, but three of these produced results that were not very useful. For FAA analysis of the liver, one reported  $<0.5 \mu\text{g/g}$ , the second  $<1.6 \mu\text{g/g}$ , and the third a mean of  $<0.05 \mu\text{g/g}$  with a range from  $<0.05$  to  $0.17 \mu\text{g/g}$ ! However, results such as these were excluded from calculation of the overall means.

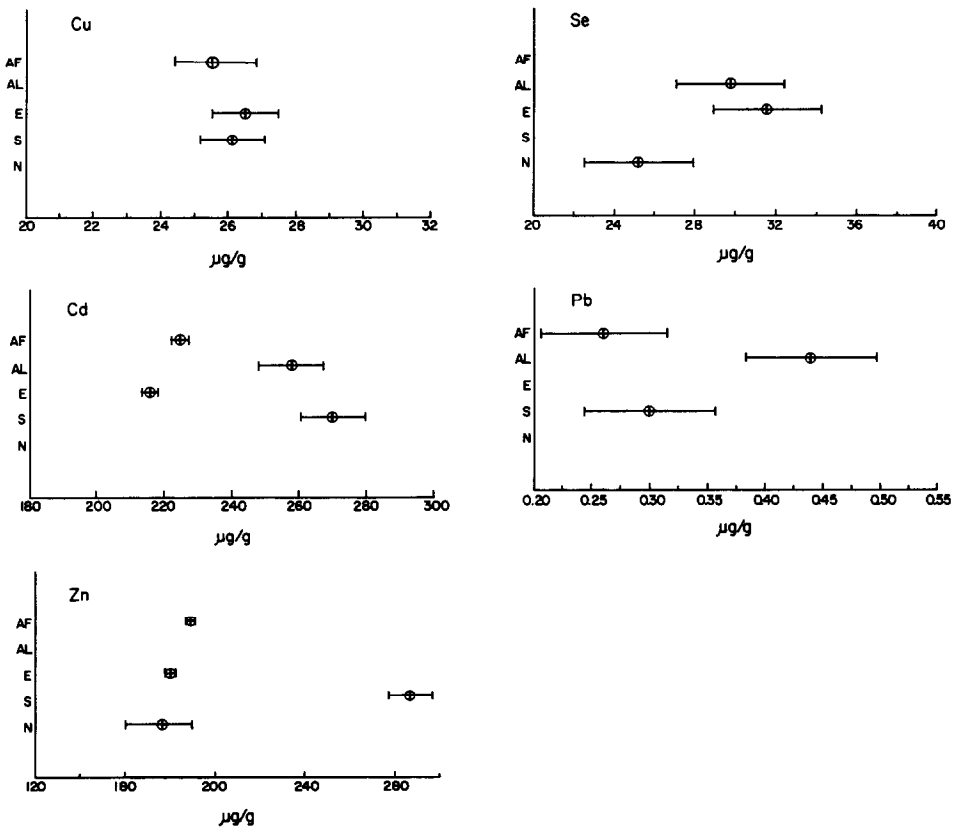


Fig. 2. Multimeans comparison (Scheffe's test), at the 90% confidence level, of metal concentrations in liver. Bars indicate the outcome of the test: only where they do not overlap is there a significant difference between the respective means.

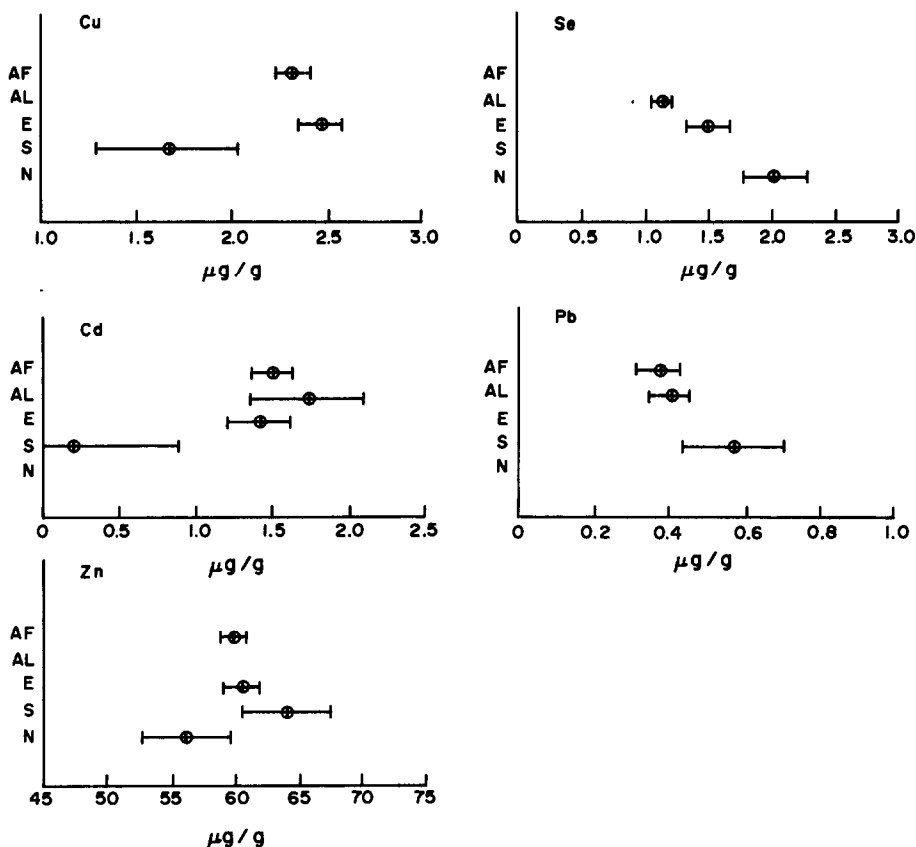


Fig. 3. Multimeans comparison (Scheffe's test), at the 90% confidence level, of metal concentrations in muscle. Bars indicate the outcome of the test: only where they do not overlap is there a significant difference between the respective means.

Tables of means for individual laboratories are available on request from the senior author.

#### Precision

Interlaboratory precision (expressed as coefficient of variation) for Cu, Cd, Hg, and Zn in liver ranged from 2 to 5% except for ASV and NAA, for which it was 6 and 7% respectively for zinc. The overall precision, regardless of method, for these four metals was 3–5% (Table 4). The precision for zinc in muscle was similar to that for liver (Table 5). This was not

unexpected in view of the high concentration of zinc in muscle.

For copper in muscle the overall precision was poorer than for liver (8.8 and 3.4% respectively, Tables 4 and 5), no doubt because of the much lower concentration.

Cadmium in muscle was determined generally with much poorer overall precision than in liver (19 and 3.6% respectively), probably because the concentration was more than two orders of magnitude lower than in liver. AE yielded the poorest precision for muscle (37%). At 1.5  $\mu\text{g/g}$  the limit of reliability

Table 4. Interlaboratory precision, in terms of coefficient of variation, %, for the determination of metals in liver by various methods

Method	Cu	Cd	Zn	Pb	Hg	Se
FAA	3.9	3.2	1.9	31	—	—
CVAA	—	—	—	—	5.4	—
ETAA	—	3.9	—	11	—	5.7
AE	2.6	2.4	4.6	—	—	6.6
ASV*	2.3	1.5	5.6	23	—	—
NAA	—	—	6.8	—	—	21
GC*	—	—	—	—	—	4.1
Overall	3.4	3.6	3.2	15	5.4	6.6

\*Performed by one laboratory only.

Table 5. Interlaboratory precision, in terms of coefficient of variation, %, for the determination of metals in muscle by various methods

Method	Cu	Cd	Zn	Pb	Hg	Se
FAA	6.4	6.7	4.0	27	—	—
CVAA	—	—	—	—	4.8	—
ETAA	—	13	—	15	—	5.3
AE	11	37	2.5	—	—	6.7
ASV*	3.0	26	6.3	1.8	—	—
NAA	—	—	7.5	—	—	26
GC*	—	—	—	—	—	5.6
Overall	8.8	19	3.7	21	4.8	5.7

\*Performed by one laboratory only.

by direct measurement was being approached. For cadmium in liver at over 200  $\mu\text{g/g}$ , the precision by AE was, at 2.4%, better than or as good as that obtained by other methods.

Lead was determined with an overall precision of 15 and 21% in liver and muscle respectively; FAA yielded the poorest precision for both tissues (see comments at the end of the previous section).

Selenium was determined with a precision of approximately 6% in both tissues by all methods except NAA which was notably less precise at 21% and 26% (Tables 4 and 5).

The interlaboratory errors, as reflected by the coefficients of variation in Tables 4 and 5, or the standard deviations accompanying each mean in Tables 2 and 3, represent the total error for a particular instrumental method. There were too many variations in the work-up of samples for further analysis of the errors to be attempted.

#### DISCUSSION

In this study the results obtained for most of the elements by the various laboratories were concordant (Tables 2 and 3), and remarkably so for copper in liver, despite the variety of digestion procedures and instrumental techniques. The least familiar method used was DCP atomic-emission spectrometry, but the results obtained compared well with those of the atomic-absorption methods, except for cadmium at 1.5  $\mu\text{g/g}$ .

The within-laboratory precision for the various methods was only marginally lower than the between-laboratories precision; this was unexpected since in earlier reports the latter was usually a good deal worse than the within-laboratory precision.<sup>4,15</sup>

The between-laboratory precision obtained for trace metal determinations in similar comparative studies in the past has sometimes been disappointingly poor,<sup>16</sup> and the adoption of a single method for use by participating laboratories has been suggested as a way of improving performance.<sup>17</sup> The better results of our study, with its variety of methods, may be a consequence of the experience of the participating laboratories in trace metal analysis.

The results were all blank-corrected by the individual laboratories. Some laboratories stated explicitly that they used a certified reference material to verify accuracy or calibrate their instruments, and others may have done this without mentioning it. The best that can be done without use of absolute methods is to make measurements with methods based on different principles and to assume that the better the results agree, the more likely it is that they are correct.

Contamination may be difficult to avoid or even detect. In such a study as this, variation between laboratories owing to contamination cannot be separated from variations between methods. Airborne

contamination may be revealed for some metals by paying attention to air quality as a variable. In a comparative study of trace metal analyses in a conventional and a class 100 clean laboratory, Adejolu and Bond<sup>18</sup> found that lead concentrations in bovine liver (NBS) and veal samples came out 38 and 58% higher in the conventional than in the clean laboratory. They found no such differences for cadmium.

It was not our purpose in this study to establish true concentrations in the original samples, but only to find out how analyses by experienced laboratories would compare for two homogeneous samples having trace metal concentrations near to the natural ones. To establish the accuracy of the metal values would be another matter, requiring great certainty that no contamination of the sample had occurred before analysis (or knowledge of the level of any such contamination), and similar knowledge of any contamination occurring during the analysis. However, where there is agreement between different methods we think that the results may approach the true value. Comparisons of results obtained by conventional laboratories with those from clean laboratories would be valuable in a more direct study concerned with accuracy.

#### CONCLUSIONS

Of the different instrumental methods used for this work, the most versatile seem to be FAA, CVAA, ETAA, AE, and ASV, which were each used to determine four (though not the same four) of the six elements. As judged by the agreement of the means for each method with the overall mean for all methods, FAA did well for Cu, Cd, and Zn at both "high" and "low" levels, CVAA did well for Hg at both levels, and ETAA for Cd at low level. AE did quite well for Cu and Zn at both levels and for Cd at higher levels. ASV and NAA produced some "good" values and some outliers, but were used by only two or three of the laboratories. At the low level of 0.39  $\mu\text{g/g}$ , Pb was determined with tolerable precision by FAA, ETAA and ASV. ETAA, AE, NAA, and GC were able to determine Se at the high level and with good agreement but for the low level, one of the two determinations by NAA appeared as an outlier.

The precision and possibly the accuracy of the results show an improvement on earlier inter-laboratory studies. Of the 90 or so results reported, only four qualified as outliers.

*Acknowledgements*—First, we extend our strongest thanks to all heads and analytical chemists of participating laboratories for their work in this study, and their comments on it. The support and assistance of G. D. Koshinsky is gratefully acknowledged. We thank several unknown Inuit hunters and R. Walker for providing the narwhal and the tissues, and A. Lutz for valuable analytical work. We also thank D. Povoledo and G. Boila for assisting in the dissection, P. V. Cassidy for typing the manuscript, and Drs.

R. A. Chalmers and B. Johnston for helpful comment. We were fortunate to have the help of M. J. Sala, who undertook the long drying process with understanding of the need to avoid contamination. This study was funded by the Office of Energy Research and Development, Department of Energy, Mines and Resources, Government of Canada.

#### REFERENCES

1. G. Wernimont, *Anal. Chem.*, 1951, **23**, 1572.
2. D. E. King, in *Methods and Standards for Environmental Measurement*, W. H. Kirchnoff (ed.) *Natl. Bur. Std., Spec. Publ. 464*, 1977, p. 581.
3. K. I. Aspila and J. M. Carron, *Interlaboratory Quality Control Study No. 18*, Report Series No. 61, Inland Waters Directorate, Burlington, Ontario, Canada, 1979.
4. T. S. Koh, T. H. Benson and G. J. Judson, *J. Assoc. Off. Anal. Chem.*, 1980, **63**, 809.
5. S. G. Capar, R. J. Gajan, E. Madzsar, R. H. Albert, M. Sanders and J. Zyren, *ibid.*, 1982, **65**, 978.
6. H. Brix, J. E. Lyngby and H-H. Schierup, *Mar. Chem.*, 1982, **12**, 69.
7. W. B. Galloway, J. L. Lake, D. K. Phelps, P. F. Rogerson, V. T. Bowen, J. W. Farrington, E. D. Goldberg, J. L. Laseter, G. C. Lawler, J. H. Martin and R. W. Risebrough, *Environ. Toxicol. Chem.*, 1983, **2**, 395.
8. B. M. Slabyj, R. D. Koons, H. E. Bradbury and R. E. Martin, *J. Food Prot.*, 1983, **46**, 122.
9. G. Topping, in *Trace Metals in Sea Water*, C. S. Wong, E. Boyle, K. W. Bruland, J. D. Burton and E. D. Goldberg (eds.), pp. 155-173, Plenum Press, New York, 1980.
10. J. C. Sherlock, W. H. Evans, J. Hislop, J. J. Kay, R. Law, D. J. McWeeny, G. A. Smart, G. Topping and R. Wood, *Chem. Brit.*, 1985, **21**, 1019.
11. W. J. Youden, *Ind. Qual. Control.*, 1959, **15**, 24.
12. H. Scheffe, *Analysis of Variance*, Wiley, New York, 1959.
13. R. Wagemann, N. B. Snow, A. Lutz and D. P. Scott, *Can. J. Fish. Aquat. Sci.*, 1983, **40**, 206.
14. M. Burnett and C. C. Patterson, in *Lead in the Marine Environment*, M. Branica and Z. Konrad (eds.), pp. 15-30, Pergamon Press, Oxford, 1980.
15. M. R. Hendzel, B. W. Fallis, and B. G. E. Demarch, *J. Assoc. Off. Anal. Chem.*, 1986, **69**, 71.
16. G. H. Morrison, in *Accuracy in Trace Analysis: Sampling, Sample Handling, Analysis*. Vol. 1, P. D. LaFleur (ed.), p. 65. *Natl. Bur. Stand., Spec. Publ. 422*, 1976.
17. A. V. Holden, G. Topping and J. F. Uthe, *Can. J. Fish. Aquat. Sci.*, 1983, **40**, 100.
18. S. B. Adeloju and A. M. Bond, *Anal. Chem.*, 1985, **57**, 1728.

#### APPENDIX

##### Participating Laboratories

Dept. of Agriculture and Fisheries  
Marine Laboratory, P.O. Box 101, Victoria Rd.  
Aberdeen AB9 3DB, Scotland

Analytical Science Branch, Atomic Energy of Canada Ltd.  
Whiteshell Nuclear Research Establishment  
Pinawa, Manitoba, Canada, R0E 1L0

Ministry of the Environment  
Laboratory Services and Applied Research, I.T.C. Section  
Box 213, Rexdale, Ontario, Canada

National Swedish Environmental Protection Board  
Water Research Laboratory, Box 1302, S-171 25 Solna,  
Sweden

Water Quality Laboratory, Inland Waters Directorate,  
CCIW  
867 Lakeshore Rd., P.O. Box 5050  
Burlington, Ontario, Canada, L7R 4A6

Ministry of Agriculture, Fisheries and Food  
Directorate of Fisheries Research  
Fisheries Laboratory, Remembrance Ave.  
Burnham-on-Crouch, Essex CM0 8HA, England

Central Institute for Industrial Research, Forskningsv. 1  
P.O. Box 350 Blinden, Oslo 3, Norway

Dept. of Fisheries and Oceans, Central & Arctic Region  
Physical & Chemical Sciences Directorate  
Contaminants and Toxicology Research Division  
Freshwater Institute Science Lab, 501 University Cresc.  
Winnipeg, Manitoba, Canada R3T 2N6

Statens Naturvardsverk  
The National Swedish Environment Protection Board  
Research Laboratory  
S-170 11 Drottningholm, Sweden

Analytical Chemistry Branch  
National Research Council Canada  
Ottawa, Ontario, Canada K1A 0R6

Washington State University, Nuclear Radiation Center  
Pullman, Washington 99164, U.S.A.

Institute of Hygiene, University of Aarhus  
Universitetsparken, DK-8000 Aarhus C, Denmark

Dept. of Fisheries and Oceans, Central & Arctic Region  
Inspection and Field Services Branch  
501 University Crescent  
Winnipeg, Manitoba, Canada R3T 2N6

## FLUORIMETRIC DETERMINATION OF ULTRATRACES OF LEAD BY ION-PAIR EXTRACTION WITH CRYPTAND 2.2.1 AND EOSIN

D. BLANCO GOMIS, P. ARIAS ABRODO, A. M. PICINELLI LOBO and A. SANZ MEDEL  
Departamento de Química Física y Analítica, Facultad de Química, Universidad de Oviedo, Oviedo, Spain

(Received 21 October 1987. Revised 12 January 1988. Accepted 28 January 1988)

**Summary**—A spectrofluorimetric study of the extraction of lead into 1,2-dichloroethane, as an ion-pair formed between the cryptand 2.2.1-lead complex and the eosinate counter-ion is described. Optimum conditions for the extraction have been established and a new spectrofluorimetric determination of ultratraces of lead is proposed (detection limit 0.8 ng/ml; relative standard deviation 2.4% at the 60 ng/ml level). The metal:ligand:counter-ion molecular ratio in the extracted mononuclear ion-pair is 1:1:1. The equilibrium constants involved in the extraction have been estimated and refined by the Letagrop-DISTR program.

The diazopolyoxamacrocyclics or cryptands, first synthesized by Lehn,<sup>1</sup> are well known for their ability to form inclusion complexes, called cryptates, with metal ions, which are readily extractable as ion-pairs with strongly coloured or fluorescent hydrophobic anions into suitable organic solvents.

In an earlier work, we reported a highly sensitive and selective spectrofluorimetric method for the determination of ultratraces of lead, based on solvent extraction with chloroform of the ion-pair formed between the positively-charged cryptate of lead with cryptand 2.2.2, and the eosinate anion.<sup>2</sup> However, the cryptand forming the most stable complex with lead is cryptand 2.2.1 ( $\log \beta_{\text{PbL}} = 13.12$ , in water). Moreover, this ligand offers a selectivity spectrum intrinsically different from that of cryptand 2.2.2, as shown by the stability constants reported for the cryptates.<sup>3,4</sup> Therefore, we have undertaken a comparative study of the extraction of the Pb(II)-2.2.1 cryptate complex with several fluorescein derivatives as counter-ions and different organic solvents. As a result we have found that eosin and 1,2-dichloroethane provide the most convenient extraction system for this lead cryptate.

Here we report on the extraction and fluorimetric determination of lead with cryptand 2.2.1 and the above-mentioned extraction system and compare the results with those previously reported<sup>2</sup> for the corresponding cryptand 2.2.2 system. The equilibrium constants of the extraction process have also been determined, and refined by using the Letagrop-DISTR program.<sup>5</sup>

### EXPERIMENTAL

#### Apparatus

Fluorescence intensity measurements and spectra were obtained with an LS-5 Perkin-Elmer spectrofluorimeter equipped with a Model 3600 data-station. The excitation

and emission slit-widths were both 2.5 mm and standard 1.00-cm silica cells were used. The temperature of the sample cell was kept constant within  $\pm 0.2^\circ$  by using a Julabo (Paratherm III) thermostat system.

A WTW-D812 pH-meter Model 319, calibrated against Radiometer buffers, was used for pH-measurements of the aqueous phases.

For the voltammetric measurements of lead, a Metrohm E-506 polarograph equipped with a Metrohm EA-410 hanging mercury drop electrode (HMDE) was used.

#### Reagents

All reagents were of analytical grade, and doubly distilled and demineralized water was used throughout.

**Pb(II) stock solution (1000 ppm).** Prepared by dissolving 1.598 g of lead nitrate in water, and diluting the solution to 1 litre; standardized gravimetrically by precipitation of lead sulphate. All working standard solutions were freshly prepared by appropriate dilution of the stock solution.

**Cryptand 2.2.1.** The commercial product (Kryptofix, Merck reagent) was used as received. It was dissolved in water to which perchloric acid had been added and through which argon had been passed in order to remove carbon dioxide and avoid carbonation of the cryptand. The ligand concentration used when the solution was stored in polyethylene flasks was  $1.54 \times 10^{-2} M$ , and the perchloric acid concentration used was 1.5 times that of the ligand. This solution was diluted 100-fold before use.

**Acidic eosin solution,  $3.86 \times 10^{-5} M$ .** Pure eosin was synthesized by reaction of  $\text{Br}^-/\text{BrO}_3^-$  with fluorescein in acidified aqueous acetone as described elsewhere.<sup>6</sup>

**Buffer solution (pH 6.5).** Prepared by dissolving 0.976 g of 2-(*N*-morpholino)ethanesulphonic acid (MES) in about 80 ml of doubly distilled and demineralized water. The pH of the solution was adjusted with tetramethylammonium hydroxide (TMA) (pH-meter control). Finally, the solution was diluted to 100 ml with water.

*1,2-Dichloroethane, Carlo Erba RPE-Analyticals.*

#### General procedure

Pipette standard lead solutions (containing up to 400 ng of the metal) into a series of 10-ml centrifuge tubes. To each tube add 0.1 ml of the diluted cryptand 2.2.1 stock solution, 1 ml of buffer solution and 0.2 ml of eosin solution, and dilute to 5 ml with doubly distilled and demineralized water (final pH  $6.5 \pm 0.1$ ). After mixing, add 5 ml of 1,2-dichloro-



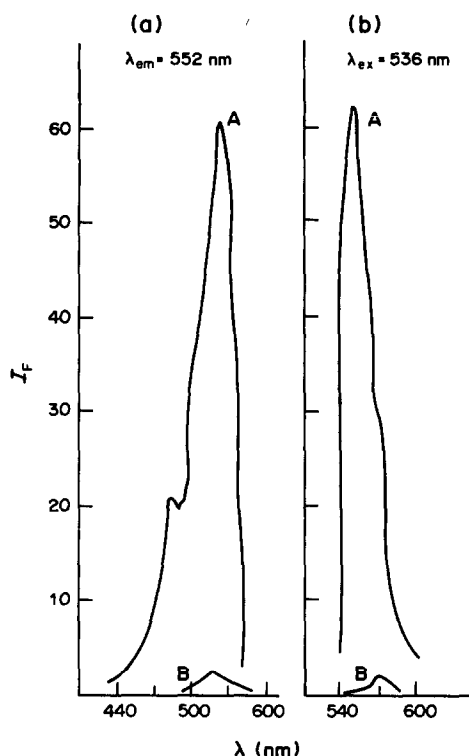


Fig. 1. Excitation (a) and emission (b) spectra of blank (B) and ion-association lead complex (A).

ethane (previously equilibrated with lead-free buffered aqueous phase) and extract the complex by shaking the stoppered tube for 15 min. Allow the phases to separate and measure the fluorescence intensity,  $I_f$ , of the organic layer at 552 nm (excitation wavelength 536 nm). Prepare and measure in the same way a reagent blank without Pb(II). Keep the temperature constant throughout. Analyse samples similarly. Soak all glassware in concentrated nitric acid after conventional cleaning, and finally wash it with doubly distilled and demineralized water to avoid lead contamination.<sup>2</sup>

## RESULTS AND DISCUSSION

### Preliminary investigations

The acidic fluorescent dyes tested as counter-ions for the binary cryptand 2.2.1-Pb<sup>2+</sup> complex were fluorescein and its derivatives, including 2',7'-dichlorofluorescein, dichlorotetraiodofluorescein (Rose Bengal), tetrabromofluorescein (eosin) and tetraiodofluorescein (erythrosin). As expected, virtually no extraction was observed, over the pH range 4–11.5, with fluorescein or dichlorofluorescein. Erythrosin and Rose Bengal produced good analytical fluorimetric signals but were discarded because of their high reagent blank fluorescence. Eosin, however, not only gave good analytical signals but also negligible blank fluorescence values. This behaviour, as we have mentioned elsewhere,<sup>2</sup> agrees with the general extraction behaviour of ion-association ternary complexes with fluorescein dyes. Therefore,

eosin was selected as the counter-ion for the extraction of the lead-2.2.1 cryptate complex.

Benzene, toluene, chloroform, dichloromethane and 1,2-dichloroethane were examined as organic solvents for the ion-pair formed with eosin. The efficiency of extraction of 0.4  $\mu$ g of lead into these solvents decreases in the order 1,2-dichloroethane > chloroform > dichloromethane > benzene > toluene. The best corrected fluorescence intensities were observed when 1,2-dichloroethane or chloroform was used. Photochemical decomposition after 3 min of radiation exposure was observed when chloroform was used, but use of 1,2-dichloroethane produced stable and reproducible intensity measurements. Therefore, 1,2-dichloroethane was chosen as the organic solvent. This behaviour differs from that observed for cryptand 2.2.2 where the extraction efficiency decreased in the order chloroform > 1,2-dichloroethane > dichloromethane and no photochemical decomposition of the chloroform extract was noticed.

### Absorption and emission spectra

The absorption and emission spectra of the ion-pair and of the reagent blank, extracted by the general procedure, are given in Fig. 1. As expected, the excitation maximum appears at 536 nm and the emission maximum at 552 nm.

### Effect of pH

The pH-dependence of the ion-association lead-cryptand 2.2.1-eosin ternary complex is complicated owing to the possible secondary reactions affecting the cation, the ligand and/or the counter-ion. Taking into account all these possible reactions, we have calculated the conditional stability constant of the lead binary complex in aqueous solution at different pH-values (Fig. 2, curve A), from the stability constant of the cryptand 2.2.1-Pb<sup>2+</sup> complex,<sup>4</sup> the  $pK_a$  values<sup>3</sup> of the mono- and diprotonated cryptand 2.2.1, and the stability constants of the lead-hydroxide complexes.<sup>7</sup> Considering the actual reagent concentration used in the procedure it can be said that the formation of the lead-cryptand 2.2.1 complex is quantitative between pH 6.0 and 11.5.

To determine the optimal pH for the formation and extraction of the ion-pair we studied the influence of pH on the fluorescence intensity due to 80 ng/ml lead over the pH range 5.5–11.5 (fixed by addition of acetic acid or tetramethylammonium hydroxide). The results are shown in Fig. 2, curve B, and indicate that the maximum extraction takes place at pH 6.3, in agreement with the presence of the doubly charged eosinate anion at pH 5–6.<sup>8</sup> Nevertheless, the signal unexpectedly decreases rapidly at about pH 7, so a final pH of 6.5 (MES-TMA buffer) was selected for subsequent work.

The pH-dependence of the extraction of this lead-cryptand 2.2.1-eosin ion-pair has a different trend from that observed for the lead-cryptand

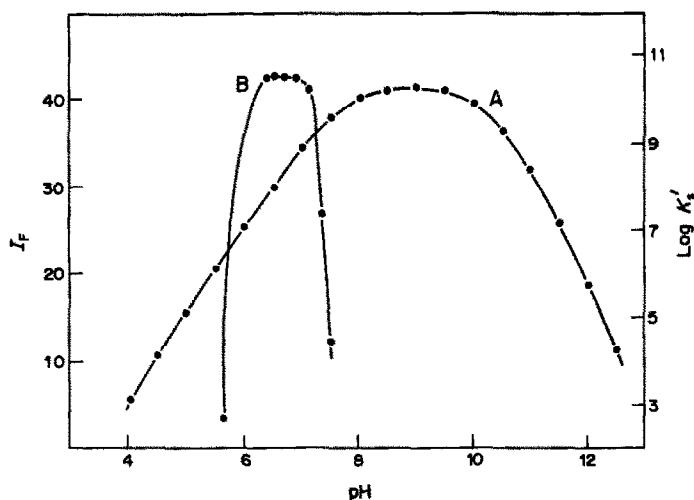


Fig. 2. (A) Effect of pH on the conditional stability constant  $K'_c$  of the lead-cryptate complex. (B) Influence of pH on the fluorescence intensity of the lead complex (80 ng/ml).

2.2.2-eosin ion-pair:<sup>2</sup> the fluorescence of the lead complex with cryptand 2.2.2 is pH-independent in the range 6.8–9.5, which is in accordance with the conditional stability constant of the binary complex as a function of the pH in the aqueous solution. In our opinion the formation of dimer species in the organic phase when cryptand 2.2.2 is used is the possible reason for the pH-range for extraction of the ion-pair being wider.<sup>2</sup> As we will see later, when cryptand 2.2.1 was used, no extractable polynuclear species could be detected, so the absence of secondary reactions in the organic phase would render the overall extraction constant smaller and hence make the lead extraction more critically dependent on pH.

#### Reagent concentrations

The effects of variation of the cryptand 2.2.1 and eosin concentrations on the fluorescence signal of the extract for a fixed level of lead (80 ng/ml) are shown in Fig. 3. As can be seen, the fluorescence becomes constant at a cryptand 2.2.1:lead molar ratio of about 4:1 (for a fixed eosin concentration of  $1.16 \times 10^{-6}M$ ). A maximum and constant signal was observed for an eosin:lead molar ratio of about 2:1 (for a fixed cryptand 2.2.1 concentration of  $3.09 \times 10^{-6}M$ ).

The results are similar to those obtained with cryptand 2.2.2, where the excesses required were of the same order.<sup>2</sup>

#### Rate of extraction and stability of the extract

The effect of variation of mechanical shaking time on the fluorescence intensity shows that equilibrium is achieved after 10 min of mechanical shaking (15 min were used in subsequent work), and the fluorescence of a given organic extract remains constant for at least 20 hr under the usual laboratory conditions. Different orders of addition of the re-

agents were tested and a slight influence of this factor on the fluorescence signal was noticed, similar to that already observed with cryptand 2.2.2.<sup>2</sup>

#### Effect of ionic strength

The results of varying the ionic strength ( $I$ ) (from  $10^{-3}$  to  $0.1M$ , fixed with lithium perchlorate) on the lead extraction are plotted in Fig. 4. Ionic strengths higher than  $10^{-2}M$  produce a sharp decrease in the analytical signal. Only for low values of  $I$  does the fluorescence of the organic layer remain constant. The reason for this behaviour has to be searched for in the influence of ionic strength on the association, and subsequent extraction, of the binary complex with the counter-ion. Increase in the ionic strength promotes poorer association of the metal-macrocycle complex with the eosinate anion, as we have demonstrated in a similar research on the extraction of strontium with cryptand 2.2.2. and eosin.<sup>2,9</sup> This

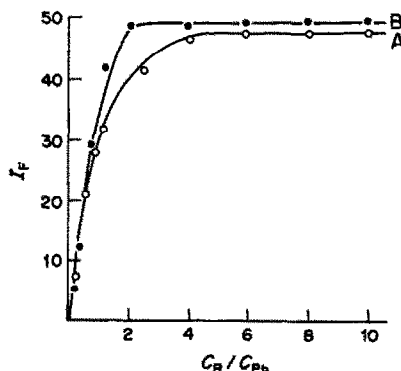


Fig. 3. Variation of fluorescence intensity as a function of reagent concentration of: (A) molar concentration ratio cryptand 2.2.1/lead, for a fixed eosin concentration of  $1.16 \times 10^{-6}M$ ; (B) molar concentration ratio eosin/lead, for a fixed cryptand concentration of  $3.09 \times 10^{-6}M$ .

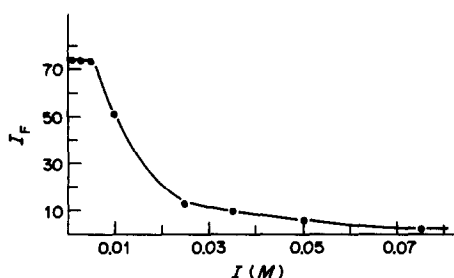


Fig. 4. Influence of ionic strength ( $\text{LiClO}_4$ ) on the fluorescence intensity: 80 ng/ml  $\text{Pb}^{2+}$ ,  $C_L = 3.09 \times 10^{-6} M$ ,  $C_E = 1.54 \times 10^{-6} M$ .

weaker interaction results in a decrease in the extractability of the ion-pair.

In contrast, a different behaviour was observed in the extraction of lead with cryptand 2.2.2 and eosin,<sup>2</sup> where no significant effect of increasing ionic strength was noticed. This could be attributed to the strong tendency of the lead ion-pair to form polymeric species in the organic phase.

Of course, the variation of fluorescence with the ionic strength poses a serious analytical disadvantage since this parameter has to be controlled rigorously for reliable fluorescence measurements to be made.

#### Calibration graph, limit of detection and precision

The calibration graph is linear from the detection limit up to 80 ng/ml lead, the limit of detection being 0.8 ng/ml, (evaluated as twice the standard deviation of the blank value).

The precision (relative standard deviation) of the determination, estimated by analysing 11 replicates containing 0.3  $\mu\text{g}$  of lead, was 2.4%.

#### Selectivity

To evaluate the selectivity, the effect of several ions capable of forming stable complexes with cryptand 2.2.1 (*e.g.*, those of the alkali and alkaline-earth metals, and some other metals associated with lead, such as Hg, Cd, Zn) was investigated. The effect of 1000-fold molar ratio of alkali and alkaline-earth metal ions and 500-fold ratio of other potential interferents on the determination of lead by the recommended procedure was initially tested, and further investigated at lower levels for those cations which were found to interfere (*e.g.*, producing an error greater than  $\pm 5\%$  in the apparent recovery of 0.3  $\mu\text{g}$  of lead).

The results are summarized in Table 1. It can be seen that alkali-metal ions do not interfere, as expected from the values of the stability constants of the corresponding  $\text{ML}^+$  complexes in aqueous solution.<sup>3,4</sup>

Among the alkaline-earth metals, calcium and barium up to the 500-fold level, and magnesium and strontium up to the 100- and 5-fold levels, respectively, can be tolerated. This behaviour differs from that previously reported for the determination

of lead with cryptand 2.2.2, where barium and magnesium could be tolerated up to 1000-fold and calcium and strontium up to 100- and 0.5-fold ratio to the lead, and these two last interferences could be easily eliminated by increasing the ionic strength of the aqueous phase.<sup>2</sup>

A look at the stability constants of the binary complexes<sup>3,4</sup> with cryptand 2.2.1 and cryptand 2.2.2 shows that the stability constant of the calcium-cryptand 2.2.1 complex ( $\log K_f = 6.95$ ) is greater than that of the calcium-cryptand 2.2.2 complex ( $\log K_f = 4.40$ ), yet calcium is less well tolerated in the second case. The opposite effect is observed with barium, and strontium exhibits a lower stability constant with cryptand 2.2.1 than with cryptand 2.2.2 but interferes only at ten times higher levels when cryptand 2.2.1 is used. These results indicate that the extractability of the ion-pair complexes is also a decisive factor.

Cadmium and mercury interfere at any level because they are extracted at pH 6.5. In our previous work<sup>2,10</sup> on the extraction of toxic heavy metal ions with conventional crown and cryptand polyethers (the donor hetero-atoms fundamentally being oxygen) we never found an extraction as efficient for these two metals as we have observed here with cryptand 2.2.1. This opens the possibility of applying this ligand to the separation and possible spectrophotometric and/or fluorimetric determination of these elements. Aluminium, chromium and iron interfere because they produce a depressive effect on the lead extraction, probably owing to the adsorption of lead on the corresponding hydroxides at the pH of extraction (hindering the formation and extraction of the lead complex). In any case, it is possible to minimize this effect as reported previously.<sup>10</sup>

#### Stoichiometry of the extracted complex

The cryptate structure of the lead-cryptand 2.2.1

Table 1. Effect of foreign ions (M) on the determination of 0.3  $\mu\text{g}$  of lead

Cation	M:Pb (molar ratio)	Apparent recovery, %
$\text{Li}^+$	1000	100.0
$\text{Na}^+$	1000	100.0
$\text{K}^+$	1000	105.0
$\text{Mg}^{2+}$	1000	—
	100	96.5
$\text{Ca}^{2+}$	500	102.8
$\text{Sr}^{2+}$	5	103.0
$\text{Ba}^{2+}$	500	102.8
$\text{Zn}^{2+}$	500	104.3
$\text{Cu}^{2+}$	500	105.0
$\text{Co}^{2+}$	500	104.9
$\text{Ni}^{2+}$	500	101.0
$\text{Al}^{3+}$ , $\text{Cr}^{3+}$ , $\text{Fe}^{3+}$	—	Interfere
$\text{Cd}^{2+}$	10	136.3
	1	108.0
$\text{Hg}^{2+}$	1	141.7
	0.5	102.0

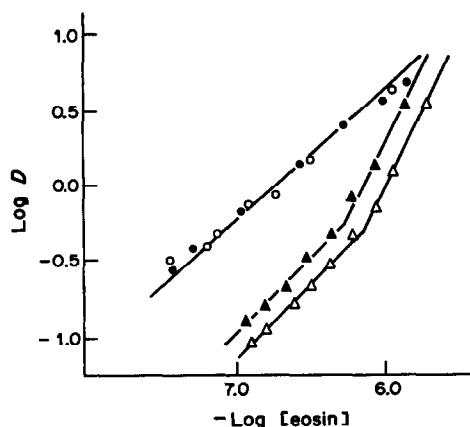


Fig. 5. Dependence of the lead distribution ratio on the eosin concentration in the aqueous phase. For lead-cryptand 2.2.1-eosin complex: (●)  $C_{Pb} = 9.65 \times 10^{-7} M$ ,  $C_L = 7.72 \times 10^{-6} M$ ,  $C_E = (5.01-39.8) \times 10^{-6} M$ . (○)  $C_{Pb} = 1.93 \times 10^{-6} M$ ,  $C_L = 7.72 \times 10^{-6} M$ ,  $C_E = (4.92-31.6) \times 10^{-6} M$ . For lead-cryptand 2.2.2-eosin complex: (▲)  $C_{Pb} = 7.25 \times 10^{-5} M$ ,  $C_L = 9.66 \times 10^{-5} M$ ,  $C_E = (4.06-72.5) \times 10^{-6} M$ . (△)  $C_{Pb} = 9.66 \times 10^{-5} M$ ,  $C_L = 9.66 \times 10^{-5} M$ ,  $C_E = (9.66-172) \times 10^{-6} M$ .

complex and therefore the 1:1 metal:ligand stoichiometry have been clearly established.<sup>4,11,12</sup>

In our previous papers dealing with the extraction of lead with 18-crown-6 or cryptand 2.2.2 and eosin we have determined, in both cases, that the stoichiometry is 1:1:1 metal:ligand:counter-ion. Here, the dissociation constants of eosin<sup>8</sup> and the pH value of 6.5 also suggest that only a neutral complex (lead: cryptand 2.2.1: eosin, 1:1:1) should be extracted.

To confirm this hypothesis we have studied the dependence of the distribution ratio of lead on the eosin concentration. We performed two sets of experiments for two different total lead concentrations, 200 and 400 ng/ml. In each case the lead concentration in the organic and aqueous phases was measured by anodic stripping voltammetry. Free eosin concentrations were determined in the aqueous layer fluorimetrically at 535 nm (excitation wavelength 509 nm). The results obtained, plotted in Fig. 5, clearly demonstrate on the one hand the 1:1:1 metal:ligand:counter-ion stoichiometry and on the other hand the non-existence of polymerization reactions. This behaviour is clearly different from that observed for the ion-pairs extracted with 18-crown-6 or cryptand 2.2.2 and eosin, where the existence of the 1:1:1 complex extracted at low eosin concentration and the  $(1:1:1)_2$  dimer formed at higher eosin concentration has been established.<sup>2</sup> This polymerization reaction could be responsible for these extraction systems not being affected by changes in ionic strength.

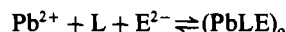
We have already demonstrated elsewhere that ionic strength may strongly affect the association and extraction of the ion-pair, that is, the partition

coefficient,  $P_{CT}$ ,<sup>13</sup> as well as the extraction constant,  $K_{ext}$ , if no secondary polymerization reactions occur.<sup>9</sup> Thus, the case of the lead-2.2.1-eosin complex proves clearly that when mononuclear complexes are extracted, the ionic strength plays an important role.

#### Extraction constants

From the data obtained in the determination of the stoichiometry we can calculate the partition coefficient and the extraction constant of the ion-pair.

According to the established stoichiometry, the overall extraction equilibrium between the aqueous phase (containing the metal cation, the ligand and the counter-ion) and the organic phase may be formulated as



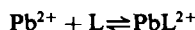
where the subscript "o" and the absence of a subscript indicate the organic and the aqueous phase respectively.

The extraction constant can be defined as:

$$K_{ext} = [PbLE]_o / [Pb^{2+}][L][E^{2-}]$$

For treatment of the data, this overall extraction equilibrium may be analysed in terms of two constituent equilibria:

(a) the formation of the binary complex:

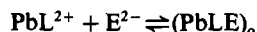


$$K_s = [PbL^{2+}] / [Pb^{2+}][L]$$

for which the conditional constant is

$$K'_s = [PbL^{2+}] / [Pb^{2+}][L];$$

(b) the association of the binary complex with the counter-ion and the subsequent extraction of the ion-pair:



$$P_{CT} = [PbLE]_o / [PbL^{2+}][E^{2-}]$$

and thus,

$$K_{ext} = P_{CT} K_s$$

The distribution ratio of the bivalent metal can be defined as:

$$D = \frac{\sum [Pb^{2+}]_o}{\sum [Pb^{2+}]} \\ = \frac{[PbLE]_o}{([Pb^{2+}] + [PbL^{2+}])}$$

assuming that the association between  $PbL^{2+}$  and  $E^{2-}$  in the aqueous phase, and the dissociation of the ion-pair in the organic phase, are negligible.

Under the experimental conditions used, we may assume that  $[PbL^{2+}] \gg [Pb^{2+}]$  and thus:

$$\log D = \log P_{CT} + \log [E^{2-}]$$

The data obtained in the two sets of determinations of the distribution ratio of lead for different eosin concentrations and two total lead concentrations, have been refined by the Letagrop program DISTR,<sup>5</sup> which provides the equilibrium constant values  $\pm 2\sigma$

Table 2. Equilibrium constants for the lead-cryptand 2.2.1-eosin system in 1,2-dichloroethane

$\log K_s$	$12.76 \pm 0.42$
$\log K'_s$	$8.03 \pm 0.07$
$\log P_{CT}$	$6.23 \pm 0.20$
$\log K_{ext}$	$18.99 \pm 0.11$

$\sigma$  ( $\sigma$  = standard deviation) summarized in Table 2.

The values of  $P_{CT}$  and  $K_{ext}$  indicate the high tendency of the binary complex to associate with the counter-ion and to be extracted into an organic phase.

### Conclusions

The present method is superior in reproducibility, similar in sensitivity but inferior in selectivity to the similar method<sup>2</sup> based on use of cryptand 2.2.2. Furthermore, the fluorescence signal with cryptand 2.2.1 is critically affected by the ionic strength, whereas that of the  $Pb^{2+}$ -cryptand 2.2.2 system is not. Therefore for determination of ultratraces of lead the best choice is the cryptand 2.2.2 method.

On the other hand, the studies with cryptand 2.2.1 provide a deeper understanding of the chemistry involved in the extraction of metal ions with macrocyclic compounds.

Finally, from the interference studies made we can

deduce that it is possible to determine some other elements of toxicological interest (*i.e.*, mercury and cadmium) with cryptand 2.2.1. Further studies on the determination of these metal ions are in progress.

*Acknowledgement*—Acknowledgement is made to the "Comisión Asesora de Investigación Científica y Técnica (CAICYT)", which supported this research.

### REFERENCES

1. B. Dietrich, J. M. Lehn and J. P. Sauvage, *Tetrahedron Lett.*, 1969, 2885.
2. D. Blanco Gomis, E. Fuente Alonso and A. Sanz Medel, *Talanta*, 1985, **32**, 915.
3. J. M. Lehn and J. P. Sauvage, *J. Am. Chem. Soc.*, 1975, **97**, 6700.
4. F. Arnaud-Neu, B. Spiess and M. J. Schwing-Weill, *Helv. Chim. Acta*, 1977, **60**, 2633.
5. D. H. Siem, *Acta Chem. Scand.*, 1971, **25**, 1521.
6. D. Fompeydie, F. Onur and P. Sevilain, *Bull. Soc. Chim. France*, 1982, II-5.
7. A. Ringbom, *Complexation in Analytical Chemistry*, (Spanish translation), p. 348. Alhambra, Madrid, 1979.
8. N. O. Mchedlov-Petrosyan, L. B. Adanovich and L. E. Nikishima, *Zh. Analit. Khim.*, 1980, **35**, 1495.
9. J. L. Arias Alvarez, *Master's Thesis*, University of Oviedo, 1986.
10. A. Sanz Medel, D. Blanco Gomis, E. Fuente Alonso and S. Arribas Jimeno, *Talanta*, 1981, **31**, 515.
11. B. Spiess, D. Martin-Faber, F. Arnaud-Neu and M. J. Schwing-Weill, *Inorg. Chim. Acta*, 1981, **54**, L91.
12. F. Arnaud-Neu, B. Spiess and M. J. Schwing-Weill, *J. Am. Chem. Soc.*, 1982, **104**, 5641.
13. H. K. Frensdorff, *J. Am. Chem. Soc.*, 1971, **93**, 4684.

## SEDIMENT ANALYSIS—LABILITY OF SELECTIVELY EXTRACTED FRACTIONS

T. U. AUALIITIA and W. F. PICKERING

Department of Chemistry, University of Newcastle, N.S.W. 2308, Australia

(Received 5 October 1987. Accepted 28 January 1988)

**Summary**—Contaminated sediment samples and wastes were extracted with a series of chemical solutions widely used in soil and sediment analyses. The Cu, Pb and Cd contents of the extracts were then determined by both AAS and ASV, and it was found that not all of the metal ion retrieved was “labile”. Differences between selected extraction values were compared with the bonding-mode category values obtained by using a well-known sequential extraction procedure, and it was found that the series and sequential approaches yielded different results for Pb and Cu. The advantages and limitations of ASV monitoring in sediment studies are considered and the inappropriateness of some operationally defined fraction categories is indicated.

It is widely recognized that only a fraction of the total metal content of contaminated materials (*e.g.*, wastes, sediments and soils) is “labile”, “mobile” or “biologically available”. For species in solution there is support for a close link between ASV-labile contents and the “biologically available” fraction; for ions associated with suspended particulates or sediment beds, “mobility” is often related to modes of bonding, *e.g.*, ion-exchangeable, associated with carbonate, or associated with the hydrous oxides of Fe and Mn.<sup>1-3</sup> The fractions are usually evaluated by selective extraction procedures, but views differ<sup>4,5</sup> on the most appropriate reagents and sequence of attack to use.

Metal ions released by reagent attack can be partially re-adsorbed by residual solid surfaces, and this leads to underestimation of the amount of metal released. The analytical procedures adopted (often AAS) tend to evaluate total metal contents in solution, and this approach ignores the fact that only part of the metal content may be in a labile form. Phase analysis studies have also indicated that the operationally defined categories used (*e.g.*, “associated with carbonates”) are convenient labels which do not necessarily correspond to reality.

As a preliminary to studies on contaminated sediments, a detailed investigation of the effect of colloidal particles on the ASV signals of Cd, Pb and Cu at ng/ml levels was undertaken.<sup>6-8</sup> This approach provided background information about metal-colloid interactions and modes of bonding, as well as indicating that ASV analyses of suspensions can release some labile ions (*e.g.*, Cd) held on particulate surfaces.

This article describes a study in which some contaminated materials were exposed to a range of chemical extractant solutions, and the extracts were analysed by ASV and AAS. The results obtained by sequential attack have been compared with those for

individual attack by the same set of reagents and the release of matrix elements (Ca, Fe and Mn) has been evaluated.

### EXPERIMENTAL

#### *Metal-contaminated samples*

A series of samples used previously in an interlaboratory comparison study was made available by one of the industries involved. The material examined included two process wastes and seven estuarine sediments, all having different metal contents.

The *calcine sample* (a product of oxidative heating of ore concentrate at ~1000°) had residual total metal levels (g/kg) of ~13 (Pb), 4 (Cu) and <0.08 (Cd). At the high temperature used, most of the Cd is volatilized along with other impurities, such as As, S and C. The oxidation also ensures that the Fe (3.5%) and Mn (0.2 g/kg) present, are converted into their higher oxidation state oxides.

The *jarosite residue* (formed during Fe removal from oxidized Zn concentrate leachates) was predominantly a basic double salt  $[KFe_3(SO_4)_2(OH)_6]$  which contained about 50% Fe, 0.2% Mn and 10, 1 and 0.2 g/kg of Pb, Cu and Cd, respectively.

The *estuarine sediments* varied in heavy-metal content and Fe and Mn levels, as shown in Table 1.

#### *Analytical techniques*

All standard solutions were prepared from analytical-grade chemicals and for calibration purposes were mixed with appropriate base solutions (*i.e.*, the various extractant solutions, also prepared from analytical grade chemicals).

Total metal contents of the aqueous phases were determined by atomic-absorption spectroscopy (AAS) with a Varian® AA875 unit and an air-acetylene flame.

The “labile” metal content of the aqueous phases (and in some cases suspensions) was determined by differential pulse anodic stripping voltammetry (DPASV) at a hanging mercury drop electrode (P.A.R. Model 303 SMDE) connected to an Amel Polarographic Analyser (Model 473), with signals recorded on a fast-response X-Y recorder (Yew Model 3022 A4). The instrumental settings used were deposition time 90 sec, deposition potential -900 mV, scan-speed 20 mV/sec, pulse height 50 mV, cut-off potential between -10 and -50 mV (the value required to resolve the peaks for Cu stripping and Hg dissolution varied with the ligand present). The test solutions were deaerated by passage of nitrogen.

Table 1. Metal content of sediment samples (g/kg)

Code No.	Cd	Cu	Pb	Zn	Mn	Fe
(a) S1	0.9	4.0	15	80	5.3	125
(b) S2	1.0	3.8	13	90	7.0	120
(c) S3	0.06	0.48	2	8.5	0.8	61
(d) S4	0.005	0.07	0.17	0.6	0.4	24
(e) S5	0.01	0.04	0.27	0.9	0.4	28
(f) S6	0.005	0.04	0.09		0.2	35
(g) S7	0.01	0.04	0.06	0.6	0.3	32

### Extraction studies

**ASV response in extractant solutions.** One-gram samples of solid were placed in 30-ml vials, together with 20 ml of chemical extractant solution. The vials were sealed, transferred to a sample agitator, equilibrated overnight, then centrifuged, and the phases were separated. The metal content in the supernatant liquid was then determined by both AAS and ASV. For the ASV measurements aliquots were mixed with an equal volume of 0.13M acetate buffer (pH 5) prior to deaeration and analysis.

The extractants tested included solutions of acids, ligands capable of reversing chemisorption equilibria, and simple salts to displace loosely bound metal ions. The results are summarized in Fig. 1. Variation in ASV peak shape or position with different extractants was evident only with Cu,

in the presence of chloride or complexing ligand (as shown later in Fig. 7).

**Rate of pollutant leaching.** The effect of extraction time on the Cd, Pb and Cu leached by magnesium chloride and hydroxylamine solutions was studied with one example each of a highly polluted (HP) and a mildly polluted (MP) sediment.

One-gram samples of S1 and S5 were extracted with 8 ml of 1M magnesium chloride (unbuffered, pH 7) over time periods varying between 0.5 and 20 hr. At the end of each selected time interval, the suspensions were centrifuged and the metals in the supernatant solutions determined by both ASV and AAS. The results are summarized in Fig. 2.

To evaluate the desorption rates of metals associated with the hydrous oxides of Fe and Mn, 20 ml of 40mM hydroxylamine hydrochloride in 25% v/v acetic acid solution were added to 1-g samples of S1 and S5 in 30-ml glass vials. The vials were capped and the mixtures equilibrated at 90°. At each selected time interval, the vials were quickly cooled under a tap and the labile metal fraction present was determined (by direct ASV measurement of the deaerated sediment suspensions). For total metal determinations, the samples were then centrifuged and the liquid phase analysed by AAS. The results for Cd, Pb and Cu are summarized in Fig. 3.

Because of the increasingly brown colour of the sample suspensions (tentatively attributed to dissolution of organic matter), the supernatant solutions were also irradiated

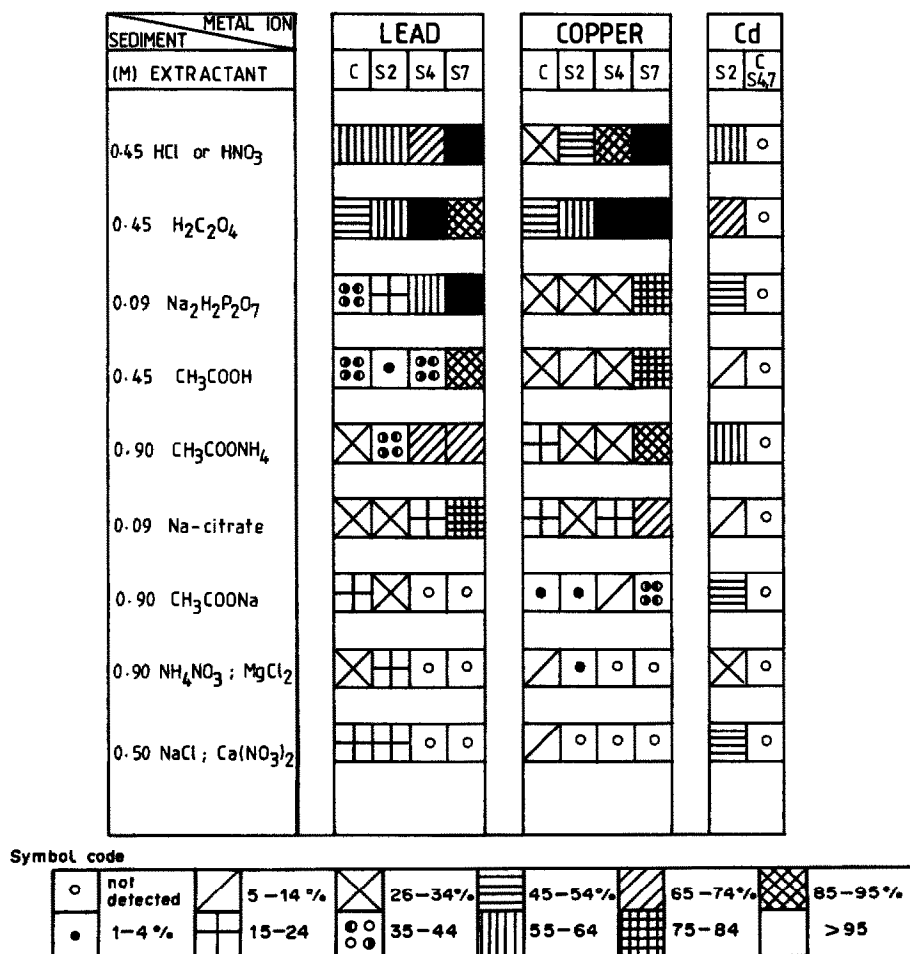


Fig. 1. Schematic representation of the fraction (%) of total Pb, Cu or Cd content of a calcine (C) and three sediments (S2, S4, S7) extracted by different reagents and found to be "ASV-labile".

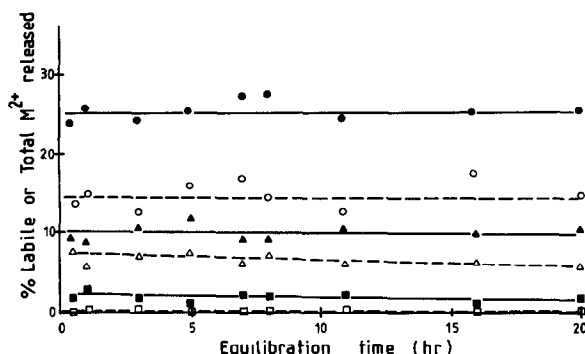


Fig. 2. Effect of extraction time on the Cd (●, ○), Pb (▲, △) and Cu (■, □) contents of 1.0M MgCl<sub>2</sub> leachates from sediment samples S1 (highly polluted, filled symbols) and S5 (mildly polluted, open symbols). Both AAS and ASV analysis gave similar values for % displaced (values quoted are the "ASV labile" values).

under an ultraviolet lamp before re-analysis by ASV. The results thus obtained are indicated by the symbol ▲ in Fig. 3.

The rates of release of Fe and Mn from these two samples into the hydroxylamine reagent were also studied, and these results are summarized in Fig. 4.

*Comparison of sequential and individual extraction approaches to speciation.* Three samples (the calcine, jarosite

residue and sediment S3) were subjected to the sequential extraction scheme proposed by Tessier *et al.*<sup>9</sup> (coded as SEQ). In this procedure, after extraction with one reagent the solid phase is isolated, washed with water and then exposed to the next reagent in the sequence. The metal content of each extract was determined by flame AAS, with check analysis by ASV wherever possible.

One-g samples (in quadruplicate) were placed in 50-ml polyethylene centrifuge tubes and were first extracted by continuous agitation with 8 ml of water for 1 hr (A). After centrifugation the supernatant solution was removed and analysed.

The residue from (A) was similarly leached for 1 hr with 1M magnesium chloride (B). After centrifugation and removal of the supernatant solution, the residue was washed with 8 ml of water to remove residual extractant, and after centrifugation the water-wash was combined with the initial extract, for analysis.

The extraction/wash sequence was repeated, with the other named reagents, on the residues from each step. The extraction times and temperatures were 6 hr at 25° with 8 ml of 0.13M acetate buffer (pH 5), 6 hr at 95° with 20 ml of 40mM hydroxylamine hydrochloride in 25% acetic acid solution, and finally for 2 hr and then 3 at 85° with two 20-ml portions of 0.020M nitric acid plus 5 ml of 30% hydrogen peroxide to release metal ions associated with organic matter. The final residue was transferred to a platinum crucible and attacked with a hot mixture of 10 ml each of concentrated nitric acid and hydrofluoric acid and 2 ml of concentrated perchloric acid.

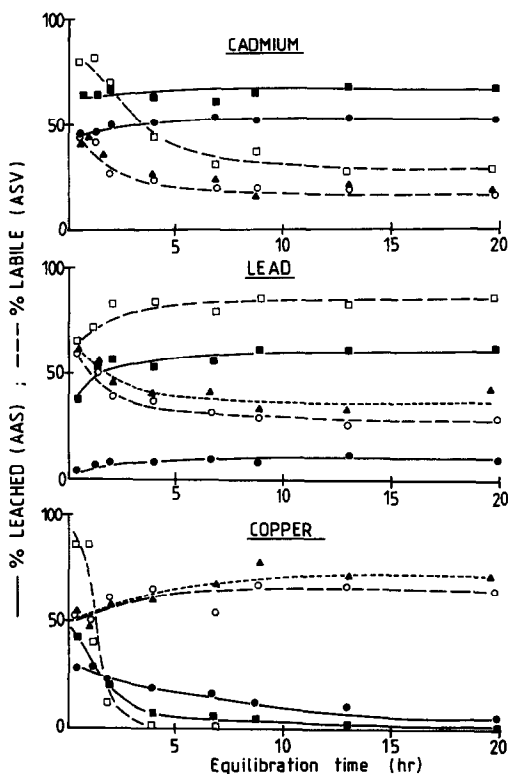


Fig. 3. Effect of extraction time on the Cd, Pb and Cu contents of the 0.04M NH<sub>2</sub>OH.HCl/25% CH<sub>3</sub>COOH leachates from sediment samples S1 (■, □) and S5 (●, ○). The percentages detected by AAS (*i.e.*, total extract values) are shown by full lines; the ASV (*i.e.*, labile metal) values are indicated by broken lines. Curve symbol ▲ indicates ASV-labile values found after UV irradiation.

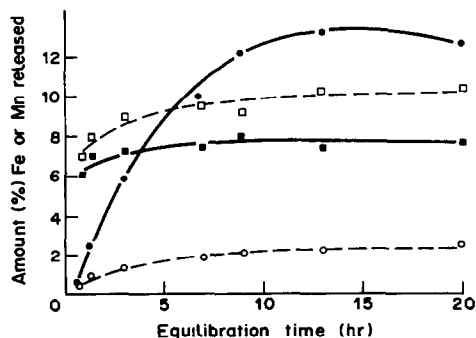


Fig. 4. Effect of equilibration time on the Fe (●, ○) and Mn (■, □) contents of 0.04M NH<sub>2</sub>OH.HCl/25% CH<sub>3</sub>COOH leachates from sediment samples S1 (solid lines) and S5 (broken lines); (expressed as a percentage of total sediment content detected by AAS).



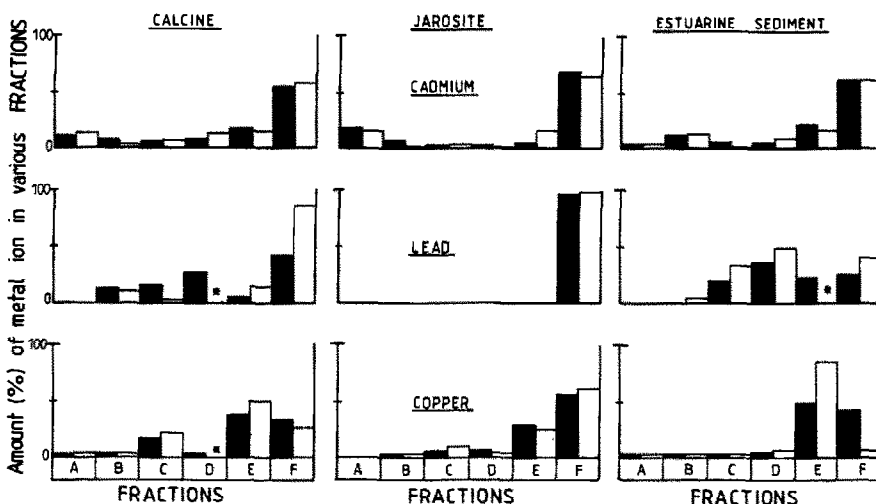


Fig. 5. Diagram showing the distribution of metal ion between six operationally defined categories, found either by a sequential analysis procedure (■) or from the differences between individual extractions (□). A, water-soluble; B,  $MgCl_2$ -displaceable; C,  $CH_3COONa$  (pH 5) extractable; D, released by  $NH_2OH \cdot HCl$  in  $CH_3COOH$ ; E, released by  $HNO_3/H_2O_2$ ; F, residual content. The additive total metal values ( $\mu g/g$ ) in the calcine were Cd, 82.5; Pb, 9750 and Cu, 3170; for the jarosite the contents were 240 (Cd), 10300 (Pb) and 970 (Cu); for sediment S3 the values were Cd 75; Pb 2240; Cu 400.

The aqueous phase from each step in the sequence was analysed for its Cu, Pb and Cd contents and results are shown as filled rectangles in Fig. 5.

In the individual-leach (IL) experiments, separate 1-g samples of the solid materials were taken and each was treated with one of the reagents used in the sequential study. After equilibration for the appropriate time, the aqueous phase was analysed for Cu, Pb and Cd content. If it is assumed that each reagent can fulfil the same role as all those preceding it in the sequential scheme, then the difference between the values obtained with two consecutive reagents should be similar to those obtained for the corresponding step of the sequential scheme. These "difference" values are shown as open rectangles in Fig. 5.

**Matrix attack.** To test the ability of the various reagents to release cations normally associated with matrix components, each of the sequential series extracts was analysed for Ca, Fe and Mn content. The distribution patterns observed are summarized in Fig. 6.

**Analytical precision.** The reproducibility of the replicates in the various studies varied with the element being studied, its level, and the matrix. In the best situations the relative standard deviations were 2-3% and in the worst cases 15-20%, leading to average spreads of  $\pm 10\%$ .

## RESULTS AND DISCUSSION

Natural sediments contain varying amounts of different substrate components (e.g., hydrous oxides, organic matter, clay minerals and silicates), each retaining different amounts of metal ions, possibly by different bonding modes. With sediment samples, therefore, the amount displaced by any selected reagent can be expected to vary with the adsorbate mix and total loading. With low contamination, lattice-bound and specifically sorbed fractions should predominate, whereas ion-exchangeable species are more likely to abound in highly polluted areas.

To evaluate the amount of metal ion loosely

bonded, or associated primarily with a particular component, it is customary to extract the sample with chemical reagents having different interaction strengths.

### Leaching capacity of reagents

Figure 1 summarizes the fraction (%) of the total metal content released from three estuarine sediments, as detected by ASV (i.e., the "labile" fraction). The sediments varied in total Cu + Pb + Cd bound (from 18 g/kg to 0.3 or 0.1 g/kg) and the fraction detected varied with the loading level and metal ion considered. Included in this diagram for comparison are the results obtained for a calcine (Pb + Cu + Cd  $\approx 17$  g/kg), a material which should be fully oxidized and contain no organic phase.

The amount of metal ion released by acid treatment can be a measure of the non-detrital fraction, i.e., the fraction not bound in the crystal lattices of rock mineral fragments. This assignment has to be made cautiously, however, since recent studies<sup>10</sup> have shown that exposure of sediments to air can enhance the apparent value, owing to partial oxidation of sulphides and increased solubility of an element because of formation of surface carbonates, oxyhydroxides, silicates or oxides.

It can be observed from Fig. 1 that cold acid extraction retrieved most of the Cu and Pb present in the slightly contaminated sediments (S4, S7), which indicates little contamination with ore body particles. For sample S2 and the calcine, the recoveries were much lower, indicative of the presence of significant amounts of lattice-bound Cu or Pb. Contributing to the low values, however, was the fact that only a fraction of the total metal extracted may be "ASV-labile" (cf. Figs. 3, and 4 and Table 2).

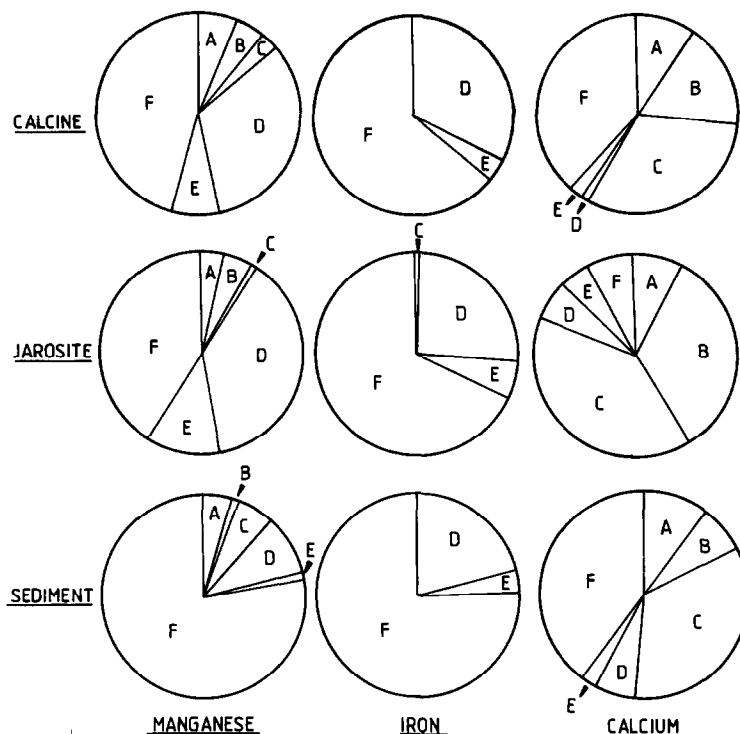


Fig. 6. Diagram showing the relative proportions of Mn, Fe and Ca in the "operationally defined" extracts described in Fig. 5. Total element contents (determined by AAS) for the test samples were: calcine, Ca 25  $\mu\text{g/g}$ , Mn 1.9 mg/g, Fe 17.3 mg/g; jarosite, Ca 60  $\mu\text{g/g}$ , Mn 3.0 mg/g, Fe 28.9 mg/g; sediment S3, Ca 26.0  $\mu\text{g/g}$ , Mn 0.6 mg/g, Fe 36.1 mg/g.

Variations in the leachate values were expected, since each reagent group displaces metal ions from the substrates by a different mechanism. For example, salt solutions displace loosely sorbed (and ion-exchangeable) fractions (aided at times by complex formation); pyrophosphate should promote dispersion of the organic fraction, and oxalic acid should reduce any amorphous iron and manganese hydrous oxide phases. Similarly, the four samples were expected to bind metal ions in different ways, leading to different degrees of recovery with any particular reagent.

Figure 1 indicates that displacement by electrolytes (e.g., magnesium chloride and ammonium nitrate) can be as high as 30% or non-detectable, depending on the sample and metal ion considered. This ion-exchangeable, or loosely bonded fraction, was most apparent in the calcine and highly polluted sediment material. Higher recoveries were observed with other reagents, because of greater attack on some of the component substrates.

#### Leaching rates

For a heterogeneous reaction, the rate of attack can be influenced by temperature, time and the physical properties of the solid phase. To gain some indication of the kinetic effect, time responses were examined at ambient temperature for two estuarine

sediment samples (highly polluted, S1, and slightly contaminated, S5) and two extractants, namely magnesium chloride solution (to displace loosely bound ions) and acidified hydroxylamine hydrochloride (which should release exchangeable metal ions plus the fractions bound to carbonates or associated with amorphous hydrous oxides). As shown by Fig. 2, displacement (or ion-exchange) was almost instantaneous, as expected for a process which does not involve any matrix dissolution or fracture of strong bonds. Analysis of the leachates by both AAS and ASV yielded similar values (i.e., all released metal ion was present in labile form). The fraction displaced decreased in the sequence  $\text{Cd} > \text{Pb} > \text{Cu}$ , with higher fractions coming from the more contaminated sample.

With the hydroxylamine solutions both total and labile values varied with time, generally becoming constant after about 8 hr, and also varied according to the metal ion considered and its total concentration in the substrate, as shown in Fig. 3. The amount of Fe and Mn released through reagent attack on the sediments also varied with time, as shown in Fig. 4. The percentage of the total Fe or Mn released varied between samples and was relatively small e.g., < 12% of the higher Fe level.

The relationship between labile and total Cd, Pb and Cu in the extractant solutions varied with the metal ion concerned. Comparison of the AAS

analytical plots (full lines) with the ASV results (dashed lines) shows that the labile Cd fraction, and labile Pb and Cu from the mildly polluted material, declined with equilibration time (cf. Fig. 3). This indicates that some of the metal ion initially displaced slowly formed an ASV non-labile species, and it is interesting to note that the final value approached the value for displacement by magnesium chloride. It may be suggested that part of the metal ion released during substrate attack was re-adsorbed on new surface sites (exposed through loss of surface coating) or on dispersed colloidal matter. To test whether the sorption sites were associated with organic matter, the solutions were exposed to ultraviolet light prior to re-analysis. As shown by the points ▲ in Fig. 3, this step increased the labile metal content only marginally.

At first glance, the results for labile Pb and Cu appear to be in error, since they are higher than the quoted total values. This apparent anomaly arises from a small difference in experimental approach. For the AAS determination, the solid phase was first separated by centrifuging; in the ASV study the particles remained suspended in the test solution. This allowed any labile metal ion loosely bound to particle surfaces to migrate to the electrode during the electrodeposition step of the ASV procedure. The existence of labile surface-bound species has been demonstrated in an earlier study,<sup>8</sup> and the differences between the full and dashed lines in Fig. 4 highlight the additional information that can be gleaned from inclusion of ASV analysis of suspensions.

Re-adsorption of leached metals on fresh sites has been proposed in several studies. For example, Guy *et al.*<sup>11</sup> extracted mixtures of humic acid, bentonite clay and manganese dioxide and observed that recovery from humic acid or clay (with metal ion) was lower in the presence of the other two components than from the humic acid or clay alone. Similarly, Tipping *et al.*<sup>12</sup> found direct evidence of "redistribution" or re-adsorption when manganese oxide in a mine-wall deposit was selectively separated from iron oxide with a hydroxylamine solution. Microprobe analysis before extraction indicated that lead was present in the manganese phase but not in the iron phase. After the extraction, however, Pb was present in the iron phase but not in the extraction solution. To minimize metal ion re-adsorption, Robbins *et al.*<sup>13</sup> proposed that sodium citrate should be included in the 1M hydroxylamine hydrochloride reagent (pH 5), on the assumption that the citrate ion would form metal complexes and also enhance dissolution of amorphous and poorly crystalline iron oxyhydroxides.

#### *Comparison of sequential and individual extraction schemes*

The data summarized in Fig. 5 show the difference in distribution patterns (with a range of extractants)

observed when the metals Cd, Pb and Cu were associated with three vastly different types of base matrix, namely a calcine (oxidized material, organic-free), jarosite (a basic double sulphate rich in Fe) and a contaminated estuarine sediment. The data also highlight the occasional major differences between the "fraction values" obtained by sequential analysis (filled rectangles) and the "difference values" obtained by extraction of separate samples with the individual reagents (open rectangles).

In many of the studies, the percentage of the total element recovered in a given fraction was similar in both the sequential and series procedures. Notable exceptions were for Pb and Cu in the calcine (fractions C, E, and F), Cd in the jarosite (fraction E), and Pb (fractions D and F) and Cu (fractions E and F) in the contaminated sediment. In a number of these cases, the difference value for fraction E was higher than the sequential value, the corresponding difference for fraction F being lower to a similar extent. This suggests that attack by nitric acid/hydrogen peroxide was more effective on the original sample than on a residue that had already undergone a sequence of different chemical interactions. It is equally logical to suggest that the sequential value (filled block) was lower because the previous treatments had exposed new active sorption sites, leading to retention of some of the metal ion released by partial attack on other matrix components.

Except for Pb and Cu in the sediment, most of the sample metal ion content was found in the residue fraction (F) and thus could not be classified as biologically available. Conversely, about 10% of the Cd in the calcine and jarosite was water-soluble, and would be extremely mobile and "available." A similar amount of Pb in the calcine and Cd in the sediment was "ion-exchangeable" (fraction B) and likely to be "available".

The Cu content of the sediment was found mainly in the "organic phase" (E), a conclusion consistent with the results of earlier soil studies.<sup>14</sup> A similar conclusion could be drawn for Cu in the calcine, except that it would be invalid because of the absence of organic matter after the initial oxidative ignition at 1000°. In this case, it can merely be concluded that the copper oxide was reasonably soluble in the nitric acid/hydrogen peroxide mixture. It seems equally unlikely that the jarosite sample contained a significant organic phase (or sulphides to oxidize), yet nearly 40% of the copper was found in fraction E. The distribution of Pb in the sediment was fairly even between four fractions, the association with amorphous Fe and Mn hydrous oxides (fraction D) being marginally more important. From the calcine, some Pb was released by the hydroxylamine reagent, but none was detected from the jarosite, even though iron constituted 50% of the matrix.

The amount of metal ion released by a given reagent appears to bear little relationship to the

Table 2. Amount (%) of labile metal ion in each selectively extracted fraction\*

Fraction	Calcine			Jarosite			Sediment S3		
	Cd	Pb	Cu	Cd	Pb	Cu	Cd	Pb	Cu
Water-soluble	92 (84)	86 (80)	22 (16)	82 (80)	28 (54)	10 (16)	82 (86)	74 (86)	8 (8)
MgCl <sub>2</sub> -exchangeable	78 (90)	50 (54)	26 (12)	78 (85)	36 (46)	11 (20)	92 (90)	66 (74)	4 (4)
Acetate buffer extractable	38 (54)	44 (46)	36 (28)	86 (80)	34 (55)	33 (20)	60 (79)	76 (82)	18 (8)
Hydrous oxide reduction	34 (62)	40 (38)	44 (64)	70 (50)	43 (34)	45 (36)	33 (37)	54 (68)	42 (53)

\*Values in parentheses correspond to differences in individual leach (IL) values.

amount of Ca, Fe and Mn co-extracted by the same system (cf. the distribution diagrams in Fig. 6).

When the various extracts were analysed by DPASV, it was found that the "labile" material in solution could be as low as 10% or as high as 90% (as shown in Table 2) of the total found by AAS. In many cases, the labile fractions detected in the sequential procedure were different from those found by direct attack on fresh samples (the IL series). This could have arisen by displacement from metal-bearing colloidal material or release from stable complex ions (e.g., metal humates). If the argument is accepted that only labile metal ions released by reagents of limited reactivity (e.g., fractions A-C) are likely to be "biologically available", then the levels in the materials examined are very low indeed.

#### Terminology of extraction studies

By comparison of the responses obtained with two popular trace-analysis techniques applied to three greatly different types of sample, the limitations of the operationally defined fraction names became obvious. Reagents are not necessarily selective in their attack, and sequential procedures can yield residues having higher surface activity than the original material (with consequent marked re-adsorption). Some of the released metal ion remains in a non-labile form, and is thus unlikely to have any significant biological activity (cf. Table 2). As shown by Fig. 1, changes in the reagent used to release a specific fraction (e.g., use of 0.05M calcium chloride instead of magnesium chloride) produce different recoveries. Figure 6 indicates that many reagents are capable of displacing small amounts of guideline matrix ions such as Ca, Fe and Mn, which indicates that these ions are also bound in a variety of ways.

A number of authors justify their choice of extractant and this trend is to be encouraged, because it is unwise to transfer even proven procedures from one matrix to another (e.g., from soil to sediment) without some assessment of the possible limitations. Before any speciation scheme is undertaken, the analytical objectives must be carefully defined and the method and techniques adopted should meet these objectives.

#### Evaluation of labile content by ASV

When definition of the problem requires evaluation of "labile" metal levels, analysis by ASV can provide the appropriate information. Provided the solid suspensions are de-aerated prior to admission to the measuring cell, the analysis can be performed in the presence of the particle and the result will include metal ions loosely held to the surfaces (and often lost during an intermediate filtration step).<sup>8</sup> Other advantages of ASV measurements include the high sensitivity of the procedure ( $\mu\text{g/l.}$  levels of Cd, Pb and Cu) and evidence of new labile chemical forms (as indicated by changes in ASV peak positions). Some peak shifts reflect interaction between the metal ion and extractant (as shown by the variations in Cu peak positions in the "blank" curves shown in Fig. 7). The substrate also introduces new peaks (or shoulders), indicating that some released species do not react so readily with the extractant ligands. Figure 7 indicates how the presence of the calcine split the Cu peaks for four different base solutions. Similarly, the presence of the sediment samples split the Cu-oxalato peaks in a pattern indicative of stabilization of a Cu(I) intermediate. The ASV approach also has some distinct limitations. For example, the chloride ion introduced with the hydroxylamine altered the Cu ASV response through the formation of chloro-complexes. The hydroxylamine on the other hand, minimized the interfering effect of redox cycling of soluble Fe(II)/(III) at the electrode.

Other limitations associated with the technique and noted in our studies include the following.

(a) Restriction on base solution composition (e.g., not suitable for use with strong acids, or with hydrogen peroxide present).

(b) Peak shifts and broadening due to complex formation (e.g., Cu in chloride or oxalate media).

(c) Signals lost owing to redox cycling of matrix element at the electrodes (e.g., Fe and Mn systems).

(d) Signals lost owing to formation of soluble non-labile complexes (e.g., with added EDTA or DTPA).

(e) Presence of some particulate materials may influence electrode response.

The limitations are of concern, and means of minimizing their effects will have to be developed, but

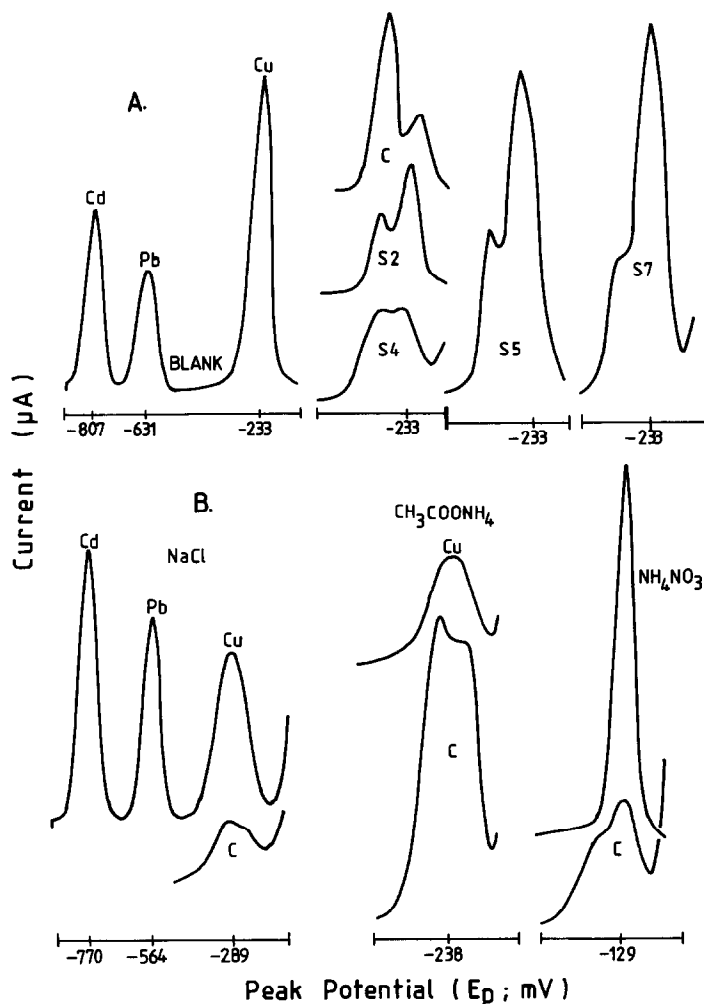


Fig. 7. Voltamperograms showing the position and shape of Cu peaks in different base solutions, particularly in the presence of suspended particles. *A*: 0.45M (COOH)<sub>2</sub> base solution; standard mixture (100 µg/l. M<sup>2+</sup>) blank curves (recorder full scale deflection 5 µA) and Cu curves with solids present [recorder f.s.d. 2 (S4, S5, S7) or 5 µA (S2, calcine)]. *B*: standard mixture blank curves in NaCl, CH<sub>3</sub>COONH<sub>4</sub> or NH<sub>4</sub>NO<sub>3</sub> (f.s.d. 5 µA) and Cu curves derived from calcine treated with each of these extractants (f.s.d. 2, 5 and 10 µA, respectively).

the advantage of obtaining labile (as distinct from total) values warrants the additional effort. A recent review<sup>5</sup> emphasized that most current approaches to soil and sediment analysis are open to criticism of one kind or another. Despite these limitations, the approach yields some interesting data and provides a fresh outlook on sediment and soil studies.

#### REFERENCES

1. J. O. Leckie and R. O. James, in *Aqueous-Environmental Chemistry of Metals*, A. J. Rubin, (ed.), Chap. 1. Ann Arbor Science, Ann Arbor, 1974.
2. G. A. Parks, in *Chemical Oceanography*, J. P. Riley and G. Skirrow (eds), Vol. 1, 2nd Ed., pp. 241-308. Academic Press, London, 1975.
3. W. Salomons and U. Förstner, *Metals in the Hydro-cycle*, Chap. 1. Springer-Verlag, Berlin, 1984.
4. W. F. Pickering, *CRC Crit. Rev. Anal. Chem.*, 1981, **12**, 233.
5. *Idem*, *Ore Geol. Rev.*, 1985, **1**, 83.
6. T. U. Aualititia and W. F. Pickering, *Water Res.*, 1986, **20**, 1397.
7. *Idem*, *Talanta*, 1987, **34**, 231.
8. *Idem*, *Water, Air Soil Pollut.*, 1987, **35**, 171.
9. A. Tessier, P. G. C. Campbell and M. Bisson, *Anal. Chem.*, 1979, **51**, 844.
10. M. Kersten and U. Förstner, *Water Sci. Technol.*, 1986, **18**, 121.
11. R. D. Guy, C. L. Chakrabarti and D. C. McBain, *Water Res.*, 1978, **12**, 21.
12. E. Tipping, N. B. Hetherington, J. Hilton, D. W. Thompson, E. Bowles and J. Hamilton-Taylor, *Anal. Chem.*, 1985, **57**, 1944.
13. J. M. Robbins, M. Lyle and G. R. Heath, *College of Oceanography Report 84-3*, Oregon State University, 1984.
14. R. G. McLaren and D. V. Crawford, *J. Soil. Sci.*, 1973, **24**, 172.

## PRECONCENTRATION OF GASEOUS ORGANIC POLLUTANTS IN THE ATMOSPHERE

J. NAMEŚNIK

Institute of Inorganic Chemistry and Technology, Technical University, 11/12 Majakowski St.,  
80-952 Gdańsk, Poland

(Received 19 September 1984. Revised 12 November 1987. Accepted 22 January 1988)

**Summary**—Three basic methods of preconcentration of organic atmospheric pollutants, *viz.* by cold trap, absorption in solutions and adsorption on solids at ambient temperature, and methods of liberating the trapped components, are discussed. Adsorption on solids is becoming more widely employed because of its advantages, and selection of the most appropriate sorbent for a given group of pollutants is of major importance. The characteristics of individual types of sorbents are presented, as well as the basic methods of determination of sorption capacity.

In analysis of gaseous atmospheric pollutants, especially in industrial hygiene, portable instruments may be used for *in situ* measurements, or samples may be collected for subsequent examination in the laboratory.

The fundamental advantage of *in situ* analysis is the possibility of continuous monitoring of variations in pollutant concentration and investigation of their causes, but this requires use of a variety of instruments at each sampling site. The alternative approach requires fewer instruments and makes it more economical to use a large number of sample collection points, but certain requirements must be met to make the results analytically valid: (a) the sample collected must be representative; (b) the sample volume must be compatible with the sensitivity of the analyser for a given concentration range; (c) the sample must not undergo any changes between collection and analysis.

For a long time, sampling was done with containers of defined volume, made of steel or glass (sample collection with an evacuated container or by flushing the container with sample) or with flexible plastic bags (made of PVC, polyethylene, *etc.*). This method, successfully used for the vapours of a large number of compounds (mainly volatile and of low polarity), has two main disadvantages: (a) the sample volume is limited to several tens of litres at most, so the absolute amount of a sample component may be quite low, making the analysis difficult; (b) preservation of the sample unchanged is sometimes in doubt, because of adsorption on the container walls, or chemical reactions, which makes the method impossible to use for compounds of low volatility or high polarity (alcohols, amines, acids, *etc.*).

To eliminate these problems, various methods have been developed for preconcentration of trace components. According to a generally accepted definition<sup>1</sup> a trace component is one which has an

average concentration of less than about 100  $\mu\text{g/ml}$  or 100  $\mu\text{g/g}$ .

Preconcentration, generally defined by IUPAC<sup>2</sup> as "an operation (process) as a result of which the ratio of the concentration or the amount of micro-components (trace constituents) and macro-components (matrix) increases", not only improves the analytical detection limit; it also reduces matrix effects and so enhances the accuracy of the results and facilitates calibration. Furthermore, preconcentration allows the sample volume taken to be increased and so improves the representative nature of the results.

By preconcentration, the concentration ( $C_i$ ) of determinand (X) in the initial sample of size  $S_i$  is increased to a concentration ( $C_f$ ) in a preconcentrated sample size  $S_f$  (same units as  $S_i$ ) in accordance with the equation<sup>3</sup>

$$C_f = \frac{C_i f_r S_i}{S_f} \quad (1)$$

where  $f_r$  is the chemical recovery of X in the preconcentration step. The ratio  $S_i/S_f$  is called the preconcentration factor, and  $C_f$  should be high enough for accurate determination of X.

This equation can be used to calculate the initial sample size needed, if the other terms are known or can be estimated:

$$S_i = \frac{C_f S_f}{C_i f_r} \quad (2)$$

$S_f$  is generally fixed (within certain limits) by the analytical procedure to be used. Ideally,  $f_r$  will approach unity and  $C_f$  should be at least 5–10 times the limit of detection (LD) of X in the final sample by the method of determination used (LD being the concentration equivalent to three times the noise or standard deviation of the measurements).

The atmosphere may be polluted by a large number of organic compounds. For example, 41–126

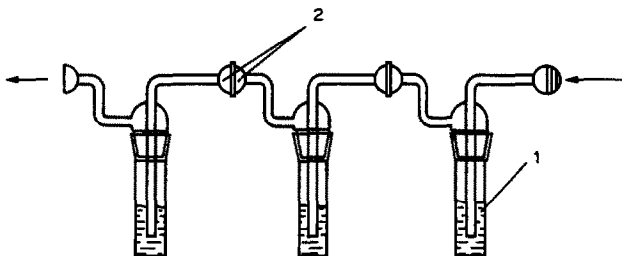


Fig. 1. Absorption train: 1—bubbler with absorbing solution; 2—ball joint. (Reprinted by permission, from E. Kissa, *Anal. Chem.*, 1983, **54**, 2622. Copyright 1983, American Chemical Society.)

volatile organic compounds have been identified in urban air, depending on sampling place, sample volume and determination technique,<sup>4,5</sup> and during the Skylab-4 mission<sup>6</sup> over 300 organic compounds were detected in the atmosphere. This was all made possible by use of preconcentration.

Preconcentration can be useful in the determination of both the time-weighted average (TWA) concentration (long-term exposure) and the short-term exposure level (STEL)<sup>7</sup> for particular compounds, as well as the elemental spectrum of organic atmospheric pollutants,<sup>8</sup> expressed as the normalized total elemental contents of the pollutants. A total elemental content can be defined<sup>9</sup> as the total amount of the element found in the gaseous components of an occupational exposure sample which are detected (or immobilized) by the detector (or collector) used and contribute to the assay value. An example is total organic carbon (TOC). To determine the elemental spectrum, direct methods utilizing appropriately sensitive detectors<sup>10-13</sup> (flame-ionization, infrared, flame-photometry, microwave plasma) or indirect methods incorporating a preconcentration step are employed. In the latter case either the organic compounds themselves,<sup>14-18</sup> or the products of their mineralization (e.g., CO<sub>2</sub> in the case of TOC determination<sup>19-23</sup>) are preconcentrated.

#### Classification of preconcentration methods

Three basic techniques are employed for preconcentration of organic atmospheric pollutants.<sup>24-26</sup>

(1) *Absorption in a suitable solution.*<sup>27-29</sup> Figure 1 presents a schematic diagram of a train of bubblers for the determination of hexachloroacetone in air.<sup>30</sup> This technique has the following advantages: (a) the possibility of using reaction with the absorption medium to convert the concentrated component into a less volatile or more stable compound; (b) high efficiency for preconcentration of compounds of low volatility; (c) it can be used for sampling moist atmospheres, whereas other techniques experience problems caused by condensation; (d) it is particularly suitable for use in conjunction with photometric methods of determination.

On the other hand, it has some drawbacks: (a) ease of loss of volatile components as a result of evaporation and stripping by the sample gas-stream passing through the absorption medium; (b) dilution of the

sample in the course of washing out the bubblers; (c) need to use absorption media of low volatility; (d) specific requirements concerning the shape and size of bubblers, depending on the type of component to be preconcentrated; (e) need to use a train of bubblers; (f) impracticability of use in personal monitors.

These disadvantages limit the usefulness of the technique, but it is successfully employed in certain cases (preconcentration of aldehydes, organic acids, isocyanates, etc.), sampling of moist atmospheres, collection of compounds of intermediate volatility.

(2) *Cold trapping.* The sample is passed through an empty tube cooled to a sufficiently low temperature by liquid nitrogen, helium, argon, oxygen or air,<sup>31-40</sup> or through a cooled tube containing a solid sorbent or a support coated with a suitable liquid phase.<sup>45-48</sup> A temperature gradient can also be used.<sup>49</sup> The advantages of this technique are (a) the possibility of sample clean-up by selective trapping or by subsequent fractional distillation, (b) trapping of all components (including very volatile compounds), (c) lack of side-reactions. The disadvantages are (a) difficulties in recovery of the preconcentrated sample (particularly of compounds of high molecular weight) and (b) serious interference in subsequent analysis because of entrapment of water, unless a means of handling it is included.

This technique is employed for preconcentration of very volatile components. In the modification employing a sorbent, the trap need not be cooled so far below ambient temperature. Figure 2 shows a schematic diagram of an apparatus used for preconcentration of light hydrocarbons at  $-80^{\circ}$ .<sup>50</sup> In general, traps filled with a liquid<sup>51</sup> or solid sorbent<sup>4,14,52-57</sup> or a chromatographic phase coated on a support,<sup>58,59</sup> are cooled to temperatures ranging from 0 to  $-80^{\circ}$ . Sequential trapping can be used to eliminate at least some of the disadvantages and limitations<sup>60,61</sup> of the method. To liberate the preconcentrated components the cooling agent is removed and the trap is rapidly heated to the desired temperature.

(3) *Adsorption on solids at ambient temperature.* The trap is filled with a solid sorbent, or a support carrying an appropriate liquid phase support.

Over 15 years ago, activated charcoal tubes (CT) were used for collection of the samples, and gas chromatography for the analysis of mixtures of organic vapours in industrial atmospheres.<sup>62</sup> Tubes of

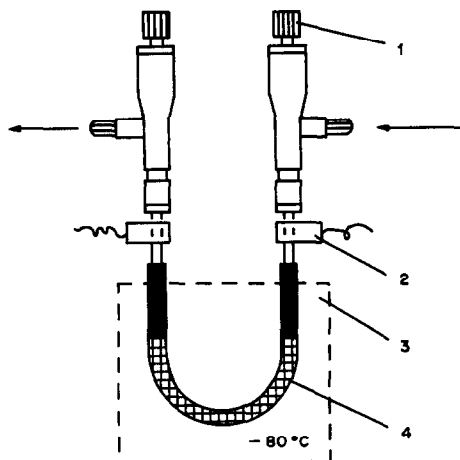


Fig. 2. Schematic diagram of an apparatus for preconcentration at lowered temperature: 1—control valve; 2—power supply (during heating); 3—cryostat; 4—solid sorbent.<sup>50</sup> (Reproduced by permission of the copyright holder, Société Française de Chimie.)

this design are still recommended by NIOSH and are commercially available.<sup>63,64</sup> Figure 3 presents the design of a typical charcoal sorbent tube.<sup>65,66</sup> Since 1970 the technique of preconcentration on solids has been extensively developed and has found many applications. The primary advantages of this technique include: (a) simplicity and low cost; (b) possibility of use of mixed packings or sequential selective packings; (c) selectivity (through selection of a suitable sorbent). The major drawbacks are (a) loss of components of low molecular weight; (b) possibility of chemical reaction on the sorbent surface; (c) limited range of gas flow-rate (particularly when the packing is a chromatographic phase coated on a support); (d) limited efficiency of desorption of very high molecular-weight compounds; (e) unsuitability for sampling moist atmospheres.

Use of light-weight, portable, battery-powered, constant-flow pumps (developed in the early 1970s) together with charcoal sampling-tubes permits the determination of individual exposures (expressed as TWA concentration or STEL); this is called "personal monitoring"<sup>67</sup> for vapours of organic compounds in workplaces. Such a combination of a constant-flow pump and an adsorption tube or de-

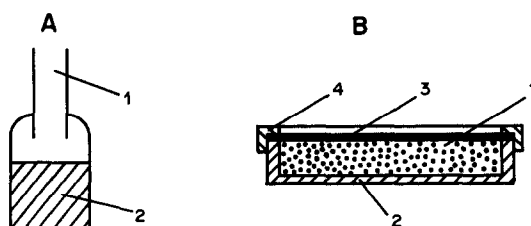


Fig. 4. Passive devices utilizing preconcentration on solid sorbents. A—Schematic design of the first diffusion-type passive sampler: 1—diffusion zone; 2—solid sorbent. B—Schematic design of a permeation-type passive personal monitor: 1—sorbent bed (charcoal, porous polymers); 2—impermeable casing; 3—permeable membrane (silicone); 4—cover.<sup>71</sup> (Reproduced by permission. Copyright 1973, American Industrial Hygiene Association.)

tector tube can be called an active device. In recent years, "passive" devices have become more frequently used as personal or area monitors, however. These collect a compound (or compounds) of interest from their immediate surroundings by diffusion or permeation of these compounds to the interior of the tube where they are trapped by means of adsorbent, adsorbent or reactive material. The design of the two basic types of passive sampler<sup>68</sup> is presented in Fig. 4. The theory, design and application of various types of passive dosimeters have been comprehensively reviewed.<sup>69-73</sup> Passive dosimeters have a number of advantages over the active type. They are simple, small and light in weight, have no batteries or pumps, and since they determine the TWA concentration of analyte, only the exposure time is needed, not the volume of sample. They are similar in size, weight and convenience to the familiar radiation dosimeters. They are of special importance to health professionals, who use them for the determination of exposure to waste anaesthetics.

Compounds trapped on a solid sorbent must be released as quantitatively as possible before determination. Solvent extraction or thermal desorption can be used for this purpose. Carbon disulphide is often employed as the solvent,<sup>74-82</sup> but diethyl ether,<sup>83-91</sup> acetonitrile,<sup>82,92,93</sup> methanol,<sup>94-97</sup> n-hexane,<sup>97-100</sup> ethyl acetate,<sup>10</sup> chloroform,<sup>10</sup> toluene,<sup>103</sup> n-pentane,<sup>104</sup> cyclohexane,<sup>105</sup> acetone,<sup>53,106</sup> naphtha ether,<sup>107</sup> *N,N*-dimethylformamide,<sup>108</sup> benzyl alco-

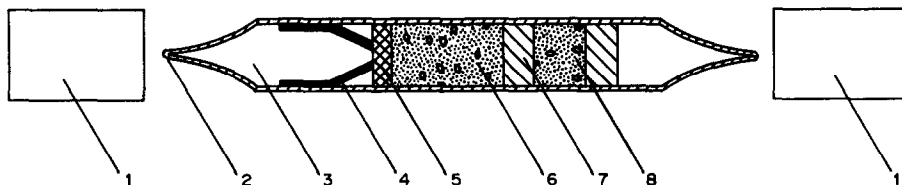


Fig. 3. A typical NIOSH batch-test charcoal sorbent tube (CT): 1—NIOSH approved sealing caps (to prevent contamination); 2—precise sealed tips (to permit safe, easy breaking to the specified opening size); 3—glass tube ( $L = 75$  mm,  $\phi_e = 4$  mm,  $\phi_i = 3$  mm; especially drawn to very close tolerances for repeatable results); 4—precision lock spring (to hold charcoal layers securely in place to prevent sample channeling, and allow transport without damaging sample); 5—high-purity glass wool (precise amount for uniform pressure drop); 6—100-mg sorbent layer (precisely controlled surface area, pore size, adsorptive characteristics, particle size); 7—foam separator (for uniform pressure drop); 8—50-mg back-up sorbent layer.



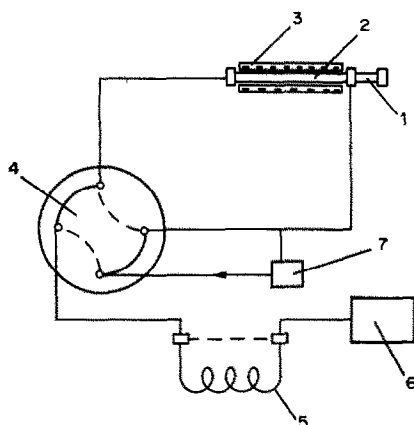


Fig. 5. Schematic diagram of an apparatus for thermal desorption and chromatographic determination of organic compounds preconcentrated on a solid sorbent: 1—injector; 2—trap; 3—oven; 4—four-way valve; 5—GC column; 6—detector; 7—carrier gas tank.<sup>122</sup> (Reproduced by permission of the copyright holders.)

hol,<sup>109</sup> carbon tetrachloride,<sup>110</sup> benzene,<sup>111</sup> water<sup>112-116</sup> or mixtures of solvents, such as methanol-water,<sup>117,118</sup> acetone-water,<sup>119</sup> propanol-water<sup>120</sup> and hexane-naphtha ether,<sup>121</sup> have also been used, as has 0.1M sodium hydroxide.<sup>122</sup> The extraction efficiency and the effect of various factors on the recovery have been extensively investigated.<sup>123-126</sup> Desorption with CS<sub>2</sub> is used mainly for compounds trapped on charcoal. The use of a solvent for desorption has several disadvantages: (a) decreased sensitivity, depending on the volume of solvent and size of aliquot used; (b) interference by solvent components in chromatographic separation of the sample compounds; (c) solvent toxicity; (d) need for adsorbent regeneration before further use of the sorbent tube.

Thermal desorption<sup>127-134</sup> substantially simplifies automation of the analysis and has several advantages.<sup>135</sup> Figure 5 shows a typical scheme for thermal desorption and chromatographic determination of atmospheric pollutants.<sup>122</sup> The main advantage is that the entire amount of preconcentrated material may be recovered for determination. To obtain sufficiently high enrichment factors, in the desorption step the trap should be heated to the required temperature (which depends on the thermal stability of the sorbent and the preconcentrated compounds) as quickly as possible (preferably in a few seconds, or at most a few minutes), and the carrier-gas flow-rate should be minimized. The sorbent trap can be heated with a movable furnace, a resistance wire supplied through a transformer with a high electric current at low voltage, by a spiral made of Fe-Ni alloy (Curie-point spirals)<sup>136-152</sup> or by microwaves.<sup>153</sup> However, none of these desorption techniques is suitable for direct interfacing with a gas chromatograph.

Analysis for organic air pollutants by use of preconcentration at ambient temperature can be divided into four operations: the sampling step; sample storage; recovery of the preconcentrated components; the

final determination step. Each of these steps introduces a number of factors which can influence the final result, and these have been reviewed.<sup>25,26,154</sup> As in all other methods of analysis, unless the sampling step is correctly executed, the final results will be biased. The main purpose of the present review is therefore to assist in avoiding such errors, and because the use of solid sorbents at ambient temperature is probably the most widespread, this aspect will be stressed.

#### Choice of sorbent

Conventional gas-liquid chromatography compositions have been used for many years for sampling gases and vapours at ambient temperature, and although interest has turned to the solid sorbents, later workers have continued to use a variety of columns, listed in Table 1. The outstanding feature of all these columns is the very high loading used. A significant development was the appearance of materials in which the liquid phase was chemically bonded to the stationary phase (e.g., Porasil C), yielding a column material with a liquid phase of virtually zero vapour pressure.

Some properties of various solid sorbents which can be utilized for preconcentration of gases and vapours from the atmosphere are listed in Tables 2-4. Porous polymers are a new class of material used almost as widely as charcoal. Figure 6 presents the chemical structure of two sorbents from this group, Tenax-GC<sup>174,175</sup> and XAD-2.<sup>175</sup> In selection of a solid sorbent, the following factors<sup>155,176</sup> should be considered: (a) the volume of air sample which can be passed through the sorbent without breakthrough of the compounds present; (b) the degree of decomposition of sample components during preconcentration, storage and liberation; (c) any background signal due to the sorbent; (d) affinity of the sorbent for water; (e) simplicity, speed and completeness of desorption of the concentrated compounds; (f) the enrichment factor; (g) the degree of adsorption of gaseous inorganic pollutants (CO, CO<sub>2</sub>, H<sub>2</sub>S, SO<sub>2</sub>, NO, NO<sub>2</sub>), which is particularly important in determination of the elemental spectrum of organic air pollutants.

In Table 5 the applications of solid sorbents to particular types of compounds are collated.<sup>155,177,178</sup> The results are gleaned from the literature and a blank can indicate either no data or a negative result.

The changes which can occur in the sorbent layer because of reaction with the sample components<sup>170,201-203</sup> or exposure to sunlight,<sup>204</sup> or thermal treatment<sup>205</sup> have been studied, and the type and level of organic residues in synthetic porous polymers have been determined.<sup>172,206</sup>

#### MATHEMATICAL DESCRIPTION OF ADSORPTION ON SOLIDS

A simple mathematical model describing the adsorption process was presented in 1946.<sup>207</sup> Let us

Table 1. Loaded gas chromatographic columns used for air sampling<sup>45-49,59,86,91,96,111,134,155-158</sup>

Stationary phase	Support	Loading
Silicone E 301	Celite 545 or silica gel	3:7
PEG 400	Celite 545 or silica gel	3:7
Carbowax 1540	Firebrick	10%
Dimethyl sulpholane	Firebrick C-22	10%
Silicone oil	Celite C-22	20%
Apiezon L	Chromosorb W	20%
Apiezon K	Sterchamol	25%
SE 30 or OV 17	Chromosorb W	10%
Cottonseed oil	Pyrex glass beads	2.2% v/v
Carbowax 600	Chromosorb W	20%
Didecyl phthalate	Chrom P	25%
Tricresyl phosphate	Chrom W	20%
Carbowax 400	Porasil C	Bonded
Oxypropionitrile	Porasil C	Bonded
Phenyl isocyanate	Porasil C	Bonded
Durapak n-octane	Porasil C	Bonded
TCEP	Shimalite	25%
Tritolyl phosphate	Shimalite	1%
3,3,3-Trifluoropropyl-(methyl) cyclotrisiloxane	Chromosorb WAW	10%
DC-200	Chromosorb WAW-DMCS	10%
Apiezon M	Chromosorb PAW-DMCS	4%
SP-100	Carbopack B	0.4%
2,4-Dinitrophenyl-hydrazine (DNPH)	XAD-2	1%
Durapak-Carbowax 400	Porasil F	Bonded
Potassium 2,4,6-tri-chlorophenate	GLC-110	1.5%
OV-101	Pt (powder)	
KOH	Porasil A	5%
SP-100	Tenax-GC or graphitized carbon black	0.3%
SE-54	Capillary column	2.3 μm layer
Bondapack C-18	Porasil B	

suppose<sup>207-209</sup> that when a pulse of air contaminated with a vapour at concentration  $C_i$  passes through a sorbent bed at a linear velocity  $L$ , the contaminant concentration  $C$  falls at a rate corresponding to a first-order reaction:

$$\frac{dC}{dt} = -KC \quad (3)$$

which on integration gives

$$\ln \frac{C_i}{C} = Kt \quad (4)$$

where  $K$  is the overall rate constant for the system. If the bed has a finite depth  $d_1$ , then the emergent concentration  $C_1$  is given by

$$\ln \frac{C_i}{C_1} = K d_1/L \quad (5)$$

Table 2. Properties of various solid sorbents<sup>101,155,159-166</sup>

Sorbent	Composition	Specific surface area, $m^2/g$	Mean pore size, $\text{Å}$
Silica gel	$\text{SiO}_2$	300-800	20-40
Alumina	$\text{Al}_2\text{O}_3$		
Charcoals:			
coconut-based	Carbon	800-1000	20
petroleum-based	Carbon	800-1000	18-22
wood-based	Carbon		
Foamed plastics	Porous polyurethane foam (PPF)*		
Florasil	Magnesium silicate		

\*Usually a foam of open-cell polyether type (density  $0.022 \text{ g/cm}^3$ ) in which the bubbles (cells) occupy 97% of the volume (97% void).

Table 3. Physical properties of some graphitized carbon black sorbents used for preconcentration of organics<sup>148</sup>

Sorbent	Specific surface area, $m^2/g$	Mean pore diameter, $\text{Å}$
Carbosieve B	1000	—
Carbosieve G	1000	—
Carbopack B	100	3000
Carbopack BHT	100	—
Carbopack C	12	2000
Carbopack CHT	12	—
Ambersorb XE-340	400	300
Ambersorb XE-347	350	300
Ambersorb XE-348	500	300
Sterling FT	15	1500
Carbosphere	20	1200
Carbochrome K-5	110	3500
Carbosil	130-400	40-60

Table 4. Physical properties of porous polymers used as adsorbents for preconcentration of trace organic volatiles<sup>101,148,155,161,163,167-173</sup>

Sorbent	Composition*	Specific surface area, m <sup>2</sup> /g	Mean pore diameter, Å	Temperature limit, °C
Tenax-GC	Poly(2,6-diphenyl- <i>p</i> -phenylene oxide)	19-30	720	450
Chromosorb 101	S-DVB copolymer	50	3500	300
Chromosorb 102	S-DVB copolymer	300-400	90	250
Chromosorb 103	Cross-linked poly-S	15-25	3500	250
Chromosorb 104	ACN-DVB copolymer	100-200	700	250
Chromosorb 105	Polyaromatic type	600-700	500	200
Chromosorb 106	Poly-S	700-800	50	250
Chromosorb 107	Poly-AE	400-500	80	250
Chromosorb 108	Cross-linked AE	100-200	250	200
Porapak N	Polyvinylpyrrolidone	225-300	120	200
Porapak P	S-DVB copolymer	100-200	150	250
Porapak Q	EVD-DVB copolymer	630-840	75	250
Porapak QS	Silaned Q			
Porapak PS	Silaned P			
Porapak R	Polyvinylpyrrolidone	550-700	76	250
Porapak S	Polyvinylpyridine	450-600	76	300
Porapak T	EGDMA	300-450	91	200
XAD-1	Polymethyl-MTC resin	100	200	150
XAD-2	S-DVB copolymer	290-300	85-90	200
XAD-4	S-DVB copolymer	750	50	200
XAD-7	S-DVB copolymer	450	80	150
XAD-8	Poly-MTC resin	140	250	150
XAD-9	Sulphoxide	70	370	
XAD-11	Amide	69	35	200-250
XAD-12	Very polar N,O group	20	1300	
Ostion SP-1	S-DVB copolymer	350	86	200
Spheron MD 30/70	Methyl-MTC-DVB copolymer	70	3800	230
Spheron SE	S-ethylenedi-MTC copolymer	70	3800	280
Cekachrom 1	Ethyl-S-DVB copolymer	520	170	250
Cekachrom 2	Ethyl-S-DVB copolymer	300	650	250
Cekachrom 3	Ethyl-S-DVB copolymer	120	780	250
Synachrom	S-DVB-EVB copolymer	520-620	75	340
Polysorbimide	PMDA-DADPE copolymer	70	3500	300

\*S—styrene; DVB—divinylbenzene; ACN—acrylonitrile; AE—acrylic ester; MTC—methacrylate; EVB—ethylvinylbenzene; EGDMA—ethylene glycol dimethyl adipate; PMDA—pyromellitic dianhydride; DADPE—4,4-diaminodiphenyl ether.

If the pulse is then regarded as the start of a steady flow of air with contaminant concentration  $C_1$  it will be apparent that the contaminant concentration in the effluent will increase from zero and will reach  $C_1$

when the bed is completely spent. For analytical purposes we need to select a value of  $C_1$  which we regard as the highest tolerable, and discard the filter when this concentration is reached. We can denote this critical concentration by  $C'_1$ . A number of important aspects of this simple picture are to be noted.

1. If the bed is sufficiently shallow for the emergent concentration of the initial pulse to be  $C'_1$ , the bed depth is known as the critical depth  $d'_1$ , since a filter with this or a smaller depth has zero life. For a given system, the critical bed depth is thus inversely proportional to  $K$  since:

$$d'_1 = \frac{L}{K} \ln \frac{C_1}{C'_1} \quad (6)$$

Note that we may also refer to a critical residence time  $R'_1$ , since  $R = d/L$ .

2. When  $d_1$  is greater than  $d'_1$ , the additional depth is available for trapping, and the time needed for the emergent concentration to reach  $C'_1$  is proportional to  $(d_1 - d'_1)$ , the proportionality constant being directly related to the equilibrium sorptive capacity  $N_1$  of the sorbent.

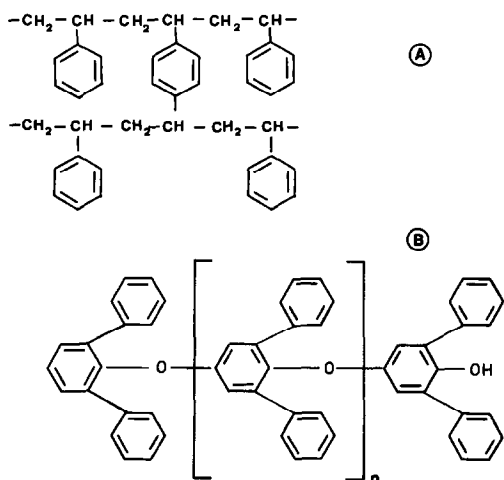


Fig. 6. Chemical structure of sorbent resins: A—XAD-2; B—Tenax-GC.

3. The shape of the wave front is dependent on the rate constant  $K$ ; a high value gives a flat wave front (adsorption front) and a low value a diffuse front. Points 1 and 2 above are more formally expressed in the Mecklenburg equation:

$$T = \frac{n_i(d_1 - d'_1)}{C_i LA} = \frac{N_i(V - V')}{C_i F} \quad (7)$$

where  $T$  is the penetration time (breakthrough time, BTT);  $n_i$  and  $N_i$ —are the equilibrium sorptive capacities of unit length and unit volume of bed, respectively;  $A$  is the cross-sectional area of the bed;  $V$  and  $V'$  are the bed volume and critical bed volume, respectively;  $F$  is the volumetric flow-rate of the air sample.

It will be observed from equation (7) that the capacity ( $N_i$ ) of the sorbent is of great importance, especially when  $V \gg V'$ .

#### *The course of adsorption on solids*

Adsorption refers to the physical interaction between a molecule of gas or liquid and a solid surface. If the adsorptive forces are strong,<sup>208</sup> about 1 mg of vapour is held on 1 m<sup>2</sup> of solid surface; thus for microporous solids (charcoal, porous polymers) possessing an internal surface area of hundreds of square metres per gram the amount of vapour adsorbed can be in the range of 10–70% w/w.<sup>135,208</sup> There is also an appreciable energy decrease—the heat of adsorption.

The adsorption process on a solid sorbent has been represented by various schemes.<sup>106,154,167,191,210–213</sup> That for a single carbon granule is shown in cross section<sup>214</sup> in Fig. 7. The air–vapour mixture is shown flowing across the granule. As the vapour diffuses into the pores, it migrates to the carbon surface and condenses in the pores. The pores continue to fill until some maximum value is achieved, depending on the prevailing conditions. There is a high degree of pore filling at high concentrations of relatively non-volatile solvent vapours.

An assemblage of solvent-adsorbing granules produces the situation shown<sup>214</sup> in Fig. 8. Here, the concentration at any point in the sorbent bed is shown as a function of bed depth, diagrammatically by shading, and also in graphical form. The incident concentration is  $C_i$  and the concentration profile is generally termed the adsorption wave (wave front). *A* shows the first layer of the sorbent bed adsorbing the first fraction of vapour, the process taking place similarly to frontal chromatography. An equilibrium is then established between adsorption and desorption processes, and *B* shows the first layer of the sorbent completely saturated and the intermediate layer partially saturated. Initial breakthrough is just beginning at the downstream sorbent boundary. *C* shows the sorbent bed almost completely saturated at 50% breakthrough. The breakthrough curve, which shows the vapour concentration in the effluent as a function of time, is a mirror image of the adsorption

wave. The overall adsorption efficiency, calculated from the ratio of the amount of adsorbate retained on the bed to the amount of adsorbate required to fully saturate the bed, depends on the distribution of adsorbate across the bed. Under ideal conditions of mass transfer the adsorbate front in the bed remains sharp and the sample stream can be completely depleted of vapour until the sorbent bed is fully saturated. In practice, however, under non-ideal mass-transfer conditions breakthrough occurs before the bed is fully saturated,<sup>211</sup> and the sorbent has to be discarded before it is. Figure 9 shows the breakthrough curve as a function of time.<sup>214</sup> Typically, only 2% of the solvent vapour has penetrated the sorbent trap at 10% breakthrough.

There is a direct relationship between the shape of a chromatographic profile (either in elution or frontal analysis) and the shape of the equilibrium adsorption isotherm. Figure 10 illustrates<sup>175,215</sup> this correspondence for linear, Langmuir and anti-Langmuir isotherms. Thus, if an elution peak or frontal profile is strongly skewed, the type of sorption isotherm governing the phase equilibrium can be immediately identified. However, there are traps for the unwary. For example, unfavourable adsorption/desorption kinetics can contribute to a skewed profile. Chromatography with a mobile-phase flow-rate far from the minimum indicated by the van Deemter equation can cause excessive band-broadening, particularly at high flow-rate where resistance to mass-transfer is maximal. It is also possible to begin at an input concentration which corresponds to an isotherm section that contains an inflection point. A different input concentration may be in a different portion of the isotherm, and give a skew in the opposite direction.

#### *Evaluation of adsorption capacity of solids*

A number of standard criteria for a successful sampling procedure have been suggested.<sup>155,191,216</sup>

- accuracy and precision of combined analytical and collection procedures for concentration ranges from 0.1 TLV to 2 TLV not worse than  $\pm 16\%$  relative at the 95% confidence level;
- total recovery efficiency at least 75%;
- the difference between total recovery and adsorption efficiency less than  $\pm 10\%$  relative;
- able to take samples for 10–15 min at maximum and average levels;
- minimum sampling time 1 hr, preferably 4–8 hr for TWA concentration;
- samples stored for 14 days should agree to within  $\pm 10\%$  relative with initial samples;
- the flow-rate of the sampling pump should be known within  $\pm 5\%$ ;
- the sorbent granules should retain their shape and size, and not crush;
- high capacity for contaminant adsorption;
- ability to sorb contaminant at high rate.

Table 5. Application of various sorbents to different types of compounds

Compound type	Charcoal	Porous polymers	Liquid phases	Silica gel	Molecular sieve	Alumina	Other sorbents	References
<b>HYDROCARBONS</b>								
Saturated								
Methane	+	+	+	+		+		25, 56, 136, 179-181 65, 182-186
Ethane	+							65, 182, 185-187
Unsaturated	+			+				25, 39, 56, 180, 187
Ethylene	+			+				65, 182, 185-187
Acetylene	+			+				65, 184-187
Alicyclic	+			+				25, 39, 56, 180, 184, 188, 189
Aromatics	+	+	+	+				25, 41, 56, 136, 179, 181, 190
<b>ALCOHOLS</b>								
Saturated	+	+	+	+				25, 39, 41, 56, 136, 179, 191
Unsaturated	+	+						25, 41, 56, 179, 191
Aromatic	+	+						25, 41, 56, 179, 191
<b>PHENOLS</b>	+	+		+				39, 41, 166, 184, 188, 189
<b>ALDEHYDES</b>								
Saturated		+	+	+		+		36, 39, 41, 179, 181, 192
Unsaturated	+	+		+				36, 39, 179, 181, 192
Aromatic			+					36, 39, 179, 181, 192
<b>KETONES</b>	+	+	+	+				25, 56, 136, 179-181, 190, 192
<b>ACIDS</b>	+	+						39, 41, 163, 189
<b>ESTERS</b>	+	+	+	+				25, 56, 136, 179-181, 190
<b>ETHERS</b>								
Saturated	+	+	+					25, 56, 163, 180, 181, 191
Unsaturated	+							25, 56, 163, 180, 181, 189
Aromatic	+	+						25, 56, 163, 180, 181, 189
<b>ORGANIC OXIDES</b>								
<b>ORGANOHALIDES</b>	+	+						65, 163, 181
Alkyl	+							
Aromatic	+	+		+				25, 56, 136, 179, 181, 193
Organochlorine pesticides	+	+	+	+				25, 56, 136, 179, 181, 193
<b>ORGANIC NITROGEN COMPOUNDS</b>								
Alkyl amines	+	+	+	+		+	+	91, 106, 160, 166, 181, 194, 195
Alicyclic amines		+						39, 118, 161, 163, 179, 196
Aromatic amines	+	+	+	+				65, 179, 184, 189
Azo compounds		+						65, 179, 184, 189
Hydrazines		+		+				65, 184, 189, 197
Nitrates	+	+						65, 184, 189, 197
Nitriles	+	+		+				25, 184, 188, 197, 198
Nitro compounds alkyl	+	+						65, 184, 189, 197
Nitro compounds aromatic	+	+	+					65, 160, 179, 181, 189
Nitrosamines	+	+						65, 179, 181, 189, 194
	+	+						65, 184, 189, 194, 198

<b>ORGANIC SULPHUR COMPOUNDS</b>								
Mercaptans	+	+						39, 41, 56, 180, 189
Sulphides, alkyl	+	+	+					39, 41, 56, 180, 189
Sulphorates, alkyl		+						39, 41, 180, 197, 198
Sulphates, alkyl		+						25, 39, 41, 180, 189
<b>ORGANOPHOSPHORUS COMPOUNDS</b>								65, 186, 197, 199
<b>ORGANOSILICATES</b>								155, 177, 178
<b>HETEROCYCLICS</b>								
Nitrogen-containing	+	+	+					65, 163, 186, 188, 195, 197, 198
Oxygen-containing	+	+						65, 163, 166, 189, 197
Nitrogen- and sulphur-containing		+						65, 163, 186, 193
<b>ORGANOMETALLICS</b>								
Organolead								
Organomercury	+		+					155, 163, 177, 178
<b>MISCELLANEOUS COMPOUNDS</b>								
Ammonia	+ <sup>f</sup>							41, 65, 163, 185, 186
Carbon dioxide	+ <sup>f</sup>		+					65, 182, 183, 185
Carbon disulphide	+		+					25, 41, 65, 163, 185, 191
Carbonyl sulphide	+							65, 184, 185, 187
Cyanogen chloride	+							65, 184, 187
Hydrogen cyanide	+							65, 184, 185, 187
Hydrogen fluoride	+							41, 183-185
Hydrogen sulphide	+							65, 166, 184, 187
Iodine	+							65, 184, 187
Mercuric chloride			+					65, 163, 166, 184
Mercury	+							65, 183-185
Nitric oxide								65, 163, 184, 185, 200
Nitrogen dioxide								65, 184, 185, 187
Nitrous oxide			+					65, 184, 185, 193
Phosgene								65, 163, 184
Phosphine			+					65, 163, 184
Phosphorus (white)			+					65, 163, 184
Sulphur dioxide								65, 183-185, 187

<sup>1</sup>Formaldehyde; <sup>2</sup>includes polyurethane foam (PUF); <sup>3</sup>iodine crystals; <sup>4</sup>gold beads; <sup>5</sup>modified charcoal; <sup>6</sup>sodium hydroxide flakes; <sup>7</sup>silver wool; <sup>8</sup>copper shot; <sup>9</sup>silver nitrate.

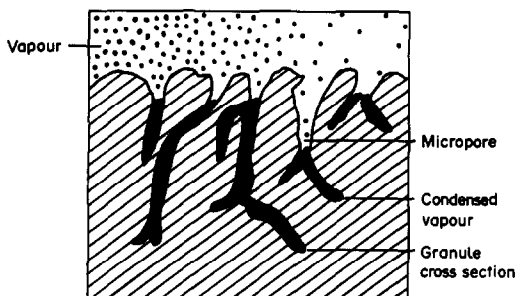


Fig. 7. The adsorption process.<sup>214</sup> (Reproduced by permission. Copyright 1976, American Industrial Hygiene Association.)

To be analytically useful, the preconcentration process must be quantitative. Hence, evaluation of the sorptive capacity of a given sorbent under defined conditions prior to its use is mandatory. One of the most frequently used measures of capacity of a sorbent bed is the breakthrough volume (BTV) or the corresponding breakthrough time (BTT). The BTV is the volume of gas passed through a sorbent bed before the compound of interest begins to be eluted from the sorbent. Passing larger volumes of gas results in incomplete recovery. For comparing the adsorption capacities of various sorbents, the BTV should be expressed in units of gas volume per unit mass of sorbent. The breakthrough of the sorbent bed is variously defined as corresponding to  $C_1'$  being 50%,<sup>193,217</sup> 10%,<sup>26,159,179,180,212,218</sup> 5%,<sup>101,210,219-222</sup> or 1%<sup>162,223-225</sup> of  $C_1$ , or the detection limit obtainable with the detector used.<sup>8,139,167,226-230</sup>

\*References 8, 80, 97, 101, 139, 154, 161, 167, 191, 219, 220, 222, 223, 226-230, 251-255.

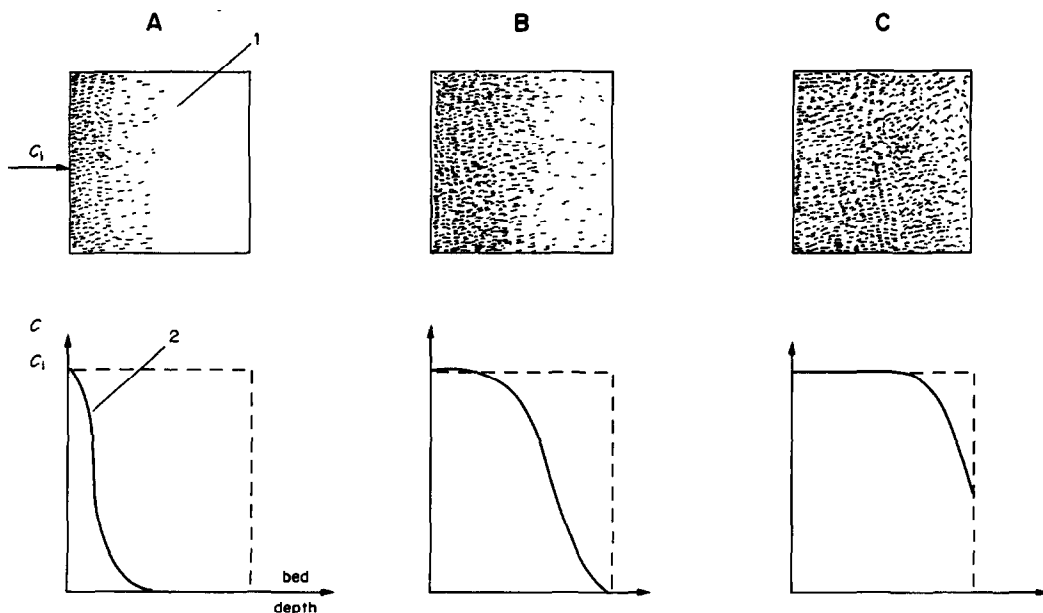


Fig. 8. Cartridge loading patterns and migration of the adsorption front through the sorbent trap as a function of time: 1—organic vapour cartridge; 2—adsorption front.<sup>214</sup> (Reproduced by permission. Copyright 1976, American Industrial Hygiene Association.)

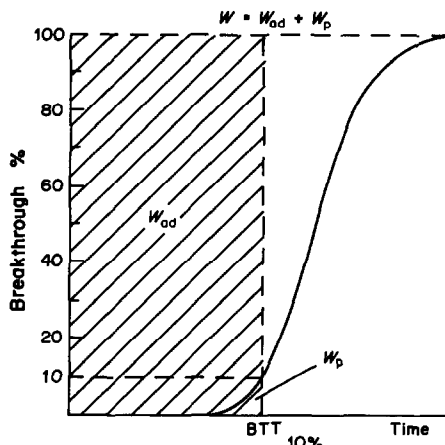


Fig. 9. Percentage breakthrough as a function of time:  $W_{ad}$ —amount of vapour actually adsorbed;  $W_p$ —amount which passes through the cartridge unadsorbed;  $W$ —amount of vapour which contacts the adsorbent in time  $t$ .<sup>214</sup> (Reproduced by permission. Copyright 1976, American Industrial Hygiene Association.)

The BTV and BTT can be determined in various ways.

(1) From theoretical calculations utilizing appropriate mathematic equations,<sup>81,82,97,112,132,224,225,231-245</sup> particularly for active carbon beds,<sup>159,179,212,214,218,246-249</sup> or statistical-moment theory.<sup>211,215,250</sup>

(2) From experimental data. Figure 11 illustrates three methods. In the direct, continuous method, a stream of gas containing a known concentration of a compound (or compounds) is passed through a tube packed with a known amount of a sorbent, and the compound is detected in the effluent by a suitable detector.\* In the direct discrete method a fixed volume of effluent is sampled periodically with a

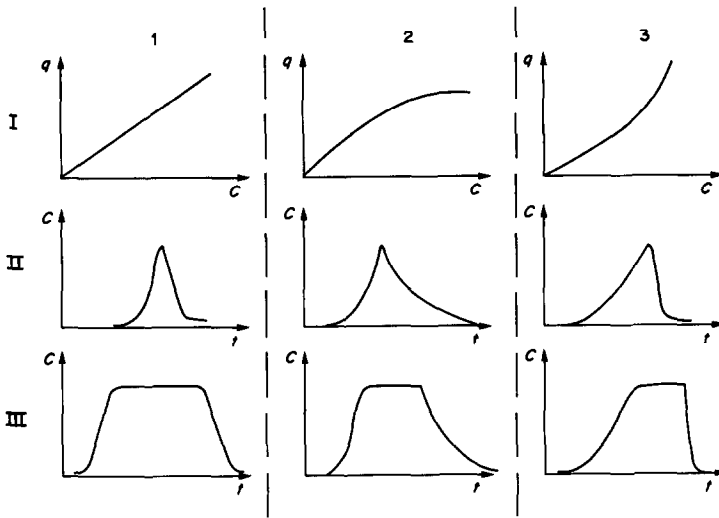


Fig. 10. Relationship between adsorption isotherm, elution and frontal analysis:  $q$ —capacity of sorbent bed;  $C$ —concentration;  $t$ —time. I. Sorption isotherms: 1—linear; 2—Langmuir; 3—anti-Langmuir. II. Elution analysis. III. Frontal analysis. (Reproduced by permission, from O. Grubner and W. A. Burgess, *Environ. Sci. Technol.*, 1981, 15, 1346. Copyright 1981, American Chemical Society.)

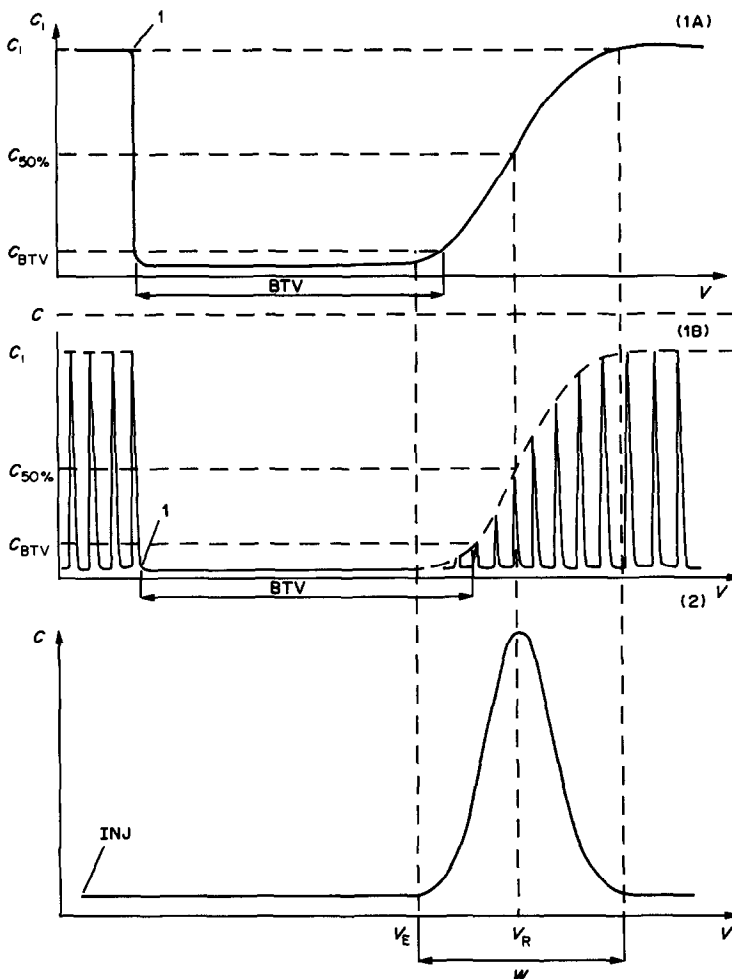


Fig. 11. Graphical illustration of methods of determination of breakthrough volume (BTV) and elution volume ( $V_E$ ): 1—A, direct continuous method; B, direct discrete method; 2—indirect method.



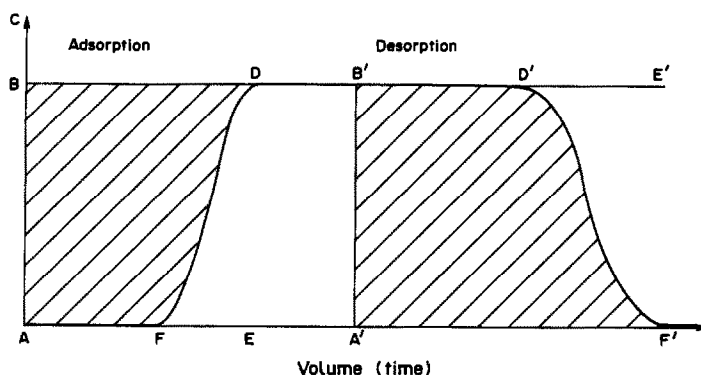


Fig. 12. Graphical evaluation of weight capacity of sorbent resin (g/g) from frontal analysis adsorption and desorption curves.

syringe or sampling loop and analysed.<sup>25,26,180,256</sup> The indirect methods treat the sorbent bed as a chromatographic column (frontal analysis) and apply chromatographic theory. The retention volume gives access to much useful information. First, the retention volumes of the various compounds studied indicate the ability of different sorbents to separate them completely. Secondly, the retention volumes at ambient temperature indicate the efficiency of the trap: the maximum sample volume without breakthrough at ambient temperature; the enrichment factor; and (by extrapolation to higher temperatures) the flushing time necessary for the total recovery of the trapped compounds. The net retention volume ( $V_N$ ) is derived from the retention time of the compound ( $t_R$ ) and of an unretained compound ( $t_0$ ) and the carrier-gas flow-rate ( $F_c$ ) at the outlet pressure and the absolute temperature of the column ( $T_c$ ):

$$V_N = j(t_R - t_0)F_c \quad (8)$$

where  $j$  is the compressibility correction factor

$$j = 1.5 \left[ \frac{(p_i/p_o)^2 - 1}{(p_i/p_o)^3 - 1} \right] \quad (9)$$

$p_i$  and  $p_o$  being the inlet and outlet pressures, respectively. If the flow-rate is measured at absolute temperature  $T$  with an aqueous bubble meter, and denoted by  $F$ , then  $F_c$  is related to it by

$$F_c = \frac{FT_c}{T} \frac{(p_A - p_w)}{p_o} \quad (10)$$

where  $p_w$  is the water-vapour pressure at temperature  $T$  and  $p_A$  is the atmospheric pressure.

We can also use the corrected retention volume ( $V_R^0$ ) which is the effective volume of gas at the column temperature and outlet pressure necessary to elute the compound:

$$V_R^0 = jt_R F_c = V_N + V_G \quad (11)$$

where  $V_G = jt_0 F_c$ .

This volume is used to calculate the sample volume of the gas which can be passed through the sorbent bed without loss of the analyte in the gas (break-

through volume). In practice,<sup>164,170,171,179,182,213,257-259</sup> retention parameters are measured at elevated temperatures and the values at ambient temperature are calculated by an extrapolation of the relationship  $\log V_R^0 = f(1/T)$ . The maximum sample volume (MSV) is given by:<sup>257</sup>

$$\text{MSV} = V_R^0 \left[ 1 - \frac{2}{\sqrt{N}} \right] \quad (12)$$

where  $N$  is the number of theoretical plates. Some workers<sup>176,262,263</sup> recommend use of  $V_R$  instead of  $V_R^0$  in this equation.

For a sorbent trap, the number of theoretical plates does not usually exceed 50,<sup>176,262,263</sup> so the precision of the results is limited. On the other hand, the method is very simple and no additional equipment is required, and it can be successfully used for preliminary selection of sorbents.

Another measure of the adsorptive capacity is the weight capacity of the sorbent ( $q$ , in g/g). Figure 12 shows<sup>175</sup> the evaluation of weight capacity for both the adsorption and desorption branches of a frontal analysis chromatogram. Here,  $q$  is determined by graphical integration, so  $q_{ads}$  is given by

$$q_{ads} = \left( \frac{\text{Area ABDF}}{\text{Area ABDEF}} \right) V_{DE} C_B \quad (13)$$

and  $q_{des}$  by

$$q_{des} = \left( \frac{\text{Area of A'B'D'F'}}{\text{Area of A'B'D'E'F'}} \right) V_{A'F'} C_B \quad (14)$$

where  $V_{DE}$  is the eluent volume required for complete adsorption and  $V_{A'F'}$  is the volume of eluent required for complete desorption.

Point A indicates the first entrance of sorbate into the sample cartridge, and B' marks the point at which flow of the sample mixture is stopped and desorption is begun by passage of eluting gas. If the experiment is done in the Henry's law region, then the area of ABDF = area of A'B'D'F' and

$q_{ads} = q_{des}$ .

The weight capacity can also be calculated from frontal analysis experiments by using the

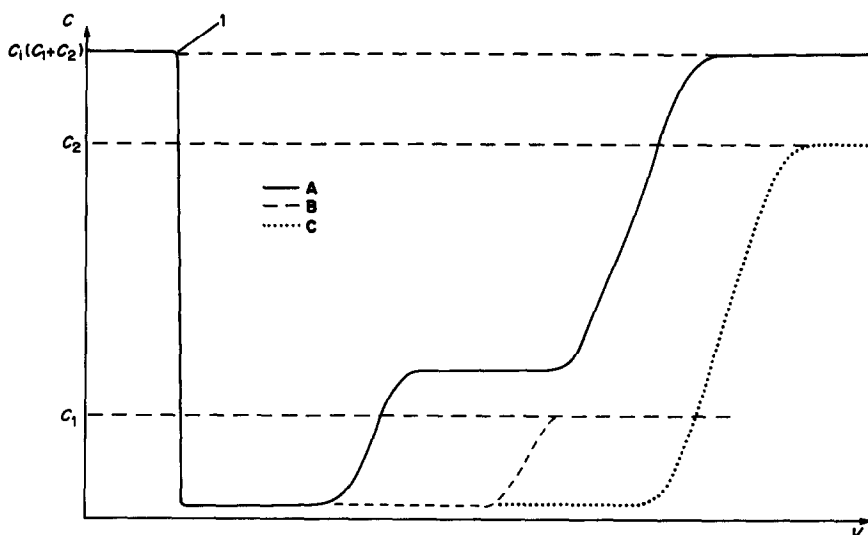


Fig. 13. The effect of presence of other components on the BTV value: A—breakthrough curve for a mixture of two components (A + B); B—breakthrough curve for component A; C—breakthrough curve for component B.<sup>191</sup> (Reproduced by permission. Copyright 1978, American Industrial Hygiene Association.)

expression:<sup>253</sup>

$$q_{\text{ads}} = \frac{(t - t_0)F_c C}{w} \quad (15)$$

where

- $t$  is the time (sec) needed to saturate the adsorbent,
- $t_0$  the retention time (sec) of an unretained compound,
- $w$  the weight (g) of adsorbent,
- $F$  the carrier-gas flow-rate (ml/sec) and
- $C$  the concentration of adsorbate in the carrier gas (g/ml).

The sorption capacity can also be determined by passing a known volume of standard mixture containing an amount  $M_1$  of analyte through the sorbent bed, then desorbing the analyte and measuring its amount  $M_p$ .<sup>123,264-266</sup> The collection efficiency (CE) can be calculated<sup>265</sup> from

$$CE = 100M_p/M_1\% \quad (16)$$

The adsorption capacity can be determined graphically from the relationship  $CE = f(V)$ . A sorbent trap is frequently divided into two sections packed with sorbent (front and back sections; see Fig. 3). In such a case the capacity of a sorbent cartridge can be determined graphically from a plot of  $100M_2/M_1$  vs.  $V$  where  $M_1$  and  $M_2$  are the masses found in the front and back sections respectively and  $V$  is the volume of a gas containing a known concentration of the analyte.

Irrespective of the method of determination of the sorption capacity, the choice of sorbent is usually

based on comparative measurements.\* There is a growing use of passive devices for evaluation of atmospheric pollution (mainly in workplaces), and these also need determination of the sorption capacity.<sup>268,269</sup>

The primary disadvantage of indirect methods of determination of sorption capacity (by means of  $V_R$  and  $w$ ) is their inapplicability for investigation of the effect of various parameters on the BTV or BTT values. The effect of these factors then has to be taken into account by means of empirical correction terms,<sup>251</sup> to give the "safe sampling volume". The effect of various factors on breakthrough parameters has been comprehensively discussed in a number of papers.<sup>25,26,161,191,216</sup> Some factors known to have important effects on the BTV<sup>25,26,161,191,216</sup> include the rate and type of flow (steady state, cyclic or pulsating, laminar or turbulent), the relative humidity of the air and the water content of the sorbent, the concentration of contaminant, the temperature, the physico-chemical properties of the sorbent (surface area, porosity, surface characteristics), size of the granules and its relationship to surface area, activity and capacity of the sorbent, the physical and chemical properties of the gases and vapours (polarizability, dipole moment, quadrupole moment, etc), the desorption characteristics, the void fraction, and the presence of other components in the mixture (co-adsorption). By far the most extensive treatment of the subject is the series of papers by Nelson *et al.*<sup>159,179,212,214,246-249</sup> concerning the testing of organic vapour and gas cartridges (packed with charcoal) for their breakthrough (penetration, service life) characteristics.

Figure 13 depicts<sup>22,26,191,270</sup> the mutual effect of the mixture components on the BTV value of a given component. For two- or multi-component mixtures

\*References 8, 25, 26, 53, 77, 101, 167, 171-176, 179, 182, 193, 223, 226-230, 252, 255, 257, 260-263, 266, 267.

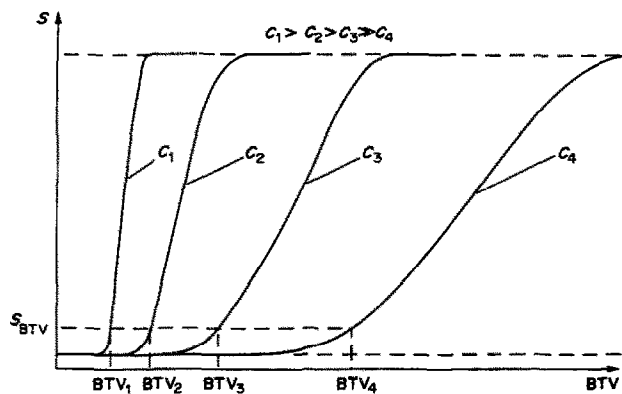


Fig. 14. The effect of concentration of preconcentrated compound on the shape of the breakthrough curve and BTV value.

the breakthrough curve initially has the usual form, but later reaches a plateau at a concentration considerably higher than the concentration of the component with lower BTV value, and finally becomes the breakthrough curve of the second component. This can be explained as due to competitive adsorption of the two compounds present in the mixture. The molecules of the more strongly adsorbed compound (higher BTV) displace those of the more feebly adsorbed compound. The first plateau corresponds to enrichment of the gas phase with the more feebly adsorbed component, and gives the sum of the inlet concentration  $C_{IA}$  of this compound and the concentration of it produced by its displacement from the sorbent layer by the more strongly adsorbed compound. The degree of enrichment (the difference between  $C_{IA}$  and the plateau concentration) is proportional to the concentration of the compound more strongly adsorbed.

Figure 14 shows the shape of the breakthrough curves and the dependence of the BTV value on the concentration of a preconcentrated compound.<sup>25,26,161</sup> In a number of papers\* much attention was paid to the effect of various factors on the adsorption capacity. Suitable standard gaseous mixtures are necessary for this type of investigation. Many general reviews<sup>275-285</sup> have dealt with the preparation and use of calibration standards, so there is no need to discuss this problem in detail. However, generation of standard gaseous mixtures containing the analyte at very low concentrations always creates difficulties, but air pollutant concentrations of this order are necessary for model investigations of preconcentration on various sorbents (if the investigations are to reflect realistic levels of the pollutants). For this reason, it would be useful if the sorptive capacity at relatively high concentration levels could be related to that at low. The breakthrough parameters (BTV or BTT) can be related to the concentration ( $c$ ) of the compound in air, and for charcoal, the em-

pirical Freundlich isotherm appears to apply. This equation<sup>159,222</sup> takes the form:

$$\log \text{BTT} = \log a + b \log C \quad (17)$$

where  $a$  and  $b$  are constants. A similar equation giving the possibility of extrapolation to low levels, and used for other sorbents, has the form:<sup>228,270</sup>

$$\text{BTV} = -K \log C + B \quad (18)$$

where  $K$  and  $B$  are constants.

#### *Practical aspects of preconcentration on solid sorbents*

References to application of the most widely used sorbents are listed in Table 6. Tenax-GC is widely used, mainly<sup>304</sup> because its thermal stability allows thermal desorption of high-boiling organic compounds. Moreover, it is hydrophobic and does not react with the majority of organic pollutants.

Another sorbent of widespread application (Table 6) is polyurethane foam. Its large available surface area and cellular structure make it very suitable as an adsorbent and absorbent and as a column filling material. In microspherical form it has excellent capacity for firmly retaining various loading and extracting agents. The hydrodynamic properties of foam-filled columns have been shown to be very favourable, and relatively high flow-rates can be attained by gravity flow. In general, the membrane-like structure of polyurethane foam makes adsorption and extraction (solid-liquid, solid-gas and liquid-liquid) with it fairly rapid. Its very low resistance to gas flow enables its application in high-volume air samplers.<sup>315</sup>

Obviously, other types of sorbents, such as various types of charcoal, carbon molecular sieves and other carbon sorbents are also widely employed (Table 6). Of the porous polymers the following have found practical application as sorbents: Chromosorb 101, Chromosorb 102, Chromosorb 105, Porapak N, Porapak Q, Porapak R, Porapak S, Porapak QS, XAD-2, XAD-4 and XAD-7.

Several other sorbents, the properties of which are listed in Tables 2-4, have been employed in practice (Table 6). Combinations of two or more sorbents

\*References 49, 53, 75, 80, 82, 94, 96, 101, 107, 108, 130, 134, 161, 167, 180, 183, 228, 252, 260, 264, 271-274.

Table 6. References to the most important sorbents

Sorbent	References
Tenax GC	6, 36, 53, 82, 130, 131, 149, 180, 193, 260, 267, 268, 271, 286-305
Polyurethane foam	98-100, 105, 108, 111, 121, 266, 306
Charcoal	74, 75, 78-80, 128, 139, 162, 264, 307
Carbon molecular sieves	52, 138, 151
Other carbon sorbents	54, 60, 129, 156, 308
Chromosorb 101	309
Chromosorb 102	84, 310-312
Chromosorb 105	313
Porapak N	59, 97, 194, 314
Porapak Q	56, 61, 104, 138, 315, 316
Porapak QS	59
Porapak R	138, 255
Porapak S	317
XAD-2	85, 89, 90, 107, 110, 318
XAD-4	83
XAD-7	318
Silicalite	319
Molecular sieve 10A	222
Molecular sieve 13X	113, 256, 320
Al <sub>2</sub> O <sub>3</sub>	57, 321, 322
Florisil	255, 323
Silica gel	92-94, 102, 112, 115, 119, 120, 180, 220, 324, 325

(successive layers in a sorbent trap) have also found practical application.<sup>255,265,273,274,326,327</sup>

In analytical practice, important parameters of the preconcentration are the flow-rate of gas through a sorbent bed and the volume of sample used. The literature values of the flow-rates and volumes used are listed in Table 7.

Several commercially available and laboratory devices for the preconcentration of organic compounds have been described.\* Figure 15 gives<sup>334</sup> a schematic diagram of an apparatus for the measurement of concentrations of various organic compounds in air by means of the so-called simultaneous direct reading

indicator tube system (SDRITS). The system, which concurrently draws air through up to 10 separate colorimetric direct-reading detector tubes, has been developed for qualitative analysis for hazardous substances in air. The identification is limited to various defined groups of substances, such as acidic compounds, amines, alcohols, etc.

#### CONCLUSIONS

In the case of a tube having two separate sorbent sections, or of two tubes connected in series, the appearance of the contaminant in the second section indicates that some of it had penetrated through the front section, which was nearing saturation when

\*References 137, 143, 144, 147, 154, 191, 314, 332, 333.

Table 7. Sample flow-rates and volumes

Flow-rate, l./min	Volume, l.	References
≤0.1		49, 56, 74-76, 88, 90-93, 96, 97, 110, 122, 183, 194, 264, 290, 291, 320, 303, 305, 308, 320, 328
0.1-0.5		6, 53, 77, 85, 86, 89, 101, 102, 117, 120, 127, 129, 130, 134, 156, 180, 220, 255, 287, 291, 294, 304, 318
0.5-10.0		80, 100, 106, 113, 115, 158, 203, 265, 288, 299, 311
10.0-1000		98, 99, 105, 107, 266, 273, 323, 329
	≤1.0	36, 130, 290, 320, 322, 328
	1.0-5.0	49, 52, 53, 77, 86, 88, 89, 96, 115, 117, 138, 305, 318, 326
	5.0-10.0	7, 56, 75, 76, 85, 94, 120, 264, 302
	10.0-100	59, 74, 78, 79, 82, 84, 91-93, 102, 108, 110, 113, 116, 118, 127, 151, 158, 267, 288, 291, 304, 330
	100-1000	47, 98, 100, 111, 128, 129, 203, 255, 273
	10 <sup>4</sup> -10 <sup>5</sup>	99, 105-107
	>10 <sup>6</sup>	121, 266, 306, 323, 331

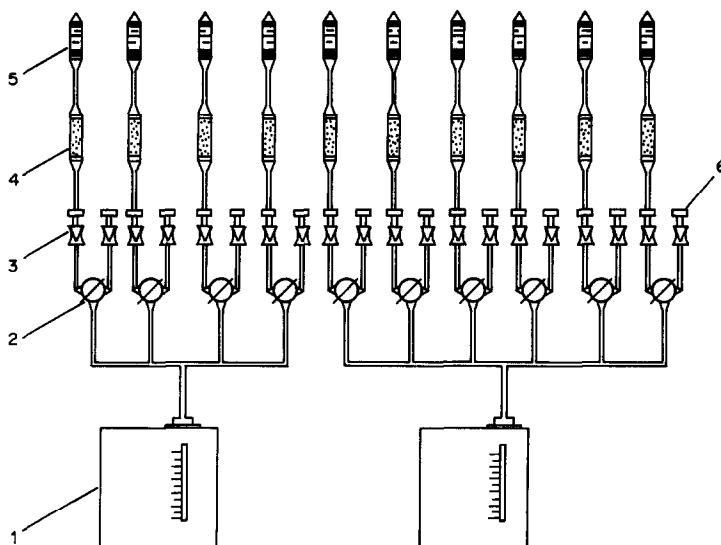


Fig. 15. Schematic diagram of the simultaneous direct reading indicator tube system (SDRITS): 1—battery-powered pump; 2—three-way stopcock; 3—needle valve; 4—filter charcoal tubes; 5—Dräger tubes; 6—blank needle valve.<sup>334</sup> (Reproduced by permission. Copyright 1983, American Industrial Hygiene Association.)

sampling stopped. Unfortunately, nothing is known about the state of the second section—whether it was saturated or not or whether contaminant had penetrated through that section as well. A method has been proposed<sup>335</sup> for calculating the amount of contaminant loss that may have occurred, which can be added to the amount found in the two sections to give the total. Let the mass of contaminant adsorbed in the first section of a sorbent tube (or in the first tube in series) be  $M_1$  and in the second section  $M_2$ , and the loss (the mass not adsorbed in either section)  $M_3$ . Over the duration of sampling the amount of material entering the tube is  $M = M_1 + M_2 + M_3$ . In either section the fraction retained ( $r$ ) is:

$$r = (\text{input} - \text{output})/\text{input} \quad (19)$$

For the first section the input is  $M$  and the output  $M_2 + M_3$  and, therefore:

$$\begin{aligned} r_1 &= \frac{M_1 + M_2 + M_3 - (M_2 + M_3)}{M_1 + M_2 + M_3} \\ &= \frac{M_1}{M_1 + M_2 + M_3} \end{aligned} \quad (20)$$

and for the second section:

$$\begin{aligned} r_2 &= \frac{M_2 + M_3 - M_3}{M_2 + M_3} \\ &= \frac{M_2}{M_2 + M_3} \end{aligned} \quad (21)$$

In practice, the second section usually contains only half the amount of sorbent in the front section. Let us assume that the fractional retention on the second section is half that of the first section (this assumption

is conservative); hence  $r_2 = r_{1/2}$  and

$$\frac{M_2}{M_2 + M_3} = \frac{M_1}{2(M_1 + M_2 + M_3)} \quad (22)$$

Cross-multiplying, collecting terms and solving for  $M_3$  results in

$$M_3 = \frac{M_2(M_1 + 2M_2)}{M_1 - 2M_2} \quad (23)$$

A conservative estimate of the total mass of contaminant the adsorption tube should have collected is

$$M = M_1 + M_2 + \left[ \frac{M_2(M_1 + 2M_2)}{M_1 - 2M_2} \right] \quad (24)$$

$$= M_1^2 / (M_1 - 2M_2) \quad (25)$$

This reasoning is valid only when  $M_3$  is a small fraction (not more than a few per cent) of  $M$ .

The aim of this paper was a general discussion of preconcentration methods and not detailed presentation of the application of particular methods and techniques for preconcentration of vapours of specific compounds. Special attention is paid to use of solid sorbents for this purpose and to discussion of the basic parameters influencing the preconcentration (collection) process.

The article is based on research papers published within the last few years. Most of the papers published during this period concern the application of various kinds of solid sorbent as collecting media. This does not mean, however, that other techniques are being abandoned—there is still wide scope for their application.

Since the article was completed, several papers have appeared, and references to many of these may be found in the review articles by Fox<sup>336</sup> and especially that by Langhorst and Coyne.<sup>337</sup>

## REFERENCES

1. G. H. Morrison, K. L. Cheng and M. Grasserbauer, *Pure Appl. Chem.*, 1979, **51**, 2243.
2. E. Jackwerth, A. Mizuike, Yu. A. Zolotov, H. Berndt, R. Hohn and N. M. Kuzmin, *ibid.*, 1979, **51**, 1105.
3. K. Othmer, *Encyclopedia of Chemical Technology*, 3rd Ed., Vol. 23, p. 310. Wiley, New York, 1983.
4. D. Ullrich and B. Seifert, *Z. Anal. Chem.*, 1978, **291**, 299.
5. B. V. Joffe, V. A. Isidorov and I. G. Zenkevich, *J. Chromatog.*, 1977, **142**, 786.
6. W. Bertsch, A. Zlatkis, H. M. Liebich and H. J. Schneider, *ibid.*, 1974, **99**, 673.
7. G. E. Podolak, R. M. McKenzie, D. S. Rinehart and J. F. Mazur, *Am. Ind. Hyg. Assoc. J.*, 1981, **42**, 734.
8. J. Namieśnik and E. Kozłowski, *Chem. Anal. Warsaw*, 1980, **25**, 301.
9. J. G. Montalvo, Jr., *Am. Ind. Hyg. Assoc. J.*, 1979, **40**, 1046.
10. J. S. Hobbs, C. A. Mannan and B. E. P. Beeston, *Int. Lab.*, 1979, **9**, No. 5, 25.
11. A. Hadjitofi and M. J. G. Wilson, *Atmos. Environ.*, 1979, **13**, 755.
12. F. W. Sexton, R. M. Michie, Jr., F. F. McElroy and V. L. Thompson, *Report* 1982, EPA-600/4-82-046.
13. T. E. Graedel and J. E. McRae, *Atmos. Environ.*, 1982, **16**, 1119.
14. S. Allie and R. J. Ranchoux, *Air Pollut. Control Assoc. J.*, 1980, **30**, 792.
15. *Idem*, *Proc. Ann. Meet. Air Pollut. Control Assoc.*, 1981, Vol. 3, Paper 80-41.3.
16. D. Kuroda, *Akushu no Kenkyo*, 1981, **10**, 38; *Chem. Abstr.*, 1981, **95**, 208660.
17. E. R. Stephens and O. P. Hellrich, *Environ. Sci. Technol.*, 1980, **14**, 836.
18. R. D. Cox, M. A. Devitt, K. W. Lee and G. K. Tannahill, *ibid.*, 1982, **16**, 57.
19. E. Kozłowski and J. Namieśnik, *Mikrochim. Acta*, 1978 II 435.
20. *Idem*, *ibid.*, 1978 II 473.
21. *Idem*, *ibid.*, 1979 I, 1.
22. *Idem*, *ibid.*, 1979 I, 317.
23. *Idem*, *ibid.*, 1979 I, 345.
24. G. A. Junk and B. A. Jerome, *Am. Lab.*, 1983, **15**, No. 12, 16.
25. J. P. Guenier and J. Muller, *Cah. Notes Doc.*, 1981, **103**, 197.
26. *Idem*, *Ber. Int. Kolloq. Verhuetung Arbeitsunfaellen Berufskr. Chem. Ind.*, 8th, 1982, p. 355.
27. R. Kuntz, W. Lonneman, G. Namie and L. A. Hull, *Anal. Lett.*, 1980, **13**, 1409.
28. R. Morales, J. F. Stampfer and R. E. Hermes, *Anal. Chem.*, 1982, **54**, 340.
29. P. Biscard, L. Malhave, B. Rietz and P. Wilhardt, *Anal. Lett.*, 1983, **16**, 1457.
30. E. Kissa, *Anal. Chem.*, 1983, **55**, 1222.
31. C. A. M. Brenninkmeijer, *ibid.*, 1982, **54**, 2622.
32. D. Kalman, R. Dills, C. Perera and F. DeWalle, *ibid.*, 1980, **52**, 1993.
33. S. Jacobsen and S. Berg, *J. High Resol. Chromatog., Chromatog. Commun.*, 1982, **5**, 236.
34. K. Fushimi and Y. Sugimura, *Papers Meteorol. Geophys. Tokyo*, 1981, **32**, 313.
35. M. A. Ferman, *Ann. Meet. Air Pollut. Control Assoc., Montreal, Quebec, 22-27 June 1980*, Paper 80-39.2.
36. M. Holdren, S. Humrickhouse, S. Truitt, H. Westberg and H. Hill, *Ann. Meet. Air Pollut. Control Assoc., Cincinnati, Ohio, 24-29 June 1979*, Paper 79-52.2.
37. M. Deimel and W. Dulson, *Staub-Reinhalt Luft*, 1979, **39**, 332.
38. M. E. Parrish, C. T. Higgins, D. R. Douglas and D. C. Watson, *J. High Resol. Chromatog., Chromatog. Commun.*, 1979, **2**, 551.
39. Y. Hoshika, *Takiki Osen Gakkaishi*, 1979, **14**, 210; *Chem. Abstr.*, 1980, **92**, 10476.
40. R. A. Rasmussen, *Am. Lab.*, 1972, **4**, No. 7, 19.
41. Y. Hoshika and G. Muto, *Bunseki Kagaku*, 1980, **29**, T10.
42. J. Rudolph and C. Jebsen, *Int. J. Environ. Anal. Chem.*, 1983, **13**, 129.
43. W. Schneider, J. C. Frohne and H. Bruderreck, *J. Chromatog.*, 1978, **155**, 311.
44. B. Seifert and D. Ullrich, *Atmos. Pollut.*, April 1978, p. 25.
45. I. Kifune and T. Shirai, *Eisei Kagaku*, 1979, **25**, 155.
46. Y. Hoshika, *Analyst*, 1981, **106**, 683.
47. *Idem*, *Bunseki Kagaku*, 1981, **30**, 15.
48. J. W. Graydon and K. Grob, *J. Chromatog.*, 1983, **254**, 265.
49. A. Jonsson and S. Berg, *ibid.*, 1983, **279**, 307.
50. D. Tourres and H. Vessely, *Analisis*, 1981, **9**, 340.
51. A. Keussner, *Chromatographia*, 1982, **16**, 207.
52. J. Rudolph, D. H. Ekhalt, A. Khedim and C. Jebsen, *J. Chromatog.*, 1981, **217**, 301.
53. R. D. Barnes, L. M. Law and A. J. MacLeod, *Analyst*, 1981, **106**, 412.
54. F. Bruner, G. Crescentini and F. Mangani, *Anal. Chem.*, 1981, **53**, 798.
55. T. Dumas, *J. Assoc. Off. Anal. Chem.*, 1982, **65**, 913.
56. B. I. Brookes and P. J. Young, *Talanta*, 1983, **30**, 665.
57. E. Neuber, J. Müller and R. Sartorius, *Mikrochim. Acta*, 1979 II, 131.
58. M. Selucký, J. Novák and J. Janák, *J. Chromatog.*, 1967, **28**, 285.
59. T. Nielsen, H. Egsgaard and E. Larsen, *Anal. Chim. Acta*, 1981, **125**, 1.
60. F. Bruner, G. Bertoni and G. Crescentini, *J. Chromatog.*, 1978, **167**, 399.
61. J. Becka and L. Feltl, *ibid.*, 1977, **131**, 179.
62. L. D. White, D. G. Taylor, P. A. Mauer and R. E. Kupel, *Am. Ind. Hyg. Assoc. J.*, 1970, **31**, 225.
63. R. F. Mindrup, Jr., *Supelco Bulletin*, No. 769.
64. M. Fracchia, L. Pierce, R. Gravl and R. Stanley, *Am. Ind. Hyg. Assoc. J.*, 1977, **38**, 144.
65. *SKC 1984 Catalogue and Guide to Air Sampling Standards*, SKC Ltd., Poole, England.
66. B. E. Saltzman, *J. Assoc. Off. Anal. Chem.*, 1978, **62**, 214.
67. M. Freifeld, *J. Chem. Educ.*, 1982, **59**, A351.
68. E. D. Palmes and A. F. Gunnison, *Am. Ind. Hyg. Assoc. J.*, 1973, **34**, 78.
69. P. W. West, *Am. Lab.*, 1980, **12**, No. 7, 35.
70. V. Vitols, *Report* 1982, NILV-OR-1/82.
71. V. E. Rose and J. E. Perkins, *Am. Ind. Hyg. Assoc. J.*, 1983, **44**, 605.
72. W. K. Fowler, *Int. Lab.*, 1982, **12**, December, 80.
73. J. Namieśnik, T. Górecki, E. Kozłowski, L. Torres and J. Mathieu, *Sci. Total. Environ.*, in the press.
74. B. Miller, P. O. Kane, D. B. Robinson and P. J. Whittingham, *Analyst*, 1978, **103**, 1165.
75. K. S. Sidhu, *J. Appl. Toxicol.*, 1981, **1**, 300.
76. *Idem*, *J. Anal. Toxicol.*, 1980, **4**, 266.
77. K. Andersson, J. O. Levin, R. Lindhal and C. A. Nilsson, *Chemosphere*, 1981, **10**, 143.
78. M. Lorincz, *J. Chromatog.*, 1978, **166**, 141.
79. S. Thorburn and B. A. Colenutt, *Int. J. Environ. Stud.*, 1979, **13**, 265.
80. L. W. Severs and K. K. Skory, *Am. Ind. Hyg. Assoc. J.*, 1974, **35**, 669.
81. L. Pozzoli and D. Cottica, *G. Ital. Med. Lav.*, 1979, **1**, 133.
82. R. W. Bishop, T. A. Ayers and D. S. Rinehart, *Am. Ind. Hyg. Assoc. J.*, 1981, **42**, 586.
83. B. W. Hermann and J. N. Seiber, *Anal. Chem.*, 1981, **53**, 1077.

84. B. Zimmerli and H. Zimmermann, *Z. Anal. Chem.*, 1980, **304**, 23.
85. K. Andersson, J. O. Levin and C. A. Nilsson, *Chemosphere*, 1981, **10**, 137.
86. K. Andersson, C. Hallgren, J. O. Levin and C. A. Nilsson, *Scand. J. Work. Environ. Health*, 1981, **7**, 282.
87. K. Andersson, J. O. Levin and C. A. Nilsson, *Chemosphere*, 1983, **12**, 821.
88. *Idem*, *ibid.*, 1983, **12**, 377.
89. K. Andersson, C. Hallgren, J. O. Levin and C. A. Nilsson, *ibid.*, 1981, **10**, 275.
90. M. L. Lanhorst, *Am. Ind. Hyg. Assoc. J.*, 1980, **41**, 328.
91. R. G. Melcher, W. L. Garner, L. W. Severs and J. R. Vaccaro, *Anal. Chem.*, 1978, **50**, 251.
92. Y. G. Raffin and J. Damour, *Ber. Int. Kollog. Verhuetung Arbeitsunfaellen Berufskr. Chem. Ind.*, **8th**, 1982, p. 347.
93. R. K. Beasley, C. E. Hoffman, M. L. Rueppel and J. W. Worley, *Anal. Chem.*, 1980, **52**, 1110.
94. C. J. Purnell and C. J. Warwick, *Analyst*, 1980, **105**, 861.
95. *Idem*, *IARC Sci. Publ.*, 1981, **40**, 133.
96. M. L. Langhorst, R. G. Melcher and G. J. Kallos, *Am. Ind. Hyg. Assoc. J.*, 1981, **42**, 47.
97. S. VanTassel, N. Amalfitano and R. S. Narang, *Anal. Chem.*, 1981, **53**, 2130.
98. K. E. MacLeod, *Environ. Sci. Technol.*, 1981, **15**, 926.
99. C. L. Stratton, *Spec. Conf. Specific Control (Toxic) Pollut.*, *Proc.*, 1979, p. 159.
100. R. Grover and L. A. Kerr, *J. Environ. Sci. Health*, 1981, **16**, 59.
101. R. A. Glaser and W. J. Woodfin, *Am. Ind. Hyg. Assoc. J.*, 1981, **42**, 18.
102. R. J. Hunt, N. R. Neubauer and R. F. Picone, *ibid.*, 1980, **41**, 592.
103. G. T. Taylor, T. E. Redington, M. J. Bailey and F. Buddingh, *ibid.*, 1980, **41**, 819.
104. G. Müller, K. Norpoth and S. Z. M. Travenius, *Int. Arch. Occup. Environ. Health*, 1981, **48**, 325.
105. K. E. Thrané and A. Mikalsen, *Atmos. Environ.*, 1981, **15**, 909.
106. N. F. Burdick and T. F. Bidleman, *Anal. Chem.*, 1981, **53**, 1926.
107. G. J. Hollod and S. J. Eisenreich, *Anal. Chim. Acta*, 1981, **124**, 31.
108. K. Andersson, A. Gudehn, J. O. Levin and C. A. Nilsson, *Chemosphere*, 1982, **11**, 3.
109. B. Kolb and L. Pospisil, *Chromatog. Newslett.*, 1980, **8**, 35.
110. M. L. Langhorst and T. J. Nestricks, *Anal. Chem.*, 1979, **51**, 2018.
111. J. L. Lindgren, H. J. Krauss and M. A. Fox, *Air Pollut. Control Assoc. J.*, 1980, **30**, 166.
112. H. Frind and R. Hensel, *Z. Anal. Chem.*, 1982, **312**, 237.
113. T. G. Matthews and T. C. Howell, *Anal. Chem.*, 1982, **54**, 1495.
114. K. E. Williams, G. G. Esposito and D. S. Rinchart, *Am. Ind. Hyg. Assoc. J.*, 1981, **42**, 476.
115. J. C. Cage, V. Lagesson and A. Tunek, *Ann. Occup. Hyg.*, 1977, **20**, 127.
116. D. L. Haynes, *Ion Chromatog. Anal. Environ. Pollut.*, 1979, **2**, 157.
117. M. Waldman and M. Vaněček, *Ann. Occup. Hyg.*, 1982, **25**, 5.
118. K. Kuwata, E. Akiyama, Y. Yamazaki, H. Yamasaki, Y. Kuge and Y. Kiso, *Anal. Chem.*, 1983, **55**, 2199.
119. J. C. Gilland, G. T. Johnson and W. A. McGee, *Am. Ind. Hyg. Assoc. J.*, 1981, **42**, 630.
120. S. P. Tucker and G. J. Deye, *Anal. Lett.*, 1981, **14**, 959.
121. T. F. Bidleman, *Atmos. Environ.*, 1981, **15**, 619.
122. S. Fuselli, G. Benedetti and R. Mastrangeli, *ibid.*, 1982, **16**, 2943.
123. J. Krajewski, J. Gromiec and M. Dobiecki, *Am. Ind. Hyg. Assoc. J.*, 1980, **41**, 531.
124. J. C. Posner and J. R. Okenfuss, *ibid.*, 1981, **42**, 643.
125. J. C. Posner, *ibid.*, 1981, **42**, 647.
126. S. T. Rodriguez, D. W. Gosselink and H. E. Mullins, *ibid.*, 1982, **43**, 569.
127. Y. Hoshika and G. Muto, *Analyst*, 1982, **107**, 855.
128. D. W. Oblas, D. L. Dugger and S. I. Lieberman, *IEEE Trans. Components, Hybrids, Manuf. Technol.*, CHMT-3, 1980, 17.
129. A. Raymond and G. Guiochon, *Environ. Sci. Technol.*, 1974, **8**, 143.
130. N. Kashihira, K. Kirita, Y. Watanabe and K. Tanaka, *Bunseki Kagaku*, 1980, **29**, 853.
131. R. Hageman, H. Virelizier and D. Gaudin, *Analysis*, 1978, **6**, 401.
132. Z. Dębowski, *Ochrona Powietrza*, April 1979, 94.
133. L. Pozzoli and A. Berri, *Med. Lav.*, 1977, **68**, 469.
134. K. Kuwata, Y. Yamazaki and M. Uebori, *Bunseki Kagaku*, 1980, **29**, 170.
135. J. Delcourt, J. P. Guenier and J. Muller, *Chromatographia*, 1983, **17**, 88.
136. B. A. Colenutt and S. Thorburn, *ibid.*, 1979, **12**, 519.
137. B. A. Colenutt, *Int. J. Environ. Anal. Chem.*, 1980, **7**, 315.
138. R. G. Melcher and V. J. Coldecourt, *Anal. Chem.*, 1980, **52**, 875.
139. B. E. Wilkes, L. J. Priestley, Jr. and L. K. Scholl, *Microchem. J.*, 1982, **27**, 420.
140. L. J. Priestley, Jr. and B. E. Wilkes, *ibid.*, 1979, **24**, 88.
141. J. M. Purcell and P. Magidman, *Anal. Lett.*, 1983, **16**, 465.
142. J. F. Pankow and T. J. Kristensen, *Anal. Chem.*, 1983, **55**, 2187.
143. A. G. Gargus and C. R. Watterson, *Am. Lab.*, 1980, **12**, No. 2, 133.
144. A. G. Gargus, S. A. Liebman and C. R. Watterson, *ibid.*, 1981, **13**, No. 5, 114.
145. H. J. Neu, W. Merz and H. Panzel, *J. High Resol. Chromatog., Chromatog. Commun.*, 1982, **5**, 382.
146. *EMS Thermal Desorber*, Technical Brochure, MDA Scientific Inc., Glenview, IL, USA, 1982.
147. *CDS-320 GC Sample Concentrator*, Technical Brochure, Chemical Data Systems Inc., Oxford, PA, USA, 1981.
148. A. J. Nuñez, L. F. Gonzalez and J. Janák, *J. Chromatog.*, 1984, **300**, 127.
149. L. J. Rigby, *Ann. Occup. Hyg.*, 1981, **24**, 331.
150. L. Wennrich, T. Welsch and W. Engewald, *J. Chromatog.*, 1982, **241**, 49.
151. H. Schlitt, H. Knoeppel, B. Versino, A. Peil, H. Schauenburg and H. Vissers, *ASTM Spec. Tech. Publ.*, 1981, No. **721**, p. 22.
152. E. D. Pellizzari, B. H. Carpenter, J. E. Bunch and E. Sawicki, *Environ. Sci. Technol.*, 1975, **9**, 556.
153. J. Sevcik, *Int. Lab.*, 1984, **14**, June, 62.
154. J. Namieśnik, L. Torres and J. Mathieu, *Sci. Total Environ.*, in the press.
155. S. Crisp, *Ann. Occup. Hyg.*, 1980, **23**, 47.
156. G. Crescentini and F. Bruner, *Ann. Chim. (Rome)*, 1978, **68**, 343.
157. K. Watabe, S. Iida, T. Ichikawa and M. Kondo, *Eisei Kagaku*, 1979, **25**, 343; *Anal. Abstr.*, 1980, **39**, 1H14.
158. M. Krzymen, *J. Chromatog.*, 1981, **204**, 453.
159. G. O. Nelson and Ch. A. Harder, *Am. Ind. Hyg. Assoc. J.*, 1976, **37**, 205.
160. R. G. Melcher, P. W. Langwardt, M. L. Langhorst and S. A. Bouyoucos, in *Chemical Hazards in the Workplace*, G. Choudhary (ed.), p. 155. ACS, Washington, 1981.
161. R. J. Sydor and D. J. Pietrzyk, *Anal. Chem.*, 1978, **50**, 1842.
162. Y. Matsumura, *Ind. Health*, 1980, **18**, 61.

163. E. C. Gunderson and E. L. Fernandes, in *Chemical Hazards in the Workplace*, G. Choudhary (ed.), p. 179. ACS, Washington, 1981.
164. G. A. Eiceman and F. W. Karasek, *J. Chromatog.*, 1980, **200**, 115.
165. K. Urano, S. Omori and E. Yamamoto, *Environ. Sci. Technol.*, 1982, **16**, 10.
166. T. Braun and A. B. Farag, *Anal. Chim. Acta*, 1978, **99**, 1.
167. J. Namieśnik, L. Torres, E. Kozłowski and J. Mathieu, *J. Chromatog.*, 1981, **208**, 239.
168. O. L. Hollis, *J. Chromatog. Sci.*, 1973, **11**, 335.
169. M. Dressler, *J. Chromatog.*, 1979, **165**, 167.
170. C. H. Lochmuller, M. W. Ewalt and E. C. Jensen, *Int. J. Environ. Anal. Chem.*, 1980, **8**, 37.
171. L. D. Butler and M. F. Burke, *J. Chromatog. Sci.*, 1976, **114**, 117.
172. G. T. Hunt and N. Pangaro, *Anal. Chem.*, 1982, **54**, 369.
173. L. D. Johnson and R. G. Merrill, *Toxicol. Environ. Chem.*, 1983, **6**, 109.
174. R. Van Wijk, *J. Chromatog. Sci.*, 1970, **8**, 418.
175. R. F. Gallant, J. W. King, P. L. Levins and J. F. Pieciewicz, *Report* 1978, EPA-600/7-78/054.
176. J. Namieśnik and E. Kozłowski, *Z. Anal. Chem.*, 1982, **311**, 581.
177. Yu S. Drugov, *Zavodsk. Lab.*, 1982, **48**, No. 1, 3.
178. A. B. Belikov and Yu. S. Drugov, *Zh. Analit. Khim.*, 1981, **36**, 1624.
179. G. O. Nelson and C. A. Harder, *Am. Ind. Hyg. Assoc. J.*, 1974, **35**, 391.
180. T. Kuwata, T. Uemura, I. Kifune, Y. Tominaga and K. Oikawa, *Bunseki Kagaku*, 1982, **31**, 453.
181. J. P. Guenier and J. Muller, *Ann. Occup. Hyg.*, 1984, **28**, 61.
182. G. Castello and G. D'Amato, *J. Chromatog.*, 1980, **196**, 245.
183. C. D. Chriswell and D. T. Gjerde, *Anal. Chem.*, 1982, **54**, 1911.
184. Yu. S. Drugov, *Metody ochenkii proizvodstvennoi sredy promyshlennykh predpriyatii*, p. 66. Moscow, 1980.
185. R. Mindrup, *J. Chromatog. Sci.*, 1978, **16**, 380.
186. Yu. S. Drugov and V. G. Berezkin, *Russ. Chem. Rev.*, 1979, **48**, 1006.
187. K. I. Sakodynskii and L. I. Panina, *Polimernye sorbenty dlya molekulyarnoi khromatografi*, Nauka, Moscow, 1977.
188. K. Andersson, J. O. Levin, R. Lindhal and C. A. Nilsson, *Chemosphere*, 1984, **13**, 437.
189. P. S. Ramanathan, *Indian J. Environ. Prot.*, 1982, **2**, 23.
190. D. G. Parkes, C. R. Ganz, A. Polinsky and J. Schulze, *Am. Ind. Hyg. Assoc. J.*, 1976, **37**, 165.
191. R. G. Melcher, R. R. Langner and R. O. Kagel, *ibid.*, 1978, **39**, 349.
192. J. P. Guenier, P. Simon, J. Delcourt, M. F. Didierjean, C. Lefevre and J. Muller, *Chromatographia*, 1984, **18**, 137.
193. K. J. Krost, E. D. Pellizzari, S. G. Walburn and S. A. Hubbard, *Anal. Chem.*, 1982, **54**, 810.
194. M. W. Dietrich, L. M. Chapman and J. P. Mieure, *Am. Ind. Hyg. Assoc. J.*, 1978, **39**, 385.
195. T. F. Bidleman, in *Trace Analysis*, Vol. 4, p. 51. Academic Press, New York, 1985.
196. P. Lovkvist and J. A. Jonsson, *J. Chromatogr.*, 1984, **286**, 279.
197. M. T. Dmitriev, E. G. Rastiannikov and S. A. Volkov, *Gig. Sanit.*, 1980, No. 5, 42.
198. E. D. Pellizzari, J. E. Bunch, B. H. Carpenter and E. Sawicki, *Environ. Sci. Technol.*, 1975, **9**, 552.
199. M. E. Krzymien, *ASTM Spec. Tech. Publ.*, 1982, No. 786, 35.
200. L. A. Wallace and W. R. Ott, *J. Air Pollut. Control Assoc.*, 1982, **32**, 601.
201. G. Devitofrancesco, C. Furnari, A. Bacaloni and B. M. Petronio, *J. Chromatog.*, 1981, **210**, 261.
202. J. E. Bunch and E. D. Pellizzari, *ibid.*, 1979, **186**, 811.
203. R. L. Hanson, Ch. R. Clark, R. L. Carpenter and C. H. Hobbs, *Environ. Sci. Technol.*, 1981, **15**, 701.
204. Y. Hanai, K. Takahashi and T. Katou, *Bull. Inst. Environ. Sci. Technol.*, 1981, **7**, 35.
205. S. Coppi, A. Betti, G. Blo and C. Bighi, *J. Chromatog.*, 1983, **267**, 91.
206. G. T. Hunt, N. Pangaro and S. G. Zelensky, *Anal. Lett.*, 1980, **13**, 521.
207. C. J. Danby, J. G. Davoud, D. H. Everett, C. N. Hinshelwood and R. M. Lodge, *J. Chem. Soc.*, 1946, 918.
208. F. A. P. Maggs, *Filtr. Sep.*, 1983, **20**, No. 3, 192.
209. F. J. Weisenhorn, *Chem. Ztg.*, 1982, **106**, 339.
210. Z. S. Jarda, *Chimia*, 1978, **32**, 484.
211. O. Grubner and D. W. Underhill, *Sepr. Sci.*, 1970, **5**, 555.
212. G. O. Nelson and C. A. Harder, *Am. Ind. Hyg. Assoc. J.*, 1972, **33**, 97.
213. J. Schaefer, *Proc. Flavour 81 Wuerman Symp.*, 1981, p. 301.
214. G. O. Nelson and A. N. Correia, *Am. Ind. Hyg. Assoc. J.*, 1976, **37**, 514.
215. O. Grubner and W. A. Burgess, *Environ. Sci. Technol.*, 1981, **15**, 1346.
216. E. S. Moyer, *Am. Ind. Hyg. Assoc. J.*, 1983, **44**, 46.
217. M. S. Black, R. P. Herbst and D. R. Hitchcock, *Anal. Chem.*, 1978, **50**, 848.
218. N. W. Henry III and R. S. Wilhelme, *Am. Ind. Hyg. Assoc. J.*, 1979, **40**, 1017.
219. D. R. Hemenway, B. J. Fitzgerald and T. Paret, *ibid.*, 1982, **43**, 686.
220. P. D. Cobos and J. B. Toha, *Med. Segur. Trab.*, 1982, **30**, 189.
221. K. W. Boyd, M. B. Emory and H. K. Dillon, in *Chemical Hazards, in the Workplace*, G. Choudhary (ed.), p. 49. ACS, Washington, 1981.
222. R. H. Hill, Jr., C. S. McCammon, A. T. Saalwaechter, A. W. Teass and W. J. Woodfin, *Anal. Chem.*, 1976, **48**, 1395.
223. J. W. Russell, *Environ. Sci. Technol.*, 1975, **9**, 1175.
224. L. A. Jonas and W. J. Svirbely, *J. Catal.*, 1972, **24**, 446.
225. E. B. Sansone, Y. B. Tewari and L. A. Jonas, *Environ. Sci. Technol.*, 1979, **13**, 1511.
226. J. Namieśnik and E. Kozłowski, *Chem. Anal. Warsaw*, 1980, **25**, 999.
227. J. Namieśnik, E. Kozłowski, L. Torres and J. Mathieu, Paper presented at 2nd Congrès de Chimie Analytique, 34th Congrès du G.A.M.S., 8-12 December, 1980.
228. J. Namieśnik, E. Kozłowski, L. Torres and J. Mathieu, *Proc. VIIth World Congress on Air Quality*, 1983, Vol. 1, p. 377.
229. L. Torres, M. Frihka, J. Mathieu, M. L. Riba and J. Namieśnik, *Int. J. Environ. Anal. Chem.*, 1983, **13**, 155.
230. M. L. Riba, L. Torres, E. Randrianalimanana, J. Mathieu and J. Namieśnik, *Proc. VIIth World Congress on Air Quality*, 1983, Vol. 1, p. 147.
231. A. Golovoy and J. Braslav, *Environ. Prog.*, 1982, **1**, 89.
232. L. A. Jonas and E. B. Sansone, *Environ. Sci. Technol.*, 1981, **15**, 1367.
233. C. L. Fraust and E. R. Hermann, *Am. Ind. Hyg. Assoc. J.*, 1969, **30**, 499.
234. L. A. Jonas and J. A. Rehrmann, *Carbon*, 1973, **11**, 59.
235. A. Wheeler and A. J. Robell, *J. Catal.*, 1969, **13**, 299.
236. E. B. Sansone and L. A. Jonas, *Am. Ind. Hyg. Assoc. J.*, 1981, **42**, 688.
237. G. I. Senum, *Environ. Sci. Technol.*, 1981, **15**, 1073.
238. A. Golovoy and J. Braslav, *Air Pollut. Control Assoc. J.*, 1981, **31**, 861.



239. L. A. Jonas, E. B. Sansone and T. S. Farris, *Am. Ind. Hyg. Assoc. J.*, 1983, **44**, 716.
240. H. Kitegawa, *Kogai*, 1980, **15**, 112.
241. *Idem*, *ibid.*, 1980, **15**, 118.
242. *Idem*, *Carbon*, 1980, **18**, 448.
243. P. B. Meyer and H. Steenweg van Witteloostuyn, *Am. Ind. Hyg. Assoc. J.*, 1977, **38**, 46.
244. M. Vaněček and M. Waldman, *Collection Czech. Chem. Commun.*, 1979, **44**, 519.
245. M. Waldman and M. Vaněček, *ibid.*, 1978, **43**, 2905.
246. W. E. Ruch, G. O. Nelson, C. L. Lindeken, R. G. Johnsen and D. J. Hodgkins, *Am. Ind. Hyg. Assoc. J.*, 1972, **33**, 105.
247. G. O. Nelson, A. N. Correia and C. A. Harder, *ibid.*, 1976, **37**, 280.
248. G. O. Nelson, R. E. Johnsen, C. L. Lindeken and R. D. Taylor, *ibid.*, 1972, **33**, 745.
249. G. O. Nelson and D. J. Hodgkins, *ibid.*, 1972, **33**, 110.
250. O. Grubner, A. Zikanova and M. Ralek, *J. Chromatog.*, 1967, **28**, 209.
251. R. H. Brown and C. J. Purnell, *ibid.*, 1979, **178**, 79.
252. M. L. Riba, E. Randrianalimanana, J. Mathieu, L. Torres and J. Namieśnik, *Int. J. Environ. Anal. Chem.*, 1985, **19**, 133.
253. V. Patzelová, M. Wurst and V. Čatská, *J. Chromatog.*, 1980, **193**, 137.
254. A. T. Saalwaechter, C. S. McCammon, C. P. Roper and K. S. Carlberg, *Am. Ind. Hyg. Assoc. J.*, 1978, **39**, 476.
255. R. G. Lewis and M. D. Jackson, *Anal. Chem.*, 1982, **54**, 592.
256. A. Gold, C. E. Dube and R. B. Perni, *ibid.*, 1978, **50**, 1839.
257. C. Vidal-Madjar, M. F. Gonnord, F. Benchah and G. Guiochon, *J. Chromatog. Sci.*, 1978, **16**, 190.
258. F. Raschdorf, *Chimia*, 1978, **32**, 478.
259. K. J. Saunders, in *Analytical Techniques in Environmental Chemistry*, J. Albaiges (ed.), Vol. 2, p. 287. Pergamon Press, Oxford, 1982.
260. S. Seshedri and J. W. Bozzelli, *Chemosphere*, 1983, **12**, 809.
261. T. Tanaka, *J. Chromatog.*, 1978, **153**, 7.
262. A. Raymond and G. Guiochon, *J. Chromatog. Sci.*, 1975, **13**, 173.
263. A. Raymond and G. Guiochon, *Analisis*, 1973, **2**, 357.
264. K. S. Sidhu, *Arch. Environ. Contam. Toxicol.*, 1983, **12**, 747.
265. R. G. Lewis and K. E. MacLeod, *Anal. Chem.*, 1982, **17**, 383.
266. W. N. Billings and T. F. Bidleman, *Atmos. Environ.*, 1983, **17**, 383.
267. J. W. Bozzelli and B. B. Kebbekus, *J. Environ. Sci. Health*, 1982, **A17**, 693.
268. Y. Hanai, T. Katou and H. Nanya, *Bull. Inst. Environ. Sci. Technol.*, 1980, **6**, 3.
269. T. Hirayama and M. Ikeda, *Am. Ind. Hyg. Assoc. J.*, 1979, **40**, 1091.
270. G. Bertoni, F. Bruner, A. Liberti and C. Perrino, *J. Chromatog.* 1981, **203**, 263.
271. K. Kuwata, Y. Yamazaki, M. Uebori and Y. Eguchi, *Taiki Osen Gakkaishi*, 1979, **14**, 197; *Chem. Abstr.*, 1980, **92**, 10475.
272. A. D. Snyder, N. F. Hodgson, M. A. Kemmer and J. R. McKendree, *U.S. NTIS, PB. REP.*, PB-257131, 1976; *Chem. Abstr.*, 1977, **86**, 176254.
273. M. D. Jackson and R. G. Lewis, *ASTM Spec. Tech. Publ.*, 1981, No. **721**, 36.
274. R. G. Oldham, R. L. Spraggins, J. R. Parr and K. W. Lee, *Spec. Conf. Control Specific (Toxic) Pollut., Proc.*, 1979, p. 130.
275. H. D. Axelrod and J. P. Lodge, Jr., *Air Pollution*, A. C. Stern, (ed.), 3rd Ed., Vol. 3, p. 145. Academic Press, New York, 1976.
276. *Methods for the Preparation of Gaseous Mixtures*, BSI Report, BS 4559, British Standard Institution, London, 1970.
277. R. S. Barratt, *Analyst*, 1981, **106**, 817.
278. I. Delespaul, H. Paperstraete and T. Ryman, *U.S. NBS Special Publication*, 1977, No. 464, p. 464.
279. R. T. Drew and M. Lippman, in *Air Sampling Instruments for the Evaluation of Atmospheric Contamination*, M. Lippman (ed.), 4th Ed., 1972, Am. Conf. Gov. Ind. Hyg., Cincinnati, OH, USA, 1972.
280. N. R. McQuaker, H. Haboosheh and W. Best, *Int. Lab.*, 1981, **11**, Jan./Feb., 61.
281. J. P. Lodge, in *Air Pollution*, A. C. Stern (ed.), 2nd Ed., Vol. 2, Academic Press, New York, 1968.
282. K. Leichnitz, *Pure Appl. Chem.*, 1983, **55**, 1239.
283. *Selected Methods for Measuring Air Pollutants*, WHO Report, Publication No. 24, Geneva, 1976.
284. J. Namieśnik, *J. Chromatog.*, 1984, **300**, 79.
285. J. Szulc and Z. Witkiewicz, *Chem. Anal. Warsaw*, 1981, **26**, 375.
286. B. B. Kebbekus and J. W. Bozzelli, *J. Environ. Sci. Health*, 1982, **A7**, 713.
287. W. Bertsch, R. C. Chang and A. Zlatkis, *J. Chromatog. Sci.*, 1974, **12**, 175.
288. B. E. Bowen, *Anal. Chem.*, 1976, **48**, 1584.
289. R. E. Berkeley and E. D. Pellizzari, *Anal. Lett.*, 1978, **11**, 327.
290. J. L. Beveridge and H. J. Duncan, *ibid.*, 1981, **14**, 689.
291. G. Holzer, H. Shanfield, A. Zlatkis, W. Bertsch, P. Juarez, H. Mayfield and H. M. Liebich, *J. Chromatog.*, 1977, **142**, 755.
292. R. Jelts and T. R. Thijsee, *Atmos. Environ.*, 1978, **12**, 1567.
293. F. H. Jarke and S. M. Gordon, *Proc. Ann. Meet. Air Pollut. Control Assoc.*, 1981, Paper 81-57.2.
294. J. S. Parsons and S. Mitzner, *Environ. Sci. Technol.*, 1975, **9**, 1053.
295. E. D. Pellizzari, J. E. Bunch, R. E. Berkeley and J. McRae, *Anal. Chem.*, 1976, **48**, 803.
296. *Idem*, *Anal. Lett.*, 1976, **9**, 45.
297. E. D. Pellizzari, J. E. Bunch, I. T. Bursey, R. E. Berkeley, E. Sawicki and K. Krost, *ibid.*, 1976, **9**, 579.
298. D. S. Walker, *Analyst*, 1978, **103**, 397.
299. A. Zlatkis, H. A. Lichtenstein and A. Tishbee, *Chromatographia*, 1973, **6**, 67.
300. Y. Hoshika and G. Muto, *Bunseki Kagaku*, 1978, **27**, 273.
301. W. V. Ligon, Jr. and R. L. Johnson, Jr., *Anal. Chem.*, 1976, **48**, 481.
302. M. Mattson and G. Petersson, *Int. J. Environ. Anal. Chem.*, 1982, **11**, 211.
303. B. Versino, M. De Groot and F. Geiss, *Chromatographia*, 1974, **7**, 302.
304. B. Versino, H. Knoppel, M. De Groot, A. Peil, J. Poelman, H. Schauenburg, H. Vissers and F. Geiss, *J. Chromatog.*, 1976, **122**, 373.
305. E. Tsani-Bazaca, A. E. McIntyre, J. N. Lester and R. Perry, *Environ. Technol. Lett.*, 1981, **2**, 303.
306. M. Oehme and H. Stray, *Z. Anal. Chem.*, 1981, **311**, 665.
307. A. Borroni, B. Maza and G. Nano, *AES*, 1982, **4**, 94.
308. P. Ciccio, G. Bertoni, E. Brancaleoni, R. Fratarcangeli and F. Bruner, *J. Chromatog.*, 1976, **126**, 757.
309. G. C. Fabiano, *Chim. Ind.*, 1978, **60**, 111.
310. X. Guardiano, J. Bartual and M. J. Berenguer, *Afinidad*, 1979, **36**, 9.
311. A. Dravnieks, B. K. Krotoszyński, J. Whitfield, A. O'Donnell and T. Burgwald, *Environ. Sci. Technol.*, 1971, **5**, 1220.
312. M. Krejci and M. Rusek, *Int. J. Environ. Anal. Chem.*, 1981, **9**, 159.
313. K. E. Murray, *J. Chromatog.*, 1977, **135**, 49.

314. D. N. Campbell and R. H. Moore, *Am. Ind. Hyg. Assoc. J.*, 1979, **40**, 904.
315. A. G. L. Burm and J. Spierdijk, *Anesthesiology*, 1979, **50**, 230.
316. B. I. Brookes, S. M. Jickells and R. S. Nicolson, *J. Assoc. Public Anal.*, 1978, **16**, 101.
317. J. De Greef, M. De Proft and F. De Winter, *Anal. Chem.*, 1976, **48**, 38.
318. K. Anderson, J. O. Levin, R. Lindhal and C. A. Nilsson, *Chemosphere*, 1982, **11**, 1115.
319. G. M. W. Sibbel-Schultz, D. T. Gjerde, C. D. Chriswell, J. S. Fritz and W. E. Coleman, *Talanta*, 1982, **29**, 447.
320. Y. Yokouchi, T. Fujii, Y. Ambe and K. Fuwa, *J. Chromatog.*, 1979, **180**, 133.
321. A. Kettrup, H. Stenner and H. Weber, *Erdol Kohle, Erdgas Petrochem.*, 1982, **35**, 475.
322. J. Kasche and K. Schroeter, *Chem. Tech.*, 1979, **31**, 311.
323. J. Adams, E. L. Atlas and C. S. Giam, *Anal. Chem.*, 1982, **54**, 1515.
324. K. Miyoshi and M. Okamura, *Shin Nippon Denki Giho*, 1979, **14**, 4; *Chem. Abstr.*, 1980, **93**, 100653.
325. R. G. Williams, *J. Chromatog.*, 1982, **245**, 381.
326. E. Heil, H. Oser, R. Hatz and H. Kalker, *Z. Anal. Chem.*, 1979, **297**, 357.
327. P. M. Houpt and F. Langeweg, *Anal. Chim. Acta*, 1981, **124**, 15.
328. G. Holzer, J. Oro and W. Bertsch, *J. Chromatog.*, 1976, **126**, 771.
329. C. L. Stratton, S. A. Whitlock and J. M. Allan, *Spec. Conf. Control Specific (Toxic) Pollut., Proc.*, 1979, p. 159.
330. R. Tatsukawa, T. Okamoto and T. Wakimoto, *Bunseki Kagaku*, 1978, **27**, 164.
331. T. F. Bidleman, W. N. Billings and C. G. Simon, *Report 1980, EPA-600/2-80-67*.
332. R. S. Marano, W. S. Updegrova and R. C. Machen, *Anal. Chem.*, 1982, **54**, 1947.
333. J. Snell, *Pollut. Eng.*, 1982, **14**, 36.
334. M. V. King, P. M. Eller and R. J. Costello, *Am. Ind. Hyg. Assoc. J.*, 1983, **44**, 615.
335. J. E. Peterson, *ibid.*, 1980, **41**, 450.
336. D. L. Fox, *Anal. Chem.*, 1987, **59**, 280R.
337. M. L. Langhurst and L. B. Coyne, *ibid.*, 1987, **59**, IR.

## SHORT COMMUNICATIONS

# A PVC-COATED CARBON ROD ION-SELECTIVE ELECTRODE FOR THALLIUM AND ITS APPLICATION TO THE ANALYSIS OF ROCKS AND MINERALS

DEZHONG DAN and YALAN DONG

Department of Applied Chemistry, Chengdu College of Geology, Chengdu, Sichuan, People's Republic of China

(Received 22 July 1987. Revised 28 January 1988. Accepted 5 February 1988)

**Summary**—A new Tl(III) ion-selective electrode prepared by coating a graphite rod with a PVC membrane has been made and investigated. The optimum membrane composition is Butylrhodamine B-TlCl<sub>4</sub> 5 mg, chlorobenzene 0.1 ml, dioctyl phthalate 0.4 ml, PVC 0.17 g. The electrode exhibits Nernstian response to Tl(III) over the concentration range  $6.5 \times 10^{-7}$ – $2.5 \times 10^{-3}M$ . The detection limit is  $3.5 \times 10^{-7}M$  and the slope of the electrode response is  $53 \pm 1$  mV per decade. The electrode shows high stability and selectivity. The electrode is easy to make and store, and inexpensive.

Thallium, which shows crystallochemical affinities with the geochemically important elements potassium and rubidium, is an element of geological interest. It has been proposed as a geochemical indicator in problems such as petrogenesis, rock-sea-water interaction, and evaluation of the degree of sulphur saturation in a silicate melt.<sup>1,2</sup>

The abundance of thallium in geological material is very low so its determination requires highly sensitive analytical methods, such as fluorimetry, neutron activation, atomic-absorption spectrometry (AAS) and anodic stripping voltammetry (ASV). Fluorimetry has severe limitations due to interference, neutron activation requires expensive facilities and a long time for irradiation and cooling of samples, and AAS and ASV often require enrichment methods.

We have already developed a PVC membrane electrode based on the Butylrhodamine B-AuCl<sub>4</sub><sup>-</sup> ion-pair as electroactive agent,<sup>3</sup> and now propose Butylrhodamine B-TlCl<sub>4</sub> as an electroactive agent for use in a PVC coating on a carbon rod electrode. This electrode, which needs no internal reference solution and internal reference electrode, is easier and cheaper to make than conventional PVC membranes or all solid-state PVC membranes.<sup>4</sup> The electrode has been used successfully for the determination of Tl(III) in geological reference samples.

### EXPERIMENTAL

#### Reagents

Analytical-reagent grade chemicals were used. Tl(III) stock solution,<sup>5</sup>  $1 \times 10^{-2}M$ , diluted as required, with 0.5M sodium chloride and 0.5M hydrochloric acid. Carbon rod, spectroscopically pure, 8 mm diameter.

#### Preparation of electrode

Weigh 0.2 g of Butylrhodamine B and dissolve it in 5 ml of demineralized water, then add 1 ml of concentrated hydrochloric acid, 0.7 g of sodium chloride and 10 ml of

$10^{-2}M$  Tl(III) stock solution dropwise. Centrifuge and wash the red precipitate with two 5-ml portions of 20% hydrochloric acid. Dry the product at 80°.

The optimum membrane composition has been found to be 5 mg of Butylrhodamine B-TlCl<sub>4</sub>, 0.1 ml of chlorobenzene, 0.4 ml of dioctyl phthalate and 0.17 g of PVC. Mix these reagents in the ratios stated, add 10 ml of tetrahydrofuran, stir, and let stand for 10 hr. Coat the carbon rod by immersing it in the solution, removing it and allowing it to dry. Repeat the coating, taking care to get a well-distributed membrane. Leave the membrane in the air for about 12 hr. A thin membrane has poor stability and a short lifetime, but the response is slow if the membrane is too thick. A four-layer membrane is a suitable compromise. Figure 1 shows the structure of the coated carbon rod PVC membrane electrode.

Before use, the electrode should be activated for 2 hr by immersion in  $10^{-3}M$  Tl(III) solution in 0.5M hydrochloric acid/0.5M sodium chloride. Rinse the electrode in demineralized water until the potential relative to an SCE is stable.

The cell is

carbon rod || PVC sensor | unknown soln. || SCE

### RESULTS AND DISCUSSION

#### Response characteristics of the electrode

Tl(III) hydrolyses and precipitates at pH > 5. A reasonable pH range for use is 0–5. The membrane resistance measured by the parallel resistance method is 0.1 MΩ. The electrode response is immediate if the concentration of Tl(III) is  $> 10^{-6}M$ . The response time is about 30 sec in  $10^{-7}$ – $10^{-6}M$  Tl(III). The potential reading taken every 30 min over a period of 3 hr had a drift of only  $\pm 1$  mV. Potential readings taken five times in  $10^{-5}M$  and  $10^{-6}M$  Tl(III) alternately, showed no memory effect. Table 1 shows the reproducibility of the electrode response over a period of 4 days.

Figure 2 shows a typical Tl(III) calibration graph. The response is Nernstian ( $53 \pm 1$  mV/decade at 18°) over the concentration range  $6.3 \times 10^{-7}$ – $2.5 \times 10^{-3}M$ . The detection limit is  $3.5 \times 10^{-7}M$ .

Table 1. Reproducibility of electrode response

Day	Response, mV			
	$1 \times 10^{-3} M$ Tl	$1 \times 10^{-4} M$ Tl	$1 \times 10^{-5} M$ Tl	$1 \times 10^{-6} M$ Tl
1	-271	-321	-375	-428
2	-271	-324	-378	-430
3	-271	-323	-373	-427
4	-271	-323	-374	-429

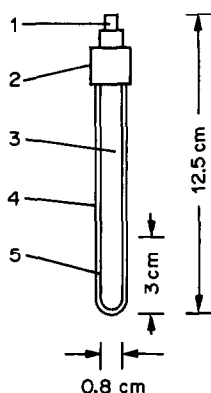


Fig. 1. Diagram of coated carbon rod PVC membrane electrode. 1, Electrical connection; 2, electrode cap; 3, carbon rod; 4, PVC insulator; 5, PVC sensor.

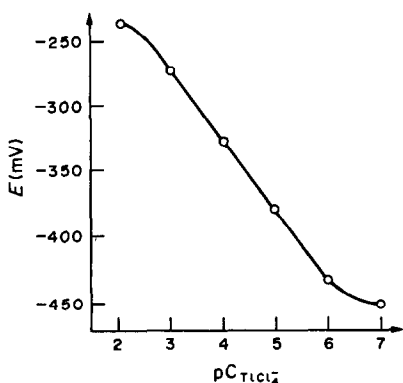


Fig. 2. Typical calibration graph for Tl(III).

The potentiometric selectivity coefficients of the electrode for some interferent ions, measured by the separate solution method, are listed in Table 2. The interference of other ions is negligible except for Au(III).

#### Analysis of geological samples

Weigh 0.2 g of sample into a 100-ml beaker, and add 20 ml of freshly prepared *aqua regia*. Heat on a steam-bath until a moist residue remains, add 5 drops of concentrated hydrofluoric and perchloric acids, then heat on a hot-plate to fumes of perchloric acid. Heat with hydrochloric acid to drive off nitric acid, repeating the treatment twice, cool, transfer the sol-

Table 2. Potentiometric selectivity coefficients (separate solution method)

Foreign ion (j)	$K_{TlCl_4}^{Pot, j}$	Foreign ion (j)	$K_{TlCl_4}^{Pot, j}$
Na <sup>+</sup>	$3.9 \times 10^{-4}$	As <sup>3+</sup>	†
K <sup>+</sup>	$3.4 \times 10^{-4}$	Au <sup>3+</sup>	*
Mg <sup>2+</sup>	†	NO <sub>3</sub> <sup>-</sup>	$4.5 \times 10^{-4}$
Zn <sup>2+</sup>	†	PO <sub>4</sub> <sup>3-</sup>	$1.2 \times 10^{-6}$
Bi <sup>3+</sup>	$5.2 \times 10^{-6}$	ClO <sub>4</sub> <sup>-</sup>	$6.4 \times 10^{-2}$
Ga <sup>3+</sup>	$1.2 \times 10^{-5}$	I <sup>-</sup>	$2.6 \times 10^{-2}$
In <sup>3+</sup>	$6.7 \times 10^{-5}$	Br <sup>-</sup>	$9.5 \times 10^{-4}$
Al <sup>3+</sup>	$4.7 \times 10^{-6}$		

\*Severe interference.

†No interference.

Table 3. Determination of thallium

Sample*	Recommended value, ppm	Found, ppm	RSD, %
GBW07302	1.90	1.92	1.0
GBW07304	1.16	1.05	9.5
GBW07305	1.08	1.07	1.0
GBW07306	1.20	1.20	0.0

\*Chinese reference standard (formerly Chinese stream-sediment reference standard).

ution to a 50-ml standard flask, and dilute to volume with 0.5M sodium chloride/0.5M hydrochloric acid. Analyse for Tl(III). Table 3 shows typical results.

#### CONCLUSIONS

The carbon-coated PVC membrane electrode is a new type of PVC membrane electrode with good characteristics. The electrode is easy to prepare, convenient to use and preserve, inexpensive and reliable, and has a long lifetime. There is good adherence of the PVC membrane to the carbon rod, and the rod can be used repeatedly. The technique is extremely economical.

*Acknowledgement*—We thank Mr Xu Peifan and Mr Chang Huijun for experimental work.

#### REFERENCES

- P. J. McGoldrick, R. R. Keays and B. B. Scott, *Geochim. Cosmochim. Acta*, 1979, **43**, 1303.
- J. Hertogen, M. J. Janssen and H. Palme, *ibid.*, 1980, **44**, 2125.
- Dan Dezhong, Xu Peifang and Liu Lun, *Fenxi Huaxue*, 1987, **8**, 706.
- J. L. F. C. Lima and A. A. S. C. Machado, *Analyst*, 1986, **111**, 799.
- A. G. Fogg, A. A. Al-Sibai and N. Burgess, *Anal. Lett.*, 1975, **8**, 129.

# POTENTIAL RESPONSE OF LIQUID ION-EXCHANGE MEMBRANE ELECTRODES WITH A WEAK-ACID ANION AS PRIMARY ION, AND ITS DEPENDENCE ON pH

Z. MALÁ

Institute of Analytical Chemistry, Czechoslovak Academy of Sciences, Leninova 82, 611 42 Brno, Czechoslovakia

J. ŠENKÝŘ\*

Analytical Chemistry Department, J. E. Purkyně University, Kotlářská 2, 611 37 Brno, Czechoslovakia

(Received 10 August 1987. Revised 14 January 1988. Accepted 29 January 1988)

**Summary**—The potential of a liquid ion-exchange membrane electrode with a weak-acid primary anion has been studied in the pH range 1–12. A mathematical model has been designed for describing the dependence of the potential on pH and including changes of the activity of the primary anion  $A^-$  (of a mono- or dibasic acid) in a test solution, extraction of the membrane ion-exchanger into the test solution by protonation in the acidic region, and interference by  $HSO_4^-$  during adjustment of pH with sulphuric acid.

This paper is a part of a larger study dealing with the influence of pH on the potential response of liquid ion-selective electrodes (ISEs). The earlier studies concentrated on the interference of  $HSO_4^-$  on anion-exchange electrodes<sup>1</sup> and the influence, on the membrane potential response, of trace impurities in nitrobenzene used as a membrane solvent.<sup>2</sup> This paper is concerned with the potential response of anion-sensitive electrodes with a weak-acid anion as their primary ion, as a function of pH. Benzoic acid was chosen as the model of a monobasic acid, phthalic acid as a model dibasic acid. The dependence of the potential on pH has already been reported for benzoic and phthalic acids,<sup>3,4</sup> but has not been studied in detail. This work is concentrated on a mathematical description of the effect of pH changes on the potential of such ISEs. Thus it is necessary not only for understanding how such electrodes function at different pH values but also for selection of the optimal pH for their analytical use.

redistilled water, shaken with 1M ammonia solution, washed with water again, dried with an activated mixture of an aluminosilicate molecular sieve 4A and alumina and distilled under reduced pressure.

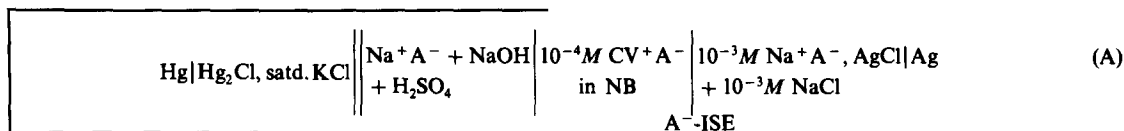
Crystal Violet ( $CV^+Cl^-$ ) was refined repeatedly by conversion into the free base with alkali, extraction into chloroform and stripping with an equivalent amount of hydrochloric acid. A membrane solution containing  $10^{-4}M$   $CV^+A^-$  ( $A^-$  represents the anion of the corresponding organic acid) was prepared by shaking 10 ml of purified NB with an aqueous mixture of 10 ml of  $10^{-4}M$   $CV^+Cl^-$  and 10 ml of  $10^{-2}M$   $Na^+A^-$ . After separation of the phases, the membrane solution was washed with redistilled water.

Sodium benzoate ( $Na^+Benz^-$ ) and sodium hydrogen phthalate ( $Na^+HPhthal^-$ ) were prepared from the corresponding acids of analytical reagent grade by neutralization with sodium hydroxide.

Sulphuric acid and sodium hydroxide of analytical reagent grade were used without further purification. The sodium hydroxide was used in the form of a 50% solution, containing only a negligible amount of sodium carbonate.

## Apparatus

The emf of the cell



The presence of weak acids in the test solution or in the membrane may be a source of serious interferences and distort the pH-characteristics of strong-acid anions.

## EXPERIMENTAL

### Reagents

Nitrobenzene (NB) of analytical reagent grade was shaken with 20% v/v sulphuric acid, then washed with

and the pH were measured with an MV 88 Präcitronic precision pH-meter (GDR).  $A^-$ -ISE in cell A was an electrode with a liquid membrane of  $10^{-4}M$   $CV^+A^-$  in NB ( $A^- = Benz^-$  or  $HPhthal^-$ ). The electrode body, which allows good reproducibility, has already been described.<sup>5</sup> A Radiometer K 401 saturated calomel electrode, and G 202 B glass electrode were used.

### Procedure

The 50% sodium hydroxide solution was added by micropipette to  $10^{-3}$ ,  $10^{-4}$  or  $10^{-5}M$   $Na^+A^-$  solution to give a pH of ca. 12.3. The pH was then decreased stepwise by addition of 50% v/v sulphuric acid from a micropipette, so

\*Author for correspondence.

that the total volume of the measured solution remained practically unchanged. The emf of cell A was then measured at each pH value (at  $25 \pm 1^\circ$ , in unstirred solution).

#### Relationships used

The equilibrium concentrations of the ions  $[L^-]$  (a monobasic acid anion) or  $[HL^-]$  (a dibasic acid anion) can be expressed by means of the total analytical concentration:

$$c_{HL} = [HL] + [L^-] \quad (1)$$

$$c_{H_2L} = [H_2L] + [HL^-] + [L^{2-}] \quad (2)$$

and corresponding dissociation constants  $K'_1$  or  $K''_1$  and  $K''_2$ :

$$K'_1 = \frac{[H^+][L^-]}{[HL]} f_{H^+} f_{L^-} \quad (3)$$

$$K''_1 = \frac{[H^+][HL^-]}{[H_2L]} f_{H^+} f_{HL^-} \quad (4a)$$

$$K''_2 = \frac{[H^+][L^{2-}]}{[HL^-]} \frac{f_{H^+} f_{L^{2-}}}{f_{HL^-}} \quad (4b)$$

By combination of (1) and (3), or (2), (4a) and (4b), expressions for  $[L^-]$  or  $[HL^-]$  can be obtained:

$$[L^-] = \frac{c_{HL}}{1 + [H^+] f_{H^+} f_{L^-} / K'_1} \quad (5)$$

$$[HL^-] = \frac{c_{H_2L}}{1 + K''_2 f_{HL^-} / [H^+] f_{H^+} f_{L^{2-}} + [H^+] f_{H^+} f_{HL^-} / K''_1} \quad (6)$$

The total ionic strength  $I$  in the measured solution changes during evaluation of  $E = f(\text{pH})$  by about an order of magnitude. The relationship for  $I = f(\text{pH})$  was derived earlier:<sup>1</sup>

$$I = \frac{(10^{-m} - 10^{m-pK_w} + [Na^+] - [A^-])(1 + 3 \times 10^9)}{1 + 2 \times 10^9 + [A^-] + 10^{m-pK_w}} \quad (7)$$

where  $m = \text{pH} + \log f_{H^+}$ ,  $n = \text{pH} - pK_{2(H_2SO_4)} + \log f_{HSO_4^-} - \log f_{SO_4^{2-}}$ ,  $K_w$  is the ionic product for water and  $[A^-]$  is the equilibrium concentration of the primary anion. The contribution of  $[L^{2-}]$  to the total ionic strength is negligible and it is not taken into account in equation (7).

The values of the molar activity coefficients  $f_i$  for ionic strengths  $I$  up to  $0.2M$  were calculated from the extended Debye-Hückel equation

$$-\log f_i = \frac{0.509 \sqrt{I}}{1 + 0.33 a_i \sqrt{I}} \quad (8)$$

where  $a_i$  is the Kieland parameter for ion  $i$  and  $I$  is expressed by equation (7) for  $f_i = 1$ . The values were obtained by iteration.

Provided that undissociated HL or  $H_2L$ , and  $L^{2-}$  do not give a potential response with the corresponding ISE, it is possible to express the emf of the cell A in the presence of interfering bisulphate anions by the Nikolskii equation

$$E = E_0 - S \log(a_A^* - + k_{A^-, HSO_4^-}^{\text{Pot}}(\text{app.}) a_{HSO_4^-}) \quad (9)$$

where  $a_A^*$  is the activity of the primary anion ( $L^-$  or  $HL^-$ ) in the measured solution close to the membrane surface,  $E_0$  is the emf for  $a_{A^-, HSO_4^-} = 1$  and  $a_{HSO_4^-} = 0$ ,  $S$  is the response slope of the A<sup>-</sup>-ISE and  $k_{A^-, HSO_4^-}^{\text{Pot}}(\text{app.})$  is an apparent concentration-dependent selectivity coefficient,<sup>6</sup> the value of which can be calculated from the equation<sup>7</sup>

$$k_{A^-, HSO_4^-}^{\text{Pot}}(\text{app.}) = \frac{1}{2} \{A(1 - B) - C + \{[A(1 - B) + C]^2 + 4AB(C + U_{HSO_4^-}/U_{A^-})\}^{1/2}\} \quad (10)$$

where  $A = k_{A^-, HSO_4^-}^{\text{Pot}}$ ,  $B = Q/a_{HSO_4^-}$ ,  $C = a_A^*/a_{HSO_4^-}$ ;  $A$  is a concentration-independent selectivity coefficient,  $Q$  is the critical concentration of the membrane,<sup>7</sup>  $U$  is the mobility (in water) of the ion indicated by subscript. The calculation was done with the following values:

$$k_{\text{Benz}^-, HSO_4^-}^{\text{Pot}} = 1.52 \times 10^{-2}, \quad k_{\text{HPhthal}^-, HSO_4^-}^{\text{Pot}} = 5.62 \times 10^{-5},$$

$$Q = 5 \times 10^{-5} M, \quad \text{and} \quad U_{HSO_4^-}/U_{\text{Benz}^-} = U_{HSO_4^-}/U_{\text{HPhthal}^-} = 2.$$

The activity  $a_A^*$  of the primary anion  $A^-$  close to the membrane surface includes the equilibrium activity  $a_{A^-}$  of the anion  $A^-$  in the bulk of the measured solution, increased by a quantity extracted from the membrane,  $a_D^*$ , and a contribution caused by protonation of  $CV^+$  at low pH.  $a_A^*$  can be expressed approximately by the relationship derived earlier,<sup>1</sup>

$$a_A^* = \frac{1}{2} \{a_{A^-} + [a_{A^-}^2 + 4(K_{\text{prot}} 10^{-\text{pH}} + 1)a_D^{*2}]^{1/2}\} \quad (11)$$

where  $a_{A^-} = [A^-] f_{A^-}$  and  $[A^-]$  is given by relationship (5) or (6), and similarly

$$a_D^* = a_D \left/ \left( 1 + \frac{[H^+]}{K'_{HL}} f_{H^+} f_{L^-} \right) \right. \quad (12)$$

or

$$a_D^* = a_D \left/ \left( 1 + \frac{K''_{2, H_2L} f_{HL^-}}{[H^+] f_{H^+} f_{L^{2-}}} + \frac{[H^+]}{K''_{1, H_2L}} f_{H^+} f_{HL^-} \right) \right. \quad (13)$$

where  $a_D$  is the detection limit<sup>8</sup> of the A<sup>-</sup>-ISE used,  $K_{\text{prot}}$  is the protonation constant of  $CV^+ + H^+ \rightleftharpoons HCV^{2+}$  in the aqueous medium; for calculations the value  $K_{\text{prot}} = 21$ , determined photometrically, was used.

The following relationship<sup>1</sup> was derived for the  $HSO_4^-$  activity as a function of pH

$$a_{HSO_4^-} = \frac{10^{-m}(10^{-m} + [Na^+] - [A^-])}{(10^{-m} - \log f_{HSO_4^-} + 2K_2/f_{H^+} f_{SO_4^{2-}})} \quad (14)$$

where  $m = \text{pH} + \log f_{H^+}$  and  $K_2$  is the dissociation constant

$$K_2 = a_{H^+} a_{SO_4^{2-}} / a_{HSO_4^-}$$

The values<sup>9</sup> of the thermodynamic dissociation constants  $K_A$  and the experimentally determined detection limits  $a_D$  are given in Table 1.

## RESULTS AND DISCUSSION

Figure 1 shows the dependence of the Benz<sup>-</sup>-ISE potential on pH for  $c_{HL} = 10^{-3}M$  (curve 1),  $10^{-4}M$  (curve 2) and  $10^{-5}M$  (curve 3). (Individual curves are, for easier reading, shifted along the potential axis.) At  $\text{pH} > 5.7$  the potential is constant with reproducibility of  $\pm 0.5$  mV, benzoic acid is dissociated completely and the electrode may be used for analytical determinations. This experimental result is in accordance with the theory: if the Benz<sup>-</sup>-ISE potential is expressed (in a simplified way) by means of relationship (5),  $E = E_0 - S \log\{c_{HL}/(1 + [H^+]/K'_1)\}$ , the significant change of  $\Delta E > 1$  mV (*i.e.*, increasing potential with decreasing pH) is given by  $S \log(1 + [H^+]/K'_1) > 1$ , and the solution of this inequality for  $S = 59$  mV/pH is the relationship  $\text{pH} < pK'_1 + 1.4$  (*i.e.*, for the Benz<sup>-</sup>-ISE  $\text{pH} < 5.6$ ), which is valid generally for all the weak monobasic acids.

With decreasing pH the potential increases in the same way as the primary anion activity decreases, owing to formation of the non-dissociated acid [the dashed line calculated according to relationship (5)]. With further decrease in pH the  $HSO_4^-$  anion inter-

Table 1. Constants used

Anion	$pK_A$	$pa_D$
$HSO_4^-$	1.99	—
Benz <sup>-</sup>	4.19	4.62
HPhthal <sup>-</sup>	2.95	5.95
	5.41	

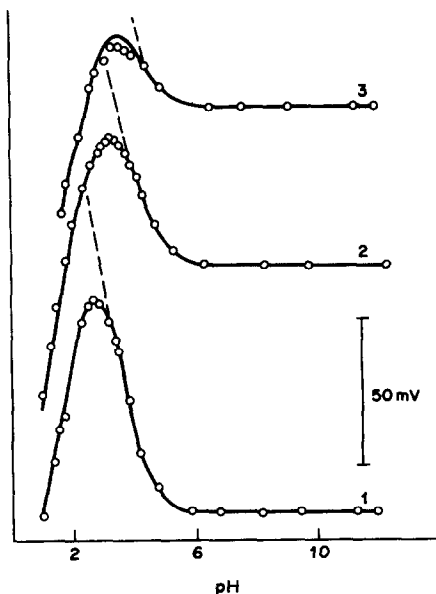


Fig. 1. Dependence of the emf of the Benz<sup>-</sup>-ISE as a function of pH. Membrane  $1 \times 10^{-4} M$  CV<sup>+</sup>Benz<sup>-</sup> in NB. Measured solution: (1)  $1 \times 10^{-3} M$  Na<sup>+</sup>Benz<sup>-</sup>; (2)  $1 \times 10^{-4} M$  Na<sup>+</sup>Benz<sup>-</sup>; (3)  $1 \times 10^{-3} M$  Na<sup>+</sup>Benz<sup>-</sup>.

ference (due to addition of H<sub>2</sub>SO<sub>4</sub>) appears as well as, at lower values of  $c_{HL}$ , extraction of the CV<sup>+</sup>Benz<sup>-</sup> ion-exchanger (determining  $a_D^*$ ) from the membrane into the measured solution, and protonation of CV<sup>+</sup>.<sup>1</sup> The circles mark the points obtained experimentally, the full line is the theoretical dependence calculated according to relationship (9) by using relationships (10)–(12) and (14), including all the mentioned influences. For the solution with  $c_{HL} = 10^{-3} M$ , only the HSO<sub>4</sub><sup>-</sup> interference appears. The influence of extraction and protonation is negligible because  $c_{HL}$  is approximately two orders of magnitude higher

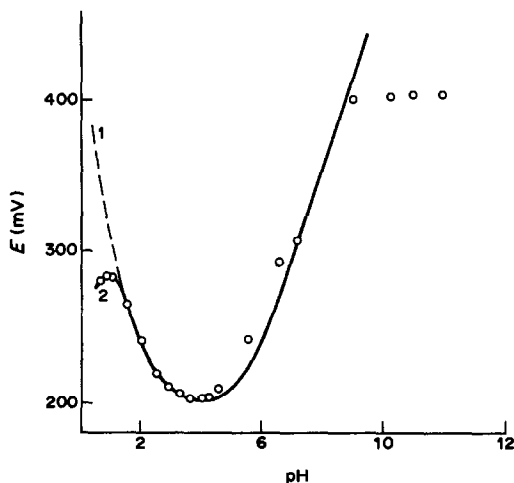


Fig. 2. Dependence of the emf of the HPhthal<sup>+</sup>-ISE as a function of pH. Membrane:  $1 \times 10^{-4} M$  CV<sup>+</sup>HPhthal<sup>-</sup> in NB. Measured solution:  $1 \times 10^{-4} M$  Na<sup>+</sup>HPhthal<sup>-</sup>.

than the detection limit  $a_D$  of the Benz<sup>-</sup>-ISE. With decreasing  $c_{HL}$  the influence of the extraction and interference of HSO<sub>4</sub><sup>-</sup> is more marked. The influence of CV<sup>+</sup> protonation appears at pH  $\leq 3$  in those cases when the influence of extraction on  $a_D^*$  cannot be neglected. The necessity of correcting  $k_{Benz^-, HSO_4^-}^{Pot}$  according to relationship (10) appears at pH = 2.3–3.2 where  $a_{HSO_4^-}$  is close to the critical value of  $Q = 5 \times 10^{-3} M$ . The value of  $k_{Benz^-, HSO_4^-}^{Pot}$  was determined indirectly by means of a Cl<sup>-</sup>-ISE and calculation from:

$$\log k_{Benz^-, HSO_4^-}^{Pot} = \log k_{Benz^-, Cl^-}^{Pot} + \log k_{Cl^-, HSO_4^-}^{Pot}^{-1}$$

Good correspondence between the theoretical and experimental curves certifies that the given mathematical model includes all the important factors influencing the Benz<sup>-</sup>-ISE potential. At the curve maximum, where various contradictory influences act most sensitively, the theoretical curve differs from the experimental one by only 0.5 mV for  $c_{HL} = 10^{-3} M$ , 1.3 mV for  $c_{HL} = 10^{-4} M$  and 6 mV for  $c_{HL} = 10^{-5} M$ .

Figure 2 shows the pH-dependence of the HPhthal<sup>-</sup>-ISE potential for  $c_{HL} = 10^{-4} M$ . Phthalic acid, as a dibasic acid, shows the maximum of the function  $[HL^-] = f(pH)$  according to equation (6) at pH =  $(pK_1 + pK_2)/2 = 4.18$ , to which the minimum on curves 1 and 2 corresponds. Curve 1 represents the theoretical dependence where the primary ion activity is expressed by relationship (6). The full curve 2 includes the influence of HSO<sub>4</sub><sup>-</sup> interference, extraction of CV<sup>+</sup> from the membrane and the consequent protonation of CV<sup>+</sup>. It was calculated from relationships (9)–(11), (13) and (14). It is in very good agreement with the experimentally obtained points (circles) in the acidic region. Towards the alkaline region, the correspondence between experiment and theory is less satisfactory. At pH > 9 and in the absence of HPhthal<sup>-</sup>, the potential response is influenced by traces of impurities from the NB, most probably by the anion of nitrophenol.<sup>2</sup> For practical purposes, this electrode can be used if the pH in the measured solution is adjusted precisely to the value at the minimum of the curve.

#### REFERENCES

1. J. Šenkýř and Z. Malá, *J. Electroanal. Chem.*, 1987, **233**, 267.
2. Z. Malá and J. Šenkýř, *Talanta*, in the press.
3. C. J. Coetzee and H. Freiser, *Anal. Chem.*, 1969, **41**, 1128.
4. A. Jyo, M. Yonemitsu and N. Ishibashi, *Bull. Chem. Soc. Japan*, 1973, **46**, 3734.
5. J. Šenkýř and J. Petr, *Chem. Listy*, 1979, **73**, 1097.
6. R. P. Buck, *Anal. Chim. Acta*, 1974, **73**, 321.
7. J. Šenkýř and J. Petr, in *Ion Selective Electrodes*, E. Pungor and I. Buzás (eds.), p. 327. Akadémiai Kiadó, Budapest, 1981.
8. *Pure Appl. Chem.*, 1976, **48**, 128.
9. L. G. Sillén and A. E. Martell, *Stability Constants of Metal-Ion Complexes*, 2nd Ed., The Chemical Society, London, 1964.

## SEPARATION OF SELENIUM(IV) AND TELLURIUM(IV) FROM MIXTURES BY EXTRACTION CHROMATOGRAPHY WITH TRIOCTYLPHOSPHINE OXIDE

R. B. HEDDUR and S. M. KHOPKAR

Department of Chemistry, Indian Institute of Technology, Bombay-400 076, India

(Received 22 May 1986. Revised 18 January 1988. Accepted 28 January 1988)

**Summary**—The reversed-phase extraction chromatographic separation of selenium(IV) and tellurium(IV) from several elements with trioctylphosphine oxide as extractant is reported. Selenium was extracted from 6M hydrochloric acid containing 7M lithium chloride and was stripped with 4M hydrochloric acid, and tellurium was extracted from either the same medium as selenium or from 4M hydrochloric acid, and stripped with 1–2M hydrochloric acid. Selenium and tellurium can be separated from multicomponent mixtures.

Extraction chromatography with TBP has been used for the separation of selenium(IV) and tellurium(IV) from other species.<sup>1–3</sup> Trioctylamine<sup>4,5</sup> has been utilized for the separation of tellurium(IV) from tin, lead and antimony(V), and Amberlite LA-2<sup>6</sup> for its separation from indium. Bis(2-ethylhexyl)phosphoric acid (HDEHP) has also been used for the separation of tellurium and antimony. However, the chromatographic behaviour of selenium(IV) and tellurium(IV) with trioctylphosphine oxide has not hitherto been reported.

### EXPERIMENTAL

#### Apparatus

The chromatographic column was made of a borosilicate glass tube, bore 8 mm, length 20 cm, fitted with a glass-wool plug at the base.

#### Reagents

A 0.1M trioctylphosphine oxide (TOPO) solution was prepared by dissolving 1.94 g of the reagent (Merck) in 100 ml of toluene.

Silica gel (BDH) (60–120 mesh) was dried at 120° for 2 hr and stored in a desiccator. Some of the silica gel was packed in a U-tube through which was passed a stream of dry nitrogen that had been bubbled through a small Durand bottle containing about 20 ml of dimethyldichlorosilane (DMCS). The passage of DMCS vapour was continued for 2–3 hr. The silica gel was then washed with anhydrous methanol and dried. A 3-g portion of the silanated silica gel was soaked in 5 ml of 0.1M TOPO in toluene for 24 hr. The solvent was then evaporated till the gel was nearly dry. A slurry of the coated silica gel in distilled water was prepared by centrifugation at 2000 rpm and the coated silica gel was packed into the chromatographic column to give a bed height of 8 cm. The bed was then covered with a glass wool plug and the column covered with opaque paper to avoid photochemical degradation of the extractant.

The stock solution of selenium(IV) was prepared by fusing 500 mg of powdered selenium with sodium hydroxide. The fused mass, after cooling, was extracted with water and the solution made up to 100 ml with addition of sufficient hydrochloric acid to give a final 1% v/v concentration of the acid. The solution was standardized by precipitation of elemental selenium<sup>7</sup> and found to contain

4.50 mg/ml selenium(IV). A 60 µg/ml solution was then prepared by appropriate dilution.

The stock solution of tellurium was prepared by dissolving 500 mg of powdered tellurium in *aqua regia*. The solution was evaporated to dryness and the residue taken up in water, and the solution made up to 100 ml to contain 1% v/v hydrochloric acid. The solution was standardized gravimetrically<sup>8</sup> with weighing as elemental tellurium. It contained 5.00 mg/ml tellurium(IV). A 50 µg/ml solution was prepared by appropriate dilution.

#### General procedure

An aliquot of solution was made 6M in hydrochloric acid and 7M in lithium chloride for extraction of selenium, or 4M in hydrochloric acid for extraction of tellurium. The solution was passed through the coated silica gel column at 0.5 ml/min. The selenium or tellurium extracted was stripped with mineral acids and salt solutions. Twenty 2-ml fractions were collected, which were analysed for selenium spectrophotometrically at 345 nm with 3,3'-diaminobenzidine<sup>9</sup> and tellurium(IV) as its iodide complex at 340 nm.<sup>10</sup>

### RESULTS AND DISCUSSION

#### Extraction studies

It was observed that there was no extraction of selenium(IV) from 1–6M hydrochloric acid. Addition of lithium chloride (as salting-out agent) to 6M hydrochloric acid increased the retention of selenium(IV). Extraction of selenium(IV) was quantitative from 6M hydrochloric acid containing 7M lithium chloride.

Similar studies showed that retention of tellurium(IV) on the column was quantitative from 4–6M hydrochloric acid and also from 6M hydrochloric acid containing 7M lithium chloride. At lower concentration of hydrochloric acid (1–3M) tellurium(IV) was not isolated on the column.

#### Stripping agents

Selenium was found to be stripped by 1–6M solutions of all mineral acids or their salts and tellu-



Table 1

Metal ion ( $\mu\text{g}$ )	Extraction conditions, [HCl], M.	Stripping agents
Gallium (15)	1.5-6	0.1-1M HCl, HNO <sub>3</sub> , H <sub>2</sub> SO <sub>4</sub> ; NaCl, NH <sub>4</sub> NO <sub>3</sub> and H <sub>2</sub> O
Indium (75)	2-6	0.01-0.5M HCl; 0.01-1M HNO <sub>3</sub> , H <sub>2</sub> SO <sub>4</sub> ; 0.5-2M NaCl, NH <sub>4</sub> NO <sub>3</sub> and H <sub>2</sub> O
Germanium (22)	4-6	0.1-4M HCl; 0.25-3M HNO <sub>3</sub> , H <sub>2</sub> SO <sub>4</sub> ; 0.5-2M NaCl, NaNO <sub>3</sub> ; NH <sub>4</sub> Cl and H <sub>2</sub> O
Tin(IV) (59)	0.5-6	0.5-4M HNO <sub>3</sub>
Antimony(III) (60)	0.25-0.75	2-5M HCl, HNO <sub>3</sub> , H <sub>2</sub> SO <sub>4</sub>
Bismuth (96)	0.5	1.5-4M HCl; 3-7M HNO <sub>3</sub> ; 1-4M H <sub>2</sub> SO <sub>4</sub>
Selenium(IV) (60)	6 + 7M LiCl	1.6M HCl, HNO <sub>3</sub> , H <sub>2</sub> SO <sub>4</sub> ; 1-7M LiCl, NaNO <sub>3</sub>
Tellurium(IV) (50)	4-8	0.1-3M HCl, HNO <sub>3</sub> , H <sub>2</sub> SO <sub>4</sub> ; 1-3M LiCl, NaNO <sub>3</sub> and H <sub>2</sub> O

rium(IV) with 1-3M solutions of the mineral acids or salts (Table 1).

*Separation of selenium(IV) or tellurium(IV) from binary mixtures with other ions*

Selenium(IV) was extracted from 6M hydrochloric acid containing 7M lithium chloride [or tellurium(IV) with 4M hydrochloric acid] in the presence of any of the other ions added, the latter passing through the

column. The selenium(IV) or tellurium(IV) extracted could be stripped with 6M or 1M hydrochloric acid respectively. It was possible to separate selenium(IV) or tellurium(IV) from any of the elements in the binary mixtures in concentration ratios of 1:200.

*Applications*

Separation schemes can be worked out from the following information. Cu(II), Cd, Mn(II), Co, Tl(I),

Table 2. Separation of selenium(IV) from multicomponent mixtures

Mixture	Taken, $\mu\text{g}$	Found, $\mu\text{g}$	Recovery, %	Eluent	Eluent volume ml	
1	Cu	51	50.5	99	6M HCl/7M LiCl*	10
	Se(IV)	60	60.2	100.3	6M HCl	10
	Te(IV)	180	178	98.9	1M HCl	12
2	Cd/Mn	70	69	98.6	6M HCl/7M LiCl*	8
	Se(IV)	60	59.5	99.2	6M HCl	10
	Sc	50	50.5	101	2M HCl	10
3	Co/Tl(I)	80	80.5	100.6	6M HCl/7M LiCl*	8
	Se(IV)	60	59	98.3	6M HCl	10
	Th	50	50	100	2M HCl	10
	Ga	15	14.7	98	0.1M HCl	8
4	Ni	50	48.5	99	6M HCl/7M LiCl*	8
	Se(IV)	60	60.2	100.3	6M HCl	10
	Ge	22	22.1	100.5	2M HCl	12
	Fe(III)	62.5	63	100.8	0.25M HCl	16
	Mo(VI)	50	49.6	99.2	0.1M HCl	16
5	Pb/Mg	75	75.5	100.7	6M HCl/7M LiCl*	8
	Se(IV)	60	59.8	99.7	6M HCl	10
	Zr	75	75	100	2M HCl	10
	Ga	75	74.8	98.8	0.1M HCl	8
	Cr(VI)	51	50	98	H <sub>2</sub> O	22
6	Al	70	71	101.4	6M HCl/7M LiCl*	8
	Se(IV)	60	60.5	100.8	6M HCl	10
	Te(IV)	180	180	100	1M HCl	12
	Sn(IV)	59	59.2	100.3	2M HNO <sub>3</sub>	10
	Au(III)	100	99	99	7M HNO <sub>3</sub>	14

\*Sample solution medium.

Table 3. Separation of tellurium(IV) from multicomponent mixtures

	Mixtures	Taken, μg	Found, μg	Recovery, %	Eluent	Eluent volume, ml
1	Pb	75	76	101.3	6M HCl/7M LiCl*	8
	Se(IV)	60	59.5	99.2	6M HCl	10
	Te(IV)	50	49.8	99.6	1M HCl	12
2	Ni/As(III)	50	49.5	99	4M HCl	8
	Te(IV)	50	50.1	100.2	2M HCl	16
	Fe(III)	62.5	63	110.8	0.25M HCl	14
	Mo(VI)	50	51	102	0.1M HCl	16
3	Co	80	80.3	100.6	5M HCl	8
	Ge	22	21.8	99.1	4M HCl	30
	Te(IV)	50	49.8	99.6	2M HCl	16
	Ga	15	15.3	102	0.1M HCl	8
	Sn(IV)	59	59.2	100.3	2M HNO <sub>3</sub>	10
4	Cu	51	50.5	99	6M HCl/7M LiCl	10
	Se(IV)	60	60.2	100.3	6M HCl	10
	Te(IV)	50	50.2	100.4	1M HCl	12
	Cr(VI)	51	50	98	H <sub>2</sub> O	22
5	Mg	75	75.5	100.7	4M HCl	8
	Te(IV)	50	50	100	2M HCl	16
	In	75	74.1	98.8	0.25M HCl	20
	Mo(VI)	50	50.5	101	0.1M HCl	16
	Cr(VI)	51	50	98	H <sub>2</sub> O	22
	Tl(III)	100	99	99	5% hydrazine sulphate/ 0.5M H <sub>2</sub> SO <sub>4</sub>	12
6	Cu	51	50.2	98.4	6M HCl/7M LiCl	10
	Se(IV)	60	59.5	99.2	6M HCl	10
	Ge	22	22.2	101.9	4M HCl	30
	Te(IV)	50	49.5	99	1M HCl	12
	Sn(IV)	59	59.2	100.3	2M HNO <sub>3</sub>	10
	Au(III)	100	101	101	7M HNO <sub>3</sub>	14

Ni, Pb, Mg and Al are not extracted by the column from 6M hydrochloric acid/7M lithium chloride medium, but Sc, Th, Zr, Ge, Ga, Fe(III), Mo(VI), Cr(VI), In, Se(IV) and Te(IV) are quantitatively extracted and can be stripped in the following order: Se(IV) with 6M hydrochloric acid, Ge with 4M hydrochloric acid, Te(IV), Sc, Th, and Zr with 2M hydrochloric acid, Fe(III) and In with 0.25M hydrochloric acid, Mo(VI) and Ga with 0.1M hydrochloric acid, Cr(VI) with water. Ge can be quantitatively extracted from 5M hydrochloric acid and stripped with the 4M acid.

Sn(IV), Au(III) and Tl(III) are also quantitatively extracted and can be stripped (after Se, Ge and Te) with 2M nitric acid, 7M nitric acid and 0.5M sulphuric acid/5% hydrazine sulphate solution respectively.

Te(IV) cannot be separated from Sc, Th and Zr; it can be stripped with 1–3M hydrochloric acid.

Some results for analysis of various multicomponent mixtures are given in Tables 2 and 3 to illustrate the efficiency of the system. All elements were determined spectrophotometrically.<sup>11</sup>

The separation of selenium from iron, lead, arsenic, bismuth, copper, nickel and cobalt is im-

portant, as they are associated with selenium in minerals. The separation of tellurium from lead, bismuth, iron, copper and antimony is of significance as they are present in tellurium minerals. The time required for separation and determination is about 2 hr.

#### REFERENCES

1. L. N. Moskvina, *Radiokhimiya*, 1964, **6**, 110.
2. J. Mikulski and I. Stronski, *Nukleonika*, 1961, **6**, 775.
3. R. Denning, N. Trautmann and G. Herrmann, *J. Radioanal. Chem.*, 1970, **6**, 331.
4. J. Mikulski, *Nukleonika*, 1966, **11**, 57.
5. I. P. Alimarin, E. V. Skobelkina, T. A. Bolshova and N. B. Zorov, *Zh. Analit. Chem.*, 1978, **33**, 1318.
6. I. Stronski, *Radiochem. Radioanal. Lett.*, 1970, **C5**, 113.
7. R. Denning, N. Trautmann and G. Herrmann, *J. Radioanal. Chem.*, 1970, **6**, 57.
8. A. I. Vogel, *A Text Book of Quantitative Inorganic Analysis*, 3rd Ed., p. 508. Longmans, London, 1961.
9. A. I. Busev, V. B. Tiptsova and V. M. Ivanov, *Analytical Chemistry of Rare Elements*, p. 359, Mir, Moscow, 1981.
10. D. F. Boltz, *Colorimetric Determination of Nonmetals*, p. 323. Interscience, New York, 1958.
11. E. B. Sandell, *Colorimetric Determination of Traces of Metals*, 3rd Ed., Interscience, New York, 1959.

## CONSTANT-CURRENT STRIPPING ANALYSIS FOR IRON(III) BY ADSORPTIVE ACCUMULATION OF ITS SOLOCHROME VIOLET RS COMPLEX ON A CARBON-FIBRE ELECTRODE

CHI HUA, DANIEL JAGNER and LARS RENMAN

Department of Technical Analytical Chemistry, Chemical Centre, University of Lund, P.O. Box 124,  
S-221 00 Lund, Sweden

(Received 2 December 1987. Revised 30 March 1988. Accepted 12 April 1988)

**Summary**—The optimum experimental conditions with respect to pH, adsorption potential and Solochrome Violet RS concentration for the constant-current stripping determination of iron(III) have been investigated. The suggested procedure has been used for the determination of iron(III) in tap water and the accuracy investigated both by analysing standard solutions and by comparison with results obtained by atomic-absorption spectrometry. The relative precision was 6–13% and the detection limit for iron(III), set by the reagent blank, was approximately 1 µg/l. The results obtained with a mercury-film coated carbon-fibre flow electrode have been compared with those obtained with a hanging mercury drop electrode. The advantages of measuring electrode potential *vs.* time instead of *vs.* current have been evaluated.

In recent years a large number of methods have been reported for the determination of various trace elements, based on adsorptive accumulation at a constant electrode potential and subsequent electrochemical reduction and desorption (stripping).<sup>1</sup> Among the main advantages of this technique are high sensitivity and simple instrumentation. The adsorbed complex of the element can be reduced according to two main principles. In that most frequently exploited, reduction is performed by means of a cathodic potential ramp during which the reduction current is monitored as a function of the electrode potential. Alternatively, the reduction can be performed by applying a constant current through the working electrode, with simultaneous monitoring of electrode potential *vs.* time. The latter approach, which is referred to here as constant-current stripping analysis, has previously been exploited in the determination of molybdenum(VI),<sup>2</sup> uranium(VI),<sup>3</sup> cobalt(II),<sup>4</sup> nickel(II)<sup>4</sup> and some electroactive drugs.<sup>5</sup> As demonstrated in those papers, computerized constant-current stripping analysis has the distinct advantage that samples can be analysed without deoxygenation, and also, when a multiple scanning mode is used, the range of linearity between analytical signal and analyte concentration is extended considerably. Furthermore, when the technique is used in the flow mode the analyses can be highly automated.

Owing to the need for sensitive methods for the determination of iron(III), various reagents likely to be suitable for adsorptive stripping analysis for iron(III) have been investigated. Van den Berg and Huang have suggested the use of catechol for the

adsorptive determination of iron(III).<sup>6</sup> This reagent, however, suffers from insufficient selectivity with respect to iron(II), lead(II) and copper(II). Consequently, the present work focuses on the use of Solochrome Violet RS (SVRS), a reagent which has previously been used by Latimer<sup>7</sup> and Rooney and McIver<sup>8</sup> for the polarographic determination of iron(III). During the final stages of this investigation Wang and Mahmoud<sup>9</sup> published an adsorptive stripping method for iron(III), based on use of this reagent. Even though their instrumental method, monitoring of current *vs.* potential, differs from the present method of constant-current stripping, and their working electrode, the hanging mercury drop electrode, differs from the present mercury-coated carbon-fibre flow electrode, the reduction mechanism at the electrode surface is the same. For this reason all mechanistic discussions have been omitted from this paper.

To demonstrate the utility of the present method and to permit comparison with the Wang and Mahmoud<sup>9</sup> approach a complete analytical procedure for the determination of iron(III) in tap water has been devised.

### EXPERIMENTAL

#### Instrumentation

A laboratory-constructed computerized potentiometric and constant-current stripping analyser was used in all investigations. With this instrument six different solutions can be drawn into the flow-cell in any selected order by means of a peristaltic pump, and the electrode potential, flow-rate, magnitude of stripping current and opening and closing of magnetic valves are all under computer control. After recording the analytical and background potential *vs.*

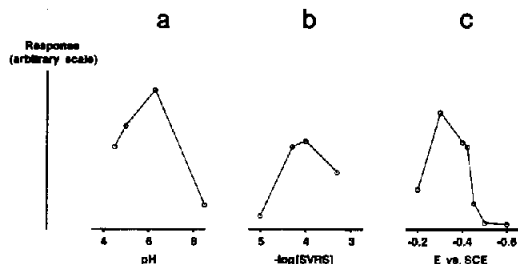


Fig. 1. Effect of (a) pH (b) SVRS concentration and (c) adsorption potential on the stripping peak area for iron(III).

time transients with a real-time sampling rate of 25.6 kHz and a potential resolution of 1 mV, the analyser performs differentiation, digital filtration, background subtraction, stripping-peak location and integration and, finally, evaluation and graphical presentation of the analytical results, obtained by either a calibration curve or standard-addition procedure. The analyser<sup>10</sup> and several applications<sup>11-13</sup> have been described in detail elsewhere. In all investigations reported here an averaging filter of 30 mV and a Savitzky-Golay filter of 15 mV were used.

The drinking water samples were also analysed by graphite-furnace atomic-absorption spectrometry (Varian AA-1475).

In the batch procedure a Princeton Research Model 303 hanging mercury drop electrode (HMDE) (small drop size) was used in combination with a platinum wire counter-electrode and a calomel reference electrode.

#### Flow electrode

A 10  $\mu\text{m}$  diameter carbon fibre, inserted perpendicular to the direction of flow in a poly(vinyl chloride) tube with an inner diameter of 0.80 mm, was used as the working electrode.<sup>14</sup> Downstream from this electrode a platinum tube and a thin-layer cell saturated calomel electrode (SCE) were used as the counter-electrode and reference electrode, respectively.<sup>10</sup> All potentials cited below are vs. SCE.

#### Reagent and solutions

All chemicals were of analytical grade except the nitric acid and sodium acetate, which were of Suprapur grade (Merck). All dilutions were made with "Millipore" water. A stock solution of SVRS ( $10^{-3}M$ ) (Pfaltz and Bauer, Inc., USA) was prepared by dissolving the reagent in water. A stock solution of iron(III) (1 g/l.) was prepared by dissolving atomic-absorption standards (pH Tamm, Sweden) in water. Drinking water samples were taken from the water tap in the laboratory after at least one minute of free running.

The mercury-film plating solution consisted of 100 mg/l. mercury(II) nitrate in 0.10M nitric acid.

#### Mercury-film surface renewal

Before each analysis the mercury-film surface was renewed by applying a potential of  $-1.80$  V with the electrode system in the mercury plating solution, for 10 sec.

#### Procedure for iron(III) in tap water

Add 0.40 ml of concentrated nitric acid to 40 ml of tap water and allow the mixture to stand at room temperature for at least 30 min in order to permit dissolution of all hydroxide particles. Add 10 ml of 1M sodium acetate, 5 ml of  $10^{-3}M$  SVRS and make up to 100 ml with water. The resulting mixture should have a pH of 4.5. Perform the same procedure with another 40-ml tap water sample to which an iron(III) spike equivalent to 25  $\mu\text{g/l.}$  has been added.

Place the solutions at two of the inlets of the analyser, perform the mercury-film renewal procedure and electrolyse

the sample at a potential of  $-0.42$  V for 8 sec and a flow-rate of 0.40 ml/min prior to stripping the sample with a constant current of 1.5  $\mu\text{A}$  until a potential of  $-1.30$  V is reached. After 5 sec at this potential apply a potential of  $-0.42$  V for 1 sec and record a background scan over the same potential interval. Repeat the recording of the analytical and the background scans seven times.

In the digital evaluation procedure, the analyser subtracts the accumulated background scans from the accumulated analytical scans, locates the stripping peak potential by searching the potential interval from  $-0.58$  to  $-0.80$  V and, finally, integrates the peak over an interval of  $\pm 0.09$  V around the peak potential. The stripping time thus obtained is displayed on the printer/plotter together with a graph of the stripping curve. The analytical procedure is repeated on the sample to which iron(III) has been added and the sample concentration of iron(III) is automatically evaluated by use of the standard-addition equation.

## RESULTS

### Optimum pH, SVRS concentration and adsorptive deposition potential

The effect of pH on the area of the stripping peak was investigated by using the procedure described above for tap water, with a solution containing 10  $\mu\text{g/l.}$  iron(III). The results, displayed in Fig. 1(a), show that the sensitivity increases as the pH is increased from 4 to 7, above which it decreases. Even so, pH 4.5 was chosen for the tap water analysis, the reason being that at this pH the conditional constants for the SVRS complexes of likely interferents are too small for these complexes to be formed in appreciable amounts.<sup>15</sup>

The effect of SVRS concentration at an adsorption potential of  $-0.45$  V and pH 4.5 is shown in Fig. 1(b). Obviously the SVRS concentration is not a very critical parameter and a concentration of  $5 \times 10^{-5}M$  was chosen for the analytical procedure.

The effect of adsorption potential on stripping peak area at pH 4.5 and  $5 \times 10^{-5}M$  total concentration of SVRS is shown in Fig. 1(c). Stripping peaks obtained with adsorption potentials more positive than  $-0.30$  V were broad and unsymmetrical, whereas those obtained after adsorption at more negative potentials were narrow and symmetrical. An adsorption potential of  $-0.42$  V was chosen as most suitable.

### Linear range, accuracy and detection limit

The range of linearity between stripping time and iron(III) concentration was investigated by analysing solutions containing 0–40  $\mu\text{g/l.}$  iron(III), according to the procedure above for tap water. No deviation from linearity was obtained in the range investigated ( $r = 0.998$ ,  $n = 8$ ). At concentrations above 50  $\mu\text{g/l.}$  deviation from linearity began, owing to surface saturation. The linear range could, of course, be extended by decreasing the electrolysis time.

The accuracy was investigated by analysing a water sample to which a 12.5- $\mu\text{g/l.}$  spike of iron had been added. Eight consecutive analyses yielded a mean

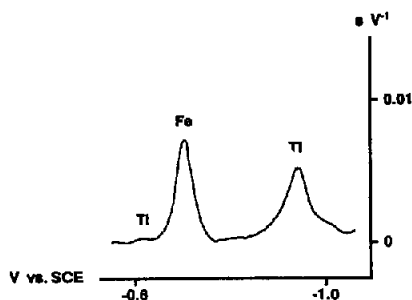


Fig. 2. Differentiated and background-corrected constant-current ( $1.5 \mu\text{A}$ ) stripping curve obtained from a solution containing  $60 \mu\text{g/l}$ . titanium(IV) and  $10 \mu\text{g/l}$ . iron(III) at pH 4.5. The sum of three scans, each obtained after 8 sec of adsorptive accumulation at  $-0.42 \text{ V}$ .

value of  $13.3 \mu\text{g/l}$ . with a standard deviation of  $0.9 \mu\text{g/l}$ .

Twenty analyses of "Millipore" water yielded an average iron(III) value of  $1.0 \mu\text{g/l}$ ., with a standard deviation of  $0.3 \mu\text{g/l}$ . In spite of the use of Suprapur sodium acetate and hydrochloric acid it was not possible to obtain lower blank values. Nor was it possible to ascertain the source of the iron(III) contamination. The relatively high blank value sets the detection limit of the technique. Judging from the shape of the stripping peaks and their reproducibility it ought to be possible to reach a detection limit below  $0.1 \mu\text{g/l}$ . in the absence of a reagent blank.

#### Interferences

Interferences in adsorptive stripping analysis can be caused either by the reduction of interfering metal complexes or by reduction of ligand adsorbed on the electrode surface. With an electrolysis potential below  $-0.40 \text{ V}$  interference from adsorbed ligand could be avoided. This was demonstrated by analysing a sample containing the SVRS reagent before and after the addition of  $10 \mu\text{g/l}$ . iron(III). Before addition of the iron(III) no stripping peak appeared in the potential interval from  $-0.58$  to  $-0.80 \text{ V}$  used for locating the iron(III) stripping peak (see above).

SVRS forms complexes with a wide range of elements.<sup>15</sup> Only a few of these, however, are capable of forming complexes at pH 4.5. The effect of likely interferents was investigated by adding nickel(II), zinc(II), cadmium(II), manganese(II), tin(IV), aluminium(III), copper(II), chromium(III) or iron(II) at  $50\text{-}\mu\text{g/l}$ . level to a sample containing  $10 \mu\text{g/l}$ . iron(III) and analysing according to the tap water procedure. Of the elements investigated, only tin(IV) and iron(II) affected the iron(III) signal significantly. In accordance with the findings of Wang and Mahmoud<sup>9</sup> iron(II) increased the signal by approximately 20%. The results were, however, poorly reproducible. Since SVRS is highly selective for iron(III) relative to iron(II) this probably reflects oxidation of iron(II) during sample manipulation. Addition of a suitable

redox buffer prior to analysis would probably overcome this interference. Tin(IV) decreased the iron(III) signal by approximately 40%, but iron(III) could be determined in the presence of tin(IV) by the standard addition procedure.

It is well known that SVRS forms strong complexes with titanium(IV), zirconium(IV) and some rare-earth elements. This has also recently been made the basis for an electrochemical stripping determination of titanium(IV)<sup>16</sup> and zirconium(IV)<sup>17</sup> by current *vs.* electrode potential monitoring techniques. That titanium(IV) can also be determined by constant-current stripping analysis was confirmed by analysing a solution containing  $60 \mu\text{g/l}$ . titanium(IV) and  $10 \mu\text{g/l}$ . iron(III) in acetate buffer of pH 5, to which SVRS had been added to give a concentration of  $5 \times 10^{-5} \text{ M}$ . The results from three accumulated stripping scans, each obtained after electrolysis for 8 sec at  $-0.42 \text{ V}$ , are shown in Fig. 2. In constant-current stripping analysis titanium(IV) yields two stripping peaks, one at  $-0.58 \text{ V}$  and one at  $-0.93 \text{ V}$ , the latter peak yielding higher sensitivity (cf. Fig. 2).

#### Comparison between the carbon-fibre electrode and the HMDE

The vast majority of published adsorptive stripping procedures are based on the use of the HMDE in combination with current *vs.* electrode potential monitoring techniques.<sup>1</sup> That the HMDE can also be used in the constant-current stripping mode was confirmed by analysing a solution containing  $10 \mu\text{g/l}$ . iron(III), by the tap water procedure above except that the reducing current was  $20 \mu\text{A}$ . The solution was stirred with a magnetic bar throughout the experiment. Figure 3 shows the constant-current stripping curve. The peak potential obtained with the HMDE,  $-0.62 \text{ V}$ , is the same as that obtained with the mercury-film coated carbon-fibre electrode, showing that the reduction is the same at the

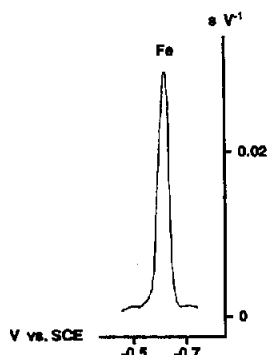


Fig. 3. Differentiated and background-corrected constant-current ( $20 \mu\text{A}$ ) stripping curve obtained with an HMDE in a solution containing  $10 \mu\text{g/l}$ . iron(III) at pH 4.5. The sum of eight stripping scans, each obtained after 8 sec of adsorptive accumulation at  $-0.42 \text{ V}$ . The solution was stirred with a magnetic bar throughout the experiment.

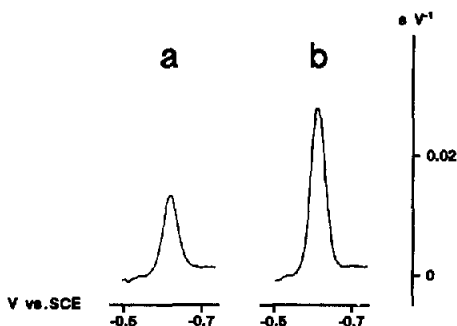


Fig. 4. Differentiated and background-corrected constant-current ( $1.5 \mu\text{A}$ ) stripping curves obtained in the analysis for iron(III) in tap water (a) before and (b) after the standard addition of  $25 \mu\text{g/l}$ . iron(III). The sum of eight scans, each obtained after 8 sec of absorptive accumulation at  $-0.42 \text{ V}$ .

two electrodes. Figure 3 also shows that the HMDE can be successfully used for the determination of iron(III) in air-saturated solutions provided that the constant-current stripping mode is used.

#### Analysis of tap water

Figure 4 shows the constant-current stripping curves obtained in the analysis for iron(III) in a tap water sample before [Fig. 4(a)] and after [Fig. 4(b)] the standard addition of  $25 \mu\text{g/l}$ . iron(III). Eight analyses of this sample gave an average value of  $22.2 \mu\text{g/l}$ . for the iron(III) concentration, with a standard deviation of  $2.9 \mu\text{g/l}$ . The value obtained from the atomic-absorption analysis was  $25 \mu\text{g/l}$ . (no standard deviation reported).

#### DISCUSSION AND CONCLUSION

The present paper is part of an investigation into the possibilities of using time *vs.* electrode potential monitoring techniques (*e.g.*, potentiometric or constant-current stripping) instead of current *vs.* electrode potential monitoring techniques (*e.g.*, linear or differential anodic stripping voltammetry) in electrochemical stripping analysis. The results confirm previous findings<sup>3-5</sup> that adsorptive stripping procedures using various current *vs.* electrode potential modes can be transformed into the constant-current stripping mode. The main advantages thus obtained are the possibility of analysing air-saturated samples, and the extended linear range in the multiple scanning mode. Also the procedures can be more automatized,

since the computerized measurement of time is considerably simpler than the computerized measurement of current. The present results also show that adsorptive constant-current analysis can be performed both on a mercury-film coated carbon-fibre electrode and on an HMDE. Obviously the mercury drop provides a more perfect mercury surface than that produced by the mercury droplets adhering to the carbon fibre. From a practical point of view, however, the flow carbon-fibre electrodes are simpler to handle than the drop electrodes, particularly in the flow-analysis mode. The mercury-film plating procedure, recently introduced in this laboratory, based on the use of very reducing potentials (typically from  $-1.5$  to  $-2.0 \text{ V}$ ), improves the quality of the mercury-film surface considerably, making the difference between the two types of electrode much smaller.<sup>18</sup> In addition, the very negative potentials applied free the mercury film surface from adsorbed species, making the long-term stability of the fibre electrodes surprisingly good.

#### REFERENCES

1. J. Wang, *Stripping Analysis*, VCH Publishers, Deerfield Beach, Florida, 1985.
2. Chi Hua, D. Jagner and L. Renman, *Anal. Chim. Acta*, 1987, **192**, 103.
3. *Idem, ibid.*, 1987, **197**, 2650.
4. H. Eskilsson, C. Haraldsson and D. Jagner, *ibid.*, 1985, **175**, 79.
5. Chi Hua, D. Jagner and L. Renman, *Talanta*, 1988, **35**, 525.
6. C. M. G. van den Berg and Z. Qianghuang, *J. Electroanal. Chem.*, 1984, **177**, 269.
7. G. W. Latimer, *Talanta*, 1968, **15**, 1.
8. R. C. Rooney and P. J. McIver, *Analyst*, 1962, **87**, 895.
9. J. Wang and J. S. Mahmoud, *Z. Anal. Chem.*, 1987, **327**, 789.
10. L. Renman, D. Jagner and R. Berglund, *Anal. Chim. Acta*, 1987, **188**, 137.
11. L. Almestrand, D. Jagner and L. Renman, *ibid.*, 1987, **193**, 71.
12. Huang Huiliang, D. Jagner and L. Renman, *Talanta*, 1987, **34**, 539.
13. L. Almestrand, D. Jagner and L. Renman, *ibid.*, 1986, **33**, 991.
14. Huang Huiliang, Chi Hua, D. Jagner and L. Renman, *Anal. Chim. Acta*, 1987, **193**, 61.
15. A. Ringbom, *Complexation in Analytical Chemistry*, Wiley, New York, 1963.
16. J. Wang and J. S. Mahmoud, *J. Electroanal. Chem.*, 1986, **208**, 383.
17. J. Wang, P. Tuzhi and K. Varughese, *Talanta*, 1987, **34**, 561.
18. Huang Huiliang, D. Jagner and L. Renman, *Anal. Chim. Acta*, in the press.

## DETERMINATION OF PENTACHLOROPHENOL BY FLOW-INJECTION ANALYSIS WITH SPECTROPHOTOMETRIC DETECTION

M. RODRIGUEZ-ALCALA, P. YAÑEZ-SEDEÑO and L. MA. POLO DIEZ

Department of Analytical Chemistry, Faculty of Chemistry, University Complutense of Madrid,  
E-28040 Madrid, Spain

(Received 30 March 1987. Revised 1 September 1987. Accepted 12 April 1988)

**Summary**—Two FIA methods for the determination of pentachlorophenol, based on its oxidizing-condensation reaction with 4-aminoantipyrine in aqueous medium and spectrophotometric detection in the conventional and stopped-flow modes, are described. In both cases the calibration graphs are linear in the range from 1.0 to 60.0  $\mu\text{g/ml}$  pentachlorophenol, with sampling rates of 48 and 28 samples/hr for triplicate analysis, respectively. Interferences from phenol and other chlorophenols have been evaluated. The stopped-flow method is particularly useful for determining pentachlorophenol in commercial formulations containing no more than 15% of other chlorophenols.

Chlorophenols are pollutants commonly found in the environment, arising from degradation or metabolism of pesticides, chlorination of water and from industrial sources.<sup>1</sup> Pentachlorophenol (PCP) and its water-soluble sodium salt are used mainly as wood preservatives, the most toxic of which are those of the chlorophenol series.

Several methods for PCP determination have been reported. Most of the chromatographic procedures are based on formation of derivatives with diazomethane or diazoethane and GC with electron-capture (EC) detection;<sup>2-4</sup> HPLC<sup>5-7</sup> has been used for analysis of complex samples. The spectrophotometric methods are based on direct measurement of the ultraviolet absorption of PCP in alkaline medium<sup>8-10</sup> and on either formation of ion-pair compounds<sup>11,12</sup> or an oxidizing-condensation product with 4-aminoantipyrine (4-AAP).<sup>13-16</sup> The latter reaction, performed in basic medium, yields a bluish-green 4-AAP dye. In the conventional spectrophotometric method, the absorbance changes significantly within 1-10 min, which causes problems even if the reaction product is extracted into organic solvents.<sup>15</sup> In the present work, these inconveniences are minimized by using the FIA technique, the selectivity being improved by applying the stopped-flow mode.

### EXPERIMENTAL

#### Apparatus

A Tecator model FIAstar 5020 flow-injection analyser, equipped with an injector valve of variable volume and two peristaltic pumps synchronized with the injector system, was used in conjunction with a spectrophotometric detector model FIAstar 5023 and a FIAstar 5022 recorder. A Metrohm E 510 pH-meter equipped with a combined Metrohm AG 9100 electrode was also used.

#### Reagents

A 100  $\mu\text{g/ml}$  aqueous pentachlorophenol stock solution was prepared by dissolving 100 mg of the chemical (Aldrich,

99% pure) in 2 ml of 1M sodium hydroxide and diluting to 1 litre with distilled water.

From a 0.1M aqueous stock solution of 4-aminoantipyrine (Aldrich, 99% pure), working solutions were prepared in 0.1M  $\text{NH}_4\text{Cl}/\text{NH}_3$  buffer (pH 9.0).

A 0.05M aqueous stock solution of potassium ferricyanide (Merck) and a Britton-Robinson buffer solution (0.2M in each acid component) were also used; the pH was adjusted with sodium hydroxide.

Other chlorophenols and chemicals used were of analytical grade. The sample analysed was a commercial fungicide, "Cryptogil Na", with the following composition: pentachlorophenate 78%; tetrachlorophenate 6.5%; other chlorophenates 6%; water 9%.

#### Procedure

Figure 1 shows the manifolds used for the determination of pentachlorophenol by conventional FIA and by the stopped-flow mode, indicating the optimum experimental conditions for the chemical and FIA variables. The sample solution, containing PCP in the concentration range 1.0-60.0  $\mu\text{g/ml}$  was injected directly into the 4-AAP carrier solution and the peak height (conventional FIA) or the signal increment (stopped-flow mode) detected at 637 nm was measured. For the determination of PCP in the solid commercial formulation, an amount of sample giving a concentration in the working range was weighed and dissolved in distilled water. The stopped-flow method indicated in Fig. 1 was applied.

### RESULTS AND DISCUSSION

In a simple two-channel FIA system, best results were found with 4-AAP as carrier solution. To select the optimum detection wavelength, absorption spectra were obtained by using the FIA system under the stopped-flow conditions specified in Fig. 1b. When distilled water was injected, the spectrum registered showed a band with its maximum at 540 nm, corresponding to the red oxidized 4-AAP.<sup>17</sup> When PCP was injected, maximum absorbance values were obtained at 610 nm, which indicates that it is possible to determine PCP in aqueous medium. The spectrum

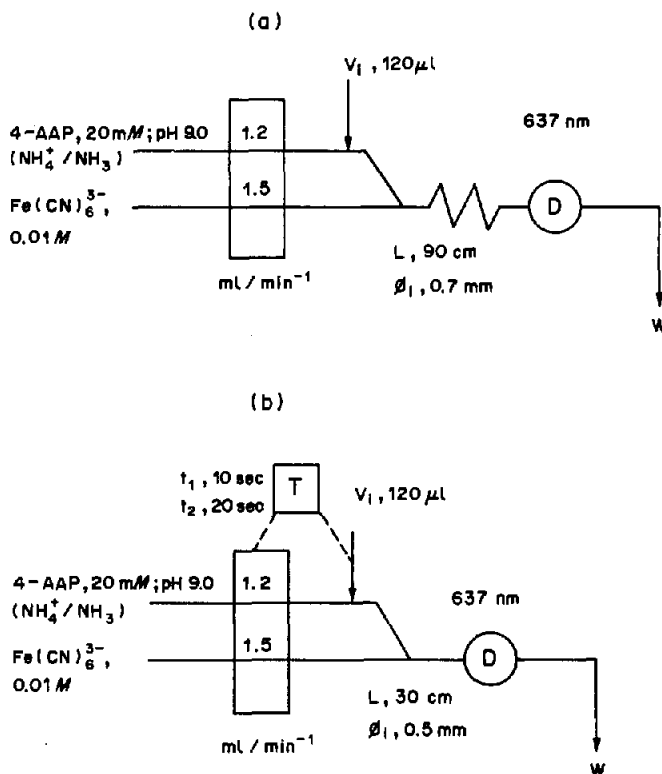


Fig. 1. Manifolds used for the determination of pentachlorophenol: (a) conventional FIA; (b) stopped-flow mode.

of the PCP dye could not be obtained under the usual spectrophotometric working conditions, owing to the rapid change of the colour. As can be seen in Fig. 2 the maximum difference between the dye and blank spectra is at around 637 nm.

#### Optimization of chemical variables

To test different pH values a 0.2M Britton–Robinson buffer was used, and the optimum pH for measurement was found to be 9.0. At pH values lower than this, a shift of the 637 nm band to shorter wavelengths was observed; higher pH values produced a decrease of the absorbance at this wavelength. Maximum signals were obtained when the 4-AAP carrier solution was prepared in 0.1M  $\text{NH}_4\text{Cl}/\text{NH}_3$  buffer (pH 9.0). Under these conditions, signals from the blank obtained by injecting distilled water were negligible. The spectra of the dye at different pH values showed an isosbestic point at 585 nm, indicating equilibrium between species having acid–base properties.

The influence of the 4-AAP and  $\text{Fe}(\text{CN})_6^{3-}$  concentrations was studied in the range  $5.0 \times 10^{-3}$ – $4.0 \times 10^{-2}M$ . The highest peaks were obtained with  $2.0 \times 10^{-2}M$  4-AAP; the optimum  $\text{Fe}(\text{CN})_6^{3-}$  concentration was found to be  $1.0 \times 10^{-2}M$ , and higher concentrations give rise to 4-AAP oxidation and hinder the PCP reaction.<sup>17</sup>

#### Optimization of the FIA variables

The FIA variables of the conventional technique were first optimized. Under these optimum conditions, an increase in the absorbance was observed when the sample plug was stopped in the flow-cell. Conditions were therefore further modified to give maximum response in the stopped-flow mode.

**Conventional technique.** The flow-rate of the  $\text{Fe}(\text{CN})_6^{3-}$  channel was kept constant at 1.5 ml/min, and the flow-rate of the 4-AAP carrier stream was varied between 0.8 and 3.2 ml/min. The signal decreased when the flow-rate was increased, because of the shorter reaction time and the greater dispersion. A value of 1.2 ml/min was chosen to give a good compromise between residence time and sampling frequency. Under these conditions, there was no significant variation of signal when the flow-rate of the  $\text{Fe}(\text{CN})_6^{3-}$  channel was varied between 1.5 and 2.8 ml/min.

The signal increased linearly with the length (42–120 cm) and internal diameter (up to 0.7 mm) of the reactor tube. A reactor length ( $L$ ) of 90 cm and i.d. of 0.7 mm were chosen to give a compromise between maximum peak height and sampling frequency. The optimum volume of injected sample was found to be 120  $\mu\text{l}$ .

**Stopped-flow mode.** In this technique, the sample plug is kept in the flow-cell by stopping the pump for an appropriate period of time, thus allowing the



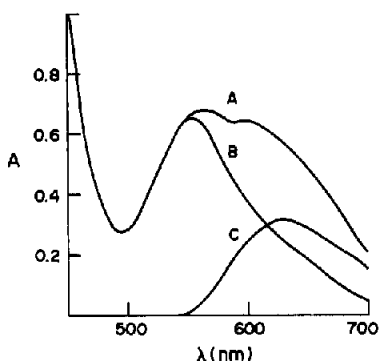


Fig. 2. Absorption spectra: (A) 30 ppm PCP; (B) distilled water; (C) difference between spectra (A) and (B). Experimental conditions as in Fig. 1.

degree of reaction to be increased. Under the same chemical conditions as those used in the conventional mode, optimization of the FIA variables yielded the following values:  $L = 30$  cm; i.d. = 0.5 mm; delay time = 10 sec and stop time = 20 sec.

#### Determination of pentachlorophenol

The analytical characteristics of the two FIA methods are summarized in Table 1. Linear calibration graphs were obtained for the PCP determination at two concentration ranges and two gain levels by both the conventional and the stopped-flow methods. These results were similar to those obtained by the

standard spectrophotometric method,<sup>15</sup> but the upper concentration limit was higher. The spectrophotometric procedures require extraction of the coloured product into organic solvents, such as benzene or chloroform, whereas the FIA method allows the determination of PCP directly in aqueous medium because the reaction product is detected quickly. The critical effect of time on the absorbance measurements is thereby avoided; the sampling speed is also enhanced, allowing up to 48 samples per hour to be analysed in triplicate by the conventional FIA method. The relative standard deviation (8 replicates) for determination of 30  $\mu\text{g/ml}$  PCP was 0.98% by conventional FIA, and 2.6% by the stopped-flow method.

#### Interferences

A systematic study of potential interferences in the two proposed methods was made. Phenol and several chlorophenols, which are often found as impurities in PCP commercial formulations, were tested. All these compounds also react with 4-aminoantipyrine in the presence of  $\text{Fe}(\text{CN})_6^{3-}$ , yielding red or bluish 4-AAP dyes.<sup>13</sup> The absorption spectra of these reaction products, obtained under the conditions used for PCP determination (Fig. 1), show bands with maximum absorption at between 514 and 533 nm for phenol, 3-chlorophenol, 2,4-dichlorophenol and 2,4,6-trichlorophenol. The small absorbances of these products at 637 nm cause an increase in the signal corresponding to PCP and give rise to positive errors

Table 1. Analytical characteristics of the FIA methods for pentachlorophenol

	FIA mode	
	Conventional	Stopped-flow
Calibration equations* for PCP (ppm)	$S$ (mV) = 11.4 [PCP] - 0.67 $S$ (mV) = 18.1 [PCP] - 1.4	$\Delta S$ (mV) = 7.4 [PCP] - 3.0 $\Delta S$ (mV) = 14.7 [PCP] - 0.8
Linear range, ppm	5.0-60.0; 1.0-10.0	5.0-60.0; 1.0-10.0
Correlation coefficient	0.9999	0.9988
Relative std. devn., %	0.98 (30 ppm); 1.4 (5 ppm)	2.6 (30 ppm); 1.4 (5 ppm)
Detection limit ( $3\sigma$ ), ppm	0.15; 0.18	0.21; 0.15
Sampling frequency, $\text{hr}^{-1}$	48	28

\*With our equipment.

Table 2. Interferences from other phenolic compounds in the PCP determination\*

Species	Added, ppm	PCP found, ppm†		Error, %	
		Conventional FIA	Stopped-flow mode	Conventional FIA	Stopped-flow mode
Phenol	5.0	31.0	29.9	+3.3	-0.3
	10.0	31.6	29.6	+5.3	-1.3
3-Chlorophenol	5.0	31.9	29.6	+6.3	-1.3
	10.0	33.0	29.6	+10.0	-1.3
2,4-Dichlorophenol	5.0	32.1	29.9	+7.0	-0.3
	10.0	32.4	30.8	+8.0	+2.7
2,4,6-Trichlorophenol	5.0	31.2	30.0	+4.0	0.0
	10.0	32.7	30.5	+9.0	+1.7
2,3,5,6-Tetrachlorophenol	5.0	35.4	25.6	+18.0	-14.7
	10.0	38.3	20.4	+27.7	-32.0

\*30.0 ppm PCP added.

†Mean of three determinations.

Table 3. Determination of pentachlorophenol in a commercial formulation by the stopped-flow procedure

Sample	PCP content, %	
	FIA method	D.P.V. method
1	76.2	75.4
2	74.1	73.8
3	76.2	76.7
4	74.6	75.4
5	74.9	74.1

	PCP, ppm*		
	Total	Found†	Recovery, %
6	10	9.4 ± 1	94 ± 1
7	20	19.6 ± 0.2	98 ± 1
8	30	29.2 ± 0.2	97.4 ± 0.6
9	40	39.9 ± 0.2	99.6 ± 0.6
10	50	49.1 ± 0.4	98.2 ± 0.7

\*Initial concentration, 7.5 ppm of pentachlorophenol.

†Mean ± s.d. of three determinations.

of up to 10% in the determination of 30.0 ppm of PCP by conventional FIA, but when the stopped-flow mode is used the error is much smaller, as shown in Table 2. The major interfering species in both methods was found to be 2,3,5,6-tetrachlorophenol, because the absorption band of the reaction product has its maximum at close to 637 nm. This compound can be tolerated only at a concentration up to a tenth of that of PCP, even by the stopped-flow procedure. When the standard spectrophotometric method is applied,<sup>13</sup> the 2,3,5,6-tetrachlorophenol product is also extracted into the organic phase and interferes seriously in the PCP determination, thus requiring a previous separation by anion-exchange procedures.<sup>15</sup> However, the stopped-flow method may be useful for the direct determination of PCP in commercial fungicides, which usually contain between 10 and 15% of lower phenols.

#### Analysis of commercial formulations

To test the applicability of the FIA method, the PCP content in a commercial fungicide, "Criptogil Na", was determined. Owing to the presence of lower chlorophenols in the sample, the stopped-flow method was used because of its better selectivity. A reference method based on PCP oxidation at a glassy-carbon electrode and measurement by differential pulse voltammetry was used for comparison purposes (Table 3). The mean value was  $75 \pm 1\%$  PCP by both methods, in good agreement with the nominal value, 78%. Recovery studies with different PCP concentrations in the range 10–50  $\mu\text{g/ml}$  in the final solutions gave good results, the mean value being  $97.4 \pm 0.8\%$  (Table 3).

#### REFERENCES

1. A. J. Fatiadi, *Environ. Int.*, 1984, **10**, 175.
2. T. R. Edgerton, R. F. Moseman, R. E. Linder and L. H. Wright, *J. Chromatog.*, 1979, **170**, 331.
3. M. Sackmauerová-Veningerová, J. Uhnák, A. Szokolay and A. Kočan, *ibid.*, 1981, **205**, 194.
4. H. J. Hoben, S. A. Ching, L. J. Casarett and R. A. Young, *Bull. Environ. Cont. Toxicol.*, 1976, **15**, 78.
5. H. C. Smit, T. T. Lub and W. J. Vloon, *Anal. Chim. Acta*, 1980, **122**, 267.
6. D. E. Mundy and A. F. Machin, *J. Chromatog.*, 1981, **216**, 229.
7. K. D. McMurtrey, A. E. Holcomb, A. V. Ekwenchi and N. C. Fawcett, *J. Liq. Chromatog.*, 1984, **7**, 953.
8. B. K. Afghan, P. E. Belliveau, R. H. Larose and J. F. Ryan, *Anal. Chim. Acta*, 1974, **71**, 355.
9. J. E. Fontaine, P. E. Joshipura, P. N. Keliher and J. D. Johnson, *Anal. Chem.*, 1975, **47**, 157.
10. R. S. Carr, P. Thomas and J. M. Neff, *Bull. Environ. Cont. Toxicol.*, 1982, **28**, 477.
11. W. T. Haskins, *Anal. Chem.*, 1951, **23**, 1672.
12. K. Kotsuji, T. Sakurai and Y. Yamamoto, *J. Chem. Soc. Japan*, 1965, **86**, 519; *Anal. Abstr.*, 1967, **14**, 4342.
13. K. Bencze, *Analyst*, 1963, **88**, 622.
14. A. Tatsuo, *Bunseki Kagaku*, 1965, **14**, 101; *Anal. Abstr.*, 1966, **13**, 6570.
15. A. I. Williams, *Analyst*, 1971, **96**, 296.
16. Z. Bardodej, *Acta Hyg. Epidem. Microb.*, 1985, **4**, 35.
17. F. W. Ochynski, *Analyst*, 1960, **85**, 278.

## STUDY OF AN ACTINOMYCIN COMPLEX BY MASS SPECTROMETRY—MASS SPECTROMETRY

M. BARBER, D. BELL, M. MORRIS, L. TETLER\* and M. WOODS  
Department of Chemistry, UMIST, Manchester, England

B. W. BYCROFT

Department of Pharmacy, University of Nottingham, England

J. J. MONAGHAN and W. E. MORDEN

ICI C&P Group, Runcorn Heath, Cheshire, England

B. N. GREEN

VG Analytical, Floats Road, Wythenshawe, England

(Received 26 January 1988. Accepted 12 April 1988)

**Summary**—The characterization of components within actinomycin complexes may often be complicated by the lack of material and standards of known actinomycins. Mass spectrometry—mass spectrometry can be employed both as a separatory device and as a means of structural analysis. This technique has been applied to an actinomycin complex obtained from a previously unidentified *Streptomyces* strain. The method involved initial work on a known material, in this case actinomycin D, and application to the unknown material. Three major components within the unknown complex were characterized as actinomycins D, F<sub>2</sub> and F<sub>3</sub>.

Some years ago, in a study related to the biosynthesis of actinomycin D, actinomycin complexes from two unidentified *Streptomyces* strains were isolated. Although it was possible to identify actinomycin D as a major component in both mixtures by comparative chromatography, the identification of the other compounds in the mixtures was not possible because of lack of material and of the various standards of the known actinomycins.

Comprehensive reviews of the structural variations and methods employed for identification have been published.<sup>1,3</sup> It is well established that the actinomycins are produced as mixtures of closely related compounds differing only in the amino-acid residues at the sites indicated in Fig. 1. The most useful techniques that have been employed to identify unknown actinomycins by comparison with known samples are paper<sup>4</sup> and thin-layer<sup>5</sup> chromatography. In addition, amino-acid analysis<sup>6</sup> of the hydrolysates of the separated components, as well as gas chromatographic analysis<sup>7</sup> of the dioxapiperazines formed on thermolysis, has been employed to identify the various amino-acid residues.

Until recently, mass spectrometry had not figured significantly as a tool for the characterization of these molecules, because of their involatility and thermal instability. We have recently utilized fast atom bombardment (FAB) mass spectrometry—mass

spectrometry (MS/MS) to characterize previously unidentified components of the Tyrothricin complex.<sup>8</sup> We now report our initial findings on the application of this method to one of the actinomycin complexes.

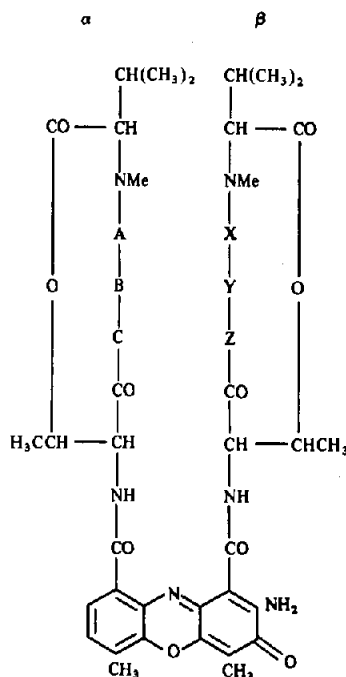


Fig. 1. Structural variations in the actinomycin family. A, X = site 4, B, Y = site 3, C, Z = site 2.

\*Author to whom correspondence should be addressed.

## EXPERIMENTAL

MS/MS data were acquired with two instruments, namely a VG Analytical ZAB-4F and a VG Analytical ZAB-HSQ. The geometries of these instruments have been described elsewhere.<sup>9,10</sup>

With both instruments, the parent ion of interest was preselected by using the magnetic and electric field of the first instrument (MS I). Collisional activation (CA) with inert gas atoms to enhance fragmentation was then undertaken, the resulting daughter ions being subjected to mass analysis by the second instrument (MS II). The ZAB-4F provides daughter ions arising from high (8 keV) energy collisions, and the ZAB-HSQ, those from low (up to 500 eV) energy collisions.

Standard FAB mass spectra were obtained with a VG updated MS902 mass spectrometer.

Samples were prepared by dissolution of 1–2  $\mu\text{g}$  of the solid in 3–5  $\mu\text{l}$  of a suitable liquid matrix directly on the probe tip of the sample-introduction system. The liquid matrices employed were thioglycerol, *m*-nitrobenzyl alcohol and a 2:1 v/v glycerol and thioglycerol mixture containing 1% v/v trifluoroacetic acid.

The samples were ionized by FAB with xenon atoms at a discharge current of 1 mA and a potential of 8 kV.

Actinomycin D was isolated as described by Roussos and Vining,<sup>11</sup> from cultures of *Streptomyces parvullus* (ATCC, 12434).

The two unidentified *Streptomyces* strains, isolated from soil and provided by the Boots Company, Nottingham, England, were grown on the same medium in rapidly shaken submerged culture at 27°. After four days of growth, the mycelium was filtered off and the filtrate repeatedly extracted with ethyl acetate. Removal of the solvent afforded a red solid which was further purified by dissolution in ethyl acetate-methanol (9:1 v/v) and filtration through a short column of silica; evaporation of the effluent gave the actinomycin complexes. Paper chromatography (Whatman No. 3 paper, ethyl acetate as mobile phase) revealed several components, including actinomycin D, which was identified by comparison with an authentic sample.

## RESULTS AND DISCUSSION

To evaluate the structural information available in the MS/CA/MS spectra, it was decided to use actinomycin D as a standard compound<sup>1</sup> of well established structure.

The FAB mass spectrum of actinomycin D is characterized by an intense line for the protonated molecular ion  $(M + H)^+$ , observed at  $m/z$  1255, together with limited fragment ions leading to incomplete sequence information concerning the identity of the peptide rings.

The application of CA, in conjunction with MS/MS, leads to enhancement of those peaks which are of importance in characterizing the structure. Furthermore, the ratio of these analytical signals to the ubiquitous background associated with FAB is considerably enhanced.

The daughter ion spectra obtained from the protonated molecular ion with the ZAB-4F and ZAB-HSQ are shown in Fig. 2. These prove to be complementary in that the high-mass ions are more pronounced when high-energy collisions are used. These ions clearly indicate the fragmentation of the desipeptide ring, and allow sequencing of the

amino-acid residues. The relevant fragmentation can be interpreted as due to initial opening of one of the lactone linkages at the bond between the bridging oxygen atom and the threonine side-chain, followed by sequential loss of amino-acid residues by cleavage at the appropriate peptide bonds.

Towards lower masses, fragments derived by the breakdown of both peptide rings are apparent, providing information concerning the amino-acid sequence and assisting in the identification of the subsequent amino-acid replacements for the other components of the actinomycin complex. These fragmentations are listed in Table 1.

It appears that there is no discrimination as to which of the two lactone bonds is opened first. Furthermore, no significant fragmentation of the chromophore is observed.

When it had been established that this method afforded not only molecular weight information, but also data that are structurally significant within a defined mass range for the standard compound, the technique was applied to a total actinomycin complex.

The molecular ion region of the actinomycin "SA" complex is depicted in Fig. 3, and reveals three major components [as  $(M + H)^+$ ] at  $m/z$  1255, 1229 and 1203. Species of lower intensity, interpreted as the  $(M + Na)^+$  ions from these components, can be observed at  $m/z$  1277, 1251 and 1225. Spectra obtained from specimens in *m*-nitrobenzyl alcohol and other matrices indicate the presence of minor components of low intensity at  $m/z$  1189, 1215, 1243 and 1269.

In application of MS/MS to this mixture, the first mass spectrometer allows passage of one ionic species, thus effectively acting as a separatory device. This is then followed by collisional activation, and subsequent analysis of the resultant daughter ions. The MS/MS spectrum of  $(M + H)^+$  at  $m/z$  1255 was identical to that obtained from actinomycin D.

Both high and low collision-energy daughter-ion spectra were obtained for the ions occurring at  $m/z$  1229 and 1203. These are shown in Figs. 4 and 5. Again, the MS/MS spectra recorded for high and low energy collisions are complementary, with the high-mass ions being more pronounced at high collision energy (8 keV). Interpretations of the spectra are given in Figs. 4 and 5, and Table 2. The spectra reveal

Table 1

$m/z$	Interpretation
956	Loss of (H-Pro-Sar-MeVal-OH)
857	Loss of (H-Val-Pro-Sar-MeVal-OH)
657	Loss of (H-Pro-Sar-MeVal-OH) from both rings
558	Loss of (H-Pro-Sar-MeVal-OH) from one ring and (H-Val-Pro-Sar-MeVal-OH) from the other
459	Loss of (H-Val-Pro-Sar-MeVal-OH) from both rings
399	(H-Val-Pro-Sar-MeVal-OH + H) <sup>+</sup>
300	(H-Pro-Sar-MeVal-OH + H) <sup>+</sup>

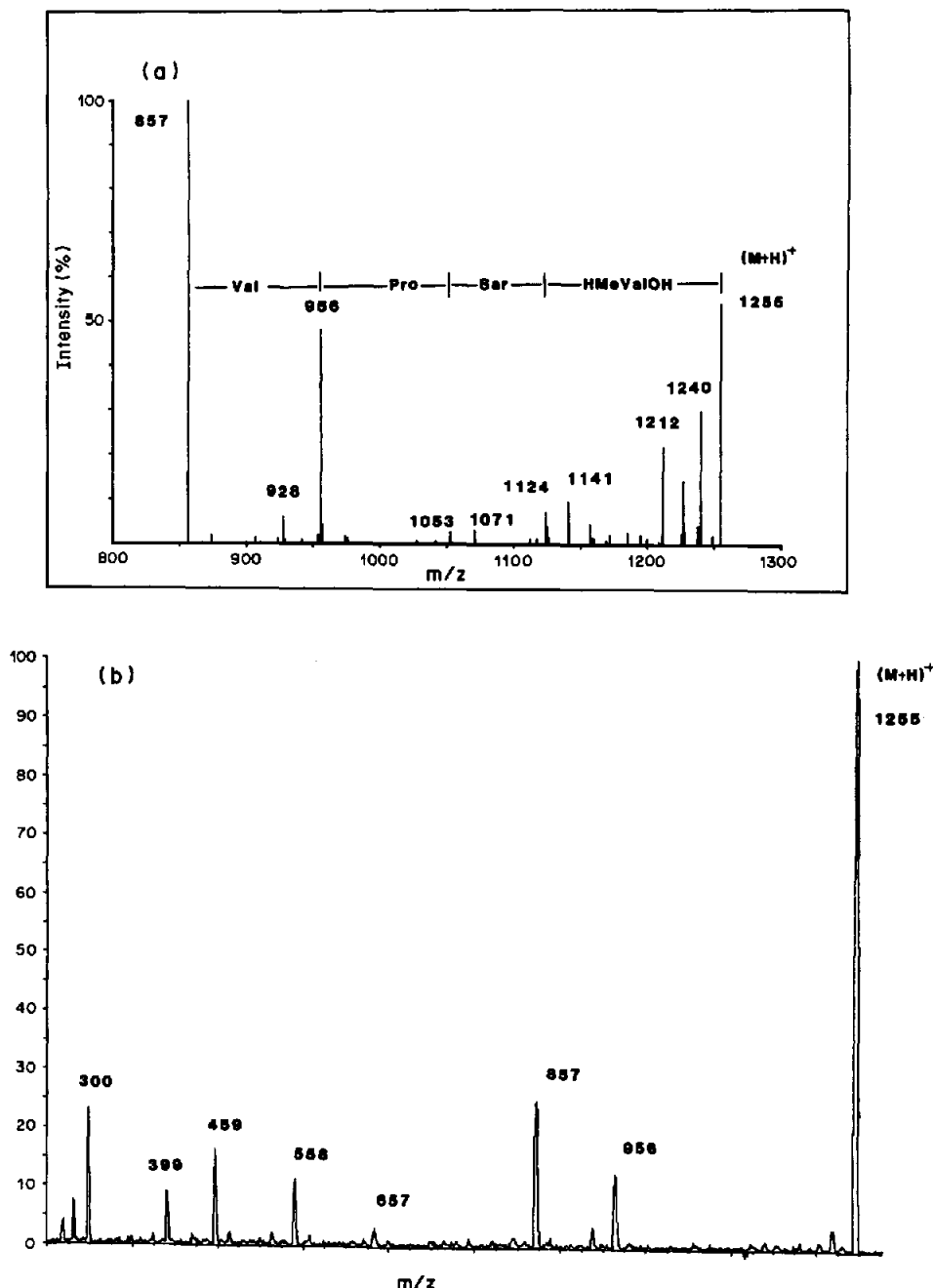


Fig. 2. (a) Daughter-ion spectra of  $m/z$  1255 obtained at high energy (8 keV) collision with He; (b) daughter-ion spectra of  $m/z$  1255 obtained at low-energy (59 eV) collision with Ar.

the replacement of one or both proline residues by a group with 'molecular weight' 71 (presumably sarcosine, since alanine has not been observed as a replacement at this site). This would identify these components as actinomycins  $F_7$  and  $F_8$ , respectively.

To date, the minor components have only been characterized by molecular weight. Although, at present, the concentration of these actinomycins is low, proving problematic for MS/MS, chromatographic enrichment is currently under study. However, in view of the known site replacements within

the actinomycins, it is possible to tentatively assign the structures shown in Table 3.

#### CONCLUSIONS

It has been shown that FAB ionization can produce high-quality molecular weight information from microgram quantities of the actinomycins. The fragmentation, however, is sparse, and this combined with the multicomponent nature of the sample material makes interpretation impracticable. By use

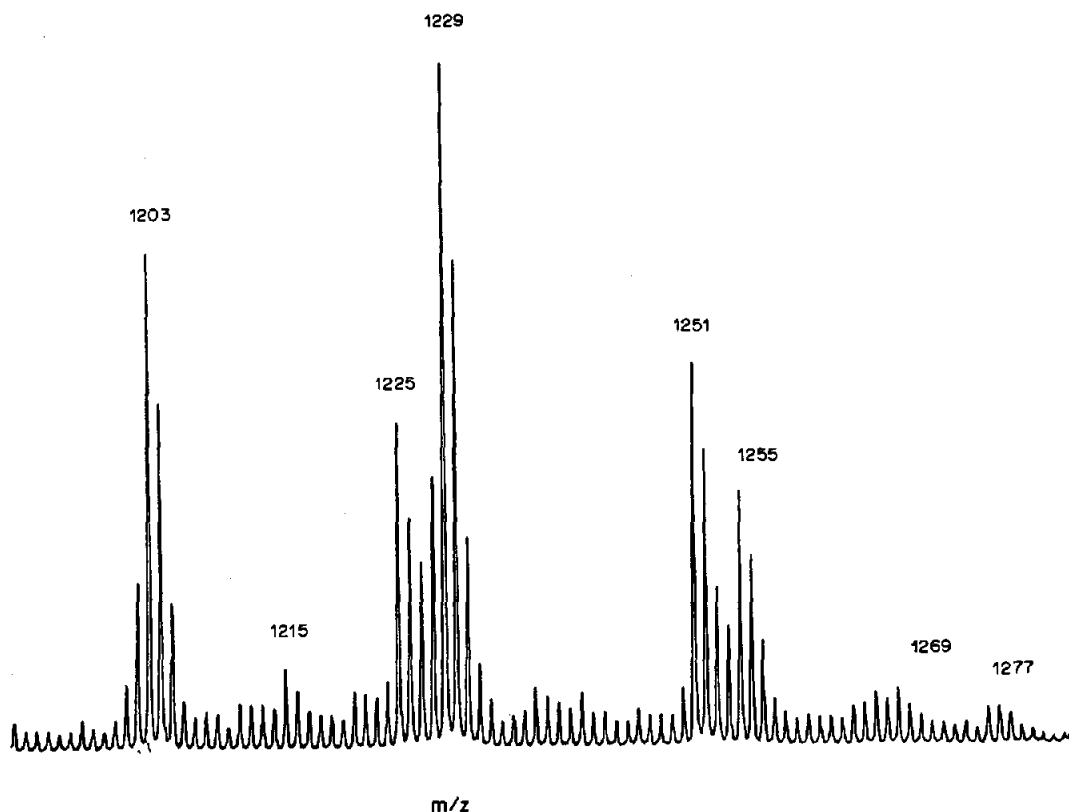


Fig. 3. Molecular-ion region of actinomycin 'SA' complex obtained by FAB-MS, with *m*-nitrobenzyl alcohol as matrix.

of MS/MS techniques, the molecular ions of the individual components of complex mixtures may be selected from the high-mass region of the total spectrum for the complex. These selected ions can then be subjected to collisional activation, enhancing the fragmentation, to give sequence information about the depsipeptide rings. This technique has been successfully applied to one actinomycin complex, resulting in facile characterization of the major com-

ponents. It has also provided important information concerning the amino-acid composition of the minor components, which needs to be confirmed by additional information from amino-acid analysis and a further combination of MS/MS and degradative studies (to be described later). The potential of this method for monitoring biosynthesis, and the production of semi-synthetic actinomycins by controlled biosynthesis is currently under investigation.

Table 2

<i>m/z</i>	Interpretation
(a) Parent ion <i>m/z</i> 1229	
956	Loss of (H-Sar-Sar-MeVal-OH)
930	Loss of (H-Pro-Sar-MeVal-OH)
857	Loss of (H-Val-Sar-Sar-MeVal-OH)
831	Loss of (H-Val-Pro-Sar-MeVal-OH)
657	Cleavages from both rings to give same products as actinomycin D
558	
459	
399	as Table 1
373	(H-Val-Sar-Sar-MeVal-OH + H) <sup>+</sup>
300	as Table 1
274	(H-Sar-Sar-MeVal-OH + H) <sup>+</sup>
(b) Parent ion <i>m/z</i> 1203	
930	Loss of (H-Sar-Sar-MeVal-OH)
831	Loss of (H-Val-Sar-Sar-MeVal-OH)

The following ions offer the same interpretation as above:  
*m/z* 657, 558, 459, 373 and 274

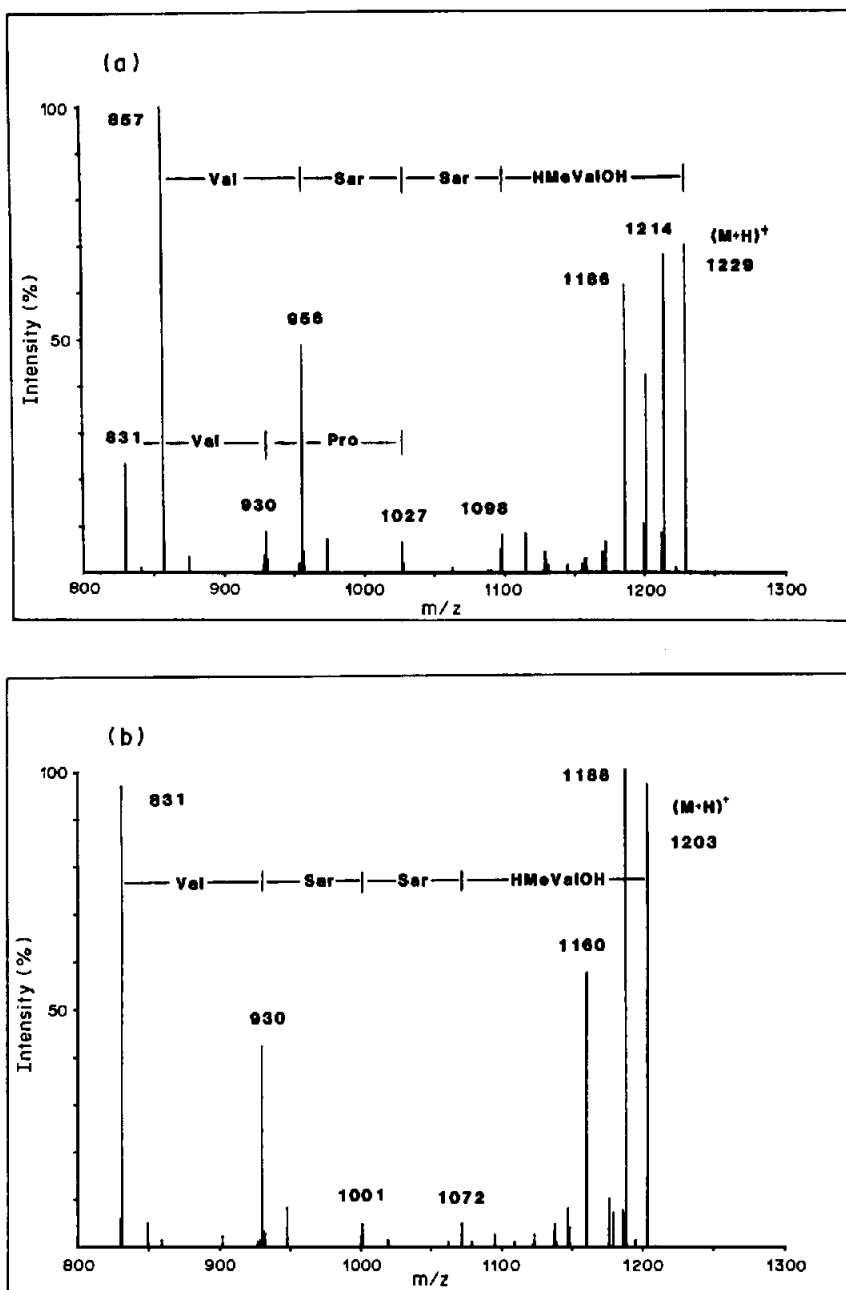


Fig. 4. (a) Daughter-ion spectra of  $m/z$  1229 obtained after high-energy (8 keV) collision with He; (b) daughter-ion spectra of  $m/z$  1203 obtained after high-energy (8 keV) collision with He.

Table 3

$M_R$	Trivial name	A	B	C	X	Y	Z
<i>Actinomycin 'SA' complex—major components</i>							
1254	Actinomycin D, C <sub>2</sub>	Sar	Pro	Val	Sar	Pro	Val
1228	Actinomycin F <sub>9</sub>	Sar	Pro	Val	Sar	Sar	Val
1202	Actinomycin F <sub>8</sub>	Sar	Sar	Val	Sar	Sar	Val
<i>Actinomycin 'SA' complex—minor components</i>							
1268	Actinomycin C <sub>2</sub>	Sar	Pro	Val	Sar	Pro	alle
	and/or						
	Actinomycin iso-C <sub>2</sub>	Sar	Pro	alle	Sar	Pro	Val
1242	Actinomycin F <sub>2</sub>	Sar	Pro	Val	Sar	Sar	alle
1214	—	Sar	Pro	Val	Gly	Sar	Val
1188	—	Sar	Sar	Val	Gly	Sar	Val
1174	—	Gly	Sar	Val	Gly	Sar	Val

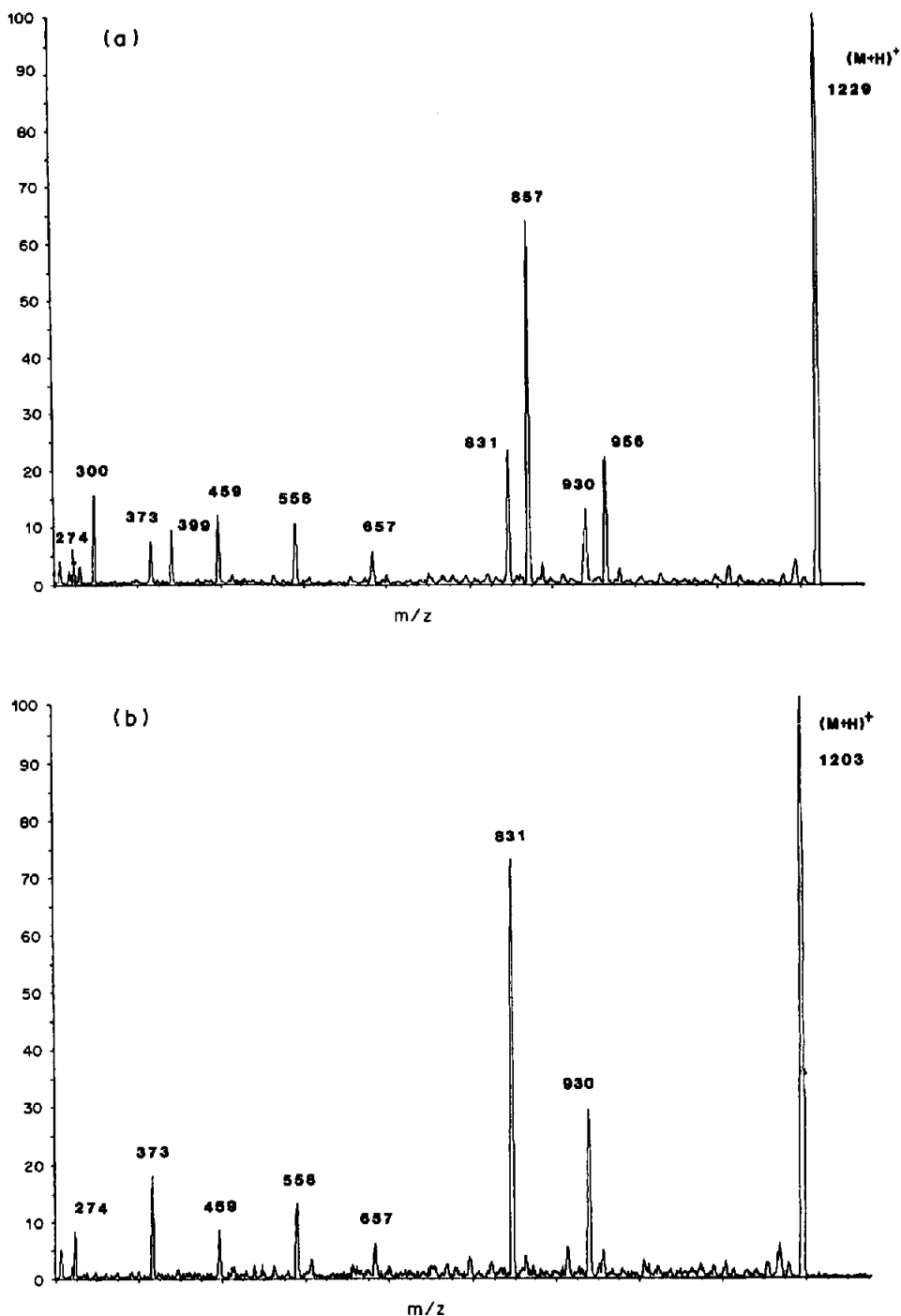


Fig. 5. (a) Daughter-ion spectra of  $m/z$  1229 obtained after low-energy (41 eV) collision with Ar; (b) daughter-ion spectra of  $m/z$  1203 obtained after low-energy (41 eV) collision with Ar.

*Acknowledgements*—M.M. and M.W. would like to thank SERC for financial support and D.B. to thank ICI for funding. Thanks are also due to S. Evans for assistance with the data analysis.

#### REFERENCES

1. A. B. Mauger, *The Actinomycins, Topics In Antibiotic Chemistry*, Vol. 5, P. Sammes (ed.), pp. 225–257. Horwood, Chichester, 1980.
2. W. A. Remers, *Actinomycin, Chemistry of Antitumour Antibodies*, Vol. 1, Wiley, New York, 1979.
3. V. Hollstein, *Chem. Rev.*, 1980, **74**, 625.
4. K. Zepf, *Experimentia*, 1958, **14**, 207.
5. E. Katz, W. K. Williams, K. T. Mason and A. B. Mauger, *Antimicrob. Agents Chemother.*, 1977, **11**, 1056.
6. A. B. Mauger and E. Katz, *Antibiotics, Isolation, Separation and Purification*, M. J. Weinstein and G. H. Wagman (eds.), Elsevier, New York, 1978.
7. A. B. Mauger, *J. Chem. Soc. Perkin Trans. I*, 1975, 1320.



8. M. Barber, L. Tetler, D. Bell, J. J. Monaghan, W. E. Morden, B. Bycroft and B. N. Green, *Presented at the 35th ASMS Conference on Mass Spectrometry and Allied Topics*, Denver, Colorado, 24-29 May 1987.
9. J. R. Hass, B. N. Green, R. H. Bateman and P. A. Bott, *Presented at the 32nd Annual Conference on Mass Spectrometry and Allied Topics*, San Antonio, Texas, 27 May-1 June 1984.
10. A. E. Harrison, R. S. Mercer, E. J. Reiner, A. B. Young R. K. Boyd, R. E. March and C. J. Porter, *Int. J. Mass Spectrom. Ion Phys.*, 1986, 74, 213.
11. G. G. Roussos and L. C. Vining, *J. Chem. Soc.*, 1956, 2469.

## STUDY OF THE PHYSICOCHEMICAL PROPERTIES OF AQUEOUS DANTROLENE SOLUTIONS BY DIFFERENTIAL PULSE POLAROGRAPHY

M. H. LIVERTOUX\*, Z. JAYYOSI and A. M. BATT

Université de Nancy I, Centre du Médicament, U.A. CNRS No. 597, 30 rue Lionnois, F-54000 Nancy, France

(Received 23 March 1987. Revised 2 March 1988. Accepted 25 March 1988)

**Summary**—Dantrolene is a skeletal-muscle relaxant which exists in three different forms over the pH range 0–14, corresponding to the cation  $H_2A^+$ , neutral species HA and anion  $A^-$ . Dantrolene is slightly soluble in water and is polarographically reducible over the whole pH range. The acid dissociation constants of the ionic species were investigated by means of differential pulse polarography ( $H_2A^+/HA$  equilibrium with  $pK_{a1} = 2.02 \pm 0.05$ ) and potentiometry ( $HA/A^-$ ,  $pK_{a2} = 7.49 \pm 0.05$ ). It was shown that differential pulse polarography is a valid alternative method when the  $pK_a$  values of an electroactive drug cannot be determined by potentiometric or spectrophotometric methods. Polarography was also used to monitor the stability of the drug in acidic media and its extraction by chloroform.

Dantrolene, 1- $\{[5-(p\text{-nitrophenyl})\text{furfurylidene}]\text{-amino}\}$ imidazolidine-2,4-dione trihydrate, sodium salt, is a peripherally acting skeletal-muscle relaxant used mainly to decrease muscle spasticity resulting from serious chronic disorders such as multiple sclerosis, spinal cord injury, stroke and cerebral palsy.<sup>1</sup> Recently it has also been recommended for the prevention and treatment of malignant hyperthermia.<sup>2</sup> The use of this drug is limited by its side-effect of hepatic damage, which is related to long-term dantrolene therapy and the dose used. The metabolism of dantrolene has been investigated in our laboratory by *in vitro* incubation with rat-liver microsomes. The enzymatic reaction was stopped by the addition of hydrochloric acid to the incubation medium, and after extraction the drug and its metabolites were detected by high-performance liquid chromatography (HPLC) coupled with spectrophotometric detection.<sup>3</sup> The work also involved determination of the two acidity constants of dantrolene and the optimal extraction conditions. No equilibrium constant has previously been reported for protonation of dantrolene.

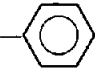
Many methods have been used for determination of dantrolene and its metabolites in biological fluids: colorimetry,<sup>4</sup> spectrofluorimetry<sup>5</sup> and HPLC.<sup>6,7</sup> The reduction of dantrolene and of its acetylated metabolite at the mercury electrode have been reported by Cox *et al.*<sup>8</sup> At pH 4, the differential pulse (DP) polarogram of  $10^{-5}M$  dantrolene showed two peaks attributed to reduction of both the nitro group and the azomethine linkage.<sup>8</sup> Several works have been devoted to the electroreduction of compounds

that contain the  $—HC=N—N<$  group,<sup>9–12</sup> and are electrochemically active substances conveniently determinable by DP polarography. This electro-analytical technique has high sensitivity and selectivity. The mechanism of the polarographic reduction of nitrofurantoin in acidic media has been reported,<sup>11,12</sup> and we supposed that dantrolene has a similar polarographic reduction mechanism, owing to its chemical similarity (Table 1). The variation of the reduction half-wave potential of the azomethine group with pH has been observed in structurally related compounds.<sup>11,14</sup>  $pK_a$  values can be determined from the shift of potential with pH, as intersections of the linear portions on  $E_p$ -pH plots.<sup>15,16</sup> This method was used for the determination of the approximate value of the dissociation constant of the azomethine group of dantrolene.

The drug undergoes degradation of the azomethine bond in acidic solutions to give 5-(*p*-nitrophenyl)-furfural and 1-aminohydantoin as shown spectrophotometrically by Inotsume *et al.*<sup>17</sup> Such degradation reactions may cause errors in the measurement of the drug and its metabolites by extraction from the incubation mixture. To determine whether such degradation might occur, we have examined the rate and extent of the hydrolytic reactions of dantrolene in acidic solutions, by using DP polarography, which allows the changes of the azomethine bond signal to be followed directly. We have also tried to demonstrate that the acidity constant values ( $pK_a$ ) of dantrolene can conveniently be measured with satisfactory precision and accuracy for routine applications by DP polarography. We have also used DP polarography to monitor the solubility at pH 7.4, the stability in acidic media and the extraction of dantrolene by chloroform at various pH values.

\*Author to whom reprint requests should be directed.

Table 1. Formulae and acid-base constants of dantrolene and other similar nitrofuran derivatives; literature data

Compound	R	Acidity constant ( $pK_a$ )			References
		$N_2$	$N_1$	$N_3$	
Dantrolene		NVR	NVR	7.5	13
Nitrofurantoin	$-\text{NO}_2$	3.5	7.8	opening of cycle	12

NVR: no value reported in the literature.

## EXPERIMENTAL

### Chemicals

Dantrolene sodium ( $\text{DtNa} \cdot 3\text{H}_2\text{O}$ ), and nitrofurantoin were a gift from Oberval Laboratories (Lyon, France). Stock solutions ( $5 \times 10^{-3} M$ ) were freshly prepared in dimethylsulphoxide (DMSO) and 10–50  $\mu\text{l}$  portions were diluted in an appropriate buffer to the desired concentrations. Dantrolene was also used as an internal standard added to the solution in the solubility determination. When methanol was used as solvent, partial precipitation of dantrolene sodium was observed a few hours after preparation of the solution.

Citrate (pH 3) and phosphate (pH 5) buffers were prepared from Merck Titrisol materials. Borate solution ( $I = 0.1 M$ ) was prepared by dissolving the sodium salt. The pH values of solutions were adjusted by addition of 0.1 M sodium hydroxide. The physiological-pH solution was 0.1 M Tris buffer. All reagents used were of analytical grade.

### Apparatus

The polarograph was a Solea-Tacussel PRG, connected to a three-electrode cell system. The dropping mercury electrode (DME) had a flow-rate of 0.843 mg/sec and a controlled drop-time of 1 sec. All potentials were referred to a saturated calomel electrode (SCE). The scan rate was 1 mV/sec with a modulation amplitude of 50 mV. The pH measurements were made with a digital Metrohm 632 pH-meter with a glass combination electrode, and magnetic stirring during titration.

### Polarography

Samples (10 ml) of  $10^{-5} M$  solution were studied at each pH value. All samples were deaerated by passage of pure nitrogen for 5 min. The solutions were assayed immediately and/or at timed intervals.

### Measurements of $pK_a$

The acid dissociation constants  $pK_{a1}$  and  $pK'_{a1}$  of protonated dantrolene were measured by DP polarography from the shift of the azomethine peak to more negative potentials with increasing pH. The effect of pH on the current-voltage curve was investigated by recording DP polarograms of  $10^{-5} M$  dantrolene in HCl-KCl (pH 0–3), citrate (pH 3–5), phosphate (pH 6–8) and borate (pH 9–11) buffered media. The  $pK_a$  values were calculated from the intersection of two successive linear relations of the form

$$\Delta E_p = a \text{ pH} + b$$

where  $a$  and  $b$  are constants. The potential shifts are given by

$$E_p = c + (RT/\alpha n F) \ln\{[H^+]^m/K_1 + [H^+]^n\}$$

where  $\alpha$ ,  $m$ , and  $n$  are the transfer-coefficient, the number of protons transferred before the potential-determining step, and the total number of electrons consumed per molecule of electroactive species.

From plots of  $E_p$  against pH it is possible to determine the ratio  $m/\alpha n$ , corresponding to the slope  $\alpha$  in the  $E_p$ -pH plots.

### Potentiometry

Potentiometric pH-titration of dantrolene sodium with 0.1 M hydrochloric acid was performed at a concentration ( $C_0$ ) of  $5 \times 10^{-4} M$  in  $10^{-3} M$  potassium nitrate electrolyte. The HA form of dantrolene is only slightly soluble in water, so precipitation of the weak acid occurred during the titration. The  $pK_{a2}$  value was calculated by using the relationship given by Levy and Rowland,<sup>18</sup> adapted from the equation developed by Leeson and Brown:

$$Z' = C_T - [\text{H}_3\text{O}^+] = C_0 - (K_a [\text{HA}]_{\text{sol}} / [\text{H}_3\text{O}^+])$$

where  $Z'$  is the concentration of conjugate acid formed during titration,  $C_0$  is the total concentration of all the drug species in solution and  $C_T$  the concentration of the hydrochloric acid used as titrant. It was necessary to determine the solubility of the un-ionized species  $[\text{HA}]_{\text{sol}}$ .<sup>19</sup> At the end of each run (pH  $\sim 5.6$ ), the solution was separated by centrifugation and  $[\text{HA}]_{\text{sol}}$  was measured by DP polarography. Near pH 5.6 dantrolene is essentially in the form HA (99%) and the concentration of the uncharged molecules remains constant throughout the precipitation.

### Spectrophotometry

Experimental solutions (10 ml) were prepared by dilution of stock solution with the appropriate buffer to give a drug concentration of  $2 \times 10^{-5} M$ . Spectra were recorded at 22°C with a Uvikon 810–820 double-beam spectrophotometer. Matched 1-cm path-length silica cells were used. The wavelength region scanned was from 200 to 500 nm and the reference was a blank of buffer solution (2 ml) containing the same amount of DMSO as the samples (20  $\mu\text{l}$ ). The range from about pH 1 to 11 was scanned at unit pH-intervals to determine the approximate value of  $pK_{a2}$ . The regions around the other  $pK_a$  values defined by

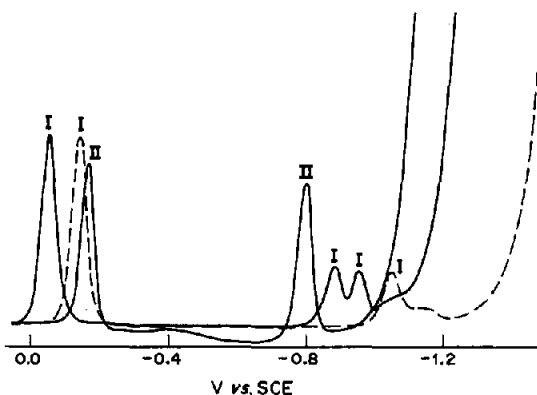


Fig. 1. Differential pulse polarogram of  $10^{-5}M$  nitrofurantoin (I) and dantrolene (II) in citrate buffer at pH 3.0 (—) and pH 5.0 (---).

DP polarography were then studied in more detail with solutions buffered at pH intervals of 0.3.

#### Solubility determination

Solubility measurements were made at pH 7.4 (0.1M Tris buffer). Excess of dantrolene was shaken with aqueous buffer at room temperature for 24 hr. The undissolved drug was separated by centrifugation, then 1 ml of the supernatant liquid was diluted with the same buffer (10 ml) and analysed polarographically, before and after addition of known quantities ( $10 \mu\text{l}$ ) of the  $5 \times 10^{-3}M$  stock dantrolene solution.

#### Stability studies

Dantrolene sodium was dissolved in hydrochloric acid solutions at various pH values, the ionic strength being adjusted to 0.1M with potassium chloride. The final concentrations of dantrolene were  $10^{-5}M$ . The solutions (10 ml) were assayed immediately and at time intervals from 5 min to 1 hr. The degree of hydrolysis was estimated by measuring the azomethine peak height and comparing it with that for the initial solution.

#### Extraction procedure

Dantrolene solutions ( $10^{-5}M$ ) were extracted at various pH values. The extraction ratios ( $R$ ) were determined by shaking equal volumes (10 ml) of the organic (chloroform) and aqueous phases (10 ml) for 2 min. The mixture was centrifuged for 5 min, then 5 ml of the organic layer were transferred into a polarographic cell and evaporated to dryness under a gentle stream of nitrogen. The residue was dissolved in 10 ml of the appropriate buffer solution and polarographed.  $R$  was calculated as  $200 i_{p2}/i_{p1} \%$ , where  $i_{p1}$  and  $i_{p2}$  are the azomethine reduction peak intensities in the sample before and after extraction, respectively.

## RESULTS AND DISCUSSION

### Polarographic behaviour of dantrolene

At pH 3 dantrolene was reduced in two steps at the DME (Fig. 1), with two peaks with potentials ( $E_p$ ) of  $-0.18$  and  $-0.81$  V vs. SCE, and similar heights, the first corresponding to the 4-electron reduction of the nitro group to a hydroxylamine group and the second either to simultaneous reduction of the azomethine and hydroxylamine groups, as in the case of nitrobenzodiazepine derivative (nitrazepam<sup>20</sup>), or to simultaneous reductive rupture of the  $-\text{HC}=\text{N}-\text{N}<$  group and the reduction of the imine formed,<sup>11</sup> as in the case of hydrazones.<sup>21</sup> Even in acidic solutions, the reduction of the protonated hydroxylamine group to an amino group in a 2-electron step was not detected. In acidic media (pH < 2), the second peak decreased with time, which indicates breaking of the  $-\text{HC}=\text{N}-\text{N}<$  group under these conditions. Polarograms of the hydrolysate obtained from a saturated dantrolene solution in 2M hydrochloric acid were recorded at various pH values (from 2 to 5). No peak corresponding to a 2-electron reduction of hydroxylamine to an amino group was observed. This may prove that the second hypothesis for the reaction leading to the peak at  $-0.81$  V is the more probable.

The  $E_p$  values are pH-dependent. The first peak shows a linear variation of potential with pH, while the second has two breaks near pH 2 and 5.3. The pH-dependent changes of the  $-\text{HC}=\text{N}-\text{N}<$  signal in the polarograms are illustrated in Fig. 2. These changes are due to protonation of the nitrogen atom in the azomethine group.

The peak height for reduction of the azomethine linkage ( $i_p$ ) was proportional to the dantrolene concentration between pH 3 and 7.5 over the entire concentration range  $10^{-7}$ – $6 \times 10^{-5}M$ .

The polarographic behaviour of dantrolene was different from that of other nitrofurane derivatives such as nitrofurantoin. The various waves observed in this last case can be related to the rate of the protonation and are pH-dependent (Fig. 1).

### Ionization constants

We believed that the  $pK_{a2}$  value corresponds to deprotonation at position 3, by analogy with the results obtained for hydantoin compounds.<sup>12</sup> The

Table 2. Polarographic data related to acid-base reactions for dantrolene at 22° ( $I = 0.1M$ )

Equilibrium	pH range	$-dE_p/dpH$ , $mV/pH, (r)$	$pK_a$ values	Method
$A^-/HA$ $pK_{a2}$	6–9	43 (0.998)	$7.49 \pm 0.05$ $7.50 \pm 0.06$	potentiometry spectrophotometry
$HA/H_2A^+$ $pK_{a1}$	3–5	85 (0.999)	$5.33 \pm 0.02$	DP polarography
$pK_{a1}$	–0.3–2	61 (0.999)	$2.02 \pm 0.05$	DP polarography

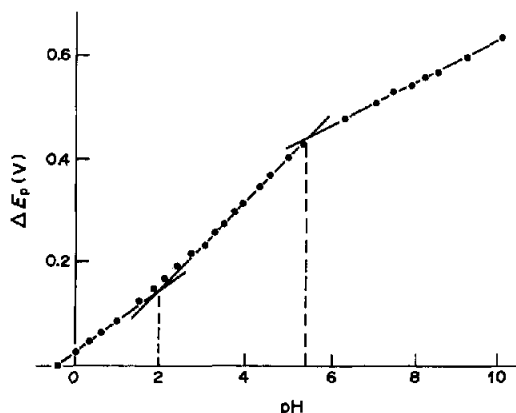


Fig. 2. Dependence, on pH, of the DP polarographic peak potentials of  $10^{-5}M$  dantrolene ( $-\text{HC}=\text{N}-\text{N}<$ ) in hydrochloric acid solution (from  $H_0 = -0.3$  to  $\text{pH} = 2$ ) and in aqueous buffers (from  $\text{pH} = 3$  to  $\text{pH} = 10.3$ ) ( $I = 0.1M$ ).

$\text{p}K_{a2}$  value of 7.5 reported in the literature<sup>13</sup> was not evident from Fig. 2. We have corroborated this value by potentiometric titration of  $10^{-5}M$  and  $5 \times 10^{-4}M$  dantrolene with  $0.1M$  hydrochloric acid (Fig. 3). The constant of the acid-base  $\text{HA}/\text{A}^-$  equilibrium was calculated after polarographic determination of the un-ionized species solubility near  $\text{pH} 5.6$  ( $[\text{HA}]_{\text{sol}} = 0.85 \times 10^{-6}M$ ). The  $\text{p}K_{a2}$  value ( $7.49 \pm 0.05$ ) thus obtained is in good agreement with the literature value.<sup>13</sup> The titrimetric method was excluded for determination of  $\text{p}K_{a1}$  owing to the low solubility of the drug in the protonated form  $\text{H}_n\text{A}^{(n-1)+}$ .

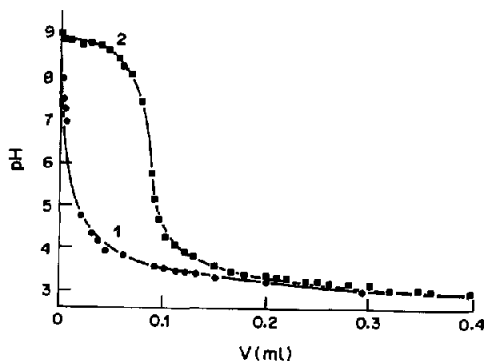


Fig. 3. Potentiometric titration of dantrolene (1)  $10^{-5}M$  and (2)  $5 \times 10^{-4}M$  in  $10^{-3}M$   $\text{KNO}_3$  with  $0.1M$   $\text{HCl}$ .

The spectral changes of dantrolene with pH are shown in Fig. 4. Three absorption bands were found and the second band (310 nm) can be attributed to absorption by the  $-\text{HC}=\text{N}-\text{N}<$  group.<sup>12,17</sup> The spectra exhibited three isosbestic points, at 288, 332 and 394 nm, owing to the shift of the 383 nm band in alkaline solutions. Deprotonation at position 3 of dantrolene would cause a 10 nm shift of the 383 nm band. The plots of absorbance *vs.* pH are shown as an inset of Fig. 4 and the point of inflexion gives the  $\text{p}K_{a2}$  value  $7.5 \pm 0.06$ . The absorbance was constant from  $\text{pH} 1$  to  $\text{pH} 6$ . The pH regions around the two breaks in the  $E_p$ -pH plots shown in Fig. 2 were then studied in more detail from  $\text{pH} 1.1$  to  $\text{pH} 2.9$  and from  $\text{pH} 4.36$  to  $\text{pH} 6.23$ . The absorbance at 310 nm

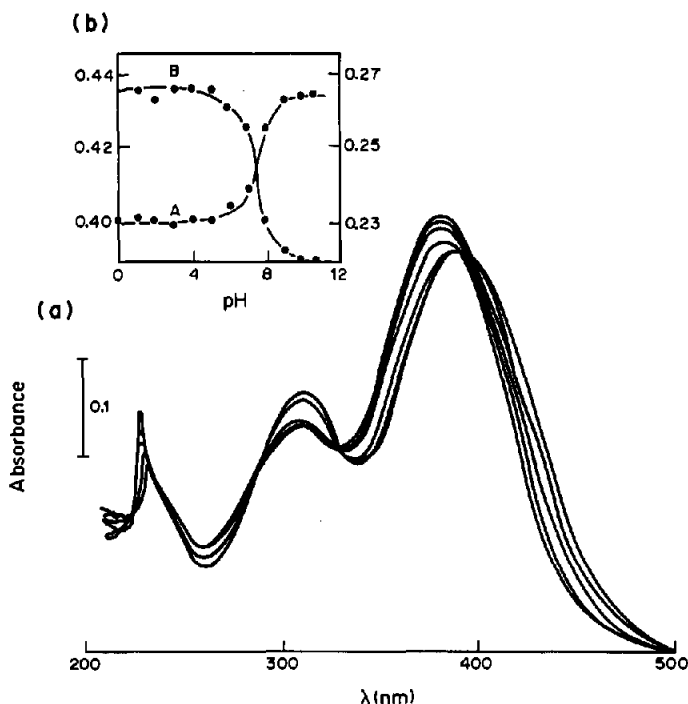


Fig. 4. Absorption spectra of  $2 \times 10^{-5}M$  dantrolene. (a) pH dependence of spectra. (b) Plots of absorbance *vs.* pH at 310 nm (A) and 383 nm (B).

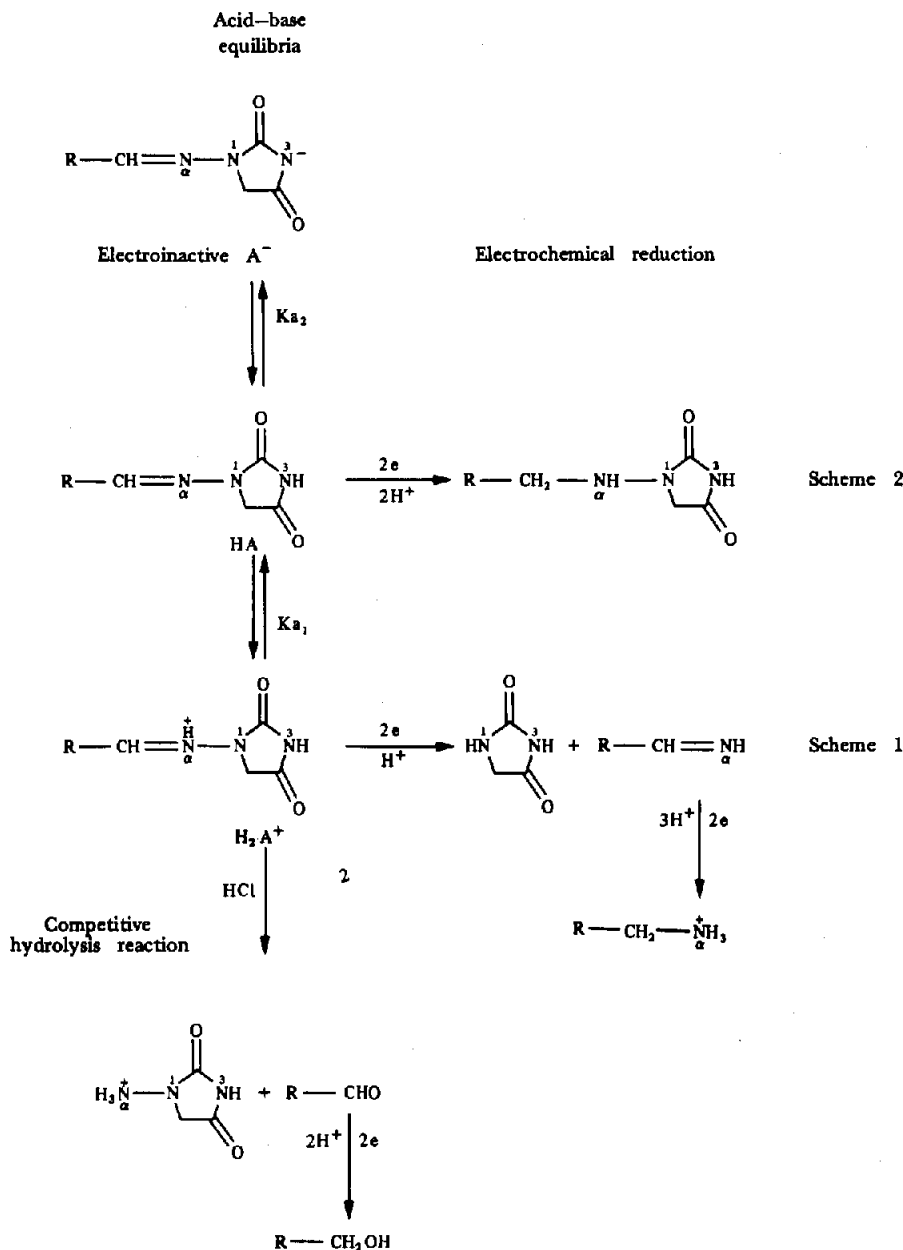


Fig. 5. Proposed acid-base equilibria and reduction mechanisms of the dantrolene azomethine group.

was found to be unaffected by these pH changes. Protonation of the azomethine group would not be expected to cause any spectral changes of the 310 nm band. The absorption of the ionic form should not differ from that of the neutral molecule in wavelength and in intensity.

Nevertheless, it is possible to estimate the  $pK_{a1}$  value corresponding to the acid dissociation constant of the protonated azomethine group, from the measurements of the peak potentials ( $E_p$ ) and polarographic currents ( $i_p$ ), and their pH plots offer information about the chemical reactions accompanying the electrode process.

Reduction of the  $-HC=N-N<$  group results in a two- or four-electron signal and is accompanied by an acid-base equilibrium which results in changes of the polarographic curves with pH.<sup>11,12,20</sup> A mechanism can be proposed for the general reduction of hydrazones.<sup>21</sup> After proton uptake, hydrazones may be reduced to amines in a 4e-reduction or to hydrazines in a 2e-reduction, depending on the pH (Fig. 5). In strongly acid solution, a four-electron reduction was found and the first step was the hydrogenolysis of the nitrogen-nitrogen bond. The imine thus formed was then protonated and further reduced (scheme 1). In alkaline solution, a two-electron reduction was

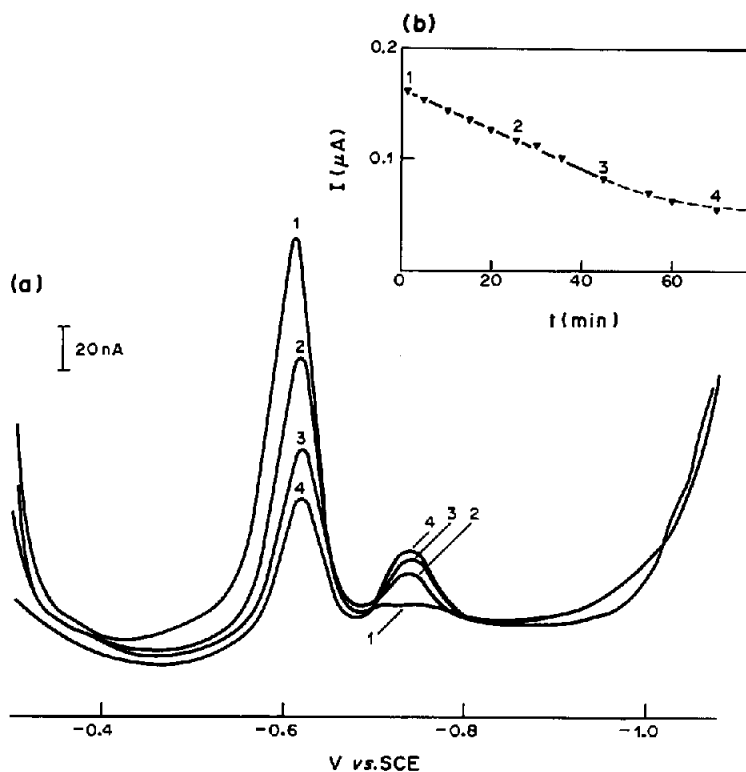


Fig. 6. Stability of dantrolene in acidic media. (a) Typical polarogram changes for the hydrolysis of  $10^{-5}M$  dantrolene in  $2M$  HCl media, at  $22^\circ$ . (b) Variation of the current peak intensity (azomethine group) with time, in the same solution as for (a).

found, which resulted primarily in saturation of the carbon–nitrogen double bond to yield the hydrazine (scheme 2). At intermediate pH values both reduction paths may be followed simultaneously and the relative importance of the two routes depends on the pH.

If we regard the  $pK_a$  values of 2.0 and 7.5 as the true values, and calculate the distribution curve as a function of pH, we find that at  $pH \sim 5$  the dantrolene is practically entirely in the neutral form HA. Since the dissociated species  $A^-$  is non-electroactive, we conclude that the change in  $\Delta E_p$  vs. pH at about pH 5.3 is due to the involvement of protons in the rate-determining step in the electroreduction of HA, and/or slow establishment of the  $HA/A^-$  equilibrium, so that the apparent  $pK_a$  value of 5.3 is an artifact related to  $pK_{a1}$  ( $=2.0$ ).

The peak height remained unchanged in the acidity range from  $H_0 -0.3$  to pH 5, then showed a slight decrease with an inflexion point at  $pH \sim 5.3$  (corresponding to the artifact break in Fig. 2), then decreased significantly at  $pH > 7$  with an inflexion point at  $pH 7.5$ , corresponding to the predominance of the non-electroactive anionic form  $A^-$ . This result is in agreement with the  $pK_{a2}$  value obtained by potentiometry (Fig. 3) and spectrophotometry (Fig. 4).

#### Solubility in buffered solution (pH 7.4)

This can be determined by DP polarography.

Preliminary assays showed that dantrolene is slightly soluble in  $0.1M$  Tris buffer at room temperature. Because of hydrolysis the solubility of the sodium salt  $S_{(DTN_8,3H_2O)}$  at  $pH 7.4$  is the sum of the solubility of both the undissociated acid molecule and the anionic form.

At  $20^\circ$  and physiological pH,  $S_0$  was  $0.7 \times 10^{-4}M$  (21 mg/l.) in the Tris buffer ( $I = 0.1M$ ). A solubility of 15 mg/l. for  $A^-$  and 1 mg/l. for HA in distilled water was reported by Wuis *et al.*<sup>7</sup> Thus the ionic strength affects the solubility.

#### Stability of dantrolene in acidic media

The advantage of the polarographic method is the possibility of directly following the changes in the azomethine group signal with time, which is impossible with a less specific method such as spectrophotometry.<sup>22</sup> A study of the stability of dantrolene solutions between  $H_0 -0.3$  and pH 3 showed that the peak current  $i_p$  decreased appreciably with time. Polarograms for the reactant and the possible reaction product 5-(*p*-nitrophenyl)furfural were obtained for  $10^{-5}M$  solutions in  $2M$  hydrochloric acid at  $22^\circ$  (Fig. 6). At  $pH > 1$  the changes in  $i_p$  were smaller and slower than those in  $2M$  hydrochloric acid, indicating that the equilibrium tended in favour of intact dantrolene. At  $pH > 2$ , the current changed negligibly with time (3% after 5 days). The stability

Table 3. Extraction ratios ( $R$ ) of dantrolene between chloroform and aqueous buffered solutions, at various pH values

Media ( $I = 0.1M$ )	Extraction pH	$i_{p1}$ arbitrary units	$2i_{p2}$ arbitrary units	$R$ , %
HCl	2	13.8	12.7	92
Citrate	3	13.2	10.4	82
	4	13.4	11.3	82
	5	14.1	11.4	83
Phosphate	6	15	12.4	83
	7.4	13.8	12.6	86
	7.5	12.4	12.0	92

In all cases, approximate standard deviation to be expected is 5%.

of dantrolene in a solution containing the microsomal suspension (10 ml) and 1M hydrochloric acid (1 ml) was examined by extraction with chloroform at various times (from 1 to 5 min) after the addition of hydrochloric acid to the medium. The absorption spectra and DP polarographic peak heights of the azomethine group in buffered solutions (pH 4.1) were constant during this time period. Thus, dantrolene was not degraded during analysis of the microsomal preparations treated with hydrochloric acid (pH 1.8).

#### Solvent extraction

The extraction procedure was developed in establishing a method for the measurement of dantrolene in microsomal preparations. Partition of the dantrolene between the solvent and a buffer of appropriate pH in the range from pH 2 to 8.5 (corresponding to the stability range of dantrolene in aqueous solutions) was determined by DP polarography. Citrate, phosphate and borate buffers were used and the ionic strength was kept at 0.1M, which gave a buffer concentration greater than that of the solute used in the experiments.

The results in Table 3 prove that pH changes had a limited effect on the extraction at a drug concentration in the  $10^{-5}M$  range. Consequently, no special pH precautions are necessary and the extraction can be performed at the pH of the aqueous solutions of the drug.

#### CONCLUSION

Potentiometry and spectrophotometry are the most widely used techniques for determination of protonation constants.<sup>13</sup> Potentiometry is usually considered to be the more precise, but it cannot be used for the study of slightly soluble substances or for those with low or high  $pK_a$  values. Sometimes these problems have been resolved by using polarography, when the protonated and uncharged forms of

the drugs are reducible at the dropping mercury electrode.

It can be concluded from the stability assays and from the  $pK_a$  values that all the forms of dantrolene are extractable into chloroform, analogously to extraction of nitrofurantoin into nitromethane, presumably owing to formation of ion-pairs with ionic species of the buffer. Extraction into chloroform at pH near 2 or at physiological pH can be performed for the determination of dantrolene and its metabolites in studies of metabolism of the drug by liver microsomes.

*Acknowledgements*—We are grateful to Professors J. Bessière and A. Nicolas (Université de Nancy 1) for stimulating discussions. We are thankful to Dr. H. Laisné (Laboratoires Oberval, Lyon, France) for his generous gift of the drugs.

#### REFERENCES

1. A. Ward and M. O. Chaffman, *Drugs*, 1986, **32**, 130.
2. S. K. Pandit, S. P. Kothary and P. J. Cohen, *Anaesthesiology*, 1979, **50**, 156.
3. Z. Jayyosi, J. Villoutreix, J. M. Ziegler, A. M. Batt, F. de Maack and G. Siest, submitted for publication.
4. J. D. Conklin and R. J. Sobers, *J. Pharm. Sci.*, 1973, **62**, 102.
5. R. D. Hollifield and J. D. Conklin, *ibid.*, 1973, **62**, 271.
6. S. J. Saxena, I. L. Honogberg, J. T. Stewart and J. J. Vallner, *ibid.*, 1977, **66**, 751.
7. E. W. Wuis, A. C. L. M. Grutters, T. B. Vree and E. van der Kleyn, *J. Chromatog.*, 1982, **231**, 401.
8. P. L. Cox, J. P. Heotis, D. Polin and G. M. Rose, *J. Pharm. Sci.*, 1969, **58**, 987.
9. L. Vignoli and B. Cristau, *Chim. Anal. (Paris)*, 1963, **45**, 439, 499.
10. J. T. Brown, in *Polarography of Molecules of Biological Significance*, W. F. Smyth (ed.), p. 111. Academic Press, London, 1979.
11. J. Chodkowski and D. Gralewska-Ludwicka, *Polish J. Chem.*, 1980, **54**, 567.
12. J. S. Burmicz, W. F. Smyth and R. F. Palmer, *Analyst*, 1976, **101**, 986.
13. A. Albert and E. P. Serjeant, *The Determination of Ionization Constants*, p. 168. Chapman & Hall, London, 1984.
14. P. Surman and P. Aswakun, *Arch. Pharm. (Weinheim)*, 1985, **318**, 14.
15. P. Zuman, in *Progress in Polarography*, P. Zuman, L. Meites and I. M. Kolthoff (eds.), Vol. III, p. 73. Wiley-Interscience, New York, 1972.
16. M. Heyrovský and S. Vavříčka, *J. Electroanal. Chem.*, 1972, **36**, 203, 223.
17. N. Inotsume and M. Nakano, *Intern. J. Pharm.*, 1983, **17**, 357.
18. R. H. Levy and M. Rowland, *J. Pharm. Sci.*, 1971, **60**, 1155.
19. L. Z. Benet and J. E. Goyan, *ibid.*, 1967, **56**, 665.
20. J. M. Clifford and W. F. Smyth, *Z. Anal. Chem.*, 1973, **264**, 149.
21. L. G. Feoktistov and H. Lund, in *Organic Electrochemistry*, M. M. Baizer (ed.), p. 378. Dekker, New York, 1973.
22. J. A. Goldsmith, A. Jenkins, J. Grant and W. F. Smyth, *Anal. Chim. Acta*, 1973, **66**, 427.



## SPECTROPHOTOMETRIC DETERMINATION OF SOME BENZOTHIADIAZINE DIURETICS WITH 7,7,8,8-TETRACYANOQUINODIMETHANE

ABDEL-MABOUD I. MOHAMED

Department of Pharmaceutical Chemistry, Faculty of Pharmacy, Assiut University, Assiut, Egypt

(Received 24 August 1987. Revised 2 February 1988. Accepted 25 March 1988)

**Summary**—A new spectrophotometric method for the determination of some benzothiadiazine drugs is presented, based on reaction with 7,7,8,8-tetracyanoquinodimethane in sodium acetate medium and measurement at 578 nm. Beer's law is obeyed in the concentration range 0.7–6.0  $\mu\text{g/ml}$  for all eight drugs tested.

Benzothiadiazines are important as diuretics and antihypertensives, used alone or in combination with other compounds. The assay procedures listed in official compendia<sup>1,2</sup> mostly describe titrimetric methods for determination of the pure drugs with sodium methoxide, lithium methoxide or tetrabutylammonium hydroxide. Other methods described include non-aqueous titrimetry,<sup>3,4</sup> complexometry,<sup>5</sup> amperometry,<sup>6</sup> polarography,<sup>7,8</sup> liquid chromatography,<sup>9-12</sup> thin-layer chromatography,<sup>13-16</sup> gas chromatography,<sup>17-19</sup> spectrophotometry<sup>3,20-28</sup> and fluorimetry.<sup>14,29</sup>

7,7,8,8-Tetracyanoquinodimethane (TCNQ) is a strong electron-acceptor and has been used for the determination of electron-donors such as alkaloids,<sup>30</sup> procaine,<sup>31</sup> some nitrogen bases,<sup>32</sup> vitamin A,<sup>33</sup> antihistamines,<sup>34</sup> pentazocaine<sup>35</sup> and some sulpha drugs.<sup>36</sup>

In the present study, TCNQ is used for determination of eight benzothiadiazine diuretics in pure or in tablet form. The proposed method is simple, sensitive and accurate.

### EXPERIMENTAL

#### Apparatus

A Zeiss PM2DL spectrophotometer and a Unicam SP 1750 spectrophotometer were used

#### Reagents

All chemicals and solvents used were of analytical grade. **TCNQ solution.** Dissolve 150 mg of TCNQ in 100 ml of acetonitrile. Prepare fresh daily.

**Sodium acetate solution.** Dissolve 3 g of sodium acetate in 100 ml of distilled water.

**Standard benzothiadiazine solutions.** Dissolve 40 mg of the benzothiadiazine drug (as the free base) in 100 ml of acetonitrile. Dilute a 5-ml portion accurately to 100 ml with acetonitrile to obtain a working standard 20- $\mu\text{g/ml}$  solution.

#### Procedure

Pipette 5 ml of standard benzothiadiazine solution into a 50-ml standard flask. Add 5 ml of TCNQ solution and 5 ml of sodium acetate solution. Mix and leave for about 5 min. Make up to volume with acetonitrile and then let stand for

20 min. Measure the absorbance at 578 nm in 1-cm cells against a reagent blank treated concurrently.

#### Analysis of benzothiadiazine tablets

Weigh and powder 20 tablets. Transfer an accurately weighed amount of powder equivalent to 40 mg of the drug (2 mg for cyclopentiazide) into a 100-ml standard flask. Add 70 ml of acetonitrile and shake the mixture well for 10 min, then dilute to volume with acetonitrile. Filter through a dry paper, discarding the first portion of filtrate. Dilute a 5-ml portion accurately to 100 ml with acetonitrile to obtain a final solution containing 20  $\mu\text{g}$  of the drug per ml. Use the cyclopentiazide filtrate without further dilution, as the final 20- $\mu\text{g/ml}$  sample solution. Apply the procedure above to 5 ml of the 20- $\mu\text{g/ml}$  solution.

### RESULTS AND DISCUSSION

Benzothiadiazines react with TCNQ to form intensely blue products at pH 9.0–9.6. These products exhibit five main absorption peaks at 436, 578, 603, 735 and 805 nm, with different intensities. Figure 1 shows the absorption spectra of the coloured products from chlorothiazide and hydrochlorothiazide as representative examples of the benzothiadiazines studied. Absorbance measurements were made at the 578 nm peak, where the reagent blank has negligible absorbance when measured against pure solvent. The absorbance, however, depends on the nature of the buffer system used (Table 1).

Figure 2 shows that at least 0.12% TCNQ solution must be used for maximum and reproducible colour intensity of the reaction products of chlorothiazide and hydrochlorothiazide to be obtained, and a concentration of 0.15% is recommended.

Figure 3 shows that the absorbance is maximal and constant when at least 5 ml of 3% sodium acetate solution is used.

Acetonitrile, dimethylformamide, dimethyl sulphoxide, isobutyl methyl ketone, methylene chloride, 1,2-dichloroethane, chloroform, dioxan, methanol and ethanol were examined as solvents. Acetonitrile

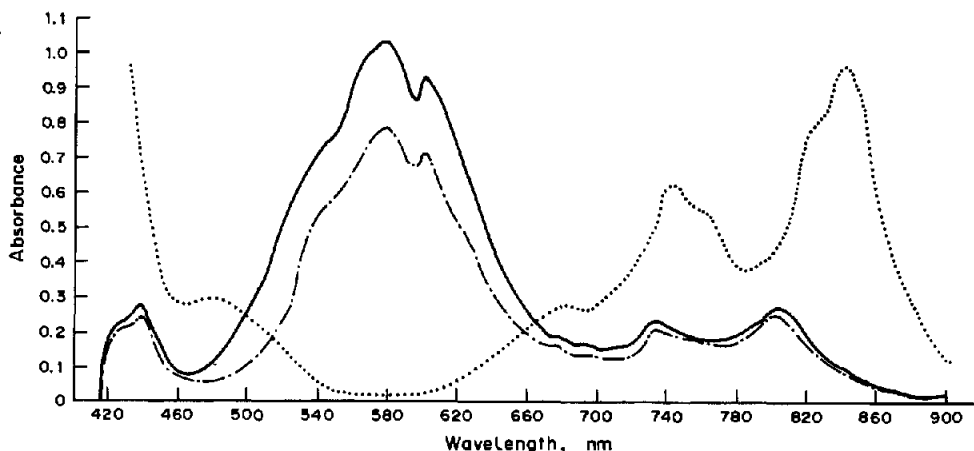


Fig. 1. Absorption spectra of the coloured products of TCNQ and sodium acetate with hydrochlorothiazide (5  $\mu\text{g/ml}$ ) —, chlorothiazide (5  $\mu\text{g/ml}$ ) - - - - and reagent blank .....

Table 1. Effect of pH on the absorbance (at 578 nm) of the reaction product of hydrochlorothiazide (4  $\mu\text{g/ml}$ ) with TCNQ in aqueous acetonitrile solution

pH	Absorbance		
	(1)	(2)	(3)
7.0	0.000	0.000	—
7.5	0.050	0.045	—
8.0	0.095	0.075	—
8.5	0.140	0.125	—
9.0	0.710	0.650	—
9.2	0.712	0.650	0.780
9.4	0.708	0.642	0.782
9.6	0.705	0.640	0.773
9.8	0.672	0.623	0.731
10.0	0.578	0.560	0.630
10.5	0.500	0.470	0.603
11.0	0.485	0.464	0.592

(1) Britton and Robinson buffer, pH 2.40–12.02.

(2) Teorell and Stenhagen buffer, pH 2.0–12.0.

(3) Kolthoff and Vleschhouwer buffer, pH 9.2–11.0.

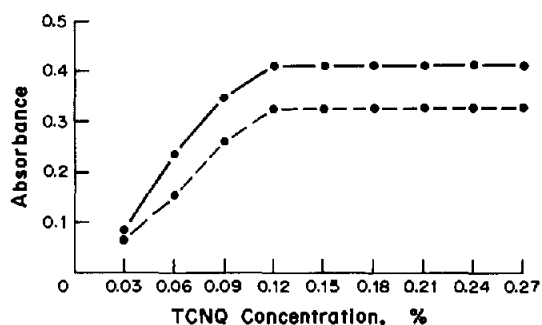


Fig. 2. Effect of TCNQ concentration on the absorbance of the hydrochlorothiazide (2  $\mu\text{g/ml}$ ) —●— and chlorothiazide (2  $\mu\text{g/ml}$ ) - -●- products.

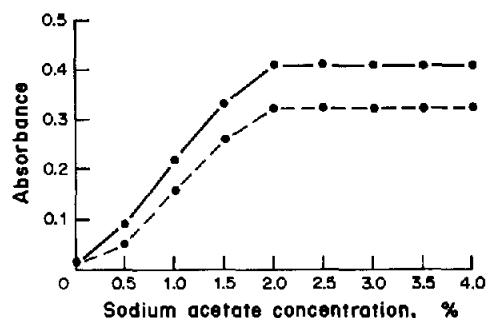


Fig. 3. Effect of sodium acetate concentration on the absorbance of the hydrochlorothiazide (2  $\mu\text{g/ml}$ ) —●— and chlorothiazide (2  $\mu\text{g/ml}$ ) - -●- products.

Table 2. Comparative summary of statistical data for determination of some benzothiadiazine drugs with TCNQ and sodium acetate

Compound	$\epsilon$ at 578 nm, $l. \text{mole}^{-1}. \text{cm}^{-1}$	Beer's law linearity range, $\mu\text{g/ml}$	Slope	Intercept	Correlation coefficient
Hydrochlorothiazide	$6.07 \times 10^4$	0.4–6	0.202	0.011	0.9935
Hydroflumethiazide	$5.96 \times 10^4$	0.4–7	0.179	0.005	0.9990
Benzthiazide	$4.84 \times 10^4$	0.7–10	0.112	0.003	0.9950
Bendroflumethiazide	$6.24 \times 10^4$	0.5–8	0.150	0.010	0.9997
Trichloromethiazide	$6.09 \times 10^4$	0.4–7	0.159	0.005	0.9990
Cyclothiazide	$5.77 \times 10^4$	0.5–8	0.148	0.000	0.9943
Cyclopenthiazide	$5.47 \times 10^4$	0.5–8	0.145	–0.005	0.9958

Table 3. Analysis of some benzothiadiazine diuretics in commercial preparations by the proposed method and official methods (mean  $\pm$  standard deviation of 5 determinations)

Product	Content	Proposed method				Found by B.P. 1980, mg/tablet
		Nominal content, mg/tablet	Found,* mg/tablet	Added, mg/tablet	Recovery, %	
Esidrex tablets	Hydrochlorothiazide	50	48.8 $\pm$ 0.5 $t = 1.85, F = 1.65$	50	98.6 $\pm$ 0.6	49.6 $\pm$ 0.4
Hydrex tablets	Hydrochlorothiazide	25	25.4 $\pm$ 0.3 $t = 2.72, F = 1.78$	25	99.4 $\pm$ 0.8	24.6 $\pm$ 0.2
Reserpine-hydrochlorothiazide tablets†	Reserpine Hydrochlorothiazide	0.125 25	25.4 $\pm$ 0.3 $t = 0.52, F = 1.21$	25	100.2 $\pm$ 0.6	25.5 $\pm$ 0.2
Saluron tablets	Hydroflumethiazide	50	48.8 $\pm$ 0.5 $t = 0.45, F = 1.49$	50	98.4 $\pm$ 1.2	48.7 $\pm$ 0.5
Fovane tablets	Benzthiazide	50	49.9 $\pm$ 0.5 $t = 0.13, F = 1.00$	50	101.0 $\pm$ 0.9	49.6 $\pm$ 0.6§
Navidrex tablets	Cyclopentthiazide	0.5	0.482 $\pm$ 0.003 $t = 1.25, F = 0.30$	—	—	0.484 $\pm$ 0.005

\*Theoretical values at 95% confidence limit:  $t = 2.78, F = 6.39$ ; Comparison with official method.

†Laboratory-prepared tablets.

§Analysed according to USP 1980.

as diluent afforded maximum stability and intensity of colour. It also has fairly good solvent power for TCNQ (0.3% maximum solubility) and for all studied benzothiadiazines. None of the other solvents is a good substitute for it.

The colour develops completely in 15 min at 30°, and remains stable for at least 90 min. At 20° the corresponding times are 35 min and 2 hr. Heating increases the reaction rate but also decreases the stability of the colour, and use of temperatures above 35° is not recommended. There is marked loss of colour at temperatures above 50°.

For all the benzothiadiazine drugs studied, under the conditions described the Beer's law plots were linear in the general concentration range of 0.7–6.0  $\mu\text{g/ml}$  (Table 2). Separate determinations at different concentration levels of each drug gave coefficients of variation not exceeding 2%.

To assess the selectivity of the method for benzothiadiazines, several drugs and related compounds were tested under the recommended reaction conditions. Substituted sulphonamides, sulphonacetamides, sulphonyl ureas and acetanilide gave zero absorbance at 578 nm. Primary aromatic amines give yellow to orange products with absorption maxima at 330 and 475 nm, but negligible absorbance at 578 nm. The reaction products formed with different benzothiadiazines and unsubstituted sulphonamides have approximately similar spectral characteristics. Thus the method is not suitable for analysis of their mixtures without prior separation, or of hydrolysed benzothiadiazine samples containing 4-amino-6-chloro-1,3-disulphonamide. However, most benzothiadiazines are commercially available in plain dosage forms and the problem of interference does not then arise.

Commercial tablets of hydrochlorothiazide, hydroflumethiazide, benzothiazide and cyclopentthiazide were successfully analysed by the method. Recovery experiments were performed for each drug in tablet forms. The results (Table 3) were compared statistically with those obtained by applying the compendial methods.<sup>1,37</sup> Commonly encountered excipients and additives did not interfere with the colour development.

Job's method of continuous variation<sup>38</sup> showed that the benzothiadiazines and TCNQ reacted in 1:1 molar ratio under the recommended conditions. Attempts to characterize the products failed, however; although they were readily isolated by solvent extraction or column chromatography, they were too unstable for identification to be possible.

## REFERENCES

1. *British Pharmacopoeia*, Her Majesty's Stationery Office, London, 1980.
2. *United States Pharmacopoeia XXI, and National Formulary XVI*, U.S. Pharmacopoeial Convention, Rockville, 1985.
3. E. F. Salim and W. W. Hilty, *J. Pharm. Sci.*, 1967, **56**, 518.

4. H. C. Chiang, *ibid.*, 1961, **50**, 885.
5. L. Przyborowski and G. Pionka, *Farm. Pol.*, 1976, **32**, 399; *Anal. Abstr.*, 1976, **31**, SE64.
6. M. Madgeara, H. Beral and E. Cuciureanu, *Farmacia (Bucharest)*, 1968, **16**, 471; *Chem. Abstr.*, 1969, **70**, 6558e.
7. A. L. Woodson and D. E. Smith, *Anal. Chem.*, 1970, **42**, 242.
8. E. Kkolos and J. Walker, *Anal. Chim. Acta*, 1975, **80**, 17.
9. R. H. Barbhaiya, T. A. Phillips and P. G. Welling, *J. Pharm. Sci.*, 1981, **70**, 291.
10. J. Kirschbaum and S. Perlman, *ibid.*, 1984, **73**, 686.
11. S. Perlman, M. Szyper and J. Kirschbaum, *ibid.*, 1984, **73**, 259.
12. A. G. Butterfield, E. G. Lovering and R. W. Sears, *ibid.*, 1978, **67**, 651.
13. M. Schaefer, H. E. Geissler and E. Mutschler, *J. Chromatog.*, 1977, **143**, 615.
14. Y. Garceau, I. Davis and J. Hasegawa, *J. Pharm. Sci.*, 1974, **63**, 1793.
15. G. Misztal, M. Przyborowska and L. Przyborowski, *Pharmazie*, 1983, **38**, 67.
16. G. B. Osborne, *J. Chromatog.*, 1972, **70**, 190.
17. W. J. A. Vandenneuvel, V. F., Gruber, R. W. Walker and F. J. Wolf, *J. Pharm. Sci.*, 1975, **64**, 1309.
18. B. Lindstroem, M. Molander and M. Groschinsky, *J. Chromatog.*, 1975, **114**, 459.
19. C. Fagerlund, P. Hartvig and B. Lindstroem, *ibid.*, 1979, **168**, 107.
20. B. Pérez, C. Danhier and A. J. Brieva, *An. Real Acad. Farm.*, 1967, **33**, 233; *Intern. Pharm. Abstr.*, 1968, **5**, 1270.
21. P. Bulut and F. Tureli, *Turk. Hij. Deneyisel Biyol. Derg.*, 1983, **40**, 206; *Anal. Abstr.*, 1984, **46**, 1E36.
22. H. Abdine, M. A-H. El-Sayed and Y. M. El-Sayed, *J. Assoc. Off. Anal. Chem.*, 1978, **61**, 695.
23. R. Chu, *ibid.*, 1971, **54**, 603.
24. H. Kala, *Pharmazie*, 1965, **20**, 82.
25. D. Suria, *Clin. Biochem.*, 1978, **11**, 222.
26. F. Namigohar, J. Khorrami and A. Soltani, *J. Pharm. Belg.*, 1977, **32**, 162.
27. M. A.-H. El-Sayed and C. O. Nwakanma, *Pharmazie*, 1979, **34**, 251.
28. B. A. Moussa and N. M. El-Kousy, *Pharm. Weekbl. Sci. Ed.*, 1985, **7**, No. 2, 79.
29. R. B. Smith, R. V. Smith and G. J. Yakatan, *J. Pharm. Sci.*, 1976, **65**, 1208.
30. A. Taha and A. Ruecker, *Arch. Pharm. (Weinheim)*, 1977, **310**, 485.
31. K. A. Kovar, W. Mayer and H. Auterhoff, *ibid.*, 1981, **314**, 447.
32. S. I. Obtemperanskaya and E. A. El-Kafravi, *Zh. Analit. Khim.*, 1982, **37**, 1894.
33. F. U. Lichti and J. A. Lucy, *Biochem. J.*, 1969, **112**, 221.
34. M. M. Abdel-Khalek, M. E. Abdel-Hamid and M. S. Mahrous, *J. Assoc. Off. Anal. Chem.*, 1985, **68**, 1057.
35. M. E. Abdel-Hamid, M. S. Mahrous M. M. Abdel-Khalek and M. A. Abdel-Salem, *J. Pharm. Belg.*, 1985, **40**, 237; *Anal. Abstr.*, 1986, **48**, 7E26.
36. S. I. Obtemperanskaya, E. A. El-Kafravi and N. V. Zhmurova, *Vestn. Mosk. Univ., Ser. 2, Khim.*, 1985, **26**, 327; *Anal. Abstr.*, 1986, **48**, 3E51.
37. *United States Pharmacopeia XX and National Formulary XV*, p. 77. U.S. Pharmacopeial Convention, Rockville, 1980.
38. P. Job, *Ann. Chim. (Paris)*, 1936, **16**, 97.

## A STUDY OF THE CHEMILUMINESCENCE OF SOME ACIDIC TRIPHENYLMETHANE DYES

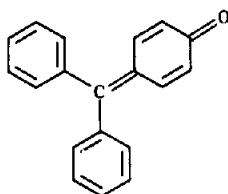
G. N. CHEN\* and C. S. HUANG

Chemistry Department of Fuzhou University, Fuzhou, Fujian, People's Republic of China

(Received 24 June 1987. Revised 18 February 1988. Accepted 23 March 1988)

**Summary**—Chemiluminescence was observed when some acidic triphenylmethane dyes were oxidized with hydrogen peroxide in alkaline solution. Trace amounts of Co(II) catalysed this chemiluminescent reaction strongly, especially in the presence of the cationic surfactant cetyltrimethylammonium bromide. The chemiluminescence spectra of some compounds and the absorption spectra of some products of the chemiluminescent reactions were investigated, and some acidic triphenylmethane dyes were studied by the Hückel molecular orbital method. On the basis of these investigations, a possible mechanism for this chemiluminescent reaction, and an initial explanation for the relationship between the structure of the reagents and their chemiluminescent behaviour were proposed. The optimum conditions for use of some of the chemiluminescent reaction systems were selected by means of the modified simplex method, and a chemiluminescent analytical method for determination of ultratrace amounts of cobalt was established, with a detection limit of 5 pg/ml. It was used for analysis of natural water samples, and good results were obtained.

Acidic triphenylmethane dyes are an important type of organic reagent. All examples of this kind of reagent have the following basic structure:



These dyes are principally used in analytical chemistry as indicators for complexometric titrations and as reagents for spectrophotometric analysis, especially in the presence of surfactants, their sensitivity then being greatly increased, the molar absorptivity of their complexes generally being  $> 1 \times 10^5 \text{ l. mole}^{-1} \cdot \text{cm}^{-1}$ .

We have found that when certain acidic triphenylmethane dyes were oxidized with hydrogen peroxide in alkaline solution, chemiluminescence could be observed, and that trace Co(II) strongly catalysed this chemiluminescent reaction, especially in the presence of the cationic surfactant cetyltrimethylammonium bromide (CTMAB). However, chemiluminescence could not be observed for some other acidic triphenylmethane dyes under the same conditions. We have tried to discover the relationship between the chemiluminescent behaviour and the structural character of the reagent molecules. We studied some acidic triphenylmethane dyes by the Hückel molecular orbital (HMO) method, and also

investigated the chemiluminescence spectra of some compounds and the absorption spectra of some products of chemiluminescent reactions. On the basis of these investigations, we have identified the structural character of the reagents which are able to produce chemiluminescence, and proposed a possible mechanism for this chemiluminescent reaction.

We have also examined the application of these chemiluminescent systems in analytical chemistry. All of them can be used for the determination of ultratrace amounts of cobalt; the detection limit found was 5 pg/ml with the Pyrogallol Red system, and this is so far one of the most sensitive methods for determination of cobalt.<sup>1-4</sup>

### EXPERIMENTAL

#### Apparatus

FG83-1 chemiluminescence spectrophotometer (made in our laboratory). 751G spectrophotometer (Analytical Instrumental Plant, Shanghai).

#### Reagents

*Standard solution of Co(II)*. High-purity (99.99%) cobalt powder was dissolved in pure concentrated hydrochloric acid, then diluted to the required concentration with water.

*Solutions of acidic triphenylmethane dyes*. The analytical grade dyes were dissolved in absolute ethanol, and the solutions diluted to the required concentration with water.

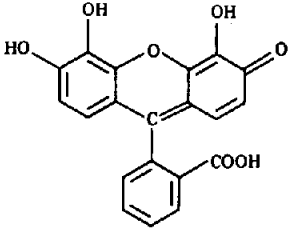
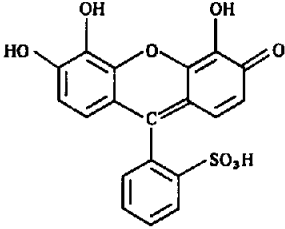
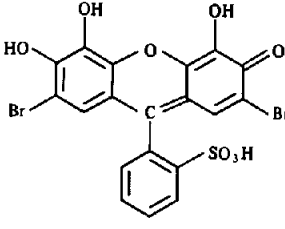
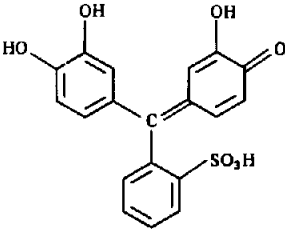
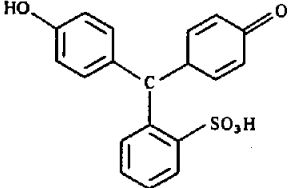
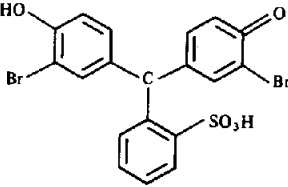
All other reagents were analytical grade or better and all water used was doubly distilled in fused-silica apparatus.

#### Procedures

*Detection of chemiluminescence*. One ml of Pyrogallol Red (or other dye) solution, 0.5 ml of CTMAB solution, 0.5 ml of hydrogen peroxide solution, 2.5 ml of water and 0.5 ml of sodium hydroxide solution were added in turn by pipette to the reaction cell and mixed. The cell was then put into the camera, the shutter was opened and the zero point of the

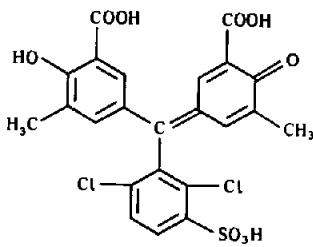
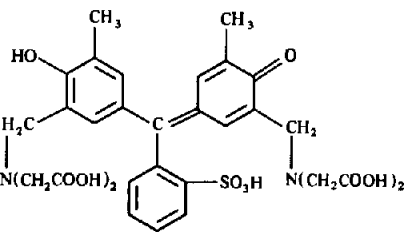
\*Present address: Chemistry Department, La Trobe University, Bundoora, Victoria 3083, Australia.

Table 1. The chemiluminescent characters of some acidic triphenylmethane dyes

Reagent	Structural formula	CL signal*	Catalytic ions
4,5-Dihydroxyfluorescein		Strongest	Co(II) Fe(III) Ni(II)
Pyrogallol Red		Very strong	Co(II) Fe(III) Ni(II)
Bromopyrogallol Red		Strong	Co(II) Fe(III) Ni(II)
Pyrocatechol Violet		Less strong	Co(II) Fe(III) Ni(II) Cu(II) Cr(III)
Phenol Red		No signal	
Bromophenol Red		No signal	

*continued*

Table 1—continued

Reagent	Structural formula	CL signal*	Catalytic ions
Chrome Azurol S		No signal	
Xylenol Orange		No signal	

\*CL = chemiluminescence.

recorder was adjusted. Then standard Co(II) standard solution (or a water sample) was injected into the reaction cell and the chemiluminescence signal was recorded.

*For measurement of absorption spectra.* After detection of the chemiluminescence, the absorption spectrum in the ultraviolet region was measured against a reagent blank solution in 1-cm silica cells.

## RESULTS AND DISCUSSION

From the many acidic triphenylmethane dyes, we selected Pyrogallol Red, Bromopyrogallol Red, Pyrocatechol Violet, Phenol Red, Bromophenol Red, 4,5-dihydrofluorescein, Chrome Azurol S and Xylenol Orange for investigation. Their chemiluminescence characteristics are shown in Table 1.

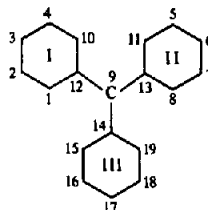
### *Mechanism of the chemiluminescence*

*Chemiluminescence spectra.* Figure 1 shows that the chemiluminescence spectra produced on oxidation of Pyrogallol Red, Pyrocatechol Violet, Bromopyrogallol Red, pyrogallol, catechol and gallic acid are very similar, with a band at 520 nm and another at 580 nm, which suggests that when these acidic triphenylmethane dyes are oxidized, polyphenols, such as pyrogallol, catechol and gallic acid may be produced during the reactions, and that the chemiluminescence occurs on further oxidation of these intermediates.

*Absorption spectra of some reaction products.* During the chemiluminescent reactions of the acidic triphenylmethane dyes studied, the solutions gradu-

ally became colourless. Figure 2 shows that the final reaction products of the acidic triphenylmethane dyes and polyphenols tested all gave very similar ultraviolet absorption spectra, with maximal absorbance at about 300 nm. This again suggests that the polyphenols are involved in the reaction mechanism.

*Mechanism.* The electron-density distribution in the acidic triphenylmethane dyes studied was calculated by the Hückel molecular orbital method. For convenience in discussion, the carbon atoms and benzene rings of the dye molecules are numbered as follows:



The calculation shows that for all the dyestuffs tested the  $\pi$ -electron density at  $C_9$  is lower than at the other carbon atoms. Of the three atoms connected with  $C_9$ , the  $C_{14}$  atom has the lowest  $\pi$ -electron density. It is generally recognized that in alkaline solution, hydrogen peroxide produces the  $O_2^-$  ion radical. This should attack the  $C_9$  position first, with possible production of a peroxide bridge between  $C_9$  and  $C_{14}$ , followed by formation of the polyphenols. The scheme is shown below for Pyrogallol Red as an example.

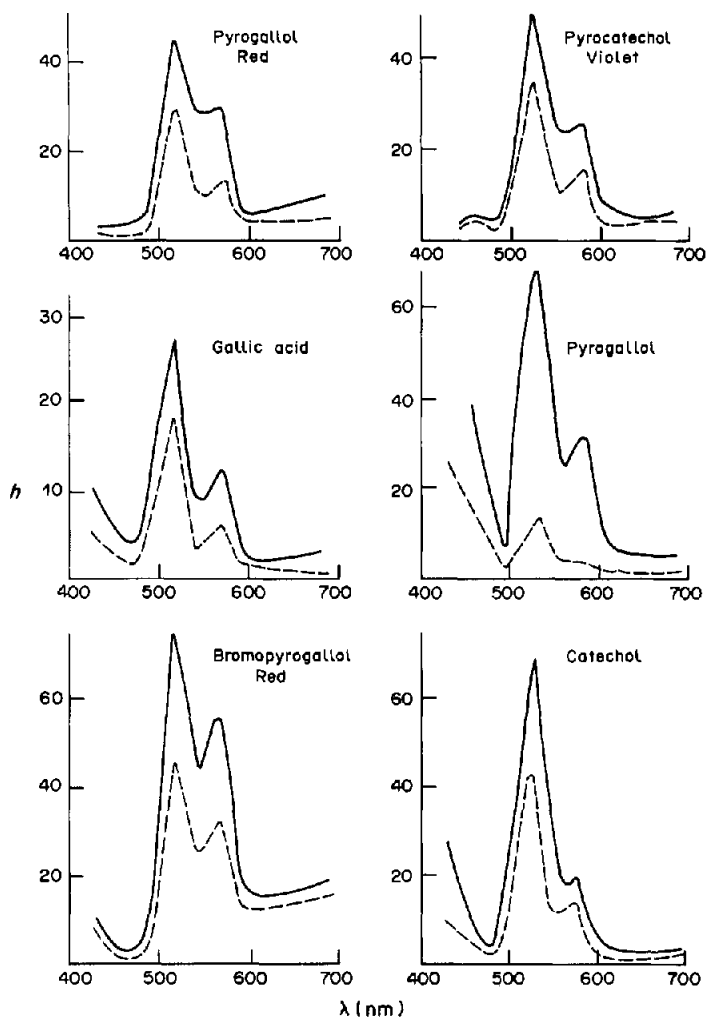
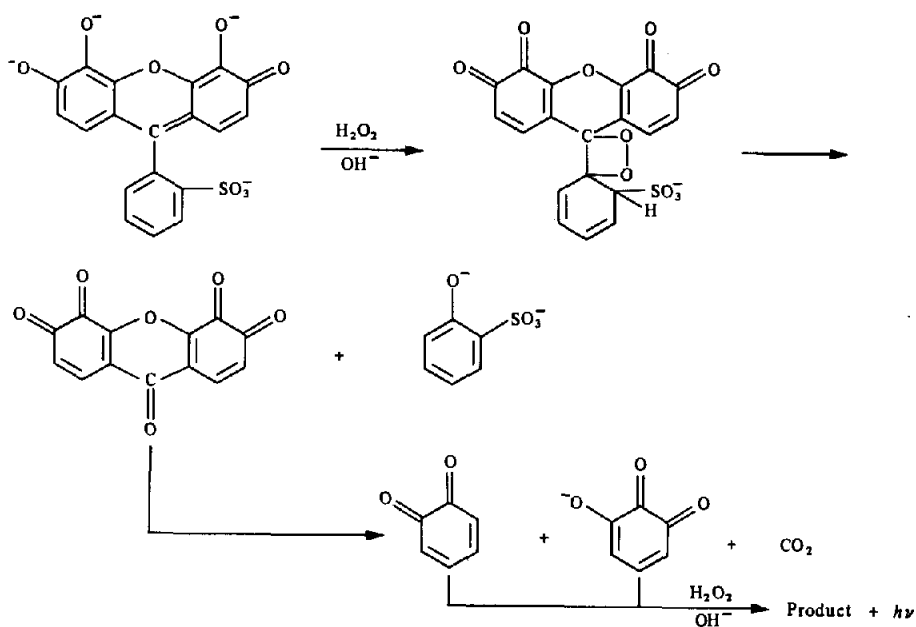


Fig. 1. Chemiluminescence spectra from some compounds: (—) with CTMAB; (---) without CTMAB.



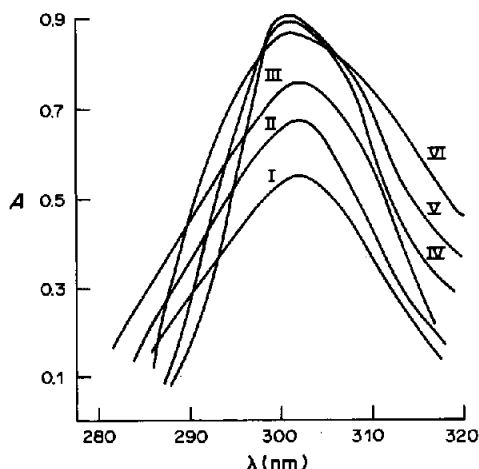


Fig. 2. Absorption spectra of reaction products from I, Bromopyrogallol Red; II, Pyrogallol Red; III, Pyrocatechol Violet; IV, catechol; V, pyrogallol; VI, gallic acid.

The production of  $\text{CO}_2$  was confirmed by experiment, and the mechanism of the chemiluminescent oxidation of polyphenols has been shown<sup>5</sup> to proceed in several stages to produce low molecular-weight, water-soluble polymers, and several other as yet unidentified products, and the chemiluminescence is due to emission from singlet oxygen and intermolecular energy-transfer.

The results of our quantum calculation also show that the chemiluminescence intensity obtained by oxidation of these reagents is also related to the difference in  $\pi$ -electron density between positions 9 and 14 (denoted by  $\delta$ ), and in general increases with it (Table 2). 4,5-Dihydroxyfluorescein has a carboxyl group at  $\text{C}_{19}$ , which not only greatly decreases the  $\pi$ -electron density at positions  $\text{C}_9$  and  $\text{C}_{14}$  but also greatly increases  $\delta$ , so the chemiluminescence intensity obtained with 4,5-dihydroxyfluorescein is the strongest.

#### Relationship between the chemiluminescence behaviour and structure of acidic triphenylmethane dyes

Pyrocatechol Violet gives quite strong chemiluminescence on oxidation by hydrogen peroxide in alkaline solution, but Phenol Red is decolorized without production of chemiluminescence. The two dyes differ in structure by only the two additional hydroxyl groups at  $\text{C}_4$  and  $\text{C}_5$  in Pyrocatechol Violet (Table 1). The quantum mechanical calculations

show that the  $\pi$ -electron density at  $\text{C}_9$  is even lower in Phenol Red than in Pyrocatechol Violet. Moreover, the rate of disappearance of the colour shows that Phenol Red is oxidized as rapidly as Pyrocatechol Violet, so the oxidation mechanism is likely to be the same for both, only the products being different: a catechol from Pyrocatechol Violet and a phenol from Phenol Red. Many experiments have shown that no chemiluminescence is produced from a phenol under the conditions used. From the structural formulae of Chrome Azurol S and Xylenol Orange, we know that there are no polyphenols among their oxidation products, so no chemiluminescence is observed. Comparison of the structures of Pyrogallol Red and Pyrocatechol Violet shows that the former has an "oxo bridge" between positions 10 and 11, whereas the latter does not, so when Pyrogallol Red is oxidized there is a pyrogallol among the products. The chemiluminescence from Pyrogallol Red is therefore more intense than that from Pyrocatechol Violet (the chemiluminescence intensity from pyrogallol is stronger than that from catechol).

Several initial conclusions can be drawn, as follows. (1) When an acidic triphenylmethane dye containing an "oxo bridge" between positions 10 and 11 is oxidized, chemiluminescence occurs. (2) The occurrence of a chemiluminescence reaction and the intensity of any chemiluminescence produced will depend on the numbers of hydroxyl groups on the benzene rings of the molecule; if there is no "oxo bridge" between positions 10 and 11, chemiluminescence will occur only if there are two or more hydroxyl groups on benzene rings I and II, the chemiluminescence intensity generally increasing with the number of hydroxyl groups, and that of an *ortho*-dihydroxyl compound being stronger than that of a *meta*-dihydroxyl compound. (3) The  $\pi$ -electron density at positions 9 and 14 will be decreased and the  $\delta$  value increased by introduction of an electron-withdrawing group at position 19, and the chemiluminescence will be intensified. (4) The  $\delta$  value will be decreased by introduction of a halogen atom at positions 2 and 7, so this will not improve the chemiluminescent performance.

#### Application in analytical chemistry

$\text{Co(II)}$  is one of the most commonly studied ions in chemiluminescence analysis. In general, its detection limit is 0.01–1 ng/ml.<sup>1-4</sup> The chemiluminescence reaction of acidic triphenylmethane dyes in alkaline solution is strongly catalysed by trace  $\text{Co(II)}$ , especially in the presence of the cationic surfactant CTMAB, and the chemiluminescence intensity is proportional to the concentration of  $\text{Co(II)}$ . Thus these chemiluminescence systems are suitable for determination of trace  $\text{Co(II)}$ . We have therefore tried to find the best conditions for determination of trace  $\text{Co(II)}$  in natural water.

The chemiluminescence intensity from acidic triphenylmethane dyes is dependent on the concen-

Table 2. Relationships between  $\delta$  value and chemiluminescence intensity

Reagent	$\delta$	Intensity
4,5-Dihydroxyfluorescein	0.106	Strongest
Pyrogallol Red	0.086	Very strong
Bromopyrogallol Red	0.076	Strong
Pyrocatechol Violet	0.068	Less strong

Table 3. Optimum conditions for some reaction systems

System	[Reagent], <i>M</i>	[CTMAB], <i>M</i>	[H <sub>2</sub> O <sub>2</sub> ], <i>M</i>	[NaOH], <i>M</i>
4,5-Dihydroxyfluorescein	$1 \times 10^{-5}$	$2 \times 10^{-5}$	0.10	0.25
Pyrogallol Red	$5 \times 10^{-5}$	$5 \times 10^{-4}$	0.20	0.25
Bromopyrogallol Red	$1 \times 10^{-4}$	$8 \times 10^{-5}$	0.30	0.15
Pyrocatechol Violet	$5.5 \times 10^{-5}$	$5 \times 10^{-4}$	0.12	0.24

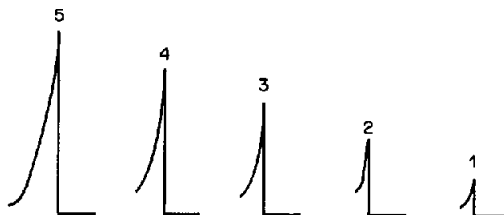


Fig. 3. Typical chemiluminescence signals for determination of cobalt: 1, blank; 2, 0.1 ng/ml; 3, 0.2 ng/ml; 4, 0.3 ng/ml; 5, 0.4 ng/ml.

trations of the dye, hydrogen peroxide, CTMAB and sodium hydroxide used. These systems are not easy to optimize by the traditional methods. The modified simplex method (MSM), however, is readily adaptable to solving such problems,<sup>6,7</sup> and was therefore used for the purpose, and the conditions found for Pyrogallol Red, Pyrocatechol Violet, Bromopyro-

gallol Red and 4,5-dihydroxyfluorescein are listed in Table 3.

Under the optimized conditions for use of Pyrogallol Red, the relative standard deviation found (10 replicates) for 2 ng/ml Co(II) was 3.3%. The standard deviation of the peak height (10 replicates) for the blank was 0.20 mm. Typical chemiluminescence signals are shown in Fig. 3. For the range 0.05–0.4 ng/ml Co(II) the calibration equation found was

$$H = 0.2 + 80.5[\text{Co(II)}]$$

where  $H$  is the peak height (mm) and [Co(II)] is in ng/ml. The correlation coefficient was 0.9998, and the detection limit was 0.005 ng/ml (defined as three times the concentration corresponding to the standard deviation of the blank signal).

An investigation of interference in the determination of 2 ng/ml Co(II) gave the results shown in Table 4. It is evident that the selectivity of the

Table 4. Effect of diverse ions on determination of 2 ng/ml Co(II)

Ion	Added, ng/ml	Co(II) recovery, %	Ion	Added, ng/ml	Co(II) recovery, %
Ni(II)	40	105	Bi(III)	1000	102
Ca(II)*	10,000	97	Nb(V)	300	108
Mg(II)*	10,000	96	Rh(III)	25	109
Al(III)	200	108	Ir(III)	50	106
Cu(II)	200	110	V(V)	200	91
Cr(III)	200	98	Ge(III)	500	96
Pb(II)	200	98	Mn(II)	200	101
Cd(II)	200	107	Fe(III)	10,000	103
Mo(VI)	200	99	Ga(III)	20	102
Ti(III)	200	91	Cl <sup>-</sup>	$9.0 \times 10^7$	86
W(VI)	200	99	NO <sub>3</sub> <sup>-</sup>	$6.2 \times 10^6$	101
Zn(II)	200	98	PO <sub>4</sub> <sup>3-</sup>	$1.9 \times 10^5$	86
Ti(IV)	1000	106	ClO <sup>-</sup>	$8.8 \times 10^{-4}$ M	91

\*In presence of tartaric acid.

Table 5. Results of determination of Co(II) in natural waters (10 replicates)

Sample	[Co(II)] ± s.d., ng/ml	Co(II) recovery,* %	[Co(II)] found by GFAAS, ng/ml
Ming river 1	$0.62 \pm 0.02$	97	0.68
Ming river 2	$0.57 \pm 0.01$	98	0.55
West lake 1	$1.24 \pm 0.03$	96	1.30
West lake 2	$1.08 \pm 0.02$	102	1.12
Hot spring 1	$0.35 \pm 0.01$	97	0.41
Tap water	$0.48 \pm 0.02$	102	0.46

\*Of 1 ng/ml added Co(II).

Pyrogallol Red system is adequate for determination of Co(II) in natural water. The method is very simple. The water sample is adjusted to pH 3–4 with hydrochloric acid, then filtered through a 0.45  $\mu\text{m}$  membrane, and analysed as described above.

The measurement takes only 2 min for each sample. The results for analysis of some natural water samples are shown in Table 5.

#### REFERENCES

1. F. Zhang and G. N. Chen, *Fenxi Huaxue*, 1985, **13**, 790.
2. M. Yamada and S. Suzuki, *Chem. Lett.*, 1983, 783.
3. R. J. Miller and J. D. Ingle, Jr., *Talanta*, 1982, **29**, 303.
4. D. F. Marino and J. D. Ingle, Jr., *Anal. Chem.*, 1981, **53**, 292.
5. D. Slawinska and J. Slawinski, *ibid.*, 1975, **47**, 2101.
6. G. N. Chen and F. Zhang, *Gaodeng Xuexiao Huaxue Xuebao*, in the press.
7. *Idem*, *Acta Chim. Sinica*, 1987, **45**, 139.

# DETERMINATION OF SELENIUM IN ORES, CONCENTRATES AND RELATED MATERIALS BY GRAPHITE-FURNACE ATOMIC-ABSORPTION SPECTROMETRY AFTER SEPARATION BY EXTRACTION OF THE 4-NITRO-*o*-PHENYLENEDIAMINE COMPLEX

ELSIE M. DONALDSON

Mineral Sciences Laboratories, Canada Centre for Mineral and Energy Technology, Department of  
Energy, Mines and Resources, Ottawa, Canada

(Received 1 December 1987. Accepted 17 February 1988)

**Summary**—A method for determining  $\sim 0.01 \mu\text{g/g}$  or more of selenium in ores, concentrates, rocks, soils, sediments and related materials is described. After sample decomposition selenium is reduced to selenium(IV) by heating in 4M hydrochloric acid and separated from the matrix elements by toluene extraction of its 5-nitropiazselenol complex from  $\sim 4.2M$  hydrochloric acid. After the extract has been washed with 2% nitric acid to remove residual iron, copper and chloride, the selenium in the extract is oxidized to selenium(VI) with 20% bromine solution in cyclohexane and stripped into water. This solution is evaporated to dryness in the presence of nickel, and selenium is ultimately determined in a 2% v/v nitric acid medium by graphite-furnace atomic-absorption spectrometry at 196.0 nm with the nickel functioning as matrix modifier. Common ions, including large amounts of iron, copper and lead, do not interfere. More than 1 mg of vanadium(V) and 0.25 mg each of platinum(IV), palladium(II) and gold(III) causes high results for selenium, and more than 1 mg of tungsten(VI) and 2 mg of molybdenum(VI) causes low results. Interference from chromium(VI) is eliminated by reducing it to chromium(III) with hydroxylamine hydrochloride before the formation of the selenium complex.

The accurate determination of trace and  $\mu\text{g}$  amounts of selenium in ores, concentrates, rocks, soils, processing products and related materials is an important requirement in many CANMET projects, including the Canadian Certified Reference Materials Project (CCRMP). With the recent acquisition by the CANMET Chemical Laboratory of graphite-furnace instrumentation, it was considered that it might be possible to develop a suitably sensitive graphite-furnace atomic-absorption spectrometric (GFAAS) method for selenium that would be applicable to all these materials and that would involve a reasonably selective solvent-extraction separation step.

Probably the most selective solvent-extraction procedures for selenium are those involving the extraction of piazselenol complexes with 1,2-diaminobenzene and its derivatives<sup>1,2</sup> and, in recent years, numerous gas-chromatographic methods with electron-capture detection (GCECD)<sup>3-6</sup> and GFAAS methods<sup>7-13</sup> for the determination of small amounts of selenium in a variety of materials have been based on this type of separation. In most of these methods, particularly the more recent ones, the 4-nitro substituted *o*-phenylenediamine derivative was used for complex formation either because of its greater sensitivity in gas-chromatographic work and its high selectivity and stability or because it reacts with selenium at relatively high acidity.<sup>1,2</sup> This last

property gives it a definite advantage over other commonly used reagents such as 2,3-diaminonaphthalene, 3,3'-diaminobenzidine and the 4-chloro substituted reagent, which require either one or two pH adjustments for complex formation,<sup>2</sup> because it facilitates and expedites the complex formation step. For this reason 4-nitro-*o*-phenylenediamine was also chosen for the present work and complex formation was further hastened by heating the selenium solution after the addition of the reagent.<sup>1,3</sup> Although the extract and, in most cases, a matrix modifier are injected directly into the graphite furnace in all the GFAAS methods mentioned above, an aqueous medium was chosen for this work because of the greater reproducibility and sensitivity.

In the proposed method, selenium is separated from matrix elements by extraction of the 5-nitropiazselenol complex into toluene from  $\sim 4M$  hydrochloric acid in the presence of hydroxylamine hydrochloride as a reductant for chromium(VI). Selenium in the extract is oxidized to selenium(VI) with bromine solution in cyclohexane, stripped into water and ultimately determined by GFAAS in a 2% v/v nitric acid medium in the presence of nickel as matrix modifier.

## EXPERIMENTAL

### Apparatus

A Perkin-Elmer model 5000 atomic-absorption spectrometer, equipped with an HGA-400 graphite furnace, an AS-40 autosampler, a Data System 10 and HGA graphics

software, was used with a selenium hollow-cathode lamp operated at 8 mA. The 196.0 nm resonance line was used with a spectral band-pass of 0.7 nm. Pyrolytically-coated graphite tubes with solid pyrolytic graphite platforms were employed and 20- $\mu$ l aliquots of the appropriate solutions, containing 0.01% nickel as matrix modifier, were injected. Measurements were made in the peak-height mode, with deuterium-arc background correction. The instrumental conditions for the dry, char and atomization steps are given in Table 1.

#### Reagents

**Standard selenium solution, 1000  $\mu$ g/ml.** Dissolve 0.5476 g of pure sodium selenite in water, add  $\sim$ 12.5 ml of concentrated nitric acid and dilute the solution to 250 ml with water. Prepare a 100- $\mu$ g/ml solution in  $\sim$ 5% v/v nitric acid and a 1- $\mu$ g/ml solution in  $\sim$ 2% v/v nitric acid by appropriate dilution of the stock and 100- $\mu$ g/ml solutions, respectively. The diluted solutions are stable for at least one week. Verify the selenium content of the sodium selenite gravimetrically by precipitation with sulphur dioxide.<sup>14</sup>

**Nickel solution, 10 mg/ml.** Dissolve 1 g of high-purity nickel metal in  $\sim$ 20 ml of water containing 3 ml of concentrated nitric acid. Cool and dilute to 100 ml with water.

**4-Nitro-*o*-phenylenediamine solution, 0.5% w/v.** Dissolve 125 mg of the reagent by heating in a water-bath with  $\sim$ 15 ml of water containing 2 ml of concentrated hydrochloric acid. Cool, transfer the solution to a 60-ml separatory funnel, dilute to  $\sim$ 20 ml with water, then shake the solution for  $\sim$ 1 min with  $\sim$ 15 ml of toluene. Transfer the aqueous phase to a 25-ml standard flask and dilute to volume with water. Prepare a fresh solution weekly.

**Hydroxylamine hydrochloride solution, 20% w/v.** Store in a plastic bottle and prepare fresh weekly.

**Bromine solution, 20% v/v in cyclohexane.**

**Nitric acid, 2% v/v.**

**Hydrochloric acid, 5M.**

**Toluene.** Analytical-reagent grade.

Doubly demineralized water was used throughout and all acids employed were analytical-reagent grade.

#### Calibration solutions

Prepare 0.02-, 0.04-, 0.06-, 0.08- and 0.10- $\mu$ g/ml selenium solutions by adding 1, 2, 3, 4 and 5 ml, respectively, of 1- $\mu$ g/ml standard selenium solution to 50-ml standard flasks containing 1 ml of concentrated nitric acid and 500  $\mu$ l of 10-mg/ml nickel solution and dilute to volume with water. Prepare a blank calibration solution in a similar manner. These solutions should be prepared fresh weekly.

#### Procedure

Transfer up to 2 g of powdered sample, containing up to  $\sim$ 40  $\mu$ g of selenium, to a 250-ml Teflon beaker. Add  $\sim$ 5 ml of water, 1 ml of 10-mg/ml nickel solution and  $\sim$ 1 g of sodium chlorate (Note 1), then cover the beaker with a watch-glass and add 15 ml of concentrated nitric acid and 7 ml of concentrated perchloric acid. Heat the solution until the evolution of oxides of nitrogen ceases, then remove the cover and wash down the sides of the beaker with water.

Add 10 ml of concentrated hydrofluoric acid and carefully evaporate the solution to  $\sim$ 3 ml. Add 35 ml of water and 20 ml of concentrated hydrochloric acid, cover the beaker with a watch-glass, heat the solution to the boiling point and boil gently for  $\sim$ 10 min to dissolve the soluble salts and to reduce selenium(VI) to selenium(IV). Transfer the solution to a 100-ml standard flask containing 23 ml of concentrated hydrochloric acid, cool it to room temperature, then dilute to volume with water and allow the solution to stand until any insoluble material has settled. Run a blank through the whole procedure.

Pipette 5–25 ml of the resulting solution, containing not more than  $\sim$ 2  $\mu$ g of selenium, into a 50-ml beaker. If necessary, dilute the solution to  $\sim$ 25 ml with 5M hydrochloric acid, then add 1 ml of 20% hydroxylamine hydrochloride solution, mix and let stand for  $\sim$ 5 min. Add 1 ml of 0.5% 4-nitro-*o*-phenylenediamine solution, mix and heat the solution in a boiling water-bath for 15 min. Cool the solution to room temperature, then transfer it to a 60-ml separatory funnel, marked at 30 ml, and dilute to the mark with water. Add 10 ml of toluene, shake the solution for 2 min, allow the layers to separate, then drain off and discard the aqueous phase. Wash the extract twice, by shaking it for  $\sim$ 30 sec each time, with 10 ml of 2% nitric acid. Drain off the acid phase, then add 2 ml of 20% bromine solution in cyclohexane to the extract, mix, and allow the solution to stand for  $\sim$ 10 min to ensure the complete destruction of the selenium complex (Note 2). Add 5 ml of water and shake the funnel for  $\sim$ 30 sec. Allow the layers to separate, then drain the aqueous phase into a 50-ml beaker. Wash the stem of the funnel with water and collect the washings in the beaker. Repeat the stripping step twice more, with 5 and 3 ml of water, and wash the stem of the funnel with water each time (Note 3).

Add 200  $\mu$ l of concentrated nitric acid and sufficient 10-mg/ml nickel solution to the resulting blank and sample solutions for 50  $\mu$ l (*i.e.* 50  $\mu$ g of nickel) to be present for each 5 ml. to be present per ml of final solution (Note 4), then gently evaporate the solutions to dryness on a hot-plate maintained at  $\leq$ 200°. Cool, wash down the sides of the beakers with a few ml of water and evaporate to dryness again. Add sufficient concentrated nitric acid to each beaker for the final solutions to contain 2% by volume, then add 2 or 3 ml of water and heat gently for  $\sim$ 2 min to dissolve the salts. Allow the solutions to cool to room temperature, then transfer them to standard flasks of appropriate size (5–25 ml) and dilute to volume with water.

Measure the peak-height absorbance of the sample and blank solutions under the conditions described under "Apparatus" and in Table 1 (Note 5). Determine the selenium concentration of the solutions by reference to peak-height values obtained concurrently for the calibration solutions. Calculate the selenium content of the solutions (in ng) and correct the result obtained for the sample solution by subtracting that obtained for the blank solution.

#### Notes

1. Sodium chlorate is not required if sulphides are absent.
2. On standing, or during the subsequent stripping step, the extract containing bromine may become colourless because of the reaction between toluene and bromine to

Table 1. Instrumental conditions for the determination of selenium

Step function	1	2	3	4
	Dry	Char	Char	Atomize
Temperature ( $^{\circ}$ C)	110	200	900	2600
Ramp time (sec)	10	5	5	0
Hold time (sec)	10	10	20	5
Internal argon flow (ml/min)	300	300	300	0
Read	—	—	—	—1 sec
Base-line	—	—	—	—2 sec

produce bromotoluene. However, this does not interfere with the stripping of selenium.

3. After the stripped extract has been drained into a waste bottle the funnel should be shaken with ~20–30% hydroxylamine hydrochloride solution and then left open in a fume-hood to air out for several hr before re-use. This helps to eliminate corrosive fumes which cause eye discomfort during subsequent washing of the funnel.

4. For final sample solution volumes of 5, 10 or 25 ml, add 50, 100 or 250  $\mu\text{l}$  of nickel solution, respectively. The corresponding volumes of concentrated nitric acid to be added in the subsequent part of the procedure are 100, 200 or 500  $\mu\text{l}$ .

5. If dilution is necessary, dilute suitable aliquots of both the blank and sample solutions directly in the autosampler cup with the blank calibration solution and correct the result (ng of selenium) obtained for the diluted sample solution by subtracting that obtained for the diluted blank solution.

## RESULTS AND DISCUSSION

### GFAAS determination of selenium

Previous investigators,<sup>7–13</sup> who used a GFAAS finish after extraction of various selenium piaszelenol complexes into different organic solvents (decahydronaphthalene,<sup>8</sup> chloroform,<sup>13</sup> butyl acetate,<sup>9</sup> or toluene<sup>7,10–12</sup>), have determined selenium directly in the organic phase, using wall-atomization either in the absence of a matrix modifier<sup>7,10,13</sup> or in the presence of nickel<sup>9,11,12</sup> or copper.<sup>8</sup> Although nickel is usually recommended as a modifier for selenium, recent work has shown that, depending on the acid present, palladium is also very effective.<sup>15–18</sup> Consequently, both nickel and palladium were investigated in this work and platform-atomization was ultimately chosen because of the greater sensitivity and better reproducibility. Initial work involving direct injection of the selenium 5-nitropiazselenol-toluene extract into the graphite furnace showed that in this medium the approximate maximum charring temperature for selenium for peak-height measurement was ~1000° for both nickel and palladium, and that under these conditions the sensitivity for selenium in the presence of palladium was at least four times that obtained with nickel. However, in these tests, both palladium and nickel, which were added as 5- $\mu\text{l}$  portions of dilute nitric acid solutions of the nitrates to 20  $\mu\text{l}$  of extract, yielded very erratic base-lines and extremely poor reproducibility. This was attributed mostly to the non-uniform spread of the aqueous modifier solution (lower phase) and the toluene extract (upper phase) over the bottom of the sample cavity of the graphite platform during the drying step, because increasing, but still very erratic, peak-height values were obtained in further tests with palladium when the volume ratio of palladium solution to 10  $\mu\text{l}$  of extract was increased from 0.25:1 to 1:1. In most earlier work at least a 1:1 volume ratio and very small volumes ( $\leq 5 \mu\text{l}$ ) of both the aqueous modifier solution and the extract were used but this limits the practical detection limit of the method. Furthermore, in platform analysis, the use of

large volumes of modifier solution in conjunction with a suitably large volume of extract (e.g., 20  $\mu\text{l}$ ) is not feasible because the capacity of the platform cavity (~30–35  $\mu\text{l}$  in this work) may be exceeded. For these reasons, an aqueous medium, in which the modifier and selenium solution are fully miscible, was chosen for this work, and preliminary tests done with a 2% v/v nitric acid medium (Fig. 1) showed that, at the optimum charring temperature found for peak-height measurements (900–1000°), palladium and nickel in small amounts ( $\leq 2 \mu\text{g}$ ) are about equally effective as modifiers; with large amounts the sensitivity decreases. These tests also showed that the sensitivities in the presence of palladium and nickel were greater in the aqueous medium, particularly for nickel (~10 times greater), than in the toluene medium. Reduced palladium modifiers, in which an organic reducing agent such as hydroxylamine hydrochloride<sup>16</sup> or ascorbic acid,<sup>16,18</sup> or an organic compound such as albumin,<sup>17</sup> is used in conjunction with palladium, have been found to be more effective than palladium alone for selenium, presumably because palladium is either reduced to the metal early in the temperature programme<sup>16</sup> and/or because of the conversion of the added compound into graphite, which forms a new graphite surface in the graphite tube.<sup>17</sup> This could explain the much greater sensitivity obtained for toluene extracts of the organic "carbon-producing" selenium complex in the presence of palladium than in the presence of nickel. However, these organic compounds are not very effective in dilute nitric acid media, presumably because nitric acid or nitrate interferes with the reduction of the palladium during the drying and charring steps.<sup>18</sup> In the presence of palladium no significant increase in sensitivity was obtained for 2% nitric acid solutions of selenium containing ascorbic acid. Peak-area results obtained with these modifiers, including palladium in the presence of ascorbic acid, were very similar, showing, as found in previous work on arsenic,<sup>19</sup> that there is no significant difference between these modifiers when peak-area is measured. Because subsequent work

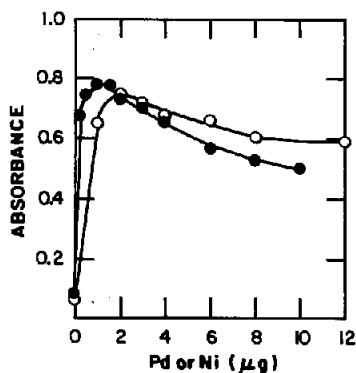


Fig. 1. Effect of Pd (●) and Ni (○) on peak-height absorbance for selenium. Se taken, 20  $\mu\text{l}$  (2 ng) of 0.10  $\mu\text{g}/\text{ml}$  solution in 2%  $\text{HNO}_3$ ; Pd and Ni solutions (in 2%  $\text{HNO}_3$ ) taken, 5  $\mu\text{l}$ .

showed that the addition of nickel to the strip solutions was necessary to prevent loss of selenium during the evaporation of the solutions to dryness, and because the reproducibility in the presence of nickel was much better than that with palladium, nickel was used as the matrix modifier in this work. The use of nickel is also advantageous compared with palladium because it is inexpensive and can be added directly to the final sample solution, as mentioned above. For economic reasons, palladium is usually separately injected into the furnace. Figure 1 shows that the optimum amount of nickel required is  $\sim 2 \mu\text{g}$  which is considerably less than the optimum amount ( $\geq 16 \mu\text{g}$ ) found for wall-atomization under essentially the same conditions.

#### *Separation of selenium by extraction of 5-nitropiaz-selenol*

In most previous work the selenium 5-nitropiaz-selenol complex was formed in  $\leq 2M$  hydrochloric acid and extracted into toluene at the same acid concentration after allowing  $\sim 2$  hr for complex formation.<sup>1-6,11</sup> However, preliminary work, in which for convenience selenium was determined spectrophotometrically<sup>1</sup> by measuring the absorbance of the extract at 350 nm, the wavelength of maximum absorption ( $\epsilon = 1.42 \times 10^3 \text{ l. mole}^{-1} \cdot \text{mm}^{-1}$ ), showed that, at the  $50\text{-}\mu\text{g}$  selenium level, the complex is completely formed in hydrochloric acid ranging from 0.1 to at least  $6M$  in concentration. It is completely or almost completely extracted into toluene in one extraction under the same conditions when the volume ratio of the aqueous to organic phase varies from 1:1 to 3:1.

Although the extraction step is reasonably specific as far as small amounts of most other elements are concerned, the effect of large amounts of iron had to be considered in this work because it is a principal constituent of most ores and related materials. Previous investigators found that iron(III) produces a positive error in the spectrophotometric result for selenium extracted as the 5-nitropiazselenol, because of the yellow colour imparted to the extract, and that this error increases as the acidity decreases.<sup>1</sup> This was confirmed by tests which showed that the positive error in the presence of 50–100 mg of iron(III) was greatest when selenium was extracted from  $\leq 2M$  hydrochloric acid, and that the spectrophotometric error from up to at least 100 mg of iron(III) can be reduced significantly by extracting selenium from  $\sim 4\text{--}5M$  hydrochloric acid, followed by washing the extract once or twice with an equal volume of  $\sim 5M$  hydrochloric acid. This also reduces positive error from up to at least the same amount of copper(II), which reacts similarly. Further work indicated that the positive spectrophotometric error obtained in the presence of these ions is most probably caused by the catalytic oxidation of 4-nitro-*o*-phenylenediamine<sup>20</sup> and the subsequent co-extraction of the oxidized compound. The co-extraction of this compound

would be expected to decrease with increasing hydrochloric acid concentration because the extraction of the reagent itself decreases under these conditions and becomes minimal at hydrochloric acid concentrations  $> 3M$ . Although the co-extraction of neither the reagent nor the oxidized compound would be expected to be critical for a GFAAS finish, complex formation in, and extraction from,  $\sim 4\text{--}5M$  hydrochloric acid was chosen for this work for convenience and to minimize the unnecessary co-extraction of these compounds. To hasten complex formation, the piaszelenol complex was formed by heating the solution in a boiling water-bath<sup>1,3,4</sup> for  $\sim 15$  min in the presence of 1 ml of 0.5% 4-nitro-*o*-phenylenediamine solution. This amount of reagent is sufficient for the complexation of up to at least  $50 \mu\text{g}$  of selenium(IV). An added advantage of the heating step is that, at the high hydrochloric acid concentration used for complex formation, any selenium(VI) present in the solution will be largely reduced to selenium(IV) during the complex formation step; selenium(VI) does not form a piaszelenol complex.<sup>2</sup> Subsequent GFAAS work showed that under the chosen conditions of acidity and reagent concentration, up to at least  $2 \mu\text{g}$  of selenium is  $\geq 99\%$  extracted into toluene in one extraction when the organic/aqueous phase volume-ratio is 1:3.

#### *Stripping of the selenium complex*

Initial stripping tests with nitric acid solutions of increasing concentration showed that the 5-nitropiaz-selenol complex is very stable and not readily destroyed under relatively strong oxidizing conditions. No selenium was stripped when extracts were shaken for  $\sim 5$  min with up to 50% v/v nitric acid, and only  $\sim 30\%$  was recovered by shaking for 10 min with concentrated nitric acid. Complete stripping of selenium could be obtained by treating the extracts with bromine solution in carbon tetrachloride, as described previously for arsenic(III) xanthate extracts,<sup>19</sup> followed by back-extraction of the resultant selenium(VI) into water. However, low results were obtained when the strip solutions were acidified with nitric acid and evaporated to a low volume to remove the excess of bromine before the GFAAS determination of selenium. This was attributed to the suppressive effect of small amounts of residual hydrochloric and/or hydrobromic acid in the solutions. Complete recovery of selenium was obtained when the solutions were evaporated to dryness in the presence of nitric acid and nickel, which had previously been found<sup>13</sup> to prevent selenium from being lost, presumably by volatilization, during the evaporation step. For the same reason, nickel was added to the samples before the decomposition step. A bromine solution in cyclohexane, rather than in carbon tetrachloride, was used for subsequent work because the lower specific gravity ( $< 1$ ) of this solvent facilitated the stripping step. With a carbon tetrachloride (specific gravity  $> 1$ ) solution of bromine it

was necessary to add a solvent of specific gravity  $< 1$  during the second stripping step, for the organic phase to be the upper layer. A bromine solution in toluene cannot be prepared because bromine reacts with toluene to form bromotoluene.

#### *Effect of diverse ions*

Early work involving spectrophotometric<sup>1</sup> and GCECD<sup>2</sup> measurement of the 5-nitropiazselenol extract showed that, except for iron(III), molybdenum(VI), chromium(VI), vanadium(V) and tin(IV), moderate amounts of most common ions<sup>1</sup> and large amounts of copper, arsenic and tellurium do not interfere in the extraction of selenium.<sup>2</sup> Recent work, based on chloroform extraction of the complex and a GFAAS finish using wall-atomization in a zirconium-coated tube and direct injection of the extract, has shown that  $\mu\text{g}$ -quantities ( $\leq 30 \mu\text{g}$ ) of various metal ions that occur in soil samples, including most of those mentioned above, do not interfere in the extraction or determination of selenium.<sup>13</sup> However, because considerably larger amounts of most matrix elements, particularly iron, copper and lead, would be expected to be present in the largest aliquot of the sample solution taken for extraction in this work, tests were done to determine the effects of large amounts of these elements and mg-amounts of various other elements on the determination of selenium under the proposed extraction and GFAAS conditions. These tests showed that up to at least 100 mg each of iron(III) and copper(II), 100 mg of lead, 5 mg of arsenic(V), antimony(V), bismuth, tin(IV), manganese(II) and indium, 2 mg of molybdenum(VI), 1 mg of vanadium(V) and tungsten(VI) and up to 250  $\mu\text{g}$  each of platinum(IV), palladium(II) and gold(III) will not cause significant error in the result. Larger amounts of molybdenum and tungsten will produce low results for selenium and larger amounts of vanadium, platinum, palladium and gold will produce high results. Whether or not the high results obtained in the presence of gold, platinum and palladium are caused by some co-extraction of these elements was not investigated, but the residues obtained after evaporation of the strip solutions to dryness indicated little or no co-extraction. Vanadium(V) is not significantly co-extracted because, at the 5-mg level, only  $\sim 25 \mu\text{g}$  was found in the wash solution; none was found in the final strip solution. More than  $\sim 0.5 \text{ mg}$  of chromium(VI) interferes seriously by oxidizing 4-nitro-*o*-phenylenediamine, producing a reddish colour and a very low result, but up to at least 10 mg can be present if it is reduced to chromium(III) with hydroxylamine hydrochloride before the addition of the reagent. Although this reductant also reduces vanadium(V) to vanadium(IV), it does not eliminate the interference from vanadium. Also, it reduces the catalytic oxidation by iron(III) but not that by copper(II). Washing the extract twice with 2% nitric acid removes residual hydrochloric acid, iron, copper and other elements.

#### *Applications*

Table 2 shows that the mean results obtained for selenium in various diverse CCRMP, National Research Council Canada, National Bureau of Standards and United States Geological Survey reference materials are in excellent agreement with the certified values, with values given for information only, or with the consensus mean values obtained during interlaboratory certification programmes or in recent compilations of existing data. In most cases they also agree reasonably well with other reported values obtained by a variety of instrumental methods. The results obtained for CCU-1 and CCU-1a are in good agreement with those obtained spectrophotometrically in this laboratory by measuring the absorbance of the 5-nitropiazselenol complex after washing the extract twice with 5M hydrochloric acid, as mentioned previously, to remove residual iron, copper and most of the co-extracted oxidized reagent. For this analysis, about the same amounts of copper and iron present in these concentrates were added to the blank solution to compensate approximately for the small increase in the absorbance ( $\sim 0.02$ ) of the sample extracts that was caused by the remainder of the co-extracted oxidized compound. The results obtained for CZN-I and CPB-I are slightly lower than, but still in reasonably good agreement with, previous results obtained in this laboratory during the respective interlaboratory certification programmes by a spectrophotometric method involving the extraction of the selenium 3,3'-diaminobenzidine complex into toluene after the preliminary separation of selenium by extraction as the xanthate.<sup>32</sup> Each of the individual results obtained for the reference materials in Table 2 was the mean of 3–5 GFAAS runs, each involving a single measurement. The resulting peak-height absorbance values were compared with, and the selenium concentration calculated from, absorbance values obtained for each run for selenium calibration solutions covering the linear response range of 0–0.10  $\mu\text{g}/\text{ml}$ .

In the proposed method, the detection limit, calculated as three times the standard deviation of the reagent blank, based on a 25-ml aliquot (equivalent to a 0.5-g sample) of sample solution taken through the extraction step and a final volume of 5 ml, is  $\sim 10 \text{ ng}$  of selenium per g of sample. The sensitivity (or characteristic mass) is  $\sim 12 \text{ pg}$  for 0.0044 absorbance. In this work no high-temperature cleaning step was required after atomization and the reagent blank for 25-ml aliquots of sample solution varied from  $\sim 4$  to 10 ng of selenium. The method has some definite advantages over previously reported GFAAS methods based on the separation of selenium by extraction of piasselenol complexes followed by direct injection of the extracts.<sup>7–13</sup> In this method, relatively large amounts of copper and iron do not interfere, no long waiting period is required for formation of the complex and, as mentioned pre-



Table 2. Determination of selenium in CCRMP and other reference ores, concentrates and related materials

Sample*	Nominal composition, %	Selenium, µg/g		
		Certified value and 95% confidence limits	This work†	Other reported values‡
CCU-1 Copper concentrate	24.7 Cu, 3.2 Zn, 30.9 Fe, 35.4 S, 2.6 SiO <sub>2</sub>	120 ± 9	113.3 ± 2.4	113.7§
CCU-1a Copper concentrate	~27 Cu, ~27 Fe, ~3 Zn, ~35 S	192 ± 32	188.1 ± 4.2(S)	193.3§
CZN-1 Zinc concentrate	44.7 Zn, 10.9 Fe, 7.5 Pb, 30.2 S	5.5 ± 1.1	4.3 ± 0.1	5.0¶
CPB-1 Lead concentrate	64.7 Pb, 8.4 Fe, 4.4 Zn, 17.8 S, 0.4 Sb	30 ± 3	28.0 ± 0.6	32.5¶
SO-1 Regosolic soil	25.7 Si, 9.4 Al, 6.0 Fe, 2.3 Mg, 1.8 Ca, 0.5 Ti	0.088 ± 0.007 <sup>a</sup>	0.098 ± 0.018	0.087, <sup>21</sup> 0.10, 0.094, <sup>22</sup> 0.09, <sup>23</sup> 0.091, <sup>24</sup>
SO-2 Podzolic soil	25.0 Si, 8.1 Al, 5.6 Fe, 2.0 Ca, 0.9 Ti	0.36 ± 0.06 <sup>a</sup>	0.42 ± 0.00	0.44, <sup>21</sup> 0.54, 0.48, <sup>22</sup> 0.04 <sup>b</sup> , <sup>23</sup> 0.47, <sup>24</sup>
SO-3 Calcareous C Horizon soil	15.9 Si, 3.1 Al, 1.5 Fe, 5.0 Mg, 14.6 Ca	0.040 ± 0.015 <sup>a</sup>	0.028 ± 0.002	0.03, <sup>21</sup> 0.020, 0.022, <sup>22</sup> 0.05, <sup>23</sup> 0.028, <sup>24</sup>
SO-4 Calcareous A Horizon soil	32.0 Si, 5.5 Al, 2.4 Fe, 1.1 Ca	0.44 ± 0.08 <sup>a</sup>	0.55 ± 0.03	0.55, <sup>21</sup> 0.54, 0.55, <sup>22</sup> 0.47, <sup>23</sup> 0.63, <sup>24</sup>
MRG-1 Gabbro	39.3 SiO <sub>2</sub> , 8.5 Al <sub>2</sub> O <sub>3</sub> , 8.3 Fe <sub>2</sub> O <sub>3</sub> , 8.6 FeO, 13.5 MgO, 14.8 CaO, 3.7 TiO <sub>2</sub>	0.2 <sup>c</sup>	0.20 ± 0.01	0.19, <sup>21</sup> 0.19, <sup>22</sup> 0.19, <sup>23</sup> 0.19, <sup>24</sup>
NRCC MESS-1 Marine sediment	67.5 SiO <sub>2</sub> , 11.0 Al <sub>2</sub> O <sub>3</sub> , 4.4 Fe <sub>2</sub> O <sub>3</sub> , 1.4 MgO, 0.9 TiO <sub>2</sub> , 0.7 S	0.34 ± 0.06	0.37 ± 0.03	0.36, 0.35, 0.33, <sup>5</sup> 0.33, 0.35, <sup>25</sup>
NRCC BCSS-1 Marine sediment	66.1 SiO <sub>2</sub> , 11.8 Al <sub>2</sub> O <sub>3</sub> , 4.7 Fe <sub>2</sub> O <sub>3</sub> , 2.4 MgO, 0.7 TiO <sub>2</sub> , 0.4 S	0.43 ± 0.06	0.44 ± 0.03	0.45, 0.44, 0.40, <sup>5</sup> 0.42, 0.44, <sup>25</sup>
NBS 1633a Coal fly ash	22.8 Si, 14.3 Al, 9.4 Fe, 1.1 Ca, 0.8 Ti	10.3 ± 0.6	9.8 ± 0.1	9.4, <sup>21</sup> 10.8, <sup>22</sup> 9.4, <sup>26</sup> 10.6, <sup>24</sup>
NBS 1645 River sediment	2.3 Al, 11.3 Fe, 3.0 Cr, 2.9 Ca, 1.1 S	1.5 <sup>d</sup>	1.3 ± 0.1	1.5, <sup>21</sup> 0.85, <sup>26</sup>
NBS 1646 Estuarine sediment	~31 Si, 6.3 Al, 3.4 Fe, 1.1 Mg, 1.0 S, 0.5 Ti	0.6 <sup>d</sup>	0.49 ± 0.02	0.58, 0.59, <sup>5</sup> 0.61, 0.59, <sup>25</sup>
USGS PCC-1 Peridotite	42.0 SiO <sub>2</sub> , 0.7 Al <sub>2</sub> O <sub>3</sub> , 2.7 Fe <sub>2</sub> O <sub>3</sub> , 5.2 FeO, 43.3 MgO	0.028 ± 0.008 <sup>e</sup>	0.015 ± 0.006	0.03, <sup>21</sup> 0.025, <sup>27</sup> 0.040, <sup>28</sup> 0.018, <sup>24</sup>
USGS GSP-1 Granodiorite	67.4 SiO <sub>2</sub> , 15.2 Al <sub>2</sub> O <sub>3</sub> , 1.7 Fe <sub>2</sub> O <sub>3</sub> , 2.3 FeO, 1.0 MgO, 2.0 CaO, 0.7 TiO <sub>2</sub>	0.067 ± 0.009 <sup>e</sup>	0.057 ± 0.008	0.11, <sup>21</sup> 0.073, <sup>27</sup> 0.079, <sup>28</sup>
USGS BCR-1 Basalt	54.5 SiO <sub>2</sub> , 13.6 Al <sub>2</sub> O <sub>3</sub> , 3.5 Fe <sub>2</sub> O <sub>3</sub> , 8.9 FeO, 3.5 MgO, 7.0 CaO, 2.2 TiO <sub>2</sub>	0.086 ± 0.008 <sup>e</sup>	0.061 ± 0.004	0.12, <sup>21</sup> 0.092, <sup>27</sup> 0.087, <sup>24</sup>

\*CCRMP reference materials except where indicated otherwise.

†Mean and standard deviation for 3 values except where indicated otherwise in parentheses.

‡Two or more results reported by the same authors were obtained by different methods or by using different decomposition procedures.

§Mean value obtained by the author using a spectrophotometric finish after extraction of selenium as described in this work.

¶Current consensus mean value.

||Mean value obtained by the author during the interlaboratory certification programme.

<sup>a</sup>1983 compilation of data.<sup>29</sup><sup>b</sup>Questionable result compared with those obtained by the same authors for the other soils—numbers probably transposed.<sup>c</sup>Most recent usable value.<sup>30</sup><sup>d</sup>NBS value given for information only (not certified).<sup>e</sup>1982 compilation of data.<sup>31</sup>

viously, at the high acidity and temperature used for complex formation, any selenium(VI) present is largely reduced to selenium(IV). The hydroxylamine hydrochloride used to reduce chromium(VI) to chromium(III) before the addition of the 4-nitro-*o*-phenylenediamine may also promote this reduction.<sup>33</sup> Although the stripping and final evaporation steps require some additional time, the aqueous calibration solutions are stable and can be used for at least one week, whereas selenium extracts for calibration should preferably be prepared fresh each day to minimize error from evaporation. As mentioned previously, the reproducibility for selenium was found to be much better in an aqueous medium than in toluene. Furthermore, with an aqueous medium larger aliquots can usually be used for injection.

The possible application of an alternative hydride-generation AAS finish, after the separation and stripping of selenium as described in the proposed method, was investigated but found to be unfeasible. Tests in which the strip solutions were evaporated to ~3 or 4 ml to remove bromine, followed by the addition of water and sufficient concentrated hydrochloric acid to give a 4M solution, and heating to reduce selenium(VI) to selenium(IV) (required for the hydride-generation step), yielded extremely low results for selenium. Subsequent work indicated that this was most probably caused by the simultaneous stripping of an organic compound, possibly oxidized 4-nitro-*o*-phenylenediamine, which interferes with the reduction of selenium(VI), since similarly low results were obtained when selenium(VI) was added to strip solutions derived from blank solutions taken through the extraction and stripping steps. This unknown compound is also extremely resistant to oxidative destruction with nitric and perchloric acids, because not all, but increasingly larger amounts, of the added selenium was recovered in tests in which the strip solutions were treated with these acids, evaporated to fumes of perchloric acid in the presence of ~0.5 mg of nickel and then covered and refluxed vigorously for increasing time intervals up to 1 hr. About 85–95% of the selenium was recovered after refluxing for 1 hr. During this hydride-generation work it was also found that the extract may not be washed with 4–5M hydrochloric acid or 2% perchloric acid to remove residual iron, copper and other elements, instead of with 2% nitric acid as recommended in the procedure, because, for some unknown reason, this appears to accelerate the reaction between bromine and toluene. Under these conditions, the mixed toluene–bromine–cyclohexane phase is decolorized almost immediately or within

1 or 2 min after the addition of the bromine–cyclohexane solution. When the extract is washed with 2% nitric acid the mixed organic phase can stand for at least 20 min without being decolorized. Longer time intervals were not investigated.

*Acknowledgement*—The author thanks Maureen E. Leaver for performing most of the hydride-generation AAS work.

#### REFERENCES

1. M. Tanaka and T. Kawashima, *Talanta*, 1965, **12**, 211.
2. K. Tōei and Y. Shimoishi, *ibid.*, 1981, **28**, 967 (and references therein).
3. Y. Shimoishi and K. Tōei, *ibid.*, 1970, **17**, 165.
4. C. I. Measures and J. D. Burton, *Anal. Chim. Acta*, 1980, **120**, 177.
5. K. W. M. Slu and S. S. Berman, *Anal. Chem.*, 1983, **55**, 1603.
6. *Idem*, *ibid.*, 1984, **56**, 1806.
7. K. Ohta and M. Suzuki, *Anal. Chim. Acta*, 1975, **77**, 288.
8. F. J. Szydłowski, *At. Abs. Newsl.*, 1977, **16**, 60.
9. N. L. Fishkova, I. I. Nazarenko, V. A. Vilenkin and Z. A. Petrakova, *J. Anal. Chem. USSR*, 1980, **36**, 83.
10. J. Nève and M. Hanocq, *Anal. Chim. Acta*, 1977, **93**, 85.
11. J. Nève, M. Hanocq and L. Molle, *ibid.*, 1980, **115**, 133.
12. *Idem*, *Z. Anal. Chem.*, 1981, **308**, 448.
13. Shan Xiao-quan, Jin Long-zhu and Ni Zhe-ming, *At. Spectrosc.*, 1982, **3**, 41.
14. A. I. Vogel, *A Textbook of Quantitative Inorganic Analysis*, 2nd Ed., pp. 441–442. Longmans, London, 1951.
15. Shan Xiao-quan and Hu Kai-jing, *Talanta*, 1985, **32**, 23.
16. L. M. Voth-Beach and D. E. Shrader, *Spectroscopy*, 1986, **1**, 10.
17. J. E. Teague-Nishimura, T. Tominaga, T. Katsura and K. Matsumoto, *Anal. Chem.*, 1987, **59**, 1647.
18. M. Knowles, *Varian Instruments at Work*, No. AA-70, 1987.
19. E. M. Donaldson, *Talanta*, 1988, **35**, 47.
20. P. F. Lott, P. Cukor, G. Moriber and J. Solga, *Anal. Chem.*, 1963, **35**, 1159.
21. E. S. Gladney and D. Knab, *Geostds. Newsl.*, 1981, **5**, 67.
22. N. Imai, S. Terashima and A. Ando, *ibid.*, 1984, **8**, 39.
23. H. Agemian and E. Bedek, *Anal. Chim. Acta*, 1980, **119**, 323.
24. C. C. Y. Chan, *Anal. Chem.*, 1985, **57**, 1482.
25. E. de Oliveira, J. W. McLaren and S. S. Berman, *ibid.*, 1983, **55**, 2047.
26. H. A. van der Sloot, D. Hoede, Th. J. L. Klinkers and H. A. Das, *J. Radioanal. Chem.*, 1982, **71**, 463.
27. J. Erzinger and H. Puchelt, *Geostds. Newsl.*, 1980, **4**, 13.
28. V. Lavrakas, T. J. Golembeski, G. Pappas, J. E. Gregory and H. L. Wedlick, *Anal. Chem.*, 1974, **46**, 952.
29. E. S. Gladney, C. E. Burns and I. Roelandts, *Geostds. Newsl.*, 1985, **9**, 35.
30. S. Abbey and E. S. Gladney, *ibid.*, 1986, **10**, 3.
31. E. S. Gladney, C. E. Burns and I. Roelandts, *ibid.*, 1983, **7**, 3.
32. E. M. Donaldson, *Talanta*, 1977, **24**, 441.
33. M. Ishizaki, *ibid.*, 1978, **25**, 167.

## SOLUTION NEBULIZATION OF AQUEOUS SAMPLES INTO THE TUBULAR-ELECTRODE TORCH CAPACITATIVELY-COUPLED MICROWAVE PLASMA

B. M. PATEL\*, J. P. DEAVOR† and J. D. WINEFORDNER‡

Department of Chemistry, University of Florida, Gainesville, FL 32611, U.S.A.

(Received 23 September 1987. Revised 26 January 1988. Accepted 5 February 1988)

**Summary**—This work shows the feasibility of using nebulization for introduction of aqueous samples into the tubular-torch capacitatively-coupled microwave plasma (CMP). Previously, solid electrodes were used with this type of plasma, in which analyte carrier and plasma support gases are premixed and swept around the electrode tip. With the new design, the analyte carrier gas passes through the centre of the hollow tubular electrode and mixes with the plasma support gas at the tip of the electrode where the plasma is formed. Sample solutions are nebulized with a Meinhard nebulizer and a laboratory-constructed spray chamber and desolvation system. The tubular torch is made of tantalum. Plasma gases investigated include argon, helium and nitrogen. Typical operating powers are 300–350 W. Elements studied include Ag, Al, Ba, Ca, Cd, Cr, Cs, Cu, K, Li, Na, Pb, Pd, Sr and Zn.

There are two main types of microwave plasmas employed in analytical chemistry. By far the most commonly used is the microwave-induced plasma (MIP).<sup>1-4</sup> The MIP is confined within a silica or alumina tube and sustained by coupling microwave power to the gas within such a tube by means of a resonant cavity. The second type of microwave plasma, the focus of this paper, is the capacitatively-coupled microwave plasma (CMP), also referred to as the single-electrode plasma (SEP). This discharge features a plasma produced at the tip of a metal electrode to which microwave power is coupled by a coaxial waveguide.

Dahmen<sup>5</sup> gave an extensive bibliography of the CMP in his 1981 review and has annually updated it.<sup>6-10</sup> Much work has since been accomplished by several groups in Japan, Europe and the United States.

Akatsuka and Atsuya have used the CMP to analyse steels for manganese,<sup>11</sup> molybdenum,<sup>12</sup> nickel<sup>13</sup> and vanadium,<sup>14</sup> and also arsenic by hydride generation.<sup>15</sup> They have optimized the procedures and looked for possible interferences. A high concentration of iron was found to provide a convenient spectrochemical buffer.

Wunsch and co-workers have performed analysis for tungsten<sup>16-18</sup> and ten other elements.<sup>19</sup> Feuerbacher<sup>20</sup> introduced a 120-mm long plasma

torch and minimized condensation problems by having the nebulizer very close to the plasma. Disan *et al.*<sup>21</sup> determined 21 metals in trace concentrations in aqueous solutions, using nitrogen as a second mantle gas to stabilize the plasma and improve excitation conditions, and also made an interference study.

Winefordner and co-workers have performed both applied and fundamental studies of their CMP. Inorganic and organometallic mercury was determined by vaporizing these species thermally from standard reference orchard leaves and tuna and detecting them by atomic emission as a function of vaporization appearance temperature for various chemical species.<sup>22</sup> A platinum-clad tungsten electrode was found to be thermally stable and chemically inert, giving longer electrode life.<sup>23</sup> The CMP was characterized with regard to spectroscopic and electron temperatures and density for various plasma gases.<sup>24</sup> In another study, the CMP was optimized to determine trace water in evolved-gas samples.<sup>25</sup> Trace hydrogen and oxygen in NBS/SRM titanium was determined by heating the metals in a helium atmosphere at reduced pressure and sweeping the evolved gas into the CMP.<sup>26</sup> An air plasma using a solid electrode was optimized for use with aqueous solutions for determination of calcium, potassium and sodium in SRM oyster tissue and glass.<sup>27</sup> The total lead content of gasoline engine exhaust gases was determined and compared with the amount of particulate lead.<sup>28</sup> Tin has also been determined by means of hydride generation and the tubular electrode CMP.<sup>29</sup> The tubular electrode facilitated mixing of the analyte with the plasma support gas. The increase in sensitivity was over two orders of magnitude for tin. The present study was performed to show the possibilities of nebulizing solutions into the tubular-torch CMP.

Research supported by EPA-CR-813017-01-1.

\*On leave from the Atomic Energy Commission, India; Department of Atomic Energy, Bhabha Atomic Research Centre, Radiochemistry Division, Bombay 400085, India.

†On leave from Department of Chemistry, College of Charleston, Charleston, SC 29424, U.S.A.

‡Author to whom correspondence should be addressed.

Table 1. Instrumentation used for solution nebulization into the tubular electrode torch microwave plasma emission spectrometer system

Apparatus	Model	Manufacturer
Magnetron output frequency 2.450 GHz; Plate voltage (max) 4.5 kV; Plate current (max) 350 mA; Output power, 885 W	H 3032 L (for microwave oven)	Hitachi Ltd., Tokyo, Japan
Power supply (for magnetron) constant current, regulation 15%; output voltage (max), 3 kV; output current (max), 400 mA	803-330	Hipotronics Inc., Brewster, NY
Plasma torch		Laboratory constructed <sup>29</sup>
Nebulizer	Meinhard concentric glass nebulizer, TR-30-A3	J. E. Meinhard Associates, Santa Ana, CA
Spray chamber and desolvation system		Laboratory constructed
Monochromator 0.35 m focal length, 1200 grooves/mm grating scanning spectrometer	EU-700	GCA/McPherson Instrument Corp., Acton, MA
Photomultiplier tube	R-955	Hamamatsu Corp., Bridgewater, NJ
High-voltage power supply (for photomultiplier tube)	226	Pacific Instruments, Concord, CA
Differential amplifier	26A2	Tektronix Inc., Beaverton, OR
Recorder	Series 5000	Fisher Sci. Co., Pittsburgh, PA

## EXPERIMENTAL

*Apparatus*

The single-channel electrode and the electrode-holder assembly have been described elsewhere.<sup>29</sup> The central electrode is made of tantalum and is held within an aluminium electrode holder which screws into a brass tube. Carrier gas passes through the central channel and sheath gas flows around the electrode but within the silica tube.

The electrode assembly is water-cooled, and the magnetron is air-cooled. The instrumental components are listed in Table 1. The plasma is attached to the tip of the tubular tantalum electrode. When helium is used as both carrier and sheath gas, the plasma is self-igniting. Other gases or combinations of gases require the insertion of the metal tip of an insulated screwdriver to cause arcing and initiate the plasma. The gas flow-rates have been optimized to yield the

best signal. Use of argon as the analyte carrier gas and nitrogen as the plasma sheath gas gives a stable plasma, without the plasma-displacement found when an all-helium or helium-nitrogen plasma is used.

A schematic diagram of the system is given in Fig. 1 and the operating conditions are given in Table 2.

*Procedure*

Standard solutions of various metals were used to determine analytical figures of merit. They were prepared by dissolution of the metals in acid, or from the metal halides. Blank determinations were made with demineralized distilled water. A Meinhard C-2 concentric nebulizer was used to generate an aerosol in a laboratory-built spray chamber, and the aerosol was carried through a water-cooled condenser to the plasma. The connection between the condenser and the plasma was kept warm with a heating tape. Blank

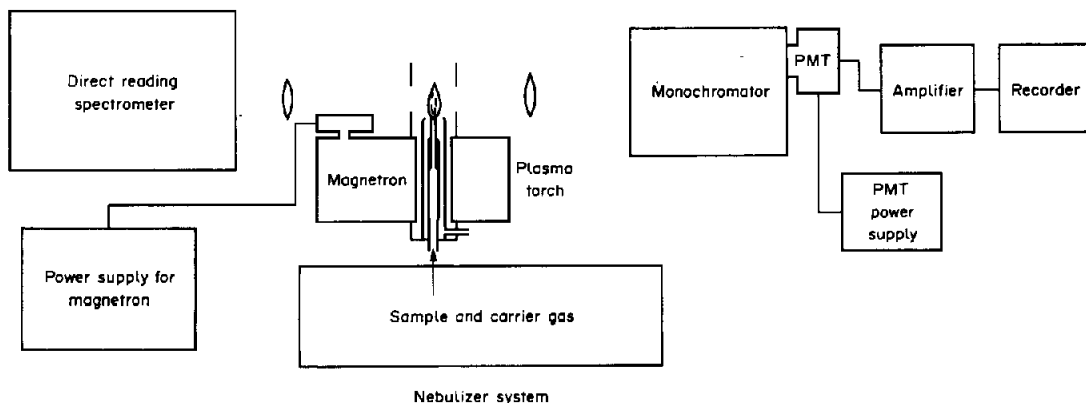


Fig. 1. Block diagram of the experimental system.

Table 2. Operating conditions of spectrometric system

Microwave frequency	2.450 GHz
Magnetron anode voltage	2.1 kV dc
Magnetron anode current	155 mA dc
Microwave power output	325 W
Plasma viewing mode	radial
Plasma viewing position	3 mm above the electrode tip
Plasma gas (N <sub>2</sub> ) flow-rate	6.5 l/min
Sample nebulizer gas (Ar) flow-rate	0.6 l/min
Solution uptake rate	1.75 l/min
Slit width	0.35 mm
Slit height	10 mm

and sample solutions were run alternately, each being sampled for a minimum of 30 sec. The plasma was observed by means of a 0.35-m Czerny-Turner monochromator/photomultiplier system with focusing of an unmagnified image on the entrance slit. A current-to-voltage amplifier/filter system was optimized for each element to yield the maximum signal-to-noise and signal-to-background ratios. The observation zone was 2–6 mm above the tip of the electrode. Molecular-band emission in certain regions of the spectrum added to the background. The plasma was operated at a power yielding the optimum signal-to-background ratio.

## RESULTS AND DISCUSSION

### Effects of microwave power on emission intensity

An increase in microwave power increased the emission signal for chromium (Fig. 2) but also increased the background emission signal. Similar effects were found for the other elements studied. For each element, an optimum power level was established, based on the signal-to-background ratio, as depicted in Fig. 3 for chromium. Because the sheath or plasma gas and nebulizer gas flow-rates had minimal effect on the signal-to-background ratios for all the element lines studied (see below), univariate searches could be made for finding the operating (not optimized) parameters given in Table 2.

### Effects of different gases and flow-rates

Variation of the type of plasma-sheath or carrier gas had little effect on the emission intensity when the tubular-torch configuration was used with desolvation. Large changes in the plasma-sheath gas flow changed the overall plasma size and influenced the emission signal. Additionally, changes in this parameter cause an upward shift of the plasma, necessitating a change in observation height.

### Linearity and detection limits

Linear analytical ranges and detection limits were determined, under the experimental conditions given in Table 2, for several metal ions in aqueous solutions. Standard solutions (0.01–1000 µg/ml) of several elements were used to measure the emission intensities. Limits of detection were calculated as the concentration of the element in solution which gave a signal three times the standard deviation of the blank<sup>30</sup> (16 replicate measurements of the signal from

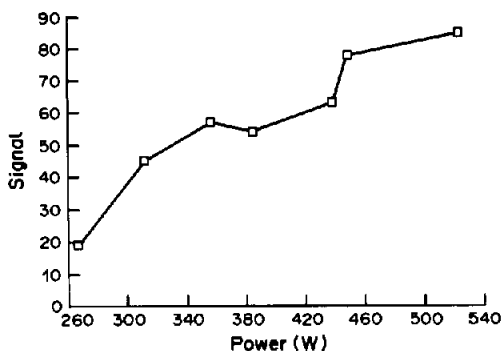


Fig. 2. Plot of emission signal intensity vs. microwave power, for 100-µg/ml Cr(III) solution.

aspiration of demineralized distilled water). Solutions were analysed in triplicate, blanks being alternated with samples, and a cleaning period was allowed before each measurement. Detection limits, useful analytical ranges, and precision (relative standard deviation, RSD) for each element are listed in Table 3. The precisions depend on the spectral background in the region of each line. Table 4 lists the statistics for log-log calibration plots over the linear range for several elements, including the linear dynamic range (as orders of magnitude) from the detection limit to the concentration at which the slope is reduced to 0.95.

The limits of detection obtained with the system are compared in Table 5 with those previously reported<sup>27</sup> for use of the W-Pt solid-electrode torch. Although the microwave power, nebulizer flow-rate and aspiration efficiency used in the present work are lower, the detection limits are better and lower by factors of 2–10 for the elements studied (except for Sr for which the detection limit is lower by a factor of 100). The large improvement factors for Sr and Al are probably a result of the greater efficiencies of sample introduction into the plasma core, which would be expected to increase the dissociation of stable molecular species such as monoxides. However, the detection limit for Ca with the W-Pt solid-electrode

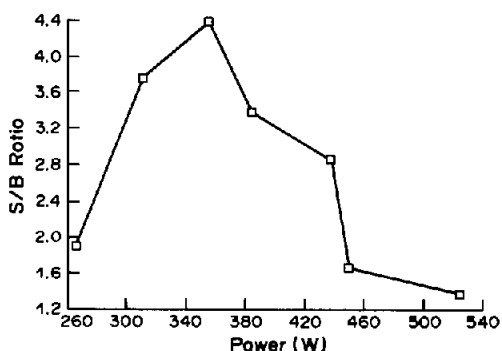


Fig. 3. Plot of signal-to-background ratio vs. microwave power, for 100-µg/ml Cr(III) solution.

Table 3. Detection limits, analytical ranges and precision (relative standard deviation, RSD) for several elements determined with the use of solution nebulization into the microwave plasma

Element	Wavelength, <i>nm</i>	Linear		RSD, %
		analytical range, $\mu\text{g/ml}$	Limit of detection,* $\mu\text{g/ml}$	
Ag	328.07	2-100	0.47	1.6
Al	396.15	3-500	0.5	1.1
Ba	553.56	10-100	3.1	2.0
Ca	422.67	2-200	0.65	6.5
Cd	228.80	4-250	0.62	1.2
Cr	425.43	1-200	0.26	1.7
Cs	852.11	10-100	4.0	2.8
Cu	324.75	0.5-200	0.09	6.0
K	766.49	2-500	0.26	3.5
Li	670.78	0.03-20	0.005	1.7
Na	588.99	0.05-15	0.01	1.8
Pb	405.78	20-1000	2.9	1.0
Pd	342.12	10-200	2.1	2.1
Sr	460.73	0.05-100	0.01	1.9
Zn	213.86	10-100	5.0	4.3

\*Limit of detection is defined as the concentration giving a signal equivalent to 3 times the standard deviation of 16 repetitive measurements of the background when demineralized water is nebulized into the microwave plasma.

Table 4. Statistics for log-log calibration plots

Element	Slope	Std. devn. of slope	Intercept	Std. devn. of intercept	Corr. coeff.	Linear range orders of magnitude
Ag	1.03	4.40E-04	1.32E-02	4.10E-04	0.997	2.5
Cd	0.97	4.21E-04	-0.38	4.50E-04	0.996	3
Cr	0.97	9.96E-05	-0.29	1.07E-04	0.999	2
Cu	0.98	1.18E-03	0.55	1.41E-03	0.997	2
Li	1.02	1.80E-04	0.89	1.72E-04	0.999	3
Na	1.11	9.66E-04	1.14	1.22E-03	0.998	2.5
K	1.13	3.73E-03	-0.14	2.91E-03	0.994	2
Pb	1.05	3.45E-04	-0.91	3.10E-04	0.998	3

Table 5. Limits of detection for several elements measured by use of solution nebulization for Ta tubular-torch and W-Pt solid-electrode torch microwave plasma emission spectrometry

Element	Wavelength, <i>nm</i>	Limit of detection, <i>ppm</i>		Improvement factor
		Ta tubular-torch (present work)	W-Pt solid-electrode torch <sup>27</sup>	
Al	396.15	0.5	4.9	9.8 ×
Ca	422.67	0.65	0.4	0.6 ×
Cd	228.80	0.62	3.2	5.2 ×
K	766.49	0.26	0.9	3.5 ×
Li	670.78	0.005	0.008	1.6 ×
Na	588.99	0.01	0.03	3.0 ×
Pb	405.78	2.9	7.6	2.6 ×
Sr	460.73	0.01	1.0	100 ×
Zn	213.86	5.0	6.8	1.4 ×

Other experimental conditions:

Microwave power, <i>W</i>	325	520
Plasma type	N <sub>2</sub> -Ar plasma	air-plasma
Nebulizer gas flow-rate, <i>l./min</i>	0.6	2.2
Solution uptake rate, <i>ml/min</i>	1.65	1.2
Aspiration efficiency, %	3.5	12.0

torch was about 40% lower than that obtained with the tubular torch.

#### CONCLUSION

Direct nebulization of aqueous sample solutions into the tubular-electrode torch capacitatively-coupled microwave plasma emission-spectrometer provides low detection limits and wide linear responses for a broad range of metals. The technique appears particularly attractive in view of its lower power requirements, reduced gas consumption, more robust character and lower cost when compared to the ICP. Further studies are in progress to evaluate interference effects, including those from easily ionized elements and of phosphate and aluminium on Ca.

#### REFERENCES

1. R. K. Skogerboe and G. N. Coleman, *Anal. Chem.*, 1976, **48**, 611A.
2. C. I. M. Beenakker, P. W. J. M. Boumans and P. J. Rommers, *Philips Tech. Rev.*, 1980, **39**, 65.
3. A. T. Zander and G. M. Hieftje, *Appl. Spectrosc.*, 1981, **35**, 357.
4. J. P. Matousek, B. J. Orr and M. Selby, *Prog. Anal. At. Spectrosc.*, 1984, **7**, 275.
5. J. Dahmen, *ICP Inform. Newsl.*, 1981, **6**, 576.
6. *Idem, ibid.*, 1982, **7**, 441.
7. *Idem, ibid.*, 1983, **9**, 81.
8. *Idem, ibid.*, 1984, **10**, 71.
9. *Idem, ibid.*, 1985, **11**, 71.
10. *Idem, ibid.*, 1986, **12**, 7.
11. I. Atsuya and K. Akatsuka, *Anal. Chim. Acta*, 1976, **81**, 61.
12. *Idem, ibid.*, 1978, **99**, 351.
13. *Idem, ibid.*, 1980, **119**, 341.
14. *Idem, Bunseki Kagaku*, 1980, **29**, 714.
15. *Idem, Spectrochim. Acta*, 1981, **36B**, 747.
16. G. Wunsch, *ICP Inform. Newsl.*, 1982, **8**, 133.
17. G. Wunsch, N. Czech and G. Hegenberg, *Z. Anal. Chem.*, 1982, **310**, 62.
18. G. Wunsch and N. Czech, *ibid.*, 1984, **317**, 5.
19. G. Wunsch, G. Hegenberg and N. Czech, *Spectrochim. Acta*, 1983, **38B**, 1135.
20. H. Fuererbacher, *ICP Inform. Newsl.*, 1981, **6**, 571.
21. A. Disam, P. Tschöpel and G. Tölg, *Z. Anal. Chem.*, 1982, **310**, 131.
22. S. Hanamura, B. W. Smith and J. D. Winefordner, *Anal. Chem.*, 1983, **55**, 2026.
23. *Idem, Can. J. Spectrosc.*, 1984, **29**, 13.
24. B. Kirsch, S. Hanamura and J. D. Winefordner, *Spectrochim. Acta*, 1984, **39B**, 955.
25. S. Hanamura, B. Kirsch and J. D. Winefordner, *Anal. Chem.*, 1985, **57**, 9.
26. *Idem, Can. J. Spectrosc.*, 1985, **30**, 46.
27. Y. K. Zhang, S. Hanamura and J. D. Winefordner, *Appl. Spectrosc.*, 1985, **39**, 226.
28. H. Vermaak, O. Kujirai, S. Hanamura and J. D. Winefordner, *Can. J. Spectrosc.*, 1986, **31**, 95.
29. B. M. Patel, E. Heithmar and J. D. Winefordner, *Anal. Chem.*, 1987, **59**, 2374.
30. G. L. Long and J. D. Winefordner, *ibid.*, 1983, **55**, 712A.

## A BECQUEREL-DISC PHOSPHOROSCOPE FOR THE MEASUREMENT OF LIFETIMES IN ROOM-TEMPERATURE PHOSPHORIMETRY\*

BRADLEY T. JONES, BENJAMIN W. SMITH, ALAIN BERTHOD† and JAMES D. WINEFORDNER‡  
Chemistry Department, University of Florida, Gainesville, FL 32611, U.S.A.

(Received 20 January 1988. Accepted 30 January 1988)

**Summary**—A Becquerel-disc phosphoroscope is constructed from a commercially available optical chopper with variable frequency and digital read-out. By use of a continuous source, phosphorescence lifetimes in the range 1–1000 msec can be measured with better than 4% relative standard deviation.

In 1858, Becquerel reported the invention of the first phosphoroscope.<sup>1</sup> A phosphorescent material was mounted between two revolving discs each carrying four evenly spaced slots near the edge (and each slot has a width of  $\pi/8$  radian). The discs were arranged so that light passing through a hole in the first disc and striking the sample could not be seen by looking through a hole in the second disc. A fraction of a second later, depending on the rate of revolution of the discs, the exciting light was cut off by the first disc and a hole in the second disc permitted observation of phosphorescent light emitted from the sample.<sup>2</sup> Becquerel's disc was capable of measuring phosphorescence with a lifetime as short as  $10^{-4}$  sec. Later, he cemented a solid phosphor to the surface of a revolving cylinder.<sup>3</sup> Upon excitation at one point on the cylinder, different stages of decay were observed at different distances around the can.

Later, Wood cemented several solid phosphors to the surface of a revolving disc.<sup>4</sup> The lifetimes of these phosphors were estimated by observing the width of the phosphorescent band on the face of the disc. Lifetimes were reported as fractions of a revolution of the disc. More precise measurements were prevented by speed fluctuations in the driving motor and the error involved in estimating the band widths. A few years later, similar experiments were performed with a photocell detector, allowing lifetime measurements in the range  $10^{-5}$ –5 sec.<sup>5,6</sup> The method was still limited by uncertainty in the measurement of the disc's angular velocity.

Recently, most measurements of phosphorescent lifetimes have been performed with pulsed excitation sources and gated detectors.<sup>7–11</sup> These systems are complex and more expensive but produce more precise results. The relative standard deviations (RSD)

are between 2 and 10%, and the lifetimes measured vary from 0.5 to 800 msec. This communication describes a Becquerel-disc phosphoroscope which provides more precise lifetime measurements (<4% RSD) over a broad range (1–1000 msec).

### THEORY

Normally, when phosphorescence lifetimes ( $\tau_L$ ) are determined, the phosphorescence intensity measured at some delay time ( $t_D$ ) after a period of excitation and its abrupt termination is assumed to follow a simple exponential decay:

$$I_{pt} = I_{po} \exp(-t_D/\tau_L) \quad (1)$$

where  $I_{po}$  is the phosphorescence intensity which would be measured if the excitation period was long enough to allow it to reach a steady-state value and  $I_{pt}$  is the intensity at time  $t_D$ . It is assumed that the exposure time ( $t_E$ ) and the time between successive exposures ( $t_C$ ) remain constant for measurements of  $I_{pt}$  at different delay times. Figure 1 is a graphical representation of two cycles of excitation with subsequent phosphorescence decay.

An equation for the phosphorescence intensity which accounts for the excitation and measurement processes was reported by O'Haver and Winefordner<sup>12</sup> and is

$$I_{pt} = I_{po} \exp(-t_D/\tau_L) \frac{[1 - \exp(-t_E/\tau_L)]}{[1 - \exp(-t_C/\tau_L)]} \quad (2)$$

This equation accounts for the diminished phosphorescence intensity growth when a shorter exposure time,  $t_E$ , is used for a particular measurement of  $I_{pt}$ . It also accounts for changes in the phosphorescence intensity, prior to exposure, due to changes in time between exposures,  $t_C$ . For lifetimes measured with a variable-speed phosphoroscope, equation (2) must be considered. If a pulsed-source system is employed equation (1) is suitable, since the pulse width ( $t_E$ ) and the source-repetition rate ( $1/t_C$ ) may be held constant, while the delay time may be

\*Research supported by NIH-GM11373-25.

†Present address: Laboratoire des Sciences Analytiques, Université de Lyon, 1, 69622 Villeurbanne cedex, France.

‡Author to whom correspondence should be sent.



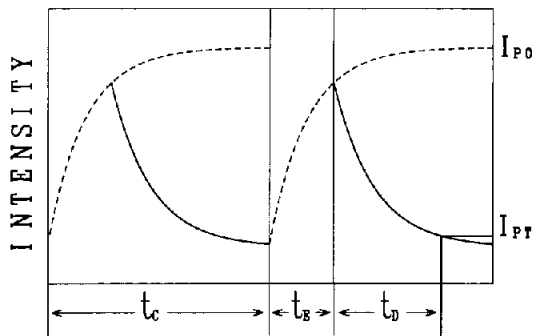


Fig. 1. Graphical representation of the operation of a Becquerel-disc phosphoroscope.

varied by changing the delay time on a gated detector, or by viewing the entire signal *vs.* time trace directly from an oscilloscope.

In the particular case of a rotating-disc phosphoroscope with a phosphor covering the entire front surface of the disc, some simplifications can be made for equation (2). The times  $t_c$ ,  $t_E$  and  $t_D$  are determined by the angular velocity of the disc. Expressions for  $t_E$  and  $t_c$  may be found in terms of  $t_D$  and then substituted into equation (2). In our case, with a 1-inch disc, excitation of the phosphor occurs at a single point near the edge of the disc, producing a ring of phosphorescence 25 mm in diameter (Fig. 2). For a given angular velocity, the time between exposures corresponds to the distance between successive exposures, *i.e.* to the length of the phosphorescent ring (80 mm). The exposure time corresponds to the size of the excitation beam (1 mm) focused onto the surface of the disc. Phosphorescence is collected at a point  $90^\circ$  away from the excitation point in the direction of the rotation, so  $t_D$  corre-



Fig. 2. Photograph showing the luminescence decay of a solid phosphor on a rotating disc.

sponds to 1/4 revolution of the disc, or a 20-mm length of the phosphorescent ring. Taking these factors into account results in the decay expression

$$I_{pt} = I_{po} \exp(-t_D/\tau_L) \frac{[1 - \exp(-t_D/20\tau_L)]}{[1 - \exp(-4t_D/\tau_L)]} \quad (3)$$

Further reduction of equation (3) is difficult. At this point, it is useful to compare some hypothetical results for lifetimes calculated by equation (3), with those calculated by using equation (1). With equation (1), the phosphorescence lifetime is determined by taking the inverse of the slope of a plot of  $\ln(I_{pt})$  *vs.*  $t_D$  where:

$$\ln(I_{pt}) = \ln(I_{po}) - \frac{t_D}{\tau_L} \quad (4)$$

Equation (4) can be rearranged to show that a plot of  $\ln(I_{pt}/I_{po})$  *vs.*  $t_D/\tau_L$  will be linear, with a slope of  $-1$ . By assuming values for  $t_D/\tau_L$ , values for  $I_{pt}/I_{po}$  can be calculated by using equation (3). A plot of  $\ln(I_{pt}/I_{po})$  *vs.*  $t_D/\tau_L$  is found to be a curve with a maximum at  $t_D/\tau_L \sim 1$ , and approaching linearity with a slope of  $-1$  at  $t_D/\tau_L > 5$  (Fig. 3). Unfortunately, at  $t_D/\tau_L > 5$ , the phosphorescence intensity of most samples is too weak to measure. On the other hand, measurements are easily made in the region  $1 < t_D/\tau_L < 3$ , where the average slope of the curve is  $-0.54$ . This implies that a phosphorescence lifetime ( $\tau_L^m$ ) measured by using equation (4) for a variable-speed rotating disc phosphoroscope must be multiplied by a factor of 0.54 to obtain the correct luminescence lifetime  $\tau_L$

$$\tau_L^m = 0.54 \tau_L \quad (5)$$

The factor relating  $\tau_L^m$  to  $\tau_L$  is independent of  $\tau_L^m$  as long as that portion of the plot is used where  $\tau_L^m < t_D < 3\tau_L^m$ . This region is easily located experimentally without previous knowledge of  $\tau_L^m$ , by beginning measurements at a delay time corresponding to the peak phosphorescence intensity and continuing to a delay time three times as large.

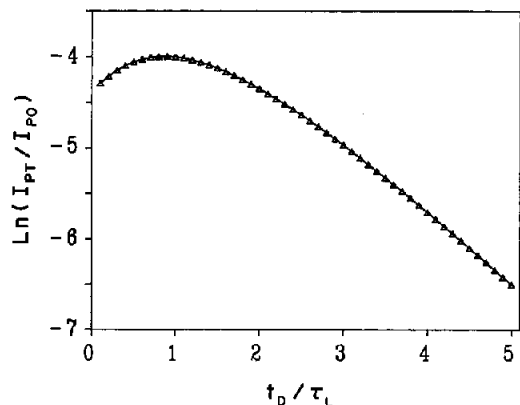


Fig. 3. Theoretical plot of the natural logarithm of relative phosphorescence intensity *vs.* relative delay time as calculated by using equation (3).

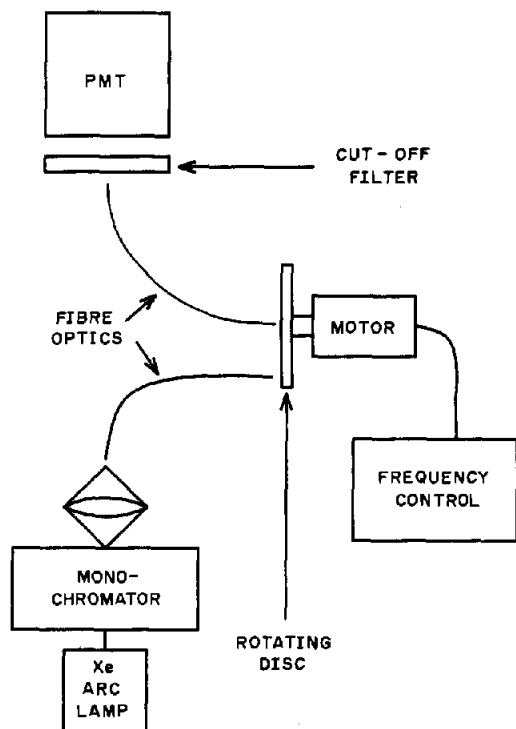


Fig. 4. Instrumental arrangement used to measure lifetimes with a Becquerel-disc phosphoroscope. As stated in the text, the two fibre optics are positioned 5 mm in from the edge of the disc, at 90° and 180° from top dead centre.

#### EXPERIMENTAL

A diagram showing the instrumental arrangement for the Becquerel-disc phosphoroscope is given in Fig. 4. The excitation source was a 150-W xenon arc lamp (Varian Assoc., Palo Alto, CA). Source radiation was passed through a 0.1-m monochromator (ISA, Metuchen, NJ). A 16-nm band of radiant flux leaving the exit slit of the monochromator was focused into a fibre optic with a microscope objective. The exit end of the fibre optic was placed 2 mm away from the surface of the rotating disc carrying the sample. The fibre optic was positioned opposite the bottom centre of the disc, 5 mm from the edge. The excitation beam covered a 1-mm diameter circle on the disc surface. Phosphorescence from the sample was collected by a second fibre optic opposite a point 5 mm in from the right-hand side of the disc, at the upper edge of the quadrant starting from the excitation point. The exit end of the emission fibre optic was coupled to a cooled photomultiplier tube (EMI Model 9789, Plainview, NY). A coloured glass cut-off filter blocking light of wavelength shorter than 450 nm was positioned between the fibre optic and the photomultiplier tube (PMT). The signal from the PMT was recorded directly on a strip-chart recorder (Houston Instruments, Austin, TX).

The rotating-disc phosphorescence consisted of a commercially available optical chopper with a 35-mm diameter aluminium disc. The chopper used was the Model OC 4000 (Photon Technology, Inc., Princeton, NJ) and could turn the disc at variable rates between 0.133 and 133 Hz. The frequency was recorded manually from a six-digit LED display on the controller. The aluminium disc was home-built and easily removable for sample application.

The lifetimes of several phosphorescent species were measured to demonstrate the useful range of the phosphoroscope. Three solid phosphors were obtained from the

National Bureau of Standards. They were: standard reference material (SRM) No. 1023—a zinc cadmium sulphide phosphor with silver as activator, SRM No. 1028—a zinc silicate phosphor with manganese as activator and SRM No. 1030—a magnesium arsenate phosphor with manganese as activator. About 0.1 g of each phosphor was applied to the surface of the rotating disc with 0.5 ml of clear optical cement. The mixture was spread evenly so that it covered the entire face of the disc.

Three molecular samples known to produce room-temperature phosphorescence when adsorbed on filter paper were also tested. Pyrene, quinine, and fluoranthene (Aldrich, Milwaukee, WI) were dissolved in absolute ethanol (1 mg/ml); a 250- $\mu$ l portion of sample solution was spotted onto 1-inch discs of filter paper (Schleicher and Schüll 593-C) previously treated with 250  $\mu$ l of 0.5M lead acetate. The filter paper was allowed to dry in air for 15 min before being glued to the rotating disc.

Finally, a "glow in the dark" phosphorescent paint was applied to the disc. The yellow paint was purchased at a local hobby store and was used to demonstrate that the phosphoroscope was capable of measuring lifetimes of the order of 1 sec. The paint was applied directly to the disc and allowed to dry for 15 min.

The measurement process was as follows. After a sample had been applied to the disc, a range of disc speeds was selected. The speeds corresponded to delay times of 2–2000 msec between excitation and observation of phosphorescence. The signal for each delay time was recorded and a plot of signal *vs.*  $t_D$  was generated (Fig. 5). Each plot was fitted with a simple exponential decay function [equation (1)]. The linear region of a plot of  $\ln(I_{pi})$  *vs.*  $t_D$  had a slope equal to  $-1/\tau_L^n$  where  $\tau_L^n$  was the measured lifetime of the luminescence. The actual phosphorescence lifetime,  $\tau_L^i$ , was calculated by using equation (5). The precision of the  $\tau_L^i$  measurements was calculated by finding the standard deviation of the slope of the line.

Lifetimes determined with the Becquerel-disc phosphoroscope were compared with those determined by using a pulsed-source system. The instrumental arrangement used for the pulsed-source measurements was constructed from parts obtained commercially. The excitation source was a 300-W xenon arc flashlamp (Xenon Corp, Wilmington, MA). Source radiation was passed through a 0.33-m monochromator (GCA/McPherson, Acton, MA) onto the sample. Phosphorescence was collected through a similar monochromator with a photomultiplier tube attachment. The signal from the PMT was amplified and directed to a digital storage oscilloscope (Tektronix Model 2430A, Beaverton, Oregon). A decay curve averaged over 256 excitation pulses was stored. Data points ( $t_D$ ,  $I_{pi}$ ) were read directly from the oscilloscope display. Lifetimes were calcu-

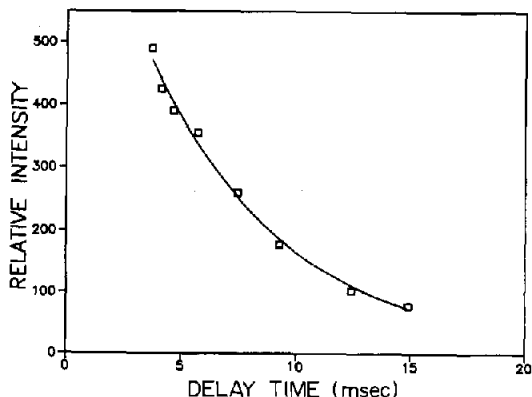


Fig. 5. Exponential decay curve for the luminescence of a solid phosphor (NBS SRM No. 1030).

Table 1. Phosphorescence lifetimes measured with a Becquerel-disc phosphoroscope

Phosphor	System*	$\lambda_{\text{ex}}$ , nm	$\lambda_{\text{em}}$ , nm	Lifetime,† msec	RSD, %	Correlation‡ coefficient
SRM No. 1023	A	380	Yellow	3.1 ± 0.2	2.1	0.9983
	B	380	590	3.7 ± 1.5	8.4	0.9695
SRM No. 1028	A	375	Yellow/Green	2.3 ± 0.1	1.3	0.9987
	B	375	540	2.7 ± 0.2	2.5	0.9952
SRM No. 1030	A	420	Red	3.2 ± 0.4	3.2	0.9971
	B	420	695	2.8 ± 0.2	1.9	0.9989
Fluoranthene	A	365	Yellow/Green	11.1 ± 0.8	2.1	0.9981
	B	365	545	14.3 ± 5.5	8.2	0.9733
Pyrene	A	340	Orange	9.9 ± 0.9	2.5	0.9972
	B	340	595	7.7 ± 1.1	3.9	0.9925
Quinine	A	335	Green	22.0 ± 1.4	1.8	0.9987
	B	335	510	25 ± 15	16.3	0.9944
Phosphorescent§ paint	A	400	Yellow	813 ± 10	1.3	0.9993
	B	400	570	—	—	—

\*System A is the Becquerel-disc phosphoroscope; System B is a pulsed-source system.

†Lifetimes are reported along with 99% confidence limits.

‡Correlation coefficients are reported for a linear plot of delay time *vs.*  $\ln(\text{signal})$ .

§The lifetime of the phosphorescent paint could not be measured with the pulsed-source system.

lated from a plot of equation (4). The same number of data points, with the same delay times, were used for both pulsed-source and Becquerel-disc measurements.

## RESULTS AND DISCUSSION

A photograph of the phosphorescence decay of NBS SRM No. 1023 is shown in Fig. 2. Excitation light from the fibre optic strikes the sample at the bottom of the rotating disc as it moves in an anti-clockwise direction. The decaying phosphorescence can be seen along the periphery of the disc. The "emission" (collection) fibre optic has been removed from the photo for clarity.

Table 1 gives the lifetimes measured for seven phosphors by the two methods. The good agreement between the two methods suggests that the assumptions made in the derivation of equation (5) are valid. The precision (relative standard deviation) is better by a factor of  $\sim 2$  for the Becquerel-disc measurements. The Becquerel-disc phosphoroscope is also capable of measuring longer lifetimes than the flashlamp system can. This is a result of the fixed pulse-rate of the flashlamp, 4 Hz, which restricts lifetime measurements to below 250 msec.

The Becquerel-disc phosphoroscope is ideally suited to the measurement of lifetimes of phosphorescence analytes on solid substrates; such information is not readily available in the literature. A few lifetimes have been reported for several indoles,<sup>10</sup> and for several organic acids<sup>7</sup> absorbed on filter paper,

but no extensive tables of lifetimes covering a wide range of compounds have been published. The Becquerel-disc phosphoroscope described here could be used to generate such data easily and reliably. Such an endeavour would benefit those interested in the analysis of complex mixtures by time-resolved phosphorimetry.

*Acknowledgement*—One of us (B.T.J.) acknowledges support by a Merck Fellowship.

## REFERENCES

1. E. Becquerel, *Ann. Chim. Phys.*, 1859, **55**, 1 (see p. 79 and Plate II).
2. E. N. Harvey, *A History of Luminescence*, p. 349. American Philosophical Society, Philadelphia, 1957.
3. E. Becquerel, *Ann. Chim. Phys.*, 1861, **62**, 5 (see p. 10 and Plate I).
4. R. W. Wood, *Proc. Roy. Soc. London*, 1921, **A99**, 362.
5. V. W. Büniger and W. Flechsig, *Z. Phys.*, 1931, **67**, 42.
6. P. Pringsheim and M. Vogel, *Luminescence of Liquids and Solids*, p. 63. Interscience, New York, 1943.
7. E. M. Schulman and C. Walling, *J. Phys. Chem.*, 1973, **77**, 902.
8. D. E. Goering and H. L. Pardue, *Anal. Chem.*, 1979, **51**, 1054.
9. G. Scharf and J. D. Winefordner, *Talanta*, 1986, **33**, 17.
10. J. J. Aaron, M. Andino and J. D. Winefordner, *Anal. Chim. Acta*, 1984, **160**, 171.
11. G. Scharf and J. D. Winefordner, *Spectrochim. Acta*, 1985, **41A**, 899.
12. T. C. O'Haver and J. D. Winefordner, *Anal. Chem.*, 1988, **38**, 602.

## SHORT COMMUNICATIONS

# DETERMINATION OF SOME CARBOHYDRATES WITH *N*-BROMOPHTHALIMIDE AND *N*-BROMOSACCHARIN

K. GIRISH KUMAR, C. MOHANA DAS and P. INDRASENAN\*

Department of Chemistry, University of Kerala, Trivandrum 695 034, India

(Received 1 March 1988. Accepted 25 March 1988)

**Summary**—Two better titrimetric methods have been developed for determination of carbohydrates such as glucose, fructose, lactose and sucrose, and sugars present in honey and milk. They involve reduction of Cu(II) to Cu(I) by the carbohydrate concerned, and oxidative titration of the Cu(I) with a standard solution of *N*-bromophthalimide or *N*-bromosaccharin.

Determination of carbohydrates is of much importance because of their wide natural distribution. Of the current methods, those based on reduction are the most significant.<sup>1-4</sup> In these Cu(II) is first reduced to Cu(I) by the carbohydrate and the Cu(I) so formed is determined either gravimetrically or titrimetrically, the latter being the better. In all these methods the Cu(I) should be free from excess of Cu(II) and other reagents, such as sodium potassium tartrate, present in the reaction mixture. Therefore these methods are relatively slow because of the time needed for washing the Cu<sub>2</sub>O precipitate free from Cu(II) and other impurities, and for the titration or drying and weighing of the product. We have found that *N*-bromophthalimide and *N*-bromosaccharin are useful for several redox titrations.<sup>5-7</sup> Therefore, we thought it worthwhile to investigate whether use of these *N*-bromoinimides would provide rapid determination of carbohydrates by avoiding washing of the Cu<sub>2</sub>O precipitate. The results are reported in this paper.

### EXPERIMENTAL

#### Reagents

*N*-Bromophthalimide (NBP) and *N*-bromosaccharin (NBSA) were prepared by brominating phthalimide and saccharin, respectively and their standard solutions (~0.05*N*) were prepared in anhydrous glacial acetic acid as reported earlier.<sup>5,6</sup> Glucose, fructose and lactose were all analytical-reagent grade. Cane sugar (sucrose), honey and milk were obtained from the local market. Standard solutions were prepared by dissolving glucose (0.5 g), fructose (0.5 g), lactose (0.5 g), sucrose (2.0 g), honey (15 g) or milk (30 g) in water and diluting to 250 ml. The strengths of these solutions were checked by reported methods.<sup>1,2</sup> Fehling's solutions A and B and Methyl Red indicator were prepared as usual.<sup>1,8</sup> Cuprous oxide was prepared by adding excess of saturated glucose solution to a boiling solution of cupric acetate, filtered off, washed with alcohol, and dried under reduced pressure over phosphorus pentoxide.

#### Preliminary studies

To test the feasibility of the proposed methods a known weight (10-35 mg) of Cu<sub>2</sub>O was dissolved in 20 ml of 2*M* hydrochloric acid and 2 drops of Methyl Red indicator were added. The solution was titrated with standard NBP (or NBSA) solution until the red colour of the solution changed to a permanent bluish green. A blank titration was also done. The experiments were repeated in the presence of added impurities such as Cu(II), sodium chloride, sodium acetate and sodium potassium tartrate, and it was found that none of these affected the titrations.

#### Procedure

To a measured portion (5-20 ml) of carbohydrate solution (glucose, fructose or lactose), Fehling's solutions A and B were added in excess (as indicated by the colour developed) and the resulting solution was boiled for 3 min for the Cu(II) to oxidize the carbohydrate. The solution was cooled and 20 ml of 2*M* hydrochloric acid were added to dissolve the cuprous oxide. To this solution 2 drops of Methyl Red indicator were added and the solution was titrated with standard NBP (or NBSA) solution until the red colour changed to permanent bluish green. A blank titration was also done, but it was found that no blank correction was necessary. For sucrose prior hydrolysis was necessary. A measured portion (5-20 ml) of sucrose solution was boiled with 10 ml of 2*M* hydrochloric acid for 5 min, cooled, and titrated as described above. Honey and milk were clarified with alumina suspension and cupric sulphate, respectively, as reported earlier.<sup>1,2</sup> The clarified solutions were used for analysis as described for carbohydrates.

The amount of Cu(I) formed was calculated from 1 ml of 0.05*N* NBP (or NBSA) ≡ 3.175 mg of Cu, and the amount of carbohydrate was then directly read from the Munson and Walker sugar table.<sup>1,2</sup>

### RESULTS AND DISCUSSION

Typical results are presented in Table 1. During the titration Cu(I) is oxidized to Cu(II), NBP being reduced to phthalimide and NBSA to saccharin as suggested earlier.<sup>5,6</sup> This was confirmed by identification of the reaction products in the titrated solution.

\*Author for correspondence.

Table 1. Titrimetric determination of some carbohydrates with *N*-bromophthalimide and *N*-bromosaccharin (averages of ten replicates)

Carbohydrate	NBP method			NBSA method			Thiosulphate method		
	Amount taken, mg	Amount found, %	C.V., %	Amount taken, mg	Amount found, %	C.V., %	Amount taken, mg	Amount found, %	C.V., %
Glucose	10.3–28.8	100.0	0.3	16.8–35.8	99.7	0.5	17.8–34.9	99.7	0.5
Lactose	12.9–32.2	100.1	0.3	10.7–30.1	100.1	0.4	10.7–30.1	99.5	0.7
Fructose	10.4–32.4	99.8	0.2	10.4–32.4	99.9	0.4	10.4–32.4	100.3	1.5
Sucrose (Cane sugar)	5.10–28.6	100.0	0.5	5.10–28.6	99.9	0.4	5.10–28.6	96.1	1.5
Milk (Lactose)	453–483	4.8	2.4	248–472	4.9	2.6	248–472	4.9	2.6
Honey (Fructose)	10.7–113	61.9	0.3	10.7–113	62.0	0.4	10.7–113	62.0	0.8
Honey (Total sugar)	10.4–72.5	64.1	0.8	10.4–56.9	64.4	0.7	10.4–56.9	64.3	0.8

The results show that the proposed methods are accurate and precise. The presence of Cu(II) and sodium potassium tartrate (from the Fehling's solutions), sodium chloride and sodium acetate does not affect the results. However, Fe(II), cysteine, glutamic acid and hydrazines interfere severely. Both titrations are simple and the end-points are very clear.

The proposed methods have clear advantages over the existing methods based on use of sodium thio-sulphate and potassium permanganate, and requiring washing of the cuprous oxide formed. In the new methods there is no need to isolate cuprous oxide from the reaction mixture after the reduction step. Instead, it is dissolved by adding hydrochloric acid to the reaction mixture itself. The new methods are thus simpler, faster and better than the earlier methods for the determination of carbohydrates and related compounds.

*Acknowledgements*—The authors are thankful to Prof. C. G. R. Nair for his helpful suggestions and to the State Committee on Science, Technology and Environment, Government of Kerala, Trivandrum, for financial assistance.

#### REFERENCES

1. H. O. Tribold and L. W. Avrand, *Food Composition and Analysis*, p. 218. Van Nostrand, Princeton, 1963.
2. A. G. Woodman, *Food Analysis*, p. 262. McGraw-Hill, New York, 1941.
3. T. H. Khan, *Analyst*, 1979, **104**, 261.
4. B. B. Dey and M. V. Sitaraman, *Laboratory Manual of Organic Chemistry*, 3rd Ed., p. 363. Viswanathan, Central Act Press, Madras, 1957.
5. C. M. Das and P. Indrasenan, *Indian J. Chem.*, 1984, **23A**, 869.
6. *Idem, ibid.*, 1987, **26A**, 55.
7. *Idem, J. Food Sci. Tech.*, 1987, **22**, 339.
8. A. I. Vogel, *A Text-book of Quantitative Inorganic Analysis*, 3rd Ed., p. 237. Longmans, London, 1964.

## INDIRECT ATOMIC-ABSORPTION SPECTROPHOTOMETRIC DETERMINATION OF PHOSPHORUS IN STEEL BY USE OF THE BISMUTH PHOSPHOMOLYBDATE COMPLEX

R. RAMCHANDRAN and P. K. GUPTA

Division of Material Characterization, National Physical Laboratory, New Delhi 110 012, India

(Received 20 November 1986. Revised 30 October 1987. Accepted 10 December 1987)

**Summary**—An indirect method for determination of phosphorus by atomic-absorption spectrophotometry has been developed, based on formation of the bismuthophosphomolybdate complex and its extraction by methyl isobutyl ketone. Bismuth is determined in the extract and correlated with the phosphorus content. The method is applicable to different kinds of steel.

Phosphorus in steel or cast iron is usually determined spectrophotometrically as phosphomolybdate either in the reduced or unreduced form.<sup>1,2</sup> The complex is selectively extracted into an organic solvent, resulting in removal of interfering ions. Titrimetric methods<sup>3</sup> have also been employed, based on careful washing of an insoluble phosphomolybdate and its dissolution in excess of alkali, the surplus of which is titrated with standard acid.

Atomic-absorption spectrometry cannot be applied directly for determination of phosphorus, as the principal resonance line of phosphorus lies in the vacuum ultraviolet region (177.5 nm) where atmospheric absorbance causes serious interference. Most of the methods are therefore indirect, based on selective extraction of the heteropoly acid into a suitable solvent and determination of molybdenum in the organic phase<sup>4</sup> or in the aqueous phase after stripping with acid.<sup>5,6</sup>

We showed earlier<sup>7</sup> that phosphorus can be determined by formation of the ternary bismuthophosphomolybdate, its extraction into methyl isobutyl ketone, and measurement of bismuth in the organic phase. This procedure can conveniently be used for determination of phosphorus in iron and steel.

### EXPERIMENTAL

#### Apparatus

A Pye Unicam SP 1900 double-beam atomic-absorption spectrophotometer with digital read-out and deuterium lamp background-correction was used with the experimental conditions given earlier.<sup>7</sup>

#### Reagents

The bismuth, molybdate and phosphate solutions were prepared as described earlier.<sup>7</sup> A 10% ascorbic acid solution was used. Two g of electrolytic grade iron powder (free from phosphorus) was dissolved in *aqua regia*, then 10–15 ml of 60% perchloric acid were added, the solution was evaporated until perchloric acid fumes were evolved, then cooled and diluted to 250 ml.

#### Procedure

Weigh a 2-g sample into a 250-ml conical flask and add 20–25 ml of *aqua regia*. When the sample has dissolved add 10–15 ml of 60% perchloric acid and heat until the perchloric acid starts refluxing and thick white fumes appear. If more than 0.05% arsenic is present, cool the solution and add 5 ml of concentrated hydrobromic acid to volatilize the arsenic, and heat again until dense white fumes have been expelled for about 1 min. Cool the flask, dissolve the residue in water, filter if necessary, and make up to volume in a 250-ml standard flask. Take a 10-ml aliquot in a 100-ml beaker and a 10-ml aliquot of the phosphorus-free iron solution (as a reagent blank) in another 100-ml beaker. Add 5 ml of 10% sodium sulphite ( $\text{Na}_2\text{SO}_3$ ) solution to each, heat to boiling for about a minute, cool to room temperature, add 2.5 ml of 0.12M sodium molybdate and 2 ml of 0.001M bismuth solution to both solutions and dilute them to about 45 ml. Add 5 ml of ascorbic acid solution to each. Let the solutions stand for 10 min, then extract each with 25 ml of isobutyl methyl ketone in a 100-ml separating funnel. Measure the absorbance of the bismuth at the 223.1 nm resonance line and subtract the absorbance for the reagent blank.

Prepare a calibration graph by taking different known volumes of suitable standard phosphate solutions, adding to each an amount of phosphorus-free iron solution equivalent to about 0.08 g of iron and apply the reduction and extraction procedure followed by the AAS measurement and correction for the blank. The graph is linear up to 1.4  $\mu\text{g/ml}$  phosphorus in the 25-ml extract.

### RESULTS AND DISCUSSION

The method is a modification of an earlier method<sup>8</sup> based on formation of antimonylphosphomolybdate and determination of antimony by atomic-absorption spectrophotometry. The use of bismuthophosphomolybdate is advantageous because the principal resonance line of bismuth (223.6 nm) lies nearer to the visible region than the antimony line (206.8 nm) does, and the sensitivity for bismuth is better by a factor of almost 3 on a w/w basis and 6 on an atomic-ratio basis. The method has been applied to

Table 1. Analysis of standards

No.	Sample	Sample wt., g	Aliquot taken, ml	Phosphorus found, %	Certified value, %
1	BCS 218/1	2	10	0.014	0.014
2	BCS 225 (Ni, Cr, Mo steel)	2	10	0.021	0.021
3	BCS 214 mild steel	2	10	0.016	0.016
4	Mild steel NML Jamshedpur	1	5 10	0.075 0.076	0.078
5	BCS 232 mild steel	1	5	0.076	0.076
6	BCS 235 stainless steel	2	10	0.020	0.020
7	BCS 241/1 high speed tungsten steel	2	10	0.020	0.021
8	BCS 234/3	0.499	2	0.33	0.33
9	BCS 206/2 cast iron	0.15	2	1.36	1.38
10	BCS 247/1 cast iron	0.2	2	1.14	1.13

the determination of phosphorus in different kinds of standard iron and steel samples and the results are given in Table 1. The results obtained by the present method compare well with the certified values for the standard samples.

Most of the steel-making elements do not interfere in the application of the present method in the analysis of cast iron and steel. Nickel does not cause interference even if present in amounts 400 times that of the phosphorus; this has been confirmed by an analysis of BCS 225 (Table 1). Antimony interferes by competitive formation of antimonophosphomolybdate, but this does not cause any practical problems as antimony is generally not found in steel. Titanium does not interfere if it is treated with excess of ascorbic acid.<sup>9</sup> Niobium and tantalum, if present, are readily removed during the fuming with perchloric acid, by precipitation of the corresponding acids (or hydrous oxides). The standard deviations for samples 4, 6, 7 and 10 in Table 1 were found to be 0.006, 0.0022, 0.0017 and 0.03% phosphorus

respectively. The results obtained by the present method compare well with the certified values.

*Acknowledgement*—The authors wish to thank Dr. Krishan Lal, Head of Materials Characterization Division, for his encouragement and keen interest in this work.

#### REFERENCES

1. Z. Marczenko, *Separation and Spectrophotometric Determination of Elements*, Horwood, Chichester, 1986.
2. M. Halmann (ed.), *Analytical Chemistry of Phosphorus Compounds*, Wiley, New York, 1972.
3. T. S. Harrison, *Handbook of Analytical Control of Iron and Steel Production*, Horwood, Chichester, 1979.
4. T. V. Ramakrishna, J. W. Robinson and P. W. West, *Anal. Chim. Acta*, 1969, **45**, 43.
5. T. R. Hurford and D. F. Boltz, *Anal. Chem.*, 1968, **40**, 379.
6. C. Riddle and A. Turek, *Anal. Chim. Acta*, 1977, **92**, 49.
7. P. K. Gupta and R. Ramchandran, *J.A.S.*, 1987, **2**, 413.
8. P. K. Gupta and A. K. Sarkar, *Indian J. Chem.*, 1979, **17A**, 317.
9. D. F. Boltz and J. A. Howell, *Colorimetric Determination of Nonmetals*, p. 362. Wiley, New York, 1978.

## SPECTROPHOTOMETRIC DETERMINATION OF FORMALDEHYDE

GHAZI AL-JABARI and BRUNO JASELSKIS

Department of Chemistry, Loyola University of Chicago, 6525 N. Sheridan Road, Chicago,  
IL 60626, U.S.A.

(Received 17 March 1988. Accepted 12 April 1988)

**Summary**—A new spectrophotometric method for the determination of micro amounts of formaldehyde in aqueous and methanol solutions is based on the oxidation of formaldehyde by hydrous silver oxide at pH 11–12.5 and oxidation of the metallic silver produced, with iron(III) in the presence of Ferrozine. The absorbance of the resulting iron(II)–Ferozine complex at 562 nm is proportional to the amount of formaldehyde and corresponds to an apparent molar absorptivity of  $5.58 \times 10^4$  l.mole<sup>-1</sup>.cm<sup>-1</sup>.

Large volume production and usage of formaldehyde and its possible exposure-related health effects have caused much concern over the sensitivity and accuracy of analytical methodology for this compound.

In general, large amounts of formaldehyde or other aliphatic aldehydes have been determined titrimetrically by reaction with alkaline silver(I) and back-titration of the excess of silver(I)<sup>1-4</sup> or by the Ripper method with sulphite and back-titration of the excess of sulphite with standard iodine solution.<sup>5</sup>

Small amounts of formaldehyde are determined by gas chromatography,<sup>6,7</sup> high-performance liquid chromatography,<sup>8,9</sup> electrochemical<sup>10,11</sup> and spectrophotometric<sup>12-18</sup> methods. Spectrophotometric methods are commonly used and one of these, the chromotropic acid method, is recommended by NIOSH in its P&CAM 125 and P&CAM 235 reference methods.<sup>19</sup>

This study describes a colorimetric procedure for the determination of formaldehyde and aliphatic aldehydes in aqueous and methanolic solutions, by use of a modified Ponndorf method (hydrous silver oxide) coupled with the iron(III)–Ferozine system.

### EXPERIMENTAL

#### Instrumentation

A Cary 14 spectrophotometer and a Corning model XII pH-meter were used. A PAR 170 A polarographic analyser with a dropping mercury electrode in a three-electrode system was operated in the differential mode at a scan-rate of 5 mV/sec, a modulation amplitude of 25 mV, a drop-rate of 1 drop per sec, recorder sensitivity of 1  $\mu$ A/25 cm, and scan-range from -1.5 to -2.0 V.

#### Reagents

All chemicals were analytical or primary grade. Formaldehyde standard stock solution ( $2.58 \times 10^{-3}$  M) was prepared from 37% formalin and standardized argentometrically.<sup>4</sup> Approximately 1.24 g of Ferrozine [3-(2-pyridyl)-5,6-diphenyl-1,2,4-triazine-*p,p*-disulphonic acid monosodium salt monohydrate (Aldrich)] was dissolved in 250 ml of demineralized water. Stock solutions of 0.004 M iron(III) and 0.05 M silver nitrate were prepared by dissolving 1.932 g of ammonium ferric sulphate dodecahydrate

in 1 litre of 0.1 M sulphuric acid and 2.12 g of silver nitrate in 250 ml of demineralized water. Acetate buffer of pH 3.5 was prepared by adding concentrated sodium hydroxide dropwise to 0.5 M acetic acid. Polarographic determinations were performed with a 0.1 M lithium hydroxide, 0.01 M lithium chloride supporting electrolyte.

#### Procedures

**Standardization and determination of formaldehyde in aqueous solutions.** Suitable aliquots (0.050–0.500 ml) of  $2.58 \times 10^{-3}$  M standard formaldehyde solution, 0.25 ml of 0.05 M silver nitrate and 0.1 ml of 0.1 M sodium hydroxide were added to 25-ml test-tubes, in that order. The solutions were stirred for 10 min, then 2 ml of 0.004 M iron(III) solution, 2 ml of Ferrozine solution, and 5 ml of acetate buffer were added, and the mixtures were transferred to 50-ml standard flasks and diluted to volume. The absorbances at 562 nm were measured after 10 min against a blank. The same standard formaldehyde solution was used for a comparative study of the chromotropic acid and polarographic methods.

**Determination of formaldehyde in dilute ( $3-10 \times 10^{-5}$  M) aqueous and methanolic solutions.** Dilute formaldehyde solutions were analysed in a similar manner to the more concentrated samples. The conditions were changed to 5 or 10 ml of sample, 0.5 ml of silver nitrate solution, 2–3 ml of sodium hydroxide solution, and 25 min reaction time before the addition of iron(III), Ferrozine, and acetate buffer. Very dilute samples were analysed by the standard-addition method, as described below for methanol.

The amount of formaldehyde (or other aliphatic aldehyde) in technical and reagent grade methanol was determined by the standard-addition method. Three 0.500-ml samples of the methanol were placed in 50-ml standard flasks, and diluted with 6 ml of demineralized water, then two of the samples were spiked with known amounts of standard formaldehyde solution. The other reagents were added in the same order as for dilute solutions.

The absorbance was measured against a blank containing all the reagents used in the analysis of the sample, except the silver nitrate.

### RESULTS

The amount of formaldehyde in the sample can be determined by several methods: (i) calibration curve, (ii) calculation by using the apparent molar absorp-



Table 1. Determination of formaldehyde in aqueous and methanolic solutions by the proposed method and the chromotropic acid and differential pulse polarography (DPP) methods

Final CH <sub>2</sub> O concentration, $\mu\text{M}$	Ag <sub>2</sub> O-Fe(III)		Chromotropic acid		DPP peak height, mm
	A*	$\epsilon$ , $10^4 \text{ l. mole}^{-1} \cdot \text{cm}^{-1}$	A*	$\epsilon$ , $10^4 \text{ l. mole}^{-1} \cdot \text{cm}^{-1}$	
<i>Water</i>					
6.3	0.350	5.56	0.097	1.55	13
12.6	0.705	5.59	0.194	1.54	25
18.9	1.055	5.59	0.292	1.55	37
25.2	1.403	5.57	0.390	1.55	49
<i>10% Methanol-water</i>					
6.3	0.349	5.56	—	—	13
12.6	0.701	5.56	—	—	25
18.9	1.050	5.55	—	—	38
25.2	1.400	5.56	—	—	50

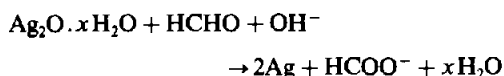
\*Average of four determinations, corrected for the blank.

tivity of  $5.58 \times 10^4 \text{ l. mole}^{-1} \cdot \text{cm}^{-1}$ , and (iii) the standard-addition method (used with very dilute solutions). In the calculation method, the amount of formaldehyde in the 50 ml of final solution is  $26.9A \mu\text{g}$ , where  $A$  is the absorbance measured in a 1-cm cell.

Results for determination of formaldehyde in standard aqueous and methanolic solutions and in methanol samples and the comparison experiments are summarized in Tables 1 and 2.

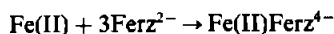
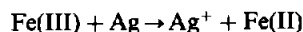
#### DISCUSSION

Ponndorf<sup>1</sup> reported that hydrous silver oxide oxidizes formaldehyde to formate:



In the Ponndorf procedure the excess of silver ion is determined by titration with standard thiocyanate solution, whereas in the proposed method the

amount of metallic silver is obtained colorimetrically from the amount of iron(II)-Ferrozine complex<sup>20</sup> produced:



Siggia and Segal<sup>2</sup> used an ammoniacal silver ion solution instead of hydrous silver oxide. However, ammoniacal silver solution (Tollen's reagent) presents a potential danger of explosion, particularly when the solution becomes concentrated or dries out. Because of this, Mayes *et al.*<sup>3</sup> modified the method by replacing the ammonia with *tert*-butylamine. The use of ammoniacal silver solution does not prevent aldehydes from undergoing the Cannizzaro reaction, whereas in the Ponndorf method the side-reactions of aldehydes such as the Cannizzaro reaction or aldol condensation do not occur, since the solutions are strongly basic and dilute. However, the pH must be kept in the range 11–12.4. Below pH 11 the reaction is too slow, while with pH above 12.5 the results are low.

Table 2. Determination of formaldehyde in methanol and simulated samples

Sample	Aliquot, ml	CH <sub>2</sub> O added, $\mu\text{g}$	Net absorbance	CH <sub>2</sub> O found in the original sample, $\mu\text{g}$
<i>Bulk methanol</i>				
	0.500	0.00	0.055	$1.7 \pm 0.2^*$
	0.500	8.80	0.390	
	0.500	17.60	0.720	
<i>Aqueous dilute sample†</i>				
	0.030†	0.00	0.110	$3.5 \pm 0.2^*$
	0.030†	8.80	0.440	
	0.030†	17.60	0.755	
<i>Aqueous</i>				
	0.050	9.4	0.350	$9.4 \pm 0.2$
	0.100	18.9	0.710	$19.1 \pm 0.3$
	0.150	28.3	1.060	$28.5 \pm 0.3$

\*Value obtained by the standard-addition graphical method.

†Formaldehyde concentration  $5.93 \times 10^{-3} \text{M}$ .

Hydrous silver oxide does not oxidize alcohols, ketones, carboxylic acids, phenols and acetals. Aliphatic aldehydes react readily with it, the reactivity decreasing with increasing molecular weight. Aromatic aldehydes are considerably less reactive than aliphatic aldehydes and their interference is not serious as long as their concentration is not much greater than that of the formaldehyde and the reaction time is kept to 25 min or less. Monosaccharides and citric, tartaric and ascorbic acids interfere, and formaldehyde must be separated from them by distillation or other methods. Sulphite and sulphide reduce iron(III) to iron(II) and must be eliminated when present in amounts greater than that of the formaldehyde. The sulphite-formaldehyde addition compounds do not react readily with hydrous silver oxide.

Trioxan does not react with hydrous silver oxide, whereas paraformaldehyde is quantitatively oxidized.

The absorbance of the iron(II)-Ferrozine complex produced in the method is directly proportional to the formaldehyde concentration in the sample. The apparent molar absorptivity of  $5.58 \times 10^4$  l. mole<sup>-1</sup>. cm<sup>-1</sup> corresponds to the oxidation of formaldehyde to formate, with transfer of two electrons.

The modified Ponndorf method coupled with the iron(III)-Ferrozine reaction is approximately 3.5 times more sensitive than the chromotropic acid method and can be used with aqueous methanol solutions provided that the methanol concentration is less than approximately 10% v/v. Otherwise, the reaction of formaldehyde with silver oxide is slow and incomplete. However, the procedure cannot be used with formaldehyde absorbed in sulphite solutions, unless the sulphite is eliminated. On the other hand, chromotropic acid can be used with sulphite solutions but not with methanolic solutions.

The reproducibility has been checked for various levels of formaldehyde by quadruplicate analysis. The relative standard deviations of individual sets varied from 1.5 to 3.5% depending on the concentration of formaldehyde.

The procedure does not differentiate between individual aliphatic aldehydes and in a mixture they are all determined as though they are formaldehyde.

Also, alcoholic beverages containing sucrose, citric, tartaric acids and hemiacetals cannot be analysed by this procedure, since these as well as formaldehyde reduce hydrous silver oxide to metallic silver. The proposed method allows the determination of formaldehyde in amounts from 9 to 40 µg when 50-ml standard flasks are used. Also, the concentration of formaldehyde in the original sample must be greater than  $3 \times 10^{-5}M$ , or the reaction time will be long and the results low. However samples more dilute than  $3 \times 10^{-5}M$  can be analysed by the standard addition method.

#### REFERENCES

1. W. Ponndorf, *Ber.*, 1931, **64**, 1913.
2. S. Siggia and E. Segal, *Anal. Chem.*, 1953, **25**, 640.
3. J. Mayes, E. Kuchar and S. Siggia, *ibid.*, 1964, **36**, 934.
4. M. Ripper, *Monatshefte*, 1900, **21**, 1079.
5. E. R. Kennedy and R. Hill, Jr., *Anal. Chem.*, 1982, **54**, 1739.
6. *National Institute for Occupational Safety and Health Manual of Analytical Methods*, D. G. Taylor (ed.), NIOSH Cincinnati, Ohio, DHHS (NIOSH) Publication No. 80-125, P&CAM 318.
7. K. Kuwata, M. Uebori and Y. Yamazaki, *J. Chromatog. Sci.*, 1979, **17**, 264.
8. F. Lipari and J. S. Swarin, *J. Chromatog.*, 1982, **247**, 297.
9. *National Institute for Occupational Safety and Health Manual of Analytical Methods*, D. G. Taylor (ed.), NIOSH, Cincinnati, Ohio, 1978, DHHS (NIOSH) Publication No. 80-125, P&CAM 327.
10. C. J. Septon and C. J. Ku, *Am. Ind. Hyg. Assoc. J.*, 1982, **43**, 845.
11. A. C. Rayner and C. M. Jephcott, *Anal. Chem.*, 1961, **33**, 627.
12. D. R. Ekberg and E. C. Silver, *ibid.*, 1966, **38**, 1421.
13. P. W. West and B. Sen, *Z. Anal. Chem.*, 1956, **153**, 12.
14. D. E. Jordan, *Anal. Chem.*, 1980, **113**, 189.
15. P. W. West and G. C. Gaeke, *ibid.*, 1986, **28**, 1816.
16. R. R. Miksch, D. W. Anthon, L. Z. Fanning, C. D. Hollowell, K. Revzan and J. Glanville, *ibid.*, 1981, **53**, 2118.
17. P. E. Georghiou, L. Harlick, L. Winsor and D. Snow, *ibid.*, 1983, **55**, 567.
18. C. E. Bricker and W. A. Vail, *ibid.*, 1950, **22**, 720.
19. *National Institute for Occupational Safety and Health Manual of Analytical Methods*, D. G. Taylor (ed.), NIOSH, Cincinnati, Ohio, 1977, DHHS (NIOSH) Publication No. 77-157A, P&CAM 125 and P&CAM 235.
20. G. Al-Jabari and B. Jaselskis, *Talanta*, 1987, **34**, 479.

## SILVER-GELATIN METHOD FOR DETERMINATION OF INORGANIC PEROXIDES IN ALKALINE SOLUTION

T. PAL\*, D. S. MAITY and A. GANGULY

Department of Chemistry, Indian Institute of Technology, Kharagpur 721 302, India

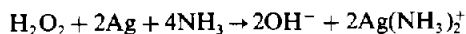
(Received 29 April 1985. Revised 12 February 1988. Accepted 25 March 1988)

**Summary**—An aqueous solution of gelatin binds silver(I) at pH >7 and a yellow silver sol can be produced from this by reduction. The sol reacts with peroxide in strongly ammoniacal medium to give a colourless solution. The reaction may be used for photometric and visual titration of peroxide with relative standard deviations of 0.4 and 1.5% respectively and also for its spectrophotometric determination.

We have developed a new and simple method for determination of inorganic peroxides in alkaline solution. Until recently,<sup>1,2</sup> most titrimetric methods for determining peroxide involved an acidification before the titration,<sup>3-6</sup> which can result in evolution of heat and hence partial decomposition of the peroxide solutions. Addition of boric acid retards the decomposition of peroxide in the acidification step.<sup>6</sup> Ethanol will also inhibit thermal decomposition of peroxides.<sup>7</sup> It would seem best to determine peroxides in alkaline solution whenever possible. There are few reagents which can be used in alkaline medium for determination of peroxide, and of these hydrazine and chromium(II) deserve mention. However, both are strong reducing agents and can be oxidized by air, making it difficult to preserve their standard solutions; the chromium(II) method also involves some rather lengthy steps.

We now report a new, simple and sensitive method for the determination of peroxide by spectrophotometry or titration. The spectrophotometric method is more sensitive than the indirect determinations of peroxide based on oxidation of iodide to iodine,<sup>8</sup> Mn<sup>2+</sup>-catalysed Hydroxynaphthol Blue oxidation,<sup>9</sup> the Hantzsch reaction<sup>10</sup> and chemiluminescence,<sup>11</sup> and is not susceptible to interference by Mn(II) and Fe(III), which limit utilization of the commonly used luminol-hydrogen peroxide chemiluminescence method.<sup>12</sup>

The principle is dissolution of the coloured silver sol produced by reaction of the silver-gelatin complex<sup>13</sup> with various reducing agents.<sup>14,15</sup> Peroxide reacts quantitatively with the sol in presence of ammonia, which accelerates the reaction.



### EXPERIMENTAL

#### Reagents

All reagents were of analytical grade except where otherwise specified. Carbon monoxide was prepared from con-

centrated sulphuric acid and formic acid and was purified by passage through alkali.

The silver nitrate solution was made by dissolving 0.850 g of silver nitrate in 500 ml of distilled water, standardized by Volhard's method<sup>16</sup> and diluted to exactly 0.01M. A 5 g/l. gelatin solution was made by dissolving 1 g of gelatin in 200 ml of warm distilled water. The hydrogen peroxide solution was made by diluting 0.1 ml of 30% solution to 250 ml and standardized by the permanganate method.<sup>6</sup>

**Sodium peroxide solution.** About 0.4 g of sodium peroxide was dissolved in 100 ml of water; 2.5 ml of the solution were diluted to volume in a 250-ml standard flask, and standardized by the permanganate method.

**Silver sol ( $4 \times 10^{-4}$ M).** Fifty ml of warm (~50°) gelatin solution were mixed with 10 ml of the 0.01M silver nitrate with stirring, and the pH was then adjusted to about 8 with 0.2M sodium hydroxide. Carbon monoxide was passed through the solution at room temperature for 20 min and the solution was then left for 2 hr. Dissolved carbon monoxide was removed by blowing air through the solution. The resulting sol was diluted to volume with water in a 250-ml standard flask.

#### Procedures

**Spectrophotometric.** An aliquot of 1.5 ml of  $4 \times 10^{-4}$ M silver sol was pipetted into a series of 10-ml standard flasks, each containing 2 ml of 6M ammonia solution. Various volumes of  $5 \times 10^{-6}$ M hydrogen peroxide were introduced from a microburette into the flasks, which were then shaken for 15 min. The solutions were diluted to volume and the absorbances were measured at 415 nm against water, and the calibration graph of corrected absorbance of the silver sol vs. hydrogen peroxide concentration was plotted. Depending on the make of spectrophotometer used, the corrected absorbance can be obtained automatically or manually by taking the difference between the absorbances of the silver sol in the presence and absence of the peroxide solution. The graph is linear over the 0.10-10.0 µg/ml hydrogen peroxide range.

Hydrogen peroxide samples can be similarly analysed, provided suitable volumes of the reagents are present and the amount of peroxide is not too high. Alternatively, the method can be used as a photometric titration, increasing volumes of hydrogen peroxide sample being added to the same amount of reagent solution (1.25 ml of  $4 \times 10^{-4}$ M silver sol and 2.0 ml of 6M ammonia); the mixtures are diluted to volume in 10-ml standard flasks and the absorbances are measured and plotted against the volumes of sample added (Fig. 1). The end-point is given by the point at which the extrapolation of the absorbance line cuts the

\*Author for correspondence.

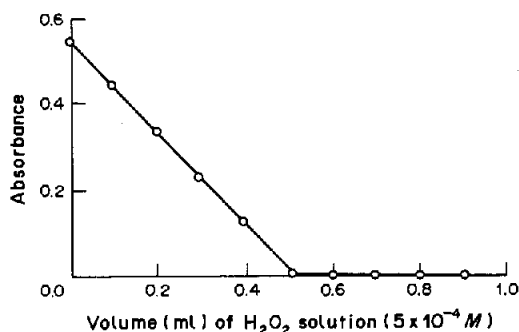


Fig. 1. Spectrophotometric titration of silver sol.

$x$ -axis. The peroxide concentration of the sample (mole/l.) is then calculated from

$$[\text{H}_2\text{O}_2] = M_{\text{sol}} V_{\text{sol}} / 2V_{\text{ep}}$$

where  $M_{\text{sol}}$  and  $V_{\text{sol}}$  are the molarity and volume (ml) of the silver sol used, and  $V_{\text{ep}}$  is the volume (ml) of sample needed to reach the end-point.

**Visual titration.** A measured amount of silver sol solution is taken in a 250-ml Erlenmeyer flask, made strongly ammoniacal, and titrated with the peroxide solution. The reaction is slow and goes to completion only with vigorous shaking. The end-point is indicated by the solution becoming colourless. Detection of the end-point is easier with starch-iodide paper or acidified starch-iodide solution as external indicator.

## RESULTS AND DISCUSSION

Of the two methods the most sensitive is the spectrophotometric one. The reproducibility of this method is 0.4% and a reduction of 0.011 in the

absorbance of the 10 ml of solution measured is equivalent to 0.10  $\mu\text{g}$  of hydrogen peroxide, indicating the suitability of the method for trace analysis. Moreover, the results obtained by the spectrophotometric procedure were found to be in good agreement with those of the standard iodometric method.<sup>8</sup> The results obtained by the photometric and visual titration methods were comparable to those from the permanganate method<sup>6</sup> (Tables 1 and 2).

The addition of boric acid as stabilizer does not affect the results, and hence its addition appears unnecessary. The value obtained for sodium peroxide solution was significantly closer to the nominal value than that obtained by the permanganate method, which appears to confirm the disadvantage of using an acidification step.

The reproducibilities of the results were good for the spectrophotometric methods (rsd 0.4%) and visual titrations (rsd 1.5%). At the low concentrations used the peroxide solutions did not decompose in a burette.

Interferences include any species that are oxidizing or strongly complexing in alkaline solution (such as hypochlorite and cyanide, which can be determined<sup>17,18</sup> by a slightly modified version of the procedure).

It was established that a 10-fold excess (50  $\mu\text{g}/\text{ml}$  for spectrophotometry and 200  $\text{mg}/\text{l}$ . for visual titration) of alkaline-earth metal ions and Mn(II), Cu(II), Ni(II), Zn(II) and Pb(II) did not hinder the determination if 0.1 ml of 0.1M Na<sub>2</sub>EDTA solution was added. Hence, peroxide solutions containing such metal ions can be analysed if these ions are masked with Na<sub>2</sub>EDTA.

Table 1. Analysis of peroxide solutions

Peroxide	Nominal H <sub>2</sub> O <sub>2</sub> taken, $\mu\text{g}/\text{ml}$	H <sub>2</sub> O <sub>2</sub> found, $\mu\text{g}/\text{ml}$	
		Iodometric method <sup>8</sup>	Present method
H <sub>2</sub> O <sub>2</sub>	1.170	1.170	1.170
H <sub>2</sub> O <sub>2</sub>	0.930	0.929	0.930
H <sub>2</sub> O <sub>2</sub>	0.520	0.520	0.519
Na <sub>2</sub> O <sub>2</sub> *	0.870	0.865	0.862

\*Calculated as hydrogen peroxide.

Table 2. Analysis of peroxide solutions

Peroxide	Nominal H <sub>2</sub> O <sub>2</sub> taken, $\text{mg}/\text{l}$ .	H <sub>2</sub> O <sub>2</sub> found, $\text{mg}/\text{l}$ .		
		Permanganate method	Visual titration (Ag sol)	Visual titration (Ag sol) with H <sub>3</sub> BO <sub>3</sub> present
H <sub>2</sub> O <sub>2</sub>	76.4	75.9	76.4	76.4
H <sub>2</sub> O <sub>2</sub>	42.3	42.1	42.3	42.3
H <sub>2</sub> O <sub>2</sub>	19.2	19.04	19.20	19.20
H <sub>2</sub> O <sub>2</sub>	10.54	16.64	10.52	10.56
Na <sub>2</sub> O <sub>2</sub> *	16.78	16.24	16.76	16.76

\*Calculated as hydrogen peroxide.

## REFERENCES

1. R. W. Lynch, *Anal. Chem.*, 1980, **52**, 347.
2. R. W. Lynch and M. R. Smith, *ibid.*, 1980, **52**, 1998.
3. J. W. Mellor, *A Comprehensive Treatise on Inorganic and Theoretical Chemistry*, Vol. 1, pp. 944-945. Longmans, London, 1952.
4. W. C. Schumb, C. N. Satterfield and R. L. Wentworth, *Hydrogen Peroxide*, pp. 553-560. Reinhold, New York, 1955.
5. *Standard Methods of Chemical Analysis*, 6th Ed., F. J. Welcher (ed.), Vol. IIB, 1318. Van Nostrand, Princeton, 1963.
6. A. I. Vogel, *A Text Book of Quantitative Inorganic Analysis*, 3rd Ed, p. 296. Longmans, London, 1973.
7. A. Meffert and H. Meier-Ewert, *Z. Anal. Chem.*, 1963, **198**, 325.
8. A. Magill and A. R. Beeker, *J. Pharm. Sci.*, 1984, **73**, 1663.
9. T. Yamane, *Bunseki Kagaku*, 1984, **33**, E 203.
10. S. Kawai and C. Tsutsui, *ibid.*, 1984, **33**, E 73.
11. T. Ibusuki, *Atmos. Environ.*, 1983, **17**, 393.
12. G. L. Kok, T. P. Holler, M. B. Lopes, H. A. Nachtrieb and M. Yuan, *Environ. Sci. Technol.* 1978, **12**, 1072.
13. T. Pal, *Inorg. Chim. Acta*, 1983, **79**, 283.
14. T. Pal and D. S. Maity, *Anal. Lett.*, 1985, **18**, 1131.
15. T. Pal, A. Ganguly and D. S. Maity, *Bull. Chem. Soc. Japan*, 1987, **60**, 3001.
16. A. I. Vogel, *op. cit.*, p. 259.
17. T. Pal, A. Ganguly and D. S. Maity, *Anal. Chem.*, 1986, **58**, 1564.
18. *Idem*, *Chem. Anal. Warsaw*, in the press.

## SPECTROPHOTOMETRIC DETERMINATION OF COBALT IN A VITAMIN, ALLOYS AND AN ORE BY EXTRACTION OF ITS 3-HYDROXY-2-METHYL-1,4-NAPHTHOQUINONE 4-OXIME COMPLEX INTO MOLTEN NAPHTHALENE

R. K. SHARMA and S. K. SINDHWANI\*

Department of Chemistry, University of Delhi, Delhi 110 007, India

(Received 17 December 1986. Revised 19 April 1987. Accepted 25 March 1988)

**Summary**—A selective spectrophotometric method has been developed for the determination of cobalt after extraction of its 3-hydroxy-2-methyl-1,4-naphthoquinone 4-oxime (HMNQM) complex into molten naphthalene. The optimum pH range for the extraction is 5.0–7.5. The solidified naphthalene, containing the cobalt–HMNQM complex, is separated by filtration and dissolved in *N,N*-dimethylformamide. The absorbance is measured at 430 nm against a reagent blank. Beer's law is obeyed up to 1.90 ppm cobalt. The molar absorptivity is  $2.09 \times 10^4$  l. mole<sup>-1</sup>. cm<sup>-1</sup>.

In this work, the technique of extraction into molten naphthalene is used in conjunction with 3-hydroxy-2-methyl-1,4-naphthoquinone 4-oxime (HMNQM) for the determination of cobalt.

### EXPERIMENTAL

#### Reagents

Doubly distilled water and analytical reagent grade acids and salts were used throughout, unless otherwise stated.

**Standard cobalt solution.** A standard solution of cobalt sulphate heptahydrate was prepared and standardized by one of the usual methods.<sup>2</sup>

**Sodium acetate–acetic acid buffer.** Mix 0.2M sodium acetate and 0.2M acetic acid in suitable proportions.

***N,N*-Dimethylformamide (DMF) and naphthalene.** Check the purity spectrophotometrically before use.

**3-Hydroxy-2-methyl-1,4-naphthoquinone 4-oxime.** Preparation of the reagent was reported earlier.<sup>3</sup>

#### General procedure

To an aliquot of sample solution (containing 1.2–18.0 µg of cobalt) in a 100-ml beaker add 1 ml of  $5 \times 10^{-4}$ M HMNQM. Adjust the pH to 5.0–7.5 with 5 ml of pH-6 acetate buffer and 0.2M sodium hydroxide. Transfer the solution into a 100-ml round-bottomed flask and heat to 60° in a water-bath. Add 2.0 g of naphthalene, stopper the flask and continue to heat until the naphthalene melts. Remove the flask from the water-bath and shake it vigorously until the naphthalene separates out as a solid mass. Repeat the melting and solidification once more. Filter off the naphthalene on paper. Dissolve the solid mass in DMF and dilute to volume with DMF in a 10-ml standard flask. Dry the solution with 2 g of anhydrous sodium sulphate and measure the absorbance in a 1-cm cell at 430 nm against a reagent blank. Prepare a calibration graph similarly.

### RESULTS AND DISCUSSION

#### Absorption spectra

The absorption spectra of HMNQM and its cobalt

complex in naphthalene–DMF solutions were recorded against water and the reagent blank, respectively (Fig. 1). The absorbance is maximal at 430 nm, and all measurements are made at this wavelength.

#### Reaction conditions

The shape of the spectrum is independent of the pH of extraction, indicating formation of only one complex. The extraction is quantitative in the pH range 5.0–7.5 and with 0.6–4.0 ml of  $5 \times 10^{-4}$ M HMNQM, provided the aqueous phase volume does not exceed

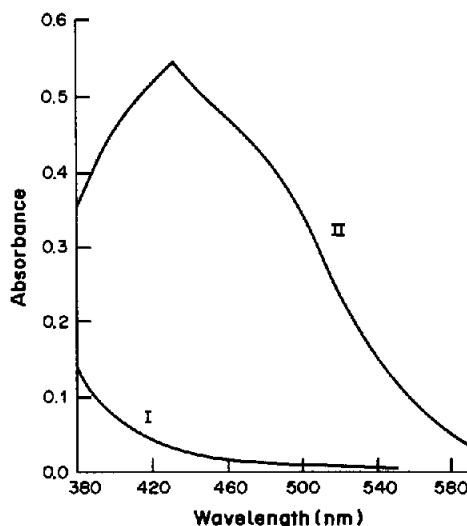


Fig. 1. Absorption spectra of HMNQM and the Co–HMNQM complex in naphthalene–DMF solution containing 14.7 µg of Co, 0.5 ml of  $5 \times 10^{-3}$ M HMNQM and 2 g of naphthalene; shaking time 1 min, pH 6.0. Reference: (I) water for HMNQM; (II) reagent blank for Co–HMNQM.

\*To whom correspondence should be addressed.

Table 1. Effect of diverse anions on determination of 14  $\mu\text{g}$  of cobalt; amount of naphthalene, 2 g; pH, 6.0

Anion added	Amount of anion added, $\mu\text{g}$	Absorbance
None	—	0.524
Fluoride	3000	0.521
Chloride	5000	0.523
Bromide	5000	0.521
Iodide	2000	0.525
Nitrate	2000	0.523
Nitrite	1500	0.524
Sulphate	4000	0.526
Sulphite	2000	0.523
Thiourea	2000	0.520
Thiosulphate	3000	0.526
Citrate	2500	0.524
Tartrate	2500	0.521
Oxalate	2000	0.525
Phosphate	5000	0.523
Thiocyanate	5000	0.526

Table 2. Effect of diverse metal ions on determination of 14  $\mu\text{g}$  of cobalt; amount of naphthalene, 2 g; pH, 6.0

Metal ion added	Amount of metal ion added, $\mu\text{g}$	Absorbance
None	—	0.524
$\text{Ca}^{2+}$	1000	0.523
$\text{Ba}^{2+}$	1000	0.524
$\text{Sr}^{2+}$	1000	0.523
$\text{Fe}^{2+}$	500	0.523
$\text{Zn}^{2+}$	800	0.525
$\text{Cd}^{2+}$	800	0.523
$\text{Hg}^{2+}$	500	0.521
$\text{Pb}^{2+}$	1000	0.521
$\text{Mg}^{2+}$	800	0.528
$\text{Al}^{3+}$	1000	0.526
$\text{Mn}^{2+}$	1000	0.523
$\text{W(VI)}$	1000	0.521
$\text{Cu}^{2+}$	150	0.521
$\text{Ni}^{2+}$	500	0.524
$\text{Sn}^{2+}$	600	0.525
$\text{Mo(VI)}$	1000	0.523
$\text{As}^{3+}$	400	0.523
$\text{Ag}^+$	500	0.526
$\text{Ru}^{3+}$	100	0.525
$\text{Rh}^{3+}$	100	0.526
$\text{UO}_2^{2+}$	2000	0.520
$\text{Be}^{2+}$	2000	0.521
$\text{Cr}^{3+}$	1000	0.522
$\text{Cr(VI)}$	500	0.521
$\text{Pd}^{2+}$	80	0.526
$\text{Os(VIII)}$	80	0.528
$\text{Os(VI)}$	30	0.526
$\text{Ir}^{3+}$	80	0.521
$\text{Pt}^{4+}$	80	0.522
$\text{V(V)}$	600	0.523
$\text{Th}^{4+}$	400	0.525
$\text{Sb}^{3+}$	1000	0.524
$\text{Bi}^{3+}$	500	0.523
$\text{Ce}^{3+}$	2000	0.526

60 ml, and the amount of naphthalene is in the range 1.25–3.5 g. With less than 1.25 g the extraction is in complete, and with more than 4.0 g it is difficult to dissolve the naphthalene in the limited amount of DMF (10 ml).

The absorbance of the extract remains unchanged

Table 3. Determination of cobalt in alloys, an ore and a vitamin injection

Sample	Co present	Co found
Tata 66/4 alloy	5.30%	5.24, 5.28, 5.32%
'K' Monelwire	0.51%	0.50, 0.53, 0.53%
Limonite	0.06%	0.059, 0.063, 0.064%
Macraberin Forte injection (vitamin)	36.0 ppm	36.2, 36.3, 36.4 ppm

for up to 15 hr. The extraction into molten naphthalene is very rapid, and complete within 1 min.

#### Spectral data

Beer's law is obeyed up to 19  $\mu\text{g}$  of cobalt in 10 ml of DMF solution. A Ringbom plot shows that the optimum range is 1.2–18  $\mu\text{g}$  of cobalt per 10 ml of DMF solution. The molar absorptivity is  $2.09 \times 10^4 \text{ l. mole}^{-1} \text{ cm}^{-1}$ . Eight replicates containing 14.7  $\mu\text{g}$  of cobalt gave a mean absorbance of 0.524 with a standard deviation of 0.003.

#### Interferences

Sample solutions containing 14.7  $\mu\text{g}$  of cobalt and various amounts of various salts were prepared and the cobalt was determined. The results are given in Tables 1 and 2.

#### Determination of cobalt in alloys, ore and vitamin

The accuracy of the method was checked by the determination of cobalt in alloys, an ore and a vitamin formulation.

The ore (limonite) was decomposed by the standard method.<sup>4</sup> A 0.2–1.2 g sample was dissolved by boiling with 40 ml of concentrated nitric acid; the solution was then cooled, potassium chlorate (8 g) was added to it, and the mixture was evaporated to dryness. The residue was treated with 10 ml of concentrated hydrochloric acid and the solution evaporated to dryness. This step was repeated twice and finally the residue was heated with dilute hydrochloric acid and the solution was filtered. The residue was fused with potassium hydrogen sulphate, the cooled melt was dissolved in dilute hydrochloric acid, and the two solutions were combined and made up to volume in a 100-ml standard flask with dilute hydrochloric acid. A 5-ml aliquot was used for the determination of cobalt, with 0.2 g of ammonium fluoride added as masking agent.

The contents of two 2-ml ampoules of Macraberin Forte injection (Glaxo, Bombay) were decomposed in a covered beaker by heating with concentrated nitric acid, first at low temperature to avoid violent reaction, then more strongly (with more acid), until the acid had evaporated. Finally the residue was heated to about 400° on a hot-plate, then cooled and dissolved in nitric acid (1 + 1) to give a solution which was slowly evaporated (1–2 hr) on a steam-bath. The residue was taken up in water (25 ml) to which concentrated nitric acid was added in 0.25-ml portions until a clear solution was obtained on gentle

heating. The cobalt content of this solution was determined by the recommended procedure. The results are presented in Table 3.

#### REFERENCES

1. B. K. Puri, K. W. Jackson and M. Katyal, *Microchem. J.*, 1987, **36**, 135.
2. A. I. Vogel, *A Text Book of Quantitative Inorganic Analysis*, 3rd Ed., Longmans, London, 1969.
3. R. K. Sharma, K. Shrivah, S. K. Singh and S. K. Sindhwani, *Thermochim. Acta*, 1985, **86**, 149.
4. K. Kodama, *Methods of Quantitative Inorganic Analysis*, pp. 263, 269. Interscience, New York, 1963.



# SEQUENTIAL POTENTIOMETRIC MICRODETERMINATION OF CHLORIDE AND PHOSPHATE AND ITS APPLICATION TO THE DETERMINATION OF PHOSPHORUS AND CHLORINE IN ORGANIC COMPOUNDS

AGOSTINO PIETROGRANDE and MIRELLA ZANCATO

Department of Pharmaceutical Sciences, University of Padua, Via Marzolo 5, I-35131 Padua, Italy

(Received 21 January 1987. Revised 12 February 1988. Accepted 18 February 1988)

**Summary**—Orthophosphate has been determined at the micro level in the presence of chloride by argentimetric potentiometric titration. Chloride is titrated first, at pH 3 in water-propan-2-ol (1:1 v/v), and phosphate in the same solution, buffered at pH 8.5–9.0. Under these conditions, the titration error from partial co-precipitation of silver oxide near the equivalence point is minimized. A procedure for performing the titration with an automatic apparatus is described. The method has been applied to the determination of phosphorus and chlorine in the same organic compound after mineralization by the Schöniger method.

In an earlier paper<sup>1</sup> on argentimetric potentiometric titration of orthophosphate, we reported that correct results are obtained when the solvent is a water-propan-2-ol mixture, buffered at pH 9. This procedure gave satisfactory results for phosphorus (mg-scale) in organic compounds after decomposition and oxidation to orthophosphoric acid by the Schöniger method.

We now report how this titration is affected by the presence in the solution of interfering species, such as chloride, which can also be precipitated with silver.

Few reports on this topic have been published. Christian *et al.*<sup>2</sup> found that titration of orthophosphate in the presence of iodide or bromide leads to large negative errors (23 and 60% respectively) owing to co-precipitation of orthophosphate with the silver halides. McColl and O'Donnell<sup>3</sup> reported that chloride as well as bromide or iodide can be sequentially determined together with phosphate in a single titration. They gave an experimental plot but no detail of the procedure or results. Selig<sup>4</sup> has claimed that the sequential titration of halide and phosphate is possible, but he, too, reported no experimental data.

## EXPERIMENTAL

### Apparatus

A Metrohm 636 Titroprocessor connected to a Model 635 automatic burette and a Metrohm EA 246 combined massive silver electrode was used. The pH values were measured by a Metrohm EA 120 combined glass pH-electrode connected to a Model 632 Metrohm pH-meter. The volumes added were measured with a precision of  $\pm 0.001$  ml.

### Reagents

All chemicals were of analytical-reagent grade. Silver nitrate solutions, 0.02M, were standardized against potassium chloride (relative standard deviation 0.05%).

### Procedure for phosphate and chloride samples

The aqueous sample (containing 5–10 mg of phosphate and 1–10 mg of chloride) is diluted to 15 ml with distilled water, then 15 ml of propan-2-ol are added. The silver and glass electrodes, and the burette tip, are inserted in the titration beaker and magnetic stirring is started. Nitric acid (1M) is added dropwise until the pH is 3.

The "control cards" are inserted and automatic titration with 0.02M silver nitrate, to a prefixed end-point of 100 mV, is started.

The "control card" recommended is "dynamic titration, kinetic T at value 3". With this card the volume of titrant added is progressively decreased automatically as the end-point is approached. The preset end-point was selected on the basis of results of preliminary tests. This titration yields the percentage of chloride present.

Sodium tetraborate solution (3–5 ml, 0.125M) is then added, and a sufficient volume of propan-2-ol (6–8 ml) to restore the 1:1 v/v water:alcohol ratio. If necessary, the pH is adjusted to 8.5–9.0 by addition of some drops of dilute acetic acid. The appropriate "control card" is inserted and the automatic titration with 0.02M silver nitrate restarted. The end-point is taken here as the point corresponding to the maximum potential/volume slope.

### Procedure for the determination of phosphorus and chlorine in organic compounds

The absorption solution is 10 ml of water plus 0.7 ml of 30% hydrogen peroxide. Samples (10–15 mg) are weighed, wrapped in a piece of Schleicher and Schüll 589 paper,<sup>2</sup> and placed in the platinum basket. The combustion in the oxygen flask is performed in the usual manner. After about 30 min, the flask is opened and the stopper and the basket are rinsed with 10 ml of water. The solution is transferred quantitatively to a 60-ml beaker. Four ml of 0.1M sodium hydroxide are added and the solution is boiled for 30 min. The solution is boiled down to a volume of 15 ml, then maintained at that volume by addition of water, as required, up to a mark on the beaker. The solution is cooled, 15 ml of propan-2-ol are added, and the titration is done as described already.

Table 1. Determination of chloride in the presence of  $K_2HPO_4 \cdot 3H_2O$ 

Compound	Weight* range, mg	Chloride expected, %	Chloride range found, %	s, %†
Levamisole hydrochloride $C_{11}H_{12}N_2S \cdot HCl$	3.351–9.743	14.74	14.65–14.84	0.06
Potassium chloride	2.932–8.341	47.56	47.4–47.8	0.14

\*In all cases 10 mg of  $K_2HPO_4 \cdot 3H_2O$  was added to the sample.

†s = standard deviation.

Table 2. Sequential microdetermination of chloride and phosphate in aqueous propan-2-ol solutions

Sample	Chloride		Phosphate	
	Weight taken, mg	Found, mg	Weight taken, mg	Found, mg
Potassium monohydrogen phosphate 3-hydrate	7.421	7.43 <sub>2</sub>	5.575	5.63
+ potassium chloride	2.575	2.56 <sub>5</sub>	6.271	6.32
	4.529	4.53 <sub>3</sub>	5.919	5.98
	3.930	3.94 <sub>9</sub>	7.008	6.97
	1.915	1.93 <sub>1</sub>	6.915	6.98
	3.434	3.43 <sub>8</sub>	9.002	9.07
Potassium monohydrogen phosphate + potassium chloride	3.627	3.64 <sub>5</sub>	5.982	5.99
	5.271	5.29 <sub>2</sub>	6.821	6.86
	6.081	6.10 <sub>3</sub>	7.927	7.98
	2.915	2.91 <sub>2</sub>	8.342	8.38
	1.899	1.89 <sub>5</sub>	9.261	9.23
	6.538	6.53 <sub>1</sub>	8.767	8.72
Potassium monohydrogen phosphate + levamisole hydrochloride	6.822	6.78 <sub>1</sub>	8.411	8.39
	5.238	5.23 <sub>8</sub>	7.344	7.39
	4.933	4.89 <sub>3</sub>	9.228	9.30
	3.001	3.01 <sub>6</sub>	6.189	6.24
	4.718	4.74 <sub>6</sub>	9.866	9.85
	2.017	2.03 <sub>3</sub>	9.142	9.10

Table 3. Results from sequential microdetermination of chloride and phosphate derived from oxygen-flask of some phosphorus and chlorine-containing organic compounds

Compound	Chlorine, %		Phosphorus, %	
	Expected	Found	Expected	Found
Pyridoxamine-5- phosphate hydrochloride		12.32		10.69
	12.28	12.40	10.97	10.67
		12.26		11.25
5-Chloro-4- hydroxy-3-methoxybenzil isothiourea phosphate		10.04		9.20
	10.29	10.04	8.99	9.28
		10.03		8.83
Triphenylphosphine + <i>p</i> -chlorobenzoic acid		22.83*		11.56*
	22.65	22.68*	11.81	11.71*
		22.47*		11.46*

\*Calculated on basis of individual weights of the compounds mixed to form the sample.

## RESULTS AND DISCUSSION

Preliminary attempts at sequential determination of chloride and phosphate by titration with silver directly in aqueous solution gave unsatisfactory results. Thus, even titrations of solutions buffered with 0.025*M* sodium tetraborate to pH 8.5–9.0 gave high values for chloride and low values for phosphate.

Theory suggests that sequential titration of chloride and phosphate ought to be possible at pH 8.5–9.0, but the poorly reproducible and incorrect results actually obtained suggest that appreciable co-

precipitation of silver phosphate occurs in the chloride titration. Addition of surface-active alcohols (*e.g.*, butyl or isopentyl) gave no improvement.

We therefore decided to employ two different pH values in the titration of the two anions with the same silver nitrate titrant.

At pH less than 3, phosphate is protonated to such an extent that silver phosphate does not precipitate, so this pH was adopted for titration of chloride ions. pH values lower than 3 were avoided because they could have necessitated addition of large amounts of buffer to raise the pH to that needed for the phos-

phate determination. The results obtained at this pH for synthetic solutions are summarized in Table 1.

Phosphate ions were then titrated in the same solution after adjustment to an "apparent" pH in the range 8.5–9.0 by addition of suitable amounts of sodium tetraborate.

The presence of propan-2-ol is not expected to affect significantly the solubility sequence  $\text{AgCl}$ ,  $\text{Ag}_3\text{PO}_4$ ,  $\text{AgOH}$ . It is known<sup>5</sup> that a propan-2-ol content of 50% causes the solubility product for  $\text{AgCl}$  to change from  $10^{-9.8}$  to  $10^{-10.44}$ . Our own measurements have shown that the solubility of silver phosphate changes correspondingly.

The "control card" operation of the Titroprocessor caused a problem in that the two titrations were regarded by the machine as being completely separate. If chloride was titrated to the point of maximum potential/volume slope, titrant was added after the equivalence point, and this excess of course remained available to react with phosphate when the pH was raised. Since the machine believed that the phosphate titration actually started when the new program was inserted, the results then had a bias of  $-4\%$ .

The difficulty was avoided by choosing to titrate chloride to a preset potential, so that no excess of

titrant would be added. Table 2 shows results obtained by the proposed procedure.

The proposed procedure is simple and allows a clear differentiation of the two anions to be achieved. A relatively critical step is the pH adjustment at the end of the chloride titration; if the solution is made too alkaline, silver oxide could also precipitate.

#### *Determination of chlorine and phosphorus in the same organic compound*

The method was used for determination of chlorine and phosphorus in some organic compounds. The results, obtained after oxygen-flask combustion, are reported in Table 3. Satisfactory accuracy and precision were obtained.

#### REFERENCES

1. A. Pietrogrande and M. Zancato, *Analyst*, 1987, **112**, 129.
2. G. D. Christian, E. C. Knoblock and W. C. Purdy, *Anal. Chem.*, 1963, **35**, 1869.
3. D. H. McColl and T. A. O'Donnell, *ibid.*, 1964, **36**, 848.
4. W. Selig, *Mikrochim. Acta*, 1976 **II**, 9.
5. E. Högfeltdt, *Stability Constants of Metal-Ion Complexes*, Part A, pp. 219, 220. Pergamon Press, Oxford, 1982.

## VALGRAN, A PROGRAM FOR POTENTIOMETRIC TITRATIONS WITH A VERSATILE AUTOMATIC MODULAR SYSTEM

V. CERDA, J. MAIMO, J. M. ESTELA and A. SALVA

Càtedra de Química Anàlitica, Departament de Química, Universitat de les Illes Balears, E-07071 Palma de Mallorca, Spain

G. RAMIS

Departament de Química Analítica, Universitat de València, E-46100 Burjasot, València, Spain

(Received 30 October 1987. Revised 18 February 1988. Accepted 12 April 1988)

**Summary**—A very flexible modular system for use with a portable IBM PC for potentiometric titrations is described. The appropriate software has been developed in order to obtain automatic end-points, and conventional, first-derivative, second-derivative and Gran curves, as well as a listing of the potentiometric points expressed in different ways. All these alternatives are selectable on menu presentations. The potentiometric system has been applied both the research and routine problems.

The use of microcomputers for the automation of analytical techniques has been of growing interest in recent years. They can be adapted to perform many routine laboratory tasks. Even a single time-shared microcomputer can fulfil the requirements of many different analytical techniques, with a high degree of versatility. In automated procedures, experimental conditions are better controlled and a great number of data can be obtained rapidly and accurately,<sup>1-3</sup> and the calculations can be done on-line or off-line.

Additional advantages accrue from use of the popular IBM or IBM-compatible microcomputers, since the data can be directly fed to a great variety of powerful programs, ranging from the commercial dBase III or Lotus 1-2-3 to typical scientific programs.<sup>4-6</sup>

Descriptions of the use of cheap microprocessors for automation are readily available,<sup>7-14</sup> but assembler language, which has the disadvantage of requiring specific training, is frequently used. Personal microcomputers (PCs) are far more popular and can be easily programmed in BASIC, and increasingly powerful PCs are currently available at very low prices.

In this work, a modular system for automatic potentiometric titrations controlled by a portable IBM PC microcomputer is presented. Powerful and versatile menu-driven software has been developed. Many experimental conditions and schemes for treatment of the data can easily be selected from several menus.

### EXPERIMENTAL

#### Apparatus

A portable IBM PC microcomputer with 256 kbyte of RAM, and a graphic screen, connected to a Seikosha SP-800 printer, was used. A Crison Digilab 517 potentiometer, with a precision of  $\pm 0.1$  mV, and a Crison model 738 automatic burette, were serially connected to the microcomputer through RS232C interfaces. Orion combined glass and silver 94-16A electrodes with a Crison electrode adaptor were also used.

The modular system is shown in Fig. 1. Since the external ports of the portable IBM PC microcomputer work at the RS232C standard potential, direct connection to the instruments is possible.

### THE PROGRAM

#### Characteristics of the program VALGRAN\*

The logical support of the system is provided by the program VALGRAN, which was developed to meet the following criteria.

No specific training should be required to run the program, which is driven by very simple menus.

The titration rate is to match the requirements of the experiment. For study of chemical equilibria, the electrode must reach equilibrium after each titrant addition, whereas for routine work the analysis time is minimized by automatic adjustment of the addition rate in accordance with the slope of the titration curve.

Input options include experimental acquisition of data, input from previously diskette-stored data and manual input through the keyboard.

Output options are diskette-storage, printing of data and numerical and/or graphical screen presentation.

\*VALGRAN is available from SCIWARE, Bank of Programs, Chemistry Dept., Universitat de les Illes Balears, E-07071 Palma de Mallorca, Spain.

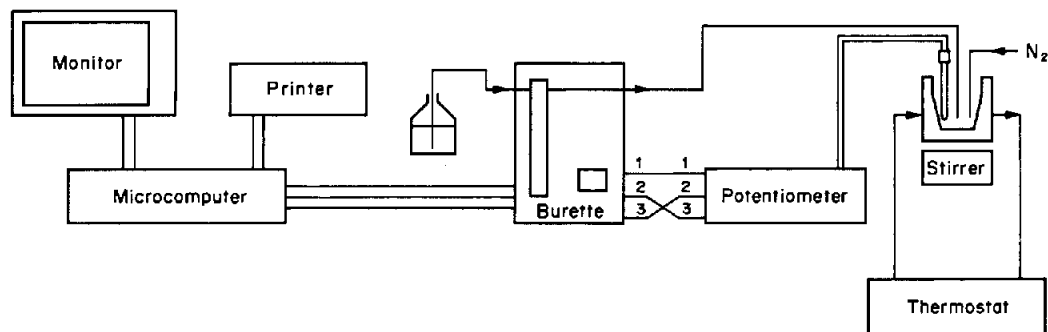


Fig. 1. Modular system for potentiometric titrations.

As an option, first and second derivative and Gran linearization treatments can be applied to the data.

The system can handle any type of potentiometric titration, only the titrant and the electrodes need be changed. Metallic or membrane electrodes can be used.

The main parts of the program are as follows.

#### Main menu

*Option 1: experimental titration.* Two types of titrations are possible.

The first corresponds to titrations performed for chemical equilibrium studies, so a fixed waiting time is allowed between consecutive potential measurements. A measurement is accepted only when the difference from the previous one is smaller than a given value. When a measurement has been accepted, a new addition of titrant is triggered and another sequence of measurements is carried out. Stability constants can be determined with a high degree of accuracy by this type of titration. Accurate data are easily obtained all along the titration curve, even when a very long time is necessary for the solution-electrode equilibrium to be reached. Times as long as several hours are frequently required near the equivalence point and sometimes even over the whole titration (e.g., acid-base titrations with a glass electrode in DMSO).

Different criteria must be used to control the titration rate in routine work, since stabilization of the electrode potential is not necessary. In this case, a compromise between accuracy of the equivalence point and analysis time is established. To achieve a high titration rate, only a fixed short waiting time is allowed between the end of an addition and the measurement of the potential, but the volume added is automatically modified, in inverse proportion to the slope of the titration curve. Far away from the equivalence point the slope is small and large volumes are added. Near the equivalence point, increasingly higher slopes are found and thus smaller volumes of titrant are used. Finally, after the equivalence point, the volume added increases again. In this way, the system works as a skilled analyst would, and accurate determinations can be performed in 5 min or less.

In addition, some further modifications save a considerable amount of time. At the beginning of the titration some time is needed to fill the syringe of the burette, but there is a considerable waste of time between consecutive additions if a fixed delay time is employed. Instead, the current state of the syringe is continuously checked during the filling operation. When the plunger travel is found to have stopped, the program understands that the syringe is full and the titration begins immediately.

Because of the difference in execution speed between interpreter-executed and compiled programs, the use of FOR-NEXT-based idle delay loops is not advisable. In the program VALGRAN all the delay loops have been replaced by clock-based delay times.

The possibility of the equivalence volume being larger than the syringe volume has also been considered. When the syringe is empty, it is automatically refilled. If the end-point has not been found after a given number of fillings, a message is issued indicating that dilution of the sample is advisable.

Experimental titration, printing of the data and graphic representation of the titration curve on the monitor screen can be carried out simultaneously. In this way, any irregularity can be immediately detected and better quality-control achieved.

When a titration is finished, the data are stored in a diskette file. By means of the WORDPERFECT word processor, these files can be easily converted into files that can be handled by powerful programs for data refinement such as MINIPOT or MINIQUAD. We have adapted these programs for the IBM PC microcomputer.

*Options 2, 3 and 4: manual introduction of the data, retrieval of stored data and return to DOS.* By means of option 2, data which have not been obtained by the system can be manually introduced through the keyboard and stored in a file. Option 3 permits the retrieval of any stored data for printing or for application of mathematical treatments. Option 4 returns the computer to DOS.

#### Treatment of the data

Several options for treatment of the data have been introduced in the program VALGRAN.

*Option 1.* Representation of the titration curve as electrode potential vs. titrant volume.

*Option 2.* Calculation of the equivalence volume and concentration of the sample by means of the second-derivative method. Also, as an option, the first and second derivative curves can be plotted on the screen.

*Option 3.* Calculation of the Gran functions. This has been adapted from a previous program.<sup>15</sup> The Gran functions are independently calculated, before and after the equivalence point, by linear regression. The two fitted straight lines and the corresponding experimental points are presented on the monitor screen. In this way, the regions of the lines containing the best experimental points can easily be selected, and the calculation repeated as many times as necessary. Independent values of the equivalence volume, as well as the two standard electrode potentials, before and after the equivalence point, can be obtained from the extrapolation of both straight lines. For acid-base titrations, the values of the standard potentials allow the calculation of the ionic product of the water under the conditions of the experiment. This is a very useful parameter when titrations for the study of ionic equilibria are performed.

#### APPLICATIONS

##### *Example 1—Acid-base titration with stabilized potential readings*

A 150-ml sample of hydrochloric acid was titrated with 0.1110M sodium hydroxide at 23.7 ± 0.1°, with a glass electrode. The equivalence volume calculated by the second-derivative method was 3.800 ml, which differed from the expected value, 3.793 ml, by 0.2%. Larger errors were obtained when the Gran functions were used, the results being 3.876 ± 0.044 and 3.901 ± 0.014 ml by extrapolation of the functions before and after the equivalence point, respectively. From the corresponding electrode potentials,  $E'_0 = 374.3 \pm 1.1$  mV in the acid region and  $E'_0 = -430.9 \pm 0.0$  mV in the basic region, the value  $pK_w = 13.607$  was obtained.

##### *Example 2—Routine acid-base titration*

A 150-ml volume of hydrochloric acid was titrated with 0.1110M sodium hydroxide at 24.1°, with a combined glass electrode. The second-derivative method led to the value 7.645 ml, within 0.6% of the expected value of 7.595 ml. The waiting time between the addition and reading of the potential was set at 5 sec and total increment time of 2 min 25 sec was necessary for the titration.

##### *Example 3—Titration of chloride with silver*

A 150-ml volume of potassium chloride was titrated with 0.1000M silver nitrate at 25.6°, with an Orion 94-16A silver electrode. As in example 2, only the analyte concentration is to be measured.

The equivalence volume was 7.403 ml (second-derivative method), and the expected value was 7.500 ml. The titration took 4 min 10 sec, with a waiting time of 10 sec between titrant addition and the corresponding potential reading.

#### CONCLUSIONS

Modular systems, built up by using PCs and RS232C interfaces, have several advantages over commercial automatic instruments. Increasingly compact, light, quick, powerful and cheap PCs are available. No specific training is needed to build up an automatic system with RS232C connections and supported by a program written in BASIC. All the elements are versatile and can be devoted to many laboratory tasks. The system can quickly and easily be adapted. No professional assistance is necessary.

*Acknowledgement*—Thanks are due to the DGICYT (Spanish Council for Research in Science and Technology) for financial support (PA 86-0033).

#### REFERENCES

1. R. R. Samrdzewski, *Microprocessor Programming and Applications for Scientists and Engineers*, Elsevier, Amsterdam, 1984.
2. M. Margoshes and D. A. Burns, in *Treatise on Analytical Chemistry*, 2nd Ed., P. J. Elving, V. G. Mossotti and I. M. Kolthoff (eds.), Part I, Vol. 4, p. 413. Wiley-Interscience, New York, 1984.
3. M. B. Denton, *Analyst*, 1987, **112**, 347.
4. F. Gaizer and A. Puskás, *Talanta*, 1981, **28**, 565.
5. F. R. Hartley, C. Burgess and R. M. Alcock, *Solution Equilibria*, Horwood, Chichester, 1980.
6. Bank of Programs, Chemistry Dept., University of Illes Balears, Palma de Mallorca, Spain.
7. A. H. B. Wu and H. V. Malmstadt, *Anal. Chem.*, 1978, **50**, 2090.
8. I. R. Bonnell and R. J. Dalle-Molle, *Anal. Chim. Acta*, 1982, **134**, 189.
9. H. Y. Cheng, W. White and R. N. Adams, *Anal. Chem.*, 1980, **52**, 2445.
10. D. J. Leggett, *Talanta*, 1982, **29**, 189.
11. I. R. Bonnell and R. J. Dalle-Molle, *Anal. Chim. Acta*, 1982, **134**, 179.
12. L. Petros, L. Sváb, V. Hynek and V. Svoboda, *Chem. Listy*, 1982, **76**, 241.
13. E. D. Salin, M. W. Blades and G. Horlick, *Talanta*, 1981, **28**, 519.
14. E. B. Buchanan, Jr. and M. L. Buchanan, *Talanta*, 1980, **27**, 947.
15. J. Cantalalops, J. M. Estela and V. Cerdá, *Anal. Chim. Acta*, 1985, **169**, 397.

## SOFTWARE SURVEY SECTION

---

### Software package TAL-006/88

#### FLUOPAC2

Contributors: M.T. Oms and V. Cerda, University of Baleares, E-07071 Palma de Mallorca, Spain; and F. Garcia Sanchez and A.L. Ramos, University of Malaga, Faculty of Sciences, The University, Malaga 29071, Spain.

Brief description: FLUOPAC2 is a software package designed to control the Perkin-Elmer LS-5 spectrofluorimeter with an IBM PC or PS/2 30-50, with use of the Perkin-Elmer RS232C interface. The program permits acquisition of data from the optical unit, data manipulation and storage on disk, display of spectra on the VDU, and plotting on a printer connected by a parallel interface. All user instructions are entered by single key strokes of the function keys (f1 - f10). The key functions are as follows: prescan, scan, autozero, directory of disk, save on disk, label graph, add and subtract, multiply and divide, axis and grid, clear, cursors, expand, GOTO wavelength, intensity, merge, mode, ordinate, peak, phosphorescence mode, print graph, set mode (scale factor, response factor), smooth, status, tdrive (time), view, differentiate, and change. There is also a special help key. Some other functions are available from a menu.

Potential users: Analytical chemists, molecular luminescence spectroscopists

Fields of interest: Analytical and environmental chemistry

This package has been developed for the IBM PC and PS/2, and is written in BASIC (compiled), to run under PC-DOS. It is available on 360K 5.25-in disc. The memory required is 640K.

Distributed by the contributors.

An IBM-PC computer, or clone, is required, along with a Perkin-Elmer LS-5 Spectrofluorimeter with RS232C interface, and a suitable printer. No modifications are required to the instrument or computer. The package is self-documenting. The source code is not available. The package has been fully operational for about 6 months. The contributors are willing to deal with enquiries.

## A NEW ELECTROCHEMICAL METHOD BASED ON TRANSFER AT A LIQUID/LIQUID INTERFACE: DETERMINATION OF BARIUM AND STRONTIUM

ZHISHENG SUN and ERKANG WANG

Changchun Institute of Applied Chemistry, Chinese Academy of Sciences, Changchun, Jilin 130021,  
People's Republic of China

(Received 24 June 1987. Revised 15 December 1987. Accepted 24 May 1988)

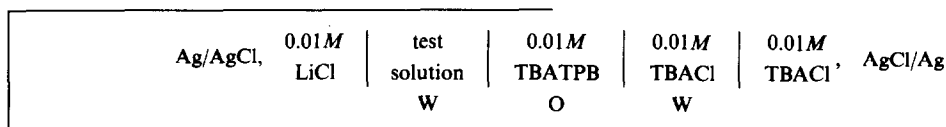
**Summary**—A new kind of polyoxyethylene ionophore is introduced to facilitate metal ion transfer across a liquid/liquid interface. The transfer of  $Ba^{2+}$  and  $Sr^{2+}$ , facilitated by polyethylene glycol 400 across the interfaces of water/nitrobenzene and water/1,2-dichloroethane, has been studied in detail by cyclic voltammetry, and a new method for the determination of barium and strontium established. Both metals can be determined by cyclic voltammetry with good selectivity and reproducibility.

The analytical applications of electrochemistry at liquid/liquid (L/L) interfaces have attracted much interest.<sup>1-5</sup> Although the transfer behaviour and the mechanism of transfer across the L/L interface facilitated by a neutral carrier have been studied for many years,<sup>1,2,6</sup> the determination of metal ions based on

used as received. Doubly distilled water was used to prepare the aqueous electrolyte solution.

### Measurements

Electrochemical measurements were performed with a Solartron 1286 Electrochemical Interface by using an electrolytic cell with four electrodes.<sup>1,11</sup> The cell can be expressed as follows:



electrochemistry at the L/L interface is still a perplexing question because of the poor selectivity of ion-transfer processes when other metal ions are present. Mareček *et al.*<sup>7</sup> determined  $Ca^{2+}$  with the help of a selective synthetic ionophore, and some papers have dealt with the determination of antibiotics.<sup>5,8,9</sup> The peak current for dye transfer has been shown to decrease linearly as the concentration of metal ions increases, owing to complexation between the dye and metal ion,<sup>10</sup> but this effect does not allow a convenient and practical method of metal determination. In the present study, we found that polyoxyethylene compounds, such as polyethylene glycol 400, are good ionophores and can facilitate selective transfer of  $Ba^{2+}$  or  $Sr^{2+}$  ions across the L/L interface, giving clear and stable cyclic voltammetry peaks and allowing these metals to be determined at  $10^{-5}M$  concentration by cyclic voltammetry. This is very interesting not only for the trace determination of barium and strontium, but also as an example of the application of electrochemistry at an L/L interface to metal-ion determination.

### EXPERIMENTAL

#### Chemicals

Polyethylene glycol 400 (PEG 400), tetrabutylammonium chloride (TBACl), tetrabutylammonium tetraphenylborate (TBATPB), nitrobenzene (NB), 1,2-dichloroethane (1,2-DCE),  $BaCl_2$ ,  $SrCl_2$ , LiCl and other analytical reagents were

used as received. Doubly distilled water was used to prepare the aqueous electrolyte solution.

### RESULTS AND DISCUSSION

#### The cyclic voltammetric behaviour of $Ba^{2+}$ and $Sr^{2+}$ with transfer across the L/L interface, assisted by PEG 400

Figure 1 shows the cyclic voltammetry (CV) for the transfer of  $Ba^{2+}$  and  $Sr^{2+}$  ions across the water-nitrobenzene interface, assisted by PEG 400. Clear CV peaks appear within the "potential window" when 0.01M TBATPB and 0.01M lithium or magnesium chloride are used as electrolytes in the organic and aqueous phases respectively. It can be seen that the peak potential  $\Delta_0^* \phi_p$  is independent of scan-rate over the range 10-200 mV/sec, the peak separation  $\Delta(\Delta_0^* \phi_p)$  is about 30 mV and the peak current  $i_p$  is proportional to the square root of the scan-rate and to the metal ion concentration in the aqueous phase when  $C_p(w) \gg C_M(w)$ , where  $C_p$  and  $C_M$  are the PEG 400 and metal ion concentrations. Calibration plots for barium and strontium are linear over the range  $1 \times 10^{-5}$ - $5 \times 10^{-4}M$ . (Fig. 2).

When dichloroethane is used as the organic solvent the transfer behaviour of  $Ba^{2+}$  and  $Sr^{2+}$ , assisted by PEG 400, also shows reversible characteristics with peak current  $i_p$  proportional to the aqueous metal-ion



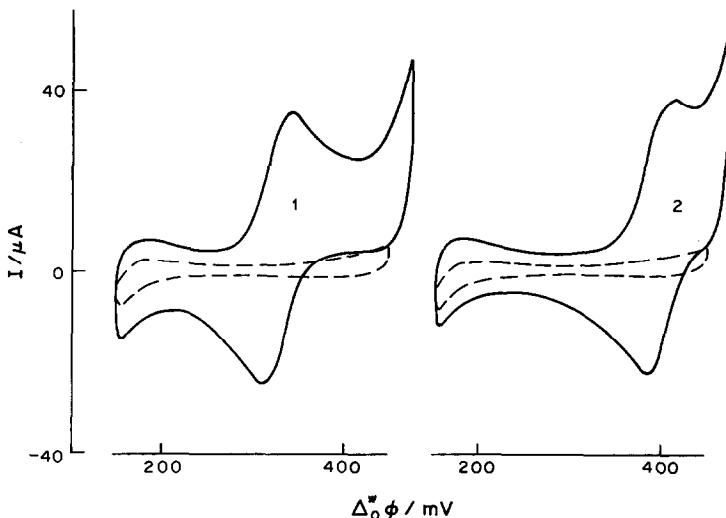


Fig. 1. CV curves for  $\text{Ba}^{2+}$  and  $\text{Sr}^{2+}$  with transfer across the W/NB interface facilitated by PEG 400. W:  $0.01\text{M}$  LiCl,  $5.6\text{mM}$  PEG 400, solid line; (1)  $5 \times 10^{-5}\text{M}$   $\text{Ba}^{2+}$ , (2)  $5 \times 10^{-5}\text{M}$   $\text{Sr}^{2+}$ , scan-rate  $60\text{ mV/sec}$ ; dashed line; without  $\text{Ba}^{2+}$  and  $\text{Sr}^{2+}$ , Scan-rate  $30\text{ mV/sec}$ . NB:  $0.01\text{M}$  TBATPB in nitrobenzene.

concentration and to the square root of the scan-rate over the range  $10\text{--}200\text{ mV/sec}$ . The peak separation  $\Delta(\Delta_0^* \phi_p)$  is about  $30\text{ mV}$ , but the peak potential shifts to more positive values than in the case of nitrobenzene. Figure 3 shows the  $i_p\text{--}C_{\text{Ba}^{2+}}$  plots for  $\text{Ba}^{2+}$  transfer across the water/dichloroethane interface, assisted by PEG 400, which are reasonably linear at different scan-rates. For the determination

of barium or strontium, a scan-rate of  $50$  or  $60\text{ mV/sec}$  was selected.

#### Effect of pH

The effect of pH on the transfer behaviour was studied by using Britton–Robinson buffer solutions. In the pH range  $2\text{--}4$ , the interfacial potentials shift negatively somewhat with increasing pH, and then

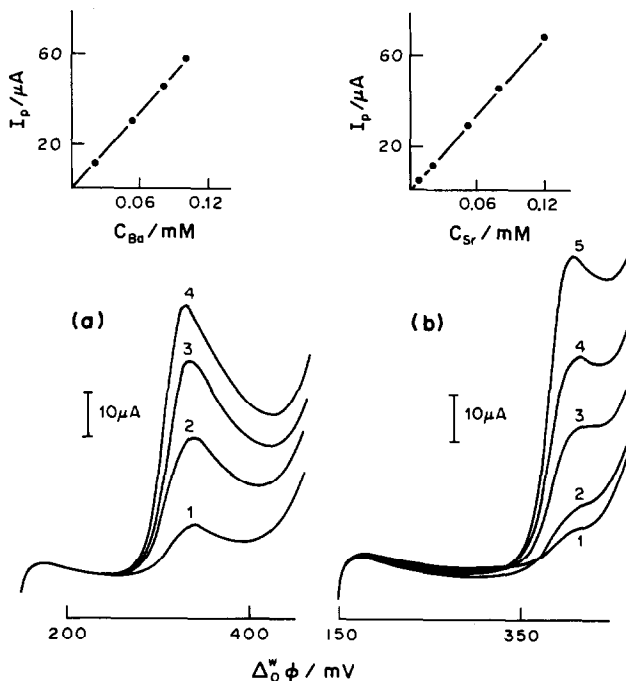


Fig. 2. Voltammetric curves obtained for aqueous solutions of increasing  $\text{Ba}^{2+}$  and  $\text{Sr}^{2+}$  concentration. W:  $0.01\text{M}$  LiCl,  $5.6\text{mM}$  PEG 400. NB:  $0.01\text{M}$  TBATPB in nitrobenzene. Scan-rate  $60\text{ mV/sec}$ . (a)  $\text{Ba}^{2+}$  concentration (mM): 1,  $0.020$ ; 2,  $0.050$ ; 3,  $0.080$ ; 4,  $0.100$ . (b)  $\text{Sr}^{2+}$  concentration (mM): 1,  $0.008$ ; 2,  $0.020$ ; 3,  $0.050$ ; 4,  $0.080$ ; 5,  $0.120$ .

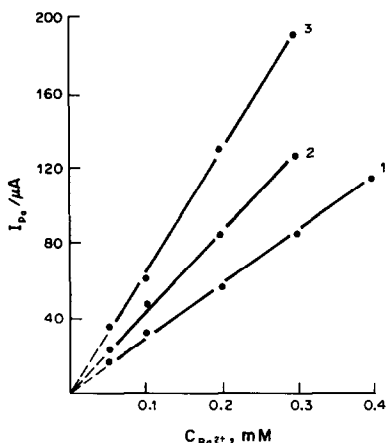


Fig. 3.  $i_p$ - $C_{Ba^{2+}}$ (w) curves for  $Ba^{2+}$  with transfer facilitated by PEG 400, at different scan-rates. W: 0.01M LiCl, 5.6mM PEG 400. 1,2-DCE: 0.01M TBATPB in 1,2-dichloroethane. Scan-rates (mV/sec): 1, 20; 2, 40; 3, 100.

remain constant, the transfer current being independent of pH. This means that barium and strontium can be determined over a wide pH range, as shown in Fig. 4. It should be noted, however, that an increase in sodium ion concentration can cause interference in the measurement of  $Ba^{2+}$  and  $Sr^{2+}$  transfer, by increasing the pH of the buffer solutions. The pH range suitable for the determination is ca. 2-8.

**Selectivity**

It can be concluded that PEG 400 can facilitate selective transfer of  $Ba^{2+}$  and  $Sr^{2+}$  across the L/L interface. Among the alkali and alkaline-earth metal ions,  $Li^+$  and  $Mg^{2+}$  cannot transfer in the range of the "potential window" of the electrolytes which can be used for the determination of  $Ba^{2+}$  and  $Sr^{2+}$ . The

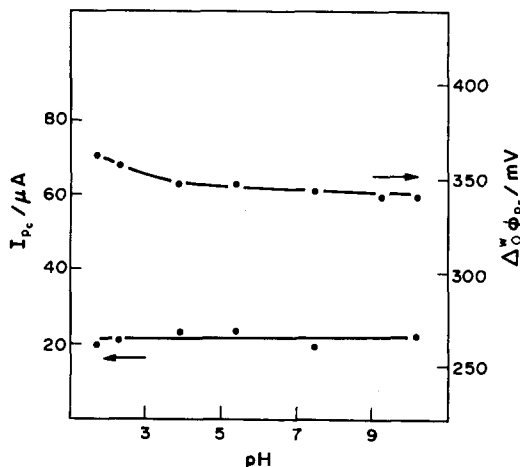


Fig. 4. Effect of pH on the peak currents and potentials for  $Ba^{2+}$ . W: 0.01M LiCl, 0.15mM  $Ba^{2+}$ , 5.6mM PEG 400; B-R buffer. NB: 0.01M TBATPB in nitrobenzene. Scan-rate 30 mV/sec.

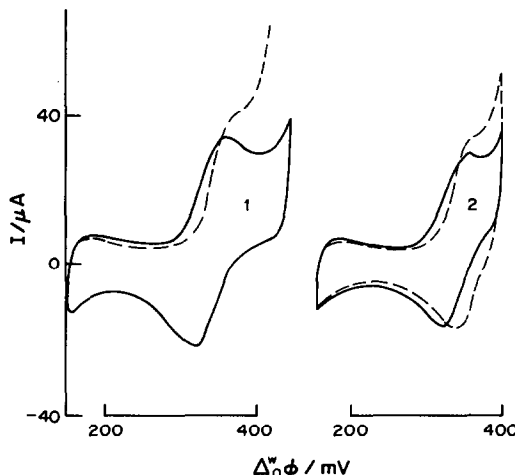


Fig. 5. CV curves for  $Ba^{2+}$  with PEG 400 in different solvents in the presence of  $K^+$  and  $Ca^{2+}$ . W: 0.01M LiCl. (1) 0.050mM  $Ba^{2+}$ , 2mM  $Na^+$ , 2.8mM PEG 400. (2) 0.040mM  $Ba^{2+}$ , 1mM  $Ca^{2+}$ , 2.5mM PEG 400. NB: 0.01M TBATPB in nitrobenzene. Solid line, W/NB; dashed line, W/1,2-DCE. Scan-rate 60 mV/sec.

transfer current for  $5 \times 10^{-5}M$   $Ba^{2+}$  in the presence of interfering ions  $Na^+$ ,  $Ca^{2+}$  and  $K^+$  remains constant when the concentrations of  $Na^+$  and  $Ca^{2+}$  are lower than 4 mM and that of  $K^+$  is lower than 1 mM. Other metal ions tested ( $Zn^{2+}$  and  $Cu^{2+}$  etc.) do not interfere.

**Improvement in selectivity by changing the organic solvent**

Figure 5 shows the cyclic voltammetry curves for  $Ba^{2+}$  with transfer assisted by PEG 400 at the interfaces with different solvents, in the presence of the interfering ions  $K^+$  and  $Ca^{2+}$ . It can be seen that distinct CV peaks for  $Ba^{2+}$  appear when nitrobenzene is used, but there is overlap with the post-wave of the interfering ions  $K^+$  and  $Ca^{2+}$  when dichloroethane is used.

**Effect of PEG 400 concentration on the selectivity**

It can be concluded from our experiments that the interfacial potentials of the transferring ions  $Ba^{2+}$ ,  $Sr^{2+}$  and the interfering ions  $K^+$ ,  $Ca^{2+}$ ,  $Na^+$  shift negatively with increasing concentration of PEG 400, but with different slopes for different kinds of ions. For bivalent ions the slope is 30 mV/ $pC_p$ , while for the univalent ion  $K^+$ , the slope is about 60 mV/ $pC_p$ , so we can improve the selectivity of the barium determination by controlling the PEG concentration. Figure 6 shows the CV curves for  $Ba^{2+}$ , with transfer assisted by different concentrations of PEG 400, in the presence of  $K^+$  ions. When the concentration of PEG 400 is too high or too low, the interference by potassium is increased. The suitable range of PEG 400 concentration is about 0.28-10 mM.

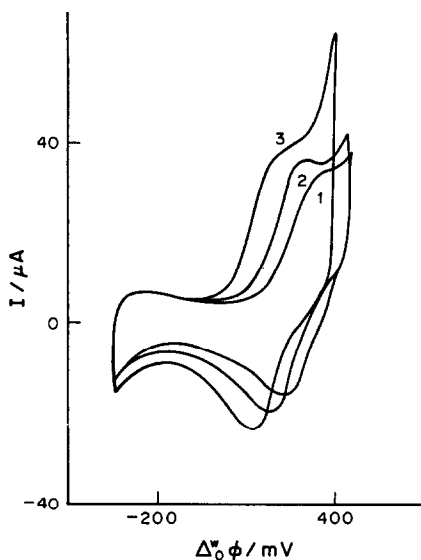


Fig. 6. CV curves for  $\text{Ba}^{2+}$  for different PEG 400 concentrations. W:  $0.01M$  LiCl,  $0.04mM$   $\text{Ba}^{2+}$ ,  $0.40mM$   $\text{K}^+$ , PEG 400 concentration ( $mM$ ): (1) 0.28, (2) 1.4, (3) 12. NB:  $0.01M$  TBATPB in nitrobenzene. Scan-rate  $60$  mV/sec.

#### Stability of the interface

Figure 7 shows the CV curves for  $\text{Ba}^{2+}$ , with transfer assisted by PEG 400, at different time intervals. The measured peak currents  $i_p$  (6 runs) were  $33 \pm 1 \mu\text{A}$ , suggesting that the interface has good stability and reproducibility.

#### Determination of $\text{Ba}^{2+}$ in the presence of $\text{Na}^+$

Table 1 lists results for the determination of barium in the presence of  $1$  mM sodium by the calibration graph method, suggesting that the method has good precision and accuracy.

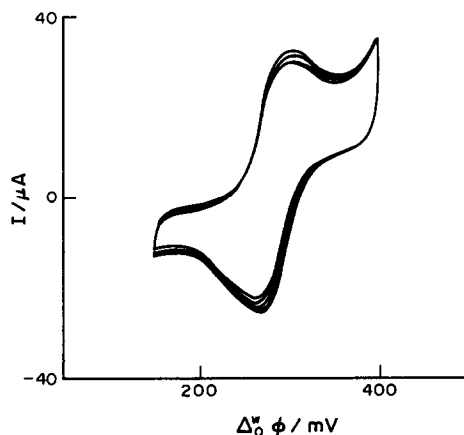


Fig. 7. Stability of  $\text{Ba}^{2+}$  transfer across the W/NB interface, facilitated by PEG 400. W:  $0.01M$  LiCl,  $0.14mM$  PEG 400,  $10^{-4}M$   $\text{Ba}^{2+}$ . NB:  $0.01M$  TBATPB in nitrobenzene. Scan-rate  $25$  mV/sec, 6 scans during  $50$  min.

Table 1. Determination of barium in the presence of sodium\*

Taken, mM	Found, mM	Average found, mM	CV, %
0.035	0.0349, 0.0384	0.0364	5
	0.0358, 0.0341		
	0.0367, 0.0384		
0.065	0.0688, 0.0662	0.0659	2.6
	0.0653, 0.0636		
	0.0653, 0.0662		

\* $1$  mM  $\text{Na}^+$ ; CV = coefficient of variation.

#### Determination of $\text{Ba}^{2+}$ in the presence of $\text{Ca}^{2+}$

Table 2 shows results for the determination of barium in the presence of  $1$  mM calcium; the coefficient of variation was  $<3\%$  and the error  $<2\%$ .

#### Determination of $\text{Ba}^{2+}$ in the presence of $\text{Sr}^{2+}$

When strontium is present in the sample, barium can be determined correctly and precisely (Table 3), but strontium cannot be determined by the calibration graph method, owing to the interference by the prior  $\text{Ba}^{2+}$  wave. Barium and strontium can be determined in the same solution when their concentrations are similar. For voltammetry, the current<sup>12</sup> is

$$i = kC \quad (1)$$

and the currents are additive when two peaks overlap. Therefore, we can obtain a set of linear equations for the voltammetric curves with linear potential sweep when  $\text{Ba}^{2+}$  and  $\text{Sr}^{2+}$  are both present (Fig. 8):

Table 2. Results for determination of barium in the presence of calcium\*

Taken, mM	Found, mM	Average found, mM	CV, %
0.040	0.040, 0.040	0.0392	2.3
	0.0382, 0.040		
	0.0386, 0.0382		
0.060	0.0585, 0.0594	0.0590	1.6
	0.0594, 0.0603		
	0.0585, 0.0576		

\* $\text{Ca}^{2+}$   $1$  mM.

Table 3. Determination of barium in the presence of strontium\*

$\text{Ba}^{2+}$		Average found, mM	CV, %
Taken, mM	Found, mM		
0.050	0.0504, 0.0525	0.0496	4.5
	0.0477, 0.0477		
	0.0469, 0.0490		
	0.0493, 0.0529		

\* $0.050$  mM  $\text{Sr}^{2+}$ .

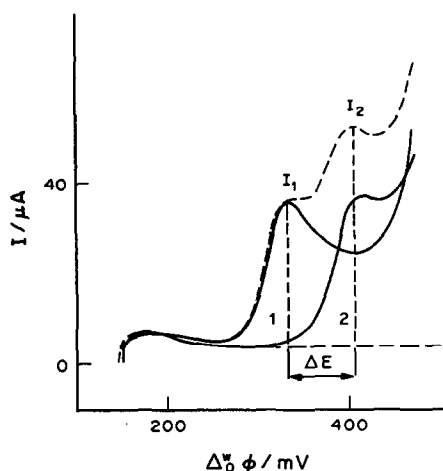


Fig. 8. Voltammetric curves for the determination of  $\text{Ba}^{2+}$  and  $\text{Sr}^{2+}$ . W: 0.01M LiCl, 5.6mM PEG 400; solid line, (1) 0.050mM  $\text{Ba}^{2+}$ , (2) 0.050mM  $\text{Sr}^{2+}$ ; dashed line; 0.050mM  $\text{Ba}^{2+}$  + 0.050mM  $\text{Sr}^{2+}$ . NB: 0.01M TBATPB in nitrobenzene. Scan-rate 60 mV/sec.

$$I_1 = K_{11} C_1 + K_{12} C_2 \quad (2)$$

$$I_2 = K_{21} C_1 + K_{22} C_2 \quad (3)$$

where  $I_1$  and  $I_2$  are the currents on the  $I-\Delta_0^* \phi$  curve in the presence of  $\text{Ba}^{2+}$  and  $\text{Sr}^{2+}$  corresponding to the peak potentials of  $\text{Ba}^{2+}$  and  $\text{Sr}^{2+}$ , respectively:

$$I_1 = i'_1 + i''_1 \quad (4)$$

$$i'_1 = i_p(\text{Ba}^{2+}) = K_{11} C_1 \quad (5)$$

$$i''_1 = K_{12} C_2 (\text{Sr}^{2+}) \quad (6)$$

$$I_2 = i'_2 + i''_2 \quad (7)$$

$$i'_2 = K_{21} C_1 (\text{Ba}^{2+}) \quad (8)$$

$$i''_2 = i_p(\text{Sr}^{2+}) = K_{22} C_2 \quad (9)$$

So the concentrations of  $\text{Ba}^{2+}$  and  $\text{Sr}^{2+}$  ( $C_1$  and  $C_2$ ) can be obtained:

$$C_1 = \frac{I_2 - K_{22} I_1 / K_{12}}{K_{12} - K_{22} K_{11} / K_{12}} \quad (10)$$

$$C_2 = \frac{I_2 - K_{21} I_1 / K_{11}}{K_{22} - K_{21} K_{12} / K_{11}} \quad (11)$$

The values of  $K_{11}$ ,  $K_{12}$ ,  $K_{21}$ ,  $K_{22}$  were calculated from equations (5), (6), (8), (9) based on the individual

Table 4. The simultaneous determination of barium and strontium

No.	Ion determined	Taken, mM	Found*, mM	CV, %
I	$\text{Ba}^{2+}$	0.035	0.0327	3
	$\text{Sr}^{2+}$	0.065	0.0630	1.3
II	$\text{Ba}^{2+}$	0.050	0.0498	2
	$\text{Sr}^{2+}$	0.050	0.0487	2.2
III	$\text{Ba}^{2+}$	0.075	0.0723	2.4
	$\text{Sr}^{2+}$	0.035	0.0378	3.6

\*Average of 6 determinations.

voltammetric curves of  $\text{Ba}^{2+}$  and  $\text{Sr}^{2+}$  and found to be:

$$K_{11} = 601$$

$$K_{21} = 364$$

$$K_{12} = 10.88$$

$$K_{22} = 605$$

Table 4 shows the results for the determination of barium and strontium have good precision and reproducibility.

*Acknowledgement*—The project was supported by the National Natural Science Foundation of China.

#### REFERENCES

- D. Homolka, L. Q. Hung, A. Hofmanová, M. W. Khalil, J. Koryta, V. Mareček, Z. Samec, S. K. Sen, P. Vanýsek, J. Weber, M. Brezina, M. Janda, and I. Stibor, *Anal. Chem.*, 1980, **52**, 160.
- J. Koryta, *Ion-Selective Electrode Rev.*, 1983, **5**, 131.
- P. Vanýsek and R. P. Buck, *J. Electroanal. Chem.*, 1984, **163**, 1.
- T. Osakai, T. Kakutani and M. Senda, *Bunseki Kagaku*, 1984, **33**, 371.
- J. Koryta, W. Ruth, P. Vanýsek and A. Hofmanová, *Anal. Lett.*, 1983, **15**, 1686.
- X. Lin, Z. Zhao and H. Freiser, *J. Electroanal. Chem.*, 1986, **210**, 137.
- V. Mareček and Z. Samec, *Anal. Chim. Acta*, 1983, **151**, 265.
- Idem, ibid.*, 1982, **141**, 65.
- E. Wang, Y. Liu and Y. Jiang, *Proc. Electrochem. Soc.*, 1986, 86-14, 35; *Chem. Abstr.*, 1987, **106**, 162668h.
- Z. Sun and E. Wang, *Electrochim. Acta*, 1988, **33**, 603.
- X. Teng, Z. Pang, D. Guo and E. Wang, *Fenxi Yiqi*, 1985, No. 3, 9.
- A. J. Bard and L. R. Faulkner, *Electrochemical Methods, Fundamentals and Applications*, p. 217. Wiley, New York, 1980.

## DETERMINATION OF SELENIUM AND TELLURIUM IN AIR BY ATOMIC-ABSORPTION SPECTROMETRY

SIRINART MUANGNOICHAROEN, KUEN-YUAN CHIOU and OLIVER KEITH MANUEL\*  
Chemistry Department, University of Missouri, Rolla, MO 65401, U.S.A.

(Received 3 February 1988. Accepted 15 May 1988)

**Summary**—Elemental selenium and tellurium, and gaseous inorganic forms of Se(IV), Se(VI), Te(IV) and Te(VI) have been determined after their adsorption on gold-coated beads. After leaching, with water and dilute hydrochloric and nitric acids, the different chemical species in each acid fraction were separated with an anion-exchange resin (Bio-Rad AG-1X8) and a cation-exchange resin (Amberlite IR-120 Plus) by varying the acidity of the leaching agent. Subsequent analysis was by graphite-furnace atomic-absorption spectrometry. The lower detection limit for Se and Te was 0.03 ng/m<sup>3</sup> with a precision of  $\pm 5\%$ . The average amounts of selenium in interior and exterior air samples were about 4.73 and 1.93 ng/m<sup>3</sup> respectively. For tellurium the corresponding values were about 0.78 and 0.24 ng/m<sup>3</sup>.

Sulphur oxides are believed to be primarily responsible for the dramatic increase in the acidity of precipitation in the north-eastern United States, although nitrogen oxides and carbon dioxide also contribute significantly to it.<sup>1</sup> A recent study<sup>2</sup> indicates that electricity power stations, industrial combustion operations, non-ferrous smelters and other industrial processes are major emission sources of sulphur oxides in the United States. The 1980 emission inventory by NAPAP<sup>2</sup> shows the annual emission of SO<sub>2</sub> from such sources, in the 48 contiguous states and the District of Columbia, is about 27.1 million tons per year.

Selenium and tellurium are usually associated with sulphur in nature. The Se:S and Te:S weight ratios in coal samples are reported to be about  $1.1 \times 10^{-4}$  and  $0.3 \times 10^{-4}$  respectively, and in bulk aerosols collected in the central part of the United States these weight ratios are about  $9 \times 10^{-4}$  and  $1 \times 10^{-4}$ , respectively.<sup>3,4</sup> Thus, significant amounts of Se and Te accompany the 27 million tons of SO<sub>2</sub> that are released into the atmosphere each year.

These elements are of environmental interest because (i) the oxides of sulphur contribute significantly to the acidity of precipitation;<sup>1</sup> (ii) although at the ppm level selenium is an element essential to animals, slightly higher concentrations of selenium or tellurium are highly toxic;<sup>5,6</sup> (iii) the average concentrations of S, Se, and Te in bulk aerosols are higher than those in the earth's crust by factors of 780, 2200 and 12000, respectively;<sup>4</sup> and (iv) the chalcogen elements are highly concentrated on very fine aerosol particles (< 1.1  $\mu\text{m}$ ) which have long atmospheric residence times and are readily inhaled. On such fine aerosols, the chalcogen elements exhibit enrichment factors of  $10^4$ – $10^6$  relative to their abundances.<sup>7</sup>

Up to 50% of atmospheric selenium has been reported to pass through filters capable of collecting 99% of particles having diameters > 0.1  $\mu\text{m}$ ,<sup>8</sup> but we have been unable to find similar reports on tellurium other than our own.<sup>9</sup> In addition to organic species such as the methyl-, dimethyl-, ethyl- and diethyl-compounds, the atmosphere may contain elemental Se and Te and inorganic compounds in oxidation states (IV) and (VI).<sup>8-14</sup> The atmospheric component of Se and Te in aerosols was recently reported.<sup>7</sup> The present study was undertaken to obtain additional information on the species of these elements present in air.

### EXPERIMENTAL

#### Apparatus

A Perkin Elmer model 560 atomic-absorption spectrometer with an HGA 500 graphite furnace, a deuterium background corrector and Se and Te hollow-cathode lamps (Fisher Scientific Co., New Jersey, U.S.A.) were used. Argon was used as carrier gas at a flow-rate of 30 ml/min, with "auto-stop" during atomization. The drying temperature was 120°, charring temperature 700° and atomizing temperature 2700°. Peak heights for Se at 196.0 nm and Te at 214.3 nm were recorded (Perkin-Elmer model 023 recorder).

#### Reagents

Unless otherwise stated, all the chemicals used were of analytical grade. A standard stock solution of 1000 ppm Se(IV) was prepared from SeO<sub>2</sub> (99.99%, Gallard Schlesinger Chemicals, New York) in 6M hydrochloric acid. The working solution was obtained by dilution with 1M hydrochloric acid. A standard 1000 ppm Se(VI) solution was prepared by dissolving selenic acid (96%, BDH Chemicals, Poole, England) in water and diluting with 1M hydrochloric acid. A 1000 ppm Te(IV) solution was prepared by dissolving TeO<sub>2</sub> (> 99%, Fisher Laboratory Chemicals, New Jersey) in a minimal amount of concentrated hydrochloric acid and diluting with 1M hydrochloric acid. The Te(VI) stock solution (1000 ppm) was prepared by dissolving H<sub>2</sub>TeO<sub>4</sub> · 2H<sub>2</sub>O (99.5%, BDH Chemicals) in water and diluting with 1M hydrochloric acid. Periodic checks

\*To whom correspondence should be addressed.

of the standard solutions were made as a precaution against deterioration and change in oxidation state during storage.<sup>15</sup> Standards for atomic-absorption measurement were prepared from Se powder (99.99%, Alfa Products, Massachusetts) and Te powder (99.999%, Johnson Matthey Chemicals, London), dissolved in a minimal amount of concentrated nitric acid. After evaporation of the solution almost to dryness, water was added and the evaporation was repeated, this step being repeated. Stock solutions of 1000 ppm were made by dilution with 1M hydrochloric acid. Palladium solution, for use as a matrix modifier for the determination of Se, was prepared by dissolving anhydrous PdCl<sub>2</sub> (99.5%, Research Organic/Inorganic Chemicals Corp., California) in a minimal amount of concentrated hydrochloric acid and diluting with water.

#### Adsorption procedure

In our earlier work,<sup>9</sup> adsorption yields for selenium and tellurium on a column of gold-coated quartz beads at a flow-rate of 5 l./min were found to be about 88 and 67%, respectively. In that experiment, the gold coating was about 10% of the total weight of the beads. In the work reported here, the gold coating on the beads was increased to about 15% of the total weight in order to enhance the adsorption efficiency. We also used four successive columns of gold-coated quartz beads instead of the three successive columns used in the previous work. The gold coating was achieved by dissolving gold powder (99.95%, Johnson Matthey) in a minimal amount of *aqua regia* and then adding 20–80 mesh quartz beads that had been washed successively in hydrochloric and nitric acids. The slurry was evaporated to near dryness, and then packed into a silica tube (9 mm o.d., 150 mm length) with a silica wool plug at each end of the column. Finally, the gold was reduced to the metal by gentle heating under a nitrogen atmosphere to minimize loss of AuCl<sub>3</sub> by volatilization.<sup>16,17</sup>

The air samples were collected (and subsequent adsorption yields obtained) with an air flow-rate of 7 l./min. Se and Te in the vapour phase were generated from standard solutions by gradually raising the temperature with an electric tube furnace to 1000° and maintaining that temperature for 12 hr while passing air over the standards and through the adsorber train by means of a vacuum pump with a variable flow-control.

#### Leaching procedure

The adsorbed species were leached successively with (i) warm distilled water (60°) for Se(IV), Se(VI) and Te(VI), (ii) 1M hydrochloric acid for Te(IV), and (iii) 3M nitric acid for elemental Se and Te. The reagent flow-rate was kept constant at 10 ml/min by means of a variable speed pump. After each acid leach, about 100 ml of distilled water was used to remove all acid from the column, the resulting eluate being added to the acid solution.

#### Separation procedure

The first two fractions, (i) and (ii) above, were mixed and diluted to 0.05M hydrochloric acid concentration to prevent any change in the oxidation state of the Se and Te species. This solution was loaded onto an AG-1X8 (100–200 mesh, Cl<sup>-</sup> form) anion-exchange column (7.0 mm bore, 60 mm length) and washed with 20 ml of 0.05M hydrochloric acid, at a flow-rate of 0.6 ml/min. Se(VI) was retained on the column; Se(IV), Te(IV) and Te(VI) were eluted. The eluate was passed through a cation-exchange column (10 mm bore, 120 mm length) packed with Amberlite IR-120 (60–80 mesh, H<sup>+</sup> form), and 80 ml of 0.05M hydrochloric acid at a flow-rate of 1.0 ml/min were used to remove Se(IV) and Te(VI) from the column, Te(IV) being retained. The eluate was evaporated to near dryness, and Te(VI) was reduced to Te(IV) by heating with 1 ml of concentrated hydrochloric acid. The solution was then taken up in 0.05M hydrochloric

acid and Se(IV) was separated from Te(IV) with a cation-exchange resin, as in the previous step.

Se(VI) was subsequently eluted from the anion-exchange column with 30 ml of 0.3M hydrochloric acid, and the Te(IV) was eluted from the cation-exchange column with 150 ml of 0.3M hydrochloric acid.<sup>18</sup>

The nitric acid leach dissolved elemental Se and Te from the adsorber column, and this solution was evaporated to near dryness. Concentrated hydrochloric acid was then added dropwise to remove all nitrate and also to reduce Se(VI) and Te(VI) to Se(IV) and Te(IV) for separation on the cation-exchange column by the procedures given above.

Each fraction was analysed for Se and Te by atomic-absorption spectrometry after evaporation to near dryness to prevent any loss by volatilization. After the determination of Te, 2 µg of Pd were added per ml of sample solution as a matrix modifier prior to the determination of Se. This enhanced the signal by a factor of about three.<sup>19</sup> The amounts of Se and Te species in each fraction were read off from calibration plots prepared with standard solutions.

## RESULTS AND DISCUSSION

### Adsorption yield

Table 1 shows that the adsorption of Se seems to be quantitative on the first gold column at a flow-rate of 7 l./min. Similar results were observed for Te (Table 2), with about 97% retained on the first gold column. However, the entire four-column train was used to ensure quantitative adsorption of Se and Te from air during the long period of sample collection.

Table 1. Adsorption efficiency of Se\* on a train of 4 gold columns at a flow-rate of 7 l./min (*n* = 3)

	Se found, µg	Retained, %
Column 1	0.98 ± 0.02	97.5 ± 2.0
Column 2	nil	nil
Column 3	nil	nil
Column 4	nil	nil

\*1.0 µg of Se was heated to generate selenium vapour which was then passed through 4 successive columns of gold-coated beads at a constant flow-rate. The amount of Se in each column was investigated.

Table 2. Adsorption efficiency of Te\* on a train of 4 gold columns at a flow-rate of 7 l./min (*n* = 3)

	Te found, µg	Retained, %
Column 1	0.71 ± 0.02	96.6 ± 2.8
Column 2	nil	nil
Column 3	nil	nil
Column 4	nil	nil

\*0.73 µg of Te was heated to generate tellurium vapour which was then passed through 4 successive columns of gold-coated beads at a constant flow-rate. The amount of Te in each column was investigated.

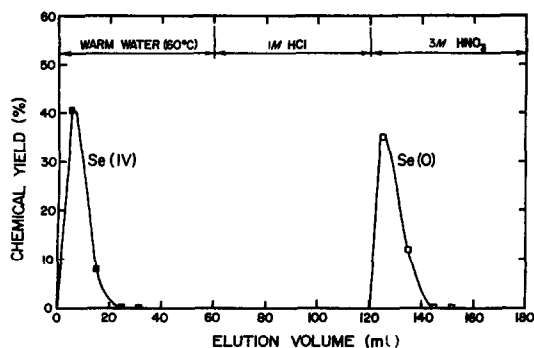


Fig. 1. Sequential leaching of Se from a gold column with water, hydrochloric acid and nitric acid. The total recovery of Se was  $97.5 \pm 2.0\%$  ( $n = 3$ ).

#### Leaching efficiency

The leaching procedures for Se, Se(IV), Se(VI), Te, Te(IV) and Te(VI) were based on the chemical properties of the various species.

Figures 1 and 2 show the net adsorption plus leaching yields observed when vapours from standard solutions of Se(IV) and Te(VI) were drawn over the train. The results shown in Fig. 1 for selenium demonstrate that Se(IV) can be eluted quantitatively with 20 ml of warm water ( $60^\circ$ ); no selenium was found in the hydrochloric acid leaching solution. Another species that we propose was elemental Se was quantitatively removed with 25 ml of 3M nitric acid. At the elevated temperatures (up to  $1000^\circ$ ) used to drive off Se vapours, there was apparently appreciable reduction of Se(IV) to Se.

The net adsorption plus leaching efficiency for tellurium is shown in Fig. 2. The species Te(VI), Te(IV) and Te are quantitatively eluted with 15 ml of warm water, 20 ml of 1M hydrochloric acid and 15 ml of 3M nitric acid, respectively. We attribute this to the dissolution of the tellurium oxides and/or acidic species in warm water and dilute hydrochloric acid, and the dissolution of elemental Te in the 3M nitric acid. Our results suggest that there was significant reduction of Te(VI) to Te(IV) and Te at

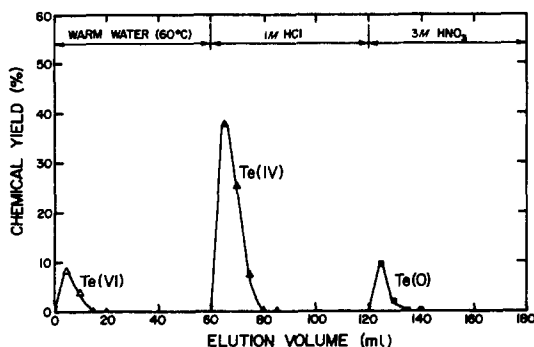


Fig. 2. Sequential leaching of Te from a gold column with water, hydrochloric acid and nitric acid. The total recovery of Te was  $96.7 \pm 2.8\%$  ( $n = 3$ ).

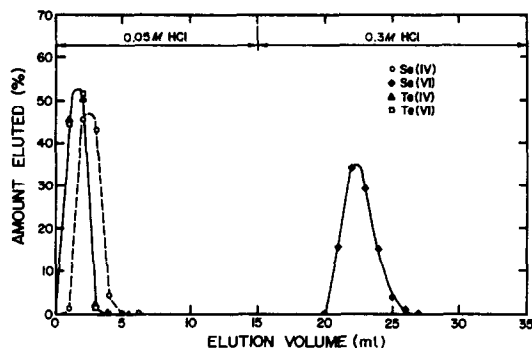


Fig. 3. Elution curve of Se(IV), Se(VI), Te(IV) and Te(VI) from an AG-1X8 anion-exchange column. Se(VI) is separated from the other species on this column by variation of the eluent concentration. Se(IV), Te(IV) and Te(VI) are then separated by means of an Amberlite IR-120 cation-exchange resin.<sup>18</sup>

the temperatures used to generate tellurium vapours from the standard.

#### Separation procedure

Chiou and Manuel<sup>18</sup> have demonstrated the separation of Se(IV) and Te(IV) on Amberlite IR-120 plus and the separation of Te(IV) from Te(VI) with this resin.<sup>20</sup> In addition, we studied the separation of Se(VI) from Se(IV), Te(IV) and Te(VI) with AG-1X8 anion-exchange resin. The results shown in Fig. 3 clearly demonstrate that Se(VI) is the only one of these species that is retained on the column in the presence of 0.05M hydrochloric acid. Se(IV), Te(IV) and Te(VI) were quantitatively eluted with 5 ml of 0.05M hydrochloric acid, and the Se(VI) was subsequently leached with 15 ml 0.3M hydrochloric acid.

This method permits the determination of 1 ng/ml Se or Te with a precision of about  $\pm 5\%$ . At its upper end, the calibration graph is not linear if the concentration of Se or Te exceeds about 50 ng/ml. For an air sample of 40 m<sup>3</sup> or larger, as little as 0.03 ng/m<sup>3</sup> Se or Te can be determined with a precision of  $\pm 5\%$ .

#### Interferences

We investigated the possibility of interference from some elements commonly found in air. Chiou and Manuel<sup>18,20</sup> have shown that the presence of some foreign species, e.g., As(III), Hg(II), Cu(II), Ni(II) and Ag(I), will decrease the atomic-absorption signals of Te. In the present study, the addition of 10  $\mu$ g of Hg(II), 10  $\mu$ g of As(III) and 10  $\mu$ g of Sb(III), 25  $\mu$ g of Au(III), 25  $\mu$ g of Cd(II), 25  $\mu$ g of Ag(I), 25  $\mu$ g of Pb(II) and 50  $\mu$ g of Zn(II) to the solution containing 1.0  $\mu$ g of standard Se(IV), Se(VI), Te(IV) or Te(VI) prior to the ion-exchange separation had no effect on the determination of Se or Te by atomic-absorption spectrometry. Other common ions that are normally found in air, e.g., ammonium, sulphate and nitrate, were also studied. We found that the addition of up to 1000  $\mu$ g of these ions per 1.0  $\mu$ g of each Se and

Table 3. Amount of inorganic species of Se found in local air in Rolla, Missouri

Location*	Sample volume, $m^3$	Se, $ng/m^3$	Se(IV), $ng/m^3$	Se(VI), $ng/m^3$	Se total, $ng/m^3$
a	52.08	2.21	2.64	0.75	5.60
b	65.73	1.54	2.09	0.58	4.22
b	88.80	1.57	2.30	0.51	4.38
c	142.59	1.12	0.81	0.10	2.03
c	102.78	0.97	0.75	0.08	1.80
c	182.25	1.05	0.78	0.10	1.93
c	162.46	1.13	0.72	0.10	1.95
blank		0.24	0.20	n.d.	0.44

\*Location a is indoor air from a laboratory working with Se and Te. Location b is indoor air from a general chemistry laboratory. Location c is outdoor air from the third floor of a chemistry building.

Table 4. Amount of inorganic species of Te found in local air in Rolla, Missouri

Location*	Sample volume, $m^3$	Te, $ng/m^3$	Te(IV), $ng/m^3$	Te(VI), $ng/m^3$	Te total, $ng/m^3$
a	52.08	0.47	0.20	0.26	0.93
b	65.73	0.36	0.19	0.20	0.75
b	88.80	0.34	0.18	0.15	0.67
c	142.59	0.06	0.06	0.13	0.25
c	102.78	0.05	0.05	0.11	0.21
c	182.25	0.07	0.06	0.13	0.26
c	162.40	0.07	0.05	0.13	0.25
blank		0.03	0.03	0.03	0.09

\*As for Table 3.

Te species does not interfere in the analysis. In all cases, the chemical yields of Se(IV), Se(VI), Te(IV) and Te(VI), found after adsorption, leaching and separation by the anion- and cation-exchange procedures, were over 90%. This demonstrates that our separation scheme is capable of removing the interferences of these foreign ions.

#### Local air analysis

Tables 3 and 4 give the results of our analyses for Se and Te in local air samples collected at three campus locations: location a is in a laboratory where experiments on Se and Te have been conducted for several years, location b is in a general chemistry laboratory, and location c is on the north-east side of a chemistry building, at third floor level. The air was drawn through a 0.2- $\mu$ m pore membrane filter and then through the train of four gold-coated bead columns.

Our results show that several chemical species contribute to the total burden of Se and Te in air. As shown in Tables 3 and 4, the total concentrations of Se and Te in outside air were in the range 1.80–2.03  $ng/m^3$  and 0.21–0.26  $ng/m^3$ , respectively. The highest total concentrations of Se (5.60  $ng/m^3$ ) and Te (0.93  $ng/m^3$ ) were found in the laboratory where these elements are routinely used. Intermediate total concentrations of Se (4.22–4.38  $ng/m^3$ ) and Te (0.67–0.75  $ng/m^3$ ) were observed in the general chemistry laboratory.

Table 3 shows that elemental Se is the dominant species of selenium in outside air, and Se(IV) is the

dominant species in laboratory air. In both cases the concentration of Se(IV) exceeds that of Se(VI). Differences in the volatility of the different chemical species may determine the ratio of the selenium forms at the emission source. Andren *et al.*<sup>21</sup> have noted that SO<sub>2</sub> generated during combustion of coal may act to reduce other forms of selenium to elemental Se, which may thus be the dominant species close to the emission source. Since SeO<sub>2</sub> is more volatile than Se,<sup>22</sup> preferential deposition of Se on aerosol particles decreases the Se:SeO<sub>2</sub> ratio as the sampling distance from the emission increases. Some SeO<sub>2</sub> may also react with oxidants in the troposphere, *e.g.* hydroxyl radicals, O<sub>3</sub> and H<sub>2</sub>O<sub>2</sub> *etc.*, and be oxidized to Se(VI).

Table 4 shows the concentrations and species of tellurium found in local air. In outdoor air Te(VI) is the major component. During its atmospheric cycle, Te(VI) emitted from coal combustion may undergo reduction to Te(IV) and elemental Te, not only by SO<sub>2</sub> but also by some other reactive species such as nitrogen oxides, *e.g.* NO, NO<sub>2</sub>, *etc.*,<sup>23</sup> especially as the residence time increases.

*Acknowledgements*—Special thanks are due to T. J. O'Keefe and Sami Cuzmar for their kindness in making the AAS instrument available for the study.

#### REFERENCES

1. J. N. Galloway, G. E. Likens and M. E. Howley, *Science*, 1984, **226**, 829.
2. D. A. Toothman, J. C. Yates and E. J. Sabo, *Status Report on the Development of the NAPAP Emission Inventory for the 1980 Base Year and Summary of Preliminary Data*, EPA-600/7-84-091, 1984.



3. Y. Hashimoto and J. W. Winchester, *Environ. Sci. Technol.*, 1967, **1**, 338.
4. K. Y. Chiou and O. K. Manuel, in *Coal Science and Technology, Processing and Utilization of High Sulfur Coals*, Y. A. Attia (ed.), p. 89. Elsevier, New York, 1985.
5. W. C. Cooper, *Tellurium*, Chapter 7. Van Nostrand Reinhold, New York, 1971.
6. S. E. Raptis, G. Kaiser and G. Tölg, *Z. Anal. Chem.*, 1983, **316**, 105.
7. K. Y. Chiou and O. K. Manuel, *Environ. Sci. Technol.*, 1986, **20**, 987.
8. D. C. Reamer and W. H. Zoller, *Science*, 1980, **208**, 500.
9. S. Muangnoicharoen, K. Y. Chiou and O. K. Manuel, *Anal. Chem.*, 1986, **58**, 2811.
10. D. S. Lee and J. M. Edmond, *Nature*, 1985, **313**, 782.
11. M. O. Andreae, *Anal. Chem.*, 1984, **56**, 2064.
12. C. H. Chung, E. Iwamoto, M. Yamamoto and Y. Yamamoto, *Spectrochim. Acta*, 1984, **39B**, 459.
13. S. N. Willie, R. E. Sturgeon and S. S. Berman, *Anal. Chem.*, 1986, **58**, 1143.
14. C. I. Measure, B. Grant, M. Khadem, D. S. Lee and J. M. Edmond, *Earth Planet. Sci. Lett.*, 1984, **71**, 1.
15. T. W. May and D. A. Kane, *Anal. Chim. Acta*, 1984, **161**, 387.
16. R. S. Braman and D. L. Johnson, *Environ. Sci. Technol.*, 1974, **8**, 996.
17. R. Dumary, R. Dams and J. Hoste, *Anal. Chem.*, 1985, **57**, 2638.
18. K. Y. Chiou and O. K. Manuel, *ibid.*, 1984, **56**, 2721.
19. Shan Xiao-Quan and Hu Kai-Jing, *Talanta*, 1985, **32**, 23.
20. K. Y. Chiou and O. K. Manuel, *Determination of inorganic tellurium species in natural water using cation-exchange graphite furnace atomic absorption spectrometry*, Presentation at the 20th ACS Great Lakes Regional Meeting, Milwaukee, Wisconsin, 2-4 June 1986.
21. A. W. Andren, D. H. Klein and Y. Talmi, *Environ. Sci. Technol.*, 1975, **9**, 856.
22. R. C. Weast, *CRC Handbook of Chemistry and Physics* 62nd Ed., p. D-172. CRC Press, Boca Raton, 1981-1982.
23. G. Gschwandtner, K. Gschwandtner, K. Eldridge, C. Mann and D. Mobley, *J. Air Pollut. Control Assoc.*, 1986, **36**, 139.

## REVERSED-PHASE HPLC SEPARATION OF COMPLEX MIXTURES OF TRACE METALS AS DIBENZYL-DITHIOCARBAMATE CHELATES

C. BAIOCCHI\*, A. MARCHETTO, G. SAINI and P. BERTOLO

Dipartimento di Chimica Analitica, Università di Torino, Via P. Giuria 5, 10125 Torino, Italy

G. PETTITI

Laboratorio di Anestesiologia e Rianimazione, Università di Torino, C.so Bramante 90,  
10100 Torino, Italy

(Received 14 June 1987. Revised 29 April 1988. Accepted 12 May 1988)

**Summary**—The dibenzyl-dithiocarbamate chelates of Cd(II), Pb(II), Bi(III), Hg(II), Ni(II), Cu(II), As(III), Fe(III), Co(III) and In(III) are separated by reversed-phase HPLC in isocratic conditions. The procedure is simple, rapid, and gives satisfactory separations with high efficiency and sensitivity at mobile phase compositions very rich in organic modifier (85–88% CH<sub>3</sub>CN). The detection limits range from 1.4 to 14 µg/l. The elution order is correlated with the ability of the central metal atom to affect the electronic distribution of the ligand, which has readily polarizable donor atoms. Infrared spectroscopy data corroborate this assumption.

An especially promising approach for quantitative multi-element determinations of trace metals involves pre-column formation of chelates followed by reversed-phase liquid chromatographic separation. The dithiocarbamates form thermodynamically stable complexes readily extractable from aqueous systems into organic solvents.<sup>1</sup> With such characteristics they have long been used for analysis by extraction followed by spectrophotometric or atomic-absorption spectrometric determination. For the same reasons these complexes are particularly suitable for HPLC separation, allowing the determination of trace levels of metal ions even in complex matrices such as sea-water and other marine samples.

Separations of various dialkyldithiocarbamate chelates on hydrocarbon stationary phases have been reported.<sup>2-14</sup> Chelates of pyrrolidinedithiocarbamate,<sup>15</sup> *N*-methyl-2-naphthylmethyl-dithiocarbamate,<sup>16</sup> bis(2-hydroxyethyl)dithiocarbamate,<sup>17,18</sup> *N*-methyl-*N*-2-sulphoethyl-dithiocarbamate<sup>19</sup> and tetramethylenedithiocarbamate<sup>20</sup> have also been studied. The detection technique was mainly ultraviolet spectrophotometry, but some attention was also paid to electrochemical detection, because many metal dithiocarbamate complexes are electroactive at various working electrodes.

A limitation of the method arises from the possible decomposition of the complexes in the column, particularly when very low concentrations are involved, as in trace analysis. The ligand used in the present work is sodium dibenzyl-dithiocarbamate (DBzDTC).

The presence of the two benzyl groups ensures high absorptivity and their relative bulkiness contributes to the stability of the complexes formed. An excess of ligand was added to the mobile phase in order to minimize decomposition during the separation.

### EXPERIMENTAL

#### Instrumentation

The liquid chromatograph was a Varian LC 5060, with a UV 100 spectrophotometric detector and a VISTA 401 Data System. The detector was operated at 254 nm.

The analytical columns used were a Varian MCH-10 (10-µm particles, 300 × 4.6 mm, carbon load 8%, no end-capping) and an Alltech Adsorbosphere (10-µm particles, 250 × 4.6 mm, carbon load 19%, fully end-capped) indicated hereafter as columns A and B, respectively.

The ultraviolet spectroscopic properties of the samples were monitored in the range 190–600 nm. The chromatographic analysis had to be performed as soon as possible after preparation of the sample.

All glassware was conditioned with 1.0M nitric acid and rinsed several times with water from the Milli-Q system to minimize contamination.

The infrared spectra were obtained with solid samples of the metal complexes after crystallization from chloroform. The spectral range explored was 4000–400 cm<sup>-1</sup> at a scan speed of 10 cm<sup>-1</sup>/sec, with a resolution of 4 cm<sup>-1</sup> at an absorbance of 0.50.

#### Reagents

HPLC-grade acetonitrile (Merck) and water purified with the Millipore Milli-Q system were used as the mobile phase constituents. Analytical grade sodium dibenzyl-dithiocarbamate was obtained from Fluka.

Individual 0.01M solutions of each metal salt were made by dilution of stock 1000-mg/l. standard solutions (C. Erba "For atomic absorption", Merck "Titrisol"). The ligand stock solution (1.0 × 10<sup>-3</sup>M) was prepared by dissolving the

\*To whom all correspondence should be addressed.

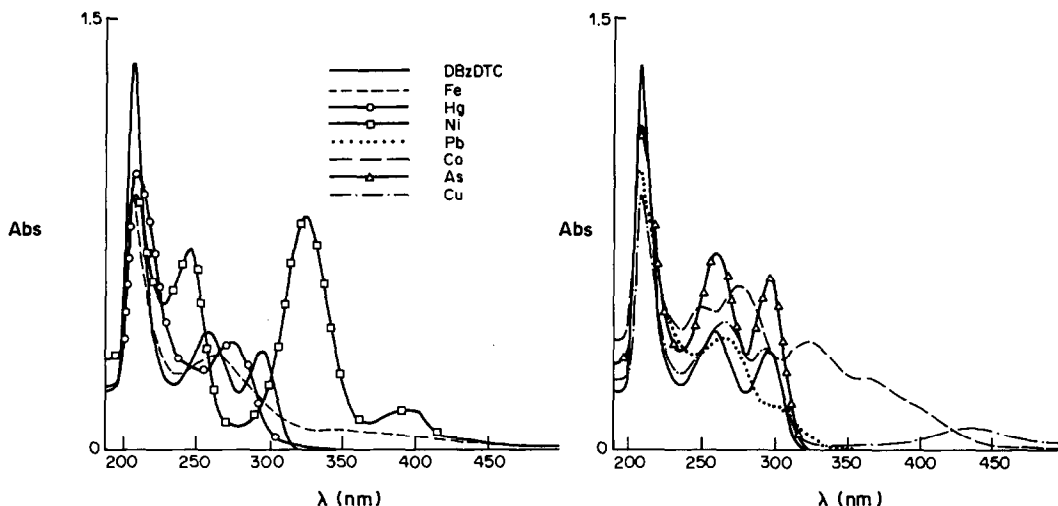


Fig. 1. Spectra of DBzDTC and its metal chelates.

appropriate amount of reagent in 100.0 ml of chromatography grade acetonitrile that had been deoxygenated by passage of gentle stream of nitrogen through it. DBzDTC chelates in concentrations varying in the range  $1.0 \times 10^{-5}$ – $1.0 \times 10^{-7} M$  were formed by adding appropriate amounts of metal ion stock solutions to 50.0 ml of a 1:1 v/v water–acetonitrile mixture that was  $4.0 \times 10^{-5} M$  in DBzDTC.

#### RESULTS AND DISCUSSION

The ultraviolet spectroscopic properties of DBzDTC and its complexes are shown in Fig. 1. The spectra differ from metal to metal. In the absence of a common wavelength of maximum absorbance for all the chelates, it was decided to use 254 nm as the detection wavelength, to make the method easily applicable to chromatographic systems equipped with a fixed wavelength detector.

The chromatographic studies were performed with either 1:1 v/v acetonitrile–water solutions of the DBzDTC complexes or acidic solutions (pH 2.5) of salts of the following species: Cd(II), Pb(II), Bi(III), Zn(II), Hg(II), Ni(II), Cu(II), As(III), Fe(III), Co(II). The Co(II) was rapidly aerielly oxidized to Co(III) species stabilized by complexation with the dithiocarbamate. Few of the complexes were inert enough to give adequate resolution of peaks in a simple water–acetonitrile mixture. The addition of a tertiary amine (triethylamine, TEA) to give a 0.05M concentration in the aqueous component in order to shield the free silanol groups of the stationary phase,<sup>21</sup> and of an excess of ligand ( $2.0 \times 10^{-4} M$ ) to the organic component of the mobile phase, resulted in very satisfactory chromatographic results. The pH of the final solution containing TEA was adjusted to 4.5 with 0.05M acetate buffer. The mobile phase composition providing the best resolution was different for the two columns used and the shapes and resolution of the peaks showed significant differences, depending on the stationary phase.

In Fig. 2, chromatograms corresponding to injections of (a) freshly prepared and (b) 24 hr old solutions of DBzDTC and Pb(DBzDTC)<sub>2</sub> are shown. The

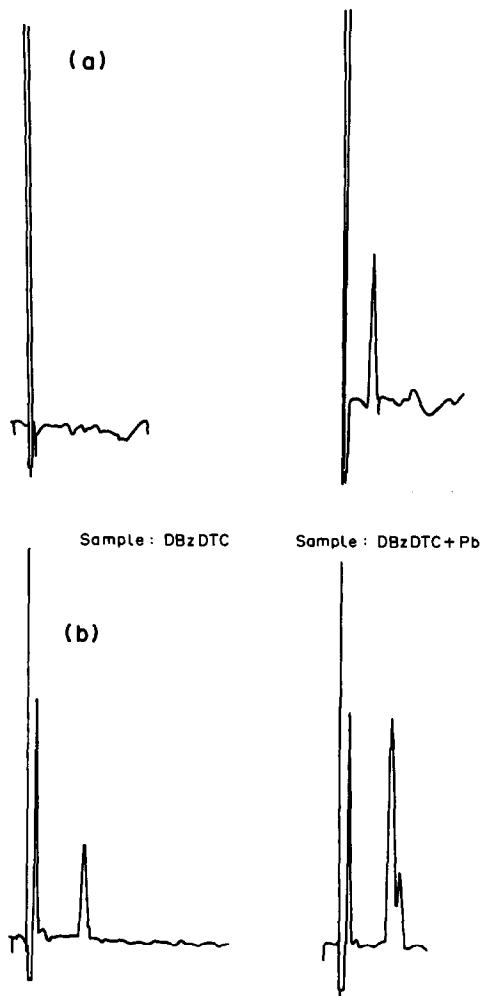
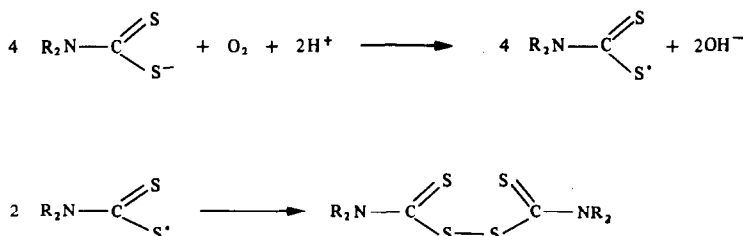


Fig. 2. Chromatograms of the ligand and its Pb(II) complex: (a) freshly prepared, (b) after 24 hr.

retention time of the chelate is very long and a new peak with a retention time of 5.0 min appears; by analogy with similar cases,<sup>15</sup> this peak may be attributed to the formation of a dimer of the free ligand by oxidation according to the scheme



It is difficult to identify what change in the structure or composition of the complex gives rise to the change in retention time.

The chelates of all the other metal ions examined showed similar changes in the peaks after aging of their solutions. Moreover, chromatographic runs of samples that had undergone extraction, evaporation to dryness and reconstitution in an acetonitrile–water mixture gave the same chromatograms as the aged solutions. The solvent extraction obviously facilitates oxidation by dissolved and/or aerial oxygen.

The instability of the solutions necessitated frequent preparation of new standards. To avoid this, *in situ* formation of complexes by direct injection of slightly acidic solutions of the metal ions was tried. The efficiency and selectivity of the separation of DBzDTC complexes formed *in situ* was exactly the same as for those formed prior to injection. A possible difficulty with *in situ* complex formation is that during the residence time in the column the less reactive ions in an injected mixture might not be able to react completely with the ligand in the mobile phase. The example in Fig. 3 shows that this was the case for the Sn(IV) and Cd(II) complexes. In the same figure it can be seen that the detection sensitivity obtained in the case of the pre-column chelation was better, mainly for the peaks in the middle of the chromatogram (chromatogram A was recorded at a sensitivity eight times greater than that for chromatogram B). This effect may also be due to incomplete reaction.

The solutions for the pre-column system could be made more stable by careful degassing (for about 15 min), but the resulting increase in sensitivity did not seem large enough to justify the work and careful handling involved.

The simpler option of *in situ* formation of the complexes was adopted as our standard procedure and Fig. 4 shows typical chromatograms obtained with the two columns used. In Table 1 the chromatographic data and detection limits for the two

types of column are reported. As expected, the efficiency and selectivity were different in the two cases. Columns A and B differed in carbon load (8 and 19% respectively) and column B was end-capped with trimethylsilane. Both factors affect the number

of free silanol groups, which may complicate the retention mechanism and influence the separation efficiency and selectivity. In the absence of tertiary amine in the mobile phase, column A (which was richer in free silanol groups) was not able to provide peaks of acceptable shape for most of the complexes. In contrast, for column B the presence of a buffer to control the pH was enough to give very good peaks for all the complexes examined. However, aqueous solutions of TEA were used in both cases for uniformity.

Calibration plots for all the metal ions examined exhibit satisfactory linearity in the concentration range examined. Table 2 lists the numerical results.

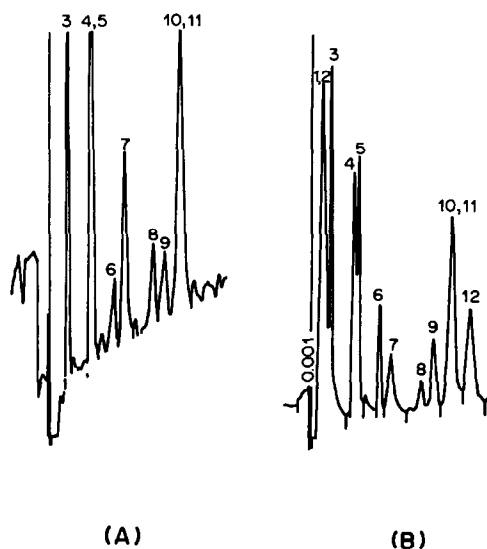


Fig. 3. Effect of reactivity competition on the *in situ* chelation of a mixture of metal ions. Chromatogram A: *in situ* chelation (detector sensitivity 0.0156 absorbance for full scale deflection). B: pre-column chelation (detector sensitivity 0.125). (1) Cd(II), (2) Sn(IV), (3) Pb(II), (4) Zn(II), (5) Hg(II), (6) Se(IV), (7) Ni(II), (8) Cu(II), (9) As(III), (10) Co(III), (11) Fe(III) and (12) In(III) in B only. Flow-rate 1.5 ml/min. All metal concentrations  $1.0 \times 10^{-5} M$ .

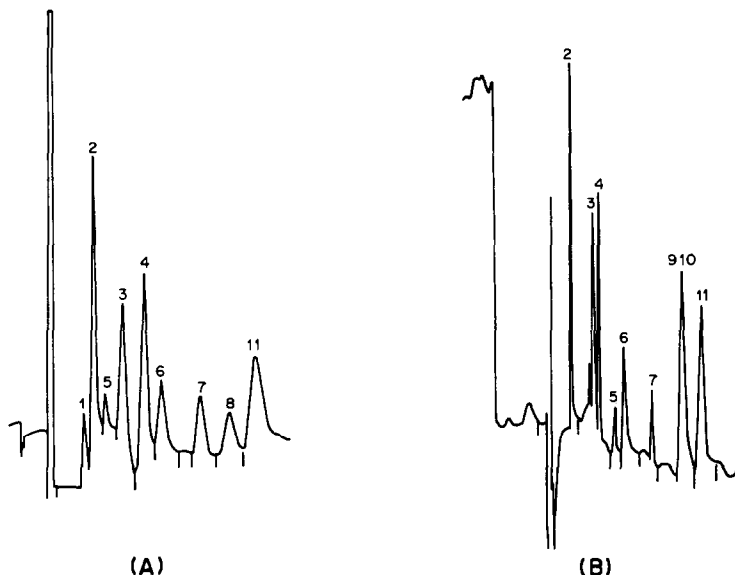


Fig. 4. Comparison of separations performed on different columns. A: column A,  $\text{CH}_3\text{CN}$  ( $+2.0 \times 10^{-4} M$  DBzDTC)/ $\text{H}_2\text{O}$  ( $+0.01 M$  TEA) (85:15); flow-rate 1.2 ml/min, detector sensitivity 0.0156. B: column B,  $\text{CH}_3\text{CN}$  ( $+2.0 \times 10^{-4} M$  DBzDTC)/ $\text{H}_2\text{O}$  ( $+0.01 M$  TEA) (88:12); flow-rate 1.5 ml/min, detector sensitivity 0.031. The metals common to both experiments were (2) Pb(II), (3) Zn(II), (4) Hg(II), (5) Se(IV), (6) Ni(II), (7) Cu(II), (11) In(III). Fe(III) (9) and Co(III) (10) were used only in B, and Bi(III) (1) and As(III) (8) only in A. All concentrations were  $5.0 \times 10^{-6} M$ .

Table 1. Chromatographic retention and efficiency parameters and detection limits of the metal complexes

Column	Parameter	Bi	Pb	Se	Zn	Hg	Ni	Cu	As	In	Fe	Co
A*	$k'$	1.23	1.59	2.05	2.65	3.47	4.10	5.51	6.58	7.49		
	Plate height, mm		0.11	0.12	0.32	0.16	0.16	0.10	0.15	0.18		
	DL, $\mu\text{g/l}$ .	14.0	1.8	1.4	1.8	5.8	2.8	3.1	2.2	5.4		
B†	$k'$		1.38	5.08	2.93	3.33	4.43	7.02		10.71	9.28	9.28
	Plate height, mm		0.051	0.040	0.048	0.049	0.039	0.039		0.036	0.042	0.042
	DL, $\mu\text{g/l}$ .		1.4	1.4	1.5	4.4	2.0	3.1		3.4	—	—

\*Column A:  $\text{CH}_3\text{CN}$  85%; flow-rate 1.2 ml/min.

†Column B,  $\text{CH}_3\text{CN}$  88%; flow-rate 2.0 ml/min.

All the chromatographic runs were done in triplicate and the relative standard deviations of the peak heights were at worst [Se(IV) and As(III) chelates] about 3%.

Table 1 also lists the detection limits, which were evaluated as the concentrations corresponding to a signal to noise ratio of two. As can be seen, they were satisfactorily low, taking into account that they were obtained under the separation conditions for the mixture. Since real samples containing all the metals examined are unlikely to be common, it is possible to improve the detection sensitivity of single ions by choosing more suitable operating conditions (*e.g.*, different organic modifier concentration, lower flow velocity, more suitable wavelength). In this connection, the chromatographic behaviour of the  $\text{Cd}(\text{DBzDTC})_2$  chelate did not allow its determination in conditions compatible with those for the other chelates. However, its determination was possible with a suitable mobile phase (70:30 v/v  $\text{CH}_3\text{CN}/\text{NH}_4\text{OAc}$  buffer).

It is worth noting that very good selectivity was

achieved at high organic modifier concentrations in the mobile phase, though such compositions normally give poor selectivity.

Table 2. Calibration plot parameters

Column	Complex	Slope, $\text{mm. l. mg}^{-1}$	Intercept, mm	Correlation coefficient
A	Bi(III)	3.3	0.1	0.989
	Pb(II)	18.0	0.1	0.971
	Se(IV)	2.6	0.1	0.981
	Zn(II)	10.6	0.1	0.984
	Hg(II)	10.7	0.1	0.988
	Ni(II)	4.8	0.1	0.987
	Cu(II)	4.5	0.1	0.985
	As(III)	3.0	0.1	0.979
	In(III)	6.3	0.1	0.983
B	Pb(II)	27.7	0.2	0.978
	Zn(II)	12.6	0.2	0.986
	Hg(II)	15.4	0.2	0.965
	Ni(II)	3.3	0.2	0.966
	Se(IV)	7.7	0.2	0.981
	Cu(II)	4.9	0.2	0.975
	In(III)	11.9	0.2	0.985

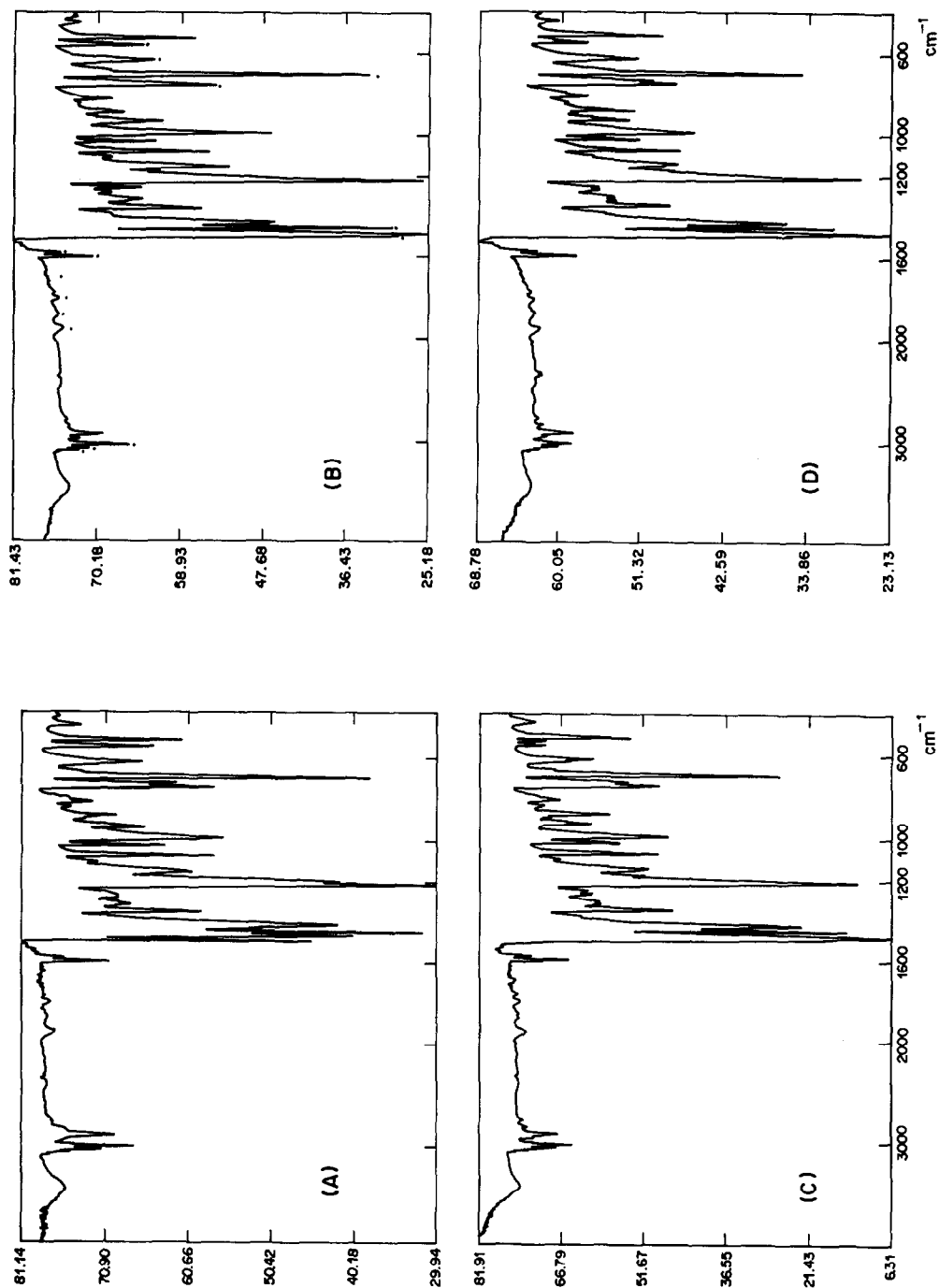


Fig. 5. Infrared spectra of solid DBzDTC chelates. (A)  $\text{Pb}(\text{DBzDTC})_2$ , (B)  $\text{Cu}(\text{DBzDTC})_2$ , (C)  $\text{Co}(\text{DBzDTC})_3$ , (D)  $\text{Fe}(\text{DBzDTC})_3$ .

A rationalization of the results may be attempted in terms of the electron-density distribution in the chelating ring, which is the part of a metal complex molecule that is mainly responsible for differences in the chromatographic properties of this type of compound.<sup>22</sup> The central metal ion can affect the proton-acceptor ability of the donor atoms of the ligands (*i.e.*, their ability to give dipolar interaction with the solvent molecules) as a consequence of the more or less ionic character of the metal–ligand bond. In addition, it can alter the electronic distribution of the ligand molecules (which are generally highly conjugated) and so influence the lipophilicity of the non-polar part of the compound. This influence is rather small for nitrogen and oxygen as donor atoms, since these are strongly electronegative and not easily polarized, so in such cases only small differences in chromatographic behaviour are caused by the different metal ions. To separate the metal complexes it is then necessary to employ a mobile phase with a low organic content, which often results in very long retention times and poor peak shapes. In contrast, the donor sulphur atoms of DBzDTC are only weakly electronegative and the central metal ions can markedly affect the electronic distribution and character of the metal–ligand bond and hence govern the chromatographic selectivity.

The degree of ionic character of the metal–ligand bonds depends on the effective positive charge localized on the metal ion. However, the values obtained for this charge by means of parameters such as the covalency index values  $X_m^2 r$  (where  $X_m^2$  and  $r$  are the electronegativity and radius of the metal ion) do not correlate with the elution order of the chelates examined. Information obtained from the infrared spectra is more useful.

It is well known that in dithiocarbamates the C–N bond is partly double-bond in character owing to the shift of a nitrogen electron-pair toward the chelate ring. Such a shift affects the ability of the nitrogen atom to interact with polar solvent molecules and obviously depends on the nature of the central metal ion. The position of the absorption band assigned to the stretching vibrations of the C–N bond in the infrared spectra of dibenzylidithiocarbamate complexes, such as those shown in Fig. 5, confirms an intensification of double-bond character. The larger the  $\nu_{CN}$  value, the smaller the ability of the nitrogen atom to interact with mobile phase molecules, and the larger the retention times. Table 3 shows that the proposed correlation is strictly observed for trivalent metal ions, but the elution order of bivalent ions is not as expected in the case of Ni and Zn. The Ni and Zn chelates differ from the others in being co-ordination unsaturated. Two co-ordination positions are ligand-free and can be occupied by mobile phase molecules that are then in the inner co-ordination sphere of the metal ion. The resulting stronger interactions with the solvent cause shorter retention times than expected. The Co(III) and Fe(III) complexes,

Table 3. Frequencies of the stretching vibrations of the C–N bond in the infrared spectra, and the retention volumes of the DBzDTC chelates

Chelate	$\nu_{CN}, \text{cm}^{-1}$	$V_R, \text{ml}$	
		Column A	Column B
Bi(III)	1476	7.6	5.2
Fe(III)	1480	23.8	17.7
Co(III)	1480	23.8	17.7
In(III)	1485	27.4	20.0
Pb(II)	1465	5.6	5.4
Hg(II)	1473	10.0	10.0
Zn(II)	1479	9.2	9.0
Cu(II)	1482	19.2	15.6
Ni(II)	1486	14.4	12.0

which have identical vibration frequencies for the C–N bond, have identical retention times at all mobile phase compositions examined.

Figure 5 shows examples of some of the spectra. The frequency range typical of C–N bond vibrations in the dithiocarbamates is known<sup>23</sup> to be 1490–1470  $\text{cm}^{-1}$ . In the present case the peak at 1493  $\text{cm}^{-1}$ , occurring in all the spectra, is typical of the benzyl group, and the adjacent peak is typical of the C–N bond vibration. The pair of peaks in the range 1455–1410  $\text{cm}^{-1}$  are outside the range usually attributed to  $\nu_{CN}$  vibration, and in any case are not affected by the presence of different metal ions. A similar situation was found in the case of metal complexes with diethyldithiocarbamate.<sup>22</sup>

## CONCLUSIONS

The structural factors examined above show the fundamental role played by the central metal ions in characterizing the chromatographic behaviour of DBzDTC complexes. The resulting high selectivity of separation (together with the favourable spectroscopic properties of the chelates) makes this method suitable for trace-metal determination. Furthermore, *in situ* formation of the complexes is simple and rapid, allowing a large number of samples to be analysed in a reasonable time.

## REFERENCES

1. B. J. Mueller and R. J. Lovett, *Anal. Chem.*, 1987, **59**, 1405.
2. A. M. Bond and G. G. Wallace, *ibid.*, 1981, **53**, 1209.
3. S. R. Hutchins, P. R. Haddad and S. Dilli, *J. Chromatog.*, 1982, **252**, 185.
4. G. Schwedt, *Chromatographia*, 1979, **12**, 613.
5. E. B. Edward-Inatimi, *J. Chromatog.*, 1983, **256**, 253.
6. A. R. Timerbaev, O. M. Petrukhin and Yu. A. Zolotov, *Zh. Analit. Khim.*, 1986, **41**, 2135.
7. H. Irth, G. J. de Jong, U. A. Th. Brinkman and R. W. Frei, *Anal. Chem.*, 1987, **59**, 98.
8. G. Drasch, *Z. Anal. Chem.*, 1986, **325**, 285.
9. T. Tetsumi, M. Sumi, M. Tanaka and T. Shono, *J. Chromatog.*, 1985, **348**, 389.
10. B. J. Mueller and R. J. Lovett, *Anal. Lett.*, 1985, **18**, 2399.
11. *Idem*, *Anal. Chem.*, 1985, **57**, 2693.

12. R. M. Smith, A. M. Butt and A. Thakur, *Analyst*, 1985, **110**, 35.
13. S. Inoue, S. Hoshi and M. Mathubara, *Talanta*, 1985, **32**, 44.
14. M. Kaniwa, *J. Chromatog.*, 1987, **405**, 263.
15. A. M. Bond and G. G. Wallace, *Anal. Chem.*, 1982, **54**, 1706.
16. Young-Tzung Shih and P. W. Carr, *Anal. Chim. Acta*, 1982, **142**, 55.
17. J. King and J. S. Fritz, *Anal. Chem.*, 1987, **59**, 703.
18. A. Munder and K. Ballschmiter, *Z. Anal. Chem.*, 1986, **323**, 869.
19. G. Schwedt and P. Schneider, *ibid.*, 1986, **325**, 116.
20. S. Leharne, *J. Chem. Educ.*, 1986, **63**, 727.
21. J. S. Kiel, S. L. Morgan and R. K. Abramson, *J. Chromatog.*, 1985, **320**, 313.
22. A. R. Timerbaev and O. M. Petrukhin, *Anal. Chim. Acta*, 1984, **159**, 229.
23. L. J. Bellamy, *The Infrared Spectra of Complex Molecules*, p. 401. Methuen, London, 1975



## THE SPECIATION OF TRACE AMOUNTS OF ORGANOMETALLICS IN MARINE ORGANISMS BY GEL-PERMEATION HIGH-PRESSURE LIQUID CHROMATOGRAPHY WITH PAR DERIVATIZATION\*

AMBROGIO MAZZUCOTELLI and ROBERTO FRACHE

Cattedra di Chimica Analitica, Istituto di Chimica Generale, Università di Genova, Genoa, Italy

ALDO VIARENGO

Istituto di Fisiologia Generale, Università di Genova, Genoa, Italy

GABRIELLA MARTINO

Istituto di Scienze Ambientali Marine, Università di Genova, Genoa, Italy

(Received 2 July 1986. Revised 22 March 1988. Accepted 23 April 1988)

**Summary**—A high-pressure liquid chromatograph equipped with an off-column colorimetric reactor was used for the determination of metallorganic compounds such as metallothioneins. The stainless-steel gel-permeation column used was first tested with ultraviolet detection of a standard protein mixture. The metallothioneins were determined by absorbance measurements at 520 nm after an off-column reaction of the metal-containing eluates with a buffered 4-(2-pyridylazo)resorcinol (PAR) solution. The eluates were also tested by flame and electrothermal atomic-absorption spectrometry; a correlation between AAS and ICP results and the peak areas of the colorimetric detection was also made. A zinc-inhibiting reagent was also added to the PAR solution in order to find the colorimetric error due to the presence of other metals such as copper or cadmium.

The molecular characterization, or speciation, of organometallic compounds in environmental samples has received increasing attention. These metal-containing substances occur at very low concentrations in highly polar solvents, such as biotic fluids or natural waters. Thus the necessity of determining the chemical form of the metal when examining the environmental impact of such compounds, has in recent years given an impetus to trace metal studies.<sup>1</sup> Several authors have studied different media from the point of view of the metallorganic speciation of trace elements.<sup>2-4</sup> A particular aspect is the study of the low molecular-weight (< ~ 6000) organometallic compounds called metallothioneins, which have been particularly studied in marine organisms inhabiting coastal and estuarine waters which can be exposed to elevated levels of trace metals through both biogeochemical processes and pollution. Whilst some trace metals are potentially toxic (*e.g.*, Cd, Ag, Pt, Hg, Pb and Cr) to marine organisms, others are essential in nutrition and growth (*e.g.*, Cu, Zn, Mn and Co).<sup>5,6</sup> Since metallothionein in mammals was initially described,<sup>7</sup> this low molecular-weight

sulphur-containing and metal-binding protein has been characterized as the primary protein responsible for trace-metal detoxification of both invertebrates and vertebrates.<sup>8,9</sup> In our laboratories, samples containing metallothioneins were early analysed on Sephadex gel-permeation macro-columns (100 cm length and 1.5 cm diameter) with fraction collection and determination of the metal by electrothermal atomization atomic-absorption spectrophotometry (ETA-AAS)<sup>10-13</sup> but such a procedure is time-consuming and does not allow direct recording of the elution. The use of a high-speed separation technique such as HPLC coupled with a high-resolution detection technique such as AAS has been suggested by several authors.<sup>1,14-17</sup>

Unfortunately, ETA-AAS, which would be the most useful technique owing to its high sensitivity, cannot be coupled in-line to the chromatograph, because it has a discontinuous sampling system. Suzuki and co-workers<sup>15-17</sup> have described the direct coupling of AAS with gel-permeation HPLC for metalloprotein determination in rat liver, but the technique cannot be described as a true HPLC separation: the initial use<sup>15</sup> of a gel-permeation column of large dimensions (2.1 × 60 cm), a sample volume of 200 or 1000 μl and a flow-rate of 3.5 ml/min is more similar to a classic than an HPLC separation; the flow-rate was later reduced to

\*This work was performed with a contribution from Gruppo Ricerche Oceanografiche Genova (GROG) and with the financial contribution of the Ministero Pubblica Istruzione (Fondi 40%) of Italy.

1 ml/min<sup>16,17</sup> but we have found that flame AAS for Cd and Zn at such flow values is less sensitive by a factor of 10 than our proposed colorimetric method of detection. Moreover, Suzuki and co-workers applied their method to animal samples (rat liver, rat kidney, quail liver, frog) which contain higher amounts of metallothioneins that our mussel samples do. For these reasons we think that a more economic (in equipment and sample) and more sensitive technique is needed to evaluate the metallothionein content of marine organisms such as mussels.

In another communication<sup>18</sup> we described an HPLC method with colorimetric detection with 4-(2-pyridylazo)resorcinol (PAR), which has been used for the HPLC separation and colorimetric detection of trace amounts of rare earths in phosphors and silicate rocks.<sup>19-21</sup>

### EXPERIMENTAL

#### Reagents

PAR solution (0.005%), buffered at pH 5.0 with an acetic acid-sodium acetate buffer (300 ml of 0.2M acetic acid plus 700 ml of 0.2M sodium acetate). PAR/masking-agent solution; prepared as above, plus 3% sodium pyrophosphate. Eluent: 0.05M potassium monohydrogen phosphate and potassium dihydrogen phosphate, adjusted to pH 7. Mercaptoethanol.

#### Apparatus

Laboratory Data Control (LDC) high-pressure liquid chromatograph, equipped with two isocratic pumps (models Constametric II and III); Rheodyne M 7125 injection valve (40- $\mu$ l loop); Perkin-Elmer LC5 variable wavelength spectrophotometric detector equipped with LC autocontrol; Kipp and Zonen B5 strip-chart recorder; LDC 10 calculating integrator; Waters Millipore gel-permeation column equipped with guard column, both filled with "I-125 Protein Analysis" recommended bulk material, (300 mm length, 9 mm bore).

#### Procedure

The samples were mussels (*Mytilus Galloprovincialis* Lam.) 4-6 cm long; they were exposed to a 0.1 ppm zinc environment for 4 days in a static sea-water system as described by Viarengo *et al.*<sup>12</sup> The digestive glands were removed from the mussels and homogenized in 4 volumes of 0.5M sucrose in 20mM Tris hydrochloride solution (pH 8.6) containing sodium chloride, 6  $\mu$ g of leupetin and 50mM phenylmethylsulphonyl fluoride (PMSF). The tissue debris was removed by centrifugation at  $2 \times 10^4$  rpm for 10 min. The supernatant liquid was heated at 60° for 10 min then the heat-stable fraction was applied directly to the gel-permeation column. Before the injection, one of the isocratic pumps was connected to the pH-7 eluent reservoir and the other to either the PAR solution or the PAR/masking-agent solution reservoir; both pumps were set to 1 ml/min constant flow, and started. The detector was set at 520 nm. After the system had been run for about 1 hr to stabilize all the fluxes, the sample was injected.

### RESULTS AND DISCUSSION

The chromatographic separation was first tested by passing through the gel-permeation column a standard mixture (ferritin, egg-albumin, ribonuclease and guanosine), to verify the molecular-weight distribution. Figure 1 shows this elution and that

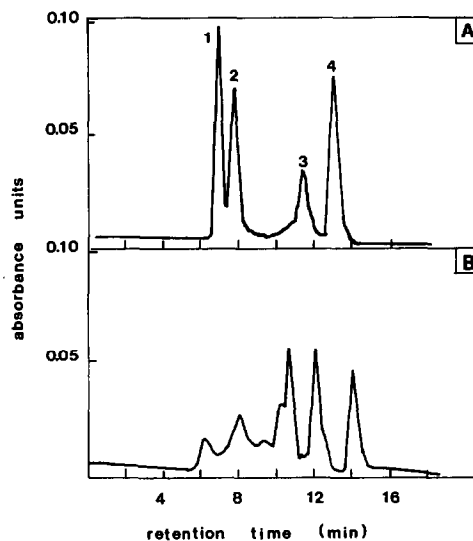


Fig. 1. HPLC-UV (280 nm) calibration profiles on gel-permeation chromatographic column. (A): standard mixture of proteins (1, ferritin, M.W.  $5.4 \times 10^5$ ; 2, egg-albumin, M.W.  $2.5 \times 10^4$ ; 3, ribonuclease, 4, guanosine, M.W. 280). (B): heat-treated cytosol fraction from mussel digestive gland.

performed under the same conditions for the analytical sample. To make the conditions completely comparable, when PAR was not needed in the detection system, eluent was pumped by the PAR pump at 1.00 ml/min, so that the eluate passed through the detector cell at the same speed whether PAR was used or not. The detection wavelength for the standard mixture was 280 nm. Figure 2 shows the

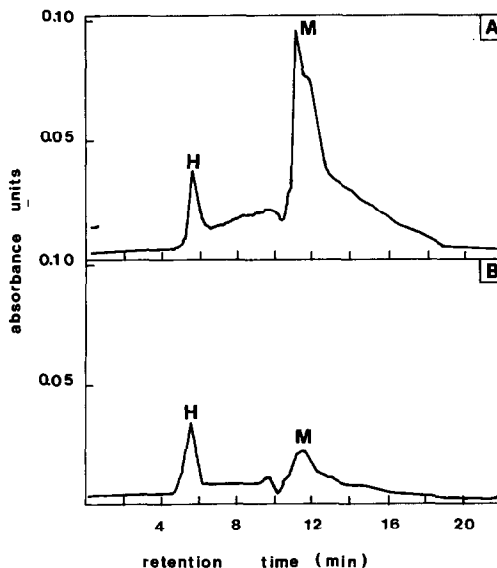


Fig. 2. HPLC (520 nm) elution profiles on gel-permeation chromatographic column. Enriched Zn-thionein fractions from mussel digestive gland. (A): after reaction with PAR solution, (B): after reaction with PAR-pyrophosphate zinc-inhibiting solution. H = high molecular-weight compounds; M = metallothioneins.

Table 1. Peak areas (mm<sup>2</sup>) and metal concentrations ( $\mu\text{g/ml}$ ) found by various methods for the HMWC and MT in mussel-gland extracts

	Glands	Tissues
HMWC		
Areas		
PAR	420	600
PAR + PY	400	580
Concs. (median value)		
Zn VIS-HPLC	0.15	0.42
Zn FAAS	0.13	0.38
Cu VIS-HPLC	0.09	0.10
Cu ETA-AAS	0.08	0.10
MT		
Areas		
PAR	400	3000
PAR + PY	100	500
Concs. (median value)		
Zn VIS-HPLC	0.41	1.08
Zn FAAS	0.33	1.20
Cu VIS-HPLC	0.05	0.26
Cu ETA-AAS	0.05	0.28

chromatograms for the same analytical sample, one for the reaction with PAR solution and the other for reaction with PAR/masking-reagent solution.

The test solution was prepared from zinc-enriched mussel glands as described in the experimental section. The peak for the zinc metallothioneins in chromatogram (A) is apparently not completely eliminated by use of the PAR/masking-reagent solution. The residual peak was shown by ETA-AAS to be due to copper present in the glands. Table 1 shows the relation between the chromatographic peak area and the zinc and copper concentrations found by FAAS or ETA-AAS (as appropriate). In the total collected fractions of high molecular-weight compounds (HMWC) and metallothioneins (MT) of the digestive gland cells and remaining total tissue, Zn was determined by flame AAS with an air-acetylene flame at 213.8 nm, and Cu by ETA-AAS at 324.8 nm. As can be observed, the peak related to the HMWC is the same whichever PAR reagent is used.

This effect cannot be ascribed to the copper content because this is too low to produce such a peak. The zinc content is also low, which suggests that the particular structure of these organic compounds may interfere with the inhibiting reaction. Injection of a 1000 ppm standard Zn solution showed that free ionic zinc is very strongly retained by the column. However, the correlations in Table 1 show that no dissociation of zinc metallothioneins appeared to take place. The Zn-PAR methods were compared with those in the literature.<sup>22-25</sup> The proposed method appears more sensitive and selective than the classical procedure based on macro-column separation with subsequent fraction collection and AAS determination, and is much faster, taking less than one hour, compared with about a day for the classical method. The HPLC-PAR method appears to

be more sensitive than the HPLC-AAS method. This is important because high sensitivity is needed to monitor separation of metallothioneins. From a biological point of view, the importance of the results is that it has never previously been demonstrated that Zn *per se* can stimulate the neosynthesis of metallothioneins in marine organisms. The Zn/Cu-binding proteins prepared from mussel tissues have been characterized, after purification by gel-filtration and ion-exchange chromatography, as typical of chelatin, but additional purification by denaturing polyacrylamide-gel electrophoresis was necessary to obtain a homogeneous copper-binding protein with the general characteristics of metallothioneins.<sup>12,26</sup> In addition, it has been demonstrated that the Cd/Zn-binding proteins isolated from mussel tissues belong to the class of metallothioneins. It is important to stress that Zn, which is always present in metallothioneins, can be displaced by exposure of the animals to metals such as Cu, Cd, Hg *etc.*, which have much stronger affinity than Zn for -SH residues.<sup>27</sup> Such data demonstrate that the metal content of MT is directly related to the concentrations of the different metals in the cytosol of the cells,<sup>13,28</sup> and that any increase in the zinc content of the extract cannot be due to displacement of other metals by zinc. Hence it is concluded that the effect of the zinc is to stimulate synthesis of the metallothioneins.

#### REFERENCES

1. S. Hill and L. Ebdon, *Eur. Spectrosc. News*, 1985, **58**, 20.
2. D. J. Mackey, *Mar. Chem.*, 1983, **13**, 169.
3. J. W. Foote and H. T. Delves, *Analyst*, 1983, **108**, 192.
4. *Idem, ibid.*, 1984, **109**, 709.
5. D. W. Engel and M. Brower, *Mar. Environ. Res.*, 1984, **13**, 177.
6. A. J. Zelarowsky, J. S. Garvej and J. D. Hoeschele, *Arch. Biochem. Biophys.*, 1984, **229**, 246.
7. M. Margoshes and B. Vallee, *J. Am. Chem. Soc.*, 1957, **79**, 4813.
8. J. H. R. Kagi and M. Nordberg (eds.), *Metallothionein*, Birkhauser, Boston, 1979.
9. G. Roesijadi, *Mar. Environ. Res.*, 1981, **4**, 167.
10. A. Viarengo, M. Pertica, G. Mancinelli, G. Zanichchi and M. Orunesu, *Comp. Biochem. Physiol.*, 1980, **67**, 215.
11. A. Viarengo, M. Pertica, G. Mancinelli, S. Palmero, G. Zanichchi and M. Orunesu, *Mar. Environ. Res.*, 1980, **4**, 145.
12. A. Viarengo, M. Pertica, G. Mancinelli, G. Zanichchi, G. Bioquegneau and M. Orunesu, *Mol. Physiol.*, 1984, **5**, 41.
13. A. Viarengo, *Mar. Poll. Bull.*, 1985, **16**, 153.
14. L. Brown, S. J. Haswell, H. M. Rhead, P. O'Neill and K. C. C. Bancroft, *Analyst*, 1983, **108**, 1511.
15. K. Y. Suzuki, *Anal. Biochem.*, 1980, **102**, 31.
16. K. T. Suzuki, H. Sunaga, Y. Aoki and M. Yamamura, *J. Chromatog.*, 1983, **281**, 159.
17. K. T. Suzuki, H. Sunaga and T. Yajima, *ibid.*, 1984, **303**, 131.
18. A. Mazzucotelli, A. Viarengo and R. Frache, *XV Congr. Naz. Soc. Chim. Ital.*, Grado (Italy), 1985.
19. A. Mazzucotelli, A. Dadone, R. Frache and F. Baffi, *Chromatographia*, 1982, **15**, 697.

20. A. Dadone, A. Mazzucotelli, R. Frache and F. Baffi, *Ann. Chim. (Rome)*, 1984, **74**, 289.
21. A. Mazzucotelli, A. Dadone, R. Frache and F. Baffi, *J. Chromatog.*, 1985, **349**, 137.
22. G. Goldstein, W. L. Maddox and M. T. Kelley, *Anal. Chem.* 1974, **46**, 485.
23. D. Nonova, V. Nonov and N. Lihareva, *Talanta*, 1976, **23**, 679.
24. F. D. Snell, *Photometric and Fluorometric Methods of Analysis*, Wiley, New York, 1978.
25. Q. Wenbin and Z. Lihong, *Talanta*, 1985, **32**, 1013.
26. A. Viarengo, M. Pertica, G. Mancinelli, G. Zanicchi, J. M. Boiquegneau and M. Orunesu, *Int. Symp. Acta*, 1983.
27. A. Viarengo, S. Palmero, G. Zanicchi, R. Capelli, R. Vaissiere and M. Orunesu *Mar. Environ. Res.*, 1985, **16**, 23.
28. S. G. George and A. Viarengo, *Mar. Poll. Physiol.*, recent advances 1985, 125.

## GOLD CHLORIDE ELECTRODES AS ELECTROCHEMICAL SENSORS FOR LIQUID CHROMATOGRAPHY

M. S. TUNULI

Department of Chemistry, California State University, Northridge, CA 91330, U.S.A.

(Received 25 November 1987. Revised 7 February 1988. Accepted 23 April 1988)

**Summary**—A fast, simple, inexpensive and reproducible method for the fabrication of a gold chloride electrode is presented. The response of this electrode is highly stable and it leads to improved detection for various redox species. Experiments demonstrating the utility of the gold chloride electrode as a sensitive sensor for liquid chromatography are described.

In everyday practice an analyst deals with the selective and sensitive detection of the components of mixtures that may be quite complex. Often, prior to detection, a chromatographic separation is needed, which dilutes the trace analytes. Thus there is always a need for better detection methods that are fast, sensitive, selective, and offer stable responses. One such method for use with liquid chromatography (LC) is electrochemical detection (ED). The hybrid of LC and ED (called LCED) combines the excellent selectivity of the chromatography and high sensitivity of electrochemical detection.<sup>1</sup> The selectivity of the detector itself, obtained by varying the potential, is usually poor, and for compounds which exhibit irreversible electrochemical behaviour (*i.e.*, compounds with slow charge-transfer kinetics at the electrode-solution interface) the sensitivity is also low. A useful approach for overcoming these difficulties involves modification of the electrode surface by physical, chemical, or electrochemical means.<sup>2-15</sup>

Most of the reported electrode-surface modifications were aimed at enhancing the reversibility to provide significant improvements in detection. Santos and Baldwin<sup>2</sup> showed that the overvoltage for oxidation of oxalic acid is reduced by 0.4 V by incorporation of cobalt phthalocyanine into a carbon-paste electrode. Improved response of carbon-paste electrodes for electrochemical detection after pretreatment with surfactants was demonstrated by Albahadily and Mottola.<sup>3</sup> One of the most interesting chemical modifications was reported by Price and Baldwin,<sup>4</sup> who used a platinum electrode modified with ferrocene carboxaldehyde for the determination of aromatic amines. In another novel approach Ravichandran and Baldwin<sup>5</sup> and Rice *et al.*<sup>6</sup> utilized electrochemical pretreatment to achieve electrocatalysis. Falat and Cheng, using an electrochemically treated graphite/epoxy electrode, have clearly demonstrated a voltammetric differentiation between ascorbic acid and dopamine.<sup>7</sup>

The prime requirements of a sensor for routine use with LC are: (1) fast and simple fabrication, (2) stable

and highly reproducible response, and (3) enhancement of selectivity and sensitivity. This paper reports the fabrication of a gold chloride electrode and its utility as a sensitive electrochemical sensor in LC. The results indicate that the electrode has most of the attributes of a good sensor for voltammetric analysis.

### EXPERIMENTAL

#### Apparatus

For cyclic voltammetry a PAR Model 173 potentiostat-galvanostat was used in conjunction with a PAR Model 175 universal programmer. A BAS voltammetry gold electrode (0.02 cm<sup>2</sup> area), a BAS model RE-1 Ag/AgCl electrode and a platinum wire were used as working, reference and counter electrodes, respectively.

The LC system consisted of a Beckman model 110 pump, an Altex model 210 injector with 20- $\mu$ l loop, a Biophase ODS 3  $\mu$ m phase 2 analytical column (100  $\times$  3 mm) and a BAS model LC4B/17AT electrochemical detector. The electrochemical transducer employed a BAS gold working electrode, a BAS model RE-4 Ag/AgCl/gel reference electrode, a stainless-steel counter-electrode and a BAS model TG-2M Teflon gasket. The mobile phase consisted of 0.05M monochloroacetic acid containing 15 mg/l. sodium octylsulphate and 150 mg/l. Na<sub>2</sub>EDTA. The detector temperature was set at 25°.

#### Reagents

Sodium octylsulphate (Sigma), L(+)-ascorbic acid (M&B) and Na<sub>2</sub>EDTA (Fisher) were used as received. All solutions were prepared by dissolving the reagents in 0.1M sulphuric acid or the mobile phase, and were made up just before use. The mobile phase was filtered through a 0.22- $\mu$ m Durapore membrane (Millipore). 3,4-Dihydroxybenzylamine (DHBA) and sodium sulphide 9-hydrate were purchased from BAS and M&B respectively.

#### Modification procedure

Prior to use, all electrodes were hand-polished to a mirror finish on a pad of microcloth (Buehler) by sequential use of 1- $\mu$ m and 0.3- $\mu$ m alumina suspensions (Buehler micropolish II). They were then cleaned ultrasonically for 10 min, with frequent changes of water. Polished electrodes were either used unmodified or were modified as follows. The electrodes were placed in 0.37M HCl and subjected over a period of 300 sec to oxidation-reduction cycles from 0.0 to 1.15  $\pm$  0.05 V (the anodic limit cannot be extended beyond 1.2 V because the onset of chlorine evolution prevents the formation of a smooth and reproducible gold chloride film)

at a scan-rate of 100 mV/sec in the anodic direction and 1100 mV/sec in the cathodic direction, the first cycle being initiated, and the last terminated, at +0.4 V. Since attachment of gold chloride mainly takes place at the higher positive potentials, *i.e.*, towards the end of the anodic scan, a slow forward (anodic) scan ensures a fixed deposition time, and a fast cathodic reversal reduces the desorption time. The net result is the formation of a smooth and reproducible chloride film on the gold electrode. This film is visible as a glassy copper-coloured layer.

## RESULTS AND DISCUSSION

Cyclic voltamperograms (CVs) obtained with the gold chloride electrode in 0.1M sulphuric acid with and without 1 mM ascorbic acid are shown in Fig. 1. For comparison Fig. 2 shows CVs obtained with an unmodified gold electrode in corresponding conditions. These cyclic voltamperograms clearly demonstrate that the heterogeneous electron-transfer rates for ascorbic acid have been significantly increased by the chloride film electrochemically deposited on the gold electrode. Significant differences in the shapes of

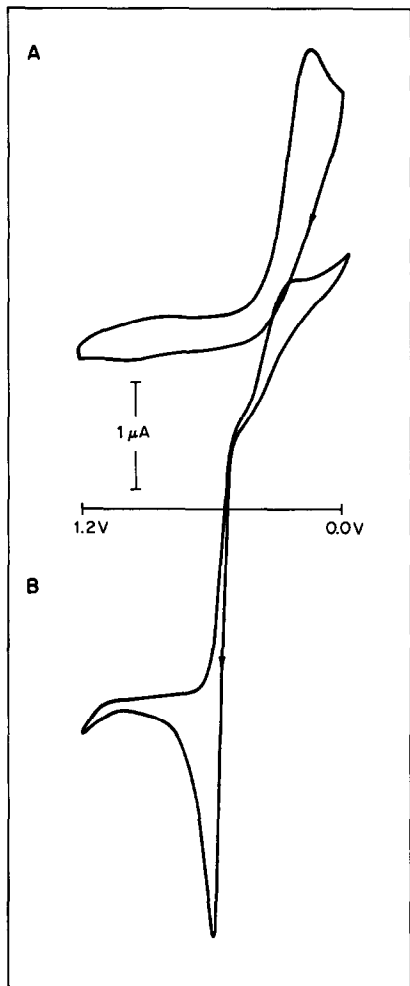


Fig. 1. Cyclic voltamperograms of 0.1M  $\text{H}_2\text{SO}_4$  (A) and 1mM ascorbic acid dissolved in 0.1M  $\text{H}_2\text{SO}_4$  (B) at an AuCl electrode. Scan-rates were 50 mV/sec (A) and 10 mV/sec (B).

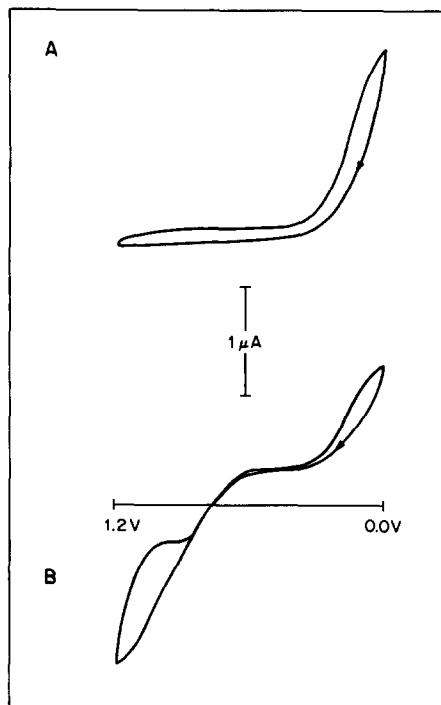


Fig. 2. Cyclic voltamperograms of 0.1M  $\text{H}_2\text{SO}_4$  (A) and of 1mM ascorbic acid dissolved in 0.1M  $\text{H}_2\text{SO}_4$  (B) at a gold electrode. Scan-rates were 50 mV/sec (A) and 10 mV/sec (B).

the CVs obtained with the modified and unmodified electrodes in 0.1M sulphuric acid are a clear demonstration that the modification procedure indeed led to the desired surface alteration. Amperometric, flame-emission, ion-chromatography, and Raman scattering experiments (to be described elsewhere) have unequivocally demonstrated the presence of gold chloride on the modified surface. In the Raman experiments, for example, the modified electrode gives a well-defined Raman band centred at  $265\text{ cm}^{-1}$  at an applied potential of +0.8 V *vs.* Ag/AgCl. This band is not given by the unmodified electrode, and corresponds to the gold-chloride stretching mode.<sup>16</sup>

As shown in Figs. 1B and 2B, when ascorbic acid is oxidized at the gold chloride electrode, there is a 600 mV cathodic shift in the anodic peak and the current is enhanced compared with the results for the unmodified electrode. The analytical advantages associated with these observations are enhanced sensitivity (increased current) and improved selectivity (potential shift). Furthermore, the potential shift allows the use of extremely low detection potentials where fewer species are expected to interfere. A further minimization of interferences is associated with the fact that the oxidation peak at the AuCl electrode is narrower and sharper than the corresponding peak at the unmodified electrode. Thus, interferences can be easily "tuned-out" at the modified electrode. Similar results were obtained for DHBA (Fig. 3) and sulphide (Fig. 4).

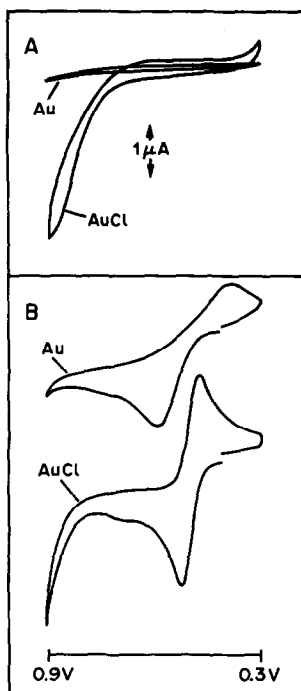


Fig. 3. Cyclic voltamperograms of Au and AuCl in the LC mobile phase without (A) and with (B)  $5.0 \times 10^{-4} M$  DHBA. Scan-rate 10 mV/sec.

The hydrodynamic voltamperograms of 1mM ascorbic acid dissolved in the LC mobile phase are shown in Fig. 5 for AuCl and Au electrodes. As expected from the CVs above, the modified electrode exhibits a plateau current at substantially lower potentials than the unmodified electrode. Furthermore, to establish the superior performance of the AuCl electrode in amperometric detection after liquid chromatography of ascorbic acid, the chromatographic

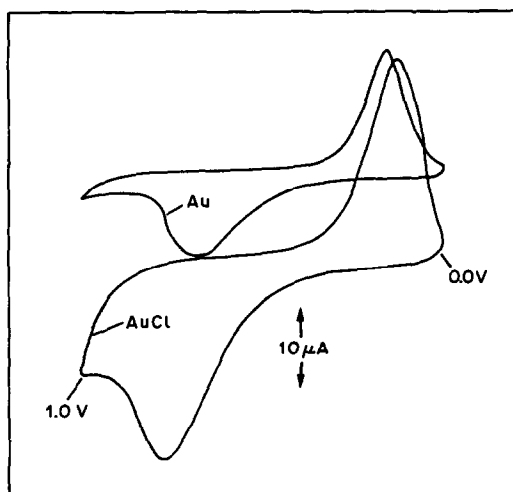


Fig. 4. Cyclic voltamperograms of Au and AuCl electrodes in 0.005M NaOH containing  $1.0 \times 10^{-4} M$   $Na_2S \cdot 9H_2O$ . Scan-rate 100 mV/sec. The anodic peak on the left clearly indicates catalysis of the sulphide oxidation at the AuCl electrode.

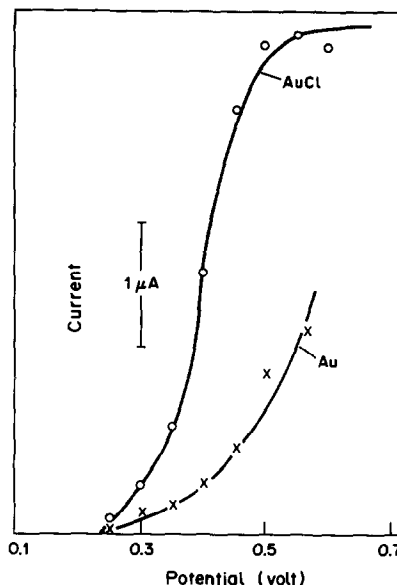


Fig. 5. Hydrodynamic voltamperograms for 5-nmole injections of ascorbic acid (dissolved in mobile phase) at Au and AuCl electrodes.

peak heights obtained at the two electrodes at an applied potential of 0.45 V were compared. The peak height with the AuCl electrode was about six times that with the Au electrode.

To be useful for routine analysis, the response of the modified electrode should be stable over an extended period of time. Excellent stability of the AuCl electrode in 36 successive cycles between 0.0 and 1.0 V in a solution of 1mM ascorbic acid in 0.1M sulphuric acid was observed. Similar stability was observed for 1mM ascorbic acid dissolved in the mobile phase. Furthermore, in LCED experiments the mobile phase that flows past the electrode has excellent cleaning power, which further enhances the stability of the electrode response. Thus for 25 repetitive injections of 0.2 nmole ascorbic acid the stability of the response at an applied potential of 0.45 V had a relative standard deviation of 5%. By and large, the stability of the AuCl electrode response seems excellent.

In conclusion, a fast, simple, reproducible, and inexpensive method for the fabrication of AuCl electrodes is reported. The stability of the response of these electrodes is excellent for cyclic voltammetric and LCED experiments. The modified electrode catalyses the oxidation of ascorbic acid and therefore leads to its improved electrochemical detection after liquid chromatography.

*Acknowledgements*—This work was supported by the California State University Foundation, Northridge. I wish to thank Mr Louis Armendariz for checking the reproducibility of the work presented here.

#### REFERENCES

1. P. T. Kissinger, *Anal. Chem.*, 1977, **49**, 447A.

2. L. M. Santos and R. P. Baldwin, *ibid.*, 1986, **58**, 848.
3. F. N. Albahadily and H. A. Mottola, *ibid.*, 1987, **59**, 958.
4. J. F. Price and R. P. Baldwin, *ibid.*, 1980, **52**, 1940.
5. K. Ravichandran and R. P. Baldwin, *ibid.*, 1984, **56**, 1744.
6. M. E. Rice, Z. Galus and R. N. Adams, *J. Electroanal. Chem.*, 1983, **143**, 89.
7. L. Falat and H.-Y. Cheng, *Anal. Chem.*, 1982, **54**, 2108.
8. F. G. Gonon, C. M. Fombarlet, M. J. Buda and J. F. Pujol, *ibid.*, 1981, **53**, 1386.
9. J. Wang and P. Tuzhi, *ibid.*, 1986, **58**, 1787.
10. J. Wang and B. Freiha, *ibid.*, 1984, **56**, 2266.
11. C. Urbaniczky and K. Lundstrom, *J. Electroanal. Chem.*, 1984, **176**, 169.
12. M. K. Halbert and R. P. Baldwin, *Anal. Chim. Acta*, 1986, **187**, 89.
13. J. Zak and T. Kuwana, *J. Electroanal. Chem.*, 1983, **150**, 645.
14. J. A. Cox and M. Majda, *Anal. Chem.*, 1980, **52**, 861.
15. R. F. Lane and A. T. Hubbard, *ibid.*, 1976, **48**, 1287.
16. B. H. Loo, *J. Phys. Chem.*, 1982, **86**, 433.



## UNTERSUCHUNGEN ZUR ANWENDUNG TERNÄRER KOMPLEXE IN DER PHOTOMETRIE—V

### SPEKTRALPHOTOMETRISCHE BESTIMMUNG UND NACHWEIS VON PHENOLEN MIT $\text{FeY}^-$ ( $\text{H}_4\text{Y} = \text{EDTE}$ )

S. KOCH, G. ACKERMANN und I. BRUNNE

Sektion Chemie, Bergakademie Freiberg, 9200 Freiberg, DDR

(Eingegangen am 11. November 1987. Revidiert am 20. Januar 1988. Angenommen am 23. April 1988)

**Zusammenfassung**—Zur Bewertung der Verwendbarkeit ternärer Komplexe in der Photometrie organischer Verbindungen wurden Systeme Eisen(III)/EDTE/Phenol mit Unterschub sowie Überschub an Phenolen nach gegebenen Arbeitsvorschriften analytisch charakterisiert. Neben der Ermittlung der Kennzahlen Arbeitsbereich, relative Standardabweichung, Eichfunktion und Korrelationskoeffizient erfolgte auch eine Untersuchung der entsprechenden Nachweisreaktionen (Erfassungsgrenze bzw. Empfindlichkeitsexponent). Es zeigte sich, daß Phenole mit isolierter OH-Gruppe gegenüber der *o*-OH-Gruppierung weniger empfindlich reagieren.

**Summary**—To assess the usefulness of ternary complexes in the photometry of organic compounds, iron(III)/EDTA/phenol systems with a deficit or excess of phenol were examined analytically under different conditions. Besides determination of the working range, relative standard deviation, calibration function and correlation coefficient, an investigation was made of the corresponding qualitative reactions (detection limit and sensitivity exponent). It was found that phenols with an isolated OH-group gave less sensitive reactions than those with *o*-OH-groups.

Im Rahmen systematischer Untersuchungen zur Anwendung ternärer Komplexe in der Photometrie<sup>1</sup> konnte nachgewiesen werden, daß dieser Komplexotyp auch in der organischen Analyse von Bedeutung sein kann. Wie sich am Beispiel der häufig auftretenden aromatischen funktionellen Hydroxylgruppe  $-\text{OH}$  zeigen läßt, treten mit Eisen(III) in Gegenwart von Ethylendiamintetraessigsäure (EDTE,  $\text{H}_4\text{Y}$ ) analytisch wertvolle Reaktionen auf. Das Chelat  $\text{FeY}^-$  bildet dabei mit Phenolen je nach deren Struktur farbige ternäre oder binäre Komplexe, welche die Ausarbeitung von Nachweis- oder Bestimmungsverfahren gestatten. Vom analytischen Standpunkt aus ist diese Variante den bisherigen Reaktionen mit einfachen binären Komplexen überlegen.

In der vorliegenden Arbeit soll deshalb über Ergebnisse zur spektralphotometrischen Bestimmung und zum Nachweis einiger typischer Phenole mit dem Reagens  $\text{FeY}^-$  berichtet werden.

#### EXPERIMENTELLES

Die photometrischen Messungen erfolgten mit einem Beckman Spektralphotometer DU, und zur Kontrolle der pH-Werte diente ein pH-Meter MV 88 (VEB Präcitrone, Dresden). Für die Herstellung der 1M Eisen-Stammlösung (0,1M an  $\text{HClO}_4$ , gravimetrisch kontrolliert) wurde  $\text{Fe}(\text{NO}_3)_3 \cdot 9\text{H}_2\text{O}$  (p.a. Reachim, UdSSR) verwendet. Als Eichlösungen, welche täglich frisch hergestellt wurden, ka-

men methanolische Lösungen (maximal 5 ml/Probe) zum Einsatz. Für die Lösungen der EDTE fand  $\text{Na}_2\text{H}_2\text{Y} \cdot 2\text{H}_2\text{O}$  (rein, VEB Feinchemie Sebnitz) Verwendung. Alle verwendeten Phenole waren handelsübliche Produkte; ihre Reinheit wurde nach Umkristallisation durch Schmelzpunkt bzw. Brechungsindex sowie Elementaranalyse kontrolliert. Die Messungen erfolgten in Abhängigkeit von der Löslichkeit der Phenole in Wasser oder Methanol/Wasser (50 Vol. %).

#### KOMPLEXBILDUNG IM SYSTEM EISEN(III)/EDTE/PHENOL

Wegen der unterschiedlichen komplexchemischen Eigenschaften von Phenolen mit isolierter Hydroxylgruppe oder mit der *o*-OH-Gruppierung gibt es eine Reihe von Koordinationsmöglichkeiten, die im folgenden kurz erörtert werden sollen. Zur Beschreibung der Gleichgewichte,<sup>2-8</sup> welche mit Hilfe physikalisch-chemischer Methoden (Spektralphotometrie, Papierelektrophorese) aufgeklärt wurden, sollen nachstehende Symbole dienen:  $\text{H}_4\text{Y}$ (EDTE),  $\text{H}_n\text{R}$ (Phenole).

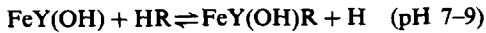
Die Gleichgewichte gelten für Systeme (Wasser bzw. Methanol/Wasser) mit EDTE-Überschub ( $C_Y/C_{\text{Fe}} = 5$ ) und einer Ionenstärke von  $I = 0,1$  ( $\text{NaClO}_4$ ).

#### Die isolierte OH-Gruppe

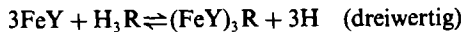
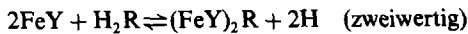
Zur Bildung ternärer Komplexe\* kommt es neben  $\text{FeY}^-$  hauptsächlich mit dem davon abgeleiteten

\*Die Ladungen sollen hierbei unberücksichtigt bleiben.

Teilchen  $[\text{FeY}(\text{OH})]^{2-}$ :

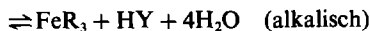
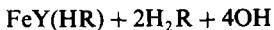
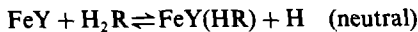


Der jeweilige Mechanismus wird dabei durch die Säure-Base-Eigenschaften der Phenole und somit vom pH-Wert des Mediums festgelegt. Während es sich mit  $\text{FeY}^-$  um eine Anlagerungsreaktion des Liganden  $\text{R}^-$  handelt, stellt die zweite Variante eine innerkomplexe Verdrängungsreaktion einer Carboxylatgruppe des  $\text{Y}^{4-}$  aus der Koordinationssphäre dar. Die angegebenen einfachen Reaktionen, welche für ein-, zwei- und dreiwertige Phenole zutreffen, laufen dabei aber nur in Systemen mit Phenolüberschuß ab. Bei  $\text{FeY}$ -Überschuß kommt es mit mehrwertigen Phenolen auch zur Bildung zwei- bzw. dreikerniger Species.<sup>9</sup>

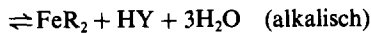
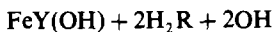
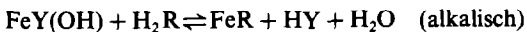


#### Die o-OH-Gruppierung

Die Bildung ternärer Species stellt hierbei eine Anlagerungsreaktion des Liganden  $\text{HR}^-$  dar, wobei folgende Reaktionen ablaufen:



Da die Komplexe  $\text{FeY}(\text{HR})$  aus verschiedenen Gründen zur analytischen Anwendung nicht geeignet sind,<sup>1</sup> kommen hierfür die entsprechenden binären Chelate ( $\text{FeY}$ -Überschuß)



in Frage.

#### Statistische Bewertung

Zur Festlegung des Arbeitsbereiches wurde als untere Grenze  $A = 0,05$  und als obere Grenze  $A = 1,5$  bzw. der Bereich bis zum Abknicken der Eichfunktion festgelegt. Die Berechnung des Schätzwertes der Standardabweichung mittlerer Konzentrationen ( $A \approx 0,4$ ) mit  $f = 20$  Freiheitsgraden erfolgte wie üblich nach

$$s_{\text{rel}} = \frac{100 \sqrt{\frac{\sum (A_i - \bar{A})^2}{(n-1)}}}{\bar{A}} \%$$

Bei der Ermittlung der Eichfunktionen (Korrelationskoeffizient  $r$ ) mittels Regressionsanalyse mit  $f = 8$  Freiheitsgraden wurde von der Geradengleichung

$$A = bc + a$$

bzw. für gekrümmte Eichfunktionen von einem Polynom zweiten Grades

$$A = b_0 + b_1c + b_2c^2$$

ausgegangen.

Die Charakterisierung der Nachweisreaktionen erfolgte mit Hilfe der Erfassungsgrenze als kleinste noch sicher nachweisbare Menge (Arbeitsvolumen: 1 ml) und des Empfindlichkeitsexponenten:

$$D = \frac{\text{Erfassungsgrenze } [\mu\text{g}]}{\text{Arbeitsvolumen } [\text{ml}] \times 10^6}$$

$$\text{p}D = -\lg D$$

#### ERGEBNISSE

Aus den komplexchemischen Eigenschaften der Systeme  $\text{FeY}/\text{R}$  lassen sich nun mehrere Varianten zum Nachweis sowie zur Bestimmung von Phenolen ableiten.

#### Phenole mit isolierter OH-Gruppe

Für diesen Analyttyp ergeben sich zwei Möglichkeiten zur spektralphotometrischen Bestimmung. Während man bei der ersten Variante (lineare Eichfunktion) mit  $\text{FeY}$ -Überschuß arbeitet, erfordert die zweite (gekrümmte Eichfunktion) einen Analytüberschuß. Bei der zweiten Variante liegt der seltene Fall vor, daß sich der Komplex nicht vollständig bildet.

#### Arbeitsvorschriften

*Variante mit  $\text{FeY}$ -Überschuß.* Zu 25 ml einer 0,4M EDTE-Lösung ( $\text{pH} = 10$ ) gibt man unter Rühren 2 ml einer 1M Eisen(III)-Lösung (0,1M an  $\text{HClO}_4$ ) und 10 ml Analyt-Lösung entsprechend des Arbeitsbereiches. Die Einstellung des pH-Wertes erfolgt mit Ammoniak sowie mit Perchlorsäure geeigneter Konzentration. Nach Überführung der Lösung in einen 50-ml Meßkolben und Auffüllen mit dem Lösungsmittel wird die Probe gegen eine Vergleichsprobe ohne Analyt, nach einer Stunde, bei  $d = 1$  cm gemessen.

*Variante mit Phenol-Überschuß.* Zu 5 ml einer 0,05M EDTE-Lösung ( $\text{pH} = 10$ ) gibt man unter Rühren 1 ml einer 0,05M Eisen(III)-Lösung (0,05M an  $\text{HClO}_4$ ) und 10 ml Analyt-Lösung entsprechend dem Arbeitsbereich. Die Einstellung des pH-Wertes erfolgt mit verd. Ammoniak bzw. Perchlorsäure. Nach Überführung der Lösung in einen 50-ml Meßkolben und Auffüllen mit dem Lösungsmittel wird die Probe nach einer Stunde gegen Wasser bei  $d = 1$  cm gemessen. Die Meßparameter dazu sowie die ermittelten Kennzahlen beider Varianten sind in den Tabellen 1 und 2 zusammengestellt.

#### Phenole mit o-OH-Gruppierung

Bei solchen Phenolen ist nur die Variante mit  $\text{FeY}$ -Überschuß geeignet, weil sonst wegen der vollständigen Bildung des Chelates  $\text{FeR}_3$  keine

Tabelle 1. Spektralphotometrische Bestimmungen mit FeY-Überschuß (isolierte OH-Gruppe)

Analyt	Medium	$\lambda_{\max}$ , nm	pH <sub>max</sub>	Arbeitsbereich, mg	$s_{\text{rel}}$ , % (mg)*	Eichfunktion†	$\epsilon'$ , l.mole <sup>-1</sup> .cm <sup>-1</sup>	r
Phenol	H <sub>2</sub> O	520	8,0	2–110	1,24 (25)	$b = 0,0136$ $a = 0,020$	68	0,9999
2-Chlorphenol	H <sub>2</sub> O	510	7,4	1–50	1,67 (15)	$b = 0,0302$ $a = 0,054$	211	0,9989
4-Chlorphenol	H <sub>2</sub> O	525	7,8	4–80	0,99 (25)	$b = 0,0193$ $a = -0,017$	119	0,9995
2-Cresol	H <sub>2</sub> O	530	8,5	4–130	1,45 (30)	$b = 0,0113$ $a = 0,005$	68	0,9999
3-Cresol	H <sub>2</sub> O	520	8,3	4–120	0,69 (40)	$b = 0,0124$ $a = 0,004$	66	0,9998
4-Cresol	H <sub>2</sub> O	530	8,1	5–100	0,88 (30)	$b = 0,0147$ $a = -0,018$	81	0,9999
2,5-Xylenol	CH <sub>3</sub> OH	540	8,8	8–180	1,34 (60)	$b = 0,0082$ $a = -0,011$	47	0,9999
Resorcinol	H <sub>2</sub> O	520	7,8	2–60	1,00 (20)	$b = 0,0250$ $a = 0,000$	137	0,9998
Phloroglucinol	H <sub>2</sub> O	515	7,4	1–60	4,25 (15)	$b = 0,0258$ $a = 0,059$	191	0,9995
1-Naphthol	CH <sub>3</sub> OH	610	8,6	4–90	1,16 (25)	$b = 0,0170$ $a = -0,007$	120	0,9987
2-Naphthol	CH <sub>3</sub> OH	550	8,4	4–130	1,65 (30)	$b = 0,0116$ $a = 0,002$	85	0,9999

\*Probekonzentration.

†Lineare Regressionsanalyse,  $A = bc + a$ ;  $c = [\text{Analyt}]$  (mg/50 ml).

Tabelle 2. Spektralphotometrische Bestimmungen mit Phenol-Überschuß (isolierte OH-Gruppe)

Analyt	Medium	$\lambda_{\max}$ , nm	pH <sub>max</sub>	Arbeitsbereich, M	$s_{\text{rel}}$ , % (M)*	Eichfunktion†	r
Phenol	H <sub>2</sub> O	495	8,7	0,005–0,1	1,31 (0,05)	$b_0 = 0,0164$ $b_1 = 8,23$ $b_2 = -20,15$	0,9998
2-Chlorphenol	CH <sub>3</sub> OH	490	8,6	0,002–0,1	0,37 (0,05)	$b_0 = 0,0310$ $b_1 = 15,31$ $b_2 = -59,83$	0,9986
4-Chlorphenol	CH <sub>3</sub> OH	500	8,8	0,001–0,1	0,73 (0,05)	$b_0 = 0,0132$ $b_1 = 11,70$ $b_2 = -33,32$	0,9996
2-Cresol	CH <sub>3</sub> OH	520	9,2	0,009–0,1	1,21 (0,05)	$b_0 = 0,0056$ $b_1 = 5,29$ $b_2 = -10,72$	0,9986
3-Cresol	CH <sub>3</sub> OH	500	9,2	0,007–0,1	0,80 (0,05)	$b_0 = 0,0048$ $b_1 = 6,03$ $b_2 = -12,51$	0,9988
4-Cresol	CH <sub>3</sub> OH	520	9,0	0,006–0,1	0,82 (0,05)	$b_0 = 0,0084$ $b_1 = 6,42$ $b_2 = -12,18$	0,9996
2,5-Xylenol	CH <sub>3</sub> OH	530	9,6	0,006–0,1	0,62 (0,05)	$b_0 = -0,0035$ $b_1 = 6,26$ $b_2 = -15,70$	0,9988
Resorcinol	H <sub>2</sub> O	500	8,4	0,002–0,1	0,82 (0,05)	$b_0 = 0,0255$ $b_1 = 14,35$ $b_2 = -51,17$	0,9992
Phloroglucinol	H <sub>2</sub> O	505	8,1	0,002–0,1	0,91 (0,05)	$b_0 = 0,0373$ $b_1 = 15,53$ $b_2 = -60,52$	0,9991
1-Naphthol	CH <sub>3</sub> OH	600	9,3	0,004–0,1	1,13 (0,05)	$b_0 = 0,0194$ $b_1 = 12,65$ $b_2 = -40,99$	0,9982
2-Naphthol	CH <sub>3</sub> OH	550	9,2	0,003–0,1	1,06 (0,05)	$b_0 = 0,0038$ $b_1 = 11,14$ $b_2 = -34,35$	0,9993

\*Probekonzentration.

†Gekrümmte Eichfunktion  $A = b_0 + b_1c + b_2c^2$ ;  $c = [\text{Analyt}]$  (M).

Tabelle 3. Spektralphotometrische Bestimmungen mit FeY-Überschuß (*o*-OH-Gruppierung, Medium: H<sub>2</sub>O)

Analyt	Zeit, min	Arbeitsbereich, mg	$\epsilon'$ , l. mole <sup>-1</sup> . cm <sup>-1</sup>	$S_{rel}$ , %	Eichfunktion*	<i>r</i>
Brenzcatechin	60	0,1–4,5	2010	1,10	$b = 0,3241$ $a = 0,019$	0,9997
4-Nitrobrenzcatechin	30	0,1–8,3	1520	0,74	$b = 0,1748$ $a = 0,050$	0,9994
Tiron	120	0,5–25,0	1400	1,40	$b = 0,0512$ $a = 0,157$	0,9891
Gallussäure	60	1,0–9,4	1220	1,39	$b = 0,1749$ $a = -0,139$	0,9994
Pyrogallolcarbonsäure	30	0,9–7,3	1510	1,64	$b = 0,2296$ $a = -0,17$	0,9995
2,3-Dihydroxynaphthalen	60	0,1–3,0	3810	0,85	$b = 0,4748$ $a = 0,002$	0,9999

\* $A = bc + a$ ;  $c = [\text{Analyt}]$  (mg/50 ml).

Abhängigkeit  $A = f(C_A)$  resultiert ( $C_A = \text{Analytkonzentration}$ ).

*Arbeitsvorschrift.* Zu 25 ml einer 0,4M EDTE-Lösung (pH = 10) gibt man unter Rühren 2 ml einer 1M Eisen(III)-Lösung (0,1M an HClO<sub>4</sub>). Zur Verhinderung der Oxydation der Phenole durch Luftsauerstoff setzt man der Lösung eine Spatelspitze Natriumsulfit zu. Anschließend wird der pH-Wert mit verd. Ammoniak und Perchlorsäure auf etwa 9 gebracht, und es erfolgt entsprechend des Arbeitsbereiches die Zugabe von 10 ml Analyt-Lösung. Nach Einstellung des pH-Wertes auf 9,0 überführt man die Lösung in einen 50-ml Meßkolben und füllt mit Wasser auf. Die Probe wird bei 600 nm und  $d = 1$  cm gegen eine Vergleichsprobe ohne Analyt nach entsprechender Reaktionszeit gemessen.

Tabelle 3 enthält die einzelnen Reaktionszeiten sowie die dazugehörigen Kennzahlen.

#### Nachweisreaktionen

Wie bereits dargelegt, reagiert das Chelat FeY<sup>-</sup> mit Phenolen je nach deren Struktur zu unterschiedlichen Koordinationsverbindungen. Da es sich bei allen diesen Teilchen um Komplexe mit intensiven Charge-Transfer-Banden im sichtbaren Spektralbereich

handelt, sind diese Reaktionen als Nachweisreaktionen für Phenole geeignet.

*Arbeitsvorschrift.* In einem Halbmikroreagenzglas gibt man zur neutralen Probelösung (maximal 1 ml) 1 ml Reagens ( $C_{Fe} = 0,02M$ ,  $C_{EDTE} = 0,04M$ , pH = 8,5) und vergleicht den Ansatz mit einer Reagens-Probe.

Die nach der angegebenen Vorschrift für eine Reihe von Phenolen ermittelten Kennzahlen enthält Tabelle 4.

#### DISKUSSION

Das Chelat FeY<sup>-</sup> stellt praktisch ein universelles Reagens für Phenole unterschiedlicher Struktur dar, wobei gegenüber den klassischen Reaktionen mit Eisen(III) die schon beschriebenen Vorteile<sup>1</sup> bestehen.

Bei den hier untersuchten Reaktionen mit FeY findet man generell eine höhere Selektivität. So zeigen Oxime, Alkohole, Carbonsäuren, Aminosäuren, aromatische Amine und viele Enole keine Farbreaktionen. Nach den vorliegenden Ergebnissen wird jedoch deutlich, daß die angegebenen Verfahren auf Einzelbestimmungen beschränkt bleiben. Dabei stören *o*-Diphenole die Bestimmung einfacher Phenole stark. Andererseits findet man für *o*-Diphenole

Tabelle 4. Nachweis von Phenolen mit FeY

Analyt	Farbe	Erfassungsgrenze, $\mu\text{g}$	pD-Wert
Phenol	orange	268	3,6
2-Chlorphenol	weinrot	30	4,5
4-Chlorphenol	weinrot	67	4,2
2-Cresol	rot	318	3,5
3-Cresol	weinrot	69	4,2
4-Cresol	rot	209	3,7
2,5-Xylenol	rot	238	3,6
Resorcinol	weinrot	318	3,5
Hydrochinon	violett	176	3,7
Phloroglucinol	weinrot	295	3,5
1-Naphthol	türkis	318	3,5
2-Naphthol	rosa	223	3,6
Brenzcatechin	grün	13	4,9
Tiron	blau	35	4,4
Pyrogallol	violett	16	4,8
Gallussäure	violett	18	4,7
2,3-Dihydroxynaphthalen	violett	5	5,3
Chromotropsäure	grün	318	3,5

durch Phenole mit isolierter OH-Gruppe nur eine geringe Überlagerung. Da die Komplexbildung nicht nur durch die phenolischen OH-Gruppen bestimmt wird, sondern eine Funktion des gesamten Moleküls darstellt, ist auch eine Summenbestimmung nicht möglich.

Die Empfindlichkeit der einzelnen Varianten wird naturgemäß vom Mechanismus der dazugehörigen Reaktionen bestimmt. Während die Variante (isolierte OH-Gruppe) bei Phenolüberschuß mit nicht-linearer Kalibrationsfunktion für hohe, die mit FeY-Überschuß für mittlere Konzentrationen geeignet ist, erlaubt das Verfahren zur Bestimmung von Phenolen mit der *o*-OH-Gruppierung die Erfassung kleiner Gehalte. Die Ursache für diese höhere Empfindlichkeit, welche auch bei den Nachweisreaktionen zu sehen ist, liegt in der binären Komplexbildung mit zweizähligen Phenolliganden und der damit verbundenen hohen Übergangswahrscheinlichkeit. Phenole mit isolierter OH-Gruppe bilden dagegen ternäre Species mit einzähligen wirksamen Liganden, deren Reaktionen deshalb weniger empfindlich sind. Wie man den Steigungen der Eichfunktionen und den *pD*-Werten entnehmen kann, werden die Reaktionen in üblicher Weise<sup>9</sup> durch Substituenten im aromatischen System aufgrund von Induktions- sowie Mesomerieeffekten beeinflusst. Interessant ist in diesem Zusammenhang das Verhalten der Chromotropsäure als Verbindung mit Hydroxylgruppen in *peri*-Stellung. Der für Liganden mit benachbarten OH-Gruppen kleine Empfindlichkeitsexponent von

$pD = 3,5$  sowie komplexchemische Untersuchungen<sup>9</sup> machen deutlich, daß hier der ternäre Komplex  $[\text{FeY}(\text{OH})\text{R}]^{6-}$  wegen eines extrem stabilen Protonenchelates und der damit verbundenen Einschränkung der Zweizähligkeit keine Bildung binärer Species  $\text{FeR}_n$  zuläßt.

Vom Vorteil ist das Reagens FeY auch für die Präzision, da Störreaktionen wie Hydrolyse und/oder Oxydation nicht auftreten. Die erarbeiteten Varianten weisen bei guter Zeitstabilität die für photometrische Verfahren üblichen relativen Standardabweichungen auf.

Mit Hilfe der vorgestellten Verfahren ist es prinzipiell möglich, weitere Derivate von Phenolen, Cresolen, Xylenolen und Naphtholen zu bestimmen. Ausgenommen davon sind aber phenolische Nitroverbindungen sowie Phenole mit einer Carboxylgruppe in *o*-Stellung, da diese Produkte mit FeY keine Farbreaktionen zeigen.

#### LITERATUR

1. S. Koch und G. Ackermann, *Talanta*, 1987, **34**, 313.
2. *Idem*, *Z. Anorg. Allg. Chem.*, 1973, **400**, 29.
3. *Idem*, *Z. Chem.*, 1983, **23**, 436.
4. *Idem*, *ibid.*, 1985, **25**, 444.
5. S. Koch, G. Ackermann und M. Bartušek, *ibid.*, 1986, **26**, 181.
6. S. Koch, und G. Ackermann, *ibid.*, 1986, **26**, 300.
7. S. Koch, G. Ackermann und M. Bartušek, *Z. Anorg. Allg. Chem.*, 1987, **554**, 231.
8. S. Koch und G. Ackermann, *Z. Chem.*, in Vorbereitung.
9. S. Koch, *ibid.*, 1987, **27**, 309.

## ASPECTS OF APPLICATION OF KALMAN FILTERING IN MULTICOMPONENT SPECTROPHOTOMETRY\*

YI-MING LIU and RU-QIN YU†

Department of Chemistry and Chemical Engineering, Hunan University, Changsha,  
People's Republic of China

(Received 5 January 1988. Accepted 23 April 1988)

**Summary**—It is shown theoretically and experimentally that the reliability of the analytical results obtained by Kalman filtering in multicomponent spectrophotometry can be judged by means of the normalized autocorrelation coefficient (NAC) of the innovation sequence. Variations of the initial values of the concentration vector  $X(0)$ , the error covariance matrix  $P(0)$ , and the measurement noise variance  $R$  over a wide range do not show a substantial effect on the computed results. The effect of the rounding-off errors associated with application of different forms of the equation for calculation of the error covariance matrix is also discussed.

Kalman filtering as a chemometrics tool has been used to estimate concentrations from multicomponent spectrophotometric measurements. A Kalman filter relies on two models: one describing the dynamic system and the other expressing the measurement process. The system model can be formulated as

$$X(k) = \Phi(k, k-1) \cdot X(k-1) + \Gamma(k) \cdot w(k) \quad (1)$$

where  $X(k)$  is the vector of state variables,  $\Gamma(k)$  the model noise matrix, and  $w(k)$  the vector of model noise at time  $k$ . The state transition matrix,  $\Phi(k, k-1)$ , describes how the states propagate from time  $k-1$  to time  $k$ . The model describing the behaviour of the measurement process is given as

$$Z(k) = H(k) \cdot X(k) + v(k) \quad (2)$$

where  $Z(k)$  is the vector of measurables,  $v(k)$  the measurement noise, and  $H(k)$  describes the functional relationship of the states  $X(k)$  to the measurements,  $Z(k)$ , at time  $k$ . In multicomponent spectrophotometry, measurements are made at various wavelengths, so we can consider the variable  $k$  in the equations above as referring to wavelength rather than time. Since the state variables, *i.e.*, the concentrations of the components, are invariant at various wavelengths and there is only one measurable (absorbance of the solution), equation (1) reduces to

$$X(k) = I \cdot X(k-1) \quad (3)$$

where  $X(k)$  is the vector of concentrations at wavelength  $k$ , and  $I$  the identity matrix. The measurement model can also be rewritten as

$$z(k) = S^T(k) \cdot X(k) + v(k) \quad (4)$$

Here the measured absorbance,  $z(k)$ , and the noise of the absorbance measurement,  $v(k)$ , at wavelength  $k$  are both scalars.  $S(k)$  is no longer a matrix but a vector consisting of the absorptivities of the components involved, at wavelength  $k$ . Table 1 shows a summary of the Kalman filtering algorithm equations for interpretation of multicomponent spectrophotometric measurements. The sequence of the residuals,  $v(k)$  for  $k = 1, 2, \dots$ ,  $v(k) = z(k) - S^T(k) \cdot X(k|k-1)$ , in equation (8) is known as the innovation sequence.

The use of Kalman filtering to estimate concentrations from multicomponent spectrophotometric and electrochemical measurements has been reviewed.<sup>1-4</sup> In the present work some aspects concerning the application of Kalman filtering to multicomponent spectrophotometry are investigated; these include the evaluation of reliability of the analytical results obtained, the effect of the values of the initial guess on the computed results, and selection of the equation for computation of error covariance matrix.

### EXPERIMENTAL

#### Simulated spectra

Gaussian peaks containing 30 data points each were generated by using a computer program written in BASIC. All of these peaks had standard deviations of 5 units and the separations between them were 2 units. Individual responses and normally distributed random noise with zero mean and standard deviation of 0.3% (relative to the value of multicomponent response) were added together to form a synthetic multicomponent response (Fig. 1).

#### Data analysis

The spectral data were treated by using a Kalman filter program in BASIC running under single precision on an IBM PC-XT. Equation (10) was used for calculating the covariance matrix  $P$ , unless specified otherwise.

\*Project supported by National Natural Science Foundation of China.

†Author for correspondence.

Table 1. Kalman filter algorithm equations

State-estimate extrapolation: $X(k k-1) = X(k-1 k-1)$	(5)
Error covariance extrapolation: $P(k k-1) = P(k-1 k-1)$	(6)
Kalman gain: $K(k) = P(k k-1) \cdot S(k) \cdot [S^T(k) \cdot P(k k-1) \cdot S(k) + R(k)]^{-1}$	(7)
State-estimate update: $X(k k) = X(k k-1) + K(k) \cdot [z(k) - S^T(k) \cdot X(k k-1)]$	(8)
Error covariance update: $P(k k) = [I - K(k) \cdot S^T(k)] \cdot P(k k-1)$	(9)
or $P(k k) = [I - K(k) \cdot S^T(k)] \cdot P(k k-1) \cdot [I - K(k) \cdot S^T(k)]^T + K(k) \cdot R(k) \cdot K^T(k)$	(10)

## RESULTS AND CONCLUSION

*Evaluation of the analytical results by means of the NAC of the innovation sequence*

One of the outstanding features of Kalman filtering as applied to analytical chemistry is that during the filtering process the analyst can obtain information concerning the reliability of the analytical results obtained. Seeling and Blount<sup>5</sup> proposed some criteria for evaluation of the performance of the Kalman filter as applied to linear-sweep anodic-stripping voltammetry. They tested whether the innovation sequence converged to values uniformly distributed about a zero mean. In our previous work<sup>6</sup> it was reported that examination of the nature of the innovation sequence would provide information concerning the presence of a third (impurity) component in the analysis of a two-component drug mixture.

There are many reasons for bias in analytical results. In spectrophotometry, for example, unknown absorbing species may be present in the solution; recording the absorbance before completion of the colour reaction, and the instability of absorbing complex species may lead to deviation from the proposed system model, equation (1), and/or the measurement model, equation (2).

A biased estimator of the autocorrelation coefficients of the innovation sequence,  $C(k)$ , at point  $k$  is given<sup>5,7</sup> by:

$$C(k) = (1/N) \sum_{i=k+1}^N v(i) \cdot v(i-k)^T$$

$$k = 0, 1, 2, \dots, N-1 \quad (11)$$

where  $N$  is the number of data points. In the case described here the normalized autocorrelation coefficients (NAC) denoted by  $\rho(k)$ , can be calculated from

$$\rho(k) = C(k)/C(0) \quad k > 0 \quad (12)$$

The range of variation for  $\rho(k)$  is  $\pm 1.00$ . If less than 5.0% of the calculated NAC values fall outside the confidence limits of  $\pm(1.96/N^{1/2})$ , the innovation sequence is taken as a white-noise sequence, with 95% confidence.<sup>7</sup> Otherwise the analytical results must be considered as unreliable.

Figure 2a shows the NAC sequence for the innovation sequence obtained when Kalman filtering was used to deconvolute the simulated three-component mixture spectrum (depicted in Fig. 1). If this three-component system was treated as a two-component system with a third interfering absorbing species, the

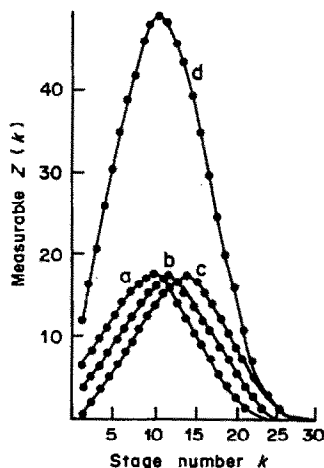


Fig. 1. Simulated spectra. Spectrum of component I (a); component II (b); component III (c); a mixture of components I, II, III in a concentration proportion of 1.5:0.5:1.0 (d).

NAC sequence for the innovation sequence obtained during the filtering process was that depicted in Fig. 2b. In this case 23% of the NAC values fell outside the 95% confidence limits of  $\pm(1.96/N^{1/2})$ , indicating the unreliability of the analytical results. Even in this case, however, the concentration estimates converged as described in Fig. 3, and the two diagonal elements of  $P(k)$  decreased monotonically as described in Fig. 4, which gave no information about the biased results.

When biased results are caused by measurement of the absorbance before the completion of the colour

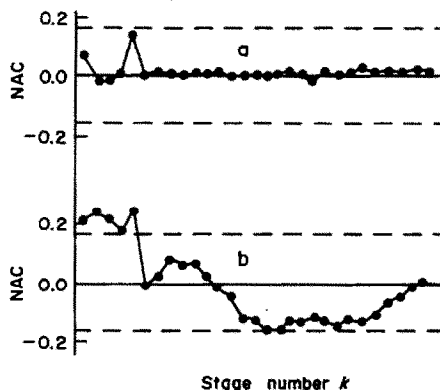


Fig. 2. NAC sequences for reliable analytical results (a) and for unreliable ones caused by an interfering absorbing component present in the system (b).

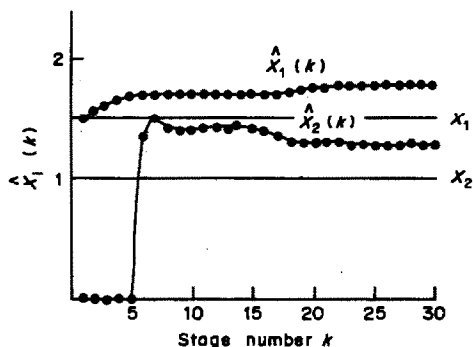


Fig. 3. Estimates  $X_i(k)$ . Kalman filtering used for system containing an unknown absorbing component. Initial values:  $X(0) = 0$ ,  $P(0) = I$ .  $R(k) = 10^{-3}$  for all  $k$ . The true values are indicated by the horizontal lines.

reaction, the NAC sequence is also very helpful. Suppose that the true system model is

$$X(k) = X(k - 1) + \alpha$$

i.e., the concentrations of the absorbing species increase by  $\alpha$  during the time period between two measurements. During the filtering process we still use the system model described by

$$X(k) = X(k - 1)$$

For simplicity, assume that the measurement function,  $S(k)$ , consists of unit absorptivities, i.e.  $S(k) = 1$ , and the measurement-noise variance  $R(k)$  is  $\beta^2$  for all measurement points. Take  $X(0) = 0$ ,  $P(0) = \infty$  as the initial values. That is to say, we do not have any *a priori* knowledge about the state. Using the expressions for  $P(k|k)$  and  $K(k)$  in the following modified forms<sup>8</sup>

$$P(k|k)^{-1} = P(k|k - 1)^{-1} + S(k) \cdot R(k)^{-1} \cdot S^T(k)$$

and

$$K(k) = P(k) \cdot S(k) \cdot R(k)^{-1},$$

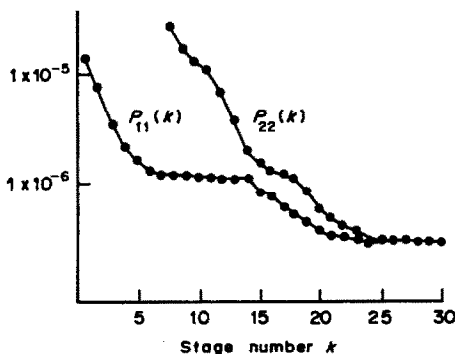


Fig. 4. Estimated variances. Kalman filtering used for system containing an unknown absorbing component. Initial values:  $X(0) = 0$ ,  $P(0) = I$ . Measurement noise variance  $R(k) = 0.001$  for all  $k$ .

we obtain

$$\begin{aligned} P(1|1)^{-1} &= P(1|0)^{-1} + S(1) \cdot R(1)^{-1} \cdot S^T(1) \\ &= P(0|0)^{-1} + S(1) \cdot R(1)^{-1} \cdot S^T(1) \\ &= \beta^{-2} \end{aligned}$$

$$\begin{aligned} P(k|k)^{-1} &= P(k|k - 1)^{-1} + S(k) \cdot R(k)^{-1} \cdot S^T(k) \\ &= P(k - 1|k - 1)^{-1} \\ &\quad + S(k) \cdot R(k)^{-1} \cdot S^T(k) \\ &= P(k - 1|k - 1)^{-1} + \beta^{-2} \\ &= P(k - 2|k - 2)^{-1} + 2\beta^{-2} \\ &= \dots = k\beta^{-2} \end{aligned}$$

$$\begin{aligned} K(k) &= P(k|k) \cdot S(k) \cdot R(k)^{-1} \\ &= P(k|k)\beta^{-2} = 1/k \end{aligned}$$

$$\begin{aligned} X(k) &= X(k - 1) \\ &\quad + K(k) \cdot [z(k) - S^T(k) \cdot X(k - 1)] \\ &= X(k - 1) + \frac{1}{k} [z(k) - X(k - 1)] \\ &= \left(\frac{k - 1}{k}\right) X(k - 1) + \frac{1}{k} z(k) \\ &= \left(\frac{k - 2}{k}\right) X(k - 2) + \frac{1}{k} z(k - 1) \\ &\quad + \frac{1}{k} z(k) \\ &= \dots = \frac{1}{k} \sum_{l=1}^k z(l) \end{aligned}$$

Note that the measurable  $z(k)$  is given as

$$z(k) = X_0 + k \cdot \alpha + v(k)$$

Then

$$\begin{aligned} X(k) &= \frac{1}{k} \sum_{l=1}^k [X_0 + l \cdot \alpha + v(l)] \\ &= X_0 + \left(\frac{k + 1}{2}\right) \alpha + \frac{1}{k} \sum_{l=1}^k v(l) \end{aligned}$$

where  $X_0$  is the true value of the state at measurement point  $k = 0$ . The expectation of  $X(k)$  is

$$E[X(k)] = X_0 + \left(\frac{k + 1}{2}\right) \alpha$$

The true value of the state at measurement point  $k$ , however, is

$$X_k = X_0 + k \cdot \alpha$$

The error in the estimate is

$$\Delta X_k = \left(\frac{k - 1}{2}\right) \alpha.$$

As shown above, the error covariance matrix  $P(k)$  is given as

$$P(k|k) = \frac{\beta^2}{k}$$



Table 2. Effect of initial guess on the estimates

Expt. No.	X(0)	Initial guess		R	Estimates		
		P(0)			x <sub>1</sub>	x <sub>2</sub>	x <sub>3</sub>
1	0	1 · I <sub>n</sub>		0.1	1.498	0.504	0.995
2	0	1 · I <sub>n</sub>		10 <sup>-3</sup>	1.498	0.502	0.996
3	0	1 · I <sub>n</sub>		10 <sup>-5</sup>	1.498	0.502	0.996
4	0	10 · I <sub>n</sub>		10 <sup>-3</sup>	1.498	0.502	0.996
5	0	10 <sup>-3</sup> · I <sub>n</sub>		10 <sup>-3</sup>	1.498	0.502	0.996
6	5	1 · I <sub>n</sub>		10 <sup>-3</sup>	1.498	0.502	0.996

True values: x<sub>1</sub> = 1.5, x<sub>2</sub> = 0.5, x<sub>3</sub> = 1.0

which decreases monotonically, not providing any information about the biased analytical results. For the NAC of the innovation sequence we have

$$\begin{aligned}
 v(k) &= z(k) - S^T(k) \cdot X(k-1) \\
 &= z(k) - \left(\frac{k}{k-1}\right) \left[\left(\frac{k-1}{k}\right) X(k-1)\right] \\
 &= z(k) - \left(\frac{k}{k-1}\right) \cdot \left(\frac{1}{k}\right) \sum_{l=1}^{k-1} z(l) \\
 &= z(k) - \left(\frac{1}{k-1}\right) \sum_{l=1}^{k-1} [X_0 + l \cdot \alpha + v(l)] \\
 &= X_0 + k \cdot \alpha + v(k) - X_0 \\
 &\quad - \frac{1 + 2 + 3 \dots + (k-1)}{k-1} - \frac{1}{k-1} \sum_{l=1}^{k-1} v(l)
 \end{aligned}$$

Thus the mean value of the innovation v(k) is  $\frac{k}{2} \alpha$ . Then the NAC of the innovation sequence can be written as

$$\begin{aligned}
 \rho(k) &= \frac{1(k+1) + 2(k+2) + 3(k+3) + \dots + (N-k)N}{1^2 + 2^2 + 3^2 + \dots + N^2} \\
 &= \frac{1(k+1) + 2(k+2) + 3(k+3) + \dots + (N-k)(k+N-k)}{1^2 + 2^2 + 3^2 + \dots + N^2} \\
 &= \frac{k[1 + 2 + 3 + \dots + (N-k)]}{1^2 + 2^2 + 3^2 + \dots + N^2} + \frac{1^2 + 2^2 + 3^2 + \dots + (N-k)^2}{1^2 + 2^2 + 3^2 + \dots + N^2}
 \end{aligned}$$

It is obvious that the innovation sequence does not have the character of white noise and so the results obtained must be considered as unreliable.

*Effect of errors in the initial guess*

When no *a priori* information is available, the filter is generally initiated with X(0) = 0 and P(0) = σ<sup>2</sup> · I<sub>n</sub>.

Poullisse<sup>1</sup> suggested that choosing the largest possible value for σ was preferable for obtaining unbiased estimates, and gave an empirical equation for estimating σ. The measurement noise variable R is also taken as an initial value, because it is often assumed to be invariant at all wavelengths in Kalman-filtering spectrophotometry and must be given in advance. The simulated three-component spectrophotometric system (depicted in Fig. 1) was treated by a Kalman filter initiated with various initial guesses. Changes in the X(0), P(0) and R values over quite a wide range do not affect the computed results (Table 2). It was found that larger σ<sup>2</sup> caused more rapid convergence of the estimates to the true values, but with larger R values the convergence rate slowed down.

*Effect of rounding-off errors*

In the routine applications of Kalman filtering it is possible to use pocket computers for experimental

convenience. In such cases care should be taken concerning the rounding-off errors and some alternative algorithms of the original Kalman filter, such as square-root Kalman filtering algorithms, are preferable.<sup>9</sup> With the original Kalman filter, we should be careful, for instance, in choosing the equation for

Table 3. Effect of the rounding-off errors—comparison between equations (9) and (10)

No. of the simulated system	True values				Estimated values							
					KF* based on equation (9)				KF* based on equation (10)			
	x <sub>1</sub>	x <sub>2</sub>	x <sub>3</sub>	x <sub>4</sub>	x <sub>1</sub>	x <sub>2</sub>	x <sub>3</sub>	x <sub>4</sub>	x <sub>1</sub>	x <sub>2</sub>	x <sub>3</sub>	x <sub>4</sub>
1	1.5	1.0			1.49	1.0			1.49	1.0		
2	1.5	0.5	1.0		1.59	-575	0.98		1.51	0.49	1.0	
3	1.5	0.5	1.0	0.5	58.6	-169	5.7	0.53	1.5	0.49	1.0	0.5

Initial values: X(0) = 0, P(0) = 1 · I<sub>n</sub>. Measurement noise variance R = 10<sup>-3</sup> for all k.

\*KF program run on a SHARP PC-1500 pocket computer.

calculation of the error covariance matrix. Two equations [(9) and (10)] are most frequently cited in the chemical literature. It has been noticed that for the calculation of  $P(k)$  during the filtering process, equation (9) is much more sensitive to the rounding-off errors produced by a pocket computer than is equation 10 (Table 3). It should be mentioned that both equations (9) and (10) can give satisfactory results when a microcomputer such as an IBM PC is used, especially with double precision.

## REFERENCES

1. H. N. J. Poullisse, *Anal. Chim. Acta*, 1979, **112**, 361.
2. S. D. Brown, *ibid.*, 1986, **181**, 1.
3. S. C. Rutan, *J. Chemomet.*, 1987, **1**, 7.
4. T. Lilley, *Anal. Proc.*, 1984, **21**, 147.
5. P. F. Seeling and H. N. Blount, *Anal. Chem.*, 1979, **51**, 327.
6. Y. M. Liu and R. Q. Yu, *Acta Pharm. Sinica*, 1987, **22**, 913.
7. R. K. Mehra, *IEEE Trans. Automatic Control*, 1970, **15**, 175.
8. R. G. Brown, *Introduction to Random Signal Analysis and Kalman Filtering*, p. 218, Wiley, New York, 1983
9. T. F. Brown, D. M. Caster and S. D. Brown, *Anal. Chem.*, 1984, **56**, 1214.

## A RAPID ALGORITHM FOR SOLUTION OF THE EQUATIONS OF MULTIPLE EQUILIBRIUM SYSTEMS—RAMESES

V. W.-H. LEUNG, B. W. DARVELL and A. P.-C. CHAN

Dental Materials Science Unit, University of Hong Kong, Prince Philip Dental Hospital,  
34 Hospital Road, Hong Kong

(Received 18 November 1987. Accepted 23 April 1988)

**Summary**—The solution of systems of equilibrium equations is an important though commonplace operation, rendered difficult by non-linearity. Previous methods of numerical solution have suffered from slow convergence, unreliability, and inefficient structure. An algorithm, RAMESES, is presented in matrix algebra terms, which is both simple in structure and efficient, involving only one matrix inversion per system and giving an exact solution of the set of dependent equilibrium equations at each iteration.

The calculation of the distribution of species in a solution according to the various equilibria involved is tractable by classical methods only for relatively simple systems, with few components. The manual solution of the problem is discussed and illustrated in many elementary textbooks<sup>1,2</sup> and serves to explain such common concepts as buffers and titration. Briefly, the problem is one of solving a set of simultaneous equations, namely the equilibrium equations, and the mass and charge balances. An explicit solution may be obtained by the usual method of successive substitution in some simple cases, but this rapidly becomes unmanageable or frankly impossible as the size of the system increases. To reduce the difficulties (which are in terms of effort and not theory) reliance is often placed on assumptions of the insignificance of various species and thus the elimination of variables. In practical terms, for simple systems, this may be satisfactory, but it has the disadvantages that a different set of assumptions must be made in each of several pH regions, for example, and that the concentrations of the minor (ignored) species are not well defined. This latter point may be particularly significant when a reactive species is in the discarded group. However, for polyelectrolyte systems in general such assumptions are dangerous and do not appreciably reduce the labour.

Various computational methods for calculating the distribution of species at equilibrium in multi-component electrolytes have been reviewed and utilized.<sup>3–6</sup> The existing general procedures can be divided into two main categories: free-energy minimization and equilibrium-constant methods. These are essentially routines for (a) optimization, and (b) solution of non-linear equations, respectively. The free-energy minimization approach is based on the thermodynamic criterion that the total free energy of a system at constant temperature and pressure has a minimum value at equilibrium. However, the present discussion is restricted to the second class of methods, based on equilibrium constants.

It seems to be a common aspect of these methods that the ionic species in an aqueous solution are divided into two sets: one, the “basis” set, consists of the uncomplexed ionic species, and the other of the complexes. It is stated that the efficiency of the computation is critically dependent upon the choice of the “basis” set and the initial estimates of the equilibrium concentrations of the components,<sup>5,7</sup> two constraints which are at best inconvenient and at worst require much preliminary exploratory work.

The program HALTAFALL<sup>8</sup> used a nested routine which solved for one component at a time, feeding back estimates for each free ion concentration in turn, holding the concentration of complexes constant. When the iteration was finished the complex ion concentrations were determined. The subroutine COGS<sup>9</sup> estimated, in the one loop, complexes, free cations, and free anions in turn, before adjusting the estimates for the next iteration. MULTIREACTIONEQUILIBRIUM,<sup>10</sup> however, solved each of the equilibrium equations individually, one after another, with use of the estimates from the equations already solved, before testing the error and going back to the top of the list for another iteration. Each of these represents a rather crude programming approach to the solution of the problem, relying on the ability of machines to perform large numbers of extremely tedious calculations. None of these methods requires explicit matrix inversion, and they suffer from rather slow rates of convergence because of the stepwise-by-species adjustments. One reason for this is that every time an adjustment is made, error reappears from other sources, *i.e.*, from complex ions or ions previously considered but now needing readjustment.

The adoption of the Newton–Raphson method<sup>7,11,12</sup> gave an improvement in the rate of convergence under some limited conditions. The subroutine COGSNR<sup>12</sup> developed from COGS<sup>9</sup> is such a procedure, but it too has the assumption of no complex formation in the first part of the program, which then

parallels the procedure in HALTAFALL.<sup>8</sup> COGSNR inverts a matrix of errors to find adjustments for the next cycle. The estimated free metal and ligand concentrations are used to calculate the concentration of all other species for the next iteration. It is, however, known to be unreliable, even with double precision, for systems of more than two metals and two ligands, for which COGS<sup>9</sup> is preferred.<sup>12</sup>

COMPLX<sup>11</sup> also utilizes the Newton-Raphson method, with the use of partial derivatives of the mass-balance and charge-balance equations, expressed as Taylor series, as the coefficients of the principal matrix. The program flow differs slightly from that of COGSNR,<sup>12</sup> but not significantly. Using estimates of only the free species concentrations, a matrix inversion routine provides the next set of estimates for iteration. When the differences become less than an assigned value, the method is said to have converged. This kind of tolerance test is, in general, somewhat weak, as the rate of convergence is not known: there is a danger of premature termination at a solution which is wide of the mark by an unknown amount. A rather small tolerance would have to be imposed to prevent this. When approximations to the equilibrium concentrations of the free species have been found, the concentrations of the remaining species are calculated from the equilibrium equations.

EQUIL<sup>7</sup> has been highly recommended,<sup>5,6</sup> and uses a general numerical technique based on a modified Newton-Raphson method. Both selection of the "basis"<sup>7</sup> and making the initial estimates of the equilibrium concentrations of the main components are tedious, but it is understood that these are critical.<sup>7</sup> Since the method suffers from a substantial risk of a singular matrix and of non-convergence, various protections are adopted, including scaling the matrix, eigenvector analysis, development of an iteration matrix, and adoption of a convergence forcer, a somewhat lengthy and convoluted procedure overall.

The solution of the general problem is made difficult by the fact that the system of equations is not homogeneous: that is to say, the equilibrium equations are in the form of products, the remainder are sums. The equilibrium equations are convertible into linear form by taking logarithms, but the system remains inhomogeneous. Nevertheless, matrix solution methods can be used on the logarithmic expressions and are eminently suited to machine computation, especially with the development of both extensive libraries of good matrix routines and higher level languages capable of handling matrix mathematics directly (such as Hewlett-Packard BASIC). These methods offer considerable scope for poly-electrolyte systems. The method proposed here can handle all the species together, without the risk of matrix singularity, thus avoiding complicated manipulations.

#### NUMERICAL METHOD

If we have  $r$  equilibria, with equilibrium constants

$K$  (excluding "complete" dissociation), involving  $s$  species in solution, there are  $t = s - r$  non-explicit concentrations. The values of  $t - 1$  of these may be chosen independently (that is, these are the degrees of freedom of the system), the remaining one species being determined by the constraint of charge balance. Such a system is, of course, indeterminate and further constraints,  $t - 1$  in number, must be invoked to find the single, thermodynamic, solution. These constraints may take one of two forms: (i) the actual concentration of a species may be fixed, regardless of the total amount of the corresponding system component, for example by choosing a particular pH, but otherwise this seems to be of rather rare interest; (ii) the total concentration of the system component, irrespective of the species in which it is found, is predetermined as in working with, say, a fixed total molarity of ligand.

The solution of the system in the first case is direct, as one (ionic) species can be left available to adjust the charge balance; in the second case a guess or guesses must be refined. A general approach might then be to adjust the concentration of the other  $t - 1$  species by the proportion in which the corresponding calculated total of fixed components is in error, following the method employed in COGS,<sup>9</sup> providing successive approximation and convergence to the unique solution.

Thus the first step is to choose the minimal set of  $t$  (convenient) independent species in terms of which all others will be calculated from the equilibrium equations. These concentrations provide a vector  $\mathbf{X}_A (t \times 1)$ :

$$\mathbf{X}_A = \begin{bmatrix} X_1 \\ \vdots \\ X_t \end{bmatrix} \quad (1)$$

At the start, the values of non-preset concentrations must be guessed for  $X_{A(i)}$ . These need only be non-zero positive, *i.e.*, each  $X_{A(i)} \in \mathbb{R}^+$ , but common sense permits more sensible choices in the range from zero to the maximum notionally feasible. Informed guesses will reduce the number of iterations but are not essential.

The remaining, "dependent", species then form a second concentration vector  $\mathbf{X}_B (r \times 1)$ :

$$\mathbf{X}_B = \begin{bmatrix} X_{t+1} \\ \vdots \\ X_{t+r} \end{bmatrix} \quad (2)$$

These two vectors may be combined into the full concentration vector,  $\mathbf{X} (s \times 1)$ :

$$\mathbf{X} = \begin{bmatrix} \mathbf{X}_A \\ \mathbf{X}_B \end{bmatrix} \quad (3)$$

Corresponding to  $\mathbf{X}_B$ , we have a vector  $\mathbf{K} (r \times 1)$  of equilibrium constants. To linearize this portion of the system, these must be converted into their logarithms to yield the vector  $\mathbf{L} (r \times 1)$ , with the  $i$ th element given by:

$$L_i = \log(K_i) \quad (4)$$

Similarly, for  $\mathbf{P}_A (r \times 1)$ :

$$\mathbf{P}_{Ai} = \log(X_{Ai}) \quad (5)$$

The corresponding matrix of coefficients is  $\mathbf{C} (r \times s)$ , the coefficients being the powers to which the species are raised in the equilibrium equations, with note taken of sign. The columns of the submatrix  $\mathbf{C}_A (r \times t)$  are identified and deleted from  $\mathbf{C}$  to form  $\mathbf{C}_B (r \times r)$ ; then  $\mathbf{Z} (r \times 1)$  is found from:

$$\mathbf{Z} = \mathbf{L} - \mathbf{C}_A \mathbf{P}_A \quad (6)$$

The columns of  $\mathbf{C}_A$  are chosen to correspond to the species of the rows of  $\mathbf{X}_A$ , the implication being that these can be any subset of size  $t$ : the choice depends only on need and convenience. The corresponding log (concentrations) of the remaining  $r$  species are given by the vector  $\mathbf{P}_B$ :

$$\mathbf{P}_B = \mathbf{C}_B^{-1} \mathbf{Z} \quad (7)$$

Then:

$$\mathbf{X}_{B_i} = \log^{-1}(\mathbf{P}_{B_i}) \quad (8)$$

$\mathbf{X}_{(n)}$  is then the first ( $n = 1$ ) approximation to the solution if  $\mathbf{X}_A$  contains any guessed values.

Charge balance is next checked by using  $\mathbf{Q} (s \times 2)$ , the matrix of the (signed) species charges  $z$ :

$$\mathbf{Q} = \begin{bmatrix} q_{1,1} & q_{1,2} \\ \vdots & \vdots \\ q_{s,2} & q_{s,2} \end{bmatrix}; \quad \begin{array}{l} q_{i,1} = z_i, \quad z_i > 0 \\ q_{i,2} = z_i, \quad z_i < 0 \\ = 0 \text{ otherwise} \end{array} \quad (9)$$

(the order of the rows of  $\mathbf{Q}$  corresponds to the order in  $\mathbf{X}$ ). Then, the matrix of total positive and negative charges  $\mathbf{D} (1 \times 2)$  is given by:

$$\mathbf{D} = \mathbf{X}^T \mathbf{Q} \quad (10)$$

(we use superscript T to mean "transpose"), so that the charge error,  $\Delta$ , is obtained from  $\Delta = D_1 + D_2$  (i.e., the sum of the elements of  $\mathbf{D}$ ). Similarly, a matrix  $\mathbf{M} (s \times t)$  of component multiplicities in all solution species is constructed (ignoring  $\text{OH}^-$  and  $\text{H}^+$  if combined with any species, i.e., setting  $m_j$  to zero):

$$\mathbf{M} = \begin{bmatrix} m_{1,1} & \dots & m_{1,t} \\ \vdots & \ddots & \vdots \\ m_{s,1} & \dots & m_{s,t} \end{bmatrix} \quad (11)$$

Then  $\mathbf{S} (1 \times t)$ , the current component totals matrix, is given by:

$$\mathbf{S} = \mathbf{X}^T \mathbf{M} \quad (12)$$

There is also a corresponding matrix  $\mathbf{T} (1 \times t)$  of required total component values, one of which, the  $j$ th, is undefined (required for the charge balance).

If the approximation is made that the adjustment required in the guessed values of the species in vector  $\mathbf{X}_A$  with preset component totals is proportional to the error, we form a diagonal matrix of correction factors,  $\mathbf{F} (t \times t)$ , where:

$$F_{ii} = \frac{T_i}{S_i}, \quad F_{ik} = 0, \quad i \neq k \quad (13)$$

The  $j$ th, and necessarily charged, species in  $\mathbf{X}_A$  for which no value in  $\mathbf{T}$  is defined, is adjusted according to the charge balance, but in proportion to the concentration of that species relative to the sum of concentrations of all species having the same charge sign, weighted by the charge number. This correction factor is then:

$$F_{jj} = \left\{ 1 - \frac{\Delta}{D_z} \frac{f}{z_j} \right\} \quad (14)$$

Here,  $D_z$  means either  $D_1$  or  $D_2$  as appropriate to the value of  $z_j$ , the charge of the species being adjusted, introduced to correct the direction and equivalence of the adjustment which is to be made. The scalar,  $f$ , is a damping factor introduced in an *ad hoc* fashion to avoid uncontrolled oscillation, particularly in the early iterations, where the approximation may be poor. In one sense,  $f$  represents the sensitivity of the system to perturbation and a general optimum value cannot be given. Values in the range 0.7–2.5 have been found to work in practice; some programming refinement is required to optimize this if necessary.

The success or otherwise of the approximation at each iteration is tested by comparing each error,  $E_{ii}$ , defined by

$$\mathbf{E} = \mathbf{F} - \mathbf{I} \quad (15)$$

where  $\mathbf{I}$  is the identity matrix, against a tolerance,  $\epsilon$ , thus requiring  $|E_{ii}| < \epsilon$ , any difference exceeding the tolerance forcing a further iteration. Then the elements of  $\mathbf{X}_{A(n)}$  can be corrected for the next,  $(n + 1)$ th, iteration:

$$\mathbf{X}_{A(n+1)} = \mathbf{F} \mathbf{X}_{A(n)} \quad (16)$$

The adjusted vector  $\mathbf{X}_{A(n+1)}$  is then reinserted at equation (5) for the  $(n + 1)$ th iteration. When the initial approximations are poor, the values of the correction factors,  $F_{ii}$ , from equation (14) may become negative (corresponding to negative concentrations in the following step, purely because of the simplicity of the adjustment rule itself), and it is suggested that  $F_{ii}$  be then given a nominal default value near to 0, say 0.01 or 0.001, to permit the approximation to proceed. Even if this turns out to be excessively conservative, self-correction usually appears to be rapid, and no more sophisticated procedure is necessary. Certainly, no problem has been observed.

A rather faster convergence is achieved by use of a slight calculation refinement, without affecting the principle of the procedure. Since in any iteration, the change in an estimated complex concentration will be strongly positively correlated with the changes in its free component concentrations (allowing that it is frequently convenient to choose the independent species in  $\mathbf{X}_A$  as "free" species and not themselves complexes), there is a tendency for the corrections to

be overdone. However, calculating the  $(t-1)$   $F_{ij}$  values (*i.e.*, excluding the  $j$ th, charge-adjustment, species), and then making the approximation that all complexes containing  $X_{A_j}$  are adjusted in proportion to the change in  $X_j$  required for charge balance, makes the adjustments to those independent species a little more conservative, the solution a little more stable, and consequently the convergence faster.

The conditional adjustment is set up in a temporary matrix  $M^*$  ( $s \times t$ ):

$$\begin{aligned} M_{ki}^* &= M_{kj} F_{ij} \quad \text{if } M_{kj} > 0 \\ M_{ki}^* &= M_{ki} \quad \text{otherwise} \end{aligned} \quad (17)$$

Then, analogously to equations (12) and (13),

$$L = \begin{bmatrix} 7.68 \\ 7.40 \\ 4.07 \\ 5.62 \\ 4.34 \\ 2.91 \\ 10.82 \\ 14.00 \\ 25.20 \\ 17.20 \\ 9.20 \end{bmatrix}, \quad C_A = \begin{bmatrix} 0 & 0 & 2 \\ 0 & -1 & 0 \\ 0 & 0 & 0 \\ 0 & -1 & -1 \\ 0 & 0 & -1 \\ 0 & 0 & -1 \\ 0 & 1 & -1 \\ 0 & 0 & -1 \\ 0 & 0 & 0 \\ 1 & 0 & 0 \\ 0 & 0 & 0 \end{bmatrix}, \quad C_B = \begin{bmatrix} 0 & 0 & -2 & 0 & 0 & 1 & -2 & 0 & 0 & 0 & 0 \\ 0 & 0 & -1 & 1 & 0 & 0 & 0 & 0 & 0 & 0 & 0 \\ 0 & 0 & 0 & -2 & 1 & 0 & 0 & 0 & 0 & 0 & 0 \\ 0 & 0 & 0 & 0 & 0 & 0 & 1 & 0 & 0 & 0 & 0 \\ 0 & 0 & 0 & 0 & 0 & 0 & -1 & 1 & 0 & 0 & 0 \\ 0 & 0 & 0 & 0 & 0 & 0 & 0 & -1 & 1 & 0 & 0 \\ 0 & 0 & 0 & 0 & 0 & 0 & 0 & 0 & 0 & -1 & 0 \\ 0 & 0 & 0 & 0 & 0 & 0 & 0 & 0 & 0 & 0 & -1 \\ 0 & 1 & -1 & 0 & 0 & 0 & 0 & 0 & 0 & 0 & -3 \\ 0 & 0 & -1 & 0 & 0 & 0 & 0 & 0 & 0 & 0 & -2 \\ 1 & 0 & -1 & 0 & 0 & 0 & 0 & 0 & 0 & 0 & -1 \end{bmatrix}$$

$$S^* = X^T M^* \quad (18)$$

and

$$F_{ij} = \frac{T_i}{S_i^*}; \quad F_{ij} = 0, \quad i \neq j \quad (19)$$

The procedure continues with equation (16) as before.

The routine, programmed in Hewlett-Packard BASIC, is given in the Appendix. This language is used for the illustration primarily because of its readability. The "housekeeping" part of the program, *i.e.*, data input, array dimensioning and manipulation, as well as the utilities for scans and data output, have been omitted since they are matters of style and installation rather than critical to the present proposal. As far as possible, the notation of the text has been retained, except as noted; cross-references to the equations have been inserted to reduce the documentation.

#### EXAMPLE

The aqueous uranyl-citrate system is used as an example of application of the method. Fourteen species are considered, and the behaviour of the system containing  $10^{-5}M$  total uranium is examined as a function of pH, *i.e.*, total citrate is allowed to vary. The choice of species for the vectors  $X_A$  and  $X_B$  (based on the treatment<sup>13</sup> of citric acid as  $H_4L$ ) is as follows

$$X_A = \begin{bmatrix} [UO_2(OH)_2] \\ [HL^{3-}] \\ [H^+] \end{bmatrix}$$

$$X_B = \begin{bmatrix} [UO_2(OH)^+] \\ [UO_2(OH)_3^{-1}] \\ [UO_2^{2+}] \\ [UO_2HL^-] \\ [(UO_2HL)_2^{2-}] \\ [(UO_2)_2(H_2L)_2(OH)_2^{2-}] \\ [H_2L^{2-}] \\ [H_3L^-] \\ [H_4L] \\ [L^{4-}] \\ [OH^-] \end{bmatrix}$$

The vector of the log  $K$  values<sup>13-15</sup> and the coefficient matrices are:

For example, the first row corresponds to the equilibrium:

$$[H^+]^2 = \frac{K[UO_2)_2(H_2L)_2(OH)_2^{2-}]}{[UO_2^{2+}]^2[H_2L^{2-}]^2}; \quad K = 4.79 \times 10^7$$

Notice that some rows in  $C_A$  are allowed to contain only zeros, but that no row or column in  $C_B$  may.

The corresponding charge and multiplicity matrices are:

$$Q = \begin{bmatrix} 0 & 0 \\ 0 & -3 \\ 1 & 0 \\ 1 & 0 \\ 0 & -1 \\ 2 & 0 \\ 0 & -1 \\ 0 & -2 \\ 0 & -2 \\ 0 & -2 \\ 0 & -1 \\ 0 & 0 \\ 0 & -4 \\ 0 & -1 \end{bmatrix}, \quad M = \begin{bmatrix} 1 & 0 & 0 \\ 0 & 1 & 0 \\ 0 & 0 & 1 \\ 1 & 0 & 0 \\ 1 & 0 & 0 \\ 1 & 0 & 0 \\ 1 & 1 & 0 \\ 2 & 2 & 0 \\ 2 & 2 & 0 \\ 0 & 1 & 0 \\ 0 & 1 & 0 \\ 0 & 1 & 0 \\ 0 & 1 & 0 \\ 0 & 0 & 0 \end{bmatrix}$$

remembering that the columns of  $M$  and  $C_A$  correspond to the elements of  $X_A$ .

Figure 1 shows the calculated distribution of all species except  $H^+$  and  $OH^-$  over a range which shows clearly the kind of complexity that can be readily handled. The program was written in Turbo Pascal, using for the matrix solution a Gauss-Jordan Elimination Method<sup>16</sup> subroutine,

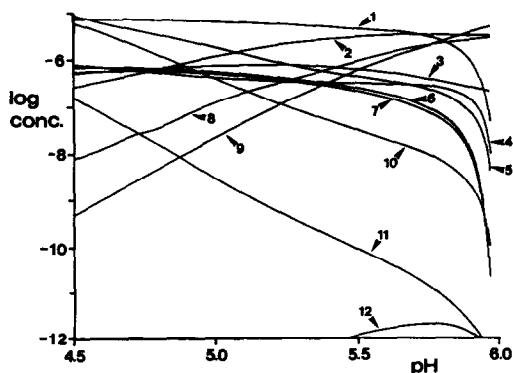


Fig. 1. Log (concentration) vs. pH for each species in the uranyl-citrate (L) system for a total uranyl concentration of  $10^{-5}M$ , calculated by using RAMESES. The narrow range in pH was chosen to illustrate the resolution of a difficult region. The right-hand limit corresponds to no citrate [i.e.,  $UO_2(OH)_2$  in water]. The species are as follows: 1.  $[UO_2HL^-]$ , 2.  $[UO_2(OH)^+]$ , 3.  $[UO_2^{2+}]$ , 4.  $[HL^{3-}]$ , 5.  $[H_2L^{2-}]$ , 6.  $[(UO_2)_2(H_2L)_2(OH)_2^{2-}]$ , 7.  $[(UO_2HL)_2^{2-}]$ , 8.  $[UO_2(OH)_2]$ , 9.  $[UO_2(OH)_3^-]$ , 10.  $[H_3L^-]$ , 11.  $[H_4L]$ , 12.  $[L^{4-}]$ .

and run on an IBM PC XT with 8087 and 8088 processors. The running time for each set of results was between about 3 and 5 sec, usually with between 20 and 40 iterations for pH steps of 0.1 and the results of the previous run used as the "guess" for  $X_A$ . The tolerance,  $\epsilon$ , was set at  $10^{-10}$ , to demonstrate the general stability of the solution and the lack of need to compromise accuracy for non-inherent reasons.

#### DISCUSSION

The proposed algorithm offers a great improvement in the numerical analysis of equilibrium systems in that the computational route is very direct and free from arbitrary simplifications or approximations. It is efficient, giving complete solution in relatively few iterations, and has the advantage of procedural clarity.

An immediate and major advantage apparent is the need to invert the matrix  $C_B$  only once (usually matrix inversion is the slowest and therefore rate-limiting procedure, especially for large systems). This is true even when many calculations on the same system are required, since  $C_B$  is the equilibrium equation coefficient matrix which is, of course, unchanging, so this step can be taken outside the main loop.  $C_B$  is also always non-singular. There is thus no possibility of failure to converge [provided that  $f$  in equation (14) is chosen appropriately] for chemically feasible systems.

It is noteworthy that equation (7) represents a complete and exact algebraic solution of the  $r$  simultaneous equations for the  $n$ th estimate of dependent species concentrations. This is in contrast to previous methods, which all involve some degree of approximation at this stage, primarily because of the stepwise solution of the equations.

The remark above, concerning chemical feasibility,

needs some elaboration. It is obvious that for a given acid-base system with, say, the concentration of the base given, there is a corresponding upper limit to the pH when the end concentration of acid is zero. No solution exists beyond that point (see Fig. 1). Similarly, there is a lower pH-limit. There is also the question of overall solubility limits, which must be determined separately. Care must therefore be taken when setting up scans in pH, for example, which will produce nonsensical answers (e.g.,  $10^{33}M$ ) or failure to converge because of the simple impossibility of satisfying the equilibrium equations.

The example given is a demonstration of the method and is only a first approximation, because the concentrations and not the activities of the ions were used. This computational example is not necessarily complete or accurate as a description of the system, since the constants have been taken uncritically from the literature.

Further refinements are possible, such as the use of activities<sup>17</sup> rather than concentrations, and consideration of the "concentration" of solvent (for high molality calculations). In addition, the efficiency of the convergence can be increased by modifying the adjustment factor calculation.

It is important to recognize that because of the efficiency of the calculation very small tolerances are easily attained (no difficulty has been experienced in obtaining algebraically stable solutions at tolerances of  $10^{-12}$  and smaller), but that although this is beneficial in ensuring that spurious solutions are not found, especially for very large systems, no more significance should be attached to the results than is allowed by the reliability of the equilibrium constants themselves (which is usually not very good<sup>14,15</sup>).

The method may find wide applicability in solution chemistry in general, for example in the field of environmental pollution: risk assessment for radioactive waste disposal<sup>18</sup> routinely involves such calculations.

*Acknowledgement*—This work was done in partial fulfillment of the degree of Ph.D for one of us (V.W.-H.L.) at, and supported by, the Faculty of Dentistry, University of Hong Kong.

#### REFERENCES

1. J. N. Butler, *Ionic Equilibrium, A Mathematical Approach*, Addison-Wesley, Reading, Mass., 1964.
2. F. J. C. Rossotti and H. Rossotti, *The Determination of Stability Constants and other Equilibrium Constants in Solution*, McGraw-Hill, New York, 1961.
3. W. E. Brown, in *Environmental Phosphorus Handbook*, E. J. Griffith (ed.), Wiley, New York, 1973.
4. C. W. Childs, *Inorg. Chem.*, 1970, 9, 2465.
5. G. H. Nancollas, Z. Amjad and P. Koutsoukos, in *Chemical Modeling in Aqueous Systems*, E. A. Jenne (ed.), p. 475. ACS, Washington DC, 1979.
6. D. K. Nordstrom, L. N. Plummer, T. M. L. Wigley, T. J. Wolery, J. W. Ball, E. A. Jenne, R. L. Bassett, D. A. Crerar, T. M. Florence, B. Fritz, M. Hoffman, G. R. Holdren, Jr., G. M. Lafon, S. V. Mattigod, R. E. McDuff, F. Morel, M. M. Reddy, G. Sposito and

- J. Thrailkill, in *Chemical Modeling in Aqueous Systems*, E. A. Jenne (ed.), p. 857. ACS, Washington DC, 1979.
7. T. P. I and G. H. Nancollas, *Anal. Chem.*, 1972, **44**, 1940.
  8. N. Ingri, W. Kakolowicz, L. G. Sillén and B. Warnqvist, *Talanta*, 1967, **14**, 1261; errata, 1968, **15**, No. 3, ix.
  9. D. D. Perrin and I. G. Sayce, *Talanta*, 1967, **14**, 833.
  10. P. Benedek and F. Olti, *Computer-Aided Chemical Thermodynamics of Gases and Liquids*, Wiley, New York, 1985.
  11. K. J. Johnson, *Numerical Methods in Chemistry*, p. 226. Dekker, New York, 1980.
  13. A. Okáč and Z. Kolařík, *Collection Czech. Chem. Commun.*, 1959, **24**, 1.
  14. E. Högfeldt, *Stability Constants of Metal-Ion Complexes*, Part A, *Inorganic Ligands*, Pergamon Press, Oxford, 1982.
  15. D. D. Perrin, *Stability Constants of Metal-Ion Complexes*, Part B, *Organic Ligands*, Pergamon Press, Oxford, 1979.
  16. *Numerical Methods, Toolbox*, Turbo Pascal, IBM Version, Borland International, Inc., 1986.
  17. A. L. Horvath, *Handbook of Aqueous Electrolyte Solutions*, Horwood, Chichester, 1985.
  18. P. A. H. Saunders and J. D. Wilkins, *Chem. Brit.*, 1987, **23**, 448.

## APPENDIX

Listing of the RAMESES algorithm as a subroutine in Hewlett-Packard BASIC. Equation numbers (eqn) refer to the main text. Data input and matrix manipulation are omitted.

```

1000 ! RAMESES
1010 !
1020 ! matrix X1 = XA @ eqn(1)
1030 ! matrix X2 = XB @ eqn(2)
1040 ! matrix C1 = CA @ eqn(6)
1050 ! matrix C2 = CB @ eqn(7)
1060 ! matrix P1 = PA @ eqn(5)
1070 ! matrix P2 = PB @ eqn(7)
1080 ! matrix M0 = M* @ eqn(17)
1090 ! matrix S0 = S* @ eqn(18)
1100 ! matrix I = identity
1110 ! E = tolerance
1120 ! F = f @ eqn(15)
1130 ! J = index of charge balance sp.
1140 ! R = r: no. equilibria
1150 ! S = s: no. of spp.
1160 ! T = t: independent spp.
1170 !
1180 T(J) = 0
1190 MAT C3 = INV(C2)
1200 FOR I = 1 TO R
1210 L(I) = LGT(K(I)) ! eqn(4)
1220 NEXT I
1230 !
1240 FOR N = 1 TO 500 ! iteration
1250 !
1260 FOR I = 1 TO T
1270 P1(I) = LGT(X1(I)) ! eqn(5)
1280 NEXT I
1290 MAT Z = C1 * P1
1300 MAT Z = L - Z ! eqn(6)
1310 MAT P2 = C2 * Z ! eqn(7)
1320 FOR I = 1 TO R
1330 X2(I) = 10 ^ P2(I) ! eqn(8)
1340 NEXT I
1350 MAT X(1:T) = X1 ! eqn(3)
1360 MAT X(T+1:S) = X2 ! eqn(3)
1370 !
1380 ! totals
1390 MAT S = TRN(M) * X ! eqn(12)
1400 FOR I = 1 TO T
1410 F(I, I) = T(I) / (S(I) ! eqn(13)
1420 NEXT I
1430 !
1440 ! charge correction
1450 MAT D = TRN(Q) * X ! eqn(11)
1460 F0 = 1 - F * (D(1) + D(2)) / (D(1) * Q(J, 1) - D(2)
    * Q(J, 2)) ! eqn(14)
1470 IF F0 < 0 THEN F0 = .01
1480 F(J, J) = F0
1490 !
1500 ! tolerance check
1510 MAT E = F - I ! eqn(15)
1520 IF MAXAB(E) < E THEN 1730
1530 !
1540 ! independent | charge
1550 FOR K = 1 TO S
1560 FOR L = 1 TO T
1570 IF M(K, L) AND M(K, J) THEN M0(K, L) =
    M(K, L) * F0 ELSE M0(K, L) = M(K, L) ! eqn(17)
1580 NEXT L
1590 NEXT K
1600 !
1610 ! charge adjusted totals
1620 MAT S0 = TRN(M0) * X ! eqn(18)
1630 FOR I = 1 TO T
1640 F(I, I) = T(I) / S0(I) ! eqn(19)
1650 NEXT I
1660 F(J, J) = F0
1670 !
1680 IF AMIN(F) < 0 THEN F(AMINROW,
    AMINROW) = .01 @ GOTO 1680
1690 MAT X1 = F * X1 ! eqn(16)
1700 IF N > 20 AND X1(J) < 1.E-25 THEN 1720
1710 NEXT N
1720 PRINT "NO SOLUTION"
1730 RETURN
1740 END

```



## SHORT COMMUNICATIONS

# COMPLEXOMETRIC DETERMINATION OF MERCURY(II) WITH 2-IMIDAZOLIDINETHIONE AS A SELECTIVE MASKING AGENT

B. NARAYANA and M. R. GAJENDRAGAD\*

Department of Post-Graduate Studies and Research in Chemistry, Mangalore University,  
Mangalagangothri 574 199, Karnataka, India

(Received 25 March 1987. Revised 26 December 1987. Accepted 24 May 1988)

**Summary**—A simple, rapid and selective complexometric method is proposed for the determination of mercury(II). Mercury(II) is first complexed with a known excess of EDTA and the surplus EDTA is back-titrated at pH 5.0–6.0 with lead nitrate, Xylenol Orange being used as indicator. 2-Imidazolidinethione is then added to displace EDTA from the Hg–EDTA complex quantitatively and the EDTA released is titrated with lead nitrate. Reproducible and accurate results are obtained for 2–75 mg of mercury, with a relative error of less than 0.3% and standard deviation of less than 0.04 mg.

Körbl and Přibil<sup>1</sup> reported the determination of Hg(II) by complexation with EDTA in presence of associated cations, followed by selective decomposition of the Hg–EDTA complex with a masking agent such as thiosemicarbazide, and titration of the EDTA liberated. In this method Cu(II) interferes severely. Volf<sup>2</sup> titrated Ca<sup>2+</sup> and Mg<sup>2+</sup> with EDTA in presence of Hg(II), Pb(II) and Zn(II) by masking these three ions with unithiol. Ueno<sup>3</sup> suggested potassium iodide as releasing agent in alkaline medium for indirect complexometric determination of Hg(II) in the presence of Cu(II), but found that several cations interfered. Singh<sup>4</sup> described the determination of Hg(II) in presence of various cations with thiourea as releasing agent; the interference of copper was avoided by controlling the pH at 5.5 and cooling the solution to below 15°. Good results in presence of Cu(II) are obtainable with thiourea as releasing agent provided it is added in only slight excess, relative to the mercury, which suggests that a preliminary estimation would be needed for completely unknown concentrations of mercury. Barcza and Körös<sup>5</sup> used thiocyanate to mask Hg(II) during the determination of Bi(III) at pH 1.0. The mercury thiocyanate complex could then be decomposed by silver ions and the liberated mercury(II) titrated with EDTA at pH 5.0–6.0 in the same solution. Chickerrur and Venugopalam<sup>6</sup> suggested a method for the determination of Hg(II) in the presence of Ca<sup>2+</sup> by masking Ca<sup>2+</sup> with ammonium fluoride. The selective determination of Hg(II) suggested by Vasilikiotis and Apostotopoulou<sup>7</sup> with *N*-allylthiourea as releasing agent is inconvenient because it involves heating for decomposition of the Hg–EDTA complex, and some

precipitation of HgS occurs. 4-Amino-5-mercapto-1,2,4-triazole<sup>8</sup> and thiocyanate<sup>9</sup> have been found to be reliable and convenient as replacing reagents.

This paper demonstrates the merits of 2-imidazolidinethione (IMT) as a selective releasing agent for the indirect complexometric determination of Hg(II) by EDTA titration.

## EXPERIMENTAL

### Reagents

*2-Imidazolidinethione (IMT)*. Synthesized as reported in the literature<sup>11</sup> and used as a 0.5% solution in acetone.

*Mercuric chloride solution*. Prepared from analytical grade material and standardized by the ethylenediamine method.<sup>12</sup>

*Lead nitrate solution, 0.02M*. Standardized by the salicylaldoxime method.<sup>12</sup>

*EDTA solution, 0.04M*. Prepared by dissolving the disodium salt in distilled water.

*Xylenol Orange (XO) indicator solution (0.5%)*.

### Procedure

To an aliquot of acidic solution [containing 2–75 mg of Hg(II)], an excess of 0.04M EDTA is added and the mixture is diluted to about 100 ml. The pH is adjusted to 5.0–6.0 by adding hexamine, a few drops of XO indicator are added and the excess of EDTA is back-titrated with the standard lead nitrate solution. An excess of IMT solution in acetone is added, and after 3–5 min the EDTA liberated is titrated with the lead nitrate solution. This second volume of titrant is equivalent to the Hg(II) present in the aliquot taken.

### Analysis of mercury complexes

A number of mercury(II) complexes with some sulphur-containing ligands were prepared by conventional methods and their purity checked by elemental analysis. About 0.2–0.4 g of complex was decomposed by evaporation to near dryness with *aqua regia*. The residue was then cooled, dissolved in water and the solution made up accurately to 100 ml. Aliquots of 100 ml were used for titration by the procedure above.

\*Author for correspondence.

Table 1. Determination of mercury(II) in mercuric chloride solution

Hg taken, mg	Hg found,* mg	Standard deviation, mg
1.92	1.92	0.02
3.83	3.82	0.02
9.58	9.56	0.02
19.17	19.18	0.02
28.75	28.73	0.04
38.33	38.36	0.03
47.91	47.89	0.03
67.08	67.19	0.04
76.66	76.62	0.04

\*Average of five determinations.

### RESULTS AND DISCUSSION

The fact that IMT displaces EDTA quantitatively from the Hg-EDTA complex indicates that the Hg-IMT complex is more stable than the Hg-EDTA complex. The reaction takes place quantitatively and rapidly at room temperature. Further, unlike many thio-ligands, IMT forms a highly soluble (1:2 metal:ligand)<sup>10</sup> mercury complex. The absence of a precipitate in the reaction mixture favours sharpness of the end-point. At least 100% excess of IMT is required for complete release of EDTA from its mercury complex, but a larger excess has no adverse effect. A high concentration of chloride and sulphate should be avoided, since they may tend to form a precipitate with the titrant.

Table 1 shows that accurate and reproducible results are obtainable for analysis of mercuric chloride with a maximum relative error of  $\pm 0.3\%$ . The effects of various metal ions and anions on the determination of mercury(II) was studied. It is noteworthy that copper(II) can be tolerated even at above three fold w/w ratio to mercury, without the need for secondary masking agents and cooling to below room temperature, unlike some earlier methods. However, the presence of Pd(II), Fe(II) or Fe(III) results in

sluggish end-points and a positive error, possibly because of slow partial demasking of their EDTA complexes by IMT. No interference in the determination of 20 mg of mercury was observed when any of the following ions were present, in the amounts stated in brackets: Zn, citrate, chloride, oxalate, sulphate, tartrate (100 mg); Cd (80 mg); Bi, Co, Cu, Ni (60 mg); Zr (50 mg); Al, Cr(III), La, Ti(IV) (25 mg), Mn(II) (12 mg), Au(III) (8 mg); Sn(IV) interferes severely.

A special feature of the reagent is that it does not form any precipitate with either Hg(II) or Pb(II) under the experimental conditions; this results in a sharp end-point without the need for addition of other chemicals. The method works well for up to 75 mg of mercury. A further advantage of the method is that it does not require heating or cooling before or during the titration, or extraction of the mercury complex.

*Acknowledgement*—One of the authors (B.N.) is grateful to Mangalore University, Mangalore for providing a Research Fellowship.

### REFERENCES

1. J. Körbl and R. Pribil, *Chem. Listy*, 1957, **51**, 667.
2. L. A. Volf, *Zavodsk. Lab.*, 1959, **25**, 1438.
3. K. Ueno, *Anal. Chem.*, 1957, **29**, 1669.
4. R. P. Singh, *Talanta*, 1969, **16**, 1447.
5. L. Barcza and E. Kőrös, *Chemist-Analyst*, 1959, **48**, 94.
6. N. S. Chickerrur and R. Venugopalam, *J. Inst. Chem. India*, 1974, **46**, 11.
7. G. S. Vasilikiotis and C. D. Apostolopoulou, *Microchem. J.*, 1975, **20**, 66.
8. H. R. A. Gadiyar, R. V. Gadag and M. R. Gajendra-gad, *Talanta*, 1982, **29**, 941.
9. K. N. Raoot, S. Raoot and L. Kumari, *ibid.*, 1983, **30**, 611.
10. B. Singh, D. K. Sharma, U. S. P. Sharma and B. K. Sharma, *J. Indian Chem. Soc.*, 1979, **46**, 964.
11. J. Van Allan, *Organic Synthesis*, Coll. Vol. 3, p. 394. Wiley, New York, 1955.
12. A. I. Vogel, *A Text Book of Quantitative Inorganic Analysis*, 3rd Ed., p. 482. Longmans, London, 1951.

## COMPLEXOMETRIC TITRATION OF THALLIUM(III), BY USE OF 4-AMINO-5-MERCAPTO-3-PROPYL-1,2,4-TRIAZOLE AS REPLACING REAGENT

NITYANANDA SHETTY A. and R. V. GADAG

Department of Chemistry, Karnataka Regional Engineering College, Surathkal, Srinivasnagar, 574 157,  
India

M. R. GAJENDRAGAD\*

Department of Chemistry, Mangalore University, Mangalagangothri, 574 199, Karnataka, India

(Received 1 September 1986. Revised 26 December 1987. Accepted 24 May 1988)

**Summary**—A simple and selective EDTA method using a masking and demasking technique is proposed for the determination of thallium(III). The thallium is complexed with excess of EDTA, the surplus being back-titrated (pH 5–6, hexamine buffer) with zinc sulphate solution (Xylenol Orange as indicator). 4-Amino-5-mercapto-3-propyl-1,2,4-triazole is then added and the mixture heated on a water-bath for 5–10 min to displace EDTA from its thallium complex. The EDTA liberated is titrated with zinc sulphate solution. Reproducible and accurate results are obtained in the range 5–75 mg of thallium with both the relative error and coefficient of variation not exceeding 0.4%.

4-Amino-5-mercapto-3-propyl-1,2,4-triazole (HPAMT) has been used as a displacing reagent in the complexometric determination of Hg(II) and Pd(II).<sup>1,2</sup> Although sodium thiosulphate,<sup>3</sup> ascorbic acid,<sup>4</sup> diethylenetriamine-*N,N,N',N'',N''*-penta-acetic acid,<sup>5</sup> EDTA, *etc.*, have been used for indirect complexometric titration of Tl(III), complexometric determination of Tl(III) by the demasking technique is rare. Thiopyrine<sup>6</sup> is one such reagent used in chelatometric titration of Tl(III). Here we report on the use of HPAMT for the purpose.

### EXPERIMENTAL

#### Reagents

**HPAMT.** The reagent was synthesized by the method reported in the literature.<sup>7</sup> The product was recrystallized twice and the purity of the sample checked by elemental analysis and the m.p. (104°). The reagent was used as a 1% solution in acetone.

**Thallium(III) chloride solution.** Prepared from analytical grade thallium(I) nitrate<sup>8</sup> and standardized by the chromate method.<sup>9</sup>

**Zinc sulphate solution, 0.02M.** Prepared from analytical grade material and standardized by a gravimetric method.<sup>10</sup>

**EDTA solution, 0.04M.** Made from the disodium salt and demineralized water.

**Xylenol Orange, 0.5% aqueous solution.**

#### Procedure

To a known volume of acidic sample containing 5–75 mg of Tl(III), an excess of 0.04M EDTA was added and the mixture was heated to about 80° to ensure complexation of species such as Al(III), which react slowly with EDTA. The solution was diluted to 30 ml with distilled water and the pH adjusted with solid hexamine to 5–6. The surplus EDTA was titrated with 0.02M zinc sulphate to the sharp colour change of Xylenol Orange to red-violet. A 1% solution of HPAMT in acetone (1 ml for every 3 mg of Tl) was added, and the

reaction mixture was heated on a water-bath for 5–10 min, then cooled to room temperature and the EDTA released was titrated with zinc solution as before, the volume needed corresponding to the thallium present.

#### Analysis of thallium complexes

A number of Tl(I) complexes with some sulphur-donor ligands were prepared and their purity was checked by elemental analysis. About 0.3 g of the complex was decomposed by evaporation nearly to dryness with *aqua regia*. The residue was cooled, dissolved in 3 ml of 2M hydrochloric acid, and made up to volume in a 250-ml standard flask with demineralized water, and 25-ml aliquots were used for titration by the procedure above.

### RESULTS AND DISCUSSION

#### Effect of excess of HPAMT

Experiment showed that 1 ml of 1% solution of HPAMT for every 3 mg of Tl(III) was sufficient for quantitative displacement of EDTA from the Tl-EDTA complex, but no adverse effects were observed when a larger ratio was used.

#### Effect of heat

The displacement of EDTA from the Tl-EDTA complex by HPAMT at room temperature was rather slow and the end-point of the titration not sharp. Quantitative release and a sharp end-point were obtained when the reaction mixture was heated on a water-bath for 5–10 min before the second titration.

#### Accuracy and precision

Six titrations of thallium at each of eight levels ranging from 7.6 to 76 mg, gave coefficients of variation not exceeding 0.4% and a maximum mean error of 0.4%.

\*Author for correspondence.

Table 1. Analysis of thallium complexes

Complex	Tl theoretically present, %	Tl found, %
Tl(C <sub>3</sub> H <sub>7</sub> N <sub>4</sub> S)*	61.27	61.4
Tl(C <sub>11</sub> H <sub>11</sub> N <sub>4</sub> S)†	46.97	46.0
Tl(C <sub>2</sub> H <sub>2</sub> N <sub>3</sub> S <sub>2</sub> )‡	60.73	60.5
Tl(C <sub>2</sub> H <sub>3</sub> N <sub>4</sub> S <sub>2</sub> )‡	58.13	58.4

\*Thallium complex of 4-amino-5-mercapto-3-methyl-1,2,4-triazole.

†Thallium complex of 4-benzylidene-3-ethyl-5-mercapto-1,2,4-triazole.

‡Thallium complex of 5-amino-2-mercapto-1,3,4-thiadiazole.

‡Thallium complex of 4-amino-3,5-dimercapto-1,2,4-triazole.

#### Effect of foreign ions

The effect of other metal ions on the accuracy and precision of the method was examined by determining 20 mg of Tl(III) in presence of each of these cations. The tolerance levels found were 200 mg for Au(III) and Pb, 100 mg for Co, 60 mg for Cu and Cd, 40 mg for Ni and Fe(III), and 20 mg for Mn(II). However, Hg(II), Pd(II), Bi(III), Sn(IV) and Cr(III) interfere severely. The interference of Cr(III) is due to the deep purple colour of its EDTA complex. It is important to add the indicator only *after* the addition of excess of EDTA and heating of the solution, otherwise the indicator may be "blocked" by any aluminium, gallium or indium present.

#### Application

The proposed method is useful for the determination of thallium in its complexes with sulphur-containing ligands and also in mixtures of salts of thallium(III). It can also be used for the determination of the composition of alloys containing Tl as an alloying element. Same results are summarized in Table 1.

#### Composition of the Tl-HPAMT complex

Whereas Tl(I) shows little tendency for complexation<sup>11</sup> with EDTA, Tl(III) forms a stable chelate<sup>12</sup> (log *K* = 22.5). Like many mercapto compounds, HPAMT is a powerful reducing agent. It also forms stable complexes with soft metal ions.<sup>13,14</sup> It can therefore be expected that it would first reduce Tl(III) to Tl(I) and then form a stable chelate with the latter. This is the principle underlying the displacement of EDTA from the Tl-EDTA complex by

Table 2. Analysis of HPAMT and its thallium complex\*

		C*	H*	N*	S†	Tl†
C <sub>3</sub> H <sub>10</sub> N <sub>4</sub> S	Theory, %	37.9	6.3	35.4	20.3	—
	Found, %	38.3	6.1	35.5	20.3	—
TlC <sub>5</sub> H <sub>9</sub> N <sub>4</sub> S	Theory, %	16.6	2.5	15.5	8.9	56.5
	Found, %	16.5	2.6	15.5	8.8	56.3

\*Microanalysis done at CDRI, Lucknow.

†Semimicroanalysis.

HPAMT. To confirm this and determine the composition of the complex, solid Tl-HPAMT complex was prepared and analysed. The results (Table 2) are in agreement with a 1:1 molar ratio of thallium to HPAMT. The oxidation state of thallium in the complex was further confirmed by a spot-test for Tl(I),<sup>15</sup> a red precipitate being produced when a solution of the complex in dilute hydrochloric acid was treated with one drop each of bismuth nitrate and sodium iodide. The cause for the slow displacement of EDTA from the Tl-EDTA complex by HPAMT in the cold is presumably due to a slow rate of reduction, which should increase on heating.

*Acknowledgements*—The authors are thankful to Professors B. S. Basavarajaiah and T. Ramchandran, Principals, and Professor S. B. Akki, Head of the Chemistry Department, Karnataka Regional Engineering College, for providing laboratory facilities and all-round help.

#### REFERENCES

- H. R. A. Gadiyar, R. V. Gadag and M. R. Gajendragad, *Talanta*, 1982, **29**, 941.
- Idem*, *J. Indian Chem. Soc.*, 1983, **60**, 889.
- M. M. Amer, R. Přibil, M. S. Tawakkol, *Egypt. J. Pharm. Sci.*, 1976, **17**, 21.
- L. Erdey, K. Vigh and I. Buzás, *Acta Chem. Acad. Sci. Hung.*, 1961, **26**, 85.
- F. Ya, Kulba and N. B. Platonova, *Zh. Analit. Khim.*, 1973, **28**, 1009.
- T. Tanaka, *Yakugaku Zasshi*, 1973, **93**, 252.
- K. S. Dhaka, J. Mohan, V. K. Chadha and H. K. Pujari, *Indian J. Chem.*, 1974, **12**, 288.
- R. C. Agarwal and A. K. Srivastava, *ibid.*, 1966, **4**, 359.
- A. I. Vogel, *A Text Book of Quantitative Inorganic Analysis*, 2nd Ed., p. 478. Longmans, London, 1951.
- R. Přibil, *Talanta*, 1967, **14**, 613.
- K. Saito and H. Jerry, *J. Chem. Soc.*, 1956, 4701.
- R. G. Pearson, *J. Am. Chem. Soc.*, 1963, **83**, 3533.
- Idem*, *Science*, 1966, **151**, 172.
- Idem*, *Chem. Brit.*, 1967, **3**, 103.
- C. J. Van Nieuwenburg and J. Gillis, *Reagents for Qualitative Inorganic Analysis*, p. 160. Elsevier, Amsterdam, 1948.

# A HIGHLY SENSITIVE SPECTROPHOTOMETRIC DETERMINATION OF CADMIUM WITH $\alpha,\beta,\gamma,\delta$ -TETRAKIS(4-*N*-TRIMETHYLAMINOPHENYL)- PORPHINE

MASASHI KOMATA and JUN-ICHI ITOH\*

Department of Environmental Chemistry, Kitami Institute of Technology, Koen-cho 165, Kitami-shi,  
Hokkaido, 090 Japan

(Received 9 December 1987. Accepted 24 May 1988)

**Summary**—A new and highly sensitive reagent is proposed for spectrophotometric determination of cadmium.  $\alpha,\beta,\gamma,\delta$ -Tetrakis (4-*N*-trimethylaminophenyl) porphine forms a chelate with cadmium in alkaline solution with a molar absorptivity of  $5.77 \times 10^5$  l. mole<sup>-1</sup>. cm<sup>-1</sup>, the largest value reported to date for a cadmium complex. An extraction method is described for selective separation of cadmium.

Extensive studies have been made of the complexation of metal ions with water-soluble porphyrins and its application to spectrophotometric determination.<sup>1-3</sup> Three tetraphenylporphines have been proposed as sensitive reagents for cadmium.<sup>4,5</sup> We have previously reported that  $\alpha,\beta,\gamma,\delta$ -tetrakis(4-*N*-trimethylaminophenyl)porphine (I) is the most sensitive reagent for copper.<sup>6,7</sup> Further investigation has shown that it is also the most sensitive reagent for cadmium, allowing its determination at levels as low as 10 ng/ml without preconcentration.

## EXPERIMENTAL

### Reagents

The *p*-toluenesulphonate of I was prepared by the method described in a previous paper,<sup>6</sup> and an  $8 \times 10^{-5}M$  solution was prepared by dissolving 0.063 g of it in water and diluting to 500 ml. The solution was standardized by photometric titration with a standard copper solution. A 0.01M cadmium solution was prepared by dissolving 1.54 g of cadmium nitrate tetrahydrate in water containing a small amount of nitric acid and diluting to 500 ml, and was standardized by titration with EDTA. Other reagents were of reagent grade. The water used was distilled twice and then subjected to Milli-Q purification.

### Apparatus

Measurements were made with a Hitachi 200-10 type spectrophotometer equipped with a 1-cm cell.

### Separation of cadmium

The method previously reported for selective separation of cadmium<sup>4</sup> was modified. To the sample solution (500 ml, containing less than 9  $\mu$ g of cadmium) 10 ml of 0.25M hydrobromic acid/0.25M potassium bromide and 10 ml of 5% triethylamine/xylene solution are added. The solution is shaken for 10 min in a separatory funnel, the aqueous phase is discarded, and the cadmium is stripped with two 10-ml portions of sodium hydroxide.

### Spectrophotometric determination

A 40-ml portion of sample containing not more than 9  $\mu$ g of cadmium is transferred to a 100-ml amber-coloured flask. Then 5 ml of 2M sodium hydroxide are added (this is not necessary if the sample is prepared by extraction), and the mixture is brought to the boil. Then 1 ml of  $8 \times 10^{-5}M$  reagent solution is added, and after 2 min the solution is cooled to room temperature and diluted accurately to 50 ml with water. The absorbance at 433 nm is measured against water.

## RESULTS AND DISCUSSION

In alkaline solution, I forms a 1:1 complex with cadmium. The absorption spectra of the Soret bands of I and the complex are shown in Fig. 1. In alkaline solution, I is reddish-purple and has a Soret band absorption peak at 411 nm ( $\epsilon = 5.2 \times 10^5$  l. mole<sup>-1</sup>. cm<sup>-1</sup>); the cadmium complex is green and has a Soret band absorption peak at 433 nm ( $\epsilon = 5.77 \times 10^5$  l. mole<sup>-1</sup>. cm<sup>-1</sup>). The molar absorptivity of I is larger in alkaline medium in neutral solution.<sup>7</sup> The molar absorptivity for the complex is the largest so far reported for a cadmium complex. The absorbances of the reagent and the complex are unaffected by the alkali concentration in the range 0.1-1M sodium hydroxide. At room temperature, the complex formation reaction proceeds instantaneously to about 90% completion and then stops, so heating is necessary for quantitative reaction, and is complete after heating for over 1 min at 90°. Bases such as imidazole, pyridine and 2,2'-bipyridyl, which have been reported as effective catalysts for formation of cadmium complexes with other porphyrins,<sup>4</sup> do not accelerate the reaction with I. Like other cadmium-porphyrin complexes, the Cd-I complex is decomposed by light; the absorbance is decreased by 15% after 1 hr under room lighting, but is not

\*Author to whom correspondence should be addressed.

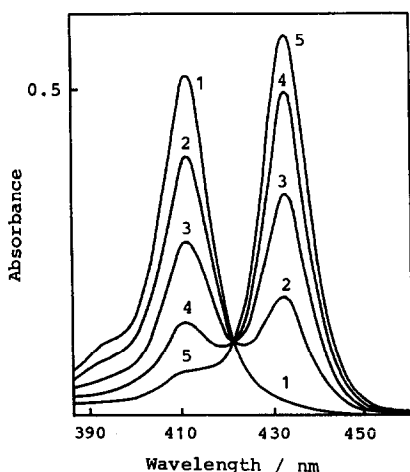


Fig. 1. Absorption spectra of I and its cadmium complex.  $[I] = 10^{-6}M$ ;  $[Cd(II)]$ : 1, 0; 2,  $2.7 \times 10^{-7}$ ; 3,  $5.4 \times 10^{-7}$ ; 4,  $8.1 \times 10^{-7}$ ; 5,  $1.08 \times 10^{-6}M$ .

changed at all after 8 hr if the complex is kept in an amber-coloured flask.

The calibration curve is linear for up to  $9 \mu\text{g}$  of cadmium. By use of a spectrophotometer with an expanded full-scale absorbance range of 0.1, a cadmium concentration of  $10 \text{ ng/ml}$  can be directly determined. The relative standard deviation found for 5 determinations of  $67 \text{ ng/ml}$  cadmium was 2.4%.

The interference of various ions with the direct determination without extraction was examined, the criterion for interference being a deviation of  $\pm 5\%$ .  $Au(III)$ ,  $Bi(III)$ ,  $Mo(VI)$ ,  $Pb(II)$ ,  $Pd(II)$ ,  $Sn(II)$ ,  $V(V)$  and  $V(IV)$  could be tolerated at 300:1 w/w ratio to Cd, but  $Ag(I)$ ,  $Co(II)$ ,  $Cr(III)$ ,  $Cu(II)$ ,  $Fe(II)$ ,  $Fe(III)$ ,  $Hg(II)$ ,  $Ni(II)$ ,  $Mn(II)$  and  $Zn(II)$  interfered at this level. However, cadmium could be selectively separated from  $1000 \mu\text{g}$  of each of these interfering ions, except  $Hg(II)$  and  $Zn(II)$ , by the extraction system described above. The tolerance limit thus obtained for  $Zn(II)$  was  $50 \mu\text{g}$ , and the interference of  $50 \mu\text{g}$  of  $Hg(II)$  could be avoided by adding 2 ml of  $10^{-3}M$  thiourea as masking reagent.

#### REFERENCES

1. J. Itoh, T. Yotsuyanagi and K. Aomura, *Anal. Chim. Acta*, 1975, **74**, 53.
2. T. Makino and J. Itoh, *Rinshou Kagaku*, 1979, **8**, 296.
3. J. Itoh, M. Yamahira, T. Yotsuyanagi and K. Aomura, *Bunseki Kagaku*, 1976, **25**, 781.
4. S. Igarashi, J. Itoh, T. Yotsuyanagi and K. Aomura, *Nippon Kagaku Kaishi*, 1978, 212.
5. H. Koh, K. Kawamura and H. Ishii, *ibid.*, 1979, 591.
6. T. Makino and J. Itoh, *Clin. Chim. Acta*, 1981, **111**, 1.
7. J. Itoh, M. Komata and H. Oka, *Bunseki Kagaku*, 1988, **37**, T1.

## ALKALIMETRIC DETERMINATION OF MERCURY BY USE OF ITS REACTION WITH 1-MERCAPTOPROPAN-2,3-DIOL

KRISHNA K. VERMA, PRAMILA TYAGI and SUNIL K. SANGHI  
Department of Chemistry, Rani Durgavati University, Jabalpur 482001, India

(Received 3 October 1986. Revised 18 February 1988. Accepted 16 May 1988)

**Summary**—The reaction of mercury(II) with 1-mercaptopropan-2,3-diol to form its mercaptide and protons, and alkalimetric titration of the acid produced is proposed as a simple and rapid method for determination of mercury. Any acid already present is first neutralized to Phenol Red indicator after complexation of the mercury(II) with iodide to avoid precipitation of mercuric oxide. Mercury metal, its insoluble salts in both oxidation states, complexes and organomercury compounds have been determined after digestion with nitric acid and persulphate to produce mercury(II). The interference of copper(II) is avoided by its reduction and solvent extraction with 2-benzoxazolethiol. The method is unaffected by the presence of large amounts of halides, oxalate, tartrate, citrate, fluoride, EDTA, thiocyanate and thiourea, which all interfere severely in complexation titrations.

Most of the titrimetric procedures for mercury are applicable only to ionized mercury(II) salts<sup>1</sup> and cannot be applied to those which are either feebly dissociated such as mercuric chloride, or contain a masking anion such as cyanide or thiocyanate. Mercuric chloride is usually determined by reduction to mercurous chloride, which is titrated with iodine<sup>1</sup> or iodate.<sup>2,3</sup> The same method is also applicable to other salts of mercury(II) such as the acetate and phosphate and the tetraiodo complex, but not to the cyanide, which fails to undergo reduction even after several hours of heating with a reducing agent.<sup>2</sup> Direct EDTA titration of mercury(II) has poor selectivity and its modifications still suffer interference from masking anions and copper(II).<sup>4</sup>

Recently, 2-mercaptopropionic acid has been used for the alkalimetric determination of mercury(II)<sup>5</sup> but has the disadvantage that the reagent is acidic and that acid or basic impurities and copper(II) interfere. However, we have found that mercury(II) can be determined by reacting it with an excess of 1-mercaptopropan-2,3-diol and titrating the liberated acid with sodium hydroxide. Any free acid present cannot be directly neutralized (with phenolphthalein or Phenol Red as indicator) since precipitation of mercuric hydroxide (or oxide) begins near the equivalence point, but this can be circumvented by first complexing the mercury with excess of iodide; the tetraiodomercurate anion does not react with alkali, and any concomitant acidity can be completely neutralized. Elemental mercury, mercurous salts and organomercury compounds are oxidized to give mercury(II), which is then determined. The interference of copper(II) is avoided by solvent extraction of its 2-benzoxazolethiol mercaptide.

### EXPERIMENTAL

#### Reagents

*1-Mercaptopropan-2,3-diol*, 1% solution in water. The solution is stable for several months.

*Sodium hydroxide*, 0.02 and 0.04M. Standardized with furoic acid.

*Phenol Red*, 0.05% solution in 95% ethanol.

#### Samples

All mercury compounds tested were analytical reagent grade chemicals and their mercury content was determined by established procedures (Tables 1 and 2).

#### Determination of mercury(II)

Shake a weighed quantity of sample containing 5–40 mg of mercury(II) with about 0.5 g of potassium iodide and 25 ml of demineralized water until dissolution is complete, then add 3 or 4 drops of Phenol Red indicator and neutralize any acid or base impurity present with 0.02M sodium hydroxide or hydrochloric acid. Add 5 ml of 1% 1-mercaptopropan-2,3-diol solution with swirling and titrate the liberated acid with 0.02M sodium hydroxide for up to 20 mg of mercury or with 0.04M sodium hydroxide for larger amounts. The end-point is shown by appearance of the pink colour of the indicator.  $Hg \text{ (mg)} = 1.00.3VM$  where  $V$  is the volume used (ml) of sodium hydroxide of molarity  $M$ . To analyse mercury(II) oxide or cyanide, digest the sample with 5 ml of hydrochloric acid (1 + 1), evaporate just to dryness, dissolve the residue in demineralized water and proceed as for mercury(II) determination.

#### Determination of mercury(II) in the presence of copper(II)

Acidify the test solution with 2 ml of 1% hydrochloric acid, dilute to 25 ml with water, add 5 ml of 0.5% 2-benzoxazolethiol solution in chloroform, followed by 5 ml of aqueous 4% thiourea solution, and shake the mixture in a separatory funnel. The copper complex is extracted, while the mercury(II) thiourea complex remains in the aqueous phase. Discard the chloroform layer, and repeat the extraction with 5-ml portions of chloroform until the extracts are colourless (three extractions are sufficient). Analyse the aqueous phase for mercury(II) as above.

Table 1. Determination of mercury without involving any pre-digestion

Mercury(II) salt	Mercury, mg, found by	
	Present method*	Comparison method†
Chloride	4.99 ± 0.01	5.00 a
	10.16 ± 0.02	10.01 a
	12.75	12.13 a
	25.49 ± 0.05	25.03 a
	35.82 ± 0.09	35.04 a
	38.05 ± 0.11	37.55 a
Acetate	4.95 ± 0.01	5.02 b
	5.95 ± 0.01	6.01 b
	7.43 ± 0.02	7.50 a
	10.00 ± 0.02	9.90 c
	14.95	15.01 b
	19.53	19.96 c
Bromide	24.32 ± 0.06	25.01 b
	34.44	34.98 b
	6.07 ± 0.01	5.98 a
	7.43	7.47 c
	10.13 ± 0.02	9.97 a
	19.58 ± 0.02	19.95 c
Nitrate	24.54	24.93 c
	34.66 ± 0.06	34.84 a
	48.84 ± 0.15	49.85 a
	10.54	10.01 b
	15.34 ± 0.03	15.05 b
	20.08	19.97 a
Thiocyanate	25.31 ± 0.06	25.02 a
	35.34 ± 0.06	35.25 b
	10.07 ± 0.02	9.92 c
	19.95 ± 0.04	20.14 c
	25.62	25.17 c
	30.10 ± 0.07	30.21 c
	35.68 ± 0.07	35.52 c

\*Average of six determinations ± standard deviation.

†Comparative results were produced by (a) reduction and iodate titration,<sup>3</sup> (b) EDTA back-titration,<sup>16</sup> and (c) digestion with nitric acid/peroxydisulphate and EDTA back-titration.<sup>16</sup>

#### Determination of elemental mercury, mercurous salts and organomercury compounds

Boil a known amount of sample, containing 5–40 mg of mercury, with 5 ml of concentrated nitric acid, then with two successive 5-ml portions of nitric acid (1 + 1) containing about 2 g of potassium peroxydisulphate, evaporate gently, cool the residue, take up soluble salts with 20 ml of water, filter off any insoluble material on a Whatman No. 41 filter paper, and analyse the filtrate for mercury(II).

### RESULTS AND DISCUSSION

Most of the methods for the analysis of biological and environmental materials require decomposition of the sample. In analysis of biological samples for toxic elements, especially mercury, to avoid loss of analyte the sample decomposition has usually been conducted in closed systems,<sup>6–8</sup> or in open systems coupled with means of trapping the volatile elements.<sup>9,10</sup> In many instances a simple open decomposition procedure would be of advantage. One such method<sup>11</sup> provides quantitative recovery of mercury, but the resulting chloric acid medium is often not

Table 2. Determination of mercury after pre-digestion

Test substance	Mercury found, mg	
	Present method*	Comparison method†
Mercury metal	5.36 <sup>a</sup> ± 0.01	5.30
	9.73 <sup>b</sup>	9.75
	13.16 <sup>c</sup> ± 0.03	13.20
	19.71 <sup>d</sup>	19.76
	24.80 <sup>e</sup> ± 0.06	24.62
	29.13 <sup>f</sup>	29.21
	35.28 <sup>g</sup> ± 0.11	35.35
Mercurous nitrate	5.06 ± 0.01	4.98
	7.52	7.48
	10.10 ± 0.02	9.97
	12.02	12.22
Mercurous chloride	13.88 ± 0.04	13.49
	10.03 ± 0.02	10.14
	19.97	20.02
	24.97 ± 0.05	24.94
Mercuric oxide	29.58	29.63
	34.90 ± 0.07	34.86
	49.48 ± 0.13	49.15
	5.08 ± 0.01	4.99
Mercuric cyanide	9.93	10.03
	19.08	19.97
	25.17 ± 0.06	25.00
	34.78 ± 0.10	35.02
Mercurous nitrate	5.17 ± 0.01	5.29
	9.86	10.12
	20.14 ± 0.05	20.30
	25.43	25.25
	30.39 ± 0.09	30.14

\*Average of six determinations ± standard deviation. The weights of mercury taken for analysis were (a) 5.32 mg, (b) 9.78 mg, (c) 13.25 mg, (d) 19.82 mg, (e) 24.70 mg, (f) 29.28 mg, and (g) 35.46 mg.

†Comparative results for mercurous chloride by iodate titration,<sup>3</sup> and for the other substances by digestion with nitric acid/peroxydisulphate and EDTA back-titration.<sup>16</sup>

suitable for the determination procedure. It has been experimentally confirmed<sup>12,13</sup> that losses of mercury from hydrochloric acid/hydrogen peroxide and nitric acid/hydrochloric acid/hydrogen peroxide mixtures at temperatures up to 220–250° are undetectable, but the decomposition of organic matter is reported not to be complete.<sup>14</sup> In the present work a nitric acid/peroxydisulphate mixture is employed for open wet decomposition and the recovery of mercury has been found to be quantitative. Being a very powerful oxidizing agent, peroxydisulphate quickly decomposes organic matter and oxidizes mercury to its bivalent state. Concentrated nitric acid alone was found to be a better reagent for the oxidation of elemental mercury.

Aromatic thiols and those which contain a carboxyl group are themselves acidic<sup>15</sup> and not suitable for use as releasing agents in the alkalimetric determination of mercury. 1-Mercaptopropane-2,3-diol is the reagent of choice, because it does not have an offensive odour, is miscible with water to give solutions of excellent stability, and though it has an acid reaction towards phenolphthalein it is neutral to Phenol Red. The following mercaptide formation



Table 3. Determination of mercury in organic compounds

Test material	Theory, %	Found,* %	RSD, %
Sodium 4-chloromercuribenzoate	52.64	53.2	0.3
Bis-(2-mercaptobenzoic acid)mercury(II)	39.64	39.5	0.3
Sodium 2-ethylmercurithiobenzoate	49.58	50.0	0.3
Bis-(diethyldithiocarbonato)mercury(II)	40.39	40.5	0.2

\*Average of six determinations; RSD = relative standard deviation.

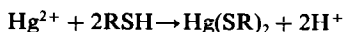
Table 4. Determination of mercury in the presence of copper

Mercury(II) taken,* mg	Copper(II) added, mg	Mercury(II) found,† mg	RSD %
8.25	30.5	8.29	0.6
15.39	25.0	15.42	0.7
20.16	20.3	20.25	0.5
22.55	15.4	22.80	0.4
25.89	10.2	25.67	0.6
31.68	5.6	31.56	0.5

\*Stock solutions standardized by EDTA back-titration.<sup>16</sup>

†Average of five determinations; RSD = relative standard deviation.

reaction occurs with mercury(II):



The protons liberated can be titrated with alkali.

The present method can only determine total mercury. A wide variety of compounds have been analysed by it and the results obtained (Tables 1–3) compared with those found by reduction to mercury(I) and iodate titration,<sup>3</sup> and by EDTA back-titration.<sup>16</sup> Test substances which contain anions that interfere in the EDTA back-titration methods,<sup>16–18</sup> or mercury(I), were digested with nitric acid/peroxydisulphate and analysed by EDTA back-titration<sup>16</sup> to produce comparative results. Mercury(II) undergoes mercaptide formation with 2-benzoxazolethiol but copper(II) is reduced by the reagent to give a disulphide and the copper(I) mercaptide:



The separation of copper is based on the fact that on treatment with thiourea the copper(I) mercaptide remains unaffected whereas the mercury(II) mercaptide decomposes to give a water-soluble mercury(II)-thiourea complex. Results for the determination of mercury in the presence of copper are presented in Table 4.

Large amounts of chloride, bromide, iodide, fluoride, borate, phosphate, acetate, tartrate, oxalate, thiocyanate, thiourea and EDTA do not effect the results.

*Acknowledgement*—Thanks are due to the Council of Scientific and Industrial Research (New Delhi) for award of a Senior Research Fellowship to PT.

#### REFERENCES

1. I. M. Kolthoff and P. J. Elving (eds.), *Treatise on Analytical Chemistry*, Part II, Vol. 3, pp. 198–286. Interscience, New York, 1966.
2. S. Bose, *J. Indian Chem. Soc.*, 1958, **35**, 641.
3. J. Bessett, R. C. Denney, G. H. Jaffery and J. Mendham, *Vogel's Textbook of Quantitative Inorganic Analysis*, p. 388. Longmans, London, 1978.
4. R. Přibil, *Applied Complexometry*, Pergamon Press, Oxford, 1982.
5. K. K. Tiwari and R. M. Verma, *Talanta*, 1984, **31**, 1018.
6. L. Kotz, G. Henze, G. Kaiser, S. Pahlke, M. Veber and G. Tölg, *ibid.*, 1979, **26**, 681.
7. L. Kotz, G. Kaiser, P. Tschöpel and G. Tölg, *Z. Anal. Chem.*, 1972, **260**, 207.
8. W. Zmijewska, *J. Radioanal. Chem.*, 1977, **35**, 389.
9. G. Knapp, S. E. Raptis, G. Kaiser, G. Tölg, P. Schramel and B. Schreiber, *Z. Anal. Chem.*, 1981, **308**, 97.
10. H. B. Han, G. Kaiser, and G. Tölg, *Anal. Chim. Acta*, 1982, **135**, 3.
11. G. Knapp, B. Sadjadi and H. Spitzzy, *Z. Anal. Chem.*, 1975, **274**, 275.
12. L. Lendero and V. Krivan, *Anal. Chem.*, 1982, **54**, 579.
13. H. F. Hass and V. Krivan, *Talanta*, 1984, **31**, 307.
14. O. W. Lau, P. K. Hon, C. Y. Cheung and M. H. Chau, *Analyst*, 1985, **110**, 483.
15. K. K. Verma, *Talanta*, 1975, **22**, 920.
16. J. Körbl and R. Přibil, *Chem. Listy*, 1957, **51**, 667.
17. R. P. Singh, *Talanta*, 1969, **16**, 1447.
18. K. N. Raoot, S. Raoot and V. L. Kumari, *ibid.*, 1983, **30**, 611.

## RESPONSE OF AMMONIUM-SELECTIVE MICROELECTRODES BASED ON THE NEUTRAL CARRIER NONACTIN

D. DE BEER and J. C. VAN DEN HEUVEL

Department of Chemical Engineering and Biotechnological Centre, University of Amsterdam, Nieuwe  
Achtergracht 166, 1018 WV Amsterdam, The Netherlands

(Received 10 December 1987. Revised 19 April 1988. Accepted 12 May 1988)

**Summary**—Ammonium-selective microelectrodes made with an ion-exchanger based on nonactin and having a tip diameter of  $1\ \mu\text{m}$  have been developed. The response of the electrode is linear from  $10^{-5}$  to  $10^{-1}\text{M}$   $\text{NH}_4^+$  and the response time is 1 min. Applications of these electrodes can be found in biotechnology and microbial ecology, but the low selectivity with respect to  $\text{K}^+$  and  $\text{Na}^+$  limits their use to low salt environments. Concentration gradients in gels containing cross-linked urease were measured and found to be in accord with macrokinetic measurements.

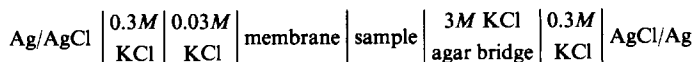
Microelectrodes are unique tools for the measurement of concentrations in extremely small volumes, and of concentration gradients over  $\mu\text{m}$  distances. They were first used for intracellular analysis by animal physiologists and neurophysiologists. Nowadays their application has reached the fields of microbial ecology and biotechnology, for use in microenvironmental studies. Interesting results have been obtained for sediments and microbial films with pH and oxygen microelectrodes.<sup>1</sup> Besides their complicated construction, oxygen microelectrodes have the disadvantage of disturbing the oxygen distribution patterns because of their size of  $5\ \mu\text{m}$  and their consumption of oxygen.<sup>2</sup> Until now, no other microelectrodes have been available to measure the substrates relevant in this context.

In order to study kinetics and mass transfer in bacterial aggregates, microelectrodes have been constructed with an ammonium-selective liquid membrane. The electrodes have a tip diameter of about  $1\ \mu\text{m}$  and are relatively simple to prepare. To test the

### EXPERIMENTAL

Two types of liquid ion-exchanging membrane (LIX) were used: type A was a saturated solution of  $\text{NH}_4^+$ -selective ligand (75% nonactin + 25% monactin, Fluka AG) in tris(ethylhexyl) phosphate (TEHP), and type B was a solution of 10% of the same ligand and 1% of tetraphenylborate (tPB) in *o*-nitrophenyl *n*-octyl ether (NPOE). Glass capillaries  $1.2\ \text{mm}$  in diameter (Clark GC120F-15) were drawn with an automatic horizontal puller (Anna puller, Biological Centre Amsterdam) into micropipettes. During the pulling procedure air was blown at  $1\ \text{ml/sec}$  along the capillaries to reduce the ratio of the outer and inner diameters of the tip of the micropipettes. The outer tip diameter of the micropipettes was about  $1\ \mu\text{m}$ , and their resistance when filled with  $3\text{M}$  potassium chloride was  $5\ \text{m}\Omega$ . Immediately after being pulled, the tips were silanized by dipping them in a 20% solution of trimethylchlorosilane in carbon tetrachloride for 15 sec, followed by baking at  $130^\circ$  for 15 min. The electrode tips were filled with sensor through capillary attraction by dipping the tips in the sensor at  $40^\circ$ . The electrode shafts were subsequently filled with  $0.03\text{M}$  potassium chloride as electrolyte solution by means of a small tube. Air bubbles were removed by heating the electrodes locally with a heating loop.

The cell used for calibration was



reliability of these microelectrodes under experimental conditions, product gradients have been measured in a well-defined model system. For this purpose, spherical gel beads were prepared containing immobilized urease, which catalyses the hydrolysis of urea to ammonium and carbonate. The product gradients were compared with data obtained from macrokinetic measurements.

Urease-containing gels may be employed for the treatment of urea containing waste water from fertilizer industries etc.<sup>3</sup>

The electrode assembly was placed inside a Faraday cage. Measurements were made with a continuous-flow cell at  $20 \pm 0.5^\circ$ . The solutions inside and outside the Faraday cage were electrically separated by drip chambers. The potential difference between the Ag/AgCl wires was transmitted through a triaxial input cable (Keithley 6011) to an electrometer (Keithley 617) placed outside the Faraday cage.

Selectivity factors were determined by the separate solution method.<sup>4,5</sup>

The urease-containing gels were prepared as follows. Urease was cross-linked with bovine serum albumin.<sup>6</sup> A 0.75% suspension of the cross-linked enzyme in demineralized water containing 0.001% Triton X-100 was pre-

pared by sonification ( $2 \times 30$  sec, 8 W/ml). One part of the suspension was mixed with four parts of a 2.5% agar solution at  $40^\circ$ . The enzyme-agar suspension was dripped into oil at  $10^\circ$  to form spherical gel beads with a diameter of 3.2 mm. The homogeneous distribution of the enzyme was verified colorimetrically with Coomassie Brilliant Blue. The gels were kept at pH 9.0 in a buffer consisting of 0.02M triethylethylenediamine (TEEDA) and 0.001M ethylenediaminetetra-acetic acid (EDTA).

The gel beads were fixed in the flow cell with two entomological-specimen needles. Electrodes were positioned in the gels by a micromanipulator driven by a stepper motor. During concentration measurements on the gel, buffer supplied with the desired concentration of urea was pumped through the flow cell. Before each experiment the gels were incubated in this buffer for 40 min to achieve a steady state.

The maximum reaction rate ( $V_{max}$ ) and Michaelis constant ( $K_m$ ) of the cross-linked enzyme were determined by measuring the rate of ammonium carbonate production with an ammonium-selective macroelectrode.<sup>7</sup> The apparent kinetic parameters of the immobilized enzyme in the gel beads were measured in the same way.

When the conversion in a homogeneous gel bead is reaction-limited, it can be deduced that the product concentration gradient in the gel near the interface with the bulk liquid is given by

$$\left[ \frac{dc}{dr} \right]_{r=R} = \frac{V_{max}SR}{3(S + K_m)D} \quad (1)$$

where  $c$  is the product concentration,  $S$  the substrate concentration,  $R$  the radius of the gel bead,  $D$  the diffusion coefficient, and  $r$  the distance from the centre. The nature of the limitation was determined by calculating the modified Thiele modulus  $\phi_p$ .<sup>8</sup> If  $\phi_p$  is  $< 1$  the conversion is not limited by diffusion.

## RESULTS

The responses of both types of microelectrodes to concentrations of  $10^{-5}$ – $10^{-1}$ M ammonium carbonate in demineralized water were linear, with slopes of 50–55 mV/log[NH<sub>4</sub><sup>+</sup>] (Fig. 1).

The resistance of the electrodes with LIX type A depended on the NH<sub>4</sub><sup>+</sup> concentration and varied from 20 GΩ at  $10^{-1}$ M NH<sub>4</sub><sup>+</sup> to 90 GΩ at  $10^{-5}$ M NH<sub>4</sub><sup>+</sup>. The 90% response time ( $t_{90}$ ) was about 10 sec. The resistances of the electrodes with LIX type B ranged from 10 to 40 GΩ and were independent of the NH<sub>4</sub><sup>+</sup> concentration. The response time ( $t_{90}$ ) was 60 sec. The drift of the signal after a stabilization period of about 0.5 hr was 1–2 mV/hr. The response of the electrode was independent of pH in the range from 5 to 8 but at higher pH values the response decreased because of the shift in the ammonia/ammonium equilibrium.

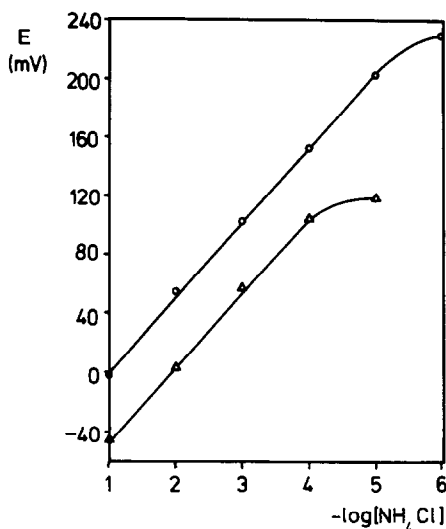


Fig. 1. Calibration curves of microelectrodes with LIX type B. (○) demineralized water, (△) pH 9.0 buffer, 0.02M TEEDA and 0.001M EDTA.

In a 0.02M TEEDA buffer at pH 9.0 the lower limit of linear response increased to  $10^{-4}$ M NH<sub>4</sub><sup>+</sup>.

The selectivity factors of the different types of electrode are given in Table 1. Electrodes with NPOE as solvent (type B) for the ion-exchanger showed a higher selectivity than those with TEHP (type A). Addition of 1% tPB did not influence the selectivity with respect to Na<sup>+</sup> and K<sup>+</sup>, but increased that with respect to Ca<sup>2+</sup>.

The electrodes could be used for 12 hr, during which the detection limit and the slope factor remained constant. However, after 24 hr the detection limit had sometimes increased by a factor of 10. As a consequence, freshly prepared electrodes were used for each experiment.

Product gradients in gel beads containing cross-linked urease were measured with electrodes of type B. They were almost symmetrical, and their size depended on the substrate concentration, as shown in Fig. 2. The results of four experiments are summarized in Table 2. The measured slopes show good agreement with those calculated by means of equation (1) from macrokinetic measurements. In the buffer used, the  $K_m$  value for the cross-linked enzyme, and also the apparent  $K_m$  for the gel beads, was 0.0058M. In all experiments the modified Thiele

Table 1. Selectivity factors  $K_{\text{NH}_4^+,j}$  for microelectrodes with different types of liquid membranes and a macroelectrode

$j$	Microelectrode			
	Macroelectrode <sup>7</sup>		LIX type B	
	LIX type A	LIX type A	(no tPB)	(with tPB)
K <sup>+</sup>	0.12	0.85	0.4	0.38
Na <sup>+</sup>	0.002	0.67	0.02	0.02
Ca <sup>2+</sup>	0.00017	0.07	0.07	0.002

Table 2. Product concentration gradient ( $dc/dr$ ) at  $r = R$  in different conditions

Parameter	Experimental			
	1	2	3	4
$V_{max}$ , mole.l <sup>-1</sup> .sec <sup>-1</sup>	$5 \times 10^{-7}$	$8.8 \times 10^{-8}$	$3 \times 10^{-7}$	$6.8 \times 10^{-8}$
$R$ , mm	1.68	1.64	1.68	1.64
$S$ , M	0.1	0.1	0.004	0.004
$\Phi_p$	0.053	0.015	0.165	0.055
$dc/dr^*$ , mole.l <sup>-1</sup> .m <sup>-1</sup>	0.332	0.057	0.086	0.019
$dc/dr^\dagger$ , mole.l <sup>-1</sup> .m <sup>-1</sup>	0.340	0.051	0.080	0.018

\* Calculated from macrokinetic data by equation (1).

† Measured with microelectrodes.

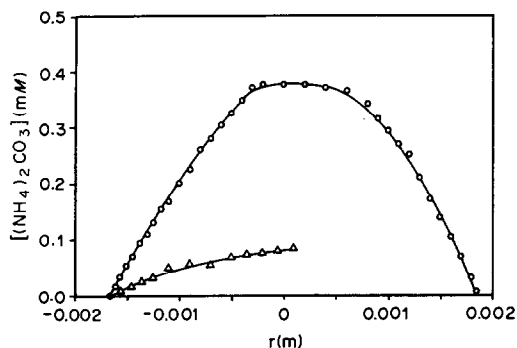


Fig. 2. Measured product concentration gradients in agar gels containing immobilized urease. Gels were incubated in (O) 0.1M and (Δ) 0.004M urea.

modulus  $\Phi_p$  was less than 1 so the reaction rate was not limited by diffusion, and equation (1) holds.

#### DISCUSSION

The electrode developed is a modification of the macroelectrode described by Scholer and Simon.<sup>7</sup> Simple miniaturization, however, was unsatisfactory because the resulting microelectrodes showed poor selectivity (Table 1) and often shed their membranes. Both selectivity and stability could be improved by the use of NPOE (type B) instead of TEHP (type A) as the membrane solvent, although the response time was longer. Furthermore, addition of tPB increased the selectivity with respect to bivalent cations and resulted in a resistance that was independent of the ammonium ion concentration. The selectivity of the microelectrodes with LIX type B was sufficient for our purposes, although lower than the selectivity of macroelectrodes.<sup>7</sup> It should be noted that miniaturization increases the role of shunt resistances between the glass-membrane interface and the glass wall, generally leading to a decrease of selectivity.<sup>5</sup>

The measuring range of the electrodes for ammonium ions is limited by the presence of interfering ions. As a rule of thumb the detection limit for  $\text{NH}_4^+$  is  $0.1[\text{Na}^+]$  or  $10[\text{K}^+]$ . The electrode is therefore not suitable for physiological experiments or use in marine environments. During measurements in dilute

salt solutions no concentration changes of interfering ions should occur. Measurements can be made in media such as freshwater sediments, nitrifying bacterial granules<sup>9</sup> and gels with immobilized enzymes, since in these systems no concentration gradients or concentration changes of  $\text{Na}^+$  and  $\text{K}^+$  are to be expected. In our experiments the electrode proved to be reliable, since the measured gradients corresponded quite well with macrokinetic data.

In biotechnology much effort is directed to the development of mathematical models to quantify the conversion inside a biofilm or a catalyst particle containing immobilized enzymes.<sup>10</sup> The value of these models depends heavily on the assumed structure of the biological system, i.e., the distribution of organisms and kinetic parameters. With microelectrodes it is possible to obtain direct information from measurements inside heterogeneous biological systems. Therefore, it is to be expected that the electrode developed may have wider applications in microbial ecology and biotechnology.

*Acknowledgement*—The authors wish to thank Dr. J. Siegenbeek van Heukelom (Department of Zoology, University of Amsterdam) for technical facilities and expert advice.

#### REFERENCES

1. N. P. Revsbech and B. B. Jorgensen, *Adv. Microb. Ecol.*, 1986, **9**, 293.
2. R. A. Albanese, *J. Theor. Biol.*, 1973, **38**, 143.
3. H. J. Vos, D. J. Groen, J. J. M. Potters and K. Ch. A. M. Luyben, in O. M. Neijssel, R. R. van der Meer and K. Ch. A. M. Luyben (eds.), *Proc. 4th European Congr. Biotechnol.* Vol. 1, p. 188. Elsevier, Amsterdam, 1987.
4. D. Ammann, *Ion-selective Microelectrodes: Principles, Design and Application*, Springer, Berlin, 1986.
5. W. McD. Armstrong and J. F. Garcia-Diaz, *Fed. Proc., Fed. Am. Soc. Exp. Biol.*, 1980, **39**, 2851.
6. G. Broun, D. Thomas, G. Gelff, D. Domurado, A. M. Berjonneau and C. Guillon, *Biotechnol. Bioeng.*, 1973, **15**, 359.
7. R. P. Scholer and W. Simon, *Chimia*, 1970, **24**, 372.
8. B. Atkinson and F. Ur-Rahman, *Biotechnol. Bioeng.*, 1979, **21**, 221.
9. Z. Lewandowski, R. Bakke and W. G. Characklis, *Water Sci. Technol.*, 1987, **19**, 175.
10. J. C. Kissel, P. L. McCarthy and R. L. Street, *J. Environ. Eng.*, 1984, **110**, 393.

## FLUOROMETRIC DETERMINATION OF RESERPINE IN DOSAGE FORMS

M. I. WALASH, F. BELAL\* and F. A. ALY

Department of Analytical Chemistry, Faculty of Pharmacy, University of Mansoura,  
Mansoura 35516, Egypt

(Received 18 January 1988. Revised 16 April 1988. Accepted 28 April 1988)

**Summary**—A rapid and highly sensitive fluorometric procedure has been developed for the routine determination of reserpine, in bulk and in dosage forms. The method is based on the fluorescence induced by oxidation of reserpine with hexa-amminecobalt(III)tricarbonatocobaltate in aqueous acetic acid. The oxidation product exhibits a greenish yellow fluorescence with its emission maximum at around 420 nm. The fluorescence intensity is a linear function of reserpine concentration over the range 0.01–0.24  $\mu\text{g/ml}$  in the solution finally measured. The advantages and disadvantages of the proposed method are discussed, and its applicability to different formulations is demonstrated.

The double therapeutic effect of reserpine as an antihypertensive and a tranquilizer is well known. Because of its therapeutic importance, several methods have been developed for the determination of reserpine. Most of these methods require separation steps, by extraction, paper and column chromatography, paper electrophoresis, *etc.* Schirmer<sup>1</sup> has reviewed the methods reported up to 1975 for the determination of reserpine. Since then spectrophotometric,<sup>2-6</sup> densitometric,<sup>7</sup> polarographic,<sup>8</sup> radio-immunoassay,<sup>9</sup> gas-chromatographic<sup>10</sup> and HPLC<sup>11</sup> methods have appeared.

Reserpine has been determined fluorometrically in tablets after oxidation with nitrite.<sup>12,13</sup> Reagents other than nitrite have also been used to induce the fluorescence, including hydrogen peroxide,<sup>14</sup> selenious acid,<sup>15</sup> *p*-toluenesulphonic acid,<sup>16</sup> "sulphovanadic" acid<sup>17</sup> and vanadium pentoxide.<sup>18</sup>

The goal of this study was to develop a fluorescence method which would be as sensitive as the published methods, but simpler. The method is based on the formation of a greenish yellow fluorescence on oxidation with hexa-amminecobalt(III)tricarbonatocobaltate(III), HCTC, in aqueous acetic acid, and can be used for the determination of reserpine when high sensitivities are desired.

### EXPERIMENTAL

#### Apparatus

Aminco-Bowman spectrofluorometer, model J4-8960, with excitation and emission slit controls set at 5 mm, and the intensity scale control set at 3. The excitation and emission wavelengths used were 370 and 420 nm respectively. Measurements were performed with 1-cm silica cells.

#### Materials

Reserpine (Ciba) pharmaceutical grade, was used as the working standard. Dosage forms were collected from commercial sources.

#### Reagent

HCTC was prepared as described by Baur and Bricker,<sup>19</sup> and a  $5 \times 10^{-3}M$  solution was made by stirring 3.0 g of the pure compound with 1 litre of water (saturated with sodium bicarbonate) for 2-3 hr, then filtering, and standardizing iodometrically.

#### Sample preparation

A 1.0-mg/ml stock solution of reserpine in glacial acetic acid was prepared. This solution was further diluted with 10% acetic acid to give a 1- $\mu\text{g/ml}$  reserpine working solution.

#### Calibration graph

Known volumes of 1- $\mu\text{g/ml}$  reserpine solution were transferred to 25-ml standard flasks. Five ml of 10% v/v acetic acid were added to each followed by 0.2 ml of  $5 \times 10^{-3}M$  HCTC. After 20 min, the fluorescence was measured. The fluorescence intensity was plotted against amount of reserpine.

#### Procedures for dosage forms

**Tablets.** Weigh and pulverize 20 tablets. Transfer an accurately weighed amount of the powder equivalent to ~2.5 mg of reserpine into a small conical flask, add 30 ml of glacial acetic acid, stir for 15 min, filter into a 100-ml standard flask, washing the residue with 10% v/v acetic acid, and dilute the combined solution and washings to volume with the same solvent. Analyse a suitable volume as described above.

**Ampoules.** Mix the contents of 20 ampoules. Transfer an accurately measured volume equivalent to ~2.5 mg reserpine into a 100-ml standard flask, and make up to the mark with 10% v/v acetic acid. Analyse as described above.

**Tablets containing reserpine and dihydralazine sulphate.** Weigh and pulverize 20 tablets. To a quantity of the powder equivalent to ~1.0 mg of reserpine add 10 ml of 2% citric acid solution, and extract the reserpine with three 25-ml portions of chloroform, shaking for 20 min each time. Wash

\*To whom correspondence should be addressed.

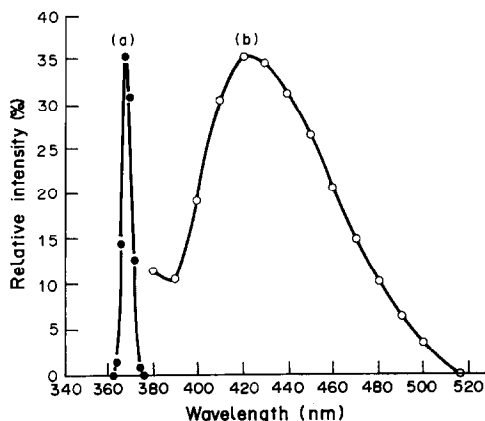


Fig. 1. Fluorescence spectra of the oxidation product of reserpine (0.14  $\mu\text{g/ml}$ ). (a) Excitation spectrum. (b) Emission spectrum.

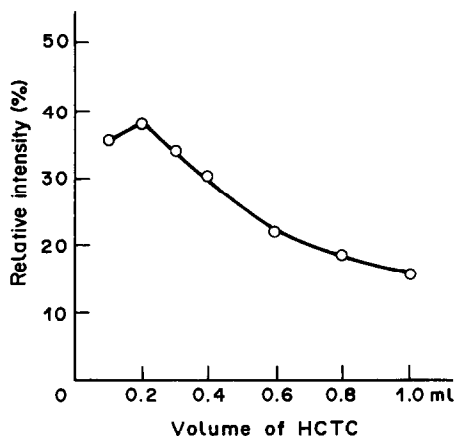


Fig. 2. Effect of volume of HCTC ( $5 \times 10^{-3} M$ ) on the fluorescence of reserpine (0.15  $\mu\text{g/ml}$ ).

the combined extracts with 10 ml of 1% sodium bicarbonate solution. Place the chloroform extract in an evaporating dish, and evaporate to dryness on a water-bath. Dissolve the residue in 10 ml of glacial acetic acid. Transfer the solution into a 50-ml standard flask, make up to the mark with 10% v/v acetic acid, filter through a dry paper, transfer 25 ml of the filtrate into a 100-ml standard flask and make up to the mark with 10% v/v acetic acid. Transfer an aliquot containing a suitable quantity of reserpine into a 25-ml standard flask and analyse as described above.

#### DISCUSSION

HCTC is a stable trivalent cobalt complex. In acid medium, it releases free  $\text{Co}^{3+}$ , a strong oxidizing agent with an oxidation potential of 1.18 V in 0.9M hydrochloric acid.<sup>20</sup> It has been used for the determination of phenothiazines<sup>21</sup> and antimony(III) compounds.<sup>22</sup> In this work, it has been tested as a reagent for inducing fluorescence from reserpine. Figure 1 shows the excitation and emission spectra obtained.

The effect of various experimental conditions on the fluorescence intensity was studied. The volume of HCTC solution was found to be critical, 0.2 ml of the  $5 \times 10^{-3} M$  reagent producing the maximum reading, but larger volumes giving a much lower value. This may be due to further oxidation to give a less fluorescent (or even non-fluorescent) product. The

fluorescence develops immediately, reaches maximum intensity after 20 min and remains stable for 1.5 hr (Fig. 3). The fluorescence intensity is linearly related to the reserpine concentration in the measured solution over the range 0.01–0.24  $\mu\text{g/ml}$ .

The precision of the method was evaluated by analysing reserpine solutions in triplicate at three levels (0.1, 0.16, 0.2  $\mu\text{g}$ ). The mean recoveries ranged from 98.8 to 100.8%, with standard deviations ranging from 0.8 to 1.4%.

The method was also applied to some dosage forms containing reserpine, either alone or in combination

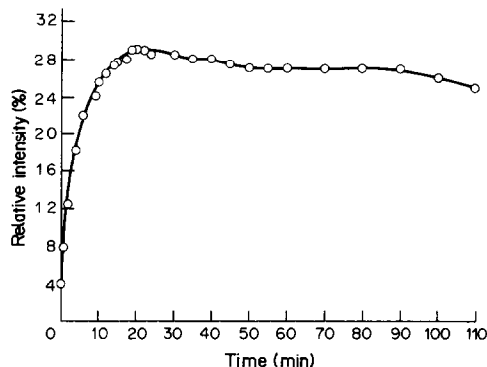


Fig. 3. Effect of time on the stability of oxidation product of reserpine (0.12  $\mu\text{g/ml}$ ).

Table 1. Analysis of some Ciba-Geigy dosage forms containing reserpine by the proposed and official methods\*

Preparation	Recovery, %	
	Proposed method	Official method <sup>2,3</sup>
Serpasil ampoules (1.0 mg reserpine/ml)	99.1 $\pm$ 0.1	99.0 $\pm$ 1.1
Serpasil ampoules (2.5 mg reserpine/ml)	101.6 $\pm$ 1.4	100.8 $\pm$ 0.7
Serpasil tablets (0.1 mg reserpine/tablet)	100.2 $\pm$ 1.4	101.3 $\pm$ 0.6
Serpasil tablets (0.25 mg reserpine/tablet)	99.0 $\pm$ 0.9	99.8 $\pm$ 1.2
Adelphan tablets (0.1 mg reserpine + 10 mg dihydralazine sulphate/tablet)	99.9 $\pm$ 1.3	100.0 $\pm$ 1.3

\*The results are the averages ( $\pm$  standard deviations) of 6 separate determinations and are expressed relative to the nominal reserpine content.

with other drugs. The results in Table 1 are in accordance with those obtained by the official method.<sup>2,3</sup> Statistical analysis<sup>23</sup> of these results by the Student-*t* test and the variance-ratio *F*-test showed no significant difference between the performances of the two methods as regards accuracy and precision.

Interference from drugs likely to be co-formulated with reserpine was studied. Phenobarbitone, caffeine, barium chloride, ferric chloride, potassium chloride and calcium chloride in 100 times amount relative to reserpine did not interfere. Ascorbic acid and aspirin decreased fluorescence when present in amounts 50 times greater than that of reserpine, hydralazine and hydrochlorothiazide caused quenching of the fluorescence.

The proposed method is simpler than any of the reported fluorimetric methods. The experimental conditions are very mild, neither corrosive acids nor heating being required. The nitrite method involves heating for 30 min<sup>12</sup> and the proposed method is slightly more sensitive. In the nitrate method the decomposition products of reserpine, particularly 3,4-dehydroreserpine, are estimated as reserpine unless corrections are applied. Similarly, the *p*-toluenesulphonic acid method<sup>16</sup> involves heating in glacial acetic acid for 10 min. The method using a mixture of sulphuric, hydrochloric and acetic acids<sup>24</sup> is tedious and much less sensitive than the proposed method. The product from oxidation of reserpine with vanadium pentoxide in phosphoric acid was reported to be identical to that produced by the nitrite method,<sup>18</sup> and so the vanadium method should also be subject to interference by the decomposition products.

Although the chemical structure of the product in the proposed method is not yet known, it is neither 3,4-dehydro reserpine nor 3,4,5,6-tetrahydroreserpine. Its ultraviolet absorption spectrum and fluorescence spectrum are not identical with those of these decomposition products,<sup>18</sup> and as these do not fluoresce at the wavelengths used in the proposed method, this can be considered as a stability-indicating assay for reserpine.

Analysis of one sample takes 30 min, whereas the official methods<sup>2,3</sup> need more than 2 hr. With the exception of the volume of HCTC, the condition are not critical. Thus the method is simple and easy to use.

#### REFERENCES

1. R. E. Schirmer, in *Analytical Profile of Drug Substances*, F. Klaus (ed.), Vol. 4, p. 380. Academic Press, New York, 1975.
2. *The British Pharmacopoeia*, H.M. Stationary Office, London, 1980.
3. *The United States Pharmacopoeia XXI*, American Pharmaceutical Association, Washington, D.C., 1985.
4. D. S. Mangala, B. S. Reddy and C. S. P. Sastry, *Indian Drugs*, 1984, **21**, 526.
5. M. S. Karawya, A. A. Sharaf and A. A. Diab, *J. Assoc. Off. Anal. Chem.*, 1976, **59**, 795.
6. Y. Fujita, I. Mori and S. Kotano, *Bunseki Kagaku*, 1984, **33**, 1985.
7. J. Jarzebinski, M. Ciszewska and P. Suchocki, *Acta Pol. Pharm.*, 1980, **37**, 69.
8. A. Taira and D. E. Smith, *J. Assoc. Off. Anal. Chem.*, 1978, **61**, 641.
9. E. Thacker, *Anal. Proc.*, 1985, **22**, 136.
10. L. Di Simone, G. Portelli, M. R. Del Giudice, F. Gatta and G. Settimj, *Farmaco, Ed. Prat.*, 1980, **35**, 223.
11. U. R. Cieri, *J. Assoc. Off. Anal. Chem.*, 1985, **68**, 542.
12. D. Banes, *J. Am. Pharm. Assoc.*, 1957, **46**, 601.
13. B. N. Kabad, *J. Pharm. Sci.*, 1971, **60**, 1862.
14. E. B. Dechene, *J. Am. Pharm. Assoc.*, 1955, **44**, 657.
15. R. B. Poet and J. M. Kelly, *Abstr. 120th Meeting Am. Chem. Soc.*, 1954, p. 83c.
16. I. M. Jakovljevic, J. M. Fose and N. R. Kuzel, *Anal. Chem.*, 1962, **34**, 410.
17. R. Stainier, *J. Pharm. Belg.*, 1973, **28**, 115.
18. T. Urbanyi and H. Staber, *J. Pharm. Sci.*, 1970, **59**, 1824.
19. J. E. Baur and C. E. Bricker, *Anal. Chem.*, 1965, **37**, 1461.
20. M. Hanif, M. Saeed, M. Z. Iqbal and J. Zýka, *Pakistan J. Sci. Ind. Res.*, 1979, **19**, 14.
21. M. I. Walsh, F. Belal and F. A. Aly, *Talanta*, 1988, **35**, 320.
22. *Idem*, *Analyst*, 1988, **111**, 955.
23. D. H. Sanders, A. F. Murph and R. J. Eng, *Statistics*, McGraw Hill, New York, 1976.
24. W. H. McMullen, H. J. Pazdera, S. R. Missan, L. L. Ciaccio and T. G. Grenfell, *J. Am. Pharm. Assoc.*, 1955, **44**, 446.

## OSTERYOUNG SQUARE-WAVE VOLTAMMETRIC DETERMINATION OF NICARBAZIN IN CHICKEN TISSUE

DEAN K. ELLISON and WILLIAM TAIT

Merck Sharp & Dohme Research Laboratories, P.O. Box 2000, Rahway, NJ 07065, U.S.A.

(Received 15 March 1988. Accepted 12 May 1988)

**Summary**—Osteryoung square-wave voltammetric analysis is a rapid technique that can be used to determine nicarbazin residues in chicken tissue. The method is reproducible and can be applied to samples containing as little as 1–10  $\mu\text{g/g}$  nicarbazin. This level of sensitivity is more than adequate for meeting governmental regulations. Osteryoung square-wave voltammetry is significantly faster than classical differential pulse polarography.

Nicarbazin is widely administered to poultry as an effective coccidiostat.<sup>1</sup> Several assays are currently in use to detect nicarbazin in tissue or in feed. Since nicarbazin is a 1:1 complex of 2-hydroxy-4,6-dimethylpyrimidine (HDP) and 4,4'-dinitrocarb-anilide (DNC), either the HDP or the DNC moiety is assayed to determine the total nicarbazin content in poultry feed. HDP, however, is excreted from chickens more rapidly than DNC and tissue residue analysis for nicarbazin is therefore most commonly based on the DNC moiety.<sup>2</sup>

Colorimetric procedures are generally employed to determine nicarbazin in feed, but the sample preparation is tedious and the assay is subject to interference.<sup>3</sup> Nicarbazin in feed can also be measured by liquid chromatographic (LC) methods and an LC method for nicarbazin determination in tissue is also available.<sup>3,4</sup> Gas chromatography is also used to assay nicarbazin.<sup>5</sup> The current FDA method for measuring nicarbazin levels is differential pulse polarography, based on two-electron reduction of the DNC moiety at a mercury electrode.<sup>6</sup> This method is direct (no separation is required), sensitive (below 1  $\mu\text{g/ml}$  detection limit), and selective (only a limited sample clean-up is required), but differential pulse polarography is a relatively slow electroanalytical method.<sup>7</sup>

We have applied a new electroanalytical approach, Osteryoung square-wave polarography (OSWP),<sup>8</sup> to assay nicarbazin in chicken tissue. We have found OSWP has the same advantages as differential pulse polarography, yet is an order of magnitude faster.

### EXPERIMENTAL

A Princeton Applied Research model 303A static mercury drop electrode and a BAS-100 electrochemical analyser were used for all the electroanalytical work. The counter-electrode was made of platinum wire. The reference electrode consisted of a silver wire (previously coated with silver chloride) immersed in 0.1M potassium chloride. Current-voltage curves were recorded either on a Houston

Instrument DMP-40 series digital plotter or a Bioanalytical System printer. An internal program of the BAS-100 was used to measure peak heights, which were mainly used as the analytical signal (exceptions are noted below).

The solution preparation and tissue residue analysis were as described by Wood and Downing.<sup>9</sup> Nicarbazin standards and samples were prepared in 0.1M tetraethylammonium perchlorate in DMSO containing 0.24 mg/ml benzoic acid. All solutions were deaerated with nitrogen for 4 min before a scan was started, and no precautions were taken with regard to solution temperature. Instrumental parameters used throughout are initial potential = -800 mV, final potential = -1400 mV, square-wave amplitude = 25 mV, frequency = 15 Hz, potential increment = 4 mV.

### RESULTS

Figure 1 shows a typical set of current-voltage curves obtained from Osteryoung square-wave voltammetric analysis of nicarbazin standards ranging from 0 to 10  $\mu\text{g/ml}$ . The nicarbazin is reduced at a

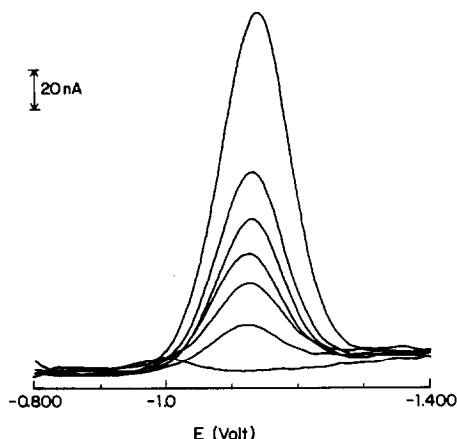


Fig. 1. Square-wave voltammetry of 0, 1, 2, 3, 4, 5 and 10  $\mu\text{g/ml}$  nicarbazin standards in 0.1M tetraethylammonium perchlorate and 0.24 mg/ml benzoic acid solution in DMSO. Instrumental parameters as in text.



Table 1. Precision of OSWV (mean of 5 runs, conditions as for Fig. 1)

Nicarbazin, $\mu\text{g/ml}$	1	2	3	4	5	10
Peak height, $nA$	18.4*	36.6	53.9	71.4	91.8	180
RSD, %	5	1.4	0.7	1.0	3	0.8

\*The internal program of the BAS-100 did not recognize the nicarbazin reduction wave at this low level, so this value was taken directly from plots of the current-voltage curve.

peak potential of  $-1.1\text{ V vs. Ag/AgCl}$ . Previous studies with differential pulse polarography (DPP) demonstrated that nicarbazin is reduced in a single wave at  $-1.0\text{ V vs. SCE}^9$  (same solution conditions as those described in the experimental section). The nicarbazin reduction peak obtained by OSWV, as shown in Fig. 1, is symmetrical with peak height proportional to the concentration of nicarbazin. Both the peak symmetry and the concentration dependence in Fig. 1 are consistent with OSWV theory.<sup>8</sup> Table 1 shows the average values obtained in five runs for the peak currents. The relative standard deviations for five different nicarbazin concentrations were all below 5%, demonstrating the precision of the procedure.

The calibration graph for the measurement of nicarbazin is linear from 0 to 10  $\mu\text{g/ml}$ , with a slope (sensitivity) of  $18\text{ nA}\cdot\text{ml}\cdot\mu\text{g}^{-1}$  and correlation coefficient 0.9996. These data demonstrate that this technique is sensitive enough to detect nicarbazin reliably at the 1  $\mu\text{g/ml}$  level.

To establish whether the OSWV technique could be applied to assaying nicarbazin in chicken tissue, we spiked liver homogenates, from non-medicated chicken, with different levels of nicarbazin. A typical Osteryoung square-wave voltammogram for nicarbazin in chicken liver homogenates (spiked at the 3.8  $\mu\text{g/ml}$  level) is shown in Fig. 2. The peak is symmetrical and appears at the characteristic peak potential of  $-1.1\text{ V vs. Ag/AgCl}$  for nicarbazin. There is only one symmetrical peak, which suggests that the assay is specific for the nicarbazin in the

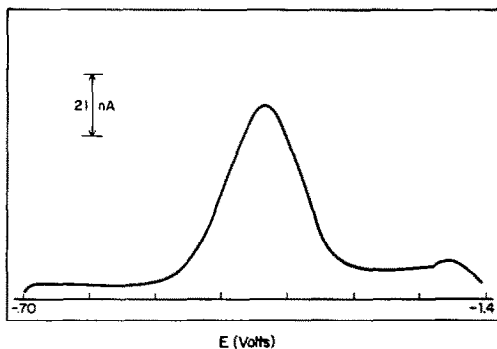


Fig. 2. Osteryoung square-wave voltammogram of nicarbazin recovered from non-medicated chicken liver (spiked at the 3.8- $\mu\text{g}$  level). Conditions as for Fig. 1.

Table 2. Recovery experiments for nicarbazin in chicken liver

Spike, $\mu\text{g/ml}$	Found, $\mu\text{g/ml}$	Recovery, %
Control (0 $\mu\text{g/ml}$ )	0	—
3.88	3.40	88
7.76	7.00	90
11.64	10.30	88

Nicarbazin was measured by OSWV under the conditions for Fig. 1.

homogenate. Additions of nicarbazin to chicken tissue resulted in a similar reduction wave to that shown in Fig. 2, with an increase in peak height that was proportional to the amount added.

Tissue homogenates from non-medicated chickens were spiked with nicarbazin and analysed by OSWV, and the nicarbazin levels read from the calibration graph (Table 2). Most of the nicarbazin was recovered (88–90%), demonstrating that OSWV can be used to measure accurately the amount of nicarbazin contained in chicken tissue (provided an empirical recovery factor is employed). The results are in good agreement with those previously reported for measurements by DPP.<sup>9</sup> Jacobsen and Lindseth have suggested that low recoveries in a polarographic assay of nicarbazin might be due to matrix effects such as adsorption of the tissue components on the electrode.<sup>11</sup>

## DISCUSSION

We have demonstrated that OSWV is a useful technique for measuring nicarbazin residues in chicken tissue at levels as low as 1  $\mu\text{g/g}$ . This sensitivity is more than adequate to meet U.S. governmental regulations, which stipulate that the nicarbazin concentration in chicken tissue must be below 4  $\mu\text{g/g}$ .

The major advantage in using OSWV rather than differential pulse polarography to measure nicarbazin is the shortened analysis time. Only about 8.5 min instrument time was required to collect the data in Table 1. To collect the same information by differential pulse polarography requires considerably longer (about 2 hr).

There is also another advantage to using OSWV. An occasional splitting of the nicarbazin reduction waves is observed when differential pulse polarography is used as the detection method (and is attributed to the phenomenon of a polarographic

maxima).<sup>10</sup> This problem was not encountered with OSWV, probably because this method is insensitive to convective diffusion currents, which can cause polarographic maxima.<sup>8</sup> Finally, OSWV requires only a single drop of mercury per voltage scan, compared to about 50 drops of mercury per voltage scan for the DPP technique.

These advantages, combined with the specificity and sensitivity of the OSWV nicarbazin assay, suggest use of this assay when nicarbazin residues must be quickly and routinely measured. This assay might also be used to measure nicarbazin residues in different milieux and also be adapted to detect residues of similar drugs.

*Acknowledgement*—We would like to thank Dr. T. Wehner for her help in the sample preparation.

## REFERENCES

1. A. C. Cuckler, C. M. Malanga and W. H. Ott, *Poultry Sci.*, 1956, **35**, 98.
2. C. C. Porter and J. J. Gilfillan, *ibid.*, 1955, **34**, 995.
3. T. D. Macy and A. Loh, *J. Assoc. Off. Anal. Chem.*, 1984, **67**, 1115.
4. J. A. Hurlbut, C. T. Nightengale and R. G. Burkepile, *ibid.*, 1985, **68**, 596.
5. N. Nose and S. Kawauchi, *Shokuhin Eiseigaku Zasshi*, 1981, **22**, 449.
6. R. F. Michielli and G. V. Downing, *J. Agric. Food Chem.*, 1974, **22**, 449.
7. *Laboratory Techniques in Electroanalytical Chemistry*, P. T. Kissinger and W. R. Heineman (eds.), pp. 155–160. Decker, New York, 1984.
8. J. G. Osteryoung and R. A. Osteryoung, *Anal. Chem.*, 1985, **57**, 101A.
9. J. S. Wood and G. V. Downing, *J. Agric. Food Chem.*, 1980, **28**, 452.
10. A. J. Bard and L. R. Faulkner, *Electrochemical Methods*, p. 151. Wiley, New York, 1980.
11. E. Jacobsen and H. Lindseth, *Anal. Chim. Acta*, 1976, **86**, 123.

# DETERMINATION OF GALLIUM IN GEOLOGICAL MATERIALS BY GRAPHITE-FURNACE ATOMIC-ABSORPTION SPECTROMETRY

FUMIYASU TAKEKAWA and ROKURO KURODA

Laboratory for Analytical Chemistry, Faculty of Engineering, University of Chiba, Yayoi-cho, Chiba, Japan

(Received 28 December 1987. Accepted 10 May 1988)

**Summary**—A graphite-furnace atomic-absorption spectrometric method has been worked out for the determination of traces of gallium in silicate rocks and minerals. The samples are opened up by fusion with a lithium carbonate-boric acid mixture and the cake is taken up with 2M nitric acid. Addition of nickel nitrate to this solution eliminates the severe matrix effects, allowing gallium solutions in nitric acid to be used as calibration standards. No separations are necessary. Results are quoted for 14 standard silicate rocks and two minerals. The RSD is 2.9%, and the sensitivity is 27 pg of gallium for 1% absorption.

The concentration of gallium in silicate rocks is normally in the range 10–100  $\mu\text{g/g}$ , and the crustal abundance is 18  $\mu\text{g/g}$ .<sup>1</sup> Some papers on application of atomic-absorption spectrometry (AAS) to the analysis of environmental and complex inorganic materials deal with separation and concentration of gallium after acid dissolution.<sup>2-4</sup> Because of serious interferences encountered in the electrothermal AAS of gallium, various techniques such as use of standard additions,<sup>5-7</sup> the L'vov platform,<sup>4,8</sup> a metal microtube atomizer,<sup>2</sup> a zirconium-impregnated graphite tube,<sup>3</sup> matrix modifications<sup>4,5,9-11</sup> etc. have been employed for complex inorganic materials. A combined use of a matrix modifier (magnesium nitrate) and the standard-addition method for determination of gallium in phosphorus flue dust and other materials by Zeeman-corrected graphite-furnace AAS has been reported.<sup>5</sup> A similar electrothermal method has been developed for gallium in environmental samples,<sup>10</sup> with both nickel and ammonium sulphate introduced into sample solutions to modify the matrix and to remove severe perchloric acid interference, respectively. These methods are efficient for analysis for traces of gallium, but take considerable time and effort and sometimes require specialized techniques. Solid sampling with electrothermal atomization has also been used for gallium in bauxite, flint clay etc., but authentic solid standard samples are essential for calibration.

There is scant information about the analysis of silicate rocks for traces of gallium.<sup>2</sup> Therefore, we attempted to develop a simple, rapid method for gallium in a variety of silicate rocks and minerals, with direct calibration with aqueous gallium standard solutions.

## EXPERIMENTAL

### Instrument

A Shimadzu AA-646 atomic-absorption spectrometer with microcomputer-based control and logic software was

used. The instrument was fitted with a deuterium background corrector, a GFA-4 furnace atomizer and a U-135 chart recorder. Background correction was performed for all measurements. The radiation source used was a Hamamatsu Photonics HTV-L233 single-element hollow-cathode lamp for gallium. The settings were lamp current 2.5 mA, wavelength 294.4 nm and spectral band-width 0.19 nm. A regular high-density graphite tube (200-54520, Shimadzu) was used throughout. The atomization programmes are summarized in Table 1. The sheath gas used was argon.

### Reagents

A standard solution of gallium (1.00 mg/ml in 1M nitric acid) for atomic-absorption spectrometry was obtained from Kanto Chemical Co. (Tokyo, Japan). Nickel solution was prepared by dissolving 10.0 g of nickel nitrate hexahydrate in 100 ml of 2M nitric acid and diluting to 100 ml with the same acid. Lithium carbonate and boric acid were of Suprapur grade (Merck). "Poisonous metal analysis grade" nitric acid was used throughout.

### Procedure

Place a 100-mg sample in a platinum crucible, add 250 mg of 1:1 lithium carbonate-boric acid mixture and mix. Dry the mixture for a few minutes with a gentle flame and then fuse the mixture for 15 min at 1000°. Dissolve the cooled melt in 2M nitric acid (magnetic stirring) and dilute accurately to 25 ml with the same acid. Place a 5-ml aliquot of the solution in a 10-ml standard flask, add 2.00 ml of the nickel solution, and dilute to the mark with 2M nitric acid. Inject 20  $\mu\text{l}$  of the mixture into the furnace with an Oxford P-7000 sampler (or equivalent) and proceed according to the programme given in Table 1. Construct the calibration curve by use of a series of gallium standard solutions which are 2M in nitric acid and contain the same amount of nickel as the sample solutions do.

Table 1. Recommended furnace programmer settings

	Dry	Ash	Atomize	Cleaning
Temperature °C	150	800	2200	2500
Time, sec	30	20	4	3
Mode	ramp	step	step	step
Internal gas*				
flow-rate, l./min	1.5	1.5	0	1.5

\*Argon.

## RESULTS AND DISCUSSION

It is often necessary to modify sample matrices to avoid interferences in graphite-furnace atomic-absorption spectrometry. In the present study a uniform content of lithium borate appeared to make it possible to minimize interferences due to differences in the matrices. However, the AAS signal for gallium is poor when lithium borate-nitric acid media are used, and the calibration graphs obtained with gallium standards in blank flux solution/2M nitric acid did not give accurate results for standard rocks with known gallium contents. Therefore, we decided to modify the matrices further and tested ammonium fluoride, magnesium nitrate, ascorbic acid and nickel nitrate for the purpose. The first three turned out not to be sufficiently effective to eliminate matrix effects, but the nickel yielded an enhanced gallium signal, thus reducing the matrix effects. Figure 1 illustrates the effect of the nickel concentration on the absorbance of gallium (40 ng/ml) in aqueous 2M nitric acid and a rock sample solution (JB-1, basalt, a standard rock of the Geological Survey of Japan) prepared according to the procedure given above (Ga ~ 40 ng/ml). The gallium signals increase with increasing concentration of nickel nitrate, reaching a plateau in the range 2–5 mg/ml nickel, and then decrease again. A silicate rock standard (GSP-1, granodiorite, U.S. Geological Survey) yielded a curve similar to that of JB-1. At a nickel content of 4 mg/ml, the two curves in Fig. 1 approach each other, permitting the determination of gallium by means of the calibration curve constructed with a series of aqueous gallium standard solutions in 2M nitric acid.

Figure 2 shows the effect of the ashing and atomization temperatures on the response from gallium in (A) 2M nitric acid (Ga 45 ng/ml) and (B) a rock

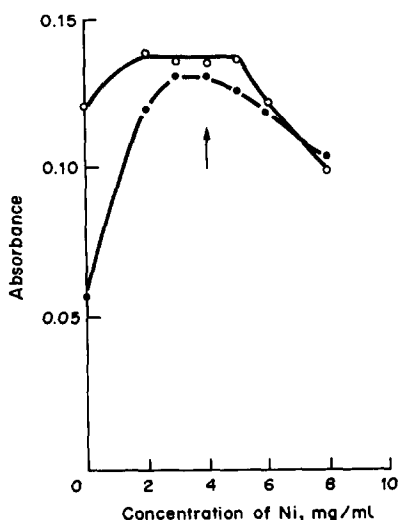


Fig. 1. Effect of nickel nitrate concentration on the signal from gallium. ○ Gallium standard solution (Ga 40 ng/ml in 2M nitric acid). ● A rock solution as prepared by the procedure (JB-1, Ga 40 ng/ml).

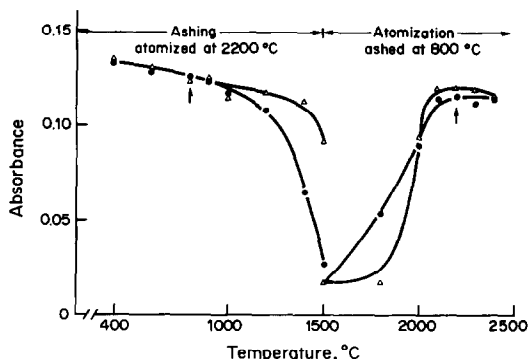


Fig. 2. Effect of ashing temperature (atomization at 2200°C) and atomization temperature (ashing at 800°C) on the signal from gallium. (A) △ Gallium standard solution. The solutions contained 45 ng/ml Ga and 4 mg/ml Ni in 2M nitric acid. (B) ● A rock sample (GSP-1) solution as prepared by the procedure. The solutions contained 4 mg/ml Ni and 43 ng/ml Ga in 2M nitric acid. Gallium concentration calculated from the literature value.<sup>14</sup>

sample solution that is 2M in nitric acid and contains flux and 43 ng/ml gallium. In both instances nickel nitrate was added prior to the atomic-absorption measurements. It appears that the ashing and atomization of gallium proceed similarly in the presence of nickel for (A) gallium alone and (B) a rock sample solution (GSP-1). The peak height for the rock solution atomized at 2200° (ashing at 800°C), when referred to the calibration with the standard solution (A) accounts reasonably well for the gallium content calculated from the recommended composition.

The results obtained for many different types of standard silicate rocks of the Geological Survey of Japan are given in Table 2 (duplicate independent determinations). The fused masses from these rocks always dissolved completely in 2M nitric acid to give clear solutions and the solutions remained unchanged for a long period of time. For comparison purposes reported values for these standard rocks are also

Table 2. Determination of gallium in standard rocks

Rock	Ga found,* μg/g	Reported values, μg/g	
		Ando <sup>12</sup>	Koshima <sup>13</sup>
JA-1 (Andesite)	16.8, 17.1	17.3	17.3
JA-2 (Andesite)	16.6, 16.6	16.4	16.4
JA-3 (Andesite)	16.3, 16.4	17	16.7
JB-1 (Basalt)	18.3, 18.3	18.1	18.1
JB-1a (Basalt)	18.0, 18.1	18	18.0
JB-2 (Basalt)	16.9, 17.3	17	17.1
JB-3 (Basalt)	20.4, 20.6	20.7	20.3
JGB-1 (Gabbro)	18.9, 18.8	18.9	18.9
JF-1 (Feldspar)	17.2, 17.9	18.1	18.1
JF-2 (Feldspar)	17.7, 17.5	18	17.5
JG-1 (Granodiorite)	16.6, 17.1	17	16.9
JG-1a (Granodiorite)	16.9, 16.3	17	17.0
JG-2 (Granite)	18.5, 18.5	19	19.0
JG-3 (Granodiorite)	16.6, 16.9	17	16.6
JR-1 (Rhyolite)	17.0, 17.2	17.6	17.6
JR-2 (Rhyolite)	18.4, 17.7	18.2	18.2

\*Samples taken independently.

given in Table 2; there are only a few data on gallium because most of the rocks became available only recently. The present results are in excellent agreement with the reported values. The precision (RSD,  $n = 5$ ) ranges from 1.2 to 6.4%, averaging 2.9%.

The proposed method is rapid, simple and accurate, because it uses the fusion technique instead of prolonged acid digestion, and involves no separation steps; it takes 20 min to complete the fusion and about the same time to dissolve the melt in 2M nitric acid. The sensitivity of the method is 27 pg of gallium for 1% absorption.

#### REFERENCES

1. J. D. Burton and F. Culkin, in K. H. Wedepohl (ed.), *Handbook of Geochemistry*, Vol. II/3, p. 31-E-7. Springer, Berlin, 1972.
2. K. Ohta and M. Suzuki, *Anal. Chim. Acta*, 1976, **85**, 83.
3. K. Kuga, *Bunseki Kagaku*, 1981, **30**, 529.
4. S. Hasegawa, T. Kobayashi, F. Hirose and H. Okochi, *ibid.*, 1987, **36**, 371.
5. D. C. Barron and B. W. Haynes, *Analyst*, 1986, **111**, 19.
6. F. J. Langmyhr and S. Rasmussen, *Anal. Chim. Acta*, 1974, **72**, 79.
7. K. Nakamura, M. Fujimori, H. Tsuchiya and H. Orii, *ibid.*, 1982, **138**, 129.
8. T. Kobayashi, F. Hirose, S. Hasegawa and H. Okochi, *Nippon Kinzoku Gakkaishi*, 1985, **49**, 656.
9. K. Kuga, S. Ooyu, E. Kitazume and K. Tsujii, *Bunseki Kagaku*, 1984, **33**, E29.
10. Shan Xiao-quan, Yuan Zhi-neng and Ni Zhe-ming, *Anal. Chem.*, 1985, **57**, 857.
11. P. V. Botha and J. Zazakas, *Anal. Chim. Acta*, 1984, **162**, 413.
12. A. Ando and S. Terashima, *Minor Elements in GSJ Rock RMS*, Geological Survey of Japan, 1986.
13. H. Koshima and H. Onishi, *Analyst*, 1987, **112**, 335.
14. K. Govindaraju, *Geost. Newsl.*, 1984, **VIII**.

## ANALYTICAL DATA

# METAL COMPLEXES OF 1-OXA-4,7,10-TRIAZACYCLODODECANE-*N,N',N''*-TRIAACETIC ACID

M. T. S. AMORIM, RITA DELGADO, J. J. R. FRAÚSTO DA SILVA, M. CÂNDIDA T. A. VAZ  
and M. FERNANDA VILHENA

Centro de Química Estrutural, Instituto Superior Técnico, Lisbon, Portugal

(Received 27 January 1988. Accepted 15 May 1988)

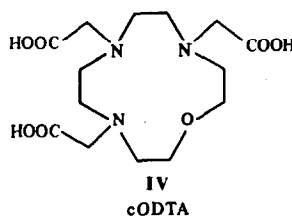
**Summary**—The macrocyclic complexone 1-oxa-4,7,10-triazacyclododecane-*N,N',N''*-triacetic acid (cDOTA) has been synthesized and its protonation constants, stability constants of metal complexes and enthalpy changes for the formation of alkaline-earth complexes have been determined. Although it is not so powerful a complexing agent as the *N*-acetate derivative of the corresponding tetra-aza macrocycle, cDOTA, this is still one of the strongest complexones known, particularly towards the alkaline-earth metals. The complexes of the transition metals are also very stable and there is an inversion of the Irving-Williams order of stability for the complexes of cobalt and nickel.

The development of macrocyclic complexones, i.e., *N*-acetate derivatives of polyaza-oligo-oxa, oligo-oxa-oligoaza macrocycles containing donor atoms other than nitrogen or oxygen, is a fairly recent field of research which has attracted the attention of a number of groups.

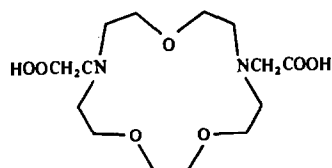
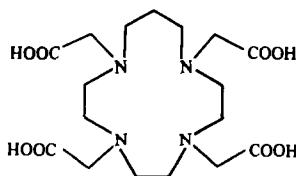
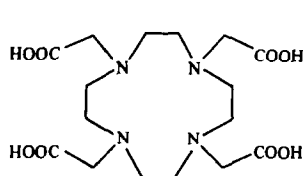
The aim of the work was to combine the selectivity associated with macrocyclic ligands (crown ethers, polyazamacrocycles, etc.) with the convenient properties of the aminopolycarboxylate compounds (stable water-soluble solids, easy to purify, yielding metal complexes of definite stoichiometry and large formation constants) to obtain new complexones that might exhibit interesting or unusual properties.

The most interesting of these macrocyclic complexones, from the analytical point of view, is probably 1,4,7,10-tetra-azacyclododecane-*N,N',N'',N'''*-tetraacetic acid (N-ac<sub>4</sub>[12]aneN<sub>4</sub> or cDOTA), I, the calcium complex of which is the most stable (in aqueous solution) known to date for a synthetic ligand,<sup>1,2</sup> but several other compounds of this family have properties of interest, e.g., 1,4,7,10-tetra-azacyclotridecane-*N,N',N'',N'''*-tetraacetic acid (N-ac<sub>4</sub>[13]aneN<sub>4</sub> or cTRITA), II, which gives a copper complex with unusually high molar absorptivity<sup>3</sup> or

1,4,10-trioxa-7,13-diazacyclopentadecane-*N,N'*-diacetic acid (K21DA or cTOPDA), III, which shows an unusual inverted U-shaped trend for the stability constants of its rare-earth metal complexes.<sup>4</sup> Minor variations in the structure of the macrocycle may lead to considerable differences in behaviour that cannot be anticipated, as in the case of the two ligands cDOTA and cTRITA, so it is not surprising that the difficult synthesis of compounds of this type still appeals to researchers, even though no spectacular new findings or very substantial improvements over the non-cyclic complexones appear to have been achieved.



In this paper we report results for a new member of the series of complexones derived from oligo-oxa oligo-aza macrocycles: the *N*-acetate derivative of 1-oxa-4,7,10-triazacyclododecane, i.e. the compound



1-oxa-4,7,10-triazacyclododecane-*N,N',N''*-triacetic acid (*N*-ac<sub>3</sub>[12]aneN<sub>3</sub>O or cODTA), IV, which has proved to be almost as powerful as the corresponding tetra-aza complexone cDOTA.

## EXPERIMENTAL

### Synthesis and characterization of the ligand

1-Oxa-4,7,10-triazacyclododecane-*N,N',N''*-triacetic acid (cODTA) was prepared by reaction of the corresponding cyclic amine in the trihydrobromide form with monochloroacetic acid in alkaline aqueous solution.

The cyclic amine was synthesized by the Richman-Atkins procedure<sup>5</sup> involving condensation of the disodium salt of tri(*p*-toluenesulphonyl)diethylenetriamine with di(*p*-toluenesulphonyl)diethyleneglycol, at 110° in dry dimethylformamide as solvent (yield 52%).

The *p*-toluenesulphonyl groups were removed by reductive cleavage with a mixture of glacial acetic acid, 48% hydrobromic acid and phenol<sup>6</sup> for 5 hr (yield 82%, M.W. 415.7; m.p. 253–255°). Found: C, 23.0%; N, 10.2%; H, 5.4%; C<sub>8</sub>H<sub>22</sub>N<sub>3</sub>OBr<sub>3</sub> requires C, 23.11%; N, 10.11%; H, 5.33%. <sup>1</sup>H-NMR spectrum (D<sub>2</sub>O, DSS): δ 3.94 (triplet, 4H, –OCH<sub>2</sub> protons), δ 3.50 (multiplet, 8H), δ 3.42 (triplet, 4H).

For the condensation of the cyclic amine with monochloroacetic acid, which took several days, the temperature was kept between 40 and 60° and the pH below 12. After the reaction, the pH was adjusted to 2.0 with 5*M* hydrochloric acid; the reaction mixture was concentrated and the precipitated inorganic salts were filtered off.

The ligand was purified by anion-exchange chromatography on Dowex 1 × 8. The fractions eluted with 0.1*M* hydrochloric acid were selected and after evaporation to dryness and several washes with ethanol, a white solid was obtained (yield 70%, M.W. 401.8; m.p. 132–134°). Found: C, 41.9; H, 7.0; N, 10.5; C<sub>14</sub>H<sub>26</sub>N<sub>3</sub>O<sub>7</sub>Cl·H<sub>2</sub>O requires C, 41.85%; H, 7.02%; N, 10.46%. <sup>1</sup>H-NMR spectrum (D<sub>2</sub>O, DSS, pD1.9): δ 4.03 (singlet, 4H, acetate groups), δ 3.95 (triplet, 4H, –OCH<sub>2</sub> ring protons), δ 3.73 (triplet, 4H), δ 3.64 (singlet, 2H, acetate group), δ 3.58 (triplet, 4H), δ 3.10 (triplet, 4H).

### Other reagents and standard solutions

Metal nitrates of analytical-reagent grade were used and solutions were prepared in demineralized water and standardized by EDTA titrations.

The ionic strength was adjusted with a solution of tetramethylammonium nitrate, Me<sub>4</sub>NNO<sub>3</sub>, prepared from Me<sub>4</sub>NOH and nitric acid and recrystallized from 80% ethanol.

Carbonate-free solutions of the titrant, tetramethylammonium hydroxide, were prepared by reacting freshly prepared silver oxide with tetramethylammonium iodide solution, under nitrogen as described in the literature.<sup>7</sup> The solutions were standardized by titration with 0.010*M* hydrochloric acid and regularly tested for carbonate; they were discarded when the concentration of carbonate reached 0.5% of the concentration of the hydroxide.

### Potentiometric titrations

The experimental set-up has been described previously;<sup>2</sup> a Crison Digilab 517 measuring instrument was used together with an Ingold U1330 glass electrode and a U1335 saturated calomel reference, with a Wilhelm-type salt bridge containing 0.10*M* Me<sub>4</sub>NNO<sub>3</sub> solution. The ionic strength of the titrated solutions was kept at 0.10*M* with Me<sub>4</sub>NNO<sub>3</sub> and the temperature was controlled at 25.0 ± 0.1° by circulating water through the jacketed titration cell, from a thermostat. The emf of the cell is given by  $E = E^0 + Q \log[H^+] + E_j$  and both  $E^0$  and  $Q$  were determined by titrating a solution of known hydrogen-ion concentration at the same ionic strength.  $E_j$ , the liquid-junction potential, was found to be

negligible in the experimental conditions used. The ionic product of water,  $K_w$ , was determined from data obtained in the alkaline zone of the titrations.

### Calorimetric determinations

The calorimetric measurements were made with an LKB model 2107 microcalorimeter. The ionic strength of the solutions of the metal nitrate and of the deprotonated complexones (with a slight excess of base—pH 12.6) was adjusted to 0.10*M* with Me<sub>4</sub>NNO<sub>3</sub> and the distribution of the species present before and after mixing was calculated at equilibrium for the actual conditions in the calorimeter; these were such that only the ML complex and the free non-protonated form of the ligand were present. Corrections for the enthalpy of dilution of the ligand were made for each experiment.

### Calculation of the stability constants

The stability constants of the various species formed were obtained from the experimental titration data with the aid of the program SUPERQUAD.<sup>8</sup> The results were obtained from a minimum of two titrations for which the  $C_M/C_L$  ratios were 1:1 and 2:1. The errors quoted were calculated by the propagation rules from the standard deviations of the overall constants obtained for about 50 readings in each set of titrations, given by the program, and do not represent the total experimental errors, which can be estimated as equivalent to ±0.25–0.45 in log  $K$  for work of this nature.<sup>9</sup>

## RESULTS AND DISCUSSION

The new ligand, cODTA, can be considered to be derived from cDOTA by replacing one of the nitrogen atoms (and its *N*-acetate pendant group) by an ether oxygen atom. This change must have an effect on the complexation properties of cODTA relative to cDOTA, but the extent of the effect is not easily predictable since not all the nitrogen atoms and acetate groups are necessarily co-ordinated to the metal ion; an experimental study of the properties of cODTA is therefore necessary. Table 1 lists the values of the protonation constants (log  $K_{H,L}$ ) and of the stability constants of its MHL and ML complexes with alkali-, alkaline-earth and some first-series transition metal ions. For comparison, the values for the corresponding cDOTA complexes are also presented.

The data in Table 1 show that cODTA is less basic than cDOTA, but the main difference is in the value of log  $K_{H_2L}$  rather than that of log  $K_{HL}$ . This suggests that in the species HL and H<sub>2</sub>L of cDOTA each proton bonds with one nitrogen atom and forms a hydrogen bond with the adjacent nitrogen atom (which may also involve the attached acetate group). For cODTA this is possible for HL but not for H<sub>2</sub>L, since there are only three nitrogen atoms, so the value of log  $K_{H_2L}$  for this ligand may be lower for this reason.

An NMR study of the protonation sequence of cDOTA and other complexones derived from tetraazamacrocycles clearly shows that the first two protons added to the ionized ligands L<sup>4-</sup> bind to diagonally opposite atoms<sup>10</sup> but gives no information on hydrogen bonding, although this might be expected.

All the reactions with the metal ions studied are rapid except for iron and nickel, in the titration of

Table 1. Protonation constants ( $\log K_{H_iL}$ ) and stability constants ( $\log K_{MHL}$  and  $\log K_{ML}$ ) of the metal complexes of 1-oxa-4,7,10-triazacyclododecane-*N,N',N''*-triacetic acid (cODTA) and corresponding values for cDOTA [ $T = 25.0 \pm 0.1^\circ\text{C}$ ;  $\mu = 0.10M$  ( $\text{Me}_4\text{MNO}_3$ )]

Ion	Species	Formation constants ( $\log K_{H_iL}$ , $\log K_{MHL}$ and $\log K_{ML}$ )*	
		cODTA†	cDOTA‡
$\text{H}^+$	LH	$11.61 \pm 0.03$	12.09
	$\text{LH}_2$	$7.70 \pm 0.05$	9.680
	$\text{LH}_3$	$4.05 \pm 0.07$	4.548
	$\text{LH}_4$	$2.77 \pm 0.1$	4.130
$\text{Na}^+$	ML	$3.266 \pm 0.006$	4.38
$\text{K}^+$	ML	$2.78 \pm 0.02$	1.64
$\text{Mg}^{2+}$	MHL	$4.31 \pm 0.06$	3.917
	ML	$10.254 \pm 0.006$	11.915
$\text{Ca}^{2+}$	MHL	$5.30 \pm 0.02$	8.68
	ML	$12.984 \pm 0.009$	17.226
$\text{Sr}^{2+}$	MHL	$4.48 \pm 0.04$	7.80
	ML	$11.370 \pm 0.007$	15.22
$\text{Ba}^{2+}$	MHL	$4.34 \pm 0.02$	6.415
	ML	$9.915 \pm 0.007$	12.873
$\text{Mn}^{2+}$	MHL	$8.62 \pm 0.05$	—
	ML	$16.09 \pm 0.03$	—
$\text{Fe}^{2+}$	MHL	$8.94 \pm 0.04$	—
	ML	$16.55 \pm 0.01$	—
$\text{Co}^{2+}$	MHL	$10.57 \pm 0.05$	12.08
	ML	$19.54 \pm 0.04$	20.17
$\text{Ni}^{2+}$	MHL	$10.09 \pm 0.05$	11.45
	ML	$18.04 \pm 0.05$	20.03
$\text{Cu}^{2+}$	MHL	$11.66 \pm 0.07$	14.416
	ML	$20.17 \pm 0.07$	22.21
$\text{Zn}^{2+}$	MHL	$9.90 \pm 0.03$	13.145
	ML	$18.66 \pm 0.02$	21.049

\* $\log K_{H_iL} = [\text{H}_i\text{L}]/[\text{H}_{i-1}\text{L}][\text{H}^+]$ ;  $\log K_{MHL} = [\text{MHL}]/[\text{M}][\text{HL}]$ ;  $\log K_{ML} = [\text{ML}]/[\text{M}][\text{L}]$ .

†Present work.

‡Reference 2.

which the potentials take about 5–10 min to stabilize after each addition of titrant. The only metal for which cODTA gives a more stable complex than cDOTA is potassium, but the differences in favour of cDOTA complexes are higher for the alkaline-earth metals (magnesium excepted) than for the transition metals. For the latter metals the differences can be ascribed to the higher basicity of cDOTA and correspond to the difference (ca. 2) between the values of  $\log K_{H_2L}$  for the two ligands; this suggests that the oxygen atom of the macrocyclic ring of cODTA and one nitrogen atom and one acetate group of cDOTA (forming an iminoacetate grouping) are not involved

in the co-ordination to these metals or interact only very weakly with them, owing to the strict stereochemical requirements for covalent bonding.

The decrease in stability of the alkaline-earth complexes of cODTA relative to the complexes of cDOTA cannot be explained simply in terms of basicity: the noble-gas electronic structure of these cations allows an optimal adjustment to all donor atoms of cDOTA to maximize the electrostatic interactions and the loss of a charged iminodiacetate moiety is not compensated by the uncharged ether oxygen atom of cODTA. This is reflected in the enthalpy and entropy changes on formation of the alkaline-earth metal

Table 2. Thermodynamic functions\* for the formation of 1:1 metal-to-ligand complexes of alkaline-earth metal ions with cODTA and cDOTA [ $T = 25.0 \pm 0.1^\circ\text{C}$ ;  $\mu = 0.10M$  ( $\text{Me}_4\text{NNO}_3$ )]

Metal ion	cODTA			cDOTA		
	$\Delta G$	$\Delta H$	$\Delta S$	$\Delta G$	$\Delta H$	$\Delta S$
$\text{Mg}^{2+}$	-13.9	+2.4	55	-16.3	+1.9	61
$\text{Ca}^{2+}$	-17.5	-10.1	25	-23.5	-11.7	40
$\text{Sr}^{2+}$	-15.5	-9.6	20	-20.8	-10.5	35
$\text{Ba}^{2+}$	-13.5	-8.1	18	-17.6	-8.5	30

\* $\Delta G$ ,  $\Delta H$ , kcal/mole;  $\Delta S$  cal. mole $^{-1}$ . K $^{-1}$ .

†Present work.

‡Reference 12.



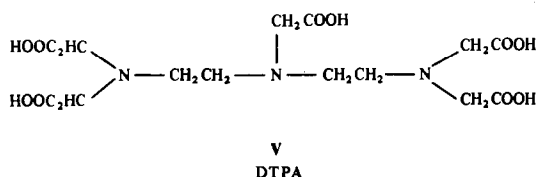
Table 3. Entropy changes (cal. mole<sup>-1</sup>.K<sup>-1</sup>) for the formation of alkaline-earth metal complexes of cODTA and DTPA

	cODTA	DTPA
Mg <sup>2+</sup>	55	53
Ca <sup>2+</sup>	25	29
Sr <sup>2+</sup>	20	20
Ba <sup>2+</sup>	18	16

complexes of the two ligands (see Table 2), both of which are favourable for the cDOTA complexes.

The differences in the entropy changes for the formation of the alkaline-earth metal complexes of cDOTA and cODTA are very close for the complexes of Ca<sup>2+</sup>, Sr<sup>2+</sup> and Ba<sup>2+</sup> (~15 cal. mole<sup>-1</sup>.K<sup>-1</sup>) and should correspond approximately to the formation of an iminoacetate chelate ring. The only available  $\Delta S$  value in the literature is that for the magnesium complex<sup>11</sup> and this is indeed of the right order of magnitude.

Note also that the entropy changes on formation of the alkaline-earth metal complexes of cODTA are quite close to the values given in Table 3 for the corresponding complexes of diethylenetriaminepentaacetic acid (DTPA, V) a non-cyclic complexone which has structural similarities with cODTA and, probably, co-ordinates to the alkaline-earth metal ions through three nitrogen atoms and three carboxylate groups.



Although it is potentially octadentate, DTPA (like all the common non-cyclic complexones), forms complexes with the alkaline-earth metals that are less stable than those of cODTA and cDOTA.

Since the entropy changes are not very different,<sup>12</sup> the increase in stability must be due to the more favourable heats of reaction for the macrocyclic complexones; hence a moderate interaction with the ether oxygen of cODTA and a favourable "cage" structure may be the reasons for the enhanced stabilities of its complexes.

With reference to the inversion of the Irving-Williams order of stability for the complexes of Co<sup>2+</sup> and Ni<sup>2+</sup> of the new ligand, deviation was already apparent for the complexes of cDOTA (though not for higher members of the family of tetra-aza complexones), but is quite significant in the present case, meaning that the complexes do not have regular octahedral co-ordination, a requisite for the rule to be obeyed.

By analogy with other cases in which the Irving-

Williams order is not followed,<sup>13,14</sup> it might be proposed that the transition metal complexes of cODTA have a pentaco-ordinated square pyramidal or trigonal bipyramidal structure; the same argument would be valid for the cobalt and nickel complexes of cDOTA and the fact that the entropy changes on formation of these complexes are smaller than for the corresponding complexes of cTRITA and the other members of this family of ligands (which we have considered an anomaly<sup>12</sup>), could be explained on this basis.

However, an X-ray diffraction study<sup>15</sup> gives evidence for a (distorted) octahedral geometry involving four amino nitrogen atoms and two carboxylate groups for the Ni<sup>2+</sup>, Cu<sup>2+</sup> and Zn<sup>2+</sup> complexes of cDOTA, and the electronic spectrum of the Co<sup>2+</sup> complex of this ligand exhibits the features of six-co-ordinated cobalt complexes<sup>16</sup> (although some degree of asymmetry is apparent) both in the position and structure of the absorption bands and in the values of the maximum molar absorptivity.<sup>17</sup>

The electronic spectrum of the Co<sup>2+</sup> complex of cODTA is not very dissimilar from that of the Co<sup>2+</sup> complex of cDOTA, but it has a higher maximum molar absorptivity, approaching the values for five-co-ordinated complexes. Still, the possibility of a six-co-ordinated complex cannot be dismissed, perhaps involving the ether oxygen atom of the macrocycle (a rather weak interaction) or a co-ordinated water molecule.

It is likely, therefore, that the inversion of the Irving-Williams order derives from a change in the ligand-field symmetry in the complexes, to be closer to pentaco-ordinated, relative to that of the octahedrally co-ordinated aqueous ions, as a consequence both of stereochemical constraints and non-equivalent donor atoms, but until more direct evidence is obtained on the actual structure (when in solution) of the complexes of the transition metals with the new ligand, this idea cannot be confirmed.

*Acknowledgements*—The authors thank the Instituto Nacional de Investigação Científica (INIC, Portugal) for financial assistance and Professors P. Paoletti and M. Micheloni (Department of Chemistry, University of Florence, Italy) for kindly providing facilities for the calorimetric determinations.

#### REFERENCES

- H. Stetter and W. Frank, *Angew. Chem., Intern. Ed. Engl.*, 1976, **15**, 686.
- R. Delgado and J. J. R. Fraústo da Silva, *Talanta*, 1982, **29**, 815.
- R. Delgado, J. J. R. Fraústo da Silva and M. Cândida T. A. Vaz, *ibid.*, 1986, **33**, 285.
- C. A. Chang and V. O. Ochaya, *Inorg. Chem.*, 1986, **25**, 355.
- J. R. Richman and T. J. Atkins, *J. Am. Chem. Soc.*, 1974, **96**, 2268.
- G. H. Searle and R. J. Geue, *Aust. J. Chem.*, 1984, **37**, 959.
- G. Schwarzenbach and W. Biedermann, *Helv. Chim. Acta*, 1948, **31**, 331.

8. P. Gans, A. Sabatini and A. Vacca, *J. Chem. Soc. Dalton Trans.*, 1985, 1195.
9. P. A. Overvoll and W. Lund, *Anal. Chim. Acta*, 1982, **143**, 153.
10. J. Ascenso, R. Delgado and J. J. Fraústo da Silva, *J. Chem. Soc. Perkins Trans.*, 1985, 781.
11. A. Martell and R. Smith, *Critical Stability Constants*, Vol. 1, Plenum Press, New York, 1974.
12. R. Delgado, J. J. R. Fraústo da Silva and M. Cândida T. A. Vaz, *Inorg. Chim. Acta*, 1984, **90**, 185.
13. A. Bianchi and P. Paoletti, *ibid.*, 1985, **96**, 137.
14. R. Delgado, J. J. R. Fraústo da Silva and M. Cândida T. A. Vaz, *Polyhedron*, 1987, **6**, 29.
15. A. Riesen, M. Zehnder and T. A. Kaden, *Helv. Chim. Acta*, 1986, **69**, 2067.
16. R. Delgado, J. J. R. Fraústo da Silva and M. Cândida T. A. Vaz, *7<sup>o</sup> Encontro Anual of S.P.Q.*, Lisbon, July 1984.
17. I. Bertini and C. Luchinat, *Adv. Inorg. Biochem.*, 1984, **6**, 71.

## INSTRUMENTAL NEUTRON-ACTIVATION DETERMINATION OF PHOSPHORUS IN BIOLOGICAL MATERIALS BY BREMSSTRAHLUNG MEASUREMENT

S. BAJO and A. WYTENBACH  
 Paul Scherrer Institut, CH-5303 Würenlingen, Switzerland

(Received 6 March 1987. Revised 9 November 1987. Accepted 23 June 1988)

**Summary**—The determination of phosphorus in biological materials by instrumental neutron-activation analysis by the reaction  $^{31}\text{P}(n, \lambda)^{32}\text{P}$  is described. The bremsstrahlung produced by  $^{32}\text{P}$  is measured in a well-type NaI(Tl) detector. The samples are measured in the polyethylene irradiation container with no additional handling between irradiation and measurement. The sources of error have been studied and the proposed method has been applied to the determination of phosphorus in ten internationally certified materials.

Neutron activation analysis is a sensitive method for the determination of phosphorus by means of the reactions  $^{31}\text{P}(n, \gamma)^{32}\text{P}$  and  $^{31}\text{P}(n, \alpha)^{28}\text{Al}$  (Table 1).

Because  $^{32}\text{P}$  ( $t_{1/2} = 14.3$  d) emits no gamma rays and  $^{28}\text{Al}$  has a very short half-life ( $t_{1/2} = 2.2$  min) many workers have developed other radioanalytical methods such as derivative neutron-activation analysis,<sup>34-37</sup> isotopic exchange,<sup>38</sup> radioreagents,<sup>38-40</sup> and isotopic dilution with substoichiometric liquid-liquid extraction,<sup>41-44</sup> for the determination.

In our laboratory, about 25 elements are routinely determined in plants by instrumental neutron-activation analysis. The importance of phosphorus in plant physiology justified extension to include determination of this element. The reaction

$^{31}\text{P}(n, \gamma)^{32}\text{P}$  and measurement of the bremsstrahlung produced in a well-type NaI(Tl) detector by the beta rays of  $^{32}\text{P}$  could be easily added to the existing procedure and required no additional equipment. The method has been applied previously, but without discussion.<sup>12, 13, 18, 21, 22</sup> This paper presents the factors affecting the accuracy of the method and reports the results of its application to standard reference materials.

### EXPERIMENTAL

#### *Samples and standards*

For irradiation, powdered materials were encapsulated in clean high-purity polyethylene containers ("Spronk" containers: Hart Woolresearch Foundation, Vondelstraat 47,

Table 1. Determination of phosphorus by neutron-activation analysis

	Methods of detection	Applications
<b>(A) Analytical reaction: <math>^{31}\text{P}(n, \gamma)^{32}\text{P}</math>.</b>		
Potential interferences: $^{32}\text{S}(n, p)^{32}\text{P}$ , $^{35}\text{Cl}(n, \alpha)^{32}\text{P}$		
Irradiation facility: nuclear reactor.		
With radiochemical separation of $^{32}\text{P}$	Measurement of beta radiation (Geiger-Müller detector)	Biological materials, <sup>1-6</sup> rocks, <sup>7-10</sup> water <sup>11</sup>
	Measurement of bremsstrahlung [NaI(Tl), detector]	Biological materials, <sup>12, 13</sup>
	Cerenkov radiation (photomultiplier, detector)	Biological materials <sup>14, 15</sup>
Without radiochemical separation of $^{32}\text{P}$	Measurement of beta radiation (Geiger-Müller detector)	Biological materials, <sup>3, 16-19</sup> rocks <sup>20</sup>
	Measurement of bremsstrahlung [NaI(Tl) or Ge(Li) detectors]	Biological materials <sup>18, 21, 22</sup>
	Measurement of bremsstrahlung (plastic scintillator)	Rocks <sup>23</sup>
	Measurement of Cerenkov radiation (photomultiplier detector)	Biological materials <sup>15, 24, 25</sup>
<b>(B) Analytical reaction: <math>^{31}\text{P}(n, \alpha)^{28}\text{Al}</math>.</b>		
Potential interferences: $^{27}\text{Al}(n, \gamma)^{28}\text{Al}$ , $^{28}\text{Si}(n, p)^{28}\text{Al}$		
Irradiation facility: neutron generator (14 MeV) or nuclear reactor (epithermal neutrons).		
Radiochemical separation of $^{28}\text{Al}$ is excluded because of its short half-life (2.2 min)		
Neutron source	Applications	
14 MeV neutrons	Biological materials, <sup>26-28</sup> synthetic mixtures. <sup>29</sup>	
Epithermal neutrons	Biological materials, <sup>30-32</sup> synthetic mixtures. <sup>33</sup>	

Amsterdam). Containers of type D (capacity, 0.85 ml; weight, 0.37 g; height, 19 mm; diameter, 9.4 mm) were used. The same type of container and weight of material ( $550 \pm 55$  mg) were taken for samples and standards.

**Phosphorus standard.** To reproduce the apparent density of the samples, spruce needles (*Picea abies* (L.) Karst) were used as a phosphorus standard. Twigs were collected and washed with chloroform to remove wax and other adhering material,<sup>45</sup> then dried at 65° for three days. The needles were pulverized in a coffee grinder, then kept in an open container for one week to permit their moisture content to equilibrate with that of the atmosphere. Analysis of this material gave, on a dry basis (drying at 85°) 1900 ppm for phosphorus (colorimetry), 920 ppm for sulphur (nephelometry) and 842 ppm for chlorine (neutron-activation analysis).

**Anion-exchange resin loaded with <sup>32</sup>P.** An anion-exchange resin (Dowex 1 × 8, 50–100 mesh) was loaded with <sup>32</sup>PO<sub>4</sub><sup>3-</sup> by the batch technique, washed with water, and air-dried at 20°. The loaded resin was used to simulate activated biological materials containing <sup>32</sup>P. The apparent density of the air-dried resin was 0.71 g/cm<sup>3</sup>. Its small beads are incompressible and behave like a liquid.

To prepare samples with different apparent densities, an easily compressible and homogeneous material was obtained by grinding a mixture of the <sup>32</sup>P-loaded resin and spruce needles in 1:2.5 w/w ratio.

#### Irradiation

Samples and standards were irradiated simultaneously in the rotating facility of the Saphir reactor for 0.4–1.5 hr at a flux of  $3.3 \times 10^{13}$  n.cm<sup>-2</sup>.sec<sup>-1</sup>.

#### Counting equipment

Counting was done with a well-type NaI(Tl) detector linked to a single-channel gamma-spectrometer; the well had a diameter of 17 mm and was 37 mm deep. The window of the amplifier was set to integrate the gamma-radiation in the energy range 100–200 keV; this setting was somewhat arbitrary. The radiation measured was the bremsstrahlung generated by the beta rays ( $E_{\max} = 1.7$  MeV) of <sup>32</sup>P in the sample, the polyethylene container, and the detector itself. An aluminium absorber 3.00 mm thick (810 mg/cm<sup>2</sup>) was used in some cases; the range of the 1.7 MeV beta rays in aluminium is 800 mg/cm<sup>2</sup>.

## RESULTS AND DISCUSSION

Various factors may affect the determination of phosphorus in biological materials by neutron-activation.

#### Linearity

Mixtures of resins loaded and non-loaded with <sup>32</sup>P were encapsulated in the polyethylene containers. The weight of the mixture was kept constant at 328 mg, which represents about half the container capacity. Good linearity was obtained for plots of the specific count-rate as a function of the weight of loaded resin in the mixture (Table 2). The slope of the straight line obtained when the aluminium absorber was used was not significantly different from zero, whereas that obtained without the aluminium absorber was different from zero at the  $P = 0.10$  level. The presence of the aluminium absorber lowers the count-rate by a factor of 2.7. With the aluminium absorber, all the beta rays are absorbed in the sample and the aluminium. Without the absorber, most of the beta rays enter the detector itself and are

Table 2. Factors affecting the determination of phosphorus in biological materials by measurement of the bremsstrahlung of <sup>32</sup>P

Factor	Absorber	Range of x	Straight line fitted ( $y = a + bx$ )*				Sample parameters			
			a	b	RSD, %†	Contents	Weight	Volume	Density	
Linearity	None	50–328	3.67 ± 0.04	(4.87 ± 2.11) × 10 <sup>-4</sup>	1.4	<sup>32</sup> P-loaded resin and non-loaded resin	Constant	Constant	Constant	
	Al	50–328	1.37 ± 0.02	(1.20 ± 1.01) × 10 <sup>-4</sup>	1.8	<sup>32</sup> P-loaded resin and non-loaded resin	Constant	Constant	Constant	
Sample weight	None	150–600	5.74 ± 0.04	-(1.22 ± 0.10) × 10 <sup>-3</sup>	0.9	<sup>32</sup> P-loaded resin	Variable	Variable	Constant	
	Al	150–600	2.21 ± 0.01	-(4.20 ± 0.35) × 10 <sup>-4</sup>	0.8	<sup>32</sup> P-loaded resin	Variable	Variable	Constant	
Sample density	None	250–650	1.60 ± 0.01	-(1.07 ± 0.03) × 10 <sup>-3</sup>	1.0	Ground mixture	Variable	Constant	Variable	
	Al	250–650	0.432 ± 0.007	-(1.15 ± 0.16) × 10 <sup>-4</sup>	1.6	Ground mixture	Variable	Constant	Variable	

\*y is the specific count rate (cps/mg), and x is the weight (mg).

†Residual standard deviation.

‡Total weight is constant, but the content of <sup>32</sup>P-loaded resin varies.

absorbed there; the bremsstrahlung is then produced in higher yield.

#### *Sample weight (volume)*

The variation of the specific count-rate with sample weight (volume) was followed by introducing different quantities of the  $^{32}\text{P}$ -loaded resin into the containers. The results are also shown in Table 2. The specific count-rate decreases as the sample weight increases, because of the increase in sample volume and self-absorption in the sample.

#### *Sample density*

Samples with different apparent densities were prepared from the ground mixture ( $^{32}\text{P}$ -loaded resin plus spruce needles). The containers (all of which had the same capacity) were filled up with different amounts of this mixture by applying pressure as required.

The variation of the specific count-rate with the apparent sample density is shown in Table 2. Increasing the sample density increases the fraction of beta rays absorbed within the sample and decreases the fraction reaching the detector. Because the main constituents of the sample (C, O, and H) have low atomic numbers, they yield less bremsstrahlung than do the heavier components (Na and I) of the detector.

The equations in Table 1 may be used to refer the specific activity of samples of different weights to a common weight. The ratio of the specific activities with and without the aluminium absorber present may be used to detect the presence of gamma-emitting nuclides.

#### *Blank*

In the proposed method, samples and standards are counted in the polyethylene container in which they were irradiated. Trace amounts of bromine and chromium are present in these containers, but measurements made 10–50 days after irradiation showed that the interfering emission from the radionuclides  $^{82}\text{Br}$  and  $^{51}\text{Cr}$  was equivalent to less than 1  $\mu\text{g}$  of phosphorus per container, corresponding to an apparent concentration of <2 ppm in a 550 mg sample. As the phosphorus content of most biological materials is about 1000 ppm, this error can be neglected.

#### *Interferences*

The interferences introduced by the reactions  $^{32}\text{S}(n, p)^{32}\text{P}$  and  $^{35}\text{Cl}(n, \alpha)^{32}\text{P}$  were determined by irradiating known quantities of diammonium hydrogen phosphate, potassium chloride and potassium sulphate in the position used for the phosphorus analysis. After a waiting period for the decay of some small gamma activities, the samples were dissolved in water and matched for their salt content. Aliquots of 2.0 ml were then counted in the NaI(Tl) detector under the conditions used for routine phosphorus sample analysis. Phosphorus produced 37.5 times as

much activity as sulphur and 108 times as much as chlorine, per unit mass. Thus, for most materials, the correction for sulphur amounts to a few per cent of the phosphorus content and the correction for the chlorine content is much smaller and can usually be neglected.

#### *Analysis of real samples*

*Decay time.* Any radioactivity contributed by the short-lived nuclides  $^{24}\text{Na}$ ,  $^{42}\text{K}$ , and  $^{82}\text{Br}$  decays to an insignificant level within 8 days after irradiation of the sample. After this waiting period, the decay of the count rate was dependent only on the half-life of  $^{32}\text{P}$ . A standard cooling period of 14–20 days was chosen.

*Sensitivity.* A typical 550-mg plant sample containing 1000 ppm phosphorus irradiated at an integrated flux of  $1.5 \times 10^{17}$  n.cm $^{-2}$  gives a count rate of  $1.6 \times 10^3$  cps when measured without an aluminium absorber two weeks after irradiation. This is equivalent to a specific phosphorus count-rate of 5.7 cps/ $\mu\text{g}$  at the end of irradiation. The background count rate is 1.3 cps.

*Sources of error.* The production of  $^{32}\text{P}$  from  $^{35}\text{Cl}$  and  $^{32}\text{S}$  interferes directly with the determination of phosphorus. Contributions from these sources can be subtracted after calculation by using the factors quoted in the section on interferences if the concentrations of chlorine and sulphur in the sample are known. The determination of chlorine by neutron-activation through the  $^{37}\text{Cl}(n, \gamma)^{38}\text{Cl}$  reaction is a straightforward task. Sulphur however, yields no useful gamma-emitter. Irradiations of samples with and without thermal-neutron shielding should allow the simultaneous determination of P and S,<sup>5,11</sup> but this procedure was not tested.

No interference by long-lived radionuclides<sup>23</sup> or high-energy beta-emitters<sup>20</sup> was detected from the shape of the decay curves. This is undoubtedly because the content of phosphorus in most biological materials is very much higher than that of any potentially interfering elements.

The error introduced by comparing the specific activities of samples and standards of different weight can be corrected by using equations of the type presented in Table 2. However, in the routine analysis of very similar materials it is worthwhile simply to match the standard to the sample in weight, volume, and composition.

#### *Results*

The results obtained are shown in Table 3. Each replicate and the corresponding standard were measured, without an aluminium absorber, eight times over a period of 10–39 days after the irradiation. The phosphorus content of each sample was calculated for each measurement. The coefficient of variation of these eight determinations was always less than 2% for all 3 replicates. The post-irradiation decay period is thus shown to be non-critical, and a single measurement will suffice for routine work.

Table 3. Analysis of biological materials with known phosphorus contents

Material	Found*			Phosphorus			Sulphur		
	ppm	C.V., %	Known content, ppm	Found		Known content, ppm	Known content, ppm	Correction for S, %†	References
				Known content, ppm	ppm				
"Feuilles d'olivier"	818	1.1	830 ± 60	0.99	1970	6.4	46		
"Feuilles de pêcher"	2720	0.43	2920 ± 100	0.93	2390	2.3	46		
"Feuilles d'oranger"	1550	1.4	1500 ± 100	1.03	2660	4.6	46		
Orchard leaves, NBS-SRM-1571	1930	1.1	2100 ± 100	0.92	2080	2.9	47		
Bowen's Kale	4590	0.78	4540 ± 1600	1.01	15800	9.2	48		
Bovine liver NBS-SRM-1577	11300	1.4	11000	1.03	7100	1.7	49		
Milk powder IAEA-A-11	9140	0.44	9100 ± 1020	1.00	18000	5.2	50		
Milk powder BCR-63	9720	1.4	10400 ± 300	0.94	§	—	51		
Citrus leaves NBS-SRM-1572	1250	2.0	1300 ± 200	0.96	4070	8.7	52		
Pine needles NBS-SRM-1570	1170	0.85	1200 ± 200	0.98	§	—	53		

\*Three replicate samples were analysed in every case except Milk powder BCR-63 where  $n = 6$ . The mean includes the correction for the sulphur content:  $P_{\text{true}} = P_{\text{measured}} - (\text{ppm S})/37.5$ .

† ppm P after correction for the contribution from S

§ Not available.

### Accuracy and precision of the method

Table 3 shows that the method is accurate. The ratio of content found to known content ( $n = 10$ ,  $\bar{x} = 0.98$ ,  $s = 0.04$ ) is very close to 1, especially when account is taken of the uncertainty associated with the reference values.

Whenever new biological materials are analysed, phosphorus should be determined with and without an aluminium absorber present, in order to detect any contribution from gamma-emitters. For example, the results obtained for beech leaves ( $n = 12$ ) and spruce needles ( $n = 20$ ) for the ratio of the phosphorus contents ( $\bar{x} \pm 1s$ ) determined without and with an aluminium absorber were  $1.03 \pm 0.01$  and  $1.01 \pm 0.01$ , respectively. The contribution of gamma-emitters could therefore be neglected in these cases.

The precision was tested by analysing many samples in duplicate. A typical run with 21 samples of beech leaves analysed in duplicate showed a coefficient of variation of 0.8% for phosphorus contents ranging from 800 to 1400 ppm.

The reproducibility, or long-term standard deviation, was determined by including two samples of NBS-SRM-1571 Orchard Leaves in each of 13 irradiations spread over one year. The result was  $\bar{x} = 1950$  ppm, C.V. = 1.3%, and a range of 1910–1990 ppm phosphorus.

*Acknowledgement*—The authors are indebted to Thomas F. Campbell for his help with the English manuscript.

### REFERENCES

- H. J. M. Bowen and P. A. Cawse, *Analyst*, 1961, **86**, 506.
- R. C. Koch and J. Roesmer, *Modern Trends in Activation Analysis, Proc. 1961 International Conference*, December 1961, College Station, Texas (1961), pp. 95–101.
- P. Kruger and I. J. Gruverman, *Int. J. Appl. Rad. Isotop.*, 1962, **13**, 106.
- R. C. Koch and J. Roesmer, *J. Food Sci.*, 1962, **27**, 309.
- A. G. Souliotis, *Anal. Chem.*, 1964, **36**, 811.
- S. S. Krishnan and R. C. Gupta, *ibid.*, 1970, **42**, 557.
- P. Henderson, *Anal. Chim. Acta*, 1967, **39**, 512.
- A. O. Brunfelt and E. Steinnes, *ibid.*, 1968, **41**, 155.
- E. Steinnes, *J. Radioanal. Chem.*, 1972, **10**, 65.
- S. O. Khalil, *Acta Chim. Acad. Sci. Hung.*, 1974, **83**, 223.
- C. H. Wayman, *Anal. Chem.*, 1964, **36**, 665.
- K. Samsahl and R. Soremark, *Modern Trends in Activation Analysis, Proc. 1961 International Conference*, December 1961, College Station, Texas (1961), pp. 149–154.
- K. Samsahl, D. Brune and P. Wester, *Int. J. Appl. Rad. Isotop.*, 1965, **16**, 273.
- F. Girardi, V. Camera and E. Sabbioni, *Radiochem. Radioanal. Lett.*, 1969, **2**, 195.
- K. Rengan, *Int. Biotechnol. Lab.* 1986, **4**, No. 3, 20.
- L. Reiffel and C. A. Stone, *J. Lab. Clin. Med.*, 1957, **49**, 286.
- M. Rakovič and H. Talpová, *Chem. Zvesti*, 1964, **18**, 669.
- E. Steinnes, *Talanta*, 1967, **14**, 753.
- E. Damsgaard and K. Heydorn, *7th International Conference Modern Trends in Activation Analysis*, Copenhagen, June 23–27 1986.

20. E. Steinnnes, *Anal. Chim. Acta*, 1971, **57**, 451.
21. W. A. Haller, R. H. Filby, L. A. Rancitelli and J. A. Cooper, *Modern Trends in Activation Analysis, Proc. 1968 International Conference*, Vol. 1, pp. 177-183. NBS, Washington DC, 1969.
22. W. A. Haller, R. H. Filby and L. A. Rancitelli, *Nuclear Applications*, 1969, **6**, 365.
23. H. A. Das, J. Zonderhuis and R. Rose, *J. Radioanal. Chem.*, 1972, **11**, 273.
24. E. Sabbioni, L. Clerici, F. Girardi and F. Campagnari, *ibid.*, 1973, **14**, 159.
25. R. Guzzi, R. Pietra and E. Sabbioni, *ibid.*, 1976, **34**, 35.
26. A. A. Prapuolenis and J. M. Bakes, *Radiochem. Radioanal. Lett.*, 1969, **1**, 19.
27. Chr. Segebade, *Z. Anal. Chem.*, 1977, **284**, 23.
28. R. E. Williams, P. K. Hopke and R. A. Meyer, *J. Radioanal. Chem.*, 1981, **63**, 187.
29. M. To-on, F. Sicilio and R. E. Wainerdi, *Trans. Am. Nucl. Soc.*, 1964, **7**, 328.
30. W. Gatschke and D. Gawlik, *J. Radioanal. Chem.*, 1980, **56**, 203.
31. *Idem*, *J. Clin. Chem. Clin. Biochem.*, 1980, **18**, 403.
32. H. Bem and D. E. Ryan, *Anal. Chim. Acta*, 1982, **135**, 129.
33. Z. B. Alfassi and N. Lavi, *Analyst*, 1984, **109**, 959.
34. H. E. Allen and R. B. Hahn, *Environ. Sci. Technol.*, 1969, **3**, 844.
35. J. D. Jones, P. B. Kaufman and W. L. Rigot, *J. Radioanal. Chem.*, 1979, **50**, 261.
36. E. W. Kleppinger, E. H. Brubaker, R. C. Young, W. D. Ehmann and S. W. Yates, *J. Chem. Educ.*, 1984, **61**, 262.
37. W. D. Ehmann, R. C. Young, D. W. Koppenaar, W. C. Jones and M. N. Prasad, *7th International Conference on Activation Analysis*, Copenhagen, June 23-27 1986.
38. A. Zeman and K. Kratzer, *Radiochem. Radioanal. Lett.* 1976, **27**, 217.
39. R. B. Hahn and T. M. Schmitt, *Anal. Chem.*, 1969, **41**, 359.
40. J. E. Kenney and M. P. Menon, *ibid.*, 1972, **44**, 2093.
41. G. A. Perezhogin and L. P. Sidorova, *J. Anal. Chem. USSR*, 1969, **24**, 435.
42. R. B. Heslop and A. C. Ramsey, *Anal. Chim. Acta*, 1969, **47**, 305.
43. T. Shigematsu and K. Kudo, *J. Radioanal. Chem.*, 1981, **67**, 25.
44. *Idem*, *ibid.*, 1981, **67**, 307.
45. A. Wyttenbach, S. Bajo and L. Tobler, *Plant Soil*, 1985, **85**, 313.
46. M. Pinta, *Analisis*, 1975, **3**, 345.
47. U.S. National Bureau of Standards, Certificate of Analysis, Standard Reference Material 1571, Washington, 31 August 1977.
48. H. J. M. Bowen, *Atomic Energy Review*, 1975, **13**, 451.
49. U.S. National Bureau of Standard, Certificate of Analysis Standard Reference Material 1577, Washington, 14 June 1977.
50. International Atomic Energy Agency, Information Sheet, Reference Material A-11, Vienna, 20 July 1980.
51. Commission of the European Communities, Community Bureau of Reference, BCR Information, BCR No. 63, Report EUR 9138 EN, Luxembourg, 1983, p. 25.
52. U.S. National Bureau of Standards, Certificate of Analysis, Standard Reference Material 1572, Washington, 22 February 1982.
53. U.S. National Bureau of Standards, Certificate of Analysis, Standard Reference Material 1575, Washington, 18 October 1976.

## DERIVATIVE ULTRAVIOLET-VISIBLE REGION ABSORPTION SPECTROPHOTOMETRY AND ITS ANALYTICAL APPLICATIONS

F. SANCHEZ ROJAS, C. BOSCH OJEDA and J. M. CANO PAVON

Department of Analytical Chemistry, Faculty of Sciences, University of Málaga, 29071 Málaga, Spain

(Received 29 May 1987. Revised 14 June 1988. Accepted 21 June 1988)

**Summary**—Theoretical aspects, instrumental devices and analytical applications of derivative ultraviolet-visible region absorption spectrophotometry are reviewed.

Derivative spectrophotometry is an analytical technique of great utility for extracting both qualitative and quantitative information from spectra composed of unresolved bands. Although it was introduced more than thirty years ago,<sup>1-3</sup> and has demonstrable advantages for the solution of specific analytical problems, this technique has been accepted only hesitantly, because of the initial lack of reasonably priced instrumentation and original limitation to the first derivative. However, in recent years, the introduction of electronic differentiation by a micro-computer interfaced with the spectrophotometer makes possible the plotting of the first, second or higher order derivatives of a spectrum with respect to wavelength.

The derivative method has found application not only in ultraviolet-visible region spectrophotometry, but also in infrared,<sup>4</sup> atomic-absorption and flame emission spectrometry,<sup>5,6</sup> and also in fluorimetry (normal<sup>7</sup> and synchronous scanning<sup>8</sup>). The use of derivative spectrometry is not restricted to special cases, but may be of advantage whenever quantitative study of normal spectra is difficult. Its disadvantage is that the differentiation degrades the signal-to-noise ratio, so that some form of smoothing is required in conjunction with the differentiation.<sup>9</sup>

Reviews dealing with the properties of derivative spectra,<sup>10-18</sup> and their practical applications,<sup>19-21</sup> are available. Reviews in foreign languages have been presented by Kubiak<sup>22</sup> (Polish), Dubrovkin<sup>23</sup> (Russian) and Wang<sup>24</sup> (Chinese).

The purpose of this paper is to review general aspects of derivative spectrometry (DS), and its use in chemical analysis, clinical chemistry and other areas of application.

### THEORETICAL ASPECTS

#### Basic properties of derivative spectra

For a single-peak spectrum, the first-derivative is a plot of the gradient  $dA/d\lambda$  of the absorption envelope *vs.* wavelength and features a maximum and a min-

imum; the vertical distance between these is the amplitude, which is proportional to the analyte concentration; theoretically,  $dA/d\lambda$  is zero at  $\lambda_{\max}$  for the band in the normal spectrum. The second-derivative spectrum,  $d^2A/d\lambda^2$  *vs.*  $\lambda$ , has two maxima with a minimum between them, at  $\lambda_{\max}$  of the normal absorption band.<sup>25</sup> In principle, both peak-heights (measured from  $d^2A/d\lambda^2 = 0$ ) are proportional to the analyte concentration but the amplitude can also be measured by the so-called tangent method, in which a tangent is drawn to the maxima and the amplitude is measured vertically from the tangent to the minimum.<sup>10</sup> Other possibilities have been considered,<sup>26</sup> and background absorbance can be eliminated.

The differentiation discriminates against broad bands, emphasizing sharper features to an extent that increases with increasing derivative order, because for bands (Gaussian or Lorentzian) the amplitude  $D_n$  of the  $n$ th derivative is related to the  $n$ th power of the inverse of the band-width,  $w$ , of the normal spectrum:<sup>27</sup>

$$D_n \propto \left(\frac{1}{w}\right)^n$$

Thus, for two bands A and B of equal absorbance but different width, the derivative amplitude of the sharper band (A, for example) is greater than that of the broader (B) by a factor that increases with increasing derivative order:<sup>28,29</sup>

$$\frac{D_{n,A}}{D_{n,B}} \propto \left(\frac{w_B}{w_A}\right)^n$$

For this reason, the use of derivative spectra can increase the detection sensitivity<sup>16,30,31</sup> of minor spectral features.

For quantitative analysis, if Beer's law is obeyed for the normal spectrum, the following equation can be obtained:

$$\frac{d^n A}{d\lambda^n} = \frac{d^n \epsilon}{d\lambda^n} lc$$

where  $A$  = absorbance,  $\epsilon$  = molar absorptivity,



$l$  = cell path-length and  $c$  = concentration of the analyte, and this forms the basis for analytical determinations.<sup>32</sup>

#### *Effect of differentiation on signal-to-noise ratio*

An inconvenience of the derivative technique is that the signal-to-noise ratio (SNR) becomes worse for progressively higher orders. The noise of a normal spectrum may be expressed as the standard deviation<sup>33</sup>  $\sigma_0$  of the absorbance of a blank; for the  $n$ th order derivative, the standard deviation  $\sigma_n$  can be calculated from  $\sigma_0$  by the usual rules for error propagation.

The SNR of derivative signals depends on the shape of the spectrum, and has been evaluated<sup>34</sup> for different bands. In Gaussian bands, for example, if we suppose an SNR of 1 in the normal spectrum, the SNR is given by  $2.02/M$  in the first derivative,  $3.26/M^2$  in the second,  $8.10/M^3$  in the third,  $17.8/M^4$  in the fourth, *etc.*, where  $M$  is the number of points in the peak full-width at half maximum. For example, if  $M = 12$ , the SNR values for the first four derivatives are 0.168, 0.022, 0.0047 and 0.00086; that is to say, if  $n$  is large, the SNR of the derivatives will be very small.

For this reason, practical derivative techniques include some degree of low-pass filtering or smoothing to control the increase in noise. The process of smoothing involves a convolution of the data series with a smoothing function consisting of a set of weighting coefficients. The various smoothing methods differ only in the way that the coefficients are calculated.

The effect of smoothing depends on two variables: (a) the smoothing ratio, which is the ratio of the width of the smoothed peak to the number  $M$  of data points corresponding to the peak full-width at half-maximum, and (b) the number of times that the smoothing is done. Moreover, the attenuation factor is determined by the smoothing ratio. A detailed study of the influences of these variables on the derivative spectra has been reported by O'Haver.<sup>34</sup>

The ratio of the SNR of the unsmoothed  $n$ th derivative  $(\text{SNR})_n$  to that of the unsmoothed normal SNR  $(\text{SNR})_0$  is given by<sup>9</sup>

$$\frac{(\text{SNR})_n}{(\text{SNR})_0} = \alpha_n C_n r^{(n+0.5)} \sqrt{M}$$

where  $C_n$  is a constant which increases with derivative order  $n$ , and  $\alpha_n$  is the attenuation factor of the  $n$ th derivative for a smoothing ratio  $r$ . Values of  $(\text{SNR})_n/(\text{SNR})_0$  have been calculated as a function of  $r$ ; the SNR ratios of all derivatives, including the zeroth, increase with  $r$ , but tend to converge at high  $r$  values; it can be concluded that the commonly observed degradation of SNR accompanying differentiation is not a necessary consequence and can be avoided if sufficient smoothing is employed. In general, the selection of the optimum smoothing ratio depends on the purpose for which the derivative

technique is used. Thus, for quantitative applications, in which the derivative technique is used to reduce a broad-band background, significantly larger smoothing ratios (0.5, for example) may be profitably employed. In contrast, when the technique is used only to enhance resolution, relatively small smoothing ratios ( $\sim 0.2$ ) will ensure very little loss of resolution, but a significant loss in SNR will have to be tolerated.

#### *Multicomponent analysis*

Spectrophotometry in the ultraviolet-visible region can be used for simultaneous determination of several components; however, the determination of the area or height of overlapping bands can be very difficult. Various theoretical and practical methods evaluating overlapping peaks have been suggested. Morrey<sup>35</sup> describes the limiting conditions for the detection of overlapping peaks; information obtained by use of a derivative spectrum is sufficient to place accurately peaks which appear only as shoulders on stronger peaks. Two reviews<sup>36,37</sup> on the computer resolution of overlapping electronic absorption bands have been published; both mention differentiation of spectra, but give little indication of the care necessary in obtaining and interpreting such spectra.

Various attempts have been made to assess the potential utility of DS for quantitative analysis of mixtures. A microcomputer has been to calculate the resolution obtainable with the 2nd and 4th derivatives of two overlapping Gaussian bands of equal or differing heights, widths and separation intervals.<sup>38</sup> O'Haver and Green<sup>39</sup> have evaluated, on a rather general basis, the utility of the technique in reducing band-overlap errors of the type often encountered in quantitative spectrometry. The approach was based on computer-generated overlapping Gaussian band pairs, one of which was an interfering band to be discriminated against; the success of a measurement was indicated by its total error, defined as the sum of the systematic error plus twice the random error. From the results obtained it can be concluded that the methods developed by these authors would be useful for reduction of band-overlap errors if the systematic error caused by the overlap is large compared to the random error and the interfering band is either known and constant or is broader than the analyte band. In general, the derivative technique reduces the total error by a factor of at least 3, and usually by much more.

Griffiths *et al.*<sup>40</sup> made a theoretical study of some relationships between absorption spectra and their second and fourth derivatives, including the limitation arising from fortuitous overlap of neighbouring peaks, and the possibilities of resolving spectra into overlapping bands; it was concluded that the practice of computing a least-squares fit of overlapping bands to a spectral profile must be changed, because the minimization step often produces a result involving excess or negative absorbances; the spectral profile should be regarded as a

boundary limit and any absorbance excess assessed as possible evidence for an additional band. On the other hand, Kvaratskheli and Demin have developed a formula for evaluating the optimum selectivity of conventional and derivative spectrophotometric determinations, including those involving higher-order derivatives.<sup>41</sup> Problems arising in the determination of spectral parameters of complex spectra contours by use of high-order derivatives have been discussed recently.<sup>42</sup>

#### *Effects of temperature*

The effects of temperature variations on derivative spectra have been investigated.<sup>43,44</sup> The absorbances of most of the substances examined exhibited a temperature coefficient of  $-0.07\%/degree$ , and the second-derivative amplitude had temperature coefficients (ranging from  $-0.1$  to  $-0.5\%/degree$ ) that bore no significant relationship to those of the corresponding absorbances. These effects can be attributed to the small reduction in curvature at the corresponding wavelengths of the fundamental spectra, that occurs with increasing temperature. The precise and accurate assay of substances by DS requires that the temperature of the standard and sample solutions are identical at the time of measurement.

### INSTRUMENTATION

Various instrumental arrangements have been used for obtaining derivative spectra, from the initial attempts<sup>45,46</sup> to the use of direct reading spectrophotometers and desk top calculators.<sup>47,48</sup> Williams and Hager<sup>49</sup> described a portable second-derivative spectrophotometer for gas analysis. Modern microcomputer-operated spectrophotometers are easy to set up and yield more accurate results.

In general, the methods can be classified according to Talsky *et al.*<sup>30</sup> as follows.

**Electromechanical systems.** A tachometer generator and a lock-in amplifier followed by a filter have been used for first-derivative spectra.<sup>50</sup> Similar arrangements have been devised, in which the signal, after amplification by a lock-in amplifier, is rectified, smoothed and filtered.<sup>51,52</sup>

**Modulation systems.** Modulation of the wavelength induces a synchronous modulation of the signal. If these signals are expanded as a Taylor series and the powers of the sine functions are expressed as sine and cosine functions, the derivatives can be obtained from the Fourier coefficients of this series.<sup>53</sup> The modulation is achieved in various ways<sup>54-59</sup> with quartz plates, vibrating lattices, mirrors, vibrating exit slits and optical wobblers. Cook *et al.*<sup>60,61</sup> described a vidicon-based rapid-scan spectrophotometer; the wavelength modulation used to produce the derivative signal was created by the electron-beam scan pattern; the system operated in the visible region over a selectable range of 40 or 400 nm and was interfaced to a minicomputer. A second-derivative tunable di-

ode laser spectrophotometer has been described;<sup>62</sup> spectra with adequate signal-to-noise ratio could only be measured when the modulation amplitude was equal to the half-width of the band at half-height.

**Two-wavelength spectrophotometry.** In this method the light is divided between two monochromators and its intensity measured by two identical photomultipliers. The signals are then directed (after amplification) to a subtraction unit with its output connected to the *Y*-input of a recorder; the *X*-axis of the recorder is driven synchronously with the wavelength scan. If the difference between the wavelength scans is sufficiently small,  $dA/d\lambda$  is obtained. The time constant can be adjusted by altering the wavelength difference of the monochromators.<sup>63-66</sup> The principal disadvantage is that the higher derivatives cannot be obtained directly by this method.

**Subtraction of delayed spectra.** The output of the photomultiplier is divided into two equal parts. One passes directly to the subtraction unit, the other is first delayed in time or space by an electronic or electro-optical circuit. The output signal from the subtraction is passed to the recorder and is directly proportional to the first derivative of the spectrum.<sup>67</sup>

In another technique the signal delay is produced by tape recording with two recording heads arranged in tandem; the time constant is regulated by the separation between the recording heads.<sup>68</sup> In general, higher order derivatives cannot be obtained by these methods.

**Digital differentiation.** The derivatives are numerically calculated by digital computers in this method.<sup>69-73</sup> The output signal of the spectrophotometer is fed to an analogue-digital converter, the signals at each given wavelength are accumulated and smoothed, and the mean value is calculated. Less complicated digital differentiators, generally based on microcomputers, have recently been used.<sup>74-76</sup> Since the development of microprocessor-controlled spectrophotometers, DS by the convolution method is often used. The relation between the derivative band characteristics and the data-processing span in the convolution operation has been investigated.<sup>77</sup> Recently, a Fourier transform algorithm was used to obtain higher-order derivative spectra; it offers high reproducibility.<sup>73</sup>

**Electronic differentiation.** This method<sup>29</sup> offers numerous advantages: higher derivatives can be obtained relatively simply without modification of the optical system, the instrumental variables can be easily optimized and the costs are, in general, relatively low. A condenser ( $c_c$ ) and a resistance ( $R_r$ ) are combined with an operational amplifier, and the differentiation time constant ( $\tau$ ) is obtained from  $\tau = c_c R_r$ , and can be adjusted by varying either the capacitive or the ohmic component. The practical resolution of the derivative spectrum depends not only on the slit-width but also to a large extent on the rate of the wavelength scan ( $s_\lambda$ ) and on  $\tau$ . In general, the best resolution is obtained with a small band-pass

(0.5–2 nm), slow scan (1–5 nm/sec) and  $\tau$  between 0.1 and 1 sec. The principal disadvantage of the electronic differentiation is that the derivative spectra are somewhat delayed with respect to the fundamental spectrum; this phase shift depends on the differentiation time constant and on the rate of the wavelength scan. For this reason, it is convenient to measure a series of samples containing the analyte and other accompanying substances, to observe the variation of the derivative peak when different experimental variables are used.

In recent years, the use of diode-array spectrophotometers, the data from which are easily converted into  $n$ th derivatives, has facilitated the use of the derivative technique in a wide field of applications.<sup>78</sup>

## APPLICATIONS

### *Pharmaceutical analysis*

DS has been used in the analysis of many pharmaceutical formulations;<sup>79,80</sup> it has proved particularly useful in eliminating matrix interferences,<sup>81</sup> including that of aromatics,<sup>20</sup> which have feeble absorption in the near ultraviolet. An accurate and precise method for the assay of ephedrine or its diastereoisomer pseudoephedrine has been described; the method was applied to tablets, capsules and nasal drops, containing also aminophylline and amylobarbitone, and also to coloured syrups containing triprolidine hydrochloride and codeine phosphate. The method has been extended recently to assay of 18 drugs in tablet and capsule formulations<sup>85</sup> and suppositories.<sup>86</sup> Other compounds, *e.g.* diphenhydramine hydrochloride,<sup>87</sup> have been determined in the same way. Mixtures of antazoline, phenylephrine and andophedrine in eye drops and acepifylline–cinchocaine–phenylbutazone and oxyphenbutazone in pharmaceuticals have been resolved satisfactorily.<sup>88,89</sup> DS has also been used in the assay of thiamine and pyridoxine in commercial solid dosage forms, and in aged commercial samples.<sup>90,91</sup> A combination of derivative and least-squares methods has been used to analyse tablets containing pseudoephedrine, triprolidine and dextromethorphan.<sup>92</sup>

Another application is the determination of salicylic acid in aspirin. The second-derivative spectrum of salicylic acid showed a trough at 292 nm, and a satellite peak at 316 nm; in presence of large amounts of aspirin, the trough disappeared, but the height of the satellite peak was not altered even at an aspirin concentration  $2 \times 10^4$  times that of the salicylic acid.<sup>93</sup>

Olson and Alway demonstrated the usefulness of first-derivative spectra in the qualitative characterization of testosterone, progesterone and some of their  $\alpha$ - and  $\beta$ -substituted derivatives.<sup>94</sup> More recently, mixtures of prednisolone, norgestrel, hydrocortisone and ethinyloestradiol have been analysed

by using the second and fourth derivative spectra.<sup>95</sup> Although ethinyloestradiol is readily distinguished from other steroids in the normal spectrum, prednisolone and norgestrel have similar normal spectra, but may readily be distinguished in the second-derivative spectrum. Hydrocortisone is not readily distinguished from norgestrel in normal or second-derivative spectra, but the fine structure in the norgestrel fourth-derivative spectrum satisfactorily discriminates between the two. Other mixtures of oestrogens and progestins have been analysed, after prior separation by thin-layer chromatography.<sup>96</sup> Some other pharmaceutical formulations (aspirin tablets, vitamin B, cortisone acetate, prednisone acetate, hydrocortisone and hydroprednisone) have also been systematically analysed by second-derivative spectrometry.<sup>97</sup>

The caffeine content of tablets can be assayed by extraction of the caffeine into alcohol and measurement of the peak–trough amplitude of the broad second-derivative spectrum, between 270 and 290 nm.<sup>20</sup> A more complicated problem is the analysis of hyoscine hydrobromide eyedrops (0.25–2%) containing 0.01% of chlorhexidine acetate as preservative. This mixture presents difficulty in conventional spectrophotometry: although the concentration of hyoscine hydrobromide is 25–200 times that of the preservative, its absorptivity is lower by a factor of 100 so its spectrum is almost completely obscured by the broad-band spectrum of the preservative. However, the amplitude of the second-derivative spectrum is linearly related to the hyoscine hydrobromide concentration, and can be used in the routine analysis of batches of the eyedrops, the coefficient of variation being 1–20%.<sup>20</sup> A similar method for analysis of the three-component system pilocarpine– eserine–benzalkonium chloride has been developed.<sup>20</sup> The assay of tropane derivatives in formulations by second-derivative ultraviolet spectrophotometry has also been described.<sup>98</sup>

The derivative technique has been used for determination of phenol in oily phenol injections (usually prepared in almond oil), and of aromatic alcohols (benzyl alcohol, 2-phenylethanol, 3-phenylpropanol and 4-phenylbutanol) used as preservatives in nutrient broth seeded with *Staphylococcus aureus*; the analysis by normal spectrophotometry is complicated by the high matrix absorbance, but the second-derivative method is applicable to a simple dilution of the sample. The amplitude is independent of the proportion of nutrient broth and bacterial concentration.<sup>99</sup>

DS has been used for the rapid determination of many food colours used in pharmaceuticals (Amaranth, Camoisine, Tartrazine, Sunset Yellow, Green S, *etc.*). A mixture of Tartrazine and Green S in a methadone elixir can be resolved by the second-derivative method.<sup>100</sup> Recently some 1,4-benzodiazepines and their degradation products have been determined in mixtures.<sup>101,102</sup>

### Forensic toxicology

DS has been used in the analysis of illicit drugs, especially for the identification of compounds which have very similar spectra, such as amphetamines<sup>103</sup> and related drugs (meperidine, ephedrine, etc.)<sup>104</sup> Mixtures of heroin and morphine have also been analysed by DS.<sup>105</sup>

### Amino-acid and protein analysis

The determination of aromatic amino-acids in proteins by ultraviolet spectrometry is based on the assumption that the absorption spectra of fully denatured proteins can be considered as the sum of the spectra of the aromatic amino-acids which they contain. DS can extract more information than would be obtained from direct measurements and, properly applied, can eliminate or reduce the effect of much spectral interference.

A method for the direct determination of phenylalanine and tryptophan has been developed by Balestrieri *et al.*<sup>106</sup> Phenylalanine was measured at 250–265 nm, where there are no significant contributions from other aromatic chromophores; tryptophan was determined at 290–295 nm, the values being corrected for the presence of tyrosine. Another procedure for phenylalanine (as the *N*-acetyl ethyl ester) residues in proteins utilizes second-derivative spectra at 245–270 nm, where tyrosine and tryptophan have no influence.<sup>107</sup> Fell has made a systematic study of mixtures of phenylalanine, tryptophan and tyrosine by second- and fourth-derivative methods; the fourth-derivative spectra gave sharper peaks for phenylalanine and tryptophan, but none for tyrosine.<sup>108</sup> A similar procedure was used for the determination of these amino-acids in the liver microsomal mono-oxidation system.<sup>109</sup> Fourth-derivative spectra have been used for the determination of tyrosine and phenylalanine residues; the two main vibrational bands of tyrosine are resolved, giving rise to two peaks which are sensitive to changes in the environment of the phenolic rings. The parameters obtained from the fourth-derivative spectra were found to depend on the strength of the hydrogen bonds formed by the OH-group of tyrosine, and on the heterogeneity of the tyrosine environment. The peaks for phenylalanine, although less sensitive than those for tyrosine, also depend on the polarity of the environment. Both amino-acids have been determined in calf thymus histone and bovine pancreatic ribonuclease.<sup>110</sup> Mixtures of tyrosine and tryptophan residues in proteins have also been considered, with reference to the mutual interference between the second-derivative bands in terms of the ratio *r* between pairs of peak-to-peak distances. The *r* values were found to be correlated, although not linearly, to the tyrosine/tryptophan ratio. The polarity of the medium modifies the *r* value appreciably.<sup>111,112</sup> A ternary mixture of *N*-acetyl ethyl esters of tryptophan, tyrosine and phenylalanine has been anal-

ysed by second-derivative spectrometry at pH 7 and 13.<sup>113</sup> Applications of derivative spectrometry in the study of the characteristics of aromatic amino-acids in proteins have been reviewed.<sup>114</sup>

The advantages of higher-order derivative spectrophotometry have been demonstrated with lactate dehydrogenase isoenzymes, myoglobins, tyrosine, phenylalanine, trypsin and tryptophan in proteins, nucleic acids and synthetic polymers. The sensitivity was good, and residual monomers could be detected in polymers at levels as low as 0.02%.<sup>115</sup>

The near infrared absorption spectrum (between 800 and 900 nm) has been used in the study of the pigment-protein complexes from *Rhodopseudomonas capsulata*, by use of the second- and fourth-order derivatives.<sup>116</sup> A significant splitting of the 870-nm band was observed in all the derivative spectra. Fourth-order spectrometry has been used as a detection system in the molecular weight determination of trypsin, chymotrypsin and their oligomers by gel chromatography.<sup>117</sup>

### Clinical chemistry

The potential clinical applications of derivative spectrometry were discussed by O'Haver, along with the analysis of porphyrins.<sup>118</sup> The determination of urinary porphyrins as described by Jones and Sweeny<sup>119</sup> is an excellent example of the advantages of derivative spectral measurements in clinical analysis. The procedure simply involves acidification of a sample of urine and recording the second derivative spectrum from 380 to 430 nm. The amplitude of the second derivative signal was linearly related to porphyrin concentration, and the wavelength (400–430 nm) of the central peak gave an estimate of the ratio of uroporphyrin to coproporphyrin; the limit of determination was 8 nM. A similar procedure was described by Schmitt;<sup>120</sup> the determination limit was 10 nM; a dilution is required for higher concentrations.

A rapid, direct and non-destructive method has been described for the determination of methaemalbumin in human blood serum.<sup>121</sup> The second-derivative spectrum of undiluted serum was recorded (560–700 nm); the difference between the signals at 636 nm (max) and 600 nm (min) was calculated, and the haematin concentration from a calibration equation. Other procedures have been described for the determination of haemoglobin in plasma<sup>122</sup> and methaemoglobin in the presence of a light-scattering suspension.<sup>123</sup>

Kullmann *et al.* have described the direct determination of phenylalanine in serum by second-order DS;<sup>124</sup> after the removal of protein and uric acid, a 100- $\mu$ l portion of serum was analysed directly for phenylalanine (by use of the maximum at 257 nm and the minimum at 254 nm); the sensitivity obtained was 5 mg/l. An interesting use of DS is the determination of bilirubin and haemoglobin.<sup>125</sup> The method may be

useful for determination of the two substances in amniotic fluid, urine and other biological fluids.

A simple and precise method, based on the second- and fourth-order derivative spectra has been established for the determination of paraquat dichloride in serum, plasma or dialysis fluid, the detection limit being 2  $\mu\text{g/l.}$  (at 396 nm); results obtained in cases of paraquat poisoning correlate well with those obtained by radioimmunoassay. The method has been applied to routine haemodialysis control.<sup>126</sup>

The determination of benzodiazepines in biological fluids by means of DS has been described. Diazepam, chlordiazepoxide, nitrazepam and chlorazepate may be determined directly at  $\geq 0.2$  mg/l.<sup>127</sup> DS has also been used to determine epinephrine/norepinephrine and metanephrine/normetanephrine ratios in urine, after a prior separation of these compounds by ion-exchange.<sup>128</sup>

### Environmental analysis

Derivative spectrometry has been used in environmental analysis for some inorganic pollutants. Strojek<sup>129</sup> describes the determination of traces of sulphur dioxide. Second-order derivative spectra have been tested for rapid determination of nitrogen oxides and sulphur dioxide.<sup>130</sup> Phenolic compounds in waste water have been determined.<sup>131</sup> Continuous determination of sulphur dioxide in gases has been described,<sup>132</sup> and the use of a repetitive-scanning spectrophotometer to monitor air for sulphur dioxide and nitrogen oxides.<sup>133</sup> In analysis for polynuclear aromatic compounds, second-derivative spectrometry was coupled with linear least-squares fitting;<sup>134</sup> detection limits of a few ng/ml were attainable for many compounds. The method was used to determine naphthalene vapour and to analyse a mixture of anthracene, phenanthrene, chrysene and pyrene in cyclohexane; polynuclear aromatic hydrocarbons have been determined in the range 0.2–2.0  $\mu\text{g/ml.}$ <sup>135</sup> A prototype instrument for field monitoring of polynuclear aromatic hydrocarbons has been described.<sup>136</sup> Matthews *et al.*<sup>137</sup> determined inorganic compounds ( $\text{HNO}_2$ ,  $\text{SO}_2$ ,  $\text{NO}$ ,  $\text{NO}_2$ ,  $\text{O}_3$ ,  $\text{NH}_3$ ) in smoke plumes, by use of the second-derivative spectrum in the ultraviolet region. Uric acid has been detected in waste water.<sup>138</sup> Stream samples polluted by coloured substances have been compared with samples from suspected sources of pollution.<sup>139</sup>

Sensitive detection of hydrogen chloride at concentrations below 50  $\mu\text{g/m}^3$  in the atmosphere has been achieved by derivative spectrometry with a diode laser spectrophotometer; the method has been used to monitor incineration plumes for HCl.<sup>140</sup>

The use of higher-order derivative spectrophotometry for environmental analysis was proposed by Talsky,<sup>141,142</sup> on account of its fine resolution and better interpretation of such electric signals. These techniques have been tested for the determination of phenols in air.

### Inorganic analysis

Talsky *et al.* used the derivative technique for trace metal analysis; by means of the fifth-derivative spectrum it is possible to determine cadmium and zinc as dithizonates simultaneously.<sup>143</sup> Third-derivative spectra have been used for rapid determination of small amounts of Nd, Ho, Er and Tm in a mixture of rare earths, with thenoyltrifluoroacetone as a mixture of Sm and Eu,<sup>145</sup> and for the determination of zirconium in the presence of hafnium with Picramine E.<sup>146</sup>

The sum of nitrate and nitrite has been determined in sea-water by use of a continuous flow system; samples are pumped through a converter containing cadmium-copper powder to convert nitrate into nitrite; the effluent is mixed with a reducing agent (sodium iodide), which reduces nitrite to NO, and the mixture is fed through a gas-liquid separator; the NO thus separated is carried by nitrogen into a heated optical cell, where the second-derivative absorbance at 214 nm is recorded.<sup>147</sup> A simpler determination of nitrite alone was described earlier.<sup>148</sup>

High-order derivative spectrometry has been used to study the chemical and structural changes in the surface layers of ferruginous bentonite containing montmorillonite as a result of the action of various acids, alkalis and chelating agents;<sup>149</sup> the method can be used as a supplement to IR, EPR, ESCA, NMR and Mössbauer spectroscopy.

### Other applications

Second-order spectra have been used for direct identification of ketones (cyclohexanone, cycloheptanone, 2-octanone, 2-butanone, 3-heptanone and acetone) at 270–300 nm; no formation of semicarbazones or nitrophenylhydrazones was necessary.<sup>150</sup> Phenols in essential oils have been determined similarly.<sup>151</sup>

Naphthalene and some homologues have been determined together and separately in a series of petroleum fractions by means of the second-derivative signals at 311, 314, 319, 322 and 324 nm; the method may be useful in the preparation of suitable heart-cuts from cracked petroleum products to obtain naphthalene.<sup>152</sup>

The method has been used for measurement of acetanilide (the substrate) and aniline (the product) in a culture of *Pseudonoma fluorescens*; the method offers appreciable advantages over other techniques.<sup>153</sup> Urea has also been determined, and saccharin in soft drinks and dyes in solution (with a prior adsorption on a thin layer of alumina).<sup>154</sup>

Olson and Alway<sup>50</sup> use derivative spectrometry as an auxiliary method for steroid structure determination; the effects of structure on the derivative ultraviolet spectra of the  $n \rightarrow \pi$  transition of some ketosteroids show that it is possible to distinguish between  $\alpha$  and  $\beta$  epimers, and to locate the position of substitution in some cases.

Second-derivative ultraviolet spectrometry has been used as an excellent method for arson investigation. The second-derivative spectra of accelerants are relatively uncomplicated even for multicomponent substances such as gasoline. This simplicity allows good visual comparison between standard and sample and generally facilitates identification of accelerants. The fire debris (matrix material) is extracted with cyclohexane. Few of these matrix materials give second-derivative spectra when treated in this manner. The method devised is both sensitive and rapid.<sup>155</sup>

The technique has been used recently in the interpretation and exploitation of data obtained from rapid-scan absorbance detectors for ascertaining the purity of chromatographic peaks. Two types of derivative were examined. The derivative of the elution curve with respect to the specific wavelength at which the major compound has a zero derivative was shown to be rapid and useful for the determination of co-eluting peaks of impurities which might form in solution or during the chromatography of compounds otherwise known to be pure. The derivatives of the spectral curves obtained during chromatography have been also examined; the results showed that derivative spectrometry has considerable potential in screening compounds for possible impurities giving overlapping peaks in HPLC. It was possible to detect, under suitable conditions, as little as a 0.1% impurity that was co-eluted with the major component.<sup>156</sup>

Use of the derivative technique in astronomical spectroscopy has recently been considered.<sup>157,158</sup>

## REFERENCES

- V. J. Hammond and W. C. Price, *J. Opt. Soc. Am.*, 1953, **43**, 924.
- J. D. Morrison, *J. Chem. Phys.*, 1953, **21**, 1767.
- A. T. Giese and C. S. French, *Appl. Spectrosc.*, 1955, **9**, 78.
- I. G. McWilliams, *Anal. Chem.*, 1969, **41**, 674.
- W. Snelleman, T. C. Rains, K. W. Yee, H. D. Cook and O. Menis, *ibid.*, 1970, **42**, 394.
- W. K. Fowler, D. O. Knapp and J. D. Winefordner, *ibid.*, 1974, **46**, 601.
- T. C. O'Haver, in E. L. Wehry (ed.), *Modern Fluorescence Spectroscopy*, Vol. 1, pp. 65-81. Plenum Press, New York, 1976.
- P. John and I. Soutar, *Anal. Chem.*, 1976, **48**, 520.
- T. C. O'Haver and T. Begley, *ibid.*, 1981, **53**, 1876.
- A. Schmitt, *Tech. Lab.*, 1978, **5**, 1207.
- B. P. Chadburn, *Anal. Proc.*, 1982, **19**, 42.
- C. T. Cottrell, *ibid.*, 1982, **19**, 43.
- T. Motokawa, *Nihacho Bunto Kodoho to Sono Oyo*, 1979, 176.
- M. Furukawa and S. Shibata, *Bunseki*, 1980, 608.
- D. Botter, *Instrum. News*, 1975, **25**, 14.
- T. C. O'Haver, *Anal. Chem.*, 1979, **51**, 91A.
- G. Talsky, *GIT Fachz. Lab.*, 1982, **26**, 929.
- J. N. Miller, T. A. Ahmad and A. F. Fell, *Anal. Proc.*, 1982, **19**, 37.
- R. N. Hager, *Anal. Chem.*, 1973, **45**, 1131A.
- A. F. Fell, *Anal. Proc.*, 1978, **15**, 260.
- J. E. Cahill and F. G. Padera, *Am. Lab.*, 1980, **12**, No. 4, 101.
- Z. Kubiak and W. Hendrich, *Wiad. Chem.*, 1981, **35**, 701.
- I. M. Dubrovkin, *Zh. Prikl. Spektrosk.*, 1983, **39**, 885.
- B. Wang, *Fenxi Huaxue*, 1983, **11**, 149.
- G. L. Green and T. C. O'Haver, *Anal. Chem.*, 1974, **46**, 2191.
- V. M. Osipov and N. F. Borisova, *Zh. Prikl. Spektrosk.*, 1985, **42**, 603.
- A. F. Fell and G. Smith, *Anal. Proc.*, 1982, **19**, 28.
- W. L. Butler and D. W. Hopkins, *Photochem. Photobiol.*, 1970, **112**, 439.
- B. A. Gulyaev and F. F. Litvin, *Biofizika*, 1970, **15**, 670.
- G. Talsky, L. Mayring and H. Kreuzer, *Angew. Chem., Int. Ed. Engl.*, 1978, **17**, 785.
- A. F. Fell, D. R. Jarvie and M. J. Stewart, *Clin. Chem.*, 1981, **27**, 286.
- A. F. Fell, *Anal. Chem.*, 1983, **2**, 1.
- J. E. Cahill, *Am. Lab.*, 1979, **11**, No. 3, 79.
- T. C. O'Haver, *Anal. Proc.*, 1982, **19**, 22.
- J. R. Morrey, *Anal. Chem.*, 1968, **40**, 905.
- B. F. Barker and M. F. Foz, *Chem. Soc. Rev.*, 1980, **9**, 143.
- W. F. Maddams, *Appl. Spectrosc.*, 1980, **34**, 245.
- P. Chen, L. Qingyao and Y. Zeng, *Guanpuxue Yu Guangpu Fenxi*, 1985, **5**, 5.
- T. C. O'Haver and G. L. Green, *Anal. Chem.*, 1976, **48**, 312.
- T. R. Griffiths, K. King, V. J. Hubbard, M. J. Schwing-Weill and J. Meullemeestre, *Anal. Chim. Acta*, 1982, **143**, 163.
- Yu. K. Kvaratskheli and Yu. V. Demin, *Zh. Analit. Khim.*, 1983, **38**, 1427.
- V. I. Sidelmikov, *Vestn. Mosk. Univ. Fiz. Astron.*, 1985, **26**, 61.
- A. G. Davidson, *J. Pharm. Biomed. Anal.*, 1985, **3**, 329.
- Idem*, *Analyst*, 1983, **108**, 728.
- E. Tannebauer, P. B. Merkel and W. H. Hamill, *J. Phys. Chem.*, 1953, **21**, 311.
- J. P. Pemsler, *Rev. Sci. Instrum.*, 1957, **28**, 274.
- J. S. Challice, *Spectrochim. Acta*, 1964, **20**, 675.
- C. Rodriguez Pichiling, *Bol. Soc. Quim. Perú*, 1984, **50**, 353.
- D. T. Williams and R. W. Hager, *Appl. Opt.*, 1970, **9**, 1597.
- E. C. Olson and C. D. Alway, *Anal. Chem.*, 1960, **32**, 370.
- M. P. Klein and E. A. Dratz, *Rev. Sci. Instrum.*, 1968, **39**, 397.
- R. Cook, *Cary Instruments Tech. Memo*, UV-70, 1970, 8.
- R. N. Hager and R. C. Andersen, *J. Opt. Soc. Am.*, 1970, **60**, 1444.
- G. Bonfiglioli and P. Provetto, *Appl. Opt.*, 1964, **3**, 1417.
- M. J. Milano, H. L. Pardue and T. E. Cook, *Anal. Chem.*, 1974, **46**, 374.
- M. J. Milano and H. L. Pardue, *ibid.*, 1975, **47**, 25.
- F. S. French, A. B. Church and R. W. Eppley, *Carnegie Inst. Washington Yearbk.*, 1945, **53**, 182.
- F. Asrmu and A. Rucci, *Rev. Sci. Instrum.*, 1966, **37**, 1696.
- I. Baslev, *Phys. Rev.*, 1966, **143**, 636.
- T. E. Cook, H. L. Pardue and R. E. Santini, *Anal. Chem.*, 1976, **48**, 451.
- T. E. Cook, R. E. Santini and H. L. Pardue, *ibid.*, 1977, **49**, 871.
- D. L. Griebel, M. L. Olson, N. P. Jeffrey and P. R. Griffiths, *Appl. Spectrosc.*, 1980, **34**, 56.
- C. S. French, *Proc. Instrum. Soc. Am.*, 1957, **8**, 83.

64. L. J. Sidel, *Arch. Biochem. Biophys.*, 1970, **54**, 185.
65. S. Shibata, *Angew. Chem.*, 1976, **88**, 750.
66. S. Shibata, M. Furukawa and K. Goto, *Anal. Chim. Acta*, 1973, **65**, 49.
67. F. Grum, D. Paine and L. Zoeller, *Appl. Opt.*, 1972, **65**, 49.
68. Y. Inoue, T. Ogawa, T. Kawai and K. Shibata, *Physiol. Plant.*, 1973, **29**, 390.
69. A. Savitzky and M. Golay, *Anal. Chem.*, 1964, **36**, 1627.
70. D. Lewis, *J. Chem. Phys.*, 1970, **53**, 2750.
71. A. Matsui and K. Tomioka, *J. Phys. Chem.*, 1976, **9**, 529.
72. J. Kandrnál, V. Lipus and B. Huvar, *Chem. Listy*, 1983, **77**, 95.
73. G. Heidecke, J. Kropf and G. Stock, *Z. Anal. Chem.*, 1983, **316**, 405.
74. K. Kitamura, E. Morita and K. Hozumi, *Yakugaku Zasshi*, 1985, **105**, 161.
75. J. Gartzke, K. Nolte and K. Berka, *Jena Rev.*, 1984, **4**, 170.
76. D. D. Schuresko, A. R. Hawthorne, T. Vo-Dinh, R. B. Gammage, W. G. Dreibleis and J. D. Van Hoesen, *Energy Res. Abstr.*, 1984, **9**, 3269.
77. T. Ichikawa and H. Terada, *Yakugaku Zasshi*, 1983, **103**, 878.
78. B. Grego, E. C. Nice and R. J. Simpsons, *J. Chromatog.*, 1986, **352**, 359.
79. Y. Cao, *Yaouxue Tongbao*, 1985, **20**, 224.
80. Y. Xu and R. Gan, *Yaown Fenxi Zazhi*, 1984, **4**, 124.
81. A. F. Fell, *UV Spectrom. Bull.*, 1980, **8**, 5.
82. R. Jones and G. J. Marnham, *J. Pharm. Pharmacol.*, 1981, **33**, 458.
83. M. M. Abdel-Khalek, M. E. Abdel-Hamid, M. S. Mahrous and M. A. Abdel-Salam, *Anal. Lett.*, 1985, **18**, 781.
84. A. G. Davidson and H. Elsheik, *Analyst*, 1982, **107**, 879.
85. A. G. Davidson and S. M. Hassan, *J. Pharm. Sci.*, 1984, **73**, 413.
86. M. A. Korany, A. M. Wahbi, M. A. Elsayed and S. Mandour, *Anal. Lett.*, 1984, **17**, 1373.
87. A. F. Fell and A. G. Smith, *Anal. Proc.*, 1982, **19**, 28.
88. M. A. Korany, A. M. Wahbi, S. Mandour and M. A. Elsayed, *Anal. Lett.*, 1985, **18**, 21.
89. M. A. Korany, A. M. Wahbi, M. A. Elsayed and S. Mandour, *Farmaco, Ed. Prat.*, 1984, **17**, 1353.
90. V. Such, J. Traveset, R. Gonzalo and E. Gelpi, *Anal. Chem.*, 1980, **52**, 412.
91. J. Traveset, V. Such, R. Gonzalo and E. Gelpi, *J. Pharm. Sci.*, 1980, **69**, 269.
92. R. Jones, M. J. Orchard and K. Hall, *J. Pharm. Biomed. Anal.*, 1985, **3**, 335.
93. K. Kitamura and R. Majima, *Anal. Chem.*, 1983, **55**, 54.
94. E. C. Olson and C. D. Alway, *ibid.*, 1960, **32**, 370.
95. A. F. Fell, *Proc. Symp. Analysis of Steroids*, Eger, Hungary, 1981, 455.
96. P. Corti, E. Lencioni and G. F. Sciana, *Boll. Chim. Farm.*, 1983, **122**, 281.
97. Z. Gao, *Yaown Fenxi Zazhi*, 1983, **3**, 102.
98. S. M. Hassan and A. G. Davidson, *J. Pharm. Pharmacol.*, 1984, **36**, 7.
99. A. F. Fell, *ibid.*, 1978, **30** (Supp.).
100. A. F. Fell and J. G. Allan, *Anal. Proc.*, 1981, **18**, 291.
101. M. E. Abdel-Hamid, M. M. Abdel-Khalek and M. S. Mahrous, *Anal. Lett.*, 1984, **17**, 135.
102. M. E. Abdel-Hamid, M. Korany and M. Beduir, *Acta Pharm. Jugosl.*, 1984, **34**, 183.
103. R. Gill, T. S. Bal and A. C. Moffat, *J. Forensic. Sci.*, 1982, **22**, 165.
104. A. H. Lawrence and J. D. MacNeil, *Anal. Chem.*, 1982, **54**, 2385.
105. A. H. Lawrence and J. Kover, *ibid.*, 1984, **56**, 1731.
106. C. Balestrieri, G. Colonna, A. Giovane, G. Irace and L. Servillo, *Eur. J. Biochem.*, 1978, **90**, 433.
107. T. Ichikawa and H. Terada, *Biochim. Biophys. Acta*, 1977, **494**, 267.
108. A. F. Fell, *J. Pharm. Pharmacol.*, 1979, **31** (Supp.).
109. K. Ruckpaul, H. Rein, D. P. Bullou and M. J. Coon, *Int. Symp. Microsomes Drug Oxid.*, 74th, 1979, **1**, 37.
110. E. Padrós, A. Morros, J. Mañosa and M. Duñach, *Eur. J. Biochem.*, 1982, **127**, 117.
111. R. Ragone, G. Colonna, C. Balestrieri, L. Servillo and G. Irace, *Biochemistry*, 1984, **23**, 1781.
112. L. Servillo, G. Colonna, C. Balestrieri, R. Ragone and G. Irace, *Anal. Biochem.*, 1982, **126**, 251.
113. T. Ichikawa and H. Terada, *Chem. Pharm. Bull.*, 1981, **29**, 438.
114. E. Padrós, M. Duñach, A. Morros, M. Sabes and J. Manosa, *Trends Biochem. Sci.*, 1984, **9**, 508.
115. G. Talsky, J. Dostal, M. Glasbrenner and S. Goetz-Maler, *Angew. Makromol. Chem.*, 1982, **105**, 49.
116. G. Talsky, C. P. Rygersberg, R. Van Grondelk, R. Feick and G. Drews, *Z. Naturforsch. C, Biosci.*, 1980, **35**, 722.
117. G. Talsky and J. Dostal, *J. Chromatog.*, 1983, **282**, 487.
118. T. C. O'Haver, *Clin. Chem.*, 1979, **25**, 1548.
119. K. G. Jones and G. D. Sweeney, *ibid.*, 1979, **25**, 71.
120. A. Schmitt, *J. Clin. Chem. Clin. Biochem.*, 1977, **15**, 303.
121. A. Bertrand, C. Cox, P. Foucart and J. Buret, *Clin. Chim. Acta*, 1982, **123**, 121.
122. G. J. Sanderink and H. J. M. Van Rijn, *ibid.*, 1985, **146**, 65.
123. W. E. Weiser and H. L. Pardue, *Clin. Chem.*, 1983, **29**, 1673.
124. K. H. Kullmann, W. Endres, S. Kirzinger and H. L. Schmidt, *J. Clin. Chem. Clin. Biochem.*, 1982, **20**, 181.
125. M. F. Merrick and H. L. Pardue, *Clin. Chem.*, 1986, **32**, 598.
126. A. F. Fell, D. R. Jarvie and M. J. Stewart, *ibid.*, 1981, **27**, 286.
127. D. Martínez and M. P. Giménez, *J. Anal. Toxicol.*, 1981, **5**, 10.
128. R. H. Christenson and C. D. McGlothlin, *Anal. Chem.*, 1982, **54**, 2015.
129. J. W. Strojek, D. Yates and T. Kuwana, *ibid.*, 1975, **47**, 1050.
130. E. Falanga, *Inquinamento*, 1978, **20**, 43.
131. A. R. Hawthorne, S. A. Morris, R. L. Moody and R. B. Gammage, *J. Environ. Sci. Health*, 1984, **19**, 253.
132. K. Nagashima and S. Suzuki, *Bunseki Kagaku*, 1983, **32**, 251.
133. T. Izumi and N. Takeda, *Appl. Opt.*, 1983, **32**, 251.
134. A. R. Hawthorne, J. H. Thorngate, R. B. Gammage and T. Vo-Dinh, *Int. Symp. Chem. Biol. Carcinogen Mutagen*, 3rd, 1978, 299.
135. Y. R. Tahboub and H. L. Pardue, *Anal. Chem.*, 1985, **57**, 38.
136. A. R. Hawthorne, S. A. Morris, R. L. Moody and R. B. Gammage, *J. Environ. Sci. Health*, 1984, **19**, 253.
137. T. G. Matthews, A. R. Hawthorne and R. B. Gammage, *Oak Ridge Report*, ORNL/TM8007, 1982; *Chem. Abstr.*, 1982, **97**, 114408x.
138. W. Maurer and J. Storp, *GIT Fachz. Lab.*, 1980, **24**, 124.
139. W. A. McCrum, *Water Res.*, 1984, **18**, 1249.
140. P. Pokrowsky and W. Herrmann, *Opt. Eng.*, 1984, **23**, 88.
141. G. Talsky, *Intern. J. Environ. Anal. Chem.*, 1983, **14**, 81.

142. *Idem*, *Technisches Messentm.*, 1981, **48**, 211.
143. G. Talsky, S. Götz-Maler and H. Betz, *Mikrochim. Acta*, 1981 **II**, 1.
144. Y. Ren, Z. Lin and H. Zhou, *Fenxi Huaxue*, 1985, **13**, 6.
145. A. A. Kucher, N. S. Poluektov, V. T. Mishchenko and N. N. Alesandrova, *Zavodsk. Lab.*, 1983, **49**, No. 10, 11.
146. Yu. K. Kvaratskheli, Yu. V. Demin, V. A. Pchelkin, G. R. Kukushkin and N. V. Melchakova, *Zh. Analit. Khim.*, 1983, **38**, 1434.
147. K. Nagashima, M. Matsumoto and S. Suzuki, *Anal. Chem.*, 1985, **57**, 2065.
148. K. Nagashima, S. Suzuki, *Anal. Chim. Acta*, 1981, **151**, 113.
149. G. Talsky, O. Hanbensak and E. E. Kohler, *Keram. Z.*, 1982, **34**, 573.
150. L. Meal, *Anal. Chem.*, 1983, **55**, 2448.
151. M. A. Korany, A. A. El-Din, A. Seif and A. Nabil, *Anal. Lett.*, 1984, **17**, 483.
152. L. Dixit, S. Ram, R. B. Gupta, H. C. Chandola and P. Kumar, *Analyst*, 1986, **111**, 101.
153. J. Woodrow and K. Spear, *Appl. Microbiol. Biotechnol.*, 1984, **19**, 177.
154. K. Nagashima, M. Matsumoto and S. Suzuki, *Bunseki Kagaku*, 1985, **34**, 91.
155. L. Meal, *Anal. Chem.*, 1986, **58**, 834.
156. A. Grant and P. K. Bhattacharyya, *J. Chromatog.*, 1985, **347**, 219.
157. C. Bonoli, *Astrophys. Space. Sci.*, 1983, **89**, 377.
158. S. I. Gandzha, *Astron. Astrofiz.*, 1984, **52**, 49.



## A CHEMICAL STUDY OF 2-BUTYNE-1,4-DIOL

M. D'AMBOISE\*

Département de Chimie, Université de Montréal, C.P. 6128, Succ. A, Montréal, Canada

D. MATHIEU and D. L. PIRON

Département de génie métallurgique, École Polytechnique, C.P. 6079, Succ. A, Montréal, Canada

(Received 6 May 1988. Accepted 15 June 1988)

**Summary**—Commercial grade 2-butyne-1,4-diol has been used in electroplating for several years. In laboratory experiments, its presence in the electrolyte increases the current efficiency of zinc electro-winning. Its chemical behaviour in solution is not well known. The present paper indicates that the brownish technical grade 2-butyne-1,4-diol contains the monomer, the dimer and some trimer. Pure monomeric 2-butyne-1,4-diol is a white solid obtained by evaporation of the technical grade product. The monomer is slowly transformed into dimer and possibly into a trimer when dissolved in water. Various analytical techniques were used in the study of this system. Factor analysis with column cross-validation was applied to chromatographic data to help in the resolution of the system.

The compound 2-butyne-1,4-diol (abbreviated to BD) is used as a brightening agent in nickel plating.<sup>1,2</sup> Most of the literature concerning this chemical deals with the morphology of nickel deposited in its presence. The diol is a grain refiner and a levelling agent which reduces dendrite formation.<sup>2-5</sup> It has also been shown<sup>5,6</sup> that BD slows down nickel plating by constant-current deposition from solutions rich in nickel ions (about 60 g/l.). This experimental fact is in agreement with the change in polarization curves for nickel, on a nickel surface, in the presence of BD.<sup>5</sup> Volk and Fisher<sup>7</sup> have proposed the presence of a thin film of BD on the nickel surface. Thus, they report that an increase in the 2-butyne-1,4-diol concentration causes a decrease of the differential capacity of a nickel electrode, so that the surface coverage by the organic material is increased. Other researchers<sup>8-10</sup> have studied the kinetics of deposition of nickel in the presence of BD. They also have observed a reduction of the differential capacity of the electrode and have shown that BD reduces the rate of the different reactions associated with the nickel deposition. Moreover, in zinc electro-winning, it has been observed that the presence of BD in the electrolyte decreases the nickel content of the cathodic deposit. This result, as yet unexplained, offers the possibility of increasing current efficiency in the presence of impurities.<sup>11,12</sup> The compound also finds widespread application in organic synthesis.<sup>13-17</sup> Neither the exact nature of the diol in solution nor that of the adsorbed substance on the electrode surface has ever been thoroughly studied. The present work was undertaken to achieve a better understanding of the chemical behaviour of 2-butyne-1,4-diol in electrolytic solutions.

### EXPERIMENTAL

Ultraviolet-visible region spectra were recorded between 200 and 600 nm, against water, with a Perkin-Elmer model 552 spectrophotometer and 1.00-cm path-length matched silica cells. Gas chromatograms were obtained with a Hewlett Packard F&M Scientific 700 Laboratory Chromatograph, using a flame ionization detector and helium as carrier gas. The column temperature was varied between 135 and 200°. The liquid chromatograph system consisted of an Altex pump, model 100 (Altex Scientific, Berkeley, CA), coupled to a Perkin-Elmer LC-55 or Hitachi model 100-20 variable wavelength detector. A universal injector, Altex model 905-19, was used. The stainless-steel column (15 cm long, 4.2 mm bore) was packed with either Lichrosorb RP-8 (10 µm; Merck) or with Si-60 (5 µm) by a balanced-density slurry method. The chromatograms were obtained with eluents of different polarities.

Technical grade 2-butyne-1,4-diol was obtained from Eastman Kodak. HPLC grade acetonitrile and HPLC grade methanol were from Burdick and Jackson (Muskegon, MI 49442). Dimethylformamide, methylene chloride and hexane were Fisher chemical reagents.

Commercial 2-butyne-1,4-diol was purified through a slow (18 hr) sublimation at 45°, or evaporation at 70° (5 hr) under reduced pressure (ca. 10 mmHg). Both methods gave a compound with similar properties. Purified 2-butyne-1,4-diol (m.p. 58°; literature value 57.5°) was recovered as a white solid. A small quantity of residue, highly soluble in water, was also recovered. When exposed to light for a long period of time (many weeks), the purified compound is slowly transformed into a yellowish substance very similar in appearance to the technical grade chemical.

A small amount of the commercial BD was dissolved in a minimum of hot methanol. A brownish precipitate was obtained upon addition of dichloromethane. The ultraviolet and infrared spectra of this compound were similar to those of the unpurified reagent.

### RESULTS AND DISCUSSION

The ultraviolet spectrum (Fig. 1) of purified 2-butyne-1,4-diol in an unbuffered aqueous solution is featureless; it merely shows a sharp increase of absorbance for wavelengths shorter than 250 nm.

\*To whom correspondence should be addressed.

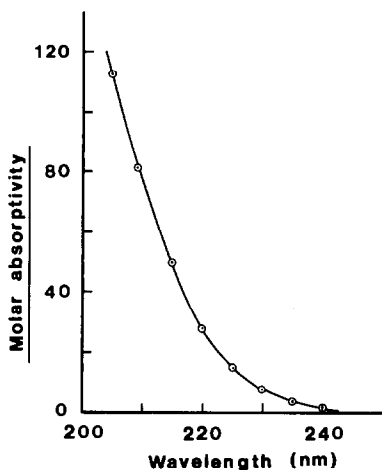


Fig. 1. Absorption spectra for fresh solutions of pure monomeric 2-butyne-1,4-diol in water, at room temperature.

This fact contradicts the report by Balyatinskaya and Babankova<sup>18</sup> of absorbance maxima at 260–279 and 284 nm. The single triple-bond structure of the butyne diol is not compatible with these absorption bands, which we attribute to different species (see below). The absorbance of the pure monomer at 210 nm deviates from Beer's law for concentrations larger than *ca.*  $6\text{--}7 \times 10^{-3}M$  (Fig. 2); it was verified that under the measurement conditions, stray light was not responsible for the deviations. A simple model involving the formation of a dimer explains the deviations, but these are too small, and not sufficiently accurate, to allow the establishment of a more precise chemical model for the system.

The absorptivities (in  $l.g^{-1}.cm^{-1}$ ) of technical 2-butyne-1,4-diol in water are shown in Fig. 3; Beer's law is obeyed at all wavelengths examined in the concentration range studied (as for the pure compound). This fact indicates that the proportions of the various species present in solution are constant, relative to each other, or that the contribution of a given species is too small to affect the absorption of

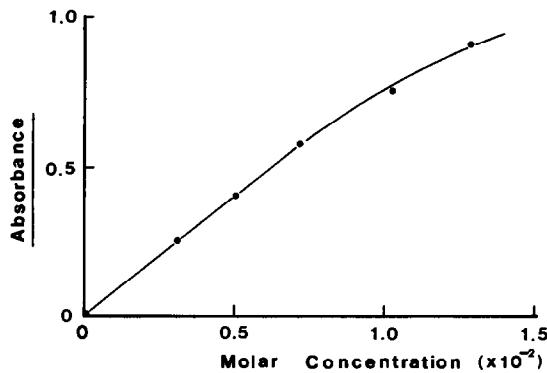


Fig. 2. Beer's law plot for purified 2-butyne-1,4-diol at 210 nm.

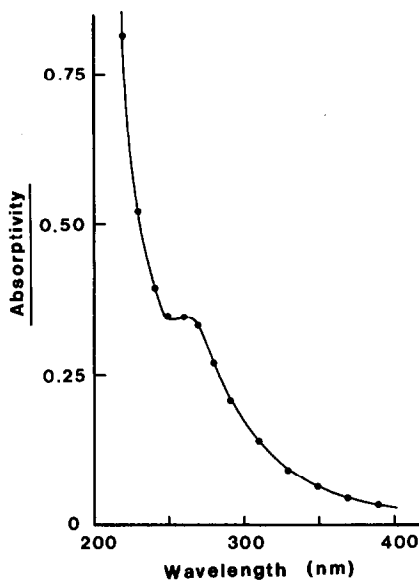


Fig. 3. Absorption spectra for technical grade 2-butyne-1,4-diol in water, at room temperature

light in the wavelength range studied. The technical reagent was shown<sup>12</sup> to mainly contain the dimer and some trimer of butyne-2-diol-1,4. Therefore, its properties should resemble those of the dimer. Spectra of the compound recrystallized from dichloromethane were very similar to those of the technical reagent. Hence, we conclude that the recrystallization procedure produces the dimer. A complete characterization is now under investigation.

Gas chromatography of the purified BD shows a single sharp peak which is attributed to the monomer. Under the chromatographic conditions (injector temperature  $>100^\circ$ ), substances such as the dimer or trimer, if present, would be converted into the

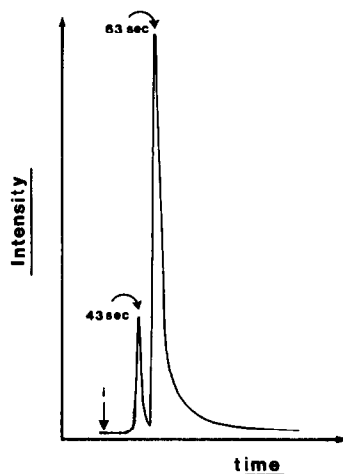


Fig. 4. Gas chromatogram for technical grade 2-butyne-1,4-diol. Column, Apiezon b, 3%, 90 cm long  $\times$  8 mm bore,  $170^\circ C$ ; detector, FID, range  $10^2$ , att. 5; carrier gas, helium, 30 ml/min. Amount injected, 250  $\mu g$ .

monomer in the injector, and thus would escape detection (*N.B.*, the monomer is obtained by evaporation of the solid).

The technical reagent produces a chromatogram with two peaks, which is very similar to the chromatograms obtained with aged solutions of the purified samples. A representative gas chromatogram ( $T_{\text{col}} = 170^\circ$ ) is shown in Fig. 4. An intense peak, having the same retention time ( $t_r = 63$  sec) as the pure monomer, is observed along with a small peak at a shorter retention time, 43 sec. This result may be explained by the arguments given above: dimer and trimer are converted into monomer in the injector, but owing to the large proportion of dimer in the technical reagent, some of it is still unconverted when it reaches the column. The gas chromatograms were obtained at different temperatures; the retention time of the large peak, 63 sec at  $170^\circ$ , increases to 116 sec at  $140^\circ$ . A van't Hoff plot of  $\log k'$  for the large peak *vs.* the inverse of the absolute temperature was linear with a slope corresponding to a heat of absorption of  $-56$  kJ/mole  $\pm 3\%$ . This value is twice as large as that for a common hydrogen bond. This suggests that a molecule of the substance retained is able to form two hydrogen bonds with the material of the stationary phase. This is possible with the monomeric form of 2-butyne-1,4-diol. Similar results (1 and 2 peaks respectively for the purified and the technical grade reagent) were obtained with a polar column (DEGS, 3%; temperature range,  $160$ – $200^\circ$ ). Therefore, the gas chromatograms do not permit firm conclusions as regards the composition of the solid or the solutions of commercial 2-butyne-1,4-diol.

HPLC was used in an attempt to separate the constituents of a solution of technical 2-butyne-1,4-diol. Chromatograms of freshly prepared and aged solutions of the purified 2-butyne-1,4-diol were obtained by reversed-phase chromatography (Lichrosorb, RP-8,  $10 \mu\text{M}$ ). Acetonitrile was used as eluent at a flow-rate of  $1.0$  ml/min. The detection

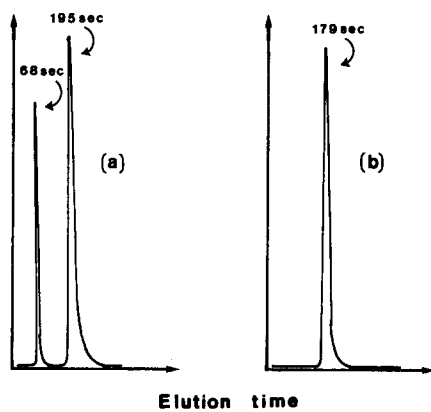


Fig. 5. HPLC chromatogram for 2-butyne-1,4-diol. Column, RP-8,  $10 \mu\text{M}$ ; eluent, acetonitrile,  $1.0$  ml/min; detector,  $260$  nm;  $0.008$  AUFS; (a) technical grade; (b) purified reagent, aged.

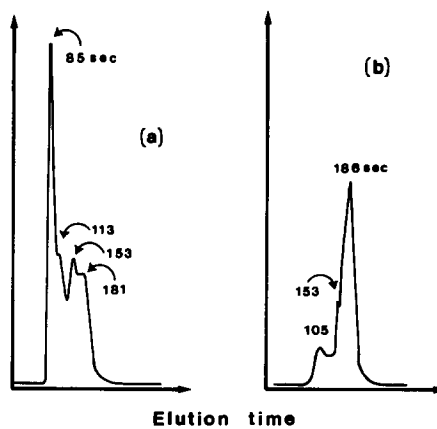


Fig. 6. HPLC chromatogram of 2-butyne-1,4-diol solution. Column, RP-8,  $10 \mu\text{M}$ ; eluent, methanol,  $1.0$  ml/min.; detector,  $250$  nm,  $0.004$  AUFS: (a) solution of technical grade 2-butyne-1,4-diol; (b) aged solution of purified 2-butyne-1,4-diol.

wavelength was  $260$  nm. Freshly prepared solutions of purified BD in acetonitrile produced a single peak. The same behaviour was observed for methanol solutions. Two peaks were observed for the technical product in acetonitrile (Fig. 5a). The peak with the longer retention time was similar in retention time to the peak observed with an old solution (not shown) of purified BD. Although a single peak (Fig. 5b) is observed on the chromatogram of old solutions of 2-butyne-1,4-diol in acetonitrile, more peaks (Fig. 6b) are observed when methanol is used as the solvent and eluent. The chromatograms of technical BD (Figs. 5a and 6a) may be compared with those of the old solutions (Figs. 5b and 6b) of purified BD. The intense peak at  $t_r \approx 180$ – $195$  sec is attributed to the dimer, on the basis of mass spectrometry.<sup>12</sup> The peak with  $t_r \approx 70$  sec in the acetonitrile chromatograms is attributed to a trimer, possibly the cyclotrimer. This trimer contains six  $\text{CH}_2\text{OH}$  groups which would interact strongly with the polar eluents and very little with the aliphatic chain of the stationary phase. Therefore it is not expected to be retained significantly under those chromatographic conditions. Elution with solvents containing an increasing proportion of methanol in acetonitrile (*i.e.*, a decreasing polarity), increased the number of peaks appearing in the chromatogram. The best separation was achieved with pure methanol. Typical chromatograms obtained with this solvent are shown in Fig. 6; they are more complex than those for the acetonitrile system. The attribution of the peaks is as follows: monomer at  $\approx 180$  sec, dimer at  $\approx 150$  sec, and trimer at  $\approx 80$  sec. The other peaks may correspond to impurities in the commercial chemical or to some yet unidentified compounds or intermediates present in the system. The chromatograms of old methanol solutions of 2-butyne-1,4-diol (Fig. 6b) are compatible with a model in which the monomer is slowly transformed into the dimer and some trimer.

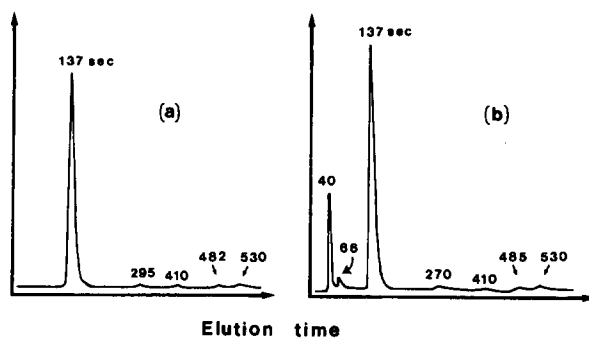


Fig. 7. HPLC chromatogram of 2-butyne-1,4-diol. Column, RP-8, 10  $\mu$ m; eluent, water, 2.0 ml/min; detector, 220 nm, 0.002 AUFS: (a) purified reagent; (b) technical grade.

This model agrees with the previous observation that the reagent is slowly transformed into a dimer when dissolved in water. It is noteworthy that the same transformation does not seem to take place to any significant extent in acetonitrile; hence a proton-donor solvent seems to be required for the transformation.

Pure 2-butyne-1,4-diol was also examined under the same conditions as those described above for the technical reagent: a single peak was observed.

The dark brownish residue remaining after a 5-hr evaporation cycle was also examined by HPLC. The chromatograms were very similar to those of the technical BD under the same experimental conditions. Longer wavelengths, 350–400 nm, can be used for the detection of these species. This last observation shows that the residue contains a higher proportion of trimer.

A final series of chromatograms was obtained with water as eluent. Both purified and technical grade BD give numerous peaks when the RP-8 column is used. The technical product shows (Fig. 7b) two more peaks (40 and 66 sec) than the purified reagent (Fig. 7a). The intensity of the larger peak (137 sec) decreases rapidly to zero at detection wavelengths longer than 280 nm; the intensity of the 40-sec peak remains high for those wavelengths. The use of methanol–water mixtures as eluent decreases the number of peaks appearing on the chromatogram of the technical grade BD; furthermore, the intensities of the various peaks decrease with increase in detection wavelength.

Chromatograms obtained by HPLC, with various methanol–water eluents, were also studied carefully by factor analysis to establish the number of significant species independently of the number and shape of the peaks; in some cases factor analysis also permits identification of some or all components of the system.

Abstract factor analysis (AFA) and column cross-validation were used to evaluate the number of chemical species present in the system responsible for the data matrix. The matrix contained data from chromatograms obtained by detection at different

wavelengths. It contained 24 rows and 18 columns. The matrix was transposed and factor-analysed according to previously described methods.<sup>19–21</sup>

Column cross-validation of the data (Fig. 8) shows that 5 factors are required to explain the data within experimental error. The diagram shows the function SREP as a function of the number of factors. This function is defined<sup>21</sup> as follows:

$$\text{SREP}(k) = \left[ \frac{1}{m} \right] \sum_{i=1}^m \text{REP}(i)$$

The real errors in the predicted vector,  $\text{REP}(i)$ , are calculated with the AFA models. The latter were obtained from the experimental data after removing successively each and every column of the original data matrix, and using the removed column as the test vector. Thus,  $m$  REP values are generated for each of the  $k$  factors tested. These REP values are summed and averaged. We thus obtain an SREP value for each factor tested; the function SREP *vs.* number of factors tested shows a minimum when the correct number of factors is used. The minimum value must take into account the error in the SREP function itself. The stippled rectangles represent SREP values which are not statistically different. A one-tail (Student) value is established, and the correct number of factors is taken as the smallest number which gives an SREP minimal value that is smaller than or equal to the maximal value (one-tail test) of

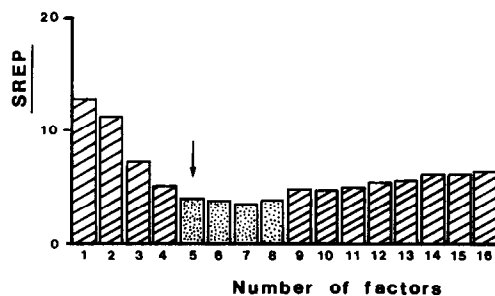


Fig. 8. Column cross-validation of a data matrix from the HPLC chromatograms of technical grade butyne-2-diol-1,4.

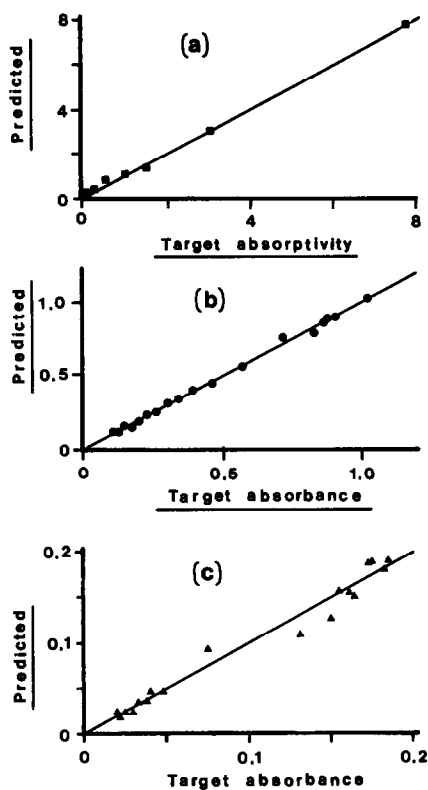


Fig. 9. Target factor analysis: predicted spectra vs. target spectra: (a) monomer; (b) dimer; (c) trimer.

the smallest SREP value on the graph. Figure 8 shows that the absolute minimum is observed with 7 factors; the 5% one-tailed maximal value is 3.87. With 5 factors, the one-tailed minimum is 3.71; with 4 factors it is 4.68. Therefore, at the 5% confidence level, it can be said that there are 5 species in the system. At the 1% confidence level, we have respectively: for 7 factors, a maximal value of 3.99; for 5 factors, a minimum of 3.58, and for 4 factors, a minimum of 4.52. Again, at the 1% confidence level, we can say that there are 5 species in the technical grade butyne-2-diol-1,4. Therefore, the technical reagent contains 5 significant chemical species when in water and methanol solution.

Target factor analysis (TFA) complements abstract factor analysis. Whereas AFA gives an evaluation of the number of factors which are necessary to explain the experimental data, TFA confirms the identification of some or all of the factors. In the present experiment, the factors are identical to the chemical species present in the system. Identification of the factors is achieved by testing one of its target vectors against the factor-analysed model. The test vectors to be used with the matrix studied consisted of the absorption spectra of the species suspected to be present in the solution. The spectra of the monomer and dimer were obtained directly by spectrophotometry. The spectrum of the trimer was

evaluated from a series of aqueous chromatograms obtained with detection at different wavelengths. The height of the peak assigned to the trimer was measured as a function of the detection wavelength. Thus, a graph showing the peak height vs. detection wavelength represents a qualitative spectrum of the species.

TFA calculates a spectrum based on the AFA model; the calculated values are compared with the spectrum tested. If both spectra are statistically equivalent, the species corresponding to that vector is present in the solution. Various statistical parameters<sup>20</sup> may be used in order to test for the statistical acceptability of a given factor (or chemical species). Accordingly, the functions AET (apparent error in the target), RET (real error in the target), REP (real error in the predicted vector), and SPOIL ( $\approx \text{RET}/\text{REP}$ ) were evaluated with the vectors of various suspected factors.

Values of the functions defined above, for three of the species believed to be present in the system, are given in Table 1; a 5-factor model was used in the calculations. Plots of the predicted values against experimental values for the spectra of the three species are shown in Fig. 9. A linear least-squares analysis of the plots gave the results in Table 1, which clearly show that monomer, dimer and trimer are likely substances in the system. SPOIL values of 4.3, 4.2 and 2.8 respectively for the monomer, dimer and trimer definitely show that these species are present in the system. The two other species present in the technical grade are as yet unidentified; these may be different oligomers of butyne-2-diol-1,4 or unknown impurities.

## CONCLUSION

Sublimation of technical grade 2-butyne-1,4-diol, a brownish solid, produces the pure monomer, a white solid. The solid technical compound contains the dimer, some trimer, and some monomer. Spectrophotometric data support the hypothesis that the monomer is slowly transformed into a dimer (and possibly a trimer) when dissolved in water and

Table 1. Target factor analysis (TFA) of the chromatographic data

Parameter	Monomer	Dimer	Trimer
AET	0.136	0.018	0.011
RET	0.132	0.017	0.010
REP	0.030	0.004	0.004
SPOIL	4.3	4.2	2.8
<i>a</i>	-0.033	-0.002	0.000
<i>b</i>	$1.002 \pm 0.017$	$1.002 \pm 0.014$	$0.99 \pm 0.04$
$R^2$	0.995	0.996	0.973
<i>F</i>	3363	4819	576

N.B.: The *a* and *b* values are the least-squares parameters for the data in Fig. 9; *a* is the intercept, *b* is the slope with its standard error.  $R^2$  is the coefficient of determination and *F* is the Fisher coefficient.

methanol. At room temperature, monomer, dimer and trimer can clearly be identified by liquid chromatography under various elution conditions. Since the dimer and trimer are transformed into monomer in the gas phase at temperatures above room temperature, only the last is detected under gas chromatographic conditions. Factor analysis by AFA and TFA supports the hypotheses resulting from the different analytical techniques.

*Acknowledgements*—We thank Martin Lachapelle for the preliminary study on the recrystallization and spectrophotometry of the dimer. The financial support of the Ministère de l'éducation du Québec-FCAC and the NSERCC is also acknowledged.

#### REFERENCES

1. E. Raub, N. Boba, M. Knobler and M. Stalzer, *Trans. Inst. Met. Finish.*, 1963, **42**, 108.
2. I. Epelboin, M. Froment and R. Wiart, *Compt. Rendus*, 1962, **254**, 4021.
3. N. Atanassov, H. R. Borzhkov, S. Vitkova and S. Rashkov, *Surf. Technol.*, 1982, **17**, 291.
4. I. Epelboin, M. Froment and G. Maurin, *Plating*, 1969, **56**, 1356.
5. O. Volk and H. Fisher, *Electrochim. Acta*, 1961, **5**, 112.
6. E. Raub and P. Müller, *Metall.*, 1964, **18**, 6.
7. O. Volk and H. Fisher, *Electrochim. Acta*, 1961, **4**, 251.
8. E. Chassaing, M. Jousselein and R. Wiart, *J. Electroanal. Chem.*, 1983, **157**, 75.
9. J. Bressan and R. Wiart, *J. Appl. Electrochem.*, 1979, **9**, 615.
10. I. Epelboin and R. Wiart, *J. Electrochem. Soc.*, 1971, **118**, 1577.
11. D. Mathieu and D. L. Piron, *Can. Met. Quart.*, 1983, **22**, 327.
12. D. L. Piron, D. Mathieu and M. d'Amboise, *Can. J. Chem. Eng.*, 1987, **65**, 685.
13. U. Rosenthal and W. Schulz, *Z. Chem.*, 1985, **25**, 227.
14. A. D. Miller, *S. African Patent*, 76 06, 188, 19 August 1977.
15. H. Koenig, F. Graf and V. Weberdoerfer, *Liebigs Ann. Chem.*, 1981, 668.
16. M. Utaka, M. Akiyama and A. Takeda, *Bull. Chem. Soc. Japan*, 1977, **50**, 1980.
17. J. V. Schloss and F. C. Hartman, *Bioorg. Chem.*, 1980, **9**, 217.
18. L. N. Balyatinskaya and L. G. Babankova, *Zh. Analit. Khim.*, 1978, **33**, 842.
19. M. d'Amboise and D. Noel, *Anal. Chim. Acta*, 1985, **170**, 255.
20. E. R. Malinowski and D. S. Howey, *Factor Analysis in Chemistry*, Wiley-Interscience, New York, 1980.
21. M. d'Amboise and B. Lagarde, *Computers & Chemistry*, in the press.

## POTENTIOMETRIC TITRATIONS IN METHANOL/WATER MEDIUM: INTERTITRATION VARIABILITY

E. FISICARO\* and A. BRAIBANTI

Istituto di Chimica Fisica Applicata, Facolta' di Farmacia Universita' di Parma, Parma, Italy

(Received 22 January 1988. Revised 12 May 1988. Accepted 15 June 1988)

**Summary**—Homogeneous sets of data from strong acid–strong base potentiometric titrations in a mixed solvent medium (9:1 v/v methanol/water), performed by means of the glass electrode, at various constant ionic strengths and with different reference electrodes, have been analysed by statistical criteria. A standardized procedure has been established to obtain reliable potentiometric data in mixed solvents. It has been demonstrated how, with the aid of a proper linearized model, analysis of variance (ANOVA) applied to the standardization titrations can be used to test the reliability of a potentiometric chain in a medium other than pure water. The error expected in the stability constants thus evaluated is related to the intertitration error of the operational  $pK_w^*$ , for the same medium and the same chain. The results obtained by applying ANOVA to the mixed solvent data substantially confirm the trend found for aqueous media, the intertitration error being larger than the intratitration error for all the parameters investigated ( $E_0$ ,  $pK_w^*$ , mean equivalence volume). The stochastic error thus obtained depends on the ionic medium used and on the kind of reference electrode employed in the electrochemical chain.

Our preceding studies on the assessment of models for the investigation of metal–proton–ligand equilibria in aqueous solution<sup>1-3</sup> have shown that the formation constant,  $\beta_{pqr} = [M_p H_q L_r]/[M]^p [H]^q [L]^r$ , for a given species  $M_p H_q L_r$ , is affected by an error which is randomly distributed between the titrations performed rather than between the individual points of the titrations. In other words, the largest source of error in the potentiometric determination of equilibrium constants in aqueous solution is the variability from one titration to another.

Because the parameters specific for each titration, such as  $E_0$ , the standard potential,  $E_j$ , the liquid-junction potential, and the operational ionic product of water,  $K_w^*$ , usually derived by a strong acid–strong base standardization titration, seem to be the major source of errors in evaluating the formation constants, we have applied analysis of variance to sets of standardization data, in order to ascertain whether they are affected by the same kind of errors as the formation constants are.<sup>3</sup>

Some methods proposed for testing the performance of glass electrodes in aqueous media and for calibration purposes use a suitable series of standard buffers. The correction for the liquid-junction potential is empirically evaluated either by the Biedermann and Sillén method<sup>4,5</sup> or by measurements in cells with and without liquid junction.<sup>6</sup> Otherwise, the glass electrode is calibrated on the concentration scale against the hydrogen electrode, by measurement of the potentials of the two electrodes immersed in the same buffer.<sup>7</sup>

It is also possible to obtain the measurements in terms of emf, by standardizing the chain by means of a previous calibration titration: provided the ionic strength of the test solution remains constant, the emf at each point of the titration is related to the concentration of free hydrogen ions,  $h$ , by the Nernst equation

$$E = E_0 + (RT/F) \ln h$$

where  $E_0$  accounts for all the constant potentials in the cell, disregarding any possible junction potentials  $E_j$ .

More recently,<sup>8-10</sup> an iterative procedure using the computer program MAGEC has been proposed in order to optimize simultaneously any or all of the titration parameters pertinent to the calibration of the glass electrode, even if limitations arise from the correlations of errors between the parameters.

The potentiometric method has been scarcely used in the past to study equilibria in non-aqueous and mixed solvents. In recent years, however, the number of thermodynamic studies of metal complexes in solvents other than water (pure solvents or binary or ternary mixtures) has been considerably increasing.<sup>11,12</sup>

Recently, in order to overcome some experimental difficulties (low solubility of ligands and/or of Cu(II)-complexes in water)<sup>13</sup> and to obtain information about solute–solvent and solvent–solvent interactions, we have chosen to study solution equilibria by potentiometric titrations in mixed solvents, particularly in 9:1 v/v methanol/water. This choice is justified by the fact that the alcohols are similar to water in the nature of their protolytic behaviour and

\*To whom correspondence should be addressed.

can be studied by the same experimental techniques, though they differ in physical properties (dielectric constant, lipophilicity, *etc.*).<sup>14</sup> The solvent can indeed influence the equilibria in solution by long-range electrostatic interactions and through short-range factors, such as solute-solvent interactions, the importance of which is not yet well understood.<sup>15,16</sup>

Binary mixed solvents containing water as one component are able to react protolytically both with protic acids and their conjugate bases. The acid-base behaviour of many of these mixed solvents is qualitatively comparable with that of water, even though wide quantitative differences are observed.

In non-aqueous and mixed solvents, the glass electrode is widely used in combination with an Ag/AgCl or a commercial aqueous saturated calomel electrode as reference. From a practical point of view, this choice is very attractive, notwithstanding the large liquid-junction potentials introduced.

However, no definitively recommended procedure for handling the potentiometric data for solvents other than pure water has yet been established.

To evaluate the response of different electrode chains and achieve a satisfactory standardization of potentiometric titrations in mixed solvents, we have applied analysis of variance (ANOVA) to homogeneous sets of strong acid-strong base potentiometric titrations, once a suitable model to interpret the data was chosen.

It is the purpose of this work to demonstrate how, with the aid of a proper linearized model, ANOVA can be applied to strong acid-strong base potentiometric titrations to test the reliability of the potentiometric technique in a solvent other than pure water. The error evaluated by this treatment of the data should be related to the accuracy to be expected in determination of stability constants in the same medium.<sup>2,3</sup>

## EXPERIMENTAL

### Reagents

Freshly boiled doubly distilled water, stored under nitrogen, was used throughout. Doubly distilled methanol was boiled, and stored in CO<sub>2</sub>-free conditions. Hydrochloric acid (*ca.* 0.15*M*) and potassium hydroxide solution (*ca.* 0.20*M*) were prepared by diluting the contents of Merck Titrisol ampoules with the proper quantity of water and methanol to achieve a methanol/water ratio of 9:1 v/v. The potassium hydroxide solutions were standardized with potassium hydrogen phthalate (C. Erba; dried at 120°).

Appropriate weights of potassium chloride (C. Erba) or of tetrabutylammonium bromide (Fluka; dried under vacuum) were added to the acidic solution to give an ionic strength of 0.1*M*.

### Measurements

The potentiometric measurements were performed with an automated titration system based on a Radiometer PHM 64 digital voltmeter (nominal error 0.1 mV) and an Ingold H6336 glass electrode. The reference electrodes were: (a) Ingold saturated KCl/calomel; (b) Ingold 0.1*M* aqueous KCl/calomel; (c) K4078 Radiometer 0.1*M* KCl (in 9:1 v/v methanol/water)/calomel. Titrant was added by means of a 5-ml Metrohm Dosimat E535 motor burette (nominal

error 0.005 ml). The whole system was controlled by an Apple IIe Personal Computer. The starting volume in the cell ( $V_0 = 50$  ml) contained 0.4–0.5 mmole of hydrogen chloride. The titration vessel was kept at  $25.0 \pm 0.1^\circ$  under a stream of nitrogen, pre-equilibrated by bubbling through a 0.1*M* solution of potassium chloride or tetrabutylammonium bromide in the same mixed solvent.

## DATA PROCESSING

As already outlined,<sup>3</sup> once the starting  $V_0$  and the concentration  $N$  of the titrant (or of the acid titrated) are known, a strong acid-strong base potentiometric titration curve is completely defined when the parameters  $E_0$ ,  $K_w^*$  and the equivalence volume are defined. In the following, when the parameters  $E_0$  and  $K_w^*$  refer to the mixed solvent, they will be marked by a prime. To evaluate these parameters and their relative standard deviations, a suitable model for treating the experimental data must be chosen. A titration curve can be linearized in two ways: by using the Nernst equation or by using the Gran plot.<sup>17</sup> We have chosen to use the latter, as we did for investigations of aqueous media.<sup>3</sup>

The potentiometric data were processed by computer programs assembled in our laboratory, with an IBM XT PC. The data automatically collected by the Apple IIe PC were transferred to the IBM through the communication interface. The program GRAPPLE processes the data according to the Gran method (or, optionally, the Nernst equation) by a least-squares fit and determines the values and the relative standard deviations of the parameters  $E_0$ , the standard potential of the electrode chain,  $K_w^*$ , the ion product of water, the acidic and basic equivalence volumes and the difference ( $\Delta$  and  $\Delta/2$ ) between the two values, and its relative value with respect to the mean value of the equivalence volume (VEM). These parameters are collected in a file for the subsequent application of ANOVA. The program GRAPPLE evaluates the junction potentials by the Gran method modified by Rossotti and Rossotti.<sup>18</sup> The program STATGRAN applies the analysis of variance to the files of the parameters collected as described above.

## STANDARDIZATION OF THE METHOD

As regards potentiometric titration in methanol-water solutions, the literature generally<sup>11</sup> refers to the studies of Bates *et al.*:<sup>19,20</sup> the electrode chain of glass and calomel electrodes is calibrated by means of aqueous buffer solutions. The "pH" read on the pH-meter is referred to the standard state in the mixed solvent by means of the parameter  $\delta$ , accounting for the differences in activity coefficients and liquid-junction potentials.

Rossotti and Rossotti<sup>18</sup> stressed the importance of keeping constant the activity coefficients of species participating in the cell reaction, and the potentials at



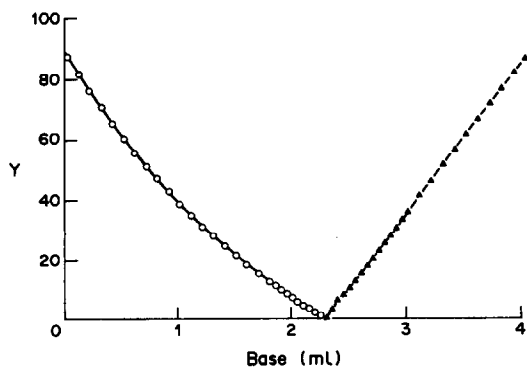


Fig. 1. Gran plot for a strong acid-strong base titration in 9:1 v/v methanol/water with a saturated KCl/calomel reference electrode and aqueous potassium hydroxide as titrant, without pretreatment of methanol;  $I = 0.1M$  KCl. (Scale factors: basic range  $1 \times 10^{-3}$ ; acid range  $2.85 \times 10^{13}$ .)

any liquid-liquid junction, in order to get better potentiometric data for complexation equilibria in solution.

To obtain a reliable electrochemical technique for use in methanol/water systems, we have performed a set of strong acid-strong base titrations, paying attention principally to three experimental aspects: (a) pretreatment of the organic solvent, (b) preparation of the reactants, (c) the electrode chain.

The pretreatment and storage of the methanol as described in the experimental section appears to be absolutely necessary if good linearity of the Gran plot is to be obtained.

During the whole titration, the water/methanol ratio must be kept perfectly constant to ensure constancy of the junction potentials, activity coefficients<sup>18</sup> and  $K_w^*$ , the operational ionic product of water in the mixed solvent used. This means that the titrants must be prepared in the same solvent as that used in the potentiometric cell. If the titration is done by means of aqueous potassium hydroxide without pre-

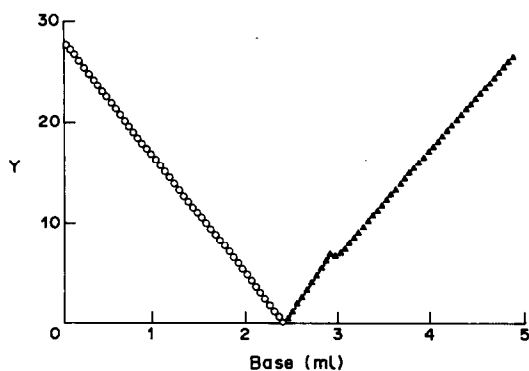


Fig. 2. Gran plot for a strong acid-strong base titration in 9:1 v/v methanol/water with a commercial aqueous saturated KCl/calomel reference electrode;  $I = 0.1M$  KCl. (Scale factors: basic range  $4.6 \times 10^{-3}$ ; acid range  $1 \times 10^{13}$ .)

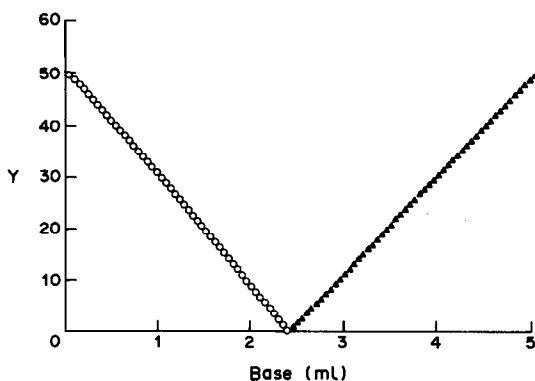


Fig. 3. Gran plot for a strong acid-strong base titration in 9:1 v/v methanol/water with a 0.1M KCl/calomel reference electrode;  $I = 0.1M$  KCl. (Scale factors: basic range  $1 \times 10^{-3}$ , acid range  $2.6 \times 10^{13}$ .)

treatment of the methanol, the Gran plot is non-linear in the acid region, as shown in Fig. 1.

When the important requirements mentioned above were fulfilled, the use of a saturated KCl/calomel electrode with a porous diaphragm gave a Gran plot like that shown in Fig. 2: the Gran model did not agree with the experimental data in the alkaline region, the plot showing two branches with different slopes after the equivalence point. We ascribe this behaviour to precipitation of potassium chloride at the liquid junction between the mixed solvent and the aqueous saturated potassium chloride solution in the reference electrode, resulting in a sudden variation of the liquid-junction potential.

The use of a 0.1M solution of potassium chloride in 9:1 v/v methanol/water in the calomel electrode overcomes this difficulty, and results in a Gran plot like that shown in Fig. 3.

## DISCUSSION

The sets of standardization titrations examined by ANOVA allow evaluation of the general behaviour of the electrode chain in 9:1 v/v methanol/water, and the effect of a different liquid-junction potential (realized by using 0.1M potassium chloride solution in 9:1 v/v in methanol/water) and of a different ionic medium.

(1) Reference electrode 0.1M aqueous KCl/calomel; ionic medium 0.1M KCl

The intratitration error can be evaluated by means of the standard deviations of the parameters  $E'_0$ ,  $K_w^*$ ,  $pK_w^*$ ,  $\Delta/2$ ,  $\Delta/2\%$ , obtained from the output of the program GRAPPLE. Table 1 gives the values obtained and the relative standard deviations for the set of titrations under examination. It has been demonstrated<sup>3</sup> that the variance of  $\Delta/2$  is the same as that of VEM, so  $\sigma(\Delta/2\%)$  is an estimate of the relative error in VEM. The intratitration variance of  $\Delta/2\%$ ,  $E'_0$ ,  $K_w^*$  and  $pK_w^*$  can be evaluated from the

Table 1. Set 1 of titrations: intratitration variability

	$\Delta/2\%$	$E'_0$	$pK_w^{*'} $
1	$-0.277 \pm 0.075$	$338.488 \pm 0.029$	$14.4109 \pm 0.0006$
2	$-0.374 \pm 0.064$	$336.721 \pm 0.021$	$14.4422 \pm 0.0005$
3	$-0.266 \pm 0.051$	$334.655 \pm 0.023$	$14.4272 \pm 0.0005$
4	$-0.296 \pm 0.070$	$334.025 \pm 0.025$	$14.4296 \pm 0.0006$
5	$-0.231 \pm 0.057$	$333.301 \pm 0.024$	$14.4249 \pm 0.0005$
6	$-0.179 \pm 0.112$	$332.834 \pm 0.045$	$14.4128 \pm 0.0014$
7	$-0.351 \pm 0.232$	$335.516 \pm 0.057$	$14.4056 \pm 0.0007$
8	$-0.279 \pm 0.097$	$333.272 \pm 0.038$	$14.4227 \pm 0.0007$
9	$-0.113 \pm 0.122$	$334.317 \pm 0.049$	$14.4406 \pm 0.0009$
10	$-0.283 \pm 0.074$	$335.623 \pm 0.030$	$14.4608 \pm 0.0006$
11	$-0.744 \pm 0.122$	$334.734 \pm 0.047$	$14.4448 \pm 0.0009$
12	$-0.183 \pm 0.076$	$331.416 \pm 0.032$	$14.4241 \pm 0.0006$
13	$-0.139 \pm 0.117$	$331.717 \pm 0.048$	$14.4278 \pm 0.0009$
14	$-0.041 \pm 0.094$	$331.395 \pm 0.040$	$14.4209 \pm 0.0007$
15	$-0.140 \pm 0.072$	$331.905 \pm 0.047$	$14.4301 \pm 0.0006$
16	$-0.020 \pm 0.090$	$331.905 \pm 0.038$	$14.4305 \pm 0.0007$
17	$-0.011 \pm 0.075$	$329.917 \pm 0.028$	$14.4106 \pm 0.0006$
18	$-0.045 \pm 0.099$	$330.415 \pm 0.044$	$14.4102 \pm 0.0008$
19	$-0.140 \pm 0.102$	$330.106 \pm 0.041$	$14.4124 \pm 0.0007$

Solvent: 9:1 v/v methanol/water  
Reference electrode: aqueous calomel in 0.1M KCl  
Ionic medium: 0.1M KCl  
Temperature:  $25.0 \pm 0.1^\circ\text{C}$

laws of error propagation as

$$\sigma^2(\Delta/2\%) = \frac{10^4}{\text{VEM}^2} \sigma^2(\text{VEM}) \left[ 1 + \left( \frac{\Delta/2}{\text{VEM}} \right)^2 \right]$$

$$\sigma^2(E'_0) = (\beta/b)^2 \sigma^2(b) + (\beta/N)^2 \sigma^2(N)$$

$$\sigma^2(K_w^{*'}) = e^{-2E_0/\beta} / a^2 [\sigma^2(E'_0) N^2 / \beta^2 + \sigma^2(a) N^2 / a^2 + \sigma^2(N)]$$

$$\sigma^2(pK_w^{*'}) = \sigma^2(K_w^{*'}) / (-K_w^{*'} \ln 10)^2$$

where  $\beta = RT/F$ ,  $b$  is the slope of the acidic branch of the Gran function, with standard deviation  $\sigma(b)$ ,  $a$  is the alkaline branch slope with standard deviation  $\sigma(a)$ , and  $N$  is the normality of the base, with standard deviation  $\sigma(N)$ .

It is easy to see that the model fits the experimental data very well, the standard deviations of VEM and  $E'_0$  being comparable with the instrumental error, and the ionic product of water showing a very small standard deviation.

If we compare the behaviour in mixed solvent with that in water,<sup>3</sup> the intratitration errors seem to be greater for the latter medium: the greater accuracy when the mixed solvent is used is, in our opinion, probably due to the automated collection of the data and to the greater number of points so collected for

each titration (about 60 points for mixed solvent, a maximum of 30 points for water).

Table 2 reports the results of ANOVA applied to the set of 19 titrations of Table 1 to assess the reliability of both the equipment and the titration system. Comparison of the variance of the mean values with the estimated interpoint average variance indicates (at a chosen confidence level) whether the titrations belong to the same normal population ( $H_0$  hypothesis) or not ( $H_1$  hypothesis). The  $F$ -test applied to the mean values of  $E'_0$  and  $pK_w^{*'}$  (or  $K_w^{*'}$ ) indicates a behaviour similar to that in the aqueous environment: the  $H_0$  hypothesis must be rejected, at a very high level of confidence. This fact confirms once more what we found earlier:<sup>1-3</sup> the intertitration errors are much larger than the intratitration errors, so a correct evaluation of the precision of the above mentioned parameters can be obtained only from the intertitration variability. The standard deviation of  $E'_0$  is 2.3 mV, about three times that found for the water system: such a large value can be due either to a non-reproducible liquid-junction potential, independent of the hydrogen-ion concentration, or to a less stable standard potential of the 0.1M KCl electrode. On the other hand, it is generally accepted that the value of  $E_0$  can change from one titration to another, by inclusion of any systematic error.

The mean value of  $\Delta/2\%$  is 0.15, corresponding to a systematic error of 0.15% in the evaluation of VEM: this value is small and insignificant, as demonstrated by the value of 0.94 for  $t$ , compared with the tabular value  $t_{0.95} = 2.10$  for 18 degrees of freedom.

The  $F$ -test applied to the evaluated and estimated variances of  $\Delta/2\%$  seems to indicate that the  $H_1$  hypothesis could be accepted at only a moderately significant confidence level, the value being between the tabular values for 95% and 99% confidence (18 and 30 degrees of freedom).

(2) Reference electrode 0.1M KCl (in 9:1 v/v methanol/water)/calomel; ionic medium 0.1M KCl

The data reported in Table 3 for 11 titrations show that the intratitration errors are of the same order of magnitude as in the set obtained with the aqueous reference electrode. When ANOVA is applied to this set of data, the same arguments as before can be applied to the parameters shown in Table 4. Again the titrations belong to different populations. The intratitration errors, however, are smaller: the standard potential  $E'_0$  is the parameter most sensitive to the change in the kind of liquid junction and it can

Table 2. Set 1 of titrations: intertitration analysis of variance

	$\bar{x}$	$\sigma$	$\sigma^2$	$\sigma_0^2$	$F$
$\Delta/2\%$	-0.15	0.16	0.025	0.010	2.35
$E'_0$	333.28	2.33	5.44	$1.40 \times 10^{-3}$	3875
$K_w^{*'} $	$3.73 \times 10^{-15}$	$1.29 \times 10^{-16}$	$1.67 \times 10^{-32}$	$4.23 \times 10^{-35}$	395
$pK_w^{*'} $	14.429	0.015	$2.31 \times 10^{-4}$	$5.81 \times 10^{-7}$	398
$\bar{x}$ = mean of the parameter, with estimated standard deviation $\sigma$					
$\sigma_0^2$ = estimated intertitration variance					

Table 3. Set 2 of titrations: intratitration variability; effect of change of reference electrode

	$\Delta/2\%$	$E'_0$	$pK_w^{*'}$
1	$-0.058 \pm 0.056$	$406.421 \pm 0.034$	$14.4404 \pm 0.0007$
2	$-0.152 \pm 0.040$	$406.812 \pm 0.026$	$14.4415 \pm 0.0006$
3	$-0.103 \pm 0.034$	$407.125 \pm 0.027$	$14.4409 \pm 0.0006$
4	$-0.102 \pm 0.079$	$406.862 \pm 0.029$	$14.4355 \pm 0.0008$
5	$-0.181 \pm 0.045$	$406.185 \pm 0.030$	$14.4388 \pm 0.0007$
6	$-0.210 \pm 0.032$	$407.211 \pm 0.025$	$14.4560 \pm 0.0006$
7	$-0.252 \pm 0.063$	$407.878 \pm 0.035$	$14.4479 \pm 0.0007$
8	$-0.046 \pm 0.059$	$407.067 \pm 0.034$	$14.4369 \pm 0.0007$
9	$-0.090 \pm 0.039$	$406.499 \pm 0.029$	$14.4371 \pm 0.0006$
10	$-0.127 \pm 0.038$	$407.025 \pm 0.028$	$14.4444 \pm 0.0006$
11	$-0.137 \pm 0.064$	$406.250 \pm 0.035$	$14.4392 \pm 0.0007$

Solvent: 9:1 v/v methanol/water  
Reference electrode: 0.1M KCl/calomel in 9:1 v/v methanol/water  
Ionic medium: 0.1M KCl  
Temperature:  $25.0 \pm 0.1^\circ\text{C}$

Table 5. Set 3 of titrations: intratitration variability; effect of change of background electrolyte

	$\Delta/2\%$	$E'_0$	$pK_w^{*'}$
1	$-0.442 \pm 0.133$	$422.083 \pm 0.047$	$14.5054 \pm 0.0009$
2	$-0.431 \pm 0.126$	$421.974 \pm 0.041$	$14.5107 \pm 0.0008$
3	$-0.443 \pm 0.100$	$418.055 \pm 0.029$	$14.5105 \pm 0.0007$
4	$-0.592 \pm 0.142$	$416.077 \pm 0.031$	$14.5277 \pm 0.0008$
5	$-0.450 \pm 0.115$	$415.395 \pm 0.042$	$14.5229 \pm 0.0008$
6	$-0.642 \pm 0.097$	$406.488 \pm 0.043$	$14.3841 \pm 0.0008$
7	$-0.682 \pm 0.135$	$408.354 \pm 0.041$	$14.3858 \pm 0.0009$
8	$-0.900 \pm 0.091$	$409.951 \pm 0.016$	$14.3967 \pm 0.0006$
9	$-0.996 \pm 0.078$	$409.441 \pm 0.025$	$14.4064 \pm 0.0006$
10	$-0.772 \pm 0.078$	$408.969 \pm 0.029$	$14.3919 \pm 0.0006$
11	$-0.836 \pm 0.066$	$408.938 \pm 0.031$	$14.4046 \pm 0.0006$
12	$-0.899 \pm 0.054$	$408.963 \pm 0.016$	$14.3974 \pm 0.0004$

Solvent: 9:1 v/v methanol/water  
Reference electrode: 0.1M KCl/calomel in 9:1 v/v methanol/water  
Ionic medium: 0.1M N(But)<sub>4</sub>Br  
Temperature:  $25.0 \pm 0.1^\circ\text{C}$

be evaluated with a standard deviation of 0.48 mV, larger than the instrumental error, but comparable with that for the aqueous system. The error in the determination of  $pK_w^{*'}$  decreases to 0.006.

(3) Reference electrode: 0.1M KCl (in 9:1 v/v methanol/water)/calomel; ionic medium 0.1M N(But)<sub>4</sub>Br

The effect of the ionic medium was examined by means of a set of 12 titrations in which 0.1M N(But)<sub>4</sub>Br was employed as background electrolyte: the results are reported in Tables 5 and 6. The intertitration standard deviations are much worse than in the preceding two sets, even though the intratitration errors of  $E'_0$  and  $pK_w^{*'}$  are of the same order of magnitude.

The mean value of  $\Delta/2\%$  is  $-0.67$  and the *t*-test shows that the presence of a systematic error in the determination of VEM within each titration is highly probable. The variability of  $E'_0$  is very large and  $pK_w^{*'}$  can be evaluated with an error of 0.06.

This behaviour is comparable with that when potassium nitrate solution in water is used as ionic medium,<sup>3</sup> and appears to be due to a sort of noise, probably due to junction potentials. In this case, however, we cannot exclude the possibility that the difficulty of obtaining certain quaternary ammonium salts in highly purified form could play an important role, even though organic nitrogen bases partially neutralized with hydrochloric acid have been suggested<sup>21</sup> as stable compounds for the preparation of standard buffer solutions to determine the sodium error of the glass electrode.

#### (4) Mean values of $pK_w^{*'}$

The mean values of  $pK_w^{*'}$  reported in Tables 2, 4, and 6 do not differ significantly, the grand mean being  $14.438 \pm 0.009$ . The error introduced by using different reference electrodes or ionic media is comparable with the intertitration error. An inspection of the data in Tables 1, 3, and 5 could suggest that the distribution of these values is not normal. Therefore the mean values of  $pK_w^{*'}$  obtained by assuming a Gaussian (normal) distribution and by calculating the best Poisson distribution fitting the data have been compared (Table 7). The grand means are very close. Because of the limited number of determinations, however, it is hard to say whether the  $pK_w^{*'}$  values always have a Poisson distribution. The answer can be obtained by examining a large number of data from different laboratories.

## CONCLUSIONS

The possibility of obtaining reliable results when potentiometric methods are used to evaluate the formation constants of a given metal–ligand–proton system in a mixed solvent, depends on accurate standardization of the method. When a suitable model is used to fit the experimental data, statistical parameters can be derived and the classical statistical tests applied to the analysis of the results. Application of ANOVA to three sets of potentiometric strong acid–strong base titrations in 9:1 v/v methanol/water

Table 4. Set 2 of titrations: intertitration analysis of variance

	$\bar{x}$	$\sigma$	$\sigma^2$	$\sigma_0^2$	<i>F</i>
$\Delta/2\%$	-0.13	0.06	$3.9 \times 10^{-3}$	$2.7 \times 10^{-3}$	1.46
$E'_0$	406.85	0.48	0.23	$9.2 \times 10^{-4}$	246
$K_w^{*'}$	$3.62 \times 10^{-15}$	$4.89 \times 10^{-17}$	$2.39 \times 10^{-33}$	$3.26 \times 10^{-35}$	73
$pK_w^{*'}$	14.442	0.006	$3.5 \times 10^{-5}$	$4.7 \times 10^{-7}$	75

$\bar{x}$  = mean of the parameter, with estimated standard deviation  $\sigma$   
 $\sigma_0^2$  = estimated intertitration variance

Table 6. Set of 3 titrations: intertitration analysis of variance

	$\bar{x}$	$\sigma$	$\sigma^2$	$\sigma_0^2$	$F$
$\Delta/2$	-0.67	0.21	0.042	0.011	3.84
$E_0'$	412.89	5.55	30.78	$1.14 \times 10^{-3}$	26868
$K_w^{*'} $	$3.62 \times 10^{-15}$	$5.06 \times 10^{-16}$	$2.56 \times 10^{-31}$	$3.54 \times 10^{-35}$	7244
$pK_w^{*'} $	14.445	0.063	$3.93 \times 10^{-3}$	$5.26 \times 10^{-7}$	7418

$\bar{x}$  = mean of the parameter, with estimated standard deviation  $\sigma$   
 $\sigma_0^2$  = estimated intertitration variance

substantially confirms the trend found in aqueous systems, as follows.

(a) The parameters  $E_0'$  and  $pK_w^{*'}$  show a distribution where the intertitration error is larger than the intratitration error. The titrations of a set must therefore be individually refined and the mean values of the set evaluated.

(b) The distribution of  $\Delta/2\%$  is also not normal, though the confidence level for this statement is lower than for the other parameters. Its value, compared with the standard deviation, however, is not significant.

(c) The use of a reference electrode with the same solvent as that in the potentiometric cell gives a more reproducible liquid-junction potential, thus decreasing the intertitration error.

(d) The potentiometric method is considerably affected by the background salt added to keep the ionic strength constant. Very good results are obtained with 0.1M potassium chloride; the use of N(But)<sub>4</sub>Br results in a remarkable increase in the errors of any parameter. In our opinion, apart from the problem of impurities or decomposition, some salts lead to differences in concentration and density which make the galvanic cell unstable.

It is important to stress that the analysis of strong acid-strong base potentiometric titrations implies evaluation of an equilibrium constant, the ionic product of water,  $pK_w^{*'}$ : the intertitration error of  $pK_w^{*'}$  gives us a measure of the accuracy we can expect in the potentiometric determination of the stability constants. On the other hand, the use of an iterative procedure like that proposed by May and Williams<sup>8,10</sup>

Table 7. Analysis of the distribution of  $pK_w^{*'}$ ; titration sets 1, 2 and 3

Table	Mean values	
	Gauss	Poisson
1	14.428	14.423
3	14.442	14.439
5	14.445	14.434
Grand mean	14.438	14.432

Normal distribution: mean =  $\Sigma pK_w^{*'}/n$  for  $n$  titrations  
Poisson distribution: mean =  $(pK_w^{*'})_{\min} + md$   
 $d$  = sampling interval for the histogram  
 $m$  from  $P(X=k) = e^{-m} m^k/k!$ , fitting the observed frequencies

does not allow a distinction to be made between the inter- and intratitration errors, and though it may confirm the variability among titrations, it does not give a real estimate of the error in the stability constants, this error being minimized by variation of the other parameters ( $E_0'$ , titrant and titrand concentration and so on).

The application of the classical statistical tests to the standardization titrations therefore appears to be a good tool for fast and complete evaluation of the reliability of an electrochemical system in mixed solvents as well as in purely aqueous media.

## REFERENCES

1. A. Braibanti, F. Dallavalle, G. Mori and B. Veroni, *Talanta*, 1982, **29**, 725.
2. A. Braibanti, F. Dallavalle, G. Mori and M. Pasquali, *Gazz. Chim. Ital.*, 1983, **113**, 407.
3. A. Braibanti, C. Bruschi, E. Fisicaro and M. Pasquali, *Talanta*, 1986, **33**, 471.
4. G. Biedermann and L. G. Sillén, *Arkiv Kemi*, 1953, **5**, 425.
5. H. S. Dunsmore and D. Midgley, *Anal. Chim. Acta*, 1972, **61**, 115.
6. H. K. J. Powell and M. C. Taylor, *Talanta*, 1983, **30**, 885.
7. I. Aggeryd, Yi-Chang Liang and Å. Olin, *Anal. Chim. Acta*, 1985, **169**, 231.
8. P. M. May and D. R. Williams, *Talanta*, 1982, **29**, 249.
9. P. M. May, *ibid.*, 1983, **30**, 899.
10. P. M. May and D. R. Williams, in *Computational Methods for the Determination of Formation Constants*, D. J. Leggett, (ed.), pp. 37-70. Plenum Press, New York, 1985.
11. I. Ziogas, I. Moutzisz and G. Papanastasiou, *Ann. Chim. (Rome)*, 1986, **76**, 143.
12. S. Ishiguro and I. Ohtaki, *J. Coord. Chem.*, 1987, **15**, 237.
13. E. Fisicaro, *Ateneo Parmense, Acta Nat.*, 1986, **22**, 65.
14. R. G. Bates, in *Solute-Solvent Interactions*, J. F. Coetzee and C. D. Ritchie (eds.), p. 53. Dekker, New York 1969.
15. R. Aruga, *Can. J. Chem.*, 1986, **64**, 780.
16. *Idem, ibid.*, 1986, **64**, 785.
17. G. Gran, *Analyst*, 1952 **77**, 661.
18. F. J. C. Rossotti and H. Rossotti, *J. Phys. Chem.*, 1964, **68**, 3773.
19. R. G. Bates, M. Paabo and R. A. Robinson, *ibid.*, 1963, **67**, 1833.
20. K. C. Ong, R. A. Robinson and R. G. Bates, *Anal. Chem.*, 1964, **36**, 1971.
21. M. Filomena, G. F. C. Camoes and A. K. Covington, *ibid.*, 1974, **46**, 1547.

## IDENTIFICATION AND DETERMINATION OF VOLATILES DERIVED FROM PHENOL-FORMALDEHYDE MATERIALS

ROMAN GRZESKOWIAK and GRAHAM D. JONES\*

School of Chemistry, Thames Polytechnic, Wellington St., London SE18 6PF, England

ALLAN PIDDUCK

RSRE, Malvern, Worcestershire, England

(Received 21 April 1987. Revised 6 June 1988. Accepted 15 June 1988)

**Summary**—Volatile substances derived from moulding compounds, resins and fillers used in the formulation of phenol-formaldehyde materials have been identified, isolated and determined. The amounts of the volatiles are related to the type of resins, fillers, curing agents and degree of cure used in the formulation.

There is interest in the potential corrosivity and toxicity of the volatile species derived from organic polymers. Corrosion by polymers is of particular concern within the electronics industry,<sup>1-3</sup> as is induced failure of polymers due to metal-polymer contact,<sup>4</sup> where such materials are applied extensively for encapsulation of integrated circuits. Reasons for their use include humidity control, protection against atmospheric contaminants, and buffering against temperature and pressure fluctuations. Any release of aggressive species by the encapsulants themselves can be disastrous, owing to the small dimensions of the circuits enclosed.<sup>1</sup> Phenolic polymers are generally considered to be particularly corrosive,<sup>5-8</sup> because they are known to break down to produce phenol, formaldehyde, ammonia and formic, acetic and hydrochloric acids.<sup>3,6,7</sup> However, one reviewer<sup>9</sup> has stated that fully cured phenolics containing only "inert" fillers do not release such species and are non-corrosive. Few detailed studies have been reported.

Various fillers, including cellulose (cotton) and lignin (wood, olivestone), are often incorporated in phenolic compositions, to impart particular physical and mechanical properties, and reduce the cost of the final article. Such materials are known to be a further source of harmful volatiles. Zinc, cadmium and other metals readily corrode in the vicinity of wood<sup>6,8,10</sup> owing to the release of formic and acetic acids. Possible factors affecting the acidity and consequent corrosivity of wood include the species and type of wood, season of felling, and subsequent chemical treatment.<sup>11,12</sup>

This report is concerned with the identification of volatiles evolved from commercial phenolics of known formulation and history, together with the determination of the major species. The materials were selected as representative of those phenolics currently available.

### EXPERIMENTAL

Table 1 summarizes the materials investigated. These were the moulding compounds (MC), cured to approximately 95%, together with the individual resins and fillers used in their formulation. Resol resins are prepared under basic conditions, with excess of formaldehyde, and novolak resins are prepared under acidic conditions with an excess of phenol. Consequently, the chemistry of resol materials is such that they may be referred to as "self-curing" whilst novolaks require the addition of a curing agent, hexamethylenetetramine (HMT) being by far the most commonly used.<sup>13</sup> Full-cured mouldings (M) were prepared from these moulding compounds, according to British Specification BS 771, as follows.

Precure heating is optional in BS 771, but was always applied in this work: a known weight of MC was heated at 95° for 15 min, then immediately transferred to the moulding die (5-cm diameter, preheated to 160 ± 3°) and a pressure of 25 MPa was applied for the time required for full-cure, which was dependent on the amount of material used, *i.e.*, on the thickness of the moulding.

Weight of moulding compound, g	Time for full-cure, min
5.0	4
10.0	6
30.0	12

### Extraction of volatiles

**Cold-trap collection.** A schematic diagram of the apparatus used is shown in Fig. 1. The helium carrier gas (flow-rate 30 ml/min) was purified by passage through a moisture trap (A), an oxygen trap (B) and a 5- $\mu$ m dust filter (C), placed immediately before the flow-controllers (D). The gas was

\*Enquiries should be addressed to: Dr. G. D. Jones, Rhone-Poulenc Ltd., Biopharmaceutical Research, Rainham Road South, Dagenham, Essex, England.

Table 1. Summary of materials used

Moulding compound reference	Resin(s) used and type	Catalyst used for resin preparation	Filler(s) incorporated in moulding compound	Curing agent and approximate percentage (w/w MC)
MC1	R1—Resol	Sodium hydroxide	Glass fibre	None required
MC2	*R2.1—Resol	Ammonia solution	Cotton fibre	HMT—1
	R2.2—Novolak	Oxalic acid	(cellulose-based)	
MC3	R3—Novolak	Sulphuric acid and calcium sulphate	Wood flour and olivestone (both lignin-based)	HMT—12
MC4	R4—Novolak	Oxalic acid	Olivestone and nylon	HMT—12
MC5	*R5.1—Novolak	Hydrochloric acid and sodium chloride	Glass fibre	HMT—12
	R5.2—Novolak	Acetic acid and zinc acetate		
MC6	*R6.1—Resol	Ammonia solution	Wood flour and glass fibre	HMT—1
	R6.2—Novolak	Unknown		

\*Indicates the major resin component of the moulding compound.

then heated in a series of metal coils (E) before entering the sample compartments (F), all held at 103° in the oven. Species volatilized from the sample (which was typically 20 g of moulding compound or 100 g of moulding, crushed and sieved to pass an 80-mesh but not a 120-mesh sieve) were carried through heated transfer lines (G) maintained at 15° above the oven temperature to a cold trap (H) immersed in liquid nitrogen. The trap consisted of a U-tube of 15 mm internal diameter containing crushed glass helices (1 g) to provide a large cold-surface area. Both the inlet and outlet of the trap were sealed by Teflon-backed silicone rubber washers. After a collection period of approximately 8 hr for examination of moulding compounds and up to 42 hr for that of mouldings, the trap was removed from the liquid nitrogen. Distilled water (10 ml) was then immediately added to wash the trap and transfer line. The frozen water was thawed, the trap and transfer line were rinsed out with more water, and the combined washings were analysed.

“Flash” distillation. This method was adapted from normal steam distillation, previously used for the extraction of volatiles from polymers.<sup>14,15</sup> Approximately 20 g of moulding compound were sieved, then loaded into a round-

bottomed flask, together with 100 ml of distilled water. Distillation was continued for several hours, the water level in the flask being maintained by dropwise addition of water from a dropping funnel at a rate matching the distillation rate. The remaining solution was decanted from the sample and distilled, and this distillate was combined with that previously obtained. This process of collecting fractions was repeated until no further volatiles could be detected, each fraction being analysed separately.

*Aqueous reflux.* This was performed in a twin-necked round-bottomed flask to which 80–100 g of moulding, crushed and sieved, together with 100 ml of distilled water, were added. After several hours of reflux the solution was decanted, and the residue similarly extracted with a fresh 100-ml volume of water, the process being repeated until no further volatiles were detected in the extract. This method was also applied to the extraction of volatiles from filler materials.

The complete removal of volatiles by the distillation and reflux techniques was confirmed by analysis of the remaining sample residues by low-temperature solid-probe mass spectrometry.

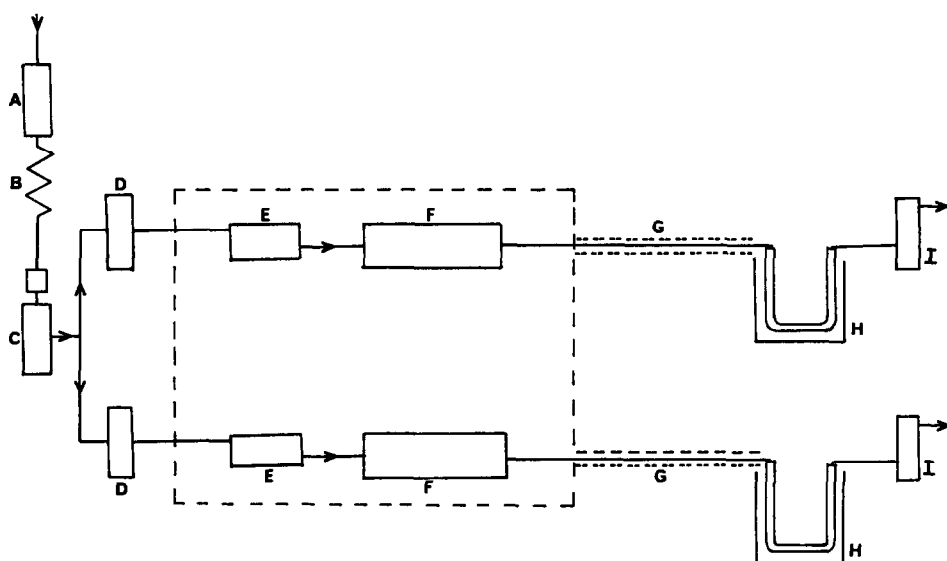


Fig. 1. Schematic diagram of cold-trap apparatus: (A) moisture trap, (B) oxygen trap, (C) dust filter, (D) flow controller, (E) gas heating coils, (F) sample compartments, (G) heated transfer lines, (H) cold-trap, (I) flow monitors.

### Identification of volatiles

**Gas chromatography-mass spectrometry (GC-MS).** The GC-MS system consisted of a Perkin-Elmer Sigma 3 gas chromatograph, interfaced through a jet separator to a single-focusing VG 305F mass spectrometer, operated in the electron impact mode at 70 eV. Data-acquisition, calibration and processing were performed with a VG Multi-Spec 8 data system.

Chromatographic separation was achieved with either a moderately polar free fatty-acid phase (FFAP) or a basic Chromosorb 103 packed column, both 1 metre in length. Detected species were identified on the basis of retention times and spectral interpretation, with selected ion monitoring applied to confirm the association between molecular and fragment ions. To minimize any memory effects, distilled water was injected alternately with the sample solutions.

**Head-space gas chromatography-mass spectrometry (HS-GC-MS).** Identification of the volatiles evolved directly from the materials was performed with a semi-automated Perkin-Elmer HS6 unit,<sup>16</sup> combined with the GC-MS system described above. The finely powdered sample (3-4 g) was loaded into a glass head-space vial, which was then sealed with a silicone-backed septum. The vial was heated in an oven at 100° for at least 24 hr before insertion into the heated head-space unit, also at 100°. After a pressurization time of 1 min, the head-space atmosphere above the sample was automatically injected into the chromatographic column, packed with either FFAP or Poropak QS.

**High-performance ion chromatography (HPIC).** This was performed with an unsuppressed anion-exchange column (Vydac 302: 25 cm × 4.2 mm bore) and detection by on-line ion conductance or indirectly by ultraviolet absorbance measurement.<sup>17</sup> Concomitant separation of anionic species extracted from the samples was achieved by using a mobile phase of aqueous phthalic acid solution (1 mM, pH 3.5) at a flow-rate of 1.5 ml/min and ambient temperature.

### Quantitative analysis

The ammonia content of the distillate and reflux fractions

was determined by means of an ammonia gas-sensitive electrode (Orion Research Inc), which was both sensitive and selective in the absence of volatile amines;<sup>18</sup> no evidence had been found by GC-MS for the presence of such amines. Working standards, adjusted to pH 13 by dropwise addition of concentrated sodium hydroxide solution, were prepared from a stock solution of ammonium chloride, which contained the equivalent of 1000 µg/ml free ammonia.

Formaldehyde was determined gravimetrically as its dimedone derivative,<sup>14,19</sup> which was found to be the method providing the most consistent results.<sup>20</sup>

Phenol was determined by gas chromatography with a flame ionization detector. The FFAP packed column was maintained at 180° and the carrier gas flow-rate was 50 ml/min. Working standards were prepared by sequential dilution of a 0.1M aqueous stock solution of phenol.

Acetate, formate and chloride were determined by the HPIC procedure described. Working standards were prepared on a daily basis for both acetate and formate, owing to their observed instability even when stored under refrigeration.

For each of the species determined, the total water-extractable volatiles (TWEV) content in the sample was expressed in µmole/g.

## RESULTS AND DISCUSSION

### Qualitative analysis

GC-MS was used for the identification of species, primarily in samples obtained by cold-trap collection, owing to the relatively large amounts of volatiles released. Species evolved directly from the materials under investigation were detected by HS-GC-MS. A typical HS-GC-MS trace obtained for the head-space analysis of olivestone filler is shown in Fig. 2. Table 2 summarizes the results obtained for moulding compounds, resins and filler materials. With the

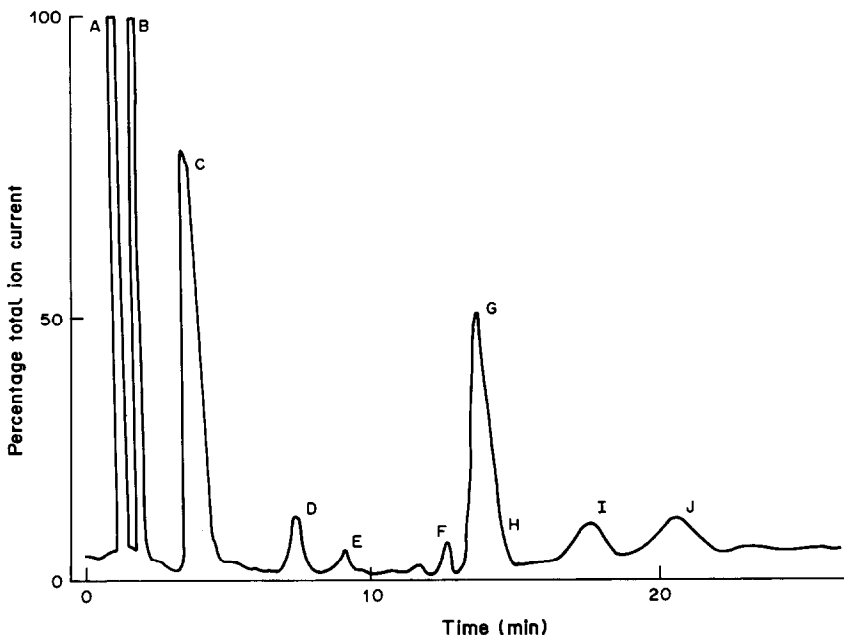


Fig. 2. HS-GC-MS trace for olivestone (Poropak Q-S column). (A) air, (B) carbon dioxide, (C) water, (D) methanol, (E) acetaldehyde, (F) acetone, (G) methyl acetate, (H) acetic acid, (I) alkane-alkene, (J) alkane.

Table 2. Species identified in moulding compounds, selected resins and fillers

Species identified	Material investigated											
	MC1	MC2	MC3	MC4	MC5	MC6	R2.1	R4	Cotton	Nylon	Olivestone	Wood
Acetaldehyde												
Acetic acid			*†	*		*					†	
Acetone										*†	*†	*†
Alkane/alkene											*†	
Ammonia		*	*	*	*	*	*	*		*		
Benzaldehyde	*	*	*	*	*	*	*	*				
Carbon dioxide	†	†	†	†	†	†			†	†	†	†
Formaldehyde	*		*	*	*	*						
Furfuraldehyde		*		*	*	*						
Hexamethylenetetramine			*	*	*							
Methanol				†							†	
Methyl acetate											†	
Methylfuran						*						
Methylphenol	*	*	*	*	*	*	*	*				
Methylpropanol						*						
Naphthalene			*									
Phenol	*†	*†	*†	*†	*†	*†	*†	*†			*	*
Salicylaldehyde	*	*	*	*	*	*	*	*				
Species A	*	*		*	*	*	*	*				
Species B			*	*	*	*		*				
Toluene			*	*	*	*						
Water	†	†	†	†	†	†	†	†	†	†	†	†

Identified by GC-MS(\*) and HS-GC-MS(†).

exception of the fillers, phenol was the major component in all cases and probably originated from unreacted starting material. Other components, such as benzaldehyde, methylphenol and salicylaldehyde, were observed in all MC extracts, being either impurities in the starting materials or degradation products produced during cure.

Hexamethylenetetramine was identified only in those formulations which contained novolak resin as a major component (*i.e.*, MC3, MC4, MC5). Ammonia was also detected whenever HMT was used for curing and in resins R2.1 and R6.1, for which ammonia solution was used as a catalyst. Formaldehyde was difficult to detect with certainty, owing to a relatively high background of low-mass fragments. However, its presence was positively confirmed in a range of formulations by selected ion monitoring at the retention time previously determined by the injection of aqueous formaldehyde standards. Both ammonia and formaldehyde can be produced by the hydrolysis of HMT,<sup>21</sup> particularly under acidic conditions. Toluene and 2-methylpropanol, detected in only a few samples, are commonly used solvents and were probably processing residues. Naphthalene, detected only in MC3, is a commonly used plasticizer for phenolics, and furfuraldehyde (MC2, MC4, MC6 and R2.1) may be incorporated to aid flow characteristics during moulding. Neither of these species was detected in the full-cured mouldings themselves. Species A, the mass spectrum of which is shown in Fig. 3a, is considered to be a mono-substituted aromatic compound of molecular weight 136. Species B (Fig. 3b) was interpreted from the mass spectrum as an alkyl ether

derivative of diethylene glycol, although exactly which homologue remains uncertain.

Although GC-MS was not applied quantitatively, the relative amounts of those species detected by using the FFAP column were estimated by normalizing to the peak area for phenol, the major component. As shown by Table 3, significant amounts of salicylaldehyde, furfuraldehyde and Species A were also present in certain samples.

The HPIC results (Table 4) showed that formate and chloride were present in all MC samples, and acetate in all but MC1. Oxalate was detected in MC2, probably as a result of its use for the catalysis of resin R2.2. Sulphate anions in MC3 originated from the sulphuric acid-calcium sulphate catalyst used in the preparation of resin R3. Fillers based on lignin and cellulose were shown to contain acetate, formate and chloride ions.

#### Quantitative analysis

Investigations into the recoveries by "flash" distillation showed that the average losses were ammonia 7.3%, phenol 4.2% and formaldehyde 32.2%. Those found by aqueous reflux were ammonia 15.2%, phenol 1.4%, formaldehyde 49.7%, formic acid 9.0%. The reason for the high loss of formaldehyde could not be established. The results given are those which were experimentally determined and have not been corrected for losses incurred during extraction.

Table 5 summarizes the results obtained by steam distillation for moulding compounds, selected resins and fillers. The levels of formaldehyde and ammonia in the moulding compounds are comparable to those



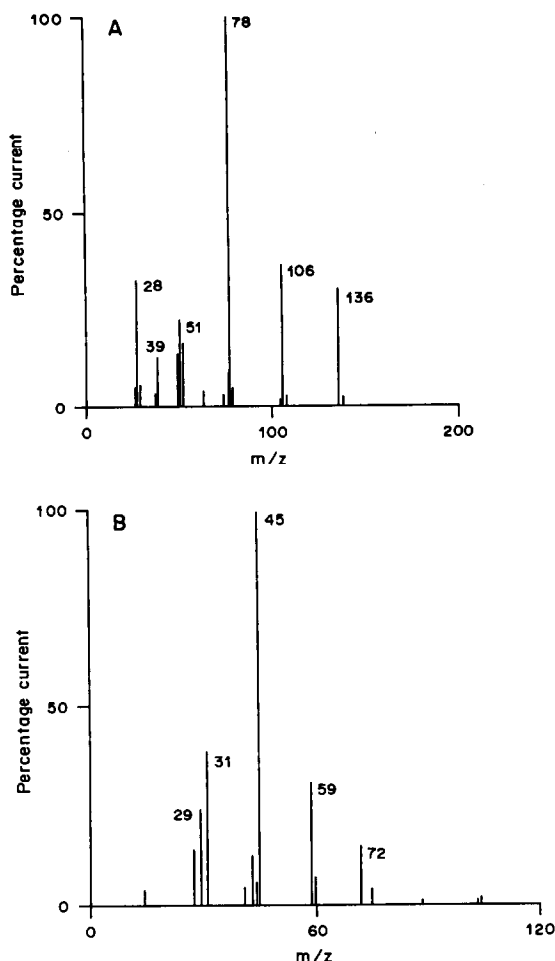


Fig. 3. A: averaged mass spectrum of Species A, considered to be a mono-substituted aromatic compound of molecular weight 136. B: averaged mass spectrum of Species B, considered to be an alkyl ether derivative of diethylene glycol.

previously given for "phenolic plastics".<sup>15</sup> The ammonia and formaldehyde values are higher for novolak-based materials, in which a greater amount of HMT is employed (up to 12% w/w). The TWEV

value for ammonia in MC2 is increased because of the use of ammonia solution as a catalyst in the preparation of the constituent resin R2.1. The concentration of phenol in the moulding compounds is apparently unrelated to the resin type, although the novolak resin R4 did show a substantially higher level than resol resin R2.1. In both cases, the phenol content of the resins was found to be greater than that for the moulding compounds although it should be remembered that approximately 50% of each moulding compound is filler. The amounts of anionic species are closely related to the nature of the filler, particularly for acetate and formate. Thus glass-filled materials (MC1) contained no acetate and little formate and chloride. Acetate in particular is present in fair quantity in those moulding compounds filled with olivestone and wood (e.g., MC3). Comparable results were obtained for the fillers themselves, although direct comparisons are difficult to make.

The cumulative extraction *vs.* time profiles for ionic species in MC4 and olivestone filler by aqueous reflux are shown in Fig. 4. From the linear section of each curve, as estimated by linear regression, the rates of extraction of acetate, formate and chloride ions from MC4 are 21.0, 2.3 and 1.5  $\mu\text{mole.g}^{-1}.\text{hr}^{-1}$ , respectively, compared with 2.5, 0.5 and 1.0  $\mu\text{mole.g}^{-1}.\text{hr}^{-1}$  for the filler. Therefore, despite the greater porosity of the filler, the rate of removal of acetate and formate from it was lower than that from the moulding compound, by a factor of 5–10. One explanation is that these acidic species exist as free entities within the moulding compounds, but only as hydrolysable esters within the lignin-based fillers themselves. It is possible that the free acids are produced within the moulding compounds during the initial cure process (160°, 5 MPa pressure) as a result of partial filler degradation, perhaps through hydrolysis by the water produced during the curing process. A similar effect has been reported in connection with the kiln drying of wood.<sup>10</sup>

Table 6 summarizes the TWEV values obtained by aqueous reflux for mouldings and also provides a comparison with the results obtained for the associated moulding compounds. Certain volatiles were

Table 3. Estimation of amounts of volatile species detected by GC-MS (FFAP column)

Species identified	Material investigated							
	MC1	MC2	MC3	MC4	MC5	MC6	R2.1	R4
Benzaldehyde	D	D	D	D	D	C		D
Formaldehyde	D		B	C		C		
Furfuraldehyde		D		A		C	D	
Hexamethylenetetramine			C	C	C			
Methylphenol	C	C	C	C	C	C	C	C
Naphthalene			C					
Phenol	100	100	100	100	100	100	100	100
Salicylaldehyde	C	B	D	C	C	C	B	C
Species A	C	D		B	D	C	C	D
Species B			D	B		D		D
Toluene			D	D		D		

Relative to phenol (100%): greater than 60% (A), 60–30% (B), 30–5% (C), less than 5% (D).

Table 4. Species identified by HPIC in steam distillate and aqueous reflux solutions

Species identified	Material investigated											
	MC1	MC2	MC3	MC4	MC5	MC6	R2.1	R4	Cotton	Nylon	Olivestone	Wood
Acetate	*	*	*	*	*	*			*		*	*
Chloride	*	*	*	*	*	*	*T	*T	*		*	*
Formate	*	*	*	*	*	*					*	*
Oxalate		*										
Sulphate			*									

Tentative assignment (T).

Table 5. Determination of TWEV ( $\mu\text{mole/g}$ ) of major species in moulding compounds, resins and fillers

Species determined*	Moulding compounds						Resins		Fillers			
	MC1	MC2	MC3	MC4	MC5	MC6	R2.1	R4	Cotton	Nylon	Olivestone	Wood
Ammonia	193	263	593	738	674	248	58	44	ND	ND	ND	ND
Acetate	ND	2	253	369	17	123	—	—	NQ	ND	319	189
Chloride	9	19	22	29	17	22	—	—	8	ND	20	11
Formaldehyde	87	167	471	574	545	96	8	46	ND	ND	ND	ND
Formate	NQ	28	48	42	26	39	—	—	13	ND	54	46
Phenol	188	234	326	208	207	169	333	655	ND	ND	NQ	NQ

\*Volatiles extracted by steam distillation.

NQ: Not quantifiable.

ND: Not detected.

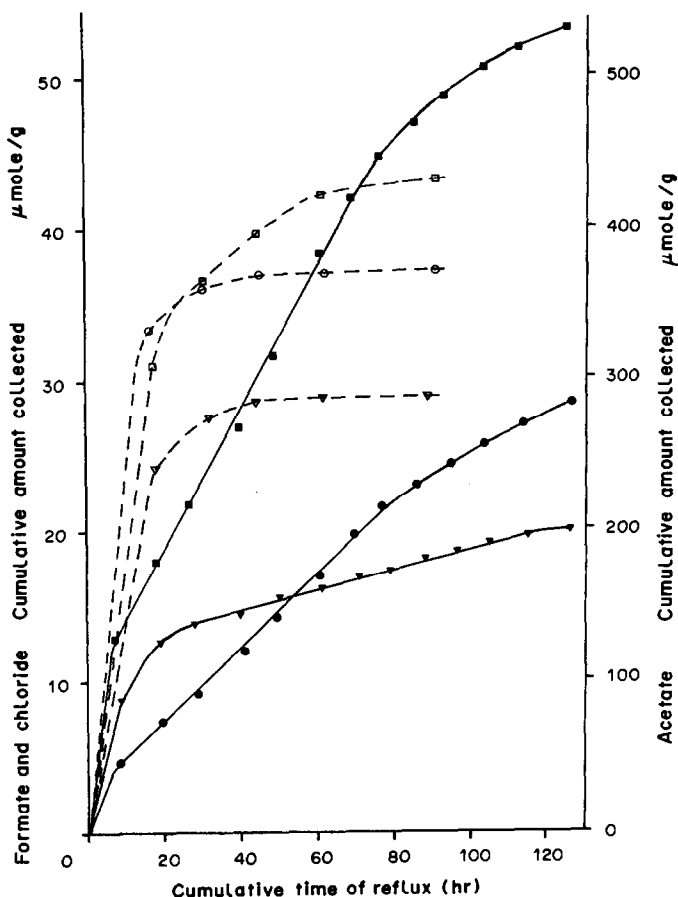


Fig. 4. Plot of cumulative amounts of ionic species extracted from MC4 (----) and olivestone filler (—) by aqueous reflux. Acetate (● and ○), formate (■ and □) and chloride (▼ and ▽) ions.

Table 6. TWEV ( $\mu\text{mole/g}$ ) of major species in mouldings

Species determined*	Material investigated†					
	M1	M2	M3	M4	M5	M6
Ammonia	NQ	9 (3.4)	231 (39.0)	239 (32.4)	265 (39.3)	8 (3.2)
Acetate	ND	NQ	164 (64.8)	96 (26.0)	ND	59 (48.0)
Chloride	NQ	14 (73.7)	23 (104.5)	22 (75.9)	NQ	20 (90.9)
Formaldehyde	2 (2.3)	NQ	2 (4.2)	NQ	ND	ND
Formate	ND	NQ	27 (56.2)	23 (54.8)	NQ	15 (38.5)
Phenol	5 (2.7)	29 (12.4)	20 (6.1)	42 (20.2)	20 (9.7)	21 (12.4)

\*Volatiles extracted by aqueous reflux; the percentage of the value for moulding compounds is given in parenthesis.

†M1 Denotes the moulding derived from MC1, etc.

NQ: Not quantifiable.

ND: Not detected.

substantially reduced in amount, although for ammonia this was dependent upon resin type. These losses may be explained in terms of volatilization during full-cure, although the argument is less convincing for phenol, formaldehyde and ammonia (resol only), which may suggest that these species are active in the curing mechanism. Conversely, the comparatively small reduction in ammonia for novolak mouldings may indicate minimal involvement in curing.

### CONCLUSIONS

It has been shown that a complex range of volatiles exists within phenol-formaldehyde polymeric materials, arising from a variety of sources: unreacted starting compounds (phenol, formaldehyde), catalyst residues (ammonia, oxalic acid), decomposition of HMT curing agent in novolak-containing formulations (ammonia, formaldehyde), processing residues (toluene, 2-methylpropanol), additives (naphthalene, furfuraldehyde), resin degradation (salicylaldehyde) and lignin fillers (acetic, formic acids).

The determination of selected major compounds has indicated that the amount of residual phenol is independent of the resin type, whereas the levels of ammonia and formaldehyde are greater with novolak-based materials. The use of olivestone and wood fillers in the formulation of moulding compounds and mouldings leads to increased levels of acetic and formic acids and, to a lesser extent, of chloride ions. The acidic species probably arise from the partial degradation of the fillers' lignin structure during the cure process, although cotton, which is cellulose-based, appeared not to follow this behaviour.

It has been shown that the degree of cure is important with regard to the level of volatiles. The most striking result was for ammonia, which was

present in the resol mouldings at approximately 1% of the moulding compound, but at approximately 40% of the moulding compound in novolak mouldings. The greater level of ammonia trapped in the novolak mouldings might be expected as the result of degradation of the remaining HMT. However, such degradation would also be expected to result in the production and retention of formaldehyde in the polymer, which is not the case, as seen in Table 6. This may indicate that formaldehyde is possibly more important than ammonia in the curing of novolaks. Possibly paraformaldehyde, which would evolve formaldehyde only on full-cure, could be used instead of HMT,<sup>21</sup> particularly where sensitivity towards ammonia is important.

*Acknowledgements*—We would like to thank the Ministry of Defence (DQA/TS) for financial support to GDJ during the period October 1981–January 1985, and also Drs. B. King and J. Hodson (MOD), and J. Mendham (Thames Polytechnic), for helpful discussions and guidance.

### REFERENCES

1. W. Macleod-Ross. *Proc. Conf. on Protection of Metals in Storage and Transit*, Braintree Exhibitions Ltd., London, 1970.
2. A. J. Brown, T. Logan and L. Allison. *Br. Aerospace Dynamics Groups Report*, No. CMLR 35/2100, 1981.
3. A. C. Kennett, *Chem. Ind., New Zealand*, March 1971, 19.
4. S. G. Kiryushkin, T. B. Kovalev, G. M. Panchenkov, A. E. Chebotarevskii and Y. A. Shlyapnikov, *Int. Polym. Sci. Technol.*, 1982, 9, T/62.
5. J. S. Bora, *Corros. Sci.*, 1974, 14, 503.
6. D. Knotková-Čermáková and J. Vicková, *Br. Corros. J.*, 1971, 6, 17.
7. D. Knotková-Čermáková, *Plastics-Fire-Corrosion Int. Symp., Swedish Fire Protection Association*, 1969, L1.
8. V. R. Rance and H. G. Cole, *Corrosion of Metals by Vapour From Organic Materials*. HMSO, London, 1958.

9. P. D. Donovan and J. Stringer, *Br. Corros. J.*, 1971, **6**, 132.
10. S. G. Clark and E. E. Longhurst, *J. Appl. Chem.*, 1961, **11**, 435.
11. P. C. Arni, G. C. Cochrane and G. D. Gray, *ibid.*, 1965, **15**, 305.
12. *Idem, ibid.*, 1965, **15**, 463.
13. A. A. K. Whitehouse and E. G. K. Pritchett, *Phenolic Resins: Plastic Monograph No. C3*, 2nd Ed., Guthrie, Glasgow, 1955.
14. J. Haslam, H. A. Willis and D. C. M. Squirrell, *Analysis and Identification of Plastics*, Heyden, London, 1980.
15. N. A. Zavorovskaya, E. V. Nekhorosheva and L. P. Artemeva, *Int. Polym. Sci. Technol.*, 1983, **10**, T/1.
16. M. House, *Anal. Proc.*, 1983, **20**, 423.
17. R. A. Cochrane and D. E. Hillman, *J. Chromatog.*, 1982, **241**, 392.
18. M. E. Lopez and G. A. Rechnitz, *Anal. Chem.*, 1982, **54**, 2085.
19. J. F. Walker, *Formaldehyde*, Reinhold, New York, 1964.
20. G. D. Jones, *Ph. D. Thesis*, Thames Polytechnic, London, 1985.
21. H. Zowall, *Int. Polym. Sci. Technol.*, 1983, **10**, T/96.

## APPLICATION OF A SULPHIDE-SELECTIVE ELECTRODE IN THE ABSENCE OF A pH-BUFFER

IMRE TÓTH\*, PIROSKA SOLYMOSSI and ZOLTÁN SZABÓ†

Department of Inorganic and Analytical Chemistry, Kossuth University, H-4010 Debrecen, Hungary

(Received 22 January 1988. Accepted 31 May 1988)

**Summary**—Calibration of a sulphide electrode in the pH-range 9–12 has been studied as an e.m.f. vs. (pH – p[HS<sup>-</sup>]) function by measuring e.m.f. and pH in parallel. Calibration can also be done in this pH range by using a differential amplifier with a three-electrode measuring cell (glass, sulphide-selective and reference electrodes). The effects of an antioxidant (ascorbic acid) and a complexing agent (DCTA) on the calibration of the glass-sulphide electrode cell at pH < 5 were studied. The applicability of this end-point indicator cell has been demonstrated for titrations of Ag<sup>+</sup>, Pb<sup>2+</sup> and Bi<sup>3+</sup> with Na<sub>2</sub>S.

Sulphide-selective electrodes are widely used for the rapid determination of S<sup>2-</sup> in many kinds of samples.<sup>1,2</sup> Alkaline pH buffers are commonly added in order to avoid the loss of H<sub>2</sub>S and to keep the pH constant. Since S<sup>2-</sup> is a strong base, the potential of the indicator electrode is strongly affected by the effect of pH changes on the protonation equilibria of S<sup>2-</sup>.<sup>3</sup>

The equilibrium concentrations of the protonated species can be calculated if the potentials of a sulphide-selective electrode and a pH glass electrode are measured, by using the protonation constants of S<sup>2-</sup>, but these constants are the subject of considerable debate.<sup>4,5</sup>

In this paper we present some speculations (based on equilibrium chemistry) on the effect of pH on the measured sulphide-electrode potentials, together with experimental evidence supporting these speculations. The calibration of the sulphide-electrode-Ag/AgCl reference electrode measuring cell in the pH-range 9–12 without a pH-buffer is discussed. A method is suggested for direct potentiometry with a sulphide-selective-pH-sensing glass electrode measuring cell at pH < 5, and the application of this special cell for end-point detection in the Ag<sup>+</sup>-S<sup>2-</sup>-H<sup>+</sup>, Pb<sup>2+</sup>-S<sup>2-</sup>-H<sup>+</sup> and Bi<sup>3+</sup>-S<sup>2-</sup>-H<sup>+</sup> systems is presented.

### EXPERIMENTAL

The following electrodes were used: an OP-S 07110 sulphide-selective electrode, an OP-0718P glass electrode, an OP-8202 Ag/AgCl double-junction reference electrode (Radelkis) and a 6202B glass electrode (Radiometer).

The e.m.f. measurements were made with OP 208 and OP 208/1 precision digital pH-meters (Radelkis). In the case of

the sulphide-selective electrode-glass electrode measuring cell, the sulphide electrode was connected to socket R and the glass electrode to the high-impedance input G.

The circuit diagram of the home-made amplifier used for the experiments with three electrodes (sulphide-glass-reference) is shown in Fig. 1.

The direct potentiometric experiments were performed with 0.5M potassium nitrate media. To protect S<sup>2-</sup> from oxidation by air, deoxygenated argon was passed over the test solutions. Sodium sulphide solution was added to the sample from a microburette. For mixing, a magnetic stirrer was used. Since the presence of air was not observed to affect the titrations of the Ag<sup>+</sup>, Pb<sup>2+</sup> and Bi<sup>3+</sup> solutions, the use of an argon atmosphere was not needed for these.

A stock solution of sodium sulphide (about 0.5M) was prepared from recrystallized Na<sub>2</sub>S·9H<sub>2</sub>O (*p.a.* Merck) dissolved in deaerated distilled water, and 1% v/v isoamyl alcohol was added to inhibit the activity of any sulphur bacteria. The solution was stored under argon. The potassium hydrogen sulphide stock solution was prepared by absorption of a weighed quantity of H<sub>2</sub>S in potassium hydroxide solution, and was stored similarly to the sodium sulphide stock solution.

The S<sup>2-</sup> concentrations of the stock solutions were determined by oxidation with potassium iodate in acidic medium,<sup>6</sup> and also by potentiometric precipitation titration of acidified silver nitrate solution with the sodium sulphide solution. The concentrations of the sulphide stock solution remained constant for weeks. Diluted sulphide solutions were prepared daily.

The AgNO<sub>3</sub>, Pb(NO<sub>3</sub>)<sub>2</sub> and Bi(NO<sub>3</sub>)<sub>3</sub> (Reanal) used were of reagent grade. Silver nitrate solutions were prepared from accurately weighed portions of the recrystallized and dried chemical. The lead and bismuth solutions were standardized by complexometric titration.<sup>7</sup>

The points of maximum slope (inflection points) on the potentiometric titration curves were evaluated by the standard graphical method and the Gran method<sup>8</sup> modified for precipitation titrations, with a computer program.<sup>9</sup> The results obtained by the two methods agreed well.

### RESULTS AND DISCUSSION

At 25° and at constant ionic strength the electrode potential<sup>3</sup> of the sulphide electrode (*E<sub>s</sub>*) is given by

$$E_s = \text{const}_1 - 0.0296 \log [S^{2-}] \quad (1)$$

\*Author for correspondence.

†Present address: Alkaloida Pharmaceutical Works, H-4440 Tiszavasvári, Hungary.

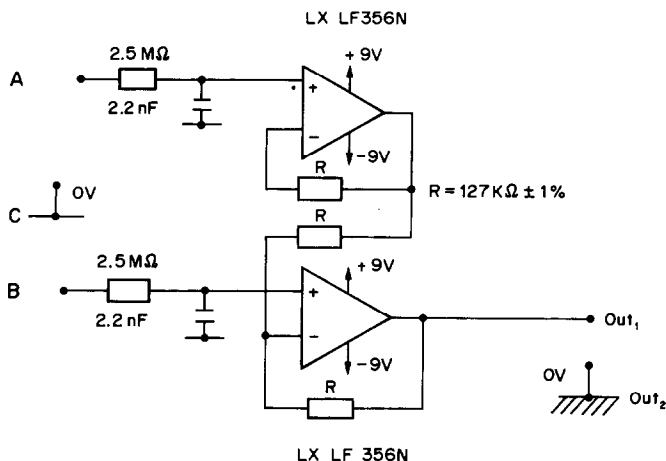


Fig. 1. Circuit diagram of the amplifier. The electrodes were connected as follows: (A) glass electrode, (B) sulphide-selective electrode, (C) Ag/AgCl double-junction reference electrode.

The equilibrium concentration of  $S^{2-}$  can be expressed as

$$[S^{2-}] = \frac{T_S}{1 + K_1^H [H^+] + K_1^H K_2^H [H^+]^2} \quad (2)$$

where  $T_S = [S^{2-}] + [HS^-] + [H_2S]$ ,  $K_1^H = [HS^-]/([S^{2-}][H^+])$  and  $K_2^H = [H_2S]/([HS^-][H^+])$ . The pH-dependence of the electrode potential is frequently eliminated by using a pH-buffer. This is obviously not possible in many cases in co-ordination chemistry, where the other equilibria of the system are generally influenced by both the pH value and the components of the buffer.<sup>10</sup> Here, we suggest an alternative route to avoid these problems.

#### Calibration in the pH-range 9–12

Equation (2) can be simplified for work within a restricted pH range. Since  $\log K_2^H = 7.0$  and  $\log K_1^H = 13.9$ ,<sup>11</sup> at pH above about 9,  $K_1^H K_2^H [H^+]^2 \ll K_1^H [H^+]$  and  $K_1^H [H^+] \gg 1$ ; thus, equations (1) and (2) give the expression

$$E_S = \text{const}_1 - 0.0296 \log \frac{T_S}{K_1^H [H^+]} \quad (3)$$

(The value of  $\log K_1^H$  has recently been debated again, but use of the proposed values  $\log K_1^H = 19 \pm 2$ ,<sup>4</sup> or  $\log K_1^H = 17.6 \pm 0.3$ ,<sup>5</sup> simply correspondingly extends the upper limit of validity of the following derivation.)

If we consider the range  $(\log K_2^H + 2) < \text{pH} < (\log K_1^H - 2)$ , i.e.  $9 < \text{pH} < 12$ ,  $T_S$  is  $[HS^-]$ , and thus equation (3) can be written in the form:

$$E_S = \text{const}_2 - 0.0296 (\text{pH} - \text{p}[HS^-]) \quad (4)$$

A linear calibration plot based on equation (4) was obtained by titrating 20 ml of 0.5M potassium nitrate with 0.05M sodium sulphide. The potential difference between the sulphide-selective electrode and an Ag/AgCl double-junction reference electrode was measured. The pH increased during the titration because of the hydrolysis of  $S^{2-}$ , and was measured

with a glass electrode against the same reference electrode. The very good linearity, and the almost theoretical slope of  $-28.8 \pm 0.05 \text{ mV}/(\text{pH} - \text{p}[HS^-])$  recorded at five different times, demonstrate the applicability of the method. The intercept was found to be very reproducible, with a mean value of  $-502.5 \pm 0.3 \text{ mV}$ . The linear response range was  $\text{p}T_S = 2\text{--}4.5$  for pH values in the range 9.0–11.5. Note that  $[HS^-]$  can be found from the calibration curve without direct use of the debated values of  $\log K_1^H$ .

These experiments were repeated with use of the amplifier system (Fig. 1). The e.m.f. was measured between the glass electrode (input A, electrode potential  $E_G = \text{const}_3 + 0.0591 \log[H^+]$ ), and the sulphide electrode (input B). The potential of the sulphide electrode was amplified with a gain of 2. Both potentials were referred to the potential of the Ag/AgCl reference electrode (input C). The e.m.f. between socket out<sub>1</sub> and socket out<sub>2</sub> is

$$\text{e.m.f.} = E_G - 2E_S \quad (5)$$

and substituting equation (4) into (5) gives

$$\text{e.m.f.} = \text{const}_4 - 0.0591 \text{p}[HS^-] \quad (6)$$

The e.m.f. given by equation (6) is independent of pH when the differential amplifier is used in the appropriate pH-range 9–12.

The calibration plots were both linear, with a slope of  $-56 \text{ mV}/\text{p}[HS^-]$  for the Radelkis and  $-58 \text{ mV}/\text{p}[HS^-]$  for the Radiometer glass electrode. These values are close to the theoretical value of  $-59.1 \text{ mV}/\text{p}[HS^-]$  given by equation (6). The method also gives the equilibrium concentration of  $HS^-$ , but does not require a separate pH measurement.

#### Calibration of the glass-sulphide-selective electrode measuring cell in acidic solution

The advantages of an  $H^+$ -selective glass-sulphide-selective measuring cell have been studied indepen-

dently by Frevert<sup>12</sup> and Gulens.<sup>13</sup> At  $\text{pH} < 5$ ,  $T_s$  is  $\sim [\text{H}_2\text{S}]$  and equation (2) can be simplified to

$$[\text{S}^{2-}] = \frac{T_s}{K_1^H K_2^H [\text{H}^+]^2} \quad (7)$$

The e.m.f. measured between the glass and sulphide electrodes can then be expressed as

$$\text{e.m.f.} = \text{const}_5 - 0.0296 \text{p}[\text{H}_2\text{S}] \quad (8)$$

Although the only condition required for the validity of this equation is  $\text{pH} < 5$ , the behaviour of this special cell when there are significant changes in  $\text{pH}$  was not investigated in detail. In the case of natural water samples, the glass electrode has a constant potential because of the nearly constant  $\text{pH}$ .<sup>12</sup> In the samples measured by Gulens,<sup>13</sup> the  $\text{pH}$  was adjusted to the same value by a diffusion process.

In our work, standard sodium sulphide solution was added to  $0.5M$  potassium nitrate/ $0.03M$  ascorbic acid mixture. The  $\text{pH}$  was adjusted with concentrated hydrochloric acid or sodium hydroxide solution and the e.m.f. measured with the glass electrode-sulphide electrode cell. At  $T_s = 10^{-3}M$ , the e.m.f. was constant for  $\text{pH} < 5$ .

Various sulphide antioxidant buffers have been investigated in alkaline solutions. To increase the sensitivity of the sulphide-selective electrodes,<sup>14</sup> we repeated the experiments in acidic solutions. Calibration graphs were obtained for  $0.5M$  potassium nitrate with and without ascorbic acid and diamino-cyclohexanetetra-acetic acid (DCTA) present, by titration with sodium sulphide solution to cover the range  $\text{p}T = 2.5-7$  (Fig. 2). The concentration of the acids was kept low, allowing a definite change in  $\text{pH}$  during the titration, from  $\text{pH} \sim 2.5$  to  $\text{pH} \sim 4.5$ .

The calibration graphs have a Nernstian response at  $\text{p}T_s < 5$  for each system, but a deviation was found at lower concentrations of sulphide. The range of Nernstian response was extended by the addition of

ascorbic acid (2) or DCTA (3). The calibration graph was linear up to  $\text{p}T_s \sim 6$  in the solution containing both ascorbic acid and DCTA (4). The nearly theoretical slope,  $-30.5 \text{ mV/p}T_s$ , demonstrates the advantage of using a cell without liquid-junction potential.<sup>15</sup> It should be stressed that the potentials of both electrodes of the cell change during the titration, but their changes are parallel and the e.m.f. depends only on  $T_s$  (or  $[\text{H}_2\text{S}]$ ).

#### Potentiometric titrations with the glass electrode-sulphide electrode measuring cell in acidic solution

For the determination of  $\text{S}^{2-}$  concentration by potentiometric titration or by direct potentiometry with an ion-selective electrode, several methods are available.<sup>3,16-18</sup> Since a number of metal ions form insoluble sulphides<sup>19</sup> there is a possibility of determining them by precipitation titration monitored with a sulphide-selective indicator electrode. However, most of these metal ions form hydroxo-complexes or hydroxides in the alkaline solutions which are normally considered best when the sulphide electrode is used. A glass electrode-sulphide electrode measuring cell working in acidic solution can overcome this problem.

Acidified silver nitrate solutions were titrated with sodium sulphide (Fig. 3) and with potassium hydrogen sulphide solutions (Fig. 4). There is practically no  $\text{pH}$  change until the end-point of the precipitation reaction ( $2\text{Ag}^+ + \text{S}^{2-} \rightleftharpoons \text{Ag}_2\text{S}$ ) in the case of sodium sulphide as titrant, but the acid concentration increases throughout the titration with potassium hydrogen sulphide ( $2\text{Ag}^+ + \text{HS}^- \rightleftharpoons \text{Ag}_2\text{S} + \text{H}^+$ ). When the precipitation is complete, there is a  $\text{pH}$  increase due to hydrolysis of  $\text{S}^{2-}$  ( $\text{S}^{2-} + \text{H}_2\text{O} \rightleftharpoons \text{HS}^- + \text{OH}^-$ ) or  $\text{HS}^-$  ( $\text{HS}^- + \text{H}_2\text{O} \rightleftharpoons \text{H}_2\text{S} + \text{OH}^-$ ). To keep the  $\text{pH}$  below 5 until about 100% excess of titrant has been

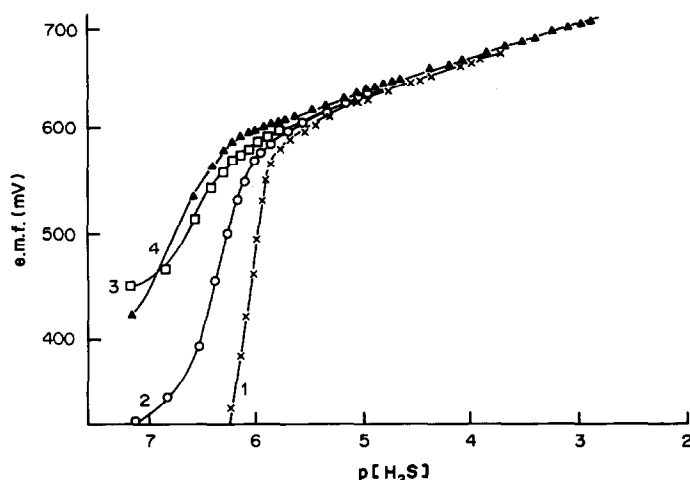


Fig. 2. E.m.f. values between glass and sulphide-selective electrodes vs.  $\text{p}[\text{H}_2\text{S}]$  in  $0.5M$   $\text{KNO}_3$  with (1)  $0.01M$  acetic acid, (2)  $0.01M$  ascorbic acid, (3)  $0.01M$  acetic acid +  $0.05M$  DCTA, (4)  $0.01M$  ascorbic acid +  $0.05M$  DCTA.

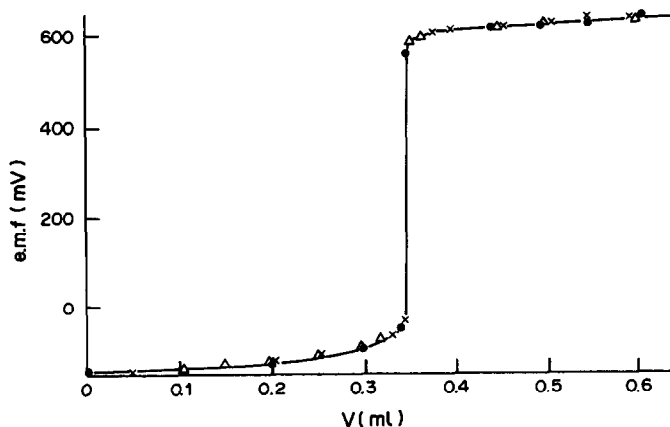


Fig. 3. Titrations of 20 ml of 0.01840M  $\text{AgNO}_3 + 0.03\text{M HNO}_3$  with  $\text{Na}_2\text{S}$  titrant.

added, nitric acid (0.03M) was added to the samples. Figures 3 and 4 show sharp breaks and good reproducibility, demonstrating the applicability of the measuring cell. The sulphide concentrations calculated from the inflexion points were found to be close to the results of iodometric titrations<sup>6</sup> and these concentrations were used for the potentiometric titrations of lead and bismuth solutions.

To compare the titration curve recorded with a conventional sulphide electrode–Ag/AgCl double-junction reference electrode measuring cell, silver nitrate solutions with different excesses of nitric acid were titrated with sodium sulphide. Typical titration curves are shown in Fig. 5. In the case of titration curve 1, the excess of nitric acid is relatively high and the shape of the curve is not strongly affected by the pH change resulting from the excess of  $\text{S}^{2-}$ . When the acid concentration was decreased (titration curves 2 and 3), the pH increased markedly during the titration and the titration curves became more complicated. The second and third inflexion points at about  $-400$  and  $-700$  mV relate to the protonation reactions of  $\text{S}^{2-}$  ( $2\text{H}^+ + \text{S}^{2-} \rightleftharpoons \text{H}_2\text{S}$  and  $\text{H}_2\text{S} + \text{S}^{2-} \rightleftharpoons 2\text{HS}^-$ , respectively). (These curves

demonstrate the operation of the sulphide electrode as a pH-sensor).

Lead nitrate solutions were also titrated in acidic solution. Typical titration curves are shown in Fig. 6. The starting potentials are different for the 0.01M lead solutions (curves 1–3) because of the slightly different concentrations of acetic acid used, but the end-points are very close to each other. The calculated concentration of lead agrees well with the concentration measured by complexometric titration.

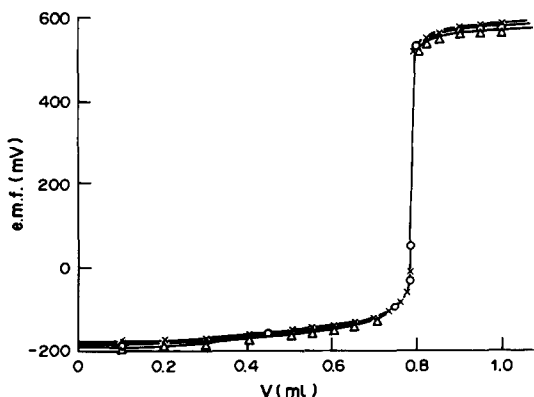


Fig. 4. Titrations of 20 ml of 0.01905M  $\text{AgNO}_3 + 0.03\text{M HNO}_3$  with KHS titrant.

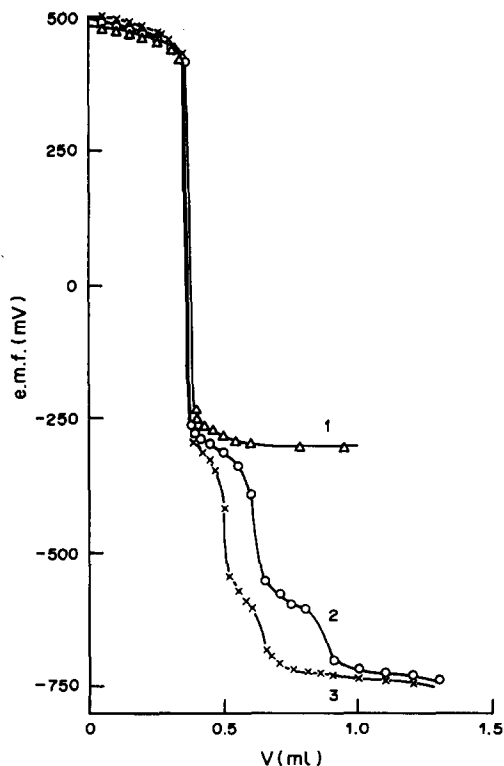


Fig. 5. Titration of 20 ml of 0.01905M  $\text{AgNO}_3$  with  $\text{Na}_2\text{S}$ . Measuring cell: sulphide–Ag/AgCl reference electrodes (connected to socket R). Approximate concentration of  $\text{HNO}_3$ : (1)  $3 \times 10^{-2}\text{M}$ , (2)  $1 \times 10^{-2}\text{M}$ , and (3)  $5 \times 10^{-3}\text{M}$ .



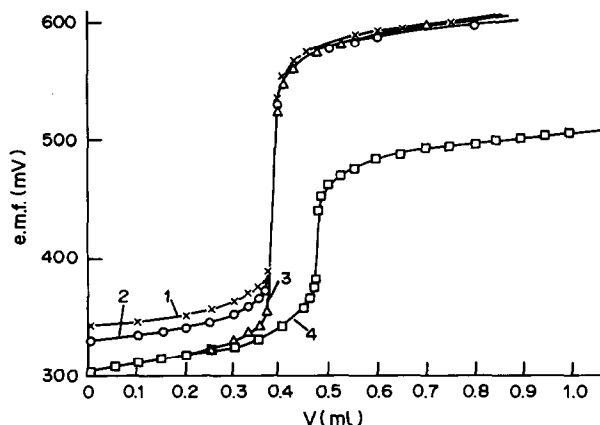


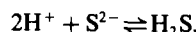
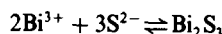
Fig. 6. Titration of 20 ml of  $0.01019M$   $Pb(NO_3)_2 + 7 \times 10^{-3}M$  acetic acid with  $0.5294M$   $Na_2S$  (1-3). Calculated concentration of  $Pb^{2+}$  is  $0.01017M$ , and the error is  $-0.2\%$ . Titration of 210 ml of  $4.76 \times 10^{-5}M$   $Pb(NO_3)_2 + 0.04M$  acetic acid with  $0.01M$   $Na_2S$  (4). Calculated concentration of  $Pb^{2+}$  is  $4.84 \times 10^{-5}M$ , and error is  $+1.7\%$ .

The inflexion point of the titration curve coincides with the end-point of the reaction  $Pb^{2+} + S^{2-} \rightleftharpoons PbS$ , and thus the cell is suitable for end-point indication.<sup>20,21</sup>

Acceptable titration curves could also be recorded for very dilute solutions, as shown in Fig. 6 (curve 4, for a lead concentration that is 1-2 orders of magnitude lower than that determinable by conventional titration methods).

To demonstrate the application of this cell to the determination of an easily hydrolysed metal ion, bismuth solutions were titrated at different pH values (Fig. 7). The position of the inflexion point varied with the pH, and an increasing positive error was found with increasing pH. Bismuth(III) is known to form very complicated multinuclear hydroxo-complexes,<sup>22</sup> and the following competing reactions

can be considered to occur during the titration:



The optimum pH for the determination was found to be  $\sim 1$ , because at this pH the hydrolysis of  $Bi^{3+}$  is suppressed and the formation of  $Bi_2S_3$  is stoichiometric. The end-point of the titration then coincides with the inflexion point of the titration curve. This low pH is optimum even though the equilibrium concentration of  $S^{2-}$  in the system is decreased by protonation.

Determination of bismuth in the range  $10^{-3}$ - $10^{-2}M$  at pH  $\sim 1$  was possible with a relative error of 1%.

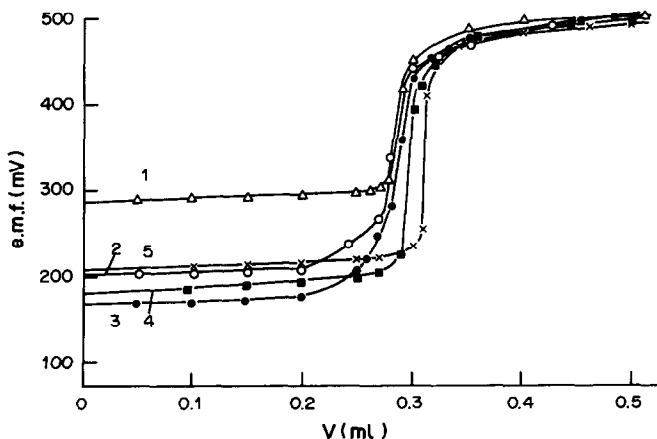


Fig. 7. Titration of 20 ml of  $0.005M$   $Bi(NO_3)_3$  with  $0.5681M$   $Na_2S$ . Starting pH of the samples: (1) 0.581, (2) 0.972, (3) 1.295, (4) 4.374 and (5) 4.61.

## REFERENCES

1. J. Koryta, *Anal. Chim. Acta*, 1986, **183**, 1.
2. E. Pungor and K. Tóth, *Analyst*, 1970, **95**, 1132.
3. T. Hseu and G. A. Rechnitz, *Anal. Chem.*, 1968, **40**, 1054.
4. R. J. Myers, *J. Chem. Educ.*, 1986, **63**, 687.
5. S. Licht and J. Manessen, *J. Electrochem. Soc.*, 1987, **134**, 918.
6. P. O. Bethge, *Anal. Chim. Acta*, 1954, **10**, 310.
7. A. I. Vogel, *Quantitative Inorganic Analysis*, 3rd Ed., Longmans, London, 1962.
8. G. Gran, *Analyst*, 1952, **77**, 661.
9. L. Zékány and T. Kiss, personal communication.
10. I. Tóth, L. Zékány and E. Brücher, *Polyhedron*, 1985, **4**, 279.
11. A. J. Ellis and R. M. Golding, *J. Chem. Soc.*, 1959, 127.
12. T. Frevert and H. Galster, *Schweiz. Z. Hydrol.*, 1978, **40**, 199; T. Frevert, *ibid.*, 1980, **42**, 255.
13. J. Gulens, H. D. Herrington, J. W. Thorpe, G. Mainprize, M. G. Cooke, P. D. Bello and S. MacDougall, *Anal. Chim. Acta*, 1982, **138**, 65.
14. M. G. Glaister, G. J. Moody, T. Nach and J. D. R. Thomas, *ibid.*, 1984, **165**, 281.
15. M. J. Brand and G. A. Rechnitz, *Anal. Chem.*, 1970, **42**, 616.
16. M. Mascini and A. Liberti, *Anal. Chim. Acta*, 1970, **51**, 231.
17. S. Ikeda, H. Satake, T. Hisano and T. Terazawa, *Talanta*, 1972, **19**, 1654.
18. T. M. Florence and Y. J. Farrer, *Anal. Chim. Acta*, 1980, **116**, 175.
19. *Comprehensive Inorganic Chemistry*, Vol. 2, p. 932. Pergamon Press, Oxford 1973.
20. L. Meites and J. A. Goldman, *Anal. Chim. Acta*, 1964, **30**, 18.
21. P. W. Carr, *Anal. Chem.*, 1971, **43**, 425.
22. C. F. Baes, Jr. and R. E. Mesmer, *The Hydrolysis of Cations*, Wiley, New York, 1976.

# A COMPARATIVE STUDY OF THE EFFECT OF *o*-NITROPHENYL OCTYL ETHER AND *o*-NITROPHENYL PENTYL ETHER AS PLASTICIZERS ON THE RESPONSE AND SELECTIVITY OF CARRIER-BASED LIQUID MEMBRANE ION-SELECTIVE ELECTRODES

ABDULRAHMAN S. ATTIYAT

Department of Chemistry, Yarmouk University, Irbid, Jordan

GARY D. CHRISTIAN

Department of Chemistry, BG-10, University of Washington, Seattle, WA 98195, U.S.A.

JOHNNY L. HALLMAN and RICHARD A. BARTSCH

Department of Chemistry and Biochemistry, Texas Tech University, Lubbock, TX 79409, U.S.A.

(Received 12 February 1988. Accepted 14 May 1988)

**Summary**—Lithium, potassium and caesium-selective microelectrodes were prepared by coating the tips of preconditioned silver wires, incorporated in a flow-cell, with PVC membranes containing four different ionophores. A dicarboxamide, a 14-crown-4 carboxylic acid, benzo-18-crown-6 and di-(*tert*-butylbenzo)-21-crown-7 ionophores were used in the electrode matrix. The first two ionophores were used in lithium ion-selective electrodes, the third in a potassium ion electrode and the fourth in a caesium ion electrode. Two different plasticizers, *o*-nitrophenyl octyl ether (NPOE) and *o*-nitrophenyl pentyl ether (NPP'E) were used. Enhancement of the signal and the slope of the calibration curve and improvement of the curve linearity were observed in all cases when NPP'E was used as plasticizer. A general trend of enhanced selectivity of the electrodes incorporating crown ether ionophores was also observed when NPP'E was the plasticizer.

Ion-selective electrodes based on neutral carriers have attracted the attention of many researchers in the last decade. Neutral carriers have been utilized to prepare electrodes selective for certain metal ions, especially the alkali and alkaline-earth metal cations.<sup>1-5</sup> Different neutral ionophores have been used for different cations.<sup>3-6</sup> The electrode response and selectivity for a certain metal ion relative to another depend on the nature and characteristics of the ionophore and on the exact composition of the electrode matrix.<sup>4</sup> The selectivity coefficient values also depend on the composition of the solution to which the membrane is exposed and the method of measurement and calculation of the selectivity coefficients.<sup>4,5</sup>

It has been found that the selectivity of a certain ionophore for lithium ion changes with variation of the plasticizer and whether potassium tetrakis(*p*-chlorophenyl)borate is present.<sup>4,6</sup> Discussion of the influence of the electrode composition has been presented.<sup>1,2,7</sup> The selectivity can be significantly altered by changing the relative proportions of the electrode components.<sup>7</sup> One of the major components of the electrode membrane is the plasticizer, which mainly acts as a solvent for the membrane.<sup>2</sup> Various plasticizers have been used in different metal ion-selective electrode matrices. *o*-Nitrophenyl octyl

ether (NPOE), a widely used plasticizer, has been employed in ion-selective electrodes for hydrogen, sodium,<sup>3</sup> lithium,<sup>8-12</sup> potassium,<sup>13,14</sup> calcium,<sup>3</sup> strontium and lead ions.<sup>15</sup> Dipentyl phthalate (DPP) has been used for potassium ion-selective electrodes.<sup>16-18</sup> Dioctyl phenyl phosphate (DOPP), dioctyl 3-nitrophenyl phosphonate (N-DOPP),<sup>19</sup> dipentyl phthalate (DPP), tris-(2-ethylhexyl) phosphate (TEHP), dioctyl phthalate (DOP) and bis-(2-ethylhexyl) sebacate<sup>12,18</sup> have been used in membranes selective for lithium ions. *o*-Nitrophenyl phenyl ether (NPPE) has been used in membranes selective for lithium<sup>12</sup> and barium ions.<sup>20</sup> Dioctyl sebacate has been used with different ring-size crown ethers in ion-selective electrodes for sodium and potassium ions.<sup>21</sup>

In this study, two plasticizers, *o*-nitrophenyl octyl ether (NPOE) and *o*-nitrophenyl pentyl ether (NPP'E) were used with four ionophores (1-4) to construct electrode membranes. A comparative study was made of the performance of the electrodes made with the two plasticizers.

## EXPERIMENTAL

The 14-crown-4 carboxylic acid (ionophore 1) was synthesized according to the reported procedure.<sup>22</sup> The ionophore *N,N*-dicyclohexyl-,*N',N'*-disobutyl-*cis*-cyclo-

hexane-1,2-dicarboxamide (ionophore 2) was supplied by Professor W. Simon. Ionophore 3, benzo-18-crown-6, was synthesized according to the reported procedure.<sup>23</sup> Ionophore 4, di-(*tert*-butylbenzo)-21-crown-7 synthesis will be reported elsewhere.<sup>24</sup> Tetrahydrofuran (THF), obtained from EM Science, Cherry Hill, NJ, was used to dissolve the electrode matrix. Poly(vinyl chloride) (PVC) (high molecular weight) was obtained from Fluka AG, and *o*-nitrophenyl octyl ether (NPOE) and potassium tetrakis-(*p*-chlorophenyl)borate were from Specialty Organics, Inc., Irwindale, California. *o*-Nitrophenyl pentyl ether (NPP'E) was synthesized as described below. Caesium, rubidium, potassium, sodium, lithium, strontium, calcium, and magnesium chlorides were dried at 140° for 48 hr prior to the preparation of standard solutions. Distilled demineralized water was used to prepare all standard solutions.

#### Synthesis of *o*-nitrophenyl pentyl ether

To 75.0 g (0.54 mole) of dry *o*-nitrophenol dissolved in 550 ml of dry acetone, 75 g of anhydrous potassium carbonate and 89.8 g (0.59 mole) of 1-bromopentane were added. The reaction mixture was refluxed for 60 hr and then evaporated under reduced pressure. To the residue 0.6 l. of water was added and the mixture was extracted with dichloromethane solution (3 × 200 ml). The organic layer was washed with 10% aqueous sodium hydroxide solution (3 × 350 ml) and then water (400 ml). After drying over anhydrous magnesium sulphate, the dichloromethane was evaporated under reduced pressure. Vacuum distillation of the residue gave 67.5 g (60%) of a yellow liquid with b.p. 137–140°/0.5 mmHg, literature value<sup>25</sup> b.p. 150–153°/9 mmHg.

#### Apparatus

A flow-injection analysis system with a flow-cell incorporating a series of silver wire electrodes, similar to that reported earlier,<sup>26</sup> was used in this study. A set of electrode membranes was prepared by completely dissolving 1.4 mg of each ionophore, 65 mg of NPOE, 33 mg of PVC, and an amount of potassium tetrakis(*p*-chlorophenyl)borate equivalent to half the molar amount of the ionophore, in 350  $\mu$ l of tetrahydrofuran (THF). Another set of electrode matrices was similarly prepared with 65 mg of NPP'E. Three 2- $\mu$ l portions of the matrix solution were applied to the tip of a preconditioned<sup>12</sup> silver wire, by means of a capillary pipette to give a thin membrane. After the solvent had evaporated, the flow channel was sealed by a plastic sheet with double-sided adhesive tape. The flow-cell was then introduced into the flow system and the electrodes were conditioned before use, by being left in contact with a static carrier-stream solution (14mM sodium chloride) overnight. A silver chloride electrode mounted downstream in the flow-cell was used as a reference electrode.

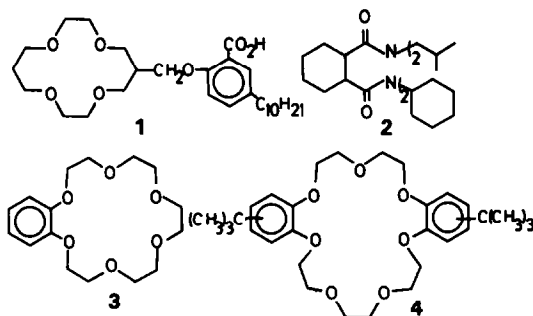
A Beckman 3500 digital pH-meter was used to monitor the potentials of the electrodes. It was connected to a strip-chart recorder (Linear Co.) to record the FIA signals. Air-pressurized reference and carrier-stream reservoirs were used in connection with flowmeters and debubblers.

#### Procedure

A measurement procedure similar to that reported earlier<sup>26</sup> was used except that the carrier stream and the reference stream were both 14mM sodium chloride, and the flow-rates were 1 ml/min for the carrier stream and 0.2 ml/min for the reference stream. The 14 mM sodium chloride carrier was chosen to represent the sodium background corresponding to injection of a ten-fold diluted serum sample. The sample volume was 200  $\mu$ l, to eliminate dispersion at the middle of the sample plug, as previously demonstrated.<sup>9</sup>

Standard solutions of 0.2, 0.5, 10, 20, 50, 100 and 200 mM lithium chloride in distilled demineralized water were injected and the potentiometric FIA signals of each solution were

recorded for electrodes incorporating ionophores 1 and 2, and used to construct calibration curves for lithium. Similar standard solutions of potassium chloride and caesium chloride were used to construct calibration curves for electrodes containing ionophores 3 and 4, respectively. For determination of selectivity coefficients, standard solutions of 100mM caesium chloride, rubidium chloride, potassium chloride, sodium chloride, lithium chloride, strontium chloride, calcium chloride and magnesium chloride were used.



#### Calculation of the potentiometric selectivity coefficients

The selectivity coefficients were calculated by two methods.<sup>26,27</sup> In method 1 (the separate solution method), equal concentrations of pure solutions of the primary and the interfering ions were injected separately into the carrier stream. The potentiometric FIA signal of each solution was recorded. The selectivity coefficient was calculated from the equation:<sup>27</sup>

$$\log k_{A,B}^{\text{pot}} = \frac{E_B - E_A}{S} + \left(1 - \frac{Z_A}{Z_B}\right) \log [A] \quad (1)$$

where  $E_B$  and  $E_A$  are the FIA signals for the primary (A) and the interfering (B) ions, respectively,  $S$  is the slope of the calibration curve for the primary ion,  $Z_A$  and  $Z_B$  are the charges of the primary and the interfering ions, respectively. Since the sample volume is large enough to prevent dispersion at the middle of the sample plug, the height of the FIA signal represents the signal of the pure solutions.

In method 2,<sup>26</sup> pure solutions of the interfering ions of known concentrations were injected into the carrier streams and the potential responses were recorded. The primary ion concentrations corresponding to these potentials were obtained from the calibration graphs for the primary ions. The selectivity coefficients were then calculated according to the equation:<sup>26</sup>

$$k_{A,B}^{\text{pot}} = \frac{C_A}{C_B^{1/Z_B}} \quad (2)$$

## RESULTS AND DISCUSSION

#### Calibration graphs

Figure 1 depicts the calibration graphs for lithium, obtained by using electrodes made with ionophore 1 and the two plasticizers. The use of NPP'E enhanced both the FIA potentiometric signal and the slope of the calibration plot. Figure 2 shows the corresponding lithium calibration graphs for electrodes made with ionophore 2 and the two plasticizers. The use of NPP'E again increases the slope and slightly improves the signal. Figure 3 shows the calibration graphs for the determination of potassium ion with electrodes made with ionophore 3. The linearity and the slope of the curve are preserved when the plas-

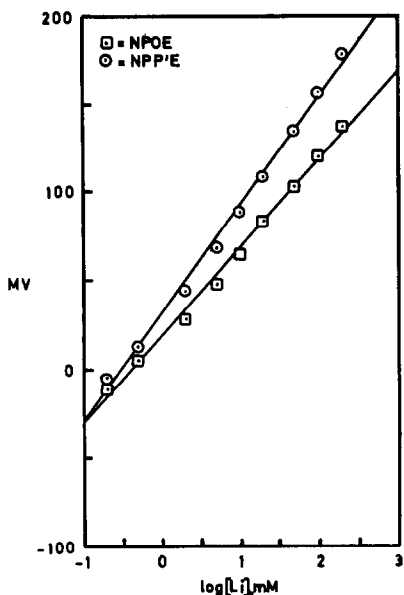


Fig. 1. Calibration graphs for lithium, with ionophore 1, and NPOE (□) and NPP'E (○) as plasticizers.

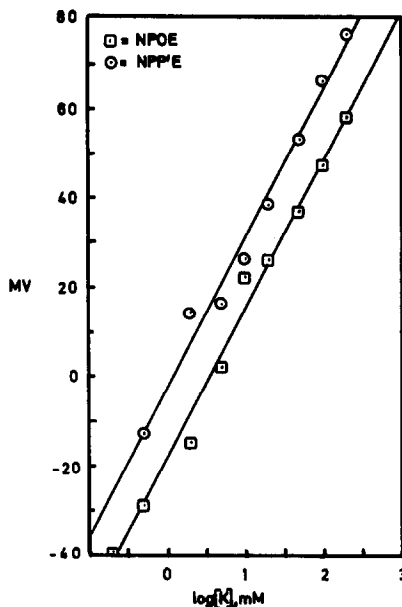


Fig. 3. Calibration graphs for potassium, with ionophore 3, and NPOE (□) and NPP'E (○) as plasticizers.

ticizer is changed from NPOE to NPP'E, but the signal is enhanced. Figure 4 depicts the calibration graphs for the determination of caesium ion by use of electrodes made with ionophore 4. It is seen that the use of NPP'E greatly improves the linearity, increases the slope and enhances the potentiometric FIA signal.

It is clear from these results that the use of NPP'E as a plasticizer instead of NPOE improves the sensitivity of the sensors.

#### Selectivity coefficients

Table 1 shows the selectivity coefficients and their reciprocals for lithium relative to caesium, rubidium, potassium, sodium, strontium, calcium and magnesium with ionophores 1 and 2. The values of the selectivity coefficients determined by the two methods are reasonably similar in most instances. With ionophore 1, the selectivity for lithium relative to the large ions (Cs, Sr, Rb) is decreased by the use of NPP'E as plasticizer, but increased with respect to the smaller ions (K, Na and Mg). This indicates an enhancement

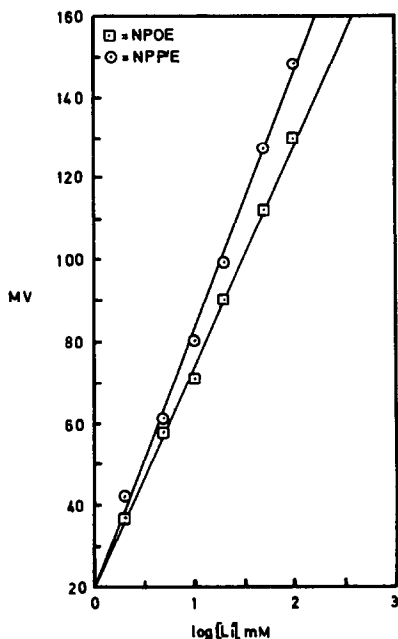


Fig. 2. Calibration graphs for lithium, with ionophore 2, and NPOE (□) and NPP'E (○) as plasticizers.

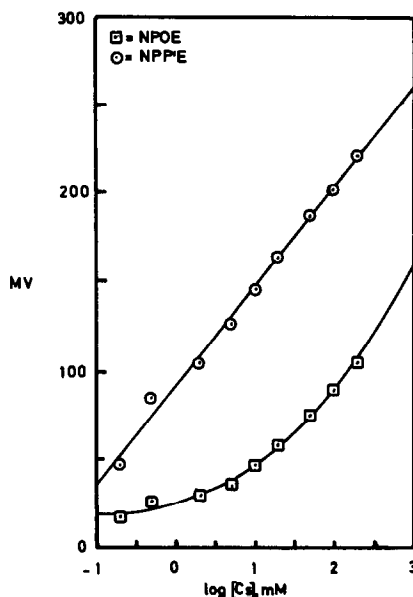


Fig. 4. Calibration graphs for caesium, with ionophore 4, and NPOE (□) and NPP'E (○) as plasticizers.

Table 1. Selectivity coefficients and their reciprocals for lithium ion with respect to other metal cations, with ionophores 1 and 2 and NPOE and NPP'E plasticizers

Ionophore	Plasticizer	Selectivity	Cs		Rb		K		Na		Sr		Ca		Mg	
			M <sub>1</sub>	M <sub>2</sub>	M <sub>1</sub>	M <sub>2</sub>	M <sub>1</sub>	M <sub>2</sub>	M <sub>1</sub>	M <sub>2</sub>	M <sub>1</sub>	M <sub>2</sub>	M <sub>1</sub>	M <sub>2</sub>	M <sub>1</sub>	M <sub>2</sub>
1	NPOE	$k_{Li^+M}^{pot}$	$1.6 \times 10^{-2}$	$1.9 \times 10^{-2}$	$1.3 \times 10^{-2}$	$1.3 \times 10^{-2}$	$1.4 \times 10^{-2}$	$1.7 \times 10^{-2}$	$2.3 \times 10^{-2}$	$2.9 \times 10^{-2}$	$2.5 \times 10^{-3}$	$2.8 \times 10^{-3}$	$5.0 \times 10^{-3}$	$6.2 \times 10^{-3}$	$4.6 \times 10^{-4}$	$3.2 \times 10^{-4}$
		$\frac{1}{k_{Li^+M}^{pot}}$	62	53	77	77	71	59	43	34	400	360	200	160	2200	3100
1	NPP'E	$k_{Li^+M}^{pot}$	$3.3 \times 10^{-3}$	$4.5 \times 10^{-3}$	$2.0 \times 10^{-3}$	$1.0 \times 10^{-3}$	$1.3 \times 10^{-3}$	$1.6 \times 10^{-3}$	$2.0 \times 10^{-3}$	$2.8 \times 10^{-3}$	$3.0 \times 10^{-3}$	$3.6 \times 10^{-3}$	$1.0 \times 10^{-2}$	$1.4 \times 10^{-2}$	$3.3 \times 10^{-4}$	*
		$\frac{1}{k_{Li^+M}^{pot}}$	30	22	50	100	77	62	50	36	330	280	100	71	3000	*
2	NPOE	$k_{Li^+M}^{pot}$	$1.8 \times 10^{-2}$	$5.7 \times 10^{-3}$	$1.2 \times 10^{-2}$	$6.8 \times 10^{-3}$	$1.0 \times 10^{-2}$	$4.3 \times 10^{-3}$	$1.3 \times 10^{-2}$	$1.1 \times 10^{-2}$	$7.9 \times 10^{-3}$	$8.4 \times 10^{-3}$	$8.6 \times 10^{-3}$	$9.0 \times 10^{-3}$	$2.6 \times 10^{-3}$	*
		$\frac{1}{k_{Li^+M}^{pot}}$	56	180	83	150	100	230	77	90	130	120	110	380	†	
2	NPP'E	$k_{Li^+M}^{pot}$	$3.7 \times 10^{-2}$	$1.6 \times 10^{-2}$	$2.2 \times 10^{-2}$	$1.4 \times 10^{-2}$	$1.5 \times 10^{-2}$	$1.3 \times 10^{-2}$	$2.0 \times 10^{-2}$	$2.0 \times 10^{-2}$	$2.7 \times 10^{-2}$	$3.2 \times 10^{-2}$	$3.8 \times 10^{-2}$	$4.6 \times 10^{-2}$	$1.3 \times 10^{-2}$	$1.4 \times 10^{-3}$
		$\frac{1}{k_{Li^+M}^{pot}}$	27	62	45	71	67	77	50	50	37	31	26	22	77	710

M<sub>1</sub>: Method 1.M<sub>2</sub>: Method 2.\*Less than  $2.0 \times 10^{-4}$ .

†Greater than 5000.

Table 2. Selectivity coefficients and their reciprocals for potassium ion with respect to other metal cations, with ionophore 3 and NPOE and NPP'E plasticizers

Ionophore	Plasticizer	M		Cs		Rb		Na		Li		Sr		Ca		Mg	
		Selectivity	$k_{K,M}^{pot}$	$M_1$	$M_2$	$M_1$	$M_2$	$M_1$	$M_2$	$M_1$	$M_2$	$M_1$	$M_2$	$M_1$	$M_2$	$M_1$	$M_2$
3	NPOE	$k_{K,M}^{pot}$	7.6	8.3	1.6	1.4	1.4	0.28	0.24	0.53	0.45	2.8	4.0	1.4	1.6	$6.8 \times 10^{-3}$	$5.9 \times 10^{-2}$
		$\frac{1}{k_{K,M}^{pot}}$	0.13	0.12	0.62	0.71	3.6	4.2	1.9	2.2	0.36	0.25	0.71	0.62	15	17	
3	NPP'E	$k_{K,M}^{pot}$	6.6	5.3	1.6	1.6	$1.9 \times 10^{-2}$	$2.0 \times 10^{-2}$	$4.0 \times 10^{-2}$	$3.9 \times 10^{-2}$	15	9.3	2.9	3.0	$1.6 \times 10^{-3}$	$3.2 \times 10^{-3}$	
		$\frac{1}{k_{K,M}^{pot}}$	0.15	0.19	0.62	0.62	53	50	25	26	$6.6 \times 10^{-2}$	0.11	0.34	0.33	620	310	

M<sub>1</sub>: Method 1.  
M<sub>2</sub>: Method 2.

Table 3. Selectivity coefficients and their reciprocals for caesium ion, with respect to other metal cations, with ionophore 4 and NPOE and NPP'E plasticizers

Ionophore	Plasticizer	M		Rb		K		Na		Li		Sr		Ca		Mg	
		Selectivity	$k_{Cs,M}^{pot}$	$M_1$	$M_2$	$M_1$	$M_2$	$M_1$	$M_2$	$M_1$	$M_2$	$M_1$	$M_2$	$M_1$	$M_2$	$M_1$	$M_2$
4	NPOE	$k_{Cs,M}^{pot}$	0.31	0.30	0.17	0.19	0.19	$5.9 \times 10^{-3}$	$3.9 \times 10^{-3}$	$2.5 \times 10^{-3}$	$1.6 \times 10^{-3}$	$6.0 \times 10^{-3}$	$6.6 \times 10^{-3}$	$1.6 \times 10^{-3}$	$8.9 \times 10^{-4}$	$9.3 \times 10^{-4}$	
		$\frac{1}{k_{Cs,M}^{pot}}$	3.2	3.3	5.9	5.3	170	260	400	620	170	150	620	1100			
4	NPP'E	$k_{Cs,M}^{pot}$	1.0	1.0	0.35	0.35	$2.0 \times 10^{-3}$	$2.5 \times 10^{-3}$	*	$4.3 \times 10^{-4}$	*	$3.3 \times 10^{-4}$	*	$2.0 \times 10^{-4}$			
		$\frac{1}{k_{Cs,M}^{pot}}$	1.0	1.0	2.8	2.8	500	400	†	2300	†	3000	†	5000			

M<sub>1</sub>: Method 1.  
M<sub>2</sub>: Method 2.  
\*Less than  $2.0 \times 10^{-4}$ .  
†Greater than 5000.

of the selectivity for the larger ions when NPP'E is used as plasticizer. With ionophore **2**, the selectivity for lithium ion with respect to all other ions is poorer when NPP'E plasticizer is used.

Table 2 records the selectivity coefficients and their reciprocals for potassium relative to caesium, rubidium, sodium, lithium, strontium, calcium and magnesium ions, with ionophore **3** in the electrode matrix with both plasticizers. The selectivity for potassium is improved by using NPP'E as the plasticizer.

Table 3 shows the selectivity coefficients and their reciprocals for caesium with respect to rubidium, potassium, sodium, lithium, strontium, calcium and magnesium ions with electrodes incorporating ionophore **4** and both plasticizers. The selectivity for caesium relative to the other metal cations studied (except rubidium and potassium) was enhanced by the use of NPP'E as plasticizer.

#### CONCLUSION

The use of *o*-nitrophenyl pentyl ether (NPP'E) enhanced the signal, slope and linearity of the calibration graphs for all four ionophores used in the electrode matrices. However, the selectivity of ionophore **2** (a dicarboxamide) for lithium ion was decreased when NPP'E was used as plasticizer. On the other hand, this plasticizer generally enhanced the primary ion selectivity when used with crown ether ionophores. The combination of increased signal, better linearity and larger slope of the curve and enhanced selectivity leads to improved electrode performance.

*Acknowledgements*—The authors gratefully acknowledge the gift of ionophore **2** from Professor W. Simon. A. S. Attiyat gratefully acknowledges the support from the Council for International Exchange of Scholars (Fulbright Scholarship) and from Yarmouk University, Irbid, Jordan. R. A. Bartsch acknowledges support by the Division of Basic Chemical Sciences of the United States Department of Energy (Contract DE-AS05-30ER-10604).

#### REFERENCES

- D. Amman, W. E. Morf, P. Anker, P. C. Meier, E. Pretsch and W. Simon, *Ion-Selective Electrode Rev.*, 1983, **5**, 3.
- V. P. Y. Gadzekpo, G. J. Moody, J. D. R. Thomas and G. D. Christian, *ibid.*, 1986, **8**, 173.
- Neutral Ionophores for Ion-Selective Electrodes*, Fluka Chemical Corp., Ronkonkoma, New York.
- V. P. Y. Gadzekpo, J. M. Hungerford, A. M. Kadry, Y. A. Ibrahim, R. Y. Xie and G. D. Christian, *Anal. Chem.*, 1986, **58**, 1948.
- A. S. Attiyat, G. D. Christian, R. Y. Xie, X. Wen and R. A. Bartsch, *ibid.*, in the press.
- E. Metzger, D. Ammann, E. Pretsch and W. Simon, *Chimia*, 1984, **38**, 440.
- P. C. Meier, W. E. Morf, M. Laubli and W. Simon, *Anal. Chim. Acta*, 1984, **156**, 1.
- A. F. Zhukov, D. Erne, D. Ammann, M. Guggi, E. Pretsch and W. Simon, *ibid.*, 1981, **131**, 117.
- R. Y. Xie and G. D. Christian, *Anal. Chem.*, 1986, **58**, 1806.
- K. Kimura, H. Yano, S. Kitazawa and T. Shono, *J. Chem. Soc. Perkin Trans. II*, 1986, 1945.
- E. Metzger, R. Dohner, W. Simon, D. J. Vonderschmitt and K. Gautschi, *Anal. Chem.*, 1987, **59**, 1600.
- S. Kitazawa, K. Kimura, H. Yano and T. Shono, *Analyst*, 1985, **110**, 295.
- M. Yamauchi, A. Jyo and N. Ishibashi, *Anal. Chim. Acta*, 1982, **136**, 399.
- A. S. Attiyat, G. D. Christian, C. V. Cason and R. A. Bartsch, unpublished results.
- A. S. Attiyat, G. D. Christian, B. Strzelbicka, Z.-y. Yu, J. A. McDonough and R. A. Bartsch, unpublished results.
- O. Ryba and J. Petraněk, *Talanta*, 1976, **23**, 158.
- Idem*, *Electroanal. Chem. Interfac. Electrochem.*, 1973, **44**, 425.
- J. Petraněk and O. Ryba, *Anal. Chim. Acta*, 1974, **72**, 375.
- V. P. Y. Gadzekpo, G. J. Moody and J. D. R. Thomas, *Anal. Proc.* 1986, **23**, 62.
- P. H. V. Alexander, G. J. Moody and J. D. R. Thomas, *Analyst*, 1987, **112**, 113.
- T. M. Fyles and C. A. McGavin, *Anal. Chem.*, 1982, **54**, 2103.
- P. Czech, A. Czech, B. Son, H. K. Lee and R. A. Bartsch, *J. Heterocyclic Chem.*, 1986, **23**, 465.
- D. N. Reinhoudt, F. de Jong and H. P. M. Tomassen, *Tetrahedron Lett.*, 1979, 2067.
- R. A. Bartsch, Z.-y. Yu and J. A. McDonough, unpublished results.
- R. Nodzu, H. Watanabe, S. Kuwata, C. Nagaishi, K. Shibuya, T. Teramatsu, H. Arima, K. Kobayashi and M. Maizura, *J. Pharm. Soc. Japan*, 1952, **72**, 543.
- R. Y. Xie, V. P. Y. Gadzekpo, A. M. Kadry, Y. A. Ibrahim, J. Růžicka and G. D. Christian, *Anal. Chim. Acta*, 1986, **184**, 259.
- IUPAC, *Pure Appl. Chem.*, 1976, **48**, 129.



## METHODS FOR ANALYSIS OF THE MONONUCLEAR AND BINUCLEAR MANGANESE(III) CYANO-COMPLEXES

G. LOPEZ-CUETO\*

Analytical Chemistry Division, University of Alicante, Apdo. 99, 03080 Alicante, Spain

A. ALONSO-MATEOS

Department of Analytical Chemistry, University of Salamanca, 37008 Salamanca, Spain

C. UBIDE and G. DEL CAMPO-MARTINEZ

Department of Analytical Chemistry, University of Pais Vasco, 20017 San Sebastián, Spain

(Received 18 January 1988. Revised 27 May 1988. Accepted 10 July 1988)

**Summary**—Simple titrimetric methods are described for the analysis of potassium hexacyanomanganate(III) and of heptapotassium  $\mu$ -oxo-bis[pentacyanomanganate(III)] cyanide.  $Mn_2O(CN)_{10}^{6-}$  is determined by potentiometric titration with hexacyanoferrate(III). Cyanide is determined in both complexes by back-titration with Hg(II) and  $SCN^-$ , and manganese(III) is determined by back-titration with Fe(II) and  $MnO_4^-$ . The absorption spectra of both cyano-complexes in cyanide and in acidic solutions are also described, and their molar absorptivities are reported.

Two manganese(III) cyano-complexes are known as potassium salts. Potassium hexacyanomanganate(III) is obtained by the action of potassium cyanide on manganese(III) phosphate, according to the method of Lower and Fernelius,<sup>1</sup> and heptapotassium  $\mu$ -oxo-bis[pentacyanomanganate(III)] cyanide is obtained when potassium permanganate is reduced by potassium cyanide under appropriate conditions.<sup>2,3</sup> Cyanate appears to be the oxidation product of cyanide in the basic medium used.<sup>4</sup> Alternatively, both complexes may be prepared from the same solution by following the method reported by Brauer for obtaining potassium hexacyanomanganate(III).<sup>5,6</sup>

Analysis of  $K_3Mn(CN)_6$  and  $K_7[Mn_2O(CN)_{10}]CN$  gives very similar manganese, cyanide and potassium contents. This may be the reason why, before being characterized,<sup>2,3,7,8</sup> the binuclear compound was confused for a long time with the mononuclear one.<sup>9-14</sup> On the other hand, the preparation of the binuclear compound by oxidation of cyanide with permanganate gives a highly impure product.<sup>2</sup> This is why it would be useful to have analytical methods accurate enough to characterize these two manganese(III) cyano-complexes.

Cyanide in metal cyano-complexes is usually determined by decomposition with acid and distillation of HCN.<sup>15-17</sup> When applied to manganese(III) cyano-complexes, this method gives low results,<sup>12</sup> apparently because of partial oxidation of cyanide, probably to cyanogen, by manganese(III) during the acidic treatment at the high temperature used since the reaction is relatively slow at room temperature.<sup>6</sup> Manganese is generally determined by oxidation to permanganate

and titration with standard iron(II) solution. Obviously, this method gives the total manganese content, not the manganese(III) content.

In this paper we report simple titrimetric methods for determining the purity of the binuclear compound and for determining the cyanide and the manganese(III) in the two manganese(III) cyano-complexes. The purity of  $\mu$ -oxo-bis[pentacyanomanganate(III)] is determined by potentiometric titration with hexacyanoferrate(III) standard solution. Distillation is not necessary to determine the cyanide, and cyanide oxidation is avoided by prior reduction of the manganese(III). Manganese(III) is determined by addition of excess of iron(II) and back-titration with permanganate. The absorption spectra of both compounds in cyanide and in acidic solutions, as well as their molar absorptivities, are also reported, as they may be useful for both characterization and quantification.

### EXPERIMENTAL

#### Reagents

$K_3Mn(CN)_6$  and  $K_7[Mn_2O(CN)_{10}]CN$  were prepared by the procedure previously reported.<sup>6</sup> Solutions of  $Hg(NO_3)_2$ ,  $H_2O_2$ ,  $HNO_3$ ,  $Fe_2(SO_4)_3$ ,  $KSCN$ ,  $Fe(NH_4)_2(SO_4)_2 \cdot 6H_2O$ ,  $H_2SO_4$ ,  $H_3PO_4$ ,  $KMnO_4$ ,  $KCN$ ,  $NaCl$  and  $K_3Fe(CN)_6$  were prepared from analytical grade reagents. Distilled water was used throughout.

#### Apparatus

A Radiometer PHM 82 potentiometer with platinum and calomel electrodes was used for potentiometric titrations, and a Varian 634-S spectrophotometer with 1.0-cm silica cells, coupled with a Radiometer REC 80 Servograph recorder, was used for the spectrophotometric measurements.

\*Author for correspondence.

### Procedures

**Titration of  $\mu$ -oxo-bis[pentacyanomanganate(III)].** Dissolve 0.1–0.2 g of sample in 50 ml of 4M sodium cyanide/0.5M sodium chloride solution at a temperature of about 15° and titrate immediately with 0.01M potassium hexacyanoferrate(III), using potentiometric end-point detection with a platinum indicator electrode.

**Cyanide determination.** Weigh accurately 0.1 g of the sample and dissolve it in a few ml of distilled water. A brown precipitate of manganese(III) oxide will appear. Add 25 ml of 0.05M mercuric nitrate solution in 0.12M nitric acid, and then one drop of 10% hydrogen peroxide solution. Warm at 50–60° until the precipitate is completely dissolved. Cool to room temperature, add 1 ml of saturated iron(III) sulphate solution and titrate with 0.1M potassium thiocyanate. Near the end-point, add 5 ml of 6M nitric acid and continue the titration to the end-point.

**Manganese(III) determination.** Weigh accurately 0.1–0.2 g of sample and add it to 25 ml of 0.03M iron(II) solution. If a blue precipitate of mixed Mn–Fe cyanide compounds of the Prussian Blue type is formed,<sup>18</sup> warm slowly until the precipitate is redissolved. Cool, add 4–5 ml of concentrated phosphoric acid and titrate with 0.006M potassium permanganate. Iodometric titration can be used as an alternative for determining the manganese(III) content in the binuclear complex, but not in the mononuclear one.

**Other determinations.** The total manganese content can be determined by oxidation to permanganate, addition of excess of iron(II) and back-titration with permanganate. Potassium can be determined gravimetrically as potassium tetraphenylborate.

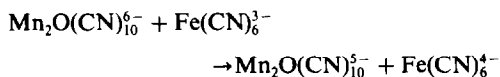
## RESULTS AND DISCUSSION

### Titrimetric determination of $\mu$ -oxo-bis[pentacyanomanganate(III)]

The binuclear complex is readily oxidized by hexacyanoferrate(III) in cyanide medium. A stoichiometric ratio close to 2:1 Mn(III):Fe(III) has been reported for this reaction.<sup>7</sup> The anodic oxidation of  $\text{Mn}_2\text{O}(\text{CN})_{10}^{6-}$  at a platinum electrode in cyanide solution gives two one-electron reversible waves which are due to the following electrode reactions:<sup>8</sup>



The half-wave potentials are about 0.03 and 0.60 V *vs.* SCE respectively. From these values and from the standard potential of the  $\text{Fe}(\text{CN})_6^{3-}/\text{Fe}(\text{CN})_6^{4-}$  couple, it can easily be deduced that, thermodynamically, the Mn(III) binuclear cyano-complex may be oxidized by hexacyanoferrate(III) only to the Mn(III)·Mn(IV) mixed oxidation state complex, according to the equation



but the further oxidation to the Mn(IV)·Mn(IV) complex is not possible. Since both systems are reversible, equilibrium potentials during the course of the reaction may easily be measured with the platinum indicator electrode, and the end-point may be conveniently located by potentiometry.

Two parallel reactions may act as sources of inter-

ference. On the one hand, the manganese(III) binuclear complex is unstable in cyanide solution, and slowly decomposes into the mononuclear complex. It has been found that the rate of this reaction decreases at high cyanide concentration and at high ionic strength, as well as at low temperature. On the other hand, free cyanide ion may be oxidized by hexacyanoferrate(III), the rate of this reaction being increased when the cyanide concentration as well as the ionic strength increase.<sup>19</sup> These two reactions cause interferences which have opposite effects, and therefore the experimental conditions for the titration must be selected so that the experimental errors are minimized. The results obtained by use of a 4.0M sodium cyanide/0.5M sodium chloride medium at about 15° were in good agreement with the coulometric value,<sup>20</sup> and this may be a useful rapid procedure for finding the purity of the binuclear complex. In Table 1 the results for seven different samples are shown. As can be seen, the compound is not pure, its  $\text{K}_7[\text{Mn}_2\text{O}(\text{CN})_{10}]\text{CN}$  content ranging between 92.5 and 97.0%. It has been detected, by voltammetric measurements in fresh cyanide solutions of  $\text{K}_7[\text{Mn}_2\text{O}(\text{CN})_{10}]\text{CN}$ , that the amount of  $\text{K}_3\text{Mn}(\text{CN})_6$  present is close to the impurity content of the solid binuclear complex, so  $\text{K}_3\text{Mn}(\text{CN})_6$  appears to be the principal impurity. Therefore, it can be expected that the analysis of impure samples for individual constituents does not give very significant differences from the theoretical values, in view of the very similar elemental composition of the two manganese(III) cyano-complexes.

### Analysis of the manganese(III) cyano-complexes

The proposed procedure for cyanide determination is based on addition of an excess of mercury(II) and back-titration with thiocyanate.<sup>21</sup> Decomposition of the Mn(III) cyano-complexes starts when the sample is dissolved in water, and proceeds rapidly with precipitation of manganese(III) oxide, while cyanide remains mostly in solution. The addition of mercury(II) completes the decomposition by complexation with the cyanide. Finally, Mn(III) is reduced in acidic medium with hydrogen peroxide to avoid both its oxidation of cyanide, and the presence of a precipitate, because manganese(II) remains in

Table 1. Determination of the  $\text{K}_7[\text{Mn}_2\text{O}(\text{CN})_{10}]\text{CN}$  content in samples of the binuclear complex (each result is the average of 3 determinations)

Sample	$\text{K}_7[\text{Mn}_2\text{O}(\text{CN})_{10}]\text{CN}$ , %
1	96.3 ± 0.2
2	92.5 ± 0.2
3	95.8 ± 0.2
4	96.1 ± 0.2
5	96.3 ± 0.3
6	93.8 ± 0.3
7	97.0 ± 0.2

Table 2. Determination of cyanide and manganese in manganese(III) cyano-complexes (each result is the average of 3-6 determinations)

Complex	CN <sup>-</sup> , %		Mn(III), %		Total Mn, %	
	Calc.	Found	Calc.	Found	Calc.	Found
K <sub>3</sub> Mn(CN) <sub>6</sub>	47.54	47.10 ± 0.03	16.73	16.76 ± 0.01	16.73	16.70 ± 0.01
K <sub>7</sub> [Mn <sub>2</sub> O(CN) <sub>10</sub> ]CN	41.74*	40.54 ± 0.13	16.02*	15.98 ± 0.01§	16.02*	15.94 ± 0.03
	41.95†		16.05†		16.05†	

\*Calculated for a pure sample.

†Calculated for a sample with 96.3% K<sub>7</sub>[Mn<sub>2</sub>O(CN)<sub>10</sub>]CN and 3.7% K<sub>3</sub>Mn(CN)<sub>6</sub>.

§Iodometric value: 15.99 ± 0.01 (3 determinations).

solution in acidic medium. In this way, the separation of HCN by distillation is made unnecessary and the procedure is simpler. The results obtained (Table 2) indicate that the method gives good reproducibility, and is more accurate for analysis of K<sub>3</sub>Mn(CN)<sub>6</sub> than of K<sub>7</sub>[Mn<sub>2</sub>O(CN)<sub>10</sub>]CN. Presumably, the oxidation of cyanide by manganese(III) cannot be completely avoided in the decomposition of the binuclear complex.

The results for determination of manganese(III) in pure K<sub>3</sub>Mn(CN)<sub>6</sub> and in the 96.3% pure K<sub>7</sub>[Mn<sub>2</sub>O(CN)<sub>10</sub>]CN (sample 1 in Table 1) by the back-titration method are given in Table 2, and are in good agreement with those obtained in the determination of total manganese. Furthermore, iodometric determination gave practically the same manganese(III) content in the K<sub>7</sub>[Mn<sub>2</sub>O(CN)<sub>10</sub>]CN. However, when iodometry was applied to K<sub>3</sub>Mn(CN)<sub>6</sub> significantly high results were obtained, which seems to indicate that iodide then undergoes aerial oxidation, probably by an induced reaction.

Gravimetric determination of potassium as the tetraphenylborate gives precise and accurate results: 35.69 ± 0.08% for K<sub>3</sub>Mn(CN)<sub>6</sub> (calc. 35.72%) and 39.81 ± 0.04% for K[Mn<sub>2</sub>O(CN)<sub>10</sub>]CN (calc. 39.81%).

#### Absorption spectra

The absorption spectra of cyanide and acid solutions of the two manganese(III) cyano-complexes are summarized in Table 3. When K<sub>3</sub>Mn(CN)<sub>6</sub> is dis-

solved in acidic medium, the spectrum obtained in the fresh solution is similar to that obtained in cyanide medium but rapidly changes owing to the formation of Mn(CN)<sub>6</sub><sup>2-</sup> and of Mn(H<sub>2</sub>O)<sub>6</sub><sup>3+</sup> by disproportionation of Mn(CN)<sub>6</sub><sup>3-</sup>. This reaction is rapid,<sup>6</sup> and therefore the spectrum described in Table 3 actually corresponds to the Mn(CN)<sub>6</sub><sup>2-</sup> complex. K<sub>7</sub>[Mn<sub>2</sub>O(CN)<sub>10</sub>]CN is unstable in both cyanide and acidic solutions. Nevertheless, the decomposition in acidic medium is very slow, and the decomposition rate in cyanide medium may be made conveniently low by use of high cyanide concentration. The spectra of the binuclear complex in both cyanide and acidic media have been recorded under conditions giving slow decomposition. The differences observed between the cyanide and acidic solutions of the binuclear complex are probably due to the predominance of protonated species in the acid medium. In fact, at low acidities the absorption bands at 231 and 373 nm decrease, the band at 462 nm increases and a band at 290 nm appears. Three isosbestic points at 235, 320 and 410 nm are produced in this spectral change. A value of about 0.1 may be estimated for the acid dissociation constant, although no attempt has been made to calculate a more precise value, because the experimental data have been obtained in only a narrow acidity range (between 0.05 and 1.0M sulphuric-acid), as the complex is hydrolysed at lower acidities. In view of the rather high acidity constant, it may be assumed that the proton is linked to one of the co-ordinated cyanide ions.

Table 3. Spectral characteristics of hexacyanomanganate(III) and  $\mu$ -oxo-bis[pentacyanomanganate(III)]. K<sub>3</sub>Mn(CN)<sub>6</sub>: 0.27M NaCN (cyanide solution); 0.05M H<sub>2</sub>SO<sub>4</sub> (acidic solution). K<sub>7</sub>[Mn<sub>2</sub>O(CN)<sub>10</sub>]CN: 1.0M NaCN/4.0M NaCl (cyanide solution); 1.0M H<sub>2</sub>SO<sub>4</sub> (acidic solution)

Complex	Cyanide solution		Acidic solution	
	$\lambda$ , nm	$\epsilon$ , l. mole <sup>-1</sup> . cm <sup>-1</sup>	$\lambda$ , nm	$\epsilon$ , l. mole <sup>-1</sup> . cm <sup>-1</sup>
K <sub>3</sub> Mn(CN) <sub>6</sub>	324	2.99 × 10 <sup>3</sup>	387	2.03 × 10 <sup>3</sup>
	268	1.63 × 10 <sup>3</sup>	292	3.78 × 10 <sup>3</sup>
	238	3.86 × 10 <sup>3</sup>	244	8.6 × 10 <sup>3</sup>
K <sub>7</sub> [Mn <sub>2</sub> O(CN) <sub>10</sub> ]CN	500	1.59 × 10 <sup>3</sup>	462	1.72 × 10 <sup>3</sup>
	370	3.93 × 10 <sup>4</sup>	373	1.32 × 10 <sup>4</sup>
	235	1.09 × 10 <sup>4</sup>	231	1.83 × 10 <sup>4</sup>

The spectrum described for the acidic solution of K<sub>3</sub>Mn(CN)<sub>6</sub> corresponds in fact to that of an Mn(IV) cyano-complex (see text).

## REFERENCES

1. J. A. Lower and W. C. Fernelius, *Inorg. Syn.*, 1946, **2**, 213.
2. R. F. Ziolo, R. H. Stanford, G. R. Rossman and H. B. Gray, *J. Am. Chem. Soc.*, 1974, **96**, 7910.
3. G. Trageser and H. H. Eysel, *Inorg. Nucl. Chem. Lett.*, 1978, **14**, 65.
4. A. M. Qureshi and S. A. Zubairi, *J. Chem. Soc. Pak.*, 1984, **6**, 83.
5. G. Brauer, *Química Inorgánica Preparativa*, Reverté, Barcelona, 1958.
6. G. López-Cueto and C. Ubide, *Can. J. Chem.*, 1986, **64**, 2301.
7. G. López-Cueto, A. Alonso-Mateos, J. Hernández-Méndez and F. Lucena-Conde, *An. Quim.*, 1975, **71**, 245.
8. G. López-Cueto and A. Alonso-Mateos, *Anal. Lett.*, 1978, **11**, 43.
9. O. T. Christensen, *J. Prakt. Chem.*, 1885, **31**, 163.
10. J. Meyer, *Z. Anorg. Allg. Chem.*, 1913, **81**, 385.
11. A. W. Adamson, J. P. Welker and W. B. Wright, *J. Am. Chem. Soc.*, 1951, **73**, 4786.
12. A. G. MacDiarmid and N. F. Hall, *ibid.*, 1953, **75**, 5204.
13. I. D. Chawla and M. J. Frank, *J. Inorg. Nucl. Chem.*, 1970, **32**, 555.
14. G. López-Cueto and J. Hernández-Méndez, *Quim. Anal.*, 1974, **28**, 160.
15. J. M. Kruse and N. G. Mellon, *Sewage Ind. Wastes Engng.*, 1951, **23**, 1402.
16. F. J. Ludzack, W. A. Moore and C. C. Ruchhoft, *Anal. Chem.*, 1954, **26**, 1784.
17. N. Burger, *Talanta*, 1985, **32**, 49.
18. D. B. Brown and D. F. Shriver, *Inorg. Chem.*, 1969, **8**, 37.
19. G. López-Cueto and J. A. Casado-Riobó, *Talanta*, 1979, **26**, 127.
20. G. López-Cueto and A. Alonso-Mateos, *Rev. Roum. Chim.*, 1986, **31**, 9.
21. G. Charlot, *Les Méthodes de la Chimie Analytique: Analyse Quantitative Minérale*, Masson, Paris, 1966.

## DETERMINATION OF AMMONIUM ION IN SEA-WATER BY CAPILLARY ISOTACHOPHORESIS

KEIICHI FUKUSHI

Kobe University of Mercantile Marine, Fukae, Higashinada, Kobe 658, Japan

KAZUO HIRO

Government Industrial Research Institute, Osaka, Midorigaoka, Ikeda, Osaka 563, Japan

(Received 15 March 1988. Accepted 2 May 1988)

**Summary**—A new procedure for determination of ammonium ion in sea-water by means of capillary isotachophoresis and a gas-liquid separator with a tubular microporous polytetrafluoroethylene membrane for preliminary enrichment has been developed. Ammonia generated by adding sodium hydroxide solution to the sea-water samples is allowed to permeate through the membrane and then dissolve in sulphuric acid. A linear calibration graph has been obtained with artificial sea-water samples containing up to 300  $\mu\text{g/l}$ . ammonium ion. The method has been applied to the determination of ammonium ion in surface and bottom sea-water samples.

It is important to determine the concentration of ammonium ion in sea-water, because the ion is closely related to marine-life production.<sup>1</sup> The indophenol blue method<sup>2-7</sup> is widely applied for the purpose, but is complex and time-consuming and subject to several interferences.

Recently, separation with a gas-permeable membrane has been applied to the determination of volatile substances in water samples, and also to the determination of ammonium ion in river and lake-waters,<sup>8-10</sup> blood and urine,<sup>11,12</sup> and condensed steam and boiler feed-water,<sup>13</sup> but has been little applied to the determination of ammonium ion in sea-water.<sup>14,15</sup> There is no report of the analysis of sea-water by capillary isotachophoresis with use of a gas-permeable membrane for prior separation.

We have already described the isotachophoretic determination of sulphide,<sup>16</sup> total carbon dioxide<sup>17</sup> and bromide<sup>18</sup> in sea-water after preliminary enrichment by use of a gas-liquid separator with a tubular microporous polytetrafluoroethylene (PTFE) membrane, and now report extension of the technique to the determination of ammonium ion in sea-water.

### EXPERIMENTAL

#### Apparatus

A Shimadzu IP-2A isotachophoretic analyser was used, with a potential gradient detector. The main column was a fluorinated ethylene-propylene (FEP) copolymer tube, 15 cm long, 0.5 mm inner diameter; the precolumn was a PTFE tube, 30 cm long, 1.0 mm inner diameter. A Hamilton 1725-N microsyringe was used for the injection of samples. Two kinds of gas-liquid separator were used. One was the double-tube structure used in our previous studies;<sup>16-18</sup> it consisted of an inner microporous PTFE tube (20 cm long, 2.0 mm i.d., 2.8 mm o.d.) and an outer glass tube (3.5 mm i.d., 6.0 mm o.d.). The second was similar, but had an inner

microporous PTFE tube (100 cm long, 1.0 mm i.d., 1.8 mm o.d.) and an outer FEP tube (2.4 mm i.d., 3.2 mm o.d.). Both PTFE tubes (Japan Goretex Inc.) had maximum pore size of 2  $\mu\text{m}$ , and 50% porosity. The flow system is shown in Fig. 1. The gas-liquid separators, wound round a cylindrical PVC former, were immersed in a Tokyo-Rikakikai SB-35 water-bath. The sample solution (the pH of which was raised by addition of sodium hydroxide solution) was circulated through the outer tube; sulphuric acid was circulated through the inner PTFE tube by means of an Atto SJ-1220 peristaltic pump. The temperature, pH, salinity and dissolved oxygen (DO) content of sea-water were measured as already described.<sup>16-18</sup> Sea-water samples were filtered through a 0.45- $\mu\text{m}$  membrane and stored in polyethylene bottles inside a refrigerator as soon as possible after the sample was collected.<sup>18</sup>

#### Reagents

All solutions were prepared from analytical reagent grade chemicals. 18-Crown-6 was obtained from the Aldrich Chemical Co. Standard solutions of ammonium ion were prepared by dissolving ammonium chloride in water from a Yamato-Kagaku WA-22 automatic still and a Nihon Millipore-Kogyo Milli QII system. The preparation of the artificial sea-water was based on a Japanese Standard.<sup>19</sup>

#### Procedure

Sea-water samples were analysed by the following procedure as soon as possible after collection. Add 0.5 ml of 5M sodium hydroxide to 45 ml of sea-water sample to convert ammonium ion into ammonia. Centrifuge the suspension at 3000 rpm for 5 min to remove the magnesium hydroxide precipitate. With the water-bath temperature set at 60°, circulate 40 ml of the supernatant solution through the outer FEP tube and 2.0 ml of  $2.0 \times 10^{-4}\text{M}$  sulphuric acid through the inner PTFE tube, both at a flow-rate of 6 ml/min, for 20 min. Ammonia permeates through the wall of the inner PTFE tube and dissolves in the sulphuric acid. Pump out the sulphuric acid and inject 150  $\mu\text{l}$  of it into the isotachophoretic analyser. Maintain the migration current at 200  $\mu\text{A}$  for the first 16 min and then reduce it to 50  $\mu\text{A}$ . As leading electrolyte use 5mM hydrochloric acid/2mM 18-crown-6/0.01% Triton X-100, and as terminating electrolyte 10mM lithium chloride/0.01% Triton X-100. Prepare a calibration graph by applying the method to synthetic standards.

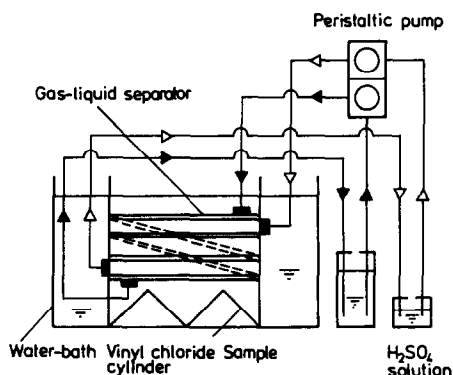


Fig. 1. Schematic diagram of flow system.

## RESULTS AND DISCUSSION

### Electrolyte system

It was necessary to select an electrolyte system by which the ammonium ion could be isotachophoretically separated from the potassium ion present as an impurity in the reagents. We have already described<sup>20</sup> how the isotachophoretic separation of low concentrations of these ions can be achieved with a leading electrolyte containing 1–3 mM 18-crown-6, with linear response for ammonium ion up to 1.0 mg/l.

### Gas-liquid separator

Artificial sea-water samples containing 100  $\mu\text{g/l}$ . ammonium ion were analysed by use of both the gas-liquid separators described above. The recovery of ammonium ion was 20% when the older (glass) type was used and 69% with the modified (FEP) type, *i.e.*, the increase in the surface area of the inner PTFE tube resulted in a corresponding increase in the recovery factor. The modified gas-liquid separator was, therefore, used in all subsequent experiments.

### Volume of sodium hydroxide solution

The zone length for ammonium ion in the isotachopherograms was almost constant irrespective of the volume of 5M sodium hydroxide added (over the

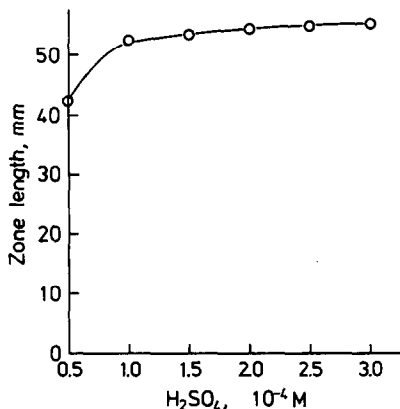


Fig. 2. Effect of sulphuric acid concentration.

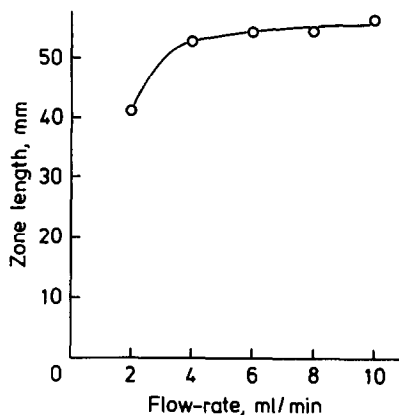


Fig. 3. Effect of the flow-rate of sample solution.

range 0.3–0.7 ml). During the circulation, magnesium hydroxide precipitated when the volume of alkali added was below the range above, because significant amounts of the magnesium ion remained in solution, and calcium carbonate precipitated when volumes  $>0.7$  ml were used. Therefore, 0.5 ml of 5M sodium hydroxide was selected as the volume to be added to the 45 ml of sample solution.

### Concentration of sulphuric acid

The concentration of the sulphuric acid was varied in the range  $0.5\text{--}3.0 \times 10^{-4} \text{ M}$ . The zone length for ammonium ion increased with the sulphuric acid concentration, but only slightly when this was  $>1.0 \times 10^{-4} \text{ M}$ , as shown in Fig. 2. The isotachophoretic measurement took longer when the sulphuric acid concentration was higher than  $2.5 \times 10^{-4} \text{ M}$ , because of the excess of hydrogen ion in the treated solution. Therefore,  $2.0 \times 10^{-4} \text{ M}$  was adopted as the optimum sulphuric acid concentration.

### Flow-rate of sample circulation

The flow-rate of sample solution was varied in the range 2–10 ml/min. The zone length for ammonium

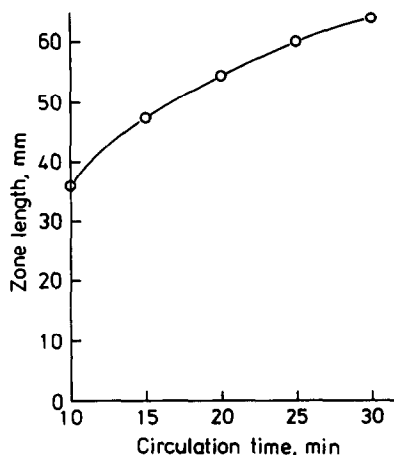


Fig. 4. Effect of circulation time.

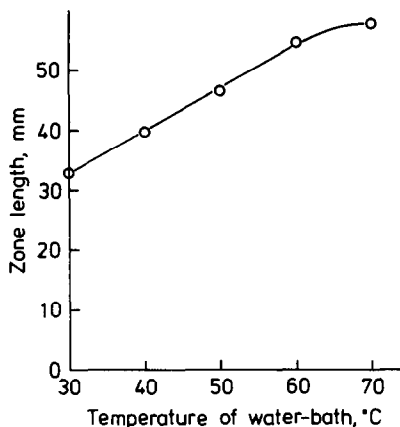


Fig. 5. Effect of temperature.

ion increased with flow-rate up to 4 ml/min, but then almost levelled off, as shown in Fig. 3. At higher flow-rate, sample solution as well as ammonia is liable to permeate through the wall of the inner PTFE tube, so 6 ml/min was adopted as the optimum flow-rate for sample circulation.

#### Duration of sample circulation

The circulation time was varied in the range 10–30 min. The zone length for ammonium ion increased with circulation time, but not linearly, as shown in Fig. 4. To shorten the analysis time, 20 min was adopted as the circulation time.

#### Effect of temperature

The temperature of the water-bath was varied in the range 30–70°. The zone length for ammonium ion increased linearly with temperature up to 60°, as shown in Fig. 5, because of decreased solubility of ammonia in the alkaline solution.<sup>21</sup> Although the recovery of ammonia was greater when a temperature of 70° was used, 60° was preferred because temperature control was easier.

#### Calibration graph

A linear calibration graph was obtained for 12 artificial sea-water samples containing 25–300 µg/l. ammonium ion. The regression equation was

$y = 0.395x - 0.8$  (correlation coefficient 1.000) where  $x$  is the ammonium concentration in µg/l. and  $y$  the zone length in mm. The performance was estimated from the variation in zone length per 1.0 µg/l., calculated for each point on the calibration graph. The standard deviation was found to be 0.033 mm ( $n = 12$ ). The lower determination limit for ammonium ion was calculated by substituting 0.1 mm for  $y$  in the regression equation, and was taken as 0.25 µg/l. The recovery of ammonium ion, at  $67 \pm 3\%$ , was less than complete, but this does not matter in practice, because the recovery is almost constant in the range 0–300 µg/l. It may, however, be increased by use of a longer microporous PTFE tube.

In addition, a similar calibration was obtained for sea-water samples appropriately diluted with artificial sea-water. The regression equation of this graph was  $y = 0.379x + 0.6$  (correlation coefficient 0.999).

#### Analysis of sea-water samples

The proposed method was applied to the determination of ammonium ion in surface and bottom sea-water samples collected around the coastal area of Osaka Bay between Port of Amagasaki and Rokko Island on 6 February 1988. The concentrations of ammonium ion in these samples were so high that

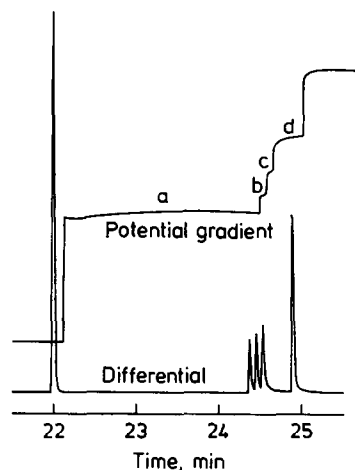


Fig. 6. Isotachopherogram of sea-water sample treated by the proposed method. a,  $\text{NH}_4^+$ ; b,  $\text{K}^+$ ; c,  $\text{Ca}^{2+}$ ; d,  $\text{Na}^+$ .

Table 1. Results for ammonium ion in sea-water

Sampling site	Depth, m	Temp., °C	pH	Salinity, ‰	DO, mg/l.	$\text{NH}_4^+$ found, µg/l.
Port of Amagasaki	0	10.5	7.50	15.1	7.11	3750
Port of Amagasaki	5.0	10.7	7.64	24.0	7.00	1740
Mouth of Muko river	0	9.5	7.79	26.0	10.05	1060
Mouth of Muko river	3.0	9.2	7.85	26.5	9.09	1060
Nishinomiya harbour	0	10.1	7.78	25.6	8.85	1200
Nishinomiya harbour	1.5	9.6	7.83	26.6	8.25	987
Pond at KUMM	0	9.3	7.82	22.6	9.89	4580
Pond at KUMM	5.0	9.2	7.80	26.1	7.89	1040
Rokko Island	0	9.2	8.01	27.6	10.77	1010
Rokko Island	5.5	9.1	8.08	27.9	9.80	970

Sampling date: 6 February 1988; KUMM = Kobe University of Mercantile Marine.

they were diluted with artificial sea-water before analysis. An isotachopherogram of surface sea-water from the mouth of the Muko river is shown in Fig. 6. The concentrations of ammonium ion listed in Table I were calculated by use of the calibration graph prepared with artificial sea-water samples. From these results, it was found that eutrophication was progressing rapidly in these sea-areas.

Tanaka *et al.*<sup>9</sup> found that methylamine interfered positively with the determination of ammonium ion by the automated measuring apparatus with a gas-permeable membrane. In the proposed method, this interference can be eliminated because methylammonium, dimethylammonium and trimethylammonium ions are separated from the ammonium ion by isotachopheresis with the electrolyte system described above.<sup>22</sup>

For the determination of ammonium ion in sea-water, the proposed method is simple, has a high sensitivity and precision and no interferences.

*Acknowledgements*—The authors express their gratitude to Drs. E. Sekido, Y. Masuda and T. Tanaka for their kind encouragement and suggestions, and to Mr. S. Miyamichi for his experimental help.

#### REFERENCES

1. S. Tsunogai and S. Noriki, in *Kaiyo-Kagaku*, M. Nishimura (ed.), p. 106. Sangyo-Tosho, Tokyo, 1986.
2. K. Matsunaga and M. Nishimura, *Bunseki Kagaku*, 1971, **20**, 993.
3. J. D. H. Strickland and T. R. Parsons, *A Practical Handbook of Seawater Analysis*, 2nd Ed., p. 87. Fisheries Research Board of Canada, Ottawa, 1972.
4. F. Koroleff, in *Methods of Seawater Analysis*, 2nd Ed., K. Grasshoff, M. Ehrhardt and K. Kremling (eds.), p. 150. Verlag Chemie, Weinheim, 1983.
5. Y. Miyake and Y. Kitano, *Shin-Suishitsu-Kagaku-Bunseki-Ho*, p. 135. Chijin-Shokan, Tokyo, 1985.
6. M. A. Brzezinski, *Mar. Chem.*, 1987, **20**, 277.
7. G. Catalano, *ibid*, 1987, **20**, 289.
8. T. Aoki, S. Uemura and M. Munemori, *Anal. Chem.*, 1983, **55**, 1620.
9. T. Tanaka, A. Kawahara, S. Wakida and K. Hiiro, *Kankyo Gijutsu*, 1986, **15**, 46.
10. R. Nakata and H. Sakashita, *Proc. 35th Annual Meeting Japan Society for Analytical Chemistry*, Okayama, 11–14 October 1986, p. 556.
11. Y. M. Fraticelli and M. E. Meyerhoff, *Anal. Chem.*, 1981, **53**, 992.
12. T. Aoki, S. Uemura and M. Munemori, *Bunseki Kagaku*, 1984, **33**, 505.
13. D. Midgley and K. Torrance, *Analyst*, 1972, **97**, 626.
14. T. R. Gilbert and A. M. Clay, *Anal. Chem.*, 1973, **45**, 1757.
15. Y. Takase, H. Hashitani and M. Okumura, *Proc. Symposium Chemical Society of Japan (Chugoku-Shikoku Branch)*, Matsue, 22–23 November 1987, p. 228.
16. K. Fukushi and K. Hiiro, *J. Chromatog.*, 1987, **393**, 433.
17. *Idem*, *Z. Anal. Chem.*, 1987, **328**, 247.
18. *Idem*, *Bunseki Kagaku*, 1987, **36**, 712.
19. *Test Method for Rust-Preventing Characteristics of Lubricating Oil*, JIS K 2510—1987, p. 7. Japanese Standards Association, Tokyo, 1987.
20. K. Fukushi and K. Hiiro, *Talanta*, 1988, **35**, 55.
21. W. E. van der Linden, *Anal. Chim. Acta*, 1983, **151**, 359.
22. *Kagaku-Binran*, 3rd Ed., p. 460. Chemical Society of Japan, Tokyo, 1984.



## SHORT COMMUNICATIONS

# SPECTROPHOTOMETRIC DETERMINATION OF BISMUTH AND EDTA BY MEANS OF THE REACTION OF BISMUTH WITH PYROCATECHOL VIOLET IN THE PRESENCE OF SEPTONEX

DAGMAR HONOVÁ, IRENA NĚMCOVÁ and VÁCLAV SUK

Department of Analytical Chemistry, Charles University, Albertov 2030, 128 40 Prague 2, Czechoslovakia

(Received 29 January 1988. Accepted 21 June 1988)

**Summary**—The reaction of bismuth(III) with Pyrocatechol Violet in the presence of the cationic surfactant Septonex was studied and the optimal conditions for its analytical use were found ( $\lambda = 612$  nm, pH = 3.1,  $c_{PV} = 4 \times 10^{-5} M$ ,  $c_{Sept} = 5 \times 10^{-4} M$ ). The Lambert–Beer law is obeyed over the bismuth range 0.1–7.5  $\mu\text{g/ml}$ . Decomposition of the Bi–PV–Septonex complex was utilized for indirect determination of ethylenediaminetetra-acetic acid at concentrations of 0.3–7.4  $\mu\text{g/ml}$ .

Pyrocatechol Violet (PV) is one of the most common metallochromic indicators<sup>1</sup> and has often been used as a spectrophotometric reagent. Its reaction with bismuth<sup>2</sup> was studied soon after it had been introduced in analytical practice and a method for spectrophotometric determination of bismuth was developed later.<sup>3</sup> This method has been modified by use of diphenylguanidine in the procedure.<sup>4</sup> Methods of spectrophotometric determination of bismuth have been reviewed.<sup>5</sup>

The present paper deals with the effect of the cationic surfactant carboxypentadecyltrimethylammonium bromide (Septonex) on the reaction of bismuth with Pyrocatechol Violet. The results obtained have been used in the development of a spectrophotometric method for the determination of bismuth, with reasonably high sensitivity. It has further been found that the complex of bismuth with Pyrocatechol Violet and Septonex is decomposed by ethylenediaminetetra-acetic acid, EDTA, similarly to the Bi(III)–PV binary complex;<sup>6</sup> on this basis, a highly sensitive, indirect method has been developed for the determination of EDTA.

### EXPERIMENTAL

#### Apparatus

A Pye-Unicam SP 800 spectrophotometer with 1.00-cm path-length silica cuvettes, and a Radiometer PHM 64 pH-meter with GK 2401B combined electrode were used.

#### Reagents

A 0.01M stock solution of bismuth was prepared by dissolving 2.090 g of the 99.999% pure metal in nitric acid and diluting with redistilled water to 1000 ml. A  $3 \times 10^{-4} M$  working solution was obtained by diluting the stock solution with redistilled water.

A  $1 \times 10^{-3} M$  stock solution of Pyrocatechol Violet (PV) was prepared by dissolving 0.1081 g of the substance, purified by recrystallization from ethanol, in 250 ml of redistilled water.

A  $5 \times 10^{-3} M$  stock solution of Septonex was prepared by dissolving 0.5281 g of the substance in 250 ml of distilled water.

A  $5 \times 10^{-2} M$  stock solution of EDTA was prepared by dissolving 18.61 g of the free acid in water and diluting to 1000 ml, and standardized by titration of copper.

The pH was adjusted with a solution prepared by mixing 50 ml each of 0.1M sodium acetate and 0.1M nitric acid and diluting to 250 ml with distilled water.

Analytical grade reagents were used whenever possible.

#### Procedures

**Determination of bismuth.** The sample solution, containing not more than 200  $\mu\text{g}$  of bismuth, is placed in a 25-ml standard flask, two drops of 1% Pentamethoxyl Red solution are added and 0.5M sodium acetate is added until the indicator becomes colourless. Then 5 ml of the sodium acetate–nitric acid mixture are added, followed by 3.5 ml of a mixture of Pyrocatechol Violet and Septonex (prepared by mixing 1 part of  $1 \times 10^{-3} M$  PV and 2.5 parts of  $5 \times 10^{-3} M$  Septonex). The solution is made up to the mark with distilled water and after 5 min the absorbance is measured at 612 nm against a reagent blank.

**Determination of EDTA.** A 2.5-ml volume of  $3 \times 10^{-4} M$  bismuth and 5 ml of the mixture of sodium acetate and nitric acid are placed in a 25-ml standard flask, Pentamethoxyl Red solution is added, the pH is adjusted by addition of 0.5M sodium acetate until the colour is discharged, then 3.5 ml of the mixture of Pyrocatechol Violet and Septonex are added. After 5 min (allowed for formation of the Bi(III)–PV–Septonex complex), the test solution, containing a maximum of 170  $\mu\text{g}$  of EDTA, is added, the mixture is diluted to 25 ml and the absorbance at 612 nm is measured immediately against a similarly prepared blank.

### RESULTS AND DISCUSSION

#### Bismuth determination

The absorption spectra of Pyrocatechol Violet and its binary complex with bismuth are given in Fig. 1;  $\lambda_{\text{max}} = 440$  and 450 nm respectively. The spectrum of the complex has a plateau at 550–580 nm. The spectra of the same solutions in the presence of Septonex are shown as curve 1' ( $\lambda_{\text{max}} = 440$  nm) and curve 2':

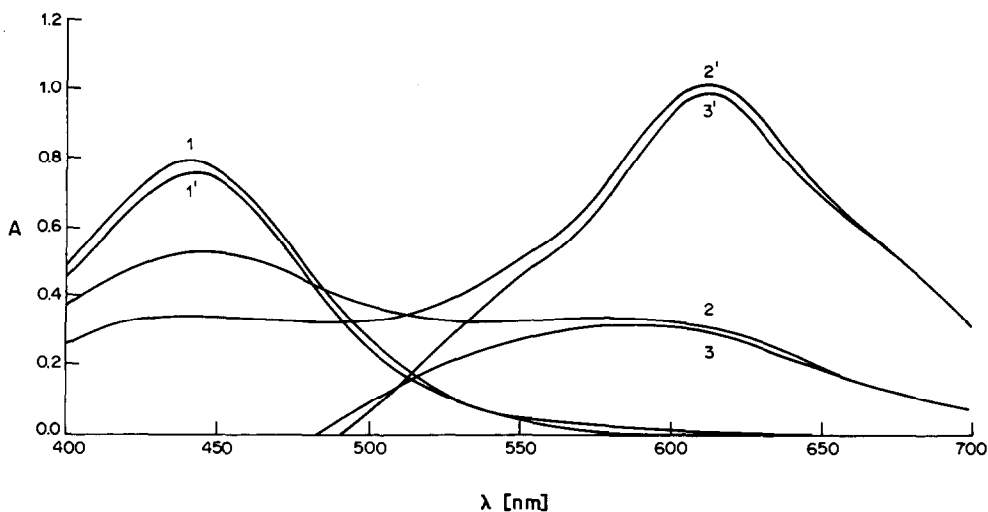


Fig. 1. Absorption curves: (1) PV, (2) Bi(III)-PV, (3) the difference curve (2-1), (1') PV-Septonex, (2') Bi(III)-PV-Septonex, (3') difference curve (2'-1');  $c_{\text{Bi(III)}} = 3 \times 10^{-5} M$ ,  $c_{\text{PV}} = 4 \times 10^{-5} M$ ,  $c_{\text{Sept}} = 5 \times 10^{-4} M$ , pH = 3.1.

( $\lambda_{\text{max}} = 612 \text{ nm}$ ). The cationic surfactant thus produces a maximum in the spectrum of the complex, at 612 nm, and a large hyperchromic shift; the molar absorptivity calculated for  $\lambda_{\text{max}}$  of the corresponding difference curves (3 and 3') increases from  $\epsilon_{580} = 1.13 \times 10^4 \text{ l.mole}^{-1}.\text{cm}^{-1}$  for the binary complex to  $\epsilon_{612} = 3.36 \times 10^4 \text{ l.mole}^{-1}.\text{cm}^{-1}$  for the ternary system containing Septonex.

Maximal and constant absorbance of the complex in the presence of Septonex is attained in the pH range 2.8-3.9. The colour is fully developed within 5 min, and is stable for 24 hr, whereas the colour in the absence of Septonex is stable for only 15 min. The complex formation is not affected by changes in temperature. For complete complex formation, a Pyrocatechol Violet concentration greater than  $3.5 \times 10^{-5} M$  is required for a bismuth concentration of  $3 \times 10^{-5} M$ ; a PV concentration of  $4 \times 10^{-5} M$  is recommended. Under these conditions, maximal colour is attained with a Septonex concentration of  $5 \times 10^{-4} M$ . It has been found that the best reproducibility of measurement is obtained if the time interval between the additions of PV and Septonex is as small as possible, so it is best to add a mixture of the two reagents in the appropriate ratio.

**Composition of the complex.** It was found by the Job method and the molar ratio method, that the stoichiometric ratio of Bi(III) and PV in the complex is 1:1; in these tests the Septonex concentration was maintained constant at  $5 \times 10^{-4} M$ .

**Calibration and interferences.** Under the optimal conditions found ( $\lambda = 612 \text{ nm}$ , pH = 3.1,  $c_{\text{PV}} = 4 \times 10^{-5} M$ ,  $c_{\text{Sept}} = 5 \times 10^{-4} M$ ), the calibration graph was linear from 0.1 to 7.5  $\mu\text{g}$  of Bi(III) per ml. The relative standard deviation was 1% for 5.0  $\mu\text{g}/\text{ml}$  Bi(III) (7 parallel determinations).

$\text{Na}^+$ ,  $\text{K}^+$ ,  $\text{Mg}^{2+}$ ,  $\text{Ca}^{2+}$ ,  $\text{Sr}^{2+}$ ,  $\text{Ba}^{2+}$ ,  $\text{NO}_3^-$ ,  $\text{SO}_4^{2-}$  and

$\text{CH}_3\text{COO}^-$  do not interfere up to a w/w ratio to  $\text{Bi}^{3+}$  of 5000. The tolerance ratios for other ions are  $\text{NH}_4^+$  3000,  $\text{Zn}^{2+}$  1000,  $\text{Cd}^{2+}$ ,  $\text{Pb}^{2+}$ ,  $\text{Mn}^{2+}$  300,  $\text{Ni}^{2+}$ ,  $\text{Cr}^{2+}$ ,  $\text{Cu}^{2+}$ ,  $\text{Al}^{3+}$  100, and  $\text{Fe}^{2+}$  50. Ions that form complexes with Pyrocatechol Violet under the given conditions will interfere; these are  $\text{Sb}^{3+}$ ,  $\text{Sn}^{4+}$ ,  $\text{Fe}^{3+}$ ,  $\text{Zr}^{4+}$ ,  $\text{Ti}^{4+}$ ,  $\text{Th}^{4+}$ ,  $\text{MoO}_4^{2-}$ ,  $\text{WO}_4^{2-}$ .

#### Determination of EDTA

Addition of EDTA to the Bi(III)-PV-Septonex ternary system leads to a decrease in the absorbance at 612 nm, as the Bi(III) complex with EDTA is more stable than that with PV. This decrease is a linear function of the EDTA concentration and can be used for the determination of EDTA.

The optimal conditions for the reaction (pH,  $c_{\text{PV}}$ ,  $c_{\text{Sept}}$ ) are the same as above. The colour is decreased immediately on addition of EDTA and the residual absorbance is stable for more than 24 hr.

**Calibration and interferences.** The calibration graph, constructed with  $c_{\text{Bi(III)}} = 3 \times 10^{-5} M$ ,  $c_{\text{PV}} = 4 \times 10^{-5} M$ ,  $c_{\text{Sept}} = 5 \times 10^{-4} M$ , pH = 3.1, is linear from 0.3 to 7.4  $\mu\text{g}/\text{ml}$  EDTA. The relative standard deviation, obtained for 7 parallel determinations, is 1.6% for 6.0  $\mu\text{g}/\text{ml}$  EDTA.

The interferences are the same as those in the determination of Bi(III) with PV and Septonex.

#### REFERENCES

1. V. Suk and M. Malát, *Chemist-Analyst*, 1956, **45**, 30.
2. M. Malát, V. Suk and O. Ryba, *Collection Czech. Chem. Commun.*, 1954, **19**, 258.
3. M. Malát, *Z. Anal. Chem.*, 1962, **186**, 418.
4. N. L. Shestidesyatnaya, N. M. Milyaeva and L. I. Kotelyanskaya, *Zh. Analit. Khim.*, 1975, **30**, 522.
5. Z. Marczenko, *Separation and Spectrophotometric Determination of Elements*, Horwood, Chichester, 1986.
6. M. Malát, *Chemist-Analyst*, 1962, **51**, 74.

## DETERMINATION OF METHOTREXATE IN HUMAN BLOOD PLASMA BY ADSORPTIVE STRIPPING VOLTAMMETRY\*

AYTEKIN TEMIZER† and A. NUR ONAR

Department of Analytical Chemistry, Faculty of Pharmacy, Hacettepe University, 06100 Ankara, Turkey

(Received 13 October 1987. Revised 12 April 1988. Accepted 24 May 1988)

**Summary**—The use of adsorptive stripping voltammetry to measure sub-micromolar concentrations of methotrexate in plasma has been investigated. A simple clean-up procedure has been developed in which methotrexate is extracted from blood plasma with Amberlite XAD-2, which is a non-ionic resin, and eluted with methanol. Recovery for plasma analysis was 80%.

Methotrexate (4-amino-*N*<sup>10</sup>-methylpteroyl glutamic acid MTX) is one of the most widely used anti-cancer drugs. High-dose MTX therapy has been effectively employed in chemotherapy for a variety of neoplasms. The clinical usefulness of MTX is, however, limited because of its marked toxicity. It has been shown that MTX toxicity increases in some patients if its elimination is delayed and that the routine monitoring of MTX levels in blood plasma may allow early detection of patients at high risk.<sup>1</sup> It is, therefore, important to have a reliable method for determining the amount of MTX in plasma. There are several methods for measuring the drug concentration in plasma: fluorimetry,<sup>2</sup> radioassay, radio-immunoassay and enzyme inhibition assay,<sup>3</sup> and HPLC.<sup>4,5</sup>

The electrochemical behaviour of MTX has been studied<sup>6</sup> and an adsorptive stripping voltammetric method developed<sup>7</sup> for its determination down to  $2 \times 10^{-9} M$ . The purpose of the present study was to examine the applicability of adsorptive stripping voltammetry to the assay of the drug in plasma, where pretreatment is required. The work described here shows that a non-ionic resin can be used to separate MTX in aqueous solution. Some minor changes to the adsorptive stripping voltammetry procedure itself are also proposed.

### EXPERIMENTAL

#### Apparatus

A PAR 174A voltammetric analyser with a PAR 303A static mercury drop electrode was used. Other equipment was as previously described.<sup>8</sup> The sample cell (PAR model 0057) was fitted with a saturated calomel reference electrode and a platinum wire auxiliary electrode. The hanging mercury drop mode was used throughout. Instrumental parameters were as follows: drop size, "large;" potential scan-rate 5 mV/sec; pulse amplitude 50 mV; pulse repetition 0.5 sec; equilibrium time 15 sec. A magnetic stirrer and a

Teflon-coated stirrer bar provided the mixing during the accumulation step.

#### Reagents

A stock solution of MTX (1000 mg/l.) was prepared by dissolving the drug in 0.1M sodium hydroxide. Dilute solutions of MTX were prepared daily. The supporting electrolyte was Britton–Robinson (BR) pH-4.5 buffer.

#### Plasma samples

Plasma samples were obtained from patients undergoing high-dose MTX therapy in the Pediatric Oncology Department of the Faculty of Medicine, Hacettepe University. MTX was extracted from the plasma by use of Amberlite XAD-2 non-ionic resin.

#### Extraction procedure

Amberlite XAD-2 (2.1 µg) was placed in a plastic tube and washed with 5 ml of 0.2M sodium hydroxide. After introduction of 1 ml of plasma into this column, it was washed in succession with 5 ml of pH-6.5 phosphate buffer, 3 ml of chloroform, 3 ml of diethyl ether and again with 5 ml of pH-6.5 phosphate buffer. MTX was eluted from the column with 3 ml of methanol in 0.5-ml portions. Application of suction to the column speeded up the extraction. The methanolic extract was evaporated at 60° and the residue was dissolved in 1 ml of water. Portions (0.1 ml) of this solution were analysed in the electrochemical cell.

#### Stripping procedure

BR buffer solution (5 ml) was used as the supporting electrolyte and was deaerated by passage of nitrogen for 8 min. The preconcentration potential ( $-0.54 V$  vs. SCE) was applied to the HMDE for a known time (1–3 min) while the solution was stirred at a reproducible rate. Stirring was then stopped and after a 15-sec rest period the voltamperogram was recorded, with application of a negative-going differential pulse scan. First a background voltamperogram was recorded, then further voltamperograms for addition of a 10-µl portion of the plasma extract, and subsequent successive 100-µl additions of 1-µg/ml standard MTX solution, the adsorptive stripping cycle being repeated with a new drop for each addition. All data were obtained at room temperature ( $20.0 \pm 0.1^\circ$ ).

### RESULTS AND DISCUSSION

There has been increasing interest in the electro-analytical determination of anti-cancer drugs in recent years,<sup>7,9–13</sup> including the use of adsorptive stripping voltammetry.<sup>7,12,13</sup> MTX has been studied by

\*This work was presented at the International Symposium on Pharmaceutical and Biomedical Analysis, Barcelona, 23–25 September 1987.

†To whom correspondence should be addressed.

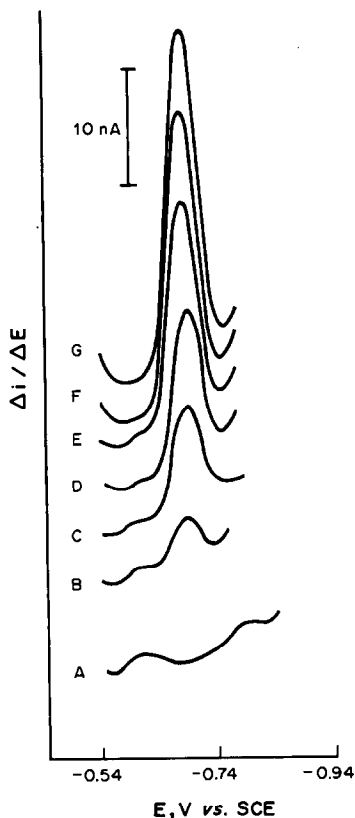


Fig. 1. Adsorptive stripping voltamperograms of MTX extracted from plasma samples. (A) supporting electrolyte, (B) plasma sample, (C)–(G) 100- $\mu$ l additions of 1 mg/l MTX.

cyclic voltammetry<sup>6</sup> and adsorptive stripping voltammetry<sup>7</sup> and shown to exhibit three cathodic peaks in the low-neutral pH range. The adsorption of MTX on mercury can be used as a preconcentration step prior to voltammetric determination and the resulting adsorptive stripping procedure offers a convenient means of analysing for submicromolar and nanomolar levels of the drug.

Because of the high sensitivity of this method, the possibility of applying the adsorptive stripping procedure for the determination of MTX in plasma was tested. A linear calibration plot has been reported<sup>7</sup> for  $2.5 \times 10^{-9}$ – $1.25 \times 10^{-7}$  M MTX in 0.05 M phosphate buffer at pH 2.5. By using a large drop size, a different electrolyte (pH-4.5 BR buffer) and a different preconcentration potential ( $-0.54$  V), we have extended the linear calibration plot to cover the range from  $8.8 \times 10^{-10}$  to  $1.0 \times 10^{-6}$  M (using 3 min adsorption at the lower levels and 1 min at the higher levels). A typical adsorptive stripping voltamperogram of MTX at the hanging mercury drop electrode is shown in Fig. 1. After voltamperograms had been taken for the supporting electrolyte before and after addition of the extract, known amounts of MTX were added to the solution. The concentration of MTX in the plasma sample was calculated as being  $4.3 \times 10^{-8}$  M. This plasma sample belonged to a

patient having high-dose MTX chemotherapy and was taken 48 hr after injection of the drug. The results show that there was no risk of toxicity from the MTX because it was below the  $1 \times 10^{-7}$  M level considered to be "safe".<sup>14</sup> Folic acid and citrovorum factor (*N*-formyltetrahydrofolic acid), which may be present in some samples, did not interfere with the determination of MTX in plasma, nor did other drugs less commonly used in conjunction with MTX: chlorpromazine, oxytetracycline, metachloropramidine, vincristine and dixyrazine. Metabolites of MTX have not been detected in man and other animals,<sup>15</sup> so no interference from this source is expected. The procedure is, therefore, highly selective for MTX.

Clinical application of the adsorptive stripping approach required a clean-up procedure to minimize the possible interferences. The plasma sample containing MTX was passed through a properly conditioned column, allowing selective retention of the MTX. The column was washed to remove undesirable matrix components, such as proteins, salts and pigments, and the MTX was then selectively eluted from the column. Determination was based on standard addition. The recovery obtained was nearly 80%. The loss occurs during the washing of the XAD-2 column, and can be allowed for in calculating the results. The correction factor can be determined by adding an MTX standard to an MTX-free plasma sample and applying the whole procedure to it.

In conclusion, the assay of plasma MTX reported here provides an effective way of monitoring MTX excretion and should be useful in helping to prevent development of renal toxicity.

*Acknowledgement*—This work was supported by Hacettepe University Research Foundation, Grant 85-01-013-07.

#### REFERENCES

1. Y.-M. Wang, E. Lantin and W. W. Sutow, *Clin. Chem.*, 1976, **22**, 1053.
2. M. M. Kincade, W. R. Vogler and P. G. Dayton, *Biochem. Med.*, 1974, **10**, 337.
3. R. Virtanen, E. Iisalo, M. Parvinen and E. Nordman, *Acta Pharmacol. Toxicol.*, 1979, **44**, 296.
4. J. L. Wisnicki, W. P. Tong and D. B. Ludlum, *Cancer Treat. Rep.*, 1978, **62**, 529.
5. A. C. Garcia, A. J. M. Ordieres, M. A. G. Fernández and P. T. Blanco, *Anal. Proc.*, 1985, **22**, 349.
6. R. C. Gurira and L. D. Bowers, *J. Electroanal. Chem.*, 1983, **146**, 109.
7. J. Wang, P. Tuzhi, Meng-shan Lin and T. Tapia, *Talanta*, 1986, **33**, 707.
8. A. N. Onar and A. Temizer, *Analyst*, 1987, **112**, 227.
9. J. Barek, A. Berka and J. Zima, *Talanta*, 1985, **32**, 987.
10. A. Temizer, *ibid.*, 1986, **33**, 791.
11. G. M. Schmid and D. R. Atherton, *Anal. Chem.*, 1986, **58**, 1956.
12. E. N. Chaney and R. P. Baldwin, *Anal. Chem.*, 1982, **54**, 2556.
13. J. Wang, Meng Shan Lin and V. Villa, *Anal. Lett.*, 1986, **19**, 2293.
14. M. H. N. Tattersall, L. M. Parker, S. W. Pitman and E. Frei, *Cancer Chemother. Rep., Part 3*, 1975, **6**, 25.
15. E. S. Henderson, R. H. Adamson, C. Denham and V. T. Oliverio, *Cancer Res.*, 1965, **25**, 1008, 1018.

## ION-SELECTIVE ELECTRODES IN ORGANIC ANALYSIS—DETERMINATION OF XANTHATE

WING HONG CHAN, ALBERT W. M. LEE and KAM TONG FUNG

Department of Chemistry, Hong Kong Baptist College, 224 Waterloo Road, Kowloon, Hong Kong

(Received 19 August 1987. Revised 31 May 1988. Accepted 22 June 1988)

**Summary**—A PVC membrane xanthate-selective electrode has been developed for the direct determination of xanthates of primary and secondary alcohols. The xanthate electrode is highly selective and exhibits a Nernstian response in the range  $5.0 \times 10^{-2}$ – $7.1 \times 10^{-5}M$  xanthate with a slope of 58.6 mV per concentration decade. The electrode has a wide working pH range (5.0–11.5), a fast response time (less than 30 sec) and is stable for at least two months.

Alkyl xanthates are important analytical, agricultural and industrial chemicals. They are widely used as chelating reagents in analytical chemistry, as fungicides for soil treatment<sup>1</sup> and as collection agents in the mining industry.<sup>2</sup> Although many analytical methods such as titrimetry, gravimetry, polarography and photometry are available for the determination of xanthate,<sup>3</sup> most of them are rather tedious, unselective and inapplicable to low concentrations of xanthates. On the other hand, ion-selective electrodes (ISEs), which have been successfully used in direct potentiometric determination of many ionic organic species,<sup>4</sup> have many advantages in terms of simplicity, selectivity and sensitivity. An indirect ISE method using a Cu-salicylaldehyde electrode for end-point detection in the titration of xanthate with copper sulphate solution had been reported.<sup>5</sup> However, direct ISE determination of xanthate has not received much attention.<sup>6</sup> The aim of our study was to develop a general PVC membrane xanthate-selective electrode for the direct determination of various xanthates derived from primary and secondary alcohols. The performance and application of this electrode are reported.

### EXPERIMENTAL

#### Apparatus

Potentiometric measurements were made at constant temperature in the range 20–25° with an Orion digital "ion-analyser" (model 601A). A platinized platinum electrode (model 3401) from Yellow Spring Instrument Co. Inc. was used as an internal reference electrode. A saturated calomel electrode (SCE) from Orion (model 9006) was used as external reference electrode. A Senonex combined pH electrode model (5200C) was used for pH measurements.

#### Reagents

High molecular-weight PVC was obtained from Aldrich Chemical Company. Analytical grade reagents and demin-

eralized distilled water were used throughout. Potassium ethyl xanthate was recrystallized once from acetone before use. Other alkyl xanthates were prepared by reacting the corresponding potassium alkoxides with carbon disulphide.<sup>7</sup>

#### Preparation of the sensing material

A mixture of 0.2 g of purified potassium ethyl xanthate in 20 ml of distilled water and 0.6 g of tetraheptylammonium bromide in 20 ml of dichloromethane was stirred magnetically in a 100-ml round-bottomed flask for 1 hr. The organic layer was separated and the aqueous layer was extracted with two 10-ml portions of dichloromethane. The combined organic layers were dried over anhydrous magnesium sulphate. Evaporation of solvent by a rotary evaporator gave the sensor, tetraheptylammonium ethyl xanthate [ $C_2H_5OCSS^- \cdot N(n-C_7H_{15})_4^+$ ], as a white solid.

#### Fabrication of the tetraheptylammonium ethyl xanthate-PVC matrix membrane

A mixture of 0.14 g of tetraheptylammonium ethyl xanthate and 0.35 g of PVC powder with 0.32 g of plasticizer (dioctyl phthalate) was dissolved in 20 ml of tetrahydrofuran (THF). The solution was poured into a Petri dish (diameter 7.5 cm) and covered with a filter paper. After all the THF had evaporated, a sheet of tetraheptylammonium ethyl xanthate-PVC matrix membrane remained.

#### Assembly of the ISE

The electrode body was made from a screwcap adapter.<sup>8</sup> A circular PVC matrix membrane with a diameter of ca. 0.8 cm was placed in the space between the plastic screwcap and the glass adapter. With the aid of an O-ring, the membrane was held tightly without leakage of the internal solution (Fig. 1). The electrode was filled with the internal solution, a 0.01M solution of potassium ethyl xanthate at pH 9. A platinized platinum electrode was used as the internal reference electrode. The electrode, filled with the internal solution, was conditioned (for 2 hr) and stored in distilled water before and after use.

#### Electrode calibration

A series of standard potassium ethyl xanthate solutions in the concentration range  $1 \times 10^{-5}$ – $5 \times 10^{-2}M$  was obtained by appropriate dilution of a 0.1M stock solution. Fifty ml of each standard solution were used for calibration after adjustment to pH 9 by addition of a few drops of concentrated sodium hydroxide solution. With an SCE as external reference electrode, the experimental cell is

internal reference electrode (Pt-Pt) electrode)	internal reference solution 0.01M EtOCSSK at pH 9	PVC matrix membrane with tetraheptylammonium ethyl xanthate	standard xanthate solution at pH 9	saturated KCl solution	external reference electrode (SCE)
---	---	---	------------------------------------	------------------------	------------------------------------

The two half cells, the PVC-matrix membrane electrode in standard xanthate solution and the external reference electrode in saturated potassium chloride solution were electrically linked by a potassium nitrate salt bridge. The measured potentials of the standard solutions were plotted as a function of the logarithm of the xanthate concentration.

## RESULTS AND DISCUSSION

### Nature and composition of the membrane

The 1:1 ion-pair nature of the sensor has been established by means of its NMR spectrum in  $\text{CDCl}_3$ . Of the quaternary ammonium salts considered for the sensor preparation, tetraheptylammonium bromide emerged as the best; others considered included n-hexadecyltrimethylammonium bromide and Aliquat S336. Addition of plasticizer in the membrane fabrication greatly improved the performance and the lifetime of the membrane. After some experimentation, the optimum amount of plasticizer to be

used in the membrane fabrication was found to be 40%.

### Response characteristics of the electrode

A typical calibration graph for the tetraheptylammonium ethyl xanthate-PVC membrane electrode, as depicted in Fig. 2, showed a Nernstian response in the range  $5.0 \times 10^{-2}$ – $7.1 \times 10^{-5}M$  ethyl xanthate. The response characteristics of the electrode, obtained from nine determinations over a period of two months, are summarized in Table 1. The slope, correlation coefficient and detection limit all demonstrated the suitability and sensitivity of this membrane for the determination of ethyl xanthate. In addition, the response of the electrode was sufficiently rapid for routine analysis. The time required for the electrode to reach a value within  $\pm 1$  mV of the final equilibrium potential, was less than 30 sec for successive immersions in ethyl xanthates of different concentrations. Also, the aging of the membrane was not a serious problem, the performance of the electrode in terms of linearity and Nernstian response being reproducible over a period of two months.

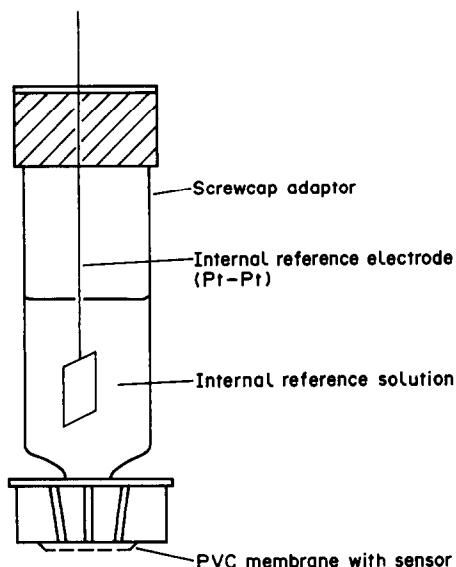


Fig. 1. Schematic diagram of the electrode.

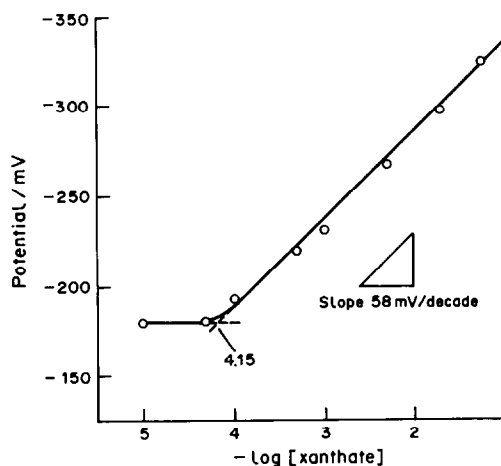


Fig. 2. Calibration graph for potassium ethyl xanthate at pH 9.

Table 1. Response characteristics of tetraheptylammonium ethyl xanthate-PVC membrane for different xanthates

Xanthate	$\text{C}_2\text{H}_5\text{OCSSK}$	$\text{C}_7\text{H}_{15}\text{OCSSK}$	cyclohexyl —OCSSK
Slope, mV/log [xanthate]	58.6*	57.1†	55.3†
Correlation coefficient	0.9997	0.9993	0.9993
Detection limit, $M$	$7.1 \times 10^{-5}$	$5.8 \times 10^{-5}$	$1.5 \times 10^{-5}$

\*Average of nine determinations at pH 9.

†Average of five determinations at pH 11.

Table 2. Selectivity coefficients for tetraheptylammonium ethyl xanthate-PVC membrane electrode

Interfering compound	Concentration of interfering compound, M	Selectivity coefficient, $K_{ij}$
Sodium chloride	$2.1 \times 10^{-3}$	$3.3 \times 10^{-2}$
Potassium nitrate	$2.0 \times 10^{-3}$	*
Sodium carbonate	$1.8 \times 10^{-3}$	*
Sodium acetate	$2.0 \times 10^{-3}$	$3.6 \times 10^{-2}$
Ammonium pyrrolidinedithiocarbamate	$9.6 \times 10^{-4}$	*

\*No interference was observed by the fixed interference method.<sup>9</sup>

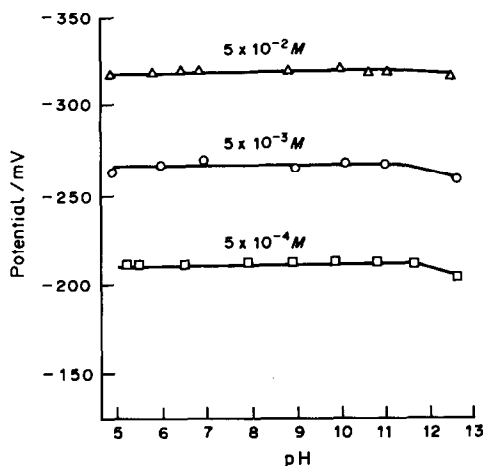


Fig. 3. Effect of pH on the potential of the tetraheptylammonium ethyl xanthate-PVC membrane electrode at different xanthate concentrations.

#### Effect of pH and interfering ions

The effect of pH on the response of the electrode at three different concentrations of ethyl xanthate is shown in Fig. 3. Evidently, the electrode exhibits a wide pH working range. Within the pH range 5.0–11.5, the potential difference for the solutions varied by less than 1 mV. In practice, the potential measurement is best made between pH 9 and pH 11 (Table 1).

To study the selectivity of the electrode, the response of the electrode to ethyl xanthate was examined in the presence of some foreign organic and inorganic species, by the fixed interference method.<sup>9</sup> The selectivity coefficients found are reported in Table 2. Common inorganic ions found in water, such as  $\text{Na}^+$ ,  $\text{K}^+$ ,  $\text{NH}_4^+$ ,  $\text{CO}_3^{2-}$ ,  $\text{NO}_3^-$ , do not interfere with xanthate determination, and acetate and chloride interfere only slightly. It is interesting that

1-pyrrolidinecarbodithiocarbamate, which has a very similar structure to xanthate, did not interfere.

#### Response characteristics of the electrode to other xanthates

At the outset of this study, we considered that an electrode with a tetra-alkylammonium ethyl xanthate as the sensing material should be a general sensing device for xanthates derived from alcohols other than ethanol. To prove this supposition, the electrode was calibrated with standard solutions of potassium n-heptyl and cyclohexyl xanthates derived from n-heptanol and cyclohexanol respectively. Linear Nernstian calibration graphs resulted, with detection limits comparable to that for ethyl xanthate. The response characteristics of the tetraheptylammonium ethyl xanthate PVC membrane toward various xanthates are summarized in Table 1, and show that the application of the electrode, can be extended to the determination of xanthates derived from other primary and secondary alcohols besides ethanol.

#### REFERENCES

1. K. H. Buchel (ed.), *Chemistry of Pesticides*, pp. 158, 273. Wiley, New York, 1983.
2. W. K. Lewis, L. Squires and G. Broughton, *Industrial Chemistry of Colloidal and Amorphous Materials*, p. 268. Macmillan, New York, 1942.
3. I. M. Kolthoff and P. J. Elving (eds.), *Treatise on Analytical Chemistry*, Part II, Vol. 15, Wiley-Interscience, New York, 1976.
4. T. S. Ma and S. S. M. Hassan, *Organic Analysis Using Ion Selective Electrodes*, Vols. 1 and 2, Academic Press, London, 1982.
5. V. V. Coşofreţ and P. G. Zugravescu, *Rev. Chim. (Bucharest)*, 1977, **28**, 785.
6. A. Kowal, E. Krauss and A. Pomianowski, *Chem. Anal. (Warsaw)*, 1981, **26**, 441; *Chem. Abstr.* 1982, **97**, 103644v.
7. A. I. Vogel, *Elementary Practical Organic Chemistry*, Part III, p. 839. Wiley, New York, 1958.
8. W. H. Chan, M. S. Wong and C. W. Yip, *J. Chem. Educ.* 1986 **63**, 915.
9. G. G. Guilbault, *Ion-Selective Electrode Rev.*, 1979, **1**, 139.

## CONFIGURATION WITH INTERNALLY COUPLED VALVES TO OVERCOME SHORTCOMINGS IN THE SIMULTANEOUS DETERMINATION OF NITRITE AND NITRATE BY FLOW-INJECTION ANALYSIS

B. BERMUDEZ, A. RIOS, M. D. LUQUE DE CASTRO and M. VALCARCEL

Department of Analytical Chemistry, Faculty of Sciences, University of Córdoba, Córdoba, Spain

(Received 21 October 1987. Revised 20 March 1988. Accepted 21 June 1988)

**Summary**—A configuration with internally coupled valves and a reductant column located in the loop of the secondary valve is proposed for the simultaneous determination of nitrite and nitrate. Depending on the column characteristics, a washing stream flowing in the opposite direction to the sample may or may not be required. The washing step may conveniently be performed by use of the proposed configuration.

In implementing an automatic FIA method for routine determination of nitrite and nitrate, based on earlier methods, namely the direct determination of nitrite by the modified Griess reaction and the sum of nitrite and nitrate after passage of the sample through a column of copper-coated cadmium,<sup>1-5</sup> we found that when the redox column was used, the signal for a fixed amount of nitrate increased in the first 40-50

min and then remained essentially constant (Fig. 1). After searching the literature, we found no clear reference to this phenomenon, nor to the expected column life-time, but only indirect information ("copperized cadmium filings were prepared daily";<sup>2</sup> "The reaction column can be activated by replacing the distilled water with EDTA-copper sulphate solution"<sup>3</sup>) which indicated the problem. A recent paper<sup>5</sup>

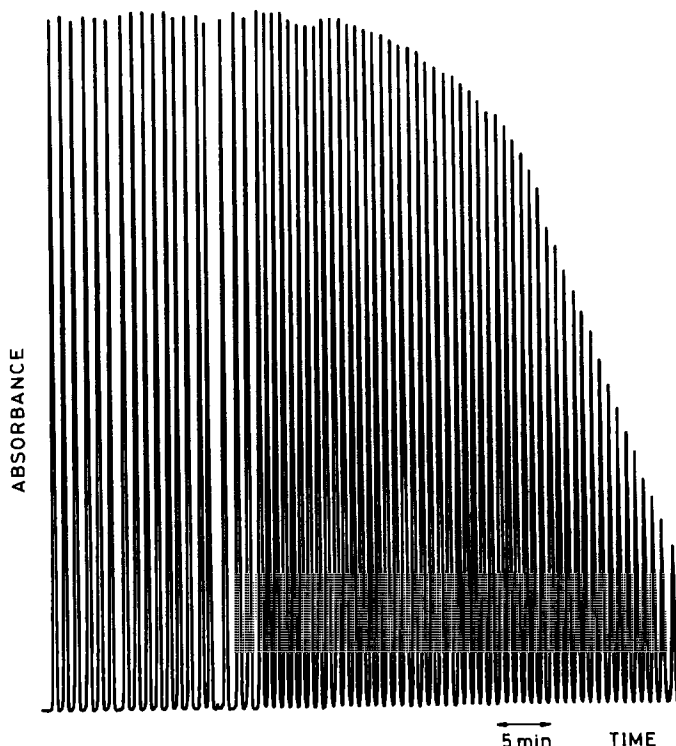


Fig. 1. Reproducibility of the signals obtained with a column of copper-coated cadmium and a normal FIA configuration.



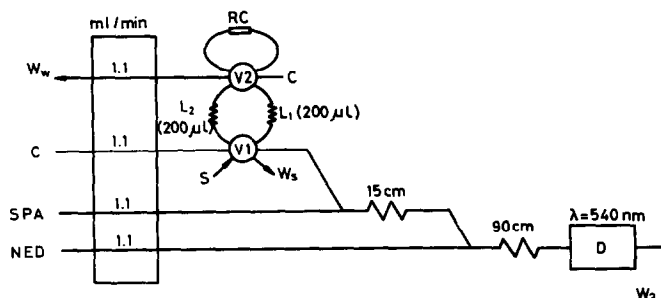


Fig. 2. FIA configuration used for the determination of nitrite and nitrate. Ww, washing waste; C, carrier; SPA, sulphaniamide; NED, *N*-(1-naphthyl)ethylenediamine; RC, redox column; V1 and V2, primary and secondary valves, respectively; L<sub>1</sub> and L<sub>2</sub> sub-loops of secondary valve; S, sample; Ws sample waste; D, detector; Wg general waste.

reported the use of two columns (copper and copper-coated cadmium) to overcome it.

Having found that the effect was due to the continuous increase in column compactness caused by the uninterrupted flow in the same direction, we have tried to solve this problem and achieve a completely simultaneous determination (both analytes with a single sample injection<sup>6</sup>) by using a configuration with internally coupled valves<sup>7,8</sup> such as that shown in Fig. 2.

#### EXPERIMENTAL

##### Apparatus

A Pye Unicam SP6-500 spectrophotometer equipped with a Hellma 178.12QS flow-cell, a Gilson Minipuls-2 peristaltic pump, a Tecator type I chemiford and a home-made dual-injection valve were used.

##### Reagents

**Sulphanilamide solution.** Prepared by dissolving 0.95 g of the chemical in 10 ml of concentrated hydrochloric acid and diluting to 250 ml with distilled water.

***N*-(1-Naphthyl)ethylenediamine dihydrochloride solution.** Prepared by dissolving 0.36 g of the chemical and 2.8 g of sodium chloride in 250 ml of distilled water.

**Standard nitrite and nitrate solutions, 1.000 g/l.**

##### Column package

The reduction column was made by packing a glass capillary (8.5 cm long, 1.8 mm bore) with cadmium granules

of various sizes, coated with copper by passage of a 0.1% cupric sulphate/0.1M copper-EDTA solution. In the assembly shown in Fig. 2, the sample (containing both analytes) fills the two sub-loops (L<sub>1</sub> and L<sub>2</sub>) of the primary valve (V1), and the reduction column is contained in the loop of the secondary valve (V2).

##### Procedure

The loop of the primary valve is filled during a time interval in which the washing solution (the carrier, 10<sup>-3</sup>M acetic acid) circulates through the loop of the secondary valve (and hence through the reduction column) from right to left. When both valves are switched simultaneously to the emptying position, the sample volume contained in L<sub>1</sub> passes through the reactor section, merges with the reagents and, on arrival at the detector, provides a peak due to the presence of nitrite in the sample; meanwhile, the sample volume in L<sub>2</sub> passes through the reduction column in the

Table 1. Classification of the columns according to grain-size distribution

Grain diameter, mm	Type I, %	Type II, %	Type III, %
> 1	2.0	6.0	10.0
1-0.84	3.5	8.5	20.3
0.84-0.50	32.0	59.5	53.4
0.50-0.42	26.5	18.5	15.1
0.41-0.21	25.5	7.5	1.2
0.21-0.17	3.0	0.0	0.0
0.17-0.149	7.5	0.0	0.0

Table 2. Behaviour of the different types of column

Column type	Grain size	Features	Time needed to attain re-producible signals	Effect of reversal of flow	Column life-time
I	small	uncoppered	≥ 60 min (progressive increase of the signal)	critical; mandatory control of flow in each direction	at least 15 days
		coppered	>> 60 min (progressive decrease of the signal)	critical; mandatory control of flow in each direction	1 day
II	medium	uncoppered	15-20 min	significant; reversal advisable	at least 15 days
		coppered	15-20 min (poorer stability than for uncoppered)	significant	1 day
III	medium-large	uncoppered	3-4 min	not useful	at least 15 days
		coppered	3-4 min	not useful	1 day

Table 3. Features of the method

	NO <sub>3</sub> <sup>-</sup>	NO <sub>2</sub> <sup>-</sup>	
		first peak	second peak
<i>(a) Uncoppered column</i>			
Linear range, µg/ml	0.1–16.0	0.025–16.0	
Intercept	0.004	-0.007	-0.005
Slope	0.0725	0.327	0.272
Regression coefficient	0.999	0.999	0.999
RSD, % (mixtures)*	0.9	1.1	
<i>(b) Coppered column</i>			
Linear range, µg/ml	0.2–18.0	0.1–3.5	
Intercept	0.001	0.002	0.004
Slope	0.0705	0.326	0.266
Regression coefficient	0.999	0.999	0.999
RSD, % (mixtures)*	1.3	1.5	

\*[NO<sub>2</sub><sup>-</sup>] 1.0 µg/ml; [NO<sub>3</sub><sup>-</sup>] 5 µg/ml (11 samples, each injected in triplicate).

secondary valve, where nitrate is reduced to nitrite, and when this plug reaches the detector, the signal produced is due to the sum of nitrite and nitrate initially present in the sample.

#### RESULTS AND DISCUSSION

After study of the FIA manifold variables with the reagent concentrations described in the literature (resulting in the optimum values shown in Fig. 2) the influence of the grain size and nature of the reductant was examined. Three types of particle-size distribution (Table 1) were tested. The results given in Table 2 show that:

(1) when small or medium-sized grains are used (easier column packing and higher reduction yield) reversal of flow between the washing and reduction steps is necessary to preserve the degree of compactness and yield reproducible signals (use of only small grain sizes even requires accurate control of the duration of passage in both directions);

(2) use of medium to large grain sizes does not require reversal of the flow, and the signal stabilizes rapidly, though it is always smaller than that achieved with small grain-sizes;

(3) there is no clear gain in copper-coating the cadmium beads.

The features of the method were determined by using a column made with type II particle-size distribution (with and without copper coating). Table 3 summarizes the results.

The sampling frequency is 65 per hr. The proposed configuration allows determination of both nitrite and nitrate in the same sample, elimination of the effect of changes in the column compactness, and elimination of loss of activity of the reductant (non-coated).

#### REFERENCES

1. B. C. Madsen, *Anal. Chim. Acta*, 1981, **124**, 437.
2. M. F. Giné, H. Bergamin F<sup>o</sup>, E. A. G. Zagatto and B. F. Reis, *ibid.*, 1980, **114**, 191.
3. J. F. van Staden, *ibid.*, 1982, **138**, 403.
4. L. Anderson, *ibid.*, 1979, **110**, 123.
5. J. F. van Staden, A. E. Joubert and H. R. van Vliet, *Z. Anal. Chem.*, 1986, **325**, 150.
6. M. D. Luque de Castro and M. Valcárcel, *Trends Anal. Chem.*, 1986, **5**, 71.
7. A. Ríos, M. D. Luque de Castro and M. Valcárcel, *Anal. Chem.*, 1986, **58**, 663.
8. *Idem*, *Anal. Chim. Acta*, 1986, **187**, 139.

## DETERMINATION OF QUATERNARY AMMONIUM SURFACTANTS IN PHARMACEUTICAL FORMULATIONS BY THE HYPOCHROMIC EFFECT

SONIA Z. EL-KHATEEB and EZZAT M. ABDEL-MOETY

King Saud University, College of Pharmacy, P.O. Box 2457, Riyadh 11451, Saudi Arabia

(Received 18 November 1987. Revised 31 May 1988. Accepted 15 June 1988)

**Summary**—A spectrophotometric procedure for determination of the quaternary ammonium salts cetrimide (*N,N,N*-trimethyl-1-hexadecylammonium bromide), cetylpyridinium chloride (1-hexadecylpyridinium chloride) and sapamine [*N*-(2-dimethylaminoethyl)oleamide acetate] in bulk form and some pharmaceutical formulations, such as eye-drops, disinfectant solutions, creams and tablets, is described. Following TLC separation when necessary, addition of an aqueous solution of the active surfactant to a standard amount of Bromothymol Blue, buffered at pH 7.5, leads to an equivalent decrease of the absorbance at 610 nm, which can be taken as an analytical measure of the drug concentration. Good mean recoveries have been obtained for standard additions of these analytes to pharmaceutical formulations containing them.

Quaternary ammonium salts are commonly used in galenicals, owing to their emulsifying properties, *i.e.*, their surface activity, and/or their antibacterial effects. Such compounds are normally used in very low concentrations, and are then difficult to determine with high precision and reproducibility. Most methods for their determination are based on complexation with an acid dye followed by extraction of the coloured complex into a chlorinated hydrocarbon.<sup>1-3</sup> Formation of an emulsion in the extraction system leads to inaccuracy and poor reproducibility. A survey of dye-surfactant interactions has recently been made, including the influence of the cationic, anionic or non-ionic character of a surfactant on the absorption and/or fluorescence behaviour.<sup>4</sup> Ion-exchange separation and automated determination of commercial detergent formulations has also been investigated.<sup>5</sup>

The present work overcomes the problem of incomplete extraction of the dye-surfactant products, by use of a spectrophotometric method that measures the hypochromic effect caused by the action of cationic surfactants on the acid dye Bromothymol Blue.

### EXPERIMENTAL

#### Apparatus

A Varian DMS 100 double-beam spectrophotometer with matched 1-cm glass cuvettes was used. TLC was performed on 0.3-mm thick layers of silica gel G (Merck) prepared and activated according to Stahl;<sup>6</sup> the developing solution was a 1:9 v/v mixture of concentrated ammonia solution (s.g. 0.88) and acetone.

#### Reagents

Phosphate buffer, pH 7.5, was prepared from 0.05M dipotassium hydrogen phosphate and 0.05M potassium dihydrogen phosphate.<sup>7</sup> A 10<sup>-3</sup>M solution of Bromothymol Blue (Riedel-DeHaën) was prepared according to BP 1980.<sup>8</sup> Modified Dragendorff's reagent<sup>9</sup> was freshly prepared. Pure

CP-grade samples of cetrimide (ICI), cetylpyridinium chloride (Prolabo) and sapamine (Ciba-Geigy) were used without further treatment, to prepare 10<sup>-3</sup>M solutions in water. Corresponding 10<sup>-4</sup>M solutions were made by dilution with the pH 7.5 phosphate buffer.

#### Pharmaceutical preparations

Samples of pharmaceutical formulations containing the surfactants were randomly purchased from local pharmacies in Cairo and Riyadh.

#### Procedures

**Calibration graph.** Transfer suitable volumes (in the range 1-10 ml) of standard 10<sup>-4</sup>M surfactant solution in phosphate buffer (pH 7.5) into 25-ml standard flasks. To each add about 5 ml of the buffer solution followed by 1 ml of Bromothymol Blue solution, mix, and dilute to volume with the buffer. Measure the absorbance (*A*) at 610 nm against the buffer solution. Measure the corresponding absorbance (*B*) of a reagent (buffer + Bromothymol Blue) solution similarly prepared. Plot *B* - *A* vs. concentration. Use the same procedure for assay of the bulk analytes.

**Disinfectant solutions.** Mix the contents of at least 3 bottles, transfer accurately a known volume equivalent to about 30 mg of surfactant into a 100-ml standard flask and dilute it to the mark with 95% ethanol. Apply a 0.5 ml portion of the solution in band form, 2 cm above the lower edge of an activated TLC plate. Apply 10- $\mu$ l of 1% alcohol solutions of the authentic surfactant and other ingredients beside the sample band. Develop the plate in the acetone/ammonia system and let it dry in air (under a fume hood). Cover the sample and spray the reference spots with modified Dragendorff's reagent, locate the surfactant band, scrape it off and transfer it to a small beaker. Extract the surfactant with two 5-ml portions of 5% aqueous ethanol and then with 10 ml of phosphate buffer (pH 7.5), collecting the extracts in a 25-ml standard flask. Add 1 ml of Bromothymol Blue reagent, mix and dilute to volume with buffer solution. Run a blank with 1 ml of the indicator in the same phosphate buffer, without surfactant. Record the absorbance at 610 nm.

**Creams.** Mix the contents of at least three tubes and weigh accurately an amount equivalent to 2.5-5 mg of surfactant. Transfer it to a 150-ml separating funnel with 50 ml of water and 30 ml of petroleum ether (b.p. 60-80°) and shake the

funnel mechanically for about 5 min. If an emulsion forms, centrifuge the mixture (3–5 min). Repeat the extraction with 30 ml of petroleum ether, and centrifuge if necessary, then wash the combined organic extracts with two 10-ml portions of water. Combine the aqueous phase and washings in a 100-ml standard flask and dilute to the mark with distilled water. Transfer 2 ml of this solution to a 25-ml standard flask and complete the analysis as for authentic samples.

**Eye-drops.** Mix the contents of 3–5 bottles, transfer 5 ml into a flat-bottomed dish, and evaporate the solvent over concentrated sulphuric acid in a vacuum desiccator. Dissolve the residue in 1 ml of ethanol, and apply the TLC separation *etc.*, as for disinfectant solutions.

**Tablets.** Weigh and powder at least ten tablets and calculate the average weight of one tablet. Extract an amount of powdered tablet equivalent to 3–12 mg of surfactant, with 10, 5 and 5 ml of ethanol, and dilute the combined extracts to volume in a 25-ml standard flask, with ethanol. Apply the TLC separation *etc.*, as for disinfectant solutions.

## RESULTS

The results are calculated from calibration graphs prepared with solutions of the authentic surfactant or from the corresponding linear regression equation, or from the apparent absorptivities for the surfactants.

Table 1 shows the results of analyses of the three model surfactants and their statistical comparison with those obtained by the BP 1980 procedure.<sup>10</sup>

Table 2 shows results of pharmaceutical assays and recoveries of different amounts of added pure surfactants.

## DISCUSSION

Analytical applications of surfactants to alter reaction pathways and equilibria are based mainly on the characteristics of micelles. Addition of a cationic detergent to an indicator in anionic form produces spectral changes due to solubilization of the anion in the surfactant micelles.<sup>4,11</sup>

Formation of true ion-association complexes between ionic surfactants and dyes with opposite charges has been suggested,<sup>12,13</sup> but not yet satisfactorily explained. A possible mechanism recently discussed<sup>4</sup> is that in the presence of cationic surfactants, an aromatic compound containing  $-\text{SO}_3^-$  or  $-\text{COO}^-$  groups, such as a dyestuff, may be incorporated into the water-rich Stern layer of the micelles in a sandwich arrangement. This permits not only hydration of the hydrophilic groups but also solubilization of the aromatic part of the dye by means of the  $-\text{NR}_3^+$  groups and participation of van der Waals interactions between adjacent surfactant chains and the organic dye moiety. This will lead to a change in the micro-environment of the chromophore.

Indirect methods based on the acid dye technique<sup>1-3</sup> have the disadvantage that the ion-association complex must be extracted, which may reduce the accuracy and reproducibility. Procedures similar to the one described here were developed by Lowry for determination of benzalkonium chloride, benzethonium chloride and chlorohexidine gluconate.<sup>14</sup>

Table 1. Purity assessment of authentic samples of cetrимide, cetylpyridinium chloride and sapamine by applying the proposed acid dye technique and a pharmacopoeial procedure (BP 1980)<sup>10</sup>

Sample	Proposed method			Official (BP 1980) method	
	Amount taken*		Recovery, † %	Amount taken, g	Recovery, † %
	mg	µg/ml			
Cetrимide	75–300	3–12	99.9 ± 0.9 ( <i>n</i> = 8) <i>t</i> = 0.367 (2.365)§	~2	100.2 ± 0.1 ( <i>n</i> = 8)
Cetylpyridinium chloride	75–300	3–12	99.8 ± 0.7 ( <i>n</i> = 8) <i>t</i> = 1.785 (2.365)§	~2	100.1 ± 0.1 ( <i>n</i> = 9)
Sapamine®	120–350	4.8–14	99.8 ± 0.5 ( <i>n</i> = 8) <i>t</i> = 0.644 (2.365)§	~2	100.4 ± 0.8 ( <i>n</i> = 9)

\*Samples and working solutions: see experimental part.

†Mean percent recovery ± standard deviation for *n* experiments.

§Figures in parentheses are the corresponding theoretical *t*-values at *p* = 0.05.

Table 2. Assay and recovery of cetrимide and sapamine in some pharmaceutical formulations by the described acid dye procedure

Pharmaceutical formulations	Surfactant	Nominal content	Assay*, %	Amount added, mg	Recovery	
					%	SD, §
Savlon <sup>®</sup> solution	cetrимide	30 mg/ml	97.6	15–30 mg	99.4	0.95 ( <i>n</i> = 6)
Cetazole <sup>®</sup> cream	cetrимide	5 mg/g	99.2	5–12 mg	99.2	0.60 ( <i>n</i> = 5)
Prisoline <sup>®</sup> drops	cetrимide	20 µg/ml	104.3	50–140 µg	99.7	0.76 ( <i>n</i> = 5)
Enterovioform <sup>®</sup> tablets	sapamine	not stated	(8.64 mg/g)†	2–5 mg	100.2	0.31 ( <i>n</i> = 5)

\*Relative to nominal content, average of at least 5 replicates.

†Actual content found.

§SD, is the relative standard deviation.

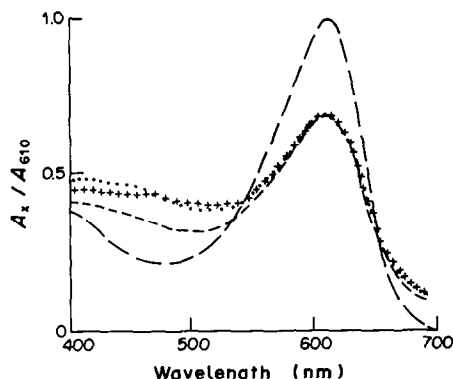


Fig. 1. Effect of equal molar amount of cetrimide (----) cetylpridinium chloride (.....) and sapamine (+ + + +) on the colour of Bromothymol Blue (—), expressed as ratio of absorbance to that of Bromothymol Blue at 610 nm ( $A_x/A_{610}$ ).

Optimization of the conditions for the acid dye technique included choice of pH, dye:drug ratio, etc. Different buffers in the pH range 5–9 were tried, and use of phosphate buffer, pH 7.5, was found to give the highest absorbances of the Bromothymol Blue–surfactant complexes. Bromothymol Blue gives higher absorbances than Bromophenol Blue and Phenol Red.<sup>3</sup>

The change in absorbance was found to be greatest at 610 nm (Fig. 1). Application of Job's method<sup>15</sup> showed that all three surfactants react with Bromothymol Blue in 1:1 molar ratio. The calibration graph was linear over the range  $0.5\text{--}3 \times 10^{-3}M$ .

Table 1 shows that there are no significant differences between the results obtained by the present method and the pharmacopoeial method.

Table 2 shows acceptable recovery values for standard additions of the appropriate surfactant to pharmaceutical preparations containing cetrimide or

sapamine. For samples containing more than one surfactant of the same type, the acid dye technique can only be applied after separation of the analytes.<sup>4,5</sup> Also, when the surfactant is present in minute quantities, a separation and preconcentration step may be necessary for an acceptable degree of sensitivity and accuracy to be achieved. The TLC method recommended by Bey<sup>16</sup> is suitable for the purpose.

The method described is preferred when extraction difficulties arise with other methods, and its sensitivity allows the low concentration of surfactants in pharmaceutical formulations to be determined with good precision and confidence.

#### REFERENCES

1. R. S. Santoro, *J. Am. Pharm. Assoc. Sci. Ed.*, 1960, **49**, 666.
2. L. C. Chatten and K. O. Okamura, *J. Pharm. Sci.*, 1973, **62**, 1328.
3. S. Z. El-Khateeb, Z. H. Mohamed and L. El-Sayed, *Tenside-Detergents*, 1988, **25**, 236.
4. M. E. Diaz Garcia and A. Sanz-Medel, *Talanta*, 1986, **33**, 255.
5. L. S. MacDonald, B. G. Cooksey, J. M. Ottaway and W. C. Campbell, *Anal. Proc.*, 1986, **23**, 448.
6. E. Stahl (ed.), *Thin-layer Chromatography*, 2nd Ed., p. 55. Springer Verlag, Heidelberg, 1969.
7. *Documenta Geigy Scientific Tables*, Part 3, p. 59, Ciba-Geigy, Basel, 1984.
8. *British Pharmacopoeia* 1980, A47. HMSO, Cambridge, 1980.
9. R. Munier, *Bull. Soc. Chem. Biol.*, 1953, **35**, 1225.
10. *British Pharmacopoeia* 1980, p. 91, HMSO, Cambridge, 1980.
11. G. S. Hartley, *Trans. Faraday Soc.*, 1934, **30**, 44.
12. J. Rosendorfova and L. Čermáková, *Talanta*, 1980, **27**, 705.
13. V. Skarydová and L. Čermáková, *Collection Czech. Chem. Commun.*, 1982, **47**, 776.
14. J. B. Lowry, *J. Pharm. Sci.*, 1979, **68**, 110.
15. P. Job, *Ann. Chim. Paris*, 1928, **9**, 113.
16. K. Dey, *Fette Seifen Anstrichmittel*, 1965, **67**, 25.

## DETERMINATION OF CYADOX AND ITS METABOLITES IN PLASMA BY ADSORPTIVE VOLTAMMETRY

IVANA ŠESTÁKOVÁ

Research Institute for Feed Supplements and Veterinary Drugs, 254 49 Jilové u Prahy, Czechoslovakia

MILOSLAV KOPANICA

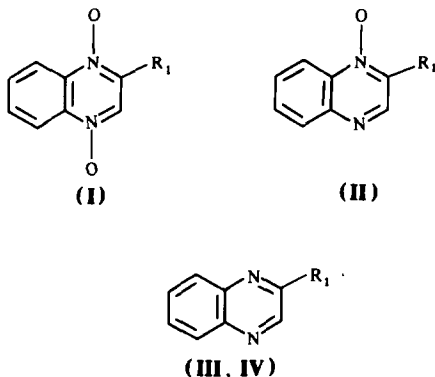
UNESCO Laboratory of Environmental Electrochemistry, J. Heyrovský Institute of Physical Chemistry and Electrochemistry, Czechoslovak Academy of Sciences, Dolejškova 3, 182 23 Prague 8, Czechoslovakia

(Received 11 April 1988. Accepted 14 June 1988)

**Summary**—Adsorptive stripping voltammetry was combined with separation of the surfactants by gel chromatography or solvent extraction for determination of the growth promotor, cyadox, and its metabolites in the plasma from pig blood. The procedure permits determination of the substance at concentrations from units to hundreds of ng per ml of plasma. The accuracy of the results was checked by comparison with radiochemical measurements.

Studies of the adsorptive voltammetry of some derivatives with the quinoxaline-*N*-dioxide structure<sup>1,2</sup> have indicated that these substances can be determined at the nanomolar level after adsorptive accumulation on the surface of a mercury electrode. The detection limit for the growth stimulant cyadox<sup>3,4</sup> is  $3 \times 10^{-10} M$ . Owing to this high sensitivity, adsorptive stripping voltammetry can be applied to monitoring cyadox and its metabolites in the plasma from pigs reared with fodder containing cyadox. Such determinations have hitherto been made only radiometrically, with a tritiated cyadox derivative.<sup>5</sup>

On the basis of our knowledge of cyadox (I) metabolism,<sup>6</sup> the adsorptive voltammetric determination has also been applied to cyadox monoxide (II), deoxycyadox (III) and the final metabolite isolated from pig's blood, quinoxaline-2-carbonylglycine (IV). The interference from surfactants was eliminated by removal of the surfactants from plasma samples by gel chromatography<sup>7</sup> or by extraction of the test substances and back-extraction into a pure electrolyte.



I, II and III:  $R_1 = CH=NNHCOCH_2CN$   
IV:  $R_1 = CONHCH_2COOH$

### EXPERIMENTAL

#### Apparatus

The measurements were made with a PA-3 polarographic analyser and a three-electrode circuit consisting of a static mercury drop electrode, SMDE-1, a saturated calomel reference electrode (SCE) and a platinum counter-electrode (all from Laboratorní Přístroje, Prague). The solutions were deaerated by passage of nitrogen.

The extractions were performed with a Mixxor liquid extractor (Cole Palmer, USA). Preseparations were done with a Sep-Pak C 18 microcolumn (Waters, USA). Sephadex G-25 Medium (Pharmacia, Uppsala, Sweden) columns ( $200 \times 10$  mm) were used for gel-chromatography separations.

#### Chemicals

Cyadox (I), cyadox monoxide (II), deoxycyadox (III) and quinoxalinecarbonyl glycine (IV) were prepared in the Research Institute of Pharmacy and Biochemistry, Prague, and analysis showed that their active component content was at least 99%. Solutions of the substances ( $200 \mu g/ml$ ) were prepared in freshly redistilled dimethylformamide, and were used within three days of preparation; more dilute solutions were prepared immediately before use.

Dimethylformamide (DMF) was purified by distillation and kept at  $6^\circ$ . All the chemicals used were of p.a. purity and the water was distilled twice in a silica apparatus.

#### Procedures

**Sample preparations.** The plasma was obtained from the blood taken from the animal *vena cava cranialis*. Heparin was added, and the sample was centrifuged and then frozen until used for analysis.

The samples for monitoring the metabolic changes as a function of time, were collected at the required time intervals from 10 experimental and 4 control animals that were fed with a fodder mixture commonly used for a weight category of 35 kg. The experimental animals were fed 100 mg of cyadox per kg of the mixture, according to a programme involving first 4 weeks of the use of the pure mixture, followed by 10 days of feeding with the mixture containing cyadox and then again using the pure mixture. The control group of pigs was fed with only the pure mixture. The initial weight of the piglets was 16 kg and the average consumption of fodder was 1.63 kg per pig per day.

**Separation of surfactants by gel chromatography.** Sephadex (0.5 g) was stirred with 10 ml of a Britton-Robinson

buffer of pH 2.2. After swelling, the Sephadex was packed in a 200 × 10 mm column and washed with 10 ml of the buffer. A 100- $\mu$ l plasma sample was added to the column and eluted with the pH 2.2 buffer containing 10% v/v DMF, at a flow-rate of 1.5 ml/min. The first 5 ml of the eluate were discarded and then 10-ml fractions were collected and used for the voltammetric determination. A fresh Sephadex column must be prepared for each sample.

**Extraction separation.** A 1-ml portion of the plasma was acidified with 1 ml of hydrochloric acid (1 + 4) and extracted with acetone in the Mixxor liquid extractor. The acetone layer was separated, the acetone evaporated in a vacuum rotary evaporator and the residue immediately dissolved in 10 ml of Britton–Robinson buffer (pH 2.2). This solution was applied to a Sep-Pak microcolumn pre-washed with 10 ml of methanol and 10 ml of water. The substances retained in the column were eluted with 10 ml of methanol and the solvent was evaporated in a rotary vacuum evaporator. The resultant residue was dissolved in 10 ml of the pH 2.2 buffer, filtered through a fine-pore ashless paper filter (e.g., Whatman No. 44 or Schleicher and Schüll blue band) and used for the voltammetric determination.

**Voltammetric determination.** The measurement was performed with the SMDE used as a hanging mercury drop electrode, and a potential scan from +0.10 to -0.70 V (SCE) at 20 mV/sec, by the differential pulse technique (100-msec pulses with 100-msec intervals between them). The accumulation was done at a potential  $E_{ac} = +0.10$  V in stirred solution, and was followed by a 15-sec rest period.

## RESULTS AND DISCUSSION

### Adsorptive stripping voltammetry of cyadox and its metabolites

Cyadox (I) and cyadox monoxide (II) are reduced in two steps, corresponding to the reduction of the N–O groups and the quinoxaline nucleus, respectively. Deoxycyadox (III) and quinoxaline-2-carboxylglycine (IV) are reduced in a single step, at the quinoxaline nucleus.<sup>8</sup> It has been found that accumulation at +0.10 V increases the height of the peaks corresponding to both reduction steps, as described for cyadox and other quinoxaline-N-dioxide derivatives.<sup>1</sup> For analytical purposes it is more suitable to measure the heights of the peaks corresponding to the reversible reduction of the quinoxaline ring; the peak potential varies from -0.26 to -0.37 V. The dependence of the peak current on the accumulation time is given in Fig. 1.

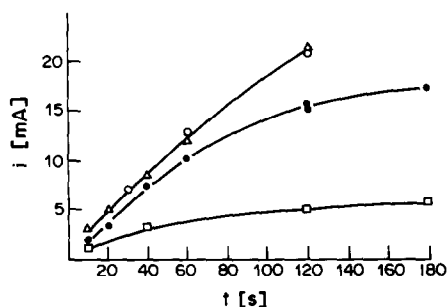


Fig. 1. Dependence of the peak height for the reduction of the quinoxaline ring on the accumulation time: Britton–Robinson buffer, pH 2.2,  $E_{ac}$  +0.10 V, DPV,  $\Delta E$  25 mV, ○—cyadox, △—cyadox monoxide, ●—deoxycyadox, □—quinoxaline-2-carboxylglycine.

The peak current is proportional to concentration for all four substances from 5 to 250 ng/ml, with an accumulation time of 40 sec.

### Adsorptive stripping determination after separation of surfactants from the plasma

The separation of surfactants from the plasma by gel chromatography was verified for cyadox (I) and deoxycyadox (III). To 100- $\mu$ l samples of the plasma from the control animals, 400 ng of cyadox or deoxycyadox were added. After the chromatographic separation, recoveries of 70% of the cyadox and 93% of the deoxycyadox were obtained in the 5–15 ml fraction of the eluate. This fraction was further treated and the linearity of the dependence of the height of the quinoxaline reduction peak on the substance concentration was verified. The measurements were performed for concentrations from 5 to 200 ng/ml, with 40-sec accumulation at +0.10 V. The plots were always linear and the slopes for cyadox and cyadox monoxide were the same, 1.25 nA · ml · ng<sup>-1</sup>, similar to the value obtained for cyadox in sodium perchlorate medium.<sup>1</sup> The values obtained for deoxycyadox and quinoxalinecarbonyl glycine were 3.25 and 0.25 nA · ml · ng<sup>-1</sup>, respectively; hence the method is unsuitable for determination of quinoxalinecarbonyl glycine.

### Plasma analysis

In analyses of samples from the test animals, peaks corresponding to the reduction of the N–O groups were not found, only those corresponding to the reduction of the quinoxaline ring. The peak heights depended on the accumulation time. The results were evaluated by standard addition of deoxycyadox (20 ng/ml); when the gel chromatographic separation was used the 5–15 ml fraction was measured. The peak heights were evaluated by comparison of the current responses for the test and control animals, with the same sampling technique and both separation methods. In view of biological variability, the mean values were used. The values of the current for the control samples confirmed that the samples were not changed by aging or exposure to higher temperatures. The results for the two separation procedures are given in Table 1.

Table 1. Deoxycyadox level in the plasma of pigs

Number of days after termination of cyadox application	Separation	
	Gel chromatography, ng/ml	Extraction, ng/ml
1	446	434
2	261	300
3	215	—
7	154	—
8	92	—
14	0	0
15	0	—
21	0	—
28	0	0

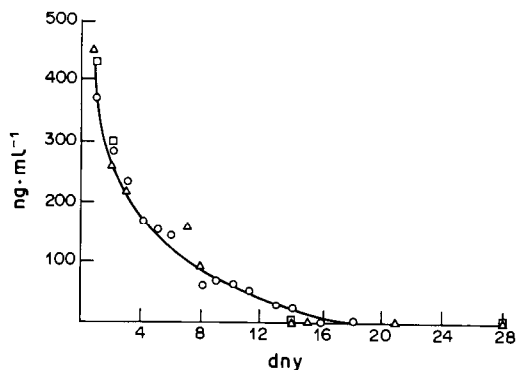


Fig. 2. The levels of the cyadox metabolites in the plasma from pigs (ng/ml) as a function of the number of days elapsed from the termination of cyadox application:  $\triangle$ —adsorptive stripping voltammetry with gel chromatography;  $\square$ —adsorptive stripping voltammetry with extraction;  $\circ$ —radiometric measurements.<sup>5</sup>

The data in Table 1 show that the two separation procedures yield comparable results; the use of gel chromatography is less tedious and time-consuming. It follows from Fig. 2 that the results obtained are in good agreement with those for radiometric determination of the plasma level after administration (at 80 mg/day for 7 days) of cyadox labelled with tritium on the benzene ring.<sup>5</sup>

## CONCLUSION

It has been demonstrated that adsorptive stripping voltammetry, combined with gel chromatography or solvent extraction, is applicable to determination of cyadox, cyadox monoxide and deoxycyadox in the plasma from pigs. Another metabolite, quinoxaline-2-carbonylglycine, cannot be determined in this way, as the accumulation step is insufficient.

## REFERENCES

1. V. Stará and M. Kopanica, *Anal. Chim. Acta*, 1986, **186**, 21.
2. M. Kopanica and V. Stará, *J. Electroanal. Chem.*, 1986, **214**, 115.
3. J. Hebký, V. Lupínek, Z. Sova, B. Ševčík and J. Brož, *Czech Patents*, Nos. 189 915/PV 1788-75; 195 508/PV 5118-77.
4. B. Ševčík, J. Straková, J. Paulová, J. Nastuneak, J. Dvořák, F. Reichel and E. Ševčíková, *Biol. Chem. Vet.*, 1983, **19**, 517.
5. K. Ráž, Z. Franc, A. Selecká, D. Pichová, J. Pícha and P. Minařík, *The Fate of Cyadox Labelled by the <sup>3</sup>H Radionuclide in Pigs*, VUFB Report, Prague 1983.
6. Z. Franc, J. Grimová, J. Holubek, B. Kakáč, E. Kasafírek, E. Kleinerová, I. Koruna, E. Kraus, K. Ráž, Z. Loubal, M. Ryska, J. Sluka and V. Zikán, *A Metabolic Study of Cyadox*, VUFB, Prague 1985.
7. R. Kalvoda, *Anal. Chim. Acta*, 1984, **162**, 197.
8. I. Šestáková and P. Škarka, *Biol. Chem. Vet.*, 1987, **23**, 455.



## ANODIC STRIPPING VOLTAMMETRIC DETERMINATION OF TRACE LEAD WITH A NAFION/CROWN-ETHER FILM ELECTRODE

SHAOUJUN DONG\* and YUDONG WANG

Changchun Institute of Applied Chemistry, Academia Sinica, Changchun, Jilin 130021,  
People's Republic of China

(Received 23 September 1987. Revised 25 February 1988. Accepted 16 May 1988)

**Summary**—An electrode for the anodic stripping voltammetric determination of trace lead has been made by coating glassy carbon with a film of Nafion in which a crown ether is incorporated. The sensitivity is increased because of continuous transfer of lead from solution to the electrode surface by complexation with the crown ether and reduction during the deposition period. A detection limit of  $5 \times 10^{-10} M$  has been obtained by electrodeposition for 3 min. The method is sensitive, simple and relatively rapid, with a relative standard deviation of 8% at the  $2 \times 10^{-9} M$  level.

Chemically modified electrodes (CMEs) are now widely used in analytical chemistry.<sup>1-3</sup> Typical applications include determination of metal ions,<sup>4-7</sup> organic molecules,<sup>8</sup> inorganic anions,<sup>9,10</sup> and *in vivo* monitoring of neurotransmission materials.<sup>11</sup> It has been suggested<sup>12,13</sup> that a film consisting of redox centres and metal co-ordination sites may be used for analysis and for indication of saturation of the electrodes. A carbon-paste electrode prepared from graphite powder coated with dimethylglyoxime (DMG) has been used to detect nickel at the 50 ng/ml level.<sup>6</sup> Wang and Huchins<sup>14</sup> have shown that base hydrolysis of a cellulose acetate coating on an electrode opens up the pores in the film while still inhibiting electrode fouling by proteins. Polta and Johnson<sup>15</sup> have exploited the influence of non-electroactive adsorbed anions such as  $Cl^-$  and  $CN^-$  on the formation of platinum oxide, as the basis for flow-injection analysis. In our previous studies,<sup>16,17</sup> thallium and silver were determined by anodic stripping voltammetric analysis with a Nafion/crown-ether polymer film electrode. The sensitivity was enhanced, and saturation of the modified electrode could be overcome, mainly by releasing the active sites during the deposition step of the anodic stripping voltammetry (ASV). The present paper continues the work with a study of the determination of trace lead by ASV with a Nafion/DC18C6 film electrode. DC18C6 (dicyclohexyl-18-crown-6) forms a lead complex which can be strongly attracted to the electrode surface by Nafion in the cation-exchange mode. This electrochemical method is simple, reliable and quite sensitive, and avoids the use of mercury in ASV. It can be used for the determination of trace lead in water samples. A detection limit of  $5 \times 10^{-10} M$  (0.1 ng/ml) has been achieved by electrodeposition at  $-1.10 V$  for 3 min. Even higher sensi-

tivity can be reached by using longer deposition times and higher purity reagents (in our previous work<sup>16,17</sup> the detection limit for thallium and silver was  $10^{-12} M$  with a deposition time of 30 min).

### EXPERIMENTAL

#### Apparatus

A BAS Model CV-47 instrument (Bioanalytical Systems, Inc., U.S.A.) was used with a Model ATA-1A rotating disk electrode (Jiangsu Electroanalysis Instruments Factory, China). Data were recorded on a Model LZ3-204 X-Y recorder (Dahua Meters Factory, China). A three-electrode cell configuration was employed, which had a saturated calomel electrode (SCE) with double salt bridges as reference electrode, a platinum wire as auxiliary electrode, and the CME as working electrode. All electrode potentials were measured and reported with respect to the SCE.

#### Reagents

DC18C6 was obtained from Fluka. A dry Nafion 117 (Du Pont, U.S.A.) membrane was dissolved according to the method of Martin<sup>18</sup> to give a 0.4% solution in ethanol-water (1:1 v/v). Other reagents were of analytical or guaranteed reagent grade. All reagents were used without further purification. All solutions were prepared with doubly distilled water.

#### Modification procedure

Five  $\mu l$  of 0.1M DC18C6 solution in acetonitrile were added to 500  $\mu l$  of 0.4% Nafion solution to make the modifier solution. The CME was prepared by dip-coating as described previously.<sup>16</sup>

#### Procedure

Before the analysis the CME was immersed in the supporting electrolyte solution, and the background voltamperograms were recorded to examine its performance. The CME was then placed in a cell containing 10 ml of sample or standard lead solution containing 0.1M lithium nitrate as supporting electrolyte. After deaeration of the solution by purging with water-saturated argon (or nitrogen) for 10 min, a deposition potential of  $-1.10 V$  was imposed on the CME [which was rotated at 1100 rpm under an argon (or nitrogen) atmosphere], for an adequate time. This was followed by a 15-sec rest period and a linear potential scan at 100 mV/sec from  $-1.10$  to  $-1.50 V$  and then back again while anodic stripping voltamperograms

\*To whom correspondence should be addressed.

were recorded. The potential was next kept at +0.40 V for 1–2 min, then the CME was placed in 1M nitric acid (and rotated) to release the lead cation. After 5 min the electrode was rinsed with doubly distilled water and was ready for the next deposition–stripping cycle. The performance of the CME was found to deteriorate with use, owing to the loss of DC18C6 from the Nafion film on the electrode surface. After about 60 determinations the sensitivity of the modified electrode was very low, so at this point the DC18C6-Nafion film was removed by wiping the electrode face with a soft tissue wetted with ethanol and the modification procedure was repeated.

## RESULTS AND DISCUSSION

### Effects of supporting electrolyte and pH

Lithium nitrate was chosen as supporting electrolyte because the ability of lithium ion to form a complex with DC18C6 is relatively low. The effect of its concentration on the anodic stripping peak current at the CME was examined. The peak current increases with the lithium nitrate concentration and is maximal at a concentration of 0.1–0.2M. A concentration of 0.1M was selected for use.

The solution pH has a large effect on the anodic stripping peak current (Fig. 1). Although the peak current for lead is higher at low pH, the peak often splits and is not well defined. A pH of 5–6, where the peak current remains unaffected by small changes in pH, was chosen for use.

### Deposition potential and electrode rotation speed

The deposition potential can affect the efficiency of deposition to some extent in ASV. The anodic stripping peak current was observed to increase with shift of the deposition potential from –0.80 to –1.10 V (Fig. 2), with little further change at deposition potentials more negative than –1.20 V. A deposition potential of –1.10 V was selected to obtain a high stripping current and to avoid many interferences.

Under the selected conditions the peak current of lead is a linear function of the square root of the CME rotation speed in the range 0–1600 rpm, showing that the deposition is diffusion-controlled. An electrode rotation speed of 1100 rpm was used in all further work.

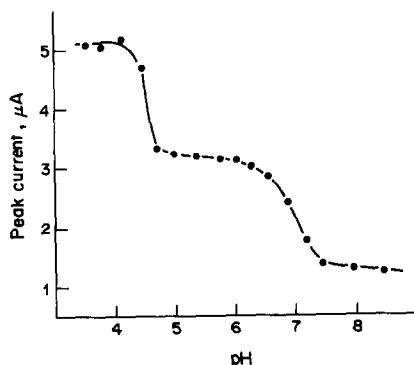


Fig. 1. Effect of solution pH. Solution composition, 0.1M  $\text{LiNO}_3$  and  $2 \times 10^{-7}\text{M}$   $\text{Pb(II)}$ ; deposition time, 1 min; deposition potential, –1.10 V vs. SCE; scan-rate: 100 mV/sec.

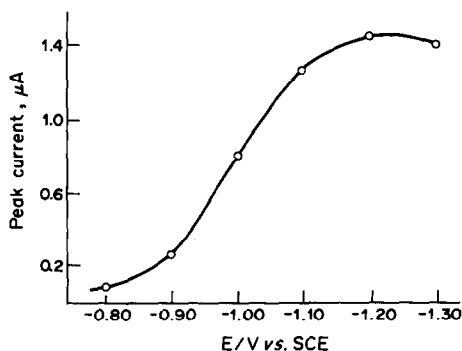


Fig. 2. Effect of the deposition potential. Conditions are the same as for Fig. 1 except the deposition potential.

### Effects of scan-rate and of other elements

The relationship between the anodic stripping peak current and the potential scan-rate is not conventional. The peak current increases with the scan-rate up to about 100 mV/sec and then begins to decline. This is because the lead cation readily forms a cationic DC18C6 complex which is strongly adsorbed on the electrode surface by the Nafion cation-exchanger film. At the deposition potential chosen the strongly adsorbed complex is not completely reduced, so before the anodic stripping step the electrode is first scanned towards more negative potentials to reduce the complex cation completely, but if the scan-rate is too high the complex cations are still incompletely reduced, resulting in a lower peak current. A scan-rate of 100 mV/sec is recommended.

Under these experimental conditions, there is a linear relationship between the anodic stripping peak current and deposition time over the range 0–180 sec. The effect of deposition times longer than 180 sec was not examined because the reagent purity was not high enough.

We have noticed<sup>16,17</sup> that when the concentration of DC18C6 in the Nafion film on the electrode surface is too high the film often splits, so a concentration of 0.5M (estimated from the density of dry Nafion 117 membrane, about 2 g/cm<sup>3</sup>) was used.

### Interferences

Under the recommended experimental conditions, no interferences appear from common cations such as Sn(II), Zn(II), In(III), Ni(II) and Co(II). In the presence of  $1 \times 10^{-6}\text{M}$  Fe(II) the peak current for lead can be reduced by 10%. At Cd(II) concentrations above  $1 \times 10^{-6}\text{M}$  there is a positive shift in the stripping peak potential, but little effect on the peak current. Copper(II) above  $10^{-6}\text{M}$  interferes by causing a positive shift of 70 mV and broadening the stripping peak, increasing the peak current by 50%. The peak current is slightly decreased by more than  $10^{-6}\text{M}$  Tl(I) or Ag(I), but the peak shape and position do not change. The same effect on the anodic

stripping peak is caused by the presence of  $>10^{-2}M$  alkali-metal ions such as  $K^+$  or  $Na^+$  which can form complexes with DC18C6, but the interference is not serious.

#### Cyclic voltammetry

Figure 3 compares the cyclic voltamperograms of  $2 \times 10^{-4}M$  Pb(II) obtained with the CME and a bare GC electrode. Both voltamperograms were recorded after the electrode had been rotated in the solution for 1 min. The anodic and cathodic peaks obtained with the CME are higher than those with the bare GC electrode, and the ratio of anodic to cathodic peak current approaches 1:1 for the CME but is very high for the bare GC electrode. The overpotential of lead reduction is lower on the CME. The cyclic voltamperogram of lead with a Nafion/GC electrode is similar to that for the (DC18C6-Nafion)/GC CME but the peak height is lower. All these phenomena show that the Nafion film on the electrode surface has some affinity for the Pb(II), and this is enhanced by incorporating DC18C6 in the Nafion film because the DC18C6 complex cation is immobilized on the electrode surface as soon as it forms, owing to the strong electrostatic force between Nafion and large organic cations. At the deposition potential at which the Pb(II) in the complex cation is reduced to the metal (which is deposited on the electrode surface), the DC18C6 molecule is released, then becoming a free complexing centre to collect more Pb(II) in the solution. Therefore the analysis sensitivity is apparently raised.

#### Sensitivity and limit of detection for lead

Under the experimental conditions, a detection

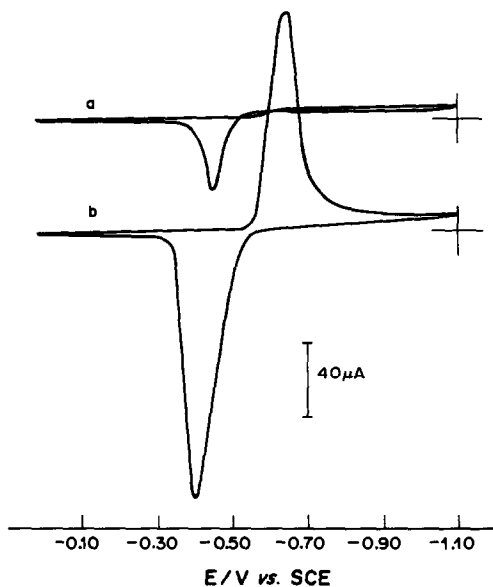


Fig. 3. Cyclic voltamperograms of lead on different electrodes. Solution composition,  $0.1M$   $LiNO_3$  and  $2 \times 10^{-4}M$  Pb(II); scan-rate,  $100$  mV/sec. (a) Bare GC electrode. (b) (DC18C6-Nafion)/GC electrode.

limit of  $5 \times 10^{-10}M$  ( $0.1$  ng/ml; peak current  $0.1 \mu A$ ) was obtained after a preconcentration time of 3 min. The relationship between peak current and lead concentration is linear over the range  $1 \times 10^{-9}$ – $1 \times 10^{-7}M$  (correlation coefficient  $>0.999$ ) and the graph passes through the origin.

The relative standard deviation found for nine determinations of  $3 \times 10^{-7}M$  Pb(II) was 3.3%. Lead in the tap water in Changchun (Jilin, China) was determined by the single standard-addition method, with the CME. A  $0.1M$  lithium nitrate solution prepared in tap water was used as the sample solution and  $1.00 \times 10^{-5}M$  standard  $Pb^{2+}$  solution was used as the standard addition made to 10 ml of sample. A relative standard deviation of 8% was obtained for seven determinations of  $2.1 \times 10^{-9}M$  lead.

#### CONCLUSIONS

The results above demonstrate the feasibility of using a crown ether incorporated in Nafion polymer to make a film electrode for the determination of trace lead in water by anodic stripping voltammetry. The detection limit is  $0.1$  ng/ml. The method is sensitive, simple and relatively rapid. The electrode is stable and can be used repeatedly.

*Acknowledgements*—This project was supported by the National Natural Science Foundation of China, the aid from which is gratefully acknowledged.

#### REFERENCES

1. D. C. Johnson, M. D. Ryan and G. S. Wilson, *Anal. Chem.*, 1986, **58**, 33R.
2. R. W. Murray, A. G. Ewing and R. D. Durst, *ibid.*, 1987, **59**, 379A.
3. Shaojun Dong, *Fenxi Huaxue*, 1985, **13**, 870.
4. G. T. Cheek and R. F. Nelson, *Anal. Lett.*, 1978, **11**, 393.
5. K. Izutsu, T. Nakamura, R. Takizawa and H. Hanawa, *Anal. Chim. Acta*, 1983, **149**, 147.
6. R. P. Baldwin, J. K. Christensen and L. Kryger, *Anal. Chem.*, 1986, **58**, 1790.
7. Hulin Li, Zhixing Su, Ming Yang and Jianzhong Feng, *Fenxi Huaxue*, 1986, **14**, 85.
8. J. F. Price and R. P. Baldwin, *Anal. Chem.*, 1980, **52**, 1940.
9. N. Oyama and F. C. Anson, *J. Electrochem. Soc.*, 1980, **127**, 247.
10. J. A. Cox and B. K. Das, *Anal. Chem.*, 1985, **57**, 2739.
11. G. A. Gerhardt, A. F. Oke, G. Nagay, B. Mughaddum and R. N. Adams, *Brain Res.*, 1984, **290**, 390.
12. A. R. Guadalupe and H. D. Abruña, *Anal. Chem.*, 1985, **57**, 142.
13. L. M. Wier, A. R. Guadalupe and H. D. Abruña, *ibid.*, 1985, **57**, 2009.
14. J. Wang and L. D. Hutchins, *ibid.*, 1985, **57**, 1536.
15. J. A. Polta and D. C. Johnson, *ibid.*, 1985, **57**, 1373.
16. Yudong Wang and Shaojun Dong, *Fenxi Huaxue*, in the press.
17. Shaojun Dong and Yudong Wang, *Pittsburgh Conference Abstracts*, No. 659, 1988.
18. C. R. Martin, T. A. Rhoades and J. A. Ferguson, *Anal. Chem.*, 1982, **54**, 1639.

## ANALYSIS OF GALLIUM ARSENIDE BY SPARK-SOURCE MASS-SPECTROMETRY

GREGORY P. MAKLAE

GTE Laboratories Incorporated, Waltham, MA 02254, U.S.A.

(Received 15 December 1987. Revised 25 March 1988. Accepted 12 May 1988)

**Summary**—A method has been developed for analysing gallium arsenide with a resistance of greater than  $10^9 \Omega$  by spark-source mass-spectrometry, without the need for pelleting, which introduces a prohibitively high level of contamination and lowers the detection limit for a given exposure. It uses a gold evaporation technique, whereby a thin layer of 99.999% pure gold is deposited on one surface of the GaAs electrodes, in a chamber mounted on the ion-source. No contamination, other than gold, is introduced into the sample at a level of 50 ng/g or greater. It is possible to detect carbon in the sample at the 1–2  $\mu\text{g/g}$  level. The sample preparation time is less than 30 min, and more than one set of samples can be gold-coated at a time.

Spark-source mass-spectrometry (SSMS) is an extremely useful tool for the determination of impurities or dopants in GaAs, for several reasons. First, it is possible to obtain detection limits in the low mid parts per billion atomic range for most elements, the most notable exceptions being carbon, oxygen and elements near the matrix isotopes which are "lost in the fog" of long exposures. SSMS also has the benefit of recording in a single exposure all elements from lithium to uranium, except for those giving lines covered by multiply-charged ions or molecular clusters. The results are "correct" within a factor of five when no standards are available, and the analysis time per element detected is good.

The only major restriction is that the samples should be electrically conductive. The higher the conductivity, the more reliable the analysis, in that the sparking parameters are kept to the minimum values, which keeps the temperature of the electrodes as low as possible. Therefore, preferential ionization of the more volatile species is minimized.<sup>1</sup> High conductivity may be achieved in three ways. If the sample is very conductive, it may be analysed directly, as is commonly the case with pure metals. In the second method, the sample is ground to a powder, mixed with a conductive pelleting agent, usually silver or graphite, and analysed. This method is commonly employed in oxide analysis, and has several shortcomings: the signal from the sample elements is decreased by the dilution caused by the pelleting material, thus raising the impurity detection limit for a given exposure; more importantly, contamination can be introduced into the sample in several ways. For example, the pelleting medium may constitute 50% or more of the mixture with the sample and any impurities in it will show up in the mass spectrum. Also, the grinding process introduces impurities, not only from the material of the mortar and pestle, but also by contamination from previous samples ground

in the same apparatus. The shaking necessary to homogenize the sample, and the pelleting material will introduce organic material if a plastic vial is used for the shaking, resulting in doublet lines (Fig. 1). Using graphite for pelleting is not advantageous, because even though it is available in higher purity than silver,  $C_x$  clusters further complicate the spectra, interfering with Mg, K and Ti determination. Pressing a metal backing onto the sample and sparking with a counter-electrode has several disadvantages. First the signal of the sample is decreased because of dilution by both the backing material and the counter-electrode. Secondly, there may be preferential sparking of the backing material, leading to an inhomogeneous signal. Also, the pressing procedure may introduce contamination onto the sample. Therefore, a third method of inducing conductivity has been developed for semiconductor samples. In this procedure, high-purity gold is evaporated and a thin layer of it deposited on one surface of the GaAs to provide a conductive path, so that the sample can readily be sparked. The effective bulk concentration of the gold is less than 100  $\mu\text{g/g}$  so it does not attenuate the sample impurity signals or introduce additional measurable impurities. Gold was chosen

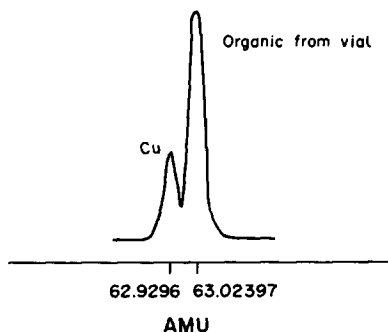


Fig. 1. Organic doublet interference.

because it is mono-isotopic and has an odd mass number, minimizing the effect of multiply-charged interferences, is available as high-purity wire, (5N material was used in this work), and its signal is at the end of the photoplate where typical impurities or dopants in GaAs are not found. It is also easily evaporated. Other metals considered for evaporation were indium and aluminium. Indium was not tried because its low melting point may cause it to flow from the sample during sparking, breaking the conductive path to the sample holder. Aluminium was tried but is not a good choice because of the possibility of it being present in GaAs.

### EXPERIMENTAL

An AEI MS-702 spark-source mass-spectrometer with photoplate detection was employed. The magnet current was 265 mA and the accelerating voltage 20 kV. The pulse length was 200  $\mu$ sec and the pulse rate 300/sec. The RF power was set at a meter reading of 35%, or approximately 28 kV. The vacuum was in the  $10^{-8}$ – $10^{-7}$  mmHg range. Kodak SWR photoplates were used to record the spectra.

Sections suitable for electrodes ( $1.5 \times 5$  mm) were cut from a GaAs wafer with a diamond scribe. These were degreased in methanol, etched in a mixture of 5 ml each of concentrated hydrochloric and nitric acids and 90 ml of water, for 5 min, rinsed several times in distilled water, rinsed for 3 min in a 10% solution of bromine in methanol, then rinsed several times in pure methanol and dried under an infrared lamp.<sup>1</sup> All the cleaning was done in a Teflon beaker. The resistance of these electrodes was greater than  $10^9 \Omega$ , and they could not be sparked directly, even at full power of the spark source. Therefore, following the second method, commonly used for insulators, the sample was ground to a powder with a boron carbide mortar and pestle. Grinding the gallium arsenide, and/or the silver power used for pelleting, introduced several impurities at concentrations which would be critical with respect to the functionality of the GaAs device, including carbon, boron and zinc. When the grinding was done with an alumina mortar and pestle, impurities were again introduced. Therefore, new electrodes were cut and cleaned and the new technique was employed.

A layer of 5N gold, 0.1–0.2  $\mu$ m thick, was deposited on one side of the electrodes, by the following procedure. A chamber for evaporation of the gold was mounted on a port of the ion-source chamber (Fig. 2). Since the original source diffusion pump was replaced with a 6-in. one, the additional load did not affect the pumping speed or ultimate vacuum,

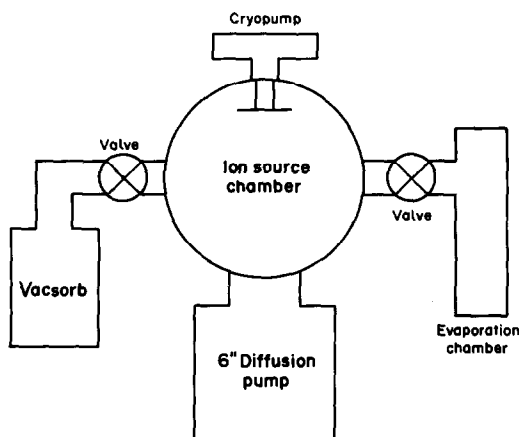


Fig. 2. Ion-source housing.

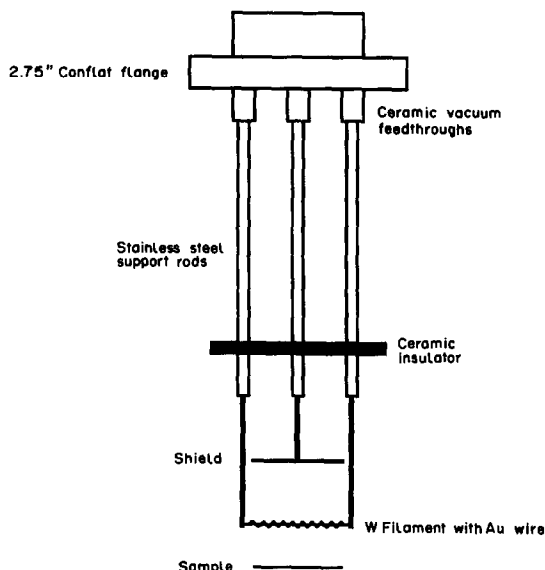


Fig. 3. Evaporation apparatus.

and an additional pumping unit was not needed. A pressure of  $5 \times 10^{-7}$  mmHg was obtained within 20 min of loading the sample. The evaporation apparatus was constructed from a modified sublimation-pump titanium filament holder which was mounted on a  $2\frac{1}{2}$ -in. Conflat flange. (Fig. 3). The holder was fitted with 1.5 mm copper wire to support a  $0.33 \times 25$  mm tungsten filament around which were wrapped several turns of 0.5 mm gold wire. Passage of a current of 10 A for 5 sec deposited an adequate layer of gold on a sample placed approximately 20 mm from the filament. The system was then vented and the samples were removed from the evaporation chamber and mounted in the source chamber of the mass spectrometer, in previously redesigned sample holders. The source was evacuated, with a modified ion-source housing and pumping system<sup>2</sup> utilizing a combination of diffusion pumping and cryopumping, to  $10^{-8}$  mmHg. The cryopanel achieved a temperature of 18 K. The source chamber was not baked with the samples in place, because it was found that baking deposited contaminants on the sample surfaces, which interfered with the determination of carbon levels. The samples were very easily sparked and were pre-sparked for 10 min to ensure that the gold had been removed from the tips of the electrodes, but retained on the sides of the samples to keep the conductive path intact, and to coat the source parts with gallium arsenide. Slight vibration was applied to the right-hand electrode and little further adjustment was necessary during the experiment. The exposures, of less than 0.003 nC, were very homogeneous. This is not always the case if gold wire is either wrapped around the sample or placed next to it.<sup>3</sup> It was possible to collect data at the rate of 5 nC/min.

The photoplate was evaluated by means of an Apple IIe computer interfaced to a Photometric Data Systems micro-densitometer by an ADALAB card (Interactive Microware). The recorded transmissions, backgrounds and exposures were entered into the IBM 3081 mainframe and processed by the Hull equation and the Seidel function.<sup>4</sup> Sensitivity factors were based on a combination of theoretical calculations and measurements made in this laboratory.

### RESULTS AND DISCUSSION

Table 1 summarizes the analysis of the gold wire employed, and the results of the GaAs wafer analysis

Table 1. Gold wire analysis

Element	$\mu\text{g/g}$	Element	$\mu\text{g/g}$
Na	4.2	Cu	0.54
Mg	0.11	Zn	0.14
Al	1.1	Rh	4.6
Si	1.5	Ag	3.9
Ca	2.2	In	2.2
K	3.1	C	4.4
Cr	2.4	N	0.36
Fe	6.0	O	1.9
Ni	4.9		

are shown in Table 2. Since one of the impurities of interest was zinc, exposures were limited to 50 nC because of severe fogging in the  $m/z$  64 region. This gave a detection limit of 0.1–0.5  $\mu\text{g/g}$  or lower for most elements, and 0.6  $\mu\text{g/g}$  for zinc. If lower detection limits for elements below mass 60 and above mass 85 are desired, the emulsion on the lower half of the plate can be either masked or removed in the mass range 60–80. This will eliminate the fogging of the background and allow exposures of 300 nC or more in an hour.<sup>5</sup> This would produce detection limits of 20 ng/g for many elements. Masking will not remove the arsenic exposures of interest, 0.0003–0.003 nC, which are recorded on the upper half of the photoplate and used as the internal reference. A correlation coefficient of 0.999 was achieved for the arsenic calibration, in a plot of exposure in (nC) vs. the Seidel function of the trans-

Table 2. Analysis of GaAs

Element	Found, $\mu\text{g/g}$			
	Method 2a	Method 2b	Method 3a	Method 3b
B	76	25	$8.7 \pm 3^*$	3.1
C	$14 \times 10^3$	$14 \times 10^3$	$2.0 \pm 0.9^*$	2.9
Mg	4.0	24	nd	nd
Al	2.7	$0.82 \times 10^3$	nd	7.5
Si	31	$0.52 \times 10^3$	nd	2.1
P	1.5	0.1	nd	nd
S	26	1.5	nd	nd
Cl	16	43	nd	nd
K	1.6	14	nd	nd
Ca	17	34	nd	nd
Mn	0.24	0.23	nd	nd
Fe	3.2	13	$0.5 \pm 0.1^*$	2.8
Cu	0.15	1.3	nd	nd
Zn	0.45	1.4	nd	nd

nd = not detected.

Method 2a: ground with boron carbide mortar and pestle and compacted with silver.

Method 2b: ground with alumina mortar and pestle and compacted with silver.

Method 3a: gold-plated wafer.

Method 3b: aluminium-plated wafer.

\*Based on three analyses.

mission. The background level of carbon found by this method appeared to be 1  $\mu\text{g/g}$  (based on the fact that the electrically active carbon in the GaAs was calculated from resistivity measurements to be below this level. Because of the probability of oxidation of the surface during sample preparation, oxygen concentrations were not calculated. Potassium was observed but not reported, because of severe inhomogeneity. Sodium levels could not be determined, owing to  $^{69}\text{Ga}^{3+}$  interference. With a difference of 0.015  $m/z$  between this and  $^{23}\text{Na}^+$ , and a mass-spectrometer resolution of only 1550, no doublet could be observed.

The results demonstrate the reduction in the levels and numbers of impurities when the gold-plated samples are used instead of compacted samples. The precision of the results for the gold plated samples is good. The additional time for sample preparation is more than offset by the shorter sparking time needed to achieve a given detection limit.

#### CONCLUSIONS

Future semiconductor devices will require extremely pure substrate materials. As the purity of the material increases, the conductivity decreases, so direct analysis by spark source is not possible. Treating the sample as an insulator and using the standard methods introduces prohibitively high contamination and reduces the sensitivity. Deposition of gold onto the sample is a satisfactory alternative, however. Its merits are that no contamination is introduced into the sample, the sample remains at a low temperature during sparking, 99.99% of the ions formed are from the sample and only 0.01% from the gold, so impurities in the sample are not diluted, and the background level of carbon is low. This method has also been applied to the analysis of an insulating film on a conductive substrate, for example a ZnS film deposited on a silicon wafer has been analysed for chromium and aluminium.

*Acknowledgements*—I wish to thank James Kafalas for supplying the GaAs wafers that were used in the experiment and Drs Joseph Lester and Donald L. Dugger for their guidance and support.

#### REFERENCES

1. J. C. Brice, J. A. Roberts and G. Smith, *J. Materials Sci.* 1967, 2, 132.
2. D. L. Dugger and D. W. Oblas, *Talanta*, 1977, 24, 248.
3. A. J. Ahearn, *Trace Analysis by Mass Spectrometry*, Chapter 9, Academic Press, New York, 1972.
4. *Idem*, *op. cit.* Chapter 6.
5. D. L. Dugger, *Texas Instruments Technical Report*, TR 08-71-24, 1972.

## THE USE OF GLASS ELECTRODES FOR THE DETERMINATION OF FORMATION CONSTANTS—III\*

### OPTIMIZATION OF TITRATION DATA: THE ESTA LIBRARY OF COMPUTER PROGRAMS

PETER M. MAY†

School of Mathematical and Physical Sciences, Murdoch University, Western Australia 6150

KEVIN MURRAY

Processing and Chemical Manufacturing Technology Division, Council for Scientific and Industrial  
Research, Pretoria, South Africa 0001

DAVID R. WILLIAMS

Department of Applied Chemistry, UWIST, Cardiff, Wales

(Received 22 August 1988. Accepted 30 August 1988)

**Summary**—Difficulties with the analysis of titration data for the determination of formation constants are discussed. Considerable differences between published values can, in part, be attributed to incorrect "model selection", *i.e.*, incorrect selection of chemical species. Experimental errors also contribute to the problem in ways that are neither well understood nor easy to overcome. The library of computer programs described, called ESTA (Equilibrium Simulation for Titration Analysis), has been written to investigate better methods of optimizing formation constants from potentiometric titration data.

#### SYMBOLS

$\bar{Z}$ —formation function  
 $U$ —objective function to be minimized  
 $R^H$ —Hamilton factor  
 $n_p$ —number of parameters to be optimized  
 $p_a$ —parameter  $a$   
 $\beta_j$ —thermodynamic formation constant of complex  $j$   
 $E_k^\circ$ —electrode  $k$  response intercept  
 $s_k$ —electrode  $k$  response slope  
 $V^0$ —initial volume in titration vessel  
 $C_i^v$ —initial concentration of component  $i$  in vessel  
 $C_{im}^B$ —concentration of component  $i$  in solution in burette  $m$   
 $N$ —total number of experimental titration points  
 $n_c$ —total number of electrodes  
 $w_{nq}$ —weight of  $q$ th residual at  $n$ th point  
 $y_{nq}^{obs}$ —observed variable of  $q$ th residual at  $n$ th point  
 $y_{nq}^{calc}$ —calculated variable of  $q$ th residual at  $n$ th point  
 $T_{nq}$ —total concentration of electrode ion  $q$  at  $n$ th point  
 $E_{nq}$ —emf of electrode  $q$  at  $n$ th point  
 $\bar{a}$ —Gauss-Newton quadratic parameter vector

$\bar{b}$ —Gauss-Newton quadratic parameter vector  
 $\bar{p}$ —optimization parameter vector  
 $\bar{p}^t$ —transpose of  $\bar{p}$   
 $H$ —Hessian  
 $\bar{g}$ —Gauss-Newton gradient vector  
 $\bar{s}$ —Gauss-Newton shift vector  
 $I$ —unit matrix  
 $\mu$ —Levenberg-Marquardt factor  
 $G$ —inverse Hessian  
 $\sigma_r$ —standard deviations of the  $r$ th optimized parameter  
 $I$ —ionic strength  
 $r_{sr}$ —correlation coefficient of parameters  $s$  and  $r$

Nowadays, the measurement of metal-ligand formation constants is often regarded as routine—a view which greatly underestimates the difficulties still involved in determination of reliable values. It takes many years to acquire the skills which are today expected of competent workers in this area and, therefore, most investigations are carried out by research groups that are very highly specialized in the necessary experimental and computational techniques.

However, neither this specialization nor the intricate procedures which have been evolved to determine formation constants guarantee good results. Considerable discrepancies between the values published for the same chemical system by various authors frequently occur. So worrying had this become that, some years ago, a collaborative

\*Part II: P. M. May, K. Murray and D. R. Williams, *Talanta*, 1985, **32**, 483.

†Author for correspondence.

investigation of nickel(II)–glycinate equilibria compared the results from many laboratories working under the same conditions.<sup>1</sup> Even with this relatively simple and well-behaved chemical system, worrying differences emerged between the results. With trickier systems such as aluminium(III)–citrate, a comparison made by Martin<sup>2</sup> of published results<sup>3–5</sup> clearly shows how problematical the matter remains. Reported formation constants often differ by orders of magnitude, and agreement, even regarding the set of most-predominant complexes, is rare.

This widespread lack of reproducibility is attributed by many of those working in this field to difficulties associated with the computer analysis of the titration data. Most concern is focused on the problem of “model selection”, *i.e.*, the methods for choosing the set of complex species which best describes the chemical system investigated. Almost all the computer programs available for calculation of formation constants require a “model” to be specified *ab initio* (although the HOSK approach provides an interesting, albeit limited, exception<sup>6</sup>). Thus, formation constants can only be evaluated by refining a set of initial estimates on the assumption that all the predominant complexes in the experimental solutions are already known.

Various techniques and strategies for identifying these major complexes do exist; the most commonly used is based on the so-called formation function,  $\bar{Z}$ .<sup>7</sup> However, such methods seldom (if ever) give unequivocal results, so it is often necessary to make chemically informed guesses about which species it is most reasonable to consider. Searches are then made with the aim of finding the correct set of species, defined as that which gives the “best agreement” between the calculated and experimental data. Unfortunately, there are usually too many possibilities for these searches to be performed exhaustively and, most importantly, it is extraordinarily difficult to know what sort of agreement between observed and calculated data constitutes a genuinely good fit.

The unfortunate but widely appreciated fact is that conventional measures of agreement between observed and calculated data cannot be trusted. Thus, an *apparent* improvement in the goodness-of-fit can often be obtained simply by refining an extra parameter (for example, as happens when an additional chemical species is included in the model). Optimization calculations can, almost always, exploit another degree of freedom but, of course, this does not necessarily indicate that the newly postulated species is actually present in the solution: the improved agreement between calculated and observed data (as reflected, for example, in a lowered objective function,  $U$ , or Hamilton factor,  $R^H$ ,<sup>8</sup>) may merely result from accommodation of experimental errors.

Since, in the experimental context, neither the model nor the actual errors can ever be known with complete certainty, this problem has proved intractable. Methods for judging (i) the quality of experi-

mental data, (ii) the overall goodness-of-fit and (iii) the best model have become profoundly subjective. It seems clear that better ways must be found if the serious discrepancies between published sets of formation constants are ever to be satisfactorily resolved.

This paper describes a library of computer programs collectively called ESTA (Equilibrium Simulation for Titration Analysis). These programs were developed to provide a flexible investigative tool for the quantitative characterization of chemical interactions in solution, especially those pertaining to the determination of formation constants. The programs are used to calculate equilibrium distributions of chemical species, to analyse potentiometric titration data and to manipulate titration data for a variety of other purposes. The underlying aim in their development was to produce a set of self-consistent programs that would permit easy simulation of a well-defined system and then optimization of the resulting data in a variety of ways. Accordingly, the best choice of objective function, the effects of various kinds of error and the most successful model selection strategy could be unequivocally ascertained (because, when simulated data are used, the true result is known). It was hoped sufficient insight into the optimization process would be gained to allow methods to be devised that could then confidently be applied to the analysis of experimental data.

## THEORY

An approach towards the simulation of titration data has already been described in Part II of this series.<sup>9</sup> It thus remains only to outline the algorithms for optimization.

Simultaneous optimization of  $n_p$  parameters  $p_r$  (where  $p_r$  may be  $\beta_j$ ,  $E_k^\circ$ ,  $s_k$ ,  $V^\circ$ ,  $C_i^\circ$  or  $C_{im}^\circ$ ) is performed by minimizing an objective function,  $U$ , defined as

$$U = (N - n_p)^{-1} \sum_{n=1}^N n_c^{-1} \sum_{q=1}^{n_c} w_{nq} (y_{nq}^{\text{obs}} - y_{nq}^{\text{calc}})^2 \quad (1)$$

where  $y_{nq}^{\text{obs}}$  and  $y_{nq}^{\text{calc}}$  may be either a  $T_{nq}$  or an  $E_{nq}$ . The use of weights,  $w_{nq}$ , will be discussed in detail later (Part IV).<sup>10</sup>

A Gauss–Newton method is the most frequent approach used for minimizing  $U$ , and this has been adopted in ESTA as the main means of optimization. The method assumes that  $U$  is quadratic with respect to the parameters,  $p_r$ , *i.e.*,

$$U = \bar{a} + \bar{p}^T \bar{b} + (\bar{p}^T \mathbf{H} \bar{p})/2 \quad (2)$$

where the Hessian,  $\mathbf{H}$ , is defined by

$$\mathbf{H}_{sr} = \frac{\delta^2 U}{\delta p_s \delta p_r} \quad (3)$$

The gradient,  $\bar{g}$ , is simply

$$\bar{g} = \frac{\delta U}{\delta \bar{p}} = \bar{b} + \mathbf{H} \bar{p} \quad (4)$$



and the solution,  $\bar{p}^{\text{min}}$ , occurs when

$$\bar{g}^{\text{min}} = \bar{b} + \mathbf{H} \bar{p}^{\text{min}} = 0 \quad (5)$$

Hence

$$\bar{b} = -\mathbf{H} \bar{p}^{\text{min}} \quad (6)$$

Substituting into equation (4) leads to

$$\bar{g} = -\mathbf{H} \bar{p}^{\text{min}} + \mathbf{H} \bar{p} = -\mathbf{H} \bar{s} \quad (7)$$

where the shift vector  $\bar{s} = \bar{p}^{\text{min}} - \bar{p}$ .

Thus, given some initial estimates of the parameters, the set of linear equations  $\bar{g} = -\mathbf{H} \bar{s}$  can be solved for  $\bar{s}$  to provide an improved estimate of the parameters.

The elements of the Hessian, equation (3), are obtained as follows. Differentiation of equation (1) with respect to  $p_r$  leads to

$$\frac{\delta U}{\delta p_r} = 2(N - n_p)^{-1} \sum_{n=1}^N n_c^{-1} \sum_{q=1}^{n_c} w_{nq} \times (y_{nq}^{\text{obs}} - y_{nq}^{\text{calc}}) \frac{\delta(y_{nq}^{\text{obs}} - y_{nq}^{\text{calc}})}{\delta p_r} \quad (8)$$

where it is assumed that  $w_{nq} \neq f(p_r)$ . Then differentiating equation (8) with respect to  $p_s$  and ignoring second-order derivatives, leads to

$$\frac{\delta^2 U}{\delta p_s \delta p_r} = 2(N - n_p)^{-1} \sum_{n=1}^N n_c^{-1} \sum_{q=1}^{n_c} w_{nq} \times \frac{\delta(y_{nq}^{\text{obs}} - y_{nq}^{\text{calc}})}{\delta p_s} \cdot \frac{\delta(y_{nq}^{\text{obs}} - y_{nq}^{\text{calc}})}{\delta p_r} \quad (9)$$

In general, given good initial estimates and a reasonably well behaved system, the Gauss-Newton method described above performs extremely well. It often converges in 3-6 cycles.

Unfortunately, the solution of equation (7) is sometimes obviously unsatisfactory. It may, for example, produce a shift vector with an upward gradient. Alternatively, one or more parameter shifts may be unreasonably large. If the shifts are not too excessive a Levenberg-Marquardt method<sup>11</sup> may be applied to reduce them. Otherwise, they are almost certainly indicative of an ill-conditioned system and, hence, the program should be made to terminate. In the Levenberg-Marquardt approach, equation (7) is modified as follows

$$(\mathbf{H} + \mu \mathbf{I}) \bar{s} = -\bar{g} \quad (10)$$

This aims to modify the shift vector towards the direction of steepest descent and to reduce the size of the shift. Initially, we have used

$$\mu = \left[ \sum_{r=1}^N g_r^2 / H_{rr} \right] U^{-1} \times 10^{-5} \quad (11)$$

If this does not satisfy the requirements of a downward gradient and reasonably-sized shifts,  $\mu$  can be repeatedly multiplied by 2 until it does.

Even when the gradient and parameter shifts are controlled in this way, applying the shift may still

result in an increase in objective function. This often indicates that the system is poorly conditioned, but occasionally it may mean that the objective function minimum has been overshoot. Accordingly, to help ensure convergence, an attempt should be made to make a linear optimization of the shift.<sup>12</sup> When non-unit weighting is applicable, it is simplest to make successive bisections of the shift; otherwise a combination of bisection and Davidson's cubic interpolation<sup>13</sup> can be used. If linear optimization is unable to decrease the objective function before the shift is reduced below a threshold value (*i.e.*, a preset minimum fraction of the original shift or the internal convergence tolerance, whichever is the larger), the program should terminate.

When the estimates of the parameter being refined are judged to be sufficiently close to the solution, standard deviations of the parameters may be calculated from

$$\sigma_r = \left[ \frac{U \times \mathbf{G}_{rr}}{N - n_p} \right]^{1/2} \quad (12)$$

where  $\mathbf{G} = \mathbf{H}^{-1}$ .

Correlation coefficients can be calculated by using the formula

$$r_{sr} = \frac{\mathbf{G}_{sr}}{(\mathbf{G}_{ss} \mathbf{G}_{rr})^{1/2}} \quad (13)$$

and the Hamilton R-factor,  $R^{\text{H}}$ , is given by

$$R^{\text{H}} = \left[ \frac{U}{\sum_{n=1}^N n_c^{-1} \sum_{q=1}^{n_c} w_{nq} (y_{nq}^{\text{obs}})^2} \right]^{1/2} \quad (14)$$

and its limit by

$$R_{\text{lim}}^{\text{H}} = \left[ \frac{N}{\sum_{n=1}^N n_c^{-1} \sum_{q=1}^{n_c} w_{nq} (y_{nq}^{\text{obs}})^2} \right]^{1/2} \quad (15)$$

## PROGRAM DESCRIPTION

ESTA accommodates chemical systems of up to 10 components forming up to 99 complexes. Titrations involving up to three electrodes and three burettes are permitted. The programs can take into account variations in ionic strength and the associated changes in activity coefficients. They also permit corrections of titration data affected by liquid-junction potentials and imperfect ion-selectivity of electrodes.

The ESTA library contains the following program modules, many of which perform more than one kind of calculation (specified as a different "task"). Interested readers can obtain details of how to acquire copies of the latest version (Version 3.0) of these programs by writing to one of the authors (PMM).

### ESTA1: the simulation module

By setting up and solving the mass-balance equations, ESTA1 can determine, on a point-by-point basis, single values for almost any titration parameter. The calculations fall into two categories: (i)

species-distribution calculations and (ii) potentiometric titration calculations. The former are specified by the task SPEC. The latter include determination of emf values (task SIME), formation constant estimates (task BETA), total analytical concentrations (task TOTL), initial vessel concentrations (task VESL) and initial burette concentrations (task BURT). Other kinds of titration analysis are also possible; at each point the following can be obtained:

- (a) percentage distributions of species for both SIME- and SIMV-type calculations (task ERR%)
- (b) formation function values (task ZBAR)
- (c) deprotonation function values (task QBAR), and
- (d) appropriate weights, an overall objective function value and the relative contribution of the most important errors based on residuals in both emf and total concentrations (tasks OBJE and OBJT respectively).

A file of simulated titration data, with a format identical to ESTA input, can be generated as output.

#### *ESTA2: the optimization modules*

There are two optimization programs, ESTA2A and ESTA2B, differing only in the way the weights are calculated (see Part IV<sup>10</sup> of this series). They are used when it is desired to determine, for one or more parameters, the "best" values, based on a least-squares procedure applied to a whole system of titrations. The following parameters can thus be refined: formation constants, vessel and burette concentrations, electrode intercept, electrode slope and initial vessel volume. It is possible to group together, over any combination of titrations, local parameters of the same type and with the same value so that they are refined together as a single parameter. The objective functions may be weighted or unweighted. The sum of squares of residuals may be minimized with respect to either emf—task OBJE—or total concentrations—task OBJT. The total number of titrations is dimensioned to 20 and the total number of points to 1000 but these can readily be varied if necessary. A file of titration data containing the optimized parameter values and with a format identical to ESTA input can be generated as output.

#### *ESTA3: the Monte Carlo analysis modules*

These are mentioned here only for completeness. There are two programs, ESTA3A and ESTA3B, corresponding to the ESTA2 programs and again differing only in the way in which the weights are calculated. A full description of the theory and use of ESTA3 will be given in Part V of this series.<sup>14</sup>

#### *ESTA4: the experimental conditions optimization module*

This module is still under development and will be published in due course.

#### *ESTA5: the graphical display module*

Data for production of graphics are produced by ESTA1 as a separate output file in a standardized format. The ESTA5 program is used to process this file and to generate various kinds of display. This two-stage approach isolates the system-specific code which graph-plotting necessitates. Subroutines suitable for the GINO and CALCOMP systems are available.

#### *ESTA6: the foreign program formatting module*

This program creates (from data in ESTA format) input files for a number of the more commonly used formation-constant programs. These include program MINQUAD,<sup>15</sup> task MINI, and program MAGEC,<sup>16</sup> task MGEC. Similar capabilities for programs SCOGS<sup>17</sup> DALSF EK<sup>18</sup> and SUPERQUAD<sup>19</sup> have been planned but are not yet completed.

#### *ESTA7: the error imposition module*

This program produces an ESTA input file which can be used to examine the effects of random experimental errors on the values of optimized parameters. Emf values are calculated from parameters and titration volumes into which random errors (of known standard deviation) have been introduced.

#### *ESTA8: the interactive input module*

This program facilitates the preparation of ESTA input files. Data are supplied interactively by the user in response to specific prompts. A comprehensive on-line "HELP" facility is available to guide the user at every stage. An attempt is made to provide sensible defaults at each prompt in order to minimize typing.

### PROGRAM TESTING

It is impossible to be entirely rigorous when testing a body of software of the size and complexity of ESTA. However, we have gone to considerable lengths to ensure that the programs do not contain major errors. For example, in one case, a system of three components and about ten complexes was solved manually (*i.e.*, by using a calculator) and shown to yield a species distribution in exact agreement with that computed by ESTA. For those tasks where it is reasonable to make a comparison, ESTA gives results that are satisfactorily similar to those of other published programs such as PSEUDOPLOT,<sup>20</sup> SCOGS<sup>17</sup> and MINQUAD.<sup>15</sup> [Refinement of formation constants by using an unweighted objective function based on total analytical concentrations, *i.e.*, the ESTA2 task OBJT without any corrections switched on (see below), is comparable to the calculations performed by SCOGS and MINQUAD.] Nevertheless, this approach is not possible when it comes to many of ESTA's other facilities: none of the previous programs permits calculations that involve corrections for activity-coefficient (Debye-Hückel)

effects, liquid-junction potentials and imperfect ion-selectivity of electrodes; neither are they as versatile in respect of the parameters which can be determined, or of the titration set-up (number of electrodes, number of burettes *etc.*).

Since many aspects of the programs cannot be tested manually, we have often had to resort to checking thoroughly for internal consistency. Such checks warrant more confidence than might initially be imagined, because, often, ESTA calculations can be performed in opposite directions independently. Obvious examples of this encompass the paired tasks SIME/SIMV and OBJE/OBJT (in those cases where both can be performed). A less apparent but none the less important instance of forward and backward calculation occurs with Debye-Hückel corrections when titration points actually have the reference ionic strength. This is because values (say, of emf) identical to those determined without Debye-Hückel corrections must be obtained. Recall that activity coefficient calculations first convert all the user-supplied conditional constants into their "thermodynamic" counterparts (*i.e.*, values at  $I = 0$ ) and then back again on a point-by-point basis to the actual ionic strength that is calculated during the simulation.<sup>9</sup> Finally, note that all calculations can be fairly well checked for internal consistency just by working with simulated data (for which, of course, the answer will be known).

A third and rather different kind of test has arisen in implementing the ESTA programs on a variety of computers. Aside from considerations of FORTRAN standardization (which lie outside the scope of the present paper), this tends to reveal certain programming errors which would otherwise be very difficult or impossible to detect. We have prepared a set of eight data files containing input for the purpose of testing most aspects of the programs when they are loaded onto a new kind of machine. For example, when we first ported ESTA onto an ICL 2900 computer, we obtained different results on successive executions with the same data! This was because we had not initialized every variable within the programs (a failure which has of course now been corrected). Unlike the VAXen on which the software was developed, the ICL 2900 does not automatically initialize all program variables. The point is that this error had not previously manifested itself in any way. To our knowledge, the ESTA programs are now successfully implemented on computers from at least ten different manufacturers, including two kinds of micro-computer. Probably the most important requirement of a computer is that arithmetic should be done with a minimum precision of 32 bits.

#### PROGRAM LIMITATIONS

It was originally intended that ESTA should perform all of its various calculations regardless of the kinds of corrections desired for changes in activity

coefficients, electrode selectivity or liquid-junction potential. Unfortunately, this has not been entirely achieved.

The most significant difficulty concerns the evaluation of certain analytical derivatives in those ESTA tasks where solving the electrode equation requires knowledge of all the free concentrations and where it is thus necessary to solve this equation and the mass-balance equations iteratively (see Part II<sup>9</sup> of this series). The problem occurs only when the above-mentioned corrections are required. Whilst it is possible, in principle, to overcome this obstacle, *e.g.*, by evaluating the necessary derivatives numerically, this is tedious to do well, and would make for very sluggish processing performance. Since we now see little benefit in going to these lengths, we have not done so. Accordingly, the task OBJT (both in ESTA1 and ESTA2) is not permitted to make Debye-Hückel, liquid-junction or ion-selectivity corrections.

Another limitation arises with those tasks which either calculate total analytical concentrations (TOTL, VESL and BURT) or in which such totals are not always well defined because a free instead of a total concentration is specified (SPEC). In these cases, the mass-balance equations are solved in a way that does not ensure mathematically that the charge balance is maintained. In other words, a total concentration of a charged component, say citrate, can be calculated without constraining (through the mass-balance equations) the concentration of its inert counter-ion, say sodium. This is a consequence solely of the conventional way in which the mass-balance equations are set up, *e.g.*, in introducing a mass-balance equation for hydrogen ion instead of considering the solution's charge balance. Once again, however, the problem is of little consequence apart from the exceptions it creates in ESTA's capabilities. It is worth noting that in the important context of determining total analytical concentrations by optimization, charge balance can easily be maintained for the purpose of activity calculations by simultaneously adjusting the concentration of a corresponding inert ion.

#### CONCLUSION

The ESTA programs have been under development for several years. During this time they have been applied in the treatment of potentiometric data by a number of researchers studying a variety of chemical systems<sup>21-27</sup> and have been favourably compared with other programs.<sup>28,29</sup> As intended at the outset, they have been used to explore many different approaches to optimization. Some of the ideas we investigated have proved unfruitful but others have fared better. The stage has only recently been reached at which an overall picture has emerged and a definitive strategy for optimizing formation constants can be recommended.

With hindsight, it is not surprising to find that all

of our more important results concern the effects of errors on the data analysis. For example, we have published some preliminary findings showing that quite large errors may arise, at least with certain glass electrodes, owing to neglect of the sodium ion interference from the background electrolyte often used in bio-inorganic studies.<sup>22</sup> Large errors may also occur, in particular circumstances, from changes during a titration of ionic strength and/or of liquid-junction potential.<sup>1</sup> The only proper way to deal with these effects, when they cannot be suppressed experimentally, is to characterize them (more or less empirically, as needs be) and then to correct for them in all calculations, along the lines taken in ESTA. Much experimental work will need to be done to quantify these effects before they can be handled entirely satisfactorily,<sup>9</sup> and this, undoubtedly, presents a formidable challenge.

However, the most pronounced influence on the analysis of titration data for the determination of formation constants stems not from the above-mentioned effects, but from the more important experimental errors in titration parameters such as the known analytical concentrations, any "fixed" formation constants (especially the protonation constants) and the electrode calibration parameters (if either set of these is not refined simultaneously). Methods of dealing with such errors have now been developed and these will be described in Parts IV and V of this series.<sup>10,14</sup> These techniques, discovered by using ESTA to quantify and reduce the effects of experimental errors, have considerable implications for future computational analyses of potentiometric titration data. They can substantially reduce what we assess has been the main source of the discrepancies in published sets of formation constants; namely, inadequate assessment of, and hence inability to avoid, the ill-effects of such experimental errors on the optimization procedures adopted.

#### REFERENCES

1. E. Bottari, A. Braibanti, L. Ciavatta, A. M. Corrie, P. G. Daniele, F. Dallavalle, M. Grimaldi, A. Mastroianni, G. Mori, G. Ostacoli, P. Paoletti, E. Rizzarelli, S. Sammartano, C. Severini, A. Vacca and D. R. Williams, *Ann. Chim. (Roma)*, 1978, **68**, 813.
2. R. B. Martin, *J. Inorg. Biochem.*, 1986, **28**, 181.
3. G. E. Jackson, *S. Afr. J. Chem.*, 1982, **35**, 89.
4. L.-O. Öhman and S. Sjöberg, *Acta Chem. Scand.*, 1983, **A37**, 875.
5. R. J. Motekaitis and A. E. Martell, *Inorg. Chem.*, 1984, **23**, 18.
6. D. J. Leggett, in *Computational Methods for the Determination of Formation Constants*, D. J. Leggett (ed.), Chapter 1, p. 12, Plenum Press, New York, 1985.
7. G. Berthon, P. M. May and D. R. Williams, *J. Chem. Soc. Dalton Trans.*, 1978, 1433.
8. A. Vacca in *Proc. Summer School on Stability Constants*, Bivigliano, Florence, June 1974, p. 105. Edizioni Scuola Universitaria, Firenze, Italy.
9. P. M. May, K. Murray and D. R. Williams, *Talanta*, 1985, **32**, 483.
10. P. M. May and K. Murray, *ibid.*, in the press.
11. M. Davies and I. J. Whiting in *Numerical Methods for Non-Linear Optimization*, F. A. Lootsma (ed.), p. 191. Academic Press, London, 1972.
12. P. Gans, *Coord. Chem. Rev.*, 1976, **19**, 99.
13. G. R. Walsh, *Methods of Optimisation*, p. 97. Wiley, London, 1975.
14. P. M. May and K. Murray, *Talanta*, in the press.
15. A. Sabatini, A. Vacca and P. Gans, *ibid.*, 1974, **21**, 53.
16. P. M. May, D. R. Williams, P. W. Linder and R. G. Torrington, *ibid.*, 1982, **29**, 249.
17. I. G. Sayce, *ibid.*, 1968, **15**, 1397.
18. R. M. Alcock, F. R. Hartley and D. E. Rogers, *J. Chem. Soc. Dalton Trans.*, 1978, 115.
19. P. Gans, A. Sabatini and A. Vacca, *ibid.*, 1985, 1195.
20. A. M. Corrie, G. K. R. Makar, M. L. D. Touche and D. R. Williams, *ibid.*, 1975, 105.
21. M. Otto, P. M. May, K. Murray and J. D. R. Thomas, *Anal. Chem.*, 1985, **57**, 1511.
22. P. M. May, K. Murray and D. Peaper, *Rev. Port. Quim.*, 1985, **27**, 312.
23. M. Filella, A. Izquierdo and E. Casassas, *J. Inorg. Biochem.*, 1986, **28**, 1.
24. M. Filella, E. Casassas and D. R. Williams, *Inorg. Chim. Acta*, 1987, **136**, 177.
25. L. Lambs and G. Berthon, *ibid.*, 1988, **151**, 33.
26. G. E. Jackson, *ibid.*, 1988, **151**, 273.
27. F. Marsicano, C. Monberg, B. S. Martincigh, K. Murray, P. M. May and D. R. Williams, *J. Coord. Chem.*, 1988 **16**, 321.
28. E. Casassas, R. Tanler and M. Filella, *Anal. Chim. Acta*, 1986, **191**, 399.
29. E. Casassas, M. Filella and R. Tanler, *ibid.*, 1986, **191**, 413.

## ELIMINATION OF INTERFERENCES IN ELECTROTHERMAL-ATOMIZATION ATOMIC-ABSORPTION SPECTROMETRY OF CADMIUM

KIYOHISA OHTA\*, WATARU AOKI and TAKAYUKI MIZUNO

Department of Chemistry, Faculty of Engineering, Mie University, Tsu, Mie 514, Japan

(Received 1 June 1988. Accepted 30 August 1988)

**Summary**—The determination of cadmium by use of a molybdenum-tube atomizer and atomic-absorption spectrometry has been investigated. The absorption profiles for various cadmium compounds and the interferences caused by large amounts of concomitants were evaluated. Sulphur was tested as a matrix modifier for removal of interference and found to be effective at the interferent levels likely to be found in biological samples. A simple, precise and convenient method for determination of cadmium in biological materials has been established.

Numerous investigators have reported determinations of cadmium in various types of sample by electrothermal atomization atomic-absorption spectrometry (ETA-AAS).<sup>1-48</sup>

However, in most cases there is the problem of matrix interference, and the AAS determination has been combined with a prior separation by electro-deposition, ion-exchange, co-precipitation or solvent extraction to eliminate the interference.<sup>49-53</sup> Various matrix modifiers, including sodium phosphate, diammonium hydrogen phosphate, ammonium dihydrogen phosphate-EDTA-thiourea, ammonium dihydrogen phosphate-nitric acid, diammonium hydrogen phosphate-ammonium nitrate, ammonium nitrate, palladium nitrate-ammonium nitrate, nitric acid, lanthanum, and thiourea have been used in the graphite-furnace or metal-tube AAS determination of cadmium.<sup>1-14</sup> Yoshimura *et al.* have studied the de-oxidation effect of sulphur powder on zinc oxide in flame and on beryllium oxide in ETA-AAS,<sup>54,55</sup> and found that the sensitivities for zinc and beryllium were improved by the addition of sulphur powder dispersed in water. However, relatively little information has so far been reported on the usefulness of sulphur as a matrix modifier for determination of cadmium by ETA-AAS.

This report discusses the use of sulphur for the elimination of interferences in the ETA-AAS determination of cadmium with a molybdenum-tube atomizer and reports a simple, precise, and convenient method for determining cadmium in biological materials. The molybdenum-tube atomizer was chosen for use on account of its various advantages<sup>56</sup> and long experience with it.

### EXPERIMENTAL

#### Apparatus

All atomic-absorption measurements were made with a Nippon Jarrell-Ash 0.5 m Ebert-type monochromator fitted

with an R943 photomultiplier tube (Hamamatsu Photonics Co.) and a fast-response amplifier.

A molybdenum tube (20 mm long, 1.8 mm i.d., 0.05 mm wall thickness, 0.060 ml volume), made from high-purity molybdenum sheet (99.95% purity, Rembar Co.), was used as the atomizer. A cadmium hollow-cathode lamp (Hamamatsu Photonics Co.) was used at the cadmium resonance line of 228.8 nm, and molecular-background correction was achieved with a deuterium lamp (Original Hanau D200F).

The light-beam from the source was collimated with two apertures (1 mm diameter) in front of and at the rear of the atomizer tube to reduce the intensity of the radiation from the surface of the atomizer, to increase the sensitivity and improve the reproducibility of the signals. The atomic-absorption signal from the amplifier and the atomizer-temperature signal from a photodiode (Hamamatsu Photonics Co. S641) were monitored with an Iwatsu Memoriscopes (MS-5021) and fed simultaneously to a micro-computer (Sord M223). The temperature read-out was calibrated beforehand with an optical pyrometer (Chino Works). Both signals were displayed on a cathode-ray tube and recorded on a plotter (Graphtec WX4675) after mathematical processing by a program already described.<sup>56</sup>

A Rotaflex (Rigaku RU-200B) X-ray diffraction apparatus fitted with a copper tube operated at 40 kV and 150 mA, and a proportional detector, was used.

#### Reagents

A 1-mg/ml standard stock cadmium solution was prepared by dissolving the high-purity metal (optical grade) in 7M nitric acid and diluting the solution to known volume with demineralized distilled water. Solutions of cadmium chloride, sulphate, phosphate and acetate were prepared by heating cadmium nitrate with the corresponding acid.

Solutions of the matrix elements were prepared from the nitrates as needed.

A sulphur solution (10 mg/ml) was prepared by dissolving high-purity sulphur in carbon disulphide. All test solutions were prepared immediately before use, by dilution with demineralized distilled water.

All chemicals used were of analytical grade.

#### Procedures

An argon (480 ml/min)-hydrogen (20 ml/min) mixture was used to purge the atomization chamber.

Accurately weighed portions of biological sample (about 0.1 g) were digested with 8 ml of 14M nitric acid and 2 ml of 30% hydrogen peroxide for 3 hr in a Uni-seal decomposition vessel placed in an electric oven at 390 K. After

\*To whom correspondence should be addressed.

digestion, the solutions were transferred to Teflon beakers and evaporated to dryness in a poly(ethylene glycol) bath at 380 K. The residues were dissolved in about 2 ml of 1M nitric acid, transferred to 10-ml standard flasks and made up to the mark with water. These solutions were further diluted with demineralized distilled water as required.

For the measurement step a 1- $\mu$ l aliquot, containing 2.5 pg of cadmium for the interference studies, was injected into the metal-tube atomizer with a glass pipette and dried at 370 K for 10 sec. A 1- $\mu$ l aliquot of the sulphur solution (10  $\mu$ g of S) was added to the atomizer with another glass pipette. After standing for 10 sec the residue was pyrolysed at 570 K for 10 sec and atomized at 2170 K.

The atomic-absorption profile and the background signal were measured. The background was subtracted from the absorption profile, and the baseline variation with time was compensated to give zero baseline absorption. After smoothing, the data were accumulated automatically in a disk memory by the microcomputer. These steps were repeated at least three times. The position of the peak on each atomic-absorption profile was then established and the signals at other points away from the peak were accumulated. The averaged absorption profiles are shown in Figs. 1-10.

Samples for X-ray diffraction measurement were prepared by heating about 1 mg of cadmium nitrate, containing 10 mg of sulphur, on a molybdenum sheet (5.5  $\times$  50 mm) at 570 K in the reducing argon-hydrogen atmosphere. The X-ray diffraction patterns were obtained by measurement at  $2\theta = 26.5^\circ$  ( $d = 3.36 \text{ \AA}$ ).

## RESULTS AND DISCUSSION

### Effect of the counter-ion

For a simple and direct analysis of various samples for cadmium by ETA-AAS it is important to investigate the atomization profiles of various stable cadmium compounds, because differences in the combined form of the cadmium would be expected to influence the profiles. Therefore, the signals from cadmium nitrate, chloride, sulphate, phosphate, acetate and sulphide in the metal-tube atomizer were measured, in a flow of 480 ml/min argon plus 20 ml/min hydrogen, which is the best experimental condition for cadmium atomization,<sup>14</sup> and are shown in Fig. 1. The signals from these compounds were all

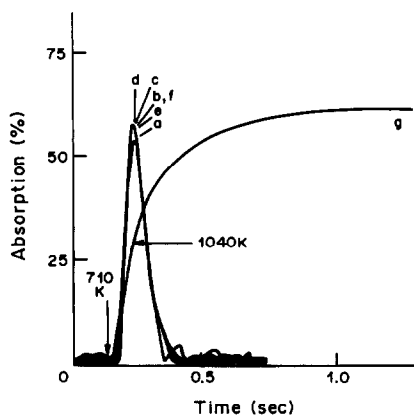


Fig. 1. Effect of particular cadmium salts on the atomic-absorption signal in 480 ml/min Ar and 20 ml/min H<sub>2</sub>: (a) acetate; (b) chloride; (c) nitrate; (d) sulphate; (e) sulphide; (f) phosphate; (g) temperature increase; Cd 2.5 pg.

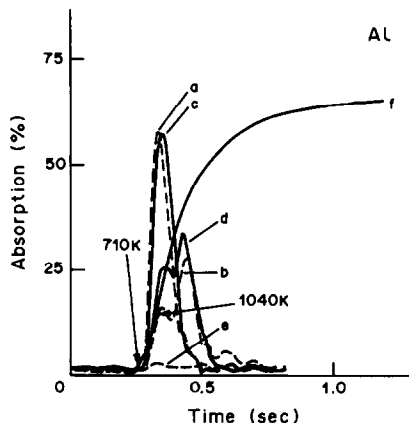


Fig. 2. Atomization profiles of cadmium in presence of large amounts of aluminium with and without sulphur present, in 480 ml/min Ar and 20 ml/min H<sub>2</sub>. Solid line, sulphur added; broken line, without sulphur: (a) 2.5 pg of cadmium; (b) 2.5 pg of cadmium and 250 ng of aluminium; (c) 2.5 pg of cadmium with sulphur; (d) 2.5 pg of cadmium and 250 ng of aluminium with sulphur; (e) 250 ng of aluminium; (f) temperature increase.

similar. Also, the signal for a given compound with added sulphur was similar to that for cadmium nitrate in the presence of sulphur. It was established by X-ray analysis that when heated in the presence of sulphur these compounds were converted into the sulphide at the pyrolysis temperature in the argon-hydrogen atmosphere.

### Interference study

The effects of large amounts ( $10^3$ - $10^5$  fold) of Al, Ca, Cr, Cu, Fe, K, Na and Pb on the cadmium absorption profile were investigated with the metal-tube atomizer. These elements were selected for examination on the basis of known interference

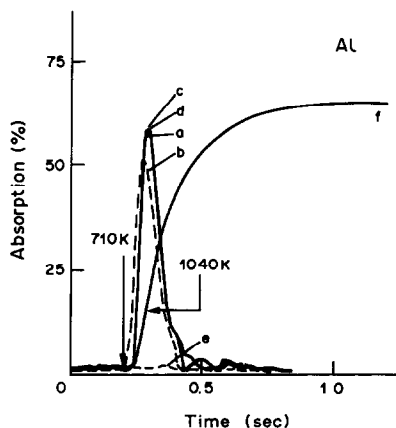


Fig. 3. Atomization profiles of cadmium in presence of 2.5 ng of aluminium with and without sulphur added, in 480 ml/min Ar and 20 ml/min H<sub>2</sub>. Solid line, sulphur added; broken line, without sulphur: (a) 2.5 pg of cadmium; (b) 2.5 pg of cadmium and 2.5 ng of aluminium; (c) 2.5 pg of cadmium with sulphur; (d) 2.5 pg of cadmium and 2.5 ng of aluminium with sulphur; (e) 2.5 ng of aluminium; (f) temperature increase.

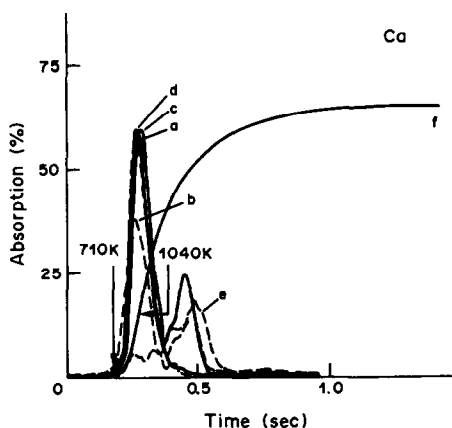


Fig. 4. Atomization profiles of cadmium in presence of large amounts of calcium with and without sulphur added, in 480 ml/min Ar and 20 ml/min  $H_2$ . Solid line, sulphur added; broken line, without sulphur: (a) 2.5 pg of cadmium; (b) 2.5 pg of cadmium and 250 ng of calcium; (c) 2.5 pg of cadmium with sulphur; (d) 2.5 pg of cadmium and 250 ng of calcium with sulphur; (e) 250 ng of calcium; (f) temperature increase.

effects for cadmium<sup>14</sup> and in accordance with their abundances in biological materials.

The interference effects of 250, 25 and 2.5 ng of aluminium in the absence and presence of sulphur were examined. The presence of 250 or 25 ng of aluminium depressed the cadmium signal considerably, as shown in Fig. 2, and the addition of sulphur did not modify this effect. The effect of 2.5 ng of aluminium on the signal for 2.5 pg of cadmium in the presence and absence of sulphur is illustrated in Fig. 3. Sulphur completely eliminated the interference.

The effect of 250 ng of calcium on the cadmium signal, with and without sulphur present, is shown in

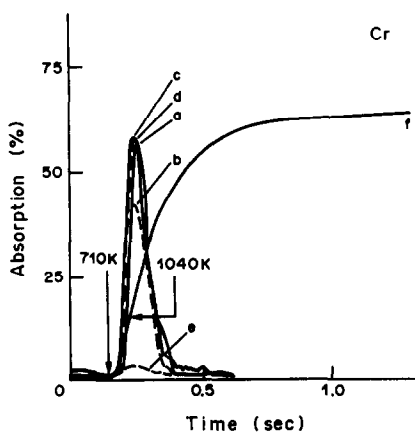


Fig. 5. Atomization profiles of cadmium in presence of large amounts of chromium with and without sulphur added, in 480 ml/min Ar and 20 ml/min  $H_2$ . Solid line, sulphur added; Broken line, without sulphur: (a) 2.5 pg of cadmium; (b) 2.5 pg of cadmium and 250 ng of chromium; (c) 2.5 pg of cadmium with sulphur; (d) 2.5 pg of cadmium and 250 ng of chromium with sulphur; (e) 250 ng of chromium; (f) temperature increase.

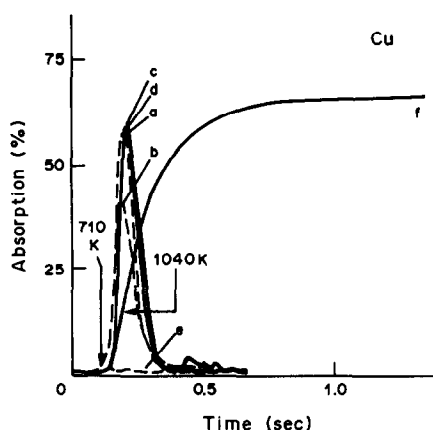


Fig. 6. Atomization profiles of cadmium in presence of large amounts of copper with and without sulphur added, in 480 ml/min Ar and 20 ml/min  $H_2$ . Solid line, sulphur added; broken line, without sulphur: (a) 2.5 pg of cadmium; (b) 2.5 pg of cadmium and 250 ng of copper; (c) 2.5 pg of cadmium with sulphur; (d) 2.5 pg of cadmium and 250 ng of copper with sulphur; (e) 250 ng of copper; (f) temperature increase.

Fig. 4. An additional peak appeared in the higher temperature region of the absorption profile of cadmium in both cases. The melting points of calcium oxide and sulphide are 2845 and 1823 K, respectively and the boiling point of calcium oxide is 3123 K.<sup>59</sup> Thus, the peak must result from molecular absorption by calcium. The original cadmium absorption profile was restored (when calcium was present) by the addition of sulphur, but not by addition of thiourea.<sup>14</sup>

Figure 5 illustrates the effect of 250 ng of chromium on 2.5 pg of cadmium, and the effect of sulphur as matrix modifier. The chromium depressed the

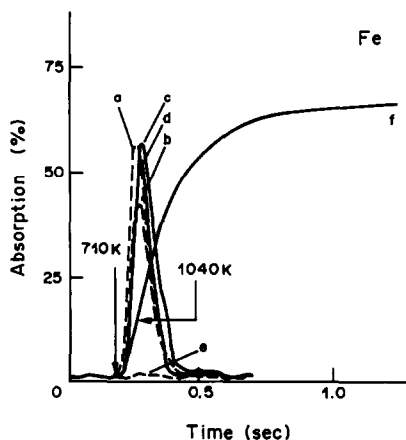


Fig. 7. Atomization profiles of cadmium in presence of large amounts of iron with and without sulphur in 480 ml/min Ar and 20 ml/min  $H_2$ . Solid line, sulphur added; broken line, without sulphur: (a) 2.5 pg of cadmium; (b) 2.5 pg of cadmium and 250 ng of iron; (c) 2.5 pg of cadmium with sulphur; (d) 2.5 pg of cadmium and 250 ng of iron with sulphur; (e) 250 ng of iron; (f) temperature increase.

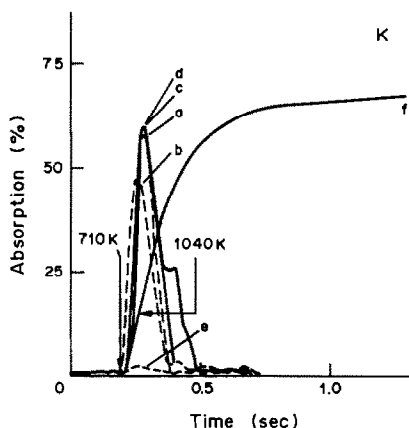


Fig. 8. Atomization profiles of cadmium in presence of large amounts of potassium with and without sulphur added, in 480 ml/min Ar and 20 ml/min  $H_2$ . Solid line, sulphur added; broken line, without sulphur: (a) 2.5 pg of cadmium; (b) 2.5 pg of cadmium and 250 ng of potassium; (c) 2.5 pg of cadmium with sulphur; (d) 2.5 pg of cadmium and 250 ng of potassium with sulphur; (e) 250 ng of potassium; (f) temperature increase.

cadmium signal, without shifting the peak temperature, but addition of sulphur eliminated the interference.

The absorption signal for cadmium in the presence of 250 ng of copper was lower and at lower temperature than in the absence of copper. The interference, however, was sufficiently modified by adding sulphur, as shown in Fig. 6.

The interference by 250 ng of iron and the modifying effect of sulphur are illustrated in Fig. 7. Iron depressed the absorption signal, but sulphur eliminated this effect.

The effect of 250 ng of potassium on the cadmium absorption, and its modification with sulphur are shown in Fig. 8. The signal in the presence of potassium shifted to a lower temperature and was lower than for cadmium alone. Addition of sulphur completely removed this effect. However, two absorption peaks appeared when both potassium and sulphur were present, though not in the presence of potassium alone. This is reasonable, considering that potassium oxide decomposes at 623 K and that the melting point of potassium sulphide is 1113 K.<sup>57</sup> Absorption measurements with a deuterium lamp indicated that the second peak resulted from molecular absorption (maybe by potassium sulphide).

The effect of 250 ng of sodium on the cadmium signal was investigated in the absence and presence of sulphur, as illustrated in Fig. 9. The cadmium signal was depressed by the addition of a  $10^5$ -fold amount of sodium. The signal in the presence of sodium was poorly reproducible and appeared at a lower temperature than for cadmium alone. When sulphur was also added, the cadmium signal was the same as that for cadmium in the presence of sulphur and absence of sodium and was reproducible. Small peaks were

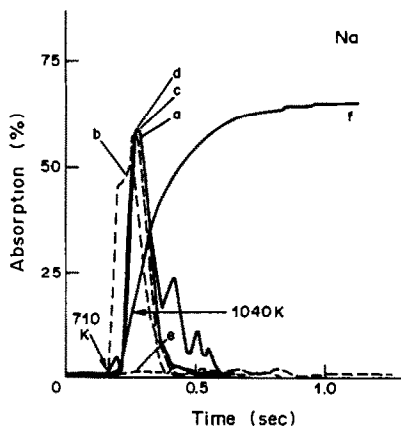


Fig. 9. Atomization profiles of cadmium in presence of large amounts of sodium with and without sulphur added in 480 ml/min Ar and 20 ml/min  $H_2$ . Solid line, sulphur added; broken line, without sulphur: (a) 2.5 pg of cadmium; (b) 2.5 pg of cadmium and 250 ng of sodium; (c) 2.5 pg of cadmium with sulphur; (d) 2.5 pg of cadmium and 250 ng of sodium with sulphur; (e) 250 ng of sodium; (f) temperature increase.

observed on the tail of the cadmium profile when sodium and sulphur were both present, but not when only sodium was added. Measurements with the deuterium lamp indicated that these peaks were due to molecular absorption. The melting point of sodium sulphide is 1453 K.<sup>57</sup> On the other hand, sodium oxide decomposes to give sodium and sodium peroxide at temperatures above 673 K and the peroxide then decomposes at 930 K.<sup>57</sup> Since the peaks appeared at temperatures above 1500 K, they were probably due to sodium sulphide.

The interference by 250 ng of lead was investigated in the absence and presence of sulphur. The lead depressed the cadmium signal considerably, and sul-

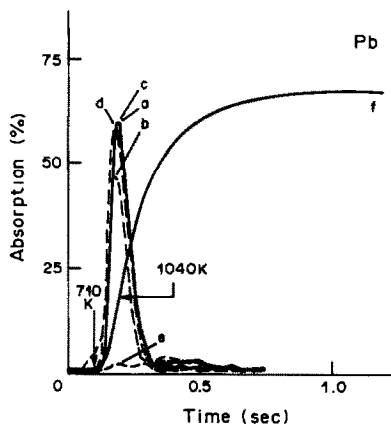


Fig. 10. Atomization profiles of cadmium in presence of 25 ng of lead with and without sulphur added, in 480 ml/min Ar and 20 ml/min  $H_2$ . Solid line, sulphur added; broken line, without sulphur: (a) 2.5 pg of cadmium; (b) 2.5 pg of cadmium and 25 ng of lead; (c) 2.5 pg of cadmium with sulphur; (d) 2.5 pg of cadmium and 25 ng of lead with sulphur; (e) 25 ng of lead; (f) temperature increase.



Table 1. Determination of cadmium in biological samples

Sample	Cadmium, $\mu\text{g/g}$	
	Found	Certified value
Bovine liver*	0.26, 0.25, 0.24	$0.27 \pm 0.04$
Oyster tissue*	3.2, 3.2, 3.5	$3.5 \pm 0.4$
Orchard leaves*	0.11, 0.11, 0.10	$0.11 \pm 0.01$
Pepper bush†	6.6, 6.3, 6.6	$6.7 \pm 0.5$

\*NBS standard.

†NIES standard.

phur could not modify the signal sufficiently. However, the interference of 25 ng of lead could be eliminated completely by the addition of sulphur, as seen in Fig. 10.

In general, the cadmium absorption profile in the presence of sulphur was shifted to a slightly higher temperature than that for cadmium alone even though the dissociation energy of the sulphide is lower than that of the oxide. The sublimation temperature of cadmium sulphide is 1253 K which is higher than that of the oxide (973 K).<sup>57,58</sup> Thus the shift may be due to this difference in the sublimation temperatures of the two compounds. Modification with sulphur for dealing with large amounts of the matrix interferences was more satisfactory than modification with thiourea.<sup>14</sup>

#### Determination of cadmium in biological matrices

Li and Zhang digested biological samples with concentrated nitric acid and hydrogen peroxide for cadmium determination and obtained recoveries of 88.4–99.6% by graphite-furnace atomic-absorption spectrometry.<sup>59</sup> The same decomposition method was therefore used in the present work. Table 1 shows the results obtained for some biological materials with certified values. The relative standard deviations estimated by the range method were 2.7–5.4%. The method can be considered satisfactory for the determination of cadmium in biological materials.

**Acknowledgement**—This work was supported financially by the Ministry of Education, Science and Culture of Japan.

#### REFERENCES

- H. Berndt, J. Baasner and J. Messerschmidt, *Anal. Chim. Acta*, 1986, **180**, 389.
- W. Calmano, W. Ahlf and T. Schilling, *Z. Anal. Chem.*, 1986, **323**, 865.
- D. T. E. Hunt and D. A. Winnard, *Analyst*, 1986, **111**, 785.
- J. R. Clark, *J. Anal. At. Spectrom.*, 1986, **1**, 301.
- S. Lin, *Fenxi Huaxue*, 1986, **14**, 611.
- A. Kumar, A. L. Aggarwal and B. T. Deshmukh, *Indian J. Pure Appl. Phys.*, 1987, **25**, 197.
- A. Stelz, *Lebensmittel Chem. Gerichtl. Chem.*, 1987, **1**, 110.
- M. Hoening, *Int. Clin. Prod. Rev.*, 1987, **6**, 38.
- X. Yin, G. Schlemmer and B. Welz, *Anal. Chem.*, 1987, **59**, 1462.
- H. Han, X. Le and X. Ni, *Huanjing Huaxue*, 1986, **5**, No. 6, 34.
- J. Fleckenstein, *Z. Anal. Chem.*, 1987, **328**, 396.
- L. Chen, Y. Yan and W. Zhou, *Guangpuxue Yu Guangpu Fenxi*, 1987, **7**, No. 3, 63.
- K. S. Subramanian, *Clin. Chem.*, 1987, **33**, 1298.
- M. Suzuki and K. Ohta, *Anal. Chem.*, 1982, **54**, 1686.
- F. Fagioli, S. Landi, C. Locatelli and C. Bigli, *At. Spectrosc.*, 1986, **7**, 49.
- N. Fudagawa, A. Hioki, M. Kubota and A. Kawase, *Bunseki Kagaku*, 1986, **35**, T62.
- K. Hirokawa, M. Namiki, J. Kimura and A. Kawase, *ibid.*, 1986, **35**, 701.
- K. O. Olayinka, S. J. Haswell and R. Grzeskowiak, *J. Anal. At. Spectrom.*, 1986, **1**, 297.
- I. P. Kharlamov, V. I. Lebedev, V. Yu. Persits and G. V. Eremina, *Zh. Analit. Khim.*, 1986, **41**, 1004.
- D. A. Batistoni, L. H. Erijman and A. L. Pazos, *An. Asoc. Quim. Argent.*, 1986, **74**, 265.
- S. J. Nagourney, H. Heit and D. C. Bogen, *Spectroscopy*, 1986, **1**, 41.
- F. Jin and F. Liu, *Guangpuxue Yu Guangpu Fenxi*, 1986, **6**, No. 4, 45.
- D. J. Halls, M. M. Black, G. S. Fell and J. M. Ottaway, *J. Anal. At. Spectrom.*, 1987, **2**, 305.
- M. Vačková, L. Smirnová and E. Kozáková, *Chem. Listy*, 1986, **80**, 635.
- K. R. Lun and M. Callaghan, *Anal. Chim. Acta*, 1986, **187**, 157.
- I. C. Clurea, Y. F. Lipka and B. E. Humbert, *Mitt. Geb. Lebensmittelunters. Hyg.*, 1986, **77**, 509.
- M. Hoening and P. Van Hoeyweghen, *Anal. Chem.*, 1986, **58**, 2614.
- M. M. Reddy, M. A. Benefiel and H. C. Claassen, *Mikrochim. Acta*, 1986, **1**, 159.
- G. R. Dulude, J. J. Sotera and D. L. Pfeil, *Spectroscopy*, 1987, **2**, 49.
- Standards Association of Australia, *Australia Standard*, 1987, **2**, 8.
- U. Voellkopf, R. Lehman and D. Weber, *J. Anal. At. Spectrom.*, 1987, **2**, 455.
- G. Rygh and K. W. Jackson, *ibid.*, 1987, **2**, 397.
- I. Atsuya, K. Itoh and K. Akatsuka, *Z. Anal. Chem.*, 1987, **328**, 338.
- A. M. de Kersabiec and M. F. Benedetti, *ibid.*, 1987, **328**, 342.
- A. A. Brown, M. Lee, G. Küllemer and A. Rosopulo, *ibid.*, 1987, **328**, 354.
- E. Lücker, A. Rosopulo and W. Kreuzer, *ibid.*, 1987, **328**, 370.
- M. van Son and H. Muntau, *ibid.*, 1987, **328**, 390.
- J. Fleckenstein, *ibid.*, 1987, **328**, 396.
- V. A. Letourneau, B. M. Joshi and L. C. Butler, *At. Spectrosc.*, 1987, **8**, 145.
- H. Berndt and D. Scopczak, *Z. Anal. Chem.*, 1987, **329**, 18.
- K. Akatsuka and I. Atsuya, *ibid.*, 1987, **329**, 453.
- S. J. Nagourney, M. Heit and D. C. Bogen, *Talanta*, 1987, **34**, 465.
- H. van Beek, H. C. A. Greefkes and A. J. Baars, *ibid.*, 1987, **34**, 580.
- J. R. Castillo, I. Concha and C. Martinez, *At. Spectrosc.*, 1987, **8**, 172.
- S. C. Apte and A. M. Gunn, *Anal. Chim. Acta*, 1987, **193**, 147.
- N. Khalid, S. Rahman, R. Ahmed and I. H. Qureshi, *Int. J. Environ. Anal. Chem.*, 1987, **28**, 133.
- J. C. Amiard, A. Pineau, H. L. Boiteau, C. Metayer and C. Amiard-Triquet, *Water Res.*, 1987, **21**, 693.
- G. Strübel, V. Rzepka-Glinder and K. H. Grobecker, *Z. Anal. Chem.*, 1987, **328**, 382.
- W. Lund, B. V. Larsen and N. Gundersen, *Anal. Chim. Acta*, 1976, **81**, 319.
- M. D. Vensand and R. Lawerys, *Arch. Mal. Prof. Trav. Secur. Soc.*, 1972, **33**, 97.

51. H. M. Kingston, I. L. Barnes, T. J. Brady, T. C. Rains and M. A. Champ, *Anal. Chem.*, 1978, **50**, 2064.
52. K. L. Iu, I. D. Pulford and H. J. Duncan, *Anal. Chim. Acta*, 1979, **106**, 319.
53. R. W. Dabeka and A. D. Mckenzie, *Can. J. Spectrosc.*, 1986, **31**, 44.
54. C. Yoshimura and Y. Noda, *Nihon Kagaku Kaishi*, 1978, 1098.
55. C. Yoshimura and T. Fujino, *ibid.*, 1983, 659.
56. M. Suzuki and K. Ohta, *Prog. Anal. At. Spectrosc.*, 1983, **6**, 49.
57. R. C. Weast (ed.), *Handbook of Chemistry and Physics*, 61st ed., pp. B86, B135, B137, B149, B151, F222-F226, CRC Press, Ohio, 1980.
58. S. Mizushima (ed.), *Encyclopedia Chimica*, Vol. 3, pp. 990, 991; Vol. 9, pp. 651, 653. Kyoritsu Shuppan KK, Tokyo, 1963.
59. S. Li and Z. Zhang, *Fenxi Shiyanshi*, 1986, **5**, 63.

## ADSORPTIVE VOLTAMMETRY OF LIPOIC ACID AND LIPOAMIDE, BASED ON USE OF A CATALYTIC HYDROGEN WAVE

SHUNITZ TANAKA and HITOSHI YOSHIDA

Department of Chemistry, Faculty of Science, Hokkaido University, Nishi-8, Kita-10, Kita-ku, Sapporo-shi, Hokkaido, Japan

(Received 10 February 1987. Revised 28 April 1988. Accepted 29 August 1988)

**Summary**—The adsorptive voltammetry of lipoic acid and lipoamide was investigated with a hanging mercury drop electrode. These compounds produced a catalytic hydrogen wave at  $-1.35$  V in ammonia buffer solution containing cobalt(II), and the peak current increased with adsorptive accumulation at the electrode. Thus adsorptive voltammetry with the catalytic hydrogen wave could provide a sensitive method for determining trace amounts of lipoic acid and lipoamide. The calibration graphs for both compounds were linear over the range  $2$ – $10$  nM with accumulation for 5 min at  $-0.6$  V, and the detection limit was ca.  $0.5$  nM.

Lipoic acid (6,8-dithio-octanoic acid) is a biologically important substance and widely distributed in many animal, plant and microbial cells.<sup>1</sup> It plays an important role in a number of biochemical reactions involving hydrogen transfer. Lipoamide is also an important substance, as the electron-acceptor of lipoamide dehydrogenase. Both substances have the disulphide group in their structure. The biochemical reaction is accompanied by conversion of the disulphide into a dithiol grouping, and it has been reported that this redox reaction occurs reversibly at the mercury electrode.<sup>2,3</sup> The polarographic behaviour of lipoic acid has been studied in detail.<sup>4-8</sup>

A few electroanalytical methods for determining lipoic acid and lipoamide have been reported. Polarographic methods based on measurement of the wave for reduction from disulphide to dithiol,<sup>6,7</sup> the catalytic hydrogen wave produced by the disulphide in the presence of cobalt(II), the so-called Brdička current,<sup>7</sup> and cathodic stripping voltammetry have been attempted, but were not sensitive enough.

In this study, an investigation was made of determination of trace amounts of lipoic acid and lipoamide by means of the catalytic hydrogen wave produced by lipoic acid and lipoamide accumulated adsorptively on the hanging mercury drop electrode (HMDE) in an ammonia buffer solution containing cobalt(II). It was expected that the sensitivity, already high for the catalytic hydrogen wave, would be further increased by the adsorptive preconcentration of the analytes on the HMDE.

### EXPERIMENTAL

#### Apparatus

A PAR 174A polarographic analyser was used for voltammetric measurements. An Omnigraphic model 2000H X-Y recorder (Houston Instrument Co.) was used for

recording voltamperograms. The working electrode was a Metrohm model E 410 HMDE and the counter-electrode was a glassy-carbon rod. A saturated calomel electrode with a diaphragm tube containing 1M potassium nitrate was used as reference electrode. Stirring for accumulation was performed with a magnetic stirrer. The measurements were made at  $25 \pm 0.1^\circ$ . A potentiostat (Hokuto Denki Co.) was used for potentiostatic experiments. Cyclic voltammetry was performed with a manually operated PAR 174A instrument.

#### Reagents

Lipoic acid and lipoamide were obtained from Sigma Co. and used without further purification. The 0.01M stock solutions were made in 50% v/v ethanol-water mixture. The solution of cobalt(II) was prepared from  $\text{Co}(\text{NO}_3)_2$  (Wako Pure Chemical Industry Co.) and the solution of cobalt(III) from  $[\text{Co}(\text{NH}_3)_6]\text{Cl}_3$  (Eastman Kodak Co.). The supporting electrolyte was ammonium chloride/ammonia buffer. High-purity nitrogen was used for deaeration. Other reagents were analytical reagent grade.

### RESULTS AND DISCUSSION

Cyclic voltamperograms of lipoamide in 0.1M ammonia buffer solution (pH 8.5) at the HMDE are shown in Fig. 1(a). The waves of the redox reaction corresponding to the transformation from disulphide into dithiol and *vice versa* appear at about  $-0.7$  V as sharp peaks, and indicate that lipoamide is adsorbed on the mercury electrode surface. In the presence of cobalt(II), the cyclic voltamperograms of lipoamide show a new reduction wave at about  $-1.35$  V, Fig. 1(b-f). The peak current is very large and proportional to the concentration of cobalt(II) when this is lower than  $200 \mu\text{M}$ . This wave seems to be a catalytic hydrogen wave since it is located at only slightly more positive potential than that of the hydrogen reduction wave in the same ammonia buffer solution and the peak current is very much larger than that expected from diffusion of cobalt(II) or

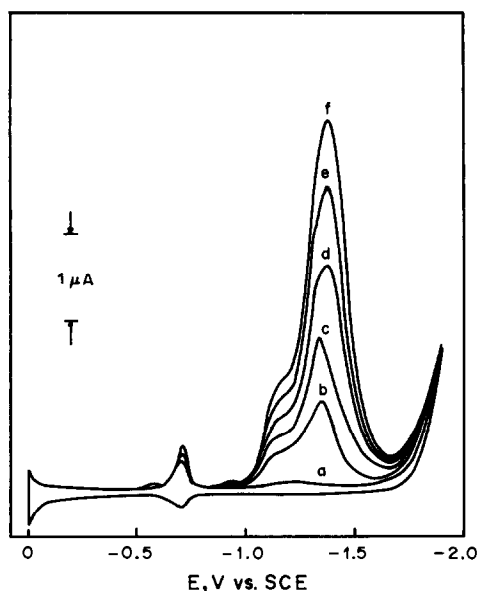


Fig. 1. Cyclic voltamperograms of  $10\mu\text{M}$  lipoamide. Supporting electrolyte,  $0.1\text{M}$  ammonia buffer solution (pH 8.5); with (a) 0, (b) 1, (c) 2, (d) 3, (e) 4, (f)  $5\mu\text{M}$  Co(II). Scan-rate;  $50\text{ mV/sec}$ .

lipoamide. Furthermore, it was confirmed by the potentiostatic investigations with a mercury pool electrode that gas was evolved at the electrode surface when the electrode potential was kept at  $-1.35\text{ V}$ .

Cyclic voltamperograms similar to that of lipoamide were observed for lipoic acid, and a catalytic hydrogen wave appeared at about  $-1.30\text{ V}$  when cobalt(II) was present.

The effects of the adsorptive accumulation of lipoic acid or lipoamide on the HMDE are shown in Fig. 2. The peak height of the catalytic hydrogen

wave at  $-1.35\text{ V}$  is increased by adsorptive accumulation of lipoic acid or lipoamide at  $-0.6\text{ V}$ . The catalytic hydrogen wave obtained after the adsorptive accumulation is sharper than that without accumulation. It is considered that the lipoic acid or lipoamide adsorbed on the HMDE but not that diffusing from the bulk solution is concerned in the catalytic hydrogen evolution. The catalytic hydrogen wave is also influenced by the concentration and pH of the supporting electrolyte. The half-peak width of the catalytic hydrogen wave decreases with increase in the concentration of the ammonia buffer, from  $220\text{ mV}$  at  $0.1\text{M}$  to  $70\text{ mV}$  at  $1\text{M}$ , though the peak current remains constant. The peak current is maximal in the pH region 8–9.5.

The relation between peak current and accumulation potential is shown in Fig. 3. When lipoic acid (at  $0.1\mu\text{M}$  concentration) is accumulated for 2 min at various potentials, the peak current of the catalytic hydrogen wave is constant over the accumulation potential range from  $-0.5$  to  $-0.8\text{ V}$ . For  $0.1\mu\text{M}$

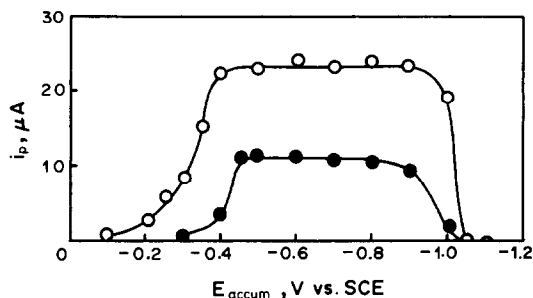


Fig. 3. Effect of accumulation potential on peak current. Supporting electrolyte,  $1\text{M}$  ammonia buffer solution (pH 9.0) containing  $200\mu\text{M}$  Co(II); (—○—)  $0.1\mu\text{M}$  lipoamide accumulated for 1 min; (—●—)  $0.1\mu\text{M}$  lipoic acid accumulated for 2 min.

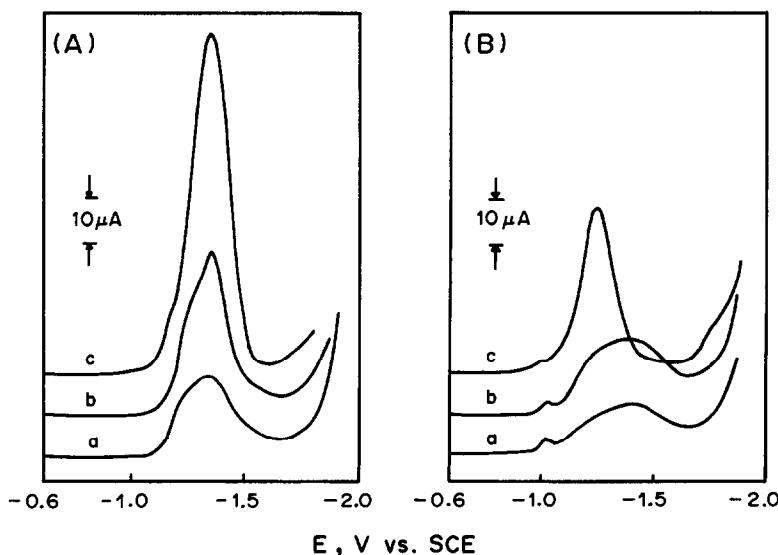


Fig. 2. Effect of accumulation. Supporting electrolyte:  $0.1\text{M}$  ammonia buffer solution (pH 8.5). (A)  $1\mu\text{M}$  lipoamide, (B)  $1\mu\text{M}$  lipoic acid: (a) not accumulated, (b) accumulated at  $-0.6\text{ V}$  for 1 min without stirring, (c) accumulated at  $-0.6\text{ V}$  for 1 min with stirring.

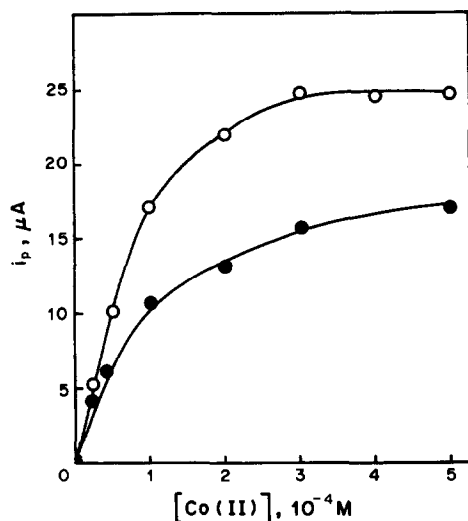


Fig. 4. Effect of concentration of Co(II) on peak current. Supporting electrolyte, 1M ammonia buffer solution (pH 9.0); (—○—) 0.1  $\mu$ M lipoamide accumulated at  $-0.6$  V for 1 min; (—●—) 0.1  $\mu$ M lipoic acid accumulated at  $-0.6$  V for 2 min.

lipoamide the peak current is constant for accumulation for 1 min at a potential from  $-0.4$  to  $-0.9$  V. In this potential range, a constant amount of lipoic acid or lipoamide is adsorbed on the HMDE. Since the reduction potential from disulphide to dithiol is about  $-0.7$  V, it is suggested that both the oxidized and the reduced form could be accumulated adsorptively to a similar extent.

The relation between the peak currents of the catalytic hydrogen wave and the concentration of cobalt(II) is shown in Fig. 4. The peak current increases non-linearly with cobalt(II) concentration; approaching a maximum asymptotically, and is proportional to the square root of the potential scan-rate. This behaviour suggests that the catalytic hydrogen wave is produced by cobalt(II) diffusing to the electrode.

At low concentrations of lipoamide and lipoic acid, the peak current of the catalytic hydrogen wave increases linearly with accumulation time but tends to approach a constant value at high concentrations. This is presumably due to saturation of the adsorptive sites on the mercury electrode. The trend towards saturation can also be seen in the calibration graphs of lipoic acid and lipoamide; with accumulation at  $-0.6$  V for 5 min there is linearity over the range from 1 to 10 nM with correlation coefficients of 0.986 and 0.997 for lipoic acid and lipoamide respectively. The precisions for 5 runs at various concentrations of lipoic acid and lipoamide are shown in Table 1. The relative standard deviations at all the concentrations were ca. 6%.

The catalytic hydrogen waves in the polarography of lipoic acid and lipoamide are observed at the same potential in the presence of not only Co(II) but also Co(III), and also occur for many other compounds containing disulphide and thiol groups. Further, the presence of Fe(II) or Fe(III) also produces the catalytic hydrogen wave; in this case, however, the reproducibility of the peak current is reduced by

Table 1. Precision

Concentration, $\mu$ M	Lipoic acid			Lipoamide		
	Accumulation time, min	$i_p$ , $\mu$ A	RSD, %	Accumulation time, min	$i_p$ , $\mu$ A	RSD, %
0.1	2	12.4	6.0	1	22.9	5.4
0.02	2	2.3	4.2	2	6.2	6.4
0.005	5	1.4	5.3	5	2.9	6.6

Supporting electrolyte: 1M ammonia buffer solution (pH 9.0) containing 200  $\mu$ M Co(II). Accumulation at  $-0.6$  V.

Table 2. Influences of other substances

Substance	Concn.	$\Delta i_p$ , %	Substance	Concn., $\mu$ M	$\Delta i_p$ , %
Cysteine	50 $\mu$ M	-2	Cu(II)	50	+2
	100 $\mu$ M	-10		100	-6
Cystine	50 $\mu$ M	0	Pb(II)	50	-11
	100 $\mu$ M	-31		100	-19
BSA	$1 \times 10^{-5}$ %	-17	Cd(II)	50	-13
	$5 \times 10^{-5}$ %	-46		100	-17
Gelatin	$5 \times 10^{-5}$ %	-2	Mn(II)	50	-25
	$1 \times 10^{-4}$ %	-37		100	-30
Triton X-100	$1 \times 10^{-5}$ %	-5	Ni(II)	50	+10
	$2 \times 10^{-5}$ %	-30		100	+14
SDS	$1 \times 10^{-4}$ %	-100	Fe(II)	50	-7
	10 $\mu$ M	-11		100	-25
	50 $\mu$ M	-24			

Supporting electrolyte 1M ammonia buffer (pH 9.0) containing 200  $\mu$ M Co(II); 0.1  $\mu$ M lipoamide accumulated at  $-0.6$  V for 1 min.

formation of the hydroxides. The presence of Ni(II) does not produce a catalytic hydrogen wave.

The influence of other substances on the catalytic hydrogen wave was investigated. In Table 2, the extent of interference is shown as the relative change in the peak current of the catalytic hydrogen wave of lipoamide, caused by the presence of the potential interferent. Cysteine and cystine, typical compounds containing a thiol or disulphide group, do not interfere up to  $50\mu M$  concentration. They produce a catalytic hydrogen wave in the presence of cobalt(II), but their adsorptivity on the mercury electrode at  $-0.6$  V is lower than that of lipoamide, and they are not accumulated on the HMDE. BSA (bovine serum albumin), however, decreased the peak current even at  $1 \times 10^{-5}\%$  concentrations. This seems to be due to the strong adsorptivity of BSA on the mercury electrode, which prevents the accumulation of lipoamide.

Surface-active substances such as gelatin, Triton X-100 and SDS (sodium dodecyl sulphate) interfered strongly by adsorption on the electrode. In particular, the peak of the catalytic hydrogen wave of lipoamide disappeared in the presence of  $1 \times 10^{-4}\%$  Triton X-100.

Many metal ions did not interfere, not even Cu(II), which is accumulated and forms an amalgam with the mercury electrode. The presence of Fe(III) or Mn(II) reduced the peak current slightly, owing to the formation of their hydroxides.

#### REFERENCES

1. I. C. Gunsalus, in *The Mechanism of Enzyme Action*, W. D. McElroy and B. Glass (eds.), Johns Hopkins Press, Baltimore, 1954.
2. L. J. Reed, B. G. DeBusk, I. C. Gunsalus and G. H. F. Schnakenberg, *J. Am. Chem. Soc.*, 1951, **73**, 5920.
3. L. J. Reed, I. C. Gunsalus, G. H. F. Schnakenberg, Q. F. Soper, H. E. Boaz, S. F. Kern and T. V. Parke, *ibid.*, 1953, **75**, 1267.
4. Y. Asahi, *Yakugaku Zasshi*, 1960, **80**, 684.
5. M. Senda, S. Shibabe and E. Okada, *Rev. Polarog. (Japan)*, 1967, **14**, 392.
6. J. Šponar and M. Jirsa, *Biochem. Biophys. Acta*, 1958, **29**, 434.
7. B. Ke, *ibid.*, 1957, **25**, 650.
8. G. T. Rogers and D. N. Mallett, *Bioelectrochem. Bioenerg.*, 1983, **10**, 269.
9. H. Sawamoto and M. Kawazoe, *Rev. Polarog. (Japan)*, 1985, **31**, 126.

# EXTRACTIVE PHOTOMETRIC DETERMINATION OF GALLIUM WITH 8-QUINOLINOL IN LAYERED CRYSTALS OF BISMUTH TELLURIDE—ESTIMATION OF THE DETERMINATION LIMIT

JITKA ŠRÁMKOVÁ and STANISLAV KOTRLÝ

Department of Analytical Chemistry, University of Chemical Technology, 532 10 Pardubice, Czechoslovakia

(Received 16 June 1988. Accepted 29 July 1988)

**Summary**—A method for determining microgram amounts of gallium in milligram samples of layered monocrystals of the type  $A_2^{\text{VB}}B_3^{\text{VI}}$  is described. For the separation of 1–5  $\mu\text{g}$  of gallium(III) from a large excess of bismuth in a single extraction the recommended conditions are pH 3.6–4.2 (acetate buffer,  $V_{\text{aq}}$  40 ml), an adequate excess of 8-quinolinol for complete extraction and of thiosulphate for masking bismuth. The absorbance of a chloroform extract ( $V_{\text{org}} = 10$  ml) is measured at 392.5 nm in a 50-mm cell against a blank extract concurrently obtained with a solution of pure  $\text{Bi}_2\text{Te}_3$ . Reference polycrystalline materials are used to check the precision and accuracy of the method. In routine analysis of layered monocrystals a relative standard deviation of 4–8% is to be expected for about 1  $\mu\text{g}$  of gallium in the extraction system. Estimation of the limit of determination, based on two statistical models, is discussed with respect to the error of the method and the fluctuation of the blank.

As part of a research programme investigating the optical and other physical parameters of bismuth telluride monocrystals doped with gallium atoms<sup>1</sup> it was necessary to determine gallium at the 0.01% level in milligram samples of the crystals. Bismuth telluride forms monocrystals with a tetradymite structure in which gallium is distributed with a marked concentration gradient; therefore, every crystal segment taken for physical measurements is an individual and non-replaceable sample. The attainable precision and reliability of the method has to conform with the requirements of determination of the non-stoichiometry in correlation with the physical parameters. A survey of the literature shows that the problem of microgram analysis of milligram samples is a new challenge in this field.

Information on the applicability of 8-quinolinol in extraction of trace amounts of metals<sup>2–5</sup> led us to believe that a suitable method for gallium could be developed. A calculation, based on the equilibrium constants for the gallium(III)–8-quinolinol system,<sup>6,7</sup> confirmed that between pH 3 and 4 the extraction into chloroform is practically complete in a single step if a suitable excess of the reagent is used. Basic data for the determination of gallium(III) with this reagent have also been published.<sup>8–10</sup> Keil<sup>11</sup> recommended 8-quinolinol for spectrophotometric determinations of gallium because the extraction is almost specific if suitable masking reagents are used. However, the problem of how to mask a large excess of bismuth had not yet been solved adequately. In our preliminary experiments thiosulphate was found to be a promising masking agent for bismuth.

A search of the literature also revealed that 8-quinolinol, despite the amount of work invested in fundamental studies of its analytical properties, has found only few applications in the determination of gallium in real samples. In most cases it was used only in the final reaction, e.g., in fluorimetric determinations in silicate rocks<sup>12</sup> and bauxites<sup>13</sup> or in a spectrophotometric determination of gallium in pure germanium and germanium dioxide<sup>14</sup> after a prior separation based on the extraction of chlorogallate species with ether. Some new applications of 8-quinolinol can be illustrated by the determination of trace gallium in iron ores,<sup>15</sup> in which gallium is separated by extraction into chloroform and determined by graphite furnace AAS.

Evidently little attention has been given to the investigation of all the factors influencing the precision and reproducibility of the extraction of the tris(8-quinolinolato)gallium(III) chelate from a more complicated matrix. In this respect it is also important to tackle the problem of the effect of the blank on the error of an extractive determination. Statistical analysis of results obtained in a large number of experiments is used in the present paper to illustrate the influence of compensation of blanks on the limit of determination.

## EXPERIMENTAL

### Reagents

Standard gallium(III) solution, 0.01M in 0.01M nitric acid, was prepared from analytical-grade  $\text{Ga}(\text{NO}_3)_3 \cdot 3\text{H}_2\text{O}$ . This stock solution was standardized by back-titration of EDTA added in sufficient excess. Precise results can be

obtained with visual end-point detection if a standard 0.01M solution of bismuth is used as titrant at pH 2.5 (chloroacetate buffer) and with Xylenol Orange as indicator ( $s_r = 0.1\%$ ,  $n = 5$ ). The concentration of a standard  $10^{-4}M$  gallium(III) solution, prepared by appropriate dilution, can be checked by a photometric microtitration (the same titrant, pH 1.5, Xylenol Orange,  $\lambda$  535 nm). In this way sufficient precision can be achieved even with a very dilute titrant [e.g., 0.0025M bismuth(III),  $s_r = 0.2\%$ ,  $n = 5$ ].

8-Quinolinol of analytical reagent quality (Lachema, Brno) was twice recrystallized from hot ethanol. An approximately 0.25% w/v solution was prepared by dissolving 0.5 g of purified 8-quinolinol in 50 ml of water acidified with 1 ml of glacial acetic acid and heated to 50–60°, and diluting to 200 ml. This reagent solution should not be kept for more than 1 week.

A sodium acetate solution (0.22M) was used for pH adjustment of the aqueous phase. Sodium thiosulphate solution (~2%  $\text{Na}_2\text{S}_2\text{O}_3 \cdot 5\text{H}_2\text{O}$ ) was stabilized by addition of sodium carbonate (0.1 g/l).

All reagents were reagent-grade quality. Distilled chloroform and redistilled water were used in all experiments.

#### Apparatus

A Zeiss double-beam M40 spectrophotometer was used to record the absorption spectra of the chloroform solutions. For routine photometry a Zeiss precise single-beam VSU 2G spectrophotometer was used. The absorbance of the chloroform extracts was measured at 392.5 nm (slit-width 0.2 mm) in 50-mm glass cells fitted with PTFE caps, against a blank extract and pure chloroform as references.

A Radelkis Model OP-211/1 pH-meter with an OP-0808P combined glass electrode (Radelkis, Budapest) was calibrated with the buffer solutions of the operational pH scale.<sup>16</sup>

Burettes and pipettes were calibrated.

#### Procedures

**Decomposition of samples.** Two extreme situations should be avoided when bismuth telluride materials are dissolved: (a) addition of an undefined amount of nitric acid—after dilution to volume the resulting acid concentration should be about 0.3M; (b) hydrolysis of bismuth(III), which may be caused by a local decrease in acidity during a dilution. As the final dilution of the sample solution has to be chosen with respect to the available mass of the sample and the actual content of gallium, the dissolution procedure has to be modified accordingly. For the sake of convenience, the amounts of reagents are given here for a sample of 50–120 mg and final dilution to 100 ml.

Add 10.0 ml of dilute nitric acid (1 + 4) to a sample (>0.02% Ga) in a tall-form 150-ml beaker and heat on a steam-bath for 10–20 min till dissolution is complete and oxides of nitrogen are expelled. Allow the solution to cool, dilute with 20 ml of 0.2M nitric acid and transfer it to a 100-ml calibrated standard flask. Use  $5 \times 10^{-3}M$  nitric acid for washings and dilution to the mark. Whenever a substantial modification of the procedure is necessary, check the resulting acidity alkalimetrically.

**Extraction.** Transfer 10 ml of 0.22M sodium acetate, 5 ml of 0.25% solution of 8-quinolinol, and 5 ml of 2% sodium thiosulphate solution to a 100-ml separating funnel, in that order, and mix well. Then add by pipette a 5-ml aliquot of the sample solution, containing more than 1  $\mu\text{g}$  of Ga(III), mix again and dilute the aqueous phase with water to about 40 ml. Extract with 10.0 ml of chloroform by shaking for 4 min. Allow the phases to separate and after discarding about 0.5 ml of the chloroform extract insert the funnel stem into a filter-tube containing a small dry filter paper to retain water droplets. Transfer the chloroform extract into a clean, dry 50-mm cell provided with a well fitting PTFE cap. Measure the absorbance at 392.5 nm against a blank extract as reference.

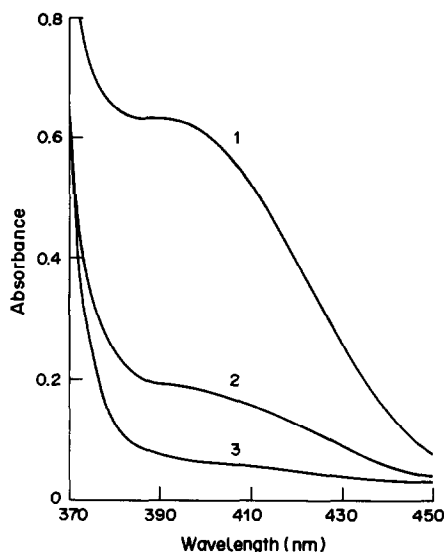


Fig. 1. Absorption spectra of extracts measured against chloroform as reference (pH 4.2, 50-mm cell). Aliquots of solutions from the following materials [with amount of Ga(III) per 5 ml] taken for extractions: 1—reference material (Ga 10  $\mu\text{g}$ ); 2—sample of a monocrystal (Ga 1.54  $\mu\text{g}$ ); 3—blank (pure  $\text{Bi}_2\text{Te}_3$ , 2.5 mg/5 ml).

For a blank extraction use the same procedure but, instead of the sample solution, take a 5-ml aliquot of a matrix solution obtained by dissolving an appropriate weight of pure bismuth telluride.

## RESULTS AND DISCUSSION

#### Choice of wavelength

The yellow chelate  $\text{Ga}(\text{ox})_3$  in chloroform has an absorption maximum at 390–396 nm (Fig. 1) located close to the descending part of a broad maximum ( $\lambda_{\text{max}} = 318$  nm) of the free form  $\text{Hox}$  of 8-quinolinol. Thus only a shoulder on the absorbance curve reveals the presence of a microgram amount of gallium (curve 2, Fig. 1). Therefore, the background absorbance due to the uncomplexed 8-quinolinol, which is present in large excess, and the traces of impurities (curve 3) must be carefully compensated by means of a blank extraction.

#### Effect of pH

In preliminary experiments suitable conditions for the extraction of microgram amounts of Ga(III) were found, namely the phase ratio (water: $\text{CHCl}_3 = 4:1$ ) and the excess of 8-quinolinol and thiosulphate adequate to separate and concentrate gallium(III) in a single extraction from a great amount of bismuth(III). These experimental conditions were then used in further investigations.

The partition of tris(8-quinolinolato)gallium(III) was studied in more detail within the pH range 2.2–4.2. A reference polycrystalline material with a high gallium content of 0.429% was used for prepa-



Table 1. Determination of gallium in reference polycrystalline materials and in samples of layered monocrystals

Sample	Taken,* mg	Number of detns.	Absorbance‡	Ga found			
				$m_{\text{Ga}}$ , μg	$s(m_{\text{Ga}})$ , μg	%	$s_r$ , %
RM-1	18.825†	4	0.062 ± 0.004	1.10	0.044	0.029 ± 0.002	3.9
RM-2	129.1¶	8	0.052 ± 0.005	0.923	0.099	0.036 ± 0.003	10.7
RM-3	11.782†	4	0.052 ± 0.006	0.941	0.078	0.040 ± 0.005	8.3
RM-4	128.3¶	6	0.080 ± 0.005	1.43	0.093	0.056 ± 0.004	6.5
MC-1	37.1§	6	0.075 ± 0.005	1.34	0.090	0.036 ± 0.003	6.7
MC-2	39.9§	6	0.089 ± 0.004	1.60	0.063	0.040 ± 0.002	3.9
MC-3	58.0#	5	0.077 ± 0.005	1.39	0.077	0.048 ± 0.003	5.6
MCS-1	48.414§	4	0.052 ± 0.006	0.923	0.070	0.019 ± 0.002	7.5
MCS-2	31.00†	4	0.103 ± 0.008	1.84	0.096	0.030 ± 0.002	5.2
MCS-3	22.326†	4	0.153 ± 0.008	2.75	0.096	0.062 ± 0.003	3.5

\*Total volume of the sample solution: †25; ¶250; §50; # 100 ml.

‡Measured against a simultaneous blank extract (see the text). For  $n \leq 5$  the confidence intervals and standard deviations were calculated by the Dean and Dixon method.

ration of the test solutions. An aliquot of 5 ml contained about 10 μg of gallium(III). The aqueous phase was buffered with acetic acid-acetate and adjusted to a constant ionic strength of 0.1M with sodium nitrate. Two extractions of the test solution and one of the matrix blank were performed concurrently for each pH value of the aqueous solution.

Between pH 3 and 4.2 the absorbances, measured against the matrix blank as reference, reached practically a constant level with a mean value of  $0.542 \pm 0.010$  ( $n = 20$ ,  $\alpha = 0.05$ ). When the whole set was divided into two parts, a statistically significant difference was found between the relevant mean values (pH 3.0–3.5,  $0.556 \pm 0.015$ ,  $n = 8$ ; pH 3.7–4.2,  $0.533 \pm 0.011$ ,  $n = 12$ ). This indicated that a narrower pH range should be chosen and, moreover, that the pH-dependence of the blanks should also be taken into consideration. A plot of absorbance of the blanks, measured against chloroform as reference, showed a sharp increase in absorbance at above pH 4, from a flat minimum between pH 3.3 and 3.6; however, in this region of low blanks a greater scatter of values was observed, which affected unfavourably the results of determinations. Reagent blanks prepared without addition of the matrix solution had a similar pH-dependence but the absorbance values were different and began to increase even at below pH 3. The pH range 3.8–4.0 was thus considered as an optimum for the matrix under investigation. It was also possible to use sodium acetate for a safe pH adjustment.

#### Calibration and testing of the method

The range of concentration for the calibration was chosen to cover the amounts of gallium expected in the analysis of the telluride monocrystals. For a calibration solution 52–55 mg of powdered pure bismuth telluride was dissolved in dilute nitric acid and the solution was transferred together with washings to a 100-ml calibrated standard flask. Then a known volume of the standard  $10^{-4}M$  gallium(III)

was added (e.g., 3, 4 or 6 ml) and the solution was diluted to the mark with  $5 \times 10^{-3}M$  nitric acid.

In the course of calibration extractions, all experimental details (see the procedure) were carefully controlled to maintain optimum conditions. With each two calibration extractions one matrix blank was always run concurrently. The chloroform extracts were measured in 50-mm cells in order to reach a measurable level of absorbance, always with the relevant blank as reference.

The calibration was repeated several times. In all calibrations the Student's *t*-test at 5% significance level led to acceptance of a zero intercept for the regression line.

The calibration, which was used in most determinations listed in Tables 1 and 2, yielded the regression equation

$$A = (5.58 \pm 0.18) \times 10^{-2} m_{\text{Ga}} \quad (1)$$

where  $m_{\text{Ga}}$  is the amount of gallium(III) within the range 1–5 μg per 10 ml of the chloroform extract ( $n = 19$ ,  $s_{y,x} = 0.0070$ ). The slope of this calibration agreed well with the preceding calibrations.

The method was tested with powdered polycrystalline bismuth telluride doped with various amounts of gallium, prepared so as to obtain a more homogeneous distribution of the gallium than that in the monocrystals. These reference materials (RM) allowed examination of the applicability of the method to different weights of sample. Also, some larger pieces of monocrystals (MC) were taken to prepare test solutions (see Table 1) with final volumes of 50, 100 and even 250 ml. Thus it was possible to check the precision attainable in series of 5–8 extractions.

#### The blank extractions

As all blank extracts were also measured against chloroform as reference, large sets of absorbance values of the blanks were obtained under the same conditions. For example, a set of 49 blanks corre-

Table 2. Determination of gallium in milligram samples of layered monocrystals

Sample	Taken,* mg	Number of detns.	Absorbance†	Ga found		
				$m_{\text{Ga}}$ , μg	$s_{\text{extr}}$ , μg	%
MCS-4	21.469‡	3	0.056	1.00	0.13	0.023
MCS-5	6.166§	1	0.045	0.81	0.13	0.026
MCS-6	5.028§	2	0.090	1.61	0.13	0.064
MCS-7	9.291§	2	0.194	3.48	0.15	0.075

\*Total volume of the sample solution: ‡25 ml; §10 ml.

†Mean absorbance ( $\bar{y}$ ) against blank as reference (see the text). Estimated by inverse interpolation based on results of the calibration ( $n$  points of  $x_i$  values of the concentration):

$$s_{\text{extr}} = \frac{s_{j,v}}{b^*} \left( 1 + \frac{n_s \bar{y}^2}{b^{*2} \sum_{i=1}^n x_i^2} \right)^{1/2}$$

The symbols are explained in the text.

sponded to the calibrations represented by equation (1) and the majority of extractions listed in Table 1. These blank extracts (measured in 50-mm cells at 392.5 nm) were obtained under carefully controlled experimental conditions, as demonstrated by the reliability interval of the mean absorbance,  $0.092 \pm 0.002$ . This set was tested for normality with the use of a complex statistical computer program. An estimate of  $\chi^2$  with partitioning into 8 classes was 3.73, whereas the critical value is 12.60 ( $\nu = 6$ ,  $P = 0.95$ ). The computed estimates of the moments of skewness  $A_3$  and curtosis  $A_4$  were also much lower than the calculated critical values:  $|A_3| = 0.002$  ( $< 0.646$ );  $|A_4 - 3 + 6/(n+1)| = 0.322$  ( $< 1.180$ ). A plot of ordered blank values *vs.* corresponding values of the standard normal variate gave a straight line, passing through a random scatter of points, with practically theoretical values of the parameters. All this indicated that it was not possible to reject a hypothesis of normal distribution for these blanks.

Spectrophotometric measurements of the blank extracts revealed that the absorbance values at the beginning of the visible region were predominantly influenced by the large excess of the free, neutral form Hox of 8-quinolinol. This fact was also confirmed by calculation of the distribution of all forms of 8-quinolinol in the extraction system at pH 4.0. The blank value is thus influenced by the purity of the reagent and by all complicating factors which affect partitioning of the form Hox between water and chloroform.

The composition of the aqueous phase (even at constant pH and ionic strength) also has a significant effect; therefore, the matrix solution for blank extractions should be prepared by dissolving a weight of pure  $\text{Bi}_2\text{Te}_3$  corresponding to that of an average sample to be analysed. In routine applications it is also important to watch systematically the trends and fluctuations of the blanks.

#### Determination of gallium in layered monocrystals

For measurement of the physical properties a small

rectangle of about  $6 \times 8$  mm is cut out from a thin plate of the monocrystal, which is several tenths of a millimetre thick. As there is a considerable concentration gradient of gallium along the monocrystal, every such little crystal chip is an individual specimen with a weight of 5–25 mg (cf. MCS-3 in Table 1 and Table 2). As the amount of sample taken limits the total volume available for replication of the determination, the reliability of the method must be adequate to provide safe results even for a small number of measurements.

The samples of monocrystals were dissolved in dilute nitric acid according to the general procedure, modified according to the weight of the sample. For matrix blanks a matching amount of pure bismuth telluride was always dissolved and a 5-ml aliquot taken for a concurrent blank extraction.

The results of determinations of gallium in some telluride monocrystals are listed in Table 2. If the reliability intervals and the standard deviations are compared with those of the test solutions, it may be concluded that the method gives reproducible results despite the low gallium content.

#### Estimating the limit of detection

A more detailed analysis of the results obtained in the series of repeated determinations at low concentration levels has revealed that the random error cannot be considered as uncorrelated with the error of the blank extracts measured against chloroform as reference. This fact is also indicated by the values of particular standard deviations for the absorbance. For example, in the case of 8 sample series with net mean absorbance values ranging between 0.05 and 0.08 the pooled standard deviation was 0.0050 ( $n_s = 40$ ,  $\nu = 32$ ), whereas the standard deviation for the relevant set of blanks ( $n_b = 49$ , see above) had a value of 0.0075 which was significantly different (by *F*-test at 5% significance level)—and larger.

If the hypothesis is accepted that the influence of the blank is fully compensated, there are two main sources of error contributing to the error of the

determination expressed as a standard deviation  $s_x$ : (a) error ( $s_y$ ) incurred in  $n_s$  measurements of the absorbance ( $y$ ) in a given series; (b) the scatter of  $n$  points along a calibration regression line, e.g.,  $y = b^*x$ , which is characterized by a standard deviation  $s_{yx}$ . It has often been assumed that  $s_y = s_{yx}$ . If the error of the slope  $b^*$  is neglected, then an estimate of the limit of determination  $x_{LD}$  is related to a chosen permissible level of the relative standard deviation  $s_r$ :

$$x_{LD} = \frac{s_y}{b^*s_r} \quad (2)$$

Considering that  $s_y = 0.005$  and  $s_r = 0.1$ ,  $x_{LD}$  of the method is  $0.90 \mu\text{g}$  of Ga(III). This value agrees well with the results listed in Table 1. For example, if the standard deviations  $s(m_{\text{Ga}})$  are pooled for 7 series ( $n_g = 37$ ), which fall close to the limit of determination, then  $s_g = 0.083$ , so for  $s_r = 0.1$  an estimate of  $x_{LD}$  is  $0.83 \mu\text{g}$  of Ga(III). Evidently the results in Table 1 correspond to the case of a "well-known" blank, as mentioned by Currie,<sup>17</sup> for which  $y_{LD} = 10\sigma$ . If inverse interpolation is used to estimate  $s_x$  on the basis of the calibration line in Eq. (1),  $x_{LD}$  is about  $1.3 \mu\text{g}$  of Ga(III) (see Table 2).

Now consider the opposite case, in which the error incurred in  $n_s$  measurements of samples against a blank as reference (cf. Currie<sup>17</sup>) is uncorrelated with the error of the blank itself. The variance of a mean absorbance  $s_{\bar{y}}^2$  can be expressed by the law of propagation of errors as:

$$s_{\bar{y}}^2 = \frac{s_s^2}{n_s} + \frac{s_B^2}{n_B} \quad (3)$$

where the variances  $s_s^2$  of the samples and  $s_B^2$  of the blanks refer to absorbance. There is usually a constant ratio of the number of determinations to that of the blanks ( $n_B$ ) in a series,  $n_s = kn_B$ ; thus the variance of absorbance corresponding to a given series of determinations is estimated by:

$$s_{\bar{y}}^2 = n_s s_{\bar{y}}^2 = s_s^2 + k s_B^2 \quad (4)$$

which clearly shows that it is advisable to choose a reasonably low value of  $k$ . If a certain relative error is chosen as acceptable and the error of the slope  $b^*$  is negligible, the limit of determination is given by:

$$x_{LD} = \frac{y_{LD}}{b^*} = \frac{1}{b^*s_r} \sqrt{s_s^2 + k s_B^2} \quad (5)$$

If  $s_s = s_g = 0.005$ ,  $s_B = 0.0075$  and  $k = 2$ , the estimate of the limit of determination is  $2.1 \mu\text{g}$  of Ga(III), which is evidently somewhat high. Evidently the blank is less likely to fluctuate within a series than between subsequently reproduced series of analyses.

## Conclusions

The proposed method is applicable in routine analysis of milligram samples of monocrystals and can provide results which are useful for interpretations of optical and other physical properties of the crystals (cf. Lošťák *et al.*<sup>1</sup>).

For calibration with known amounts of the analyte a reasonably "pure" matrix should be chosen.

The blank extracts, which are used as reference, are to be obtained by use of a solution containing a matching amount of pure matrix. The background absorbance, which is mainly due to the excess of extracted free 8-quinolinol, is very largely compensated. The deviations, which are caused by random changes in composition of the extraction system *etc.* and affect the error of the blank, are more clearly evident between series of analyses than within a certain series of extractions.

*Acknowledgement*—The authors wish to thank Professor J. Horák from their University for an inspiring research project. Thanks are also due to his co-workers for providing the polycrystalline materials and the samples of monocrystals, and to Miss Y. Kalischová, Eng.M., for her valuable assistance in some experiments.

## REFERENCES

1. P. Lošťák, R. Novotný, J. Navrátil and J. Šrámková, *Phys. Stat. Sol.*, 1988, **106A**, 619.
2. E. Sandell, *Colorimetric Determination of Traces of Metals*, 3rd Ed., Interscience, New York, 1959.
3. J. Starý, *The Solvent Extraction of Metal Chelates*, p. 86. Pergamon Press, Oxford, 1964.
4. A. K. De, S. M. Khopkar and R. A. Chalmers, *Solvent Extraction of Metals*, p. 79. Van Nostrand Reinhold, London, 1970.
5. O. G. Koch and G. A. Koch-Dedic, *Handbuch der Spurenanalyse*, Vol. 1, p. 728. Springer-Verlag, Berlin, 1974.
6. A. P. Savostin, *Zh. Neorgan. Khim.*, 1965, **10**, 2565.
7. J. Starý, Yu. A. Zolotov and O. M. Petrukhin, *IUPAC Chem. Data Ser.*, 1979, No. 24.
8. T. Moeller and A. J. Cohen, *Anal. Chem.*, 1950, **22**, 686.
9. *Idem*, *J. Am. Chem. Soc.*, 1950, **72**, 3546.
10. K. Motojima and H. Hashitani, *Bunseki Kagaku*, 1960, **9**, 151.
11. R. Keil, *Z. Anal. Chem.*, 1970, **249**, 172.
12. E. B. Sandell, *Anal. Chem.*, 1947, **19**, 63.
13. S. Lacroix, *Anal. Chim. Acta*, 1948, **2**, 167.
14. C. L. Luke and M. E. Campbell, *Anal. Chem.*, 1956, **28**, 1340.
15. S. Hasegawa, T. Kobayashi, F. Hirose and H. Okochi, *Bunseki Kagaku*, 1987, **36**, 371.
16. *Pure Appl. Chem.*, 1983, **55**, 1467.
17. L. A. Currie, *Anal. Chem.*, 1968, **40**, 586.

## QUENCHING AND LIQUID CHROMATOGRAPHIC DETERMINATION OF POLYTHIONATES IN NATURAL WATER

BOKUICHIRO TAKANO\* and KUNIIHIKO WATANUKI

Department of Chemistry, The College of Arts and Sciences, The University of Tokyo, Komaba,  
Meguro-ku, Tokyo 153, Japan

(Received 1 March 1988. Revised 5 June 1988. Accepted 29 July 1988)

**Summary**—Polythionates in highly acidic, crater-lake water have been determined by ion-chromatography and high-performance microbore liquid chromatography. The first technique allows the determination of tri-, tetra- and pentathionate in excess of 10 ppm, and the second allows analysis for tetra-, penta- and hexathionate in excess of 0.2 ppm. The methods for preserving polythionates in natural solutions are also discussed. The recommended procedures for storage are to add hydroxylamine hydrochloride to sample solutions or to exclude atmospheric oxygen by using Winkler oxygen-determination bottles, followed by storage in a refrigerator at 5°.

Oxy-anions containing various oxidation states of sulphur have been reported as present in environments such as volcanic fumaroles,<sup>1,2</sup> hot springs,<sup>3,4</sup> crater-lake waters,<sup>5,6</sup> lake sediments,<sup>7,8</sup> and waste waters from mineral smelting industries.<sup>9</sup> Many of the solutions containing these oxy-anions are acidic through the oxidation of sulphur species of lower valence or the disproportionation of unstable sulphur species of intermediate oxidation states.<sup>10</sup> Detailed oxidation mechanisms for these reactions, however, are far from being understood, mainly because most intermediate sulphur oxy-anions are labile and therefore difficult to determine. Polythionates are examples of such oxy-anions, but they are rather stable under some conditions, compared with the other unstable sulphur compounds. Considerable numbers of papers have been published on the determination of each member of the homologous series, most of the methods using indirect, often tedious and time-consuming, complicated analytical procedures.<sup>11-13</sup>

The recent development of high-performance liquid chromatography (HPLC) provides a technique for simple and rapid determination of the first four polythionates with a single injection. Takano *et al.* used an anion-exchange column to separate the thionates but the method was not fully successful.<sup>14</sup> A CN-bonded silica HPLC column has been successfully used for the separation of tri-, tetra- and pentathionate,<sup>15</sup> but equilibration with the mobile phase containing hexadecyltrimethylammonium bromide took a long time. Later, by a similar approach, Rabin and Stanbury<sup>16</sup> and Steudel and Holdt<sup>17</sup> were able to separate the polythionates, from the dithionate to

pentathionate and from tri- to tridecathionate, respectively. Because of the rapid progress in the analytical chemistry of polythionates, it has become much more important to stabilize sulphur species in natural waters.

This paper will present methods for stabilization and rapid determination of polythionates (trithionate to hexathionate) in natural waters such as hot springs; crater lakes and mine drainages.

### EXPERIMENTAL

#### Reagents

Potassium trithionate was synthesized by the procedure of Stamm *et al.*<sup>18</sup> Potassium tetrathionate (Merck) was recrystallized once. Potassium pentathionate and hexathionate were both synthesized by the method of Goehring and Feldman.<sup>19</sup> Purities of all polythionate reagents were checked by gravimetry and chromatography and found to be >99%. They were all stored as dry solids in a refrigerator at 5°. A standard solution of each was prepared as necessary for each series of analyses, with demineralized water (16 MΩ.cm resistivity) from a Millipore Milli-QII system.

#### Cation-exchange columns

Columns (8 × 50 mm) of Dowex 50 W × 8 (100–200 mesh) cation-exchanger, in the Tl(I) and Ba(II) forms, were prepared in disposable plastic hypodermic syringe barrels and connected in that order to remove most of the chloride and sulphate ions which interfere with the ion-chromatographic determination of tri- and hexathionate ions.

#### Mobile phases

The ion-pairing eluent for the ion-chromatography was prepared by diluting a mixture of 100 ml of 10mM phthalic acid, 12.5 ml of 40mM tetra-n-butylammonium hydroxide solution, and 33 ml of tetrahydrofuran (chromatographic grade) to 1 litre and had a pH of 3.5. The mobile phase for the microbore HPLC was prepared by mixing 750 ml of 0.1M potassium dihydrogen phosphate with 250 ml of

\*Author for correspondence.

chromatographic-grade acetonitrile and adjusting the pH to 3.5 by dropwise addition of concentrated reagent grade phosphoric acid. Both mobile phases were filtered through 0.45  $\mu\text{m}$  Millipore filters, type HV.

#### Chromatography

The ion-chromatograph system was composed of a pump with dual reciprocating pistons (LDC/Milton Roy Consta-Metric III), an injector (Rheodyne 7125 with a 20  $\mu\text{l}$  sampling loop), a polystyrene gel column (Showa Denko IC I-613, 6 mm i.d.  $\times$  150 mm), and a detector (Shodex IC CD-2 conductometer). The flow-rate of the mobile phase was 1.5 ml/min. The column temperature was kept at 40° by circulation of warm water through a water jacket.

The Microbore HPLC system (LDC/Milton Roy) comprised a syringe pump of 5 ml total volume (microMetric metering pump, a UV detector set at 220 nm (spectro-Monitor D with a microflow cell of 2  $\mu\text{l}$  volume and 3 mm path-length), a sample injector (Rheodyne 7520, 0.5  $\mu\text{l}$  sampling volume), and an ODS column (Spherisorb S30DS2, 1 mm i.d.  $\times$  100 mm, particle size 3  $\mu\text{m}$ ). The flow-rate of the phosphate-buffered mobile phase was 25  $\mu\text{l}/\text{min}$ . The column was kept at 30° to reduce the applied column pressure. Both mobile phases were continuously degassed by an instrument which eliminates gases in the mobile phase by diffusion through the wall of a plastic tubing coil housed in an evacuated compartment (ERMA Optical Works, ERC-3310). The detector was interfaced with an NEC PC 9801 personal computer. The peak areas of both conductivity and UV signals were calculated by using CDS software, provided by Nippon Chromatographic Industries Co.

## RESULTS AND DISCUSSION

### Ion-pair chromatography

Takano *et al.*<sup>14</sup> concluded that an anion-exchange column is not sufficient for separation of polythionates even if a long column were used, because the applied pressure in the column becomes too high when the mobile phase is delivered through it. Reeve<sup>15</sup> reported that reversed-phase chromatography is effective for the separation of polythionates with a column of CN-bond type, but a long time is necessary to equilibrate the 1-bromo-hexadecane in the mobile phase with the column packing material. In the present study we tried a polystyrene gel column (10  $\mu\text{m}$  particle size) for the separation of polythionates with tetra-*n*-butylammonium hydroxide (TBAOH) as ion-pairing reagent. Tri-, tetra- and pentathionate were easily separated by this column under the conditions described above, but the hexathionate peak overlapped with a negative peak due to the phthalate anion in the mobile phase. This negative peak appeared at a retention time of 20 min. The maximum column capacity for loading of each anion is only 1  $\mu\text{g}$ . However, a higher column capacity is occasionally necessary, when the sample solutions contain traces

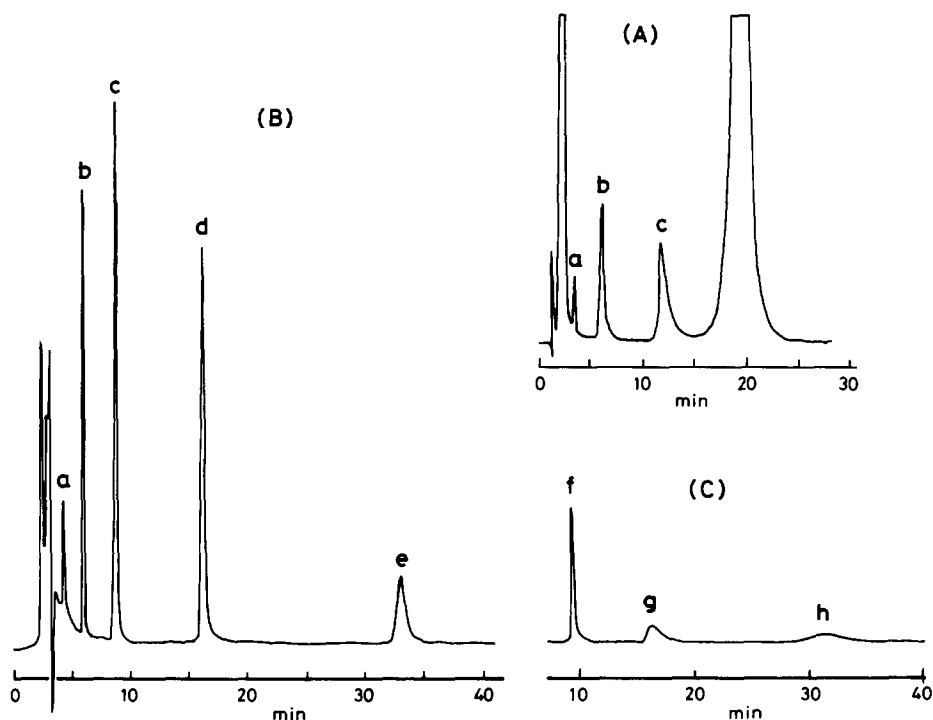


Fig. 1. Ion-chromatogram (A) and microbore-column HPLC (B, C) of the highly acidic (pH = 1.2) crater-lake water. Chromatogram C was obtained with the same mobile phase as for B except for the  $\text{CH}_3\text{CN}/\text{aq.}$  solution ratio (3/7), flow-rate (50  $\mu\text{l}/\text{min}$ ) and sensitivity (2.5  $\times$  that for B). The conditions for C makes the presence of higher polythionates clearer. a,  $\text{S}_3\text{O}_6^{2-}$ ; b,  $\text{S}_4\text{O}_6^{2-}$ ; c,  $\text{S}_5\text{O}_6^{2-}$ ; d,  $\text{S}_6\text{O}_6^{2-}$ ; e,  $\text{S}_7\text{O}_6^{2-}$ ; f,  $\text{S}_8\text{O}_6^{2-}$ ; g,  $\text{S}_9\text{O}_6^{2-}$ ; h,  $\text{S}_{10}\text{O}_6^{2-}$ ; unlabelled peak, phthalic acid. The  $\text{S}_3\text{O}_6^{2-}$  was added to the water to test its retention time. See text for details on identification of polythionate ions e, f, g, and h.

of polythionates and are not diluted; in this case, the negative phthalate peak becomes a large positive peak as shown in Fig. 1A.

Consequently, hexathionate could not be easily determined by this method. In addition, the sensitivity for hexathionate is too low, compared with that for the other three thionates, probably because the dissociation constant of hexathionic acid is much lower than those of the lower homologues.<sup>20</sup> Raising the pH of the mobile phase may lower the detection limit for hexathionate, but it is unfavourable for quantitative work because hexathionate decomposes rapidly at higher pH.

To improve the analytical performance, interfering chloride and sulphate ions are first eliminated by cation-exchange. Sulphate can be removed with a cation-exchanger (Dowex 50W X-8, 100–200 mesh) in barium-form. Chloride can usually be removed on a similar column in silver-form but silver ions decompose polythionates, with precipitation of silver sulphide. Therefore a column in thallium(I)-form is used. This technique is quite convenient for removing much of the saturation peak due to phthalic acid (Fig. 1A) and avoids partial superimposition of a trithionate peak on the sulphate peak. A Tl(I)-form column was connected with a Ba(II)-form column. These columns were prepared for each sample. No appreciable decomposition of polythionate and no poor reproducibility of the data were observed when this procedure was used (Table 1). A dilution factor of four was used in washing the column for analysis of the crater-lake water, which will be described later in the text. It should be noted here that owing to the low solubility of thallium and barium thiosulphate,<sup>21</sup> thiosulphate ions were also eliminated from the eluate.

#### Microbore column HPLC

Column efficiencies for the system ranged from  $6.0 \times 10^4$  to  $1.2 \times 10^5$  theoretical plates/m for tetra- to hexathionate ions, which proved excellent for the polythionate determination, compared with those ( $5.0 \times 10^3$ – $1.0 \times 10^4$ ) arrived at by Rabin and Stanbury.<sup>16</sup> Figure 1B shows a chromatogram of polythionates in the crater-lake water, which contains a high concentration of chloride, sulphate and cations

Table 1. Recovery of tetra- and pentathionate after removal of chloride and sulphate by Tl(I)-form and Ba(II)-form ion-exchange columns

$S_4O_6^{2-}$ , $\mu\text{g/ml}$		$S_5O_6^{2-}$ , $\mu\text{g/ml}$	
added	found	added	found
880	900	1510	1540
880	880	1510	1560
880	840	1510	1430
880	890	1510	1530
880	910	1510	1550
Mean 884		Mean 1522	

Table 2. Retention times and capacity factors ( $k'$ ) of polythionates ions

	$t_R^*$ , min	$k'^{\dagger}$
$S_3O_6^{2-}$ †	1.26	0.49
$S_4O_6^{2-}$	1.60	0.90
$S_5O_6^{2-}$	2.33	1.768
$S_6O_6^{2-}$	3.63	3.31
$S_7O_6^{2-}$ §	5.97	6.08
$S_8O_6^{2-}$ §	9.39	10.14
$S_9O_6^{2-}$ §	16.46	18.53
$S_{10}O_6^{2-}$ §	31.24	36.00
Dead time	0.84	

\*Retention times were measured with a new column and a mobile buffer solution slightly different in  $\text{CH}_3\text{CN}$ /aqueous solution ratio (3/7) from the buffer solution (2.5/7.5) used for the quantitative polythionate analysis.

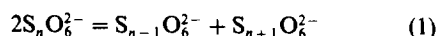
†Trithionate (1mM) added to the crater-lake water.

‡ $\ln k'$  is linearly related to the number of sulphur atoms ( $n$ ) in the polythionates:  $\ln k' = -2.50 + 0.67 n$  (correlation coefficient  $r = 0.9996$ ).

§Polythionate ions not directly identified but suspected to be present, from the indirect evidence described in the text.

but no appreciable amount of trithionate ions. However, the sensitivity is at least an order of magnitude lower for trithionate than for tetra- and pentathionate,<sup>22</sup> owing to the lower molar absorptivity for this ion. Twenty minutes are required to determine tetra-, penta and hexathionate. Four more peaks were found beyond the hexathionate peak, probably attributable to the higher polythionate homologues (Fig. 1C).

The logarithm of the capacity factor ( $k'$ ) was found to be a linear function of the number of sulphur atoms in the thionate ions (Table 2). A similar relation has also been reported for the anion-exchange column chromatography of polythionates up to hexathionate.<sup>23</sup> It is also known that  $\log k'$  for  $n$ -alkanes,  $n$ -alkylcarboxylic acids and sulphur homocycles in reversed-phase liquid chromatography can be readily predicted from a plot of  $\log k'$  vs. the number of carbon or sulphur atoms.<sup>24,25</sup> Table 2 shows such a linear relation for the tetra-, penta- and hexathionate, and the retention times of the unknown substances (Fig. 1C) corresponding to 7, 8, 9 and 10 sulphur atoms. Furthermore, chromatograms of a concentrated hexathionate solution that had been left for a few hours at ambient temperature showed peaks at exactly the same retention times as those of the suspected higher polythionates detected in the crater-lake water. According to Weitz and Spohn,<sup>26</sup> hexathionate, in the presence of hydrochloric acid, disproportionates into penta-, hepta- and further higher polythionate homologues in which the sulphur numbers are less than 20.



Therefore, we believe that the unknown substances in the lake water are hepta-, octa-, nona- and decathionate. Recently, Steudel and Holdt<sup>17</sup> claimed that a parabolic relationship exists between  $\log k'$  and the number ( $n$ ) of sulphur atoms ( $n > 4$ ) in a polythionate ion. Scrutiny of their results reveals that the data can be fitted to two straight lines which intersect at between  $n = 8$  and  $n = 9$ . According to Strauss and Steudel,<sup>27</sup> a plot of  $\log k'$  for sulphur homocycles and the sulphur numbers ( $n = 6-28$ ) consists of three lines which intersect at  $n = 10$  and  $n = 20$ . It is therefore possible that the chromatographic behaviour of sulphur homologues changes with every ten or so sulphur atoms in an ion or molecule.

#### Sampling, stabilization and storage of samples

Polythionates have long been known in the form of salts that are rather unstable in aqueous solution,<sup>28</sup> but their decomposition in solution has been a matter of controversy, though the final decomposition products are clearly sulphate and elemental sulphur. Accordingly, for the determination of polythionates their degradation must be suppressed.

We have mainly sampled solutions of volcanic origin, which are usually highly acidic and contain various salts. Currently it is not possible to determine polythionates *in situ* in sample solutions; therefore the preservation of polythionates in sample solutions is quite important in investigating geochemistry of sulphur in volcanic waters. The stability of these compounds was checked under various conditions with different containers for storing the solutions, reagents for stabilization, and storage temperatures. The solution used for these screening tests was an acidic (pH 1.2) volcanic water from Kusatsu-Shirane crater lake, Japan. The chemical composition of the water was reported earlier (for example:  $\text{Cl}^-$  2100,  $\text{SO}_4^{2-}$  2880,  $\text{Na}^+$  34,  $\text{K}^+$  15,  $\text{Ca}^{2+}$  255,  $\text{Mg}^{2+}$  37,  $\text{Fe}^{2+}$  151,  $\text{Al}^{3+}$  206,  $\text{SiO}_2$  173 ppm, sampled 30 August 1987).<sup>6</sup> According to Kurtenacker *et al.*,<sup>29</sup> aqueous polythionates other than trithionate are most stable in the pH range 0-2, at which thiosulphate is decomposed into bisulphite and elemental sulphur. We accordingly examined the stabilities of polythionates in this pH range.

**Stability of polythionates in various containers.** Polyethylene and glass containers of various sizes were used, to find the effect of their walls on polythionate stability. Transparent and amber glass bottles with air-tight plastic screw-caps were used to determine the effect of light on the stability. Contrary to our expectation, polythionates were less stable in the amber glass bottles than in transparent bottles. For example, 11 days after sampling, tetrathionate and hexathionate in an amber glass bottle have decomposed by about 60 and 80% respectively, relative to storage in a transparent glass bottle. It is possible that transition-metal ions such as Fe(III) or Mn(II) in the amber glass accelerate the decomposition, but the mechanism is not clear. No significant difference in

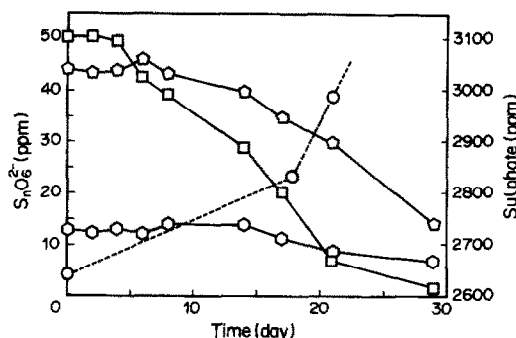


Fig. 2. Stabilities of tetra-, penta- and hexathionate in crater-lake water stored in polyethylene bottles. (□),  $\text{S}_4\text{O}_6^{2-}$ ; (○),  $\text{S}_5\text{O}_6^{2-}$ ; (△),  $\text{S}_6\text{O}_6^{2-}$ ; (○),  $\text{SO}_4^{2-}$ .

stability was found between solutions stored in tightly sealed polyethylene and transparent glass bottles. As will be shown later, no catalytic decomposition by  $\text{Fe}^{3+}$  in solution can be detected in the first few days. To determine the rate of decomposition of polythionates in the absence of additives, eight bottles of crater-lake water were collected, without air bubbles, in air-tight polyethylene bottles, and the polythionates were determined at regular intervals. Each bottle was opened only immediately prior to the first analysis. Figure 2 shows that polythionates in the crater-lake water are stable, within experimental error, for four days after the container is opened for analysis. Tetrathionate is completely decomposed within one month after opening of the container. Penta- and hexathionate are much more stable than tetrathionate, the extent of their decomposition in one month being 68 and 67%, respectively; the sulphate content increases during the same period.

In particular cases, however, polythionates in acidic solutions can be preserved for much longer times. A 0.1M hydrochloric acid solution of tetra- and pentathionate (445 and 304  $\mu\text{g}/\text{ml}$  respectively) showed only slight decomposition of either polythionate during three years. Also, the crater-lake waters sampled in the 1960s and stored without any additives have retained polythionates at about 2000  $\mu\text{g}/\text{ml}$  concentration for more than 20 years. These curious phenomena will be discussed elsewhere in the near future.

**Addition of formaldehyde or oxalaldehyde solution.** Formaldehyde forms an addition compound (hydroxymethane sulphonic acid) with bisulphate and/or sulphite ions<sup>30</sup> and is used as a stabilizing agent for these ions in solution.<sup>31</sup> Oxalaldehyde is a reagent which stabilizes hydrogen sulphide and sulphite in aqueous solution.<sup>32,33</sup> We have examined the efficiency of both compounds as fixatives for polythionates in sample solutions. All test solutions were sampled from the lake at the same time and stored in tightly sealed polyethylene bottles, each of which was used for a polythionate determination at a given time

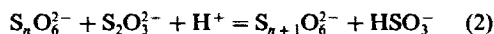
Table 3. Effect of formaldehyde on the stability of polythionate ions in crater-lake water

Polythionate	35% HCHO soln., ml	Concentration found, $\mu\text{g/ml}$			
		Day 0	Day 3	Day 17	Day 63
$\text{S}_4\text{O}_6^{2-}$	0.1	49.2	48.1	44.7	39.7
	0.2		46.4	44.0	36.7
	0.5		47.8	45.0	37.2
	1.0		48.3	43.5	35.4
	2.0		46.9	32.0	13.7
$\text{S}_5\text{O}_6^{2-}$	0.1	47.7	38.3	45.8	52.0
	0.2		40.1	43.5	48.4
	0.5		39.8	44.2	48.4
	1.0		38.2	41.5	47.2
	2.0		39.1	33.2	18.5
$\text{S}_6\text{O}_6^{2-}$	0.1	18.2	15.6	14.4	17.3
	0.2		16.7	16.7	15.2
	0.5		15.5	17.0	17.7
	1.0		14.9	15.8	19.9
	2.0		17.3	12.6	7.9

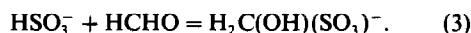
interval. During the test, each solution was left open to the air in the bottle after the first determination of polythionates. The results are listed in Table 3. Three days after sampling with *in situ* addition of 0.1–2.0 ml of 35% formaldehyde solution per 100 ml of sample solution, no change in each thionate concentration was observed in the lake water. Seventeen days after addition of the reagent, 10–35% of the tetrathionate had decomposed. The effect was most pronounced in the sample with 2 ml of aldehyde added. However, the pentathionate concentration increased by 12% over the same period of time, and hexathionate showed no significant change. Twenty-one days after sampling, the concentration of sulphate had increased by 6% from 2760 to 2930  $\mu\text{g/ml}$ . The amount of sulphate which would be produced through decomposition of the polythionates is less than the observed increase in sulphate content. This strongly suggests that sulphur species other than polythionates (for example, hydrogen sulphide and bisulphite ions) are responsible for at least part of the increase in sulphate content in the crater-lake water. In fact, the chromatogram of the lake water shows a peak due to hydrogen sulphide and/or the  $\text{HS}^-$  ion, just before the tetrathionate peak.

Sixty-three days after sampling, 20–28% of the tetrathionate in samples containing 0.1–1.0 ml of 35% formaldehyde solution per 100 ml of sample had decomposed, whereas 73% had decomposed in a 100-ml sample containing 2.0 ml of the formaldehyde solution (see Table 3). These facts indicate that too much (probably more than 0.4% in the sample solution) formaldehyde leads to decomposition of polythionates in solution. Furthermore, formaldehyde added to the solution affects the polythionate speciation. Oxalaldehyde shows an even more pronounced effect on the polythionate speciation. Seven days after sampling, the tetrathionate concentrations have considerably decreased, and those of penta- and hexathionate have increased (Fig. 3).

The behaviour of both additives suggests that they shift the reaction,



to the right, by forming adducts, e.g.,



Consequently, formaldehyde and oxalaldehyde are unsuitable for retaining the sulphur speciation of the natural water.

*Addition of hydroxylamine hydrochloride.* Hydroxylamine hydrochloride (HAH), a strong reducing agent, was added to the sample solution to prevent oxidation of the sulphur oxyanions by atmospheric oxygen. No change in polythionate concentrations was observed for the sample solutions containing HAH, even 3 weeks after sampling. During month-long storage, only 14% of the tetrathionate was lost, and penta- and hexathionate were completely preserved when more than 0.5 g of HAH was added per

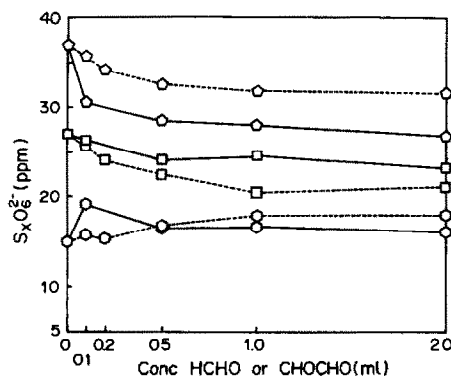


Fig. 3. Efficacies of formaldehyde and oxalaldehyde as fixatives for polythionate ions. The solid line denotes polythionate ions with various volumes of 35% formaldehyde solution; dotted line denotes those with 45% oxalaldehyde solution. (□),  $\text{S}_4\text{O}_6^{2-}$ ; (○),  $\text{S}_5\text{O}_6^{2-}$ ; (○),  $\text{S}_6\text{O}_6^{2-}$ .



Table 4. Effect of hydroxylamine hydrochloride on the stability of polythionate ions in crater-lake water

Polythionate	NH <sub>2</sub> OH·HCl, g	Polythionate found, µg/ml					
		Day 0	Day 7	Day 14	Day 21	Day 29	Day 63
S <sub>4</sub> O <sub>6</sub> <sup>2-</sup>	0.2	49.2	42.6; 40.4	1.6	—	—	—
	0.4		40.8; 41.3	1.9	—	—	—
	0.6		50.9; 50.1	2.5	—	—	0
	1.0		50.1; 47.7	49.7	45.6	45.6	0
	2.0		49.0; 49.3	49.8	48.8	48.8	36.3
S <sub>5</sub> O <sub>6</sub> <sup>2-</sup>	0.2	47.7	42.7; 43.5	4.3	—	—	—
	0.4		44.9; 46.0	6.8	—	—	—
	0.6		49.7; 48.7	13.3	—	—	0
	1.0		47.0; 45.4	46.0	45.8	45.8	0
	2.0		48.0; 48.0	47.3	46.9	46.5	45.0
S <sub>6</sub> O <sub>6</sub> <sup>2-</sup>	0.2	18.2	13.8; 12.1	3.7	—	—	—
	0.4		—; 12.8	6.1	—	—	—
	0.6		12.9; 12.8	10.3	—	—	0
	1.0		11.7; 11.8	12.8	11.4	12.5	0
	2.0		11.6; 11.6	13.2	12.8	13.0	13.1

100 ml of sample water. Two months later, a solution containing 2 g of HAH per 100 ml showed considerable decomposition of the tetrathionate (26%), but little or no decomposition of penta- or hexathionate (Table 4).

Gutmann<sup>34</sup> found qualitatively that HAH (ca. 4 g/100 ml) oxidized tetrathionate, but this conclusion was based on an experiment in which a tetrathionate solution in 25% v/v hydrochloric acid was heated for 45 min. It is well known that both heating and hydrochloric acid accelerate tetrathionate decomposition, and therefore Gutmann's conclusion is not tenable.<sup>30</sup> The pH of the solution in our work is not nearly as low as in Gutmann's experiment, and HAH is suitable for retaining the original distribution of sulphur oxyanions in the sample water, presumably by making the sample solutions oxygen-free and preventing abiotic and/or biotic oxidation of polythionates. Addition of both HAH and formaldehyde to a sample is undesirable, because both react to produce some unidentified ultraviolet-absorbing material which interferes in the determination of polythionates with an ultraviolet detector.

**Cold storage.** Three different storage methods were tested with the crater-lake water when it was sampled on 25 December 1986. The temperature of the water at the sampling site was 0.4° and that of the atmosphere during transport (a one-day trip) to a laboratory refrigerator (5°) was less than 10°. The sample solutions were stored in (a) five polythelene bottles, without additives, (b) five polyethylene bottles with the addition of HAH (1 g/100 ml), and (c) six glass Winkler oxygen-determination bottles (a variety of incubator flasks for biological oxygen demand) without additives, and analysed for polythionates at given intervals. For at least five weeks no detectable decomposition was observed for any type of storage. The samples stored in the Winkler bottles did not show any significant decomposition for at least 50 days (Fig. 4). These tests suggest that if samples are

taken without air, transported in a cooled container and kept refrigerated in the laboratory, polythionates from tetra- to hexathionate are stable for more than 35 days.

**Effect of ferric ion.** Moses *et al.*<sup>31</sup> have emphasized that some transition-metal ions, especially ferric ions, catalyse the oxidation of thiosulphate. This may lead indirectly to the chain-shortening of polythionates through reaction (2). To examine this effect of ferric ion on the stability of polythionates, we added Fe<sup>3+</sup> at 50 and 200 µg/ml levels to the crater-lake water, in which the initial Fe<sup>3+</sup> is as low as 0.3 µg/ml.<sup>35</sup> Figure 5 shows that in presence of 200 µg/ml Fe<sup>3+</sup> the polythionates are stable for more than 60 hr. About 120 hr later 30% of the hexathionate has been degraded, but only about 10% of the tetra- and pentathionate at low enough pH (in this case pH = 2.2). Two months after the addition of ferric ion, the polythionates were completely decomposed to sulphate and elemental sulphur. These results

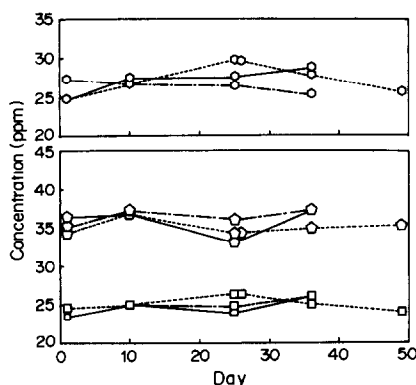


Fig. 4. Inhibition of polythionate degradation at 5° by various additives. Solid line: no additive, in polyethylene bottles; dotted line: no additive, in Winkler bottles; broken line: with hydroxylamine hydrochloride, in polyethylene bottles.

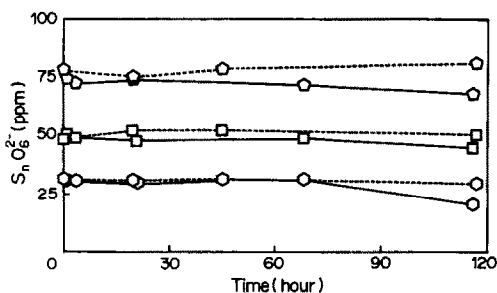


Fig. 5. Stabilities of polythionate ions in the presence of 200  $\mu\text{g/ml}$   $\text{Fe}^{3+}$ . Solid line: solutions with  $\text{Fe}^{3+}$ ; broken line: control solutions without  $\text{Fe}^{3+}$ . ( $\square$ ),  $\text{S}_4\text{O}_6^{2-}$ ; ( $\circ$ ),  $\text{S}_5\text{O}_6^{2-}$ ; ( $\circ$ ),  $\text{S}_6\text{O}_6^{2-}$ .

suggest that the catalytic degradation of polythionates through thiosulphate to sulphate *etc.* is slow enough for sample-storage not to be a problem at a ferric ion concentration as low as that in the crater-lake water.

**Biological activity in the lake water.** Satake<sup>36</sup> reported microbial sulphate reduction in the Katanuma volcanic acid crater lake (pH 1.8–2.0). However, he found no indication of carbon uptake in the Yugama lake water which was used for this research.<sup>37</sup> Takayanagi *et al.*<sup>38</sup> found sulphur-oxidizing bacteria (*Thiobacillus thiooxidans*) in lake-shore water. Until now it is unknown to what extent bacteria affect the sulphur cycle in the crater lake. The bacteria consume atmospheric oxygen, but the availability of oxygen is limited in this strongly reducing environment. Therefore, it seems unlikely that bacterial activity affects the sulphur cycle in a major way. As recommended by Moses *et al.*,<sup>31</sup> however, abiotic samples should be taken *in situ* by filtration through a 0.22- $\mu\text{m}$  membrane filter.

#### Interferences

No other natural solutes interfere with the determination of polythionates by microbore HPLC. A large amount of chloride and sulphate, however, interferes with the determination of tri- and hexathionate by ion-chromatography, as described in the text. Thiosulphate and bisulphite, if present, overlap the negative water peak in the HPLC, which appears at a retention time of 2–3 min. Ferric ion, which is one of the common ultraviolet-absorbing cations in natural water, does not interfere with the determination, because it forms a complex with the phosphate in the eluent, and is eluted before the polythionates.

#### CONCLUSIONS

Ion-pair chromatography and microbore HPLC methods have been developed for the direct determination of polythionates in volcanic waters. The former method is conveniently used for tri-, tetra- and pentathionate. The latter method has proved to

be simple and rapid for the determination of these compounds from trithionate to hexathionate and perhaps also higher homologues if pure salts of these higher members are available for calibration.

Formaldehyde and oxalaldehyde, if used as quenching reagents for polythionate reactions, change the original distribution of sulphur oxyanions. Hydroxylamine hydrochloride is adequate for preserving the initial distribution of species for at least three weeks, even if the sample is open to air. Abiotic and/or biotic oxidation by atmospheric oxygen may be the dominant reaction in the decomposition of polythionates. Excluding air from the sampling bottles, using Winkler oxygen-determination bottles, or adding 2 g of hydroxylamine hydrochloride per 100 ml of sample are recommended as methods for prolonging the safe storage periods for the sample solutions.

**Acknowledgements**—The authors are grateful for comments by M. Ichikuni of the Department of Environmental Chemistry and Engineering, Tokyo Institute of Technology, and for review of the manuscript by M. Schoonen and H. L. Barnes at Pennsylvania State University.

#### REFERENCES

1. A. L. Day and E. T. Allen, in *The Volcanic Activity and Hot Springs of Lassen Peak*, p. 115. Carnegie Institute, Washington, 1925.
2. V. I. Vlodavetz and B. I. Piip, in *Catalogue of the Active Volcanoes of the World including Sulfatara Fields, Part III, Kamchatka and Continental Areas of Asia*, Intern. Volcanol. Assoc., Naples, 1959.
3. J. Boulegue, J. P. Clabrin, C. Fouillac, G. Michard and G. Ouzounian, *Chem. Geol.*, 1979, **25**, 19.
4. J. Boulegue, *J. Geochem. Explor.*, 1981, **15**, 21.
5. J. S. MacLaurin, *Proc. Chem. Soc.*, 1911, **27**, 10.
6. B. Takano, *Science*, 1987, **235**, 1633.
7. Y. M. Nor and M. A. Tabatabai, *Soil Sci.*, 1976, **122**, 171.
8. J. O. Nriagu, R. D. Coker and A. L. K. Kemp, *Limnol. Oceanog.*, 1979, **24**, 383.
9. R. Makhija and A. Hitchen, *Talanta*, 1978, **25**, 79.
10. D. K. Nordstrom, in L. R. Hossaer, J. A. Kittrick and D. F. Faming, *Acid Sulfate Weathering: Pedo-geochemistry and Relationship to Manipulation of Soil Materials*, p. 37. Soil Sci. Soc. of America Press, Madison, Wisconsin, 1982.
11. D. P. Kelly, L. A. Chambers and P. A. Trudinger, *Anal. Chem.*, 1969, **41**, 898.
12. T. Koh and K. Taniguchi, *ibid.*, 1973, **45**, 2018.
13. T. Mizoguchi and T. Okabe, *Bull. Chem. Soc. Japan*, 1975, **48**, 1799.
14. B. Takano, M. A. McKibben and H. L. Barnes, *Anal. Chem.*, 1984, **56**, 1594.
15. R. N. Reeve, *J. Chromatog.*, 1979, **177**, 393.
16. S. B. Rabin and M. Stanbury, *Anal. Chem.*, 1985, **57**, 1130.
17. R. Steudel and G. Holdt, *J. Chromatog.*, 1986, **361**, 379.
18. H. Stamm, M. Goehring and U. Feldmann, *Z. Anorg. Allg. Chem.*, 1942, **250**, 226.
19. M. Goehring and U. Feldmann, *ibid.*, 1948, **257**, 223.
20. B. Meyer, L. Peter and K. Spitzer, *Inorg. Chem.*, 1977, **10**, 23.
21. M. Schmidt and N. Siebert, *Comprehensive Inorganic Chemistry*, Vol. 2, p. 885. Pergamon Press, Oxford, 1973.
22. M. Schmidt and T. Sand, *J. Inorg. Nucl. Chem.*, 1964, **26**, 1173.

23. W. Wolkoff and R. H. Larose, *J. Chromatog. Sci.*, 1976, **14**, 353.
24. N. Tanaka and E. R. Thornton, *J. Am. Chem. Soc.*, 1977, **99**, 7300.
25. R. S. Steudel, H.-J. Mausle, D. Rosenbauer, H. Mockel and T. Freyhold, *Angew. Chem. Int. Ed. Eng.*, 1981, **20**, 394.
26. E. Weitz and K. Spohn, *Chem. Ber.*, 1956, **89**, 2332.
27. R. Strauss and R. Steudel, *Z. Anal. Chem.*, 1987, **326**, 543.
28. M. Goehring, *Fortschr. Chem. Forsch.*, 1952, **2**, 444.
29. V. A. Kurtenacker, A. Mutschin and F. Stastny, *Z. Anorg. Allg. Chem.*, 1935, **224**, 399.
30. S. D. Boyce and M. R. Hoffman, *J. Phys. Chem.*, 1984, **88**, 4740.
31. C. O. Moses, D. K. Nordstrom and A. L. Mills, *Talanta*, 1984, **31**, 331.
32. Y. Shiina, *Bunseki Kagaku*, 1987, **36**, 184.
33. M. Wroński, *Z. Anal. Chem.*, 1961, **180**, 185.
34. A. Gutmann, *Chem. Ber.*, 1920, **53**, 444.
35. J. Ossaka, in *Field Excursion Guide to Fuji, Asama, Kusatsu-Shirane and Nantai Volcanoes. Symposium on Arc Volcanism*, p. 61. Volcanol. Soc. Japan, Int. Assoc. Volcanol. Chem. Earth Interior, Tokyo and Hakone, 1981.
36. K. Satake, *Japan J. Limnol.*, 1977, **38**, 33.
37. *Idem*, *Limnol. Oceanog.*, 1974, **19**, 331.
38. S. Takayanagi, K. Sugimori and B. Tanano, *Abstract, Annual Meeting Balneological Society of Japan*, 1987.

## COMPARATIVE STUDY OF A THIN-LAYER CELL FOR ANALYSIS OF STATIONARY AND STREAMING SOLUTIONS

G. FARSANG\*, T. DANKHÁZI, J. LÓRÁNTH and L. DARUHÁZI

Institute of Inorganic and Analytical Chemistry of L. Eötvös University, Muzeum krt. 4/B,  
1088 Budapest VIII, Hungary

(Received 22 January 1988. Revised 18 July 1988. Accepted 27 July 1988)

**Summary**—A comparative study with a home-built Kissinger-type twin-electrode thin-layer cell has been made, with the cell either filled with quiescent solutions or used as a flow-through detector. In both modes the cell was polarized by a slow linear potential sweep. The current-voltage curves recorded showed a limiting current region in both cases, in spite of the different types of transport process (steady-state diffusion caused by the redox cycling effect of the counter-electrode in the quiescent solution and convective diffusion in the flowing solution). The sensitivities and also the lower detection limits were found to be nearly the same for the two different modes of operation of the same cell, for which an explanation is given. The main analytical advantage of the thin-layer twin-electrode cell filled with quiescent solution is that only a few  $\mu\text{l}$  of analyte solution are necessary for the measurement. It was proved experimentally that this type of cell, used as a flow-through detector, gives the expected limiting current, but this current is dependent on the cube root of the linear flow-rate, in agreement with Weber's theoretical prediction, rather than on the square root of the flow-rate (commonly quoted in the literature).

The twin-electrode thin-layer cell is a voltammetric signal transducer which is a popular flow-through detector in high-performance liquid chromatography,<sup>1,2</sup> flow-injection analysis (FIA)<sup>3</sup> and concentration monitoring techniques.<sup>4</sup> The micrometer-type twin-electrode thin-layer cell was introduced by Reilly and co-workers.<sup>5-7</sup> The cell volume was adjusted by means of a micrometer screw and the electrodes were polarized by a bipotentiostat, which enabled them to be polarized independently to the desired potentials relative to a reference electrode connected to the cell by a Luggin capillary. The theory of this type of cell shows that if the solution film contains one form of a reversible system, then a steady-state limiting current region is developed on the current-potential curve, although both the electrodes and the solution layer are stationary during the recording of the polarization curve. According to this treatment, the steady-state limiting current is proportional to the concentration. This concept was proposed for precise measurement of diffusion coefficients and electrode reaction kinetic parameters.

A twin-electrode thin-layer cell with extremely large glassy-carbon electrodes with an area of several  $\text{cm}^2$  was suggested as a coulometric detector for HPLC by Lankelma and Poppe.<sup>8,9</sup> The first modern twin-electrode thin-layer cells having identical and opposing glassy-carbon electrodes of small area (a few  $\text{mm}^2$ ), with the possibility of  $iR$  compensation, were made by Blank<sup>10</sup> and by Brunt and Bruins.<sup>11</sup> Kissinger *et al.*<sup>12,13</sup> constructed the first such cell

suitable for commercial production (Bioanalytical Systems Inc).

This type of cell required not a bipotentiostat, but a simple and inexpensive potentiostat with a built-in current-voltage converter, and its application spread extremely rapidly. One of the twin electrodes is kept at a constant potential against the reference electrode and the potential of the other (counter) electrode is polarized to the potential at which the electrode reaction of the solvent or base-electrolyte component takes place.

The aims of the present paper are as follows.

(i) To demonstrate the applicability of a home-built Kissinger-type thin-layer twin-electrode cell for the analysis of a few  $\mu\text{l}$  of analyte by linear sweep voltammetry.

(ii) To compare the analytical parameters of the cell when used with quiescent and streaming analyte solutions.

(iii) To prove experimentally that with the cell geometry used, the current is proportional to the cube root of the linear streaming velocity of the solution, in accordance with Weber's theoretical prediction,<sup>14</sup> as opposed to the generally accepted square root relationship<sup>2</sup> based on the treatment by Blaedel *et al.* for streaming in a tubular electrode.<sup>15,16</sup>

### EXPERIMENTAL

#### Apparatus

The cell used was a home-built Kissinger-type twin-electrode thin-layer cell slightly modified as follows. The cell body was built from two "Plexiglas" rectangles. Tokai glassy-carbon plates,  $5 \times 7$  mm, were embedded in the cell

\*Author to whom correspondence should be addressed.

body with epoxy resin and positioned exactly opposite each other. In the upper half of the cell body a hole was drilled for connection of the salt bridge solution of the reference electrode to the cell solution by means of a porous Vycor<sup>®</sup> rod. The reference electrode was a chloride-coated silver wire immersed in 1M sodium chloride saturated with silver chloride.

The stainless-steel inlet and outlet tubes were led through two "Plexiglas" screws positioned at equal distances from the centre of the working electrode, which was always the electrode in the lower cell body. These connections were made leak-proof by use of PTFE ferrules. The two surfaces of the cell body with the embedded electrodes were polished to a mirror finish, the final polishing being done with Buehler alumina, of 0.01  $\mu\text{m}$  average grain-size, suspended in doubly distilled water. A 65  $\mu\text{m}$  thick Teflon spacer with a 6.0  $\times$  30 mm channel cut in it was positioned between the two halves of the cell and the whole sandwich was held together with stainless-steel screws at the four corners. In some cases, to decrease the volume of the cell, a 25  $\mu\text{m}$  thick poly(vinyl chloride) spacer was used, with a channel of the same size as before.

For measurements of quiescent solutions, the cells were flushed and then filled with the analyte solution by means of an Agla micrometer syringe with its glass needle fitted to the inlet tube through a very short polyethylene tube (bore 0.25 mm). Both the inlet and outlet tubes were then closed with polyethylene caps.

For measurements of streaming solutions an MMG AM 0885 pneumatic low-pressure control valve fed high-purity (99.98%) nitrogen into a stainless-steel buffer chamber, to give a pressure which could be varied precisely and continuously in the range 0–2.5 bar. On the lid of the chamber up to three liquid-stream connections were mounted with soft copper and rubber O-ring gaskets. In this way the liquid pumping lines could be used simultaneously, the main advantage being fine control of flow-velocity and pulsation-free liquid stream(s) in the streaming solution line(s). The carrier solutions were contained in glass beakers in the pressurized chamber, each equipped with a polyethylene tube with one end near the bottom of the solution, and the other end attached to the stream connection in the lid of the vessel. The flow apparatus and cell are shown in Fig. 1.

A Radelkis OH-105 type Universal Polarograph was used to polarize the cell and record the signal. Either am-

perometric ( $E_w = \text{constant}$ ) or potentiodynamic [ $i = f(E_w)$ ] curves were recorded ( $E_w = \text{working electrode potential}$ ). In each case, a three-electrode arrangement was used. The instrument had a built-in potentiostat providing  $\pm 50$  V output voltage for compensating the  $iR$  drop.

A further instrument used was a Radelkis OP 208/1 precision digital pH-mV meter, with a Metrohm EA-120X combined glass electrode, to check the pH of the base electrolytes used.

#### Reagents

Chlorpromazine [10-(3'-dimethylaminopropyl)-2-chlorophenothiazine hydrochloride], EGIS Pharmaceutical Factory, Pharmacopeia Hungarica VII quality, dissolved in 0.01M hydrochloric acid; Variamine Blue-HCl, 4-amino-4'-methoxydiphenylamine hydrochloride, freshly dissolved in 0.2M pH 4.6 acetic acid/sodium acetate buffer; dopa (3,4-dihydroxyphenylalanine), EGIS, Pharmacopeia Hungarica VII quality, dissolved in 0.1M phosphoric acid adjusted with disodium hydrogen phosphate to pH 2.40.

Unless otherwise stated, all chemicals were of analytical reagent grade (Reanal) and used without further purification.

## RESULTS AND DISCUSSION

### *Voltammetric measurements with cells filled with quiescent solutions*

One of the most significant characteristics of the measuring cell is the concentration-dependence of the signal, which was determined in the  $10^{-7}$ – $10^{-3}$ M analyte range. With a thin quiescent layer of solution between the twin electrodes, the product formed at the working electrode is converted back into its original oxidation state at the counter-electrode if the system being investigated is electrochemically reversible. During polarization, the diffusion profiles formed will be similar to those in Anderson and Reilly's special thin-layer cell.<sup>5-7</sup> It is expected, therefore, that in spite of the solution being quiescent, a limiting current region will be found on the  $i = f(E_w)$

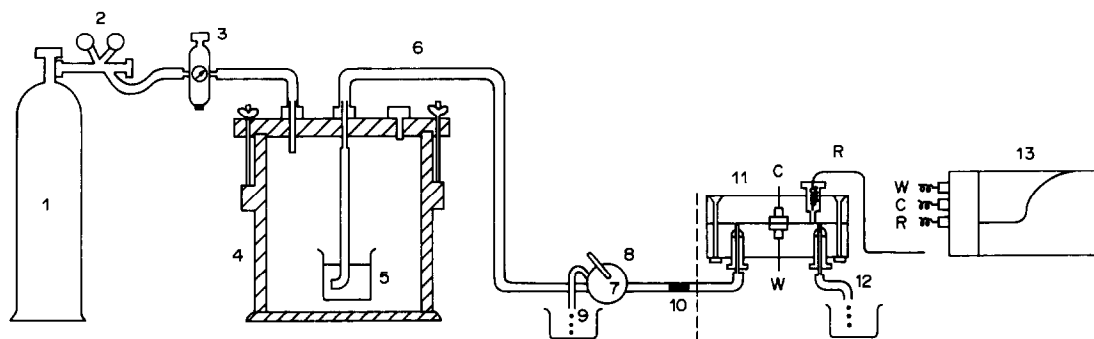


Fig. 1. Stabilized low-pressure pneumatic-flow apparatus for analysis of streaming solutions by methods sensitive to fluctuations of the flow-rate, with a voltammetric detector. The system shown includes a sample injector for FIA but results obtained with this method are not given in this paper. 1, N<sub>2</sub> gas cylinder; 2, pressure control valve; 3, MMG AM (Hungary) 0885 pneumatic pressure controller; 4, buffer vessel for pressure stabilization within  $\pm 0.5\%$ ; 5, the solution to be pumped out from the glass beaker through a 0.25-mm bore soft silicone-rubber tube connected to a stainless-steel tube sealed into the lid of the buffer vessel; 6, a similar silicone rubber tube connected to the outlet of the stainless-steel tube in the lid; 7, Labor MIM (Hungary) OE 320 HPLC injector in "load" position; 8, in FIA operation the filling connection of the injector loop; 9, waste receiver vessel; 10, porous frit for mixing the carrier and injected solutions; 11, cross section of the thin-layer cell, where W is the working electrode, C the counter-electrode and R the reference electrode; 12, outlet tube of the cell; 13, Radelkis OH-105 Universal Polarograph.

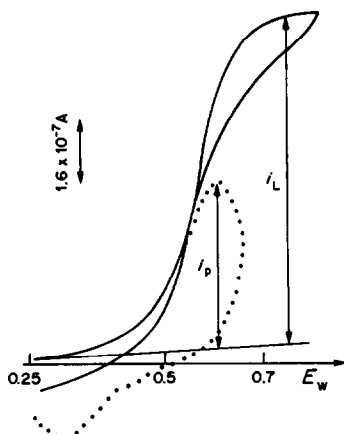


Fig. 2. Voltammetric  $i = f(E_w)$  curves recorded with the cell filled with quiescent solution. Depolarizer,  $1 \times 10^{-5} M$  dopa in pH-2.64 phosphate buffer;  $d = 65 \mu m$  (Teflon spacer),  $i_L$ , the stationary limiting current;  $i_p$ , anodic peak current. The solid line shows the curve recorded with the redox-cycling counter-electrode and the broken line the curve when the outlet tube of the cell was used as the counter-electrode.

curve, and be completely different from the symmetrical peak-shaped  $i-E_w$  curves of classical thin-layer cells, where the counter-electrodes do not reduce the product. The rate of polarization,  $v$ , must be slow enough to allow the development of stationary diffusion profiles between the two electrodes. A further condition needed for this behaviour is electrochemical reversibility of the system under study.

Figure 2 shows cyclic voltammetric curves for dopa, recorded in the twin-electrode cell in two ways: (a) with the counter-electrode opposite the working electrode to act as a redox-cycling electrode and (b) with the stainless-steel outlet tube as the counter-electrode, and the glassy-carbon electrode opposite the working electrode acting only as a diffusion-limiting barrier. Hysteresis was found on the reverse sweep, which can be explained by the electrode reaction mechanism of dopa<sup>17</sup> and its tendency to slight filming on the electrodes. The effect of the reducing counter-electrode is quite unambiguous when the cyclic voltammetric curve is compared with that obtained with the outlet tube as counter-electrode, where the irreversible shape is explained by

the presence of a coupled chemical reaction in the electrode reaction of dopa.<sup>17</sup> Similar measurements were made with two other reversible redox systems with well known electrode reaction mechanisms, Variamine Blue<sup>18</sup> and chlorpromazine.<sup>19,20</sup> The shape of the signal in each case showed a limiting current region when the counter-electrode worked as a redox-cycling electrode. The current was a linear function of the concentration in the range  $1 \times 10^{-7}$ – $1 \times 10^{-4} M$ . The coefficients of the linear calibration curves  $i_L = mC + b$  measured in the  $1 \times 10^{-6}$ – $1 \times 10^{-4} M$  are summarized in Table 1. From the results of Table 1 and experimental work done in the  $1 \times 10^{-7}$ – $1 \times 10^{-6} M$  concentration range, the following analytical consequences can be inferred.

(a) The thin-layer cell with a redox-cycling counter-electrode and a quiescent analyte layer can be used as a sensitive electrochemical detector (see the slopes obtained).

(b) The sensitivity and the lower detection limit depend on the thickness of the spacer used; with the  $25 \mu m$  spacer the detection limit is found to be approximately  $1 \times 10^{-7} M$ .

In the micromolar concentration range, the residual current is reproducible and can be easily compensated.

To a first approximation, the relationship derived by Anderson and Reilley<sup>5</sup> for the limiting current can be used:

$$i_L = \frac{nFAD_{ss}C_T}{d} \quad (1)$$

where  $A$  is the surface area of the working electrode,  $C_T$  the sum of the concentrations of the oxidized and reduced forms in the diffusion layer,  $d$  the thickness of the solution film,  $n$  and  $F$  have their usual meanings, and  $D_{ss}$  is given by

$$D_{ss} = \frac{2D_o D_r}{D_o + D_r} \quad (2)$$

where  $D_o$  and  $D_r$  are the diffusion coefficients of the oxidized and reduced forms of the reversible redox system. For  $n = 2$ ,  $F = 96485 \text{ C/eq}$ ,  $A = 0.350 \text{ cm}^2$ ,  $D_o = D_r = 1 \times 10^{-5} \text{ cm}^2/\text{sec}$ ,  $C_T = 10^{-7} M$  and  $d = 25 \mu m$ , the value of  $i_L$  calculated by use of (1) is  $27 \text{ nA}$  at the limit of detection.

Table 1. The coefficients of the analytical calibration curves for three reversible systems measured with redox-cycling counter-electrodes at two spacer thicknesses\*

Compound measured	Base electrolyte	Concentration range, $M$	Slope ( $m$ ), $\text{mA.l.mole}^{-1}.\text{mm}^{-2}$	Intercept ( $b$ ), $\text{nA/mm}^2$	Correlation coefficient	$d$ , $\mu m$
L-Dopa	0.2M phosphate buffer, pH 2.64	$1 \times 10^{-6}$ – $1 \times 10^{-4}$	21.2	2.88	0.9956	65
L-Dopa	0.2M phosphate buffer, pH 2.64	$1 \times 10^{-6}$ – $1 \times 10^{-4}$	37.8	6.77	0.9868	25
Chlorpromazine	$10^{-2} M$ HCl	$1 \times 10^{-6}$ – $1 \times 10^{-4}$	0.878	0.780	0.9989	65
Chlorpromazine	$10^{-2} M$ HCl	$1 \times 10^{-6}$ – $1 \times 10^{-4}$	2.24	2.35	0.9979	25
Variamine Blue	0.2M acetate buffer, pH 4.60	$1 \times 10^{-6}$ – $1 \times 10^{-4}$	1.58	0.642	0.9998	65

\*The  $d$  values are only approximate: the thickness of the solution layer is always smaller because of deformation of the spacers under pressure.

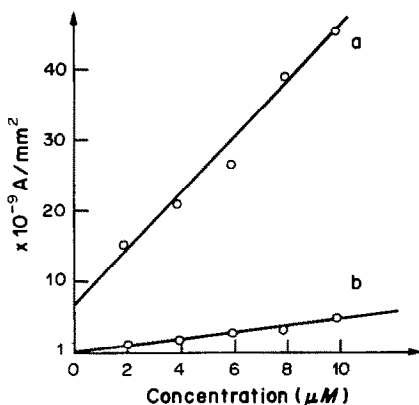


Fig. 3. The sensitivity of the cell filled with quiescent solutions of dopa dissolved in phosphate buffer of pH 2.64. Curve a, redox-cycling counter-electrode; curve b, non-redox-cycling counter-electrode.

The charging current,  $i_c$ , can be calculated<sup>21</sup> from

$$i_c = AC_d v \quad (3)$$

where  $C_d$  is the differential capacity ( $F/cm^2$ ) and  $v$  the rate of polarization ( $V/sec$ ).

With  $A$  as above,  $C_d = 20 \mu F/cm^2$  and  $v = 8.33$  mV/sec,  $i_c = 58$  nA/V. According to this the charging current interferes at the detection limit, which emphasizes the need to apply as low a polarization rate as possible during the recording of the  $i = f(E_w)$  curve.

In the course of the measurements there was no difficulty in achieving a detection limit of  $10^{-7}M$  for all the analytes investigated, which was helped by the fact that the twin electrodes worked not in a circular film of solution (Anderson and Reilley's construction<sup>6</sup>) but in a rectangular layer with an area larger than  $A$ . Hence besides strictly linear diffusion between the twin electrodes, there was diffusion towards the working electrode from the rest of the film.

(c) The method shows outstanding characteristics as a microanalytical technique. Only a 50–100  $\mu l$  volume of analyte solution is needed for the measurement, including flushing the cell with new solution. This is especially advantageous when the volume of sample for analysis is extremely small, e.g., some samples of blood and other body fluids, especially when these contain drugs or metabolites.

Chlorpromazine<sup>22</sup> and diazepam<sup>23</sup> in biological fluids have been determined by differential pulse voltammetry.

(d) A pulse-free pumping system is needed only when flow analytical methods are to be used.

(e) The limiting currents are additive, so this method is more convenient than simple linear-sweep voltammetric batch analysis.<sup>21</sup> Figure 3 shows that the sensitivity of the method is much higher in the redox-cycling mode than when the thin-layer cell is used with the twin electrode acting only to limit diffusion.

#### *Voltammetric measurements with twin-electrode thin-layer cells with flowing sample solutions*

If the cell is operated as a flow-through detector, two kinds of measurement may be made: (a) the sample concentration varies continuously in the carrier stream and can be monitored, or (b) samples are injected into the carrier stream in sequence, as in FIA, and are separately analysed. Both techniques are widely used.<sup>2-4</sup> It was surprising to find that the lower detection limits were much the same whether the cell was used as a flow-through detector in streaming solutions or as a detector with quiescent solutions. Table 2 shows results obtained with the cell as a flow-through detector.

Comparison of the results in Tables 1 and 2 shows that the most characteristic analytical parameters are at least of the same order of magnitude at the moderate flow-rate applied. The sensitivity values are about five times higher in flowing solutions than in quiescent solution and the correlation coefficients are also better. This can be explained by the cleaning effect of the streaming solution, which reduces the filming effect and so results in better reproducibility of the signals.

No dramatic improvement of the analytical performance was observed in flowing solutions, and this can be attributed to two main factors. In agreement with other authors' observations, when the cell is used as a flow-through detector, there is little, if any, contribution from the redox-cycling caused by the counter-electrode. The relatively small increase in the convective-diffusion limiting current compared to the redox-cycling diffusion limiting current is due to the

Table 2. Analytical signal-concentration dependence obtained with a twin-electrode thin-layer cell as a flow-through detector with  $d = 65 \mu m$

Compound measured	Base electrolyte (carrier stream*)	Measuring mode	Coefficient of the calibration curve		
			Slope ( $m$ ), $mA \cdot l \cdot mole^{-1} \cdot mm^{-2}$	Intercept ( $b$ ), $nA/mm^2$	Correlation coefficient
Variamine Blue	0.2M acetate buffer, pH 4.60	Amperometric monitoring†	7.21	39.9	0.9998
Variamine Blue	0.2M acetate buffer, pH 4.60	Linear sweep voltammetry§	8.35	2.53	0.9996
Chlorpromazine	$10^{-2}M$ HCl	Linear sweep voltammetry§	4.56	8.16	0.9996

\*Volume flow-rate 0.8 ml/min.

† $E_w = +0.35$  V vs. Ag/AgCl.

§Rate of polarization 0.5 V/min.

Table 3. The current efficiency ( $q\%$ ) of a thin-layer cell in streaming solution for (a)  $1 \times 10^{-4}M$  and (b)  $6 \times 10^{-4}M$  analyte

Variamine Blue in the carrier stream			
(a)		(b)	
$v, \text{ ml/min}$	$q, \%$	$v, \text{ ml/min}$	$q, \%$
0.8	8.67	0.8	7.90
2.1	4.80	2.0	4.40
3.5	3.43	3.3	3.27
5.3	2.62	5.0	2.51
6.8	2.16	6.2	2.17

very poor current efficiency of the thin-layer cell as a flow-through detector, as shown in Table 3.

The current efficiency of the cell was measured with streaming Variamine Blue solutions in the  $1 \times 10^{-4}$ – $6 \times 10^{-4}M$  concentration range. For a given concentration of Variamine Blue at different flow-rates, potential steps of 0.35 V were applied starting at 0 V and the current was recorded as a function of time. After a wait of 20–30 sec for the capacitive current to decay, the stabilized current,  $i$ , was integrated as a function of time for a given period,  $t$ :  $it = Q$ . With a known flow-rate, and concentration of Variamine Blue in the carrier stream, the current efficiency of the cell can be readily calculated for the 2-electron reaction.

#### Dependence of the current on the linear flow-rate in a Kissinger-type thin-layer cell

The literature differs as to the dependence of the current on the flow-rate, but it is accepted that the relationship has the following general form

$$i_L = kD^{2/3}\nu^{-1/6}\bar{V}^\alpha C$$

where  $i_L$  is the limiting current density ( $A/cm^2$ ),  $k$  is a constant,  $D$  the diffusion coefficient of the analyte ( $cm^2/sec$ ),  $\nu$  the kinematic viscosity ( $cm^2/sec$ ),  $C$  the analyte concentration in the flowing solution ( $mM$ ),

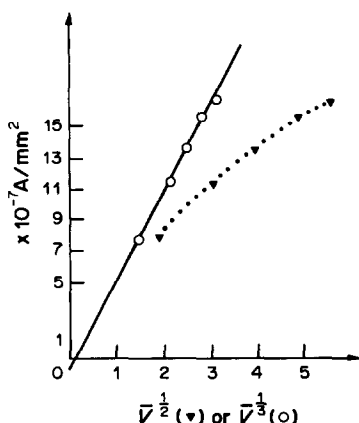


Fig. 4. The current density as a function of linear flow-rate in a twin-electrode thin-layer cell. Solid line, plotted against  $\bar{V}^{1/3}$ ; broken line, plotted against  $\bar{V}^{1/2}$ . Depolarizer:  $1 \times 10^{-4}M$  Variamine Blue in 0.2M acetate buffer, pH 4.60.  $E_w = +0.35$  V vs. Ag/AgCl/1M NaCl reference electrode.

$\bar{V}$  the linear flow velocity of the solution contacting the electrode surface (cm/sec) and  $\alpha$  an exponent depending on the geometry of the flow and governed mainly by the cell geometry. According to Levich,<sup>24,25</sup> if the flow is not turbulent and the fluid is streaming between two parallel plates in a rectangular flow channel, then  $\alpha = 0.5$ .

The cell used in this work is stated in the literature<sup>26</sup> to behave with  $i \propto \bar{V}^{1/2}$  but  $i \propto \bar{V}^{1/3}$  can also be found.<sup>27</sup> According to Weber,<sup>14</sup> if the flow profile is completely developed in the cell, i.e., the velocity profile is parabolic in the cell channel, the current is proportional to  $L\bar{V}^{1/3}$  where  $L$  is the length of the electrode in the direction of flow, but when the flow-rate profile is unable to develop completely in the cell, then the limiting current  $i_L$  is proportional to  $L\bar{V}^{1/2}$ . Applying Weber's calculations to a thin-layer cell with flow channel 0.0065 cm high and 0.6 cm wide, with a volume flow-rate of 0.017 ml/sec, the distance needed for the full development of a parabolic flow profile is 7.4  $\mu m$ . This means that most of the thin-layer cells used will show dependence of the limiting current on  $\bar{V}^{1/3}$ .

The validity of this theoretical treatment was tested for the cell used throughout this work, by measuring the limiting current dependence in the 0.8–6.5 ml/min flow-rate range ( $\bar{V} = 3.4$ – $27.8$  cm/sec) for a carrier stream containing  $5 \times 10^{-5}$ – $6 \times 10^{-4}M$  Variamine Blue as depolarizer. From the limiting currents, the current densities were calculated and plotted as functions of  $\bar{V}^{1/3}$  and  $\bar{V}^{1/2}$  (Fig. 4). The plots show that the cell behaves in accordance with Weber's prediction. The erroneous  $\bar{V}^{1/2}$  dependences reported in the literature may often be due to mechanical application of the Levich theory and the use of peristaltic pumps that do not provide flow-rate changes of wide enough range, such as that which can easily be achieved by pneumatic flow-rate control. With a narrow range of flow-rates it is easy to obtain a plot of  $i_L$  vs.  $\bar{V}^{1/2}$  that has acceptable linearity. The statistical evaluation of a large number of measured flow-rate dependences shows a clear dependence on  $\bar{V}^{1/3}$ .

**Acknowledgements**—The authors express their thanks to Mr. Mihaly Fazekas for his careful work in building the pneumatic flow-rate controller system and the thin-layer cell, and also to the Institute of General and Analytical Chemistry of the Technical University of Budapest for supplying the Variamine Blue.

#### REFERENCES

1. P. T. Kissinger, in *Laboratory Techniques in Electro-analytical Chemistry*, P. T. Kissinger and W. R. Heineman (eds.), pp. 611–630. Dekker, New York, 1984.
2. K. Štulík and V. Pacáková, *C.R.C. Crit. Rev. Anal. Chem.*, 1984, **14**, 297.
3. D. C. Johnson, S. G. Weber, A. M. Bond, R. M. Wightman, R. E. Shoup and I. S. Krull, *Anal. Chim. Acta*, 1986, **180**, 187.
4. E. Pungor, Zs. Fehér and G. Nagy, *Pure Appl. Chem.*, 1975, **44**, 595.



5. L. B. Anderson and C. N. Reilley, *J. Electroanal. Chem.*, 1965, **10**, 295.
6. *Idem*, *ibid.*, 1965, **10**, 538.
7. L. B. Anderson, B. McDuffie and C. N. Reilley, *ibid.*, 1966, **12**, 477.
8. J. Lankelma and H. Poppe, *J. Chromatog.*, 1976, **125**, 375.
9. J. Lankelma, *Ph.D. Thesis*, University of Amsterdam, 1976.
10. C. L. Blank, *J. Chromatog.*, 1976, **117**, 35.
11. K. Brunt and C. H. P. Bruins, *ibid.*, 1978, **161**, 310.
12. D. A. Roston and P. T. Kissinger, *Anal. Chem.*, 1981, **53**, 1695.
13. D. A. Roston, R. E. Shoup and P. T. Kissinger, *ibid.*, 1982, **54**, 1417A.
14. S. G. Weber, *J. Electroanal. Chem.*, 1983, **145**, 1.
15. W. J. Blaedel, C. L. Olson and L. R. Sharma, *Anal. Chem.*, 1963, **35**, 2100.
16. W. J. Blaedel and L. N. Klatt, *ibid.*, 1966, **38**, 879.
17. L. H. Piette, P. Ludwig and R. N. Adams, *ibid.*, 1962, **34**, 916.
18. G. Farsang, L. Adorjan and L. Ladanyi, *Proc. 2nd Conf. Appl. Phys. Chem.*, Vol. 1, p. 461. Akadémiai Kiadó, Budapest, 1971.
19. P. Kabasakalian and J. McGlotten, *Anal. Chem.*, 1959, **31**, 431.
20. M. D. Hawley, S. W. Tatwawadi, S. Piekarski and R. N. Adams, *J. Am. Chem. Soc.*, 1967, **89**, 447.
21. A. M. Bond, *Modern Polarographic Methods in Analytical Chemistry*, pp. 197-209. Dekker, New York, 1980.
22. T. W. Jarbawi, W. R. Heineman and G. J. Patriarche, *Anal. Chim. Acta*, 1981, **126**, 57.
23. T. P. DeAngelis, R. E. Bond, E. E. Brooks and W. R. Heineman, *Anal. Chem.*, 1977, **49**, 1792.
24. E. Pungor, Zs. Fehér and M. Varadi, *C.R.C. Crit. Rev. Anal. Chem.*, 1980, **9**, 97.
25. V. G. Levich, *Physicochemical Hydrodynamics*, Chapters 2 and 12. Prentice-Hall, Englewood Cliffs, 1962.
26. K. Brunt and C. H. P. Bruins, *J. Chromatog.*, 1979, **172**, 37.
27. Y. Hirata, P. T. Lin, M. Novotny and R. M. Wightman, *ibid.*, 1980, **181**, 287.

## RECIPROCAL DERIVATIVE CONSTANT-CURRENT STRIPPING ANALYSIS

XIANGYUAN RUAN

Department of Chemistry, Xiangtan University, Hunan, People's Republic of China

HSIANGPIN CHANG\*

750 Pammel Court, Ames, IA 50010, U.S.A.

(Received 4 May 1988. Accepted 14 July 1988)

**Summary**—Reciprocal derivative constant-current stripping analysis (RD-CCSA) is based on the measurement of  $dt/dE$  converted from a derivative signal,  $dE/dt$ , vs. electrode potential ( $E$ ) during the stripping of analyte under galvanostatic conditions from a mercury-film electrode after preconcentration. The potential transient signal ( $E-t$ ) in normal chronopotentiometric stripping analysis (CPSA) is converted in RD-CCSA into a stripping peak ( $dT/dE$ ), the height of which is proportional to the bulk concentration of analyte in solution. The theory of RD-CCSA has been derived, and validated by the good correlation obtained between the theory and experimental data. Compared with normal CPSA, RD-CCSA is more sensitive and has higher resolution. The detection limit for cadmium is  $6 \times 10^{-10} M$ . Simultaneous determination of  $Cd^{2+}$ ,  $In^{3+}$ , and  $Tl^{+}$  (for which the differences between the stripping peak potentials are 58 and 50 mV, respectively) which is impossible for normal CPSA, voltammetry or differential pulse polarography, has become possible with RD-CCSA.

Chronopotentiometric stripping analysis (CPSA) has been known for a long time.<sup>1-12</sup> A constant current, like the potential sweep in voltammetric stripping analysis and the chemical reagent in potentiometric stripping analysis, is applied in CPSA to strip the analyte from the electrode surface where it has been preconcentrated. Along with the stripping time ( $t$ ) the electrode potential ( $E$ ) is measured. The analytical signal is the transition time ( $\tau$ ) beginning and ending when the stripping is started and completed, respectively. A typical  $E-t$  curve for CPSA is shown in Fig. 1a.

Although CPSA has some advantages over voltammetric and potentiometric stripping analysis,<sup>2</sup> it has not been as popular as the other stripping techniques, mainly because of its moderately low sensitivity. One apparent limitation to the sensitivity of CPSA is that it is difficult to measure a small time signal precisely, when the potential change during stripping is small. This is especially true for analysis of mixtures. Use of a derivative technique, by measuring  $dE/dt$ , has been proposed to overcome this shortcoming,<sup>13</sup> and a typical derivative chronopotentiogram is shown in Fig. 1b. Apparently this  $dE/dt$  vs.  $t$  curve makes the measurement of  $\tau$  easier than from Fig. 1a but without significant improvement in the sensitivity. Actually, when the transition time is very small, the  $(dE/dt)-t$  curve becomes valley-like and much less well defined than that in Fig. 1b,<sup>13</sup> so this method has not been widely

used. Recently, Jagner and co-workers<sup>14-21</sup> have adopted a new technique to handle CPSA signals with a computerized system. The  $E$  signal is measured and stored in a computer. After the experiment, the  $E$  data are converted into  $dt/dE$  digitally and  $dt/dE$  is plotted against  $E$ , to give a peak as shown in Fig. 1c. This scheme of measurement has been used in flow constant-current<sup>14-16</sup> and potentiometric stripping analysis (PSA)<sup>17-21</sup> with much increased sensitivity and resolution compared to normal CPSA and PSA. However, no theoretical analysis has been given to describe the shape of the  $(dt/dE)-E$  curves. Recently, Hussam and Gunaratna<sup>22</sup> have published their work on chronopotentiometry by measuring current transients. Differential chronopotentiograms are obtained by measuring the relaxation time differences ( $\Delta t$ ) after application of potential pulses. This measurement is, however, no longer a truly galvanostatic experiment, although the shape of the signal ( $\Delta t-E$ ) obtained is similar to that of  $(dt/dE)-E$  obtained by Jagner *et al.* A brief study has also been made of applications of this technique to stripping analysis.

In this paper we report a much simplified analogue method for obtaining the  $(dt/dE)-E$  signal for constant-current stripping analysis. The potential signal in Fig. 1a is first differentiated to give  $dE/dt$  and then  $dE/dt$  is inverted to  $(dt/dE)$  which is plotted against  $E$  with an  $X-Y$  recorder. This new method is called reciprocal derivative constant-current stripping analysis (RD-CCSA) instead of chronopotentiometric stripping analysis, since the actual signal obtained is no longer a chronopotentiogram. A theoretical analysis of the  $(dt/dE)$  vs.  $E$  signals for

\*Permanent address: c/o Department of Chemistry, Iowa State University, Ames, IA 50011, U.S.A.

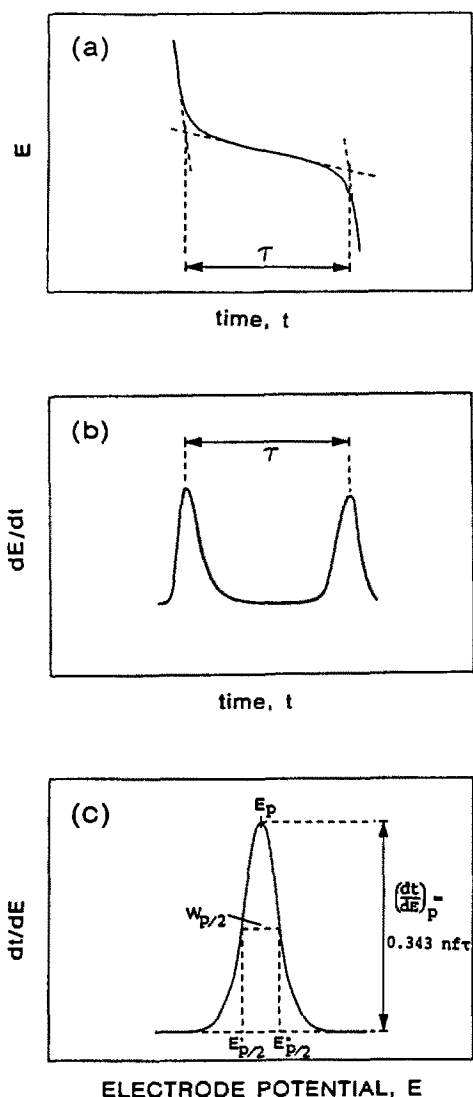


Fig. 1. Comparison of schematic CPSA, D-CPSA and RD-CCSA signals. Curves: (a) normal chronopotentiogram; (b) derivative chronopotentiogram; (c)  $(dt/dE)$  vs.  $E$ . For the definitions of the symbols, see the context.

constant-current stripping will be made and the theory validated with experimental results obtained by using this simple RD-CCSA instrument.

## THEORY

### Reciprocal derivatization measurement

The potential-time equation describing the  $E-t$  curve in Fig. 1a for the normal CPSA at a mercury film electrode can be written<sup>9</sup> as

$$E = E^0 + \frac{RT}{nF} \ln \frac{2l}{(\pi D)^{1/2}} + \frac{RT}{nF} \ln \left( \frac{t^{1/2}}{\tau - t} \right) \quad (1)$$

where  $l$  is the thickness of the mercury film,  $\tau$  is the transition time,  $D$  is the diffusion coefficient of the

metal ion ( $M^{n+}$ ) in solution,  $t$  is the stripping time, and other symbols have their normal electrochemical meanings;  $dE/dt$  is obtained by rearranging and differentiating equation (1):

$$\frac{dE}{dt} = \frac{1}{2nf} \left[ \frac{\tau + t}{t(\tau - t)} \right] \quad (2a)$$

in which  $f = F/RT$ . The measurement of  $dE/dt$  has been discussed before.<sup>13</sup> A typical  $(dE/dt)-t$  curve is shown in Fig. 1b. The reciprocal of equation (2a) yields:

$$\frac{dt}{dE} = 2nf \left[ \frac{t(\tau - t)}{\tau + t} \right] \quad (2b)$$

which is called the reciprocal derivative signal, and shown in Fig. 1c. When

$$t = t_p = 0.4142\tau \quad (3)$$

the value of  $dt/dE$  in equation (2b) is at a maximum, denoted by  $(dt/dE)_p$  and called the "stripping peak", as shown in Fig. 1c. It is noted that the stripping peak potential ( $E_p$ ) does not correspond to  $\tau/2$ . This is due to the fact that the  $E-t$  curve as described in equation (1) is asymmetric. The value of  $(dt/dE)_p$  is obtained by substituting equation (3) into (2b):

$$\left( \frac{dt}{dE} \right)_p = 0.343 nF \tau = 13.35 n\tau \quad (\text{at } 25^\circ) \quad (4)$$

Exactly the same parameter is measured in differential potentiometric stripping analysis (DPSA),<sup>23</sup> so  $dt/dE$  can easily be measured with the differential potentiometric stripping instrument working in the constant-current mode. The principle of this instrument is based on the measurement of a derivative signal  $dE/dt$  followed by inversion of  $dE/dt$  to obtain  $dt/dE$ , the final output being  $(dt/dE)$  plotted against  $E$  with an  $X-Y$  recorder. A block diagram is shown in Fig. 2 to illustrate the principle of the instrumental set-up. The potentiostat/galvanostat is used for constant-potential preconcentration and constant-current stripping. Since it is  $(dt/dE)-E$  that is obtained instead of  $E-t$ , the curve, as shown in Fig. 1c, actually resembles a pseudovoltamperogram, rather than a chronopotentiogram.

Apparently, the measuring technique for  $dt/dE$  presented here is totally different from that described by Hussam and Gunaratna,<sup>22</sup> in which a potentiostat is actually used. RD-CCSA is based on a true galvanostatic measurement and it does not involve signal differentiation procedures. The shape of the  $(dt/dE)-E$  curve in Fig. 1c is similar to that of the  $\Delta t-E$  curve (Hussam and Gunaratna) because the  $\Delta t$  values measured by these authors can be regarded as equivalent to  $\Delta t/\Delta E$  with  $\Delta E$  kept constant. Compared to the computer system used by Jagner *et al.*<sup>14-21</sup> to measure  $(dt/dE)-E$  the instrument presented here is simpler and represents a real-time  $dt/dE$  measurement.

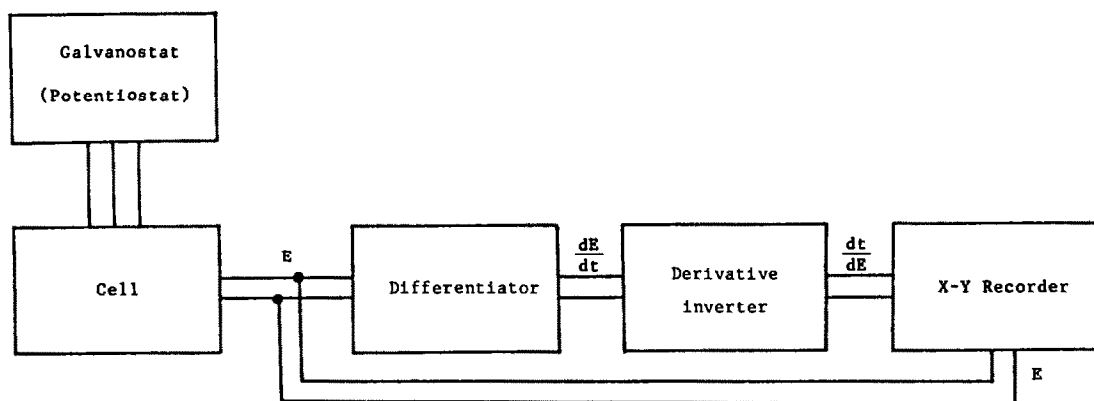


Fig. 2. Block diagram of the instrument set-up for RD-CCSA.

### Factors affecting the stripping peak height

It is known that  $\tau$  is related to the concentration of metal M ( $C_M$ ) in a mercury film of thickness  $l$ :

$$\tau = \frac{lC_M}{\lambda} \quad (5)$$

in which  $\lambda = i_s/nFA$  and  $i_s$  is the stripping current. In turn,  $C_M$  can be expressed according to the Levich equation:<sup>24</sup>

$$C_M = 0.62 \omega^{1/2} D^{2/3} \mu^{-1/6} l^{-1} t_d C^0 \quad (6)$$

where  $\omega$  is the angular rotational velocity during preconcentration,  $\mu$  is the viscosity of the solution,  $t_d$  is the deposition time, and  $C^0$  is the bulk concentration of the analyte ( $M^{n+}$ ) in solution. Substitution of equations (5) and (6) into (4) yields

$$\left(\frac{dt}{dE}\right)_p = 0.21 nf(nFA)\omega^{1/2} D^{2/3} \mu^{-1/6} t_d C^0 / i_s = 7.89 \times 10^5 n^2 A \omega^{1/2} D^{2/3} \mu^{-1/6} t_d C^0 / i_s \quad (\text{at } 25^\circ) \quad (7)$$

where  $A$  is the electrode area. From equation (7), it can be seen that the height of the stripping peak  $(dt/dE)_p$  is proportional to the bulk concentration of the analyte in solution ( $C^0$ ), which is the basis for the quantitative application of RD-CCSA.

### Stripping equation

Rearrangement and differentiation of equation (1) also yields

$$\frac{dt}{dE} = nf \left[ \frac{2\tau + e^{-x}}{(4\tau e^x + 1)^{1/2}} - e^{-x} \right] \quad (8)$$

where

$$x = 2nf(E - E') \quad (9)$$

with

$$E' = E^0 + \frac{RT}{nF} \ln \frac{2l}{(\pi D)^{1/2}} \quad (10)$$

The stripping equation describing the RD-CCSA curve shown in Fig. 1c is thus obtained by substi-

tution of equation (4) into equation (10):

$$\frac{dt}{dE} = nF \left\{ \frac{\frac{5.83}{nf} \left(\frac{dt}{dE}\right)_p + e^{-x}}{\left[\frac{11.66}{nf} \left(\frac{dt}{dE}\right)_p e^x + 1\right]^{1/2} - e^{-x}} \right\} \quad (11)$$

### Peak potential and specific potential

The peak potential equation is obtained by combination of equations (3) and (4) and substitution into equation (1):

$$E_p = E' + 1.39 \frac{RT}{nF} + \frac{RT}{2nF} \ln(n) - \frac{RT}{2nF} \ln \left(\frac{dt}{dE}\right)_p \quad (12)$$

Apparently  $E_p$  is a function of peak height.

The specific potential  $E_M$  for element M is defined as

$$E_M = E_p + \frac{RT}{2nF} \ln \left(\frac{dt}{dE}\right)_p \quad (13)$$

Substitution of (12) into (13) yields

$$E_M = E^0 + \frac{RT}{nF} \ln \frac{2l}{(\pi D)^{1/2}} + 1.39 \frac{RT}{nF} + \frac{RT}{2nF} \ln(n) \quad (14)$$

According to equation (14),  $E_M$  is a function of the standard potential of the  $M^{n+}/M$  couple ( $E^0$ ) and the mercury film thickness ( $l$ ), but independent of  $C_M$  and the stripping conditions. Therefore  $E_M$  can be used as a parameter for qualitative identification.

### Peak width and resolution

At half peak height

$$\frac{dt}{dE} = \frac{1}{2} \left(\frac{dt}{dE}\right)_p \quad (15)$$

Substitution of equation (15) into (2b) and application of (4) yields the time at half peak height ( $t_{p/2}$ ):

$$t_{p/2} = (0.4571 \pm 0.3508)\tau \quad (16)$$

Two values of the half peak potential ( $E_{p/2}$ ) are obtained by combination of equations (1), (7), and

(16):

$$E'_{p/2} = E_p + 1.46 \frac{RT}{nF} \quad (17)$$

$$E''_{p/2} = E_p - 1.10 \frac{RT}{nF} \quad (18)$$

The width of the peak at half its maximum height ( $W_{p/2}$ ) (see Fig. 1c) can then be obtained as follows:

$$W_{p/2} = E'_{p/2} - E''_{p/2} = 2.56 \frac{RT}{nF} \\ = \frac{65.5}{n} \text{ (mV at } 25^\circ\text{)} \quad (19)$$

Equation (19) indicates that the resolution of RD-CCPA is apparently higher than that of linear sweep voltammetry,  $173 \text{ mV}/n^{24a}$ , and differential pulse polarography,  $90.4 \text{ mV}/n^{24b}$ , and is close to that of semidifferential stripping voltammetry,  $54.4 \text{ mV}/n^{25}$ .

### EXPERIMENTAL

#### Apparatus

A Model DPSA-1 electroanalyser (The Seventh Electronic Factory of Shandong, China) re-equipped with a galvanostatic circuit with multilevel control of constant current between 1 and  $20 \mu\text{A}$  was used as the potentiostat/galvanostat. The  $dt/dE$  signal was measured by using the differentiation mode of the DPSA-1 instrument, originally designed for differential potentiometric stripping analysis. The working, reference, and counter electrodes were glassy carbon (GC), Ag/AgCl, and platinum, respectively. The GC disc electrode was mounted on a JCZ-A rotator (The Seventh Electronic Factory of Shandong, China). A thermostat system was used to control the temperature of the solution.

#### Reagents

All chemicals were of analytical grade and solutions were prepared with water doubly-distilled in silica apparatus. Cadmium and lead standard solutions were prepared from the nitrates and those of indium and thallium from the pure metals. Sodium nitrate ( $0.2M$ ) was used as the supporting electrolyte. Nitric acid was used to adjust the solution pH to about 4.

#### Procedure

The glassy-carbon electrode was first polished with alumina powder, then cleaned consecutively with ammonia solution (1 + 1) and 95% ethanol, and finally rinsed with distilled water before use. The mercury-film electrode was prepared by depositing mercury from  $2.0 \times 10^{-4}M$  mercuric chloride at  $E_d = -1.0 \text{ V}$ . The preconcentration of analyte in sample solutions was done with rotational velocity  $\omega = 2000 \text{ rpm}$  and stripping was done in quiescent solution. Before the deposition the solution was deaerated by passage of nitrogen for 15 min. All experiments were done at  $25.0 \pm 0.2^\circ$ .

### RESULTS AND DISCUSSIONS

#### Factors affecting the stripping peak height

The dependences of the stripping peak height  $(dt/dE)_p$  for the RD-CCSA of  $\text{Cd}^{2+}$ , on deposition

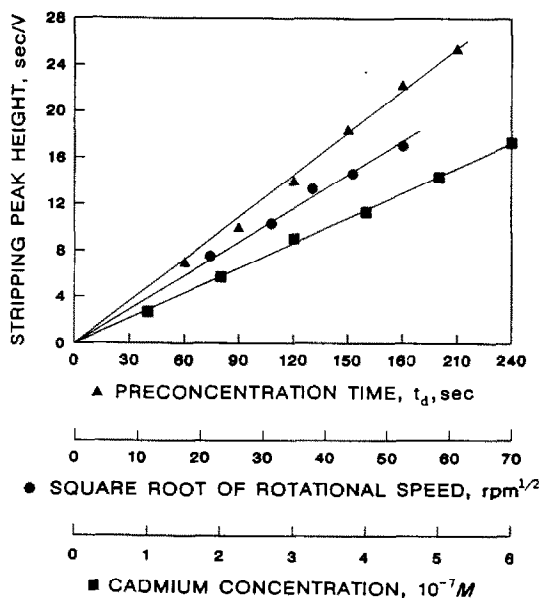


Fig. 3. Dependences of  $(dt/dE)_p$  on  $\omega^{1/2}$ ,  $t_d$  and  $[\text{Cd}^{2+}]$ . Curves: (●)  $(dt/dE)_p$  vs.  $\omega^{1/2}$ ;  $2 \times 10^{-7}M$  cadmium,  $i_s = 2 \mu\text{A}$ , and  $t_d = 2 \text{ min}$ . (▲)  $(dt/dE)_p$  vs.  $t_d$ ;  $2 \times 10^{-7}M$  cadmium and  $i_s = 2 \mu\text{A}$  (■)  $(dt/dE)_p$  vs.  $[\text{Cd}^{2+}]$ ;  $i_s = 5 \mu\text{A}$  and  $t_d = 2 \text{ min}$ .

time ( $t_d$ ), electrode rotational speed during preconcentration ( $\omega$ ), bulk concentration of cadmium ( $C^0$ ), and stripping current ( $i_s$ ) were studied independently one by one, while keeping the others constant. The  $(dt/dE)_p$  values are plotted vs.  $t_d$ ,  $\omega^{1/2}$  and  $C^0$  in Fig. 3. The linear relations in these results are consistent with the predictions from equation (7). According to equation (7),  $(dt/dE)_p i_s$  should be a constant which is independent of  $i_s$ . However, the plot of  $(dt/dE)_p i_s$  against  $i_s$ , as shown in Fig. 4, indicates that  $(dt/dE)_p i_s$  increases with  $i_s$ , but less so at larger  $i_s$  values. This may be caused by chemical stripping of the analyte, which is more effective when smaller  $i_s$  is used. The correctness of equation (7) can also be justified by

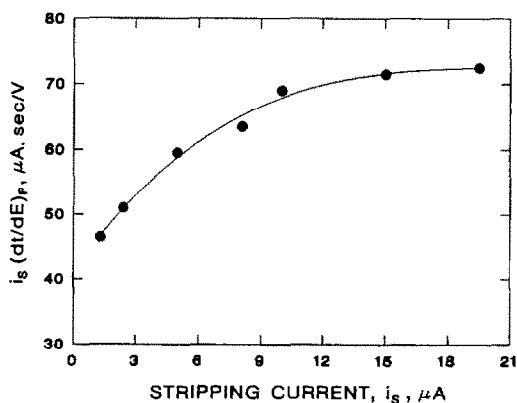


Fig. 4. Plot of  $(dt/dE)_p i_s$  vs.  $i_s$ ;  $4 \times 10^{-7}M$  cadmium and  $t_d = 2 \text{ min}$ .

comparing the slopes in Fig. 3. Rearranging equation (7) yields

$$\begin{aligned} \frac{\left(\frac{dt}{dE}\right)_p i_s}{\omega^{1/2} t_d C} &= \left[ \frac{\Delta\left(\frac{dt}{dE}\right)_p}{\Delta(\omega^{1/2})} \right] \frac{i_s}{t_d C} \\ &= \left[ \frac{\Delta\left(\frac{dt}{dE}\right)_p}{\Delta t_d} \right] \frac{i_s}{\omega^{1/2} C} \\ &= \left[ \frac{\Delta\left(\frac{dt}{dE}\right)_p}{\Delta C} \right] \frac{i_s}{\omega^{1/2} t_d} \\ &= 7.89 \times 10^5 n^2 AD^{2/3} \mu^{-1/6} \\ &= \text{constant} \end{aligned} \quad (20)$$

in which the three items in square brackets represent the slopes of the straight lines in Fig. 3. The values of the slopes are  $0.12 \text{ V}^{-1}$ ,  $0.317 \text{ sec} \cdot \text{V}^{-1} \cdot \text{rpm}^{-1/2}$ , and  $2.8 \times 10^7 \text{ sec} \cdot \text{V}^{-1} \cdot \text{l. mole}^{-1}$ , respectively. The constants as defined in equation (20) were calculated by applying these three slope values and other parameters. The results are  $2.68 \times 10^4$ ,  $2.64 \times 10^4$ , and  $2.80 \times 10^4 \mu\text{A} \cdot \text{V}^{-1} \cdot \text{rpm}^{-1/2} \cdot \text{l. mole}^{-1}$  respectively. The first two values are very close to each other, just as predicted. However, the third value is slightly larger than the others, probably because a larger value of  $i_s$  is used for  $C^0$  studies.

#### Validation of the stripping equation

A simulation method was used to validate equation (11) as follows. The  $E_p$  and  $(dt/dE)_p$  values obtained from the stripping curves were first substituted into equation (12) to calculate the corresponding theoretical values of  $E'$ . Then the  $E'$  and  $(dt/dE)_p$  values were substituted into equation (11) to calculate the  $(dt/dE)_p$  and  $E$  values for the theoretical curve, which was compared with the experimental one. One of the results is depicted in Fig. 5. The theoretical values are in good coincidence with the experimental ones in the peak region, but slightly different at the bottom of the peak owing to the capacitance effect when the electrode potential changes rapidly, which is not taken into account in the theoretical treatment.

#### Comparison of RD-CCSA and normal CPSA signals

The theoretical value of the signal ratio for RD-CCSA and normal CPSA, *i.e.*,  $(dt/dE)_p/\tau$ , is  $13.35n$  according to equation (5). The experimental  $(dt/dE)_p/\tau$  values for  $\text{Cd}^{2+}$ ,  $\text{Pb}^{2+}$ ,  $\text{Tl}^+$ , and  $\text{In}^{3+}$  are listed in Table 1 and compared with the theoretical ones. Apparently, the  $(dt/dE)_p/\tau$  values for  $\text{Cd}^{2+}$ ,  $\text{Pb}^{2+}$ , and  $\text{Tl}^+$  are very close to those predicted from the theory, but a noticeable difference is observed for

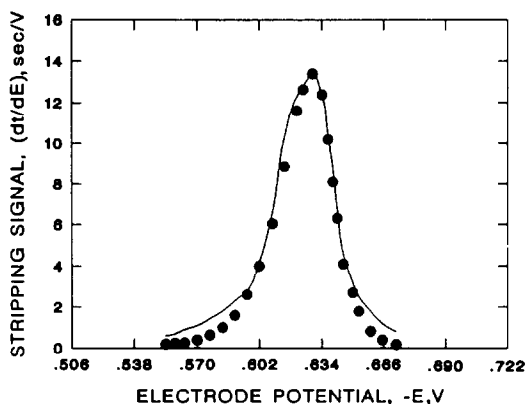


Fig. 5. Reciprocal derivative constant-current stripping signal of cadmium. Solid line: experimental result; dots indicate the theoretical responses;  $5 \times 10^{-7} M$  cadmium,  $t_d = 1.5 \text{ min}$  and  $i_s = 5 \mu\text{A}$ .

$\text{In}^{3+}$ . This may be caused by the lower reversibility of the  $\text{In}^{3+}/\text{In}$  couple.

#### Validation of the $E_M$ equation

The specific potential for metal M,  $E_M$ , defined in equation (13), is predicted by equation (14) to be a constant which is independent of stripping peak height, *i.e.*, the concentration of the metal ion and other experimental variables. The  $E_M$  values for  $\text{Cd}^{2+}$ ,  $\text{In}^{3+}$ ,  $\text{Tl}^+$ , and  $\text{Pb}^{2+}$  at four different  $(dt/dE)_p$  values obtained by changing  $t_d$  were calculated by substituting the experimental  $E_p$  and  $(dt/dE)_p$  data into equation (13). The results are listed in Table 2, and are in good agreement with the theory. For instance, when the  $(dt/dE)_p$  values for  $\text{In}^{3+}$  change from 6.2 to 46.8 sec/V, the calculated  $E_M$  values remain constant (0.528 V) within 0.4%. For other elements, the maximum relative deviation is also smaller than 1%.

#### Half-height peak-width and resolution

The theoretical  $W_{1/2}$  values for  $\text{Cd}^{2+}$ ,  $\text{In}^{3+}$ ,  $\text{Tl}^+$ , and  $\text{Pb}^{2+}$  are close to their experimental ones as shown in Table 3, indicating the correctness of equation (19).

The RD-CCSA signal for a mixed solution containing  $10^{-7} M$  levels of  $\text{Cd}^{2+}$ ,  $\text{In}^{3+}$ , and  $\text{Tl}^+$  is shown in Fig. 6. The peaks for these ions are well separated from each other, and therefore

Table 1. Comparison between RD-CCSA signal,  $(dt/dE)_p$ , and CPSA signal,  $\tau$

Element	$\tau$ , sec	$(dt/dE)_p$ , sec/V	$(dt/dE)_p/\tau$ ,	
			Experimental	Theoretical
$\text{Cd}^{2+}$	0.9	23.4	26.0	26.7
$\text{Pb}^{2+}$	1.0	25.9	25.9	26.7
$\text{In}^{3+}$	0.8	27.9	34.9	40.1
$\text{Tl}^+$	0.7	8.8	11.5	13.4

Table 2.  $E_M$  values at different peak heights  $(dt/dE)_p$

	$Cd^{2+}$			$In^{3+}$			$Tl^+$			$Pb^{2+}$						
	$-E_p, V$	0.605	0.608	0.612	0.615	0.535	0.540	0.542	0.546	0.486	0.496	0.502	0.508	0.336	0.342	0.345
$(dt/dE)_p, sec/V$	9.2	14.4	23.6	31.6	6.2	15.2	27.9	46.8	8.8	16.4	23.9	38.3	7.7	16.8	25.9	35.6
$-E_M^*, V$	0.591	0.591	0.592	0.593	0.527	0.528	0.528	0.529	0.458	0.460	0.461	0.461	0.323	0.324	0.324	0.326
$-E_M, V$			0.592			0.528				0.460				0.324		
Relative maximum deviation, %			+0.5			+0.4				+0.9				+0.9		

\*Calculated according to equation (13).

Table 3.  $W_{p/2}$  values (mV)

	$Cd^{2+}$	$In^{3+}$	$Tl^+$	$Pb^{2+}$
Experimental value	32.0	24.9	68.9	33.4
Theoretical value*	32.8	21.8	65.5	32.8
Relative error, %	+3	-12	-5	-2

\*Calculated according to equation (19).

simultaneous determination of these metal ions with RD-CCSA becomes possible, whereas it is impossible for normal CPSA. Considering that the  $E_p$  differences for the Cd-In and In-Tl couples are 58 and 50 mV, respectively, the increase of resolution for CPSA by the reciprocal differentiation technique is significant.

Detection limit

The RD-CCSA signal for  $6 \times 10^{-10}M$  cadmium was obtained under the following optimal conditions: deaeration for 30 min, deposition for 10 min,  $i_s = 1 \mu A$ . The result is 0.55 sec/V, about 3 times the value for the blank solution, 0.21 sec/V. This limit of detection is comparable to those for voltammetric and potentiometric stripping analysis.

CONCLUSION

Both theory and the experimental results prove that the sensitivity and resolution of CPSA are greatly enhanced by measuring the reciprocal derivative signal. The theories derived to describe the shape and change of the  $(dt/dE)-E$  signals for constant-current stripping analysis are consistent with the experimental results. It is believed that the improvements in signal measurement can broaden the acceptance of constant-current stripping analysis. The instrumentation reported for measuring  $(dt/dE)-E$  is different from, and, in some sense, simpler than that in the literature,<sup>14-21</sup> though the same in principle. However, although the simple analogue instrument works reasonably well, as proved, and is useful under some circumstances, it

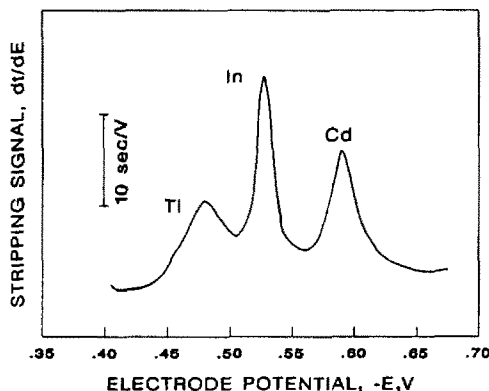


Fig. 6. Reciprocal derivative constant-current stripping signal of cadmium, indium, and thallium mixture solution:  $4 \times 10^{-7}M$  cadmium, indium, and thallium,  $t_d = 1.5$  min and  $i_s = 5 \mu A$ .

by no means represents the future of RD-CCSA. Instead, computerized systems should certainly be the choice.

It should be pointed out that the applications of the reciprocal differentiation technique in measuring chronopotentiometric signals need not be limited to stripping analysis. The technique may be used in any constant-current chronopotentiometric experiments, as it can be more generally called reciprocal derivative chronopotentiometry.

*Acknowledgement*—The authors wish to thank Lianghong Lu and Shanggui Wen for assistance in collecting some of the data, and William R. LaCourse for many suggestions on the manuscript. Special thanks are also due to Dennis C. Johnson for assistance in preparing the manuscript.

#### REFERENCES

1. F. Vydra, K. Štulík and E. Juláková, *Electrochemical Stripping Analysis*, Ellis Horwood, Chichester, 1976.
2. D. G. Davis, in *Electroanalytical Chemistry*, A. J. Bard (ed.), Vol. 1. Dekker, New York, 1967.
3. H. Eskilsson, C. Haraldsson and D. Jagner, *Anal. Chim. Acta*, 1985, **175**, 79.
4. V. J. Jennings and J. E. Morgan, *Analyst*, 1985, **110**, 121.
5. J. Adam, *Talanta*, 1982, **29**, 939.
6. T. V. Nghi and F. Vydra, *J. Electroanal. Chem.*, 1976, **71**, 325.
7. L. Luong and F. Vydra, *Collection Czech. Chem. Commun.*, 1975, **40**, 1490.
8. Z. Galus, W. Kemula and S. Sacha, *J. Polarog. Sci.*, 1968, **14**, 59.
9. S. P. Perone and A. Brumfield, *J. Electroanal. Chem.*, 1967, **13**, 124.
10. M. Paunovic, *ibid.*, 1967, **14**, 447.
11. A. R. Nisbet and A. J. Bard, *ibid.*, 1963, **6**, 332.
12. X. Ruan and D. Zhou, *Xiangtan Daxue Ziran Kexue Xuebao*, 1987, No. 3, 71.
13. D. G. Peters and S. L. Burden, *Anal. Chem.*, 1966, **38**, 530.
14. H. Huiliang, D. Jagner and L. Renman, *Anal. Chim. Acta*, 1987, **202**, 117, 123; 1987, **201**, 1.
15. C. Hua, D. Jagner and L. Renman, *ibid.*, 1987, **197**, 257, 265.
16. L. Renman, D. Jagner and R. Berglund, *ibid.*, 1986, **188**, 137.
17. L. Almestrand, D. Jagner and L. Renman, *ibid.*, 1987, **193**, 71.
18. H. Huiliang, C. Hua, D. Jagner and L. Renman, *ibid.*, 1987, **193**, 61.
19. D. Jagner and K. Årén, *ibid.*, 1982, **141**, 157.
20. D. Jagner, M. Josefson and K. Årén, *ibid.*, 1982, **141**, 147.
21. L. Anderson, D. Jagner and M. Josefson, *Anal. Chem.*, 1982, **54**, 1371.
22. A. Hussam and G. Gunaratna, *ibid.*, 1988, **60**, 503.
23. X. Ruan, *Xiangtan Daxue Ziran Kexue Xuebao*, 1986, No. 4, 71; *Chem. Abstr.*, 1987, **106**, 168057.
24. A. J. Bard and L. R. Faulkner, *Electrochemical Methods*, (a) p. 195; (b) p. 219. Wiley, New York, 1980.
25. J. Mo, P. Cai, W. Huang and F. Yun, *Huaxue Xuebao*, 1984, **42**, 556; *Chem. Abstr.*, 1984, **101**, 162712.



## UNITE D'ACQUISITION ECONOMIQUE POUR LE TRAITEMENT ELABORE DE DONNEES SPECTRO-CINETIQUES ISSUES D'UN SPECTROPHOTOMETRE UV-VISIBLE

J. J. MEYER, J. L. PAUMARD, D. MILIN, P. LEVOIR et J. C. FONTAINE  
ITODYS, Université Paris VII, Paris, France

(Reçu le 30 juin 1988. Accepté le 11 juillet 1988)

**Résumé**—Nous avons étudié et construit une unité d'acquisition numérique économique, destinée à un spectrophotomètre UV-visible CARY-210. Le flux de données est contrôlé par un microprocesseur 6809 qui commande quatre adaptateurs d'interface parallèle. Deux liaisons "série" au standard RS232-C permettent de communiquer avec un terminal et une mémoire de masse. Les données acquises sont traitées par un ordinateur personnel. Le logiciel comprend plusieurs modules, développés dans notre laboratoire, qui utilisent des algorithmes de traitement de signal très efficaces et particulièrement utiles en cinétique chimique.

**Summary**—A low-cost digital acquisition unit for a CARY-210 spectrophotometer has been designed and constructed. The data-flow is controlled by a 6809 microprocessor driving four parallel interface adapters. Two RS232-C serial links are provided for communication with a terminal and a mass storage unit. The acquired data are processed by a personal computer. Included are several software modules, based on powerful signal-processing algorithms, which are highly useful in kinetic studies.

Ces dernières années ont vu l'apparition d'une nouvelle génération de spectrophotomètres UV-visible entièrement numérisés et informatisés permettant la mise en oeuvre de différentes méthodes de traitement de signaux. Cependant, ces appareils très complexes constituent souvent des systèmes fermés et figés au niveau informatique et nécessitent toujours un investissement important. Or, de nombreux laboratoires de recherche sont équipés de spectromètres de grande qualité optique, fiables et d'emploi facile qu'il serait intéressant de munir d'une interface autorisant le transfert des données vers un micro-ordinateur en vue de leur traitement ultérieur.

Cet article décrit la réalisation d'une telle interface, originale et économique, destinée à un spectromètre UV-visible CARY-210<sup>1</sup> (Fig. 1). Le système d'acquisition numérique associé à un terminal (clavier-écran) assure l'acquisition des données et contrôle leur enregistrement sur une unité tampon à cartouches magnétiques. La lecture par un micro-ordinateur des données ainsi enregistrées s'effectue par l'intermédiaire d'une liaison "série" au standard RS232C. Cette façon de procéder permet de ne pas mobiliser l'ordinateur pendant la période d'acquisition. Un programme interactif de traitement et de visualisation des données spectroscopiques a été écrit en Turbo-Pascal. Ce logiciel, outre les modules classiques de traitement numérique, intègre des modules originaux, en particulier celui d'analyse des signaux multi-exponentiels par la méthode de Padé-Laplace.<sup>2,3</sup>

### Unité d'acquisition (Fig. 2)

Le modèle de base du CARY-210<sup>1</sup> est équipé d'un affichage numérique à 5 chiffres, avec virgule, de la densité optique. Cette information est disponible sur le connecteur J13 sous forme de dix neuf lignes (Dxx) pour la densité optique et de cinq lignes pour la position de la virgule (DP). L'indication de densité optique (DO) négative est fournie par la ligne MINS.

Notre appareil est de plus équipé des accessoires suivants:

—le module 954100 "Wavelength Programmer" qui fournit l'information longueur d'onde sur cinq chiffres; les vingt lignes (Wxx) y afférentes se trouvent sur les connecteurs J202 et J203 (résolution de 0,1 nm);

—le module 954300 "Temperature Readout" qui affiche la température sur quatre chiffres; le connecteur J502 fournit les seize lignes (Txx) correspondantes (résolution de 0,01 degré);

—le module 954000 "Timer" permettant à l'utilisateur de programmer différentes séquences d'opérations; toutes ces informations sont codées en BCD, à l'exception de la position de la virgule. Les données sont échantillonnées à la fréquence de 12,5 Hz par le signal SYNC disponible sur le connecteur J13. Toute la logique interne est réalisée en technologie CMOS (0–12 V).

La réalisation en TTL de l'unité d'acquisition nous a conduits à utiliser des convertisseurs de niveau

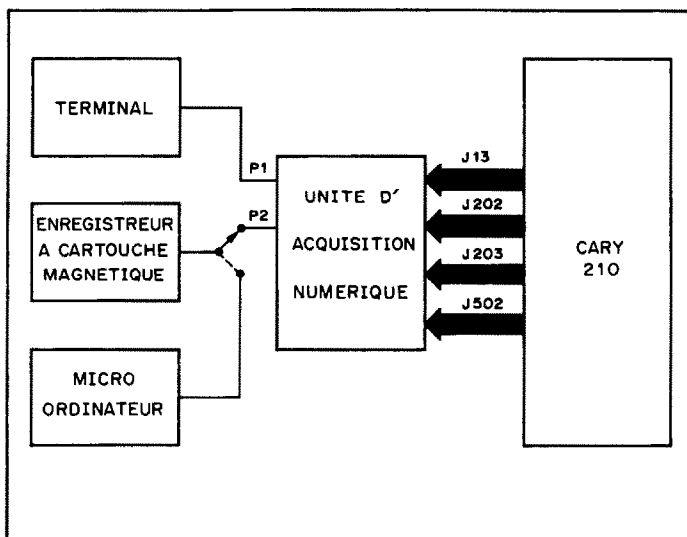


Fig. 1. Schéma fonctionnel.

MC14049 et MC14050. Les soixante deux lignes de données sont ensuite connectées aux ports d'entrée des quatre adaptateurs d'interface parallèle (PIA MC6821). Le front de descente du signal SYNC (CA2) positionne le sixième bit du registre de commande CRA de PIA1 et indique que les données densité optique, longueur d'onde et température sont valides et disponibles sur les ports d'entrée.

Un microprocesseur MC6809 constitue le coeur du système. Le programme, implanté dans une mémoire morte de 8 Koctets (ROM 2764), contrôle le flux des données en provenance des PIA. Ces données sont stockées lors de l'acquisition dans deux mémoires vives de 8 Koctets (RAM TC5565). La charge importante du bus de données a nécessité l'implantation d'un transmetteur bidirectionnel de bus 74LS245 activé par la ligne PIASEL; de même un circuit 74LS241 amplifie les lignes A0, A1, E et R/W. Un double émetteur-récepteur asynchrone universel (DUART SC2681) assure les communications "série" vers le terminal (P1) et vers l'enregistreur magnétique (P2) par l'intermédiaire d'un convertisseur de niveau au standard RS232C (MAX 232). Le clavier du terminal est branché en mode interruptible (IRQ).

#### Logiciel d'acquisition

Un logiciel de 8 Koctets écrit en langage d'assemblage symbolique 6809 permet:

- d'initialiser et de tester le système à sa mise sous tension;
- de gérer les périphériques;
- de saisir et de valider les différentes commandes et d'exécuter les modules associés décrits ci-après.

**Module CINE.** L'acquisition des données cinétiques  $DO = f(t)$  à longueur d'onde  $\lambda$  fixée est réalisée à l'aide d'un algorithme original. Son principe con-

siste à acquérir les 1024 premières données avec le pas initial d'échantillonnage de 80 msec (signal SYNC), puis de conserver une donnée sur deux et d'acquérir les 512 valeurs suivantes avec un pas double. Ce processus est répété jusqu'à une valeur maximale du pas ( $2^{16}$  fois 80 msec) ou jusqu'à une interruption de l'opérateur (fin de la cinétique). Cette méthode présente l'avantage de ne pas nécessiter la connaissance préalable de la durée de la cinétique.

**Module SPEC.** Ce module gère l'acquisition automatique d'une série de spectres  $DO = F(\lambda)$  dans le même domaine de longueur d'onde, avec un intervalle de temps prédéterminé entre les balayages. L'opérateur doit tout d'abord fournir un certain nombre d'informations: données générales (date, nom du composé, ...), paramètres expérimentaux (domaine spectral, nombre de spectres, vitesse de balayage, ...). Des tests de validité sont effectués sur certaines informations. Le pas est ensuite calculé en fonction du domaine spectral choisi, du pas minimal et du nombre de points maximal autorisé. L'acquisition est alors déclenchée par l'opérateur. Tout spectre acquis est enregistré entre chaque balayage.

Des modules supplémentaires permettent à l'utilisateur de réaliser des opérations telles que l'enregistrement des données (ENRE), l'affichage des valeurs acquises (AFFI) et la visualisation des différentes commandes (MENU).

#### Logiciel de traitement

Le développement de cette unité d'acquisition numérique performante nous a permis d'entreprendre l'étude de systèmes chimiques complexes. En particulier, nous nous sommes intéressés à la réaction de transimination des bases de Schiff;<sup>4</sup> réaction qui présente deux phénomènes cinétiques remarquables.<sup>5</sup> Ainsi, avec une amine bi-fonctionnelle observe-t-on

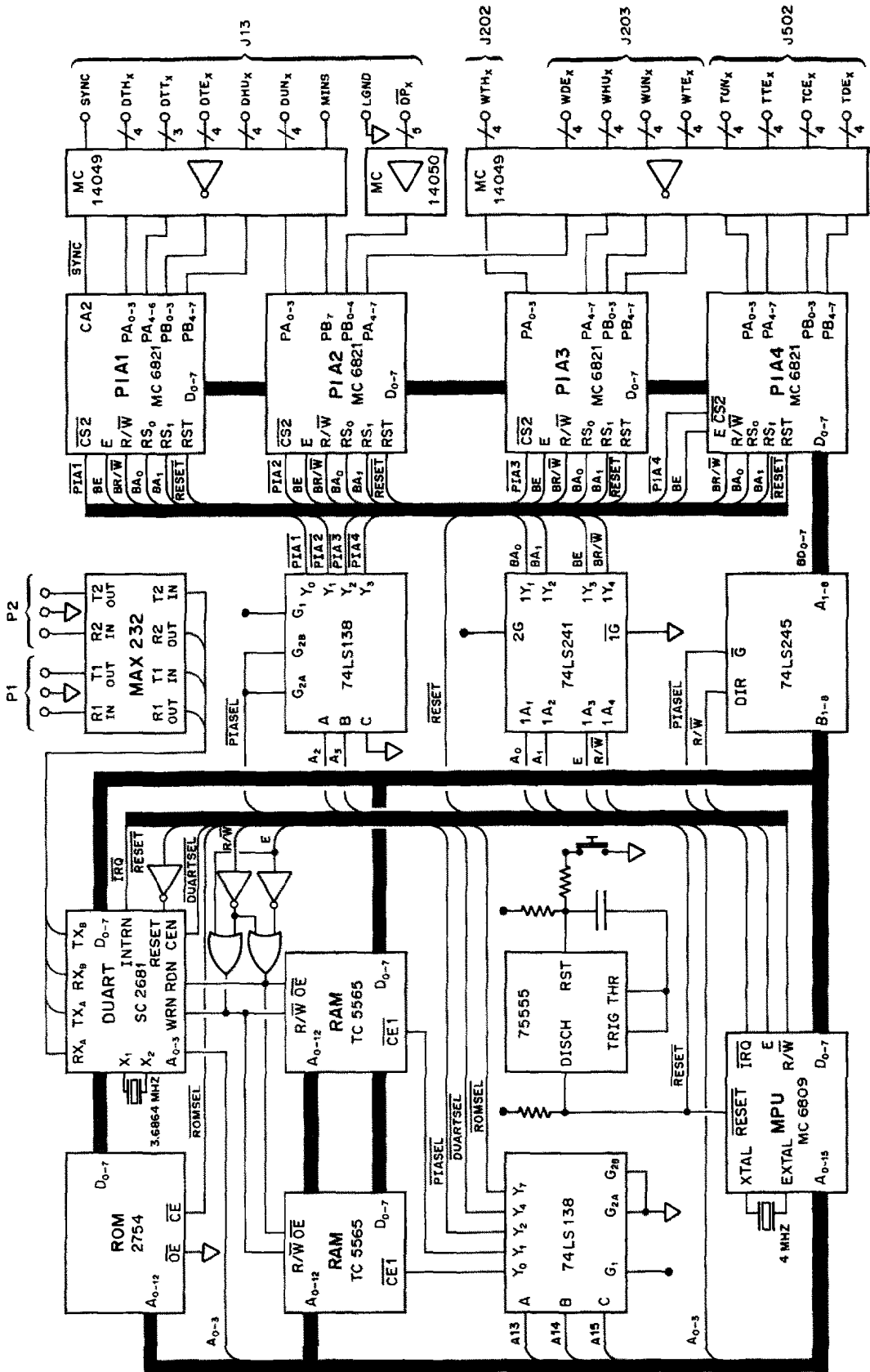


Fig. 2. Unité d'acquisition (le symbole  $\nabla$  représente l'alimentation +5V).

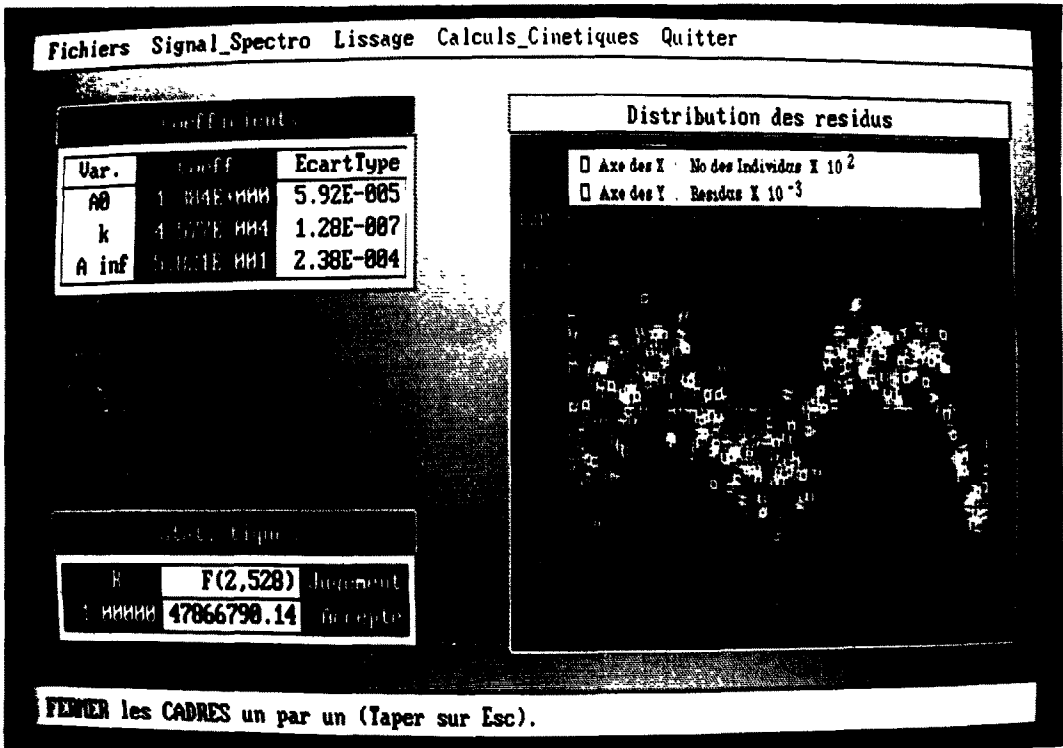


Fig. 3. Analyse statistique d'un signal mono-exponentiel par la méthode dite "du plan de phase".  
Distribution des écarts entre données calculées et données expérimentales.

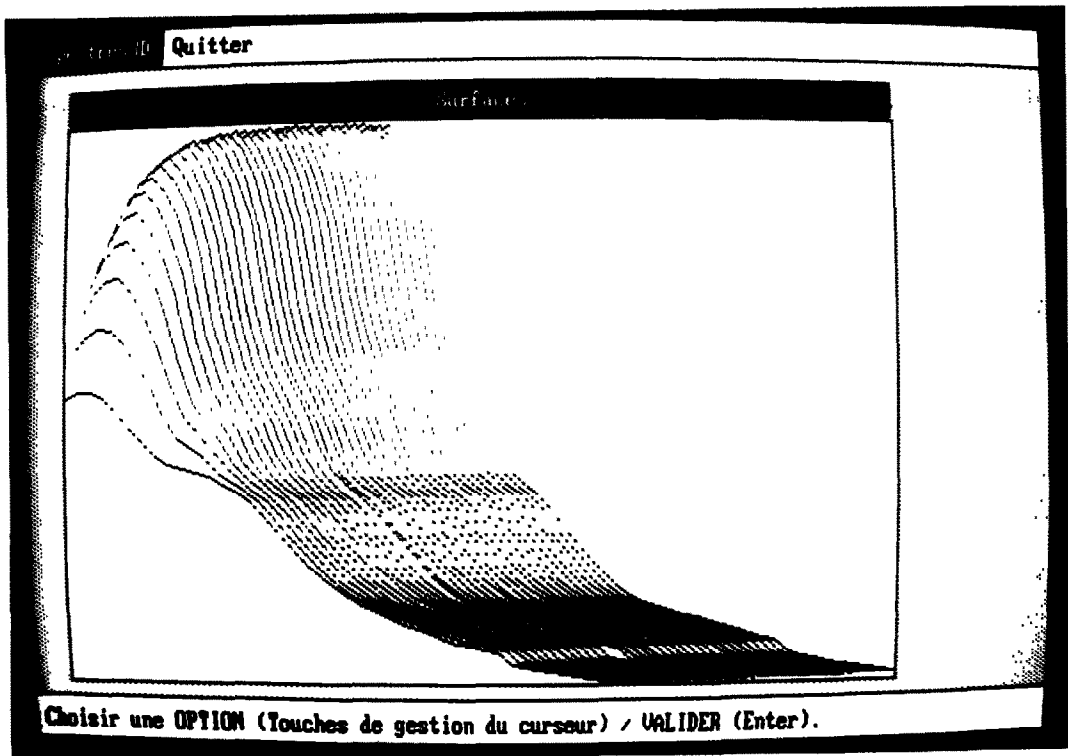


Fig. 4. Visualisation tri-dimensionnelle des spectres évolutifs de formation de l'arylidènepropylamine.

un signal cinétique mono-exponentiel correspondant à une cinétique classique du premier ordre, alors que dans le cas d'une amine mono-fonctionnelle le signal cinétique est plus complexe et correspond à la somme de deux exponentielles couplées. L'étude de tels systèmes chimiques nous a donc amenés à concevoir un logiciel de traitement numérique du signal souple et convivial. Des techniques de multi-fenêtrage et l'emploi généralisé de menus déroulants et de boîtes de dialogue apportent à ce logiciel une grande facilité d'emploi, même et surtout pour des utilisateurs non avertis (Fig. 3).

La partie analyse du logiciel est dotée de diverses méthodes de lissage dont le lissage binomial;<sup>6</sup> d'autre part, l'utilisateur a la possibilité de tronquer le signal à sa convenance et dispose d'une vaste panoplie de méthodes permettant d'extraire les composantes de signaux mono- ou multi-exponentiels. La visualisation en trois dimensions des spectres d'absorption fournit une aide à l'interprétation des signaux spectroscopiques (Fig. 4). L'analyse des signaux mono-exponentiels peut s'effectuer soit par la méthode classique de Guggenheim, soit par celle plus puissante dite "du plan de phase",<sup>7</sup> qui permet d'atténuer le bruit par intégration directe du signal. D'autre part, pour des signaux multi-exponentiels, la détermination des paramètres peut s'effectuer au moyen de deux méthodes:

—une méthode classique des moindres carrés non linéaires;

—une méthode dite "de Padé-Laplace"<sup>2,3</sup> qui permet, outre le calcul des paramètres des exponentielles, la détermination sans a priori du nombre des composantes du signal.

Ces techniques servent également à traiter des problèmes de recombinaison de bandes, dans le cas de spectres d'absorption, en partant d'un modèle basé sur une somme de lorentziennes ou de gaussiennes. Enfin, nous avons développé un module de visualisation en trois dimensions de spectres d'absorption

provenant de l'évolution dans le temps du système réactionnel. Ce module permet aussi de reconstituer le spectre au temps zéro par extrapolation des absorbances.

#### CONCLUSION

Grâce à la liaison "série" standard, la configuration décrite dans cet article est facilement modifiable. Par exemple, l'ensemble clavier-écran ainsi que l'enregistreur à cartouches magnétiques peuvent être remplacés par un micro-ordinateur dédié muni d'une mémoire de masse (disquette, disque dur, ...).

Au niveau du logiciel, d'autres modules sont actuellement en développement au laboratoire; entre autre, un module d'acquisition de la densité optique en fonction de la température permettra de déterminer les grandeurs thermodynamiques des équilibres chimiques. Les auteurs sont à la disposition de toute personne qui souhaiterait des détails complémentaires concernant le matériel et le logiciel.

*Remerciements*—Les auteurs remercient particulièrement Monsieur R. S. Razafindralambo pour sa contribution aux études cinétiques.

#### LITTÉRATURE

1. Varian Instrument Division, Model 210/219 spectrophotometer: Schematics, assembly drawings and parts lists.
2. E. Yeramian and P. Claverie, *Nature*, 1987, **326**, 169.
3. J. Aubard, P. Levoir and A. Denis, *Comput. Chem.*, 1987, **3**, 163.
4. J. L. Hogg, D. A. Jencks and W. P. Jencks, *J. Am. Chem. Soc.*, 1977, **99**, 4772.
5. R. S. Razafindralambo, D.E.A. de Chimie Organique, Université Paris VII, Paris, 1985.
6. P. Marchand and L. Marmet, *Rev. Sci. Instrum.*, 1983, **54**, 1034.
7. J. R. Bacon and J. N. Demas, *Anal. Chem.*, 1983, **55**, 653.

## DEGRADATION OXYDATIVE DES SULFAMIDES A USAGE THERAPEUTIQUE

### ISOLEMENT STRUCTURE ET METHODES D'ANALYSE DES PRODUITS FORMES

A. DE SOUZA, D. BAYLOCOQ et F. PELLERIN

Laboratoire de Chimie Analytique—Centre d'Etudes Pharmaceutiques de l'Université de Paris XI, 1, Rue  
J.B. Clément, F.92296—Chatenay-malabry, France

(Reçu le 26 janvier 1988. Accepté le 10 juillet 1988)

**Résumé**—L'oxydation douce de sulfamides antibactériens est menée à la température ambiante et à la lumière du jour, au moyen de peroxyde d'hydrogène en milieu acide. Les produits d'oxydation formés sont isolés par chromatographie classique sur colonne et après purification leur pureté est déterminée par chromatographie liquide. Ces produits sont identifiés à l'aide de méthodes spectrales d'analyse, plus particulièrement par spectrophotométrie infra-rouge et par spectrométrie de masse. Un produit d'oxydation, jusqu'à présent non isolé et rapporté, a été isolé et identifié. La cinétique de formation est établie, et un mécanisme d'oxydation est proposé.

**Summary**—The mild oxidation of bactericidal sulphonamides by hydrogen peroxide in acidic medium at room temperature in daylight, is reported. The oxidation products have been isolated by classical chromatography and purified, and their purity has been determined by HPLC. They have been identified by spectroscopy, chiefly by infrared and mass spectroscopy. An oxidation product not previously reported has been isolated and identified. An oxidation mechanism and the kinetics are discussed.

Depuis la découverte de l'action antibactérienne des sulfamides<sup>1-3</sup> et des études de Fourneau *et al.*<sup>4</sup> sur l'activité d'une série de dérivés sulfamidés, une gamme de sulfamides à activité diverse a été synthétisée et mise sur le marché.

La littérature apporte des études diversifiées, soit sur le mécanisme d'action antibactérienne des sulfamides,<sup>5-8</sup> soit sur les méthodes d'analyse.<sup>9-14</sup>

Pour étudier la conservation et la stabilité des solutés injectables et des suspensions de sulfamides, des méthodes d'analyse ont été mises au point dans le but de mettre en évidence les éventuels produits de dégradation. Les résultats obtenus ne sont pas toujours concluants. Dans certains cas, ils restent au stade d'hypothèse, dans d'autres, des produits de dégradation sont décelés.<sup>15,16</sup>

Dans cette étude, les auteurs suivent la cinétique d'oxydation de trois sulfamides par chromatographie liquide haute performance, isolent les produits d'oxydation par chromatographie sur colonne et les identifient par des méthodes spectrales d'analyse; un mécanisme d'oxydation à l'aide d'inhibiteurs de radicaux est ensuite proposé.

Une application particulière envisagée concerne le comportement des préparations pharmaceutiques à base de sulfamides et leur stabilité dans les climats tropicaux. Pour simuler ces conditions et isoler la nature des produits formés, une oxydation douce est envisagée selon une technique bien définie.

#### PARTIE EXPERIMENTALE

Trois sulfamides sont étudiés: le sulfanilamide, le sulfametoxazole et le sulfadoxine (tableau 1).

##### *Préparation: isolement des produits de dégradation des sulfamides*

Une solution de sulfamides de 0,2 à 0,5%, selon la solubilité, est préparée dans l'acide sulfurique 0,5M. Après addition de peroxyde d'hydrogène (0,176M) les échantillons sont homogénéisés et abandonnés à la température ambiante, à la lumière du jour. Après cinq jours de contact, les produits d'oxydation formés sont isolés par chromatographie sur colonne de gel de silice 15 à 40  $\mu\text{m}$ , à l'aide du mélange méthanol/2-propanol/toluène/ammoniaque concentré (12:3:3:4).

##### *Identification des produits formes*

Les produits bruts sont recristallisés puis identifiés par des méthodes spectrales d'analyse.

*Spectrophotométrie infra-rouge.* Perkin-Elmer modèle 297, et pastillage avec du bromure de potassium.

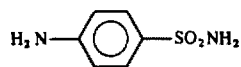
*Spectrométrie de masse.* Spectromètre Nermag 10-10 C à analyseur type quadripolaire; spectrométrie par impact électronique et par ionisation chimique, traitement de données par ordinateur PDP-11.

##### *Etude de la cinétique de dégradation*

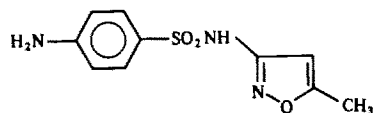
La cinétique de dégradation est étudiée par CLHP dans les conditions suivantes: pompe Chromatem M 380, vanne à boucle Rhéodyne 7125, colonne en acier inox de 200 mm de longueur sur 4 mm de diamètre interne, remplie d'une phase C18 Lichrosorb RP de granulométrie 7  $\mu\text{m}$ , détecteur Shimadzu modèle SPD-2 A à longueur d'onde variable, enregistreur Kipp et Zonen BD-40-04/06. Un étalon interne,

Tableau 1

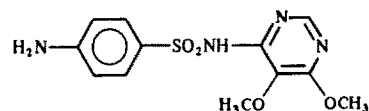
## Sulfanilamide

*p*-Amino benzène sulfonamide

## Sulfaméthoxazole

Amino-4 *N* (méthyl-5-isoxazolyl-3) benzène sulfonamide

## Sulfadoxine

Amino-4 *N* (diméthoxy-5,6, pyrimidinyl-4) benzène sulfonamide

le nitro-4-benzènesulfonamide synthétisé par les auteurs, est utilisé.

*Proposition du mécanisme d'oxydation*

Un mécanisme d'oxydation est étudié selon une série de réactions chimiques utilisant deux modèles organiques, et l'addition d'un inhibiteur de radicaux.

## RESULTATS

*Identification et structure des produits d'oxydation*

Le sulfanilamide après cinq jours de contact avec le mélange d'oxydation a donné trois dérivés d'oxydation révélés par CLHP. Ces dérivés isolés par chromatographie préparative ont été identifiés par analyse spectrale, en particulier par spectrométrie de masse et par spectrophotométrie infra-rouge.

L'analyse systématique des spectres de masse a mis en évidence les pics des fragments les plus importants de l'hydroxylamino-4-benzènesulfonamide, du *N,N'*-dihydroxyhydrazobenzènesulfonamide-4,4' et de l'azoxybenzènesulfonamide-4,4', comme l'indiquent les schémas de fragmentation correspondants (schémas 1, 2 et 3) (tableau 2).

Les spectres infra-rouge confirment la présence des groupements fonctionnels de chaque produit identifié, particulièrement les vibrations de valence à  $3450\text{ cm}^{-1}$  ( $-\text{N}-\text{O}-\text{H}$ ), à  $1340$  et à  $1150\text{ cm}^{-1}$  ( $\text{SO}_2$  sym et asym), à  $1260\text{ cm}^{-1}$  ( $-\text{N}=\text{N}-\text{O}^-$ ).

En ce qui concerne le dérivé *N,N'*-dihydroxyhydrazobenzènesulfonamide-4,4', l'analyse par ionisation chimique avec l'ammoniaque a donné des fragments permettant d'analyser plus précisément l'ion moléculaire et la fragmentation formée. La présence d'un fragment de masse 356 est due à la perte d'une molécule d'eau à partir de l'ion moléculaire, ce qui a été confirmé par l'analyse thermogravimétrique.

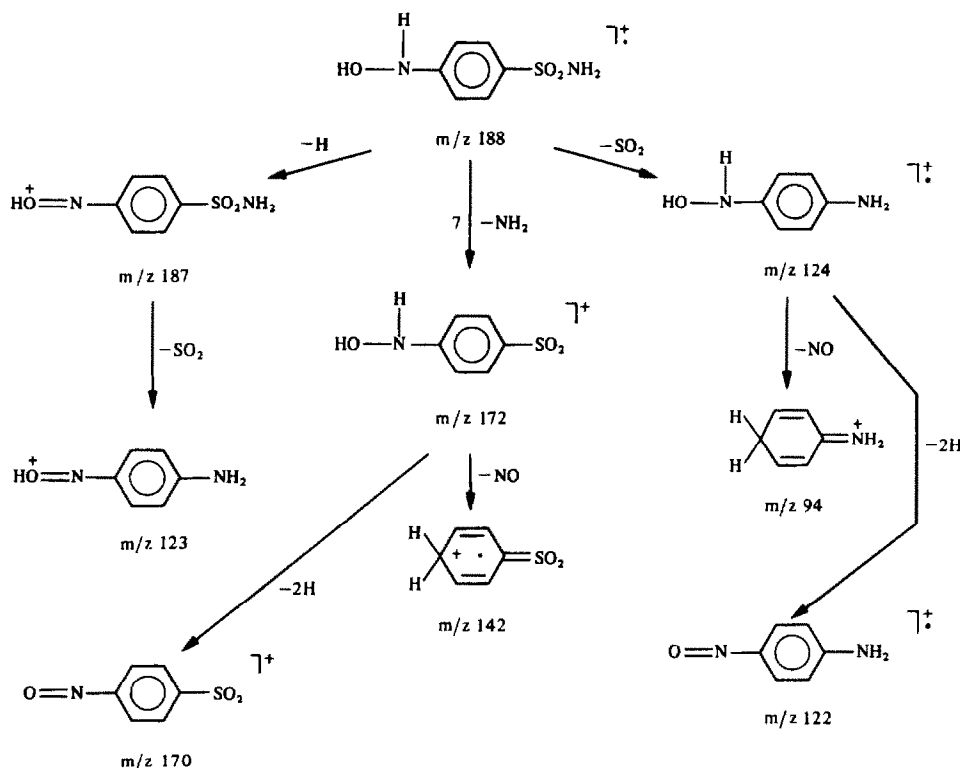
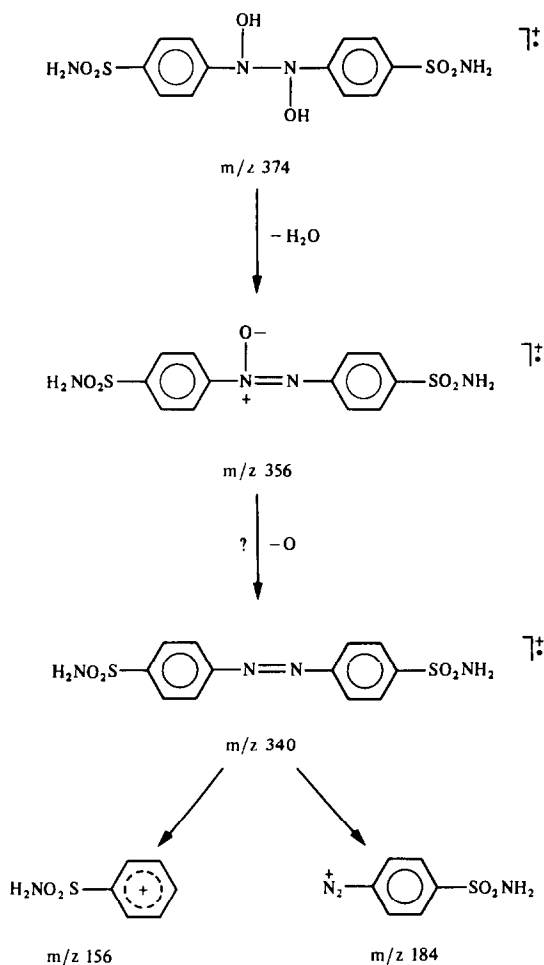


Schéma 1



Il s'agit d'un produit, jusqu'à présent non isolé et rapporté, comme un produit intermédiaire de l'oxydation des sulfamides en milieu alcalin.<sup>17</sup>

Le *sulfamétoazole* soumis au même traitement oxydatif pendant le même temps, a donné trois produits d'oxydation détectés par CLHP. L'analyse spectrale a permis d'identifier l'hydroxylamino-4-benzène-*N*-(méthyl-5-isoxazolyl-3)-sulfonamide, le nitro-4-benzène-*N*-(méthyl-5-isoxazolyl-3)-sulfonamide et l'azoxybenzène-*N*-(méthyl-5-isoxazolyl-3)-disulfonamide-4,4'.

Pour les spectres de masse, les pics qui résultent de la perte de SO<sub>2</sub> à partir de l'ion moléculaire sont toujours présents. Les dérivés azoxy sont fragmentés suivant le modèle bien connu.<sup>18</sup> Pour les dérivés nitro, on observe la perte de NO, caractéristique de l'isomérisation du groupement nitro du groupement nitrile. Dans le cas de l'hydroxylamine dérivée, les pics M<sup>+</sup> - 1 et M<sup>+</sup> - 16 sont aisément identifiés.

Les spectres infra-rouge permettent d'identifier les groupements hydroxylamino, nitro et azoxy particulièrement par les vibrations de valence à 3430 cm<sup>-1</sup>

(-N-O-H), 1300 et 1150 cm<sup>-1</sup> (SO<sub>2</sub> sym et asym) et 1250 cm<sup>-1</sup> (-N=H-O<sup>-</sup>).

Le *sulfadoxine* dans les mêmes conditions d'oxydation a formé deux dérivés d'oxydation indiqués par CLHP et isolés par chromatographie sur colonne. L'analyse spectrale a permis une fois de plus d'identifier l'hydroxylamino-4-benzène-*N*-(diméthoxy-5,6-pyrimidinyl-4)-sulfonamide et le nitro-4-benzène-*N*-(diméthoxy-5,6-pyrimidinyl-4)-sulfonamide.

Les caractéristiques spectrales des dérivés hydroxylamino et nitro sont confirmées par l'analyse des spectres de masse et infra-rouge.

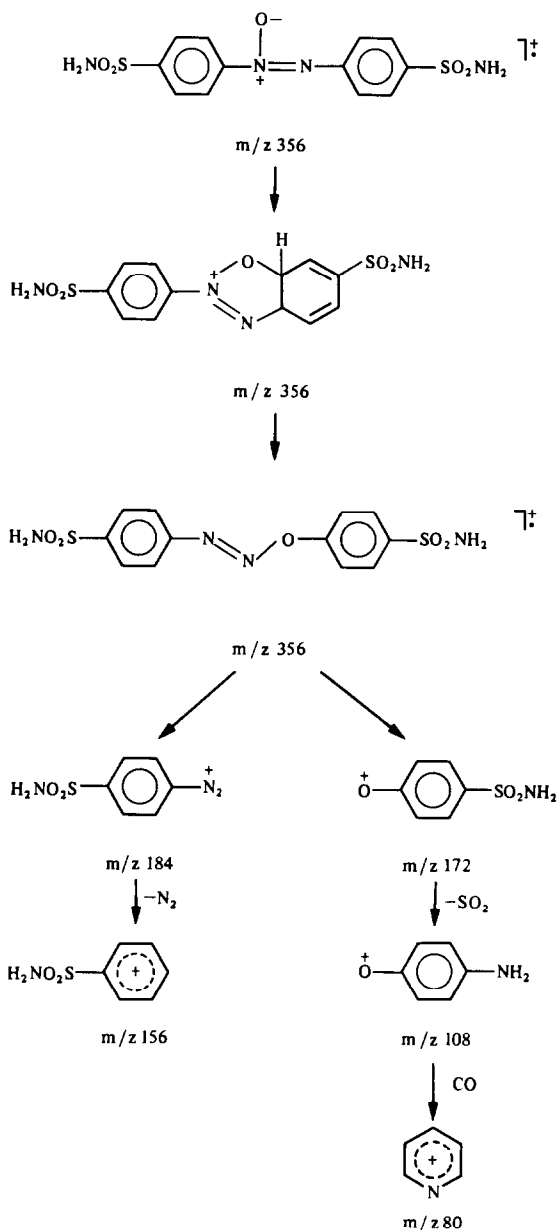


Schéma 3



Tableau 2

Produit de départ	Dérivés formés	Constante de vitesse, $10^{-6}$ hr/l.
<i>Sulfanilamide</i>	Hydroxylamino-4-benzène sulfonamide	1,790
	<i>N,N'</i> -Dihydroxyhydrazobenzène-disulfonamide-4,4'	0,505
	Azobenzènedisulfonamide-4,4'	1,604
<i>Sulfamétoxazole</i>	Hydroxylamino-4-benzène	
	<i>N</i> -(methyl-5-isoxazoly-3)-sulfonamide	1,490
	Nitro-4-benzène- <i>N</i> -(methyl-5-isoxazoly-3)-sulfonamide	1,286
<i>Sulfadoxine</i>	Azoxybenzène- <i>N</i> -(methyl-5-isoxazoly-3)-disulfonamide-4,4'	0,499
	Hydroxylamino-4-benzène- <i>N</i> -(diméthoxy-5,6-pyrimidinyl-4)-sulfonamide	0,724
	Nitro-4-benzène- <i>N</i> -(diméthoxy-5,6-pyrimidinyl-4)-sulfonamide	0,242

### Cinétique d'oxydation

La cinétique a été suivie par CHLP sur des échantillons oxydés dans les mêmes conditions. Pour chaque sulfamide étudié la constante de vitesse d'oxydation et l'ordre de la réaction ont été déterminés. Une séquence de dégradation oxydative a été établie en vue d'étudier le mécanisme.

Les constantes de vitesse sont indiquées dans le tableau 2.

### Mécanisme d'oxydation

A partir de la séquence d'oxydation déterminée par la cinétique, un mécanisme d'oxydation a été étudié en utilisant un thiol—l'acide amino-2-mercapto-3-propanoïque—comme inhibiteur de radicaux pour déceler la formation de l'hydroxylamine. L'inhibition de la réaction est totale en fonction de la quantité d'inhibiteur additionné et du temps ce qui confirme un mécanisme radicalaire pour la première étape de la réaction d'oxydation de sulfamides dans les conditions décrites.

L'étude du mécanisme de formation du dérivé *N,N'*-dihydroxyhydrazobenzènedisulfonamide-4,4' a été faite à partir d'une série de réactions entre le *N,N'*-diméthylamino-4-nitrobenzène et l'hydroxylamino-4-benzène sulfonamide, synthétisé par les auteurs. Ces réactions ont été réalisées en milieu acide avec ou sans peroxyde d'hydrogène et en l'absence de l'acide amino-2-mercapto-3-propanoïque.

Le *N,N'*-diméthylamino-4-nitrobenzène a été choisi en fonction de la stabilité de la forme monomère du groupement nitroso.

Les résultats de ces essais autorisent à conclure à une condensation ionique entre le nitroso-4-benzènesulfonamide et l'hydroxylamino-4-benzène-sulfonamide en milieu acide.

### CONCLUSION

Le comportement des médicaments en présence d'agents oxydants est prescrit dans les réglementations internationales, en vue de préciser leur stabilité et leur conservation; l'intérêt de l'oxydation par le perhydrol réside dans la douceur relative de l'oxydation qui permet de mieux situer les conditions de stabilité et sur le plan expérimental d'arrêter aisément son action et de simplifier les opérations d'extraction des produits formés.

### LITTÉRATURE

1. J. Trefouel, F. Nitti et D. Bouet, *Compt. Rend. Soc. Biol.*, 1935, **120**, 756.
2. G. Domagk, *Dtsch. Med. Wschr.* 1943, **69**, 379.
3. C. Levaditi et A. Vaisman, *Compt. Rend. Soc. Biol.*, 1935, **120**, 1077.
4. E. Fourneau, J. Trefouel, F. Nitti et D. Bouet, *ibid.*, 1936, **122**, 258.
5. R. L. Mayer, *Bull. Acad. Med.* 1937, **117**, 727.
6. E. R. Main, L. E. Shinn et R. R. Mellon, *Proc. Soc. Exp. Biol. Med.* 1938, **39**, 272; 1939, **42**, 115; 1940, **43**, 593.
7. G. V. James, *Biochem. J.*, 1940, **34**, 640.
8. D. D. Woods, *B. J. Exp. Path.*, 1940, **21**, 74.
9. A. C. Bratton et E. K. Marshall, Jr., *J. Biol. Chem.*, 1939, **128**, 537.
10. J. S. Fritz et S. S. Yamamura, *Anal. Chem.*, 1957, **29**, 1079.
11. J. Turczan, *J. Pharm. Sci.*, 1968, **57**, 142.
12. T. C. Kram, *ibid.*, 1972, **61**, 254.
13. B. Blessington, *Org. Mass. Spectrom.*, 1972, **6**, 347.
14. J. Turczan et T. Medwick, *J. Pharm. Sci.*, 1972, **61**, 434.
15. P. A. Clarke, *Pharm. J.*, 1965, **194**, 375.
16. M. Zajac, *Pol. J. Pharmacol. Pharm.*, 1977, **29**, 445, 455, 683, 689.
17. S. Oae, T. Fukumoto et M. Yamagami, *Bull. Chem. Soc. Japan*, 1963, **36**, 728.
18. J. H. Bowie, R. G. Cooks et G. E. Lewis, *Aust. J. Chem.*, 1967, **20**, 1601.

## SPECTROPHOTOMETRIC DETERMINATION OF BISMUTH(III) WITH *o*-HYDROXYHYDROQUINONEPHTHALEIN IN THE PRESENCE OF BRIJ 58

ITSUO MORI\*, YOSHIKAZU FUJITA, KINUKO FUJITA, RIKA FUJITA, YOSHIHIRO NAKAHASHI  
and KEIJI KATO

Osaka University of Pharmaceutical Sciences, Matsubara-shi, Osaka 580, Japan

(Received 29 December 1987. Revised 28 June 1988. Accepted 9 July 1988)

**Summary**—A simple and sensitive spectrophotometric determination of bismuth(III) is based on the reaction between bismuth(III) and *o*-hydroxyhydroquinonephthalein in the presence of Brij 58 in acidic media. The calibration graph is linear over the range 0–3.5 µg/ml bismuth(III) in the final solution, and the apparent molar absorptivity at 520 nm is  $9.03 \times 10^4$  l. mole<sup>-1</sup>. cm<sup>-1</sup>. The proposed method is 2–10 times more sensitive than other methods, and simpler. It has been applied to the assay of bismuth(III) in pharmaceutical preparations, such as dermatol and bismuth subnitrate, with good results.

Bismuth and its pharmaceutical preparations, such as bismuth subnitrate, subcarbonate, subgallate (dermatol), *etc.*, are used as antidiarrhoeics and local astringents. Numerous methods are available for the spectrophotometric determination of bismuth(III), *e.g.*, with dithizone, diethyldithiocarbamate, thiourea, Xylenol Orange, potassium iodide, Methylthymol Blue (MTB), Bromopyrogallol Red, Phenylfluorone and Gallein derivatives.<sup>1–9</sup>

We have already reported that *o*-hydroxyhydroquinonephthalein (Qnph), an analogue of phenylfluorone, is a useful xanthene dye for the spectrophotometric determination of various metal ions, such as tin(IV).<sup>9,10</sup> In addition, the effect of the presence of various surfactants—hexadecylpyridinium chloride (HPC) as a cationic surfactant, poly(oxyethylene)sorbitan monolaurate (Tween 20) as a non-ionic surfactant, sodium laurylsulphate (SLS) as an anionic surfactant, and sodium *N*-lauroylsarcosine (LS) as an amphoteric surfactant, on the assay for various metals, such as aluminium, thorium, copper, palladium and molybdenum, and the effectiveness of these surfactants alone or in combination have already been reported.<sup>11–14</sup> The effect of a cationic surfactant on the colour reaction between various fluorone or Pyrogallol Red derivatives and bismuth has also been investigated.<sup>6–8,13,16</sup> In most cases, since the pH range for maximum colour development between these dyes and bismuth is restricted to around the neutral region, these reactions tend to be affected by foreign-ion interference. Systematic studies of the effect of surfactants on these reaction systems have not hitherto been made.

This paper describes the effect of various surfactants—alone or in combination—on the colour reaction between Qnph and bismuth(III) in weakly acidic media, and gives a simple, rapid and sensitive spectrophotometric method for determination of bismuth by means of the reaction with Qnph in the presence of the non-ionic surfactant, Brij 58 [poly(oxyethylene) cetyl ether], without the need for solvent extraction.

### EXPERIMENTAL

#### Reagents

All reagents were of analytical reagent grade. A standard 0.01M bismuth(III) stock solution was prepared by dissolving 209.0 mg of the 99.999% pure metal in 5 ml of concentrated nitric acid by heating, and diluting accurately to 100 ml with water. A working bismuth solution ( $5.0 \times 10^{-4}$ M) was prepared by dilution of the stock standard solution. A  $1.0 \times 10^{-3}$ M Qnph solution was prepared as previously described.<sup>9,10</sup> Aqueous non-ionic surfactant solutions (1.0%) of Triton X-100 [poly(oxyethylene) iso-octylphenyl ether], Tween 20 [poly(oxyethylene)sorbitan monolaurate], PVP [poly(*N*-vinyl-2-pyrrolidone)], PVA [poly(vinyl alcohol)], Brij 35 [poly(oxyethylene)dodecyl ether], or Brij 58 solutions were prepared by dissolving the commercially available compounds without purification. For the pH adjustments, 1.0% v/v nitric acid was used. Demineralized water was used throughout.

#### Procedure

To a solution containing up to 35 µg of bismuth(III), in a 10-ml standard flask, appropriate amounts (about 0.75 ml) of 1.0% v/v nitric acid (to give a pH of 1.7–2.1), 1.0 ml of 1.0% surfactant solution and 1.0 ml of  $1.0 \times 10^{-3}$ M Qnph were added. The mixture was diluted to volume with water (solution A), and kept at room temperature (15–25°C) for 10 min, together with a reagent blank (solution B). The absorbance of solution A was measured at 520 nm against solution B.

\*To whom correspondence should be addressed.

## RESULTS AND DISCUSSION

*Colour reaction with and without surfactants*

The colour reactions between various xanthene dyes and bismuth(III) in acidic media were systematically investigated in the absence of surfactant. As shown in Table 1, the reaction between Qnph and bismuth(III) gave the largest bathochromic shift, and high and stable absorbance. The effect of surfactants, alone or in combination, on the Qnph/bismuth system was then investigated (Table 2).

The absorption spectra of the Qnph-bismuth complex (solution A) in the presence and absence of Brij 58 or hexadecyltrimethylammonium chloride (HTAC) are shown in Figs. 1 and 2, together with those of the reagent blanks (solution B).

The presence of a cationic surfactant, such as HTAC or zephiramine, gave a large absorbance for the Qnph/bismuth system, but the colour developed was remarkably unstable, and gradually gave way to formation of a precipitate. The combination of cationic and non-ionic surfactants did not give the effect reported for other systems.<sup>17,18</sup> Stabilization of the Qnph-bismuth-cationic surfactant ternary complex by micelle stabilization was unsatisfactory with cationic and non-ionic surfactant combinations. On the other hand, the Qnph-bismuth binary complex in the

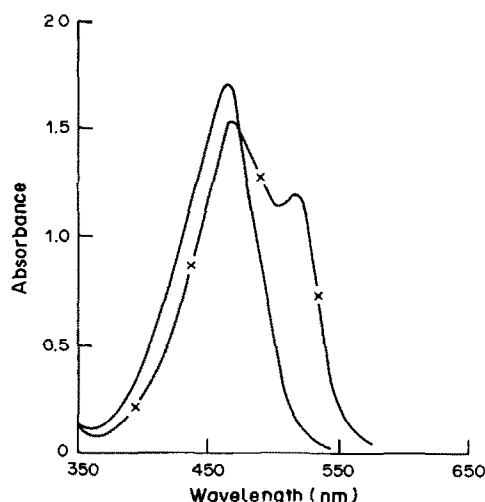


Fig. 1. Absorption spectra of Qnph and Qnph-bismuth(III) solution in the presence of Brij 58 as non-ionic surfactant. Bismuth(III), 26.1  $\mu\text{g}/10\text{ ml}$ ; Qnph,  $5.0 \times 10^{-5}\text{ M}$ ; Brij 58, 0.1%; pH, 1.8; reference, water; —, Qnph; —x—, Qnph-bismuth(III).

presence of a non-ionic surfactant such as Brij 58 was very stable, and its absorbance was relatively high, with good reproducibility.

Table 1. Colour reaction between xanthene dyes and bismuth(III) in the absence of surfactant

Xanthene dyes	$\lambda_{\text{max}}$ nm	Absorbance at $\lambda_{\text{max}}$
<i>o</i> -Hydroxyhydroquinonephthalein (Qnph)	505	0.292
Pyrogallolphthalein (Gall)	570	0.126
Pyrogallol Red (PR)	585	0.069
Bromopyrogallol Red (BPR)	590	0.040
Pyrocatechol Violet (PV)	550	0.200
Xylenol Orange (XO)	540	0.145
Methylthymol Blue (MTB)	525	0.087

Bismuth(III) taken, 20.9  $\mu\text{g}/10\text{ ml}$ ; dyes,  $1.0 \times 10^{-4}\text{ M}$ ; pH 1.8; reference, reagent blank.

Table 2. Effect of surfactants on the colour reaction between Qnph and bismuth(III)

Surfactants			$\lambda_{\text{max}}$ nm	Absorbance at $\lambda_{\text{max}}$
cationic	anionic	non-ionic		
—	—	—	505	0.146
HTAC	—	—	520	0.320*
—	SLS	—	500	0.266
—	—	Brij 35	520	0.445
—	—	Brij 58	520	0.471
—	—	Tween 20	520	0.362
—	—	Triton x 100	515	0.274
—	—	PVP	510	0.267
HTAC	—	Brij 35	520	0.397
—	SLS	Brij 35	520	0.384

Bismuth(III) taken, 10.5  $\mu\text{g}/10\text{ ml}$ ; Qnph,  $1.0 \times 10^{-4}\text{ M}$ ; HTAC,  $1.0 \times 10^{-3}\text{ M}$ ; anionic and non-ionic surfactant, 0.1%; pH, 1.8; reference, reagent blank.

\*Unstable.

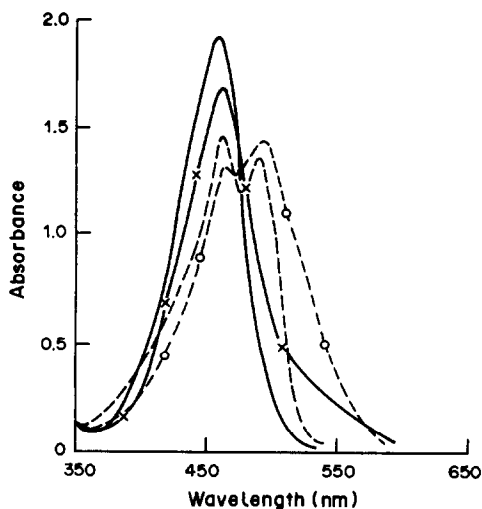


Fig. 2. Absorption spectra of Qnph-bismuth(III) and Qnph in the presence or absence of cationic surfactant. Bismuth(III), 26.1  $\mu\text{g}/10\text{ ml}$ ; Qnph,  $5.0 \times 10^{-5}\text{ M}$ ; HTAC, 0.1%; pH, 1.8; reference, water; —, Qnph; —x—, Qnph-bismuth(III); - - -o- - -, Qnph-HTAC; ---o---, Qnph-HTAC-bismuth(III).

#### Effect of non-ionic surfactant

The addition of a non-ionic surfactant of poly-(oxyethylene) alkyl ether type, such as Brij 35 or 58, especially the latter, was particularly effective, giving good sensitivity and stability. Maximal and practically constant absorbance was obtained in the presence of 0.75–3.0 ml of 1.0% Brij 58 solution in a final volume of 10 ml. Hence, all further work was done with a final concentration of 0.1% Brij 58.

#### Effect of pH

Maximal and constant absorbance was obtained in the pH range from 1.7 to 2.1, with 0.5–1.0 ml of 1.0%

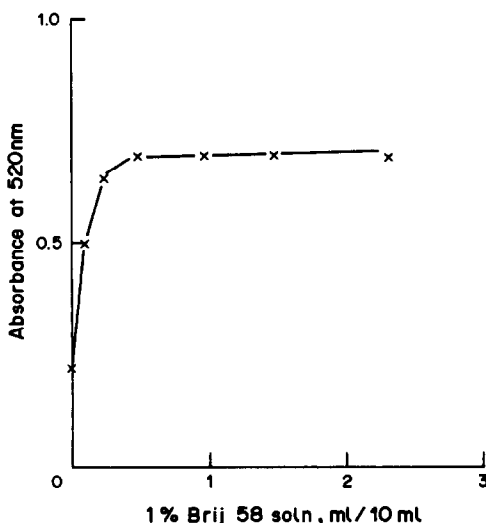


Fig. 3. Effect of Brij 58 concentration. Bismuth(III), 15.7  $\mu\text{g}/10\text{ ml}$ ; Qnph,  $5.0 \times 10^{-5}\text{ M}$ ; pH, 1.8; reference, reagent blank.

v/v nitric acid used for pH adjustments. Further investigations were made at pH 1.8.

#### Effect of Qnph concentration

The absorbances for  $7.5 \times 10^{-6}$  and  $1.0 \times 10^{-5}\text{ M}$  bismuth were practically constant when 0.5–1.0 ml of  $1.0 \times 10^{-3}\text{ M}$  Qnph was present in the final solution, and 1.0 ml was chosen as the optimum reagent volume.

#### Calibration data

Beer's law was obeyed up to 35  $\mu\text{g}$  of bismuth in the final volume of 10 ml. The apparent molar absorptivity was  $9.03 \times 10^4\text{ l.mole}^{-1}\text{.cm}^{-1}$  at 520 nm. The relative standard deviation (5 replicates) was 0.5% for 21  $\mu\text{g}$  of bismuth. The sensitivity was 10 times that of the potassium iodide or diethyl-dithiocarbamate methods and twice that of the MTB methods.<sup>1-5,7,8</sup> The absorbance was unaffected by temperature in the range investigated (15–25°), and stable for a considerable time.

#### Interferences

Iron(III), thorium, tin(IV), zirconium, molybdenum(VI), antimony(III) and other ions giving colour reactions with Qnph in acidic media caused large positive errors even at low concentrations (Table 3).

Aluminium could be tolerated at about 50  $\mu\text{g}/\text{ml}$  in the final solution, copper at about 30  $\mu\text{g}/\text{ml}$  and cobalt at about 150  $\mu\text{g}/\text{ml}$ . The proposed method is somewhat superior to the Phenylfluorone derivative or other methods<sup>1-8</sup> in terms of interferences.

Of the anions tested, only oxalate caused serious interference. The high tolerance for fluoride was useful, since the interference of aluminium or thorium could be eliminated by masking with fluoride. For example, addition of 2.5 ml of 0.02M sodium fluoride eliminated the interference of about 400  $\mu\text{g}$  of aluminium or 200  $\mu\text{g}$  of thorium. Table 4 shows the results for assay of bismuth-aluminium and bismuth-thorium solutions with masking by addition of sodium fluoride.

#### Composition of the complex

The molar ratio of Qnph to bismuth in the presence of Brij 58 was estimated to be 3:1 by the molar-ratio method and Job's method.

#### Application

The proposed method was applied to assay of bismuth pharmaceutical preparations, such as bismuth subnitrate, bismuth subcarbonate or dermatol, as antidiarrhoeic drugs. The results are shown in Table 5 and compared with those obtained by ICP-AES and EDTA titration.

ICP-AES is generally insensitive for the determination of bismuth, but the proposed method is very sensitive and simple and shows satisfactory agreement with certified values.

Table 3. Effect of foreign ions

Foreign ions	Added as	Added		Absorbance at 520 nm
		$\mu\text{g}/10\text{ ml}$	mole ratio to Bi	
—	—	—	—	0.471
Fe(III)	alum	2.8	1	0.654
Th(IV)	nitrate	11.6	1	0.558
Sn(IV)	sulphate	6.0	1	0.558
Sb(III)	sulphate	6.1	1	0.720
Al(III)	sulphate	135	100	0.492
Zr(IV)	chloride	4.6	1	0.634
Cu(II)	nitrate	318	100	0.472
Co(II)	nitrate	1470	500	0.477
$\text{MoO}_4^{2-}$	$\text{Na}_2\text{MoO}_4$	4.3	1	1.034
$\text{I}^-$	KI	634	100	0.470
$\text{F}^-$	NaF	950	1000	0.487
$\text{NO}_2^-$	$\text{NaNO}_2$	2300	1000	0.561
$\text{SO}_3^{2-}$	$\text{Na}_2\text{SO}_3$	2002	500	0.483
L-Ascorbic acid	—	8800	1000	0.470
Tartaric acid	—	8500	1000	0.452
Oxalate	$\text{Na}_2\text{C}_2\text{O}_4$	44.0	10	0.430

Bismuth(III) taken, 10.5  $\mu\text{g}/10\text{ ml}$ ; Qnph,  $1.0 \times 10^{-4}\text{M}$ ; Brij 58, 0.1%; pH, 1.8; reference, reagent blank.

Table 4. Assay of bismuth(III) in a mixed solution of bismuth(III) and aluminium(III) or thorium(IV)

Bi, $\mu\text{g}/10\text{ ml}$	Ion added	Amount, $\mu\text{g}/10\text{ ml}$	Mole ratio Bi:ion added	Absorbance		Bi found, $\mu\text{g}/10\text{ ml}$	
				no masking	masking with NaF	no masking	masking with NaF
10.5	—	—	—	0.471	0.473	10.5	10.5
10.5	Al(III)	404	1:300	0.526	0.473	12.0	10.5
10.5	Al(III)	539	1:400	0.534	0.473	12.5	10.5
10.5	Al(III)	809	1:600	0.670	0.480	14.5	10.9
10.5	Th(IV)	232	1:10	0.674	0.471	14.5	10.4
10.5	Th(IV)	464	1:20	0.705	0.473	15.5	10.5

Qnph,  $1.0 \times 10^{-4}\text{M}$ ; Brij 58, 0.1%; pH, 1.8; reference, reagent blank; NaF,  $1.0 \times 10^{-2}\text{M}$ .

Table 5. Assay of bismuth-containing pharmaceutical preparations, and recovery tests

Samples	Bismuth(III) found, %			Recovery* by proposed method	
	ICP-AES	EDTA titn.	Proposed†	%	R.S.D., %
Bismuth subnitrate	74.9	73.2	73.9	103.8	0.7
Bismuth subcarbonate	77.1	81.4	84.4	98.1	0.4
Dermatol	50.5	48.1	49.8	96.3	0.4
detr.§	48.0	48.2	48.8	99.0	0.4

\*Bismuth(III) taken, 10.5  $\mu\text{g}$ .

†R.S.D. ( $n = 5$ ) 0.4–0.7%.

§detr. = destruction by heating with nitric acid.

## REFERENCES

- H. Onishi, *Photometric Determination of Traces of Metals*, 4th Ed., Part IIA, p. 248. Wiley, New York, 1985.
- Muki Oyohisyoku Bunseki, Vol. 1, p. 343. Kyoritu, Tokyo, 1973.
- D. Kantcheva, P. Nenova and B. Karadakov, *Talanta*, 1972, **19**, 1450.
- T. Enoki, I. Mori and Y. Izumi, *Bunseki Kagaku*, 1969, **18**, 963.
- I. Mori, *Yakugaku Zasshi*, 1966, **96**, 173.
- S. Feng and J. Lu, *Fenxi Shiyanshi*, 1987, **6**, 26; *Anal. Abstr.*, 1987, **49**, 11B187.
- V. P. Antonovich, E. N. Suvorova and E. I. Shelikhina, *Zh. Analit. Khim.*, 1982, **37**, 429; *Anal. Abstr.*, 1982, **43**, 16B79.
- I. Němcová, H. Pešínová and V. Suk, *Microchim. J.*, 1984, **30**, 27.
- Y. Fujita, I. Mori and T. Enoki, *Bunseki Kagaku*, 1975, **24**, 253.
- I. Mori, Y. Fujita and T. Enoki, *ibid.*, 1977, **26**, 480.
- I. Mori, Y. Fujita, K. Sakaguchi and S. Kitano, *ibid.*, 1982, **31**, E239.

12. S. Kitano, I. Mori, Y. Fujita and Y. Kamada, *ibid.*, 1984, **33**, E153.
13. I. Mori, Y. Fujita, H. Kawabe, K. Fujita, Y. Koshiyama, T. Tanaka and N. Kawado, *Anal. Sci.*, 1985, **1**, 429.
14. I. Mori, Y. Fujita, K. Fujita, T. Tanaka, Y. Koshiyama and H. Kawabe, *Chem. Pharm. Bull.* 1986, **34**, 4836.
15. Xu Qiheng and Xu Xiujun, *Huaxue Xueba*, 1982, **40**, 419; *Anal. Abstr.*, 1983, **44**, 2B108.
16. C. Wyganowski, *Chem. Anal. (Warsaw)*, 1982, **40**, 419; *Anal. Abstr.*, 1983, **44**, 2B108.
17. I. Mori, Y. Fujita, K. Fujita, T. Tanaka, Y. Nakahashi and M. Iizuka, *Anal. Lett.*, 1988, **21**, 279.
18. I. Mori, Y. Fujita, K. Fujita, Y. Nakahashi and Y. Kishida, *ibid.*, 1988, **21**, 563.

## MANUAL AND FIA METHODS FOR THE DETERMINATION OF CADMIUM WITH MALACHITE GREEN AND IODIDE

I. LOPEZ GARCIA, P. NAVARRO and M. HERNANDEZ CORDOBA

Department of Analytical Chemistry, Faculty of Sciences, University of Murcia, 30001 Murcia, Spain

(Received 27 November 1987. Revised 4 April 1988. Accepted 9 July 1988)

**Summary**—A sensitive and rapid spectrophotometric method for the determination of cadmium is described, based on the formation of a blue complex at pH 4 between the anionic iodide complex of cadmium(II) and Malachite Green; the colour is stabilized with poly(vinyl alcohol). The calibration graph for measurement at 685 nm is linear over the range 1–50  $\mu\text{g}$  of cadmium per 25 ml of final solution, with a relative standard deviation of  $\pm 1.7\%$  for 1  $\mu\text{g}/\text{ml}$  cadmium. The molar absorptivity is  $6.1 \times 10^4 \text{ l. mole}^{-1} \cdot \text{cm}^{-1}$ . The method can be successfully adapted for FIA, the peak height being proportional to the cadmium concentration over the range 0.1–3  $\mu\text{g}/\text{ml}$ ; a two-channel manifold is used and an improvement in selectivity is obtained. The use of a gradient tube is demonstrated to give a good calibration for Cd(II) over the range  $2 \times 10^{-2}$ – $2 \times 10^{-6} M$ .

The determination of traces of cadmium has attracted considerable attention owing to the toxicity of cadmium and its compounds. In addition to the AAS and ICP methods, the use of ternary complex formation provides an attractive alternative to the conventional extraction with dithizone.<sup>1</sup> The procedures so far described are sensitive, but as a general rule, separation of the complex into an organic solvent is needed.<sup>2–4</sup> However, certain dyes show spectral shifts on formation of ion-association systems involving cadmium.<sup>5–7</sup> If this occurs, a solvent extraction step is unnecessary. With this in mind, we have studied the interaction of Malachite Green with cadmium in the presence of large amounts of iodide, and have developed a new method for the spectrophotometric determination of cadmium without extraction.

The characteristics of the proposed method make it suitable for use in flow-injection analysis (FIA). Although several FIA methods have been proposed for cadmium, with electrometric,<sup>8–13</sup> atomic-absorption<sup>14,15</sup> and fluorimetric<sup>20</sup> detection, very few spectrophotometric procedures have been developed either with<sup>21–23</sup> or without<sup>24</sup> extraction. In this study the cadmium–iodide–Malachite Green system has been used as the basis for a FIA-spectrophotometric method for the routine determination of cadmium. A very simple manifold is proposed: good selectivity is obtained from peak height measurements.

The use of peak width as a quantitative parameter in FIA was first demonstrated by Růžička *et al.*<sup>25,26</sup> and since then, the method has been studied and applied by various workers.<sup>27–29</sup> Recently an accurate equation relating peak width to analyte concentration, when FIA manifolds with mixing chambers or other gradient-forming devices are used, has been studied in depth by Tyson.<sup>30,31</sup> When advantage is taken of the peak-width method to extend the

working range, cadmium can be determined by FIA in the range  $2 \times 10^{-6}$ – $2 \times 10^{-2} M$ .

The aim of our work was to develop a rapid method for the routine determination of cadmium, for industrial purposes. We report here our findings on the interaction of the anionic iodo-complex of cadmium with Malachite Green, as the basis for a spectrophotometric method involving no extraction step. To decrease the analysis time the batch procedure has been adapted to FIA systems. The use of simple FIA manifolds allows a high sampling rate with good reproducibility and moderate selectivity.

### EXPERIMENTAL

#### Apparatus

A Pye-Unicam SP8-200 spectrophotometer with 10-mm path-length glass cells was used for recording spectra and making absorbance measurements, and a Radiometer PHM63 pH-meter was used for pH measurements.

The flow injection system (see Fig. 1) consisted of a Gilson HP8 peristaltic pump, an Omnifit injection valve and a Perkin-Elmer 550 SE spectrophotometer as detector. Connecting tubing was 0.5 mm bore PTFE tubing and various end fittings and connectors (Omnifit) were used. The output from the detector was monitored either by a Perkin-Elmer 561 chart recorder or a Perkin-Elmer Sigma 15 chromatography data station.

A gradient tube consisting of a straight "Perspex" tube approximately 50 mm long and 2 mm in bore was used.

#### Reagents

All inorganic chemicals used were of analytical-reagent grade and were used without further purification. Doubly distilled water was used throughout. Malachite Green solution ( $2 \times 10^{-3} M$ ) was prepared from a commercial product. Potassium iodide–ascorbic acid solution was prepared by dissolving 16.6 g of potassium iodide and 2 g of ascorbic acid in water and diluting to 100 ml; a fresh solution was prepared every week. Poly(vinyl alcohol) (PVA) solution, 1%, was prepared from commercially available PVA. Standard cadmium solution was prepared by dissolving 3.00 g of

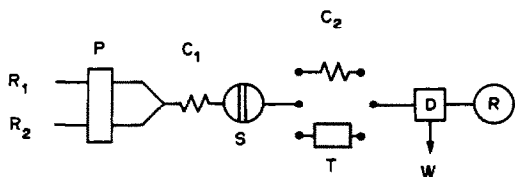


Fig. 1. Two-line FIA manifold where the carrier solution (see text for details) is a mixture of two solutions each propelled at 0.7 ml/min by the peristaltic pump P; S = sample injector (135  $\mu$ l loop size), C<sub>1</sub> and C<sub>2</sub> = coils (0.5 mm bore, lengths 1 m and 0.25 m, respectively), D = detector operating at 685 nm; R = recorder; T = gradient tube for peak-width measurements (2 mm bore, 50 mm length), R<sub>1</sub> and R<sub>2</sub> = reagent solutions; W = waste.

high-purity cadmium in 10 ml of concentrated hydrochloric acid and accurately diluting to 1 litre with water. Acetic acid/sodium acetate buffer solution, 2M, with pH 4.0, was made.

#### Manual batch procedure

Transfer up to 20 ml of sample containing no more than 50  $\mu$ g of cadmium into a 25-ml standard flask and dilute to 20 ml with water if necessary. Add 1 ml of iodide/ascorbic acid solution, 1 ml of buffer solution, 2 ml of PVA solution, mix and add 1 ml of Malachite Green solution. Mix thoroughly and measure the absorbance at 685 nm after 15 min, against a reagent blank. Beer's law is obeyed over the concentration range 1–50  $\mu$ g of cadmium in 25 ml of solution.

#### FIA procedure

Use the two-channel manifold shown in Fig. 1. The peak height at 685 nm is proportional to cadmium concentration between 0.1 and 3  $\mu$ g/ml (135- $\mu$ l sample loop). If the peak-width method is preferred, use the gradient tube instead of the coil. Prepare cadmium solutions covering the range  $2 \times 10^{-6}$ – $2 \times 10^{-2}$  M by dilution of the stock solution and inject 1500  $\mu$ l of each into the manifold. Plot a graph of the time interval between the doublet peaks ( $t_{eq}$ ) vs. the logarithm of the initial cadmium concentration ( $\log C_0$ ).

## RESULTS AND DISCUSSION

#### Batch method

Preliminary studies indicated that a major problem was the gradual precipitation of the complex on standing, which made absorbance measurements difficult. The complex was colloidal in nature and could be stabilized by addition of the protective colloid PVA, which successfully retarded precipitation of the complex, even on standing overnight. As a matter of routine, PVA was therefore added before the other reagents, for stabilization purposes.

Figure 2 shows the absorption spectra of Malachite Green with different amounts of cadmium in the presence of an excess of potassium iodide at pH 4. It is evident that the interaction between the cadmium iodide complex and the Malachite Green results in a considerable red shift and that the complex shows maximum absorption at 685 nm, compared with 615 nm for the reagent.

The optimum pH was found by using universal buffer solutions over the range 2–8. Measurements of the absorbances of the complex and the reagent blank

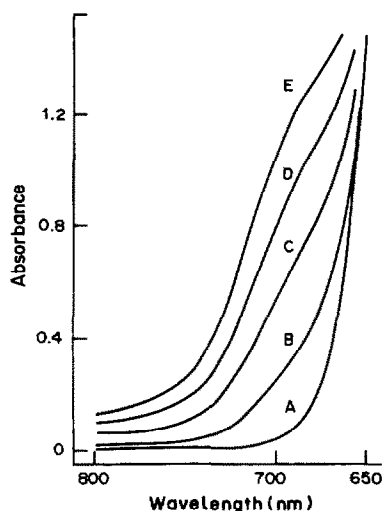


Fig. 2. Absorption spectra: (A) reagent blank; (B)–(E) as for (A) with the addition of 14, 18, 42 and 56  $\mu$ g of cadmium.

showed that the colour system is unaffected by pH over the range 2–5, but iodine is liberated at below pH 2. Although the reaction proceeds over a wide pH range, the pH of the sample and the blank should not be widely different, as the blank absorbance varies slightly with pH (Fig. 3). The pH was maintained at 4.0 in all subsequent investigations. To avoid the use of the complex universal buffer solution, simpler buffers for pH 4.0 were tested. Either potassium hydrogen phthalate or an acetate buffer could be used without affecting the colour system; varying the buffer concentration in the range 0.04–0.12 M did not affect the absorbance. All subsequent investigations were done with the acetate buffer.

Two series of experiments were performed to investigate the influence of the concentration of the reagents on the development of the colour. In one, various amounts of 0.2 M potassium iodide were added to a mixture of 1 ml of 20  $\mu$ g/ml cadmium solution and 5 ml of  $5 \times 10^{-4}$  M Malachite Green. The optimum amount was found to be 5 ml (Fig. 4). In the second series, various amounts of Malachite

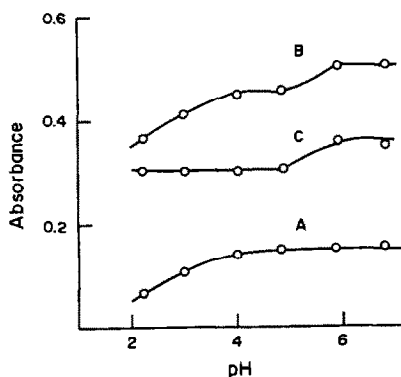


Fig. 3. Effect of pH on absorbance at 685 nm: (A) reagent blank (reference water); (B) and (C) with 15  $\mu$ g of cadmium [(B) reference water and (C) reference reagent blank].



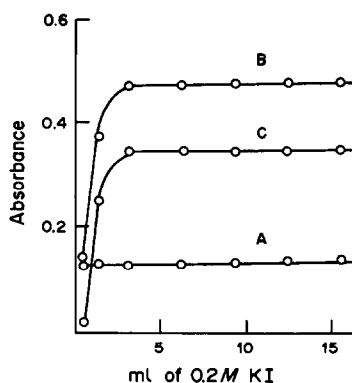


Fig. 4. Effect of iodide concentration on absorbance at 685 nm: (A) reagent blank (reference water); (B) and (C) with 15  $\mu\text{g}$  of cadmium [(B) reference water and (C) reference reagent blank].

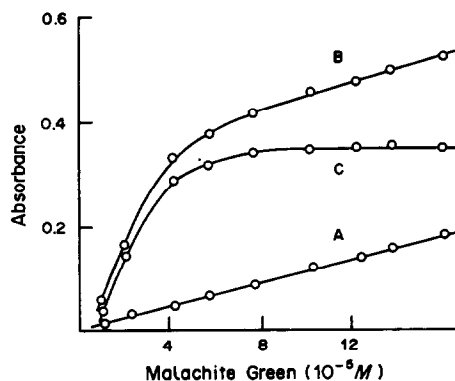


Fig. 5. Effect of Malachite Green concentration on absorbance at 685 nm: (A) reagent blank (reference water); (B) and (C) with 15  $\mu\text{g}$  of cadmium [(B) reference water and (C) reference reagent blank].

Green were added to 1 ml of 1M potassium iodide. The colour development reached a maximum at  $5 \times 10^{-5}M$  Malachite Green and remained the same for Malachite Green concentrations up to  $10^{-4}M$  (Fig. 5).

Poly(vinyl alcohol), PVA, plays an important role as stabilizing agent and its position in the order of addition of the reagents significantly affects the development of the colour. In the absence of PVA the colour faded gradually, and if PVA was added after the dye the absorbances were poorly reproducible. The best results were obtained when the PVA was added before the dye, as in the procedure. Under these conditions a standing time of 15 min was necessary in order to obtain constant absorbance measurements. The PVA concentration could be varied over the range 0.06–0.12% without effect.

The ratio of cadmium to Malachite Green in the complex in the presence of an excess of iodide was established as 1:3 by the conventional Job method. The ratio of cadmium to iodide in the complex was investigated in the presence of an excess of Malachite Green, and evidence for formation of the pentaiodo-cadmate(II) anion was found. Since the method uses a large excess of both iodide and dye, it is concluded that the complex formed is  $[\text{CdI}_5]^{3-}[\text{R}^+]_3$  where  $\text{R}^+$  is the Malachite Green cation.

Beer's law is obeyed over the range 1–50  $\mu\text{g}$  of

cadmium in a final volume of 25 ml. Under the conditions described, the molar absorptivity is  $6.1 \times 10^{-4} \text{ l. mole}^{-1} \text{ cm}^{-1}$ . A series of 10 standard solutions each containing 25  $\mu\text{g}$  of cadmium was analysed; the standard deviation and relative standard deviation (RSD) of the absorbances were 0.008 and 1.7%, respectively.

Numerous cations and anions were examined as potential interferences. The results are given in Table 1, column A. The tolerance limit for the foreign ion was taken as the concentration causing an error of  $\pm 3\%$  in the absorbance. The selectivity can be enhanced by using the FIA system, where kinetic effects play an important role (Table 1, column B).

#### Flow-injection method

Since the absorbance for the blank is low and the reaction is fast, the method described here is suitable for the routine determination of cadmium.

A simple manifold using a mixture of Malachite Green and iodide as carrier is not suitable, because the Malachite Green/iodide ion-pair precipitates in the reagent reservoir. When a two-channel FIA manifold (Fig. 1) is used, there are no problems of precipitation in the coil or in the flow-cell, owing to the very short time of contact between the reagents. As a consequence, it is not necessary to add PVA, and the development of the colour is then faster.

Table 1. Effect of diverse ions on the determination of 0.7  $\mu\text{g}/\text{ml}$  cadmium

Species added	Tolerance ratio [Ion]/[Cd(II)]	
	A, Spectrophotometry	B, FIA
Fluoride, nitrate, citrate	4000*	4000*
Sulphate	2000	5000
Mg, Ca, Ba, Co(II), Ni, Zn, Al, Mn(II)	2000	3000
Bromide, U(VI), Fe(III), Cr(III)	1000	3000
NTA, Cr(VI), V(V)	200	500
As(V), Tl(III), Mo(VI), Pb(II)	10	100
EDTA, perchlorate, Pd(II), Pt(IV), Cu, Hg(II), Ag, Au(III)	1	5

\*Maximum molar ratio tested.

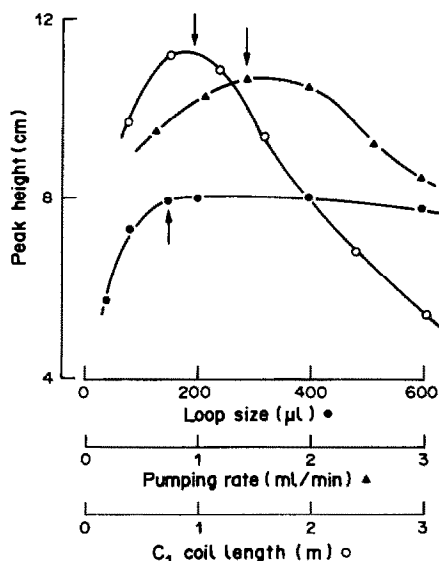


Fig. 6. Effect of loop size (●), pumping rate (▲) and  $C_1$  coil length (○) on peak height at 664 nm. Sample injected 1  $\mu\text{g/ml}$  Cd(II). The arrows mark the selected values for these parameters.

Figure 6 shows the effect of pumping rate, loop size and length of coil  $C_1$ . From these results it seems clear that a coil length of 1 m is best if a decrease in sensitivity is to be avoided. On the other hand, the tube  $C_2$  has to be as short as possible, to avoid dispersion effects.

The optimum values for the FIA variables are as follows: flow-rate ( $q$ ) = 1.4 ml/min; injected volume ( $v_1$ ) = 135  $\mu\text{l}$ ; reactor lengths,  $C_1$  = 1 m and  $C_2$  = 25 cm; inner diameter of the reactors ( $\phi$ ) = 0.5 mm. These values allow the cadmium-iodide-Malachite Green complex to be formed by the time the sample plug passes through the detector, where it is monitored at 685 nm.

The optimum concentrations for the carrier solutions were found to be 0.08M for the potassium iodide ( $R_1$ ) and  $2.5 \times 10^{-4}$ M Malachite Green ( $R_2$ ), both in 0.1M sodium acetate-acetic acid buffer (pH 4).

With the manifold described, a plot of peak absorbance (corrected for the blank) vs. concentration of cadmium in the sample injected was linear over the range 0.1–3  $\mu\text{g/ml}$ , with a small negative intercept

on the ordinate. The RSD ( $P = 0.05$ ) for the determination of 1.5  $\mu\text{g/ml}$  cadmium was 1.8%, at a sampling frequency of 120 samples per hour.

#### Peak-width FIA Method

The mathematical model used<sup>30,31</sup> assumes a molar reagent concentration  $C_0^R$  in the carrier flow-rate  $Q$  ( $\mu\text{l/sec}$ ), an injected sample volume of  $V_1$   $\mu\text{l}$ , with molar concentration  $C_0^S$ , and a mixing chamber of volume  $V$   $\mu\text{l}$ . The time interval  $t_{eq}$  (sec) between the doublet peaks is given by:

$$t_{eq} = (V/Q)\ln(C_0^S/C_0^R) + (V/Q)\ln[\exp(V_1/V) - 1]$$

In order to strike a compromise between linearity of calibration and the sampling frequency a gradient tube was included in the manifold. Solutions containing cadmium in the range  $2 \times 10^{-6} - 2 \times 10^{-2}$ M were prepared and a 1500- $\mu\text{l}$  volume of each was injected into the carrier. A least-squares regression analysis of the graph of  $t_{eq}$  vs.  $\ln C_0^S$  gave a slope of  $14.5 \pm 0.5$  and a correlation coefficient of 0.9976.

#### Conclusion

The procedure described provides a simple means for the determination of trace amounts of cadmium. The sensitivity, similar to that of the standard dithizone method, is adequate for routine purposes but the procedure shows limited sensitivity. To validate the method, four samples of liquids from an electrolysis plant manufacturing zinc and cadmium were analysed by the batch procedure without any pretreatment. The results, shown in Table 2, were compared with those obtained by AAS. Recovery tests for cadmium were also made.

*Acknowledgement*—The authors are grateful to the CAICYT (project no 84-0374) for financial support. Thanks are also extended to the Española del Zinc Company for supplying the liquid samples.

#### REFERENCES

1. Z. Marczenko, *Spectrophotometric Determination of Elements*, pp. 177, 322. Horwood, Chichester, 1976.
2. P. P. Kish and I. S. Balog, *Zh. Analit. Khim.*, 1977, **32**, 482.
3. S. Hoshi, T. Hirai, S. Inoue and M. Matsubara, *Bunseki Kagaku*, 1984, **33**, 565.

Table 2. Determination of cadmium in liquid samples from zinc production

Cadmium found, $\mu\text{g/ml}$	Recovery test*			Cadmium found by AAS, $\mu\text{g/ml}$	
	Taken, $\mu\text{g}$	Found, $\mu\text{g}$	Recovery, %		
Sample I	825	16.5	26.4	99	827
Sample II	640	12.8	23.0	102	637
Sample III	1.6	16.0	25.9	99	1.52
Sample IV	180	9.0	19.1	101	182

\*10  $\mu\text{g}$  of cadmium added.

4. J. Courtot-Coupez and P. Geurder, *Bull. Soc. Chim. France*, 1961, 1942.
5. Liu Shaopu, Liu Yi and Liu Zhonfan, *Mikrochim. Acta*, 1983 **III**, 355.
6. T. R. Prasada and T. V. Ramakrishna, *Analyst*, 1982, **107**, 704.
7. B. Huang, S. Yu and B. Pu, *Fenxi Huaxue*, 1986, **14**, 279.
8. W. Frenzel and P. Braetter, *Anal. Chim. Acta*, 1986, **179**, 389.
9. A. Hu, R. E. Dessy and A. Granelli, *Anal. Chem.*, 1983, **55**, 320.
10. J. Wang, H. D. Dewald and B. Greene, *Anal. Chim. Acta*, 1983, **146**, 45.
11. P. W. Alexander and U. Akapongkul, *ibid.*, 1983, **148**, 103.
12. J. Wang and H. D. Dewald, *ibid.*, 1983, **153**, 325; 1984, **162**, 189; *Anal. Chem.*, 1984, **56**, 156; *Talanta*, 1984, **31**, 387.
13. G. Schulze, M. Husch and W. Frenzel, *Mikrochim. Acta*, 1984 **I**, 191.
14. Z. Fang, S. Xu and S. Zhang, *Anal. Chim. Acta*, 1984, **164**, 41.
15. S. Olssen, L. C. R. Pessenda, J. Růžicka and E. H. Hansen, *Analyst*, 1983, **108**, 905.
16. K. E. Lawrence, G. W. Rice and V. A. Fassel, *Anal. Chem.*, 1984, **56**, 289.
17. K. Bäckström, L. G. Danielsson and L. Nord, *Analyst*, 1984, **109**, 323.
18. Z. Fang, J. Růžicka and E. H. Hansen, *Anal. Chim. Acta*, 1984, **164**, 23.
19. S. D. Hartenstein, J. Růžicka and G. D. Christian, *Anal. Chem.*, 1985, **57**, 21.
20. J. L. Burguera, M. Burguera and A. Townshend, *Anal. Chim. Acta*, 1981, **127**, 199.
21. O. Klinghoffer, J. Růžicka and E. H. Hansen, *Talanta*, 1980, **27**, 169.
22. J. L. Burguera and M. Burguera, *Anal. Chim. Acta*, 1983, **153**, 207.
23. E. A. Jones, *Tech. Rep. Mintek*, 1983, **M111**, 32.
24. E. Bylund, R. Andersson and J. A. Carlsson, *Pharmacia*, Uppsala, Sweden, 1978.
25. J. Růžicka and E. H. Hansen, *Flow Injection Analysis*, 1st Ed., pp. 137, 138 and Fig. 6.6. Wiley, New York, 1981.
26. A. U. Ramsing, J. Růžicka and E. H. Hansen, *Anal. Chim. Acta*, 1981, **129**, 1.
27. K. K. Stewart and A. G. Rosenfeld, *Anal. Chem.*, 1982, **54**, 2368.
28. J. F. Tyson, *Analyst*, 1984, **109**, 319.
29. H. L. Pardue and B. Fields, *Anal. Chim. Acta*, 1981, **124**, 39.
30. J. F. Tyson, *ibid.*, 1986, **179**, 131.
31. *Idem*, *Analyst*, 1987, **112**, 523.

## DETERMINATION OF POLYNUCLEAR AROMATIC HYDROCARBONS IN WATER BY FLOTATION ENRICHMENT AND HPLC

XU BO-XING and FANG YU-ZHI\*

Great Lakes Laboratory, State University College at Buffalo, 1300 Elmwood Avenue, Buffalo,  
NY 14222, U.S.A.

(Received 9 July 1986. Revised 17 March 1988. Accepted 9 July 1988)

**Summary**—A method of concentration and determination of several polynuclear aromatic hydrocarbons (PAHs) in water by flotation enrichment and HPLC is described. Triton X-100 was used as the foaming agent to extract the PAHs from water by passage of nitrogen. Reversed-phase liquid chromatography with coupled fluorescence detection was applied to separate and determine these PAHs. Various factors which may affect the recovery of PAHs from water, including pH, temperature and the concentration of Triton X-100 added, are discussed. This simplified method of concentrating PAHs from water has been applied to determine PAHs in water from Lake Erie. The method has practical value for the determination of PAHs in large volumes of water.

Polynuclear aromatic hydrocarbons (PAHs) are widely distributed throughout the environment from both natural and man-made sources. Because of the strong carcinogenic activity of several PAHs, considerable attention has been paid to their detection, identification and determination in a variety of matrices.<sup>1,2</sup> To regulate the consumption of PAHs in drinking water, it is necessary to monitor their presence and concentration in natural waters. Since this concentration is very low, owing to the extremely low solubility of PAHs in water, the conventional analytical methods are laborious, and often give poor recoveries.

Many techniques have been developed to extract and concentrate PAHs from water, including solvent extraction<sup>3-6</sup> and adsorption on solids.<sup>7-10</sup> Both these approaches have certain disadvantages which affect the recovery and reproducibility. For example, the solvent extraction techniques require large amounts of both water and solvent, thus resulting in poor recovery of PAHs. In the adsorption technique, recovery becomes increasingly poor as the number of aromatic rings increases, probably owing to the decreasing aqueous solubility, resulting in increasing adsorption of the PAHs on the container surfaces. As a more convenient alternative, a rapid and simple extraction technique has been developed in our laboratory, with a foam flotation method. The procedure involves the enrichment of the PAHs by means of a foam obtained by bubbling nitrogen through a solution of non-ionic surfactant, Triton X-100, followed by collection of the foam in a small volume of

methylene chloride. This solution is then analysed by reversed-phase HPLC.

The combination of the flotation technique and HPLC offers a convenient method for the determination of ng/l. levels of PAHs in water samples. We have used the method for determining PAHs in Lake Erie. It can be readily adapted for the routine monitoring of PAHs in natural waters.

### EXPERIMENTAL

#### Reagents

Methylene chloride, methanol and acetonitrile were HPLC grade (J. T. Baker Chemical Co.). The Triton X-100 was analytical grade (Fisher Scientific Company).

#### Standards

The individual PAH standards and a standard solution of mixed PAHs were obtained from Supelco Inc. The standard mix contained anthracene, benz(a)anthracene, benzo(a)pyrene, benzo(e)pyrene, chrysene, fluoranthene, perylene, phenanthrene, pyrene and triphenylene, at a concentration of 0.5 mg/ml each, in toluene. The standard PAH solutions were prepared in methanol. In some cases, complete dissolution required treatment in a sonic bath. The stock solutions were stored in the refrigerator at 7°.

#### Glassware

All glassware was soaked in "Alconot", then rinsed with demineralized water and finally with methanol. Sample blanks confirmed that this washing procedure was adequate for the removal of PAHs and other contamination from the glassware.

#### Instrumentation

A Varian VISTA series 5000 liquid chromatograph, coupled with a Fluorichrom detector, was interfaced with a 401 data-station printer and plotter. The chromatographic conditions are given in Table 1.

#### Extraction of PAHs by flotation with Triton X-100

The water sample (1 litre) was filtered (glass fibre GF/F, Whatman Ltd.) into a flotation vessel (Fig. 1) to remove any

\*Visiting scholars from the Department of Chemistry, East China Normal University, Shanghai, China (which is their present address).

Table 1. Chromatographic conditions

Column	Supelco C <sub>18</sub> column, 15 cm × 4.0 mm, particle size 5 μm
Mobile phase	Water/acetonitrile linear gradient from 65/35 to 15/85 (v/v) over 40 min then held.
Flow-rate	1.2 ml/min
Detector	Fluorichrom detector (FD) with filters set for λ <sub>ex</sub> = 340–380 nm (filters 7–54, 7–60) and λ <sub>em</sub> = 460–650 nm (filters 4–76, 3–71)

turbidity. The pH of the filtered water was adjusted to 3 with 6M hydrochloric acid. Triton X-100 (0.2 ml of 5% v/v solution in water) was added. Nitrogen was bubbled at 250 ml/min through this mixture, which was stirred magnetically. The foam thus formed was collected in a separatory funnel containing 15 ml of methylene chloride. The foam was collapsed and extracted by shaking the separatory funnel for 1 min. The methylene chloride extract was transferred into a vial and evaporated to dryness under reduced pressure. The residue was dissolved in 0.2 ml of methanol. Aliquots (50 μl) were analysed by HPLC (see Table 1 for HPLC conditions).

### RESULTS AND DISCUSSION

Flotation is a well known technique for separating and concentrating particles from aqueous systems<sup>11</sup> and has been used for many years to separate minerals from a rock matrix. The process is usually accomplished by bubbling air through the solution, resulting in the suspension of the solid particles as they come into contact with the bubble film, the particles and bubbles then being carried to the surface and skimmed off with the foam. Researchers have applied this technique in analytical chemistry to improve trace analysis.<sup>12–15</sup> However, the use of the non-ionic surfactant, Triton X-100, as a collector for extraction of PAHs from water has not been previously reported. It is a new approach to the determination of PAHs in natural waters, and may have practical value in routine analysis for PAHs.

#### Parameters influencing recovery

*Amount of Triton X-100 added.* Maximum recoveries of benzo(a)pyrene added to distilled water were

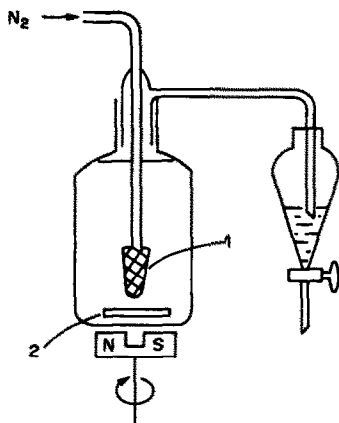


Fig. 1. Flotation apparatus. 1—sintered-glass frit; 2—stirrer bar.

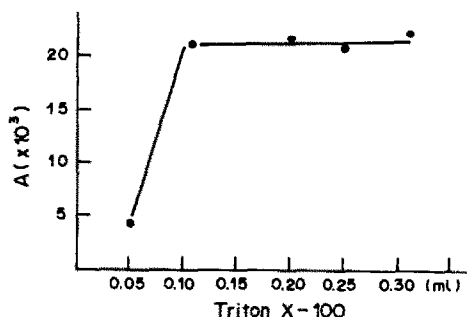


Fig. 2. Effect of amount of Triton X-100.

obtained with the addition of 0.1–0.3 ml of 5% Triton X-100 solution per litre of water (Fig. 2). The volume selected for subsequent experiments was 0.2 ml. The use of larger volumes is disadvantageous because a longer flotation time (and hence longer analysis time) is required. Of the various solvents (methanol, acetonitrile, methylene chloride, etc.) used for subsequent treatment of the Triton X-100 foam, methylene chloride was found to be superior to methanol and acetonitrile, because using a hydrophobic solvent, methylene chloride, facilitates the drying and concentration of the extract. These results demonstrate that the flotation technique is useful not only for the concentration of suspended particles, but also for the quantitative extraction of trace quantities of organic material from water.

*pH and temperature.* The recovery of PAHs was highest at pH 3–4 (see Fig. 3) and progressively decreased at higher pH. A possible interpretation is that since the Triton X-100 is a macromolecule with a hydroxyl group, it may be partially ionized at high pH, thus partially losing its binding affinity for PAHs.

The effect of a minor change in the water temperature on the recovery of PAHs was not significant.

#### Chromatographic separation and determination

Five PAHs (out of the total of 10) (5 ng of each) were resolved from the mixed PAH standard, and detected with a fluorimetric detector under the conditions used (Fig. 4). The failure to detect the remaining 5 PAHs [benzo(e)pyrene, chrysene, phenanthrene

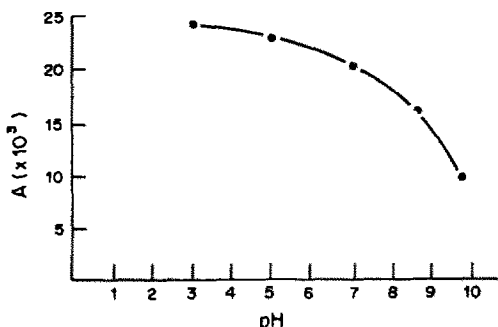


Fig. 3. Effect of pH value.

Table 2. The results for the water sample analysis (sample volume 1000 ml)

Compound	PAH added, ng	PAH found,* ng	RSD, %	Recovery,† %
Benzo(a)pyrene	0	0.3	56.7	
	10	9.6	2.7	93
Perylene	0	1.6	41.3	
	10	12.3	13.6	107
Fluoranthene	0	10.6	2.5	
	10	21.0	10.3	104

\*Average of 5 determinations.

†Average of 4 determinations.

pyrene and triphenylene] apparently resulted from their relatively low fluorescence response under these conditions. Calibration curves (FD response vs. concentration) were obtained for five of the PAHs [perylene, benzo(a)anthracene, anthracene, fluoranthene and benzo(a)pyrene]. Those for anthracene, fluoranthene and benzo(a)anthracene were linear for 10–100 ng of PAH in 0.2 ml of methanol; the linear range for benzo(a)pyrene and perylene was 0–80 ng in 0.2 ml of methanol.

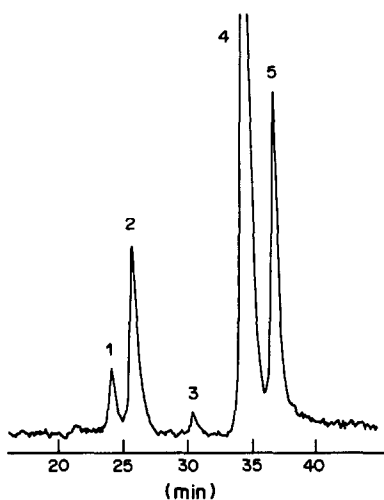


Fig. 4. The chromatogram of the standard mixture of PAHs. 1—Anthracene; 2—fluoranthene; 3—benz(a)anthracene; 4—perylene; 5—benzo(a)pyrene.

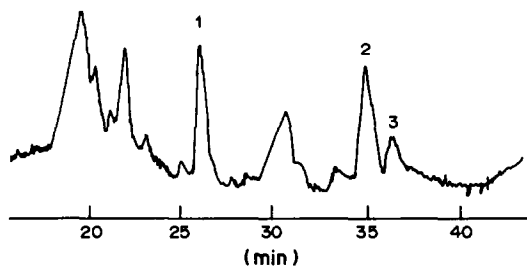


Fig. 5. The chromatogram of the PAH extract from the sample. 1—fluoranthene; 2—perylene; 3—benzo(a)pyrene.

#### Determination and recoveries of PAHs in water samples

The recoveries of perylene (10 ng), benzo(a)pyrene (10 ng), anthracene (50 ng), fluoranthene (50 ng) and benz(a)anthracene (50 ng) from 1 litre of distilled water that had been spiked with these compounds were 102, 86, 87, 95 and 96% respectively.

Samples of water collected from Times Beach, Buffalo (Lake Erie), a site containing dredged sediments with a high level of PAHs (Army Corps of Engineers, unpublished data) were subjected to Triton X-100 foam flotation and HPLC analysis as described above. Three PAHs were identified by comparison of their retention times with those of standards: perylene (1.6 pg/ml), fluoranthene (10.6 pg/ml) and benzo(a)pyrene (0.3 pg/ml) (Fig. 5, Table 2). The concentration of anthracene was below the limit of detection of the method (about 2 pg/ml). The failure to detect benz(a)anthracene could have resulted from interference by one or more unidentified compounds (Fig. 5). It should be noted that the samples were collected in December and January (water temperature 0°) under conditions that would minimize the aqueous solubilities of these compounds.

#### CONCLUSIONS

Application of the Triton X-100 flotation technique to concentrate PAHs from water, followed by HPLC identification and determination is a new approach for the determination of PAHs in natural water. It is a simplified analytical procedure with high sensitivity for PAHs and can be used for monitoring trace levels of PAHs in large volumes of water.

*Acknowledgements*—We are very grateful to Dr. Harish C. Sikka, Dr. Subodh Kumar and Dr. A. Ruth Steward of the Great Lakes Laboratory for their enthusiastic help in finishing this work.

#### REFERENCES

- IARC (International Agency for Research on Cancer), *Monographs on Evaluation of Carcinogenic Risk of Chemicals to Man: Certain Polycyclic Aromatic Hydrocarbons and Heterocyclic Compounds*, Vol. 3, Geneva, 1973.

2. R. F. Freudenthal and P. W. Jones, *Polynuclear Aromatic Hydrocarbons: Chemistry, Metabolism and Carcinogenesis*, Raven Press, New York, 1976.
3. S. R. Smith, J. Tanaka, R. Collins and J. Johnson, *Report 1982*, W83-03591, OWRT-A-084-CONN(1); Order No. PB 83-235259; *Chem. Abstr.*, 1983, **99**, 200261s.
4. W. C. Glaze and C. C. Lin, *Report 1983*, EPA-600/4-83-052; Order No. PB 84-112937; *Chem. Abstr.*, 1984, **100**, 144718w.
5. G. A. Junglauss, L. M. Games and R. A. Hites, *Anal. Chem.*, 1976, **48**, 1894.
6. *US EPA Method 610, Federal Register, Dec. 1979*, **44**, 233.
7. H. Thielemann and H. Grahneis, *Z. Gesamte Hyg. Grenzgeb.*, 1983, **29**, 268.
8. J. Saxena, J. Kozuchowski and D. K. Basu, *Environ. Sci. Technol.*, 1978, **12**, 791.
9. R. K. Symons and I. Crick, *Anal. Chim. Acta*, 1983, **151**, 237.
10. P. Van Rossum and R. G. Webb, *J. Chromatog.*, 1978, **150**, 381.
11. E. W. Berg, *Physical and Chemical Methods of Separation*, McGraw-Hill, New York, 1963.
12. R. S. S. Murthy and D. E. Ryan, *Anal. Chem.*, 1983, **55**, 682.
13. International Union of Pure and Applied Chemistry, *Pure Appl. Chem.*, 1982, **54**, 1555.
14. T. Nozaki, K. Kato, M. Uchida, M. Doi, N. Mise and Y. Soma, *Bunseki Kagaku*, 1983, **32**, 145.
15. Z. Skorko-Trybula and E. Koinska, *Chem. Anal. (Warsaw)*, 1981, **26**, 581.

## SPECTROPHOTOMETRIC DETERMINATION OF CHLORDIAZEPOXIDE AND NITRAZEPAM

M. I. WALASH, M. RIZK and A. EL-BRASHY\*

Analytical Chemistry Department, Faculty of Pharmacy, Mansoura University, Mansoura, Egypt

(Received 6 January 1988. Revised 15 June 1988. Accepted 25 June 1988)

**Summary**—The use of ethyl acetoacetate in the spectrophotometric determination of chlordiazepoxide and nitrazepam has been investigated. The procedure is based on coupling the diazotized drugs with ethyl acetoacetate, which possesses an active methylene group. The products have absorption maxima at 408 and 482 nm and apparent molar absorptivities of  $2.74 \times 10^4$  and  $4.11 \times 10^4$  l. mole<sup>-1</sup>. cm<sup>-1</sup>, respectively. The method is simple, highly sensitive and suitable for 1–16 µg/ml concentrations of the two compounds, with mean recoveries of  $100.3 \pm 1.2$  and  $99.8 \pm 1.0\%$  respectively.

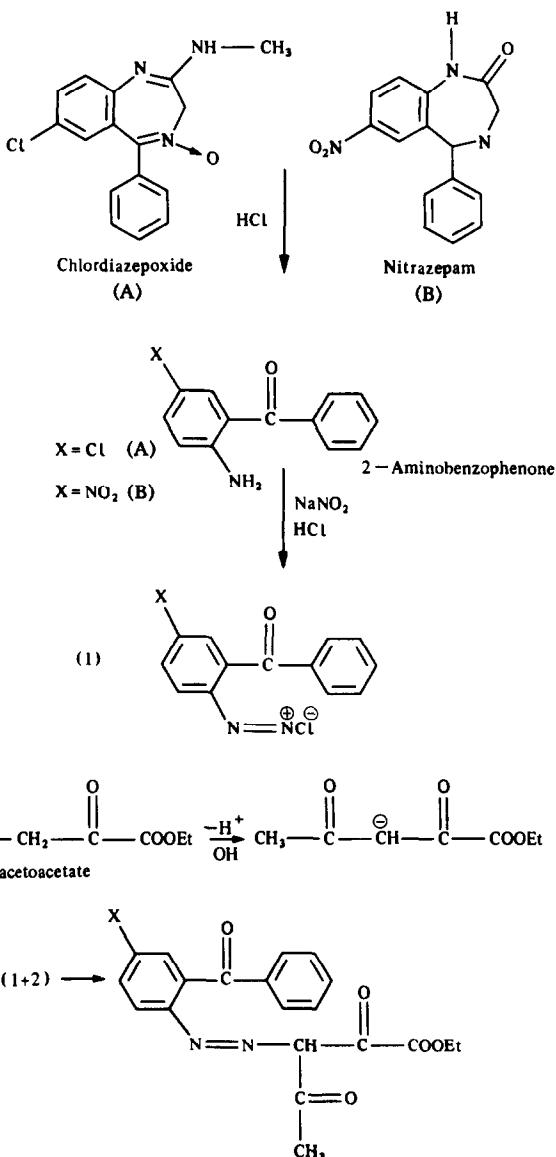
Chlordiazepoxide and nitrazepam are 1,4-benzodiazepines and are used as tranquillizers and sedatives. Several methods have been reported for their assay, including non-aqueous titration,<sup>1,2</sup> complexometry,<sup>3,4</sup> spectrophotometry,<sup>5-7</sup> colorimetry,<sup>8-14</sup> fluorimetry,<sup>15,16</sup> polarography,<sup>17,18</sup> gas chromatography<sup>19,20</sup> and high-performance liquid chromatography.<sup>21,22</sup>

The colorimetric methods are based on acid hydrolysis of the drugs, resulting in their corresponding aminobenzophenones. Determination is by measurement of the absorbance of the hydrolysis products or the compound produced by diazotizing them and coupling with thiocol,<sup>8</sup> 1-naphthol,<sup>9</sup> Thymol Blue,<sup>10</sup> *N*-(1-naphthyl)ethylenediamine<sup>11,12</sup> or 8-hydroxyquinoline.<sup>13,14</sup>

Coupling of the diazonium salt is an electrophilic substitution and may take place with carbanions associated with an active hydrogen atom.<sup>23</sup> Thus ethyl acetoacetate, which gives a measurable coloured product with diazonium derivatives of 4-nitroaniline<sup>24</sup> has been used as a coupling reagent for determination of pharmaceutical primary aromatic amines<sup>25</sup> and benzothiazines.<sup>26</sup>

This work presents a simple and sensitive procedure for the estimation of chlordiazepoxide and nitrazepam. It is based on coupling the corresponding diazotized hydrolysis product with ethyl acetoacetate, followed by alkalization to obtain absorption maxima at 408 and 482 nm for chlordiazepoxide

and nitrazepam respectively.



and nitrazepam respectively. The proposed method is compared with the *N*-(1-naphthyl)ethylenediamine,<sup>11,12</sup> 8-hydroxyquinoline<sup>13,14</sup> and official<sup>2</sup> methods.

### RESULTS AND DISCUSSION

The scheme presented below shows the reac-

\*To whom correspondence should be addressed.



### Study of the experimental conditions

Chlordiazepoxide is completely hydrolysed to 5-chloro-2-aminobenzophenone when heated with 3*M* hydrochloric acid in a boiling water-bath for 15 min. Nitrazepam is converted completely into 5-nitro-2-aminobenzophenone when boiled with concentrated hydrochloric acid for 15 min. For either drug 0.5 ml of 0.05% sodium nitrite solution is sufficient for diazotization. Sulphamic acid is required to remove the excess of nitrous acid, and stabilize the colour; 1 ml of 0.2% solution is adequate. One ml of 5% ethyl acetoacetate solution in ethanol is enough to ensure complete reaction.

Addition of 2 ml of 50% sodium hydroxide solution was needed to produce a high colour intensity. The absorption maxima are at 408 and 482 nm, with molar absorptivities of  $2.74 \times 10^4$  and  $4.11 \times 10^4$  l. mole<sup>-1</sup>. cm<sup>-1</sup> for chlordiazepoxide and nitrazepam respectively.

Beer's law is obeyed over the concentration range 1–16 µg/ml. Table 1 shows the results of a study of the proposed method and the *N*-(1-naphthyl)-ethylenediamine dihydrochloride<sup>11,12</sup> and 8-hydroxyquinoline<sup>13,14</sup> methods and Table 2 shows results obtained by the proposed method, the other two colorimetric methods and the official method.<sup>2</sup>

The proposed method was then applied to analysis of certain commercial formulations (Table 3). Lactose, starch, magnesium stearate and talc, which are commonly incorporated as excipients, did not interfere.

Statistical analysis of the results by the variance-ratio test and the Student *t*-test showed there was no significant difference between the performances of the three colorimetric methods (Table 4). The suggested method has the advantages of being simple and sensitive and may be considered as a general method for spectrophotometric determination of benzodiazepines. It also has the advantage that the coloured products are soluble in the aqueous alkaline medium and do not require extraction.

### EXPERIMENTAL

#### Reagents

Ethyl acetoacetate, 5% solution in ethanol. *N*-(1-Naphthyl)ethylenediamine dihydrochloride, 0.2% solution in water. 8-Hydroxyquinoline, 5% in 1% sodium hydroxide solution in ethanol. Sodium nitrite, 2 and 0.05% solutions in water. Sulphamic acid, 0.2% solution in water. Sodium hydroxide, 50% aqueous solution.

#### Drugs

*Chlordiazepoxide*. The drug is hydrolysed by dissolving it in 3*M* hydrochloric acid and heating the solution in a boiling water-bath for 15 min.

*Nitrazepam*. The drug is hydrolysed by dissolving it in concentrated hydrochloric acid and heating in a boiling water-bath for 15 min.

#### Procedures

*Ethyl acetoacetate method*. Transfer suitable volumes (in the range 1–5 ml) of solution (containing 25–400 µg of the drug) into 25-ml standard flasks and add 0.5 ml of 0.05%

Table 1. Results obtained by the ethyl acetoacetate, *N*-(1-naphthyl)ethylenediamine<sup>11,12</sup> and 8-hydroxyquinoline<sup>13,14</sup> methods

Compound	Ethyl acetoacetate			<i>N</i> -(1-Naphthyl)ethylenediamine			8-Hydroxyquinoline		
	$\lambda_{\max}$ nm	$\epsilon$ , 10 <sup>4</sup> l. mole <sup>-1</sup> . cm <sup>-1</sup>	Working range, µg/ml	$\lambda_{\max}$ nm	$\epsilon$ , 10 <sup>4</sup> l. mole <sup>-1</sup> . cm <sup>-1</sup>	Working range, µg/ml	$\lambda_{\max}$ nm	$\epsilon$ , 10 <sup>4</sup> l. mole <sup>-1</sup> . cm <sup>-1</sup>	Working range, µg/ml
Chlordiazepoxide	408	2.74	1–16	545	1.28	5–40	515	2.45	2–20
Nitrazepam	482	4.11	1–12	536	1.90	5–30	585	2.45	2–20

Table 2. Determination of the two compounds by the proposed and other methods

Compound	Ethyl acetoacetate		<i>N</i> -(1-Naphthyl)-ethylenediamine		8-Hydroxyquinoline		Official	
	Taken, $\mu\text{g/ml}$	Mean recovery, %*	Taken, $\mu\text{g/ml}$	Mean recovery, %*	Taken, $\mu\text{g/ml}$	Mean recovery, %*	Taken, mg	Mean recovery, %*
Chlordiazepoxide	1	101.1	5	100.7	2	98.5	100	100.7
	2	99.9	10	99.6	5	100.7	150	102.8
	4	101.7	15	98.9	10	100.9	200	101.8
	8	100.9	20	100.0	15	98.9		
	10	98.8	25	101.1	20	100.3		
	12	98.6	30	100.3				
16	101.1	35	99.9					
40			99.7					
Mean recovery $\pm$ SD		100.3 $\pm$ 1.2		100.0 $\pm$ 0.7		99.9 $\pm$ 1.1		101.8 $\pm$ 1.1
Nitrazepam	1	98.8	5	99.2	2	101.3	100	101.4
	2	99.1	10	100.3	5	99.6	150	102.6
	4	100.3	15	99.6	10	98.6	200	100.4
	8	101.6	20	101.7	15	100.0		
	10	99.2	25	101.6	20	100.4		
	12	99.8	30	98.5				
Mean recovery $\pm$ SD		99.8 $\pm$ 1.0		100.2 $\pm$ 1.3		100.0 $\pm$ 1.0		101.5 $\pm$ 1.1

\*Results are the average of at least 3 separate experiments.

Table 3. Determination of chlordiazepoxide and nitrazepam in their tablets

Tablets	Proposed method		<i>N</i> -(1-Naphthyl)-ethylenediamine method <sup>11,12</sup>		8-Hydroxyquinoline method <sup>13,14</sup>		Official method <sup>2</sup>	
	Taken, $\mu\text{g/ml}$	Mean recovery, %*	Taken, $\mu\text{g/ml}$	Mean recovery, %*	Taken, $\mu\text{g/ml}$	Mean recovery, %*	Taken, $\mu\text{g/ml}$	Mean recovery, %*
Libran-5†	4	100.9	5	98.8	5	98.9	16	101.3
(5 mg of chlordiazepoxide per tablet)	8	100.2	8	99.0	10	101.5	16	98.9
	10	99.0	10	101.3	20	100.1	16	99.2
Mean recovery $\pm$ S.D.		100.0 $\pm$ 1.0		99.7 $\pm$ 1.4		100.2 $\pm$ 1.3		99.8 $\pm$ 1.3
Mogadon§	4	99.8	5	101.9	5	99.2	5	98.9
(5 mg of nitrazepam per tablet)	8	101.6	8	102.5	10	98.5	5	99.3
	10	102.2	10	102.9	20	99.0	5	98.5
Mean recovery $\pm$ S.D.		101.2 $\pm$ 1.3		102.4 $\pm$ 0.5		98.9 $\pm$ 0.3		98.9 $\pm$ 0.4

\*Results are the average of at least 3 separate experiments.

†Memphis Chemical Co.

§F. Hoffmann-La Roche.

Table 4. Statistical analysis of the proposed and other methods

	Chlordiazepoxide			Nitrazepam		
	<i>N</i> -(1-Naphthyl)-ethylenediamine method <sup>12</sup>	Proposed method	Oxine method <sup>13</sup>	<i>N</i> -(1-Naphthyl)-ethylenediamine method <sup>11</sup>	Proposed method	Oxine method <sup>14</sup>
No. of variates	8	7	5	6	6	5
Mean recovery, %	100.0	100.3	99.9	100.2	99.8	100.0
Variance	0.5	1.5	1.2	1.7	1.0	1.0
Student <i>t</i> -test <sup>27</sup>	0.544 (2.160)	0.553 (2.228)		0.409 (2.228)	0.231 (2.262)	
Variance ratio <sup>27</sup> ( <i>F</i> -test)	3.244 (2.870)	1.217 (6.160)		1.651 (5.050)	1.056 (6.260)	

The values in brackets are the tabulated values (at  $P = 0.05$ ).<sup>27</sup>

sodium nitrite solution. After 2 min, add 1 ml of 0.2% sulphamic acid solution, 1 ml of 5% ethyl acetoacetate solution and 2 ml of 50% sodium hydroxide solution and dilute to the mark with water. Measure the absorbance at 408 nm for chlordiazepoxide and 482 nm for nitrazepam, against a blank similarly prepared.

*N*-(1-Naphthyl)ethylenediamine dihydrochloride method.<sup>11,12</sup> Transfer suitable volumes (in the range 0.8–5 ml) of solution (containing 20–400 µg of the drug) into 10-ml standard flasks and add 0.2 ml of 0.05% sodium nitrite solution. After 5 min add 1 ml of 0.2% sulphamic acid solution, wait for 5 min, then add 1 ml of 0.2% *N*-(1-naphthyl)ethylenediamine dihydrochloride solution. Wait for 10 min and dilute to volume with water. Measure the absorbance at 545 nm for chlordiazepoxide and 536 nm for nitrazepam, against a blank similarly prepared.

8-Hydroxyquinoline method.<sup>13,14</sup> Transfer suitable volumes (in the range 2–5 ml) of solution (containing 50–500 µg of the drug) into 25-ml standard flasks and add 1 ml of 2% sodium nitrite solution. After 5 min add 10 ml of 5% 8-hydroxyquinoline solution and dilute to volume with ethanol. Measure the absorbances at 515 nm for chlordiazepoxide and 585 nm for nitrazepam against blanks prepared in the same manner.

*Determination of the compounds in commercial tablets.* Weigh and powder 20 tablets. Take a weight equivalent to 50 mg of the pure drug and extract with three successive 20-ml portions of ethanol. Filter the combined extracts and evaporate to dryness. Hydrolyse the residue with hydrochloric acid as described for the pure drug. Dilute to 50 ml with 3*M* hydrochloric acid for chlordiazepoxide tablets and concentrated hydrochloric acid for nitrazepam tablets, and analyse the solution by the procedures described above.

#### REFERENCES

1. F. Barbato, C. Grieco, C. Silipo and A. Vittoria, *Farmaco Ed. Prat.*, 1979, **34**, 187.
2. *British Pharmacopoeia*, 1980, p. 98. HMSO, Cambridge, 1980.
3. M. Gajewska, M. Ciszewska, E. Lugowska and B. Kwiatkowska, *Chem. Anal. (Warsaw)*, 1979, **24**, 119.
4. M. Gajewska, E. Lugowska, J. M., Ciszewska and M. Rzedowski, *ibid.*, 1981, **26**, 517.
5. E. V. Rao and K. S. Reddy, *Indian Drugs*, 1983, **20**, 409.
6. A. G. Davidson, *J. Pharm. Sci.*, 1984, **73**, 55.
7. I. Popovici, V. Dorneanu, R. Cuciureanu and E. Stefanescu, *Rev. Chim. (Bucharest)*, 1983, **34**, 554.
8. J. F. Magalhaes and M. G. Piroos, *Rev. Brasil. Farm.*, 1970, **51**, 195.
9. H. Raber and J. Gruber, *Sci. Pharm.*, 1972, **40**, 35.
10. A. R. E. Ossman and A. H. El-Hassany, *Pharmazie*, 1975, **30**, 257.
11. H. Sawada and K. Shinohara, *Eisei Kagaku*, 1970, **16**, 318.
12. K. Antczak, *Diagn. Lab.*, 1974, **10**, 412.
13. A. R. E. Ossman and A. H. El-Hassany, *Pharmazie*, 1976, **31**, 744.
14. Z. Kosa, *Gyogyszereszet*, 1977, **21**, 287.
15. H. Sawada, A. Hara, T. Nakayama, M. Hayashibara and T. Saeki, *Gifu Yokka Daigaku Kiyo*, 1979, **28**, 4.
16. J. Troschuetz, *Arch. Pharm.*, 1981, **314**, 204.
17. A. K. Mishra and K. D. Gode, *Analyst*, 1985, **110**, 1105.
18. W. F. Smyth and A. Ivaska, *ibid.*, 1985, **110**, 1377.
19. M. Werner, R. J. Mohrbacher and C. J. Riendeau, *Clin. Chem.*, 1979, **25**, 2020.
20. S. Barazi and M. Bonini, *J. Chromatog.*, 1980, **202**, 473.
21. C. Violon and A. Vercreyusse, *ibid.*, 1980, **189**, 94.
22. S. E. Roberts and M. F. Delaney, *ibid.*, 1984, **283**, 265.
23. A. K. Connors, *Reaction Mechanisms in Organic Chemistry*, p. 244. Wiley-Interscience, New York, 1973.
24. M. S. Rosenthal, *J. Biol. Chem.*, 1949, **179**, 1235.
25. S. Belal, E. A. El-Neaey and S. Soliman, *Talanta*, 1978, **25**, 290.
26. F. Belal, M. Rizk, F. A. Ibrahim and M. K. Sharaf El-Din, *ibid.*, 1986, **33**, 170.
27. R. Caulcutt and R. Boddy, *Statistics for Analytical Chemists*, Chapman & Hall, London, 1983.

## NABTIT—A COMPUTER PROGRAM FOR NON-AQUEOUS ACID-BASE TITRATION

O. BUDEVSKY, T. ZIKOLOVA\* and J. TENCHEVA

Academy of Medicine, Faculty of Pharmacy, Ekz. Josif St. 15, Sofia-1000, Bulgaria

(Received 23 March 1988. Accepted 14 May 1988)

**Summary**—A program NABTIT written in BASIC has been developed for the treatment of data (ml/mV) obtained from potentiometric acid-base titrations in non-aqueous solvents. No preliminary information on equilibrium constants is required for the input. The treatment of the data is based on known equations and uses least-squares procedures. The essence of the method is to determine the equivalence volume ( $V_e$ ) accurately, and to use the data acquired by adding titrant after  $V_e$  for the pH\*-calibration of the non-aqueous potentiometric cell. As a by-product of the calculations, the  $pK^*$  value of the substance titrated is also obtained, and in some cases the autoprotolysis constant of the medium ( $pK_s^*$ ). Good agreement between experiment and theory was found in the treatment of data obtained for water and methanol-water mixtures.

Non-aqueous acid-base titration finds many applications in the analysis of organic and inorganic substances. This useful method could find even greater application if there existed a universal approach to the determination of pH in non-aqueous solvents. Potentiometric titration in these media is therefore mainly done by using the mV scale of pH-meters to detect the inflection point on the titration curve, perhaps with application of derivative methods. These methods of end-point (e.p.) determination cause some problems, especially in the determination of substances with weak acid-base properties.

In aqueous solutions, the pH "problem" was resolved by definition of the so-called "operational pH-scale", in which a number of pH-standards are used. Many difficulties connected with potentiometric acid-base titration in water (including that of very weak acids and bases) were thus successfully removed, especially after Ingman and Still<sup>1</sup> enlarged the method of Gran<sup>2</sup> in deriving a non-approximate equation for evaluating titration of acids and bases. The same equation was rearranged later into linear form,<sup>3,4</sup> yielding thus not only the equivalence volume ( $V_e$ ) but also the  $pK$  value for the substance titrated. It was also shown that the equation in question was almost identical with that derived by Hofstee,<sup>5</sup> applied by Benet and Goyan,<sup>6</sup> and enlarged and modified by Leeson and Brown.<sup>7</sup>

Ingman and co-workers<sup>8-10</sup> have given a critical survey of the determination of bases and acids, and proposed a new approach and a basic idea for a computer program. Besides the use of linear plots (the method of Gran), computer treatment of data for determination of acids and bases in water and some non-aqueous media has been reviewed

recently.<sup>11</sup> It seems that the FORTRAN program "ACBA"<sup>12</sup> and its BASIC version "ESAB"<sup>13</sup> are especially effective. These programs use the basic idea, developed by Sillén in his program LETAGROP,<sup>14,15</sup> of multiparametric minimization.

From the work discussed, it can be concluded that the accurate determination of weak acids and bases depends on reliable pH data and even on accurate autoprotolysis ( $pK_s$ ) values. The difficulty of obtaining reliable pH data for organic and aqueous-organic media creates serious problems for potentiometric acid-base non-aqueous titrations. It should be added that the computer treatments usually use non-linear regression, so some parameters must be known in order to solve the problem.

We propose here a straightforward method for the determination of acids and bases in non-aqueous media, in which no preliminary pH-calibration or knowledge of constants is needed. Since it involves rather tedious calculations, a BASIC computer program for its implementation has also been developed. The method is based on our earlier proposal to calibrate the glass electrode non-aqueous cell during the potentiometric titration itself.<sup>16</sup> Once highly reliable pH-values in the non-aqueous medium are available, application of the exact equations already mentioned leads to very accurate and precise results for the determination of acids and bases of various strengths. As a by-product from the calculations, the respective acid or base constant is also obtained. When the acid or base titrated is moderately strong ( $pK < 5$ ), the value of the autoprotolysis constant ( $pK_s$ ) can also be calculated.

### OUTLINE OF THE METHOD

Before the principles of the proposed method are outlined, a very important limitation must be men-

\*Present address: Chemical Pharmaceutical Research Institute, Kliment Ohridsky St. 3, Sofia-1156, Bulgaria.

tioned, namely, the titrant must be fully dissociated in the non-aqueous medium used. It may seem that this limitation is rather severe, since some very important solvents such as glacial acetic acid and pyridine must be excluded. However, as will be shown later, the highly accurate pH determinations obtained mean that analytical problems more complicated than with these solvents can be resolved. The most suitable medium for the application of the proposed approach is a solvent with properties close to those of water. Methanol is perhaps the ideal non-aqueous solvent, having a relatively high dielectric constant, hydrogen-bonding ability, compatibility with strong titrants *etc.* Still better properties are shown by some water-organic solvent mixtures. At constant ionic strength and with a standard solution of a strong acid (*e.g.*, hydrochloric) as titrant, the galvanic cell, consisting of a glass electrode (GE) and a saturated calomel reference electrode (SCE-aqueous), has the following potential in such media (see list of symbols in Appendix I).

$$E = E^0 + s \log c_{H^+} \quad (1)$$

At this point it must be clearly stated that here pH is defined in terms of concentration, not of activity as it is in the formal definition for water. In order to differentiate between our definition (concentration of  $H^+$  in the non-aqueous medium at constant ionic strength) and the activity definition, ours will be denoted by an asterisk. Then equation (1) can be rewritten in the form:

$$pH^* = (E^0 - E)/s \quad (2)$$

As seen from equation (2) an accurate value of  $E^0$  is very important for obtaining reliable  $pH^*$  data. This value is calculated as a mean from the potentials for a series of titration points with known concentrations of hydrogen ions, *i.e.*,

$$E^0 = E + s \text{ pH}^* \quad (3)$$

The titration of a base is considered first, and the accurate determination of  $V_c$  will be the main aim. The strong-acid titrant added after the end-point defines accurately the concentration of hydrogen ions in equation (3), thus allowing an accurate determination of the  $E^0$  value. It was mentioned above that Pehrsson *et al.*<sup>8</sup> showed that the determination of

$V_c$ , especially for weak acids and bases, is not easy, and that the knowledge of some constants is essential. To deal with titrations in an arbitrary non-aqueous solvent or water-organic solvent mixture for which the appropriate constants are unavailable, we propose the following treatment of the primary data (mV/ml) obtained from an acid-base titration. For the titration of a base with a standard solution of a strong acid (see the flow-diagram in Fig. 1 and the equations in Table 1), step (i) is to apply Gran's mV functions to obtain the equivalence volumes  $V'_c$  and  $V''_c$  from data before and after the end-point respectively. A least-squares procedure (LSQ) is used, after division of the data into two groups of  $i$  and  $j$  data points, before and after the end-point respectively. Only  $V''_c$  is used later in the calculations. In step (ii) the titrant added after  $V''_c$  is used to determine a rough mean value for  $E^0$  from equation (3), along with its standard deviation (SD). When the base is not very weak, the SD of both  $V''_c$  and  $E^0$  is very small and they hold the same values throughout the whole calculation procedure. In step (iii), by means of equation (2) all the original mV data are recalculated into  $pH^*$  data; then in (iv), by means of a least-squares procedure and the Hofstee subroutine, rough values for  $K_a^*$  and  $V'_c$  are calculated (note that  $K_a^*$ , not  $K_b^*$ , is found). In the determination of moderately strong bases ( $pK_b^* < 5$ ), the standard deviation is highly sensitive to the value of the autoprotolysis constant  $pK_s^*$ , so a minimization procedure  $\Delta pK_s^*$  is used, and this yields quite accurate  $pK_s^*$  values. In step (v), the calculated  $K_a^*$  values are used in the Ingman subroutine to find an accurate  $V''_c$  value, from which highly accurate  $E^0$  and  $pH^*$  values are obtained. When the base is very weak ( $pK^* > 7$ ), the standard deviation of  $V''_c$  is very sensitive to the  $E^0$ -value. A minimization procedure  $\Delta E^0$  is applied in this case. In step (vi) the Hofstee equation is used again to calculate the final  $V'_c$  and  $K_a^*$  values, which are printed along with the  $V''_c$  and  $E^0$  values and their SD. When the base is moderately strong, further data are available and  $pK_s^*$  and  $pK_b^*$  ( $= pK_s^* - pK_a^*$ ) are also calculated.

At this point a minor detail should be discussed: when the titration is done with an acid titrant, the characteristic constant of the galvanic cell  $E^0$  defines the  $pH^*$  scale from its acidic range, and the constant

Table 1. Equations used in NABTIT; symbols are given in Appendix I

Name of subroutine	Equations	Remarks
Gran mV acids	$V_i 10^{E_i/s}; (V_0 + V_i) 10^{E_i/s}; (V_0 + V_i)/10^{E_i/s}$	Using LSQ yields $V'_c, V''_c$ .
bases	$V_i/10^{E_i/s}; (V_0 + V_i)/10^{E_i/s}; (V_0 + V_i) 10^{E_i/s}$	Actually only $V''_c$ is used.
Hofstee	$y_i = V_i + (V_0 + V_i)(H_i - K_a^*/H_i)/T$ $x_i = -[V_i H_i + (V_0 + V_i)(H_i^2 - K_s^*/T)]$	Using LSQ yields $V'_c$ and $K_a^*$ or $V'_c$ and $K_b^*$
Ingman	$V''_c = V_j + \frac{1}{K_a^*} [V_j H_j + H_j^2 (V_0 + V_j)/T - K_s^* (V_0 + V_j)/T] + (V_0 + V_j)(H_j - K_a^*/H_j)$	Yields mean value of $V''_c$ from $j$ data points, with the standard deviation

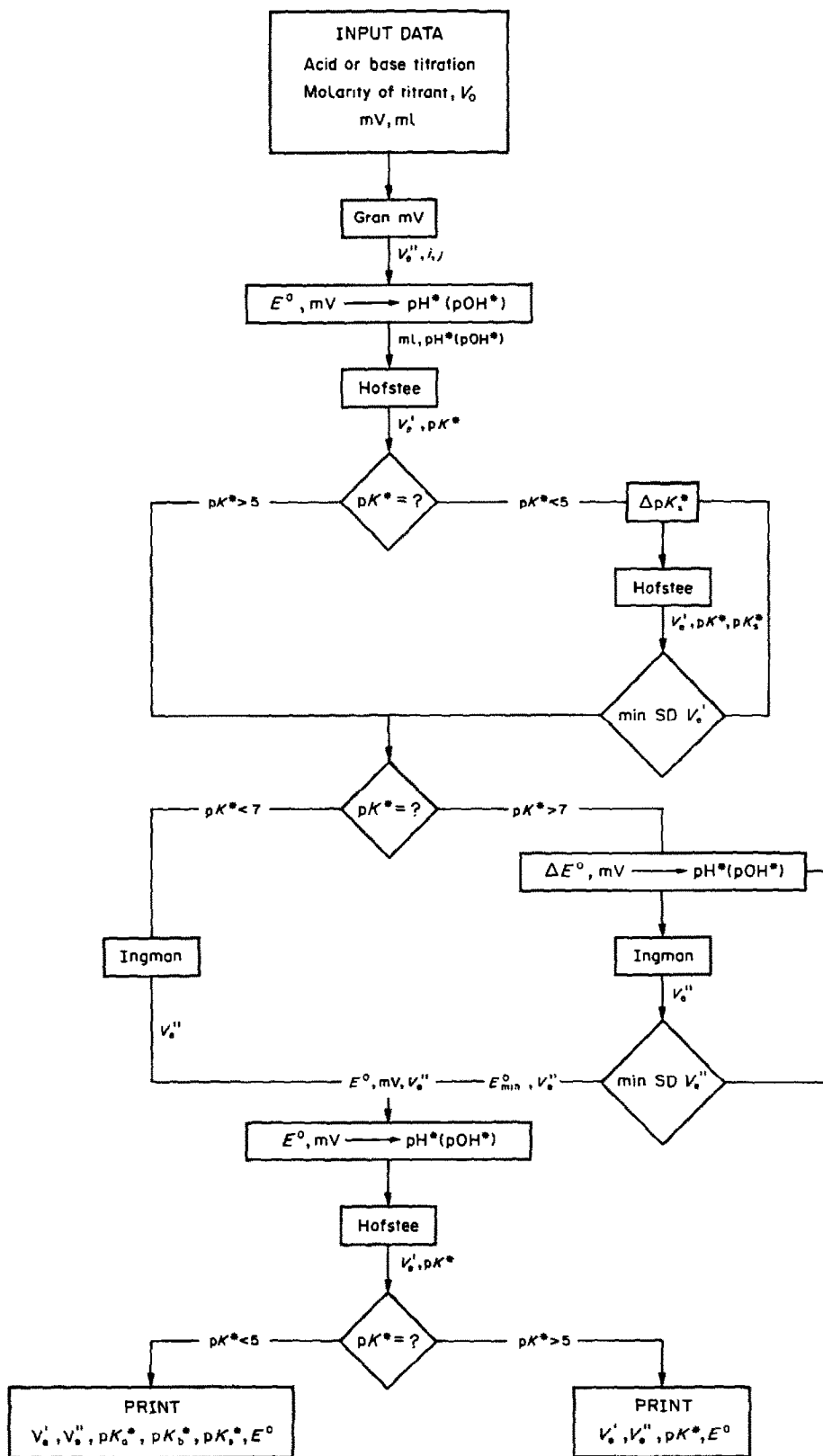


Fig. 1. Flow diagram of NABTIT program.

is denoted as  $E_{\text{acid}}^0$  or  $E_a^0$ . When an acid is titrated with a strong base, the calculated constant is the basic one,  $E_b^0$ , which defines the basicity scale, that is the  $\text{pS}^*$  scale (note that  $\text{S}^-$  is the analogue of  $\text{OH}^-$  for non-aqueous solvents, the so-called lyate ion;  $\text{SH}_2^+$  is the analogue of  $\text{H}_3\text{O}^+$ , the so-called lyonium ion). The calculations in the case of a titration of an acid are very similar to those already described (and use the same equations) but the constants obtained are now  $K_a^*$  and  $E_b^0$ , and these are printed together with  $V_c'$  and  $V_c''$ . When the acid is moderately strong ( $\text{p}K_a^* < 5$ ),  $\text{p}K_s^*$  and  $\text{p}K_a^*$  are also calculated.

Of special interest is the accurate value obtained for the autoprotolysis constant  $\text{p}K_s^*$ , which occurs in the equations for both the Hofstee and the Ingman subroutines (see Table 1). Preliminary investigations showed that this accurate value is necessary only in the determination of  $V_c'$  with the Hofstee subroutine in the special case when the titrated acid or base is moderately strong. The determination of  $V_c''$  in this case with the Ingman subroutine is not affected by the  $\text{p}K_s^*$  value, unless its value is higher than the true one. The influence of  $\text{p}K_s^*$  in Hofstee's equation was investigated in detail by use of simulated data for hypothetical titrations of acids of various strengths, by a BASIC computer program TIAB (Titration of Acids and Bases)<sup>17</sup> similar to Sillén's HALTA-FALL.<sup>18</sup> The results of these investigations are presented in Fig. 2, which shows the error-square sum

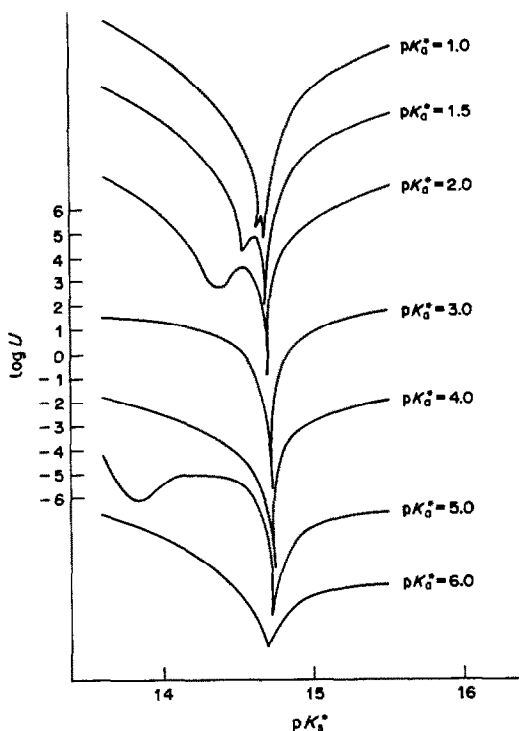


Fig. 2. Error-square sum as a function of  $\text{p}K_s^*$  from the Hofstee subroutine, for acids with  $\text{p}K_a^* = 1-6$  in a hypothetical solvent with  $\text{p}K_s^* = 14.7$ . (The  $\log U$  scale is valid for  $\text{p}K_a^* = 3.0$ .)

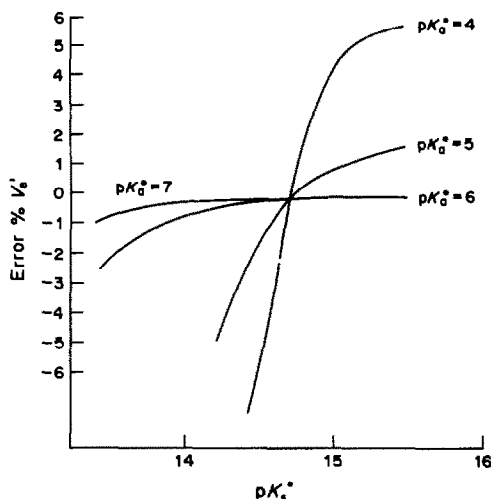


Fig. 3. Percentage error in the determination of  $V_c'$  as a function of  $\text{p}K_s^*$  for acids with  $\text{p}K_a^* = 4-7$  in a hypothetical solvent with  $\text{p}K_s^* = 14.7$ .

$U = \sum (K_a^* x_i + V_c' - y_i)^2$  as a function of the value assumed for  $\text{p}K_s^*$ , for titration of acids ( $\text{p}K_a^* = 1-6$ ) in a hypothetical solvent with  $\text{p}K_s^* = 14.7$ . The error-square sum can be seen to be highly sensitive to variations in  $\text{p}K_s^*$ . This behaviour explains the success of the method for determination of the autoprotolysis constant by finding the minimum of the  $U$ -function. Since local minima are observed in some cases ( $\text{p}K_s^* < 3$ ) the minimization procedure is started from higher  $\text{p}K_s^*$  values. It can also be seen that with  $\text{p}K_a^*$  values above 6, the minimum is not so definite, so in these cases it cannot be used for the determination of  $\text{p}K_s^*$ .

Similar investigations were made of the error in the determination of  $V_c'$  (with the Hofstee subroutine) as a function of  $\text{p}K_s^*$  (see Fig. 3 where the "true" value of  $\text{p}K_s^*$  is 14.7). As expected, the error in  $V_c'$  was highly dependent on the  $\text{p}K_s^*$  value only for a moderately strong acid. Since in these cases  $\text{p}K_s^*$  is determined as a by-product of the calculations, the value of  $V_c'$  is determined accurately. For acids with  $\text{p}K_a^* > 6$  the error is very small and quite independent of  $\text{p}K_s^*$ , so the lack of  $\text{p}K_s^*$  data will not prevent the determination of an accurate value for  $V_c'$ . As already mentioned, high starting values should be used for  $\text{p}K_s^*$ , moreover this is a requirement for the successful application of the Ingman subroutine in the case of a very weak acid.

## EXPERIMENTAL

### Reagents

Methanol (Merck) was used without purification. Water-methanol (50%) solution was prepared by weight with doubly distilled water.

Sodium chloride was recrystallized from water and dried at 105°.

Tris(hydroxymethyl)aminomethane hydrochloride (Merck) and sulphanic acid (Chemapol, Czechoslovakia), both reagent grade (99% purity), were used without

purification. Tris(hydroxymethyl)aminomethane (Merck) was recrystallized from water and dried at 105°.

Sodium hydroxide (0.1M) solution in water-methanol mixture was purified by addition of barium chloride (0.01M) to precipitate carbonate. Aqueous hydrochloric acid (0.1M) was used.

#### Measurements

The potentiometric titrations were performed in a cell kept at 25 ± 0.2°. The potential was measured with a PHM 84 pH-meter (Radiometer), to ± 0.1 mV. Glass G202 B and saturated calomel K401 electrodes (Radiometer) were used. The ionic strength ( $I = 0.2$  or 0.1M) was maintained with sodium chloride.

### RESULTS AND DISCUSSION

To check the validity of the proposed method and the function of the program NABTIT, several titrations were performed with standard substances often used in acid-base investigations. Since the method can in principle be applied in water, the first test was done with aqueous medium and tris-(hydroxymethyl)aminomethane (TRIS). The titration was done with standard hydrochloric acid at constant ionic strength. The data, the output and some specific details are presented in Table 2.

As seen from the output of NABTIT, first the Gran mV plot is calculated, then the value of the specific constant of the potentiometric cell is found ( $E_a^0$ ). All quantities are printed with their standard deviations. Based on  $E_a^0$ , all the original data are recalculated into pH\* values, and the Hofstee subroutine is used to calculate  $V_c'$ . Since the substance titrated is a weak base, no difference was found from  $V_c'$  calculated by

Gran's mV equation, and little difference was found when the Ingman subroutine was used to calculate  $V_c''$ . This small correction did not alter  $E_a^0$ , so no change was observed in the final Hofstee  $V_c'$ . This final result was used to calculate the content of TRIS, which was found to be very near to that expected—99.9 ± 0.4%. The concentration acidity constant of TRIS was calculated to be  $pK_a^* = 8.054 \pm 0.004$ . By using the extended Debye-Hückel equation with  $a = 2.8 \text{ \AA}$  for  $H_3O^+$  and  $a = 4 \text{ \AA}$  for  $TRIS.H^+$ ,<sup>19</sup> a correction term of  $\log(f_{H_3O^+}/f_{TRIS.H^+}) = 0.018$  was found. The thermodynamic constant,  $pK_a^T = 8.072$ , calculated with this, coincides fairly well with that obtained by Bates and Hefzer<sup>20</sup> ( $pK_a^T = 8.075$ ) (we think the good agreement is perhaps accidental).

Good coincidence between experiment and theory was also found in the calibration of the potentiometric cell. This is demonstrated clearly in Table 2 where the experimentally determined pH\* values (column 3) can be seen alongside the values calculated by program TIAB (column 4) and the differences  $\Delta pH^* = 100(pH_{exp}^* - pH_{theor}^*)$  in column 5.

It is obvious that the error of the pH\* data found by NABTIT is less than ± 0.01. Two points near to the end-point (Nos. 7 and 8) differ considerably from the theoretical values, and these two points are rejected by the program. This clearly demonstrates the advantage of linear plots over the use of the inflection point or derivative methods to estimate  $V_c'$  from data only in the vicinity of the end-point, as is common with automatic titrators.

The second step in this investigation was to check

Table 2. Titration of 0.02M TRIS with hydrochloric acid in water

Output from NABTIT			Output from TIAB		
Gran mV $V_c' = 5.127 \pm 0.02$					
Gran mV $V_c'' = 5.128 \pm 0.01$					
$E_{acid}^0 = +388.1 \pm 0.2$					
Experimental data, mV	Volume, ml	pH* <sub>exp</sub>	pH* <sub>theor</sub>	100 $\Delta pH^*$ 100 (pH* <sub>exp</sub> - pH* <sub>theor</sub> )	
-99.7	2.00	8.246	8.246	0.0	
-89.6	2.50	8.075	8.074	+0.1	
-79.5	3.00	7.905	7.903	+0.2	
-69.2	3.50	7.730	7.720	+0.1	
-55.7	4.00	7.502	7.504	-0.2	
-37.0	4.50	7.186	7.200	-1.4	
+10.9	5.00	6.376	6.478	-10.2	
+212.3	5.50	2.972	2.932	+4.0	
+236.0	6.00	2.571	2.565	+0.6	
+247.9	6.50	2.370	2.374	-0.4	
+255.5	7.00	2.241	2.246	-0.5	
+261.2	7.50	2.145	2.149	-0.5	
+265.6	8.00	2.071	2.073	-0.2	
+269.3	8.50	2.008	2.009	-0.4	
+272.4	9.00	1.956	1.956	0.0	
Hofstee $V_c' = 5.127 \pm 0.02$					
Ingman $V_c'' = 5.125 \pm 0.01$					
$pK_a^* = 8.054 \pm 0.04$					

Conditions: titrant 0.0974M HCl;  $V_0 = 25.00$  ml;  $I = 0.2$  (0.2M NaCl); temperature = 25°; TRIS taken = 60.50 mg; found = 60.44 mg; purity = 99.9%.



Table 3. Titration of TRIS.HCl with sodium hydroxide solution in 50% w/w methanol-water

Experimental data, <i>mV</i>		Volume, <i>ml</i>	Output from TIAB		
			$\text{pH}_{\text{exp}}^*$	$\text{pH}_{\text{theor}}^*$	100 $\Delta\text{pH}^*$
Output from NABTIT					
Gran $mV V_e' = 2.872 \pm 0.02$					
Gran $mV V_e'' = 2.818 \pm 0.01$					
$E_{\text{base}}^0 = -447.09 \pm 0.13$					
-57.8	0.50	7.319	7.316	+0.3	
-81.4	1.00	7.718	7.720	-0.2	
-99.5	1.50	8.024	8.031	-0.7	
-119.0	2.00	8.353	8.353	$\pm 0.0$	
-147.3	2.50	8.832	8.818	+1.4	
-254.3	3.00	10.641	10.540	+10.1	
-274.2	3.20	10.977	10.920	+5.7	
-284.9	3.40	11.158	11.120	+3.8	
-292.3	3.60	11.283	11.256	+2.7	
-302.6	4.00	11.457	11.439	+1.8	
-311.5	4.50	11.608	11.590	+1.8	
-317.5	5.00	11.709	11.699	+2.0	
-322.5	5.50	11.793	11.784	+0.9	
-326.5	6.00	11.861	11.852	+0.9	
-329.6	6.50	11.913	11.909	+0.4	
Hofstee $V_e' = 2.869 \pm 0.018$					
Ingman $V_e'' = 2.817 \pm 0.011$					
$\text{p}K_s^* = 5.908 \pm 0.05$					
Conditions: titrant 0.08867M NaOH; 50% w/w MeOH-H <sub>2</sub> O; $V_0 = 25.00$ ml; $I = 0.1$ (0.1M NaCl); temperature = 25°; TRIS.HCl taken = 40.35 mg; found = 40.09 mg; purity = 99.3 <sub>5</sub> %.					

Table 4. Titration of sulphanilic acid with sodium hydroxide solution in 50% w/w methanol-water

Experimental data, <i>mV</i>		Volume, <i>ml</i>	Output from TIAB		
			$\text{pH}_{\text{exp}}^*$	$\text{pH}_{\text{theor}}^*$	100 $\Delta\text{pH}^*$
Output from NABTIT					
Gran $mV V_e' = 3.277 \pm 0.23$					
Gran $mV V_e'' = 2.873 \pm 0.01$					
$E_{\text{base}}^0 = -450.64 \pm 0.17$					
+208.4	0.80	2.719	2.718	+0.1	
+204.2	1.00	2.790	2.790	0.0	
+199.7	1.20	2.866	2.866	0.0	
+194.8	1.40	2.949	2.949	0.0	
+189.5	1.60	3.039	3.039	0.0	
+183.5	1.80	3.140	3.139	+0.1	
+176.6	2.00	3.257	3.255	+0.2	
+168.3	2.20	3.397	3.393	+0.4	
+157.8	2.40	3.575	3.572	+0.3	
+142.3	2.60	3.837	3.837	0.0	
-243.6	3.00	10.360	10.477	-11.7	
-272.1	3.20	10.842	10.873	-3.1	
-289.6	3.50	11.138	11.148	-1.0	
-304.6	4.00	11.391	11.393	-0.2	
-313.7	4.50	11.545	11.545	0.0	
-320.1	5.00	11.653	11.653	0.0	
-325.1	5.50	11.738	11.738	0.0	
-329.2	6.00	11.807	11.806	+0.1	
-332.4	6.50	11.861	11.864	-0.3	
Hofstee $V_e' = 2.865 \pm 0.002$					
Ingman $V_e'' = 2.871 \pm 0.009$					
$\text{p}K_s^* = 11.10$					
$\text{p}K_s^* \text{min} = 13.90$					
$\text{p}K_s^* = 2.80$					
Conditions: Titrant 0.08739M NaOH; 50% w/w MeOH-H <sub>2</sub> O; $V_0 = 25.00$ ml; $I = 0.1$ (0.1M NaCl); temperature = 25°; SA taken = 44.15 mg; found = 43.36 mg; purity 98.2%.					

the program by titrations with non-aqueous solutions. Because reliable data for 50% methanol media are available, this solvent was used, with TRIS.HCl and sulphanic acid (SA). The first was chosen because of the reliable data obtained by Schindler *et al.*<sup>19</sup> and the second because it is moderately strong so would allow determination of the  $pK_a^*$  value for the mixture, in addition to  $V_e$  and  $K_a^*$ . The input data, the output and other details are given in Tables 3 and 4. The quantity of TRIS.HCl found was close to the expected value (equivalent to 99.3% purity). From the base constant  $pK_b^* = 5.908$ , the acid constant was calculated to be  $pK_a^* = pK_b^* - 5.908 = 7.982$  ( $pK_s^* = 13.90$ —see below). By use of the extended Debye-Hückel equation, with specific gravity  $d_0 = 0.9125$ ,<sup>21</sup> and dielectric constant  $\epsilon = 56.3$ ,<sup>19</sup> for the methanol-water mixture,  $pK_a^T = 8.00$  was found, which correlates quite well with the literature value<sup>22</sup> of  $pK_a^T = 7.818$ . Column 5 in Table 3 shows a relatively good calibration of the glass electrode cell in this medium. The results in Table 4 also show a very good coincidence for  $pH^*$  between theory and experiment. Because SA is a moderately strong acid, the  $pK_b^*$  and  $pK_a^*$  values were found. No data for  $pK_a^*$  were found in the literature for this medium. The calculated  $pK_s^*$  value is 13.90, which agrees well with the result ( $pK_s^* = 13.86$ ) obtained from a titration of hydrochloric acid with a standard solution of sodium hydroxide in the same non-aqueous medium ( $I = 0.1M$ ). The purity of the SA was found to be 98.2%, which was near to the specification.

In conclusion, in contrast to other published programs, the main advantage of NABTIT is the absence of any requirements for input information concerning equilibrium constants. This allows the program to be used for non-aqueous acid-base titrations (e.g. in water-organic solvent mixtures) for which equilibrium constants are scarce. A second interesting use of NABTIT might be to supply preliminary input data for non-linear regression programs for which the input of equilibrium constants as starting values is imperative.

## REFERENCES

1. F. Ingman and E. Still, *Talanta*, 1966, **13**, 1431.
2. G. Gran, *Analyst*, 1952, **77**, 661.
3. A. Johansson, *Analyst*, 1970, **95**, 535.
4. T. Briggs and J. Stuehr, *Anal. Chem.*, 1974, **46**, 1517.
5. H. J. Hofstee, *Science*, 1960, **131**, 39.
6. L. Z. Benet and J. E. Goyan, *J. Pharm. Sci.*, 1965, **54**, 1179.
7. L. J. Leeson and M. Brown, *ibid.*, 1966, **55**, 431.
8. L. Pehrsson, F. Ingman and A. Johansson, *Talanta*, 1976, **23**, 769.
9. *Idem. ibid.*, 1976, **23**, 781.
10. L. Pehrsson and F. Ingman, *ibid.*, 1977 **24**, 79.
11. M. Meloun, J. Havel and E. Högföldt, *Computation of Solution Equilibria*. Ellis Horwood, Chichester, 1988.
12. G. Arena, E. Rizzarelli, S. Sammartano and C. Rigano, *Talanta*, 1979, **26**, 1.
13. C. Rigano, M. Grasso and S. Sammartano, *Ann. Chim. (Rome)*, 1984, **74**, 537.
14. L. G. Sillén, *Acta Chem. Scand.*, 1962, **16**, 159.
15. N. Ingri and L. G. Sillén, *ibid.*, 1962, **16**, 173.
16. J. Tencheva, G. Velinov and O. Budevsky, *J. Electroanal. Chem.*, 1976, **68**, 65.
17. O. Budevsky, unpublished program.
18. N. Ingri, W. Kakałowicz, L. G. Sillén and B. Warnqvist, *Talanta*, 1967, **14**, 1261; Errata, 1968, **15**, No. 3, ix.
19. P. Schindler, R. A. Robinson and R. Bates, *J. Res. Natl. Bur. Stds.*, 1968, **72A**, 141.
20. R. Bates and H. Hefzer, *J. Phys. Chem.*, 1961, **65**, 667.
21. B. R. Staples and R. S. Carter, Jr., *NBS Technical Note*, 1969, **503**, 45.
22. R. Bates, *ibid.*, 1965, **271**, 53.

## APPENDIX I

$pH^*$ —negative logarithm of hydrogen ion concentration in the non-aqueous medium at constant ionic strength ( $I = \text{const.}$ ).

$pK_s^*$ ,  $pK_a^*$ ,  $pK_b^*$ —autoprotolysis, acid and base equilibrium constants defined for the same conditions.

$s$ —the Nernst factor  $2.303RT/F = 59.155 \text{ mV/decade}$  at  $25^\circ$ .

$E^0$ —characteristic constant of a galvanic cell consisting of a glass electrode (GE) and saturated calomel electrode (SCE).

$V_0$ —initial volume, ml.

$i, j$ —number of points before and after the equivalence point.

$V_i, V_j$ —volume of standard solution, ml.

$V_e'$ —equivalence volume calculated by means of data before the end-point.

$V_e''$ —equivalent volume obtained from data after the end-point.

$E_i, E_j$ —measured potential, mV.

$H_i, H_j$ —molar concentration of  $H^+$ .

$T$ —molarity of titrant.

## SHORT COMMUNICATIONS

# A MICROWAVE DISSOLUTION TECHNIQUE FOR THE DETERMINATION OF ARSENIC IN SOILS

J. HUANG, D. GOLTZ and F. SMITH\*

Chemistry Department, Laurentian University, Sudbury, Ontario, Canada

(Received 1 February 1988. Accepted 4 August 1988)

**Summary**—A procedure has been developed for rapid dissolution of soil samples by heating with various acid mixtures in sealed vessels in a microwave oven, without risk of loss of arsenic through volatilization.

The decomposition of soil samples for analysis for arsenic is traditionally time-consuming. Great care must be taken to ensure that all the arsenic is released from the soil matrix into the solution, but that none is lost as volatile compounds.<sup>1,2</sup> In our laboratory, we have achieved excellent dissolution results with a wide range of soil types, using the method proposed by Maher,<sup>3</sup> followed by arsine generation and atomic-absorption spectrophotometry. Recently however, we have developed a two-stage microwave dissolution procedure which cuts down the time taken for sample preparation from 15 hr or so, to 2 hr.

This communication describes the procedure, and reports the results of arsenic determination in four standard soil samples.

### EXPERIMENTAL

#### Apparatus

A domestic microwave oven (Toshiba model ER-855BTC) with nine power settings (starting at 72 W and increasing by 81-W increments to 720 W) was used. The Teflon-PFA vessels used for the dissolutions had a volume of approximately 150 ml and tight-fitting screw cap lids. Arsine was generated with sodium borohydride in a Perkin-Elmer MHS-10 system, and introduced into a silica cell, 16.5 cm long and 1.2 cm in diameter, heated in the air-acetylene flame of a Perkin-Elmer model 5000 atomic-absorption spectrophotometer.

#### Reagents

All the chemicals used were of analytical-reagent grade. The standard soil samples were drawn from a variety of environments:

- SO-1: Regosolic C Horizon Soil
- SO-2: Podzolic B Horizon Soil
- SO-3: Calcareous C horizon Soil
- SO-4: Black Chernozemic A Horizon Soil

The origin and preparation of these materials is detailed elsewhere,<sup>4</sup> and the results of round-robin analyses for a number of elements in the samples have been reported.<sup>5</sup>

#### Procedure for microwave dissolution

The soil sample (0.1–0.5 g) was weighed into a 150-ml Teflon-PFA vessel and 3.5 ml of concentrated nitric acid were added. The vessel was then sealed with the screw cap (tightened with the wrench supplied by the makers) and placed in the microwave oven (set at power level 9) for 2.5 min. The vessel was then removed from the oven and placed in a tray of ice-water for 30 min. Next, the cap was carefully removed and 3.5 ml of concentrated nitric acid, 1.5 ml of 70% perchloric acid and 1.0 ml of concentrated sulphuric acid were added. The vessel was then re-capped and replaced in the microwave oven for three intervals of heating at power level 9, each of 2.5 min duration, with a break of 2 min without heating between each of the intervals. After this, the vessel was removed from the oven and placed in the ice-water bath for a further 30 min. Then the cap was removed, the contents of the vessel were washed through a Whatman No. 40 filter paper into a 50-ml standard flask and made up to volume with 1.5% v/v hydrochloric acid and the solution was stored in a plastic bottle to await analysis.

#### Safety precautions

Since considerable pressures are generated in the vessels during the microwave heating process, gloves and a visor were used when removing the vessels from the oven, and when releasing the caps.

\*Author to whom correspondence should be addressed.

Table 1. Results of arsenic analyses on standard soil samples\*

Soil	Sample weight, g	n	As found, µg/g	CANMET value, µg/g	n
SO-1	0.3	8	1.9 (0.1)	1.9 (0.3)	5
SO-2	0.5	8	1.1 (0.1)	1.2 (0.2)	5
SO-3	0.2	8	2.6 (0.1)	2.6 (0.1)	5
SO-4	0.1	12	7.1 (0.5)	7.1 (0.7)	6

\*(Standard deviations are given in parentheses, for n replicates).

### RESULTS AND DISCUSSION

The results of the determinations of arsenic in the standard soils, following the microwave dissolution procedure, are given in Table I.

The results are in very good agreement with the CANMET<sup>5</sup> values for each of the different soil types, and the precisions obtained are excellent. We therefore have confidence in recommending this relatively rapid procedure for routine laboratory use.

*Acknowledgements*—We thank the Centre in Mining and Mineral Exploration Research (CIMMER) of Laurentian University for the provision of facilities and financial sup-

port, and John Labrecque of Kidd Creek Mines Ltd., for the gift of standard soil samples.

### REFERENCES

1. J. F. Uthe, H. C. Freeman, J. R. Johnston and P. Michalik, *J. Assoc. Anal. Chem.*, 1974, **57**, 1363.
2. J. E. Portmann and J. P. Riley, *Anal. Chim. Acta*, 1964, **31**, 509.
3. W. A. Maher, *Talanta*, 1983, **30**, 534.
4. W. S. Bowman, G. H. Faye, R. Sutarno, J. A. McKeage and H. Kodama, *Geostds. Newsl.*, 1978, **3**, 109.
5. *Idem*, *CANMET Rep.* 79-3, Energy, Mines and Resources, Canada, 1979.

## A TITRIMETRIC METHOD FOR ESTIMATION OF FLUORINE IN ORGANIC COMPOUNDS

PARTHA S. DAS, BASUDAM ADHIKARI, MRINAL M. MAITI and SUKUMAR MAITI  
Materials Science Centre, Indian Institute of Technology, Kharagpur 721 302, India

(Received 1 March 1988. Revised 28 May 1988. Accepted 11 July 1988)

**Summary**—A simple and rapid titrimetric method for estimation of fluorine in organic compounds and fluoropolymers is reported. It involves combustion of the sample in oxygen, absorption of the combustion products in an aqueous solution of Ce(III) nitrate and glycerol, containing hexamethylenetetramine, and finally titration with EDTA, with Xylenol Orange and Methylene Blue as screened indicator.

Many organic fluoro-compounds are widely used in industry, as aerosol propellants, refrigerants, insulators, agrochemicals, drugs, fluoroplastics, etc., but there are few satisfactory, simple and rapid methods for determination of fluorine in these materials. The procedures reported suffer from various drawbacks, such as poor accuracy or reproducibility, lengthiness, complexity and hazard. The major steps are decomposition to yield fluoride, removal of various interferences, and finally estimation of the fluoride by various methods, titrimetry, photometry, potentiometry etc. The main sources of error arise from the difficulty in decomposing the fluoro-compound, separation of the fluoride from the interfering species, and the estimation methods themselves.

Procedures for decomposition of organic fluoro-compounds were reviewed up to 1958 by Ma and Gwirtsman.<sup>1,2</sup> They were based on catalytic oxidation, reduction with sodium in liquid ammonia, alkaline fusion, and hydrolysis to fluoride. The determination was by titration with thorium nitrate, alkalimetric determination of hydrogen fluoride, or gravimetric determination of fluoride.

Light and Mannion<sup>3</sup> reported a microdetermination by potentiometric titration, with a fluoride-selective electrode as the end-point detector, and compared the combustion of the fluoro-compound in a borosilicate flask with that in a polycarbonate flask, with or without a combustion aid.

Here we report the estimation of fluorine in organic compounds after decomposition in a glass Schöniger flask without a combustion aid.

### EXPERIMENTAL

#### Apparatus

A Heraeus Schöniger combustion apparatus was used.

#### Reagents

All chemicals used were of analytical reagent grade.

Ce(III) nitrate solution (0.005*M*) was prepared by dissolving 2.75 g of ceric ammonium nitrate in 1000 ml of water containing 2 ml of concentrated nitric acid, then gradually adding solid hydroxylamine hydrochloride until the solution

was decolorized, and finally a further 2 g of hydroxylamine hydrochloride.

EDTA solution (0.002*M*) was prepared by dissolving 3.722 g of EDTA (disodium salt) in 1000 ml of water and diluting 200 ml of this solution to 1000 ml with water, and standardized by an appropriate titration.

#### Procedure

Weigh about 5–10 mg of the fluorocarbon compound, containing 1–3 mg of fluorine, into the usual L-shaped piece of Whatman No. 40 filter paper, fold the packet, and place it in the platinum basket of the combustion flask. Place the absorption solution, consisting of water (5 ml), cerium(III) nitrate solution (exactly 15 ml) and 10% glycerol solution (5 ml) in the combustion flask, then fill the flask with pure oxygen. If apparatus with a built-in ignition system is used, insert the stopper/sample-holder assembly, invert the flask to seal the joint with absorption solution, and place it in the combustion chamber. Otherwise, light the paper and insert the stopper as usual. After ignition, allow the flask to cool for 10 min and then vigorously shake it for complete absorption of the combustion products. Open the flask, rinse the stopper assembly with a little water and add 20 ml of ethanol. Add 3 drops of 0.2% Xylenol Orange solution and 2 drops of 0.1% Methylene Blue solution followed by ~70 mg of hexamethylenetetramine to develop a violet colour for the indicator and maintain the pH in the range 5.5–6.5. Titrate with 0.002*M* EDTA to a sharp colour change to green at the end-point ( $V_1$  ml). Run a blank ( $V_2$  ml) in the same way.

The percentage of fluorine in the sample is calculated from

$$\% F = 5700(V_2 - V_1)M/W$$

where  $M$  is the molarity of the EDTA and  $W$  is the weight of sample in mg.

### RESULTS AND DISCUSSION

Repeated attempts to analyse organic fluoro-compounds according to the manual for the combustion apparatus<sup>4</sup> failed to give reliable results. We have therefore modified the method as follows.

1. Three drops of 0.2% Xylenol Orange solution and 70–75 mg of solid hexamethylenetetramine and three drops of 0.1% Methylene Blue solution were used as a screened indicator system and buffer,

Table 1. Determination of fluorine in organic compounds by a modified Schöniger combustion flask method

Sample	Weight, mg	Found, %
<i>p</i> -Fluorobenzoic acid (Theory 13.56% F)	6.9	13.5 <sub>2</sub>
	8.3	13.5 <sub>9</sub>
	9.3	13.4 <sub>9</sub>
	7.2	13.5 <sub>9</sub>
2-(Trifluoromethyl)phenothiazine (Theory 21.33% F)	9.3	21.4 <sub>3</sub>
	9.1	21.5 <sub>0</sub>
	9.5	21.2 <sub>4</sub>
	9.2	21.6 <sub>8</sub>
3-Trifluoromethylbenzoic acid (Theory 29.98% F)	9.5	30.1 <sub>5</sub>
	9.9	29.7 <sub>6</sub>
	9.4	29.8 <sub>5</sub>
	2,6-Dinitro- <i>N,N'</i> -dipropyl-4-(trifluoromethyl)benzenamine (Theory 16.99% F)	8.2
10.4		16.8 <sub>7</sub>
8.4		17.1 <sub>8</sub>
Teflon (commercial) (Theory 76% F)		4.4
	3.9	72.3
	3.2	72.1

instead of 1 g of Xylenol Orange/hexamine mixture (1:2 w/w) recommended.<sup>4</sup>

2. A pH of 5.5–6.5 was used for the absorption solution to avoid any protonation of the fluoride.

3. The recommended<sup>4</sup> boiling of the absorption solution was eliminated.

In this modified method a clear end-point is obtained. The results obtained for fluorine in four standard organic compounds by this method are presented in Table 1. It is evident that the combustion of the organic fluoro-compounds is complete. There is practically no interaction of the combustion products with the glass vessel. In earlier reports<sup>2,3,5-7</sup> the low results were attributed to incomplete combustion and the use of combustion aids was recommended. It was also reported that the results may be low because the hydrogen fluoride produced during the combustion reacts with the borosilicate glass of the combustion flask. Some authors claimed better results could be obtained by using a polycarbonate flask. Others<sup>5,8,9</sup> suggested the use of polypropylene and polyethylene flasks.

Since Light and Mannion<sup>3</sup> used only pure water as the absorption solution, there was ample scope for interaction of hydrogen fluoride with the borosilicate glass flask, so the major reason for error with their method may not have been due solely to the combustion problem. In the present method, since the absorption solution contains Ce(III) nitrate, the hydrogen fluoride produced in the combustion reacts

immediately to produce insoluble cerous fluoride.<sup>10</sup> The possibility of interaction of hydrogen fluoride with the glass flask is thus minimized. The function of the glycerol is not clear; if it is not present, low and irreproducible results are obtained. It may assist in rapid dissolution of the hydrogen fluoride, or prevent its interaction with the glass.

This modified method is simple as well as rapid both in the decomposition and estimation steps and gives results within 15 min, with not more than  $\pm 0.3\%$  absolute error.

#### REFERENCES

1. T. S. Ma and J. Gwirtzman, *Anal. Chem.*, 1957, **29**, 140.
2. T. S. Ma, *ibid.*, 1958, **30**, 1557.
3. T. S. Light and R. F. Mannion, *ibid.*, 1969, **41**, 107.
4. W. Schöniger, *Methods of Analysis Relating to the Schöniger Method*, in Operation Manual of Combustion Apparatus, Heraeus, Hanau.
5. A. M. G. Macdonald, in *Advances in Analytical Chemistry and Instrumentation*, C. N. Reilly (Ed.), Vol. 4, pp. 75–116. Wiley-Interscience, New York, 1965.
6. A. Steyermark, R. R. Kaup, D. A. Petras and E. A. Bass, *Microchem. J.*, 1959, **3**, 523.
7. B. Z. Senkowski, E. G. Wollish and E. G. E. Shafer, *Anal. Chem.*, 1959, **31**, 1574.
8. M. E. Fernandopulle and A. M. G. Macdonald, *Microchem. J.*, 1966, **11**, 41.
9. J. E. Burroughs, W. G. Kator and A. I. Attia, *Anal. Chem.*, 1968, **40**, 657.
10. *Kirk-Othmer Encyclopedia of Chemical Technology*, 3rd Ed., Vol. 5, p. 322. Wiley-Interscience, New York, 1979.

## EXAMINATION OF GUANOSINE AND XANTHOSINE NUCLEOTIDES BY HPLC AND ELECTROCHEMICAL DETECTION

ANNA MARIA GHE, GIUSEPPE CHIAVARI and CECILIA BERGAMINI

Scuola di Specializzazione in Chimica Analitica, Dipartimento di Chimica "G. Ciamician", Università de Bologna, via Selmi, 2-40126 Bologna, Italy

(Received 8 April 1988. Revised 27 May 1988. Accepted 24 August 1988)

**Summary**—The suitability of electrochemical detection (ECD) following HPLC separation of guanosine, xanthosine and adenosine nucleotides has been evaluated. Separation of five monophosphates of guanosine was achieved by using a reversed-phase column; di- and triphosphates have also been separated from monophosphates. Adenosine compounds are insensitive to ECD.

Purine and pyrimidine bases are important components of nucleic acids, coenzymes, and the media of hormone action. Thus qualitative and quantitative analyses for these bases are under continuous development.

Recent studies have demonstrated that in certain pathological situations there is a change in the concentration of nucleotides, nucleosides, and the corresponding purine bases in biological fluids. We can therefore think of these substances as biological markers.<sup>1</sup> Particular importance from this point of view attaches to guanosine and its compounds, especially as neoplastic disease markers.<sup>2</sup>

A rapid and easily reproducible method for determination of guanosine and its nucleotides is desirable. Several methods are available, but it is the chromatographic techniques which are preferred when separation of components is necessary—as from a complex biological matrix—prior to determination. HPLC can be used successfully in the analysis of nucleotides and nucleosides and no derivatization is necessary.<sup>3,4</sup> The possibility of coupling HPLC and electrochemical detection (ECD) should reduce the effect of interferences. Previous work related to HPLC/ECD examination of purine and pyrimidine bases has been reported.<sup>5,6</sup> We have studied<sup>5</sup> bases and related nucleosides by HPLC/ECD, both in reversed-phase and ion-exchange chromatography, and verified that not all bases and related nucleosides are electrochemically active.

The aim of this work is to complete the study, examining the nucleotides of guanosine, adenosine and xanthosine by HPLC/ECD. We have used both reversed-phase and ion-exchange columns with the aim of establishing the optimum isocratic conditions. Use of the gradient technique with an electrochemical detector is not advised, as unacceptable noise is generated by the changes in polarity and composition of the eluents during the analysis.

### EXPERIMENTAL

#### Apparatus

A Hewlett-Packard model 1010A liquid isochromatograph with a Rheodyne 7120 sample injector (20  $\mu$ l loop, Varian model 2150) was used. The detectors were a Varian model 2550 variable wavelength detector and an ESA Coulochem electrochemical detector (model 5100) equipped with a model 5010 analytical cell. The output was recorded with a Houston Omniscrite or a Varian model 4290 integrator recorder. The columns used were an Erbasil C18 10  $\mu$  (250 mm  $\times$  4.6 mm) and a Whatman Partisil PXS 10/25 SAX (250 mm  $\times$  4.6 mm).

#### Reagents

The eluents used were: (a)  $\text{KH}_2\text{PO}_4$  (0.02M) and methanol (95:5 v/v), pH 5.8; (b)  $\text{KH}_2\text{PO}_4$  (0.02M), pH 7; and (c)  $\text{KH}_2\text{PO}_4$  (0.25M), pH 6.8.

The pH was adjusted by addition of acid or base to the buffer solution and measured with an Orion Research pH-meter (model 201) with an accuracy of  $\pm 0.01$ . Carlo Erba solvents (HPLC grade) and reagents (RPE grade) were used to prepare the eluents.

The standards were 5'-guanosine monophosphate (5'-GMP), 3'-guanosine monophosphate (3'-GMP), 2'-guanosine monophosphate (2'-GMP), cyclic 2',3'-guanosine monophosphate (2',3'-GMPC), cyclic 3',5'-guanosine monophosphate (3',5'-GMPC), 5'-guanosine diphosphate (5'-GDP), 5'-guanosine triphosphate (5'-GTP), guanosine, 5'-xanthine monophosphate (5'-XMP), 5'-xanthosine diphosphate (5'-XDP), 5'-xanthosine triphosphates (5'-XTP), 5'-adenosine monophosphate (5'-AMP), 5'-adenosine diphosphate (5'-ADP) and 5'-adenosine triphosphate (5'-ATP), supplied by Sigma, and of the highest purity available.

#### Procedure

The standard solutions and eluents were filtered through a 0.45- $\mu$ m plastic Millipore filter. For ultraviolet measurements a wavelength of 250 nm was chosen because the substances examined give maximum absorption at this wavelength. All experiments were done at room temperature, and at least in triplicate. Voltammetric measurements were made with an AMEL model 556 potentiostat equipped with a Hewlett-Packard model 7040A x-y recorder. A three-electrode cell was used with an AMEL GC492 glassy-carbon working electrode, a platinum counter-electrode and a saturated calomel reference electrode.

Table 1

Nucleotides	$k = (t_R - t_M)/t_M$		
	C18	PXS 10/25 SAX	
	Eluent (a)	Eluent (b)	Eluent (c)
5'-GMP	0.3	25.4	0
3'-GMP	0.9	25.4	0
2',3'-GMPc	1.3	12.6	0
2'-GMP	2.0	30.2	0
3',5'-GMPc	2.3	12.6	0
5'-GDP	0	—	1.7
5'-GTP	0	—	26.5
Guanosine	5.2	—	—
5'-XMP	0.4	—	0
5'-XDP	0	—	1.4
5'-XTP	0	—	23.2
5'-AMP*	1.3	—	0
5'-ADP*	0	—	—
5'-ATP*	0	—	—

Flow-rate 1 ml/min.

Ultraviolet detection at 250 nm.

\*Electrochemically inactive.

## RESULTS AND DISCUSSION

### HPLC separation of nucleotides

Nucleotides of guanosine, xanthine and adenosine were considered. Table 1 gives the capacity factors ( $k$ ) of these compounds on the Erbasil C18 and Partisil PXS 10/25 SAX columns. It appears that an isocratic separation of the mono-, di-, and triphosphates of guanosine and xanthosine is not practicable. The reversed-phase column, however, gives a good separation of the five guanosine monophosphates.

With the ion-exchange column PXS 10/25 SAX and eluent (b) (Table 1) there is a predictable inversion of the retention times of the different substances, but the separation between the five guanosine monophosphates is poorer. 5'-GMP and 2'-GMP are co-eluted and so are the two cyclic monophosphates 2',3'-GMPc and 3',3'-GMPc.

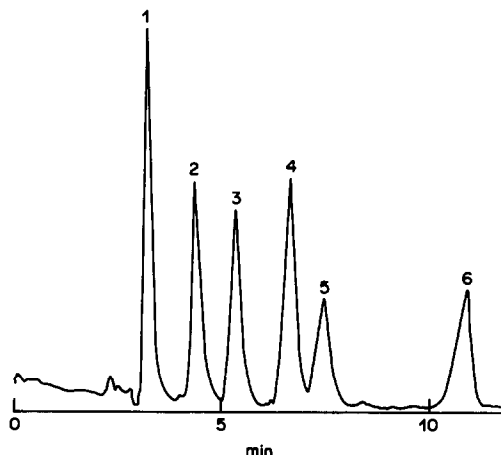


Fig. 1. Separation of guanosine monophosphates on an Erbasil C18 column, eluent (a). Electrochemical detection (oxidation potential +1.0 V). 1 = 5'-GMP, 2 = 3'-GMP, 3 = 2',3'-GMPc, 4 = 2'-GMP, 5 = 3',5'-GMPc, 6 = guanosine.

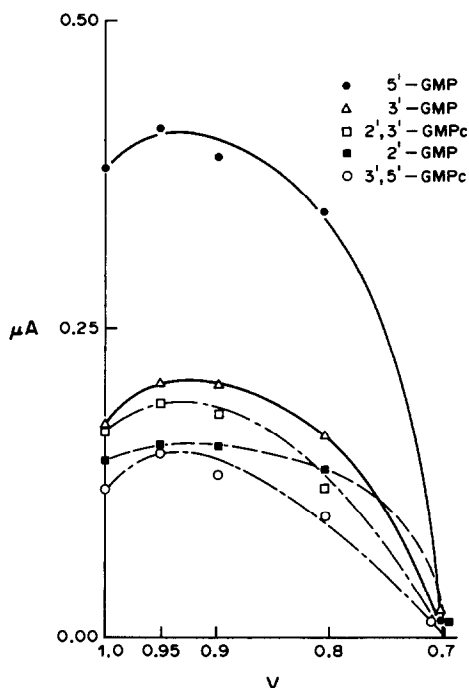


Fig. 2. Monophosphates: relationship between electrochemical detector response and applied potential. Erbasil C18 column, eluent (a); sample solutions  $10^{-5}M$ .

With eluent (c) (Table 1) it is possible to separate the di- and triphosphates from the monophosphates, which all have  $k = 0$ . Figure 1 shows the separation (Erbasil C18 column) of guanosine from its five monophosphates.

### Electrochemical detection of nucleosides

The change in oxidation state during ECD of nucleotides and nucleosides is related to the structure

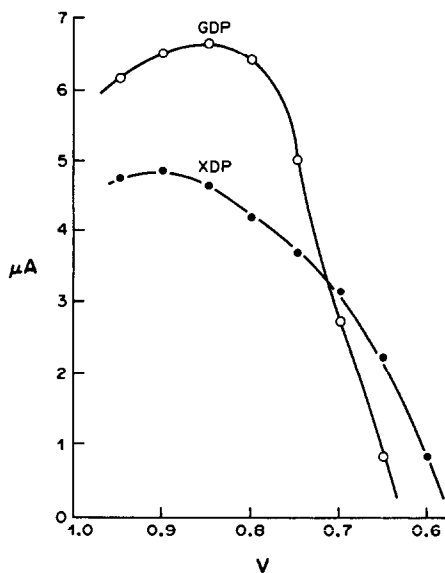


Fig. 3. Diphosphates: relationship between electrochemical detector response and applied potential. Erbasil C18 column, eluent (c); sample solutions  $10^{-5}M$ .



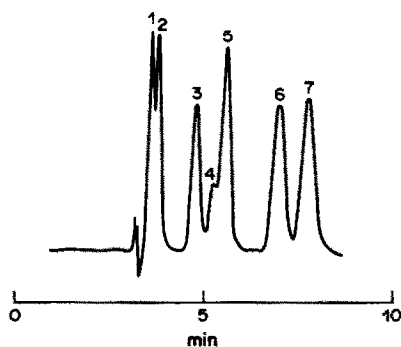


Fig. 4. Electrochemical detection at +1.00 V; 1, 5'-GMP; 2, 5'-XMP; 3, 3'-GMP; 4, 5'-AMP; 5, 2',3'-GMPc; 6, 2'-GMP; 7, 3',5'-GMPc.

of the corresponding base. Our previous work<sup>5</sup> showed that when the purine base was electrochemically active, the related nucleotides were oxidizable and therefore detectable by ECD. The present study, extended to nucleotides, confirms this behaviour.

The electroactivity of the test compounds was investigated to find the best working potentials for use of LSV (linear sweep voltammetry) methods. An anodic peak with an  $E_p$  of about +1.0 V, showing irreversibility characteristics under the experimental conditions (20 mV/sec), was observed. Over the range of potentials examined (down to -1.0 V) no reduction was apparent. Figure 2 shows the response (current vs. applied potential) for the guanosine and xanthosine monophosphates, and Fig. 3 gives the corresponding results for the diphosphates. The electrochemical response of the monophosphates begins at +0.7 V (with a maximum at about +0.95 V) whereas a lower potential is sufficient for the diphosphates (+0.6 V). Adenosine and related nucleotides do not give oxidation curves. Figures 4 and 5 show the ultraviolet and ECD responses for a mixture of

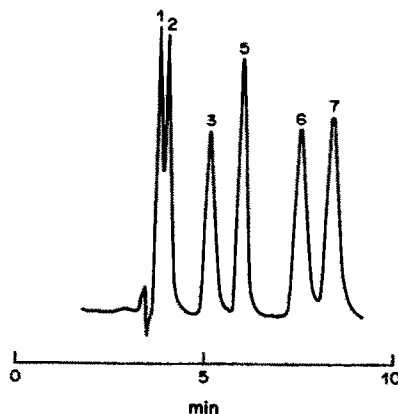


Fig. 5. Ultraviolet detection at 250 nm; identification of peaks as in Fig. 4.

monophosphates. The detection of 2',3'-GMPc in the presence of 5'-AMP is difficult with an ultraviolet detector but possible by ECD because the adenosine compounds do not give an ECD signal. The detection limits found for the mono- and diphosphates are around 10 pmole with either detector. The sensitivity for the triphosphates is poorer, toward 5 nmole, with both detectors, because of the "flattening" of the peaks owing to the higher retention times of these substances.

#### REFERENCES

1. R. A. Hartwich and P. R. Brown, *J. Chromatog.*, 1976, **126**, 769.
2. Chaghrou Yi, J. L. Fasching and P. R. Brown, *ibid.*, 1985, **339**, 75.
3. J. Stadler, *Anal. Biochem.*, 1987, **86**, 477.
4. J. B. Kafil, H. Y. Cheng and T. A. Last, *Anal. Chem.*, 1986, **58**, 285.
5. A. M. Ghe, G. Chiavari and J. Evgenidis, *Talanta*, 1986, **33**, 379.
6. R. J. Henderson and C. A. Griffin, *J. Chromatog.*, 1984, **298**, 231.

## SPECTROPHOTOMETRIC DETERMINATION OF MUZOLIMINE

C. S. P. SASTRY, M. V. SURYANARAYANA, A. S. R. P. TIRNENI  
and T. N. V. PRASAD

Foods and Drugs Laboratory, School of Chemistry, Andhra University, Waltair 530 003, India

(Received 16 May 1988. Accepted 11 July 1988)

**Summary**—Five simple, rapid and sensitive spectrophotometric procedures for the determination of muzolimine in bulk samples and pharmaceutical dosage forms are described. The methods are based on the formation of coloured species when muzolimine is reacted with 3-methyl-2-benzothiazolinone hydrazone hydrochloride, *p*-*N,N*-dimethylphenylenediamine dihydrochloride or *p*-*N*-methylaminophenol sulphate and a suitable oxidant or with 2,6-dichloroquinone chlorimide. The results obtained are reproducible with a coefficient of variation of less than 1.5%.

Muzolimine [MZ, 3-amino-1-(3,4-dichloro- $\alpha$ -methylbenzyl)-2-pyrazolin-5-one] is a new diuretic which differs structurally from other diuretics.<sup>1,2</sup> Investigations with dogs and humans have shown it to be a potent loop diuretic combining high ceiling activity with prolonged duration of action<sup>3-5</sup> similar to thiazides. In healthy volunteers, a single 30-mg dose of MZ was as effective a diuretic as a similar dose of frusemide.<sup>6</sup> Currently, MZ and its formulations are not to be found in any pharmacopoeia. Only two chromatographic procedures (TLC<sup>7</sup> and HPTLC<sup>8</sup>) have been reported for the determination of MZ in biological fluids. A sensitive and precise spectrophotometric method would greatly aid in its determination in bulk samples and pharmaceutical dosage forms. 3-Methyl-2-benzothiazolinone hydrazone,<sup>9,10</sup> *p*-*N,N*-dimethylphenylenediamine<sup>11</sup> and *p*-*N*-methylaminophenol,<sup>12-14</sup> each in conjunction with an appropriate oxidizing agent, and 2,6-dichloroquinone chlorimide<sup>15,16</sup> have been suggested as chromogenic agents for the determination of aromatic amines and enols. In this work we have utilized these reagents for the determination of MZ in bulk samples and pharmaceutical dosage forms.

### EXPERIMENTAL

#### Apparatus

A Systronics model 105 (MK1) spectrophotometer with 1-cm matched glass cells and an Elico model LI-120 digital pH-meter were used.

#### Reagents

All the reagents were of analytical or pharmacopoeial grade and all solutions were prepared in doubly distilled water unless otherwise specified. Freshly prepared solutions were used.

Aqueous solutions of 3-methyl-2-benzothiazolinone hydrazone hydrochloride (MBTH; Fluka; 0.2%), *p*-*N,N*-dimethylphenylenediamine dihydrochloride (DMPD; Fluka; 0.05%), *p*-*N*-methylaminophenol sulphate (PMAP; BDH; 0.4%), chloramine-T (CAT; Loba;  $7.1 \times 10^{-3}$  M),

ceric ammonium sulphate [Ce(IV); BDH;  $1.58 \times 10^{-2}$  M in 4% v/v sulphuric acid], sodium hypochlorite (OCl<sup>-</sup>; Burgoyne;  $4.6 \times 10^{-3}$  M), potassium dichromate [Cr(VI); Reechem;  $1.02 \times 10^{-2}$  M] were prepared. All the oxidants except Cr(VI) were standardized.

2,6-Dichloroquinone chlorimide solution (DCQC; Loba; 0.05%) was prepared in isopropyl alcohol.

Buffer solutions of pH 3.0 (potassium hydrogen phthalate-hydrochloric acid) and pH 7.0 (potassium dihydrogen phosphate-disodium hydrogen phosphate) were prepared according to Lurie.<sup>17</sup>

**Standard drug solution.** MZ (Bayer), 25 mg, was dissolved in 50 ml of methanol. Working solutions were prepared by further dilution with the same solvent.

#### Procedures for bulk samples

The procedures are given for preparation of the calibration graphs. The same methods are used for samples.

**Method A.** Transfer suitable volumes (0.2–2.0 ml) of MZ solution (50  $\mu$ g/ml) into a series of 10-ml standard flasks. To each add 2 ml of MBTH and 2 ml of CAT and dilute to the mark with methanol. Measure the absorbances at 430 nm after 1 min, against a reagent blank.

**Method B.** Transfer suitable volumes (0.25–3.0 ml) of the drug solution (200  $\mu$ g/ml) into a series of 10-ml standard flasks. To each add 1 ml of MBTH and 1 ml of Ce(IV) and dilute to the mark with distilled water. Allow a 1-min wait, then measure the absorbances at 620 nm within the next 15 min against a reagent blank.

**Method C.** Transfer suitable volumes (0.25–3.0 ml) of the drug solution (400  $\mu$ g/ml) into a series of 25-ml standard flasks. To each add 15 ml of pH-3.0 buffer solution, 1 ml of PMAP and 1 ml of Cr(VI) and dilute to the mark with distilled water. Measure the absorbances at 620 nm after not less than 10 or more than 60 min, against a reagent blank.

**Method D.** Transfer suitable volumes (0.25–2.0 ml) of the drug solution (100  $\mu$ g/ml) into a series of 10-ml standard flasks. To each add 1 ml of DMPD and 1 ml of OCl<sup>-</sup> and maintain at 70° for 5 min. Cool, then dilute to the mark with methanol. After a 1-min wait, measure the absorbances at 500 nm during the next 60 min against a reagent blank.

**Method E.** Transfer suitable volumes (0.25–3.0 ml) of the drug solution (200  $\mu$ g/ml) into a series of 25-ml standard flasks. To each add 1 ml of DCQC followed by 2 ml of pH 7.0-buffer solution and dilute to the mark with distilled water. Allow 1 min for colour development then measure the absorbances at 500 nm against a reagent blank during the next 30 min.

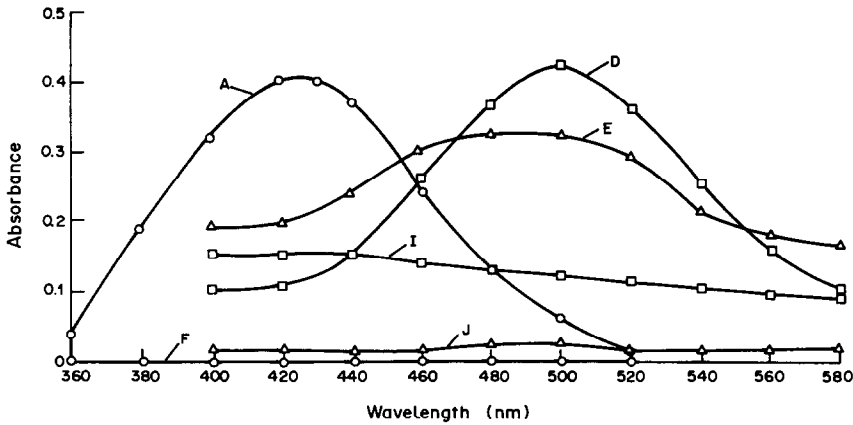


Fig. 1. Absorption spectra of A, MZ-(MBTH-CAT); D, MZ-(DMPD-OCI<sup>-</sup>); E, MZ-DCQC; F, (MBTH-CAT) vs. distilled water; I, (DMPD-OCI<sup>-</sup>) vs. distilled water; J, DCQC vs. distilled water. Concentration of MZ: A,  $2.76 \times 10^{-3}M$ ; D,  $5.51 \times 10^{-3}M$ ; E,  $5.85 \times 10^{-3}M$ ; MBTH,  $1.71 \times 10^{-3}M$ ; CAT,  $1.42 \times 10^{-3}M$ ; DMPD,  $2.39 \times 10^{-4}M$ ; OCI<sup>-</sup>,  $4.6 \times 10^{-4}M$ ; DCQC,  $9.5 \times 10^{-5}M$ .

#### Analysis of pharmaceutical preparations

Treat a suitable amount of powdered tablet or volume of injection (equivalent to about 25 mg of MZ) with 50 ml of methanol and determine the concentration of drug by the procedures for assay of the bulk drug.

#### RESULTS AND DISCUSSION

The spectral characteristics obtained with different reagents are shown in Figs. 1 and 2. Several oxidants, Cr(VI), OCI<sup>-</sup>, S<sub>2</sub>O<sub>8</sub><sup>2-</sup>, CAT, Ce(IV), Fe(CN)<sub>6</sub><sup>3-</sup>, Fe(III) and I<sub>2</sub> were tested. The combinations best suited for the determination of MZ were Ce(IV) and CAT with MBTH in acidic or neutral conditions, OCI<sup>-</sup> with DMPD in neutral conditions and Cr(VI) with PMAP at pH 3.0.

The effect of the reagent concentrations, buffer (pH 1-13), temperature and order of addition of reagents,

on the blank, stability and adherence to Beer's law was studied and the optimal conditions were identified. The optical characteristics and figures of merit are given in Table 1. The values obtained by the proposed methods and a reference method<sup>18</sup> for dosage forms are compared in Table 2, together with the results of recovery experiments. Because these formulations were not available commercially in India, we prepared our own according to literature methods.<sup>19,20</sup>

Commonly used tablet excipients such as starch, lactose, gelatin, talc and magnesium stearate and commonly used injection preservatives did not interfere in the procedures.

The proposed methods were found to be simple, rapid, accurate and sensitive for the assay of bulk MZ and its dosage forms.

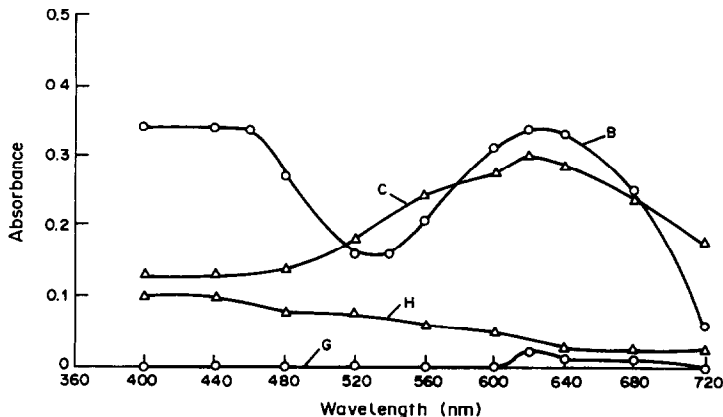


Fig. 2. Absorption spectra of B, MZ-[MBTH-Ce(IV)]; C, MZ-[PMAP-Cr(VI)]; G, MBTH-Ce(IV) vs. distilled water; H, PMAP-Cr(VI) vs. distilled water. Concentration of MZ: B,  $1.47 \times 10^{-4}M$ ; C,  $5.88 \times 10^{-5}M$ ; MBTH,  $8.56 \times 10^{-4}M$ ; Ce(IV),  $1.58 \times 10^{-3}M$ ; PMAP,  $4.65 \times 10^{-4}M$ ; Cr(VI),  $4.08 \times 10^{-4}M$ .

Table 1. Optical characteristics, precision and accuracy

	Proposed methods				
	A	B	C	D	E
Beer's law range, $\mu\text{g/ml}$	1-10	5-60	4-48	2.5-20	2-24
$\epsilon$ , $10^3 \text{ l. mole}^{-1} \text{ cm}^{-1}$	14.7	2.31	5.10	7.34	5.44
RSD, %	1.2	1.2	1.4	1.4	1.4
Error,* %	-0.3	+0.4	-0.6	-0.4	-0.8

\*Sample size: 100  $\mu\text{g}$  in methods A and D and 200  $\mu\text{g}$  in methods B, C and E.  
Average error for three determinations.

Table 2. Assay of muzolimine in pharmaceutical preparations by proposed and reference methods

Product	Nominal MZ content	Found,* mg					Reference method†	Recovery by proposed methods,§ %				
		Proposed methods						A	B	C	D	E
		A	B	C	D	E						
Tablet	10 mg	9.9	10.1	9.8	9.8	10.1	9.8	99	100	98	98	101
Tablet	30 mg	29.8	29.5	30.2	29.6	29.7	29.5	99	98	100	98	98
Injection	15 mg/ml	14.9	15.1	14.8	14.9	15.1	14.8	99	101	98	99	101

\*Average of three determinations.

†Titrimetric method.

§Of 5 mg of MZ added to the pharmaceutical preparation.

#### Nature of the coloured species

The reaction pathways leading to the formation of the coloured species in methods A-E may be postulated by analogy. MBTH,<sup>9,10</sup> DMPD<sup>11</sup> and PMAP<sup>21,22</sup> undergo oxidation in the presence of an appropriate oxidant to yield less stable and highly reactive species. These species and DCQC<sup>15,16</sup> react with MZ (through involvement of either the amino group or the enolic hydroxyl group) by an electrophilic attack on the most nucleophilic site on the 1,2-azole of the coupler. The resulting leuco dye is oxidized to the indo dye. The probable pathway in method C appears to be the formation of a charge-transfer complex<sup>21,22</sup> involving the reactive species *p*-N-methylbenzoquinone monoimine (acceptor) and MZ (donor). The variation in  $\lambda_{\text{max}}$  and  $\epsilon_{\text{max}}$  of the coloured species formed on treating MZ with MBTH and CAT or Ce(IV) appears to be due to the involvement of Ce(III) in complex formation with the oxidative coupling product initially formed in the latter case.

**Acknowledgements**—The authors are grateful to Bayer AG Germany for their generous gift of MZ and also to the authorities of Andhra University for providing research facilities.

#### REFERENCES

- E. Moller, H. Horstmann, K. Meng and D. Loew, *Experientia*, 1977, **33**, 382.
- Martindale Extra Pharmacopoeia*, 28th Ed., J. E. F. Reynolds (ed.), p. 608. Pharmaceutical Press, London, 1982.
- K. Meng, D. Loew, K. Stoepel and F. Hoffmeister, *Curr. Med. Res. Opin.*, 1977, **4**, 555.
- K. J. Berg, S. Jörstad and A. Tromsdal, *Pharmatherapeutica*, 1976, **1**, 319.
- G. Hoppe-Seyler, A. Heissler, M. Coppencastrop, M. Schindler, P. Schollmeyer and W. Ritter, *ibid.*, 1977, **1**, 422.
- D. Loew, W. Ritter and J. Dycka, *Eur. J. Clin. Pharmacol.*, 1977, **12**, 341.
- W. Ritter, *J. Chromatog.*, 1977, **142**, 431.
- Idem*, *Methodol. Surv. Biochem. Anal.*, 1983, **12**, 231.
- E. Sawicki, T. W. Stanley, T. R. Hauser, W. Elbert and J. L. Noe, *Anal. Chem.*, 1961, **33**, 722.
- M. Pays, R. Bourdon and M. Beljean, *Anal. Chim. Acta*, 1969, **47**, 101.
- D. N. Kramer and L. U. Tolentino, *Anal. Chem.*, 1971, **43**, 834.
- R. Ramakrishna and C. S. P. Sastry, *Talanta*, 1979, **26**, 861.
- R. Ramakrishna, P. Siraj and C. S. P. Sastry, *Acta Ciencia Indica*, 1980, **60**, 140.
- Idem*, *Indian J. Pharm. Sci.*, 1979, **41**, 200.
- G. R. Rao, S. S. N. Murty and E. V. Rao, *Indian Drugs*, 1985, **22**, 484.
- A. A. Abou Ouf, S. M. Hassan and M. E. S. Metwally, *Analyst*, 1980, **105**, 1113.
- J. Lurie, *Handbook of Analytical Chemistry*, p. 253. Mir, Moscow, 1975.
- R. Ramakrishna, P. Siraj and C. S. P. Sastry, *Acta Ciencia Indica*, 1978, **4**, 345.
- Pharmaceutical Dosage Forms: Tablets*, Vol. I, H. A. Liberman and L. Lachman (eds.), Dekker, New York, 1980.
- Pharmaceutical Dosage Forms: Parenteral Medications*, Vol. I, K. E. Avis, L. Lachman and H. A. Liberman (eds.), Dekker, New York, 1984.
- C. S. P. Sastry, B. G. Rao, B. S. Reddy and S. S. N. Murthy, *J. Indian Chem. Soc.*, 1981, **57**, 665.
- C. S. P. Sastry, T. M. K. Reddy and B. G. Rao, *Indian Drugs*, 1984, **21**, 145.

## DETERMINATION OF SULPHIDE BY ANION-EXCHANGE WITH LEAD IODATE

KRISHNA K. VERMA\*, DAYASHANKER GUPTA, SUNIL K. SANGHI  
and ARCHANA JAIN

Department of Chemistry, Rani Durgavati University Jabalpur 482 001, Madhya Pradesh, India

(Received 22 April 1988. Accepted 14 June 1988)

**Summary**—A quick anion-exchange reaction, suitable for the determination of sulphide, has been found to occur on stirring a suspension of lead iodate (solubility product,  $K_{so} = 1.2 \times 10^{-13}$ ) with sulphide solution at pH 5–8. After removal of the precipitates of lead iodate and lead sulphide ( $K_{so} = 3.4 \times 10^{-28}$ ), the iodate released can be determined by its reaction with acidified iodide to give tri-iodide which is either titrated with thiosulphate or measured spectrophotometrically as its blue complex with starch. Chloride, bromide, iodide, fluoride, oxalate, sulphate, thiocyanate and phosphate do not interfere. Thiosulphate, sulphite, nitrite and thiols do not give an anion-exchange reaction but do interfere in the redox reaction of iodate with acidified iodide. However, this is avoided if they are first oxidized with bromine (the liberated iodate remains unaffected) before iodometry.

Sulphide commonly occurs in a variety of waste effluents, e.g., septic sewage, oil refinery wastes, viscose rayon wastes, either free or as heavy-metal salts. Its presence in waste water is usually indicated by the characteristic odour of hydrogen sulphide, which is a toxic nuisance and may be taken as a measure of the prevalence of anaerobic conditions.<sup>1</sup> The control authorities tend to determine sulphide species in terms of their capacity to yield hydrogen sulphide. In the traditional acid displacement procedure<sup>2</sup> hydrogen sulphide, liberated on acidification, is removed by a stream of carbon dioxide, absorbed in zinc acetate solution and determined iodometrically.<sup>3,4</sup> Interference from sulphite is minimized by addition of formaldehyde to the zinc sulphide suspension. In the spectrophotometric method,<sup>4–8</sup> which is applicable to fresh waters and lightly polluted effluents, the sample is treated with 4-*N,N*-diethylaminoaniline and an oxidizing agent [iron(III) or dichromate] in acid medium to produce Ethylene Blue, which is measured. Sulphite, thiosulphate and iodide interfere. A field method for the determination of gaseous hydrogen sulphide in equilibrium with dissolved sulphide by using gas analysis tubes<sup>9</sup> has formed the basis of a gas chromatographic method<sup>10</sup> in which solution-gas equilibrium is achieved at an acidity that approximates to that used in the standard acid displacement procedure.

Except for ion-selective electrode methods,<sup>2,4</sup> no analytical procedure is available that is specific

for free sulphide, or can tolerate the interference of reducing agents, e.g., sulphite, thiosulphate and thiols, when present in effluents. The following method is proposed.

### EXPERIMENTAL

#### Reagents

Lead iodate (made by the reaction of lead nitrate with potassium iodate) and starch-iodide reagent solution were prepared as described earlier.<sup>11</sup>

**Acetanilide solution.** Dissolve 10 g of acetanilide in 50 ml of glacial acetic acid and dilute to 100 ml with water.

**Standard sulphide solution, approximately 100 mg/l.** Dissolve about 0.9 g of sodium sulphide nonahydrate in 1 litre of water, and standardize iodometrically.<sup>10</sup> Dilute a 25-ml portion of the stock solution to volume with water in a 250-ml standard flask to give a 10-mg/l. sulphide solution. Standardize the stock solution frequently and dilute it freshly as required.

#### Procedure

**Titrimetric determination in the absence of reducing agents.** To a 5-ml aliquot of test solution, containing 30–300  $\mu\text{g}$  of sulphide, in a 20-ml beaker, add 2 ml of 10% sodium acetate solution and about 50 mg of powdered lead iodate, then stir the mixture for 10 min. Filter off the lead iodate and lead sulphide on a Whatman No. 41 filter paper and wash with three 4-ml portions of ethanol-water mixture (40:60, v/v). Mix the combined filtrate and washings with 0.5 g of potassium iodide, 2 ml of 5% sulphuric acid and 25 ml of water, then titrate the liberated iodine with 0.01M thiosulphate, using starch solution as indicator. Concurrently run a blank determination with approximately the same amount of lead iodate (the blank titration is usually about 0.3 ml).

$$S^{2-} (\mu\text{g}) = 2667 VM$$

where  $V$  is the difference in the volume (ml) of thiosulphate (molarity  $M$ ) used in the sample and blank titrations.

\*Present address: Department of Biochemistry and Nutrition, Virginia Polytechnic Institute and State University, Blacksburg, VA 24061, U.S.A.

Table 1. Titrimetric and spectrophotometric determination of sulphide at the  $\mu\text{g}$  level

Titrimetric determination		Spectrophotometric determination	
Taken*	Found† (% RSD)	Taken‡	Found† (% RSD)
28.6	28.3 (1.5)	1.98	1.96 (1.5)
48.2	48.7	2.47	2.49 (0.8)
63.7	63.1 (0.8)	3.55	3.52
101.5	100.2	4.90	4.93 (0.5)
138.9	137.5	5.72	5.68
160.1	161.4 (0.5)	6.03	6.09 (0.4)
198.7	199.0	7.54	7.49
230.0	228.1 (0.6)	8.12	8.18 (1.2)
259.6	257.4		
276.9	279.2		
296.4	298.8 (1.0)		

\*The test solution was standardized by iodometry.<sup>10</sup>

†Average of six determinations.

‡The test solution was standardized by the Ethylene Blue method.<sup>4</sup>

*Titration in the presence of reducing substances.* Stir the test solution with lead iodate, filter and wash as before. Treat the combined filtrate and washings with 2–4 ml of saturated bromine water, allow to stand for 10 min (add more bromine if there is complete decolorization during standing), add 5 ml of 10% acetanilide solution and shake vigorously until the bromine is decolorized; then add 0.5 g of potassium iodide and 2 ml of 5% sulphuric acid and titrate the liberated iodine with 0.01M thiosulphate. Run a blank determination simultaneously.

*Spectrophotometric determination.* To construct the calibration graph, mix 0.5–3.0 ml of 25.0-mg/l. potassium

iodate solution with 2 ml of starch-iodide reagent solution, 1 ml of 1M sulphuric acid and 6 ml of ethanol-water mixture in a 25-ml standard flask, shake, make up to the mark with water, and after 5 min measure the absorbance at 580 nm against water, and plot it against the weight ( $\mu\text{g}$ ) of iodate taken.

Combine a 5-ml portion of test solution, containing 2–8  $\mu\text{g}$  of sulphide, with 1 ml of 10% sodium acetate solution and 20 mg of powdered lead iodate, stir the mixture for 10 min, filter into a 25-ml standard flask and wash the residue with three 2-ml portions of ethanol-water mixture. Mix the combined filtrate and washings with 2 ml of

Table 2. Titrimetric determination of sulphide in the presence of reducing agents and other substances

S <sup>2-</sup> taken,* $\mu\text{g}$	Foreign substance	Amount added, $\mu\text{g}$	S <sup>2-</sup> found,† $\mu\text{g}$ (% RSD)
25.0	hydrogen sulphite	5	25.2 (0.5)
		10	25.1
		50	25.3
		100	25.4 (1.0)
50.0	thiosulphate	10	50.2 (0.6)
		50	50.2
		100	50.5
		150	50.4 (1.1)
75.0	nitrite	20	75.1 (0.4)
		50	75.4
		100	75.7 (0.8)
100.0	phenol	20	100.5 (0.5)
		40	99.6
		60	100.8 (0.5)
		5	149.6 (0.6)
150.0	2-mercaptoethanol	10	150.8
		20	151.0 (0.9)
		10	175.9 (0.5)
175.0	cysteine hydrochloride	20	176.4
		30	178.3 (0.7)
		5	199.4 (0.8)
		10	200.9
200.0	toluene- $\alpha$ -thiol	20	201.4 (0.9)
		5	248.1 (0.6)
		20	252.1
250.0	hydrazinium chloride	50	252.2 (0.8)
		10	298.1 (0.6)
		30	302.6
		50	297.4 (1.0)

\*The test solution was standardized by iodometry.<sup>10</sup>

†Average of six determinations.

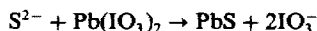
starch-iodide reagent solution and 1 ml of 1M sulphuric acid, dilute to volume with water, and after 5 min measure the absorbance at 580 nm against a reagent blank. Reference to the calibration graph gives the amount of iodate liberated, which is related to that of sulphide in the sample aliquot by the equation:

$$S^{2-}(\mu\text{g}) = 0.09143 m$$

where  $m$  is the amount of iodate ( $\mu\text{g}$ ) liberated.

## RESULTS AND DISCUSSION

The high sensitivity of metal iodate methods,<sup>12-17</sup> and the good selectivity of lead iodate,<sup>11</sup> prompted us to examine the analytical potential of lead iodate for the determination of sulphide. The anion-exchange reaction that occurs when sulphide is stirred with a suspension of lead iodate is:



The solubility products ( $K_{s0}$ ) for lead iodate and lead sulphide are  $1.2 \times 10^{-13}$  and  $3.4 \times 10^{-28}$  respectively.<sup>18</sup> The most suitable pH for the exchange reaction is 5-8.

The results, given in Table 1, were found not to be affected by the presence of as much as a 100-fold molar ratio (to sulphide) of chloride, bromide, fluoride, iodide, phosphate, oxalate, tartrate, thiocyanate or sulphite. Chromate also reacts quantitatively<sup>11</sup> but, being oxidizing in nature is not found along with sulphide. Thiosulphate, sulphite, nitrite, phenol, hydrazine, aniline, unsaturated organic compounds and thiols do not undergo any reaction with lead iodate in the present method but interfere in the redox reaction of iodate with acidified iodide. This interference can be avoided by oxidizing these species with bromine (the liberated iodate remains unaffected) before iodometry (Table 2). Tribromophenyl hypobromite ( $C_6H_2Br_3OBr$ ), which is formed from phenol on reaction with an excess of bromine, remains unaffected when the residual bromine is reduced by formic acid<sup>19-22</sup> and also liberates iodine on reaction with iodide to give a positive bias for sulphide. This error was circumvented in the present method by replacing the formic acid by acetanilide, which reacts rapidly with residual bromine as well as with any hypobromite formed, to give 4-bromoacetanilide. Neither acetanilide nor its bromo derivative interferes in iodometry. Cyanide, hexacyanoferrate(II) and molybdate ions vitiate the analysis by

giving an analogous exchange reaction. Ammonium, alkali metal and other cations which do not form insoluble salts with sulphide or iodate cause no interference.

Lead iodate is more selective in its action than barium<sup>16</sup> or mercuric iodate<sup>12-15</sup> and can be used for the selective and sensitive determination of sulphide in the presence of a large number of substances.

*Acknowledgement*—Thanks are due to the Council of Scientific and Industrial Research, New Delhi, for a Senior Research fellowship to A.J.

## REFERENCES

1. R. D. Pomroy, *The Problem of Hydrogen Sulphide in Sewers*, p. 8. Clay Pipe Development Association, London, 1977.
2. K. H. Mancy and W. J. Weber, Jr., *Analysis of Industrial Waste Waters*, I. M. Kolthoff, P. J. Elving and F. H. Stross (eds), p. 526. Wiley-Interscience, New York, 1971.
3. W. Wang and W. J. Barcelona, *Environ. Inst.*, 1983, **9**, 129.
4. Standing Committee of Analysts, *Sulphide in Water and Effluents*, HMSO, London, 1983.
5. R. Pomroy, *Sewage Works J.*, 1936, **8**, 572.
6. D. J. Leggett, N. H. Chen and D. S. Mahadevappa, *Anal. Chim. Acta*, 1981, **128**, 163.
7. A. Rios, M. D. Luque de Castro and M. Valcárcel, *Analyst*, 1984, **109**, 1487.
8. M. O. Babiker and J. A. W. Dalziel, *Anal. Proc.*, 1983, **20**, 609.
9. D. Ballinger and A. Lloyd, *Water Pollut. Control*, 1981, **80**, 648.
10. D. J. Hawke, A. Lloyd, D. M. Martinson, P. G. Slater and C. Excell, *Analyst*, 1985, **110**, 269.
11. K. K. Verma, P. Tyagi and M. G. P. Ekka, *Talanta*, 1986, **33**, 1009.
12. F. D. Snell, *Photometric and Fluorimetric Methods of Analysis: Non-metals*, p. 254. Wiley-Interscience, New York, 1981.
13. R. E. Humphrey, R. R. Clark, L. Houston and D. J. Kippenburger, *Anal. Chem.*, 1972, **44**, 1299.
14. W. L. Hinze and R. E. Humphrey, *ibid.*, 1973, **45**, 385.
15. R. E. Humphrey and W. L. Hinze, *ibid.*, 1973, **45**, 1747.
16. W. L. Hinze and R. E. Humphrey, *ibid.*, 1973, **45**, 814.
17. K. Katoh and S. Takahashi, *Kenkyu Hokoku-Niigata Diagaku Kogakubu*, 1985, **34**, 21; *Anal. Abstr.*, 1985, **47**, 10H72.
18. F. J. Welcher and R. B. Hann, *Semimicro Qualitative Analysis*, p. 212. Van Nostrand, New York, 1969.
19. D. Amin and W. A. Bashir, *Talanta*, 1984, **31**, 283.
20. D. Amin and K. Y. Saleem, *Int. J. Environ. Anal. Chem.*, 1984, **17**, 275.
21. D. Amin, F. M. El-Samman and H. Abdulahmed-Malalla, *Talanta*, 1985, **32**, 66.
22. D. Amin, *Analyst*, 1985, **110**, 211.

## ANALYTICAL DATA

# POLAROGRAPHIC STUDY OF THE DIPROPYLDITHIOPHOSPHINATE COMPLEXES OF Pd(II), Pb(II), Cd(II), AND Zn(II) IONS

ZHIVKO I. DENCHEV and NIKOLA K. NIKOLOV  
Central Research Laboratory, University of Plovdiv, 4000 Plovdiv, Bulgaria

(Received 10 June 1987. Revised 22 February 1988. Accepted 20 June 1988)

**Summary**—The complexes of the dithiophosphinic acids with Pd(II), Pb(II), Cd(II), and Zn(II) in a toluene-ethanol medium produce single polarographic waves. The half-wave potential is a linear function of the ligand concentration. The stabilities of these chelates, which are characterized by a sulphur-metal bond, are in the order: Pd(II) > Pb(II) > Cd(II) > Zn(II).

The polarographic behaviour of various bidentate chelate reagents containing a donor sulphur atom, such as dithiocarbamates, xanthates and dithiophosphates, has been reported in the literature.<sup>1-4</sup> Because of the electron-density distribution on the sulphur atom, the relative stability of their complexes is dithiocarbamates > xanthates > dithiophosphates.<sup>4,5</sup>

The objective of the present paper is to compare the polarographic characteristics and conditional stability constants of the Pb, Pd, Cd and Zn complexes of another sulphur-containing complexing reagent, dipropylldithiophosphinic acid (DTPH).

### EXPERIMENTAL

#### Apparatus

A Radelkis OH-105 polarograph, with a dropping mercury electrode (DME, drop-time 4.4 sec, mercury flow 1.51 mg/sec, at a column height of 95 cm and potential of -1.00 V) and a saturated calomel electrode. A toluene-ethanol medium (2:3 v/v) containing 0.2 mole of lithium perchlorate per litre and 0.01% Triton X-100 was used. A Specord spectrophotometer was used with 0.997 cm path-length silica cuvettes.

#### Reagents

Sodium dipropylldithiophosphinate was obtained by the usual method and recrystallized from acetone.<sup>6</sup>

#### Procedure

The polarography was performed at  $25 \pm 0.1^\circ$ . The test solutions were deaerated by passage of argon for 15 min. The half-wave potentials were determined in the presence and absence of the ligand. The ionic strength of 0.2 was kept constant with lithium perchlorate.

### RESULTS AND DISCUSSION

The metal complexes obtained are reduced according to the equation



The DME potential for an irreversible electro-reduction is given by

$$E_{\text{DME}} = E_{1/2} - \frac{RT}{\alpha nF} \ln \left( \frac{i}{i_d - i} \right) \quad (1)$$

where  $i_d$  is the limiting current,  $i$  the observed current, and  $\alpha$  is the transfer coefficient.

The number of ligands ( $p$ ) in the metal complex  $\text{MeL}_p$ , is calculated from the change in half-wave potential ( $\Delta E_{1/2}$ ) with change in ligand concentration ( $\Delta C_L$ ) by means of the equation

$$\frac{\Delta \log C_L}{\Delta E_{1/2}} = - \frac{\alpha nF}{2.30pRT} \quad (2)$$

The conditional stability constants are calculated<sup>7</sup> from

$$E_{1/2(\text{MeL}_p)} - E_{1/2(\text{Me}^{n+})} = \frac{RT}{\alpha nF\beta_p} - \frac{pRT \ln C_L}{\alpha nF} \quad (3)$$

where

$$\beta_p = [\text{MeL}_p] / [\text{Me}^{n+}] [\text{L}^-]^p$$

When  $\alpha n$  is a constant, equation (3) is applicable to irreversible electroreduction of metal chelates.<sup>7</sup>

Palladium(II), lead(II), cadmium(II) and zinc(II) produce single polarographic waves in a toluene-ethanol medium containing DTPH. Maxima on the reduction waves can be suppressed with Triton X-100.

The wave-heights in the presence of  $4 \times 10^{-3} M$  DTPH are a linear function of the metal-ion concentration over the range  $2 \times 10^{-5}$ – $4 \times 10^{-4} M$ . The ratio of the wave-height to the square root of the height of the mercury column is constant, indicating that the reduction is diffusion-limited. It was found that a plot of  $\log [i/(i_d - i)]$  vs. applied potential was linear with a slope of 0.034–0.036 V for Pd(II), Pb(II) and Cd(II), and 0.042 V for Zn(II), the values remaining constant



Table 1. Stability constants calculated from variation of  $E_{1/2}$  with concentration of ligand

[DTPH], M	Cd		Zn		Pd		Pb	
	$E_{1/2}$ , V vs. SCE	$\log \beta_2$	$E_{1/2}$ , V vs. SCE	$\log \beta_2$	$E_{1/2}$ , V vs. SCE	$\log \beta_2$	$E_{1/2}$ , V vs. SCE	$\log \beta_2$
—	-0.630	—	-1.00	—	-0.095	—	-0.450	—
0.0012	-0.800	7.70	-1.156	6.86	-0.345	9.85	-0.645	8.24
0.0020	-0.815	7.64	-1.170	6.54	-0.360	10.17	-0.660	8.45
0.0032	-0.825	7.68	-1.181	6.81	-0.372	10.05	-0.675	8.61
0.0040	-0.838	7.71	-1.188	6.75	-0.377	10.18	-0.682	8.28
0.0048	-0.845	7.74	-1.194	6.78	-0.383	10.08	-0.690	8.42
0.0060	-0.853	7.83	-1.200	6.78	-0.388	10.04	-0.695	8.43
0.0080	-0.860	7.79	—	—	-0.392	10.07	-0.700	8.47

with increase in ligand concentration. Hence  $an$  was constant, indicating the reduction processes were reversible or close to reversible. For all four metals the value of  $p$  was found to be 2.

Application of equation (3) gave  $\log \beta_2 = 10.1, 8.5, 7.8$  and  $6.8$  for the Pd, Pb, Cd and Zn complexes respectively. The extrapolation method<sup>8</sup> gave  $\log \beta_2$  for the Pd and Pb complexes as 10.5 and 9.1, respectively.

The absorption spectra of the complex and the reagent were employed for the estimation of the conditional stability constant for Pd(II) by the molar-ratio method and the equation:

$$\beta_2 = \frac{A/\epsilon}{(C_{Me} - A/\epsilon)(C_L - 2A/\epsilon)^2}$$

where  $A$  is the absorbance of the solution at 315 nm,  $C_{Me}$  and  $C_L$  are the total concentrations of the metal ion and ligand respectively, and  $\epsilon = 1.50 \times 10^4 \text{ l. mole}^{-1} \text{ cm}^{-1}$  at  $\lambda_{\max} = 315 \text{ nm}$  and the composition of the complex is Pd(II):DTPH = 1:2. The

value obtained for  $\log \beta_2$  (9.4) is reasonably close to the value 10.1 obtained polarographically.

The relative order of stability of the dithio-phosphinate complexes is the same as that for the other sulphur-containing complexes<sup>1-4</sup> of the four metals examined.

#### REFERENCES

1. P. S. Setty and Q. Fernando, *J. Inorg. Nucl. Chem.*, 1966, **28**, 2873.
2. Q. Fernando and C. D. Green, *ibid.*, 1967, **29**, 647.
3. P. S. Setty and Q. Fernando, *ibid.*, 1967, **29**, 1921.
4. V. F. Toropova, G. K. Budnikov and N. A. Ulalehovich, *Zh. Obshch. Khim.*, 1975, **45**, 653.
5. D. Concovanis, *Prog. Inorg. Chem.*, 1970, **11**, 233.
6. W. A. Higgins, P. W. Vogel and W. G. Graig, *J. Am. Chem. Soc.*, 1955, **77**, 1864.
7. R. S. Subrachmanya, *Advances in Polarography*, Vol. 2, p. 647, Pergamon Press, Oxford, 1960.
8. M. I. Bulatov and I. P. Kalinkin, *Prakticheskoe rukovodstvo po fotokolorimetriceskimi i spektrofotometriceskimi metodam analiza*, p. 247. Izd. Khimiya, Moscow, 1976.

## PRELIMINARY COMMUNICATION

### COLORIMETRIC DETERMINATION OF CYCLOBUTYLPHENYLGLYCOLLIC ACID AND ITS KETONE

Harvey W. Yurow and Samuel Sass ✝

U.S. Army Chemical Research, Development and Engineering Center, SMCCR-RSL,  
Aberdeen Proving Ground, Maryland 21010-5423, USA

(Received 5 September 1988. Accepted 9 September 1988)

A number of anticholinergic esters contain the benzilate moiety in combination with an amino-alcohol, e.g., benactyzine.<sup>1</sup> Benzilic acid yields an intense red colour in concentrated sulphuric acid, owing to the forming of various arylfluorene carbonium ions, and this serves as a fairly specific test.<sup>2,3</sup> In the search for more potent drugs, researchers have replaced one of the phenyl rings in benzilic acid by various groups,<sup>4</sup> including cycloalkyls (C<sub>3</sub>-C<sub>6</sub>). These acids fail to produce a colour in sulphuric acid alone. However, when *p*-anisaldehyde is added to the mixture followed by brief heating, a strong violet hue is given both by cyclobutylphenylglycollic acid and its ketone.

The reaction is not produced by the cyclopropyl or cyclohexyl homologue and only weakly by the cyclopentyl compound. Interestingly enough, a deep orange fluorescence (near ultraviolet excitation) accompanies the violet colour, and has some value as a spot-test.

In the analytical procedure 1 ml of aqueous solution of the test compound is treated with 1 mg of *p*-anisaldehyde (1% solution in methanol) and concentrated sulphuric acid (4 ml) is added dropwise, followed by heating for 15 min in a boiling water-bath (45 min for the ketone). The sample is cooled and its absorbance at 580 nm measured against a reagent blank. Beer's law is followed in the range 0.5 - 2.5 µg/ml, and the colour is relatively stable. The molar absorptivity is  $5 \times 10^4 \text{ l.mole}^{-1} \text{ cm}^{-1}$ .

Heating of cyclobutylphenylglycollic acid with 80% sulphuric acid followed by addition of *p*-anisaldehyde and further heating also gave a positive result. In another experiment, brief refluxing of the ketone with *p*-anisaldehyde in trifluoroacetic acid and water, 9:1 v/v, followed by cooling and addition of excess of methanol, precipitated a tan solid, (m.p. 142 - 144°) which dissolved in concentrated trifluoroacetic acid to give the characteristic colour.

The mechanism of these reactions may involve initial carbonium ion formation followed by intramolecular cyclization and subsequent reaction with *p*-anisaldehyde. Aromatic aldehydes are known to condense at low pH with active methylene groups or with activated hydrogen atoms on phenyl rings. There appears to be a correlation between the intensity of colour produced and the stability of the cycloalkyl carbonium ion, which decreases in the sequence: cyclobutyl > cyclopentyl > cyclohexyl > cyclopropyl.<sup>5</sup>

A reaction similar to that for cyclobutylphenylglycollic acid is given by 1-methoxy-bicyclo[3,2,0]hepta-3,6-diene, a compound containing a cyclobutene ring, which is formed by short-wave ultraviolet irradiation of 1-methoxy-1,3,5-cycloheptatriene in methanol.<sup>6</sup> In contrast, of the cycloalkanols, only the cyclohexyl compound condenses with the aromatic

✝ Deceased.

aldehyde in strong acid to give an analytically useful procedure.<sup>7</sup>

A relatively unselective test for various substituted glycollic acids involves reaction with 2-diphenylacetyl-1,3-indanedione-1-hydrazone to produce fluorescence.<sup>8</sup>

A considerable number of photochemical reactions involving unsaturated organic compounds result in the formation of cyclobutyl derivatives.<sup>9</sup> For detection of these, and of any other cyclobutyl compounds, the technique that is described in this report should be considered in any investigation.

#### References

1. The Merck Index, M. Widholz (ed.), 9th Ed., p. 133, Merck, Rahway, NJ, 1976.
2. H. Klinger and C. Lonnes, Chem. Ber., 1896, 29, 734.
3. H. Dobeneck and R. Kiefer, Ann. Chem., 1965, 684, 115.
4. G.R. Treves and B.M. Baum, U.S. Patent 4,467,095; Chem. Abstr., 1984, 101, 637.
5. A. Streitwieser Jr., Solvolytic Displacement Reactions, pp. 49, 95, 181. McGraw-Hill, New York, 1962.
6. H.W. Yurow and S. Sass, Anal. Chim. Acta, 1987, 194, 323.
7. Idem, Microchem. J., 1970, 15, 428.
8. E.J. Poziomek, E.V. Crabtree and R.A. Mackay, Anal. Lett., 1980, 13, 1249.
9. N.J. Turro, Molecular Photochemistry, pp. 196-208. Benjamin, New York, 1967.

## SOFTWARE SURVEY SECTION

---

### Software package TAL-007/88

#### CONSTRUCTION OF SMALL BIBLIOGRAPHIC DATABASES BY USING "LOTUS 1-2-3"

Contributors: M.J. Gomez\*, H. Torres, Z. Benzo, M. de le Guardia and H. Schorin, Centro de Quimica, I.V.I.C., Apartado 21827, Caracas 1020-A, Venezuela.

Brief description: The authors have developed a way of using a popular spreadsheet to construct databases, each of which summarizes, schematically, the specific content of a set of references. Specialist scientists who are already using a spreadsheet (here, Lotus 1-2-3) for numerical data-handling, may be interested to apply the same program for bibliographic data handling. Careful design is necessary for such a database. The data items to be included must be carefully chosen in order to facilitate bibliographic searching, but without leaving too many blank spaces to consume memory unnecessarily. The data items and the form in which to record the information must be planned by the whole user group, especially for commonly used items such as keywords. The content of the references can be coded by mnemonic symbols, as an aid to subsequent searching, and also show schematically the content of the references. The entire information base can also be represented by a printed summary table.

New data items are added as a single step procedure. Data extraction is quick and versatile. When the information becomes greatly diversified, derived databases can readily be generated.

Potential users: scientists.

Fields of interest: bibliographic data storage and retrieval for scientists of all kinds.

This application has been developed for the IBM-PC and compatibles, and it involves use of the commercial package LOTUS 1-2-3 (Lotus Development Corp., 161 First Street, Cambridge, MA 02142). The minimum memory required is 256Kb. LOTUS 1-2-3 is user-friendly and well documented. For this special application, extensive documentation is available to help users to develop and improve the design of a bibliographic database. This information can be supplied free of charge by the contributor.

The application is fully operational, and is in use by two laboratory teams. The contributor is willing to deal with enquiries, and suggestions are welcome too.

-----  
\*Contributor for correspondence.

## THE USE OF GLASS ELECTRODES FOR THE DETERMINATION OF FORMATION CONSTANTS—IV\*

### MATTERS OF WEIGHT

PETER M. MAY†

School of Mathematical and Physical Sciences, Murdoch University, Murdoch, Western Australia 6150

KEVIN MURRAY

Processing and Chemical Manufacturing Technology Division, Council for Scientific and Industrial Research, Pretoria, South Africa 0001

(Received 22 August 1988. Accepted 8 September 1988)

**Summary**—Implicit and explicit methods of weighting titration data for the purpose of determining formation constants are considered. Many current computer programs make no provision at all for weighting and the exceptions do so in ways that have unknown effects. It is shown that formation constants obtained by optimization can, in practice, vary significantly when different methods of weighting are employed. However, none of these methods consistently yields the best results. Whenever possible, it is advisable to use several approaches to check for agreement between them.

It is a well established statistical principle that, in general, least-squares analyses ought not to treat every data point as having identical importance. Homoscedasticity, the condition of uniform variance over all the data,<sup>1</sup> must be fulfilled. Thus, to obtain unbiased results, the data ought to be "weighted" so that those points likely to be distorted most by experimental error are correspondingly reduced in their effect on the optimized values of parameters.

However, in the determination of formation constants from titration data, the issue of weighting is often completely ignored. It is noteworthy that many of the most popular generalized formation constant programs (including MINIQUAD,<sup>2</sup> SCOGS,<sup>3</sup> ACREF3A<sup>4</sup> and TITFIT<sup>5</sup>) make no allowance for it. What impact has this had on the great number of formation constants published from these programs?

The neglect of weighting can, undoubtedly, have very detrimental consequences. As anyone who attempts to use an unweighted objective function based on residuals in emf soon discovers, manifestly bad results can be obtained because of the excessive influence of unbuffered regions in the data (for example, the points that occur near end-points, where small errors in titration volumes, *etc.*, produce large errors in emf).

Evidently such problems do not always arise. Programs like those above, which treat every point as being equally affected by error (*i.e.*, apply so-called unit weights by default) are widely regarded as satis-

factory. This can presumably be credited to the particular objective functions which they employ. For example, it might be predicted that by formulating residuals in terms of titration volumes or analytical concentrations, these programs limit the ill-effects of unbuffered titration regions. It seems, therefore, that an acceptable weighting can sometimes be achieved implicitly, because of the way in which the simulation calculations are performed. The precise consequences of this, however, are again unknown. How does expressing the residuals in different variables by transforming the calculation so that it is carried out in different "directions" (*e.g.*, from emf to residuals in titration volume or *vice versa*) affect the resulting values of optimized formation constants?

The effectiveness of weighting even in those programs which use it explicitly is also unclear. For example, MIQUV<sup>6</sup> and SUPERQUAD<sup>7</sup> both calculate objective functions based on residuals in emf. They apply weights,  $w$ , at each point, calculated from estimated standard deviations in titration volume,  $\sigma_v$ , and emf,  $\sigma_e$ , by a standard error-propagation formula, namely

$$w = \left[ \left( \frac{dE^{\text{obs}}}{dV} \right)^2 \sigma_v^2 + \sigma_e^2 \right]^{-1} \quad (1)$$

where the derivative is obtained from the slope of the titration curve. Similar weighting functions are applied by STBLTY,<sup>8</sup> MUCOMP<sup>9</sup> and MICMAC.<sup>10</sup> However, errors from many sources other than titration volumes and emf will contribute to the probable size of the residual. Ought these to be taken into account in calculating the weights, particularly since errors in analytical concentrations will often be the

\*Part III—*Talanta*, 1988, 35, 825.

†Author for correspondence.

dominant ones? Is a weighting scheme which neglects such factors satisfactory or even worthwhile?

Other approaches to weighting have also been mentioned in the literature, *e.g.*, with programs such as LETAGROP VRID,<sup>1</sup> DALSEK<sup>12</sup> and ABLET<sup>13</sup> but, typically, implementation details are left obscure. Certainly, the consequences of these various adaptations have not been described.

Questions concerning the weighting of titration data in the determination of formation constants thus abound. More generally, the whole matter of how best to deal with experimental errors in titration data needs to be elucidated. Is a better approach to weighting all that is necessary? The discrepancies between published sets of values described in the introduction to Part III of this series<sup>14</sup> may well be attributed to these problematical issues. Moreover, it is doubtful whether sound methods for model selection can be agreed before the matter of weighting is properly settled. This paper describes an investigation of various possible weighting procedures, with the ESTA programs.

### THEORY

The purpose of weighting is to reduce, as much as possible, the adverse influences on optimized parameters that arise because errors in values held constant during the calculation tend to propagate differently at different points. This is quite distinct from the effects of systematic errors discussed in Part V of this series.<sup>15</sup> Proper weighting prevents the optimization process from reducing a large residual (that is probably due to errors in the "known" titration parameters) at the expense of increasing other residuals less affected by such errors. In other words, in extracting information from the data, we must allow for the fact that some points will be more reliable and informative than others, because they are relatively less distorted by experimental errors.

Since the origin of the errors in the titration data may reasonably be considered as random, we can assess how they are likely to affect each point individually, by using a Taylor-series propagation formula. The appropriate weight would thus be the reciprocal of the variance of the residual ( $y_{nq}^{\text{obs}} - y_{nq}^{\text{calc}}$ ). With the same symbols as in Part III<sup>14</sup>

$$w_{nq} = \left[ \sum_p \left( \frac{\delta(y_{nq}^{\text{obs}} - y_{nq}^{\text{calc}})}{\delta p} \right)^2 \sigma_p^2 \right]^{-1} \quad (2)$$

where  $\sigma_p$  is the standard deviation of the titration parameters held constant during the optimization. These parameters may include the titration volume,  $v_m$ , the initial volume  $V^\circ$ , the formation constants  $\beta_j$ , the initial vessel concentrations,  $C_i^0$ , the burette concentrations,  $C_{im}^0$ , the electrode intercept,  $E_k^0$ , the electrode response slope,  $s_k$ , and the measured emf at the point,  $E_k$ .

The main reason why considerations of errors have often been restricted just to those in  $v_m$  and  $E_k$  is that,

when everything else is neglected, the weights can be calculated directly from the experimental data (as described above for MIQUV and SUPERQUAD). Without this simplification, matters are much trickier. This is because the weights become dependent on the nature of the chemical system itself, *e.g.*, whether it is buffered or not. Their correct evaluation involves the postulated chemical model: they are affected by the particular equilibria operating in the system and by the magnitude of the titration parameters, including those being optimized.

At first sight, trying to evaluate the weights in a model-dependent way appears to be extremely awkward. Since the objective function is a sum of weighted terms, this would make comparisons between the results from different optimizations (say for the purpose of model selection) meaningless. Even worse, the important assumption made in deriving equation (8) of Part III, namely that  $w_{nq} \neq f(p_k)$ , is rendered invalid. Calculating the Hessian without making this assumption is, if not impossible, a very formidable task. Moreover, it would be necessary to ensure that iterative changes in weighting did not subvert the location of the objective function minimum—the optimization would not be wanted to find those formation constants which give the largest (or even the smallest) error propagations! The fact is that, in measuring formation constants, the problem of how to handle real errors goes beyond the bounds of conventional least-squares theory. It can thus be concluded that, at least for now, weights cannot be evaluated in a rigorous manner.

However, a rigorous evaluation may not actually be necessary. The aim of weighting is simply to obtain better (numerical) answers from the optimization than would otherwise be the case. Starting with any satisfactory estimates of the parameters to be optimized, perhaps obtained without weighting, we can calculate what is likely to be an excellent set of weights based on the particular model chosen. These may then be applied as constants in a subsequent optimization. The difference which this might produce in the results would be indicative of the importance of weighting in the particular system being investigated. If the difference happened to be significant, the procedure could be repeated until convergence was obtained. In principle, this should be an improvement over methods of weighting hitherto adopted.

### METHODS AND RESULTS

Weighting procedures based on the principles outlined above have therefore been incorporated throughout the suite of ESTA programs. In particular, weights are calculated by equation (2) from errors in any or all titration parameters specified by the user. Default standard deviations are provided automatically by ESTA8.<sup>14</sup> These correspond to the precision which might reasonably be expected in routine



Table 3. Example of results for titration of strong acid vs. strong base: 1 titration only, 101 points (exact simulated values were  $\log K_w = 14.000$ ,  $E^0 = 400.00$  mV and  $C_m^V = 20.000$  mM)

Parameter	Task OBJE			Task OBJT		
	Unit weights	Weighted method A	Weighted method B	Weighted method A	Weighted method B	Unit weights
$\log K_w$	-13.996	-13.996	-13.996	-13.996	-13.996	-13.995
$E^0$	399.60	399.62	399.62	399.62	399.62	399.62
$C_m^V$	20.030	20.024	20.024	20.024	20.024	20.020
$U$	$9.10 \times 10^{-3}$	$5.5 \times 10^{-2}$	$5.5 \times 10^{-2}$	$4.1 \times 10^{-2}$	$4.2 \times 10^{-2}$	$7.8 \times 10^{-10}$
Convergence	Yes	Yes	Yes	Yes	Yes	1(94%)

weighting is applied and, if it is not, which objective function (*viz.* OBJE or OBJT) is chosen. It is interesting and relevant to note that agreement often occurs between the weighted optimizations regardless of which objective function is calculated. Furthermore the weighted results often coincide within the precision of the optimization. These observations are in accord with the theoretical view that it does not matter which variable is chosen for expression of the residuals, *provided that the residuals are correctly weighted*. When such agreement is not observed it may mean either that the errors have been incorrectly estimated or that systematic effects dominate. Although not specifically evident in the examples chosen, it is also pertinent to point out that the weighted results generally fall somewhere between the unweighted results but frequently lie closest to the unweighted OBJT values. Apparently, unweighted objective functions based on residuals in analytical concentrations (or titration volumes) are frequently not much different from (and possibly not inferior to) weighted objective functions. Indeed they have some distinct advantages, the most important being that they provide an absolute measure of agreement between the calculated and observed data (which, unlike a weighted objective function, does not depend on assessment of experimental errors). On the other hand, OBJT calculations are not possible if it is desired to make Debye-Hückel, liquid-junction or ion-selectivity corrections.<sup>14</sup>

3. None of the options distinguishes itself as an unerring means of obtaining optimized values close to the "true" formation constants used in the ESTA7 simulations. Pronounced differences, much larger than might be expected from the conventional standard deviations, affect most results. It seems clear that the unweighted OBJE calculations are sometimes especially prone to error. Otherwise, no general pattern emerges. Whilst certain options may perform significantly better than others in particular cases, none does so consistently. We have been unable to draw infallible conclusions regarding the best method of weighting to apply when the answer is unknown.

4. The weighted objective function values generally do not tend to minimize to unity. Convergence to unity is expected and, reassuringly, is observed when the errors introduced by ESTA7 are confined to the experimental variables (titration volumes and emfs).

However, when titration parameters are also perturbed, the effects are unpredictable.

## DISCUSSION

The results described above strongly suggest that all attempts at weighting are being confounded by errors in titration parameters that are held constant during the calculation. These account for the differences observed between the optimized and the "true" values (point 3) and for the final weighted objective function values typically being greater than unity (point 4). The systematic nature of such errors is notorious for the difficulties it creates in formation constant determinations and it is not surprising to find adverse effects occurring in the present context.

None of the weighting methods based on random error propagations is thus capable, by itself, of yielding satisfactory results. Unless and until the systematic effects of errors can be eliminated, the way the data are weighted is largely irrelevant. Accordingly, with many systems, we have investigated whether the problem can be solved by optimizing various titration parameters simultaneously with the formation constants. In particular, we wondered whether a particular set of titration parameters could be selected which would effectively eliminate the systematic influences at the root of all the trouble.

This idea did not have the desired result as far as weighting was concerned, *i.e.*, the question of which weighting method to use was not answered. However, the outcome of optimizing various parameters together with the formation constants proved rewarding in another respect. As an example of this, Tables 4 and 5 show the results for the chemical system used in Table 1. First, note that as the number of parameters being optimized is increased, an increasing degree of correlation becomes evident, as expected. This is reflected in both the number of correlations reported by ESTA2 and the extent of individual correlations (where the maximum percentage of each set is given in parentheses). However, associated with the increasing number of parameters being optimized (and, hence, with increasing correlation) is a second, very striking effect. The formation constant values are progressively and dramatically improved towards their "true" values (which are  $\log \beta_1 = 10.500$ ,  $\log \beta_2 = 18.000$  and  $\log$



Table 4. Example of results from weighted OBJE tasks when increasing numbers of parameters are refined simultaneously with the formation constants (the simulated data were the same as those of Table 1; systems with reported correlations have the highest percentage correlation given in parentheses)

Parameters refined	$\beta$ only	$\beta + E^0$	$\beta + C_H^Y$	$\beta + C_H^B$	$\beta + E^0 + C_H^Y$	$\beta + C_H^Y + C_H^B$	$\beta + E^0 + C_H^B$	$\beta + C_H^Y + s$	$\beta + E^0 + C_H^Y + s$
$\beta_1$	10.541	10.552	10.506	10.497	10.512	10.497	10.500	10.496	10.509
$\beta_2$	18.097	18.114	18.002	17.992	18.013	17.993	17.998	17.985	18.010
$\beta_3$	20.111	20.162	19.982	19.984	20.006	19.982	19.993	19.954	20.003
$U$	2.46	2.23	0.263	0.334	0.320	0.0705	0.0311	0.176	0.0284
Weighted OBJE									
Number of correlations reported	0	0	0	1 (97%)	1 (95%)	0	2 (95%)	3 (99%)	4 (97%)
Parameters refined	$\beta + E^0 + C_H^Y + C_L^Y$	$\beta + E^0 + C_H^Y + C_L^Y$	$\beta + E^0 + C_H^Y + C_L^Y + s$	$\beta + E^0 + C_H^B + C_L^Y$	$\beta + E^0 + C_H^Y + C_L^Y + s$	$\beta + E^0 + C_H^Y + C_H^B + C_L^Y$	$\beta + E^0 + C_H^B + C_L^Y + s$		
$\beta_1$	10.502	10.507	10.498	10.501	10.492	10.501	14.492		
$\beta_2$	18.002	17.999	17.997	18.000	17.988	18.000	17.988		
$\beta_3$	19.998	19.995	19.992	19.996	19.988	19.996	19.988		
$U$	0.0241	0.0235	0.0251	0.0244	0.0244	0.0244	0.0244		
Weighted OBJE									
Number of correlations reported	3 (96%)	1 (94%)	3 (98%)	9 (100%)	9 (100%)	19 (100%)			

Table 5. Example of results from unweighted OBJT tasks, for titrations of a ligand, when increasing numbers of parameters are refined simultaneously with the formation constants (the simulated data were the same as those of Tables 1 and 4; systems with reported correlations have the highest percentage correlations given in parentheses)

Parameters refined	$\beta$ only	$\beta + E^0$	$\beta + C_H^V$	$\beta + C_H^V + C_H^B$	$\beta + C_H^V + C_H^B + E^0$	$\beta + C_H^V + C_M^B + C_L^V + E^0$
$\beta_1$	10.528	10.533	10.505	10.497	10.505	10.512
$\beta_2$	18.047	18.054	17.998	17.994	18.005	18.018
$\beta_3$	20.050	20.070	19.979	19.985	20.002	20.020
$U$	$9.1 \times 10^{-9}$	$1.4 \times 10^{-9}$	$4.7 \times 10^{-9}$	$1.3 \times 10^{-9}$	$8.3 \times 10^{-10}$	$8.6 \times 10^{-10}$
Unweighted OBJT						
Number of correlations reported	1 (96%)	0	2 (98%)	0	5 (99%)	10 (100%)

$\beta_3 = 20.000$ ). At the end of Table 4, when six parameters are being optimized in addition to the formation constants, the result suddenly gets much worse but, before this, there are benefits in optimizing more and more parameters. Why is this? Evidently, error which would otherwise be transferred into the optimized formation constant values is instead being squeezed into other parameters (of less interest). This general pattern of behaviour has been observed in all cases that we have studied.

This discovery forms the basis of the method for dealing with systematic errors described in Part V of this series.<sup>15</sup> It suffices here to say that the Monte Carlo analysis proposed therein provides an opportunity for evaluating more rigorously the methods of weighting discussed in this paper. The results thus obtained conform, in all respects, to the general observations outlined above. Individually, there are significant differences produced by the various methods of weighting. However, we can discern no general rule which is certain, or even likely, to yield the best results.

This conclusion does not mean that there are no advantages in weighting the data properly. Improving the information content of the data by giving greater emphasis where it is due remains a theoretically desirable goal. There will always be errors that propagate differently at different points and cannot be taken into account in any other way. It remains to be seen how useful this notion can be in practice since this can only be investigated once the adverse effects of systematic errors on the optimization calculations have been dealt with.

For the present, the main advantage in using different methods of weighting is precisely that, when

systematic errors are significant, they may well give rise to markedly different formation constant results. It is thus advisable to use several approaches whenever possible and to check for agreement between them. Results which do not much depend on the particular method of weighting obviously merit more confidence than those which do.

#### REFERENCES

1. D. L. Massart, B. G. M. Vandeginste, S. N. Deming, Y. Michotte and L. Kaufman, *Chemometrics: A Textbook*, p. 84. Elsevier, Amsterdam, 1988.
2. A. Sabatini, A. Vacca and P. Gans, *Talanta*, 1974, **21**, 53.
3. I. G. Sayce, *ibid.*, 1968, **15**, 1397.
4. M. Cromer-Morin, J. P. Scharff and R. P. Martin, *Analisis*, 1982, **10**, 92.
5. A. D. Zuberbühler and T. A. Kaden, *Talanta*, 1982, **29**, 201.
6. A. Vacca and A. Sabatini in *Computational Methods for the Determination of Formation Constants*, D. J. Leggett (ed.), p. 99. Plenum Press, New York, 1985.
7. P. Gans, A. Sabatini and A. Vacca, *J. Chem. Soc. Dalton Trans.*, 1985, 1195.
8. A. Avdeef, S. R. Sofen, T. L. Bregante and K. N. Raymond, *J. Am. Chem. Soc.*, 1978, **100**, 5362.
9. M. Wozniak and G. Nowogrocki, *Talanta*, 1978, **25**, 643.
10. A. Laouenan and E. Suet, *ibid.*, 1985, **32**, 245.
11. N. Ingri and L. G. Sillén, *Ark. Kemi*, 1964, **23**, 97.
12. R. M. Alcock, F. R. Hartley and D. E. Rogers, *J. Chem. Soc. Dalton*, 1978, 115.
13. J. Havel and M. Meloun in *Computational Methods for the Determination of Formation Constants*, D. J. Leggett (ed.), p. 221. Plenum Press, New York, 1985.
14. P. M. May, K. Murray and D. R. Williams, *Talanta*, 1988, **35**, 825.
15. P. M. May and K. Murray, *ibid.*, 1988, **35**, 933.

## THE USE OF GLASS ELECTRODES FOR THE DETERMINATION OF FORMATION CONSTANTS—V\*

### MONTE CARLO ANALYSIS OF ERROR PROPAGATION

PETER M. MAY†

School of Mathematical and Physical Sciences, Murdoch University, Western Australia 6150

KEVIN MURRAY

Processing and Chemical Manufacturing Technology Division, Council for Scientific and Industrial Research, Pretoria, South Africa 0001

(Received 22 August 1988. Accepted 8 September 1988)

**Summary**—The precision with which formation constants are calculated can be quantified by a Monte Carlo technique from realistic estimates of the experimental errors in titration parameters. The resulting standard deviations are invariably much poorer than those obtained conventionally because they reflect the true effects of systematic errors on the formation constant calculation. Such effects probably account for many of the discrepancies in the formation constant literature. Better assessment of errors makes it possible to select the set of titration parameters which, when optimized, yields the result with greatest probable accuracy. It is shown that this approach can markedly reduce the differences between formation constants determined by independent observers.

There are two distinct ways, random and systematic, in which errors in titration data can affect the optimization of formation constants. Although many kinds of error originate from unpredictable variations in experimental procedure, only a few act randomly on a least-squares calculation. More often, because parameters in the calculation are held at either too large or too small a value, the resulting errors operate in the same sense over ranges of data. Accordingly, in these cases the errors do not tend to cancel out as the number of titration points increases (which they would if they were random). This is so even if the residuals caused by them tend to change sign periodically. Such errors can thus have a systematic influence on any or all of the optimized formation-constant values.

Indeed, in titration data, the only errors that can reasonably be treated as random are those made in estimating titration volumes and emf readings. These observations should tend to distribute themselves evenly around the true values. On the other hand, the errors acting systematically include those in "local" parameters such as analytical concentrations and electrode calibration constants (*i.e.*, quantities affecting all points within individual titrations) and those in "global" parameters such as the dissociation constant of water and any ligand protonation constants. The so-called global parameters apply, more or less, at every point in all titrations in the data set.

Although these systematic errors may be kept to a minimum by good experimental technique, their actual magnitude can never be exactly determined. Consequently, they tend to propagate into the calculated values of the parameters chosen to be optimized. This happens in ways which are generally obscure and which differ markedly from case to case. The end result is that formation constants determined by titrimetry are often subject to substantial and unsuspected error.

The main problem is that conventional standard deviations of formation constants [as calculated, for example, by equation (12) of Part III of this series<sup>1</sup>] take no account of possible systematic errors. A quite misleading view of the precision is therefore obtained from all current generalized computer programs which determine formation constants by the usual least-squares methods. Their statistical analyses always significantly underestimate the spread of results likely to be obtained if the measurements were repeated independently many times.<sup>2,3</sup>

This paper describes a novel approach, based on an analysis by a Monte Carlo technique, which attempts to overcome this problem. The method aims to quantify how much "information" may reasonably be obtained by optimization of titration data, given standard deviations of certain experimentally determined titration parameters. This permits the selection of those parameters which it is most beneficial to optimize. By such means it becomes possible to suppress the ill-effects of systematic errors in parameters held constant during the optimization. We believe that by adopting a proper Monte Carlo

\*Part IV—*Talanta*, 1988, **35**, 927.

†Author for correspondence.

analysis, the differences between published sets of formation constants can be substantially reduced. These differences have hitherto been a marked and very disturbing phenomenon in the literature.<sup>1</sup>

### THEORY

The effects of errors in titration parameters held constant during an optimization cannot generally be assessed by an error propagation formula based on a Taylor-series expansion. Their influence depends on the whole body of data. This includes the various mathematical inter-relationships between all titration parameters, those being optimized as well as those being held constant. Accordingly, the sensitivity of any particular optimized parameter towards errors in another depends, at least in part, on the number and type of all the parameters that are being calculated simultaneously.

This kind of interaction between parameters in an optimization may be called correlation. Unfortunately, the term is used in a variety of ways in the literature and it is not always made clear exactly what is intended by it. Here it will be used to mean the tendency of optimized values to vary in response to changes in other parameters, whether or not they be optimized. In the following discussion it is only possible to mention those aspects of correlation with a particular bearing on the present objective. A more detailed, general treatment is available.<sup>4</sup>

The degree of correlation between two or more parameters being optimized governs the possibility, mathematically, of determining the values independently. Highly correlated parameters cannot be so determined; in the calculation their values vary in concert, giving rise to sets of nearly equivalent answers, all with approximately the same objective-function sum. In contrast, the correlation between fixed and optimized parameters determines how errors in the former propagate into the latter.

The effects of correlation most relevant to optimization processes are well illustrated by considering a linear least-squares regression. If the data points are well spread out, it is possible to obtain good, and reasonably independent, estimates of both the intercept and the gradient. On the other hand, if the points lie too close to one another (say, falling almost on the same spot), the data can only be used reliably to determine one of the two parameters—the other must be known accurately or it will cause the (single) optimized value to be in considerable error. In this second case, the parameters are said to be highly correlated. This example introduces two other pertinent points. The first is that the extent of correlation is not inherent solely in the mathematical relationship between the parameters; it depends on the number of data points and, crucially, on the range over which they are collected. Secondly, the extent of correlation depends on errors in the data. The larger the scatter of data points, the more blurred is the optimized

result and the more dependent will become the optimized value of one parameter on the exact value of the other if it is held constant.

Sillén described the correlation between two parameters in terms of a "skewed pit".<sup>5</sup> By this he meant that the objective function forms an elongated valley or pit (with a flattish bottom) oriented diagonally to the orthogonal axes representing the parameters. This picture clearly illustrates how fixing one parameter at an incorrect value may cause error in the optimized result (which corresponds to the objective-function minimum in the restricted dimension). Note that if the pit runs parallel to an axis or if it has concentric contours, there is no correlation. Note also that, if errors even slightly distort the bottom of a diagonally-oriented pit (*i.e.*, of a correlated system), they can dramatically alter the optimized outcome because a displacement of one value can be compensated for by a displacement in the other, without necessarily causing much of an increase in the final objective-function value.

This explains why, in the analysis of experimental data, it is not possible to optimize for all titration parameters simultaneously. In general, determining all parameters is only possible with perfectly simulated data, *i.e.*, where errors arise only from round-off in the computer and happen to be insignificant. If larger (but still random) errors are introduced into the data, *e.g.*, by using ESTA7,<sup>1</sup> it is observed that certain titration parameters must be held constant for correct results still to be obtained. It can be said that the errors reduce the "information content" of the data. Which parameters have to be known (and hence fixed) varies somewhat from system to system, depending on the chemical model and the correlations which are established.

### Monte Carlo analysis

As a prerequisite to limitation of their ill-effects, the important correlations affecting formation-constant determinations must be quantified. The easiest and, perhaps, the only way of tackling this problem is to use a Monte Carlo technique. This examines the effects of errors by successively imposing randomly generated perturbations on all the appropriate parameter values and repeating the optimization many times. The perturbations need to be applied with the correct (say Gaussian) distribution and they must be given a magnitude reflecting the error in each respective parameter (estimated, say, as a standard deviation). The spread of optimized results obtained in this manner from the repeated calculations will reflect the way all the errors are propagated. The probable error in an individual optimized answer can thus be determined from the observed variation and expressed as a standard deviation, 95% confidence interval or whatever other statistical measure is deemed appropriate.

What is particularly noteworthy about the Monte Carlo method here is its ability to encompass the

entire procedure for optimizing formation constants. This includes, for example, any method chosen to derive a set of weights (see Part IV). Given a particular chemical model, the Monte Carlo analysis quantifies the effects of errors whether or not they act in a systematic way on the optimization. Indeed, every kind of error which can possibly be represented in setting up the calculations can be taken into account.

Another way of looking at the proposed Monte Carlo method is to regard it as a means of simulating the measurements which might be made on a system if the whole practical exercise were to be repeated by a large number of independent investigators. On each such occasion, different experimental errors would be introduced: the determinations of titrand and titrant concentrations, of electrode calibration parameters, or previously measured protonation constants *etc.* would give final results scattered around the true values.

Of course, these experimental errors only affect the result of each optimization if the respective parameters in error are held constant during the calculation, *i.e.*, are not optimized. Also, the extent to which they have an influence will differ from case to case, depending on the chemical system and on the range of experimental conditions, as described above. However, all these relevant factors are taken into account by using the same mathematical relationships and data ranges in the repeated Monte Carlo simulations as in calculations with the real data. By using standard deviations that represent a realistic experimental precision (to determine probabilistically the effect of each simulated error), it is possible in this way to predict the variation in optimized formation constants which would be obtained by many independent investigators.

In addition to this measure of how precisely a particular optimized parameter can be determined, the Monte Carlo method also provides a criterion for selecting which parameters to optimize. The set chosen should be the one that is found to give the smallest variation in the parameters of particular interest. The smaller the Monte Carlo spread, the less likely is it that the optimization of the parameters is significantly affected by errors in values held constant during the calculation. In other words, by using the Monte Carlo analysis, it is possible to judge quite accurately the extent to which the information content of the data justifies optimizing any chosen set of parameters.

#### METHODS AND RESULTS

The practical benefits of the proposed Monte Carlo analysis have been assessed by recomputing formation constants for the nickel(II)-glycine system with data taken from the benchmark interlaboratory study published in 1978.<sup>7</sup> With commendable far-sightedness, it was agreed that participants in this

"challenge project" would tabulate their experimental details in full. This makes it possible for anyone to confirm for themselves the results obtained by the original calculations and to try out new computational methods on established data.<sup>3</sup> Sufficient information for this purpose is rarely to be found in the formation-constant literature and, to our knowledge, it was unique for several independent laboratories to contribute data on the same equilibrium system under identical conditions of temperature, ionic strength and background electrolyte. Accordingly, we have been able to test the ESTA Monte Carlo analysis on real data to establish its effectiveness.

Three sets of data were selected from the seven tabulated in the "challenge project" publication. These were from the research groups in St. Andrews (STA), Firenze (FI) and Parma (PR). The choice was made simply on the grounds that the raw data could be set up in ESTA format almost exactly as provided. There were just two minor exceptions: (i) electrode gradients were not explicitly stated by FI and PR so the theoretical Nernstian value was used and (ii) the amount of hydrogen ion reported by FI for curve 3 is in error; analysis with the ESTA task VESL suggested that the value should be 11.7523 not 1.7523, a misprint which was confirmed by the authors (P. Paoletti and A. Vacca, personal communication). Other participants did not report their measurements in a form that could be processed directly by ESTA, *i.e.*, they did not specify their titrations wholly in terms of titration volumes, emfs and amounts or concentrations in vessel and burette.

Two programs, ESTA3A and ESTA3B were developed to perform the Monte Carlo analyses. These differ only in the way the titration data are weighted, as described in Part IV of this series.<sup>6</sup> The procedure by which they calculate the standard deviations of refined formation constants is as follows. In every Monte Carlo cycle, a new set of randomly generated errors is imposed on those parameters which are to be held constant in the subsequent optimization. A simulation is then performed in which the emf at each point is determined on the basis of the perturbed titration-parameter values. A further error, based on the standard deviation of the emf readings, is randomly generated and imposed on this calculated emf. Finally, the formation constants are optimized with the simulated error-loaded data. If the optimization succeeds, the resulting values are stored for subsequent averaging over all Monte Carlo cycles and evaluation of the corresponding standard deviations.

The number of Monte Carlo cycles employed determines the precision with which the standard deviations are obtained and is set by the user, as the ESTA print option (IPRT). Fewer than 25 cycles is never recommended. In this work, we have used 75 in determining all standard deviations that are actually reported.

Table 1. Results from ESTA calculations of protonation constants without simultaneous refinement of titration parameters;  $pK_w = 13.690$  in all cases, for comparability

Laboratory	ESTA task	$\log \beta_{011}$	$\log \beta_{012}$
STA	Weighted OBJE	$9.562 \pm 0.026$	$11.972 \pm 0.049$
	Unweighted OBJT	$9.636 \pm 0.009$	$12.042 \pm 0.016$
FI	Weighted OBJE	$9.656 \pm 0.020$	$12.072 \pm 0.030$
	Unweighted OBJT	$9.643 \pm 0.016$	$12.054 \pm 0.031$
PR	Weighted OBJE	$9.685 \pm 0.026$	$12.101 \pm 0.039$
	Unweighted OBJT	$9.667 \pm 0.014$	$12.078 \pm 0.026$

The appropriate number of Monte Carlo cycles to use depends on the reproducibility of the standard deviations calculated. We have found that this number varies widely according to the chemical system being considered. Highly correlated systems, such as strong-acid *vs.* strong-base titrations, appear to need many more cycles than less correlated ones. This has major practical implications because the Monte Carlo calculations require prodigious amounts of computation—CPU times on a MicroVax II and a Sperry 1100 of many hours, and even of days, are typically needed for large metal–ligand systems like some of those dealt with in this paper. An investigation into the causes of this variability is presently under way.

The Monte Carlo procedure described above covers those instances in which a single set of user-specified titration parameters is optimized simultaneously with the formation constants (as well as the case in which the formation constants are refined alone). Initially, however, it is necessary to consider many possible combinations of various selected parameters since it is not known *a priori* which of these will yield the smallest standard deviation in the formation constants. This search is made by specifying a special print option (IPRT = 11). All combinations of flagged titration parameters are then automatically computed in turn. Thus, by comparison of the standard deviations obtained in the various cases, the most promising combinations of parameters to optimize can be identified.

Unfortunately, this criterion for selecting parameters is not always clear-cut. Fairly frequently, we have obtained two or more sets of optimized parameters with standard deviations that are too alike for one set to be confidently preferred. Moreover, the alternatives may rank differently when different formation-constant values are granted the highest

relative precision. In such cases, we have chosen to optimize those parameters for which it appears there is most "information content" in the data. This means optimizing as many parameters as possible, so long as it does not cause either too many optimization failures (say, more than 2 in 10), or too much correlation between optimized parameters (say, more than one or two parameters with correlation coefficients greater than 95% and none greater than 99%).

The rationale behind this strategy is to minimize the effects of errors in parameters held constant during the optimization, yet not to permit correlation to become so widespread that the uniqueness of the mathematical solution is lost. This is done by seeking the best trade-off between over-specifying information (which has harmful, systematic effects) and under-specifying it (which lets the formation constants deviate too readily from their true values).

The subjectivity involved in these secondary selection criteria is unfortunate but cannot be avoided. It is reassuring to remember that the choice has only to be made between sets of parameters which the Monte Carlo analysis shows are either the best or almost the best in terms of achievable precision. Consistent with this view, we have found that when the grounds for preferring one alternative to another are shaky, the two optimized results rarely differ by much. Presumably, this is because correlations which make it difficult to pick out the best set of parameters inherently tend to blur other distinctions. For example, it is not surprising to find that, when each is optimized separately, parameters such as the initial vessel volume and the vessel acid concentration frequently have very similar effects.

The results of the ESTA3B calculations from the three sets of "challenge project" data are given in Tables 1–4. Formation-constant values and the corresponding standard deviations determined by Monte

Table 2. Results from ESTA calculations of metal–ligand formation constants without simultaneous refinement of titration parameters;  $pK_w = 13.690$ ,  $\log \beta_{011} = 9.634$  and  $\log \beta_{012} = 12.034$  in all cases, for comparability

Laboratory	ESTA task	$\log \beta_{110}$	$\log \beta_{120}$	$\log \beta_{130}$
STA	Weighted OBJE	$5.946 \pm 0.011$	$10.672 \pm 0.019$	$14.534 \pm 0.060$
	Unweighted OBJT	$5.827 \pm 0.018$	$10.612 \pm 0.022$	$14.393 \pm 0.074$
FI	Weighted OBJE	$5.598 \pm 0.014$	$10.325 \pm 0.026$	$13.705 \pm 0.060$
	Unweighted OBJT	$5.598 \pm 0.017$	$10.315 \pm 0.040$	$13.667 \pm 0.091$
PR	Weighted OBJE	$5.595 \pm 0.015$	$10.335 \pm 0.023$	$13.691 \pm 0.072$
	Unweighted OBJT	$5.594 \pm 0.013$	$10.334 \pm 0.019$	$13.668 \pm 0.077$

Table 3. Results obtained from ESTA calculations of protonation constants with simultaneous refinement of given titration parameters;  $pK_w = 13.690$

Laboratory	ESTA task	Parameters co-refined	$\log \beta_{011}$	$\log \beta_{012}$
STA	Weighted OBJE	$C_H^V, C_L^V$ $V^O, C_H^V, C_L^V$	$9.632 \pm 0.003$ $9.634 \pm 0.002$	$12.020 \pm 0.005$ $12.027 \pm 0.005$
	Unweighted OBJT	$V^O, C_L^V$ $E^O, V^O, C_L^V$	$9.641 \pm 0.003$ $9.628 \pm 0.002$	$12.045 \pm 0.007$ $12.016 \pm 0.006$
FI	Weighted OBJE	$C_H^V$ $C_H^V, V^O, E^O$	$9.639 \pm 0.004$ $9.627 \pm 0.003$	$12.038 \pm 0.008$ $12.028 \pm 0.005$
	Unweighted OBJT	$E^O, C_H^B$	$9.639 \pm 0.003$	$12.053 \pm 0.006$
PR	Weighted OBJE	$C_H^V, C_H^B$ $E^O, V^O, C_H^V$	$9.635 \pm 0.003$ $9.632 \pm 0.003$	$12.065 \pm 0.008$ $12.032 \pm 0.005$
		$E^O, V^O, C_H^V, C_L^V$	$9.635 \pm 0.002$	$12.032 \pm 0.007$
	Unweighted OBJT	$E^O, C_H^V, C_L^V, C_H^B$	$9.636 \pm 0.002$	$12.025 \pm 0.006$

Carlo analysis are presented. Optimizations have been performed by ESTA with a variety of objective functions. Some results from the original "challenge project" calculations are also given, for ease of comparison, in Table 5.

Tables 1 and 2 show the values obtained when the formation constants are optimized alone. Significant differences are apparent between the results from the different laboratories. Reasonable agreement is achieved between FI and PR but not between them and STA. This is in accord with the findings tabulated in the "challenge project" report as a whole: the STA formation-constant values lay markedly outside the grouping of results from all the other laboratories. At the time, it was suggested that detection of hydroxo-nickel(II)-hydroxy-glycinate complexes in the STA titrations might have been responsible for the difference but this now seems unlikely for several reasons: (i) the discrepancy did not disappear when the titration points at high pH were removed from the STA calculation, (ii) evidence for complexes other than the three stepwise species was not obtained even

when the other "challenge project" participants specifically extended their searches to find them and (iii) there was no indication of the "curls" in the STA formation function,  $Z$ , in repeated investigations of the nickel(II)-glycinate system by Ph.D. students from the Bioinorganic Group at UWIST in Cardiff (who, over a number of years, used it as a test of their experimental technique).<sup>8</sup> It can thus be concluded that, in all probability, the formation-constant values from the STA data differ from the others simply because of the accumulated effect of experimental errors.

Tables 3 and 4 show the values of the formation constants obtained after each set of data has been analysed (by the Monte Carlo method described above) to determine one or more combinations of titration parameters for simultaneous refinement. The improvement obtained in the agreement between the results from STA and those from FI and PR is striking. There is even a slightly better match between the results of FI and PR. It is important to record that no attempt was made to select titration parame-

Table 4. Results obtained from ESTA calculations of metal-ligand formation constants with simultaneous refinement of given titration parameters;  $pK_w = 13.690$ ,  $\log \beta_{011} = 9.634$  and  $\log \beta_{012} = 12.034$

Laboratory	ESTA task	Parameters co-refined	$\log \beta_{110}$	$\log \beta_{120}$	$\log \beta_{130}$
STA	Weighted OBJE	$V^O, C_H^V$ $C_H^V, C_H^B$	$5.623 \pm 0.007$ $5.626 \pm 0.007$	$10.343 \pm 0.009$ $10.358 \pm 0.010$	$13.698 \pm 0.012$ $13.733 \pm 0.019$
		$V^O, C_H^V$ $C_H^V, C_H^B$	$5.595 \pm 0.010$ $5.597 \pm 0.011$	$10.331 \pm 0.012$ $10.338 \pm 0.013$	$13.725 \pm 0.020$ $13.737 \pm 0.016$
	Unweighted OBJT	$E^O, C_H^V, C_H^B$ $E^O, C_H^V, C_H^B$	$5.603 \pm 0.009$ $5.610 \pm 0.017$	$10.304 \pm 0.015$ $10.358 \pm 0.026$	$13.630 \pm 0.018$ $13.793 \pm 0.035$
		$E^O, C_H^V, C_H^B$ $C_H^V, C_L^V$	$5.615 \pm 0.010$ $5.618 \pm 0.006$	$10.364 \pm 0.018$ $10.356 \pm 0.015$	$13.799 \pm 0.039$ $13.787 \pm 0.023$
FI	Weighted OBJE	$E^O, C_H^B, C_H^B$ $E^O, C_H^V, C_H^B$	$5.610 \pm 0.017$ $5.615 \pm 0.010$	$10.358 \pm 0.026$ $10.364 \pm 0.018$	$13.793 \pm 0.035$ $13.799 \pm 0.039$
	Unweighted OBJT	$C_H^V, C_L^V$ $E^O, C_L^V, C_H^B$	$5.618 \pm 0.006$ $5.617 \pm 0.005$	$10.356 \pm 0.015$ $10.367 \pm 0.009$	$13.787 \pm 0.023$ $13.797 \pm 0.014$
PR	Weighted OBJE	$E^O, C_L^V, C_H^B$	$5.617 \pm 0.007$	$10.359 \pm 0.012$	$13.805 \pm 0.020$
	Unweighted OBJT	$E^O, C_H^V$ $E^O, C_H^V, C_H^B$	$5.618 \pm 0.008$ $5.615 \pm 0.006$	$10.365 \pm 0.015$ $10.357 \pm 0.010$	$13.801 \pm 0.027$ $13.808 \pm 0.016$

Table 5. Results obtained in the original study<sup>7</sup> for comparison with those obtained by ESTA and given in Tables 1-4

Laboratory	$pK_w$	$\log \beta_{011}$	$\log \beta_{012}$	$\log \beta_{110}$	$\log \beta_{120}$	$\log \beta_{130}$
STA	13.680	9.629	12.036	5.800	10.588	14.308
FI	13.704	9.654	12.067	5.625	10.356	13.750
PR	13.700	9.659	12.071	5.625	10.381	13.805

ters for optimization other than by the criteria listed above and that all optimizations for which results were obtained are shown in Tables 1-4.

#### DISCUSSION

The great disadvantage of using simulated data (with a known answer) to investigate strategies for the determination of formation constants is that the resulting test inherently conforms to all underlying assumptions regarding the source and magnitude of errors in the data. With real data, unexpected effects of varying degree are very likely to occur. If these happen to be significant, they may well confound the proposed strategy and, in particular, do so in a way that does not become apparent because the true answer is not known. In one sense, this is the problem with conventional least-squares programs: in determining the formation constants, they implicitly neglect the effects of systematic errors in titration parameters. The consequence is that, in processing experimental data, the results are distorted and all the statistical analyses are rendered entirely invalid.

There is no general remedy for this. New methods can be tested by using real data only if a reliable answer is already available. In the present context, however, since potentiometry is by far the most precise technique for measuring formation constants for more than three or four chemical species in solution, it is impossible for us to establish categorically that the methods proposed in this paper invariably lead to more accurate results.

However, there are some good reasons for believing that a Monte Carlo analysis by ESTA3 will prove effective. These are of both a practical and a theoretical nature. In practice, we have obtained consistently reasonable results with the dozen or so chemical systems thus far studied. The agreement in results achieved with the data from the three different "challenge project" laboratories is most impressive. This is especially so since it is in contrast with the results obtained by the original participants, who analysed their data by the best computational procedures then available. The values obtained by us also lie very close to the middle of the ranges given in the IUPAC report on the recommended procedure for testing potentiometric apparatus used in the measurement of metal-complex equilibrium constants.<sup>1</sup>

This assessment can be consolidated only by much more time and testing than has been possible to date but the experience we have had, albeit limited, has been good. The prospects also seem satisfactory on theoretical grounds. There is no doubt that determinations of formation constants with no attempt made to deal with the systematic effects of errors in titration parameters are subject to substantial inaccuracy. Through optimization of appropriate titration parameters and effective weighting of data, the effects of experimental errors can surely be reduced.

It follows that finding better ways to calculate formation constants depends mainly on avoiding the dangers of false optimization. The object of the Monte Carlo analysis done by ESTA3 is to find those sets of parameters to refine which, in this sense, holds the least risk. Predicting the "best" optimization(s) to perform on titration data really means finding those that are least likely to suffer from the adverse effects of systematic errors or correlations. Whilst this does not (and cannot) provide a guarantee, there is every likelihood that the results will be better than values obtained by previous methods of computation.

#### *Matters resolved*

With any simulation method (such as the proposed Monte Carlo analysis) it is obviously important to consider what happens when the assumed model does not conform exactly to reality. There are three areas of possible concern that, in our view, do not constitute serious problems.

First, there are questions about the correctness of the chemical model. These need to be dealt with in two parts, concerning the choice of chemical species and the values of their formation constants.

(a) It is necessary to state explicitly that throughout this paper it is assumed that the identities of the chemical species in solution are already known. Although, later, we will show that a Monte Carlo analysis can help to resolve the problem of model selection raised in Part III of this series,<sup>1</sup> this remains outstanding for the time being. Selection of titration parameters to optimize, before deciding which chemical species are present, is totally inappropriate. Correlations between formation constants and titration parameters can act to reduce the objective function of an optimization in which a species has been neglected; consequently, minor species will be hidden and may be lost if titration parameters are optimized before the species have been identified.

Notwithstanding this important disclaimer, the effects of an incorrect model on the Monte Carlo analysis and subsequent optimization of titration parameters need to be considered. Whilst it is not easy to predict with complete certainty what would happen, it is reasonable to expect that omitting from the model a species that is present in solution, or including one that is not actually present, will introduce a systematic error. This will have many characteristics in common with the systematic errors that have already been considered. For example, correlations with titration parameters being optimized will tend to reduce any ill-effects on other formation constants. However, this also means that the standard deviations calculated by the Monte Carlo analysis will be incorrect (to an extent that depends on the importance of the erroneous species in the calculation). In this respect, the Monte Carlo analysis is like all methods of formation-constant optimization: if the model is wrong, the results may or



may not be useful but they can never wholly be trusted.

(b) The use of incorrect values of formation constants in the Monte Carlo analysis will, of course, distort the calculation of the standard deviations. In general, however, this is not going to be a serious problem. Optimizing the formation constants alone, can be expected to yield values which are sufficiently accurate to give satisfactory results. In any event, if there is any uncertainty about this, the Monte Carlo analysis could be repeated with the improved formation constants made available by titration-parameter optimization.

Secondly, it is necessary to consider how the Monte Carlo analysis will fare if the actual errors in titration parameters are not correctly quantified. If users are unduly pessimistic about their experimental precision, the calculated standard deviations of the formation constants will be higher than they should be. Conversely, if their specified standard deviations are unrealistically small, the final error estimates will also be too small. In so far as the search for the titration parameters to be optimized is concerned, the exact size of the perturbations, provided they are not too excessive, is unlikely to alter the *kind* of correlations which occur.

On the other hand, these estimates of errors are critical in determining the magnitude of the standard deviations calculated by the Monte Carlo method, so there will be a problem if they are not assessed correctly on those (relatively rare) occasions when the absolute size of the error in formation constants is important. However, judging the experimental precision is sometimes rather subjective, since not all investigators are willing to undertake calibration of all their apparatus and repeat everything a sufficient number of times to identify outliers. Furthermore, the value of much repetition is questionable, because it neglects the most damaging kind of error—the single, careless mistake producing an error lying well outside the normal distribution expected of a competent worker. In other words, real errors may not be distributed in a Gaussian manner. For these reasons, it has been recommended<sup>6</sup> that the default error estimates supplied by ESTA8 be used in routine circumstances. This, at least, will provide standard deviations that can be compared meaningfully.

It is noteworthy that optimizing as many titration parameters as possible tends to reduce the untoward effects of gross experimental mistakes or of entirely unsuspected systematic errors. Of course, this cannot be relied on, because often the effects of such errors will not be entirely eliminated, and will still distort the answer to some extent. The point is, however, that in these circumstances, optimizing only the formation constants will generally yield even worse results.

Thirdly, there is a matter which is, perhaps, most likely to concern those who do not grasp how correlations affect all optimization calculations. Fre-

quently, in the optimization of titration parameters, it is observed that the optimized values clearly lie outside the bounds established by realistic estimates of the experimental precision. Worries of this kind led Gans *et al.* to describe optimized titration parameters as “dangerous”.<sup>9</sup> It is understandable but incorrect to regard optimizations with suspicion solely for this reason. It must be remembered that optimizers attempt to squeeze as much of the error as possible into the optimized values. In other words, errors are being propagated into the optimized titration parameters from many sources, especially those other titration parameters which are being held constant in the calculation. It is thus perfectly feasible for optimizations to loosen the connection between calculated the value of the parameter and the real value. The extent to which this happens is quantified by the Monte Carlo standard deviation. Hence, it is possible to check that the answers obtained by optimization are consistent with knowledge of the real system and how all the errors are propagated, but simply comparing the optimized values of titration parameters with a range estimated analytically does not do this.

On the contrary, the use of Monte Carlo analysis to select titration parameters for optimization will increase the number of instances in which titration parameters have optimized values lying outside plausible analytical limits. Making this choice of parameters solely on the grounds of reducing the standard deviations of the formation constants (if these are the only values it is actually desired to determine) means sacrificing interest in other parameters. Indeed, the proposed strategy is specifically designed to find ways by which errors can propagate into these unimportant values instead of the formation constants. A different choice would have to be made if the object of the optimization was to determine titration parameters as well as, or rather than, formation constants.

#### *Matters unresolved*

Although the approaches described in this paper can be applied immediately and, in our view, with benefit, the work has exposed certain fundamental difficulties in the construction of ESTA and other programs for determining formation constants. This prevents them from utilizing the Monte Carlo technique in a strictly proper manner.

The main problem arises from an effect which we have termed “linkage of systematic errors”. This means that certain experimental errors in local titration parameters, *i.e.*, ones applicable to individual titrations, act systematically for more than one titration or more than one parameter within titrations. For example, if a single stock solution is used to prepare every solution being titrated, the error in its concentration affects all titrations in the same sense. As is widely understood, this practice is undesirable because it magnifies the effect of the single analytical error. In contrast, the use of independent stock solutions in different titrations tends to reduce the

effects of errors through cancellation. Ironically, the way in which standard deviations are conventionally calculated makes it seem that the data obtained in the first way give the more precise formation constants. (This is because the method leads to better internal consistency). Yet the formation constant values so determined are undoubtedly less reliable than those obtained by the second, more punctilious, method.

A Monte Carlo analysis will not create this misleading impression if the randomly generated perturbations are imposed in a way that mirrors the experimental procedure. If the same simulated error in analytical concentration is imposed in several places, the consequence would generally be to increase the Monte Carlo standard deviations of the optimized formation constants.

In fact, ESTA and some other programs do allow titration parameters to be refined collectively over a range of titrations, so the linkage of some systematic errors, *e.g.*, those arising through the use of a single stock solution, can, to a certain extent, be accommodated. However, the problem goes deeper than this. All current computer programs for determining equilibrium constants of reactions in solution are based on certain conventions as to how the problem is formulated mathematically. Mass-balance equations are set up in terms of "components" and all complexes are described by overall formation reactions. There is no fundamental reason for this;<sup>10</sup> it is merely a matter of convenience in programming and, especially, in helping the user to specify the chemical system to be evaluated. Avdeef has found that these conventions can cause difficulties with refinement.<sup>11</sup> The point, here, is that they are not appropriate when it comes to handling experimental errors correctly. This is for two reasons.

(a) The total analytical concentrations of components (upon which each mass-balance equation is based) will often contain errors that have been generated in complicated ways—a correct error-propagation analysis requires that these ways are all faithfully reproduced in the Monte Carlo simulation. For example, the error in total concentration of the component  $H^+$  will often stem from experimental manipulations both with ligand and with mineral acid. The way in which the errors propagate into formation constants depends very much on how the solutions were prepared. The same can sometimes be said of different solutions used in the same titration, *e.g.*, if the metal ion is dissolved in acid, an error in pipetting this solution affects the total concentration of both  $M^{n+}$  and  $H^+$  in a directly related way. These linkages of systematic errors are likely to have a significant impact on the optimization process and, notably, on which titration parameters ought to be refined. However, since they introduce entangled ratios into the total analytical concentrations, none of the present computer programs for determining

formation constants (including ESTA) can easily be modified to deal with these effects.

(b) The formulation of equilibrium constants in a particular general way (*e.g.*, as overall formation constants) means that correlations are set up between them which will often be unnecessarily high.<sup>11</sup> This is readily illustrated by considering the dependence of  $\beta_{ML_2}$  on  $\beta_{ML}$ . When the equilibrium  $M + L \rightleftharpoons ML$  is less amenable to characterization than  $ML + L \rightleftharpoons ML_2$ , an uncertainty is associated with  $\beta_{ML_2}$  (from its dependence on  $\beta_{ML}$ ) that could be avoided by determining the stepwise equilibrium constants instead of the overall formation constants.

ESTA3 currently has a capability that permits the user to deal with systems in which previously determined formation constants (held constant in a subsequent calculation) are highly correlated amongst themselves. This is achieved by storing the successive sets of values for the constants determined during the Monte Carlo calculation of their standard deviations. These sets of (correlated) values are used instead of values with (independently) generated random errors. This propagates the effects of their correlation into the subsequent optimization. However, this merely allows the errors which arise to be estimated. If, instead, the chemical equilibria could be reformulated to minimize these correlations, the result would be better formation constants rather than a better idea of their poor precision.

It is clear from these difficulties that an entirely new approach to the computation of solution equilibria is needed in order to extract the maximum information possible from experimental titration data by using the Monte Carlo technique. For this and other reasons, we have begun development of a new computer package called JESS (for *JOINT EXPERT SPECIATION SYSTEM*). About 50000 lines of FORTRAN code have been written so far.<sup>12</sup> Prototype versions of the programs for accessing a large thermodynamic database have been completed. Interested readers can obtain details of how to acquire copies of JESS by writing to the authors.

#### CONCLUSION

Nearly 30 years ago Sillén<sup>5</sup> wrote 'It would be deplorable if the use of . . . computer methods should lead to an overestimate of the significance of "best" [formation constant] values'. Sadly, there is little doubt that this has occurred. The Monte Carlo calculations (for systems we have studied so far) suggest that errors in published values commonly exceed those expected (from the reported standard deviations) by one or even two orders of magnitude. The effects of propagating systematic errors are, virtually alone, capable of causing the kinds of discrepancies which commonly afflict the formation-constant literature. In spite of the difficulties outlined

above, the Monte Carlo analysis described in this paper can begin to rectify this underestimation.

Our approach also provides a means for selecting titration parameters for simultaneous optimization with formation constants. It seems likely that this will yield more accurate values of formation constants than have been obtained hitherto. Until even more effective computational techniques are developed, the ESTA library of programs can be used, within the constraints imposed by existing conventions, to apply these new ideas forthwith.

Although proper selection of the titration parameters to be optimized can thus now enhance the chances of reporting good constants, this ought not to detract from the importance, in itself, of having better estimates of the standard deviations. This capability of Monte Carlo analysis has potential implications for model selection and for assessing experimental design, which will be considered more fully in a later paper.

*Acknowledgements*—Thanks are due to those many colleagues with whom discussions have helped to develop our ideas. The perceptive comments of Dr. Glenn Hefter (Murdoch University) and Prof. Peter Linder (University of Cape Town) are particularly appreciated.

## REFERENCES

1. P. M. May and K. Murray, *Talanta*, 1988, **35**, 825.
2. A. Braibanti, F. Dallavalle, G. Mori and B. Veroni, *ibid.*, 1982, **29**, 725.
3. A. Braibanti, G. Ostacoli, P. Paoletti, L. D. Pettit and S. Sammartano, *Pure Appl. Chem.*, 1987, **59**, 1721.
4. D. L. Massart, B. G. M. Vandeginste, S. N. Deming, Y. Michotte and L. Kaufman, *Chemometrics: A Textbook*, Chapter 14, Elsevier, Amsterdam, 1988.
5. L. G. Sillén, *Acta Chem. Scand.*, 1962, **16**, 159.
6. P. M. May and K. Murray, *Talanta*, 1985, **35**, 927.
7. E. Bottari, A. Braibanti, L. Ciavatta, A. M. Carrie, P. G. Daniele, F. Dallavalle, M. Grimaldi, A. Mastroianni, G. Mori, G. Ostacoli, P. Paoletti, E. Rizzarelli, S. Sammartano, C. Severini, A. Vacca and D. R. Williams, *Ann. Chim. (Roma)*, 1978, **68**, 813.
8. University of Wales, Institute of Science and Technology, *Ph.D. Theses*, J. R. Duffield, 1982; W. J. Trott, 1982; G. L. Smith, 1983; D. C. Jones, 1983; K. M. Quinlan, 1984.
9. P. Gans, A. Sabatini and A. Vacca, *J. Chem. Soc. Dalton Trans.*, 1985, 1195.
10. F. M. M. Morel, *Principles of Aquatic Chemistry*, p. 5. Wiley, New York, 1983.
11. A. Avdeef, in *Computational Methods for the Determination of Formation Constants*, D. J. Leggett (ed.), Chapter 9, p. 359. Plenum Press, New York, 1985.
12. P. M. May and K. Murray, *Talanta*, 1987, **34**, 821.

## STOPPED-FLOW DETERMINATION OF CARBARYL AND ITS HYDROLYSIS PRODUCT IN MIXTURES IN ENVIRONMENTAL SAMPLES

M. C. QUINTERO, M. SILVA and D. PEREZ-BENDITO

Department of Analytical Chemistry, Faculty of Sciences, University of Córdoba, 14004 Córdoba, Spain

(Received 5 May 1988. Revised 22 June 1988. Accepted 30 August 1988)

**Summary**—A kinetic method for determination of carbaryl and its hydrolysis product in mixtures, by a modular stopped-flow system, is reported. The method involves the formation of the coupling product formed between 1-naphthol, the hydrolysis product of carbaryl and diazotized sulphanilic acid in a weak acid medium. With one hydrolysed and one unhydrolysed sample aliquot both carbaryl and 1-naphthol can be determined in their mixtures, with a relative standard deviation of 0.8%. The method is highly selective and free from interference by other pesticides tested and has been applied to the analysis of environmental samples for carbaryl and 1-naphthol.

Pesticides of the carbamate family have become increasingly important in recent years because of their broad spectrum of biological activity. They are employed as insecticides, fungicides, nematocides, miticides and molluscicides.<sup>1</sup> Of these pesticides, carbaryl (1-naphthyl methylcarbamate) is a broad-spectrum insecticide used extensively because of its effectiveness and low acute mammalian toxicity (the oral LD<sub>50</sub> for rats is 560 mg/kg). However, recent studies have indicated that carbaryl may be a viral enhancer and a teratogen.<sup>2</sup> Because of this new information about its chronic toxicity and its wide use near water supplies and soil, evaluation of water pollution with carbaryl necessitates observation of the concentrations of both carbaryl and its hydrolysis product, 1-naphthol, in natural waters.

Although chromatographic methods are very useful for determining and estimating pesticides, the throughput capability of a stopped-flow method, requiring only a few seconds per sample, is much superior to that of a chromatograph. Furthermore, the susceptibility of many carbamates to thermal decomposition complicates their gas chromatography.<sup>3,4</sup> The spectrophotometric methods used are generally based on coupling of the 1-naphthol obtained by hydrolysis of carbaryl to a diazotized compound,<sup>5-8</sup> but the joint spectrophotometric determination of carbaryl and 1-naphthol in mixtures has not been reported so far. Such mixtures have been analysed, however, on the basis of the native fluorescence of the two compounds.<sup>9-11</sup>

A method for the kinetic determination of this pesticide, both alone and in mixtures with its hydrolysis product, is presented in this paper. It is based on the rate of coupling between 1-naphthol and diazotized sulphanilic acid and the use of the photometric stopped-flow technique. The substitution of a semi-automatic kinetic method for the equilibrium methods, which involve several steps prior to the absorb-

ance measurements, results in a considerably simpler and faster procedure for the determination of these substances. For this purpose, a modular stopped-flow system<sup>12</sup> has been used. It is inexpensive and provides a useful means for routine analysis of pesticides. It was earlier used in clinical analysis<sup>13</sup> with good results.

### EXPERIMENTAL

#### Reagents

The reagents used were of analytical-reagent grade and distilled water and dioxan were used to prepare the solutions. Carbaryl and 1-naphthol solutions (1000 µg/ml) were prepared by dissolving 100.0 mg of the chemical in 100 ml of dioxan, and were stored in a PTFE bottle in the refrigerator. Sulphanilic acid solution was prepared by dissolving 500 mg of the reagent in 100 ml of 30% v/v acetic acid. A sodium nitrite solution (0.1%) was prepared with distilled water.

#### Apparatus

The stopped-flow system<sup>12</sup> marketed by QuimiSur Instrumentation was fitted to a Perkin-Elmer Lambda 5 spectrophotometer. Kinetic data were collected and treated by a Hewlett-Packard 98561AE computer and a 16-bit Hewlett-Packard 98640A analogue-to-digital converter provided with a program written by us for application of the initial-rate method (readers can obtain a copy of the program from us). This data-acquisition system was also coupled on-line to the spectrophotometer.

#### Procedure

**Kinetic determination of carbaryl.** Two solutions were prepared and placed in the drive syringes. For solution A, the volume of carbaryl solution required to ensure a final concentration of pesticide between 0.7 and 70 µg/ml, 1 ml of 2M sodium hydroxide and 0.2 ml of ethanol (in order to ensure complete hydrolysis of carbaryl) were added to a 10-ml standard flask, then 1 ml of 2M hydrochloric acid and 2 ml of 1M acetic acid/sodium acetate buffer (pH 4.14) were added and the mixture was diluted to the mark with distilled water. Solution B was prepared by mixing 0.5 ml of 0.5% sulphanilic acid solution and 1.5 ml of 0.1% sodium nitrite solution in a 10-ml standard flask and diluting to the mark with acetic acid/sodium acetate buffer (pH 4.14).

Equal volumes of both solutions (0.2 ml) were mixed in the stopped-flow system and the reaction was monitored at 475 nm. The temperature was kept constant at  $45 \pm 0.1^\circ$  throughout. The kinetic curve, the initial rate measurement (in the first 1.5 sec) and the concentration of the analyte were automatically obtained by means of the computer system.

**Analysis of carbaryl/1-naphthol mixtures.** Synthetic samples containing various trace concentrations of carbaryl and 1-naphthol were analysed in two kinetic runs. Samples containing 30–600  $\mu\text{g}$  of carbaryl and 21.5–250  $\mu\text{g}$  of 1-naphthol were reacted by the procedure described above. The initial rate calculated was proportional to the carbaryl plus 1-naphthol concentration in the sample. In the second run, the sodium hydroxide and ethanol were omitted from the samples in order to avoid the hydrolysis of carbaryl, and the procedure was followed as above. The difference between the two rates represented the carbaryl content.

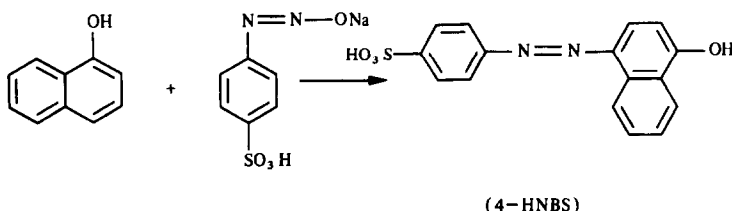
#### Preparation and analysis of environmental samples

**Extraction of water samples.** After collection of the water samples (minimum volume 100 ml) their pH was adjusted to below 5.0 with 5 ml of sodium acetate/acetic acid buffer (pH 4.14) and 3 g of sodium chloride were dissolved in each 100-ml sample. For spiking of the samples, several known amounts of carbaryl and 1-naphthol from stock solutions in dioxan were added to the water samples. Next, each sample was shaken with 50 ml of methylene chloride in a 250-ml separating funnel for 4 min. The resulting organic extract was transferred into a 250-ml beaker and the aqueous phase was shaken with a further 25 ml of methylene chloride. The second organic extract was added to the first and this solution was evaporated almost to dryness. The residue was dissolved in 4 ml of dioxan and diluted accurately to 10 ml with distilled water for determination of the carbaryl content, or was previously hydrolysed as described above for determination of the carbaryl plus 1-naphthol content by the procedure above.

**Extraction and clean-up of vegetable samples.** Fifty g of blended vegetable were spiked with 50–100  $\mu\text{g}$  of carbaryl in dioxan and extracted with 100 ml of methylene chloride for 5 min. The organic layer was filtered through a Whatman No. 1 filter paper and the residue was washed with two 50-ml portions of methylene chloride. The solvent in the combined organic extract was evaporated, and the residue was dissolved and analysed for carbaryl by the above-described procedure.

## RESULTS AND DISCUSSION

Weakly acidic solutions of diazotized sulphanilic acid react with 1-naphthol to yield a coupling product *p*-(4-hydroxyl-1-naphthylaza)benzenesulphonic acid (4-HNBS):



Since this reaction is time-dependent and fast, the determination of carbaryl must be performed by using the stopped-flow technique with monitoring of the reaction rate spectrophotometrically at 475 nm

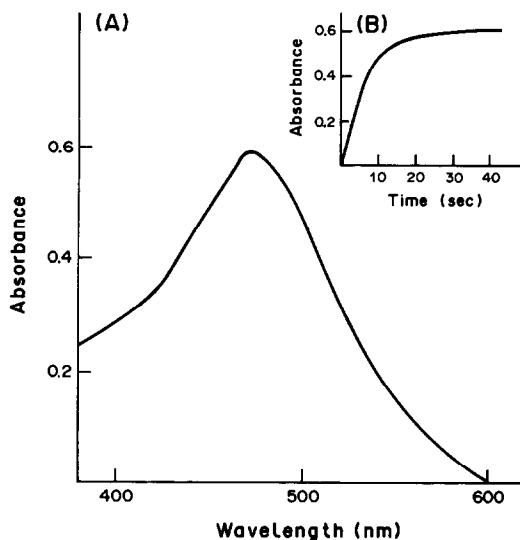


Fig. 1. (A) Absorption spectrum of the coupled product formed between 1-naphthol (from 10  $\mu\text{g}/\text{ml}$  carbaryl) and diazotized sulphanilic acid. (B) Typical absorbance *vs.* time plot for the reaction under study. Conditions as described under experimental.

(absorption maximum of the coupling product formed). The spectral features of the reaction product are given in Fig. 1A, which also shows a typical absorbance *vs.* time plot for a carbaryl concentration of 10  $\mu\text{g}/\text{ml}$  (Fig. 1B).

As stated in the literature, the rate of hydrolysis of carbaryl is a function of pH and the solvent used.<sup>11</sup> In our method, carbaryl is instantaneously and quantitatively hydrolysed to sodium 1-naphtholate with ethanolic sodium hydroxide. On the other hand, since the coupling reaction takes place in a weakly acidic medium in which carbaryl is inactive, the method allows carbaryl to be distinguished from 1-naphthol. Thus, a kinetic study of the influence of the variables on the rate of the coupling reaction was made in order to develop a kinetic method for the determination of carbaryl alone or in mixtures with 1-naphthol.

#### Effect of reaction variables

In this study of the effect of variables, all concentrations indicated are the initial concentrations in the

syringes (*i.e.*, twice the actual concentrations in the reaction mixture at time zero after mixing).

The effect of temperature on the reaction rate was examined between 15 and 50°. The absorbance *vs.* time curves show an increase in reaction rate with increase in temperature up to 40°, above which the initial rate remains practically constant. Therefore, a temperature of 45° was chosen as optimal. A plot of the logarithm of the rate constant against the inverse of the absolute temperature gave the activation energy as 34.4 kJ/mole.

In the study of the other variables, the kinetic data were obtained from the initial rate *vs.* concentration plots. Likewise, the partial orders for each variable were calculated from the resulting log-log plots. The influence of the sulphanilic acid concentration was evaluated over the range  $0.15\text{--}1.5 \times 10^{-3}M$ ; the reaction rate was found to increase with sulphanilic acid concentration up to  $1.15 \times 10^{-3}M$  and remains constant above it. A sulphanilic acid concentration of  $1.45 \times 10^{-3}M$  (0.5 ml of 0.5% solution) was selected. For the kinetic dependence on the sulphanilic concentrations outside the plateau region, a partial order of 1 was found. The effect of varying the sodium nitrite concentration over the range  $3.7 \times 10^{-5}\text{--}5.8 \times 10^{-3}M$  was also studied. The reaction rate does not depend on nitrite concentration when this is above  $1.45 \times 10^{-3}M$ , which corresponds to a sulphanilic acid/nitrite ratio of about 1. At lower concentrations, the reaction rate decreases linearly with decreasing nitrite concentration. The concentration advocated in the procedure (1.5 ml of 0.1% sodium nitrite in 10 ml) is  $2.17 \times 10^{-3}M$ .

The influence of the pH of solution B was studied between 2.75 and 5.88 (Fig. 2). The initial rate increased with increasing pH (partial order with respect to  $[H^+]$ , from a log-log plot was  $-1.0$ ). Since no zero-order kinetic region was found in this study, the optimal pH was chosen according to the following reasoning. Obviously the kinetic determination of

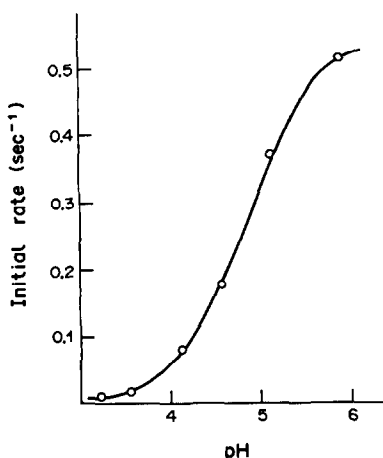


Fig. 2. Effect of pH on the initial rate. Carbaryl concentration 10  $\mu\text{g/ml}$ , other conditions as described under experimental.

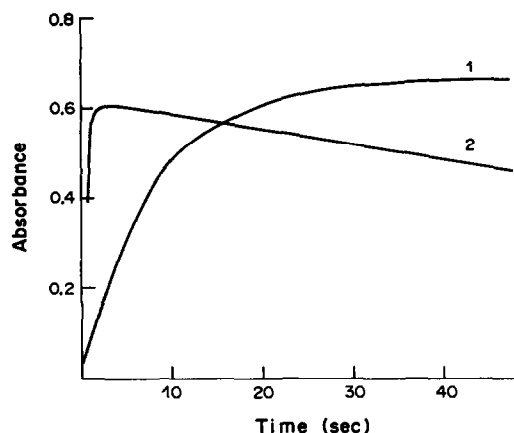


Fig. 3. Stability of the reaction product at pH 4.10 (1) and 5.88 (2). Other conditions as described under experimental.

carbaryl is more favourable at higher reaction rates (higher pH values). However, at pH about 6.0, several factors exert a negative effect on this kinetic determination. (a) The instability of the reaction product (see Fig. 3) gives rise to more irreproducible results in the initial rate measurement. Thus, the relative standard deviations ( $n = 11$ ) for the initial rate at pH 5.88 and 4.10 were 5.9 and 0.8%, respectively. (b) The stability of solution B was greatly affected by the pH, *e.g.*, at pH 4.10 it was stable for at least one day, whereas at pH 5.88 it had to be prepared every 2 hr. A pH value of 4.10 was therefore selected. This pH was achieved in solution B by using 1.0M sodium acetate/acetic acid buffer (pH 4.14) to dilute the selected amounts of sulphanilic acid and sodium nitrite added to the 10-ml standard flask. Under these selected conditions, the diazotization of sulphanilic acid was instantaneous.

Two important variables which affect the preparation of solution A were studied. The pH of this solution over the range 2.0–12.0 did not affect the initial rate. However, even at pH 12.0, it was necessary to add some ethanolic sodium hydroxide solution to hydrolyse the carbaryl instantaneously. The influence of several water-miscible organic solvents, such as methanol, dioxan and dimethylsulphoxide, at up to 50% v/v concentration was also studied because of the practical interest in application of the method (the residue of pesticides extracted from real samples must be dissolved in water-miscible organic solvents). At the highest concentration tested, 50% v/v, dioxan had no effect on development of the reaction; however, methanol and dimethylsulphoxide exerted opposite effects, methanol increasing the initial rate by about 50%, and dimethylsulphoxide decreasing it by about 25%.

Absorbance *vs.* time curves were recorded for solutions containing different amounts of carbaryl, under the above-described experimental conditions. The reaction was found to be first-order with respect to 1-naphthol. By using the linear plot of  $\ln(A_\infty - A_t)$

Table 1. Analysis of synthetic mixtures of carbaryl and 1-naphthol\*

Taken, † 10 <sup>-5</sup> M		Carbaryl		1-Naphthol	
Carbaryl	1-Naphthol	Found, 10 <sup>-5</sup> M	Error, %	Found, 10 <sup>-5</sup> M	Error, %
1.50	1.50	1.46	-2.7	1.43	-4.6
3.00	1.50	3.09	3.0	1.46	-2.7
7.50	1.50	7.66	2.1	1.49	-0.7
15.0	1.50	15.4	2.7	1.47	-2.0
22.5	1.50	23.3	3.6	1.51	0.7
30.0	1.50	28.7	-4.3	1.52	1.4
3.50	7.00	3.48	-0.6	7.02	0.3
3.50	17.5	3.35	-4.3	16.8	-4.0

\*Experimental conditions as in procedure.

†These concentrations refer to the initial concentrations in solution B.

*vs.* time (where  $A_{\infty}$  is the final absorbance and  $A_t$  the absorbance at time  $t$ ) a first-order rate constant of 0.12 sec<sup>-1</sup> was computed, the half-life being 5.8 sec.

The following simplified kinetic equation can be applied under the conditions recommended in the procedure for the determination of carbaryl:

$$d[4\text{-HNBS}]/dt = k[1\text{-naphthol}]/[H^+]$$

where  $k$  is the rate constant of the coupling reaction.

#### Kinetic determination of carbaryl

The absorbance *vs.* time curves recorded for different amounts of carbaryl by the stopped-flow technique were analysed by the initial-rate method. The calibration graph was linear over the concentration range 0.35–35 µg/ml carbaryl. Pearson's correlation coefficient ( $r$ ) was 0.998. These concentrations refer to the actual concentrations in the reaction mixture (in the observation chamber). The slope of the calibration plot was  $(2.85 \pm 0.05) \times 10^{-3}$  ml. µg<sup>-1</sup>. sec<sup>-1</sup>, and this value was taken as the analytical sensitivity. The detection limit was calculated on the basis of the variation of the analyte response at low concentrations<sup>14</sup> because no blanks were used in this determination, and was defined as the concentration of carbaryl yielding an initial rate equal to 3 times the standard deviation of the initial rate (20 determinations) on a sample containing 3.5 µg/ml carbaryl. The value found was 0.17 µg/ml. The precision (RSD) ( $P = 0.05$ ,  $n = 11$ ) for 3.5 µg/ml carbaryl was 0.8%. The sampling rate, calculated from the time corresponding to three replicates performed for the same sample, was about 120/hr.

#### Kinetic analysis of carbaryl/1-naphthol mixtures

The simultaneous determination of carbaryl and its hydrolysis product, 1-naphthol, in aqueous media is of great interest because 1-naphthol is as toxic as the original pesticide carbaryl to a number of aquatic species.<sup>15</sup> The half-life of carbaryl in aqueous systems is strongly dependent on the pH, 15 min at pH 10 and 10.5 days at pH 7, and the rate of hydrolysis increases 2–3 times as the temperature increases from 20 to 30°. In summary, the simultaneous rapid determination of carbaryl and 1-naphthol would permit

the direct examination of the effect of environmental conditions such as temperature, pH, sunlight, *etc.* on the degradation of carbaryl.

The carbaryl and 1-naphthol concentrations in several standard mixtures were assessed from the initial rates obtained under two sets of experimental conditions and by using the calibration graph obtained with standards. Table 1 lists the results obtained; the analysis of carbaryl/1-naphthol mixtures was feasible over the molar ratio range from 1:5 to 20:1 (maximum relative error  $\pm 5\%$ ). These results are very satisfactory and more advantageous than those provided by the fluorimetric equilibrium method,<sup>9,10</sup> because the proposed method allows the resolution of this mixture for lower degrees of hydrolysis of carbaryl in the sample to be analysed (down to 4.8%).

The mean of the results from 11 samples each containing  $3.5 \times 10^{-5}M$  carbaryl and 1-naphthol gave the overall relative standard deviation of the method as 0.9%.

A study of interferences was made to determine the tolerance limit for various compounds commonly associated with carbaryl and 1-naphthol in environmental samples, especially in water samples. For a mixture of  $3.5 \times 10^{-5}M$  carbaryl and 1-naphthol the maximum level of foreign compound studied was

Table 2. Influence of foreign species on the kinetic determination of  $3.5 \times 10^{-5}M$  carbaryl and 1-naphthol.

Compound added	Tolerance ratio
Malathion, parathion, parathion-methyl, paraoxon, fenitrothion, dieldrin, $\alpha$ -HCH, lindane, carbofuran, propoxur, 2-isopropoxyphenol, carbofuranphenol, 4-nitrophenol, phenol, 2-chlorophenol, <i>o</i> -cresol, <i>m</i> -cresol, benzene, toluene, cyclohexane, Manoxol O. T., dodecyltrimethylammonium bromide, sodium dodecylsulphate	40*
Aldrin†, ethylbenzene†, Triton X-100, Brij	20
Cyclohexane†	10
2-Naphthol, naphthalene†	5

\*Maximum foreign compound/analyte molar ratio tested.

†Maximum ratio assayed owing to its low solubility in water.

Table 3. Recovery of carbaryl and 1-naphthol added to water samples

Sample	Carbaryl content, ng/ml			Mean recovery, %	1-Naphthol content, ng/ml			
	Added	Found*			Added	Found*		Mean recovery, %
Distilled water	70	61, 71, 76		99.0	250	248, 241, 246		98.0
	140	148, 148, 141		104.0	100	98, 105, 96		99.6
	280	279, 260, 274		96.8	20	19, 21, 19		98.3
Drinking water	70	72, 72, 68		101.1	250	240, 240, 249		97.2
	140	128, 126, 139		93.6	100	97, 98, 97		97.3
	280	277, 275, 276		98.6	20	18, 19, 19		93.3
River water	70	70, 71, 69		100.0	250	240, 251, 243		97.9
	140	138, 140, 141		99.8	100	98, 104, 96		99.3
	280	277, 279, 274		98.8	20	21, 19, 20		100.0
		Mean		99.1		Mean		97.9
		Standard deviation		2.8		Standard deviation		1.9

\*For three separate determinations.

$1.4 \times 10^{-3}M$  (tolerance limit 40-fold molar ratio) when the solubility of the test compound in water allowed. The tolerance limit for the foreign compound was taken as the largest amount yielding an error less than  $\pm 3\%$  in the initial-rate measurements.

The substances assayed in this study of interferences can be classified into four groups: (a) other pesticides such as chlorinated, phosphorated and carbamate compounds; (b) phenol and its derivatives as well as phenolic hydrolysis products of other pesticides commonly found in water samples; (c) aromatic and saturated hydrocarbons; (d) different types of surfactants (anionic, cationic and non-ionic).

As can be seen from Table 2, the method offers much greater selectivity insofar as, of the tested compounds, the most serious interference was caused by 2-naphthol, but at a moderately high concentration level (5 times that of carbaryl or 1-naphthol).

#### Applications

To obtain an indication of the efficiency of the proposed procedure for the analysis of carbaryl/1-naphthol mixtures, water samples to which known amounts of carbaryl and 1-naphthol had been added were analysed. Water samples (100 ml each) were spiked at levels of 70–280 ng/ml carbaryl and 20–250 ng/ml 1-naphthol, extracted with methylene chloride and analysed for carbaryl and 1-naphthol as described above. The results given in Table 3 indicate that recoveries ranged from 93.6 to 104.0%, with an average of 99.1% for carbaryl and 97.9% for 1-naphthol. The relative standard deviation for the whole procedure was 2.8% and 1.9% for carbaryl and 1-naphthol, respectively, for 9 determinations. These recoveries show the good performance of the trace-enrichment technique used.

According to literature data, no free 1-naphthol is found in vegetables polluted with carbaryl. Thus, to check the recovery from vegetable samples, these were spiked only with carbaryl. Thus, 50–100  $\mu\text{g}$  of pesticide were added to 50 g of vegetable (string bean, pepper and squash) and extracted with methylene

chloride. The recovery was 95.5–100.5% (Table 4) with a standard deviation of 1.4%.

#### CONCLUSIONS

The results reported above show that the stopped-flow technique is suitable for the routine determination of carbaryl and 1-naphthol in environmental samples. The method offers several advantages which can be classified into two groups.

(1) Those inherent in the stopped-flow technique: (a) low sample and reagent consumption; (b) ease of automation; (c) high sampling frequency; (d) low cost per determination.

(2) Specific advantages over other classical photometric methods: (a) resolution of carbaryl and 1-naphthol mixtures; (b) wider determination range and higher selectivity, which allow its application to environmental samples; (c) no blank is required, which is of interest in determination of carbaryl in vegetable samples, because the colour of the extracts has no effect on the kinetic determination; (d) higher stability of the colour-developing reagent in contrast to others such as *p*-nitrobenzenediazonium fluoroborate, which is proposed in the AOAC standard methods and must be prepared immediately

Table 4. Recovery of carbaryl added to vegetable samples

Sample	Carbaryl, $\mu\text{g}^*$		Mean recovery, %
	Added	Found†	
Pepper	50.0	47.8, 49.6, 49.5	97.9
	75.0	71.9, 71.5, 71.4	95.5
	100.0	96.4, 95.0, 101.2	97.5
Bean	50.0	49.0, 49.9, 49.4	98.9
	75.0	76.1, 69.8, 74.0	97.7
Squash	100.0	100.4, 100.2, 100.8	100.5
	50.0	48.1, 50.8, 49.8	99.1
	75.0	73.1, 73.6, 72.7	97.5
	100.0	97.4, 98.9, 98.3	98.2
		Mean	98.1
		Standard deviation	1.4

\*Amount added to 50 g of vegetable.

†For three separate determinations.



prior to use,<sup>17</sup> (e) because of the dynamic nature of many of these coupling reactions, equilibrium methods are troublesome as exact timing of the addition of reagents and of the instrumental measurement is required. The proposed kinetic method is therefore a suitable, faster and simpler alternative for the determination of carbaryl and 1-naphthol.

*Acknowledgement*—The authors are grateful to the C.A.I.C.y T. (Project No. 0979/84) for financial support.

#### REFERENCES

1. J. H. A. Ruzicka, *Proc. Soc. Anal. Chem.*, 1973, **10**, 32.
2. R. J. Bushway, *J. Chromatog.*, 1981, **211**, 135.
3. H. W. Dorough and J. H. Thorstenson, *J. Chromatog. Sci.*, 1975, **13**, 212.
4. R. C. Hall and D. E. Harris, *J. Chromatog.*, 1979, **169**, 245.
5. J. R. Rangaswamy and S. K. Majumder, *J. Assoc. Off. Anal. Chem.*, 1974, **57**, 592.
6. M. Chiba, *J. Agric. Food Chem.*, 1981, **29**, 118.
7. K. M. Appaiach, R. Ramakrishna, K. R. Subbarao and O. Kapur, *J. Assoc. Off. Anal. Chem.*, 1982, **65**, 32.
8. K. M. Appaiach, U. C. Nag, O. P. Kapur and K. V. Nagaraja, *J. Food Sci. Technol.*, 1983, **20**, 252.
9. R. J. Argauer and W. Bontayan, *J. Assoc. Off. Anal. Chem.*, 1970, **53**, 1166.
10. M. L. Larkin and M. J. Day, *Anal. Chim. Acta*, 1979, **108**, 425.
11. J. J. Aaron and N. Some, *Analysis*, 1982, **10**, 481.
12. A. Loriguillo, M. Silva and D. Pérez-Bendito, *Anal. Chim. Acta*, 1987, **199**, 29.
13. M. C. Gutierrez, A. Gómez-Hens and D. Pérez-Bendito, *Z. Anal. Chem.*, 1987, **328**, 120.
14. J. A. Glaser, D. L. Foerst, G. D. Mckee, S. A. Quave and W. L. Budde, *Environ. Sci. Technol.*, 1981, **15**, 1426.
15. G. Kahnt, *Phytochemistry*, 1967, **6**, 755.
16. O. M. Aly and M. A. El-Dib, *Water Res.*, 1971, **5**, 1191.
17. *Methods of Analysis of the AOAC*, W. Horwitz (ed.), AOAC, pp. 537–538. Washington, DC, 1975.

## SOLVENT EXTRACTION EQUILIBRIA OF THE NICKEL-3-(2-FURYL)-2-MERCAPTOPROPENOIC ACID COMPLEX AS AN ION-PAIR WITH THE DIPHENYLGUANIDINIUM ION

A. IZQUIERDO, M. D. PRAT and A. GARBAYO

Department of Analytical Chemistry, Faculty of Chemistry, University of Barcelona, Barcelona, Spain

(Received 24 April 1987. Revised 13 July 1988. Accepted 29 August 1988)

**Summary**—The extraction of nickel from aqueous media (0.1M NaClO<sub>4</sub>) with 3-(2-furyl)-2-mercaptopropenoic acid (FMPA) in dichloroethane at 25° has been studied. The extraction is efficient only if a suitable counter-ion is present to form an ion-associate with the Ni-FMPA complex. The diphenylguanidinium ion has been found suitable as the counter-ion.

3-(2-Furyl)-2-mercaptopropenoic acid (FMPA) and other 3-aryl-2-mercapto propenoic acids form chelates with various metal ions,<sup>1</sup> and with Ni(II), Co(II), Mn(II) and Zn(II) form the mononuclear complexes ML and ML<sub>2</sub><sup>2-</sup>.<sup>2,3</sup> No evidence of polynuclear complexes has been found. These complexes are partially or quantitatively extracted into solvating organic solvents, such as alcohols or ketones, and several 2-mercaptopropenoic acids have been used for the extraction and colorimetric determination of some metal ions. Although the 2-mercaptopropenoate chelates are not extractable into non-solvating solvents, they can be effectively extracted into dichloroethane or chloroform when a large organic cation is added to the system to form an ion-association complex.

The extraction equilibria for the Ni-FMPA-diphenylguanidinium system in water/1,2-dichloroethane are reported in this paper. Diphenylguanidine is a fairly strong base that exists as the guanidinium ion in acidic and neutral media and has been used in the extraction of a wide variety of metal ions,<sup>4-6</sup> and was chosen in this case because it was a more effective counter-ion than other organic cations tested.

### EXPERIMENTAL

#### Apparatus

A Beckman Acta VII spectrophotometer with 10-mm silica cells, a Perkin-Elmer 4000 atomic-absorption spectrophotometer, and a Radiometer PHM64 pH-meter equipped with glass-calomel electrodes were used.

#### Reagents

Analytical-reagent grade chemicals were used throughout without further purification, unless stated otherwise.

**Standard nickel solution.** A stock aqueous solution of nickel(II) chloride was prepared (1 g/l.), and standardized gravimetrically with dimethylglyoxime. Working solutions were prepared daily by appropriate dilution.

**FMPA solution in 1,2-dichloroethane.** FMPA was synthesized and purified as described previously.<sup>2</sup> To prevent oxidation of FMPA, the dichloroethane was shaken with an aqueous solution of sodium bisulphite and then several

portions of distilled water before use. The solution is stable for at least 8 hr.

**Diphenylguanidinium chloride solution.** Diphenylguanidine (DPG), recrystallized from diethyl ether, was dissolved in the stoichiometric amount of hydrochloric acid of the desired concentration.

#### Procedure

Ten ml of aqueous solution, saturated with dichloroethane, and 10 ml of organic solution, saturated with water, were shaken in 30-ml glass-stoppered vials in a water-bath kept at 25.0 ± 0.1°. The organic phase was dichloroethane or a solution of FMPA in dichloroethane, and the aqueous phase contained various amounts of Ni(II) and diphenylguanidinium ion. The pH of the aqueous phase was adjusted by addition of small amounts of sodium formate, acetate, phosphate or borate. All solutions were made 0.1M in sodium perchlorate, unless stated otherwise. After equilibrium was attained (shaking for 10 min was found enough), the phases were separated by centrifugation. The concentration of DPG in the aqueous phase was measured spectrophotometrically at 235 nm. The concentration of nickel in the aqueous phase was determined by atomic-absorption spectrophotometry. The concentration of FMPA in both phases was determined spectrophotometrically at 330 nm. The pH of the aqueous phase was measured after the extraction.

### RESULTS AND DISCUSSION

#### Distribution of FMPA

The distribution of FMPA between dichloroethane and aqueous 0.1M sodium perchlorate, at pH 1-7, is illustrated in Fig. 1. Assuming no formation of polymeric species, the distribution ratio,  $D_R$ , is given by

$$D_R = \frac{[RH_2]_o}{[RH_2] + [RH^-] + [R^{2-}]} = K_{DR} / (1 + K_1/[H^+] + K_1K_2/[H^+]^2) \quad (1)$$

where  $K_{DR}$  is the distribution constant of FMPA,  $K_1$  and  $K_2$  are the acid dissociation constants, and  $RH_2$  is undissociated FMPA. Species in the organic phase are denoted by the subscript "o".

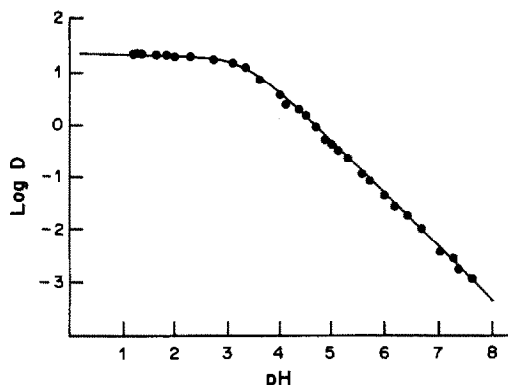


Fig. 1. Distribution of FMFA in the water-dichloroethane system.  $I = 0.1M$   $\text{NaClO}_4$ ;  $C_R = 3 \times 10^{-3}M$ .

As  $K_2$  is less than  $10^{-8}$ ,  $[\text{R}^{2-}]$  is negligible at  $\text{pH} < 7$ , and equation (1) can be simplified to

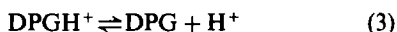
$$D_R = \frac{K_{DR}}{1 + K_1/[\text{H}^+]} \quad (2)$$

The constancy of  $D_R$  at  $\text{pH} 1-2$ , over the FMFA range  $4 \times 10^{-4}$ – $4 \times 10^{-3}M$ , agrees with the assumption that there is no association in the organic phase.  $K_{DR}$  and  $K_1$  were determined by Sillén's graphical method,<sup>7</sup> and also by the Letagrop-Distribution program.<sup>8</sup> The values found were  $\log K_{DR} = 1.45 \pm 0.03$ ,  $\text{p}K_1 = 3.31 \pm 0.05$ .

The latter is in close agreement with that obtained potentiometrically (3.51) in 10% v/v ethanol-water medium.<sup>2</sup> The equilibrium constants in this ethanol-water medium are approximately the same as those in aqueous medium.

#### Extraction of $\text{DPGH}^+$ with $\text{ClO}_4^-$ into dichloroethane

The system can be described by



Assuming that the concentration of the ion-pair in the aqueous phase and the dissociation of the ion-pair in the organic phase can be neglected, the distribution ratio of diphenylguanidine,  $D_{\text{DPG}}$ , is given by

$$D_{\text{DPG}} = \frac{[\text{DPGH}^+ \text{ClO}_4^-]_o + [\text{DPG}]_o}{[\text{DPGH}^+] + [\text{DPG}]} \quad (6)$$

The distribution of DPG was found to be independent of  $\text{pH}$  at  $\text{pH} < 6$ , and to increase rapidly at higher  $\text{pH}$ . This indicates that for extraction from acid medium  $\text{DPGH}^+ \text{ClO}_4^-$  is the only significant species present in the organic phase; the concentration of DPG in the aqueous phase is also negligible ( $\text{p}K_a$  for  $\text{DPGH}^+$  in water<sup>9</sup> is  $\sim 10$ ). Therefore, at  $\text{pH} 1-6$ , the extraction may be described by equation (5),

and the extraction constant,  $K_{\text{BHClO}_4}$ , will be given by

$$K_{\text{BHClO}_4} = \frac{[\text{DPGH}^+ \text{ClO}_4^-]_o}{[\text{DPGH}^+][\text{ClO}_4^-]} = \frac{D_{\text{DPG}}}{[\text{ClO}_4^-]} \quad (7)$$

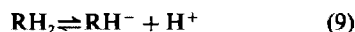
Results obtained at  $\text{pH} \sim 4$ , with  $[\text{ClO}_4^-]$  constant ( $0.1M$ ) and initial  $[\text{DPGH}^+]$  in the range  $10^{-3}$ – $10^{-2}M$ , showed that the distribution ratio is independent of  $[\text{DPGH}^+]$ , confirming that there is no appreciable dissociation of the ion-pair in the organic phase.

When  $[\text{DPGH}^+]$  was held constant,  $\log D_{\text{DPG}}$  was found to be a linear function of  $\log [\text{ClO}_4^-]$  over the range examined ( $0.04$ – $0.13M$ ). The slope of the  $\log D_{\text{DPG}}$  vs.  $\log [\text{ClO}_4^-]$  plot was 0.96. From the extraction data, the extraction constant at ionic strength 0.1 was calculated. Values obtained from perchlorate concentrations other than  $0.1M$  were corrected by means of the Debye-Hückel equation, with  $a = 3.5$  for the perchlorate ion,<sup>10</sup> and 7 for the diphenylguanidinium ion ( $a$  for  $\text{DPGH}^+$  is not known, and was taken as 7 because analogous substances have about this value).

The extraction constant was found to be  $\log K_{\text{BHClO}_4} = 1.13 \pm 0.04$ .

#### Extraction of diphenylguanidine with FMFA

At  $\text{pH} < 6$ , the predominant FMFA species in the aqueous phase are  $\text{RH}_2$  and  $\text{RH}^-$ . The latter can react with diphenylguanidinium to form an ion-pair extractable into dichloroethane:



A quantitative description of the extraction of the  $\text{DPGH}^+ \text{RH}^-$  ion-pair requires consideration of the extraction equilibria of the  $\text{DPG}^+ \text{Cl}^-$  and  $\text{DPGH}^+ \text{X}^-$  ion-pairs ( $\text{X}^-$  is the anion used to adjust the  $\text{pH}$  or ionic strength). We have found that, in the presence of sodium chloride ( $0.1M$ ) and sodium formate ( $0.01M$ ), there is less than 1% extraction of  $\text{DPGH}^+ \text{Cl}^-$  and  $\text{DPGH}^+ \text{HCOO}^-$ . To avoid the competitive extraction of  $\text{DPGH}^+ \text{ClO}_4^-$  in the study of extraction of the  $\text{DPGH}^+ \text{RH}^-$  ion-pair, the ionic strength was adjusted to 0.1 with sodium chloride instead of sodium perchlorate, and the  $\text{pH}$  was kept in the range 3–4 with a formic acid-formate buffer. Under these conditions, the distribution ratio of diphenylguanidine will be

$$D_{\text{DPG}} = \frac{[\text{DPGH}^+ \text{RH}^-]_o}{[\text{DPGH}^+]} \quad (11)$$

and the extraction constant,  $K_{\text{BHRH}}$ , for equation (10) is

$$K_{\text{BHRH}} = \frac{[\text{DPGH}^+ \text{RH}^-]_o}{[\text{DPGH}^+][\text{RH}^-]} = \frac{D_{\text{DPG}}}{[\text{RH}^-]} \quad (12)$$

$D_{\text{DPG}}$  was calculated from the absorbance of the aqueous phase at 235 nm. For aqueous solutions at

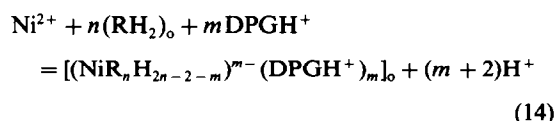
pH 3–4 and  $10^{-3} M$  initial concentration of DPG, and organic phases containing FMFA at initial concentration in the range  $5 \times 10^{-4}$ – $5 \times 10^{-3} M$ , a plot of  $\log D_{\text{DPG}}$  vs.  $\log[\text{RH}^-]$  was a straight line with a slope of  $\sim 1$  ( $\log D_{\text{DPG}} = 3.51 + 0.94 \log[\text{RH}^-]$ ).  $[\text{RH}^-]$  was calculated from the material balances for DPG and FMFA, the pH, and the distribution constant of FMFA, by means of the equation

$$[\text{RH}^-] = \frac{C_R - (C_B - [\text{DPGH}^+]) K_1}{K_1 + [\text{H}^+](1 + K_{\text{DR}})} \quad (13)$$

where  $C_R$  and  $C_B$  are the initial concentrations of FMFA and DPG respectively. From the values of  $D_{\text{DPG}}$  and  $[\text{RH}^-]$ , and also by the Letagrop-Distribution program, the extraction constant was found to be  $\log K_{\text{BHRH}} = 3.67 \pm 0.06$ .

#### Extraction of nickel with FMFA and $\text{DPGH}^+$

The extraction of nickel from aqueous solutions containing diphenylguanidium, with an organic phase containing FMFA, can be described by the equation



The extraction constant,  $K_{\text{ext}}$ , is given by

$$K_{\text{ext}} = \frac{[(\text{NiR}_n \text{H}_{2n-2-m})^{m-} (\text{DPGH}^+)_m]_o [\text{H}^+]^{m+2}}{[\text{Ni}^{2+}] [\text{RH}_2]_o^n [\text{DPGH}^+]^m} \quad (15)$$

Assuming that the ion-pair is the only nickel species extracted, and that the presence of hydroxo-complexes can be neglected,<sup>11</sup> the distribution ratio for nickel will be:

$$D_{\text{Ni}} = \frac{[(\text{NiR}_n \text{H}_{2n-2-m})^{m-} (\text{DPGH}^+)_m]_o}{[\text{Ni}^{2+}] + [\text{NiR}] + [\text{NiR}_2^-]} \quad (16)$$

From the formation constants<sup>2</sup> ( $\log \beta_1 = 7.5$  and  $\log \beta_2 = 16.4$ ) for  $\text{NiR}$  and  $\text{NiR}_2^-$ , we conclude that, for the conditions used in this study, the concentrations of  $\text{NiR}$  and  $\text{NiR}_2^-$  in the aqueous phase are

$$[\text{RH}_2]_o = \frac{C_R K_{\text{DR}} [\text{H}^+]}{K_{\text{DR}} (\text{H}^+) + [\text{H}^+] + K_1 K_{\text{BHRH}} [\text{DPGH}^+] + K_1} \quad (19)$$

$$[\text{DPGH}^+] = \frac{C_B K_{\text{DR}} [\text{H}^+]}{K_{\text{DR}} [\text{H}^+] (1 + K_{\text{BHClO}_4} [\text{ClO}_4^-]) + K_{\text{BHRH}} K_1 [\text{RH}_2]_o} \quad (20)$$

negligible. Thus equation (16) can be simplified to:

$$D_{\text{Ni}} = \frac{[(\text{NiR}_n \text{H}_{2n-2-m})^{m-} (\text{DPGH}^+)_m]_o}{[\text{Ni}^{2+}]} \quad (17)$$

Substituting from equation (15) and taking logarithms gives

$$\log D_{\text{Ni}} = \log K_{\text{ext}} + n \log [\text{RH}_2]_o \\ + m \log [\text{DPGH}^+] + (m+2) \text{pH} \quad (18)$$

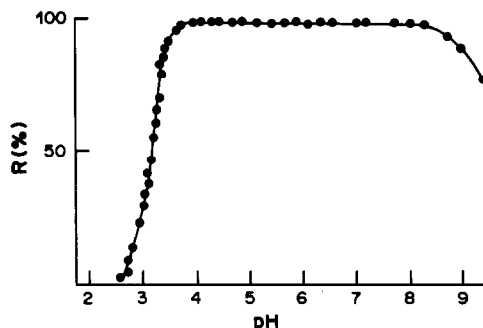


Fig. 2. Nickel extraction as a function of pH.  $C_{\text{Ni}} = 7 \times 10^{-5} M$ ;  $C_R = 3 \times 10^{-3} M$ ;  $C_B = 10^{-2} M$ .

From this equation, which relates the distribution ratio to the experimental variables, the coefficients  $m$  and  $n$  and the extraction constant can be calculated.

The effect of pH on the extraction of nickel from aqueous solutions containing a large excess of DPG (0.01M) into an organic phase containing a large excess of FMFA (0.003M) is shown in Fig. 2. The extraction is almost quantitative (99.3%) at pH 4.0–8.3.

The slope of the plot of  $\log D_{\text{Ni}}$  vs. pH, at constant ligand and  $\text{DPGH}^+$  concentrations, will give  $(m+2)$ , the number of protons liberated per metal ion complexed. However, if a fixed initial concentration of DPG and FMFA is used, the  $[\text{DPGH}^+]$  and ligand concentrations cannot be kept constant if the pH is varied, because of the pH-dependence of the extraction of  $\text{DPGH}^+$   $\text{RH}^-$  and of the FMFA distribution. For example, the equilibrium concentrations of  $\text{DPGH}^+$  and  $(\text{RH}_2)_o$ , in the pH range 2.7–3.4, vary by up to 9 and 25% respectively. Therefore  $\log D_{\text{Ni}} - 2 \log (\text{DPGH}^+) - 2 \log [\text{RH}_2]_o$  was plotted against pH in order to calculate  $(m+2)$ ; values of  $n$  and  $m$  are not yet known at this stage, but these values seem to be the most probable ones, and data obtained in further experiments agreed with this assumption. The  $[\text{RH}_2]_o$  and  $[\text{DPGH}^+]$  values used were calculated from the material balances for DPG, FMFA and perchlorate, the pH, the distribution constant of FMFA, and the extraction constants  $K_{\text{BHClO}_4}$  and  $K_{\text{BHRH}}$ , by means of the equations

$$[\text{ClO}_4^-] = \frac{C_{\text{ClO}_4^-}}{1 + K_{\text{BHClO}_4} [\text{DPGH}^+]} \quad (21)$$

These equations were derived with the assumption that the amounts of FMFA and DPG in the complex are negligible.

A set of experiments done with initial concentrations of nickel, DPG and FMFA of  $7 \times 10^{-5}$ ,  $10^{-2}$ , and  $3 \times 10^{-3} M$ , respectively, gave a straight line with a slope of  $\sim 4$  ( $\log D_{\text{Ni}} - 2 \log [\text{RH}_2]_o -$

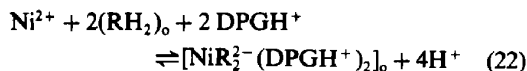
$2 \log[\text{DPGH}^+] = -2.31 + 3.99 \text{ pH}$ ). This indicates the liberation of four protons per metal ion.

From the values of  $\log D_{\text{Ni}}$  and  $\log[\text{RH}_2]_0$ , at constant pH and  $\text{DPGH}^+$  concentration, the coefficient  $n$  can be calculated. Although the initial pH was the same for all samples, differences of as much as 0.1 in the equilibrium pH values were found. Furthermore with constant initial DPG concentration, the equilibrium  $\text{DPGH}^+$  concentration decreased with increasing  $\text{RH}_2$  concentration. Therefore, to calculate  $n$ ,  $\log D_{\text{Ni}} - 4 \text{ pH} - 2 \log(\text{DPGH}^+)$  was plotted over the range 3.4–3.5, with initial concentrations of nickel and DPG of  $7 \times 10^{-5}$  and  $10^{-2} M$ , respectively. The plot was linear with a slope of  $\sim 2$  ( $\log D_{\text{Ni}} - 2 \log[\text{DPGH}^+] - 4 \text{ pH} = -2.51 + 1.96 \log[\text{RH}_2]_0$ ), which indicates that the value of  $n$  is 2.

Similarly,  $\log D_{\text{Ni}} - 2 \log[\text{RH}_2] - 4 \text{ pH}$  was plotted *vs.*  $\log[\text{DPGH}^+]$ , for a set of experiments at pH 3.4–3.5 and constant initial ligand concentration ( $C_{\text{R}} = 3 \times 10^{-3} M$ ). The initial DPG concentration was varied over the range  $2 \times 10^{-3} - 10^{-2} M$ . A straight line with slope of  $\sim 2$  was obtained ( $\log D_{\text{Ni}} - 2 \log[\text{RH}_2]_0 - 4 \text{ pH} = -2.23 + 2.04 \log[\text{DPGH}^+]$ ), indicating that two  $\text{DPGH}^+$  ions are required for each metal ion in the extracted species. The value obtained for  $m$  agrees with that obtained before for the number of protons liberated per metal ion.

From these results, we conclude that the extraction

equilibria can be described by



$$\log D_{\text{Ni}} = \log k_{\text{ext}} + 2 \log[\text{RH}_2]_0 + 2 \log[\text{DPGH}^+] + 4\text{H}^+ \quad (23)$$

To calculate the extraction constant, the experimental values from the determination of  $n$ ,  $m$  and  $(m + 2)$  were substituted in equation (23), and also treated by the Letagrop-Distribution program. The value of the extraction constant was found to be  $\log K_{\text{ext}} = -2.36 \pm 0.04$ .

#### REFERENCES

1. A. Izquierdo and J. Calmet, *Quim. Anal.*, 1974, **28**, 148.
2. A. Izquierdo, L. Garcia-Puignou and J. Guasch, *Polyhedron*, 1986, **5**, 1253.
3. M. Filella, N. Garriga and A. Izquierdo, *J. Chim. Phys.*, 1987, **84**, 93.
4. K. L. Cheng, K. Ueno and T. Imanura, *Handbook of Organic Analytical Reagents*, CRC Press, Boca Raton, 1982.
5. A. I. Busev and G. P. Rudzit, *Zh. Analit. Khim.*, 1963, **18**, 840.
6. *Idem*, *ibid.*, 1965, **20**, 76.
7. L. G. Sillén, *Acta Chem. Scand.*, 1956, **10**, 186.
8. D. H. Liem, *ibid.*, 1971, **25**, 152.
9. D. D. Perrin, *Dissociation Constants of Organic Bases in Aqueous Solution*, Butterworths, London, 1965.
10. J. Kielland, *J. Am. Chem. Soc.*, 1937, **59**, 1675.
11. E. Högfeldt, *Stability Constants of Metal-Ion Complexes, Part A: Inorganic Ligands*, Pergamon Press, Oxford, 1982.

## DETERMINATION OF THE LABILE SPECIES OF ZINC BY ANODIC STRIPPING STAIRCASE VOLTAMMETRY, WITH SPECIAL REFERENCE TO CORRELATION WITH THE TOXICITY TO *TETRAHYMENA*

BO SVENSMARK\*

Department of General and Organic Chemistry, The H. C. Ørsted Institute, University of Copenhagen, Universitetsparken 5, DK-2100 Copenhagen Ø, Denmark

JØRGEN LARSEN

Institute of Cell Biology and Anatomy, The Zoological Institute, University of Copenhagen, Universitetsparken 15, DK-2100 Copenhagen Ø, Denmark

(Received 26 April 1988. Revised 9 June 1988. Accepted 27 August 1988)

**Summary**—Anodic stripping staircase voltammetry (ASSV) has been tested as a method to determine the concentration of “free” ions and very labile complexes of zinc. These species are thought to be primarily responsible for the toxic effect of zinc on the ciliated protozoan *Tetrahymena pyriformis*. ASSV and toxicological experiments were performed in an inorganic salt medium and the effects of Cu interference were studied. Even though the ASSV results were encumbered with problems, the results agreed well with the toxicological effects. In contrast, calculations based on the solubility product of  $Zn_3(PO_4)_2 \cdot 4H_2O$  could lead to erroneous results because kinetic and other effects result in very slow precipitation of zinc phosphate at the concentration levels in the salt medium used. In this medium there is a dose-dependent effect of zinc on *Tetrahymena* which is in agreement with the ASSV data, which indicate that all the zinc is in a labile form. The study emphasizes the importance of using experimental determinations in preference to theoretical models, which may predict quite erroneous results.

There is increasing interest in the chemical speciation of heavy metals because several studies have indicated the importance of the chemical forms of a metal with regard to its toxicity.<sup>1-4</sup> Several methods for the determination of the different species formed by heavy metals in natural waters have been proposed, including anodic stripping voltammetry.<sup>5-9</sup> With this technique it is possible to resolve species according to their reduction potential and thus determine various levels of labile or electroactive complexes, and also “free” ions.

Rapid-scan anodic stripping staircase voltammetry,<sup>10</sup> ASSV, is a variety of stripping analysis whereby heavy metal ions can be determined without deaeration of the solution. Normally, deaeration is necessary because the oxygen reduction wave interferes during the reoxidation step of anodic stripping voltammetry. Deaeration may, however, change the natural conditions of complex media and seriously disturb the results of the anodic stripping determination.<sup>11</sup>

To assess the ASSV results in terms of toxicity we have investigated the toxic effects of zinc on a unicellular organism, *Tetrahymena*. This freshwater ciliate is commonly used in biochemical and cell physiology studies, and it seems particularly suitable for toxicity bioassays.<sup>12-15</sup> The toxic effect and the

electrochemistry were studied in an inorganic salt medium.

The ASSV method has two principal drawbacks: (1) there is deterioration of the electrode by organic components, an effect which is common with many natural liquids,<sup>16-20</sup> and (2) copper interferes strongly by forming an insoluble intermetallic compound with zinc in the mercury of the working electrode.<sup>21,22</sup> These interferences were eliminated in the present study.

At equilibrium in the inorganic medium used, zinc should precipitate as the phosphate, because the medium is mainly a phosphate buffer. Zinc phosphate is fairly insoluble [ $K_{sp}$  for  $Zn_3(PO_4)_2 \cdot 4H_2O$  is  $5 \times 10^{-36}$ ].<sup>23</sup> Thus the highest concentration of free  $Zn^{2+}$  under the present experimental conditions is below  $1 \mu M$  according to calculations, but the ASSV experiments revealed that  $Zn^{2+}$  concentrations of at least  $100 \mu M$  are possible in this medium. This can be explained by the kinetics of precipitation. The activation energy of nucleation (the start of precipitation in homogeneous solutions) depends strongly on the supersaturation, i.e., initiation of the precipitation may take a very long time in highly diluted solutions.<sup>24</sup>

The purpose of this part of our work on the toxic effects of heavy metals on living organisms is to stress the importance of the chemical speciation of a metal in toxicity bioassays. Furthermore, we will argue that the determination of chemical speciation purely by

\*To whom correspondence should be addressed.

calculation from published constants is inadequate and may lead to erroneous conclusions. The ASSV method seems, however, to be a promising experimental method for identifying the toxic species of a heavy metal.

## EXPERIMENTAL

### Electrochemical measurements

The instrumentation and the anodic stripping staircase voltammetric method have been described elsewhere.<sup>10</sup> The electrochemical instrumentation was a home-made potentiostat controlled by an M6800 microcomputer connected to an RC8000 mainframe computer. The working electrode was a glassy-carbon rotating disc electrode, made from a 2.5 mm V10 Le Carbone-Lorraine glassy-carbon rod, and rotated at a rate of 40.0 rps. A mercury film was formed on this electrode by reduction of a 100 ppm  $\text{Hg}^{2+}$  solution in 0.29M nitric acid at  $-1.00$  V vs. SCE for 35.0 sec. The reference electrode was a Radiometer Standard Calomel Electrode and the counter-electrode a platinum wire. The cell was a fused-silica cup.

The ASSV-labile zinc was determined in the following way. Potassium nitrate was added as neutral electrolyte to give a concentration of 0.2M. The mercury-film electrode was immersed in the solution, and zinc was plated out for 10.0 sec at a potential of  $-1200$  mV vs. SCE, without deaeration or use of a protecting gas. At the end of the plating time an anodic staircase scan was initiated immediately. A normal scan consists of steps 10 mV in height and 256  $\mu\text{sec}$  in duration. A single measurement (plating and stripping) thus takes less than 11 sec.

The concentrations were calculated by simple proportion from the response for a zinc standard in 0.2M potassium nitrate ( $i_{\text{H}_2\text{O}}$ ) measured with the same film-electrode before measurement of the sample solution ( $i_x$ ) ( $C_x = c_{\text{H}_2\text{O}} i_x / i_{\text{H}_2\text{O}}$ ). This procedure introduces a possibility of minor errors, because the electrode is transferred from one solution (the standard) to another (the sample) between measurements. On the other hand, calibration by standard additions to the sample solution may give quite erroneous results, because the added standard may also become complexed,<sup>25</sup> and at an unknown rate. Our procedure gives good accuracy but the precision may be reduced.

### Toxicological experiments

*Tetrahymena pyriformis* GL<sup>26</sup> was grown at 28° in sterile solutions of 2% proteose peptone (PP) and 0.1% yeast extract enriched with salts.<sup>27</sup> Cells were used in the exponentially multiplying growth phase ( $5 \times 10^6$  cells/ml). The cells were transferred to the starvation medium containing inorganic salts<sup>28</sup> (0.68 g of  $\text{K}_2\text{HPO}_4$ , 0.15 g of  $\text{KH}_2\text{PO}_4$ , 2.75 g of NaCl and 0.25 g of  $\text{MgSO}_4 \cdot 7\text{H}_2\text{O}$  in 1000 ml of  $\text{H}_2\text{O}$ ), 1 hr prior to experimental use. The pH of the medium was 7.1.

The stock solutions of zinc chloride used were 1, 10, or 100mM, kept in polyethylene bottles and at least 0.1mM in nitric acid. When addition of a zinc solution to the culture medium caused a reduction in the pH, the pH was readjusted with sodium hydroxide.

For determination of the effect of zinc on cell mortality, 2-ml cell samples were withdrawn from the culture after 1 hr of starvation, placed in 30-ml conical flasks, exposed to zinc, and then returned to a temperature of 28°.

The cell density of the cultures was determined after fixation of a 0.5 ml cell sample with 0.5 ml of 1% glutaraldehyde in an inorganic salt medium; an electronic particle counter (Coulter Counter model ZB) was used. When cell mortality was observed, the cell density was determined manually in triplicate with a Fuchs-Rosenthals cell chamber; the electronic particle counter could not be used because it does not differentiate between living and dead cells.

Identical values for the cell numbers of untreated control cultures were found by the two methods. When a large number of dead and partly dissolved cells were seen, 100  $\mu\text{l}$  of 1M hydrochloric acid were added to the cell sample before the cell density was determined to ensure a homogeneous sample for counting.

## RESULTS

Electrochemical measurements of zinc in the inorganic salt medium by ASSV showed that the anodic oxidation current was a linear function of the zinc concentration with an intercept on the ordinate. The current was the same for zinc in the inorganic salt medium and in water (both 0.2M in potassium nitrate) in concentrations up to 1000 $\mu\text{M}$ . Thus the speciation of zinc is similar in both media. The negative intercept of the calibration line with the abscissa corresponded to a background level of 0.5 $\mu\text{M}$  zinc for both media, and this therefore could come from impurities in the potassium nitrate or from the electrodes etc.

Since the inorganic salt medium used is mainly a phosphate buffer, zinc phosphate ought to precipitate under the conditions used. To show that this is the case under equilibrium conditions, the experiments listed in Table 1 were performed. Zinc solution and solid  $\text{Zn}_3(\text{PO}_4)_2 \cdot 4\text{H}_2\text{O}$  were added to 0.2M potassium nitrate solutions in the inorganic medium and demineralized water, the solutions were stirred overnight and the ASSV-labile zinc was measured. Table 1 shows that the final concentrations of free zinc in solutions containing solid zinc phosphate are the same for both starting concentrations, 0 and 90 $\mu\text{M}$ .

To avoid deterioration of the working electrode surface caused by organic components, the experiments were performed in an inorganic medium. To study the interference of copper in the zinc determinations, the interaction of Cu and Zn was studied. In Fig. 1 the ASSV sensitivity ( $\mu\text{A}/\mu\text{M}$ ) for Cu and Zn is plotted as a function of amount of added Zn and Cu, respectively. There is a strong decrease in sensitivity with increasing levels of the other metal. Both plots are linear. To eliminate this interference, a copper-free inorganic medium was used.

The rate of cell mortality was determined after a 1-hr exposure to different concentrations of zinc. Some mortality appeared after 1-hr exposure to 2.5 $\mu\text{M}$  zinc. Above this concentration, a dose-dependent increase in cell mortality was found,

Table 1. Effect of solid  $\text{Zn}_3(\text{PO}_4)_2 \cdot 4\text{H}_2\text{O}$  on ASSV-labile Zn in the inorganic medium (IM) used

Solution*	$\text{Zn}_3(\text{PO}_4)_2 \cdot 4\text{H}_2\text{O}$	Zn added, $\mu\text{M}$	ASSV-labile Zn, $\mu\text{M}$
$\text{H}_2\text{O}$	—	1.4	1.4
IM	—	1.4	0.9
IM	+	0.0	1.5
IM	+	90.0	1.4

\*0.2M in  $\text{KNO}_3$ .

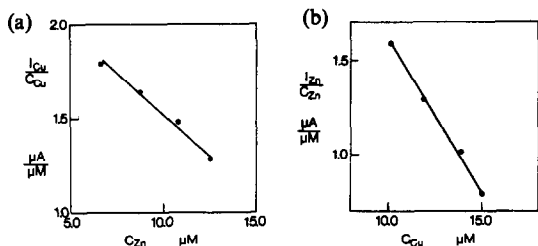


Fig. 1. The ASSV sensitivity in 0.2M KNO<sub>3</sub> for Cu (Fig. 1a) and Zn (Fig. 1b) as a function of the concentration of Zn and Cu respectively. In Fig. 1a the concentration of Cu is 11.8–10.2 μM; in Fig. 1b the concentration of Zn is 12.5–11.0 μM. This small variation in concentration is due to the volume increase on addition of Zn or Cu solution.

Fig. 2. From the linear portions of the curve an LC<sub>50</sub> value of 8 μM can be calculated for 1-hr exposure in this medium.

DISCUSSION

The toxicological experiments show a dose-dependent effect of zinc on *Tetrahymena* in the inorganic salt medium at zinc concentrations above 2.5 μM. These results were unexpected, because from its solubility product zinc phosphate should precipitate from the inorganic medium when the zinc concentration is above 1 μM. However, the toxicological data are in agreement with the results from the ASSV method, which revealed that all the zinc is present as labile species in this medium.

The inorganic medium used is essentially a 5mM phosphate buffer with pH 7.1. From the solubility product,  $5 \times 10^{-36}$  for Zn<sub>3</sub>(PO<sub>4</sub>)<sub>2</sub>·4H<sub>2</sub>O,<sup>23</sup> and the acid dissociation constants for phosphoric acid, pK<sub>a2</sub> = 7.2 and pK<sub>a3</sub> = 12.35, the solubility of zinc ions in this medium is calculated to be 0.6, 0.4 and 0.2 μM at pH 6.8, 7.0 and 7.2 respectively. The

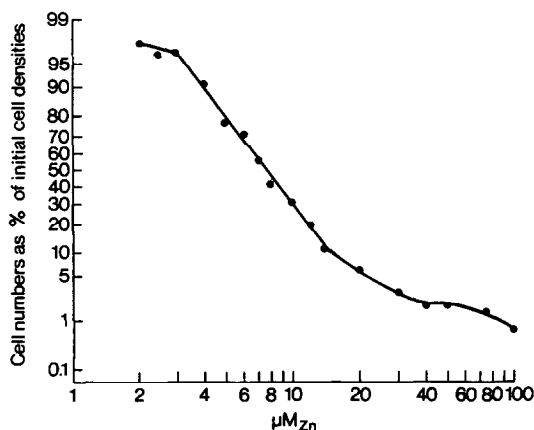


Fig. 2. A log-normal plot of the cell density in per cent of initial density as a function of the concentration of Zn in the inorganic salt medium. The cell densities were determined after 1 hr exposure in the inorganic medium.

medium has a ionic strength of 0.064, and calculations taking activity factors into account did not indicate a higher solubility. Similar values (0.4, 0.3 and 0.2 μM Zn<sup>2+</sup> at pH 6.8, 7.0 and 7.2) are obtained by using the extended Debye-Hückel theory.<sup>24</sup> Thus all calculations indicate equilibrium zinc concentrations below 1 μM in the pH range used.

Experiments in which solid zinc phosphate was added to solutions containing 0 or 90 μM zinc gave zinc concentrations of 1.5 and 1.4 μM respectively. Thus, at equilibrium the ASSV-labile concentration is independent of the initial zinc concentration and in fair agreement with the concentration calculated from the solubility product.

The reason why zinc phosphate does not precipitate is most likely the precipitation kinetics under the given circumstances. Formation of precipitates in homogeneous solutions requires that nuclei of sufficient size are formed, i.e., a certain number of the relevant ions should encounter each other in the solution. At very low concentrations this may be a slow process. Generally, the rate of nucleation is determined by the degree of supersaturation,<sup>24</sup>  $a/a_0$ , where  $a = (C_{Zn}^3 C_{PO_4}^2)^{1/5}$ , and  $a_0 = (5 \times 10^{-36})^{1/5}$ . For  $C_{Zn} = 100 \mu M$  and  $C_{PO_4}$  = the free PO<sub>4</sub><sup>3-</sup> concentration in the inorganic medium at pH 7.1, the degree of supersaturation can be calculated to be 39 and 21, with and without correction for activity effects, respectively. According to nucleation theory<sup>24</sup> these values indicate that one nucleus per ml is formed after about 10<sup>10</sup> sec (3000 years). Experimentally, an expression of the form  $ta^j = \text{const.}$  has been found to represent the induction time ( $t$ ) for precipitation of simple salts such as BaSO<sub>4</sub> and Ag<sub>2</sub>CrO<sub>4</sub>.<sup>29</sup> The exponent  $j$  is interpreted as the number of ions required to build the nucleus and was found to be 7 and 5 for these two salts. Zinc phosphate has not been studied, but estimates based on values similar to those for BaSO<sub>4</sub> and Ag<sub>2</sub>CrO<sub>4</sub> ( $ta^5 = 10^{-12}$ ) result in induction times of the order of 10<sup>14</sup> sec (3 million years).

These calculations indicate that the precipitation of zinc by phosphate under the conditions used is likely to require a very long time. On the other hand, such exponential relations cause errors orders of magnitude in size, even for small errors in the concentrations and constants. Another complication is that precipitation may be initiated by other particles or impurities in the solution, especially in the toxicological experiments, where the chemical and physical conditions change with time.<sup>30</sup> High local concentrations or other precipitates may also initiate the reaction. We have observed that zinc was not precipitated in the phosphate buffer at pH around 7.1. This result suggests that calculations based on equilibria for ions at trace levels are unsatisfactory and may lead to erroneous conclusions. Therefore the speciation should be determined experimentally under the actual conditions in each case.

The power of anodic stripping voltammetry for



speciation studies is due to the selectivity in the preconcentration step—only species reducible at potentials lower than the plating potential are determined. Complex formation between the metal ion and ligands in solution shifts the reduction potential towards more negative values. For a complex  $MeL_m$  with a conditional stability constant  $\beta$ , the reduction potential for the metal is shifted cathodically:

$$\begin{aligned} \Delta E_{1/2} &= E_{1/2}(\text{with ligand}) \\ &\quad - E_{1/2}(\text{without ligand}) \\ &= -(RT/nF)\ln(1 + \beta[L]^m) \end{aligned} \quad (1)$$

By proper selection of the reduction potential relative to  $E_{1/2}$  we can select the species to be determined. In this work we used the lowest plating potential at which all  $Zn^{2+}$  in 0.2M potassium nitrate is reduced. In this medium there are weak, very labile, zinc complexes with nitrate,  $\beta_1 = 0.62$  and  $\beta_2 = 0.24$ .<sup>31</sup> The potential shift in 0.2M potassium nitrate due to these complexes can be calculated from equation (1) to be 1.6 mV. Thus the ASSV-labile species in our study include labile complexes such as  $ZnNO_3^-$  and  $Zn(NO_3)_2$ .

In this way we have demonstrated that all the zinc in the inorganic salt medium is completely available in ASSV-labile form.

The interference by copper is clearly seen in Fig. 1. Since copper will always be plated out together with zinc we cannot avoid this interference. It is due to formation of CuZn, which is sparingly soluble in the mercury electrode,<sup>21,22</sup> and the effect is seen to be quite pronounced. Since this effect is caused by copper in the electrode film, it is important to strip the copper off the electrode between zinc determinations. Otherwise copper would accumulate in the mercury, an effect which would increase with time. This problem could be circumvented by the use of an inorganic medium free from copper.

The classical method for measuring the toxicity of a metal to *Tetrahymena* and other aquatic organisms in an inorganic medium is by the  $LC_{50}$  test. The  $LC_{50}$  value is the metal concentration at which 50% of the organisms are killed after a given time of exposure. The relationship between metal concentration and per cent survival is typically a log-normal distribution,<sup>31</sup> and this can be utilized for determination of the  $LC_{50}$  values. By measuring the percentage response in terms of response probits, a linear relation between response and log of the dose can be obtained,<sup>31</sup> as demonstrated in the present study. It must be noted, however, that the curve obtained is sigmoid.

In an inorganic medium the toxicity of zinc to *Tetrahymena* may vary greatly. Chapman and Dunlop<sup>33</sup> reported an  $LC_{50}$  value of about  $8\mu M$  for 5-hr exposure, in agreement with the results obtained in the present study. However, Carter and Cameron<sup>13</sup> found  $LC_{50}$  values exceeding  $150\mu M$  after 1, 3, and 24 hr of exposure. This difference may be explained by

the use of different strains of *Tetrahymena* or by differences in the culture conditions. However, the discrepancy may also be due to dissimilarity of the physiological state of the cells; Carter and Cameron's experiments were done with cells from a stationary growth phase, whereas we used cells from an exponentially multiplying culture. That the toxicity of a heavy metal may depend on the physiological state of the cells prior to starvation has been demonstrated for copper.<sup>34</sup>

## CONCLUSION

The present study showed that it may be a very risky approach to calculate the distribution of metal species in solution from the given or assumed composition of the solution. The difficulty associated with such calculations may be due to either the kinetics or to the complexity of the medium. The difficulties increase with the complexity of the solution and may prove insurmountable for natural aquatic environments.

For these reasons we find it worthwhile to continue attempts to optimize the ASSV method for determination of toxic species of heavy metals. Though still far from perfect, it is the best method available at present.

*Acknowledgements*—Our sincere thanks to Professor Christian Overgaard Nielsen for critical reading of the manuscript. Financial support from the Danish Natural Science Research Council, grant no. 511-15013, for the instrumentation, is gratefully acknowledged.

## REFERENCES

1. H. Babich and G. Stotzky, *Appl. Environ. Microbiol.*, 1978, **36**, 906.
2. G. S. Canterford and D. R. Canterford, *J. Mar. Biol. Assoc., U.K.*, 1980, **60**, 227.
3. D. W. Engel and B. A. Fowler, *Environ. Health Perspect.*, 1979, **28**, 81.
4. W. G. Sunda, D. W. Engel and R. M. Thuottle, *Environ. Sci. Technol.*, 1978, **12**, 409.
5. B. Raspor, H. W. Nürnberg, P. Valenta and M. Branica, *Mar. Chem.*, 1984, **15**, 231.
6. G. E. Batley and T. M. Florence, *ibid.*, 1976, **4**, 347.
7. T. M. Florence, B. G. Lumsden and J. J. Fardy, *Anal. Chim. Acta*, 1983, **151**, 281.
8. D. P. H. Laxen and R. M. Harrison, *Sci. Total Environ.*, 1981, **19**, 59.
9. T. M. Florence, *Analyst*, 1986, **111**, 489.
10. B. Svensmark, *Anal. Chim. Acta*, 1987, **197**, 239.
11. J. Lecomte, P. Mericam, A. Astruc and M. Astruc, *Anal. Chem.*, 1981, **53**, 2372.
12. L. E. Tingle, W. A. Pavlat and I. L. Cameron, *J. Protozool.*, 1973, **20**, 301.
13. J. W. Carter and I. L. Cameron, *Water Res.*, 1973, **7**, 951.
14. J. Larsen and J. R. Nilsson, *Protoplasma*, 1983, **118**, 140.
15. J. R. Nilsson, *ibid.*, 1986, **135**, 1.
16. P. L. Brezonik, P. A. Brauner and W. Stumm, *Water Res.*, 1976, **10**, 605.
17. J. Wang, *J. Electroanal. Chem.*, 1982, **139**, 225.
18. P. Sagberg and W. Lund, *Talanta*, 1982, **29**, 457.

19. F. Wahdat and R. Neeb, *Z. Anal. Chem.*, 1983, **316**, 770.
20. A. M. Bond and R. B. Reust, *Anal. Chim. Acta*, 1984, **162**, 389.
21. F. Vydra, K. Štulík and E. Juláková, *Electrochemical Stripping Analysis*, Horwood, Chichester, 1976.
22. J. Wang, *Stripping Analysis. Principles, Instrumentation and Applications*, VCH Publishers, Deerfield Beach, 1985.
23. A. E. Martell and R. M. Smith, *Critical Stability Constants*, Vol. 4, Plenum Press, New York, 1976.
24. W. Stumm and J. J. Morgan, *Aquatic Chemistry. An Introduction Emphasizing Chemical Equilibria in Natural Waters*, Wiley-Interscience, New York, 1970.
25. W. C. Gorman and R. K. Skogerboe, *Anal. Chim. Acta*, 1986, **187**, 325.
26. D. L. Nanney and J. W. McCoy, *Trans. Am. Microsc. Soc.*, 1976, **95**, 664.
27. P. Plesner, L. Rasmussen and E. Zeuthen, *Synchrony in Cell Division and Growth*, E. Zeuthen (ed.), p. 543. Interscience, New York, 1964.
28. K. Hamburger and E. Zeuthen, *Exp. Cell Res.*, 1957, **13**, 443.
29. J. A. Christiansen and A. E. Nielsen, *Acta Chem. Scand.*, 1951, **5**, 673.
30. J. Larsen, B. Svensmark and J. R. Nilsson, *J. Protozool.*, 1988, **35**, 541.
31. S. Komorsky-Lovric, M. Lovric and M. Branica, *J. Electroanal. Chem.*, 1986, **214**, 37.
32. P. S. Hewlett and R. L. Plackett, *The Interpretation of Quantal Responses in Biology*, Edward Arnold, London, 1979.
33. G. Chapman and S. Dunlop, *Environ. Res.*, 1981, **26**, 81.
34. J. R. Nilsson, *Protoplasma*, 1981, **109**, 359.

## POLAROGRAPHIC DETERMINATION OF 9,10-ANTHRAQUINONE AND ITS 1,2-, 1,4- AND 1,8-DIHYDROXY DERIVATIVES IN CHLOROFORM

### APPLICATION TO THE ANALYSIS OF PAPERS AND BLACK LIQUORS

M. H. POURNAGHI-AZAR\* and S. M. GOLABI

Electroanalytical Chemistry Laboratory, Faculty of Science, University of Tabriz, Tabriz, Iran

(Received 15 February 1988. Revised 8 August 1988. Accepted 27 August 1988)

**Summary**—The polarographic behaviour of 9,10-anthraquinone (I) and some of its dihydroxy derivatives, such as alizarin (II), quinizarin (III) and chrisazin (IV) has been studied in the presence of proton donors of HA and HB<sup>+</sup> type. After optimization of conditions for reversible reduction of the anthraquinones, various polarographic techniques were used for the determination of anthraquinones in chloroform. In the dc method, the relative standard deviation for the determination of 1mM concentrations was about 1.5%. In the ac method, the detection limit was 0.1 µg/ml and the relative standard deviation for determination at the 0.2 µg/ml level was 2%. The proposed methods are usable for the simultaneous determination of I and II, II and III, II and IV, and have been applied to the determination of 9,10-anthraquinone in papers and black liquors.

Anthraquinones, particularly the 9,10-compounds, are of great importance in chemistry, mainly in connection with production of dyestuffs and pharmaceuticals. Recently, anthraquinones have become of considerable interest in pulp and paper production.<sup>1,2</sup> Ethylantraquinone and its tetrahydro derivative are present in the solution used in the autoxidation process for production of hydrogen peroxide.<sup>3</sup>

Because of the pronounced oxidation-reduction properties of anthraquinones, electrochemical methods are convenient for their determination. Several polarographic studies of these compounds have been reported and quantitative methods developed, with dimethylformamide<sup>4,5</sup> or alcohol-water mixed solvents, (where the alcohol was either methanol<sup>6,7</sup> or ethanol<sup>8</sup>) or chloroform-methanol-hydrochloric acid mixture<sup>9</sup> as the medium. Differential pulse polarography has been applied to the determination of 9,10-anthraquinone at trace levels in aqueous systems<sup>6</sup> and in polygonum bulbs.<sup>10</sup>

Polarographic analysis of mixtures of 2-ethylanthraquinone and its tetrahydro derivative has been proposed by Jennings.<sup>7</sup>

In view of the high dissolution and extraction properties of chloroform for quinone compounds, and on the basis of our previous works,<sup>11-15</sup> we have examined the use of dc, ac and differential pulse polarography for the determination of 9,10-anthraquinone and its dihydroxy derivatives, with a supporting electrolyte of 0.75M piperidinium perchlorate

(PPC) + 0.25M piperidine (P) in chloroform. The methods developed were applied to the determination of anthraquinone in papers and black liquors.

#### EXPERIMENTAL

##### Reagents

The chloroform, piperidine and perchloric acid were Merck *p.a.* grade. The anthraquinones were obtained from Aldrich and used without further purification. Piperidinium perchlorate was prepared by gradual addition of the required amount of perchloric acid to a given volume of piperidine at room temperature; the yellowish crystals obtained were purified by crystallization from aqueous acetone.

##### Apparatus

A Polarecord E506 was used with an E505 mercury drop electrode (Metrohm). An E524 coulostat connected to an E525 integrator (Metrohm) was used for coulometry. The necessary glassware was made in our laboratory. An Ag/AgI electrode in 0.05M (But)<sub>4</sub>NI + 0.5M (But)<sub>4</sub>NClO<sub>4</sub> in chloroform was used as reference electrode.<sup>16</sup>

##### Procedures

In all experiments, the test solution was protected from light and deaerated by a stream of nitrogen that had been passed through chloroform.

**Analysis of papers.** Cut the sample (*ca.* 10 g) into strips, place it in a 250-ml separating funnel and shake it with 25 ml of chloroform for 2 hr. Withdraw 10 ml of the chloroform extract, add 1.40 g of piperidinium perchlorate and 0.25 ml of piperidine as supporting electrolyte (0.75M PPC + 0.25M P). Bubble nitrogen through the solution for 20 min, then record the ac polarogram by sweeping the potential from -100 to -400 mV *vs.* Ag/AgI, at 2 mV/sec.

\*To whom correspondence should be addressed.

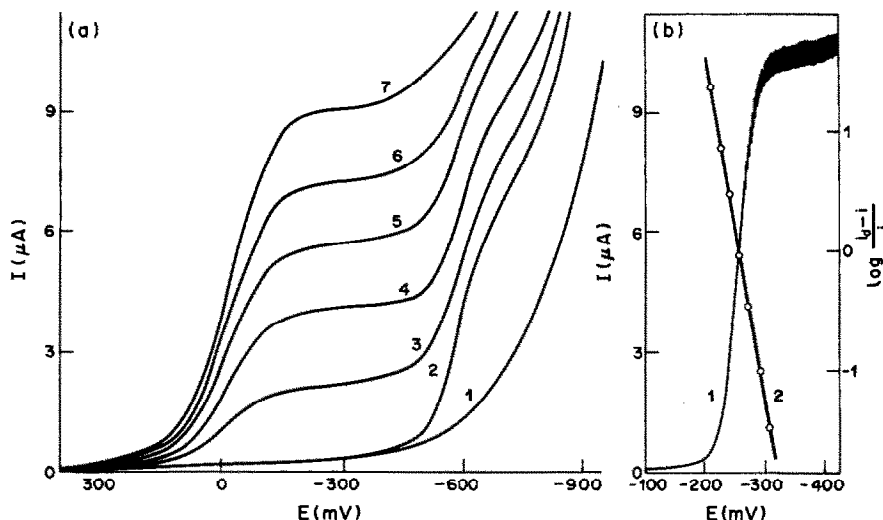


Fig. 1. Direct current polarograms of (a) 1, 0.50*M* TBAPC; 2, 1 + 1*mM* 9,10-anthraquinone; 3, 2 + 0.4*mM* CCl<sub>3</sub>COOH (TCAA); 4, 2 + 0.8*mM* TCAA; 5, 2 + 1.2*mM* TCAA; 6, 2 + 1.6*mM* TCAA; 7, 2 + 2*mM* TCAA; (b) 1, 1*mM* 9,10-anthraquinone in the presence of 0.75*M* PPC + 0.25*M* P as supporting electrolyte; 2,  $dE = d\log[(i_d - i)/i]$ .

**Analysis of black liquor by dc polarography.** Place 5 ml of black liquor in a 200-ml separating funnel and extract with two 10-ml portions of chloroform, by shaking for 10 min with each (on a shaker to avoid the formation of an emulsion) and leaving for 10 min for phase separation. Collect and combine the chloroform phases. Use 10 ml of the solution for recording the dc polarogram as for analysis of papers.

**Analysis of black liquor by ac polarography.** Add 4 ml of water to 1 ml of black liquor in a 200-ml separating funnel and extract as for the dc method.

## RESULTS AND DISCUSSION

### Direct current polarography

In chloroform, in the absence of a proton donor and with (But)<sub>4</sub>NClO<sub>4</sub> as the supporting electrolyte, the reduction of 9,10-anthraquinone (AQ) and its 1,4-dihydroxy (quinizarin) and 1,8-dihydroxy (chrisazin) derivatives gives one reduction wave which nearly coalesces with the reduction wall of the solvent (Fig. 1a, curve 2) and corresponds to reduction of the anthraquinones to semiquinones (radical anions).<sup>12</sup> 1,2-Dihydroxyanthraquinone (alizarin) is not reducible in this medium.

On the addition of a proton donor, such as benzoic or trichloroacetic acid (HA type) or piperidinium perchlorate (HB<sup>+</sup> type) to a chloroform solution of AQ and its dihydroxy derivatives, a new wave appears at less negative potentials. As the concentration of added acid increases from zero to a value equal to twice the AQ bulk concentration, the new wave grows at the direct expense of the original wave (Fig. 1a). At  $C_{\text{acid}}/C_{\text{AQ}} = 2$ , the original one-electron wave is completely replaced by a single two-electron wave. The height of this new wave is twice that of the wave obtained in the absence of the acid and the degree of reversibility of this wave increases with

increasing concentration of the proton-donor (particularly of HB<sup>+</sup> type). With 0.75*M* PPC + 0.25*M* P as supporting electrolyte, a well defined and reversible two-electron reduction wave is obtained (Fig. 1b). Cyclic voltamperograms of AQ and its dihydroxy derivatives in the presence of this last supporting electrolyte are shown in Fig. 2.

The half-wave potentials for AQ and its dihydroxy-compounds are given in Table 1. Controlled potential coulometry shows that the single cathodic wave of AQ and its dihydroxy derivatives corresponds to a 2-electron reduction. A plot of  $\log[(i_d - i)/i]$  vs.  $E$  gives a straight line with a slope of about 32 mV (Table 1).

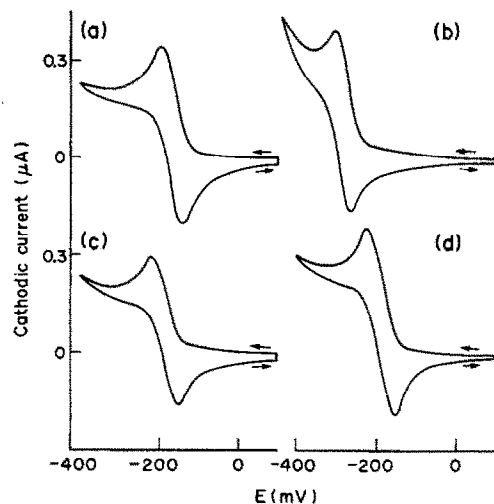


Fig. 2. Cyclic voltamperograms of (a) 1*mM* 1,8-dihydroxy-AQ, (b) 1*mM*, 1,2-dihydroxy-AQ, (c) 1*mM* 1,4-dihydroxy-AQ, (d) 1*mM* AQ, in the presence of 0.75*M* PPC + 0.25*M* P as supporting electrolyte. Scan-rate for (a) and (c) 5 mV/sec; for (b) and (d) 10 mV/sec.

Table 1\*

Anthraquinones	$E_{1/2}, V$	$s, \dagger V$	$k, \S$	rsd, %
9,10-Anthraquinone (AQ)	-0.248	0.032	0.9995	1.1
1,2-Dihydroxy-AQ (alizarin)	-0.342	0.032	0.9993	1.1
1,4-Dihydroxy-AQ (quinizarin)	-0.266	0.032	0.9994	1.1
1,8-Dihydroxy-AQ (chrisazin)	-0.240	0.032	0.9994	1.0

\*Data obtained for  $10^{-5}M$  solutions of anthraquinones.

$\dagger$ Slope =  $dE/d\log[(i_d - i)/i]$ .

$\S$ Correlation coefficient.

The calibration graphs are linear over the range  $10^{-5}$ – $10^{-3}M$ . At the 1 mM concentration level, the polarograms of five separate solutions had  $i_d$  values with a relative standard deviation of about 1% (Table 1).

#### Alternating current polarography

Polarograms for  $4 \times 10^{-5}M$  anthraquinone solutions in the presence of 0.75M PPC + 0.25M P as supporting electrolyte, were recorded under several different conditions (scan-speed, drop-time, voltage amplitude, and frequency of the alternating current) and the optimal parameters were selected: scan-speed 2 mV/sec, drop-time 1 sec, voltage amplitude 10 mV, frequency 75 Hz.

Figure 3 shows ac polarograms of AQ and its 1,4-dihydroxy derivative (quinizarin). The values of  $E_p$  and other characteristic data are given in Table 2. An 8-point calibration graph was linear over the

range  $10^{-6}$ – $6 \times 10^{-5}M$ . At the  $10^{-5}M$  level, the relative standard deviation of the peak current was 1.4%.

#### Differential pulse polarography

A solution of  $10^{-5}M$  AQ and its 1,8-dihydroxy derivative, in 0.75M PPC + 0.25M P as supporting electrolyte, gave a reduction peak nearly coalescing with the reduction wall of the solvent. The scan-rate, pulse width, modulation amplitude and drop-time were optimized. Figure 4 shows the differential pulse polarograms of AQ. The calibration levels examined were between  $10^{-6}$  and  $5 \times 10^{-5}M$  for anthraquinone.

#### Analysis of papers and black liquors

Anthraquinone was extracted from the samples of papers and black liquors according to the procedures given above and determined by ac or dc polarography with the standard addition method. Table 3

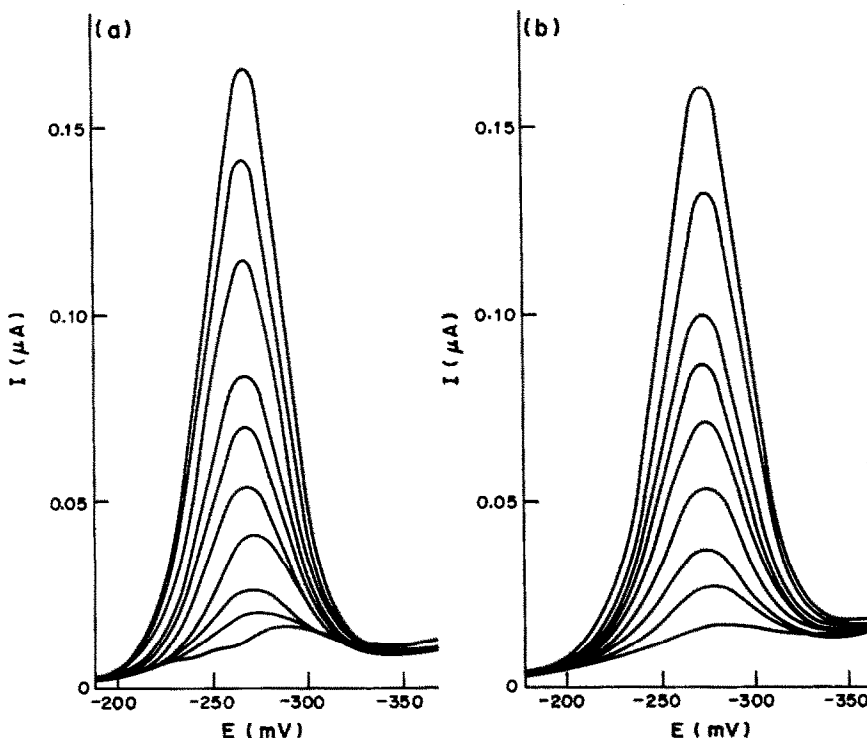


Fig. 3. Alternating current polarograms of (a) AQ, (b) 1,4-dihydroxy-AQ (from  $10^{-6}$  to  $2 \times 10^{-5}M$ ), in the presence of 0.75M PPC + 0.25M P as supporting electrolyte;  $t = 1$  sec,  $V_- = 10$  mV,  $f = 75$  Hz.

Table 2\*

Anthraquinones	$E_p, V$	$E_{p/2}, \dagger V$	$k \S$	rsd, %
9,10-Anthraquinone (AQ)	-0.266	0.048	0.9995	1.4
1,2-Dihydroxy-AQ (alizarin)	-0.360	0.050	0.9994	1.4
1,4-Dihydroxy-AQ (quinizarin)	-0.284	0.049	0.9996	1.4
1,8-Dihydroxy-AQ (chrisazin)	-0.258	0.050	0.9995	1.4

\*Data obtained for  $10^{-5}M$  solutions of anthraquinones.

†Half-peak width.

§Correlation coefficient.

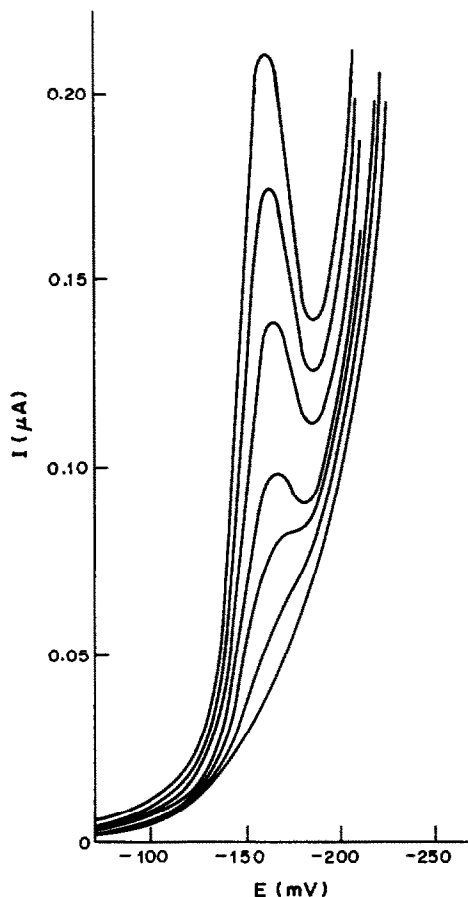


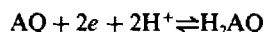
Fig. 4. Differential pulse polarograms of  $10^{-6}$ – $2 \times 10^{-5}M$  AQ in the presence of  $0.75M$  PPC +  $0.25M$  P as supporting electrolyte;  $t = 1$  sec, pulse height =  $50$  mV.

gives the results for the polarographic determination of 9,10-anthraquinone in papers and black liquors. Figure 6 shows the ac and dc polarograms of the extracts.

#### CONCLUSIONS

On the basis of results obtained from the dc and ac polarography and controlled-potential coulometry, the reduction of anthraquinones in the presence of  $0.75M$  PPC +  $0.25M$  P in chloroform can be shown

to be



The plot of  $\log [(i_d - i)/i]$  vs.  $E$  for the dc polarograms, the half-peak widths in the ac polarograms and the  $\Delta E_p$  values in the cyclic voltammetry are the criteria which indicate that the reduction of anthraquinones is a two-electron reversible process at sufficiently slow potential scan-speed (cf. Tables 1 and 2). From the data in Tables 1 and 2, it can be concluded that  $\Delta E_{1/2}$  and  $\Delta E_p$  between 9,10-anthraquinone and its 1,2-dihydroxy derivative are large enough (about  $100$  mV) to allow determination of both these anthraquinones in a mixture (Fig. 5). The separation between the two half-wave or peak potentials for 1,2-dihydroxyanthraquinone and the other dihydroxy derivatives, is also about  $100$  mV, permitting the determination of 1,2-dihydroxyanthraquinone and one (but not both) of the other two compounds in a mixture (Fig. 6, a and b).

The behaviour of anthraquinones in ac and dp polarography has shown that the selection of the correct instrumental parameters is of importance. The detection limit of the ac method is acceptably low ( $0.5 \mu\text{g/ml}$ ) and the method could be used for anthraquinone in the  $\mu\text{g/ml}$  concentration range. As can be seen from Fig. 4, the dp polarograms of anthraquinone derivatives coalesce with the reduction wall for the solvent. Therefore an accurate and quantitative measurement of these peaks cannot be made.

The correlation coefficients show a linear relationship between  $i_d$  or  $i_p$  and the concentration of

Table 3

Sample	Amount	Procedure*	AQ, ppm
Paper I†	11.25 g	(i)	1.73
Paper II†	9.82 g	(i)	2.42
Liquor I§	1 ml	(iii)	95.7
Liquor II§	5 ml	(ii)	95.8

\*A solution of 9,10-anthraquinone in chloroform was used as standard: (i) ac polarography method for papers, (ii) dc polarography method for black liquors, (iii) ac polarography method for black liquors.

†Samples from Pars Paper Industry, Iran.

§Sample from Tchouka Paper Industry, Iran.

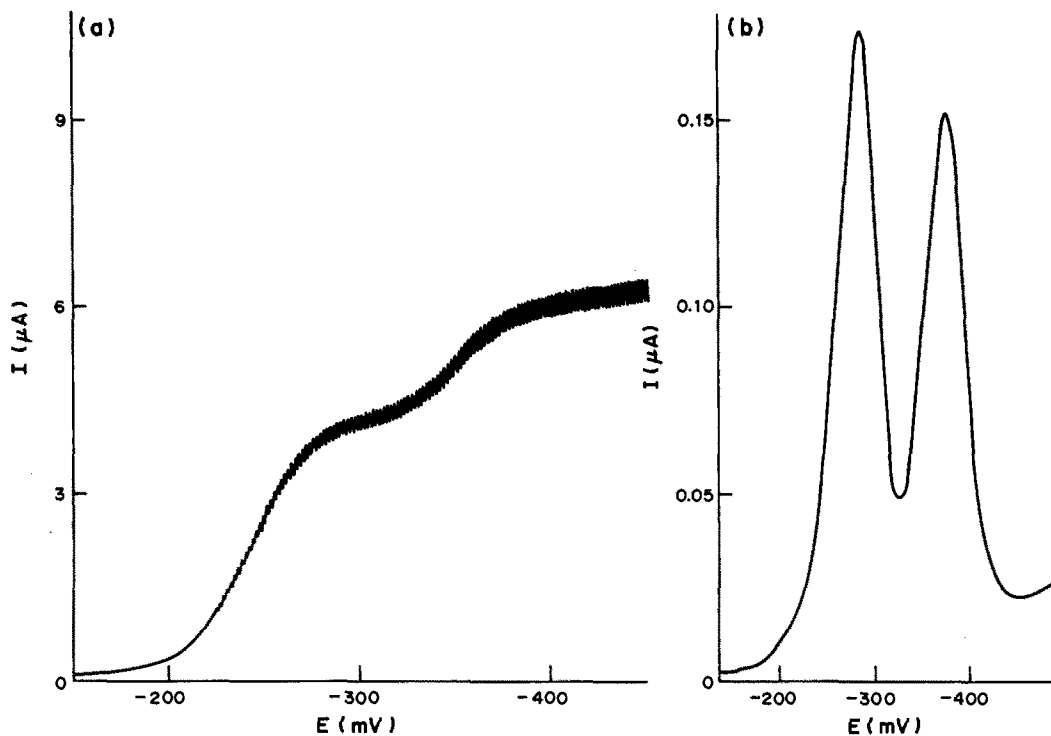


Fig. 5. (a) Direct current polarogram of  $10^{-3}M$  1,8-dihydroxy-AQ +  $5 \times 10^{-4}M$  1,2-dihydroxy-AQ. (b) Alternating current polarogram of a mixture of  $2 \times 10^{-5}M$  1,8-dihydroxy-AQ and 1,2-dihydroxy-AQ.  $t = 1$  sec ( $V_{\omega} = 10$  mV,  $f = 75$  Hz. Supporting electrolyte in both cases was  $0.75M$  PPC +  $0.25M$  P.

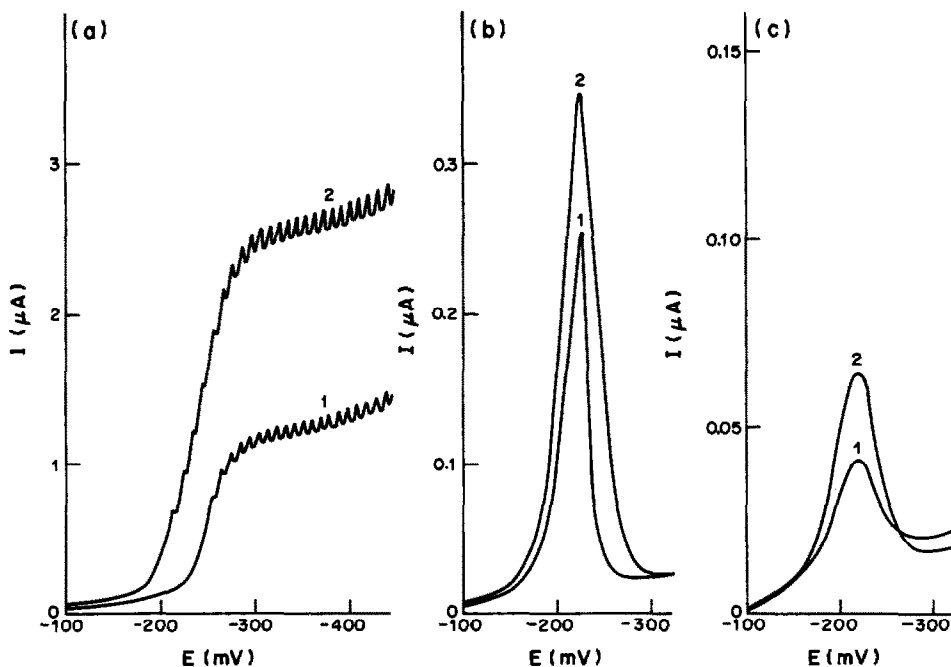


Fig. 6. Polarograms of black liquor extracts in chloroform, (a) dc and (b) ac, and of paper extract in chloroform (c), ac. (1) Extracted phases, (2) after standard addition.

the anthraquinones. All the anthraquinones should be individually determinable by means of a calibration graph and the method of standard additions can be used.

It is evident from the results that chloroform as solvent with piperidinium perchlorate plus piperidine as supporting electrolyte is a suitable medium for the determination of anthraquinones by dc and ac polarography, with an error of about 2%. The methods are directly applicable for the determination of these compounds after their extraction into chloroform from aqueous (e.g., black liquor) and solid samples (e.g., papers).

#### REFERENCES

1. H. H. Holton, *Pulp Pap. Can.*, 1977, **78**, 10.
2. G. Geijersted, *S. Trärförkningsinst. Stockholm Rept.*, B529, 1979.
3. C. S. Cronon, *Chem. Eng.*, 1959, **66**, 118.
4. R. L. Edsberg, D. Eichlin and J. J. Garis, *Anal. Chem.*, 1953, **25**, 798.
5. E. I. Klabunovskii and N. A. Ezerskaya, *Zh. Analit. Khim.* 1963, **18**, 989; *J. Anal. Chem. USSR*, 1963, **18**, 855.
6. J. O. Brønstad, K. H. Schröder and H. O. Friestad, *Anal. Chim. Acta*, 1980, **119**, 243.
7. V. J. Jennings, *Anal. Proc.*, 1985, **22**, 359.
8. G. A. Qureshi, G. Svehla and M. A. Leonard, *Analyst*, 1979, **104**, 705.
9. P. D. Garn and M. C. Bott, *Anal. Chem.*, 1961, **33**, 84.
10. Xiuquin Zhang and Lixin Xu, *Yaoxue Xuebao*, 1984, **19**, 519; *Chem. Abstr.*, 1984, **101**, 198270 h.
11. S. M. Golabi and M. H. Pournaghi-Azar, *Proc. 6th Intern. Conf. Non-Aqueous Solutions*, Canada, 1978, p. 97.
12. *Idem*, *Electrochim. Acta*, 1987, **32**, 425.
13. M. H. Pournaghi-Azar and S. M. Golabi, *J. Pharm. Belg.*, 1987, **42**, 315.
14. S. M. Golabi and M. H. Pournaghi-Azar, *Bull. Res. Dept. Univ. Tabriz*, 1980, **1**, 10.
15. M. H. Pournaghi-Azar and S. M. Golabi, *Proc. 2nd Intern. Symposium Drug Analysis, Brussels*, 1986, p. 309.
16. M. E. Peover, *Proc. Chem. Soc.*, 1963, 167; *Trans. Faraday Soc.* 1964, **60**, 417.



## CATALYTIC-ADSORPTIVE STRIPPING VOLTAMMETRIC MEASUREMENTS OF HYDRAZINES

JOSEPH WANG\* and ZIAD TAHA

Department of Chemistry, New Mexico State University, Las Cruces, NM 88003, U.S.A.

(Received 3 August 1988. Accepted 24 August 1988)

**Summary**—Hydrazine compounds can be determined by voltammetry, based on their hydrogen catalytic wave in formaldehyde-platinum-sulphuric acid media. Adsorption of the platinum-formazone complex on the hanging mercury drop electrode enhances the sensitivity, allowing convenient measurement of micromolar and submillimolar concentrations of simple hydrazines. The selectivity is better than that of conventional (anodic) measurements of hydrazines, as oxidizable compounds do not interfere. The sensitivity is also greatly improved. The hydrazine response is evaluated with respect to preconcentration time, concentration dependence, platinum and formaldehyde concentrations, reproducibility and other variables. The relative standard deviation (at  $2 \times 10^{-5}M$ ) is 1.6%.

Because of the industrial and toxicological significance of hydrazine compounds, a highly sensitive method is required for their determination. Spectrophotometric measurements of these compounds usually require preliminary derivative formation, owing to the modest absorptivities of simple hydrazines.<sup>1,2</sup> Electrochemical measurements, based on direct oxidation of the hydrazine group, have been attempted.<sup>3</sup> Because of the substantial overpotential for this process at conventional electrodes, modified (catalytic) electrodes are usually employed to facilitate the determination, including phthalocyanine-containing carbon paste<sup>4</sup> and electrochemically treated glassy carbons.<sup>5</sup> However, unless used as the detection mode for liquid chromatography, voltammetry at such activated surfaces permits quantification of only millimolar concentrations.

This paper reports a sensitive and selective voltammetric approach for determining simple hydrazines, based on their adsorption-dependent catalytic effect on hydrogen-ion reduction in the presence of platinum and formaldehyde. It has been shown recently that extremely low levels of platinum can be determined by means of the sensitive catalytic hydrogen wave obtained in its presence in formaldehyde-hydrazine medium.<sup>6,7</sup> This wave was attributed to the lowering of the hydrogen overpotential on adsorption of the platinum-formazone complex onto the mercury electrode (formazone is formed by the reaction of hydrazine with formaldehyde). Detection limits as low as  $1 \times 10^{-10}$  and  $1 \times 10^{-12}M$  platinum were reported as obtained by pulse polarography<sup>6</sup> and adsorptive stripping voltammetry,<sup>7</sup> respectively. The catalytic wave was shown to depend strongly on the hydrazine concentration. Hence, the current work is intended to examine the utility of catalytic-adsorptive stripping voltammetry of simple hydraz-

ines in the presence of platinum and formaldehyde. It has been shown that by reversing the role of platinum and hydrazine, sensitive and selective voltammetric measurements of hydrazines can be attained.

### EXPERIMENTAL

#### Apparatus

The instrumentation used, a PAR 264A voltammetric analyser with a PAR 303 static mercury drop electrode, has already been described in detail.<sup>8</sup> Anodic measurements were made with a stationary glassy-carbon disk and a 10-ml voltammetric cell (Bioanalytical Systems Models MF2012 and VC-2, respectively).

#### Reagents

All solutions were prepared with demineralized water. Hydrazine solutions were prepared from hydrazine sulphate (Baker). Methylhydrazine, 1,2-dimethylhydrazine and the 1000-ppm platinum stock solution were purchased from Aldrich; formaldehyde was purchased from Fisher.

#### Procedure

Ten ml of 1M sulphuric acid containing 0.1% w/v formaldehyde and 20  $\mu\text{g/l}$ . platinum, were pipetted into the cell and purged with nitrogen for 8 min. The preconcentration potential ( $-0.3$  V) was applied to a fresh mercury drop while the solution was stirred (400 rpm). Following the preconcentration step, the stirring was stopped and after 15 sec the voltamperogram was recorded by applying a linear scan terminating at  $-1.30$  V. After the background voltamperogram had been obtained, aliquots of the standard hydrazine solution were introduced. The solution was stirred and purged for 4 min to allow the formation of the platinum-formazone complex. The accumulation/stripping cycle was repeated with a new drop. All measurements were made at room temperature.

### RESULTS AND DISCUSSION

Figure 1 shows cyclic voltamperograms for  $2 \times 10^{-5}M$  hydrazine in a sulphuric acid medium containing 20  $\mu\text{g/l}$ . platinum and 0.1% w/v formaldehyde, obtained after (A) 0 and (B) 60 sec accumulation at  $-0.3$  V. Two cathodic peaks are

\*Author for correspondence.

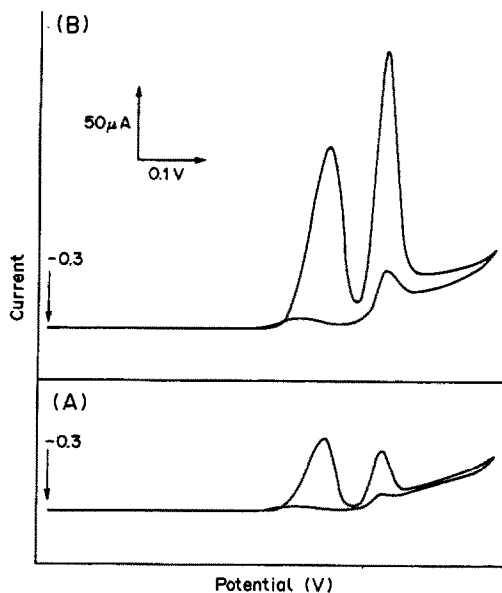


Fig. 1. Cyclic voltamperograms for  $2.5 \times 10^{-5} M$  hydrazine in  $1 M$  sulphuric acid containing  $20 \mu\text{g/l.}$  platinum and  $0.1\%$  w/v formaldehyde, after (A) 0 and (B) 60 sec accumulation at  $-0.3 \text{ V}$ . Scan-rate  $50 \text{ mV/sec}$ .

observed, at  $-0.85$  and  $-0.95 \text{ V}$ . The first is the catalytic response of the platinum-formazone complex; the second is the platinum catalytic response in the presence of formaldehyde [observed also in the absence of hydrazine (not shown)]. Scanning in the reverse direction exhibits also cathodic peaks indicative of hydrogen catalytic processes. The response increases dramatically when an accumulation period precedes the potential scan (compare A and B), indicating enhancement by adsorption. No significant change in the magnitude of the peaks is observed when scans are repeated (not shown). The effect of the potential scan-rate on the characteristics of the first peak—used for the hydrazine determination—was also evaluated ( $2.5 \times 10^{-5} M$  hydrazine, 30 sec accumulation). The peak potential shifted from  $-0.83$  to  $-0.87 \text{ V}$  when the scan-rate was increased from  $10$  to  $100 \text{ mV/sec}$ ; no further change in the potential was observed at scan-rates between  $100$  and  $500 \text{ mV/sec}$ . Unlike the direct proportionality between the current and the scan-rate expected for an ideal redox couple immobilized on electrode surfaces, the catalytic/adsorptive current here first increased for scan-rates between  $10$  and  $50 \text{ mV/sec}$  and then rapidly decayed.

Adsorption of the formazone complex can be used as a preconcentration step, prior to the voltammetric measurement of hydrazine, and makes possible a sensitive determination. Figure 2 shows linear scan voltamperograms for  $1 \times 10^{-5} M$  hydrazine, after different preconcentration periods [0–120 sec (a–d)]. The Pt-formazone stripping peaks are well defined, with a peak potential of  $-0.84 \text{ V}$  and peak half-width

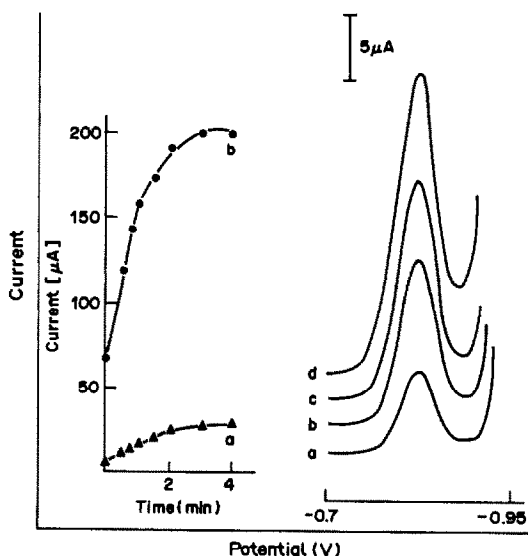


Fig. 2. Effect of preconcentration period on the voltamperogram for  $1 \times 10^{-5} M$  hydrazine. Preconcentration period: (a) 0, (b) 30, (c) 60, (d) 120 sec. Preconcentration potential,  $-0.3 \text{ V}$ . Also shown are current-deposition time plots for (a)  $1 \times 10^{-5} M$  and (b)  $2 \times 10^{-5} M$  hydrazine. Other conditions as for Fig. 1.

of  $53 \text{ mV}$ . The longer the preconcentration time, the more formazone complex is adsorbed on the surface, and the larger is the peak current. As a result, convenient measurement at the micromolar concentration level is possible. Also shown in Fig. 2 are plots of peak current *vs.* preconcentration time at (A)  $1 \times 10^{-5}$  and (B)  $2 \times 10^{-5} M$  hydrazine. In both cases,

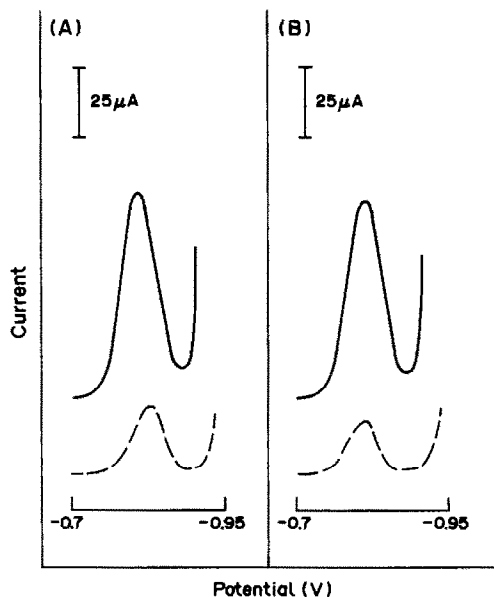


Fig. 3. Voltamperograms for (A)  $2 \times 10^{-5} M$  methylhydrazine and (B)  $2 \times 10^{-5} M$  1,2-dimethylhydrazine after 120 sec accumulation. The responses without accumulation are shown as dashed lines. Other conditions as for Fig. 1.

the current increases rapidly at first with deposition time (up to 120 sec) and then levels off.

Other hydrazine compounds which form complexes with platinum and formaldehyde can be measured in a similar manner. For example, Fig. 3 shows catalytic-adsorptive stripping peaks for  $2 \times 10^{-5} M$  methylhydrazine (A) and 1,2-dimethylhydrazine (B). A similar response is observed. The adsorptive accumulation of the corresponding complexes on the mercury electrode is indicated by comparison with the response without preconcentration (shown as a dashed line).

The data in Figs. 2 and 3 have several important analytical implications. Besides the enhanced response associated with the catalytic-adsorptive process, these data indicate the feasibility of measuring oxidizable hydrazine compounds indirectly by reductive voltammetry. Such use of a different detection principle affords a wider range of selectivity compared to conventional (anodic) measurements of hydrazines. The improved selectivity is illustrated in Fig. 4. When the voltammetric measurement is performed by a positive-going scan at the glassy-carbon electrode, the large phenol peak completely masks the hydrazine peak of interest (A, curve b). In contrast, no such effects are observed when the catalytic-adsorptive approach (B) is used, and hydrazine can thus be determined without interference. Similar improvements in selectivity (over anodic measurements) were observed in analogous measurements in the presence of *m*-aminophenol, 2,4-dichlorophenol, catechol and *p*-nitroaniline (not shown). Comparison of the curves in Fig. 4 indicates also the significant improvements in the sensitivity, and overall signal-to-background characteristics, when the adsorptive-catalytic scheme is used.

The hydrazine catalytic response depends strongly on the solution conditions. For example, Fig. 5 shows the effect of the platinum concentration on the catalytic current for (a) 5 and (b)  $8 \mu M$  hydrazine. At the lower hydrazine level, the peak current increases

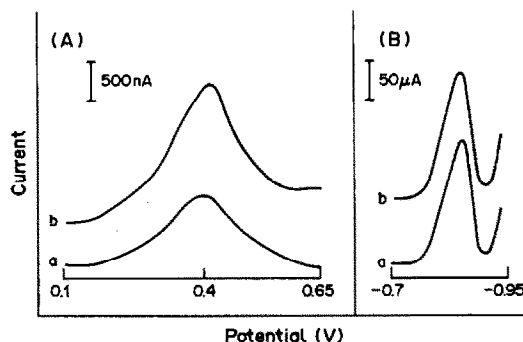


Fig. 4. Response for  $2.5 \times 10^{-5} M$  hydrazine in (a) the absence and (b) the presence of  $5 \times 10^{-5} M$  phenol, as recorded at the glassy carbon (A) and hanging mercury drop (B) electrodes. Conditions: (A) differential pulse waveform with 10 mV/sec scan-rate and 25 mV amplitude; (B) as for Fig. 1 except that the preconcentration period was 30 sec.

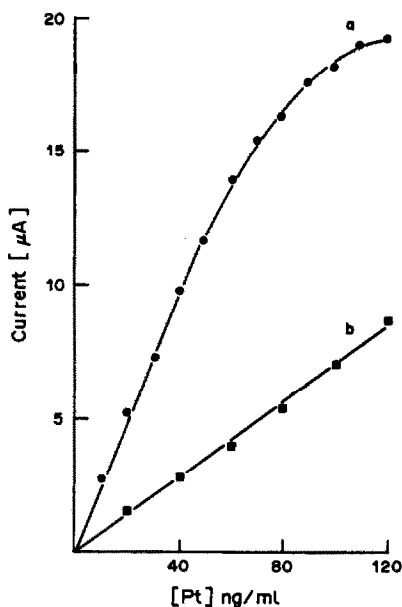


Fig. 5. Effect of platinum on the catalytic-adsorptive stripping response for (a)  $5 \times 10^{-5}$  and (b)  $8 \times 10^{-3} M$  hydrazine. Other conditions as for Fig. 1B.

linearly with change in platinum concentration over the 0–120  $\mu g/l.$  range. With  $8 \mu M$  hydrazine, the current increases linearly with the platinum level at first (up to 50  $\mu g/l.$ ) and then starts to level off. Thus, full surface coverage is approached on forming higher concentrations of the complex. The effect of formaldehyde on the catalytic current was also investigated (not shown,  $5 \times 10^{-6} M$  hydrazine; 60  $\mu g/l.$  platinum; 60 sec preconcentration). The hydrazine peak increased rapidly at first (up to 0.1% w/v formaldehyde) and then levelled off. Measurements of  $2.5 \times 10^{-5} M$  hydrazine were used to evaluate the effects of the accumulation potential, convective mass-transport and potential waveform (30 sec accumulation). The peak current remained unchanged on varying the accumulation potential between  $-0.1$  and  $-0.3$  V; a gradual decrease of the current was observed at higher potentials. Convective mass-transport (during accumulation) has only a mild effect on the adsorptive/catalytic current. For example, a stirring rate of 400 rpm resulted in almost two-fold enhancement of the response, as compared to that obtained in a quiescent solution. The linear scan mode was preferred to use over the differential pulse waveform, because of its faster response, improved resolution (from the neighbouring platinum-formazone peak), and slightly improved signal-to-background characteristics.

Figure 6 shows the dependence of the catalytic current on the hydrazine concentration, for different preconcentration times [(a) 15, (b) 30 and (c) 60 sec]. All the plots exhibit the same profile, with curvature at concentrations lower than  $2 \times 10^{-5} M$  and linearity over the  $(2-8) \times 10^{-5} M$  range [the slopes of the linear portions are (a) 17.2, (b) 20.7 and

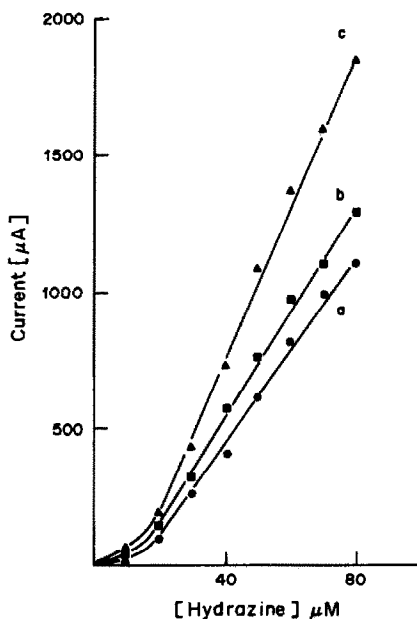


Fig. 6. Calibration plots for hydrazine over the  $(1-8) \times 10^{-3}M$  concentration range, following (a) 15, (b) 30 and (c) 45 sec accumulation. Other conditions as for Fig. 1.

(c)  $28.7 \text{ nA} \cdot 1. \mu\text{mole}^{-1}$ ; correlation coefficients, 0.997, 0.992 and 0.997, respectively]. The profiles shown in Fig. 6 differ from those commonly obtained for adsorptive stripping measurements (where the curvature usually occurs at higher concentrations), and

appear to relate to the formation of the formazone complex. (This is supported by the fact that the trend in Fig. 6 is independent of the adsorption time.) Nevertheless, the concentration dependence is well defined and reproducible, allowing convenient determination at the micromolar and submillimolar levels. The reproducibility was estimated by ten successive measurements on a stirred  $2 \times 10^{-5}M$  hydrazine solution (30 sec preconcentration). The mean peak current was 149 nA, with a range of 147–151 nA, and a relative standard deviation of 1.6%. Such excellent reproducibility is of great significance, considering the irreproducible response of anodic measurements at solid electrodes.

*Acknowledgement*—This work was supported by the National Institutes of Health (Grant No. GM30913-05) and Battelle Pacific Northwest Laboratory.

#### REFERENCES

1. H. M. Abdou, T. Medwick and L. C. Bailey, *Anal. Chim. Acta*, 1974, **93**, 221.
2. Y. Liu, I. Schemeltz and D. Hoffmann, *Anal. Chem.*, 1974, **46**, 885.
3. E. S. Fiala and C. Kulakis, *J. Chromatog.*, 1981, **214**, 229.
4. K. K. Korfhage, K. Ravichandran and R. P. Baldwin, *Anal. Chem.*, 1984, **56**, 1514.
5. K. Ravichandran and R. P. Baldwin, *ibid.*, 1983, **55**, 1782.
6. Z. Zhao and H. Freiser, *ibid.*, 1986, **58**, 1498.
7. J. Wang, J. Zadeii and M. S. Lin, *J. Electroanal. Chem.*, 1987, **237**, 281.
8. J. Wang, P. A. Farias and J. Mahmoud, *Anal. Chim. Acta*, 1985, **172**, 57.

## A NEW METHOD FOR THE IODOMETRIC DETERMINATION OF SULPHOXIDES

W. CIESIELSKI, W. JEDRZEJEWSKI, Z. H. KUDZIN\* and R. SKOWROŃSKI  
 Institute of Chemistry, University of Łódź, Narutowicza 68, 90-136 Łódź, Poland

J. DRABOWICZ

Centre of Molecular and Macromolecular Studies, Polish Academy of Sciences, Boczna 5, 90-362 Łódź, Poland

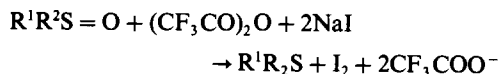
(Received 6 November 1987. Revised 20 July 1988. Accepted 24 August 1988)

**Summary**—A method is described for determination of sulphoxides through their reaction with iodide in a trifluoroacetic acid/acetone medium to produce iodine, which is then titrated with thiosulphate.

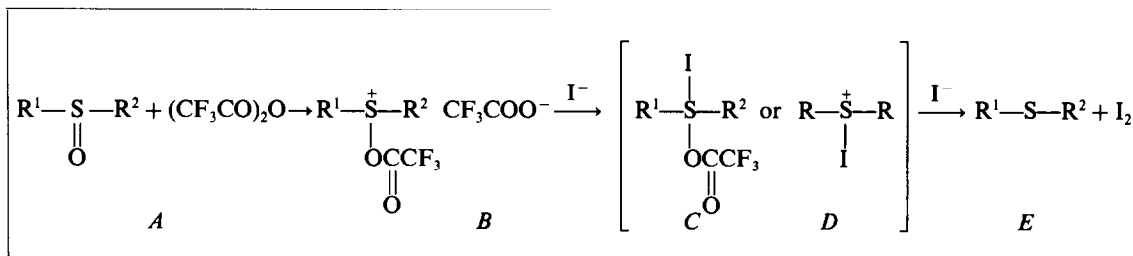
The determination of sulphoxides is of great interest owing to the role which this class of sulphanyl derivatives plays in modern organic synthesis<sup>1,2</sup> as well as in the field of bio-organic and biological chemistry.<sup>3,4</sup> The significance of this topic is reflected by the number of procedures which have been reported during more than fifty years.<sup>5,6</sup>

Although in the last decade mainly GLC techniques have been introduced for the determination of volatile sulphoxides the non-volatile and unstable

converts sulphoxides into the corresponding sulphides according to the general equation



The preparative scale deoxygenation of sulphoxides by means of this reagent has been found to be fast and quantitative even at temperatures around 0.<sup>18</sup> The reaction may be rationalized as shown in the mechanistic scheme below.



derivatives must still be determined by classical titrimetric methods. The first of these procedures were based on reduction with stannous<sup>7</sup> or titanous<sup>8,9</sup> salts and back-titration of the excess of reducing agent with a standard ferric iron solution. The sulphoxides have also been reduced with iodide in hydrochloric acid,<sup>10</sup> hydrochloric acid-acetic acid,<sup>11</sup> or acetic acid-acetyl chloride mixtures<sup>12</sup> with subsequent determination of the iodine released.

Later, methods based on the oxidation of sulphoxides by potassium permanganate,<sup>13</sup> potassium dichromate,<sup>14</sup> chloramine-T<sup>15</sup> or chloramine-B<sup>16</sup> were introduced. The sulphoxides were also determined by potentiometric titration with perchloric acid in anhydrous dioxan-acetic anhydride solution.<sup>17</sup>

Here we present a new procedure for the iodometric determination of sulphoxides, which is based on the use of trifluoroacetic anhydride-sodium iodide (TFAA-I) mixture as a reducing agent, which

The first step of the reaction is undoubtedly the formation of the acyloxysulphonium salt *B*.<sup>12,19</sup> In the subsequent step either the sulphonium salt *D* or the sulphurane intermediate *C* may be formed. Decomposition of *C* or *D* by iodide will lead to the final reduction product with simultaneous release of iodine in a quantitative reaction. The reactivity of TFAA-I also recommends this reagent for other deoxygenations (e.g., of *N*-oxy compounds) as already described by us.<sup>20,21</sup>

### EXPERIMENTAL

#### Materials

DMSO (Aldrich) was standardized by the permanganate method.<sup>13</sup> Phosphonoethionine sulphoxide (C<sub>3</sub>H<sub>14</sub>NO<sub>4</sub>PS·2H<sub>2</sub>O) was synthesized<sup>22</sup> and standardized by the permanganate method.<sup>13</sup> The other sulphoxides listed in Table 1 were prepared as previously described<sup>23</sup> and had the purity reported. Trifluoroacetic anhydride was purchased from Aldrich. Acetone was distilled from phosphorus pentoxide and stored over 13 Å molecular sieve. Sodium iodide (Aldrich) was dried in vacuum over phosphorus pentoxide before use.

\*Author to whom correspondence should be addressed.

Table 1. Results for determination of various sulphoxides

Compounds			Taken, $\mu\text{mole}$	Found, $\mu\text{mole}$	Std. devn., $\mu\text{mole}$ ( $n = 6$ )	Solvent
R <sup>1</sup>	R <sup>2</sup>					
1a	Me	Me	20	19.93	0.1	acetone
			50	49.9	0.1	acetone
			90	89.7	0.2	acetone
			20	19.94		AcOH-Ac <sub>2</sub> O (5%)
			50	49.9	0.1	AcOH-Ac <sub>2</sub> O (5%)
			90	89.8		AcOH-Ac <sub>2</sub> O (5%)
1b	nBu	nBu	50	49.9	0.1	acetone
1c	Ph	Ph	50	49.9	0.2	acetone
1d	Ph	Bu	50	50.10	0.1	acetone
1e	Ph	<i>p</i> Tol	50	49.7	0.1	acetone
1f	Ph	<i>p</i> MeO-C <sub>6</sub> H <sub>4</sub>	50	49.8	0.1	acetone
			20	19.8		AcOH-Ac <sub>2</sub> O (5%)
1g	Et	H <sub>2</sub> N-CH(CH <sub>2</sub> ) <sub>2</sub> -   PO <sub>3</sub> H <sub>2</sub>	50	49.8	0.3	AcOH-Ac <sub>2</sub> O (5%)
			100	99.0		AcOH-Ac <sub>2</sub> O (5%)

**Solutions**

*Sodium iodide.* A 0.5M solution in anhydrous acetone.

*TFAA.* A 0.8M solution in anhydrous acetone, prepared immediately before use.

*Sulphoxides.* Solutions (0.1M) of compounds 1a-1f (Table 1) in anhydrous acetone, and of 1g in a 95:5 v/v mixture of glacial acetic acid and acetic anhydride.

*Aqueous potassium iodide solution,* 0.1M.

Table 2. Yields of the reaction of TFAA-iodide with compounds containing semipolar X-O bonds

Compounds					Amount of iodine, $\mu\text{mole}$	
Structure	R <sup>1</sup>	R <sup>2</sup>	R <sup>3</sup>	Taken, $\mu\text{mole}$	1 min	20 min
1a	Me	Me		50	49.9*	
1b	Bu	Bu		50	49.9*	
1c	Ph	Ph		50	49.9*	
2a	Ph	Ph		50	0.0	0.0
2b	Bu	Bu		50	0.0	0.0
3a	Ph	Me	H	50	0.0	0.0
4a	Me	Me	Me	50	0.0	0.0
4b	Ph			50	25	49.5
5a	Me			50	0.0	0.0
5b	Et			50	0.0	0.0
5c	Ph			50	0.0	0.0
6a	<i>p</i> ClC <sub>6</sub> H <sub>5</sub> -	H		50	45	45
6b	<i>p</i> O <sub>2</sub> NC <sub>6</sub> H <sub>5</sub> -	H		50	45	45
7a	Ph	Me		50	0.0	0.0
7b	PhCH <sub>2</sub>	PhCH <sub>2</sub>		50	0.0	0.0
8a	Ph			50	0.0	0.0
8b	Naph			50	0.0	0.0
9a	Ph			50	0.0	0.0

\*These amounts of iodine were released after a few seconds of reaction time and did not increase over a period of 1 min.

Table 3. Comparison with representative methods of sulphoxide determination

Method	Time, min	Range, mmole	Accuracy, %	Standard used
A. Potentiometric titration with standardized solution of HClO <sub>4</sub> in Ac <sub>2</sub> O-dioxan solution	30	1.0	99.5 ± 0.1 99.2 ± 0.2 99.7 ± 0.4	DMSO <sup>17</sup> DPSO DBSO <sup>19</sup>
B. Oxidation with excess of standardized solution of K <sub>2</sub> Cr <sub>2</sub> O <sub>7</sub> in H <sub>2</sub> SO <sub>4</sub> . Redox back-titration with 0.1M Fe(II)	45	0.5–1.5	99.9 ± 0.1 95.7 ± 7.4	DMSO, DPSO <sup>14</sup> DBSO <sup>19</sup>
C. Oxidation with excess of standardized solution of KMnO <sub>4</sub> in H <sub>2</sub> SO <sub>4</sub> . Redox back-titration with 0.1M Fe(II)	35	4.0	99.4 ± 0.6	DMSO, DPSO <sup>13</sup>
D. Oxidation with standardized solutions of chloramine-T, <sup>15</sup> or chloramine-B. <sup>16</sup> Iodide reduction and iodometric determination of chloramine excess (0.05M Na <sub>2</sub> S <sub>2</sub> O <sub>3</sub> )	5–10	0.2–1.0	99.5 ± 0.5	DMSO <sup>15,16</sup>
E. Reduction with excess of standardized solution of SnCl <sub>2</sub> . Redox back-titration with 0.1M Fe(III)	80	2.5–6.0	98.8 ± 10	DBSO <sup>19</sup>
F. Reduction with standardized solution of TiCl <sub>3</sub> . Redox back-titration with 0.1M Fe(III)	95	2.0–5.0	99.3 ± 4.9	DBSO <sup>19</sup>
G. Reduction with KI in 10M HCl. Titration of iodine with 0.05M Na <sub>2</sub> S <sub>2</sub> O <sub>3</sub>	5–10	0.5	99.7 ± 0.3	AMSP <sup>11</sup>
H. Acetylation-reduction with AcCl–AcOH–NaI. Iodometric titration with 0.1M Na <sub>2</sub> S <sub>2</sub> O <sub>3</sub>	20	0.5–1.0	100.2 ± 1.3	DBSO <sup>19</sup>
I. Acylation-reduction with TFAA–I. Iodometric titration with 0.02M Na <sub>2</sub> S <sub>2</sub> O <sub>3</sub>	5	0.02–0.1	99.8 ± 0.2	1a–1g (Table 1)

\*DMSO—dimethyl sulphoxide, DBSO—dibenzyl sulphoxide, DPSO—diphenyl sulphoxide, AMPS—3-amino-6-methylsulphoxy pyrazine.

Sodium thiosulphate solution, 0.02M. Standardized by coulometric titration with iodine.

Starch, 0.5% aqueous solution.

#### Procedure

A known volume of sample solution (containing 20–100  $\mu$ mole of the sulphoxide) is placed in a 100-ml Erlenmeyer flask and 1 ml of 0.5M solution of sodium iodide in acetone is added, followed by 0.5 ml of 0.8M solution of TFAA in acetone. Iodine is immediately formed. After gentle swirling for 0.5 min, the mixture is diluted with 20 ml of 0.1M potassium iodide and titrated at once with 0.02M sodium thiosulphate. Starch indicator is added towards the end of the titration.

#### RESULTS AND DISCUSSION

The method of sulphoxide determination presented is characterized by the results summarized in Table 1. The reductive deoxygenation of sulphoxides is very fast and affords the stoichiometric amount of iodine over the broad range of sulphoxide concentrations from  $10^{-3}$  to 0.1M. Sulphoxide concentrations as low as  $10^{-6}$ M can be determined with ultraviolet spectrometric determination of the iodine released.

The sensitivity of the method results from the final determination system, namely the thiosulphate titration of iodine with starch as indicator in the presence of excess of iodide to enhance the colour change. This system allows determination of sulphoxides at micromole level (20–100  $\mu$ mole in the titrated sample) with visual detection of the endpoint.

The low acidity of the reaction mixture (0.4 mmole of TFAA, 4–20-fold molar ratio of TFAA to sul-

phoxide) practically eliminates the side-reaction of aerial oxidation of iodide, and the need for a blank titration (though this can always be performed). In comparison, the Allenmark procedure,<sup>12</sup> involving titration in 1M hydrochloric acid medium, gives a blank of about 5  $\mu$ mole, for which a correction must be applied. The selectivity of the method is illustrated by the results for application of the method to sulphoxides and other class of compounds bearing semipolar functions (Table 2). It is interesting that there is no interference by sulphides and sulphones. Thus, the determination of diphenyl sulphoxide (50  $\mu$ mole) alone or in a mixture with diphenyl sulphide (50  $\mu$ mole) or diphenyl sulphone (50  $\mu$ mole), under the prescribed conditions, always gave the same results.

A comparison of this method with other representative procedures, experimentally verified by Moravek and Vláčil,<sup>19</sup> is presented in Table 3.

*Acknowledgement*—This project was financially supported by the Polish Academy of Sciences, National Committee of Chemistry.

#### REFERENCES

1. T. Durst, in *Comprehensive Organic Chemistry*, D. N. Jones (ed.), Vol. 3, pp. 121ff. Pergamon Press, Oxford, 1979.
2. *Special Periodical Reports, Organic Compounds of Sulphur, Selenium and Tellurium*, Vols. 1–9, Chemical Society, London, 1970–1986.
3. A. Kajaer, *Tetrahedron*, 1974, **30**, 1551.
4. R. L. Whistler, *Carbohydrates, Nucleotides, Nucleosides*, 1979, **16**, 199.

5. M. R. F. Ashworth, *Determination of Sulphur-containing Groups*, Vol. 1, p. 30. Academic Press, London, New York, 1972.
6. J. H. Karchmer, *The Analytical Chemistry of Sulfur and its Compounds*, Part II, Chapter 11, Wiley-Interscience, New York, 1972.
7. E. Glynn, *Analyst*, 1947, **72**, 248.
8. D. Barnard and K. R. Hargrave, *Anal. Chim. Acta*, 1951, **5**, 536.
9. R. R. Legault and K. Groves, *Anal. Chem.*, 1957, **29**, 1945.
10. E. N. Karaulova and G. D. Galpern, *Zh. Obshch. Khim.*, 1959, **29**, 3033.
11. F. Jančík and J. Körbl, *Cesk. Farm.*, 1962, **11**, 305.
12. A. Allenmark, *Acta Chem. Scand.*, 1955, **20**, 910.
13. V. Krishnan and C. C. Patel, *Inorg. Chim. Acta*, 1967, **1**, 165.
14. V. Savant, C. C. Patel and J. Gopalakrishnan, *Z. Anal. Chem.*, 1968, **238**, 273.
15. T. B. Douglas, *Talanta*, 1968, **15**, 704.
16. C. Rangajwamy, H. C. Yathirajan and P. S. Mahadevappa, *Indian J. Chem.*, 1979, **17A**, 682.
17. D. C. Wimer, *Anal. Chem.*, 1958, **30**, 2060.
18. J. Drabowicz and S. Oae, *Synthesis*, 1977, 402.
19. J. Moravek and F. Vláčil, *Chem. Listy*, 1979, **73**, 750.
20. W. Ciesielski, J. Drabowicz, W. Jedrzejewski, Z. H. Kudzin and R. Skowroński, Papers presented at 31st IUPAC International Congress, Sophia, 1987.
21. *Idem*, Paper presented at IVème Colloque Franco-Polonais Chimie Organique, Łódź, 1987.
22. M. Tishler, C. C. Tam and K. L. Mattocks, *Synthesis*, 1982, 188.
23. J. Drabowicz, H. Midura and M. Mikolajczyk, *ibid.*, 1979, 39.



## STUDIES OF 7-HYDROXYCOUMARINS

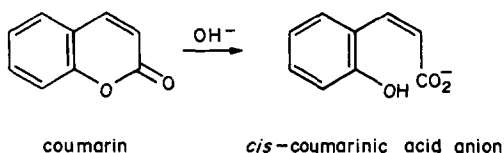
GERALDINE M. HUITINK

Department of Chemistry, Indiana University at South Bend, South Bend, IN 46634, U.S.A.

(Received 19 July 1988. Accepted 23 August 1988)

**Summary**—Spectral studies of a series of 7-hydroxycoumarins substituted at positions 3 and 4 with methyl and phenyl groups are reported. Rates of ring opening in 0.7M potassium hydroxide at 25.5° have been determined fluorometrically, and rate constants and half-lives are reported.

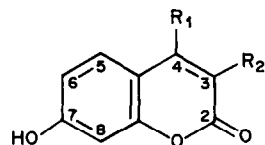
A great many investigations have been conducted on derivatives of 7-hydroxycoumarin (umbelliferone), a 7-hydroxybenzo-2-pyrone. Among these are the investigations of Balaiah *et al.*<sup>1</sup> and of Sherman and Robins<sup>2</sup> who found that electron-withdrawing substituents such as carbethoxy, cyano, and phenyl dramatically enhance the fluorescence of 7-hydroxycoumarins when they are located at position 3 of the benzo-2-pyrone ring. Other investigators have studied the hydrolysis of coumarin derivatives in a variety of solvents by spectrophotometric,<sup>3-5</sup> polarographic,<sup>6-7</sup> and conductometric<sup>8</sup> methods. When coumarin is attacked by hydroxide the anion of *cis*-coumarinic acid is formed.<sup>9</sup> Bowden *et al.*<sup>8</sup> have shown that the mechanism of this reaction consists of hydroxide attack on the carbonyl carbon atom (rate-determining step) followed by fast fission of the cyclic oxygen-carbonyl bond. Under conditions of limited basicity, the singly charged anion is produced. The doubly charged anion is produced in the presence of excess of base.



The present investigation was undertaken to determine whether substitution patterns might be found which would provide the 7-hydroxybenzo-2-pyrone nucleus with high relative fluorescence as well as with resistance to ring opening in alkaline solution. These properties are necessary for molecules employed as the fluorescent moieties in metallofluorescent indicators which are to be used in spectrofluorometric analyses at high pH. This investigation, an extension of an earlier work,<sup>10</sup> followed essentially the same course as the investigation of derivatives of 7-hydroxybenzo-4-pyrone, and the calculations and reasoning follow the pattern presented in the earlier paper.

### EXPERIMENTAL

Eight 7-hydroxycoumarins differing in substitution at the 3- and 4- positions were synthesized.



7-hydroxycoumarin  
(7-hydroxybenzo-2-pyrone)

- I  $R_1 = \text{H}, R_2 = \text{H}$   
(7-hydroxycoumarin)
- II  $R_1 = \text{H}, R_2 = \text{CH}_3$   
(7-hydroxy-3-methylcoumarin)
- III  $R_1 = \text{CH}_3, R_2 = \text{H}$   
(7-hydroxy-4-methylcoumarin)
- IV  $R_1 = \text{CH}_3, R_2 = \text{CH}_3$   
(7-hydroxy-3,4-dimethylcoumarin)
- V  $R_1 = \text{H}, R_2 = \text{C}_6\text{H}_5$   
(7-hydroxy-3-phenylcoumarin)
- VI  $R_1 = \text{C}_6\text{H}_5, R_2 = \text{H}$   
(7-hydroxy-4-phenylcoumarin)
- VII  $R_1 = \text{C}_6\text{H}_5, R_2 = \text{C}_6\text{H}_5$   
(7-hydroxy-3,4-diphenylcoumarin)
- VIII  $R_1 = \text{CH}_3, R_2 = \text{C}_6\text{H}_5$   
(7-hydroxy-4-methyl-3-phenylcoumarin)

References to compound preparation methods, melting points (uncorrected) and elemental analysis data are given in Table 1.

All chemicals used were of reagent grade. Buffers were prepared according to the method of Bates<sup>10</sup> and were of constant ionic strength. All water was distilled and demineralized by passage through Amberlite MB-1.

### Procedures

**Absorption spectra.** Absorption spectra over the pH range 3.0–12.0 at intervals of 0.5 pH were obtained with a Cary Model 219 spectrophotometer. Stock solutions ( $3.11 \times 10^{-3}M$ ) of substituted 7-hydroxycoumarin, were prepared by dissolving appropriate amounts of each compound in 100 ml of 95% ethanol. Solutions for which spectra were recorded were prepared by delivering 375  $\mu\text{l}$  of stock solution into 25-ml standard flasks from a Micro Metric SB 2 microburette and a model S5Y syringe and diluting to the mark with the appropriate buffer. Spectra were run as soon as possible after solution preparation in order to avoid precipitation of the compounds from acid solution and hydrolysis of the compounds in alkaline solution.

**Fluorescence spectra.** Fluorescence spectra were obtained for the pH range 3.0–12.0 at intervals of 0.5 pH by using an Aminco-Bowman spectrofluorometer and were uncorrected

Table 1. Literature references to preparation, melting points, and elemental analyses of 3- and 4- substituted 7-hydroxycoumarins

Compound	Reference	m.p. (lit.), °C	Elemental analysis*	
			Carbon, %	Hydrogen, %
I	11	236-238 (227-228)	66.6 (66.67)	3.8 <sub>3</sub> (3.73)
II	12	228-229 (218)	68.0 (68.17)	4.6 <sub>3</sub> (4.58)
III	13	192-193 (194-195)	68.3 (68.17)	4.6 <sub>0</sub> (4.58)
IV	14	269-271 (256)	69.4 (69.47)	5.4 <sub>9</sub> (5.29)
V	15	214-216 (209-210)	75.7 (75.62)	4.2 <sub>3</sub> (4.23)
VI	16	255-256 (256.5-257)	75.6 (75.62)	4.3 <sub>3</sub> (4.23)
VII	17	298-300 (287-289)	80.0 (80.24)	4.5 <sub>7</sub> (4.49)
VIII	18	231-233 (228-229)	75.7 (76.18)	4.9 <sub>3</sub> (4.79)

\*Theoretical values in parentheses.

for variations in the emission characteristics of the lamp and response characteristics of the photomultiplier tube. The stock solutions were  $1.55 \times 10^{-3} M$  for compounds V and VIII and  $3.11 \times 10^{-3} M$  for the others. Solutions were prepared by delivering between 5 and 25  $\mu$ l of stock solution into 25-ml standard flasks from a Micro Metric SB 2 microburette and a model S5Y syringe and diluting to the mark with appropriate buffers. Measurements were made as soon as possible after solution preparation.

**Acid dissociation constants.** The acid dissociation constant of 7-hydroxy-3,4-diphenylcoumarin was determined from solubility data by the method of Krebs and Speakman.<sup>19</sup> Acid dissociation constants for the other compounds were determined from absorbance and fluorescence measurements of the acid and base forms of the compounds, and of solutions containing a mixture of both forms, at  $pH = pK_a \pm 0.0, \pm 0.2, \pm 0.4$  and  $\pm 0.6$ , by using methods described before.<sup>10</sup>

**Hydrolysis study.** The rate of hydroxide attack on the 3-methyl, 3-phenyl-, and 4-methyl-derivatives of 7-hydroxybenzo-2-pyrone was followed fluorometrically by means of a Turner Model 110 filter fluorometer equipped with a flow-through cell. The filters used were: primary, 7-60; secondary, 110-828 (4), with a 1% neutral-density filter. For monitoring the hydrolysis of the feebly fluorescent 4-phenyl derivatives, the neutral density filter was removed. The hydrolyses were investigated by adding sufficient coumarin stock solution to 50 ml of 0.7M potassium hydroxide to provide an initial reading of 80-100% relative fluorescence. Plots of the logarithm of the difference in fluorescence at any time,  $F$ , and the final fluorescence,  $F_{\infty}$ , as a function of time, gave straight lines in accord with

$$\log|F - F_{\infty}| = \frac{-kt}{2.303} + \log|F_0 - F_{\infty}| \quad (1)$$

where  $F_0$  is the fluorescence of the completely unhydrolysed compound. Rate constants and half-lives were determined

from the slopes of these straight lines. Hydrolyses were repeated a minimum of five times per compound, at different concentrations of coumarin. All hydrolyses were followed for a minimum of 3.5 half-lives and, in most cases, for 5 half-lives.

## RESULTS AND DISCUSSION

### Absorption data

The parent compound, 7-hydroxycoumarin, has absorption maxima at 323.3 nm in pH 4.0 solution and 365.7 nm in pH 10.5 solution, with molar absorptivities of  $1.52 \times 10^4$  and  $1.98 \times 10^4$   $l. mole^{-1}. cm^{-1}$ , respectively. A similar shift to longer wavelength, accompanied by a 5-30% increase in molar absorptivity, is observed for each of the compounds studied and is attributed to neutralization of the phenolic proton. Table 2 lists the wavelengths of maximum absorbance, and the molar absorptivities in acid and base solution. Phenyl substitution at position 3 or 4 results in an increase in the wavelength of maximum absorbance in both acid and alkaline solution, the shift being greater for compounds having a 3-phenyl substituent conjugated to the hydroxyl group at position 7. Methyl substitution at position 3 or 4 produces a slight blue shift in the wavelength of maximum absorbance. Acid dissociation constants given in Table 3 and determined by changes in both absorbance and fluorescence are in excellent agreement, and are attributed to ground-state dissociation of the phenolic proton.

Table 2. Absorption maxima and molar absorptivities of 3- and 4-substituted 7-hydroxybenzo-2-pyrones at pH 4.0 and 10.5

Compound	pH 4.0		pH 10.5	
	Absorption maximum, nm	Molar absorptivity, $l. mole^{-1}. cm^{-1}$	Absorption maximum, nm	Molar absorptivity, $l. mole^{-1}. cm^{-1}$
I	323.3	$1.52 \times 10^4$	365.7	$1.98 \times 10^4$
II	321.2	$1.62 \times 10^4$	361.2	$1.91 \times 10^4$
III	320.4	$1.63 \times 10^4$	359.9	$2.11 \times 10^4$
IV	320.7	$1.56 \times 10^4$	357.4	$1.80 \times 10^4$
V	338.0	$1.12 \times 10^4$	382.6	$1.39 \times 10^4$
VI	329.1	$1.37 \times 10^4$	375.1	$1.77 \times 10^4$
VII		insoluble	251.8	$1.70 \times 10^4$
VIII	326.1	$1.85 \times 10^4$	378.5	$2.31 \times 10^4$
			365.8	$2.25 \times 10^4$

Table 3. Acid dissociation constants ( $\pm$  standard deviation) obtained from absorbance, fluorescence, and solubility data

Compound	$pK_a$	Method
I	$7.74 \pm 0.03$	Absorbance
	$7.65 \pm 0.03$	Fluorescence
II	$8.02 \pm 0.03$	Absorbance
	$7.97 \pm 0.05$	Fluorescence
III	$7.80 \pm 0.02$	Absorbance
	$7.83 \pm 0.03$	Fluorescence
IV	$8.09 \pm 0.02$	Absorbance
	$8.04 \pm 0.04$	Fluorescence
V	$7.73 \pm 0.02$	Absorbance
	$7.70 \pm 0.02$	Fluorescence
VI	$7.64 \pm 0.05$	Absorbance
	$7.52 \pm 0.03$	Fluorescence
VII	7.67	Solubility
VIII	$7.86 \pm 0.05$	Absorbance
	$7.86 \pm 0.08$	Fluorescence

### Fluorescence study

The wavelengths of maximum fluorescence excitation in acid and base solution correspond to the wavelengths of maximum absorbance (Table 4). The wavelength of maximum fluorescence emission of 7-hydroxy-3-phenylcoumarin exhibits a 5-nm shift to longer wavelength on neutralization of the ground-

Table 4. Wavelengths of maximum fluorescence excitation and emission at pH 4.0 and 10.5

Compound	pH	Fluorescence	
		Excitation $\lambda_{max}$ , nm	Emission $\lambda_{max}$ , nm
I	4.0	324	455
	10.5	366	455
II	4.0	322	464
	10.5	363	464
III	4.0	322	448
	10.5	360	448
IV	4.0	321	460
	10.5	358	460
V	4.0	339	466
	10.5	382	472
VI	4.0	328	504
	10.5	374	504
VII	4.0	insoluble	
	10.5	374	483
VIII	4.0	332	464
	10.5	368	462

state phenolic proton. For the remaining compounds, the wavelength of maximum fluorescence emission remains unchanged over the pH range studied and, in all cases, emission is attributed to the phenolate form of the compounds. Phenyl substitution for hydrogen at either the 3- or 4-position of 7-hydroxycoumarin increases the wavelength of maximum emission, 4-phenyl substitution producing the compound with the longest emission wavelength. Addition of a second phenyl group at position 3 of 7-hydroxy-4-phenylcoumarin results in an emission maximum of shorter wavelength than that of the 4-phenyl derivative and is due presumably to crowding of the two adjacent phenyl groups. Of the compounds studied, 4-phenylumbelliferone exhibits the most feeble fluorescence.

### Hydrolysis study

Attack by hydroxide on the carbonyl carbon atom of 7-hydroxycoumarin results in opening of the benzo-2-pyrone ring. Because ring-opening is accompanied by loss of fluorescence, hydrolyses were conveniently followed by monitoring fluorescence as a function of time. Pseudo first-order rate constants and half-lives are given in Table 5. Consistent with inductive effects, an electron-withdrawing phenyl group at position 3 results in accelerated rate of hydroxide attack on the carbonyl carbon atom (compare compounds I and V, III and VIII, and VI and VII). Phenyl substitution at position 4 has little, if any, effect on the rate of ring cleavage of 7-hydroxycoumarin (compare compounds I and VI), while substitution of phenyl for hydrogen at position 4 of 7-hydroxy-3-phenylcoumarin slows the rate of ring cleavage (compare compounds V and VII), presumably because the phenyl at position 3 is forced out of the plane of the benzo-2-pyrone ring, thus reducing the positive charge at the carbonyl carbon atom.

It is surprising that introduction of the electron-donating methyl group at position 3 also results in accelerated ring-opening (compare compounds I and II, and III and IV), but Lippold and Garrett<sup>5</sup> report a similar effect for 3-methylcoumarin at 25°; at temperatures below 15°, 3-methylcoumarin is less susceptible to attack by hydroxide than the unsubstituted coumarin, but at 17.5° and 25.0° the

Table 5. Pseudo first-order rate constants and half-lives ( $\pm$  standard deviation) for 7-hydroxybenzo-2-pyrones differing in substitution at positions 2 and 3; solvent 0.7M potassium hydroxide ( $25.5 \pm 0.1^\circ$ )

Compound	$k$	$t_{1/2}$
I	$0.00831 \pm 0.00006 \text{ sec}^{-1}$	$83.1 \pm 0.6 \text{ sec}$
II	$0.0117 \pm 0.0001 \text{ sec}^{-1}$	$59.1 \pm 0.3 \text{ sec}$
III	$0.123 \pm 0.002 \text{ min}^{-1}$	$5.63 \pm 0.10 \text{ min}$
IV	$0.146 \pm 0.005 \text{ min}^{-1}$	$4.74 \pm 0.15 \text{ min}$
V	$0.0144 \pm 0.0002 \text{ sec}^{-1}$	$47.9 \pm 0.5 \text{ sec}$
VI	$0.00855 \pm 0.00007 \text{ sec}^{-1}$	$80.9 \pm 0.6 \text{ sec}$
VII	$0.0116 \pm 0.0000 \text{ sec}^{-1}$	$59.6 \pm 0.3 \text{ sec}$
VIII	$0.165 \pm 0.001 \text{ min}^{-1}$	$4.18 \pm 0.03 \text{ min}$

system can supply the activation energy for 3-methylcoumarin and accelerated attack by hydroxide occurs. The present study shows that methyl substitution at position 4 greatly increases resistance of the 7-hydroxybenzo-2-pyrone nucleus to alkaline hydrolysis in 0.7*M* potassium hydroxide at 25° (compare compounds I and III, II and IV, and V and VII).

The half-lives of 7-hydroxybenzo-2-pyrones in the present study are shorter (between 47.4 sec and 5.63 min) than half-lives of compounds in a similar series of 7-hydroxybenzo-4-pyrones substituted at positions 2 and 3 with methyl and phenyl groups (between 6.98 min and 16.6 days),<sup>10</sup> indicating that the benzo-2-pyrone nucleus is more susceptible to alkaline hydrolysis than the benzo-4-pyrone nucleus. The approximately one order of magnitude range of half-lives exhibited by the 7-hydroxycoumarins is about one quarter of that exhibited by similarly substituted 7-hydroxybenzo-4-pyrones, indicating that methyl and phenyl substituents exert a lesser influence of 7-hydroxycoumarin stability than on 7-hydroxychromone stability.

Although the compound in the present study that is most resistant to alkaline hydrolysis, 7-hydroxy-4-methylcoumarin (III), is very fluorescent and has been used as the fluorescent moiety in the metallofluorescent indicator Calcein Blue, it is very susceptible to attack by hydroxide ( $t_{1/2} = 5.63 \pm 0.10$  min) and thus exhibits too rapid a decay of the fluorescence signal to be recommended for incorporation into spectrofluorometric reagents that will be used in highly alkaline solution. Furthermore, it appears unlikely that a structurally simple, readily synthesized, highly fluorescent 7-hydroxycoumarin could be prepared that would display significantly greater resistance to alkaline hydrolysis than 7-hydroxy-4-methylcoumarin (4-methylumbelliferone).

*Acknowledgements*—This research was made possible by financial assistance in the form of Summer Faculty Fellowships and Grant-in-Aid of research funds from Indiana University at South Bend and is gratefully acknowledged. The author also thanks Dr. Harvey Diehl of Iowa State University and Dr. Kenneth W. Street, Jr., formerly of Loyola University, Chicago, who made Aminco-Bowman spectrofluorometers available for her use.

#### REFERENCES

1. V. Balaiah, T. R. Seshadri and V. Venkateswarlu, *Proc. Indian Acad. Sci.*, 1942, **16A**, 68.
2. W. R. Sherman and E. Robins, *Anal. Chem.*, 1968, **40**, 803.
3. B. N. Mattoo, *Trans. Faraday Soc.*, 1957, **53**, 760.
4. E. R. Garrett, B. C. Lippold and J. B. Mielck, *J. Pharm. Sci.*, 1971, **60**, 396.
5. B. C. Lippold and E. R. Garrett, *ibid.*, 1971, **60**, 1019.
6. G. Giacometti, *Atti. Accad. Naz. Lincei, Rend. Classe Sci. Fis. Mat. Nat.*, 1954, **17**, 379.
7. A. Foffani, *ibid.*, 1953, **14**, 281.
8. K. Bowden, M. J. Hanson and G. R. Taylor, *J. Chem. Soc. (B)*, 1962, 174.
9. H. Decker and P. Becker, *Chem. Ber.*, 1922, **55**, 375.
10. G. M. Huitink, *Talanta*, 1980, **27**, 977.
11. R. G. Bates, *Determination of pH; Theory and Practice*, pp. 156–162. Wiley, New York, 1964.
12. *Organic Reactions*, Vol. VII, p. 20. Wiley, New York, 1953.
13. E. Cingolani, A. Schiavello and C. Sebasitani, *Gazz. Chim. Ital.*, 1953, **83**, 647.
14. *Organic Syntheses*, Collective Vol. I, p. 23. Wiley, New York, 1941.
15. F. W. Canter, F. H. Curd and A. Robertson, *J. Chem. Soc.*, 1931, 1264.
16. Ng. Ph. Buu-Hoi, B. Ekert and R. Royer, *J. Org. Chem.*, 1954, **19**, 1548.
17. L. L. Woods and J. Sapp, *ibid.*, 1962, **27**, 3703.
18. D. Lednicer, *U.S. Patent* 3,275,658 (Cl 260-343.2), 27 September 1966.
19. T. R. Seshadri and S. Varadarajan, *J. Sci. In. (India) Res.*, 1952, **11A**, 48.
20. H. A. Krebs and J. C. Speakman, *J. Chem. Soc.*, 1945, 593.

## SIMULTANEOUS SPECTROPHOTOMETRIC DETERMINATION OF FURAZOLIDONE AND BERBERINE IN TABLET FORM

S. M. HASSAN, F. BELAL\* and M. SULTAN

Department of Analytical Chemistry, Faculty of Pharmacy, University of Mansoura,  
Mansoura 35516, Egypt

(Received 10 August 1987. Revised 29 June 1988. Accepted 23 August 1988)

**Summary**—Two spectrophotometric procedures are suggested for the analysis of mixtures of furazolidone and berberine in tablets. No preliminary separation step is required. The first procedure is based on the use of the modified Vierordt equation as developed by Glenn. The second depends on the spectral changes induced for both components by reduction with zinc and hydrochloric acid. The methods have been applied to the assay of mixtures of the two compounds in tablets and the results obtained compared favourably with those obtained by other methods, but the proposed methods are more accurate and precise and less time-consuming.

Berberine is an alkaloid present in various species of berberis (*Berberidaceae*) and is reported to have antimalarial and antipyretic action.<sup>1</sup> Numerous methods have been reported for its determination in plant extracts and in dosage forms, *viz.* titrimetric,<sup>2,3</sup> spectrophotometric,<sup>4-7</sup> fluorometric,<sup>8</sup> TLC,<sup>9</sup> HPLC<sup>10</sup> and HPTLC.<sup>11</sup>

Furazolidone is a synthetic nitrofur derivative, therapeutically effective as a bactericidal agent.<sup>1</sup> It has been determined in bulk and dosage forms and in biological fluids by titrimetric,<sup>12</sup> spectrophotometric,<sup>13</sup> fluorometric,<sup>14</sup> TLC,<sup>15</sup> HPLC<sup>16</sup> and GLC<sup>17</sup> methods.

Furazolidone and berberine are frequently formulated together, but only one method for analysis of such mixtures, based on TLC separation and subsequent spectrophotometric determination,<sup>18</sup> seems to have been reported, and is tedious, time-consuming and not sufficiently accurate. Neither the British Pharmacopoeia nor the United States Pharmacopoeia has reported on the analysis of mixtures of the two species in formulations. This led us to search for a simple, rapid and accurate method for the purpose. Two spectrophotometric methods are suggested, the first the two-component method developed by Glenn<sup>19</sup> and the second the absorbance ratio method. Both give accurate and precise results.

### EXPERIMENTAL

#### Procedures

**The two-component method.** The accuracy obtainable from Vierordt's method<sup>20</sup> largely depends on establishment of the required numerical coefficients for the particular instrument used at the time of the analysis. For the special

case of a two-component mixture, Glenn has formulated the method in terms of absorbance ratios, which can be determined with solutions of unknown concentration, thus facilitating the task of obtaining the currently valid numerical coefficients. This enables the analyst to avoid use of wavelength pairs and concentration ratios that are unsatisfactory for precision.

Prepare separate stock solutions of furazolidone and berberine sulphate, in dimethylformamide and water respectively. Prepare mixtures of the two and dilute with water, so that the concentration of each compound is in the range 0.4–1.5 mg/100 ml. Measure the absorbances ( $A_1$  and  $A_2$ ) of the mixtures in a 1-cm cell at 365 and 342 nm respectively, and calculate the concentration of the two compounds from the equations:

$$C_x = -\frac{A_1}{\alpha_1} (b - m) / (b - a)$$

$$C_y = \frac{A_2}{\beta_2} [b(m - a) / (b - a)]$$

where  $C_x$  and  $C_y$  are the concentrations of furazolidone and berberine sulphate respectively, in g/100 ml,  $\alpha_1$  and  $\alpha_2$  are  $A_{1\text{cm}}^{1\%}$  values for furazolidone at 365 and 342 nm respectively,  $\beta_1$  and  $\beta_2$  are the  $A_{1\text{cm}}^{1\%}$  values for berberine sulphate at 365 and 342 nm respectively,  $m = A_2/A_1$ ,  $a = \alpha_2/\alpha_1$  and  $b = \beta_2/\beta_1$ .

**The absorbance-ratio method.** The theory of this method is that a two-component mixture can be analysed by measuring its total absorbance at a wavelength at which both components absorb, and then again after a reaction which reduces the absorbance of one component to zero, but yielding an absorbance for the other component that is linked by a constant factor to the absorbance of that component at the first wavelength.

Mix volumes of the 1.0 mg/ml stock solutions of furazolidone and berberine (in the range 0.5–1.4 mg/100 ml) in 100-ml standard flasks and dilute the mixtures to volume with water. Measure the absorbance of each mixture at 260 nm ( $A_1$ ). In a separate set of 100-ml standard flasks, place the combinations of the standard solutions as above, add 300 mg of zinc powder, 10 ml of water and 2 ml of concentrated hydrochloric acid and let stand for 10 min. Dilute to the mark with water, mix, filter through a dry

\*To whom correspondence should be addressed.

Table 1. Data for determination of furazolidone and berberine by Glenn's method

Compound	Concentration range, $\mu\text{g/ml}$	$\lambda = 365 \text{ nm}$			$\lambda = 342 \text{ nm}$				
		$A_{1\text{cm}}^{1\%}$ *	Correlation coefficient	Slope	Intercept	$A_{1\text{cm}}^{1\%}$	Correlation coefficient	Slope	Intercept
Furazolidone	4–15	720 (0.4%)	0.999	0.0702	0.001	524 (0.5%)	0.9997	0.0524	0.001
Berberine sulphate	8–15	131 (1.2%)	0.9998	0.131	0.001	538 (0.6%)	0.9997	0.054	0.003

The figures in parentheses are the coefficients of variation.

\*Average of 15 separate determinations.

paper, reject the first 10 ml of filtrate and measure the absorbance of the next 10–20 ml at 265 nm ( $A_2$ ).

Calculate the concentration of berberine sulphate from a calibration graph prepared by treating suitable standards with zinc and hydrochloric acid as just described.

To calculate the concentration of furazolidone, multiply  $A_2$  by the ratio of the absorbance of pure berberine sulphate solution at 260 nm to that of the same solution at 265 nm, and subtract the product from  $A_1$  to obtain the absorbance

(at 260 nm) of the furazolidone in the mixture; read the concentration from a previously plotted calibration graph.

*Analysis of tablets.* Weigh and pulverize 20 tablets. Extract an accurately weighed amount of the powder equivalent to ~50 mg of each drug, with three 15-ml portions of DMF followed by three 15-ml portions of water. Filter, and wash the filter with water. Make up the filtrate and washings to volume in a 100-ml standard flask. Transfer an accurately measured volume of this solution into a 100-ml standard

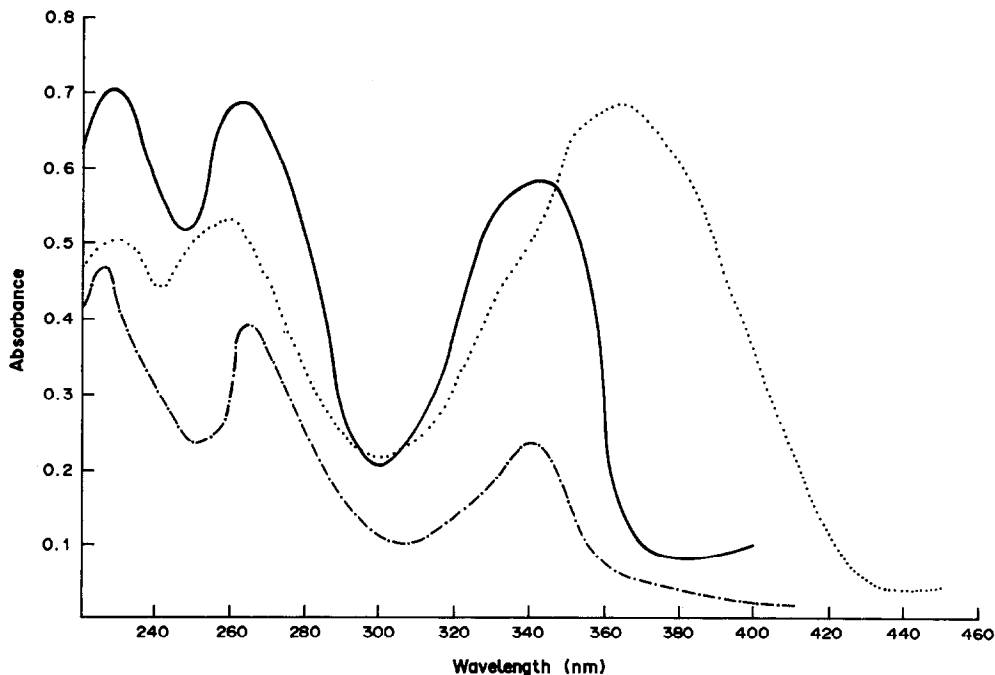


Fig. 1. Absorption spectra of berberine sulphate (—), its reduction product (---) and furazolidone (···), 10  $\mu\text{g/ml}$  concentration.

Table 2. Data for determination of furazolidone and berberine by the absorbance ratio method

Compound	$A_{1\text{cm}}^{1\%}$ *	Concentration range, $\mu\text{g/ml}$	$\lambda$ max, nm	Correlation coefficients	Slope	Intercept
Berberine sulphate	712 (0.2%)	5–15	260	0.9999	0.0713	0.003
Reduced berberine	364 (0.5%)	5–15	265	0.9999	0.0364	-0.002
Furazolidone	501 (0.3%)	5–15	260	0.9999	0.0500	-0.001

The figures in parentheses are the coefficients of variation.

\*Average of 15 separate determinations.

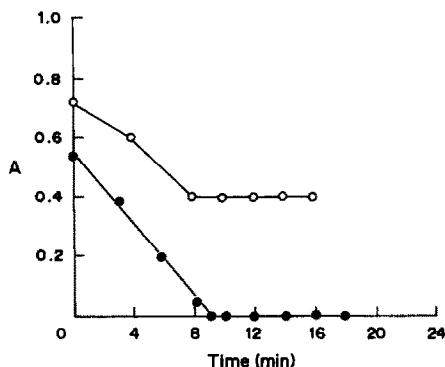


Fig. 2. Effect of reduction time on absorbance of 10 µg/ml furazolidone (●) and berberine sulphate (○) at 265 nm.

flask, so that the concentrations of the analytes are in the calibration range, then apply procedure A or B.

### RESULTS AND DISCUSSION

Table 1 shows the data needed for analysis of mixtures of furazolidone and berberine sulphate by Glenn's method.<sup>19</sup> Figure 1 shows that 365 and 342 nm are suitable wavelengths for the measurements.

The absorbance ratio method is based on the fact that on reduction with zinc in hydrochloric acid medium, the absorption spectrum of furazolidone completely disappears. The nitro group is reduced to the amine group, and the conjugated double bonds may become saturated, resulting in loss of absorption. Berberine, on the other hand, suffers only a hypochromic effect, its absorbance decreasing. This may be due to saturation of the ring containing a quaternary nitrogen atom, with consequent decrease in absorption. The ratio of absorbance of berberine at 260 nm before reduction to that at 265 nm after reduction is constant, and multiplying the absorbance of the reduced berberine by the appropriate factor gives the absorbance for the original unreduced berberine. The absorbance of furazolidone is obtained

by subtracting the absorbance of berberine from the total absorbance of the mixture at 260 nm. The necessary data are given in Table 2.

#### Study of the reduction conditions

Concentrated hydrochloric acid will react with the zinc powder immediately and too rapidly to effect the reduction. Therefore water is added first, followed by the hydrochloric acid. It was found that addition of 10 ml of water and 2 ml of concentrated hydrochloric acid is adequate. Variation of the reduction time showed that 10 min is sufficient for complete disappearance of the absorbance of furazolidone and for that of berberine (at 265 nm) to reach a constant value (Fig. 2).

Varying the quantity of zinc powder showed that 30 mg will suffice (Fig. 3).

#### Application to tablets

Both methods were applied to the determination of furazolidone and berberine sulphate in the medicinally recommended ratio (1:1). The results in Tables 3 and 4 show that the methods are accurate and precise. The TLC-spectrophotometric method<sup>18</sup> was also tried, but gave lower recovery of furazolidone and berberine ( $96.1 \pm 0.2$  and  $97.1 \pm 0.8\%$

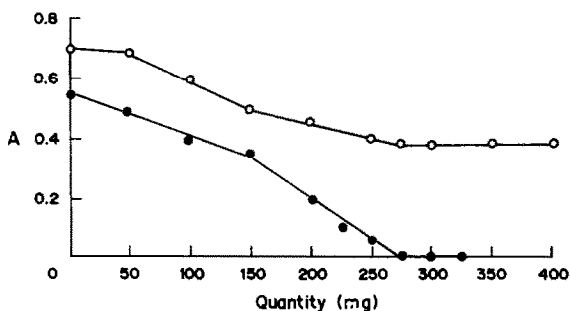


Fig. 3. Effect of amount of zinc powder on absorbance of reduced furazolidone (●) and berberine sulphate (○) at 265 nm, (10 µg/ml initial concentration).

Table 3. Application of Glenn's method

	No.	Added, mg/100 ml		Recovery, %	
		Furazolidone	Berberine sulphate	Furazolidone	Berberine sulphate
Authentic samples	1	1.0	1.0	99.5	100.1
	2	2.0	0.8	101.1	98.6
	3	0.8	1.0	101.9	97.2
	4	0.5	1.0	98.8	101.6
	5	0.5	1.2	101.0	98.6
	6	0.6	0.8	100.8	100.1
	$\bar{x}$			100.5	99.4
	S.D.			1.1	1.5
Tablets					
(50 mg furazolidone		1.0	1.0	99.7 (0.3)	99.1 (0.5)
+ 50 mg berberine		0.8	0.8	99.7 (0.6)	99.9 (0.5)
sulphate per tablet)		0.6	0.6	98.7 (0.3)	100.5 (0.4)
		0.5	0.5	99.6 (0.4)	99.1 (0.2)

Each result is the average of 4 separate determinations. The figures in parentheses are the range of error,  $p = 0.05$ .

Table 4. Application of the absorbance ratio method

	No.	Added, mg/100 ml		Recovery, %	
		Furazolidone	Berberine sulphate	Furazolidone	Berberine sulphate
Authentic samples	1	0.5	0.5	99.0	100.0
	2	1.0	0.5	100.6	100.0
	3	0.5	0.8	99.0	99.6
	4	0.8	0.5	99.4	101.7
	5	0.8	0.8	101.5	99.0
	6	0.5	1.0	98.2	100.3
	$\bar{x}$			99.6	100.1
S.D.			1.2	0.9	
Tablets					
(50 mg furazolidone		0.8	0.8	101.3 (0.7)	98.9 (0.7)
+ 50 mg berberine		0.7	0.7	100.1 (0.6)	98.1 (0.5)
sulphate per tablet)		0.6	0.6	99.5 (0.5)	98.5 (0.4)
		0.5	0.5	100.6 (0.4)	97.8 (0.4)

Each result is the average of 4 separate determinations.

The figures in parentheses are the range of error,  $p = 0.05$ .

respectively), and was slow, analysis of one sample taking more than an hour. Analysis by either of the proposed methods takes less than 25 min, needs no special skill, and is reliable for control work.

#### REFERENCES

1. E. G. C. Clarke, *Isolation and Identification of Drugs*, Vol. I, Pharmaceutical Press, London, 1974.
2. M. Tsubouchi, *Bull. Chem. Soc. Japan*, 1979, **52**, 2581.
3. Jingfen Zhong, Shuqin Sun, Jiuji Fan and Weihua Xin, *Yaoxue Tongbao*, 1982, **17**, 603; *Anal. Abstr.*, 1983, **45**, 3E15.
4. T. Sakai, *Analyst*, 1983, **108**, 608.
5. T. Sakai, I. Hera and M. Tsubouchi, *Chem. Pharm. Bull.*, 1977, **25**, 2451.
6. S. El-Masry, M. A. Korany and A. H. A. Abou Donia, *J. Pharm. Sci.*, 1980, **69**, 597.
7. S. Tadao, *ibid.*, 1979, **68**, 875.
8. A. L. Ramo Rubio, C. Cruces Blanco and F. García Sánchez, *Z. Anal. Chem.*, 1986, **323**, 153.
9. Y. Lu, Q. Xu and A. Shao, *Yaowu Fenxi Zazhi*, 1985, **5**, 290; *Anal. Abstr.*, 1986, **48**, 8E16.
10. K. Sagara, Y. Ito, M. Oimal, T. Oshima, K. Suto, T. Misaki and H. Itokawa, *Chem. Pharm. Bull.*, 1985, **33**, 5369.
11. M. Wang and M. Zhu, *Yaowu Fenxi Zazhi*, 1984, **4**, 12; *Anal. Abstr.*, 1985, **47**, 6E16.
12. I. P. Koka, *Farm. Zh. (Kiev)*, 1982, No. 3, 55; *Anal. Abstr.*, 1983, **44**, 1E7.
13. A. Biswas and S. Ghosh, *Indian J. Pharm. Sci.*, 1980, **42**, 60.
14. N. Sugimoto, S. Kashiwagi and T. Matsuda, *Nippon Suisan Gakkaishi*, 1979, **45**, 353; *Chem. Abstr.*, 1979, **91**, 124x.
15. J. P. Hoetis, J. L. Mertz, R. J. Herrett, J. R. Diaz, D. C. Van Hart and J. Olivard, *J. Assoc. Off. Anal. Chem.*, 1980, **63**, 720.
16. G. F. Ernst and A. van der Kaaden, *J. Chromatog.*, 1980, **198**, 526.
17. M. Kamikura and H. Eguchi, *Eisei Shikensho Hokoku*, 1979, **97**, 135; *Anal. Abstr.*, 1981, **41**, 1F30.
18. N. H. Paik, M. K. Park and B. R. Lim, *Soul Taehakkyo Yakha Nonmurjip*, 1976, **1**, 121; *Chem. Abstr.*, 1977, **87**, 122840r.
19. A. L. Glenn, *J. Pharm. Pharmacol.*, 1960, **12**, 595.
20. L. Heilmeyer, *Spectrophotometry in Medicine*, p. 7. Hilger, London, 1943.
21. M. Parnarowski, A. M. Knevel and J. E. Christian, *J. Pharm. Sci.*, 1961, **50**, 943.



## MULTIPARAMETRIC CURVE FITTING—XIII

### RELIABILITY OF FORMATION CONSTANTS DETERMINED BY ANALYSIS OF POTENTIOMETRIC TITRATION DATA

MILAN MELOUN and MICHAL BARTOŠ

Department of Analytical Chemistry, College of Chemical Technology, CS-532 10 Pardubice,  
Czechoslovakia

ERIK HÖGFELDT

Department of Inorganic Chemistry, The Royal Institute of Technology, S-100 44 Stockholm, Sweden

(Received 24 April 1987. Revised 29 June 1988. Accepted 12 August 1988)

**Summary**—The formation (protonation) constants  $\log K_i$  of the acid  $H_jL$  are determined by regression analysis of potentiometric titration data when common parameters ( $\log K_i, i = 1, \dots, j$ ) and group parameters ( $E^0, L_0, H_T$ ) are refined. The influence of three kinds of error on the protonation constants has been investigated: error from the strategy of minimization, random error, and error from uncertain estimates of group parameters. An analysis of variance of the  $\log K_i$  matrix was made for 7 identical titrations and 8 computational strategies, or of 7 identical titrations and 8 different options of group parameters to be refined. The influence of the standard potential  $E^0$  of the glass-electrode cell on the systematic error in  $\log K$  is greater than that of the acid concentration ( $L_0$ ) or the concentration of titrant used ( $H_T$ ). The ill-conditioned group parameters should be refined together with the common parameters ( $K_i$ ), otherwise the estimates of  $\log K_i$  are not accurate enough. Two ways of calibrating the glass electrode cell were compared. *Internal* calibration (performed during titration) was more accurate than *external* calibration done separately. Of the programs tested ESAB and ACBA are the most powerful because they permit refinement of group parameters and internal calibration. Citric acid was chosen as model substance.

The protonation constants of acid(s) can be estimated by analysis of acid-base titrations, and the methods have been reviewed.<sup>1-3</sup> In simple cases normalized graphs might give a fair estimate, but if the influence of various systematic errors has to be taken into account computer methods are necessary.

The first attempt to use least-squares methods for refining both formation constants (common parameters) and analytical concentrations (group parameters) was made by Sillén *et al.*<sup>4</sup> More recently non-linear regression programs for analysing potentiometric data for both common and group parameters have been constructed such as ACBA,<sup>5</sup> ESAB<sup>6</sup> and SUPERQUAD.<sup>7</sup> In this paper the notation introduced by Sillén *et al.*<sup>4</sup> is used. Common parameters are those that are the same for all the experiments, such as formation constants. Group parameters are those that vary from one experiment to another, such as  $E^0$ , analytical concentrations, calibration of the electrode used. To limit the number of group parameters the experiments must be done as titrations, each with its own set of group parameters. Batch experiments create too many group parameters to be handled by present-day methods. In selecting the group parameters to be refined, Sillén<sup>4</sup> kept constant those having little or no influence on the common parameters (formation constants) searched for, since if these are varied, rather large compensating errors may arise in them and in other par-

ameters, and sometimes quite unrealistic values are obtained. For that reason group parameters are sometimes termed *dangerous* parameters.<sup>7</sup> Only when the correct chemical model has been identified can these hitherto constant parameters be refined. For acid-base titrations the chemical model is often known and the group parameters can be refined directly. On the other hand for systems where the model is unknown and only guessed, this difficulty should be kept in mind and group parameters refined after the correct model has been obtained by graphical or numerical methods.

The reliability of formation constants obtained by regression analysis of potentiometric data is dependent upon (i) calibration of the glass electrode cell, (ii) the algorithm used, (iii) the parameters selected for refinement.

In order to have a well-known but not too trivial system, citric acid was chosen as the test substance. From the literature<sup>8,9</sup> the following values for the protonation constants were chosen:

$$\log K_1 = 5.65$$

$$\log K_2 = 4.34$$

$$\log K_3 = 2.87 \quad (I = 0.1, 298 K)$$

In the treatment below these constants are formally taken as "true" values.

## THEORY

The emf of a cell containing a reference electrode (half-cell) and a glass electrode (in the measuring half-cell) can be written

$$E_{\text{cell}} = E_{\text{H}} + E_{\text{j}} - E_{\text{ref}} = E^0 + \frac{RT}{F} \ln h + \frac{RT}{F} \ln \gamma_{\text{H}} + j_{\text{a}}h - j_{\text{b}}K_{\text{w}}/h - E_{\text{ref}} = E^0 + S \log h \quad (1)$$

where  $E^0$  is the standard potential of the glass electrode plus other constant terms such as the asymmetry potential, *etc.*,  $h = [\text{H}^+]$ ,  $E_{\text{j}}$  is the liquid-junction potential ( $j_{\text{a}}h - j_{\text{b}}K_{\text{w}}/h$ ), and  $S$  is the slope of the electrode response,  $RT/F \ln 10$ , for Nernstian response.

An explicit equation for the titration volume, expressing the relation between the volume of titrant added,  $v_i$ , monitored emf,  $E_{\text{cell},i}$ , and the common ( $\beta$ ) and group parameters ( $p$ ), is given by

$$v_i = f(E_{\text{cell},i}; \beta, p) \quad (2a)$$

in which the vector of common parameters  $\beta = (\beta_1, \dots, \beta_m)$  contains the formation constants of the acid  $\text{H}_i\text{L}$  or a sum of acids. There is also a vector of group parameters

$$p = (E^0, S, K_{\text{w}}, E_{\text{j}}, L_0, L_{\text{T}}, H_0, H_{\text{T}}) \quad (2b)$$

containing, besides the constants of the Nernst equation, the total ligand concentration,  $L_0$ , and the hydrogen-ion concentration in the titrand,  $H_0$ , as well as the corresponding quantities for the titrant,  $L_{\text{T}}$  and  $H_{\text{T}}$ . Note that for the titrant, the concentration of hydroxide ions is expressed as a negative hydrogen-ion concentration.  $K_{\text{w}}$  is the operational ion product of water. In most cases group parameters cannot be determined independently with sufficient accuracy. However, in work with high ionic concentration media of constant ionic strength,  $K_{\text{w}}$ ,  $j_{\text{a}}$  and  $j_{\text{b}}$  may be determined by separate experiments.

Group parameters can be refined individually or with certain constraints introduced in the computation.

## Algorithms

In most regression programs for treating emf data the task is to find the model and set of formation constants that give the "best" fit to the experimental data. In ESAB<sup>6</sup> (or ACBA<sup>7</sup>) the parameters  $\beta$  and  $p$  are refined by minimizing the residual-square sum ( $U_v$ )

$$U_v = \sum_{i=1}^n w_i (v_{\text{exp},i} - v_{\text{calc},i})^2 = \text{minimum} \quad (3)$$

where  $w_i$  is the statistical weight, in which ACBA is set equal to unity, whereas in ESAB the following expression is used

$$w_i = \frac{1}{\sigma_i^2} = \frac{1}{\sigma_v^2} + \left( \frac{\partial v}{\partial E} \right)_i \sigma_E^2 \quad (4)$$

In MINIQUAD<sup>2a,10</sup> only the parameters  $\beta$  are refined, by minimizing the residual-square sum  $U_c$ , given by

$$U_c = \sum_{i=1}^n w_i (C_{\text{exp},i} - C_{\text{calc},i})^2 = \text{minimum} \quad (5)$$

where  $C_i$  is the total concentration of ligand ( $L$ ) or proton ( $H$ ) at the  $i$ th point of the titration curve.

In PSEQUAD<sup>2b</sup> only the parameters  $\beta$  are refined, by minimizing with respect to volume ( $U_v$ ) or emf ( $U_E$ ) or both.

## Accuracy of the protonation constants

The value of a certain protonation constant ( $K$ ) from a certain ( $i$ )th titration can be written

$$\log K(i) = \log K(t) + \epsilon_{\text{cell}} + \epsilon_{\text{conc}} + \epsilon_{\text{alg}} + \epsilon_i \quad (6)$$

where  $\log K(t)$  is the "true" value of  $K$  in a statistical analysis of variance, often denoted by  $\mu$ , and  $\epsilon_{\text{cell}}$  is a systematic error due to an imprecise estimate of the group parameters,  $E^0$ ,  $S$ ,  $j_{\text{a}}$ ,  $j_{\text{b}}$  and  $K_{\text{w}}$ . These parameters may be improved by calibration of the glass electrode.  $\epsilon_{\text{conc}}$  is a systematic error due to estimates of the group parameters  $L_0$ ,  $L_{\text{T}}$ ,  $H_0$  and  $H_{\text{T}}$ , which might be evaluated by independent chemical analysis.  $\epsilon_{\text{alg}}$  is a systematic error due to poor quality of the minimization procedure in the algorithm used, and  $\epsilon_i$  is the random error in the  $i$ th titration.

The accuracy of  $K(i)$  can be expressed by the systematic deviation  $e(\log K)$  given by

$$e(\log K) = (\log K_{\text{lit}} - \log K_{\text{exp}}) \quad (7)$$

where  $\log K_{\text{lit}}$  is the "best" value available in the literature, for the experimental conditions used. In the case of simulated data  $\log K_{\text{lit}}$  is the preselected value from which the data have been generated.

## Precision of the protonation constants

The protonation constant  $K$  (one of the protonation constants of the acid  $\text{H}_i\text{L}$ ) is affected by an error which is randomly distributed between the titrations performed rather than between individual titration points. Braibanti *et al.*<sup>11</sup> proved that  $\sigma_K^2 \approx \sigma_{\text{tit}}^2$  in the relation

$$\sigma_K^2 = \sigma_i^2 + \sigma_{\text{tit}}^2 + \sigma_{\text{lab}}^2 \quad (8)$$

where  $\sigma_K$  is the standard deviation of  $\log K$  as determined experimentally,  $\sigma_i$  is the intratitration (point-to-point) standard deviation,  $\sigma_{\text{tit}}$  is the intertitration (titration-to-titration) standard deviation, and  $\sigma_{\text{lab}}$  is the intralaboratory standard deviation.

Analysis of variance applied to  $n$  points of the  $k$ th titration in one laboratory may prove whether (*i*) all the points in each titration belong to the same data population; (*ii*) all the titrations in each laboratory belong to the same data population; (*iii*) the algorithm used has no influence on the parameters estimated; (*iv*) a certain number of group parameters (to be refined) has no influence on the common parameters. Equation (8) can be extended to include also

the influence of the algorithm used,  $\sigma_{alg}^2$ , and the computation strategy for the parameters to be refined,  $\sigma_{par}^2$ , *i.e.*,

$$\sigma_K^2 = \sigma_i^2 + \sigma_{tit}^2 + \sigma_{lab}^2 + \sigma_{alg}^2 + \sigma_{par}^2 \quad (9)$$

The precision of the constant  $\log K$  can be expressed by the standard deviation  $s(\log K)$  found by the regression algorithm used.

**EXPERIMENTAL**

*Reagents*

Citric acid, 0.030M, and sodium citrate, 0.030M, were made from analytical-grade chemicals that were not further purified. Sodium hydroxide, 1M, was prepared from metallic sodium and carbon dioxide-free water under cooling and vigorous stirring with argon. This solution was standardized by titration against a solution of potassium hydrogen phthalate by using the Gran method in the MAGEC program<sup>12</sup> or by the non-linear regression program ACBA.<sup>5</sup>

Perchloric acid, 1M, was prepared by dilution of the 70% acid *p.a.* quality, with distilled water, and standardized against HgO and KI, with a reproducibility of  $\pm 0.2\%$ . Demineralized or doubly distilled water was used in the preparation of the solutions.

*Apparatus*

All emf measurements were made at  $298.0 \pm 0.1$  K, by means of an OP-208/1 digital voltmeter (Radelkis, Budapest) with a G202B glass electrode (Radiometer, Copenhagen) and an OP-0830P SCE reference electrode (Radelkis, Budapest). A waterjacketed 100-ml glass vessel, closed with a Teflon bung carrying the electrodes argon inlet, thermometer, stirrer and the microburette capillary tip, was used for the titrations.

During the titrations a stream of argon was bubbled through the solution both for stirring and for maintaining an inert atmosphere. The argon was passed through the pure ionic medium before entering the equilibrium solution.

The burettes used were home-made syringe microburettes of 2500  $\mu$ l or 1250  $\mu$ l capacity, with a 25.00 mm micrometer screw. The polyethylene capillary tip of the microburette was immersed in the solution during addition of titrant and then pulled out to avoid leakage of titrant during the pH reading.

The microburettes were calibrated by weighing water delivered from them, with a precision of  $\pm 0.015\%$  over the volume range.

*Calibration of glass electrode cell*

The potentiometric titrations of citric acid with sodium hydroxide were performed with use of two pH scales.

(i) The proton activity (pH) was obtained by calibrating (by Irving's method<sup>13</sup>) with standard buffers (S1500, 1510, 1316, Radiometer, Copenhagen), assigned the pH values 6.865, 7.410 and 4.010 at 298 K. The operating temperature and Nernstian slope,  $S$ , were compensated for by adjustment of the pH-meter.

(ii) The hydrogen concentration  $[H^+] = h$  was known from the preparation of the solution and the measured emf,  $E_{cell}$ . From equation (1),  $E_{cell} = E^0 + S \log h$ , and with a set of experimental data ( $E_{cell}, h$ ) obtained by titrating a known concentration of perchloric acid with standard sodium hydroxide, the group parameters  $E^0$  and  $S$  can be estimated in the range where  $E_j$  is practically constant and can be included in  $E^0$ .

Two calibration methods were used: *internal* and *external* calibration, *cf.* Fig. 1. Both the precision and accuracy of the protonation constants of citric acid can be investigated. The actual values of the group parameters  $H_0$ ,  $H_T$ ,  $E^0$ ,  $S$  and  $pK_w$  are estimated by the MAGEC program from a separate

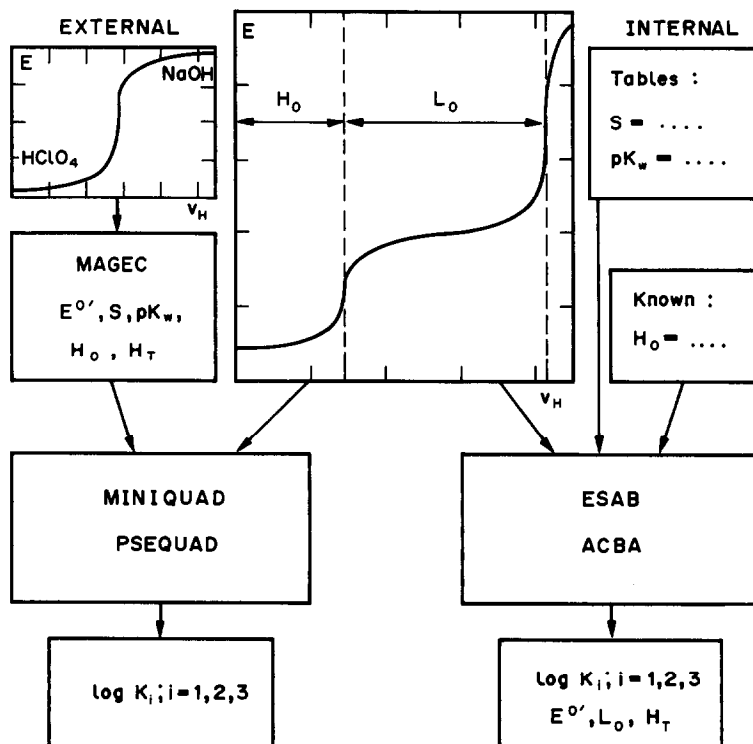


Fig. 1. Scheme of external and internal calibration of glass electrode and an estimation of the common parameters  $\log K_1$ ,  $\log K_2$ ,  $\log K_3$  of citric acid simultaneously with the three group parameters  $L_0$ ,  $H_T$  and  $E^0$ .

acid-base titration, the *external* calibration, and the program ESAB estimates  $H_T$ ,  $L_0$  and  $E^{0'}$  from the actual titration of a mixture of citric and perchloric acids with sodium hydroxide, the *internal* calibration.

Some group parameters are given in the input data for ESAB, such as the Nernstian slope and  $pK_w$ , both of which are available from the literature, *etc.* Group parameters can be estimated by regression analysis of both branches of a titration curve or from the acid branch only, because the basic might be affected by any carbonate and silicate in the alkali.

The program MAGEC offers a choice of group parameters to be estimated. The most accurate results were obtained by estimation of only  $E^{0'}$  and  $S$ , *cf.* part B of Table 1. With ESAB the three group parameters  $E^{0'}$ ,  $H_0$  and  $H_T$  were refined, and gave the best fit as expressed by the Hamilton *R*-factor, *cf.* part C in Table 1. Since  $E^{0'}$  might slightly change from one titration to another because of  $E_j$ , the internal calibration is more accurate and to be preferred.

#### Titration procedure

A mixture of 20.0 ml of 0.015*M* citric acid and 0.100*M* perchloric acid was titrated with 1.00*M* sodium hydroxide and the pH or  $E_{\text{cell}}$  was read, depending on which pH-scale that was used. As mentioned earlier the temperature was kept constant at  $298 \pm 0.1$  K.

#### Computation

The influence of the regression algorithm on the precision and accuracy of the three protonation constants was investigated. A set of seven titration curves was analysed by the eight regression programs: ESAB( $v_H$ ), ACBA( $v_H$ ), MINQUAD( $L, H$ ), MAGEC( $v_H, E_{\text{cell}}$ ), MIQUV( $E_{\text{cell}}$ ), PSEQUAD( $v_H$ ), PSEQUAD( $E_{\text{cell}}$ ), PKAS(pH). The variable(s) within brackets are those minimized in the residual-squares sum. Here  $v_H$  is the volume of acid or base added.

All computations were performed on the EC 1033 computer at the Computing Centre of the College of Chemical Technology, CS-532 10 Pardubice, Czechoslovakia.

### DISCUSSION

Seven titrations ( $k = 7$ , *cf.* Table 3) of a mixture of perchloric and citric acids with sodium hydroxide were performed. The data were treated with seven different programs but eight computational strategies ( $m = 8$ , *cf.* Table 3). Besides the three common parameters (the protonation constants) the three group parameters (the concentration of citric acid in the titrand,  $L_0$ , of sodium hydroxide in the titrant,  $H_T$ , and the constant  $E^{0'}$ ) were also refined.

Table 2 gives the results of one particular titration analysed by several programs, by use of both external and internal calibration. In part (A), besides the original data ( $v_H, E_{\text{cell}}$ ) and  $-\log h$ , the statistical weight [ $w$ , *cf.* equation (4)], the Bjerrum formation function ( $Z$ ), the calculated ionic strength ( $I$ ) at each point, and the relative concentrations of the species  $HL^{2-}$ ,  $H_2L^-$  and  $H_3L$  are given. The fourth species  $L^{3-}$  is obtained by subtracting the values in Table 2 from 100.

Part (B) compares the influence of the programs on the accuracy and precision of the estimated protonation constants. The accuracy is expressed by the systematic deviation in  $\log K$  related to the "best" literature value for the experimental conditions used.

Table 1. Reproducibility of external calibration of the glass electrode cell by standardization titration of  $HClO_4$  with NaOH and evaluation by programs MAGEC and ESAB; experimental conditions:  $v_0 = 20.0$  ml,  $H_0 = 0.09869M$ ,  $H_T = -1.071M$ ,  $pK_w = 13.78$ ,  $I = 0.1$ , 298 K, cell used G202B-SCE (Radiometer, Copenhagen); standard deviations (in parentheses) refer to corresponding last figures

Titration	1	2	3	4	5	6	7
Part (A): Program MAGEC, all points of titration curve used.							
$v_e$ (ml)	1.823	1.832	1.833	1.834	1.833	1.833	1.831
$E^{0'}$ (mV)	375.4(5)	378.9(2)	379.8(1)	377.6(1)	378.6(1)	377.4(1)	377.4(2)
$S$ (mV/pH)	58.50(9)	58.82(2)	58.63(2)	58.39(2)	58.53(2)	58.55(2)	58.39(3)
Part (B): Program MAGEC, points of acid branch of titration curve used only.							
$v_e$ (ml)	1.818	1.830	1.830	1.832	1.830	1.831	1.828
$E^{0'}$ (mV)	389.4(11)	381.6(4)	381.8(2)	379.4(2)	380.6(1)	379.3(1)	381.3(1)
$S$ (mV/pH)	65.54(55)	60.15(18)	59.64(12)	59.30(9)	59.52(6)	59.54(7)	60.38(7)
$R$ -factor (%)	0.263	0.087	0.057	0.041	0.027	0.033	0.034
Part (C): Program ESAB, points of acid branch of titration curve used only.							
$H_0$ ( $10^{-2}M$ )	9.875(916)	10.013(985)	9.847(925)	9.988(874)	9.756(992)	9.981(890)	9.883(889)
$-H_T$ (M)	1.079(99)	1.088(127)	1.069(105)	1.084(96)	1.058(116)	1.084(121)	1.074(94)
$E^{0'}$ (mV)	378.5(24)	379.5(42)	381.0(29)	378.9(26)	380.2(28)	378.4(22)	379.2(18)
$R$ -factor (%)	0.017	0.068	0.028	0.036	0.023	0.018	0.025

$v_e$  means volume at equivalence point.

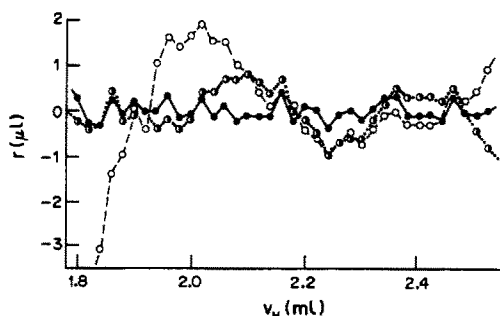


Fig. 2. Response of an option of group parameters to be refined on the degree-of-fit and accuracy of three protonation constants of citric acid. The standard deviation  $s(\log K_i)$  is written in brackets and refers to the last decimal place of  $\log K_i$ .

Circle	$\log K_1$	$\log K_2$	$\log K_3$	$L_0, 10^{-2}M$	$-H_T$	$E^0, mV$	$ \bar{r} , \mu l$	$R, \%$
○	5.607(3)	4.305(3)	2.844(3)	1.517	1.091	378.5	1.47	0.068
●	5.579(9)	4.324(7)	2.927(8)	1.453(5)	1.080(1)	378.5	1.23	0.022
●	5.631(7)	4.332(4)	2.895(4)	1.512(5)	1.092(1)	381.3(2)	0.20	0.009

Table 2. Estimation of the protonation constants of citric acid by various regression programs  
Part (A): Shortened output of the results from the ESAB program.

$\log K_1 = 5.667 \pm 0.010, \log K_2 = 4.361 \pm 0.005, \log K_3 = 2.932 \pm 0.005$  (common parameters)  
 $L_0 = (1.499 \pm 0.007) \times 10^{-2}M, E^0 = 381.5 \pm 0.3$  mV,  $-H_T = 1.089 \pm 0.0013M$  (group parameters)

$i$	$v_H, \mu l$	Residual $\mu l$	$E, mV$	$-\log h$	$w$	$Z$	$I$	HL, %	H <sub>2</sub> L, %	H <sub>3</sub> L, %
1	1800	0.0	237.4	2.436	0.77	2.75	0.095	0.29	24.38	75.33
2	1820	0.1	233.2	2.507	0.81	2.72	0.095	0.38	27.49	72.13
3	1840	-0.3	228.9	2.579	0.84	2.68	0.096	0.51	30.90	68.59
4	1860	0.7	224.1	2.661	0.87	2.64	0.096	0.69	34.95	64.36
5	1880	-0.1	219.6	2.737	0.89	2.60	0.097	0.92	38.92	60.16
6	1900	-0.6	214.9	2.816	0.90	2.55	0.097	1.22	43.19	55.59
7	1920	-0.3	209.9	2.901	0.92	2.49	0.098	1.64	47.76	50.60
8	1940	-0.1	204.8	2.987	0.94	2.44	0.099	2.19	52.33	45.47
9	1960	0.4	199.5	3.076	0.96	2.38	0.100	2.93	56.87	40.20
10	1980	0.2	194.2	3.166	0.98	2.32	0.101	3.87	61.03	35.10
11	2000	0.1	188.7	3.259	1.00	2.25	0.102	5.08	64.81	30.09
12	2020	0.1	183.0	3.355	1.03	2.19	0.103	6.66	68.01	25.29
13	2040	0.0	177.1	3.455	1.05	2.12	0.104	8.68	70.45	20.82
14	2060	0.4	170.9	3.560	1.06	2.05	0.105	11.28	71.93	16.70
15	2080	-0.3	164.9	3.661	1.07	1.99	0.106	14.32	72.26	13.29
16	2100	-0.4	158.7	3.766	1.07	1.92	0.107	18.02	71.45	10.32
17	2120	0.0	152.4	3.872	1.06	1.85	0.109	22.38	69.43	7.85
18	2140	-0.1	146.4	3.974	1.05	1.78	0.111	27.06	66.47	5.95
19	2160	0.2	140.4	4.075	1.03	1.71	0.112	32.18	62.60	4.44
20	2180	0.0	134.7	4.172	1.01	1.63	0.114	37.36	58.21	3.30
21	2200	-0.5	129.2	4.265	1.00	1.56	0.116	42.50	53.46	2.45
22	2220	-0.1	123.5	4.361	1.00	1.49	0.118	47.82	48.18	1.77
23	2240	0.1	117.9	4.456	1.00	1.42	0.119	52.85	42.82	1.26
24	2260	-0.1	112.4	4.549	1.00	1.35	0.121	57.41	37.55	0.89
25	2280	-0.2	106.8	4.643	1.01	1.28	0.123	61.51	32.35	0.62
26	2300	0.2	101.0	4.741	1.02	1.20	0.125	65.00	27.28	0.42
27	2320	0.2	95.2	4.839	1.03	1.13	0.128	67.58	22.63	0.28
28	2340	0.3	89.3	4.939	1.04	1.06	0.130	69.16	18.41	0.18
29	2360	0.4	83.3	5.041	1.04	0.98	0.132	69.63	14.67	0.11
30	2380	-0.2	77.5	5.139	1.05	0.91	0.134	68.99	11.60	0.07
31	2400	0.3	71.4	5.242	1.04	0.84	0.137	67.17	8.91	0.04
32	2420	0.4	65.4	5.343	1.04	0.77	0.139	64.33	6.75	0.03
33	2440	-0.2	59.6	5.441	1.05	0.70	0.142	60.72	5.09	0.02
34	2460	-0.2	53.6	5.543	1.05	0.62	0.145	56.26	3.73	0.01
35	2480	-0.3	47.5	5.646	1.07	0.55	0.147	51.18	2.68	0.01
36	2500	-0.2	41.1	5.754	1.10	0.48	0.150	45.51	1.86	0.00
37	2520	0.1	34.2	5.870	1.15	0.40	0.153	39.31	1.23	0.00

Degree-of-fit test:  $|\bar{r}| = 0.23 \mu l, s(r) = 0.28 \mu l, R = 0.013\%$ .

Table 2 continued overleaf

Table 2. (contd.)

Part (B): External calibration of glass electrode cell and MAGEC evaluation of group parameters:  $S = 58.40$  mV/pH,  $E^0 = 379.5$  mV,  $L_0 = 1.501 \times 10^{-2} M$ ,  $-H_T = 1.089 M$ ; systematic error in  $\log K_i$  is  $e_i = 10^i \epsilon(\log K_i)$ ,  $i = 1, 2, 3$ ; standard deviations (in parentheses) refer to the corresponding last figures; values from literature:  $\log K_1 = 5.65$ ,  $\log K_2 = 4.34$ ,  $\log K_3 = 2.87$  [for  $I = 0.1$  (NaClO<sub>3</sub>), 298.0 K].

Program	Group parameters	$e_3$	$e_2$	$e_1$	$E^0$ , mV	$L_0$ , $10^{-2} M$	$-H_T$ , M	$s(r)$	$ \bar{r} $	$R$ , %
ACBA( $v_H$ )	—	112(1)	82(1)	105(1)	379.5	1.501	1.089	0.5 $\mu$ l	0.4 $\mu$ l	0.023
	$L_0$	102(2)	54(4)	52(8)	379.5	1.480(3)	1.089	0.4 $\mu$ l	0.3 $\mu$ l	0.021
	$H_T$	65(6)	40(5)	51(6)	379.5	1.501	1.093(1)	0.4 $\mu$ l	0.3 $\mu$ l	0.018
	$L_0, H_T$	75(4)	38(3)	38(5)	379.5	1.489(2)	1.092(1)	0.3 $\mu$ l	0.2 $\mu$ l	0.013
	$E^0, S = 59.31$ mV/pH	0	0	0	377.8(3)	1.501	1.089	2.0 $\mu$ l	1.5 $\mu$ l	0.091
	$L_0, H_T, E^0$	75(5)	38(3)	37(7)	379.4(3)	1.487(6)	1.091(5)	0.3 $\mu$ l	0.2 $\mu$ l	0.013
MINIQUAD(L, H)	—	113(2)	80(2)	108(2)	379.5	1.501	1.089	1.8E-5M	1.0E-5M	0.088
MAGEC( $v, E_{cell}$ )	—	92(X)	91(X)	53(X)	379.5	1.501	1.089	not calculated	not calculated	—
MIQUV( $E_{cell}$ )	—	113(2)	81(1)	108(1)	379.5	1.501	1.089	1.88 mV	1.21 mV	1.20
PSEQUAD( $v_H$ )	—	112(1)	82(1)	105(1)	379.5	1.501	1.089	0.5 $\mu$ l	0.5 $\mu$ l	—
PSEQUAD( $E_{cell}$ )	—	112(1)	82(1)	105(1)	379.5	1.501	1.089	0.1 mV	0.1 mV	—
PKAS(pH)	—	110(3)	81(1)	105(4)	379.5	1.501	1.089	0.002 pH	0.001 pH	0.052

Part (C): Internal calibration of the glass electrode cell using ESAB:  $S = 59.159$  mV/pH,  $E^0 = 378.5$  mV,  $L_0 = 1.517 \times 10^{-2} M$ ,  $-H_T = 1.091 M$ ; (X) means that standard deviation could not be estimated; modified version of MINIQUAD program for estimation of  $E^0$  was used.

Programs	Group parameters	$e_3$	$e_2$	$e_1$	$E^0$ , mV	$L_0$ , $10^{-2} M$	$-H_T$ , M	$s(r)$	$\bar{r}$	$R$ , %
ESAB( $v_H$ )	—	23(7)	-20(7)	-15(8)	378.5	1.517	1.091	1.9 $\mu$ l	1.2 $\mu$ l	0.088
	$E^0$	65(3)	35(2)	48(2)	382.1(1)	1.517	1.091	0.3 $\mu$ l	0.2 $\mu$ l	0.015
	$L_0$	43(7)	-66(13)	109(27)	378.5	1.480(0)	1.091	1.6 $\mu$ l	1.0 $\mu$ l	0.076
	$H_T$	138(18)	123(16)	169(21)	378.5	1.517	1.076(2)	1.3 $\mu$ l	1.1 $\mu$ l	0.060
	$E^0, L_0$	57(4)	21(5)	23(9)	381.9(1)	1.508(3)	1.091	0.3 $\mu$ l	0.2 $\mu$ l	0.013
	$E^0, L_0, H_T$	63(5)	21(5)	17(10)	381.5(3)	1.499(7)	1.089(1)	0.3 $\mu$ l	0.2 $\mu$ l	0.013
	—	188(4)	23(3)	-11(2)	378.5	1.517	1.091	2.8E-5M	1.8E-5M	0.135
MINIQUAD(L, H)	$E^0$	66(2)	34(1)	51(1)	372.1(X)	1.517	1.091	1.3E-5M	6.9E-6M	0.062

The precision is expressed by the standard deviation (given in parentheses after each value, and referred to the last digit of the value). The fit obtained is expressed by the mean residual,  $|\bar{r}|$ , the standard deviation  $[s(r)]$ , and the Hamilton  $R$ -factor (in %).

The lowest values of the systematic error were obtained when the program ESAB was used in

combination with the internal calibration of the glass electrode [part (C) in Table 2].

Refinement of the group parameters  $E^0$ ,  $L_0$  and  $H_T$  leads to the lowest systematic error in the protonation constants, as shown in Fig. 2. The most important group parameter seems to be the constant  $E^0$ , as its refinement leads to  $R = 0.015\%$ , cf. Table 2(C).

Table 3. Effect of choice of group parameters to be refined, and reproducibility, on accuracy and precision of the protonation constants:  $\log K_1$ ,  $\log K_2$ ,  $\log K_3$ : the refined group parameters are, for various M: (1) none, (2)  $L_0$ , (3)  $H_T$ , (4)  $L_0, H_T$ , (5)  $E^0$ , (6)  $H_T, E^0$ , (7)  $L_0, E^0$ , (8)  $L_0, H_T, E^0$ ; in brackets are the standard deviations, referring to the last figures: initial guess of group parameters:  $L_0^{(0)} = 0.01517M$ ,  $H_T^{(0)} = 1.091M$ ,  $E^{0(0)} = 378.5 \text{ mV}$ ,  $S^{(0)} = 59.159 \text{ mV/pH}$ ,  $pK_w^{(0)} = 13.78$ , at  $I = 0.1$  (NaClO<sub>4</sub>) and 298 K

	$k = 1$	Repeated titrations						Average titration	Weighted mean	
		2	3	4	5	6	7			
$\log K_1$	$m = 1$	2.905(0)	2.675(8)	2.836(3)	2.844(3)	2.855(3)	2.847(4)	2.974(4)	2.847(3)	2.889(21)
	2	2.906(1)	2.657(13)	2.820(6)	2.826(5)	2.835(6)	2.827(7)	2.783(8)	2.825(6)	2.895(36)
	3	2.911(3)	3.096(28)	2.981(18)	2.950(19)	2.995(20)	3.009(18)	2.965(15)	2.970(15)	2.921(27)
	4	2.911(3)	2.963(17)	2.946(8)	2.927(8)	2.955(10)	2.961(8)	2.929(12)	2.930(7)	2.924(10)
	5	2.906(2)	2.962(4)	2.916(3)	2.912(2)	2.939(3)	2.935(3)	2.874(6)	2.914(1)	2.912(8)
	6	2.911(4)	2.847(7)	2.915(5)	2.897(4)	2.919(5)	2.927(5)	2.908(11)	2.913(3)	2.907(7)
	7	2.910(3)	2.853(5)	2.914(4)	2.903(3)	2.928(4)	2.927(4)	2.906(9)	2.913(3)	2.909(7)
	8	2.911(4)	2.848(7)	2.917(6)	2.899(4)	2.916(6)	2.932(5)	2.906(11)	2.913(3)	2.907(8)
$\log K_2$	$m = 1$	4.323(0)	4.233(7)	4.305(3)	4.305(3)	4.321(3)	4.320(4)	4.233(3)	4.302(3)	4.319(7)
	2	4.326(3)	4.156(22)	4.267(13)	4.265(10)	4.274(12)	4.274(13)	4.209(16)	4.249(13)	4.309(25)
	3	4.329(3)	4.599(25)	4.433(16)	4.399(17)	4.443(18)	4.463(16)	4.381(14)	4.410(13)	4.346(38)
	4	4.330(3)	4.330(17)	4.343(8)	4.324(7)	4.345(10)	4.354(8)	4.303(14)	4.320(8)	4.333(4)
	5	4.324(1)	4.342(2)	4.354(2)	4.347(2)	4.373(2)	4.375(2)	4.281(4)	4.342(1)	4.320(16)
	6	4.330(3)	4.327(6)	4.353(5)	4.333(3)	4.353(5)	4.367(5)	4.314(10)	4.342(3)	4.339(5)
	7	4.331(4)	4.328(7)	4.352(5)	4.332(4)	4.355(5)	4.361(5)	4.333(14)	4.341(4)	4.342(5)
	8	4.331(4)	4.327(7)	4.352(5)	4.331(4)	4.355(5)	4.361(5)	4.332(15)	4.341(4)	4.342(5)
$\log K_3$	$m = 1$	5.617(0)	5.555(9)	5.605(4)	5.607(3)	5.629(4)	5.635(4)	5.502(4)	5.599(3)	5.611(12)
	2	5.623(5)	5.399(45)	5.529(26)	5.525(21)	5.534(25)	5.541(27)	5.454(33)	5.497(26)	5.605(38)
	3	5.625(4)	6.018(33)	5.769(20)	5.729(22)	5.780(23)	5.819(21)	5.697(18)	5.737(16)	5.650(54)
	4	5.627(6)	5.535(32)	5.599(14)	5.579(12)	5.599(17)	5.615(13)	5.551(24)	5.571(14)	5.610(13)
	5	5.619(1)	5.682(3)	5.661(2)	5.656(2)	5.689(3)	5.698(2)	5.558(5)	5.647(1)	5.645(18)
	6	5.625(4)	5.663(8)	5.660(6)	5.636(4)	5.662(6)	5.687(7)	5.604(14)	5.646(4)	5.645(8)
	7	5.630(7)	5.657(12)	5.657(9)	5.627(6)	5.656(10)	5.673(9)	5.653(25)	5.644(7)	5.644(7)
	8	5.629(8)	5.661(13)	5.655(11)	5.631(7)	5.669(10)	5.667(10)	5.651(29)	5.643(9)	5.650(3)
$H_T$ (M)	$m = 1$	—	—	—	—	—	—	—	—	—
	2	—	—	—	—	—	—	—	—	—
	3	1.090(0)	1.055(2)	1.078(2)	1.081(2)	1.878(2)	1.086(2)	1.075(1)	1.080(1)	1.080(6)
	4	1.090(0)	1.058(1)	1.078(1)	1.080(1)	1.078(1)	1.077(1)	1.076(1)	1.080(1)	1.077(5)
	5	—	—	—	—	—	—	—	—	—
	6	1.090(0)	1.093(1)	1.091(1)	1.093(0)	1.094(1)	1.092(1)	1.086(1)	1.091(0)	1.091(1)
	7	—	—	—	—	—	—	—	—	—
	8	1.091(1)	1.092(1)	1.090(1)	1.092(1)	1.095(1)	1.089(1)	1.091(3)	1.091(1)	1.091(1)
$E^0$ (mV)	$m = 1$	—	—	—	—	—	—	—	—	—
	2	—	—	—	—	—	—	—	—	—
	3	—	—	—	—	—	—	—	—	—
	4	—	—	—	—	—	—	—	—	—
	5	378.6(1)	385.7(1)	381.7(1)	381.3(1)	381.9(1)	382.1(1)	381.7(2)	381.2(1)	381.9(12)
	6	378.5(1)	385.8(1)	381.7(1)	381.5(1)	382.3(1)	382.2(1)	381.1(3)	381.2(1)	382.0(12)
	7	378.6(1)	385.5(2)	381.7(1)	381.1(1)	381.7(1)	381.9(1)	382.2(2)	381.1(1)	381.3(9)
	8	378.6(2)	385.7(3)	381.5(3)	381.3(2)	382.5(3)	381.5(3)	382.2(6)	381.1(2)	381.3(12)
$L_0$ ( $10^{-2}M$ )	$m = 1$	—	—	—	—	—	—	—	—	—
	2	1.519(2)	1.456(17)	1.485(10)	1.485(8)	1.480(10)	1.480(10)	1.498(13)	1.475(10)	—
	3	—	—	—	—	—	—	—	—	—
	4	1.518(0)	1.348(11)	1.449(5)	1.453(5)	1.443(6)	1.440(5)	1.461(9)	1.453(5)	—
	5	—	—	—	—	—	—	—	—	—
	6	—	—	—	—	—	—	—	—	—
	7	1.521(2)	1.508(4)	1.515(3)	1.507(2)	1.505(3)	1.508(3)	1.551(9)	1.516(3)	—
	8	1.520(5)	1.515(8)	1.512(7)	1.512(5)	1.524(7)	1.499(7)	1.550(18)	1.515(5)	—
$R$ (%)	$m = 1$	0.009	0.192	0.080	0.068	0.084	0.088	0.087	0.067	—
	2	0.009	0.166	0.071	0.057	0.071	0.076	0.083	0.055	—
	3	0.009	0.132	0.055	0.054	0.064	0.060	0.049	0.043	—
	4	0.009	0.057	0.024	0.022	0.030	0.024	0.034	0.018	—
	5	0.009	0.018	0.013	0.012	0.017	0.014	0.031	0.007	—
	6	0.009	0.017	0.013	0.010	0.013	0.014	0.026	0.007	—
	7	0.009	0.016	0.013	0.010	0.015	0.013	0.026	0.007	—
	8	0.009	0.016	0.013	0.009	0.013	0.013	0.025	0.007	—

continued overleaf

Table 3. (*contd.*)

	$k = 1$	Repeated titrations						Average titration	Weighted mean
		2	3	4	5	6	7		
$m = 1$	0.202	4.168	1.725	1.469	1.819	1.913	1.877	1.448	
2	0.199	3.604	1.530	1.229	1.541	1.650	1.798	1.192	
3	0.191	2.861	1.202	1.169	1.384	1.297	1.057	0.932	
$s(r)$	0.190	1.240	0.524	0.485	0.660	0.513	0.741	0.391	
$(\mu)$	0.199	0.394	0.285	0.262	0.369	0.319	0.664	0.150	
6	0.191	0.358	0.285	0.173	0.282	0.305	0.564	0.149	
7	0.190	0.363	0.284	0.209	0.315	0.287	0.539	0.149	
8	0.189	0.357	0.283	0.203	0.277	0.279	0.539	0.149	
$m = 1$	0.153	2.600	1.092	0.962	1.203	1.182	1.244	0.891	
2	0.147	2.389	1.053	0.830	1.079	1.046	1.232	0.778	
3	0.134	2.273	1.016	0.206	1.140	1.074	0.862	0.771	
$ \bar{r} $	0.133	1.024	0.445	0.425	0.556	0.433	0.528	0.338	
$(\mu)$	0.152	0.331	0.218	0.204	0.310	0.253	0.518	0.123	
5	0.133	0.293	0.218	0.173	0.218	0.250	0.385	0.124	
7	0.136	0.304	0.218	0.157	0.261	0.232	0.395	0.123	
8	0.134	0.295	0.218	0.163	0.205	0.227	0.393	0.123	
$m = 1$	0.202	4.168	1.725	1.469	1.819	1.913	1.877	1.448	
2	0.199	3.604	1.530	1.229	1.541	1.650	1.798	1.192	
3	0.191	2.861	1.202	1.169	1.384	1.297	1.057	0.932	
$s(r)$	0.190	1.240	0.524	0.485	0.660	0.513	0.741	0.391	
$(\mu)$	0.199	0.394	0.285	0.262	0.369	0.319	0.664	0.150	
6	0.191	0.358	0.285	0.173	0.282	0.305	0.564	0.149	
7	0.190	0.363	0.284	0.209	0.315	0.287	0.539	0.149	
8	0.189	0.357	0.283	0.203	0.277	0.279	0.539	0.149	
$m = 1$	0.153	2.600	1.092	0.962	1.203	1.182	1.244	0.891	
2	0.147	2.389	1.053	0.830	1.079	1.046	1.232	0.778	
3	0.134	2.273	1.016	0.206	1.140	1.074	0.862	0.771	
$ \bar{r} $	0.133	1.024	0.445	0.425	0.556	0.433	0.528	0.338	
$(\mu)$	0.152	0.331	0.218	0.204	0.310	0.253	0.518	0.123	
5	0.133	0.293	0.218	0.173	0.218	0.250	0.385	0.124	
7	0.136	0.304	0.218	0.157	0.261	0.232	0.395	0.123	
8	0.134	0.295	0.218	0.163	0.205	0.227	0.393	0.123	

When  $L_0$  and  $H_T$  are also refined,  $R$  decreases to 0.013%.

When a modified version of MINQUAD is used that allows  $E^0$  to be refined, more accurate estimates of the protonation constants are obtained as well as an improved fit [*cf.* Table 2(C)].

When  $E^0$ ,  $L_0$ ,  $H_T$  and  $S$  are estimated from an independent determination the log  $K$  values are still loaded by some systematic error, *cf.* Table 2(C), uppermost row for ESAB. Table 3 gives the reproducibility of log  $K$  values for various choices of group parameters.

$E^0$  has the greatest influence on the accuracy, and hence should always be refined. As further group parameters are refined the fit is improved, as demonstrated in Table 3.

The influence of different factors on the protonation constants is obtained by analysis of the matrix of these constants (*cf.* Table 3). When this matrix for various computational strategies and repeated titrations is analysed, the influence of a given choice of group parameters and of the reproducibility on log  $K$  may be tested.

The Fisher-Snedecor test in analysis of variance (ANOVA) is applied to test the variance  $\sigma_{\text{par}}^2$  arising from different sets of refined group parameters in comparison with the variance,  $\sigma_{\text{tit}}^2$ , from the reproducibility. The test is performed by comparing the

experimental value  $F_{\text{exp}}$  with the critical value  $F_{\text{crit}}[\alpha, m-1, (m-1)(k-1)]$  where  $\alpha$  is the significance level and  $F_{\text{exp}}$  is the ratio of the variance tested ( $\sigma^2$ ) to the residual variance  $\sigma_{\text{res}}^2$ , and when  $F_{\text{exp}}$  is larger than  $F_{\text{crit}}$ , the variance  $\sigma^2$  is significantly different from that of the residuals.

Table 4 shows the results of an ANOVA test. It shows that while the variance from the reproducibility is not significant, but the variances from the algorithm used or the choice of group parameters are significant, the latter being the more important of the two.

The parameters can be divided into two groups: well-conditioned and ill-conditioned. Ill-conditioned parameters have little influence on the residual-squares sum function  $U$ , which makes their determination rather uncertain. This is illustrated in Fig. 3 where  $(1-U)$  is plotted against each common parameter and various ill-conditioned group parameters. As seen in Fig. 3, none of the ill-conditioned parameters  $E^0$ ,  $L_0$  and  $H_T$  leads to a pronounced maximum in  $(1-U)$ , so their determination is uncertain, and might sometimes lead to false estimates of the common parameters. This is the reason why such parameters are sometimes called dangerous parameters. On the other hand, well-conditioned parameters have great influence on the hyperparaboloid ( $U$ -surface), as shown in Fig. 4, where a



Table 4. Analysis of variance in the protonation constants of citric acid for: (i) influence of algorithm used in comparison with reproducibility of titration for (a) external calibration using MAGEC, (b) internal calibration using ESAB; (ii) influence of group parameters compared to reproducibility in titration: both matrices have the same size  $7 \times 8$  ( $= k \times m$ , cf. Table 3); the values for  $F_{crit}$  are  $F_{crit}(0.05, 6, 36) = 2.68$ ,  $F_{crit}(0.05, 6, 42) = 2.25$ ,  $F_{crit}(0.05, 7, 42) = 2.17$

		(i) Influence of algorithm used and reproducibility, on $\log K_i$ , $i = 1, 2, 3$			
		Algorithm used		Reproducibility	
$\log K_1$	(a)	$F_{exp} = 5.37$	$F_{crit} = 2.68$	$F_{exp} = 0.41$	$F_{crit} = 2.68$
	(b)	2.50		4.45	
$\log K_2$	(a)	2.85		0.58	
	(b)	4.05		1.50	
$\log K_3$	(a)	6.16		2.18	
	(b)	1.11		6.20	

		(ii) Influence of group parameters refined and reproducibility, on $\log K_i$			
		Reproducibility		Group parameters	
$\log K_1$		$F_{exp} = 12.81$	$F_{crit} = 2.17$	$F_{exp} = 1.88$	$F_{crit} = 2.25$
$\log K_2$		10.16		1.41	
$\log K_3$		8.80		2.03	

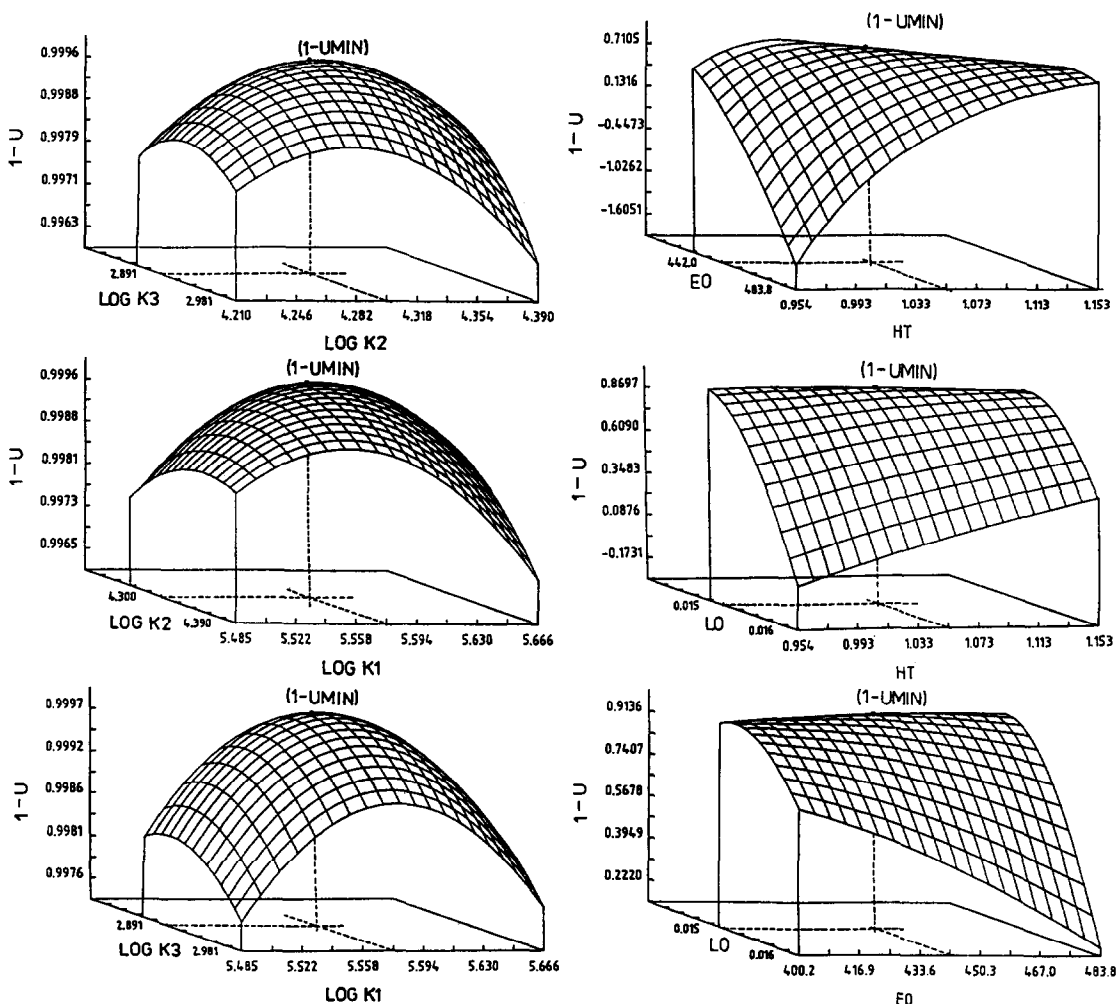


Fig. 3. Three-dimensional representation of the  $(1 - U)$  surface for the well-conditioned parameters (left half of figure) and ill-conditioned parameters (right half) indicates which parameters are rather uncertainly estimated by the regression program.

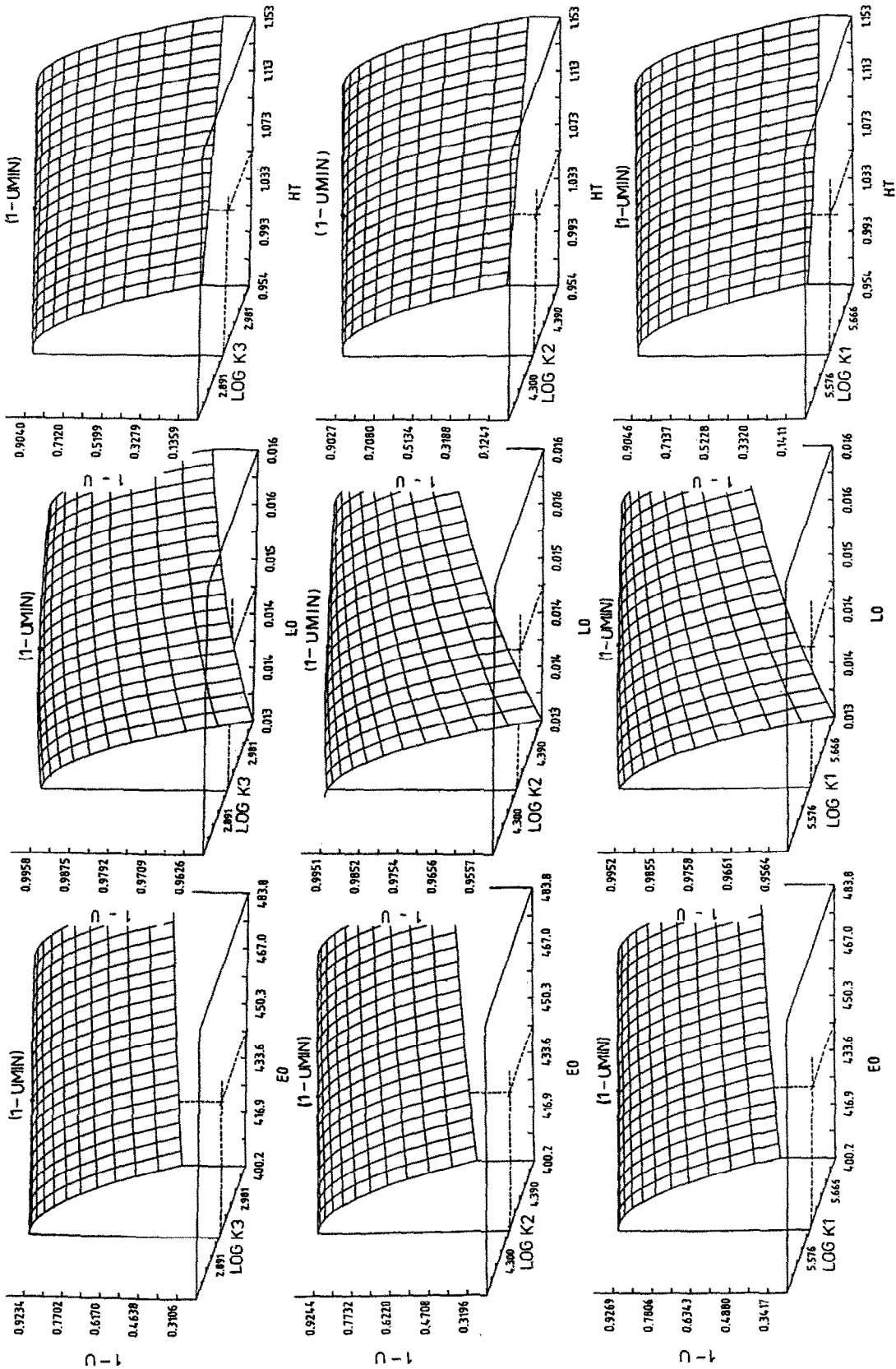


Fig. 4. The minimum of  $U$  for 6 parameters [ $\log K_i$ ,  $i = 1, 2, 3$ ],  $L_0$ ,  $H_T$ ,  $E^{(0)}$ ] may be represented by a pit in the hyperparaboloid surface in  $(6 + 1)$ -dimensional space. Three-dimensional representation of the  $(1 - U)$  surface is drawn for the ill-conditioned parameters where determination leads to rather uncertain estimates.

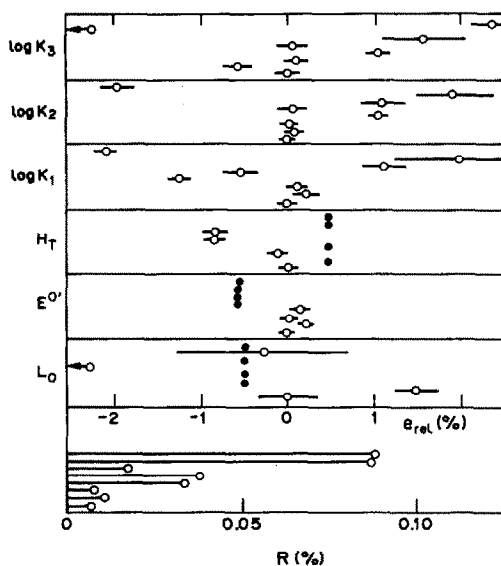


Fig. 5. Influence of group parameters on the relative systematic error defined by  $e_{rel} = e(\log K)/\log K$  [cf. equation (7)]. In each part the uppermost points refer to runs 1, 2, down to 8. Parameters kept constant are marked (●). The circles (○) express the accuracy, and the linear segment the precision of each parameter. Run 1: no group parameters refined. Run 2:  $L_0$  refined. Run 3:  $H_T$  refined. Run 4:  $L_0$  and  $H_T$  refined. Run 5:  $E^{0'}$  refined. Run 6:  $H_T$  and  $E^{0'}$  refined. Run 7:  $L_0$  and  $E^{0'}$  refined. Run 8:  $L_0$ ,  $H_T$  and  $E^{0'}$  refined.

good maximum is obtained for the three protonation constants, whereas various group parameters are ill-conditioned in relation to each other.

Various sets of synthetic data were constructed by using random errors generated so that they should have a normal distribution, and different values were assumed for the instrumental error,  $s_{inst}(E_{cell}) = 0.04, 0.28, 2.80$  mV, etc. Refinement of these simulated data gave residuals which did not show any systematic trends. Figure 5 shows the influence of various group parameters on the log  $K$  values obtained with  $s_{inst}(E_{cell}) = 0.04$  mV. Group parameters, which were not refined, were kept constant at values about 0.5% from the true ones.

In the first runs there was refinement of one or more of the group parameters, and the common parameters then always had a systematic error of 1–2%. In the sixth and seventh runs two group parameters were refined and the systematic error decreased to about 0.1%. In the eighth run all three group parameters were refined and the systematic error in log  $K_i$  was practically zero. The goodness-of-fit, as indicated by the Hamilton  $R$ -factor, decreased each time and became smallest, cf. Fig. 5, for run 8.

## CONCLUSIONS

Three kinds of errors in determination of protonation constants have been investigated: error from the minimization strategy, the random error, and error from group parameters. Of these the group parameters have the greatest influence on the systematic errors in log  $K_i$ . By variation of one or two etc. of the parameters such as  $E^{0'}$ ,  $L_0$  and  $H_T$ , the systematic errors in the log  $K$  values can be minimized or practically disappear. Of the group parameters studied,  $E^{0'}$  has the greatest influence and an attempt should always be made to refine this parameter together with the formation constants, in spite of the fact that it might be ill-conditioned and therefore make the computational strategy (i.e., choice of program) important.

Of the programs tested, ESAB and ACBA are the most powerful, because they permit refinement of the group parameters. A very interesting program for the same purpose is SUPERQUAD,<sup>7</sup> which we intended to include in this comparison, but could not manage because the program was never received.

*Acknowledgements*—This paper is part of a program supported in part by the Swedish and Czech Academies of Sciences (E.H.). Dipl.-Ing. M. Javůrek made the computer drawn Figs 3 and 4.

## REFERENCES

1. F. R. Hartley, C. Burgess and R. M. Alcock, *Solution Equilibria*, Horwood, Chichester, 1980.
2. D. J. Leggett (ed.), *Computational Methods for the Determination of Formation Constants*, Plenum Press, New York 1985. (a) pp. 99–157. (b) pp. 291–353.
3. M. Meloun, J. Havel and E. Högföldt, *Computation of Solution Equilibria*, Horwood, Chichester, 1988.
4. L. G. Sillén and B. Warnqvist, *Arkiv Kemi*, 1968, **31**, 315.
5. G. Arena, E. Rizzarelli, S. Sammartano and C. Rigano, *Talanta*, 1979, **26**, 1.
6. C. Rigano, M. Grasso and S. Sammartano, *Ann. Chim. Rome*, 1984, **74**, 537.
7. P. Gans, A. Sabatini and A. Vacca, *J. Chem. Soc. Dalton Trans.*, 1985, 1195.
8. S. Kotrlý and L. Šůcha, *Handbook of Chemical Equilibria in Analytical Chemistry*, Horwood, Chichester, 1985.
9. E. P. Serjeant and B. Dempsey, *Ionisation Constants of Organic Acids in Aqueous Solution*, Pergamon Press, Oxford, 1979.
10. A. Sabatini, A. Vacca and P. Gans, *Talanta*, 1974, **21**, 53.
11. A. Braibanti, F. Dallavalli, G. Mori and B. Veroni, *ibid.*, 1982, **29**, 725.
12. P. M. May, D. R. Williams, P. W. Linder and R. G. Torrington, *ibid.*, 1982, **29**, 249.
13. H. M. Irving, M. G. Miles and L. D. Pettit, *Anal. Chim. Acta*, 1967, **38**, 475.

## ELECTROCHEMICAL STUDY OF CARMINOMYCIN AT SOLID ELECTRODES

F. MEBSOUT, J.-C. VIRE and G. J. PATRIARCHE

Institut de Pharmacie, Université Libre de Bruxelles, Campus Plaine, C.P. 205/6, Boulevard du Triomphe,  
B-1050 Bruxelles, Belgium

G. D. CHRISTIAN

Department of Chemistry, University of Washington, Seattle, WA 98195-9550, U.S.A.

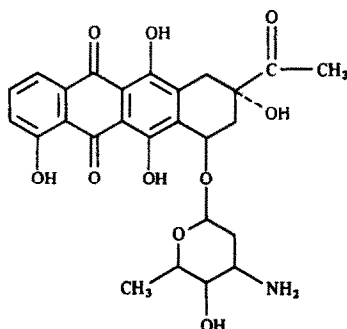
(Received 8 June 1988. Accepted 12 August 1988)

**Summary**—The electrochemical behaviour of carminomycin at carbon-paste, glassy-carbon and composite carbon-polymer electrodes has been compared. Three electroactive sites on the molecule have been identified. Two sites are involved in the oxidation processes, the first corresponding to the hydroquinone structure in the C-6/C-11 positions, the second attributed to the C-4 phenolic function. Applying a negative-going scan allows reduction of the quinone moiety in the C-5/C-12 positions. Both the quinone and hydroquinone functions exhibit quasi-reversible electrochemical reactions in acidic medium, becoming irreversible in alkaline solution. Adsorption phenomena accompany both the oxidation and reduction processes, primarily in neutral and alkaline media. The adsorption can be decreased by using the composite electrode, which is less sensitive to surface phenomena. This working electrode is proposed as the most suitable for the determination of carminomycin at pH 1. A linear calibration plot can be obtained over the range  $1 \times 10^{-6}$ – $1 \times 10^{-4}M$ , with a limit of detection of  $6 \times 10^{-8}M$ .

Carminomycin<sup>1-3</sup> belongs to the anthracycline family of compounds, which are used in the chemotherapeutic treatment of cancer, alone or associated with other cytostatic agents.<sup>4,5</sup> This antitumour activity is due to the presence of the quinone function in their structures.<sup>1,2</sup> The quinone function also gives rise to electrochemical activity, which has been the subject of several investigations.<sup>6-9</sup>

Pursuant to the voltammetric study of these anthracycline derivatives,<sup>10-13</sup> the aim of this work was to compare the redox behaviour of carminomycin at the carbon-paste, glassy-carbon, and carbon-polymer electrodes. Each of these electrodes offers unique electrochemical characteristics due to differences in the electrode material.<sup>13,14</sup> These characteristics have been exploited in this study for both mechanistic and quantitative studies.

The structure of carminomycin is represented below:



### EXPERIMENTAL

#### Apparatus

The electrochemical instrumentation used has already been described.<sup>13</sup> The working electrodes were a Metrohm EA 267 carbon-paste electrode, a Metrohm glassy-carbon electrode, and a composite electrode prepared in our laboratory by mixing poly(vinyl acetate) with 30% by weight of activated carbon.<sup>14</sup> Potentials are referred to the saturated calomel electrode.

#### Reagents

Carminomycin, kindly provided by Bristol Meyers (Brussels), was used without further purification. Solutions for voltammetric study were prepared as previously described.<sup>12</sup>

### RESULTS AND DISCUSSION

#### Oxidation

The electrochemical oxidation of carminomycin was studied in the pH range 1–12, with aqueous solutions containing  $1 \times 10^{-4}M$  depolarizer. A comparison of the results obtained by using the three electrodes allowed more ready identification of the types of recorded currents.

*Influence of pH for the carbon-paste electrode.* Differential pulse voltammetry with linear potential scan gave two oxidation peaks, A and B (Fig. 1a). The variation of peak potential with pH is shown in Fig. 2a. The first peak, A, remains well defined over the entire pH range. Its potential changes by 60 mV/pH up to pH 6 and by 75 mV/pH in alkaline medium. This peak, corresponding to a two-electron

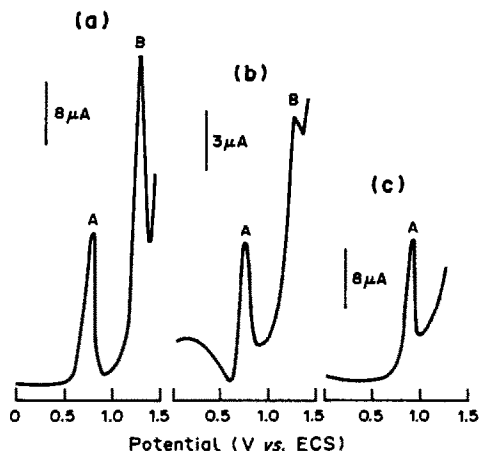


Fig. 1. Differential pulse voltammetry of carminomycin with different electrodes. Carminomycin  $1 \times 10^{-4} M$ ; pH 1; methanol 20% v/v. Working electrode: (a) carbon paste; (b) glassy carbon; (c) carbon-polymer.

transfer, as shown by controlled potential coulometric measurements, is due to oxidation of the hydroquinone function to the corresponding quinone. The values of  $E_{pa} - E_{pa}/2$  are between 40 and 50 mV up to pH 9, which indicates a quasi-reversible process in acidic and weakly alkaline medium. Such behaviour has been observed for the oxidation of marcellomycin,<sup>13</sup> and confirmed by a cyclic voltammetric study of carminomycin (see below).

The second peak, B, can be observed up to pH 8 when the carbon-paste electrode is used. The height of the peak decreases rapidly above pH 8, and the peak disappears between pH 9 and 10. This peak is very close to the solvent oxidation potential at all pH values, making quantitative measurements difficult. Its potential decreases by 44 mV/pH. Peak B results from the oxidation of the phenolic group in the C-4 position. This is in agreement with results for the oxidation of marcellomycin.<sup>13</sup> It is, however, impossible in the present case to reach a sufficiently alkaline pH to produce the corresponding phenolate

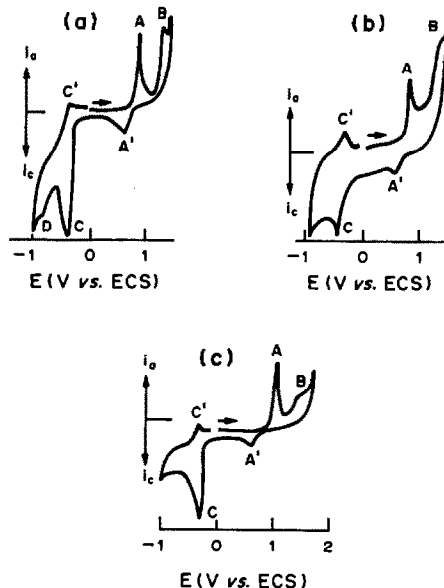


Fig. 3. Cyclic voltammetry in acid solution. Carminomycin  $2 \times 10^{-4} M$ ; pH 1; methanol 20% v/v; scan-rate 20 mV/sec. Working electrode: (a) carbon paste; (b) glassy carbon; (c) carbon-polymer.

anion.<sup>15,16</sup> This electrochemical process remains totally irreversible in acidic and alkaline media, as shown by the absence of a reduction peak in the cyclic voltamperograms (Figs. 3a and 4a). However, the reversibility of the hydroquinone/quinone couple in acidic medium is evident from cyclic voltammetry (A and A', Fig. 3a), as is its irreversibility in alkaline medium (peak A, Fig. 4a).

Several factors indicate the presence of both diffusion and adsorption currents, which are resolved. These factors are the abnormal increase in the peak height when the pH is increased, the non-linearity of the relation between peak height and the square root of the scan-rate in cyclic voltammetry, and the large slope of the mV/pH plot. Further confirmation is given by the shift of the peak poten-

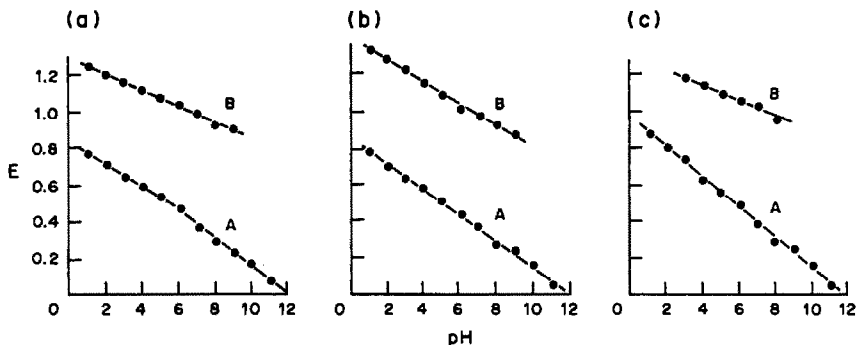


Fig. 2. Dependence of the DPV peak potential on pH. Carminomycin  $1 \times 10^{-4} M$ ; methanol 20% v/v; working electrode: (a) carbon paste; (b) glassy carbon; (c) carbon-polymer. A, oxidation of the C-6/C-11 hydroquinone function; B, oxidation of the C-4 phenolic function.

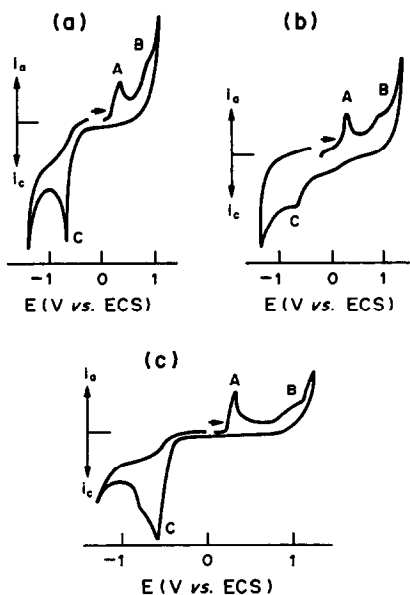


Fig. 4. Cyclic voltammetry in alkaline solution. Carminomycin  $2 \times 10^{-4} M$ ; pH 8, methanol 20% v/v; scan-rate 20 mV/sec. Working electrode: (a) carbon paste; (b) glassy carbon; (c) carbon-polymer.

tial to less positive values when the concentration of the depolarizer is increased.

**Influence of pH for the glassy-carbon electrode.** The electrochemical characteristics for the oxidation of carminomycin at the glassy-carbon electrode are very similar to those observed with the carbon-paste electrode (Fig. 1b). The potential of peak A is shifted by 70 mV/pH (Fig. 2b), and the hydroquinone/quinone couple remains partially reversible in acidic and neutral media, as shown by the  $E_p - E_p/2$  values of 30–40 mV and by the cyclic voltamperograms (Fig. 3b). The irreversibility of the electrochemical reaction in alkaline medium is confirmed (Fig. 4b).

Owing to the more rapid kinetics of solvent oxidation at the glassy-carbon electrode, peak B appears only as a shoulder on the solvent current. The shoulder is better defined in neutral medium, and disappears above pH 9, as with the carbon-paste electrode. Its potential is also shifted by 58 mV/pH unit (Fig. 2b). According to the criteria noted for the carbon-paste electrode, the glassy-carbon electrode also exhibits adsorption phenomena in neutral and weakly alkaline medium, but to a lesser extent.

**Influence of pH for the composite carbon-polymer electrode.** This electrode is characterized by a wide potential range and low residual current.<sup>14</sup> Despite these favourable properties, peak B resulting from oxidation of the phenolic function overlaps with the solvent current in very acidic media, but can be detected above pH 3 (Fig. 1c). Its potential is shifted by 42 mV/pH up to pH 8, and the peak disappears at higher pH (Fig. 2c). The hydroquinone/quinone couple always gives rise to peak A, which is quasi-reversible in acidic medium (Fig. 3c). Its potential is shifted by 80 mV/pH unit (Fig. 2c) until the solution is alkaline, and then becomes irreversible (Fig. 4c). Though the composite electrode offers a wider positive potential range than the glassy-carbon electrode, this is not a real advantage because the phenolic oxidation (peak B) is more difficult with this electrode (by 0.1 V). However, this electrode does offer the advantage of lower adsorption currents. Peak A remains well defined over the entire pH range with this electrode and its height varies by only a few per cent, as opposed to the results obtained with the other two electrodes.

**Influence of concentration.** Because the degree of adsorption depends on both the analyte concentration and the electrode material, it is expected that the range of linear response will vary with each electrode. This is confirmed by the results shown in Table 1. The concentration range is more restricted with the carbon-paste electrode, on which the adsorption is stronger, and is extended when the composite electrode is used. Moreover, a better correlation coefficient is obtained with the latter electrode. This comparative study was performed at pH 1, where the adsorption phenomena are less pronounced. Calculated as the concentration corresponding to a signal equal to three times the standard deviation of the supporting electrolyte current,<sup>17,18</sup> the detection limits obtained average between  $1 \times 10^{-6}$  and  $6 \times 10^{-8} M$ , depending on the nature of the working electrode (Table 1).

#### Reduction

Because quite large negative potentials can be reached with these three electrodes, it is possible to study the characteristics of the reduction of the quinone group of carminomycin. We have compared the reduction results with those obtained previously for the polarographic reduction of this compound.<sup>11</sup> The use of solid electrodes does not change the reduction behaviour from that observed with mer-

Table 1. Linear range and detection limit as a function of the working electrode material, for differential pulse voltammetry at pH 1

Working electrode material	Linear range, $M$	Correlation coefficient	Detection limit, $M$
Carbon paste	$1 \times 10^{-5} - 2 \times 10^{-4}$	0.982	$1 \times 10^{-6}$
Glassy carbon	$2 \times 10^{-6} - 8 \times 10^{-5}$	0.987	$8 \times 10^{-7}$
Composite carbon-polymer	$1 \times 10^{-6} - 1 \times 10^{-4}$	0.995	$6 \times 10^{-8}$

cury electrodes. A well defined peak due to a two-electron two-proton transfer appears over the entire pH range 1–12 with each electrode. The potential is shifted by 50 mV/pH in acidic medium, and by only 20 mV/pH in alkaline solution. As in polarography, adsorption phenomena affect the voltamperograms obtained for neutral solutions. An adsorption peak precedes the faradaic process, and a very sharp peak follows it that is apparently due to desorption of the reduced compound, which causes a disturbance of the double layer; a similar phenomenon is observed with cyclic voltammetry at a hanging mercury drop electrode.<sup>11</sup> The adsorption is more significant with the carbon-paste electrode.

A second peak, which has been attributed to the cleavage of the sugar moiety from the molecule,<sup>4,6</sup> is observed with a mercury electrode,<sup>11</sup> but of the three electrodes reported on here, only the carbon-paste electrode gives this peak (Fig. 3a, peak D).

The reversibility of the hydroquinone/quinone couple in reduction is similar to that noted for oxidation. It has low reversibility in acid solution (Fig. 3a, b, c, peaks C and C') and becomes irreversible in alkaline medium (Fig. 4a, b, c, peak C).

*Acknowledgements*—We are indebted to Bristol Meyers (Brussels) who provided us with samples of carminomycin. Thanks are also expressed to Le Fonds National de la Recherche Scientifique FNRS (Belgium) for help to one of us (G.J.P.) and to the Ministry of Superior Teaching of the Republic of Algeria (F.M.) and to SPPS (Belgium Politic Research ARC) Contract No. 86/91-89.

## REFERENCES

1. S. T. Crooke and A. W. Prestayko, *Cancer and Chemotherapy*, Vol. 3, *Antineoplastic Agents*, Chap. 8, Academic Press, New York, 1981.
2. R. C. Young, R. F. Ozols and C. E. Meyers, *New Engl. J. Med.*, 1981, **305**, 139.
3. F. M. Schabel, M. W. Trader, W. R. Laster, T. H. Corbett and D. P. Griswold, *Cancer Treat. Rep.*, 1979, **63**, 1459.
4. R. T. Eagan, S. Frytak, E. T. Creagan, J. N. Ingle, L. K. Kvols and D. T. Coles, *ibid.*, 1979, **63**, 1589.
5. H. W. Bruckner, C. J. Cohen, J. D. Goldberg, B. Kabakow, R. C. Wallach, G. Deppe, E. M. Greenspan, S. B. Gusberg and J. F. Holland, *Cancer*, 1981, **47**, 2288.
6. A. Anne and J. Moiroux, *Nouv. J. Chim.*, 1984, **8**, 259.
7. R. P. Baldwin, D. Packett and T. M. Woodcock, *Anal. Chem.*, 1981, **53**, 540.
8. E. N. Chaney and R. P. Baldwin, *ibid.*, 1982, **54**, 2556.
9. J. Pursley, *Current Sepns.*, 1982, **4**, 11.
10. M. Chateau-Gosselin, J. C. Vire and G. J. Patriarche, *Mikrochim. Acta*, 1983 **III**, 457.
11. F. Mebsout, J. C. Vire and G. J. Patriarche, *Anal. Lett.*, 1984, **17**, 805.
12. *Idem, ibid.*, 1985, **18**, 1431.
13. F. Mebsout, J.-M. Kauffmann and G. J. Patriarche, *Analysis*, 1987, **15**, 243.
14. M. P. Prete, J. M. Kauffmann, J. C. Vire and G. J. Patriarche, *Anal. Lett.*, 1984, **17**, 1391.
15. J. M. Kauffmann, G. J. Patriarche, M. Chateau-Gosselin and B. Gallo-Hermosa, *Talanta*, 1986, **33**, 733.
16. B. Gallo-Hermosa, J.-M. Kauffmann, G. J. Patriarche and G. G. Guilbault, *Anal. Lett.*, 1986, **19**, 2011.
17. G. E. Batley and T. M. Florence, *J. Electroanal. Chem.*, 1974, **55**, 23.
18. H. Baiser, *Anal. Chem.*, 1970, **42**, 26A.

## SQUARE-WAVE ADSORPTIVE STRIPPING VOLTAMMETRY OF MENADIONE (VITAMIN K<sub>3</sub>)

J.-C. VIRE, N. ABO EL MAALI\* and G. J. PATRIARCHE

Institut de Pharmacie, Université Libre de Bruxelles, Campus Plaine, C.P. 205/6, Boulevard du Triomphe,  
B-1050, Bruxelles, Belgium

G. D. CHRISTIAN

Department of Chemistry, University of Washington, Seattle, WA 98195-9550, U.S.A.

(Received 8 June 1988. Accepted 12 August 1988)

**Summary**—Menadione (vitamin K<sub>3</sub>) undergoes a reversible two-electron transfer involving the quinone structure in acidic medium. As demonstrated by using cyclic voltammetry, the reduced form is more strongly adsorbed than the oxidized one. Stripping voltammetry of an adsorbed layer has been applied to the determination of this molecule after preconcentration of the reduced compound and scanning the potential towards less negative values. Adsorption, which is highly effective when stirring is used, approaches an equilibrium process in quiescent solution, as evidenced by a loss of part of the adsorbed material when stirring is stopped. A square-wave mode has been selected owing to its high sensitivity (the current is 20 times that for the differential pulse mode), but also to its high scan-rate, which minimizes the slow desorption process occurring during the scan. A concentration range from  $2 \times 10^{-10}$  to  $5 \times 10^{-7} M$  is easily investigated, the detection limit being  $1.3 \times 10^{-10} M$ . The influence of several operational parameters has also been considered.

Vitamins of the K group have long been recognized as essential constituents for blood coagulation and, owing to the reversible redox character of quinones, as electron mediators in the respiratory processes of the cells.<sup>1</sup> The electrochemical activity of these compounds, mainly the polarographic reduction of their quinone structure, is well known.<sup>2-4</sup> From an analytical point of view, the reversible two-electron transfer allows d.c. and d.p. polarographic determination of these vitamins in the  $10^{-6}$ – $10^{-5} M$  range.<sup>2</sup> However, the a.c. signal cannot be used for this purpose as the current does not increase linearly with concentration, owing to the sensitivity of this method to the adsorption currents which accompany the faradaic process. As illustrated by numerous examples,<sup>5</sup> these usually undesirable interfacial interactions may become very useful in enhancing, by an adsorptive preconcentration step, the performances of voltammetric techniques. Such a procedure, made very sensitive by applying a square-wave potential scan, has been adapted to the determination of vitamin K<sub>3</sub> (menadione, 2-methyl-1,4-naphthoquinone).

### EXPERIMENTAL

#### Instrumentation

Cyclic and square-wave voltamperograms were recorded with a PAR Model 384 B Polarographic Analyzer coupled with a PAR 303 A Static Mercury Drop Electrode (medium-size drop) and a Houston "HILOT" DMP 40 Digital

Plotter. The potentials were referred to the Ag/AgCl/saturated KCl reference electrode and a platinum wire was used as counter-electrode. A PAR 305 stirrer was connected to the 303 SMDE. The peak heights were automatically measured by using the "tangent fit" capability of the instrument.

#### Reagents

Stock solutions of vitamin K<sub>3</sub> (Merck 5793, used without further purification) were prepared by dissolving the appropriate amount in a methanol–water (20:80 v/v) mixture, and stored in the dark. Supporting electrolytes were made from doubly distilled water and analytical grade reagents.

#### Procedure

Ten ml of the supporting electrolyte are deaerated with nitrogen for 12 min. The deposition potential is then applied to a new mercury drop, the solution being stirred at 400 rpm. A positive-going scan is performed after the equilibration period. Unless otherwise stated, the following parameters are used: deposition potential (and initial potential),  $-0.100 V$  vs. Ag/AgCl/saturated KCl; equilibration time, 10 sec; scan-rate, 200 mV/sec; pulse amplitude, 20 mV; frequency, 100 Hz. The same procedure is repeated after spiking the solution with increasing concentrations of the analyte.

### RESULTS AND DISCUSSION

#### Preliminary experiments

A preliminary investigation of the adsorption stripping procedure for vitamin K<sub>3</sub> showed that performing the preconcentration step at a potential less negative than that of the reduction peak results in a very low reduction signal on scanning to more negative potentials, even with  $5 \times 10^{-7} M$  solutions. This indicates a weak adsorption of the oxidized form of

\*On leave of absence from Department of Chemistry, Faculty of Science, Assiut University, Assiut, Egypt.



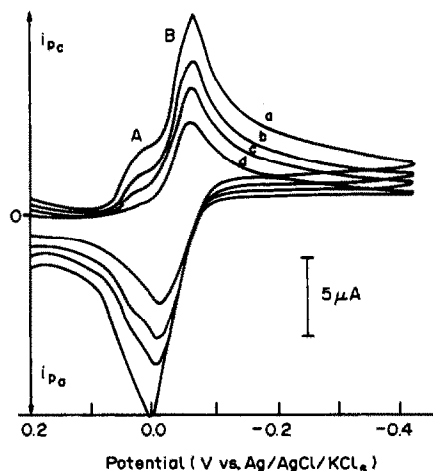


Fig. 1. Cyclic voltammetry of vitamin K<sub>3</sub>, Vitamin K<sub>3</sub>,  $5 \times 10^{-4}M$ ; HClO<sub>4</sub>, 0.3M; starting potential, +0.20 V; scan-rate (mV/sec); (a) 500; (b) 300; (c) 200; (d) 100. A: capacitive shoulder; B: faradaic reduction peak.

the vitamin. Such a behaviour was expected, from a.c. polarography, in which the baseline following the reduction process falls below the residual current of the supporting electrolyte, indicating adsorption of the reduced form.<sup>6</sup> This observation has been confirmed by cyclic voltammetry, where a shoulder precedes the faradaic reduction peak (Fig. 1). The intensity of this shoulder is proportional to the scan-rate, demonstrating its capacitive origin.

These results led us to expect that owing to the high reversibility of the quinone–hydroquinone system, there should be stronger adsorption of the compound and thereby a better sensitivity if the preconcentration step were performed at a potential more negative than the reduction one, followed by a positive-going potential scan. This hypothesis has been verified by cyclic voltammetry with a  $5 \times 10^{-7}M$  solution.

As illustrated by Fig. 2A, a cyclic scan starting at +0.175 V, performed after a 60 sec deposition time at a potential corresponding to the oxidized form (+0.175 V), exhibits a small reduction peak (peak a, 25 nA). The re-oxidation peak (peak a') on the back-scan is of the same magnitude. When the 60-sec deposition time is used at a potential corresponding to the reduced form (-0.100 V), which is also the starting potential for the scan, the resulting oxidation peak is enhanced by a factor of 10 (Fig. 2B, peak b, 250 nA). The reduction peak, however, has a lower intensity (peak b', 78 nA), indicating that the strongly adsorbed reduced form is partially released after its oxidation. On the basis of these results, this second procedure has been adopted for analytical application.

#### Selection of the wave-form

A  $5 \times 10^{-8}M$  vitamin K<sub>3</sub> solution was used in order to compare the electrochemical response ob-

tained with three techniques: linear scan stripping (DCS), differential pulse stripping (DPS) and square-wave stripping (SWS) voltammetry (Fig. 3). A 60-sec deposition time is applied at -0.100 V in each case. DCS exhibits a small peak (5 nA), poorly defined on a large background current. The baseline and sensitivity are improved by using DPS, the recorded peak height (25 nA) being increased by a factor of five. However, SWS appears to be the method of choice, as 20-fold and 100-fold enhancement of the peak height (525 nA) is observed, relative to DPS and DCS, respectively. This study clearly demonstrates the suitability of SWS voltammetry for the determination of low concentrations, thanks to the applied wave-form and the high scan-rates which can be used.

#### Supporting electrolyte

The nature, pH and concentration of the supporting electrolyte all influence the voltammetric response. Among five buffers tested, an acetic acid–sodium acetate mixture resulted in the highest signal. However, because the peak increases with the proton concentration, sulphuric and perchloric acid media were used for studying the effect of high acidity. The latter acid was preferred owing to its lower background current. Taking into account the shape and definition of the peak, which is at a potential very close to that for oxidation of mercury, a 0.3M perchloric acid medium was adopted for further investigations.

It should be mentioned that similar sensitivities can be obtained in weakly alkaline buffered solutions but with lower reproducibility. Very alkaline media are

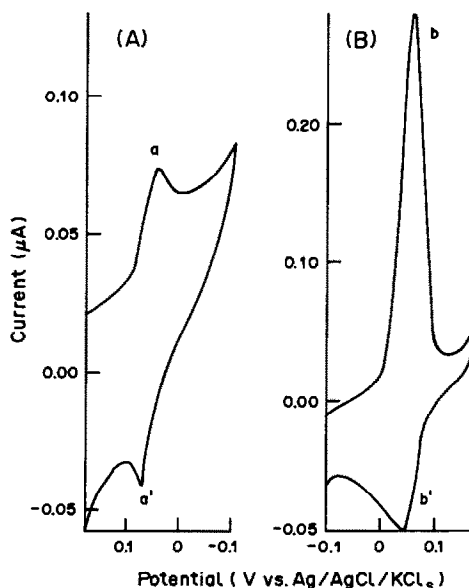


Fig. 2. Cyclic voltammetry with deposition time of 60 sec before scan. Vitamin K<sub>3</sub>,  $5 \times 10^{-7}M$ ; HClO<sub>4</sub>, 0.3M; scan-rate 100 mV/sec. A: deposition and initial potential +0.175 V, negative-going scan; B: deposition and initial potential -0.100 V, positive-going scan.

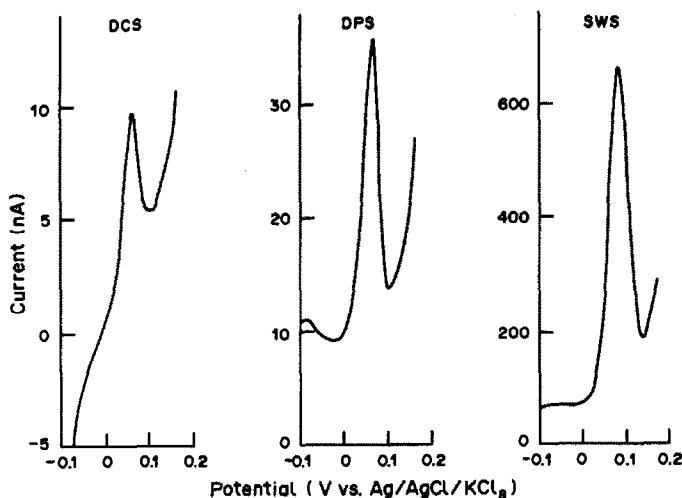


Fig. 3. Comparison of the voltammetry responses by DCS, DPS and SWS. Vitamin  $K_3$ ,  $5 \times 10^{-8} M$ ;  $HClO_4$ ,  $0.3 M$ ; deposition time 60 sec; deposition potential  $-0.100 V$ ; scan-rate (mV/sec): DCS, 20; DPS, 10; SWS, 200; DPS and SWS pulse amplitude, 20 mV; SWS frequency, 100 Hz.

to be avoided, as vitamin  $K_3$  then undergoes a degradation reaction.<sup>3</sup>

#### Operational parameters

The peak height is maximal and constant when the deposition potential lies between  $-0.100$  and  $-0.300 V$ . It decreases markedly when this potential is made more negative, indicating a lower extent of adsorption. A decrease in the current is also observed when the equilibration time after stopping the stirrer exceeds 20 sec, showing that adsorption takes place under stirring conditions but is subject to an equilibration process in quiescent solutions. The high scan-rate of square-wave voltammetry makes the effect of this desorption during the reduction step much smaller than it is in differential pulse polarography.

A 20 mV pulse amplitude is applied, since the current increases linearly with the amplitude up to this value and becomes constant at amplitudes above 30 mV. A linear relationship is also observed between the peak current and the frequency of the signal up to 100 Hz, which is the frequency chosen to improve the sensitivity without any distortion of the peak or of the baseline.

#### Influence of the deposition time

As seen in Fig. 4, curve A, the current recorded for a  $2 \times 10^{-8} M$  solution does not increase linearly with deposition time. This non-linearity cannot be attributed to saturation of the drop surface, since the lack of linearity occurs at very low deposition times. Moreover, a similar relationship is obtained with a  $4 \times 10^{-9} M$  solution (Fig. 4, curve C). Such a behaviour may be indicative of equilibrium between the adsorbed and dissolved species. This process depends only on the deposition time, not on the vitamin concentration, since working at a fixed accumulation

time with increasing concentrations results in linear relationships, as is seen below. Similar properties have already been observed with vitamin  $K_1$ ,<sup>7</sup> and 9,10-phenanthrenequinone.<sup>8</sup> However, the two curves were obtained after a deposition step performed with stirring. Curve B in Fig. 4 shows that a linear relationship is obtained for a  $2 \times 10^{-8} M$  quiescent solution. Since these currents and thus the amount of adsorbed compound are higher than those for curve C, the equilibrium alone cannot be evoked to explain the stable (linear) current. Rather, a rearrangement of the molecules after their adsorption at the electrode

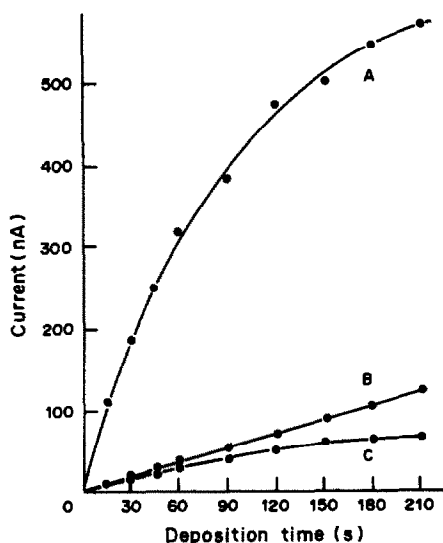


Fig. 4. Influence of the deposition time on the peak current of vitamin  $K_3$ .  $HClO_4$ ,  $0.3 M$ ; SWS. (A) Vitamin  $K_3$ ;  $2 \times 10^{-8} M$ ; deposition with stirring. (B) Vitamin  $K_3$ ;  $2 \times 10^{-8} M$ ; deposition without stirring. (C) Vitamin  $K_3$ ;  $4 \times 10^{-9} M$ ; deposition with stirring.

Table 1. Characteristics of the vitamin K<sub>3</sub> calibration plots (0.3M HClO<sub>4</sub> medium)

Deposition time, sec	Linearity range, M	Equation*	Correlation coefficient
30	$1.0 \times 10^{-9}$ – $4.8 \times 10^{-7}$	$Y = 60.7x - 3.5$	0.9999
60	$5.0 \times 10^{-10}$ – $2.5 \times 10^{-7}$	$Y = 105.2x - 13.3$	0.9999
120	$3.0 \times 10^{-10}$ – $1.1 \times 10^{-7}$	$Y = 178.6x + 13.0$	0.9998
300	$2.0 \times 10^{-10}$ – $2.6 \times 10^{-8}$	$Y = 234.2x - 7.3$	0.9995

\*Y in nA, x in  $10^{-8}M$ , slope in nA/ $10^{-8}M$ , intercept in nA.

surface may occur, this final state being immediately established in quiescent solution, leading to a more stable adsorbed state. An alternative explanation may be that for the quiescent solution, the adsorption/desorption will be diffusion-controlled, and might be expected to be linear for the initial fraction of a "half-life". With stirred solutions, however, the "half-life" would be shorter and so the current-deposition time curve would be more closely exponential in form.

Figure 4 (curves A and B) also indicates that a marked increase in sensitivity results from stirring the solution during the preconcentration step. Owing to the particular properties described above, the current enhancement varies with the deposition time, from a tenfold increase for shorter times to fivefold for longer times.

#### Influence of concentration

Reproducibility was evaluated by performing 10 measurements on a  $2 \times 10^{-8}M$  solution after a 60 sec deposition, with stirring. A mean value of 189 nA was found, with a range of 183–195 nA and a relative standard deviation of 2.3%.

Table 1 summarizes the characteristics of the calibration plots established with different deposition times. In spite of the adsorption equilibrium described above, linearity can be obtained for a constant preconcentration time, as indicated by the correlation coefficients. The effect of this equilibrium, however, appears on comparing the slopes of the plots, which are not directly proportional to the deposition time, the non-linearity increasing with increase in deposition times.

The upper limit of the calibration linearity range indicates the complete coverage of the electrode

surface. The current corresponding to saturation of the drop decreases linearly with increasing deposition time. This effect is also related to the adsorption equilibrium, as in ideal cases the saturation current is independent of the preconcentration time.

As described above, the 0.3M perchloric acid supporting electrolyte gives a low and reproducible background current. This allows a detection limit of  $1.3 \times 10^{-10}M$  (based on a signal-to-noise ratio of 3) to be attained, with 300 sec deposition time. This value means that 0.22 ng can be detected in the 10-ml capacity cell. Measurements made at these low concentrations are made possible by the capability of the instrument to subtract the blank signal.

*Acknowledgements*—Thanks are expressed to the Fonds National de la Recherche Scientifique (FNRS Belgium) for help to one of us (G. J. Patriarche) and to the SPSS (Belgium Politic Research, ARC) contract no. 86/91-89.

#### REFERENCES

1. W. H. Sebrell, Jr. and R. S. Harris, *The Vitamins*, 2nd Ed., Vol. III, Academic Press, New York, 1971.
2. J.-C. Vire and G. J. Patriarche, *Analisis*, 1978, **6**, 395.
3. J.-C. Vire, G. J. Patriarche and G. D. Christian, *Anal. Chem.*, 1979, **51**, 752.
4. G. J. Patriarche, M. Chateau-Gosselin, J. Vandenbalck and P. Zuman, in *Electroanalytical Chemistry*, A. J. Bard (ed.), Vol. 11, p. 141. Dekker, New York, 1979.
5. J. Wang, *Stripping Analysis. Principles, Instrumentation and Applications*, Verlag Chemie, Deerfield Beach, FL, 1985.
6. G. Dryhurst, *Electrochemistry of Biological Molecules*, Academic Press, New York, 1977.
7. J.-C. Vire, V. Petra Lopez, G. J. Patriarche and G. D. Christian, unpublished work.
8. H. Y. Cheng, L. Falat and R. L. Li, *Anal. Chem.*, 1982, **54**, 1384.

## EXTRACTION-SPECTROPHOTOMETRIC DETERMINATION OF VANADIUM WITH 3,5-DINITROCATECHOL AND BRILLIANT GREEN

Z. MARCZENKO and R. ŁOBIŃSKI

Department of Analytical Chemistry, Technical University, Warsaw, Poland

(Received 22 January 1988. Accepted 10 July 1988)

**Summary**—The formation and extraction of the ion-associates of the vanadium(V)–3,5-dinitrocatechol (DNC) anionic chelate complex with various basic dyes have been studied and a new sensitive extraction-spectrophotometric method for the determination of vanadium based on the system V(V)–DNC–Brilliant Green has been developed. Beer's law is obeyed up to a vanadium concentration of 0.3 µg/ml and the molar absorptivity is  $1.7 \times 10^5 \text{ l. mole}^{-1} \text{ cm}^{-1}$  at 630 nm. The molar ratios of the components and the form of the vanadium(V) cation in the extracted compound have been determined, and the formula  $[\text{VO}(\text{OH})(\text{DNC})_2]^- [\text{BG}^+]_2$  is proposed. Titanium, molybdenum, tungsten, EDTA and thiocyanate interfere seriously. The method becomes specific after a preliminary separation of vanadium by its extraction as the BPHA complex from  $\text{H}_2\text{SO}_4$ –HF medium, and is 40 times more sensitive than the spectrophotometric BPHA method. The proposed method has been applied to determination of traces of vanadium (about  $10^{-5}\%$ ) in alums.

Many sensitive extraction-spectrophotometric methods for the determination of metals and non-metals are based on extraction of the ion-associates of basic dyes with anionic (mostly halide) complexes. Anionic complexes with chelating reagents (e.g. oxine, benzoic acid, 3,5-dinitrocatechol) are seldom applied although they allow a sensitive determination of the metals which do not form sufficiently stable anionic complexes with halides (e.g., Ti, Th, U, V, W, Zr, lanthanides).<sup>4</sup>

There is a lack of very sensitive spectrophotometric methods for the determination of vanadium and therefore the present work is devoted to the development of such a method based on the extraction of the ion-associate of a basic dye with the doubly charged anionic complex of vanadium(V) with 3,5-dinitrocatechol.

Hitherto, the 3,5-dinitrocatechol complex/basic dye system has been restricted to the extractive spectrophotometric determination of germanium, tin, titanium and lanthanides.<sup>5-9</sup>

### EXPERIMENTAL

#### Reagents

*Vanadium(V) standard solution (1 mg/ml)*. Dissolve 1.786 g of  $\text{V}_2\text{O}_5$ , previously ignited at 500°, in dilute sodium hydroxide solution. Acidify the solution with sulphuric acid and dilute to volume with water in a 1-litre standard flask. Dilute further with water as required.

*3,5-Dinitrocatechol (DNC) solution,  $8 \times 10^{-4}\text{M}$ , in 20% ethanol medium*. DNC was synthesized<sup>6</sup> and its purity confirmed by melting point measurement, elemental analysis, thin-layer chromatography, and infrared and NMR spectroscopy.

*Brilliant Green (BG) (Reakhim, USSR) solution,  $8 \times 10^{-4}\text{M}$ , in ethanol*. The commercial preparation was purified according to Fogg *et al.*<sup>10</sup>

*N-Benzoyl-N-phenylhydroxylamine (BPHA) solution, 0.1%, in chloroform*.

Doubly distilled water was used throughout. All other chemicals used were of analytical-reagent grade.

#### Apparatus

A Specord UV-VIS recording spectrophotometer and a VSU2-P spectrophotometer with 10-mm glass cells were used. Polypropylene separatory funnels were used for the extraction from fluoride medium.

#### Procedure

Place the sample solution (pH 5–7), containing not more than 3 µg of vanadium(V), in a separatory funnel, and add 1 ml of 3,5-dinitrocatechol solution, followed by 1 ml of 0.25M sulphuric acid. Make up with water to about 10 ml, add 5 ml of carbon tetrachloride, then 0.5 ml of Brilliant Green solution and shake for 1 min. After separation of the phases, transfer the organic layer to a 10-ml standard flask containing 1 ml of ethanol and one drop of 0.01M sulphuric acid. Make up to the mark with carbon tetrachloride, mix, and measure the absorbance at 630 nm against a reagent blank prepared in the same way.

### RESULTS AND DISCUSSION

#### Preliminary investigations

In an acidic (pH 1–3) medium vanadium(V) reacts with 3,5-dinitrocatechol (DNC) to form an anionic yellow complex ( $\lambda_{\text{max}} = 428 \text{ nm}$ ). In the presence of a suitable basic dye an ion-associate is formed.

The following basic dyes were examined: Brilliant Green, Malachite Green, Methyl Violet, Crystal Violet (triphenylmethane dyes), Methylene Blue, Nile Blue A (azine dyes), Rhodamine B and Rhodamine 6G (xanthene dyes). The possibility of the extraction of the vanadium–DNC–basic dye ion-associate from a sulphuric acid medium (pH 0–4) into various organic solvents [benzene, toluene, carbon tetra-

chloride, chloroform, n-pentyl acetate, cyclohexane, methyl isobutyl ketone (MIBK), di-isopropyl ether and petroleum ether] was studied.

Ion-associates are formed with all the basic dyes examined (apart from Methylene Blue) and are either extracted into the organic phase (benzene, toluene, chloroform, MIBK, n-pentyl acetate) or floated (cyclohexane, di-isopropyl ether and petroleum ether). Carbon tetrachloride extracts the Brilliant Green ion-associate but floats the ion-associates of all the other dyes tested.

From the analytical point of view the extraction solvent should completely extract the vanadium ion-associate but not the dye itself or its ion-pair with DNC. These conditions were fulfilled only by the Malachite Green-toluene and Brilliant Green-carbon tetrachloride systems. As the latter gave the higher sensitivity, it seemed the more promising and was further investigated in detail.

#### Formation and extraction of the $V(V)$ -DNC-BG ion-associate

From Fig. 1 it is evident that maximum absorbance is obtained when the sulphuric acid concentration is about  $0.025M$  (pH  $1.3 \pm 0.1$ ). From more acidic media, the vanadium(V) ion-associate is not extracted quantitatively, and with progressively less acidic ones the blank absorbance increases considerably owing to the greater dissociation of DNC, the resulting increasing concentration of the DNC anion, and consequently greater probability of DNC-BG ion-pair formation. Because the pH of the aqueous phase is practically constant during the extraction, no buffer solution is needed. The required acidity is established by adding a suitable amount of sulphuric acid to a sample solution of pH 5-7. This way of establishing the acidity gives more reproducible results and is faster than adjustment with pH-meter control.

Figure 2 shows the dependence of the absorbance of the extract and of the blank on the DNC concentration. A DNC concentration of at least  $8 \times 10^{-5}M$  (16-fold molar excess with respect to  $2.5 \mu\text{g}$  of vanadium) gives maximal and reproducible absorbance values.

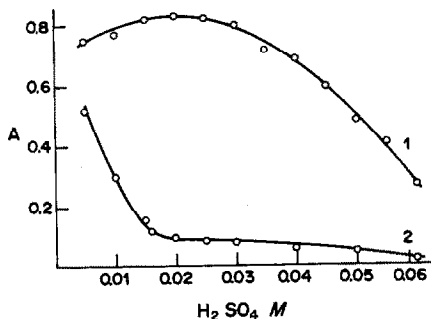


Fig. 1. Effect of the sulphuric acid concentration on formation and extraction of the vanadium ion-associate: curve 1, absorbance of the extract measured against the blank; 2, blank absorbance measured against  $\text{CCl}_4$ -ethanol (9 + 1) mixture.

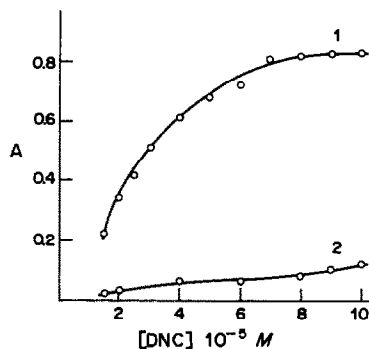


Fig. 2. Dependence of the absorbance of the extract on the DNC concentration: curve 1, absorbance of the vanadium ion-associate measured against the blank; 2, blank absorbance measured against  $\text{CCl}_4$ -ethanol (9 + 1) mixture.

Figure 3 shows that maximal absorbance readings are obtained with a Brilliant Green concentration of at least  $4 \times 10^{-5}M$  (about 8-fold molar excess with respect to  $2.5 \mu\text{g}$  of vanadium). Because of the dimerization of Brilliant Green in more concentrated (about  $1 \times 10^{-3}M$ ) aqueous solutions, and then dissociation into monomer after dilution,<sup>11</sup> an ethanolic solution of the dye was used. It was observed that maximal and well reproducible absorbances were obtained when the Brilliant Green solution was introduced after addition of the extracting solvent. The extraction should then be done as soon as possible because of the protonation of Brilliant Green in acidic (pH < 2) aqueous solutions.<sup>10</sup>

The vanadium is completely extracted by shaking the aqueous phase and one 5-ml portion of carbon tetrachloride for 1 min.

The colour of the extract fades after separation of the layers and therefore the extract itself is useless for analytical purposes, but it has been found that the presence of a small amount of acid prevents the fading of the colour. The addition of even one drop of  $0.01M$  sulphuric acid makes the extract turbid, but subsequent addition of ethanol or methanol clears the turbidity. This addition also causes a significant increase in the absorbance of the extract and a change

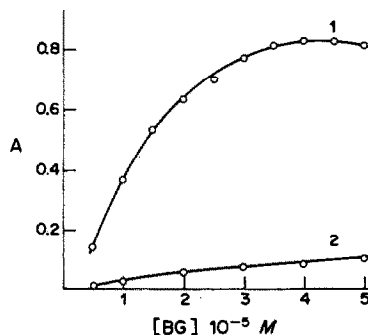


Fig. 3. Dependence of the absorbance of the extract on the Brilliant Green concentration: curve 1, absorbance of the vanadium ion-associate measured against the blank; 2, blank absorbance measured against  $\text{CCl}_4$ -ethanol (9 + 1) mixture.

in colour from green to blue. A final concentration of 10% ethanol or methanol is optimal.

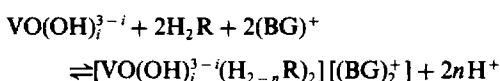
Although the molar absorptivity is higher ( $1.94 \times 10^5 \text{ l. mole}^{-1} \cdot \text{cm}^{-1}$ ) for the methanol than the ethanol ( $1.70 \times 10^5$ ) system, the latter is preferred because the blank value is lower (0.08 instead of 0.12 with methanol).

#### Composition of the $V(V)$ -DNC-BG ion-associate

The molar ratios of vanadium to DNC and to Brilliant Green were determined by the Bent and French logarithmic method<sup>12</sup> and both found to be 1:2. These results were confirmed by the Job method and are the same for both the methanol and ethanol systems.

An extract containing a known amount of vanadium was evaporated and the residue was dissolved in a 1:4 v/v mixture of water and methanol. The absorbance of the solution was almost equal to the absorbance of a solution (in the same solvent) of an amount of Brilliant Green that was in 2:1 molar ratio to the amount of vanadium in the extract.

Attempts were made to determine the form in which vanadium(V) is present in the ion-associate. The molar ratios DNC:V and BG:V found for the ion-associate permit postulation of the following equation for its formation and extraction (DNC is denoted by  $H_2R$ ):



The equilibrium constant is

$$K = \frac{[\text{VO}(\text{OH})_i^{3-i}(\text{H}_{2-n}\text{R})_2(\text{BG})_2^+][H^+]^{2n}}{[\text{VO}(\text{OH})_i^{3-i}][H_2R]^2[(\text{BG})^+]^2}$$

Hence

$$-\log B = -pK + 2n\text{pH}$$

where

$$B = \frac{[\text{VO}(\text{OH})_i^{3-i}][H_2R]^2[(\text{BG})^+]^2}{[\text{VO}(\text{OH})_i^{3-i}(\text{H}_{2-n}\text{R})_2(\text{BG})_2^+]}$$

The relationship  $-\log B = f(\text{pH})$  was investigated for all possible vanadium cation forms ( $i = 0, 1, 2, 3$ ). All the constants necessary for the calculations are known.<sup>8,13</sup> The values of  $-\log B$  plotted *vs.* pH give a straight line with a slope that is an even number ( $n$  should be an integer) only for  $i = 2$ , which corresponds to the cation  $\text{VO}(\text{OH})_2^+$ .

We conclude from this that the ion-associate has the formula

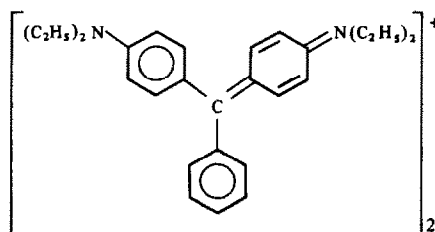


Table 1. Statistical evaluation of the results for determination of vanadium by the proposed method

Vanadium, $\mu\text{g}$		Standard deviation,* $\mu\text{g}$	Confidence limits (probability level 0.95), $\mu\text{g}$
Added	Found		
1.00	1.01	0.032	$1.01 \pm 0.03$
2.00	1.99	0.030	$1.98 \pm 0.03$
3.00	2.98	0.036	$2.98 \pm 0.04$

\*For seven determinations.

It must be emphasized that, in contrast to the extraction-spectrophotometric methods based on the ion-associates formed by singly charged anionic metal-halide complexes with basic dyes, in the present method a doubly charged anion is extracted in association with two singly charged dyestuff cations, which increases the sensitivity.

#### Determination of vanadium

The calibration graph obeys Beer's law over the range 0.005–0.3  $\mu\text{g/ml V}$ . The molar absorptivity is  $1.70 \times 10^5 \text{ l. mole}^{-1} \cdot \text{cm}^{-1}$  at 630 nm (specific absorptivity  $a = \epsilon/at \cdot \text{wt} \times 1000 = 3.3$ ). Thus, the proposed method is 30–40 times more sensitive than the well-known BPHA and 8-hydroxyquinoline methods and about 5 times more sensitive than the PAR method.<sup>3</sup>

The statistical evaluation of determination of trace amounts of vanadium at three concentration levels shows the good precision and accuracy of the proposed method (Table 1).

The effects of many cations and anions on the determination were examined. Titanium, molybdenum and tungsten interfere at any level. Gallium and indium can be tolerated when present in 1:1 w/w ratio to vanadium, and iron(III) in 100-fold ratio. Aluminium and bismuth give 10% positive error at 1000-fold w/w ratio to vanadium. Cr(III), Mn, Co, Ni, Cu, Zn, Cd, Sb(V), and alkali and alkaline-earth metal ions do not interfere at all.

Anions can interfere either by forming extractable ion-pairs with the dye cation, thus influencing the blank, or by complexing the vanadium cation. Chloride, bromide, nitrate and acetate do not interfere at 1000-fold molar ratio to vanadium; 10-fold molar ratio of fluoride, iodide, perchlorate, oxalate, tartrate and citrate can be tolerated. Thiocyanate and EDTA interfere at any level.

Thus the proposed method, like most of the sensitive methods based on ion-associates with basic dyes,

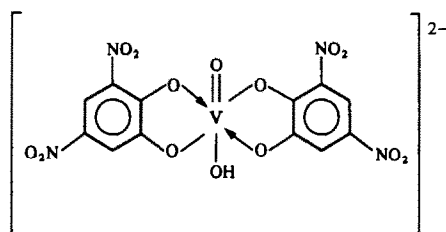


Table 2. Results for determination of vanadium in the presence of other metals (enumerated in the text; 100  $\mu\text{g}$  of each metal)

Vanadium			Standard deviation,* $\mu\text{g}$	Confidence limits (probability level 0.95), $\mu\text{g}$
Added, $\mu\text{g}$	Found, $\mu\text{g}$	Recovery, %		
1.00	0.94	94.0	0.061	$0.95 \pm 0.06$
2.00	1.89	94.3	0.066	$1.89 \pm 0.07$
3.00	2.85	94.8	0.074	$2.85 \pm 0.07$

\*For seven determinations.

Table 3. Results for determination of vanadium in alums

Salt	Sample weight, g	Vanadium, $\mu\text{g}$		Standard deviation,* $\mu\text{g}$	Vanadium content, %	Confidence limits (probability level 0.95), $\mu\text{g}$
		Added	Found			
Iron(III) ammonium alum	5.0	—	1.18	0.066	$2.4 \times 10^{-5}$	$1.18 \pm 0.07$
		1.50	2.60	0.075		
Aluminium ammonium alum	5.0	—	0.84	0.057	$1.7 \times 10^{-5}$	$0.84 \pm 0.06$
		1.50	2.28	0.071		

\*For seven determinations.

is poorly selective and a preliminary separation of vanadium is necessary. The method becomes specific after the extraction of vanadium as its complex with BPHA from a mixture of sulphuric and hydrofluoric acids.<sup>14</sup> Because stripping of the vanadium proved difficult, the organic solvent was evaporated, the BPHA complex thermally decomposed, and the vanadium(V) oxide obtained was dissolved in a small amount of sodium hydroxide solution. If a sulphuric-hydrofluoric acid medium is used, Nb, Ta, Mo, W, and Ti at 1000-fold w/w ratio to V, as well as all other metals which do not form complexes with BPHA in a strongly acidic medium, do not interfere.

The precision and accuracy of the method employing separation of vanadium with BPHA were verified for synthetic samples containing a known amount of vanadium (1, 2 or 3  $\mu\text{g}$ ) as well as Nb, Ta, Mo, W, Ti, Zr, Cr, Mn, Fe, Co, Ni, Cu, Zn, Cd, Al, Ga, In, Sn, Pb, Sb, Bi (100  $\mu\text{g}$  of each element). The results are shown in Table 2.

The method was applied to the determination of trace amounts of vanadium (ca.  $10^{-5}\%$ ) in ferric and aluminium alums, by the following procedure.

Dissolve the sample in 2M sulphuric acid plus 0.2 g of ammonium persulphate, and place the solution in a polypropylene separatory funnel. Add 5 ml of concentrated hydrofluoric acid, dilute with water to 50 ml and mix. Shake the solution with three successive portions (10, 10 and 5 ml) of BPHA solution, each time for 2 min. Transfer the combined extracts into a platinum crucible. Evaporate the solvent on a water-bath and heat the crucible to ash the residue. After cooling the crucible, add 1 ml of 0.1M sodium hydroxide, dilute with water and heat to boiling. After cooling, adjust the pH to 5–7 and continue as already described. Run a blank in parallel.

*Note.* As some commercially available ammonium persulphate and sulphuric acid can contain traces of vanadium, these reagents should be checked for vanadium content before use, and purified if necessary by shaking the mixture (to be used for dissolving the alum sample) with a suitable amount of BPHA solution.

The results for the determination of vanadium in the alums are shown in Table 3. The recovery of known added amounts of vanadium was about 95%.

*Acknowledgement*—This work was supported by Research Programme CPBP-01.17.

## REFERENCES

1. E. B. Sandell and H. Onishi, *Photometric Determination of Traces of Metals*, 4th Ed., *General Aspects*, Wiley, New York, 1978.
2. K. L. Cheng, K. Ueno and T. Imamura, *Handbook of Organic Analytical Reagents*, CRC Press, Boca Raton, 1982.
3. Z. Marczenko, *Separation and Spectrophotometric Determination of Elements*, Horwood, Chichester, 1986.
4. *Idem*, *Microchim. Acta*, 1977 II, 651.
5. V. A. Nazarenko, N. V. Lebedeva and L. I. Vinarova, *Zh. Analit. Khim.*, 1973, **28**, 1100.
6. *Idem*, *ibid.*, 1972, **27**, 128.
7. J. Chwastowska and E. Grzegorzółka, *Chem. Anal. (Warsaw)*, 1975, **20**, 1065.
8. V. A. Nazarenko, E. A. Biryuk, L. I. Vinarova and K. A. Mukelo, *Zh. Analit. Khim.*, 1982, **27**, 252.
9. N. S. Poluektov, R. S. Lauer, L. A. Ovchar and S. F. Potapova, *ibid.*, 1975, **30**, 1513.
10. A. G. Fogg, C. Burgess and D. T. Burns, *Analyst*, 1970, **95**, 1012.
11. A. G. Fogg, A. Willcox and D. T. Burns, *ibid.*, 1976, **101**, 67.
12. H. Bent and C. French, *J. Am. Chem. Soc.*, 1941, **63**, 568.
13. V. A. Nazarenko, V. P. Antonovich and E. M. Nevskaya, *Metal Ion Hydrolysis in Dilute Solutions* (in Russian), Atomizdat, Moscow, 1979.
14. E. M. Donaldson, *Talanta*, 1970, **17**, 583.

## SHORT COMMUNICATIONS

# THE REACTION OF *N*-NITROSAMINES WITH PYRIDINIUM SALTS

O. R. IDOWU\*

Department of Chemistry, University of Ibadan, Ibadan, Nigeria

(Received 4 May 1988. Revised 18 July 1988. Accepted 8 September 1988)

**Summary**—*N*-Nitrosamines react readily with pyridinium salts containing an activated methylene group to give hydrazones. This reaction may serve as the basis for the routine determination of *N*-nitrosamines.

*N*-Nitrosamines are a formidable group of carcinogens, more than 300 of which are known to be carcinogenic in one or more of some 40 animal species.<sup>1</sup> As *N*-nitrosamines are ubiquitous,<sup>2</sup> it is desirable to detect their presence in food, biological and environmental samples by a routine screening procedure.

The best methods for the determination of *N*-nitrosamines require specialized and expensive equipment which is not widely available. The limitations of the more accessible gas chromatographic methods, based on the measurement of derivatives of *N*-nitrosamines, have been discussed in a recent communication in which two new derivatives suitable for routine determination of *N*-nitrosamines were reported.<sup>3</sup>

Further studies have shown that *N*-nitrosamines react with pyridinium salts which have an activated methylene group attached to the pyridinium nitrogen atom, to give hydrazones. These products may be suitable derivatives for the determination of *N*-nitrosamines by gas chromatography or liquid chromatography, with ultraviolet or fluorescence detection. Details of these reactions are presented here.

### EXPERIMENTAL

*N*-Nitrosodimethylamine (NDMA), *N*-nitrosodibutylamine (NDiBA) and *N*-nitrosodiphenylamine (NDPhA) were chosen for the present study.

9-Methylacridine was synthesized according to the method of Poral-Koshits *et al.*,<sup>4</sup> 2-methylbenzoxazole was prepared as described by Theilacker<sup>5</sup> and 2,4-dinitrotoluene was prepared by nitration of 4-nitrotoluene.

#### Preparation of pyridinium salts

Dissolve 5 g of 9-methylacridine (or 2,4-dinitrotoluene or 2-methylbenzoxazole) in 10 ml of dry pyridine and add 20 ml of pyridine containing a corresponding number of moles of iodine. Heat the mixture on a boiling water-bath for 3 hr to precipitate the *N*-(9-acridylmethyl)pyridinium, *N*-(2,4-dinitrotolyl)pyridinium or *N*-(2-benzoxazolyl-

methyl)pyridinium iodide. The yield of *N*-(2,4-dinitrotolyl)pyridinium iodide is improved if benzene is added to the cooled reaction mixture with vigorous stirring. Filter off the pyridinium salt by suction, wash it with 25 ml of pyridine and recrystallize it from 50% aqueous ethanol.

#### Reaction of *N*-nitrosamines with pyridinium salts

To 200 mg of pyridinium iodide, dissolved in ethanol, add a solution of the equivalent amount of *N*-nitrosamine in ethanol and 5 drops of 10% potassium hydroxide solution. Allow to stand at room temperature for 30 min, then heat the mixture on a boiling water-bath for 20 min. Cool, then extract the mixture with three 6-ml portions of chloroform, and dry the combined extracts over anhydrous potassium carbonate. Filter and evaporate the filtrate to dryness.

All work with *N*-nitrosamines should be performed in a well-ventilated fume cupboard, with suitable protection for the hands and with use of a disposable surgical mask.

### RESULTS AND DISCUSSION

#### Product identification

*Thin-layer chromatography (TLC)*. Suitable amounts of the products were chromatographed on silica gel with hexane:chloroform (5:2) or chloroform:ethanol (9:1), with detection by examination under ultraviolet light and also by exposure to iodine vapour. The results are summarized in Table 1.

*Test for N-nitrosamines*. Ethanol solutions of the products were examined for *N*-nitrosamines by use of the Griess reagent and sulphamic acid tests.<sup>6</sup> No residual nitrosamine was detected in any of the tests.

*Acid hydrolysis and test for aldehyde*. Each of the nine products was hydrolysed by heating about 100 mg of the substance with 2 ml of 2*M* hydrochloric acid in a boiling water-bath for 30 min. On cooling, the acid solution was extracted with three 5-ml portions of chloroform, and the extracts were combined and dried over anhydrous potassium carbonate. After filtration, the chloroform was evaporated and the residue dissolved in 2 ml of ethanol. The ethanol solution was treated with an equal volume of a solution of 2,4-dinitrophenylhydrazine to test for the presence of aldehyde. Positive tests were obtained in all cases.

*Spectral analysis*. The proton magnetic resonance

\*Present address: Department of Pharmacology and Therapeutics, The University of Liverpool, Liverpool, England.



Table 1. Nature and yield (%) of products formed from the reaction of *N*-nitrosamines with pyridinium salts (fluorescence colours in parentheses)

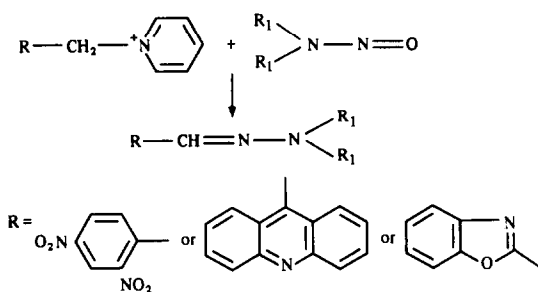
Pyridinium iodide	<i>N</i> -Nitrosamine		
	NDPhA	NDiBA	NDMA
Acridylmethyl-	Solid (47.7) (Violet)	Solid (72.2) (Yellow-green)	Solid (51.0) (Blue-green)
Benzoxazolymethyl-	Solid (65.4) (Violet)	Liquid (45.1) (Violet)	Liquid (40.1) (Blue)
Dinitrotolyl-	Solid (40.7)	Solid (60.0)	Liquid (55.0)

spectra of the compounds were measured. The mass spectra of five of the solid products were obtained by both electron impact and chemical ionization. The compounds were analysed for C, H and N.

The condensation of aromatic *C*-nitroso compounds with activated methyl or methylene groups is a well-known reaction.<sup>7</sup> When a methylene group activated by a quaternary pyridinium group is condensed with an aromatic *C*-nitroso compound under basic conditions to give a nitron and/or anil, the reaction is referred to as the Kröhnke reaction.<sup>8-11</sup> Aromatic *C*-nitroso compounds have also been condensed with compounds possessing activated methyl groups under acidic conditions to give nitrones,<sup>12</sup> and a similar reaction with *N*-nitrosamines has been reported to result in fission of the *N*-nitroso bond and formation of an oxime from the activated methylene compound.<sup>13</sup> This latter reaction is not useful in analysis as all *N*-nitrosamines would give the same oxime on reaction with a particular activated methylene compound. Furthermore, aliphatic *N*-nitrosamines take part in this reaction only with difficulty.

The condensation of *N*-nitrosamines under basic conditions with compounds having activated methyl or methylene groups was studied as a possible method for the formation of suitable analytical derivatives of *N*-nitrosamines.

No reaction was observed between *N*-nitrosamines and a compound with an activated methyl group such as nitromethane. However, pyridinium salts containing a methylene group activated by the ring nitrogen atom, and also by an additional group as in the pyridinium salts described here, react with *N*-nitrosamines to give hydrazones, as shown in Scheme 1:



R<sub>1</sub> = methyl, or *n*-butyl or phenyl

TLC analysis of the nine products showed they were different from the starting pyridinium salts and from the *N*-nitrosamines. The type and yields of the products obtained are shown in Table 1. The hydrazones formed from reaction of *N*-(9-acridylmethyl)pyridinium iodide with the *N*-nitrosamines gave fluorescent spots on the TLC plate when examined under ultraviolet light, listed in Table 1. This pyridinium salt may be useful as a spray reagent for TLC detection of *N*-nitrosamines. Similarly, the *N*-(2-benzoxazolymethyl)pyridinium salt also reacts with the *N*-nitrosamines to give hydrazones which fluoresce under ultraviolet light, and the hydrazone formed from nitrosodiphenylamine gives bright yellow-green fluorescence in daylight when dissolved in carbon tetrachloride.

The results of elemental analysis and the proton magnetic spectra were consistent. The chemical ionization mass spectra of the products gave fragmentation patterns that confirmed their identity, but the electron impact mass spectra of the compounds were found to be less diagnostic, because the prominent ions in the spectra result from an initial fission of the N-N bond of the molecular ion, whereas the ions in which the N-N bond is preserved are of very low intensities.

*Acknowledgement*—The author is grateful to Dr J. L. Maggs for the mass spectral data.

#### REFERENCES

1. P. Bogovski and S. Bogovski, *Intern. J. Cancer*, 1981, **27**, 471.
2. W. Ljinsky and S. S. Epstein, *Nature*, 1970, **225**, 21.
3. O. R. Idowu and O. O. P. Faboya, *Talanta*, 1987, **34**, 441.
4. A. E. Porai-Koshits and A. A. Kharkarov, *Bull. Acad. Sci. URSS, Classe Sci. Chim.*, 1944, 243; *Chem. Abstr.*, 1945, **39**, 1631.
5. W. Thielacker, *J. Prakt. Chem.*, 1939, **153**, 54; *Chem. Abstr.*, 1939, **33**, 6307.
6. F. Feigl, *Spot Tests in Organic Analysis*, 7th Ed., p. 292. Elsevier, Amsterdam, 1966.
7. P. Ehrlich and F. Sachs, *Chem. Ber.*, 1899, **32**, 2341.
8. F. Kröhnke and E. Borner, *ibid.*, 1936, **69**, 2006.
9. F. Kröhnke, *ibid.*, 1938, **71**, 2583.
10. F. Kröhnke and W. Zecher, *Angew. Chem. (Intern. Ed. English)*, 1962, **1**, 626.
11. F. Kröhnke, *ibid.*, 1963, **2**, 225.
12. O. Tsuge, M. Nishionohara and M. Tashiro, *Bull. Chem. Soc. Japan*, 1963, **36**, 1477.
13. C. H. Schmidt, *Angew. Chem. (Intern. Ed. English)*, 1963, **2**, 101.

## SPECTROPHOTOMETRIC DETERMINATION OF MOLYBDENUM IN STEELS WITH *o*-NITROPHENYLFLUORONE AND CETYLTRIMETHYLAMMONIUM BROMIDE

HSU ZHANG-FA and LIAO XI-MAN

Department of Chemistry, East China Normal University 3663 Chung Shan Road (N), Shanghai,  
People's Republic of China

(Received 21 June 1988. Accepted 29 August 1988)

**Summary**—A method has been developed for determining microamounts of molybdenum(VI) in aqueous solution by means of the Mo-*o*-nitrophenylfluorone-cetyltrimethylammonium bromide system, in which micellar solubilization is applied. A red complex is formed in 0.2-0.6M hydrochloric acid medium. The sensitivity of the method is high, and the apparent molar absorptivity is  $1.55 \times 10^5 \text{ l. mole}^{-1} \text{ cm}^{-1}$ . The absorption peak of the complex appears at 530 nm. The colour of the complex develops quickly and is stable for more than 24 hr. The composition of the complex is Mo:*o*-NPF = 1:1, and the system obeys Beer's law in the range 0-10  $\mu\text{g}$  of Mo per 25 ml. The method has been used for the rapid determination of molybdenum in alloy steels with satisfactory results.

The method usually used for determination of trace amounts of molybdenum in steels is extraction of the thiocyanate complex and spectrophotometric measurement after reduction.<sup>1-4</sup> It suffers from interference by tungsten and requires fairly rigid control of conditions. The methods based on other reagents also have several drawbacks.

Dranitskaya *et al.*<sup>5</sup> have determined molybdenum in food and soil with *o*-nitrophenylfluorone (*o*-NPF) as chromogenic reagent, but prior extraction was required and no results for steels were reported.

In the present paper, a spectrophotometric method for determining trace amounts of molybdenum in steels with *o*-NPF is proposed. In the presence of cetyltrimethylammonium bromide (CTAB), *o*-NPF reacts instantaneously with molybdate to form a red 1:1 (Mo: *o*-NPF) complex in 0.3M hydrochloric acid. The CTAB is used as a micellar solubilizing and sensitizing agent. The proposed method has been applied to the spectrophotometric determination of trace amounts of molybdenum in steels and offers the advantages of high sensitivity, simplicity, good repeatability and high stability of the coloured solution, and needs no heating or prior extraction.

### EXPERIMENTAL

#### Reagents

**Molybdenum(VI) solution.** A stock solution of molybdenum(VI) was prepared from analytical grade sodium molybdate dihydrate and standardized gravimetrically with 8-hydroxyquinoline.<sup>6</sup> The working solution (10  $\mu\text{g/ml}$ ) was prepared by appropriate dilution just before use.

***o*-Nitrophenylfluorone solution,**  $1 \times 10^{-3} \text{ M}$ . Freshly prepared by dissolving 36.7 mg of *o*-NPF in 1.7 ml of concentrated hydrochloric acid and diluting to 100 ml with ethanol. The solution can be kept for several weeks when stored in a refrigerator.

**Cetyltrimethylammonium bromide solution,**  $2 \times 10^{-3} \text{ M}$ . Analytical grade reagents and demineralized water were used throughout.

#### Standard procedure

Take an aliquot of standard solution, containing up to 10  $\mu\text{g}$  of molybdenum, in a 25-ml standard flask and, with swirling, add 2.0 ml of 4M hydrochloric acid, 3 ml of  $2 \times 10^{-3} \text{ M}$  CTAB, 2 ml of  $1 \times 10^{-3} \text{ M}$  *o*-NPF, make up to volume with water and mix well. Measure the absorbance at 530 nm in a 1-cm glass cell, with a reagent blank as reference.

#### Procedure for steel analysis

Take a 0.1-g sample in a 100-ml fused-silica beaker, and dissolve it in 10 ml of hydrochloric acid (1 + 1) by heating gently, uncover the beaker, and evaporate the solution to dryness. Heat the residue with a few drops of concentrated nitric acid, evaporate almost to dryness, cool, take up the residue in 1-2 ml of 4M hydrochloric acid, transfer the solution into a 250-ml standard flask and dilute to the mark with water. Take an aliquot (containing not more than 10  $\mu\text{g}$  of molybdenum) in a 25-ml standard flask and determine molybdenum as described in the standard procedure above, after addition of 5 ml of 10% ascorbic acid solution and 2 ml of 5% sodium fluoride solution.

If hydrochloric acid is not satisfactory as the solvent, which is especially the case for steels containing high levels of Cr, W, Ti and Ni, dissolve the sample with 5-7 ml of 70% perchloric acid and 5 ml of concentrated hydrochloric acid, heat till the fumes of chromyl chloride have been evolved, cool, reduce Cr(VI) to Cr(III) with ascorbic acid, add 2-4 ml of sulphuric acid (1 + 1), and heat the solution to expel excess of perchloric acid. Cool, add 2 ml of hydrochloric acid (1 + 1) and 1 ml of 2M tartaric acid to obtain a clear solution, and dilute it to volume in a 250-ml standard flask with water. Take two aliquots (containing not more than 10  $\mu\text{g}$  of molybdenum) in 25-ml standard flasks, add to each 1 ml of 10% hydroxylamine chloride-5% EDTA solution and two drops of *p*-nitrophenol indicator and sufficient hydrochloric acid to discharge the colour of the indicator. Heat one flask in a boiling water-bath for about 10 min and cool it; use this as the reference solution in the standard

procedure described above. Add 2 ml of 20% Rochelle salt/4% sodium fluoride solution to the other, and follow the standard procedure above.

## RESULTS AND DISCUSSION

### Spectral characteristics

The absorption spectra of the solubilized complex, binary complex and the reagent blank are shown in Fig. 1. When CTAB is present the absorption peak has its maximum at 530 nm, a red-shift of 70 nm. *o*-NPF has negligible absorption at this wavelength.

### Experimental variables

The order of addition of the reagents was found to have no effect on the absorbance. Despite this, it is advisable to add the hydrochloric acid and CTAB before the *o*-NPF reagent, to avoid precipitation. However, any precipitate formed on addition of the *o*-NPF reagent will redissolve on addition of the CTAB solution, and there is no adverse effect on the results. Maximum and constant absorbance of the solubilized complex was obtained over the hydrochloric acid range 0.2–0.6M and 0.3M hydrochloric acid was chosen as optimal. *o*-NPF and its binary complex with molybdenum are only sparingly soluble in water, and have low absorbance, but their solubility can be increased and the sensitivity enhanced by addition of 2–7 ml of  $2 \times 10^{-3}$  M CTAB. It was found that 3 ml of  $2 \times 10^{-3}$  M CTAB and 2 ml of  $1 \times 10^{-3}$  M *o*-NPF are sufficient to complex 10  $\mu$ g of molybdenum. The normal variation in laboratory temperature has negligible effect on the determination of molybdenum. The complex forms instantaneously and the absorbance remains stable for at least 24 hr.

### Calibration graph, sensitivity and repeatability

The calibration graph obtained by the standard procedure was linear over the range of 0–10  $\mu$ g of

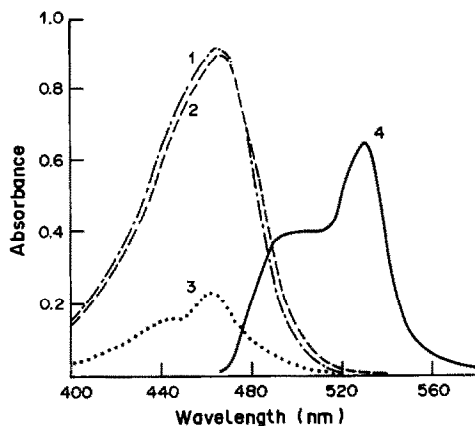


Fig. 1. Absorption spectra. 1: Reagent blank. 2: *o*-NPF-CTAB. 3: Mo-*o*-NPF; reference reagent blank. 4: Mo-*o*-NPF-CTAB; reference reagent blank; Mo  $4.17 \times 10^{-6}$  M, CTAB  $1.6 \times 10^{-3}$  M, *o*-NPF  $2 \times 10^{-5}$  M, HCl 0.3M.

Table 1. Interference of foreign ions in the determination of 6  $\mu$ g of molybdenum

Ion, mg	Ion/Mo, w/w	Mo recovery, %	
Zn(II)	15	2500	102
Mg(II)	15	2500	100
Ca(II)	15	2500	100
Cu(II)	15	2500	101
Ni(II)	15	2500	102
Co(II)	15	2500	101
Ba(II)	15	2500	101
K(I)	15	2500	103
Na(I)	15	2500	102
NH <sub>4</sub> (I)	15	2500	100
Cd(II)	15	2500	102
Fe(III)*	6	1000	97
Pb(II)	6	1000	100
Hg(II)	6	1000	101
Be(II)	1.5	250	98
Al(III)	3.0	500	100
Cr(III)	0.18	30	98
La(III)	4.8	800	97
Y(III)	4.2	700	98
Nb(V)	0.06	10	102
Ta(V)	0.06	10	103
Nd(III)	0.45	75	99
Ti(IV)	0.015	2.5	100
	0.06	10	102
Zr(IV)	0.3	50	99
W(VI)	0.03	5	100
Sb(III)	0.15	25	101
V(V)	0.12	20	100
Mn(VII)†	1.5	250	97
Sn(IV)	0.03	5	99
Sn(II)	0.6	100	102
Th(IV)	0.15	25	102
U(IV)	0.3	50	103
Nitrate	15	2500	100
Chloride	15	2500	100
Sulphate	15	2500	98
Phosphate	15	2500	99
Carbonate	10	1670	101
Oxalate	6	1000	97
Tartrate	6	1000	98
Citrate	5	830	100
EDTA	6	1000	97
Ascorbic acid	15	2500	97
Fluoride	0.6	100	98
Dichromate	6	100	103
Thiocyanate	0.3	50	97
Hydroxylamine	0.15	25	100

\*Masked with ascorbic acid and hydroxylamine.

†Reduced by ascorbic acid.

molybdenum in 25 ml of solution, at 530 nm. The optimum concentration range evaluated from a Ringbom plot<sup>7</sup> was 0.3–10  $\mu$ g per 25 ml. The apparent molar absorptivity at 530 nm calculated from the slope of the graph was  $1.55 \times 10^5$  l.mole<sup>-1</sup>.cm<sup>-1</sup>. Thus, *o*-NPF is one of the most sensitive chromogenic reagents for molybdenum. Ten parallel determinations of 6  $\mu$ g of molybdenum gave a mean absorbance of 0.387 and a standard deviation of 0.03  $\mu$ g.

### Composition of the complex

The ratio of molybdenum to *o*-NPF and CTAB in

Table 2. Determination of molybdenum in steel alloys

Sample	Certified composition,* %	Mo certified, %	Mo found, %
BH0501	Mn 0.625; Cr 0.22; Ni 0.195; Cu 0.31; W 0.20	0.47	0.46, 0.47, 0.47, 0.48, 0.48
BH0502	Mn 0.74; Cr 0.26; Ni 0.31; Cu 0.38; W 0.335	0.77	0.77, 0.78, 0.76, 0.76, 0.76
BH0504	Mn 0.225; Cr 0.033; Ni 0.034; Cu 0.096; W 0.044	0.034	0.04, 0.04, 0.03, 0.04, 0.04
BH0505	Mn 0.18; Cr 0.105; Ni 0.11; Cu 0.13; W 0.135	0.205	0.21, 0.22, 0.20, 0.22, 0.21
BH111-1	Mn 0.0277; Cr 1.90; V 0.398; Cu 0.232; W 0.517; Ti 0.040	0.536	0.54, 0.55, 0.54, 0.55, 0.53

\*These compositions were given by the suppliers of the samples, Wuhan Steel Union Company, China.

Table 3. Comparison of the sensitivities of methods for spectrophotometric determination of molybdenum

Reagent	Molar absorptivity, $10^4 \text{ l. mole}^{-1} \text{ cm}^{-1}$	$\lambda_{\text{max}}$ , nm	Reference
SCN <sup>-</sup> + hexamethylphosphotriamide	1.76	460	3
SCN <sup>-</sup> + ethylisobutrazide hydrochloride	3.86	460	4
SCN <sup>-</sup> + Sn <sup>2+</sup> + Fe <sup>2+</sup> + adogen*	2.13	467	10
Malachite Green + <i>p</i> -chloromandelic acid	10.6	630	11
3,4-Dithiol + tributyl phosphate	1.84	705	12
2-Aminobenzenethiol	1.28	500	13
Pyrocatechol + NTC†	1.43	420	14
	0.98	650	
Dithioamide	0.022	600	15
<i>o</i> -NPF‡ + <i>N</i> -phenylbenzohydroxamic acid	7.0	520	16
<i>o</i> -NPF + gelatine	not stated	584	5
<i>o</i> -NPF + CTAB	15.5	530	Present method

\*Adogen: methyltrioctylammonium chloride.

†NTC: neotetrazolium chloride.

‡*o*-NPF: *o*-nitrophenylfluorone.

the complex was determined by Job's method of continuous variations.<sup>8</sup> The most probable composition of the complex was found to be 1:1:0 for Mo:*o*-NPF:CTAB. The molar ratio method<sup>9</sup> confirmed these results, so CTAB serves only to enhance the solubility and sensitivity, presumably by the usual micellar effects.

### Interferences

The effect of diverse ions which often accompany molybdenum was studied with 6  $\mu\text{g}$  of molybdenum per 25 ml, and an error of  $\pm 2\%$  in the absorbance readings was considered tolerable. The results summarized in Table 1 show that molybdenum can be selectively determined in the presence of a large excess of many cations and anions, most probably because of the high acidity used.

### Determination of molybdenum in steel samples

The proposed method was applied to the determination of molybdenum in alloy steels. Table 2 shows that the values obtained are in good agreement with the certified values. Recoveries of 97–103% were obtained by the standard addition method.

### Comparison with other methods

Thiocyanate is the most widely explored reagent for the determination of molybdenum by spectrophotometry,<sup>1-4</sup> and during the last 10 years, the method has been refined to give good sensitivity and improved selectivity, but the working conditions are

not simple and additional steps such as extraction or reduction are needed. The sensitivities of the most sensitive spectrophotometric reagents for molybdenum reported during the last decade are compared in Table 3. Our method compares favourably with the reagents listed in Table 3 in sensitivity and has better selectivity.

### REFERENCES

1. E. B. Sandell and H. Onishi, *Photometric Determination of Traces of Metals*, 4th Ed., Part I, Wiley, New York, 1978.
2. A. I. Busev, *Analytical Chemistry of Molybdenum*, Israel Program for Scientific Translations, Jerusalem, 1964.
3. M. Mitra and B. K. Mitra, *Talanta*, 1977, **24**, 698.
4. A. T. Gowda and N. M. M. Gowda, *Analyst*, 1985, **110**, 743.
5. R. M. Dranitskaya and E. I. Frum, *Pochwovedenie*, 1968, **10**, 127.
6. A. I. Vogel, *Quantitative Inorganic Analysis*, 3rd Ed., p. 506. Longmans, London, 1968.
7. A. Ringbom, *Z. Anal. Chem.*, 1938, **115**, 332.
8. P. Job, *Compt. Rend.*, 1925, **180**, 928.
9. J. H. Yoe and A. L. Jones, *Ind. Eng. Chem., Anal. Ed.*, 1944, **16**, 111.
10. F. Salinas, J. J. Berzas-Nevaldo and M. I. Acedo-Valenzuela, *Talanta*, 1985, **32**, 63.
11. S. Sato, M. Iwamoto and S. Uchikawa, *ibid.*, 1987, **34**, 419.
12. M. E. M. S. Desiva, *Analyst*, 1975, **100**, 517.
13. A. K. Chakrabarti and S. P. Bag, *Talanta*, 1976, **23**, 736.
14. A. K. Singh and D. Kumar, *Analyst*, 1985, **110**, 751.
15. D. A. Williams, I. J. Holcomb and D. F. Boltz, *Anal. Chem.*, 1975, **47**, 20.
16. A. T. Pilipenko, A. I. Samchuk and O. S. Zul'figarov, *Zh. Analit. Khim.*, 1985, **40**, 1262.

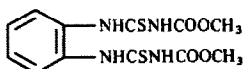
## AN OXIDIMETRIC METHOD FOR THE DETERMINATION OF THIOPHANATE-METHYL IN COMMERCIAL FORMULATIONS

B. C. VERMA\*, D. K. SHARMA, H. K. THAKUR, BH. GOPALA RAO and N. K. SHARMA  
Chemistry Department, Himachal Pradesh University, Shimla-5, India

(Received 8 March 1988. Revised 10 August 1988. Accepted 24 August 1988)

**Summary**—A simple, accurate and reliable titrimetric method is described for the determination of thiophanate-methyl, an important commercial fungicide. The method is based on its direct titration at room temperature with ammonium hexanitratocerate(IV) in sulphuric acid medium in the presence of potassium iodate as catalyst. The method permits detection of the end-point visually, potentiometrically or spectrophotometrically. The proposed method is recommended for routine determination of the fungicide in its commercial formulations.

Thiophanate-methyl, 1,2-bis(3-methoxycarbonyl-2-thioureido)benzene, is a systemic fungicide based on a bis-thiourea derivative.



It exhibits a rather broad antifungal spectrum and is extensively used against various fruit and vegetable diseases. Its wide use necessitates convenient, reliable and rapid methods for its determination.

In the course of our investigations on the oxidimetric determination of thiourea and its derivatives,<sup>1</sup> we have found cerium(IV) an excellent reagent for the purpose.<sup>2,3</sup> The ease with which thioureas are smoothly and quantitatively oxidized with this oxidant in sulphuric acid medium in the presence of potassium iodate (as catalyst) to the corresponding substituted formamidine disulphides, prompted us to extend the advantages of this cerimetric method to thiophanate-methyl.

purposes the visual end-point is adequate, the potentiometric method is of use when coloured solutions are encountered. For more dilute solutions, the visual end-point is difficult to detect, and the spectrophotometric titration is useful.

### EXPERIMENTAL

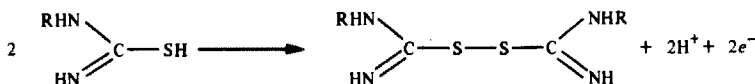
#### Apparatus

Potentiometric titrations were performed with a Toshniwal (India) potentiometer equipped with a platinum and saturated calomel electrode assembly. Spectrophotometric measurements were made with Beckman DU-6 and Bausch and Lomb spectrophotometers.

#### Reagents

*Ammonium hexanitratocerate(IV) solution (0.04M) in 0.5M sulphuric acid.* Prepared by dissolving a little more than the calculated amount of dried analytical grade reagent in 0.5M sulphuric acid and standardized by titration with ferrous ammonium sulphate in sulphuric acid medium, with ferroin as indicator.

*Ferroin solution in water, 0.01M.* Prepared by dissolving 0.594 g of 1,10-phenanthroline and 0.278 g of analytical grade ferrous sulphate heptahydrate in 100 ml of water.



The fungicide may be directly titrated with the reagent at room temperature, with visual, potentiometric or spectrophotometric end-point detection. Ferroin is a suitable indicator for the visual titration. The spectrophotometric titrations are monitored at 340 nm, the wavelength of maximum absorbance of the oxidant, the absorbance being virtually zero until the equivalence point is reached, and then increasing linearly with excess of reagent. Though for most

*Thiophanate-methyl.* Standard material was supplied by courtesy of the Environmental Protection Agency, N.C., U.S.A.

#### Procedures

*Visual and potentiometric titration.* Aliquots of acetonitrile solutions of the pure compound were placed in titration vessels and diluted to 20 ml with acetonitrile. Each solution was mixed with 20 ml of 1M sulphuric acid, 1 or 2 drops of 0.0025M potassium iodate, and 1 or 2 drops of ferroin indicator (for visual titrations) and titrated at room temperature (~23°) with 0.04M ammonium hexanitratocerate(IV) visually and potentiometrically. In the

\*Author for correspondence.

Table 1. Determination of thiophanate-methyl with ammonium hexanitratocerate(IV) (visual and potentiometric titrations)

Thiophanate-methyl taken, mg	Thiophanate-methyl found,* mg	
	Visual method	Potentiometric method
2.00	2.02 ± 0.02	2.01 ± 0.02
4.00	3.97 ± 0.03	4.02 ± 0.03
6.00	6.04 ± 0.04	5.95 ± 0.04
8.00	8.08 ± 0.04	8.03 ± 0.04
10.00	10.08 ± 0.05	9.94 ± 0.05

\*Mean and standard deviation of ten determinations.

visual titrations, the end-point was marked by a sharp colour change from red to very light blue. In the potentiometric titrations, a sharp break in potential was observed at the equivalence point. The results are given in Table 1.

**Spectrophotometric titration.** Aliquots of acetonitrile solutions of the pure compound were diluted to 3 ml with acetonitrile, mixed with 3 ml of 1M sulphuric acid and titrated at room temperature (~23°) at 340 nm, with standard oxidant. The absorbance at 340 nm was monitored. A dilution correction was applied and the titration curve plotted in the usual way. The results are given in Table 2.

**Formulation analysis.** A wettable powder formulation containing 70% active ingredient was used. A single large sample of the formulation was weighed, shaken with acetonitrile and filtered. The residue (if any) was washed 2 or 3 times with acetonitrile. The filtrate and washings were diluted to known volume with the same solvent. Aliquots were then taken for titrations. The visual, potentiometric and spectrophotometric titrations were performed as described above. The results are given in Tables 3 and 4.

## RESULTS AND DISCUSSION

Ammonium hexanitratocerate(IV) is a versatile oxidimetric reagent. This is due to its high redox

Table 2. Determination of thiophanate-methyl with ammonium hexanitratocerate(IV) (spectrophotometric titration)

Thiophanate-methyl taken, µg	Thiophanate-methyl found,* µg
20.0	19.9 ± 0.1
40.0	39.7 ± 0.2
60.0	59.6 ± 0.4
80.0	80.8 ± 0.5
100.0	99.0 ± 0.6

\*Mean and standard deviation of five determinations.

potential, and the availability of a good number of visual indicators. It also has good stability and high equivalent weight. The results in Table 1 show that the thiophanate-methyl in the range 2–10 mg can be determined by visual and potentiometric titrations with the reagent with a maximum relative standard deviation (rsd) of 0.8%. With photometric titrations, the compound could be determined in the range 20–100 µg with a maximum rsd of 0.6% (Table 2). For the commercial formulation the visual and potentiometric titration procedures gave values corresponding to 98.1–99.3% of the nominal content, with rsd values in the range 0.3–0.5% (Table 3). The spectrophotometric titration gave 98.2–99.3% of the nominal content, with rsd values in the range 0.3–0.4% (Table 4). Analysis of the formulation by an independent method<sup>4</sup> gave comparable results (Tables 3 and 4). Ureas, thiosemicarbazides, xanthates, mercaptans and dithiocarbamates have been found to interfere in the proposed method.

The results indicate that each molecule of thiophanate-methyl consumes 4 equivalents of the

Table 3. Determination of thiophanate-methyl from commercial formulation nominally containing 70% active ingredient

Nominal amount taken,* mg	Found,† mg					
	Visual method	Recovery, %	Potentiometric method	Recovery, %	Comparison method†	Recovery, %
3.00	2.97	99.0 ± 0.4	2.98	99.3 ± 0.3	2.96	98.7 ± 0.9
5.00	4.93	98.6 ± 0.4	4.94	98.8 ± 0.4	4.93	98.6 ± 0.6
7.00	6.89	98.4 ± 0.5	6.90	98.6 ± 0.4	6.90	98.6 ± 0.9
10.00	9.81	98.1 ± 0.3	9.83	98.3 ± 0.3	9.80	98.0 ± 0.7

\*Based on 70.0% content in formulation.

†Mean and standard deviation of ten determinations.

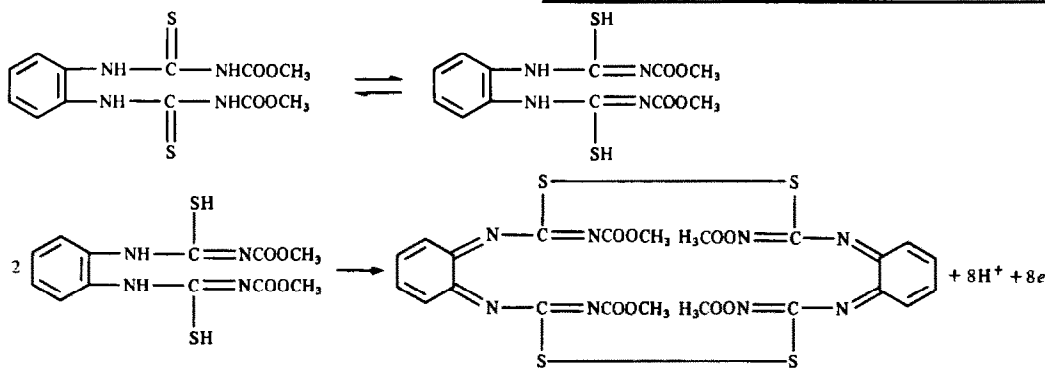
Table 4. Determination of thiophanate-methyl in commercial formulation nominally containing 70% active ingredient

Nominal amount taken,* µg	Amount found,† µg			
	Spectrophotometric titration	Recovery, %	Comparison method†	Recovery, %
25.0	24.8	99.3 ± 0.4	24.8	99.0 ± 0.6
50.0	49.4	98.8 ± 0.3	49.3	98.6 ± 0.7
75.0	73.7	98.3 ± 0.4	73.6	98.1 ± 0.5
100.0	98.2	98.2 ± 0.3	98.1	98.1 ± 0.4

\*Based on 70.0% content formulation.

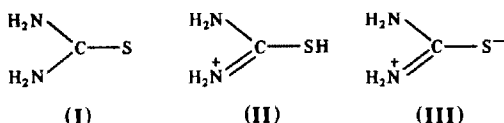
†Mean and standard deviation of five determinations.

reagent. In other words, the compound is oxidized with a four-electron change by the reagent. The most plausible reaction mechanism is:



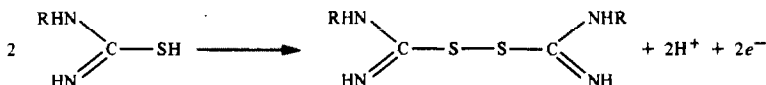
This is supported by the following observations and experiments.

(1) Thiourea (I), in the presence of an acid, exists as a cation (II) derived from the zwitterion structure (III).



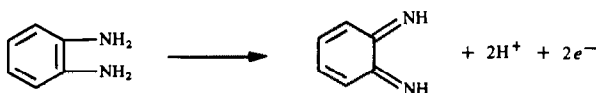
This is in conformity with its property of being a neutral substance but reacting with acids as a mono-acidic base, forming stable salts.

(2) Thioureas are oxidized in acid medium to the corresponding substituted formamidine disulphides with a single-electron change per thiourea group<sup>1</sup> (thiophanate-methyl is a bis-thiourea and consequently involves a two-electron change).



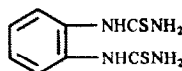
That thioureas are indeed oxidized to substituted formamidine disulphides is supported by the fact that these disulphides have been synthesized by the oxidation of thioureas in acid medium.<sup>5</sup>

(3) Thiophanate-methyl may be considered as an *o*-phenylenediamine derivative. That such diamines are oxidized to the corresponding *o*-di-imines with a two-electron change is well known.<sup>6</sup>



Hence the oxidation of thiophanate-methyl involves an overall four-electron change (the bis-thiourea and *o*-phenylenediamine moieties each

contributing a two-electron change). It may be mentioned here that the following bis-thiourea



(a related compound which we prepared and purified in the laboratory) could be similarly titrated with cerium(IV), being oxidized with a four-electron change.

*Acknowledgements*—The authors thank the Indian Council of Agricultural Research (ICAR), New Delhi, for financial assistance.

#### REFERENCES

1. B. Singh and B. C. Verma, *J. Sci. Ind. Res. India*, 1965, **24**, 536.
2. *Idem*, *J. Indian Chem. Soc.*, 1963, **40**, 39.
3. *Idem*, *Mikrochim. Acta*, 1974, 123.
4. V. L. Miller, E. Csonka and C. J. Gould, *J. Assoc. Off. Anal. Chem.*, 1977, **60**, 1154.
5. P. W. Preisler and L. Berger, *J. Am. Chem. Soc.*, 1947, **69**, 322.
6. R. Adams and J. W. Way, *ibid.*, 1954, **76**, 2763.

## ANALYTICAL DATA

### ACID-BASE INDICATORS IN ACETONITRILE: THEIR $pK_a$ VALUES AND CHROMATIC PARAMETERS

J. BARBOSA, M. ROSES and V. SANZ-NEBOT

Department of Analytical Chemistry University of Barcelona, Barcelona, Spain

(Received 10 August 1987. Revised 16 February 1988. Accepted 29 August 1988)

**Summary**—A series of acid–base indicators in acetonitrile has been studied. Their chromaticity co-ordinates,  $pK_a$  values, transition pH ranges, pH of maximum colour change, optimum concentration for titration, and quality of colour change in acetonitrile have been determined, together with the effect of ionic strength on their properties. Various bases and their mixtures have been titrated to test the practical usefulness of the indicators.

For many years, acetic acid has been a popular medium for the titration of weak bases, but the pH change at the end-point is much greater in many aprotic protophobic solvents, such as acetonitrile.

Acetonitrile owes its many applications in diverse fields to its physical characteristics;<sup>1</sup> it is a considerably weaker base and a much weaker acid than water and has a relatively high dielectric constant ( $\epsilon = 36.0$ ). The cumulative effect of these factors is that acetonitrile is a good differentiating solvent for acids and bases, as is reflected by its small autoprotolysis constant ( $pK_{HS} > 33$ ).<sup>2</sup>

Nevertheless it is not a very suitable medium for the successive titration of acids in mixtures, because of homo- and heteroconjugation.<sup>3</sup> On the other hand, its low ability to solvate anions means that conjugation in it is negligible for bases<sup>4</sup> so it is a very suitable solvent for titration of bases, especially very weak bases and their mixtures.<sup>3</sup>

Many indicators have been recommended for acid–base titrations<sup>5</sup> because visual end-point detection is very precise and accurate for bases. Because the neutralization curves for bases can be calculated, if the indicator dissociation constants are known, it is possible to predict which indicators will give a sharp colour change at the end-point.

The  $pK_a$  values of a large number of indicators have been reported<sup>6,7</sup> but the information about their properties is not enough to allow the selection of the one most suitable for a particular acid–base titration, because an objective method of describing the quality of the indicator colour changes has not been applied.

In this work, a series of commercially available indicators with pronounced colour change was studied over the most useful acidity range and the dissociation constants of several indicators, not previously reported, were determined. The colour changes were characterized by the chromatic parameters in both the CIE and complementary chromaticity systems.<sup>8–10</sup> The optimum concentrations for the indicators were determined by the Vytřas<sup>11</sup>

and Kotrlý and Vytřas<sup>12</sup> methods. In accordance with CIE recommendations, the CIELAB ( $L^*$ ,  $a^*$ ,  $b^*$ ) and CIELUV ( $L^*$ ,  $u^*$ ,  $v^*$ ) co-ordinates were used to calculate the index of colour change perceptibility. The sensitivity, sharpness of colour change, pH corresponding to maximum colour change, and the transition ranges of each indicator were determined.<sup>13,14</sup>

In this paper we report the pH value at which an indicator would show a specific colour, at zero ionic strength, taking into account the activity coefficients, as reported earlier.<sup>15</sup> Finally the behaviour of the indicators was tested by titration of different bases and mixtures of bases.

#### EXPERIMENTAL

##### Apparatus

A Beckman Acta M-VII spectrophotometer with 10-mm cells, a Hewlett-Packard 9816 computer, a CRISON Digilab 517 pH-meter, with a Radiometer G202C glass electrode and a reference electrode similar to the one described by Pleskov,<sup>16</sup> with 0.1M tetraethylammonium perchlorate in acetonitrile serving as a double salt-bridge similar to that used by Coetzee *et al.*<sup>17</sup> and Kolthoff *et al.*<sup>18</sup> were used.

This system gives stable and reproducible potentials within 5–10 min.

##### Reagents

Picric acid (Doesder R. A. grade) vacuum-dried, 0.1M tetrabutylammonium hydroxide in 2-propanol (Carlo Erba, RPE grade), acetonitrile for chromatography (Merck), tetraethylammonium perchlorate (Carlo Erba, R.S. grade) perchloric acid (Carlo Erba, RPE-ACS grade), *p*-toluenesulphonic acid (Merck, A. R. grade), monochloroacetic acid (Scharlau, A. R. grade) and dichloroacetic acid (Carlo Erba, RPE grade) were used. The indicators were *p*-naphtholbenzein (pNB) and Neutral Red (NR) (Merck, analytical grade), Tropaeolin 00 (TROP), Quinaldine Red (QR), Brilliant Green (BG) and Malachite Green (MG) (Carlo Erba, RPE grade), and Bromocresol Green (BCG) (Scharlau, analytical grade).

##### Determination of the standard potential and autoprotolysis constant

The glass electrode was calibrated by titration of 0.005M picric acid in acetonitrile, ( $K_{HP} = 10^{-11}$  in acetonitrile)<sup>18,19</sup> with 0.1M tetrabutylammonium hydroxide. This method is suitable for calibration of the glass electrode, because



Table 1. Standard potentials in acid and basic medium and autoprotolysis constant values

Titration	$E_a^0, mV$	$E_b^0, mV$	$pK_{HS}$
1	998.2	-986.6	33.6
2	994.7	-988.2	33.5
3	998.5	-996.0	33.7
4	995.8	-998.3	33.7
5	994.0	-1008.4	33.8
6	993.8	-986.2	33.5
7	994.0	-978.4	33.3
Average	995.6	-991.7	33.6

conjugation in acetonitrile is very low for ions with a delocalized charge such as picrate and can be neglected. Moreover, the presence of water or alcohols, which are usually present in the titrants in up to 0.5M concentration, has little or no effect on the pH picrate buffer solutions in acetonitrile because the picrate ion is not a strong hydrogen-bond acceptor.<sup>20</sup>

On the other hand, the dielectric constant of acetonitrile is sufficiently high to allow complete dissociation of ionic solutes such as tetrabutylammonium picrate at concentrations up to  $10^{-2}M$ .<sup>21</sup>

A computer program written in Basic, ACETERISO,<sup>22</sup> was used to calculate the standard potentials in acidic and basic medium. From these values, the autoprotolysis constant of the medium can be calculated. A reliable value for the autoprotolysis constant of pure acetonitrile has not yet been reported, because even very small quantities of impurities greatly decrease the  $pK_{HS}$  value. The determination from the measured standard potentials gives the true value of the autoprotolysis constant, which is needed for computation of acid-base equilibria.

Table 1 shows the standard potentials and autoprotolysis constant values obtained in seven titrations. The average value of  $pK_{HS} = 33.6 \pm 0.2$  is in agreement with the value  $pK_{HS} > 33$  reported by Kolthoff *et al.*<sup>2</sup>

#### Determination of the chromatic parameters and $pK_a$ values

Indicator solutions (approximately  $10^{-5}M$ ) were titrated with 0.1M tetrabutylammonium hydroxide solution, in the presence of an appropriate acid to keep the solutions buffered over the pH range of the colour change (monochloroacetic acid for BCG, perchloric and dichloroacetic acid mixture for NR and QR, *p*-toluenesulphonic acid for TROP, and perchloric and *p*-toluenesulphonic acid mixture for BG, MG and PNB).

The titrations were monitored by continuous measurement of the absorbance values at 10-nm intervals between 380 and 770 nm, and simultaneously by potentiometric measurement.

The test solution was stirred with a stream of nitrogen and continuously circulated between the titration vessel and the spectrophotometer cell by means of a peristaltic pump. The temperature was  $25 \pm 0.2^\circ$ .

#### Computation

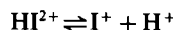
To calculate the chromaticity parameters, the weighted ordinate method,  $\Delta\lambda = 10$  nm, with the coefficients for the standard illuminant C and "10° standard observer"<sup>8</sup> was used, with the SUPERCOLOR program.<sup>23</sup> This program, written in Basic, allows the computation of the optimum concentration of the indicator in titrations, the calculation of the chromaticity co-ordinates in a variety of colour spaces, and determination of the  $pK_a$  value of the indicator.

### RESULTS AND DISCUSSION

The criteria for selection of the indicators were commercial availability, widespread use, solubility in

acetonitrile, sharpness of colour change and availability of  $pK_a$  values.<sup>6</sup>

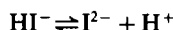
The indicators studied represent four kinds of dissociation equilibria,



$$pK = pH + \log(\gamma_{HI^{2+}}/\gamma_{I^+}) - \log([I^+]/[HI^{2+}])$$



$$pK = pH + \log \gamma_{HI^+} - \log([I]/[HI^+])$$



$$pK = pH + \log(\gamma_{HI^-}/\gamma_{I^{2-}}) - \log([I^{2-}]/[HI^-])$$



$$pK = pH - \log \gamma_{I^-} - \log([I^-]/[HI])$$

where HI represents the acid form and I the basic form of the indicator.

The indicator colour is related to the concentrations of the acid and basic forms of the indicator, and hence to the pH and the ionic strength of the indicator system. The influence of ionic strength is different for each dissociation model and could be important at high ionic strengths for indicators of models (1) and (3) (Table 2).

Because of the high dielectric constant of acetonitrile, the activity coefficients have less influence than in other solvents, such as 2-propanol and 2-methyl-2-propanol.

If the indicator were at infinite dilution, the colour would not depend on activity coefficients. Thus, we use the pH value at zero ionic strength ( $pH_0$ ) to specify a reference indicator colour:<sup>15</sup>

$$(1) pH_0 = pH + \log(\gamma_{HI^{2+}}/\gamma_{I^+})$$

$$(2) pH_0 = pH + \log \gamma_{HI^+}$$

$$(3) pH_0 = pH + \log(\gamma_{HI^-}/\gamma_{I^{2-}})$$

$$(4) pH_0 = pH - \log \gamma_{I^-}$$

These relationships allow chromaticity parameters to be referred to  $pH_0$  values, and the comparison of

Table 2. Influence of ionic strength ( $I$ ) on activity coefficients in acetonitrile

$I$	$\log(\gamma_{HI^{2+}}/\gamma_{I^+})$	$\log \gamma_{HI^+}$ or $\log \gamma_{I^-}$	$\log(\gamma_{HI^-}/\gamma_{I^{2-}})$
$10^{-6}$	0	0	0
$10^{-5}$	-0.02	0	0.02
$10^{-4}$	-0.05	-0.02	0.05
$5 \times 10^{-4}$	-0.11	-0.04	0.11
$10^{-3}$	-0.16	-0.05	0.16
$5 \times 10^{-3}$	-0.35	-0.12	0.35
$10^{-2}$	-0.49	-0.16	0.49
$10^{-1}$	-1.56	-0.52	1.56

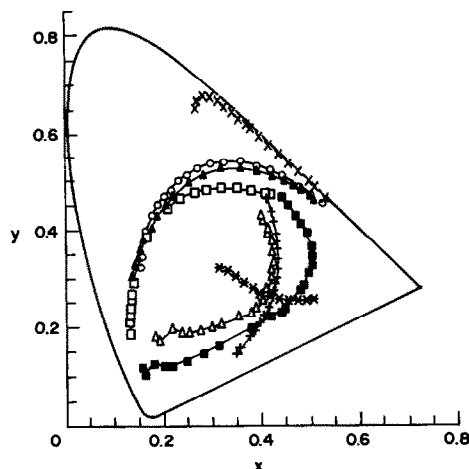


Fig. 1. CIE chromaticity co-ordinates ( $x, y$ ) of indicator solutions at optimum concentration.  $\times$ , pNB;  $+$ , TROP;  $*$ , QR;  $\circ$ , BG;  $\blacktriangle$ , MG;  $\square$ , BCG;  $\triangle$ , NR - 1;  $\blacksquare$ , NR - 2. The symbols for NR - 1 and NR - 2 correspond to complete transitions of the indicator at optimum concentration for equilibria 1 and 2 respectively.

colour transitions at different ionic strengths for the various types of indicator.

To calculate the  $\text{pH}_0$  values, the relationships above are applied to the experimental pH values and the activity coefficients calculated by means of the Debye-Hückel equations.<sup>17</sup> In a practical titration, the true pH range of a colour transition can be calculated from the  $\text{pH}_0$  range and the ionic strength of the solution.

The sequence of colour changes of the indicators can be described by the traditional 1931 CIE system ( $x, y, Y$ ) or by the latest colour spaces CIELAB ( $L^*, a^*, b^*$ ) and CIELUV ( $L^*, u^*, v^*$ ) recommended by the CIE.<sup>24</sup>

The indicator colour changes at optimum concentration are shown in Figs. 1 and 2. In these plots, the  $Y$  and  $L^*$  co-ordinates, which measure colour luminosity, not chroma,<sup>8</sup> have been omitted.

The CIELAB and CIELUV systems can be used to calculate the colour differences by using the relations:

$$\Delta E = [(\Delta L^*)^2 + (\Delta a^*)^2 + (\Delta b^*)^2]^{1/2}$$

$$\Delta E = [(\Delta L^*)^2 + (\Delta u^*)^2 + (\Delta v^*)^2]^{1/2}$$

The complementary chromaticity co-ordinates ( $Q_x, Q_y$ ), which are colour physical constants, were used to describe the colour sequence of the indicators, Fig. 3. For all the indicators tested, straight lines denoting mixtures of two pure coloured forms were obtained. The fact that NR gives two linear segments shows the presence of two equilibria, each involving a particular colour change, the first from blue to red and the second to yellow.

Although pNB, BG and MG show a second colour change at very high pH values, this is of no analytical interest; likewise, the protonated red form ( $\text{H}_2\text{I}^+$ ) of TROP cannot be distinguished by eye from the

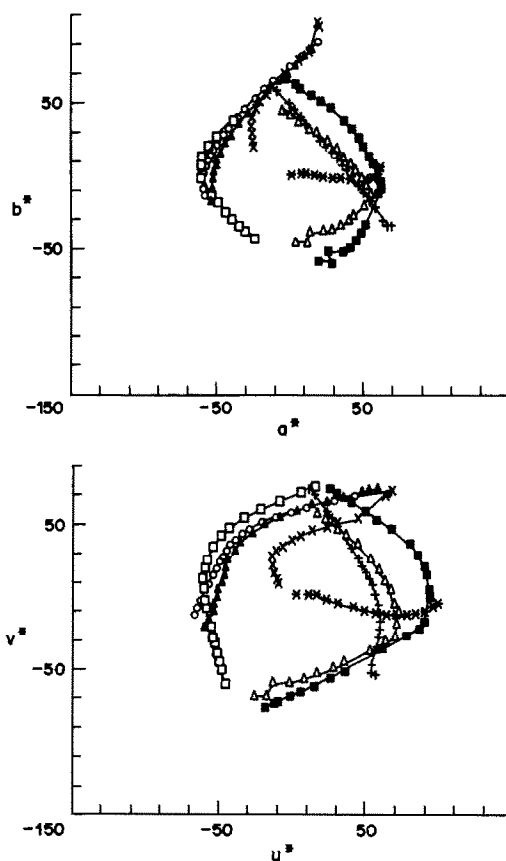


Fig. 2. CIELAB ( $a^*, b^*$ ) and CIELUV ( $u^*, v^*$ ) chromaticity co-ordinates of indicator solutions at optimum concentration. Symbols as for Fig. 1.

neutral form (HI) and the colour transition of BCG at low pH is poor,<sup>6</sup> and of no practical interest. We have therefore studied only the useful transition in each case.

The indicator dissociation constants were determined from the complementary chromaticity co-ordinates according to Reilley *et al.*<sup>25,26</sup> and also

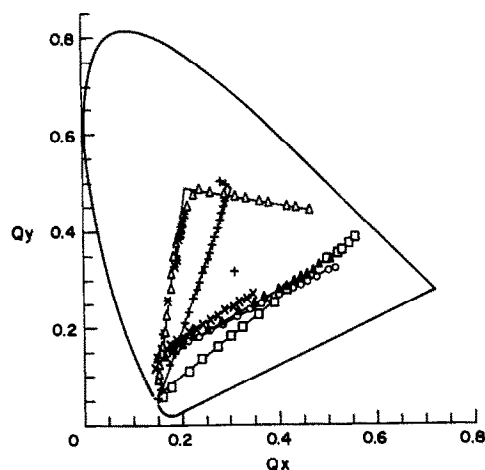


Fig. 3. Colour transitions in the complementary chromaticity diagram. Symbols as for Fig. 1.

Table 3.  $pK$  values of the indicators

Indicator	Chromatic method*	Standard method	Average
pNB	$7.20 \pm 0.13$	$7.15 \pm 0.10$	$7.18 \pm 0.12$
TROP 00	$8.96 \pm 0.10$	$8.96 \pm 0.12$	$8.96 \pm 0.11$
QR	—	$9.41 \pm 0.04$	$9.41 \pm 0.04$
MG	$5.98 \pm 0.05$	$5.99 \pm 0.04$	$5.98 \pm 0.05$
BG	$6.65 \pm 0.05$	$6.64 \pm 0.11$	$6.64 \pm 0.09$
BCG	$18.80 \pm 0.02$	$18.80 \pm 0.04$	$18.80 \pm 0.03$
NR - 1	$4.68 \pm 0.07$	$4.66 \pm 0.04$	$4.67 \pm 0.08$
NR - 2	$16.33 \pm 0.08$	$16.36 \pm 0.08$	$16.34 \pm 0.08$

\*Average  $pK_a \pm s$  values obtained from  $Q_x$ ,  $Q_y$  and  $Q_z$  co-ordinates. For QR, the  $pK_a$  values from  $Q_z$  co-ordinates were not considered because of the small variation of  $Q_z$  in the pH range, Fig. 4.

spectrophotometrically by a procedure described by Albert and Serjeant.<sup>27</sup> The results of the two methods agree (Table 3). In the case of TROP the second protonation equilibrium, perceptible as a short line in the complementary chromaticity diagram, was taken into account in the  $pK_a$  computation. The colour point of the pure form of TROP (HI) can be found from the intersection of the two linear segments in Fig. 3.<sup>25,28</sup> The colour point of the pure form of pNB (I), was found in a similar way.

The quality of the colour change of an indicator depends on the distance between the colour points of its acidic and basic forms in the complementary chromaticity diagram. However, the colour distribution on this diagram is not uniform and does not allow direct evaluation of the quality of colour changes, because distances in different regions of the diagram have non-equivalent physical meanings.<sup>10</sup>

However, we can deduce that the colour change of BCG is of better quality than that of MG, BG and pNB, all of which give complementary chromatic transitions with similar orientation. In the same way, TROP shows a better quality of colour change than QR and the second transition of NR. As the orientation of the segments in the complementary chromaticity diagram is very different, the two groups of indicators cannot be compared and neither can the first colour change of NR. Furthermore, the complementary chromaticity data give no information about the ideal indicator concentration, and to find this the method of Kotrlý and Vytřas<sup>12</sup> was used. In this, the minimum of the plot of  $\Delta pH/\Delta E$  (index of colour change perceptibility) *vs.*  $\log(c/c_{ref})$  gives the

optimum indicator concentration;  $c_{ref}$  is the reference experimental value of the indicator concentration,  $c$  is the indicator concentration and  $E$  is the total difference between two colours, calculated by using the CIELAB and CIELUV systems. The data obtained for both systems agree and the results, referred to 1-cm path-length, are given in Table 4.

To describe objectively the quality of colour change of the indicators, a modification<sup>14</sup> of the method of Bhuchar and Agrawal,<sup>13</sup> based on a plot of  $\Delta E/\Delta pH$  [or the specific colour discrimination (SCD) values] *vs.* pH (Fig. 4), was used.

In this plot, the band-width of each peak is the transition pH range, and the pH value at the maximum is the pH for the maximum change of colour ( $pH_{mcc}$ ). The half band-width ( $\Delta pH_{1/2SCD}$ ) is also related to the sharpness of the chromatic transition, and the maximum of each peak (in SCD units) is taken as the sensitivity of the colour change. Table 4 gives the average obtained by both CIELAB and CIELUV, except for the SCD values, which are not comparable for different chromatic systems.

From the SCD values (Fig. 4) it can be deduced that MG, BG, TROP and BCG show very pronounced colour changes in acetonitrile and the other indicators give smaller colour changes but still have adequate sensitivity. These conclusions all agree with visual observations.

Table 4 shows the difference between the  $pK_a$  and  $pH_{mcc}$  values that do not agree, as a result of the different sensitivity of human eye to different colours.

The  $pH_{mcc}$  values are displaced, relative to the  $pK_a$  values, towards pH values at which the concentration

Table 4. Colour changes of indicators

Indicator	$c_{ref}$ , M	Optimum concn. for 1-cm path-length,		$pH_{mcc}$	Transition pH range	$\Delta pH_{1/2SCD}$	$pK - pH_{mcc}$
		$c_{ref}$ , M	M				
pNB	$9.57 \times 10^{-5}$	$6 \times 10^{-4}$		8.2	6.8-10.5	2.0	-1.0
TROP	$2.30 \times 10^{-5}$	$5 \times 10^{-5}$		9.5	7.5-10.5	1.5	-0.5
QR	$3.96 \times 10^{-5}$	$9 \times 10^{-5}$		9.0	7.6-10.0	1.1	0.6
MG	$1.11 \times 10^{-5}$	$6 \times 10^{-5}$		5.4	3.8-7.2	1.8	0.6
BG	$1.11 \times 10^{-5}$	$7 \times 10^{-5}$		6.1	4.2-7.9	2.2	0.5
BCG	$1.66 \times 10^{-5}$	$1 \times 10^{-4}$		18.2	17.1-19.2	1.1	0.6
NR - 1	$2.17 \times 10^{-5}$	$4 \times 10^{-5}$		4.7	3.4-6.4	1.3	0
NR - 2	$2.17 \times 10^{-5}$	$7 \times 10^{-5}$		16.9	15.1-18.4	1.9	-0.6

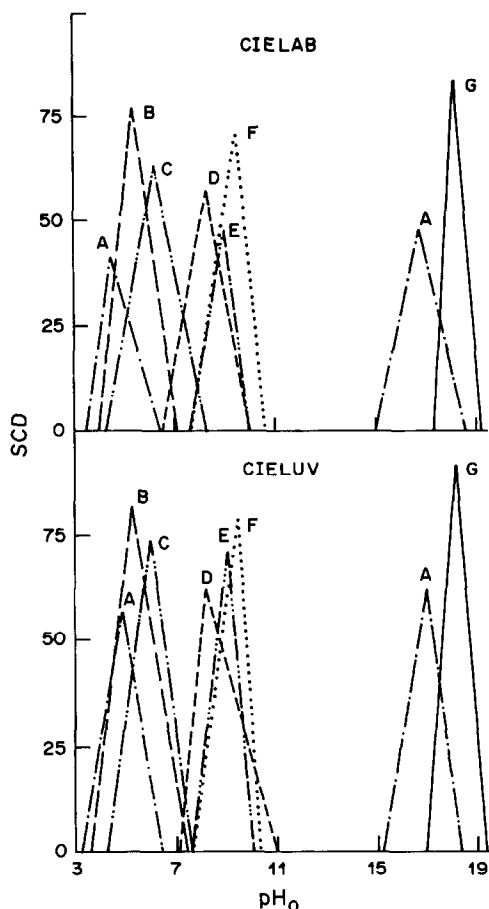


Fig. 4. Changes of SCD values, in CIELAB and CIELUV systems, with pH at zero ionic strength ( $pH_0$ ). A, NR; B, MG; C, BG; D, pNB; E, QR; F, TROP; G, BCG.

of the less intensely coloured form is the higher. Thus, the  $pH_{mcc}$  value of pNB is higher than its  $pK_a$  value, because the green acidic form is more intensely coloured than the yellow basic form, and in the same

way the  $pH_{mcc}$  value of the first transition of Neutral Red agrees with the  $pK_a$  value, since the chromatic transition occurs between two almost equally strongly coloured forms.  $pH_{mcc}$  values are very important because they allow selection of the most suitable indicator for a specific titration.

Figure 5 gives the colour-change pH ranges of the indicators studied, the colours before and after the  $pH_{mcc}$  value.

The most important use of acetonitrile in acid-base titrations is as a medium for titrations of weak bases and their mixtures. The series of indicators studied covers the necessary pH range completely, as can be inferred from Fig. 5.

To test the usefulness of the indicators examined, some bases in acetonitrile medium were visually titrated with 0.1M perchloric acid. The results are given in Table 5. Solutions of perchloric acid in acetonitrile are unsuitable as titrants because their hydrogen-ion activity decreases rapidly on aging,<sup>5</sup> so perchloric acid in anhydrous acetic acid was used as the titrant. However, this solution cannot be used for visual titration of bases when indicators with  $pK_a$  values  $\geq 14$  are used, and is also not suitable for titrations of mixtures of bases in acetonitrile because the acetic acid decreases the potential break, especially on the basic side, and levels the difference in basic strength by reaction with the free bases.<sup>5</sup>

We have found that a solution of perchloric acid monohydrate in nitromethane, which is more viscous than sulpholane, is very suitable for titrations in acetonitrile. This solution, recommended by Kolthoff *et al.*,<sup>5</sup> permits titration of bases with use of indicators having a transition interval in the basic region, such as BCG and NR, with very low errors (Table 5) and can be used for resolving mixtures of bases.

A binary mixture of tetramethylguanidine (TMG) and pyridine, has been titrated, with NR or a mixture of BCG and TROP as indicators, with errors less than 1%. Both these indicators are especially suitable

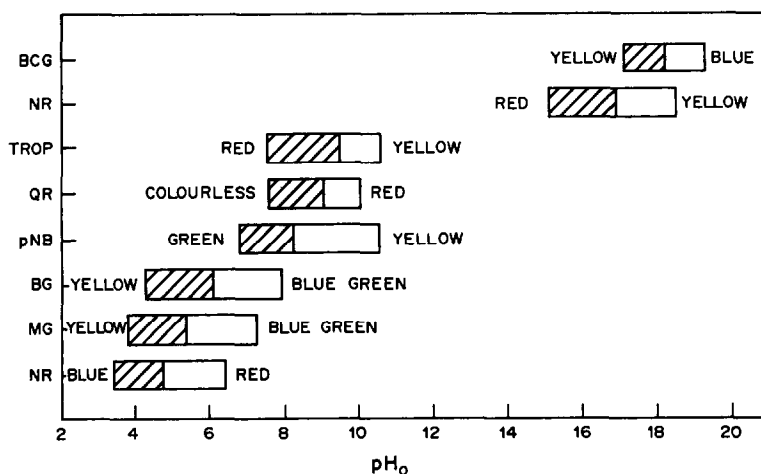


Fig. 5. Indicator transition ranges, at zero ionic strength, for the indicators in acetonitrile. Diagonal hatching, before the  $pH$  of maximum colour change; no hatching, after the  $pH$  of maximum colour change.

Table 5. Error (%) in titration of different substances in acetonitrile with 0.1M HClO<sub>4</sub> in acetic acid or nitromethane (means of 5 determinations of 10–50 mg of substance, RSD ≤ 0.5%)

Indicators Base	BCG	NR-2	RQ	TROP	pNB	BG	MG	NR - 1
Tetramethylguanidine			0.4 0.3	0.3 0.6	0.4 0.4	0.9 0.4	0.9 0.8	1.1 0.9
pK = 23.3 <i>n</i> -Butylamine	-1.7*	-1.17*			-0.7*			0.6*
			0.2 0.6	0.2 0.6	-0.0 <sub>3</sub> 0.6	0.6 0.9	0.4 0.9	0.5 0.8
pK = 18.26 1,3-DFG		-1.8*	0.2*	1.6 1.5	1.3 0.6	1.5 1.1	1.5 1.3	1.6 1.5
pK = 17.90 Morpholine			0.4 0.7	-0.0 <sub>4</sub> 0.7	0.1 0.9	0.3 0.8	0.1 0.8	0.6 0.8
pK = 16.61 Pyridine			0.9 0.8	0.7 0.6	0.9 0.7	1.1 1.2	1.3 1.4	1.5 1.0
pK = 12.33 Aniline			0.1 0.3	-0.2 -0.3	0.7 0.8	0.4 0.7	0.5 0.9	0.7 1.1
pK = 10.56 Urea				-0.8*				1.7* 0.3*
pK = 7.7								

\*Titration with perchloric acid solution in nitromethane.

for titrating mixtures of bases, because there is no colour interference between their pure forms.

The indicators studied give very sharp end-points in titrations of bases with dissociation constants of the order of 10<sup>-10</sup> or lower. Urea is more difficult to titrate and requires the most acidic indicator, NR, and perchloric acid in nitromethane as titrant, Table 5.

## REFERENCES

- J. F. Coetzee and M. W. Martin, *Recomm. Methods Purif. Solvents Tests Impurities*, 1982, 10.
- I. M. Kolthoff and P. J. Elving (eds.), *Treatise on Analytical Chemistry*, 2nd Ed., Part 1, Vol. 2, p. 243. Wiley-Interscience, New York, 1979.
- I. M. Kolthoff, *Anal. Chem.*, 1974, **46**, 1992.
- J. F. Coetzee and G. R. Padmanabhan, *J. Am. Chem. Soc.*, 1965, **87**, 5005.
- I. M. Kolthoff, M. K. Chantooni, Jr. and S. Bhowmik, *Anal. Chem.*, 1967, **39**, 1627.
- Idem, ibid.*, 1967, **39**, 315.
- M. Blanco and J. Barbosa, *Talanta*, 1982, **30**, 61.
- F. W. Billmeyer and M. Saltzmann, *Principles of Colour Technology*, 2nd Ed., Wiley, New York, 1981.
- G. J. Chamberlin and D. F. Chamberlin, *Colour*, Heyden, London, 1980.
- C. N. Reilley, H. A. Flaschka, S. Laurent and B. Laurent, *Anal. Chem.*, 1960, **32**, 1218.
- K. Vytřas, *Chem. Zvesti*, 1974, **28**, 252.
- S. Kotrlý and K. Vytřas, in *Essays on Analytical Chemistry*, (E. Wänninen (ed.)), pp. 259–280. Pergamon Press, Oxford, 1977.
- V. M. Bhuchar and A. K. Agrawal, *Analyst*, 1982, **107**, 1439.
- J. Barbosa, E. Bosch and R. Carrera, *Talanta*, 1985, **32**, 1077.
- J. Barbosa, E. Bosch and M. Rosés, *Analyst*, 1987, **112**, 179.
- V. A. Pleskov, *Zh. Fiz. Khim.*, 1948, **22**, 351.
- J. F. Coetzee and G. R. Padmanabhan, *J. Phys. Chem.*, 1962, **66**, 1708.
- I. M. Kolthoff and M. K. Chantooni, Jr., *J. Am. Chem. Soc.*, 1965, **87**, 4428.
- I. M. Kolthoff, M. K. Chantooni, Jr. and S. Bhowmik, *ibid.*, 1966, **88**, 5430.
- I. M. Kolthoff, M. K. Chantooni, Jr. and H. Smargowski, *Anal. Chem.*, 1970, **42**, 1622.
- J. F. Coetzee, G. R. Padmanabhan and G. P. Cunningham, *Talanta*, 1964, **11**, 93.
- M. Rosés, *Ph.D. Thesis*, University of Barcelona, 1986.
- Idem, Anal. Chim. Acta*, submitted for publication.
- J. Barbosa, D. Barron and E. Bosch, *Analyst*, 1987, **112**, 1717.
- C. Reilley and E. Smith, *Anal. Chem.*, 1960, **32**, 1233.
- H. Flaschka, *Talanta*, 1961, **8**, 342.
- A. Albert and E. P. Serjeant, *The Determination of Ionization Constants*, Chapman and Hall, London, 1974.
- J. Barbosa, J. Sánchez and E. Bosch, *Talanta*, 1984, **31**, 279.

# Talanta

The International Journal of Pure and Applied Analytical Chemistry



The illustration of a Greek balance from one of the Hope Vases is reproduced here by kind permission of Cambridge University Press

---

## Editor-in-Chief

DR R.A.CHALMERS, Department of Chemistry, University of Aberdeen, Old Aberdeen, Scotland

## Assistant Editors

DR J.R.MAJER, University of Birmingham, England

DR I.L.MARR, University of Aberdeen, Scotland

DR D.MIDGLEY, Central Electricity Research Laboratories, Leatherhead, England

## Computing Editor

DR MARY R.MASSON, University of Aberdeen, Scotland

## Regional Editors

PROFESSOR I.P.ALIMARIN, Vernadsky Institute of Geochemistry and Analytical Chemistry, U.S.S.R. Academy of Sciences, Kosygin St., 19, Moscow V-334, U.S.S.R.

PROFESSOR J.S.FRITZ, Department of Chemistry, Iowa State University, Ames, IA 50010, U.S.A.

PROFESSOR T.HORI, Department of Chemistry, Kyoto University, Kyoto, Japan

DR K.-H. KOCH, Hoesch Stahl AG, Dortmund, G.F.R.

PROFESSOR E.PUNGOR, Institute for General and Analytical Chemistry, Technical University, Gellért tér 4, 1502 Budapest XI, Hungary

PROFESSOR J.D.WINEFORDNER, Department of Chemistry, University of Florida, Gainesville, FL 32611, U.S.A.

## Editorial Board

Chairman: PROFESSOR J.D.WINEFORDNER

DR R.A.CHALMERS

DR J.R.MAJER

DR I.L.MARR

DR M.R.MASSON

DR D.MIDGLEY

---

## Publishing Office

Journals Production Unit, Pergamon Journals Ltd, Hennock Road, Marsh Barton, Exeter, Devon EX2 8NE, England [Tel. Exeter (0392) 51558; Telex 42749].

## Subscription and Advertising Offices

North America: Pergamon Journals Inc., Maxwell House, Fairview Park, Elmsford, NY 10523, U.S.A.

Rest of the World: Pergamon Journals Ltd, Headington Hill Hall, Oxford OX3 0BW, England [Tel. Oxford (0865) 64881].

## Published Monthly. Annual Subscription Rates (1988)

Annual institutional subscription rate (1988) DM 1045.00; 2-year institutional rate (1988/89) DM 1985.50; personal subscription rate for those whose library subscribes at the regular rate (1988) DM 204.00. Prices are subject to amendment without notice.

### Microform Subscriptions and Back Issues

Back issues of all previously published volumes are available in the regular editions and on microfilm and microfiche. Current subscriptions are available on microfiche simultaneously with the paper edition and on microfilm on completion of the annual index at the end of the subscription year.

Copyright © 1988 Pergamon Journals Limited

It is a condition of publication that manuscripts submitted to this journal have not been published and will not be simultaneously submitted or published elsewhere. By submitting a manuscript, the authors agree that the copyright for their article is transferred to the publisher if and when the article is accepted for publication. However, assignment of copyright is not required from authors who work for organizations which do not permit such assignment. The copyright covers the exclusive rights to reproduce and distribute the article, including reprints, photographic reproductions, microform or any other reproductions of similar nature and translations. No part of this publication may be reproduced, stored in a retrieval system or transmitted in any form or by any means, electronic, electrostatic, magnetic tape, mechanical, photocopying, recording or otherwise, without permission in writing from the copyright holder.

Photocopying information for users in the U.S.A. The Item-fee Code for this publication indicates that authorization to photocopy items for internal or personal use is granted by the copyright holder for libraries and other users registered with the Copyright Clearance Center (CCC) Transactional Reporting Service provided the stated fee for copying beyond that permitted by Section 107 or 108 of the U.S. Copyright Law is paid. The appropriate remittance of \$3.00 per copy per article is paid directly to the Copyright Clearance Center Inc., 27 Congress Street, Salem, MA 01970.

Permission for other use. The copyright owner's consent does not extend to copying for general distribution, for promotion, for creating new works or for resale. Specific written permission must be obtained from the publisher for such copying.

The Item-fee Code for this publication is: 0039-9140/88 \$3.00 + 0.00

## PUBLICATIONS RECEIVED

---

**Chromatographic Theory and Basic Principles:** J. A. JÖNSSON (Editor), Marcel Dekker, New York, 1987. Pages xi + 396. \$79.75 (U.S. and Canada); \$95.50 (elsewhere).

This is another book in the Chromatographic Science Series (Volume 38). It begins with a brief, but concise, review of the basic terminology common to all forms of chromatography. This is followed by an excellent chapter which deals with, in the main, the origins and theoretical aspects of dispersion and peak shapes in chromatography. Empirical peak shape equations are given which will facilitate the simulation and computerized handling of chromatographic data. In subsequent chapters the basic principles and the theoretical aspects of retention in GLC, GS, LC, IC and SEC are all covered. The general approach used throughout is one of the development of mathematically based model systems which can be used to predict or explain real chromatographic behaviour. The text is well referenced and the excellent bibliography is extensive and appropriate. The book is a must for those chromatographers who wish to optimize their chromatographic systems on the basis of a sound understanding of the underlying theoretical principles involved.

R. R. MOODY

## PUBLICATIONS RECEIVED

---

**Practical High-Performance Liquid Chromatography:** V. R. MEYER, Wiley, Chichester, 1988. Pages xiii + 310. £29.50.

The aim of this book is to show the possibilities and problems associated with modern HPLC. The text appears to be suitable for a wide readership, including beginners, laboratory technicians with a working knowledge of the subject and even experts in the field.

There are 25 small sections in the book, which include theory, equipment, chromatographic separation modes and analytical and preparative HPLC. The theoretical background is restricted to the principles of HPLC, and several problems are presented and worked through to enhance the clarity of the presentation. An extensive bibliography on HPLC is also included.

Practical aspects of the book are very much in evidence; indeed, the initial manuscript of the textbook was written for a training course in HPLC for laboratory technicians. Potential problems are mentioned and practical hints are given. The applied nature of the book is demonstrated by sections on preparation of equipment, column packing and regeneration, HPLC column tests, choice of method and solving the elution problem. In each of the nine sections on a particular separation mode, such as reversed-phase chromatography or size-exclusion chromatography, applications of the technique are mentioned.

There are small sections on the separation of enantiomers and on some relatively new HPLC techniques concerning columns, speed and mobile phase. A number of review papers on the separation of individual classes of compounds is given and extensive lists of commercially available stationary phases and manufacturers concludes the text.

As the book attempts to cover nearly all aspects of HPLC, some topics are mentioned only briefly. For example a little more detail on photodiode array detectors and on coupling techniques for improved specificity of detection would have been beneficial. However, this is an extremely useful book packed full of information that will be a valuable addition to any laboratory using HPLC. Highly recommended.

P. J. Cox

**High Resolution Solid State NMR of Silicates and Zeolites:** G. ENGELHARDT and D. MICHEL. Wiley, Chichester, 1987. Pages xiv + 485. £55.00 (cloth bound).

This book describes the principles, techniques and applications of high-resolution solid state NMR methods, especially as applied to silicates and aluminosilicates. It provides a very good and authoritative account of the subject and will be of value both to researchers in the field and to all interested in silicates, their structures and applications. The chapter on principles and techniques assumes the reader has a general familiarity with NMR and concentrates on the theory behind NMR line-widths, and techniques, such as magic angle spinning, which are used to reduce line-widths and obtain high-resolution spectra of solid samples. The remaining five chapters deal more with applications and fall into two groups. One group treats  $^{29}\text{Si}$  and  $^{27}\text{Al}$  NMR. A short chapter on silicate solutions reviews silicate anions, the  $Q$  notation for silicate polymers and the kind of information on structures, chemical reactions and equilibria in solution obtained by using  $^{29}\text{Si}$  NMR. This is a useful preliminary to the main purpose of the book. Two major chapters on silicates and aluminosilicates deal with the factors that influence chemical shifts, intensities and line-widths and how NMR may be used as a local structure probe of, *e.g.*, Al, Si ordering in zeolites. Hundreds of examples are given, all post-1980, illustrating the power and utility of the method for obtaining structural information that is frequently unobtainable by conventional diffracton techniques.

The other group deals with various other nuclei such as  $^{17}\text{O}$ ,  $^{13}\text{C}$  (for looking at the structure of the "organic template" in zeolite syntheses),  $^1\text{H}$  (for probing Si-OH groups),  $^{11}\text{B}$  (for borosilicates), and various nuclei present in molecules which can be adsorbed on zeolites, silicas, *etc.* and which are involved in catalytic processes.

A. R. WEST



## TALANTA MEDAL

---

### PROFESSOR H. A. LAITINEN



The Publisher and Editorial Board of *Talanta* take great pleasure in announcing that, with the approval of the Advisory Board, the Twelfth Award of the Talanta Medal has been made to Professor Herbert A. Laitinen, of the Department of Chemistry, University of Florida.

Professor Laitinen's name is universally known in the world of analytical chemistry, not only for his researches in electrochemistry and other branches of chemistry, but also for the profound influence he has had on research and teaching, first through his classic text *Chemical Analysis*, and then through his distinguished editorship of *Analytical Chemistry*, and the penetrating observations made in his editorials. In a research career that has spanned more than 50 years he has published over 200 papers and is still active in the field. He is a truly outstanding analytical chemist.

## CORRIGENDUM

---

In the paper by J. Namieśnik, *Talanta*, 1988, **35**, 567, the acknowledgement of copyright in certain figures should read as follows.

- Figure 4 Reprinted with permission by *American Industrial Hygiene Association Journal*: Vol. 34:78, Fig. 1 (1973). Permission granted by Paul D. Halley.
- Figure 7 Reprinted with permission by *American Industrial Hygiene Association Journal*: Vol. 37:514, Fig. 9 (1976). Permission granted by Paul D. Halley.
- Figure 8 Reprinted with permission by *American Industrial Hygiene Association Journal*: Vol. 37:514, Fig. 10 (1976). Permission granted by Paul D. Halley.
- Figure 9 Reprinted with permission by *American Industrial Hygiene Association Journal*: Vol. 37:514, Fig. 12 (1976). Permission granted by Paul D. Halley.
- Figure 13 Reprinted with permission by *American Industrial Hygiene Association Journal*: Vol. 39:349, Fig. 5 (1978). Permission granted by Paul D. Halley.
- Figure 15 Reprinted with permission by *American Industrial Hygiene Association Journal*: Vol. 44:615, Fig. 3 (1983). Permission granted by Paul D. Halley.

Note also that in Fig. 4, the reference number should have been 68, not 71.

## PUBLICATIONS RECEIVED

---

**Analytical Chemistry in the Exploration, Mining and Processing of Materials:** L. R. P. BUTLER (Editor), Blackwell Scientific Publications, Oxford, 1986. Pages 254. £24.00.

This very informative book contains most of the invited lectures presented at the Second International Symposium on Analytical Chemistry in the Exploration, Mining and Processing of Materials, which was held in Pretoria, South Africa, in 1985 under the auspices of the IUPAC Analytical Chemistry Division and the Council for Scientific and Industrial Research. These lectures, many by well-known researchers in their fields, deal with the theory and practice and advantages and disadvantages of various instrumental techniques, *viz.* inductively-coupled plasmas (including ICP-AES, ICP-OES and ICP-MS), X-ray fluorescence and diffraction, atomic-absorption spectrometry, neutron activation and ion-beam analysis, pulse voltammetry and laser-excited atomic-fluorescence spectrometry, used for the analysis of materials associated with the mining industry. However, the greatest emphasis is on ICP, XRF and AAS techniques. Some specific applications of these techniques are to the analysis of ferrous and non-ferrous materials, coal, high-temperature reactor core materials, ceramic materials and gold, silver and platinum-group geological materials. Other important themes are the application of surface analysis techniques in material development, automation and on-line analysis for process control in extractive metallurgy, flow-injection analysis, environmental analysis, chemometrics, reference materials, wet chemistry and separation techniques and the use of gas anomalies in geochemical exploration.

The book contains a wealth of information on present-day instrumental practice in the analytical sciences connected with the exploration, mining and processing of materials and should be of interest to all those engaged in these fields.

ELSIE M. DONALDSON

**Assay and Analytical Practice in the South African Mining Industry:** W. C. LENAHAN and R. DE L. MURRAY-SMITH, South African Institute of Mining and Metallurgy, Johannesburg, 1986. Pages xix + 640, \$80.00.

This book is a revised, updated and considerably improved version of the 1955 second edition, *Assay Practice in the Witwatersrand*, by V. S. Dillon. It has essentially the same format, with the same emphasis on gold and the gold mining industry, and deals with all aspects of the South African mining industry, including laboratory design and safety, fire-assay practice, preparation of samples and sampling, particle size analysis, treatment and analysis of water and effluents, analysis and testing of coal and coke and analysis of mine air, uranium-prospecting, mining and plant samples, gold bullion, cyanide solutions, geological prospecting samples and ores and related materials. Older "classical" methods of analysis for gold and other elements have been retained in this third edition but many new alternative instrumental methods involving atomic-absorption, emission and X-ray spectrometric and UV and visible spectrophotometric finishes have been added, notably for the determination of impurities in water and effluents and in gold bullion and high-purity silver, for base metals in ores and related materials and for gold in cyanide solutions and geological prospecting samples. A chapter on statistical control in analytical practice has also been included.

The book is a comprehensive and informative guide to present-day methods of assaying. The presentation is clear and concise and it is relatively free of typographical errors. The methods are described in adequate detail and include notes on potential problems and sources of error. Small criticisms are the use of the rather antiquated units, cm<sup>3</sup> and dm<sup>3</sup>, rather than the more universally-accepted millilitre (ml) and litre (l), which were used in the second edition, and the unnecessary inclusion in Chapter 17 of sections describing the basic theory and practice of atomic-absorption spectrometry and various other instrumental techniques. These can be found in many other reference books. It is also not clear what the treatment and/or analysis of swimming pool water, sewage effluents and sorghum beer have to do with the mining industry. However, these are only minor points and do not detract from the overall quality and usefulness of the book. It should be of value to all technical staff in mining laboratories.

ELSIE M. DONALDSON

**High Performance Liquid Chromatography:** SANDY LINDSAY, Wiley, Chichester, 1987. Pages xx + 244. £28.00 (cloth-bound); £9.95 (paper-back).

This book in the Analytical Chemistry Open Learning series was written to explain the principles of HPLC to people who have had no practical experience of the technique in chemistry. The first two chapters deal with the instrumentation commonly found in HPLC, and the factors determining its performance. Later chapters give a general outline of experimental applications commonly used in the laboratory. Although the book deals with very simple applications of the techniques, the basic methods described can be adapted to allow more complicated separations to be achieved. Throughout the book problems and examples are given with their solutions to allow self assessment. The book's emphasis is more on the theoretical side of HPLC. Although the book is adequate as a textbook on HPLC, it would be more useful as a reference work if more practical examples were given instead of concentrating so much on the hardware, and if it had an index.

HILARY SMITH

## TALANTA ADVISORY BOARD

---

The Publisher and Editorial Board of *Talanta* take great pleasure in announcing the appointment of Dr. B. Ya. Spivakov as an additional member of the Advisory Board of the journal.

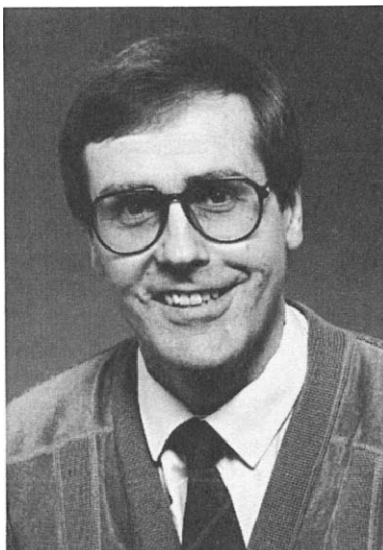


Doctor B. Ya. Spivakov was born in 1941 in Moscow. He holds the degrees of Candidate of Science and Doctor of Science obtained from the Vernadsky Institute of Geochemistry and Analytical Chemistry, USSR Academy of Sciences, Moscow. He joined the staff of the Vernadsky Institute in 1964, and is currently the head of a research group of the Analytical Department. His research interests are in separation and enrichment methods and their combinations with instrumental techniques of analysis for determination of small and trace amounts of elements in various materials. He has published over 100 research papers in these fields. He is head of the Commission on Separation and Preconcentration, of the Scientific Council on Analytical Chemistry of the USSR Academy of Sciences, and currently a member of the Commission on Microchemical Techniques and Trace Analysis, in the Analytical Division of IUPAC.

## TALANTA ADVISORY BOARD

---

The Publisher and the Editorial Board of *Talanta* welcome Professor Ari Ivaska as a member of the Advisory Board of the journal.



Professor Ari U. Ivaska was born on 8 May 1946 at Kuopio, Finland, and gained his M.Sc. in Chemical Engineering, at Åbo Akademi, Turku (Åbo), Finland in 1971, followed by a Ph.D. in Analytical Chemistry in 1975 and a Docent degree in 1980. He has been successively Assistant (1971–1975) and Lecturer (1975–1979) in General Chemistry, then Lecturer (1979–1987) in Analytical Chemistry and is now Professor of Analytical Chemistry at Åbo Akademi. He has been a British Council Scholar at Chelsea College, London (1978–1979), UNESCO expert in electroanalytical chemistry at Universidade Estadual de Campinas, Campinas, Brazil (1980–1981), NSF Postdoctoral Fellow at Northwestern University, Evanston, Illinois (1982–1983) and Special Research Fellow at the Research Centre of Neste Ltd, Kulloo, Finland (1985–1986). His awards include the Finnish Chemical Society Komppa Prize for the best doctoral thesis in chemistry in Finland (1975) and the Åbo Akademi German Prize for meritorious research (1985). He is the author or co-author of over 50 scientific papers, and his main research interests are continuous and automatic analytical methods, process analytical chemistry, electrochemical methods in analysis, and use of fast Fourier Transform methods in analysis of electrochemical data, especially in ac polarography. Recently he has become interested in simultaneous spectroscopic and electrochemical studies on conductive polymers. His hobbies are sailing and carpentry.

## OBITUARY

---



**PROFESSOR HANS EWALD BLASIUS**  
(1921–1987)

Professor Hans Ewald Blasius, of the University of the Saarland, died on 15 August 1987 after a short illness. Born in Berlin in 1921, he graduated in the Institute of J. D'Ans in the Technical University of Berlin, with investigations on the rare earths. In 1958, under G. Jander at the same university, he received his habilitation with a thesis on chromatographic methods in analytical and preparative chemistry, with special regard to ion-exchange. In 1964 he was made Director of the Institute of Analytical Chemistry and Radiochemistry of the University of the Saarland, at Saarbrücken. He became well known to German-speaking chemists through two course-books and two textbooks on analytical chemistry. His investigations in the field of ion-exchange, electrophoresis and special problems of radiochemistry broadened over the ensuing 24 years to cover a wide field, such as application of cross-linked macrocyclic polyethers in analytical and preparative chemistry, sulphur chemistry, archeometry, and separations of fission products from radioactive waste of the nuclear fuel cycle. His scientific activity is documented in 170 publications, monographs and books. Professor Blasius was a member of numerous national and international organizations, and invited to lecture extensively all over the world. He will be missed not only by his family and friends, but also by the students to whom he was a popular teacher of analytical chemistry.

K.-P. JANZEN

## PUBLICATIONS RECEIVED

---

**Occurrence, Properties and Utilization of Natural Zeolites:** edited by D. KALLO and H. S. SHERRY, Akadémiai Kiadó, Budapest, 1988. Pages XII + 857. £45.00

This volume consists of the papers (invited and submitted) presented at the 2nd International Conference on the title topic, held in Budapest in August 1985. It is divided into subject sections: Geology and Mineralogy, Synthesis and Stability; Crystal Chemistry and Physical Properties; Applications in General; Ion-Exchange; Water Purification; Adsorption; Catalysis; Agricultural Applications; Miscellaneous. The 66 papers therefore provide something for almost everyone interested in zeolites. The text is presented as camera-ready typescript, but the typing is uniform. The price is very reasonable.

R. A. CHALMERS

**Handbook of Industrial Drying:** edited by ARUN S. MAJUMDAR, Dekker, New York, 1987. Pages xii + 948. US\$150.00 (U.S.A. and Canada); \$180.00 (elsewhere).

Covering all aspects of large-scale drying processes and techniques, this volume is a mine of information for those concerned with moisture control in industrial products and raw materials, but like most mines it requires a fair amount of work to be done to extract material from it. In other words, the index is not as useful as it should be. The contents list is not all that helpful either, since it does not give the subsection headings, and the running heads indicate only the chapter title and authors, and not the chapter number or section number. The analyst needing to use the book frequently will probably make up his own specialist index.

R. A. CHALMERS

**Manual of Fertilizer Processing:** edited by FRANCIS T. NIELSSON, Dekker, New York, 1987. Pages xv + 525. US\$125.00 (U.S.A. and Canada); \$150.00 (elsewhere).

The book covers the major developments in the fertilizer industry over the past 30 years or so, dealing with the production of single and mixed fertilizers. The emphasis throughout is on the production aspects, and the only section likely to be of interest to the analyst is the chapter on environmental regulations.

R. A. CHALMERS

**Principles of Colloid and Surface Chemistry:** 2nd Edition, PAUL C. HIEMENZ, 2nd Ed., Dekker, New York, 1986. Pages xv + 815. US\$39.75 (U.S.A. and Canada); \$47.70 (elsewhere).

The first edition of this book has served well a generation of colloid and surface science students. With the field of these topics continually expanding, in depth and in breadth, it was inevitable that a new edition was necessary to encompass recent advances. Hiemenz has managed to produce a reasonably-sized book including more topics, without sacrificing the elementary introduction to each topic. The result overall is a reasonably good first text-book, but it has strong and weak points.

If students wish to know the state-of-the-art, then sufficient background material is provided in the book to enable them to tackle current journals and monographs. Students and teachers will appreciate the large number of solved problems throughout the book, and the care that Hiemenz has taken in selecting, for inclusion at the end of each chapter, problems originating from recent research publications is welcome. It would have been more helpful if answers to the numerical problems had been included. There are a number of problems of the type... "criticize or defend the following propositions:..." which are effective in a tutorial mode but which may overwhelm a distance learner.

The topics are arranged in a semi-arbitrary order with chapters on surfaces (6, 7, 9, 10) lying between those on colloids (1-5, 8, 11-13). It is unfortunate that Chapter 1, "Colloid and Surface Chemistry: Their Scope and Variables" is the least satisfactory. It includes an unusual array of subjects, with some explanations more perplexing than informative. Readers should not be deterred by this, as later chapters are of a higher standard.

There are a number of mathematical and typographical errors, and debatable points of view, so teachers using this book as a basis for their courses will need to scrutinize each part carefully. Some parts of this edition could have been omitted without serious loss: other parts could have included recent advances with added benefit. In spite of these criticisms, this edition is a good, readable, comprehensive "first text-book" for the next generation of students of colloid and surface chemistry.

JAMES B. CRAIG

**Surfactant Solutions: New Methods of Investigation:** edited by RAOUL ZANA, Dekker, New York, 1987, Pages xii + 479. US\$99.75 (U.S.A. and Canada); \$119.50 (elsewhere).

This volume is a review, written by fourteen authors and edited by Raoul Zana, of the theory and application of some modern techniques to the study of surfactant-containing systems.

Chapter 1, *Thermodynamic Systems*, deals with the application of the thermodynamics of solutions to binary, tertiary, and multicomponent systems. Trends of thermodynamic functions in the pre- and post-micellar concentration ranges are treated mathematically to extract relevant parameters. Mathematical models, pseudo-phase and mass-action, are described with their general equations, and their application to ionic and non-ionic surfactant solutions critically assessed. This chapter is of particular interest to those working with complex, multi-solute systems. Classical thermodynamics cannot provide structural information, whereas the subjects of Chapter 2, *Small-Angle Scattering Methods*, and Chapter 3, *Light-Scattering*, do. Both chapters are complementary and reading them requires a knowledge of vectors: the former requires a knowledge of statistical mechanics and Fourier components.

In Chapter 4, *Rheology of Surfactant Solutions*, the viscosity-concentration relationships for globular and rod-like micelles are examined and their flow behaviour explained. The variations in viscoelasticity with temperature, concentration, and chemical structure are used to describe the size, shape, and motion of micellar aggregates in solution. *Luminescence Probing Methods*, Chapter 5, describes how the aggregation number may be determined under actual experimental conditions by steady-state and decay methods. Information on the distribution of reactants among particles, micropolarity, microviscosity, dynamics, and partition coefficients, obtained by luminescence probing methods, is also provided.

*NMR Studies of Surfactant Systems*, Chapter 6, shows how the technique of nuclear magnetic resonance may be applied to surfactant chemistry to determine molecular transport, phase diagrams and structure, self-association, micelle size and shape, chain-packing and dynamics, counter-ion binding, hydration, and solubilization. Chapter 7, *Spin Labels*, describes how electron spin resonance may be used to give precise information on local state conformation in lamellar amphiphilic films, on special effects with curved films, and on localization effects in micelles. The use, synthesis, and need for critical selection of appropriate spin labels are clearly described. The theoretical aspects of ESR are treated in a simplified, though not over-simplified, way. The basic ideas of computer simulation of spectra are applied to the effects of geometrical distribution and slow molecular motions.

Chapter 8, *Chemical Relaxation Methods*, is a comprehensive treatment of the theoretical aspects of this technique when applied to the kinetics of micellization. A brief review is given of the temperature and pressure jump, shock tube, ultrasonic, and stopped-flow methods. Results on the dynamics of pure micellar solutions, mixed micelles, microemulsions, and micelles with added polymers, are assessed. Chapter 9, *Miscellaneous Methods*, deals with a collection of other techniques, birefringence, Rayleigh scattering, polarography, and ion-specific electrodes, which may be used in conjunction with established methods of examining surfactant properties.

Every chapter is well-written, comprehensive, up-to-date, and relatively error-free. Current research is critically assessed by each of the authors, who, with the editor, are to be congratulated for distilling a wealth of information into this moderately-sized, moderately-priced book. Those working in the field of surfactant science will find this volume a valuable addition to their own or establishment library.

J. B. CRAIG



## PUBLICATIONS RECEIVED

**Visible and Ultraviolet Spectroscopy:** RONALD C. DENNEY and ROY SINCLAIR, Wiley, Chichester, 1987. Pages xvii + 197. £28.50 (cloth), £9.95 (softback).

This is a small book in the Analytical Chemistry by Open Learning (ACOL) series. It serves as a basic introduction to colorimetry and to spectroscopy in the UV and visible regions of the spectrum. Nearly all aspects of the subjects are covered at an elementary level in an informal literary style. Several self-assessment questions and answers are included and the book is directed at the self-study market. As with other ACOL units it is a combination of a text book and a work book. In this respect there is more to be gained by purchasing the book than borrowing it from a library.

It is divided into four sections: Introduction, Quantitative Methodology, Spectrometric Determinations, and Qualitative Analysis and Structural Relationships. There is an overlap of subject material, such as the Beer-Lambert law and spectra-structure relationships, between these sections and the omission of an index is regrettable.

As expected, the emphasis throughout the book is placed on analytical applications. There is mention of the variables encountered with both instrumentation and solutions and the effects of these on analysis. Plenty of examples are given, including the determination of iron in water and in reagent chemicals, and the determination of sucrose and glucose in foodstuffs. Analysis by visual colorimetry and the analysis of binary systems are both well covered in the text.

As in any small book covering a wide topic, some aspects are given only a cursory treatment. This is particularly true with respect to the effect of temperature, elimination of interferences, nature of a complex (e.g., Job's method is not mentioned) and the importance of accuracy and precision. I would like to have seen the latter pair of topics treated more fully and specifically listed on the "Contents" page. It is also of limited value to simplify chemical equations, such as those for some of the colour tests, to the extent that they are not balanced.

Some Woodward rules for diene absorption are given along with calculation examples. The quoted value of 222 nm for the parent  $\alpha,\beta$ -unsaturated carbonyl is confusing, as this value varies with the type of carbonyl (e.g., aldehyde, ketone, ester, etc.). The reader is asked here to calculate absorption values for some aromatic molecules, which are not covered in the text, and for a molecule without a chromophore (presumably a misprint).

The book is good value for money but I imagine most potential customers would be willing to pay a little extra for an improved, extended version.

P. J. COX

**BASIC Programming for Chemists: An Introduction:** PETER C. JURIS, THOMAS L. ISENHOUR and CHARLES L. WILKINS. Wiley-Interscience, New York, 1987. Pages ix + 313. £30.50.

This book offers a comprehensive collection of some 40 chemical topics suitable for treatment by short computer programs, with example programs provided for each. It will serve as a valuable source book for instructors designing courses in computing for chemistry students, and it will also be useful for more advanced students, who should be able to make progress by working through the programs and problems. Examples of the topics included are: molar masses, gas laws, empirical formulae from analysis data, titration simulation and end-point location, phase diagrams, X-ray diffraction, Monte Carlo calculations, least squares, function fitting, and matrix operations.

However, I was most surprised to find a book published in 1987 to be so old-fashioned and main-frame orientated. For example the introductory discussion of high-level languages mentions only "compiler languages", and lists BASIC, FORTRAN, ALGOL, COBOL and PL1 as typical examples. The BASIC described is a mainframe BASIC, so the "Introduction to BASIC" would not be very suitable for use with microcomputers. There is no attempt to introduce computer graphics (except line-printer graphics), and there is no mention of real-time applications and data acquisition. It almost seems that the authors have not noticed the microcomputer revolution, which is a great pity.

MARY MASSON

**Introduction to Computer-Assisted Experimentation:** KENNETH L. RATZLAFF, Wiley, New York, 1987. Pages xv + 438. £41.25.

This book offers a comprehensive introduction to the many topics that concern the scientist wanting to be involved in computer-assisted experimentation. The author points out that manufacturers no longer expect the people who use small computers to be computer professionals, and this book is written for scientists, not computer specialists, nor yet electronic engineers. It begins with a general discussion of computers and their modes of operation, then moves on to look at the computer representation of numbers (binary, octal, hex, BCD, integers, floating point, double precision etc.) and alphanumeric codes (ASCII, EBCDIC, etc.). (But does Table 2.1 really demonstrate 2's complement numbers?)

Next comes a description of the hardware components, including the CPU, memory (ROM, RAM, PROM, EPROM, EEPROM), input-output ports, mass storage (floppy and hard discs, magnetic tape, optical methods), the system bus, user-interface peripherals. Anyone confused by computer jargon (such as the many acronyms included in this review) will find in Ratzlaff's book clear explanations of what the terms mean, and what the components actually do.

A section on operating systems and computer languages gives clear and helpfully critical descriptions and comparisons of many high-level languages, along with some discussion of the usefulness of "business software" such as databases and spreadsheets.

A detailed section on interfaces follows, in which the topics include input-output registers, parallel interfaces, analogue interfaces (i.e., analogue-to-digital converters), timing of data acquisition, and remote interface controllers.

The author then passes on to two chapters giving introductions to analogue and digital electronics (requiring only a general physics course as background), then to the important topic of transducers: first for temperature, light,

electrochemistry, and electrical power control; then for strain, pressure, and translation (including a section on laboratory robotics). A minor irritation here is the author's inability to spell "Celsius"—it appears incorrectly on several figures.

Later chapters cover data communications (RS232-C, X.25, IEE-488, Centronics parallel), graphics, computational techniques for data and signal processing, and there is a final chapter on 'The Overall Task', that considers how to choose a computer, develop the system, and maintain it.

This is a most useful reference book and handbook: it should be in every scientific library, and also at the bench in any laboratory involved, or intending to be involved, in computer-assisted experimentation.

MARY MASSON

**Reactions of Acids and Bases in Analytical Chemistry:** A. HULANICKI, Ellis Horwood, Chichester, 1987. Pages 308. £47.50

This book is derived from a Polish text first published in 1971 and has thus been thoroughly debugged; I found no errors apart from a dozen typographical ones and the writing is clear and easy to understand. The title is somewhat unspecific, however: the subject is more truly pH calculations in analytical chemistry, with the emphasis on calculations. Methodology is not touched on at all. The book is intended as a student text, with usefully illustrative worked examples in each section and a set of problems at the end of each chapter, but it could be used with profit by anyone concerned with titration curves and pH calculations. The basic concepts are covered in the first 80 pages and the book ends with 30 pages covering structural aspects and the various theories of acid-base reactions. In the middle we learn how to handle pH calculations of varying degrees of complexity including polyprotic acids, mixtures, the effect of metal ions, buffers and logarithmic diagrams (95 pages) and how to predict and interpret titration curves (55 pages). The arguments are developed gradually and in a well integrated way that aids comprehension. My only criticism is that the treatment of titration end-points and errors, although correct in as far as it goes, is restricted to rather old-fashioned procedures. In the modern laboratory the auto-titrator is the norm and analysts should know what is involved in the various methods of instrumental end-point detection, with their respective errors and advantages, which is not something they will ever find in an instruction manual. There is, however, much that is useful in the book and it is recommended to a wide readership.

DEREK MIDGLEY

## PUBLICATIONS RECEIVED

**Visible and Ultraviolet Spectroscopy:** RONALD C. DENNEY and ROY SINCLAIR, Wiley, Chichester, 1987. Pages xvii + 197. £28.50 (cloth), £9.95 (softback).

This is a small book in the Analytical Chemistry by Open Learning (ACOL) series. It serves as a basic introduction to colorimetry and to spectroscopy in the UV and visible regions of the spectrum. Nearly all aspects of the subjects are covered at an elementary level in an informal literary style. Several self-assessment questions and answers are included and the book is directed at the self-study market. As with other ACOL units it is a combination of a text book and a work book. In this respect there is more to be gained by purchasing the book than borrowing it from a library.

It is divided into four sections: Introduction, Quantitative Methodology, Spectrometric Determinations, and Qualitative Analysis and Structural Relationships. There is an overlap of subject material, such as the Beer-Lambert law and spectra-structure relationships, between these sections and the omission of an index is regrettable.

As expected, the emphasis throughout the book is placed on analytical applications. There is mention of the variables encountered with both instrumentation and solutions and the effects of these on analysis. Plenty of examples are given, including the determination of iron in water and in reagent chemicals, and the determination of sucrose and glucose in foodstuffs. Analysis by visual colorimetry and the analysis of binary systems are both well covered in the text.

As in any small book covering a wide topic, some aspects are given only a cursory treatment. This is particularly true with respect to the effect of temperature, elimination of interferences, nature of a complex (e.g., Job's method is not mentioned) and the importance of accuracy and precision. I would like to have seen the latter pair of topics treated more fully and specifically listed on the "Contents" page. It is also of limited value to simplify chemical equations, such as those for some of the colour tests, to the extent that they are not balanced.

Some Woodward rules for diene absorption are given along with calculation examples. The quoted value of 222 nm for the parent  $\alpha,\beta$ -unsaturated carbonyl is confusing, as this value varies with the type of carbonyl (e.g., aldehyde, ketone, ester, etc.). The reader is asked here to calculate absorption values for some aromatic molecules, which are not covered in the text, and for a molecule without a chromophore (presumably a misprint).

The book is good value for money but I imagine most potential customers would be willing to pay a little extra for an improved, extended version.

P. J. COX

**BASIC Programming for Chemists: An Introduction:** PETER C. JURTS, THOMAS L. ISENHOUR and CHARLES L. WILKINS. Wiley-Interscience, New York, 1987. Pages ix + 313. £30.50.

This book offers a comprehensive collection of some 40 chemical topics suitable for treatment by short computer programs, with example programs provided for each. It will serve as a valuable source book for instructors designing courses in computing for chemistry students, and it will also be useful for more advanced students, who should be able to make progress by working through the programs and problems. Examples of the topics included are: molar masses, gas laws, empirical formulae from analysis data, titration simulation and end-point location, phase diagrams, X-ray diffraction, Monte Carlo calculations, least squares, function fitting, and matrix operations.

However, I was most surprised to find a book published in 1987 to be so old-fashioned and main-frame orientated. For example the introductory discussion of high-level languages mentions only "compiler languages", and lists BASIC, FORTRAN, ALGOL, COBOL and PL1 as typical examples. The BASIC described is a mainframe BASIC, so the "Introduction to BASIC" would not be very suitable for use with microcomputers. There is no attempt to introduce computer graphics (except line-printer graphics), and there is no mention of real-time applications and data acquisition. It almost seems that the authors have not noticed the microcomputer revolution, which is a great pity.

MARY MASSON

**Introduction to Computer-Assisted Experimentation:** KENNETH L. RATZLAFF, Wiley, New York, 1987. Pages xv + 438. £41.25.

This book offers a comprehensive introduction to the many topics that concern the scientist wanting to be involved in computer-assisted experimentation. The author points out that manufacturers no longer expect the people who use small computers to be computer professionals, and this book is written for scientists, not computer specialists, nor yet electronic engineers. It begins with a general discussion of computers and their modes of operation, then moves on to look at the computer representation of numbers (binary, octal, hex, BCD, integers, floating point, double precision etc.) and alphanumeric codes (ASCII, EBCDIC, etc.). (But does Table 2.1 really demonstrate 2's complement numbers?)

Next comes a description of the hardware components, including the CPU, memory (ROM, RAM, PROM, EPROM, EEPROM), input-output ports, mass storage (floppy and hard discs, magnetic tape, optical methods), the system bus, user-interface peripherals. Anyone confused by computer jargon (such as the many acronyms included in this review) will find in Ratzlaff's book clear explanations of what the terms mean, and what the components actually do.

A section on operating systems and computer languages gives clear and helpfully critical descriptions and comparisons of many high-level languages, along with some discussion of the usefulness of "business software" such as databases and spreadsheets.

A detailed section on interfaces follows, in which the topics include input-output registers, parallel interfaces, analogue interfaces (i.e., analogue-to-digital converters), timing of data acquisition, and remote interface controllers.

The author then passes on to two chapters giving introductions to analogue and digital electronics (requiring only a general physics course as background), then to the important topic of transducers: first for temperature, light,

electrochemistry, and electrical power control; then for strain, pressure, and translation (including a section on laboratory robotics). A minor irritation here is the author's inability to spell "Celsius"—it appears incorrectly on several figures.

Later chapters cover data communications (RS232-C, X.25, IEE-488, Centronics parallel), graphics, computational techniques for data and signal processing, and there is a final chapter on 'The Overall Task', that considers how to choose a computer, develop the system, and maintain it.

This is a most useful reference book and handbook: it should be in every scientific library, and also at the bench in any laboratory involved, or intending to be involved, in computer-assisted experimentation.

MARY MASSON

**Reactions of Acids and Bases in Analytical Chemistry:** A. HULANICKI, Ellis Horwood, Chichester, 1987. Pages 308. £47.50

This book is derived from a Polish text first published in 1971 and has thus been thoroughly debugged; I found no errors apart from a dozen typographical ones and the writing is clear and easy to understand. The title is somewhat unspecific, however: the subject is more truly pH calculations in analytical chemistry, with the emphasis on calculations. Methodology is not touched on at all. The book is intended as a student text, with usefully illustrative worked examples in each section and a set of problems at the end of each chapter, but it could be used with profit by anyone concerned with titration curves and pH calculations. The basic concepts are covered in the first 80 pages and the book ends with 30 pages covering structural aspects and the various theories of acid-base reactions. In the middle we learn how to handle pH calculations of varying degrees of complexity including polyprotic acids, mixtures, the effect of metal ions, buffers and logarithmic diagrams (95 pages) and how to predict and interpret titration curves (55 pages). The arguments are developed gradually and in a well integrated way that aids comprehension. My only criticism is that the treatment of titration end-points and errors, although correct in as far as it goes, is restricted to rather old-fashioned procedures. In the modern laboratory the auto-titrator is the norm and analysts should know what is involved in the various methods of instrumental end-point detection, with their respective errors and advantages, which is not something they will ever find in an instruction manual. There is, however, much that is useful in the book and it is recommended to a wide readership.

DEREK MIDGLEY

## NOTICES

---

### 1989 EUROPEAN WINTER CONFERENCE ON PLASMA SPECTROCHEMISTRY

8-14 January 1989  
Reutte, Tyrol/Austria

The Austrian Society for Analytical Chemistry and Microchemistry (Working Group for Atomic Spectroscopy) in co-operation with the German Working Group on Applied Spectroscopy (DASp) are planning to organize the next European Plasma Winter Conference.

The original scientific and social format created by this conference series will be taken up again. A series of plenary lectures and extensive presentations of original research, mainly in poster form, are expected.

The location in the western part of Austria was chosen for its good accessibility from north and south. The city of Reutte is surrounded by magnificent mountains with great opportunities for practising all kinds of winter sports. At the same time Reutte's character is influenced very much by one of the best known hard metal and refractory metal producers worldwide, Metallwerke Plansee, which has its major production centre and company headquarters in this city. The newly built Chamber of Commerce will provide superb conference facilities, the hotels for good food and lodging. The first circular will be issued later in Spring 1988.

An instrument exhibition for plasma-related apparatus and spectrometers is being organized.

For information please contact:

Dr. Wolfhard Wegscheider, Graz Institute of Technology, Technikerstraße 4, A-8010 Graz/Austria: Telex 311221; Telefax +43 (316) 77 6 85

---

Name .....

Address .....

.....

.....

Please send to:

Dr. Wolfhard Wegscheider  
Inst. f. Analytische Chemie  
Technische Universität Graz  
Technikerstraße 4  
A-8010 Graz

I plan to attend the Plasma Winter Conference

I want to give a paper; tentative title .....

.....

I want to participate in the Instrument Exhibition

**J. HEYROVSKÝ CENTENNIAL CONGRESS ON POLAROGRAPHY  
and  
41st MEETING OF THE INTERNATIONAL SOCIETY OF  
ELECTROCHEMISTRY**

20–25 August 1990  
Prague, Czechoslovakia

The congress is organized to commemorate the 100th anniversary of the birth of Professor J. Heyrovský (born 20.12.1890) jointly by the Czechoslovak Academy of Sciences and the ISE.

New developments in polarography and other electrochemical methods and their applications to various fields of human activities will be discussed.

The major topics of the Congress will be:

1. Polarography and other electroanalytical methods in industrial, biomedical and environmental applications
2. Theory of charge transfer
3. Molecular electrochemistry
4. Non-metallic electrodes
5. Conversion and energy storage

Five plenary lectures and about 15 section lectures are foreseen. All scientific contributions will be presented in poster form.

Those interested in attending the Congress or getting further information are requested to write to:

Secretariat of the J. HEYROVSKÝ CENTENNIAL CONGRESS ON POLAROGRAPHY

J. Heyrovský Institute of Physical Chemistry and Electrochemistry, Czechoslovak Academy of Sciences,  
Vlašská 9, 118 40 Prague 1, Czechoslovakia

---

**3rd INTERNATIONAL SYMPOSIUM ON DRUG ANALYSIS**

16–19 May 1989  
Antwerp, Belgium

**BELGISCH GENOOTSCHAP VOOR  
FARMACEUTISCHE WETENSCHAPPEN**

---

**SOCIETE BELGE DES SCIENCES  
PHARMACEUTIQUES**

The International Symposium will be held in the University of Antwerp (UIA), Universiteitsplein 1, 2610 Wilrijk, from Tuesday 16 till Friday 19 May 1989.

*Scope*

The purpose of the Symposium is to bring together people from Industry, Universities, Control Laboratories and Hospitals to discuss the current status of analytical techniques, including instrumental applications and theoretical developments.

*Topics*

1. Fundamental aspects of drug analysis
2. Quality control of natural and synthetic raw materials
3. Analysis of pharmaceutical preparations
4. Determination of drugs in biological media
5. Automation in drug analysis

*Programme*

Plenary and keynote lectures will be given by invited speakers. Oral presentations will be limited. Preference will be given to poster presentations. Panel discussions could be organized.

For further information, please contact the Secretary of the Organizing Committee:

Dr. Apr. G. Laekeman

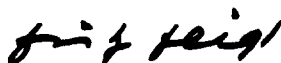
3rd International Symposium on Drug Analysis-Antwerp, Universitaire Instelling Antwerpen, Departement Farmaceutische Wetenschappen, Universiteitsplein 1, B-2610 WILRIJK, Belgium

# Foreword

THE importance of chemical analysis in all branches of pure and applied chemistry has always been fully recognized, and has resulted in constant efforts to meet their increasing demands. However new analytical methods are not found by chance or empirically: they are the fruits of experimental research based on the principles of analytical chemistry: they are oriented to them. These principles are related to all branches of chemistry. It was, and sometimes still is, a widespread belief that analytical chemistry owes its advancement exclusively to the progress made in other fields of chemistry. The pertinent literature shows us how far this is from the truth. Analytical papers frequently include statements and observations whose importance may exceed their analytical interest, and these have often become the starting point for further investigations in specific branches of chemistry.

The present high standard of chemical and physical analysis could never have been achieved without research which, in respect of originality, intensity and utility, ranks as high as any research work carried out in other fields of chemistry. Evidence of this is shown by the enormous number of analytical papers dealing with new discoveries, with critical examinations of, and improvements in, previously described methods and, last but not least, with applications of appropriate methods of testing materials in biological and other sciences. This unending flow of new contributions will certainly continue and increase in the future. Existing journals are not sufficient to ensure the rapid publication which is demanded both by authors and readers. It is therefore highly opportune that TALANTA, this new international journal of analytical chemistry in its broadest sense, is being introduced. The high standards and the tradition of analytical chemistry in education and research in the United Kingdom fully justify this enterprise.

The roll of eminent colleagues from many countries who have agreed to act on the editorial and advisory boards shows clearly the enthusiastic echo which is to be found all over the world when international scientific collaboration is the goal.



## PUBLICATIONS RECEIVED

**Secondary Ion Mass Spectrometry:** A. BENNINGHOVEN, F. G. RÜDENAUER and H. W. WERNER, Wiley, New York, 1987. Pages XXXV + 1227. £143.00.

This book contains over 2100 references and a wealth of information of value both to the beginner who requires a survey of the basic concepts and to the expert who will find in-depth treatments of all aspects of the subject. The coverage is comprehensive and includes the basic concepts, instrumental aspects, applications and trends.

Following a detailed discussion of the ion-solid interactions that occur, aspects of quantitative elemental analysis are covered, with description and assessment of the thermodynamic models used. The chapter on instrumentation not only covers the ion-optics and components of the mass spectrometer in considerable detail but also describes the commercially-available instruments, major laboratory-built instruments and other selected instruments which include novel or unusual design features. Although this last 100-page section cannot by its nature be up-to-date, it is of considerable value to those who wish to compare instruments or to see what features are available.

After a description of the operational modes (surface analysis, depth-profile analysis, lateral analysis and sputtered-neutral mass spectrometry) the experimental and technical considerations for application of SIMS are covered with some examples of application to biology and medicine, electronic materials, geology, metallurgy and other studies. The relatively modern technique of fast atom bombardment is given only two brief mentions and perhaps more should have been included of this important development, especially its applications.

The text is completed by consideration of SIMS combined with other techniques and by a preview of future developments. The appendices contain tables of data which make this a useful handbook as well as a general reference book.

J. R. BACON

**Personal Computers for Scientists. A Byte at a Time:** GLENN I. OUCHI, American Chemical Society, Washington, DC, 1987. pp. x + 278. USA and Canada \$34.95 (cloth), \$22.95 (paper); export \$41.95 (cloth), \$27.95 (paper).

This is a book written to help the new generation of computer users to make good use of the personal computers that are taking over all our lives. With especial reference to the IBM PC and its many clones, the author shows how scientists can make use of commercial applications packages for solving problems, organizing information, and plotting data. In non-technical language, he gives much useful information about PC hardware, explains all the jargon terms that a user is likely to encounter, and offers help to would-be purchasers (e.g., find an application program to do what you want, then buy some hardware that will run it.) Operating systems and computer languages are discussed critically, as are utility packages. In more detail, the author discusses the uses of word-processing packages, spreadsheets, graphics packages, database management systems, statistical analysis programs, data communication interfaces, and scientific interfacing packages. Most of the examples used to illustrate the uses of commercial packages consist of analytical data, especially chromatographic data. It seems that spreadsheets and databases have a lot to offer to the chromatographer. The text is well provided with the most useful kind of references, namely the details, including prices, of all the packages mentioned in the text, along with the names and addresses of the suppliers.

I found this book to be a most refreshing look at how computers can be used in laboratories, full of hints and tips of the kind that are never found in the manufacturers' handbooks, and with much to offer both to complete novices and to experienced hackers. I enjoyed it greatly.

MARY MASSON

**Nuclear Environmental Chemical Analysis:** J. TÖLGYESSY and E. H. KLEHR, Ellis Horwood, Chichester, 1987. Pages iv + 176. £35.00.

The obscure title is defined by the authors to cover indicator methods, activation methods, and interaction methods (e.g., scattering and fluorescence) as applied to environmental analysis, as well as measurement of radionuclides (both natural and man-made) in the environment. The book consists of the following chapters: the philosophy of N.E.C.A. (20 p., 27 refs.); environmental sampling (27 p., 25 refs.); preparation of standards and sample pretreatment (9 p., 14 refs.); analysis of radioactive environmental samples—(here is meant the measurement of radioactivity in environmental samples)—(17 p., 74 refs.); isotope dilution analysis (18 p., 42 refs.); radio-reagent methods (22 p., 81 refs.); activation analysis (31 p., 247 refs.); non-activation interaction analysis (21 p., 118 refs.); sources of information (7 p.), and an index (5 p.).

With such a wide subject matter, coverage in this slimish volume is necessarily concise. It is thus crucial to strike a reasonable balance between the fields considered, and unfortunately this is not always achieved. As evident from the page and reference listings above, isotope dilution analysis and radio-reagent methods receive more space than they merit on the basis of their usefulness in environmental analysis.

The weakest chapter is that on environmental radioactivity. While four diagrams are lavished on emanometric apparatus (though track etch methods are not mentioned), the section "Determination of Natural Radioactive Elements" consists, apart from some well known tables, of only 18 lines of text and one reference, while the section "Analysis of Transuranium Nuclides" receives 9 lines and 3 references. Tritium is not considered. Additionally the word "radioecology" is not in evidence, and the reader will search in vain for  $K_d$  values, uptake and transfer factors, models and modelling of pathways, etc.

It is not clear why sampling and sample treatment are split between two chapters. Some sampling techniques receive (over) detailed attention, but the use of clean benches or clean rooms is not described for biological materials, and several



important references are missing (e.g. Heydorn's book on Clinical Activation Analysis, Wolf's book of Biological Reference Materials, IAEA Technical Report 197 on biological materials). In Table 3.3, three sets of trace element values for Bowen's Kale from 1967, 1974 and 1975 are given, but not the 1979 IUPAC recommended values, or Bowen's 1985 values given in Wolf.

The chapter on activation analysis is comprehensive, contains many data in tabular form and is well referenced. Surprisingly, however, neutron-induced prompt gamma techniques (PGAA) are not mentioned. The listing of sources is very welcome, but the index is poor.

The style of the book is academic and in contrast to the more "hands-on" approach of "Environmental Radioanalysis" by Das, Faanhof and Van der Sloot, which is, however, more limited in scope. It is rather free of misprints and has only a few infelicitous expressions.

In summary, in spite of its drawbacks, this book could be useful to those seeking a concise guide to current nuclear analytical techniques in the environmental field.

A. R. BYRNE

**Computer Software Applications in Chemistry:** PETER C. JURTS, Wiley, New York, 1986. pp. xiv + 253. £33.70.

This book provides an excellent introduction to a wide range of applications of computer software in chemistry. The major divisions of the book are (1) Numerical Methods, which includes chapters on curve fitting, regression, numerical integration, solution of differential equations, matrix methods, Monte Carlo methods, and Simplex optimization; (2) Nonnumerical Methods, which includes chemical structure information handling, graph theory, substructure searching, molecular mechanics, pattern recognition, artificial intelligence and expert systems, and spectroscopic library searching; and (3) Graphics, which includes graphical display of data, and graphical display of molecules. Despite the wide range of areas covered, topics are treated in some depth, and are well referenced. Also, FORTRAN examples are often provided. I can strongly recommend this book to anyone who wants to get actively involved in chemical computing.

MARY MASSON

**Chemistry by Computer. An Overview of the Applications of Computers in Chemistry:** STEPHEN WILSON, Plenum Press, New York, 1986. pp. xi + 233. £37.50.

From the subtitle of this book, I expected it to be rather similar to the book by Jurts, but in reality, the subtitle is most misleading. The main title is quite correct, since this book is about computational chemistry, that is, chemistry done entirely by computation, and not about the uses of computers as an aid to "real" chemistry. The topics covered include quantum chemistry, molecular mechanics, prediction of chemical reactions, simulation of liquids and solids, interstellar chemistry, computational pharmacology, molecular biology, and molecular electronics. I found it fascinating to read in this clear and illuminating account about how much of chemistry can now be predicted by computation, but this is a theoretical sort of book, and not really quite right for practical folk like analytical chemists.

MARY MASSON

## PUBLICATIONS RECEIVED

---

**Applied Geochemical Analysis:** C. O. INGAMELLS and F. F. PITARD, Wiley-Interscience, New York, 1986. Pages ix + 733. Price £86.00.

This book contains valuable information on the sampling and analysis of rocks, ores and minerals. Sampling, as the authors state in their preface, is "already part of the analytical process . . . and is too often overlooked . . ."

Chapter 1 discusses sampling and sample preparation in detail, and describes and relates various sampling theories. Sampling is also discussed in subsequent chapters, for example, in connection with noble metals (Chapter 4) and in Chapter 6 entitled "Basic Calculations and Recommendations".

Also in their preface the authors state: "Some topics in this book reflect an audacity that could disturb old habits in some circles. Innovations are many and have been carefully selected. The difficulty in preparing the text has not been what to include, but what to leave out. Much of the material cannot be found elsewhere—it has been drawn from our lifetime experience."

Chapters 2–4 deal with the classical analysis of rocks and minerals, stressing the importance of such analyses of reference materials used as calibration and/or control samples in rapid instrumental procedures. As the authors state in Chapter 3, the term "classical analysis" signifies "the hard core of well-tried methods of maximum accuracy"; and "whenever a primary method is developed and is proven more accurate than the old, it is incorporated in the "classical scheme".

Surprisingly, in the first section of Chapter 2, entitled "Tools of the Art", no mention is made of plastic laboratory ware and the usefulness of modern (electronic) balances in enabling solutions to be measured by mass rather than volume. This would necessitate qualification of the statement "Volumetric flasks are indispensable" (p. 105).

Chapter 5 recommends an excellent approach to devising rapid analytical methods for particular sample types. This approach results in adequate documentation of the method in a form similar to that of, for example, international standard analytical methods.

Details are given of various dissolution procedures. More than 40 complete mineral analyses are given along with procedural details. Unusual elements or minerals, for which literature information is often lacking, are emphasized.

Chapter 7 discusses the preparation and use of geochemical reference materials, and stresses their importance. Each chapter ends with a list of useful references.

Analytical chemists in laboratories worldwide should benefit from the wisdom contained in this wide-ranging book.

T. D. RICE

**Aquatic Surface Chemistry—Chemical Processes at the Particle–Water Interface:** WERNER STUMM (ed.), Wiley, New York, 1987. Pages 520. £64.15.

This multi-authored book springs from a workshop held in Switzerland in 1986, but is not the usual conference proceedings publication. The 18 chapters, by well-known authors from several countries, are rather more reflective than that. The first third of the book is devoted to the physical chemistry of surface processes, including adsorption, double-layer theory and spectroscopic investigation of molecular structures on surfaces. The middle third deals with the formation of solid phases by hydrolysis of iron and the dissolution of oxides and silicates. Finally, the role of particles in regulating the composition of lakes and sea-water is discussed, including the behaviour of colloids and heterogeneous complexants and heterogeneous reactions of organic species. In a book intended primarily for geochemists, this last section, together with Marinsky's chapter on polyelectrolytes, is of the most immediate interest to analytical chemists. Consideration of the processes discussed in Part 2, however, must give pause for thought when speciation is at issue and Parsons' chapter in Part 1 hints at transfers from fundamental electrochemical studies to the more complicated real world. The many who use the other books edited by Stumm will doubtless wish to read the latest in the series.

DEREK MIDGLEY

**Electroanalytical Measurements in Flowing Liquids:** KAREL ŠTULÍK and VĚRA PACÁKOVÁ, Ellis Horwood, Chichester, 1987. Pages 290. £45.00.

It would be best to regard this book as a text on electrochemical detectors in HPLC and, to a lesser extent, flow-injection analysis. Other types of sample streams are mentioned, but industrial on-line monitoring is specifically excluded as a major theme. A 50-page chapter summarizes the equations describing the hydrodynamic principles relevant to the detectors discussed in the next 80 pages. The relationship between these two chapters is not developed particularly closely, however, nor is the final chapter on HPLC applications (75 pages) specially illuminated by what has gone before. Instrumentation is dealt with very briefly and electronics not at all. A brief chapter on analytical methods concentrates on rather uncommon arrangements, e.g. for direct potentiometry and potentiometric titration. This is no bad thing in itself, but the treatment is insufficiently critical. This attitude permeates the whole book: success looks too assured. In a hand-book of analytical methods such an approach would matter less, but I see this book as a source for those developing detectors for HPLC and FIA in particular and perhaps as an aid to those who are engaged in routine analysis by these techniques and wish to have a deeper understanding of the various detectors. There is no doubt that the book is of value for such purposes. The text is clearly written and well illustrated.

DEREK MIDGLEY

**X-Ray Methods:** CLIVE WHISTON, Wiley, Chichester, 1987. Pages xxi + 426. £36.00 (Cloth), £13.75 (Softback).

This is a book in the Analytical Chemistry by Open Learning (ACOL) series and as such has been written with a view to self-study. It is, for example, used as one of 12 such books that are associated with a course leading to an LRSC qualification. One aspect of these books is that numerous Self Assessment Questions (SAQs) and associated answers are included, often occupying one third of the book. I assume the omission of an index is common to all ACOL books, that study objectives of a particular section appear after, rather than before, the appropriate text and that tables are referred to as figures.

The literary style of *X-Ray Methods* is informal without being patronizing and this is appreciated by students using the book. The first chapter covers production and properties of X-rays, including details of health hazards and safety precautions. The treatment of theoretical aspects is limited to the "need to know" essentials and is presented very clearly.

There are two chapters on X-ray powder diffraction techniques that cover both camera and diffractometer methods and many varied examples involving qualitative and quantitative analysis are given. X-Ray fluorescence analysis receives a similar treatment with a discussion of both wavelength-dispersive and energy-dispersive techniques. I particularly liked the explanations given for use of the powder diffraction file and the X-ray spectrometry tables. Other related techniques such as  $\beta$ -probe X-ray analysis, radioisotope X-ray fluorescence, electron-probe microanalysis and scanning electron microscopy are covered briefly. (There is a separate ACOL book entitled "Scanning Electron Microscopy and X-Ray Microanalysis" by Graham Lawes.) Structure elucidation by single crystal diffraction is not included and there is no treatment of symmetry or space groups.

There are very few errors (an unbalanced equation on page 221 is an example) but nothing to distract from the valuable practical information that exudes from this book. The examples given are very relevant and reader participation in SAQs proves to be very rewarding.

B. J. Cox

**Atomic Absorption and Emission Spectroscopy:** ED METCALF, Wiley, Chichester, 1987. Pages xxi + 289. £32.00 (Cloth), £11.50 (Softback).

This is another of the ACOL series of books (or "units") that are designed for self-study and assessment. The SAQs in this book are fewer than usual and the literary style is formal.

It is assumed that the reader has very little or no knowledge of spectroscopy and hence the introductory chapter is very basic. This is followed by elementary theory of atomic spectroscopy and a clear and informative discussion of instrumental optics, although I would like to have seen a little more on multi-element hollow-cathode lamps.

Flame and non-flame AAS techniques are covered, including details of instrumentation, sample preparation, interferences and calibration methods. Other less common AAS methods are included and comparisons between all AAS procedures are made. Details of background corrections are given in a separate chapter.

Atomic emission spectroscopy is well covered and includes both flame and plasma methods.

As the author admits, a very wide, possibly bewildering, variety of atomic spectroscopic methods are given. These are all compared at the end of the book on the basis of cost, detection limits and precision, speed of analysis, susceptibility to interference and background, and ease of sample preparation. Possible future developments are also considered. Very clear definitions of precision, accuracy and detection limit are presented in an Appendix.

There are few errors in the book, for example 'Nz' for zirconium and the odd incorrect word making nonsense of a sentence. All in all I consider this a very useful book on the basis that it should be dipped into for information rather than studied conscientiously from cover to cover.

B. J. Cox

**Thermal Methods:** JAMES W. DODD and KENNETH H. TONGE, Wiley, Chichester, 1987. Pages xxi + 337. £36.00 (Cloth), £13.75 (Softback).

This is another book in the ACOL series which is keenly priced and aimed at the self-study market. The authors here really do give the impression that they are acting as substitute tutors as there are plenty of encouraging remarks and interesting illustrative applications. For example, thermal data are given to distinguish between butter, and two brands of margarine. Also, the importance of thermal data in determining the merits of Navy underwear is explained!

The introduction, which contains some minor typographical errors, is an overview of the subject that whets the appetite for further study. The techniques of TG, DTG, DTA, DSC, EGD and EGA are mentioned in this opening chapter.

Two chapters on thermogravimetry are then followed by two chapters on DTA/DSC techniques and many practical aspects are included. The authors adopt the convention that DSC exotherms are represented by an up peak and endotherms by a down peak. Multiple techniques are sensibly emphasized and a full paper from *Talanta*, dealing with a ternary oxalate mixture, is reproduced. This paper, which is explained further in the text, deals with an analysis of Ca, Sr and Ba ions by DTA/DTG/TG techniques.

The final chapter is devoted to the practical, thermal analysis of high-alumina cement. Several DTA curves related to this problem are supplied in a separate envelope. A thorough explanation of their use is given and extra curves are included as part of a final SAQ. A very useful book for those new to the subject.

B. J. Cox

## PUBLICATIONS RECEIVED

**Computerized Quality Control: Programs for the Analytical Laboratory:** T. F. HARTLEY, Ellis Horwood, Chichester, 1987, pp. 165. £

Quality control analysis is normally seen as a necessary but tedious and time-consuming exercise. Dr. Hartley demonstrates that with the aid of a personal computer it is possible to reduce the tedium and to obtain a fuller analysis.

In the first chapter (Calibration graphs) the author identifies 6 possible shapes of calibration graphs (linear, concave or convex to either axis, sigmoid) and gives three programs (LINCALIB, SPLINE, CURVEFIT) one of which should give a reasonable fit to any set of results. The second chapter (batch quality control) deals with within-batch quality control, and in it the special problems that arise because small batch size and small number of quality controls are highlighted. Two programs are given, the first (OCCURVE) is a program that calculates and plots the operating characteristic of the user's proposed batch quality control scheme. The second (GMREG) performs  $y$  on  $x$ ,  $x$  on  $y$  and geometric-mean regressions. Estimates of fixed and relative bias errors can be obtained. In Chapter 3 the problem of trend detection is considered. Computerized versions of Cusum V-Mask Scanning, Trigg Tracking Signal and Standard Normal Deviate Plot are given.

This book contains 11 Basic programs, all of which could be useful to an analyst. There is a full listing of every program and in the accompanying text an adequate description of the purpose of each line or group of lines. The programs have been written in a user-friendly style and could be quite easily modified to suit a particular situation. They are available in various floppy disk formats, including IBM PC, Apple II and BBC. A word of warning to those who will type in the listings. The author has tried as far as possible to use no uncommon features of the Basic Language, but he has used LOG, which in some dialects is  $\log_3$  and in others is  $\log_{10}$ .

W. A. J. BRYCE

**Binding Constants: The Measurement of Molecular Complex Stability:** KENNETH A. CONNORS, Wiley-Interscience, New York, 1987, pp. 411. £64.15.

The outstanding feature of this book is the way it unifies different techniques by relating the experimental observations and the stability constants and ligand concentrations through functions (isotherms) of the same mathematical form whenever possible. These preferred isotherms are represented by the equation of a rectangular hyperbola and are applied to all types of binding: acid-base, ion-pairing, metal-ligand complexing and molecular (including macromolecular) association. Emphasis on molecular complexing, with its often weak interactions, gives the book a useful distinction. The first 140 pages are devoted to general matters such as reference states, the binding isotherm concept and the statistical treatment of data. This section could be read profitably by anyone intending to measure stability constants. The rest of the book, under the heading "The Methods", elaborates the author's approach in regard to specific methods of studying complexing, with a decided bias towards "molecular" rather than "ionic" examples. This section is concerned with using the results, not with obtaining them; experimentalists will not discover how to use their apparatus, but they will learn about experimental design. The calculation of results emphasizes the graphical approach, computers being dismissed in a few references; while this is obviously done for positive reasons, a little more guidance would have been useful. The presentation is generally very clear, apart from a very few typographical errors: p. 67,  $y = 2 - \sqrt{2}$ ; p. 96 SM not SL; equations (2.88) and (2.89), right-hand terms should be added. In summary, this is a useful and distinctive text that can be recommended particularly for beginners who need an overview of the subject.

DEREK MIDGLEY

**Analytical Chemistry by Open Learning—Electroanalytical Chemistry, Instrumentation, and Gas Chromatography:** ACOL Series

There is no doubt—this is a series with a difference, both as regards approach and coverage. The project is a bold one, and all concerned are to be congratulated on producing such an extensive high-quality series in so short a time. It remains to be seen where the market lies—who, at work by day, is going to buy these volumes and find the time at home at night to follow this mammoth course of self-instruction. Some of the individual volumes will prove valuable for courses taught in polytechnics—and in universities—but which students, even post-graduate, can afford the number of volumes relevant to an advanced taught course?

I am a little unhappy that there are plans to back up these books with computer-assisted learning material and simulation programs. There is no substitute for real hands-on experience in becoming a practising analytical chemist, because only in this way does the student meet the day to day problems associated with instrumentation as well as seeing what the equipment can achieve. However, I would be happier leaving students alone with their instruments if I knew they had copies of the relevant ACOL volumes beside them.

I have a few comments on the style of the series. The quality of the type-setting and the art work is very high, and all three of these volumes are readable, presenting the material soundly, and concisely. The texts are frequently interspersed with rhetorical questions, the answers to which, both right and wrong, form the basis of the ensuing discussions. There is careful cross-referencing to other sections and to other volumes of the series. There are also self-assessment questions

at the end of each section, with answers and discussions taking up typically 20% of each volume. All in all, I find these volumes to be very carefully put together.

I find two general omissions. First, references to more detailed or advanced reference material, monographs and original papers are very few, and some of those given are far out of date. Surely, having taken the reader so far, the authors should give him the necessary directions for him to find the way further into the field if he so wishes. Secondly, and this is serious, none of the volumes I have seen has an index. How do we find those answers tantalising hidden away in the text inside these little encyclopaedias? I hope this will be rectified in any reprinting. And now for the three volumes on hand for review.

**Principles of Electroanalytical Methods:** T. RILEY and C. TOMLINSON. ACOL Series, Wiley, Chichester, 1987, pp. 252. £28 in cloth, £9.95 in soft-back.

In spite of what I have just said, I find this volume a disappointment. It is an introduction to two further volumes, and I feel that there have been problems in deciding just how far this volume should go. So it follows the traditional physical chemist's approach, but without getting deeply involved in the theory, and also without pointing out the practical consequences for analytical chemistry. Some examples may illustrate the point.

- (i) Activity coefficients decrease then increase again as the ionic strength increases. True. But what matters is that they are least variable in the salt concentration range 0.1–1M, which is most commonly used in practical work, so conditional constants for this range are very useful.
- (ii) The temperature coefficient of the 0.1M calomel electrode is small. True. So why is the saturated calomel electrode used so widely?
- (iii) Redox electrodes are said to be inert. False, or they would not respond to ionic equilibria in solution.
- (iv) The fluoride ion-selective electrode is used with TISAB. True. But why is it needed and what does it do?
- (v) AC polarography and DPP give peaks, not waves. True. But why?

So often we are left dangling when one or two more sentences would bridge the gap between theory and practice. This book does not bridge that gap, and therefore partly fails in its purpose.

**Instrumentation:** GRAHAM CURRELL. ACOL Series, Wiley, Chichester, 1987, pp. 401. £36 in cloth, £13.75 in soft-back.

I am much more taken by this volume, which fills a vacant spot in the literature, and does so excellently. The author presents the concepts of instrumentation, signals and noise, detectors and amplifiers, modulation and signal handling with ease and authority, obliging the reader to clarify his own thoughts: some of the rhetorical questions made me sit up and think more about concepts I thought I understood. The emphasis is on explaining the background to the problems we all meet in the laboratory when working with electronic or optical equipment, or when considering purchase of a new item and faced with specifications of rival instruments. Subtle effects such as those of "aliasing" are discussed because they are relevant not just to computer sampling of signals, but also to simple measurement with a digital voltmeter. The author's experience pervades all chapters of this book, tempting the reader to continue always just a little further... and further. This is excellent and will be an essential for my own post-graduate students.

**Gas Chromatography:** J. E. WILLETT. ACOL Series, Wiley, Chichester, 1987, pp. 253. £28.00 in cloth. £9.95 in soft-back.

I like this one too—a splendid blend of principles and practice answering so many questions from the beginner and from the experienced gas chromatographer as well. The discussions on sample injection, column packings, detectors, and "so, what else can go wrong?" are very good, and will be appreciated by novices and experts alike. The chapter on the hyphenated techniques GS-MS and CG-FTIR is thorough and informative—much more detailed than those in most texts on instrumental analysis. I would complain about the lack of modern references (one article in 1967 for detectors is not adequate for 1987) and also that van Deemter's equation gets no more than a cross-reference to another volume. On the plus side, the author's sense of humour frequently lightens the discussion in a natural and entertaining way and at the same time helps to reinforce the important points. Warmly recommended, and to be chained to the bench beside each gas chromatograph!

IAIN L. MARR

## PUBLICATIONS RECEIVED

**Scanning Electron Microscopy and X-Ray Microanalysis:** GRAHAME LAWES, Wiley, New York, 1987. Pages xviii + 103. £28.00 (cloth), £9.95 (softback)

This book is one of the series "Analytical Chemistry by Open Learning", intended for use by students working towards BTEC levels IV and V, RSC Certificates of Applied Chemistry and similar qualifications. It gives an introduction to the principles of scanning electron microscopy and X-ray microanalysis in an informal style which makes the information presented easy to assimilate. Self-assessment questions are provided at intervals throughout the text; they are well thought out and an important feature of the book. Although little theory is given, there is a useful bibliography of more rigorous textbooks. The text is divided into three main sections, SEM Instrumentation, Specimen Preparation and X-Ray Microanalysis-Instrumentation.

The description of the mechanical construction of the SEM is clear and comprehensive, but, because theory is kept to an absolute minimum, the mechanisms of image formation, particularly by secondary electrons, are largely neglected. A simple diagram might have been a useful addition. Similarly the factors affecting resolution have been treated in a manner which I feel has been over-simplified. Specimen preparation methods and the reasons for using them are well described, with the emphasis placed on the problems associated with biological material.

Both wavelength-dispersive and energy-dispersive X-ray detection methods are treated, and their relative merits are clearly discussed. In spite of the claim in section 3.6 that the effects of mass thickness and specimen topography on X-ray production are described in section 3.5, this is not the case. It is a fairly serious omission in an otherwise excellent chapter. The difficulties encountered in making quantitative analyses are particularly well dealt with, within the necessarily limited theoretical framework provided.

There are a number of typographical errors (including misspelling the author's name). In addition, the syntax is occasionally poor.

Overall, in spite of the limitations described above, the book succeeds as a primer. It will be extremely useful to students approaching SEM for the first time.

ERIC E. LACHOWSKI

**Potentiometry and Ion Selective Electrodes:** ALUN EVANS, Wiley, Chichester, 1987. Pages xvi + 304. £11.50 (paper), £32.00 (cloth).

This book is in the Analytical Chemistry by Open Learning (ACOL) series and takes the student in easy stages from an outline of the basic principles of galvanic cells and electrolytes, through the construction, properties and basic mechanism of ISEs to devising methods for typical applications. Each section is followed by one or two "Self-Assessment Questions" (answers at the back) to reinforce what has been learnt. As an instructional book on this subject, this is unrivalled in the clarity of its approach, the principle of which is admirable. While emphasizing that most things are right, I have the following criticisms to offer. I suspect that the space left for the answers will remain blank and the cost of these pages would have been better devoted to an index. The bibliography could list more than 2 books on ISEs. There are a number of typographical errors, most of which would not confuse the reader, but on p. 154 the  $K_p$  value for CuS should be  $10^{-35}$ . The mechanism given for the cyanide ISE (pp. 167/282) needs revision. I dislike the suggestion that multiple standard additions can overcome the problems of interferences. The fragility of glass electrodes is over-emphasized and sounds a little old-fashioned, as does the preference for ion-exchange over neutral carrier Ca-ISEs (p. 216). A table bringing together, in one place, all the types of electrodes worthy of commercial production, and their principal characteristics, would be useful. It is to be hoped that the ACOL project is successful as a whole, but his book deserves a good life in its own right as a student text.

DEREK MIDGLEY

**Aquatic Surface Chemistry—Chemical Processes at the Particle–Water Interface:** WERNER STUMM (editor), Wiley, New York, 1987. Pages xix + 520. £64.15.

This multi-authored book springs from a workshop held in Switzerland in 1986, but is not the usual conference proceedings publication. The 18 chapters, by well-known authors from several countries, are rather more reflective than that. The first third of the book is devoted to the physical chemistry of surface processes, including adsorption, double-layer theory and spectroscopic investigation of molecular structures on surfaces. The middle third deals with the formation of solid phases by hydrolysis of iron and the dissolution of oxides and silicates. Finally, the role of particles in regulating the composition of lakes and sea-water is discussed, including the behaviour of colloids and heterogeneous complexants and heterogeneous reactions of organic species. In a book intended primarily for geochemists, this last section, together with Marinsky's chapter on polyelectrolytes, is of the most immediate interest to analytical chemists. Consideration of the processes discussed in Part 2, however, must give pause for thought when speciation is at issue and Parsons' chapter in Part 1 hints at transfers from fundamental electrochemical studies to the more complicated real world. The many who use the other books edited by Stumm will doubtless wish to read the latest in the series.

DEREK MIDGLEY

**Mass Spectrometry in the Analysis of Large Molecules:** C. J. McNEAL (editor), Wiley, Chichester, 1986. Pages x + 221. £24.00.

The material in this book is an account of the lectures given at a Symposium on the Mass Spectrometry of Large Molecules, held in Texas in April 1986. The thirteen contributions deal with the desorption and ionization of molecules of high molecular weight by energetic particles, either fast atoms or ions produced in accelerators, or  $^{232}\text{Cf}$  plasmas. The molecules studied are most commonly polypeptides or other biopolymers and the mass range has been extended to above 20000. Some attention is given to the mass analysis process and to the interpretation of the mass spectra so produced. Results from such studies are compared critically with those which might be obtained by more conventional methods for the analysis of large molecules. The book is provided with an epilogue which summarizes the successes and failures of the participants in creating and resolving, as well as identifying, large molecule-ions. It was suggested that the mass range of most interest, the lower limit of which is double that currently achieved, will be reached in the not too distant future, so opening up the possibility of the analysis of many small proteins.

J. R. MAJER

**Gaseous Ion Chemistry and Mass Spectrometry:** J. H. FUTRELL (editor), Wiley, New York, 1986. Pages xii + 335. £57.50.

This book is a modified record of a Workshop held at the University of Utah in 1983, and devoted to the subject of Gas Phase Ion Chemistry. The theory of ion dissociation and of ion molecule reactions is discussed and the techniques of mass and ion energy analysis are reviewed. There are accounts of the instrumentation used in studying ion dissociation and of its application to biomedical problems. This is a book with a limited appeal to mass spectrometric experts and the intimate details of ion dissociation will hold little interest for the practising analytical chemist.

J. R. MAJER

**Fluorescence and Phosphorescence Spectroscopy:** DAVID RENDELL, Wiley, Chichester, 1987. Pages xix + 419. £36.50 (cloth), £13.95 (softback).

This is another book in the ACOL series and as such has been written with a view to self-study. Numerous Self-Assessment Questions (SAQs) are included throughout the text, which insures that one section is understood before another is started. For ease of reference all the SAQs with the associated answers are included at the end of the book.

The introduction gives a simple, clear, well illustrated account of the origin of fluorescence and phosphorescence spectra. Some basic knowledge of absorption spectrophotometry is required. Particular attention has been paid to processes that are likely to compete with fluorescence, to the importance of molecular structure, and the choice of solvent. Temperature effects have not been included.

The chapter on instrumentation is to be particularly recommended. In it, filter fluorimeters, spectrofluorimeters and phosphorimeters are all covered in sufficient detail to allow the reader to obtain a good basic understanding of how a particular instrument works, its limitations, and how to optimize its performance in terms of the possible practical results obtained.

The last three chapters deal with quantitative aspects. A general approach pertinent to any fluorescence assay is adopted in the first chapter. I particularly liked the clear derivation of the quantitative fluorescence equation and the manner in which its limitations are highlighted. In the subsequent chapters the breadth of the applications of photoluminescence methods is demonstrated. Included are direct, derivative and chromatographic methods, fluoroimmunoassay and room-temperature phosphorescence. By using a few selected literature examples and considering them in great detail, the author has succeeded in focusing attention on the importance of a good practical technique coupled with a sound understanding of the theoretical aspects of each step, and the possible sources of error in a particular analysis. However, I feel a simpler example than the complex four-component analysis of opium might have been more appropriate.

The book could be improved by the inclusion of the quantitative equation for phosphorescence and a section on fluorescence polarization and its applications.

There are very few errors: Figs. 2.2a, 2.5b, 2.5c have unlabelled ordinates; in Fig. 5.5b narcotine is incorrectly spelt; p. 194 has spectrophotometer instead of spectrofluorimeter.

Overall this is a most worthwhile basic text book. It would be a valuable asset to those who wish to gain a rapid, working knowledge of the theory, instrumentation and practice of fluorescence and phosphorescence.

R. R. MOODY

**Analytical Applications of Lasers:** E. H. PIEPMEIER (editor), Wiley, New York, 1986. Pages xiii + 703. £85.95

The first experimental demonstration of lasers was conducted in 1960. It was another 10 years, however, before analytical applications were described in the literature, derived from their intrinsic properties of high directionality, radiance, monochromaticity and coherence. Since then, as optical sources in spectroscopy, the use of lasers in analytical science has grown and developed at a rapid rate, embracing a wide range of techniques. This book, volume 87 in this successful series of monographs on the methodology and application of analytical chemistry, provides a thorough overview of contemporary laser technology and laser-assisted analytical methods. For the general reader and non-specialist in laser theory, the editor has thoughtfully provided a useful introductory chapter covering the basic principles of lasers and non-linear optical effects fundamental to the applications discussed and described in the subsequent 18 chapters. The number and variety of these applications has prompted the editor to further subdivide the book into several parts, based on prominent characteristics of the methods. Sections are devoted to selected methods using various detection schemes, methods utilizing the improved spectral resolution offered by lasers, multiphoton and multiwavelength methods and methods based on special laser characteristics. Laser-excited fluorescence spectrometry provides the basis for some of the most selective and sensitive analytical techniques available. Detailed accounts of such methods are well represented in this book, with individual

chapters devoted to atomic and ionic fluorescence in flames and plasma cells, cryogenic molecular fluorescence (including Shpol'skii spectrometry) and two-photon excited fluorescence spectroscopy for the study of molecular symmetry. Complementing luminescence methods, the techniques of laser-assisted optoacoustic spectroscopy, infrared transmission and Raman spectroscopies are reviewed. A number of analytical techniques have been developed which effectively exploit the unique characteristics of laser radiation and a section devoted to some is presented. Topics covered include laser remote sensing, intracavity-enhanced spectroscopy, the thermal lens effect, picosecond spectroscopy, electrophoretic light scattering and laser flow cytometry. The final section in the book is concerned with the use of laser sources combined with other, more established, analytical techniques. Three examples are discussed, laser systems in chromatographic detectors, laser ionization techniques for mass spectrometry and laser ablation for atomic spectrometry.

The extensive range and detail of the topics described and reviewed ensure, that for the expert and non-specialist alike, this book provides a valuable reference and guide to advances in the application of laser systems to analytical science. It will undoubtedly stimulate further studies in this rapidly expanding and exciting field of research and application.

M. J. ADAMS

**Thin Layer Chromatography, (Analytical Chemistry By Open Learning):** RICHARD HAMILTON and SHIELA HAMILTON, Wiley, Chichester, 1987. Pages xix + 129. Price £28.00 (cloth), £9.95 (softback).

This small volume contains more than sufficient information to allow the student to attempt to tackle his/her own problems with confidence. The book covers the basic principles of selection of stationary and mobile phases. The eluotropic series for solvents is explained by using the solvent strength parameter  $\epsilon^0$  and a table is given showing how two different solvents can be used to produce a mixed solvent of suitable eluotropic strength. Chapters on practical techniques and general applications of TLC are included, as are discussions on recent developments such as reverse-phase and high-performance TLC. Self-assessment questions spaced throughout the book are very helpful in improving understanding of the main points taught. Although this book is aimed at the trainee technician, sixth year, A-level students and undergraduates will find it both instructive and informative.

R. E. MASSON

**Flavour Science and Technology: Proceedings of the 5th Weurman Flavour Research Symposium, Oslo, Norway, 23-25 March 1987:** M. MARTENS, G. A. DALEN and H. RUSSWURM, JR, (editors) Wiley, Chichester, 1987. Pages xvi + 566. £40.00

This book deals with a wide range of subjects, both traditional and topical, in the flavour forum. It is conveniently subdivided into four sections, namely chemistry, biotechnology, sensory science and data analysis in flavour research. Each section is preceded by a keyword index to the papers, which helps identify specific subject areas. This is followed by an introductory lecture setting the scene on each topic.

This publication, in the growing tradition of the Weurman Symposium, provides an up to date account of work in the flavour/food area. It is impossible to comment on individual papers, though the introductory lectures are well written and provide a good summary of current thinking in the appropriate areas. The papers exhibit an individuality in format which is refreshing; one common feature which is lacking, however, is an abstracted version of each paper below the title and authors name(s), and there is a paucity of listing in the subject index. Chemistry in flavour research still dominates this symposium, in terms of the number of papers submitted, many of the contributions still relating to the characterization of flavour compounds. We are lacking in our knowledge of flavour/ingredient interaction and should encourage developments in this direction through this forum. The articles by Overbosch and Dumont are of interest in this area.

This compilation will be of prime interest to flavour and food specialists in academic and industrial environments and to students with an interest in flavour science.

P. J. DUNPHY



## SUBJECT INDEX

Acidity constants, of nitric and nitrous acids . . . . .	205
Actinides, Separation by HPLC. . . . .	461
Actinomycin complex, Study by MS . . . . .	605
Algorithm, for multiple equilibrium systems . . . . .	713
Aluminium, Determination by FAAS. . . . .	403
Ammonium ions, Determination by isotachopheresis . . . . .	55, 799
Anion-exchange, Determination of sulphide . . . . .	917
Antimony, Determination by AAS. . . . .	443
—, — by AAS and FAAS . . . . .	406
—, — by neutron-activation analysis . . . . .	183
Anthraquinones, Determination, polarographic . . . . .	959
Aromatic amines, Determination, spectrophotometric . . . . .	409
— hydrochlorides, Determination by electrochemical methods . . . . .	379
— hydrocarbons, polynuclear (PAH), Determination by HPLC. . . . .	891
—, —, Phosphorimetry of. . . . .	41
Arsenic, Determination after microwave dissolution . . . . .	907
—, — by FAAS . . . . .	47, 297
—, — by NAA . . . . .	183
Atomic-absorption spectrometry (AAS), Determination of P . . . . .	653
—, — of Pb . . . . .	337
—, — of Sb . . . . .	406, 443
—, —, Elimination of interferent effects . . . . .	465
—, —, flameless (FAAS), Determination of Al . . . . .	403
—, — of As . . . . .	47, 297
—, — of Cd . . . . .	831
—, — of Ga . . . . .	737
—, — of organotin compounds . . . . .	539
—, — of Sb . . . . .	406
—, — of Se. . . . .	633
—, — of Se and Te . . . . .	679
—, — of Sn(IV) and organotin compounds . . . . .	519
Barium, Determination by new electrochemical method . . . . .	673
Bentonite suspensions, Kerr effect . . . . .	369
Benzothiadiazine diuretics, Determination, spectrophotometric . . . . .	621
Berberine, Determination, spectrophotometric . . . . .	977
Bismuth, Determination, spectrophotometric . . . . .	311, 803, 879
Borate ion-pair stability constants . . . . .	271
Boron, Determination, spectrophotometric . . . . .	351
Cadmium, Determination by FAAS . . . . .	831
—, — spectrophotometric . . . . .	723, 885
—, —, Extraction of complexes . . . . .	413
Calcium, Determination, amperometric . . . . .	231
Carbaryl, Determination, kinetic . . . . .	943
Carbohydrates, Determination, titrimetric . . . . .	651
Carbon dioxide, fibre-optic sensor for . . . . .	109
Carminomycin, electrochemical study of. . . . .	993
Cell, for analysis of solutions . . . . .	855
Chemiluminescence, of triphenylmethane dyes . . . . .	625
Chlordiazepoxide, Determination, spectrophotometric . . . . .	895
Chloride, Determination by ISE . . . . .	173
—, — by ion-selective field-effect transistor. . . . .	326
—, —, Titration, potentiometric . . . . .	664
Chlorpromazine, Determination, alkalimetric . . . . .	211
Chromatography, extraction, Separation of Se(IV) and Te(IV) . . . . .	594
—, —, high-pressure liquid (HPLC), Detector for . . . . .	179, 697
—, —, —, Determination of metal ions . . . . .	187
—, —, —, — of organometallics . . . . .	693
—, —, —, — of polythionates . . . . .	847

—, ———, Separation of metal chelates . . . . .	461, 685
—, ———, — of nucleotides . . . . .	911
—, ———, — of PAHs . . . . .	891
—, ion, Determination of Fe(II) and Fe(III) . . . . .	15
—, —, — of nitrate and sulphate . . . . .	245
—, —, — of S oxyanions . . . . .	307
Cobalt, Determination, spectrophotometric . . . . .	661
Complexes, ternary, Use in Spectrophotometry . . . . .	701
Computer evaluation, of ionization constants . . . . .	249
— programs, ESTA library of . . . . .	825
——, for non-aqueous acid-base titrations . . . . .	899
——, for potentiometric titrations . . . . .	667
Copper, Determination by ASV . . . . .	329
Copper, —, catalytic . . . . .	199
Curve fitting, multiparametric . . . . .	981
Cyadox, Determination by adsorptive SV . . . . .	816
Cyclobutylphenylglycollic acid, Determination, spectrophotometric . . . . .	923
Cysteine, Determination, polarographic . . . . .	68
Dantrolene solutions, Study, polarographic . . . . .	613
Degradation, oxidative, of sulphonamides . . . . .	875
Detector, drop-fall, for polarography . . . . .	401
Dibenzofuran and derivatives, Luminescence of . . . . .	267
Diethazine, Determination, alkalimetric . . . . .	211
Digital acquisition unit for spectrophotometric data . . . . .	869
Dimethyl sulphoxide, Determination, voltammetric . . . . .	323
Dissociation constants, of phenothiazine derivatives . . . . .	211
Drainage profiles, of thin liquid films . . . . .	221
Drop-time, Effect of interfacial tension . . . . .	365
Drugs, antiameobic and anthelmintic, Determination, spectrophotometric . . . . .	23
—, psychoactive, Determination by adsorptive SV . . . . .	287
EDTA, Determination, spectrophotometric . . . . .	799
Electrochemical study, of carminomycin . . . . .	993
Electrochromic dyes, in optode technology . . . . .	123
Electrode, carbon-paste, for voltammetry . . . . .	277
—, combination-pH . . . . .	447
—, copper, for amperometric flow detection . . . . .	455
—, glass, Determination of formation constants . . . . .	825
—, glassy-carbon, for HPLC detector . . . . .	179
—, gold chloride, as sensor for HPLC . . . . .	697
—, ion-selective (ISE), for ammonium ion . . . . .	728
—, —, for F and Cl . . . . .	173
—, —, for hydralazine . . . . .	487
—, —, for sulphide . . . . .	783
—, —, for Tl . . . . .	589
—, —, for xanthate . . . . .	807
—, —, Selectivity and detection limit . . . . .	281
—, —, Use of multiple electrodes . . . . .	215
—, liquid-membrane, Dependence on pH . . . . .	591
—, —, Determination of perrhenate . . . . .	361
—, —, Effect of plasticizer . . . . .	789
Elements, Distribution coefficients on cation-exchange resin . . . . .	385
Enzyme reactions, in optode technology . . . . .	123
Erbium, Determination, spectrophotometric . . . . .	293
Erythromycin, Determination by adsorptive SV . . . . .	525
Ethanol, Sensing by fibre-optic biosensor . . . . .	151
Extraction, of As . . . . .	47
—, of Fe(II) . . . . .	253
—, of Fe(III) . . . . .	57
—, of ginsenosides . . . . .	314
—, of Ni . . . . .	949
—, of sediments . . . . .	559
—, ion-pair, of Pb ultratraces . . . . .	553
—, —, of trace metal ions . . . . .	167
Fibre-optic biosensor, based on fluorescence . . . . .	145
——, for ethanol . . . . .	151
Field-effect transistor, ion-selective, for chloride . . . . .	326
Flotation, of PAHs . . . . .	891
Flow detection, amperometric . . . . .	455
Flow-gradient function, in FIA . . . . .	425
Flow-injection analysis (FIA), Determination of Cd . . . . .	885
——, — of nitrite and nitrate . . . . .	810
——, — of pentachlorophenol . . . . .	601

-----, — of rare-earth elements . . . . .	259
-----, — of water . . . . .	59
-----, Flow-gradient function . . . . .	425
Fluoride, Determination by ISE . . . . .	173
—, — complexometric . . . . .	909
—, Sensing with optical fibres . . . . .	83
Fluorimetry, Determination of Pb ultratraces . . . . .	553
—, — of reserpine . . . . .	731
—, fibre-optic, for immunoassays . . . . .	139
Formaldehyde, Determination, spectrophotometric . . . . .	655
Formation constants, Determination with glass electrodes. . . . .	825, 927, 933
—, Reliability of . . . . .	981
Furazolidone, Determination, spectrophotometric . . . . .	977
Gallium, Determination by FAAS . . . . .	737
—, — spectrophotometric. . . . .	343, 841
—, Indium and thallium, Separation . . . . .	357
— arsenide, Analysis by spark-source MS . . . . .	822
Ginsenosides, Extraction of . . . . .	314
Herbicides, Determination, polarographic . . . . .	235
Hormone-protein interactions, in optode technology . . . . .	123
Hydrazines, Determination by adsorptive SV . . . . .	965
7-Hydroxycoumarins, spectral study of . . . . .	973
Immunoassays, by fibre-optic fluorimetry . . . . .	139
Indicators, acid-base, for determination of pH . . . . .	103
—, —, in acetonitrile . . . . .	1013
Indium, Gallium and thallium, Separation . . . . .	357
Instrumentation, for optical fibre sensors . . . . .	157
Interfacial tension, Effect on drop time . . . . .	365
Interferent effects in flame AAS, Elimination of . . . . .	465
Ionic strength, fibre-optic sensor . . . . .	119
Ions, fibre-optic sensor for . . . . .	113
Ionization constants, Evaluation by computer . . . . .	249
Iron(II), Determination, spectrophotometric . . . . .	253
Iron(III), Determination by adsorptive SV . . . . .	597
—, — spectrophotometric. . . . .	57
— and iron(II), Analysis of mixtures . . . . .	15
Isotachopheresis, Determination of $\text{NH}_4^+$ ion . . . . .	799
—, — of $\text{NH}_4^+$ and $\text{K}^+$ ions. . . . .	55
Isoxsuprine hydrochloride, Determination, spectrophotometric . . . . .	237
Kalman filtering, Use in multicomponent spectrophotometry. . . . .	707
Kerr effect, in bentonite suspensions . . . . .	369
Lanthanides, Determination, Review . . . . .	1
—, Separation by HPLC . . . . .	461
Lead, Determination by AAS and XRF . . . . .	337
—, — by ASV . . . . .	819
—, — by X-ray photoelectron spectroscopy . . . . .	68
—, — of ultratraces. . . . .	553
Letter to the Editor. . . . .	333
Lipoic acid and lipoamide, Determination by adsorptive SV . . . . .	837
Louis Gordon Memorial Award . . . . .	No. 8, III
Luminescence, of dibenzofuran and derivatives . . . . .	267
Magnesium ion, Behaviour, polarographic . . . . .	239
Manganese(III), Analysis of cyano-complexes . . . . .	795
Masking, electrochemical, of Ti. . . . .	191
Matrix, Air, Determination of Se and Te . . . . .	679
—, Alloys, Determination of Co . . . . .	661
—, —, — of Ga . . . . .	343
—, —, — of Ni . . . . .	485
—, Animal tissues, Determination of trace metals . . . . .	545
—, Bacterial cells, Determination of . . . . .	227
—, Biological materials, Determination as As and Sb . . . . .	183
—, —, — of P . . . . .	747
—, Bismuth telluride, Determination of Ga. . . . .	841
—, Blood plasma, Determination of cyadox and metabolites. . . . .	816
—, —, — of methotrexate. . . . .	805
—, Bryophytes, Determination of Pb . . . . .	68
—, Chicken tissue, Determination of nicarbazin . . . . .	734
—, Copper, Determination of oxygen. . . . .	479
—, Drugs, Assay of tetracyclines . . . . .	375

—, Environmental samples, Determination of carbaryl . . . . .	943
—, Fly-ash, Determination of Ga . . . . .	343
—, —, — of Pb . . . . .	337
—, Geological materials, Determination of F and Cl . . . . .	173
—, —, — of Ga . . . . .	737
—, —, — of lanthanides . . . . .	1
—, Lead, Determination of Sb . . . . .	443
—, Marine organisms, Determination of organometallics . . . . .	693
—, Minerals, Determination of Tl . . . . .	589
—, Natural waters, Determination of organotin compounds . . . . .	539
—, —, — of polythionates . . . . .	847
—, Ores, Determination of Co . . . . .	661
—, — and concentrates, Determination of As . . . . .	47, 297
—, —, —, — of Se . . . . .	633
—, Organic compounds, Determination of Bi . . . . .	311
—, —, — of F . . . . .	909
—, — solvents, Determination of water . . . . .	59
—, Pharmaceuticals, Determination of isoxsuprine hydrochloride . . . . .	237
—, —, — of surfactants . . . . .	813
—, Rocks, Determination of Tl . . . . .	589
—, — and ores, Determination of Sb . . . . .	406
—, Sea-water, Determination of $\text{NH}_4^+$ ion . . . . .	799
—, —, —, — of Sn(IV) and organotin compounds . . . . .	519
—, Soils, Determination of As . . . . .	907
—, Steels, Determination of Mo . . . . .	1007
—, —, — of P . . . . .	653
—, Tap and sea-water, Determination of Mc(VI) . . . . .	301
—, Urine, Determination of drugs . . . . .	287
—, —, — of erythromycin . . . . .	525
—, Vitamins, Determination of Co . . . . .	661
—, Water, Determination of PAHs . . . . .	891
—, Zinc concentrates, Determination of Sb . . . . .	443
Menadione, Determination by adsorptive SV . . . . .	997
Mercury, Determination, alkalimetric . . . . .	725
—, —, voltammetric . . . . .	277
Mercury(II), Determination, complexometric . . . . .	719
—, —, kinetic . . . . .	397
Metal chelates, Separation by HPLC . . . . .	685
— complexes, Polarography of . . . . .	921
— ions, Determination by HPLC . . . . .	187
—, —, Preconcentration by extraction . . . . .	167
—, —, Separation by chelating resin . . . . .	65
—, —, Sorption by anion-exchange resin . . . . .	431
— ligand equilibria, Non-linear regression analysis . . . . .	507
Methotrexate, Determination by adsorptive SV . . . . .	805
Molybdenum, Determination, spectrophotometric . . . . .	1007
Molybdenum(VI), Determination in mixtures with Se(IV) . . . . .	496
—, —, polarographic . . . . .	301
Multi-element optical waveguide sensor . . . . .	95
Multiple equilibrium systems, Algorithm for . . . . .	713
Muzolimine, Determination, spectrophotometric . . . . .	914
Nebulization, of aqueous samples into plasma . . . . .	641
Neutron-activation analysis (NAA), Determination of As and Sb . . . . .	183
—, —, — of P . . . . .	747
—, —, — of U . . . . .	161
New electrochemical method for Ba and Sr . . . . .	673
Nicarbazin, Determination, voltammetric . . . . .	734
Nickel, Determination, spectrophotometric . . . . .	485
—, Extraction of complex . . . . .	949
Nickel(III) complexes, Mass spectrometry of . . . . .	27
Nitrate, Determination by ion-chromatography . . . . .	245
— and nitrite, Determination of FIA . . . . .	810
Nitrazepam, Determination, spectrophotometric . . . . .	895
Nitric and nitrous acids, Acidity constants . . . . .	205
N-Nitrosamines, Reaction with pyridinium salts . . . . .	1005
Nucleotides, Determination by HPLC . . . . .	911
Obituary: Prof. Hans Ewald Blasius . . . . .	No. 1, I
Optical fibres, for process control . . . . .	75
—, —, Sensing of fluoride ions . . . . .	83
—, — of polar solvent vapours . . . . .	89
— sensors, Instrumentation for . . . . .	157
Optical waveguide sensor, multi-element . . . . .	95
Optimum working range, Determination in spectrophotometry . . . . .	531

Optode, fluorescent chemoreceptive . . . . .	129
Organometallics, Speciation by HPLC . . . . .	693
Organotin compounds, Determination by FAAS . . . . .	519, 539
Oxygen, Determination in Cu by reductive fusion . . . . .	479
Penicillamine, Determination, polarographic . . . . .	68
Pentachlorophenol, Determination by FIA . . . . .	601
pH, Determination with acid-base indicators . . . . .	103
Pergamon Press 1948-1988 and Talanta 1958-1988: two anniversaries . . . . .	No. 5, III
Peroxides, inorganic, Determination by silver-gelatin method . . . . .	658
Perrhenate, Determination by liquid-membrane electrode . . . . .	361
Phenols, Determination, spectrophotometric . . . . .	701
— formaldehyde materials, Determination of volatiles . . . . .	775
Phenothiazine derivatives, Determination, titrimetric . . . . .	320
Phosphate, Titration, potentiometric . . . . .	664
Phosphorimetry, of PAHs . . . . .	41
—, with Becquerel-disc phosphoroscope . . . . .	647
Phosphorus, Determination by AAS . . . . .	653
—, — by NAA . . . . .	747
Plasma, microwave, tubular-torch capacitatively-coupled, Determination of elements . . . . .	641
Plasticizers, Effect on ISEs . . . . .	789
Polarography, of anthraquinones . . . . .	959
—, of metal complexes . . . . .	921
—, differential-pulse, of dantrolene solutions . . . . .	613
—, —, of herbicides . . . . .	235
—, —, of Mo(VI) . . . . .	301
—, Drop-fall detector for . . . . .	401
—, reverse-pulse, Determination of Mg . . . . .	239
—, —, — of penicillamine . . . . .	68
Pollutants, gaseous organic, Preconcentration . . . . .	567
Polythionates, Determination by HPLC . . . . .	847
Potassium ions, Determination by isotachopheresis . . . . .	55
Praseodymium, Determination, spectrophotometric . . . . .	293
Preconcentration, of gaseous organic pollutants . . . . .	567
Process control, with optical fibres . . . . .	75
Protons, Sorption by anion-exchange resin . . . . .	431
Purines and pyrimidines, Analysis of mixtures . . . . .	513
Pyridinium salts, Reaction with <i>N</i> -nitrosamines . . . . .	1005
Rare-earth elements, Determination by FIA . . . . .	259
Reagent, Arsenazo III, for rare-earth elements . . . . .	259
—, <i>N</i> -Bromophthalimide and <i>N</i> -bromosaccharin, for carbohydrates . . . . .	651
—, 5-Bromo-2-(2-pyridylazo)-5-diethylaminophenol, for rare-earth elements . . . . .	259
—, —, for Zr . . . . .	502
—, 2-Butyne-1,4-diol, chemical study of . . . . .	763
—, Chrome Azurol S, for rare-earth elements . . . . .	259
—, 3,5-Dinitrocatechol, for V . . . . .	1001
—, 4,6-Di- <i>tert</i> -butyl-3-methoxycatechol, for B . . . . .	351
—, Dithio-oxamide, for Re . . . . .	62
—, Hexa-amminecobalt(III) tricarbonatocobaltate(III), for pharmaceuticals . . . . .	320
—, <i>o</i> -Hydroxyhydroquinonephthalein, for Bi(III) . . . . .	879
—, 3-Hydroxy-2-naphthoic acid, for Cu(II) . . . . .	199
—, 2-Imidazolindinethione, as masking agent . . . . .	719
—, Iodine, for terfenadine . . . . .	242
—, Karl Fischer, for water . . . . .	59
—, Malachite Green, for Cd . . . . .	885
—, 1-Mercaptopropan-2,3-diol, for Hg . . . . .	725
—, 4- <i>N</i> -Methylaminophenol, for aromatic amines . . . . .	409
—, 1,2-Naphthoquinone-2-thiosemicarbazone, as acid-base indicator . . . . .	419
—, <i>o</i> -Nitrophenylfluorone, for Mo . . . . .	1007
—, Nitrous acid, for tryptophan . . . . .	35
—, 1-Oxa-4,7,10-triazacyclododecane- <i>N,N',N''</i> -triacetic acid, for metals . . . . .	741
—, Oxazine dyes, as redox indicators . . . . .	490
—, Pentacyanoferrate(II), for dimethyl sulphoxide . . . . .	323
—, 1-(2-Pyridylazo)-2-naphthol, for Er and Pr . . . . .	293
—, 4-(2-Pyridylazo)resorcinol, for rare-earth elements . . . . .	259
—, Pyrocatechol Violet, for Bi and EDTA . . . . .	799
—, —, for Fe(II) . . . . .	253
—, 8-Quinolinol, for Ga . . . . .	841
—, 7,7,8,8-Tetracyanoquinodimethane, for benzothiadiazine diuretics . . . . .	621
—, —, for terfenadine . . . . .	242
—, $\alpha$ , $\beta$ , $\gamma$ , $\delta$ -Tetrakis(4- <i>N</i> -trimethylaminophenyl)-porphine, for Cd . . . . .	723
—, 2-(2-Thiazolylazo)- <i>p</i> -cresol, for Ni . . . . .	485
—, Thiocarbonylhydrazides, for Ga . . . . .	343
—, —, for spectrophotometry . . . . .	493

Regression analysis, non-linear, of metal-ligand equilibria . . . . .	507
Reserpine, Determination, fluorometric . . . . .	731
Resin, anion-exchange, Sorption of protons and metal ions . . . . .	431
—, cation-exchange, Distribution coefficients of elements . . . . .	385
—, chelating, Separation of metal ions . . . . .	65
—, —, Synthesis and characterization . . . . .	439
Review: Determination of lenthanides . . . . .	1
Rhenium, Determination, spectrophotometric . . . . .	62
Ronald Belcher Memorial Award . . . . .	No. 8, IV
Sediment analysis . . . . .	559
Selectivity, of ISEs . . . . .	281
Selenium, Determination by FAAS . . . . .	623, 679
Selenium(IV), Determination in mixtures with Mo(VI) . . . . .	496
—, Separation from mixtures . . . . .	594
Sensor, fibre-optic, for CO <sub>2</sub> . . . . .	109
—, —, for ions . . . . .	113
—, —, for ionic strength . . . . .	119
—, optochemical, based on fluorescence . . . . .	123
Silver-gelatin method, Determination of inorganic peroxides . . . . .	658
Software survey, Construction of Small Bibliographic Databases by Using "Lotus 1-2-3" . . . . .	925
—, Fleet Street Editor/Fleet Street Publisher . . . . .	335
—, FLUOPAC1 . . . . .	335
—, FLUOPAC2 . . . . .	671
—, GHS . . . . .	336
—, Multivariate Linear Regression for Calibration and Testing of Analytical Methods . . . . .	505
—, SOPHD . . . . .	336
Solutions, Stationary and streaming, Analysis of . . . . .	855
Solvent vapours, polar, Sensing with optical fibres . . . . .	89
Spectral study, of 7-hydroxycoumarins . . . . .	973
— line intensity-ratio fluctuations, of elements . . . . .	317
Spectrophotometry, Determination of optimum working range . . . . .	531
—, Digital data acquisition unit . . . . .	869
—, Use of ternary complexes . . . . .	701
—, atomic-fluorescence, Determination of Sn . . . . .	499
—, derivative, analytical applications . . . . .	753
—, mass, of actinomycin complex . . . . .	605
—, —, of nickel(III) complexes . . . . .	27
—, —, spark-source, of Ga arsenide . . . . .	822
—, multicomponent, Use of Kalman filtering . . . . .	707
—, UV derivative, Analysis of purines and pyrimidines . . . . .	513
—, X-ray fluorescence (XRF), Determination of Pb . . . . .	337
—, X-ray photoelectron, Determination of Pb . . . . .	68
Stability constants, Borate ion-pair . . . . .	271
Stripping analysis, Reciprocal derivative constant-current . . . . .	861
Strontium, Determination by new electrochemical method . . . . .	673
Sulphate, Determination by ion chromatography . . . . .	245
Sulphide, Determination by anion-exchange . . . . .	917
Sulphonamides, oxidative degradation . . . . .	875
Sulphoxides, Determination, iodometric . . . . .	969
Sulphur, Separation of oxyanions . . . . .	307
Surfactants, Quaternary ammonium, Determination, spectrophotometric . . . . .	813
Talanta Advisory Board . . . . .	No.3, I, No. 4, I, No. 12, V
Talanta Editorial and Advisory Boards . . . . .	No. 1, III
Talanta Medal . . . . .	No. 11, I
Tellurium, Determination by FAAS . . . . .	679
Tellurium(IV), Separation from mixtures . . . . .	594
Terfenadine, Determination, spectrophotometric . . . . .	242
Tetracyclines, Assay, spectrophotometric . . . . .	375
Thallium, Determination by ASV . . . . .	191
—, Indium and gallium, Separation . . . . .	357
Thallium(III), Determination, spectrophotometric . . . . .	721
Thin liquid films, Drainage profiles of . . . . .	221
Thiophanate-methyl, Determination, oxidimetric . . . . .	1010
Tin, Determination by atomic-fluorescence spectrometry . . . . .	499
Tin(IV), Determination by FAAS . . . . .	519
Titanium, Removal of matrix effect . . . . .	191
Titration, of metal ions with Fe(II) . . . . .	490
—, acid-base, non-aqueous . . . . .	899
—, alkalimetric, of Hg . . . . .	725
—, complexometric, of F . . . . .	909
—, —, of Hg(II) . . . . .	719
—, —, of Tl(III) . . . . .	721
—, iodometric, of sulphoxides . . . . .	969

—, oxidimetric, of thiophanate-methyl . . . . .	1010
—, potentiometric, in methanol/water medium . . . . .	769
—, —, of chloride and phosphate . . . . .	664
—, —, of two metals . . . . .	473
—, —, with automatic modular system . . . . .	667
— data, Linearization of . . . . .	271
Trace metals, Determination by different methods . . . . .	545
Transition metals, Separation by HPLC . . . . .	461
Triphenylmethane dyes, Chemiluminescence of . . . . .	625
Tryptophan, Determination, spectrophotometric . . . . .	35
Tubular-torch capacitatively-coupled microwave plasma, Determination of elements . . . . .	641
Uranium, Determination by NAA . . . . .	161
—, —, radiometric . . . . .	227
Vanadium, Determination, spectrophotometric . . . . .	1001
Volatiles from phenol-formaldehyde materials, Determination . . . . .	775
Voltammetry, Determination of Hg . . . . .	227
—, adsorptive stripping, Determination of cyadox and metabolites. . . . .	816
—, —, — of drugs . . . . .	287
—, —, — of Fe(III). . . . .	597
—, —, — of hydrazines . . . . .	965
—, —, — of lipoic acid and lipoamide . . . . .	837
—, —, — of menadione . . . . .	997
—, —, — of methotrexate. . . . .	805
—, —, — of organic compounds . . . . .	525
—, anodic stripping (ASV), Determination of Cu . . . . .	329
—, —, — of Pb . . . . .	819
—, —, — of Tl . . . . .	191
—, — staircase, Determination of Zn species . . . . .	953
—, Cyclic, Determination of dimethyl sulphoxide . . . . .	323
—, differential-pulse, of aromatic amine hydrochlorides . . . . .	379
—, Osteryoung square-wave, Determination of nicarbazin. . . . .	734
Water, Determination by FIA . . . . .	59
Xanthate, Determination by ISE . . . . .	807
Zinc species, Determination by ASV . . . . .	953
Zirconium, Determination, spectrophotometric . . . . .	502

## EDITORIAL

---

As already announced in the Editorial in the July issue, there is to be a change in the organization of *Talanta*. Starting on the 1st of January 1989, I shall cease to be Editor-in-Chief, although I shall continue my association with the journal for some time. In my place, Professor G. D. Christian, University of Washington, Seattle, and Professor D. Littlejohn, University of Strathclyde, Glasgow, will be joint Editors-in-Chief. The present Regional Editors will continue their duties, but will become known as Regional Advisers. The technical editing of papers accepted for publication will continue to be done by the present team of Assistant Editors and the Computing Editor, with assistance from me, until a permanent full-time Technical Editor is appointed to replace me. In this way it is hoped that there will be the minimum of inconvenience to contributors to the journal, and that they can rest assured that our present standards will be maintained.

To divide the work reasonably evenly between the two Editors-in-Chief, authors in the North and South Americas, Japan, China, Australia, India and other countries in that half of the world should send their papers to

Professor G. D. Christian  
Department of Chemistry  
University of Washington  
Seattle, WA 98195  
U.S.A.

and those in Europe, the Middle East and Africa should send theirs to

Professor D. Littlejohn  
Department of Pure and Applied Chemistry  
259 Cathedral Street  
Glasgow G1 1XL  
Scotland

Papers already in my hands (and any arriving before this notification has its intended effect) will be dealt with by me.

A further change is that the Editorial Board, after consultation with the Advisory Board, has decided that in the future only papers written in English will be considered for publication. There are various reasons for this decision, the most cogent being that English is the *lingua franca* of the scientific world, and that there is less likelihood of papers written in it being misunderstood because of problems in translation. (There is a story of an English-Swahili dictionary being checked for accuracy by translation back into English: the phrase "out of sight, out of mind" came back as "invisible idiot".) It may be argued that the policy is unfair to those whose native tongue is French or German, but it is no more unfair to them than to others (including native English-speakers, some of whom speak more grammatically than they write). Any polishing necessary will be done editorially as it is now.

During the 23 years I have been Editor-in-Chief, I have learned a great deal of chemistry from the papers submitted to the journal. In return I have tried to give good advice when necessary and to ensure that the journal has been as error-free as human frailty will allow. I believe that with the wise and penetrating advice given by the referees, and the skilled assistance of the editorial staff and the production team, *Talanta* has set a standard that may be rivalled but not surpassed by the other journals of analytical chemistry. I heartily thank all the contributors and my assistants for the part they have played in the success of the journal, and wish them and it a long and happy future.

R. A. CHALMERS



## ERRATUM

---

In the paper by E. M. Donaldson, *Talanta*, 1988, **35**, No. 8, 633, on p. 634 the first sentence in the third paragraph of the procedure should read as follows.

Add 200  $\mu\text{l}$  of concentrated nitric acid and sufficient 10-mg/ml nickel solution to the resulting blank and sample solutions for 50  $\mu\text{l}$  (*i.e.*, 500  $\mu\text{g}$  of nickel) to be present for each 5 ml of final solution (Note 4), then gently evaporate the solutions to dryness on a hot-plate maintained at  $\leq 200^\circ$ .

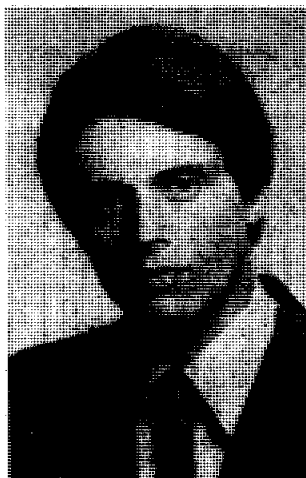
## THE RONALD BELCHER MEMORIAL AWARD

---

As with the first Ronald Belcher Memorial Award it proved difficult to choose between the candidates, and again it was decided to obtain maximum benefit from the award by dividing it between two of the candidates, Dr. Peter D. Wentzell and Dr. Spas D. Kolev.



Dr. Wentzell, of Vancouver, Canada, is particularly interested in chemometrics, kinetic methods of analysis, and analytical instrumentation.



Dr. Kolev, of Sofia, Bulgaria, is especially interested in mathematical modelling of analytical systems, particularly in flow-injection analysis, chemical and biological reactors, and spectrophotometry.

The two winners of the first award made good use of it, Dr. Macdonald travelling to the United States and visiting various academic and industrial laboratories and attending conferences, and Dr. Cruces Blanco visited universities in England and Scotland.

## EDITORIAL

---

At the end of this month, *Talanta* will be just 30 years old, the first issue having appeared in August 1958. Various changes in the format, style and policy of the journal have taken place in that time, and will continue to be made in the future. The most recent changes are the appointment of Professor M. Valcárcel, of the University of Córdoba, as Regional Editor for Spain, and of two additional Assistant Editors for the journal, Dr. W. A. J. Bryce, Department of Chemistry, University of Aberdeen, and Dr. P. J. Cox, Department of Pharmacy, Robert Gordon's Institute of Technology, Aberdeen, whose fields of interest will complement those of the rest of the editorial team. Amongst changes planned for the future the most important will be the establishment of an international consortium of Editors who will be responsible for the general policy and conduct of the journal, and give it even wider scope in its coverage of analytical chemistry. Professor G. D. Christian, University of Washington, has already agreed to join the group, and the names of his fellow Editors will be announced as soon as possible. One of the reasons for the change is that the present Editor-in-Chief is not immortal and feels he should not try to prove the opposite; it is therefore deemed important to ensure continuity in the day-to-day affairs of the journal, and a smooth transition to the new regime. Until the transfer is complete, editorial business will be conducted as usual, by the present editorial staff. All changes will be announced in the journal.

R. A. CHALMERS

## EDITORIAL

---

At the end of this month, *Talanta* will be just 30 years old, the first issue having appeared in August 1958. Various changes in the format, style and policy of the journal have taken place in that time, and will continue to be made in the future. The most recent changes are the appointment of Professor M. Valcárcel, of the University of Córdoba, as Regional Editor for Spain, and of two additional Assistant Editors for the journal, Dr. W. A. J. Bryce, Department of Chemistry, University of Aberdeen, and Dr. P. J. Cox, Department of Pharmacy, Robert Gordon's Institute of Technology, Aberdeen, whose fields of interest will complement those of the rest of the editorial team. Amongst changes planned for the future the most important will be the establishment of an international consortium of Editors who will be responsible for the general policy and conduct of the journal, and give it even wider scope in its coverage of analytical chemistry. Professor G. D. Christian, University of Washington, has already agreed to join the group, and the names of his fellow Editors will be announced as soon as possible. One of the reasons for the change is that the present Editor-in-Chief is not immortal and feels he should not try to prove the opposite; it is therefore deemed important to ensure continuity in the day-to-day affairs of the journal, and a smooth transition to the new regime. Until the transfer is complete, editorial business will be conducted as usual, by the present editorial staff. All changes will be announced in the journal.

R. A. CHALMERS

## NOTICE

---

### 1988 PITTSBURGH CONFERENCE MEMORIAL NATIONAL COLLEGE GRANTS AWARD PROGRAM

(15th Year of Funding)

The Pittsburgh Conference on Analytical Chemistry and Applied Spectroscopy, Inc., and its cosponsoring technical societies, the Spectroscopy Society of Pittsburgh (SSP) and The Society for Analytical Chemists of Pittsburgh (SACP), are happy to announce the 15th year of funding for The Pittsburgh Conference Memorial National College Grants Award Program. At least eight (8) colleges will be selected to receive awards (\$2,500 maximum), based on their submitted proposals, for the purchase of scientific equipment, audio-visual and other teaching aids, and/or library materials for use in the teaching of science at the undergraduate level.

To be eligible for an award, the school must meet these criteria:

- (1) A school must have an enrollment of not more than 2,500 students, and
- (2) Receive no more than 25% of its operating budget from national or state governments. Two-year community colleges sponsored by political subdivisions of a state are not bound by these requirements.
- (3) Requests for materials to be used only for research purposes shall not be funded.
- (4) Previous awardee schools are not eligible for an award for a three-year period following their award. (For example, the 1985, 1986 and 1987 awardee schools are not eligible for the 1988 program).
- (5) This award may be used as part of a "Matching Grant" program for undergraduate studies as described above. In fact, generating "MATCHING FUNDS" is recommended.

Any interested faculty member is urged to participate by completing an APPLICATION FORM and submitting it with a PROPOSAL (original and 3 copies of each), by 1 April 1988, to

Richard S. Danchik,  
The Pittsburgh Conference, Inc.  
12 Federal Drive,  
Suite 322,  
Pittsburgh,  
PA 15235,  
U.S.A.

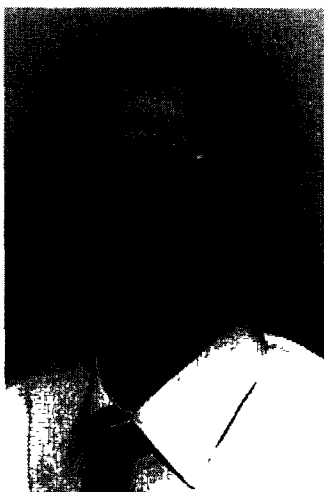
Award-winning schools will be announced by 1 May 1988, joining the list of 80 previous award-winning schools.

PLEASE WRITE NOW FOR APPLICATION/PROPOSAL INFORMATION AT THE ADDRESS ABOVE.

## TALANTA EDITORIAL AND ADVISORY BOARDS

---

The Publisher and Editorial Board of *Talanta* deeply regret the death of Professor Hans Ewald Blasius, who had served as a Regional Editor of the journal since 1965. They are also sorry to lose the services of Dr. M. Williams, as Consultant Editor. Dr. Williams has been associated with the journal since 1960, first as Assistant Editor, then as Associate Editor (1961–1964) and Editor-in-Chief (1965), after which he was Journals Manager at Pergamon Press until his present position in charge of the IUPAC Secretariat in Oxford. A further loss has been suffered through the retirement of Dr. M. Pesez, who joined the Advisory Board in 1960 and has been a Regional Editor since 1965. Professor Blasius will be replaced as Regional Editor by Dr. K.-H. Koch, to whom manuscripts from German-speaking countries may be sent. The Publisher and Editorial Board welcome Professor A. Corsini to membership of the Advisory Board, and wish to extend their thanks to Professor E. Wänninen, who has now retired from university work and from the Advisory Board (after membership of it since 1963).



**PROFESSOR A. CORSINI** (a member of the Advisory Board from 1972 to 1981) gained his Ph.D. at McMaster University in 1961, after which he was a Research Associate at the University of Arizona, with Professor Freiser, until 1963, when he joined the Department of Chemistry at McMaster University, becoming full professor in 1973. He served as Associate Dean of Science Studies from 1977 to 1981. He was a member of the Executive of the Analytical Chemistry Division of the Chemical Institute of Canada from 1965 to 1980, and was its Chairman in 1968. He was named Fellow of the Institute in 1972, and received its Fisher Scientific Lecture Award for Analytical Chemistry in 1985. In 1973 he was awarded the *Talanta* Louis Gordon Memorial Award. His research interests are many and varied. Over the years, an abiding interest in structural and reactivity factors that govern the selectivity of organic analytical reagents; the design and synthesis of such reagents, measurement of solution thermodynamic parameters and application to trace metal analysis. Present interests involve the development of new solvent-extraction systems and chelating resins, particularly for the concentration of environmentally significant metal ions; metal-ion speciation in natural waters; and fundamental studies on the atomization behaviour of certain metal ions in electrothermal AA spectrometry.

## PERGAMON PRESS 1948-1988 AND TALANTA 1958-1988

### TWO ANNIVERSARIES

ROBERT A. CHALMERS

Department of Chemistry, University of Aberdeen, Old Aberdeen, Scotland

Like many of the important developments in analytical chemistry, *Talanta* partly owes its existence to serendipity. It happened (as far as can be traced) that at a time when Ronald Belcher was becoming increasingly dissatisfied with the policies and standards of some of the analytical journals then current, and wondering what could be done about that and the rapidly increasing number of papers arising from the upsurge in analytical research, he chanced to meet in a London pub an employee of Pergamon Press who mentioned that Robert Maxwell was considering expanding his list of scientific journals to include one on analytical chemistry. Belcher not only expressed immediate interest but also said he knew someone who would make an excellent editor for such a journal. There thus came about a meeting between Belcher and Maxwell, which resulted in the appearance of a new journal on the analytical scene—*Talanta*, with Cecil Wilson as Editor-in-Chief.

The first issue appeared in August 1958, with a Foreword by Fritz Feigl (see Frontispiece), a highly distinguished international band of analytical chemists as the Advisory Board, and Louis Gordon, Rudolf Přibil and Takeo Takahashi as Regional Editors. The new journal was so successful in attracting work for publication that in spite of a double-size first issue there was an editorial apology for failure to include *all* the papers submitted for it and accepted for publication. The initial policy was to publish full papers, short communications, preliminary communications (with publication given priority), critical reviews, book reviews, notices of meetings, letters to the editor, and summaries in English, French and German for each paper. The papers themselves could be written in any of these three languages. Later, Russian summaries were added, and the English and Russian versions were repeated at the end of each issue so that they could be cut out and used for the compilation of card indexes. A notable early feature was the publication of specially commissioned "Talanta Reviews" (later supplemented by updating in "Mini-Reviews"), some 60 of which appeared.

As time went on, further features were added to the journal, in keeping with the ideals behind its foundation. The "Analytical Data" section was added to deal with the numerous papers on determination of stability constants, protonation constants *etc.*, which convey data vital to the understanding and inter-

pretation of analytical chemistry, but do not necessarily require detailed descriptions, since the methods used are more or less standard. The "Annotations" feature was created to allow publication of those papers which offer a critical commentary on existing ideas, or attempt to resolve controversy and polemic, and all too frequently have been refused publication elsewhere on the grounds that they do not constitute "research", even though in fact they may be far more valuable than many of the papers that are readily accepted as "research" despite the fact that their authors may well be the only people ever to use the methods described in them. This question of what to accept and what to reject is often a difficult one. Many workers struggle to do research under highly adverse circumstances, often having to cope with lack of finance and equipment, and shortage of library funds, and are dependent on publication for promotion or even continuation of tenure. The inevitable consequence is that all too often, through no fault of their own, their work may not meet the standards set by the journal to which they submit it, though it may well have been soundly conceived and executed. It was to try to help research workers in general that an earlier feature was introduced in *Talanta*, in the form of papers on the development and publication of new methods using a particular technique. These were intended to lay down a set of requirements for the thorough investigation of the proposed method and to provide guidelines for writing up the results for publication. Starting with the classic paper by Kirkbright in 1966, several of these papers appeared (Table 1), until the idea was taken over by IUPAC for publication in *Pure and Applied Chemistry*.

A further extension of the range of services offered by *Talanta* has been the establishment of "paper symposia" in the form of special issues devoted to a particular research topic, the contributors being selected from the leaders in their field and specially invited to write for the issue. The issues to date are listed in Table 2. The most recent development has arisen from the widespread use of computer facilities in analysis, and has taken the form of the "Software Survey" which offers rapid publication of basic information about software designed for use in analytical chemistry.

Besides this unusually broad range of publication features, *Talanta* has at its command two prestigious

Table 1. Research guideline papers

Topic	<i>Talanta</i> reference
Spectrophotometry	G. F. Kirkbright, 1966, 13, 1
Gravimetry	L. Erdey, L. Pólos, R. A. Chalmers, 1970, 17, 1143
Ion-selective electrodes	G. J. Moody, J. D. R. Thomas, 1972, 19, 623
Titrimetry	A. Berka, J. Ševčík, R. A. Chalmers, 1972, 19, 747
Kinetic methods	H. B. Mark, Jr., 1973, 20, 257
Atomic-absorption spectrometry	J. Ramirez-Muñoz, 1973, 20, 705
Stability constants	H. S. Rossotti, 1974, 21, 809
Solvent extraction	Y. Marcus, 1976, 23, 203
Polarography	L. Meites, B. H. Campbell, P. Zuman, 1977, 24, 709

awards. One is the "Honour Issue" which can be dedicated to an individual or a country in recognition of eminence in the analytical world, and the other—thanks to the generosity of Robert Maxwell—is the "Talanta Medal", awarded in recognition of an outstanding contribution to analytical chemistry. Neither is awarded at regular time intervals, but only when a suitably worthy occasion arises. The Honour Issues are, of course, the equivalent of the German "Festschrift" issues. This article, like similar ones in other Pergamon journals, will in fact form part of a Festschrift planned for presentation to Robert Maxwell in June this year in celebration of his 65th birthday and the 40th anniversary of the establishment of Pergamon Press (and incidentally the 30th anniversary of the founding of *Talanta*). A list of the Honour Issues is given in Table 3, and a list of recipients of the Talanta Medal in Table 4. A picture of the medal itself is shown in Plate I.

These are not the only awards associated with *Talanta*, however. When Louis Gordon, who had served as Regional Editor for the United States since *Talanta* was started, died in 1966, it was decided to institute the Louis Gordon Memorial Award in his honour. This is awarded for the paper judged to be the best written of those published in the journal in the year of award, and takes the form of a specially bound copy of the volume in which the award-winning paper appeared. A list of the winners shows that the ability to write well knows few geographical boundaries. It should be pointed out the Award can be made only once to the same person, otherwise at least one of the winners would possess several bound copies of *Talanta*!

An award of similar nature is the Pharmacia Prize, funded by Pharmacia AB, Uppsala, Sweden, for the

best research paper published in *Talanta* by an industrial research laboratory. It is a biennial award and consists of a specially commissioned piece of Swedish ceramic, accompanied by a scroll citing the award. It is perhaps not surprising that so far the Prize has always gone to a laboratory in the United States.

Finally, to commemorate Ronald Belcher, the original inspiration behind the journal, who served as Chairman of the Advisory and Editorial Boards from the beginning of the journal to his death in 1985, Pergamon Press has established the Ronald Belcher Memorial Award, designed to assist young research workers to undertake travel they might otherwise not be able to afford.

There has often been speculation about the meaning of the title of the journal. This was explained in the correspondence reprinted below, from *Talanta*, 1962, 9, 1063.

Table 3. Honour Issues

1961	H. H. Willard
1963	Hungary
1964	I. M. Kolthoff
1966	G. F. Smith
1968	A. A. Smales
1969	R. Belcher
1972	Japan
1975	Scandinavia
1979	Germany
1980	H. Diehl
1985	H. Freiser
1987	Soviet Union

Table 4. Talanta Medal winners

1961	F. Feigl
1963	G. Schwarzenbach
1965	I. P. Alimarin
1967	E. Stahl
1969	A. Walsh
1971	R. Přibil
1974	B. V. L'vov
1977	R. Belcher
1981	J. Růžička
1983	T. Fujinaga
1986	E. Pungor

Table 2. Paper symposia\*

Topic	<i>Talanta</i> issue
Errors in trace analysis	1982, November
Analytical methods in clinical chemistry	1984, October
Fiber optic chemical sensors	1988, February

\*A precursor was a special issue on microprocessors, July 1981.



## NOTICES

---

### THE 40th PITTSBURGH CONFERENCE & EXPOSITION ON ANALYTICAL CHEMISTRY AND APPLIED SPECTROSCOPY

6-10 March 1989  
Exposition—6-9 March 1989

Georgia World Congress Center  
Atlanta, Georgia, U.S.A.

Original papers may be contributed in all areas of Analytical Chemistry, Spectroscopy and associated fields.

Details from:

Pittsburgh Conference  
Dept. CFP  
12 Federal Drive, Suite 322  
Pittsburgh, PA 15235, U.S.A.

---

### INTERNATIONAL UNION OF BIOLOGICAL SCIENCES

#### Workshop on Methods of Assessment and Evaluation of Element Concentration Cadastrers in Ecosystems (ECCE)

13-15 March 1989  
Osnabrück, F.R.G.

The major goals for this IUBS/ECCE project are:

- Assessment of the global distribution pattern of all chemical elements in ecosystems
- Study of element fluxes through the ecosystem from rain and dust or soil and waters to plants and animals
- Study of functional impacts of all elements, especially of those not yet commonly investigated.

The workshop will deal with basic problems for the assessment and evaluation of element concentration cadastrers.

Four topics require foremost attention:

1. Representative sampling in ecosystems
2. Sample preparation, preconcentration, separation
3. Instrumental multi-element analysis
4. Data handling, evaluation and interpretation

The discussions will be based on the books "Kurze Einführung in die Erstellung und Anwendung ökosystemarer Element-Konzentrations-Kataster", by Lieth and Markert, soon to be published by Springer Verlag, and "Instrumentelle Multielementanalyse", by Sansoni (ed.), VCH-Verlagsgesellschaft, D-6940 Weinheim, 1985.

The registration fee of DM200,—will cover all services provided including the publication of workshop proceedings.

Further information from:

International IUBS-ECCE-Workshop  
Dr. B. Markert  
Arbeitsgruppe Systemforschung  
University of Osnabrück  
P.O. Box 4469  
4500 Osnabrück, F.R.G.

---

## IIIrd INTERNATIONAL SYMPOSIUM ON QUANTITATIVE LUMINESCENCE SPECTROMETRY IN BIOMEDICAL SCIENCES

23–26 May 1989  
State University of Ghent, Belgium

Details from:

Dr. Willy R. G. Baeyens  
Symposium Chairman  
Laboratory of Pharmaceutical Chemistry and Drug Quality Control  
Institute of Pharmacy  
State University of Ghent  
Harelbekestraat 72  
B-9000 Ghent  
Belgium

---

## THE XXVI COLLOQUIUM SPECTROSCOPICUM INTERNATIONALE (CSI)

2–9 July 1989  
Sofia, Bulgaria

The scientific program of the Colloquium will be distributed between plenary lectures, oral presentation in parallel sessions and predominantly poster sessions.

### PROGRAM TOPICS

Basic theory, methods and applications of:

1. Atomic-emission spectroscopy
2. Atomic-absorption spectrometry
3. Atomic-fluorescence spectrometry
4. X-Ray emission and fluorescence spectrometry
5. Vibrational spectroscopy
6. Molecular electron spectroscopy
7. Mass spectroscopy
8. Non-linear spectroscopy
9. Magnetic resonance spectroscopy
10.  $\gamma$ -Ray and Mössbauer spectroscopy
11. Surface spectroscopy
12. Astrophysical spectroscopy
13. Molecular interactions
14. Molecular structure

15. Sample preparation, introduction and standard reference materials
16. Radiation sources and detectors
17. Spectra acquisition and processing

Special emphasis will be placed on the following analytical applications

1. Analysis of metals
2. Analysis of geological materials
3. Analysis of industrial products
4. Biological, clinical and pharmaceutical analysis
5. Food and agricultural analysis
6. Analysis of high purity materials
7. Environmental analysis

The working languages of CSI are English, French and German. There will be no simultaneous translation.

Address for correspondence

XXVI CSI'89

Sofia University, Faculty of Physics

Dept. of Optics and Spectroscopy

5, A. Ivanov Blvd., 1126-30 Sofia, BULGARIA

Tel. (3592) 62-74-75, Telex SUKO 23296 R BG

---

## THE 5th INTERNATIONAL CONFERENCE ON PARTICLE INDUCED X-RAY EMISSION AND ITS ANALYTICAL APPLICATIONS

21-25 August 1989  
Amsterdam, The Netherlands

### Scope of the Conference

Although, of course, the main emphasis will be on PIXE (both its methodology and its applications in various fields), attention will be paid to other accelerator-based analytical techniques such as those using nuclear reactions or using synchrotron radiation as the primary source. A special session on microprobe techniques will be included. Sessions will consist of both invited and contributed papers and posters. Workshops on special items such as data acquisition, reduction and analysis are also planned. Given sufficient interest, ion source development and quadrupole systems will also be covered in workshops.

Contact address:

Department of Physics and Astronomy  
Free University  
De Boelelaan 1081  
1081 HV Amsterdam  
The Netherlands  
*Telephone: 020-5486224.*

---

## ROYAL SOCIETY OF CHEMISTRY, LONDON, ENGLAND

### Anniversary Fellowship for Analytical Chemistry

Council of the Analytical Division of The Royal Society of Chemistry has approved proposals for a ROBERT BOYLE FELLOWSHIP IN ANALYTICAL CHEMISTRY to mark the 150th Anniversary in 1991 of the founding of The Chemical Society. The Fellowship will be awarded by the Trustees of the Analytical Chemistry Trust Fund.

It is intended that the Fellowship be awarded to an applicant making the most prestigious proposal within the realm of and of direct benefit to the advancement of Analytical Chemistry in the modern world.

Although the initiative for the Fellowship arises from the desire to mark the 150th Anniversary of The Chemical Society, founded in 1841, it is noted that 1991 marks the tercentenary of the death of ROBERT BOYLE (1627–91) in whose work were to be seen the beginnings of modern chemical analysis. Therefore, the Fellowship is also dedicated to him.

It is expected that the Fellow appointed will be at work at the time of the 150th Anniversary Celebrations of The Royal Society of Chemistry (within which are amalgamated The Chemical Society, The Royal Institute of Chemistry, The Society for Analytical Chemistry and The Faraday Society) to be held at Imperial College, University of London between April 9th and 12th, 1991.

The Fellowship will be tenable at a British university, polytechnic, or research establishment having facilities to meet the approval of the Trustees. Prospective applicants should register their interest with the Secretary of the Analytical Division at the address given below.

## LIST OF CONTENTS

### JANUARY

<b>Obituary</b>	I
<i>Talanta Editorial and Advisory Boards</i>	III
<b>Chiran J. Kantipuly and Alan D. Westland</b>	1 Review of methods for the determination of lanthanides in geological samples
<b>Carl O. Moses, Alan T. Herlihy, Janet S. Herman and Aaron L. Mills</b>	15 Ion-chromatographic analysis of mixtures of ferrous and ferric iron
<b>C. S. P. Sastry, M. Aruna and A. Rama Mohana Rao</b>	23 Spectrophotometric determination of some antiamoebic and anthelmintic drugs with metol and chromium(VI)
<b>B. Corain, B. Longato, A. M. Maccioni, B. Pelli, P. Traldi and F. R. Kreissl</b>	27 Mass spectrometric behaviour of pentachlorophenyl $\beta$ -carbonylenolate phosphino nickel(II) complexes: an example of thermal generation of a nickel(III) species
<b>Krishna K. Verma, Archana Jain and J. Gasparič</b>	35 Spectrophotometric determination of tryptophan by reaction with nitrous acid
<b>G. Ramis Ramos, I. M. Khasawneh, M. C. García-Alvarez-Coque and J. D. Winefordner</b>	41 Room-temperature phosphorimetry of polyaromatic hydrocarbons with organized media and paper substrate: a comparative study
<b>Elsie M. Donaldson</b>	47 Determination of arsenic in ores, concentrates and related materials by graphite-furnace atomic-absorption spectrometry after separation by xanthate extraction
<i>Short Communications</i>	
<b>Keiichi Fukushi and Kazuo Hiroy</b>	55 Simultaneous determination of low concentrations of ammonium and potassium ions by capillary type isotachopheresis
<b>K. C. Bayan and H. K. Das</b>	57 Extractive spectrophotometric determination of trace amounts of iron(III) with benzyltriethylammonium chloride
<b>Chen Liang, Pavel Vácha and Willem E. van der Linden</b>	59 Determination of water in organic solvents by flow-injection analysis with Karl Fischer reagent and a biampometric detection system
<b>O. D. Bozhkov, N. Jordanov and L. V. Borisova</b>	62 Spectrophotometric determination of rhenium with dithio-oxamide in strongly alkaline medium
<b>Krystyna Brajter, Ewa Olbrych-Sleszyńska and Mieczysław Stąskiewicz</b>	65 Preconcentration and separation of metal ions by means of Amberlite XAD-2 loaded with Pyrocatechol Violet
<b>M. Soma, H. Seyama and K. Satake</b>	68 X-Ray photoelectron spectroscopic analysis of lead accumulated in aquatic bryophytes
<b>J. M. López Fonseca, A. Otero and J. C. García Monteagudo</b>	71 Application of reverse pulse polarography to the determination of substances which form films electrochemically on the mercury electrode
<i>Publications Received</i>	i
<i>Notice</i>	iii
<i>Questionnaire: Software Survey Section</i>	v

### FEBRUARY

## FIBER OPTIC CHEMICAL SENSORS

<b>Mark A. Arnold</b>	V Foreword
<b>Gilbert Boisdé, Floreal Blanc and Jean-Jacques Perez</b>	75 Chemical measurements with optical fibers for process control

<b>R. Narayanaswamy, D. A. Russell and F. Sevilla, III</b>	83	Optical-fibre sensing of fluoride ions in a flow-stream
<b>Hermann E. Posch, Otto S. Wolfbeis and Johannes Pusterhofer</b>	89	Optical and fibre-optic sensors for vapours of polar solvents
<b>Richard R. Smardzewski</b>	95	Multi-element optical waveguide sensor: general concept and design
<b>T. E. Edmonds, N. J. Flatters, C. F. Jones and J. N. Miller</b>	103	Determination of pH with acid-base indicators: implications for optical fibre probes
<b>Christiane Munkholm, David R. Walt and Fred P. Milanovich</b>	109	A fiber-optic sensor for CO <sub>2</sub> measurement
<b>Frank V. Bright, Greg E. Poirier and Gary M. Hieftje</b>	113	A new ion sensor based on fiber optics
<b>Lynn M. Christian and W. Rudolf Seitz</b>	119	An optical ionic-strength sensor based on polyelectrolyte association and fluorescence energy transfer
<b>N. Opitz and D. W. Lübbers</b>	123	Electrochromic dyes, enzyme reactions and hormone-protein interactions in fluorescence optic sensor (optode) technology
<b>Ulrich J. Krull, R. S. Brown, R. F. DeBono and B. D. Hougham</b>	129	Towards a fluorescent chemoreceptive lipid membrane-based optode
<b>Randy D. Petrea, Michael J. Sepaniak and Tuan Vo-Dinh</b>	139	Fiber-optic time-resolved fluorimetry for immunoassays
<b>David Meadows and Jerome S. Schultz</b>	145	Fiber-optic biosensors based on fluorescence energy transfer
<b>Bonnie S. Walters, Timothy J. Nielsen and Mark A. Arnold</b>	151	Fiber-optic biosensor for ethanol, based on an internal enzyme concept
<b>A. J. Guthrie, R. Narayanaswamy and N. A. Welti</b>	157	Solid-state instrumentation for use with optical-fibre chemical-sensors
<i>Publications Received</i>	i	
<i>Questionnaire: Software Survey Section</i>	iii	

## MARCH

<i>Talanta Advisory Board</i>	I	
<b>A. R. Byrne and L. Benedik</b>	161	Determination of uranium at trace levels by radiochemical neutron-activation analysis employing radioisotopic yield evaluation
<b>Valerio Porta, Edoardo Mentasti, Corrado Sarzanini and Maria Carla Gennaro</b>	167	Ion-pair liquid-solid extraction for the preconcentration of trace metal ions. Optimization of experimental conditions
<b>T. Denis Rice</b>	173	Determination of fluorine and chlorine in geological materials by induction furnace pyrohydrolysis and standard-addition ion-selective electrode measurement
<b>J.-M. Kauffmann, C. R. Linders, G. J. Patriarche and Malcolm R. Smyth</b>	179	A comparison of glassy-carbon and carbon-polymer composite electrodes incorporated into electrochemical detection systems for high-performance liquid chromatography
<b>W. M. Mok and C. M. Wai</b>	183	Determination of arsenic and antimony in biological materials by solvent extraction and neutron activation
<b>Ninus Simonzadeh and A. A. Schilt</b>	187	Metal-ion chromatography on silica-immobilized 2-pyridinecarboxy-aldehyde phenylhydrazone
<b>Aleksander Ciszewski and Zenon Lukaszewski</b>	191	Electrochemical masking for removal of the titanium matrix effect in DPASV determination of thallium
<b>E. Casassas, A. Izquierdo-Ridorsa and L. Puignou</b>	199	Catalytic spectrophotometric determination of trace amounts of copper(II) with 3-hydroxy-2-naphthoic acid
<b>A. Boughriet and M. Wartel</b>	205	Chemical and electrochemical behaviour of nitric and nitrous acids in sulpholane
<b>P. Rychlovský and I. Němcová</b>	211	The effect of surfactants on the dissociation constants of phenothiazine derivatives. Alkalimetric determination of diethazine and chlorpromazine

<b>Scott A. Glazier, Mark A. Arnold and Jeffery P. Glazier</b>	215	Evaluation of an overdetermined system based on multiple ion-selective electrodes of the same type
<b>Ray von Wandruszka and James D. Winefordner</b>	221	Fluorescence drainage profiles of thin liquid films
<b>M. Chwistek, J. Chmielowski and I. Tomza</b>	227	Radiometric determination of uranium accumulated in bacterial cells
<b>Nirmal Maitra, Albert W. Herlinger and Bruno Jaselskis</b>	231	Determination of semimicro amounts of calcium in the presence of other alkaline-earth metals
<i>Short Communications</i>		
<b>M. T. Lippolis and V. Concialini</b>	235	Differential pulse polarographic determination of the herbicides atrazine, prometryne and simazine
<b>C. V. Rajeswari, D. V. Naidu, N. V. S. Naidu and P. R. Naidu</b>	237	A simple spectrophotometric method for determination of isoxsuprine hydrochloride in pharmaceuticals
<b>Minoru Hara and Noboru Nomura</b>	239	Modified reverse pulse polarographic behaviour of magnesium ion in aqueous solution
<b>Mohamed E. Abdel-Hamid and Mustafa A. Abuirjeie</b>	242	Utility of iodine and 7,7,8,8-tetracyanoquinodimethane for determination of terfenadine
<b>Jarl M. Pettersen, Hanne G. Johnsen and Walter Lund</b>	245	The determination of nitrate and sulphate in 50% sodium hydroxide solution by ion-chromatography
<i>Publications Received</i>	i	
<i>Corrigenda</i>	v	
<i>Notes for Authors</i>	vii	
<i>Questionnaire: Software Survey Section</i>	ix	

#### APRIL

<i>Talanta Advisory Board</i>	I	
<b>A. Gustavo González, Daniel Rosales, José L. Gómez Ariza and A. Guiraúm Pérez</b>	249	A computational method for approximate evaluation of ionization constants from potentiometric data
<b>M. Tarek M. Zaki, W. H. Mahmoud and A. Y. El-Sayed</b>	253	Extraction-spectrophotometric determination of iron(II) by ternary complex formation with Pyrocatechol Violet and cetyltrimethylammonium bromide
<b>D. B. Gladilovich, V. Kubán and L. Sommer</b>	259	Determination of the sum of rare-earth elements by flow-injection analysis with Arsenazo III, 4-(2-pyridylazo)resorcinol, Chrome Azurol S and 5-bromo-2-(2-pyridylazo)-5-diethylaminophenol spectrophotometric reagents
<b>I. M. Khasawneh and J. D. Winefordner</b>	267	Luminescence characteristics of dibenzofuran and several polychlorinated dibenzofurans and dibenzo- <i>p</i> -dioxins
<b>Howard R. Rogers and Constant M. G. van den Berg</b>	271	Determination of borate ion-pair stability constants by potentiometry and non-approximative linearization of titration data
<b>Joseph Wang and Mojtaba Bonakdar</b>	277	Preconcentration and voltammetric measurement of mercury with a crown-ether modified carbon-paste electrode
<b>Magdalena Maj-Żurawska, Tomasz Sokalski and Adam Hulanicki</b>	281	Interpretation of the selectivity and detection limit of liquid ion-exchanger electrodes
<b>Lucas Hernández, Antonio Zapardiel, José Antonio Pérez López and Esperanza Bermejo</b>	287	Measurement of nanomolar levels of psychoactive drugs in urine by adsorptive stripping voltammetry
<b>J. Hernández Méndez, B. Moreno Cordero and J. L. Pérez Pavón</b>	293	Simultaneous spectrophotometric determination of erbium and praseodymium with 1-(2-pyridylazo)-2-naphthol in the presence of octylphenol poly(ethyleneglycol) ether (TX-100)
<b>Elsie M. Donaldson and Maureen E. Leaver</b>	297	Determination of arsenic in ores, concentrates and related materials by continuous hydride-generation atomic-absorption spectrometry after separation by xanthate extraction
<b>J. L. Hidalgo, M. A. Gomez, M. Caballero, R. Cela and J. A. Pérez-Bustamante</b>	301	Determination of Mo(VI) in tap-water and sea-water by differential-pulse polarography and co-flotation
<b>A. Beveridge, W. F. Pickering and J. Slavek</b>	307	Separation of oxyanions of sulphur by single-column ion-chromatography

<i>Short Communications</i>	
H. N. A. Hassan, M. E. M. Hassouna and Y. A. Gawargjous	311 Spectrophotometric microdetermination of bismuth in organic compounds after oxygen-flask combustion
J. R. Kim und H. Lentz	314 Extraktion von Ginsenosiden mit Ammoniak und Kohlensäure unter erhöhtem Druck
Bo Thelin	317 Correlation of spectral-line intensity-ratio fluctuations of different elements
M. I. Walash, F. Belal and F. A. Aly	320 Evaluation of certain pharmaceuticals with hexa-amminecobalt(III) tricarbonatocobaltate(III)—I. Determination of some <i>N</i> -substituted phenothiazine derivatives
Henrique E. Toma, Denise Oliveira and Americo T. Meenochite	323 Analytical determination of dimethyl sulphoxide by complex formation with the pentacyanoferrate(II) ion
Shin-ichi Wakida, Masataka Yamane and Kazuo Hiiro	326 A novel Urushi matrix chloride ion-selective field effect transistor
Aleksander Ciszewski	329 Determination of copper in the presence of a large excess of bismuth by differential-pulse anodic-stripping voltammetry without preliminary separation
<i>Letter to the Editor</i>	
Pier G. Daniele, Alessandro De Robertis, Concetta De Stefano, Silvio Sammartano and Carmelo Rigano	333
Software Survey Section	335 FLUOPAC1; Fleet Street Editor/Fleet Street Publisher; SOPHD; GHS
<i>Publications Received</i>	i
<i>Questionnaire: Software Survey Section</i>	iii

## MAY

<i>Frontispiece</i>	I The Foreword in the first issue of <i>Talanta</i>
Robert A. Chalmers	III Pergamon Press 1948–1988 and <i>Talanta</i> 1958–1988. Two anniversaries
Marit Andersson, Christina Ericzon and Åke Olin	337 Determination of lead in fly-ash from a garbage incinerator by atomic-absorption and X-ray fluorescence spectrometry
F. J. Barragán de la Rosa, R. Escobar Godoy and J. L. Gómez Ariza	343 Spectrophotometric determination of gallium in alloys and fly-ash with pyridoxal derivatives of thiocarbohydrazide and carbohydrazide
Mitsuko Oshima, Kiyomi Shibata, Takako Gyouten, Shoji Motomizu and Kyoji Tôei	351 Extraction-spectrophotometric determination of boron with 4,6-di- <i>tert</i> -butyl-3-methoxycatechol and Ethyl Violet
Shashikant R. Kuchekar and Manohar B. Chavan	357 Separation of gallium, indium and thallium by extraction with <i>n</i> -octyl-aniline in chloroform
Saad S. M. Hassan and M. A. Hamada	361 A new liquid membrane electrode for the selective determination of perchlorate
James B. Craig and Carlann Mackay	365 A simple operational relationship between drop-time and interfacial tension at a charged mercury/aqueous solution interface
James B. King and Roger Stephens	369 Some observations on the Kerr effect in suspensions of bentonite
Salah M. Sultan, Ibrahim Z. Alzamil and Nawal A. Alarfaj	375 Complexometric-spectrophotometric assay of tetracyclines in drug formulations
Paolo Ugo, Salvatore Daniele, Gino Bontempelli and Antonio Beccari	379 Determination of residual aromatic amine hydrochlorides in process samples of di-isocyanate used in the manufacture of polyurethane. A comparison of electroanalytical methods
Franz W. E. Strelow	385 Distribution coefficients and ion-exchange selectivities for 46 elements with a macroporous cation-exchange resin in hydrochloric acid-acetone medium
C. Sánchez-Pedreño, M. I. Albero and M. S. Garcia	397 Kinetic determination of Hg(II) in different materials, based on its inhibitory effect on a catalysed process



<i>Short Communications</i>	
J. B. Craig, D. Hopkins and R. A. Howie	401 A precision drop-fall detector for polarographic and electrocapillary work
János Fazakas and Michel Hoenig	403 The influence of atomization pressure on the behaviour of aluminium in electrothermal atomic-absorption spectrometry
N. K. Roy and A. K. Das	406 Determination of antimony in rocks and sulphide ores by flame and electrothermal atomic-absorption spectrometry
Krishna K. Verma, Sunil K. Sanghi and Archana Jain	409 Spectrophotometric determination of primary aromatic amines with 4- <i>N</i> -methylaminophenol and 2-iodylbenzoate
<i>Analytical Data</i>	
G. Rauret, L. Pineda, R. Casas, R. Compañó and A. Sanchez-Reyes	413 Solvent extraction of Cd(II) with <i>N</i> -cyclohexyl- <i>N</i> -nitrosohydroxylamine and 4-methylpyridine into methyl isobutyl ketone
Elisabeth Bosch and Martí Rosés	419 1,2-Naphthoquinone-2-thiosemicarbazone as a new acid-base indicator in isopropyl and <i>tert</i> -butyl alcohol media
<i>Publications Received</i>	i
<i>Questionnaire: Software Survey Section</i>	iii

## JUNE

Jun'ichi Toei	425 Potential of the flow-gradient function in FIA with a multifunction pump delivery system
Maria Pesavento, Antonella Profumo and Raffaella Biesuz	431 Sorption of protons and metal ions from aqueous solutions by a strong-base anion-exchange resin loaded with sulphonated azo-dyes
J. Chwastowska and E. Kosiarska	439 Synthesis and analytical characterization of a chelating resin loaded with dithizone
S. S. Murti, S. C. S. Rajan and J. Subrahmanyam	443 Determination of antimony in lead, zinc concentrates and other smelter products by atomic-absorption spectrophotometry after separation by <i>n</i> -butyl acetate extraction of the chloro-complex
Derek Midgley	447 Combination pH electrodes of special design: temperature characteristics and performance in poorly-buffered waters
Karel Štulík, Věra Pacáková, Kang Le and Bas Hennissen	455 Amperometric flow detection with a copper working electrode—response mechanism and application to various compounds
Raul Morales, C. S. Bartholdi and P. T. Cunningham	461 HPLC separation of heterocyclic $\beta$ -diketonates of actinide, lanthanide and transition metals
L. Pszonicki, A. Lechotycki and M. Krupiński	465 Computational elimination of interferent effects in flame atomic-absorption spectrometry
A. Parczewski	473 Determination of two metals from a single potentiometric titration curve. The application of two indicator electrodes
Li Manling, Tang Meier, Sun Zhengcai, Wu Lingye, Tang Sunming, Wang Guowei, He Huannan, Yan Ronghua, Zhao Gunadi and Lu Qingren	479 Influence of carbon dioxide in the determination of oxygen in copper by reduction fusion
<i>Short Communications</i>	
Sérgio Luis Costa Ferreira	485 Spectrophotometric determination of nickel in copper-base alloy with 2-(2-thiazolylazo)- <i>p</i> -cresol
S. S. Badawy, A. F. Shoukry, M. S. Rizk and M. M. Omar	487 Hydralazine-selective PVC membrane electrode based on hydralazinium tetraphenylborate
K. Vijaya Raju and G. Madhu Gautam	490 Iron(II) titration of some metal ions, with oxazine dyes as redox indicators
Fernando Alvarez, Fernando de Pablos and José Luis Gómez Ariza	493 Evaluation of two new asymmetric derivatives of thiocarbonylhydrazide as spectrophotometric analytical reagents
M. Yusuf, A. C. Sarki, S. B. Idris, G. A. Ayoko and K. Singh	496 Separation and determination of selenium(IV) and molybdenum(VI) in mixtures by selective precipitation with potassium thiocarbonate

<b>Alessandro D'Ulivo</b>	499	On the determination of total dissolved tin in natural waters by direct hydride generation and non-dispersive atomic-fluorescence spectrometry
<b>G. V. Rathaiah and M. C. Eshwar</b>	502	Rapid spectrophotometric determination of zirconium with 2-(5-bromo-2-pyridylazo)-5-diethylaminophenol
<b>Software Survey Section</b>	505	Multivariate linear regression for calibration and testing of analytical methods
<i>Notices</i>	i	
<i>Questionnaire: Software Survey Section</i>	iii	

## JULY

<b>Editorial</b>	III	
<b>Paul D. Taylor, Ian E. G. Morrison and Robert C. Hider</b>	507	Microcomputer application of non-linear regression analysis to metal-ligand equilibria
<b>Jean-Jacques Aaron and Mame Diabou Gaye</b>	513	Analysis of mixtures of purines and pyrimidines by first- and second-derivative ultraviolet spectrometry
<b>M. Chamsaz, I. M. Khasawneh and J. D. Winefordner</b>	519	Speciation and determination of tin(IV) and organotin compounds in sea-water by hydride generation-atomic-absorption spectrometry with an electrically heated long absorption cell
<b>Chi Hua, Daniel Jagner and Lars Renman</b>	525	Computerized flow constant-current stripping analysis for some electro-active organic compounds. Application to the determination of erythromycin in urine
<b>A. G. Asuero, G. González, F. de Pablos and J. L. Gómez Ariza</b>	531	Determination of the optimum working range in spectrophotometric procedures
<b>S. C. Apte and M. J. Gardner</b>	539	Determination of organotins in natural waters by toluene extraction and graphite furnace AAS
<b>R. Wagemann and F. A. J. Armstrong</b>	545	Trace metal determination in animal tissues: an interlaboratory comparison
<b>D. Blanco Gomis, P. Arias Abrodo, A. M. Picinelli Lobo and A. Sanz Medel</b>	553	Fluorimetric determination of ultratracés of lead by ion-pair extraction with cryptand 2.2.1 and eosin
<b>T. U. Aualiitia and W. F. Pickering</b>	559	Sediment analysis—lability of selectively extracted fractions
<b>J. Namieśnik</b>	567	Preconcentration of gaseous organic pollutants in the atmosphere
<i>Short Communications</i>		
<b>Dezhong Dan and Yalan Dong</b>	589	A PVC-coated carbon rod ion-selective electrode for thallium and its application to the analysis of rocks and minerals
<b>Z. Malá and J. Šenkýř</b>	591	Potential response of liquid ion-exchange membrane electrodes with a weak-acid anion as primary ion, and its dependence on pH
<b>R. B. Heddur and S. M. Khopkar</b>	594	Separation of selenium(IV) and tellurium(IV) from mixtures by extraction chromatography with trioctylphosphine oxide
<i>Publications Received</i>	i	
<i>Questionnaire: Software Survey Section</i>	iii	

## AUGUST

<b>The Louis Gordon Memorial Award</b>	III	
<b>The Ronald Belcher Memorial Award</b>	IV	
<b>Chi Hua, Daniel Jagner and Lars Renman</b>	597	Constant-current stripping analysis for iron(III) by adsorptive accumulation of its Solochrome Violet RS complex on a carbon-fibre electrode

<b>M. Rodríguez-Alcalá, P. Yáñez-Sedeño and L. Ma. Polo Díez</b>	601	Determination of pentachlorophenol by flow-injection analysis with spectrophotometric detection
<b>M. Barber, D. Bell, M. Morris, L. Tetler, M. Woods, B. W. Bycroft, J. J. Monaghan, W. E. Morden and B. N. Green</b>	605	Study of an actinomycin complex by mass spectrometry-mass spectrometry
<b>M. H. Livertoux, Z. Jayyosi and A. M. Batt</b>	613	Study of the physicochemical properties of aqueous dantrolene solutions by differential pulse polarography
<b>Abdel-Maboud I. Mohamed</b>	621	Spectrophotometric determination of some benzothiadiazine diuretics with 7,7,8,8,-tetracyanoquinodimethane
<b>G. N. Chen and C. S. Huang</b>	625	A study of the chemiluminescence of some acidic triphenylmethane dyes
<b>Elsie M. Donaldson</b>	633	Determination of selenium in ores, concentrates and related materials by graphite-furnace atomic-absorption spectrometry after separation by extraction of the 4-nitro- <i>o</i> -phenylenediamine complex
<b>B. M. Patel, J. P. Deavor and J. D. Winefordner</b>	641	Solution nebulization of aqueous samples into the tubular-electrode torch capacitatively-coupled microwave plasma
<b>Bradley T. Jones, Benjamin W. Smith, Alain Berthod and James D. Winefordner</b>	647	A Becquerel-disc phosphoroscope for the measurement of lifetimes in room-temperature phosphorimetry
<i>Short Communications</i>		
<b>K. Girish Kumar, C. Mohana Das and P. Indrasenan</b>	651	Determination of some carbohydrates with <i>N</i> -bromophthalimide and <i>N</i> -bromosaccharin
<b>R. Ramchandran and P. K. Gupta</b>	653	Indirect atomic-absorption spectrophotometric determination of phosphorus in steel by use of the bismuth phosphomolybdate complex
<b>Ghazi Al-Jabari and Bruno Jaselskis</b>	655	Spectrophotometric determination of formaldehyde
<b>T. Pal, D. S. Maity and A. Ganguly</b>	658	Silver-gelatin method for determination of inorganic peroxides in alkaline solution
<b>R. K. Sharma and S. K. Sindhvani</b>	661	Spectrophotometric determination of cobalt in a vitamin, alloys and an ore by extraction of its 3-hydroxy-2-methyl-1,4-naphthoquinone 4-oxime complex into molten naphthalene
<b>Agostino Pietrogrande and Mirella Zancato</b>	664	Sequential potentiometric microdetermination of chloride and phosphate and its application to the determination of phosphorus and chlorine in organic compounds
<b>V. Cerdá, J. Maimo, J. M. Estela, A. Salva and G. Ramis</b>	667	VALGRAN, a program for potentiometric titrations with a versatile automatic modular system
<b>Software Survey Section</b>	671	FLUOPAC2
<i>Publications Received</i>	i	
<i>Notices</i>	iii	
<i>Questionnaire: Software Survey Section</i>	vii	

## SEPTEMBER

<b>Zhisheng Sun and Erkang Wang</b>	673	A new electrochemical method based on transfer at a liquid/liquid interface: determination of barium and strontium
<b>Sirinart Muangnoicharoen, Kuen-Yuan Chiou and Oliver Keith Manuel</b>	679	Determination of selenium and tellurium in air by atomic-absorption spectrometry
<b>C. Baiocchi, A. Marchetto, G. Saini, P. Bertolo and G. Pettiti</b>	685	Reversed-phase HPLC separation of complex mixtures of trace metals as dibenzylidithiocarbamate chelates

<b>Ambrogio Mazzucotelli, Roberto Frache, Aldo Viarengo and Gabriella Martino</b>	693	The speciation of trace amounts of organometallics in marine organisms by gel-permeation high-pressure liquid chromatography with PAR derivatization
<b>M. S. Tunuli</b>	697	Gold chloride electrodes as electrochemical sensors for liquid chromatography
<b>S. Koch, G. Ackermann und I. Brunne</b>	701	Untersuchungen zur Anwendung ternärer Komplexe in der Photometrie—V. Spektralphotometrische Bestimmung und Nachweis von Phenolen mit $\text{FeY}^-$ ( $\text{H}_4\text{Y} = \text{EDTE}$ )
<b>Yi-Ming Liu and Ru-Qin Yu</b>	707	Aspects of application of Kalman filtering in multicomponent spectrophotometry
<b>V. W.-H. Leung, B. W. Darvell and A. P.-C. Chan</b>	713	A rapid algorithm for solution of the equations of multiple equilibrium systems—RAMESES
<i>Short Communications</i>		
<b>B. Narayana and M. R. Gajendragad</b>	719	Complexometric determination of mercury(II) with 2-imidazolidinethione as a selective masking agent
<b>Nityananda Shetty A., R. V. Gadag and M. R. Gajendragad</b>	721	Complexometric titration of thallium(III), by use of 4-amino-5-mercapto-3-propyl-1,2,4-triazole as replacing reagent
<b>Masashi Komata and Jun-ichi Itoh</b>	723	A highly sensitive spectrophotometric determination of cadmium with $\alpha,\beta,\gamma,\delta$ -tetrakis(4- <i>N</i> -trimethylaminophenyl)porphine
<b>Krishna K. Verma, Pramila Tyagi and Sunil K. Sanghi</b>	725	Alkalimetric determination of mercury by use of its reaction with 1-mercaptopropan-2,3-diol
<b>D. de Beer and J. C. van den Heuvel</b>	728	Response of ammonium-selective microelectrodes based on the neutral carrier nonactin
<b>M. I. Walash, F. Belal and F. A. Aly</b>	731	Fluorometric determination of reserpine in dosage forms
<b>Dean K. Ellison and William Tait</b>	734	Osteryoung square-wave voltammetric determination of nicarbazin in chicken tissue
<b>Fumiyasu Takekawa and Rokuro Kuroda</b>	737	Determination of gallium in geological materials by graphite-furnace atomic-absorption spectrometry
<i>Analytical Data</i>		
<b>M. T. S. Amorim, Rita Delgado, J. J. R. Fraústo da Silva, M. Cândida T. A. Vaz and M. Fernanda Vilhena</b>	741	Metal complexes of 1-oxa-4,7,10-triazacyclododecane- <i>N,N',N''</i> -triacetic acid
<i>Corrigendum</i>	i	
<i>Notes for Authors</i>	iii	
<i>Questionnaire: Software Survey Section</i>	v	

## OCTOBER

<b>S. Bajo and A. Wyttenbach</b>	747	Instrumental neutron-activation determination of phosphorus in biological materials by bremsstrahlung measurement
<b>F. Sanchez Rojas, C. Bosch Ojeda and J. M. Cano Pavón</b>	753	Derivative ultraviolet-visible region absorption spectrophotometry and its analytical applications
<b>M. d'Amboise, D. Mathieu and D. L. Piron</b>	763	A chemical study of 2-butyne-1,4-diol
<b>E. Fiscaro and A. Braibanti</b>	769	Potentiometric titrations in methanol/water medium: intertitration variability
<b>Roman Grzeskowiak, Graham D. Jones and Allan Pidduck</b>	775	Identification and determination of volatiles derived from phenol-formaldehyde materials
<b>Imre Tóth, Piroska Solymosi and Zoltán Szabó</b>	783	Application of a sulphide-selective electrode in the absence of a pH-buffer

- Abdulrahman S. Attiyat,  
Gary D. Christian,  
Johnny L. Hallman and  
Richard A. Bartsch
- G. López-Cueto, A. Alonso-Mateos,  
C. Ubide and  
G. del Campo-Martínez
- Keiichi Fukushi and Kazuo Hiroy
- Short Communications*
- Dagmar Honová, Irena Němcová  
and Václav Suk
- Aytekin Temizer and A. Nur Onar
- Wing Hong Chan, Albert W. M. Lee  
and Kam Tong Fung
- B. Bermúdez, A. Ríos,  
M. D. Luque de Castro and  
M. Valcárcel
- Sonia Z. El-Khateeb and  
Ezzat M. Abdel-Moety
- Ivana Šestáková and  
Miloslav Kopanica
- Shaojun Dong and Yudong Wang
- Gregory P. Maklae
- Questionnaire: Software Survey Section*
- 789 A comparative study of the effect of *o*-nitrophenyl octyl ether and *o*-nitrophenyl pentyl ether as plasticizers on the response and selectivity of carrier-based liquid membrane ion-selective electrodes
- 795 Methods for analysis of the mononuclear and binuclear manganese(III) cyano-complexes
- 799 Determination of ammonium ion in sea-water by capillary isotachopheresis
- 803 Spectrophotometric determination of bismuth and EDTA by means of the reaction of bismuth with Pyrocatechol Violet in the presence of Septonex
- 805 Determination of methotrexate in human blood plasma by adsorptive stripping voltammetry
- 807 Ion-selective electrodes in organic analysis—determination of xanthate
- 810 Configuration with internally coupled valves to overcome shortcomings in the simultaneous determination of nitrite and nitrate by flow-injection analysis
- 813 Determination of quaternary ammonium surfactants in pharmaceutical formulations by the hypochromic effect
- 816 Determination of cyadox and its metabolites in plasma by adsorptive voltammetry
- 819 Anodic stripping voltammetric determination of trace lead with a Nafion/crown-ether film electrode
- 822 Analysis of gallium arsenide by spark-source mass-spectrometry
- i

## NOVEMBER

- Talanta Medal
- Peter M. May, Kevin Murray  
and David R. Williams
- Kiyohisa Ohta, Wataru Aoki  
and Takayuki Mizuno
- Shunitz Tanaka and Hitoshi Yoshida
- Jitka Šrámková and Stanislav Kotrlý
- Bokuichiro Takano and  
Kunihiko Watanuki
- G. Farsang, T. Dankházi, J. Lóránth  
and L. Daruházi
- Xiangyuan Ruan and Hsiangpin Chang
- J. J. Meyer, J. L. Paumard,  
D. Milln, P. Levoir et  
J. C. Fontaine
- A. De Souza, D. Baylocq et  
F. Pellerin
- I
- 825 The use of glass electrodes for the determination of formation constants—III. Optimization of titration data: the ESTA library of computer programs
- 831 Elimination of interferences in electrothermal-atomization atomic-absorption spectrometry of cadmium
- 837 Adsorptive voltammetry of lipoic acid and lipoamide, based on use of a catalytic hydrogen wave
- 841 Extractive photometric determination of gallium with 8-quinolinol in layered crystals of bismuth telluride—estimation of the determination limit
- 847 Quenching and liquid chromatographic determination of polythionates in natural water
- 855 Comparative study of a thin-layer cell for analysis of stationary and streaming solutions
- 861 Reciprocal derivative constant-current stripping analysis
- 869 Unité d'acquisition économique pour le traitement élaboré de données spectro-cinétiques issues d'un spectrophotomètre UV-visible
- 875 Dégradation oxydative des sulfamides à usage thérapeutique. Isolement structure et méthodes d'analyse des produits formés

<b>Itsuo Mori, Yoshikazu Fujita, Kinuko Fujita, Rika Fujita, Yoshihiro Nakahashi and Keiji Kato</b>	879 Spectrophotometric determination of bismuth(III) with <i>o</i> -hydroxyhydroquinonephthalein in the presence of Brij 58
<b>I. López García, P. Navarro and M. Hernández Córdoba</b>	885 Manual and FIA methods for the determination of cadmium with Malachite Green and iodide
<b>Xu Bo-Xing and Fang Yu-Zhi</b>	891 Determination of polynuclear aromatic hydrocarbons in water by flotation enrichment and HPLC
<b>M. I. Walash, M. Rizk and A. El-Brashy</b>	895 Spectrophotometric determination of chlordiazepoxide and nitrazepam
<b>O. Budevsky, T. Zikolova and J. Tencheva</b>	899 NABTIT—a computer program for non-aqueous acid–base titration
<i>Short Communications</i>	
<b>J. Huang, D. Goltz and F. Smith</b>	907 A microwave dissolution technique for the determination of arsenic in soils
<b>Partha S. Das, Basudam Adhikari, Mrinal M. Maiti and Sukumar Maiti</b>	909 A titrimetric method for estimation of fluorine in organic compounds
<b>Anna Maria Ghe, Giuseppe Chiavari and Cecilia Bergamini</b>	911 Examination of guanosine and xanthosine nucleotides by HPLC and electrochemical detection
<b>C. S. P. Sastry, M. V. Suryanarayana, A. S. R. P. Tipirneni and T. N. V. Prasad</b>	914 Spectrophotometric determination of muzolimine
<b>Krishna K. Verma, Dayashanker Gupta, Sunil K. Sanghi and Archana Jain</b>	917 Determination of sulphide by anion-exchange with lead iodate
<i>Analytical Data</i>	
<b>Zhivko I. Denchev and Nikola K. Nikolov</b>	921 Polarographic study of the dipropyldithiophosphinate complexes of Pd(II), Pb(II), Cd(II), and Zn(II) ions
<i>Preliminary Communication</i>	
<b>Harvey W. Yurow and Samuel Sass</b>	923 Colorimetric determination of cyclobutylphenylglycollic acid and its ketone
<b>Software Survey Section</b>	925 Construction of small bibliographic databases by using “Lotus 1–2–3”
<i>Publications Received</i>	i
<i>Erratum</i>	iii
<i>Questionnaire: Software Survey Section</i>	v

## DECEMBER

<b>Editorial</b>	III
<i>Talanta Advisory Board</i>	V
<b>Peter M. May and Kevin Murray</b>	927 The use of glass electrodes for the determination of formation constants—IV. Matters of weight
<b>Peter M. May and Kevin Murray</b>	933 The use of glass electrodes for the determination of formation constants—V. Monte Carlo analysis of error propagation
<b>M. C. Quintero, M. Silva and D. Pérez-Bendito</b>	943 Stopped-flow determination of carbaryl and its hydrolysis product in mixtures in environmental samples
<b>A. Izquierdo, M. D. Prat and A. Garbayo</b>	949 Solvent extraction equilibria of the nickel–3-(2-furyl)-2-mercapto-propenoic acid complex as an ion-pair with the diphenylguanidinium ion
<b>Bo Svensmark and Jørgen Larsen</b>	953 Determination of the labile species of zinc by anodic stripping staircase voltammetry, with special reference to correlation with the toxicity to <i>Tetrahyena</i>

<b>M. H. Pournaghi-Azar and S. M. Golabi</b>	959	Polarographic determination of 9,10-anthraquinone and its 1,2- 1,4- and 1,8-dihydroxy derivatives in chloroform. Application to the analysis of papers and black liquors
<b>Joseph Wang and Ziad Taha</b>	965	Catalytic-adsorptive stripping voltammetric measurements of hydrazines
<b>W. Ciesielski, W. Jedrzejewski, Z. H. Kudzin, R. Skowroński and J. Drabowicz</b>	969	A new method for the iodometric determination of sulphoxides
<b>Geraldine M. Huitink</b>	973	Studies of 7-hydroxycoumarins
<b>S. M. Hassan, F. Belal and M. Sultan</b>	977	Simultaneous spectrophotometric determination of furazolidone and berberine in tablet form
<b>Milan Meloun, Michal Bartoš and Erik Högfeldt</b>	981	Multiparametric curve fitting—XIII. Reliability of formation constants determined by analysis of potentiometric titration data
<b>F. Mebsout, J.-C. Vire, G. J. Patriarche and G. D. Christian</b>	993	Electrochemical study of carminomycin at solid electrodes
<b>J.-C. Vire, N. Abo El Maali, G. J. Patriarche and G. D. Christian</b>	997	Square-wave adsorptive stripping voltammetry of menadione (vitamin K <sub>3</sub> )
<b>Z. Marczenko and R. Łobiński</b>	1001	Extraction-spectrophotometric determination of vanadium with 3,5-dinitrocatechol and Brilliant Green
<i>Short Communications</i>		
<b>O. R. Idowu</b>	1005	The reaction of <i>N</i> -nitrosamines with pyridinium salts
<b>Hsu Zhang-fa and Liao Xi-man</b>	1007	Spectrophotometric determination of molybdenum in steels with <i>o</i> -nitrophenylfluorone and cetyltrimethylammonium bromide
<b>B. C. Verma, D. K. Sharma, H. K. Thakur, Bh. Gopala Rao and N. K. Sharma</b>	1010	An oxidimetric method for the determination of thiophanate-methyl in commercial formulations
<i>Analytical Data</i>		
<b>J. Barbosa, M. Rosés and V. Sanz-Nebot</b>	1013	Acid-base indicators in acetonitrile: their p <i>K</i> values and chromatic parameters
<i>Publications Received</i>	i	
<i>Questionnaire: Software Survey Section</i>	iii	

## THE LOUIS GORDON MEMORIAL AWARD

---

The Editorial Board and Publisher of *Talanta* take great pleasure in announcing that the Louis Gordon Memorial Award for 1987 (for the paper judged to be the best written of those appearing in *Talanta* during the year) will be made to Professor Yu. A. Zolotov, of the Vernadsky Institute of Geochemistry and Analytical Chemistry, Moscow, for his paper "Analytical chemistry in the Soviet Union" (*Talanta*, 1987, **34**, 1).



---

The Louis Gordon Memorial Award for 1986 was presented to Dr. A. C. Mehta by Mrs. E. Maxwell at Headington Hall. Left to right: Dr. R. A. Chalmers, Mrs. E. Maxwell, Dr. A. C. Mehta, Professor J. D. Winefordner.

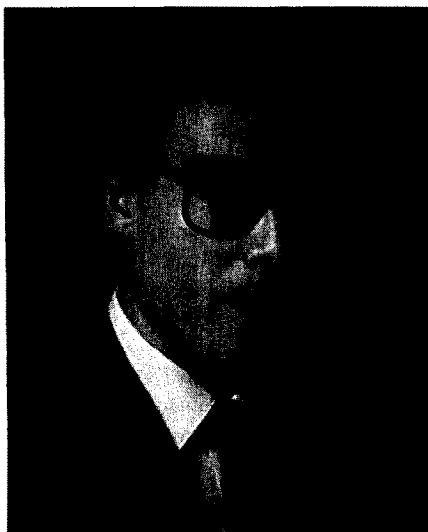




## TALANTA ADVISORY BOARD

---

The Publisher and the Editorial Board of *Talanta* welcome Professor A. Asuero and Professor I. Roelandts as members of the Advisory Board. They also wish to record their sincere thanks for the help given by Professor S. B. Savvin, who retires from the Board. These changes will be effective from January 1989.



AGUSTIN G. ASUERO was born in Huelva in 1951, and received his Thesis and Ph.D. Thesis degrees in Chemistry from the University of Seville in 1974 and 1976, respectively, under the direction of F. Pino. From 1974 to 1976 he was *Professor Ayudante* in the Faculty of Chemistry. In January 1977 he was appointed *Professor Adjunto* of Chemical Analysis and Bromatology of the Faculty of Pharmacy and since 1983 has been Professor in Charge of the Chair of Chemical Analysis of the same Faculty. He is a member of the Investigation Commission of the University of Seville, the scientific activity of which has been mainly in the field of trace analysis, including work on the spectrophotometric determination of metal ions, and reviews on trace elements and trace anions in foods, as well as in the theory and application of computation methods to overlapping equilibria. He is also interested in the analytical study of mixed aqueous-non-aqueous solvents and in the methodological aspects of analytical science. He is a member of The Royal Society of Chemistry, The British Society for the History of Science, The Royal Spanish Societies of Chemistry, Analytical Chemistry, Bromatology and Toxicology, respectively, and of the Andalusian Association of Food Scientists and Technologists. He has published over 80 research publications or review articles. To date 6 graduate students in Chemistry or Pharmacy have received Ph.D. degrees under his direction.



IWAN ROELANDTS was born on 12 November 1941 in Verviers, Belgium. He studied chemistry at the University of Liège, where he graduated in 1964. He immediately joined the Department of Geology, Petrology and Geochemistry in that university and was in charge of the analytical laboratory. His main responsibilities were the development and application of precise and accurate analytical methods for determination of major, minor and trace elements in rocks and minerals. In 1972, 1973 and 1976 he was a guest worker at the Mineralogisk Geologisk Museum at the University of Oslo. He obtained his Ph.D. from the University of Liège in 1975 for work on determination of rare-earth and other trace elements in rocks by neutron activation analysis, and in 1976 became "Chef de Travaux" and lecturer in analytical geochemistry at the university. His main research interests include classical and physical methods of analysis (XRF, AAS, NAA, PIXE, PIGE, ICP), analytical separation techniques (co-precipitation, ion-exchange, solvent extraction) and rock analysis in general. He also paid great attention to reference materials and participated actively in the certification of many of them. Another of his interests is the analysis of biological, medical and environmental specimens by the PIXE technique. He has contributed nearly a hundred scientific papers in these fields, and presented many communications at international conferences and symposia. He has been a Regional Editor of *Geostandards Newsletter* since its launch in 1977, and is currently a member of the Editorial Advisory Boards of the *Journal of Radioanalytical and Nuclear Chemistry*, and *Spectrochimica Acta, B*.

## LETTERS TO THE EDITOR

## Talanta

SIR,

Anybody with even a modicum of interest in analytical chemistry must, I think, peruse *Talanta* quite often. I wonder how many readers have been puzzled—as the writer is—by the meaning of this title. It certainly is more lively and appealing than the variety of *Archives—Memoirs—Acta—Journal—Zeitschrift* to which one has become accustomed since time immemorial—but what *does* it mean? Its editors and authors may be talented—the Journal may be worth a talent of gold—but why the plural *Talantata*? And why was this title chosen? The writer dug out his old Greek dictionary, consulted the British Encyclopedia and the Oxford Dictionary, but no explanation was forthcoming. It might therefore perhaps not be out of place if the editor would give an explanation, either as a subtitle, or somewhere on the cover or in the table of contents, either of each issue or at least from time to time, and so end this tantalising frustration. At the birth of the Journal, an explanation was probably given to midwives and bystanders but many readers may have missed this stage and so perhaps *repetitio est mater studiorum*.

In spite, however, of this etymological uncertainty, *vivat, crescat, floreat Talantata!*

I am, Sir, Yours, etc.

WILLIAM STROSS

1, Haydon Hill House  
Bicester Road  
Aylesbury, Bucks. England  
16 June 1962

Dear Dr. Stross,

Your enquiry, coupled with various other friendly enquiries in the past, leads me to believe that an explanation of the name of our Journal might be of interest to a wider public.

When we first projected the journal it was thought of as a sister journal to the already established *Tetrahedron*. It was, therefore, felt that it would be very appropriate if we had a Greek name to go with *Tetrahedron*, and one which was as closely associated with analytical chemistry as *Tetrahedron* is with organic chemistry. Apart from this, we felt that it would be a very considerable advantage to have a name which did not actually contain the terms "analysis" or "analytical"; for the purpose of indicating references, it was desirable to choose a title which could not be confused with any of the existing journals in analytical chemistry.

We consulted our Greek experts (we ourselves lay little claim to classical scholarship) and pointed out that the determination of the parts of a whole is fundamental to analytical chemistry. Their first suggestion was *Stoicheion*. We were tempted to accept this because it means quite precisely "element"; but we found that none of us could consistently spell the word correctly! The experts next said that the Greek word for a balance was *Talanta* (related to the Greek "talent" which, of course, was originally a weight of gold or silver). The rather obvious confusion with the word "talent", as used in its more conventional sense, appealed to our sense of humour, or whatever one might call it! We tried the name out on various people and they were rather intrigued by it; it seemed to fit in very well with *Tetrahedron*; and, therefore, we adopted it. I think it is true that most people do not understand the implication of it. But the cover design was, in its first rough draft, designed by us to include the Greek form of the name in order to give some sort of clue about the origin of the word.

Incidentally, the little vignette of balance which appears inside the cover is the result of a considerable amount of

searching on the part of our Greek experts for an actual picture of a Greek balance. It is surprising how hard it was to track down one—we could get Egyptian balances and Roman balances, but this must be one of the very few authentic instances of an illustration of a Greek balance.

*Tailpiece:* It is curious to find how many people cannot spell the present name of the Journal correctly. We are quite startled to find how often people refer to it as "*Tantala*" and often speculate about what *would* have happened had we settled for *Stoicheion!*

Yours sincerely,

CECIL L. WILSON  
(Editor-in-Chief)

Other variants of the name have appeared since then, of which "*Talantala*" is perhaps the most amusing—it might be transliterated into Japanese phonetics as "*Tarantara*" and will remind light opera fans of Gilbert and Sullivan's *Iolanthe*. The logo of the Greek balance, from one of the Hope vases, also led to confusion on one occasion. A manuscript was received with a request to "consider it for publication at your usual rates". It turned out to be by a lawyer, on the topic of "The Law of Contract Between Servant and Master", but the temptation to send a bill for deciding to reject it was easily resisted.

In its 30 years of existence, the journal has had only three Editors-in-Chief: Cecil Wilson from 1958 until his retirement in 1965, when he was succeeded by Maurice Williams (appointed Assistant Editor in 1960, then Associate Editor in 1961), who resigned at the end of 1965 on becoming Journals Manager at Pergamon Press. The present writer was appointed as Editor-in-Chief from January 1966, the irony being that until then he had steadfastly claimed that he could see no need for *Talanta*, and his only association with it had been to recommend for publication one of the papers that had been treated by another journal in the manner that had first caused Ronald Belcher so much concern (the paper was *not* one of Belcher's!) and thus contributed to the inception of *Talanta*. In a sense, the wheel had come full circle.

No article on the story of *Talanta* would be complete without a heartfelt tribute to the patience, loyalty and friendliness of its authors and the referees (without whose care, help and dedication the maintenance of the standards of the journal would have been impossible), the editorial assistants and the printing and production staff (without whom there would be no journal at all), the forbearance of the families of the editorial staff, and last but far from least, Robert Maxwell and Pergamon Press for unstinting help and support in continuation of the journal they had the foresight and faith to establish. It has always been the aim of the journal to serve both authors and readers to the utmost of its ability by presenting work that was as correct as possible both scientifically and linguistically. Its current position in the spectrum of analytical journals is the best evidence of the extent to which that aim has been fulfilled. *Semper floreat Talanta!*

## CORRIGENDA

---

In the paper by Drora Kaplan, Dan Raphaeli and Sam Ben-Yaakov, *Talanta*, 1987, **34**, 709, Dr. Kaplan's address was incorrect. It should be The Jacob Blaustein Institute for Desert Research, Ben-Gurion University of the Negev, Sede Boqer Campus, 84990, Israel.

## FOREWORD

This special issue of *Talanta* is dedicated to the subject of fiber optic chemical sensors (FOCSs). Manuscripts were solicited from world-renowned researchers in the area of FOCS development. These researchers were invited to submit an original manuscript that details their most recent efforts in the area. The collection of papers in this issue is the result of these invitations.

FOCS systems can be classified into the following three major groups: (1) remote, passive sensors; (2) flow-through sensing arrangements; (3) active sensing probes. The first category includes systems in which a natural optical property of the system (such as fluorescence) is continuously monitored through an optical fiber arrangement. The system is termed passive because no chemical reaction is required to generate the measured species. An example is the remote *in situ* sensing system described in the paper by Boisdé and co-workers. These researchers have worked for many years on the development of techniques for passive remote sensing. Progress in the development of a system for remote monitoring of uranium(III), (IV) and (VI) and plutonium(VI) is presented.

The second category includes flow-through arrangements in which a fiber optic-based detector cell is employed. Typically, an analytical reaction is used to generate an optically detectable species. The reagents required can be immobilized either upstream of the detector or as part of the detector. Alternatively, reagent solutions can be added to the sample stream as part of the flow arrangement. Flow-through fiber optic systems are described in the papers by Narayanaswamy, Wolfbeis and Smardzewski. Narayanaswamy and co-workers describe a novel flow-through system for the measurement of fluoride ions in solution. The chemistry is based on an immobilized cerium(III)/Alizarin Complexone complex which goes from wine-red to blue upon complexation with fluoride. The report by Wolfbeis describes a system for the detection of potentially harmful vapors. Polar solvents in gaseous samples are detected. Interaction of the solvent with a reagent that is immobilized in a fiber optic detector cell causes a change in the monitored light intensity. The Wolfbeis system is also constructed in a probe-type arrangement. A third fiber optic flow-through arrangement is detailed in the paper by Smardzewski *et al.* where preliminary results for a multicomponent analysis system are presented. Eight optical waveguides are coated with selective analytical reagents. The sample (gaseous or solution) flows past the device and the analytes of interest react differently

with each reagent. Signals from this fiber optic sensor array are processed to give the concentrations of all analytes in the sample.

Active sensing probe-type FOCSs include devices in which the analytical reagent is immobilized at the tip of a fiber optic device (single fiber or fiber bundle). The immobilized reagent provides a detectable change in the optical signal in the presence of the analyte. The system can be used by dipping the probe tip into the sample and reading the resulting sensor signal. An example of this type of FOCS is the pH probe presented in the paper by Boisdé and co-workers. Recently, the validity of fiber optic pH probes has been challenged by Professor Janata (*Anal. Chem.*, 1987, **59**, 1351) based on thermodynamic considerations. Professor Janata questions the ability of these sensors to accurately measure the hydrogen-ion activity in solutions with a varying matrix. In relation to this question, Edmonds *et al.* report here the results of their examination of the reliability of fiber optic pH sensors under typical experimental conditions. Their results indicate that current sensor designs provide poor overall reliability.

Novel FOCS probes are presented in the papers by Walt, Hieftje, and Seitz. Walt and co-workers report on development of a gas-sensing fiber optic probe for carbon dioxide measurements. In their sensor design, a pH-responsive layer and a gas-permeable layer are sequentially placed at the tip of a single optical fiber. The result is a small sensor with fast response times. Hieftje and co-workers report a novel sensing strategy for FOCSs. The rate of fluorescence quenching is measured and related to the concentration of the chemical species that causes the quenching. Alternatively, the rate of quencher removal by exchange with a non-quenching species can be used to quantify the non-quencher species. The paper by Christian and Seitz reports progress toward the development of an ionic strength sensor. The response of this last sensor is based on an energy transfer mechanism.

Considerable work in the development of fiber optic biosensing probes is indicated by the large number of papers on this topic. First, Optiz and Lübbers present a brief overview of their pioneering work with FOCS based on electrochromic dyes, enzymes, and binding proteins. The concept of energy transfer is used by Meadows and Schultz in a novel type of glucose sensor. The binding protein Concanavalin A (ConA), which is labeled with Rhodamine, and fluorescein isothiocyanate labeled dextran are employed. Competition between the sample glucose and labeled dextrose for the limited ConA

sites is the basis behind this sensor. Krull and co-workers detail their most recent progress in the development of fiber optic sensors based on fluorogenic reagents immobilized in lipid membranes. Changes in the lipid membrane structure can be monitored as a change in the fluorescence signal. Sepaniak and co-workers discuss their progress in the development of fiber optic immuno-based probes. These probes employ a layer of immobilized antibody at the tip of a signal optical fiber. In this report, rare-earth metal chelates are evaluated as possible labels for these probes. Finally, a new strategy for biosensors is introduced by Arnold and co-workers. This novel approach is termed an "internal enzyme" configuration because the enzyme is located inside the sensor body. The analyte of interest must diffuse across a gas-permeable membrane where the analytical reaction is catalyzed by the internal enzyme. The relative merits of this approach are discussed.

Many of the papers presented in this issue provide

details concerning innovative developments in the instrumentation used for FOCSs. A paper by Narayanaswamy and co-workers is dedicated to a description of their recently developed solid-state instrumentation for use with FOCSs. Their novel design is demonstrated with several pH-sensing probes.

Overall, the area of FOCSs is growing rapidly. New sensors are continually being introduced. Many of the recently reported sensors are currently being characterized and evaluated in comparison with conventional technology. Although it is too early to generalize the relative merits of FOCSs over other more established systems, it is reasonable to expect that for certain analytes, FOCSs will be the system of choice in the future. I hope the publication of this special issue stimulates progress in this exciting area of Analytical Chemistry.

MARK A. ARNOLD

Software Survey Section

JOURNAL NAME TALANTA

PERGAMON PRESS  
SOFTWARE DESCRIPTION FORM

Title of software program: \_\_\_\_\_

Type of program:  Application  Utility  Other \_\_\_\_\_

Category: \_\_\_\_\_ (ie.) stability constants,  
calibration, pattern recognition, optimization)

Developed for (name of computer/s): \_\_\_\_\_

in (language/s): \_\_\_\_\_

to run under (operating system): \_\_\_\_\_

available on:  Floppy disk/diskette. Specify:

Size \_\_\_\_\_ Density \_\_\_\_\_  Single-sided  Dual-sided

Magnetic tape. Specify:

Size \_\_\_\_\_ Density \_\_\_\_\_ Character set \_\_\_\_\_

Hardware required: \_\_\_\_\_

Memory required: \_\_\_\_\_ User training required:  Yes  No

Documentation:  None  Minimal  Self-documenting  
 Extensive external documentation

Source code available:  Yes  No

Stage of development:  Design complete  Coding complete  
 Fully operational  Collaboration welcomed

Is program in use?  Yes How long? \_\_\_\_\_ How many sites? \_\_\_\_\_  
 No

Is the contributor available for user inquiries:  Yes  No

Distributed by: \_\_\_\_\_

Cost of program: \_\_\_\_\_

Demonstration disk available?  Yes Cost: \_\_\_\_\_  
 No

(continued)

RETURN COMPLETED FORM TO:

Dr. Mary R. Masson  
Department of Chemistry  
University of Aberdeen  
Meston Walk  
Old Aberdeen AB9 2UE, Scotland

[This Software Description Form may be photocopied without permission]

Description of what software does [maximum: 200 words]:

Potential users: \_\_\_\_\_

Field/s of interest: \_\_\_\_\_

# # # # #

Name of contributor: \_\_\_\_\_

Institution: \_\_\_\_\_

Address: \_\_\_\_\_

Telephone number: \_\_\_\_\_

# # # # #

Reference No. [Assigned by Journal Editor] \_\_\_\_\_

-----

[The information below is not for publication.]

Would you like to have your program:

Reviewed? [ ] Yes [ ] No [ ] Not at this time

Marketed and distributed? [ ] Yes [ ] No [ ] Not at this time

[This Software Description Form may be photocopied without permission]



## AUTHOR INDEX

- Aaron J.-J. 513  
 Abdel-Hamid M. E. 242  
 Abdel-Moety E. M. 813  
 Abuirjeie M. A. 242  
 Ackermann G. 701  
 Adhikari B. 909  
 Alarfaj N. A. 375  
 Albero M. I. 397  
 Al-Jabari G. 655  
 Alonso-Mateos A. 795  
 Alvarez F. 493  
 Aly F. A. 320, 731  
 Alzamil I. Z. 375  
 Amorim M. T. S. 741  
 Andersson M. 337  
 Aoki W. 831  
 Apte S. C. 539  
 Arias Abrodo P. 553  
 Armstrong F. A. J. 545  
 Arnold M. A. No. 2, V, 151, 215  
 Aruna M. 23  
 Asuero A. G. 531  
 Attiyat A. S. 789  
 Aualiitia T. U. 559  
 Ayoko G. A. 496
- Badawy S. S. 487  
 Baiocchi C. 685  
 Bajo S. 747  
 Barber M. 605  
 Barbosa J. 1013  
 Barragán de La Rosa F. J. 343  
 Bartholdi C. S. 461  
 Bartoš M. 981  
 Bartsch R. A. 789  
 Batt A. M. 613  
 Bayan K. C. 57  
 Baylocq D. 875  
 Beccari A. 379  
 Belal F. 320, 731, 977  
 Bell D. 605  
 Benedik L. 161  
 Bergamini C. 911  
 Bermejo E. 287  
 Bermúdez B. 810  
 Berthod A. 647  
 Bertolo P. 685  
 Beveridge A. 307  
 Biesuz R. 431  
 Blanc F. 75  
 Blanco Gomis D. 553  
 Boisdé G. 75  
 Bonakdar M. 277  
 Bontempelli G. 379  
 Borisova L. V. 62  
 Bosch E. 419  
 Bosch Ojeda C. 753  
 Boughriet A. 205  
 Bozhkov O. D. 62  
 Braibanti A. 769  
 Brajter K. 65  
 Bright F. V. 113  
 Brown R. S. 129  
 Brunne I. 701  
 Budevsky O. 899  
 Bycroft B. W. 605  
 Byrne A. R. 161
- Caballero M. 301  
 Cano Pavón J. M. 753  
 Casas R. 413
- Casassas E. 199  
 Cela R. 301  
 Cerdá V. 667  
 Chalmers R. A. No. 5, III  
 Chamsaz M. 519  
 Chan A. P.-C. 713  
 Chan W. H. 807  
 Chang H. 861  
 Chavan M. B. 357  
 Chen G. N. 625  
 Cerdá V. 667  
 Chiavari G. 911  
 Chiou K.-Y. 679  
 Chmielowski J. 227  
 Christian G. D. 789, 993, 997  
 Christian L. M. 119  
 Chwastowska J. 439  
 Chwistek M. 227  
 Ciesielski W. 969  
 Ciszewski A. 191  
 Compañó R. 413  
 Concialini V. 235  
 Corain B. 27  
 Córdoba M. H. 885  
 Craig J. B. 365, 401  
 Cunningham P. T. 461
- d'Amboise M. 763  
 Dan D. 589  
 Daniele P. G. 333  
 Daniele S. 379  
 Dankházi T. 855  
 Daruházi L. 855  
 Darvell B. W. 713  
 Das A. K. 406  
 Das C. M. 651  
 Das H. K. 57  
 Das P. S. 909  
 Deavor J. P. 641  
 de Beer D. 728  
 DeBono R. F. 129  
 del Campo-Martinez G. 795  
 Delgado R. 741  
 Denchev Z. I. 921  
 de Pablos F. 493, 531  
 De Robertis A. 333  
 De Souza A. 875  
 De Stefano C. 333  
 Donaldson E. M. 47, 297, 633  
 Dong S. 819  
 Dong Y. 589  
 Drabowicz J. 969  
 D'Ulivo A. 499
- Edmonds T. E. 103  
 El-Brashy A. 895  
 El-Khateeb S. Z. 813  
 Ellison D. K. 734  
 El Maali N. A. 997  
 El-Sayed A. Y. 253  
 Ericzon C. 337  
 Escobar Godoy R. E. 343  
 Eshwar M. C. 502  
 Estela J. M. 667
- Fang Y.-Z. 891  
 Farsang G. 855  
 Fazakas J. 403  
 Ferreira S. L. C. 485  
 Fiscaro E. 769  
 Flatters N. J. 103
- Fonseca J. M. L. 71  
 Fontaine J. C. 869  
 Frache R. 693  
 Fraústo da Silva J. J. R. 741  
 Fujita K. 879  
 Fujita R. 879  
 Fujita Y. 879  
 Fukushima K. 55, 799  
 Fung K. T. 807
- Gadag R. V. 721  
 Gajendragad M. R. 719, 721  
 Ganguly A. 658  
 Garbayo A. 949  
 Garcia I. L. 885  
 Garcia M. S. 397  
 Garcia-Alvarez-Coque M. C. 41  
 Gardner M. J. 539  
 Gaspariç J. 35  
 Gautam G. M. 490  
 Gawargious Y. A. 311  
 Gaye M. D. 513  
 Gennaro M. C. 167  
 Ghe A. M. 911  
 Gladilovich D. B. 259  
 Glazier J. P. 215  
 Glazier S. A. 215  
 Golabi S. M. 959  
 Goltz D. 907  
 Gomez M. A. 301  
 Gómez Ariza J. L. 249, 343, 493, 531  
 González A. G. 249  
 González G. 531  
 Green B. N. 605  
 Grzeskowiak R. 775  
 Guiraúm Pérez A. 249  
 Gupta D. 917  
 Gupta P. K. 653  
 Guthrie A. J. 157  
 Gyouten T. 351
- Hallman J. L. 789  
 Hamada M. A. 361  
 Hara M. 239  
 Hassan H. N. A. 311  
 Hassan S. M. 977  
 Hassan S. S. M. 361  
 Hassouna M. E. M. 311  
 Heddur R. B. 594  
 Hennissen B. 455  
 Herlihy A. T. 15  
 Herlinger A. W. 231  
 Herman J. S. 15  
 Hernández L. 287  
 Hidalgo J. L. 301  
 Hider R. C. 507  
 Hieftje G. M. 113  
 Hiirio K. 55, 326, 799  
 Hoenig M. 403  
 Högfeldt E. 981  
 Honová D. 803  
 Hopkins D. 401  
 Hougham B. D. 129  
 Howie R. A. 401  
 Hsu Z. 1007  
 Hua C. 525, 597  
 Huang C. S. 625  
 Huang J. 907  
 Huannan H. 479  
 Hulanicki A. 281  
 Huitink G. M. 973

- Idowu O. R. 1005  
 Idris S. B. 496  
 Indrasenan P. 651  
 Itoh J. 723  
 Izquierdo A. 949  
 Izquierdo-Ridorsa A. 199
- Jagner D. 525, 597  
 Jain A. 35, 409, 917  
 Jaselskis B. 231, 655  
 Jayyosi Z. 613  
 Jędrzejewski W. 969  
 Johnsen H. G. 245  
 Jones B. T. 647  
 Jones C. F. 103  
 Jones G. D. 775  
 Jordanov N. 62
- Kang L. 455  
 Kantipuly C. J. 1  
 Kato K. 879  
 Kauffmann J.-M. 179  
 Khasawneh I. M. 41, 267, 519  
 Khopkar S. M. 594  
 Kim J. R. 314  
 King J. B. 369  
 Koch S. 701  
 Komata M. 723  
 Kopanica M. 816  
 Kosiarska E. 439  
 Kotrlý S. 841  
 Kreissl F. R. 27  
 Krull U. J. 129  
 Krupiński M. 465  
 Kubáň V. 259  
 Kuchekar S. R. 357  
 Kudzin Z. H. 969  
 Kumar K. G. 651  
 Kuroda R. 737
- Larsen J. 153  
 Leaver M. E. 297  
 Lechotycki A. 465  
 Lee A. W. M. 807  
 Lentz H. 314  
 Leung V. W.-H. 713  
 Levoir P. 869  
 Li M. 479  
 Liang C. 59  
 Liao X. 1007  
 Linders C. R. 179  
 Lippolis M. T. 235  
 Liu Y.-M. 707  
 Livertoux M. H. 613  
 Lobiński R. 1001  
 Longato B. 27  
 López-Cueto G. 795  
 Lóránth J. 855  
 Lu Q. 479  
 Lübbers D. W. 123  
 Lukaszewski Z. 191  
 Lund W. 245  
 Luque de Castro M. D. 810
- Maccioni A. M. 27  
 Mackay C. 365  
 Mahmoud W. H. 253  
 Maimo J. 667  
 Maiti M. M. 909  
 Maiti S. 909  
 Maitra N. 231  
 Maity D. S. 658  
 Maj-Żurawska M. 281  
 Maklae G. P. 822  
 Malá Z. 591
- Manuel O. K. 679  
 Marchetto A. 685  
 Marczenko Z. 1001  
 Martino G. 693  
 Mathieu D. 763  
 May P. M. 825, 927, 933  
 Mazzucotelli A. 693  
 Meadows D. 145  
 Mebsout F. 993  
 Meenochite A. T. 323  
 Meloun M. 981  
 Méndez J. H. 293  
 Mentasti E. 167  
 Meyer J. J. 869  
 Midgley D. 447  
 Milanovich F. P. 109  
 Milin D. 869  
 Miller J. N. 103  
 Mills A. L. 15  
 Mizuno T. 831  
 Mohamed A.-M. I. 621  
 Mok W. M. 183  
 Monaghan J. J. 605  
 Monteagudo J. C. G. 71  
 Morales R. 461  
 Morden W. E. 605  
 Moreno Cordero B. 293  
 Mori I. 879  
 Morris M. 605  
 Morrison I. E. G. 507  
 Moses C. O. 15  
 Motomizu S. 351  
 Muangnoicharoen S. 679  
 Munkholm C. 109  
 Murray K. 825, 927, 933  
 Murti S. S. 443
- Naidu D. V. 237  
 Naidu N. V. S. 237  
 Naidu P. R. 237  
 Nakahashi Y. 879  
 Namieśnik J. 567  
 Narayana B. 719  
 Narayanaswamy R. 83, 157  
 Navarro P. 885  
 Němcová I. 211, 803  
 Nielsen T. J. 151  
 Nikolov N. K. 921  
 Nomura N. 239
- Ohta K. 831  
 Olbrych-Sleszyńska E. 65  
 Olin Ā. 337  
 Oliveira D. 323  
 Omar A. N. 805  
 Omar M. M. 487  
 Opitz N. 123  
 Oshima M. 351  
 Otero A. 71
- Pacáková V. 455  
 Pal T. 658  
 Parczewski A. 473  
 Patel B. M. 641  
 Patriarche G. J. 179, 993, 997  
 Paumard J. L. 869  
 Pellerin F. 875  
 Pelli B. 27  
 Perez J.-J. 75  
 Pérez-Bendito D. 943  
 Pérez-Bustamante J. A. 301  
 Pérez López J. A. 287  
 Pérez Pavón J. L. 293  
 Pesavento M. 431  
 Petrea R. D. 139
- Pettersen J. M. 245  
 Pettiti G. 685  
 Picinelli Lobo A. M. 553  
 Pickering W. F. 307, 559  
 Pidduck A. 775  
 Pietrogrande A. 664  
 Pineda L. 413  
 Piron D. L. 763  
 Poirier G. E. 113  
 Polo Diez Ma. P. 601  
 Porta V. 167  
 Posch H. E. 89  
 Pournaghi-Azar M. H. 959  
 Prasad T. N. V. 914  
 Prat M. D. 949  
 Profumo A. 431  
 Pszonicki L. 465  
 Puignou L. 199  
 Pusterhofer J. 89
- Quintero M. C. 943
- Rajan S. C. S. 443  
 Rajeswari C. V. 237  
 Raju K. V. 490  
 Ramchandran R. 653  
 Ramis G. 667  
 Ramis Ramos G. 41  
 Rao A. R. M. 23  
 Rao Bh. G. 1010  
 Rathaiah G. V. 502  
 Rauret G. 413  
 Renman L. 525, 597  
 Rice T. D. 173  
 Rigano C. 333  
 Ríos A. 810  
 Rizk M. 487, 895  
 Rodríguez-Alcalá M. 601  
 Rogers H. R. 271  
 Rosales D. 249  
 Rosés M. 419, 1013  
 Roy N. K. 406  
 Ruan X. 861  
 Russell D. A. 83  
 Rychlovský P. 211
- Saini G. 685  
 Salva A. 667  
 Sammartano S. 333  
 Sánchez-Pedreño C. 397  
 Sanchez-Reyes A. 413  
 Sanchez Rojas F. 753  
 Sanghi S. K. 409, 725, 917  
 Sanz Medel A. 553  
 Sanz-Nebot V. 1013  
 Sarki A. C. 496  
 Sarzanini C. 167  
 Sass S. 923  
 Sastry C. S. P. 23, 914  
 Satake K. 68  
 Schilt A. A. 187  
 Schultz J. S. 145  
 Seitz W. R. 119  
 Šenkýř J. 591  
 Sepaniak M. J. 139  
 Šestáková I. 816  
 Sevilla III F. 83  
 Seyama H. 68  
 Sharma D. K. 1010  
 Sharma N. K. 1010  
 Sharma R. K. 661  
 Shetty N. A. 721  
 Shibata K. 351  
 Shoukry A. F. 487

- Silva M. 943  
 Simonzadeh N. 187  
 Sindhwani S. K. 661  
 Singh K. 496  
 Skowroński R. 969  
 Slavek J. 307  
 Smardzewski R. R. 95  
 Smith B. W. 647  
 Smith F. 907  
 Smyth M. R. 179  
 Sokalski T. 281  
 Solymosi P. 783  
 Soma M. 68  
 Sommer L. 259  
 Šrámková J. 841  
 Staśkiewicz M. 65  
 Stephens R. 369  
 Strelow F. W. E. 385  
 Štulík K. 455  
 Subrahmanyam J. 443  
 Suk V. 803  
 Sultan M. 977  
 Sultan S. M. 375  
 Sun Z. 673  
 Suryanarayana M. V. 914  
 Svensmark B. 953  
 Szabó Z. 783
- Taha Z. 965  
 Tait W. 734  
 Takano B. 847  
 Takekawa F. 737  
 Tanaka S. 837  
 Tang M. 479  
 Tang S. 479
- Taylor P. D. 507  
 Temizer A. 805  
 Tencheva J. 899  
 Tetler L. 605  
 Thakur H. K. 1010  
 Thelin B. 317  
 Tipirneni A. S. R. P. 914  
 Toei J. 425  
 Tōei K. 351  
 Toma H. E. 323  
 Tomza I. 227  
 Tóth I. 783  
 Traldi P. 27  
 Tunuli M. S. 697  
 Tyagi P. 725
- Ubide C. 795  
 Ugo P. 379
- Vácha P. 59  
 Valcárcel M. 810  
 van den Berg C. M. G. 271  
 van den Heuvel J. C. 728  
 van der Linden W. 59  
 Vaz M. C. T. A. 741  
 Verma B. C. 1010  
 Verma K. K. 35, 409, 725, 917  
 Viarengo A. 693  
 Vilhena M. F. 741  
 Vire J.-C. 993, 997  
 Vo-Dinh T. 139  
 von Wandruszka R. 221
- Wagemann R. 545  
 Wai C. M. 183
- Wakida S. 326  
 Walash M. I. 320, 731, 895  
 Walt D. R. 109  
 Walters B. S. 151  
 Wang E. 673  
 Wang G. 479  
 Wang J. 277, 965  
 Wang Y. 819  
 Wartel M. 205  
 Watanuki K. 847  
 Welti N. A. 157  
 Westland A. D. 1  
 Williams D. R. 825  
 Winefordner J. D. 41, 221, 267, 519, 647  
 Wolfbeis O. S. 89  
 Woods M. 605  
 Wu L. 479  
 Wyttenbach A. 747
- Xu B.-X. 891
- Yamane M. 326  
 Yan R. 479  
 Yáñez-Sedeño P. 601  
 Yoshida K. 837  
 Yu R.-Q. 707  
 Yurow H. W. 923  
 Yusuf M. 496
- Zaki M. T. M. 253  
 Zancato M. 664  
 Zapardiel A. 287  
 Zhao G. 479  
 Zikolova T. 899